ISSN 1007-9327 (print)
ISSN 2219-2840 (online)

World Journal of *Gastroenterology*

World J Gastroenterol 2023 September 7; 29(33): 4920-5019



Published by Baishideng Publishing Group Inc

World Journal of Gastroenterology

Contents

Weekly Volume 29 Number 33 September 7, 2023

OPINION REVIEW

4920 Very early onset perinatal constipation: Can it be cow's milk protein allergy?

Arakoni R, Kamal H, Cheng SX

REVIEW

4927 Non-coding RNAs: The potential biomarker or therapeutic target in hepatic ischemia-reperfusion injury

Shao JL, Wang LJ, Xiao J, Yang JF

4942 Prevention and management of hepatitis B virus reactivation in patients with hematological malignancies in the targeted therapy era

Mak JWY, Law AWH, Law KWT, Ho R, Cheung CKM, Law MF

4962 Direct oral anticoagulants for the treatment of splanchnic vein thrombosis: A state of art

Monaco G, Bucherini L, Stefanini B, Piscaglia F, Foschi FG, Ielasi L

ORIGINAL ARTICLE

Basic Study

4975 Angiotensin-converting enzyme 2 improves liver fibrosis in mice by regulating autophagy of hepatic stellate cells

Wu Y, Yin AH, Sun JT, Xu WH, Zhang CQ

4991 Diabetes exacerbates inflammatory bowel disease in mice with diet-induced obesity

Francis KL, Alonge KM, Pacheco MC, Hu SJ, Krutzsch CA, Morton GJ, Schwartz MW, Scarlett JM

5005 Novel deformable self-assembled magnetic anastomosis ring for endoscopic treatment of colonic stenosis *via* natural orifice

Zhang MM, Zhao GB, Zhang HZ, Xu SQ, Shi AH, Mao JQ, Gai JC, Zhang YH, Ma J, Li Y, Lyu Y, Yan XP

CASE REPORT

5014 Carcinoid syndrome caused by a pulmonary carcinoid mimics intestinal manifestations of ulcerative colitis: A case report

Reyes CM, Klein H, Stögbauer F, Einwächter H, Boxberg M, Schirren M, Safi S, Hoffmann H

World Journal of Gastroenterology

Weekly Volume 29 Number 33 September 7, 2023

Contents

ABOUT COVER

Editorial Board Member of *World Journal of Gastroenterology*, Luca Mastracci, MD, Full Professor, Department of Surgical Sciences and Integrated Diagnostics, University of Genoa and Ospedale Policlinico San Martino, Genoa 16132, Italy. luca.mastracci@unige.it

AIMS AND SCOPE

The primary aim of *World Journal of Gastroenterology* (*WJG*, *World J Gastroenterol*) is to provide scholars and readers from various fields of gastroenterology and hepatology with a platform to publish high-quality basic and clinical research articles and communicate their research findings online. *WJG* mainly publishes articles reporting research results and findings obtained in the field of gastroenterology and hepatology and covering a wide range of topics including gastroenterology, hepatology, gastrointestinal endoscopy, gastrointestinal surgery, gastrointestinal oncology, and pediatric gastroenterology.

INDEXING/ABSTRACTING

The *WJG* is now abstracted and indexed in Science Citation Index Expanded (SCIE, also known as SciSearch®), Current Contents/Clinical Medicine, Journal Citation Reports, Index Medicus, MEDLINE, PubMed, PubMed Central, Scopus, Reference Citation Analysis, China Science and Technology Journal Database, and Superstar Journals Database. The 2023 edition of Journal Citation Reports® cites the 2022 impact factor (IF) for *WJG* as 4.3; Quartile category: Q2. The *WJG*'s CiteScore for 2021 is 8.3.

RESPONSIBLE EDITORS FOR THIS ISSUE

Production Editor: *Hua-Ge Yu*; **Production Department Director:** *Xiang Li*; **Editorial Office Director:** *Jia-Ru Fan.*

NAME OF JOURNAL
World Journal of Gastroenterology

ISSN
ISSN 1007-9327 (print) ISSN 2219-2840 (online)

LAUNCH DATE
October 1, 1995

FREQUENCY
Weekly

EDITORS-IN-CHIEF
Andrzej S Tarnawski

EXECUTIVE ASSOCIATE EDITORS-IN-CHIEF
Xian-Jun Yu (Pancreatic Oncology), Jian-Gao Fan (Chronic Liver Disease)

EDITORIAL BOARD MEMBERS
http://www.wjgnet.com/1007-9327/editorialboard.htm

PUBLICATION DATE
September 7, 2023

COPYRIGHT
© 2023 Baishideng Publishing Group Inc

PUBLISHING PARTNER
Pancreatic Cancer Institute, Fudan University

INSTRUCTIONS TO AUTHORS
https://www.wjgnet.com/bpg/gerinfo/204

GUIDELINES FOR ETHICS DOCUMENTS
https://www.wjgnet.com/bpg/GerInfo/287

GUIDELINES FOR NON-NATIVE SPEAKERS OF ENGLISH
https://www.wjgnet.com/bpg/gerinfo/240

PUBLICATION ETHICS
https://www.wjgnet.com/bpg/GerInfo/288

PUBLICATION MISCONDUCT
https://www.wjgnet.com/bpg/gerinfo/208

POLICY OF CO-AUTHORS
https://www.wjgnet.com/bpg/GerInfo/310

ARTICLE PROCESSING CHARGE
https://www.wjgnet.com/bpg/gerinfo/242

STEPS FOR SUBMITTING MANUSCRIPTS
https://www.wjgnet.com/bpg/GerInfo/239

ONLINE SUBMISSION
https://www.f6publishing.com

PUBLISHING PARTNER's OFFICIAL WEBSITE
https://www.shca.org.cn/

© 2023 Baishideng Publishing Group Inc. All rights reserved. 7041 Koll Center Parkway, Suite 160, Pleasanton, CA 94566, USA
E-mail: bpgoffice@wjgnet.com https://www.wjgnet.com

World Journal of Gastroenterology

Submit a Manuscript: https://www.f6publishing.com

World J Gastroenterol 2023 September 7; 29(33): 4920-4926

DOI: 10.3748/wjg.v29.i33.4920

ISSN 1007-9327 (print) ISSN 2219-2840 (online)

OPINION REVIEW

Very early onset perinatal constipation: Can it be cow's milk protein allergy?

Rajalakshmy Arakoni, Hebat Kamal, Sam Xianjun Cheng

Specialty type: Gastroenterology and hepatology

Provenance and peer review: Invited article; Externally peer reviewed.

Peer-review model: Single blind

Peer-review report's scientific quality classification

Grade A (Excellent): 0
Grade B (Very good): B
Grade C (Good): C
Grade D (Fair): 0
Grade E (Poor): 0

P-Reviewer: Tang ST, China; Torres MRF, Brazil

Received: April 10, 2023
Peer-review started: April 10, 2023
First decision: June 17, 2023
Revised: July 21, 2023
Accepted: August 15, 2023
Article in press: August 15, 2023
Published online: September 7, 2023

Rajalakshmy Arakoni, Department of Pediatrics, University of Florida Shands Children's Hospital, Gainesville, FL 32608, United States

Hebat Kamal, Sam Xianjun Cheng, Department of Pediatric Gastroenterology, Hepatology, and Nutrition, University of Florida Shands Children's Hospital, Gainesville, FL 32608, United States

Corresponding author: Sam Xianjun Cheng, MD, MSc, PhD, Attending Doctor, Department of Pediatric Gastroenterology, Hepatology, and Nutrition, University of Florida Shands Children's Hospital, 1600 SW Archer Rd, HD 606, Gainesville, FL 32608, United States.
sam.cheng@ufl.edu

Abstract

Delayed passage of meconium or constipation during the perinatal period is traditionally regarded as a signal to initiate further work up to evaluate for serious diagnoses such as Hirschsprung's disease (HD), meconium ileus due to Cystic Fibrosis, *etc.* The diagnosis of HD particularly warrants invasive testing to confirm the diagnosis, such as anorectal manometry or rectal suction biopsy. What if there was another etiology of perinatal constipation, that is far lesser known? Cow's milk protein allergy (CMPA) is often diagnosed in infants within the first few weeks of life, however, there are studies that show that the CMPA allergen can be passed from mother to an infant in-utero, therefore allowing symptoms to show as early as day one of life. The presentation is more atypical, with perinatal constipation rather than with bloody stools, diarrhea, and vomiting. The diagnosis and management would be avoidance of cow's milk protein within the diet, with results and symptom improvement in patients immediately. Therefore, we discuss whether an alternative pathway to address perinatal constipation should be further discussed and implemented to potentially avoid invasive techniques in patients. This entails first ruling out CMPA with safe, noninvasive techniques with diet modification, and if unsuccessful, then moving forward with further diagnostic modalities.

Key Words: Delayed passage of meconium; Perinatal constipation; Cow's milk protein allergy; In-utero; Alternate pathway; Hirschsprung's disease

©The Author(s) 2023. Published by Baishideng Publishing Group Inc. All rights reserved.

Core Tip: Cow's milk protein allergy (CMPA) is a far lesser known cause of perinatal constipation compared to more frequently considered diagnoses such as Hirschsprung's, Cystic fibrosis related meconium ileus, *etc.* The presentation during the perinatal period is considered atypical caused by a non-immunoglobulin E (IgE) mechanism as opposed to the typical presentation caused by an IgE-mediated mechanism. The likelihood of CMPA is significant in the perinatal period, therefore should be considered more often. Here we discuss an alternative pathway for the workup of perinatal constipation focusing on CMPA as an etiology. The use of this pathway can avoid invasive tests among patients.

Citation: Arakoni R, Kamal H, Cheng SX. Very early onset perinatal constipation: Can it be cow's milk protein allergy? *World J Gastroenterol* 2023; 29(33): 4920-4926
URL: https://www.wjgnet.com/1007-9327/full/v29/i33/4920.htm
DOI: https://dx.doi.org/10.3748/wjg.v29.i33.4920

INTRODUCTION

Delayed passage of meconium or constipation is defined as failure to pass stool within the first 48 h after birth[1]. With a positive history of delayed meconium passage, providers traditionally regard this as a signal towards serious diagnoses such as Hirschsprung's disease (HD), meconium ileus (MI) due to cystic fibrosis (CF), or intestinal obstruction, and initiate work up such as barium enema, anorectal manometry, and or rectal suction biopsy per current recommendations [2]. We rarely consider cow's milk protein allergy (CMPA), even though it has been described to occur in the perinatal period[3,4] and causes disease that mimics HD[5-8]. Since there's still no available diagnostic laboratory tests, the diagnosis of CMPA has to be clinical. We recently reported 3 cases of infants who had delayed passage of meconium with subsequent early-onset perinatal constipation that did not respond to conventional therapies and required rectal stimulation to defecate. The symptoms resolved when the milk protein component was withheld and recurred when milk proteins were reintroduced for the patients. The symptoms subsequently resolved again when switched to an extensively hydrolyzed or amino acid-based formula[9]. Thus, it had not only avoided more aggressive and invasive workup, but had also significantly improved the care of this very vulnerable young patient population. Unfortunately, per our recent survey, this early-onset atypical perinatal form of CMPA was rarely recognized by a large majority of care providers including gastroenterologists, contrasting the typical form of CMPA that occurs later in life. This is not surprising; it indicates that more presentations of this condition to gastroenterology communities are necessary. In fact, even for its typical, more known counterpart of CMPA, it has taken approximately 20 years of time before it became widely recognized by providers. CMPA was rarely diagnosed before 1950, but since 1970 the condition has been further documented[10]. This paper will discuss 4 burning questions regarding the atypical CMPA, typical CMPA, and HD.

WHAT IS THE PREVALENCE OF HD *VS.* CMPA IN INFANTS WITH CONSTIPATION?

A number of conditions can cause delayed passage of meconium or early-onset perinatal constipation. This includes HD, intestinal obstruction, MI, meconium plug syndrome, functional ileus, small left colon, drug effect, hypothyroidism, and megacystis-microcolon-intestinal hypoperistalsis syndrome[2]. However, these conditions might be much less common than we think when thinking about perinatal constipation. For example, a study conducted in 2008 looked at causes of meconium plug syndrome (radiological form of perinatal constipation) in the largest cohort of a patient population to that date, which actually indicated that only about 13% were due to HD, and none were caused by CF[11]. Table 1 below summarizes the incidences in pubmed of HD, meconium plug syndrome, MI, anorectal malformation, and CMPA in infants, whereas Table 2 lists the frequencies of HD relative to CMPA. As shown, the incidences of these congenital diagnoses are extremely low, less than 0.1%[2] for all four diagnoses individually, in contrast to CMPA, which is estimated to occur in 0.5%-17%[10,12]. Thus, it is possible that the majority of the cases of perinatal constipation are not caused by HD or other congenital etiologies, but by acquired CMPA. In accordance with this, we recently observed 25 neonates/young infants referred to our clinic for intractable perinatal constipation and found 23 responded to cow's milk protein (CMP) avoidance, suggesting that this very early onset constipation is largely related to CMPA, specifically the atypical CMPA.

WHAT IS ATYPICAL CMPA AND HOW DOES IT DIFFER FROM TYPICAL CMPA?

CMPA is an abnormal immunological response to CMP. According to time of onset, CMPA can be categorized into two forms: Atypical form that occurs early in life before, during, or shortly after birth, and typical form that commonly happens later in life, typically weeks or months after birth. Table 3 compares their differences in clinical presentation, way of allergen transmission, type of allergy reaction, and intestinal tissue and brief mechanism involved as well as their diagnosis, management, and relative awareness. The development of CMPA requires exposure followed by an immunological response to the milk allergen, which can take up to months to occur. Therefore, CMPA has been thought to most

Table 1 Incidences of various diagnoses in infants with very early-onset constipation

Diagnosis	Incidence	Ref.
Hirschsprung's disease	0.025%	Loening-Baucke and Kimura[2]
Meconium plug syndrome	0.1%-0.2	Loening-Baucke and Kimura[2]
Meconium ileus	0.04	Loening-Baucke and Kimura[2]
Anorectal malformation	0.025%-0.05%	Loening-Baucke and Kimura[2]
CMPA	0.5%-17%	Høst[10], Rona *et al*[12]

CMPA: Cow's milk protein allergy.

Table 2 Relative frequencies of Hirschsprung's disease *vs* cow's milk protein allergy in infants with very early-onset constipation

Ref.	HD (%)	CMPA (%)
Burge and Drewett[18]	38.1	
Kubota *et al*[19]	34.6	65.4
Van Leeuwen *et al*[20]	25.0	
Keckler *et al*[11]	13.0	
Cheng *et al* (unpublished observation)	8.0	92.0

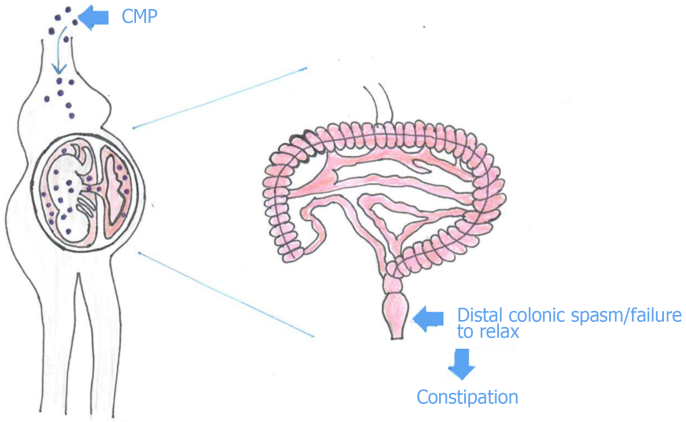
CMPA: Cow's milk protein allergy; HD: Hirschsprung's disease.

Table 3 Comparison of atypical *vs* typical cow's milk protein allergy

	Atypical CMPA	Typical CMPA
Time of onset	Perinatal period[3]	Early infancy[21,22]
Way of transmission of allergen	Vertically *via* placenta and amniotic fluid[3]	Vertically *via* breast feeding Horizontally by oral ingestion[21,22]
Typical presentation	Intractable constipation[5,6]	Vomiting and diarrhea, bloody stools[21]
Type of allergy reaction	Non IgE mediated[5]	IgE mediated[5]
Tissues involved	Enteric neurons and smooth muscle[5-8]	Intestinal mucosa[5]
Mechanism involved	Immune mediated neuromuscular dysfunction leading to persistent spasm or failure to relax of the anorectum (HD like changes)[5-8]	Allergic enterocolitis[5]
Diagnosis	CMP avoidance and challenge. Both blood and skin allergy testings are of no diagnostic value[9]	CMP avoidance and challenge with or without blood and skin allergy testing[21]
Treatment	CMP avoidance[9]	CMP avoidance[9]
Awareness to providers	Rarely aware/reported	Well known/reported

CMP: cow's milk protein; CMPA: cow's milk protein allergy; HD: Hirschsprung's disease; IgE: Immunoglobulin E.

commonly occur within weeks or months after their first postnatal feed. However, cow's milk allergens are not only transported postnatally *via* the oral route; they can also pass through the placenta and amniotic fluid to sensitize fetuses and cause allergy[3-4]. This indicates that the process of developing CMPA can occur prenatally. To support this, there are studies that show α-lactalbumin, -lactoglobulin, and α-casein were found in full-term neonates, which are indications of responses of cord blood lymphocytes to cow's milk allergen[3,13]. Figure 1 demonstrates the passage of CMP from maternal ingestion through the placenta, affecting the infant in-utero, eventually leading to perinatal constipation. The typical, late-onset form of CMPA is now well known to care providers, however the early-onset form is often overlooked, particularly when this type of CMPA presents with atypical symptoms. Most pediatricians including pediatric gastroenterologists are not aware of the early-onset CMPA. As a result, many atypical cases of neonate infants CMPA were



DOI: 10.3748/wjg.v29.i33.4920 **Copyright** ©The Author(s) 2023.

Figure 1 How cow's milk protein allergen from maternal diet passes into the fetus causing distal colon spasm or failure to relax leading to Hirschsprung's disease-like constipation. As mentioned in the text, the suspected mechanism involves neuromodulation of the enteric nervous system, with increased anal pressure at rest. CMP: Cow's milk protein.

missed, leaving them undiagnosed or misdiagnosed. This resulted in delay of initiating the appropriate treatment for this very treatable condition or led to many unnecessary workup procedures.

WHAT IS THE MECHANISM BY WHICH CMPA CAUSES PERINATAL CONSTIPATION?

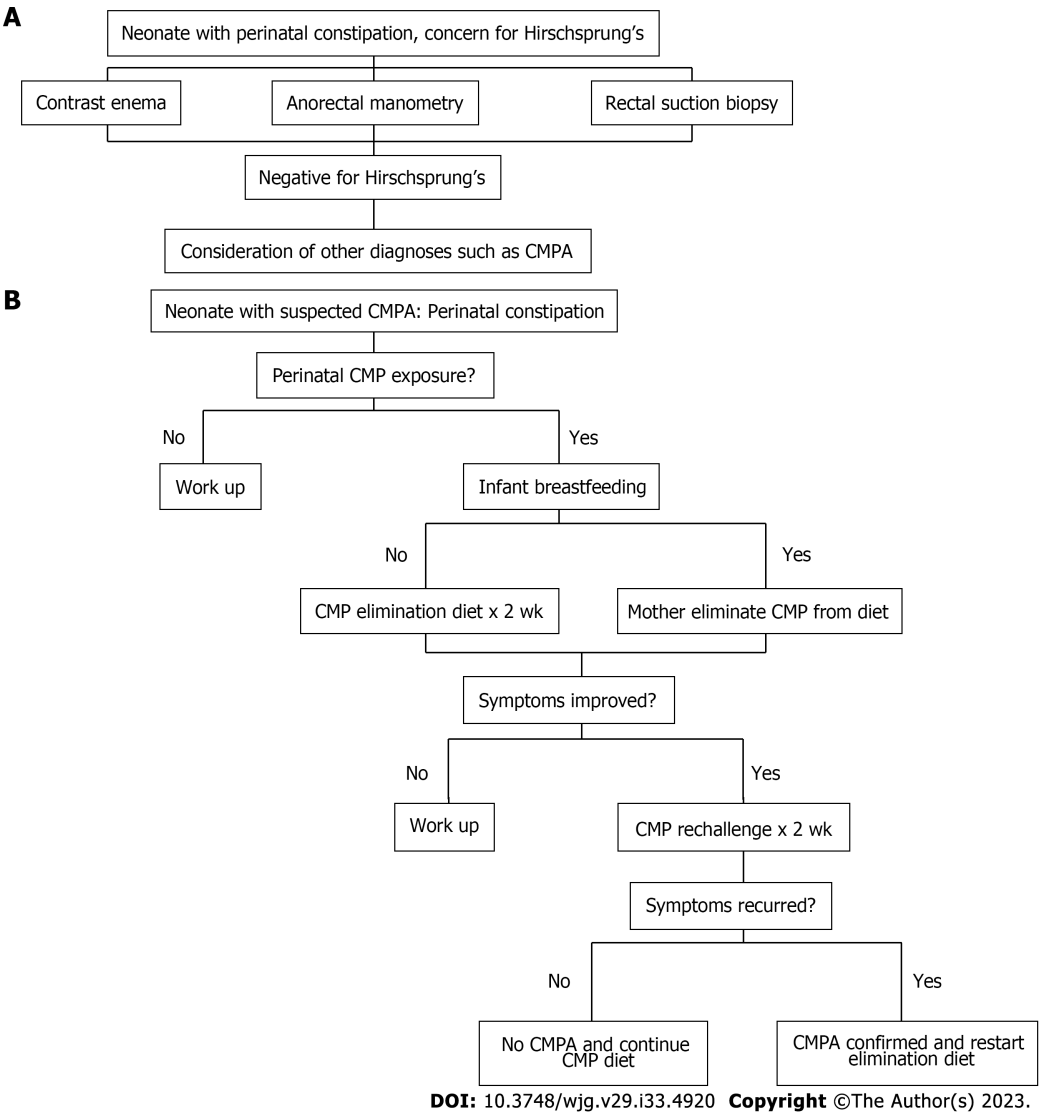
The exact mechanism by which CMPA causes perinatal constipation has remained incompletely understood. CMP can cause constipation in at least two ways: Nonspecifically through CMP constipating effect and specifically through CMPA. CMPA, rather than CMP constipation, is considered a more probable etiology for perinatal constipation, because for the CMP constipation to occur, patients will require a prolonged consumption of the CMP and this is unlikely to occur in this neonatal patient population, during the perinatal period. Then, how does CMPA lead to perinatal constipation? CMPA occurs by two primary mechanisms: an immunoglobulin E (IgE)-mediated immediate hypersensitivity reaction and a non-IgE-mediated delayed hypersensitivity reaction[9]. As shown in Table 3, the former is primarily seen in the typical CMPA, while the latter is speculated to cause the atypical CMPA. The IgE-mediated reaction is described as IgE antibodies that are secreted in response to the allergen and bind to the surface of mast cells and basophils, causing subsequent release of histamine and inflammatory mediators, leading to eosinophilia, allergic colitis and proctitis, and bloody/mucousy stools[5]. The non-IgE mediated reaction is not as well-known as compared to the IgE-mediated reaction, but hypotheses include milk antigens binding to immune complexes of immunoglobulin A or immunoglobulin G or directly binding and stimulating T cells, resulting in activation of an inflammatory cascade[14] that involves neuromodulation of the enteric nervous system[15], leading to alteration of the function of smooth muscle and intestinal motility that is functionally similar to that of HD[5], with increased anal pressure at rest[16] causing difficulties in stooling. As illustrated in one of our cases[9], early-onset constipation had normal appearing colorectal histology, with no evidence of lamina propria/muscularis mucosa eosinophilia nor increased mast cell infiltration, therefore the etiology of the perinatal constipation is likely not the IgE-mediated but more consistent with the non-IgE mediated mechanism. Also, all of our observed cases mentioned in the previous case series[9] and subsequent new cases did not respond to stool softeners but required rectal stimulation/rectal insertion for bowel movement, suggesting that the mechanism of constipation is likely not simply related to the hardness of the stool but the dysmotility of the muscle of the distal colon, either due to distal colon spasm or failure to relax (Figure 1).

WHAT IS THE BEST MANAGEMENT ALGORITHM FOR CARE PROVIDERS TO DIFFERENTIATE ATYPICAL CMPA FROM HD IN PATIENTS WITH PERINATAL CONSTIPATION?

How to effectively diagnose the infants with acquired condition from the infants with congenital disease as in HD and other anatomical obstructions without extensive testing remains clinically challenging.

Current guidelines recommend a moderate level of suspicion for HD, although practice varies regarding the evaluation of these infants. At a minimum, they should be closely observed and evaluated promptly for HD if they develop symptoms of constipation even though a great majority of those patients are not due to HD[2]. We designate this management algorithm the "top-down" approach (Figure 2A).

Our practice has adopted a new management guideline in managing these patients[9] given that CMPA rather than HD causes most of these presentations. The new guideline has recommended performing a 2-week trial of CMP avoidance as the initial diagnostic procedure before performing a contrast enema, anorectal manometry, and or suction biopsy. We designate this new management algorithm the "bottom-up" approach (Figure 2B).



DOI: 10.3748/wjg.v29.i33.4920 **Copyright** ©The Author(s) 2023.

Figure 2 Two algorithms for clinical management of patients with intractable early onset perinatal constipation. A: Top-down approach and current guideline for management of perinatal constipation. B: Bottom-up approach; new guideline to consider which suspects cow's milk protein allergy as a diagnosis. CMP: Cow's milk protein; CMPA: Cow's milk protein allergy.

The top-down approach relies on highly sophisticated investigations (*i.e.*, contrast enema, anorectal manometry or suction biopsy) to first rule out HD, which are rare and expensive; whereas the bottom-up protocol uses relatively simple food elimination diet to first rule in CMPA before rare entities are considered, which is common and inexpensive. With this new approach, we have promptly identified and successfully treated CMPA in 23 of 25 infants with intractable early-onset constipation without the need to go to any of the invasive testings (Cheng *et al*, unpublished observation). Thus, if this is validated by other clinical centers or practices, the new recommendation would largely help avert many unnecessary investigations, which are not only costly but are also invasive and expose patients to various potential complications.

CONCLUSION

Further understanding of the mechanism of CMPA makes it clear that infants can present with the manifestations immediately after birth. Therefore, shouldn't we consider CMPA in our patients who present with perinatal constipation early on? There is no doubt that the serious diagnoses such as HD and CF related MI cannot be missed, however, if there is a way to eliminate invasive tests, we should, as providers, incorporate it into our medical practice. There are many unanswered questions that have yet to be further studied. For example, in our studies, all the mothers of patients with perinatal constipation consumed dairy products during pregnancy, however, this does not mean all mothers who consume dairy products during pregnancy will necessarily give birth to infants who will develop CMPA or symptoms of perinatal constipation. What factor(s) determines who develops and who does not develop sensitization and allergy remains unclear. Also unclear is the factor(s) that determines the type of CMPA, typical *vs* atypical. Similarly, although

we know CMP allergens can pass the placenta and amniotic fluid to sensitize fetuses and cause allergy, we still do not know how long this sensitization process lasts and how long the allergens remain effective. The fact that our patients' symptoms resolved following the 2-week elimination period of the allergen, however, seems to suggest that this could approximate the timeline of allergen effectiveness. Also, the overall prognosis of typical CMPA is good, with a total recovery of 56% at 1 year, 77% at 2 years, 87% at 3 years, 92% at 5 and 10 years and 97% at 15 years of age[17]. Whether this applies to atypical CMPA in the perinatal population requires further investigation. Regardless of what the type of CMPA is, our recommendation for treatment of CMPA is the same, that is, once a diagnosis of CMPA is confirmed, a milk-free diet will be continued until a new milk challenge has shown development of tolerance. All infants with CMPA will be rechallenged at 12 mo of age and, in the event of continued clinical sensitivity to CMP, controlled rechallenges will be performed every 6 mo up to 3 years of age; and thereafter every 12 mo until tolerance develops.

ACKNOWLEDGEMENTS

We thank Joseph Neu, MD, for discussions of the objectives of this manuscript and the feedback in regards to the alternative pathway when addressing delayed passage of meconium in the neonatal population. The artwork in Figure 1 is an original drawing by Alamelu Arakoni, B.Tech.

FOOTNOTES

Author contributions: Cheng SX conceived the idea for the manuscript; Arakoni R and Cheng SX reviewed the literature and drafted the manuscript; Kamal H edited the manuscripts.

Conflict-of-interest statement: The authors declare no conflicts of interest.

Open-Access: This article is an open-access article that was selected by an in-house editor and fully peer-reviewed by external reviewers. It is distributed in accordance with the Creative Commons Attribution NonCommercial (CC BY-NC 4.0) license, which permits others to distribute, remix, adapt, build upon this work non-commercially, and license their derivative works on different terms, provided the original work is properly cited and the use is non-commercial. See: https://creativecommons.org/Licenses/by-nc/4.0/

Country/Territory of origin: United States

ORCID number: Rajalakshmy Arakoni 0009-0008-9222-201X; Sam Xianjun Cheng 0000-0003-0252-9357.

S-Editor: Lin C
L-Editor: A
P-Editor: Cai YX

REFERENCES

1 **Clark DA**. Times of first void and first stool in 500 newborns. *Pediatrics* 1977; **60**: 457-459 [PMID: 905009]
2 **Loening-Baucke V**, Kimura K. Failure to pass meconium: diagnosing neonatal intestinal obstruction. *Am Fam Physician* 1999; **60**: 2043-2050 [PMID: 10569507]
3 **Szépfalusi Z**, Nentwich I, Gerstmayr M, Jost E, Todoran L, Gratzl R, Herkner K, Urbanek R. Prenatal allergen contact with milk proteins. *Clin Exp Allergy* 1997; **27**: 28-35 [PMID: 9117877]
4 **Feiterna-Sperling C**, Rammes S, Kewitz G, Versmold H, Niggemann B. A case of cow's milk allergy in the neonatal period--evidence for intrauterine sensitization? *Pediatr Allergy Immunol* 1997; **8**: 153-155 [PMID: 9532257 DOI: 10.1111/j.1399-3038.1997.tb00170.x]
5 **Vitaliti G**, Cimino C, Coco A, Praticò AD, Lionetti E. The immunopathogenesis of cow's milk protein allergy (CMPA). *Ital J Pediatr* 2012; **38**: 35 [PMID: 22824011 DOI: 10.1186/1824-7288-38-35]
6 **Carroccio A**, Iacono G. Review article: Chronic constipation and food hypersensitivity--an intriguing relationship. *Aliment Pharmacol Ther* 2006; **24**: 1295-1304 [PMID: 17059511 DOI: 10.1111/j.1365-2036.2006.03125.x]
7 **Bloom DA**, Buonomo C, Fishman SJ, Furuta G, Nurko S. Allergic colitis: a mimic of Hirschsprung disease. *Pediatr Radiol* 1999; **29**: 37-41 [PMID: 9880614 DOI: 10.1007/s002470050530]
8 **Iacono G**, Bonventre S, Scalici C, Maresi E, Di Prima L, Soresi M, Di Gesù G, Noto D, Carroccio A. Food intolerance and chronic constipation: manometry and histology study. *Eur J Gastroenterol Hepatol* 2006; **18**: 143-150 [PMID: 16394795 DOI: 10.1097/00042737-200602000-00006]
9 **Madala A**, Lure AC, Cheng S, Cheng SX. Case Reports of Cow's Milk Protein Allergy Presenting as Delayed Passage of Meconium With Early Onset Infant Constipation. *Front Pediatr* 2022; **10**: 858476 [PMID: 35498816 DOI: 10.3389/fped.2022.858476]
10 **Høst A**. Cow's milk protein allergy and intolerance in infancy. Some clinical, epidemiological and immunological aspects. *Pediatr Allergy Immunol* 1994; **5**: 1-36 [PMID: 7704117]
11 **Keckler SJ**, St Peter SD, Spilde TL, Tsao K, Ostlie DJ, Holcomb GW 3rd, Snyder CL. Current significance of meconium plug syndrome. *J Pediatr Surg* 2008; **43**: 896-898 [PMID: 18485962 DOI: 10.1016/j.jpedsurg.2007.12.035]
12 **Rona RJ**, Keil T, Summers C, Gislason D, Zuidmeer L, Sodergren E, Sigurdardottir ST, Lindner T, Goldhahn K, Dahlstrom J, McBride D,

Madsen C. The prevalence of food allergy: a meta-analysis. *J Allergy Clin Immunol* 2007; **120**: 638-646 [PMID: 17628647 DOI: 10.1016/j.jaci.2007.05.026]

13 **Kondo N**, Kobayashi Y, Shinoda S, Kasahara K, Kameyama T, Iwasa S, Orii T. Cord blood lymphocyte responses to food antigens for the prediction of allergic disorders. *Arch Dis Child* 1992; **67**: 1003-1007 [PMID: 1520001 DOI: 10.1136/adc.67.8.1003]

14 **Brill H**. Approach to milk protein allergy in infants. *Can Fam Physician* 2008; **54**: 1258-1264 [PMID: 18791102]

15 **Undem BJ**, Taylor-Clark T. Mechanisms underlying the neuronal-based symptoms of allergy. *J Allergy Clin Immunol* 2014; **133**: 1521-1534 [PMID: 24433703 DOI: 10.1016/j.jaci.2013.11.027]

16 **Miceli Sopo S**, Arena R, Greco M, Bergamini M, Monaco S. Constipation and cow's milk allergy: a review of the literature. *Int Arch Allergy Immunol* 2014; **164**: 40-45 [PMID: 24853450 DOI: 10.1159/000362365]

17 **Høst A**, Halken S, Jacobsen HP, Christensen AE, Herskind AM, Plesner K. Clinical course of cow's milk protein allergy/intolerance and atopic diseases in childhood. *Pediatr Allergy Immunol* 2002; **13**: 23-28 [PMID: 12688620 DOI: 10.1034/j.1399-3038.13.s.15.7.x]

18 **Burge D**, Drewett M. Meconium plug obstruction. *Pediatr Surg Int* 2004; **20**: 108-110 [PMID: 14760494 DOI: 10.1007/s00383-003-1098-y]

19 **Kubota A**, Kawahara H, Okuyama H, Shimizu Y, Nakacho M, Ida S, Nakayama M, Okada A. Cow's milk protein allergy presenting with Hirschsprung's disease-mimicking symptoms. *J Pediatr Surg* 2006; **41**: 2056-2058 [PMID: 17161204 DOI: 10.1016/j.jpedsurg.2006.08.031]

20 **Van Leeuwen G**, Glenn L, Woodruff C, Riley WC. Meconium plug syndrome with aganglionosis. *Pediatrics* 1967; **40**: 665-666 [PMID: 6051066]

21 **Al-Beltagi M**, Saeed NK, Bediwy AS, Elbeltagi R. Cow's milk-induced gastrointestinal disorders: From infancy to adulthood. *World J Clin Pediatr* 2022; **11**: 437-454 [PMID: 36439902 DOI: 10.5409/wjcp.v11.i6.437]

22 **Martorell A**, Plaza AM, Boné J, Nevot S, García Ara MC, Echeverria L, Alonso E, Garde J, Vila B, Alvaro M, Tauler E, Hernando V, Fernández M. Cow's milk protein allergy. A multi-centre study: clinical and epidemiological aspects. *Allergol Immunopathol (Madr)* 2006; **34**: 46-53 [PMID: 16606545 DOI: 10.1157/13086746]

World Journal of Gastroenterology

Submit a Manuscript: https://www.f6publishing.com

World J Gastroenterol 2023 September 7; 29(33): 4927-4941

DOI: 10.3748/wjg.v29.i33.4927

ISSN 1007-9327 (print) ISSN 2219-2840 (online)

REVIEW

Non-coding RNAs: The potential biomarker or therapeutic target in hepatic ischemia-reperfusion injury

Jia-Li Shao, Li-Juan Wang, Ji Xiao, Jin-Feng Yang

Specialty type: Gastroenterology and hepatology

Provenance and peer review: Invited article; Externally peer reviewed.

Peer-review model: Single blind

Peer-review report's scientific quality classification

Grade A (Excellent): 0
Grade B (Very good): B, B
Grade C (Good): 0
Grade D (Fair): 0
Grade E (Poor): 0

P-Reviewer: Joshi MK, India; Katada K, Japan

Received: May 6, 2023
Peer-review started: May 6, 2023
First decision: July 9, 2023
Revised: July 22, 2023
Accepted: August 18, 2023
Article in press: August 18, 2023
Published online: September 7, 2023

Jia-Li Shao, Li-Juan Wang, Ji Xiao, Jin-Feng Yang, Department of Anesthesiology, The Affiliated Cancer Hospital of Xiangya School of Medicine, Central South University, Changsha 410013, Hunan Province, China

Corresponding author: Jin-Feng Yang, MD, PhD, Chief Physician, Director, Doctor, Professor, Department of Anesthesiology, The Affiliated Cancer Hospital of Xiangya School of Medicine, Central South University, No. 283 Tongzipo, Yuelu District, Changsha 410013, Hunan Province, China. yangjinfeng@hnca.org.cn

Abstract

Hepatic ischemia-reperfusion injury (HIRI) is the major complication of liver surgery and liver transplantation, that may increase the postoperative morbidity, mortality, tumor progression, and metastasis. The underlying mechanisms have been extensively investigated in recent years. Among these, oxidative stress, inflammatory responses, immunoreactions, and cell death are the most studied. Non-coding RNAs (ncRNAs) are defined as the RNAs that do not encode proteins, but can regulate gene expressions. In recent years, ncRNAs have emerged as research hotspots for various diseases. During the progression of HIRI, ncRNAs are differentially expressed, while these dysregulations of ncRNAs, in turn, have been verified to be related to the above pathological processes involved in HIRI. ncRNAs mainly contain microRNAs, long ncRNAs, and circular RNAs, some of which have been reported as biomarkers for early diagnosis or assessment of liver damage severity, and as therapeutic targets to attenuate HIRI. Here, we briefly summarize the common pathophysiology of HIRI, describe the current knowledge of ncRNAs involved in HIRI in animal and human studies, and discuss the potential of ncRNA-targeted therapeutic strategies. Given the scarcity of clinical trials, there is still a long way to go from pre-clinical to clinical application, and further studies are needed to uncover their potential as therapeutic targets.

Key Words: Hepatic ischemia-reperfusion injury; Non-coding RNAs; MicroRNAs; Long non-coding RNAs; Circular RNAs

©The Author(s) 2023. Published by Baishideng Publishing Group Inc. All rights reserved.

Core Tip: This review focuses on the recent progress in understanding non-coding RNAs (ncRNAs) in hepatic ischemia-reperfusion injury (HIRI). HIRI can alter ncRNAs expressions, which in turn modulates the pathophysiological processes that contribute to the development of HIRI. Differentially expressed ncRNAs from different sources (the liver tissues, serums and cells) are involved in oxidative stress, inflammatory responses, cell death and so on. ncRNAs are regarded as biomarkers for the diagnosis and assessment of liver damage severity, or as therapeutic targets for HIRI; however, their clinical transformation will still take a long time.

Citation: Shao JL, Wang LJ, Xiao J, Yang JF. Non-coding RNAs: The potential biomarker or therapeutic target in hepatic ischemia-reperfusion injury. *World J Gastroenterol* 2023; 29(33): 4927-4941
URL: https://www.wjgnet.com/1007-9327/full/v29/i33/4927.htm
DOI: https://dx.doi.org/10.3748/wjg.v29.i33.4927

INTRODUCTION

Hepatic ischemia-reperfusion injury (HIRI) is a common clinical issue that occurs during major liver resection, liver transplantation, and liver trauma[1-3]. HIRI usually causes liver injury, early transplantation failure, liver failure and even multiple-organ failure. Although existing studies have shown that several signaling pathways, such as oxidative stress, inflammatory response, and cell death, participate in the pathological process of HIRI[4-6], current treatments and pharmacological approaches cannot completely address this problem. Therefore, much more new molecules need to be explored for the diagnosis and treatment of HIRI.

Non-coding RNAs (ncRNAs) are a cluster of functional RNAs that cannot encode protein[7,8]. In recent years, ncRNAs have become a hot area of research and have been reported to play a significant role in various diseases, including cancers, nervous system diseases, and ischemia/reperfusion injuries[9-11]. ncRNAs mainly consist of microRNAs (miRNAs), long ncRNAs (lncRNAs), and circular RNAs (circRNAs), which have been shown to modulate genes expression, and participate in many critical biological processes at different levels (*e.g.* immune responses, oxidative stress reactions, apoptosis, autophagy, and energy metabolism)[12-14]. The role of ncRNAs in HIRI is explored in a few studies, and has attracted the attention of many researchers.

ncRNAs are regarded as potential biomarkers or therapeutic targets for assessing or attenuating HIRI development. As the present studies are mainly in the preclinical stage, and clinical investigations are lacking, there are still large research prospects for the diagnosis, prevention, and treatment of HIRI. This review briefly illustrates the well-studied molecular mechanisms of HIRI and summarizes the relevant ncRNAs and their roles in the pathological process of HIRI to provide a reference for further research.

HIRI AND THE UNDERLYING MECHANISMS

HIRI is usually classified into two types, warm IRI *in situ* and cold IRI *in vitro*, and the cells involved are different. Warm IRI is characterized by hepatocellular injury, which is mainly caused by Kupffer cells (KCs) induced oxidative stress and neutrophils recruitment[15]. Cold IRI is associated with sinusoidal endothelial cells (SECs) damage[11]. Although the initial cells are different, they do share common subsequent reactions: activation of cell death programs such as apoptosis, necrosis, pyroptosis, and autophagy, thus contributing to the development of inflammation[1,16-18].

The mechanisms involved in HIRI pathogenesis are multifactorial and complex. Numerous studies have demonstrated several molecular mechanisms that contribute to the development of HIRI[19], such as anaerobic metabolism, immune response[20], microcirculatory dysfunction[21], and gene transcription[6,21].

Oxidative stress

The most widely studied mechanism is oxidative stress, which is defined as an imbalance between the oxidant and antioxidant systems, resulting in tissue damages[22,23]. For instance, CeO2, NO, and chlorogenic acid have a liver-protective effect by reducing oxidative stress during HIRI[20,24,25]. In contrast, Han *et al*[26] found that hyperglycemia aggravates HIRI by inducing reactive oxygen species (ROS) mediated oxidative stress. ROS are the most critical reactive molecules involved in HIRI. Enormous amounts of ROS are usually generated by mitochondria and KCs during reperfusion, which can result in apoptosis, autophagy, inflammation, protein and DNA damage, and worsened hepatocyte injury[5,22]. Prussian blue scavenger is a potential therapeutic agent for treating HIRI with ROS-scavenging and anti-inflammatory properties[27]. OX40 expression in neutrophils can increase ROS production, which in turn activates neutrophils and, aggravates HIRI[28]. Dugbartey *et al*[29] designed a reversible redox probe REPOM to monitor ROS during HIRI for early diagnosis and timely intervention. Furthermore, an increasing number of studies on gene therapy for oxidative stress have attracted the attention of researchers in recent years. Therefore, strategies that are aimed at inhibiting oxidative stress or scavenging ROS may alleviate HIRI, and novel antioxidant regulatory molecules are required.

Inflammatory response and immune response

The inflammatory response is another major mechanism underlying HIRI. During HIRI development, KCs and SECs are initially activated[30,31], and generate a range of inflammatory mediators including cytokines, such as PAF, TNFα, and interleukins (*e.g.*, IL-1, IL-6, IL-12, and IL-23), which could lead to the inflammatory response involved in HIRI development[32-34]. In addition, several cytokines (*e.g.*, PAF, leukotriene B4, IL-8, and IL-17) induce neutrophil accumulation, which plays a role in the process of HIRI[35]. Furthermore, activated neutrophils can form neutrophil extracellular traps (NETs) *via* TLR-dependent pathways, that initiate inflammatory responses during HIRI[36]. This local inflammatory state can cause a systemic inflammatory response, leading to systemic inflammatory response syndrome and even multiple-organ failures.

Both innate and adaptive immune responses play important roles in HIRI[37,38]. KCs can increase the production of damage-associated molecular patterns (DAMPs), such as ATP, histones, high mobility group box 1 (HMGB1), S100, and heat shock proteins, which are released into the circulation and induce cytokine/chemokine storms to attract neutrophils and other immune cells[39]. In contrast, DAMPs can bind to Toll-like receptors (TLRs) and drive immune responses. Targeting the DAMP pathways alleviates HIRI. For example, HMGB1/NLRP3 inflammasome inhibition attenuated HIRI [40]. In addition, the complement system serves as an important contributor to the process of HIRI[41-43]. Therefore, targeting inflammation-oriented therapies may alleviate HIRI.

Cell death

Cell death is a stable pathological indicator of I/R injury, including apoptosis, necrosis, autophagy, pyroptosis, and ferroptosis. Among them, apoptosis, necrosis, and autophagy are the most common types of cell death during HIRI and may share the same stimuli and signaling pathways[44]. For example, hydrogen sulfide (H_2S) effectively alleviates HIRI by attenuating hepatocyte apoptosis *via* inhibition of the endoplasmic reticulum (ER) stress response[22]. Eucommia ulmoides polysaccharide administration notably reduced the area of liver necrosis in a rat HIRI model[45]. Cafestol preconditioning can inhibit apoptosis and autophagy in hepatocytes, thus attenuating HIRI, by suppressing the extracelluar signal-regulated/eroxisome proliferator-activated receptor gamma (ERK/PPARγ) pathway[46]. Moreover, some studies suggest that mitochondrial autophagy is a key pathological mechanism underlying age-dependent hypersensitivity to HIRI[16]. In our previous studies, we found that octreotide pretreatment mitigated HIRI and attenuated kidney injury caused by HIRI by inhibiting hepatocellular apoptosis and enhancing autophagy[47-49]. These three processes usually coexist and participate in the development of HIRI.

The role of pyroptosis in HIRI remains unclear. Pyroptosis is a form of regulated cell death driven by perturbations in extracellular or intracellular homeostasis related to innate immunity. It is usually associated with IL-1β and IL-18 secretion and hence mediates robust pro-inflammatory effects[50]. Adipose-derived mesenchymal stem cells reduce pyroptosis in HIRI by inhibiting the NF-κB pathway and activating the Wnt/β-catenin pathway[51,52]. In the hepatic tissue of HIRI mice, lncRNA KCNQ1OT1 increased, which modulated miR-142a-3p/HMGB1, thereby promoting pyroptosis[15]. Under HIRI condition, IKZF1 increased, but sirtuin 1 (SIRT1) decreased in both human and mouse livers. Further investigation indicated that IKZF1 augmented pyroptosis through negatively regulating SIRT1 expression. Hence, pyroptosis plays an important role in the development of HIRI, and targeting pyroptosis is a promising approach for attenuating HIRI. However, the role of pyroptosis in HIRI requires further investigations.

In addition to the common types of cell death, ferroptosis has recently been reported to participate in HIRI. In 2012, Dixon *et al*[53] first proposed the definition of ferroptosis, which is characterized by the iron-dependent accumulation of lethal lipid ROS. Then ferroptosis was proved contributed to HIRI pathogenesis. Deferoxamine, (an iron chelator) attenuated HIRI and lipid peroxidation, whereas iron overload was a novel risk factor for HIRI[53]. Bioinformatics analysis was conducted to predict the genes related to ferroptosis in HIRI. Five genes (ATF3, IL6, IL1B, CDKN1A, and PTGS2) and several miRNAs (miR-128-3p and miR-24-3p) were identified[54]. Subsequently, Maresin conjugate in tissue regeneration 1 ameliorated ferroptosis-induced HIRI by promoting nuclear factor erythroid-derived 2-like 2 expression [55]. However, μ opioid receptor alleviated ferroptosis in HIRI *via* the HIF-1α/ axis[56]. These results indicate that ferroptosis plays a critical role in HIRI.

Other mechanisms

Many other regulatory mechanisms, in addition to those mentioned in previous sections, are involved in the progress of HIRI. For instance, mitochondrial dysfunction (such as mitophagy and impairment of mitochondrial permeability) plays a vital role in HIRI[16]. Acidic microenvironment has been reported to be a key factor affecting HIRI through the regulation of PPAR-γ[26]. Besides, lipid metabolites[57,58], calcium overload[56], adenosine triphosphate depletion[55], gap junctions[6], dysfunctional microcirculation[5,53], and endoplasmic reticulum stress[26,29] can affect the development of HIRI.

miRNAs

miRNAs are a class of endogenous single-chain, small ncRNAs with (21-25 nucleotides in length). The first known miRNAs (lin-4 and let-7) were identified in C. elegans in 1993[59]. Subsequently, more miRNAs have been found in plants, viruses, and animals. miRNAs produced from hairpin-like precursor transcripts are regulators of posttranscriptional and transcriptional gene expression[7,60], and are involved in various biological processes, such as development, apoptosis, metabolism, and proliferation[61]. miRNAs play important roles in human diseases, such as cancer, cardiovascular diseases, and genetic diseases[62,63]. In HIRI, numerous miRNAs have been thus far identified as

biomarkers or therapeutic targets in the past decades (shown in Table 1).

In 2009, Xu *et al*[64] reported for the first time that under the criteria of fold change > 2 and *P* value < 0.5, 78 miRNAs (40 down-regulated/38 up-regulated) were identified in the liver upon I/R injury. Among them, four miRNAs (miR-23a, miR-326, miR-346_MM1, and miR-370) were significantly downregulated by ischemic preconditioning (IPC) compared to non-preconditioned controls, implying a potential role of these miRNAs in the protective mechanism of IPC against hepatic injury[64]. Subsequently, more miRNAs were identified and their specific regulatory mechanisms were reported. The rise or fall of miRNAs determines their modulatory effects on HIRI development, and the different target genes of miRNAs allow them to be involved in the different mechanisms underlying HIRI, such as inflammation, apoptosis, and oxidative stress. The relevant information is presented in Tables 1 and 2.

miR-34

During HIRI, miR-34 is upregulated and mediates several important signaling pathways involved in various biological processes, such as inflammatory responses and apoptosis. Carbon monoxide (CO) inhalation or p-coumaric acid reduces miR-34a expression in the liver tissue, thus increasing SIRT1, which in turn mitigates HIRI by alleviating inflammatory responses, hepatocellular apoptosis and autophagy[64,65]. Similarly, H_2S and crocin exerted hepatoprotective effects in a rat model of HIRI by regulating the miR-34a/Nrf-2 pathway[66,67]. H_2S significantly modulated miR-34a expression in hepatocytes, whereas crocin regulated its expression in serum. Both zinc sulfate and gallic acid decreased the miR-34a serum level of miR-34a as an anti-miR to ameliorate HIRI[68-70]. Zheng *et al*[71] revealed that high miR-34a-5p expression may reduce liver injury during hepatectomy in adults. Further, agomir-miR-34a-5p could attenuate HIRI in rats, and *in vitro* experiments indicated that miR-34a-5p/HNF4α might be the underlying mechanism.

miR-122

miR-122 is a hepato-specific miRNA that accounts for nearly 70% of the total miRNAs pool in the liver tissue and exerts modulatory effects in liver diseases[71-74]. Recent studies have implicated its role in HIRI. van Caster *et al*[75] reported that miR-122 is a potential biomarker of warm HIRI of rats. In clinical research, serum miR-122 Levels were significantly elevated in patients with acute liver failure (ALF) than in healthy individuals. Further investigation revealed higher miR-122 levels in the serum and liver tissue of ALF survivors compared with those in the non-recovered patients[75]. Furthermore, miR-122 downregulation is involved in the hepatoprotective effects of crocin, gallic acid, and zinc sulfate [67-69]. However, John *et al*[76] found that hepatocyte-specific miR122 deletion in mice exacerbated liver injury during HIRI and that nanoparticle-mediated miR122 overexpression attenuated liver injury. These controversial modulatory effects require further investigations.

miR-370

In 2009, miR-370 was detected in a mouse model of HIRI by using miRNA microarrays. Subsequent analysis revealed that miR-370 was upregulated and positively correlated with the severity of ischemic injury[63,77]. Li *et al*[78] reported that miR-370 was significantly upregulated in a mouse model of HIRI, and that miR-370 inhibition efficiently attenuated liver damage *via* TbRII. Further investigation revealed that downregulation of miR-370 reduced the levels of proinflammatory cytokines, but had no effect on the apoptosis and proliferation of hepatocytes during HIRI. Moreover, the NF-κB gene was suggested as a potential target of miR-370[78]. Mesenchymal stem cells (MSCs) display immunomodulatory functions and have been proven to alleviate HIRI[79-81]. Zare *et al*[82] revealed that bone marrow-derived mesenchymal stem cells (BM-MSCs) downregulated miR-370 and inhibited inflammatory responses and apoptosis, thus attenuating liver damage during HIRI.

miR-494

In addition, miR-494 warrants further investigation. In a mouse model of HIRI, miRNA microarrays have indicated a upregulation of miR-494[63]. Besides, miR-494 expression was reported to significantly increase during hypoxia for 4 h in L02 cells, and its overexpression protected against hypoxia-induced apoptosis[82]. Another study suggested in a rat model of HIRI, miR-494 was elevated, and reducing its expression with propofol had a protective effect during HIRI[83, 84]. However, we observed an opposite trend in miR-494 expression of in other studies. Su *et al*[85] showed that miR-494 was downregulated in a rat model of HIRI and H_2O_2-induced apoptosis in hepatic AML12 cells. Furthermore, overexpression of miR-494 attenuated HIRI by modulating the PTEN/ PI3K/AKT signaling pathway[85]. We speculated that the opposite trend of miR-494 during HIRI might be caused by the duration of ischemia and reperfusion, cell lines, and different models. Based on previous studies, the researchers chosen different durations of ischemia (75 min, 30 min, and 60 min), different durations of reperfusion (2 h, reperfusion moment, 6 h), and different cell models (hypoxia-induced apoptosis in L02 cells and H_2O_2-induced apoptosis in AML-12 cells) for their studies. Further studies are required to confirm this hypothesis.

In addition to these above miRNAs, many other miRNAs have been identified, including miR-17, miR-155, miR-223, miR-494, miR-27-5p, miR-191, miR-450-5p, and miR-218-5p. Functional tests revealed they might be involved in HIRI development by modulating various biological processes such as cell death, inflammatory immune responses, and oxidative stress by targeting different downstream genes. Tables 1 and 2 present detailed information on the upregulated miRNAs.

The downregulated miRNAs

Several miRNAs were downregulated and exhibited modulatory effects on HIRI. miR-146b, miR-124, miR-20b-5p, miR-133a-5p, miR-449b-5p, miR-9-3p, and miR-124-3p were significantly downregulated in a rat HIRI model[85]. In terms of a

Table 1 MicroRNAs and their function in hepatic ischemia-reperfusion injury

miRNAs	Change	Targets	Effect on HIRI	Models	Ref.
miR-34a	Up	Nrf-2, SIRT1	Overexpression aggravates, downregulation alleviates	Rats, mice and RAW264.7	[66,68-71]
miR-34a-5p	Up	NF-κB /JNK/ P38	Overexpression alleviates	Human, rats, 7702 cells, AML12 cells	[72]
miR-122	Up	Nrf2, PHD1	Overexpression aggravates, overexpression alleviates	Rats, mice and human	[69-71, 78]
miR-370	Up	TbRII, NF-κB, Blc2/BAX	Downregulation alleviates	Mice and AML12	[79,80, 83]
miR-17	Up	Stat3	Overexpression aggravates	Mice and AML12	[96]
miRNA-155	Up	CD80, CD86, MHC-II	Knock out alleviates	Mice, Kupffer cells, AML12 cells, primary hepatocytes	[97]
MiR-223	Up		Biomarker	Mice and human	[98]
miR-494	Up	HIF-1α/HO-1, PI3K/Akt pathway	Overexpression alleviates	Mice, L02 cells, rats	[65,84, 85]
miR-27a-5p	Up	Bach1	Overexpression alleviates, downregulation aggravates	Mice and AML12 cells	[99]
miRNA-191	Up	ZONAB/Cyclin D1	Overexpression aggravates, knock out alleviates	Mice and LO2 cells	[100]
miR-450b-5p	Up	CRYAB/NF-κB, Akt1/mTOR	Downregulation alleviates	Mice and RAW 264.7 cells	[101]
miR-218-5p	Up	GAB2/PI3K/AKT	downregulation alleviates, overexpression aggravates	mice	[102]
miR-494	Down	PTEN/PI3K/AKT	Overexpression alleviates	Rats and AML12 cells	[86]
miR-146b	Down	TRAF6, NF-κB	Downregulation aggravates	Rats	[103]
miR-330-3p	Down	PGAM5	Overexpression alleviates, downregulation aggravates	Mice and AML12 cells	[104]
miR-1246	Down	IL-6-gp130-STAT3	Downregulation aggravates	Mice and hUCB-MSCs	[105]
miR-142	Down	HMGB1/TLR4/NF-κB	Overexpression alleviates, downregulation aggravates	Mice and NCTC 1469 cells	[93]
miR-96	Down	FOXO4	Overexpression alleviates, downregulation aggravates	Mice and primary hepatocytes	[92]
miR-494	Down	PTEN/PI3K/AKT	Overexpression alleviates	L02 cells; rats, AML12 cells	[84,86]
miR-30b	Down	Atg12-Atg5	Downregulation aggravates	Mice and AML12	[106]
miR-146a	Down	IRAK1, TRAF6	Overexpression alleviates	Mice and RAW264.7	[107]
miR-124	Down	Rab38, AKT pathway	Overexpression alleviates	Rats and L02 cells	[108]
miR-20b-5p	Down	SIRT1	Overexpression alleviates	Rats	[67]
miRNA-182-5p	No detect	TLR4	Overexpression alleviates	Mice and RAW264.7	[109]
miR-192-5p	Up/Down	Zeb2	Downregulation alleviates	Mice and Hepa1-6 cells, human	[90]
125b-5p	Down	Myd88, c-Fos and A20	No functional tests	Mice	[87]
miR-501-3p	Down	Myd88, c-Fos and A20	No functional tests	Mice	[87]
miR-133a-5p	Down	MAPK6	Overexpression alleviates, downregulation aggravates	Rats and QSG-7701	[95]
miR-214	Down	TRAF1/ASK1/JNK	Overexpression alleviates	Mice and AML12 cells	[110]
miR-449b-5p	Down	HMGB1, NF-κB	Overexpression alleviates	Rats and L02 cells	[111]
miR-142-3p	Down	MARCKS	Overexpression alleviates, downregulation aggravates	Mice and AML12, HepG2 cells	[112]
miR-24-3p	Down	STING	Overexpression alleviates	Mice	[113]
miR-9-5p	Down	CXCR4	Overexpression alleviates	Liver sinusoidal endothelial cells	[114]

miR-141-3p	Down	Keap1/Nrf2	Overexpression alleviates, downregulation aggravates	Human, mice and LO2 cells	[89]
miR-194	Down	PHLDA1	Overexpression alleviates	Mice and RAW 264.7 cells	[115]
miR-9-3p	Down	FNDC3VB	Overexpression alleviates, downregulation aggravates	Rats	[94]
miR-29a-3p	No change	Ireb2	Overexpression alleviates, downregulation aggravates	Rats and BMMSC	[116]
miR-124-3p	Down	TRAF3/CREB, Steap3	Overexpression alleviates, downregulation aggravates	Mice and Normal BNL Rats, CL.2 hepatocytes, BMMSC	[117, 118]
miR-140-5p	Down	CAPN1	Overexpression alleviates, downregulation aggravates	Mice and AML12 cells	[119]

miRNAs: MicroRNAs; HIRI: Hepatic ischemia-reperfusion injury.

Table 2 MicroRNAs and the involved mechanisms in hepatic ischemia-reperfusion injury

Mechanisms	miRNAs	Ref.
Apoptosis	miR-1, miR-17, miR-133, miR-205, miR-34a, miR-124, miR-146a, miR-494, miR-192-5p, miR-133a-5p, miRNA-155, miR-146b, miR-27a-5p, miR-214, miRNA-191, miR-370, miR-449b-5p, miRNA-142-3p, miRNA-24-3p, miR-9-5p, miR-96, miRNA-141-3p, miR-9-3p, miR-218-5p, miR-124-3p, miR-34a-5p, miR-142, miR-140-5p	[68,72,83,84,86,89-95, 97,99,100,102,107,108, 110-113,114,117,119]
Inflammatory responses	miRNA-182-5p, miR-370, miR-34a, miR-146a, 125b-5p and miR-501-3p, miRNA-155, miR-146b, miR-148a, miR-1246, MiRNA-142-3p, miRNA-24-3p, miR-9-5p, miR-194, miR-9-3p, miR-124-3p, miR-218-5p, miR-450b-5p, miR-142, miR-140-5p	[68,79,80,87,93,94,97, 101-103,105,107,109, 112-115,117,119,120]
Oxidative stress	miR-34a, miR-122, miR-494, miR-9-3p, miR-218-5p, miR-142	[69,70,71,86,93,94,102]
Autophagy	miR-17, miR-30b, miR-330-3p	[96,104,106]
Ferroptosis	miR-29a-3p, miR-124-3p	[116,118]

miRNAs: MicroRNAs.

mouse HIRI model, the downregulated miRNAs, including miR-330-3p, miR-1246, miR-142, miR-30b, miR-146a, miR-96, 125b-5p , miR-501-3p, miR-214, miR-142-3p, miR-24-3p, miR-141-3p, miR-194, miR-124-3p, miR-140-5p, miR-153-3p, miR-210-5p, miR-107-3p, miR-103-3p, miR-205-5p, miR-296-5p, miR-183-3p, and miR-698-5p were detected[86,87]. Most of these miRNAs were confirmed and their functions were verified using cell models. Detailed information on the downregulated miRNAs is presented in Tables 1 and 2.

Only two miRNAs (miR-141-3p and miR-192-5p) have been identified in humans. Li *et al*[88] collected serum samples from 27 Liver transplantation patients at different time points (pre-operatively, 4 h after reperfusion, and on postoperative days 1, 2, and 3) and measured the expression of miR-141-3p, ALT, and AST. They found that 4 h after perfusion, miR-141-3p was lower than pre-operation and then gradually increased over time, which manifested a negative correlation with ALT/AST levels[87]. Roy and his colleagues detected miR-192-5p expression in the liver tissues and sera of patients with acute liver injury. The results shown that miR-192-5p decreased in liver samples, but elevated in serum levels from patients with acute hepatic injury; further investigation revealed that miR-192-5p concentrations in serum were positively correlated with AST, ALT, and miR-122 Levels, which might represent a hepatocyte-specific serum biomarker[88].

Of note, several miRNAs have been indicated to participate in the hepatoprotective effect of several pharmacological agents during HIRI, including inhaled anesthetics and propofol. For instance, sevoflurane preconditioning ameliorates liver injury by the inhibitory effects of several miRNAs (*e.g.*, miR-133 and miR-205) on the Akt–GSK–cyclin D1 pathway [89]. Others have reported that sevoflurane preconditioning promotes the expression of miR-96 and inhibits FOXO4, thus alleviating HIRI[90]. In contrast, sevoflurane postconditioning exhibited the same hepatoprotective effect by counteracting miR-142 downregulation induced by I/R[91]. Moreover, isoflurane upregulates miR-9-3p to protect rats from HIRI by inhibiting FNDC3VB[92]. In addition, propofol exhibited protective effects against HIRI in rats by increasing the expression of miR-133a-5p and decreasing that of MAPK6[93].

Collectively, HIRI alters the expression of miRNAs. In turn, differentially expressed miRNAs play vital roles in HIRI development. Currently, a lot of miRNAs have been identified and their specific modulatory roles have been verified. However, it is important to note that human trails are lacking. Future research should focus on clinical transformation, which remains a significant challenge.

LNCRNAS

lncRNAs are a subset of noncoding RNAs with over 200 nucleotides (200 nt) and are localized to both the nucleus and cytoplasm[8,119]. Typically, lncRNAs are transcribed by Pol II, and have 5′-end 7-methyl guanosine (m^7G) caps and 3′-end polyadenylated [poly(A)] tails. lncRNAs were considered transcription junks without protein-coding capacity until their modulatory effects on gene expression were established. lncRNAs modulate chromatin structure and function, transcription, post-transcription, and sponge miRNAs by interacting with DNA, RNA and proteins, and in turn participate in diverse cellular processes such as cell differentiation, cell apoptosis, stem cell pluripotency, and stress response[12,120,121]. Recent studies show that lncRNAs can affect various diseases (*e.g.*, nervous disorders, immune systems, and cancers)[122,123]. The role of lncRNAs in the pathophysiology of I/R has been explored in multiple oxygen-dependent organs, such as the heart, brain, and kidney[124-129]. In terms of HIRI, it is still at an early stage. Here, we summarize the lncRNAs that have been reported, and detailed information is shown in Table 3.

In 2013, Chen *et al*[130] first revealed that in mouse livers after I/R treatment, 71 upregulated lncRNAs (fold change ≥ 1.5, and P value < 0.5) and 27 downregulated lncRNAs (fold change ≤ 0.7, and P value < 0.5) were identified. Four up-regulated lncRNAs (AK139328, AK087277, AK054386 and AK028007) and six down-regulated lncRNAs (AK143693, NR-028310, NR-015462, NR-036616, ENSMUST00000151138 and AK143294) were validated using quantitative reverse transcription polymerase chain reaction (RT-qPCR). Further investigation suggested that silencing of AK139328 could ameliorate HIRI by activating the Akt/ NF-κB signaling pathway[128]. The same research team detected the lncRNA profile in mouse plasma after HIRI and found that under the same criteria, 64 up-regulated lncRNAs and 244 down-regulated lncRNAs were detected. The authors then conducted a comparative analysis of dysregulated lncRNA profiles between plasma and liver and revealed that all dysregulated lncRNAs in plasma remained either unchanged or absent in mice livers after HIRI, as did dysregulated lncRNAs in the livers, which strongly indicated that the source of these dysregulated lncRNAs may not be restricted to liver cells during HIRI[129]. Another study suggested that blood cells secrete large amounts of lncRNAs during heart failure[130,131].

With the development of novel technologies, an increasing number of differentially expressed lncRNAs have been identified, and their roles have been explored in HIRI models. Current studies indicate that lncRNAs participate in various biological processes involved in HIRI development. A few studies revealed that some lncRNAs, including TUG1 [132], NEAT1[133], MALAT1[134] and Hnf4αos[135], could modulate the processes of apoptosis and inflammatory response. Other lncRNAs, such as MEG3[136], Gm4419[137], CCAT1[138] and AK054386[139] were verified to regulate apoptosis, whereas AK139328 was only found to regulate the inflammatory response[130]. In addition to regulating these common biological processes, several lncRNAs participate in uncommon processes. HOTAIR expression in the liver was upregulated in a mouse model of HIRI, and further investigation indicated that HOTAIR regulates hepatocyte autophagy by targeting miR-20b-5p/ATG7[140]. Similarly, HIRI downregulates the expression of KCNQ1OT1 in mice livers, which promotes proliferation and inhibits pyroptosis by serving as a competing endogenous RNA to modulate the miR-142a-3p/HMGB1 axis[5]. Moreover, AK054386 upregulation may lead to sustained ERS and increased cell apoptosis and death in mice HIRI models[139]. Detailed information is shown in Table 4.

Li *et al*[141] successfully constructed HIRI-related lncRNA-miRNA-mRNA networks such as LOC1201029870-miRNA-331-3p/miRNA-128-5p-CDH3/UPK3B and LOC120094223-miRNA-92b-5p-KRT7, which may play an important role in HIRI. However, these specific modulatory mechanisms stay uncovered, and further investigation is needed.

In summary, these studies support the use of lncRNAs as highly attractive targets for diagnosing and treating HIRI. An increasing number of lncRNAs are known to be involved in HIRI. Overexpression and knockdown of lncRNAs attenuated or aggravated the extent of HIRI *in vivo* and *in vitro*, respectively, indicating the significance of lncRNAs in HIRI. A comprehensive understanding of lncRNAs in HIRI not only provides a new dimension to the molecular mechanisms, but also paves the way for future treatments. Indeed, future studies need more functional experiments *in vivo* and *in vitro* to reveal the specific roles of lncRNAs and to further explore its secretory and transport mechanisms in HIRI.

CIRCULAR RNAS

Circular RNA is a special subclass of ncRNAs characterized by a covalent bond joining the 3′ and 5′ ends generated by the back-splicing of exons[142-144]. Once produced, most circRNAs are exported from the nucleus to the cytoplasm[145]. Compared to their cognate linear RNAs, circRNAs are more stable and are not easily degraded by RNase L, RNase P, or RNase MRP. In addition to regulating transcription, splicing, and chromatin interactions, circRNAs act as decoys for miRNAs and proteins, interact with proteins, and function as templates for translation, and as sources of pseudogene generation[13,144]. circRNAs are involved in various biological processes, including immunity, neuronal function, cell proliferation, and transformation[146-149]. Existing evidence indicates the potential of circRNAs in treating diverse diseases.

Advances in RNA sequencing technologies have allowed the detection and exploration of many circRNAs in various pathological conditions. Currently, circRNAs have been implicated in the process of I/R injury, particularly myocardial I/R injury. For instance, circ_SMG6 deteriorates myocardial I/R injury by activating the miR-138-5p/EGR1/TLR4/TRIF signaling, whereas circ_CNEACR and circ_ACR alleviate myocardial I/R injury by suppressing autophagy[150-152]. Moreover, circ-FoxO3 attenuates blood-brain barrier damage by inhibiting mTORC1 activity during cerebral I/R[153]. circ-AKT3 aggravates renal I/R injury by regulating the miR-144-5p /Wnt/β-catenin pathway[154]. However, only few studies have investigated the role of circRNAs in HIRI.

Table 3 Long non-coding RNAs and their function in hepatic ischemia-reperfusion injury

lncRNAs	Change	Targets	Effect on HIRI	Models	Ref.
TUG1	Up	Brg1, miR-194/SIRT1	Alleviate	Mice, AML12 cells, WRL-68 cells	[133,144]
SNHG1	Up	miR-186-5p/YY1	Alleviate	AML12 cells	[145]
NEAT1	Up	-	Aggravate	HL7702 cells	[134]
Gm4419	Up	miR-455/SOX6 axis	Aggravate	Rats and BRL-3A	[138]
AK139328	Up	Akt signaling pathway and NF-κB	Aggravate	Mice and primary mouse hepatocyte	[130]
AK054386	Up	miR-199	Aggravate	Mice and BNL-CL2 cells	[140]
HOTAIR	Up	miR-20b-5p/ATG7	Aggravate	Mice and primary mouse hepatocyte	[141]
MALAT1	Up	HMGB1-TLR4	Aggravate	HL7702 cells	[135]
Hnf4αos	Up	Hnf4α/miR-23a	Aggravate	Human, mice, primary mouse hepatocyte and L02 cells	[136]
KCNQ1OT1	Up	miR-142a-3p/HMGB1	Aggravate	Mice and primary mouse hepatocyte	[15]
CCAT1	Down	caspase-3, cyclin D1	Aggravate	HL7702 cells	[139]
MEG3	Down	miR-34a/Nrf2	Aggravate	Mice and HL7702 cells	[137]

lncRNAs: Long non-coding RNAs; HIRI: Hepatic ischemia-reperfusion injury.

Table 4 Long non-coding RNAs and the involved mechanisms in hepatic ischemia-reperfusion injury

Mechanisms	lncRNAs	Ref.
Apoptosis	MEG3, TUG1, NEAT1, Gm4419, CCAT1, AK054386, MALAT1, Hnf4αos	[133-140]
Inflammatory responses	TUG1, NEAT1, AK139328, MALAT1, Hnf4αos	[130,133-136]
Oxidative stress	TUG1	[133,144]
Autophagy	HOTAIR	[141]
Pyroptosis	KCNQ1OT1	[142]
Endoplasmic reticulum stress	AK054386	[140]

lncRNAs: Long non-coding RNAs.

To date, only two studies have reported the potential role of circRNAs in HIRI. Zhang *et al*[87] conducted a circRNA microarray in mice for the first time in 2019 and found that, compared to the sham group, 706 circRNAs were differentially expressed in the I/R group, including 213 upregulated and 493 downregulated circRNAs. Compared to the ischemic postconditioning (IPO) group, 641 up-regulated and 252 down-regulated circRNAs were identified in the I/R group (fold change ≥ 2.0 and P value < 0.05). Among these, circRNA_005186 was upregulated in the I/R group, whereas IPO treatment downregulated its expression. A subsequent *in vitro* experiment showed that circRNA_005186 functioned as a miRNA sponge for miR-124-3p, thereby enhancing Epha2 expression. In other words, the circRNA_005186-miR-124-3p-Epha2 pathway might be a possible protective mechanism of IPO against HIRI[87]. The other five circRNAs (circRNA_011137, circRNA_013703, circRNA_29140, circRNA_36837, and circRNA_43819) were validated by RT-qPCR, and may be the focus of future research. In addition to IPO, IPC can attenuate HIRI. Tian *et al*[155] reported the circRNA profiles of mice with ischemic livers, with and without IPC. The data revealed that there were 77 circRNAs and 686 mRNAs in the IRI group, 50 circRNAs and 95 mRNAs in the IPC group (fold change ≥ 1.5, and P value < 0.05), respectively, when compared with those in the sham group. Next, they compared the circRNA alterations in the three groups and selected circRNA_017753 for further study. The prediction of the circRNA–miRNA–mRNA pathway implied a potential role of the circRNA_017753–miR-218-5p/miR-7002-3p/miR-7008-3p–Jade1 pathway in the mechanisms of IPC protection in HIRI. However, further investigations are required[155].

Although circRNA research in the field of HIRI is still in its infancy, the present data indicate great prospects for research. With the increasing attention of the scientific community, a thorough understanding of circRNA mechanisms will provide new insights and therapeutic targets for treating HIRI.

ADDITIONAL NCRNAS

Other ncRNAs such as PIWI-interacting RNAs (piRNAs), small nucleolar RNAs (snoRNAs) and tRNA-derived small RNAs (tsRNAs), have attracted widespread attention in recent years. For instance, some studies have revealed that piRNAs were abnormally expressed and might play a regulatory role in liver cancer, non-alcoholic fatty liver disease and liver injury[156-158]. Moreover, snoRNAs and tsRNAs are involved in several liver diseases as biomarkers and therapeutic targets[159-162]. However, only few studies have investigated their roles in HIRI. As our knowledge of these ncRNAs expands, their potential role in HIRI will be confirmed.

CONCLUSION

Although ncRNAs have not been fully identified in the development of HIRI, current data indicate that ncRNAs are important regulators of various biological processes involved in the pathology of HIRI, and can serve as biomarkers for the diagnosis and assessment of therapeutic targets for treating HIRI. However, we noticed that most of the data were collected from animal studies, and the majority of ncRNAs described in this review were isolated from total liver tissue. So, establishing large clinical trials with diverse sample sources is necessary. Meanwhile, exploring the role of lncRNAs and circRNAs in HIRI is still in the start-up phase, and more attention needs to be paid in the future. In summary, our expanding knowledge of the capabilities of ncRNAs in HIRI will pave the way for novel diagnostic indicators and therapeutic inventions for HIRI.

FOOTNOTES

Author contributions: Shao JL collected the data, prepared the tables and wrote the paper; Wang LJ collected the data; Xiao J revised the paper; Yang JF conceptualized the idea, obtained the funding, and revised the paper; all authors have read and approved the final manuscript.

Supported by the National Natural Science Foundation of China, No. 82070648; and the Science and Technology Innovation Program of Hunan Province, No. 2021SK4014.

Conflict-of-interest statement: All the authors report no relevant conflicts of interest for this article.

Open-Access: This article is an open-access article that was selected by an in-house editor and fully peer-reviewed by external reviewers. It is distributed in accordance with the Creative Commons Attribution NonCommercial (CC BY-NC 4.0) license, which permits others to distribute, remix, adapt, build upon this work non-commercially, and license their derivative works on different terms, provided the original work is properly cited and the use is non-commercial. See: https://creativecommons.org/Licenses/by-nc/4.0/

Country/Territory of origin: China

ORCID number: Jia-Li Shao 0000-0002-8291-1849; Li-Juan Wang 0000-0002-1467-7907; Ji Xiao 0000-0002-8726-9285; Jin-Feng Yang 0000-0002-0774-0496.

S-Editor: Yan JP
L-Editor: A
P-Editor: Yu HG

REFERENCES

1 **Zhai Y**, Petrowsky H, Hong JC, Busuttil RW, Kupiec-Weglinski JW. Ischaemia-reperfusion injury in liver transplantation--from bench to bedside. *Nat Rev Gastroenterol Hepatol* 2013; **10**: 79-89 [PMID: 23229329 DOI: 10.1038/nrgastro.2012.225]

2 **Teoh NC**, Farrell GC. Hepatic ischemia reperfusion injury: pathogenic mechanisms and basis for hepatoprotection. *J Gastroenterol Hepatol* 2003; **18**: 891-902 [PMID: 12859717 DOI: 10.1046/j.1440-1746.2003.03056.x]

3 **Liu H**, Man K. New Insights in Mechanisms and Therapeutics for Short- and Long-Term Impacts of Hepatic Ischemia Reperfusion Injury Post Liver Transplantation. *Int J Mol Sci* 2021; **22** [PMID: 34360975 DOI: 10.3390/ijms22158210]

4 **Huang M**, Cai H, Han B, Xia Y, Kong X, Gu J. Natural Killer Cells in Hepatic Ischemia-Reperfusion Injury. *Front Immunol* 2022; **13**: 870038 [PMID: 35418990 DOI: 10.3389/fimmu.2022.870038]

5 **Han JY**, Li Q, Ma ZZ, Fan JY. Effects and mechanisms of compound Chinese medicine and major ingredients on microcirculatory dysfunction and organ injury induced by ischemia/reperfusion. *Pharmacol Ther* 2017; **177**: 146-173 [PMID: 28322971 DOI: 10.1016/j.pharmthera.2017.03.005]

6 **Hernández-Guerra M**, Hadjihambi A, Jalan R. Gap junctions in liver disease: Implications for pathogenesis and therapy. *J Hepatol* 2019; **70**: 759-772 [PMID: 30599172 DOI: 10.1016/j.jhep.2018.12.023]

7 **Farh KK**, Grimson A, Jan C, Lewis BP, Johnston WK, Lim LP, Burge CB, Bartel DP. The widespread impact of mammalian MicroRNAs on mRNA repression and evolution. *Science* 2005; **310**: 1817-1821 [PMID: 16308420 DOI: 10.1126/science.1121158]

8 **Kapranov P**, Cheng J, Dike S, Nix DA, Duttagupta R, Willingham AT, Stadler PF, Hertel J, Hackermüller J, Hofacker IL, Bell I, Cheung E, Drenkow J, Dumais E, Patel S, Helt G, Ganesh M, Ghosh S, Piccolboni A, Sementchenko V, Tammana H, Gingeras TR. RNA maps reveal new RNA classes and a possible function for pervasive transcription. *Science* 2007; **316**: 1484-1488 [PMID: 17510325 DOI: 10.1126/science.1138341]

9 **Ghafouri-Fard S**, Shoorei H, Taheri M. Non-coding RNAs participate in the ischemia-reperfusion injury. *Biomed Pharmacother* 2020; **129**: 110419 [PMID: 32563988 DOI: 10.1016/j.biopha.2020.110419]

10 **Slack FJ**, Chinnaiyan AM. The Role of Non-coding RNAs in Oncology. *Cell* 2019; **179**: 1033-1055 [PMID: 31730848 DOI: 10.1016/j.cell.2019.10.017]

11 **Salta E**, De Strooper B. Noncoding RNAs in neurodegeneration. *Nat Rev Neurosci* 2017; **18**: 627-640 [PMID: 28855739 DOI: 10.1038/nrn.2017.90]

12 **Statello L**, Guo CJ, Chen LL, Huarte M. Gene regulation by long non-coding RNAs and its biological functions. *Nat Rev Mol Cell Biol* 2021; **22**: 96-118 [PMID: 33353982 DOI: 10.1038/s41580-020-00315-9]

13 **Kristensen LS**, Andersen MS, Stagsted LVW, Ebbesen KK, Hansen TB, Kjems J. The biogenesis, biology and characterization of circular RNAs. *Nat Rev Genet* 2019; **20**: 675-691 [PMID: 31395983 DOI: 10.1038/s41576-019-0158-7]

14 **Treiber T**, Treiber N, Meister G. Regulation of microRNA biogenesis and its crosstalk with other cellular pathways. *Nat Rev Mol Cell Biol* 2019; **20**: 5-20 [PMID: 30228348 DOI: 10.1038/s41580-018-0059-1]

15 **Liang C**, Peng Y, Sun H, Wang L, Jiang L, Zou S. Silencing lncRNA KCNQ1OT1 reduced hepatic ischemia reperfusion injury-induced pyroptosis by regulating miR-142a-3p/HMGB1 axis. *Mol Cell Biochem* 2023; **478**: 1293-1305 [PMID: 36308669 DOI: 10.1007/s11010-022-04586-y]

16 **Kim JS**, Chapman WC, Lin Y. Mitochondrial Autophagy in Ischemic Aged Livers. *Cells* 2022; **11** [PMID: 36552847 DOI: 10.3390/cells11244083]

17 **Zou Z**, Shang R, Zhou L, Du D, Yang Y, Xie Y, Li Z, Zhao M, Jiang F, Zhang L, Zhou P. The Novel MyD88 Inhibitor TJ-M2010-5 Protects Against Hepatic Ischemia-reperfusion Injury by Suppressing Pyroptosis in Mice. *Transplantation* 2023; **107**: 392-404 [PMID: 36226835 DOI: 10.1097/TP.0000000000004317]

18 **Yu C**, Chen P, Miao L, Di G. The Role of the NLRP3 Inflammasome and Programmed Cell Death in Acute Liver Injury. *Int J Mol Sci* 2023; **24** [PMID: 36834481 DOI: 10.3390/ijms24043067]

19 **Pretzsch E**, Nieß H, Khaled NB, Bösch F, Guba M, Werner J, Angele M, Chaudry IH. Molecular Mechanisms of Ischaemia-Reperfusion Injury and Regeneration in the Liver-Shock and Surgery-Associated Changes. *Int J Mol Sci* 2022; **23** [PMID: 36361725 DOI: 10.3390/ijms232112942]

20 **Li K**, Feng Z, Wang L, Ma X, Liu K, Geng X, Peng C. Chlorogenic Acid Alleviates Hepatic Ischemia-Reperfusion Injury by Inhibiting Oxidative Stress, Inflammation, and Mitochondria-Mediated Apoptosis In Vivo and In Vitro. *Inflammation* 2023; **46**: 1061-1076 [PMID: 36856879 DOI: 10.1007/s10753-023-01792-8]

21 **Vollmar B**, Menger MD. The hepatic microcirculation: mechanistic contributions and therapeutic targets in liver injury and repair. *Physiol Rev* 2009; **89**: 1269-1339 [PMID: 19789382 DOI: 10.1152/physrev.00027.2008]

22 **Chen L**, Lin B, Yang J, Zhong L, Xiong X, Wang X. Hydrogen sulfide alleviates ischemia induced liver injury by repressing the SPHK1/S1P pathway. *Ann Transl Med* 2023; **11**: 73 [PMID: 36819566 DOI: 10.21037/atm-22-6460]

23 **Elias-Miró M**, Jiménez-Castro MB, Rodés J, Peralta C. Current knowledge on oxidative stress in hepatic ischemia/reperfusion. *Free Radic Res* 2013; **47**: 555-568 [PMID: 23738581 DOI: 10.3109/10715762.2013.811721]

24 **Galaris D**, Barbouti A, Korantzopoulos P. Oxidative stress in hepatic ischemia-reperfusion injury: the role of antioxidants and iron chelating compounds. *Curr Pharm Des* 2006; **12**: 2875-2890 [PMID: 16918418 DOI: 10.2174/138161206777947614]

25 **Gobut H**, Kucuk A, Şengel N, Arslan M, Ozdemir C, Mortas T, Kasapbası E, Kurtipek O, Kavutcu M. Effects of cerium oxide (CeO(2)) on liver tissue in liver ischemia-reperfusion injury in rats undergoing desflurane anesthesia. *BMC Anesthesiol* 2023; **23**: 40 [PMID: 36737682 DOI: 10.1186/s12871-023-01999-0]

26 **Han CY**, Lim SW, Koo JH, Kim W, Kim SG. PHLDA3 overexpression in hepatocytes by endoplasmic reticulum stress *via* IRE1-Xbp1s pathway expedites liver injury. *Gut* 2016; **65**: 1377-1388 [PMID: 25966993 DOI: 10.1136/gutjnl-2014-308506]

27 **Ding W**, Duan Y, Qu Z, Feng J, Zhang R, Li X, Sun D, Zhang X, Lu Y. Acidic Microenvironment Aggravates the Severity of Hepatic Ischemia/Reperfusion Injury by Modulating M1-Polarization Through Regulating PPAR-γ Signal. *Front Immunol* 2021; **12**: 697362 [PMID: 34234785 DOI: 10.3389/fimmu.2021.697362]

28 **Huang Y**, Xu Q, Zhang J, Yin Y, Pan Y, Zheng Y, Cai X, Xia Q, He K. Prussian Blue Scavenger Ameliorates Hepatic Ischemia-Reperfusion Injury by Inhibiting Inflammation and Reducing Oxidative Stress. *Front Immunol* 2022; **13**: 891351 [PMID: 35693813 DOI: 10.3389/fimmu.2022.891351]

29 **Dugbartey GJ**, Juriasingani S, Zhang MY, Sener A. H(2)S donor molecules against cold ischemia-reperfusion injury in preclinical models of solid organ transplantation. *Pharmacol Res* 2021; **172**: 105842 [PMID: 34450311 DOI: 10.1016/j.phrs.2021.105842]

30 **Shi Z**, Song Y, Gao X, Loor JJ, Aboragah A, Yu H, Fang Z, Zhu Y, Du X, Li X, Gao W, Liu G. Disruption of endoplasmic reticulum homeostasis exacerbates liver injury in clinically ketotic cows. *J Dairy Sci* 2021; **104**: 9130-9141 [PMID: 34001360 DOI: 10.3168/jds.2021-20238]

31 **Hisama N**, Yamaguchi Y, Ishiko T, Miyanari N, Ichiguchi O, Goto M, Mori K, Watanabe K, Kawamura K, Tsurufuji S, Ogawa M. Kupffer cell production of cytokine-induced neutrophil chemoattractant following ischemia/reperfusion injury in rats. *Hepatology* 1996; **24**: 1193-1198 [PMID: 8903397 DOI: 10.1053/jhep.1996.v24.pm0008903397]

32 **Samarasinghe DA**, Farrell GC. The central role of sinusoidal endothelial cells in hepatic hypoxia-reoxygenation injury in the rat. *Hepatology* 1996; **24**: 1230-1237 [PMID: 8903403 DOI: 10.1002/hep.510240541]

33 **Zhou W**, McCollum MO, Levine BA, Olson MS. Inflammation and platelet-activating factor production during hepatic ischemia/reperfusion. *Hepatology* 1992; **16**: 1236-1240 [PMID: 1427662 DOI: 10.1002/hep.1840160521]

34 **Hoffmann F**, Sass G, Zillies J, Zahler S, Tiegs G, Hartkorn A, Fuchs S, Wagner J, Winter G, Coester C, Gerbes AL, Vollmar AM. A novel technique for selective NF-kappaB inhibition in Kupffer cells: contrary effects in fulminant hepatitis and ischaemia-reperfusion. *Gut* 2009; **58**: 1670-1678 [PMID: 19470497 DOI: 10.1136/gut.2008.165647]

35 **Kono H**, Fujii H, Ogiku M, Hosomura N, Amemiya H, Tsuchiya M, Hara M. Role of IL-17A in neutrophil recruitment and hepatic injury after warm ischemia-reperfusion mice. *J Immunol* 2011; **187**: 4818-4825 [PMID: 21949019 DOI: 10.4049/jimmunol.1100490]

36 **Al Mogrampi S**, Boumpoureka C, Afaloniati H, Lagou M, Angelopoulou K, Anestakis D, Tampouratzi ZG, Iliadis S, Antoniadis N,

Giakoustidis A, Papalois A, Papadopoulos V, Poutahidis T, Giakoustidis D. Inhibition of γδ-TcR or IL17a Reduces T-Cell and Neutrophil Infiltration after Ischemia/Reperfusion Injury in Mouse Liver. *J Clin Med* 2023; **12** [PMID: 36902538 DOI: 10.3390/jcm12051751]

37 **Huang H**, Tohme S, Al-Khafaji AB, Tai S, Loughran P, Chen L, Wang S, Kim J, Billiar T, Wang Y, Tsung A. Damage-associated molecular pattern-activated neutrophil extracellular trap exacerbates sterile inflammatory liver injury. *Hepatology* 2015; **62**: 600-614 [PMID: 25855125 DOI: 10.1002/hep.27841]

38 **Zhai Y**, Busuttil RW, Kupiec-Weglinski JW. Liver ischemia and reperfusion injury: new insights into mechanisms of innate-adaptive immune-mediated tissue inflammation. *Am J Transplant* 2011; **11**: 1563-1569 [PMID: 21668640 DOI: 10.1111/j.1600-6143.2011.03579.x]

39 **van Golen RF**, Reiniers MJ, Olthof PB, van Gulik TM, Heger M. Sterile inflammation in hepatic ischemia/reperfusion injury: present concepts and potential therapeutics. *J Gastroenterol Hepatol* 2013; **28**: 394-400 [PMID: 23216461 DOI: 10.1111/jgh.12072]

40 **Han H**, Desert R, Das S, Song Z, Athavale D, Ge X, Nieto N. Danger signals in liver injury and restoration of homeostasis. *J Hepatol* 2020; **73**: 933-951 [PMID: 32371195 DOI: 10.1016/j.jhep.2020.04.033]

41 **Du Y**, Zhong F, Cheng H, Li T, Chen Y, Tan P, Huang M, Liang T, Liu Y, Xia X, Fu W. The Dietary Supplement γ-Oryzanol Attenuates Hepatic Ischemia Reperfusion Injury *via* Inhibiting Endoplasmic Reticulum Stress and HMGB1/NLRP3 Inflammasome. *Oxid Med Cell Longev* 2021; **2021**: 4628050 [PMID: 34512864 DOI: 10.1155/2021/4628050]

42 **Arumugam TV**, Woodruff TM, Stocks SZ, Proctor LM, Pollitt S, Shiels IA, Reid RC, Fairlie DP, Taylor SM. Protective effect of a human C5a receptor antagonist against hepatic ischaemia-reperfusion injury in rats. *J Hepatol* 2004; **40**: 934-941 [PMID: 15158333 DOI: 10.1016/j.jhep.2004.02.017]

43 **Diepenhorst GM**, de Graaf W, Niessen HW, van Vliet AK, Hack CE, van Gulik TM. Immunoglobulin M, C-reactive protein and complement activation in rat hepatic ischemia-reperfusion injury. *Eur Surg Res* 2014; **52**: 50-62 [PMID: 24642533 DOI: 10.1159/000360474]

44 **Feng XB**, Ke JJ, Rao Y, Zhang ZZ, Wang YL. Effect of complement C1q expression on hepatic ischemia-reperfusion injury in rats. *J Huazhong Univ Sci Technolog Med Sci* 2014; **34**: 403-407 [PMID: 24939307 DOI: 10.1007/s11596-014-1291-3]

45 **Mao B**, Yuan W, Wu F, Yan Y, Wang B. Autophagy in hepatic ischemia-reperfusion injury. *Cell Death Discov* 2023; **9**: 115 [PMID: 37019879 DOI: 10.1038/s41420-023-01387-0]

46 **Gao W**, Feng Z, Zhang S, Wu B, Geng X, Fan G, Duan Y, Li K, Liu K, Peng C. Anti-Inflammatory and Antioxidant Effect of Eucommia ulmoides Polysaccharide in Hepatic Ischemia-Reperfusion Injury by Regulating ROS and the TLR-4-NF-κB Pathway. *Biomed Res Int* 2020; **2020**: 1860637 [PMID: 32566664 DOI: 10.1155/2020/1860637]

47 **Ji J**, Wu L, Feng J, Mo W, Wu J, Yu Q, Li S, Zhang J, Dai W, Xu X, Mao Y, Xu S, Chen K, Li J, Guo C. Cafestol preconditioning attenuates apoptosis and autophagy during hepatic ischemia-reperfusion injury by inhibiting ERK/PPARγ pathway. *Int Immunopharmacol* 2020; **84**: 106529 [PMID: 32344356 DOI: 10.1016/j.intimp.2020.106529]

48 **Yang J**, Sun H, Takacs P, Zhang Y, Liu J, Chang Y, Candiotti KA. The effect of octreotide on hepatic ischemia-reperfusion injury in a rabbit model. *Transplant Proc* 2013; **45**: 2433-2438 [PMID: 23953560 DOI: 10.1016/j.transproceed.2013.02.112]

49 **Sun H**, Zou S, Candiotti KA, Peng Y, Zhang Q, Xiao W, Wen Y, Wu J, Yang J. Octreotide Attenuates Acute Kidney Injury after Hepatic Ischemia and Reperfusion by Enhancing Autophagy. *Sci Rep* 2017; **7**: 42701 [PMID: 28205545 DOI: 10.1038/srep42701]

50 **Zou S**, Sun H, Candiotti KA, Peng Y, Zhang Q, Xiao W, Zhao S, Wu L, Yang J. Octreotide protects against hepatic ischemia/reperfusion injury *via* HO-1-mediated autophagy. *Acta Biochim Biophys Sin (Shanghai)* 2018; **50**: 316-318 [PMID: 29385400 DOI: 10.1093/abbs/gmx149]

51 **Galluzzi L**, Vitale I, Aaronson SA, Abrams JM, Adam D, Agostinis P, Alnemri ES, Altucci L, Amelio I, Andrews DW, Annicchiarico-Petruzzelli M, Antonov AV, Arama E, Baehrecke EH, Barlev NA, Bazan NG, Bernassola F, Bertrand MJM, Bianchi K, Blagosklonny MV, Blomgren K, Borner C, Boya P, Brenner C, Campanella M, Candi E, Carmona-Gutierrez D, Cecconi F, Chan FK, Chandel NS, Cheng EH, Chipuk JE, Cidlowski JA, Ciechanover A, Cohen GM, Conrad M, Cubillos-Ruiz JR, Czabotar PE, D'Angiolella V, Dawson TM, Dawson VL, De Laurenzi V, De Maria R, Debatin KM, DeBerardinis RJ, Deshmukh M, Di Daniele N, Di Virgilio F, Dixit VM, Dixon SJ, Duckett CS, Dynlacht BD, El-Deiry WS, Elrod JW, Fimia GM, Fulda S, García-Sáez AJ, Garg AD, Garrido C, Gavathiotis E, Golstein P, Gottlieb E, Green DR, Greene LA, Gronemeyer H, Gross A, Hajnoczky G, Hardwick JM, Harris IS, Hengartner MO, Hetz C, Ichijo H, Jäättelä M, Joseph B, Jost PJ, Juin PP, Kaiser WJ, Karin M, Kaufmann T, Kepp O, Kimchi A, Kitsis RN, Klionsky DJ, Knight RA, Kumar S, Lee SW, Lemasters JJ, Levine B, Linkermann A, Lipton SA, Lockshin RA, López-Otín C, Lowe SW, Luedde T, Lugli E, MacFarlane M, Madeo F, Malewicz M, Malorni W, Manic G, Marine JC, Martin SJ, Martinou JC, Medema JP, Mehlen P, Meier P, Melino S, Miao EA, Molkentin JD, Moll UM, Muñoz-Pinedo C, Nagata S, Nuñez G, Oberst A, Oren M, Overholtzer M, Pagano M, Panaretakis T, Pasparakis M, Penninger JM, Pereira DM, Pervaiz S, Peter ME, Piacentini M, Pinton P, Prehn JHM, Puthalakath H, Rabinovich GA, Rehm M, Rizzuto R, Rodrigues CMP, Rubinsztein DC, Rudel T, Ryan KM, Sayan E, Scorrano L, Shao F, Shi Y, Silke J, Simon HU, Sistigu A, Stockwell BR, Strasser A, Szabadkai G, Tait SWG, Tang D, Tavernarakis N, Thorburn A, Tsujimoto Y, Turk B, Vanden Berghe T, Vandenabeele P, Vander Heiden MG, Villunger A, Virgin HW, Vousden KH, Vucic D, Wagner EF, Walczak H, Wallach D, Wang Y, Wells JA, Wood W, Yuan J, Zakeri Z, Zhivotovsky B, Zitvogel L, Melino G, Kroemer G. Molecular mechanisms of cell death: recommendations of the Nomenclature Committee on Cell Death 2018. *Cell Death Differ* 2018; **25**: 486-541 [PMID: 29362479 DOI: 10.1038/s41418-017-0012-4]

52 **Piao C**, Sang J, Kou Z, Wang Y, Liu T, Lu X, Jiao Z, Wang H. Effects of Exosomes Derived from Adipose-Derived Mesenchymal Stem Cells on Pyroptosis and Regeneration of Injured Liver. *Int J Mol Sci* 2022; **23** [PMID: 36292924 DOI: 10.3390/ijms232012065]

53 **Dixon SJ**, Lemberg KM, Lamprecht MR, Skouta R, Zaitsev EM, Gleason CE, Patel DN, Bauer AJ, Cantley AM, Yang WS, Morrison B 3rd, Stockwell BR. Ferroptosis: an iron-dependent form of nonapoptotic cell death. *Cell* 2012; **149**: 1060-1072 [PMID: 22632970 DOI: 10.1016/j.cell.2012.03.042]

54 **Hide D**, Ortega-Ribera M, Garcia-Pagan JC, Peralta C, Bosch J, Gracia-Sancho J. Effects of warm ischemia and reperfusion on the liver microcirculatory phenotype of rats: underlying mechanisms and pharmacological therapy. *Sci Rep* 2016; **6**: 22107 [PMID: 26905693 DOI: 10.1038/srep22107]

55 **Sun S**, Xue J, Guo Y, Li J. Bioinformatics analysis of genes related to ferroptosis in hepatic ischemia-reperfusion injury. *Front Genet* 2022; **13**: 1072544 [PMID: 36531223 DOI: 10.3389/fgene.2022.1072544]

56 **Liu Q**, Wu D, Ma Y, Cao Y, Pang Y, Tang M, Pu Y, Zhang T. Intracellular reactive oxygen species trigger mitochondrial dysfunction and apoptosis in cadmium telluride quantum dots-induced liver damage. *NanoImpact* 2022; **25**: 100392 [PMID: 35559896 DOI: 10.1016/j.impact.2022.100392]

57 **Han X**, Wang R, Song X, Yu F, Lv C, Chen L. A mitochondrial-targeting near-infrared fluorescent probe for bioimaging and evaluating endogenous superoxide anion changes during ischemia/reperfusion injury. *Biomaterials* 2018; **156**: 134-146 [PMID: 29195182 DOI: 10.1016/j.biomaterials.2017.11.039]

58 **Monga SP**. Lipid metabolic reprogramming in hepatic ischemia-reperfusion injury. *Nat Med* 2018; **24**: 6-7 [PMID: 29315298 DOI:

10.1038/nm.4468]
59 **Ke B**, Kupiec-Weglinski JW. Lipid Metabolites: The Alarm Signal to Trigger Liver Ischemia-reperfusion Injury. *Transplantation* 2018; **102**: 887-889 [PMID: 29782474 DOI: 10.1097/TP.0000000000002206]
60 **Lee RC**, Feinbaum RL, Ambros V. The C. elegans heterochronic gene lin-4 encodes small RNAs with antisense complementarity to lin-14. *Cell* 1993; **75**: 843-854 [PMID: 8252621 DOI: 10.1016/0092-8674(93)90529-y]
61 **Khraiwesh B**, Arif MA, Seumel GI, Ossowski S, Weigel D, Reski R, Frank W. Transcriptional control of gene expression by microRNAs. *Cell* 2010; **140**: 111-122 [PMID: 20085706 DOI: 10.1016/j.cell.2009.12.023]
62 **Bartel DP**. Metazoan MicroRNAs. *Cell* 2018; **173**: 20-51 [PMID: 29570994 DOI: 10.1016/j.cell.2018.03.006]
63 **Mendell JT**, Olson EN. MicroRNAs in stress signaling and human disease. *Cell* 2012; **148**: 1172-1187 [PMID: 22424228 DOI: 10.1016/j.cell.2012.02.005]
64 **Xu CF**, Yu CH, Li YM. Regulation of hepatic microRNA expression in response to ischemic preconditioning following ischemia/reperfusion injury in mice. *OMICS* 2009; **13**: 513-520 [PMID: 19780683 DOI: 10.1089/omi.2009.0035]
65 **Kim HJ**, Joe Y, Yu JK, Chen Y, Jeong SO, Mani N, Cho GJ, Pae HO, Ryter SW, Chung HT. Carbon monoxide protects against hepatic ischemia/reperfusion injury by modulating the miR-34a/SIRT1 pathway. *Biochim Biophys Acta* 2015; **1852**: 1550-1559 [PMID: 25916635 DOI: 10.1016/j.bbadis.2015.04.017]
66 **Moradi M**, Farbood Y, Mard SA, Dianat M, Goudarzi G, Khorsandi L, Seyedian SS. p-Coumaric acid has pure anti-inflammatory characteristics against hepatopathy caused by ischemia-reperfusion in the liver and dust exposure. *Iran J Basic Med Sci* 2023; **26**: 164-175 [PMID: 36742142 DOI: 10.22038/IJBMS.2022.66192.14554]
67 **Huang X**, Gao Y, Qin J, Lu S. The role of miR-34a in the hepatoprotective effect of hydrogen sulfide on ischemia/reperfusion injury in young and old rats. *PLoS One* 2014; **9**: e113305 [PMID: 25405338 DOI: 10.1371/journal.pone.0113305]
68 **Akbari G**, Mard SA, Dianat M, Mansouri E. The Hepatoprotective and MicroRNAs Downregulatory Effects of Crocin Following Hepatic Ischemia-Reperfusion Injury in Rats. *Oxid Med Cell Longev* 2017; **2017**: 1702967 [PMID: 28367266 DOI: 10.1155/2017/1702967]
69 **Mard SA**, Akbari G, Dianat M, Mansouri E. The Effect of Zinc Sulfate on miR-122, miR-34a, Atioxidants, Biochemical and Histopathological Parameters Following Hepatic Ischemia/Reperfusion Injury in Rats. *Biol Trace Elem Res* 2019; **188**: 434-440 [PMID: 30014282 DOI: 10.1007/s12011-018-1425-8]
70 **Akbari G**, Savari F, Mard SA, Rezaie A, Moradi M. Gallic acid protects the liver in rats against injuries induced by transient ischemia-reperfusion through regulating microRNAs expressions. *Iran J Basic Med Sci* 2019; **22**: 439-444 [PMID: 31168350 DOI: 10.22038/ijbms.2018.31589.7605]
71 **Zheng X**, Wang G, Yuan J, Li N, Yan B, Yan J, Sheng Y. hsa-miR-34a-5p Ameliorates Hepatic Ischemia/Reperfusion Injury Via Targeting HNF4α. *Turk J Gastroenterol* 2022; **33**: 596-605 [PMID: 35879917 DOI: 10.5152/tjg.2022.21169]
72 **Chang J**, Nicolas E, Marks D, Sander C, Lerro A, Buendia MA, Xu C, Mason WS, Moloshok T, Bort R, Zaret KS, Taylor JM. miR-122, a mammalian liver-specific microRNA, is processed from hcr mRNA and may downregulate the high affinity cationic amino acid transporter CAT-1. *RNA Biol* 2004; **1**: 106-113 [PMID: 17179747 DOI: 10.4161/rna.1.2.1066]
73 **Yin S**, Fan Y, Zhang H, Zhao Z, Hao Y, Li J, Sun C, Yang J, Yang Z, Yang X, Lu J, Xi JJ. Differential TGFβ pathway targeting by miR-122 in humans and mice affects liver cancer metastasis. *Nat Commun* 2016; **7**: 11012 [PMID: 26987776 DOI: 10.1038/ncomms11012]
74 **Rheault M**, Cousineau SE, Fox DR, Abram QH, Sagan SM. Elucidating the distinct contributions of miR-122 in the HCV life cycle reveals insights into virion assembly. *Nucleic Acids Res* 2023; **51**: 2447-2463 [PMID: 36807979 DOI: 10.1093/nar/gkad094]
75 **Van Caster P**, Brandenburger T, Strahl T, Metzger S, Bauer I, Pannen B, Braun S. Circulating microRNA-122, -21 and -223 as potential markers of liver injury following warm ischaemia and reperfusion in rats. *Mol Med Rep* 2015; **12**: 3146-3150 [PMID: 25954995 DOI: 10.3892/mmr.2015.3742]
76 **John K**, Hadem J, Krech T, Wahl K, Manns MP, Dooley S, Batkai S, Thum T, Schulze-Osthoff K, Bantel H. MicroRNAs play a role in spontaneous recovery from acute liver failure. *Hepatology* 2014; **60**: 1346-1355 [PMID: 24913549 DOI: 10.1002/hep.27250]
77 **Ju C**, Wang M, Tak E, Kim B, Emontzpohl C, Yang Y, Yuan X, Kutay H, Liang Y, Hall DR, Dar WA, Bynon JS, Carmeliet P, Ghoshal K, Eltzschig HK. Hypoxia-inducible factor-1α-dependent induction of miR122 enhances hepatic ischemia tolerance. *J Clin Invest* 2021; **131** [PMID: 33792566 DOI: 10.1172/JCI140300]
78 **Li L**, Li G, Yu C, Shen Z, Xu C, Feng Z, Zhang X, Li Y. A role of microRNA-370 in hepatic ischaemia-reperfusion injury by targeting transforming growth factor-β receptor II. *Liver Int* 2015; **35**: 1124-1132 [PMID: 24351048 DOI: 10.1111/liv.12441]
79 **Zhu J**, Zhu F, Song W, Zhang B, Zhang X, Jin X, Li H. Altered miR-370 expression in hepatic ischemia-reperfusion injury correlates with the level of nuclear kappa B (NF-κB) related factors. *Gene* 2017; **607**: 23-30 [PMID: 28043920 DOI: 10.1016/j.gene.2016.12.026]
80 **Pan GZ**, Yang Y, Zhang J, Liu W, Wang GY, Zhang YC, Yang Q, Zhai FX, Tai Y, Liu JR, Zhang Q, Chen GH. Bone marrow mesenchymal stem cells ameliorate hepatic ischemia/reperfusion injuries *via* inactivation of the MEK/ERK signaling pathway in rats. *J Surg Res* 2012; **178**: 935-948 [PMID: 22658855 DOI: 10.1016/j.jss.2012.04.070]
81 **Wu R**, Fan X, Wang Y, Shen M, Zheng Y, Zhao S, Yang L. Mesenchymal Stem Cell-Derived Extracellular Vesicles in Liver Immunity and Therapy. *Front Immunol* 2022; **13**: 833878 [PMID: 35309311 DOI: 10.3389/fimmu.2022.833878]
82 **Zare MA**, Zare A, Azarpira N, Pakbaz S. The protective effect of bone marrow-derived mesenchymal stem cells in liver ischemia/reperfusion injury *via* down-regulation of miR-370. *Iran J Basic Med Sci* 2019; **22**: 683-689 [PMID: 31231497 DOI: 10.22038/ijbms.2019.32670.7812]
83 **Sun G**, Zhou Y, Li H, Guo Y, Shan J, Xia M, Li Y, Li S, Long D, Feng L. Over-expression of microRNA-494 up-regulates hypoxia-inducible factor-1 alpha expression *via* PI3K/Akt pathway and protects against hypoxia-induced apoptosis. *J Biomed Sci* 2013; **20**: 100 [PMID: 24364919 DOI: 10.1186/1423-0127-20-100]
84 **Lv J**, Zou X, Yu C, Ou W, Sun C. Effects of propofol on cardiac function and miR-494 expression in rats with hepatic ischemia/reperfusion injury. *J Int Med Res* 2021; **49**: 300060521990988 [PMID: 33682507 DOI: 10.1177/0300060521990988]
85 **Su S**, Luo D, Liu X, Liu J, Peng F, Fang C, Li B. miR-494 up-regulates the PI3K/Akt pathway *via* targetting PTEN and attenuates hepatic ischemia/reperfusion injury in a rat model. *Biosci Rep* 2017; **37** [PMID: 28842516 DOI: 10.1042/BSR20170798]
86 **Zheng W**, Men H, Li J, Xing Y, Wu B, Wang Z, Teng D, Shi Y, Jiang P, Cai J. Global MicroRNA Expression Profiling of Mouse Livers following Ischemia-Reperfusion Injury at Different Stages. *PLoS One* 2016; **11**: e0148677 [PMID: 26859886 DOI: 10.1371/journal.pone.0148677]
87 **Zhang P**, Ming Y, Ye Q, Niu Y. Comprehensive circRNA expression profile during ischemic postconditioning attenuating hepatic ischemia/reperfusion injury. *Sci Rep* 2019; **9**: 264 [PMID: 30670716 DOI: 10.1038/s41598-018-36443-8]

88 **Li T**, Chen Q, Dai J, Huang Z, Luo Y, Mou T, Pu J, Yang H, Wei X, Wu Z. MicroRNA-141-3p Attenuates Oxidative Stress-induced Hepatic Ischemia Reperfusion Injury via Keap1/Nrf2 Pathway. 2021 Preprint [DOI: 10.21203/rs.3.rs-1107846/v1]

89 **Li T**, Chen Q, Dai J, Huang Z, Luo Y, Mou T, Pu J, Yang H, Wei X, Wu Z. MicroRNA-141-3p attenuates oxidative stress-induced hepatic ischemia reperfusion injury *via* Keap1/Nrf2 pathway. *Mol Biol Rep* 2022; **49**: 7575-7585 [PMID: 35644004 DOI: 10.1007/s11033-022-07570-3]

90 **Roy S**, Benz F, Alder J, Bantel H, Janssen J, Vucur M, Gautheron J, Schneider A, Schüller F, Loosen S, Luedde M, Koch A, Tacke F, Luedde T, Trautwein C, Roderburg C. Down-regulation of miR-192-5p protects from oxidative stress-induced acute liver injury. *Clin Sci (Lond)* 2016; **130**: 1197-1207 [PMID: 27129188 DOI: 10.1042/CS20160216]

91 **Morita T**, Ishikawa M, Sakamoto A. Identical MicroRNAs Regulate Liver Protection during Anaesthetic and Ischemic Preconditioning in Rats: An animal study. *PLoS One* 2015; **10**: e0125866 [PMID: 25974021 DOI: 10.1371/journal.pone.0125866]

92 **He B**, Yang F, Ning Y, Li Y. Sevoflurane alleviates hepatic ischaemia/reperfusion injury by up-regulating miR-96 and down-regulating FOXO4. *J Cell Mol Med* 2021; **25**: 5899-5911 [PMID: 34061461 DOI: 10.1111/jcmm.16063]

93 **Xu L**, Ge F, Hu Y, Yu Y, Guo K, Miao C. Sevoflurane Postconditioning Attenuates Hepatic Ischemia-Reperfusion Injury by Limiting HMGB1/TLR4/NF-κB Pathway *via* Modulating microRNA-142 in vivo and in vitro. *Front Pharmacol* 2021; **12**: 646307 [PMID: 33935744 DOI: 10.3389/fphar.2021.646307]

94 **Wang H**, Guo L, Wang Y, Song S. Isoflurane upregulates microRNA-9-3p to protect rats from hepatic ischemia-reperfusion injury through inhibiting fibronectin type III domain containing 3B. *Cell Cycle* 2021; **20**: 1527-1539 [PMID: 34308776 DOI: 10.1080/15384101.2021.1947548]

95 **Hao W**, Zhao ZH, Meng QT, Tie ME, Lei SQ, Xia ZY. Propofol protects against hepatic ischemia/reperfusion injury *via* miR-133a-5p regulating the expression of MAPK6. *Cell Biol Int* 2017; **41**: 495-504 [PMID: 28198596 DOI: 10.1002/cbin.10745]

96 **Li S**, Zhang J, Wang Z, Wang T, Yu Y, He J, Zhang H, Yang T, Shen Z. MicroRNA-17 regulates autophagy to promote hepatic ischemia/reperfusion injury *via* suppression of signal transductions and activation of transcription-3 expression. *Liver Transpl* 2016; **22**: 1697-1709 [PMID: 27541946 DOI: 10.1002/lt.24606]

97 **Li Y**, Ma D, Wang Z, Yang J. MicroRNA-155 Deficiency in Kupffer Cells Ameliorates Liver Ischemia-Reperfusion Injury in Mice. *Transplantation* 2017; **101**: 1600-1608 [PMID: 28640790 DOI: 10.1097/TP.0000000000001765]

98 **Schueller F**, Roy S, Loosen SH, Alder J, Koppe C, Schneider AT, Wandrer F, Bantel H, Vucur M, Mi QS, Trautwein C, Luedde T, Roderburg C. miR-223 represents a biomarker in acute and chronic liver injury. *Clin Sci (Lond)* 2017; **131**: 1971-1987 [PMID: 28646120 DOI: 10.1042/CS20170218]

99 **Xing Y**, Li J, Li SP, Xi J, Ma N, Liu L, Wang JS, Cai JZ. MiR-27a-5p regulates apoptosis of liver ischemia-reperfusion injury in mice by targeting Bach1. *J Cell Biochem* 2018; **119**: 10376-10383 [PMID: 30145824 DOI: 10.1002/jcb.27383]

100 **Pan W**, Wang L, Zhang XF, Zhang H, Zhang J, Wang G, Xu P, Zhang Y, Hu P, Zhang XD, Du RL, Wang H. Hypoxia-induced microRNA-191 contributes to hepatic ischemia/reperfusion injury through the ZONAB/Cyclin D1 axis. *Cell Death Differ* 2019; **26**: 291-305 [PMID: 29769640 DOI: 10.1038/s41418-018-0120-9]

101 **Huang Z**, Mou T, Luo Y, Pu X, Pu J, Wan L, Gong J, Yang H, Liu Y, Li Z, Shen A, Wu Z. Inhibition of miR-450b-5p ameliorates hepatic ischemia/reperfusion injury *via* targeting CRYAB. *Cell Death Dis* 2020; **11**: 455 [PMID: 32532961 DOI: 10.1038/s41419-020-2648-0]

102 **Ji H**, Li H, Zhang H, Cheng Z. Role of microRNA2185p in sevofluraneinduced protective effects in hepatic ischemia/reperfusion injury mice by regulating GAB2/PI3K/AKT pathway. *Mol Med Rep* 2022; **25** [PMID: 34726254 DOI: 10.3892/mmr.2021.12517]

103 **Zhang T**, Xiu HH, Liu JX, Ma Y, Xu KQ, Huang WQ. Protective effect of aspirin-triggered resolvin D1 on hepatic ischemia/reperfusion injury in rats: The role of miR-146b. *Int Immunopharmacol* 2017; **51**: 140-147 [PMID: 28837866 DOI: 10.1016/j.intimp.2017.08.008]

104 **Sun XL**, Zhang YL, Xi SM, Ma LJ, Li SP. MiR-330-3p suppresses phosphoglycerate mutase family member 5 -inducted mitophagy to alleviate hepatic ischemia-reperfusion injury. *J Cell Biochem* 2019; **120**: 4255-4267 [PMID: 30269356 DOI: 10.1002/jcb.27711]

105 **Xie K**, Liu L, Chen J, Liu F. Exosomal miR-1246 derived from human umbilical cord blood mesenchymal stem cells attenuates hepatic ischemia reperfusion injury by modulating T helper 17/regulatory T balance. *IUBMB Life* 2019; **71**: 2020-2030 [PMID: 31433911 DOI: 10.1002/iub.2147]

106 **Li SP**, He JD, Wang Z, Yu Y, Fu SY, Zhang HM, Zhang JJ, Shen ZY. miR-30b inhibits autophagy to alleviate hepatic ischemia-reperfusion injury *via* decreasing the Atg12-Atg5 conjugate. *World J Gastroenterol* 2016; **22**: 4501-4514 [PMID: 27182160 DOI: 10.3748/wjg.v22.i18.4501]

107 **Jiang W**, Kong L, Ni Q, Lu Y, Ding W, Liu G, Pu L, Tang W. miR-146a ameliorates liver ischemia/reperfusion injury by suppressing IRAK1 and TRAF6. *PLoS One* 2014; **9**: e101530 [PMID: 24987958 DOI: 10.1371/journal.pone.0101530]

108 **Li X**, Yi S, Deng Y, Cheng J, Wu X, Liu W, Tai Y, Chen G, Zhang Q, Yang Y. MiR-124 protects human hepatic L02 cells from H2O2-induced apoptosis by targeting Rab38 gene. *Biochem Biophys Res Commun* 2014; **450**: 148-153 [PMID: 24875359 DOI: 10.1016/j.bbrc.2014.05.085]

109 **Jiang W**, Liu G, Tang W. MicroRNA-182-5p Ameliorates Liver Ischemia-Reperfusion Injury by Suppressing Toll-Like Receptor 4. *Transplant Proc* 2016; **48**: 2809-2814 [PMID: 27788822 DOI: 10.1016/j.transproceed.2016.06.043]

110 **Huang X**, Gao Y, Qin J, Lu S. miR-214 Down-Regulation Promoted Hypoxia/Reoxygenation-Induced Hepatocyte Apoptosis Through TRAF1/ASK1/JNK Pathway. *Dig Dis Sci* 2019; **64**: 1217-1225 [PMID: 30560327 DOI: 10.1007/s10620-018-5405-9]

111 **Zhang Y**, Lv J, Wu G, Li W, Zhang Z, Lei X. MicroRNA-449b-5p targets HMGB1 to attenuate hepatocyte injury in liver ischemia and reperfusion. *J Cell Physiol* 2019; **234**: 16367-16375 [PMID: 30805938 DOI: 10.1002/jcp.28305]

112 **Li Y**, Gao M, Xu LN, Yin LH, Qi Y, Peng JY. MicroRNA-142-3p attenuates hepatic ischemia/reperfusion injury *via* targeting of myristoylated alanine-rich C-kinase substrate. *Pharmacol Res* 2020; **156**: 104783 [PMID: 32224251 DOI: 10.1016/j.phrs.2020.104783]

113 **Shen A**, Zheng D, Luo Y, Mou T, Chen Q, Huang Z, Wu Z. MicroRNA-24-3p alleviates hepatic ischemia and reperfusion injury in mice through the repression of STING signaling. *Biochem Biophys Res Commun* 2020; **522**: 47-52 [PMID: 31735332 DOI: 10.1016/j.bbrc.2019.10.182]

114 **Duan Y**, Meng Y, Gao Z, Wang X, Zhang H. microRNA-9-5p protects liver sinusoidal endothelial cell against oxygen glucose deprivation/reperfusion injury. *Open Life Sci* 2021; **16**: 375-383 [PMID: 33977146 DOI: 10.1515/biol-2021-0042]

115 **Luo YH**, Huang ZT, Zong KZ, Cao ZR, Peng DD, Zhou BY, Shen A, Yan P, Wu ZJ. miR-194 ameliorates hepatic ischemia/reperfusion injury *via* targeting PHLDA1 in a TRAF6-dependent manner. *Int Immunopharmacol* 2021; **96**: 107604 [PMID: 33839577 DOI: 10.1016/j.intimp.2021.107604]

116 **Li X**, Wu L, Tian X, Zheng W, Yuan M, Zuo H, Song H, Shen Z. miR-29a-3p in Exosomes from Heme Oxygenase-1 Modified Bone Marrow

Mesenchymal Stem Cells Alleviates Steatotic Liver Ischemia-Reperfusion Injury in Rats by Suppressing Ferroptosis *via* Iron Responsive Element Binding Protein 2. *Oxid Med Cell Longev* 2022; **2022**: 6520789 [PMID: 35720183 DOI: 10.1155/2022/6520789]

117 **Wang YL**, Zhang Y, Cai DS. Hepatoprotective effects of sevoflurane against hepatic ischemia-reperfusion injury by regulating microRNA-124-3p-mediated TRAF3/CREB axis. *Cell Death Discov* 2022; **8**: 105 [PMID: 35260558 DOI: 10.1038/s41420-021-00784-7]

118 **Wu L**, Tian X, Zuo H, Zheng W, Li X, Yuan M, Song H. miR-124-3p delivered by exosomes from heme oxygenase-1 modified bone marrow mesenchymal stem cells inhibits ferroptosis to attenuate ischemia-reperfusion injury in steatotic grafts. *J Nanobiotechnology* 2022; **20**: 196 [PMID: 35459211 DOI: 10.1186/s12951-022-01407-8]

119 **Yu Q**, Chen S, Tang H, Yang H, Zhang J, Shi X, Li J, Guo W, Zhang S. miR1405p alleviates mouse liver ischemia/reperfusion injury by targeting CAPN1. *Mol Med Rep* 2021; **24** [PMID: 34296301 DOI: 10.3892/mmr.2021.12314]

120 **Zheng D**, Li Z, Wei X, Liu R, Shen A, He D, Tang C, Wu Z. Role of miR-148a in Mitigating Hepatic Ischemia-Reperfusion Injury by Repressing the TLR4 Signaling Pathway *via* Targeting CaMKIIα in Vivo and in Vitro. *Cell Physiol Biochem* 2018; **49**: 2060-2072 [PMID: 30244246 DOI: 10.1159/000493716]

121 **van Heesch S**, van Iterson M, Jacobi J, Boymans S, Essers PB, de Bruijn E, Hao W, MacInnes AW, Cuppen E, Simonis M. Extensive localization of long noncoding RNAs to the cytosol and mono- and polyribosomal complexes. *Genome Biol* 2014; **15**: R6 [PMID: 24393600 DOI: 10.1186/gb-2014-15-1-r6]

122 **Mercer TR**, Mattick JS. Structure and function of long noncoding RNAs in epigenetic regulation. *Nat Struct Mol Biol* 2013; **20**: 300-307 [PMID: 23463315 DOI: 10.1038/nsmb.2480]

123 **Noh JH**, Kim KM, McClusky WG, Abdelmohsen K, Gorospe M. Cytoplasmic functions of long noncoding RNAs. *Wiley Interdiscip Rev RNA* 2018; **9**: e1471 [PMID: 29516680 DOI: 10.1002/wrna.1471]

124 **Li W**, Wang YY, Xiao L, Ding J, Wang L, Wang F, Sun T. Mysterious long noncoding RNAs and their relationships to human disease. *Front Mol Biosci* 2022; **9**: 950408 [PMID: 36406273 DOI: 10.3389/fmolb.2022.950408]

125 **Wapinski O**, Chang HY. Long noncoding RNAs and human disease. *Trends Cell Biol* 2011; **21**: 354-361 [PMID: 21550244 DOI: 10.1016/j.tcb.2011.04.001]

126 **Wang K**, Liu F, Liu CY, An T, Zhang J, Zhou LY, Wang M, Dong YH, Li N, Gao JN, Zhao YF, Li PF. The long noncoding RNA NRF regulates programmed necrosis and myocardial injury during ischemia and reperfusion by targeting miR-873. *Cell Death Differ* 2016; **23**: 1394-1405 [PMID: 27258785 DOI: 10.1038/cdd.2016.28]

127 **Liu D**, Liu Y, Zheng X, Liu N. c-MYC-induced long noncoding RNA MEG3 aggravates kidney ischemia-reperfusion injury through activating mitophagy by upregulation of RTKN to trigger the Wnt/β-catenin pathway. *Cell Death Dis* 2021; **12**: 191 [PMID: 33602903 DOI: 10.1038/s41419-021-03466-5]

128 **Jia P**, Xu S, Ren T, Pan T, Wang X, Zhang Y, Zou Z, Guo M, Zeng Q, Shen B, Ding X. LncRNA IRAR regulates chemokines production in tubular epithelial cells thus promoting kidney ischemia-reperfusion injury. *Cell Death Dis* 2022; **13**: 562 [PMID: 35732633 DOI: 10.1038/s41419-022-05018-x]

129 **Vasudeva K**, Dutta A, Munshi A. Role of lncRNAs in the Development of Ischemic Stroke and Their Therapeutic Potential. *Mol Neurobiol* 2021; **58**: 3712-3728 [PMID: 33818737 DOI: 10.1007/s12035-021-02359-0]

130 **Chen Z**, Jia S, Li D, Cai J, Tu J, Geng B, Guan Y, Cui Q, Yang J. Silencing of long noncoding RNA AK139328 attenuates ischemia/reperfusion injury in mouse livers. *PLoS One* 2013; **8**: e80817 [PMID: 24312245 DOI: 10.1371/journal.pone.0080817]

131 **Li D**, Chen G, Yang J, Fan X, Gong Y, Xu G, Cui Q, Geng B. Transcriptome analysis reveals distinct patterns of long noncoding RNAs in heart and plasma of mice with heart failure. *PLoS One* 2013; **8**: e77938 [PMID: 24205036 DOI: 10.1371/journal.pone.0077938]

132 **Gu XX**, Xu XX, Liao HH, Wu RN, Huang WM, Cheng LX, Lu YW, Mo J. Dexmedetomidine hydrochloride inhibits hepatocyte apoptosis and inflammation by activating the lncRNA TUG1/miR-194/SIRT1 signaling pathway. *J Inflamm (Lond)* 2021; **18**: 20 [PMID: 34039367 DOI: 10.1186/s12950-021-00287-3]

133 **Wang L**, Qu P, Yin W, Sun J. Lnc-NEAT1 induces cell apoptosis and inflammation but inhibits proliferation in a cellular model of hepatic ischemia/reperfusion injury. *J Int Med Res* 2021; **49**: 300060519887251 [PMID: 33682508 DOI: 10.1177/0300060519887251]

134 **Zhang Y**, Zhang H, Zhang Z, Li S, Jiang W, Li X, Lv J. LncRNA MALAT1 cessation antagonizes hypoxia/reoxygenation injury in hepatocytes by inhibiting apoptosis and inflammation *via* the HMGB1-TLR4 axis. *Mol Immunol* 2019; **112**: 22-29 [PMID: 31075559 DOI: 10.1016/j.molimm.2019.04.015]

135 **Wang C**, Yu H, Lu S, Ke S, Xu Y, Feng Z, Qian B, Bai M, Yin B, Li X, Hua Y, Dong L, Li Y, Zhang B, Li Z, Chen D, Chen B, Zhou Y, Pan S, Fu Y, Jiang H, Wang D, Ma Y. LncRNA Hnf4αos exacerbates liver ischemia/reperfusion injury in mice *via* Hnf4αos/Hnf4α duplex-mediated PGC1α suppression. *Redox Biol* 2022; **57**: 102498 [PMID: 36242914 DOI: 10.1016/j.redox.2022.102498]

136 **Huang X**, Gao Y, Qin J, Lu S. The mechanism of long non-coding RNA MEG3 for hepatic ischemia-reperfusion: Mediated by miR-34a/Nrf2 signaling pathway. *J Cell Biochem* 2018; **119**: 1163-1172 [PMID: 28708282 DOI: 10.1002/jcb.26286]

137 **Ying D**, Zhou X, Ruan Y, Wang L, Wu X. LncRNA Gm4419 induces cell apoptosis in hepatic ischemia-reperfusion injury *via* regulating the miR-455-SOX6 axis. *Biochem Cell Biol* 2020; **98**: 474-483 [PMID: 32114773 DOI: 10.1139/bcb-2019-0331]

138 **Zhou Z**, Chen Q, Wan L, Zheng D, Li Z, Wu Z. Dexmedetomidine protects hepatic cells against oxygen-glucose deprivation/reperfusion injury *via* lncRNA CCAT1. *Cell Biol Int* 2018; **42**: 1250-1258 [PMID: 29851220 DOI: 10.1002/cbin.10996]

139 **Dai B**, Qiao L, Zhang M, Cheng L, Zhang L, Geng L, Shi C, Sui C, Shen W, Sun Y, Chen Q, Hui D, Wang Y, Yang J. lncRNA AK054386 Functions as a ceRNA to Sequester miR-199 and Induce Sustained Endoplasmic Reticulum Stress in Hepatic Reperfusion Injury. *Oxid Med Cell Longev* 2019; **2019**: 8189079 [PMID: 31827704 DOI: 10.1155/2019/8189079]

140 **Tang B**, Bao N, He G, Wang J. Long noncoding RNA HOTAIR regulates autophagy *via* the miR-20b-5p/ATG7 axis in hepatic ischemia/reperfusion injury. *Gene* 2019; **686**: 56-62 [PMID: 30367982 DOI: 10.1016/j.gene.2018.10.059]

141 **Li X**, Su Q, Li W, Zhang X, Ran J. Analysis and identification of potential key genes in hepatic ischemia-reperfusion injury. *Ann Transl Med* 2022; **10**: 1375 [PMID: 36660667 DOI: 10.21037/atm-22-6171]

142 **Ming N**, Na HST, He JL, Meng QT, Xia ZY. Propofol alleviates oxidative stress *via* upregulating lncRNA-TUG1/Brg1 pathway in hypoxia/reoxygenation hepatic cells. *J Biochem* 2019; **166**: 415-421 [PMID: 31297532 DOI: 10.1093/jb/mvz054]

143 **Sun Q**, Gong J, Wu J, Hu Z, Zhang Q, Zhu X. SNHG1-miR-186-5p-YY1 feedback loop alleviates hepatic ischemia/reperfusion injury. *Cell Cycle* 2022; **21**: 1267-1279 [PMID: 35275048 DOI: 10.1080/15384101.2022.2046984]

144 **Zhang XO**, Dong R, Zhang Y, Zhang JL, Luo Z, Zhang J, Chen LL, Yang L. Diverse alternative back-splicing and alternative splicing landscape of circular RNAs. *Genome Res* 2016; **26**: 1277-1287 [PMID: 27365365 DOI: 10.1101/gr.202895.115]

145 **Huang C**, Liang D, Tatomer DC, Wilusz JE. A length-dependent evolutionarily conserved pathway controls nuclear export of circular RNAs. *Genes Dev* 2018; **32**: 639-644 [PMID: 29773557 DOI: 10.1101/gad.314856.118]

146 **Chen LL**. The expanding regulatory mechanisms and cellular functions of circular RNAs. *Nat Rev Mol Cell Biol* 2020; **21**: 475-490 [PMID: 32366901 DOI: 10.1038/s41580-020-0243-y]

147 **Gao Y**, Zhou Y, Wei L, Feng Z, Chen Y, Liu P, Peng Y, Huang Q, Gao L, Liu Y, Han Y, Shen H, Cai C, Zeng S. Hsa_Circ_0066351 Acts as a Prognostic and Immunotherapeutic Biomarker in Colorectal Cancer. *Front Immunol* 2022; **13**: 927811 [PMID: 36405685 DOI: 10.3389/fimmu.2022.927811]

148 **Xia P**, Wang S, Ye B, Du Y, Li C, Xiong Z, Qu Y, Fan Z. A Circular RNA Protects Dormant Hematopoietic Stem Cells from DNA Sensor cGAS-Mediated Exhaustion. *Immunity* 2018; **48**: 688-701.e7 [PMID: 29625897 DOI: 10.1016/j.immuni.2018.03.016]

149 **Piwecka M**, Glažar P, Hernandez-Miranda LR, Memczak S, Wolf SA, Rybak-Wolf A, Filipchyk A, Klironomos F, Cerda Jara CA, Fenske P, Trimbuch T, Zywitza V, Plass M, Schreyer L, Ayoub S, Kocks C, Kühn R, Rosenmund C, Birchmeier C, Rajewsky N. Loss of a mammalian circular RNA locus causes miRNA deregulation and affects brain function. *Science* 2017; **357** [PMID: 28798046 DOI: 10.1126/science.aam8526]

150 **Huang C**, Qu Y, Feng F, Zhang H, Shu L, Zhu X, Huang G, Xu J. Cardioprotective Effect of circ_SMG6 Knockdown against Myocardial Ischemia/Reperfusion Injury Correlates with miR-138-5p-Mediated EGR1/TLR4/TRIF Inactivation. *Oxid Med Cell Longev* 2022; **2022**: 1927260 [PMID: 35126807 DOI: 10.1155/2022/1927260]

151 **Gao XQ**, Liu CY, Zhang YH, Wang YH, Zhou LY, Li XM, Wang K, Chen XZ, Wang T, Ju J, Wang F, Wang SC, Wang Y, Chen ZY. The circRNA CNEACR regulates necroptosis of cardiomyocytes through Foxa2 suppression. *Cell Death Differ* 2022; **29**: 527-539 [PMID: 34588633 DOI: 10.1038/s41418-021-00872-2]

152 **Zhou LY**, Zhai M, Huang Y, Xu S, An T, Wang YH, Zhang RC, Liu CY, Dong YH, Wang M, Qian LL, Ponnusamy M, Zhang YH, Zhang J, Wang K. The circular RNA ACR attenuates myocardial ischemia/reperfusion injury by suppressing autophagy *via* modulation of the Pink1/FAM65B pathway. *Cell Death Differ* 2019; **26**: 1299-1315 [PMID: 30349076 DOI: 10.1038/s41418-018-0206-4]

153 **Yang Z**, Huang C, Wen X, Liu W, Huang X, Li Y, Zang J, Weng Z, Lu D, Tsang CK, Li K, Xu A. Circular RNA circ-FoxO3 attenuates blood-brain barrier damage by inducing autophagy during ischemia/reperfusion. *Mol Ther* 2022; **30**: 1275-1287 [PMID: 34763084 DOI: 10.1016/j.ymthe.2021.11.004]

154 **Xu Y**, Jiang W, Zhong L, Li H, Bai L, Chen X, Lin Y, Zheng D. circ-AKT3 aggravates renal ischaemia-reperfusion injury *via* regulating miR-144-5p /Wnt/β-catenin pathway and oxidative stress. *J Cell Mol Med* 2022; **26**: 1766-1775 [PMID: 33200535 DOI: 10.1111/jcmm.16072]

155 **Tian X**, Hu Y, Liu Y, Yang Z, Xie H, Zhou L, Zheng S. Circular RNA Microarray Analyses in Hepatic Ischemia-Reperfusion Injury With Ischemic Preconditioning Prevention. *Front Med (Lausanne)* 2021; **8**: 626948 [PMID: 33763433 DOI: 10.3389/fmed.2021.626948]

156 **Ma X**, Huang Y, Ding Y, Shi L, Zhong X, Kang M, Li C. Analysis of piRNA expression spectra in a non-alcoholic fatty liver disease mouse model induced by a methionine- and choline-deficient diet. *Exp Ther Med* 2020; **19**: 3829-3839 [PMID: 32346447 DOI: 10.3892/etm.2020.8653]

157 **Xu J**, Yang X, Zhou Q, Zhuang J, Han S. Biological significance of piRNA in liver cancer: a review. *Biomarkers* 2020; **25**: 436-440 [PMID: 32662667 DOI: 10.1080/1354750X.2020.1794041]

158 **Xu L**, Chen W, Chen J, Jin Y, Ma W, Qi G, Sun X, Luo J, Li C, Zhao K, Zheng Y, Yu D. PIWI-interacting RNA-23210 protects against acetaminophen-induced liver injury by targeting HNF1A and HNF4A. *Biochem Pharmacol* 2022; **197**: 114897 [PMID: 34968487 DOI: 10.1016/j.bcp.2021.114897]

159 **Liu X**, Xie W, Meng S, Kang X, Liu Y, Guo L, Wang C. Small Nucleolar RNAs and Their Comprehensive Biological Functions in Hepatocellular Carcinoma. *Cells* 2022; **11** [PMID: 36078062 DOI: 10.3390/cells11172654]

160 **Huang P**, Tu B, Liao HJ, Huang FZ, Li ZZ, Zhu KY, Dai F, Liu HZ, Zhang TY, Sun CZ. Elevation of plasma tRNA fragments as a promising biomarker for liver fibrosis in nonalcoholic fatty liver disease. *Sci Rep* 2021; **11**: 5886 [PMID: 33723340 DOI: 10.1038/s41598-021-85421-0]

161 **Zhu J**, Cheng M, Zhao X. A tRNA-derived fragment (tRF-3001b) aggravates the development of nonalcoholic fatty liver disease by inhibiting autophagy. *Life Sci* 2020; **257**: 118125 [PMID: 32702444 DOI: 10.1016/j.lfs.2020.118125]

162 **Law PT**, Qin H, Ching AK, Lai KP, Co NN, He M, Lung RW, Chan AW, Chan TF, Wong N. Deep sequencing of small RNA transcriptome reveals novel non-coding RNAs in hepatocellular carcinoma. *J Hepatol* 2013; **58**: 1165-1173 [PMID: 23376363 DOI: 10.1016/j.jhep.2013.01.032]

World Journal of Gastroenterology

Submit a Manuscript: https://www.f6publishing.com

World J Gastroenterol 2023 September 7; 29(33): 4942-4961

DOI: 10.3748/wjg.v29.i33.4942

ISSN 1007-9327 (print) ISSN 2219-2840 (online)

REVIEW

Prevention and management of hepatitis B virus reactivation in patients with hematological malignancies in the targeted therapy era

Joyce Wing Yan Mak, Alvin Wing Hin Law, Kimmy Wan Tung Law, Rita Ho, Carmen Ka Man Cheung, Man Fai Law

Specialty type: Gastroenterology and hepatology

Provenance and peer review: Invited article; Externally peer reviewed.

Peer-review model: Single blind

Peer-review report's scientific quality classification

Grade A (Excellent): 0
Grade B (Very good): B
Grade C (Good): C
Grade D (Fair): 0
Grade E (Poor): 0

P-Reviewer: Gerlich W, Germany; Krygier R, Poland

Received: May 29, 2023
Peer-review started: May 29, 2023
First decision: June 20, 2023
Revised: July 22, 2023
Accepted: August 15, 2023
Article in press: August 15, 2023
Published online: September 7, 2023

Joyce Wing Yan Mak, Carmen Ka Man Cheung, Man Fai Law, Department of Medicine and Therapeutics, Prince of Wales Hospital, Hong Kong 852, China

Alvin Wing Hin Law, Kimmy Wan Tung Law, West Island School, Hong Kong 852, China

Rita Ho, Department of Medicine, North District Hospital, Hong Kong 852, China

Corresponding author: Man Fai Law, MRCP, Doctor, Department of Medicine and Therapeutics, Prince of Wales Hospital, 30-32 Ngai Shing Street, Shatin, Hong Kong 852, China. mflaw99@yahoo.com.hk

Abstract

Hepatitis due to hepatitis B virus (HBV) reactivation can be serious and potentially fatal, but is preventable. HBV reactivation is most commonly reported in patients receiving chemotherapy, especially rituximab-containing therapy for hematological malignancies and those receiving stem cell transplantation. Patients with inactive and even resolved HBV infection still have persistence of HBV genomes in the liver. The expression of these silent genomes is controlled by the immune system. Suppression or ablation of immune cells, most importantly B cells, may lead to reactivation of seemingly resolved HBV infection. Thus, all patients with hematological malignancies receiving anticancer therapy should be screened for active or resolved HBV infection by blood tests for hepatitis B surface antigen (HBsAg) and antibody to hepatitis B core antigen. Patients found to be positive for HBsAg should be given prophylactic antiviral therapy. For patients with resolved HBV infection, there are two approaches. The first is pre-emptive therapy guided by serial HBV DNA monitoring, and treatment with antiviral therapy as soon as HBV DNA becomes detectable. The second approach is prophy-lactic antiviral therapy, particularly for patients receiving high-risk therapy, especially anti-CD20 monoclonal antibody or hematopoietic stem cell transplantation. Entecavir and tenofovir are the preferred antiviral choices. Many new effective therapies for hematological malignancies have been introduced in the past decade, for example, chimeric antigen receptor (CAR)-T cell therapy, novel monoclonal antibodies, bispecific antibody drug conjugates, and small molecule inhibitors, which may be associated with HBV reactivation. Although there is limited evidence to guide the optimal preventive measures, we recommend antivi-ral prophylaxis in HBsAg-positive patients receiving novel treatments, including Bruton's tyrosine kinase inhibitors, B-cell lymphoma 2 inhibitors, and CAR-T cell

therapy. Further studies are needed to determine the risk of HBV reactivation with these agents and the best prophylactic strategy.

Key Words: Hepatitis B; Hematologic neoplasms; Chimeric antigen receptor-T cell therapy; Monoclonal antibodies; Bruton's tyrosine kinase inhibitors; Antiviral agents

©The Author(s) 2023. Published by Baishideng Publishing Group Inc. All rights reserved.

Core Tip: Patients with chronic or past resolved hepatitis B virus (HBV) infection are at risk of reactivation of the virus when they receive chemotherapy or immunosuppressive therapy. Therefore, before treatment, patients should be screened for HBV markers, specifically hepatitis B surface antigen (HBsAg) and antibody to hepatitis B core antigen. Prophylactic antiviral therapy is important for HBsAg-positive patients, and is a reasonable option for patients with resolved HBV infection who are scheduled to receive high-risk therapy such as anti-CD20 monoclonal antibodies, anti-CD79 monoclonal antibodies, bispecific antibodies, chimeric antigen receptor-T cell therapy, or hematopoietic stem cell transplantation. For other patients with resolved HBV infection, pre-emptive antiviral therapy guided by serial monitoring of HBV DNA is a reasonable option.

Citation: Mak JWY, Law AWH, Law KWT, Ho R, Cheung CKM, Law MF. Prevention and management of hepatitis B virus reactivation in patients with hematological malignancies in the targeted therapy era. *World J Gastroenterol* 2023; 29(33): 4942-4961
URL: https://www.wjgnet.com/1007-9327/full/v29/i33/4942.htm
DOI: https://dx.doi.org/10.3748/wjg.v29.i33.4942

INTRODUCTION

Patients with chronic or resolved hepatitis B virus (HBV) infection are at risk of viral reactivation during chemotherapy or immunosuppressive therapy, commonly in patients receiving anti-cancer therapy for hematological malignancies or hematopoietic stem cell transplantation (HSCT). The earliest reports of HBV reactivation were in patients with lymphoma [1], and the highest risk of HBV reactivation is in patients receiving potent anti-CD20 monoclonal antibodies such as rituximab or obinutuzumab, which result in profound B-cell depletion.

There have been major advances in the development of new targeted therapy in the treatment of hematological malignancies in the past two decades. Bruton's tyrosine kinase (BTK) inhibitors are increasingly used in chronic lymphocytic leukemia (CLL) and lymphoma. Because these agents block B-cell antigen receptor signaling and thus reduce malignant B-cell proliferation, BTK inhibitors may potentially reactivate HBV. Other examples include bispecific antibodies in the treatment of non-Hodgkin lymphoma (NHL), CD79b-targeted antibody-drug conjugate, *i.e.*, polatuzumab vedotin, for diffuse large B cell lymphoma (DLBCL), and anti-CD38 monoclonal antibodies used in multiple myeloma (MM) patients.

Chimeric antigen receptor (CAR)-T cell therapy is a promising intervention which can be applied to lymphoid malignancies and plasma cell diseases including acute lymphoblastic leukemia (ALL), NHL, and MM. There is prolonged B-cell aplasia after CAR-T cell therapy which may potentially cause fatal HBV reactivation[2]. Hence, an understanding of the risk of HBV reactivation during treatment with novel therapies is important to prevent a fatal outcome.

This article will review the current published data on the clinical course and risk factors for HBV reactivation when using these novel therapies in patients with hematological malignancies. The recommended choice and duration of antiviral prophylaxis together with monitoring after stopping antiviral prophylaxis will also be discussed.

DEFINITIONS OF HBV REACTIVATION AND CLINICAL MANIFESTATIONS

Antibody to hepatitis B core (anti-HBc) is a good marker of current and past HBV infection as it persists even after hepatitis B surface antigen (HBsAg) is no longer detectable, while anti-HBs can be present due to successful hepatitis B vaccination or previous infection.

HBV reactivation is defined as exacerbation of chronic hepatitis B (CHB) or reactivation of past resolved hepatitis B infection. In general, reactivation is characterized by an increase from baseline in the HBV DNA level in patients with CHB, but it can also be defined as reverse HBsAg seroconversion, or the appearance of HBV DNA in serum when there is absence of HBsAg. The definition of HBV reactivation varies among different international guidelines and the information is summarized in Supplementary Table 1[3-7]. Hepatitis flare is defined as a 3-fold or more rise in alanine aminotransferase (ALT) level compared with baseline and ALT level more than 100 U/L[7].

When a patient has been infected with HBV, the virus enters the hepatocytes where the viral genome is released and transported into the nucleus. Once inside the nucleus, the viral genome is then converted into plasmid-like covalently closed circular DNA (cccDNA), which can persist in the hepatocytes in a latent and stable state[8].

HBV reactivation may occur at any time during or after chemotherapy. There are five stages in the course of HBV reactivation[9]. The first stage includes an asymptomatic elevation in markers of viral replication, with detectable HBV DNA levels in patients who are HBsAg-positive or -negative, or the reappearance of HBsAg in previously HBsAg-negative patients. In the second phase, serum HBV DNA levels continue to raise, and serum ALT and aspartate aminotransferase (AST) concentrations start increasing within a few weeks or days. This stage is also regarded as hepatic flare or HBV reactivation-related hepatitis. Most patients remain asymptomatic but a small number may experience constitutional symptoms, jaundice, and right upper-quadrant pain. Patients may then enter a spontaneous or on-treatment improvement, *i.e.*, the third stage, in which the ALT and AST levels improve spontaneously or after administration of antiviral therapy. A small proportion of patients experience the fourth stage if the hepatic injury cannot be resolved, characterized by a decrease in hepatic synthetic function, deranged clotting profile, and a rise of serum bilirubin levels. Fortunately, the majority of patients will go into the fifth stage with resolution of HBV reactivation after cessation of immunosuppressive therapy and the initiation of antiviral therapy. However, some may remain in stage 4, warranting liver transplantation in some severe cases.

In patients receiving immunosuppressive therapy, the loss of immune control may result in viral replication inside the hepatocytes without any increase in ALT levels. Nevertheless, upon immune reconstitution, sometimes during immunosuppressant tapering or withdrawal, the immune system will target the hepatocytes to clear the virus, resulting in liver damage[10].

RISK FACTORS FOR HEPATITIS B REACTIVATION

Host factors

Male sex and older age were identified to be risk factors for HBV reactivation[11-13]. A study in 626 HBsAg-positive patients who were undergoing chemotherapy for a variety of malignancies showed that there was almost a 3-fold increase of the incidence of HBV reactivation in men but the exact mechanism was not clear[13]. Chen *et al*[14] analyzed the risk of HBV reactivation among 1962 patients with hematological malignancy in Taiwan. The presence of hepatocellular carcinoma (HCC) and absence of antiviral prophylaxis were independent risk factors for HBV reactivation in HBV carriers. Among patients who were HBsAg negative at diagnosis, liver cirrhosis, diabetes mellitus, allogeneic stem cell transplantation, and low anti-HBs titers were independent risk factors for HBV reactivation[14]. Lymphoma is also associated with a higher risk of HBV reactivation[15]. Both the underlying disease and the anti-cancer therapy may contribute to HBV reactivation, indicating that the immunocompromised state is an important risk factor.

Virologic factors

The identified virologic risk factors for HBV reactivation include the presence of intrahepatic cccDNA and detectable HBV DNA levels[16-18]. Signs of increased viral replication, such as HBsAg or hepatitis B e antigen (HBeAg) positivity and detectable baseline HBV DNA, before treatment, are predictive of the patient meeting the criteria for HBV reactivation during treatment with cytotoxic chemotherapy or autologous stem cell transplantation[19-22].

HBV genotype is also related to treatment response and disease severity and progression[7,9]. For example, it was found that HBV genotype B is associated with HBeAg seroconversion at an earlier age, less active hepatic necroinflammation, more prolonged remission after HBeAg seroconversion, a slower rate of cirrhotic progression, and a reduced rate of HCC development compared with genotype C[7].

Salpini *et al*[23] identified mutations in HBsAg as being risk factors for reactivation. Using population-based and ultradeep sequencing, they analyzed the genetic diversity of HBsAg in 29 patients and found that 75.9% of HBV-reactivated patients carried mutations localized in immune-active HBsAg regions compared with only 3.1% of control patients ($P < 0.001$)[23]. The majority of these mutations resided in the B-cell epitopes of the HBs antigenic loop. Some of the mutations are known to hamper HBsAg recognition by humoral response, which may explain the frequent reactivation of HBV in patients receiving immunosuppressive therapy targeting B cells.

Types of anticancer therapies

Chemotherapy: Anthracycline chemotherapy (*e.g.*, doxorubicin, daunorubicin, and idarubicin) is a common form of treatment for hematological cancers such as lymphoma and acute myeloid leukemia (AML). The risk of HBV reactivation is significant in patients receiving doxorubicin as part of the chemotherapeutic regimen[6].

Chen *et al*[24] found that there was an increase in p21 expression during treatment with doxorubicin. The increase in p21 expression promotes the expression of CCAAT/enhancer-binding protein α (C/EBPα), which helps to activate HBV replication by enhancing the binding of C/EBPα to the HBV promoter. Kostyusheva *et al*[25] studied the effects of DNA-damaging compounds such as doxorubicin and hydrogen peroxide on the replication or reactivation of HBV and found that both doxorubicin and hydrogen peroxide dose-dependently activated HBV replication[25]. If doxorubicin is planned, anti-HBV prophylaxis is recommended for patients who are receiving doxorubicin if they have either CHB or a past resolved HBV infection.

Steroids: Steroids are commonly combined with chemotherapy or immunomodulatory drugs in the treatment of many hematological malignancies such as lymphoid malignancies and MM. Steroids can increase the HBV replication through two mechanisms. First, they can prevent T and B cell proliferation by suppressing cell-mediated immunity through the inhibition of interleukins[26]. Second, they exert a direct suppressive effect on T cell-mediated immunity through the stimulation of the glucocorticoid-responsive element present in the HBV genome[27].

Cheng *et al*[28] randomized 50 lymphoma patients who were HBsAg-positive and receiving the same chemotherapeutic regimen with or without the addition of corticosteroids, and compared the rate of HBV reactivation. The cumulative incidence of HBV reactivation was significantly higher in the corticosteroid group at 9 mo (73% *vs* 38%, respectively, $P = 0.03$). In a separate prospective cohort study with 6 years of follow-up, HBV reactivation occurred at 4 to 32 mo (median 10 mo) after the administration of steroids[29]. Most patients had malignancies or rheumatologic diseases.

The risk of HBV reactivation is further increased in patients who receive high-dose steroids (> 20 mg/d of prednisolone) and/or a long duration of therapy (> 4 wk)[6]. In a recent prospective study of 1303 patients with rheumatic diseases and past resolved HBV infection, it was found that patients taking steroids at a time-weighted average dose of higher than 20 mg/d prednisone-equivalents are at high risk for HBV reactivation or even hepatitis flare[30]. Prophylactic anti-HBV therapy should be considered for these high-risk patients.

Tyrosine kinase inhibitors: Currently, treatment with tyrosine kinase inhibitors (TKIs), *e.g.*, imatinib, nilotinib, dasatinib, and ponatinib, is a standard therapy for chronic myeloid leukemia (CML). The exact mechanism for HBV reactivation with TKIs is not known but it may be related to immune restoration. There are some published data on the risk of HBV reactivation in patients receiving TKIs. One hundred and forty-two adult Taiwanese CML patients were enrolled in a study to assess the rate of HBV reactivation during TKI therapy, including imatinib ($n = 43$, 30.3%), dasatinib ($n = 48$, 33.8%), nilotinib ($n = 37$, 26.1%), ponatinib ($n = 1$, 0.7%), and two or more TKIs ($n = 13$, 9.2%)[31]. Nineteen patients were HBV carriers and the rate of HBV reactivation was 26.3%; HBV reactivation was detected between 3 and 51 mo after the use of TKIs. Three patients experienced HBV-related hepatitis with an increase in ALT of more than 100 U/L[29]. One of the patients with HBV reactivation had received antiviral prophylaxis with entecavir; he was then given tenofovir after HBV reactivation.

A Korean study involved 69 patients with CHB being assessed for HBV reactivation[30]. Forty-six patients did not receive antiviral prophylaxis and the rate of HBV reactivation was 26% in this group of patients[32]. HBV reactivation was detected in seven patients who received imatinib, two patients receiving dasatinib, one nilotinib recipient, and one patient treated with radotinib therapy.

We would recommend prophylactic antiviral therapy to HBV carriers, and monitor HBV DNA and liver enzymes every 1 to 3 mo in patients with past resolved HBV infection, during TKI treatment. If the HBV DNA level rises, pre-emptive treatment with antiviral agents should be given. TKIs may also be used in combination with chemotherapy in the treatment of Philadelphia-positive ALL[33,34]. The combination with chemotherapy will likely lead to a deeper immunosuppressive effect, so prophylactic antiviral therapy is recommended in any patient with either CHB or past resolved HBV infection.

Anti-CD20 monoclonal antibodies: Treatment for a number of different hematological malignancies, including CLL and B-cell lymphoma, often includes B cell-depleting agents such as anti-CD20 monoclonal antibodies. Rituximab, obinutuzumab, and ofatumumab target the CD20 B-lymphocyte antigen and lead to marked depletion of the B cells involved in priming specific cytotoxic T cells[35]. Rituximab also worsens the impairment of antigen-presenting B cells which is seen in patients with CHB, resulting in inadequate induction of $CD4^+$ T cell activation and proliferation, and a T cell hyporesponsive state[36]. There is more than a 5-fold increase in the risk of HBV reactivation associated with the use of rituximab[37].

Both HBsAg-positive patients and those with resolved HBV infection are susceptible to HBV reactivation when they receive rituximab[38-41]. The incidence varies from 8.3% to 25% in patients with resolved HBV infection receiving rituximab-based chemotherapy[42-46]. Rituximab is a significant risk factor for HBV reactivation.

Obinutuzumab is a second-generation anti-CD20 monoclonal antibody. It has an engineered fragment crystallizable portion and a modified elbow hinge region[47]. Obinutuzumab has shown better efficacy than rituximab in several types of lymphoid diseases, by inducing direct cell death and enhancing antibody-dependent cellular cytotoxicity[48,49]. It can potentially cause more profound suppression of CD20 than rituximab[48,49]. It is used in patients with CLL and follicular lymphoma with promising results[48,49].

Kusumoto *et al*[50] performed a prospective study in 326 B-cell lymphoma patients with past resolved HBV infection who received obinutuzumab- ($n = 155$) or rituximab-containing immunochemotherapy ($n = 171$) in the phase 3 GALLIUM [48] and GOYA[51] studies. Of the 326 patients with resolved HBV infection, 119 (36.5%) received nucleos(t)ide analog treatment (NAT). Among these 119 patients, 94 received prophylactic NAT and 25 received pre-emptive NAT. The rate of HBV reactivation was 10.8% without antiviral prophylaxis, whereas only two of the 94 patients who received prophylactic NAT (2.1%) had HBV reactivation[48]. It was shown that the baseline detectable HBV DNA was strongly associated with an increased risk of reactivation while prophylactic NAT significantly decreased the risk on multivariate Cox analysis[50].

The reactivation rate in patients receiving obinutuzumab- and rituximab-based chemotherapy was 13.2% and 6.1%, respectively[50]. Although no significant difference in the risk of HBV reactivation between these two different immunochemotherapy regimens was demonstrated in the multivariate analysis, it might be due to confounding factors including imbalance of baseline risk factors. Anti-HBV prophylaxis is recommended in patients with either CHB or past resolved infection receiving anti-CD20 monoclonal antibody.

Monoclonal antibodies other than anti-CD20

Polatuzumab vedotin: Polatuzumab vedotin is an antibody-drug conjugate targeting CD79b, which is universally expressed on the surface of malignant B cells. CD79b is a signaling component of the B-cell receptor which is located on the surface of normal B cells as well as most of the mature B-cell tumors and 95% of DLBCL[52]. Polatuzumab vedotin was found to be useful in combination with bendamustine and rituximab (pola-BR) for patients with relapsed or refrac-

tory DLBCL[53]. It can also be used in a modified regimen of polatuzumab vedotin, rituximab-cyclophosphamide, doxorubicin, and prednisolone (pola-R-CHP) with success in the frontline treatment of DLBCL[54]. The risk of disease progression, relapse, and death was all reduced among those who received pola-R-CHP than among those who received standard rituximab-cyclophosphamide, doxorubicin, vincristine, and prednisolone (R-CHOP) therapy in previously untreated DLBCL patients with an intermediate or high risk.

To date, there are no published data or reported cases of HBV reactivation in patients receiving polatuzumab vedotin. In view of the profound B-cell suppression that occurs when these regimens are used to treat lymphoma, we would recommend antiviral prophylaxis for patients receiving polatuzumab vedotin if they have either CHB or past resolved HBV infection.

Inotuzumab ozogamicin: Inotuzumab ozogamicin is an antibody conjugate in which a humanized monoclonal antibody against CD22 is conjugated to the cytotoxic antibiotic calicheamicin[55]. After binding to CD22 on the leukemic cell surface, the CD22-conjugate complex is rapidly internalized, releasing the calicheamicin. Once released, the cytotoxic portion of the conjugate binds to the minor groove of DNA in these leukemic cells, and induces double-strand cleavage and subsequent apoptosis.

More than 90% of patients with B-cell ALL express CD22 and this cell-surface glycoprotein is not shed into the extracellular matrix, making it a logical target for B-cell cancer therapy[56]. It has been used with success in the treatment of ALL and it can deplete B cells. There have been no reports to date of HBV reactivation in patients with CHB or past resolved infection receiving inotuzumab ozogamicin. However, in view of the profound B-cell depletion, we would recommend antiviral prophylaxis during inotuzumab ozogamicin in patients with either CHB or past resolved infection.

Blinatumomab: Blinatumomab is a bispecific T-cell engager, with two binding sites: One for CD3-positive cytotoxic T cells and the other for CD19-positive B cells. By drawing the two types of immune cells together, blinatumomab facilitates the recognition and destruction of CD19-positive ALL blasts by the patient's own endogenous T cells[57]. It has been used with success in the treatment of relapsed/refractory ALL or as consolidation therapy[58,59].

We did not identify any published cases of HBV reactivation in patients with CHB or past resolved infection receiving blinatumomab. HBV prophylaxis is recommended for both chronic and resolved HBV infection in patients receiving blinatumomab, in view of profound B-cell depletion seen with this agent.

Daratumumab and isatuximab: Daratumumab is a human immunoglobulin G1 monoclonal antibody which targets CD38-expressing cells. Several of the combination regimens containing daratumumab have shown promising results in the treatment of newly diagnosed and refractory/relapsed MM[60-63]. It also has an emerging role in the treatment of amy-loid light-chain amyloidosis[64,65].

The principal mechanism of daratumumab in MM is to induce death of CD38-expressing myeloma cells *via* antibody-dependent and complement-dependent cytotoxicity, as well as *via* antibody-dependent cellular phagocytosis[66]. Daratumumab also targets normal plasma cells expressing CD38, leading to a reduction in the humoral immunity against reactivation of HBV[67].

There was a report of HBV reactivation occurring on day 15 of the third course of a daratumumab-containing regimen in a MM patient with resolved HBV infection[68]. Lee *et al*[69] also conducted a retrospective study of 93 patients with resolved HBV infection who had been treated with daratumumab and found that the risk of HBV reactivation was 6.5% at a median follow-up period of 8.7 mo. One patient later died of hepatic failure despite treatment with tenofovir. These reports highlight the risk of reactivation of resolved HBV infection after daratumumab treatment in MM patients.

Isatuximab, another anti-CD38 monoclonal antibody, has demonstrated benefits in the treatment of patients with relapsed/refractory and high-risk MM[70-73]. We would recommend anti-HBV prophylaxis in both HBV carriers or those with resolved HBV infection during treatment with either daratumumab or isatuximab in view of the similar mecha-nisms of action of both drugs.

Novel therapies for hematological malignancies

CAR-T cell therapy: CAR-T cell therapy is a promising immunotherapy with curative intent for several types of hematological malignancies including NHL[74-77], ALL[78], and MM[79,80]. CAR-T cell therapy involves removal of the patient's own T cells, reprogramming these cells with a CAR construct, and then returning them to the patient's bloodstream, where these programmed T cells attack the cancer cells[81]. The activated CAR-T cells identify targets on cancer cells, specifically leading to the destruction of these cancer cells. Because it is easier to target an adequate tumor antigen in hematological malignancies (such as CD19 in lymphoid malignancies) than it is in solid cancers, CAR-T cell therapy has been first applied to hematological malignancies.

The issue of HBV reactivation in patients receiving CAR-T cell therapy remains unexplored, and the data on HBV reactivation in these patients are limited. CAR-T cells may predispose HBV immune patients to reactivation due to its cytotoxicity against B cells. The proper prevention strategy and duration of antiviral prophylaxis in patients receiving CAR-T cell therapy are still unclear and should be further investigated. There has been a fatal case of HBV reactivation after CAR-T cell therapy[2]. HBV reactivation can be a significant complication in CAR-T cell treatment and clinicians should be cautious about this complication particularly in areas where HBV is still prevalent.

Patients can also have late HBV reactivation occurring more than 1 year after CAR-T cell therapy. CAR-T cells can persist in the blood for a long time, resulting in prolonged B-cell aplasia and a persistent reduction in immunoglobulin production, thus contributing to late reactivation[82].

Table 1 summarizes the published data on the HBV reactivation in patients receiving CAR-T cell therapy[83-89]. The rate of HBV reactivation ranged from 0% to 20% for CHB patients[83-89]. We recommend that clinicians administer anti-HBV prophylaxis during the CAR-T cell therapy and for at least 1 year afterwards in patients who had CHB or past resol-

Table 1 Studies of hepatitis B virus reactivation in patients receiving chimeric antigen receptor-T cell therapy

Ref.	Indication for CAR-T	*N*	CHB, *n*	Past resolved HBV infection, *n*	Antiviral prophylaxis, % patients	Definition of HBV reactivation	Rate of HBV reactivation	HBV-related death
Prospective studies								
Liu *et al*[87], 2020	B-cell lymphoma	17	6	11	100% for CHB, and 45.5% for past infection (entecavir)	Elevation of HBV DNA levels to > 1000 IU/mL and/or HBsAg reverse seroconversion in HBsAg-negative patients	0	0
Yang *et al* [89], 2020	DLBCL	15	15	0	100% (lamivudine, entecavir, tenofovir, or adefovir dipivoxil)	Positive follow-up HBV-DNA test if the baseline HBV-DNA is undetectable/negative or > 10-fold increase from baseline	20%	0
Li *et al* [86], 2021	ALL, B-cell lymphoma	30	0	30	No prophylaxis	Elevation of HBV DNA ≥ 100 IU/mL for two consecutive measurements	6.6%	0
Wang *et al* [88], 2020	ALL, B-cell lymphoma, PCM	70	12	29	100% for CHB (entecavir, tenofovir disoproxil, or lamivudine). Nil for patients with past HBV infection	> 1 log increase in HBV DNA, HBV DNA-positive when previously negative, HBV DNA > 2000 IU/mL if no baseline level was available, or reverse sero-conversion from HBsAg-negative to positive	16.7% with chronic infection and 34.4 % with past infection	0
Retrospective studies								
Cao *et al*[83], 2020	ALL, NHL	89	19	37	100% for chronic infection, and 5.4% for past infection	100-fold increase in HBV DNA when compared with baseline or HBV DNA ≥ 10^3 IU/mL in a patient with a previously undetectable level or reverse seroconversion from HBsAg negative to HBsAg positive	5.3% for CHB	0
Han *et al*[85], 2020	Multiple myeloma	9	1	8	100% for CHB, 25% for past infection (lamivudine/entecavir)	HBsAg seroconversion or increase in HBV DNA levels by at least 10-fold or 1 × 10^9 copies/mL	12.5% for past infection	0
Cui *et al*[84], 2021	DLBCL, B-ALL	20	5	15	100% for CHB (entecavir or tenofovir), 13.3% for past HBV infection (entecavir)	For CHB: (1) ≥ 2 log increase in HBV DNA compared to the baseline level; (2) HBV DNA ≥ 3 log IU/mL in a patient with previously undetectable level; and (3) HBV DNA ≥ 4 log IU/mL if the baseline level is not available. For resolved HBV infection: HBV DNA is detectable; reverse HBsAg seroconversion	6.2% for past infection	0

AASLD: American Association for the Study of Liver Diseases; ALL: Acute lymphoblastic leukemia; CAR: Chimeric antigen receptor; CHB: Chronic hepatitis B; CLL: Chronic lymphocytic leukemia; DLBCL: Diffuse large B-cell lymphoma; HBsAg: Hepatitis B surface antigen; HBV: Hepatitis B virus; NHL: Non-Hodgkin lymphoma; PCM: Plasma cell myeloma.

ved HBV infection[82].

Bispecific antibodies: The development of bispecific antibodies has been an important advance in the treatment of relapsed or refractory B-cell lymphomas[90-92], including DLBCL[93-95] and follicular lymphoma[96]. Bispecific antibodies target both T cells and CD19 or CD20 on malignant B cells and is a promising immunotherapy in the treatment of NHL. These dual binding sites draw malignant B cells close to endogenous T cells, thereby directly activating T-cell cytotoxicity. Examples of the bispecific antibodies include glofitamab, mosunetuzumab, epcoritamab, and odronextamab. Some of these bispecific antibodies have a fixed duration of therapy and some, such as epcoritamab, are administered until disease progression.

Since there are a lack of prospective or retrospective studies on the risk of HBV reactivation in patients receiving bispecific antibodies, the real incidence of HBV reactivation is unclear. However, bispecific antibodies will profoundly suppress B-cell activity. These drugs are highly potent and the effect on B-cell depletion is expected to be significant. Therefore, we recommend antiviral prophylaxis against HBV in patients with either CHB and past resolved HBV infection.

BTK inhibitors: BTK inhibitors such as ibrutinib, acalabrutinib, and zanubrutinib have shown success in the treatment of many lymphoid malignancies including CLL[97-102], mantle cell lymphoma[103,104], marginal zone B-cell lymphoma [105], and Waldenström's macroglobulinemia[106]. Ibrutinib blocks B-cell antigen receptor signaling, thus reducing malignant proliferation of B cells and inducing cell death[107].

The effect of ibrutinib or other BTK inhibitors on HBV reactivation has not been extensively studied, and there are no guidelines on the prophylaxis and management of HBV reactivation during treatment with ibrutinib. Table 2 summarizes the current data on the risk of HBV reactivation and their outcomes in patients receiving BTK inhibitors[108-111]. Most existing data are from retrospective studies. The rate of HBV reactivation ranged from 1.9% to 8.3% for past resolved infec -tion. BTK inhibitors will induce profound B-cell suppression. Hence, we recommend anti-HBV prophylactic treatment with nucleotide analogues for lymphoma patients with positive HBsAg or resolved HBV infection with detectable HBV DNA who are receiving BTK inhibitors. For those with resolved HBV infection and negative HBV DNA, we recommend monitoring HBV DNA levels and liver function every 1 to 3 mo, and giving pre-emptive antivirals when the HBV DNA level rises.

B cell lymphoma-2 inhibitors: The B cell lymphoma (BCL)-2 inhibitor venetoclax is commonly used in the treatment of CLL[112,113] and in combination with azacitidine or low-dose cytarabine in AML patients who are not fit for intensive chemotherapy[114,115]. Venetoclax is a potent inhibitor of the antiapoptotic BCL-2 protein. AML stem cells express BCL-2 and depend on BCL-2 for survival. Venetoclax has synergistic effects when used in combination with azacitidine.

There is a lack of large retrospective or prospective studies on the incidence of HBV reactivation in patients receiving venetoclax, so the risk is unclear. Because of its mechanism of action, venetoclax will profoundly suppress B-cell activity. Thus, the same prophylactic or pre-emptive antiviral management approach used for patients receiving BTK inhibitors should be applied in patients receiving venetoclax.

Proteasome inhibitors: The proteasome inhibitors have become the backbone treatment for MM. They include bortezomib, carfilzomib, and ixazomib. Bortezomib is the most commonly used proteasome inhibitor. Bortezomib can target cellular pathways essential for the proliferation of malignant plasma cells. However, it may also negatively impact the functions of healthy B cells and plasma cells, which are important in the immune control of HBV. It can also dysregulate cell-mediated immunity and may increase HBV reactivation by affecting the number and functions of $CD8^+$ T cells and $CD56^+$ natural killer cells[116].

Ataca Atilla *et al*[117] conducted a retrospective study in 178 MM patients who had received lenalidomide and/or bortezomib. They found that the rate of HBV reactivation was 3% after bortezomib and 8% after bortezomib and lenalidomide[117]. Lee *et al*[118] reported HBV reactivation in 5.2% of 230 MM patients with past resolved HBV infection after a median follow-up of 2.4 years. One hundred and thirty-three patients (58%) had received bortezomib-based therapy. In this study, the cumulative rate of HBV reactivation was 5% at 2 years and 8% at 5 years[118].

Mya *et al*[116] reported an HBV reactivation incidence of 5.5% in 273 relapsed or refractory MM patients who had received bortezomib and dexamethasone therapy. Li *et al*[119] conducted a retrospective study of HBV reactivation in patients receiving regimens containing bortezomib. Twenty-seven of the 139 patients were HBsAg positive and 22 of them were given antiviral prophylaxis with lamivudine or entecavir. HBV reactivation occurred in six HBsAg-positive and two HBsAg-negative/anti-HBc-positive cases from a total of 139 patients[119]. Antiviral prophylaxis is recommended for both CHB patients and those with past resolved HBV infection who are receiving proteasome inhibitors.

Immune checkpoint inhibitors: Immune checkpoint inhibitors (ICI) are effective in the treatment of solid tumors, and have also shown efficacy in the treatment of lymphoma[120-124]. ICIs can block the localization and traffic of activated lymphocytes, thus inhibiting the inflammatory response associated with immune-mediated diseases[125]. They may also reduce the local immune control of HBV replication in the liver, predisposing patients to HBV reactivation.

Table 3 summarizes the data on HBV reactivation in patients receiving ICIs[126-129]. The rate of HBV reactivation among HBsAg-positive cancer patients is 0.5% to 5.3% during ICI therapy. Prophylactic antiviral treatment is recommended for HBsAg-positive patients to prevent HBV reactivation. For those with resolved HBV infection and undetectable HBV DNA levels, we recommend monitoring liver function and HBV DNA levels every 1 to 3 mo, and administering pre-emptive treatment with antiviral agents if an increase in HBV DNA levels is detected.

PREVENTION OF HEPATITIS B REACTIVATION

Existing guidelines on the drug classes and the corresponding risk of HBV reactivation are summarized in Table 4, while Table 5 summarizes the international guidelines on the management of patients with HBV infection receiving chemotherapy. The recommendations for management of HBV-infected cancer patients receiving novel agents for hematological malignancies are shown in Table 6.

Screening for hepatitis B

In order to prevent HBV reactivation among patients with hematological malignancies, it is essential to identify those with HBV infection before starting chemotherapy or immunotherapy. This starts with screening for the presence of HBsAg and anti-HBc in blood. The commercial immunoassays usually capture HbsAg, having specificity for epitopes present on the antigenic α determinant. The enzyme-linked immunosorbent assay method used in HBsAg detection has a sensitivity and specificity of both about 80%, compared with more than 90% using the immunochromatographic test [130]. Complete loss of anti-HBc with chronic and high viremic HBV infection after allogeneic stem cell transplantation has been reported[131]. However, there might be some rare scenarios where HBsAg or anti-HBc is falsely negative. For example, mutations within the α determinant may affect the conformation of the surface epitope such that it is unrecognizable to the test, or mutations in other parts of the viral genome may affect HbsAg secretion or expression, resulting in diagnostic escape[132]. Moreover, there has been a case report describing complete loss of anti-HBc after allogeneic stem

Table 2 Studies of hepatitis B virus reactivation in patients receiving Bruton's tyrosine kinase inhibitors (all studies are retrospective)

Ref.	Disease type	Therapy	*N*	CHB, *n*	Past resolved HBV infection, *n*	Antiviral prophyl-axis, % patients	Definition of HBV reactivation	Rate of HBV reactivation, % patients	HBV-related death
Hammond *et al*[108], 2018	CLL, MCL, LPL	Ibrutinib	21	0	21	4.8%	HBV DNA > 100 IU/mL on 2 consecutive measurements ± reappearance of HBsAg	9.5%	0
Innocenti *et al*[109], 2019	CLL	Ibrutinib	34	0	12	42% for past infection (lamivudine)	Increase in serum ALT and HBV DNA in HBsAg-positive patients or elevation of HBV DNA ± HBsAg recurrence in anti-HBc-positive patients	8.3%	0
Innocenti *et al*[110], 2022	CLL	Ibrutinib	108	0	108	67.6% (lamivudine)	HBsAg seroconversion and/or an increase of serum HBV DNA by ≥ 1 log above the LLD of the assay	1.9%	0
Ni *et al*[111], 2022	DLBCL	Ibrutinib or zanu-brutinib	55	4	26	100% for CHB and 34.6% for past infection (entecavir)	> 1 log increase in HBV DNA, HBV DNA-positive when previously negative, HBV DNA > 2000 IU/mL if no baseline level was available, or reverse seroconversion from HBsAg-negative to -positive	7.69% for past infection	0

CHB: Chronic hepatitis B; CLL: Chronic lymphocytic leukaemia; DLBCL: Diffuse large B-cell lymphoma; HBsAg: Hepatitis B surface antigen; HBV: Hepatitis B virus; LLD: Lower limit of detection; LPL: Lymphoplasmacytic lymphoma; MCL: Mantle cell lymphoma; ALT: Alanine aminotransferase; anti-HBc: Antibody to hepatitis B core.

cell transplantation in a patient with resolved HBV infection who previously had positive anti-HBs and anti-HBc prior to the stem cell transplant[131]. Isolated anti-HBs without anti-HBc may be present in pretreated patients without previous hepatitis B vaccination[133,134]. Thus, a more sensitive combined screening strategy is advisable, including serological testing for HBsAg, anti-HBc, and anti-HBs and a sensitive test for HBV DNA.

HBsAg-positive patients without hepatitis at baseline

A preventive strategy is more effective than a pre-emptive strategy in HBsAg-positive patients[135,136]. We recommend giving NAT for prophylaxis in all HBsAg-positive candidates prior to immunosuppressive therapy irrespective of their HBV DNA status because the risk of HBV reactivation is high in this group of patients. This approach is highly effective, with a number needed to treat to prevent one episode of HBV reactivation of three[135].

It is not always possible to prevent the development of hepatitis or hepatitis flares if antiviral therapy is started after the onset of HBV reactivation[42], since it will take some weeks or even months for the antiviral therapy to reduce viral loads, and the inflammation and necrosis of the liver will be ongoing during this period[137].

HBsAg-negative and anti-HBc-positive patients

The risk of HBV reactivation in this group varies considerably, depending on the level of viremia and the immunosuppressive regimens administered. In general, if HBV DNA is detectable, the patient would be given anti-HBV prophylaxis and treated similarly to HBsAg-positive patients. If HBV DNA is undetectable, then the risk of reactivation associated with the immunosuppressive regimen will be assessed. High-risk groups such as those receiving anti-CD20 monoclonal antibodies should receive antiviral prophylaxis with NAT. Pre-emptive treatment is recommended for moderate- and low-risk groups, with HBV DNA monitoring every 1-3 mo.

Huang *et al*[43] compared pre-emptive with prophylactic entecavir therapy during R-CHOP chemotherapy in patients with lymphoma and resolved hepatitis B. Prophylactic entecavir treatment significantly reduced the risk of HBV reactivation compared with pre-emptive antiviral therapy (17.9% *vs* 2.4%, $P = 0.027$)[43]. Therefore, the prophylactic strategy is a better option in patients receiving high-risk immunosuppressive regimens (Table 5).

HBsAg-negative/anti-HBc-negative/anti-HBs-negative patients

HBV vaccination can be considered in patients who are HBsAg-negative, anti-HBc-negative, and anti-HBs-negative[3]. Anti-HBs potentially provide a protective effect against HBV reactivation[45,138-141]. The results of a meta-analysis showed that, among patients not receiving antiviral prophylaxis, the reactivation risk was 14% in the 388 patients who had anti-HBc only *vs* 5.0% in 1284 patients with concomitant anti-HBs. The pooled odds ratio of HBV reactivation was 0.21 (95% confidence interval: 0.14-0.32) in those with anti-HBs compared with anti-HBc only[141].

Table 3 Studies of hepatitis B virus reactivation in patients receiving immune checkpoint inhibitors (all studies were retrospective)

Ref.	Disease type	Therapy	*N*	CHB, *n*	Past resolved HBV infection, *n*	Antiviral prophylaxis, % patients	Definition of HBV reactivation	Rate of HBV reactivation	HBV-related death
Zhang *et al*[129], 2019	Solid tumors, lymphoma (7%)	PD-1/PD-L1 inhibitors (pembrolizumab, nivolumab, toripalimab, camrelizumab, sintilimab, atezolizumab)	114	114	0	74.6% received prophylaxis (entecavir, tenofovir, lamivudine, telbivudine, adefovir)	AASLD 2018 guidelines	6 (5.3%)	0
Wong *et al*[127], 2021	Solid tumors	PD-1 inhibitors (nivolumab, pembrolizumab, spartal-izumab), PD-L1 inhibitors (atezolizumab, avelumab, durvalumab), CTLA-4 inhibitors (ipilimumab, tremelimumab)	990	397	225	100% for CHB, and 11.3% for past HBV infection (entecavir, TAF, TDF, lamivudine, telbivudine, ADV)	AASLD 2018 guidelines	2/397 (0.5%); none in the resolved HBV group	0
Yoo *et al* [128], 2022	Solid tumors, lymphoma (1.8%)	PD-1 inhibitors (nivolumab, pembrolizumab), PD-L1 inhibitors (atezolizumab, avelumab), CTLA-4 inhibitors (ipilimumab, tremelimumab)	3465	511	564	90.8% for CHB, 1.1% for HBsAg negative patients (entecavir, tenofovir, lamivudine, telbivudine, adefovir, clevudine)	AASLD 2018 guidelines	1% for chronic HBV infection, 0% for past HBV infection	0
Lasagna *et al* [126], 2023	Solid tumors	Pembrolizumab, nivolumab, atezolizumab	150	0	150	Nil	AASLD 2018 guidelines	0%	0

AASLD: American Association for the Study of Liver Diseases; ADV: Adefovir dipivoxil; CHB: Chronic hepatitis B; CTLA4: Cytotoxic T-lymphocyte-associated protein 4; HBsAg: Hepatitis B surface antigen; HBV: Hepatitis B virus; PD-1: Programmed cell death protein 1; PD-L1: Programmed cell death ligand 1; TAF: Tenofovir alafenamide; TDF: Tenofovir disoproxil fumarate.

Table 4 Drug classes and corresponding risk of hepatitis B virus reactivation[6]

Drug class	Drug or dose	Risk of HBV reactivation	
		For HBsAg-positive patients	For HBsAg-negative/anti-HBc-positive patients
Anti-CD20 monoclonal antibodies	Rituximab, obinutuzumab, ofatumumab	High (30%-60%)	High (> 10%)
Anthracycline chemotherapy	Doxorubicin, daunorubicin, epirubicin	High (15%-30%)	High (> 10%)
Steroids	Moderate/high dose ≥ 4 wk	High (> 10%)	Moderate (1%-10%)
	Low dose ≥ 4 wk	Moderate (1%-10%)	Low (< 1%)
	Low dose ≤ 1 wk	Low (< 1%)	Low (< 1%)
Tyrosine kinase inhibitors	Imatinib, nilotinib, dasatinib	High to moderate	Low (< 1%)
Immune checkpoint inhibitors	Nivolumab, pembrolizumab	High (> 10%)	Uncertain
Proteasome inhibitor	Bortezomib	Moderate (1%-10%)	Moderate (1%-10%)

HBV: Hepatitis B virus; HBsAg: Hepatitis B surface antigen; anti-HBc: Antibody to hepatitis B core.

HBsAg-negative/anti-HBc-negative/anti-HBs-positive patients

It is rare to have HBV reactivation in patients with isolated anti-HBs, but there have been occasional reports of HBV reactivation in patients with only anti-HBs seropositivity[133,134]. In one report, a patient with follicular lymphoma, who had not been vaccinated for hepatitis B, was positive for anti-HBs but negative for anti-HBc prior to starting chemotherapy. He subsequently developed high HBV DNA levels (1.8×10^8 copies/mL), and was found to have an HBV escape mutant, which was difficult to detect using the standard HBsAg assays[133]. HBV escape mutants harbor mutations in the essential antigenic area of HBsAg, and are capable of growing in the presence of anti-HBs. In these circumstances,

Table 5 International guidelines on prevention of hepatitis B in patients with a history of hepatitis B virus infection who are candidates for chemotherapy

Guideline	HBV screening	Screening tests	HBsAg-positive patients	HBsAg-negative, anti-HBc-positive patients	Choice of antiviral agent	Duration of antiviral therapy	Monitoring after prophylaxis	Ref.
American Gastroenterological Association 2015 guideline	High risk of HBV reactivation (> 10%) and moderate risk of HBV reactivation (1%-10%). Routine screening not recommended for low risk of HBV reactivation (< 1%)	HBsAg, anti-HBc, HBV DNA if serology positive	Prophylactic antiviral therapy	Antiviral prophylaxis over monitoring for patients if the chemotherapy is associated with high or moderate risk of HBV reactivation	Drug with high barrier to resistance is favored over LMV	6 mo after discontinuation of therapy and at least 12 mo for B-cell depleting agents	Not defined	[6]
European Association for the Study of the Liver 2017	All candidates for CT or IST	HBsAg, anti-HBc, and anti-HBs	Anti-HBV prophylaxis	Anti-HBV prophylaxis if they are at high risk of HBV reactivation. Pre-emptive therapy for moderate (10%) or low (1%) risk of HBV reactivation, and monitor HBsAg and/or HBV DNA every 1-3 mo during and after IST	ETV or TDF or TAF	At least 12 mo (18 mo for high-risk therapy) after the last course of therapy	LFT and HBV DNA every 3 to 6 mo during prophylaxis and for ≥ 12 mo after NA withdrawal	[3]
American Association for the Study of Liver Diseases 2018	All patients for CT and IST	HBsAg and anti-HBc	Anti-HBV prophylaxis	On-demand therapy except for patients receiving anti-CD20 antibody therapy or SCT (monitor ALT, HBV DNA, HBsAg every 1-3 mo)	ETV or TDF or TAF	At least 6 mo after discontinuation of IST. At least 12 mo for B cell-depleting agents	For up to 12 mo after cessation of anti-HBV therapy	[7]
American Society of Clinical Oncology 2020 update	All candidates for CT or IST	HBsAg, anti-HBc, and anti-HBs	Anti-HBV prophylaxis	High risk, *e.g.*, anti-CD20 antibody therapy or stem cell transplantation: Prophylaxis. Others: On-demend therapy (monitor HBsAg and HBV DNA every 3 mo)	ETV, TDF, TAF	At least 12 mo after cessation of IST	High risk: Monthly for the first 3 mo after NA withdrawal and then every 3 mo (duration not specified). Resolved HBV and not high risk: Not necessary	[4]
The Asian Pacific Association for the Study of the Liver 2021	All patients planned to receive IST	HBsAg, anti-HBs and anti-HBc, quanti-tative HBV DNA for HBsAg-positive patients	Anti-HBV prophylaxis in high and moderate-risk groups, and low-risk group with advanced liver fibrosis or cirrhosis. Pre-emptive treatment in low-risk group without advanced liver fibrosis or cirrhosis	Anti-HBV prophylaxis in high-risk group and moderate-risk group with advanced liver fibrosis or cirrhosis. Pre-emptive treatment in low-risk group without advanced liver fibrosis or cirrhosis	ETV, TDF or TAF	6 mo after the completion of IST for HBsAg-positive patients, without advanced liver fibrosis or cirrhosis and with low level of HBV DNA	HBV DNA every 3 mo	[5]

High risk of hepatitis B virus reactivation (> 10%), moderate risk (1%-10%), low risk (< 1%). ALT: Alanine aminotransferase; CT: Chemotherapy; ETV: Entecavir; HBV: Hepatitis B virus; HBsAg: Hepatitis B surface antigen; IST: Immunosuppresive therapy; LFT: Liver function test; LMV: Lamivudine; NA: Nucleotide analog; SCT: Stem cell transplant; TDF: Tenofovir; TAF: Tenofovir alafenamide fumarate; anti-HBc: Antibody to hepatitis B core; TAF: Tenofovir alafenamide; TDF: Tenofovir disoproxil fumarate.

Table 6 Recommendations for management strategy of hepatitis B virus-infected cancer patients receiving novel agents for hematological malignancies

Therapy	Chronic HBV infection	Past resolved HBV infection
CAR-T (*e.g.*, axicabtagene ciloleucel, tisagenlecleucel, and lisocabtagene maraleucel)	Antiviral prophylaxis	Antiviral prophylaxis
Bispecific antibodies (*e.g.*, glofitamab, mosunetuzumab)	Antiviral prophylaxis	Antiviral prophylaxis
BTK inhibitors (*e.g.*, ibrutinib, acalabrutinib, zanubrutinib)	Antiviral prophylaxis	Antiviral prophylaxis or monitoring and pre-emptive therapy[1]
BCL-2 inhibitors (venetoclax)	Antiviral prophylaxis	Antiviral prophylaxis or monitoring and pre-emptive therapy[1]
Anti-CD19 monoclonal antibody (blinatumumab)	Antiviral prophylaxis	Antiviral prophylaxis
Anti-CD22 monoclonal antibody (inotuzumab)	Antiviral prophylaxis	Antiviral prophylaxis
Anti-CD79 monoclonal antibody (polatuzumab)	Antiviral prophylaxis	Antiviral prophylaxis
Anti-CD38 monoclonal antibody (daratumumab)	Antiviral prophylaxis	Antiviral prophylaxis

[1]Pre-emptive therapy is monitoring of serum hepatitis B virus DNA every 1-3 mo during and after immunosuppression, and starting antiviral therapy with entecavir or tenofovir in the case of detectable hepatitis B virus DNA levels.
HBV: Hepatitis B virus; CAR: Chimeric antigen receptor; BTK: Bruton tyrosine kinase; BCL: B-cell lymphoma.

anti-HBc may appear very late.

In a separate report, a patient with DLBCL (also without a record of hepatitis B vaccination) had a pre-chemotherapy HBV profile that was positive for anti-HBs (127 IU/mL) but negative for HBsAg and anti-HBc. She developed HBV reactivation after completing rituximab-based chemotherapy. Antiviral treatment with entecavir was started after HBV reactivation was detected. Despite that, she had clinical deterioration with development of hepatic encephalopathy and died of liver failure finally[134]. Figure 1 shows a suggested algorithm for HBV testing and management of patients with hematological malignancies receiving anticancer therapy.

CHOICE OF ANTIVIRAL THERAPY

For the treatment of chronic HBV infection, entecavir and tenofovir are the preferred antiviral agents because they have high genetic barriers to resistance compared with lamivudine. Huang *et al*[142] performed a prospective randomized study in 121 HBsAg-positive patients with untreated DLBCL. Sixty patients received lamivudine prophylaxis and 61 received entecavir prophylaxis. Various endpoints occurred at a significantly lower rate in the entecavir than the lamivudine group, including HBV reactivation (6.6% *vs* 30%, $P = 0.001$), HBV-related hepatitis (0% *vs* 13.3%, $P = 0.003$), and chemotherapy disruption (1.6% *vs* 18.3%, $P = 0.002$)[142].

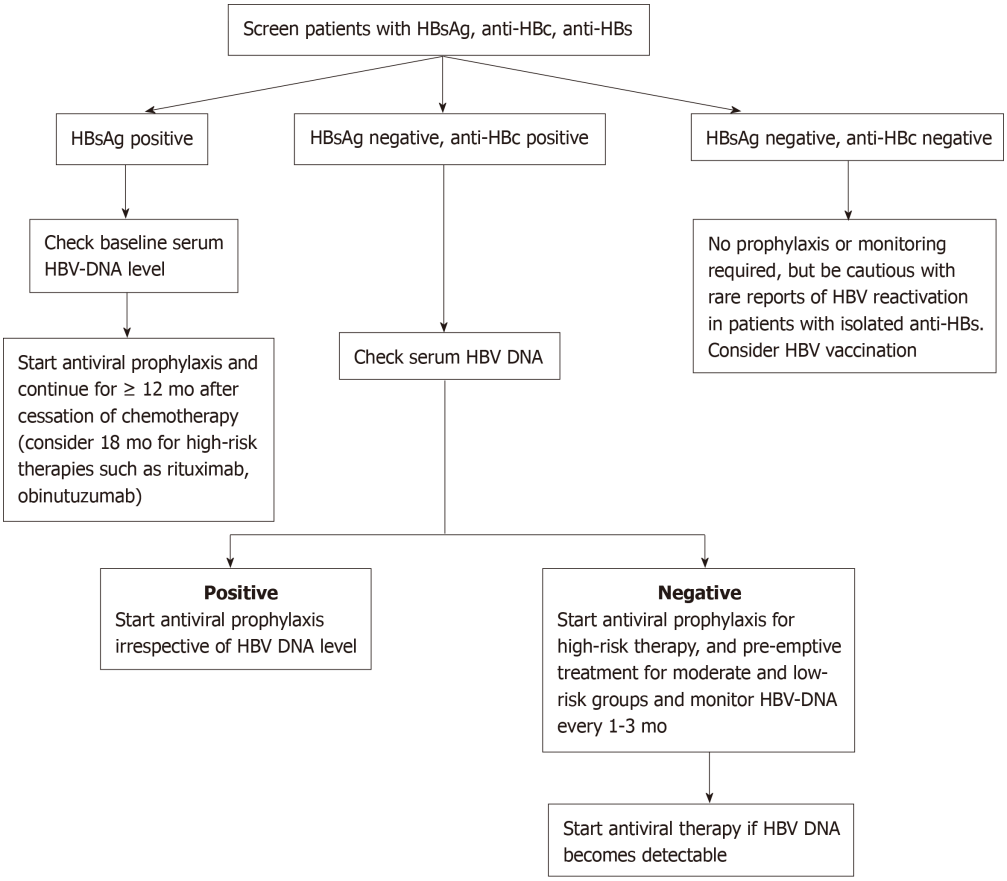
A meta-analysis of 770 patients with lymphoma showed that, in patients with CHB, the risk of HBV reactivation was significantly higher in those receiving prophylactic lamivudine compared with entecavir ($P < 0.001$)[143]. The superior prophylactic efficacy of entecavir is supported by studies in allogenic HSCT recipients and solid tumor patients, which showed a lower rate of HBV reactivation with entecavir compared with lamivudine[20,144]. Meta-analyses have also shown that tenofovir and entecavir are the most effective antiviral agents for the prevention of HBV reactivation[145,146]. Entecavir treatment of HBV patients with lamivudine-resistant viral strains is usually unsuccessful due to the rapid selection of additional mutants[147], highlighting the importance in choosing an effective initial anti-viral therapy.

Duration of antiviral therapy

Most guidelines recommend continuing antiviral therapy for 1 year after the cessation of anti-cancer therapy, and some guidelines recommend extending antiviral treatment for up to 18 mo after the last dose of cancer therapy (Table 6)[3,4,148]. Delayed HBV reactivation has been reported in patients who received anti-CD20 antibody therapy such as rituximab since rituximab will delay the immune recovery[149,150]. HBV DNA levels should be checked before stopping antiviral treatment.

Monitoring after stopping antiviral prophylaxis

HBV reactivation can develop after cessation of NAT[149,151,152], so monitoring for HBV reactivation is recommended after stopping anti-HBV prophylaxis (Table 6). In general, liver function tests and HBV DNA are monitored every 3 mo for a minimum of 12 mo after discontinuation of antiviral agents[3,4,7]. Monitoring for more than 12 mo is recommended for patients who received anti-CD20 monoclonal antibody therapy.



DOI: 10.3748/wjg.v29.i33.4942 **Copyright** ©The Author(s) 2023.

Figure 1 Recommended algorithm for hepatitis B virus testing and treatment in patients with hematological malignancies receiving anti-cancer therapy. HBsAg: Hepatitis B surface antigen; HBV: Hepatitis B virus; HBc: Hepatitis B core.

Management of HBV reactivation

Prophylaxis is better than treatment because fatal outcomes may still occur in patients with HBV reactivation even with antiviral treatment[153]. Foont and Schiff[154] performed a systematic review on the use of lamivudine for the prophylaxis of HBV reactivation in patients on chemotherapy. In the ten trials with 173 patients included in the analysis, two patients taking lamivudine prophylaxis developed fatal HBV reactivation[154]. If a patient is not on antiviral prophylaxis, treatment with an antiviral agent such as entecavir or tenofovir should be initiated. Hepatitis B flare-ups are generally uncommon in patients receiving anti-HBV prophylaxis with potent antiviral agents, but drug resistance can develop to prophylactic lamivudine. In this instance, salvage therapy such as entecavir or tenofovir may be beneficial to them. Some patients achieve biochemical and virological recovery after combination treatment with entecavir + adefovir or lamivudine + adefovir[155].

The purpose of the treatment is prevention of severe hepatitis and also hepatic failure, which are potentially fatal. It is important to closely monitor the patient's liver enzymes, clotting profile, and bilirubin levels. Patients can still progress to hepatic failure despite therapy with nucleoside analogs[42], especially when there is already a marked increase in liver enzymes or jaundice. Liver transplantation is an option for patients with liver failure and there have been reported cases of successful transplantation in patients with chemotherapy-induced HBV reactivation[156-160]. Benten *et al*[161] found a low recurrence of pre-existing extrahepatic malignancies after liver transplantation.

CONCLUSION

Many novel therapies have emerged for the treatment of hematological malignancies in the past two decades and the results are promising. The issue of prevention of HBV reactivation is an important part of the management. Hepatitis due to HBV reactivation is a potentially fatal complication of cancer chemotherapy in patients with hematological malignancies. HBV reactivation can be prevented through blood test screening and, in patients with moderate or high risk of HBV reactivation, prophylactic antiviral therapy. We recommend screening all hematology patients for HBsAg and anti-HBc prior to receipt of anticancer therapy, and risk stratification based on the types of therapies planned and the serologic status of the patients. Prophylactic antiviral therapy is important for HBsAg-positive patients. Two options are available for HBsAg-negative/anti-HBc-positive patients. One is routine prophylactic antiviral therapy. The other is serial HBV DNA monitoring, and pre-emptive antiviral drug administration as soon as HBV DNA is detected. While there is

still limited evidence on the risk of HBV reactivation with newer therapies, we recommend antiviral prophylaxis in patients with resolved HBV who are scheduled to receive high-risk therapies like anti-CD20 monoclonal antibodies, anti-CD79 monoclonal antibodies, bispecific antibodies, BTK inhibitors, BCL-2 inhibitors, CAR-T cell therapy, or HSCT.

Entecavir and tenofovir are the preferred choices for prophylactic therapy. Preventative antiviral therapy should be continued for at least 12 mo after the cessation of chemotherapy; longer durations are recommended for patients who received rituximab or those who had high levels of serum HBV DNA before starting chemotherapy. Checking the HBV DNA before the cessation of antiviral therapy is recommended. We would also recommend monitoring liver function and HBV DNA levels for at least 12 mo after the cessation of antiviral prophylaxis.

FOOTNOTES

Author contributions: Mak JWY, Law AWH, Law KWT, Ho R, Cheung CKM, and Law MF were involved in the analysis of data/references; Mak JWY revised critically the manuscript; Law AWH, Law KWT, Cheung CKM, and Law MF contributed to the acquisition of data/references; Mak JWY, Cheung CKM, and Law MF contributed to the interpretation of data/references; Cheung CKM and Law MF drafted the manuscript; and all authors approved the manuscript.

Conflict-of-interest statement: All the authors report no relevant conflicts of interest for this article.

Open-Access: This article is an open-access article that was selected by an in-house editor and fully peer-reviewed by external reviewers. It is distributed in accordance with the Creative Commons Attribution NonCommercial (CC BY-NC 4.0) license, which permits others to distribute, remix, adapt, build upon this work non-commercially, and license their derivative works on different terms, provided the original work is properly cited and the use is non-commercial. See: https://creativecommons.org/Licenses/by-nc/4.0/

Country/Territory of origin: China

ORCID number: Joyce Wing Yan Mak 0000-0001-5221-7349; Alvin Wing Hin Law 0000-0001-8376-4193; Kimmy Wan Tung Law 0000-0002-8740-0896; Rita Ho 0000-0001-5966-2680; Carmen Ka Man Cheung 0000-0001-9386-506X; Man Fai Law 0000-0003-2462-6625.

S-Editor: Wang JJ
L-Editor: Wang TQ
P-Editor: Wang JJ

REFERENCES

1 **Lok AS**, Liang RH, Chiu EK, Wong KL, Chan TK, Todd D. Reactivation of hepatitis B virus replication in patients receiving cytotoxic therapy. Report of a prospective study. *Gastroenterology* 1991; **100**: 182-188 [PMID: 1983820 DOI: 10.1016/0016-5085(91)90599-g]

2 **Wei J**, Zhu X, Mao X, Huang L, Meng F, Zhou J. Severe early hepatitis B reactivation in a patient receiving anti-CD19 and anti-CD22 CAR T cells for the treatment of diffuse large B-cell lymphoma. *J Immunother Cancer* 2019; **7**: 315 [PMID: 31753002 DOI: 10.1186/s40425-019-0790-y]

3 **European Association for the Study of the Liver**. EASL 2017 Clinical Practice Guidelines on the management of hepatitis B virus infection. *J Hepatol* 2017; **67**: 370-398 [PMID: 28427875 DOI: 10.1016/j.jhep.2017.03.021]

4 **Hwang JP**, Feld JJ, Hammond SP, Wang SH, Alston-Johnson DE, Cryer DR, Hershman DL, Loehrer AP, Sabichi AL, Symington BE, Terrault N, Wong ML, Somerfield MR, Artz AS. Hepatitis B Virus Screening and Management for Patients With Cancer Prior to Therapy: ASCO Provisional Clinical Opinion Update. *J Clin Oncol* 2020; **38**: 3698-3715 [PMID: 32716741 DOI: 10.1200/JCO.20.01757]

5 **Lau G**, Yu ML, Wong G, Thompson A, Ghazinian H, Hou JL, Piratvisuth T, Jia JD, Mizokami M, Cheng G, Chen GF, Liu ZW, Baatarkhuu O, Cheng AL, Ng WL, Lau P, Mok T, Chang JM, Hamid S, Dokmeci AK, Gani RA, Payawal DA, Chow P, Park JW, Strasser SI, Mohamed R, Win KM, Tawesak T, Sarin SK, Omata M. APASL clinical practice guideline on hepatitis B reactivation related to the use of immunosuppressive therapy. *Hepatol Int* 2021; **15**: 1031-1048 [PMID: 34427860 DOI: 10.1007/s12072-021-10239-x]

6 **Perrillo RP**, Gish R, Falck-Ytter YT. American Gastroenterological Association Institute technical review on prevention and treatment of hepatitis B virus reactivation during immunosuppressive drug therapy. *Gastroenterology* 2015; **148**: 221-244.e3 [PMID: 25447852 DOI: 10.1053/j.gastro.2014.10.038]

7 **Terrault NA**, Lok ASF, McMahon BJ, Chang KM, Hwang JP, Jonas MM, Brown RS Jr, Bzowej NH, Wong JB. Update on prevention, diagnosis, and treatment of chronic hepatitis B: AASLD 2018 hepatitis B guidance. *Hepatology* 2018; **67**: 1560-1599 [PMID: 29405329 DOI: 10.1002/hep.29800]

8 **Chang Y**, Jeong SW, Jang JY. Hepatitis B Virus Reactivation Associated With Therapeutic Interventions. *Front Med (Lausanne)* 2021; **8**: 770124 [PMID: 35096867 DOI: 10.3389/fmed.2021.770124]

9 **Loomba R**, Liang TJ. Hepatitis B Reactivation Associated With Immune Suppressive and Biological Modifier Therapies: Current Concepts, Management Strategies, and Future Directions. *Gastroenterology* 2017; **152**: 1297-1309 [PMID: 28219691 DOI: 10.1053/j.gastro.2017.02.009]

10 **Bessone F**, Dirchwolf M. Management of hepatitis B reactivation in immunosuppressed patients: An update on current recommendations. *World J Hepatol* 2016; **8**: 385-394 [PMID: 27004086 DOI: 10.4254/wjh.v8.i8.385]

11 **Tohme RA**, Bulkow L, Homan CE, Negus S, McMahon BJ. Rates and risk factors for hepatitis B reactivation in a cohort of persons in the inactive phase of chronic hepatitis B-Alaska, 2001-2010. *J Clin Virol* 2013; **58**: 396-400 [PMID: 24001884 DOI: 10.1016/j.jcv.2013.08.012]

12 **Wang B**, Mufti G, Agarwal K. Reactivation of hepatitis B virus infection in patients with hematologic disorders. *Haematologica* 2019; **104**: 435-443 [PMID: 30733266 DOI: 10.3324/haematol.2018.210252]

13 **Yeo W**, Chan PK, Zhong S, Ho WM, Steinberg JL, Tam JS, Hui P, Leung NW, Zee B, Johnson PJ. Frequency of hepatitis B virus reactivation

in cancer patients undergoing cytotoxic chemotherapy: a prospective study of 626 patients with identification of risk factors. *J Med Virol* 2000; **62**: 299-307 [PMID: 11055239 DOI: 10.1002/1096-9071(200011)62:3<299::aid-jmv1>3.0.co;2-0]

14 **Chen CY**, Tien FM, Cheng A, Huang SY, Chou WC, Yao M, Tang JL, Tien HF, Sheng WH. Hepatitis B reactivation among 1962 patients with hematological malignancy in Taiwan. *BMC Gastroenterol* 2018; **18**: 6 [PMID: 29310589 DOI: 10.1186/s12876-017-0735-1]

15 **Law MF**, Ho R, Cheung CK, Tam LH, Ma K, So KC, Ip B, So J, Lai J, Ng J, Tam TH. Prevention and management of hepatitis B virus reactivation in patients with hematological malignancies treated with anticancer therapy. *World J Gastroenterol* 2016; **22**: 6484-6500 [PMID: 27605883 DOI: 10.3748/wjg.v22.i28.6484]

16 **Yeo W**, Chan PK, Ho WM, Zee B, Lam KC, Lei KI, Chan AT, Mok TS, Lee JJ, Leung TW, Zhong S, Johnson PJ. Lamivudine for the prevention of hepatitis B virus reactivation in hepatitis B s-antigen seropositive cancer patients undergoing cytotoxic chemotherapy. *J Clin Oncol* 2004; **22**: 927-934 [PMID: 14990649 DOI: 10.1200/JCO.2004.05.161]

17 **Yeo W**, Chan PK, Hui P, Ho WM, Lam KC, Kwan WH, Zhong S, Johnson PJ. Hepatitis B virus reactivation in breast cancer patients receiving cytotoxic chemotherapy: a prospective study. *J Med Virol* 2003; **70**: 553-561 [PMID: 12794717 DOI: 10.1002/jmv.10430]

18 **Yeo W**, Johnson PJ. Diagnosis, prevention and management of hepatitis B virus reactivation during anticancer therapy. *Hepatology* 2006; **43**: 209-220 [PMID: 16440366 DOI: 10.1002/hep.21051]

19 **Shouval D**, Shibolet O. Immunosuppression and HBV reactivation. *Semin Liver Dis* 2013; **33**: 167-177 [PMID: 23749673 DOI: 10.1055/s-0033-1345722]

20 **Chen WC**, Cheng JS, Chiang PH, Tsay FW, Chan HH, Chang HW, Yu HC, Tsai WL, Lai KH, Hsu PI. A Comparison of Entecavir and Lamivudine for the Prophylaxis of Hepatitis B Virus Reactivation in Solid Tumor Patients Undergoing Systemic Cytotoxic Chemotherapy. *PLoS One* 2015; **10**: e0131545 [PMID: 26121480 DOI: 10.1371/journal.pone.0131545]

21 **Lau GK**, Leung YH, Fong DY, Au WY, Kwong YL, Lie A, Hou JL, Wen YM, Nanj A, Liang R. High hepatitis B virus (HBV) DNA viral load as the most important risk factor for HBV reactivation in patients positive for HBV surface antigen undergoing autologous hematopoietic cell transplantation. *Blood* 2002; **99**: 2324-2330 [PMID: 11895763 DOI: 10.1182/blood.v99.7.2324]

22 **Yeo W**, Zee B, Zhong S, Chan PK, Wong WL, Ho WM, Lam KC, Johnson PJ. Comprehensive analysis of risk factors associating with Hepatitis B virus (HBV) reactivation in cancer patients undergoing cytotoxic chemotherapy. *Br J Cancer* 2004; **90**: 1306-1311 [PMID: 15054446 DOI: 10.1038/sj.bjc.6601699]

23 **Salpini R**, Colagrossi L, Bellocchi MC, Surdo M, Becker C, Alteri C, Aragri M, Ricciardi A, Armenia D, Pollicita M, Di Santo F, Carioti L, Louzoun Y, Mastroianni CM, Lichtner M, Paoloni M, Esposito M, D'Amore C, Marrone A, Marignani M, Sarrecchia C, Sarmati L, Andreoni M, Angelico M, Verheyen J, Perno CF, Svicher V. Hepatitis B surface antigen genetic elements critical for immune escape correlate with hepatitis B virus reactivation upon immunosuppression. *Hepatology* 2015; **61**: 823-833 [PMID: 25418031 DOI: 10.1002/hep.27604]

24 **Chen YF**, Chong CL, Wu YC, Wang YL, Tsai KN, Kuo TM, Hong MH, Hu CP, Chen ML, Chou YC, Chang C. Doxorubicin Activates Hepatitis B Virus Replication by Elevation of p21 (Waf1/Cip1) and C/EBPα Expression. *PLoS One* 2015; **10**: e0131743 [PMID: 26121644 DOI: 10.1371/journal.pone.0131743]

25 **Kostyusheva A**, Brezgin S, Bayurova E, Gordeychuk I, Isaguliants M, Goptar I, Urusov F, Nikiforova A, Volchkova E, Kostyushev D, Chulanov V. ATM and ATR Expression Potentiates HBV Replication and Contributes to Reactivation of HBV Infection upon DNA Damage. *Viruses* 2019; **11** [PMID: 31683589 DOI: 10.3390/v11110997]

26 **Kelling M**, Sokol L, Dalia S. Hepatitis B Reactivation in the Treatment of Non-Hodgkin Lymphoma. *Cancer Control* 2018; **25**: 1073274818767879 [PMID: 29606020 DOI: 10.1177/1073274818767879]

27 **Cao X**, Wang Y, Li P, Huang W, Lu X, Lu H. HBV Reactivation During the Treatment of Non-Hodgkin Lymphoma and Management Strategies. *Front Oncol* 2021; **11**: 685706 [PMID: 34277431 DOI: 10.3389/fonc.2021.685706]

28 **Cheng AL**, Hsiung CA, Su IJ, Chen PJ, Chang MC, Tsao CJ, Kao WY, Uen WC, Hsu CH, Tien HF, Chao TY, Chen LT, Whang-Peng J; Lymphoma Committee of Taiwan Cooperative Oncology Group. Steroid-free chemotherapy decreases risk of hepatitis B virus (HBV) reactivation in HBV-carriers with lymphoma. *Hepatology* 2003; **37**: 1320-1328 [PMID: 12774010 DOI: 10.1053/jhep.2003.50220]

29 **Notsumata K**, Nomura Y, Tanaka A, Ueda T, Sanada T, Watanabe H, Toya D. Efficient Prophylactic Management of HBV Reactivation by an Information Technology Encoding System: Results of a 6-year Prospective Cohort Study. *Intern Med* 2020; **59**: 2457-2464 [PMID: 33055468 DOI: 10.2169/internalmedicine.4445-20]

30 **Zhong Z**, Liao W, Dai L, Feng X, Su G, Gao Y, Wu Q, Yang P. Average corticosteroid dose and risk for HBV reactivation and hepatitis flare in patients with resolved hepatitis B infection. *Ann Rheum Dis* 2022; **81**: 584-591 [PMID: 34933869 DOI: 10.1136/annrheumdis-2021-221650]

31 **Wang YH**, Liang JD, Sheng WH, Tien FM, Chen CY, Tien HF. Hepatitis B reactivation during treatment of tyrosine kinase inhibitors-Experience in 142 adult patients with chronic myeloid leukemia. *Leuk Res* 2019; **81**: 95-97 [PMID: 31075669 DOI: 10.1016/j.leukres.2019.05.001]

32 **Uhm J**, Kim SH, Oh S, Zang DY, Do YR, Lee WS, Chang MH, Lee SE, Kim DW. High incidence of hepatitis B viral reactivation in chronic myeloid leukemia patients treated with tyrosine kinase inhibitors. *Blood* 2018; **132**: 3010 [DOI: 10.1182/blood-2018-99-117543]

33 **Ribera JM**, García-Calduch O, Ribera J, Montesinos P, Cano-Ferri I, Martínez P, Esteve J, Esteban D, García-Fortes M, Alonso N, González-Campos J, Bermúdez A, Torrent A, Genescà E, Mercadal S, Martínez-Lopez J, García-Sanz R. Ponatinib, chemotherapy, and transplant in adults with Philadelphia chromosome-positive acute lymphoblastic leukemia. *Blood Adv* 2022; **6**: 5395-5402 [PMID: 35675590 DOI: 10.1182/bloodadvances.2022007764]

34 **Sugiura I**, Doki N, Hata T, Cho R, Ito T, Suehiro Y, Tanaka M, Kako S, Matsuda M, Yokoyama H, Ishikawa Y, Taniguchi Y, Hagihara M, Ozawa Y, Ueda Y, Hirano D, Sakura T, Tsuji M, Kamae T, Fujita H, Hiramoto N, Onoda M, Fujisawa S, Hatta Y, Dobashi N, Nishiwaki S, Atsuta Y, Kobayashi Y, Hayakawa F, Ohtake S, Naoe T, Miyazaki Y. Dasatinib-based 2-step induction for adults with Philadelphia chromosome-positive acute lymphoblastic leukemia. *Blood Adv* 2022; **6**: 624-636 [PMID: 34516628 DOI: 10.1182/bloodadvances.2021004607]

35 **Lazdina U**, Alheim M, Nyström J, Hultgren C, Borisova G, Sominskaya I, Pumpens P, Peterson DL, Milich DR, Sällberg M. Priming of cytotoxic T cell responses to exogenous hepatitis B virus core antigen is B cell dependent. *J Gen Virol* 2003; **84**: 139-146 [PMID: 12533710 DOI: 10.1099/vir.0.18678-0]

36 **Xu X**, Shang Q, Chen X, Nie W, Zou Z, Huang A, Meng M, Jin L, Xu R, Zhang JY, Fu J, Wang L, Tang Z, Xie Y, Yang X, Zhang Z, Wang FS. Reversal of B-cell hyperactivation and functional impairment is associated with HBsAg seroconversion in chronic hepatitis B patients. *Cell Mol Immunol* 2015; **12**: 309-316 [PMID: 25849120 DOI: 10.1038/cmi.2015.25]

37 **Evens AM**, Jovanovic BD, Su YC, Raisch DW, Ganger D, Belknap SM, Dai MS, Chiu BC, Fintel B, Cheng Y, Chuang SS, Lee MY, Chen TY, Lin SF, Kuo CY. Rituximab-associated hepatitis B virus (HBV) reactivation in lymphoproliferative diseases: meta-analysis and

examination of FDA safety reports. *Ann Oncol* 2011; **22**: 1170-1180 [PMID: 21115603 DOI: 10.1093/annonc/mdq583]

38 **Guo YF**, Pan JX, Zhuang WH. Concurrent and reactivation of hepatitis B virus infection in diffuse large B-cell lymphoma: risk factors and survival outcome. *Infect Agent Cancer* 2018; **13**: 40 [PMID: 30559832 DOI: 10.1186/s13027-018-0215-4]

39 **Oh MJ**, Lee HJ. A study of hepatitis B virus reactivation associated with rituximab therapy in real-world clinical practice: a single-center experience. *Clin Mol Hepatol* 2013; **19**: 51-59 [PMID: 23593610 DOI: 10.3350/cmh.2013.19.1.51]

40 **Pei SN**, Chen CH, Lee CM, Wang MC, Ma MC, Hu TH, Kuo CY. Reactivation of hepatitis B virus following rituximab-based regimens: a serious complication in both HBsAg-positive and HBsAg-negative patients. *Ann Hematol* 2010; **89**: 255-262 [PMID: 19697028 DOI: 10.1007/s00277-009-0806-7]

41 **Tsai YF**, Yang CI, Du JS, Lin MH, Tang SH, Wang HC, Cho SF, Liu YC, Su YC, Dai CY, Hsiao HH. Rituximab increases the risk of hepatitis B virus reactivation in non-Hodgkin lymphoma patients who are hepatitis B surface antigen-positive or have resolved hepatitis B virus infection in a real-world setting: a retrospective study. *PeerJ* 2019; **7**: e7481 [PMID: 31565551 DOI: 10.7717/peerj.7481]

42 **Hsu C**, Tsou HH, Lin SJ, Wang MC, Yao M, Hwang WL, Kao WY, Chiu CF, Lin SF, Lin J, Chang CS, Tien HF, Liu TW, Chen PJ, Cheng AL; Taiwan Cooperative Oncology Group. Chemotherapy-induced hepatitis B reactivation in lymphoma patients with resolved HBV infection: a prospective study. *Hepatology* 2014; **59**: 2092-2100 [PMID: 24002804 DOI: 10.1002/hep.26718]

43 **Huang YH**, Hsiao LT, Hong YC, Chiou TJ, Yu YB, Gau JP, Liu CY, Yang MH, Tzeng CH, Lee PC, Lin HC, Lee SD. Randomized controlled trial of entecavir prophylaxis for rituximab-associated hepatitis B virus reactivation in patients with lymphoma and resolved hepatitis B. *J Clin Oncol* 2013; **31**: 2765-2772 [PMID: 23775967 DOI: 10.1200/JCO.2012.48.5938]

44 **Kusumoto S**, Tanaka Y, Suzuki R, Watanabe T, Nakata M, Takasaki H, Fukushima N, Fukushima T, Moriuchi Y, Itoh K, Nosaka K, Choi I, Sawa M, Okamoto R, Tsujimura H, Uchida T, Suzuki S, Okamoto M, Takahashi T, Sugiura I, Onishi Y, Kohri M, Yoshida S, Sakai R, Kojima M, Takahashi H, Tomita A, Maruyama D, Atsuta Y, Tanaka E, Suzuki T, Kinoshita T, Ogura M, Mizokami M, Ueda R. Monitoring of Hepatitis B Virus (HBV) DNA and Risk of HBV Reactivation in B-Cell Lymphoma: A Prospective Observational Study. *Clin Infect Dis* 2015; **61**: 719-729 [PMID: 25935551 DOI: 10.1093/cid/civ344]

45 **Seto WK**, Chan TS, Hwang YY, Wong DK, Fung J, Liu KS, Gill H, Lam YF, Lie AK, Lai CL, Kwong YL, Yuen MF. Hepatitis B reactivation in patients with previous hepatitis B virus exposure undergoing rituximab-containing chemotherapy for lymphoma: a prospective study. *J Clin Oncol* 2014; **32**: 3736-3743 [PMID: 25287829 DOI: 10.1200/JCO.2014.56.7081]

46 **Yeo W**, Chan TC, Leung NW, Lam WY, Mo FK, Chu MT, Chan HL, Hui EP, Lei KI, Mok TS, Chan PK. Hepatitis B virus reactivation in lymphoma patients with prior resolved hepatitis B undergoing anticancer therapy with or without rituximab. *J Clin Oncol* 2009; **27**: 605-611 [PMID: 19075267 DOI: 10.1200/JCO.2008.18.0182]

47 **Owen C**, Stewart DA. Obinutuzumab for the treatment of lymphoproliferative disorders. *Expert Opin Biol Ther* 2012; **12**: 343-351 [PMID: 22283718 DOI: 10.1517/14712598.2012.657622]

48 **Goede V**, Fischer K, Busch R, Engelke A, Eichhorst B, Wendtner CM, Chagorova T, de la Serna J, Dilhuydy MS, Illmer T, Opat S, Owen CJ, Samoylova O, Kreuzer KA, Stilgenbauer S, Döhner H, Langerak AW, Ritgen M, Kneba M, Asikanius E, Humphrey K, Wenger M, Hallek M. Obinutuzumab plus chlorambucil in patients with CLL and coexisting conditions. *N Engl J Med* 2014; **370**: 1101-1110 [PMID: 24401022 DOI: 10.1056/NEJMoa1313984]

49 **Marcus R**, Davies A, Ando K, Klapper W, Opat S, Owen C, Phillips E, Sangha R, Schlag R, Seymour JF, Townsend W, Trněný M, Wenger M, Fingerle-Rowson G, Rufibach K, Moore T, Herold M, Hiddemann W. Obinutuzumab for the First-Line Treatment of Follicular Lymphoma. *N Engl J Med* 2017; **377**: 1331-1344 [PMID: 28976863 DOI: 10.1056/NEJMoa1614598]

50 **Kusumoto S**, Arcaini L, Hong X, Jin J, Kim WS, Kwong YL, Peters MG, Tanaka Y, Zelenetz AD, Kuriki H, Fingerle-Rowson G, Nielsen T, Ueda E, Piper-Lepoutre H, Sellam G, Tobinai K. Risk of HBV reactivation in patients with B-cell lymphomas receiving obinutuzumab or rituximab immunochemotherapy. *Blood* 2019; **133**: 137-146 [PMID: 30341058 DOI: 10.1182/blood-2018-04-848044]

51 **Vitolo U**, Trněný M, Belada D, Burke JM, Carella AM, Chua N, Abrisqueta P, Demeter J, Flinn I, Hong X, Kim WS, Pinto A, Shi YK, Tatsumi Y, Oestergaard MZ, Wenger M, Fingerle-Rowson G, Catalani O, Nielsen T, Martelli M, Sehn LH. Obinutuzumab or Rituximab Plus Cyclophosphamide, Doxorubicin, Vincristine, and Prednisone in Previously Untreated Diffuse Large B-Cell Lymphoma. *J Clin Oncol* 2017; **35**: 3529-3537 [PMID: 28796588 DOI: 10.1200/JCO.2017.73.3402]

52 **Pfeifer M**, Zheng B, Erdmann T, Koeppen H, McCord R, Grau M, Staiger A, Chai A, Sandmann T, Madle H, Dörken B, Chu YW, Chen AI, Lebovic D, Salles GA, Czuczman MS, Palanca-Wessels MC, Press OW, Advani R, Morschhauser F, Cheson BD, Lenz P, Ott G, Polson AG, Mundt KE, Lenz G. Anti-CD22 and anti-CD79B antibody drug conjugates are active in different molecular diffuse large B-cell lymphoma subtypes. *Leukemia* 2015; **29**: 1578-1586 [PMID: 25708834 DOI: 10.1038/leu.2015.48]

53 **Sehn LH**, Herrera AF, Flowers CR, Kamdar MK, McMillan A, Hertzberg M, Assouline S, Kim TM, Kim WS, Ozcan M, Hirata J, Penuel E, Paulson JN, Cheng J, Ku G, Matasar MJ. Polatuzumab Vedotin in Relapsed or Refractory Diffuse Large B-Cell Lymphoma. *J Clin Oncol* 2020; **38**: 155-165 [PMID: 31693429 DOI: 10.1200/JCO.19.00172]

54 **Tilly H**, Morschhauser F, Sehn LH, Friedberg JW, Trněný M, Sharman JP, Herbaux C, Burke JM, Matasar M, Rai S, Izutsu K, Mehta-Shah N, Oberic L, Chauchet A, Jurczak W, Song Y, Greil R, Mykhalska L, Bergua-Burgués JM, Cheung MC, Pinto A, Shin HJ, Hapgood G, Munhoz E, Abrisqueta P, Gau JP, Hirata J, Jiang Y, Yan M, Lee C, Flowers CR, Salles G. Polatuzumab Vedotin in Previously Untreated Diffuse Large B-Cell Lymphoma. *N Engl J Med* 2022; **386**: 351-363 [PMID: 34904799 DOI: 10.1056/NEJMoa2115304]

55 **Shor B**, Gerber HP, Sapra P. Preclinical and clinical development of inotuzumab-ozogamicin in hematological malignancies. *Mol Immunol* 2015; **67**: 107-116 [PMID: 25304309 DOI: 10.1016/j.molimm.2014.09.014]

56 **Kantarjian HM**, DeAngelo DJ, Stelljes M, Martinelli G, Liedtke M, Stock W, Gökbuget N, O'Brien S, Wang K, Wang T, Paccagnella ML, Sleight B, Vandendries E, Advani AS. Inotuzumab Ozogamicin versus Standard Therapy for Acute Lymphoblastic Leukemia. *N Engl J Med* 2016; **375**: 740-753 [PMID: 27292104 DOI: 10.1056/NEJMoa1509277]

57 **Hoffmann P**, Hofmeister R, Brischwein K, Brandl C, Crommer S, Bargou R, Itin C, Prang N, Baeuerle PA. Serial killing of tumor cells by cytotoxic T cells redirected with a CD19-/CD3-bispecific single-chain antibody construct. *Int J Cancer* 2005; **115**: 98-104 [PMID: 15688411 DOI: 10.1002/ijc.20908]

58 **Foà R**, Bassan R, Vitale A, Elia L, Piciocchi A, Puzzolo MC, Canichella M, Viero P, Ferrara F, Lunghi M, Fabbiano F, Bonifacio M, Fracchiolla N, Di Bartolomeo P, Mancino A, De Propris MS, Vignetti M, Guarini A, Rambaldi A, Chiaretti S; GIMEMA Investigators. Dasatinib-Blinatumomab for Ph-Positive Acute Lymphoblastic Leukemia in Adults. *N Engl J Med* 2020; **383**: 1613-1623 [PMID: 33085860 DOI: 10.1056/NEJMoa2016272]

59 **Kantarjian H**, Stein A, Gökbuget N, Fielding AK, Schuh AC, Ribera JM, Wei A, Dombret H, Foà R, Bassan R, Arslan Ö, Sanz MA, Bergeron J, Demirkan F, Lech-Maranda E, Rambaldi A, Thomas X, Horst HA, Brüggemann M, Klapper W, Wood BL, Fleishman A, Nagorsen D,

Holland C, Zimmerman Z, Topp MS. Blinatumomab versus Chemotherapy for Advanced Acute Lymphoblastic Leukemia. *N Engl J Med* 2017; **376**: 836-847 [PMID: 28249141 DOI: 10.1056/NEJMoa1609783]

60 **Dimopoulos M**, Quach H, Mateos MV, Landgren O, Leleu X, Siegel D, Weisel K, Yang H, Klippel Z, Zahlten-Kumeli A, Usmani SZ. Carfilzomib, dexamethasone, and daratumumab versus carfilzomib and dexamethasone for patients with relapsed or refractory multiple myeloma (CANDOR): results from a randomised, multicentre, open-label, phase 3 study. *Lancet* 2020; **396**: 186-197 [PMID: 32682484 DOI: 10.1016/S0140-6736(20)30734-0]

61 **Dimopoulos MA**, Oriol A, Nahi H, San-Miguel J, Bahlis NJ, Usmani SZ, Rabin N, Orlowski RZ, Komarnicki M, Suzuki K, Plesner T, Yoon SS, Ben Yehuda D, Richardson PG, Goldschmidt H, Reece D, Lisby S, Khokhar NZ, O'Rourke L, Chiu C, Qin X, Guckert M, Ahmadi T, Moreau P; POLLUX Investigators. Daratumumab, Lenalidomide, and Dexamethasone for Multiple Myeloma. *N Engl J Med* 2016; **375**: 1319-1331 [PMID: 27705267 DOI: 10.1056/NEJMoa1607751]

62 **Facon T**, Kumar S, Plesner T, Orlowski RZ, Moreau P, Bahlis N, Basu S, Nahi H, Hulin C, Quach H, Goldschmidt H, O'Dwyer M, Perrot A, Venner CP, Weisel K, Mace JR, Raje N, Attal M, Tiab M, Macro M, Frenzel L, Leleu X, Ahmadi T, Chiu C, Wang J, Van Rampelbergh R, Uhlar CM, Kobos R, Qi M, Usmani SZ; MAIA Trial Investigators. Daratumumab plus Lenalidomide and Dexamethasone for Untreated Myeloma. *N Engl J Med* 2019; **380**: 2104-2115 [PMID: 31141632 DOI: 10.1056/NEJMoa1817249]

63 **Palumbo A**, Chanan-Khan A, Weisel K, Nooka AK, Masszi T, Beksac M, Spicka I, Hungria V, Munder M, Mateos MV, Mark TM, Qi M, Schecter J, Amin H, Qin X, Deraedt W, Ahmadi T, Spencer A, Sonneveld P; CASTOR Investigators. Daratumumab, Bortezomib, and Dexamethasone for Multiple Myeloma. *N Engl J Med* 2016; **375**: 754-766 [PMID: 27557302 DOI: 10.1056/NEJMoa1606038]

64 **Kastritis E**, Palladini G, Minnema MC, Wechalekar AD, Jaccard A, Lee HC, Sanchorawala V, Gibbs S, Mollee P, Venner CP, Lu J, Schönland S, Gatt ME, Suzuki K, Kim K, Cibeira MT, Beksac M, Libby E, Valent J, Hungria V, Wong SW, Rosenzweig M, Bumma N, Huart A, Dimopoulos MA, Bhutani D, Waxman AJ, Goodman SA, Zonder JA, Lam S, Song K, Hansen T, Manier S, Roeloffzen W, Jamroziak K, Kwok F, Shimazaki C, Kim JS, Crusoe E, Ahmadi T, Tran N, Qin X, Vasey SY, Tromp B, Schecter JM, Weiss BM, Zhuang SH, Vermeulen J, Merlini G, Comenzo RL; ANDROMEDA Trial Investigators. Daratumumab-Based Treatment for Immunoglobulin Light-Chain Amyloidosis. *N Engl J Med* 2021; **385**: 46-58 [PMID: 34192431 DOI: 10.1056/NEJMoa2028631]

65 **Palladini G**, Kastritis E, Maurer MS, Zonder J, Minnema MC, Wechalekar AD, Jaccard A, Lee HC, Bumma N, Kaufman JL, Medvedova E, Kovacsovics T, Rosenzweig M, Sanchorawala V, Qin X, Vasey SY, Weiss BM, Vermeulen J, Merlini G, Comenzo RL. Daratumumab plus CyBorD for patients with newly diagnosed AL amyloidosis: safety run-in results of ANDROMEDA. *Blood* 2020; **136**: 71-80 [PMID: 32244252 DOI: 10.1182/blood.2019004460]

66 **van de Donk NWCJ**, Richardson PG, Malavasi F. CD38 antibodies in multiple myeloma: back to the future. *Blood* 2018; **131**: 13-29 [PMID: 29118010 DOI: 10.1182/blood-2017-06-740944]

67 **Zhang S**, Zhao J, Zhang Z. Humoral immunity, the underestimated player in hepatitis B. *Cell Mol Immunol* 2018; **15**: 645-648 [PMID: 29225341 DOI: 10.1038/cmi.2017.132]

68 **Kikuchi T**, Kusumoto S, Tanaka Y, Oshima Y, Fujinami H, Suzuki T, Totani H, Kinoshita S, Asao Y, Narita T, Ito A, Ri M, Komatsu H, Iida S. Hepatitis B virus reactivation in a myeloma patient with resolved infection who received daratumumab-containing salvage chemotherapy. *J Clin Exp Hematop* 2020; **60**: 51-54 [PMID: 32404569 DOI: 10.3960/jslrt.19034]

69 **Lee SK**, Sung PS, Park SS, Min CK, Nam H, Jang JW, Choi JY, Yoon SK. Reactivation of Resolved Hepatitis B After Daratumumab for Multiple Myeloma. *Clin Infect Dis* 2021; **73**: e1372-e1375 [PMID: 33846712 DOI: 10.1093/cid/ciab302]

70 **Attal M**, Richardson PG, Rajkumar SV, San-Miguel J, Beksac M, Spicka I, Leleu X, Schjesvold F, Moreau P, Dimopoulos MA, Huang JS, Minarik J, Cavo M, Prince HM, Macé S, Corzo KP, Campana F, Le-Guennec S, Dubin F, Anderson KC; ICARIA-MM study group. Isatuximab plus pomalidomide and low-dose dexamethasone versus pomalidomide and low-dose dexamethasone in patients with relapsed and refractory multiple myeloma (ICARIA-MM): a randomised, multicentre, open-label, phase 3 study. *Lancet* 2019; **394**: 2096-2107 [PMID: 31735560 DOI: 10.1016/S0140-6736(19)32556-5]

71 **Leypoldt LB**, Besemer B, Asemissen AM, Hänel M, Blau IW, Görner M, Ko YD, Reinhardt HC, Staib P, Mann C, Lutz R, Munder M, Graeven U, Peceny R, Salwender H, Jauch A, Zago M, Benner A, Tichy D, Bokemeyer C, Goldschmidt H, Weisel KC. Isatuximab, carfilzomib, lenalidomide, and dexamethasone (Isa-KRd) in front-line treatment of high-risk multiple myeloma: interim analysis of the GMMG-CONCEPT trial. *Leukemia* 2022; **36**: 885-888 [PMID: 34732857 DOI: 10.1038/s41375-021-01431-x]

72 **Moreau P**, Dimopoulos MA, Mikhael J, Yong K, Capra M, Facon T, Hajek R, Špička I, Baker R, Kim K, Martinez G, Min CK, Pour L, Leleu X, Oriol A, Koh Y, Suzuki K, Risse ML, Asset G, Macé S, Martin T; IKEMA study group. Isatuximab, carfilzomib, and dexamethasone in relapsed multiple myeloma (IKEMA): a multicentre, open-label, randomised phase 3 trial. *Lancet* 2021; **397**: 2361-2371 [PMID: 34097854 DOI: 10.1016/S0140-6736(21)00592-4]

73 **Spicka I**, Moreau P, Martin TG, Facon T, Martinez G, Oriol A, Koh Y, Lim A, Mikala G, Rosiñol L, Yağci M, Cavo M, Risse ML, Asset G, Macé S, van de Velde H, Yong K. Isatuximab plus carfilzomib and dexamethasone in relapsed multiple myeloma patients with high-risk cytogenetics: IKEMA subgroup analysis. *Eur J Haematol* 2022; **109**: 504-512 [PMID: 35871357 DOI: 10.1111/ejh.13835]

74 **Maude SL**, Laetsch TW, Buechner J, Rives S, Boyer M, Bittencourt H, Bader P, Verneris MR, Stefanski HE, Myers GD, Qayed M, De Moerloose B, Hiramatsu H, Schlis K, Davis KL, Martin PL, Nemecek ER, Yanik GA, Peters C, Baruchel A, Boissel N, Mechinaud F, Balduzzi A, Krueger J, June CH, Levine BL, Wood P, Taran T, Leung M, Mueller KT, Zhang Y, Sen K, Lebwohl D, Pulsipher MA, Grupp SA. Tisagenlecleucel in Children and Young Adults with B-Cell Lymphoblastic Leukemia. *N Engl J Med* 2018; **378**: 439-448 [PMID: 29385370 DOI: 10.1056/NEJMoa1709866]

75 **Neelapu SS**, Locke FL, Bartlett NL, Lekakis LJ, Miklos DB, Jacobson CA, Braunschweig I, Oluwole OO, Siddiqi T, Lin Y, Timmerman JM, Stiff PJ, Friedberg JW, Flinn IW, Goy A, Hill BT, Smith MR, Deol A, Farooq U, McSweeney P, Munoz J, Avivi I, Castro JE, Westin JR, Chavez JC, Ghobadi A, Komanduri KV, Levy R, Jacobsen ED, Witzig TE, Reagan P, Bot A, Rossi J, Navale L, Jiang Y, Aycock J, Elias M, Chang D, Wiezorek J, Go WY. Axicabtagene Ciloleucel CAR T-Cell Therapy in Refractory Large B-Cell Lymphoma. *N Engl J Med* 2017; **377**: 2531-2544 [PMID: 29226797 DOI: 10.1056/NEJMoa1707447]

76 **Schuster SJ**, Bishop MR, Tam CS, Waller EK, Borchmann P, McGuirk JP, Jäger U, Jaglowski S, Andreadis C, Westin JR, Fleury I, Bachanova V, Foley SR, Ho PJ, Mielke S, Magenau JM, Holte H, Pantano S, Pacaud LB, Awasthi R, Chu J, Anak Ö, Salles G, Maziarz RT; JULIET Investigators. Tisagenlecleucel in Adult Relapsed or Refractory Diffuse Large B-Cell Lymphoma. *N Engl J Med* 2019; **380**: 45-56 [PMID: 30501490 DOI: 10.1056/NEJMoa1804980]

77 **Wang M**, Munoz J, Goy A, Locke FL, Jacobson CA, Hill BT, Timmerman JM, Holmes H, Jaglowski S, Flinn IW, McSweeney PA, Miklos DB, Pagel JM, Kersten MJ, Milpied N, Fung H, Topp MS, Houot R, Beitinjaneh A, Peng W, Zheng L, Rossi JM, Jain RK, Rao AV, Reagan PM. KTE-X19 CAR T-Cell Therapy in Relapsed or Refractory Mantle-Cell Lymphoma. *N Engl J Med* 2020; **382**: 1331-1342 [PMID:

32242358 DOI: 10.1056/NEJMoa1914347]

78 **Park JH**, Rivière I, Gonen M, Wang X, Sénéchal B, Curran KJ, Sauter C, Wang Y, Santomasso B, Mead E, Roshal M, Maslak P, Davila M, Brentjens RJ, Sadelain M. Long-Term Follow-up of CD19 CAR Therapy in Acute Lymphoblastic Leukemia. *N Engl J Med* 2018; **378**: 449-459 [PMID: 29385376 DOI: 10.1056/NEJMoa1709919]

79 **Mailankody S**, Devlin SM, Landa J, Nath K, Diamonte C, Carstens EJ, Russo D, Auclair R, Fitzgerald L, Cadzin B, Wang X, Sikder D, Senechal B, Bermudez VP, Purdon TJ, Hosszu K, McAvoy DP, Farzana T, Mead E, Wilcox JA, Santomasso BD, Shah GL, Shah UA, Korde N, Lesokhin A, Tan CR, Hultcrantz M, Hassoun H, Roshal M, Sen F, Dogan A, Landgren O, Giralt SA, Park JH, Usmani SZ, Rivière I, Brentjens RJ, Smith EL. GPRC5D-Targeted CAR T Cells for Myeloma. *N Engl J Med* 2022; **387**: 1196-1206 [PMID: 36170501 DOI: 10.1056/NEJMoa2209900]

80 **Raje N**, Berdeja J, Lin Y, Siegel D, Jagannath S, Madduri D, Liedtke M, Rosenblatt J, Maus MV, Turka A, Lam LP, Morgan RA, Friedman K, Massaro M, Wang J, Russotti G, Yang Z, Campbell T, Hege K, Petrocca F, Quigley MT, Munshi N, Kochenderfer JN. Anti-BCMA CAR T-Cell Therapy bb2121 in Relapsed or Refractory Multiple Myeloma. *N Engl J Med* 2019; **380**: 1726-1737 [PMID: 31042825 DOI: 10.1056/NEJMoa1817226]

81 **Haslauer T**, Greil R, Zaborsky N, Geisberger R. CAR T-Cell Therapy in Hematological Malignancies. *Int J Mol Sci* 2021; **22** [PMID: 34445701 DOI: 10.3390/ijms22168996]

82 **Wang Y**, Li H, Song X, Qi K, Cheng H, Cao J, Shi M, Yan Z, Jing G, Pan B, Sang W, Wang X, Zhao K, Chen C, Chen W, Zheng J, Li Z, Xu K. Kinetics of immune reconstitution after anti-CD19 chimeric antigen receptor T cell therapy in relapsed or refractory acute lymphoblastic leukemia patients. *Int J Lab Hematol* 2021; **43**: 250-258 [PMID: 33112046 DOI: 10.1111/ijlh.13375]

83 **Cao W**, Wei J, Wang N, Xu H, Xiao M, Huang L, Cao Y, Li C, Xiao Y, Gu C, Zhang S, Li D, Zhang Y, Zhang T, Zhou J. Entecavir prophylaxis for hepatitis B virus reactivation in patients with CAR T-cell therapy. *Blood* 2020; **136**: 516-519 [PMID: 32291456 DOI: 10.1182/blood.2020004907]

84 **Cui R**, Lyu C, Li Q, Jiang Y, Mou N, Yang Z, Liu X, Deng Q, Li L. Humanized anti-CD19 chimeric antigen receptor-T cell therapy is safe and effective in lymphoma and leukemia patients with chronic and resolved hepatitis B virus infection. *Hematol Oncol* 2021; **39**: 75-86 [PMID: 32949412 DOI: 10.1002/hon.2807]

85 **Han L**, Zhou J, Zhou K, Zhu X, Zhao L, Fang B, Yin Q, Wei X, Zhou H, Li L, Xu B, Zhang J, Song Y, Gao Q. Safety and efficacy of CAR-T cell targeting BCMA in patients with multiple myeloma coinfected with chronic hepatitis B virus. *J Immunother Cancer* 2020; **8** [PMID: 32792360 DOI: 10.1136/jitc-2020-000927]

86 **Li P**, Zhou L, Ye S, Zhang W, Wang J, Tang X, Liu J, Xu Y, Qian W, Liang A. Risk of HBV Reactivation in Patients With Resolved HBV Infection Receiving Anti-CD19 Chimeric Antigen Receptor T Cell Therapy Without Antiviral Prophylaxis. *Front Immunol* 2021; **12**: 638678 [PMID: 34335561 DOI: 10.3389/fimmu.2021.638678]

87 **Liu W**, Huang W, Wang M, Lv R, Li J, Wang Y, Deng S, Yi S, Liu H, Rao Q, Xu Y, Lv L, Qiu L, Zou D, Wang J. Risk of hepatitis B reactivation is controllable in patients with B-cell lymphoma receiving anti-CD19 CAR T cell therapy. *Br J Haematol* 2020; **191**: 126-129 [PMID: 32671820 DOI: 10.1111/bjh.16951]

88 **Wang Y**, Liu Y, Tan X, Pan B, Ge J, Qi K, Cheng H, Cao J, Shi M, Yan Z, Qiao J, Jing G, Wang X, Sang W, Xia R, Zhang X, Li Z, Gale RP, Zheng J, Zhu F, Xu K. Safety and efficacy of chimeric antigen receptor (CAR)-T-cell therapy in persons with advanced B-cell cancers and hepatitis B virus-infection. *Leukemia* 2020; **34**: 2704-2707 [PMID: 32594100 DOI: 10.1038/s41375-020-0936-4]

89 **Yang C**, Xie M, Zhang K, Liu H, Liang A, Young KH, Qian W. Risk of HBV reactivation post CD19-CAR-T cell therapy in DLBCL patients with concomitant chronic HBV infection. *Leukemia* 2020; **34**: 3055-3059 [PMID: 32533094 DOI: 10.1038/s41375-020-0913-y]

90 **Bannerji R**, Arnason JE, Advani RH, Brown JR, Allan JN, Ansell SM, Barnes JA, O'Brien SM, Chávez JC, Duell J, Rosenwald A, Crombie JL, Ufkin M, Li J, Zhu M, Ambati SR, Chaudhry A, Lowy I, Topp MS. Odronextamab, a human CD20×CD3 bispecific antibody in patients with CD20-positive B-cell malignancies (ELM-1): results from the relapsed or refractory non-Hodgkin lymphoma cohort in a single-arm, multicentre, phase 1 trial. *Lancet Haematol* 2022; **9**: e327-e339 [PMID: 35366963 DOI: 10.1016/S2352-3026(22)00072-2]

91 **Minson A**, Dickinson M. Glofitamab CD20-TCB bispecific antibody. *Leuk Lymphoma* 2021; **62**: 3098-3108 [PMID: 34263696 DOI: 10.1080/10428194.2021.1953016]

92 **van der Horst HJ**, de Jonge AV, Hiemstra IH, Gelderloos AT, Berry DRAI, Hijmering NJ, van Essen HF, de Jong D, Chamuleau MED, Zweegman S, Breij ECW, Roemer MGM, Mutis T. Epcoritamab induces potent anti-tumor activity against malignant B-cells from patients with DLBCL, FL and MCL, irrespective of prior CD20 monoclonal antibody treatment. *Blood Cancer J* 2021; **11**: 38 [PMID: 33602901 DOI: 10.1038/s41408-021-00430-6]

93 **Dickinson MJ**, Carlo-Stella C, Morschhauser F, Bachy E, Corradini P, Iacoboni G, Khan C, Wróbel T, Offner F, Trněný M, Wu SJ, Cartron G, Hertzberg M, Sureda A, Perez-Callejo D, Lundberg L, Relf J, Dixon M, Clark E, Humphrey K, Hutchings M. Glofitamab for Relapsed or Refractory Diffuse Large B-Cell Lymphoma. *N Engl J Med* 2022; **387**: 2220-2231 [PMID: 36507690 DOI: 10.1056/NEJMoa2206913]

94 **Hutchings M**, Morschhauser F, Iacoboni G, Carlo-Stella C, Offner FC, Sureda A, Salles G, Martínez-Lopez J, Crump M, Thomas DN, Morcos PN, Ferlini C, Bröske AE, Belousov A, Bacac M, Dimier N, Carlile DJ, Lundberg L, Perez-Callejo D, Umaña P, Moore T, Weisser M, Dickinson MJ. Glofitamab, a Novel, Bivalent CD20-Targeting T-Cell-Engaging Bispecific Antibody, Induces Durable Complete Remissions in Relapsed or Refractory B-Cell Lymphoma: A Phase I Trial. *J Clin Oncol* 2021; **39**: 1959-1970 [PMID: 33739857 DOI: 10.1200/JCO.20.03175]

95 **Thieblemont C**, Phillips T, Ghesquieres H, Cheah CY, Clausen MR, Cunningham D, Do YR, Feldman T, Gasiorowski R, Jurczak W, Kim TM, Lewis DJ, van der Poel M, Poon ML, Cota Stirner M, Kilavuz N, Chiu C, Chen M, Sacchi M, Elliott B, Ahmadi T, Hutchings M, Lugtenburg PJ. Epcoritamab, a Novel, Subcutaneous CD3xCD20 Bispecific T-Cell-Engaging Antibody, in Relapsed or Refractory Large B-Cell Lymphoma: Dose Expansion in a Phase I/II Trial. *J Clin Oncol* 2023; **41**: 2238-2247 [PMID: 36548927 DOI: 10.1200/JCO.22.01725]

96 **Budde LE**, Sehn LH, Matasar M, Schuster SJ, Assouline S, Giri P, Kuruvilla J, Canales M, Dietrich S, Fay K, Ku M, Nastoupil L, Cheah CY, Wei MC, Yin S, Li CC, Huang H, Kwan A, Penuel E, Bartlett NL. Safety and efficacy of mosunetuzumab, a bispecific antibody, in patients with relapsed or refractory follicular lymphoma: a single-arm, multicentre, phase 2 study. *Lancet Oncol* 2022; **23**: 1055-1065 [PMID: 35803286 DOI: 10.1016/S1470-2045(22)00335-7]

97 **Brown JR**, Eichhorst B, Hillmen P, Jurczak W, Kaźmierczak M, Lamanna N, O'Brien SM, Tam CS, Qiu L, Zhou K, Simkovic M, Mayer J, Gillespie-Twardy A, Ferrajoli A, Ganly PS, Weinkove R, Grosicki S, Mital A, Robak T, Osterborg A, Yimer HA, Salmi T, Wang MD, Fu L, Li J, Wu K, Cohen A, Shadman M. Zanubrutinib or Ibrutinib in Relapsed or Refractory Chronic Lymphocytic Leukemia. *N Engl J Med* 2023; **388**: 319-332 [PMID: 36511784 DOI: 10.1056/NEJMoa2211582]

98 **Burger JA**, Tedeschi A, Barr PM, Robak T, Owen C, Ghia P, Bairey O, Hillmen P, Bartlett NL, Li J, Simpson D, Grosicki S, Devereux S,

McCarthy H, Coutre S, Quach H, Gaidano G, Maslyak Z, Stevens DA, Janssens A, Offner F, Mayer J, O'Dwyer M, Hellmann A, Schuh A, Siddiqi T, Polliack A, Tam CS, Suri D, Cheng M, Clow F, Styles L, James DF, Kipps TJ; RESONATE-2 Investigators. Ibrutinib as Initial Therapy for Patients with Chronic Lymphocytic Leukemia. *N Engl J Med* 2015; **373**: 2425-2437 [PMID: 26639149 DOI: 10.1056/NEJMoa1509388]

99 **Byrd JC**, Harrington B, O'Brien S, Jones JA, Schuh A, Devereux S, Chaves J, Wierda WG, Awan FT, Brown JR, Hillmen P, Stephens DM, Ghia P, Barrientos JC, Pagel JM, Woyach J, Johnson D, Huang J, Wang X, Kaptein A, Lannutti BJ, Covey T, Fardis M, McGreivy J, Hamdy A, Rothbaum W, Izumi R, Diacovo TG, Johnson AJ, Furman RR. Acalabrutinib (ACP-196) in Relapsed Chronic Lymphocytic Leukemia. *N Engl J Med* 2016; **374**: 323-332 [PMID: 26641137 DOI: 10.1056/NEJMoa1509981]

100 **Byrd JC**, Hillmen P, Ghia P, Kater AP, Chanan-Khan A, Furman RR, O'Brien S, Yenerel MN, Illés A, Kay N, Garcia-Marco JA, Mato A, Pinilla-Ibarz J, Seymour JF, Lepretre S, Stilgenbauer S, Robak T, Rothbaum W, Izumi R, Hamdy A, Patel P, Higgins K, Sohoni S, Jurczak W. Acalabrutinib Versus Ibrutinib in Previously Treated Chronic Lymphocytic Leukemia: Results of the First Randomized Phase III Trial. *J Clin Oncol* 2021; **39**: 3441-3452 [PMID: 34310172 DOI: 10.1200/JCO.21.01210]

101 **Sharman JP**, Egyed M, Jurczak W, Skarbnik A, Pagel JM, Flinn IW, Kamdar M, Munir T, Walewska R, Corbett G, Fogliatto LM, Herishanu Y, Banerji V, Coutre S, Follows G, Walker P, Karlsson K, Ghia P, Janssens A, Cymbalista F, Woyach JA, Salles G, Wierda WG, Izumi R, Munugalavadla V, Patel P, Wang MH, Wong S, Byrd JC. Acalabrutinib with or without obinutuzumab versus chlorambucil and obinutuzmab for treatment-naive chronic lymphocytic leukaemia (ELEVATE TN): a randomised, controlled, phase 3 trial. *Lancet* 2020; **395**: 1278-1291 [PMID: 32305093 DOI: 10.1016/S0140-6736(20)30262-2]

102 **Woyach JA**, Ruppert AS, Heerema NA, Zhao W, Booth AM, Ding W, Bartlett NL, Brander DM, Barr PM, Rogers KA, Parikh SA, Coutre S, Hurria A, Brown JR, Lozanski G, Blachly JS, Ozer HG, Major-Elechi B, Fruth B, Nattam S, Larson RA, Erba H, Litzow M, Owen C, Kuzma C, Abramson JS, Little RF, Smith SE, Stone RM, Mandrekar SJ, Byrd JC. Ibrutinib Regimens versus Chemoimmunotherapy in Older Patients with Untreated CLL. *N Engl J Med* 2018; **379**: 2517-2528 [PMID: 30501481 DOI: 10.1056/NEJMoa1812836]

103 **Tam CS**, Anderson MA, Pott C, Agarwal R, Handunnetti S, Hicks RJ, Burbury K, Turner G, Di Iulio J, Bressel M, Westerman D, Lade S, Dreyling M, Dawson SJ, Dawson MA, Seymour JF, Roberts AW. Ibrutinib plus Venetoclax for the Treatment of Mantle-Cell Lymphoma. *N Engl J Med* 2018; **378**: 1211-1223 [PMID: 29590547 DOI: 10.1056/NEJMoa1715519]

104 **Wang ML**, Jurczak W, Jerkeman M, Trotman J, Zinzani PL, Belada D, Boccomini C, Flinn IW, Giri P, Goy A, Hamlin PA, Hermine O, Hernández-Rivas JÁ, Hong X, Kim SJ, Lewis D, Mishima Y, Özcan M, Perini GF, Pocock C, Song Y, Spurgeon SE, Storring JM, Walewski J, Zhu J, Qin R, Henninger T, Deshpande S, Howes A, Le Gouill S, Dreyling M; SHINE Investigators. Ibrutinib plus Bendamustine and Rituximab in Untreated Mantle-Cell Lymphoma. *N Engl J Med* 2022; **386**: 2482-2494 [PMID: 35657079 DOI: 10.1056/NEJMoa2201817]

105 **Strati P**, Coleman M, Champion R, Ma S, Patti C, Levy MY, Lossos IS, Geethakumari PR, Lam S, Calvo R, Higgins K, Budde LE. A phase 2, multicentre, open-label trial (ACE-LY-003) of acalabrutinib in patients with relapsed or refractory marginal zone lymphoma. *Br J Haematol* 2022; **199**: 76-85 [PMID: 35861370 DOI: 10.1111/bjh.18368]

106 **Dimopoulos MA**, Tedeschi A, Trotman J, García-Sanz R, Macdonald D, Leblond V, Mahe B, Herbaux C, Tam C, Orsucci L, Palomba ML, Matous JV, Shustik C, Kastritis E, Treon SP, Li J, Salman Z, Graef T, Buske C; iNNOVATE Study Group and the European Consortium for Waldenström's Macroglobulinemia. Phase 3 Trial of Ibrutinib plus Rituximab in Waldenström's Macroglobulinemia. *N Engl J Med* 2018; **378**: 2399-2410 [PMID: 29856685 DOI: 10.1056/NEJMoa1802917]

107 **Cameron F**, Sanford M. Ibrutinib: first global approval. *Drugs* 2014; **74**: 263-271 [PMID: 24464309 DOI: 10.1007/s40265-014-0178-8]

108 **Hammond SP**, Chen K, Pandit A, Davids MS, Issa NC, Marty FM. Risk of hepatitis B virus reactivation in patients treated with ibrutinib. *Blood* 2018; **131**: 1987-1989 [PMID: 29490923 DOI: 10.1182/blood-2018-01-826495]

109 **Innocenti I**, Morelli F, Autore F, Corbingi A, Pasquale R, Sorà F, Pompili M, Laurenti L. HBV reactivation in CLL patients with occult HBV infection treated with ibrutinib without viral prophylaxis. *Leuk Lymphoma* 2019; **60**: 1340-1342 [PMID: 30730231 DOI: 10.1080/10428194.2018.1523401]

110 **Innocenti I**, Reda G, Visentin A, Coscia M, Motta M, Murru R, Moia R, Gentile M, Pennese E, Quaglia FM, Albano F, Cassin R, Deodato M, Ielo C, Frustaci AM, Piciocchi A, Rughini A, Arena V, Di Sevo D, Tomasso A, Autore F, Del Poeta G, Scarfò L, Mauro FR, Tedeschi A, Trentin L, Pompili M, Foà R, Ghia P, Cuneo A, Laurenti L. Risk of hepatitis B virus reactivation in chronic lymphocytic leukemia patients receiving ibrutinib with or without antiviral prophylaxis. A retrospective multicentric GIMEMA study. *Haematologica* 2022; **107**: 1470-1473 [PMID: 35199505 DOI: 10.3324/haematol.2021.280325]

111 **Ni Y**, Gao L, Lu Y, Ye S, Zhou L, Qian W, Liang A, Li P. Risk of HBV reactivation in relapsed or refractory diffuse large B-cell lymphoma patients receiving Bruton tyrosine kinase inhibitors therapy. *Front Immunol* 2022; **13**: 982346 [PMID: 36119029 DOI: 10.3389/fimmu.2022.982346]

112 **Al-Sawaf O**, Zhang C, Tandon M, Sinha A, Fink AM, Robrecht S, Samoylova O, Liberati AM, Pinilla-Ibarz J, Opat S, Sivcheva L, Le Dû K, Fogliatto LM, Niemann CU, Weinkove R, Robinson S, Kipps TJ, Tausch E, Schary W, Ritgen M, Wendtner CM, Kreuzer KA, Eichhorst B, Stilgenbauer S, Hallek M, Fischer K. Venetoclax plus obinutuzumab versus chlorambucil plus obinutuzumab for previously untreated chronic lymphocytic leukaemia (CLL14): follow-up results from a multicentre, open-label, randomised, phase 3 trial. *Lancet Oncol* 2020; **21**: 1188-1200 [PMID: 32888452 DOI: 10.1016/S1470-2045(20)30443-5]

113 **Fischer K**, Al-Sawaf O, Bahlo J, Fink AM, Tandon M, Dixon M, Robrecht S, Warburton S, Humphrey K, Samoylova O, Liberati AM, Pinilla-Ibarz J, Opat S, Sivcheva L, Le Dû K, Fogliatto LM, Niemann CU, Weinkove R, Robinson S, Kipps TJ, Boettcher S, Tausch E, Humerickhouse R, Eichhorst B, Wendtner CM, Langerak AW, Kreuzer KA, Ritgen M, Goede V, Stilgenbauer S, Mobasher M, Hallek M. Venetoclax and Obinutuzumab in Patients with CLL and Coexisting Conditions. *N Engl J Med* 2019; **380**: 2225-2236 [PMID: 31166681 DOI: 10.1056/NEJMoa1815281]

114 **DiNardo CD**, Jonas BA, Pullarkat V, Thirman MJ, Garcia JS, Wei AH, Konopleva M, Döhner H, Letai A, Fenaux P, Koller E, Havelange V, Leber B, Esteve J, Wang J, Pejsa V, Hájek R, Porkka K, Illés Á, Lavie D, Lemoli RM, Yamamoto K, Yoon SS, Jang JH, Yeh SP, Turgut M, Hong WJ, Zhou Y, Potluri J, Pratz KW. Azacitidine and Venetoclax in Previously Untreated Acute Myeloid Leukemia. *N Engl J Med* 2020; **383**: 617-629 [PMID: 32786187 DOI: 10.1056/NEJMoa2012971]

115 **Wei AH**, Montesinos P, Ivanov V, DiNardo CD, Novak J, Laribi K, Kim I, Stevens DA, Fiedler W, Pagoni M, Samoilova O, Hu Y, Anagnostopoulos A, Bergeron J, Hou JZ, Murthy V, Yamauchi T, McDonald A, Chyla B, Gopalakrishnan S, Jiang Q, Mendes W, Hayslip J, Panayiotidis P. Venetoclax plus LDAC for newly diagnosed AML ineligible for intensive chemotherapy: a phase 3 randomized placebo-controlled trial. *Blood* 2020; **135**: 2137-2145 [PMID: 32219442 DOI: 10.1182/blood.2020004856]

116 **Mya DH**, Han ST, Linn YC, Hwang WY, Goh YT, Tan DC. Risk of hepatitis B reactivation and the role of novel agents and stem-cell transplantation in multiple myeloma patients with hepatitis B virus (HBV) infection. *Ann Oncol* 2012; **23**: 421-426 [PMID: 21551005 DOI:

10.1093/annonc/mdr142]
117 **Ataca Atilla P**, Yalçıner M, Atilla E, İdilman R, Beksaç M. Hepatitis B Reactivation Rate and Fate Among Multiple Myeloma Patients Receiving Regimens Containing Lenalidomide and/or Bortezomib. *Turk J Haematol* 2019; **36**: 266-273 [PMID: 31368290 DOI: 10.4274/tjh.galenos.2019.2019.0103]
118 **Lee JY**, Lim SH, Lee MY, Kim H, Sinn DH, Gwak GY, Choi MS, Lee JH, Jung CW, Jang JH, Kim WS, Kim SJ, Kim K. Hepatitis B reactivation in multiple myeloma patients with resolved hepatitis B undergoing chemotherapy. *Liver Int* 2015; **35**: 2363-2369 [PMID: 25832927 DOI: 10.1111/liv.12838]
119 **Li J**, Huang B, Li Y, Zheng D, Zhou Z, Liu J. Hepatitis B virus reactivation in patients with multiple myeloma receiving bortezomib-containing regimens followed by autologous stem cell transplant. *Leuk Lymphoma* 2015; **56**: 1710-1717 [PMID: 25098429 DOI: 10.3109/10428194.2014.941833]
120 **Armengol M**, Santos JC, Fernández-Serrano M, Profitós-Pelejà N, Ribeiro ML, Roué G. Immune-Checkpoint Inhibitors in B-Cell Lymphoma. *Cancers (Basel)* 2021; **13** [PMID: 33430146 DOI: 10.3390/cancers13020214]
121 **Chan TSY**, Li J, Loong F, Khong PL, Tse E, Kwong YL. PD1 blockade with low-dose nivolumab in NK/T cell lymphoma failing L-asparaginase: efficacy and safety. *Ann Hematol* 2018; **97**: 193-196 [PMID: 28879531 DOI: 10.1007/s00277-017-3127-2]
122 **Kim SJ**, Lim JQ, Laurensia Y, Cho J, Yoon SE, Lee JY, Ryu KJ, Ko YH, Koh Y, Cho D, Lim ST, Enemark MB, D'Amore F, Bjerre M, Ong CK, Kim WS. Avelumab for the treatment of relapsed or refractory extranodal NK/T-cell lymphoma: an open-label phase 2 study. *Blood* 2020; **136**: 2754-2763 [PMID: 32766875 DOI: 10.1182/blood.2020007247]
123 **Meti N**, Esfahani K, Johnson NA. The Role of Immune Checkpoint Inhibitors in Classical Hodgkin Lymphoma. *Cancers (Basel)* 2018; **10** [PMID: 29914088 DOI: 10.3390/cancers10060204]
124 **Tao R**, Fan L, Song Y, Hu Y, Zhang W, Wang Y, Xu W, Li J. Sintilimab for relapsed/refractory extranodal NK/T cell lymphoma: a multicenter, single-arm, phase 2 trial (ORIENT-4). *Signal Transduct Target Ther* 2021; **6**: 365 [PMID: 34702811 DOI: 10.1038/s41392-021-00768-0]
125 **Abram CL**, Lowell CA. The ins and outs of leukocyte integrin signaling. *Annu Rev Immunol* 2009; **27**: 339-362 [PMID: 19302044 DOI: 10.1146/annurev.immunol.021908.132554]
126 **Lasagna A**, Albi G, Maserati R, Zuccarini A, Quaccini M, Baldanti F, Sacchi P, Bruno R, Pedrazzoli P. Occult hepatitis B in patients with cancer during immunotherapy with or without chemotherapy: A real-life retrospective single-center cohort study. *Front Oncol* 2023; **13**: 1044098 [PMID: 36761977 DOI: 10.3389/fonc.2023.1044098]
127 **Wong GL**, Wong VW, Hui VW, Yip TC, Tse YK, Liang LY, Lui RN, Mok TS, Chan HL, Chan SL. Hepatitis Flare During Immunotherapy in Patients With Current or Past Hepatitis B Virus Infection. *Am J Gastroenterol* 2021; **116**: 1274-1283 [PMID: 33560651 DOI: 10.14309/ajg.0000000000001142]
128 **Yoo S**, Lee D, Shim JH, Kim KM, Lim YS, Lee HC, Yoo C, Ryoo BY, Choi J. Risk of Hepatitis B Virus Reactivation in Patients Treated With Immunotherapy for Anti-cancer Treatment. *Clin Gastroenterol Hepatol* 2022; **20**: 898-907 [PMID: 34182151 DOI: 10.1016/j.cgh.2021.06.019]
129 **Zhang X**, Zhou Y, Chen C, Fang W, Cai X, Zhang X, Zhao M, Zhang B, Jiang W, Lin Z, Ma Y, Yang Y, Huang Y, Zhao H, Xu R, Hong S, Zhang L. Hepatitis B virus reactivation in cancer patients with positive Hepatitis B surface antigen undergoing PD-1 inhibition. *J Immunother Cancer* 2019; **7**: 322 [PMID: 31753012 DOI: 10.1186/s40425-019-0808-5]
130 **Navvabi N**, Khadem Ansari MH, Navvabi A, Chalipa HR, Zitricky F. Comparative assessment of immunochromatography and ELISA diagnostic tests for HBsAg detection in PCR-confirmed HBV infection. *Rev Gastroenterol Mex (Engl Ed)* 2022; **87**: 176-180 [PMID: 34776394 DOI: 10.1016/j.rgmxen.2021.11.007]
131 **Gärtner BC**, Jung W, Welsch C, Fischinger J, Schubert J, Zeuzem S, Mueller-Lantzsch N, Wend UC, Gerlich WH. Permanent loss of anti-HBc after reactivation of hepatitis B virus infection in an anti-HBs and anti-HBc-positive patient after allogeneic stem cell transplantation. *J Clin Virol* 2007; **38**: 146-148 [PMID: 17182277 DOI: 10.1016/j.jcv.2006.03.014]
132 **Osiowy C**. Detection of HBsAg mutants. *J Med Virol* 2006; **78** Suppl 1: S48-S51 [PMID: 16622877 DOI: 10.1002/jmv.20607]
133 **Awerkiew S**, Däumer M, Reiser M, Wend UC, Pfister H, Kaiser R, Willems WR, Gerlich WH. Reactivation of an occult hepatitis B virus escape mutant in an anti-HBs positive, anti-HBc negative lymphoma patient. *J Clin Virol* 2007; **38**: 83-86 [PMID: 17134939 DOI: 10.1016/j.jcv.2006.10.006]
134 **Ferreira R**, Carvalheiro J, Torres J, Fernandes A, Giestas S, Mendes S, Agostinho C, Campos MJ. Fatal hepatitis B reactivation treated with entecavir in an isolated anti-HBs positive lymphoma patient: a case report and literature review. *Saudi J Gastroenterol* 2012; **18**: 277-281 [PMID: 22824772 DOI: 10.4103/1319-3767.98436]
135 **Hsu C**, Hsiung CA, Su IJ, Hwang WS, Wang MC, Lin SF, Lin TH, Hsiao HH, Young JH, Chang MC, Liao YM, Li CC, Wu HB, Tien HF, Chao TY, Liu TW, Cheng AL, Chen PJ. A revisit of prophylactic lamivudine for chemotherapy-associated hepatitis B reactivation in non-Hodgkin's lymphoma: a randomized trial. *Hepatology* 2008; **47**: 844-853 [PMID: 18302293 DOI: 10.1002/hep.22106]
136 **Lau GK**, Yiu HH, Fong DY, Cheng HC, Au WY, Lai LS, Cheung M, Zhang HY, Lie A, Ngan R, Liang R. Early is superior to deferred preemptive lamivudine therapy for hepatitis B patients undergoing chemotherapy. *Gastroenterology* 2003; **125**: 1742-1749 [PMID: 14724827 DOI: 10.1053/j.gastro.2003.09.026]
137 **Di Bisceglie AM**, Lok AS, Martin P, Terrault N, Perrillo RP, Hoofnagle JH. Recent US Food and Drug Administration warnings on hepatitis B reactivation with immune-suppressing and anticancer drugs: just the tip of the iceberg? *Hepatology* 2015; **61**: 703-711 [PMID: 25412906 DOI: 10.1002/hep.27609]
138 **Cho Y**, Yu SJ, Cho EJ, Lee JH, Kim TM, Heo DS, Kim YJ, Yoon JH. High titers of anti-HBs prevent rituximab-related viral reactivation in resolved hepatitis B patient with non-Hodgkin's lymphoma. *J Med Virol* 2016; **88**: 1010-1017 [PMID: 26531242 DOI: 10.1002/jmv.24423]
139 **Koo YX**, Tay M, Teh YE, Teng D, Tan DS, Tan IB, Tai DW, Quek R, Tao M, Lim ST. Risk of hepatitis B virus (HBV) reactivation in hepatitis B surface antigen negative/hepatitis B core antibody positive patients receiving rituximab-containing combination chemotherapy without routine antiviral prophylaxis. *Ann Hematol* 2011; **90**: 1219-1223 [PMID: 21520001 DOI: 10.1007/s00277-011-1241-0]
140 **Matsubara T**, Nishida T, Shimoda A, Shimakoshi H, Amano T, Sugimoto A, Takahashi K, Mukai K, Yamamoto M, Hayashi S, Nakajima S, Fukui K, Inada M. The combination of anti-HBc and anti-HBs levels is a useful predictor of the development of chemotherapy-induced reactivation in lymphoma patients with resolved HBV infection. *Oncol Lett* 2017; **14**: 6543-6552 [PMID: 29151907 DOI: 10.3892/ol.2017.7012]
141 **Paul S**, Dickstein A, Saxena A, Terrin N, Viveiros K, Balk EM, Wong JB. Role of surface antibody in hepatitis B reactivation in patients with resolved infection and hematologic malignancy: A meta-analysis. *Hepatology* 2017; **66**: 379-388 [PMID: 28128861 DOI: 10.1002/hep.29082]
142 **Huang H**, Li X, Zhu J, Ye S, Zhang H, Wang W, Wu X, Peng J, Xu B, Lin Y, Cao Y, Li H, Lin S, Liu Q, Lin T. Entecavir vs lamivudine for

prevention of hepatitis B virus reactivation among patients with untreated diffuse large B-cell lymphoma receiving R-CHOP chemotherapy: a randomized clinical trial. *JAMA* 2014; **312**: 2521-2530 [PMID: 25514302 DOI: 10.1001/jama.2014.15704]

143 **Yu S**, Luo H, Pan M, Luis AP, Xiong Z, Shuai P, Zhang Z. Comparison of entecavir and lamivudine in preventing HBV reactivation in lymphoma patients undergoing chemotherapy: a meta-analysis. *Int J Clin Pharm* 2016; **38**: 1035-1043 [PMID: 27450506 DOI: 10.1007/s11096-016-0358-6]

144 **Shang J**, Wang H, Sun J, Fan Z, Huang F, Zhang Y, Jiang Q, Dai M, Xu N, Lin R, Liu Q. A comparison of lamivudine vs entecavir for prophylaxis of hepatitis B virus reactivation in allogeneic hematopoietic stem cell transplantation recipients: a single-institutional experience. *Bone Marrow Transplant* 2016; **51**: 581-586 [PMID: 26752138 DOI: 10.1038/bmt.2015.328]

145 **Zhang MY**, Zhu GQ, Shi KQ, Zheng JN, Cheng Z, Zou ZL, Huang HH, Chen FY, Zheng MH. Systematic review with network meta-analysis: Comparative efficacy of oral nucleos(t)ide analogues for the prevention of chemotherapy-induced hepatitis B virus reactivation. *Oncotarget* 2016; **7**: 30642-30658 [PMID: 27121321 DOI: 10.18632/oncotarget.8907]

146 **Zhang MY**, Zhu GQ, Zheng JN, Cheng Z, Van Poucke S, Shi KQ, Huang HH, Chen FY, Zheng MH. Nucleos(t)ide analogues for preventing HBV reactivation in immunosuppressed patients with hematological malignancies: a network meta-analysis. *Expert Rev Anti Infect Ther* 2017; **15**: 503-513 [PMID: 28317397 DOI: 10.1080/14787210.2017.1309291]

147 **Geipel A**, Seiz PL, Niekamp H, Neumann-Fraune M, Zhang K, Kaiser R, Protzer U, Gerlich WH, Glebe D; HOPE Consortium. Entecavir allows an unexpectedly high residual replication of HBV mutants resistant to lamivudine. *Antivir Ther* 2015; **20**: 779-787 [PMID: 25560463 DOI: 10.3851/IMP2928]

148 **Arora A**, Anand AC, Kumar A, Singh SP, Aggarwal R, Dhiman RK, Aggarwal S, Alam S, Bhaumik P, Dixit VK, Goel A, Goswami B, Kumar M, Madan K, Murugan N, Nagral A, Puri AS, Rao PN, Saraf N, Saraswat VA, Sehgal S, Sharma P, Shenoy KT, Wadhawan M; Members of the INASL taskforce on Hepatitis B. INASL Guidelines on Management of Hepatitis B Virus Infection in Patients receiving Chemotherapy, Biologicals, Immunosupressants, or Corticosteroids. *J Clin Exp Hepatol* 2018; **8**: 403-431 [PMID: 30568345 DOI: 10.1016/j.jceh.2018.06.010]

149 **Ceccarelli L**, Salpini R, Sarmati L, Svicher V, Bertoli A, Sordillo P, Ricciardi A, Perno CF, Andreoni M, Sarrecchia C. Late hepatitis B virus reactivation after lamivudine prophylaxis interruption in an anti-HBs-positive and anti-HBc-negative patient treated with rituximab-containing therapy. *J Infect* 2012; **65**: 180-183 [PMID: 22138369 DOI: 10.1016/j.jinf.2011.11.021]

150 **Lee IC**, Huang YH, Chu CJ, Lee PC, Lin HC, Lee SD. Hepatitis B virus reactivation after 23 months of rituximab-based chemotherapy in an HBsAg-negative, anti-HBs-positive patient with follicular lymphoma. *J Chin Med Assoc* 2010; **73**: 156-160 [PMID: 20231001 DOI: 10.1016/S1726-4901(10)70031-9]

151 **Hara T**, Oka K, Iwai N, Inada Y, Tsuji T, Okuda T, Nagata A, Komaki T, Kagawa K. Hepatitis B Virus Reactivation 55 Months Following Chemotherapy Including Rituximab and Autologous Peripheral Blood Stem Cell Transplantation for Malignant Lymphoma. *Intern Med* 2021; **60**: 417-421 [PMID: 32963163 DOI: 10.2169/internalmedicine.5678-20]

152 **Law MF**, Lai HK, Chan HN, Ha CY, Ng C, Yeung YM, Yip SF. The impact of hepatitis B virus (HBV) infection on clinical outcomes of patients with diffuse large B-cell lymphoma. *Eur J Cancer Care (Engl)* 2015; **24**: 117-124 [PMID: 25848698 DOI: 10.1111/ecc.12166]

153 **Ifuku H**, Kusumoto S, Tanaka Y, Totani H, Ishida T, Okada M, Murakami S, Mizokami M, Ueda R, Iida S. Fatal reactivation of hepatitis B virus infection in a patient with adult T-cell leukemia-lymphoma receiving the anti-CC chemokine receptor 4 antibody mogamulizumab. *Hepatol Res* 2015; **45**: 1363-1367 [PMID: 25753008 DOI: 10.1111/hepr.12513]

154 **Foont JA**, Schiff ER. Avoid the tragedy of hepatitis B reactivation in immunosuppressed patients. *Nat Clin Pract Gastroenterol Hepatol* 2007; **4**: 128-129 [PMID: 17262070 DOI: 10.1038/ncpgasthep0740]

155 **An J**, Shim JH, Kim SO, Choi J, Kim SW, Lee D, Kim KM, Lim YS, Lee HC, Chung YH, Lee YS, Suh DJ. Comprehensive outcomes of on- and off-antiviral prophylaxis in hepatitis B patients undergoing cancer chemotherapy: A competing risks analysis. *J Med Virol* 2016; **88**: 1576-1586 [PMID: 26945543 DOI: 10.1002/jmv.24512]

156 **Hung CM**, Jeng LB, Lee WC, Yu MC, Kuo LM, Chen MF. Fulminant hepatic failure caused by hepatitis B virus activation after chemotherapy for breast cancer treated with liver transplantation: a case report. *Transplant Proc* 2003; **35**: 387-388 [PMID: 12591453 DOI: 10.1016/s0041-1345(02)03780-6]

157 **Kim SG**, Chun JM, Jin R, Kim JY, Won DI, Hwang YJ. Living donor liver transplantation for acute hepatic failure caused by reactivation of hepatitis B virus infection after chemotherapy for hematologic malignancy: case reports. *Transplant Proc* 2010; **42**: 843-845 [PMID: 20430187 DOI: 10.1016/j.transproceed.2010.02.038]

158 **Noterdaeme T**, Longrée L, Bataille C, Deroover A, Lamproye A, Delwaide J, Beguin Y, Honoré P, Detry O. Liver transplantation for acute hepatic failure due to chemotherapy-induced HBV reactivation in lymphoma patients. *World J Gastroenterol* 2011; **17**: 3069-3072 [PMID: 21799656 DOI: 10.3748/wjg.v17.i25.3069]

159 **Sperl J**, Frankova S, Kieslichova E, Oliverius M, Janousek L, Honsova E, Trunecka P, Spicak J. Urgent liver transplantation for chemotherapy-induced HBV reactivation: a suitable option in patients recently treated for malignant lymphoma. *Transplant Proc* 2013; **45**: 2834-2837 [PMID: 24034061 DOI: 10.1016/j.transproceed.2013.03.047]

160 **Stange MA**, Tutarel O, Pischke S, Schneider A, Strassburg CP, Becker T, Barg-Hock H, Bastürk M, Wursthorn K, Cornberg M, Ott M, Greten TF, Manns MP, Wedemeyer H. Fulminant hepatic failure due to chemotherapy-induced hepatitis B reactivation: role of rituximab. *Z Gastroenterol* 2010; **48**: 258-263 [PMID: 20127601 DOI: 10.1055/s-0028-1109782]

161 **Benten D**, Sterneck M, Panse J, Rogiers X, Lohse AW. Low recurrence of preexisting extrahepatic malignancies after liver transplantation. *Liver Transpl* 2008; **14**: 789-798 [PMID: 18412260 DOI: 10.1002/lt.21434]

World Journal of Gastroenterology

Submit a Manuscript: https://www.f6publishing.com

World J Gastroenterol 2023 September 7; 29(33): 4962-4974

DOI: 10.3748/wjg.v29.i33.4962

ISSN 1007-9327 (print) ISSN 2219-2840 (online)

REVIEW

Direct oral anticoagulants for the treatment of splanchnic vein thrombosis: A state of art

Giovanni Monaco, Luca Bucherini, Bernardo Stefanini, Fabio Piscaglia, Francesco Giuseppe Foschi, Luca Ielasi

Specialty type: Gastroenterology and hepatology

Provenance and peer review: Invited article; Externally peer reviewed.

Peer-review model: Single blind

Peer-review report's scientific quality classification
Grade A (Excellent): A
Grade B (Very good): B, B
Grade C (Good): 0
Grade D (Fair): 0
Grade E (Poor): 0

P-Reviewer: Harmanci O, Turkey; Pintar T, Slovenia; Qi XS, China

Received: June 27, 2023
Peer-review started: June 27, 2023
First decision: July 25, 2023
Revised: August 7, 2023
Accepted: August 17, 2023
Article in press: August 17, 2023
Published online: September 7, 2023

Giovanni Monaco, Bernardo Stefanini, Fabio Piscaglia, Department of Medical and Surgical Sciences, University of Bologna, Bologna 40138, Italy

Giovanni Monaco, Bernardo Stefanini, Fabio Piscaglia, Division of Internal Medicine, Hepatobiliary and Immunoallergic Diseases, IRCCS Azienda Ospedaliero-Universitaria di Bologna, Bologna 40138, Italy

Luca Bucherini, Francesco Giuseppe Foschi, Luca Ielasi, Department of Internal Medicine, Ospedale degli Infermi di Faenza, Faenza 48018, Italy

Corresponding author: Luca Ielasi, MD, Doctor, Department of Internal Medicine, Ospedale degli Infermi di Faenza, Viale Stradone, 9, Faenza 48018, Italy. luca.ielasi.kr@gmail.com

Abstract

Splanchnic vein thrombosis (SVT) is a manifestation of venous thromboembolism in an unusual site. Portal, mesenteric, and splenic veins are the most common vessels involved in SVT which occurs mainly in patients with liver cirrhosis, although non-cirrhotic patients could be affected as well. Thrombosis of hepatic veins, also known as Budd-Chiari syndrome, is another manifestation of SVT. Prompt diagnosis and intervention are mandatory in order to increase the recalization rate and reduce the risk of thrombus progression and hypertensive complications. Traditional anticoagulation with heparin and vitamin-K antagonists is the treatment of choice in these cases. However, recent studies have shown promising results on the efficacy and safety of direct oral anticoagulants (DOACs) in this setting. Available results are mainly based on retrospective studies with small sample size, but first clinical trials have been published in the last years. This manuscript aims to provide an updated overview of the current evidence regarding the role of DOACs for SVT in both cirrhotic and non-cirrhotic patients.

Key Words: Splanchnic vein thrombosis; Portal vein thrombosis; Budd-Chiari syndrome; Direct oral anticoagulants

©The Author(s) 2023. Published by Baishideng Publishing Group Inc. All rights reserved.

Core Tip: The term splanchnic vein thrombosis (SVT) includes portal vein thrombosis and Budd-Chiari syndrome. Both conditions could occur in patients with and without an underlying liver disease. The cornerstone of treatment is anticoagulation. Direct oral anticoagulants (DOACs) are a novel class of drugs that have strongly affirmed their role in the management of patients with atrial fibrillation and venous thromboembolism. In the last few years, several studies have been published showing promising results in efficacy and safety of DOACs in patients with SVT.

Citation: Monaco G, Bucherini L, Stefanini B, Piscaglia F, Foschi FG, Ielasi L. Direct oral anticoagulants for the treatment of splanchnic vein thrombosis: A state of art. *World J Gastroenterol* 2023; 29(33): 4962-4974
URL: https://www.wjgnet.com/1007-9327/full/v29/i33/4962.htm
DOI: https://dx.doi.org/10.3748/wjg.v29.i33.4962

INTRODUCTION

Splanchnic vein thrombosis (SVT) is a rare but potentially life-threatening condition that occurs when blood clots form in the veins that drain the digestive system from the lower esophagus to the upper two-thirds of the rectum. Among different SVT, we can distinguish two main conditions: Budd-Chiari syndrome (BCS) and portal vein thrombosis (PVT).

BCS is caused by the thrombotic obstruction of hepatic venous outflow, localized anywhere from the hepatic veins to the entry of the inferior vena cava into the right atrium. BCS could also be caused by extra-vascular compression (secondary BCS), but this non-thrombotic form of the disease will not be discussed further.

There is no standardized definition of PVT. Generally, it refers to the thrombosis of the main portal trunk or its lobar branches with or without extension to the splenic or mesenteric veins.

SVT can develop both in patients with and without underlying liver disease[1].

In the first case, SVT represents a rare condition with a prevalence of less than 0.2% in the general population and it is commonly associated with strong risk factors for thrombosis[2].

In the second case, liver cirrhosis represents the mainstay of the pathogenesis of SVT and the co-presence of thrombophilic risk factors is uncommon. Cirrhotic patients generally present a PVT with an incidence that ranges from 11% to 24% at 5 years; prevalence increases according to liver disease severity (10% in compensated cirrhosis, 17% in decompensated cirrhosis, and 26% in liver transplant candidates)[3-5].

In patients with SVT, the development of portal hypertension is common; the increase of portal venous pressure could be caused by either pre-hepatic (in PVT) or post-hepatic (in BCS) venous flow obstruction.

As a thrombotic condition, anticoagulation is generally required for these patients as first line treatment. Over the last few years, interventional endovascular approaches (*e.g.* transjugular intrahepatic portosystemic shunt placement, angioplasty, suction thrombectomy, catheter-directed thrombolysis) have shown interesting results mainly in the management of acute symptomatic PVT with an inadequate response to medical treatment[6-8]. They could be used in isolation or in conjunction with systemic anticoagulation. Description of these procedures and their indications go beyond the aim of this paper, so it will not be discussed further.

Traditional anticoagulants commonly used for SVT are heparins and vitamin-K antagonists (VKA).

Low-molecular-weight heparin (LMWH) is generally preferred to unfractionated heparin (UFH) due to its lower incidence of heparin-induced thrombocytopenia, unless there are contraindications to LMWH such as severe renal failure. LMWH also has the advantage that it has a short half-life and no need of monitoring, but daily subcutaneous administration may reduce patients' compliance.

VKA are usually used for long-term anticoagulation. They have the advantage of oral administration and reversibility with vitamin K supplementation, but they require international normalized ratio (INR) monitoring and a personalized dose schedule.

Beside traditional anticoagulants, in recent years direct oral anticoagulants (DOACs) have become the first choice of treatment in several conditions, such as stroke prophylaxis in atrial fibrillation[9] and treatment of deep vein thrombosis and pulmonary embolism[10].

DOACs have the advantage of oral administration, fixed dosing schedule, predictable anticoagulant effect, and they do not require frequent monitoring.

DOACs exert their activity by directly inhibiting factor X-activated (such as rivaroxaban, apixaban and edoxaban) or factor II-activated (such as dabigatran). Their metabolism is generally both renal and hepatic, with different percentage among single drugs. Rivaroxaban, apixaban and edoxaban are metabolized by cytochromes without forming active metabolites; dabigatran is a prodrug not metabolized by cytochromes and it is the DOAC with the higher amount of renal excretion (approximatively 80%)[11].

Despite the aforementioned considerations, at present the use of DOACs for SVT remains poorly investigated. If chosen as anticoagulation therapy, they have to be prescribed off-label as they are currently not licensed for this indication in many countries.

Nevertheless, on the thrust of the advantages demonstrated in other conditions, interest on the use of DOACs in this setting is recently emerging, and data obtained by several recent reports are encouraging[12,13].

In this review, we analyzed all the studies available in the literature concerning patients with cirrhotic and non-cirrhotic PVT and BCS treated with DOACs; case reports were systematically excluded.

NON-CIRRHOTIC PVT

Causes of SVT in patients without underlying liver disease could be classified as systemic acquired risk factors for thrombosis, inherited thrombophilia and local factors. More than one risk factor is found in 10%-23% of patients[14,15].

Systemic acquired thrombophilic factors represent the cause of up to 50% of SVT[16]. The main related conditions are myeloproliferative neoplasms (mostly those related to JAK2-V617F mutation)[17,18], hormonal factors (oral contraceptive or pregnancy)[19,20], antiphospholipid antibody syndrome[21], and other systemic inflammations/infections (*e.g.* connective tissue disease, sarcoidosis, cytomegalovirus infection[22], severe acute respiratory syndrome coronavirus 2 infection[23,24], sepsis).

Inherited thrombophilic disorders could be detected in about 20% of cases[16]. The most common clotting factor alteration is factor V Leiden mutation (8% of cases), followed by G20210A prothrombin mutation and antithrombin deficiency (5% of cases each); protein S and protein C deficiency are less frequent (less than 2% and 1%, respectively)[25-27].

Local factors are involved in about 20% of cases[16]. These are represented mainly by abdominal surgery and infectious or inflammatory diseases involving abdominal organs, such as pancreatitis[28], diverticulitis, inflammatory bowel disease, abdominal vasculitis and abdominal cancers[17].

Notably, in 15%-40% of cases of SVT without cirrhosis no causative factors are identified. The treatment of the underlying disease is crucial in the management of patients, so an accurate work-up should be performed at SVT diagnosis[16].

Although not all guidelines agree on this definition, it is widely accepted that PVT can be divided in acute or chronic, based on the onset of the disease within 6 mo or beyond, respectively. The latter also includes the transformation in portal cavernoma, that is the replacement of the native portal vein with multiple tortuous collateral venous vessels that develop in response to chronic venous outflow obstruction.

In case of acute non-cirrhotic PVT, the main goal is to achieve portal recanalization and to prevent extension of the clot and sequelae such as intestinal infarction and the development of portal hypertension. Spontaneous resolution of acute PVT is rare, and early anticoagulation treatment is associated with higher rates of recanalization[29]. Therefore, full dose anticoagulation treatment should be started at diagnosis[15,29-33]. Moreover, a study showed that the risk of developing recurrent thrombotic events among subjects with non-abdominal thromboembolism and non-cirrhotic PVT is comparable [34].

Treatment should be continued for at least 3-6 mo for all patients. Similar to guideline recommendations for deep vein thrombosis occurring in typical sites, indefinite anticoagulation is recommended in all cases of persistent identified risk factors, such as acquired or congenital thrombophilia, but should also be considered in case the evidence of a persistent underlying prothrombotic factor is lacking[30,35].

As mentioned above, PVT may evolve into portal cavernoma if left untreated. In the presence of chronic PVT or portal cavernoma, even though the benefit of anticoagulation is less clear, it is recommended to treat patients as in the case of acute PVT[36-38]. However, since bleeding is the most common complication of chronic PVT[39], in patients with high risk esophageal varices anticoagulation treatment should be postponed until an adequate prophylaxis for portal hypertensive bleeding has been initiated[35].

Regarding the choice of anticoagulants, initial treatment with LMWH and subsequent switch to VKA is supported by extensive evidence and still represents the established therapy for most patients. The treatment is administered with the same therapeutic regimens and dose adjustments as for typical site venous thromboembolism.

Several studies have been recently published regarding the use of DOACs in this setting showing their efficacy and safety; at present, no randomized controlled trial has been published yet (Table 1).

Janczak *et al*[40] were the first to investigate the use of DOACs for thrombosis in atypical sites. They conducted a prospective study enrolling patients that were treated with anticoagulants for thromboembolism occurring both in typical and atypical sites. Considering the subgroup with PVT, 16 patients were treated with DOACs (rivaroxaban and apixaban), and 13 patients were treated with LMWH. The results did not reveal any statistically significant difference between DOACs and LMWH both in terms of efficacy and safety[40].

Scheiner *et al*[41] performed a retrospective study with 51 cirrhotic patients with concomitant non-malignant PVT. No anticoagulation therapy was started in 39 patients, whereas 12 patients received warfarin. Additionally, they also enrolled 10 patients treated with DOACs after traditional anticoagulation. In particular, 4 patients received edoxaban 30 or 60 mg once daily (OD), 3 apixaban 5 mg twice daily (BID), 2 rivaroxaban 10 mg OD, 1 dabigatran 100 mg BID. The mean follow-up time was 9.2 mo. In the DOAC group 70% of patients were non-cirrhotic. Regression of thrombus was observed in 20% of patients, and stability in 80%; no thrombus progression has been reported. Since cavernous transformation of the chronic PVT was already present in all patients treated with DOACs (therefore achieving recanalization could be difficult), the authors could not extrapolate data to compare the success rates of conservative or traditional therapy to DOACs. Only one bleeding episode was described in a patient in therapy with DOAC, so authors concluded that there was no statistically significant difference in bleeding events between DOAC and VKA groups[41].

Naymagon *et al*[42] published several retrospective studies comparing traditional anticoagulants *vs* DOACs for treatment of SVT in non-cirrhotic patients. In a study that compared VKA/LMWH and DOACs for non-cirrhotic PVT, recanalization rates (defined as complete radiological resolution) were higher in DOAC group compared to VKA, but similar to the group treated with enoxaparin. Nevertheless, a lower rate of bleeding was observed in patients treated with DOACs[42].

Another retrospective study from the same authors evaluated a cohort of 58 patients with inflammatory bowel disease associated-PVT who were treated either with DOACs or traditional anticoagulants. Complete radiological response rate in the DOAC group was two-fold higher than in the warfarin group; moreover, the DOAC group needed a shorter course

Table 1 Characteristics of studies on non-cirrhotic patients with portal vein thrombosis treated with direct oral anticoagulants

Study	Population	Outcomes	Adverse events	Ref.
Prospective	Non-cirrhotic, atypical sites (including PVT); Riva and Api for PVT (n = 16) *vs* enoxa for PVT (n = 13)	Riva and Apixaban are effective and safe in patients with venous thrombosis of atypical locations	No major difference in bleeding rate	Janczak *et al* [40], 2018
Retrospective	Non-malignant PVT, both cirrhotic and non-cirrhotic; Edo (n = 4), Api (n = 3), Riva (n = 2), Dabi (n = 1) *vs* traditional AC (n = 12), no AC (n = 39)	Favourable outcomes with DOACs with regression/resolution of thrombus in 20% of patients and stability or nonprogression in 80%	One bleeding episode in DOACs	Scheiner *et al* [41], 2018
Retrospective	Non-cirrhotic PVT; Riva (n = 65), Api (n = 20), Dabi (n = 8) *vs* Warf (n = 108), Enoxa (n = 70), Fondap (n = 2)	Resolution rate: Dabi (75%), Api (65%), Riva (65%), Enoxa (57%), Warf (31%); Recanalization rates are higher in DOACs compared to Warf but similar to Enoxa	Less major bleeding incidence in DOACs	Naymagon *et al*[42], 2020
Retrospective	IBD-associated PVT; DOACs (n = 23) *vs* Warf (n = 22), Enoxa (n = 13)	Resolution rate: DOACs (96%), Warf (55%); DOACs group needed a shorter course of anticoagulation (median 3.9 *vs* 8.5)	N/A	Naymagon *et al*[43] 2021
Retrospective	Intraabdominal surgery < 3 mo prior to PVT diagnosis; DOACs (n = 35) *vs* Warf (n = 31), Enoxa (n = 29), no AC (n = 12)	Complete resolution rate: DOACs (77%), Enoxa (69%), Warf (45%), no AC (17%)	N/A	Naymagon *et al*[44], 2021
Retrospective	PVT with/without cirrhosis; DOACs (n = 13; 8 non-cirrhotic) *vs* Warf (n = 20; 15 non cirrotic)	Treatment failure: DOACs (n = 0); Warf (n = 4)	Major bleedings: DOACs: n=0; VKA: n=1	Ilcewicz *et al* [45], 2021
Prospective	SVT without cirrhosis; Riva 15 BID for 3 wk + Riva 20 mg OD for 3 mo (n = 100)	Recanalization > 80% at 3 mo (47% complete)	2 major bleeding; 2 SVT recurrence	Ageno *et al* [46], 2022

AC: Anticoagulation; Api: Apixaban; BID: Twice daily; Dabi: Dabigatran; DOACs: Direct oral anticoagulants; Edo: Edoxaban; Enoxa: Enoxaparin; Fondap: Fondaparinux; IBD: Inflammatory bowel disease; OD: Once daily; PVT: Portal vein thrombosis; Riva: Rivaroxaban; SVT: Splanchnic vein thrombosis; VKA: Vitamin K antagonists; Warf: Warfarin.

of anticoagulation to achieve recanalization[43].

Similar results in terms of vein recanalization have been shown in patients who developed PVT within three months after abdominal surgery. The first group was treated with DOACs, the second with conventional anticoagulants or no anticoagulation. Recanalization rate was higher with DOAC than with VKA (77% *vs* 45%), but similar to LMWH. Of note, in the group receiving no anticoagulation treatment, only 17% of patients recanalized spontaneously[44].

Ilcewicz *et al*[45] analyzed retrospectively a cohort of 33 patients with PVT, including 10 patients with cirrhosis. Patients were treated with either warfarin or DOACs; 4 treatment failure and one major bleeding were recorded in the warfarin group but none was recorded in the DOAC group[45].

Recently, Ageno *et al*[46] conducted the first interventional study evaluating the safety and efficacy of DOACs in non-cirrhotic PVT. The study was a single-arm prospective multicentric study enrolling patients presenting with a first episode of non-cirrhotic, symptomatic, objectively diagnosed SVT who were treated with rivaroxaban 15 mg BID for 3 wk followed by 3 mo of rivaroxaban 20 mg OD. Major bleeding was the primary endpoint of the study; secondary endpoints included death, recurrent SVT, and complete vein recanalization within 3 mo. During the 6-months follow-up period, non-life-threatening major bleeding events occurred in 2 patients; recurrence of thrombosis was observed in 2 patients, and 1 death unrelated to thrombosis was recorded. The recanalization at 3 mo was achieved in more than 80% of patients, with a complete recanalization rate of 47%[46].

From what has emerged from the aforementioned studies, the use of DOACs in non-cirrhotic PVT seems to be promising; results suggest that DOACs are superior to traditional anticoagulants in terms of recanalization rate[42-44,46] although they have a similar safety profile to VKA[40].

However, it is important to emphasize that these results are affected by several limitations: Firstly, at present no randomized controlled trial has been published; secondly, the results are based on small patients cohorts, the therapeutic regimens of DOACs vary widely between studies and the duration of follow-up was also extremely heterogeneous.

CIRRHOTIC PVT

Liver cirrhosis is an irreversible end-stage liver disease characterized by the progressive deposition of fibrotic tissue and a diffuse conversion of the normal liver architecture into structurally abnormal nodules, eventually leading to impaired liver function.

The increased liver stiffness causes a reduced portal blood flow and an increase of portal pressure, (*i.e.*, portal hypertension); the blood stasis together with the pro-thrombotic status typical of cirrhotic patients lead to a higher cumulative risk of splanchnic thrombosis, mainly PVT[47,48].

A recent meta-analysis on cirrhotic PVT not treated with anticoagulation showed an improvement in 30% of cases and a progression of thrombus in approximately 25% of cases[49].

According to the Baveno VII consensus, anticoagulation is recommended in cirrhotic patients with recent (< 6 mo) and > 50% occlusive thrombosis of the main portal vein trunk, in those with symptomatic PVT or in potential candidates for liver transplantation. In the last group of patients, the aim of anticoagulation is the prevention of recurrence of thrombosis or the progression of thrombus in order to with the aim facilitate the portal anastomosis during the surgical procedure.

Anticoagulation should also be considered in patients with < 50% occlusive thrombosis of the main portal vein trunk with progression during follow-up or with extension to the superior mesenteric vein.

Once anticoagulation is started, it should be maintained until portal vein recanalization and for a minimum of 6 mo; longer anticoagulation therapy should always be considered in patients awaiting liver transplantation, even after complete portal vein recanalization[35].

Early initiation of anticoagulation seems to be related to a higher recanalization rate[50,51].

Different classifications, indications and duration of treatment, and anticoagulation of choice according to the main clinical practice guidelines[30,35,38,52] are resumed in Table 2; a deep analysis of the differences among guidelines is not the aim of this paper, so it will not be discussed further.

The assessment of the bleeding risk in cirrhotic patients is mandatory but it is always challenging. Profound alteration in coagulation pathways, related to a reduced synthesis of prothrombotic and antithrombotic clotting factors, as well as thrombocytopenia, related to hypersplenism and decreased hepatic thrombopoietin synthesis, define a hemostatic imbalance and, consequently, the management of anticoagulation therapy in cirrhotic patient could be very difficult in clinical practice[53-55].

However, anticoagulation therapy in cirrhotic patients seems to be quite safe, as demonstrated in a meta-analysis of Loffredo *et al*[56] reporting no difference in major and minor bleeding rates between patients with or without anticoagulation therapy for PVT. Moreover, a recent competing-risk meta-analysis showed that anticoagulation in patients with cirrhosis and PVT reduces all-cause mortality independently of portal recanalization[57].

The presence of hepatocellular carcinoma does not contraindicate anticoagulation for non-malignant PVT; safety and efficacy of anticoagulation seem to be similar to patients without hepatocellular carcinoma[58,59].

The choice of the best anticoagulation is still debated, and guidelines do not give strong recommendations on this topic. LMWH is the best-known treatment option, largely used and with the most solid data in the literature; for these reasons consensus panels suggest at least to start anticoagulation with this drug class[35]. Fondaparinux may be another option, although there are no significant data in the literature, especially on safety[60,61]. VKA are potentially usable[62], but physicians have to be aware that INR accuracy for treatment monitoring is significantly lower in patients with liver dysfunction[63].

Over the last few years, the clinical experience in using DOACs in patients with liver cirrhosis has been growing[64].

Despite cirrhotic patients have been excluded from phase III trials of DOACs for atrial fibrillation[65-68] and venous thromboembolism[69-72], several studies on their use in this cohort of patients have been published, demonstrating DOACs safety in patients with compensated liver disease (Child-Pugh A)[73-77]. DOACs should be used with caution in Child-Pugh B patients[78,79] and they are contraindicated in Child-Pugh C patients[80,81].

Moreover, further pharmacokinetics considerations should be considered in DOACs prescription in patients with underlying liver disease, such as altered plasma protein binding, cytochrome P450-mediated metabolism and biliary excretion[53].

Another issue is the possible hepatotoxicity of DOACs. All four available DOACs can induce hepatotoxicity with an idiosyncratic mechanism; rivaroxaban seems to have a minimally higher risk of liver injury compared to other three molecules[82]. However, recent studies have definitively shown that liver injury is a very rare adverse event and, more importantly, this rate is significantly lower than with warfarin[83-85].

Recently, several studies have been published investigating the efficacy and safety of DOAC in patients with liver cirrhosis and PVT (Table 3); In 2019, Hanafy *et al*[86] published a randomized controlled trial on rivaroxaban 10 mg BID *vs* warfarin, but it has been recently retracted for methodological issues, therefore it will not be considered in our review.

First data were obtained by Hum *et al*[87] in a single-centre retrospective cohort study of cirrhotic patients treated with anticoagulants for any indications. In the small subgroup of patients with PVT (7 patients), 4 received DOACs (rivaroxaban or apixaban) and 3 received LMWH or VKA. Of particular note, the total number of bleeding events was similar in both groups even if results are given for the entire population of study[87].

As already mentioned above, Scheiner *et al*[41] investigated a cohort of both cirrhotic and non-cirrhotic patients presenting with non-neoplastic PVT. Out of the 10 patients receiving DOACs, only 30% presented concomitant liver disease[41]. For more details about this study, refer to the previous paragraph on non-cirrhotic PVT.

De Gottardi *et al*[88] retrospectively analyzed data from 17 European centers on cirrhotic and non-cirrhotic patients all treated with DOACs (either rivaroxaban, apixaban, or dabigatran at different doses) for any indication, mainly PVT. Patients were either initially prescribed with DOACs or switched to DOACs after traditional anticoagulants. The main reasons for switching were the development of recurrent thrombosis, clinically relevant side effects, and INR instability or unreliability for monitoring cirrhotic patients. Among the entire population of 94 patients, there were 22 and 38 patients with cirrhotic and non-cirrhotic PVT, respectively. The median follow-up time was 9.6 mo. In the group of non-cirrhotic patients, bleeding event rate was 15.5% *vs* 13.9% in the cirrhotic group, suggesting that the safety of DOACs is comparable between two groups. Despite the majority of the patients presented a PVT, the results presented by the authors are referred to the entire population and actual conclusions on PVT patients alone cannot be extrapolated.

Table 2 Comparison of main clinical practice guidelines for the management of portal vein thrombosis in non-cirrhotic patients

	EASL 2016[30]	AASLD 2020[38]	ACG 2020[52]	Baveno VII 2022[35]
Classification	Acute; Chronic	Recent: < 6 mo; Chronic: > 6 mo	Acute; Chronic	Recent: < 6 mo; Chronic: > 6 mo
Treatment	Acute: AC; Chronic: Not specified	Recent PVT: AC; Chronic complete PVT or cavernous transformation: No benefit from AC	Acute PVT: AC; Chronic: thrombophilia, progression of thrombus into mesenteric veins, current or previous evidence of bowel ischemia	Recent PVT: At diagnosis; Chronic PVT: After prophylaxis for portal hypertensive bleeding in high-risk varices
Choice of anticoagulation	LMWH, VKA	LMWH, VKA, DOACs	UFH, LMWH for initiation; LMWH or VKA for maintenance (DOACs absorption limited in the presence of intestinal oedema)	LMWH, VKA, DOACs
Duration of treatment	At least 6 mo in presence of transient risk factor; long term for persistent risk factor or in case of chronic PVT with history of intestinal ischemia or recurrent thrombosis	AC for 3 mo	At least 6 mo for acute without thrombophilia; long term with thrombophilia	Recent PVT: At least 6 mo; Chronic: Long term for patient with permanent prothrombotic state
Notes				EVL can be performed safely without withdrawing VKA

AASLD: American Association for the Study of Liver Diseases; AC: Anticoagulation; ACG: American College of Gastroenterology; DOACs: Direct oral anticoagulants; EASL: European Association for the Study of the Liver; EVL: Endoscopic variceal ligation; LMWH: Low molecular weight heparin; PVT: Portal vein thrombosis; UFH: Unfractioned heparin; VKA: Vitamin K antagonists.

Another study examining DOACs safety in cirrhosis, but this time in comparison with conventional anticoagulants, was conducted by Intagliata *et al*[89]. After collecting data from a research database, a cohort of 39 cirrhotic patients treated with anticoagulants for various indications was identified. Since no patients with decompensated liver disease (Child-Pugh C) were treated with DOACs, only patients with Child-Pugh A or B cirrhosis were included. In the group treated with DOACs (apixaban or rivaroxaban, either in therapeutic or prophylactic doses) 20 patients were included, and the most common indication for treatment was PVT (60%). In contrast, most patients treated with VKA or LMWH presented non-splanchnic venous thromboembolism (63%). No statistically significant difference in bleeding rates was observed between the two groups.

Also Davis *et al*[90] investigated the safety of cirrhotic patients treated with DOACs or VKA for any indication. Since only 3 patients received DOAC for PVT, this study was not included in our review.

Nagaoki *et al*[91] conducted a retrospective cohort study to evaluate the efficacy of edoxaban as maintenance therapy in 50 cirrhotic patients with PVT. Child–Pugh classification was grade A in 29 patients, B in 16, and C in 5. All patients were initially treated with danaparoid sodium for two weeks and then switched to either warfarin or edoxaban 60 or 30 mg OD, depending on renal function (creatinine clearance < 30 mL/min), body weight (< 60 kg) and concomitant treatment with a strong P-glycoprotein inhibitor. Among study population, 17 patients had concomitant hepatocellular carcinoma, but all were diagnosed with non-neoplastic PVT. All patients were screened with endoscopy before the initiation of anticoagulation. In case of high risk esophageal and/or gastric varices, endoscopic prophylactic treatment was systematically performed. Median time from PVT to treatment was similar between edoxaban and VKA group (4.2 *vs* 4.3 mo, respectively). Complete recanalization, assessed by computed tomography (CT) scan at 6 mo, was observed in 14 of 20 patients (70%) in the edoxaban group and in 6 of 30 patients (20%) in the warfarin group. However, given the potential risk of bleeding, a target INR of 1.5–2.0 was chosen for patients undergoing warfarin treatment. This underdosing in VKA therapy, may explain the low efficacy rate in this cohort. Additionally, safety was considered comparable between edoxaban and warfarin groups with 3 and 2 gastrointestinal bleedings, respectively[91].

In a prospective cohort study performed by Ai *et al*[92] 80 patients with cirrhosis and chronic PVT were examined. Patients with history of recent bleeding (< 3 mo), high risk esophageal varices, systemic malignancies, severe renal impairment (creatinine clearance < 30 mL/min), concomitant antiplatelet therapy and low platelet count (< 50 × 10^9/L) were excluded. Of the 40 patients treated with DOACs, 26 Child-Pugh A patients were treated with rivaroxaban 20 mg OD and 14 Child-Pugh grade B or C patients with dabigatran 150 mg BID. The other 40 patients received no anticoagulation. Recanalization rates and improvements in portal vein flow velocity were analyzed at 3 and 6 mo. The recanalization rate was higher in the DOAC group than in the control group, especially after 6 mo of treatment (12.8% at 3 mo *vs* 28.2% at 6 mo), whereas the bleeding rate was similar between the 2 groups. Of note, authors considered PVT as chronic if lasting more than one month, commensurate to definition of chronic deep vein thrombosis. Overall recanalization rates were low compared to previous studies; authors suggested that the delayed initiation of anticoagulation therapy might be associated with a worse outcome[92].

Finally, Lv *et al*[93] designed a prospective observational study investigating the role of both anticoagulation and transjugular intrahepatic porto-systemic shunt (TIPS) in 396 cirrhotic patients with non-malignant PVT either acute or chronic, confirmed with CT scan. Patients with intra or extrahepatic malignancy at baseline, presence of previous TIPS, isolated mesenteric or splenic vein thrombosis, and liver transplantation recipients were excluded. Forty-eight patients

Table 3 Characteristics of studies on cirrhotic patients with portal vein thrombosis treated with direct oral anticoagulants

Study	Population	Aim of study	Doses and duration	Outcomes	Adverse events	Ref.
Retrospective	Cirrhotic, CP A/B/C; any indication (incl. PVT); subgroup with PVT: Riva or Api (n = 4) *vs* Enoxa or VKA (n = 3)	Efficacy and safety of DOACs *vs* traditional AC in cirrhosis	Riva 15 mg OD +/- 20 mg OD load; Api 5 mg BID +/- 10 mg BID load 10.6 mo (mean)	Recurrent thrombosis: DOACs (n = 1); Trad AC (n = 1)	Total bleeding events were similar in the two groups (with lesser major bleeding in the DOACs group)	Hum *et al* [87], 2017
Retrospective	Cirrhotic, CP A/BAny indication (incl. PVT); subgroup with PVT: Riva or Api (n = 12) *vs* LMWH or Warf (n = 6)	Compare the bleeding rates in cirrhotic patients	Riva 20 mg OD; Api 5 mg BID 10.6 mo (mean)	No statistical difference between therapeutic and prophylactic dosing between groups	Similar rates of major and minor bleeding in the two groups	Intagliata *et al* [89], 2016
Retrospective	Both cirrhotic and non, CP A/B; any indication (incl. PVT); subgroup with cirrhosis and PVT: Riva, Api or Dabi (n = 22)	Indication for starting or switching to DOACs and report short-term efficacy and safety	Cirrhotic: Different doses 9.6 mo (mean)	Cirrhotic: recurrent PVT (n = 1, 4.5%)	Cirrhotic group any indication: Major bleeding (n = 1), minor bleeding (n = 4)	De Gottardi *et al*[88], 2017
Retrospective	Both cirrhotic and non, CP A/B/C; non-malignant PVT; Edo (n = 4), Api (n = 3), Riva (n = 2), Dabi (n = 1) *vs* traditional AC (n = 12), no AC (n = 39)	Efficacy and safety of AC in non-malignant PVT	Edo 30/60 mg OD, Api 5 mg BID, Riva 10 mg OD, Dabi 110 mg BID 9.2 mo (median)	Favourable outcomes with DOACs: Regression/resolution 20%; stability/non-progression 80%	Portal hypertensive gastropathy bleeding	Scheiner *et al* [41], 2018
Retrospective	Cirrhotic, CP A/B; non-malignant PVT; Edo (n = 20) *vs* Warf (n = 30) (following 2 wk Danaparoid)	Compare the efficacy and safety of Edo and Warf for treatment of chronic PVT in cirrhotic patients	Edo 60 mg OD, (if CrCl > 50; n = 4) or Edo 30 mg OD (if CrCl < 50; n = 16) 6 mo (max)	Edo group had more complete resolution and less PVT progression than Warf group	Major GI bleeding: Edo (n = 3; 7%); Warf (n = 2; 15%)	Nagaoki *et al* [91], 2018
Prospective	Cirrhotic, CP A; chronic PTV; Riva (n = 26), Dabi (n = 14) *vs* no AC (n = 40)	Compare the efficacy and safety of DOACs and no AC in chronic PVT in cirrhotic patients	Riva 20 mg OD; Dabi 150 mg BID; 6 mo (max)	Recanalization rate with DOACs 28.2% (statistically higher) and improvement of liver function	No statistically significant difference between the DOACs and the control group in bleeding events	Ai *et al*[92], 2020
Prospective	Cirrhotic, CP A/B/C; non-malignant PVT; TIPS + AC (n = 197, 18 Riva) *vs* AC only (n = 63, 4 Riva) *vs* TIPS only (n = 88) *vs* nothing (n = 48)	Compare the management using a wait-and-see strategy, AC, and TIPS to treat PVT in cirrhosis	Riva 10 mg OD; 21.0 mo (median)	Recanalization: 0% with Riva only (all with PVT and SMV thrombosis), 100% with Riva + TIPS	Major bleeding events: AC only (n = 14); TIPS+AC (n = 30)	Lv *et al*[93], 2021

AC: Anticoagulation; Api: Apixaban; VKA: Vitamin K antagonists; BID: Twice daily; CP: Child-Pugh score; Dabi: Dabigatran; DOACs: Direct oral anticoagulants; Edo: Edoxaban; GI: Gastrointestinal; Enoxa: Enoxaparin; LMWH: Low molecular weight heparin; OD: Once daily; PVT: Portal vein thrombosis; Riva: Rivaroxaban; SMV: Superior mesenteric vein; TIPS: Transjugular intrahepatic portosystemic shunt; Warf: Warfarin.

received no treatment, 63 patients were treated with anticoagulants only, 88 patients received TIPS only, and 197 started anticoagulation after TIPS insertion. When patients received anticoagulation, they were treated with either VKA, LMWH, or rivaroxaban 10 mg OD, and anticoagulation treatment was extended for 12 mo after complete recanalization was achieved. A combined strategy with TIPS and subsequent anticoagulation showed the highest complete recanalization rate (188/197 patients); long-term anticoagulation with LMWH or rivaroxaban resulted in minor incidence of re-thrombosis and longer survival compared with VKA[93].

Overall, the proposed studies show that DOACs are at least non-inferior to conventional anticoagulants in cirrhotic non-malignant PVT, both in terms of efficacy and safety, but several limitations pose some issues regarding the results obtained.

First, most studies were conducted retrospectively with a limited number of patients and very heterogeneous cohorts.

Second, PVT classification, definition of bleeding events, drug dosage, and treatment duration vary widely among studies, making it difficult to compare results and to identify a standardized treatment algorithm.

Nonetheless, DOACs may represent a viable alternative to conventional anticoagulants in cirrhotic PVT, but further evidence and RCTs are needed.

BCS

Causes of primary BCS are essentially the same of non-cirrhotic PVT[16]. Compared with PVT, there is a greater prevalence of association with myeloproliferative neoplasm (30%-57% of cases)[17,94]. Some acquired thrombophilic conditions, such as paroxysmal nocturnal hemoglobinuria and Behçet's disease have also a higher causative link in BCS compared with PVT (12% *vs* < 1%, respectively)[95-97]. To the contrary, BCS caused by local factors is rare, with the only exception of hepatic hydatid cysts in countries where *Echinococcus granulosus* is endemic[98].

As for PVT, more than one risk factor could be found in 26%-46% of patients and no causative factors are identified in 10%-29% of patients[16,99].

Prompt identification and treatment of an underlying disease is mandatory for the management of BCS patients since both are positively related with outcome[96,100]. Anticoagulation is the cornerstone of BCS treatment and it should be initiated at diagnosis; long-term anticoagulation is generally recommended even in the absence of an identified prothrombotic disorder[35]. LMWH is currently the drug of choice, based on several previous studies reporting a higher rate of heparin-induced thrombocytopenia in BCS patients treated with UFH[101,102]. When a stability of the disease is achieved, a switch to VKA is usually the preferred choice in clinical practice.

The role of DOACs in BCS patients has been poorly investigated compared to PVT patients.

First data came from the aforementioned retrospective study of De Gottardi *et al*[88] about the use of DOACs in both cirrhotic and non-cirrhotic patients with SVT. In the study population (94 patients) there were 9 patients with BCS treated with DOACs (dabigatran, rivaroxaban or apixaban), but as results are presented for the entire population, it is not possible to extrapolate conclusions about efficacy and safety in this cohort of patients[88].

A recent multicentric Austrian study aimed to analyze the outcome of 22 patients treated with DOACs (all four drugs were prescribed, but almost a half of patients received edoxaban) *vs* 19 patients treated with only traditional anticoagulation (*i.e.* LMWH/VKA). Authors reported better efficacy results in the DOAC cohort (64% of complete recanalization rate and 92% of overall transplant-free survival at 5 years) and a comparable risk of major spontaneous and major procedure-related bleedings. Even though the results presented are interesting, there are some general considerations about the heterogeneity of the study population to be highlighted[103].

Firstly, in the DOAC cohort 16 patients (72.7%) were already anticoagulated with traditional drugs; among these, 8 patients (50%) had already achieved a complete response at the time of switching to DOAC.

Secondly, among the 16 patients receiving DOACs it is not known the time from LMWH/VKA start to the switch to DOACs, so it is difficult to evaluate the actual efficacy or failure of DOACs in patients previously treated with traditional anticoagulation.

Lastly, the rate of objective response to the first-line anticoagulation therapy (6 patients with DOACs *vs* 37 patients with LMWH/VKA) was comparable (66.6% *vs* 67.5%, respectively)[103].

Another retrospective monocentric study, made by Sharma *et al*[104], has investigated the role of dabigatran (36 patients) following endovascular intervention for BCS compared to VKA (62 patients). Authors concluded that stent patency rate, mortality and bleeding complication rate were comparable between dabigatran and VKA groups at 6 and 12 mo[104].

Although results from the literature are limited, DOACs seem effective and safe in patients with BCS and international guidelines have consequently added these drugs as an option of treatment, but prospective studies are needed.

CONCLUSION

In the last few years, several studies have shown promising results in the use of DOACs for the treatment of SVT in term of efficacy and, above all, safety. Unfortunately, the majority of studies are retrospective, with small sample size and with extremely heterogeneous examined populations, not allowing to give strong recommendations about the use of DOACs in this setting. Moreover, there is no conformity among studies in dosage schedule, time of initiation and duration of treatment and bleeding event definition. In some cases, it is even not specified the DOAC used.

On the other hand, international guidelines have added this new class of drugs as an option of treatment, recognizing their potential role both in cirrhotic and non-cirrhotic patients with SVT. Although in some countries there are strict limitations in prescription, more and more physicians prescribe DOACs for SVT in their clinical practice worldwide.

Further studies and clinical trials are needed in order to increase the level of evidence in this field, but current knowledge on DOAC use is already changing the therapeutic scenario of SVT.

FOOTNOTES

Author contributions: Monaco G, Bucherini L, Stefanini B and Ielasi L conceived the manuscript, reviewed the literature and wrote the original draft; Monaco G and Ielasi L reviewed and edited the manuscript; Piscaglia F and Foschi FG supervised; All authors read and agreed to the published version of the manuscript.

Conflict-of-interest statement: All authors declare no conflict of interest.

Open-Access: This article is an open-access article that was selected by an in-house editor and fully peer-reviewed by external reviewers. It is distributed in accordance with the Creative Commons Attribution NonCommercial (CC BY-NC 4.0) license, which permits others to distribute, remix, adapt, build upon this work non-commercially, and license their derivative works on different terms, provided the original work is properly cited and the use is non-commercial. See: https://creativecommons.org/Licenses/by-nc/4.0/

Country/Territory of origin: Italy

ORCID number: Bernardo Stefanini 0000-0003-3800-5678; Fabio Piscaglia 0000-0001-8264-1845; Francesco Giuseppe Foschi 0000-0002-8216-0918; Luca Ielasi 0000-0003-4162-2319.

S-Editor: Lin C
L-Editor: A
P-Editor: Yu HG

REFERENCES

1 **Di Nisio M**, Valeriani E, Riva N, Schulman S, Beyer-Westendorf J, Ageno W. Anticoagulant therapy for splanchnic vein thrombosis: ISTH SSC Subcommittee Control of Anticoagulation. *J Thromb Haemost* 2020; **18**: 1562-1568 [PMID: 32619346 DOI: 10.1111/jth.14836]

2 **Jones DEJ**, Sturm E, Lohse AW. Access to care in rare liver diseases: New challenges and new opportunities. *J Hepatol* 2018; **68**: 577-585 [PMID: 29113911 DOI: 10.1016/j.jhep.2017.11.004]

3 **Francoz C**, Valla D, Durand F. Portal vein thrombosis, cirrhosis, and liver transplantation. *J Hepatol* 2012; **57**: 203-212 [PMID: 22446690 DOI: 10.1016/j.jhep.2011.12.034]

4 **Nery F**, Chevret S, Condat B, de Raucourt E, Boudaoud L, Rautou PE, Plessier A, Roulot D, Chaffaut C, Bourcier V, Trinchet JC, Valla DC; Groupe d'Etude et de Traitement du Carcinome Hépatocellulaire. Causes and consequences of portal vein thrombosis in 1,243 patients with cirrhosis: results of a longitudinal study. *Hepatology* 2015; **61**: 660-667 [PMID: 25284616 DOI: 10.1002/hep.27546]

5 **Senzolo M**, Garcia-Tsao G, García-Pagán JC. Current knowledge and management of portal vein thrombosis in cirrhosis. *J Hepatol* 2021; **75**: 442-453 [PMID: 33930474 DOI: 10.1016/j.jhep.2021.04.029]

6 **Cheng Q**, Tree K. Systematic Review of Thrombolysis Therapy in the Management of Non-Cirrhosis-Related Portal Vein Thrombosis. *J Gastrointest Surg* 2021; **25**: 1579-1590 [PMID: 33452971 DOI: 10.1007/s11605-020-04624-4]

7 **Gadani S**, Partovi S, Levitin A, Zerona N, Sengupta S, D'Amico G, Diago Uso T, Menon KVN, Quintini C. Narrative review of portal vein thrombosis in cirrhosis: pathophysiology, diagnosis, and management from an interventional radiology perspective. *Cardiovasc Diagn Ther* 2022; **12**: 135-146 [PMID: 35282661 DOI: 10.21037/cdt-21-98]

8 **Saito H**, Sugihara F, Ueda T, Hayashi H, Shirai S, Matsumoto T, Fujitsuna R, Kumita SI. Efficacy of endovascular treatment for completely occlusive acute-subacute portal and mesenteric vein thrombosis with severe complications in patients without cirrhosis. *Jpn J Radiol* 2023; **41**: 541-550 [PMID: 36680703 DOI: 10.1007/s11604-022-01377-9]

9 **Steffel J**, Collins R, Antz M, Cornu P, Desteghe L, Haeusler KG, Oldgren J, Reinecke H, Roldan-Schilling V, Rowell N, Sinnaeve P, Vanassche T, Potpara T, Camm AJ, Heidbüchel H; External reviewers. 2021 European Heart Rhythm Association Practical Guide on the Use of Non-Vitamin K Antagonist Oral Anticoagulants in Patients with Atrial Fibrillation. *Europace* 2021; **23**: 1612-1676 [PMID: 33895845 DOI: 10.1093/europace/euab065]

10 **Konstantinides SV**, Meyer G, Becattini C, Bueno H, Geersing GJ, Harjola VP, Huisman MV, Humbert M, Jennings CS, Jiménez D, Kucher N, Lang IM, Lankeit M, Lorusso R, Mazzolai L, Meneveau N, Ní Áinle F, Prandoni P, Pruszczyk P, Righini M, Torbicki A, Van Belle E, Zamorano JL; ESC Scientific Document Group. 2019 ESC Guidelines for the diagnosis and management of acute pulmonary embolism developed in collaboration with the European Respiratory Society (ERS). *Eur Heart J* 2020; **41**: 543-603 [PMID: 31504429 DOI: 10.1093/eurheartj/ehz405]

11 **Harder S**, Graff J. Novel oral anticoagulants: clinical pharmacology, indications and practical considerations. *Eur J Clin Pharmacol* 2013; **69**: 1617-1633 [PMID: 23619611 DOI: 10.1007/s00228-013-1510-z]

12 **Gupta S**, Hidalgo J, Singh B, Iyer A, Yang Y, Short A, Singh S, Bhatt H, Gupta S. Usage of Direct Acting Oral Anticoagulants in Cirrhotic and Non-Cirrhotic Portal Vein Thrombosis: A Systematic Review. *Cureus* 2021; **13**: e16922 [PMID: 34367844 DOI: 10.7759/cureus.16922]

13 **Biolato M**, Paratore M, Di Gialleonardo L, Marrone G, Grieco A. Direct oral anticoagulant administration in cirrhotic patients with portal vein thrombosis: What is the evidence? *World J Hepatol* 2022; **14**: 682-695 [PMID: 35646264 DOI: 10.4254/wjh.v14.i4.682]

14 **Denninger MH**, Chaït Y, Casadevall N, Hillaire S, Guillin MC, Bezeaud A, Erlinger S, Briere J, Valla D. Cause of portal or hepatic venous thrombosis in adults: the role of multiple concurrent factors. *Hepatology* 2000; **31**: 587-591 [PMID: 10706547 DOI: 10.1002/hep.510310307]

15 **Plessier A**, Darwish-Murad S, Hernandez-Guerra M, Consigny Y, Fabris F, Trebicka J, Heller J, Morard I, Lasser L, Langlet P, Denninger MH, Vidaud D, Condat B, Hadengue A, Primignani M, Garcia-Pagan JC, Janssen HL, Valla D; European Network for Vascular Disorders of the Liver (EN-Vie). Acute portal vein thrombosis unrelated to cirrhosis: a prospective multicenter follow-up study. *Hepatology* 2010; **51**: 210-218 [PMID: 19821530 DOI: 10.1002/hep.23259]

16 **Elkrief L**, Payancé A, Plessier A, d'Alteroche L, Ronot M, Paradis V, Valla D, Rautou PE. Management of splanchnic vein thrombosis. *JHEP Rep* 2023; **5**: 100667 [PMID: 36941824 DOI: 10.1016/j.jhepr.2022.100667]

17 **Smalberg JH**, Arends LR, Valla DC, Kiladjian JJ, Janssen HL, Leebeek FW. Myeloproliferative neoplasms in Budd-Chiari syndrome and portal vein thrombosis: a meta-analysis. *Blood* 2012; **120**: 4921-4928 [PMID: 23043069 DOI: 10.1182/blood-2011-09-376517]

18 **Debureaux PE**, Cassinat B, Soret-Dulphy J, Mora B, Verger E, Maslah N, Plessier A, Rautou PE, Ollivier-Hourman I, De Ledinghen V, Goria O, Bureau C, Siracusa C, Valla D, Giraudier S, Passamonti F, Kiladjian JJ. Molecular profiling and risk classification of patients with myeloproliferative neoplasms and splanchnic vein thromboses. *Blood Adv* 2020; **4**: 3708-3715 [PMID: 32777065 DOI: 10.1182/bloodadvances.2020002414]

19 **Rajani R**, Björnsson E, Bergquist A, Danielsson A, Gustavsson A, Grip O, Melin T, Sangfelt P, Wallerstedt S, Almer S. The epidemiology and clinical features of portal vein thrombosis: a multicentre study. *Aliment Pharmacol Ther* 2010; **32**: 1154-1162 [PMID: 21039677 DOI: 10.1111/j.1365-2036.2010.04454.x]

20 **Bissonnette J**, Durand F, de Raucourt E, Ceccaldi PF, Plessier A, Valla D, Rautou PE. Pregnancy and vascular liver disease. *J Clin Exp Hepatol* 2015; **5**: 41-50 [PMID: 25941432 DOI: 10.1016/j.jceh.2014.12.007]

21 **Qi X**, De Stefano V, Su C, Bai M, Guo X, Fan D. Associations of antiphospholipid antibodies with splanchnic vein thrombosis: a systematic review with meta-analysis. *Medicine (Baltimore)* 2015; **94**: e496 [PMID: 25634200 DOI: 10.1097/MD.0000000000000496]

22 **De Broucker C**, Plessier A, Ollivier-Hourmand I, Dharancy S, Bureau C, Cervoni JP, Sogni P, Goria O, Corcos O, Sartoris R, Ronot M, Vilgrain V, de Raucourt E, Zekrini K, Davy H, Durand F, Payancé A, Fidouh-Houhou N, Yazdanpanah Y, Valla D, Rautou PE. Multicenter study on recent portal venous system thrombosis associated with cytomegalovirus disease. *J Hepatol* 2022; **76**: 115-122 [PMID: 34563580 DOI: 10.1016/j.jhep.2021.09.011]

23 **Buso G**, Becchetti C, Berzigotti A. Acute splanchnic vein thrombosis in patients with COVID-19: A systematic review. *Dig Liver Dis* 2021; **53**: 937-949 [PMID: 34120860 DOI: 10.1016/j.dld.2021.05.021]

24 **Baiges A**, Cerda E, Amicone C, Téllez L, Alvarado-Tapias E, Puente A, Fortea JI, Llop E, Rocha F, Orts L, Ros-Fargas O, Vizcarra P, Zekrini K, Lounes OA, Touati G, Jiménez-Esquivel N, Serrano MJ, Falgà A, Magaz M, Olivas P, Betancourt F, Perez-Campuzano V, Turon F, Payancé A, Goria O, Rautou PE, Hernández-Gea V, Villanueva C, Albillos A, Plessier A, García-Pagán JC. Impact of SARS-CoV-2 Pandemic on Vascular Liver Diseases. *Clin Gastroenterol Hepatol* 2022; **20**: 1525-1533.e5 [PMID: 34968728 DOI: 10.1016/j.cgh.2021.12.032]

25 **Qi X**, Ren W, De Stefano V, Fan D. Associations of coagulation factor V Leiden and prothrombin G20210A mutations with Budd-Chiari syndrome and portal vein thrombosis: a systematic review and meta-analysis. *Clin Gastroenterol Hepatol* 2014; **12**: 1801-12.e7 [PMID: 24793031 DOI: 10.1016/j.cgh.2014.04.026]

26 **Poisson J**, Plessier A, Kiladjian JJ, Turon F, Cassinat B, Andreoli A, De Raucourt E, Goria O, Zekrini K, Bureau C, Lorre F, Cervantes F, Colomer D, Durand F, Garcia-Pagan JC, Casadevall N, Valla DC, Rautou PE, Marzac C; French national network for vascular liver diseases. Selective testing for calreticulin gene mutations in patients with splanchnic vein thrombosis: A prospective cohort study. *J Hepatol* 2017; **67**: 501-507 [PMID: 28483676 DOI: 10.1016/j.jhep.2017.04.021]

27 **Baiges A**, de la Morena-Barrio ME, Turon F, Miñano A, Alberto Ferrusquía J, Magaz M, Reverter JC, Vicente V, Hernández-Gea V, Corral J, García-Pagán JC. Congenital antithrombin deficiency in patients with splanchnic vein thrombosis. *Liver Int* 2020; **40**: 1168-1177 [PMID: 31885188 DOI: 10.1111/liv.14342]

28 **Rebours V**, Boudaoud L, Vullierme MP, Vidaud D, Condat B, Hentic O, Maire F, Hammel P, Ruszniewski P, Lévy P. Extrahepatic portal venous system thrombosis in recurrent acute and chronic alcoholic pancreatitis is caused by local inflammation and not thrombophilia. *Am J Gastroenterol* 2012; **107**: 1579-1585 [PMID: 22825367 DOI: 10.1038/ajg.2012.231]

29 **Condat B**, Pessione F, Helene Denninger M, Hillaire S, Valla D. Recent portal or mesenteric venous thrombosis: increased recognition and frequent recanalization on anticoagulant therapy. *Hepatology* 2000; **32**: 466-470 [PMID: 10960436 DOI: 10.1053/jhep.2000.16597]

30 **European Association for the Study of the Liver**. EASL Clinical Practice Guidelines: Vascular diseases of the liver. *J Hepatol* 2016; **64**: 179-202 [PMID: 26516032 DOI: 10.1016/j.jhep.2015.07.040]

31 **Amitrano L**, Guardascione MA, Scaglione M, Pezzullo L, Sangiuliano N, Armellino MF, Manguso F, Margaglione M, Ames PR, Iannaccone L, Grandone E, Romano L, Balzano A. Prognostic factors in noncirrhotic patients with splanchnic vein thromboses. *Am J Gastroenterol* 2007; **102**: 2464-2470 [PMID: 17958760 DOI: 10.1111/j.1572-0241.2007.01477.x]

32 **Hall TC**, Garcea G, Metcalfe M, Bilku D, Dennison AR. Management of acute non-cirrhotic and non-malignant portal vein thrombosis: a systematic review. *World J Surg* 2011; **35**: 2510-2520 [PMID: 21882035 DOI: 10.1007/s00268-011-1198-0]

33 **Turnes J**, García-Pagán JC, González M, Aracil C, Calleja JL, Ripoll C, Abraldes JG, Bañares R, Villanueva C, Albillos A, Ayuso JR, Gilabert R, Bosch J. Portal hypertension-related complications after acute portal vein thrombosis: impact of early anticoagulation. *Clin Gastroenterol Hepatol* 2008; **6**: 1412-1417 [PMID: 19081529 DOI: 10.1016/j.cgh.2008.07.031]

34 **Ageno W**, Riva N, Schulman S, Beyer-Westendorf J, Bang SM, Senzolo M, Grandone E, Pasca S, Di Minno MN, Duce R, Malato A, Santoro R, Poli D, Verhamme P, Martinelli I, Kamphuisen P, Oh D, D'Amico E, Becattini C, De Stefano V, Vidili G, Vaccarino A, Nardo B, Di Nisio M, Dentali F. Long-term Clinical Outcomes of Splanchnic Vein Thrombosis: Results of an International Registry. *JAMA Intern Med* 2015; **175**: 1474-1480 [PMID: 26168152 DOI: 10.1001/jamainternmed.2015.3184]

35 **de Franchis R**, Bosch J, Garcia-Tsao G, Reiberger T, Ripoll C; Baveno VII Faculty. Baveno VII - Renewing consensus in portal hypertension. *J Hepatol* 2022; **76**: 959-974 [PMID: 35120736 DOI: 10.1016/j.jhep.2021.12.022]

36 **Intagliata NM**, Saad WE, Caldwell SH. Effects of restoring portal flow with anticoagulation and partial splenorenal shunt embolization. *Hepatology* 2015; **61**: 1088-1090 [PMID: 24867875 DOI: 10.1002/hep.27241]

37 **Chen H**, Turon F, Hernández-Gea V, Fuster J, Garcia-Criado A, Barrufet M, Darnell A, Fondevila C, Garcia-Valdecasas JC, Garcia-Pagán JC. Nontumoral portal vein thrombosis in patients awaiting liver transplantation. *Liver Transpl* 2016; **22**: 352-365 [PMID: 26684272 DOI: 10.1002/lt.24387]

38 **Northup PG**, Garcia-Pagan JC, Garcia-Tsao G, Intagliata NM, Superina RA, Roberts LN, Lisman T, Valla DC. Vascular Liver Disorders, Portal Vein Thrombosis, and Procedural Bleeding in Patients With Liver Disease: 2020 Practice Guidance by the American Association for the Study of Liver Diseases. *Hepatology* 2021; **73**: 366-413 [PMID: 33219529 DOI: 10.1002/hep.31646]

39 **Spaander MC**, Hoekstra J, Hansen BE, Van Buuren HR, Leebeek FW, Janssen HL. Anticoagulant therapy in patients with non-cirrhotic portal vein thrombosis: effect on new thrombotic events and gastrointestinal bleeding. *J Thromb Haemost* 2013; **11**: 452-459 [PMID: 23289370 DOI: 10.1111/jth.12121]

40 **Janczak DT**, Mimier MK, McBane RD, Kamath PS, Simmons BS, Bott-Kitslaar DM, Lenz CJ, Vargas ER, Hodge DO, Wysokinski WE. Rivaroxaban and Apixaban for Initial Treatment of Acute Venous Thromboembolism of Atypical Location. *Mayo Clin Proc* 2018; **93**: 40-47 [PMID: 29217335 DOI: 10.1016/j.mayocp.2017.10.007]

41 **Scheiner B**, Stammet PR, Pokorny S, Bucsics T, Schwabl P, Brichta A, Thaler J, Lampichler K, Ba-Ssalamah A, Ay C, Ferlitsch A, Trauner M, Mandorfer M, Reiberger T. Anticoagulation in non-malignant portal vein thrombosis is safe and improves hepatic function. *Wien Klin Wochenschr* 2018; **130**: 446-455 [PMID: 29916054 DOI: 10.1007/s00508-018-1351-y]

42 **Naymagon L**, Tremblay D, Zubizarreta N, Moshier E, Troy K, Schiano T, Mascarenhas J. The efficacy and safety of direct oral anticoagulants in noncirrhotic portal vein thrombosis. *Blood Adv* 2020; **4**: 655-666 [PMID: 32078681 DOI: 10.1182/bloodadvances.2019001310]

43 **Naymagon L**, Tremblay D, Zubizarreta N, Moshier E, Naymagon S, Mascarenhas J, Schiano T. The Natural History, Treatments, and Outcomes of Portal Vein Thrombosis in Patients With Inflammatory Bowel Disease. *Inflamm Bowel Dis* 2021; **27**: 215-223 [PMID: 32185400

DOI: 10.1093/ibd/izaa053]
44 **Naymagon L**, Tremblay D, Mascarenhas J, Schiano T. Characteristics, anticoagulation, and outcomes of portal vein thrombosis after intra-abdominal surgery. *Surgery* 2021; **169**: 1175-1181 [PMID: 33358635 DOI: 10.1016/j.surg.2020.11.016]
45 **Ilcewicz HN**, Martello JL, Piechowski K. Evaluation of the efficacy and safety of direct oral anticoagulants in the treatment of portal vein thrombosis. *Eur J Gastroenterol Hepatol* 2021; **33**: 911-916 [PMID: 33079786 DOI: 10.1097/MEG.0000000000001958]
46 **Ageno W**, Beyer Westendorf J, Contino L, Bucherini E, Sartori MT, Senzolo M, Grandone E, Santoro R, Carrier M, Delluc A, De Stefano V, Pomero F, Donadini MP, Tosetto A, Becattini C, Martinelli I, Nardo B, Bertoletti L, Di Nisio M, Lazo-Langner A, Schenone A, Riva N. Rivaroxaban for the treatment of noncirrhotic splanchnic vein thrombosis: an interventional prospective cohort study. *Blood Adv* 2022; **6**: 3569-3578 [PMID: 35439303 DOI: 10.1182/bloodadvances.2022007397]
47 **Intagliata NM**, Caldwell SH, Tripodi A. Diagnosis, Development, and Treatment of Portal Vein Thrombosis in Patients With and Without Cirrhosis. *Gastroenterology* 2019; **156**: 1582-1599.e1 [PMID: 30771355 DOI: 10.1053/j.gastro.2019.01.265]
48 **Prakash S**, Bies J, Hassan M, Mares A, Didia SC. Portal vein thrombosis in cirrhosis: A literature review. *Front Med (Lausanne)* 2023; **10**: 1134801 [PMID: 37181351 DOI: 10.3389/fmed.2023.1134801]
49 **Giri S**, Singh A, Kolhe K, Kale A, Shukla A. Natural history of portal vein thrombosis in cirrhosis: A systematic review with meta-analysis. *J Gastroenterol Hepatol* 2023 [PMID: 37354011 DOI: 10.1111/jgh.16263]
50 **Senzolo M**, M Sartori T, Rossetto V, Burra P, Cillo U, Boccagni P, Gasparini D, Miotto D, Simioni P, Tsochatzis E, A Burroughs K. Prospective evaluation of anticoagulation and transjugular intrahepatic portosystemic shunt for the management of portal vein thrombosis in cirrhosis. *Liver Int* 2012; **32**: 919-927 [PMID: 22435854 DOI: 10.1111/j.1478-3231.2012.02785.x]
51 **Delgado MG**, Seijo S, Yepes I, Achécar L, Catalina MV, García-Criado A, Abraldes JG, de la Peña J, Bañares R, Albillos A, Bosch J, García-Pagán JC. Efficacy and safety of anticoagulation on patients with cirrhosis and portal vein thrombosis. *Clin Gastroenterol Hepatol* 2012; **10**: 776-783 [PMID: 22289875 DOI: 10.1016/j.cgh.2012.01.012]
52 **Simonetto DA**, Singal AK, Garcia-Tsao G, Caldwell SH, Ahn J, Kamath PS. ACG Clinical Guideline: Disorders of the Hepatic and Mesenteric Circulation. *Am J Gastroenterol* 2020; **115**: 18-40 [PMID: 31895720 DOI: 10.14309/ajg.0000000000000486]
53 **Turco L**, de Raucourt E, Valla DC, Villa E. Anticoagulation in the cirrhotic patient. *JHEP Rep* 2019; **1**: 227-239 [PMID: 32039373 DOI: 10.1016/j.jhepr.2019.02.006]
54 **Lisman T**, Caldwell SH, Intagliata NM. Haemostatic alterations and management of haemostasis in patients with cirrhosis. *J Hepatol* 2022; **76**: 1291-1305 [PMID: 35589251 DOI: 10.1016/j.jhep.2021.11.004]
55 **Rautou PE**, Caldwell SH, Villa E. Bleeding and Thrombotic Complications in Patients With Cirrhosis: A State-of-the-Art Appraisal. *Clin Gastroenterol Hepatol* 2023; **21**: 2110-2123 [PMID: 37121529 DOI: 10.1016/j.cgh.2023.04.016]
56 **Loffredo L**, Pastori D, Farcomeni A, Violi F. Effects of Anticoagulants in Patients With Cirrhosis and Portal Vein Thrombosis: A Systematic Review and Meta-analysis. *Gastroenterology* 2017; **153**: 480-487.e1 [PMID: 28479379 DOI: 10.1053/j.gastro.2017.04.042]
57 **Guerrero A**, Campo LD, Piscaglia F, Scheiner B, Han G, Violi F, Ferreira CN, Téllez L, Reiberger T, Basili S, Zamora J, Albillos A; Baveno Cooperation: an EASL consortium. Anticoagulation improves survival in patients with cirrhosis and portal vein thrombosis: The IMPORTAL competing-risk meta-analysis. *J Hepatol* 2023; **79**: 69-78 [PMID: 36858157 DOI: 10.1016/j.jhep.2023.02.023]
58 **Pettinari I**, Vukotic R, Stefanescu H, Pecorelli A, Morelli M, Grigoras C, Sparchez Z, Andreone P, Piscaglia F; BO-LIVES (BOlogna LIVEr vascular Studies). Clinical Impact and Safety of Anticoagulants for Portal Vein Thrombosis in Cirrhosis. *Am J Gastroenterol* 2019; **114**: 258-266 [PMID: 30538290 DOI: 10.1038/s41395-018-0421-0]
59 **Benevento F**, Pecorelli A, Stefanescu H, Sparchez Z, Vukotic R, Pettinari I, Grigoras CA, Tovoli F, Ravaioli F, Stefanini B, Andreone P, Piscaglia F. Presence of Hepatocellular Carcinoma Does Not Affect Course and Response to Anticoagulation of Bland Portal Vein Thrombosis in Cirrhotic Patients. *J Hepatocell Carcinoma* 2023; **10**: 473-482 [PMID: 37007210 DOI: 10.2147/JHC.S390777]
60 **Zhang ZH**, Zhang JW, He P, Zhou Y, Sun CY. Fondaparinux is effective for acute portal vein thrombosis in decompensated cirrhotic patients. *Medicine (Baltimore)* 2017; **96**: e8256 [PMID: 29049216 DOI: 10.1097/MD.0000000000008256]
61 **Senzolo M**, Piano S, Shalaby S, Tonon M, Tonello S, Zanetto A, Sacerdoti D, Simioni P, Bombonato G, Burra P, Angeli P. Comparison of Fondaparinux and Low-Molecular-Weight Heparin in the Treatment of Portal Vein Thrombosis in Cirrhosis. *Am J Med* 2021; **134**: 1278-1285.e2 [PMID: 34197784 DOI: 10.1016/j.amjmed.2021.05.013]
62 **Zhou T**, Sun X, Zhou T, Li Y, Chen X, Cheng B, Gao Y. Efficacy and Safety of Nadroparin Calcium-Warfarin Sequential Anticoagulation in Portal Vein Thrombosis in Cirrhotic Patients: A Randomized Controlled Trial. *Clin Transl Gastroenterol* 2020; **11**: e00228 [PMID: 32858573 DOI: 10.14309/ctg.0000000000000228]
63 **Tripodi A**, Fracanzani AL, Primignani M, Chantarangkul V, Clerici M, Mannucci PM, Peyvandi F, Bertelli C, Valenti L, Fargion S. Procoagulant imbalance in patients with non-alcoholic fatty liver disease. *J Hepatol* 2014; **61**: 148-154 [PMID: 24657400 DOI: 10.1016/j.jhep.2014.03.013]
64 **Koh JH**, Liew ZH, Ng GK, Liu HT, Tam YC, De Gottardi A, Wong YJ. Efficacy and safety of direct oral anticoagulants *vs* vitamin K antagonist for portal vein thrombosis in cirrhosis: A systematic review and meta-analysis. *Dig Liver Dis* 2022; **54**: 56-62 [PMID: 34393072 DOI: 10.1016/j.dld.2021.07.039]
65 **Connolly SJ**, Ezekowitz MD, Yusuf S, Eikelboom J, Oldgren J, Parekh A, Pogue J, Reilly PA, Themeles E, Varrone J, Wang S, Alings M, Xavier D, Zhu J, Diaz R, Lewis BS, Darius H, Diener HC, Joyner CD, Wallentin L; RE-LY Steering Committee and Investigators. Dabigatran *vs* warfarin in patients with atrial fibrillation. *N Engl J Med* 2009; **361**: 1139-1151 [PMID: 19717844 DOI: 10.1056/NEJMoa0905561]
66 **Patel MR**, Mahaffey KW, Garg J, Pan G, Singer DE, Hacke W, Breithardt G, Halperin JL, Hankey GJ, Piccini JP, Becker RC, Nessel CC, Paolini JF, Berkowitz SD, Fox KA, Califf RM; ROCKET AF Investigators. Rivaroxaban *vs* warfarin in nonvalvular atrial fibrillation. *N Engl J Med* 2011; **365**: 883-891 [PMID: 21830957 DOI: 10.1056/NEJMoa1009638]
67 **Granger CB**, Alexander JH, McMurray JJ, Lopes RD, Hylek EM, Hanna M, Al-Khalidi HR, Ansell J, Atar D, Avezum A, Bahit MC, Diaz R, Easton JD, Ezekowitz JA, Flaker G, Garcia D, Geraldes M, Gersh BJ, Golitsyn S, Goto S, Hermosillo AG, Hohnloser SH, Horowitz J, Mohan P, Jansky P, Lewis BS, Lopez-Sendon JL, Pais P, Parkhomenko A, Verheugt FW, Zhu J, Wallentin L; ARISTOTLE Committees and Investigators. Apixaban *vs* warfarin in patients with atrial fibrillation. *N Engl J Med* 2011; **365**: 981-992 [PMID: 21870978 DOI: 10.1056/NEJMoa1107039]
68 **Giugliano RP**, Ruff CT, Braunwald E, Murphy SA, Wiviott SD, Halperin JL, Waldo AL, Ezekowitz MD, Weitz JI, Špinar J, Ruzyllo W, Ruda M, Koretsune Y, Betcher J, Shi M, Grip LT, Patel SP, Patel I, Hanyok JJ, Mercuri M, Antman EM; ENGAGE AF-TIMI 48 Investigators. Edoxaban *vs* warfarin in patients with atrial fibrillation. *N Engl J Med* 2013; **369**: 2093-2104 [PMID: 24251359 DOI: 10.1056/NEJMoa1310907]

69 **Schulman S**, Kearon C, Kakkar AK, Mismetti P, Schellong S, Eriksson H, Baanstra D, Schnee J, Goldhaber SZ; RE-COVER Study Group. Dabigatran *vs* warfarin in the treatment of acute venous thromboembolism. *N Engl J Med* 2009; **361**: 2342-2352 [PMID: 19966341 DOI: 10.1056/NEJMoa0906598]

70 **EINSTEIN Investigators**, Bauersachs R, Berkowitz SD, Brenner B, Buller HR, Decousus H, Gallus AS, Lensing AW, Misselwitz F, Prins MH, Raskob GE, Segers A, Verhamme P, Wells P, Agnelli G, Bounameaux H, Cohen A, Davidson BL, Piovella F, Schellong S. Oral rivaroxaban for symptomatic venous thromboembolism. *N Engl J Med* 2010; **363**: 2499-2510 [PMID: 21128814 DOI: 10.1056/NEJMoa1007903]

71 **Agnelli G**, Buller HR, Cohen A, Curto M, Gallus AS, Johnson M, Masiukiewicz U, Pak R, Thompson J, Raskob GE, Weitz JI; AMPLIFY Investigators. Oral apixaban for the treatment of acute venous thromboembolism. *N Engl J Med* 2013; **369**: 799-808 [PMID: 23808982 DOI: 10.1056/NEJMoa1302507]

72 **Hokusai-VTE Investigators**, Büller HR, Décousus H, Grosso MA, Mercuri M, Middeldorp S, Prins MH, Raskob GE, Schellong SM, Schwocho L, Segers A, Shi M, Verhamme P, Wells P. Edoxaban *vs* warfarin for the treatment of symptomatic venous thromboembolism. *N Engl J Med* 2013; **369**: 1406-1415 [PMID: 23991658 DOI: 10.1056/NEJMoa1306638]

73 **Hoolwerf EW**, Kraaijpoel N, Büller HR, van Es N. Direct oral anticoagulants in patients with liver cirrhosis: A systematic review. *Thromb Res* 2018; **170**: 102-108 [PMID: 30153564 DOI: 10.1016/j.thromres.2018.08.011]

74 **Menichelli D**, Ronca V, Di Rocco A, Pignatelli P, Marco Podda G; CAR. Direct oral anticoagulants and advanced liver disease: A systematic review and meta-analysis. *Eur J Clin Invest* 2021; **51**: e13397 [PMID: 32895926 DOI: 10.1111/eci.13397]

75 **Serper M**, Weinberg EM, Cohen JB, Reese PP, Taddei TH, Kaplan DE. Mortality and Hepatic Decompensation in Patients With Cirrhosis and Atrial Fibrillation Treated With Anticoagulation. *Hepatology* 2021; **73**: 219-232 [PMID: 32267547 DOI: 10.1002/hep.31264]

76 **Yoo SY**, Kim E, Nam GB, Lee D, Shim JH, Kim KM, Lim YS, Lee HC, Chung YH, Lee YS, Choi J. Safety of direct oral anticoagulants compared to warfarin in cirrhotic patients with atrial fibrillation. *Korean J Intern Med* 2022; **37**: 555-566 [PMID: 35078306 DOI: 10.3904/kjim.2020.622]

77 **Li Z**, Xu W, Wang L, Chai L, Ageno W, Romeiro FG, Li H, Qi X. Risk of Bleeding in Liver Cirrhosis Receiving Direct Oral Anticoagulants: A Systematic Review and Meta-analysis. *Thromb Haemost* 2023 [PMID: 37336474 DOI: 10.1055/s-0043-1770100]

78 **Kubitza D**, Roth A, Becka M, Alatrach A, Halabi A, Hinrichsen H, Mueck W. Effect of hepatic impairment on the pharmacokinetics and pharmacodynamics of a single dose of rivaroxaban, an oral, direct Factor Xa inhibitor. *Br J Clin Pharmacol* 2013; **76**: 89-98 [PMID: 23294275 DOI: 10.1111/bcp.12054]

79 **Violi F**, Loffredo L, Pastori D. Anticoagulation in patients with advanced liver disease: an open issue. *Intern Emerg Med* 2021; **16**: 61-71 [PMID: 33073317 DOI: 10.1007/s11739-020-02526-6]

80 **Mort JF**, Davis JPE, Mahoro G, Stotts MJ, Intagliata NM, Northup PG. Rates of Bleeding and Discontinuation of Direct Oral Anticoagulants in Patients With Decompensated Cirrhosis. *Clin Gastroenterol Hepatol* 2021; **19**: 1436-1442 [PMID: 32777555 DOI: 10.1016/j.cgh.2020.08.007]

81 **Semmler G**, Pomej K, Bauer DJM, Balcar L, Simbrunner B, Binter T, Hartl L, Becker J, Pinter M, Quehenberger P, Trauner M, Mandorfer M, Lisman T, Reiberger T, Scheiner B. Safety of direct oral anticoagulants in patients with advanced liver disease. *Liver Int* 2021; **41**: 2159-2170 [PMID: 34152697 DOI: 10.1111/liv.14992]

82 **Licata A**, Puccia F, Lombardo V, Serruto A, Minissale MG, Morreale I, Giannitrapani L, Soresi M, Montalto G, Almasio PL. Rivaroxaban-induced hepatotoxicity: review of the literature and report of new cases. *Eur J Gastroenterol Hepatol* 2018; **30**: 226-232 [PMID: 29120909 DOI: 10.1097/MEG.0000000000001030]

83 **Liakoni E**, Rätz Bravo AE, Krähenbühl S. Hepatotoxicity of New Oral Anticoagulants (NOACs). *Drug Saf* 2015; **38**: 711-720 [PMID: 26138527 DOI: 10.1007/s40264-015-0317-5]

84 **Caldeira D**, Barra M, Santos AT, de Abreu D, Pinto FJ, Ferreira JJ, Costa J. Risk of drug-induced liver injury with the new oral anticoagulants: systematic review and meta-analysis. *Heart* 2014; **100**: 550-556 [PMID: 24476812 DOI: 10.1136/heartjnl-2013-305288]

85 **Alonso A**, MacLehose RF, Chen LY, Bengtson LG, Chamberlain AM, Norby FL, Lutsey PL. Prospective study of oral anticoagulants and risk of liver injury in patients with atrial fibrillation. *Heart* 2017; **103**: 834-839 [PMID: 28057799 DOI: 10.1136/heartjnl-2016-310586]

86 **Hanafy AS**, Abd-Elsalam S, Dawoud MM. Randomized controlled trial of rivaroxaban *vs* warfarin in the management of acute non-neoplastic portal vein thrombosis. *Vascul Pharmacol* 2019; **113**: 86-91 [PMID: 29886103 DOI: 10.1016/j.vph.2018.05.002]

87 **Hum J**, Shatzel JJ, Jou JH, Deloughery TG. The efficacy and safety of direct oral anticoagulants *vs* traditional anticoagulants in cirrhosis. *Eur J Haematol* 2017; **98**: 393-397 [PMID: 28009449 DOI: 10.1111/ejh.12844]

88 **De Gottardi A**, Trebicka J, Klinger C, Plessier A, Seijo S, Terziroli B, Magenta L, Semela D, Buscarini E, Langlet P, Görtzen J, Puente A, Müllhaupt B, Navascuès C, Nery F, Deltenre P, Turon F, Engelmann C, Arya R, Caca K, Peck-Radosavljevic M, Leebeek FWG, Valla D, Garcia-Pagan JC; VALDIG Investigators. Antithrombotic treatment with direct-acting oral anticoagulants in patients with splanchnic vein thrombosis and cirrhosis. *Liver Int* 2017; **37**: 694-699 [PMID: 27778440 DOI: 10.1111/liv.13285]

89 **Intagliata NM**, Henry ZH, Maitland H, Shah NL, Argo CK, Northup PG, Caldwell SH. Direct Oral Anticoagulants in Cirrhosis Patients Pose Similar Risks of Bleeding When Compared to Traditional Anticoagulation. *Dig Dis Sci* 2016; **61**: 1721-1727 [PMID: 26725062 DOI: 10.1007/s10620-015-4012-2]

90 **Davis KA**, Joseph J, Nisly SA. Direct oral anticoagulants and warfarin in patients with cirrhosis: a comparison of outcomes. *J Thromb Thrombolysis* 2020; **50**: 457-461 [PMID: 31915998 DOI: 10.1007/s11239-019-02035-0]

91 **Nagaoki Y**, Aikata H, Daijyo K, Teraoka Y, Shinohara F, Nakamura Y, Hatooka M, Morio K, Nakahara T, Kawaoka T, Tsuge M, Hiramatsu A, Imamura M, Kawakami Y, Ochi H, Chayama K. Efficacy and safety of edoxaban for treatment of portal vein thrombosis following danaparoid sodium in patients with liver cirrhosis. *Hepatol Res* 2018; **48**: 51-58 [PMID: 28342265 DOI: 10.1111/hepr.12895]

92 **Ai MH**, Dong WG, Tan XP, Xu L, Xu C, Zhang Q, Zhang Y, Li J. Efficacy and safety study of direct-acting oral anticoagulants for the treatment of chronic portal vein thrombosis in patients with liver cirrhosis. *Eur J Gastroenterol Hepatol* 2020; **32**: 1395-1400 [PMID: 32675774 DOI: 10.1097/MEG.0000000000001846]

93 **Lv Y**, Bai W, Li K, Wang Z, Guo W, Luo B, Wang J, Wang Q, Wang E, Xia D, Li X, Yuan J, Han N, Niu J, Yin Z, Fan D, Han G. Anticoagulation and Transjugular Intrahepatic Portosystemic Shunt for the Management of Portal Vein Thrombosis in Cirrhosis: A Prospective Observational Study. *Am J Gastroenterol* 2021; **116**: 1447-1464 [PMID: 33630766 DOI: 10.14309/ajg.0000000000001194]

94 **Qi X**, Han G, Guo X, De Stefano V, Xu K, Lu Z, Xu H, Mancuso A, Zhang W, Han X, Valla DC, Fan D. Review article: the aetiology of primary Budd-Chiari syndrome - differences between the West and China. *Aliment Pharmacol Ther* 2016; **44**: 1152-1167 [PMID: 27734511 DOI: 10.1111/apt.13815]

95 **Hoekstra J**, Leebeek FW, Plessier A, Raffa S, Darwish Murad S, Heller J, Hadengue A, Chagneau C, Elias E, Primignani M, Garcia-Pagan JC, Valla DC, Janssen HL; European Network for Vascular Disorders of the Liver. Paroxysmal nocturnal hemoglobinuria in Budd-Chiari syndrome: findings from a cohort study. *J Hepatol* 2009; **51**: 696-706 [PMID: 19664836 DOI: 10.1016/j.jhep.2009.06.019]

96 **Desbois AC**, Rautou PE, Biard L, Belmatoug N, Wechsler B, Resche-Rigon M, Zarrouk V, Fantin B, de Chambrun MP, Cacoub P, Valla D, Saadoun D, Plessier A. Behcet's disease in Budd-Chiari syndrome. *Orphanet J Rare Dis* 2014; **9**: 104 [PMID: 25213625 DOI: 10.1186/s13023-014-0153-1]

97 **Sakr MA**, Reda MA, Ebada HE, Abdelmoaty AS, Hefny ZM, Ibrahim ZH, Aboelmaaty ME. Characteristics and outcome of primary Budd-Chiari syndrome due to Behçet's syndrome. *Clin Res Hepatol Gastroenterol* 2020; **44**: 503-512 [PMID: 31735495 DOI: 10.1016/j.clinre.2019.10.006]

98 **Afredj N**, Guessab N, Nani A, Faraoun SA, Ouled Cheikh I, Kerbouche R, Hannoun D, Amir ZC, Ait Kaci H, Bentabak K, Plessier A, Valla DC, Cazals-Hatem V, Denninger MH, Boucekkine T, Debzi N. Aetiological factors of Budd-Chiari syndrome in Algeria. *World J Hepatol* 2015; **7**: 903-909 [PMID: 25937867 DOI: 10.4254/wjh.v7.i6.903]

99 **Darwish Murad S**, Plessier A, Hernandez-Guerra M, Fabris F, Eapen CE, Bahr MJ, Trebicka J, Morard I, Lasser L, Heller J, Hadengue A, Langlet P, Miranda H, Primignani M, Elias E, Leebeek FW, Rosendaal FR, Garcia-Pagan JC, Valla DC, Janssen HL; EN-Vie (European Network for Vascular Disorders of the Liver). Etiology, management, and outcome of the Budd-Chiari syndrome. *Ann Intern Med* 2009; **151**: 167-175 [PMID: 19652186 DOI: 10.7326/0003-4819-151-3-200908040-00004]

100 **Plessier A**, Esposito-Farèse M, Baiges A, Shukla A, Garcia Pagan JC, De Raucourt E, Ollivier-Hourmand I, Cervoni JP, De Ledinghen V, Tazi Z, Nousbaum JB, Bun R, Bureau C, Silvain C, Tournilhac O, Gerfaud-Valentin M, Durand F, Goria O, Tellez L, Albillos A, Gioia S, Riggio O, De Gottardi A, Payance A, Rautou PE, Terriou L, Charbonnier A, Elkrief L, de la Tour RP, Valla DC, Gault N, de Fontbrune FS. Paroxysmal nocturnal hemoglobinuria and vascular liver disease: Eculizumab therapy decreases mortality and thrombotic complications. *Am J Hematol* 2022; **97**: 431-439 [PMID: 35049058 DOI: 10.1002/ajh.26474]

101 **Randi ML**, Tezza F, Scapin M, Duner E, Scarparo P, Scandellari R, Fabris F. Heparin-induced thrombocytopenia in patients with Philadelphia-negative myeloproliferative disorders and unusual splanchnic or cerebral vein thrombosis. *Acta Haematol* 2010; **123**: 140-145 [PMID: 20134155 DOI: 10.1159/000280466]

102 **Zaman S**, Wiebe S, Bernal W, Wendon J, Czuprynska J, Auzinger G. Increased prevalence of heparin-induced thrombocytopenia in patients with Budd-Chiari syndrome: a retrospective analysis. *Eur J Gastroenterol Hepatol* 2016; **28**: 967-971 [PMID: 27015137 DOI: 10.1097/MEG.0000000000000632]

103 **Semmler G**, Lindorfer A, Schäfer B, Bartl S, Hametner-Schreil S, Gensluckner S, Balcar L, Pomej K, Lampichler K, Trauner M, Aigner E, Datz C, Zoller H, Hofer H, Schöfl R, Mandorfer M, Reiberger T, Scheiner B. Outcome of Budd-Chiari Syndrome Patients Treated With Direct Oral Anticoagulants: An Austrian Multicenter Study. *Clin Gastroenterol Hepatol* 2023; **21**: 978-987.e2 [PMID: 35533994 DOI: 10.1016/j.cgh.2022.04.024]

104 **Sharma S**, Kumar R, Rout G, Gamanagatti SR, Shalimar. Dabigatran as an oral anticoagulant in patients with Budd-Chiari syndrome post-percutaneous endovascular intervention. *J Gastroenterol Hepatol* 2020; **35**: 654-662 [PMID: 31476024 DOI: 10.1111/jgh.14843]

World Journal of Gastroenterology

Submit a Manuscript: https://www.f6publishing.com

World J Gastroenterol 2023 September 7; 29(33): 4975-4990

DOI: 10.3748/wjg.v29.i33.4975

ISSN 1007-9327 (print) ISSN 2219-2840 (online)

ORIGINAL ARTICLE

Basic Study

Angiotensin-converting enzyme 2 improves liver fibrosis in mice by regulating autophagy of hepatic stellate cells

Ying Wu, Ai-Hong Yin, Jun-Tao Sun, Wei-Hua Xu, Chun-Qing Zhang

Specialty type: Gastroenterology and hepatology

Provenance and peer review: Unsolicited article; Externally peer reviewed.

Peer-review model: Single blind

Peer-review report's scientific quality classification

Grade A (Excellent): 0
Grade B (Very good): B
Grade C (Good): C, C
Grade D (Fair): 0
Grade E (Poor): 0

P-Reviewer: Durairajan SSK, India; Kreisel W, Germany

Received: May 25, 2023
Peer-review started: May 25, 2023
First decision: July 8, 2023
Revised: July 27, 2023
Accepted: August 15, 2023
Article in press: August 15, 2023
Published online: September 7, 2023

Ying Wu, Jun-Tao Sun, Wei-Hua Xu, Department of Gastroenterology, The Second Hospital, Cheeloo College of Medicine, Shandong University, Jinan 250033, Shandong Province, China

Ai-Hong Yin, Department of Gastroenterology, Shandong Second Provincial General Hospital, Jinan 250000, Shandong Province, China

Chun-Qing Zhang, Department of Gastroenterology, Shandong Provincial Hospital, Cheeloo College of Medicine, Shandong University, Jinan 250021, Shandong Province, China

Corresponding author: Wei-Hua Xu, MD, PhD, Chief Doctor, Professor, Department of Gastroenterology, The Second Hospital, Cheeloo College of Medicine, Shandong University, No. 247 Beiyuan Street, Jinan 250033, Shandong Province, China. xuweihua1967@126.com

Abstract

BACKGROUND

Liver fibrosis is the common pathological process associated with the occurrence and development of various chronic liver diseases. At present, there is still a lack of effective prevention and treatment methods in clinical practice. Hepatic stellate cell (HSC) plays a key role in liver fibrogenesis. In recent years, the study of liver fibrosis targeting HSC autophagy has become a hot spot in this research field. Angiotensin-converting enzyme 2 (ACE2) is a key negative regulator of renin-angiotensin system, and its specific molecular mechanism on autophagy and liver fibrosis needs to be further explored.

AIM

To investigate the effect of ACE2 on hepatic fibrosis in mice by regulating HSC autophagy through the Adenosine monophosphate activates protein kinases (AMPK)/mammalian target of rapamycin (mTOR) pathway.

METHODS

Overexpression of ACE2 in a mouse liver fibrosis model was induced by injection of liver-specific recombinant adeno-associated virus ACE2 vector (rAAV2/8-ACE2). The degree of liver fibrosis was assessed by histopathological staining and the biomarkers in mouse serum were measured by Luminex multifactor analysis. The number of apoptotic HSCs was assessed by terminal deoxynucleoitidyl transferase-mediated dUTP nick-end labeling (TUNEL) and immunofluorescence staining. Transmission electron microscopy was used to identify the changes in the number of HSC autophagosomes. The effect of ACE2 overexpression on

autophagy-related proteins was evaluated by multicolor immunofluorescence staining. The expression of autophagy-related indicators and AMPK pathway-related proteins was measured by western blotting.

RESULTS

A mouse model of liver fibrosis was successfully established after 8 wk of intraperitoneal injection of carbon tetrachloride (CCl_4). rAAV2/8-ACE2 administration reduced collagen deposition and alleviated the degree of liver fibrosis in mice. The serum levels of platelet-derived growth factor, angiopoietin-2, vascular endothelial growth factor and angiotensin II were decreased, while the levels of interleukin (IL)-10 and angiotensin- (1-7) were increased in the rAAV2/8-ACE2 group. In addition, the expression of alpha-smooth muscle actin, fibronectin, and CD31 was down-regulated in the rAAV2/8-ACE2 group. TUNEL and immunofluorescence staining showed that rAAV2/8-ACE2 injection increased HSC apoptosis. Moreover, rAAV2/8-ACE2 injection notably decreased the number of autophagosomes and the expression of autophagy-related proteins (LC3I, LC3II, Beclin-1), and affected the expression of AMPK pathway-related proteins (AMPK, p-AMPK, p-mTOR).

CONCLUSION

ACE2 overexpression can inhibit HSC activation and promote cell apoptosis by regulating HSC autophagy through the AMPK/mTOR pathway, thereby alleviating liver fibrosis and hepatic sinusoidal remodeling.

Key Words: Angiotensin-converting enzyme 2; Hepatic stellate cells; Autophagy; Liver fibrosis; Portal hypertension; Mice

©The Author(s) 2023. Published by Baishideng Publishing Group Inc. All rights reserved.

Core Tip: Liver fibrosis and cirrhosis are the common outcomes of most chronic liver diseases, and there is a lack of effective treatment at present. Angiotensin-converting enzyme 2 (ACE2), as the main target receptor for the coronavirus disease virus invasion into the human body, is one of the research hotspots. The involvement of autophagy in the activation mechanism of hepatic stellate cell (HSC) during liver fibrosis has attracted increasing attention. Our study found that ACE2 can inhibit the activation and proliferation of HSCs by regulating autophagy, and promote apoptosis of HSCs, providing new ideas for the treatment of liver fibrosis and hepatic sinusoidal remodeling.

Citation: Wu Y, Yin AH, Sun JT, Xu WH, Zhang CQ. Angiotensin-converting enzyme 2 improves liver fibrosis in mice by regulating autophagy of hepatic stellate cells. *World J Gastroenterol* 2023; 29(33): 4975-4990
URL: https://www.wjgnet.com/1007-9327/full/v29/i33/4975.htm
DOI: https://dx.doi.org/10.3748/wjg.v29.i33.4975

INTRODUCTION

Liver fibrosis and cirrhosis are the common pathological processes associated with the occurrence and development of various chronic liver diseases, and there is still a lack of effective prevention and treatment methods for these conditions. In liver fibrosis and cirrhosis, excessive deposition of extracellular matrix (ECM) in the liver and regenerating nodules compress blood vessels, resulting in structural changes. In addition, hepatic sinusoidal vasoconstriction and vascular remodeling cause functional changes that ultimately lead to increased intrahepatic vascular resistance and portal pressure [1]. Hepatic stellate cells (HSCs) are located in the perisinusoidal Disse space between liver sinusoidal endothelial cells (LSECs) and hepatocytes[2]. The vasomotion of hepatic sinusoids greatly affects intrahepatic blood flow and portal venous resistance, and HSCs and LSECs play key roles in increasing intrahepatic vascular resistance and portal venous pressure. Hepatic sinusoidal vascular remodeling occurs in hepatic fibrosis and is characterized by capillarization of the hepatic sinusoids and surrounded by more contractile HSCs[3]. HSC activation is a complex and coordinated process. After activation, HSCs begin to proliferate and release excess collagen, proteoglycan and other ECM components, which in turn cause changes in the intrahepatic structure; furthermore, HSCs acquire contractility, reducing the diameter of the hepatic sinusoids and increasing resistance, leading to liver fibrosis and portal hypertension[4-6].

Autophagy is a metabolic process in which eukaryotic cells eliminate disposable or potentially dangerous cytoplasmic material. It plays a critical role in cell development, differentiation, and homeostasis. In this process, some damaged proteins or organelles are wrapped by autophagic vesicles with a double membrane structure and sent to lysosomes (animals) or vacuoles (yeast and plants) for degradation and recycling[7]. Autophagy, as a cellular housekeeper, can eliminate defective proteins and organelles, clear intracellular pathogens, and prevent the accumulation of abnormal proteins. Therefore, autophagy plays an active role in the pathology of many diseases. Growing evidence suggests that an adequate autophagic response in hepatocytes and nonparenchymal cells (HSCs, LSECs, Kupffer cells) is critical for the physiological function of the liver[8]. During hepatic fibrogenesis, the study of the mechanism of autophagy involved in HSC activation has attracted increasing attention. Autophagy increases the degradation of lipid droplets in HSCs, providing energy for HSC activation[9,10]. A study showed that after reducing HSC autophagy in mice, HSC activation was inhibited, and the degree of liver fibrosis was alleviated[11]. In recent years, the study of liver fibrosis targeting HSC

autophagy has become a hot spot in this research field.

The renin-angiotensin system (RAS) is an important endocrine system that regulates vascular tone and water and electrolyte metabolism in the body. Our previous studies have confirmed that HSCs have local RAS, and activated HSCs increase the synthesis of angiotensin II (Ang II) in liver cirrhosis[12]. Under the action of angiotensin-converting enzyme 2 (ACE2), Ang II is converted to Ang- (1-7), which stimulates the Mas receptor to cause vasodilation. ACE2 is a key negative regulator of RAS, and studies have shown that it can inhibit liver fibrosis by degrading Ang II[13,14], but its specific molecular mechanism needs to be further explored. We confirmed that carvedilol could inhibit Ang II-induced HSC proliferation and contraction and improve liver fibrosis in mice[12]. The study also indicated that HSCs are the main cells expressing ACE2 in the liver. In addition, our study demonstrated that carvedilol could notably reduce HSC autophagy and inhibit HSC activation and proliferation[15]. It has been reported that ACE2 alleviates the severity of acute lung injury by inhibiting autophagy[16]. Therefore, we hypothesized that ACE2 could inhibit HSC activation and proliferation by regulating autophagy, thus improving hepatic sinusoidal remodeling and ultimately alleviating liver fibrosis and portal hypertension.

The Adenosine monophosphate activates protein kinases (AMPK)/mammalian target of rapamycin (mTOR) signaling pathway is not only an important node in the intracellular energy metabolism monitoring system but also an important upstream pathway regulating autophagy. Studies have reported that ACE2 can improve vascular endothelial dysfunction in type 2 diabetic rats with insulin resistance by regulating the AMPK/mTOR pathway[17]. In addition, ACE2 was shown to effectively modulate the AMPK/mTOR signaling pathway in a mouse model of acute lung injury[16]. Our previous study confirmed that metformin could inhibit HSC proliferation, migration and angiogenesis through the Akt/mTOR and mTOR/hypoxia inducible factor-1α (HIF-1α) pathways[18]. In this study, we evaluated the effect of ACE2 on liver fibrosis in mice and demonstrated the molecular mechanism by which ACE2 regulates HSC autophagy through the AMPK/mTOR pathway to improve liver fibrosis and hepatic sinusoidal remodeling.

The aim of this study was to determine the effect of ACE2 on HSC activation, proliferation, apoptosis and liver fibrosis by regulating autophagy. This study will provide a new direction for the prevention and targeted treatment of liver fibrosis and portal hypertension.

MATERIALS AND METHODS

Mouse model of liver fibrosis

Forty adult male C57BL/6J mice (6-8 wk, 18-20 g) were purchased from the Experimental Animal Center of Shandong University (Jinan, China). The mice were housed in an air-conditioned room at a defined temperature (23-25 °C) for one week prior to the initiation of the experiments. All experimental protocols were approved by the Animal Care Committee of the Second Hospital, Cheeloo College of Medicine, Shandong University.

The liver fibrosis mouse model was established by intraperitoneal injection of carbon tetrachloride (CCl_4, 20%, 0.5 mL/100 g) twice a week for 8 wk. To evaluate the effect of ACE2 on liver fibrosis, the liver-specific recombinant adeno-associated viral vector rAAV-ACE2 (rAAV2/8-ACE2) was injected into the tail vein 4 wk after CCl_4 administration. Mice were randomly assigned to four groups (10 in each): Group 1, normal control (olive oil); Group 2, CCl_4-induced liver fibrosis (CCl_4); Group 3, rAAV2/8-ACE2 + CCl_4; and Group 4, rAAV2/8-ACE2 + CCl_4 + rapamycin (mTOR inhibitor). Rapamycin (2 mg/kg) was administered at the 6th week after the intraperitoneal injection of CCl_4.

The mice were dissected after anesthesia administration, and liver tissues were removed and partially stored at -80 °C. Another section was fixed in 4% paraformaldehyde and embedded in paraffin.

Cytokine Enzyme Linked Immunosorbent Assay and Luminex analysis

Mouse blood samples were centrifuged at 4 °C (3000 rpm) for 10 min, and the supernatant was collected. According to the manufacturer's instructions, the serum levels of platelet-derived growth factor BB (PDGF-BB), angiopoietin-2, vascular endothelial growth factor (VEGF), interleukin (IL)-10, Ang II and Ang- (1-7) were measured using Luminex multifactor assay kits and Enzyme Linked Immunosorbent Assay kits. The data were analyzed using Graph Pad Prism 8.0.

Histopathological evaluation

The paraffin-embedded liver tissue sections were morphologically evaluated based on hematoxylin and eosin (H&E) staining. The degree of liver fibrosis in mice was measured by Masson trichrome and Sirius red staining. According to the METAVIR scale, the degree of liver fibrosis was divided into four stages from 0 to 4 (0 - No fibrosis; 1 - Portal fibrosis; 2 - Periportal fibrosis; 3 - Bridging fibrosis; 4 - Cirrhosis). The quantity of collagen production in each group after Sirius red staining was analyzed using Image-Pro Plus 6.0 software.

Immunohistochemical staining

Liver tissue sections were deparaffinized, serially dehydrated in ethanol, and then incubated overnight with primary antibody at 4 °C after antigen retrieval. The primary antibodies used in the experiment included anti-alpha-smooth muscle actin (α-SMA) antibody (1:400, Abcam, United States), anti-fibronectin (FN) antibody (1:2000, Abcam, United States), and anti-CD31 antibody (1:2000, Abcam, United States). After incubation with the appropriate biotinylated secondary antibody for 30 min, the liver sections were stained with diaminobenzidine and hematoxylin. The positive staining areas appeared brownish yellow. The sections were observed under a light microscope, photographed, and then analyzed with Image-Pro Plus 6.0 software.

Transmission electron microscopy

Fresh liver tissue sections were immobilized in electron microscopy fixative (Servicebio, Wuhan, China) for 2 h. The specimens were then immobilized in osmic acid buffer and dehydrated in ethanol. Finally, the ultrathin sections were photographed using Transmission electron microscopy (TEM) (HT7800/HT7700, Hitachi, Tokyo, Japan) after staining with 2% uranium acetate in alcohol solution. The structure of autophagosomes in each group was observed by TEM.

Apoptosis detection by TUNEL and immunofluorescence staining

Apoptotic HSCs were localized with labeled nucleotides in TUNEL staining. The mouse liver sections were stained according to the in situ cell death detection kit (Roche, Germany) protocol. The sections were then incubated with an α-SMA primary antibody (1:500, Abcam, United States) and a CY3 goat anti-rabbit fluorescence secondary antibody (1:300, Servicebio, Wuhan, China). The nuclei were counterstained with 4',6-diamidino-2-phenylindole (DAPI) and photographed under a fluorescence microscope. The relative number of apoptotic cells in each group was analyzed using Image-Pro Plus 6.0 software.

Multicolor immunofluorescence staining

Paraffin sections of mouse liver tissue were deparaffinized, subjected to antigen retrieval, and blocked with hydrogen peroxide and serum. The primary antibody, corresponding HRP-labeled secondary antibody, and fluorescently labeled tyramine were successively added. After microwave repair treatment, the first round of primary and secondary antibodies were eluted, and the fluorescently labeled tyramine was still attached to the target. When the second and third targets were detected, the previous steps were repeated for a new round of labeling and microwave repair processing. The fourth primary antibody and 594-labeled fluorescent secondary antibody were added, and the nuclei were then counterstained with DAPI. The slides were covered with anti-fade mounting medium. Finally, images were detected and collected with a slice scanner (pannoramic, 3Dhistech, Hungary). DAPI emits blue light; Fluorescein isothiocyanate (FITC-ACE2) emits green light; 647 (Desmin) is set to pink light; 594 (LC3) is set to purplish red light. The number of positive cells for each index was analyzed using Image-Pro Plus 6.0 software.

Western blot analysis

Mouse liver tissue proteins were extracted, and the concentration of each protein was determined. Equal amounts of protein samples were subjected to electrophoresis on 8%-12% sodium dodecylsulphate polyacrylamide gel electrophoresis gels and transferred to polyvinylidene fluoride membranes. The membranes were blocked in 5% nonfat dry milk for 1 h to block nonspecific sites and then incubated with the appropriate primary antibodies at 4 °C overnight. After incubation with the secondary antibody and membrane washing, the antibody-bound proteins were detected by chemiluminescence staining using an enhanced chemiluminescence assay kit (Millipore, United States). The density of each band was analyzed with ImageJ software.

Statistical analysis

The data are expressed as mean ± SD. Statistics were analyzed using GraphPad Prism 8.0 and SPSS 19.0 software. Statistical significance was determined by one-way ANOVA followed by LSD-*t* test. For all experiments, $P < 0.05$ was considered statistically significant.

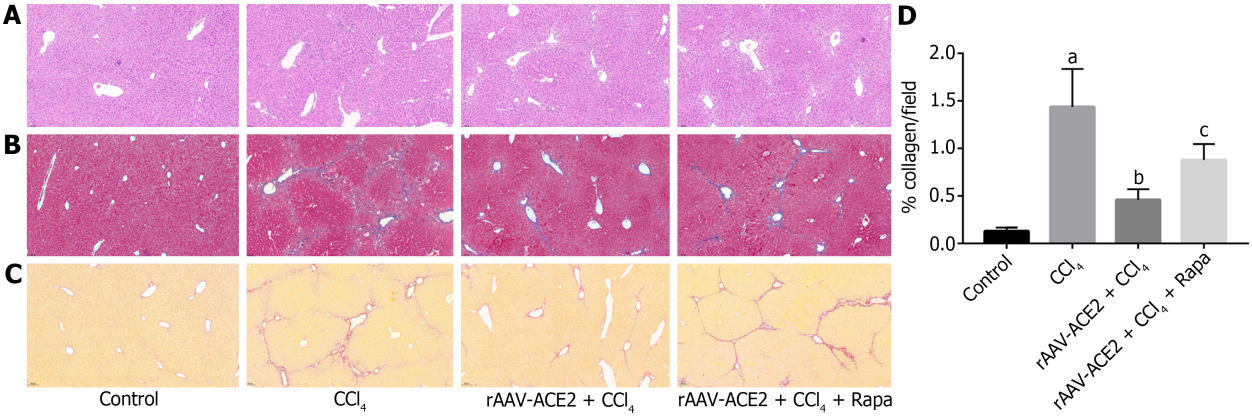
RESULTS

Effect of ACE2 on CCl_4-induced liver injury and fibrogenesis

The effect of ACE2 on CCl_4-induced liver fibrosis was evaluated by H&E (Figure 1A), Masson trichrome (Figure 1B) and Sirius red staining (Figure 1C and D). Compared with those in the control group, inflammatory cell infiltration and fibrous tissue hyperplasia in the liver tissues of mice were increased after 8 wk of CCl_4 injection (METAVIR > F2) (Figure 1A). In the CCl_4 group, the liver architecture was widely disorganized, and the hepatic sinusoids could not be distinguished. In addition, notable collagen deposition and the formation of fibrous septa bridging the portal regions were observed in the CCl_4 group. However, fibrotic tissue and inflammatory cells in the rAAV2/8-ACE2 + CCl_4 group were markedly reduced compared with those in the CCl_4 and rapamycin groups (METAVIR ≤ F2) (Figure 1B-D). Masson trichrome and Sirius red staining showed that collagen deposition was significantly increased in mice treated with CCl_4 alone ($P < 0.05$). After rAAV2/8-ACE2 treatment, the degree of collagen deposition in the perisinusoidal spaces, interlobular septum and periportal zones was reduced ($P < 0.05$) (Figure 1B-D). The results indicated that rAAV2/8-ACE2 treatment could improve liver injury and fibrosis in mice, while rapamycin treatment increased the degree of liver fibrosis compared with that in the ACE2 overexpression group. This finding suggested that mTOR inhibitor could attenuate the antifibrotic effect of rAAV2/8-ACE2.

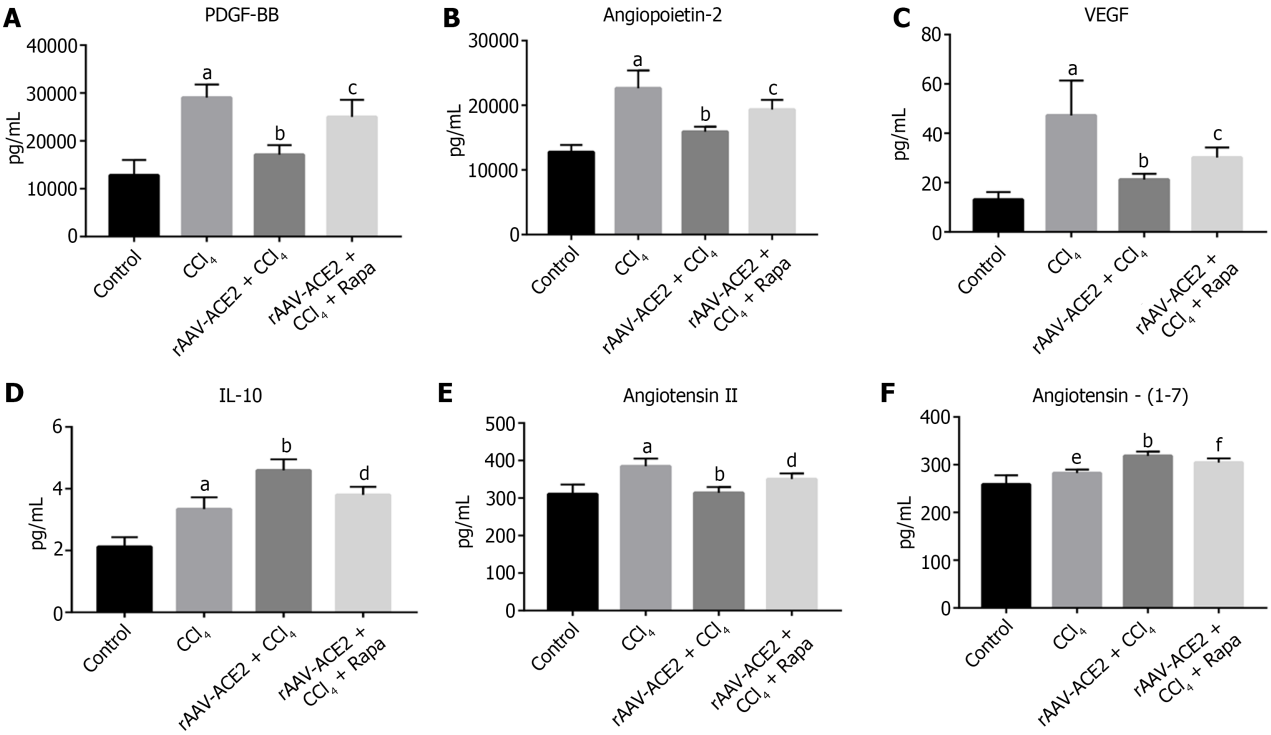
Analysis of serum biomarkers in mice with liver fibrosis

The levels of PDGF-BB, VEGF, angiopoietin-2, IL-10, Ang II and Ang- (1-7) in mouse serum were measured (Figure 2). PDGF signaling plays a vital role in HSC activation and angiogenesis[19]. VEGF and angiopoietin-2 are the most important regulators in the process of angiogenesis[20,21]. As a potential anti-inflammatory factor, IL-10 has been reported to inhibit the expression of many proinflammatory mediators[22]. The results showed that the levels of PDGF-BB, angiopoietin-2, VEGF, and Ang II in the CCl_4 group were notably higher than those in the normal control group ($P <$



DOI: 10.3748/wjg.v29.i33.4975 **Copyright** ©The Author(s) 2023.

Figure 1 Pathological changes in mouse liver tissues after rAAV-Angiotensin-converting enzyme 2 treatment (magnification × 100). A: Effect of rAAV-ACE2 treatment on liver fibrosis in mice was assessed by Hematoxylin and eosin staining; B: Effect of rAAV-ACE2 treatment on liver fibrosis in mice was assessed by Masson trichrome staining; C: Effect of rAAV-ACE2 treatment on liver fibrosis in mice was assessed by Sirius red staining; D: The quantity of collagen production in each group was analyzed using Image-Pro Plus 6.0. $^{a}P < 0.01$ *vs* Control; $^{b}P < 0.05$ *vs* CCl_4; $^{c}P < 0.05$ *vs* rAAV-ACE2 + CCl_4. Rapa: Rapamycin; ACE2: Angiotensin-converting enzyme 2.



DOI: 10.3748/wjg.v29.i33.4975 **Copyright** ©The Author(s) 2023.

Figure 2 Effect of rAAV-Angiotensin-converting enzyme 2 treatment on the levels of multiple biomarkers in mouse serum. A: The level of platelet-derived growth factor BB in each group was measured by Luminex assay; B: The level of angiopoietin-2 in each group was measured by Luminex assay; C: The level of vascular endothelial growth factor in each group was measured by Luminex assay; D: The level of interleukin-10 in each group was measured by Luminex assay; E: The level of angiotensin II in each group was measured by Enzyme Linked Immunosorbent Assay; F: The level of angiotensin- (1-7) in each group was measured by Enzyme Linked Immunosorbent Assay. $^{a}P < 0.001$ *vs* Control; $^{b}P < 0.001$ *vs* CCl_4; $^{c}P < 0.001$ *vs* rAAV-ACE2 + CCl_4; $^{d}P < 0.01$ *vs* rAAV-ACE2 + CCl_4; $^{e}P < 0.01$ *vs* Control; $^{f}P < 0.05$ *vs* rAAV-ACE2 + CCl_4. Rapa: Rapamycin; PDGF-BB: Platelet-derived growth factor BB; VEGF: Vascular endothelial growth factor; IL-10: Interleukin-10; ACE2: Angiotensin-converting enzyme 2.

0.001), and rAAV2/8-ACE2 injection reduced the expression of these cytokines ($P < 0.001$) (Figure 2A-C and E). In addition, the results demonstrated that the levels of IL-10 and Ang- (1-7) were higher in the rAAV2/8-ACE2 group than in the CCl_4 group ($P < 0.001$, $P < 0.001$), while rapamycin decreased the expression levels of these two cytokines ($P < 0.01$, $P < 0.05$) (Figure 2D and F). The results indicated that rAAV2/8-ACE2 treatment could inhibit HSC activation and angiogenesis in mice with liver fibrosis.

Effect of ACE2 on HSC activation and apoptosis

Effect of rAAV-ACE2 treatment on the expression of α-SMA, FN and CD31 in CCl_4-induced fibrotic mice was evaluated by immunohistochemistry staining (Figure 3A-C). α-SMA is a typical marker of HSC activation and proliferation. In the immunohistochemistry staining, α-SMA positive cells were distributed along the endothelium of hepatic sinusoids in the liver tissues of CCl_4-induced fibrotic mice. The number of α-SMA positive cells in the rAAV2/8-ACE2 treatment group was notably lower than that in the CCl_4 and rapamycin groups ($P < 0.05$, $P < 0.01$) (Figure 3A and D).

FN is the primary protein constituting the basement membrane, and CD31 is commonly used as a vascular endothelial marker. These proteins are rarely expressed in normal liver tissues. Immunohistochemical staining revealed that the expression of these proteins was increased in the CCl_4-induced liver fibrosis group ($P < 0.001$, $P < 0.001$) and decreased in the rAAV2/8-ACE2 treatment group ($P < 0.001$, $P < 0.001$). However, rapamycin increased the protein expression of FN and CD31 ($P < 0.01$, $P < 0.01$) (Figure 3B, C, E and F).

TUNEL and immunofluorescence staining were used to detect the number of apoptotic HSCs. Our results demonstrated that there were more apoptotic HSCs in the rAAV2/8-ACE2 treatment group than in the CCl_4 and rapamycin groups ($P < 0.05$, $P < 0.05$) (Figure 4).

The results showed that ACE2 overexpression inhibited HSC activation and induced HSC apoptosis in fibrotic mouse liver tissues, while the mTOR inhibitor attenuated the effect of rAAV2/8-ACE2 on HSCs.

Effect of ACE2 on HSC autophagy in mice

To further verify the effect of ACE2 on autophagy in liver fibrosis, a large number of autophagosomes were detected by ultrastructural analysis in the HSCs of mice in the CCl_4 group. TEM analysis showed that rAAV2/8-ACE2 injection decreased the number of autophagosomes in HSCs compared with that in the CCl_4 group ($P < 0.05$). However, autophagosomes were increased in the rAAV2/8-ACE2 + CCl_4 + rapamycin group ($P < 0.01$) (Figure 5A and B). The results of multicolor immunofluorescence staining demonstrated that the expression of the ACE2 protein was increased after rAAV2/8-ACE2 injection, and the expression of the autophagy protein LC3 was decreased compared with that in the CCl_4 group ($P < 0.01$). Treatment with rapamycin attenuated the inhibitory effect of ACE2 on LC3 protein expression ($P < 0.05$) (Figure 5C and D). These results suggested that ACE2 overexpression could reduce HSC activation and liver fibrosis by inhibiting HSC autophagy.

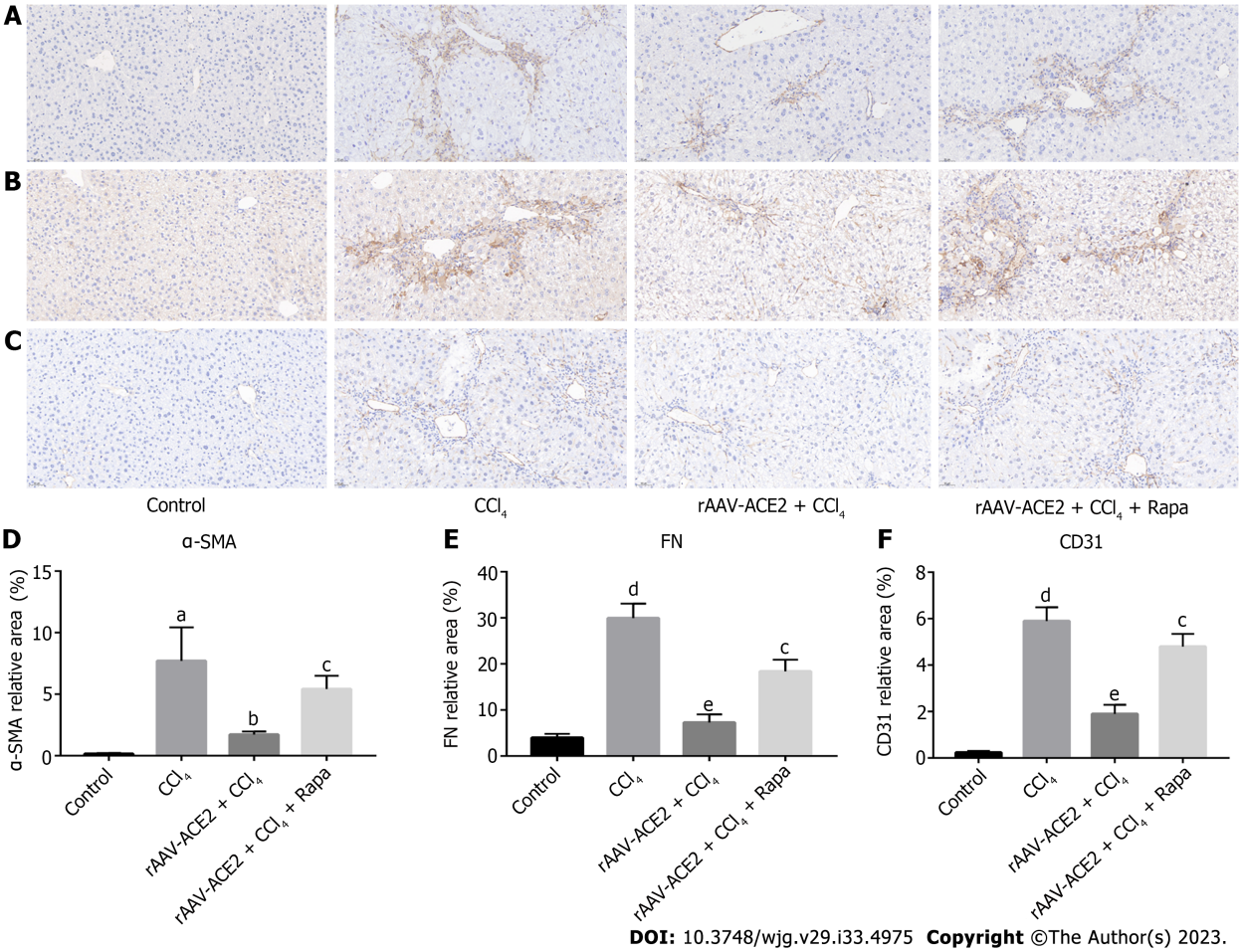
Effect of ACE2 on HSC autophagy and AMPK pathway proteins in mouse liver tissues

Autophagy is regulated by numerous autophagy-related genes, such as LC3 and Beclin-1. LC3II is a marker protein on the autophagosome membrane and is often considered an indicator of autophagy formation. As an autophagy-specific substrate, p62 interacts with LC3 to infiltrate into autophagosomes and is efficiently degraded by autophagolysosomes [23]. To determine the effect of ACE2 on HSC autophagy, we detected the expression of HSC autophagy-related indicators (LC3I, LC3II, Beclin-1) in the liver tissues of mice in each group by western blotting. Moreover, we verified the correlation of ACE2 with autophagy and the AMPK pathway by assessing the expression of AMPK pathway-related proteins (AMPK, p-AMPK, p-mTOR) and autophagy-related proteins (LC3I, LC3II, Beclin-1) in mouse liver tissues (Figure 6A and B). Compared with that in the control group, the p-AMPK/AMPK ratio was higher in the CCl_4 group ($P < 0.01$). However, the ratio of p-AMPK/AMPK in the rAAV2/8-ACE2-treated group was dramatically lower than that in the CCl_4 group ($P < 0.05$) (Figure 6A and C). In contrast, p-mTOR levels in mice in the rAAV2/8-ACE2-treated group were significantly higher than those in the CCl_4 group ($P < 0.01$) (Figure 6A and D). In addition, the results indicated that the protein levels of Beclin-1 and LC3II in the rAAV2/8-ACE2 + CCl_4 group were markedly reduced compared to those in the CCl_4 alone group ($P < 0.001$, $P < 0.05$) (Figure 6B, E and F). The m-TOR inhibitor (rapamycin) affected mTOR phosphorylation and the level of autophagy proteins in liver tissues. The present study showed that rapamycin abolished the effect of rAAV2/8-ACE2 on the expression of the autophagy proteins LC3I, LC3II and Beclin-1. Compared with those in the rAAV2/8-ACE2 group, the relative Beclin-1 and LC3II levels were increased by rapamycin treatment ($P < 0.05$, $P < 0.05$) (Figure 6B, E and F). The western blot results showed that ACE2 overexpression could inhibit the expression of autophagy-related proteins in mouse liver tissues through the AMPK/mTOR pathway.

DISCUSSION

Liver fibrosis has high morbidity and mortality worldwide, and it is a compensatory response to liver inflammation and injury caused by multiple pathogenic factors[24]. In liver fibrosis, excess fibrous ECM proteins, such as collagens I and III, are deposited in the Disse space of the hepatic sinusoids[25]. Changes in ECM composition induce LSECs to lose their fenestrae and form a basement membrane, a process known as hepatic sinusoidal capillarization[26]. The activation of HSCs plays a crucial role in the process of liver fibrosis. Upon activation due to liver injury, quiescent HSCs lose their retinoid droplets, exhibit increased α-SMA expression, and release large amounts of ECM, ultimately resulting in liver fibrosis[27].

ACE2 is expressed in human alveolar epithelial cells, esophageal epithelial cells, small intestinal epithelial cells, and vascular endothelial cells[28]. Our present study found that ACE2 was also expressed in liver HSCs. In recent years, the coronavirus disease 2019 (COVID-19) virus [severe acute respiratory syndrome coronavirus 2 (SARS-CoV-2)] that caused the outbreak has been proven to invade human alveolar epithelial cells mainly through ACE2[29]. SARS-CoV-2 infection can reduce ACE2 activity, leading to an imbalance in Ang II/ACE2 regulation[30]. ACE2, which is the main target receptor for SARS-CoV-2 invasion into the human body, is currently a research hotspot. A global registry study suggested that patients with chronic liver disease and cirrhosis had higher mortality after being infected with COVID-19[31]. The



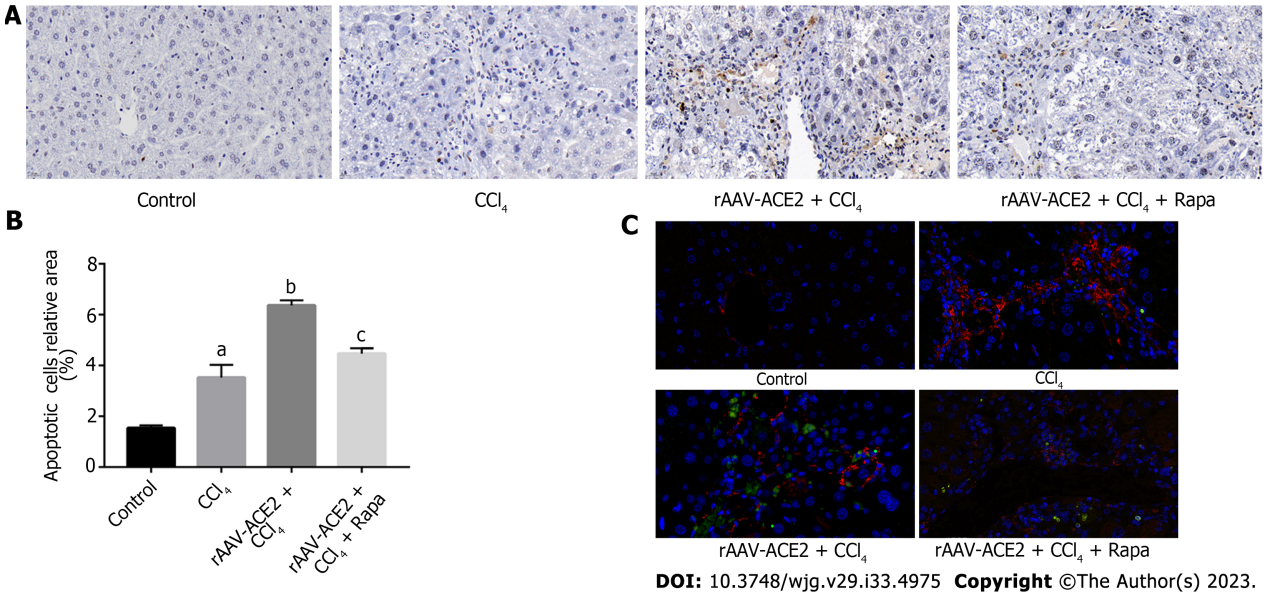
DOI: 10.3748/wjg.v29.i33.4975 **Copyright** ©The Author(s) 2023.

Figure 3 Effect of rAAV-Angiotensin-converting enzyme 2 treatment on the expression of Alpha-smooth muscle actin, Fibronectin and CD31 in CCl_4-induced fibrotic mice was evaluated by immunohistochemistry staining (magnification × 200). A: The expression level of Alpha-smooth muscle actin in the liver tissues of each group was detected; B: The expression level of Fibronectin in the liver tissues of each group was detected; C: The expression level of CD31 in the liver tissues of each group was detected; D-F: The relative expression levels of the three proteins in each group were analyzed using Image-Pro Plus 6.0. $^{a}P < 0.01$ *vs* Control; $^{b}P < 0.05$ *vs* CCl_4; $^{c}P < 0.01$ *vs* rAAV-ACE2 + CCl_4; $^{d}P < 0.001$ *vs* Control; $^{e}P < 0.001$ *vs* CCl_4. Rapa: Rapamycin; α-SMA: Alpha-smooth muscle actin; FN: Fibronectin; ACE2: Angiotensin-converting enzyme 2.

baseline liver disease severity of patients with chronic liver disease and cirrhosis is closely related to the COVID-19-related incidence rates and mortality. Therefore, SARS-CoV-2 infection may exacerbate the degree of cirrhosis and portal hypertension in patients with chronic liver disease by reducing the activity of ACE2 in the liver.

ACE2 is an endogenous negative regulator that acts as a RAS "brake" to limit fibrogenesis through Ang II degradation and Ang- (1-7) formation. It was reported that the degree of liver fibrosis in ACE2 knockout mice increased after 21 d of bile duct ligation or chronic CCl_4 treatment[13]. In addition to its effect on the RAS, whether ACE2 can affect liver fibrosis through other mechanisms remains unclear. In our study, a liver fibrosis model was induced by the intraperitoneal injection of CCl_4 to investigate the effect of ACE2 on liver fibrosis by inhibiting autophagy. In addition, the liver-specific recombinant adeno-associated viral vector rAAV2/8-ACE2 was used in this study. ACE2 is specifically overexpressed in the liver with minimal systemic effects. Moreover, enhanced expression and activity of liver tissue-specific ACE2 can reduce local Ang II levels, increase local Ang- (1-7) levels, and minimize off-target effects[32].

Autophagy is the process of degrading defective proteins, damaged organelles, excess lipids and other harmful components in cells to maintain cellular components and homeostasis[33]. Autophagy levels are elevated in conditions of inflammation and oxidative stress, and excessive autophagy is involved in inflammatory and liver diseases[24]. Studies have demonstrated that inhibiting autophagy in HSCs reduces lipid droplet degradation, thereby preventing cell activation[9]. Autophagosome is composed of a small portion of the cytoplasm surrounded by double membranes. The digested substances are various components contained in the cytoplasm, such as mitochondria and fragments of endoplasmic reticulum, and the contents are degraded by fusion with lysosomes. Autophagy generally refers to macroautophagy, which includes two consecutive stages of autophagosome formation and degradation[15]. It has been reported that IL-10 inhibits oxidative stress-induced HSC autophagosome formation, HSC activation and liver fibrosis through the mTOR/STAT3 signaling pathway[34]. The TEM results indicated that the number of autophagosomes in the rAAV2/8-ACE2-treated group was decreased. To explore the relationship between ACE2 and autophagy, we detected the expression of the autophagy proteins LC3I, LC3II and Beclin-1 in the liver tissues of mice in each group. The results indicated that ACE2 overexpression effectively inhibited autophagy during mouse liver fibrosis.



DOI: 10.3748/wjg.v29.i33.4975 **Copyright** ©The Author(s) 2023.

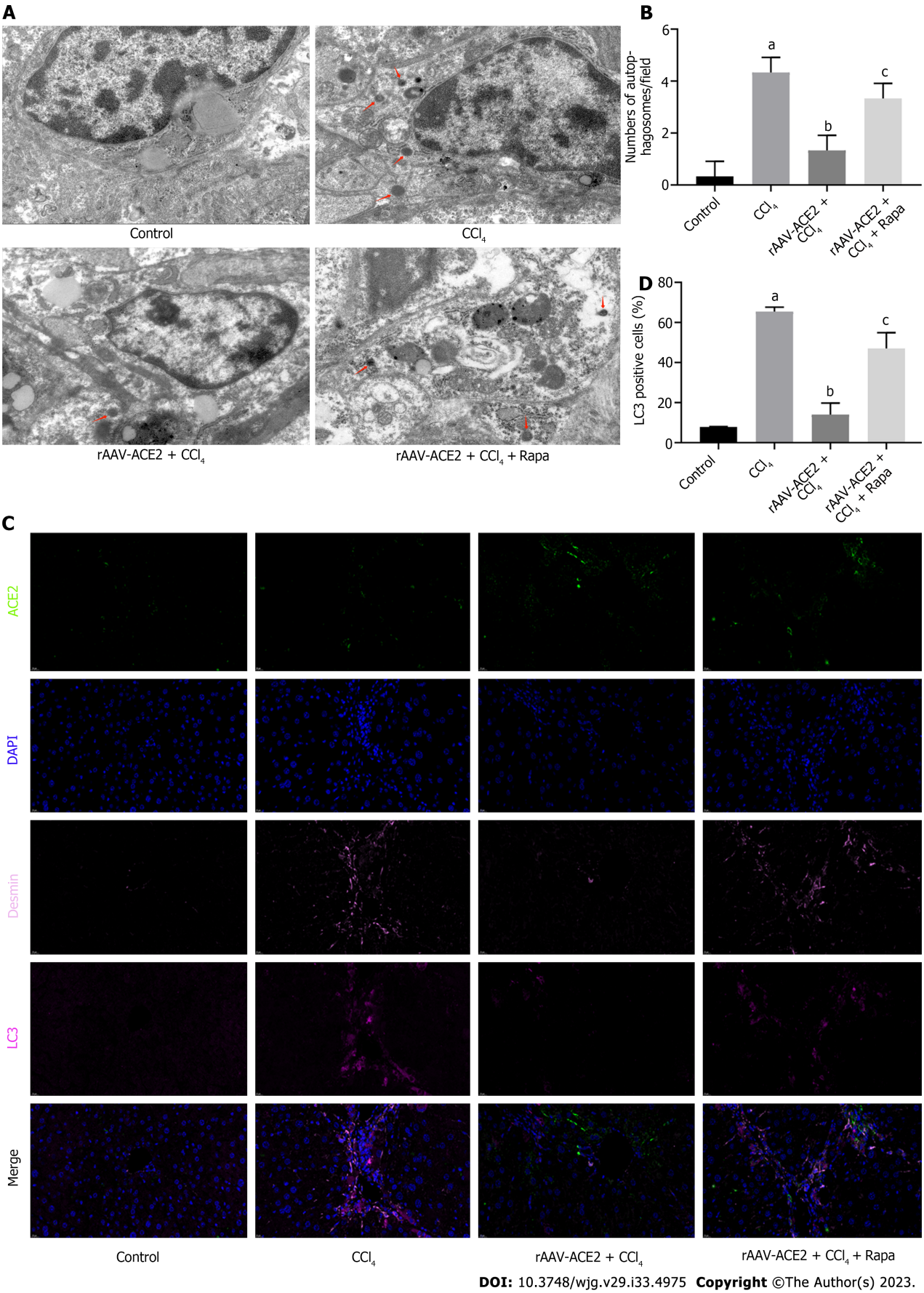
Figure 4 Effect of rAAV-Angiotensin-converting enzyme 2 treatment on hepatic stellate cell apoptosis. A: Transferase-mediated dUTP nick-end labeling (TUNEL) staining (magnification × 400); B: The relative number of apoptotic cells in each group was analyzed using Image-Pro Plus 6.0. $^{a}P < 0.05$ *vs* Control; $^{b}P < 0.05$ *vs* CCl_4; $^{c}P < 0.05$ *vs* rAAV-ACE2 + CCl_4; C: TUNEL and Alpha-smooth muscle actin (α-SMA) immunofluorescence co-localization staining (magnification × 630). The nuclei stained by DAPI were blue, FITC luciferin-labeled apoptotic cells were green, and α-SMA displayed red. Rapa: Rapamycin; ACE2: Angiotensin-converting enzyme 2; DAPI: 4',6-diamidino-2-phenylindole; FITC: Fluorescein isothiocyanate.

Autophagy regulation is intricately associated with signaling pathways such as the AMPK/mTOR pathway. AMPK can inhibit mTORC1 activity by activating the TSC1/TSC2 protein heterodimer[35,36]. mTORC1 negatively regulates the initiation of autophagy through phosphorylation at Ser757 of ULK1 upon activation[36]. Compared with that in the CCl_4 group, the p-AMPK/AMPK ratio was decreased ($P < 0.05$), while the relative expression of p-mTOR was increased in the rAAV2/8-ACE2 group ($P < 0.01$). The results showed that ACE2 overexpression could influence the AMPK/mTOR signaling pathway. We treated mice with an m-TOR inhibitor (rapamycin), which effectively inhibited m-TOR phosphorylation. The findings of the study indicated that ACE2 overexpression could inhibit HSC autophagy in mouse liver tissues through the AMPK/mTOR pathway. The results suggested that the AMPK/mTOR signaling pathway was an important node for ACE2 to regulate HSC autophagy.

Pathological staining showed the successful establishment of a mouse model of liver fibrosis after 8 wk of intraperitoneal injection of CCl_4. rAAV2/8-ACE2 injection alleviated collagen deposition and fibrosis in the liver tissues of mice. We further investigated the mechanism by which ACE2 overexpression alleviated liver fibrosis. When liver injury occurs, HSCs are activated and proliferate, and the demand for intracellular energy increases. At this time, blocking autophagy can impair HSC activation and fibrotic activity[10]. α-SMA is an important indicator for evaluating HSC activation and proliferation. In the present study, rAAV2/8-ACE2 injection inhibited α-SMA expression and HSC activation. In addition, apoptosis plays a vital role in the proliferation, differentiation and death of HSCs, and HSC apoptosis is the key to reversing liver fibrosis[37]. TUNEL and immunofluorescence staining showed that rAAV2/8-ACE2 injection increased HSC apoptosis. Our previous study demonstrated a complex relationship between autophagy and apoptosis, and the inhibition of autophagy could induce HSC apoptosis[15]. Therefore, our findings indicated that ACE2 overexpression could alleviate liver fibrosis by regulating autophagy to inhibit HSC activation and promote apoptosis.

Intrahepatic angiogenesis and sinusoidal remodeling play an important role in the development of hepatic fibrosis and portal hypertension[38]. The inhibition of pathological angiogenesis can alleviate liver fibrosis. LSEC capillarization is associated with the accumulation of interstitial collagen in the Disse space of hepatic sinusoids and is the main pathological change in liver fibrosis[26]. The reversal of LSEC capillarization has been reported to promote HSC quiescence[39]. During cirrhosis, angiogenesis-related cytokines and receptors expressed in HSCs, such as VEGF, PDGF, and angiopoietin, can induce HSC migration, angiogenesis, and collagen production[40]. Our study demonstrated that the levels of VEGF, angiopoietin-2 and PDGF-BB were elevated in liver fibrosis, resulting in increased angiogenesis. rAAV2/8-ACE2 injection inhibited the expression levels of these angiogenesis-related factors. Therefore, the results indicated that ACE2 overexpression could effectively attenuate intrahepatic angiogenesis, thus alleviating hepatic sinusoidal resistance.

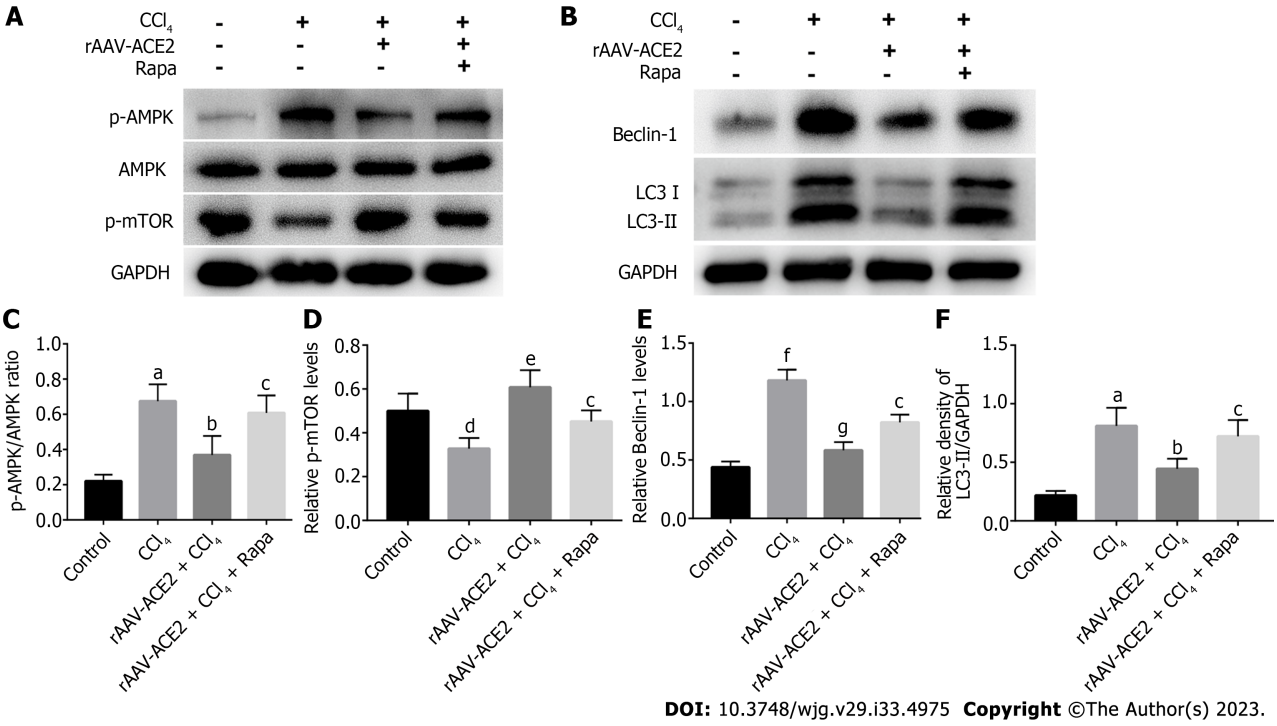
In the present study, adeno-associated viral vector technology, pathological staining, multifactor analysis, multicolor immunofluorescence staining, TEM and other advanced techniques were used to comprehensively explore the relationship and mechanism among ACE2, autophagy and liver fibrosis. However, there are still some limitations of this study. Whether ACE2 affects HSC autophagy and liver fibrosis through other pathways needs to be further explored. This study provides a new theoretical basis for the targeted treatment of liver fibrosis and portal hypertension, and its clinical application needs further research.



DOI: 10.3748/wjg.v29.i33.4975 **Copyright** ©The Author(s) 2023.

Figure 5 Effect of rAAV-Angiotensin-converting enzyme 2 administration on hepatic stellate cell autophagy in mouse liver tissues. A: Effect of rAAV-ACE2 administration on hepatic stellate cell autophagosome formation in CCl_4-induced fibrotic mice was observed by Transmission electron microscopy (magnification × 7000). As shown, red arrows indicated autophagosomes; B: The number of autophagosomes in each group was quantified. $^aP < 0.01$ *vs*

Control; [b]*P* < 0.05 *vs* CCl_4; [c]*P* < 0.01 *vs* rAAV-ACE2 + CCl_4; C: Effect of rAAV-ACE2 administration on the expression of autophagy protein LC3. Multicolor immunofluorescence staining for ACE2 (green), autophagic LC3 (Purplish red), desmin (pink), nuclear DAPI (blue), and merged signals in mouse liver tissues (magnification × 400); D: The number of LC3 positive cells in each group was analyzed using Image-Pro Plus 6.0 software. [a]*P* < 0.001 *vs* Control; [b]*P* < 0.01 *vs* CCl_4; [c] *P* < 0.05 *vs* rAAV-ACE2 + CCl_4. Rapa: Rapamycin; DAPI: 4',6-diamidino-2-phenylindole; ACE2: Angiotensin-converting enzyme 2.



DOI: 10.3748/wjg.v29.i33.4975 **Copyright** ©The Author(s) 2023.

Figure 6 Effect of rAAV-Angiotensin-converting enzyme 2 treatment on the expression of adenosine monophosphate activates protein kinases signaling pathway proteins and autophagy-related proteins in mouse liver tissues. A: The expression levels of p-AMPK, AMPK and p-mTOR were detected by western blotting; B: The expression levels of autophagy markers Beclin-1, LC3I and LC3II were detected by western blotting; C-F: The relative protein levels in each group were analyzed using ImageJ. [a]*P* < 0.01 *vs* Control; [b]*P* < 0.05 *vs* CCl_4; [c]*P* < 0.05 *vs* rAAV-ACE2 + CCl_4; [d]*P* < 0.05 *vs* Control; [e]*P* < 0.01 *vs* CCl_4; [f]*P* < 0.001 *vs* Control; [g]*P* < 0.001 *vs* CCl_4. Rapa: Rapamycin; p-mTOR: p-mammalian target of rapamycin; AMPK: Adenosine monophosphate activates protein kinases; ACE2: Angiotensin-converting enzyme 2.

CONCLUSION

In summary, the study indicates that autophagy plays a crucial role in HSC activation and liver fibrosis. ACE2 overexpression can inhibit HSC activation and promote apoptosis by regulating HSC autophagy, thereby alleviating liver fibrosis and hepatic sinusoidal remodeling. Our study also demonstrates that the AMPK/mTOR pathway is involved in the effect of ACE2 on autophagy. This study may provide new ideas for exploring the molecular mechanism by which ACE2 inhibits liver fibrosis and hepatic sinusoidal remodeling.

ARTICLE HIGHLIGHTS

Research background

Liver cirrhosis is a hallmark of end-stage chronic liver disease, which leads to millions of deaths each year. At present, the treatment options for liver fibrosis and cirrhosis are limited and often ineffective. Angiotensin-converting enzyme 2 (ACE2)-driven protective renin-angiotensin system (RAS) provides an effective therapeutic target for liver fibrosis. In addition, the study of liver fibrosis targeting hepatic stellate cell (HSC) autophagy has attracted more and more attention.

Research motivation

In addition to its effect on the RAS, whether ACE2 can affect liver fibrosis through other mechanisms remains unclear. Moreover, how to enhance the expression and activity of tissue-specific ACE2 to avoid its potential off-target effect is a problem to be solved. Using a suitable and efficient gene delivery system to achieve tissue-specific overexpression of ACE2 has pointed out a new direction for the targeted treatment of liver fibrosis.

Research objectives
The aim of this study is to determine the effect of ACE2 on HSC activation, proliferation, apoptosis and liver fibrosis by regulating autophagy. This study provides new ideas for exploring the molecular mechanism by which ACE2 inhibits liver fibrosis and hepatic sinusoidal remodeling.

Research methods
In this study, a mouse model of liver fibrosis was constructed, and adeno-associated viral vector technology, pathological staining, multifactor analysis, multicolor immunofluorescence staining, transmission electron microscopy, TUNEL apoptosis assays, western blot analysis and other experimental methods were used to comprehensively explore the relationship and mechanism among ACE2, autophagy and liver fibrosis.

Research results
In vivo experiments showed that rAAV2/8-ACE2 treatment could inhibit HSC activation and angiogenesis, induce HSC apoptosis, and alleviate HSC proliferation and liver fibrosis by inhibiting HSC autophagy. This study also demonstrated that ACE2 overexpression could inhibit HSC autophagy in mouse liver tissues through the Adenosine monophosphate activates protein kinases (AMPK)/mammalian target of rapamycin (mTOR) pathway. The completion of this study provides new ideas for the prevention and targeted treatment of liver fibrosis and portal hypertension.

Research conclusions
The study demonstrates that autophagy plays a crucial role in HSC activation and liver fibrosis. ACE2 overexpression can inhibit HSC activation and promote apoptosis by regulating HSC autophagy through the AMPK/mTOR pathway, thereby alleviating liver fibrosis and hepatic sinusoidal remodeling.

Research perspectives
The pathogenesis of liver fibrosis and cirrhosis is a complex process involving the interaction of various growth factors, cytokines, and vasoactive substances. We need further clinical research to improve patient treatment outcomes through advanced technologies such as drug carrier-targeted HSC-specific therapies.

FOOTNOTES

Author contributions: Wu Y, Xu WH, and Zhang CQ designed and coordinated the study; Wu Y, Sun JT, and Yin AH performed the experiments, acquired and analyzed data; Xu WH and Zhang CQ interpreted the data; Wu Y wrote the manuscript; All authors have read and approved the final manuscript.

Supported by Shandong Provincial Natural Science Foundation, No. ZR2021MH389.

Institutional animal care and use committee statement: All animal experiments conformed to the internationally accepted principles for the care and use of laboratory animals, NO. KYLL-2021 (KJ) A-0062, The Institutional Animal Care Committee of the Second Hospital, Cheeloo College of Medicine, Shandong University.

Conflict-of-interest statement: All the authors report no relevant conflicts of interest for this article.

Data sharing statement: No additional data are available.

ARRIVE guidelines statement: The authors have read the ARRIVE Guidelines, and the manuscript was prepared and revised according to the ARRIVE Guidelines.

Open-Access: This article is an open-access article that was selected by an in-house editor and fully peer-reviewed by external reviewers. It is distributed in accordance with the Creative Commons Attribution NonCommercial (CC BY-NC 4.0) license, which permits others to distribute, remix, adapt, build upon this work non-commercially, and license their derivative works on different terms, provided the original work is properly cited and the use is non-commercial. See: https://creativecommons.org/Licenses/by-nc/4.0/

Country/Territory of origin: China

ORCID number: Ying Wu 0000-0002-7813-7862; Ai-Hong Yin 0009-0002-4442-8343; Jun-Tao Sun 0009-0006-9448-6882; Wei-Hua Xu 0009-0002-2567-4063; Chun-Qing Zhang 0000-0001-8711-1579.

S-Editor: Li L
L-Editor: A
P-Editor: Cai YX

REFERENCES

1 **García-Pagán JC**, Gracia-Sancho J, Bosch J. Functional aspects on the pathophysiology of portal hypertension in cirrhosis. *J Hepatol* 2012; **57**: 458-461 [PMID: 22504334 DOI: 10.1016/j.jhep.2012.03.007]

2 **Deleve LD**, Wang X, Guo Y. Sinusoidal endothelial cells prevent rat stellate cell activation and promote reversion to quiescence. *Hepatology* 2008; **48**: 920-930 [PMID: 18613151 DOI: 10.1002/hep.22351]

3 **Coulon S**, Heindryckx F, Geerts A, Van Steenkiste C, Colle I, Van Vlierberghe H. Angiogenesis in chronic liver disease and its complications. *Liver Int* 2011; **31**: 146-162 [PMID: 21073649 DOI: 10.1111/j.1478-3231.2010.02369.x]

4 **Kisseleva T**. The origin of fibrogenic myofibroblasts in fibrotic liver. *Hepatology* 2017; **65**: 1039-1043 [PMID: 27859502 DOI: 10.1002/hep.28948]

5 **Mimche PN**, Lee CM, Mimche SM, Thapa M, Grakoui A, Henkemeyer M, Lamb TJ. EphB2 receptor tyrosine kinase promotes hepatic fibrogenesis in mice *via* activation of hepatic stellate cells. *Sci Rep* 2018; **8**: 2532 [PMID: 29416088 DOI: 10.1038/s41598-018-20926-9]

6 **Thabut D**, Shah V. Intrahepatic angiogenesis and sinusoidal remodeling in chronic liver disease: new targets for the treatment of portal hypertension? *J Hepatol* 2010; **53**: 976-980 [PMID: 20800926 DOI: 10.1016/j.jhep.2010.07.004]

7 **Hazari Y**, Bravo-San Pedro JM, Hetz C, Galluzzi L, Kroemer G. Autophagy in hepatic adaptation to stress. *J Hepatol* 2020; **72**: 183-196 [PMID: 31849347 DOI: 10.1016/j.jhep.2019.08.026]

8 **Ueno T**, Komatsu M. Autophagy in the liver: functions in health and disease. *Nat Rev Gastroenterol Hepatol* 2017; **14**: 170-184 [PMID: 28053338 DOI: 10.1038/nrgastro.2016.185]

9 **Hernández-Gea V**, Friedman SL. Autophagy fuels tissue fibrogenesis. *Autophagy* 2012; **8**: 849-850 [PMID: 22617442 DOI: 10.4161/auto.19947]

10 **Hernández-Gea V**, Ghiassi-Nejad Z, Rozenfeld R, Gordon R, Fiel MI, Yue Z, Czaja MJ, Friedman SL. Autophagy releases lipid that promotes fibrogenesis by activated hepatic stellate cells in mice and in human tissues. *Gastroenterology* 2012; **142**: 938-946 [PMID: 22240484 DOI: 10.1053/j.gastro.2011.12.044]

11 **Seki E**, Brenner DA. Recent advancement of molecular mechanisms of liver fibrosis. *J Hepatobiliary Pancreat Sci* 2015; **22**: 512-518 [PMID: 25869468 DOI: 10.1002/jhbp.245]

12 **Wu Y**, Li Z, Wang S, Xiu A, Zhang C. Carvedilol Inhibits Angiotensin II-Induced Proliferation and Contraction in Hepatic Stellate Cells through the RhoA/Rho-Kinase Pathway. *Biomed Res Int* 2019; **2019**: 7932046 [PMID: 31828132 DOI: 10.1155/2019/7932046]

13 **Osterreicher CH**, Taura K, De Minicis S, Seki E, Penz-Osterreicher M, Kodama Y, Kluwe J, Schuster M, Oudit GY, Penninger JM, Brenner DA. Angiotensin-converting-enzyme 2 inhibits liver fibrosis in mice. *Hepatology* 2009; **50**: 929-938 [PMID: 19650157 DOI: 10.1002/hep.23104]

14 **Mak KY**, Chin R, Cunningham SC, Habib MR, Torresi J, Sharland AF, Alexander IE, Angus PW, Herath CB. ACE2 Therapy Using Adeno-associated Viral Vector Inhibits Liver Fibrosis in Mice. *Mol Ther* 2015; **23**: 1434-1443 [PMID: 25997428 DOI: 10.1038/mt.2015.92]

15 **Meng D**, Li Z, Wang G, Ling L, Wu Y, Zhang C. Carvedilol attenuates liver fibrosis by suppressing autophagy and promoting apoptosis in hepatic stellate cells. *Biomed Pharmacother* 2018; **108**: 1617-1627 [PMID: 30372864 DOI: 10.1016/j.biopha.2018.10.005]

16 **Zhang X**, Zheng J, Yan Y, Ruan Z, Su Y, Wang J, Huang H, Zhang Y, Wang W, Gao J, Chi Y, Lu X, Liu Z. Angiotensin-converting enzyme 2 regulates autophagy in acute lung injury through AMPK/mTOR signaling. *Arch Biochem Biophys* 2019; **672**: 108061 [PMID: 31356776 DOI: 10.1016/j.abb.2019.07.026]

17 **Wang Y**, Rijal B, Xu M, Li Z, An Y, Zhang F, Lu C. Renal denervation improves vascular endothelial dysfunction by inducing autophagy *via* AMPK/mTOR signaling activation in a rat model of type 2 diabetes mellitus with insulin resistance. *Acta Diabetol* 2020; **57**: 1227-1243 [PMID: 32488498 DOI: 10.1007/s00592-020-01532-6]

18 **Li Z**, Ding Q, Ling LP, Wu Y, Meng DX, Li X, Zhang CQ. Metformin attenuates motility, contraction, and fibrogenic response of hepatic stellate cells *in vivo* and *in vitro* by activating AMP-activated protein kinase. *World J Gastroenterol* 2018; **24**: 819-832 [PMID: 29467552 DOI: 10.3748/wjg.v24.i7.819]

19 **Greuter T**, Shah VH. Hepatic sinusoids in liver injury, inflammation, and fibrosis: new pathophysiological insights. *J Gastroenterol* 2016; **51**: 511-519 [PMID: 26939970 DOI: 10.1007/s00535-016-1190-4]

20 **Fernandez M**. Molecular pathophysiology of portal hypertension. *Hepatology* 2015; **61**: 1406-1415 [PMID: 25092403 DOI: 10.1002/hep.27343]

21 **An YA**, Sun K, Joffin N, Zhang F, Deng Y, Donzé O, Kusminski CM, Scherer PE. Angiopoietin-2 in white adipose tissue improves metabolic homeostasis through enhanced angiogenesis. *Elife* 2017; **6** [PMID: 28355132 DOI: 10.7554/eLife.24071]

22 **Choi JS**, Jeong IS, Park YJ, Kim SW. HGF and IL-10 expressing ALB::GFP reporter cells generated from iPSCs show robust anti-fibrotic property in acute fibrotic liver model. *Stem Cell Res Ther* 2020; **11**: 332 [PMID: 32746905 DOI: 10.1186/s13287-020-01745-0]

23 **Klionsky DJ**, Abdel-Aziz AK, Abdelfatah S, Abdellatif M, Abdoli A, Abel S, Abeliovich H, Abildgaard MH, Abudu YP, Acevedo-Arozena A, Adamopoulos IE, Adeli K, Adolph TE, Adornetto A, Aflaki E, Agam G, Agarwal A, Aggarwal BB, Agnello M, Agostinis P, Agrewala JN, Agrotis A, Aguilar PV, Ahmad ST, Ahmed ZM, Ahumada-Castro U, Aits S, Aizawa S, Akkoc Y, Akoumianaki T, Akpinar HA, Al-Abd AM, Al-Akra L, Al-Gharaibeh A, Alaoui-Jamali MA, Alberti S, Alcocer-Gómez E, Alessandri C, Ali M, Alim Al-Bari MA, Aliwaini S, Alizadeh J, Almacellas E, Almasan A, Alonso A, Alonso GD, Altan-Bonnet N, Altieri DC, Álvarez ÉMC, Alves S, Alves da Costa C, Alzaharna MM, Amadio M, Amantini C, Amaral C, Ambrosio S, Amer AO, Ammanathan V, An Z, Andersen SU, Andrabi SA, Andrade-Silva M, Andres AM, Angelini S, Ann D, Anozie UC, Ansari MY, Antas P, Antebi A, Antón Z, Anwar T, Apetoh L, Apostolova N, Araki T, Araki Y, Arasaki K, Araújo WL, Araya J, Arden C, Arévalo MA, Arguelles S, Arias E, Arikkath J, Arimoto H, Ariosa AR, Armstrong-James D, Arnauné-Pelloquin L, Aroca A, Arroyo DS, Arsov I, Artero R, Asaro DML, Aschner M, Ashrafizadeh M, Ashur-Fabian O, Atanasov AG, Au AK, Auberger P, Auner HW, Aurelian L, Autelli R, Avagliano L, Ávalos Y, Aveic S, Aveleira CA, Avin-Wittenberg T, Aydin Y, Ayton S, Ayyadevara S, Azzopardi M, Baba M, Backer JM, Backues SK, Bae DH, Bae ON, Bae SH, Baehrecke EH, Baek A, Baek SH, Bagetta G, Bagniewska-Zadworna A, Bai H, Bai J, Bai X, Bai Y, Bairagi N, Baksi S, Balbi T, Baldari CT, Balduini W, Ballabio A, Ballester M, Balazadeh S, Balzan R, Bandopadhyay R, Banerjee S, Bánréti Á, Bao Y, Baptista MS, Baracca A, Barbati C, Bargiela A, Barilà D, Barlow PG, Barmada SJ, Barreiro E, Barreto GE, Bartek J, Bartel B, Bartolome A, Barve GR, Basagoudanavar SH, Bassham DC, Bast RC Jr, Basu A, Batoko H, Batten I, Baulieu EE, Baumgarner BL, Bayry J, Beale R, Beau I, Beaumatin F, Bechara LRG, Beck GR Jr, Beers MF, Begun J, Behrends C, Behrens GMN, Bei R, Bejarano E, Bel S, Behl C, Belaid A, Belgareh-Touzé N, Bellarosa C, Belleudi F, Belló Pérez M, Bello-Morales R, Beltran JSO, Beltran S, Benbrook DM, Bendorius M, Benitez BA, Benito-Cuesta I, Bensalem J, Berchtold MW, Berezowska S, Bergamaschi D, Bergami M, Bergmann A, Berliocchi L, Berlioz-Torrent C, Bernard A, Berthoux L, Besirli CG, Besteiro S, Betin VM, Beyaert R, Bezbradica JS, Bhaskar

K, Bhatia-Kissova I, Bhattacharya R, Bhattacharya S, Bhattacharyya S, Bhuiyan MS, Bhutia SK, Bi L, Bi X, Biden TJ, Bijian K, Billes VA, Binart N, Bincoletto C, Birgisdottir AB, Bjorkoy G, Blanco G, Blas-Garcia A, Blasiak J, Blomgran R, Blomgren K, Blum JS, Boada-Romero E, Boban M, Boesze-Battaglia K, Boeuf P, Boland B, Bomont P, Bonaldo P, Bonam SR, Bonfili L, Bonifacino JS, Boone BA, Bootman MD, Bordi M, Borner C, Bornhauser BC, Borthakur G, Bosch J, Bose S, Botana LM, Botas J, Boulanger CM, Boulton ME, Bourdenx M, Bourgeois B, Bourke NM, Bousquet G, Boya P, Bozhkov PV, Bozi LHM, Bozkurt TO, Brackney DE, Brandts CH, Braun RJ, Braus GH, Bravo-Sagua R, Bravo-San Pedro JM, Brest P, Bringer MA, Briones-Herrera A, Broaddus VC, Brodersen P, Brodsky JL, Brody SL, Bronson PG, Bronstein JM, Brown CN, Brown RE, Brum PC, Brumell JH, Brunetti-Pierri N, Bruno D, Bryson-Richardson RJ, Bucci C, Buchrieser C, Bueno M, Buitrago-Molina LE, Buraschi S, Buch S, Buchan JR, Buckingham EM, Budak H, Budini M, Bultynck G, Burada F, Burgoyne JR, Burón MI, Bustos V, Büttner S, Butturini E, Byrd A, Cabas I, Cabrera-Benitez S, Cadwell K, Cai J, Cai L, Cai Q, Cairó M, Calbet JA, Caldwell GA, Caldwell KA, Call JA, Calvani R, Calvo AC, Calvo-Rubio Barrera M, Camara NO, Camonis JH, Camougrand N; Campanella M, Campbell EM, Campbell-Valois FX, Campello S, Campesi I, Campos JC, Camuzard O, Cancino J, Candido de Almeida D, Canesi L, Caniggia I, Canonico B, Cantí C, Cao B, Caraglia M, Caramés B, Carchman EH, Cardenal-Muñoz E, Cardenas C, Cardenas L, Cardoso SM, Carew JS, Carle GF, Carleton G, Carloni S, Carmona-Gutierrez D, Carneiro LA, Carnevali O, Carosi JM, Carra S, Carrier A, Carrier L, Carroll B, Carter AB, Carvalho AN, Casanova M, Casas C, Casas J, Cassioli C, Castillo EF, Castillo K, Castillo-Lluva S, Castoldi F, Castori M, Castro AF, Castro-Caldas M, Castro-Hernandez J, Castro-Obregon S, Catz SD, Cavadas C, Cavaliere F, Cavallini G, Cavinato M, Cayuela ML, Cebollada Rica P, Cecarini V, Cecconi F, Cechowska-Pasko M, Cenci S, Ceperuelo-Mallafré V, Cerqueira JJ, Cerutti JM, Cervia D, Cetintas VB, Cetrullo S, Chae HJ, Chagin AS, Chai CY, Chakrabarti G, Chakrabarti O, Chakraborty T, Chami M, Chamilos G, Chan DW, Chan EYW, Chan ED, Chan HYE, Chan HH, Chan H, Chan MTV, Chan YS, Chandra PK, Chang CP, Chang C, Chang HC, Chang K, Chao J, Chapman T, Charlet-Berguerand N, Chatterjee S, Chaube SK, Chaudhary A, Chauhan S, Chaum E, Checler F, Cheetham ME, Chen CS, Chen GC, Chen JF, Chen LL, Chen L, Chen M, Chen MK, Chen N, Chen Q, Chen RH, Chen S, Chen W, Chen XM, Chen XW, Chen X, Chen Y, Chen YG, Chen YJ, Chen YQ, Chen ZS, Chen Z, Chen ZH, Chen ZJ, Cheng H, Cheng J, Cheng SY, Cheng W, Cheng X, Cheng XT, Cheng Y, Cheng Z, Cheong H, Cheong JK, Chernyak BV, Cherry S, Cheung CFR, Cheung CHA, Cheung KH, Chevet E, Chi RJ, Chiang AKS, Chiaradonna F, Chiarelli R, Chiariello M, Chica N, Chiocca S, Chiong M, Chiou SH, Chiramel AI, Chiurchiù V, Cho DH, Choe SK, Choi AMK, Choi ME, Choudhury KR, Chow NS, Chu CT, Chua JP, Chua JJE, Chung H, Chung KP, Chung S, Chung SH, Chung YL, Cianfanelli V, Ciechomska IA, Cifuentes M, Cinque L, Cirak S, Cirone M, Clague MJ, Clarke R, Clementi E, Coccia EM, Codogno P, Cohen E, Cohen MM, Colasanti T, Colasuonno F, Colbert RA, Colell A, Čolić M, Coll NS, Collins MO, Colombo MI, Colón-Ramos DA, Combaret L, Comincini S, Cominetti MR, Consiglio A, Conte A, Conti F, Contu VR, Cookson MR, Coombs KM, Coppens I, Corasaniti MT, Corkery DP, Cordes N, Cortese K, Costa MDC, Costantino S, Costelli P, Coto-Montes A, Crack PJ, Crespo JL, Criollo A, Crippa V, Cristofani R, Csizmadia T, Cuadrado A, Cui B, Cui J, Cui Y, Culetto E, Cumino AC, Cybulsky AV, Czaja MJ, Czuczwar SJ, D'Adamo S, D'Amelio M, D'Arcangelo D, D'Lugos AC, D'Orazi G, da Silva JA, Dafsari HS, Dagda RK, Dagdas Y, Daglia M, Dai X, Dai Y, Dal Col J, Dalhaimer P, Dalla Valle L, Dallenga T, Dalmasso G, Damme M, Dando I, Dantuma NP, Darling AL, Das H, Dasarathy S, Dasari SK, Dash S, Daumke O, Dauphinee AN, Davies JS, Dávila VA, Davis RJ, Davis T, Dayalan Naidu S, De Amicis F, De Bosscher K, De Felice F, De Franceschi L, De Leonibus C, de Mattos Barbosa MG, De Meyer GRY, De Milito A, De Nunzio C, De Palma C, De Santi M, De Virgilio C, De Zio D, Debnath J, DeBosch BJ, Decuypere JP, Deehan MA, Deflorian G, DeGregori J, Dehay B, Del Rio G, Delaney JR, Delbridge LMD, Delorme-Axford E, Delpino MV, Demarchi F, Dembitz V, Demers ND, Deng H, Deng Z, Dengjel J, Dent P, Denton D, DePamphilis ML, Der CJ, Deretic V, Descoteaux A, Devis L, Devkota S, Devuyst O, Dewson G, Dharmasivam M, Dhiman R, di Bernardo D, Di Cristina M, Di Domenico F, Di Fazio P, Di Fonzo A, Di Guardo G, Di Guglielmo GM, Di Leo L, Di Malta C, Di Nardo A, Di Rienzo M, Di Sano F, Diallinas G, Diao J, Diaz-Araya G, Díaz-Laviada I, Dickinson JM, Diederich M, Dieudé M, Dikic I, Ding S, Ding WX, Dini L, Dinić J, Dinic M, Dinkova-Kostova AT, Dionne MS, Distler JHW, Diwan A, Dixon IMC, Djavaheri-Mergny M, Dobrinski I, Dobrovinskaya O, Dobrowolski R, Dobson RCJ, Đokić J, Dokmeci Emre S, Donadelli M, Dong B, Dong X, Dong Z, Dorn Ii GW, Dotsch V, Dou H, Dou J, Dowaidar M, Dridi S, Drucker L, Du A, Du C, Du G, Du HN, Du LL, du Toit A, Duan SB, Duan X, Duarte SP, Dubrovska A, Dunlop EA, Dupont N, Durán RV, Dwarakanath BS, Dyshlovoy SA, Ebrahimi-Fakhari D, Eckhart L, Edelstein CL, Efferth T, Eftekharpour E, Eichinger L, Eid N, Eisenberg T, Eissa NT, Eissa S, Ejarque M, El Andaloussi A, El-Hage N, El-Naggar S, Eleuteri AM, El-Shafey ES, Elgendy M, Eliopoulos AG, Elizalde MM, Elks PM, Elsasser HP, Elsherbiny ES, Emerling BM, Emre NCT, Eng CH, Engedal N, Engelbrecht AM, Engelsen AST, Enserink JM, Escalante R, Esclatine A, Escobar-Henriques M, Eskelinen EL, Espert L, Eusebio MO, Fabrias G, Fabrizi C, Facchiano A, Facchiano F, Fadeel B, Fader C, Faesen AC, Fairlie WD, Falcó A, Falkenburger BH, Fan D, Fan J, Fan Y, Fang EF, Fang Y, Fanto M, Farfel-Becker T, Faure M, Fazeli G, Fedele AO, Feldman AM, Feng D, Feng J, Feng L, Feng Y, Feng W, Fenz Araujo T, Ferguson TA, Fernández ÁF, Fernandez-Checa JC, Fernández-Veledo S, Fernie AR, Ferrante AW Jr, Ferraresi A, Ferrari MF, Ferreira JCB, Ferro-Novick S, Figueras A, Filadi R, Filigheddu N, Filippi-Chiela E, Filomeni G, Fimia GM, Fineschi V, Finetti F, Finkbeiner S, Fisher EA, Fisher PB, Flamigni F, Fliesler SJ, Flo TH, Florance I, Florey O, Florio T, Fodor E, Follo C, Fon EA, Forlino A, Fornai F, Fortini P, Fracassi A, Fraldi A, Franco B, Franco R, Franconi F, Frankel LB, Friedman SL, Fröhlich LF, Frühbeck G, Fuentes JM, Fujiki Y, Fujita N, Fujiwara Y, Fukuda M, Fulda S, Furic L, Furuya N, Fusco C, Gack MU, Gaffke L, Galadari S, Galasso A, Galindo MF, Gallolu Kankanamalage S, Galluzzi L, Galy V, Gammoh N, Gan B, Ganley IG, Gao F, Gao H, Gao M, Gao P, Gao SJ, Gao W, Gao X, Garcera A, Garcia MN, Garcia VE, García-Del Portillo F, Garcia-Escudero V, Garcia-Garcia A, Garcia-Macia M, García-Moreno D, Garcia-Ruiz C, García-Sanz P, Garg AD, Gargini R, Garofalo T, Garry RF, Gassen NC, Gatica D, Ge L, Ge W, Geiss-Friedlander R, Gelfi C, Genschik P, Gentle IE, Gerbino V, Gerhardt C, Germain K, Germain M, Gewirtz DA, Ghasemipour Afshar E, Ghavami S, Ghigo A, Ghosh M, Giamas G, Giampietri C, Giatromanolaki A, Gibson GE, Gibson SB, Ginet V, Giniger E, Giorgi C, Girao H, Girardin SE, Giridharan M, Giuliano S, Giulivi C, Giuriato S, Giustiniani J, Gluschko A, Goder V, Goginashvili A, Golab J, Goldstone DC, Golebiewska A, Gomes LR, Gomez R, Gómez-Sánchez R, Gomez-Puerto MC, Gomez-Sintes R, Gong Q, Goni FM, González-Gallego J, Gonzalez-Hernandez T, Gonzalez-Polo RA, Gonzalez-Reyes JA, González-Rodríguez P, Goping IS, Gorbatyuk MS, Gorbunov NV, Görgülü K, Gorojod RM, Gorski SM, Goruppi S, Gotor C, Gottlieb RA, Gozes I, Gozuacik D, Graef M, Gräler MH, Granatiero V, Grasso D, Gray JP, Green DR, Greenhough A, Gregory SL, Griffin EF, Grinstaff MW, Gros F, Grose C, Gross AS, Gruber F, Grumati P, Grune T, Gu X, Guan JL, Guardia CM, Guda K, Guerra F, Guerri C, Guha P, Guillén C, Gujar S, Gukovskaya A, Gukovsky I, Gunst J, Günther A, Guntur AR, Guo C, Guo H, Guo LW, Guo M, Gupta P, Gupta SK, Gupta S, Gupta VB, Gupta V, Gustafsson AB, Gutterman DD, H B R, Haapasalo A, Haber JE, Hać A, Hadano S, Hafrén AJ, Haidar M, Hall BS, Halldén G, Hamacher-Brady A, Hamann A, Hamasaki M, Han W, Hansen M, Hanson PI, Hao Z, Harada M, Harhaji-Trajkovic L, Hariharan N, Haroon N, Harris J, Hasegawa T, Hasima Nagoor N, Haspel JA, Haucke V, Hawkins WD, Hay BA, Haynes CM, Hayrabedyan SB, Hays TS, He C, He Q, He RR, He YW, He YY, Heakal Y, Heberle AM, Hejtmancik JF, Helgason GV, Henkel V, Herb M, Hergovich A, Herman-Antosiewicz A, Hernández A, Hernandez C, Hernandez-Diaz S, Hernandez-Gea V, Herpin A, Herreros J, Hervás JH, Hesselson D, Hetz C, Heussler VT, Higuchi Y, Hilfiker S, Hill JA, Hlavacek WS, Ho EA, Ho IHT, Ho PW, Ho SL, Ho WY, Hobbs GA, Hochstrasser M, Hoet PHM, Hofius D, Hofman P, Höhn A, Holmberg CI, Hombrebueno JR, Yi-Ren Hong CH,

Hooper LV, Hoppe T, Horos R, Hoshida Y, Hsin IL, Hsu HY, Hu B, Hu D, Hu LF, Hu MC, Hu R, Hu W, Hu YC, Hu ZW, Hua F, Hua J, Hua Y, Huan C, Huang C, Huang H, Huang K, Huang MLH, Huang R, Huang S, Huang T, Huang X, Huang YJ, Huber TB, Hubert V, Hubner CA, Hughes SM, Hughes WE, Humbert M, Hummer G, Hurley JH, Hussain S, Hussey PJ, Hutabarat M, Hwang HY, Hwang S, Ieni A, Ikeda F, Imagawa Y, Imai Y, Imbriano C, Imoto M, Inman DM, Inoki K, Iovanna J, Iozzo RV, Ippolito G, Irazoqui JE, Iribarren P, Ishaq M, Ishikawa M, Ishimwe N, Isidoro C, Ismail N, Issazadeh-Navikas S, Itakura E, Ito D, Ivankovic D, Ivanova S, Iyer AKV, Izquierdo JM, Izumi M, Jäättelä M, Jabir MS, Jackson WT, Jacobo-Herrera N, Jacomin AC, Jacquin E, Jadiya P, Jaeschke H, Jagannath C, Jakobi AJ, Jakobsson J, Janji B, Jansen-Dürr P, Jansson PJ, Jantsch J, Januszewski S, Jassey A, Jean S, Jeltsch-David H, Jendelova P, Jenny A, Jensen TE, Jessen N, Jewell JL, Ji J, Jia L, Jia R, Jiang L, Jiang Q, Jiang R, Jiang T, Jiang X, Jiang Y, Jimenez-Sanchez M, Jin EJ, Jin F, Jin H, Jin L, Jin M, Jin S, Jo EK, Joffre C, Johansen T, Johnson GVW, Johnston SA, Jokitalo E, Jolly MK, Joosten LAB, Jordan J, Joseph B, Ju D, Ju JS, Ju J, Juárez E, Judith D, Juhász G, Jun Y, Jung CH, Jung SC, Jung YK, Jungbluth H, Jungverdorben J, Just S, Kaarniranta K, Kaasik A, Kabuta T, Kaganovich D, Kahana A, Kain R, Kajimura S, Kalamvoki M, Kalia M, Kalinowski DS, Kaludercic N, Kalvari I, Kaminska J, Kaminskyy VO, Kanamori H, Kanasaki K, Kang C, Kang R, Kang SS, Kaniyappan S, Kanki T, Kanneganti TD, Kanthasamy AG, Kanthasamy A, Kantorow M, Kapuy O, Karamouzis MV, Karim MR, Karmakar P, Katare RG, Kato M, Kaufmann SHE, Kauppinen A, Kaushal GP, Kaushik S, Kawasaki K, Kazan K, Ke PY, Keating DJ, Keber U, Kehrl JH, Keller KE, Keller CW, Kemper JK, Kenific CM, Kepp O, Kermorgant S, Kern A, Ketteler R, Keulers TG, Khalfin B, Khalil H, Khambu B, Khan SY, Khandelwal VKM, Khandia R, Kho W, Khobrekar NV, Khuansuwan S, Khundadze M, Killackey SA, Kim D, Kim DR, Kim DH, Kim DE, Kim EY, Kim EK, Kim HR, Kim HS, Hyung-Ryong Kim, Kim JH, Kim JK, Kim J, Kim KI, Kim PK, Kim SJ, Kimball SR, Kimchi A, Kimmelman AC, Kimura T, King MA, Kinghorn KJ, Kinsey CG, Kirkin V, Kirshenbaum LA, Kiselev SL, Kishi S, Kitamoto K, Kitaoka Y, Kitazato K, Kitsis RN, Kittler JT, Kjaerulff O, Klein PS, Klopstock T, Klucken J, Knævelsrud H, Knorr RL, Ko BCB, Ko F, Ko JL, Kobayashi H, Kobayashi S, Koch I, Koch JC, Koenig U, Kögel D, Koh YH, Koike M, Kohlwein SD, Kocaturk NM, Komatsu M, König J, Kono T, Kopp BT, Korcsmaros T, Korkmaz G, Korolchuk VI, Korsnes MS, Koskela A, Kota J, Kotake Y, Kotler ML, Kou Y, Koukourakis MI, Koustas E, Kovacs AL, Kovács T, Koya D, Kozako T, Kraft C, Krainc D, Krämer H, Krasnodembskaya AD, Kretz-Remy C, Kroemer G, Ktistakis NT, Kuchitsu K, Kuenen S, Kuerschner L, Kukar T, Kumar A, Kumar D, Kumar S, Kume S, Kumsta C, Kundu CN, Kundu M, Kunnumakkara AB, Kurgan L, Kutateladze TG, Kutlu O, Kwak S, Kwon HJ, Kwon TK, Kwon YT, Kyrmizi I, La Spada A, Labonté P, Ladoire S, Laface I, Lafont F, Lagace DC, Lahiri V, Lai Z, Laird AS, Lakkaraju A, Lamark T, Lan SH, Landajuela A, Lane DJR, Lane JD, Lang CH, Lange C, Langel Ü, Langer R, Lapaquette P, Laporte J, LaRusso NF, Lastres-Becker I, Lau WCY, Laurie GW, Lavandero S, Law BYK, Law HK, Layfield R, Le W, Le Stunff H, Leary AY, Lebrun JJ, Leck LYW, Leduc-Gaudet JP, Lee C, Lee CP, Lee DH, Lee EB, Lee EF, Lee GM, Lee HJ, Lee HK, Lee JM, Lee JS, Lee JA, Lee JY, Lee JH, Lee M, Lee MG, Lee MJ, Lee MS, Lee SY, Lee SJ, Lee SB, Lee WH, Lee YR, Lee YH, Lee Y, Lefebvre C, Legouis R, Lei YL, Lei Y, Leikin S, Leitinger G, Lemus L, Leng S, Lenoir O, Lenz G, Lenz HJ, Lenzi P, León Y, Leopoldino AM, Leschczyk C, Leskelä S, Letellier E, Leung CT, Leung PS, Leventhal JS, Levine B, Lewis PA, Ley K, Li B, Li DQ, Li J, Li K, Li L, Li M, Li PL, Li MQ, Li Q, Li S, Li T, Li W, Li X, Li YP, Li Y, Li Z, Lian J, Liang C, Liang Q, Liang W, Liang Y, Liao G, Liao L, Liao M, Liao YF, Librizzi M, Lie PPY, Lilly MA, Lim HJ, Lima TRR, Limana F, Lin C, Lin CW, Lin DS, Lin FC, Lin JD, Lin KM, Lin KH, Lin LT, Lin PH, Lin Q, Lin S, Lin SJ, Lin W, Lin X, Lin YX, Lin YS, Linden R, Lindner P, Ling SC, Lingor P, Linnemann AK, Liou YC, Lipinski MM, Lipovšek S, Lira VA, Lisiak N, Liton PB, Liu C, Liu CH, Liu CF, Liu F, Liu H, Liu HS, Liu HF, Liu J, Liu L, Liu M, Liu Q, Liu W, Liu XH, Liu X, Liu Y, Livingston JA, Lizard G, Lizcano JM, Ljubojevic-Holzer S, LLeonart ME, Llobet-Navàs D, Llorente A, Lo CH, Lobato-Márquez D, Long Q, Long YC, Loos B, Loos JA, López MG, López-Doménech G, López-Guerrero JA, López-Jiménez AT, López-Pérez Ó, López-Valero I, Lorenowicz MJ, Lorente M, Lorincz P, Lossi L, Lotersztajn S, Lovat PE, Lovell JF, Lovy A, Lőw P, Lu G, Lu H, Lu JH, Lu JJ, Lu M, Lu S, Luciani A, Lucocq JM, Ludovico P, Luftig MA, Luhr M, Luis-Ravelo D, Lum JJ, Luna-Dulcey L, Lund AH, Lund VK, Lünemann JD, Lüningschrör P, Luo H, Luo R, Luo S, Luo Z, Luparello C, Lüscher B, Luu L, Lyakhovich A, Lyamzaev KG, Lystad AH, Lytvynchuk L, Ma AC, Ma C, Ma M, Ma NF, Ma QH, Ma X, Ma Y, Ma Z, MacDougald OA, Macian F, MacIntosh GC, MacKeigan JP, Macleod KF, Maday S, Madeo F, Madesh M, Madl T, Madrigal-Matute J, Maeda A, Maejima Y, Magarinos M, Mahavadi P, Maiani E, Maiese K, Maiti P, Maiuri MC, Majello B, Major MB, Makareeva E, Malik F, Mallilankaraman K, Malorni W, Maloyan A, Mammadova N, Man GCW, Manai F, Mancias JD, Mandelkow EM, Mandell MA, Manfredi AA, Manjili MH, Manjithaya R, Manque P, Manshian BB, Manzano R, Manzoni C, Mao K, Marchese C, Marchetti S, Marconi AM, Marcucci F, Mardente S, Mareninova OA, Margeta M, Mari M, Marinelli S, Marinelli O, Mariño G, Mariotto S, Marshall RS, Marten MR, Martens S, Martin APJ, Martin KR, Martin S, Martín-Segura A, Martín-Acebes MA, Martin-Burriel I, Martin-Rincon M, Martin-Sanz P, Martina JA, Martinet W, Martinez A, Martinez J, Martinez Velazquez M, Martinez-Lopez N, Martinez-Vicente M, Martins DO, Martins JO, Martins WK, Martins-Marques T, Marzetti E, Masaldan S, Masclaux-Daubresse C, Mashek DG, Massa V, Massieu L, Masson GR, Masuelli L, Masyuk AI, Masyuk TV, Matarrese P, Matheu A, Matoba S, Matsuzaki S, Mattar P, Matte A, Mattoscio D, Mauriz JL, Mauthe M, Mauvezin C, Maverakis E, Maycotte P, Mayer J, Mazzoccoli G, Mazzoni C, Mazzulli JR, McCarty N, McDonald C, McGill MR, McKenna SL, McLaughlin B, McLoughlin F, McNiven MA, McWilliams TG, Mechta-Grigoriou F, Medeiros TC, Medina DL, Megeney LA, Megyeri K, Mehrpour M, Mehta JL, Meijer AJ, Meijer AH, Mejlvang J, Meléndez A, Melk A, Memisoglu G, Mendes AF, Meng D, Meng F, Meng T, Menna-Barreto R, Menon MB, Mercer C, Mercier AE, Mergny JL, Merighi A, Merkley SD, Merla G, Meske V, Mestre AC, Metur SP, Meyer C, Meyer H, Mi W, Mialet-Perez J, Miao J, Micale L, Miki Y, Milan E, Milczarek M, Miller DL, Miller SI, Miller S, Millward SW, Milosevic I, Minina EA, Mirzaei H, Mirzaei HR, Mirzaei M, Mishra A, Mishra N, Mishra PK, Misirkic Marjanovic M, Misasi R, Misra A, Misso G, Mitchell C, Mitou G, Miura T, Miyamoto S, Miyazaki M, Miyazaki T, Miyazawa K, Mizushima N, Mogensen TH, Mograbi B, Mohammadinejad R, Mohamud Y, Mohanty A, Mohapatra S, Möhlmann T, Mohmmed A, Moles A, Moley KH, Molinari M, Mollace V, Møller AB, Mollereau B, Mollinedo F, Montagna C, Monteiro MJ, Montella A, Montes LR, Montico B, Mony VK, Monzio Compagnoni G, Moore MN, Moosavi MA, Mora AL, Mora M, Morales-Alamo D, Moratalla R, Moreira PI, Morelli E, Moreno S, Moreno-Blas D, Moresi V, Morga B, Morgan AH, Morin F, Morishita H, Moritz OL, Moriyama M, Moriyasu Y, Morleo M, Morselli E, Moruno-Manchon JF, Moscat J, Mostowy S, Motori E, Moura AF, Moustaid-Moussa N, Mrakovcic M, Muciño-Hernández G, Mukherjee A, Mukhopadhyay S, Mulcahy Levy JM, Mulero V, Muller S, Münch C, Munjal A, Munoz-Canoves P, Muñoz-Galdeano T, Münz C, Murakawa T, Muratori C, Murphy BM, Murphy JP, Murthy A, Myöhänen TT, Mysorekar IU, Mytych J, Nabavi SM, Nabissi M, Nagy P, Nah J, Nahimana A, Nakagawa I, Nakamura K, Nakatogawa H, Nandi SS, Nanjundan M, Nanni M, Napolitano G, Nardacci R, Narita M, Nassif M, Nathan I, Natsumeda M, Naude RJ, Naumann C, Naveiras O, Navid F, Nawrocki ST, Nazarko TY, Nazio F, Negoita F, Neill T, Neisch AL, Neri LM, Netea MG, Neubert P, Neufeld TP, Neumann D, Neutzner A, Newton PT, Ney PA, Nezis IP, Ng CCW, Ng TB, Nguyen HTT, Nguyen LT, Ni HM, Ní Cheallaigh C, Ni Z, Nicolao MC, Nicoli F, Nieto-Diaz M, Nilsson P, Ning S, Niranjan R, Nishimune H, Niso-Santano M, Nixon RA, Nobili A, Nobrega C, Noda T, Nogueira-Recalde U, Nolan TM, Nombela I, Novak I, Novoa B, Nozawa T, Nukina N, Nussbaum-Krammer C, Nylandsted J, O'Donovan TR, O'Leary SM, O'Rourke EJ, O'Sullivan MP, O'Sullivan TE, Oddo S, Oehme I, Ogawa M, Ogier-Denis E, Ogmundsdottir MH, Ogretmen B, Oh GT, Oh SH, Oh YJ, Ohama T, Ohashi Y, Ohmuraya M, Oikonomou V, Ojha R, Okamoto K, Okazawa H, Oku M, Oliván S, Oliveira JMA, Ollmann M, Olzmann JA,

Omari S, Omary MB, Önal G, Ondrej M, Ong SB, Ong SG, Onnis A, Orellana JA, Orellana-Muñoz S, Ortega-Villaizan MDM, Ortiz-Gonzalez XR, Ortona E, Osiewacz HD, Osman AK, Osta R, Otegui MS, Otsu K, Ott C, Ottobrini L, Ou JJ, Outeiro TF, Oynebraten I, Ozturk M, Pagès G, Pahari S, Pajares M, Pajvani UB, Pal R, Paladino S, Pallet N, Palmieri M, Palmisano G, Palumbo C, Pampaloni F, Pan L, Pan Q, Pan W, Pan X, Panasyuk G, Pandey R, Pandey UB, Pandya V, Paneni F, Pang SY, Panzarini E, Papademetrio DL, Papaleo E, Papinski D, Papp D, Park EC, Park HT, Park JM, Park JI, Park JT, Park J, Park SC, Park SY, Parola AH, Parys JB, Pasquier A, Pasquier B, Passos JF, Pastore N, Patel HH, Patschan D, Pattingre S, Pedraza-Alva G, Pedraza-Chaverri J, Pedrozo Z, Pei G, Pei J, Peled-Zehavi H, Pellegrini JM, Pelletier J, Peñalva MA, Peng D, Peng Y, Penna F, Pennuto M, Pentimalli F, Pereira CM, Pereira GJS, Pereira LC, Pereira de Almeida L, Perera ND, Pérez-Lara Á, Perez-Oliva AB, Pérez-Pérez ME, Periyasamy P, Perl A, Perrotta C, Perrotta I, Pestell RG, Petersen M, Petrache I, Petrovski G, Pfirrmann T, Pfister AS, Philips JA, Pi H, Picca A, Pickrell AM, Picot S, Pierantoni GM, Pierdominici M, Pierre P, Pierrefite-Carle V, Pierzynowska K, Pietrocola F, Pietruczuk M, Pignata C, Pimentel-Muiños FX, Pinar M, Pinheiro RO, Pinkas-Kramarski R, Pinton P, Pircs K, Piya S, Pizzo P, Plantinga TS, Platta HW, Plaza-Zabala A, Plomann M, Plotnikov EY, Plun-Favreau H, Pluta R, Pocock R, Pöggeler S, Pohl C, Poirot M, Poletti A, Ponpuak M, Popelka H, Popova B, Porta H, Porte Alcon S, Portilla-Fernandez E, Post M, Potts MB, Poulton J, Powers T, Prahlad V, Prajsnar TK, Praticò D, Prencipe R, Priault M, Proikas-Cezanne T, Promponas VJ, Proud CG, Puertollano R, Puglielli L, Pulinilkunnil T, Puri D, Puri R, Puyal J, Qi X, Qi Y, Qian W, Qiang L, Qiu Y, Quadrilatero J, Quarleri J, Raben N, Rabinowich H, Ragona D, Ragusa MJ, Rahimi N, Rahmati M, Raia V, Raimundo N, Rajasekaran NS, Ramachandra Rao S, Rami A, Ramírez-Pardo I, Ramsden DB, Randow F, Rangarajan PN, Ranieri D, Rao H, Rao L, Rao R, Rathore S, Ratnayaka JA, Ratovitski EA, Ravanan P, Ravegnini G, Ray SK, Razani B, Rebecca V, Reggiori F, Régnier-Vigouroux A, Reichert AS, Reigada D, Reiling JH, Rein T, Reipert S, Rekha RS, Ren H, Ren J, Ren W, Renault T, Renga G, Reue K, Rewitz K, Ribeiro de Andrade Ramos B, Riazuddin SA, Ribeiro-Rodrigues TM, Ricci JE, Ricci R, Riccio V, Richardson DR, Rikihisa Y, Risbud MV, Risueño RM, Ritis K, Rizza S, Rizzuto R, Roberts HC, Roberts LD, Robinson KJ, Roccheri MC, Rocchi S, Rodney GG, Rodrigues T, Rodrigues Silva VR, Rodriguez A, Rodriguez-Barrueco R, Rodriguez-Henche N, Rodriguez-Rocha H, Roelofs J, Rogers RS, Rogov VV, Rojo AI, Rolka K, Romanello V, Romani L, Romano A, Romano PS, Romeo-Guitart D, Romero LC, Romero M, Roney JC, Rongo C, Roperto S, Rosenfeldt MT, Rosenstiel P, Rosenwald AG, Roth KA, Roth L, Roth S, Rouschop KMA, Roussel BD, Roux S, Rovere-Querini P, Roy A, Rozieres A, Ruano D, Rubinsztein DC, Rubtsova MP, Ruckdeschel K, Ruckenstuhl C, Rudolf E, Rudolf R, Ruggieri A, Ruparelia AA, Rusmini P, Russell RR, Russo GL, Russo M, Russo R, Ryabaya OO, Ryan KM, Ryu KY, Sabater-Arcis M, Sachdev U, Sacher M, Sachse C, Sadhu A, Sadoshima J, Safren N, Saftig P, Sagona AP, Sahay G, Sahebkar A, Sahin M, Sahin O, Sahni S, Saito N, Saito S, Saito T, Sakai R, Sakai Y, Sakamaki JI, Saksela K, Salazar G, Salazar-Degracia A, Salekdeh GH, Saluja AK, Sampaio-Marques B, Sanchez MC, Sanchez-Alcazar JA, Sanchez-Vera V, Sancho-Shimizu V, Sanderson JT, Sandri M, Santaguida S, Santambrogio L, Santana MM, Santoni G, Sanz A, Sanz P, Saran S, Sardiello M, Sargeant TJ, Sarin A, Sarkar C, Sarkar S, Sarrias MR, Sarmah DT, Sarparanta J, Sathyanarayan A, Sathyanarayanan R, Scaglione KM, Scatozza F, Schaefer L, Schafer ZT, Schaible UE, Schapira AHV, Scharl M, Schatzl HM, Schein CH, Scheper W, Scheuring D, Schiaffino MV, Schiappacassi M, Schindl R, Schlattner U, Schmidt O, Schmitt R, Schmidt SD, Schmitz I, Schmukler E, Schneider A, Schneider BE, Schober R, Schoijet AC, Schott MB, Schramm M, Schröder B, Schuh K, Schüller C, Schulze RJ, Schürmanns L, Schwamborn JC, Schwarten M, Scialo F, Sciarretta S, Scott MJ, Scotto KW, Scovassi AI, Scrima A, Scrivo A, Sebastian D, Sebti S, Sedej S, Segatori L, Segev N, Seglen PO, Seiliez I, Seki E, Selleck SB, Sellke FW, Selsby JT, Sendtner M, Senturk S, Seranova E, Sergi C, Serra-Moreno R, Sesaki H, Settembre C, Setty SRG, Sgarbi G, Sha O, Shacka JJ, Shah JA, Shang D, Shao C, Shao F, Sharbati S, Sharkey LM, Sharma D, Sharma G, Sharma K, Sharma P, Sharma S, Shen HM, Shen H, Shen J, Shen M, Shen W, Shen Z, Sheng R, Sheng Z, Sheng ZH, Shi J, Shi X, Shi YH, Shiba-Fukushima K, Shieh JJ, Shimada Y, Shimizu S, Shimozawa M, Shintani T, Shoemaker CJ, Shojaei S, Shoji I, Shravage BV, Shridhar V, Shu CW, Shu HB, Shui K, Shukla AK, Shutt TE, Sica V, Siddiqui A, Sierra A, Sierra-Torre V, Signorelli S, Sil P, Silva BJA, Silva JD, Silva-Pavez E, Silvente-Poirot S, Simmonds RE, Simon AK, Simon HU, Simons M, Singh A, Singh LP, Singh R, Singh SV, Singh SK, Singh SB, Singh S, Singh SP, Sinha D, Sinha RA, Sinha S, Sirko A, Sirohi K, Sivridis EL, Skendros P, Skirycz A, Slaninová I, Smaili SS, Smertenko A, Smith MD, Soenen SJ, Sohn EJ, Sok SPM, Solaini G, Soldati T, Soleimanpour SA, Soler RM, Solovchenko A, Somarelli JA, Sonawane A, Song F, Song HK, Song JX, Song K, Song Z, Soria LR, Sorice M, Soukas AA, Soukup SF, Sousa D, Sousa N, Spagnuolo PA, Spector SA, Srinivas Bharath MM, St Clair D, Stagni V, Staiano L, Stalnecker CA, Stankov MV, Stathopulos PB, Stefan K, Stefan SM, Stefanis L, Steffan JS, Steinkasserer A, Stenmark H, Sterneckert J, Stevens C, Stoka V, Storch S, Stork B, Strappazzon F, Strohecker AM, Stupack DG, Su H, Su LY, Su L, Suarez-Fontes AM, Subauste CS, Subbian S, Subirada PV, Sudhandiran G, Sue CM, Sui X, Summers C, Sun G, Sun J, Sun K, Sun MX, Sun Q, Sun Y, Sun Z, Sunahara KKS, Sundberg E, Susztak K, Sutovsky P, Suzuki H, Sweeney G, Symons JD, Sze SCW, Szewczyk NJ, Tabęcka-Łonczynska A, Tabolacci C, Tacke F, Taegtmeyer H, Tafani M, Tagaya M, Tai H, Tait SWG, Takahashi Y, Takats S, Talwar P, Tam C, Tam SY, Tampellini D, Tamura A, Tan CT, Tan EK, Tan YQ, Tanaka M, Tang D, Tang J, Tang TS, Tanida I, Tao Z, Taouis M, Tatenhorst L, Tavernarakis N, Taylor A, Taylor GA, Taylor JM, Tchetina E, Tee AR, Tegeder I, Teis D, Teixeira N, Teixeira-Clerc F, Tekirdag KA, Tencomnao T, Tenreiro S, Tepikin AV, Testillano PS, Tettamanti G, Tharaux PL, Thedieck K, Thekkinghat AA, Thellung S, Thinwa JW, Thirumalaikumar VP, Thomas SM, Thomes PG, Thorburn A, Thukral L, Thum T, Thumm M, Tian L, Tichy A, Till A, Timmerman V, Titorenko VI, Todi SV, Todorova K, Toivonen JM, Tomaipitinca L, Tomar D, Tomas-Zapico C, Tomić S, Tong BC, Tong C, Tong X, Tooze SA, Torgersen ML, Torii S, Torres-López L, Torriglia A, Towers CG, Towns R, Toyokuni S, Trajkovic V, Tramontano D, Tran QG, Travassos LH, Trelford CB, Tremel S, Trougakos IP, Tsao BP, Tschan MP, Tse HF, Tse TF, Tsugawa H, Tsvetkov AS, Tumbarello DA, Tumtas Y, Tuñón MJ, Turcotte S, Turk B, Turk V, Turner BJ, Tuxworth RI, Tyler JK, Tyutereva EV, Uchiyama Y, Ugun-Klusek A, Uhlig HH, Ułamek-Kozioł M, Ulasov IV, Umekawa M, Ungermann C, Unno R, Urbe S, Uribe-Carretero E, Üstün S, Uversky VN, Vaccari T, Vaccaro MI, Vahsen BF, Vakifahmetoglu-Norberg H, Valdor R, Valente MJ, Valko A, Vallee RB, Valverde AM, Van den Berghe G, van der Veen S, Van Kaer L, van Loosdregt J, van Wijk SJL, Vandenberghe W, Vanhorebeek I, Vannier-Santos MA, Vannini N, Vanrell MC, Vantaggiato C, Varano G, Varela-Nieto I, Varga M, Vasconcelos MH, Vats S, Vavvas DG, Vega-Naredo I, Vega-Rubin-de-Celis S, Velasco G, Velázquez AP, Vellai T, Vellenga E, Velotti F, Verdier M, Verginis P, Vergne I, Verkade P, Verma M, Verstreken P, Vervliet T, Vervoorts J, Vessoni AT, Victor VM, Vidal M, Vidoni C, Vieira OV, Vierstra RD, Viganó S, Vihinen H, Vijayan V, Vila M, Vilar M, Villalba JM, Villalobo A, Villarejo-Zori B, Villarroya F, Villarroya J, Vincent O, Vindis C, Viret C, Viscomi MT, Visnjic D, Vitale I, Vocadlo DJ, Voitsekhovskaja OV, Volonté C, Volta M, Vomero M, Von Haefen C, Vooijs MA, Voos W, Vucicevic L, Wade-Martins R, Waguri S, Waite KA, Wakatsuki S, Walker DW, Walker MJ, Walker SA, Walter J, Wandosell FG, Wang B, Wang CY, Wang C, Wang D, Wang F, Wang G, Wang H, Wang HG, Wang J, Wang K, Wang L, Wang MH, Wang M, Wang N, Wang P, Wang QJ, Wang Q, Wang QK, Wang QA, Wang WT, Wang W, Wang X, Wang Y, Wang YY, Wang Z, Warnes G, Warnsmann V, Watada H, Watanabe E, Watchon M, Wawrzyńska A, Weaver TE, Wegrzyn G, Wehman AM, Wei H, Wei L, Wei T, Wei Y, Weiergräber OH, Weihl CC, Weindl G, Weiskirchen R, Wells A, Wen RH, Wen X, Werner A, Weykopf B, Wheatley SP, Whitton JL, Whitworth AJ, Wiktorska K, Wildenberg ME, Wileman T, Wilkinson S, Willbold D, Williams B, Williams RSB, Williams RL, Williamson PR, Wilson RA, Winner B, Winsor NJ, Witkin SS, Wodrich H, Woehlbier U, Wollert T, Wong E, Wong JH, Wong RW, Wong VKW, Wong WW, Wu AG, Wu C, Wu J, Wu KK, Wu M, Wu

SY, Wu S, Wu WKK, Wu X, Wu YW, Wu Y, Xavier RJ, Xia H, Xia L, Xia Z, Xiang G, Xiang J, Xiang M, Xiang W, Xiao B, Xiao G, Xiao H, Xiao HT, Xiao J, Xiao L, Xiao S, Xiao Y, Xie B, Xie CM, Xie M, Xie Y, Xie Z, Xilouri M, Xu C, Xu E, Xu H, Xu J, Xu L, Xu WW, Xu X, Xue Y, Yakhine-Diop SMS, Yamaguchi M, Yamaguchi O, Yamamoto A, Yamashina S, Yan S, Yan SJ, Yan Z, Yanagi Y, Yang C, Yang DS, Yang H, Yang HT, Yang JM, Yang J, Yang L, Yang M, Yang PM, Yang Q, Yang S, Yang SF, Yang W, Yang WY, Yang X, Yang Y, Yao H, Yao S, Yao X, Yao YG, Yao YM, Yasui T, Yazdankhah M, Yen PM, Yi C, Yin XM, Yin Y, Yin Z, Ying M, Ying Z, Yip CK, Yiu SPT, Yoo YH, Yoshida K, Yoshii SR, Yoshimori T, Yousefi B, Yu B, Yu H, Yu J, Yu L, Yu ML, Yu SW, Yu VC, Yu WH, Yu Z, Yuan J, Yuan LQ, Yuan S, Yuan SF, Yuan Y, Yuan Z, Yue J, Yue Z, Yun J, Yung RL, Zacks DN, Zaffagnini G, Zambelli VO, Zanella I, Zang QS, Zanivan S, Zappavigna S, Zaragoza P, Zarbalis KS, Zarebkohan A, Zarrouk A, Zeitlin SO, Zeng J, Zeng JD, Žerovnik E, Zhan L, Zhang B, Zhang DD, Zhang H, Zhang HL, Zhang J, Zhang JP, Zhang KYB, Zhang LW, Zhang L, Zhang M, Zhang P, Zhang S, Zhang W, Zhang X, Zhang XW, Zhang XD, Zhang Y, Zhang YD, Zhang YY, Zhang Z, Zhao H, Zhao L, Zhao S, Zhao T, Zhao XF, Zhao Y, Zheng G, Zheng K, Zheng L, Zheng S, Zheng XL, Zheng Y, Zheng ZG, Zhivotovsky B, Zhong Q, Zhou A, Zhou B, Zhou C, Zhou G, Zhou H, Zhou J, Zhou K, Zhou R, Zhou XJ, Zhou Y, Zhou ZY, Zhou Z, Zhu B, Zhu C, Zhu GQ, Zhu H, Zhu WG, Zhu Y, Zhuang H, Zhuang X, Zientara-Rytter K, Zimmermann CM, Ziviani E, Zoladek T, Zong WX, Zorov DB, Zorzano A, Zou W, Zou Z, Zuryn S, Zwerschke W, Brand-Saberi B, Dong XC, Kenchappa CS, Lin Y, Oshima S, Rong Y, Sluimer JC, Stallings CL, Tong CK. Guidelines for the use and interpretation of assays for monitoring autophagy (4th edition)(1). *Autophagy* 2021; **17**: 1-382 [PMID: 33634751 DOI: 10.1080/15548627.2020.1797280]

24 **Tao Y**, Wang N, Qiu T, Sun X. The Role of Autophagy and NLRP3 Inflammasome in Liver Fibrosis. *Biomed Res Int* 2020; **2020**: 7269150 [PMID: 32733951 DOI: 10.1155/2020/7269150]

25 **Dewidar B**, Meyer C, Dooley S, Meindl-Beinker AN. TGF-β in Hepatic Stellate Cell Activation and Liver Fibrogenesis-Updated 2019. *Cells* 2019; **8** [PMID: 31718044 DOI: 10.3390/cells8111419]

26 **Ni Y**, Li JM, Liu MK, Zhang TT, Wang DP, Zhou WH, Hu LZ, Lv WL. Pathological process of liver sinusoidal endothelial cells in liver diseases. *World J Gastroenterol* 2017; **23**: 7666-7677 [PMID: 29209108 DOI: 10.3748/wjg.v23.i43.7666]

27 **Sui M**, Jiang X, Chen J, Yang H, Zhu Y. Magnesium isoglycyrrhizinate ameliorates liver fibrosis and hepatic stellate cell activation by regulating ferroptosis signaling pathway. *Biomed Pharmacother* 2018; **106**: 125-133 [PMID: 29957462 DOI: 10.1016/j.biopha.2018.06.060]

28 **Durairajan SSK**, Singh AK, Saravanan UB, Namachivayam M, Radhakrishnan M, Huang JD, Dhodapkar R, Zhang H. Gastrointestinal Manifestations of SARS-CoV-2: Transmission, Pathogenesis, Immunomodulation, Microflora Dysbiosis, and Clinical Implications. *Viruses* 2023; **15** [PMID: 37376531 DOI: 10.3390/v15061231]

29 **Zhou P**, Yang XL, Wang XG, Hu B, Zhang L, Zhang W, Si HR, Zhu Y, Li B, Huang CL, Chen HD, Chen J, Luo Y, Guo H, Jiang RD, Liu MQ, Chen Y, Shen XR, Wang X, Zheng XS, Zhao K, Chen QJ, Deng F, Liu LL, Yan B, Zhan FX, Wang YY, Xiao GF, Shi ZL. A pneumonia outbreak associated with a new coronavirus of probable bat origin. *Nature* 2020; **579**: 270-273 [PMID: 32015507 DOI: 10.1038/s41586-020-2012-7]

30 **Cheng H**, Wang Y, Wang GQ. Organ-protective effect of angiotensin-converting enzyme 2 and its effect on the prognosis of COVID-19. *J Med Virol* 2020; **92**: 726-730 [PMID: 32221983 DOI: 10.1002/jmv.25785]

31 **Moon AM**, Webb GJ, Aloman C, Armstrong MJ, Cargill T, Dhanasekaran R, Genescà J, Gill US, James TW, Jones PD, Marshall A, Mells G, Perumalswami PV, Qi X, Su F, Ufere NN, Barnes E, Barritt AS, Marjot T. High mortality rates for SARS-CoV-2 infection in patients with pre-existing chronic liver disease and cirrhosis: Preliminary results from an international registry. *J Hepatol* 2020; **73**: 705-708 [PMID: 32446714 DOI: 10.1016/j.jhep.2020.05.013]

32 **Warner FJ**, Rajapaksha H, Shackel N, Herath CB. ACE2: from protection of liver disease to propagation of COVID-19. *Clin Sci (Lond)* 2020; **134**: 3137-3158 [PMID: 33284956 DOI: 10.1042/CS20201268]

33 **Mizushima N**, Levine B, Cuervo AM, Klionsky DJ. Autophagy fights disease through cellular self-digestion. *Nature* 2008; **451**: 1069-1075 [PMID: 18305538 DOI: 10.1038/nature06639]

34 **Chen J**, Guo Q, Chen Q, Chen Y, Chen D, Chen Z, Wang X, Huang Y. Interleukin 10 inhibits oxidative stress-induced autophagosome formation in hepatic stellate cells by activating the mTOR-STAT3 pathway. *Exp Cell Res* 2022; **411**: 113001 [PMID: 34973945 DOI: 10.1016/j.yexcr.2021.113001]

35 **Cao Y**, Luo Y, Zou J, Ouyang J, Cai Z, Zeng X, Ling H, Zeng T. Autophagy and its role in gastric cancer. *Clin Chim Acta* 2019; **489**: 10-20 [PMID: 30472237 DOI: 10.1016/j.cca.2018.11.028]

36 **Zheng Q**, Zhao K, Han X, Huff AF, Cui Q, Babcock SA, Yu S, Zhang Y. Inhibition of AMPK accentuates prolonged caloric restriction-induced change in cardiac contractile function through disruption of compensatory autophagy. *Biochim Biophys Acta* 2015; **1852**: 332-342 [PMID: 24793415 DOI: 10.1016/j.bbadis.2014.04.023]

37 **Jin S**, Li H, Han M, Ruan M, Liu Z, Zhang F, Zhang C, Choi Y, Liu B. Mesenchymal Stem Cells with Enhanced Bcl-2 Expression Promote Liver Recovery in a Rat Model of Hepatic Cirrhosis. *Cell Physiol Biochem* 2016; **40**: 1117-1128 [PMID: 27960154 DOI: 10.1159/000453166]

38 **Kong LJ**, Li H, Du YJ, Pei FH, Hu Y, Zhao LL, Chen J. Vatalanib, a tyrosine kinase inhibitor, decreases hepatic fibrosis and sinusoidal capillarization in CCl4-induced fibrotic mice. *Mol Med Rep* 2017; **15**: 2604-2610 [PMID: 28447731 DOI: 10.3892/mmr.2017.6325]

39 **DeLeve LD**. Liver sinusoidal endothelial cells in hepatic fibrosis. *Hepatology* 2015; **61**: 1740-1746 [PMID: 25131509 DOI: 10.1002/hep.27376]

40 **Novo E**, Cannito S, Zamara E, Valfrè di Bonzo L, Caligiuri A, Cravanzola C, Compagnone A, Colombatto S, Marra F, Pinzani M, Parola M. Proangiogenic cytokines as hypoxia-dependent factors stimulating migration of human hepatic stellate cells. *Am J Pathol* 2007; **170**: 1942-1953 [PMID: 17525262 DOI: 10.2353/ajpath.2007.060887]

World Journal of Gastroenterology

Submit a Manuscript: https://www.f6publishing.com

World J Gastroenterol 2023 September 7; 29(33): 4991-5004

DOI: 10.3748/wjg.v29.i33.4991

ISSN 1007-9327 (print) ISSN 2219-2840 (online)

ORIGINAL ARTICLE

Basic Study

Diabetes exacerbates inflammatory bowel disease in mice with diet-induced obesity

Kendra L Francis, Kimberly M Alonge, Maria Cristina Pacheco, Shannon J Hu, Cody A Krutzsch, Gregory J Morton, Michael W Schwartz, Jarrad M Scarlett

Specialty type: Gastroenterology and hepatology

Provenance and peer review: Unsolicited article; Externally peer reviewed.

Peer-review model: Single blind

Peer-review report's scientific quality classification
Grade A (Excellent): 0
Grade B (Very good): B
Grade C (Good): C
Grade D (Fair): 0
Grade E (Poor): 0

P-Reviewer: Duan SL, China; Losurdo G, Italy

Received: June 14, 2023
Peer-review started: June 14, 2023
First decision: July 7, 2023
Revised: July 22, 2023
Accepted: August 21, 2023
Article in press: August 21, 2023
Published online: September 7, 2023

Kendra L Francis, Jarrad M Scarlett, Department of Pediatric Gastroenterology and Hepatology, Seattle Children's Hospital, Seattle, WA 98105, United States

Kendra L Francis, Kimberly M Alonge, Shannon J Hu, Cody A Krutzsch, Gregory J Morton, Michael W Schwartz, Jarrad M Scarlett, Diabetes Institute, University of Washington, Seattle, WA 98109, United States

Kimberly M Alonge, Department of Medicinal Chemistry, University of Washington, Seattle, WA 98195, United States

Maria Cristina Pacheco, Department of Laboratory Medicine and Pathology, Seattle Children's Hospital, Seattle, WA 98105, United States

Corresponding author: Jarrad M Scarlett, MD, PhD, Assistant Professor, Department of Pediatric Gastroenterology and Hepatology, Seattle Children's Hospital, 750 East Republican Street F770, Seattle, WA 98195, United States. jarrad.scarlett@seattlechildrens.org

Abstract

BACKGROUND

The increased prevalence of inflammatory bowel disease (IBD) among patients with obesity and type 2 diabetes suggests a causal link between these diseases, potentially involving the effect of hyperglycemia to disrupt intestinal barrier integrity.

AIM

To investigate whether the deleterious impact of diabetes on the intestinal barrier is associated with increased IBD severity in a murine model of colitis in mice with and without diet-induced obesity.

METHODS

Mice were fed chow or a high-fat diet and subsequently received streptozotocin to induce diabetic-range hyperglycemia. Six weeks later, dextran sodium sulfate was given to induce colitis. In select experiments, a subset of diabetic mice was treated with the antidiabetic drug dapagliflozin prior to colitis onset. Endpoints included both clinical and histological measures of colitis activity as well as histochemical markers of colonic epithelial barrier integrity.

RESULTS
In mice given a high-fat diet, but not chow-fed animals, diabetes was associated with significantly increased clinical colitis activity and histopathologic markers of disease severity. Diabetes was also associated with a decrease in key components that regulate colonic epithelial barrier integrity (colonic mucin layer content and epithelial tight junction proteins) in diet-induced obese mice. Each of these effects of diabetes in diet-induced obese mice was ameliorated by restoring normoglycemia.

CONCLUSION
In obese mice, diabetes worsened clinical and pathologic outcomes of colitis *via* mechanisms that are reversible with treatment of hyperglycemia. Hyperglycemia-induced intestinal barrier dysfunction offers a plausible mechanism linking diabetes to increased colitis severity. These findings suggest that effective diabetes management may decrease the clinical severity of IBD.

Key Words: Inflammatory bowel disease; Type 2 diabetes; Obesity; Intestinal barrier; Hyperglycemia; Colitis in mice; Tight junction proteins

©The Author(s) 2023. Published by Baishideng Publishing Group Inc. All rights reserved.

Core Tip: Metabolic syndrome affects many patients with inflammatory bowel disease (IBD). This study used mouse models of colitis to investigate how diabetes and obesity interact to impair intestinal barrier function and exacerbate IBD outcomes, highlighting the deleterious impact of sustained hyperglycemia on intestinal barrier integrity. We showed that diabetic hyperglycemia impairs the colonic mucin barrier and tight junction protein abundance in the setting of diet-induced obesity, which corresponds to worse clinical and histopathological IBD outcomes. These findings are important because as more patients with IBD are affected by obesity and/or diabetes, it is imperative to understand how these disease processes interact.

Citation: Francis KL, Alonge KM, Pacheco MC, Hu SJ, Krutzsch CA, Morton GJ, Schwartz MW, Scarlett JM. Diabetes exacerbates inflammatory bowel disease in mice with diet-induced obesity. *World J Gastroenterol* 2023; 29(33): 4991-5004
URL: https://www.wjgnet.com/1007-9327/full/v29/i33/4991.htm
DOI: https://dx.doi.org/10.3748/wjg.v29.i33.4991

INTRODUCTION

Inflammatory bowel disease (IBD), including Crohn's disease (CD) and ulcerative colitis (UC), and type 2 diabetes (T2D) are among the most challenging and costly medical disorders in modern society. Each is a chronic condition with no permanent medical cure that is increasing in prevalence globally and is associated with significant patient morbidity and economic cost[1,2]. IBD is an autoimmune condition affecting the gastrointestinal tract. The pathogenesis of IBD is multifactorial, involving genetic predisposition, immunologic abnormalities, alterations in gut microbiota, and environmental factors, particularly exposure to a Western diet[3-5]. The pathogenesis of T2D involves insulin resistance and loss of pancreatic β cell function related to risk factors including obesity, visceral adiposity, and exposure to high-fat and high-sugar diets[6,7].

There is increasing evidence that these two disease processes may be linked. Recent national cohort studies have shown that patients with IBD are at increased risk of developing T2D, even after controlling for multiple risk factors including steroid exposure, age, and body mass index[8,9]. Furthermore, the development of T2D in patients with IBD is a predictor of poor disease-related outcomes, with several studies showing higher rates of IBD-related hospitalizations in patients with IBD[10,11] as well as disease flares in patients with either CD or UC and increased IBD-related surgeries in patients with CD[11].

Obesity also constitutes a potential link between T2D and IBD. T2D is strongly associated with obesity, with the majority of T2D patients being either overweight or obese[12,13]. Obesity also affects up to 40% of adult IBD patients, with an additional 20%-40% of patients being overweight[14]. Comorbid obesity in IBD patients has been associated with higher rates of surgical complications and more severe disease that may be less responsive to standard medical therapies [15,16]. Consumption of obesity-inducing high-fat diets (HFD) is a well-known risk factor for developing IBD[17-19], and in preclinical rodent studies, diet-induced obesity (DIO) caused by consuming a HFD worsens clinical and histological IBD outcomes[20,21]. However, the mechanisms underlying the relationship among DIO, T2D, and the development of IBD are unknown.

Notably, both IBD and metabolic syndrome (of which T2D and DIO comprise two of the principle components) are associated with an altered gut microbiome, chronic systemic inflammation, and intestinal barrier dysfunction[4,22,23]. Specifically, the role of increased gut permeability leading to enhanced influx of microbial products from the gut lumen into systemic circulation has been implicated in the pathogenesis of metabolic syndrome and its many complications[22]. Increased gut permeability is also associated with active IBD, as confocal laser endomicroscopic assessment of fluorescent leakage across the intestinal barrier is increased in symptomatic patients with IBD (both CD and UC) compared to

healthy controls and asymptomatic IBD patients[24].

Currently, the mechanisms that link intestinal barrier dysfunction in diabetes, obesity, and IBD remain poorly understood. Recent work indicates that diabetic hyperglycemia may drive intestinal barrier impairments resulting in increased risk for enteric infections[25]. However, the extent to which intestinal barrier dysfunction contributes to the increased risk of IBD complications in patients with comorbid T2D and what role DIO may play in this effect is unknown.

The current work was undertaken to determine the pathogenic role of diabetes to exacerbate intestinal inflammation in a mouse model of IBD with or without coexisting DIO, highlighting intestinal barrier disruption as a mechanism that links diabetes and IBD.

MATERIALS AND METHODS

Animals

Eight-week-old C57BL/6J male mice were purchased from Jackson Laboratory (Bar Harbor, ME, United States). All animals were group-housed under specific pathogen-free conditions in a temperature-controlled environment (14:10 h lights on/off cycle; lights on at 7:00 am) in cages containing a maximum of five animals. Mice were either fed standard laboratory chow (5053 PicoLab® Rodent Diet 20; LabDiet, St. Louis, MO, United States) throughout the study or placed on an HFD (D12492; Research Diets, New Brunswick, NJ, United States) at 8 wk of age for a period of 9 subsequent weeks to induce DIO. All procedures were performed according to the National Institutes of Health Guide for the Care and Use of Laboratory Animals and approved by the Institutional Animal Care and Use Committee at the University of Washington. Body weight (BW) and food intake were recorded at least twice weekly throughout the experiment.

Streptozotocin-induced diabetes

Mice were randomly chosen to be placed on a HFD for 9 wk to induce DIO (n = 30) or maintained on standard chow (n = 20) and then received five consecutive daily intraperitoneal injections of streptozotocin (STZ; Sigma-Aldrich, St. Louis, MO, United States) at a low dose (40 mg/kg BW) to induce diabetes-range hyperglycemia (STZ-diabetes; random blood glucose levels ≥ 250 mg/dL) or sodium citrate vehicle control (Veh) at an equivalent dose (40 mg/kg)[26]. Mice were chosen randomly for the treatment groups, anesthetized with isoflurane during STZ injections, and placed immediately back into their home cage afterwards. Following STZ administration, random blood glucose levels were recorded at least twice weekly throughout the experiment.

Dextran sodium sulfate-induced colitis

Six weeks following STZ or Veh administration, 2% dextran sodium sulfate (DSS) (36-50 kDa; MP Biochemicals, Santa Ana, CA, United States) dissolved in autoclaved water or untreated autoclaved water (Veh) was provided in drinking water for 7 d, with 4-8 animals per experimental group. Animals were acclimated to the medicated water delivery system for 1 wk prior to DSS course in their home cage, with daily water and food intake recorded. To control for the observation that diabetic mice consumed more water leading up to the DSS course, paired water administration was performed during the DSS course. Disease activity index (DAI) scores were calculated daily based on the sum of the percentage of BW lost (0-4), degree of rectal bleeding (0-4), and consistency of stools (0-4)[27].

Diabetes treatment with a sodium-glucose cotransporter-2 inhibitor

A subset of C57BL/6J male mice (n = 23) was placed on an HFD to induce DIO and then received either STZ or sodium citrate Veh as described above. After 6 wk of sustained hyperglycemia, the sodium-glucose cotransporter-2 inhibitor (SGLT2i) dapagliflozin was added to the drinking water for randomly selected groups at a dose of 25 mg/kg based on ideal BW (0.03 kg) to ameliorate hyperglycemia for 3 wk in total[28]. During the last week, 2% DSS was added to drinking water for select experimental groups as detailed above. Results were compared to mice that received drinking water without dapagliflozin. There were 7-8 animals in each experimental group.

Tissue collection

Mice were sacrificed on day 7 of the DSS course by euthanasia with an anesthetic overdose. Blood, colon, small intestine, liver, mesenteric fat, spleen, and fecal samples were collected. The spleen weight was recorded. Sections of liver, spleen, and mesenteric fat were stored either fresh frozen at -80 °C or placed into 10% zinc-buffered formalin (ZBF) for fixation and histological processing. The entire colon was removed from the surrounding mesentery and excised, and the length was measured from the end of the cecum to the end of the rectum. The colon was flushed with 0.1 M phosphate-buffered saline (PBS). A small section of proximal colon was cut and flash frozen at -80 °C, and the remaining colon was fixed in ZBF for histological examination. The small intestine was divided in half and flushed with PBS. Pieces of the proximal and distal small bowel were flash frozen at -80 °C, and the remaining tissue was placed into ZBF. Tissue collection and assessment of intestinal barrier integrity were performed 7 wk after STZ administration, limiting any direct toxic effect of intraperitoneal injection of STZ on the colon.

Histopathology

After the 3 d fixation in ZBF, the intestines were cut longitudinally, swiss-rolled, pinned, and placed in 70% ethanol. Colon, proximal small bowel, and distal small bowel were paraffin embedded, sectioned at 4 μm thickness, deparaffinized, and stained with either hematoxylin and eosin or Alcian blue (AB) to stain mucins by the University of

Washington Diabetes Research Center Cellular and Molecular Imaging Core. Using a modified protocol from Wirtz *et al* [29], histopathologic scoring of the extent of tissue damage was performed by a blinded pathologist, taking into account distribution of tissue damage [0 = none, 1 = focal (less than 3 sites), 2 = moderate (3-5 sites), 3 = diffuse (> 5 sites)], severity of tissue damage (0 = none, 1 = isolated focal epithelial damage, 2 = mucosal erosions and ulcerations, 3 = extensive damage deep into the bowel wall), lamina propria inflammatory cell infiltration (0 = infrequent, 1 = increased, some neutrophils, 2 = submucosal presence of inflammatory cell clusters, 3 = transmural cell infiltrations), and presence of chronic or active inflammation (0 = none, 1 = active, 2 = chronic).

Brightfield microscopy of AB-stained colonic tissues was performed using the Keyence BZ-X800 microscope (Keyence Corp. of America, Itasca, IL, United States). Four random images at × 20 magnification were taken from each animal of intact colonic tissue, avoiding any ulceration of the epithelium, by a blinded independent investigator. Percent area of AB staining was performed using Fiji open source imaging software specific for AB imaging analysis (Color Deconvolution, Vector: AB & H, Color 1). Threshold limits were set (0, 207) and used to measure the percent area of staining across the region of interest selected (four representative crypts per image). This process was repeated for four distinct images per animal, and values were averaged per animal.

Immunofluorescence

Colon sections mounted on slides were deparaffinized with xylene, and antigen-retrieval in 10 mmol/L sodium citrate, pH 6.0 was performed. Sections were incubated in 0.1 M PBS followed by 0.2% Triton X-100 in PBS, then blocked in 2% donkey serum in 0.05% Triton X-100 at 37 °C for 1 h, and finally incubated overnight with rabbit anti-E-cadherin (24E10; Cell Signaling Technology, Danvers, MA, United States). Sections were washed, incubated for 2 h with Alexa 555-conjugated donkey anti-rabbit antibody, and then stained with DAPI.

Immunofluorescence images were captured using the Keyence BZ-X800 microscope, and four random images of intact colonic tissue at × 20 magnification were taken from each animal. Percent area of E-cadherin staining in the epithelium was performed using Fiji open source imaging software, building on prior published immunohistochemistry protein quantification methods[30]. Fluorescent images (E-cadherin: 555) were converted to 8-bit images, threshold staining limits were set (E-cadherin: 9, 255), and the region of interest outlining the entire epithelium captured in the × 20 image was selected. Percent area values were recorded for each image, repeated for a total of four images per animal, and then averaged.

Statistical analysis

Data from individual experiments including blood glucose, DAI, colon length, and spleen length data were shown as dot plots representing data from individual animals, and bar graphs represented mean ± standard error of the mean. AB and E-cadherin data were also presented as mean values ± standard error of the mean. Student's *t* test was used to compare the means in two groups, and one-way analysis of variance was used to compare multiple groups, using GraphPad Prism 5 (GraphPad software, La Jolla, CA, United States). Animals were not excluded from the study unless otherwise indicated. All differences were considered statistically significant at $P < 0.05$.

RESULTS

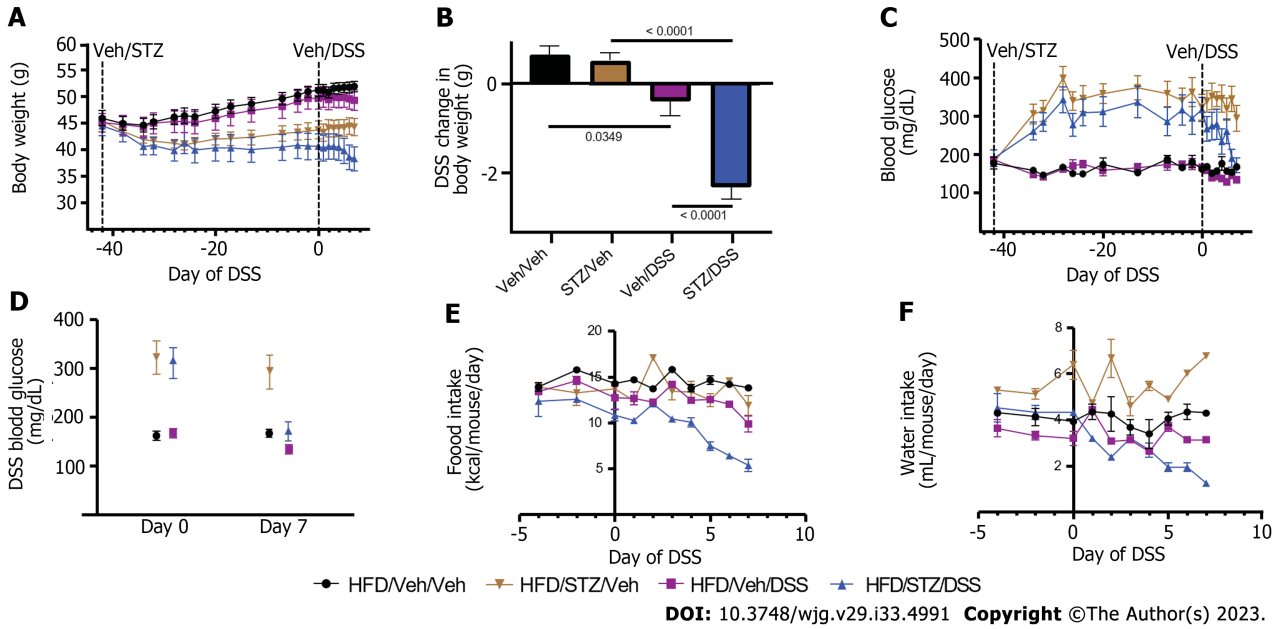
Effects of STZ-diabetes and DSS-induced colitis on BW, blood glucose, food intake, and water consumption in DIO mice

As a first step, we characterized the effects of STZ and DSS administration either alone or in combination on BW, blood glucose, food intake, and water intake in DIO mice. Mice were fed an HFD for 9 wk to induce DIO and then given either Veh or STZ to induce diabetes. After 6 wk, both STZ and Veh groups were subsequently exposed to either DSS or control drinking water (Veh), generating four study groups (Veh/Veh, STZ/Veh, Veh/DSS, and STZ/DSS). In terms of BW, all mice developed DIO after 9 wk of a HFD leading up to STZ administration, with no significant differences in BW between each group (mean BW pre-STZ: Veh/Veh 45.9 ± 3.9 g, Veh/STZ 45.4 ± 1.6 g, Veh/DSS 45.02 ± 5.0 g, STZ/DSS 44.4 ± 5.2 g; $P = 0.924$) (Figure 1A). Following STZ administration, BW decreased relative to Veh-treated controls but stabilized prior to DSS administration (Figure 1A). While BW was maintained in Veh-treated non-diabetic (Veh/Veh) and STZ-diabetic (STZ/Veh) mice, BW declined in both Veh/DSS and STZ/DSS groups throughout the 7-d DSS course but to a greater extent in STZ/DSS mice (Figure 1A and B).

As expected, STZ administration induced diabetes-range hyperglycemia across all groups relative to Veh-treated controls (30-d pre-DSS random blood glucose mean level: STZ 333 ± 31 mg/dL *vs* Veh 167 ± 10 mg/dL; $P < 0.0001$) (Figure 1C). Notably, there was a significant reduction in the blood glucose level during DSS course in the STZ/DSS group (Figure 1C and D), which was associated with a reduction in food and water intake during DSS administration (Figure 1E and F). This reduction in blood glucose during DSS course was less pronounced in non-diabetic DSS-treated mice (Veh/DSS, Figure 1C and D), as the decrease in food and water intake during the DSS course was similarly less significant in these mice (Figure 1E and F). Paired water administration between Veh/DSS-treated and STZ/DSS-treated groups ensured that hyperglycemic mice did not consume more DSS-treated water (Figure 1F).

Diabetic hyperglycemia worsens clinical and pathological outcomes of DSS colitis in DIO mice

We next determined the effects of STZ-hyperglycemia on clinical and histopathological outcomes of DSS colitis in DIO mice. Diabetic STZ/DSS mice had a more rapid onset of DSS colitis, preceding the onset of clinical colitis symptoms in



DOI: 10.3748/wjg.v29.i33.4991 **Copyright** ©The Author(s) 2023.

Figure 1 Body weight, blood glucose, food intake, and water consumption in diabetic diet-induced obese mice. A: Body weight; B: Change in body weight during dextran sodium sulfate (DSS) course; C: Blood glucose; D: Change in blood glucose during the DSS course; E: Food intake; F: Water consumption in high-fat diet-fed, diet-induced obese mice that received either vehicle (Veh) or streptozotocin to induce hyperglycemia and subsequently received Veh or DSS in the drinking water for 7 d to induce colitis. *n* = 7-8 per group, mean ± standard error of the mean. DSS: Dextran sodium sulfate; Veh: Vehicle; STZ: Streptozotocin.

Veh/DSS mice by 2 d (day 2 *vs* day 4 following DSS) (Figure 2A and B), and their DAI scores were significantly higher throughout the entire course of DSS (from days 2-7; Figure 2A and B, $P < 0.05$ on days 2 and 5, $P < 0.0001$ on days 3, 4, 6, and 7), such that by the end of the DSS course (day 7), the mean DAI score was significantly higher in diabetic STZ/DSS mice compared to normoglycemic Veh/DSS controls (Figure 2B). As disease activity was undetectable in groups that did not receive DSS (Veh/Veh and STZ/Veh), we concluded that STZ-diabetes does not independently cause colitis symptoms (Figure 2A).

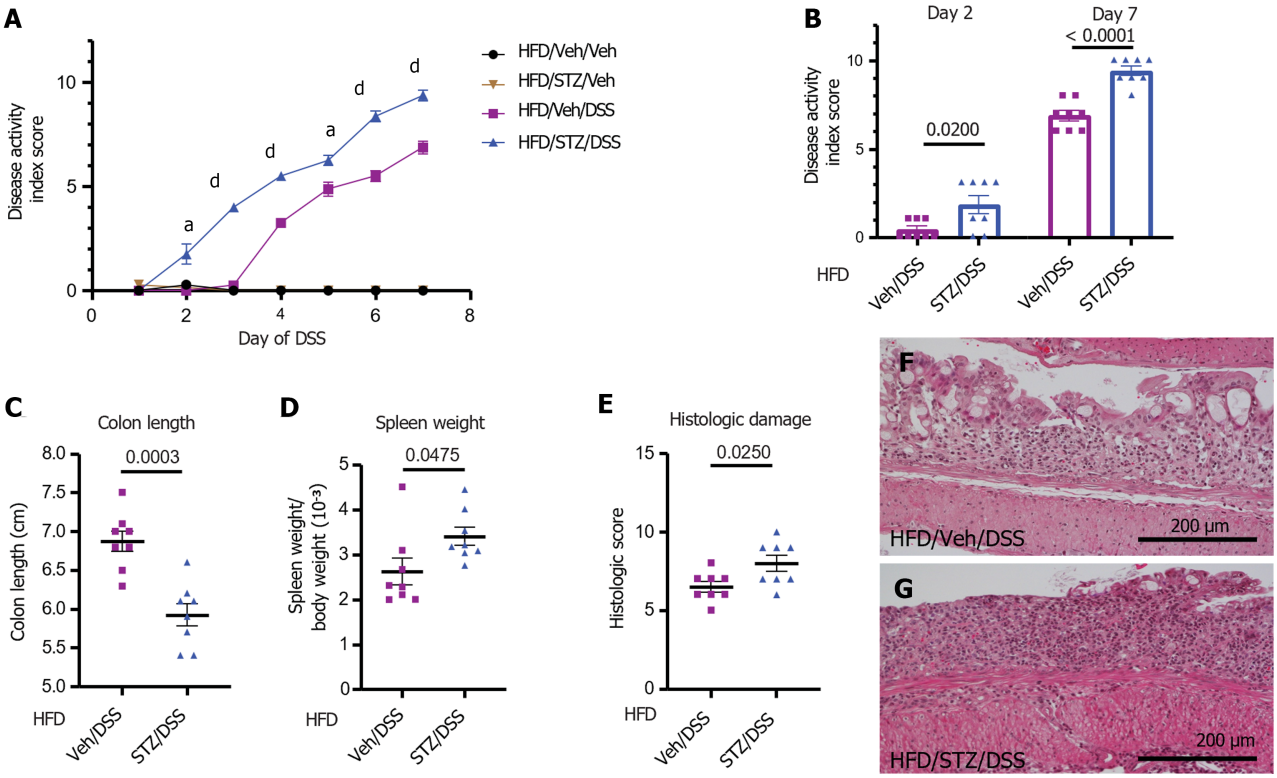
In murine models of IBD, colonic length serves as a pathologic marker of disease severity, as it shortens in response to mural inflammation in DSS colitis[20]. In STZ/DSS mice, the mean colon length at the time of sacrifice on day 7 was significantly shorter compared to Veh/DSS mice (Figure 2C). Spleen weight serves as another pathologic marker of disease severity in DSS colitis, as its weight increases in response to systemic inflammation[20]. Our finding that the spleen-to-BW ratio was significantly higher in STZ/DSS mice than Veh/DSS mice (Figure 2D) indicated greater systemic inflammation in the former group. Consistent with this interpretation, histologic damage scores assessing the degree of colonic inflammation and tissue injury were also significantly higher in STZ/DSS mice than in Veh/DSS mice (Figure 2E-G). Collectively, these findings indicated that in DIO mice, STZ-diabetes both hastens the onset of and worsens the clinical and histopathological severity of DSS-induced colitis.

Effect of hyperglycemia on the intestinal barrier in IBD in DIO mice

To investigate the mechanism by which STZ-hyperglycemia mitigates IBD outcomes in the setting of DIO, we examined the effect of STZ with and without DSS exposure on intestinal barrier function. The mucous layer of the colon and the tight junction proteins in the colonic epithelial layer are key components of the barrier that defend against pathogen entry into the bloodstream. The former is composed of mucins secreted by goblet cells in colonic crypts. By coating the colonic epithelial layer, it limits exposure of the epithelium to luminal contents[31,32]. When this mucous layer is thinned in disease states, its protective properties are diminished, placing the epithelium at greater risk of injury[31,32].

To assess the degree of mucous layer thinning, we stained postmortem colonic tissue for mucins and goblet cells with AB. Our findings showed that in DIO mice, hyperglycemia (STZ/Veh) was associated with significantly reduced AB staining compared to non-diabetic controls (Veh/Veh) (Figure 3A-C). We further showed that at the end of the DSS course in DSS-treated mice, STZ-diabetes was associated with significantly decreased colonic AB staining and sampled from areas of the colon with intact epithelium (Figure 3C). Therefore, diabetes was independently found to impair the colonic mucin barrier, with no significant effect of DSS alone when looking at areas of intact bowel without active colonic inflammation. Loss of the colonic mucin barrier, therefore, could play a causal role in the effect of diabetes to increase the rapidity of onset and severity of DSS colitis in the setting of DIO.

Tight junction proteins are an additional key component of the protective barrier of the colon, as they help to regulate the permeability of the epithelial layer[33]. Changes in the composition and concentration of tight junction proteins that occur in many disease states including IBD are associated with a more permeable epithelial barrier[33-35]. In the setting of DIO, we found that the abundance of the colonic epithelial tight junction protein E-cadherin, a key determinant of epithelial barrier integrity, was significantly decreased in hyperglycemic mice (STZ/Veh)[36] compared to non-diabetic



DOI: 10.3748/wjg.v29.i33.4991 **Copyright** ©The Author(s) 2023.

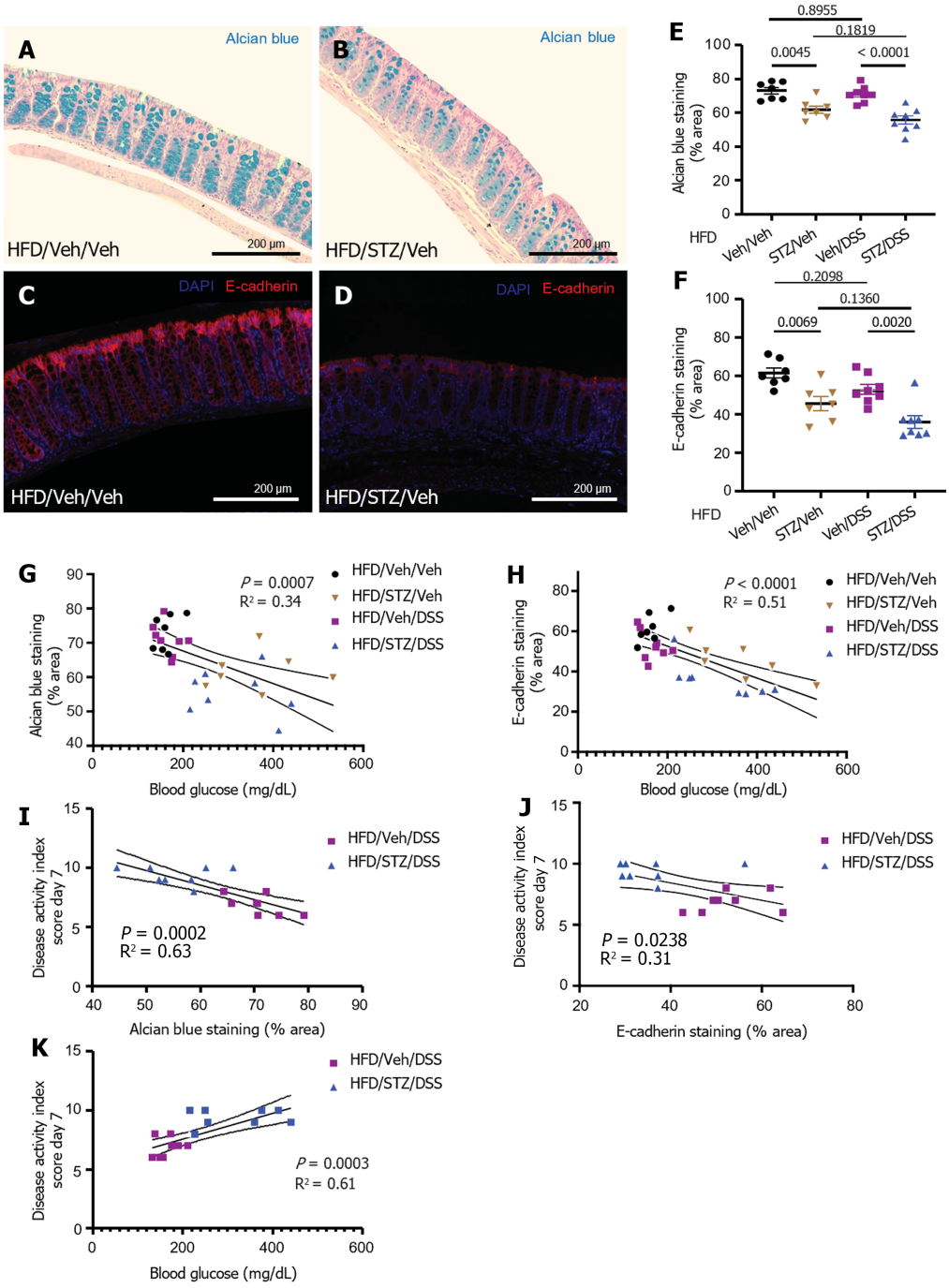
Figure 2 Clinical and pathological outcomes of dextran sodium sulfate colitis in diabetic diet-induced obese mice. A: Clinical disease activity index scores in high-fat diet (HFD)-fed mice that received either vehicle (Veh) or streptozotocin (STZ) to induce diabetes prior to the dextran sodium sulfate (DSS) course; B: Quantification on days 2 and 7; C: Colon length; D: Spleen weight-to-body weight ratio on day 7 of DSS; E: Histologic scoring of DSS damage in colonic tissues from HFD-fed normoglycemic Veh and hyperglycemic STZ mice treated with DSS; F: Representative × 20 images of normoglycemic Veh mice; G: Hyperglycemic STZ mice. n = 7-8 per group, mean ± standard error of the mean. In (A), $^{a}P < 0.05$, $^{d}P < 0.0001$ and comparison noted in (A) is between HFD/Veh/DSS and HFD/STZ/DSS groups for days 2-7 of DSS. DSS: Dextran sodium sulfate; Veh: Vehicle; STZ: Streptozotocin; HFD: High-fat diet.

controls (Veh/Veh) (Figure 3D-F). In the presence of DSS exposure, STZ-diabetes was also associated with a significant decrease of colonic E-cadherin staining (Figure 3F) when superimposed on DIO. Combined with the decrease of the protective mucous layer noted above, these data suggest that epithelial barrier integrity is impaired by diabetic hyperglycemia. Importantly, the degree of hyperglycemia correlated inversely with both AB staining and E-cadherin staining in all DIO mice regardless of exposure to STZ or DSS (Figure 3G and H). Furthermore, in DSS-treated groups, the amount of AB and E-cadherin staining correlated inversely with DAI scores on day 7 (Figure 3I and J). Finally, the degree of hyperglycemia correlated directly with IBD activity (Figure 3K). Taken together, these findings supported a mechanism whereby hyperglycemia increased the onset and severity of DSS colitis by decreasing the expression of key tight junction proteins and diminishing the colonic mucins that help maintain gut epithelial barrier integrity.

Hyperglycemia fails to worsen DSS-colitis symptoms or impair the intestinal barrier in chow-fed mice

To investigate the contribution made by DIO to the deleterious effects of STZ-diabetes on IBD outcomes in mice, we repeated the above experiments in chow-fed mice. Mice were given low-dose STZ (or Veh) to induce T2D-range hyperglycemia 6 wk prior to DSS. In contrast to HFD-fed mice (mean BW 45.1 ± 4.1 g) in the above experiments, chow-fed mice maintained normal BWs leading up to STZ administration (Figure 4A; mean BW 30.1 ± 2.1 g). STZ administration induced hyperglycemia leading up to the DSS course, which was comparable to that observed in mice fed an HFD (Figure 4B). During the course of DSS, in contrast to STZ-diabetic DIO mice, STZ-diabetic chow-fed mice (Chow/STZ/DSS) did not exhibit a more rapid onset or greater degree of severity of colitis following DSS administration compared to chow-fed mice without STZ-diabetes (Chow/Veh/DSS) (Figure 4C). Chow/Veh/DSS mice had a slightly shorter colon length on day 7 of DSS compared to Chow/STZ/DSS mice (Figure 1D), but there were no significant differences in spleen weight between both DSS-treated groups (Figure 1E).

Notably, neither AB mucin staining (Chow/Veh/Veh *vs* Chow/STZ/Veh, $P = 0.761$; Chow/Veh/DSS *vs* Chow/STZ/DSS, $P = 0.994$) (Figure 4) nor E-cadherin tight junction protein staining (Chow/Veh/Veh *vs* Chow/STZ/Veh, $P = 0.863$; Chow/Veh/DSS *vs* Chow/STZ/DSS, $P = 0.999$) (Figure 4G) was impacted by STZ administration among chow-fed mice, irrespective of DSS administration. Thus, non-obese, chow-fed mice were protected from the deleterious effects of STZ-diabetes on both colitis severity and markers of gut epithelial permeability. These findings indicated that hyperglycemia exacerbates DSS-induced colitis only in the setting of DIO.

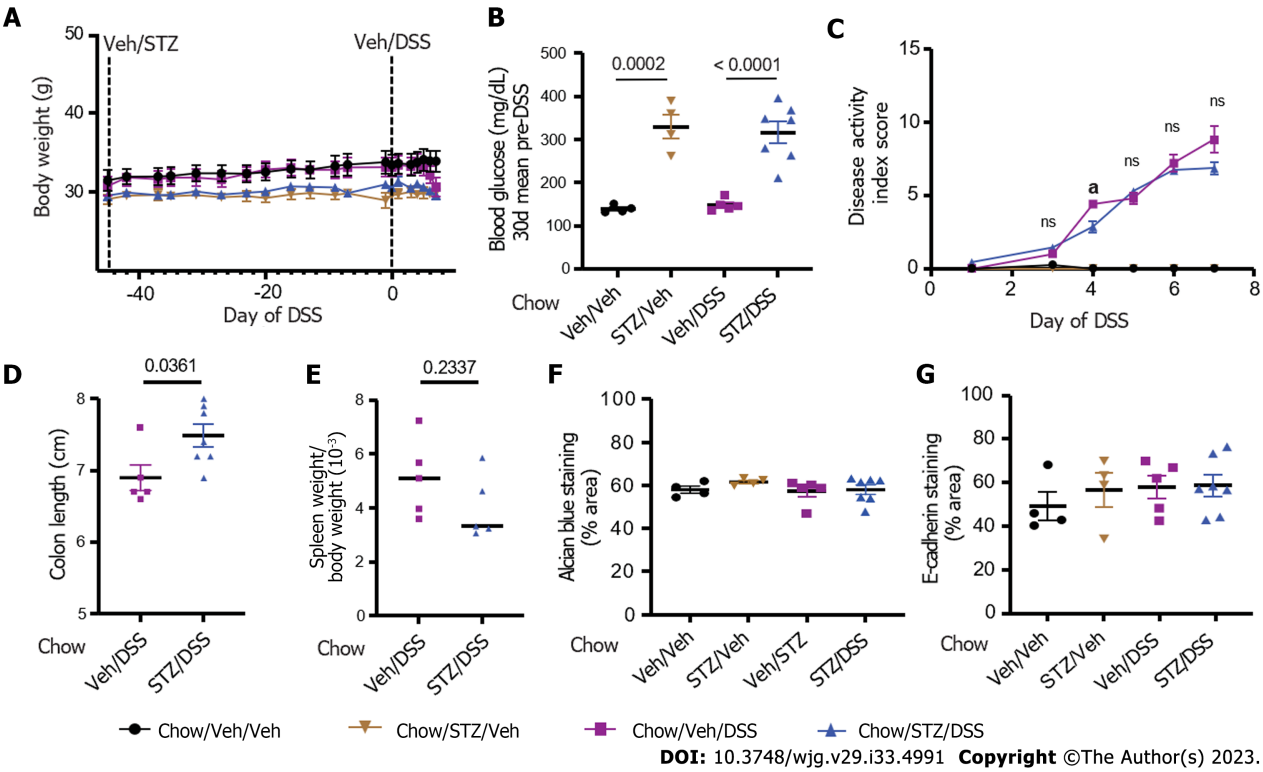


DOI: 10.3748/wjg.v29.i33.4991 **Copyright** ©The Author(s) 2023.

Figure 3 Colonic mucin barrier and tight junction protein abundance in diabetes and dextran sodium sulfate colitis in diet-induced obese mice. A: Alcian blue (AB) staining highlighted the colonic mucin barrier in normoglycemic mice; B: AB staining highlights the colonic mucin barrier in hyperglycemic mice; C: AB staining in areas of the colon with intact epithelium was quantified for each treatment group that received vehicle (Veh)/streptozotocin (STZ) and/or Veh/dextran sodium sulfate (DSS). D: Tight junction protein E-cadherin was highlighted by immunohistochemical staining in the colons of normoglycemic mice; E: Tight junction protein E-cadherin is highlighted by immunohistochemical staining in the colons of hyperglycemic mice; F: E-cadherin abundance in areas of the colon with intact epithelium was quantified for each experimental treatment group; G: Correlation of degree of hyperglycemia with AB staining; H: Correlation of degree of hyperglycemia with E-cadherin staining; I: Correlation of AB staining with clinical colitis disease severity in DSS-treated groups; J: Correlation of E-cadherin staining with clinical colitis disease severity in DSS-treated groups; K: Correlation of degree of hyperglycemia with colitis disease severity in DSS-treated groups. *n* = 7-8 per group, mean ± standard error of the mean. DSS: Dextran sodium sulfate; Veh: Vehicle; STZ: Streptozotocin; HFD: High-fat diet.

Restoring normoglycemia attenuates the deleterious effect of DSS treatment on colitis severity and intestinal barrier integrity

To determine the impact of hyperglycemia per se, independent of other elements of the diabetic state generated by STZ, on intestinal barrier function and colitis outcomes, we repeated the study with DIO mice treated with STZ and DSS, with the additional step of administering the SGLT2i dapagliflozin at a dose that normalizes glycemia to a subgroup of these mice prior to DSS administration[28]. As before, mice were given an HFD to induce DIO (mean BW 49.7 ± 6.2 g)



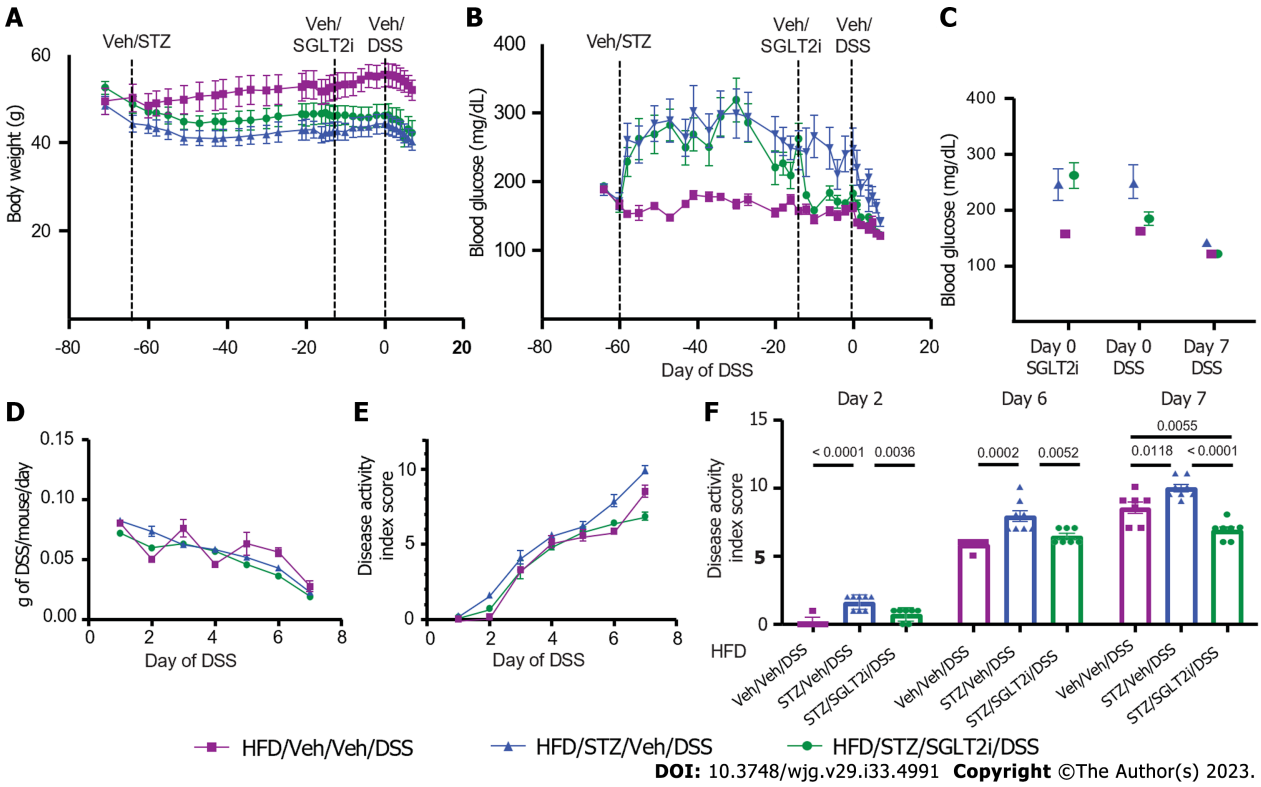
DOI: 10.3748/wjg.v29.i33.4991 **Copyright** ©The Author(s) 2023.

Figure 4 Body weight, blood glucose, clinical disease activity, histopathologic disease activity, and intestinal barrier integrity in diabetic chow-fed mice. A: Body weight; B: Blood glucose in chow-fed non-obese mice that received either vehicle (Veh) or streptozotocin (STZ) to induce diabetes and were then given dextran sodium sulfate (DSS) to induce colitis; C: Clinical DSS colitis disease activity scores in normoglycemic and hyperglycemic mice; D: Colon length; E: Spleen weight-to-body weight ratios; F: Colonic Alcian blue staining; G: Tight junction protein E-cadherin staining quantified from areas with intact colonic epithelium. n = 4-7 per group, mean ± standard error of the mean. $^{a}P < 0.05$, and comparison noted in (C) is between chow/Veh/DSS and chow/STZ/DSS groups for days 3-7 of DSS. DSS: Dextran sodium sulfate; Veh: Vehicle; STZ: Streptozotocin.

(Figure 5A) and were then given either Veh or STZ to induce diabetic-range hyperglycemia (mean post-STZ blood glucose levels: Veh 173.6 ± 15.8 *vs* STZ 282.5 ± 68.6; $P = 0.0007$) (Figure 5B). After 6 wk of sustained hyperglycemia post-STZ treatment, the SGLT2i dapagliflozin (or Veh) was added to the drinking water, which resulted in euglycemic blood glucose levels equivalent to non-STZ treated control levels (mean 10 d pre-DSS blood glucose levels: Veh/Veh/DSS 156.8 ± 11.7 mg/dL *vs* STZ/SGLT2i/DSS 172.8 ± 17.5 mg/dL; $P = 0.793$) (Figure 5B and C) and significantly lower than STZ-treated mice who did not receive dapagliflozin (STZ/Veh/DSS 242.1 ± 72.8mg/dL *vs* STZ/SGLT2i/DSS 172.8 ± 17.5 mg/dL; $P = 0.022$).

After 2 wk of SGLT2i (or Veh) exposure, DSS was added to drinking water for the last week to induce colitis in each group. Similar to our earlier observations in DIO mice (Figure 1), DSS administration caused a significant reduction in BW (Figure 5A) and blood glucose levels in all groups (Figure 5B and C). Paired DSS water administration was performed, and total DSS consumption did not differ significantly between groups (Figure 5D). As previously noted (Figure 2A), the onset of colitis symptoms was accelerated in hyperglycemic STZ/Veh/DSS mice with DIO compared to normoglycemic Veh/Veh/DSS mice, becoming evident by day 2 compared to day 3 (Figure 5E and F). This more rapid onset of symptoms was mitigated by SGLT2i treatment, as STZ/SGLT2i/DSS mice manifested clinical colitis on day 3 instead of day 2 (Figure 5E and F). While symptoms of clinical colitis severity were comparable between groups from days 3-5 (Figure 5E), STZ/Veh/DSS mice demonstrated significantly worse DAI scores on both days 6 and 7 of DSS administration than either non-STZ treated mice (Veh/Veh/DSS) or STZ-treated mice receiving SGLT2i (STZ/SGLT2i/DSS) (Figure 5F).

Similar outcomes were observed when histochemical parameters of epithelial barrier were assessed in areas of intact colon in DSS-treated mice. The effect of untreated hyperglycemia to decrease AB mucins in DIO mice (compared to non-diabetic controls) in intact areas of colonic epithelium was fully reversed by dapagliflozin treatment (Figure 6A and B). Moreover, the amount of colonic AB staining correlated inversely with the degree of hyperglycemia across the three groups (based on 1-wk average blood glucose levels prior to DSS) (Figure 6C). E-cadherin abundance similarly was decreased by STZ treatment and was partially reversed by SGLT2i administration, although this did not achieve statistical significance (Figure 6D and E, $P = 0.050$). The abundance of the colonic tight junction protein E-cadherin reached near significance with an inverse correlation to blood glucose levels as well (Figure 6F). These findings strengthened the conclusion that in DIO mice, hyperglycemia is the primary driver of both STZ-induced colonic epithelial barrier disruption and colitis severity.



DOI: 10.3748/wjg.v29.i33.4991 **Copyright** ©The Author(s) 2023.

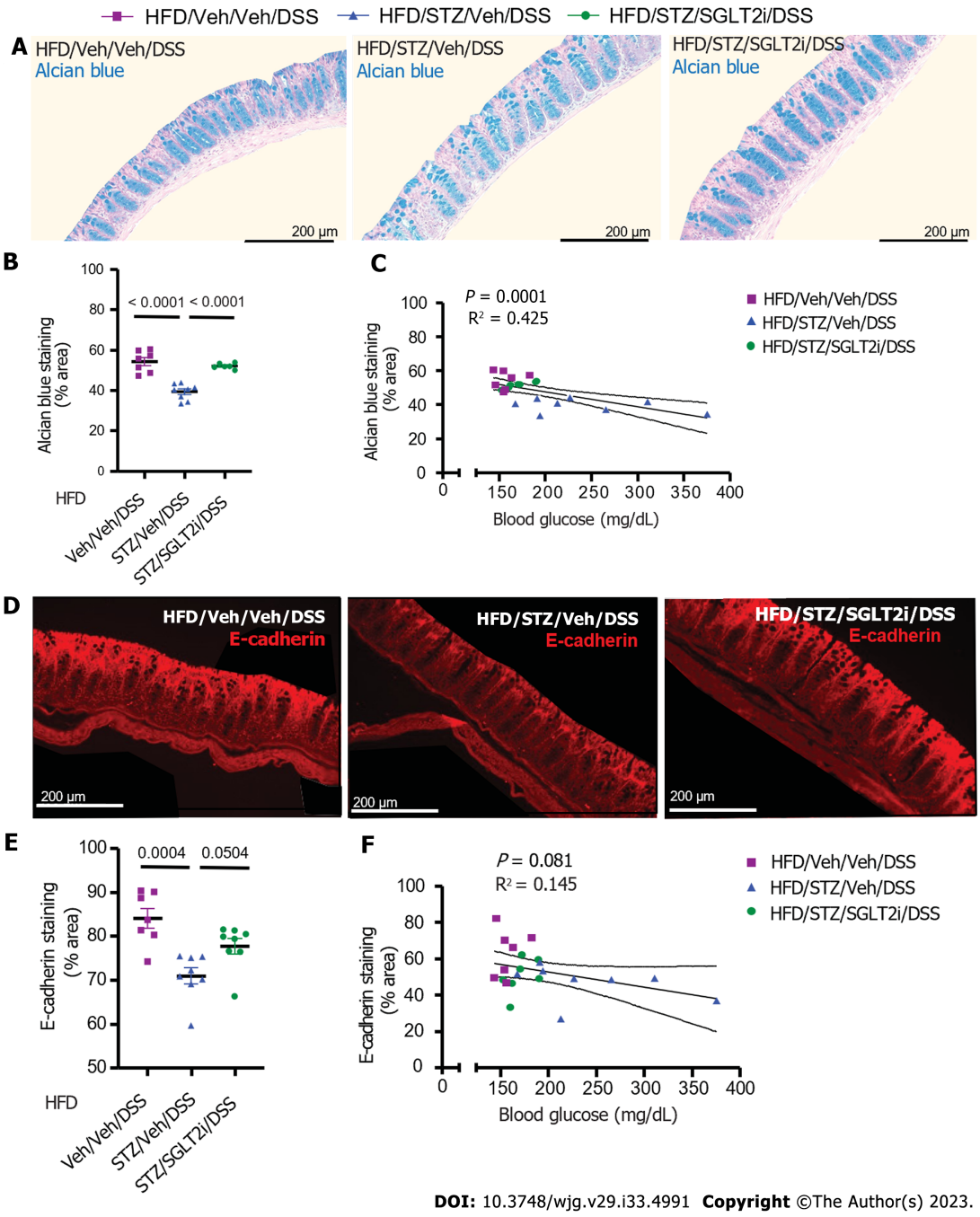
Figure 5 Body weight, blood glucose, and dextran sodium sulfate colitis activity in diabetic diet-induced obese mice on antidiabetic treatment. A: Body weight; B: Blood glucose; C: Change in blood glucose in high-fat diet-fed mice that received either vehicle (Veh) or streptozotocin to induce diabetes and were then treated with the sodium-glucose cotransporter-2 inhibitor dapagliflozin or Veh, prior to dextran sodium sulfate (DSS) colitis onset; D: Amount of DSS consumed during the DSS course; E: DSS colitis disease activity index scores through the 7 d course of DSS; F: DSS colitis disease activity index scores quantified on days 2, 6, and 7. *n* = 7-8 per group, mean ± standard error of the mean. DSS: Dextran sodium sulfate; Veh: Vehicle; STZ: Streptozotocin; HFD: High-fat diet.

DISCUSSION

In the current work, we determined whether diabetic hyperglycemia exacerbates colitis severity in a murine model of IBD. Our findings demonstrated that diabetic hyperglycemia both accelerates the onset and worsens the clinical and pathological outcomes of DSS colitis. Interestingly, each of these effects of diabetes on IBD outcomes was detected in mice with DIO but not in chow-fed, non-obese mice. Furthermore, we show that the severity of IBD increases directly in relation to the degree of hyperglycemia and that reversal of hyperglycemia with an antidiabetic medication eliminated this effect of diabetes. Taken together, these findings support a model whereby the combination of obesity and hyperglycemia predisposes to more severe outcomes of intestinal inflammation in IBD.

As a first step towards understanding the mechanisms by which diabetes and DIO influence IBD outcomes, we sought to investigate the effect of diabetes on the intestinal barrier, focusing in particular on the colonic mucin layer and tight junction proteins. Previous work had suggested that diabetic hyperglycemia impairs intestinal barrier function and increases intestinal permeability, although how this might impact IBD pathology had not been studied[25]. Importantly, it has been reported that symptomatic patients with both UC and CD have increased *in vivo* intestinal permeability[24] and decreased intestinal mucins and goblet cell depletion compared to healthy controls[37]. Additionally, in IBD colon organoid cultures, tight junction proteins are significantly reduced[38]. In our current work, we reported that STZ-induced diabetic hyperglycemia significantly impairs these two components of intestinal barrier integrity in the setting of DIO. Furthermore, the amount of mucins and tight junction protein staining correlated inversely with colitis disease activity. This supported a model in which the diabetic state acts injuriously on the intestinal barrier, making the intestines more susceptible to DSS-induced colitis. It is notable that diabetes on its own is insufficient to cause IBD pathology, but when exposed to a chemical colitic agent, the presence of diabetes and associated impaired intestinal barrier function significantly worsens IBD outcomes.

Our next goal was to determine the contribution of DIO on the effect of diabetes to exacerbate DSS-induced intestinal inflammation. Obesity is present in the vast majority of T2D patients[12,13], and patients with IBD have similar rates of obesity compared to the general population[39]. Comorbid obesity has been associated with higher hospitalization rates, more active disease, and a higher prevalence of perianal disease in patients with CD[40]. In patients with UC, elevated body mass index is associated with an increased risk of biologic therapy treatment failure[41]. Furthermore, HFD exposure exacerbates IBD outcomes in preclinical rodent models[20,21]. Conversely, severe hyperglycemia seen in uncontrolled, insulin-deficient T1D has a deleterious effect on intestinal barrier function independent of obesity[25]. To determine the contribution of DIO on the ability of a more modest, physiologic degree of hyperglycemia mimicking T2D



DOI: 10.3748/wjg.v29.i33.4991 **Copyright** ©The Author(s) 2023.

Figure 6 Colonic mucin barrier and tight junction protein abundance in diet-induced obese mice on antidiabetic treatment with dextran sodium sulfate colitis. A: Alcian blue (AB) staining highlighted the colonic mucin barrier in high-fat diet (HFD)-fed mice administered either vehicle (Veh) or streptozotocin (STZ), followed by antidiabetic treatment with Veh or a sodium-glucose cotransporter-2 inhibitor (SGLT2i) prior to the dextran sodium sulfate (DSS) course; B: AB staining following the DSS course in areas of the colon with intact epithelium was quantified for each treatment group that received Veh/STZ or Veh/SGLT2i; C: Correlation of degree of hyperglycemia with AB staining; D: Tight junction protein E-cadherin staining in the same HFD-fed, DSS-treated mice that received Veh/STZ and Veh/SGLT2i; E: E-cadherin abundance following the DSS course in areas of the colon with intact epithelium; F: Correlation of degree of hyperglycemia with E-cadherin abundance. *n* = 7-8 per group, mean ± standard error of the mean. DSS: Dextran sodium sulfate; Veh: Vehicle; STZ: Streptozotocin; HFD: High-fat diet; SGLT2i: Sodium-glucose cotransporter-2 inhibitor.

to impact intestinal barrier pathology and IBD outcomes, we tested whether low-dose STZ would worsen DSS colitis in DIO mice fed an HFD compared to non-obese, chow-fed mice. We reported here that the effect of modest hyperglycemia to impair intestinal barrier function and therefore influence IBD outcomes is dependent on coexisting DIO. One potential explanation for these findings involves an effect of the HFD exposure on the gut microbiome, shifting its composition to a more mucin-degrading and proinflammatory profile[42]. When superimposed on this change of gut flora and the state of chronic inflammation in obesity, we observed clear-cut, deleterious effects of diabetes on both intestinal permeability and colitis disease activity. Further studies are warranted to determine the exact contribution that the HFD consumption makes to worsen IBD outcomes independent of obesity.

Next, we determined the specific contribution made by hyperglycemia *per se* to the effect of diabetes on intestinal barrier pathology. To this end, we sought to normalize the blood glucose level without reversing other aspects of the uncontrolled diabetic state (*e.g.*, insulin deficiency, elevated circulating levels of ketone bodies and free fatty acids). This goal was achieved by administering an SGLT2i, which selectively normalizes glycemia without impacting insulin levels or other aspects of the diabetic state. We reported that restoring normoglycemia *via* SGLT2i administration after STZ treatment modestly improved clinical colitis outcomes. Notably, the onset of clinical colitis was delayed in mice treated with SGLT2i compared to hyperglycemic mice, and the severity of colitis at the end of the DSS course was significantly improved compared to hyperglycemic mice.

Reversal of hyperglycemia after STZ treatment with an SGLT2i resulted in significant improvement in the colonic mucin barrier, with no difference between non-STZ treated normoglycemic mice and mice treated with STZ who then received SGLT2i. The abundance of tight junction proteins also tended to improve with normalization of the blood glucose level, although it did not reach statistical significance. From these findings, we inferred that the effect of diabetes to influence intestinal barrier pathology and IBD outcomes appears to be dependent, or at least heavily reliant, on hyperglycemia. This conclusion was further supported by our findings that the degree of intestinal barrier dysfunction and colitis disease severity varied directly with the degree of hyperglycemia. These findings heightened the importance of studies to evaluate the impact of effective diabetes treatment in patients with IBD, especially given recent evidence that patients with IBD are at increased risk of developing T2D[8,9], that comorbid T2D predicts poorer IBD outcomes[11], and that high-fat, obesogenic diets are associated with a higher incidence of IBD[17-19].

The growing patient population affected by T2D, obesity, and IBD creates a compelling rationale for continued efforts to understand shared mechanisms between these disease processes, particularly in light of evidence that comorbid T2D or obesity negatively affects IBD outcomes in patients[10,11,40,41]. It is also imperative to understand how treatments for each of these conditions affect the others, particularly as corticosteroids are a mainstay of treatment to induce remission in both UC and CD and are known to both exacerbate hyperglycemia in patients with pre-existing T2D and to precipitate hyperglycemia in patients with no prior diabetes diagnosis[43]. These considerations underscore the need for clinicians to consider how these disease processes and their respective treatments affect their patients and highlight the need to investigate the potential role of antidiabetic medications in IBD management prior to hyperglycemia onset or exacerbation among those at risk.

CONCLUSION

In mice with DIO, diabetic hyperglycemia disrupts the intestinal barrier integrity and is associated with more severe clinical and pathological outcomes of colitis, highlighting the potential translational importance of ensuring optimal diabetes management in IBD patients.

ARTICLE HIGHLIGHTS

Research background

Emerging epidemiologic evidence links type 2 diabetes (T2D) and obesity to inflammatory bowel disease (IBD). However, evidence to determine the exact mechanisms by which obesity and/or diabetes influence IBD outcomes is limited. This study uses mouse models of colitis to investigate how diabetes and obesity interact to impair intestinal barrier function and exacerbate IBD outcomes, highlighting the deleterious impact of sustained hyperglycemia on intestinal barrier integrity.

Research motivation

Patients with IBD are at an increased risk of developing T2D, which serves as a predictor of poor outcomes in IBD. The rates of comorbid obesity in IBD are increasing as well, and obesity is related to a more severe IBD phenotype. As more patients with IBD are affected by obesity and/or T2D, it is imperative to understand how these disease processes interact and how treatments for each condition may impact the other.

Research objectives

In this study, we used murine models of colitis to determine the effect of T2D-range hyperglycemia on IBD outcomes and intestinal barrier function with and without coexisting diet-induced obesity (DIO).

Research methods

Mice were fed standard chow or a high-fat diet to induce DIO and then given streptozotocin (STZ) to induce sustained T2D-range hyperglycemia. Mice were then given dextran sodium sulfate (DSS) to induce colitis. Body weight and blood glucose levels were compared as well as clinical colitis scores and histopathologic assessment of intestinal injury. The effects of hyperglycemia and DIO on intestinal barrier function were interrogated by comparing colonic mucins and tight junction protein abundance. To highlight the role of hyperglycemia itself, a sodium-glucose cotransporter-2 inhibitor was subsequently used to selectively reverse hyperglycemia prior to DSS course.

Research results

In the setting of DIO, STZ-diabetes significantly worsened clinical and histopathological outcomes of DSS colitis in mice. This effect was associated with a significant reduction in the colonic mucin barrier and tight junction protein abundance and was ameliorated by the use of a sodium-glucose cotransporter-2 inhibitor to reverse hyperglycemia prior to colitis onset. Together, these findings highlighted the deleterious effect of diabetic hyperglycemia on the intestinal barrier as a mechanism by which diabetes and obesity interact to affect IBD outcomes.

Research conclusions

This study reported the novel finding that diabetic hyperglycemia disrupted intestinal barrier integrity in the setting of DIO and exacerbated DSS colitis outcomes in mice. Given the increased prevalence of T2D in patients with IBD and the negative impact of comorbid obesity on IBD outcomes, it is imperative to understand how these disease processes interact.

Research perspectives

These findings have significant translational relevance, and future research can expand on them by determining whether strict glycemic control in patients with T2D and IBD is associated with improved IBD outcomes.

ACKNOWLEDGEMENTS

The authors are grateful for the technical assistance provided by Vincent Damian, Bao Anh Phan, Tammy Doan, and Renad Sehat. The authors also thank the University of Washington Department of Comparative Medicine Histology and Imaging Core and the University of Washington Diabetes Research Center Cellular and Molecular Imaging Core for assistance with tissue processing and staining.

FOOTNOTES

Author contributions: Francis KL, Schwartz MW, and Scarlett JM conceived the study; Francis KL and Scarlett JM carried out the experiments and were responsible for the data collection, analysis, and interpretation; Hu SJ and Krutzsch CA participated in the data collection and image analysis; Pacheco MC was responsible for the pathologic analysis of tissues; Francis KL, Scarlett JM, Schwartz MW, Alonge KM, Pacheco MC, Morton GJ, Hu SJ, and Krutzsch CA participated in the study design and data interpretation; Francis KL was responsible for drafting the article; Morton GJ, Alonge KM, Schwartz MW, Pacheco MC, Scarlett SJ, Krutzsch CA, and Scarlett JM were responsible for revising and editing the manuscript.

Supported by The National Institutes of Health under the National Institute of Diabetes and Digestive and Kidney Diseases (NIH-NIDDK), No. DK114474 (JMS) and No. DK128383 (JMS), No. DK131695 (KLF), No. DK101997 (MWS), No. DK083042 (MWS), No. DK089056 (GJM) and No. DK124238 (GJM); Department of Defense (JMS), No. W81XWH2110635; The University of Washington Royalty Research Fund (JMS), No. A139339; The NIH-NIDDK T32 Training Grant (KLF), No. DK007742; The NIH-National Heart, Lung, and Blood Institute T32 Training Grant (KMA), No. HL007028; The NIH-NIDDK–funded Diabetes Research Center, No. P30DK017047; and The Nutrition Obesity Research Center at the University of Washington, No. P30DK035816.

Institutional review board statement: This study was exempted by the Ethics Committee of the University of Washington due to its not involving human subject research.

Institutional animal care and use committee statement: The experimental work involving animals conformed to the Guide for the Care and Use of Laboratory Animals. All procedures were performed according to the National Institutes of Health Guide for the Care and Use of Laboratory Animals and approved by the Institutional Animal Care and Use Committee at the University of Washington.

Conflict-of-interest statement: All authors have no conflicts of interest to declare.

Data sharing statement: There are no additional data available; all data are presented within the article.

ARRIVE guidelines statement: The authors have read the ARRIVE guidelines, and the manuscript was prepared and revised according to the ARRIVE guidelines.

Open-Access: This article is an open-access article that was selected by an in-house editor and fully peer-reviewed by external reviewers. It is distributed in accordance with the Creative Commons Attribution NonCommercial (CC BY-NC 4.0) license, which permits others to distribute, remix, adapt, build upon this work non-commercially, and license their derivative works on different terms, provided the original work is properly cited and the use is non-commercial. See: https://creativecommons.org/Licenses/by-nc/4.0/

Country/Territory of origin: United States

ORCID number: Kendra L Francis 0000-0003-2643-386X; Kimberly M Alonge 0000-0002-2171-1640; Gregory J Morton 0000-0002-8106-8386; Michael W Schwartz 0000-0003-1619-0331; Jarrad M Scarlett 0000-0003-1019-346X.

S-Editor: Fan JR
L-Editor: Filipodia
P-Editor: Cai YX

REFERENCES

1 **GBD 2017 Inflammatory Bowel Disease Collaborators**. The global, regional, and national burden of inflammatory bowel disease in 195 countries and territories, 1990-2017: a systematic analysis for the Global Burden of Disease Study 2017. *Lancet Gastroenterol Hepatol* 2020; **5**: 17-30 [PMID: 31648971 DOI: 10.1016/S2468-1253(19)30333-4]
2 **Shaw JE**, Sicree RA, Zimmet PZ. Global estimates of the prevalence of diabetes for 2010 and 2030. *Diabetes Res Clin Pract* 2010; **87**: 4-14 [PMID: 19896746 DOI: 10.1016/j.diabres.2009.10.007]
3 **Guan Q**. A Comprehensive Review and Update on the Pathogenesis of Inflammatory Bowel Disease. *J Immunol Res* 2019; **2019**: 7247238 [PMID: 31886308 DOI: 10.1155/2019/7247238]
4 **Nishida A**, Inoue R, Inatomi O, Bamba S, Naito Y, Andoh A. Gut microbiota in the pathogenesis of inflammatory bowel disease. *Clin J Gastroenterol* 2018; **11**: 1-10 [PMID: 29285689 DOI: 10.1007/s12328-017-0813-5]
5 **Xavier RJ**, Podolsky DK. Unravelling the pathogenesis of inflammatory bowel disease. *Nature* 2007; **448**: 427-434 [PMID: 17653185 DOI: 10.1038/nature06005]
6 **Kahn SE**, Hull RL, Utzschneider KM. Mechanisms linking obesity to insulin resistance and type 2 diabetes. *Nature* 2006; **444**: 840-846 [PMID: 17167471 DOI: 10.1038/nature05482]
7 **Zheng Y**, Ley SH, Hu FB. Global aetiology and epidemiology of type 2 diabetes mellitus and its complications. *Nat Rev Endocrinol* 2018; **14**: 88-98 [PMID: 29219149 DOI: 10.1038/nrendo.2017.151]
8 **Jess T**, Jensen BW, Andersson M, Villumsen M, Allin KH. Inflammatory Bowel Diseases Increase Risk of Type 2 Diabetes in a Nationwide Cohort Study. *Clin Gastroenterol Hepatol* 2020; **18**: 881-888.e1 [PMID: 31394285 DOI: 10.1016/j.cgh.2019.07.052]
9 **Kang EA**, Han K, Chun J, Soh H, Park S, Im JP, Kim JS. Increased Risk of Diabetes in Inflammatory Bowel Disease Patients: A Nationwide Population-based Study in Korea. *J Clin Med* 2019; **8** [PMID: 30862129 DOI: 10.3390/jcm8030343]
10 **Fuschillo G**, Celentano V, Rottoli M, Sciaudone G, Gravina AG, Pellegrino R, Marfella R, Romano M, Selvaggi F, Pellino G. Influence of diabetes mellitus on inflammatory bowel disease course and treatment outcomes. A systematic review with meta-analysis. *Dig Liver Dis* 2023; **55**: 580-586 [PMID: 36058820 DOI: 10.1016/j.dld.2022.08.017]
11 **Kumar A**, Teslova T, Taub E, Miller JD, Lukin DJ. Comorbid Diabetes in Inflammatory Bowel Disease Predicts Adverse Disease-Related Outcomes and Infectious Complications. *Dig Dis Sci* 2021; **66**: 2005-2013 [PMID: 32617771 DOI: 10.1007/s10620-020-06439-4]
12 **Iglay K**, Hannachi H, Joseph Howie P, Xu J, Li X, Engel SS, Moore LM, Rajpathak S. Prevalence and co-prevalence of comorbidities among patients with type 2 diabetes mellitus. *Curr Med Res Opin* 2016; **32**: 1243-1252 [PMID: 26986190 DOI: 10.1185/03007995.2016.1168291]
13 **Leitner DR**, Frühbeck G, Yumuk V, Schindler K, Micic D, Woodward E, Toplak H. Obesity and Type 2 Diabetes: Two Diseases with a Need for Combined Treatment Strategies - EASO Can Lead the Way. *Obes Facts* 2017; **10**: 483-492 [PMID: 29020674 DOI: 10.1159/000480525]
14 **Singh S**, Dulai PS, Zarrinpar A, Ramamoorthy S, Sandborn WJ. Obesity in IBD: epidemiology, pathogenesis, disease course and treatment outcomes. *Nat Rev Gastroenterol Hepatol* 2017; **14**: 110-121 [PMID: 27899815 DOI: 10.1038/nrgastro.2016.181]
15 **Swanson SM**, Harper J, Zisman TL. Obesity and inflammatory bowel disease: diagnostic and therapeutic implications. *Curr Opin Gastroenterol* 2018; **34**: 112-119 [PMID: 29356687 DOI: 10.1097/MOG.0000000000000422]
16 **Weissman S**, Patel K, Kolli S, Lipcsey M, Qureshi N, Elias S, Walfish A, Swaminath A, Feuerstein JD. Obesity in Inflammatory Bowel Disease Is Associated with Early Readmissions Characterised by an Increased Systems and Patient-level Burden. *J Crohns Colitis* 2021; **15**: 1807-1815 [PMID: 33999137 DOI: 10.1093/ecco-jcc/jjab088]
17 **Lewis JD**, Abreu MT. Diet as a Trigger or Therapy for Inflammatory Bowel Diseases. *Gastroenterology* 2017; **152**: 398-414.e6 [PMID: 27793606 DOI: 10.1053/j.gastro.2016.10.019]
18 **Owczarek D**, Rodacki T, Domagała-Rodacka R, Cibor D, Mach T. Diet and nutritional factors in inflammatory bowel diseases. *World J Gastroenterol* 2016; **22**: 895-905 [PMID: 26811635 DOI: 10.3748/wjg.v22.i3.895]
19 **Reif S**, Klein I, Lubin F, Farbstein M, Hallak A, Gilat T. Pre-illness dietary factors in inflammatory bowel disease. *Gut* 1997; **40**: 754-760 [PMID: 9245929 DOI: 10.1136/gut.40.6.754]
20 **Cheng L**, Jin H, Qiang Y, Wu S, Yan C, Han M, Xiao T, Yan N, An H, Zhou X, Shao Q, Xia S. High fat diet exacerbates dextran sulfate sodium induced colitis through disturbing mucosal dendritic cell homeostasis. *Int Immunopharmacol* 2016; **40**: 1-10 [PMID: 27567245 DOI: 10.1016/j.intimp.2016.08.018]
21 **Paik J**, Fierce Y, Treuting PM, Brabb T, Maggio-Price L. High-fat diet-induced obesity exacerbates inflammatory bowel disease in genetically susceptible Mdr1a-/- male mice. *J Nutr* 2013; **143**: 1240-1247 [PMID: 23761644 DOI: 10.3945/jn.113.174615]
22 **Winer DA**, Luck H, Tsai S, Winer S. The Intestinal Immune System in Obesity and Insulin Resistance. *Cell Metab* 2016; **23**: 413-426 [PMID: 26853748 DOI: 10.1016/j.cmet.2016.01.003]
23 **Michielan A**, D'Incà R. Intestinal Permeability in Inflammatory Bowel Disease: Pathogenesis, Clinical Evaluation, and Therapy of Leaky Gut. *Mediators Inflamm* 2015; **2015**: 628157 [PMID: 26582965 DOI: 10.1155/2015/628157]
24 **Chang J**, Leong RW, Wasinger VC, Ip M, Yang M, Phan TG. Impaired Intestinal Permeability Contributes to Ongoing Bowel Symptoms in Patients With Inflammatory Bowel Disease and Mucosal Healing. *Gastroenterology* 2017; **153**: 723-731.e1 [PMID: 28601482 DOI: 10.1053/j.gastro.2017.05.056]
25 **Thaiss CA**, Levy M, Grosheva I, Zheng D, Soffer E, Blacher E, Braverman S, Tengeler AC, Barak O, Elazar M, Ben-Zeev R, Lehavi-Regev D, Katz MN, Pevsner-Fischer M, Gertler A, Halpern Z, Harmelin A, Aamar S, Serradas P, Grosfeld A, Shapiro H, Geiger B, Elinav E. Hyperglycemia drives intestinal barrier dysfunction and risk for enteric infection. *Science* 2018; **359**: 1376-1383 [PMID: 29519916 DOI: 10.1126/science.aar3318]
26 **Scarlett JM**, Rojas JM, Matsen ME, Kaiyala KJ, Stefanovski D, Bergman RN, Nguyen HT, Dorfman MD, Lantier L, Wasserman DH, Mirzadeh Z, Unterman TG, Morton GJ, Schwartz MW. Central injection of fibroblast growth factor 1 induces sustained remission of diabetic

hyperglycemia in rodents. *Nat Med* 2016; **22**: 800-806 [PMID: 27213816 DOI: 10.1038/nm.4101]

27 **Eichele DD**, Kharbanda KK. Dextran sodium sulfate colitis murine model: An indispensable tool for advancing our understanding of inflammatory bowel diseases pathogenesis. *World J Gastroenterol* 2017; **23**: 6016-6029 [PMID: 28970718 DOI: 10.3748/wjg.v23.i33.6016]

28 **Nagareddy PR**, Kraakman M, Masters SL, Stirzaker RA, Gorman DJ, Grant RW, Dragoljevic D, Hong ES, Abdel-Latif A, Smyth SS, Choi SH, Korner J, Bornfeldt KE, Fisher EA, Dixit VD, Tall AR, Goldberg IJ, Murphy AJ. Adipose tissue macrophages promote myelopoiesis and monocytosis in obesity. *Cell Metab* 2014; **19**: 821-835 [PMID: 24807222 DOI: 10.1016/j.cmet.2014.03.029]

29 **Wirtz S**, Popp V, Kindermann M, Gerlach K, Weigmann B, Fichtner-Feigl S, Neurath MF. Chemically induced mouse models of acute and chronic intestinal inflammation. *Nat Protoc* 2017; **12**: 1295-1309 [PMID: 28569761 DOI: 10.1038/nprot.2017.044]

30 **Crowe AR**, Yue W. Semi-quantitative Determination of Protein Expression using Immunohistochemistry Staining and Analysis: An Integrated Protocol. *Bio Protoc* 2019; **9** [PMID: 31867411 DOI: 10.21769/bioprotoc.3465]

31 **Hansson GC**. Mucus and mucins in diseases of the intestinal and respiratory tracts. *J Intern Med* 2019; **285**: 479-490 [PMID: 30963635 DOI: 10.1111/joim.12910]

32 **Kim YS**, Ho SB. Intestinal goblet cells and mucins in health and disease: recent insights and progress. *Curr Gastroenterol Rep* 2010; **12**: 319-330 [PMID: 20703838 DOI: 10.1007/s11894-010-0131-2]

33 **Landy J**, Ronde E, English N, Clark SK, Hart AL, Knight SC, Ciclitira PJ, Al-Hassi HO. Tight junctions in inflammatory bowel diseases and inflammatory bowel disease associated colorectal cancer. *World J Gastroenterol* 2016; **22**: 3117-3126 [PMID: 27003989 DOI: 10.3748/wjg.v22.i11.3117]

34 **Weber CR**, Turner JR. Inflammatory bowel disease: is it really just another break in the wall? *Gut* 2007; **56**: 6-8 [PMID: 17172583 DOI: 10.1136/gut.2006.104182]

35 **Clayburgh DR**, Shen L, Turner JR. A porous defense: the leaky epithelial barrier in intestinal disease. *Lab Invest* 2004; **84**: 282-291 [PMID: 14767487 DOI: 10.1038/Labinvest.3700050]

36 **Daulagala AC**, Bridges MC, Kourtidis A. E-cadherin Beyond Structure: A Signaling Hub in Colon Homeostasis and Disease. *Int J Mol Sci* 2019; **20** [PMID: 31195621 DOI: 10.3390/ijms20112756]

37 **Kang Y**, Park H, Choe BH, Kang B. The Role and Function of Mucins and Its Relationship to Inflammatory Bowel Disease. *Front Med (Lausanne)* 2022; **9**: 848344 [PMID: 35602503 DOI: 10.3389/fmed.2022.848344]

38 **d'Aldebert E**, Quaranta M, Sébert M, Bonnet D, Kirzin S, Portier G, Duffas JP, Chabot S, Lluel P, Allart S, Ferrand A, Alric L, Racaud-Sultan C, Mas E, Deraison C, Vergnolle N. Characterization of Human Colon Organoids From Inflammatory Bowel Disease Patients. *Front Cell Dev Biol* 2020; **8**: 363 [PMID: 32582690 DOI: 10.3389/fcell.2020.00363]

39 **Losurdo G**, La Fortezza RF, Iannone A, Contaldo A, Barone M, Ierardi E, Di Leo A, Principi M. Prevalence and associated factors of obesity in inflammatory bowel disease: A case-control study. *World J Gastroenterol* 2020; **26**: 7528-7537 [PMID: 33384552 DOI: 10.3748/wjg.v26.i47.7528]

40 **Blain A**, Cattan S, Beaugerie L, Carbonnel F, Gendre JP, Cosnes J. Crohn's disease clinical course and severity in obese patients. *Clin Nutr* 2002; **21**: 51-57 [PMID: 11884013 DOI: 10.1054/clnu.2001.0503]

41 **Kurnool S**, Nguyen NH, Proudfoot J, Dulai PS, Boland BS, Vande Casteele N, Evans E, Grunvald EL, Zarrinpar A, Sandborn WJ, Singh S. High body mass index is associated with increased risk of treatment failure and surgery in biologic-treated patients with ulcerative colitis. *Aliment Pharmacol Ther* 2018; **47**: 1472-1479 [PMID: 29665045 DOI: 10.1111/apt.14665]

42 **Martinez-Medina M**, Denizot J, Dreux N, Robin F, Billard E, Bonnet R, Darfeuille-Michaud A, Barnich N. Western diet induces dysbiosis with increased E coli in CEABAC10 mice, alters host barrier function favouring AIEC colonisation. *Gut* 2014; **63**: 116-124 [PMID: 23598352 DOI: 10.1136/gutjnl-2012-304119]

43 **Elena C**, Chiara M, Angelica B, Chiara MA, Laura N, Chiara C, Claudio C, Antonella F, Nicola G. Hyperglycemia and Diabetes Induced by Glucocorticoids in Nondiabetic and Diabetic Patients: Revision of Literature and Personal Considerations. *Curr Pharm Biotechnol* 2018; **19**: 1210-1220 [PMID: 30605054 DOI: 10.2174/1389201020666190102145305]

World Journal of Gastroenterology

Submit a Manuscript: https://www.f6publishing.com

World J Gastroenterol 2023 September 7; 29(33): 5005-5013

DOI: 10.3748/wjg.v29.i33.5005

ISSN 1007-9327 (print) ISSN 2219-2840 (online)

ORIGINAL ARTICLE

Basic Study

Novel deformable self-assembled magnetic anastomosis ring for endoscopic treatment of colonic stenosis *via* natural orifice

Miao-Miao Zhang, Guang-Bin Zhao, Han-Zhi Zhang, Shu-Qin Xu, Ai-Hua Shi, Jian-Qi Mao, Jing-Ci Gai, Yu-Han Zhang, Jia Ma, Yun Li, Yi Lyu, Xiao-Peng Yan

Specialty type: Gastroenterology and hepatology

Provenance and peer review: Unsolicited article; Externally peer reviewed.

Peer-review model: Single blind

Peer-review report's scientific quality classification

Grade A (Excellent): A, A
Grade B (Very good): 0
Grade C (Good): 0
Grade D (Fair): 0
Grade E (Poor): 0

P-Reviewer: Martino A, Italy; Şurlin VM, Romania

Received: June 14, 2023
Peer-review started: June 14, 2023
First decision: August 5, 2023
Revised: August 7, 2023
Accepted: August 15, 2023
Article in press: August 15, 2023
Published online: September 7, 2023

Miao-Miao Zhang, Shu-Qin Xu, Yun Li, Yi Lyu, Xiao-Peng Yan, Department of Hepatobiliary Surgery, The First Affiliated Hospital of Xi'an Jiaotong University, Xi'an 710061, Shaanxi Province, China

Miao-Miao Zhang, Shu-Qin Xu, Ai-Hua Shi, Yi Lyu, Xiao-Peng Yan, National Local Joint Engineering Research Center for Precision Surgery & Regenerative Medicine, The First Affiliated Hospital of Xi'an Jiaotong University, Xi'an 710061, Shaanxi Province, China

Guang-Bin Zhao, State Key Laboratory for Manufacturing System Engineering, School of Mechanical Engineering, Xi'an Jiaotong University, Xi'an 710054, Shaanxi Province, China

Han-Zhi Zhang, Jing-Ci Gai, Yu-Han Zhang, Qide College, Xi'an Jiaotong University, Xi'an 710061, Shaanxi Province, China

Jian-Qi Mao, Zonglian College, Xi'an Jiaotong University, Xi'an 710061, Shaanxi Province, China

Jia Ma, Department of Surgical Oncology, Shaanxi Provincial People's Hospital, Xi'an 710068, Shaanxi Province, China

Corresponding author: Xiao-Peng Yan, MD, PhD, Associate Research Scientist, Department of Hepatobiliary Surgery, The First Affiliated Hospital of Xi'an Jiaotong University, No. 277 West Yanta Road, Xi'an 710061, Shaanxi Province, China. yanxiaopeng9966@163.com

Abstract

BACKGROUND

Although endoscope-assisted magnetic compression anastomosis has already been reported for colonic anastomosis, there is no report on a single-approach operation using the natural orifice.

AIM

To design a deformable self-assembled magnetic anastomosis ring (DSAMAR) for colonic anastomosis for use in single-approach operation and evaluate its feasibility and safety through animal experiments.

METHODS

The animal model for colonic stenosis was prepared by partial colonic ligation in

eight beagles. The magnetic compression anastomosis of their colonic stricture was performed by endoscopically assisted transanal implantation of the DSAMAR. The anastomotic specimen, obtained 2 wk after the operation, was observed by both the naked eye and a light microscope.

RESULTS

The DSAMAR was successfully inserted into the proximal end of colon stenosis through the anus. The DSAMAR of seven dogs was successfully transformed into rings, while that of the remaining dog was removed after the first deformation failed. The rings were successfully retransformed after optimization. All animals underwent colonic anastomosis using the DSAMAR. No device-related or procedure-related adverse events were observed. The colostomy specimens of the experimental dogs were obtained 2 wk after the operation. Both gross and histological observations showed good anastomotic healing.

CONCLUSION

The DSAMAR is a safe and feasible option for the treatment of colon stenosis. Its specific deformation and self-assembly capability maximize the applicability of the minimally invasive treatment.

Key Words: Magnetic surgery; Magnamosis; Colonic stenosis; Natural orifice; Endoscopy

©The Author(s) 2023. Published by Baishideng Publishing Group Inc. All rights reserved.

Core Tip: By combining magnetic compression anastomosis with endoscopic technology, we could design a deformable self-assembled magnetic anastomosis ring (DSAMAR) to perform magnetic compression anastomosis with only a single channel. We then verified the feasibility of magnetic compression anastomosis for the recanalization of colonic stenosis through animal experiments. The results showed that minimally invasive treatment of colonic stenosis can be achieved using the DSAMAR.

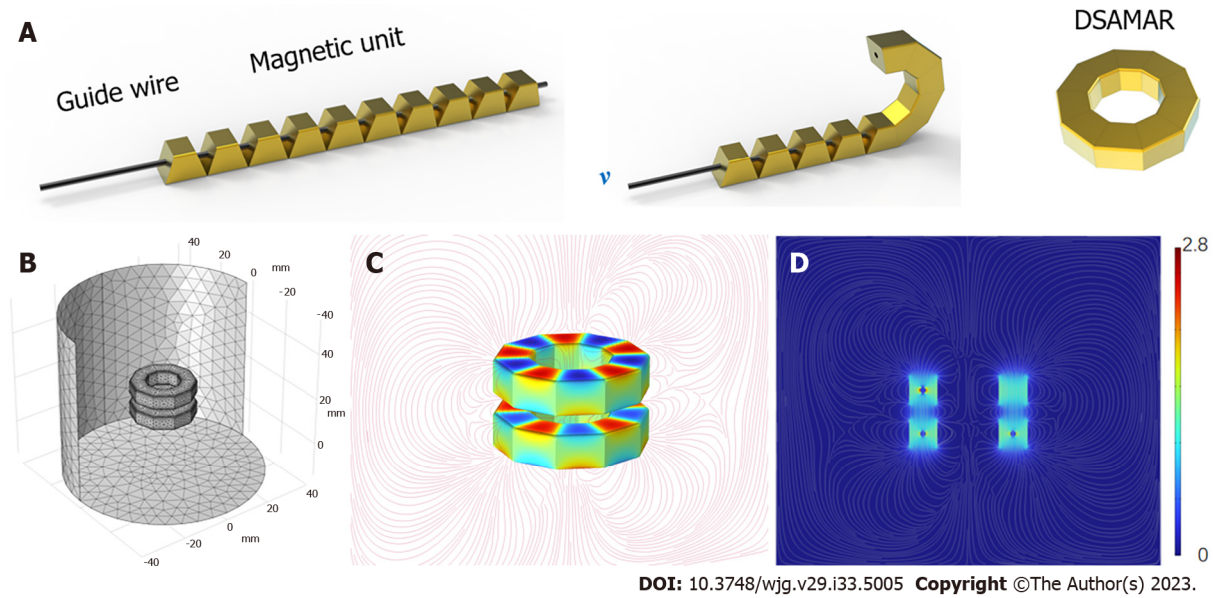
Citation: Zhang MM, Zhao GB, Zhang HZ, Xu SQ, Shi AH, Mao JQ, Gai JC, Zhang YH, Ma J, Li Y, Lyu Y, Yan XP. Novel deformable self-assembled magnetic anastomosis ring for endoscopic treatment of colonic stenosis *via* natural orifice. *World J Gastroenterol* 2023; 29(33): 5005-5013
URL: https://www.wjgnet.com/1007-9327/full/v29/i33/5005.htm
DOI: https://dx.doi.org/10.3748/wjg.v29.i33.5005

INTRODUCTION

Benign colonic stenosis is a disease with various causes, including post-colectomy anastomotic stenosis[1], transcatheter arterial embolization[2], and acute pancreatitis[3]. Benign colonic stenosis is generally treated by endoscopic balloon dilatation (EBD)[4] and surgery[5]. EBD is widely performed in clinics because of its effectiveness, technical safety, and ease of process. However, in some cases, sufficient dilatation is not achieved because of the formation of stiff fibrosis tissue at the stenosis site, which is often resistant to balloon pressure[6]. Open surgery, laparoscopic stenosis resection, and bypass anastomosis are the traditional treatment strategies for benign colonic stenosis. Although a good therapeutic effect can be obtained through surgery, it is no longer the first choice of clinicians because of trauma and various perioperative adverse events.

Magnetic compression anastomosis or magnamosis, a novel technique, can be used for managing digestive tract anastomosis[7-9], vascular anastomosis[10,11], pathologic fistula[12], and therapeutic fistula[13]. The use of magnamosis along with endoscopy for treating gastrointestinal stenosis has been reported[14]. The cylinder or circle is the most commonly used shape of the magnet in such cases. In endoscopic magnetic compression anastomosis, the daughter and parent magnets are placed at the two opposite ends of the narrow digestive duct. The patient must have two channels: A natural orifice and the digestive tract fistula[14,15]. However, some patients only have a natural orifice, making magnetic compression anastomosis very difficult to perform. Therefore, for successful magnamosis, the magnet must be designed in a way that allows efficient optimization of the operation path. The design of the magnet must meet two conditions: first, the magnet should be able to pass through the narrow digestive cavity; and second, the magnet should be able to create wide anastomoses.

This study aims to design a novel deformable self-assembled magnetic anastomosis ring (DSAMAR) that can be placed at the natural orifice of the body. It also explores the feasibility of the DSAMAR in digestive tract anastomosis using dogs as experimental animals.



DOI: 10.3748/wjg.v29.i33.5005 **Copyright** ©The Author(s) 2023.

Figure 1 A schematic of the deformable self-assembled magnetic anastomosis ring. A: Transformation of the deformable self-assembled magnetic anastomosis ring from a linear structure to a ring; B to D: Computer simulation of magnetic flux density. DSAMAR: Deformable self-assembled magnetic anastomosis ring.

MATERIALS AND METHODS

Ethical statement

The experimental protocol was approved by the Committee for Ethics of Animal Experiments of Xi'an Jiaotong University (license No. 2022-1451). Eight beagles (male = 4, female = 4) were acquired from the Laboratory Animal Center of the Xi'an Jiaotong University (Xi'an, China) as experimental animals. The research protocol and all the experimental procedures were conducted strictly in accordance with the Guidelines for the Care and Use of Experimental Animals issued by the Xi'an Jiaotong University Medical Center.

DSAMAR

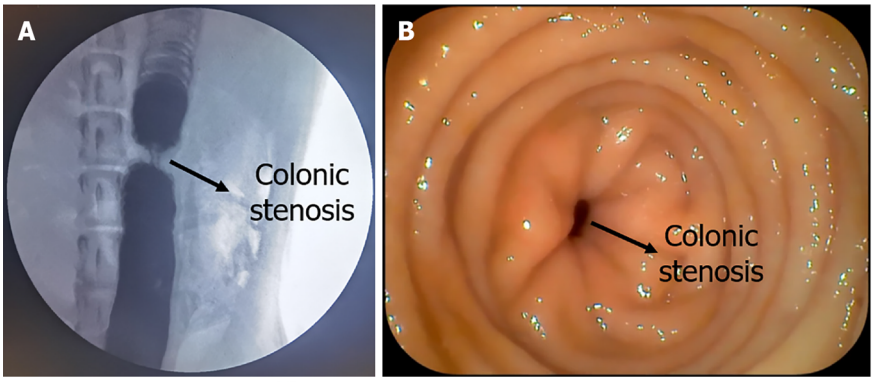
The DSAMAR consists of 10 trapezoidal magnetic units assembled in the opposite order of the N and S poles of the adjacent magnetic units. The long-axis direction of each magnetic unit contains a 1-mm diameter round hole that allows the stainless steel guide wire to pass through. Owing to the opposite N–S polarity of each magnetic unit, passing 10 sequentially arranged trapezoidal magnetic units through a hard guide wire and forming a linear arrangement is possible. When the guide wire is slowly drawn out, the inclined planes of the adjacent magnetic units attract each other and are sequentially arranged and assembled into a DSAMAR (Figure 1A) (Video 1). The magnetic unit is processed by N50-sintered neodymium-iron-boron, and its surface is coated with titanium nitride. Each magnetic unit of a DSAMAR weighs 1.25 g, the maximal magnetic field intensity at its compression surfaces is 480 mT, and the suction of two DSAMARs at zero distance can reach 184 N. The magnetic flux density can be calculated by computer simulations (Figure 1B-D).

Study design

This study aimed to verify the feasibility of the DSAMAR, an innovative surgical method. Hence, no control group was used. Eight beagles (age: > 1 year; weight: 12–15 kg) were used as experimental animals. Their operation time, postoperative adverse events, survival rate, and magnetic-ring-expel time were recorded. One month after the operation, the anastomosis was achieved and its healing was observed both by the naked eye and a light microscope.

Colonic stenosis model

The beagles were given a slag-free liquid diet 2 d before surgery. In addition, they were fasted and their water intake was restricted 6 h before surgery. They were anesthetized by an intravenous injection of 3% pentobarbital sodium (1 mL/kg) and fixed in the supine position. Repeat enemas with soapy water were conducted to clean the intestines. A 14Fr gastric tube was inserted into the colon through the anus. An approximately 10-cm-long incision in the middle of the lower abdomen was made into the abdominal cavity. The descending colon was exposed and ligated on the 14Fr gastric tube with a 1-0 silk thread in the middle part of the descending colon. The gastric tube was removed and a colon stenosis model was formed. The diameter of the colon in the narrow segment was approximately 4.5 mm. The abdomen was then closed layer by layer. The colon stenosis model was evaluated both by colonoscopy and colonography (Figure 2).



DOI: 10.3748/wjg.v29.i33.5005 **Copyright** ©The Author(s) 2023.

Figure 2 Colonic stenosis model. A: Colonic stenosis as seen by colonography; B: Colonic stenosis as seen by colonoscopy.

Endoscopic procedures

First, transanal colonoscopy was performed to determine the location and extent of colon stenosis. A guide wire was inserted through the colonoscopy biopsy hole. Under X-ray, the head end of the guide wire was passed through the colon stenosis segment. The position of the head end of the guide wire was maintained, and then the colonoscope was withdrawn (Figure 3A). Through the other end of the guide wire, 10 trapezoidal magnetic units were successively inserted in the opposite order of the N and S poles of the adjacent magnetic units. Again, under X-ray, a 5Fr push tube was used to push the magnetic units along the guide wire to make them enter the proximal end of the stenosis colon (Figure 3B and C). The magnetic units were then slowly pushed out of the guide wire one by one and transformed into a ring in the colon according to a predetermined plan. Then, the guide wire and the push tube were removed. Another DSAMAR, self-assembled in vitro, was inserted through the anus. Under X-ray, a colonoscope was used to push the magnet to the distal end of the stenosis colon. At this time, the two DSAMARs could automatically attract and compress the colon stenosis (Figure 3D and E). The two DSAMARs were then placed in the colon.

Postoperative care

All dogs were managed in a single cage after emergence from anesthesia. Pethidine hydrochloride (1 mg/kg) was intramuscularly injected every 12 h for 3 d after the operation for analgesia. The dogs were given intravenous nutritional support until the DSAMAR detached from the anus. The time that the magnets took to get expelled from all dogs was recorded. The dogs resumed oral feeding after the DSAMAR was expelled. Colonoscopy and colonography were performed to evaluate the patency of the colon.

Tissue harvest and analysis

All dogs were euthanized 2 wk after the operation, and their colonic anastomosis specimens were obtained. The healing of anastomosis was observed by the naked eye. The anastomotic specimen was then soaked overnight in 10% formalin for fixation. Then, the specimen was embedded in paraffin and a 4-μm-thick section from the anastomosis was prepared. The sections were stained with hematoxylin and eosin (H&E) and Masson trichrome and examined under a bright-field microscope.

Statistical analysis

SPSS statistical 20.0 software was used for data analysis. The quantitative data of normal distribution were described by mean ± SD, while those of non-normal distribution were described by the median. Differences between the groups were compared by an independent sample *t*-test or a nonparametric test. $P < 0.05$ indicated a significant difference.

RESULTS

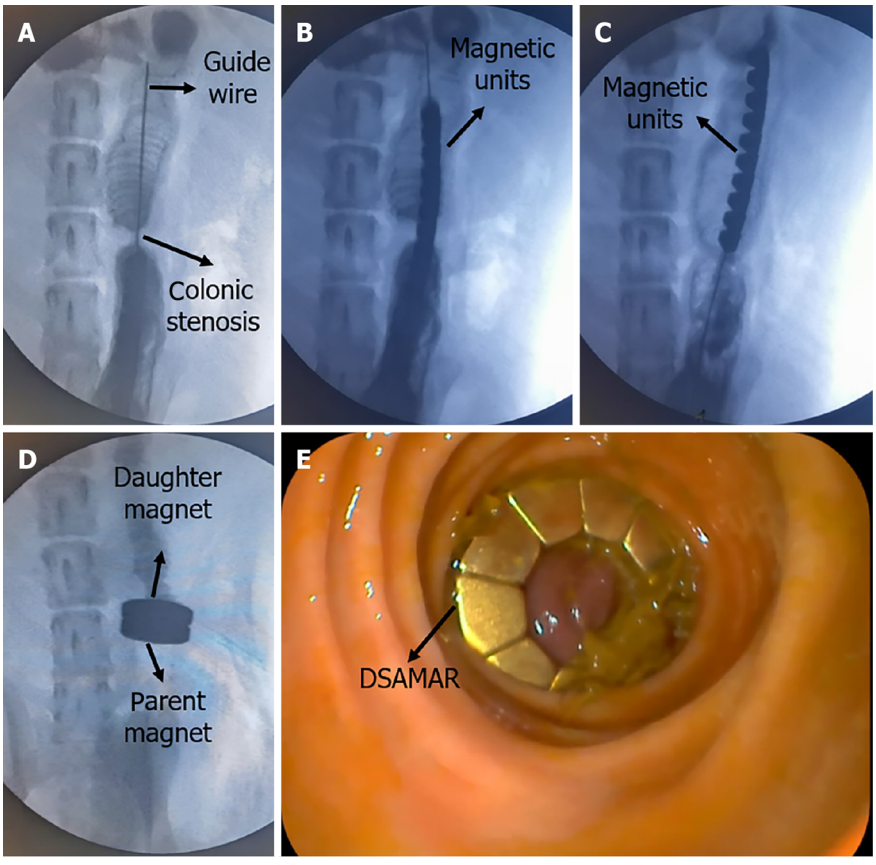
Procedural parameters

The colonic stenosis model was successfully prepared in all dogs (success rate = 100%). In seven of the eight beagles, the DSAMAR was successfully deformed only once after implantation in the proximal colon. In the remaining dog, the DSAMAR did not form during deformation, but it was successfully deformed after the removal of the magnetic ring and its re-implantation. The distal colon magnet was placed without any issue, and the DSAMARs at both ends of the stenosis were automatically attracted to each other. The endoscopic procedures (except for the model-preparation time) took 20.88 ± 5.69 min to complete, which was within the acceptable range (15–32 min). The average expulsion time of the magnets was 6.13 ± 0.99 d, again within the accepted range (5–8 d). The data related to animal experiments are listed in Table 1. The discharged DSAMARs are shown in Figure 4A-C. Colonoscopy and colonography were performed after the discharge of the magnet and a good patency of the colon was observed (Figure 4D and E).

Table 1 Data related to animal experiments

Animal	Male/female	Weight (kg)	Operation time (min)	DSAMAR expelled time (d)	Device failure (Y/N)	Device-related adverse events (Y/N)
No. 1	M	12.5	26	5	N	N
No. 2	F	12.0	18	6	N	N
No. 3	F	14.5	32	7	Y[1]	N
No. 4	M	12.0	15	6	N	N
No. 5	F	13.5	18	5	N	N
No. 6	M	14.0	20	8	N	N
No. 7	M	12.0	22	6	N	N
No. 8	F	15.0	16	6	N	N

[1]The deformable self-assembled magnetic anastomosis ring was not formed during deformation; instead, it was successfully deformed after the removal of the magnetic ring and its re-implantation.
DSAMAR: Deformable self-assembled magnetic anastomosis ring; M: Male; F: Female; Y: Yes; N: No.

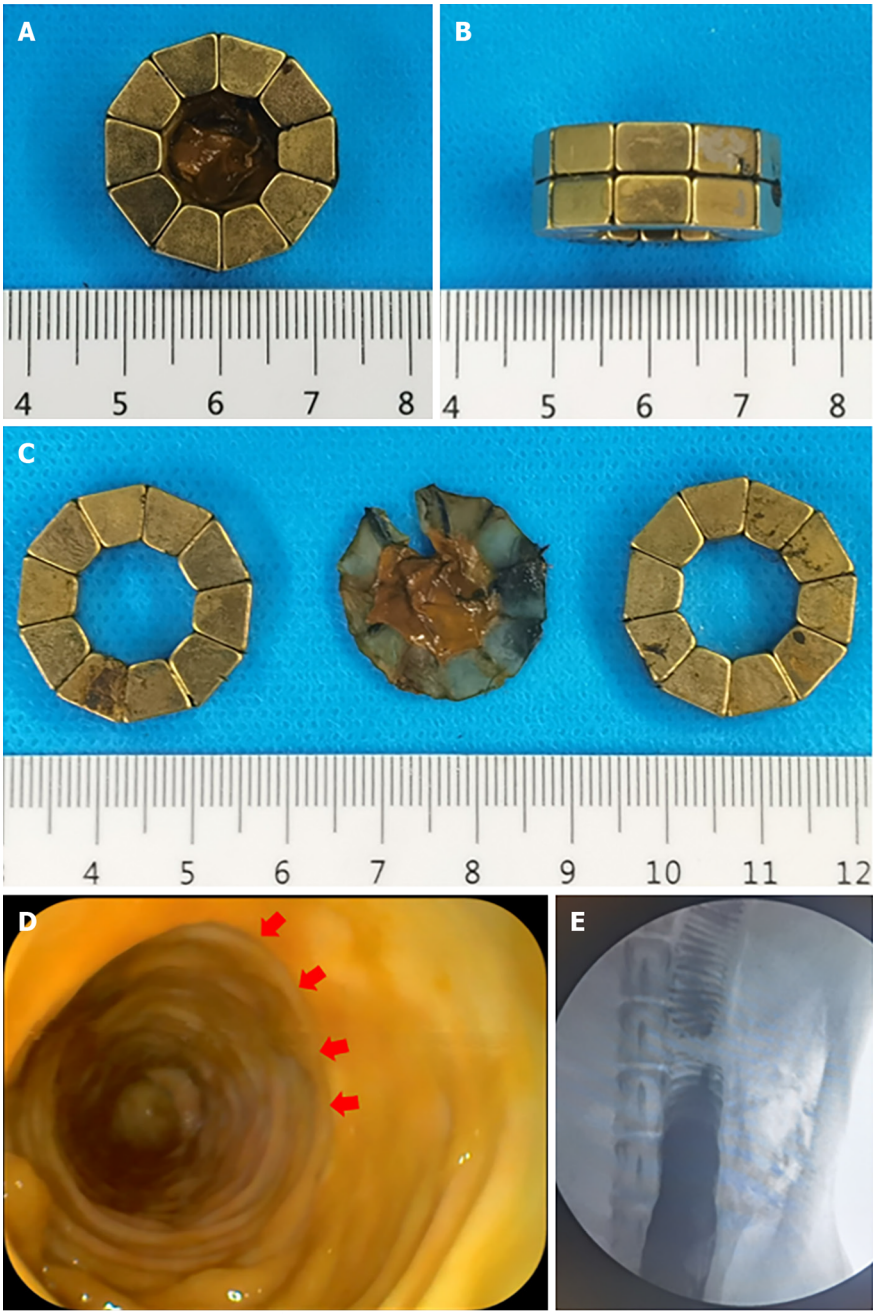


DOI: 10.3748/wjg.v29.i33.5005 **Copyright** ©The Author(s) 2023.

Figure 3 Animal experiment process. A: Hard guide wire passes through the stenosis into the proximal colon; B: Linear deformable self-assembled magnetic anastomosis ring (DSAMAR) passes through the narrow segment of the colon; C: DSAMAR enters the proximal colon completely; D: Magnetic rings at both ends of the narrow colon were attracted to each other; E: DSAMAR in the distal colon as seen by colonoscopy.

Survival rate and postoperative adverse events

The survival rate of all dogs was 100% in 2 wk after surgery. The dogs were generally in good condition after surgery, with no intestinal bleeding, perforation, obstruction, and other adverse events. After the dogs resumed normal feeding, they all excreted formed feces.



DOI: 10.3748/wjg.v29.i33.5005 **Copyright** ©The Author(s) 2023.

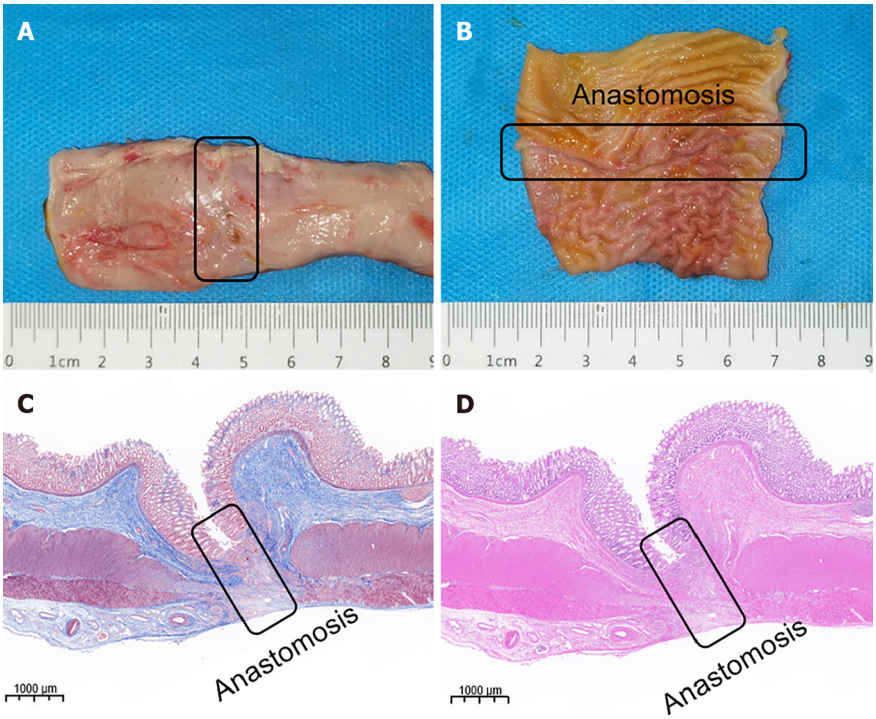
Figure 4 Magnetic compression anastomosis was established. A to C: Deformable self-assembled magnetic anastomosis rings expelled from the body; D: Magnetic compression anastomosis as seen by colonoscopy; E: Colonography showed good patency of the colon.

Gross and histological appearance of anastomosis

The experimental dogs were euthanized 2 wk after surgery, and their colonic anastomosis gross specimens were obtained by laparotomy. The colonic stenosis was not observed by the naked eye. The mucosa of the magnetic compression anastomosis was smooth and flat (Figure 5A and B). H&E and Masson staining showed good continuity and mucosal healing of the anastomotic mucosa (Figure 5C and D).

DISCUSSION

The DSAMAR along with endoscopy is a feasible treatment for gastrointestinal stenosis. Magnetic compression anastomosis is a safe technique for digestive tract anastomosis[7-9]. Non-surgical digestive tract anastomosis can be achieved when magnetic compression anastomosis is combined with endoscopy. Although most of the cases have been reported in clinical settings[14-16], the safety and feasibility of magnetic compression anastomosis are beyond doubt. To the best of our knowledge, the DSAMAR is the only magnet that can enter the narrow intestine through the natural orifice and perform the self-assembly anastomosis, which greatly increases the potential application of the magnamosis



DOI: 10.3748/wjg.v29.i33.5005 **Copyright** ©The Author(s) 2023.

Figure 5 Magnetic compression anastomosis specimen. A: Serous surface of the anastomosis; B: Colonic anastomosis seen on mucosal surface; C: Masson's staining of anastomosis; D: Hematoxylin and eosin staining of anastomosis.

technology.

The special deformation mode of the DSAMAR allows the magnet to pass through the narrow section of the digestive tract with a minimal cross-section. The DSAMAR then deforms and self-assembles into a ring, with a slimming deformation ratio of up to 1:16.35. This creates suitable conditions for the implantation of a magnet ring through the single channel of the natural orifice. Approximately 100% success rate of the deformation self-assembly of the DSAMAR *in vitro* can be achieved. Only one of the eight dogs had an unplanned deformation of the DSAMAR when failed to form a ring. This happened because the colon was not inflated enough to provide sufficient space for the DSAMAR to deform. In this case, the DSAMAR was re-inserted into the proximal colon and inflated by a colonoscope to fully expand the colon, which helped successfully complete the deformable self-assembly.

The result of animal experiments provides the best proof of the potential clinical transformation of the DSAMAR. The gross specimen and histological observation of the colonic anastomosis in dogs showed that the DSAMAR established a good anastomosis, which was not significantly different from that achieved using the conventional magnetic ring of digestive tract anastomosis reported previously. Different degrees of the narrowing of the human digestive tract after magnetic compression anastomosis have been reported, consistent with the results of previous studies[17-18]. There may be still some differences in the long-term anastomosis effect of magnetic compression anastomosis in humans and animals. This phenomenon needs to be further investigated through clinical studies with larger samples. Nevertheless, our study not only confirms the advantages of magnamosis, but also fully affirms the ingenious design of the DSAMAR. Compared with the currently available magnamosis rings, the DSAMAR can further optimize the magnetic compression anastomosis of colorectal anastomosis stenosis in postoperative patients with esophageal stenosis (non-atresia) and no fistula. This is because the DSAMAR uses only the natural orifice of a patient to successfully place the magnet.

This study has certain limitations also. The animal experiments only verified the application of the DSAMAR for the treatment of colonic stenosis. The animal sample size was small and the observation time of anastomosis was also quite short. We plan to verify the feasibility of the application of the DSAMAR in esophageal and duodenal stenoses in future studies and further observe the long-term patency of magnetic compression anastomosis. In previous studies on animal experiments[19], the colonic stenosis model was prepared by the partial ligation of silk thread, which was different from that used clinically. It may lead to differences in the anastomosis effect of the clinical application compared to that observed with animal experiments.

CONCLUSION

This study demonstrated the feasibility and safety of the DSAMAR for the treatment of digestive tract stenosis through the natural orifice by conducting animal experiments. Because of its unique deformable self-assembly, the DSAMAR can be used to handle complex gastrointestinal stenosis cases. In our next studies, we plan to further optimize the design of the DSAMAR and improve the endoscopic operation process through more animal experiments. It is expected to be used

in clinical practice in the near future.

ARTICLE HIGHLIGHTS

Research background

Magnetic compression anastomosis, or magnamosis, has been widely used for anastomotic recanalization of gastrointestinal stenosis. At present, the magnets applied to the digestive tract lumen anastomosis are usually cylindrical or circular.

Research motivation

In order to achieve magnetic anastomosis recanalization through a single-access natural orifice, we designed a deformable self-assembled magnetic anastomosis ring (DSAMAR). It is expected to provide a more minimally invasive treatment method for patients with colonic stenosis.

Research objectives

To verify the feasibility and safety of using DSAMAR to recanalize colonic stenosis through the single-approach natural orifice.

Research methods

Colonic stricture models were established in 8 beagle dogs. DSAMAR was used to achieve magnamosis recanalization of colonic stenosis and evaluate the formation of colonic anastomosis.

Research results

The results showed that the use of DSAMAR for recanalization of colonic stenosis was feasible and the anastomosis formation was good.

Research conclusions

The feasibility and safety of using DSAMAR to achieve colonic stenosis recanalization through a single-approach natural orifice were verified through animal experiments.

Research perspectives

The design of DSAMAR is ingenious. In addition to colon stenosis, it can also be used for minimally invasive treatment of digestive tract stenosis such as esophageal stricture and duodenal obstruction. It could provide a more minimally invasive treatment for patients with gastrointestinal stenosis.

FOOTNOTES

Author contributions: Lyu Y and Yan XP designed and coordinated the study; Zhang MM, Zhao GB, Zhang HZ, Xu SQ, Mao JQ, Zhang YH, Ma J, Li Y, Yan XP performed the research and acquired the data; Zhang MM, Zhao GB, Zhang HZ analyzed the data; Shi AH, Zhao GB, Zhang MM tested and analyzed the magnetic test; Zhang MM, Zhao GB, and Yan XP wrote the manuscript; Yan XP and Lyu Y conceived of the study and contributed to the study design, the interpretation of the results, and the critical revision of the manuscript; all authors read and approved the final manuscript.

Supported by the Institutional Foundation of The First Affiliated Hospital of Xi'an Jiaotong University, No. 2022MS-07; the Key Research & Development Program-Social Development of Shaanxi Province of China, No. 2023-YBSF-247.

Institutional review board statement: The experimental protocol was approved by the Committee for Ethics of Animal Experiments of Xi'an Jiaotong University (No. 2022-1451).

Institutional animal care and use committee statement: The study protocol and all experimental procedures were carried out strictly in accordance with the Guidelines for Care and Use of Experimental Animals issued by the Xi'an Jiaotong University Medical Center. This experimental study was approved by the Experimental Ethics Committee of Xi'an Jiaotong University (No. 2022-1451).

Conflict-of-interest statement: All the authors report no relevant conflicts of interest for this article.

Data sharing statement: The authors declare that the data supporting the findings of this study are available within the article or from the corresponding authors upon request.

ARRIVE guidelines statement: The authors have read the ARRIVE guidelines, and the manuscript was prepared and revised according to the ARRIVE guidelines.

Open-Access: This article is an open-access article that was selected by an in-house editor and fully peer-reviewed by external reviewers.

It is distributed in accordance with the Creative Commons Attribution NonCommercial (CC BY-NC 4.0) license, which permits others to distribute, remix, adapt, build upon this work non-commercially, and license their derivative works on different terms, provided the original work is properly cited and the use is non-commercial. See: https://creativecommons.org/Licenses/by-nc/4.0/

Country/Territory of origin: China

ORCID number: Miao-Miao Zhang 0000-0001-5679-7061; Guang-Bin Zhao 0009-0008-1730-3506; Han-Zhi Zhang 0000-0002-9972-9875; Shu-Qin Xu 0000-0002-1035-2750; Ai-Hua Shi 0000-0002-5412-1401; Jian-Qi Mao 0000-0003-2984-0102; Jing-Ci Gai 0009-0007-8844-6910; Yu-Han Zhang 0000-0001-5839-1380; Jia Ma 0000-0002-9176-0472; Yun Li 0009-0002-9270-0508; Yi Lyu 0000-0003-3636-6664; Xiao-Peng Yan 0000-0002-0335-829X.

S-Editor: Lin C
L-Editor: A
P-Editor: Yu HG

REFERENCES

1 **Zhou W**, Xia L, Wang Z, Cao G, Chen L, Chen E, Zhang W, Song Z. Transanal Minimally Invasive Surgery for Rectal Anastomotic Stenosis After Colorectal Cancer Surgery. *Dis Colon Rectum* 2022; **65**: 1062-1068 [PMID: 35421009 DOI: 10.1097/DCR.0000000000002361]
2 **Murata M**, Watanabe Y, Miyamoto S. Colonic Stenosis Caused by Transcatheter Arterial Embolization. *Clin Gastroenterol Hepatol* 2022; **20**: e645-e646 [PMID: 33781940 DOI: 10.1016/j.cgh.2021.03.032]
3 **Mandal AK**, Kafle P, Puri P, Chaulagai B, Hassan M, Bhattarai B, Kanth R, Gayam V. Acute Pancreatitis Causing Descending Colonic Stricture: A Rare Sequelae. *J Investig Med High Impact Case Rep* 2019; **7**: 2324709619834594 [PMID: 30917672 DOI: 10.1177/2324709619834594]
4 **Hirai F**. Current status of endoscopic balloon dilation for Crohn's disease. *Intest Res* 2017; **15**: 166-173 [PMID: 28522945 DOI: 10.5217/ir.2017.15.2.166]
5 **Bemelman WA**, Allez M. The surgical intervention: earlier or never? *Best Pract Res Clin Gastroenterol* 2014; **28**: 497-503 [PMID: 24913388 DOI: 10.1016/j.bpg.2014.04.013]
6 **Moroi R**, Shiga H, Nochioka K, Chiba H, Shimoyama Y, Kuroha M, Tosa M, Kakuta Y, Kayaba S, Takahashi S, Kinouchi Y, Masamune A. Endoscopic radial incision and cutting for benign stenosis of the lower gastrointestinal tract: An investigation of novel endoscopic treatment in multicenter trial. *J Gastroenterol Hepatol* 2022; **37**: 1554-1560 [PMID: 35506307 DOI: 10.1111/jgh.15882]
7 **Gagner M**, Krinke T, Lapointe-Gagner M, Buchwald JN. Side-to-side duodeno-ileal magnetic compression anastomosis: design and feasibility of a novel device in a porcine model. *Surg Endosc* 2023; **37**: 6197-6207 [PMID: 37170025 DOI: 10.1007/s00464-023-10105-x]
8 **Hornok Z**, Kubiak R, Csukas D, Ferencz A, Cserni T. Esophageal Magnetic Anastomosis Device (EMAD) to Simplify and Improve Outcome of Thoracoscopic Repair for Esophageal Atresia with Tracheoesophageal Fistula: A Proof of Concept Study. *J Pediatr Surg* 2023; **58**: 1489-1493 [PMID: 36307298 DOI: 10.1016/j.jpedsurg.2022.09.040]
9 **Muensterer OJ**, Sterlin A, Oetzmann von Sochaczewski C, Lindner A, Heimann A, Balus A, Dickmann J, Nuber M, Patel VH, Manfredi MA, Jennings RW, Smithers CJ, Fauza DO, Harrison MR. An experimental study on magnetic esophageal compression anastomosis in piglets. *J Pediatr Surg* 2020; **55**: 425-432 [PMID: 31128845 DOI: 10.1016/j.jpedsurg.2019.04.029]
10 **Obora Y**, Tamaki N, Matsumoto S. Nonsuture microvascular anastomosis using magnet rings: preliminary report. *Surg Neurol* 1978; **9**: 117-120 [PMID: 625696]
11 **Zhang M**, Ma J, An Y, Lyu Y, Yan X. Construction of an intrahepatic portosystemic shunt using the magnetic compression technique: preliminary experiments in a canine model. *Hepatobiliary Surg Nutr* 2022; **11**: 611-615 [PMID: 36016743 DOI: 10.21037/hbsn-22-209]
12 **Gao Y**, Wu RQ, Lv Y, Yan XP. Novel magnetic compression technique for establishment of a canine model of tracheoesophageal fistula. *World J Gastroenterol* 2019; **25**: 4213-4221 [PMID: 31435174 DOI: 10.3748/wjg.v25.i30.4213]
13 **Uygun I**, Okur MH, Cimen H, Keles A, Yalcin O, Ozturk H, Otcu S. Magnetic compression ostomy as new cystostomy technique in the rat: magnacystostomy. *Urology* 2012; **79**: 738-742 [PMID: 22386431 DOI: 10.1016/j.urology.2011.11.048]
14 **Kamada T**, Ohdaira H, Hoshimoto S, Narihiro S, Suzuki N, Marukuchi R, Takeuchi H, Yoshida M, Yamanouchi E, Suzuki Y. Magnetic compression anastomosis with atypical anastomosis for anastomotic stenosis of the sigmoid colon: a case report. *Surg Case Rep* 2020; **6**: 59 [PMID: 32291530 DOI: 10.1186/s40792-020-00826-9]
15 **Russell KW**, Rollins MD, Feola GP, Scaife ER. Magnamosis: a novel technique for the management of rectal atresia. *BMJ Case Rep* 2014; **2014** [PMID: 25096648 DOI: 10.1136/bcr-2013-201330]
16 **Kamada T**, Ohdaira H, Takeuchi H, Takahashi J, Ito E, Suzuki N, Narihiro S, Yoshida M, Yamanouchi E, Suzuki Y. New Technique for Magnetic Compression Anastomosis Without Incision for Gastrointestinal Obstruction. *J Am Coll Surg* 2021; **232**: 170-177.e2 [PMID: 33190786 DOI: 10.1016/j.jamcollsurg.2020.10.012]
17 **Lu G**, Li J, Ren M, Ma F, Sun X, Lv Y, He S. Endoscopy-assisted magnetic compression anastomosis for rectal anastomotic atresia. *Endoscopy* 2021; **53**: E437-E439 [PMID: 33506462 DOI: 10.1055/a-1322-1899]
18 **Ellebaek MBB**, Qvist N, Rasmussen L. Magnetic Compression Anastomosis in Long-Gap Esophageal Atresia Gross Type A: A Case Report. *European J Pediatr Surg Rep* 2018; **6**: e37-e39 [PMID: 29796381 DOI: 10.1055/s-0038-1649489]
19 **Hiratsuka T**, Inomata M. A novel animal model of colonic stenosis to aid the development of new stents for colon strictures. *Surg Endosc* 2022; **36**: 3152-3159 [PMID: 34159466 DOI: 10.1007/s00464-021-08618-4]

World Journal of Gastroenterology

Submit a Manuscript: https://www.f6publishing.com

World J Gastroenterol 2023 September 7; 29(33): 5014-5019

DOI: 10.3748/wjg.v29.i33.5014

ISSN 1007-9327 (print) ISSN 2219-2840 (online)

CASE REPORT

Carcinoid syndrome caused by a pulmonary carcinoid mimics intestinal manifestations of ulcerative colitis: A case report

Carmen Mota Reyes, Henriette Klein, Fabian Stögbauer, Henrik Einwächter, Melanie Boxberg, Moritz Schirren, Seyer Safi, Hans Hoffmann

Specialty type: Gastroenterology and hepatology

Provenance and peer review: Unsolicited article; Externally peer reviewed.

Peer-review model: Single blind

Peer-review report's scientific quality classification

Grade A (Excellent): A
Grade B (Very good): B
Grade C (Good): 0
Grade D (Fair): 0
Grade E (Poor): 0

P-Reviewer: Liu YC, China; Yan B, China

Received: May 13, 2023
Peer-review started: May 13, 2023
First decision: May 30, 2023
Revised: July 3, 2023
Accepted: July 17, 2023
Article in press: July 17, 2023
Published online: September 7, 2023

Carmen Mota Reyes, Department of Surgery, Klinikum rechts der Isar, Technical University of Munich, Munich 81675, Germany

Henriette Klein, Moritz Schirren, Seyer Safi, Hans Hoffmann, Division of Thoracic Surgery, Klinikum rechts der Isar, Technical University of Munich, Munich 81675, Germany

Fabian Stögbauer, Melanie Boxberg, Institute of Pathology, Technical University of Munich, Munich 81675, Germany

Henrik Einwächter, Department of Internal Medicine II, Technical University of Munich, Munich 81675, Germany

Corresponding author: Seyer Safi, MD, PhD, Surgeon, Division of Thoracic Surgery and Bavarian Cancer Research Center (BZKF), Klinikum rechts der Isar, Technical University of Munich, 22 Ismaningerstrasse, Munich 81675, Germany. seyer.safi@mri.tum.de

Abstract

BACKGROUND

Pulmonary carcinoids are rare, low-grade malignant tumors characterized by neuroendocrine differentiation and relatively indolent clinical behavior. Most cases present as a slow-growing polypoidal mass in the major bronchi leading to hemoptysis and pulmonary infection due to blockage of the distal bronchi. Carcinoid syndrome is a paraneoplastic syndrome caused by the systemic release of vasoactive substances that presents in 5% of patients with neuroendocrine tumors. Due to such nonspecific presentation, most patients are misdiagnosed or diagnosed late and may receive several courses of antibiotics to treat recurrent pneumonia before the tumor is diagnosed.

CASE SUMMARY

We report the case of a 48-year-old male who presented with cough, dyspnea, a history of recurrent pneumonitis, and therapy-refractory ulcerative colitis that completely subsided after the resection of a pulmonary carcinoid.

CONCLUSION

We report and emphasize pulmonary carcinoid as a differential diagnosis in patients with nonresponding inflammatory bowel diseases and recurrent pneumonia.

Key Words: Carcinoid syndrome; Paraneoplastic syndrome; Pulmonary carcinoid; Neuroendocrine tumor; Ulcerative colitis; Case report

©The Author(s) 2023. Published by Baishideng Publishing Group Inc. All rights reserved.

Core Tip: Pulmonary carcinoids are rare neuroendocrine tumors that may cause a paraneoplastic syndrome. We report the case of a 48-year-old man with a history of recurrent pneumonitis and therapy-refractory ulcerative colitis that was completely resolved after resection of a pulmonary carcinoid. Pulmonary carcinoid should be considered in the differential diagnosis of patients with unresponsive inflammatory bowel disease and recurrent pneumonia.

Citation: Reyes CM, Klein H, Stögbauer F, Einwächter H, Boxberg M, Schirren M, Safi S, Hoffmann H. Carcinoid syndrome caused by a pulmonary carcinoid mimics intestinal manifestations of ulcerative colitis: A case report. *World J Gastroenterol* 2023; 29(33): 5014-5019
URL: https://www.wjgnet.com/1007-9327/full/v29/i33/5014.htm
DOI: https://dx.doi.org/10.3748/wjg.v29.i33.5014

INTRODUCTION

Pulmonary carcinoids are rare, slow-growing neuroendocrine tumors (NETs) that account for 1%-2% of all primary lung cancers[1]. NETs arise from enterochromaffin or Kulchitsky cells lining the gastrointestinal tract (58%) and respiratory system (25%)[2]. Bronchial carcinoids commonly present with recurrent pneumonitis, cough, fever, and hemoptysis due to their central origin and hypervascularity[1]. Rarely, patients may present with features of carcinoid syndrome, a term applied to a collection of symptoms that are associated with the secretion of vasoactive substances by carcinoid tumors[3, 4]. The main symptoms of carcinoid syndrome are cutaneous flushing, diarrhea, bronchospasms and, ultimately, carcinoid heart disease[3]. Carcinoid syndrome is predominantly associated with NETs that arise from the midgut in the setting of extensive liver metastases but may be present in patients with bronchial carcinoids[3]. Early detection is crucial because surgical excision of the tumor is the only curative approach and the main determinant of the prognosis[2].

CASE PRESENTATION

Chief complaints

A 48-year-old white man with a medical history of recurrent pneumonitis and therapy-resistant ulcerative colitis over 10 years presented with fever and cough with sputum production for 10 d. He reported resting dyspnea and pain over the right thoracic wall.

History of present illness

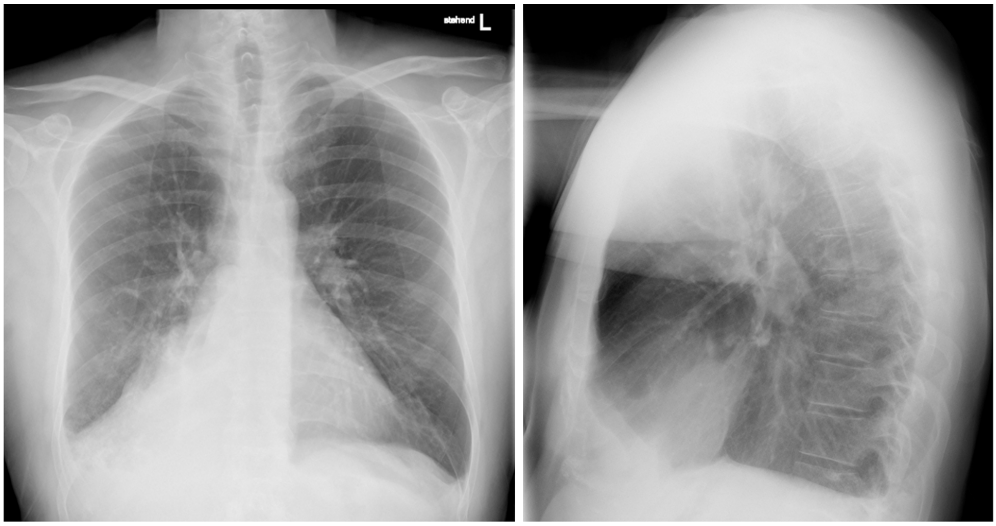
Under antibiotic therapy with moxifloxacin, no clinical improvement was reported. A chest roentgenogram showed an effaced right costo-phrenic angle and nonvisualization of the right hilar shadow suggestive of right lower lobe collapse (Figure 1).

Imaging examinations

Bronchoscopy revealed complete occlusion of the right bronchus intermedius due to a smooth-walled vascular mass with intact overlying epithelium. A computed tomography (CT) scan revealed a well-defined round-to-oval, smoothly marginated tumor measuring 43 mm × 56 mm in size located endobronchially in the proximal right main stem bronchus causing complete collapse of the right middle and lower lobe (Figure 2). A PET-CT scan showed a low metabolically active mass in the lower lobe, consistent with a carcinoid tumor, and metabolically active prominent and probably reactive mediastinal and hilar lymph nodes.

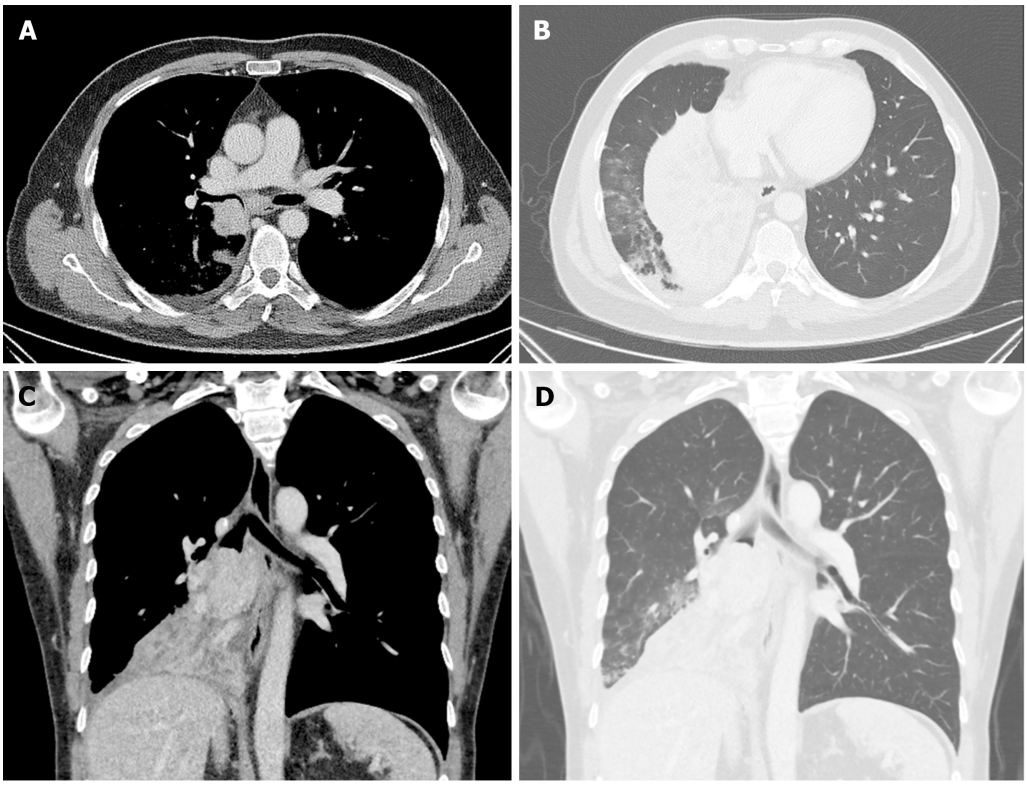
FINAL DIAGNOSIS

The definitive diagnosis of typical bronchial carcinoid was confirmed in the transbronchial biopsy of the mass.



DOI: 10.3748/wjg.v29.i33.5014 **Copyright** ©The Author(s) 2023.

Figure 1 The initial chest roentgenogram showing an unclear visualization of the right hilar shadow suggestive of right lower lobe collapse with minimal right-sided pleural effusion.

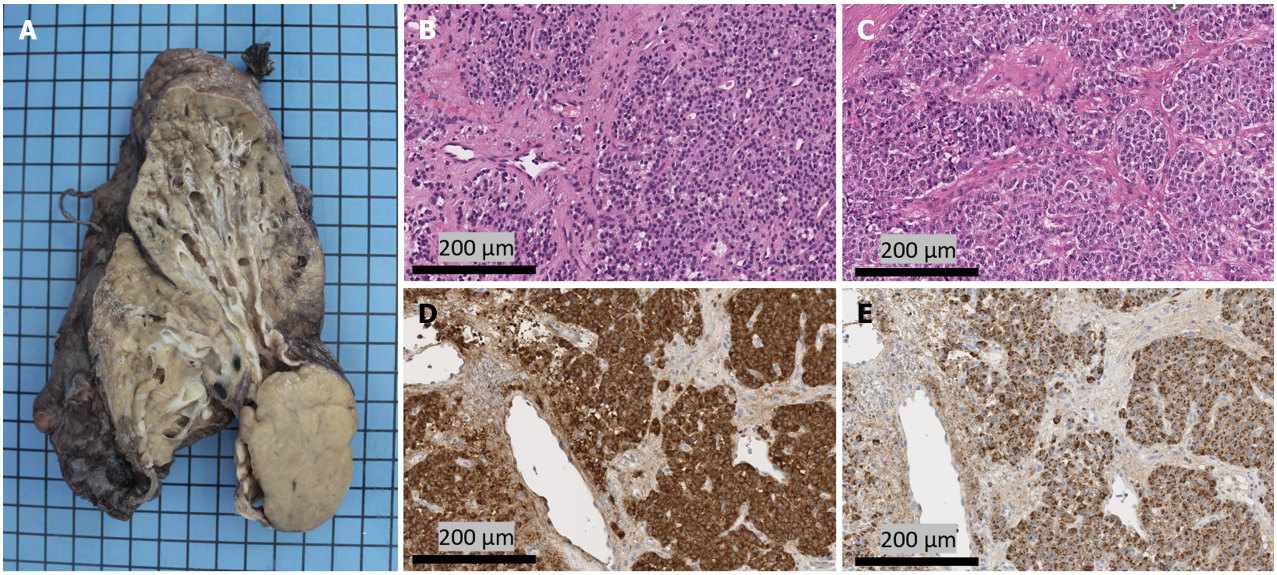


DOI: 10.3748/wjg.v29.i33.5014 **Copyright** ©The Author(s) 2023.

Figure 2 Preoperative computed tomography scan. A and B: Mediastinal window during the phase of contrast shows a well-defined 43 mm × 56 mm round bordered intraluminal growth in the right bronchus intermedius occluding the airway; C and D: Lung window shows near complete collapse of the right middle lobe with no aeration post obstruction.

TREATMENT

All pulmonary carcinoid tumors should be treated as malignancies, as the only curative approach is a margin-free surgical resection. A right middle and lower sleeve lobectomy with bronchoplastic repair and radical lymphadenectomy were performed. Histopathologic examination of the resected tumor (Figure 3) revealed a solid growth pattern of uniform tumor cells with granular chromatin. The histologic appearance of the resection specimen was consistent with the transbronchial biopsy specimen. Here, the mitotic rate was under 1%, with fewer than 2 mitoses in 2 mm^2, and necrosis was not detected. Strong immunohistochemical positivity for synaptophysin and chromogranin was detected, and



DOI: 10.3748/wjg.v29.i33.5014 **Copyright** ©The Author(s) 2023.

Figure 3 Surgical specimen. A: Macroscopic appearance of a solid, well-circumscribed intraluminal tumoral lesion in the right main stem bronchus; B and C: Representative images of tumor cells revealing round nuclei, granular chromatin and large eosinophilic cytoplasm (H&E); D: Immunohistochemistry showing positivity to chromogranin (Scale 1:100); E: The tumor demonstrates high synaptophysin expression.

somatostatin receptor subtype 2a showed strong membranous expression (score 3+). All of these features lead to the diagnosis of a typical carcinoid of the lung[5].

The patient had no postoperative complications. He was discharged home 14 d after the operation and was followed up at 3 mo, 6 mo, 10 mo, and 36 mo. On a DOTATATE PET scan performed 3 mo after the operation, there was no evidence of any lymphadenopathy or distant metastasis. At 36 mo after the operation, the patient was stable, with no evidence of recurrence in the DOTATATE PET scan. Unexpectedly, after tumor resection and in the absence of any therapy, the patient presented complete clinical remission of ulcerative colitis.

Long-standing therapy-resistant ulcerative colitis was first diagnosed in 2009. Initially, combined therapy with rectal and oral mesalazine was prescribed; however, the patient reported further persistent bloody diarrhea with acute disease flares approximately twice a year. On colonoscopy, pronounced erythema in the rectum with fibrin deposits and granularity of the mucosal surface was observed. All findings were consistent with the diagnosis of ulcerative colitis. The diagnosis of ulcerative proctitis was ultimately confirmed in the step biopsies. The addition of topical steroids did not relieve the symptoms of colitis. Furthermore, the patient reported an increased frequency of bowel movements accompanied by rectal tenesmus. After three months of remission induction therapy with high-dose systemic steroids, mild disease control was achieved; however, any attempt at dose reduction was not tolerated by the patient. For this reason, immunomodulatory therapy with azathioprine was initiated, which led to a notable alleviation of the symptoms and disease remission. Due to alterations in both ALT and AST levels, azathioprine therapy was replaced by 6-mercaptopurin in combination with systemic steroids. The intestinal manifestations responded moderately to this therapy, and the steroids were reduced over time. The therapy with 6-mercaptopurin was carried out until two weeks before the lung operation with a milder course of ulcerative colitis.

OUTCOME AND FOLLOW-UP

Remarkably, after resection of the pulmonary carcinoid, the patient presented an unaltered bowel habit with no need for therapy. In light of the clinical evolution of the intestinal symptoms, it is questionable whether the clinical manifestations of ulcerative colitis were exacerbated by the pulmonary carcinoid or whether they were part of a carcinoid syndrome.

DISCUSSION

Here, we report a case of a young adult with an over 10-year history of ulcerative colitis and concurrent pneumonitis episodes who was diagnosed with pulmonary carcinoid. After complete resection of the pulmonary carcinoid, the intestinal symptoms completely subsided with no need for further therapy even after three years of follow up. The presence of a 56 mm measuring pulmonary carcinoid suggests[6] that the carcinoid was already present at the time of the patient's ulcerative colitis diagnosis. Pulmonary carcinoids are rare neoplasms that are able to synthesize and secrete neuroendocrine peptides into the central circulation, causing many symptoms, such as flushing or diarrhea. Taken together, these facts and the timely evolution of the condition indicated that the intestinal manifestations in this patient

seemed to be exacerbated by the pulmonary carcinoid or even the result of a carcinoid syndrome. To our knowledge, this is the first reported case of pulmonary carcinoid with this clinical presentation. Interestingly, studies in mice have shown that serotonin increases the susceptibility to experimental colitis[7].

The diagnosis of pulmonary carcinoids is often overlooked even in symptomatic patients due to low clinical suspicion and the various ways in which pulmonary carcinoids can present[8,9]. Apart from symptoms such as chest pain, atelectasis or pleural effusion, common pulmonary manifestations are hemoptysis, postobstructive pneumonitis, and dyspnea, especially in centrally located tumors, as in our case[1]. Carcinoids can also be associated with a variety of hormonally induced systemic symptoms due to gastrin, vasoactive intestinal peptide, serotonin, or histamine production, and this condition is termed carcinoid syndrome[9]. The most commonly encountered symptoms are flushing of the face, severe, debilitating diarrhea, and bronchospasms[10]. Metastatic tumor spread in the liver circumvents the hepatic inactivation of these substances and leads to the development of carcinoid syndrome. Rarely, bronchial and ovarian carcinoids can release hormones directly into the systemic circulation, thereby producing symptoms in the absence of liver metastasis[4]. Carcinoid syndrome-associated diarrhea is, as in our patient, unspecific and usually described as intermittent and sporadic. It is often accompanied by mild abdominal cramping and may become continuous when complicated by bacterial overgrowth[3]. This somewhat atypical course may explain the delayed diagnosis of NETs, which can sometimes occur after many years of unspecific symptoms that result in patients being diagnosed with an advanced incurable disease.

Typical bronchial carcinoids rarely metastasize and have an excellent prognosis even when regional lymph nodes are involved[2]. Surgery has been reported to provide a 5- and 10-year survival rate of > 90% for typical pulmonary carcinoids and is the treatment of choice[4].

CONCLUSION

In conclusion, the present case highlights that localized pulmonary carcinoids can potentially cause a carcinoid syndrome even in the absence of liver metastasis. Furthermore, intestinal manifestations, among other paraneoplastic symptoms, can precede symptoms of bronchial obstruction and superinfection. Thus, in patients with a history of recurring pneumonitis, the differential diagnosis of patients with persistent diarrhea and abdominal cramping despite optimum medical treatment should include pulmonary carcinoids[2]. A strong clinical suspicion aided by radiological examinations, including chest CT scans, enables the timely and accurate diagnosis of pulmonary carcinoids, which is crucial for early surgical resection[1].

FOOTNOTES

Author contributions: Mota-Reyes C and Hoffmann H designed the study; all co-authors analyzed the data and wrote the manuscript.

Informed consent statement: Informed written consent was obtained from the patients for the publication of this report and any accompanying images.

Conflict-of-interest statement: The authors declare that they have no conflict of interest to disclose.

CARE Checklist (2016) statement: The authors have read the CARE Checklist (2016), and the manuscript was prepared and revised according to the CARE Checklist (2016).

Open-Access: This article is an open-access article that was selected by an in-house editor and fully peer-reviewed by external reviewers. It is distributed in accordance with the Creative Commons Attribution NonCommercial (CC BY-NC 4.0) license, which permits others to distribute, remix, adapt, build upon this work non-commercially, and license their derivative works on different terms, provided the original work is properly cited and the use is non-commercial. See: https://creativecommons.org/Licenses/by-nc/4.0/

Country/Territory of origin: Germany

ORCID number: Seyer Safi 0000-0002-2335-4309.

S-Editor: Chen YL
L-Editor: A
P-Editor: Cai YX

REFERENCES

1 **Bora MK**, Vithiavathi S. Primary bronchial carcinoid: A rare differential diagnosis of pulmonary koch in young adult patient. *Lung India* 2012; **29**: 59-62 [PMID: 22345917 DOI: 10.4103/0970-2113.92366]

2 **Mindaye ET**, Tesfaye GK. Bronchial carcinoid tumor: A case report. *Int J Surg Case Rep* 2020; **77**: 349-352 [PMID: 33212309 DOI: 10.1016/j.ijscr.2020.11.043]

3 **Rubin de Celis Ferrari AC**, Glasberg J, Riechelmann RP. Carcinoid syndrome: update on the pathophysiology and treatment. *Clinics (Sao Paulo)* 2018; **73**: e490s [PMID: 30133565 DOI: 10.6061/clinics/2018/e490s]

4 **Belicová M**, Prídavková D, Jankovičová V, Balážová K, Mokáň M. Bronchial carcinoid, unusual manifestation: A case report. *J Xiangya Med* 2020; **5**: 7 [DOI: 10.21037/jxym.2019.09.02]

5 **World Health Organization**. WHO classification of tumours of the lung, pleura, thymus and heart. 2015. [cited 1 July 2023]. Available from: https://www.iarc.who.int/news-events/who-classification-of-tumours-of-the-lung-pleura-thymus-and-heart-4th-edition/

6 **Russ DH**, Barta JA, Evans NR, Stapp RT, Kane GC. Volume Doubling Time of Pulmonary Carcinoid Tumors Measured by Computed Tomography. *Clin Lung Cancer* 2022; **23**: e453-e459 [PMID: 35922364 DOI: 10.1016/j.cllc.2022.06.006]

7 **Haq S**, Wang H, Grondin J, Banskota S, Marshall JK, Khan II, Chauhan U, Cote F, Kwon YH, Philpott D, Brumell JH, Surette M, Steinberg GR, Khan WI. Disruption of autophagy by increased 5-HT alters gut microbiota and enhances susceptibility to experimental colitis and Crohn's disease. *Sci Adv* 2021; **7**: eabi6442 [PMID: 34739317 DOI: 10.1126/sciadv.abi6442]

8 **Orakwe O**. Bronchial carcinoid tumor: Case report. *J Lung Pulm Respir Res* 2014; **1**: 1-3 [DOI: 10.15406/jlprr.2014.01.00001]

9 **Moraes TJ**, Langer JC, Forte V, Shayan K, Sweezey N. Pediatric pulmonary carcinoid: a case report and review of the literature. *Pediatr Pulmonol* 2003; **35**: 318-322 [PMID: 12629632 DOI: 10.1002/ppul.10249]

10 **Mota JM**, Sousa LG, Riechelmann RP. Complications from carcinoid syndrome: review of the current evidence. *Ecancermedicalscience* 2016; **10**: 662 [PMID: 27594907 DOI: 10.3332/ecancer.2016.662]



Published by **Baishideng Publishing Group Inc**
7041 Koll Center Parkway, Suite 160, Pleasanton, CA 94566, USA
Telephone: +1-925-3991568
E-mail: bpgoffice@wjgnet.com
Help Desk: https://www.f6publishing.com/helpdesk
https://www.wjgnet.com



© 2023 Baishideng Publishing Group Inc. All rights reserved.

ISSN 1007-9327 (print)
ISSN 2219-2840 (online)

World Journal of *Gastroenterology*

World J Gastroenterol 2023 September 14; 29(34): 5020-5093



Published by Baishideng Publishing Group Inc

World Journal of Gastroenterology

Contents

Weekly Volume 29 Number 34 September 14, 2023

REVIEW

5020 Perioperative immunotherapy for esophageal squamous cell carcinoma: Now and future

Liu Y

ORIGINAL ARTICLE

Basic Study

5038 Suberoylanilide hydroxamic acid upregulates reticulophagy receptor expression and promotes cell death in hepatocellular carcinoma cells

Li JY, Tian T, Han B, Yang T, Guo YX, Wu JY, Chen YS, Yang Q, Xie RJ

5054 Green tea polyphenols alleviate di-(2-ethylhexyl) phthalate-induced liver injury in mice

Shi H, Zhao XH, Peng Q, Zhou XL, Liu SS, Sun CC, Cao QY, Zhu SP, Sun SY

Retrospective Study

5075 Role of biochemical markers and autoantibodies in diagnosis of early-stage primary biliary cholangitis

Zhu YJ, Li J, Liu YG, Jiang Y, Cheng XJ, Han X, Wang CY, Li J

CASE REPORT

5082 Simultaneous rectal neuroendocrine tumors and pituitary adenoma: A case report and review of literature

Li JY, Chen J, Liu J, Zhang SZ

LETTER TO THE EDITOR

5091 Gastrointestinal microbiome and cholelithiasis: Prospect in the nervous system

Mancha Chahuara M, Lopez Tufino LDM, Mugruza-Vassallo CA

World Journal of Gastroenterology

Weekly Volume 29 Number 34 September 14, 2023

Contents

ABOUT COVER

Editorial Board of *World Journal of Gastroenterology*, Takeshi Suda, MD, PhD, Professor, Department of Gastroenterology and Hepatology, Uonuma Institute of Community Medicine, Niigata University Medical and Dental Hospital, Minami Uonuma 949-7302, Niigata, Japan. tspitt@med.niigata-u.ac.jp

AIMS AND SCOPE

The primary aim of *World Journal of Gastroenterology* (*WJG*, *World J Gastroenterol*) is to provide scholars and readers from various fields of gastroenterology and hepatology with a platform to publish high-quality basic and clinical research articles and communicate their research findings online. *WJG* mainly publishes articles reporting research results and findings obtained in the field of gastroenterology and hepatology and covering a wide range of topics including gastroenterology, hepatology, gastrointestinal endoscopy, gastrointestinal surgery, gastrointestinal oncology, and pediatric gastroenterology.

INDEXING/ABSTRACTING

The *WJG* is now abstracted and indexed in Science Citation Index Expanded (SCIE, also known as SciSearch®), Current Contents/Clinical Medicine, Journal Citation Reports, Index Medicus, MEDLINE, PubMed, PubMed Central, Scopus, Reference Citation Analysis, China Science and Technology Journal Database, and Superstar Journals Database. The 2023 edition of Journal Citation Reports® cites the 2022 impact factor (IF) for *WJG* as 4.3; Quartile category: Q2. The *WJG*'s CiteScore for 2021 is 8.3.

RESPONSIBLE EDITORS FOR THIS ISSUE

Production Editor: *Ying-Yi Yuan*; **Production Department Director:** *Xu Guo*; **Editorial Office Director:** *Jia-Ru Fan*.

NAME OF JOURNAL
World Journal of Gastroenterology

ISSN
ISSN 1007-9327 (print) ISSN 2219-2840 (online)

LAUNCH DATE
October 1, 1995

FREQUENCY
Weekly

EDITORS-IN-CHIEF
Andrzej S Tarnawski

EXECUTIVE ASSOCIATE EDITORS-IN-CHIEF
Xian-Jun Yu (Pancreatic Oncology), Jian-Gao Fan (Chronic Liver Disease), Hou-Bao Liu (Biliary Tract Disease), Naohisa Yoshida (Gastrointestinal Endoscopy)

EDITORIAL BOARD MEMBERS
http://www.wjgnet.com/1007-9327/editorialboard.htm

PUBLICATION DATE
September 14, 2023

COPYRIGHT
© 2023 Baishideng Publishing Group Inc

PUBLISHING PARTNER
Pancreatic Cancer Institute, Fudan University
Biliary Tract Disease Institute, Fudan University

INSTRUCTIONS TO AUTHORS
https://www.wjgnet.com/bpg/gerinfo/204

GUIDELINES FOR ETHICS DOCUMENTS
https://www.wjgnet.com/bpg/GerInfo/287

GUIDELINES FOR NON-NATIVE SPEAKERS OF ENGLISH
https://www.wjgnet.com/bpg/gerinfo/240

PUBLICATION ETHICS
https://www.wjgnet.com/bpg/GerInfo/288

PUBLICATION MISCONDUCT
https://www.wjgnet.com/bpg/gerinfo/208

POLICY OF CO-AUTHORS
https://www.wjgnet.com/bpg/GerInfo/310

ARTICLE PROCESSING CHARGE
https://www.wjgnet.com/bpg/gerinfo/242

STEPS FOR SUBMITTING MANUSCRIPTS
https://www.wjgnet.com/bpg/GerInfo/239

ONLINE SUBMISSION
https://www.f6publishing.com

PUBLISHING PARTNER's OFFICIAL WEBSITE
https://www.shca.org.cn
https://www.zs-hospital.sh.cn

© 2023 Baishideng Publishing Group Inc. All rights reserved. 7041 Koll Center Parkway, Suite 160, Pleasanton, CA 94566, USA

E-mail: bpgoffice@wjgnet.com https://www.wjgnet.com

World Journal of Gastroenterology

Submit a Manuscript: https://www.f6publishing.com

World J Gastroenterol 2023 September 14; 29(34): 5020-5037

DOI: 10.3748/wjg.v29.i34.5020

ISSN 1007-9327 (print) ISSN 2219-2840 (online)

REVIEW

Perioperative immunotherapy for esophageal squamous cell carcinoma: Now and future

Yong Liu

Specialty type: Gastroenterology and hepatology

Provenance and peer review: Invited article; Externally peer reviewed.

Peer-review model: Single blind

Peer-review report's scientific quality classification

Grade A (Excellent): A
Grade B (Very good): B
Grade C (Good): C
Grade D (Fair): 0
Grade E (Poor): 0

P-Reviewer: Matsuo Y, Japan; Nakano H, Japan; Viswanath Y, United Kingdom

Received: April 23, 2023
Peer-review started: April 23, 2023
First decision: July 9, 2023
Revised: July 19, 2023
Accepted: August 15, 2023
Article in press: August 15, 2023
Published online: September 14, 2023

Yong Liu, Department of Thoracic Surgery, The Central Hospital of Wuhan, Tongji Medical College, Huazhong University of Science and Technology, Wuhan 430011, Hubei Province, China

Corresponding author: Yong Liu, Doctor, MD, Chief Doctor, Surgeon, Surgical Oncologist, Department of Thoracic Surgery, The Central Hospital of Wuhan, Tongji Medical College, Huazhong University of Science and Technology, No. 26 Shengli Street, Wuhan 430011, Hubei Province, China. liuyong7575@163.com

Abstract

Esophageal cancer (EC) ranks among the most prevalent malignant tumors affecting the digestive tract. Esophageal squamous cell carcinoma (ESCC) stands as the prevailing pathological subtype, encompassing approximately 90% of all EC patients. In clinical stage II-IVA locally advanced ESCC cases, the primary approach to treatment involves a combination of neoadjuvant therapy and surgical resection. Despite concerted efforts, the long-term outcomes for ESCC patients remain unsatisfactory, with dismal prognoses. However, recent years have witnessed remarkable strides in immunotherapy, particularly in the second- and first-line treatment of advanced or metastatic ESCC, with the development of monoclonal antibodies that inhibit programmed death 1 or programmed death ligand 1 demonstrating encouraging responses and perioperative clinical benefits for various malignancies, including ESCC. This comprehensive review aims to present the current landscape of perioperative immunotherapy for resectable ESCC, focusing specifically on the role of immune checkpoint inhibitors during the perioperative period. Additionally, the review will explore promising biomarkers and offer insights into future prospects.

Key Words: Esophageal squamous cell carcinoma; Immune checkpoint inhibitors; Immunotherapy; Neoadjuvant; Randomized clinical trial

©The Author(s) 2023. Published by Baishideng Publishing Group Inc. All rights reserved.

Core Tip: Esophageal cancer ranks among the most prevalent malignant tumors affecting the digestive tract. In locally advanced esophageal squamous cell carcinoma (ESCC), the mainstay of treatment involves neoadjuvant therapy in conjunction with surgical resection. Notably, immunotherapy has achieved significant breakthroughs in the second- and first-line treatment of advanced or metastatic ESCC. This review focuses on the current landscape of perioperative immunotherapy for resectable ESCC and discusses promising biomarkers and future perspectives.

Citation: Liu Y. Perioperative immunotherapy for esophageal squamous cell carcinoma: Now and future. *World J Gastroenterol* 2023; 29(34): 5020-5037
URL: https://www.wjgnet.com/1007-9327/full/v29/i34/5020.htm
DOI: https://dx.doi.org/10.3748/wjg.v29.i34.5020

INTRODUCTION

Esophageal cancer (EC), one of the most prevalent malignancies affecting the digestive tract, originates from the epithelial lining of the esophagus. According to the International Agency for Research on Cancer's latest update on the global cancer burden, based on the GLOBOCAN 2020 projections of cancer incidence and mortality, EC ranks seventh in terms of cancer incidence worldwide and sixth in cancer-related mortality[1]. The incidence of EC varies significantly across countries and regions, with East Asia having the highest disease occurrence, being twice the global average (12.2/1000). EC can be classified into two histological subtypes: Esophageal squamous cell carcinoma (ESCC) and esophageal adenocarcinoma (EAC). EAC is the predominant pathological type in relatively low-incidence areas such as Europe and America. However, globally, ESCC accounts for approximately 90% of all EC cases[2], and more than half of the ESCC cases occur in China[3].

For many years, surgery has served as the primary treatment for early-stage ESCC. High-grade dysplasia and very early-stage tumors are amenable to local therapies such as endoscopic resection, ablation, or surgery. Surgery can improve the 5-year survival rate to 60%-85% in patients with early-stage disease[4]. However, due to the subtle nature of early symptoms, many patients present with advanced or metastatic disease at the time of diagnosis. For locally advanced disease, surgery alone has not yielded satisfactory results, with a median survival time of 12 to 18 mo and a 5-year survival rate of 15%-39%[5,6]. Furthermore, local or systemic recurrence is common, with recurrence reported in 35%-50% of patients who had underwent surgery alone[7].

Neoadjuvant therapy combined with surgery stands as a cornerstone in the treatment of locally advanced ESCC, typically encompassing clinical stages II to IVA[8]. The medical community widely acknowledges the value of neoadjuvant therapy due to its efficiency compared to postoperative adjuvant therapy. Moreover, it leads to reductions in tumor and lymph node (LN) volumes, improves the R0 resection rate, and enhances long-term survival rates[9-11]. Additionally, neoadjuvant therapy allows for the evaluation of patient response using resected specimens[12]. Numerous randomized controlled trials (RCTs) have indicated that preoperative or neoadjuvant chemoradiotherapy (nCRT) may result in longer overall survival (OS) compared to surgery alone[13-15]. The CROSS trial established nCRT as the first-line therapeutic choice for resectable locally advanced ESCC, combining radiotherapy with a chemotherapy regimen containing carboplatin and paclitaxel[16]. The NEOCRTEC5010 phase III, multi-center, open-label RCT confirmed the findings of the CROSS trial for ESCC[9]. However, the optimal neoadjuvant therapy for resectable locally advanced ESCC remains a topic of debate. Neoadjuvant chemotherapy showed improved OS over surgery alone only for EAC, whereas nCRT demonstrated considerably better OS than surgery alone for both EAC and ESCC, according to the NewEC study [17]. Several subsequent meta-analyses also supported the utility of preoperative nCRT, showing improved OS compared to other treatment modalities, including surgery alone, neoadjuvant chemotherapy, and neoadjuvant radiotherapy, albeit with increased postoperative mortality[18,19]. Postoperative morbidity was similar between the nCRT and S (surgery) groups (55.6% *vs* 52.8%; $P = 0.720$), while in-hospital postoperative mortality was significantly higher in the CRT group (11.1% *vs* 3.4%; $P = 0.049$)[20]. A Japanese study[21] examined late complications, revealing grade 2 anastomotic stricture as the most common event, occurring in 30% of the 33 patients. A total of 12 events of grade 3 or worse complications were observed in ten patients, including gastric tube ulcer, cardiac complications, and pulmonary complications. The 5-year incidence rate was 22%, and three patients succumbed to the late complications. A clear advantage of nCRT over neoadjuvant chemotherapy was not established.

Presently, both the National Comprehensive Cancer Network and the Chinese Society of Clinical Oncology guidelines recommend chemoradiotherapy (CRT) as the standard approach for locally advanced ESCC[22-24]. Despite significant efforts made by the medical community, the expected long-term outcomes for ESCC patients have seen limited improvement, remaining poor. The 5-year OS in patients undergoing nCRT and surgery is approximately 50%, and the incidence of local recurrence or distant metastasis remains high[25]. Relapse after nCRT is common and constitutes a major hurdle to overcome[26].

Immunotherapy is a therapeutic approach that involves the use of substances to stimulate or suppress the immune system, aiding the body in combating cancer, infections, and other diseases. It encompasses biologic/targeted agents that aim to enhance and restore the immune system's ability to recognize and eliminate cancer cells by modifying and/or blocking costimulatory signals[27,28]. Over the past few years, immunotherapy has achieved remarkable progress in cancer treatment, particularly with the advent of immune checkpoint inhibitors (ICIs)[29]. The development of ICIs,

which inhibit programmed death 1 (PD-1) or programmed death ligand 1 (PD-L1), has shown convincing responses and clinical benefits across various malignancies, including ESCC[30,31].

In the study "KEYNOTE-181", Pembrolizumab demonstrated superior OS, a higher objective response rate, and a lower incidence of grades 3-5 treatment-related adverse events (trAEs) compared to chemotherapy in the second-line setting [32]. Grades 3-5 trAEs occurred in 18.2% of patients treated with Pembrolizumab *vs* 40.9% in the chemotherapy group. Other trials such as "RATIONALE-302"[33], "ATTRACTION-3"[34], and "ESCORT"[35] have also reported positive outcomes. In these trials, immunotherapy showed lower rates of grades 3-5 trAEs compared to chemotherapy, with percentages of 18.8% *vs* 55.8% in "RATIONALE-302"[33], 18% *vs* 63% in "ATTRACTION-3"[34], and 19% *vs* 39% in "ESCORT"[35].

It is important to note that in studies like "JUPITER-06"[36], "CheckMate-648"[37], "ORIENT-15"[38], "ESCORT-1st"[39], and "KEYNOTE-590"[40], treating patients with advanced EC using PD-1 inhibitors in combination with chemotherapy as first-line therapy resulted in significantly longer OS and progression-free survival (PFS) compared to chemotherapy alone. The occurrence rates of grades 3-5 trAEs in these trials were relatively comparable.

Neoadjuvant immunotherapy has been explored in various other malignancies, such as lung cancer[41,42], melanoma [43], bladder cancer[44], colon cancer[45], and glioblastoma[46]. In a clinical trial (NCT02259621) investigating neoadjuvant Nivolumab, surgery was not delayed, and 45% of resected tumors showed a major pathological response (MPR). In the NADIM trial[42], patients were treated with a neoadjuvant regimen consisting of paclitaxel and carboplatin in combination with Nivolumab. Out of the initial 51 patients deemed eligible, 46 patients received neoadjuvant treatment and subsequently underwent surgery. At the 24-mo mark, the PFS rate was observed to be 77.1%. Among the 27 patients who had melanoma, eight experienced either a complete response or an MPR after receiving a single dose of the anti-PD-1 drug, Pembrolizumab. Importantly, all eight of these patients remained free from the disease[43]. In a single-arm phase II study exploring Atezolizumab before cystectomy in 95 patients with muscle-invasive urothelial cancer (NCT02662309), the pathological complete response (pCR) rate was 31%[44]. In the exploratory NICHE study (NCT03026140)[45], patients with early-stage colon cancers, categorized as mismatch repair-deficient (dMMR) or mismatch repair-proficient (pMMR) tumors, received a single dose of Ipilimumab and two doses of Nivolumab before surgery. Among dMMR tumors, 20 out of 20 displayed a pathological response, with 19 cases of MPR and 12 cases of pCR. In pMMR tumors, 4 out of 15 showed pathological responses, with three cases of MPR and one case of partial response. In a single-arm phase II clinical trial (NCT02550249)[46], a presurgical dose of Nivolumab followed by postsurgical Nivolumab until disease progression or unacceptable toxicity was tested in 30 patients. However, no significant clinical benefit was observed following salvage surgery, although two out of the three patients treated with Nivolumab before and after primary surgery remained alive 33 and 28 mo later.

Based on this background, this review aims to depict the current scenario in the field of perioperative immunotherapy for resectable ESCC, focusing in particular on an overview of the role of ICIs in this field, alongside a discussion of the promising biomarkers and forecast of future perspectives.

PERIOPERATIVE IMMUNOTHERAPY OF ESCC

Drugs for immunotherapy of ESCC

Cancer cells have the ability to evade immune surveillance by disrupting the balance of the tumor microenvironment (TME). This disruption can lead to tumor development by blocking apoptosis, promoting angiogenesis, proliferation, and distant metastasis, and evading immune detection[47]. CD8(+) T cells, also known as cytotoxic T lymphocytes, play a crucial role in killing tumor cells, and their presence in the TME is associated with improved cancer prognosis[48]. For CD8(+) T cells to effectively kill tumor cells, two signals are essential: The recognition of antigens presented by major histocompatibility complexes[49] and the stimulation or suppression of T cell activation. The second signal, acting as a co-stimulatory or co-inhibitory signal, is often referred to as an "immune checkpoint" for CD8(+) T cell function. Immune checkpoints help maintain the balance of T-cell activation, immune tolerance, and immune-mediated tissue damage[50]. Both co-stimulatory and co-inhibitory ligands and their receptors are present on T cells and antigen-presenting cells. Inhibitory checkpoint molecules displayed by CD8(+) T cells can respond to and aid the tumor in evading the immune system[51].

There are four main ICIs named after the corresponding Food and Drug Administration (FDA)-approved monoclonal antibody therapies: Cytotoxic T lymphocyte antigen-4 (CTLA-4), PD-1, PD-L1/L2, and lymphocyte activation gene-3 (LAG-3)[52]. CTLA-4 and PD-1 are members of the CD28 receptor family expressed on T-cells, which bind to their corresponding targets of the B7 family[53]. CTLA-4 is an intracellular protein often found on regulatory T cells, inhibiting CD8(+) T cell activity. Ipilimumab, approved by the FDA in 2011, targets CTLA-4[54]. PD-1 is a transmembrane protein upregulated by repeated stimulation of T cells. PD-1 has two ligands, PD-L1 and PD-L2, which are cell surface proteins expressed on tumor cells and some immune cells within the TME. When PD-1 binds to these ligands, T cell function is inhibited. Overexpression of PD-L1 is associated with tumor progression, as cancer cells exploit the PD-1/PD-L1 and PD-1/PD-L2 pathways to create an immunosuppressive environment[55]. Nivolumab and Pembrolizumab are ICIs that target the PD-1 molecule, both FDA-approved in 2014. In 2018 and 2021, Cemiplimab and Dostarlimab were also approved, respectively[56,57]. Atezolizumab, Avelumab, and Durvalumab are FDA-approved PD-L1 inhibitors[58-60]. LAG-3 is a transmembrane receptor expressed on CD8(+) T cells, further upregulated by T cell activation. Relatlimab is the only FDA-approved LAG-3 inhibitor[61].

In recent years, several domestic anti-PD-1 monoclonal antibodies have been approved as drugs for various tumors by the China National Medical Product Administration. Notably, Camrelizumab, Sintilimab, Toripalimab, and Tislelizumab are representative drugs that are currently undergoing in-depth research. Camrelizumab, a humanized anti-PD-1 monoclonal antibody developed in China, has shown promising activity and manageable toxicity when combined with Apatinib, an anti-angiogenic drug. This combination may serve as a potential second-line treatment option for patients with advanced ESCC[62] or patients with recurrent or metastatic ESCC[63].

Neoadjuvant immunotherapy of ESCC

As previously mentioned, ICI immunotherapy has demonstrated improved outcomes in terms of OS and disease-free survival (DFS) for both second-line and first-line treatments of ESCC. In the context of resectable locally advanced ESCC, there has been a growing interest in perioperative immunotherapy combined with chemotherapy or radiotherapy, representing a key research direction for this disease. Preoperative neoadjuvant immunotherapy aims to activate the patient's immune system, leading to the formation of immune memory cells, thereby enabling the immune system to assume an immune surveillance role[64,65]. This review will summarize the current status of neoadjuvant immunotherapy as a treatment for ESCC.

Completed and reported clinical studies of neoadjuvant immunotherapy

Numerous clinical studies have investigated the efficacy and safety of immunotherapy for resectable ESCC in the neoadjuvant setting, as detailed in Table 1. Most neoadjuvant immunotherapy trials are conducted in conjunction with chemotherapy or CRT. Given the high incidence of this disease in China, numerous clinical trials on this subject are carried out in the country. Specifically, six ICIs targeting PD-1/PD-L1, namely, Pembrolizumab (4 studies), Camrelizumab (10 studies), Sintilimab (4 studies), Toripalimab (5 studies), and Tislelizumab (1 study), have been studied as neoadjuvant therapy. Additionally, there is an ongoing drug-based neoadjuvant therapy RCT involving Nivolumab, the first ICI used in adjuvant immunotherapy in the CheckMate-577 study[66]. The results of this trial, known as the FRONTiER study (NCT03914443), are eagerly anticipated[67]. In Table 1, four reports were retrospective in nature, while the other 21 reports were prospective, with 20 of them being single-arm trials. Only three studies employed neoadjuvant immunotherapy in combination with concurrent CRT as an intervention. In studies involving neoadjuvant immunotherapy combined with chemotherapy, the chemotherapy drugs used included 5-fluorouracil (5-FU), cisplatin (DDP), carboplatin (CBP), nedaplatin (NDP), paclitaxel (PTX), docetaxel (DTX), albumin-bound paclitaxel (nab-PTX), and PTX liposomes. Over the past few years, the use and dosages of these chemotherapy drugs have demonstrated efficacy for ESCC treatment in clinical settings. Most surgeons have chosen an interval time of 4-6 wk from the end of neoadjuvant therapy to surgery. The primary outcomes of utmost concern to doctors are safety, feasibility, and pCR, while MPR and R0 resection rate are commonly selected as primary or secondary outcomes.

Ensuring the safety of participants is of utmost importance in clinical trials, and the occurrence of trAEs is a key indicator in assessing the safety of neoadjuvant immunotherapy[68]. When ICIs are combined with other anti-cancer therapies, such as chemotherapy, immunotherapy, targeted therapy, or radiotherapy, the incidence of trAEs is significantly higher compared to the use of ICIs alone[69]. These trAEs can affect various organs, with the most common being endocrine (hypothyroidism and hyperthyroidism), gastrointestinal (diarrhea and colitis), pulmonary (pneumonitis), dermatological (rash and pruritus), and hepatic (elevated liver enzymes) complications[70,71]. The majority of trAEs (grades 1-2) are self-limiting or can be managed with immunosuppressive therapy, such as corticosteroids. However, persistent trAEs that do not respond to corticosteroids require close monitoring and appropriate treatment. Fatal trAEs are extremely rare for anti-PD-1 antibodies, with an incidence of less than 0.5% in a meta-analysis of ICI monotherapy studies across various cancer types, most commonly associated with pneumonitis[71]. The incidence of serious trAEs (grade ≥ 3) in neoadjuvant ICI plus chemotherapy ranged from 0% to 36.7% in the studies presented in Table 1. Notably, the combination of chemotherapy with Camrelizumab and Apatinib resulted in the highest incidence of patients experiencing serious trAEs (36.7%). In another meta-analysis comparing the efficacy and safety of various ICIs for patients with advanced or metastatic ESCC, Camrelizumab and Nivolumab were found to have a lower incidence of serious trAEs in the first-line and refractory settings, respectively[72]. Close monitoring and early recognition of relevant symptoms and signs are essential to ensure appropriate management.

Feasibility can be assessed by comparing the completion rate of the trial. In a pooled analysis, the rates of completion of neoadjuvant therapy and surgery ranged from 49.4% (Camrelizumab + nab-PTX + NDP) to 100% (Sintilimab + PTX liposome, DDP, and S-1). Failures in the study were mainly attributed to trAEs[73,74], patient decisions[75-77], or disease progression[78]. As most trials achieved a treatment completion rate of over 60%, interpreting the data in the conference abstract (ChiCTR2000039170) is challenging.

The definition of pCR is the absence of any signs of cancer on a histological resection specimen. The pCR rate is a crucial efficacy-related parameter reported in all studies, with some studies choosing it as a secondary outcome. In a meta-analysis of seven clinical trials involving 815 patients, the pooled pCR rate was 32.4% (95% confidence interval [CI]: 28.2%-36.8%)[79]. Data from Table 1 shows that the pCR rate ranges from 6.7% to 46.1%. The definition of MPR is the presence of less than 10% of the remaining viable tumor cells in the resected primary tumor. In the aforementioned meta-analysis, the pooled MPR rate was 49.4% (95%CI: 42.1%-56.7%)[79]. MPR rate was chosen as the primary outcome in four studies and seemed to be a second primary outcome in the main studies verified in Table 1, with reported rates ranging from 42% to 72.3%[73,76,77,80-83]. The R0 resection rate is defined as a complete resection of the tumor with a negative microscopic edge, indicating no residual tumor. It is another crucial indicator to evaluate the effectiveness of neoadjuvant therapy. The R0 resection rate in Table 1 ranges from 80.4% to 100%, which indicates positive outcomes.

Table 1 Reported clinical results of neoadjuvant immunotherapy for resectable esophageal squamous cell carcinoma

Drug & Ref.	Trial No.	Phase	Number of enrollments	Clinical stage	Design	Chemotherapy drugs	Chemotherapy cycles	Radiotherapy	Interval time to surgery	Primary outcome	Safety (rate of grade ≥ 3 trAEs)	Feasibility (therapy completion rate)	pCR	MPR	Surgical outcome (R0 rate)
Pembrolizumab [111]	Park *et al*[111] (NR)	NA	38	IA-IVA	Retrospective	5-FU + DDP/PTX + CBP	NA	41.4 Gy/23 f	6-8 wk	Operative risk	18.75% (3/16)	100% (16/16)	NA	NA	100%
Pembrolizumab [112]	Huang *et al*[112] (NR)	NA	54	II–IVA	Retrospective	DTX + NDP	2, Q3W		4-6 wk	pCR	13.04% (4/23)	NA	30.4% (7/23)	NA	100%
Pembrolizumab [113]	NCT02844075	II	28	IB-III	Single- arm	PTX + CBP	5, Q1W	41.4 Gy/23 f	5 wk	pCR	NA	92.9% (26/28)	46.1% (12/26)	NA	NA
Pembrolizumab [80]	Keystone-001/NCT04389177	II	50	IIIA-IIIB	Single-arm	PTX + DDP	3, Q3W		4-6 wk	pCR, MPR, safety	0	69.0% (29/42)	41.4% (12/29)	72.4% (21/29)	100%
Camrelizumab [114]	Qiao *et al*[114] (NR)	NA	254	IA-IVA	Retrospective	PTX, nab-PTX/DTX	2, Q3W		NA	pCR	6.25% (3/48)	NA	41.7% (20/48)	60.4 (29/48)	NA
Camrelizumab [74]	ChiCTR1900026240	II	60	IIIA-IVA	Single-arm	nab-PTX + CBP	2, Q3W		4-6 wk	pCR	56.7% (34/60)	85.0% (51/60)	39.2% (20/51)	NA	98.0%
Camrelizumab [115]	NCT04506138	I-II	46	II-IVA	Single-arm	nab-PTX + CBP			4-6 wk	pCR	15.2% (7/46)	82.6% (38/46)	21.6% (8/37)	48.6% (18/37)	80.4%
Camrelizumab [82]	GASTO1056/ChiCTR2000028900	II	23	II-III	Single-arm	nab-PTX + CBP	2, Q3W		3-6 wk	Safety	47.8%	87.0% (20/23)	25% (5/20)	50% (10/20)	100%
Camrelizumab [116]	Yang *et al*[116] (NR)	II	12	II-III	Single-arm	nab-PTX + S1	3, Q3W		3-6 wk	pCR	0	75.0% (9/12)	33.3% (4/12)	41.7% (5/12)	100%
Camrelizumab [75]	NIC-ESCC2019/NCT04225364	II	56	II-IVA	Single-arm	nab-PTX + DDP	2, Q3W		6 wk	pCR	10.7% (6/51)	91.1% (51/56)	35.3% (18/51)	23.5% (12/21)	100%
Camrelizumab [117]	ChiCTR1900023880	Ib	30	IC-IIIB	Single-arm	nab-PTX + NDP + Apatinib	2-4, Q3W		4-8 wk	Safety, feasibility	36.7% (11/30)	96.7% (29/30)	24.1% (7/29)	51.7% (15/29)	NA
Camrelizumab [118]	ESPRIT/ChiCTR2000033761	II	48	IIA-IIIB	Single-arm	PTX + NDP	2-4, Q3W		NA	pCR	4.2%	62.5% (30/48)	35.0% (7/20)	NA	NA
Camrelizumab [119]	NCT 03917966	II	40	IC-IVA	Single-arm	DTX + NDP	2, Q3W		4-6 wk	MPR	3%	70.6% (12/17)	25.0% (3/12)	41.6% (5/12)	100%
Camrelizumab [120]	ChiCTR2000039170	II	166	Locally advanced	Single-arm	nab-PTX + NDP	NA		NA	Safety	7.8% (13/166)	49.4% (82/166)	18.5% (15/81)	63.0% (51/81)	97.5% (79/82)
Sintilimab[121]	ChiCTR1900026593	II	47	II-IVA	Single-arm	PTX liposome +	2, Q3W		3-6 wk	pCR	29.8%	95.7%	22.2%	44.4%	97.8%

						CBP					(14/47)	(45/47)	(10/45)	(20/45)	(44/45)
Sintilimab[81]	SIN-ICE study/ChiCTR2100048917	II	23	IC-IVA	Single-arm	Platinum	3, Q3W		4-6 wk	pCR, safety	30.4% (7/23)	73.9% (17/23)	35.3%, (6/17)	52.9% (9/17)	94.1% (16/17)
Sintilimab[73]	ESONICT-1/ChiCTR2100045659	II	30	IIB-IVA	Single-arm	DDP + nab-PTX	2, Q3W		4-6 wk	pCR, safety	3.3% (1/30)	76.6% (23/30)	21.7% (5/23)	52.2% (12/23)	100%
Sintilimab[88]	KEEP-G03/NCT03946969	II	30	IB-IVA	Single-arm	PTX liposom + DDP + S1	2, Q3W		Within 6 wk	Safety, feasibility	36.7%	100.0% (30/30)	20% (6/30)	50% (15/30)	100%
Toripalimab [122,123]	NCT03985670	II	30	II-IVA	Two-arm	PTX + DDP	2, Q3-4W		4-6 wk	pCR	8.33% (2/24)	80.0% (24/30)	20.8% (5/24)	NA	100%
Toripalimab [124]	ChiCTR1900025318	II	23	IIB-IVA	Single-arm	PTX + DDP	2, Q3W		4-6 wk	pCR, R0 rate	8.70% (2/23)	78.3% (18/23)	33.3% (6/18)	NA	100%
Toripalimab [77]	NCT04177797	II	20	IIIA-IVA	Single-arm	PTX + CBP	2, Q3W		4-6 wk	Safety, feasibility, MPR, pCR	20.0% (4/20)	80.0% (16/20)	18.8% (3/16)	43.8% (7/16)	87.5% (14/16)
Toripalimab [125]	ESONICT-2/ChiCTR2100052784	II	20	IIB-IVA	Single-arm	DTX + DDP	2, Q3W		4-6 wk	pCR, safety	15.0% (3/20)	60.0% (12/20)	16.7% (2/12)	41.7% (5/12)	100%
Toripalimab [126]	SCALE-1/ChiCTR2100045104	Ib	20	IIB-IVA	Single-arm	PTX + CBP	2, Q3W	30 Gy/12 f	4-7 wk	Safety	NA	87.0% (20/23)	55% (11/20)	80% (16/20)	
Tislelizumab [76]	TD-NICE/ChiCTR2000037488	II	45	IIIA-IVA	Single-arm	CBP + nab-PTX	2, Q3W		3-6 wk	MPR	33.3% (15/45)	80.0% (36/45)	50% (18/36)	72% (26/36)	97.2% (35/36)
Multiple[127]	CHICTR2100045659		27	IC-IVA	Retrospectively, two-arm	Platinum+ PTX or platinum + 5-Fu	2, Q3w		4–8 wk	30-d major complications	11.1% (3/27)	NA	NA	NA	100%

NR: Not registered; NA: Not available; 5-FU: 5-fluorouracil; DDP: Cisplatin; PTX: Paclitaxel; DTX: Docetaxel; CBP: Carboplatin; NDP: Nedaplatin; nab-PTX: Albumin bound paclitaxel; S1: Tegafur (Gimeracil and Oteracil Potassium Capsules); pCR: Pathological complete response; MPR: Major pathological response; trAEs: Treatment-related adverse events.

Ongoing clinical trials in neoadjuvant immunotherapy

This period marks a surge in clinical trials focused on neoadjuvant immunotherapy, particularly for perioperative treatment of ESCC, with a significant number of ongoing RCTs, especially led by Chinese investigators (Table 2). Eight ICIs are currently under investigation, with dozens of trials in progress. PD-1 is the primary target in seven of these trials, while Adebrelimab targets PD-L1. Camrelizumab is the most extensively studied ICI, involved in ten clinical trials, followed by Toripalimab with seven trials. Among these trials, there are 23 single-arm studies, 11 two-arm studies, two three-arm studies, and one four-arm study.

An array of combinations of new adjuvant therapies for ESCC are constantly emerging. Most ICIs are being utilized as neoadjuvant adjuncts, combined with chemotherapy in 13 trials or CRT in 18 trials. Adebrelimab, a PD-L1-targeting ICI, is used alone in one trial (NCT04215471), as is Nivolumab in another (NCT03987815). Camrelizumab, on the other hand, is being combined with radiotherapy (NCT05176002 and NCT03200691), or paired with multitargeted small molecule inhibitors and CRT or chemotherapy (NCT04666090), or further combined with both CRT and an anti-EGFR antibody

Table 2 Ongoing clinical trials of neoadjuvant immunotherapy for resectable esophageal squamous cell carcinoma

Drug & target	Trial name/No./Ref.	Phase	Sample size	Clinical stage	Design	Chemotherapy drugs	Chemotherapy cycles	Radiotherapy	Interval to surgery	Primary endpoint	Start date
Nivolumab	FRONTiER/NCT03914443[67]	I	36	IC-IVA	Two-arm	5-FU + DDP	2, Q3W		12 wk	Incidence of dose-limiting toxicities	07-May-19
	NCT03987815	II	20	NA	Single-arm	NA				MPR	01-Aug-19
	NCT05213312	II-III	90	II-III	Two-arm	PTX/5-FU + DDP	2, Q3W		4-6 wk	pCR	01-Jun-22
Pembrolizumab	PALACE-1/NCT03792347[85]	I	20	IC-IVA	Single-arm	CBP + PTX	5, Q1W	41.4 Gy/23 f	4-6 wk	Safety	21-Jan-19
	PALACE-2/NCT04435197[84]	II	143	IC-IVA	Single-arm	CBP + PTX	5, Q1 W	41.4 Gy/23 f	4-6 wk	pCR	11-Aug-20
	NCT05302011	II	30	IIB/IIIB/IVA	Single-arm	CBP/DDP + DTX	4, Q3W			Tumor response, pCR	01-Jun-20
	NCT05281003	II	128	IC-IVA	Single-arm	PTX + DDP	4, Q4W			pCR	20-Feb-23
Camrelizumab	NCT04520035	II	60	IIB-IVA	Single-arm	PTX + DDP	2, Q3W			pCR	01-Aug-20
	NCT04767295	II	28	IA-IVA	Single-arm	nab-PTX + CBP	2, Q3W		5-8 wk	pCR	01-Mar-21
	NICE-2 Study/NCT 05043688 [128]	II	204	Locally advanced	Three-arm	nab-PTX, CBP, PTX	2, Q3W	41.4 Gy/23 f	4-12 wk	pCR	14-Sep-21
	NCT05476380	II	39	IIIB-IVA	Single-arm	PTX + DDP	3, Q3W			pCR	19-Feb-21
	NCT05182944	II	130	IIB-IVA	Four-arm	nab-PTX + DDP	2, Q3W			pCR, 3-yr DFS	15-Jan-22
	NCT04937673	II	40	IIB-IVA	Two-arm	PTX/nab-PTX + DDP	3, Q3W		NA	Biomarkers related to pCR	01-Jul-21
	NCT05176002	I-II	26	II-IVA	Single-arm	NA	NA	Radiotherapy, NA	NA	Efficacy Safety	23-Sep-21
	NCT04666090	II	42	IIA-IVA	Single-arm	nab-PTX + NDP + Apatinib	2-3, Q2W		4-6wk	pCR	23-Nov-20
	NCT05355168	I-II	57	IC-IVA	Single-arm	Nimotuzumab + CRT	NA			pCR, MPR	01-Nov-21
	NCT03200691	II	21	IIA-III	Single-			40 Gy/20 f	2-4 wk	pCR	10-Aug-

					arm					17
Sintilimab	NCT03940001	I	20	IIB-IVA	Single-arm	PTX + CBP	2, Q3W	41.4 Gy/23 f	NA	Unacceptable toxicity; pCR; MPR	01-May-19
	(NICCE)NCT05028231	NA	46	IIB-IVA	Single-arm	nab-PTX + DDP	2, Q3W			pCR	05-Jun-21
	NCT05357846	III	422	IIB-IVA	Two-arm	PTX + DDP	4, Q1W	40 or 45 Gy / 20 f	6-8 wk	OS	01-Nov-22
	NCT05244798	III	420	IC-IVA	Three-arm	nab-PTX + CBP	2, Q3	41.4 Gy/23 f	6-8 wk	pCR	01-Nov-22
Toripalimab	NCT04280822	III	400	IC-IVA	Two-arm	DDP + PTX	2, Q3W		2-3 wk	3 yr EFS; 5 yr EFS	21-Apr-20
	NCT04804696	II	53	NA	Single-arm	PTX + DDP	NA		NA	pCR	10-Feb-21
	NCT04177875	II	44	IC-IIIB	Single-arm	DTX/PTX + DDP	2, Q3W	40 Gy/20 f	NA	MPR; ORR	01-May-19
	NCT04888403	II	45	IIB-IVA	Single-arm	nab-PTX + NDP	5, Q1W	41.4 Gy/23 f	Within 7 wk	pCR	31-Dec-21
	NCT04644250	II	32	IIB-IVA	Single-arm	CBP + PTX liposome	5, Q1W	41.4 Gy/23 f	2-4 wk	pCR	01-Sep-20
	NCT04848753	III	632	IC-IVA	Two-arm	DDP + PTX	NA		NA	EFS	18-Jun-21
	NCT04006041	II	44	IIB-IVA	Single-arm	PTX + DDP	4, Q1W	44 Gy/20 f	6-8 wk	pCR	25-Jun-19
Tislelizumab	iCROSS/NCT04973306	II-III	176	II-III	Two-arm	CBP + PTX	5, Q1W	41.4 Gy/23 f	NA	pCR; OS	02-Mar-22
	NCT05323890	II	15	IIB-IVA	Single-arm	nab-PTX + DDP	5, Q1W	41.4 Gy/23 f	NA	MPR, pCR	20-Apr-22
	NCT04974047	II	70	IIB-IVA	Two-arm	PTX/5-FU + DDP	2, NA	40 or 45 Gy/20 fractions	NA	pCR	17-Aug-21
	NCT05189730	II	80	II-III	Single-arm	PTX + CBP	2, Q3W	40 Gy/20 f	4-6 wk	pCR, incidence of adverse events	01-Jul-21
Adebrelimab (PD-L1)	NATION1907II/NCT04215471	II	30	Resectable	Single-arm					ORR	01-Feb-20
Durvalumab	NCT04568200	II	60	IIB-IVA	Two-arm	CBP + PTX	4, Q3W	41.4 Gy/23 f		pCR	19-Jun-20
Pembrolizumab (+ Adjuvant)	KEYSTONE-002/NCT04807673 [86]	III	342	IC-IIIB	Two-arm	PTX + DDP	3, Q3W	41.4 Gy/23 f	4-6 wk	EFS	01-Dec-21

PD-1 Inhibitor	REVO/NCT05007145	II	92	IB-IVA	Two-arm	nab-PTX + DDP	2-4, Q3W	40 Gy/20 f		pCR	15-Aug-21
Toripalimab (+ Adjuvant)	NCT 04437212	II	20	IIB-IVA	Single-arm	PTX/DDP	5, Q3W	41.4 Gy/23 f	6-8 wk	MPR	01-Jul-20

EFS: Events-free survival; DFS: Disease-free survival; OS: Overall survival; ORR: Objective response rate; NA: Not available; 5-FU: 5-fluorouracil; DDP: Cisplatin; PTX: Paclitaxel; DTX: Docetaxel; CBP: Carboplatin; NDP: Nedaplatin; nab-PTX: Paclitaxel for injection (albumin bound); pCR: Pathological complete response; MPR: Major pathological response.

(NCT05355168).

Several large medical centers are now conducting phases II and III clinical studies based on promising results from phases I and II studies. Examples include PALACE-2 (NCT04435197)[84], an advancement of PALACE-1 (NCT03792347)[85], and KEYSTONE-002 (NCT04807673)[86], another advancement based on Keystone-001 (NCT04389177)[80]. Although Pembrolizumab is the ICI being studied in both series of trials, the PALACE trial was designed as neoadjuvant immunotherapy combined with chemotherapy, while the Keystone trial was designed as neoadjuvant combined with chemotherapy and adjuvant immunotherapy. Most chemotherapy regimens include taxols and platinum, with 5-FU being chosen in only two trials. The mainstream radiotherapy method utilizes 41.4 GY divided into 23 fractions, and the interval between neoadjuvant therapy and surgery ranges from 2 to 12 wk, with 4-6 wk being the most common choice. The primary outcome sought by most ongoing trials is pCR.

Ongoing clinical trials of adjuvant immunotherapy

Despite the benefits of neoadjuvant chemoradiation in improving survival compared to surgery alone, achieving a pCR remains challenging, with persistent disease in LNs leading to decreased survival[66]. An RCT involving 346 patients with ESCC compared preoperative and perioperative chemotherapy. Both groups received two cycles of paclitaxel, cisplatin, and 5-fluorouracil before surgery, but only half received two cycles after surgery. The group receiving adjuvant chemotherapy showed an estimated 16% improvement in 5-year survival[87].

In contrast to neoadjuvant methods, adjuvant immunotherapy has received relatively little attention. The global CheckMate-577 trial, a randomized, double-blind, placebo-controlled phase III trial, demonstrated the DFS benefit of Nivolumab for ESCC (29.7 *vs* 11.0 mo)[66]. Despite the promising results of CheckMate-577 for adjuvant immunotherapy after surgery, there are currently only three ongoing trials in this area. One trial is investigating the effectiveness of Toripalimab (NCT04437212) in both neoadjuvant and adjuvant settings. The other two RCTs are assessing postoperative adjuvant therapy with Tislelizumab, with one in phase II as a single-arm study and the other in phase III with two-arm trials. The phase II trial involves adjuvant immunotherapy combined with CRT, while the phase III trial is adjuvant immunotherapy combined with chemotherapy (Table 3). Further details and results from these ongoing trials are eagerly awaited.

ISSUES SHOULD BE CONCERNED IN FUTURE

The majority of neoadjuvant immunotherapy trials in ESCC are currently single-arm, phase II clinical trials. These trials explore various combinations of different drugs and different methods of other therapies, leading to a continuous emergence of new clinical trials in this field. However, it is important to acknowledge that progress in some cases has

Table 3 Clinical trials of adjuvant immunotherapy for resectable esophageal squamous cell carcinoma

Drug	Trial name/No.	Phase	Sample size	Clinical stage	Design	Chemotherapy drugs	Chemotherapy cycles	Radiotherapy	Interval time to surgery	Primary endpoint	Start date	Outcome
Nivolumab	CheckMate-577/NCT02743494	III	784 (ESCC29%)	NA	Two-arm	NA				DFS	Completed	22.1:11.0 mo
Toripalimab (+ Neoadjuvant)	NCT 04437212	II	20	IIB-IVA	Single-arm	PTX + DDP	5, Q3W	41.4 Gy/23 f	6-8 wk	MPR	Jul 1, 2020	
Tislelizumab	AIRE/ChiCTR2100045651	III	110	High-risk resected locally advanced	Two-arm	Platinum-based doublets	2, Q3W			DFS	May 1, 2021	
Tislelizumab	CRISEC/NCT04776590	II	30	NA	Single-arm	PTX + CBP	5, Q1W	41.4 Gy/23 f		pCR	Jan 28, 2021	

DFS: Disease-free survival; NA: Not available; DDP: Cisplatin; PTX: Paclitaxel; CBP: Carboplatin; pCR: Pathological complete response; MPR: Major pathological response.

been slow or stagnant.

Ethical conduct should be a primary concern in the development of new therapies. As the development of immunotherapy is often driven by related industries, methodological, legal, and ethical frameworks can sometimes be overlooked. Currently, a significant portion of scientific research in immunotherapy is industry-driven, with various pharmaceutical companies involved in registering RCTs. Despite the existence of international research registries aimed at improving the transparency of medical research, there are still uncertainties and "not applicable" rules and regulations. Consequently, there may be a lack of control over data mining and publication bias. Even if there are significant differences between the research protocol and the reported results, most trial outcomes are still published. To ensure the reliability, quality, and expected clinical benefits of ongoing and future trials in this field, the medical community and relevant stakeholders should focus on curbing the significant increase in "feasibility" trials with unclear expected benefits. Emphasizing a few multi-center phase III trials, conducted by leading centers in ESCC research, could be a crucial approach to prevent unclear or contradictory results and uphold the integrity of the research.

The second issue of concern in clinical trials is safety, which should be carefully considered throughout the perioperative treatment of ESCC. One of the major safety risks is the occurrence of trAEs, especially immune-related adverse events. Perioperative immunotherapy trials for ESCC typically consist of three parts: Preoperative neoadjuvant therapy, surgery, and postoperative adjuvant therapy. Different immunotherapy drugs are administered at varying intervals: Pembrolizumab, Tislelizumab, Atilizumab, Toripalimab, and Sintilimab are usually given at 3-wk intervals, while Nivolumab, Camrelizumab, and Durvalumab are given at 2-wk intervals. The treatment cycles generally involve 2-4 cycles, and multiple factors such as treatment efficacy, surgical timing, economic considerations, and patient compliance are taken into account. Since most RCTs in this field are single-arm or two-arm studies within phase I or II, the safety data obtained may be limited and not fully comprehensive. This might result in an underestimation of the occurrence and severity of trAEs, especially those of grade 3 or above. Additionally, the introduction of new emerging drugs into clinical trials adds uncertain factors that could impact the results. Therefore, researchers should be attentive to the incidence and severity of trAEs, even when they are below grade 2. In cases where the trAEs are grade 3 or higher in severity, special attention should be given to the subjects to avoid fatal consequences. Furthermore, if three or more anti-cancer therapies, including immunotherapy, are administered to a subject simultaneously, researchers should exercise caution due to the

higher risk of trAEs for the patient. Vigilance and thorough monitoring are essential to ensure the safety of subjects throughout the course of treatment.

Neoadjuvant immunotherapy presents a dual challenge, aiming to achieve better treatment outcomes while minimizing harm to normal organs caused by immunotherapy. The impact of trAEs during preoperative therapy on surgery must be carefully considered. In the trial "KEEP-G 03"[88], 36.7% (11/30) of patients experienced grades 3-4 TRAEs, but fortunately, these did not result in any surgical delays. However, in another multicenter, single-arm, phase II trial using Camrelizumab and chemotherapy as neoadjuvant treatment for locally advanced ESCC[74], 34 patients (56.7%) experienced adverse events of grade 3 or worse, with one patient (1.7%) experiencing a fatal grade 5 adverse event due to pneumonia and acute respiratory failure. The risk of increased surgical complications after immunotherapy is a concern, emphasizing the importance of forming a multidisciplinary team to address trAEs and conduct comprehensive evaluations during immunotherapy. Early detection and management of trAEs can minimize the impact on subsequent treatment and related complications. Additionally, exploring biomarkers related to trAEs is crucial in the research field.

Surgery itself poses another safety concern. ESCC radical resection is a complex procedure with a high incidence of complications, and surgical team experience significantly influences the rate of complications. Patients undergoing neoadjuvant treatment may face unexpected surgical challenges. High-volume medical units with stable and mature treatment processes, including neoadjuvant therapy and operations, generally have lower complication and mortality rates[89]. Therefore, RCTs involving neoadjuvant treatment should preferably be conducted in high-volume centers to reduce surgical risks and avoid any adverse impacts. Even in multi-center clinical trials, it is advisable to select larger surgical units or include surgeons with significant experience in performing over 100 operations on ESCC, both open and minimally invasive surgeries. Such measures ensure optimal surgical outcomes and minimize potential complications.

The third issue pertains to how we can accurately assess the efficacy of chosen drugs or treatments. Imaging is a crucial tool for preoperative efficacy assessment. Circulating tumor DNA (ct-DNA) has shown promise as an effective predictive method[90]. Positron emission tomography (PET) also has reference value as an assessment method[91,92]. Typically, pCR and MPR rates are used to predict efficacy, based on the examination of residual tumor cells in postoperative pathology. However, this method has certain limitations[93,94]. First, accurately assessing the pathological conditions of ESCC before immunotherapy, especially in cases of LN metastasis, is challenging. Detection can only be done in resected specimens after neoadjuvant immunotherapy, leading to an inability to make accurate comparisons with pathological specimens before surgery. Second, there is currently no universal standard for evaluating pathological response in ESCC after neoadjuvant immunotherapy. Pathologists are relied upon for positioning, measuring, sampling, slicing, and labeling, introducing variability. The different patterns of resection after neoadjuvant treatment, involving thoracic surgeons and pathologists, may also impact ESCC prognosis[95]. Thus, there is a need for a highly sensitive, specific, and preferably repeatable, simple, and feasible biomarker to predict efficacy in clinical practice.

PET is an integral part of the standard staging for ESCC. Its utility and acceptance in initial staging and recurrence detection have led to the hypothesis that PET could be used to differentiate responders from non-responders during neoadjuvant treatment. However, the precise PET parameters with the best predictive values are still a subject of debate. Several traditional PET parameters, such as the maximum and mean standardized uptake value (SUVmax and SUVmean), metabolic tumor volume (MTV), and total lesion glycolysis (TLG)[96], have been studied to correlate with pathological response. In a study of 31 patients with resectable ESCC or EAC, PET was used prospectively during treatment with trimodality therapy, and it was found that baseline TLG and post-chemoradiotherapy TLG were associated with OS[97]. More recently, efforts have been made to develop radiomic signatures and more robust predictive models. Simoni *et al*[98] investigated multiple traditional PET parameters and identified several radiomic features, as well as tumor regression grade, which correlated with pathological response in a retrospective analysis[98]. However, further research is necessary to develop more reliable predictive models and to validate them in prospective randomized trials. The credibility of PET evaluations in the era of immunotherapy remains largely unknown. Although PET has shown promise in predicting efficacy, especially with regard to OS, its applicability to immunotherapy response assessment is not fully understood. If sufficient high-quality CT or PET data, correlating with pathological response in ESCC, can be obtained, machine learning and artificial intelligence (AI) may emerge as new methods for evaluating neoadjuvant immunotherapy in ESCC. Such advancements could potentially enhance our ability to predict treatment outcomes and optimize patient care.

As of the current writing, specific biomarkers that can precisely determine the efficacy or predict perioperative surgery outcomes of ESCC have not been identified. However, several biomarkers have been explored mainly based on immunological and genetic criteria, including PD-L1 expression, intertumoral lymphoid infiltrates, dMMR/microsatellite instable (MSI), tumor mutation burden (TMB)/tumor neoantigen burden (TNB), and human leukocyte antigen (HLA)[99]. Among these biomarkers, PD-L1 expression is one of the best characterized for anti-PD-1/PD-L1 therapy. It is assessed using immunohistochemistry (IHC) staining and evaluated by the combined positive score (CPS) or tumor proportional score (TPS). CPS is determined by dividing the number of PD-L1-positive cells (tumor cells and other lymphocytes) by the total number of tumor cells[100], while TPS is calculated by dividing the number of PD-L1-positive tumor cells by the total number of tumor cells. In general, high PD-L1 expression usually correlates with an improved objective response to anti-PD-1/PD-L1 therapy[101]. However, some clinical studies have failed to consistently demonstrate this correlation, showing that patients with tumors showing high PD-L1 expression do not always respond to PD-1/PD-L1 blockade [102]. The relationship between PD-L1 expression and clinical outcome in ESCC remains a topic of controversy[103]. While some studies have shown that PD-L1 overexpression is associated with poor clinical outcomes[104], others have indicated a favorable prognosis[105].

Studies have also shown that circulating tumor cells (CTCs) and ct-DNA have a predictive role in evaluating the treatment efficacy of PD-1/PD-L1 inhibition[106,107]. CTCs have been found to be associated with a poor response to PD-L1 inhibitors in non-small cell lung cancer (NSCLC)[106]. Similarly, ct-DNA minimal residual disease (ct-DNA MRD) is

an important indicator for monitoring the efficacy of treating NSCLC[108]. Therefore, it is worth exploring whether CTCs and ct-DNA can be introduced into the long-term follow-up of ESCC to help assess treatment response and predict patient outcomes. However, further research is needed to validate the predictive value of these biomarkers in ESCC and determine their potential role in guiding treatment decisions for patients undergoing perioperative immunotherapy.

The fourth issue pertains to the long-term benefits of perioperative immunotherapy. Many clinical trials on perioperative immunotherapy have focused on short-term or mid-term outcomes, such as safety, feasibility, and pCR. However, the true primary outcomes that need to be concerned with are long-term OS and PFS, regardless of the type of immunological drugs selected or the combination with other anti-cancer therapies. For neoadjuvant anti-PD-1 therapy in resectable NSCLC, a trial with a median follow-up of 63 mo (NCT02259621) reported promising long-term outcomes. The 5-year recurrence-free survival (RFS) and OS rates were 60% and 80%, respectively[109]. Similarly, a study evaluating neoadjuvant anti-PD-1 treatment for localized dMMR colorectal cancer (CRC) also reported positive long-term follow-up data. Among patients who underwent surgery or achieved complete response, the 2-year tumor-specific disease-free and OS rates were both 100%[110].

In the context of resectable locally advanced ESCC, neoadjuvant chemotherapy and nCRT remain the standard treatments before surgery. While immune checkpoint-based therapy shows promise, it currently benefits only a small proportion of ESCC patients. Therefore, perioperative immunotherapy should be strictly monitored with ethical confirmation and preferably conducted within clinical trials. Patients must be fully informed about the potential benefits and risks and give informed consent before participating. Accurate screening of target populations and appropriate choice of combination therapy will be crucial for future research in this field. The importance of monitoring and managing trAEs, especially when combining immunotherapies with other anti-cancer therapies, cannot be ignored. Robust predictive and prognostic biomarkers or comprehensive biomarkers need to be identified to optimize treatment strategies and ensure the most effective therapy for patients. The development of clinical consensus or guidelines based on research findings will also be necessary to ensure that patients receive the most applicable and effective immunotherapy treatments.

CONCLUSION

The utilization of immunotherapy is progressively transitioning from a second-line approach for advanced or metastatic cases to a perioperative strategy for resectable locally advanced ESCC. Despite the current results lacking comprehensiveness and robustness, substantial advancements in perioperative immunotherapy for ESCC are evident. With the assurance derived from existing outcomes, numerous EC centers are now engaged in conducting multicenter, multi-arm RCTs. These RCTs hold the promise of providing further insights into the value of perioperative immunotherapy. It is plausible that in the near future, perioperative immunotherapy will emerge as a pivotal component of comprehensive treatment for resectable locally advanced ESCC. However, the determination of the optimal drug or the most effective combination of therapies, as well as the potential role of AI as an assistant, will require further observation and investigation.

FOOTNOTES

Author contributions: Liu Y designed the paper, collected and analyzed the data in the references, and wrote the manuscript.

Conflict-of-interest statement: The author declares no conflicts of interest related to this article.

Open-Access: This article is an open-access article that was selected by an in-house editor and fully peer-reviewed by external reviewers. It is distributed in accordance with the Creative Commons Attribution NonCommercial (CC BY-NC 4.0) license, which permits others to distribute, remix, adapt, build upon this work non-commercially, and license their derivative works on different terms, provided the original work is properly cited and the use is non-commercial. See: https://creativecommons.org/Licenses/by-nc/4.0/

Country/Territory of origin: China

ORCID number: Yong Liu 0000-0002-4048-5837.

S-Editor: Yan JP
L-Editor: Wang TQ
P-Editor: Cai YX

REFERENCES

1 **Sung H**, Ferlay J, Siegel RL, Laversanne M, Soerjomataram I, Jemal A, Bray F. Global Cancer Statistics 2020: GLOBOCAN Estimates of Incidence and Mortality Worldwide for 36 Cancers in 185 Countries. *CA Cancer J Clin* 2021; **71**: 209-249 [PMID: 33538338 DOI: 10.3322/caac.21660]

2 **Rustgi AK**, El-Serag HB. Esophageal carcinoma. *N Engl J Med* 2014; **371**: 2499-2509 [PMID: 25539106 DOI: 10.1056/NEJMra1314530]

3 **Yan Y**, Feng X, Li C, Lerut T, Li H. Treatments for resectable esophageal cancer: from traditional systemic therapy to immunotherapy. *Chin Med J (Engl)* 2022; **135**: 2143-2156 [PMID: 36525602 DOI: 10.1097/CM9.0000000000002371]

4 **Plum PS**, Hölscher AH, Pacheco Godoy K, Schmidt H, Berlth F, Chon SH, Alakus H, Bollschweiler E. Prognosis of patients with superficial T1 esophageal cancer who underwent endoscopic resection before esophagectomy-A propensity score-matched comparison. *Surg Endosc* 2018; **32**: 3972-3980 [PMID: 29536160 DOI: 10.1007/s00464-018-6139-7]

5 **Omloo JM**, Lagarde SM, Hulscher JB, Reitsma JB, Fockens P, van Dekken H, Ten Kate FJ, Obertop H, Tilanus HW, van Lanschot JJ. Extended transthoracic resection compared with limited transhiatal resection for adenocarcinoma of the mid/distal esophagus: five-year survival of a randomized clinical trial. *Ann Surg* 2007; **246**: 992-1000; discussion 1000 [PMID: 18043101 DOI: 10.1097/SLA.0b013e31815c4037]

6 **Oppedijk V**, van der Gaast A, van Lanschot JJ, van Hagen P, van Os R, van Rij CM, van der Sangen MJ, Beukema JC, Rütten H, Spruit PH, Reinders JG, Richel DJ, van Berge Henegouwen MI, Hulshof MC. Patterns of recurrence after surgery alone versus preoperative chemoradiotherapy and surgery in the CROSS trials. *J Clin Oncol* 2014; **32**: 385-391 [PMID: 24419108 DOI: 10.1200/JCO.2013.51.2186]

7 **Chen G**, Wang Z, Liu XY, Liu FY. Recurrence pattern of squamous cell carcinoma in the middle thoracic esophagus after modified Ivor-Lewis esophagectomy. *World J Surg* 2007; **31**: 1107-1114 [PMID: 17426905 DOI: 10.1007/s00268-006-0551-1]

8 **Leng XF**, Daiko H, Han YT, Mao YS. Optimal preoperative neoadjuvant therapy for resectable locally advanced esophageal squamous cell carcinoma. *Ann N Y Acad Sci* 2020; **1482**: 213-224 [PMID: 33067818 DOI: 10.1111/nyas.14508]

9 **Yang H**, Liu H, Chen Y, Zhu C, Fang W, Yu Z, Mao W, Xiang J, Han Y, Chen Z, Yang H, Wang J, Pang Q, Zheng X, Li T, Lordick F, D'Journo XB, Cerfolio RJ, Korst RJ, Novoa NM, Swanson SJ, Brunelli A, Ismail M, Fernando HC, Zhang X, Li Q, Wang G, Chen B, Mao T, Kong M, Guo X, Lin T, Liu M, Fu J; AME Thoracic Surgery Collaborative Group. Neoadjuvant Chemoradiotherapy Followed by Surgery Versus Surgery Alone for Locally Advanced Squamous Cell Carcinoma of the Esophagus (NEOCRTEC5010): A Phase III Multicenter, Randomized, Open-Label Clinical Trial. *J Clin Oncol* 2018; **36**: 2796-2803 [PMID: 30089078 DOI: 10.1200/JCO.2018.79.1483]

10 **Lewis S**, Lukovic J. Neoadjuvant Therapy in Esophageal Cancer. *Thorac Surg Clin* 2022; **32**: 447-456 [PMID: 36266032 DOI: 10.1016/j.thorsurg.2022.06.003]

11 **Shah MA**, Kennedy EB, Catenacci DV, Deighton DC, Goodman KA, Malhotra NK, Willett C, Stiles B, Sharma P, Tang L, Wijnhoven BPL, Hofstetter WL. Treatment of Locally Advanced Esophageal Carcinoma: ASCO Guideline. *J Clin Oncol* 2020; **38**: 2677-2694 [PMID: 32568633 DOI: 10.1200/JCO.20.00866]

12 **Puetz K**, Bollschweiler E, Semrau R, Mönig SP, Hölscher AH, Drebber U. Neoadjuvant chemoradiation for patients with advanced oesophageal cancer - which response grading system best impacts prognostic discrimination? *Histopathology* 2019; **74**: 731-743 [PMID: 30636069 DOI: 10.1111/his.13811]

13 **Shapiro J**, van Lanschot JJB, Hulshof MCCM, van Hagen P, van Berge Henegouwen MI, Wijnhoven BPL, van Laarhoven HWM, Nieuwenhuijzen GAP, Hospers GAP, Bonenkamp JJ, Cuesta MA, Blaisse RJB, Busch ORC, Ten Kate FJW, Creemers GM, Punt CJA, Plukker JTM, Verheul HMW, Bilgen EJS, van Dekken H, van der Sangen MJC, Rozema T, Biermann K, Beukema JC, Piet AHM, van Rij CM, Reinders JG, Tilanus HW, Steyerberg EW, van der Gaast A; CROSS study group. Neoadjuvant chemoradiotherapy plus surgery versus surgery alone for oesophageal or junctional cancer (CROSS): long-term results of a randomised controlled trial. *Lancet Oncol* 2015; **16**: 1090-1098 [PMID: 26254683 DOI: 10.1016/S1470-2045(15)00040-6]

14 **Sun HB**, Xing WQ, Liu XB, Zheng Y, Yang SJ, Wang ZF, Liu SL, Ba YF, Zhang RX, Liu BX, Fan CC, Chen PN, Liang GH, Yu YK, Liu Q, Wang HR, Li HM, Li ZX; written on Henan Cancer Hospital Thoracic Oncology Group (HCHTOG). Neoadjuvant chemotherapy versus neoadjuvant chemoradiotherapy for locally advanced oesophageal squamous cell carcinoma: a single-Centre, open-label, randomized, controlled, clinical trial (HCHTOG1903). *BMC Cancer* 2020; **20**: 303 [PMID: 32293362 DOI: 10.1186/s12885-020-06824-2]

15 **Tepper J**, Krasna MJ, Niedzwiecki D, Hollis D, Reed CE, Goldberg R, Kiel K, Willett C, Sugarbaker D, Mayer R. Phase III trial of trimodality therapy with cisplatin, fluorouracil, radiotherapy, and surgery compared with surgery alone for esophageal cancer: CALGB 9781. *J Clin Oncol* 2008; **26**: 1086-1092 [PMID: 18309943 DOI: 10.1200/JCO.2007.12.9593]

16 **van Hagen P**, Hulshof MC, van Lanschot JJ, Steyerberg EW, van Berge Henegouwen MI, Wijnhoven BP, Richel DJ, Nieuwenhuijzen GA, Hospers GA, Bonenkamp JJ, Cuesta MA, Blaisse RJ, Busch OR, ten Kate FJ, Creemers GJ, Punt CJ, Plukker JT, Verheul HM, Spillenaar Bilgen EJ, van Dekken H, van der Sangen MJ, Rozema T, Biermann K, Beukema JC, Piet AH, van Rij CM, Reinders JG, Tilanus HW, van der Gaast A; CROSS Group. Preoperative chemoradiotherapy for esophageal or junctional cancer. *N Engl J Med* 2012; **366**: 2074-2084 [PMID: 22646630 DOI: 10.1056/NEJMoa1112088]

17 **Zhou HY**, Zheng SP, Li AL, Gao QL, Ou QY, Chen YJ, Wu ST, Lin DG, Liu SB, Huang LY, Li FS, Zhu HY, Qiao GB, Lanuti M, Yao HR, Yu YF. Clinical evidence for association of neoadjuvant chemotherapy or chemoradiotherapy with efficacy and safety in patients with resectable esophageal carcinoma (NewEC study). *EClinicalMedicine* 2020; **24**: 100422 [PMID: 32637899 DOI: 10.1016/j.eclinm.2020.100422]

18 **Chan KKW**, Saluja R, Delos Santos K, Lien K, Shah K, Cramarossa G, Zhu X, Wong RKS. Neoadjuvant treatments for locally advanced, resectable esophageal cancer: A network meta-analysis. *Int J Cancer* 2018; **143**: 430-437 [PMID: 29441562 DOI: 10.1002/ijc.31312]

19 **Pasquali S**, Yim G, Vohra RS, Mocellin S, Nyanhongo D, Marriott P, Geh JI, Griffiths EA. Survival After Neoadjuvant and Adjuvant Treatments Compared to Surgery Alone for Resectable Esophageal Carcinoma: A Network Meta-analysis. *Ann Surg* 2017; **265**: 481-491 [PMID: 27429017 DOI: 10.1097/SLA.0000000000001905]

20 **Mariette C**, Dahan L, Mornex F, Maillard E, Thomas PA, Meunier B, Boige V, Pezet D, Robb WB, Le Brun-Ly V, Bosset JF, Mabrut JY, Triboulet JP, Bedenne L, Seitz JF. Surgery alone versus chemoradiotherapy followed by surgery for stage I and II esophageal cancer: final analysis of randomized controlled phase III trial FFCD 9901. *J Clin Oncol* 2014; **32**: 2416-2422 [PMID: 24982463 DOI: 10.1200/JCO.2013.53.6532]

21 **Murakami Y**, Hamai Y, Emi M, Hihara J, Imano N, Takeuchi Y, Takahashi I, Nishibuchi I, Kimura T, Okada M, Nagata Y. Long-term results of neoadjuvant chemoradiotherapy using cisplatin and 5-fluorouracil followed by esophagectomy for resectable, locally advanced esophageal squamous cell carcinoma. *J Radiat Res* 2018; **59**: 616-624 [PMID: 29939306 DOI: 10.1093/jrr/rry047]

22 **Ajani JA**, D'Amico TA, Bentrem DJ, Chao J, Corvera C, Das P, Denlinger CS, Enzinger PC, Fanta P, Farjah F, Gerdes H, Gibson M, Glasgow RE, Hayman JA, Hochwald S, Hofstetter WL, Ilson DH, Jaroszewski D, Johung KL, Keswani RN, Kleinberg LR, Leong S, Ly QP, Matkowskyj KA, McNamara M, Mulcahy MF, Paluri RK, Park H, Perry KA, Pimiento J, Poultsides GA, Roses R, Strong VE, Wiesner G, Willett CG, Wright CD, McMillian NR, Pluchino LA. Esophageal and Esophagogastric Junction Cancers, Version 2.2019, NCCN Clinical Practice Guidelines in Oncology. *J Natl Compr Canc Netw* 2019; **17**: 855-883 [PMID: 31319389 DOI: 10.6004/jnccn.2019.0033]

23 **Ajani JA**, D'Amico TA, Bentrem DJ, Cooke D, Corvera C, Das P, Enzinger PC, Enzler T, Farjah F, Gerdes H, Gibson M, Grierson P,

Hofstetter WL, Ilson DH, Jalal S, Keswani RN, Kim S, Kleinberg LR, Klempner S, Lacy J, Licciardi F, Ly QP, Matkowskyj KA, McNamara M, Miller A, Mukherjee S, Mulcahy MF, Outlaw D, Perry KA, Pimiento J, Poultsides GA, Reznik S, Roses RE, Strong VE, Su S, Wang HL, Wiesner G, Willett CG, Yakoub D, Yoon H, McMillian NR, Pluchino LA. Esophageal and Esophagogastric Junction Cancers, Version 2.2023, NCCN Clinical Practice Guidelines in Oncology. *J Natl Compr Canc Netw* 2023; **21**: 393-422 [PMID: 37015332 DOI: 10.6004/jnccn.2023.0019]

24 **Muro K**, Lordick F, Tsushima T, Pentheroudakis G, Baba E, Lu Z, Cho BC, Nor IM, Ng M, Chen LT, Kato K, Li J, Ryu MH, Zamaniah WIW, Yong WP, Yeh KH, Nakajima TE, Shitara K, Kawakami H, Narita Y, Yoshino T, Van Cutsem E, Martinelli E, Smyth EC, Arnold D, Minami H, Tabernero J, Douillard JY. Pan-Asian adapted ESMO Clinical Practice Guidelines for the management of patients with metastatic oesophageal cancer: a JSMO-ESMO initiative endorsed by CSCO, KSMO, MOS, SSO and TOS. *Ann Oncol* 2019; **30**: 34-43 [PMID: 30475943 DOI: 10.1093/annonc/mdy498]

25 **Zhang W**, Wang P, Pang Q. Immune checkpoint inhibitors for esophageal squamous cell carcinoma: a narrative review. *Ann Transl Med* 2020; **8**: 1193 [PMID: 33241042 DOI: 10.21037/atm-20-4625]

26 **Eyck BM**, van Lanschot JJB, Hulshof MCCM, van der Wilk BJ, Shapiro J, van Hagen P, van Berge Henegouwen MI, Wijnhoven BPL, van Laarhoven HWM, Nieuwenhuijzen GAP, Hospers GAP, Bonenkamp JJ, Cuesta MA, Blaisse RJB, Busch OR, Creemers GM, Punt CJA, Plukker JTM, Verheul HMW, Spillenaar Bilgen EJ, van der Sangen MJC, Rozema T, Ten Kate FJW, Beukema JC, Piet AHM, van Rij CM, Reinders JG, Tilanus HW, Steyerberg EW, van der Gaast A; CROSS Study Group. Ten-Year Outcome of Neoadjuvant Chemoradiotherapy Plus Surgery for Esophageal Cancer: The Randomized Controlled CROSS Trial. *J Clin Oncol* 2021; **39**: 1995-2004 [PMID: 33891478 DOI: 10.1200/JCO.20.03614]

27 **Groom JR**. Regulators of T-cell fate: Integration of cell migration, differentiation and function. *Immunol Rev* 2019; **289**: 101-114 [PMID: 30977199 DOI: 10.1111/imr.12742]

28 **Masopust D**, Schenkel JM. The integration of T cell migration, differentiation and function. *Nat Rev Immunol* 2013; **13**: 309-320 [PMID: 23598650 DOI: 10.1038/nri3442]

29 **Baba Y**, Nomoto D, Okadome K, Ishimoto T, Iwatsuki M, Miyamoto Y, Yoshida N, Baba H. Tumor immune microenvironment and immune checkpoint inhibitors in esophageal squamous cell carcinoma. *Cancer Sci* 2020; **111**: 3132-3141 [PMID: 32579769 DOI: 10.1111/cas.14541]

30 **Janjigian YY**, Bendell J, Calvo E, Kim JW, Ascierto PA, Sharma P, Ott PA, Peltola K, Jaeger D, Evans J, de Braud F, Chau I, Harbison CT, Dorange C, Tschaika M, Le DT. CheckMate-032 Study: Efficacy and Safety of Nivolumab and Nivolumab Plus Ipilimumab in Patients With Metastatic Esophagogastric Cancer. *J Clin Oncol* 2018; **36**: 2836-2844 [PMID: 30110194 DOI: 10.1200/JCO.2017.76.6212]

31 **Kudo T**, Hamamoto Y, Kato K, Ura T, Kojima T, Tsushima T, Hironaka S, Hara H, Satoh T, Iwasa S, Muro K, Yasui H, Minashi K, Yamaguchi K, Ohtsu A, Doki Y, Kitagawa Y. Nivolumab treatment for oesophageal squamous-cell carcinoma: an open-label, multicentre, phase 2 trial. *Lancet Oncol* 2017; **18**: 631-639 [PMID: 28314688 DOI: 10.1016/S1470-2045(17)30181-X]

32 **Kojima T**, Shah MA, Muro K, Francois E, Adenis A, Hsu CH, Doi T, Moriwaki T, Kim SB, Lee SH, Bennouna J, Kato K, Shen L, Enzinger P, Qin SK, Ferreira P, Chen J, Girotto G, de la Fouchardiere C, Senellart H, Al-Rajabi R, Lordick F, Wang R, Suryawanshi S, Bhagia P, Kang SP, Metges JP; KEYNOTE-181 Investigators. Randomized Phase III KEYNOTE-181 Study of Pembrolizumab Versus Chemotherapy in Advanced Esophageal Cancer. *J Clin Oncol* 2020; **38**: 4138-4148 [PMID: 33026938 DOI: 10.1200/JCO.20.01888]

33 **Shen L**, Kato K, Kim SB, Ajani JA, Zhao K, He Z, Yu X, Shu Y, Luo Q, Wang J, Chen Z, Niu Z, Zhang L, Yi T, Sun JM, Chen J, Yu G, Lin CY, Hara H, Bi Q, Satoh T, Pazo-Cid R, Arkenau HT, Borg C, Lordick F, Li L, Ding N, Tao A, Shi J, Van Cutsem E; RATIONALE-302 Investigators. Tislelizumab Versus Chemotherapy as Second-Line Treatment for Advanced or Metastatic Esophageal Squamous Cell Carcinoma (RATIONALE-302): A Randomized Phase III Study. *J Clin Oncol* 2022; **40**: 3065-3076 [PMID: 35442766 DOI: 10.1200/JCO.21.01926]

34 **Kato K**, Cho BC, Takahashi M, Okada M, Lin CY, Chin K, Kadowaki S, Ahn MJ, Hamamoto Y, Doki Y, Yen CC, Kubota Y, Kim SB, Hsu CH, Holtved E, Xynos I, Kodani M, Kitagawa Y. Nivolumab versus chemotherapy in patients with advanced oesophageal squamous cell carcinoma refractory or intolerant to previous chemotherapy (ATTRACTION-3): a multicentre, randomised, open-label, phase 3 trial. *Lancet Oncol* 2019; **20**: 1506-1517 [PMID: 31582355 DOI: 10.1016/S1470-2045(19)30626-6]

35 **Huang J**, Xu J, Chen Y, Zhuang W, Zhang Y, Chen Z, Chen J, Zhang H, Niu Z, Fan Q, Lin L, Gu K, Liu Y, Ba Y, Miao Z, Jiang X, Zeng M, Fu Z, Gan L, Wang J, Zhan X, Liu T, Li Z, Shen L, Shu Y, Zhang T, Yang Q, Zou J; ESCORT Study Group. Camrelizumab versus investigator's choice of chemotherapy as second-line therapy for advanced or metastatic oesophageal squamous cell carcinoma (ESCORT): a multicentre, randomised, open-label, phase 3 study. *Lancet Oncol* 2020; **21**: 832-842 [PMID: 32416073 DOI: 10.1016/S1470-2045(20)30110-8]

36 **Wang ZX**, Cui C, Yao J, Zhang Y, Li M, Feng J, Yang S, Fan Y, Shi J, Zhang X, Shen L, Shu Y, Wang C, Dai T, Mao T, Chen L, Guo Z, Liu B, Pan H, Cang S, Jiang Y, Wang J, Ye M, Chen Z, Jiang D, Lin Q, Ren W, Wu L, Xu Y, Miao Z, Sun M, Xie C, Liu Y, Wang Q, Zhao L, Li Q, Huang C, Jiang K, Yang K, Li D, Zhu Z, Chen R, Jia L, Li W, Liao W, Liu HX, Ma D, Ma J, Qin Y, Shi Z, Wei Q, Xiao K, Chen X, Dai G, He J, Li J, Li G, Liu Z, Yuan X, Zhang J, Fu Z, He Y, Ju F, Tang P, Wang T, Wang W, Luo X, Tang X, May R, Feng H, Yao S, Keegan P, Xu RH, Wang F. Toripalimab plus chemotherapy in treatment-naïve, advanced esophageal squamous cell carcinoma (JUPITER-06): A multi-center phase 3 trial. *Cancer Cell* 2022; **40**: 277-288.e3 [PMID: 35245446 DOI: 10.1016/j.ccell.2022.02.007]

37 **Doki Y**, Ajani JA, Kato K, Xu J, Wyrwicz L, Motoyama S, Ogata T, Kawakami H, Hsu CH, Adenis A, El Hajbi F, Di Bartolomeo M, Braghiroli MI, Holtved E, Ostoich SA, Kim HR, Ueno M, Mansoor W, Yang WC, Liu T, Bridgewater J, Makino T, Xynos I, Liu X, Lei M, Kondo K, Patel A, Gricar J, Chau I, Kitagawa Y; CheckMate 648 Trial Investigators. Nivolumab Combination Therapy in Advanced Esophageal Squamous-Cell Carcinoma. *N Engl J Med* 2022; **386**: 449-462 [PMID: 35108470 DOI: 10.1056/NEJMoa2111380]

38 **Lu Z**, Wang J, Shu Y, Liu L, Kong L, Yang L, Wang B, Sun G, Ji Y, Cao G, Liu H, Cui T, Li N, Qiu W, Li G, Hou X, Luo H, Xue L, Zhang Y, Yue W, Liu Z, Wang X, Gao S, Pan Y, Galais MP, Zaanan A, Ma Z, Li H, Wang Y, Shen L; ORIENT-15 study group. Sintilimab versus placebo in combination with chemotherapy as first line treatment for locally advanced or metastatic oesophageal squamous cell carcinoma (ORIENT-15): multicentre, randomised, double blind, phase 3 trial. *BMJ* 2022; **377**: e068714 [PMID: 35440464 DOI: 10.1136/bmj-2021-068714]

39 **Luo H**, Lu J, Bai Y, Mao T, Wang J, Fan Q, Zhang Y, Zhao K, Chen Z, Gao S, Li J, Fu Z, Gu K, Liu Z, Wu L, Zhang X, Feng J, Niu Z, Ba Y, Zhang H, Liu Y, Zhang L, Min X, Huang J, Cheng Y, Wang D, Shen Y, Yang Q, Zou J, Xu RH; ESCORT-1st Investigators. Effect of Camrelizumab vs Placebo Added to Chemotherapy on Survival and Progression-Free Survival in Patients With Advanced or Metastatic Esophageal Squamous Cell Carcinoma: The ESCORT-1st Randomized Clinical Trial. *JAMA* 2021; **326**: 916-925 [PMID: 34519801 DOI: 10.1001/jama.2021.12836]

40 **Sun JM**, Shen L, Shah MA, Enzinger P, Adenis A, Doi T, Kojima T, Metges JP, Li Z, Kim SB, Cho BC, Mansoor W, Li SH, Sunpaweravong

P, Maqueda MA, Goekkurt E, Hara H, Antunes L, Fountzilas C, Tsuji A, Oliden VC, Liu Q, Shah S, Bhagia P, Kato K; KEYNOTE-590 Investigators. Pembrolizumab plus chemotherapy versus chemotherapy alone for first-line treatment of advanced oesophageal cancer (KEYNOTE-590): a randomised, placebo-controlled, phase 3 study. *Lancet* 2021; **398**: 759-771 [PMID: 34454674 DOI: 10.1016/S0140-6736(21)01234-4]

41 **Forde PM**, Chaft JE, Smith KN, Anagnostou V, Cottrell TR, Hellmann MD, Zahurak M, Yang SC, Jones DR, Broderick S, Battafarano RJ, Velez MJ, Rekhtman N, Olah Z, Naidoo J, Marrone KA, Verde F, Guo H, Zhang J, Caushi JX, Chan HY, Sidhom JW, Scharpf RB, White J, Gabrielson E, Wang H, Rosner GL, Rusch V, Wolchok JD, Merghoub T, Taube JM, Velculescu VE, Topalian SL, Brahmer JR, Pardoll DM. Neoadjuvant PD-1 Blockade in Resectable Lung Cancer. *N Engl J Med* 2018; **378**: 1976-1986 [PMID: 29658848 DOI: 10.1056/NEJMoa1716078]

42 **Provencio M**, Nadal E, Insa A, García-Campelo MR, Casal-Rubio J, Dómine M, Majem M, Rodríguez-Abreu D, Martínez-Martí A, De Castro Carpeño J, Cobo M, López Vivanco G, Del Barco E, Bernabé Caro R, Viñolas N, Barneto Aranda I, Viteri S, Pereira E, Royuela A, Casarrubios M, Salas Antón C, Parra ER, Wistuba I, Calvo V, Laza-Briviesca R, Romero A, Massuti B, Cruz-Bermúdez A. Neoadjuvant chemotherapy and nivolumab in resectable non-small-cell lung cancer (NADIM): an open-label, multicentre, single-arm, phase 2 trial. *Lancet Oncol* 2020; **21**: 1413-1422 [PMID: 32979984 DOI: 10.1016/S1470-2045(20)30453-8]

43 **Huang AC**, Orlowski RJ, Xu X, Mick R, George SM, Yan PK, Manne S, Kraya AA, Wubbenhorst B, Dorfman L, D'Andrea K, Wenz BM, Liu S, Chilukuri L, Kozlov A, Carberry M, Giles L, Kier MW, Quagliarello F, McGettigan S, Kreider K, Annamalai L, Zhao Q, Mogg R, Xu W, Blumenschein WM, Yearley JH, Linette GP, Amaravadi RK, Schuchter LM, Herati RS, Bengsch B, Nathanson KL, Farwell MD, Karakousis GC, Wherry EJ, Mitchell TC. A single dose of neoadjuvant PD-1 blockade predicts clinical outcomes in resectable melanoma. *Nat Med* 2019; **25**: 454-461 [PMID: 30804515 DOI: 10.1038/s41591-019-0357-y]

44 **Powles T**, Kockx M, Rodriguez-Vida A, Duran I, Crabb SJ, Van Der Heijden MS, Szabados B, Pous AF, Gravis G, Herranz UA, Protheroe A, Ravaud A, Maillet D, Mendez MJ, Suarez C, Linch M, Prendergast A, van Dam PJ, Stanoeva D, Daelemans S, Mariathasan S, Tea JS, Mousa K, Banchereau R, Castellano D. Clinical efficacy and biomarker analysis of neoadjuvant atezolizumab in operable urothelial carcinoma in the ABACUS trial. *Nat Med* 2019; **25**: 1706-1714 [PMID: 31686036 DOI: 10.1038/s41591-019-0628-7]

45 **Chalabi M**, Fanchi LF, Dijkstra KK, Van den Berg JG, Aalbers AG, Sikorska K, Lopez-Yurda M, Grootscholten C, Beets GL, Snaebjornsson P, Maas M, Mertz M, Veninga V, Bounova G, Broeks A, Beets-Tan RG, de Wijkerslooth TR, van Lent AU, Marsman HA, Nuijten E, Kok NF, Kuiper M, Verbeek WH, Kok M, Van Leerdam ME, Schumacher TN, Voest EE, Haanen JB. Neoadjuvant immunotherapy leads to pathological responses in MMR-proficient and MMR-deficient early-stage colon cancers. *Nat Med* 2020; **26**: 566-576 [PMID: 32251400 DOI: 10.1038/s41591-020-0805-8]

46 **Schalper KA**, Rodriguez-Ruiz ME, Diez-Valle R, López-Janeiro A, Porciuncula A, Idoate MA, Inogés S, de Andrea C, López-Diaz de Cerio A, Tejada S, Berraondo P, Villarroel-Espindola F, Choi J, Gúrpide A, Giraldez M, Goicoechea I, Gallego Perez-Larraya J, Sanmamed MF, Perez-Gracia JL, Melero I. Neoadjuvant nivolumab modifies the tumor immune microenvironment in resectable glioblastoma. *Nat Med* 2019; **25**: 470-476 [PMID: 30742120 DOI: 10.1038/s41591-018-0339-5]

47 **Whiteside TL**. The tumor microenvironment and its role in promoting tumor growth. *Oncogene* 2008; **27**: 5904-5912 [PMID: 18836471 DOI: 10.1038/onc.2008.271]

48 **Blessin NC**, Li W, Mandelkow T, Jansen HL, Yang C, Raedler JB, Simon R, Büscheck F, Dum D, Luebke AM, Hinsch A, Möller K, Menz A, Bernreuther C, Lebok P, Clauditz T, Sauter G, Marx A, Uhlig R, Wilczak W, Minner S, Krech T, Fraune C, Höflmayer D, Burandt E, Steurer S. Prognostic role of proliferating CD8(+) cytotoxic Tcells in human cancers. *Cell Oncol (Dordr)* 2021; **44**: 793-803 [PMID: 33864611 DOI: 10.1007/s13402-021-00601-4]

49 **Zhang N**, Bevan MJ. CD8(+) T cells: foot soldiers of the immune system. *Immunity* 2011; **35**: 161-168 [PMID: 21867926 DOI: 10.1016/j.immuni.2011.07.010]

50 **Nurieva RI**, Liu X, Dong C. Yin-Yang of costimulation: crucial controls of immune tolerance and function. *Immunol Rev* 2009; **229**: 88-100 [PMID: 19426216 DOI: 10.1111/j.1600-065X.2009.00769.x]

51 **Vinay DS**, Ryan EP, Pawelec G, Talib WH, Stagg J, Elkord E, Lichtor T, Decker WK, Whelan RL, Kumara HMCS, Signori E, Honoki K, Georgakilas AG, Amin A, Helferich WG, Boosani CS, Guha G, Ciriolo MR, Chen S, Mohammed SI, Azmi AS, Keith WN, Bilsland A, Bhakta D, Halicka D, Fujii H, Aquilano K, Ashraf SS, Nowsheen S, Yang X, Choi BK, Kwon BS. Immune evasion in cancer: Mechanistic basis and therapeutic strategies. *Semin Cancer Biol* 2015; **35** Suppl: S185-S198 [PMID: 25818339 DOI: 10.1016/j.semcancer.2015.03.004]

52 **Baldwin XL**, Spanheimer PM, Downs-Canner S. A Review of Immune Checkpoint Blockade for the General Surgeon. *J Surg Res* 2023; **281**: 289-298 [PMID: 36228339 DOI: 10.1016/j.jss.2022.08.040]

53 **Buchbinder EI**, Desai A. CTLA-4 and PD-1 Pathways: Similarities, Differences, and Implications of Their Inhibition. *Am J Clin Oncol* 2016; **39**: 98-106 [PMID: 26558876 DOI: 10.1097/COC.0000000000000239]

54 **Ribas A**, Wolchok JD. Cancer immunotherapy using checkpoint blockade. *Science* 2018; **359**: 1350-1355 [PMID: 29567705 DOI: 10.1126/science.aar4060]

55 **Sharpe AH**, Pauken KE. The diverse functions of the PD1 inhibitory pathway. *Nat Rev Immunol* 2018; **18**: 153-167 [PMID: 28990585 DOI: 10.1038/nri.2017.108]

56 **Geng Q**, Rohondia SO, Khan HJ, Jiao P, Dou QP. Small molecules as antagonists of co-inhibitory pathways for cancer immunotherapy: a patent review (2018-2019). *Expert Opin Ther Pat* 2020; **30**: 677-694 [PMID: 32715813 DOI: 10.1080/13543776.2020.1801640]

57 **Baumeister SH**, Freeman GJ, Dranoff G, Sharpe AH. Coinhibitory Pathways in Immunotherapy for Cancer. *Annu Rev Immunol* 2016; **34**: 539-573 [PMID: 26927206 DOI: 10.1146/annurev-immunol-032414-112049]

58 **Yi M**, Zheng X, Niu M, Zhu S, Ge H, Wu K. Combination strategies with PD-1/PD-L1 blockade: current advances and future directions. *Mol Cancer* 2022; **21**: 28 [PMID: 35062949 DOI: 10.1186/s12943-021-01489-2]

59 **Awadasseid A**, Wu Y, Zhang W. Advance investigation on synthetic small-molecule inhibitors targeting PD-1/PD-L1 signaling pathway. *Life Sci* 2021; **282**: 119813 [PMID: 34256042 DOI: 10.1016/j.lfs.2021.119813]

60 **Wu Q**, Jiang L, Li SC, He QJ, Yang B, Cao J. Small molecule inhibitors targeting the PD-1/PD-L1 signaling pathway. *Acta Pharmacol Sin* 2021; **42**: 1-9 [PMID: 32152439 DOI: 10.1038/s41401-020-0366-x]

61 **Maruhashi T**, Sugiura D, Okazaki IM, Okazaki T. LAG-3: from molecular functions to clinical applications. *J Immunother Cancer* 2020; **8** [PMID: 32929051 DOI: 10.1136/jitc-2020-001014]

62 **Meng X**, Wu T, Hong Y, Fan Q, Ren Z, Guo Y, Yang X, Shi P, Yang J, Yin X, Luo Z, Xia J, Zhou Y, Xu M, Liu E, Jiang G, Li S, Zhao F, Ma C, Hou Z, Li J, Wang J, Wang F. Camrelizumab plus apatinib as second-line treatment for advanced oesophageal squamous cell carcinoma (CAP 02): a single-arm, open-label, phase 2 trial. *Lancet Gastroenterol Hepatol* 2022; **7**: 245-253 [PMID: 34998471 DOI:

10.1016/S2468-1253(21)00378-2]

63 **Huang J**, Xu B, Mo H, Zhang W, Chen X, Wu D, Qu D, Wang X, Lan B, Yang B, Wang P, Zhang H, Yang Q, Jiao Y. Safety, Activity, and Biomarkers of SHR-1210, an Anti-PD-1 Antibody, for Patients with Advanced Esophageal Carcinoma. *Clin Cancer Res* 2018; **24**: 1296-1304 [PMID: 29358502 DOI: 10.1158/1078-0432.CCR-17-2439]

64 **O'Donnell JS**, Hoefsmit EP, Smyth MJ, Blank CU, Teng MWL. The Promise of Neoadjuvant Immunotherapy and Surgery for Cancer Treatment. *Clin Cancer Res* 2019; **25**: 5743-5751 [PMID: 31040150 DOI: 10.1158/1078-0432.CCR-18-2641]

65 **Topalian SL**, Taube JM, Pardoll DM. Neoadjuvant checkpoint blockade for cancer immunotherapy. *Science* 2020; **367** [PMID: 32001626 DOI: 10.1126/science.aax0182]

66 **Kelly RJ**, Ajani JA, Kuzdzal J, Zander T, Van Cutsem E, Piessen G, Mendez G, Feliciano J, Motoyama S, Lièvre A, Uronis H, Elimova E, Grootscholten C, Geboes K, Zafar S, Snow S, Ko AH, Feeney K, Schenker M, Kocon P, Zhang J, Zhu L, Lei M, Singh P, Kondo K, Cleary JM, Moehler M; CheckMate 577 Investigators. Adjuvant Nivolumab in Resected Esophageal or Gastroesophageal Junction Cancer. *N Engl J Med* 2021; **384**: 1191-1203 [PMID: 33789008 DOI: 10.1056/NEJMoa2032125]

67 **Yamamoto S**, Kato K, Daiko H, Kojima T, Hara H, Abe T, Tsubosa Y, Nagashima K, Aoki K, Mizoguchi Y, Kitano S, Yachida S, Shiba S, Kitagawa Y. Feasibility study of nivolumab as neoadjuvant chemotherapy for locally esophageal carcinoma: FRONTiER (JCOG1804E). *Future Oncol* 2020; **16**: 1351-1357 [PMID: 32396014 DOI: 10.2217/fon-2020-0189]

68 **Jia XH**, Xu H, Geng LY, Jiao M, Wang WJ, Jiang LL, Guo H. Efficacy and safety of neoadjuvant immunotherapy in resectable nonsmall cell lung cancer: A meta-analysis. *Lung Cancer* 2020; **147**: 143-153 [PMID: 32717571 DOI: 10.1016/j.lungcan.2020.07.001]

69 **Zhou X**, Yao Z, Bai H, Duan J, Wang Z, Wang X, Zhang X, Xu J, Fei K, Zhang Z, Tan F, Xue Q, Gao S, Gao Y, Wang J, He J. Treatment-related adverse events of PD-1 and PD-L1 inhibitor-based combination therapies in clinical trials: a systematic review and meta-analysis. *Lancet Oncol* 2021; **22**: 1265-1274 [PMID: 34391508 DOI: 10.1016/S1470-2045(21)00333-8]

70 **Wang Y**, Zhou S, Yang F, Qi X, Wang X, Guan X, Shen C, Duma N, Vera Aguilera J, Chintakuntlawar A, Price KA, Molina JR, Pagliaro LC, Halfdanarson TR, Grothey A, Markovic SN, Nowakowski GS, Ansell SM, Wang ML. Treatment-Related Adverse Events of PD-1 and PD-L1 Inhibitors in Clinical Trials: A Systematic Review and Meta-analysis. *JAMA Oncol* 2019; **5**: 1008-1019 [PMID: 31021376 DOI: 10.1001/jamaoncol.2019.0393]

71 **Khoja L**, Day D, Wei-Wu Chen T, Siu LL, Hansen AR. Tumour- and class-specific patterns of immune-related adverse events of immune checkpoint inhibitors: a systematic review. *Ann Oncol* 2017; **28**: 2377-2385 [PMID: 28945858 DOI: 10.1093/annonc/mdx286]

72 **Gao TT**, Shan JH, Yang YX, Zhang ZW, Liu SL, Xi M, Liu MZ, Zhao L. Comparative efficacy and safety of immunotherapy for patients with advanced or metastatic esophageal squamous cell carcinoma: a systematic review and network Meta-analysis. *BMC Cancer* 2022; **22**: 992 [PMID: 36115960 DOI: 10.1186/s12885-022-10086-5]

73 **Zhang Z**, Hong ZN, Xie S, Lin W, Lin Y, Zhu J, Yang X, Lin Z, Lin J, Kang M. Neoadjuvant sintilimab plus chemotherapy for locally advanced esophageal squamous cell carcinoma: a single-arm, single-center, phase 2 trial (ESONICT-1). *Ann Transl Med* 2021; **9**: 1623 [PMID: 34926667 DOI: 10.21037/atm-21-5381]

74 **Liu J**, Yang Y, Liu Z, Fu X, Cai X, Li H, Zhu L, Shen Y, Zhang H, Sun Y, Chen H, Yu B, Zhang R, Shao J, Zhang M, Li Z. Multicenter, single-arm, phase II trial of camrelizumab and chemotherapy as neoadjuvant treatment for locally advanced esophageal squamous cell carcinoma. *J Immunother Cancer* 2022; **10** [PMID: 35338088 DOI: 10.1136/jitc-2021-004291]

75 **Liu J**, Li J, Lin W, Shao D, Depypere L, Zhang Z, Li Z, Cui F, Du Z, Zeng Y, Jiang S, He P, Gu X, Chen H, Zhang H, Lin X, Huang H, Lv W, Cai W, Liang W, Liang H, Jiang W, Wang W, Xu K, Wu K, Lerut T, Fu J, He J. Neoadjuvant camrelizumab plus chemotherapy for resectable, locally advanced esophageal squamous cell carcinoma (NIC-ESCC2019): A multicenter, phase 2 study. *Int J Cancer* 2022; **151**: 128-137 [PMID: 35188268 DOI: 10.1002/ijc.33976]

76 **Yan X**, Duan H, Ni Y, Zhou Y, Wang X, Qi H, Gong L, Liu H, Tian F, Lu Q, Sun J, Yang E, Zhong D, Wang T, Huang L, Wang J, Chaoyang Wang, Wang Y, Wan Z, Lei J, Zhao J, Jiang T. Tislelizumab combined with chemotherapy as neoadjuvant therapy for surgically resectable esophageal cancer: A prospective, single-arm, phase II study (TD-NICE). *Int J Surg* 2022; **103**: 106680 [PMID: 35595021 DOI: 10.1016/j.ijsu.2022.106680]

77 **He W**, Leng X, Mao T, Luo X, Zhou L, Yan J, Peng L, Fang Q, Liu G, Wei X, Wang K, Wang C, Zhang S, Zhang X, Shen X, Huang D, Yi H, Bei T, She X, Xiao W, Han Y. Toripalimab Plus Paclitaxel and Carboplatin as Neoadjuvant Therapy in Locally Advanced Resectable Esophageal Squamous Cell Carcinoma. *Oncologist* 2022; **27**: e18-e28 [PMID: 35305102 DOI: 10.1093/oncolo/oyab011]

78 **van den Ende T**, de Clercq NC, van Berge Henegouwen MI, Gisbertz SS, Geijsen ED, Verhoeven RHA, Meijer SL, Schokker S, Dings MPG, Bergman JJGHM, Haj Mohammad N, Ruurda JP, van Hillegersberg R, Mook S, Nieuwdorp M, de Gruijl TD, Soeratram TTD, Ylstra B, van Grieken NCT, Bijlsma MF, Hulshof MCCM, van Laarhoven HWM. Neoadjuvant Chemoradiotherapy Combined with Atezolizumab for Resectable Esophageal Adenocarcinoma: A Single-arm Phase II Feasibility Trial (PERFECT). *Clin Cancer Res* 2021; **27**: 3351-3359 [PMID: 33504550 DOI: 10.1158/1078-0432.CCR-20-4443]

79 **Ge F**, Huo Z, Cai X, Hu Q, Chen W, Lin G, Zhong R, You Z, Wang R, Lu Y, Huang Q, Zhang H, Song A, Li C, Wen Y, Jiang Y, Liang H, He J, Liang W, Liu J. Evaluation of Clinical and Safety Outcomes of Neoadjuvant Immunotherapy Combined With Chemotherapy for Patients With Resectable Esophageal Cancer: A Systematic Review and Meta-analysis. *JAMA Netw Open* 2022; **5**: e2239778 [PMID: 36322089 DOI: 10.1001/jamanetworkopen.2022.39778]

80 **Shang X**, Zhao G, Liang F, Zhang C, Zhang W, Liu L, Li R, Duan X, Ma Z, Yue J, Chen C, Meng B, Ren X, Jiang H. Safety and effectiveness of pembrolizumab combined with paclitaxel and cisplatin as neoadjuvant therapy followed by surgery for locally advanced resectable (stage III) esophageal squamous cell carcinoma: a study protocol for a prospective, single-arm, single-center, open-label, phase-II trial (Keystone-001). *Ann Transl Med* 2022; **10**: 229 [PMID: 35280363 DOI: 10.21037/atm-22-513]

81 **Duan H**, Wang T, Luo Z, Wang X, Liu H, Tong L, Dong X, Zhang Y, Valmasoni M, Kidane B, Almhanna K, Wiesel O, Pang S, Ma J, Yan X. A multicenter single-arm trial of sintilimab in combination with chemotherapy for neoadjuvant treatment of resectable esophageal cancer (SIN-ICE study). *Ann Transl Med* 2021; **9**: 1700 [PMID: 34988209 DOI: 10.21037/atm-21-6102]

82 **Yang W**, Xing X, Yeung SJ, Wang S, Chen W, Bao Y, Wang F, Feng S, Peng F, Wang X, Chen S, He M, Zhang N, Wang H, Zeng B, Liu Z, Kidane B, Seder CW, Koyanagi K, Shargall Y, Luo H, Peng S, Cheng C. Neoadjuvant programmed cell death 1 blockade combined with chemotherapy for resectable esophageal squamous cell carcinoma. *J Immunother Cancer* 2022; **10** [PMID: 35022193 DOI: 10.1136/jitc-2021-003497]

83 **Duan H**, Shao C, Pan M, Liu H, Dong X, Zhang Y, Tong L, Feng Y, Wang Y, Wang L, Newman NB, Sarkaria IS, Reynolds JV, De Cobelli F, Ma Z, Jiang T, Yan X. Neoadjuvant Pembrolizumab and Chemotherapy in Resectable Esophageal Cancer: An Open-Label, Single-Arm Study (PEN-ICE). *Front Immunol* 2022; **13**: 849984 [PMID: 35720388 DOI: 10.3389/fimmu.2022.849984]

84 **Zheng Y**, Li C, Yu B, Zhao S, Li J, Chen X, Li H. Preoperative pembrolizumab combined with chemoradiotherapy for esophageal squamous cell carcinoma: Trial design. *JTCVS Open* 2022; **9**: 293-299 [PMID: 36003437 DOI: 10.1016/j.xjon.2021.11.003]

85 **Li C**, Zhao S, Zheng Y, Han Y, Chen X, Cheng Z, Wu Y, Feng X, Qi W, Chen K, Xiang J, Li J, Lerut T, Li H. Preoperative pembrolizumab combined with chemoradiotherapy for oesophageal squamous cell carcinoma (PALACE-1). *Eur J Cancer* 2021; **144**: 232-241 [PMID: 33373868 DOI: 10.1016/j.ejca.2020.11.039]

86 **Shang X**, Zhang W, Zhao G, Liang F, Zhang C, Yue J, Duan X, Ma Z, Chen C, Pang Q, Liu L, Ren X, Meng B, Zhang P, Ma Y, Zhang L, Li H, Kang X, Li Y, Jiang H. Pembrolizumab Combined With Neoadjuvant Chemotherapy Versus Neoadjuvant Chemoradiotherapy Followed by Surgery for Locally Advanced Oesophageal Squamous Cell Carcinoma: Protocol for a Multicentre, Prospective, Randomized-Controlled, Phase III Clinical Study (Keystone-002). *Front Oncol* 2022; **12**: 831345 [PMID: 35433421 DOI: 10.3389/fonc.2022.831345]

87 **Zhao Y**, Dai Z, Min W, Sui X, Kang H, Zhang Y, Ren H, Wang XJ. Perioperative versus Preoperative Chemotherapy with Surgery in Patients with Resectable Squamous Cell Carcinoma of Esophagus: A Phase III Randomized Trial. *J Thorac Oncol* 2015; **10**: 1349-1356 [PMID: 26287319 DOI: 10.1097/JTO.0000000000000612]

88 **Chen X**, Xu X, Wang D, Liu J, Sun J, Lu M, Wang R, Hui B, Li X, Zhou C, Wang M, Qiu T, Cui S, Sun N, Li Y, Wang F, Liu C, Shao Y, Luo J, Gu Y. Neoadjuvant sintilimab and chemotherapy in patients with potentially resectable esophageal squamous cell carcinoma (KEEP-G 03): an open-label, single-arm, phase 2 trial. *J Immunother Cancer* 2023; **11** [PMID: 36759013 DOI: 10.1136/jitc-2022-005830]

89 **Feo CV**, Villaflor VM, Patti MG. Should esophageal resections for cancer be performed in high-volume centers only? *Updates Surg* 2011; **63**: 147-150 [PMID: 21695513 DOI: 10.1007/s13304-011-0090-7]

90 **Forschner A**, Battke F, Hadaschik D, Schulze M, Weißgraeber S, Han CT, Kopp M, Frick M, Klumpp B, Tietze N, Amaral T, Martus P, Sinnberg T, Eigentler T, Keim U, Garbe C, Döcker D, Biskup S. Tumor mutation burden and circulating tumor DNA in combined CTLA-4 and PD-1 antibody therapy in metastatic melanoma - results of a prospective biomarker study. *J Immunother Cancer* 2019; **7**: 180 [PMID: 31300034 DOI: 10.1186/s40425-019-0659-0]

91 **Jreige M**, Letovanec I, Chaba K, Renaud S, Rusakiewicz S, Cristina V, Peters S, Krueger T, de Leval L, Kandalaft LE, Nicod-Lalonde M, Romero P, Prior JO, Coukos G, Schaefer N. (18)F-FDG PET metabolic-to-morphological volume ratio predicts PD-L1 tumour expression and response to PD-1 blockade in non-small-cell lung cancer. *Eur J Nucl Med Mol Imaging* 2019; **46**: 1859-1868 [PMID: 31214790 DOI: 10.1007/s00259-019-04348-x]

92 **Lv G**, Sun X, Qiu L, Sun Y, Li K, Liu Q, Zhao Q, Qin S, Lin J. PET Imaging of Tumor PD-L1 Expression with a Highly Specific Nonblocking Single-Domain Antibody. *J Nucl Med* 2020; **61**: 117-122 [PMID: 31253743 DOI: 10.2967/jnumed.119.226712]

93 **Sholl LM**. Understanding patterns of pathologic response following neoadjuvant immunotherapy for solid tumors. *Ann Oncol* 2018; **29**: 1630-1632 [PMID: 30052725 DOI: 10.1093/annonc/mdy227]

94 **Cottrell TR**, Thompson ED, Forde PM, Stein JE, Duffield AS, Anagnostou V, Rekhtman N, Anders RA, Cuda JD, Illei PB, Gabrielson E, Askin FB, Niknafs N, Smith KN, Velez MJ, Sauter JL, Isbell JM, Jones DR, Battafarano RJ, Yang SC, Danilova L, Wolchok JD, Topalian SL, Velculescu VE, Pardoll DM, Brahmer JR, Hellmann MD, Chaft JE, Cimino-Mathews A, Taube JM. Pathologic features of response to neoadjuvant anti-PD-1 in resected non-small-cell lung carcinoma: a proposal for quantitative immune-related pathologic response criteria (irPRC). *Ann Oncol* 2018; **29**: 1853-1860 [PMID: 29982279 DOI: 10.1093/annonc/mdy218]

95 **Tang H**, Jiang D, Zhang S, Zeng Z, Tan L, Hou Y, Wang Q; Zhongshan NCRT-EC working group, Wang H, Zhu J, Shen Y, Yin J, Ge D. Residual tumor characteristics of esophageal squamous cell carcinoma after neoadjuvant chemoradiotherapy. *J Thorac Cardiovasc Surg* 2021; **162**: 1632-1641 [PMID: 33268125 DOI: 10.1016/j.jtcvs.2020.09.042]

96 **van Rossum PSN**, Fried DV, Zhang L, Hofstetter WL, Ho L, Meijer GJ, Carter BW, Court LE, Lin SH. The value of (18)F-FDG PET before and after induction chemotherapy for the early prediction of a poor pathologic response to subsequent preoperative chemoradiotherapy in oesophageal adenocarcinoma. *Eur J Nucl Med Mol Imaging* 2017; **44**: 71-80 [PMID: 27511188 DOI: 10.1007/s00259-016-3478-2]

97 **Elimova E**, Wang X, Etchebehere E, Shiozaki H, Shimodaira Y, Wadhwa R, Planjery V, Charalampakis N, Blum MA, Hofstetter W, Lee JH, Weston BR, Bhutani MS, Rogers JE, Maru D, Skinner HD, Macapinlac HA, Ajani JA. 18-fluorodeoxy-glucose positron emission computed tomography as predictive of response after chemoradiation in oesophageal cancer patients. *Eur J Cancer* 2015; **51**: 2545-2552 [PMID: 26321501 DOI: 10.1016/j.ejca.2015.07.044]

98 **Simoni N**, Rossi G, Benetti G, Zuffante M, Micera R, Pavarana M, Guariglia S, Zivelonghi E, Mengardo V, Weindelmayer J, Giacopuzzi S, de Manzoni G, Cavedon C, Mazzarotto R. (18)F-FDG PET/CT Metrics Are Correlated to the Pathological Response in Esophageal Cancer Patients Treated With Induction Chemotherapy Followed by Neoadjuvant Chemo-Radiotherapy. *Front Oncol* 2020; **10**: 599907 [PMID: 33330097 DOI: 10.3389/fonc.2020.599907]

99 **Fan J**, Shen X, Wang Y, Zhou HL, Liu G, Li YL, Xu ZX. Biomarkers for immune checkpoint therapy targeting programmed death 1 and programmed death ligand 1. *Biomed Pharmacother* 2020; **130**: 110621 [PMID: 34321165 DOI: 10.1016/j.biopha.2020.110621]

100 **Shah MA**, Kojima T, Hochhauser D, Enzinger P, Raimbourg J, Hollebecque A, Lordick F, Kim SB, Tajika M, Kim HT, Lockhart AC, Arkenau HT, El-Hajbi F, Gupta M, Pfeiffer P, Liu Q, Lunceford J, Kang SP, Bhagia P, Kato K. Efficacy and Safety of Pembrolizumab for Heavily Pretreated Patients With Advanced, Metastatic Adenocarcinoma or Squamous Cell Carcinoma of the Esophagus: The Phase 2 KEYNOTE-180 Study. *JAMA Oncol* 2019; **5**: 546-550 [PMID: 30570649 DOI: 10.1001/jamaoncol.2018.5441]

101 **Aguiar PN Jr**, De Mello RA, Hall P, Tadokoro H, Lima Lopes G. PD-L1 expression as a predictive biomarker in advanced non-small-cell lung cancer: updated survival data. *Immunotherapy* 2017; **9**: 499-506 [PMID: 28472902 DOI: 10.2217/imt-2016-0150]

102 **Paz-Ares L**, Spira A, Raben D, Planchard D, Cho BC, Özgüroğlu M, Daniel D, Villegas A, Vicente D, Hui R, Murakami S, Spigel D, Senan S, Langer CJ, Perez BA, Boothman AM, Broadhurst H, Wadsworth C, Dennis PA, Antonia SJ, Faivre-Finn C. Outcomes with durvalumab by tumour PD-L1 expression in unresectable, stage III non-small-cell lung cancer in the PACIFIC trial. *Ann Oncol* 2020; **31**: 798-806 [PMID: 32209338 DOI: 10.1016/j.annonc.2020.03.287]

103 **Doroshow DB**, Bhalla S, Beasley MB, Sholl LM, Kerr KM, Gnjatic S, Wistuba II, Rimm DL, Tsao MS, Hirsch FR. PD-L1 as a biomarker of response to immune-checkpoint inhibitors. *Nat Rev Clin Oncol* 2021; **18**: 345-362 [PMID: 33580222 DOI: 10.1038/s41571-021-00473-5]

104 **Yagi T**, Baba Y, Ishimoto T, Iwatsuki M, Miyamoto Y, Yoshida N, Watanabe M, Baba H. PD-L1 Expression, Tumor-infiltrating Lymphocytes, and Clinical Outcome in Patients With Surgically Resected Esophageal Cancer. *Ann Surg* 2019; **269**: 471-478 [PMID: 29206673 DOI: 10.1097/SLA.0000000000002616]

105 **Wakita A**, Motoyama S, Nanjo H, Sato Y, Yoshino K, Sasaki T, Kawakita Y, Liu J, Imai K, Saito H, Minamiya Y. PD-L1 Expression Is a Prognostic Factor in Patients with Thoracic Esophageal Cancer Treated Without Adjuvant Chemotherapy. *Anticancer Res* 2017; **37**: 1433-1441 [PMID: 28314315 DOI: 10.21873/anticanres.11467]

106 **Tamminga M**, de Wit S, Hiltermann TJN, Timens W, Schuuring E, Terstappen LWMM, Groen HJM. Circulating tumor cells in advanced non-small cell lung cancer patients are associated with worse tumor response to checkpoint inhibitors. *J Immunother Cancer* 2019; **7**: 173 [PMID: 31291995 DOI: 10.1186/s40425-019-0649-2]

107 **Lipson EJ**, Velculescu VE, Pritchard TS, Sausen M, Pardoll DM, Topalian SL, Diaz LA Jr. Circulating tumor DNA analysis as a real-time method for monitoring tumor burden in melanoma patients undergoing treatment with immune checkpoint blockade. *J Immunother Cancer* 2014; **2**: 42 [PMID: 25516806 DOI: 10.1186/s40425-014-0042-0]

108 **Pellini B**, Chaudhuri AA. Circulating Tumor DNA Minimal Residual Disease Detection of Non-Small-Cell Lung Cancer Treated With Curative Intent. *J Clin Oncol* 2022; **40**: 567-575 [PMID: 34985936 DOI: 10.1200/JCO.21.01929]

109 **Rosner S**, Reuss JE, Zahurak M, Zhang J, Zeng Z, Taube J, Anagnostou V, Smith KN, Riemer J, Illei PB, Broderick SR, Jones DR, Topalian SL, Pardoll DM, Brahmer JR, Chaft JE, Forde PM. Five-Year Clinical Outcomes after Neoadjuvant Nivolumab in Resectable Non-Small Cell Lung Cancer. *Clin Cancer Res* 2023; **29**: 705-710 [PMID: 36794455 DOI: 10.1158/1078-0432.CCR-22-2994]

110 **Xiao BY**, Zhang X, Cao TY, Li DD, Jiang W, Kong LH, Tang JH, Han K, Zhang CZ, Mei WJ, Xiao J, Pan ZZ, Li YF, Zhang XS, Ding PR. Neoadjuvant Immunotherapy Leads to Major Response and Low Recurrence in Localized Mismatch Repair-Deficient Colorectal Cancer. *J Natl Compr Canc Netw* 2023; **21**: 60-66.e5 [PMID: 36630898 DOI: 10.6004/jnccn.2022.7060]

111 **Park SY**, Hong MH, Kim HR, Lee CG, Cho JH, Cho BC, Kim DJ. The feasibility and safety of radical esophagectomy in patients receiving neoadjuvant chemoradiotherapy with pembrolizumab for esophageal squamous cell carcinoma. *J Thorac Dis* 2020; **12**: 6426-6434 [PMID: 33282345 DOI: 10.21037/jtd-20-1088]

112 **Huang B**, Shi H, Gong X, Yu J, Xiao C, Zhou B, Liang Z, Li X. Comparison of efficacy and safety between pembrolizumab combined with chemotherapy and simple chemotherapy in neoadjuvant therapy for esophageal squamous cell carcinoma. *J Gastrointest Oncol* 2021; **12**: 2013-2021 [PMID: 34790369 DOI: 10.21037/jgo-21-610]

113 **Lee S**, Ahn BC, Park SY, Kim DJ, Lee CG, Cho J, Kim JH, Kim HR, Kim YH, Park SR, Chun YJ, Hong MH, Cho B. A phase II trial of preoperative chemoradiotherapy and pembrolizumab for locally advanced esophageal squamous cell carcinoma (ESCC). *Ann Oncol* 2019; **30**: 754 [DOI: 10.1093/annonc/mdz266.018]

114 **Qiao Y**, Zhao C, Li X, Zhao J, Huang Q, Ding Z, Zhang Y, Jiao J, Zhang G, Zhao S. Efficacy and safety of camrelizumab in combination with neoadjuvant chemotherapy for ESCC and its impact on esophagectomy. *Front Immunol* 2022; **13**: 953229 [PMID: 35911723 DOI: 10.3389/fimmu.2022.953229]

115 **Xu WL**, Jiang YH, Wang CC, Wu J, Li JQ, Hu YQ, Lu WS, Shen DJ, Wang YJ, Chen QX. The efficacy and safety of neoadjuvant camrelizumab and chemotherapy for locally advanced thoracic esophageal squamous cell carcinoma. *J Clin Oncol* 2022; **40**: 278 [DOI: 10.1200/JCO.2022.40.4_suppl.278]

116 **Yang G**, Su X, Yang H, Luo G, Gao C, Zheng Y, Xie W, Huang M, Bei T, Bai Y, Wang Z, Cai P, He H, Xiang J, Cai M, Zhang Y, Qu C, Fu J, Liu Q, Hu Y, Zhong J, Huang Y, Guo Q, Zhang X. Neoadjuvant programmed death-1 blockade plus chemotherapy in locally advanced esophageal squamous cell carcinoma. *Ann Transl Med* 2021; **9**: 1254 [PMID: 34532391 DOI: 10.21037/atm-21-3352]

117 **Wang Z**. Neoadjuvant camrelizumab combined with chemotherapy and apatinib for locally advanced thoracic esophageal squamous cell carcinoma (ESCC): A single-arm, open-label, phase Ib study. *J Clin Oncol* 2021; **39**: 4047 [DOI: 10.1200/JCO.2021.39.15_suppl.4047]

118 **Ma JQ**, Zhang JF, Yang YN, Zheng DY, Wang XY, Liang H, Zhang LQ, Xin YZ, Ling XD, Fang CY, Jiang H, Zheng W. Camrelizumab combined with paclitaxel and nedaplatin as neoadjuvant therapy for locally advanced esophageal squamous cell carcinoma (ESPRIT): A phase II, single-arm, exploratory research. *J Clin Oncol* 2021; **39**: e16033 [DOI: 10.1200/JCO.2021.39.15_suppl.e16033]

119 **Wang F**, Yu Q, Meng XG, Fan QX. Camrelizumab in combination with preoperative chemotherapy for locally advanced esophageal squamous cell carcinoma: A single-arm, open-label, phase II study. *J Clin Oncol* 2021; **39**: 222 [DOI: 10.1200/JCO.2021.39.3_suppl.222]

120 **Zhang Y**, Shen GY, Xu RY, Huang GZ, Yang SS, Zheng QF, Huang ZJ, Duan HB, Ma LY, Yang LB, Yi YF, Liu RX, Li KZ, Chen SG. Real-world effectiveness and safety of camrelizumab-based neoadjuvant therapy in resectable esophageal cancer: Initial results of a prospective multicenter observational study. *J Clin Oncol* 2022; **40**: 250 [DOI: 10.1200/JCO.2022.40.4_suppl.250]

121 **Zhang Z**, Ye J, Li H, Gu D, Du M, Ai D, Chen W, Fang Y, Xu X, Bai C, Zhao K, Zhou G. Neoadjuvant sintilimab and chemotherapy in patients with resectable esophageal squamous cell carcinoma: A prospective, single-arm, phase 2 trial. *Front Immunol* 2022; **13**: 1031171 [PMID: 36311804 DOI: 10.3389/fimmu.2022.1031171]

122 **Xing W**, Zhao L, Zheng Y, Liu B, Liu X, Li T, Zhang Y, Ma B, Yang Y, Shang Y, Fu X, Liang G, Yuan D, Qu J, Chai X, Zhang H, Wang Z, Lin H, Liu L, Ren X, Zhang J, Gao Q. The Sequence of Chemotherapy and Toripalimab Might Influence the Efficacy of Neoadjuvant Chemoimmunotherapy in Locally Advanced Esophageal Squamous Cell Cancer-A Phase II Study. *Front Immunol* 2021; **12**: 772450 [PMID: 34938292 DOI: 10.3389/fimmu.2021.772450]

123 **Xing W**, Zhao L, Fu X, Liang G, Zhang Y, Yuan D, Li Z, Gao Q, Zheng Y; written on Henan Cancer Hospital Thoracic Oncology Group (HCHTOG). A phase II, single-centre trial of neoadjuvant toripalimab plus chemotherapy in locally advanced esophageal squamous cell carcinoma. *J Thorac Dis* 2020; **12**: 6861-6867 [PMID: 33282388 DOI: 10.21037/jtd-20-2198]

124 **Liu DL**, Zhang Q, Zhu JH, Qian T, Yin R, Fan ZH, Jiang F, Li HH, Lu JW, Cao GC. Phase-II study of toripalimab combined with neoadjuvant chemotherapy for the treatment of resectable esophageal squamous cell carcinoma. *J Clin Oncol* 2021; **39**: e16029 [DOI: 10.1200/JCO.2021.39.15_suppl.e16029]

125 **Gao L**, Lu J, Zhang P, Hong ZN, Kang M. Toripalimab combined with docetaxel and cisplatin neoadjuvant therapy for locally advanced esophageal squamous cell carcinoma: a single-center, single-arm clinical trial (ESONICT-2). *J Gastrointest Oncol* 2022; **13**: 478-487 [PMID: 35557591 DOI: 10.21037/jgo-22-131]

126 **Jiang N**, Jiang M, Zhu XZ, Ren BH, Zhang JY, Guo Z, Wu YA, Song X, Zhao LJ, Kong C, Cao GC, Qian PD, Zhao Y, Li S, Luo SF. SCALE-1: Safety and efficacy of short course neoadjuvant chemo-radiotherapy plus toripalimab for locally advanced resectable squamous cell carcinoma of esophagus. *J Clin Oncol* 2022; **40**: 4063 [DOI: 10.1200/JCO.2022.40.16_suppl.4063]

127 **Hong ZN**, Zhang Z, Chen Z, Weng K, Peng K, Lin J, Kang M. Safety and feasibility of esophagectomy following combined neoadjuvant immunotherapy and chemotherapy for locally advanced esophageal cancer: a propensity score matching. *Esophagus* 2022; **19**: 224-232 [PMID: 34988773 DOI: 10.1007/s10388-021-00899-x]

128 **Yang Y**, Zhu L, Cheng Y, Liu Z, Cai X, Shao J, Zhang M, Liu J, Sun Y, Li Y, Yi J, Yu B, Jiang H, Chen H, Yang H, Tan L, Li Z. Three-arm phase II trial comparing camrelizumab plus chemotherapy versus camrelizumab plus chemoradiation versus chemoradiation as preoperative treatment for locally advanced esophageal squamous cell carcinoma (NICE-2 Study). *BMC Cancer* 2022; **22**: 506 [PMID: 35524205 DOI: 10.1186/s12885-022-09573-6]

World Journal of Gastroenterology

Submit a Manuscript: https://www.f6publishing.com

World J Gastroenterol 2023 September 14; 29(34): 5038-5053

DOI: 10.3748/wjg.v29.i34.5038

ISSN 1007-9327 (print) ISSN 2219-2840 (online)

ORIGINAL ARTICLE

Basic Study

Suberoylanilide hydroxamic acid upregulates reticulophagy receptor expression and promotes cell death in hepatocellular carcinoma cells

Jia-Yao Li, Tian Tian, Bing Han, Ting Yang, Yi-Xin Guo, Jia-Yu Wu, Yu-Si Chen, Qin Yang, Ru-Jia Xie

Specialty type: Gastroenterology and hepatology

Provenance and peer review: Unsolicited article; Externally peer reviewed.

Peer-review model: Single blind

Peer-review report's scientific quality classification

Grade A (Excellent): A
Grade B (Very good): B
Grade C (Good): C
Grade D (Fair): 0
Grade E (Poor): 0

P-Reviewer: Franci G, Italy; Rizzo A, Italy

Received: March 23, 2023
Peer-review started: March 23, 2023
First decision: June 17, 2023
Revised: July 15, 2023
Accepted: August 15, 2023
Article in press: August 15, 2023
Published online: September 14, 2023

Jia-Yao Li, Bing Han, Ting Yang, Yi-Xin Guo, Jia-Yu Wu, Yu-Si Chen, Qin Yang, Ru-Jia Xie, Guizhou Provincial Key Laboratory of Pathogenesis and Drug Research on Common Chronic Diseases, College of Basic Medical Sciences, Guizhou Medical University, Guiyang 550025, Guizhou Province, China

Jia-Yao Li, Bing Han, Ting Yang, Yi-Xin Guo, Jia-Yu Wu, Yu-Si Chen, Qin Yang, Ru-Jia Xie, Department of Pathophysiology, College of Basic Medical Sciences, Guizhou Medical University, Guiyang 550025, Guizhou Province, China

Tian Tian, Department of Eugenic Genetics, Guiyang Maternal and Child Health Care Hospital, Guiyang 550003, Guizhou Province, China

Corresponding author: Ru-Jia Xie, MD, Academic Research, Department of Pathophysiology, College of Basic Medical Sciences, Guizhou Medical University, Dongqing Road, Guiyang 550025, Guizhou Province, China. 592153968@qq.com

Abstract

BACKGROUND

Hepatocellular carcinoma (HCC) is a common clinical condition with a poor prognosis and few effective treatment options. Potent anticancer agents for treating HCC must be identified. Epigenetics plays an essential role in HCC tumorigenesis. Suberoylanilide hydroxamic acid (SAHA), the most common histone deacetylase inhibitor agent, triggers many forms of cell death in HCC. However, the underlying mechanism of action remains unclear. Family with sequence similarity 134 member B (FAM134B)-induced reticulophagy, a selective autophagic pathway, participates in the decision of cell fate and exhibits anti-cancer activity. This study focused on the relationship between FAM134B-induced reticulophagy and SAHA-mediated cell death.

AIM

To elucidate potential roles and underlying molecular mechanisms of reticulophagy in SAHA-induced HCC cell death.

METHODS

The viability, apoptosis, cell cycle, migration, and invasion of SAHA-treated Huh7 and MHCC97L cells were measured. Proteins related to the reticulophagy

pathway, mitochondria-endoplasmic reticulum (ER) contact sites, intrinsic mitochondrial apoptosis, and histone acetylation were quantified using western blotting. ER and lysosome colocalization, and mitochondrial Ca^{2+} levels were characterized *via* confocal microscopy. The level of cell death was evaluated through Hoechst 33342 staining and propidium iodide colocalization. Chromatin immunoprecipitation was used to verify histone H4 lysine-16 acetylation in the *FAM134B* promoter region.

RESULTS

After SAHA treatment, the proliferation of Huh7 and MHCC97L cells was significantly inhibited, and the migration and invasion abilities were greatly blocked *in vitro*. This promoted apoptosis and caused G1 phase cells to increase in a concentration-dependent manner. Following treatment with SAHA, ER-phagy was activated, thereby triggering autophagy-mediated cell death of HCC cells *in vitro*. Western blotting and chromatin immunoprecipitation assays confirmed that SAHA regulated FAM134B expression by enhancing the histone H4 lysine-16 acetylation in the *FAM134B* promoter region. Further, SAHA disturbed the Ca^{2+} homeostasis and upregulated the level of autocrine motility factor receptor and proteins related to mitochondria-endoplasmic reticulum contact sites in HCC cells. Additionally, SAHA decreased the mitochondrial membrane potential levels, thereby accelerating the activation of the reticulophagy-mediated mitochondrial apoptosis pathway and promoting HCC cell death *in vitro*.

CONCLUSION

SAHA stimulates FAM134B-mediated ER-phagy to synergistically enhance the mitochondrial apoptotic pathway, thereby enhancing HCC cell death.

Key Words: Suberoylanilide hydroxamic acid; Histone H4 lysine-16; Reticulophagy; Apoptosis; Autophagic cell death; Hepatocellular carcinoma

©The Author(s) 2023. Published by Baishideng Publishing Group Inc. All rights reserved.

Core Tip: Family with sequence similarity 134 member B (FAM134B) is considered to be a tumor suppressor protein that can play a pivotal role in inhibiting hepatocellular carcinoma (HCC) cells. In addition, FAM134B acts as a putative reticulophagy receptor in the regulation of the reticulophagy process. Furthermore, suberoylanilide hydroxamic acid (SAHA) upregulates FAM134B expression in HCC cells and promotes apoptosis and autophagy-mediated cell death. Thus, FAM134B-mediated reticulophagy synergizes with SAHA to induce HCC cell death. Our findings offer novel insights into the mechanism underlying SAHA-induced HCC cell death.

Citation: Li JY, Tian T, Han B, Yang T, Guo YX, Wu JY, Chen YS, Yang Q, Xie RJ. Suberoylanilide hydroxamic acid upregulates reticulophagy receptor expression and promotes cell death in hepatocellular carcinoma cells. *World J Gastroenterol* 2023; 29(34): 5038-5053

URL: https://www.wjgnet.com/1007-9327/full/v29/i34/5038.htm

DOI: https://dx.doi.org/10.3748/wjg.v29.i34.5038

INTRODUCTION

Hepatocellular carcinoma (HCC) represents the most well-known and prevalent primary liver cancer in China. The mortality rates with HCC have consistently increased annually[1]. Immune checkpoint therapies have recently emerged as noteworthy treatments for HCC[2-4]. A considerable proportion of patients, approximately 70% with advanced HCC, fail to derive benefits from immunotherapy[5]. Thus, pursuing more potent anticancer medications to combat HCC must persist. Owing to its high degree of malignancy, poor prognosis, and relatively limited range of treatment strategies, it is necessary to seek more powerful anticancer agents for treating HCC. In the past decade, accumulating evidence has validated the role that epigenetics plays in HCC tumorigenesis[6,7]. Epigenetic regulation changes the transcriptional activity of key genes without altering DNA sequences[8,9].

Epigenetic regulation occurs primarily through DNA methylation, post-translational histone modification, chromatin remodeling, and non-coding RNA-mediated gene silencing[10]. Current therapies targeting epigenetic modifications to cancer mainly include DNA methyltransferases and histone deacetylases (HDACs) as well as microRNAs (miRNAs). Due to the widespread existence of DNA methylation variation in HCC, a variety of corresponding regulators of DNA methyltransferase have been developed[11]. At the same time, miRNAs such as miRNA-148a are used in anti-HCC therapy by combining with oncolytic viruses.

Histone acetylation modification, induced by HDACs and histone acetyltransferases, is a prominent mode of epigenetic regulation[12]. The histone acetylation/deacetylation balance is dynamically regulated to maintain global chromatin structure[13]. Therefore, any dysregulation may contribute to altered gene expression, leading to pathological conditions, such as HCC. Suberoylanilide hydroxamic acid (SAHA) represents the most typical HDAC inhibitor (HDACi)

and was the first of its kind to be approved for human treatment. So far, SAHA has been found to induce the differentiation of malignant tumor cells and accelerate apoptosis *in vitro* and *in vivo*[14]. According to our previous results, SAHA may act as a potential initiator of endoplasmic reticulum (ER) stress-associated apoptosis in HepG2 hepatoma cells by activating ER stress-related apoptotic pathways[15]. However, it is still unknown whether SAHA utilizes a new mechanism to induce HCC cell death through some different therapeutic targets.

Acetylation of histone H4 lysine 16 (H4K16ac) is important for gene initiation[16]. Recently, researchers have found that H4K16ac is closely associated with autophagy induction and significantly correlated with autophagy regulation. Moreover, deacetylase inhibitors can promote the upregulation of H4K16ac and lead to autophagic death of cancer cells [17]. However, the regulatory mechanism underlying the induction of H4K16ac-mediated reticulophagy is unclear.

Family with sequence similarity 134 member B (*FAM134B*) has been proposed as a cancer suppressor gene[18,19]. Numerous researchers have demonstrated that in colorectal carcinoma, the presence of FAM134B limits the overgrowth and suppresses the proliferation of cancer cells[20,21]. In addition, FAM134B acts as a putative reticulophagy receptor in regulating ER turnover and maintaining calcium homeostasis by remodeling ER[22,23]. Recent findings have also identified that FAM134B-mediated ER-phagy may regulate ER-mitochondrion interaction[24]. As the largest cellular organelle, the ER can interact with mitochondria through multiple contact sites, termed mitochondria-ER contact sites (MERCS).

Many ER-related and mitochondria-related proteins have been discovered at MERCS, including the inositol 1, 4, 5-trisphosphate receptor type 1 (IP3R1)/glucose-regulated protein 75 (GRP75)/voltage-dependent anion channel 1 (VDAC1) complex, which is a central component of MERCS that contributes to calcium exchange regulation[25,26]. Recent research has suggested that Ca^{2+} deregulation between ER and mitochondria by MERCS led to mitochondrial calcium overload, thereby activating the mitochondria-associated apoptotic pathway[27]. In the present study, we verified that SAHA treatment augmented FAM134B expression and facilitated Huh7 and MHCC97L HCC cell apoptosis; however, the regulatory mechanisms underlying this effect remain unknown. In our study, we elucidated potential roles and underlying molecular mechanisms of reticulophagy in SAHA-induced HCC cell death. Our findings may offer new perspectives for clinical trials of HCC.

MATERIALS AND METHODS

Cell culture and treatments

The human Huh7 and MHCC97L cell lines were derived from the cell bank of the Chinese Academy of Sciences (Shanghai, China). Both cell lines were cultivated at 37 °C in a 5% CO_2-supplemented atmosphere and maintained in high-glucose Dulbecco's modified Eagle's medium (ESscience, Shanghai, China) supplemented with 10% fetal bovine serum (Gibco, Grand Island, NY, United States) and 1% penicillin-streptomycin (BioInd, Beit-Haemek, Israel). SAHA (Abcam, Cambridge, United Kingdom) was dissolved in dimethyl sulfoxide as a 5 mmol/L stock solution and then diluted with the complete medium to achieve ultimate concentrations of 0-24 μmol/L. Both cell lines were exposed to SAHA or vehicle treated with 0.1% dimethyl sulfoxide.

Cell counting kit-8 assay

Cell counting kit-8 (CCK-8) assay was applied to evaluate the anti-proliferative effects of SAHA. Briefly, MHCC97L and Huh7 cells (5×10^3) were plated onto 96-well plates and given 24 h to adhere before being treated with SAHA. The cells were then exposed to various doses of SAHA (0, 0.5, 1, 3, 6, 9, 12, 18, and 24 μmol/L) for 48 h. Subsequently, 10 μL CCK-8 reagent (Solarbio, Beijing, China) was added to each well and incubated for 4 h. Absorbance at 450 nm was recorded using a spectrophotometer (BioRad, Hercules, United States). The IC_{50} of SAHA was calculated using GraphPad Prism software (v9.0.0, GraphPad Software, La Jolla, CA, United States).

Flow cytometry

The data regarding the apoptosis and cell cycle of HCC cells treated with 0, 1, 3, 6, and 12 μmol/L SAHA were obtained *via* standard flow cytometry (NovoCyte, Agilent, Santa Clara, CA, United States). The apoptosis assay was carried out using a cellular apoptosis detection kit (KeyGEN BioTECH, Nanjing, China) following the manufacturer's protocol. Briefly, Huh7 and MHCC97L cells were plated onto 6-well plates at 1×10^5 cells per well before adding SAHA solution. Then, each group of cells was harvested, rinsed with chilled phosphate buffered saline (PBS), and loaded with binding buffer. The cells were labelled with Annexin V-FITC/propidium iodide (PI) solution, and the stained cells were calculated using the flow cytometer. Similarly, cell cycle analysis was conducted using the flow cytometer following the manufacturer's instructions. Each group of cells was collected and washed thrice with chilled PBS. The cells were fixed with 70% ethanol and stained with PI/RNase I solution (KeyGEN BioTECH), and the percentages of cells in the G1, S, and G2 stages were measured using the flow cytometer. The inbuilt software NovoExpress® 1.4.1 was used for statistical analysis.

Wound healing assay

The wound healing assay was monitored to evaluate the effect of SAHA on HCC cell migration. Briefly, Huh7 and MHCC97L cells (3×10^4) were planted onto 6-well plates, grown until they formed an optically confluent monolayer, and then wounded with a sterile 200 μL micropipette tip. Upon treatment with 0 μmol/L or 3 μmol/L SAHA for 48 h, HCC cells were photographed using a microscope (× 40).

Transwell assay

The cell invasion and migration assay *in vitro* was carried out using 24 transwell plates divided into upper and lower chambers using sterile polycarbonate with 8 μm pore size (Corning Life Science, Corning, NY, United States). The sterile polycarbonate covered 200 μL Matrigel (BD Biosciences, San Jose, CA, United States) in the cell invasion assay but not in the cell migration assay. Upon treatment with 0 μmol/L or 3 μmol/L SAHA for 48 h, cells that passed through the pore were stained with crystal violet, photographed, and quantified.

Western blot analysis

Huh7 and MHCC97L cells were exposed to 0, 1, 3, 6, and 12 μmol/L SAHA for 48 h. Then, the cells were rinsed with pre-chilled PBS, lysed in 100 μL RIPA lysis buffer with protease inhibitor (Solarbio), and collected with cell scrapers. Protein samples were boiled for 5 min, and total protein extracts were subjected to standard sodium-dodecyl sulfate gel electrophoresis and subsequently removed to polyvinylidene difluoride membranes (Merck Millipore, Burlington, MA, United States). The membranes were blocked with rapid blocking solution and stained overnight with the corresponding primary antibodies, including FAM134B (Proteintech; Wuhan, China 1:1500), CCPG1 (Proteintech; 1:1500), LC3 (Abcam; 1:2000), ATG12 (Cell Signaling Technology; Danvers, MA, United States 1:1500), H4 (Proteintech; 1:2000), total acH4 (Proteintech; 1:2000), H3K27ac (Cell Signaling Technology; 1:6000), H4K5ac (Cell Signaling Technology; 1:6000), H4K12ac (Cell Signaling Technology; 1:6000), H4K16ac (Abcam; 1:10000), GRP75 (Abcam; 1:2000), VDAC1 (Abcam; 1:2000), IP3R (Abcam; 1:1000), autocrine motility factor receptor (AMFR) (Proteintech; 1:500), cyt c (Cell Signaling Technology; 1:1500), cleaved caspase-3 (Cell Signaling Technology; 1:1500), Bax (Cell Signaling Technology; 1:1500), Bcl-2 (Cell Signaling Technology; 1;1500), and β-actin (Abcam; 1:1000), followed by incubation with the corresponding secondary antibodies (1:8000). Polyvinylidene fluoride membranes carrying proteins were treated with enhanced chemiluminescence reagent (Solarbio), and ImageLab software was used to observe the protein bands.

Live imaging of the ER and lysosomes

ER-trackers and Lyso-trackers (Beyotime; Nanjing, China), the specific organelle dyes, were applied to stain and locate ER and lysosomes, respectively. Huh7 and MHCC97L cells were exposed to 0, 1, 3, 6, and 12 μmol/L SAHA for 48 h. Then, the cells were coincubated with the two tracking dyes at 37 °C for 45 min and rinsed thrice with PBS. The stained cells were viewed at × 200 magnification under a confocal microscope (Olympus, Tokyo, Japan) and immediately imaged.

Hoechst 33342/PI double chromatin staining assay

Huh7 and MHCC97L cells (3×10^4) were seeded in confocal laser Petri dishes. The cells were pretreated with 0.5 nmol/L bafilomycin A1 (MedChemexpress, NJ, United States) for 12 h and then exposed with 12 μmol/L SAHA for 48 h. Subsequently, Hoechst 33342/PI double fluorescent chromatin staining assay was conducted using a Viastain™ Hoechst 33342/PI viability kit (Beyotime). Cells were stained with Hoechst 33342 and PI for 30 min at 25 °C in the dark. The labelled cells were observed with a confocal microscope under × 400 magnification.

Mitochondrial calcium labeling

Rhod-2 AM Red (Abcam), a specific Ca^{2+} indicator, was applied to detect the level of mitochondrial Ca^{2+}. Huh7 and MHCC97L cells were exposed to 0, 1, 3, 6, and 12 μmol/L SAHA for 48 h and rinsed thrice with Hank's balanced salt solution. The treated cells were labelled with a mixture of Mito-Tracker Green (Beyotime) and Rhod-2 AM Red (Beyotime) and incubated for 50 min. The labelled cells were observed with a confocal microscope under × 400 magnification.

Chromatin immunoprecipitation

Chromatin immunoprecipitation (ChIP) assay of Huh7 cells was conducted as described previously[28]. Huh7 cells treated with 0 μmol/L or 6 μmol/L SAHA were subjected to ChIP assay using a ChIP Kit (Thermo Fisher Scientific, Waltham, MA, United States). In brief, the Huh7 cells were cross-linked with 1% formaldehyde and lysed with sodium-dodecyl sulfate lysis buffer. The lysate was sonicated and centrifuged (9000 × g/min) to harvest chromatin fragments (200-1000 bp). Immunoprecipitation was conducted with the following antibodies: anti-H4K16ac (1:50); rabbit IgG (1:50); and anti-RNA polymerase II (1:50). A no-antibody sample was used as input control. Input DNA and ChIP DNA were detected *via* quantitative polymerase chain reaction.

JC-1 fluorescence mitochondrial imaging

The JC-1 fluorescence mitochondrial imaging technique was applied to examine the mitochondrial membrane potential of HCC cells treated with 0, 1, 3, 6, and 12 μmol/L SAHA. Briefly, Huh7 and MHCC97L cells (1×10^5) were plated onto 6-well plates before adding SAHA solution and incubated with JC-1 fluorescence solution in an incubator for 20 min. Analysis was performed using a flow cytometer.

Statistical analysis

Data were processed and analyzed, and experimental graphs were prepared using GraphPad Prism software. All experiments were conducted in biological triplicate. All data are shown as means ± standard deviation. One-way analysis of variance was conducted for multigroup comparisons. *P* values less than 0.05 were considered to indicate significance.

RESULTS

SAHA suppressed the overgrowth of HCC cells by inducing G1 phase arrest and apoptosis in vitro

In our previous study, we confirmed that SAHA suppressed the overgrowth of HepG2 cells and mediated apoptosis by promoting the ER stress-associated apoptotic pathway[15]. However, this was not demonstrated in Huh7 and MHCC97L cells. As presented in Figure 1A, HCC cell growth was notably suppressed in SAHA-treated cells; the semi-lethal dose was 12 μmol/L. Apoptosis in Huh7 and MHCC97L cells was determined using flow cytometry with different SAHA concentrations. Consistent with previous studies, SAHA induced apoptosis in Huh7 and MHCC97L cells (Figures 1B and C). The percentage of specific cell populations that were early apoptotic and late apoptotic throughout the apoptotic stage is shown in Figure 1C. In addition, cell cycle assay results showed that an increasing number of cells were blocked in the G1 phase (Figures 1D-F).

SAHA suppressed the migration and invasion of HCC cells

Both Huh7 and MHCC97L cells were tested under various treatment conditions (0 μmol/L or 3 μmol/L SAHA) to assess their ability to cross a membrane from low to high nutrient solution *in vitro*. Serum was used as an inducer, mimicking the process of tumor cell invasion into adjacent tissues *in vivo*. Cells invading through the semiporous membrane into the underlying medium containing a high serum concentration were photographed under an optical microscope (Figures 2A and B) and quantitatively analyzed (Figures 2C and D). The model cells were compared with the control sample, which was assumed to represent 100% invasion without any treatment. Huh7 and MHCC97L cells showed 78% and 68% lower migration and 44% and 30% lower invasion following treatment with 3 μmol/L SAHA, respectively. Further wound-healing tests were used to verify how cancer cells interact and move. The results showed a gradual decrease in cell migration distance after SAHA treatment (Figure 2E). Overall, SAHA resulted in reduced cell invasion and migration in HCC cells.

SAHA enhanced the level of ER-phagy and augmented autophagy-mediated cell death in HCC cells

The effect of SAHA on FAM134B-mediated ER-phagy was assessed using western blotting. In HCC cells, SAHA increases the expression of proteins linked to the reticulophagy-related signaling pathway. We found increases in the expression of FAM134B, CCPG1, and autophagy-related protein Atg12 and the LC3-II/LC3-I ratio (Figures 3A-C). In the process of reticulophagy, ER fragments were delivered to lysosomes for final degradation. To detect the final state of ER autophagic lysosome formation, we used organelle markers that could trace the ER and lysosomes to detect the colocalization of both. We found that colocalization coverage of the ER and lysosomes increased in Huh7 and MHCC97L cells under SAHA treatment (Figure 3D). The above results suggested that SAHA could enhance the level of ER-phagy in HCC cells.

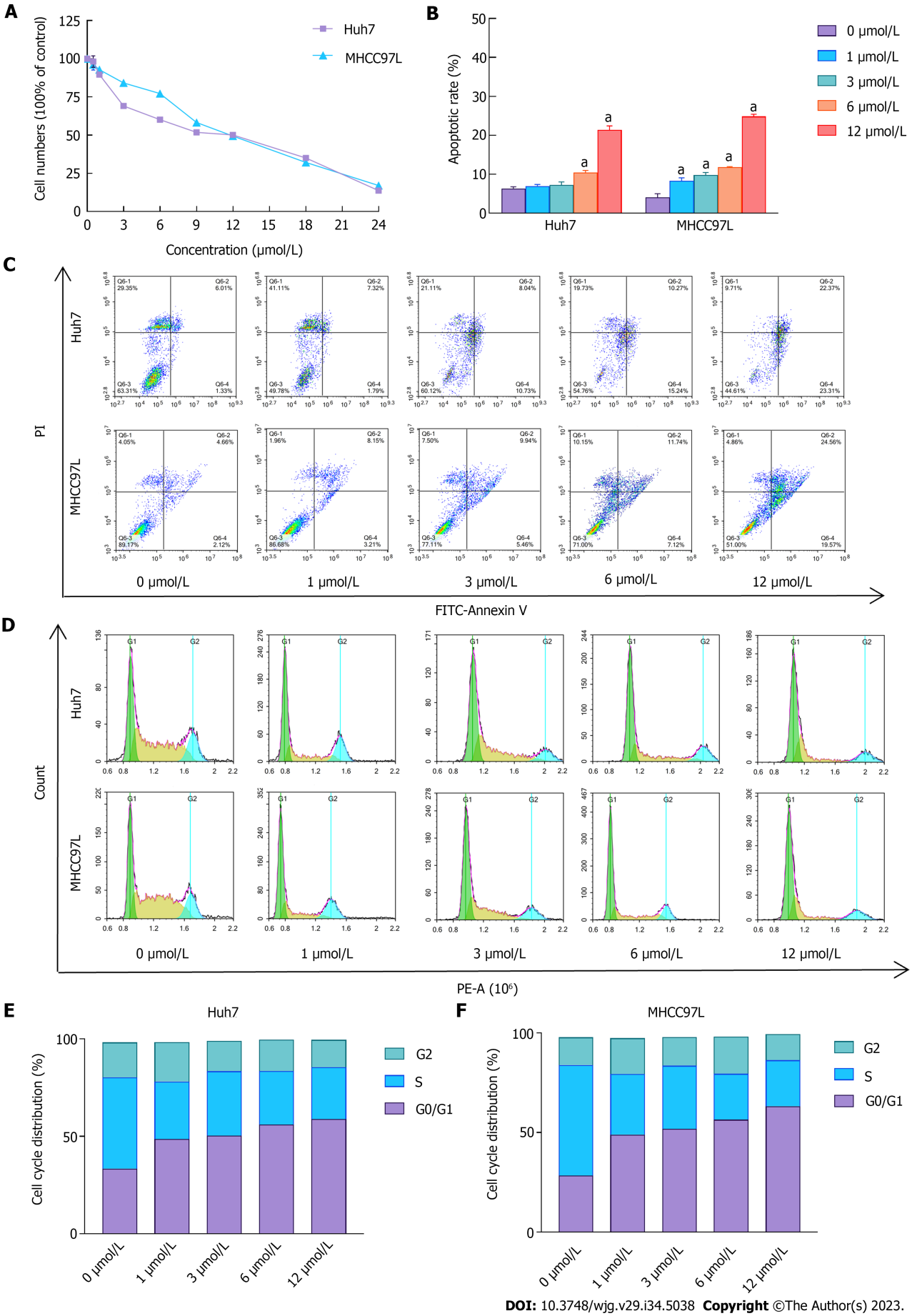
Previous research has reported that appropriate autophagy is a protective response under cellular stress conditions, but uncontrolled autophagy leads to autophagy-mediated cell death[29]. To further verify whether autophagic death mode exists in HCC cells under SAHA treatment, Huh7 and MHCC97L cells were pretreated with BafA1, a specific inhibitor of the late phase of autophagy that restrains autophagosomal fusion with lysosomes, 12 h before SAHA treatment. Nuclear double staining with Hoechst 33342 and PI was conducted to observe the level of cell death in the treated cells. The results showed that HCC cells treated with 12 μmol/L SAHA for 48 h after pretreatment with BafA1 exhibited significantly lower cell death rates compared with cells treated with 12 μmol/L SAHA alone, indicating that autophagy-mediated cell death was involved in SAHA-induced HCC cell death (Figure 3E).

SAHA upregulated the level of histone acetylation modification and enhanced H4K16ac in the promoter region of FAM134B in HCC cells

After SAHA treatment, the levels of H3K27ac, total H4ac, H4K5ac, H4K12ac, and H4K16ac in Huh7 and MHCC97L cells were determined using western blotting. We found that various doses of SAHA could upregulate the levels of these proteins (Figures 4A-C). Histone hyperacetylation results in gene transcription activation, and recent findings have shown that H4K16ac is linked to the regulation of autophagy-related genes; therefore, we further focused on the regulatory role of H4K16ac in gene expression. We conducted ChIP assays to confirm whether the regulation of *FAM134B* transcription by SAHA was mediated by H4K16ac upregulation. Our results showed that H4K16ac in the *FAM134B* promoter region was significantly increased in Huh7 cells (Figure 4D).

SAHA disturbed Ca^{2+} homeostasis and upregulated the expression of AMFR and MERCS-related proteins in HCC cells

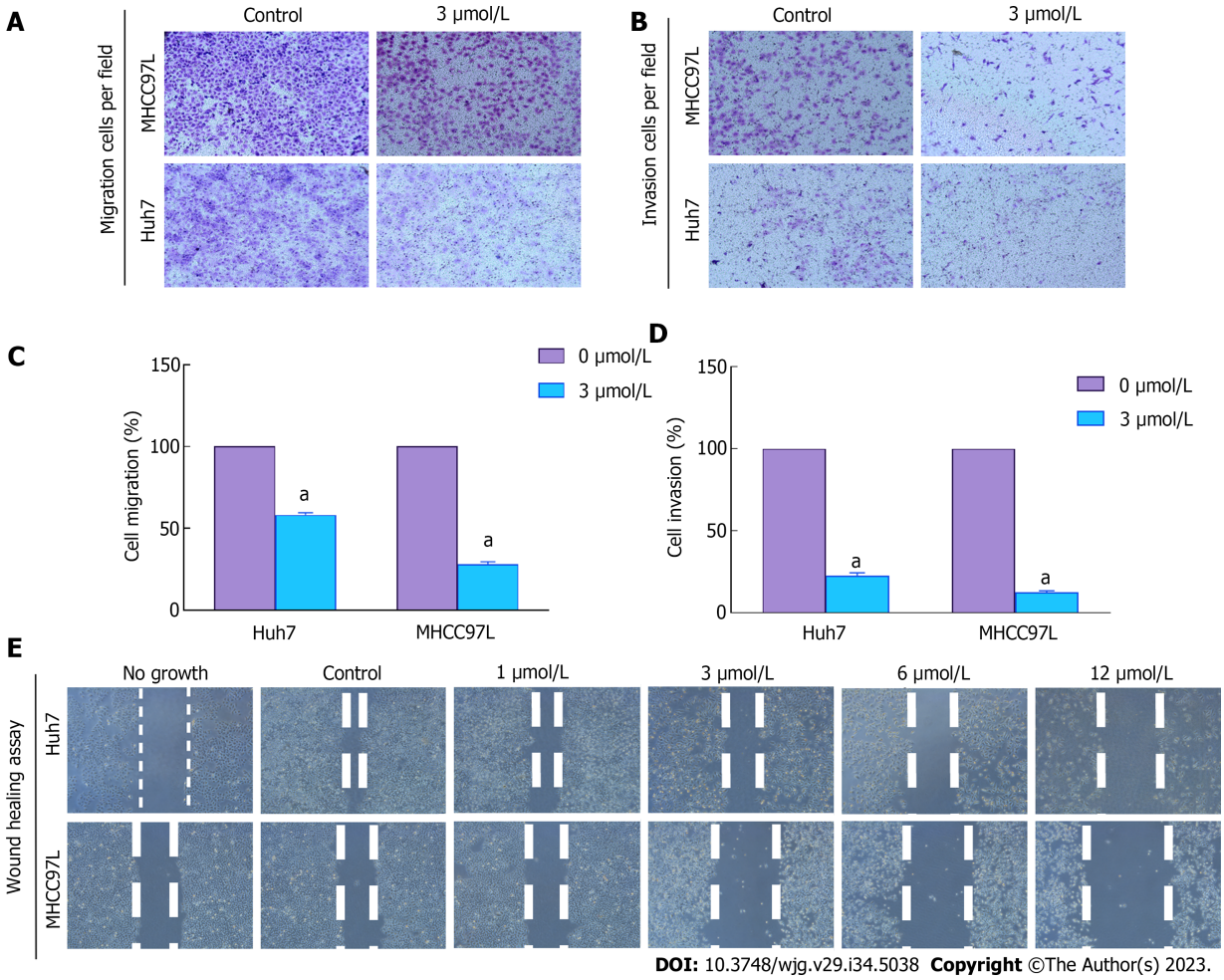
After SAHA treatment, the level of cytosolic Ca^{2+} in Huh7 and MHCC97L cells was determined using Rhod-2 AM Red staining, and mitochondrial Ca^{2+} was colocalized with Mito-Tracker Green and Rhod-2 AM Red. The results showed that SAHA markedly elevated cytosolic and mitochondrial Ca^{2+} levels (Figures 5A and B). Classical papers reported that increased cytosolic Ca^{2+} could increase the expression of AMFR, which targets the outer mitochondrial membrane (OMM) for ubiquitination and degradation[30-32]. We evaluated the protein level of AMFR in Huh7 and MHCC97L cells and found that SAHA could considerably increase AMFR protein levels. The IP3R-GRP75-VDAC1 complex is one of the most significant components of MERCS, which regulates ER-mitochondrial calcium flux. To determine the altered expression of MERCS in response to SAHA, the levels of IP3R, GRP75, and VDAC1 were examined using protein blots. Similar to our hypothesis, SAHA administration raised the protein levels of the above three proteins relative to the control group (Figures 5C-E). These findings showed that SAHA contributed to calcium buildup in the mitochondria by enhancing the interaction between the ER and mitochondria.



DOI: 10.3748/wjg.v29.i34.5038 **Copyright** ©The Author(s) 2023.

Figure 1 Impact of suberoylanilide hydroxamic acid treatment on cell viability, cell cycle dispersion, and cellular apoptosis in Huh7 and

MHCC97L cells. A: Huh7 and MHCC97L cells were treated with 0, 0.5, 1, 3, 6, 9, 12, 18, and 24 μmol/L suberoylanilide hydroxamic acid (SAHA) for 48 h. The proliferation of Huh7 and MHCC97L cells upon SAHA treatment was monitored using a cell counting kit-8 assay; B-F: Huh7 and MHCC97L cells were exposed to 0, 1, 3, 6, and 12 μmol/L SAHA for 48 h. The proportions of apoptotic cells and the cell cycle dispersion were detected using flow cytometer. Experiments were repeated thrice. Representative results from three independent replicate assays are shown. Data are exhibited as mean ± standard deviation. $^{a}P < 0.05$ *vs* 0 μmol/L group (n = 3). PI: Propidium iodide.

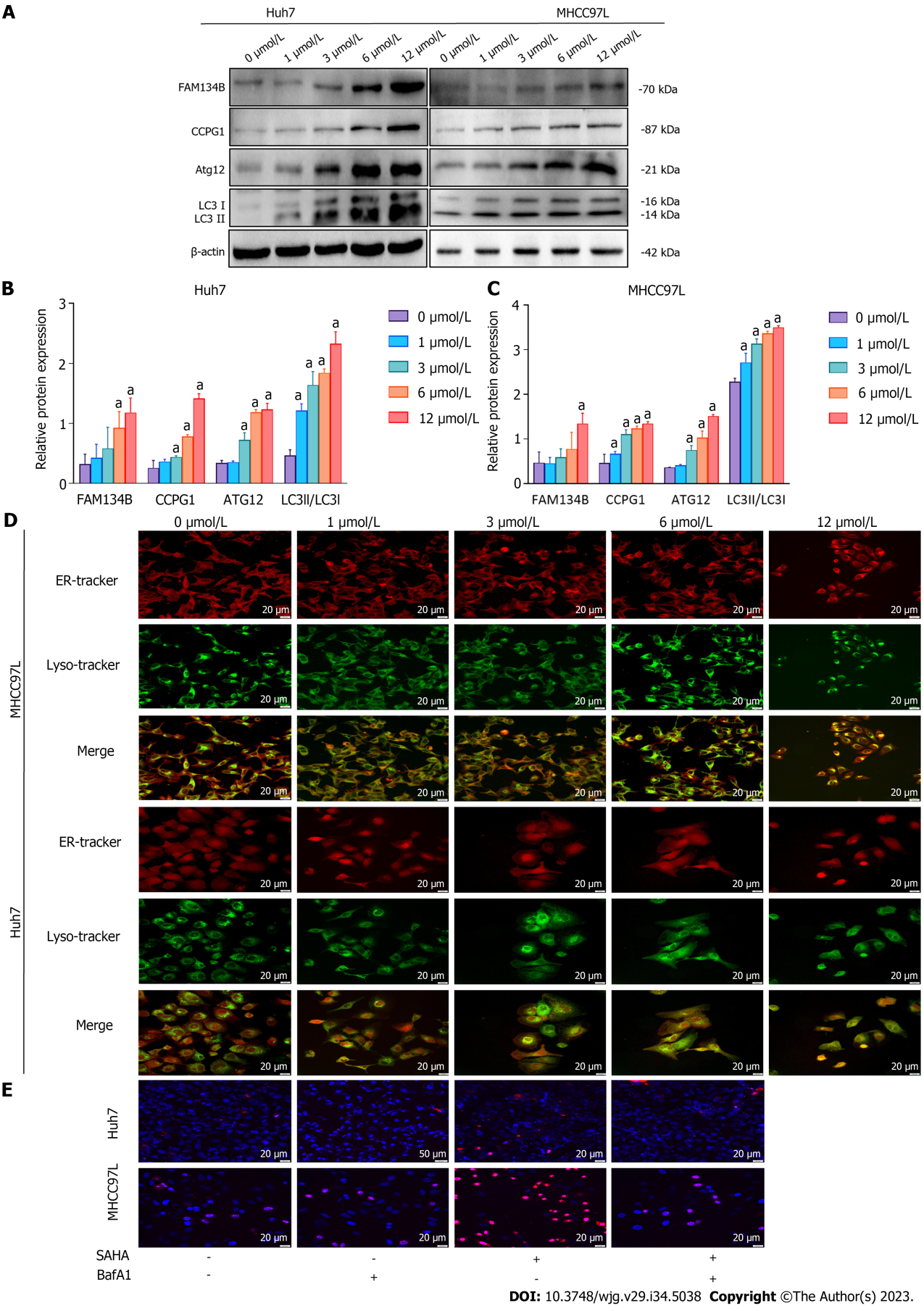


DOI: 10.3748/wjg.v29.i34.5038 **Copyright** ©The Author(s) 2023.

Figure 2 Impact of suberoylanilide hydroxamic acid treatment on the migration and invasion of Huh7 and MHCC97L cells. A and B: During experimental verification, the mobile ability of hepatocellular carcinoma cells could not be observed in the 6 μmol/L and 12 μmol/L suberoylanilide hydroxamic acid (SAHA) groups and even the cell growth was directly inhibited. Therefore, we selected 3 μmol/L SAHA to treat Huh7 and MHCC97L cells in a transwell assay. Both cell lines were vehicle-treated with 0.1% dimethyl sulfoxide or exposed to 3 μmol/L SAHA for 48 h. The migration and invasion behavior of cells was evaluated by calculating the cells stained using crystal violet. Representative pictures of invaded hepatocellular carcinoma cells from three independent replicate assays are exhibited; C and D: Statistical graphs; E: In the cell scratch experiment, the space in the middle was artificially divided into regions to observe the motility of Huh7 and MHCC97L cells upon treatment with various doses of SAHA (0, 1, 3, 6, and 12 μmol/L) for 48 h. All cells were observed under an inverted microscope with a 40-fold objective lens. Data are exhibited as mean ± standard deviation. $^{a}P < 0.05$ *vs* control group (n = 3).

SAHA treatment activated the mitochondrial apoptotic pathway by decreasing mitochondrial membrane potential

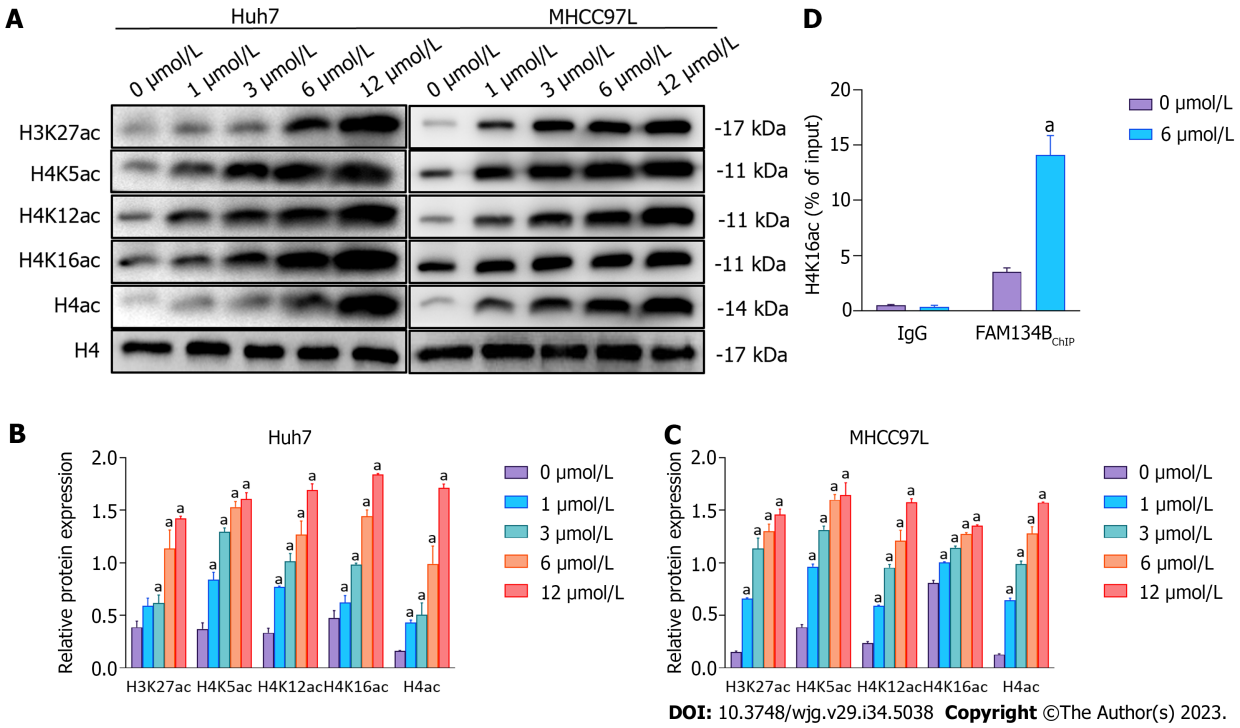
After SAHA treatment, mitochondrial membrane potential was monitored *via* JC-1 staining. We found that SAHA treatment reduced mitochondrial membrane potential (Figures 6A and B). To investigate the particular SAHA-induced apoptotic processes, the levels of cyt c, caspase-3, and proteins related to the Bcl-2 family were detected using western blotting. The experimental results revealed that SAHA upregulated the expression of cyt c, cleaved caspase-3, and Bax and downregulated the expression of Bcl-2 (Figures 6C-E). These results clearly indicated that the mitochondrial membrane potential was at a lower level, and the mitochondrial apoptotic pathway was activated under the action of SAHA.



DOI: 10.3748/wjg.v29.i34.5038 **Copyright** ©The Author(s) 2023.

Figure 3 Impact of suberoylanilide hydroxamic acid treatment on the level of endoplasmic reticulum-phagy and autophagy-mediated cell death in Huh7 and MHCC97L cells. A-C: Huh7 and MHCC97L cells were exposed to 0, 1, 3, 6, and 12 μmol/L suberoylanilide hydroxamic acid for 48 h.

Proteins related to the reticulophagy pathway were detected using western blotting. Relative protein expression levels were normalized to β-actin; D: The colocalization coverage of the endoplasmic reticulum and lysosomes were observed using a confocal microscope (× 400). Representative pictures from three independent replicate assays are exhibited; E: Huh7 and MHCC97L cells were pretreated with 0.5 nmol/L BafA1 for 12 h, followed by 12 μmol/L suberoylanilide hydroxamic acid treatment for 48 h. Hoechst 33342/propidium iodide (PI) double staining localization assay was utilized to observe nuclear coagulation. After Hoechst 33342/PI double staining, the death rate of hepatocellular carcinoma cells was quantified based on the ratio of pink cells/blue cells. Experiments were repeated thrice. Representative pictures from three independent replicate assays are shown. Data are exhibited as mean ± standard deviation. $^{a}P < 0.05$ *vs* 0 μmol/L group. SAHA: Suberoylanilide hydroxamic acid; ER: Endoplasmic reticulum; FAM134B: Family with sequence similarity 134 member B.



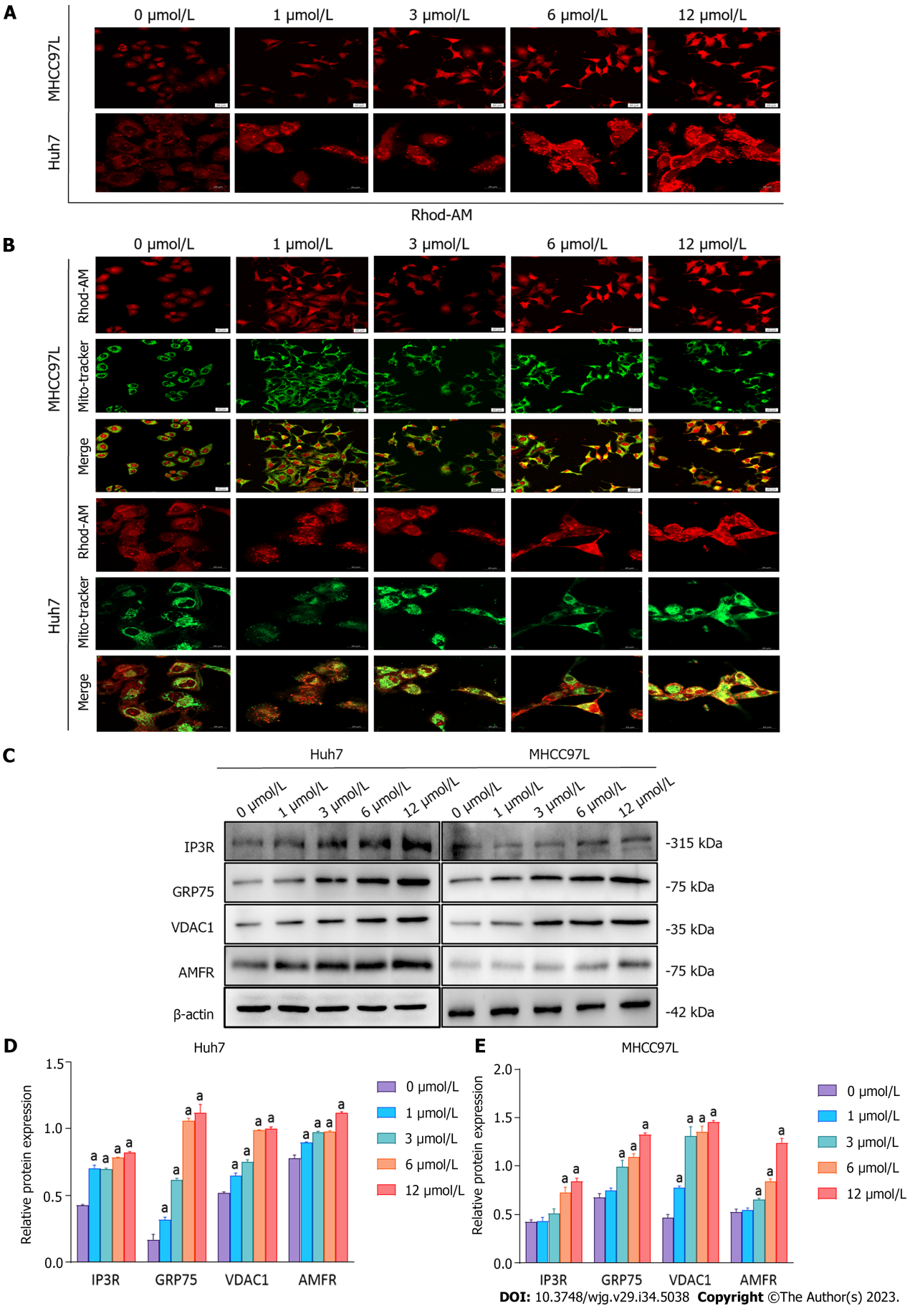
DOI: 10.3748/wjg.v29.i34.5038 **Copyright** ©The Author(s) 2023.

Figure 4 Impact of suberoylanilide hydroxamic acid treatment on the levels of histone H4 lysine 16 acetylation in the promoter region of family with sequence similarity 134 member B in Huh7 and MHCC97L cells. A-C: Huh7 and MHCC97L cells were exposed to 0, 1, 3, 6, and 12 μmol/L suberoylanilide hydroxamic acid for 48 h. Relative protein levels of histone H3 lysine 27 acetylation (H3K27ac), total H4ac, H4K5ac, H4K12ac, and H4K16ac were normalized to total histone H4. Representative western blot images from three independent replicate assays are exhibited; D: Huh7 cells were exposed to 0 μmol/L or 6 μmol/L suberoylanilide hydroxamic acid for 48 h. Quantification of the acetylated histone H4K16-related promoter region of family with sequence similarity 134 member B in Huh7 cells was measured using chromatin immunoprecipitation assay and quantitative polymerase chain reaction. Data are exhibited as mean ± standard deviation. $^{a}P < 0.05$ *vs* 0 μmol/L group ($n = 3$). FAM134B: Family with sequence similarity 134 member B; ChIP: Chromatin immunoprecipitation.

DISCUSSION

SAHA, also known as vorinostat, is an HDACi that has shown tumor-suppressive properties in clinical trials[33]. Findings have revealed that SAHA could suppress cell proliferation and accelerate apoptosis in multiple malignant tumor cells. Scholars have demonstrated that SAHA increased the expression of death receptor 5 in liver cancer cells, which led to the initiation of the death receptor-mediated apoptosis pathway[34]. Furthermore, SAHA contributed to the initiation of the mitochondria-related apoptosis pathway by enhancing the protein level of Bim and Bax[35]. Our previous study found that SAHA could initiate the ER stress-related apoptotic pathway to foster apoptosis in liver cancer cells by upregulating the protein level of CHOP, a transcription factor that accelerates proapoptotic gene transcription[15]. In the present study, we found that SAHA suppressed the proliferation and induced cell cycle arrest in Huh7 and MHCC97L cells. Moreover, SAHA initiated Huh7 and MHCC97L cell apoptosis.

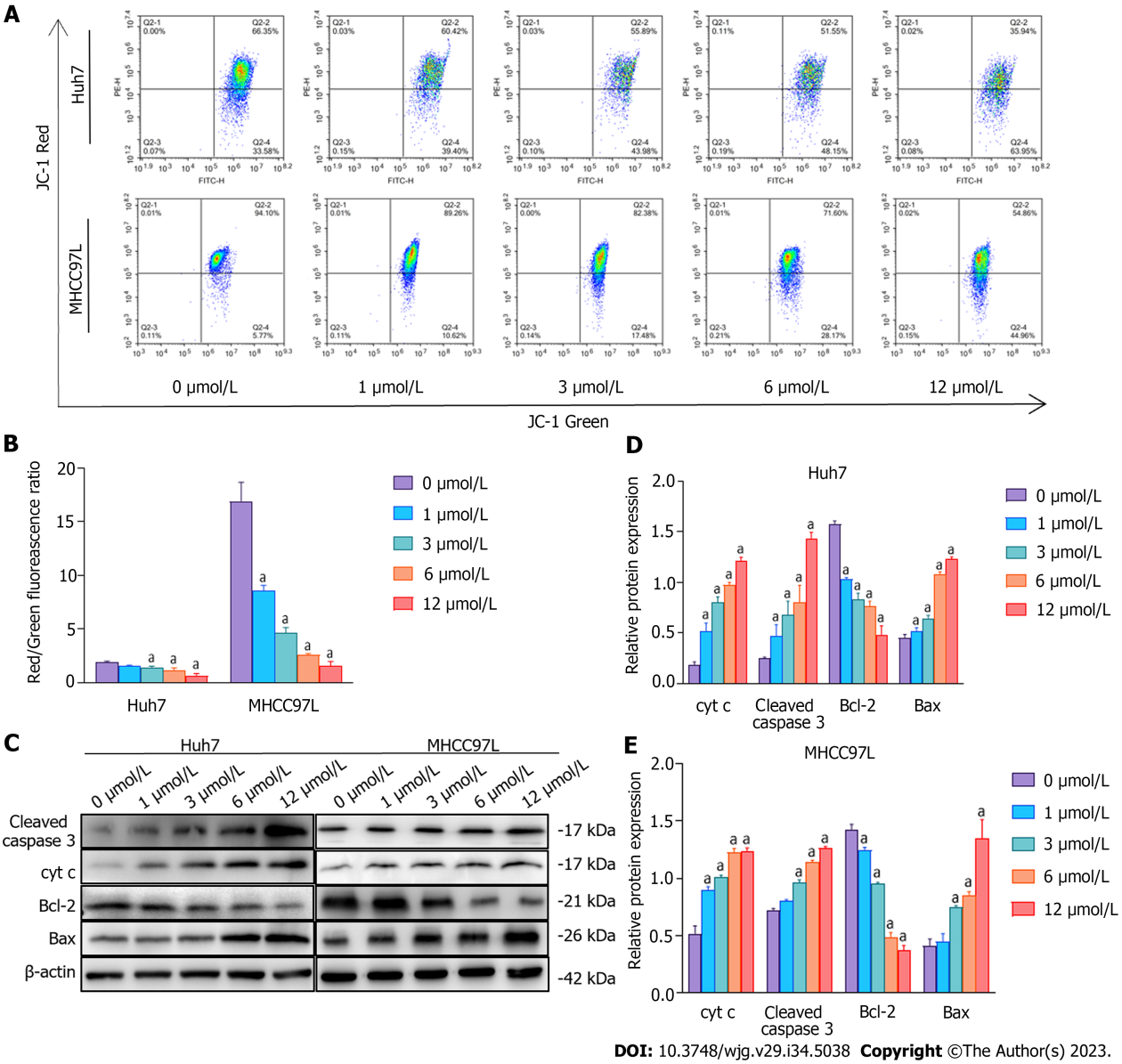
We also indicated that SAHA could augment the expression of *FAM134B*, a putative cancer suppressor gene. Studies have uncovered the pivotal role of FAM134B in multiple malignancies. Lee *et al*[20] reported that FAM134B may exert anticancer effects by influencing mitochondrial function and inducing cell cycle arrest in colon cancer. FAM134B also acts as a cancer suppressor in breast carcinoma. Upregulating FAM134B expression was significantly correlated with a higher survival in patients with breast carcinoma[36]. Zhong[37] confirmed that FAM134B was decreased in liver cancer, and its decreased expression was correlated with malignant liver cancer. In contrast, upregulation of FAM134B inhibited HepG2 cell proliferation and enhanced cell apoptosis. FAM134B was proposed as the first discovered mammalian receptor of reticulophagy[38,39], a type of selective phagocytosis. As an ER-anchored protein, FAM134B mediates the sequestration of ER fragments into phagophore membranes through its LC3-interacting region, which binds the autophagy modifier protein LC3[40-42]. In the present study, we detected the proteins related to ER-phagy in Huh7 and MHCC97L cells



DOI: 10.3748/wjg.v29.i34.5038 **Copyright** ©The Author(s) 2023.

Figure 5 Impact of suberoylanilide hydroxamic acid treatment on Ca^{2+} homeostasis and the expression of autocrine motility factor

receptor and proteins related to mitochondria-endoplasmic reticulum contact sites in Huh7 and MHCC97L cells. A: Huh7 and MHCC97L cells were exposed to 0, 1, 3, 6, and 12 μmol/L suberoylanilide hydroxamic acid (SAHA) for 48 h and stained with Rhod-2 AM. The cells were observed under a confocal microscope (× 400 magnification); B: Huh7 and MHCC97L cells were exposed to 0, 1, 3, 6, and 12 μmol/L SAHA for 48 h and simultaneously stained with Mito-Tracker Green and Rhod-2 AM Red. The cells were observed under a confocal microscope (× 400 magnification). The scale is 100 μm; C-E: Representative western blot images showed the expression of inositol 1, 4, 5-trisphosphate receptor type 1, glucose-regulated protein 75, voltage-dependent anion channel 1, and autocrine motility factor receptor in Huh7 and MHCC97L cells treated with SAHA for 48 h. Relative protein expression levels were normalized to β-actin. Data are exhibited as mean ± standard deviation. $^{a}P < 0.05$ *vs* 0 μmol/L group ($n = 3$). AMFR: Autocrine motility factor receptor; IP3R1: Inositol 1, 4, 5-trisphosphate receptor type 1; GRP75: Glucose-regulated protein 75; VDAC1: Voltage-dependent anion channel 1.



DOI: 10.3748/wjg.v29.i34.5038 **Copyright** ©The Author(s) 2023.

Figure 6 The impact of suberoylanilide hydroxamic acid treatment on mitochondrial membrane potential and the expression of proteins related to the mitochondrial apoptotic pathway in Huh7 and MHCC97L cells. A and B: After being treated with 0, 1, 3, 6, and 12 μmol/L suberoylanilide hydroxamic acid for 48 h, the mitochondrial membrane potential in Huh7 and MHCC97L cells was analyzed using flow cytometry with bivariable JC-1 dye (mitochondrial membrane potential probe). Representative pictures from three independent replicate assays are exhibited; C-E: Representative western blot images showed the related protein expression in Huh7 and MHCC97L cells treated with 0, 1, 3, 6, and 12 μmol/L suberoylanilide hydroxamic acid for 48 h. Relative protein expression levels were normalized to β-actin. Data are exhibited as mean ± standard deviation. $^{a}P < 0.05$ *vs* 0 μmol/L group ($n = 3$).

treated with various doses of SAHA. We found that the expression levels of FAM134B, Atg12, and LC3II/LC3I were considerably upregulated. Moreover, SAHA augmented the colocalization of ER and lysosomes in Huh7 and MHCC97L cells. The above results indicated that SAHA treatment enhanced the level of ER-phagy.

ER-phagy is a protective response under cellular stress conditions, but uncontrolled autophagy leads to the depletion of organelles and key proteins, which in turn lead to caspase-independent cell death, also known as autophagy-mediated

cell death[43]. Recent findings have revealed that SAHA could induce autophagy-mediated cell death in malignant tumor cells[44,45]. In fact, a decrease in cell viability detected using CCK-8 was not the same as apoptosis induction, as revealed in this study. We found that 12 μmol/L SAHA resulted in markedly reduced Huh7 and MHCC97L cell proliferation levels (Figure 1), with proliferation being inhibited by approximately 50%; however, the rate of early apoptosis was only about 25%. This phenomenon reveals that SAHA may also elicit other types of cell death to suppress the proliferation of Huh7 and MHCC97L cells, such as autophagy-mediated cell death.

To confirm this hypothesis, we investigated cells with or without pretreatment with BafA1, a specific inhibitor of the late phase of autophagy that restrains autophagosomal fusion with lysosomes. Notably, BafA1-mediated autophagy inhibition reduced SAHA-induced cell death. These results confirmed that SAHA could enhance autophagy-mediated cell death, potentially by promoting FAM134B-mediated ER-phagy. However, the specific mechanism by which SAHA regulated FAM134B expression in Huh7 and MHCC97L cells remains elusive. As an HDACi, the essential role of SAHA is the enhancement of histone acetylation. In previous research, we revealed that SAHA markedly augmented the acetylated histones H4K5 and H4K12 in HepG2 cells[15]. In the present study, SAHA was shown to augment H4K16ac. In addition, Füllgrabe *et al*[17] reported that H4K16ac was linked to altered gene expression, including the modulation of autophagy-related genes; however, it was unclear whether H4K16ac regulated *FAM134B* transcription and its associated ER-phagy. We used ChIP to detect H4K16ac in the *FAM134B* promoter region. Our findings revealed that FAM134B promoter H4K16ac was considerably elevated in Huh7 cells exposed to SAHA, which enhanced the *FAM134B* transcription.

As a key organelle in eukaryotic cells, the ER contributes to protein synthesis and maintenance of calcium homeostasis [46,47]; hence, ER dysfunction results in the agglomeration of protein aggregates and disturbance of calcium homeostasis in the ER. Moreover, the ER contributes to organelle communication[27,48]. For example, the ER can interact with mitochondria through MERCS, as the short distance (15-20 nm) between the ER and OMM enables ER-anchored proteins to interact with OMM proteins[49]. The IP3R1-GRP75-VDAC1 complex is a central component of MERCS, which is involved in regulating calcium flow[50]. Emerging evidence has indicated that the imbalance of Ca^{2+} between the ER and mitochondria by MERCS leads to calcium overload in the mitochondria, which activates the mitochondria-associated apoptotic pathway[51].

Furthermore, under ER stress conditions, increased cytosolic Ca^{2+} would elevate the level of ER E3 ligase AMFR, which targets the OMM for ubiquitination and degradation[32]. High AMFR levels accelerate OMM degradation, which brings the inner mitochondrial membrane closer to the ER, thus promoting interplay between the ER and mitochondria[30]. In the present study, we revealed that SAHA upregulated the expression of MERCS-related proteins, including IP3R1, GRP75, and VDAC1, thereby enhancing the exchange of Ca^{2+} from the ER to the mitochondria, along with mitochondrial Ca^{2+} overload. Additionally, SAHA augmented cytosolic Ca^{2+} and increased AMFR expression, thus decreasing mitochondrial membrane potential and elevating mitochondrial membrane permeability, resulting in the release of proapoptotic proteins. As expected, we found that SAHA upregulated the expression level of mitochondria-dependent apoptotic proteins, including cytochrome c, cleaved caspase-3, and Bax but downregulated the expression of Bcl-2. The above results revealed that SAHA treatment enhanced the interplay between the ER and mitochondria and promoted Ca^{2+} transmission from the ER to the mitochondria, thereby activating the mitochondria-related apoptotic pathway.

This study had a few limitations. Despite the presence of numerous reticulophagy receptors, we focused on only FAM134B in this manuscript. For comprehensive knowledge, our team will verify multiple receptors in subsequent laboratory studies. Knocking down the gene encoding FAM134B could verify if it is a key gene in the pathway leading to HCC death. In this experiment, H4K16ac, a highly relevant acetylation site, was selected for the study. However, SAHA acts as a broad-spectrum deacetylase inhibitor influencing numerous acetylation sites, which need to be further verified in subsequent experiments. Results of this study indicated that SAHA can inhibit the proliferation of liver cancer cells *in vitro*; however, *in vivo* analyses could confirm the consistency of its effectiveness. Basic medical research serves the clinic, and the clinical verification of various aspects is more persuasive. Our study provided basic information that aids ongoing and prospective *in vivo* experiment.

CONCLUSION

The HDACi SAHA initiated apoptosis and autophagy-mediated cell death in Huh7 and MHCC97L cells to exert antitumor activity in HCC. Our results underscore a crucial link between the induction of ER-phagy and H4K16ac-linked *FAM134B* gene expression, which facilitates FAM134B-mediated ER-phagy. Moreover, we presented evidence that suggested that SAHA induced the mitochondria-associated apoptotic pathway in Huh7 and MHCC97L cells by enhancing the interplay between the ER and mitochondria and promoting Ca^{2+} exchange. In summary, SAHA promoted FAM134B-mediated ER-phagy, which acted synergistically with the mitochondrial apoptotic pathway to promote HCC cell death.

ARTICLE HIGHLIGHTS

Research background

Suberoylanilide hydroxamic acid (SAHA) has been demonstrated to trigger multiple forms of cell death in hepatocellular carcinoma (HCC). Family with sequence similarity 134 member B (FAM134B), a reticulophagy receptor, has been

recognized as a cancer suppressor protein in multiple tumors, including HCC. However, few researchers have focused on the relationship between reticulophagy and SAHA-induced HCC cell death.

Research motivation

Reticulophagy is involved in a variety of human cancer pathologies. However, its specific function in the modulation of SAHA-initiated HCC cell death remains unproven.

Research objectives

To validate the potential regulatory mechanisms of the FAM134B-mediated reticulophagy in SAHA-induced HCC cell death.

Research methods

The proliferation, apoptosis, and cell cycle of SAHA-treated Huh7 and MHCC97L cells were quantified using cell counting kit-8 and flow cytometry. The migration and invasion of Huh7 and MHCC97L cells were measured using the transwell assay. Proteins related to the reticulophagy pathway, mitochondria-endoplasmic reticulum contact sites, intrinsic mitochondrial apoptosis, and histone H4K16 acetylation were detected using western blotting. ER and lysosome co-localization, and mitochondrial Ca^{2+} levels were observed *via* confocal microscopy. Autophagy-mediated cell death was validated through Hoechst33342 staining and propidium iodide colocalization. The enrichment of histone H4 lysine 16 acetylation in the *FAM134B* promoter region was determined using chromatin immunoprecipitation.

Research results

SAHA treatment augmented the expression of proteins related to the reticulophagy pathway and enhanced the level of reticulophagy in HCC cells. Chromatin immunoprecipitation experiments confirmed that SAHA regulated FAM134B expression by increasing the histone H4 lysine 16 acetylation in the *FAM134B* promoter region. SAHA interfered with Ca^{2+} homeostasis in HCC cells and upregulated the expression of autocrine motility factor receptor-related and mitochondria-endoplasmic reticulum contact sites-related proteins. Furthermore, SAHA reduced mitochondrial membrane potential and aggravated the activation of the reticulophagy-mediated mitochondrial apoptosis pathway and HCC cell death.

Research conclusions

SAHA stimulated excessive reticulophagy and induced autophagy-mediated cell death, which acted synergistically with the mitochondria-dependent apoptotic pathway to facilitate HCC cell death.

Research perspectives

FAM134B-induced reticulophagy may further provide a novel avenue for more effective interventions in HCC treatment. Our results confirmed that reticulophagy participates in SAHA-induced apoptosis and autophagy-mediated cell death in HCC cells, where SAHA-induced regulation of FAM134B expression *via* histone H4 lysine 16 is the key to HCC cell death.

ACKNOWLEDGEMENTS

The authors thank Mr. Yao Mu and Mrs. Yao Ran from the Guizhou Provincial Key Laboratory of Pathogenesis and Drug Research on Common Chronic Diseases, Guizhou Medical University (Guizhou, China) for their technical advice for using the confocal microscope and flow cytometer.

FOOTNOTES

Author contributions: Xie RJ and Yang Q contributed to the experimental conception and design; Li JY, Tian T, and Han B conducted the experiments; Yang T and Guo YX collected and assembled the experimental data; Li JY, Chen YS, and Wu JY contributed to data analysis and interpretation; Li JY and Xie RJ wrote the article; All authors approved the final manuscript. Li JY, Tian T, and Han B contributed equally to this work.

Supported by the National Natural Science Foundation of China, No. 82260127; Guizhou Provincial Science and Technology Projects, No. Qiankehe Jichu-ZK[2021]365 and Qiankehe Jichu-ZK[2021]364; National Natural Science Foundation Cultivation Project of Guizhou Medical University, No. 20NSP016; Guizhou Provincial Natural Science Foundation, No. [2021]4029 and [2022]4017; and Science and Technology Foundation of Guizhou Provincial Health Commission, No. gzwjkj2019-1-102.

Institutional review board statement: This study did not involve human subjects or living animals.

Conflict-of-interest statement: All the authors report having no relevant conflicts of interest for this article.

Data sharing statement: The data used to support the findings of this study are available from the corresponding author at 592153968@qq.com upon request.

Open-Access: This article is an open-access article that was selected by an in-house editor and fully peer-reviewed by external reviewers. It is distributed in accordance with the Creative Commons Attribution NonCommercial (CC BY-NC 4.0) license, which permits others to distribute, remix, adapt, build upon this work non-commercially, and license their derivative works on different terms, provided the original work is properly cited and the use is non-commercial. See: https://creativecommons.org/Licenses/by-nc/4.0/

Country/Territory of origin: China

ORCID number: Jia-Yao Li 0000-0003-2880-4978; Tian Tian 0000-0002-1926-2639; Bing Han 0000-0002-9577-293X; Ting Yang 0000-0001-5174-7575; Yi-Xin Guo 0000-0001-6789-8669; Jia-Yu Wu 0009-0000-8578-7778; Yu-Si Chen 0000-0003-2566-8878; Qin Yang 0000-0003-1479-6700; Ru-Jia Xie 0000-0001-5991-2678.

S-Editor: Wang JJ
L-Editor: Filipodia
P-Editor: Cai YX

REFERENCES

1 **Wang W**, Wei C. Advances in the early diagnosis of hepatocellular carcinoma. *Genes Dis* 2020; **7**: 308-319 [PMID: 32884985 DOI: 10.1016/j.gendis.2020.01.014]
2 **Santoni M**, Rizzo A, Kucharz J, Mollica V, Rosellini M, Marchetti A, Tassinari E, Monteiro FSM, Soares A, Molina-Cerrillo J, Grande E, Battelli N, Massari F. Complete remissions following immunotherapy or immuno-oncology combinations in cancer patients: the MOUSEION-03 meta-analysis. *Cancer Immunol Immunother* 2023; **72**: 1365-1379 [PMID: 36633661 DOI: 10.1007/s00262-022-03349-4]
3 **Di Federico A**, Rizzo A, Carloni R, De Giglio A, Bruno R, Ricci D, Brandi G. Atezolizumab-bevacizumab plus Y-90 TARE for the treatment of hepatocellular carcinoma: preclinical rationale and ongoing clinical trials. *Expert Opin Investig Drugs* 2022; **31**: 361-369 [PMID: 34798793 DOI: 10.1080/13543784.2022.2009455]
4 **Rizzo A**, Ricci AD, Brandi G. Atezolizumab in advanced hepatocellular carcinoma: good things come to those who wait. *Immunotherapy* 2021; **13**: 637-644 [PMID: 33820447 DOI: 10.2217/imt-2021-0026]
5 **Rizzo A**, Cusmai A, Gadaleta-Caldarola G, Palmiotti G. Which role for predictors of response to immune checkpoint inhibitors in hepatocellular carcinoma? *Expert Rev Gastroenterol Hepatol* 2022; **16**: 333-339 [PMID: 35403533 DOI: 10.1080/17474124.2022.2064273]
6 **He B**, Dai L, Zhang X, Chen D, Wu J, Feng X, Zhang Y, Xie H, Zhou L, Zheng S. The HDAC Inhibitor Quisinostat (JNJ-26481585) Supresses Hepatocellular Carcinoma alone and Synergistically in Combination with Sorafenib by G0/G1 phase arrest and Apoptosis induction. *Int J Biol Sci* 2018; **14**: 1845-1858 [PMID: 30443188 DOI: 10.7150/ijbs.27661]
7 **Ji H**, Zhou Y, Zhuang X, Zhu Y, Wu Z, Lu Y, Li S, Zeng Y, Lu QR, Huo Y, Shi Y, Bu H. HDAC3 Deficiency Promotes Liver Cancer through a Defect in H3K9ac/H3K9me3 Transition. *Cancer Res* 2019; **79**: 3676-3688 [PMID: 31097476 DOI: 10.1158/0008-5472.CAN-18-3767]
8 **Dawson MA**, Kouzarides T. Cancer epigenetics: from mechanism to therapy. *Cell* 2012; **150**: 12-27 [PMID: 22770212 DOI: 10.1016/j.cell.2012.06.013]
9 **Hogg SJ**, Beavis PA, Dawson MA, Johnstone RW. Targeting the epigenetic regulation of antitumour immunity. *Nat Rev Drug Discov* 2020; **19**: 776-800 [PMID: 32929243 DOI: 10.1038/s41573-020-0077-5]
10 **Chianese A**, Santella B, Ambrosino A, Stelitano D, Rinaldi L, Galdiero M, Zannella C, Franci G. Oncolytic Viruses in Combination Therapeutic Approaches with Epigenetic Modulators: Past, Present, and Future Perspectives. *Cancers (Basel)* 2021; **13** [PMID: 34199429 DOI: 10.3390/cancers13112761]
11 **Zhao P**, Malik S, Xing S. Epigenetic Mechanisms Involved in HCV-Induced Hepatocellular Carcinoma (HCC). *Front Oncol* 2021; **11**: 677926 [PMID: 34336665 DOI: 10.3389/fonc.2021.677926]
12 **Shvedunova M**, Akhtar A. Modulation of cellular processes by histone and non-histone protein acetylation. *Nat Rev Mol Cell Biol* 2022; **23**: 329-349 [PMID: 35042977 DOI: 10.1038/s41580-021-00441-y]
13 **Shen Y**, Wei W, Zhou DX. Histone Acetylation Enzymes Coordinate Metabolism and Gene Expression. *Trends Plant Sci* 2015; **20**: 614-621 [PMID: 26440431 DOI: 10.1016/j.tplants.2015.07.005]
14 **Eckschlager T**, Plch J, Stiborova M, Hrabeta J. Histone Deacetylase Inhibitors as Anticancer Drugs. *Int J Mol Sci* 2017; **18** [PMID: 28671573 DOI: 10.3390/ijms18071414]
15 **Yu L**, Xie R, Tian T, Zheng L, Tang L, Cai S, Ma Z, Yang T, Han B, Yang Q. Suberoylanilide hydroxamic acid upregulates histone acetylation and activates endoplasmic reticulum stress to induce apoptosis in HepG2 liver cancer cells. *Oncol Lett* 2019; **18**: 3537-3544 [PMID: 31516571 DOI: 10.3892/ol.2019.10705]
16 **Samata M**, Alexiadis A, Richard G, Georgiev P, Nuebler J, Kulkarni T, Renschler G, Basilicata MF, Zenk FL, Shvedunova M, Semplicio G, Mirny L, Iovino N, Akhtar A. Intergenerationally Maintained Histone H4 Lysine 16 Acetylation Is Instructive for Future Gene Activation. *Cell* 2020; **182**: 127-144.e23 [PMID: 32502394 DOI: 10.1016/j.cell.2020.05.026]
17 **Füllgrabe J**, Lynch-Day MA, Heldring N, Li W, Struijk RB, Ma Q, Hermanson O, Rosenfeld MG, Klionsky DJ, Joseph B. The histone H4 lysine 16 acetyltransferase hMOF regulates the outcome of autophagy. *Nature* 2013; **500**: 468-471 [PMID: 23863932 DOI: 10.1038/nature12313]
18 **Islam F**, Gopalan V, Lam AK. RETREG1 (FAM134B): A new player in human diseases: 15 years after the discovery in cancer. *J Cell Physiol* 2018; **233**: 4479-4489 [PMID: 29226326 DOI: 10.1002/jcp.26384]
19 **Kasem K**, Sullivan E, Gopalan V, Salajegheh A, Smith RA, Lam AK. JK1 (FAM134B) represses cell migration in colon cancer: a functional study of a novel gene. *Exp Mol Pathol* 2014; **97**: 99-104 [PMID: 24927874 DOI: 10.1016/j.yexmp.2014.06.002]
20 **Lee KT**, Islam F, Vider J, Martin J, Chruścik A, Lu CT, Gopalan V, Lam AK. Overexpression of family with sequence similarity 134, member B (FAM134B) in colon cancers and its tumor suppressive properties in vitro. *Cancer Biol Ther* 2020; **21**: 954-962 [PMID: 32857678 DOI: 10.1080/15384047.2020.1810535]

21 **Islam F**, Chaousis S, Wahab R, Gopalan V, Lam AK. Protein interactions of FAM134B with EB1 and APC/beta-catenin *in vitro* in colon carcinoma. *Mol Carcinog* 2018; **57**: 1480-1491 [PMID: 29964340 DOI: 10.1002/mc.22871]

22 **Jiang X**, Wang X, Ding X, Du M, Li B, Weng X, Zhang J, Li L, Tian R, Zhu Q, Chen S, Wang L, Liu W, Fang L, Neculai D, Sun Q. FAM134B oligomerization drives endoplasmic reticulum membrane scission for ER-phagy. *EMBO J* 2020; **39**: e102608 [PMID: 31930741 DOI: 10.15252/embj.2019102608]

23 **Zhu L**, Wang X, Wang Y. Roles of FAM134B in diseases from the perspectives of organelle membrane morphogenesis and cellular homeostasis. *J Cell Physiol* 2021; **236**: 7242-7255 [PMID: 33843059 DOI: 10.1002/jcp.30377]

24 **Chen W**, Ouyang X, Chen L, Li L. FAM134B-mediated ER-phagy regulates ER-mitochondria interaction through MAMs. *Acta Biochim Biophys Sin (Shanghai)* 2022; **54**: 412-414 [PMID: 35130624 DOI: 10.3724/abbs.2021020]

25 **Bao FX**, Shi HY, Long Q, Yang L, Wu Y, Ying ZF, Qin DJ, Zhang J, Guo YP, Li HM, Liu XG. Mitochondrial Membrane Potential-dependent Endoplasmic Reticulum Fragmentation is an Important Step in Neuritic Degeneration. *CNS Neurosci Ther* 2016; **22**: 648-660 [PMID: 27080255 DOI: 10.1111/cns.12547]

26 **Missiroli S**, Patergnani S, Caroccia N, Pedriali G, Perrone M, Previati M, Wieckowski MR, Giorgi C. Mitochondria-associated membranes (MAMs) and inflammation. *Cell Death Dis* 2018; **9**: 329 [PMID: 29491386 DOI: 10.1038/s41419-017-0027-2]

27 **Sterea AM**, El Hiani Y. The Role of Mitochondrial Calcium Signaling in the Pathophysiology of Cancer Cells. *Adv Exp Med Biol* 2020; **1131**: 747-770 [PMID: 31646533 DOI: 10.1007/978-3-030-12457-1_30]

28 **Liang C**, Xie RJ, Wang JL, Zhang YW, Zhang JY, Yang Q, Han B. Roles of C/EBP-homologous protein and histone H3 lysine 4 methylation in arsenic-induced mitochondrial apoptosis in hepatocytes. *Toxicol Ind Health* 2022; **38**: 745-756 [PMID: 36120900 DOI: 10.1177/07482337221127148]

29 **Denton D**, Kumar S. Autophagy-dependent cell death. *Cell Death Differ* 2019; **26**: 605-616 [PMID: 30568239 DOI: 10.1038/s41418-018-0252-y]

30 **Watanabe H**, Carmi P, Hogan V, Raz T, Silletti S, Nabi IR, Raz A. Purification of human tumor cell autocrine motility factor and molecular cloning of its receptor. *J Biol Chem* 1991; **266**: 13442-13448 [PMID: 1649192]

31 **Mo J**, Chen J, Zhang B. Critical roles of FAM134B in ER-phagy and diseases. *Cell Death Dis* 2020; **11**: 983 [PMID: 33199694 DOI: 10.1038/s41419-020-03195-1]

32 **Joshi V**, Upadhyay A, Kumar A, Mishra A. Gp78 E3 Ubiquitin Ligase: Essential Functions and Contributions in Proteostasis. *Front Cell Neurosci* 2017; **11**: 259 [PMID: 28890687 DOI: 10.3389/fncel.2017.00259]

33 **Park SJ**, Kim SM, Moon JH, Kim JH, Shin JS, Hong SW, Shin YJ, Lee DH, Lee EY, Hwang IY, Kim JE, Kim KP, Hong YS, Lee WK, Choi EK, Lee JS, Jin DH, Kim TW. SAHA, an HDAC inhibitor, overcomes erlotinib resistance in human pancreatic cancer cells by modulating E-cadherin. *Tumour Biol* 2016; **37**: 4323-4330 [PMID: 26493999 DOI: 10.1007/s13277-015-4216-2]

34 **Carlisi D**, Lauricella M, D'Anneo A, Emanuele S, Angileri L, Di Fazio P, Santulli A, Vento R, Tesoriere G. The histone deacetylase inhibitor suberoylanilide hydroxamic acid sensitises human hepatocellular carcinoma cells to TRAIL-induced apoptosis by TRAIL-DISC activation. *Eur J Cancer* 2009; **45**: 2425-2438 [PMID: 19643600 DOI: 10.1016/j.ejca.2009.06.024]

35 **Jiang X**, Tsang YH, Yu Q. c-Myc overexpression sensitizes Bim-mediated Bax activation for apoptosis induced by histone deacetylase inhibitor suberoylanilide hydroxamic acid (SAHA) through regulating Bcl-2/Bcl-xL expression. *Int J Biochem Cell Biol* 2007; **39**: 1016-1025 [PMID: 17331788 DOI: 10.1016/j.biocel.2007.01.024]

36 **Chipurupalli S**, Ganesan R, Martini G, Mele L, Reggio A, Esposito M, Kannan E, Namasivayam V, Grumati P, Desiderio V, Robinson N. Cancer cells adapt FAM134B/BiP mediated ER-phagy to survive hypoxic stress. *Cell Death Dis* 2022; **13**: 357 [PMID: 35436985 DOI: 10.1038/s41419-022-04813-w]

37 **Zhong L**. [The Expression Significance and Function of FAM134B in Hepatocellular Carcinoma Tissue]. 2020

38 **Chino H**, Mizushima N. ER-Phagy: Quality Control and Turnover of Endoplasmic Reticulum. *Trends Cell Biol* 2020; **30**: 384-398 [PMID: 32302550 DOI: 10.1016/j.tcb.2020.02.001]

39 **Grumati P**, Dikic I, Stolz A. ER-phagy at a glance. *J Cell Sci* 2018; **131** [PMID: 30177506 DOI: 10.1242/jcs.217364]

40 **Ferro-Novick S**, Reggiori F, Brodsky JL. ER-Phagy, ER Homeostasis, and ER Quality Control: Implications for Disease. *Trends Biochem Sci* 2021; **46**: 630-639 [PMID: 33509650 DOI: 10.1016/j.tibs.2020.12.013]

41 **Hübner CA**, Dikic I. ER-phagy and human diseases. *Cell Death Differ* 2020; **27**: 833-842 [PMID: 31659280 DOI: 10.1038/s41418-019-0444-0]

42 **Wilkinson S**. ER-phagy: shaping up and destressing the endoplasmic reticulum. *FEBS J* 2019; **286**: 2645-2663 [PMID: 31116513 DOI: 10.1111/febs.14932]

43 **Liao Y**, Duan B, Zhang Y, Zhang X, Xia B. Excessive ER-phagy mediated by the autophagy receptor FAM134B results in ER stress, the unfolded protein response, and cell death in HeLa cells. *J Biol Chem* 2019; **294**: 20009-20023 [PMID: 31748416 DOI: 10.1074/jbc.RA119.008709]

44 **Hrzenjak A**, Kremser ML, Strohmeier B, Moinfar F, Zatloukal K, Denk H. SAHA induces caspase-independent, autophagic cell death of endometrial stromal sarcoma cells by influencing the mTOR pathway. *J Pathol* 2008; **216**: 495-504 [PMID: 18850582 DOI: 10.1002/path.2434]

45 **Lee YJ**, Won AJ, Lee J, Jung JH, Yoon S, Lee BM, Kim HS. Molecular mechanism of SAHA on regulation of autophagic cell death in tamoxifen-resistant MCF-7 breast cancer cells. *Int J Med Sci* 2012; **9**: 881-893 [PMID: 23155362 DOI: 10.7150/ijms.5011]

46 **Kania E**, Pająk B, Orzechowski A. Calcium homeostasis and ER stress in control of autophagy in cancer cells. *Biomed Res Int* 2015; **2015**: 352794 [PMID: 25821797 DOI: 10.1155/2015/352794]

47 **Puzianowska-Kuznicka M**, Kuznicki J. The ER and ageing II: calcium homeostasis. *Ageing Res Rev* 2009; **8**: 160-172 [PMID: 19427411 DOI: 10.1016/j.arr.2009.05.002]

48 **Thoudam T**, Ha CM, Leem J, Chanda D, Park JS, Kim HJ, Jeon JH, Choi YK, Liangpunsakul S, Huh YH, Kwon TH, Park KG, Harris RA, Park KS, Rhee HW, Lee IK. PDK4 Augments ER-Mitochondria Contact to Dampen Skeletal Muscle Insulin Signaling During Obesity. *Diabetes* 2019; **68**: 571-586 [PMID: 30523025 DOI: 10.2337/db18-0363]

49 **Means RE**, Katz SG. Yes, MAM! *Mol Cell Oncol* 2021; **8**: 1919473 [PMID: 34616865 DOI: 10.1080/23723556.2021.1919473]

50 **Zhang SS**, Zhou S, Crowley-McHattan ZJ, Wang RY, Li JP. A Review of the Role of Endo/Sarcoplasmic Reticulum-Mitochondria Ca(2+) Transport in Diseases and Skeletal Muscle Function. *Int J Environ Res Public Health* 2021; **18** [PMID: 33917091 DOI: 10.3390/ijerph18083874]

51 **Xu H**, Guan N, Ren YL, Wei QJ, Tao YH, Yang GS, Liu XY, Bu DF, Zhang Y, Zhu SN. IP(3)R-Grp75-VDAC1-MCU calcium regulation axis

antagonists protect podocytes from apoptosis and decrease proteinuria in an Adriamycin nephropathy rat model. *BMC Nephrol* 2018; **19**: 140 [PMID: 29907098 DOI: 10.1186/s12882-018-0940-3]

World Journal of Gastroenterology

Submit a Manuscript: https://www.f6publishing.com

World J Gastroenterol 2023 September 14; 29(34): 5054-5074

DOI: 10.3748/wjg.v29.i34.5054

ISSN 1007-9327 (print) ISSN 2219-2840 (online)

ORIGINAL ARTICLE

Basic Study

Green tea polyphenols alleviate di-(2-ethylhexyl) phthalate-induced liver injury in mice

Heng Shi, Xin-Hai Zhao, Qin Peng, Xian-Ling Zhou, Si-Si Liu, Chuan-Chuan Sun, Qiu-Yu Cao, Shi-Ping Zhu, Sheng-Yun Sun

Specialty type: Gastroenterology and hepatology

Provenance and peer review: Unsolicited article; Externally peer reviewed.

Peer-review model: Single blind

Peer-review report's scientific quality classification

Grade A (Excellent): 0
Grade B (Very good): B, B
Grade C (Good): 0
Grade D (Fair): 0
Grade E (Poor): 0

P-Reviewer: Kuznietsova H, Ukraine; Scarfi S, Italy

Received: May 16, 2023
Peer-review started: May 16, 2023
First decision: July 10, 2023
Revised: July 19, 2023
Accepted: August 21, 2023
Article in press: August 21, 2023
Published online: September 14, 2023

Heng Shi, Xin-Hai Zhao, Xian-Ling Zhou, Chuan-Chuan Sun, Qiu-Yu Cao, Shi-Ping Zhu, Sheng-Yun Sun, Department of Traditional Chinese Medicine, The First Affiliated Hospital of Jinan University, Guangzhou 522000, Guangdong Province, China

Heng Shi, Qin Peng, Department of Gastroenterology, The Central Hospital of Shaoyang, Shaoyang 422000, Hunan Province, China

Si-Si Liu, Department of Pathology, The Central Hospital of Shaoyang, Shaoyang 422000, Hunan Province, China

Corresponding author: Sheng-Yun Sun, MD, PhD, Chief Doctor, Department of Traditional Chinese Medicine, The First Affiliated Hospital of Jinan University, No. 613 Huangpu Avenue West, Tianhe District, Guangzhou 522000, Guangdong Province, China.
shengyunsun2020@163.com

Abstract

BACKGROUND

Di (2-ethylhexyl) phthalate (DEHP) is a common plasticizer known to cause liver injury. Green tea is reported to exert therapeutic effects on heavy metal exposure-induced organ damage. However, limited studies have examined the therapeutic effects of green tea polyphenols (GTPs) on DEHP-induced liver damage.

AIM

To evaluate the molecular mechanism underlying the therapeutic effects of GTPs on DEHP-induced liver damage.

METHODS

C57BL/6J mice were divided into the following five groups: Control, model [DEHP (1500 mg/kg bodyweight)], treatment [DEHP (1500 mg/kg bodyweight) + GTP (70 mg/kg bodyweight), oil, and GTP (70 mg/kg bodyweight)] groups. After 8 wk, the liver function, blood lipid profile, and liver histopathology were examined. Differentially expressed micro RNAs (miRNAs) and mRNAs in the liver tissues were examined using high-throughput sequencing. Additionally, functional enrichment analysis and immune infiltration prediction were performed. The miRNA-mRNA regulatory axis was elucidated using the starBase database. Protein expression was evaluated using immunohistochemistry.

RESULTS

GTPs alleviated DHEP-induced liver dysfunction, blood lipid dysregulation, fatty liver disease, liver fibrosis, and mitochondrial and endoplasmic reticulum lesions in mice. The infiltration of macrophages, mast cells, and natural killer cells varied between the model and treatment groups. mmu-miR-141-3p (a differentially expressed miRNA), *Zcchc24* (a differentially expressed mRNA), and Zcchc24 (a differentially expressed protein) constituted the miRNA-mRNA-protein regulatory axis involved in mediating the therapeutic effects of GTPs on DEHP-induced liver damage in mice.

CONCLUSION

This study demonstrated that GTPs mitigate DEHP-induced liver dysfunction, blood lipid dysregulation, fatty liver disease, and partial liver fibrosis, and regulate immune cell infiltration. Additionally, an important miRNA-mRNA-protein molecular regulatory axis involved in mediating the therapeutic effects of GTPs on DEHP-induced liver damage was elucidated.

Key Words: Green tea polyphenols; Di(2-ethylhexyl) phthalate; Liver fibrosis; Fatty liver disease; Mitochondria; Immune

©The Author(s) 2023. Published by Baishideng Publishing Group Inc. All rights reserved.

Core Tip: Green tea polyphenols (GTPs) alleviated Di (2-ethylhexyl) phthalate (DEHP)-induced liver dysfunction, blood lipid dysregulation, fatty liver disease, liver fibrosis, and mitochondrial and endoplasmic reticulum lesions in mice. The infiltration of macrophages, mast cell, and natural killer cells varied between the model and treatment groups. mmu-miR-141-3p (a differentially expressed miRNA), *Zcchc24* (a differentially expressed mRNA), and Zcchc24 (a differentially expressed protein) constituted the miRNA-mRNA-protein regulatory axis involved in mediating the therapeutic effects of GTPs on DEHP-induced liver damage in mice.

Citation: Shi H, Zhao XH, Peng Q, Zhou XL, Liu SS, Sun CC, Cao QY, Zhu SP, Sun SY. Green tea polyphenols alleviate di-(2-ethylhexyl) phthalate-induced liver injury in mice. *World J Gastroenterol* 2023; 29(34): 5054-5074
URL: https://www.wjgnet.com/1007-9327/full/v29/i34/5054.htm
DOI: https://dx.doi.org/10.3748/wjg.v29.i34.5054

INTRODUCTION

Di (2-ethylhexyl) phthalate (DEHP), which is the most widely used representative phthalic acid ester, can non-covalently bind to polyolefin plastics and predominantly serves as a plasticizer, increasing the flexibility, transparency, durability, and longevity of plastics. Additionally, DEHP is extensively detected in various daily-life products (including baby toys, food packaging, and cosmetics) and several surgical and medical devices[1]. Furthermore, DEHP can be continuously released into the environment (air, soil, water, food, *etc.*), enter living organisms *via* ingestion, inhalation, or skin contact, and subsequently exert toxic effects on health[2]. A previous study reported that DEHP and its metabolites were detected in 100% of tested human urine samples, indicating persistent exposure to DEHP[3]. The DEHP exposure range of the general population is estimated to be 5.8-19 μg/kg/d, while DEHP exposure in medical environments may exceed 167.9 mg/d[4]. The development of modern chemical agriculture has increased the severity of DEHP pollution. DEHP exposure in the Pearl River Delta region of Guangdong Province, China, can reach up to 61 μg/kg/d, which is higher than the tolerable intake of DEHP[5]. Additionally, DEHP undergoes rapid degradation upon ingestion in humans. According to the United States Environmental Protection Agency, the average half-life of DEHP in the human body is 12 h. DEHP and its active metabolite mono-(2-ethylhexyl) phthalate have been detected in various human tissues, including the liver, blood, placenta, amniotic fluid, and early-pregnancy chorionic villus sample[6]. Therefore, evaluating the effect of DEHP on the environment and human health has piqued the interest of the scientific community.

The liver, an important organ involved in the synthesis, metabolism, and detoxification processes, is highly susceptible to acute or chronic damage induced by various drugs[7]. Recent studies have demonstrated that DEHP adversely affects multiple systems in the body. In particular, epidemiological and animal studies have demonstrated the hepatoxicity of DEHP[8]. The mechanism underlying the hepatotoxic effects of DEHP mainly involves oxidative stress, cell apoptosis, and signaling pathway activation. DEHP induces apoptosis in healthy human liver cells through the mitochondrial signaling pathway and/or the caspase-mediated death receptor pathway[9]. Additionally, DEHP may adversely affect gap junctional intercellular communication, peroxisome beta-oxidation activity, and DNA replication synthesis, leading to the formation of liver tumors[10]. Currently, the most extensively studied mechanism of DEHP-induced liver damage is oxidative stress in which the regulation of reactive oxygen species (ROS) production plays a critical role[11]. Excessive ROS production leads to peroxidation of the polyunsaturated fatty acids in the cell membrane. DEHP promotes lipid peroxidation in the liver, primarily through the downregulation of superoxide dismutase and catalase activity and the upregulation of malondialdehyde (MDA) concentrations[12]. Additionally, DEHP mediates the pathogenesis of non-alcoholic fatty liver disease in a high-fat diet-fed animal model by promoting lipid peroxidation[8].

Green tea is the second most widely consumed beverage worldwide after water[13]. The harvested tea leaves are steamed at high temperatures to inactivate the polyphenol oxidase in green tea, preserving most of the vitamins in tea leaves. Thus, green tea exhibits enhanced antioxidant activity. Epidemiological and clinical studies have reported that phenol compounds in tea extracts, such as green tea polyphenols (GTPs), exert a wide range of beneficial effects on human health, including anti-aging, neuroprotective[14], and therapeutic or preventive effects on various diseases, such as cancer[15], cardiovascular disease[16], and obesity[17]. Moreover, GTPs mitigate the adverse effects of poisoning with various heavy metals[18]. However, limited studies have examined the therapeutic effects of GTPs on DEHP-induced liver diseases.

Micro RNAs (miRNAs), a class of endogenous non-coding small RNAs encoded by mRNA, regulate gene expression by modulating mRNA stability. Several miRNAs are reported to play important roles in the pathogenesis of liver fibrosis [19], cirrhosis[20], and hepatocellular carcinoma[21]. Some miRNAs are diagnostic markers for drug-induced liver injury [22]. This study aimed to identify key protein nodes that may affect the expression level of miRNAs in the regulatory network of miRNA and target genes by analyzing the miRNA regulation network. Hence, this study will provide a theoretical basis for future studies on the functions and regulatory mechanisms underlying the therapeutic effects of GTPs on DEHP exposure-induced liver damage.

MATERIALS AND METHODS

Regents

DEHP was purchased from Shanghai Aladdin Biochemical Technology Co., Ltd. (Shanghai, China). GTPs were purchased from Shanghai Yuanye Bio-Technology Co., Ltd. (Shanghai, China). Corn oil was purchased from Hebei Pin Research Biotechnology Co., Ltd. (Baoding, China). Anti-ZCCHC24 antibodies were purchased from Biorbyt Ltd. (Cambridge, United Kingdom).

Animal experiments

Animal experiments were performed at the specific pathogen-free grade animal laboratory of the Medical College of Jinan University. C57BL/6J mice (n = 50) were purchased from Guangdong Yaokang Biotechnology Co., Ltd. And allowed to acclimatize to the laboratory environment for 1 wk. The animals were maintained under the following conditions: Room temperature, 20 ℃-24 ℃; relative humidity, 50%-65%; circadian cycle, 12-h light-dark cycle; access to food and water, ad libitum; diet, regular mouse chow. This study was approved by the Institutional Animal Care and Use Committee of Jinan University (ethics approval number: IACUC-20210630-15). All experimental procedures were performed according to the regulations established by the ethical committee.

Previous studies[23,24] have reported that DEHP is soluble in corn oil. Hence, this study used corn oil as the solvent for DEHP. After 1 wk of acclimatization, 50 mice were randomly assigned into the following five groups (10 mice/group): Control group, administered with 0.2 mL distilled water; model group, administered with 0.2 mL corn oil and DEHP (1500 mg/kg bodyweight); treatment group, administered with 0.2 mL corn oil and DEHP (1500 mg/kg bodyweight), followed by administration of 0.2 mL GTPs (70 mg/kg bodyweight) after 1 h; oil group, administered with 0.2 mL corn oil; GTP group, administered with 0.2 mL GTP (70 mg/kg bodyweight). Based on our previous study, DEHP [25] and GTPs[26] were gavaged. The doses were adjusted weekly based on the bodyweight of the mice. The mice were subjected to daily gavage for 8 wk. At the end of the experimental period, the blood and liver samples were obtained under anesthesia after the mice were allowed to fast overnight. Liver index = (liver weight/bodyweight) × 100%.

Evaluation of liver function and blood lipid profile

The blood from mice was collected using the retro-orbital venous plexus method. Next, the whole blood was placed in a 1.5-mL centrifuge tube and left undisturbed at room temperature for 2 h. The sample was centrifuged at 5 °C and 3000 rpm for 15 min using a high-speed refrigerated centrifuge to obtain the serum. The serum levels of liver function markers [aspartate aminotransferase (AST), alanine aminotransferase (ALT), and total bilirubin (TBIL)] and lipids [low-density lipoprotein (LDL), total cholesterol, and triglycerides (TGs)] were analyzed using a fully automated biochemical analyzer.

Hematoxylin and eosin staining

The tissue sections were fixed in 4% neutral buffered formalin, embedded in paraffin, and sectioned into 4 μm-thick sections. The sections were deparaffinized using xylene, rehydrated using a series of graded ethanol solutions, stained with hematoxylin for 5–10 min, washed with distilled water, and stained with eosin for 2-7 min. Next, the sections were dehydrated using a series of graded ethanol solutions, cleared with xylene, mounted with mounting medium, and covered with a cover slip.

Oil red O staining

The frozen sections were fixed in 4% neutral buffered formalin, rinsed with 60% isopropanol, and allowed to dry. The sections were then stained with oil red O for 15-30 min, rinsed with 60% isopropanol, counterstained with hematoxylin for 1-2 min, washed with distilled water, dehydrated, mounted with a mounting medium, and covered with a coverslip.

Periodic acid-Schiff staining

The tissue sections were deparaffinized using xylene, rehydrated using a series of graded ethanol solutions, and oxidized

with a periodic acid solution for 10-15 min. Next, the sections were rinsed with distilled water, stained with Schiff reagent for 30-60 min in the dark, counterstained with hematoxylin, washed with distilled water, dehydrated, mounted using a mounting medium, and covered with a cover slip.

Masson's trichrome staining

The tissue sections were deparaffinized using xylene, rehydrated using a series of graded ethanol solutions, stained with Weigert's iron hematoxylin for 10 min, rinsed with distilled water, stained with Biebrich scarlet-acid fuchsin solution for 5-10 min, washed with distilled water, and incubated with phosphotungstic-phosphomolybdic acid solution for 5-10 min. Next, the sections were counterstained with aniline blue for 5-10 min, washed with distilled water, dehydrated, mounted with a mounting medium, and covered with a cover slip.

Sirius red staining

The tissue sections were deparaffinized using xylene, rehydrated using a series of graded ethanol solutions, stained with Sirius red solution for 1 h, washed with distilled water, dehydrated, and cleared with xylene. Finally, the sections were mounted with a mounting medium and covered with a cover slip.

Transmission electron microscopy

One mouse from the control, treatment, and model groups was randomly selected for electron microscopy. Liver sections with a size of approximately 1 mm were treated with 2.5% glutaraldehyde (Scientific Phygene, Fuzhou, China) and rinsed thrice with phosphate-buffered saline (PBS) (PH = 7.4). The samples were fixed with 1% osmium tetroxide (Ted Pella, Redding, United States) for 2 h, rinsed thrice with PBS, and dehydrated using alcohol and acetone gradients as follows: 50% ethanol for 30 min, 70% ethanol for 30 h, 80% acetone for 30 min, and 90% acetone for 30 h. Next, the samples were washed thrice with 100% acetone and embedded in epoxy resin (Ted Pella, Redding, United States). Ultrathin sections (7 nm) were prepared using a microtome (LKB, Bromma, Sweden). The sections were stained with uranyl acetate (EMS, Hatfield, United States) for 30 min and 3% lead citrate (Ted Pella, Redding, United States) for 15 min. The target structures were observed using a transmission electron microscope (JEM-1400, Japan Electron Optics Laboratory Co., Ltd. Tokyo, Japan).

High-throughput sequencing

Liver samples (n = 3 per group) from the control, treatment, and model groups stored in liquid nitrogen were randomly selected and sent to Huada Genomics (Wuhan, China, http://www.genomics.cn) for high-throughput sequencing. For specific sequencing steps, refer to the Supplementary material.

Differentially expressed mRNAs and miRNAs

The mRNA and miRNA expression levels were measured using fragments per kilobase of transcript per million mapped reads (FPKM) values. Sequencing data were subjected to quality control. Differential expression between groups was estimated using the Limma R package (version: 3.52.2) based on the generalized linear model. To comparatively analyze the expression levels between multiple groups, the control-model and model-treatment expression profiles were regressed using the Limma package in R software (version: 4.2.1, https://posit.co/). A loose threshold was set to avoid excessive filtering of differentially expressed mRNAs and miRNAs (log fold-change > 1; P < 0.05). Differentially expressed mRNAs and miRNAs were identified.

Enrichment analysis

The mRNA expression data were subjected to Gene Ontology (GO) and Kyoto Encyclopedia of Genes and Genomes (KEGG) pathway analyses to identify the enrichment of mRNAs in the GO terms biological process (BP), cellular component (CC), and molecular function (MF) and the KEGG signaling pathways. The clusterprofiler R package (version: 4.4.4) was used for enrichment analyses with the reference files based on the org.Mm.eg.db R package (version 3.1.0) for mouse enrichment analysis. Enrichment was considered significant at P < 0.05.

Immune infiltration analysis

CIBERSORT is a gene expression-based algorithm for the accurate detection of immune cell infiltration. The "CIBERSORT" R package (CIBERSORTR script v1.03; http://cibersort.stanford.edu/) developed by Newman *et al*[27] was used to successfully quantify 22 types of immune cells, including B cells, regulatory T cells, CD4+ T, CD8+ T, natural killer (NK) cells, mast cells, plasma cells, dendritic cells, neutrophils, eosinophils, and macrophages. The reference dataset of mouse immune cells was obtained from Chen *et al*[28]. The mRNA expression data of the control, model, and treatment groups were examined using the CIBERSORT algorithm with a perm of the deconvolution algorithm set to 1000.

Regulatory network of miRNA-mRNA

miRNA, a type of non-coding RNA, negatively regulates gene expression at the posttranscriptional level. To generate a preliminary regulatory network of miRNA-mRNA in the model and treatment groups, the upregulated miRNAs or mRNAs and downregulated mRNAs or miRNAs were selected and analyzed using Cytoscape software (version: 3.7.1, https://cytoscape.org/).

The Sun Yat-sen University research team developed the starBase database (https://starbase.sysu.edu.cn/starbase2/) to analyze interaction networks between long non-coding RNA, miRNA, competitive endogenous RNAs, RNA-binding proteins, and mRNAs using cross-linked immunoprecipitation sequencing (CLIP-seq) (high-throughput sequencing of RNA using CLIP, photoactivable ribonucleoside-enhanced CLIP, individual nucleotide resolution ultraviolet CLIP, and cross-linking ligation and sequencing of hybrids) data. To obtain the final miRNA-mRNA regulatory network, the initially selected network was intersected with the mouse interaction network obtained from the starBase database. Gene expression was verified using immunohistochemical analyses. This study aimed to establish the miRNA-mRNA-protein regulatory axis.

Immunohistochemistry

The paraffin sections (4 μm) of mouse liver tissue were deparaffinized, rehydrated, and subjected to antigen retrieval in a buffer solution (pH 9.0). After blocking endogenous peroxidase activity and non-specific binding, the sections were incubated with anti-ZCCHC24 antibodies (1:100) at 4 °C overnight. The sections were then washed and incubated with horseradish peroxidase-conjugated secondary antibodies at room temperature for 1 h. Immunoreactive signals were developed using diaminobenzidine. The sections were counterstained with hematoxylin and observed under a microscope.

Statistical analyses

The average optical density (AOD) (integrated optical density/area) of positive reactions was calculated using Image-Pro Plus 6.0 software. Data were analyzed using the dplyr R package (v. 1.0.10) and visualized using the ggplot2 R package (v. 3.3.6). Categorical variables were analyzed using the Chi-squared test. Continuous variables were represented as mean ± SD. Continuous variables between two groups were compared using the Wilcoxon signed-rank test, while those between more than two groups were compared using the Kruskal-Wallis test. Differences were considered significant at $P < 0.05$.

RESULTS

Effect of GTPs on bodyweight and liver index

The flowchart of the study is shown in Figure 1. Mice in all groups survived during the experiment and did not exhibit aberrant behaviors in urination, defecation, food intake, or water consumption. As shown in Supplementary Table 1 and Figure 2A, the bodyweight of mice in all groups increased with time and was not significantly different between the groups. The liver index (Supplementary Table 2 and Figure 2B) values in the model group were significantly higher than those in the control group ($P = 0.016$) but were not significantly different between the treatment and model groups ($P = 0.51$). Additionally, the liver index values in the oil and GTP groups were not significantly different from those in the control group ($P > 0.05$).

Effect of GTPs on the serum levels of liver function markers and lipids

The serum levels of ALT, AST, TBIL, LDL, and TGs were analyzed. As shown in Figure 2C-G, the serum levels of ALT, AST, TBIL, LDL, and TGs in the model group were significantly higher than those in the control group ($P < 0.001$). Compared with those in the model group, the serum levels of liver function markers and lipids were significantly downregulated in the treatment group ($P < 0.001$). The ALT, AST, and LDL levels were not significantly different between the oil, control, and GTP groups ($P > 0.05$).

Effect of GTPs on hepatic histological characteristics

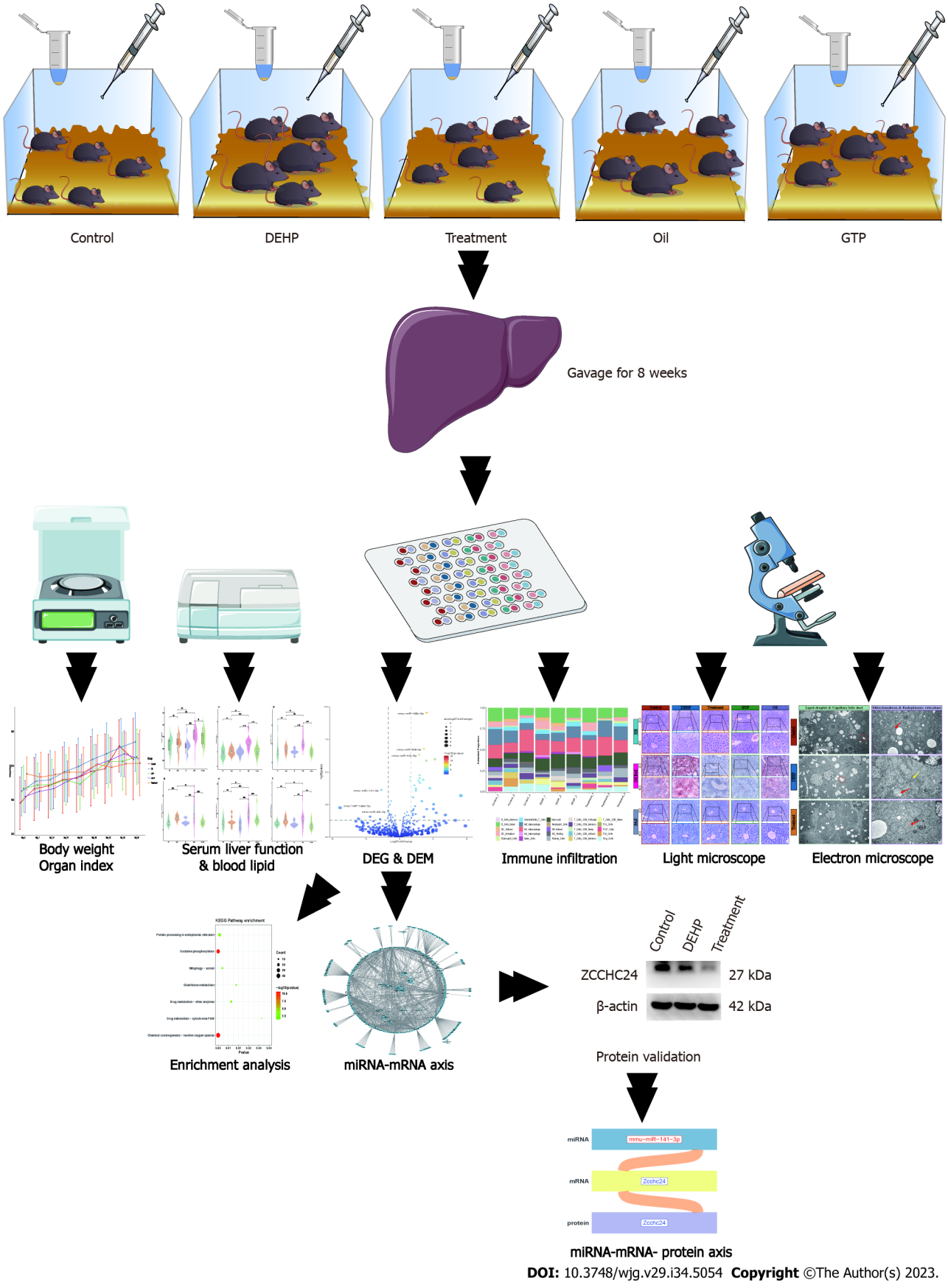
The results of liver hematoxylin and eosin staining are shown in Figure 3A. Mice in the model group exhibited significant hepatocyte ballooning degeneration, whereas those in the control, oil, and GTP groups did not exhibit hepatocyte ballooning degeneration.

Effect of GTPs on fat deposition

Oil red O staining was performed to further analyze the severity of fatty liver in different groups. As shown in Figure 3A, the model group exhibited the highest red color staining intensity in the liver, followed by the oil and control groups. Meanwhile, the liver of the treatment and GTP groups exhibited the lowest red staining intensity. Five positive staining sites in the liver of the model and treatment groups were selected to calculate the AOD. As shown in Figure 3B, the AOD in the model group (7.270 ± 1.120%) was significantly higher than that in the treatment (0.185 ± 0.061%) ($P = 0.037$) and control groups (5.760 ± 0.586%) ($P < 0.001$).

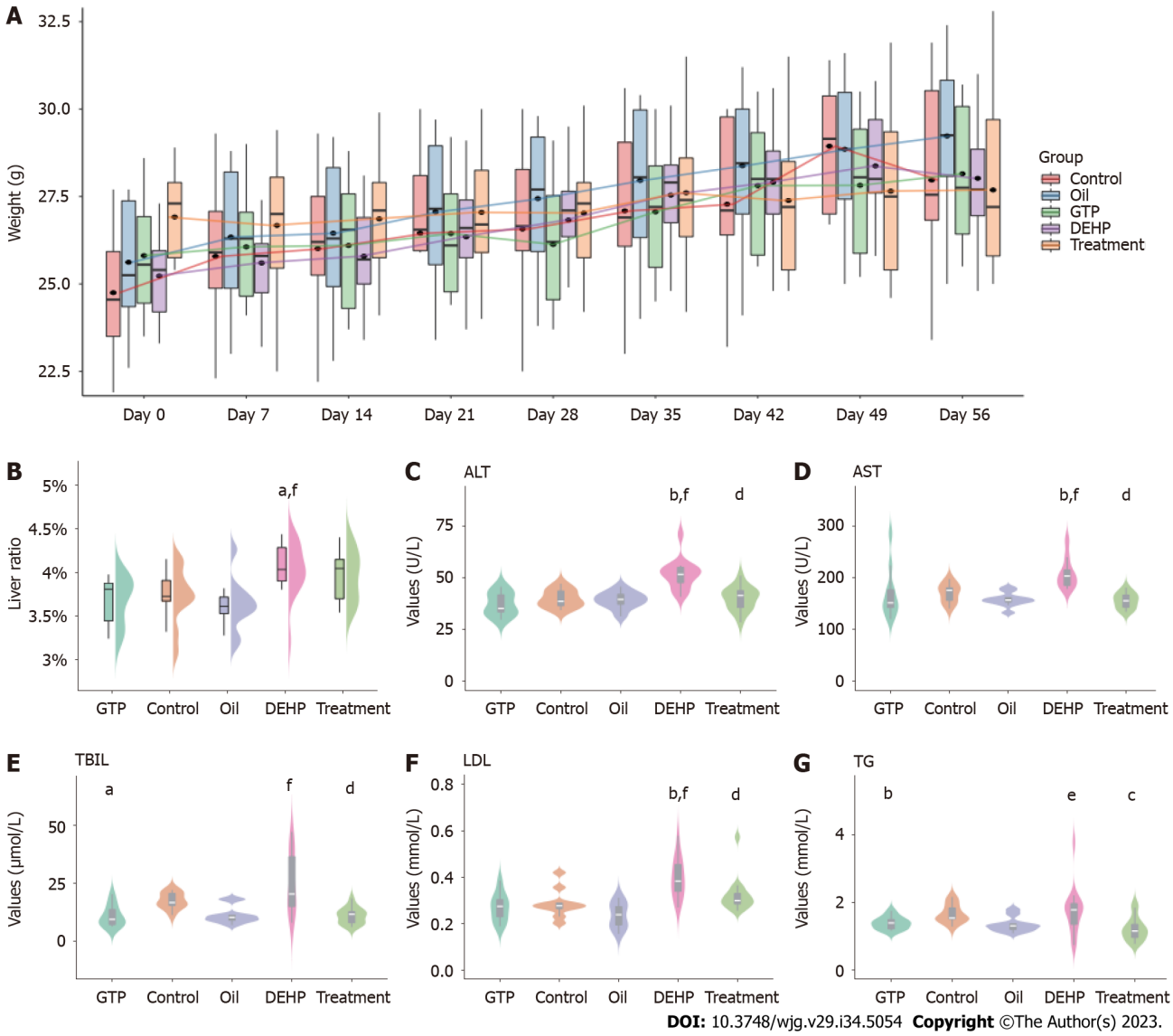
Effect of GTPs on polysaccharide accumulation

The results of Periodic acid-Schiff staining (Figure 3A) revealed the lack of red-stained areas in the liver of the model group, while the red-stained areas were upregulated in the control, oil, treatment, and GTP groups. Five positive staining sites in the liver of the model and treatment groups were selected to calculate the AOD. As shown in Figure 3C, the AOD in the model group (0.431 ± 0.083%) was significantly lower than that in the treatment (1.170 ± 0.099%) and control groups (1.360 ± 0.148%) ($P < 0.001$).



DOI: 10.3748/wjg.v29.i34.5054 **Copyright** ©The Author(s) 2023.

Figure 1 Flowchart of the study. DEG: Differentially expressed gene; DEM: Differentially expressed microRNA (miRNA).



DOI: 10.3748/wjg.v29.i34.5054 **Copyright** ©The Author(s) 2023.

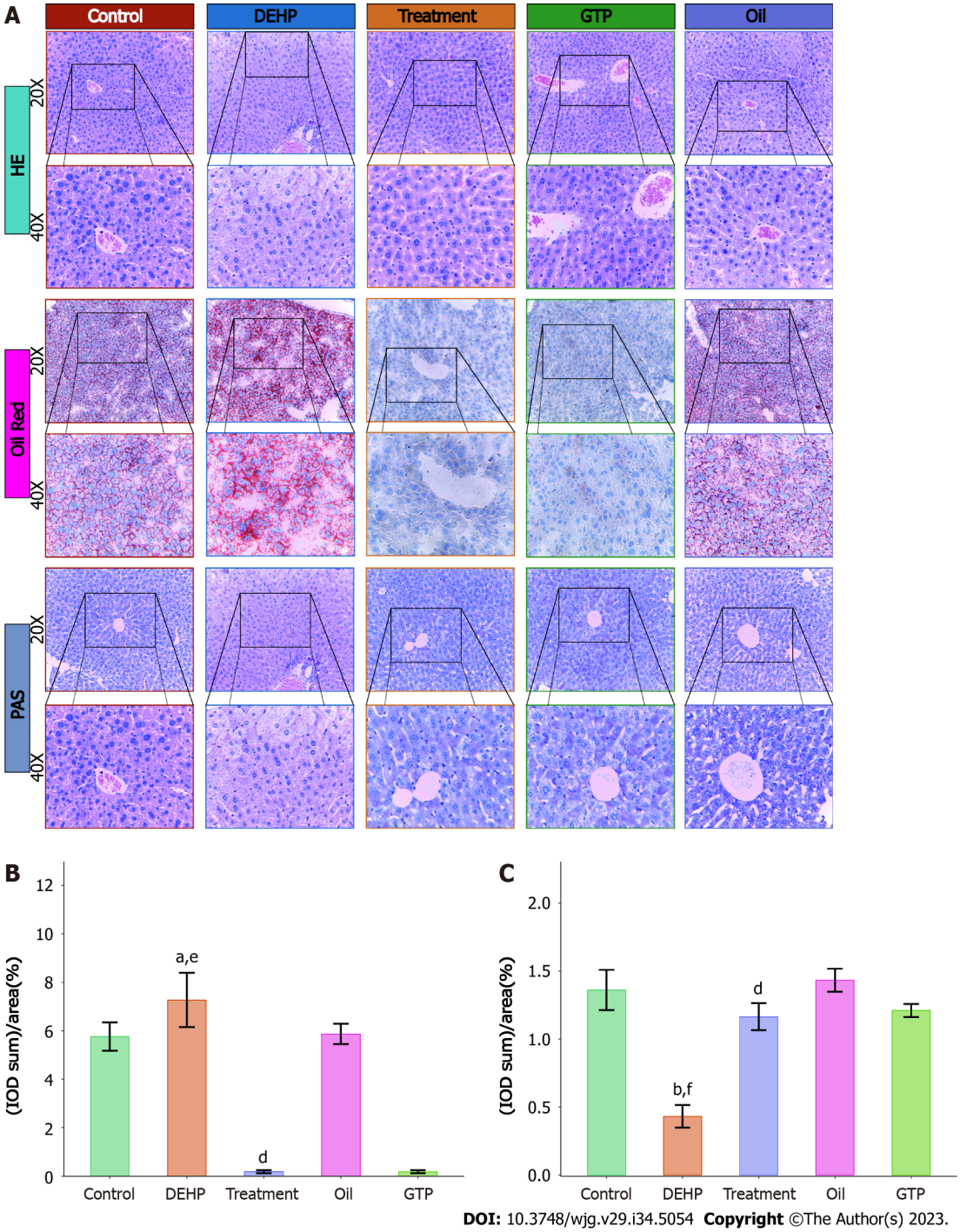
Figure 2 Mouse bodyweight and liver index and serum levels of liver function markers and lipids. A: Bodyweight changes in different groups within 8 wk; B-G: Comparative analysis of organ indices (B) and serum levels of alanine aminotransferase (C), glutamate aminotransferase (D), total bilirubin (E), low-density lipoprotein (F), and triglyceride (G) in different groups. $^{a}P < 0.05$ and $^{b}P < 0.01$ (compared to the Control group); $^{c}P < 0.05$ and $^{d}P < 0.01$ (compared to Di (2-ethylhexyl) phthalate group); $^{e}P < 0.05$ and $^{f}P < 0.01$ (compared to Oil group). ALT: Alanine aminotransferase; AST: Glutamate aminotransferase; TBIL: Total bilirubin; LDL: Low-density lipoprotein; TG: Triglyceride; DEHP: Di (2-ethylhexyl) phthalate.

Effect of GTPs on collagen fibers

The results of Masson's trichrome staining (Figure 4A) revealed blue-stained fibrous tissue around the liver blood vessels in the model group. In contrast, the area of blue-stained fibrous tissue around the liver blood vessels in the treatment group was lower than that in the model group. Fibrous tissue was not detected around the liver blood vessels in the control, oil, and GTP groups. Five positive staining sites in the liver of the model and treatment groups were selected to calculate the AOD. As shown in Figure 4B, the AOD in the model group (0.337 ± 0.113%) was significantly higher than that in the treatment group (0.183 ± 0.014%) ($P = 0.02$).

Effect of GTPs on collagen network

In Sirius red staining, type I collagen fibers exhibit strong orange-yellow or bright red colors under a polarized light microscope, whereas type III collagen fibers exhibit green color. In this study, the results of Sirius red staining (Figure 4A) revealed red-stained fibrous tissue around the blood vessels in the model group. The red-stained area around the blood vessels in the treatment group was significantly lower than that in the model group. Red-stained fibrous tissue was not detected around the blood vessels of the control, oil, and GTP groups. Next, semiquantitative analysis was performed by selecting five positive staining sites in the liver of the model and treatment groups to calculate the AOD. The AOD in the model group (1.240 ± 0.125%) was significantly higher than that in the treatment group (0.080 ± 0.025%) ($P = 0.012$) (Figure 4C).

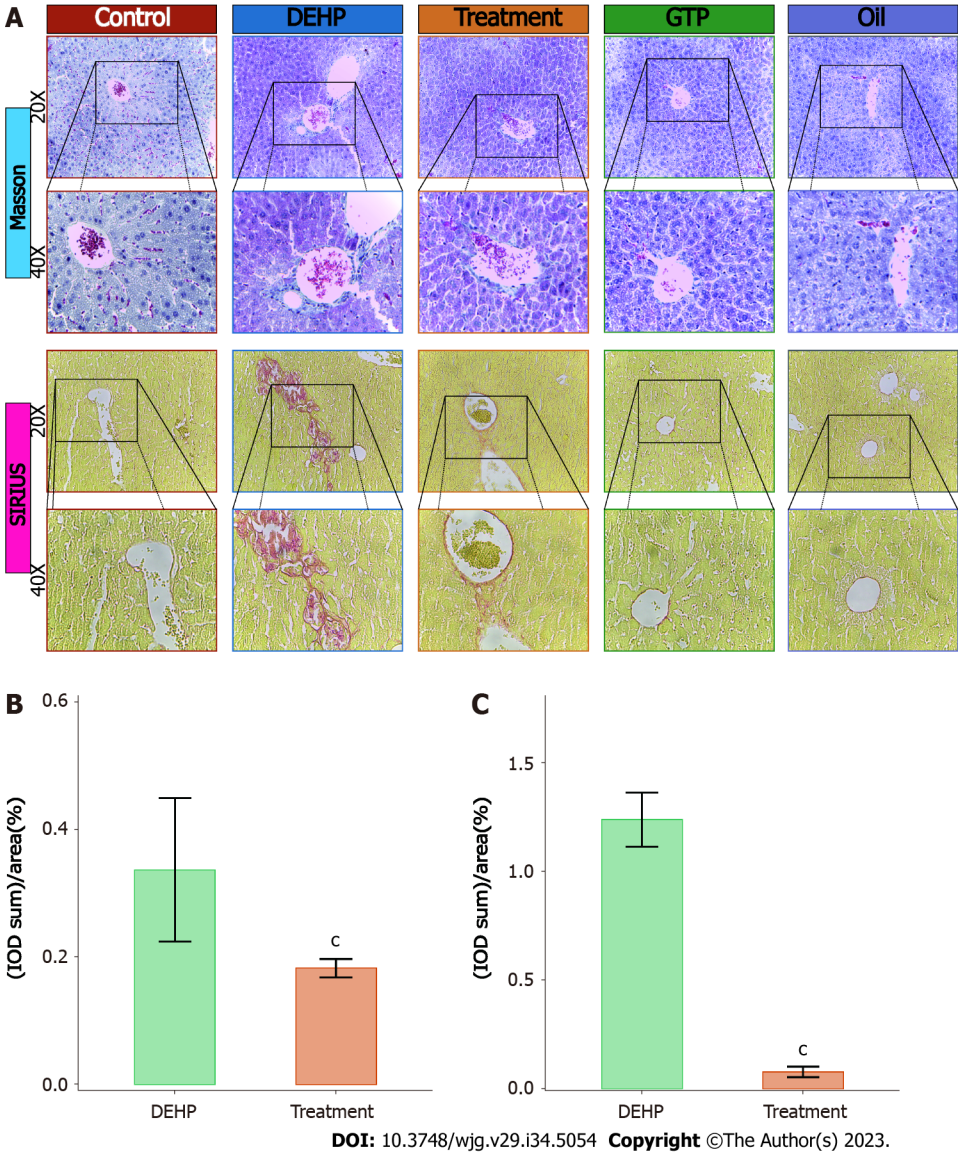


DOI: 10.3748/wjg.v29.i34.5054 **Copyright** ©The Author(s) 2023.

Figure 3 Hematoxylin and eosin, oil red O, and periodic acid-Schaff staining of liver sections and semiquantitative analysis of liver pathologies in mice from different groups. A: Hematoxylin and eosin-stained, oil red O-stained, and periodic acid-Schaff (PAS)-stained liver sections of different groups; B and C: Comparative analysis of average optical density of oil red O staining (B) and PAS staining (C) intensities between different groups. $^{a}P < 0.05$ and $^{b}P < 0.01$ (compared to the Control group); $^{d}P < 0.01$ (compared to Di (2-ethylhexyl) phthalate group); $^{e}P < 0.05$ and $^{f}P < 0.01$ (compared to Oil group). DEHP: Di (2-ethylhexyl) phthalate; HE: Hematoxylin and eosin; PAS: Periodic acid-Schaff.

Effect of GTPs on the liver microstructures

The liver tissues of the control, model, and treatment groups were subjected to transmission electron microscopy. The number and size of lipid droplets in the liver were upregulated and the capillary bile ducts were significantly dilated in the model group (Figure 5A). Additionally, the mitochondria were slightly swollen, and the arrangement of the rough endoplasmic reticulum was disordered. In contrast, the number of lipid droplets in the liver was downregulated in the treatment group, while the capillary bile ducts exhibited physiological structure. Additionally, the swelling of the mitochondria was alleviated. The results of quantitative analysis of the diameter of small bile ducts (Figure 5B) were consistent with the observations in Figure 5A. However, these findings must be carefully interpreted. Additionally, further studies with large sample sizes are needed to confirm and generalize the results.



DOI: 10.3748/wjg.v29.i34.5054 **Copyright** ©The Author(s) 2023.

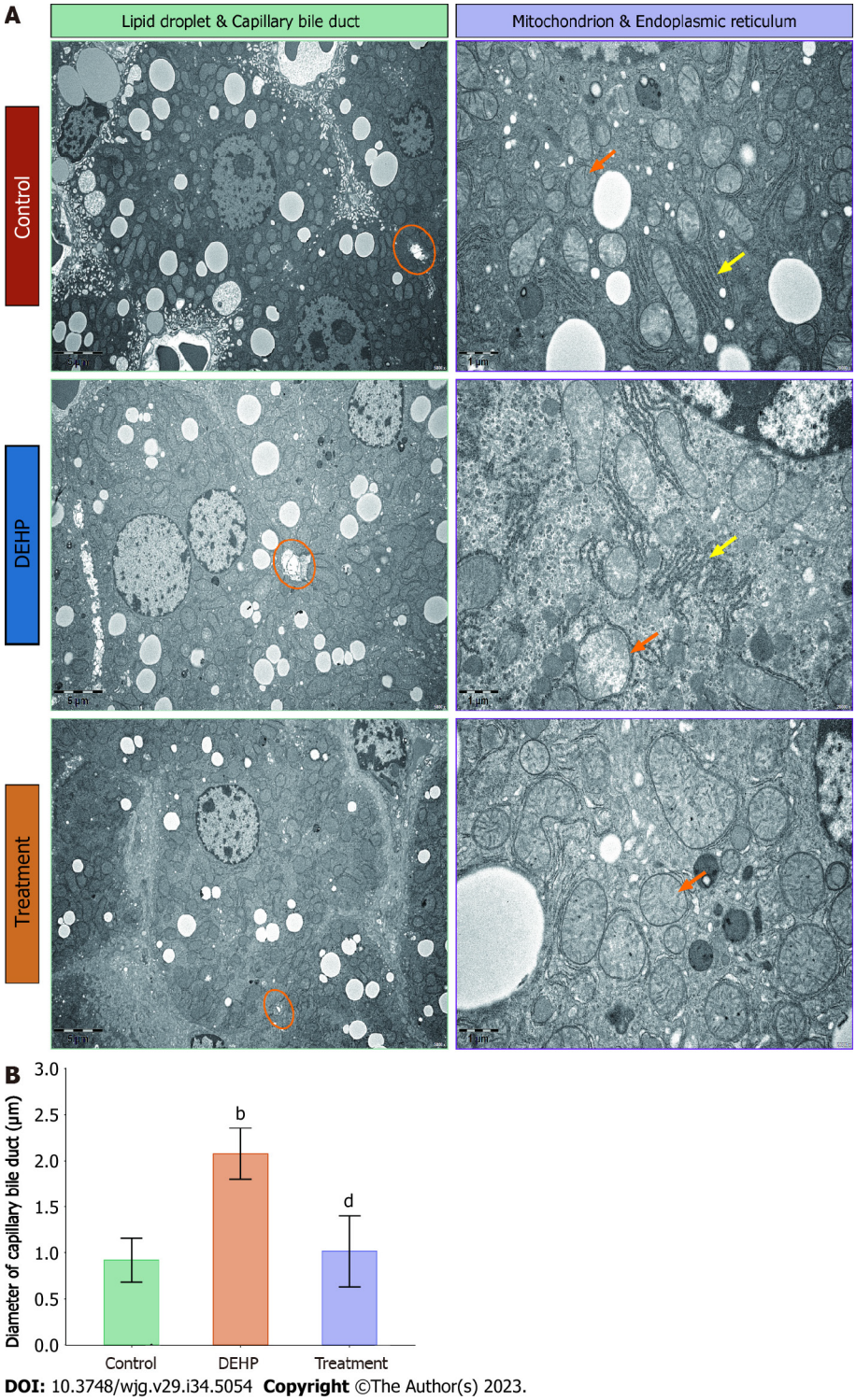
Figure 4 Masson's trichrome and Sirius red staining and semiquantitative analysis of hepatic pathologies in mice from different groups.
A: Masson's trichrome and Sirius red staining of liver samples from different groups; B and C: Comparative analysis of average optical density of Masson's trichrome staining (B) and Sirius red staining (C) intensities between the model and treatment groups. °$P < 0.05$ (compared to Di (2-ethylhexyl) phthalate group). DEHP: Di (2-ethylhexyl) phthalate.

Effect of GTPs on mRNA and miRNA expression levels

The liver samples from the control, treatment, and model groups were subjected to high-throughput screening with 3 replicate samples for each group. The mRNA and miRNA expression data were subjected to quality control analysis. The differences in the expression levels of miRNA and mRNA were minimal between the groups (Supplementary Figure 1A and B). Next, principal component analysis was performed (Supplementary Figure 1C and D). The mRNA and miRNA profiles of the control, model, and treatment groups exhibited distinct separation. Differential analysis revealed that compared with those in the model group, the number of upregulated mRNAs and miRNAs was 377 and 33, respectively, while the number of downregulated mRNAs and miRNAs was 583 and 7, respectively (Figure 6A and B). The expression levels of the significantly upregulated and downregulated mRNAs and miRNAs are shown in Figure 6C and D.

Enrichment analyses

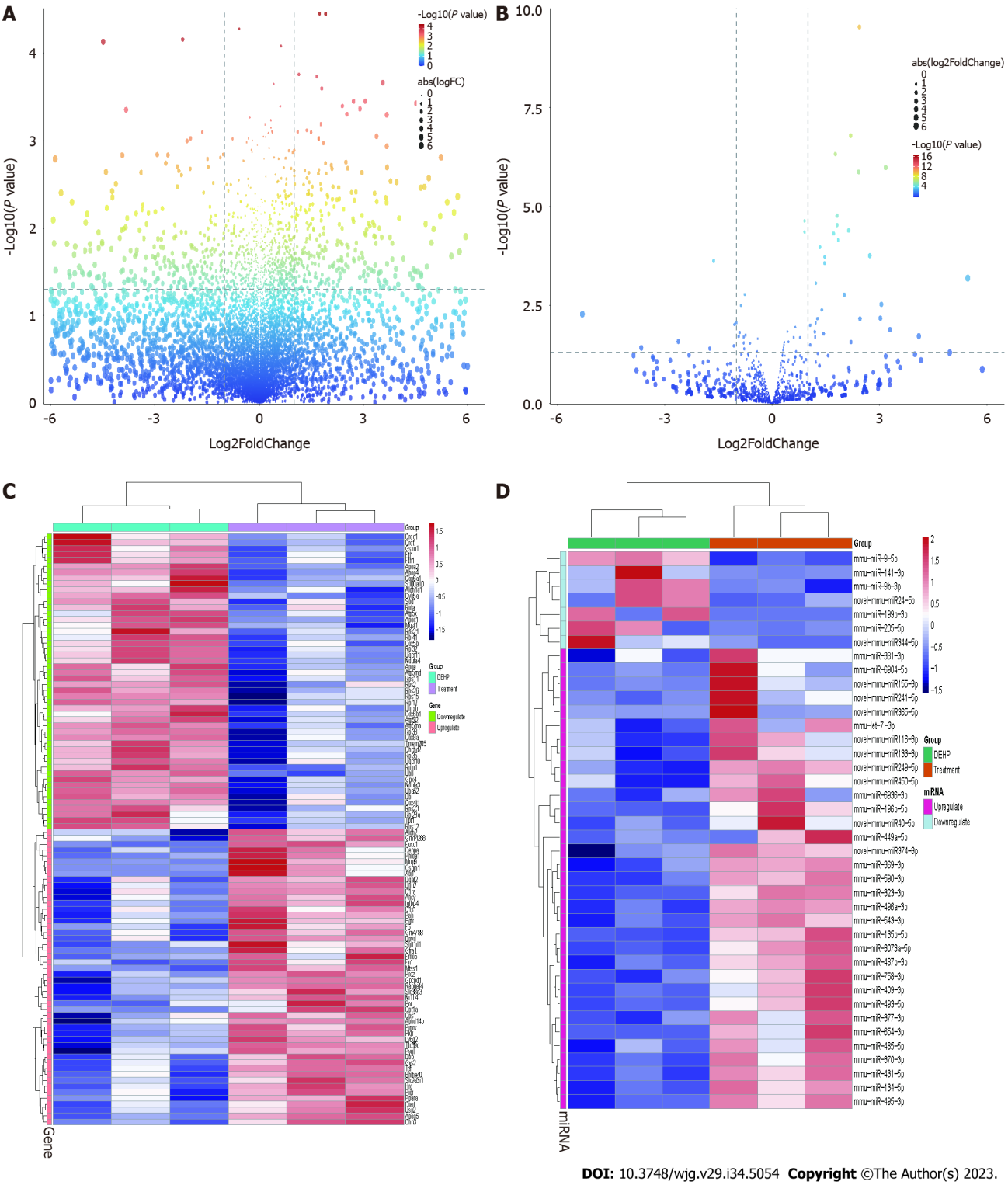
Compared with those in the control group, the differentially expressed mRNAs in the model group were enriched in the following GO terms: BP term: Fatty acid metabolic process, small molecule catabolic process, organic acid catabolic process, and carboxylic acid catabolic process (Figure 7A); CC term: Mitochondrial protein-containing complex, mitochondrial inner membrane, ribosome subunit, and ribosome (Figure 7B); MF term: Ribosome structure, electron transfer activity, oxidoreductase activity, and ubiquitin protein ligase binding (Figure 7C). Additionally, the differentially expressed mRNAs in the model group were enriched in the following KEGG pathways: Fatty acid metabolism, ferroptosis, glutathione metabolism, and PPAR signaling pathway (Figure 7D). Compared with those in the model group, the differentially expressed mRNAs in the treatment group were enriched in the following GO terms: BP term:



DOI: 10.3748/wjg.v29.i34.5054 **Copyright** ©The Author(s) 2023.

Figure 5 Comparative quantitative analysis of transmission electron microscopy results between the control, model, and treatment groups. A: Comparison of transmission electron microscopy results between the control, model, and treatment groups. In the model and control groups, increased numbers of fat droplets with enhanced size were visible. Expanded capillary bile ducts (indicated with orange circles), mildly swollen mitochondria (indicated with orange arrows), and disordered rough endoplasmic reticulum (indicated with yellow arrows) were observed in the model group. In the treatment group, the number of fat droplets decreased, capillary bile ducts appeared mostly healthy (indicated with orange circles), and mitochondrial swelling was reduced (indicated with orange arrows); B: Quantitative analysis of small bile duct diameter in mice from the control, model, and treatment groups. $^{b}P < 0.01$ (compared to the Control group); $^{d}P < 0.01$ (compared to Di (2-ethylhexyl) phthalate group). DEHP: Di (2-ethylhexyl) phthalate.

Mitochondrial organization, proteasome protein catabolic process, and oxidative phosphorylation (Figure 8A); CC term: Ribosome, ribosomal subunit, and large ribosomal subunit (Figure 8B); MF term: Structural constituent of ribosome and molecular carrier activity (Figure 8C). Additionally, the differentially expressed mRNAs in the treatment group were enriched in the following KEGG pathways: Mitochondrial autophagy, glutathione metabolism, oxidative phosphorylation, and drug metabolism (Figure 8D).

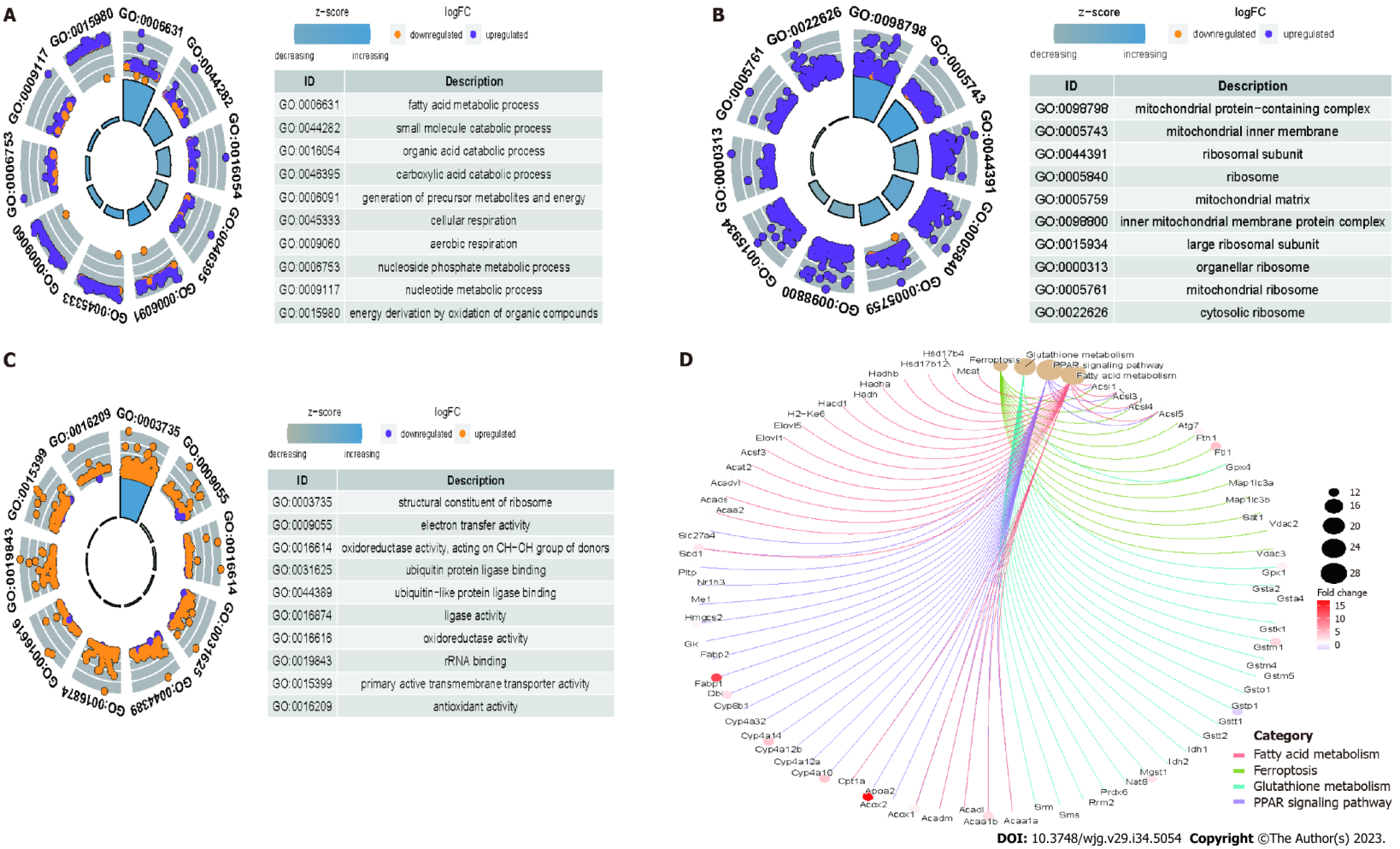


DOI: 10.3748/wjg.v29.i34.5054 **Copyright** ©The Author(s) 2023.

Figure 6 Differential expression of mRNAs and microRNAs between the treatment and model groups. A: The volcano plot of differentially expressed mRNAs between the treatment and model groups. The upper left quadrant and the upper right quadrant in the figure represent downregulated and upregulated mRNAs, respectively; B: The volcano plot of differentially expressed microRNAs (miRNAs) between the treatment and model groups. The upper left quadrant and the upper right quadrant in the figure represent downregulated and upregulated miRNAs, respectively; C: Heatmap shows the 50 mRNAs that exhibited the highest upregulation and downregulation in the treatment group relative to the model group; D: Heatmap shows the miRNAs that exhibited the highest upregulation and downregulation in the treatment group relative to the model group.

Immune infiltration analysis

The proportions and infiltration levels of immune cells in the control, model, and treatment groups are shown in Figure 9A and B. Compared with those in the control group, the infiltration levels of monocytes and immature CD8+ T cells were significantly upregulated and the infiltration levels of immature CD4+ T cells were significantly downregulated in the model group (Figure 9C). Meanwhile, compared with those in the model group, the infiltration levels of



ID	Description
GO:0006631	fatty acid metabolic process
GO:0044282	small molecule catabolic process
GO:0016054	organic acid catabolic process
GO:0046395	carboxylic acid catabolic process
GO:0006091	generation of precursor metabolites and energy
GO:0045333	cellular respiration
GO:0009060	aerobic respiration
GO:0006753	nucleoside phosphate metabolic process
GO:0009117	nucleotide metabolic process
GO:0015980	energy derivation by oxidation of organic compounds

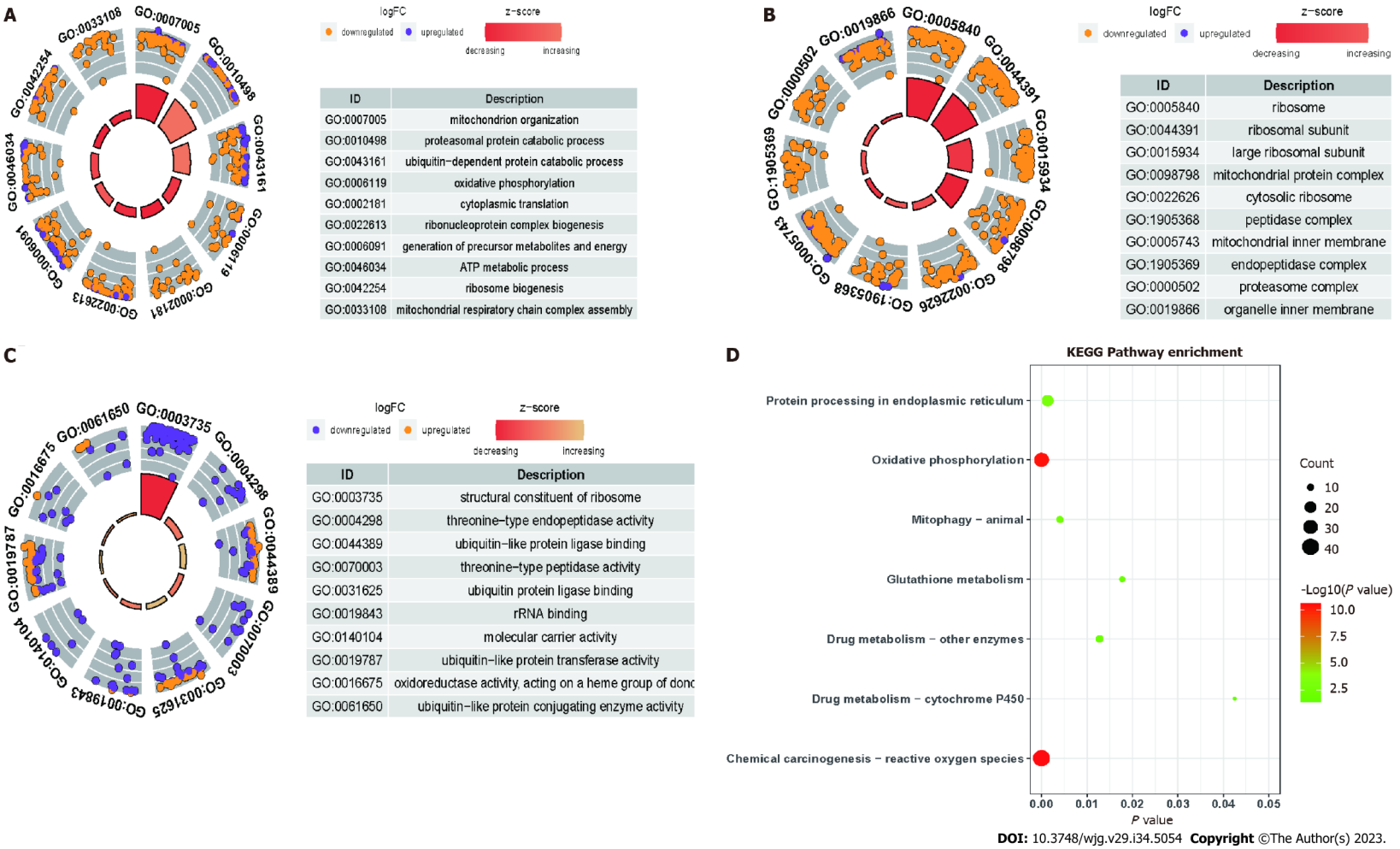
ID	Description
GO:0098798	mitochondrial protein-containing complex
GO:0005743	mitochondrial inner membrane
GO:0044391	ribosomal subunit
GO:0005840	ribosome
GO:0005759	mitochondrial matrix
GO:0098800	inner mitochondrial membrane protein complex
GO:0015934	large ribosomal subunit
GO:0000313	organellar ribosome
GO:0005761	mitochondrial ribosome
GO:0022626	cytosolic ribosome

ID	Description
GO:0003735	structural constituent of ribosome
GO:0009055	electron transfer activity
GO:0016614	oxidoreductase activity, acting on CH-OH group of donors
GO:0031625	ubiquitin protein ligase binding
GO:0044389	ubiquitin-like protein ligase binding
GO:0016874	ligase activity
GO:0016618	oxidoreductase activity
GO:0019843	rRNA binding
GO:0015399	primary active transmembrane transporter activity
GO:0016209	antioxidant activity

DOI: 10.3748/wjg.v29.i34.5054 **Copyright** ©The Author(s) 2023.

Figure 7 The differentially expressed mRNAs between the model and control groups were enriched in different Gene Ontology terms and Kyoto Encyclopedia of Genes and Genomes pathways. A: Biological processes; B: Cellular components; C: Molecular function; D: Kyoto Encyclopedia of Genes and Genomes pathways.

mast cells and active NK cells were significantly upregulated and the infiltration levels of M2 macrophages were significantly downregulated in the treatment group (Figure 9D). The correlation analysis results of various immune cells are shown in Figure 9E.

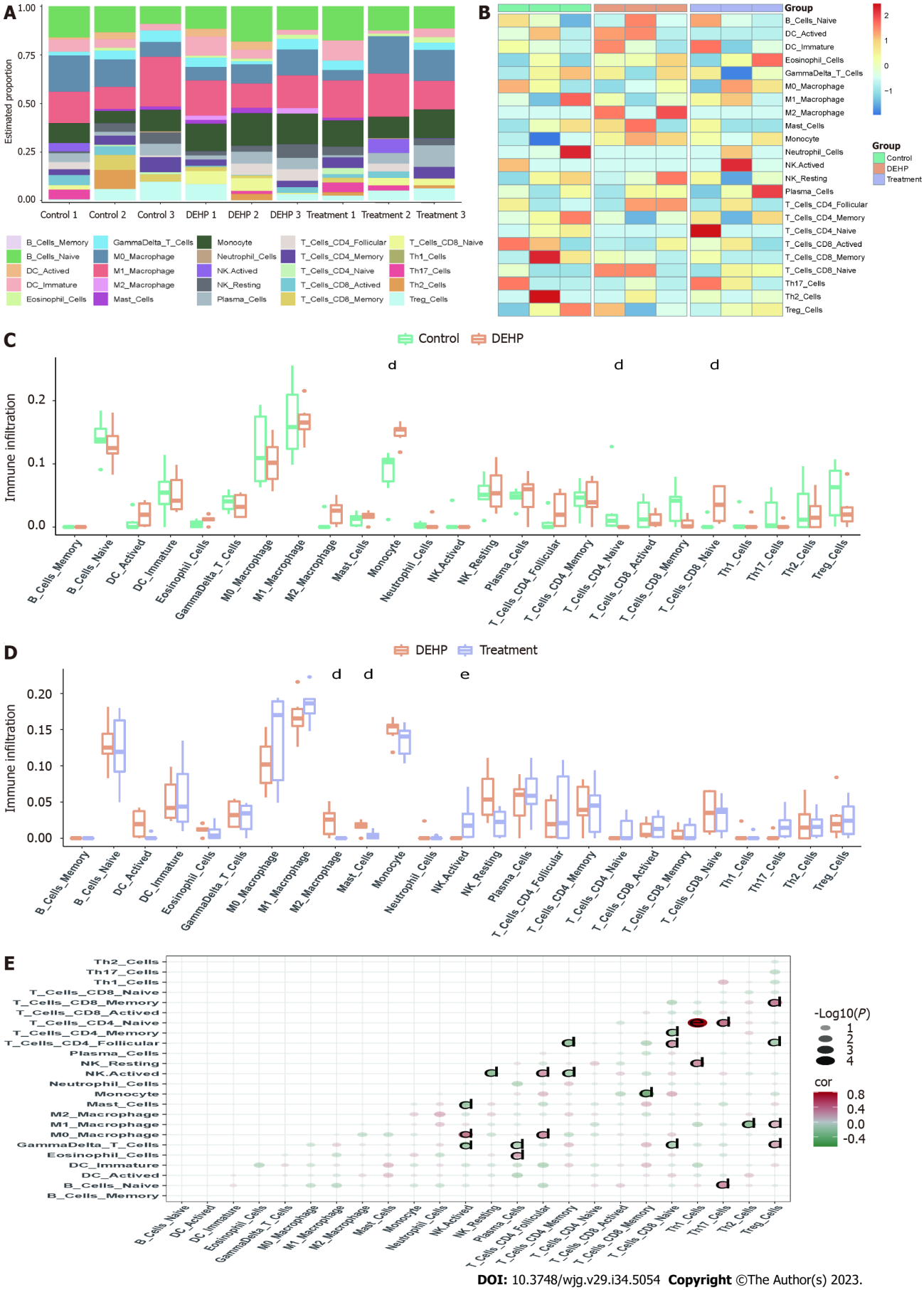


DOI: 10.3748/wjg.v29.i34.5054 **Copyright** ©The Author(s) 2023.

Figure 8 The differentially expressed mRNAs between the treatment and model groups were enriched in different Gene Ontology terms and Kyoto Encyclopedia of Genes and Genomes pathways. A: Biological processes; B: Cellular components; C: Molecular function; D: Kyoto Encyclopedia of Genes and Genomes pathways.

Construction of miRNA-mRNA-protein regulatory axis

Network diagrams (Figure 10A) of upregulated miRNAs and downregulated mRNAs, as well as that of downregulated miRNAs and upregulated mRNAs, in the treatment group were constructed. The data were matched with the miRNA-mRNA regulatory axis in the starBase database to obtain the mmu-miR-141-3p/Zcchc24 and mmu-miR-9-5p/Zbtb7a axes (Figure 10B). Correlation analysis (Figure 10C and D) revealed that the correlation coefficients of mmu-miR-141-3p/



DOI: 10.3748/wjg.v29.i34.5054 **Copyright** ©The Author(s) 2023.

Figure 9 Immune infiltration analyses. A and B: Histograms (A) and heatmaps (B) of the proportions of immune cells in the control, model, and treatment groups; C and D: Analyses of differential immune cell infiltration between the model and control groups (C), as well as between the treatment and model groups (D); E:

Correlation analyses of immune cells in different groups. [d]*P* < 0.01 (compared to Di (2-ethylhexyl) phthalate group); [e]*P* < 0.05 (compared to Oil group). DEHP: Di (2-ethylhexyl) phthalate.

Zcchc24 and mmu-miR-9-5p/Zbtb7a axes were -0.44 and -0.87, respectively. To validate these regulatory axes, the liver tissues of the control, model, and treatment groups were subjected to western blotting (Figure 10E). Compared with that in the model group, the average gray value of Zcchc24 protein was significantly downregulated in the treatment group (Figure 10F), indicating that protein expression changes were consistent with mRNA expression changes. However, Zbtb7a protein expression could not be validated using western blotting or immunohistochemical analysis due to low expression levels. These findings indicate that the mmu-miR-141-3p/*Zcchc24* (mRNA)/Zcchc24 (protein) regulatory axis plays an important role in the protective effects of GTPs on DEHP-induced liver injury in mice (Figure 10G).

DISCUSSION

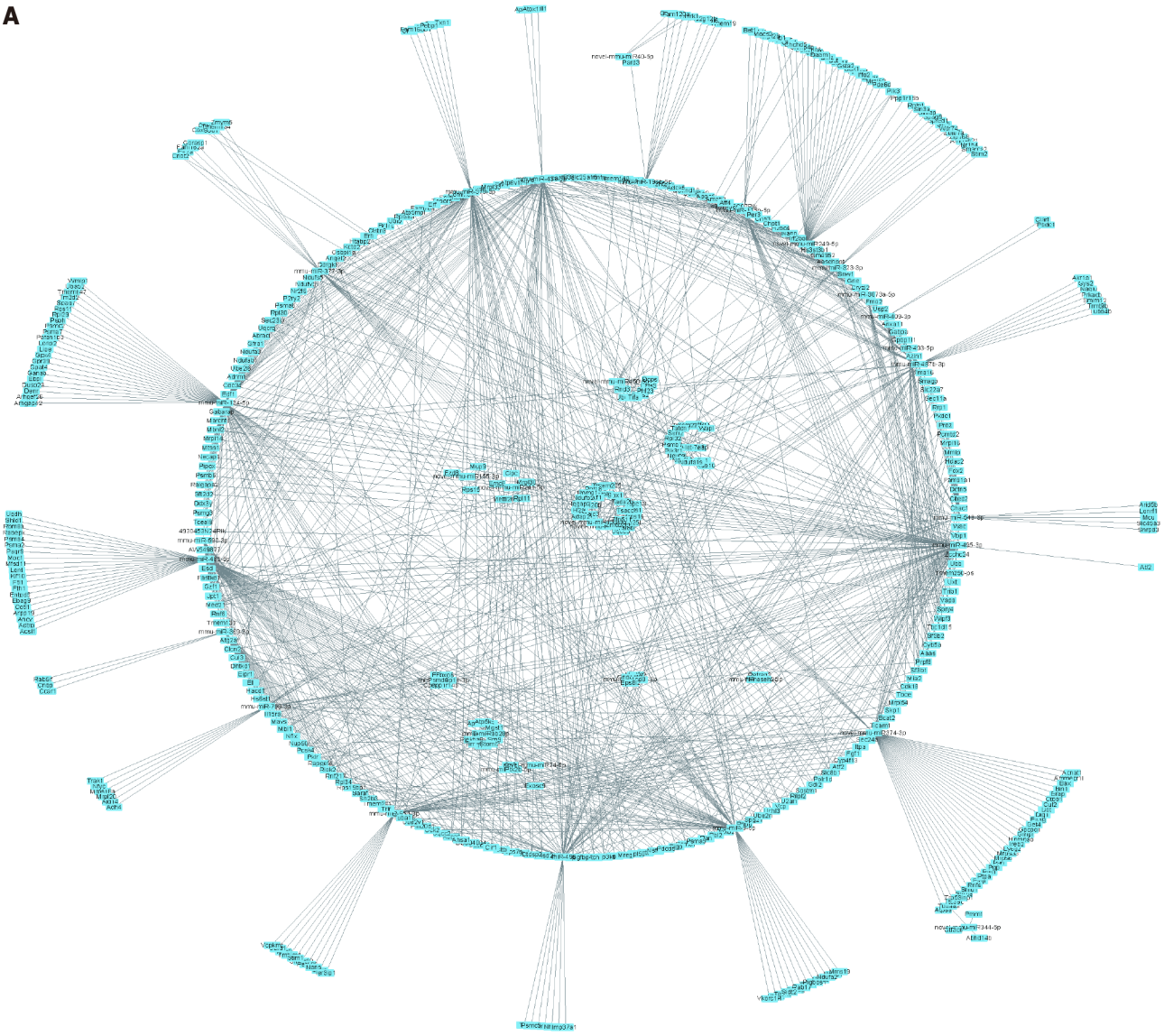
This study aimed to investigate the therapeutic mechanism of GTPs in alleviating DEHP-induced liver dysfunction, blood lipid dysregulation, non-alcoholic fatty liver, and liver fibrosis. Additionally, the role of a miRNA-mRNA-protein regulatory axis in the therapeutic effects of GTPs on DEHP-induced liver damage was elucidated (Figure 11). Thus, the findings of this study provide valuable insights into the potential therapeutic application of GTPs in DEHP-induced liver damage.

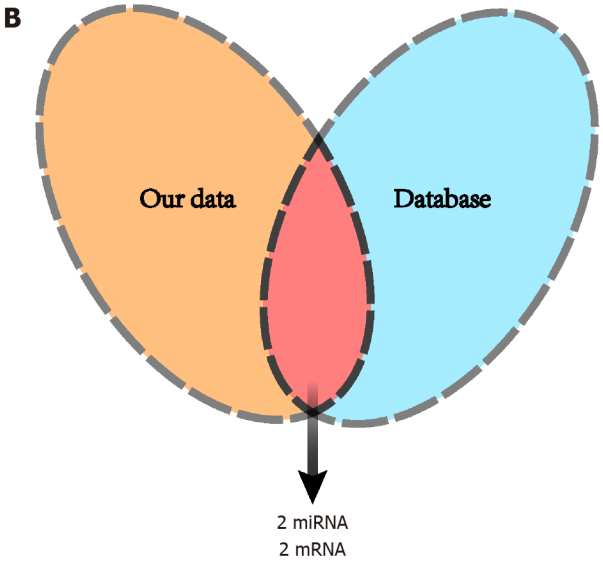
Histopathological analysis revealed that GTPs are effective in mitigating DEHP-induced non-alcoholic fatty liver disease and liver fibrosis in mice. This finding is consistent with that of previous studies, which reported the beneficial effects of GTP on liver health. For example, a meta-analysis[29] of 20 randomized controlled trials with 1536 participants revealed that green tea decreases the levels of total cholesterol and LDL. Zhao *et al*[30] reported that DEHP exposure significantly promotes inflammation, necrosis, and fibrosis in the liver and upregulates the expression of proteins associated with the development of liver inflammation and fibrosis. Kim *et al*[31] suggested that GTPs downregulate the expression of collagen content and type 1 collagen, and consequently alleviate liver fibrosis. Additionally, animal studies [32] have indicated that supplementation of green tea effectively prevented excessive accumulation of visceral and liver lipids, elevated blood glucose levels, and alleviated aberrant blood lipid levels, liver dysfunction, and hepatic steatosis in male C57BL/6 mice fed on a high-fat diet for six weeks as evidenced by the analysis of serum biochemical parameters, histological changes, lipid accumulation, inflammatory cytokines, and related indices. These findings further indicated the therapeutic potential of GTPs in liver-related conditions.

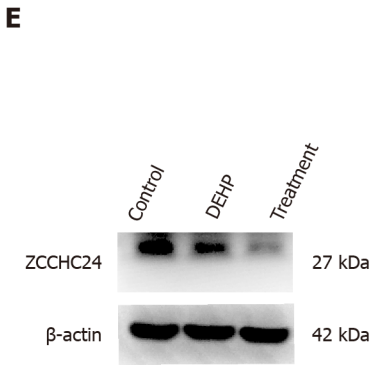
In this study, GTPs were found to ameliorate the DEHP-induced pathological damage to the liver microstructures, including the mitochondria, endoplasmic reticulum, and capillary bile ducts. These findings are consistent with those of previous studies, which reported the adverse effects of DEHP on liver microstructures. For instance, an animal study[33] indicated that DEHP induced mitochondrial and endoplasmic reticulum ultrastructural damages, characterized by increased fission and decreased fusion. Furthermore, Sun *et al*[34] suggested that DEHP promoted mitochondrial-associated endoplasmic reticulum membrane disruption, potentially through endoplasmic reticulum unfolded protein response, to induce endoplasmic reticulum stress. Consistent with the results of this study, in vitro and *in vivo* experimental studies[35] have demonstrated that GTPs effectively alleviate acetaminophen-induced liver damage and mitochondrial dysfunction. These studies have shown that GTPs possess antioxidant capacity and can prevent liver mitochondrial damage. Specifically, GTPs have been found to enhance the membrane potential and activity of liver mitochondrial respiratory chain complexes, thereby protecting against mitochondrial dysfunction. However, further research is needed to fully elucidate the underlying mechanisms and to explore the clinical applications of GTPs in protecting liver microstructures from DEHP-induced damage.

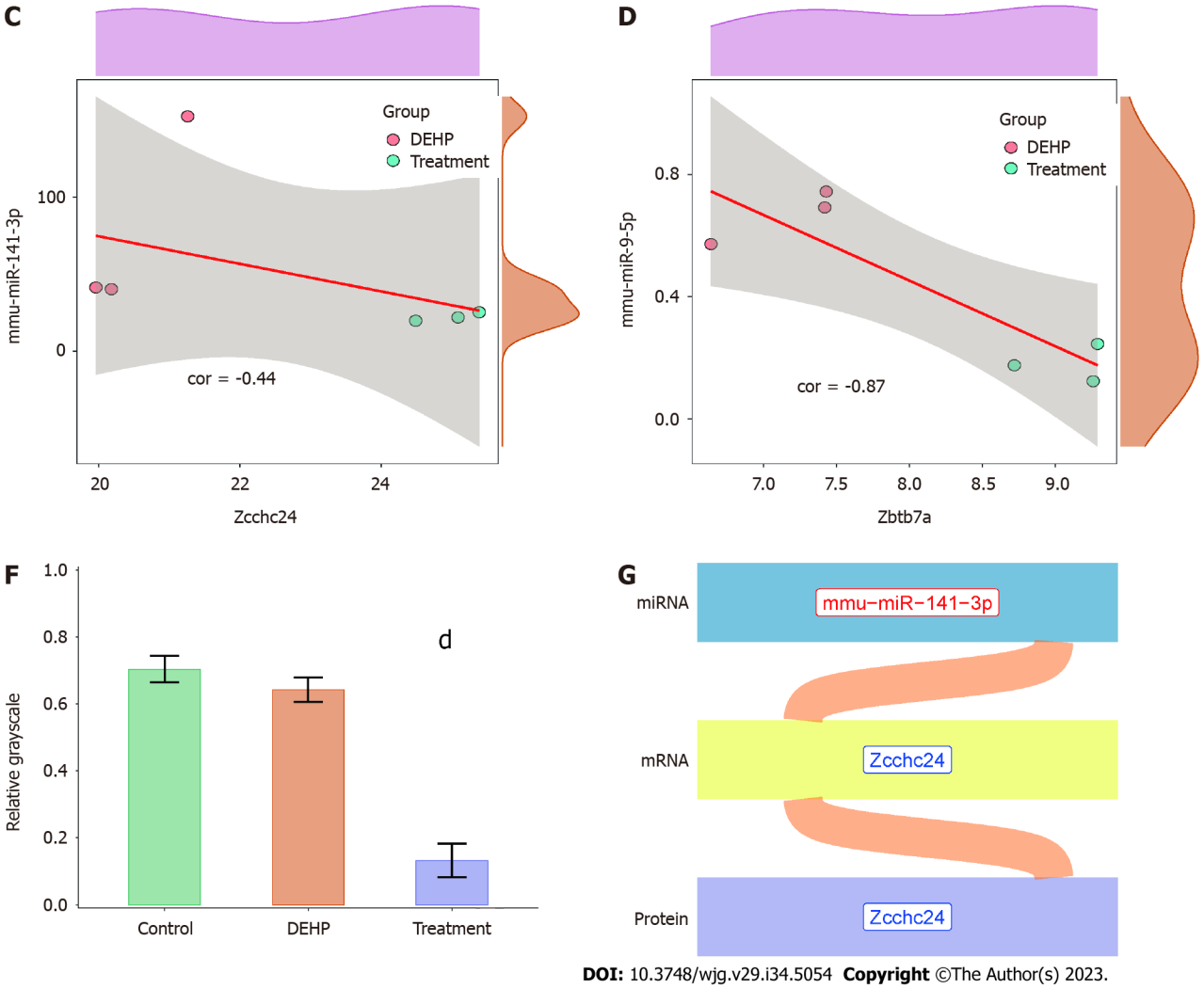
In this study, we aimed to analyze the signaling pathways involved in DEHP-induced liver damage and the hepatoprotective effects of GTPs using high-throughput sequencing. Ferroptosis, a recently discovered non-apoptotic cell death process, is induced by intracellular iron-dependent lipid peroxidation damage. Consistent with the findings of this study, Yin *et al*[36] investigated the acute toxicity of DEHP exposure in marine medaka. They conducted transcriptome analysis on the liver of DEHP-exposed medaka and reported that females were more sensitive to the immune response than males under acute DEHP exposure conditions. Furthermore, they found that DEHP exposure promoted iron depletion, leading to iron overload, increased levels of MDA and lipid peroxidation, and decreased levels of glutathione. These findings suggest that DEHP can rapidly alter certain molecular regulatory patterns and induce cell death through ferroptosis. In addition, we discussed the PPAR signaling pathway, which is a classic pathway associated with hyperlipidemia, regulates lipid metabolism and blood lipid levels by mediating various biological functions, such as the synthesis and decomposition of cholesterol and the oxidation of fatty acids[37]. Previous studies[38,39] have revealed that DEHP exposure dysregulates blood lipid levels and hepatic lipid metabolism in mice through the PPAR signaling pathway.

In this study, we utilized the CIBERSORT algorithm to identify specific alterations in immune cells. Consistent with the findings of this study, Yang *et al*[40] investigated the effect of DEHP on the immune system of male C57Bl/6 mice and reported significant atrophy of the thymus and spleen with the proportions of immature CD4+ and CD8+ populations exhibiting the highest downregulation. Additionally, they found a downregulation in the number of T and B cells in the spleen. A previous study[41] reported that green tea extract promotes macrophage phagocytic activity at a dosage of 5 mg/kg bodyweight and enhances NK cell activity and T cell proliferation at a dosage of 40 mg/kg bodyweight, supporting the potential immunomodulatory effects of GTPs demonstrated in this study.


A


B
Our data
Database
2 miRNA
2 mRNA


E
Control
DEHP
Treatment
ZCCHC24
27 kDa
β-actin
42 kDa



DOI: 10.3748/wjg.v29.i34.5054 **Copyright** ©The Author(s) 2023.

Figure 10 Construction of the microRNA-mRNA-protein regulatory axis. A: The network diagram was constructed using differentially expressed mRNAs and microRNAs (miRNAs); B: Wayne diagram indicating the intersection of the miRNA-mRNA regulatory axis and mouse interaction network from the starBase database; C: Correlation analyses of mmu-miR-141-3p and Zcchc24; D: Correlation analyses of mmu-miR-9-5p and Zbtb7a; E: Western blotting validation of Zcchc24 protein expression in the control, model, and treatment groups; F: Semiquantitative analysis of Zcchc24 protein levels in the control, model, and treatment groups; G: The Sankey plot of the miRNA-mRNA-protein regulatory axes mediating the suppressive effects of green tea polyphenols (GTPs) on di-(2-ethylhexyl) phthalate (DEHP)-induced liver damage in mice. Red and blue fonts indicate upregulated and downregulated expression, respectively. $^{d}P < 0.01$ (compared to DEHP group). DEHP: Di (2-ethylhexyl) phthalate; GTPs: Green tea polyphenols.

This study identified the mmu-miR-141-3p/*Zcchc24* (mRNA)/Zcchc24 (protein) regulatory axis, which exerted its function through Zcchc24. *Zcchc24* is reported to be involved in cell differentiation in mice. Previous studies[42] have suggested that *Zcchc24* can serve as a key gene in liver cancer prediction models, which are used to predict patient survival time. Additionally, *Zcchc24* is one of the major selective splicing factors that plays a critical role in cell fate transition, development, and disease progression.

This study has several limitations. In this study, three samples per group were analyzed using high-throughput sequencing, which may have yielded biased results. Additionally, the levels of immune cells in each group were determined using the CIBERSORT algorithm. However, immune cell infiltration was not verified using alternate methods, such as single-cell sequencing. Furthermore, the importance of *Zcchc24* was not verified using knockdown or overexpression experiments.

CONCLUSION

In conclusion, this study demonstrated that GTPs can alleviate the DEHP-induced changes in liver function and lipid profiles, improve fatty liver disease and partial liver fibrosis, and regulate immune cell infiltration. Additionally, an important miRNA-mRNA-protein molecular regulation axis that plays a crucial role in the therapeutic effects of GTPs on DEHP-induced liver damage was validated.

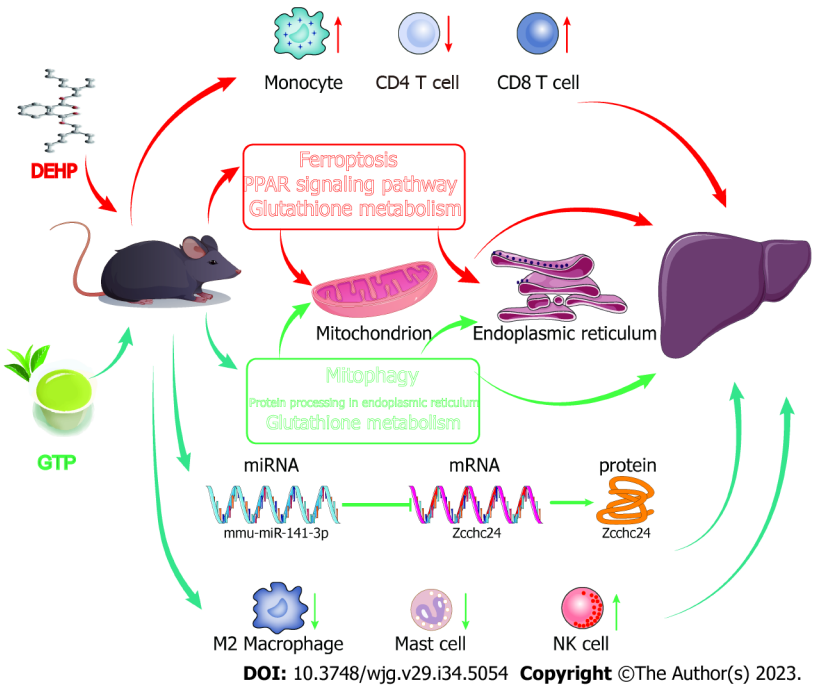


Figure 11 Mechanisms underlying di-(2-ethylhexyl) phthalate exposure-induced liver injury and the therapeutic effects of green tea polyphenols on Di (2-ethylhexyl) phthalate-indued liver injury. DEHP: Di (2-ethylhexyl) phthalate; GTPs: Green tea polyphenols.

ARTICLE HIGHLIGHTS

Research background

Di (2-ethylhexyl) phthalate (DEHP) is a widely used plasticizer that has been shown to cause liver injury. Previous studies have reported the therapeutic effects of green tea on organ damage caused by heavy metal exposure. However, there is limited research on the therapeutic effects of green tea polyphenols (GTPs) specifically on DEHP-induced liver damage.

Research motivation

Despite the known therapeutic effects of green tea on heavy metal exposure-induced organ damage, there is a lack of studies investigating the specific therapeutic effects of GTPs on DEHP-induced liver damage.

Research objectives

The research objectives of this study were to evaluate the molecular mechanism underlying the therapeutic effects of GTPs on DEHP-induced liver damage.

Research methods

In this study, C57BL/6J mice were divided into different groups and treated with DEHP and GTPs. After 8 wk, various assessments were conducted, including examination of liver function, blood lipid profile, and liver histopathology. High-throughput sequencing was used to analyze differentially expressed miRNAs and mRNAs in the liver tissues. Functional enrichment analysis and immune infiltration prediction were performed, and the miRNA-mRNA regulatory axis was elucidated using the starBase database. Protein expression was evaluated using immunohistochemistry.

Research results

The results of this study showed that GTPs had beneficial effects on DEHP-induced liver damage in mice. GTPs alleviated liver dysfunction, blood lipid dysregulation, fatty liver disease, liver fibrosis, and mitochondrial and endoplasmic reticulum lesions. The infiltration of immune cells, such as macrophages, mast cells, and natural killer cells, varied between the model and treatment groups. Furthermore, the study identified specific miRNAs, mRNAs, and proteins that constituted a regulatory axis involved in mediating the therapeutic effects of GTPs on DEHP-induced liver damage.

Research conclusions

The findings of this study indicate that GTPs have a therapeutic effect on DEHP-induced liver damage. GTPs were shown to alleviate liver dysfunction, blood lipid dysregulation, fatty liver disease, and partial liver fibrosis. Additionally, GTPs were found to regulate immune cell infiltration. The study also identified a significant miRNA-mRNA-protein regulatory axis involved in mediating the therapeutic effects of GTPs on DEHP-induced liver damage.

Research perspectives

Further studies are needed to investigate the long-term effects of GTPs on DEHP-induced liver damage and to explore the potential mechanisms underlying the regulation of immune cell infiltration. Additionally, future research should focus on optimizing the dosage and administration of GTPs to maximize their therapeutic effects and minimize potential side effects. Furthermore, clinical trials are warranted to evaluate the efficacy and safety of GTPs as a potential therapeutic intervention for DEHP-induced liver damage in humans.

ACKNOWLEDGEMENTS

We thank Bullet Edits Limited for the linguistic editing and proofreading of the manuscript. We also thank Figraw (www.figdraw.com) for the materials provided in the scientific research drawing.

FOOTNOTES

Author contributions: Shi H performed the conceptualization, software, data curation, software, writing; Zhao XH, Zhou XL, Sun CC, Cao QY, and Zhu SP contributed to the supervision and writing; Liu SS contributed to the pathology and analysis; Sun SY performed the review, editing, and supervision; all authors approved the final version of the article.

Supported by Guangdong Provincial Department of Science and Technology, Science and Technology Plan Project, Journal of Jinan University High-Level Science and Technology Journal Construction Project, No. 2021B121020012; and Guangdong Provincial Administration of Traditional Chinese Medicine, Traditional Chinese Medicine Research Project, No. 20213005.

Institutional review board statement: The study does not include Human subject research.

Institutional animal care and use committee statement: All animal experiments conformed to the internationally accepted principles for the care and use of laboratory animals (licence No. IACUC-20210630-15; protocol no. 2021621-01, The Laboratory Animal Welfare and Ethic Commettee, Jinan University, Guangzhou, China).

Conflict-of-interest statement: The authors declare no competing financial interest.

Data sharing statement: The data that support the findings of this study are openly available in the NCBI GEO database at https://www.ncbi.nlm.nih.gov/geo/ with the accession number: GSE232128.

ARRIVE guidelines statement: The authors have read the ARRIVE guidelines, and the manuscript was prepared and revised according to the ARRIVE guidelines.

Open-Access: This article is an open-access article that was selected by an in-house editor and fully peer-reviewed by external reviewers. It is distributed in accordance with the Creative Commons Attribution NonCommercial (CC BY-NC 4.0) license, which permits others to distribute, remix, adapt, build upon this work non-commercially, and license their derivative works on different terms, provided the original work is properly cited and the use is non-commercial. See: https://creativecommons.org/Licenses/by-nc/4.0/

Country/Territory of origin: China

ORCID number: Qin Peng 0000-0001-6243-3416; Sheng-Yun Sun 0000-0002-0374-8482.

S-Editor: Fan JR
L-Editor: A
P-Editor: Yuan YY

REFERENCES

1 **Liu Y**, Guo Z, Zhu R, Gou D, Jia PP, Pei DS. An insight into sex-specific neurotoxicity and molecular mechanisms of DEHP: A critical review. *Environ Pollut* 2023; **316**: 120673 [PMID: 36400143 DOI: 10.1016/j.envpol.2022.120673]

2 **Erythropel HC**, Maric M, Nicell JA, Leask RL, Yargeau V. Leaching of the plasticizer di(2-ethylhexyl)phthalate (DEHP) from plastic containers and the question of human exposure. *Appl Microbiol Biotechnol* 2014; **98**: 9967-9981 [PMID: 25376446 DOI: 10.1007/s00253-014-6183-8]

3 **Silva MJ**, Wong LY, Samandar E, Preau JL, Calafat AM, Ye X. Exposure to di-2-ethylhexyl terephthalate in a convenience sample of U.S. adults from 2000 to 2016. *Arch Toxicol* 2017; **91**: 3287-3291 [PMID: 28314884 DOI: 10.1007/s00204-017-1956-3]

4 **Kavlock R**, Boekelheide K, Chapin R, Cunningham M, Faustman E, Foster P, Golub M, Henderson R, Hinberg I, Little R, Seed J, Shea K, Tabacova S, Tyl R, Williams P, Zacharewski T. NTP Center for the Evaluation of Risks to Human Reproduction: phthalates expert panel report on the reproductive and developmental toxicity of di-n-octyl phthalate. *Reprod Toxicol* 2002; **16**: 721-734 [PMID: 12406498 DOI: 10.1016/s0890-6238(02)00031-x]

5 **Chen L**, Zhao Y, Li L, Chen B, Zhang Y. Exposure assessment of phthalates in non-occupational populations in China. *Sci Total Environ* 2012; **427-428**: 60-69 [PMID: 22578696 DOI: 10.1016/j.scitotenv.2012.03.090]

6 **Matsumoto M**, Hirata-Koizumi M, Ema M. Potential adverse effects of phthalic acid esters on human health: a review of recent studies on reproduction. *Regul Toxicol Pharmacol* 2008; **50**: 37-49 [PMID: 17983696 DOI: 10.1016/j.yrtph.2007.09.004]

7 **Jadeja RN**, Urrunaga NH, Dash S, Khurana S, Saxena NK. Withaferin-A Reduces Acetaminophen-Induced Liver Injury in Mice. *Biochem Pharmacol* 2015; **97**: 122-132 [PMID: 26212553 DOI: 10.1016/j.bcp.2015.07.024]

8 **Chen H**, Zhang W, Rui BB, Yang SM, Xu WP, Wei W. Di(2-ethylhexyl) phthalate exacerbates non-alcoholic fatty liver in rats and its potential mechanisms. *Environ Toxicol Pharmacol* 2016; **42**: 38-44 [PMID: 26773359 DOI: 10.1016/j.etap.2015.12.016]

9 **Yang G**, Zhang W, Qin Q, Wang J, Zheng H, Xiong W, Yuan J. Mono(2-ethylhexyl) phthalate induces apoptosis in p53-silenced L02 cells *via* activation of both mitochondrial and death receptor pathways. *Environ Toxicol* 2015; **30**: 1178-1191 [PMID: 24706461 DOI: 10.1002/tox.21990]

10 **Isenberg JS**, Kamendulis LM, Smith JH, Ackley DC, Pugh G Jr, Lington AW, Klaunig JE. Effects of Di-2-ethylhexyl phthalate (DEHP) on gap-junctional intercellular communication (GJIC), DNA synthesis, and peroxisomal beta oxidation (PBOX) in rat, mouse, and hamster liver. *Toxicol Sci* 2000; **56**: 73-85 [PMID: 10869455 DOI: 10.1093/toxsci/56.1.73]

11 **Ray PD**, Huang BW, Tsuji Y. Reactive oxygen species (ROS) homeostasis and redox regulation in cellular signaling. *Cell Signal* 2012; **24**: 981-990 [PMID: 22286106 DOI: 10.1016/j.cellsig.2012.01.008]

12 **Santhosh A**, Nair KG, Arun P, Deepadevi KV, Manojkumar V, Lakshmi LR, Kurup PA. Effect of DEHP [di-(2-ethyl hexyl) phthalate] on lipid peroxidation in liver in rats and in primary cultures of rat hepatocytes. *Indian J Med Res* 1998; **108**: 17-23 [PMID: 9745214]

13 **Ghosh J**, Das J, Manna P, Sil PC. Hepatotoxicity of di-(2-ethylhexyl)phthalate is attributed to calcium aggravation, ROS-mediated mitochondrial depolarization, and ERK/NF-κB pathway activation. *Free Radic Biol Med* 2010; **49**: 1779-1791 [PMID: 20854900 DOI: 10.1016/j.freeradbiomed.2010.09.011]

14 **Afzal M**, Safer AM, Menon M. Green tea polyphenols and their potential role in health and disease. *Inflammopharmacology* 2015; **23**: 151-161 [PMID: 26164000 DOI: 10.1007/s10787-015-0236-1]

15 **Mukhtar H**, Ahmad N. Tea polyphenols: prevention of cancer and optimizing health. *Am J Clin Nutr* 2000; **71**: 1698S-702S; discussion 1703S [PMID: 10837321 DOI: 10.1093/ajcn/71.6.1698S]

16 **Nagao T**, Hase T, Tokimitsu I. A green tea extract high in catechins reduces body fat and cardiovascular risks in humans. *Obesity (Silver Spring)* 2007; **15**: 1473-1483 [PMID: 17557985 DOI: 10.1038/oby.2007.176]

17 **Huang J**, Wang Y, Xie Z, Zhou Y, Zhang Y, Wan X. The anti-obesity effects of green tea in human intervention and basic molecular studies. *Eur J Clin Nutr* 2014; **68**: 1075-1087 [PMID: 25074392 DOI: 10.1038/ejcn.2014.143]

18 **Zwolak I**. Epigallocatechin Gallate for Management of Heavy Metal-Induced Oxidative Stress: Mechanisms of Action, Efficacy, and Concerns. *Int J Mol Sci* 2021; **22** [PMID: 33919748 DOI: 10.3390/ijms22084027]

19 **Zhao Z**, Lin CY, Cheng K. siRNA- and miRNA-based therapeutics for liver fibrosis. *Transl Res* 2019; **214**: 17-29 [PMID: 31476281 DOI: 10.1016/j.trsl.2019.07.007]

20 **El-Maraghy SA**, Adel O, Zayed N, Yosry A, El-Nahaas SM, Gibriel AA. Circulatory miRNA-484, 524, 615 and 628 expression profiling in HCV mediated HCC among Egyptian patients; implications for diagnosis and staging of hepatic cirrhosis and fibrosis. *J Adv Res* 2020; **22**: 57-66 [PMID: 31956442 DOI: 10.1016/j.jare.2019.12.002]

21 **Lin Q**, Zhou CR, Bai MJ, Zhu D, Chen JW, Wang HF, Li MA, Wu C, Li ZR, Huang MS. Exosome-mediated miRNA delivery promotes liver cancer EMT and metastasis. *Am J Transl Res* 2020; **12**: 1080-1095 [PMID: 32269736]

22 **Sanjay S**, Girish C. Role of miRNA and its potential as a novel diagnostic biomarker in drug-induced liver injury. *Eur J Clin Pharmacol* 2017; **73**: 399-407 [PMID: 28028586 DOI: 10.1007/s00228-016-2183-1]

23 **Hou P**, Dai W, Jin Y, Zhao F, Liu J, Liu H. Maternal exposure to di-2-ethylhexyl phthalate (DEHP) depresses lactation capacity in mice. *Sci Total Environ* 2022; **837**: 155813 [PMID: 35550907 DOI: 10.1016/j.scitotenv.2022.155813]

24 **XueXia L**, YaNan L, Zi T, YuSheng Z, ZeLin W, Peng Z, MeiNa X, FuJun L. Di-2-ethylhexyl phthalate (DEHP) exposure induces sperm quality and functional defects in mice. *Chemosphere* 2023; **312**: 137216 [PMID: 36372335 DOI: 10.1016/j.chemosphere.2022.137216]

25 **Zhou X**, Zhang Z, Shi H, Liu Q, Chang Y, Feng W, Zhu S, Sun S. Effects of Lycium barbarum glycopeptide on renal and testicular injury induced by di(2-ethylhexyl) phthalate. *Cell Stress Chaperones* 2022; **27**: 257-271 [PMID: 35362893 DOI: 10.1007/s12192-022-01266-0]

26 **Abdelrazek HM**, Helmy SA, Elsayed DH, Ebaid HM, Mohamed RM. Ameliorating effects of green tea extract on cadmium induced reproductive injury in male Wistar rats with respect to androgen receptors and caspase- 3. *Reprod Biol* 2016; **16**: 300-308 [PMID: 27840064 DOI: 10.1016/j.repbio.2016.11.001]

27 **Newman AM**, Liu CL, Green MR, Gentles AJ, Feng W, Xu Y, Hoang CD, Diehn M, Alizadeh AA. Robust enumeration of cell subsets from tissue expression profiles. *Nat Methods* 2015; **12**: 453-457 [PMID: 25822800 DOI: 10.1038/nmeth.3337]

28 **Chen Z**, Huang A, Sun J, Jiang T, Qin FX, Wu A. Inference of immune cell composition on the expression profiles of mouse tissue. *Sci Rep* 2017; **7**: 40508 [PMID: 28084418 DOI: 10.1038/srep40508]

29 **Onakpoya I**, Spencer E, Heneghan C, Thompson M. The effect of green tea on blood pressure and lipid profile: a systematic review and meta-analysis of randomized clinical trials. *Nutr Metab Cardiovasc Dis* 2014; **24**: 823-836 [PMID: 24675010 DOI: 10.1016/j.numecd.2014.01.016]

30 **Zhao ZB**, Ji K, Shen XY, Zhang WW, Wang R, Xu WP, Wei W. Di(2-ethylhexyl) phthalate promotes hepatic fibrosis by regulation of oxidative stress and inflammation responses in rats. *Environ Toxicol Pharmacol* 2019; **68**: 109-119 [PMID: 30884453 DOI: 10.1016/j.etap.2019.03.008]

31 **Kim HK**, Yang TH, Cho HY. Antifibrotic effects of green tea on in vitro and in vivo models of liver fibrosis. *World J Gastroenterol* 2009; **15**: 5200-5205 [PMID: 19891020 DOI: 10.3748/wjg.15.5200]

32 **Zhou J**, Yu Y, Ding L, Xu P, Wang Y. Matcha Green Tea Alleviates Non-Alcoholic Fatty Liver Disease in High-Fat Diet-Induced Obese Mice by Regulating Lipid Metabolism and Inflammatory Responses. *Nutrients* 2021; **13** [PMID: 34204055 DOI: 10.3390/nu13061950]

33 **Zhao Y**, Cui JG, Zhang H, Li XN, Li MZ, Talukder M, Li JL. Role of mitochondria-endoplasmic reticulum coupling in lycopene preventing DEHP-induced hepatotoxicity. *Food Funct* 2021; **12**: 10741-10749 [PMID: 34608470 DOI: 10.1039/d1fo00478f]

34 **Sun X**, Lin Y, Huang Q, Shi J, Qiu L, Kang M, Chen Y, Fang C, Ye T, Dong S. Di(2-ethylhexyl) phthalate-induced apoptosis in rat INS-1 cells is dependent on activation of endoplasmic reticulum stress and suppression of antioxidant protection. *J Cell Mol Med* 2015; **19**: 581-594 [PMID: 25418486 DOI: 10.1111/jcmm.12409]

35 **Lin Y**, Huang J, Gao T, Wu Y, Huang D, Yan F, Weng Z. Preliminary Study on Hepatoprotective Effect and Mechanism of (-)-

Epigallocatechin-3-gallate against Acetaminophen-induced Liver Injury in Rats. *Iran J Pharm Res* 2021; **20**: 46-56 [PMID: 34903968 DOI: 10.22037/ijpr.2020.112727.13918]

36 **Yin X**, Zeb R, Wei H, Cai L. Acute exposure of di(2-ethylhexyl) phthalate (DEHP) induces immune signal regulation and ferroptosis in oryzias melastigma. *Chemosphere* 2021; **265**: 129053 [PMID: 33272674 DOI: 10.1016/j.chemosphere.2020.129053]

37 **Giordano Attianese GM**, Desvergne B. Integrative and systemic approaches for evaluating PPARβ/δ (PPARD) function. *Nucl Recept Signal* 2015; **13**: e001 [PMID: 25945080 DOI: 10.1621/nrs.13001]

38 **Zhang Y**, Ge S, Yang Z, Li Z, Gong X, Zhang Q, Dong W, Dong C. Disturbance of di-(2-ethylhexyl) phthalate in hepatic lipid metabolism in rats fed with high fat diet. *Food Chem Toxicol* 2020; **146**: 111848 [PMID: 33166671 DOI: 10.1016/j.fct.2020.111848]

39 **Xu M**, Li Y, Wang X, Zhang Q, Wang L, Zhang X, Cui W, Han X, Ma N, Li H, Fang H, Tang S, Li J, Liu Z, Yang H, Jia X. Role of Hepatocyte- and Macrophage-Specific PPARγ in Hepatotoxicity Induced by Diethylhexyl Phthalate in Mice. *Environ Health Perspect* 2022; **130**: 17005 [PMID: 35019730 DOI: 10.1289/EHP9373]

40 **Yang Q**, Xie Y, Depierre JW. Effects of peroxisome proliferators on the thymus and spleen of mice. *Clin Exp Immunol* 2000; **122**: 219-226 [PMID: 11091278 DOI: 10.1046/j.1365-2249.2000.01367.x]

41 **Huang AC**, Cheng HY, Lin TS, Chen WH, Lin JH, Lin JJ, Lu CC, Chiang JH, Hsu SC, Wu PP, Huang YP, Chung JG. Epigallocatechin gallate (EGCG), influences a murine WEHI-3 leukemia model in vivo through enhancing phagocytosis of macrophages and populations of T- and B-cells. *In Vivo* 2013; **27**: 627-634 [PMID: 23988898]

42 **Apizi A**, Wang L, Wusiman L, Song E, Han Y, Jia T, Zhang W. Establishment and verification of a prognostic model of liver cancer by RNA-binding proteins based on the TCGA database. *Transl Cancer Res* 2022; **11**: 1925-1937 [PMID: 36249884 DOI: 10.21037/tcr-21-2820]

World Journal of Gastroenterology

Submit a Manuscript: https://www.f6publishing.com

World J Gastroenterol 2023 September 14; 29(34): 5075-5081

DOI: 10.3748/wjg.v29.i34.5075

ISSN 1007-9327 (print) ISSN 2219-2840 (online)

ORIGINAL ARTICLE

Retrospective Study

Role of biochemical markers and autoantibodies in diagnosis of early-stage primary biliary cholangitis

Yu-Jin Zhu, Jing Li, Yong-Gang Liu, Yong Jiang, Xiao-Jing Cheng, Xu Han, Chun-Yan Wang, Jia Li

Specialty type: Gastroenterology and hepatology

Provenance and peer review: Unsolicited article; Externally peer reviewed.

Peer-review model: Single blind

Peer-review report's scientific quality classification

Grade A (Excellent): 0
Grade B (Very good): B, B
Grade C (Good): 0
Grade D (Fair): 0
Grade E (Poor): 0

P-Reviewer: Filipec Kanizaj T, Croatia; Granito A, Italy

Received: June 4, 2023
Peer-review started: June 4, 2023
First decision: June 21, 2023
Revised: July 15, 2023
Accepted: August 25, 2023
Article in press: August 25, 2023
Published online: September 14, 2023

Yu-Jin Zhu, Jing Li, Graduate School, Tianjin Medical University, Tianjin 300041, China

Yong-Gang Liu, Department of Pathology, Clinical School of the Second People's Hospital, Tianjin 300110, China

Yong Jiang, Department of Gastroenterology, The Second Hospital of Tianjin Medical University, Tianjin 300211, China

Xiao-Jing Cheng, Xu Han, Chun-Yan Wang, Jia Li, Department of Gastroenterology, Clinical School of the Second People's Hospital, Tianjin 300110, China

Corresponding author: Chun-Yan Wang, Doctor, Chief Doctor, Department of Gastroenterology, Clinical School of the Second People's Hospital, No. 7 Sudi South Road, Nankai District, Tianjin 300110, China. wangchunyan123@tmu.edu.cn

Abstract

BACKGROUND

Primary biliary cholangitis (PBC) is a chronic progressive autoimmune cholestatic disease. The main target organ of PBC is the liver, and nonsuppurative inflammation of the small intrahepatic bile ducts may eventually develop into cirrhosis or liver fibrosis.

AIM

To explore the clinical characteristics of early-stage PBC, identify PBC in the early clinical stage, and promptly treat and monitor PBC.

METHODS

The data of 82 patients with PBC confirmed by pathology at Tianjin Second People's Hospital from January 2013 to November 2021 were collected, and the patients were divided into stage I, stage II, stage III, and stage IV according to the pathological stage. The general data, serum biochemistry, immunoglobulins, and autoimmune antibodies of patients in each stage were retrospectively analyzed.

RESULTS

In early-stage (stages I + II) PBC patients, 50.0% of patients had normal alanine aminotransferase (ALT) levels, and 37.5% had normal aspartate aminotransferase (AST) levels. For the remaining patients, the ALT and AST levels were mildly elevated; all of these patients had levels of < 3 times the upper limit of normal

values. The AST levels were significantly different among the three groups (stages I + II *vs* stage III *vs* stage IV, $P < 0.05$). In the early stage, 29.2% of patients had normal alkaline phosphatase (ALP) levels. The remaining patients had different degrees of ALP elevation; 6.3% had ALP levels > 5 times the upper limit of normal value. Moreover, γ-glutamyl transferase (GGT) was more robustly elevated, as 29.2% of patients had GGT levels of > 10 times the upper limit of normal value. The ALP values among the three groups were significantly different ($P < 0.05$). In early stage, the jaundice index did not increase significantly, but it gradually increased with disease progression. However, the above indicators were significantly different ($P < 0.05$) between the early-stage group and the stage IV group. With the progression of the disease, the levels of albumin and albumin/globulin ratio tended to decrease, and the difference among the three groups was statistically significant ($P < 0.05$). In early-stage patients, IgM and IgG levels as well as cholesterol levels were mildly elevated, but there were no significant differences among the three groups. Triglyceride levels were normal in the early-stage group, and the differences among the three groups were statistically significant ($P < 0.05$). The early detection rates of anti-mitochondria antibody (AMA) and AMA-M2 were 66.7% and 45.8%, respectively. The positive rate of anti-sp100 antibodies was significantly higher in patients with stage IV PBC. When AMA and AMA-M2 were negative, in the early stage, the highest autoantibody was anti-nuclear antibody (ANA) (92.3%), and in all ANA patterns, the highest was ANA centromere (38.5%).

CONCLUSION

In early-stage PBC patients, ALT and AST levels are normal or mildly elevated, GGT and ALP levels are not elevated in parallel, GGT levels are more robustly elevated, and ALP levels are normal in some patients. When AMA and AMA-M2 are negative, ANA especially ANA centromere positivity suggests the possibility of early PBC. Therefore, in the clinic, significantly elevated GGT levels with or without normal ALP levels and with ANA (particularly ANA centromere) positivity (when AMA and AMA-M2 are negative) may indicate the possibility of early PBC.

Key Words: Primary biliary cholangitis; Early stage; Biochemical makers; Autoantibodies; Pathology

©The Author(s) 2023. Published by Baishideng Publishing Group Inc. All rights reserved.

Core Tip: This is a retrospective study of the characteristics of early-stage primary biliary cholangitis (PBC) patients, in which we found the suggestive role of γ-glutamyl transferase as an indicator of cholestasis in the early diagnosis of PBC. We also found that when anti-mitochondria antibody (AMA) and AMA-M2 were negative, positivity for anti-nuclear antibody (ANA) especially ANA centromere indicates early-stage PBC.

Citation: Zhu YJ, Li J, Liu YG, Jiang Y, Cheng XJ, Han X, Wang CY, Li J. Role of biochemical markers and autoantibodies in diagnosis of early-stage primary biliary cholangitis. *World J Gastroenterol* 2023; 29(34): 5075-5081
URL: https://www.wjgnet.com/1007-9327/full/v29/i34/5075.htm
DOI: https://dx.doi.org/10.3748/wjg.v29.i34.5075

INTRODUCTION

Primary biliary cholangitis (PBC) is a chronic progressive autoimmune cholestatic disease. The main target organ of PBC is the liver, and nonsuppurative inflammation of the small intrahepatic bile ducts may eventually develop into cirrhosis or liver fibrosis[1]. Currently, patients who are diagnosed and treated early respond well to ursodeoxycholic acid (UDCA) and have an estimated survival rate similar to that of the general population. Based on this, we retrospectively analyzed the data of patients with PBC in our hospital, aiming to analyze the biochemical parameters and autoimmune antibody characteristics of patients with early PBC to help identify early-stage PBC, actively treat this condition, and delay disease progression.

MATERIALS AND METHODS

Study design and sample collection

This retrospective observational study was conducted at the Clinical School of the Second People's Hospital. Patients were included if they met the following criteria: (1) Confirmed PBC (detected by "APASL clinical practice guidance: The diagnosis and management of patients with primary biliary cholangitis"). The diagnosis of PBC can be established when two or more of the following three criteria are met: (a) Biochemical evidence of cholestasis based mainly on the elevation of alkaline phosphatase (ALP) and gamma glutamyl transferase (GGT) with the exclusion of extrahepatic biliary

obstruction by imaging studies; (b) presence of anti-mitochondria antibody (AMA) or other PBC-specific anti-nuclear antibodies (ANAs) including anti-sp100 or anti-gp210; and (c) histologic evidence of non-suppurative destructive cholangitis mainly affecting the interlobular bile ducts; (2) underwent liver pathology biopsy and had a clear pathological stage; (3) initially diagnosed with PBC; and (4) were not previously treated with UDCA. Exclusion was based on the following criteria: (1) Various liver tumors; (2) other autoimmune diseases; (3) alcoholic liver disease, nonalcoholic fatty liver disease, and drug-induced liver injury; (4) active viral hepatitis; (5) obstructive cholestasis; (6) repeated liver biopsy; (7) incomplete information; (8) no defined pathological stage; (9) long-term application of UDCA; and (10) rejected liver biopsy (Figure 1).

Serological analysis

For the detection of ANA, a Hep-2 kit was used, according to standard indirect immunofluorescence (IIF) protocols. Each serum sample was investigated at a starting dilution of 1:100 and titrated to zero positive; samples with positive IIF at a titer ≥ 1:100 were deemed positive. Line immunoassay was used to detect AMA (M2), anti-sp100, and anti-gp210. According to Hep-2 cell patterns, ANAs were divided into nuclear (including homogeneous, cytoplasmic speckled, nucleolar, centromere, discrete, and nuclear) and cytoplasmic (including fibrillar, cytoplasmic speckled, and reticular)[2]. Pathology readings were performed by two experienced pathologists and at least one chief pathologist.

Statistical analysis

The data were analyzed with SPSS 25.0 software. Normally distributed data were analyzed by ANOVA and are expressed as the mean ± SD. Nonnormally distributed data were analyzed by the rank sum test and are expressed as medians and ranges. Count data are expressed as the number of subjects and percentages and were compared using the chi-square test. A difference was considered statistically significant at $P < 0.05$.

RESULTS

Comparison of general information among different groups

The age distribution of PBC patients ranged from 33-71 years, with an average age of 53.7 ± 8.9 years. The mean age in the three stage groups (stages I + II, stage III, and stage IV) was 52.4 ± 9.2 years, 57.7 ± 7.3 years, and 51.5 ± 8.7 years, respectively. The 82 patients with PBC were predominantly female (68/82), and the number of females in the three stage groups was 38, 20 and 10, respectively. There were no statistically significant differences in the mean age or sex proportion among the groups ($P > 0.05$).

In early-stage patients ($n = 48$), 18 (37.5%) patients did not have significant symptoms. The major symptoms of patients were gastrointestinal symptoms (including abdominal discomfort, pain, bloating, and nausea), fatigue, yellow urine, and pruritus.

Comparison of biochemical and immunological indicators among the three groups

The alanine aminotransferase (ALT) and aspartate aminotransferase (AST) levels were normal or mildly increased in the early-stage PBC patients, and an increasing trend with the progression of the pathological stage was observed. Furthermore, the AST levels were significantly different among the three groups ($P < 0.05$). There were significant differences in total bilirubin (TBIL), direct bilirubin (DBIL), and total bile acid (TBA) levels among the three groups of PBC patients ($P < 0.05$), and the difference between the early stage group and stage IV group was statistically significant ($P = 0.002$, 0.003, and 0.009, respectively). With pathological progression, a decreasing trend for albumin and albumin/globulin levels was observed, and there were statistically significant differences among the three groups and between the early stage group and stage IV group ($P = 0.005$ and 0.001, respectively). ALP and GGT levels were trending toward an increase. While 29.2% of patients had normal ALP levels, the remaining patients had different degrees of elevation. For 6.3% of the patients, the ALP levels were elevated to > 5 times the upper limit of normal value. The elevation in GGT levels was more robust, as 29.2% of patients had elevated GGT levels of > 10 times the upper limit of normal value. The difference of ALP levels among the three groups was statistically significant ($P < 0.05$), and there was a statistically significant difference between the early stage group and stage IV group ($P = 0.006$). Triglyceride levels gradually decreased with the progression of the disease, and the differences among the different groups were statistically significant ($P < 0.05$). Cholesterol (CHO) levels showed an increasing tendency. CHO levels gradually increased but were not significantly different among the three groups. IgG, IgA, and IgM all showed an increasing trend with disease progression. IgG and IgM were predominantly elevated, while IgA and complement (C)3 and C4 were normal in the early stage. The IgA levels were significantly different among the three groups ($P < 0.05$) (Table 1).

Autoantibody levels in different groups of patients with PBC

The positive rates of AMA, AMA-M2, anti-sp100, and anti-gp210 were 52 (63.4%), 40 (48.8%), 16 (19.5%), and 13 (15.9%), respectively. The positive rate of ANA was 62 (75.6%). Cytoplasmic speckled pattern had the highest rate of 48.8%, and this was followed by nuclear pattern at 23.2% and centromere pattern at 15.9%. The positive rate of AMA-M2 significantly differed among the three groups ($P = 0.045$), but the remaining autoantibodies were not significantly different ($P > 0.05$). In early-stage PBC patients, 32 patients were positive for AMA, 22 positive for AMA-M2, 8 positive for anti-sp100, and 9 positive for anti-gp210 (Table 2). Thirty-four patients were positive for ANA, of which 24 had cytoplasmic speckled pattern, 10 had nuclear pattern, and 6 had centromere pattern (Table 3).

Table 1 Clinical and laboratory data of patients with primary biliary cholangitis

	Early-stage (stages I + II; *n* = 48)	Stage III (*n* = 22)	Stage IV (*n* = 12)	*P* value
ALT	53.5 (29.5-124.5)	54.0 (30.0-127.6)	80.0 (42.8-127.4)	0.639
AST	53.5 (34.0-97.3)[a]	68.5 (39.6-114.1)	112.2 (81.1-136.3)	0.009
TBA	9.0 (3.6-36.4)[a]	18.0 (7.0-45.1)	28.2 (18.0-111.5)	0.011
TBIL	15.4 (11.2-27.8)[a]	16.7 (13.7-24.2)[a]	61.2 (28.1-114.3)	0.002
DBIL	5.2 (3.7-16.0)[a]	8.7 (2.5-12.4)[a]	42.3 (15.8-67.3)	0.003
ALB	42.1 (38.3-44.8)[a]	39.3 (36.5-42.5)	35.8 (30. 5-41.0)	0.005
A/G	1.2 (1.1-1.4)[a]	1.0 (0.9-1.3)	0.9 (0.7-1.1)	0.001
ALP	200.4 (117.8-414.0)[a]	292.5 (162.0-421.3)	463.5 (329.6-770.5)	0.008
GGT	289.0 (133.0-668.8)	532.0 (326. 5-764.3)	336.5 (264.0-648.0)	0.070
CHO	5.8 (4.6-6.9)	6.2 (5.1-7.5)	6.8 (4.9-7.0)	0.509
TG	1.3 (1.0-1.8)	1.6 (1.2-2.1)[a]	1.1 (0.8-1.5)	0.019
IgG	16.7 ± 4.6	17.6 ± 6.7	20.6 ± 7.9	0.056
IgA	2.9 (2.1-3.3)	3.5 (2.5-4.7)	3.4 (2.4-4.4)	0.031
IgM	3.4 (1.8-5.1)	3.7 (2.1-5.0)	3.7 (1.9-6.8)	0.967
C3	1.4 (1.2-1.6)	1.6 (1.3-1.8)	1.2 (1.0-1.7)	0.126
C4	0.2 (0.2-0.3)	0.2 (0.2-0.3)	0.2 (0.2-0.3)	0.963

[a]$P < 0.05$ indicates statistically significant difference compared to stage IV.
ALT: Alanine aminotransferase; AST: Aspartate aminotransferase; TBA: Total bile acid; ALP: Alkaline phosphatase; GGT: γ-glutamyl transferase; ALB: Albumin; A/G: Albumin/globulin; TBIL: Total bilirubin, DBIL: Direct bilirubin; CHO: Cholesterol; TG: Triglycerides; IgG: Immunoglobulin G; IgM: Immunoglobulin M; IgA: Immunoglobulin A; C3: Complement 3; C4: Complement 4.

Table 2 Autoantibody positive rate in patients with early-stage primary biliary cholangitis

Autoantibody	AMA	AMA-M2	Anti-sp100	Anti-gp210	Anti-SSA/Ro52	Anti-SSA/Ro60	ANA
n	32	22	8	9	8	2	34
%	66.7	45.8	16.7	18.8	16.7	4.2	70.8

AMA: Anti-mitochondria antibody; ANA: Anti-nuclear antibody.

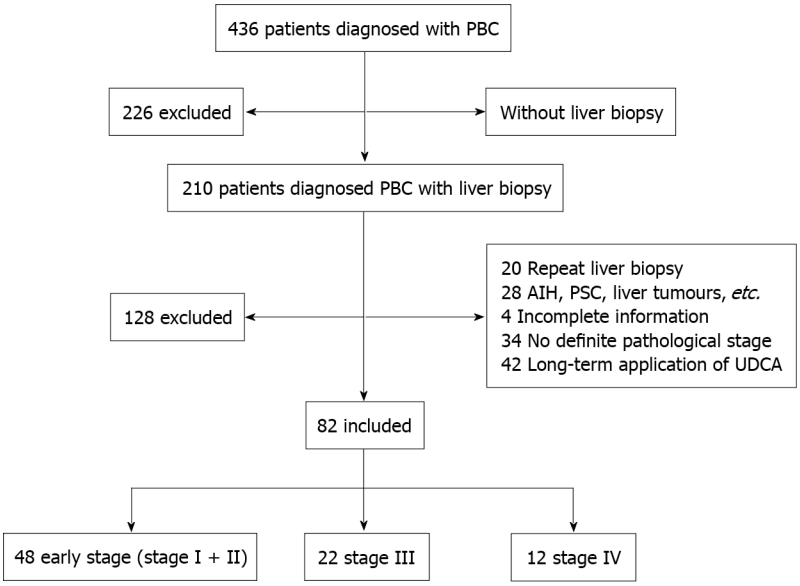
Table 3 Anti-nuclear antibody subtype positive rate in patients with early-stage primary biliary cholangitis

ANA	Cytoplasmic speckled	Fibrillar	Reticular	Discrete	Homogeneous	Centromere	Nuclear speckled	Nucleolar	Nuclear
n	24	2	6	7	1	6	5	0	10
%	50	4.2	12.5	14.6	2.1	12.5	10.4	0	20.8

ANA: Anti-nuclear antibody.

Analysis of other autoantibodies detected when AMA and AMA-M2 are negative

There were 25 PBC patients negative for both AMA and AMA-M2. These included 13 patients in the early stage, 6 patients in stage III, and 6 patients in stage IV. The autoantibody positive rates among the three groups were not significantly different ($P > 0.05$). In early-stage AMA- and AMA-M2-negative patients, the positive rate was highest for ANA (92.3%), followed by anti-SSA/RO52 (23.1%) and anti-sp100 (15.3%). In all ANA patterns, the highest was ANA centromere (38.5%).



DOI: 10.3748/wjg.v29.i34.5075 **Copyright** ©The Author(s) 2023.

Figure 1 Participant flow in the study. AIH: Autoimmune hepatitis; PSC: Primary sclerosing cholangitis; PBC: Primary biliary cholangitis; UDCA: Ursodeoxycholic acid.

DISCUSSION

PBC occurs mainly in middle-aged women, and the common clinical presentations are fatigue, splenomegaly, jaundice, and pruritus[1]. PBC may take 10-15 years to develop from the onset of illness to the symptomatic stage. Early diagnosis and treatment can improve the survival and quality of life of patients. In the early stage of PBC, patients have no obvious symptoms, but most patients have liver fibrosis or cirrhosis when they are diagnosed. Therefore, to improve PBC patient prognosis, early diagnosis and treatment are essential.

In this study, we found that GGT levels were significantly elevated in early-stage patients (29.2% of patients had elevated levels of > 10 times the upper limit of normal value) and tended to increase with the progression of illness. A study from Switzerland found elevated GGT levels in 15 of 24 PBC patients with normal ALP levels and liver biopsy results, and GGT levels were elevated in 13 patients who had early Nakanura stage histology. These findings suggest that elevated GGT levels have potential diagnostic value in PBC patients with normal ALP levels[3]. Reportedly, elevated GGT levels are closely related to the inflammation caused by fat deposition[4]. GGT is a key factor in maintaining the activity of reduced glutathione (GSH), which is an important antioxidant in the body. GGT is also involved in the production of GSH, which plays a cytoprotective role in inflammation and when an inflammatory response occurs[5]. In contrast to the levels of GGT, the levels of the cholestasis indicator ALP are not significantly elevated, and some PBC patients have normal ALP levels. Elevated ALP levels may be due to increased intracapillary pressure or to bile acids dissolving ALP from the lipid membrane into the blood[6]. A study of 67 patients with normal ALP levels and AMA positivity who underwent liver puncture biopsies found that 55 of these cases had pathology consistent with characteristic PBC presentation. Of these 55 patients, 50 were in the early stage[7]. In our study, we found that the elevation of GGT levels was more pronounced in patients with early-stage disease, which may be related to early chronic inflammation, excessive GSH depletion, and a compensatory increase in GGT.

We found that most patients had normal or mildly elevated ALT and AST levels in the early stage, and these levels increased with disease progression. These findings suggest that the degree of hepatocellular damage gradually increases. Alternatively, TBA, TBIL, and DBIL levels were not significantly elevated in the early stage but gradually increased with disease progression. In stage IV, TBIL and DBIL levels were significantly elevated, and DBIL levels were robustly elevated. This may be due to most of the hepatic parenchyma being damaged. In this study, IgM levels were predominantly elevated in early-stage PBC patients, which is consistent with previous studies[8]. A rise in IgM levels may be caused by a strong IgM secretory capacity and cellular autophagy[9].

AMA and AMA-M2 may be detectable in serum when patients are symptom-free and liver tests are normal, and they are highly specific autoantibodies for PBC. In recent years, with the development of detection methods, anti-sp100 and anti-gp210 have already been identified as PBC-specific autoantibodies. In a retrospective study of 4371 patients from Italy, the specificity of anti-sp100 and anti-gp210 for PBC was confirmed, especially in AMA-negative patients[10]. However, the reported positive rates vary widely across regions. The differences in antibody positive rates among regions could be due to different patient selection criteria and differences in technical and genetic backgrounds. In our study, the autoantibody rates of all patients were as follows: AMA, 63.4%; AMA-M2, 48.8%; and anti-gp210, 15.9%. These rates are lower than those reported in previous studies[11,12]. We found that the positive rate of anti-sp100 was 19.5%, and the positive rate of ANA was 75.6%. These rates are higher than those in other reports. One possible explanation for this is that our study did not adopt random sampling, but only patients with PBC confirmed by liver biopsy were included. This may be the main reason why the autoantibody positive rates in this study are lower than those in other

studies. The positive rates of AMA, AMA-M2, and anti-gp210 in early-stage patients with PBC were 66.7%, 45.8%, and 18.8%, respectively, which were similar to the rates of all PBC patients. The positive rate of anti-sp100 was significantly higher in stage IV PBC patients.

The number of AMA- and AMA-M2-negative PBC patients was 25, of which 13 (86.7%) were in the early stage. In early-stage AMA- and AMA-M2-negative patients, the positive rate of ANA was highest (92.3%). In all ANA patterns, the highest was ANA centromere (38.5%), which decreased with the progression of the disease. However, there were no significant differences in this parameter among the three groups ($P > 0.05$). In this article, we summarized available data on the characteristics of ANA patterns. We should be aware of the possibility of unexplained elevations in serum markers for cholestasis in AMA(M2)-negative patients, but ANA, especially centromere pattern, was positive in early-stage patients. Although those ANAs are not specific for PBC diagnostic purposes, they can still be used as auxiliary markers to reduce the rate of missed diagnoses when AMA(M2) is negative. A previous study reported that ANA centromere was almost exclusively limited to PBC patients. Thus, this antibody can still be used as an auxiliary marker to reduce the rate of missed diagnoses when AMA(M2) is negative[12].

CONCLUSION

In summary, in early-stage PBC patients, ALT and AST levels are normal or mildly elevated, GGT and ALP levels are not elevated in parallel, GGT levels are more robustly elevated, and ALP levels are normal in some patients. When AMA and AMA-M2 are negative, ANA (especially ANA centromere) positivity suggests the possibility of early PBC. Therefore, in the clinic, significantly elevated GGT levels with or without normal ALP levels and with ANA (particularly ANA centromere) positivity (when AMA and AMA-M2 are negative) may indicate the possibility of early PBC.

This study is a retrospective study with limited inclusion. Thus, it adopted nonrandom sampling with some bias. Further studies should be conducted in the future to expand the sample size and to follow up on the prognosis of patients with early-stage PBC after treatment with UDCA.

ARTICLE HIGHLIGHTS

Research background

The long course and insidious symptoms of primary biliary cholangitis (PBC) make it difficult to diagnose in the early stage.

Research motivation

To analyze clinical features and autoantibodies in patients with early-stage PBC.

Research objectives

To improve the diagnosis rates of early-stage PBC.

Research methods

We included 82 patients with PBC diagnosed by liver pathology with clear pathologic stage and divided them into three groups to compare their laboratory parameters and autoantibody positivity.

Research results

In early-stage PBC patients, alanine aminotransferase and aspartate aminotransferase levels were normal or mildly elevated, gamma glutamyl transferase (GGT) and alkaline phosphatase (ALP) levels were not elevated in parallel, GGT levels were more robustly elevated, and ALP levels were normal in some patients. When anti-mitochondria antibody (AMA) and AMA-M2 were negative, anti-nuclear antibody (ANA) (especially ANA centromere) positivity suggests the possibility of early-stage PBC.

Research conclusions

We found that GGT is elevated significantly and earlier in the early-stage PBC group. ANA and associated-ANA subtypes can be used as second-line markers for the diagnosis of early-stage PBC (particularly when specific autoantibodies are negative).

Research perspectives

We hope that this study will increase the rates of diagnosis of early-stage PBC by clinicians.

FOOTNOTES

Author contributions: Zhu YJ wrote the manuscript; Zhu YJ, Cheng XJ, and Han X contributed to data collation; Zhu YJ and Li J

contributed to statistical analysis; Liu YG contributed to liver pathology reading; Jiang Y, Wang CY, and Li J contributed to manuscript revision; Wang CY and Li J contributed to research supervision; Wang CY contributed to project design.

Institutional review board statement: The study protocol conforms to the ethical guidelines of the 1975 Declaration of Helsinki and was approved by the local Ethics Committee (Clinical School of the Second People's Hospital of Tianjin).

Informed consent statement: Patients were not required to give informed consent to the study because the analysis used anonymous clinical data that were obtained after each patient agreed to treatment by written consent.

Conflict-of-interest statement: All authors have no conflict of interest to disclose.

Data sharing statement: The data underlying this article can be available in this article and in its online supplementary material or from the first author.

Open-Access: This article is an open-access article that was selected by an in-house editor and fully peer-reviewed by external reviewers. It is distributed in accordance with the Creative Commons Attribution NonCommercial (CC BY-NC 4.0) license, which permits others to distribute, remix, adapt, build upon this work non-commercially, and license their derivative works on different terms, provided the original work is properly cited and the use is non-commercial. See: https://creativecommons.org/Licenses/by-nc/4.0/

Country/Territory of origin: China

ORCID number: Yu-Jin Zhu 0000-0003-3332-9606; Jing Li 0000-0001-5308-4146; Yong-Gang Liu 0000-0001-6165-564X; Yong Jiang 0000-0001-7402-5129; Xiao-Jing Cheng 0009-0008-8088-0103; Chun-Yan Wang 0000-0002-1074-1537; Jia Li 0000-0003-0100-417X.

S-Editor: Yan JP
L-Editor: Wang TQ
P-Editor: Yan JP

REFERENCES

1 **You H**, Ma X, Efe C, Wang G, Jeong SH, Abe K, Duan W, Chen S, Kong Y, Zhang D, Wei L, Wang FS, Lin HC, Yang JM, Tanwandee T, Gani RA, Payawal DA, Sharma BC, Hou J, Yokosuka O, Dokmeci AK, Crawford D, Kao JH, Piratvisuth T, Suh DJ, Lesmana LA, Sollano J, Lau G, Sarin SK, Omata M, Tanaka A, Jia J. APASL clinical practice guidance: the diagnosis and management of patients with primary biliary cholangitis. *Hepatol Int* 2022; **16**: 1-23 [PMID: 35119627 DOI: 10.1007/s12072-021-10276-6]

2 **Chan EK**, Damoiseaux J, Carballo OG, Conrad K, de Melo Cruvinel W, Francescantonio PL, Fritzler MJ, Garcia-De La Torre I, Herold M, Mimori T, Satoh M, von Mühlen CA, Andrade LE. Report of the First International Consensus on Standardized Nomenclature of Antinuclear Antibody HEp-2 Cell Patterns 2014-2015. *Front Immunol* 2015; **6**: 412 [PMID: 26347739 DOI: 10.3389/fimmu.2015.00412]

3 **Terziroli Beretta-Piccoli B**, Stirnimann G, Mertens J, Semela D, Zen Y, Mazzucchelli L, Voreck A, Kolbus N, Merlo E, Di Bartolomeo C, Messina P, Cerny A, Costantini S, Vergani D, Mieli-Vergani G; Swiss PBC Cohort Study Group. Primary biliary cholangitis with normal alkaline phosphatase: A neglected clinical entity challenging current guidelines. *J Autoimmun* 2021; **116**: 102578 [PMID: 33229138 DOI: 10.1016/j.jaut.2020.102578]

4 **Haring R**, Baumeister SE, Völzke H, Dörr M, Kocher T, Nauck M, Wallaschofski H. Prospective inverse associations of sex hormone concentrations in men with biomarkers of inflammation and oxidative stress. *J Androl* 2012; **33**: 944-950 [PMID: 22207707 DOI: 10.2164/jandrol.111.015065]

5 **Chen LW**, Huang MS, Shyu YC, Chien RN. Gamma-glutamyl transpeptidase elevation is associated with metabolic syndrome, hepatic steatosis, and fibrosis in patients with nonalcoholic fatty liver disease: A community-based cross-sectional study. *Kaohsiung J Med Sci* 2021; **37**: 819-827 [PMID: 34002481 DOI: 10.1002/kjm2.12395]

6 **Poupon R**. Liver alkaline phosphatase: a missing link between choleresis and biliary inflammation. *Hepatology* 2015; **61**: 2080-2090 [PMID: 25603770 DOI: 10.1002/hep.27715]

7 **Sun C**, Xiao X, Yan L, Sheng L, Wang Q, Jiang P, Lian M, Li Y, Wei Y, Zhang J, Chen Y, Li B, Huang B, Peng Y, Chen X, Fang J, Qiu D, Hua J, Tang R, Leung P, Gershwin ME, Miao Q, Ma X. Histologically proven AMA positive primary biliary cholangitis but normal serum alkaline phosphatase: Is alkaline phosphatase truly a surrogate marker? *J Autoimmun* 2019; **99**: 33-38 [PMID: 30709684 DOI: 10.1016/j.jaut.2019.01.005]

8 **Lleo A**, Liao J, Invernizzi P, Zhao M, Bernuzzi F, Ma L, Lanzi G, Ansari AA, Coppel RL, Zhang P, Li Y, Zhou Z, Lu Q, Gershwin ME. Immunoglobulin M levels inversely correlate with CD40 ligand promoter methylation in patients with primary biliary cirrhosis. *Hepatology* 2012; **55**: 153-160 [PMID: 21898485 DOI: 10.1002/hep.24630]

9 **Lian C**, Zhao Y, Sun J, Zhao L, Zhang F. Role of cell autophagy in the generation of IgM and hepatic fibrosis in primary biliary cholangitis. *Clin Rheumatol* 2020; **39**: 3499-3506 [PMID: 32382831 DOI: 10.1007/s10067-020-05111-6]

10 **Granito A**, Muratori P, Muratori L, Pappas G, Cassani F, Worthington J, Guidi M, Ferri S, DE Molo C, Lenzi M, Chapman RW, Bianchi FB. Antinuclear antibodies giving the 'multiple nuclear dots' or the 'rim-like/membranous' patterns: diagnostic accuracy for primary biliary cirrhosis. *Aliment Pharmacol Ther* 2006; **24**: 1575-1583 [PMID: 17206945 DOI: 10.1111/j.1365-2036.2006.03172.x]

11 **Lindor KD**, Bowlus CL, Boyer J, Levy C, Mayo M. Primary Biliary Cholangitis: 2018 Practice Guidance from the American Association for the Study of Liver Diseases. *Hepatology* 2019; **69**: 394-419 [PMID: 30070375 DOI: 10.1002/hep.30145]

12 **Granito A**, Muratori P, Quarneti C, Pappas G, Cicola R, Muratori L. Antinuclear antibodies as ancillary markers in primary biliary cirrhosis. *Expert Rev Mol Diagn* 2012; **12**: 65-74 [PMID: 22133120 DOI: 10.1586/erm.11.82]

World Journal of Gastroenterology

Submit a Manuscript: https://www.f6publishing.com

World J Gastroenterol 2023 September 14; 29(34): 5082-5090

DOI: 10.3748/wjg.v29.i34.5082

ISSN 1007-9327 (print) ISSN 2219-2840 (online)

CASE REPORT

Simultaneous rectal neuroendocrine tumors and pituitary adenoma: A case report and review of literature

Jing-Yi Li, Jie Chen, Jun Liu, Su-Zhen Zhang

Specialty type: Gastroenterology and hepatology

Provenance and peer review: Unsolicited article; Externally peer reviewed.

Peer-review model: Single blind

Peer-review report's scientific quality classification
Grade A (Excellent): 0
Grade B (Very good): B, B
Grade C (Good): 0
Grade D (Fair): 0
Grade E (Poor): 0

P-Reviewer: Hasan A, Egypt; Lykoudis PM, United Kingdom

Received: April 19, 2023
Peer-review started: April 19, 2023
First decision: May 27, 2023
Revised: June 9, 2023
Accepted: August 18, 2023
Article in press: August 18, 2023
Published online: September 14, 2023

Jing-Yi Li, Su-Zhen Zhang, Department of Gastroenterology, Cancer Hospital Affiliated to Shanxi Medical University, Taiyuan 030000, Shanxi Province, China

Jie Chen, Department of Neuroendocrine Tumor, Fudan University Shanghai Cancer Center, Shanghai 200032, China

Jun Liu, Department of Gastroenterology, Shanxi Bethune Hospital, Taiyuan 030032, Shanxi Province, China

Corresponding author: Su-Zhen Zhang, MM, Chief Physician, Department of Gastroenterology, Cancer Hospital Affiliated to Shanxi Medical University, No. 3 Gongxin Street, Xinghualing District, Taiyuan 030000, Shanxi Province, China. zhangsuzhen209@163.com

Abstract

BACKGROUND

Neuroendocrine tumors (NET) are rare heterogeneous tumors that arise from neuroendocrine cells throughout the body. Acromegaly, a rare and slowly progressive disorder, usually results from a growth hormone (GH)-secreting pituitary adenoma.

CASE SUMMARY

We herein describe a 38-year-old patient who was initially diagnosed with diabetes. During colonoscopy, two bulges were identified and subsequently removed through endoscopic submucosal dissection. Following the surgical intervention, the excised tissue samples were examined and confirmed to be grade 2 NET. ^{18}F-ALF-NOTATATE positron emission tomography-computed tomography (PET/CT) and ^{68}Ga-DOTANOC PET/CT revealed metastases in the peri-intestinal lymph nodes, prompting laparoscopic low anterior resection with total mesorectal excision. The patient later returned to the hospital because of hyperglycemia and was found to have facial changes, namely a larger nose, thicker lips, and mandibular prognathism. Laboratory tests and magnetic resonance imaging (MRI) suggested a GH-secreting pituitary adenoma. The pituitary adenoma shrunk after treatment with octreotide and was neuroendoscopically resected *via* a trans-sphenoidal approach. Whole-exome sequencing analysis revealed no genetic abnormalities. The patient recovered well with no evidence of recurrence during follow-up.

CONCLUSION

^{18}F-ALF-NOTATE PET/CT and MRI with pathological analysis can effectively

diagnose rare cases of pituitary adenomas complicated with rectal NET.

Key Words: Neuroendocrine neoplasm; Pituitary adenoma; Rectum; Diagnosis; Case report

©The Author(s) 2023. Published by Baishideng Publishing Group Inc. All rights reserved.

Core Tip: We herein present a rare case of rectal dual-source grade 2 neuroendocrine tumors with a pituitary growth hormone-secreting tumor that caused acromegaly and diabetes. The rarity of this combination makes an accurate diagnosis difficult to achieve. The correct diagnosis can be obtained by using ^{18}F-ALF-NOTATATE-positron emission tomography–computed tomography and magnetic resonance imaging combined with pathological analysis.

Citation: Li JY, Chen J, Liu J, Zhang SZ. Simultaneous rectal neuroendocrine tumors and pituitary adenoma: A case report and review of literature. *World J Gastroenterol* 2023; 29(34): 5082-5090
URL: https://www.wjgnet.com/1007-9327/full/v29/i34/5082.htm
DOI: https://dx.doi.org/10.3748/wjg.v29.i34.5082

INTRODUCTION

Neuroendocrine tumors (NETs) are a heterogeneous group of rare tumors that exhibit complex clinical behaviors. They typically originate from peptidergic neurons and neuroendocrine cells throughout the body, with gastroenteropancreatic NETs being the predominant form. The rectum is the most common location of these tumors, accounting for 37.4% of cases[1,2]. Acromegaly, another rare disorder that often goes undiagnosed, is a chronic, progressive endocrine and metabolic disease with an inconspicuous onset. The main cause of acromegaly is excessive production of growth hormone (GH), and > 95% of patients with enlarged limbs have pituitary adenomas that secrete GH[3]. GH stimulates the liver to produce insulin-like growth factor-1 (IGF-1), and excessive proliferation of soft tissue, bone, and cartilage can occur secondary to long-term excessive secretion of GH and IGF-1. This results in the typical symptom of enlarged limbs and can have a significant impact on various organ systems, such as the respiratory, cardiovascular, digestive, and glucose metabolism systems. Compression or invasion of pituitary adenomas can result in headaches, visual impairment, and adenohypophysis. The median age at diagnosis of acromegaly ranges from 40.5 years to 47.0 years, with delays in diagnosis lasting from 4.5 years to 9.0 years. Delayed diagnosis can significantly increase the incidence of complications and difficulty in treating patients with large limbs. In this case report, we describe a 38-year-old woman who was diagnosed with two concurrent grade 2 (G2) rectal NETs and a pituitary adenoma on the basis of ^{18}F-ALF-NOTATATE positron emission tomography-computed tomography (PET/CT) and ^{18}F-fluorodeoxyglucose (^{18}F-FDG) PET/CT findings. To the best of our knowledge, the combination of simultaneous rectal NETs and a GH-secreting pituitary adenoma has not been previously reported. To diagnose this disorder, patients may undergo both ^{18}F-ALF-NOTATATE PET/CT and ^{18}F-FDG PET/CT scans, which can reveal small lesions that cannot be detected through conventional imaging. However, routine imaging examination by CT may fail to identify pelvic metastatic lymph nodes. Because of an abnormal blood glucose concentration, a patient may initially be suspected of having diabetes and given hypoglycemic treatment. However, if the patients' blood glucose control remains poor, their clinical manifestations may be hidden, and changes in their limbs and face may only be detected long after the onset of symptoms. A multidisciplinary approach involving various specialists in the fields of endocrinology, neurosurgery, imaging, pathology, oncology, and others is required for the diagnosis and treatment of NETs. Multidisciplinary diagnosis and treatment can significantly enhance the standardization, accuracy, and individualization of patient management. Collaborative diagnosis and treatment can lead to improvement of patients' quality of life, early diagnosis of diseases, better symptom management, prevention of complications, and reduced psychological distress.

CASE PRESENTATION

Chief complaints

A 38-year-old woman was admitted to our hospital for evaluation of long-standing chronic constipation and polydipsia.

History of present illness

Upon admission to the hospital, the patient underwent colonoscopy, which revealed two masses. The masses were confirmed to be G2 NETs after endoscopic submucosal dissection and pathological examination. Peri-intestinal lymph node metastasis was detected using ^{18}F-ALF-NOTATATE PET/CT and ^{18}F-FDG PET/CT, leading to treatment by laparoscopic low anterior resection with total mesenterectomy. After surgery, the patient exhibited symptoms of poor blood glucose control, and further examination revealed the presence of a pituitary macroadenoma. The patient received three cycles of octreotide acetate before undergoing surgical intervention for the pituitary macroadenoma.

History of past illness
The patient was diagnosed with diabetes on the basis of polydipsia and abnormal blood glucose concentrations.

Personal and family history
She had no family history of NETs or psychological or genetic disorders.

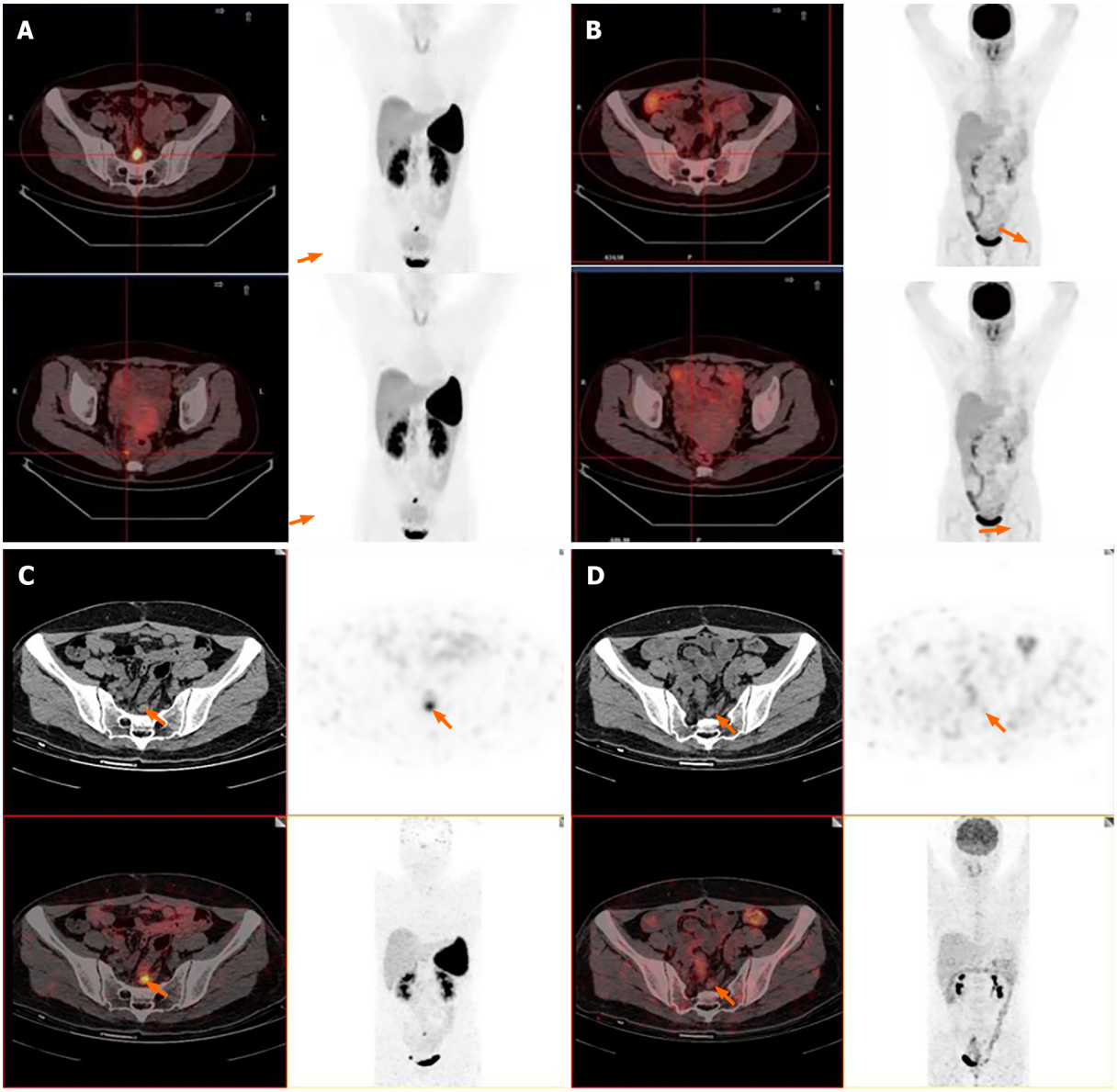
Physical examination
All vital signs were stable and physical examination revealed no notable abnormalities.

Laboratory examinations
Laboratory examinations showed that the patient had a high GH concentration at 47.79 ng/mL (reference range, 0.126-9.88 ng/mL) and high IGF-1 concentration at 497 ng/mL (reference range, 111-284 ng/mL). However, she had normal serum concentrations of sex hormones, adrenocorticotropic hormone (ACTH), thyrotropin, free thyroid hormone, and prolactin. Blood samples were collected at Peking Union Medical College Hospital 0, 30, 60, 120, and 180 min after a standard 75-g glucose test; at each of these time points, her plasma GH concentration was 29.1, 20.9, 19.2, 23.2, and 28.4 ng/mL, respectively.

Imaging examinations
^{18}F-ALF-NOTATATE PET/CT and ^{18}F-FDG PET/CT were performed to detect metastases (Figure 1A and B). ^{18}F-ALF-NOTATATE PET/CT clearly revealed metastases and high uptake in three peri-rectal and pre-sacral lymph nodes with a maximum standardized uptake value (SUV) of 13.24, 7.31, and 5.55, respectively, whereas these findings were not depicted on ^{18}F-FDG PET/CT. The patient then underwent ^{68}Ga-DOTANOC PET/CT at the First Affiliated Hospital of Sun Yat-Sen University. The ^{68}Ga-DOTANOC PET/CT findings were consistent with the ^{18}F-ALF-NOTATATE PET/CT findings, showing that the largest affected lymph node had a maximum SUV of 4.8 (Figure 1C and D).

FINAL DIAGNOSIS
The patient was diagnosed with rectal NETs with peripheral lymph node metastasis. The final pathology report listed rectal NETs, G2, stage T1N1M0 with 4/15 lymph node metastases. The patient also had acromegaly and secondary diabetes caused by a GH-secreting pituitary adenoma.

TREATMENT
Because of chronic constipation, colonoscopy was performed and revealed two lesions of 1.0 cm and 1.8 cm in diameter located 3.0 cm from the anus (Figure 2). These rectal lesions were resected by minimally invasive endoscopic submucosal dissection on 27 June 2019. Pathological examination of the two rectal specimens suggested histologic G2 NETs that were positive for synaptophysin and CD56 but negative for chromogranin A (Figure 3). The Ki67 index was 7% for the 1.8-cm-diameter tumor and 4% for the 1.0-cm-diameter tumor. Strong expression of SSTR2 (+++) suggested a predominance of the SSTR2 subtype. Only a few scattered cells were phosphorylated histone H3-positive. The larger lesion was 0.1 cm from the circumferential margin, whereas the smaller lesion was adjacent to the excision edge. ^{18}F-ALF-NOTATATE PET/CT and ^{18}F-FDG PET/CT scans in our hospital showed metastasis and high uptake in three perirectal and presacral lymph nodes. Laparoscopic low anterior resection with total mesorectal excision was performed 5 mo after diagnosis of the rectal lesions. Histological analysis of the operative specimens showed that the lymph nodes contained neuroendocrine cells. Immunohistochemical staining was positive for synaptophysin and CD56 but negative for chromogranin A. The Ki67 index was 3% (Figure 4). Four months after the rectal lesion was diagnosed by pathological examination, the patient returned to the local hospital because of hyperglycemia, and examination revealed facial changes including an enlarged nose, thickened lips, and mandibular kyphosis. A 2.4 cm × 1.3 cm × 1.3 cm pituitary adenoma was revealed by contrast-enhanced magnetic resonance imaging (MRI) (Figure 5). The GH-secreting pituitary macroadenoma was diagnosed by pathological examination. The patient was treated with long-acting octreotide (20 mg) at an interval of 28 d, and the lesion was reduced to 1.16 cm × 0.61 cm × 1.27 cm after three courses of treatment. The patient then underwent successful neuroendoscopic pituitary surgery *via* a trans-sphenoidal approach with sellar base reconstruction. Postoperative pathological examination confirmed the diagnosis of a pituitary adenoma, which was positive for GH and CAM5.2, was negative for ACTH, and had a Ki67 index of < 1%. The patients' skin condition significantly improved, becoming smoother and more refined after undergoing neuroendoscopic pituitary gland surgery. Moreover, her biochemical indicators consistently remained within the reference range postoperatively, especially with regard to her blood glucose control, which normalized without the need for hypoglycemic drugs. Given that the patients' GH-secreting pituitary tumor was a macroadenoma, direct surgery was challenging and complete removal was difficult. However, the tumor gradually decreased in size with the three cycles of octreotide acetate microsphere treatment, allowing successful R0 resection through timely surgical intervention. Thereafter, follow-up head MRI findings remained normal and the serum GH and IGF-1 concentrations consistently stayed within the reference range.



DOI: 10.3748/wjg.v29.i34.5082 **Copyright** ©The Author(s) 2023.

Figure 1 Images. A and B: ^{18}F-ALF-NOTATATE positron emission tomography-computed tomography (PET/CT) images and corresponding ^{18}F-fluorodeoxyglucose (^{18}F-FDG) PET/CT images in a patient with rectal neuroendocrine tumors in our hospital; C and D: ^{68}Ga-DOTANOC PET/CT and ^{18}F-FDG PET/CT images in the First Affiliated Hospital of Sun Yat-sen University.

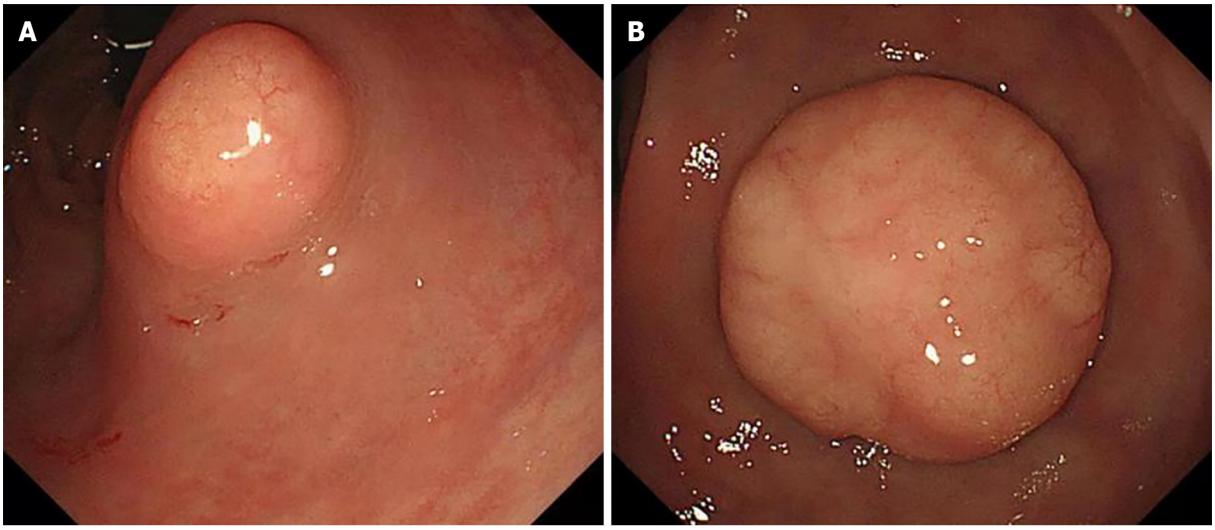
OUTCOME AND FOLLOW-UP

The patient returned for follow-up at 4, 13, and 16 mo after her pituitary surgery. No evidence of recurrence was found, and she remained asymptomatic.

DISCUSSION

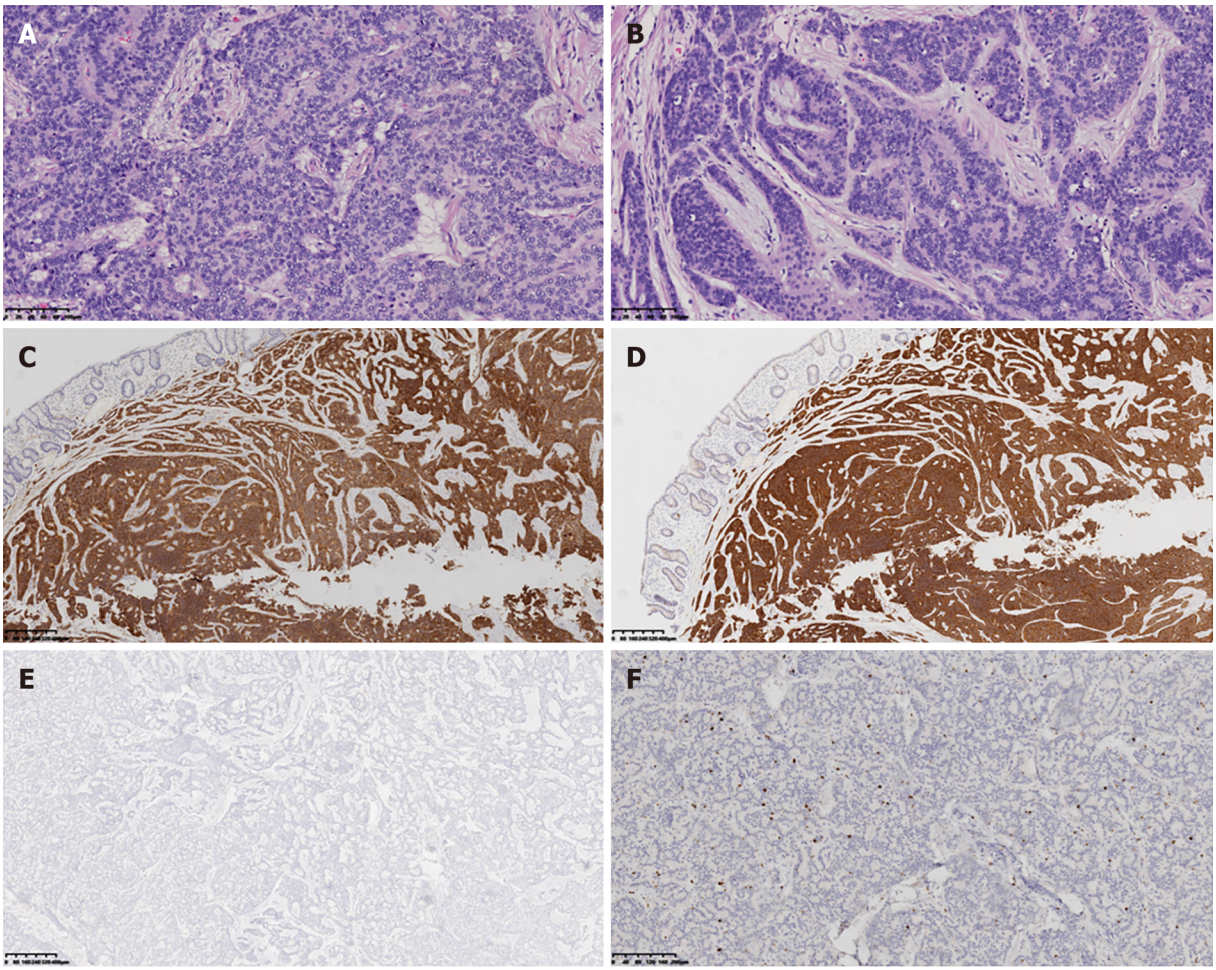
Rectal NETs can cause symptoms such as bleeding or changes in bowel habits; however, many patients are asymptomatic. The incidence of gastrointestinal NETs, including rectal NETs, is increasing, with a reported incidence of 1.04 per 100000 individuals per year according to the surveillance, epidemiology and end results database[4]. This increase is likely due to improved diagnostic endoscopy rather than a genuine increase in incidence.

Approximately 80% of rectal NETs are small (< 1 cm). There is typically no invasion or metastasis at the time of initial diagnosis. A strong correlation reportedly exists between the tumor size and spread, with only 2% of tumors under 1 cm having metastasized. The incidence of metastasis of rectal NETs ranges from 10% to 15% for 1- to 2-cm tumors but increases to 60% to 80% for tumors larger than 2 cm[5-7]. Treatment for localized G1 and G2 rectal NETs can be purely endoscopic, whereas low anterior resection of the rectum and removal of lymph nodes is necessary for advanced, localized rectal NETs. Most rectal NETs are located in the mid-section of the rectum, approximately 5 cm to 10 cm from



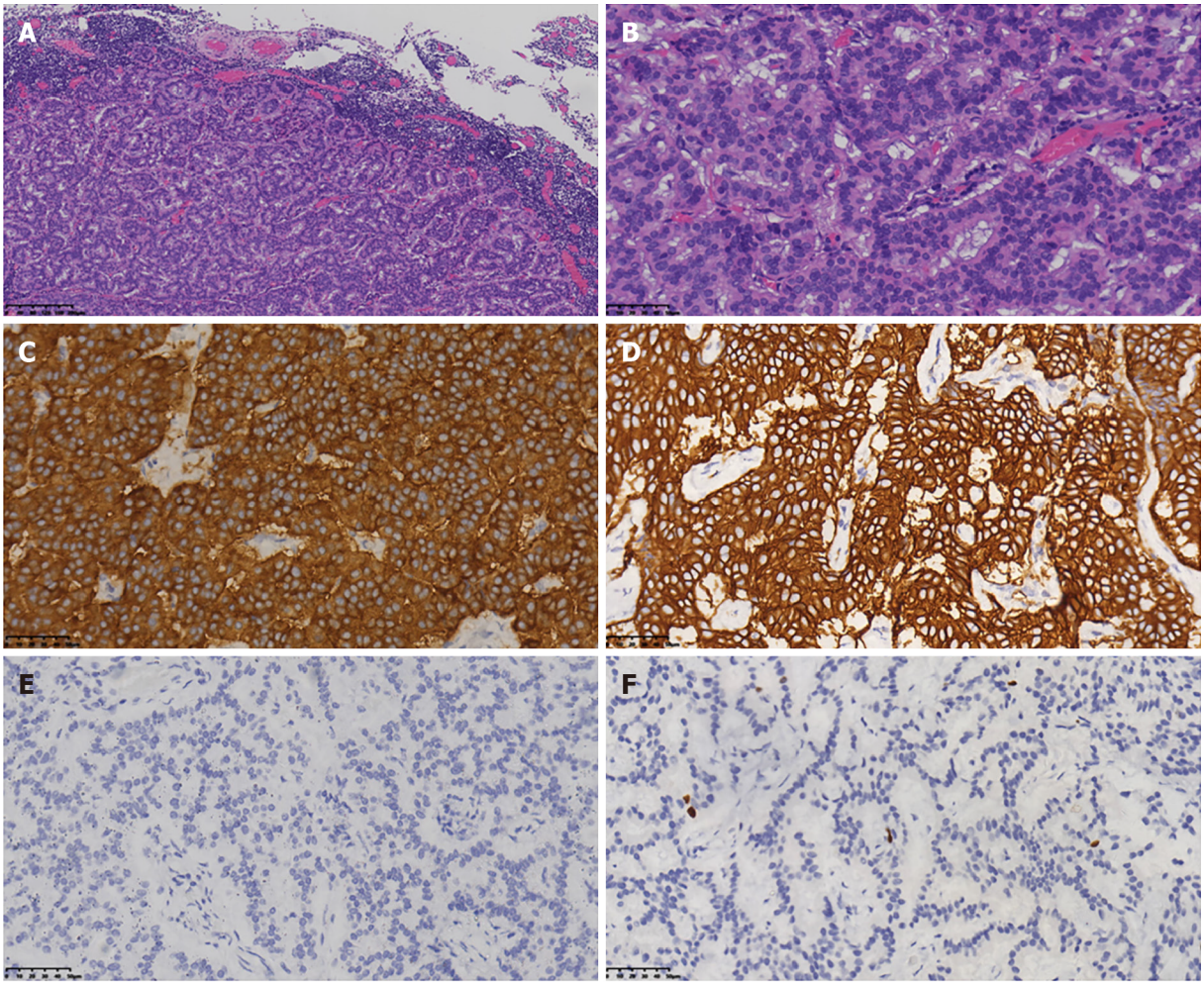
DOI: 10.3748/wjg.v29.i34.5082 **Copyright** ©The Author(s) 2023.

Figure 2 Two lesions. A: The one lesion at the lower rectum under colonoscopy; B: The second lesion at the lower rectum under colonoscopy.



DOI: 10.3748/wjg.v29.i34.5082 **Copyright** ©The Author(s) 2023.

Figure 3 Hematoxylin-eosin staining and immunohistochemical staining. A and B: Hematoxylin-eosin staining shows the pathological features of rectal neuroendocrine tumors in the larger and smaller tumor tissue specimens (20 ×); C-E: Immunohistochemical staining of neuroendocrine markers CD56, Syn, and CgA in representative tumor tissue selected by the physician (4 ×); F: Ki-67 expression in the neuroendocrine tumor at the rectum by immunohistochemistry (10 ×). Brown nuclear stain highlights Ki-67-positive tumor cells.

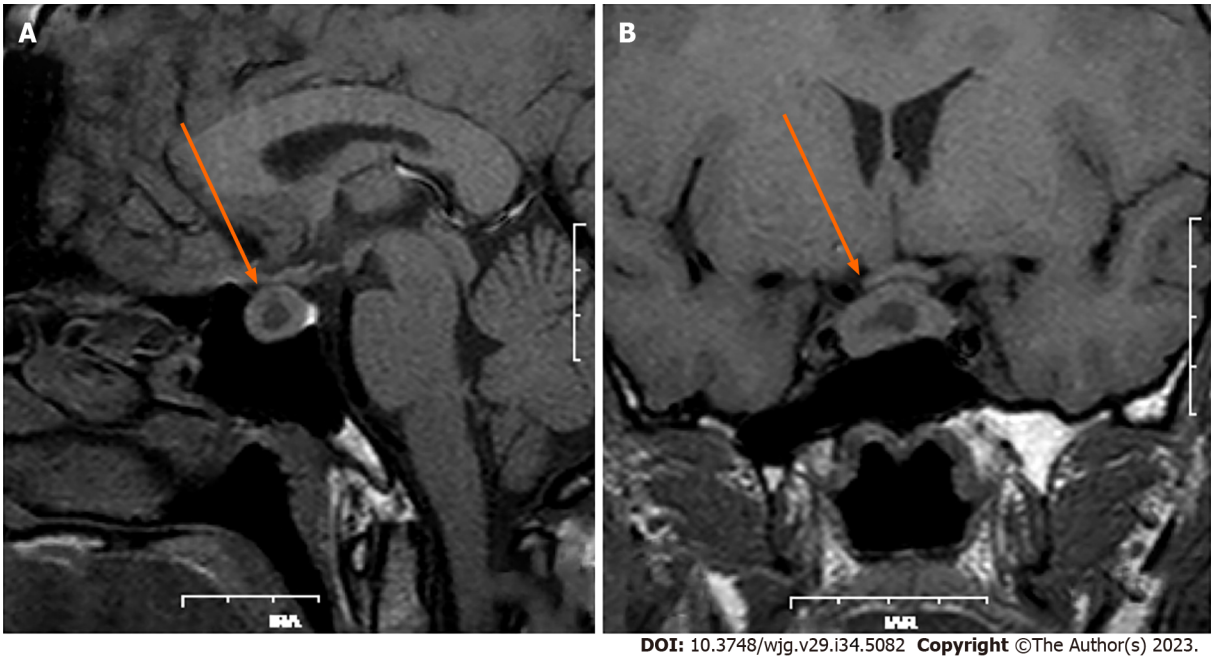


DOI: 10.3748/wjg.v29.i34.5082 **Copyright** ©The Author(s) 2023.

Figure 4 Tumor metastasis was observed in the peri-intestinal lymph nodes (4/15). A and B: Laparoscopic low anterior resection with total mesorectal excision was performed 5 mo after diagnosis of the rectal lesions. Central lymph nodes were selected from the lesion for hematoxylin–eosin staining to evaluate the metastasis of neuroendocrine cells (A: 100 ×, B: 400 ×); C-E: Immunohistochemical detection to evaluate the expression and distribution of neuroendocrine markers SSTR2, syn, and CgA in central lymph nodes (400 ×); F: Ki-67 expression in central lymph nodes by immunohistochemistry (400 ×).

the anus[5,8]. In the present case, concurrent rectal G2 NETs were detected in the distal rectum approximately 3 cm from the anus. ^{18}F-ALF-NOTATATE PET/CT showed evidence of lymph node metastases, making this the first patient to be diagnosed with NETs by a combination of ^{18}F-ALF-NOTATATE PET/CT and ^{18}F-FDG PET/CT in our hospital. To confirm these findings, we referred the patient to the First Affiliated Hospital of Sun Yat-Sen University for a ^{68}Ga-DOTANOC PET/CT scan, the results of which were consistent with our initial findings. The ^{18}F-based method is promising, with ^{18}F-octreotide being a potential alternative to ^{68}Ga-DOTA peptides. ^{18}F-AlF-NOTA-octreotide (^{18}F-OC) is a peptide imaging agent that can be rapidly synthesized and demonstrates strong uptake by tumors[9,10]. The combination of ^{18}F-FDG and ^{18}F-OC PET/CT has the potential to enhance the staging and management of neuroendocrine neoplasms [11]. At our hospital, more than 200 patients have undergone combined ^{18}F-ALF-NOTATATE PET/CT and ^{18}F-FDG PET/CT scanning to detect rectal NETs.

Pituitary adenomas are among the most common primary central nervous system tumors; their estimated prevalence is 17% of all such tumors[12-14]. Approximately half (46%-64%) of these tumors are hormone-secreting (*i.e.* functional). Frequently secreted hormones include prolactin, GH, thyrotropin, and ACTH. GH-secreting adenomas account for 13% to 20% of hormone-secreting pituitary adenomas. They cause gigantism before and acromegaly after closure of the epiphyseal growth plates[15-17]. GH hypersecretion leads to acral enlargement (77%), coarse facial features (54%), profuse sweating (52%), and insulin resistance (15%). A diagnosis of acromegaly is often confirmed by a high serum concentration of IGF-1. When the IGF-1 concentration is equivocal, an oral glucose tolerance test may be performed, and the absence of GH suppression to < 1 ng/mL is indicative of acromegaly[18]. MRI of the pituitary gland is used to assess the size and location of an adenoma. Our patient was diagnosed with a pituitary adenoma resulting in acromegaly and diabetes mellitus. Despite being histologically benign, hormone-secreting pituitary adenomas are associated with significant morbidity resulting from their direct impact on surrounding neurovascular structures and/or excessive hormone secretion, both of which may lead to a shortened lifespan[19-21]. Early diagnosis and effective management are critical for reducing morbidity and minimizing mortality.



DOI: 10.3748/wjg.v29.i34.5082 **Copyright** ©The Author(s) 2023.

Figure 5 Magnetic resonance imaging for pituitary adenoma. A: Pretreatment with long-acting octreotide (20 mg); B: Pretreatment with long-acting octreotide (20 mg) for 28 d.

The global prevalence of acromegaly, a rare and slowly progressive disorder, is approximately 60 per million. Acromegaly occurs when the pituitary gland produces too much GH[22-24]. Pituitary adenomas, which are responsible for approximately 90% of cases of acromegaly, are often very large at the time of detection because of delays in diagnosis. We have herein reported a very rare case. Although familial hereditary syndromes can be linked to the disease, our patient had no known family history of NETs, and whole-exome sequencing with an illumina genome analyzer (Illumina, San Diego, CA, United States) at Jinyu Medicine revealed no genetic abnormalities.

Krug *et al*[25] described a patient with acromegaly that was caused not by a pituitary adenoma but instead by a sporadic pulmonary NET[26]. Here, we have reported the simultaneous occurrence of rectal NETs with a GH-secreting pituitary adenomas; to the best of our knowledge, this combination of tumors has not been previously reported. The increased risk of colonic polyposis in individuals with acromegaly is well-recognized[21]. Several studies have shown that patients with acromegaly have a 2 to 14-fold increased risk of colon cancer compared with the normal population[27-30]. Furthermore, nodular thyroid disease is frequently seen in patients with acromegaly[31], some of whom have thyroid malignancies. The co-occurrence of rectal NETs and a GH-secreting pituitary adenoma in the present patient may have been coincidental. There is emerging evidence of an association between the GH/IGF-1 endocrine axis and cancer progression[32]. Excessive secretion of GH and IGF-1 by the pituitary adenoma may have stimulated the growth of our patients' rectal NETs. Surgical resection of the adenoma is the preferred treatment option for patients diagnosed with a GH-secreting pituitary adenoma. This approach can effectively eliminate or reduce the adenoma and decrease the levels of GH and IGF-1. The transsphenoidal approach is the primary method utilized to perform surgical interventions on pituitary adenomas, whereas craniotomy is only required in rare cases. Despite significant advancements in surgical techniques, there are still inherent risks associated with major extremity surgery, such as olfactory disturbance; hypopituitarism; temporary or permanent central diabetes insipidus; damage to vital nerves, blood vessels, brain tissue, and the blood supply of the skull base, resulting in postoperative cranial nerve dysfunction such as optic nerve impairment; cerebrospinal fluid rhinorrhea; meningitis; bacteremia; sepsis; hypothalamic syndrome; and even death. Patients with GH-secreting pituitary adenomas are at significantly higher risk when undergoing general anesthesia than are patients with other types of pituitary adenomas. These risks include abnormal cardiopulmonary function, increased perioperative risk, and difficulty in tracheal intubation and extubation because of soft tissue hyperplasia, making the operation more challenging for surgeons. The incidence and risk of rectal NETs in patients with acromegaly resulting from GH-secreting pituitary adenomas are unknown. Further research is necessary to elucidate the underlying mechanisms and to determine the clinical significance of this association.

CONCLUSION

We have herein presented a rare case of concurrent rectal G2 NETs combined with a pituitary adenoma. Pituitary adenomas lead to acromegaly and diabetes mellitus. Accurate diagnosis of this patients' condition was difficult. ^{18}F-ALF-NOTATATE PET/CT and pathological analysis achieved the correct diagnoses in this case.

ACKNOWLEDGEMENTS

We sincerely appreciate the patient and her family for their cooperation in information acquisition, treatment, and follow-up.

FOOTNOTES

Author contributions: Li JY drafted the manuscript and collected the data; Chen J and Liu J analyzed and collated the data; Zhang SZ guided the operation and revised the manuscript.

Informed consent statement: Informed written consent was obtained from the patient and her parents for the publication of this report and any accompanying images.

Conflict-of-interest statement: All the authors report having no relevant conflicts of interest for this article.

CARE Checklist (2016) statement: The authors have read the CARE Checklist (2016), and the manuscript was prepared and revised according to the CARE Checklist (2016).

Open-Access: This article is an open-access article that was selected by an in-house editor and fully peer-reviewed by external reviewers. It is distributed in accordance with the Creative Commons Attribution NonCommercial (CC BY-NC 4.0) license, which permits others to distribute, remix, adapt, build upon this work non-commercially, and license their derivative works on different terms, provided the original work is properly cited and the use is non-commercial. See: https://creativecommons.org/Licenses/by-nc/4.0/

Country/Territory of origin: China

ORCID number: Jing-Yi Li 0000-0002-2689-6859; Jie Chen 0000-0001-8113-3515; Jun Liu 0009-0002-7502-451X; Su-Zhen Zhang 0000-0002-0158-1420.

S-Editor: Qu XL
L-Editor: Filipodia
P-Editor: Yu HG

REFERENCES

1 **Fang C**, Wang W, Zhang Y, Feng X, Sun J, Zeng Y, Chen Y, Li Y, Chen M, Zhou Z, Chen J. Clinicopathologic characteristics and prognosis of gastroenteropancreatic neuroendocrine neoplasms: a multicenter study in South China. *Chin J Cancer* 2017; **36**: 51 [PMID: 28637502 DOI: 10.1186/s40880-017-0218-3]
2 **Andreasi V**, Partelli S, Muffatti F, Manzoni MF, Capurso G, Falconi M. Update on gastroenteropancreatic neuroendocrine tumors. *Dig Liver Dis* 2021; **53**: 171-182 [PMID: 32912771 DOI: 10.1016/j.dld.2020.08.031]
3 **AlDallal S**. Acromegaly: a challenging condition to diagnose. *Int J Gen Med* 2018; **11**: 337-343 [PMID: 30197531 DOI: 10.2147/IJGM.S169611]
4 **Dasari A**, Shen C, Halperin D, Zhao B, Zhou S, Xu Y, Shih T, Yao JC. Trends in the Incidence, Prevalence, and Survival Outcomes in Patients With Neuroendocrine Tumors in the United States. *JAMA Oncol* 2017; **3**: 1335-1342 [PMID: 28448665 DOI: 10.1001/jamaoncol.2017.0589]
5 **Hrabe J**. Neuroendocrine Tumors of the Appendix, Colon, and Rectum. *Surg Oncol Clin N Am* 2020; **29**: 267-279 [PMID: 32151360 DOI: 10.1016/j.soc.2019.11.010]
6 **Maione F**, Chini A, Milone M, Gennarelli N, Manigrasso M, Maione R, Cassese G, Pagano G, Tropeano FP, Luglio G, De Palma GD. Diagnosis and Management of Rectal Neuroendocrine Tumors (NETs). *Diagnostics (Basel)* 2021; **11** [PMID: 33923121 DOI: 10.3390/diagnostics11050771]
7 **Li YW**, He YP, Liu FQ, Peng JJ, Cai SJ, Xu Y, Wang MH. Grade G2 Rectal Neuroendocrine Tumor Is Much More Invasive Compared With G1 Tumor. *Front Oncol* 2021; **11**: 646536 [PMID: 33777809 DOI: 10.3389/fonc.2021.646536]
8 **Phan AT**, Oberg K, Choi J, Harrison LH Jr, Hassan MM, Strosberg JR, Krenning EP, Kocha W, Woltering EA, Maples WJ; North American Neuroendocrine Tumor Society (NANETS). NANETS consensus guideline for the diagnosis and management of neuroendocrine tumors: well-differentiated neuroendocrine tumors of the thorax (includes lung and thymus). *Pancreas* 2010; **39**: 784-798 [PMID: 20664476 DOI: 10.1097/MPA.0b013e3181ec1380]
9 **Laverman P**, McBride WJ, Sharkey RM, Eek A, Joosten L, Oyen WJ, Goldenberg DM, Boerman OC. A novel facile method of labeling octreotide with (18)F-fluorine. *J Nucl Med* 2010; **51**: 454-461 [PMID: 20150268 DOI: 10.2967/jnumed.109.066902]
10 **Laverman P**, D'Souza CA, Eek A, McBride WJ, Sharkey RM, Oyen WJ, Goldenberg DM, Boerman OC. Optimized labeling of NOTA-conjugated octreotide with F-18. *Tumour Biol* 2012; **33**: 427-434 [PMID: 22009690 DOI: 10.1007/s13277-011-0250-x]
11 **Long T**, Yang N, Zhou M, Chen D, Li Y, Li J, Tang Y, Liu Z, Li Z, Hu S. Clinical Application of 18F-AlF-NOTA-Octreotide PET/CT in Combination With 18F-FDG PET/CT for Imaging Neuroendocrine Neoplasms. *Clin Nucl Med* 2019; **44**: 452-458 [PMID: 30985413 DOI: 10.1097/RLU.0000000000002578]
12 **Dolecek TA**, Propp JM, Stroup NE, Kruchko C. CBTRUS statistical report: primary brain and central nervous system tumors diagnosed in the United States in 2005-2009. *Neuro Oncol* 2012; **14** Suppl 5: v1-49 [PMID: 23095881 DOI: 10.1093/neuonc/nos218]
13 **Mehta GU**, Lonser RR. Management of hormone-secreting pituitary adenomas. *Neuro Oncol* 2017; **19**: 762-773 [PMID: 27543627 DOI: 10.1093/neuonc/now130]

14 **Shih RY**, Schroeder JW, Koeller KK. Primary Tumors of the Pituitary Gland: Radiologic-Pathologic Correlation. *Radiographics* 2021; **41**: 2029-2046 [PMID: 34597177 DOI: 10.1148/rg.2021200203]

15 **Tjörnstrand A**, Gunnarsson K, Evert M, Holmberg E, Ragnarsson O, Rosén T, Filipsson Nyström H. The incidence rate of pituitary adenomas in western Sweden for the period 2001-2011. *Eur J Endocrinol* 2014; **171**: 519-526 [PMID: 25084775 DOI: 10.1530/EJE-14-0144]

16 **Agustsson TT**, Baldvinsdottir T, Jonasson JG, Olafsdottir E, Steinthorsdottir V, Sigurdsson G, Thorsson AV, Carroll PV, Korbonits M, Benediktsson R. The epidemiology of pituitary adenomas in Iceland, 1955-2012: a nationwide population-based study. *Eur J Endocrinol* 2015; **173**: 655-664 [PMID: 26423473 DOI: 10.1530/EJE-15-0189]

17 **Daly AF**, Beckers A. The Epidemiology of Pituitary Adenomas. *Endocrinol Metab Clin North Am* 2020; **49**: 347-355 [PMID: 32741475 DOI: 10.1016/j.ecl.2020.04.002]

18 **Katznelson L**, Laws ER Jr, Melmed S, Molitch ME, Murad MH, Utz A, Wass JA; Endocrine Society. Acromegaly: an endocrine society clinical practice guideline. *J Clin Endocrinol Metab* 2014; **99**: 3933-3951 [PMID: 25356808 DOI: 10.1210/jc.2014-2700]

19 **Ritvonen E**, Löyttyniemi E, Jaatinen P, Ebeling T, Moilanen L, Nuutila P, Kauppinen-Mäkelin R, Schalin-Jäntti C. Mortality in acromegaly: a 20-year follow-up study. *Endocr Relat Cancer* 2016; **23**: 469-480 [PMID: 27185871 DOI: 10.1530/ERC-16-0106]

20 **Dekkers OM**, Biermasz NR, Pereira AM, Romijn JA, Vandenbroucke JP. Mortality in acromegaly: a metaanalysis. *J Clin Endocrinol Metab* 2008; **93**: 61-67 [PMID: 17971431 DOI: 10.1210/jc.2007-1191]

21 **Clayton RN**, Raskauskiene D, Reulen RC, Jones PW. Mortality and morbidity in Cushing's disease over 50 years in Stoke-on-Trent, UK: audit and meta-analysis of literature. *J Clin Endocrinol Metab* 2011; **96**: 632-642 [PMID: 21193542 DOI: 10.1210/jc.2010-1942]

22 **McCabe J**, Ayuk J, Sherlock M. Treatment Factors That Influence Mortality in Acromegaly. *Neuroendocrinology* 2016; **103**: 66-74 [PMID: 25661647 DOI: 10.1159/000375163]

23 **Lavrentaki A**, Paluzzi A, Wass JA, Karavitaki N. Epidemiology of acromegaly: review of population studies. *Pituitary* 2017; **20**: 4-9 [PMID: 27743174 DOI: 10.1007/s11102-016-0754-x]

24 **Crisafulli S**, Luxi N, Sultana J, Fontana A, Spagnolo F, Giuffrida G, Ferraù F, Gianfrilli D, Cozzolino A, Cristina De Martino M, Gatto F, Barone-Adesi F, Cannavò S, Trifirò G. Global epidemiology of acromegaly: a systematic review and meta-analysis. *Eur J Endocrinol* 2021; **185**: 251-263 [PMID: 34061771 DOI: 10.1530/EJE-21-0216]

25 **Krug S**, Boch M, Rexin P, Pfestroff A, Gress T, Michl P, Rinke A. Acromegaly in a patient with a pulmonary neuroendocrine tumor: case report and review of current literature. *BMC Res Notes* 2016; **9**: 326 [PMID: 27349224 DOI: 10.1186/s13104-016-2132-1]

26 **Gadelha MR**, Kasuki L, Lim DST, Fleseriu M. Systemic Complications of Acromegaly and the Impact of the Current Treatment Landscape: An Update. *Endocr Rev* 2019; **40**: 268-332 [PMID: 30184064 DOI: 10.1210/er.2018-00115]

27 **Dworakowska D**, Grossman AB. Colonic Cancer and Acromegaly. *Front Endocrinol (Lausanne)* 2019; **10**: 390 [PMID: 31293513 DOI: 10.3389/fendo.2019.00390]

28 **Kasuki L**, Maia B, Gadelha MR. Acromegaly and Colorectal Neoplasm: An Update. *Front Endocrinol (Lausanne)* 2022; **13**: 924952 [PMID: 35795151 DOI: 10.3389/fendo.2022.924952]

29 **Patel GS**, Grossmann I, Rodriguez K, Soni M, Joshi PK, Patel SC, Shreya D, Zamora DI, Sange I. Acromegaly and the Colon: Scoping Beyond the Pituitary. *Cureus* 2021; **13**: e20018 [PMID: 34987906 DOI: 10.7759/cureus.20018]

30 **Terzolo M**, Puglisi S, Reimondo G, Dimopoulou C, Stalla GK. Thyroid and colorectal cancer screening in acromegaly patients: should it be different from that in the general population? *Eur J Endocrinol* 2020; **183**: D1-D13 [PMID: 32698136 DOI: 10.1530/EJE-19-1009]

31 **Uchoa HB**, Lima GA, Corrêa LL, Vidal AP, Cavallieri SA, Vaisman M, Buescu A, Gadelha MR. Prevalence of thyroid diseases in patients with acromegaly: experience of a Brazilian center. *Arq Bras Endocrinol Metabol* 2013; **57**: 685-690 [PMID: 24402013 DOI: 10.1590/s0004-27302013000900003]

32 **Werner H**, Laron Z. Role of the GH-IGF1 system in progression of cancer. *Mol Cell Endocrinol* 2020; **518**: 111003 [PMID: 32919021 DOI: 10.1016/j.mce.2020.111003]

World Journal of Gastroenterology

Submit a Manuscript: https://www.f6publishing.com

World J Gastroenterol 2023 September 14; 29(34): 5091-5093

DOI: 10.3748/wjg.v29.i34.5091

ISSN 1007-9327 (print) ISSN 2219-2840 (online)

LETTER TO THE EDITOR

Gastrointestinal microbiome and cholelithiasis: Prospect in the nervous system

Mirella Mancha Chahuara, Leidhy Dhy Maruja Lopez Tufino, Carlos Andrés Mugruza-Vassallo

Specialty type: Gastroenterology and hepatology

Provenance and peer review: Unsolicited article; Externally peer reviewed.

Peer-review model: Single blind

Peer-review report's scientific quality classification

Grade A (Excellent): 0
Grade B (Very good): B
Grade C (Good): C
Grade D (Fair): 0
Grade E (Poor): 0

P-Reviewer: Shi W, China; Sun X, China

Received: June 9, 2023
Peer-review started: June 9, 2023
First decision: July 23, 2023
Revised: July 25, 2023
Accepted: August 29, 2023
Article in press: August 29, 2023
Published online: September 14, 2023

Mirella Mancha Chahuara, Leidhy Dhy Maruja Lopez Tufino, Carlos Andrés Mugruza-Vassallo, Escuela Profesional de Medicina Humana, Universidad Privada San Juan Bautista, Lima Chorrillos 15067, Lima, Peru

Corresponding author: Carlos Andrés Mugruza-Vassallo, PhD, Senior Lecturer, Escuela Profesional de Medicina Humana, Universidad Privada San Juan Bautista, Ex Hacienda Villa, Av José Antonio Lavalle N° 302, Lima Chorrillos 15067, Lima, Peru. cmugruza@yahoo.com

Abstract

Dan and colleagues recently published research suggesting that the gastrointestinal microbiome (microorganisms and metabolites) in cholelithiasis. They reviewed gallbladder stones, choledocholithiasis, and asymptomatic gallstones. Finally, their discussion was on the gastrointestinal. We focused on complementing the effect of the S1 protein and neuroinflammatory changes caused by severe acute respiratory syndrome coronavirus 2. Our contribution was about to involve the microbiota and the nervous system. They can have similar functions because they have similar pathways and advantages, bearing in mind γ-aminobutyric acid in schizophrenia and serotonin in Parkinson's disease. Therefore in the next few years, more research should be encouraged on the microbiota consequences for development, and mobility.

Key Words: Gastrointestinal microbiome; γ-aminobutyric acid; Serotonin; Letter

©The Author(s) 2023. Published by Baishideng Publishing Group Inc. All rights reserved.

Core Tip: The microbiota and the nervous system can have similar functions because they have similar advantages. Bearing in mindγ-aminobutyric acid (GABA) in schizophrenia and serotonin in Parkinson's disease and GABA and serotonin management, we expect in the next few years, more research should be encouraged on the microbiota consequences for development, and mobility.

Citation: Mancha Chahuara M, Lopez Tufino LDM, Mugruza-Vassallo CA. Gastrointestinal microbiome and cholelithiasis: Prospect in the nervous system. *World J Gastroenterol* 2023; 29(34): 5091-5093
URL: https://www.wjgnet.com/1007-9327/full/v29/i34/5091.htm
DOI: https://dx.doi.org/10.3748/wjg.v29.i34.5091

TO THE EDITOR

Dan and colleagues recently published research suggesting that the gastrointestinal microbiome (microorganisms and metabolites) in cholelithiasis. They reviewed gallbladder stones, choledocholithiasis, and asymptomatic gallstones. Finally, their discussion was on the gastrointestinal microbiome changes and influences on cholelithogenesis[1]. This letter focuses on complementing the effect of the S1 protein and neuroinflammatory changes caused by severe acute respiratory syndrome coronavirus 2.

In the article by Garza-Velasco *et al*[2] molecular techniques were used for sequence and nucleic acids. The polymerase chain reaction in real time provided information on the importance of the microbiota in the proper functioning of the human body, *i.e.* the treatment programs associated with the administration of antibiotics affect the normal microbiota. This treatment causes the loss of sensitive members to the antimicrobial agent. Therefore, this can open the door for pathogens, which sometimes face serious competition for nutrients and oxygen. Also, both the microbiota and the nervous system may have similar functions because they have similar advantages. They argued that the microbiota may be important for the development, mobility, learning, and memory of the human brain by influencing different neurotransmitters such as serotonin and acid γ-aminobutyric acid (GABA), certain amounts of serotonin are also produced by bacteria such as Clostridium sporogenes and Ruminococcus. In addition, the microbiota synthesizes vitamins that contribute to the formation of important compounds in the metabolism of intestinal cells, including vitamin B and niacin, which are necessary for the tissues to produce Nicotinamide Adenine Dinucleotide. On the other hand, a significant part of the primary barrier prevents the free colonization of pathogens, regulates the proliferation of pathogens, and the productivity of antimicrobial agents that harm other species and/or different clones of the same species. Research on Escherichia coli colicins, with variants of the same species causing diarrhea. The protection of the intestinal microbiota also includes SCFA, for example, the acetate synthesized by Bifidobacterium longum prevents the development of Pseudomonas aeruginosa. Therefore together with propionate and butyrate, it prevents the growth of EHEC O157 and Proteus mirabilis[2]. Bearing in mind other studies with neurotransmitters involved in brain impairments GABA and serotonin. For example in the brain GABA in schizophrenic patients (modeling in brain areas by Ferrarelli and Tononi[3]; auditory cognitive properties by Mugruza-Vassallo and Potter[4]) as well as the linear association reported for the greater serotonin the lower nigral iron in Parkinson's disease patients (Jellen *et al*[5]).

Moreover, Swidsinki and Loening-Baucke[6] have shown that intestinal bacterial monocultures are resistant. They can avoid the host's immunological responses that are persistent in harsh environments and have a coordinated response to environmental stressors. The intestine is never completely sterile, and the host never has complete control over bacterial growth. The appearance, composition, and organization of the gut microbiota in each gut segment depended on whether inhibition or segregation predominates. In areas of the intestine where the microbiota was suppressed, the bacteria were sporadically present with variable composition and low concentrations. Complete separation of bacteria from the mucosa and low levels of inhibition leads to the formation of intestinal reservoirs where bacteria can grow and reach high concentrations[3]. Intestinal reservoirs where bacteria can grow and accumulate in high concentrations are formed as a result of complete separation of bacteria from the mucosa and low levels of inhibition[3]. These bacteria are native to these regions of the intestine as well as for development and mobility.

Our contribution to the types of microbiome, the locations and how the microbiome affects or favors humans. Above all, the microbiota and the nervous system can have similar functions because they have similar advantages and pathways, bearing in mind GABA in schizophrenia and serotonin in Parkinson's disease. Therefore in the next few years, more research should be encouraged on the microbiota consequences for development, and mobility.

Our objective in this work was to make a contribution to the types of microbiome, the locations and how the microbiome affects or favors us. Above all, the microbiota and the nervous system can have similar functions because they have similar advantages, it is argued that the microbiota can be important for development and mobility. All authors are in complete agreement with the information stated. The content of this manuscript is our original work and has not been published, in whole or in part, before or simultaneously with this submission.

FOOTNOTES

Author contributions: Lopez Tufino LDM drafted a study on gastrointestinal microbiome and cholelithiasis, reviewed literature, and wrote an initial version of the paper; Mancha Chahuara M drafted study on gastrointestinal microbiome and cholelithiasis, reviewed literature, and wrote initial version of the paper; Mugruza-Vassallo CA reviewed and criticized gastrointestinal microbiome and cholelithiasis, he added the prospect in the nervous systems and corrected the paper.

Conflict-of-interest statement: The authors declare no conflict of interest.

Open-Access: This article is an open-access article that was selected by an in-house editor and fully peer-reviewed by external reviewers.

It is distributed in accordance with the Creative Commons Attribution NonCommercial (CC BY-NC 4.0) license, which permits others to distribute, remix, adapt, build upon this work non-commercially, and license their derivative works on different terms, provided the original work is properly cited and the use is non-commercial. See: https://creativecommons.org/Licenses/by-nc/4.0/

Country/Territory of origin: Peru

ORCID number: Mirella Mancha Chahuara 0009-0006-7399-2030; Leidhy Dhy Maruja Lopez Tufino 0009-0002-6190-3441; Carlos Andrés Mugruza-Vassallo 0000-0002-9262-7198.

S-Editor: Fan JR
L-Editor: A
P-Editor: Fan JR

REFERENCES

1 **Dan WY**, Yang YS, Peng LH, Sun G, Wang ZK. Gastrointestinal microbiome and cholelithiasis: Current status and perspectives. *World J Gastroenterol* 2023; **29**: 1589-1601 [PMID: 36970590 DOI: 10.3748/wjg.v29.i10.1589]

2 **Garza-Velasco R**, Garza-Manero SP, Perea-Mejía LM. Microbiota intestinal: aliada fundamental del organismo humano. Gut microbiota: our fundamental allied. *Educación Química* 2021; **32(1)**: 10 [DOI: 10.22201/fq.18708404e.2021.1.75734]

3 **Ferrarelli F**, Tononi G. Reduced sleep spindle activity point to a TRN-MD thalamus-PFC circuit dysfunction in schizophrenia. *Schizophr Res* 2017; **180**: 36-43 [PMID: 27269670 DOI: 10.1016/j.schres.2016.05.023]

4 **Mugruza-Vassallo C**, Potter D. Context Dependence Signature, Stimulus Properties and Stimulus Probability as Predictors of ERP Amplitude Variability. *Front Hum Neurosci* 2019; **13**: 39 [PMID: 30863293 DOI: 10.3389/fnhum.2019.00039]

5 **Jellen LC**, Lewis MM, Du G, Wang X, Galvis MLE, Krzyzanowski S, Capan CD, Snyder AM, Connor JR, Kong L, Mailman RB, Brundin P, Brundin L, Huang X. Low plasma serotonin linked to higher nigral iron in Parkinson's disease. *Sci Rep* 2021; **11**: 24384 [PMID: 34934078 DOI: 10.1038/s41598-021-03700-2]

6 **Swidsinski A**, Loening-Baucke V. Spatial organization of intestinal microbiota in health and disease. *UpToDate on line* 2020; **18**: 214-254 [DOI: 10.1002/9781118409855.ch9]



Published by **Baishideng Publishing Group Inc**
7041 Koll Center Parkway, Suite 160, Pleasanton, CA 94566, USA
Telephone: +1-925-3991568
E-mail: bpgoffice@wjgnet.com
Help Desk: https://www.f6publishing.com/helpdesk
https://www.wjgnet.com



© 2023 Baishideng Publishing Group Inc. All rights reserved.

ISSN 1007-9327 (print)
ISSN 2219-2840 (online)

World Journal of *Gastroenterology*

World J Gastroenterol 2023 September 21; 29(35): 5094-5179



Published by Baishideng Publishing Group Inc

World Journal of Gastroenterology

Contents

Weekly Volume 29 Number 35 September 21, 2023

REVIEW

5094 Developments and challenges in neoadjuvant therapy for locally advanced pancreatic cancer

Zhou B, Zhang SR, Chen G, Chen P

ORIGINAL ARTICLE

Basic Study

5104 Regenerating gene 4 promotes chemoresistance of colorectal cancer by affecting lipid droplet synthesis and assembly

Zhang CY, Zhang R, Zhang L, Wang ZM, Sun HZ, Cui ZG, Zheng HC

Retrospective Cohort Study

5125 Clinical characteristics and outcome of autoimmune pancreatitis based on serum immunoglobulin G4 level: A single-center, retrospective cohort study

Zhou GZ, Zeng JQ, Wang L, Liu M, Meng K, Wang ZK, Zhang XL, Peng LH, Yan B, Pan F

Retrospective Study

5138 Machine learning-based decision tool for selecting patients with idiopathic acute pancreatitis for endosonography to exclude a biliary aetiology

Sirtl S, Żorniak M, Hohmann E, Beyer G, Dibos M, Wandel A, Phillip V, Ammer-Herrmenau C, Neesse A, Schulz C, Schirra J, Mayerle J, Mahajan UM

Clinical Trials Study

5154 Heparanase inhibition leads to improvement in patients with acute gastrointestinal injuries induced by sepsis

Chen TT, Lv JJ, Chen L, Li M, Liu LP

Observational Study

5166 Lowering the threshold of alanine aminotransferase for enhanced identification of significant hepatic injury in chronic hepatitis B patients

Yu HS, Jiang H, Li MK, Yang BL, Smayi A, Chen JN, Wu B, Yang YD

CORRECTION

5178 Correction to "Role of prebiotics, probiotics, and synbiotics in management of inflammatory bowel disease: Current perspectives"

Roy S, Dhaneshwar S

World Journal of Gastroenterology

Weekly Volume 29 Number 35 September 21, 2023

Contents

ABOUT COVER

Editorial Board Member of *World Journal of Gastroenterology*, Konstantinos Triantafyllou, MD, PhD, FEBGH, Full Professor, Hepatogastroenterology Unit, Second Department of Internal Medicine-Propaedeutic, Medical School, National and Kapodistrian University of Athens, ''Attikon" University General Hospital, Athens 12462, Greece. ktriant@med.uoa.gr

AIMS AND SCOPE

The primary aim of *World Journal of Gastroenterology* (*WJG*, *World J Gastroenterol*) is to provide scholars and readers from various fields of gastroenterology and hepatology with a platform to publish high-quality basic and clinical research articles and communicate their research findings online. *WJG* mainly publishes articles reporting research results and findings obtained in the field of gastroenterology and hepatology and covering a wide range of topics including gastroenterology, hepatology, gastrointestinal endoscopy, gastrointestinal surgery, gastrointestinal oncology, and pediatric gastroenterology.

INDEXING/ABSTRACTING

The *WJG* is now abstracted and indexed in Science Citation Index Expanded (SCIE, also known as SciSearch®), Current Contents/Clinical Medicine, Journal Citation Reports, Index Medicus, MEDLINE, PubMed, PubMed Central, Scopus, Reference Citation Analysis, China Science and Technology Journal Database, and Superstar Journals Database. The 2023 edition of Journal Citation Reports® cites the 2022 impact factor (IF) for *WJG* as 4.3; Quartile category: Q2. The *WJG*'s CiteScore for 2021 is 8.3.

RESPONSIBLE EDITORS FOR THIS ISSUE

Production Editor: *Yi-Xuan Cai*; **Production Department Director:** *Xiang Li*; **Editorial Office Director:** *Jia-Ru Fan.*

NAME OF JOURNAL
World Journal of Gastroenterology

ISSN
ISSN 1007-9327 (print) ISSN 2219-2840 (online)

LAUNCH DATE
October 1, 1995

FREQUENCY
Weekly

EDITORS-IN-CHIEF
Andrzej S Tarnawski

EXECUTIVE ASSOCIATE EDITORS-IN-CHIEF
Xian-Jun Yu (Pancreatic Oncology), Jian-Gao Fan (Chronic Liver Disease)

EDITORIAL BOARD MEMBERS
http://www.wjgnet.com/1007-9327/editorialboard.htm

PUBLICATION DATE
September 21, 2023

COPYRIGHT
© 2023 Baishideng Publishing Group Inc

PUBLISHING PARTNER
Pancreatic Cancer Institute, Fudan University

INSTRUCTIONS TO AUTHORS
https://www.wjgnet.com/bpg/gerinfo/204

GUIDELINES FOR ETHICS DOCUMENTS
https://www.wjgnet.com/bpg/GerInfo/287

GUIDELINES FOR NON-NATIVE SPEAKERS OF ENGLISH
https://www.wjgnet.com/bpg/gerinfo/240

PUBLICATION ETHICS
https://www.wjgnet.com/bpg/GerInfo/288

PUBLICATION MISCONDUCT
https://www.wjgnet.com/bpg/gerinfo/208

POLICY OF CO-AUTHORS
https://www.wjgnet.com/bpg/GerInfo/310

ARTICLE PROCESSING CHARGE
https://www.wjgnet.com/bpg/gerinfo/242

STEPS FOR SUBMITTING MANUSCRIPTS
https://www.wjgnet.com/bpg/GerInfo/239

ONLINE SUBMISSION
https://www.f6publishing.com

PUBLISHING PARTNER's OFFICIAL WEBSITE
https://www.shca.org.cn/

© 2023 Baishideng Publishing Group Inc. All rights reserved. 7041 Koll Center Parkway, Suite 160, Pleasanton, CA 94566, USA
E-mail: bpgoffice@wjgnet.com https://www.wjgnet.com

World Journal of Gastroenterology

Submit a Manuscript: https://www.f6publishing.com

World J Gastroenterol 2023 September 21; 29(35): 5094-5103

DOI: 10.3748/wjg.v29.i35.5094

ISSN 1007-9327 (print) ISSN 2219-2840 (online)

REVIEW

Developments and challenges in neoadjuvant therapy for locally advanced pancreatic cancer

Bo Zhou, Shi-Ran Zhang, Geng Chen, Ping Chen

Specialty type: Gastroenterology and hepatology

Provenance and peer review: Invited article; Externally peer reviewed.

Peer-review model: Single blind

Peer-review report's scientific quality classification

Grade A (Excellent): 0
Grade B (Very good): B
Grade C (Good): C
Grade D (Fair): 0
Grade E (Poor): 0

P-Reviewer: Nagaya M, Japan; Shalaby MN, Egypt

Received: June 10, 2023
Peer-review started: June 10, 2023
First decision: July 10, 2023
Revised: July 19, 2023
Accepted: August 31, 2023
Article in press: August 31, 2023
Published online: September 21, 2023

Bo Zhou, Shi-Ran Zhang, Geng Chen, Ping Chen, Department of Hepatobiliary Surgery, Daping Hospital, Army Medical University, Chongqing 400042, China

Corresponding author: Ping Chen, MD, PhD, Professor, Surgeon, Department of Hepatobiliary Surgery, Daping Hospital, Army Medical University, No. 10 Changjiang Branch Road, Yuzhong District, Chongqing 400042, China. chenpingsyd@126.com

Abstract

Pancreatic ductal adenocarcinoma (PDAC) remains a significant public health challenge and is currently the fourth leading cause of cancer-related mortality in developed countries. Despite advances in cancer treatment, the 5-year survival rate for patients with PDAC remains less than 5%. In recent years, neoadjuvant therapy (NAT) has emerged as a promising treatment option for many cancer types, including locally advanced PDAC, with the potential to improve patient outcomes. To analyze the role of NAT in the setting of locally advanced PDAC over the past decade, a systematic literature search was conducted using PubMed and Web of Science. The results suggest that NAT may reduce the local mass size, promote tumor downstaging, and increase the likelihood of resection. These findings are supported by the latest evidence-based medical literature and the clinical experience of our center. Despite the potential benefits of NAT, there are still challenges that need to be addressed. One such challenge is the lack of consensus on the optimal timing and duration of NAT. Improved criteria for patient selection are needed to further identify PDAC patients likely to respond to NAT. In conclusion, NAT has emerged as a promising treatment option for locally advanced PDAC. However, further research is needed to optimize its use and to better understand the role of NAT in the management of this challenging disease. With continued advances in cancer treatment, there is hope of improving the outcomes of patients with PDAC in the future.

Key Words: Neoadjuvant therapy; Pancreatic ductal adenocarcinoma; Locally advanced pancreatic cancer; Chemoradiotherapy; Immunotherapy; Vaccine therapy

©The Author(s) 2023. Published by Baishideng Publishing Group Inc. All rights reserved.

Core Tip: In recent years, neoadjuvant therapy (NAT) has emerged as a promising treatment option for many cancer types, including locally advanced pancreatic ductal adenocarcinoma, with the potential to improve patient outcomes. To analyze the role of NAT in the setting of locally advanced pancreatic ductal adenocarcinoma over the past decade, a systematic literature search was conducted using PubMed and Web of Science. Despite the potential benefits of NAT, there are still challenges that need to be addressed. Additionally, there is a need for better patient selection criteria to identify those who are most likely to benefit from this approach.

Citation: Zhou B, Zhang SR, Chen G, Chen P. Developments and challenges in neoadjuvant therapy for locally advanced pancreatic cancer. *World J Gastroenterol* 2023; 29(35): 5094-5103
URL: https://www.wjgnet.com/1007-9327/full/v29/i35/5094.htm
DOI: https://dx.doi.org/10.3748/wjg.v29.i35.5094

INTRODUCTION

Pancreatic ductal adenocarcinoma (PDAC) is a malignancy with a poor prognosis, and it is currently the seventh leading cause of cancer-related death worldwide. The number of deaths from PDAC (466000) is almost equal to the number of new cases (496000) each year[1-3]. Experts predict that PDAC will surpass breast cancer as the third leading cause of cancer-related deaths by 2025 in 28 European countries[4]. The 5-year survival rate for patients with PDAC is less than 5%, and locally advanced pancreatic cancer (LAPC) accounts for one-third of all pancreatic cancer cases[5-7]. Unfortunately, approximately 60% of patients with LAPC present with metastatic disease and/or poor performance status, making them ineligible for surgery[8,9]. Despite improvements in diagnosis and treatment, clinical outcomes for these patients remain poor.

In 1992, Evans *et al*[10] first proposed the use of neoadjuvant therapy (NAT) for PDAC and found that patients treated with NAT had superior outcomes compared to those treated with postsurgical adjuvant therapy[11,12]. NAT is administered before surgery to reduce tumor mass, promote tumor downstaging, or eliminate early metastatic cells, thereby improving prognosis. In the last decade, the strategy of NAT followed by conversion surgery has been increasingly employed in the treatment of LAPC[13]. The goal of this review was to summarize and discuss research exploring the use of NAT for LAPC.

DEFINITIONS OF LAPC

Pancreatic cancer is typically classified based on its resectability on preoperative imaging, according to guidelines such as the National Comprehensive Cancer Network 2022 edition, the Chinese guidelines for the Neoadjuvant Therapy of Pancreatic Cancer 2021 edition, and the International Association of Pancreatology[5,14,15]. LAPC is generally defined as local tumor growth with major involvement (> 180° circumferential) or true invasion of the superior mesenteric artery, celiac axis, or hepatic artery and/or involvement of the portal vein/superior mesenteric vein that prevents reconstruction [16]. Table 1 provides a summary of these criteria.

CHEMORADIOTHERAPY FOR LAPC

LAPC, previously thought to be an incurable disease stage and an indication for palliative treatment, is now strongly considered a potentially curable disease. Gemcitabine (GEM)-based chemoradiotherapy is the standard treatment for LAPC, with a reported median survival of 24.2 mo and progression-free survival of 15 mo[17,18]. Polychemotherapy treatment with combined leucovorin calcium (folinic acid), fluorouracil, irinotecan hydrochloride, and oxaliplatin (FOLFIRINOX) and GEM + nab-paclitaxel is recommended[19].

In a database query of patients who received induction FOLFIRINOX for LAPC between 2010 and 2016, nearly 20% responded sufficiently to undergo resection, which improved overall survival compared to that of patients who did not undergo resection[20]. Another study enrolled 485 patients with at least three cycles of first-line chemotherapy with FOLFIRINOX or GEM plus nanoparticle albumin-bound paclitaxel (GA) between 2010 and 2017 and revealed that according to the Response Evaluation Criteria in Solid Tumors a partial response was more common among patients treated with FOLFIRINOX [27 of 140 patients (19%)] than among those treated with GA [8 of 140 patients (6%); $P = 0.001$]. In this cohort of patients, FOLFIRINOX was associated with higher rates of Response Evaluation Criteria in Solid Tumors-defined partial response and subsequent pancreatectomy than GA[21]. The different types of trials evaluating NAT for LAPC in recent years are summarized in Table 2[19,22-25].

Before the administration of chemotherapy, patients diagnosed with LAPC should undergo a thorough preliminary assessment of their performance status based on the Eastern Cooperative Oncology Group (ECOG) score[26]. In addition, it is imperative to evaluate nutritional status, symptom burden, and active comorbidities (with appropriate adjustments made for treatment as warranted) and to assess biliary tract patency while considering the need for diversion or stent

Table 1 Definitions of locally advanced pancreatic cancer by different groups

Group	Definition	
	Arterial	Venous
NCCN [14]	Head/uncinate process: Solid tumor contact > 180° with the SMA or CA Body and tail Solid tumor contact of > 180° with the SMA or CA Solid tumor contact with the CA and aortic involvement	Unreconstructible SMV/PV due to tumor involvement or occlusion (can be due to tumor or bland thrombus)
IAP[15]	Tumor contact/invasion of 180 or more degree CHA Tumor contact/invasion showing tumor contact/invasion of the PHA and/or CA	Bilateral narrowing/occlusion, exceeding the inferior border of the duodenum
CMA[5]	Head Solid tumor contact of > 180° with the SMA or CA Body and tail Solid tumor contact of > 180° with the SMA or CA Solid tumor contact with the CA and aortic involvement	Unreconstructible SMV/PV due to tumor involvement or occlusion (can be due to tumor or bland thrombus). The tumor extensively involves the distal jejunal drainage branch of the superior mesenteric vein

CA: Celiac axis; CHA: Common hepatic artery; CMA: Chinese Medical Association; IAP: International Association of Pancreatology; NCCN: National Comprehensive Cancer Network; PHA: Proper hepatic artery; PV: Portal vein; SMA: Superior mesenteric artery; SMV: Superior mesenteric vein.

Table 2 Summary of trials evaluating neoadjuvant therapy for locally advanced pancreatic cancer

Ref.	Type of study	Years of accrual	No. of patients	Primary endpoint	Arms	Key findings
NCT03652428[19]	Phase 1; Phase 2	2019-2023	24	12 mo after registration or until death	Proton therapy with concurrent GEM + Nab-paclitaxel	Ongoing
NCT02578732[22]	Phase 2	2016-2024	28	Until progression, up to 5 yr	FOLFOX	Ongoing
NCT04247165[23]	Phase 1; Phase 2	2020-2024	20	12 mo	Drug: GEM; Nab-paclitaxel; Nivolumab; Ipilimumab	Ongoing
NCT02873598[24]	Phase 1	2016-2021	15	Up to 5 yr	FOLFIRINOX or GEM/abraxane followed by SBRT	Not yet publicly available
NCT02704143[25]	Phase 2	2016-2020	63	3 yr	Combination of Cyberknife with S-1	Promising efficacy

FOLFOX: Folinic acid, fluorouracil, and oxaliplatin; FOLFIRINOX: Folinic acid, fluorouracil, irinotecan hydrochloride, and oxaliplatin; GEM: Gemcitabine; S-1: Tegafur, gimeracil, and oteracil; SBRT: Stereotactic body radiation therapy.

placement. Geriatric assessment is recommended for patients who are aged 70 years and above[27]. For those patients exhibiting a good performance status (ECOG score between 0-1) along with good nutritional health, first-line chemotherapy is advised, similar to the approach for patients diagnosed with metastatic liver cancer. In contrast, for patients with higher ECOG scores, a GEM-based regimen is preferred due to its lower toxicity profile[28].

The use of stereotactic body radiation therapy (SBRT) with adjuvant chemotherapy in the treatment of LAPC has been a subject of interest among oncologists. While conventional fractionated radiation has been the standard approach, studies have explored the potential of SBRT in downstaging LAPC[29]. One recent study examined the efficacy of sequential SBRT following FOLFIRINOX chemotherapy in patients with stable but unresectable LAPC. The study authors reviewed medical records from 50 patients who were treated with induction FOLFIRINOX for a median of eight cycles, followed by SBRT. The median overall survival and progression-free survival were reported as 26.4 mo (95% confidence

interval: 22.4-30.3) and 16.7 mo (95% confidence interval: 13.0-20.3), respectively[30]. While SBRT appears to have limited utility in the treatment of LAPC compared to conventional fractionated radiation, this study suggested that it may have a role in certain cases. A multidisciplinary approach should be considered when determining optimal treatment strategies for patients with LAPC who are not surgical candidates.

In addition to SBRT, Robert R. Wilson[31] first proposed particle therapy for the treatment of tumors in 1946. After more than 70 years of development, particle therapy has become another well-established tumor treatment method after surgery, chemotherapy, traditional radiotherapy, and immunotherapy[32]. Currently, particle radiotherapy, which includes proton and heavy ion radiotherapy, has been successfully applied to the treatment of cancer. C-ion and proton radiotherapy are the most commonly used types of particle radiotherapy in clinical practice and have higher accuracy and better cell killing effects, especially in high hypoxia areas and radiation-resistant cell cycle phases[33-35]. In addition, particle radiotherapy decreases the viability, proliferation, and migration of cancer cells[36-39]. Therefore, particle therapy is used to treat deeply penetrating and radiation-resistant tumors, especially pancreatic cancers.

IMMUNOTHERAPY FOR LAPC

Currently, the use of immunotherapy for LAPC is supported by limited data. A recent immune checkpoint inhibitor trial investigating anti-PD-L1 therapy in patients with LAPC failed to demonstrate efficacy due to the poor immunogenicity and immunosuppressive tumor microenvironment of pancreatic cancer[40,41]. However, a minority of patients have genetic mutations that may be targeted with specific interventions. Ongoing clinical trials targeting these mutations have led to discoveries[42,43].

Monoclonal antibodies (mAbs) have been an integral tool in cancer treatment for several decades. They possess the ability to directly kill cells through antibody-dependent cytotoxicity and other pathways and to regulate the immune microenvironment by blocking corresponding signaling pathways, reversing immunosuppression, and enhancing the activity of antitumor effector cells. Moreover, mAbs can even be utilized for the delivery of various therapeutic reagents (Table 3)[44-50].

Mesenchymal stem cells (MSCs) are present in some solid tumors, including PDAC, where they represent almost 100% of cells[51-54]. MSCs play a pivotal role in the development of PDAC. By attenuating MSC recruitment into tumors and inhibiting their tumor-supportive activities, therapeutic outcomes for cancer patients can be improved when MSCs are combined with other anticancer drugs, such as immunotherapy[51]. Numerous clinical studies are currently assessing MSC-based cell therapies[55,56].

Mucin 1 (MUC1) is overexpressed in approximately 90% of PDAC cells[57-60]. A study demonstrated that an antibody similar to the anti-MUC1 antibody GP1.4 could inhibit the proliferation and migration of cancer cells[61]. Additionally, Muc1-c, an isoform of MUC1 with the ability to cross membranes and inhibit tumor growth, could be used as a carrier for cytotoxins in the future[62].

The overexpression of vascular endothelial growth factor mRNA is a common feature in most human tumors and is strongly associated with increased invasiveness, vascular density, metastasis, recurrence, and a poor prognosis[63]. The approval of bevacizumab, a mAb that targets vascular endothelial growth factor, has paved the way for the development of other inhibitors targeting this pathway[64,65].

Annexin A6 (AnxA6) is the largest member of the conserved annexin family of proteins and is known for its modular domain organization and interactions with a variety of proteins and lipids[66,67]. Elevated levels of AnxA6 have been documented during the progression of pancreatic cancer[48,68,69]. In a recent study, O'Sullivan *et al*[48] isolated a novel anti-AnxA6 antibody, 9E1, and demonstrated its ability to reduce the invasion capacity of pancreatic cancer cells.

The Notch signaling pathway plays a vital role in the development of embryonic and tissue homeostasis, and it has been implicated in various malignancies. One of the key ligands in mammals is Delta-like ligand 4, which contributes significantly to cancer progression[70]. Demcizumab, a humanized anti-Delta-like ligand 4 antibody, has shown potential for reversing chemotherapy resistance when used in combination with paclitaxel and GEM. However, a recent study showed that while the combination was safe, it did not improve efficacy[71].

Radioimmunotherapy is emerging as a significant treatment option for patients with PDAC[72]. Recent studies have identified CD147 and B7-H3 as potential targets for radioimmunotherapy and have demonstrated the highly promising therapeutic effects of such treatments for PDAC[73,74].

NOVEL THERAPIES FOR LAPC

Vaccine therapy for LAPC

Owing to the intertumoral and intratumoral heterogeneity of pancreatic cancer, immunotherapy, targeted therapy, and other promising treatments have been extensively tested in preclinical studies and clinical trials. However, almost all strategies have shown little significant advantage over conventional chemotherapy against pancreatic cancer, and this issue is often compounded by prevalent therapeutic resistance[75,76]. Cancer vaccines have emerged as a promising therapeutic approach for pancreatic cancer because of their multiple targets, small nonspecific effects, wide therapeutic windows, low toxicity, and induction of lasting immune memory. In particular, mRNA-based vaccines possess numerous advantages over conventional vaccines in terms of factors including efficiency, safety, increased developmental potential, and low production costs. They have facilitated significant technological and conceptual progress in personalized and precise treatment. Hence, they represent a potential choice for novel therapies for pancreatic cancer[77,78].

Table 3 Monoclonal antibody-based therapies targeting non-immune cells for pancreatic ductal adenocarcinoma

Ref.	Type of study	Years of accrual	Target	mAb
NCT01521325[44]	Phase 1	2011-2013	Mesothelin	MORAb-009
Patel *et al*[45]	Preclinical study	2013	MUC-5AC	NPC-1C
NCT03376659[46]	Phase 1/Phase 2	2018-2023	VEGF	Bevacizumab
NCT00614653[47]	Phase 1	2008-2016	VEGF	Bevacizumab
O'Sullivan *et al*[48]	Preclinical study	2017	AnxA6	9E1
Smith *et al*[49]	Phase 1	2008-2011	DLL4	Demcizumab
NCT02722954[50]	Phase 1	2016-2017	DLL4	Demcizumab

AnxA6: Annexin A6; DLL4: Delta-like ligand 4; mAb: Monoclonal antibody; MUC: Mucin; VEGF: Vascular endothelial growth factor.

Cancer gene and signaling pathway therapy for LAPC

Recent evidence has revealed that numerous genes and signaling pathways play critical roles in the pathogenesis and progression of PDAC and thus could be potential valuable therapeutic targets[79,80].

Molecular pathways

Activating mutations of *KRAS* and the phosphoinositide 3 kinase/AKT/mammalian target of rapamycin (PI3K/AKT/mTOR) signaling pathway are frequently observed in PDAC and are associated with a poor prognosis[80,81]. In addition, numerous receptor tyrosine kinases have been implicated in the development and progression of PDAC, including tropomyosin receptor kinase, epidermal growth factor receptor, insulin-like growth factor receptor, fibroblast growth factor receptor, vascular epidermal growth factor receptor, platelet-derived growth factor receptor, and others[79,82-84].

Tumor suppressor genes

Tumor suppressor genes play a vital role in regulating cell growth by preventing severe metastasis; in tumors, these genes can be altered *via* mutation or chromosomal rearrangement. In PDAC, several tumor suppressor genes, including cyclin-dependent kinase inhibitor p16, *p53*, and suppressor of mothers against decapentaplegic protein 4, are frequently mutated[80,82].

DNA repair factors

Studies have revealed that PDAC ranks as the third most common cancer associated with mutations in the BReast CAncer gene and mismatch repair genes, following breast and ovarian cancers[85-87]. Novel combination therapies evaluating immune therapies and targeted agents are being tested for patients with PDAC linked to impaired DNA damage repair [88,89].

Epithelial-mesenchymal transition

Epithelial-mesenchymal transition is a critical process in which epithelial cells acquire mesenchymal features[90,91]. In the context of PDAC, epithelial-mesenchymal transition has been associated with tumor initiation, invasion, metastasis, and resistance to therapy[92].

Cancer stem cells

Cancer stem cells (CSCs) play a critical role in tumor initiation, progression, and therapeutic resistance. In PDAC, CSCs express cell surface markers such as CD24, CD44, CD133, epithelial-specific antigen, c-Met, C-X-C motif chemokine receptor 4, and aldehyde dehydrogenase[93]. CSCs have been shown to protect tumor cells from the cytotoxic effects of chemotherapy drugs and are associated with advanced tumor recurrence. However, the mechanisms underlying CSC-mediated drug resistance remain unclear.

EVALUATION OF TREATMENT RESPONSE AFTER NAT

Evaluation of treatment response and prediction of resectability after NAT remains a challenge for patients with LAPC. Pathological assessment of response after surgical resection remains the gold standard, but this approach is limited by its invasiveness[94,95]. Multidetector computed tomography is the most commonly used imaging modality to evaluate the response of LAPC after NAT. Its advantages over other techniques include higher spatial resolution and multiplanar reconstruction capabilities[96]. Other imaging modalities, such as endoscopic ultrasound, diffusion-weighted imaging, positron emission tomography, and perfusion computerized tomography, show significant potential to become powerful tools for assessing tumor resectability and predicting survival after NAT[97]. Tumor markers are also commonly used as evaluation indicators, with carbohydrate antigen 19-9 being the only biomarker currently recommended by the National

Comprehensive Cancer Network guidelines for assessing NAT response. Other promising indicators being studied include circulating tumor cells, circulating tumor DNA, and microRNAs, among others[96].

CONCLUSION

LAPC remains a challenging disease, despite significant progress made in its treatment over the past decade. Notably, immunotherapy has shown remarkable improvements in the management of LAPC. Across all fields of pancreatic cancer research, substantial advancements have been achieved. Basic research has significantly improved the understanding of this disease. Moreover, the advent of advanced DNA and RNA sequencing technologies has enabled The Cancer Genome Atlas consortium to study both the whole genome and transcriptomes of human tumors, thereby facilitating the identification of driver mutations and transcriptional programs implicated in carcinogenesis. These efforts are poised to accelerate the application of precision medicine strategies[98-100]. Administration of NAT for the treatment of LAPC can provide important benefits, although more in-depth studies are needed. Therefore, a multidisciplinary team comprising surgeons, oncologists, radiation oncologists, and radiologists is essential for the optimal treatment of LAPC. The most urgent issues to address include identifying patients who are most suitable for NAT and evaluating treatment effects in a timely and accurate manner to achieve more precise and effective treatments for patients with LAPC.

FOOTNOTES

Author contributions: Chen P contributed to the concept, design, and drafting of the article, and approved the final revision; Zhou B drafted the article; Zhang SR and Chen G revised the manuscript critically for intellectual content; all authors approved the version to be published.

Conflict-of-interest statement: All the authors report having no relevant conflicts of interest for this article.

Open-Access: This article is an open-access article that was selected by an in-house editor and fully peer-reviewed by external reviewers. It is distributed in accordance with the Creative Commons Attribution NonCommercial (CC BY-NC 4.0) license, which permits others to distribute, remix, adapt, build upon this work non-commercially, and license their derivative works on different terms, provided the original work is properly cited and the use is non-commercial. See: https://creativecommons.org/Licenses/by-nc/4.0/

Country/Territory of origin: China

ORCID number: Bo Zhou 0000-0001-8376-3182; Geng Chen 0000-0002-1642-7098; Ping Chen 0000-0001-6575-8582.

S-Editor: Yan JP
L-Editor: Filipodia
P-Editor: Cai YX

REFERENCES

1 **Sung H**, Ferlay J, Siegel RL, Laversanne M, Soerjomataram I, Jemal A, Bray F. Global Cancer Statistics 2020: GLOBOCAN Estimates of Incidence and Mortality Worldwide for 36 Cancers in 185 Countries. *CA Cancer J Clin* 2021; **71**: 209-249 [PMID: 33538338 DOI: 10.3322/caac.21660]

2 **Park W**, Chawla A, O'Reilly EM. Pancreatic Cancer: A Review. *JAMA* 2021; **326**: 851-862 [PMID: 34547082 DOI: 10.1001/jama.2021.13027]

3 **Wood LD**, Canto MI, Jaffee EM, Simeone DM. Pancreatic Cancer: Pathogenesis, Screening, Diagnosis, and Treatment. *Gastroenterology* 2022; **163**: 386-402.e1 [PMID: 35398344 DOI: 10.1053/j.gastro.2022.03.056]

4 **Ferlay J**, Partensky C, Bray F. More deaths from pancreatic cancer than breast cancer in the EU by 2017. *Acta Oncol* 2016; **55**: 1158-1160 [PMID: 27551890 DOI: 10.1080/0284186X.2016.1197419]

5 **Study Group of Pancreatic Surgery in China Society of Surgery of Chinese Medical Association**; Pancreatic Disease Committee of China Research Hospital Association. [The guideline for neoadjuvant therapy of pancreatic cancer in China (2020 edition)]. *Zhonghua Wai Ke Za Zhi* 2020; **58**: 657-667 [PMID: 32878410 DOI: 10.3760/cma.j.cn112139-20200708-00549]

6 **Ducreux M**, Cuhna AS, Caramella C, Hollebecque A, Burtin P, Goéré D, Seufferlein T, Haustermans K, Van Laethem JL, Conroy T, Arnold D; ESMO Guidelines Committee. Cancer of the pancreas: ESMO Clinical Practice Guidelines for diagnosis, treatment and follow-up. *Ann Oncol* 2015; **26** Suppl 5: v56-v68 [PMID: 26314780 DOI: 10.1093/annonc/mdv295]

7 **Neoptolemos JP**, Kleeff J, Michl P, Costello E, Greenhalf W, Palmer DH. Therapeutic developments in pancreatic cancer: current and future perspectives. *Nat Rev Gastroenterol Hepatol* 2018; **15**: 333-348 [PMID: 29717230 DOI: 10.1038/s41575-018-0005-x]

8 **Strobel O**, Neoptolemos J, Jäger D, Büchler MW. Optimizing the outcomes of pancreatic cancer surgery. *Nat Rev Clin Oncol* 2019; **16**: 11-26 [PMID: 30341417 DOI: 10.1038/s41571-018-0112-1]

9 **Mizrahi JD**, Surana R, Valle JW, Shroff RT. Pancreatic cancer. *Lancet* 2020; **395**: 2008-2020 [PMID: 32593337 DOI: 10.1016/S0140-6736(20)30974-0]

10 **Evans DB**, Rich TA, Byrd DR, Cleary KR, Connelly JH, Levin B, Charnsangavej C, Fenoglio CJ, Ames FC. Preoperative chemoradiation and pancreaticoduodenectomy for adenocarcinoma of the pancreas. *Arch Surg* 1992; **127**: 1335-1339 [PMID: 1359851 DOI:

10.1001/archsurg.1992.01420110083017]
11 **Springfeld C**, Ferrone CR, Katz MHG, Philip PA, Hong TS, Hackert T, Büchler MW, Neoptolemos J. Neoadjuvant therapy for pancreatic cancer. *Nat Rev Clin Oncol* 2023; **20**: 318-337 [PMID: 36932224 DOI: 10.1038/s41571-023-00746-1]
12 **Wang C**, Tan G, Zhang J, Fan B, Chen Y, Chen D, Yang L, Chen X, Duan Q, Maimaiti F, Du J, Lin Z, Gu J, Luo H. Neoadjuvant Therapy for Pancreatic Ductal Adenocarcinoma: Where Do We Go? *Front Oncol* 2022; **12**: 828223 [PMID: 35785193 DOI: 10.3389/fonc.2022.828223]
13 **Gemenetzis G**, Groot VP, Blair AB, Laheru DA, Zheng L, Narang AK, Fishman EK, Hruban RH, Yu J, Burkhart RA, Cameron JL, Weiss MJ, Wolfgang CL, He J. Survival in Locally Advanced Pancreatic Cancer After Neoadjuvant Therapy and Surgical Resection. *Ann Surg* 2019; **270**: 340-347 [PMID: 29596120 DOI: 10.1097/SLA.0000000000002753]
14 **Tempero MA**, Malafa MP, Al-Hawary M, Behrman SW, Benson AB, Cardin DB, Chiorean EG, Chung V, Czito B, Del Chiaro M, Dillhoff M, Donahue TR, Dotan E, Ferrone CR, Fountzilas C, Hardacre J, Hawkins WG, Klute K, Ko AH, Kunstman JW, LoConte N, Lowy AM, Moravek C, Nakakura EK, Narang AK, Obando J, Polanco PM, Reddy S, Reyngold M, Scaife C, Shen J, Vollmer C, Wolff RA, Wolpin BM, Lynn B, George GV. Pancreatic Adenocarcinoma, Version 2.2021, NCCN Clinical Practice Guidelines in Oncology. *J Natl Compr Canc Netw* 2021; **19**: 439-457 [PMID: 33845462 DOI: 10.6004/jnccn.2021.0017]
15 **Isaji S**, Mizuno S, Windsor JA, Bassi C, Fernández-Del Castillo C, Hackert T, Hayasaki A, Katz MHG, Kim SW, Kishiwada M, Kitagawa H, Michalski CW, Wolfgang CL. International consensus on definition and criteria of borderline resectable pancreatic ductal adenocarcinoma 2017. *Pancreatology* 2018; **18**: 2-11 [PMID: 29191513 DOI: 10.1016/j.pan.2017.11.011]
16 **Kwon W**, Thomas A, Kluger MD. Irreversible electroporation of locally advanced pancreatic cancer. *Semin Oncol* 2021; **48**: 84-94 [PMID: 33648735 DOI: 10.1053/j.seminoncol.2021.02.004]
17 **Von Hoff DD**, Ervin T, Arena FP, Chiorean EG, Infante J, Moore M, Seay T, Tjulandin SA, Ma WW, Saleh MN, Harris M, Reni M, Dowden S, Laheru D, Bahary N, Ramanathan RK, Tabernero J, Hidalgo M, Goldstein D, Van Cutsem E, Wei X, Iglesias J, Renschler MF. Increased survival in pancreatic cancer with nab-paclitaxel plus gemcitabine. *N Engl J Med* 2013; **369**: 1691-1703 [PMID: 24131140 DOI: 10.1056/NEJMoa1304369]
18 **Mizusawa J**, Fukutomi A, Katayama H, Ishii H, Ioka T, Okusaka T, Ueno H, Ueno M, Ikeda M, Mizuno N, Ozaka M, Fukuda H, Furuse J; Hepatobiliary and Pancreatic Oncology Group of the Japan Clinical Oncology Group. Protocol digest of randomized phase II study of modified FOLFIRINOX versus gemcitabine plus nab-paclitaxel combination therapy for locally advanced pancreatic cancer: Japan clinical oncology group study (JCOG1407). *Pancreatology* 2018; **18**: 841-845 [PMID: 30075908 DOI: 10.1016/j.pan.2018.07.007]
19 **Department of Radiation Oncology**, University of Maryland, Baltimore. Phase I Nab-Paclitaxel Plus Gemcitabine With Proton Therapy for Locally Advanced Pancreatic Cancer (LAPC). [accessed 2023 Apr 25]. In: ClinicalTrials.gov [Internet]. Bethesda (MD): U.S. National Library of Medicine. Available from: https://ClinicalTrials.gov/show/NCT03652428 ClinicalTrials.gov Identifier: NCT03652428
20 **McIntyre CA**, Cohen NA, Goldman DA, Gonen M, Sadot E, O'Reilly EM, Varghese AM, Yu KH, Balachandran VP, Soares KC, D'Angelica MI, Drebin JA, Kingham TP, Allen PJ, Wei AC, Jarnagin WR. Induction FOLFIRINOX for patients with locally unresectable pancreatic ductal adenocarcinoma. *J Surg Oncol* 2022; **125**: 425-436 [PMID: 34719035 DOI: 10.1002/jso.26735]
21 **Perri G**, Prakash L, Qiao W, Varadhachary GR, Wolff R, Fogelman D, Overman M, Pant S, Javle M, Koay EJ, Herman J, Kim M, Ikoma N, Tzeng CW, Lee JE, Katz MHG. Response and Survival Associated With First-line FOLFIRINOX vs Gemcitabine and nab-Paclitaxel Chemotherapy for Localized Pancreatic Ductal Adenocarcinoma. *JAMA Surg* 2020; **155**: 832-839 [PMID: 32667641 DOI: 10.1001/jamasurg.2020.2286]
22 **Brown University**. FOLFOX-A For Locally Advanced Pancreatic Cancer: A Phase II Brown University Oncology Research Group Trial. [accessed 2023 Apr 25]. In: ClinicalTrials.gov [Internet]. Bethesda (MD): U.S. National Library of Medicine. Available from: https://ClinicalTrials.gov/show/NCT02578732 ClinicalTrials.gov Identifier: NCT02578732
23 **Chen I**. Nivolumab, Ipilimumab and Chemoradiation in Pancreatic Cancer. [accessed 2023 Apr 25]. In: ClinicalTrials.gov [Internet]. Bethesda (MD): U.S. National Library of Medicine. Available from: https://ClinicalTrials.gov/show/NCT04247165 ClinicalTrials.gov Identifier: NCT04247165
24 **University of Colorado**, Denver. A Dose Escalation Trial of SBRT After Induction Chemotherapy for Locally Advanced Pancreatic Cancer. [accessed 2023 Apr 25]. In: ClinicalTrials.gov [Internet]. Bethesda (MD): U.S. National Library of Medicine. Available from: https://ClinicalTrials.gov/show/NCT02873598 ClinicalTrials.gov Identifier: NCT02873598
25 **Zhu X**, Cao Y, Lu M, Zhao X, Jiang L, Ye Y, Ju X, Zhang H. Stereotactic body radiation therapy with sequential S-1 for patients with locally advanced pancreatic cancer and poor performance status: An open-label, single-arm, phase 2 trial. *Radiother Oncol* 2021; **162**: 178-184 [PMID: 34274393 DOI: 10.1016/j.radonc.2021.07.009]
26 **Stein SM**, James ES, Deng Y, Cong X, Kortmansky JS, Li J, Staugaard C, Indukala D, Boustani AM, Patel V, Cha CH, Salem RR, Chang B, Hochster HS, Lacy J. Final analysis of a phase II study of modified FOLFIRINOX in locally advanced and metastatic pancreatic cancer. *Br J Cancer* 2016; **114**: 737-743 [PMID: 27022826 DOI: 10.1038/bjc.2016.45]
27 **Tempero MA**, Malafa MP, Al-Hawary M, Asbun H, Bain A, Behrman SW, Benson AB 3rd, Binder E, Cardin DB, Cha C, Chiorean EG, Chung V, Czito B, Dillhoff M, Dotan E, Ferrone CR, Hardacre J, Hawkins WG, Herman J, Ko AH, Komanduri S, Koong A, LoConte N, Lowy AM, Moravek C, Nakakura EK, O'Reilly EM, Obando J, Reddy S, Scaife C, Thayer S, Weekes CD, Wolff RA, Wolpin BM, Burns J, Darlow S. Pancreatic Adenocarcinoma, Version 2.2017, NCCN Clinical Practice Guidelines in Oncology. *J Natl Compr Canc Netw* 2017; **15**: 1028-1061 [PMID: 28784865 DOI: 10.6004/jnccn.2017.0131]
28 **Suker M**, Beumer BR, Sadot E, Marthey L, Faris JE, Mellon EA, El-Rayes BF, Wang-Gillam A, Lacy J, Hosein PJ, Moorcraft SY, Conroy T, Hohla F, Allen P, Taieb J, Hong TS, Shridhar R, Chau I, van Eijck CH, Koerkamp BG. FOLFIRINOX for locally advanced pancreatic cancer: a systematic review and patient-level meta-analysis. *Lancet Oncol* 2016; **17**: 801-810 [PMID: 27160474 DOI: 10.1016/S1470-2045(16)00172-8]
29 **Barros AG**, Pulido CF, Machado M, Brito MJ, Couto N, Sousa O, Melo SA, Mansinho H. Treatment optimization of locally advanced and metastatic pancreatic cancer (Review). *Int J Oncol* 2021; **59** [PMID: 34859257 DOI: 10.3892/ijo.2021.5290]
30 **Jung JH**, Song C, Jung IH, Ahn J, Kim B, Jung K, Lee JC, Kim J, Hwang JH. Induction FOLFIRINOX followed by stereotactic body radiation therapy in locally advanced pancreatic cancer. *Front Oncol* 2022; **12**: 1050070 [PMID: 36620548 DOI: 10.3389/fonc.2022.1050070]
31 **Wilson RR**. Radiological use of fast protons. *Radiology* 1946; **47**: 487-491 [PMID: 20274616 DOI: 10.1148/47.5.487]
32 **Missaglia A**, Bourkadi-Idrissi A, Casamichiela F, Mazzucconi D, Carminati M, Agosteo S, Fiorini C. Prompt-gamma fall-off estimation with C-ion irradiation at clinical energies, using a knife-edge slit camera: A Monte Carlo study. *Phys Med* 2023; **107**: 102554 [PMID: 36907030 DOI: 10.1016/j.ejmp.2023.102554]
33 **Broerse JJ**, Barendsen GW, van Kersen GR. Survival of cultured human cells after irradiation with fast neutrons of different energies in

hypoxic and oxygenated conditions. *Int J Radiat Biol Relat Stud Phys Chem Med* 1968; **13**: 559-572 [PMID: 5301983 DOI: 10.1080/09553006814550621]

34 **Charalampopoulou A**, Barcellini A, Frittitta GE, Fulgini G, Ivaldi GB, Magro G, Liotta M, Orlandi E, Pullia MG, Tabarelli de Fatis P, Facoetti A. In Vitro Effects of Photon Beam and Carbon Ion Radiotherapy on the Perineural Invasion of Two Cell Lines of Neurotropic Tumours. *Life (Basel)* 2023; **13** [PMID: 36983949 DOI: 10.3390/life13030794]

35 **Wozny AS**, Rodriguez-Lafrasse C. The 'stealth-bomber' paradigm for deciphering the tumour response to carbon-ion irradiation. *Br J Cancer* 2023; **128**: 1429-1438 [PMID: 36639527 DOI: 10.1038/s41416-022-02117-6]

36 **Kanai T**, Endo M, Minohara S, Miyahara N, Koyama-ito H, Tomura H, Matsufuji N, Futami Y, Fukumura A, Hiraoka T, Furusawa Y, Ando K, Suzuki M, Soga F, Kawachi K. Biophysical characteristics of HIMAC clinical irradiation system for heavy-ion radiation therapy. *Int J Radiat Oncol Biol Phys* 1999; **44**: 201-210 [PMID: 10219815 DOI: 10.1016/s0360-3016(98)00544-6]

37 **Reese AS**, Lu W, Regine WF. Utilization of intensity-modulated radiation therapy and image-guided radiation therapy in pancreatic cancer: is it beneficial? *Semin Radiat Oncol* 2014; **24**: 132-139 [PMID: 24635870 DOI: 10.1016/j.semradonc.2013.11.003]

38 **Bittner MI**, Grosu AL, Brunner TB. Comparison of toxicity after IMRT and 3D-conformal radiotherapy for patients with pancreatic cancer - a systematic review. *Radiother Oncol* 2015; **114**: 117-121 [PMID: 25497876 DOI: 10.1016/j.radonc.2014.11.043]

39 **Naumann M**, Czempiel T, Lößner AJ, Pape K, Beyreuther E, Löck S, Drukewitz S, Hennig A, von Neubeck C, Klink B, Krause M, William D, Stange DE, Bütof R, Dietrich A. Combined Systemic Drug Treatment with Proton Therapy: Investigations on Patient-Derived Organoids. *Cancers (Basel)* 2022; **14** [PMID: 35954444 DOI: 10.3390/cancers14153781]

40 **Brahmer JR**, Tykodi SS, Chow LQ, Hwu WJ, Topalian SL, Hwu P, Drake CG, Camacho LH, Kauh J, Odunsi K, Pitot HC, Hamid O, Bhatia S, Martins R, Eaton K, Chen S, Salay TM, Alaparthy S, Grosso JF, Korman AJ, Parker SM, Agrawal S, Goldberg SM, Pardoll DM, Gupta A, Wigginton JM. Safety and activity of anti-PD-L1 antibody in patients with advanced cancer. *N Engl J Med* 2012; **366**: 2455-2465 [PMID: 22658128 DOI: 10.1056/NEJMoa1200694]

41 **Jiang Y**, Li Y, Zhu B. T-cell exhaustion in the tumor microenvironment. *Cell Death Dis* 2015; **6**: e1792 [PMID: 26086965 DOI: 10.1038/cddis.2015.162]

42 **Nevala-Plagemann C**, Hidalgo M, Garrido-Laguna I. From state-of-the-art treatments to novel therapies for advanced-stage pancreatic cancer. *Nat Rev Clin Oncol* 2020; **17**: 108-123 [PMID: 31705130 DOI: 10.1038/s41571-019-0281-6]

43 **Le DT**, Durham JN, Smith KN, Wang H, Bartlett BR, Aulakh LK, Lu S, Kemberling H, Wilt C, Luber BS, Wong F, Azad NS, Rucki AA, Laheru D, Donehower R, Zaheer A, Fisher GA, Crocenzi TS, Lee JJ, Greten TF, Duffy AG, Ciombor KK, Eyring AD, Lam BH, Joe A, Kang SP, Holdhoff M, Danilova L, Cope L, Meyer C, Zhou S, Goldberg RM, Armstrong DK, Bever KM, Fader AN, Taube J, Housseau F, Spetzler D, Xiao N, Pardoll DM, Papadopoulos N, Kinzler KW, Eshleman JR, Vogelstein B, Anders RA, Diaz LA Jr. Mismatch repair deficiency predicts response of solid tumors to PD-1 blockade. *Science* 2017; **357**: 409-413 [PMID: 28596308 DOI: 10.1126/science.aan6733]

44 **Morphotek**. A Single-Dose Pilot Study of Radiolabeled Amatuximab (MORAb-009) in Mesothelin Over Expressing Cancers. [accessed 2023 Apr 25]. In: ClinicalTrials.gov [Internet]. Bethesda (MD): U.S. National Library of Medicine. Available from: https://ClinicalTrials.gov/show/NCT01521325 ClinicalTrials.gov Identifier: NCT01521325

45 **Patel SP**, Bristol A, Saric O, Wang XP, Dubeykovskiy A, Arlen PM, Morse MA. Anti-tumor activity of a novel monoclonal antibody, NPC-1C, optimized for recognition of tumor antigen MUC5AC variant in preclinical models. *Cancer Immunol Immunother* 2013; **62**: 1011-1019 [PMID: 23591984 DOI: 10.1007/s00262-013-1420-z]

46 **Georgetown University**. Durvalumab Plus CV301 With Maintenance Chemotherapy in Metastatic Colorectal or Pancreatic Adenocarcinoma. [accessed 2023 Apr 25]. In: ClinicalTrials.gov [Internet]. Bethesda (MD): U.S. National Library of Medicine. Available from: https://ClinicalTrials.gov/show/NCT03376659 ClinicalTrials.gov Identifier: NCT03376659

47 M.D. Anderson Cancer Center. Bevacizumab, Erlotinib and Capecitabine for Advanced Pancreatic Cancer. [accessed 2023 Apr 25]. In: ClinicalTrials.gov [Internet]. Bethesda (MD): U.S. National Library of Medicine. Available from: https://ClinicalTrials.gov/show/NCT00614653 ClinicalTrials.gov Identifier: NCT00614653

48 **O'Sullivan D**, Dowling P, Joyce H, McAuley E, McCann A, Henry M, McGovern B, Barham P, Kelleher FC, Murphy J, Kennedy S, Swan N, Moriarty M, Clynes M, Larkin A. A novel inhibitory anti-invasive MAb isolated using phenotypic screening highlights AnxA6 as a functionally relevant target protein in pancreatic cancer. *Br J Cancer* 2017; **117**: 1326-1335 [PMID: 28881357 DOI: 10.1038/bjc.2017.306]

49 **Smith DC**, Eisenberg PD, Manikhas G, Chugh R, Gubens MA, Stagg RJ, Kapoun AM, Xu L, Dupont J, Sikic B. A phase I dose escalation and expansion study of the anticancer stem cell agent demcizumab (anti-DLL4) in patients with previously treated solid tumors. *Clin Cancer Res* 2014; **20**: 6295-6303 [PMID: 25324140 DOI: 10.1158/1078-0432.CCR-14-1373]

50 **OncoMed Pharmaceuticals**, Inc. A Phase 1b Study of Demcizumab Plus Pembrolizumab in Locally Advanced or Metastatic Solid Tumors. [accessed 2023 Apr 25]. In: ClinicalTrials.gov [Internet]. Bethesda (MD): U.S. National Library of Medicine. Available from: https://ClinicalTrials.gov/show/NCT02722954 ClinicalTrials.gov Identifier: NCT02722954

51 **51 Argani P**, Iacobuzio-Donahue C, Ryu B, Rosty C, Goggins M, Wilentz RE, Murugesan SR, Leach SD, Jaffee E, Yeo CJ, Cameron JL, Kern SE, Hruban RH. Mesothelin is overexpressed in the vast majority of ductal adenocarcinomas of the pancreas: identification of a new pancreatic cancer marker by serial analysis of gene expression (SAGE). *Clin Cancer Res* 2001; **7**: 3862-3868 [PMID: 11751476]

52 **Lan T**, Luo M, Wei X. Mesenchymal stem/stromal cells in cancer therapy. *J Hematol Oncol* 2021; **14**: 195 [PMID: 34789315 DOI: 10.1186/s13045-021-01208-w]

53 **Weng Z**, Zhang B, Wu C, Yu F, Han B, Li B, Li L. Therapeutic roles of mesenchymal stem cell-derived extracellular vesicles in cancer. *J Hematol Oncol* 2021; **14**: 136 [PMID: 34479611 DOI: 10.1186/s13045-021-01141-y]

54 **Timaner M**, Tsai KK, Shaked Y. The multifaceted role of mesenchymal stem cells in cancer. *Semin Cancer Biol* 2020; **60**: 225-237 [PMID: 31212021 DOI: 10.1016/j.semcancer.2019.06.003]

55 **Hassan R**, Cohen SJ, Phillips M, Pastan I, Sharon E, Kelly RJ, Schweizer C, Weil S, Laheru D. Phase I clinical trial of the chimeric anti-mesothelin monoclonal antibody MORAb-009 in patients with mesothelin-expressing cancers. *Clin Cancer Res* 2010; **16**: 6132-6138 [PMID: 21037025 DOI: 10.1158/1078-0432.CCR-10-2275]

56 **Fujisaka Y**, Kurata T, Tanaka K, Kudo T, Okamoto K, Tsurutani J, Kaneda H, Okamoto I, Namiki M, Kitamura C, Nakagawa K. Phase I study of amatuximab, a novel monoclonal antibody to mesothelin, in Japanese patients with advanced solid tumors. *Invest New Drugs* 2015; **33**: 380-388 [PMID: 25502863 DOI: 10.1007/s10637-014-0196-0]

57 **Qu CF**, Li Y, Song YJ, Rizvi SM, Raja C, Zhang D, Samra J, Smith R, Perkins AC, Apostolidis C, Allen BJ. MUC1 expression in primary and metastatic pancreatic cancer cells for in vitro treatment by (213)Bi-C595 radioimmunoconjugate. *Br J Cancer* 2004; **91**: 2086-2093 [PMID: 15599383 DOI: 10.1038/sj.bjc.6602232]

58 **Besmer DM**, Curry JM, Roy LD, Tinder TL, Sahraei M, Schettini J, Hwang SI, Lee YY, Gendler SJ, Mukherjee P. Pancreatic ductal adenocarcinoma mice lacking mucin 1 have a profound defect in tumor growth and metastasis. *Cancer Res* 2011; **71**: 4432-4442 [PMID: 21558393 DOI: 10.1158/0008-5472.CAN-10-4439]

59 **Striefler JK**, Riess H, Lohneis P, Bischoff S, Kurreck A, Modest DP, Bahra M, Oettle H, Sinn M, Bläker H, Denkert C, Stintzing S, Sinn BV, Pelzer U. Mucin-1 Protein Is a Prognostic Marker for Pancreatic Ductal Adenocarcinoma: Results From the CONKO-001 Study. *Front Oncol* 2021; **11**: 670396 [PMID: 34386419 DOI: 10.3389/fonc.2021.670396]

60 **Nagai K**, Adachi T, Harada H, Eguchi S, Sugiyama H, Miyazaki Y. Dendritic Cell-based Immunotherapy Pulsed With Wilms Tumor 1 Peptide and Mucin 1 as an Adjuvant Therapy for Pancreatic Ductal Adenocarcinoma After Curative Resection: A Phase I/IIa Clinical Trial. *Anticancer Res* 2020; **40**: 5765-5776 [PMID: 32988904 DOI: 10.21873/anticanres.14593]

61 **Hisatsune A**, Nakayama H, Kawasaki M, Horie I, Miyata T, Isohama Y, Kim KC, Katsuki H. Anti-MUC1 antibody inhibits EGF receptor signaling in cancer cells. *Biochem Biophys Res Commun* 2011; **405**: 377-381 [PMID: 21219855 DOI: 10.1016/j.bbrc.2011.01.029]

62 **Wu G**, Maharjan S, Kim D, Kim JN, Park BK, Koh H, Moon K, Lee Y, Kwon HJ. A Novel Monoclonal Antibody Targets Mucin1 and Attenuates Growth in Pancreatic Cancer Model. *Int J Mol Sci* 2018; **19** [PMID: 29987260 DOI: 10.3390/ijms19072004]

63 **Kelly PN**. The Cancer Immunotherapy Revolution. *Science* 2018; **359**: 1344-1345 [PMID: 29567702 DOI: 10.1126/science.359.6382.1344]

64 **Ferrara N**, Adamis AP. Ten years of anti-vascular endothelial growth factor therapy. *Nat Rev Drug Discov* 2016; **15**: 385-403 [PMID: 26775688 DOI: 10.1038/nrd.2015.17]

65 **Apte RS**, Chen DS, Ferrara N. VEGF in Signaling and Disease: Beyond Discovery and Development. *Cell* 2019; **176**: 1248-1264 [PMID: 30849371 DOI: 10.1016/j.cell.2019.01.021]

66 **Enrich C**, Rentero C, de Muga SV, Reverter M, Mulay V, Wood P, Koese M, Grewal T. Annexin A6-Linking Ca(2+) signaling with cholesterol transport. *Biochim Biophys Acta* 2011; **1813**: 935-947 [PMID: 20888375 DOI: 10.1016/j.bbamcr.2010.09.015]

67 **Rentero C**, Blanco-Muñoz P, Meneses-Salas E, Grewal T, Enrich C. Annexins-Coordinators of Cholesterol Homeostasis in Endocytic Pathways. *Int J Mol Sci* 2018; **19** [PMID: 29757220 DOI: 10.3390/ijms19051444]

68 **Keklikoglou I**, Cianciaruso C, Güç E, Squadrito ML, Spring LM, Tazzyman S, Lambein L, Poissonnier A, Ferraro GB, Baer C, Cassará A, Guichard A, Iruela-Arispe ML, Lewis CE, Coussens LM, Bardia A, Jain RK, Pollard JW, De Palma M. Chemotherapy elicits pro-metastatic extracellular vesicles in breast cancer models. *Nat Cell Biol* 2019; **21**: 190-202 [PMID: 30598531 DOI: 10.1038/s41556-018-0256-3]

69 **Leca J**, Martinez S, Lac S, Nigri J, Secq V, Rubis M, Bressy C, Sergé A, Lavaut MN, Dusetti N, Loncle C, Roques J, Pietrasz D, Bousquet C, Garcia S, Granjeaud S, Ouaissi M, Bachet JB, Brun C, Iovanna JL, Zimmermann P, Vasseur S, Tomasini R. Cancer-associated fibroblast-derived annexin A6+ extracellular vesicles support pancreatic cancer aggressiveness. *J Clin Invest* 2016; **126**: 4140-4156 [PMID: 27701147 DOI: 10.1172/JCI87734]

70 **Fasoulakis Z**, Koutras A, Ntounis T, Pergialiotis V, Chionis A, Katrachouras A, Palios VC, Symeonidis P, Valsamaki A, Syllaios A, Diakosavvas M, Angelou K, Samara AA, Pagkalos A, Theodora M, Schizas D, Kontomanolis EN. The Prognostic Role and Significance of Dll4 and Toll-like Receptors in Cancer Development. *Cancers (Basel)* 2022; **14** [PMID: 35406423 DOI: 10.3390/cancers14071649]

71 **Cubillo Gracian A**, Dean A, Muñoz A, Hidalgo M, Pazo-Cid R, Martin M, Macarulla Mercade T, Lipton L, Harris M, Manzano-Mozo JL, Maurel J, Guillen-Ponce C, Tebbutt N, Cooray P, Sohal D, Zalupski M, Kolevska T, Stagg R, Goldstein D. YOSEMITE: A 3 arm double-blind randomized phase 2 study of gemcitabine, paclitaxel protein-bound particles for injectable suspension, and placebo (GAP) vs gemcitabine, paclitaxel protein-bound particles for injectable suspension and either 1 or 2 truncated courses of demcizumab (GAD). *Ann Oncol* 2017; **28**: v211

72 **Sahlin M**, Bauden MP, Andersson R, Ansari D. Radioimmunotherapy--a potential novel tool for pancreatic cancer therapy? *Tumour Biol* 2015; **36**: 4053-4062 [PMID: 25926382 DOI: 10.1007/s13277-015-3479-y]

73 **Sugyo A**, Tsuji AB, Sudo H, Koizumi M, Ukai Y, Kurosawa G, Kurosawa Y, Saga T, Higashi T. Efficacy Evaluation of Combination Treatment Using Gemcitabine and Radioimmunotherapy with (90)Y-Labeled Fully Human Anti-CD147 Monoclonal Antibody 059-053 in a BxPC-3 Xenograft Mouse Model of Refractory Pancreatic Cancer. *Int J Mol Sci* 2018; **19** [PMID: 30274301 DOI: 10.3390/ijms19102979]

74 **Kasten BB**, Gangrade A, Kim H, Fan J, Ferrone S, Ferrone CR, Zinn KR, Buchsbaum DJ. (212)Pb-labeled B7-H3-targeting antibody for pancreatic cancer therapy in mouse models. *Nucl Med Biol* 2018; **58**: 67-73 [PMID: 29413459 DOI: 10.1016/j.nucmedbio.2017.12.004]

75 **Li E**, Huang X, Zhang G, Liang T. Combinational blockade of MET and PD-L1 improves pancreatic cancer immunotherapeutic efficacy. *J Exp Clin Cancer Res* 2021; **40**: 279 [PMID: 34479614 DOI: 10.1186/s13046-021-02055-w]

76 **Zhang X**, Huang X, Xu J, Li E, Lao M, Tang T, Zhang G, Guo C, Zhang X, Chen W, Yadav DK, Bai X, Liang T. NEK2 inhibition triggers anti-pancreatic cancer immunity by targeting PD-L1. *Nat Commun* 2021; **12**: 4536 [PMID: 34315872 DOI: 10.1038/s41467-021-24769-3]

77 **Huang X**, Zhang G, Tang TY, Gao X, Liang TB. Personalized pancreatic cancer therapy: from the perspective of mRNA vaccine. *Mil Med Res* 2022; **9**: 53 [PMID: 36224645 DOI: 10.1186/s40779-022-00416-w]

78 **Miao L**, Zhang Y, Huang L. mRNA vaccine for cancer immunotherapy. *Mol Cancer* 2021; **20**: 41 [PMID: 33632261 DOI: 10.1186/s12943-021-01335-5]

79 **Kang X**, Lin Z, Xu M, Pan J, Wang ZW. Deciphering role of FGFR signalling pathway in pancreatic cancer. *Cell Prolif* 2019; **52**: e12605 [PMID: 30945363 DOI: 10.1111/cpr.12605]

80 **Lai E**, Puzzoni M, Ziranu P, Pretta A, Impera V, Mariani S, Liscia N, Soro P, Musio F, Persano M, Donisi C, Tolu S, Balconi F, Pireddu A, Demurtas L, Pusceddu V, Camera S, Sclafani F, Scartozzi M. New therapeutic targets in pancreatic cancer. *Cancer Treat Rev* 2019; **81**: 101926 [PMID: 31739115 DOI: 10.1016/j.ctrv.2019.101926]

81 **Ebrahimi S**, Hosseini M, Shahidsales S, Maftouh M, Ferns GA, Ghayour-Mobarhan M, Hassanian SM, Avan A. Targeting the Akt/PI3K Signaling Pathway as a Potential Therapeutic Strategy for the Treatment of Pancreatic Cancer. *Curr Med Chem* 2017; **24**: 1321-1331 [PMID: 28176634 DOI: 10.2174/0929867324666170206142658]

82 **Polireddy K**, Chen Q. Cancer of the Pancreas: Molecular Pathways and Current Advancement in Treatment. *J Cancer* 2016; **7**: 1497-1514 [PMID: 27471566 DOI: 10.7150/jca.14922]

83 **Drilon A**, Laetsch TW, Kummar S, DuBois SG, Lassen UN, Demetri GD, Nathenson M, Doebele RC, Farago AF, Pappo AS, Turpin B, Dowlati A, Brose MS, Mascarenhas L, Federman N, Berlin J, El-Deiry WS, Baik C, Deeken J, Boni V, Nagasubramanian R, Taylor M, Rudzinski ER, Meric-Bernstam F, Sohal DPS, Ma PC, Raez LE, Hechtman JF, Benayed R, Ladanyi M, Tuch BB, Ebata K, Cruickshank S, Ku NC, Cox MC, Hawkins DS, Hong DS, Hyman DM. Efficacy of Larotrectinib in TRK Fusion-Positive Cancers in Adults and Children. *N Engl J Med* 2018; **378**: 731-739 [PMID: 29466156 DOI: 10.1056/NEJMoa1714448]

84 **Miknyoczki SJ**, Lang D, Huang L, Klein-Szanto AJ, Dionne CA, Ruggeri BA. Neurotrophins and Trk receptors in human pancreatic ductal

adenocarcinoma: expression patterns and effects on in vitro invasive behavior. *Int J Cancer* 1999; **81**: 417-427 [PMID: 10209957 DOI: 10.1002/(sici)1097-0215(19990505)81:3<417::aid-ijc16>3.0.co;2-6]

85 **Lal G**, Liu G, Schmocker B, Kaurah P, Ozcelik H, Narod SA, Redston M, Gallinger S. Inherited predisposition to pancreatic adenocarcinoma: role of family history and germ-line p16, BRCA1, and BRCA2 mutations. *Cancer Res* 2000; **60**: 409-416 [PMID: 10667595]

86 **Iqbal J**, Ragone A, Lubinski J, Lynch HT, Moller P, Ghadirian P, Foulkes WD, Armel S, Eisen A, Neuhausen SL, Senter L, Singer CF, Ainsworth P, Kim-Sing C, Tung N, Friedman E, Llacuachaqui M, Ping S, Narod SA; Hereditary Breast Cancer Study Group. The incidence of pancreatic cancer in BRCA1 and BRCA2 mutation carriers. *Br J Cancer* 2012; **107**: 2005-2009 [PMID: 23099806 DOI: 10.1038/bjc.2012.483]

87 **Macherla S**, Laks S, Naqash AR, Bulumulle A, Zervos E, Muzaffar M. Emerging Role of Immune Checkpoint Blockade in Pancreatic Cancer. *Int J Mol Sci* 2018; **19** [PMID: 30405053 DOI: 10.3390/ijms19113505]

88 **O'Reilly EM**, Lee JW, Zalupski M, Capanu M, Park J, Golan T, Tahover E, Lowery MA, Chou JF, Sahai V, Brenner R, Kindler HL, Yu KH, Zervoudakis A, Vemuri S, Stadler ZK, Do RKG, Dhani N, Chen AP, Kelsen DP. Randomized, Multicenter, Phase II Trial of Gemcitabine and Cisplatin With or Without Veliparib in Patients With Pancreas Adenocarcinoma and a Germline BRCA/PALB2 Mutation. *J Clin Oncol* 2020; **38**: 1378-1388 [PMID: 31976786 DOI: 10.1200/JCO.19.02931]

89 **Park W**, Chen J, Chou JF, Varghese AM, Yu KH, Wong W, Capanu M, Balachandran V, McIntyre CA, El Dika I, Khalil DN, Harding JJ, Ghalehsari N, McKinnell Z, Chalasani SB, Makarov V, Selenica P, Pei X, Lecomte N, Kelsen DP, Abou-Alfa GK, Robson ME, Zhang L, Berger MF, Schultz N, Chan TA, Powell SN, Reis-Filho JS, Iacobuzio-Donahue CA, Riaz N, O'Reilly EM. Genomic Methods Identify Homologous Recombination Deficiency in Pancreas Adenocarcinoma and Optimize Treatment Selection. *Clin Cancer Res* 2020; **26**: 3239-3247 [PMID: 32444418 DOI: 10.1158/1078-0432.CCR-20-0418]

90 **Pastushenko I**, Blanpain C. EMT Transition States during Tumor Progression and Metastasis. *Trends Cell Biol* 2019; **29**: 212-226 [PMID: 30594349 DOI: 10.1016/j.tcb.2018.12.001]

91 **Dongre A**, Weinberg RA. New insights into the mechanisms of epithelial-mesenchymal transition and implications for cancer. *Nat Rev Mol Cell Biol* 2019; **20**: 69-84 [PMID: 30459476 DOI: 10.1038/s41580-018-0080-4]

92 **van Mackelenbergh MG**, Stroes CI, Spijker R, van Eijck CHJ, Wilmink JW, Bijlsma MF, van Laarhoven HWM. Clinical Trials Targeting the Stroma in Pancreatic Cancer: A Systematic Review and Meta-Analysis. *Cancers (Basel)* 2019; **11** [PMID: 31035512 DOI: 10.3390/cancers11050588]

93 **Hou YC**, Chao YJ, Hsieh MH, Tung HL, Wang HC, Shan YS. Low CD8$^+$ T Cell Infiltration and High PD-L1 Expression Are Associated with Level of CD44$^+$/CD133$^+$ Cancer Stem Cells and Predict an Unfavorable Prognosis in Pancreatic Cancer. *Cancers (Basel)* 2019; **11** [PMID: 30991694 DOI: 10.3390/cancers11040541]

94 **Laura A**, Anna C, Cinquepalmi M, Giovanni M, Sole MM, Nava AK, Niccolò P, Giuseppe N, Stefano V, Paolo A, Francesco D, Giovanni R. Is Complete Pathologic Response in Pancreatic Cancer Overestimated? A Systematic Review of Prospective Studies. *J Gastrointest Surg* 2020; **24**: 2336-2348 [PMID: 32583324 DOI: 10.1007/s11605-020-04697-1]

95 **Gugenheim J**, Crovetto A, Petrucciani N. Neoadjuvant therapy for pancreatic cancer. *Updates Surg* 2022; **74**: 35-42 [PMID: 34628591 DOI: 10.1007/s13304-021-01186-1]

96 **Zhang Y**, Huang ZX, Song B. Role of imaging in evaluating the response after neoadjuvant treatment for pancreatic ductal adenocarcinoma. *World J Gastroenterol* 2021; **27**: 3037-3049 [PMID: 34168406 DOI: 10.3748/wjg.v27.i22.3037]

97 **Borhani AA**, Dewan R, Furlan A, Seiser N, Zureikat AH, Singhi AD, Boone B, Bahary N, Hogg ME, Lotze M, Zeh HJ III, Tublin ME. Assessment of Response to Neoadjuvant Therapy Using CT Texture Analysis in Patients With Resectable and Borderline Resectable Pancreatic Ductal Adenocarcinoma. *AJR Am J Roentgenol* 2020; **214**: 362-369 [PMID: 31799875 DOI: 10.2214/AJR.19.21152]

98 **ICGC/TCGA Pan-Cancer Analysis of Whole Genomes Consortium**. Pan-cancer analysis of whole genomes. *Nature* 2020; **578**: 82-93 [PMID: 32025007 DOI: 10.1038/s41586-020-1969-6]

99 **Peng L**, Bian XW, Li DK, Xu C, Wang GM, Xia QY, Xiong Q. Large-scale RNA-Seq Transcriptome Analysis of 4043 Cancers and 548 Normal Tissue Controls across 12 TCGA Cancer Types. *Sci Rep* 2015; **5**: 13413 [PMID: 26292924 DOI: 10.1038/srep13413]

100 **Traub B**, Link KH, Kornmann M. Curing pancreatic cancer. *Semin Cancer Biol* 2021; **76**: 232-246 [PMID: 34062264 DOI: 10.1016/j.semcancer.2021.05.030]

World Journal of Gastroenterology

Submit a Manuscript: https://www.f6publishing.com

World J Gastroenterol 2023 September 21; 29(35): 5104-5124

DOI: 10.3748/wjg.v29.i35.5104

ISSN 1007-9327 (print) ISSN 2219-2840 (online)

ORIGINAL ARTICLE

Basic Study

Regenerating gene 4 promotes chemoresistance of colorectal cancer by affecting lipid droplet synthesis and assembly

Cong-Yu Zhang, Rui Zhang, Li Zhang, Zi-Mo Wang, Hong-Zhi Sun, Zheng-Guo Cui, Hua-Chuan Zheng

Specialty type: Gastroenterology and hepatology

Provenance and peer review: Unsolicited article; Externally peer reviewed.

Peer-review model: Single blind

Peer-review report's scientific quality classification

Grade A (Excellent): A
Grade B (Very good): B
Grade C (Good): 0
Grade D (Fair): 0
Grade E (Poor): 0

P-Reviewer: Batyrbekov K, Kazakhstan; Osera S, Japan

Received: June 25, 2023
Peer-review started: June 25, 2023
First decision: August 8, 2023
Revised: August 10, 2023
Accepted: August 25, 2023
Article in press: August 25, 2023
Published online: September 21, 2023

Cong-Yu Zhang, Zi-Mo Wang, Hong-Zhi Sun, Hua-Chuan Zheng, Cancer Center, The First Affiliated Hospital of Jinzhou Medical University, Jinzhou 121001, Liaoning Province, China

Rui Zhang, Department of Colorectal Surgery, Liaoning Cancer Hospital, Shenyang 110042, Liaoning Province, China

Li Zhang, Department of Oncology, The Affiliated Hospital of Chengde Medical University, Chengde 067000, Hebei Province, China

Zheng-Guo Cui, Department of Environmental Health, University of Fukui School of Medical Sciences, Fukui 910-1193, Japan

Corresponding author: Hua-Chuan Zheng, MD, PhD, Professor, Cancer Center, The First Affiliated Hospital of Jinzhou Medical University, No. 2 Fifth Duan, Renmin Street, Guta District, Jinzhou 121001, Liaoning Province, China. zheng_huachuan@hotmail.com

Abstract

BACKGROUND

Regenerating gene 4 *(REG4)* has been proved to be carcinogenic in some cancers, but its manifestation and possible carcinogenic mechanisms in colorectal cancer (CRC) have not yet been elucidated. Our previous study found that the drug resistance of CRC cells may be closely linked to their fat metabolism.

AIM

To explore the role of *REG4* in CRC and its association with lipid droplet formation and chemoresistance.

METHODS

We conducted a meta-analysis and bioinformatics and pathological analyses of *REG4* expression in CRC. The effects of *REG4* on the phenotypes and related protein expression were also investigated in CRC cells. We detected the impacts of *REG4* on the chemoresistance and lipid droplet formation in CRC cells. Finally, we analyzed how *REG4* regulated the transcription and proteasomal degradation of lipogenic enzymes in CRC cells.

RESULTS

Compared to normal mucosa, *REG4* mRNA expression was high in CRC ($P < 0.05$) but protein expression was low. An inverse correlation existed between lymph

node and distant metastases, tumor-node-metastasis staging or short overall survival and *REG4* mRNA overexpression ($P < 0.05$), but vice versa for *REG4* protein expression. *REG4*-related genes included: Chemokine activity; taste receptors; protein-DNA and DNA packing complexes; nucleosomes and chromatin; generation of second messenger molecules; programmed cell death signals; epigenetic regulation and DNA methylation; transcription repression and activation by DNA binding; insulin signaling pathway; sugar metabolism and transfer; and neurotransmitter receptors ($P < 0.05$). *REG4* exposure or overexpression promoted proliferation, antiapoptosis, migration, and invasion of DLD-1 cells in an autocrine or paracrine manner by activating the epidermal growth factor receptor-phosphoinositide 3-kinase-Akt-nuclear factor-κB pathway. *REG4* was involved in chemoresistance not through de novo lipogenesis, but lipid droplet assembly. *REG4* inhibited the transcription of acetyl-CoA carboxylase 1 (ACC1) and ATP-citrate lyase (ACLY) by disassociating the complex formation of anti–acetyl (AC)-acetyl-histone 3-AC-histone 4-inhibitor of growth protein-5-si histone deacetylase;-sterol-regulatory element binding protein 1 in their promoters and induced proteasomal degradation of ACC1 or ACLY.

CONCLUSION

REG4 may be involved in chemoresistance through lipid droplet assembly. *REG4* reduces expression of de novo lipid synthesis key enzymes by inhibiting transcription and promoting ubiquitination-mediated proteasomal degradation.

Key Words: Colorectal cancer; Regenerating gene 4; Aggressive behavior; Prognosis; Chemoresistance; Lipid droplet formation; Epidermal growth factor receptor signal

©The Author(s) 2023. Published by Baishideng Publishing Group Inc. All rights reserved.

Core Tip: The roles of regenerating gene 4 (*REG4*) in colorectal cancer (CRC) and the related molecular mechanisms are still unknown. *REG4* may be involved in tumorigenesis and aggressiveness of CRC *via* the epidermal growth factor receptor-phosphoinositide 3-kinase-Akt-nuclear factor-κB pathway, and chemoresistance through lipid droplet assembly. *REG4* might be used as a useful marker for colorectal carcinogenesis and subsequent progression, as well as a potential gene therapy target.

Citation: Zhang CY, Zhang R, Zhang L, Wang ZM, Sun HZ, Cui ZG, Zheng HC. Regenerating gene 4 promotes chemoresistance of colorectal cancer by affecting lipid droplet synthesis and assembly. *World J Gastroenterol* 2023; 29(35): 5104-5124
URL: https://www.wjgnet.com/1007-9327/full/v29/i35/5104.htm
DOI: https://dx.doi.org/10.3748/wjg.v29.i35.5104

INTRODUCTION

The regenerating gene 4 (*REG4*) gene family encodes secretory calcium-dependent lectins, which act as acute phase reactants, antiapoptotic factors, and growth agents, and contributes to cellular proliferation and differentiation, inflammation, diabetes, and cancer. To date, human *REG* genes include *REG* I (*Iα* and *Iβ*), *Reg* III (III and *HIP/PAP*), and *REG4*[1-3]. Of these, *REG4* is transcriptionally activated by several transcription factors (*e.g.*, Sp1 transcription factor, GATA binding protein 6 (GATA6) and caudal type homeobox 2), and the *REG4* protein targets, epidermal growth factor receptor (EGF) (EGFR)/Akt/activator protein-1 and Akt/glycogen synthase kinase-3β/β-catenin/T cell factor-4 signaling pathways as a mitogen[4-8]. In pancreatic cancer cells, *REG4* also enhanced invasion by upregulating matrix metalloproteinase expression and macrophage polarization through the EGFR–Akt–c-AMP response element binding protein pathway[9,10]. In gastric cancer cells, the forced expression of *REG4* induced EGFR phosphorylation and inhibited 5-fluorouracil (5-FU)-induced apoptosis[11]. In ovarian cancer cells, *REG4* overexpression as well as recombinant (rh) *REG4* exposure prevented apoptosis, and enhanced proliferation, migration, and invasion with the hyperexpression of Wnt5a, p70s6k, survivin and vascular endothelial growth factor, and reduced expression of Bax[12].

In colorectal tissues, *REG4* mRNA-positive cells are mostly enteroendocrine and goblet cells. Adenomatous and cancer cells positive for *REG4* mRNA exhibited enterocyte-like, mucus-secreting, or undifferentiated features[13]. At the protein level, *REG4* expression was observed in the middle and outer parts of crypts and superficial epithelium, especially goblets[14]. Oue *et al*[15] found that the preoperative serum *REG4* concentration was not elevated in patients with colorectal cancer (CRC) at stages 0–III, but was significantly elevated in those at stage IV. Additionally, *REG4* expression was significantly linked to a worse prognosis in patients with CRC as an independent predictor[15-17]. *REG4* promoted migration and invasion of CRC cells *via* its carbohydrate-recognition domain in both autocrine and paracrine manners, which was significantly decreased by anti-*REG4* antibody[18,19]. Nanakin *et al*[20] found that *REG4* expression was stimulated by tumor necrosis factor (TNF) α, EGF, basic fibroblast growth factor, and hepatocyte growth factor in colon cancer cells, and then promoted cell proliferation and resistance to H_2O_2-induced apoptosis. As for therapy resistance, *REG4* was markedly related to chemoresistance. Violette *et al*[13] discovered that *REG4* protein was strongly expressed in

chemoresistant rectal cancer cells, but expressed weakly in drug-sensitive rectal cancer cells. *REG4* expression was found to correlate with γ-radiation sensitivity in rectal cancer patients receiving radiotherapy[21]. In radiochemotherapy-sensitive CRC cells, *REG4* expression was downregulated, while it was increased in radiochemoresistant cells[22].

Leukocytes have been found to play an important role in shaping the immune microenvironment of CRC[23-25]. Among them, the interleukin (IL)-22-mediated positive effect depended on its ability to induce neutrophil chemokines into the tumor microenvironment[24]. The proinflammatory cytokine group factors (*e.g.* TNF-α, IL-6, IL-12 and IL-23) promoted tumor cell survival, induced angiogenesis, and facilitated cell migration by exerting antiapoptotic activity[25]. Immune checkpoint molecules, including programmed death ligand ½, B7-1/2, B7-acetyl-histone 3 (H3), B7x, V-domain Ig suppressor of T cell activation and galectin-9, were found to be effective regulators of immune activation, which play a key role in immune escape of CRC[26]. Jang[27] found that T regulatory (Treg) cells gradually increased, while $CD8^+$ T cells and $CD8^+$ T cell/Treg cell ratio decreased during progression of CRC. Infiltration of T cells differed between tumor regions, and the proportion in the central region of CRC was the lowest. Unfortunately, there is no report on the relationship between *REG4* and the microenvironment in CRC.

In our previous study, *REG4* expression gradually decreased from gastric intestinal metaplasia, adenoma, and cancer to gastritis at either the mRNA or protein level[28]. Serum *REG4* levels were elevated in patients with gastric cancer, compared to those in healthy individuals. Our group subsequently developed a mouse anti-*REG4* monoclonal antibody for immunohistochemistry, and found that *REG4* was downregulated in CRC[3]. To understand the roles of *REG4* in tumorigenesis and subsequent progression of CRC, we undertook meta-analysis, and bioinformatics, pathological and serological analyses to explore the clinicopathological and prognostic significances of *REG4* in CRC. The effects of *REG4* on the phenotypes of CRC cells were also studied with the detailed mechanisms clarified. We also investigated the impacts of *REG4* on lipid droplet forma-tion and chemoresistance of CRC cells and the regulatory effect of *REG4* on the key lipogenic enzymes in CRC cells.

MATERIALS AND METHODS

Cell culture and transfection

A CRC cell line (DLD-1) was generously donated by Prof. Toshiro Sugiyama, Department of Gastroenterology, University of Toyama, Japan. This line was maintained in RPMI 1640 growth medium supplemented with 11% fetal bovine serum (FBS), 90 U/mL penicillin, and 90 μg/mL streptomycin in a humidified atmosphere of 5% CO_2 at 37 ℃. The cells were transfected at 75% confluence 20-24 h after seeding on culture dishes (Qiagen, Hilden, Germany). The cells were transfected with pcDNA3.1-*REG4* [full-length (FL)-*REG4*], pcDNA3.1-*REG4* [nonsignal peptide (NSP)-*REG4*] or siRNA against histone deacetylase [si histone deacetylase (HDAC); Santa Cruz Biotechnology, Dallas, TX, United States] using Lipofectamine 3000 (Thermo Fisher Scientific, Waltham, MA, United States). The cells were treated with high glucose (4.5 mg/L), recombinant human *REG4* protein (rh*REG4*; R and D Systems, Minneapolis, MN, United States) or anti-*REG4* antibody (R and D Systems). The cells were also exposed to 5-FU (thymidylate synthetase inhibitor); cisplatin (DDP), DNA crosslinker; suberoylanilide hydroxamic acid (SAHA); HDAC inhibitor; cycloheximide (CHX), selective inhibitor of protein synthesis to study the degradation and stability of proteins; MG132 (proteasome inhibitor to suppress proteasomal degradation of proteins); acetyl-CoA carboxylase 1 (ACC1) or ATP-citrate lyase (ACLY) inhibitor (Abmole, Chicago, United States). Centrifuged cells were washed with phosphate-buffered saline (PBS), and total protein or RNA was extracted. Some cells were subjected to proteasome extract using a Minute Nuclear or cytosolic proteasome enrichment kit (Invent Biotechnologies, Plymouth, MN, United States). For HDAC silencing, we tested at least two HDAC-specific siRNAs to control for off-target effects.

Assessment of cell proliferation by tetrazolium salt (MTT) assay

As a measure of cell proliferation, MTT was reduced to formazan in a mitochondrial-dependent manner. We seeded cells in 96-well plates. After culture for 24 or 48 h in a 37 ℃ incubator, 50 μL MTT reagent (5 mg/mL) was added to each well. After incubation for 4 h, 150 μL dimethyl sulfoxide was added to each well for coloration. After vigorous shaking of the plates for 30-min to achieve complete solubilization, the optical density was measured on a microplate reader (Model 680; Bio-Rad, Hercules, CA, United States) at a wavelength of 490 nm. We normalized the OD 490 values to the viability of control cells that were not treated with reagents or siRNA. Normalized viability (%) = (OD490 of treated cells/OD490 of untreated control cells) × 100. The normalized viability values were plotted to show the growth inhibition effects of treatments.

Apoptosis assay

We detected phosphatidylserine externalization (on the cell membrane) using fluorescein isothiocyanate (FITC)-labeled Annexin V (Immunotech, Marseille, France) and propidium iodide (PI) to identify early apoptosis. After treatment, any remaining intact cells were collected, washed with cooled PBS at 4 ℃ and centrifuged at 700 × g for 3 min. The cell suspension (490 μL) was gently mixed with FITC-labeled Annexin-V (5 μL) and PI (5 μL). After incubation at 4 ℃ for 10 min in the dark, the cell suspension was detected by flow cytometry.

Wound healing assay

Cells (5.5×10^5 per well) were plated in six-well culture plates. When the cells reached 75% confluence, they were scraped with a tip, washed four times in PBS to reduce the number of broken cells, and cultured in FBS-free RPMI 1640 medium.

We measured the area of the scratch immediately after wounding (0 h) and 24 and 48 h later using Image J. The percentage wound closure was calculated as: (Area of scratch at 0 h-area of scratch at 24 and 48 h)/area of scratch at 0 h) × 100. The values were plotted to show differences in migration between conditions.

Cell migration and invasion assays

Assays for migration were conducted by suspending 1.3 × 10^5 cells per 200 μL in FBS-free RPMI 1640 and seeding the upper chamber of each Transwell (BD Biosciences, Franklin Lakes, NJ, United States). As a chemoattractant, 11% FBS was added to each lower compartment. After incubation for 24 h, we scrubbed the upper surface of the Transwell membrane, washed the Transwell chamber with PBS three times and fixed cells in 100% cold methanol. The membrane was stained with crystal violet for several minutes. For the invasive assay, the same process as above was used except that each Transwell insert was coated with Matrigel (BD Biosciences).

Nile red staining

Cells were cultured on coverslips for 12 h, fixed in 4% paraformaldehyde for 28 min and stained with Nile red (Invitrogen, Carlsbad, CA, United States; 1: 1000) for 13 min. Finally, we stained slides with 4',6-diamidino-2-phenylindole (DAPI) and covered them with SlowFade® Gold anti-fade reagent (Thermo Fisher Scientific). The software programs, Image J and Icy, were used to acquire and analyze images.

Immunofluorescence

Cells were cultured on glass slides, fixed for 10 min with 4% formaldehyde, and permeabilized for 10 min with 0.5% Triton X-100. Cells were rinsed with PBS and treated with anti-goat *REG4* (R and D Systems; 1: 100) antibody for 3 h. The cells were incubated with Alexa Fluor 488 (green) anti-goat immunoglobulin G (IgG) (Invitrogen) for 50 min. Slides were mounted using SlowFade® Gold anti-fade reagent after being stained with DAPI.

Chromatin immunoprecipitation (ChIP)

A Magna ChIP™ G kit (Millipore, Burlington, MA, United States) was used to conduct ChIP. After IP of anti-acetyl (AC) H3, anti-AC-histone 4 (H4), anti-HDAC, anti–inhibitor of growth protein (ING) 5 or anti-sterol-regulatory element binding protein 1 (SREBP1) antibody (Supplementary Table 1), we used ACLY (*5'-AATCGCGGGGCCGTTCTC-3'*, melting temperature (TM): 57.9 ℃; *5'-CGACGAACCCCGCAAAATC-3'*, TM: 55.4 ℃, -43 bp to + 81 bp) primers or ACC1 (*5'-GCCCCGAATGGCAGATCC-3'*, TM: 55.7 ℃; *5'-GCTCAGCGGCAGCCAATG-3'*, TM: 57.4 ℃; -33 bp to + 54 bp) primers for polymerase chain reaction (PCR). IgG was used as a negative control and anti-polymerase II as a positive control. In 20 μL of mixture, DNA was amplified and separated on a 2% agarose gel.

Co-immunoprecipitation

Seven micrograms of primary antibody (Supplementary Table 1) was added to > 1 mg protein and subjected to rotation at 4 ℃ overnight. One hundred microliters of agarose A beads were added, and the mixture was rotated at 4 ℃ overnight. To exclude nonspecific binding proteins, the beads were centrifuged and washed with 1% NP40 Lysis buffer four times. The pellet was mixed using 50 μL 2 × SDS sample buffer, and heated at 100 ℃ for 10 min. The sample supernatant was used for western blotting.

Patients

Colorectal primary cancers (n = 796), adenomas (n = 62), non-neoplastic mucosa [(NNM), n = 667] and metastatic cancers in lymph nodes (n = 179) were sampled at the First Affiliated Hospital of Jinzhou Medical University between 2013 and 2022. One hundred cases of CRC and adjacent NNM were obtained from Liaoning Cancer Hospital and stored at -80 ℃ until RNA and protein extraction. Eighty patients with CRC and 50 healthy volunteers were enrolled to determinate the serum *REG4* level at Liaoning Cancer Hospital and The Affiliated Hospital of Chengde Medical University. Before surgery, none of the patients had undergone radiotherapy or chemotherapy. The ethics committee of our institution authorized the research plan after giving unanimous approval to utilize tumor tissues and patient serum for clinical research.

Pathology and tissue microarray

All tissues were preserved in 10% neutral formalin, embedded in paraffin, and sectioned into 4-mm pieces. Hematoxylin and eosin (HE) staining was used to validate the histological diagnosis and other microscopic features of these sections. In HE-stained sections, representative portions of solid tumors were selected under a microscope. Using a tissue microarray, a 2-mm tissue core from each donor block was punched out and transferred to a recipient block with a maximum of 48 cores (Azumaya kin-1, Nagoya, Japan). From the recipient block, 4-μm–thick sections were sequentially cut and placed on glass slides coated with poly-lysine.

Western blotting

One hundred and seventy microgram samples of denatured protein were separated on 12% SDS-PAGE and then transferred to a Hybond membrane (Amersham, Chicago, IL, United States). The membrane was blocked overnight in 4.5% skimmed milk in Tris-buffered saline with Tween 20 (TBST). The membrane was treated with primary antibody for immunoblotting for 1 h (Supplementary Table 1). Following a TBST rinse, it was incubated for 1 h with anti-goat, anti-mouse or anti-rabbit IgG conjugated to [horseradish peroxidase(HRP); Dako, Glostrup, Denmark]. Bands were observed

using C300 imaging system (AZURE, Peking, China) and ECL-Plus detection reagents (Santa Cruz Biotechnology).

Quantitative reverse transcription polymerase chain reaction (RT-PCR)

CRC cells or tissues were used to extract total RNA with a Qiagen RNase Mini Kit. avian myeloblastosis virus transcriptase and a random primer were used to create cDNA from 2 mg total RNA (Takara, Kusatsu, Japan). The primers for *REG4* were forward: *5′-CCTTTCCACAGTATCCTTCTTCCCT-3′*, TM: 58.4 ℃ and reverse: *5′-TATGGC-CAAAGACCCAGCTGTT-3′*, TM: 58.2 ℃ (104 bp). The primers for ACLY were forward: *5′-AAACTGTGG-GTCCTTTACTCG-3′*, TM: 53.8 ℃ and reverse: *5′-GGATGACGATACAGCCCCTG-3′*, TM: 55.6 ℃ (147 bp). The primers for ACC1 were forward: *5′-GCTGGTCCACATGAACAGG-3′*, TM: 53.8 ℃ and reverse: *5′-GCCTTCTGGATATTCAGGAC-TTT-3′*, TM: 54.5 ℃ (91 bp). The primers for GAPDH were forward: *5′-CAATGACCCCTTCATTGACC-3′*, TM: 52.0 ℃ and reverse: *5′-TGGAAGATGGTGATGGGATT-3′*, TM: 51.7 ℃ (135 bp). RT-PCR amplification was performed using a SYBR Premix Ex Taq™ II kit (Takara).

Immunohistochemistry

After deparaffinization with xylene and dehydration with alcohol, successive slices in a target retrieval solution were microwaved for 17 min (Dako). H_2O_2 at 3% in methanol was used to block endogenous peroxidase activity. To stop nonspecific binding, 4% bovine serum albumin was administered for 5 min. The sections were treated with anti-goat conjugated to horseradish peroxidase (Dako, 1: 100) antibodies for 18 min after being incubated with goat anti-human *REG4* antibody (R and D Systems, 1: 50) for 17 min. To enable previously reported intermittent irradiation, all incubations were carried out in a microwave oven[28]. *REG4* immunostaining was localized in the cytoplasm. For immunohisto-chemistry, according to the degree of color development of cell positive markers, it was divided into: Blue, negative; pale yellow, weakly positive; brown, moderately positive; dark brown, strongly positive. From five typical fields in each region, 100 cells were randomly chosen and counted by two independent observers blinded to the samples (Zhang CY and Zheng HC). Semiquantitative two-tier grading was used to determine the positive proportion of counted cells: Positive, 6%-100% and negative, 0%-5%.

ELISA

We performed an ELISA (Gelatins, Shanghai, China) to determine serum *REG4* concentration. One hundred microliters of standard or serum sample was incubated at 4 ℃ overnight on polystyrene microtiter plates coated with anti-*REG4* antibody. Following the removal of the liquid, we added 100 μL biotin-antibody working solution to each well, which was then incubated at 37 ℃ for 2 h. After aspirating the liquid, 100 μL HRP-avidin working solution was added to each well, followed by washing three times with 350 μL wash buffer, and incubation at 37 ℃ for 1 h. The plates were washed again three times with wash buffer, followed by incubation with 90 μL tetramethylbenzidine substrate at 37 ℃ for 30 min. We dispensed 50 μL stopping solution to each well and measured the absorbance at 405 nm. Recombinant *REG4* (0.312-20 ng/mL) was used as the reference standard.

Meta-analysis

PubMed, Web of Science, BIOSIS, and SciFinder were used to search the literature up to March 14, 2022. The following search phrases were entered: (Colorectal or rectal or colon or rectum) and (*REG4* or REG IV) and (cancer or carcinoma or adenocarcinoma). No limitations on language or publication year were placed on the search. Inclusion criteria for studies were: (1) Studies that used immunohistochemistry to detect changes in *REG4* expression in CRC; and (2) studies that used immunohistochemistry to relate *REG4* expression to pathobiological behavior and CRC prognosis. Exclusion criteria included: (1) Abstracts, comments, reviews and meeting reports; (2) duplication of previous publications; (3) western blotting, RT–PCR, cDNA microarray, or transcriptomic sequencing for *REG4* expression; and (4) lack of sufficient information. Two reviewers (Zhang CY and Zheng HC) independently gathered data from all relevant articles and evaluated the quality of the included studies using the Newcastle-Ottawa Scale (http://www.ohri.ca/programs/clinicalepidemiology/oxford.htm). For survival analysis, we extracted data from Kaplan-Meier curves using an Engauge Digitizer program. We calculated the hazard ratios (HRs) and accompanying 95% confidence intervals (CIs). Twelve papers regarding the correlation between *REG4* expression and cancer risk, and clinicopathological or prognostic factors of CRC were found in PubMed, Web of Science, BIOSIS Citation Index, SciFinder, and CNKI (Supplementary Table 2). Samples of normal colorectal mucosa were only included in four papers[3,29-31]. In 12 investigations, a comparison was made between *REG4* expression and the clinicopathological features of CRC[3,15,17,29-37]. Finally, we covered the importance of *REG4* expression for prognosis in five papers [15,17,30,35,36].

Bioinformatics analysis

We used Oncomine (www.oncomine.org, keywords: *REG4*, Skrzypczak, Sabates-Bellver) to analyze the *REG4* expression level. The Cancer Genome Atlas (TCGA)-assembler in R program retrieved the *REG4* expression and clinicopathological data for a total of 362 patients with CRC from the TCGA database (keywords, *REG4*). Using the Xiantao platform (https://www.xiantaozi.com/, keywords: *REG4*) and The University of Alabama at Birmingham Cancer Data Analysis Portal (UALCAN) database (http://ualcan.path.uab.edu, keywords: *REG4*), we analyzed the expression, methylation, relevant genes, and signaling pathways of the *REG4* gene. A Kaplan-Meier plotter (http://kmplot.com/, keywords: 223447_at) was used to evaluate the prognostic value of *REG4*. Additionally, we discovered the genes that were differentially expressed by Xiantao and subjected these to protein-protein interaction (PPI) network analysis and a search of critical hub genes. Subsequently, gene ontology, Kyoto Encyclopedia of Genes and Genomes (KEGG), and Gene Set Enrichment Analysis (GSEA) analyses were conducted on these genes.

Statistics analysis

Hardy-Weinberg equilibrium was assessed in each study's control group using the χ^2 test. A Z test was used to establish the statistical significance of the pooled odds ratios. A fixed effect model was applied if there was no discernible heterogeneity. Instead, a random effect model was used to analyze prognostic analysis. An I^2 test was used to quantify the heterogeneity impact. To measure the asymmetry of the funnel plot and evaluate publication bias, Begg's and Egger's tests were used to quantify this. Meta-analyses were carried out using Revman software 5.3, and Student *t* tests were used with SPSS 10.0 to handle data from the TCGA database. A log-rank statistic was used to compare survival curves and create Kaplan-Meier survival charts. Cox's hazard proportional analysis was used for multivariate survival analysis. Statistical significance was defined as two-sided $P < 0.05$.

RESULTS

Clinicopathological and prognostic significance of REG4 mRNA expression in CRC

The expression of *REG4* mRNA was higher in colorectal adenoma or CRC than in normal tissues ($P < 0.05$) using quantitative RT-PCR (Supplementary Figure 1A), Xiantao (Supplementary Figure 1B) and Oncomine (Supplementary Figure 1C) datasets. In TCGA data, *REG4* mRNA expression was higher in colonic than rectal cancer ($P < 0.05$) (Supplementary Figure 1D). A positive correlation was noted with microsatellite instability status and *BRAF* mutation, but a negative correlation was found with lymph node metastasis, distant metastasis, and tumor-node-metastasis (TNM) staging in CRC ($P < 0.05$) (Supplementary Figure 1D). Mucinous adenocarcinoma showed higher *REG4* mRNA expression than the other adenocarcinomas ($P < 0.05$) (Supplementary Figure 1E). Kaplan-Meier analysis demonstrated a significantly positive association between *REG4* mRNA expression and the overall survival rate of patients with cancer ($P < 0.05$) (Supplementary Figure 1F), even though Cox's proportional hazards analysis indicated that this relationship was not independent ($P > 0.05$) (643 patients, HR univariate/multivariate analysis 1.436, 95%CI 0.911-2.039). On the basis of a Kaplan-Meier plot, *REG4* mRNA expression had a positive correlation with overall survival of female or white patients, and those with a high mutation burden ($P < 0.05$) (Supplementary Figure 1G). *REG4* methylation [transcription start site (TSS)-289, TSS-46, TSS + 45 and TSS + 2831] and mRNA expression were negatively correlated in CRC ($P < 0.05$) (Supplementary Figure 2A). The *REG4* methylation level was lower in colon cancer than in normal mucosa ($P < 0.05$) (Supplementary Figure 2B), in stage 2 than in stage 4 cancer, in mucinous adenocarcinoma than adenocarcinoma, and in tumor protein p53 nonmutant than mutant cancer ($P < 0.05$) (Supplementary Figure 2C).

REG4-related genes and signaling pathways in CRC

We identified distinct genes in the low and high expression groups of *REG4* mRNA in CRC using a xiantao platform, and constructed a volcanic map (Supplementary Figure 3A). KEGG analysis showed that the top signaling pathway mainly included chemokine activity, taste receptor, protein-DNA and a DNA-packing complex, and nucleosome and chromatin ($P < 0.05$) (Supplementary Figure 3B). GSEA showed that the top signaling pathways were principally composed of a generation of second messenger molecules: programmed cell death protein 1 signaling, HDAC and histone acetyl transferase, and epigenetic regulation and DNA methylation ($P < 0.05$) (Supplementary Figure 3C). The upregulated genes were *CCL19*, *CCL25*, *CIDEA*, *CMA1* and *PLA2G2D*, and downregulated genes were *ANGPTL3*, *CRP*, *H2BC10*, *H4C3* and *H4C6* ($P < 0.05$) (Supplementary Figure 3D). Cytoscape software was utilized to determine the top 10 nodes by degree and STRING software to identify the PPI pairings (Supplementary Figures 4A and B). According to a Xiantao database, *CD3D*, *3D3G*, *CD4*, *HLA-DRA*, *ZAP70*, *ITK*, *CD3E*, *CD247*, *CD28* and *HLA-DRB1* were less expressed in CRC than normal tissues ($P < 0.05$) (Supplementary Figure 4C).

According to the Xiantao database, genes positively correlated with *REG4* in CRC are shown in Supplementary Figure 5A ($P < 0.05$). These genes were mainly involved in transcription repression and activation by DNA binding, and lung epithelial differentiation ($P < 0.05$) (Supplementary Figure 5B). Genes negatively correlated with *REG4* in CRC are shown in Supplementary Figure 5C ($P < 0.05$), and were principally involved in the insulin signaling pathway, sugar metabolism and transfer, and neurotransmitter receptors ($P < 0.05$) (Supplementary Figure 5D). Of the positively correlated genes (Supplementary Figure 5E), *AGR2*, *B3GNT6*, *CREB3L1*, *CTSE*, *FAM177B*, *FCGBP*, *FFAR4*, *MUC2* and *SPDEF* were less expressed in CRC than normal mucosa ($P < 0.05$), while *GRB2* was more expressed in CRC than normal mucosa ($P < 0.05$). Of the negatively correlated genes (Supplementary Figure 5F), *LY6G6E*, *LY6G6D*, *FAM27B*, *PFDN4*, *PPP1R3D*, *LY6G6F*, *RNF43*, *POFUT1* and *DDX27* were more expressed in CRC than normal mucosa ($P < 0.05$), but *MT-RNR1* was less expressed in CRC than normal mucosa ($P < 0.05$).

Relationship between REG4 mRNA expression and immune cell infiltration in CRC

According to xiantao, the infiltration of mast cells, T cells, CD8 T cells, cytotoxic T cells, T helper (Th)1, Th2 and Th17 cells, T follicular helper (TFH) cells, TReg cells, natural killer (NK) $CD56^{bright}$ cells, B cells, interstitial dendritic cells (iDCs), and activated DCs (aDCs) in CRC were positively correlated with *REG4* mRNA expression ($P < 0.05$) (Supplementary Figure 6). Meanwhile, T central memory (Tcm) cell infiltration was negatively correlated with *REG4* mRNA expression ($P < 0.05$) (Supplementary Figure 6).

Clinicopathological and prognostic significance of REG4 protein expression in CRC

Compared to normal mucosa, *REG4* protein expression was low in CRC ($P = 0.03$) (Supplementary Table 3) and positively correlated with lymph node metastasis, TNM staging, and dedifferentiation of CRC ($P < 0.05$) (Supplementary Tables 4-

6). The combined data from five datasets showed a strong correlation between *REG4* expression and overall survival in patients with CRC (Supplementary Table 7) (HR = 0.54, 95%CI: 0.41-0.72, $P < 0.0001$).

According to UALCAN (Supplementary Figure 7A), *REG4* protein expression was higher in mucinous than nonmucinous adenocarcinoma ($P < 0.05$), and negatively correlated with chromatin modifier, p53/Rb, and the HIPPO signaling pathway ($P < 0.05$). Expression of *REG4* protein was higher in CRC than in NNM, according to western blotting ($P < 0.05$) (Supplementary Figure 7B). Serum *REG4* level was higher in patients with CRC than in healthy volunteers after modification by body surface area ($P < 0.05$) (Supplementary Figure 7C). Immunohistochemically, *REG4* expression was higher in colorectal NNM than adenoma and primary cancer, and in primary than metastatic cancer ($P < 0.001$) (Supplementary Figure 7D and E). Mucinous adenocarcinoma showed higher *REG4* expression than well-, moderately and poorly differentiated adenocarcinomas ($P < 0.05$) (Supplementary Table 8).

Effects of REG4 on the phenotype of CRC cells

According to qPCR ($P < 0.05$) (Supplementary Figure 8A), western blotting (Supplementary Figure 8B), immunofluorescence (Supplementary Figure 8C), and ELISA ($P < 0.05$) (Supplementary Figure 8D), DLD-1 cells were successfully transfected with FL-*REG4* and NSP-*REG4* plasmids, as shown by higher *REG4* mRNA and protein expression in transfectants than parental cells. After treatment with rh*REG4*, the viability of DLD-1 cells was increased in a dose-dependent manner ($P < 0.05$) (Figure 1A). Exposure to anti-*REG4* antibody decreased the cell viability of FL-*REG4*-overexpressing DLD-1 cells in a dose-dependent manner ($P < 0.05$) (Figure 1B). Treatment with rh*REG4* or FL-*REG4* overexpression resulted in high viability ($P < 0.05$) (Figure 1C), antiapoptosis ($P < 0.05$) (Figure 1D), migration and invasion ($P < 0.05$) (Figures 1E and F) in comparison with untreated DLD-1 cells ($P < 0.05$). Additionally, FL-*REG4* transfection and rh*REG4* treatment enhanced the expression of *REG4*, EGFR-Tyr992, -Tyr1068, -Tyr1148, -Tyr1173, phosphorylated phosphoinositide 3-kinase (p-PI3K), p-Akt, nuclear factor (NF)-κB, p-NF-κB, Bcl-2, and Bcl-X/L compared with untreated DLD-1 cells by western blotting ($P < 0.05$) (Figure 1G). However, anti-*REG4* antibody blocked the effects of FL-*REG4* overexpression (Figure 1B-G). The effects of NSP-*REG4* on aggressive phenotypes and their related protein expression in DLD-1 cells were not detectable, which differed from the effects of FL-*REG4* expression and were similar to those of *REG4*-nontransfected CRC cells (Figure 1C-F and H).

Effects of REG4 on chemoresistance and droplet formation of CRC cells

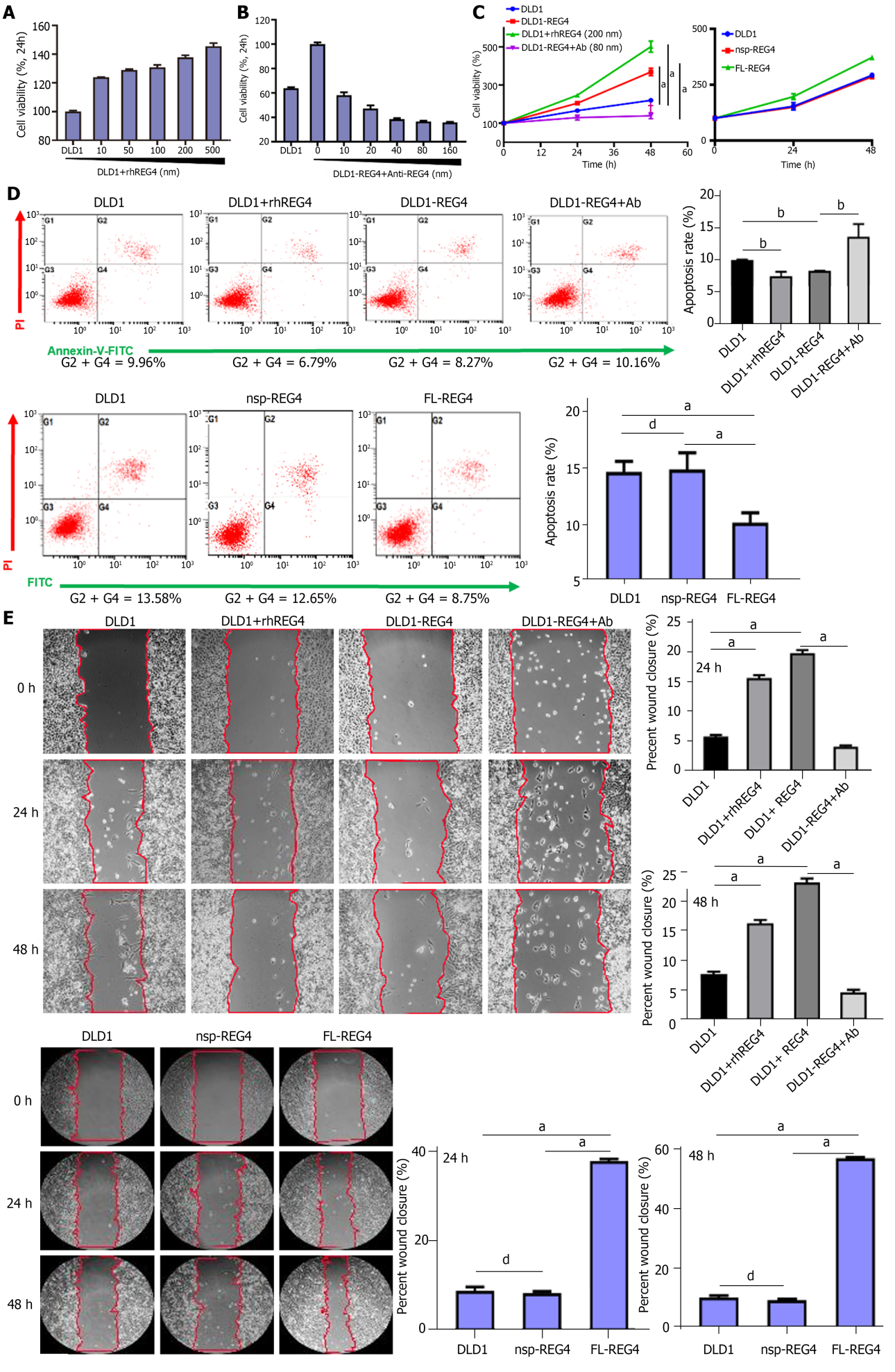
Rh*REG4* treatment and FL-*REG4* overexpression caused DLD-1 cells to become resistant to DDP and 5-FU ($P < 0.05$) (Figure 2A), while anti-*REG4* antibody reversed the chemoresistance of *REG4*-overexpressing DLD-1 cells ($P < 0.05$) (Figure 2A). rh*REG4* treatment and FL-*REG4* increased the formation of intracellular lipid droplets, as shown by Nile red staining ($P < 0.05$) (Figure 2B). *REG4* overexpression was observed in chemoresistant DLD-1 cells. FL-*REG4* overexpression enhanced the expression of acyl coenzyme A-cholesterol acyltransferase (ACAT), perilipin 5, and tail-interacting protein (TIP) 47, but weakened expression of ACLY, ACC1, p-ACC1, HDAC, adipose differentiation-related protein (ADRP), cell-death-inducing DFF45-like effector (CIDE) A, B and C, AC-H3, AC-H4, ING5, and SREBP-1 in DLD-1 cells (Figure 2C). High-glucose treatment significantly increased lipid droplet formation in DLD-1 cells, which was markedly suppressed by ACLY or ACC1 inhibitor ($P < 0.05$) (Figure 2D). DLD-1 cells treated with rh*REG4*, FL-*REG4* transfection, or high glucose had decreased chemosensitivity to 5-FU and DDP, but DLD-1 cells treated with *REG4* antibody, ACC1 inhibitor or ACLY inhibitor had increased chemosensitivity to 5-FU and DDP (Figure 2E). ACC1 or ACLY inhibitor reversed the insensitivity of cells to 5-FU and DDP in the high-glucose treatment group ($P < 0.05$).

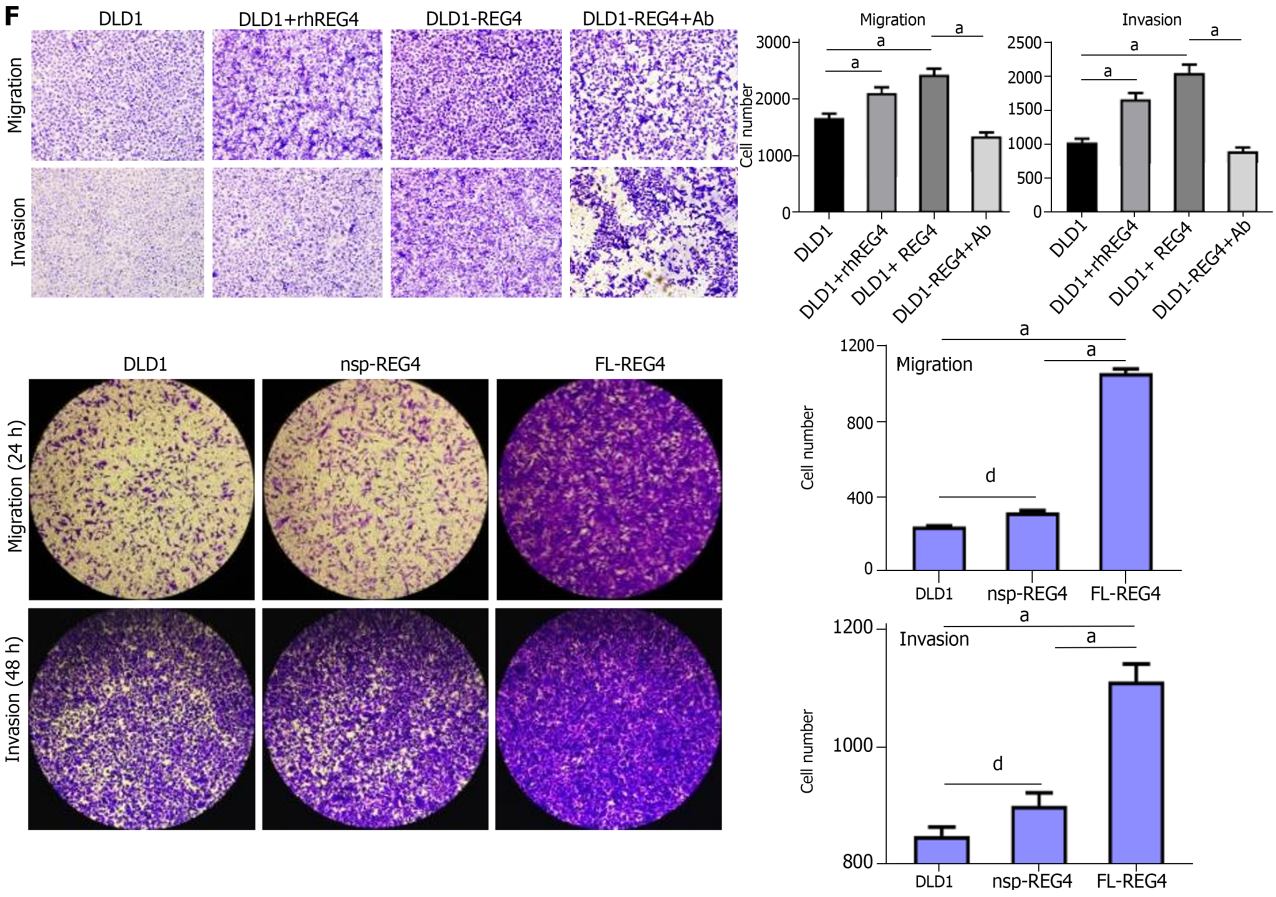
REG4 weakened transcription of ACLY and ACC1 via disassociating AC-H3-AC-H4-HDAC-ING5-SREBP1 complex

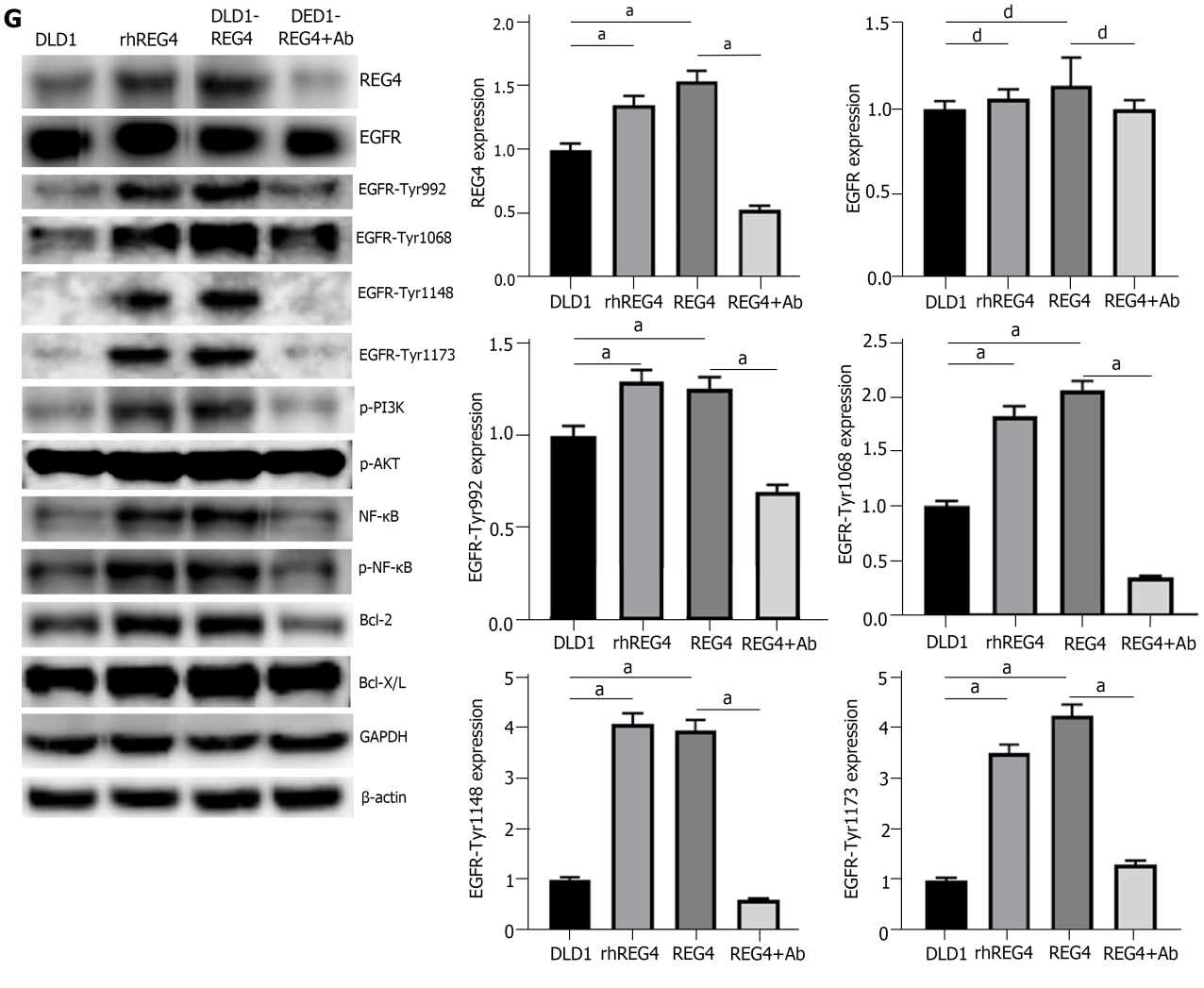
In DLD-1 cells, FL-*REG4* overexpression weakened the interaction of AC-H3, AC-H4, HDAC, SREBP1 and ING5 proteins with the ACLY or ACC1 promoter, according to ChIP ($P < 0.05$) (Figure 3A). FL-*REG4* overexpression also weakened the interaction of the five proteins ($P < 0.05$) (Figure 3B). Overexpression of FL-*REG4* decreased ACLY and ACC1 mRNA expression ($P < 0.05$) (Figure 3C), and increased lipid droplet formation ($P < 0.05$) (Figure 3D), and increased the half maximal inhibitory concentration (IC_{50}) of cells for 5-FU and DDP ($P < 0.05$) (Figure 3E). After SAHA (siHDAC inhibitor) treatment (2 μM, 24 h) and siHDAC transfection, the interaction between AC-H3, AC-H4, SREBP 1, ING5, HDAC and ACC1, ACLY promoters was weakened compared with the control group ($P < 0.05$) (Figure 3A), and the mRNA level of ACC1 and ACLY decreased ($P < 0.05$) (Figure 3B). After SAHA treatment and siHDAC transfection, the fluorescence intensity of Nile red staining decreased compared with that in the control group ($P < 0.05$) (Figure 3D), and the chemical sensitivity to 5-FU and DDP increased compared with that in the control group ($P < 0.05$) (Figure 3E).

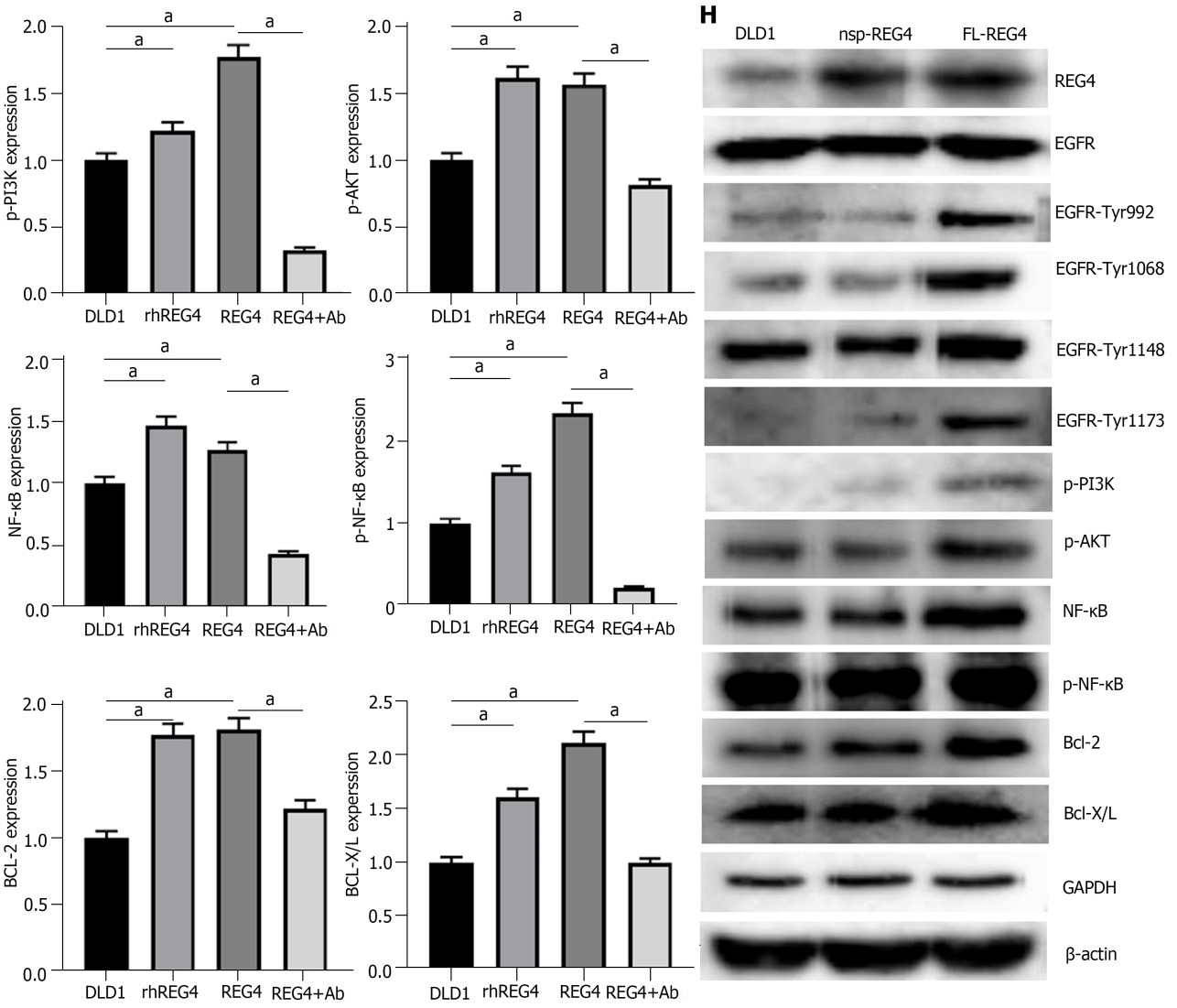
REG4 destabilized ACLY and ACC1 proteins via proteasomal degradation

After treatment with CHX (used to inhibit the synthesis of new proteins), ACC1 and ACLY protein expression was lower in FL-*REG4* transfectants than in DLD-1 cells ($P < 0.05$) (Figure 4A). MG132 (proteasome inhibitor) increased protein expression of ACC1 and ACLY in DLD-1 cells and FL-*REG4* transfectants, which was higher in DLD-1 cells than in FL-*REG4* transfectants ($P < 0.05$) (Figure 4B). Higher levels of ACC1 and ACLY proteins were noted in the nuclear proteasome of FL-*REG4* transfectants than in DLD-1 cells, but this translocation phenomenon was not enhanced by MG132 (Figure 4C). Similar levels of ACC1 and ACLY expression were noted in the cytosolic proteasome of transfectants and parental cells, even after treatment with MG132 (Figure 4C). Regarding ubiquitin ligases, expression of COP1 E3 ubiquitin ligase (COP1), Cbl proto-oncogene (CBL) and NEDD4 like E3 ubiquitin protein ligase (NEDD4L) was higher in FL-*REG4* transfectants than DLD-1 cells, but synoviolin 1 (SYVN1) and NEDD4 were lower in FL-*REG4* transfectants than DLD-1 cells (Figure 4D). Co-immunoprecipitation showed that expression of ubiquitylated ACC1 and ACLY was higher in FL-*REG4* transfectants than in DLD-1 cells, and pretreatment with a small dose of proteasome inhibitor MG132 (5 μM,


A
Cell viability (%, 24h)
DLD1
10
50
100
200
500
DLD1+rhREG4 (nm)
B
Cell viability (%, 24h)
DLD1
0
10
20
40
80
160
DLD1-REG4+Anti-REG4 (nm)
C
DLD1
DLD1-REG4
DLD1+rhREG4 (200 nm)
DLD1-REG4+Ab (80 nm)
Cell viability (%)
Time (h)
DLD1
nsp-REG4
FL-REG4
Time (h)
D
DLD1
DLD1+rhREG4
DLD1-REG4
DLD1-REG4+Ab
PI
Annexin-V-FITC
G2 + G4 = 9.96%
G2 + G4 = 6.79%
G2 + G4 = 8.27%
G2 + G4 = 10.16%
Apoptosis rate (%)
DLD1
DLD1+rhREG4
DLD1-REG4
DLD1-REG4+Ab
DLD1
nsp-REG4
FL-REG4
PI
FITC
G2 + G4 = 13.58%
G2 + G4 = 12.65%
G2 + G4 = 8.75%
Apoptosis rate (%)
DLD1
nsp-REG4
FL-REG4
E
DLD1
DLD1+rhREG4
DLD1-REG4
DLD1-REG4+Ab
0 h
24 h
48 h
Precent wound closure (%)
24 h
DLD1
DLD1+rhREG4
DLD1+ REG4
DLD1-REG4+Ab
Percent wound closure (%)
48 h
DLD1
DLD1+rhREG4
DLD1+ REG4
DLD1-REG4+Ab
DLD1
nsp-REG4
FL-REG4
0 h
24 h
48 h
Percent wound closure (%)
24 h
DLD1
nsp-REG4
FL-REG4
Percent wound closure (%)
48 h
DLD1
nsp-REG4
FL-REG4


F
DLD1
DLD1+rhREG4
DLD1-REG4
DLD1-REG4+Ab
Migration
Invasion
Cell number
DLD1
DLD1+rhREG4
DLD1+ REG4
DLD1-REG4+Ab
nsp-REG4
FL-REG4
Migration (24 h)
Invasion (48 h)


G
DLD1
rhREG4
DLD1-REG4
DED1-REG4+Ab
REG4
EGFR
EGFR-Tyr992
EGFR-Tyr1068
EGFR-Tyr1148
EGFR-Tyr1173
p-PI3K
p-AKT
NF-κB
p-NF-κB
Bcl-2
Bcl-X/L
GAPDH
β-actin
REG4 expression
EGFR expression
EGFR-Tyr992 expression
EGFR-Tyr1068 expression
EGFR-Tyr1148 expression
EGFR-Tyr1173 expression



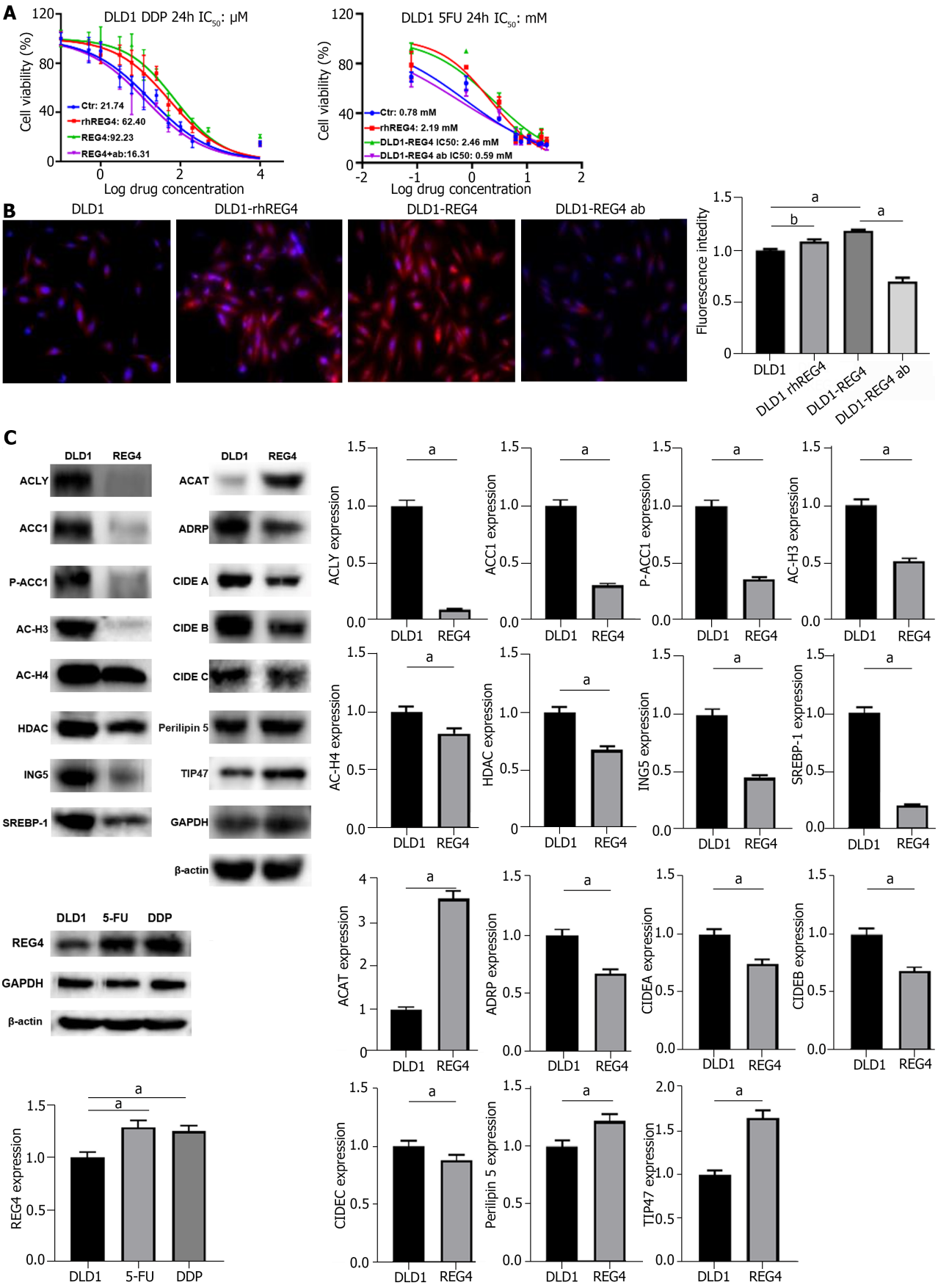
DOI: 10.3748/wjg.v29.i35.5104 **Copyright** ©The Author(s) 2023.

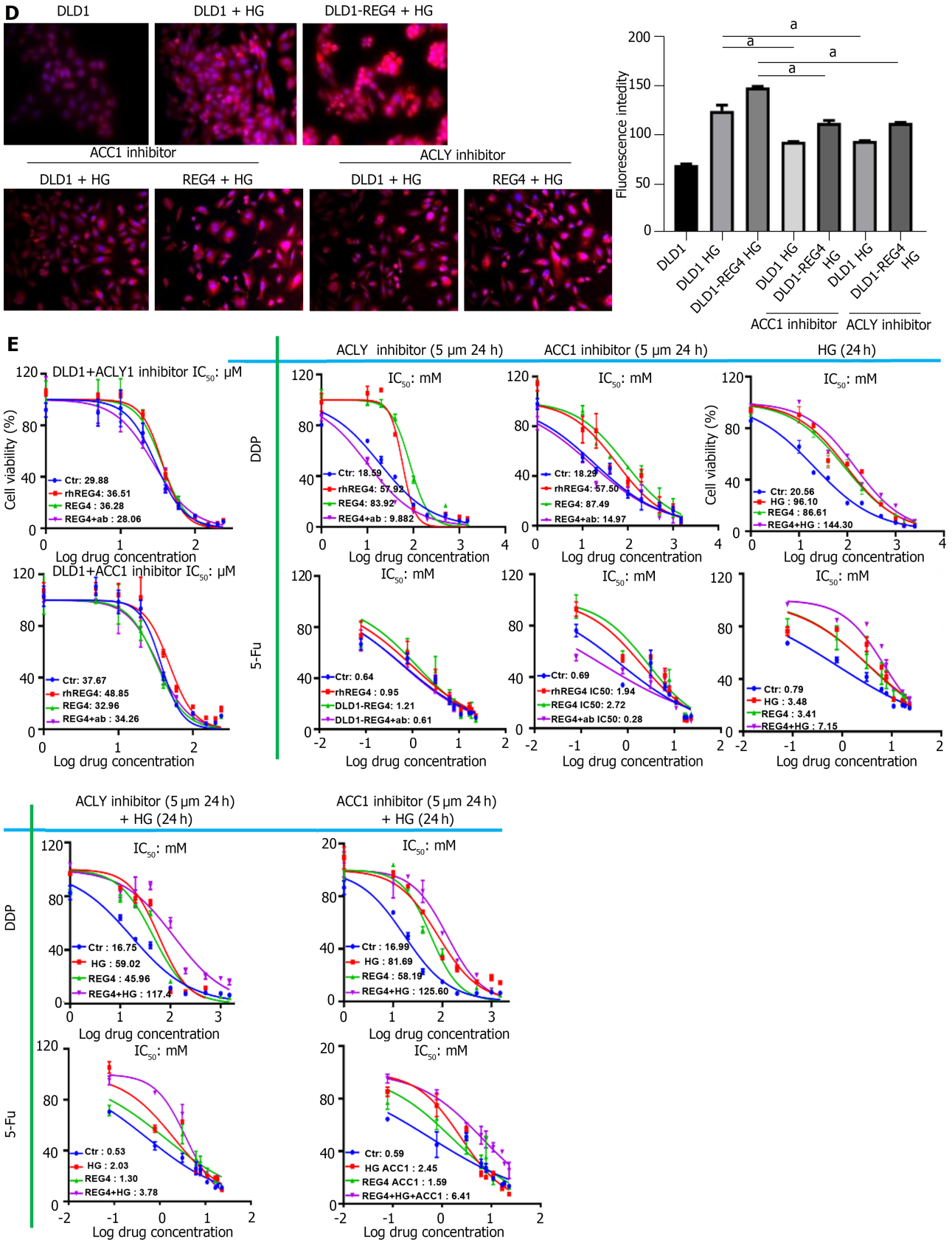
Figure 1 Effects of full-length regenerating gene 4 and nonsignal peptide regenerating gene 4 on phenotypes of DLD-1 cells. A: DLD-1 cells were incubated with increasing doses of recombinant human regenerating gene 4 (*REG4*) (rh*REG4*) (0-500 nmol/L) for 48 h and subjected to cell proliferation assay by tetrazolium salt (MTT) assay; B: Treatment with anti-*REG4* antibody produced a dose-dependent decrease in cell number of full-length (FL)-*REG4*-overexpressing DLD-1 cells; C: MTT assay was used to detect the proliferation of DLD-1 cells transfected with FL-*REG4* or nonsignal peptide (NSP)-*REG4*, and treated with rh*REG4* or *REG4* antibody; D: Apoptosis of DLD-1 cells transfected with FL-*REG4* or NSP-*REG4*, and treated with rh*REG4* or *REG4* antibody detected by flow cytometry; E: Wound healing assay was used to detect migration of DLD-1 cells transfected with FL-*REG4* or NSP-*REG4*, and treated with rh*REG4* or *REG4* antibody; F: Transwell assay was used to detect migration and invasion of DLD-1 cells transfected with FL-*REG4* or NSP-*REG4*, and treated with rh*REG4* or *REG4* antibody; G: Compared with DLD-1 cells, western blotting showed that transfection with FL-*REG4* and treatment with rh*REG4* increased expression of epidermal growth factor receptor (EGFR)-Tyr992, Tyr1068, Tyr1148, Tyr1173, Akt, p-Akt, phosphorylated phosphoinositide 3-kinase (p-PI3K), nuclear factor (NF)-κB, p-NF-KB, Bcl-2 and Bcl-X/L. *REG4* antibody inhibited the effect of FL-*REG4* transfection; H: Western blotting showed that compared with parental cells, DLD-1 cells transfected with NSP-*REG4* had no change in expression of EGFR-Tyr992, Tyr1068, Tyr1148, Tyr1173, AKT, p-AKT, p-PI3K, NF-KB, p-NF-KB, BCL-2, or BCL-XL. $^{a}P < 0.001$; $^{b}P < 0.01$; ^{d}No significance. Ab: Anti-*REG4* antibody; *REG4*: Regenerating gene 4; rh*REG4:* Recombinant human regenerating gene 4; FL: Full-length; NSP: Nonsignal peptide; EGFR: Epidermal growth factor receptor; p-PI3K: Phosphorylated phosphoinositide 3-kinase; NF: Nuclear factor.

9 h) reduced ubiquitination of ACC1 and ACLY (Figure 4E). ACLY bound more to SYVN1, NEDD4 and NEDD4L in FL-*REG4* transfectants than in DLD-1 cells, but bound less to CBL. ACC1 interacted more with COP1 in *REG4* transfectants than in DLD-1 cells, but interacted less with CBL and SYVN1 (Figure 4E). MG132 pretreatment (5 μM, 24 h) aggravated lipid droplet formation ($P < 0.05$) (Figure 4F) and chemoresistance against 5-FU and DDP ($P < 0.05$) (Figure 4G) in DLD-1 cells and FL-*REG4* transfectants.

DISCUSSION

The silencing of *REG4* reduced cellular proliferation, but rh*REG4* had the opposite effect since *REG4* downregulated p21 (Cip1/WAF1) expression and upregulated cyclin D1 expression, which might promote G_1/S transition[38,39]. Anti-*REG4*


A
DLD1 DDP 24h IC50: μM
Cell viability (%)
Ctr: 21.74
rhREG4: 62.40
REG4:92.23
REG4+ab:16.31
Log drug concentration
DLD1 5FU 24h IC50: mM
Ctr: 0.78 mM
rhREG4: 2.19 mM
DLD1-REG4 IC50: 2.46 mM
DLD1-REG4 ab IC50: 0.59 mM
B
DLD1
DLD1-rhREG4
DLD1-REG4
DLD1-REG4 ab
Fluorescence intedity
C
DLD1 REG4
ACLY
ACC1
P-ACC1
AC-H3
AC-H4
HDAC
ING5
SREBP-1
ACAT
ADRP
CIDE A
CIDE B
CIDE C
Perilipin 5
TIP47
GAPDH
β-actin
DLD1 5-FU DDP
REG4
GAPDH
β-actin
REG4 expression
ACLY expression
ACC1 expression
P-ACC1 expression
AC-H3 expression
AC-H4 expression
HDAC expression
ING5 expression
SREBP-1 expression
ACAT expression
ADRP expression
CIDEA expression
CIDEB expression
CIDEC expression
Perilipin 5 expression
TIP47 expression



DOI: 10.3748/wjg.v29.i35.5104 **Copyright** ©The Author(s) 2023.

Figure 2 Effects of regenerating gene 4 on chemoresistance and droplet formation of DLD-1 cells. A: After treatment with cisplatin (DDP) or 5-fluorouracil (5-FU), the viability was measured in DLD-1 cells, DLD-1 cells treated with recombinant human regenerating gene 4 (*REG4*) (rh*REG4*), DLD-1 cells transfected with full-length (FL)-*REG4* plasmid, and DLD-1 cells treated with anti-*REG4* antibody; B: The lipid droplet level was measured in DLD-1 cells, DLD-1 cells treated with rh*REG4*, DLD-1 cells transfected with FL-*REG4* plasmid, and DLD-1 cells treated with anti-*REG4* antibody; C: *REG4* expression was detected in DLD-1, chemoresistant DLD-1 cells to DDP and 5-FU by western blot, proteins related to de novo synthesis or assembly pathway of lipid droplets were also detected in DLD-

1 cells and DLD-1 cells transfected with FL-*REG4*; D: Nile red staining was used to detect the level of lipid droplets in DLD-1 cells and DLD-1 cells transfected with FL-*REG4* after treatment with high glucose (HG), acetyl-CoA carboxylase 1 (ACC1) inhibitor and ATP-citrate lyase (ACLY) inhibitor; E: Tetrazolium salt assay was used to detect half maximal inhibitory concentration of DLD-1 cells for 5-FU and DDP when treated with HG, ACC1 and ACLY inhibitors, alone or in combination with the above conditions. $^{a}P < 0.001$; $^{b}P < 0.01$. Ab: Anti-*REG4* antibody; *REG4*: Regenerating gene 4; rh*REG4:* Recombinant human regenerating gene 4*;* ACC1: Acetyl-CoA carboxylase 1; ACCY: ATP-citrate lyase; AC-H3: Acetyl-acetyl-histone 3; H4: Histone 4; ACC1: Acetyl-CoA carboxylase 1; HDAC: Si histone deacetylase; ING5: Inhibitor of growth protein 5; SREBP1: Sterol-regulatory element binding protein 1; ACAT: A-cholesterol acyltransferase; ADRP: Adipocyte differentiation-related protein; CIDE: Cell-death-inducing DFF45-like effector; TIP: Tail-interacting protein; DDP: Cisplatin; 5-FU: 5-fluorouracil; HG: High glucose.

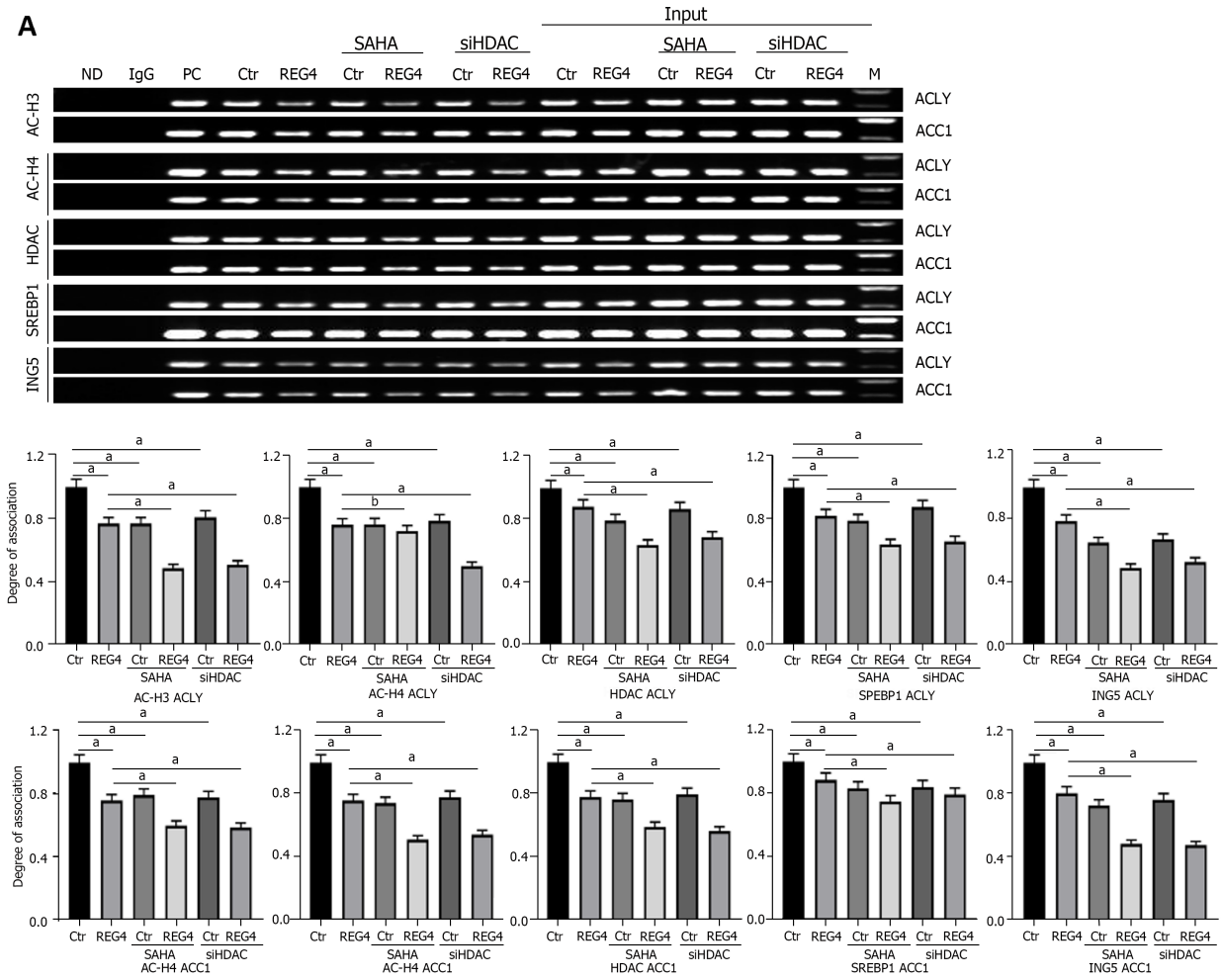
antibody dramatically reduced the autocrine and paracrine effects of secretory *REG4* on the ability of colon cancer cells to invade, migrate and proliferate[19]. *REG4* overexpression may cause resistance to the irradiation-induced apoptosis of colon cancer cells. Animal studies have shown that rh*REG4* increased the expression of the antiapoptotic genes, Bcl-2 and Bcl-xL, and survivin to shield normal intestinal crypt cells against irradiation-induced apoptosis[40].

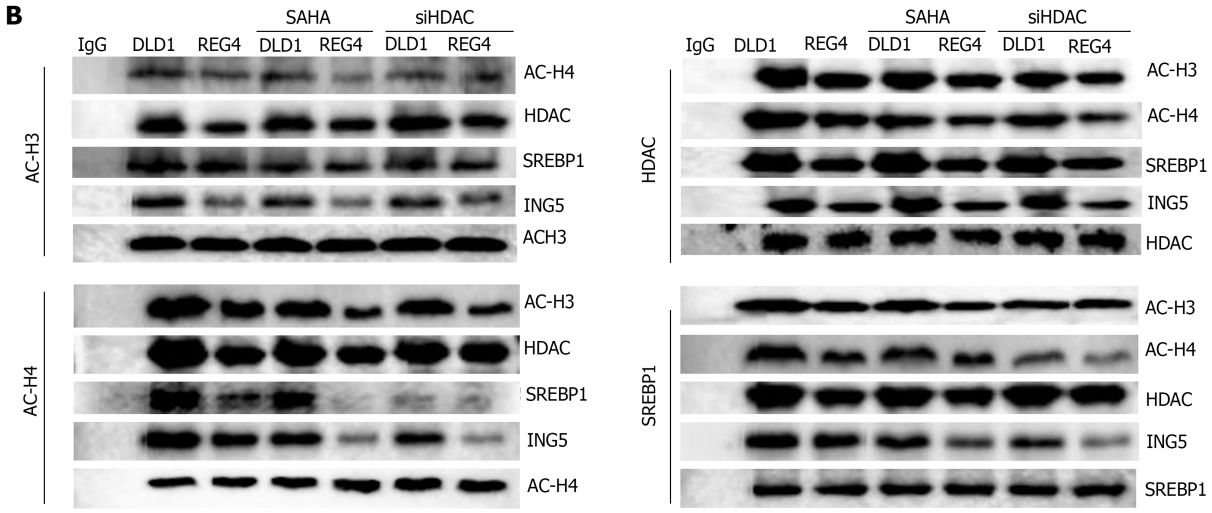
We conducted bioinformatics analysis, meta-analysis, and pathological and serological studies to evaluate the clinicopathological and prognostic significance of *REG4* expression in CRC. In bioinformatics analysis, we used data of different sizes and from different sources to ensure data heterogeneity, and we used qRT-PCR to verify the reliability of bioinformatics analysis. We discovered that *REG4* mRNA expression was upregulated in CRC, but *REG4* protein expression was downregulated, suggesting that aberrant *REG4* expression could be used as a potential biomarker for colorectal tumorigenesis. In addition, we discovered a negative correlation between *REG4* promoter methylation and mRNA expression in CRC. The correlation of *REG4* methylation with mucinous subtypes or clinicopathological staging was opposite to that of *REG4* mRNA expression. Upregulated *REG4* mRNA expression might be due to promoter hypomethylation in CRC. High *REG4* mRNA expression was discovered in colorectal, pancreatic, hepatic, and prostate malignancies as well as in inflammatory epithelium, dysplasia, and malignant lesions of ulcerative colon tissues[20,41-45], suggesting that upregulated *REG4* mRNA was involved in the early malignant transformation of epithelial cells. Although upregulated *REG4* protein expression occurred in gastric cancer, ovarian cancer, glioma, pancreatic cancer, gallbladder carcinoma, and prostate cancer[12,28,46-49], lower *REG4* expression was found in CRC. In subsequent research, we will use more databases and updated data sets to analyze the expression of *REG4* in CRC to verify the consistency between our studies and strengthen our conclusions.

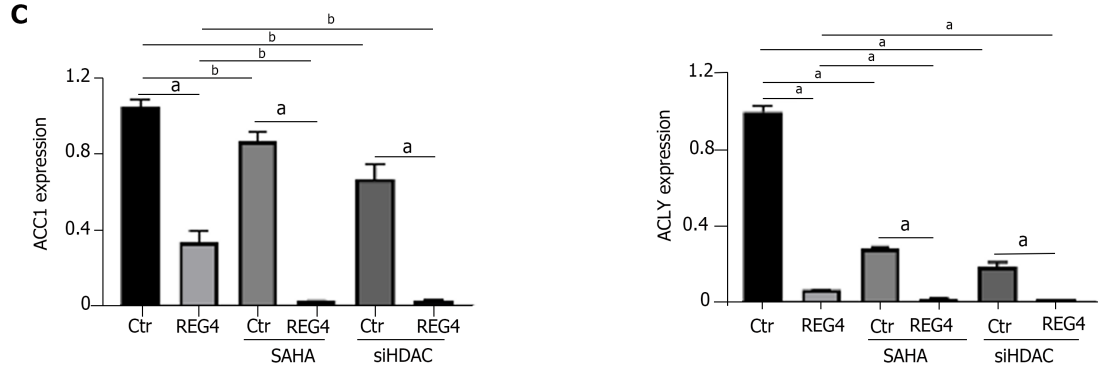
The tumor microenvironment of CRC is regulated by many factors, such as *CTLA-4*, and the altered expression of these factors can lead to changes in immune responses[50]. So far, there has been no systematic study on the relationship between *REG4* and immune microenvironment in CRC. Here, we studied the correlation between the expression of *REG4* mRNA and the infiltration of immune cells in CRC, and found that high expression of *REG4* was positively correlated with infiltration of mast cells, T cells, CD8 T cells, cytotoxic T cells, Th1, Th2 and Th17 cells, TFH cells, TReg cells, NK CD56^{bright} cells, B cells, iDCs, and aDCs. High expression of *REG4* was negatively correlated with Tcm cell infiltration. In future research, we will focus on the impact of *REG4* expression on the immune environments of primary and metastatic CRC, which is also important for immunotherapy of CRC.

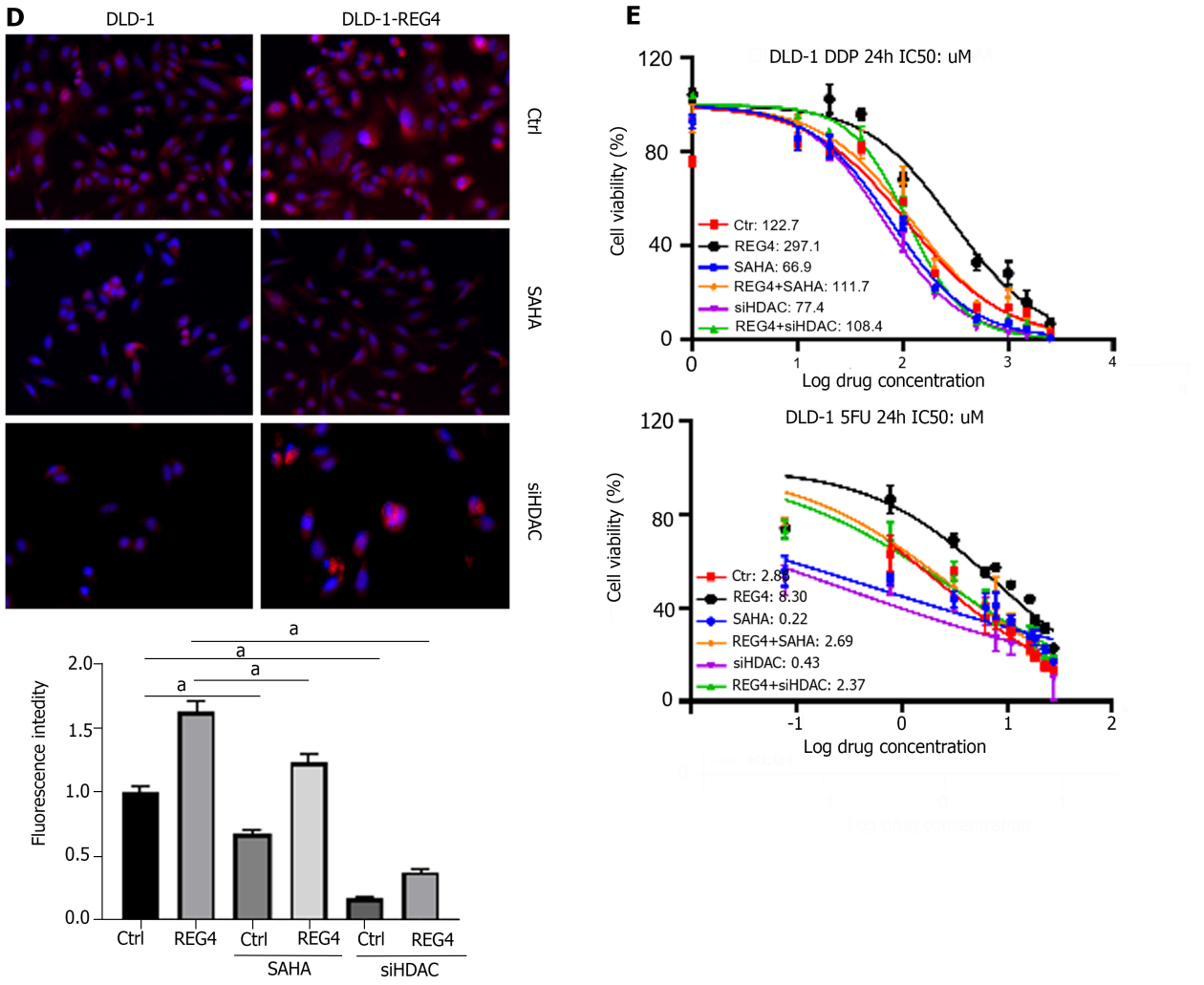
Previously, we discovered that expression of *REG4* was substantially linked with that of mucin-2 and mucin-5AC, and that it was greater in mucinous carcinoma, signet ring cell carcinoma, and intestinal metaplasia that produced mucins [28]. *REG4* was identified as a potential biomarker of mucinous ovarian cancer at both mRNA and protein levels[12,51]. Here, we also found that expression of *REG4* in mucinous adenocarcinoma was greater than that in other histological subtypes at both at the mRNA and protein levels. These findings could account for *REG4* protein overexpression in colorectal mucosa and poorly differentiated, signet ring cell carcinoma and undifferentiated carcinoma. *REG4* expression was positively correlated with lymph node metastasis, TNM staging, poorly differentiated CRC, and had a worse prognosis, in agreement with other studies[12,28,46-49]. The opposite was the case for *REG4* mRNA, suggesting that aberrant *REG4* protein expression might indicate aggressiveness and prognosis of CRC. In CRCs with reduced stroma compared to those with high stroma, *REG4* protein expression was considerably greater[52]. Previously, we performed *REG4* immunostaining on the same tissue microarrays of CRC (Supplementary Table 1), and found similar results. Therefore, the discrepancies about *REG4* mRNA and protein expression might be largely attributable to a complex process from transcription to translation and different methodologies. Serologically, the preoperative *REG4* protein level was higher in CRC than in a healthy population and postoperative patients with cancer, in agreement with the finding that serum *REG4* Levels were greater in pancreatic ductal adenocarcinoma than in chronic pancreatitis[53].

Bishnupuri *et al*[54] found that the transcriptional activator of D-type cyclins, CD44 intracytoplasmic domain, was released after *REG4* connected with transmembrane CD44 and activated γ-secretase to promote proliferation and stemness of colorectal and pancreatic cancer cells. We also found that *REG4* overexpression and rh*REG4* treatment promoted proliferation, antiapoptosis, and migration and invasion of CRC cells. Exposure to anti-*REG4* antibody inhibited the effects of *REG4* overexpression on the phenotypes of CRC cells, which is consistent with our earlier result in ovarian cancer cells[12]. We also found that *REG4* overexpression resulted in resistance of ovarian cancer cells to DDP or taxol by activating the PI3K-Akt-mTOR signaling pathway[55]. As a mutant KRAS-induced factor, *REG4* increased cancer stem cell characteristics *via* Wnt/β-catenin signaling[56]. Jin *et al*[57] showed that *REG4* increased the resistance of gastric cancer cells to 5-FU by stimulating the mitogen-activated protein kinase-ERK-Bim signaling pathway. Here, we found that expression of *REG4*, EGFR-Tyr992, -Tyr1068, -Tyr1148 and -Tyr1173, p-PI3K, p-Akt, NF-κB, p-NF-κB, Bcl-2, and Bcl-x/L was higher in DLD-1 cells treated with rh*REG4* or transfected with *REG4*-overexpressing plasmid than in parental cells. Anti-*REG4* antibody blocked the effects of *REG4* overexpression, indicating that *REG4* promoted the aggressive phenotypes by an EGFR-PI3K-Akt-NF-κB signaling pathway, in line with other studies[7,8,40]. However, the lack of effect of NSP-*REG4* on aggressive phenotypes and related signaling proteins suggested that *REG4* only functioned in


A
Input
SAHA
siHDAC
ND
IgG
PC
Ctr
REG4
M
AC-H3
AC-H4
HDAC
SREBP1
ING5
ACLY
ACC1
Degree of association
AC-H3 ACLY
AC-H4 ACLY
HDAC ACLY
SPEBP1 ACLY
ING5 ACLY
AC-H4 ACC1
HDAC ACC1
SREBP1 ACC1
ING5 ACC1


B
IgG
DLD1
REG4
SAHA
siHDAC
AC-H3
AC-H4
HDAC
SREBP1
ING5
ACH3


C
ACC1 expression
ACLY expression
Ctr
REG4
SAHA
siHDAC

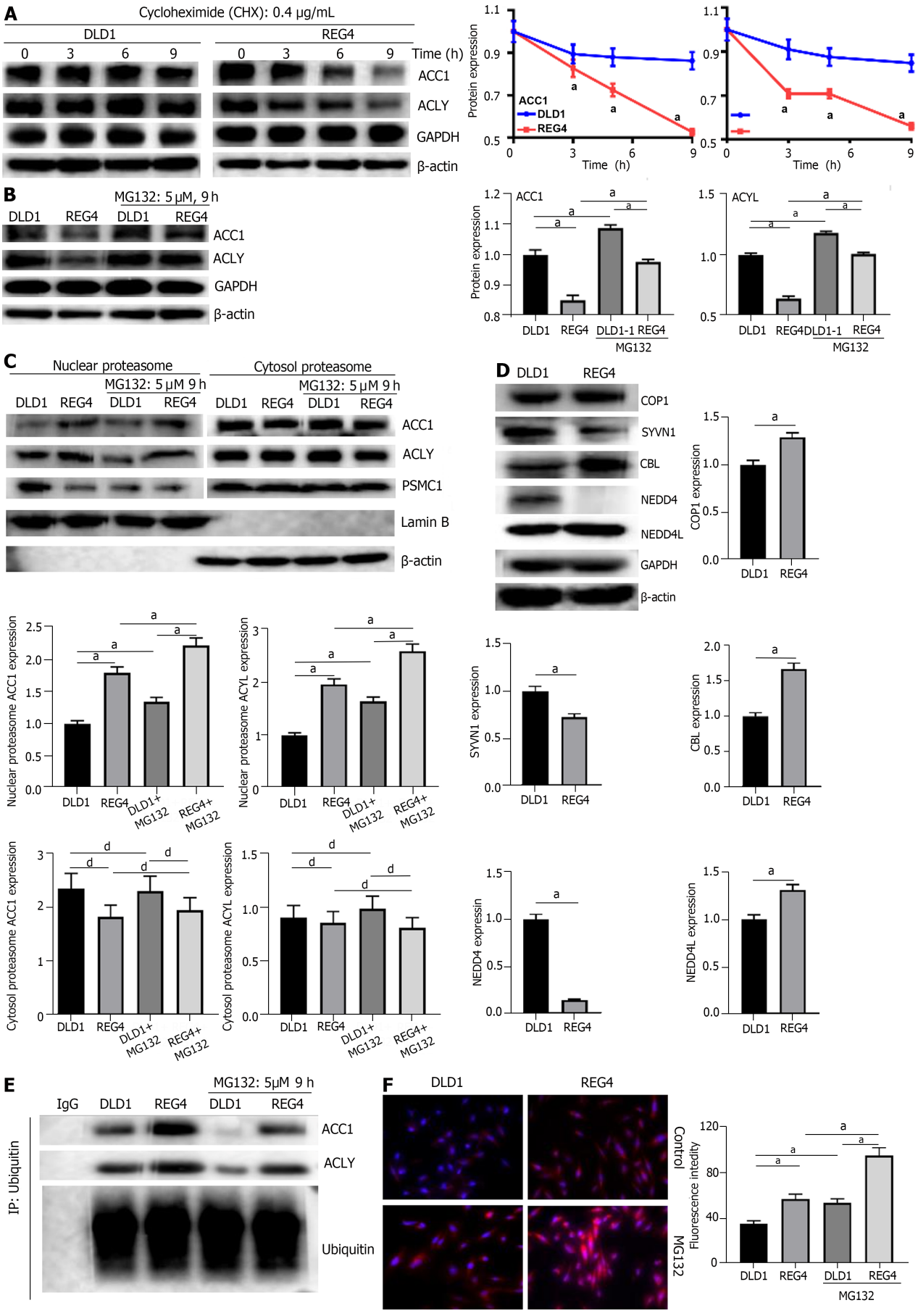


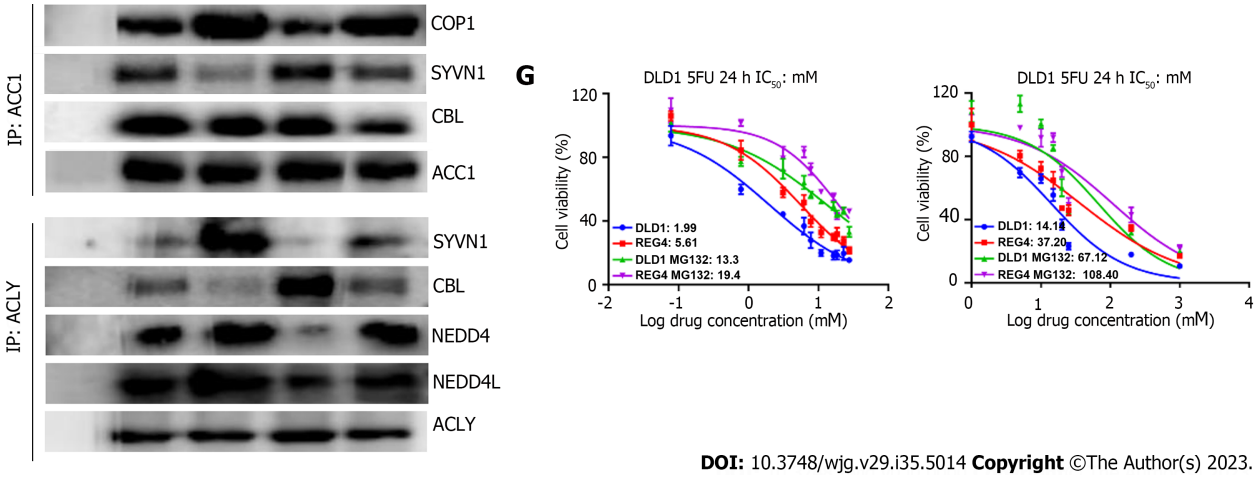
DOI: 10.3748/wjg.v29.i35.5104 **Copyright** ©The Author(s) 2023.

Figure 3 Full-length regenerating gene 4 weakened the transcription of acetyl-CoA carboxylase 1 and ATP-citrate lyase. A: DLD-1 cells and full-length-regenerating gene 4 (FL-*REG4*) transfectants were treated with suberoylanilide hydroxamic acid (SAHA) or small interfering RNA against histone deacetylase (siHDAC), and analyzed by chromatin immunoprecipitation; B: DLD-1 cells and FL-*REG4* transfectants were treated with SAHA, or siHDAC, and analyzed by co-immunoprecipitation assay using anti-anti-acetyl (AC)-acetyl-histone 3-AC-histone 4, anti-HDAC, anti-sterol-regulatory element binding protein 1 or anti-inhibitor of growth protein 5 antibody; C: DLD-1 cells and FL-*REG4* transfectants were treated with SAHA or siHDAC, and analyzed by quantitative reverse transcription polymerase chain reaction; D: DLD-1 cells and FL-*REG4* transfectants were treated with SAHA or siHDAC, and analyzed by Nile red staining; E: DLD-1 cells and FL-*REG4* transfectants were treated with SAHA or siHDAC, and analyzed by half maximal inhibitory concentration assay of 5-fluorouracil and cisplatin. $^{a}P < 0.001$; $^{b}P < 0.01$. *REG4*: Regenerating gene 4; SAHA: Suberoylanilide hydroxamic acid; siHDAC: Small interfering RNA against histone deacetylase; IgG: Immunoglobulin G; ND: No DNA; ACC1: Acetyl-CoA carboxylase 1; ACCY: ATP-citrate lyase; AC-H3: Acetyl-acetyl-histone 3; H4: Histone 4; SREBP1: Sterol-regulatory element binding protein 1; ING5: Inhibitor of growth protein 5; Ctr: Control DLD-1 cells; PC: Positive control.

CRC cells in an autocrine or paracrine manner. These findings demonstrated that *REG4* might be a potential molecular target for gene therapy of CRC.

DLD-1 cells developed resistance to 5-FU and DDP as a result of *REG4* overexpression. 5-FU- or DDP-resistant DLD-1 cells showed *REG4* overexpression, suggesting a role for *REG4* in chemoresistance, in line with previous studies[22,55]. The chemoresistance of CRC cells was produced by lysophosphatidylcholine acyltransferase 2-mediated lipid droplet formation[58], which was also aided by prothymosin α[59], and metastasis-associated in colon cancer[60] through SREBP-1- and fatty acid synthase-mediated and lipogenesis, respectively. Crucial enzymes for de novo fatty acid synthesis are ACC1 and ACLY, which are closely linked to chemoresistance[61]. In the liver and peritoneal tissues, lipid droplet assembly is mediated byadipocyte differentiation-related protein, CIDE, ACAT1, perilipin 5 and TIP47[62-66]. *REG4*-mediated lipid droplet formation might be closely linked to the upregulated expression of ACAT1, perilipin 5 and TIP47 in *REG4* transfectants, but not with de novo lipogenesis, as demonstrated by the downregulated expression of ACC1 and ACLY. *REG4*-mediated lipid droplet formation might account for *REG4*-induced resistance to 5-FU and DDP, which can be reversed by ACC1 or ACLY inhibitor, but deteriorated by high glucose exposure. In combination with these discoveries, we hypothesized that *REG4* may play an important role in chemoresistance, not through de novo lipogenesis, but by lipid droplet assembly, and might be used as a potential target for reversal of chemoresistance in CRC. According to the increased IC_{50} of DLD-1 cells after high glucose treatment, we speculate that high glucose treatment provides more glucose and increases the de novo synthesis of lipid droplets, thereby mediating the drug resistance of CRC cells.


A
Cycloheximide (CHX): 0.4 μg/mL
DLD1
REG4
0 3 6 9
Time (h)
ACC1
ACLY
GAPDH
β-actin
Protein expression
Time (h)
B
MG132: 5 μM, 9 h
DLD1 REG4 DLD1 REG4
C
Nuclear proteasome
Cytosol proteasome
PSMC1
Lamin B
Nuclear proteasome ACC1 expression
Nuclear proteasome ACYL expression
Cytosol proteasome ACC1 expression
Cytosol proteasome ACYL expression
DLD1+ MG132
REG4+ MG132
D
COP1
SYVN1
CBL
NEDD4
NEDD4L
COP1 expression
SYVN1 expression
CBL expression
NEDD4 expressin
NEDD4L expression
E
IgG
IP: Ubiquitin
Ubiquitin
F
Control
MG132
Fluorescence intedity



DOI: 10.3748/wjg.v29.i35.5014 **Copyright** ©The Author(s) 2023.

Figure 4 Full-length regenerating gene 4 destablized acetyl-CoA carboxylase 1 and ATP-citrate lyase proteins *via* proteasomal degradation. A: DLD-1 cells and full-length-regenerating gene 4 (FL-*REG4*) transfectants were treated with cycloheximide (0.4 μg/mL), followed by western blotting to detect acetyl-CoA carboxylase 1 (ACC1) and ATP-citrate lyase (ACLY) expression; B: DLD-1 cells and FL-*REG4* transfectants were treated with MG132 (5 μM, 9 h), followed by western blotting to detect ACC1 and ACLY expression; C: DLD-1 cells, FL-*REG4* transfectants, and MG132-treated DLD-1 cells and FL-*REG4* transfectants were subjected to proteasomal extract and western blotting to detect ACC1 and ACLY expression; D: Ubiquitin transferases (COP1 E3 ubiquitin ligase, synoviolin 1, Cbl proto-oncogene, NEDD4 like E3 ubiquitin protein ligase were detected by western blotting in DLD-1 cells and FL-*REG4* transfectants; E: After co-immunoprecipitation, western blotting was performed in DLD-1 cells and FL-*REG4* transfectants, with or without MG132 treatment; F: Nile red staining of DLD-1 cells, FL-*REG4* transfectants, and MG132-treated DLD-1 cells and FL-*REG4* transfectants; G: Tetrazolium salt assay was performed on DLD-1 cells, FL-*REG4* transfectants and MG132- treated DLD-1 cells and FL-*REG4* transfectants to detect half maximal inhibitory concentration of 5-fluorouracil and cisplatin. [a]*P* < 0.001; [d]No significance. *REG4*: Regenerating gene 4; ACC1: Acetyl-CoA carboxylase 1; ACCY: ATP-citrate lyase; COP1: COP1 E3 ubiquitin ligase; SYVN1: Synoviolin 1; CBL: Cbl proto-oncogene; NEDD4L: NEDD4 like E3 ubiquitin protein ligase; IgG: Immunoglobulin G.

We found that *REG4*-related signaling pathways included chemokine activity, taste receptors, protein-DNA and DNA packing complexes for transcription repression and activation, nucleosomes and chromatin, generation of second messenger molecules, HDAC and histone acetyltransferase for epigenetic regulation, and sugar metabolism. Therefore, we investigated the regulatory effects of *REG4* on the transcription of ACC1 and ACLY. *REG4* decreased expression of AC-H3, AC-H4, ING5, HDAC and SREBP1. *REG4* also weakened the interaction of the five proteins with the promoters of ACC1 or ACLY, or complex formation of the five proteins, and mRNA expression of ACC1 or ACLY. The inhibitory effect of FL-*REG4* transcription can be enhanced by low concentration SAHA (HDAC inhibitor) treatment or transfection with siHDAC. We speculated that HDAC hypoexpression or inactivation might increase the chemosensitivity of CRC cells by inhibiting the de novo lipogenesis, which suggests a potential clinical application for the antitumor drug SAHA. The decrease in lipid droplet formation and increase in chemotherapy sensitivity of DLD-1 cells after SAHA or siHDAC treatment indirectly confirm this view. We hypothesized that *REG4* inhibited the transcription of ACC1 and ACLY by disassociating the complex formation of AC-H3-AC-H4-ING5-HDAC-SREBP1 in their promoters and releasing the combination of ACC1 and ACLY promoters and complex *via* HDAC-mediated deacetylation.

To date, there has been no research about the effects of *REG4* on metabolic reprogramming, histone modification, and microenvironmental stress, and the interaction between *REG4* and metabolic or epigenetic pathways in CRC. With regard to drug resistance, Ying *et al*[67] found that upregulation of *REG4* mRNA was closely linked to the intrinsic drug resistance of gastric cancer cells to 5-FU. All 14 *REG4*-positive patients with gastric cancer showed no change or disease progression when treated with a combination of low-dose 5-FU and DDP[1]. In gastric cancer cells, *REG4* enhanced the resistance to 5-FU through the MAPK–ERK–Bim pathway[1]. Anti-*REG4* antibody significantly inhibited proliferation and chemosensitivity of gastric cancer cells to 5-FU, and *REG4* silencing caused the loss of stemness properties[68,69]. In ovarian cancer cells, *REG4* overexpression or rh*REG4* treatment promoted proliferation, G_2/S progression, antiapoptosis, migration, invasion, and DDP and paclitaxel[12,57]. In future research, we will also explore the potential interaction between *REG4* and metabolic or epigenetic pathways in CRC, which provides a new method for the early diagnosis and targeted therapy of CRC.

Finally, we also analyzed the modulatory effects of *REG4* on the protein stability of ACC1 and ACLY. Firstly, we treated DLD-1 cells and *REG4* transfectants with CHX, and found that *REG4* destabilized ACC1 and ACLY. *REG4* promoted the recruitment of ACC1 and ACLY to the nuclear proteasome for ubiquitylation-mediated degradation, during which ACLY bound to NEDD4, SYVN1 and NEDD4L, and ACC1 bound to COP1. Overexpression of *REG4* mediated lipid droplet formation and chemoresistance in DLD-1 cells. These results suggested that *REG4* facilitated proteasomal degradation of ACC1 and ACLY to suppress de novo lipogenesis. We also speculate that pretreatment of proteasome inhibitor MG132 in DLD-1 cells can increase expression of ACC1 and ACLY by reducing ubiquitination of ACC1 and ACLY, thus increasing formation of lipid droplets and leading to chemoresistance. In the future, we will explore the potential role of *REG4* from metabolic reprogramming and epigenetic regulation.

CONCLUSION

REG4 protein expression was decreased in CRC and positively linked with the degree of invasion, TNM stage, and dedifferentiation, but the converse was the case for *REG4* mRNA expression. *REG4* aggravated aggressive phenotypes in an autocrine or paracrine manner *via* the EGFR-PI3K-Akt-NF-κB signaling pathway. *REG4* may be involved in chemoresistance, not through de novo lipogenesis, but by lipid droplet assembly. *REG4* inhibited the transcription of ACC1 or ACLY by disassociating the complex formation of AC-H3-AC-H4-ING5-histone deacetylase-SREBP1 in their promoters and induced the proteasomal degradation of ACC1 and ACLY proteins. Pretreatment with high glucose might induce chemoresistance of CRC cells, which should be emphasized in clinical practice. SAHA can reverse the chemoresistance of CRC and provide a potential direction for research of DDP and 5-FU resistance of CRC. Finally, *REG4* may be used as a reliable diagnostic marker for the prognosis, aggressiveness and carcinogenesis of CRC and is a potential molecular target.

ARTICLE HIGHLIGHTS

Research background

Regulating gene 4 (*REG4*) has been proved to be carcinogenic in some cancers, but its manifestation and possible carcinogenic mechanism in colorectal cancer (CRC) have not yet been elucidated. Our previous study found that the drug resistance characteristics of CRC cells may be related to their fat metabolism.

Research motivation

With the aging of the world population, the incidence of CRC is increasing. For the treatment of CRC, chemoresistance has always been an urgent problem to be solved.

Research objectives

This study aimed to explore the role of *REG4* in CRC and its association with lipid droplet formation, and the molecular mechanisms involved.

Research methods

We conducted a meta-analysis and bioinformatics and pathological analysis of *REG4* expression in CRC. The effects of *REG4* on the phenotypes and related proteins were also investigated in CRC cells.

Research results

Compared to normal mucosa, *REG4* mRNA expression was high in CRC, but protein expression was opposite. *REG4*-related genes included epigenetic regulation, transcription repression, sugar metabolism and transfer. *REG4* exposure or overexpression promoted proliferation, antiapoptosis, migration and invasion of DLD-1 cells in an autocrine or paracrine manner by activating the epidermal growth factor receptor-phosphoinositide 3-kinase-Akt-nuclear factor-κB pathway. *REG4* was involved in chemoresistance not through de novo lipogenesis, but lipid droplet assembly, which was strengthened by high glucose treatment. *REG4* inhibited the transcription of acetyl-coA carboxylase 1 (ACC1) and ATP-citrate lyase (ACLY) by disassociating the complex formation of anti–acetyl (AC)-acetyl-histone 3-AC-histone 4-inhibitor of growth protein-5-si histone deacetylase-sterol-regulatory element binding protein 1 in their promoters and induced proteasomal degradation of ACC1 or ACLY.

Research conclusions

REG4 may be an indicator of drug resistance and metabolism of tumor cells. *REG4* might be a useful marker for colorectal carcinogenesis, as well as a potential gene therapy target.

Research perspectives

This study provides new insights into a better understanding of the pathogenesis of CRC. *REG4* may be used as a novel therapeutic target. However, the regulatory mechanism needs to be further explored.

FOOTNOTES

Author contributions: Zhang CY and Zheng HC designed the study; Zhang CY participated in data collection; Zheng HC wrote the paper; Zhang R, Zhang L, Wang ZM, Sun HZ and Cui ZG were responsible for revising the manuscript; All the listed authors have contributed and approved the final manuscript.

Supported by Natural Science Foundation of Hebei Province, No. 21377772D; No. H2022406034; National Natural Scientific Foundation of China, No. 81672700.

Institutional review board statement: The study was reviewed and approved by the Institutional Review Board at the First Affiliated

Hospital of Jinzhou Medical University.

Informed consent statement: All study participants, or their legal guardian, provided informed written consent prior to study enrollment.

Conflict-of-interest statement: All the authors report no relevant conflicts of interest for this article.

Data sharing statement: No additional data are available.

Open-Access: This article is an open-access article that was selected by an in-house editor and fully peer-reviewed by external reviewers. It is distributed in accordance with the Creative Commons Attribution NonCommercial (CC BY-NC 4.0) license, which permits others to distribute, remix, adapt, build upon this work non-commercially, and license their derivative works on different terms, provided the original work is properly cited and the use is non-commercial. See: https://creativecommons.org/Licenses/by-nc/4.0/

Country/Territory of origin: China

ORCID number: Cong-Yu Zhang 0000-0002-2089-9653; Rui Zhang 0000-0003-0197-1098; Li Zhang 0009-0004-8547-1326; Zi-Mo Wang 0000-0002-4948-8612; Hong-Zhi Sun 0009-0001-5259-1530; Zheng-Guo Cui 0000-0002-9756-9150; Hua-Chuan Zheng 0000-0003-0965-6818.

S-Editor: Qu XL
L-Editor: A
P-Editor: Cai YX

REFERENCES

1 **Zheng HC**, Xue H, Zhang CY. *REG4* promotes the proliferation and anti-apoptosis of cancer. *Front Cell Dev Biol* 2022; **10**: 1012193 [PMID: 36172286 DOI: 10.3389/fcell.2022.1012193]
2 **Hu Y**, Pan C, Hu J, Zhang S. The role of Reg IV in colorectal cancer, as a potential therapeutic target. *Contemp Oncol (Pozn)* 2015; **19**: 261-264 [PMID: 26557771 DOI: 10.5114/wo.2015.54385]
3 **Zheng HC**, Sugawara A, Okamoto H, Takasawa S, Takahashi H, Masuda S, Takano Y. Expression profile of the REG gene family in colorectal carcinoma. *J Histochem Cytochem* 2011; **59**: 106-115 [PMID: 21339177 DOI: 10.1369/jhc.2010.956961]
4 **Wang H**, Hu L, Zang M, Zhang B, Duan Y, Fan Z, Li J, Su L, Yan M, Zhu Z, Liu B, Yang Q. *REG4* promotes peritoneal metastasis of gastric cancer through GPR37. *Oncotarget* 2016; **7**: 27874-27888 [PMID: 27036049 DOI: 10.18632/oncotarget.8442]
5 **Kawasaki Y**, Matsumura K, Miyamoto M, Tsuji S, Okuno M, Suda S, Hiyoshi M, Kitayama J, Akiyama T. *REG4* is a transcriptional target of GATA6 and is essential for colorectal tumorigenesis. *Sci Rep* 2015; **5**: 14291 [PMID: 26387746 DOI: 10.1038/srep14291]
6 **Naito Y**, Oue N, Hinoi T, Sakamoto N, Sentani K, Ohdan H, Yanagihara K, Sasaki H, Yasui W. Reg IV is a direct target of intestinal transcriptional factor CDX2 in gastric cancer. *PLoS One* 2012; **7**: e47545 [PMID: 23133598 DOI: 10.1371/journal.pone.0047545]
7 **Bishnupuri KS**, Sainathan SK, Bishnupuri K, Leahy DR, Luo Q, Anant S, Houchen CW, Dieckgraefe BK. *Reg4*-induced mitogenesis involves Akt-GSK3β-β-Catenin-TCF-4 signaling in human colorectal cancer. *Mol Carcinog* 2014; **53** Suppl 1: E169-E180 [PMID: 24151146 DOI: 10.1002/mc.22088]
8 **Bishnupuri KS**, Luo Q, Murmu N, Houchen CW, Anant S, Dieckgraefe BK. Reg IV activates the epidermal growth factor receptor/Akt/AP-1 signaling pathway in colon adenocarcinomas. *Gastroenterology* 2006; **130**: 137-149 [PMID: 16401477 DOI: 10.1053/j.gastro.2005.10.001]
9 **He XJ**, Jiang XT, Ma YY, Xia YJ, Wang HJ, Guan TP, Shao QS, Tao HQ. *REG4* contributes to the invasiveness of pancreatic cancer by upregulating MMP-7 and MMP-9. *Cancer Sci* 2012; **103**: 2082-2091 [PMID: 22957785 DOI: 10.1111/cas.12018]
10 **Ma X**, Wu D, Zhou S, Wan F, Liu H, Xu X, Zhao Y, Tang M. The pancreatic cancer secreted *REG4* promotes macrophage polarization to M2 through EGFR/AKT/CREB pathway. *Oncol Rep* 2016; **35**: 189-196 [PMID: 26531138 DOI: 10.3892/or.2015.4357]
11 **Mitani Y**, Oue N, Matsumura S, Yoshida K, Noguchi T, Ito M, Tanaka S, Kuniyasu H, Kamata N, Yasui W. Reg IV is a serum biomarker for gastric cancer patients and predicts response to 5-fluorouracil-based chemotherapy. *Oncogene* 2007; **26**: 4383-4393 [PMID: 17237819 DOI: 10.1038/sj.onc.1210215]
12 **Chen S**, Gou WF, Zhao S, Niu ZF, Zhao Y, Takano Y, Zheng HC. The role of the *REG4* gene and its encoding product in ovarian epithelial carcinoma. *BMC Cancer* 2015; **15**: 471 [PMID: 26077911 DOI: 10.1186/s12885-015-1435-2]
13 **Violette S**, Festor E, Pandrea-Vasile I, Mitchell V, Adida C, Dussaulx E, Lacorte JM, Chambaz J, Lacasa M, Lesuffleur T. Reg IV, a new member of the regenerating gene family, is overexpressed in colorectal carcinomas. *Int J Cancer* 2003; **103**: 185-193 [PMID: 12455032 DOI: 10.1002/ijc.10788]
14 **Granlund Av**, Beisvag V, Torp SH, Flatberg A, Kleveland PM, Ostvik AE, Waldum HL, Sandvik AK. Activation of REG family proteins in colitis. *Scand J Gastroenterol* 2011; **46**: 1316-1323 [PMID: 21992413 DOI: 10.3109/00365521.2011.605463]
15 **Oue N**, Kuniyasu H, Noguchi T, Sentani K, Ito M, Tanaka S, Setoyama T, Sakakura C, Natsugoe S, Yasui W. Serum concentration of Reg IV in patients with colorectal cancer: overexpression and high serum levels of Reg IV are associated with liver metastasis. *Oncology* 2007; **72**: 371-380 [PMID: 18187959 DOI: 10.1159/000113147]
16 **Numata M**, Oshima T, Yoshihara K, Watanabe T, Tsuchida K, Tamagawa H, Yamamoto N, Shiozawa M, Morinaga S, Akaike M, Kunisaki C, Rino Y, Tanaka K, Masuda M, Imada T. Relationship between RegIV gene expression to outcomes in colorectal cancer. *J Surg Oncol* 2011; **104**: 205-209 [PMID: 21381041 DOI: 10.1002/jso.21906]
17 **He HL**, Lee YE, Shiue YL, Lee SW, Lin LC, Chen TJ, Wu TF, Hsing CH, Huang HY, Wang JY, Li CF. Overexpression of *REG4* confers an independent negative prognosticator in rectal cancers receiving concurrent chemoradiotherapy. *J Surg Oncol* 2014; **110**: 1002-1010 [PMID: 25155043 DOI: 10.1002/jso.23764]
18 **Guo Y**, Xu J, Li N, Gao F, Huang P. RegIV potentiates colorectal carcinoma cell migration and invasion *via* its CRD domain. *Cancer Genet*

Cytogenet 2010; **199**: 38-44 [PMID: 20417867 DOI: 10.1016/j.cancergencyto.2010.01.011]
19 **Rafa L**, Dessein AF, Devisme L, Buob D, Truant S, Porchet N, Huet G, Buisine MP, Lesuffleur T. *REG4* acts as a mitogenic, motility and pro-invasive factor for colon cancer cells. *Int J Oncol* 2010; **36**: 689-698 [PMID: 20126989 DOI: 10.3892/ijo_00000544]
20 **Nanakin A**, Fukui H, Fujii S, Sekikawa A, Kanda N, Hisatsune H, Seno H, Konda Y, Fujimori T, Chiba T. Expression of the REG IV gene in ulcerative colitis. *Lab Invest* 2007; **87**: 304-314 [PMID: 17260007 DOI: 10.1038/Labinvest.3700507]
21 **Kobunai T**, Watanabe T, Fukusato T. *REG4*, NEIL2, and BIRC5 gene expression correlates with gamma-radiation sensitivity in patients with rectal cancer receiving radiotherapy. *Anticancer Res* 2011; **31**: 4147-4153 [PMID: 22199273]
22 **Gao L**, Wu X, Zhang L, Dai Y, Zhu Z, Zhi Y, Wang K. *REG4* is a Potential Biomarker for Radiochemotherapy Sensitivity in Colorectal Cancer. *Onco Targets Ther* 2021; **14**: 1605-1611 [PMID: 33688207 DOI: 10.2147/OTT.S296031]
23 **Jou E**, Rodriguez-Rodriguez N, McKenzie ANJ. Emerging roles for IL-25 and IL-33 in colorectal cancer tumorigenesis. *Front Immunol* 2022; **13**: 981479 [PMID: 36263033 DOI: 10.3389/fimmu.2022.981479]
24 **Droeser RA**, Iezzi G. IL-22-mediates Cross-talk between Tumor Cells and Immune Cells Associated with Favorable Prognosis in Human Colorectal Cancer. *J Cell Immunol* 2021; **3**: 118-121 [PMID: 34296212 DOI: 10.33696/immunology.3.087]
25 **Djaldetti M**, Bessler H. Modulators affecting the immune dialogue between human immune and colon cancer cells. *World J Gastrointest Oncol* 2014; **6**: 129-138 [PMID: 24834143 DOI: 10.4251/wjgo.v6.i5.129]
26 **Li Y**, Liu Y, Zhao N, Yang X, Li Y, Zhai F, Zang X, Cui W. Checkpoint regulator B7x is epigenetically regulated by HDAC3 and mediates resistance to HDAC inhibitors by reprogramming the tumor immune environment in colorectal cancer. *Cell Death Dis* 2020; **11**: 753 [PMID: 32934224 DOI: 10.1038/s41419-020-02968-y]
27 **Jang TJ**. Progressive Increase of Regulatory T Cells and Decrease of CD8+ T Cells and CD8+ T Cells/Regulatory T Cells Ratio during Colorectal Cancer Development. *Korean J Pathol* 2013; **47**: 443-451 [PMID: 24255632 DOI: 10.4132/KoreanJPathol.2013.47.5.443]
28 **Zheng HC**, Xu XY, Yu M, Takahashi H, Masuda S, Takano Y. The role of Reg IV gene and its encoding product in gastric carcinogenesis. *Hum Pathol* 2010; **41**: 59-69 [PMID: 19740514 DOI: 10.1016/j.humpath.2009.06.013]
29 **Zheng SQ**, He J, Huang PL, Wang JH. Clinical significance of Reg IV protein expression in human colorectal cancer. *Shijie Huaren Xiaohua Zazhi* 2010; **18**: 3594-3598 [DOI: 10.11569/wcjd.v18.i33.3594]
30 **Li XH**, Zheng Y, Zheng HC, Takahashi H, Yang XH, Masuda S, Takano Y. REG IV overexpression in an early stage of colorectal carcinogenesis: an immunohistochemical study. *Histol Histopathol* 2010; **25**: 473-484 [PMID: 20183800 DOI: 10.14670/HH-25.473]
31 **Li FY**, Ren XB, Xu EP, Huang Q, Sheng HQ, Lv BJ, Lai MD. RegIV expression showing specificity to gastrointestinal tract and its potential role in diagnosing digestive tract neuroendocrine tumor. *J Zhejiang Univ Sci B* 2010; **11**: 258-266 [PMID: 20349522 DOI: 10.1631/jzus.B0900383]
32 **Wang LN**, Hou SP, Liu HB, Sun XL, Zhang XJ, Zhang QQ. Expression of *REG4* and surviving and clinical significance in colorectal cancer. *Shiyong Yixue Zazhi* 2015; **31**: 3347-3350 [DOI: 10.1186/s13000-015-0253-9]
33 **Wang GM**, Wang CX, Nie MN, Zhang LH, Diao WY. Expression of Reg IV in colon carcinoma and its relationship with angiogenesis. *J Med Forum* 2016; **37**: 7-9 [DOI: 10.3892/ijmm_00000007]
34 **Oue N**, Mitani Y, Aung PP, Sakakura C, Takeshima Y, Kaneko M, Noguchi T, Nakayama H, Yasui W. Expression and localization of Reg IV in human neoplastic and non-neoplastic tissues: Reg IV expression is associated with intestinal and neuroendocrine differentiation in gastric adenocarcinoma. *J Pathol* 2005; **207**: 185-198 [PMID: 16086444 DOI: 10.1002/path.1827]
35 **Sawada T**, Yashiro M, Sentani K, Oue N, Yasui W, Miyazaki K, Kai K, Fujita H, Nakamura K, Maeda K, Kakeji Y, Natsugoe S, Shirabe K, Nomura S, Shimada Y, Tomita N, Hirakawa K, Maehara Y. New molecular staging with G-factors (VEGF-C and Reg IV) by supplementing TNM classification in colorectal cancers. *Oncol Rep* 2013; **30**: 2609-2616 [PMID: 24101199 DOI: 10.3892/or.2013.2787]
36 **Zhu X**, Han Y, Yuan C, Tu W, Qiu G, Lu S, Lu H, Peng Z, Zhou C. Overexpression of *Reg4*, alone or combined with MMP-7 overexpression, is predictive of poor prognosis in colorectal cancer. *Oncol Rep* 2015; **33**: 320-328 [PMID: 25338725 DOI: 10.3892/or.2014.3559]
37 **Kaprio T**, Hagström J, Mustonen H, Koskensalo S, Andersson LC, Haglund C. *REG4* independently predicts better prognosis in non-mucinous colorectal cancer. *PLoS One* 2014; **9**: e109600 [PMID: 25295732 DOI: 10.1371/journal.pone.0109600]
38 **Takehara A**, Eguchi H, Ohigashi H, Ishikawa O, Kasugai T, Hosokawa M, Katagiri T, Nakamura Y, Nakagawa H. Novel tumor marker *REG4* detected in serum of patients with resectable pancreatic cancer and feasibility for antibody therapy targeting *REG4*. *Cancer Sci* 2006; **97**: 1191-1197 [PMID: 16918991 DOI: 10.1111/j.1349-7006.2006.00297.x]
39 **Liu CM**, Hsieh CL, He YC, Lo SJ, Liang JA, Hsieh TF, Josson S, Chung LW, Hung MC, Sung SY. In vivo targeting of ADAM9 gene expression using lentivirus-delivered shRNA suppresses prostate cancer growth by regulating *REG4* dependent cell cycle progression. *PLoS One* 2013; **8**: e53795 [PMID: 23342005 DOI: 10.1371/journal.pone.0053795]
40 **Bishnupuri KS**, Luo Q, Sainathan SK, Kikuchi K, Sureban SM, Sabarinathan M, Gross JH, Aden K, May R, Houchen CW, Anant S, Dieckgraefe BK. Reg IV regulates normal intestinal and colorectal cancer cell susceptibility to radiation-induced apoptosis. *Gastroenterology* 2010; **138**: 616-626, 626.e1 [PMID: 19900450 DOI: 10.1053/j.gastro.2009.10.050]
41 **Zhang Y**, Lai M, Lv B, Gu X, Wang H, Zhu Y, Shao L, Wang G. Overexpression of Reg IV in colorectal adenoma. *Cancer Lett* 2003; **200**: 69-76 [PMID: 14550954 DOI: 10.1016/s0304-3835(03)00460-9]
42 **Lasserre C**, Colnot C, Bréchot C, Poirier F. HIP/PAP gene, encoding a C-type lectin overexpressed in primary liver cancer, is expressed in nervous system as well as in intestine and pancreas of the postimplantation mouse embryo. *Am J Pathol* 1999; **154**: 1601-1610 [PMID: 10329612 DOI: 10.1016/S0002-9440(10)65413-2]
43 **Lasserre C**, Christa L, Simon MT, Vernier P, Bréchot C. A novel gene (HIP) activated in human primary liver cancer. *Cancer Res* 1992; **52**: 5089-5095 [PMID: 1325291]
44 **Kimura N**, Yonekura H, Okamoto H, Nagura H. Expression of human regenerating gene mRNA and its product in normal and neoplastic human pancreas. *Cancer* 1992; **70**: 1857-1863 [PMID: 1525759 DOI: 10.1002/1097-0142(19921001)70:7<1857::aid-cncr2820700708>3.0.co;2-8]
45 **Ohara S**, Oue N, Matsubara A, Mita K, Hasegawa Y, Hayashi T, Usui T, Amatya VJ, Takeshima Y, Kuniyasu H, Yasui W. Reg IV is an independent prognostic factor for relapse in patients with clinically localized prostate cancer. *Cancer Sci* 2008; **99**: 1570-1577 [PMID: 18754868 DOI: 10.1111/j.1349-7006.2008.00846.x]
46 **Takayama R**, Nakagawa H, Sawaki A, Mizuno N, Kawai H, Tajika M, Yatabe Y, Matsuo K, Uehara R, Ono K, Nakamura Y, Yamao K. Serum tumor antigen *REG4* as a diagnostic biomarker in pancreatic ductal adenocarcinoma. *J Gastroenterol* 2010; **45**: 52-59 [PMID: 19789838 DOI: 10.1007/s00535-009-0114-y]

47 **Wang Q**, Deng J, Yuan J, Wang L, Zhao Z, He S, Zhang Y, Tu Y. Oncogenic reg IV is a novel prognostic marker for glioma patient survival. *Diagn Pathol* 2012; **7**: 69 [PMID: 22713481 DOI: 10.1186/1746-1596-7-69]

48 **Tamura H**, Ohtsuka M, Washiro M, Kimura F, Shimizu H, Yoshidome H, Kato A, Seki N, Miyazaki M. Reg IV expression and clinicopathologic features of gallbladder carcinoma. *Hum Pathol* 2009; **40**: 1686-1692 [PMID: 19716164 DOI: 10.1016/j.humpath.2009.06.001]

49 **Hayashi T**, Matsubara A, Ohara S, Mita K, Hasegawa Y, Usui T, Arihiro K, Norimura S, Sentani K, Oue N, Yasui W. Immunohistochemical analysis of Reg IV in urogenital organs: Frequent expression of Reg IV in prostate cancer and potential utility as serum tumor marker. *Oncol Rep* 2009; **21**: 95-100 [PMID: 19082448]

50 **Derakhshani A**, Hashemzadeh S, Asadzadeh Z, Shadbad MA, Rasibonab F, Safarpour H, Jafarlou V, Solimando AG, Racanelli V, Singh PK, Najafi S, Javadrashid D, Brunetti O, Silvestris N, Baradaran B. Cytotoxic T-Lymphocyte Antigen-4 in Colorectal Cancer: Another Therapeutic Side of Capecitabine. *Cancers (Basel)* 2021; **13** [PMID: 34067631 DOI: 10.3390/cancers13102414]

51 **Lehtinen L**, Vesterkvist P, Roering P, Korpela T, Hattara L, Kaipio K, Mpindi JP, Hynninen J, Auranen A, Davidson B, Haglund C, Iljin K, Grenman S, Siitari H, Carpen O. *REG4* Is Highly Expressed in Mucinous Ovarian Cancer: A Potential Novel Serum Biomarker. *PLoS One* 2016; **11**: e0151590 [PMID: 26981633 DOI: 10.1371/journal.pone.0151590]

52 **Kang G**, Oh I, Pyo J, Kang D, Son B. Clinicopathological Significance and Prognostic Implications of *REG4* Immunohistochemical Expression in Colorectal Cancer. *Medicina (Kaunas)* 2021; **57** [PMID: 34577861 DOI: 10.3390/medicina57090938]

53 **Saukkonen K**, Hagström J, Mustonen H, Lehtinen L, Carpen O, Andersson LC, Seppänen H, Haglund C. Prognostic and diagnostic value of *REG4* serum and tissue expression in pancreatic ductal adenocarcinoma. *Tumour Biol* 2018; **40**: 1010428318761494 [PMID: 29542402 DOI: 10.1177/1010428318761494]

54 **Bishnupuri KS**, Sainathan SK, Ciorba MA, Houchen CW, Dieckgraefe BK. *Reg4* Interacts with CD44 to Regulate Proliferation and Stemness of Colorectal and Pancreatic Cancer Cells. *Mol Cancer Res* 2022; **20**: 387-399 [PMID: 34753802 DOI: 10.1158/1541-7786.MCR-21-0224]

55 **Xiang LW**, Xue H, Ha MW, Yu DY, Xiao LJ, Zheng HC. The effects of *REG4* expression on chemoresistance of ovarian cancer. *J Obstet Gynaecol* 2022; **42**: 3149-3157 [PMID: 35929918 DOI: 10.1080/01443615.2022.2106834]

56 **Hwang JH**, Yoon J, Cho YH, Cha PH, Park JC, Choi KY. A mutant KRAS-induced factor *REG4* promotes cancer stem cell properties *via* Wnt/β-catenin signaling. *Int J Cancer* 2020; **146**: 2877-2890 [PMID: 31605540 DOI: 10.1002/ijc.32728]

57 **Jin J**, Lv H, Wu J, Li D, Chen K, Zhang F, Han J, Feng J, Zhang N, Yu H, Su D, Ying L. Regenerating Family Member 4 (*Reg4*) Enhances 5-Fluorouracil Resistance of Gastric Cancer Through Activating MAPK/Erk/Bim Signaling Pathway. *Med Sci Monit* 2017; **23**: 3715-3721 [PMID: 28759561 DOI: 10.12659/msm.903134]

58 **Cotte AK**, Aires V, Fredon M, Limagne E, Derangère V, Thibaudin M, Humblin E, Scagliarini A, de Barros JP, Hillon P, Ghiringhelli F, Delmas D. Lysophosphatidylcholine acyltransferase 2-mediated lipid droplet production supports colorectal cancer chemoresistance. *Nat Commun* 2018; **9**: 322 [PMID: 29358673 DOI: 10.1038/s41467-017-02732-5]

59 **Jin L**, Zhu LY, Pan YL, Fu HQ, Zhang J. Prothymosin α promotes colorectal carcinoma chemoresistance through inducing lipid droplet accumulation. *Mitochondrion* 2021; **59**: 123-134 [PMID: 33872798 DOI: 10.1016/j.mito.2021.04.001]

60 **Duan J**, Chen L, Zhou M, Zhang J, Sun L, Huang N, Bin J, Liao Y, Liao W. MACC1 decreases the chemosensitivity of gastric cancer cells to oxaliplatin by regulating FASN expression. *Oncol Rep* 2017; **37**: 2583-2592 [PMID: 28339092 DOI: 10.3892/or.2017.5519]

61 **Sur S**, Nakanishi H, Flaveny C, Ippolito JE, McHowat J, Ford DA, Ray RB. Inhibition of the key metabolic pathways, glycolysis and lipogenesis, of oral cancer by bitter melon extract. *Cell Commun Signal* 2019; **17**: 131 [PMID: 31638999 DOI: 10.1186/s12964-019-0447-y]

62 **Fan H**, Diao H, Lu Y, Xie J, Cheng X. The relation between serum adipose differentiation-related protein and non-alcoholic fatty liver disease in type 2 diabetes mellitus. *Ther Adv Endocrinol Metab* 2020; **11**: 2042018820969025 [PMID: 33194172 DOI: 10.1177/2042018820969025]

63 **Kasano-Camones CI**, Takizawa M, Iwasaki W, Sasaki S, Hamada M, Morimoto A, Sakaguchi M, Gonzalez FJ, Inoue Y. Synergistic regulation of hepatic Fsp27b expression by HNF4α and CREBH. *Biochem Biophys Res Commun* 2020; **530**: 432-439 [PMID: 32553626 DOI: 10.1016/j.bbrc.2020.05.070]

64 **Ayyagari V**, Li M, Pasman Z, Wang X, Louis S, Diaz-Sylvester P, Groesch K, Wilson T, Brard L. Assessment of the diagnostic and prognostic relevance of ACAT1 and CE levels in plasma, peritoneal fluid and tumor tissue of epithelial ovarian cancer patients - a pilot study. *BMC Cancer* 2022; **22**: 387 [PMID: 35399074 DOI: 10.1186/s12885-022-09476-6]

65 **Ethem İ**, Hacıoğlu C. Effects of perilipin-5 on lipid metabolism and high-sensitivity cardiac troponin I. *Rev Assoc Med Bras (1992)* 2022; **68**: 1011-1016 [PMID: 36134829 DOI: 10.1590/1806-9282.20211377]

66 **Nose F**, Yamaguchi T, Kato R, Aiuchi T, Obama T, Hara S, Yamamoto M, Itabe H. Crucial role of perilipin-3 (TIP47) in formation of lipid droplets and PGE2 production in HL-60-derived neutrophils. *PLoS One* 2013; **8**: e71542 [PMID: 23936516 DOI: 10.1371/journal.pone.0071542]

67 **Ying LS**, Yu JL, Lu XX, Ling ZQ. Enhanced RegIV expression predicts the intrinsic 5-fluorouracil (5-FU) resistance in advanced gastric cancer. *Dig Dis Sci* 2013; **58**: 414-422 [PMID: 23010741 DOI: 10.1007/s10620-012-2381-3]

68 **Zhang XQ**, Yu LT, Du P, Yin TQ, Zhang ZY, Xu Y, Li X, Li YJ, Wang M, Luo C. Single-chain Antibody Against *Reg4* Suppresses Gastric Cancer Cell Growth and Enhances 5-FU-induced Cell Death in vitro. *Anticancer Agents Med Chem* 2019; **19**: 610-619 [PMID: 30465515 DOI: 10.2174/1871520619666181122104720]

69 **Zhou W**, Sun M, Wang DL, Wang Y, Jin F, Zhang YY, Yang L, Wu XL, Wu YZ. Silencing of RegIV by shRNA causes the loss of stemness properties of cancer stem cells in MKN45 gastric cancer cells. *Oncol Rep* 2013; **30**: 2685-2690 [PMID: 24064664 DOI: 10.3892/or.2013.2745]

World Journal of Gastroenterology

Submit a Manuscript: https://www.f6publishing.com

World J Gastroenterol 2023 September 21; 29(35): 5125-5137

DOI: 10.3748/wjg.v29.i35.5125

ISSN 1007-9327 (print) ISSN 2219-2840 (online)

ORIGINAL ARTICLE

Retrospective Cohort Study

Clinical characteristics and outcome of autoimmune pancreatitis based on serum immunoglobulin G4 level: A single-center, retrospective cohort study

Guan-Zhou Zhou, Jia-Qi Zeng, Lei Wang, Miao Liu, Ke Meng, Zi-Kai Wang, Xiu-Li Zhang, Li-Hua Peng, Bin Yan, Fei Pan

Specialty type: Gastroenterology and hepatology

Provenance and peer review: Unsolicited article; Externally peer reviewed.

Peer-review model: Single blind

Peer-review report's scientific quality classification

Grade A (Excellent): 0
Grade B (Very good): 0
Grade C (Good): C, C
Grade D (Fair): D
Grade E (Poor): 0

P-Reviewer: Cigrovski Berkovic M, Croatia; Mizushima I

Received: May 22, 2023
Peer-review started: May 22, 2023
First decision: July 8, 2023
Revised: July 21, 2023
Accepted: September 1, 2023
Article in press: September 1, 2023
Published online: September 21, 2023

Guan-Zhou Zhou, Jia-Qi Zeng, Ke Meng, Zi-Kai Wang, Xiu-Li Zhang, Li-Hua Peng, Bin Yan, Fei Pan, Department of Gastroenterology and Hepatology, The First Medical Center, Chinese PLA General Hospital, Beijing 100853, China

Guan-Zhou Zhou, School of Medicine, Nankai University, Tianjin 300071, China

Jia-Qi Zeng, Chinese PLA Medical School, Beijing 100853, China

Lei Wang, Department of Rheumatology, The First Medical Center, Chinese PLA General Hospital, Beijing 100853, China

Miao Liu, Department of Statistics and Epidemiology, Graduate School, Chinese PLA General Hospital, Beijing 100853, China

Corresponding author: Fei Pan, MD, PhD, Associate Chief Physician, Associate Professor, Department of Gastroenterology and Hepatology, The First Medical Center, Chinese PLA General Hospital, No. 28 Fuxing Road, Beijing 100853, China. panfei@plagh.org

Abstract

BACKGROUND

Autoimmune pancreatitis (AIP) has been linked with elevated immunoglobulin (Ig) G4 levels. The characteristics and outcomes of AIP based on serum markers have not been fully evaluated.

AIM

To compare clinical features, treatment efficacy, and outcome of AIP based on serum IgG4 levels and analyze predictors of relapse.

METHODS

A total of 213 patients with AIP were consecutively reviewed in our hospital from 2006 to 2021. According to the serum IgG4 level, all patients were divided into two groups, the abnormal group (n = 148) with a high level of IgG4 [> 2 × upper limit of normal (ULN)] and the normal group (n = 65). The t-test or Mann-Whitney U test was used to compare continuous variables. Categorical parameters were compared by the χ^2 test or Fisher's exact test. Kaplan-Meier curves

and log-rank tests were established to assess the cumulative relapse rates. Univariate and multivariate analyses were used to investigate potential risk factors of AIP relapse.

RESULTS

Compared with the normal group, the abnormal group had a higher average male age (60.3 ± 10.4 *vs* 56.5 ± 12.9 years, $P = 0.047$); higher level of serum total protein (72.5 ± 7.9 g/L *vs* 67.2 ± 7.5 g/L, $P < 0.001$), IgG4 (1420.5 ± 1110.9 mg/dL *vs* 252.7 ± 106.6 mg/dL, $P < 0.001$), and IgE (635.6 ± 958.1 IU/mL *vs* 231.7 ± 352.5 IU/mL, $P = 0.002$); and a lower level of serum complement C3 (100.6 ± 36.2 mg/dL *vs* 119.0 ± 45.7 mg/dL, $P = 0.050$). In addition, a lower number of cases with abnormal pancreatic duct and pancreatic atrophy (23.6% *vs* 37.9%, $P = 0.045$; 1.6% *vs* 8.6%, $P = 0.020$, respectively) and a higher rate of relapse (17.6% *vs* 6.2%, $P = 0.030$) were seen in the abnormal group. Multivariate analyses revealed that serum IgG4 [(> 2 × ULN), hazard ratio (HR): 3.583; 95% confidence interval (CI): 1.218–10.545; $P = 0.020$] and IgA (> 1 × ULN; HR: 5.908; 95%CI: 1.199–29.120; $P = 0.029$) and age > 55 years (HR: 2.383; 95%CI: 1.056–5.378; $P = 0.036$) were independent risk factors of relapse.

CONCLUSION

AIP patients with high IgG4 levels have clinical features including a more active immune system and higher relapse rate. Several factors, such as IgG4 and IgA, are associated with relapse.

Key Words: Autoimmune pancreatitis; Immunoglobulin G4; Clinical characteristics; Outcome; Relapse; Cohort study

©The Author(s) 2023. Published by Baishideng Publishing Group Inc. All rights reserved.

Core tip: Our findings suggested that patients with a high immunoglobulin (Ig) G4 level had different clinical features including a more active immune system and higher relapse rate. Patients with normal IgG4 level still require attention because they have a high incidence of jaundice and pancreatic atrophy. Some factors were identified as risk factors for relapse, such as age > 55 years [hazard ratio (HR) 2.383; 95% confidence interval (CI) 1.056-5.378; $P = 0.036$], high IgG4 level [> 2 × upper limit of normal (ULN) (HR 3.583; 95%CI 1.218-10.545; $P = 0.020$) and high IgA level (> 1 × ULN) (HR 5.908; 95%CI 1.199-29.120; $P = 0.029$).

Citation: Zhou GZ, Zeng JQ, Wang L, Liu M, Meng K, Wang ZK, Zhang XL, Peng LH, Yan B, Pan F. Clinical characteristics and outcome of autoimmune pancreatitis based on serum immunoglobulin G4 level: A single-center, retrospective cohort study. *World J Gastroenterol* 2023; 29(35): 5125-5137

URL: https://www.wjgnet.com/1007-9327/full/v29/i35/5125.htm

DOI: https://dx.doi.org/10.3748/wjg.v29.i35.5125

INTRODUCTION

Autoimmune pancreatitis (AIP) has recently become a cause of global health concern[1,2]. It is characterized by elevated serum immunoglobulin (Ig) G4 levels and an enlarged pancreas based on diagnostic imaging. AIP is a form of chronic pancreatitis that was initially introduced in 1995 by Yoshida *et al*[3]. However, understanding of the pathology was limited since then until Hamano *et al*[4] introduced the role of IgG4 in AIP.

IgG4 has unique properties, unlike other immunoglobulin subtypes. Among the four IgG subclasses, IgG4 levels are the lowest, accounting for about 5% of total IgG in a healthy adult. IgG4 inhibits the formation of immune complexes through fab-arm exchange and does not affect the classical complement pathway[5]. A correlation between the IgG4 concentration and chronic inflammatory processes and disease severity has been established; the role of IgG4 and disease pathogenicity has also been proposed in previous studies[6,7]. Elevated IgG4 levels have also been observed in autoimmune diseases, such as rheumatoid arthritis, and patients with high IgG4 levels have shown a unique clinical profile[8]. Although the etiology is not fully elucidated, the role of IgG4 in AIP pathogenesis was highlighted as a potential diagnostic marker and predictor of relapse[9-13].

A favorable response despite frequent relapse in the long term is generally seen in patients with AIP receiving steroid therapy. To date, the risk factors of relapse remain controversial. According to an epidemiological survey in Japan, > 20% of patients diagnosed with AIP experienced relapse at least once. It was less likely that the initial steroid doses and serum IgG4 level affected the appearance of relapse[1], while another study reported a higher relapse rate in patients with AIP having high IgG4 levels[14]. In addition, a cohort study highlighted IgG4-related sclerosing cholangitis as a predictor of relapse[15]. In the present retrospective cohort study, we compared the clinical characteristics of patients with AIP based on the serum IgG4 level and analyzed the potential risk factors of relapse.

MATERIALS AND METHODS

Ethics

This was a single-center retrospective study performed at the First Medical Center of Chinese PLA General Hospital. The research protocol was approved by the Ethical Committee of Chinese PLA General Hospital (S2022-330-01).

Study design and population

A total of 308 patients from 2006 to 2021 were reviewed consecutively (Figure 1). Ninety-five patients were excluded due to other chief diagnoses (n = 20), insufficient data (n = 31), and non-fulfillment of the International Consensus Diagnostic Criteria (ICDC; n = 44). Eventually, 213 patients diagnosed with AIP according to ICDC were enrolled. All enrolled patients were divided into two groups based on serum IgG4 levels: normal group [IgG4 ≤ 402 mg/dL, 2 × upper limit of normal (ULN)] and abnormal group (IgG4 > 402 mg/dL)[16].

Demographic characteristics of age, sex, and duration of hospitalization were evaluated. Clinical manifestations included predispositions, symptoms, such as abdominal pain, and involvement of other organs. Weight loss was defined as > 5 kg in the past 3 mo. Extrapancreatic lesions were diagnosed by the IgG4-RD criteria, 2021[17]. Results of blood routine examination, biochemistry, coagulation, and immunological tests were collected. Radiological findings were analyzed from computed tomography (CT), magnetic resonance imaging, and endoscopic retrograde cholangiopancreatography/magnetic resonance cholangiopancreatography. The maximum standard uptake value (SUV-max) of positron emission tomography/CT (PET/CT) was also compared. The effectiveness of treatment was based on patient symptoms and serological and radiological results. Relapse was defined as the reoccurrence of symptoms, abnormal serological results, or the presence of imaging lesions.

Statistical analysis

The t-test or Mann-Whitney U test was used to compare continuous variables, which were presented as mean ± SD or median interquartile range. Categorical parameters were compared using the χ^2 test or Fisher's exact test. Kaplan-Meier curves and log-rank tests were used to assess cumulative relapse rates and univariate and multivariate Cox regression models were performed, respectively. Baseline variables that were considered clinically relevant and showed a univariate relationship with outcome were entered into the multivariate Cox regression model. Variables for inclusion were carefully chosen, considering the number of available events, to ensure the parsimony of the final model. $P < 0.05$ was considered statistically significant. All statistical analyses were performed using GraphPad Prism 9.0 and SPSS 26.0. The statistical review of this study was performed by a biomedical statistician.

RESULTS

Demographic characteristics

Baseline data are summarized in Table 1 and Supplemental Figures 1-3. There were 65 and 148 patients in the normal and abnormal groups, respectively. There were 189 patients with type 1 AIP and 24 with type 2 AIP. The ratio of men to women was 3.06 and 3.63 in the two groups (P = 0.722), respectively. There was no significant difference in the mean age between the two groups (59.8 ± 11.0 years *vs* 57.4 ± 12.6 years, P = 0.163). However, the average age of men in the abnormal group was higher than that in the normal group (60.3 ± 10.4 years *vs* 56.5 ± 12.9 years, P = 0.047). The duration from onset to diagnosis (78.4 ± 71.7 d *vs* 93.1 ± 124.8 d, P = 0.686) and the days of hospitalization (16.5 ± 8.7 d *vs* 15.6 ± 9.0 d, P = 0.351) were similar between the normal and abnormal groups.

Clinical manifestations

Most patients in the normal and abnormal groups had no obvious causes before their onset (86.2% *vs* 84.5%, P = 0.750; Table 2). The frequency of patients' chief complaints including abdominal pain, jaundice, abdominal distension, and pruritus of patients was similar in the two groups (36.9% *vs* 42.6%, P = 0.440; 30.8% *vs* 28.4%, P = 0.724; 16.9% *vs* 20.9%, P = 0.497; 9.2% *vs* 14.9%, P = 0.263, respectively). It is noteworthy that seven patients in the abnormal group visited a doctor because of diarrhea, whereas no patient in the normal group went to the hospital for diarrhea (4.7% *vs* 0%, P = 0.104). The incidence of weight loss was 52.3% and 50.7% in the normal and abnormal groups, respectively (P = 0.826). With regard to extrapancreatic lesions, sclerosing cholangitis was the most common disease with a similar prevalence rate between the normal and abnormal groups (30.8% *vs* 37.2%, P = 0.368).

Serology results

Laboratory findings are shown in Table 3. The proportion of white blood cells was different between the two groups. Patients in the abnormal group had a higher percentage of eosinophils (6.2 ± 5.4% *vs* 3.9 ± 3.4%, P = 0.001) and a lower percentage of neutrophils (56.1 ± 10.3% *vs* 61.8 ± 11.1%, P = 0.001). The total protein level was higher in the abnormal group (72.5 ± 7.9 g/L *vs* 67.2 ± 7.5 g/L, P < 0.001) and serum albumin level was lower (36.7 ± 4.6 g/L *vs* 39.4 ± 5.8 g/L, P = 0.001). The thrombin time was also longer in the abnormal group (17.4 ± 1.6 s *vs* 16.9 ± 1.2 s, P = 0.012). With regard to the immunological tests, patients in the abnormal group had higher levels of IgE (635.6 ± 958.1 IU/mL *vs* 231.7 ± 352.5 IU/mL, P = 0.002), four IgG subtypes (IgG1, 935.8 ± 319.9 mg/dL *vs* 872.6 ± 371.8 mg/dL, P = 0.045; IgG2, 638.6 ± 241.6 mg/dL *vs* 450.4 ± 174.0 mg/dL, P < 0.001; IgG3, 53.6 ± 58.4 mg/dL *vs* 42.70 ± 43.37 mg/dL, P = 0.034; IgG4, 1420.5 ± 1110.9 mg/dL *vs* 252.7 ± 106.6 mg/dL, P < 0.001), and two subtypes of free light chain [(FLC)-κ, 569.6 ± 252.5 mg/dL *vs* 306.1 ±

Table 1 Demographic characteristics of patients in the two groups

	Normal group (*n* = 65)	Abnormal group (*n* = 148)	*P* value
Male (*n*, %)	49 (75.4)	116 (78.4)	0.722
Ratio (men to women)	3.06	3.63	0.722
Age (yr)	57.4 ± 12.6	59.8 ± 11.0	0.163
Age of men	56.5 ± 12.9	60.3 ± 10.4	0.047[a]
Age of women	60.1 ± 11.8	57.94 ± 12.9	0.572
Duration before diagnosis (d)	78.4 ± 71.7	93.1 ± 124.8	0.686
Lengths of stay (d)	16.5 ± 8.7	15.6 ± 9.0	0.351

[a]$P < 0.05$ *vs* normal group.

Table 2 Clinical symptoms of patients in the two groups (*n*, %)

	Normal group (*n* = 65)	Abnormal group (*n* = 148)	*P* value
Inducements			
No obvious cause	56 (86.2)	125 (84.5)	0.750
Greasy food intake	7 (10.8)	16 (10.8)	0.993
Alcohol intake	2 (3.1)	5 (3.4)	0.910
Initial symptoms			
Abdominal pain	24 (36.9)	63 (42.6)	0.440
Jaundice	20 (30.8)	42 (28.4)	0.724
Abdominal distension	11 (16.9)	31 (20.9)	0.497
Pruritus	6 (9.2)	22 (14.9)	0.263
Diarrhea	0 (0.0)	7 (4.7)	0.104
Accompanied symptoms			
Jaundice	46 (70.8)	86 (58.1)	0.080
Abdominal pain	28 (43.1)	70 (47.3)	0.569
Pruritus	15 (23.1)	37 (25.0)	0.764
Abdominal distension	11 (16.9)	34 (23.0)	0.319
Loss of weight	34 (52.3)	75 (50.7)	0.826
Extrapancreatic lesions			
Sclerosing Cholangitis	20 (30.8)	55 (37.2)	0.368
Salivary and lacrimal gland	7 (10.8)	26 (17.6)	0.207
Retroperitoneal fibrosis	3 (4.6)	6 (4.1)	0.851
Kidney	4 (6.2)	10 (6.8)	0.870
Lung	1 (1.5)	2 (1.4)	0.915

99.7 mg/dL, $P < 0.001$; FLC-λ, 282.5 ± 124.5 mg/dL *vs* 176.4 ± 63.4 mg/dL, $P < 0.001$)]. A lower complement C3 level (100.6 ± 36.2 mg/dL *vs* 119.0 ± 45.7 mg/dL, $P = 0.050$) and a faster erythrocyte sedimentation rate (21.1 ± 20.1 mm/h *vs* 43.4 ± 28.6 mm/h, $P = 0.002$) were noted in the abnormal group. Positive rate of serum antinuclear antibody was similar in the normal and abnormal groups (12.5% *vs* 20.0%, $P = 0.298$).

Radiology examinations

AIP can be categorized as diffuse or focal type based on the extent of pancreatic enlargement in the radiological examinations (Table 4). In the normal group, 33 of 58 (56.9%) cases were diffuse type and 16 (27.6%) were focal type. In the abnormal group, 86 (67.7%) of 127 cases were diffuse type and 24 (18.9%) were focal type. The capsule-like rim was

Table 3 Laboratory results of patients in the two groups (*n*, %)

	Normal group (*n* = 65)	Abnormal group (*n* = 148)	*P* value
Hb (g/L)	126.3 ± 16.8	126.8 ± 14.6	0.828
WBC (× 10^9/L)	6.5 ± 2.2	5.8 ± 1.8	0.026[a]
NEUT	61.8 ± 11.1	56.1 ± 10.3	0.001[a]
LY	26.8 ± 9.8	29.2 ± 8.2	0.071
EOS	3.9 ± 3.4	6.2 ± 5.4	0.001[a]
BASO	0.6 ± 0.4	0.8 ± 0.5	0.003[a]
PLT (× 10^9/L)	212.9 ± 83.3	218.6 ± 75.0	0.621
TP (g/L)	67.2 ± 7.5	72.5 ± 7.9	< 0.001[a]
ALB (g/L)	39.4 ± 5.8	36.7 ± 4.6	0.001[a]
TT (s)	16.9 ± 1.2	17.4 ± 1.6	0.012[a]
IgG1 (mg/dL)	872.6 ± 371.8	935.8 ± 319.9	0.045[a]
IgG2 (mg/dL)	450.4 ± 174.0	638.6 ± 241.6	< 0.001[a]
IgG3 (mg/dL)	42.70 ± 43.37	53.6 ± 58.4	0.034[a]
IgG4 (mg/dL)	252.7 ± 106.6	1420.5 ± 1110.9	< 0.001[a]
IgE (IU/mL)	231.7 ± 352.5	635.6 ± 958.1	0.002[a]
IgG (mg/dL)	1323.6 ± 503.9	2062.1 ± 918.9	< 0.001[a]
FLC-κ (mg/dL)	306.1 ± 99.7	569.6 ± 252.5	< 0.001[a]
FLC-λ (mg/dL)	176.4 ± 63.4	282.5 ± 124.5	< 0.001[a]
C3 (mg/dL)	119.0 ± 45.7	100.6 ± 36.2	0.050
ESR (mm/h)	21.1 ± 20.1	43.4 ± 28.6	0.002[a]
ANA (positive)	5 (12.5)	19 (20.0)	0.298
CA19-9 (abnormal)	33 (53.0)	73 (52.0)	0.887

[a]*P* < 0.05 *vs* normal group. Hb: Hemoglobin; WBC: White blood cell; NEUT: Neutrophil; LY: Lymphocyte; EOS: Eosinophil; PLT: Hemoglobin; BASO: Basophil; TP: Total protein; ALB: Albumin; TT: Thrombin time; FLC: Free light chain; ANA: Antinuclear antibody; CA19-9: Carbohydrate associated antigen 19-9; Ig: Immunoglobulin; C3: Complement C3; ESR: Erythrocyte sedimentation rate.

observed in 10 (17.2%) and 30 (23.6%) cases in the normal and abnormal groups, respectively (*P* = 0.328). Pancreatic duct images showed that the prevalence of abnormalities (stricture or dilatation) was significantly higher in the normal group (37.9% *vs* 23.6%; *P* = 0.045). Hypodense kidney lesions were seen in 11 (8.7%) cases in the abnormal group and four (6.9%) cases in the normal group (*P* = 0.683). The incidence of pancreatic atrophy was significantly higher in the normal group (8.6% *vs* 1.6%, *P* = 0.020). The two groups had similar SUV-max according to PET/CT [normal group: 4.55 (3.725–6.25) *vs* abnormal group: 5.35 (4.025–6.475), *P* = 0.260].

Remission and relapse

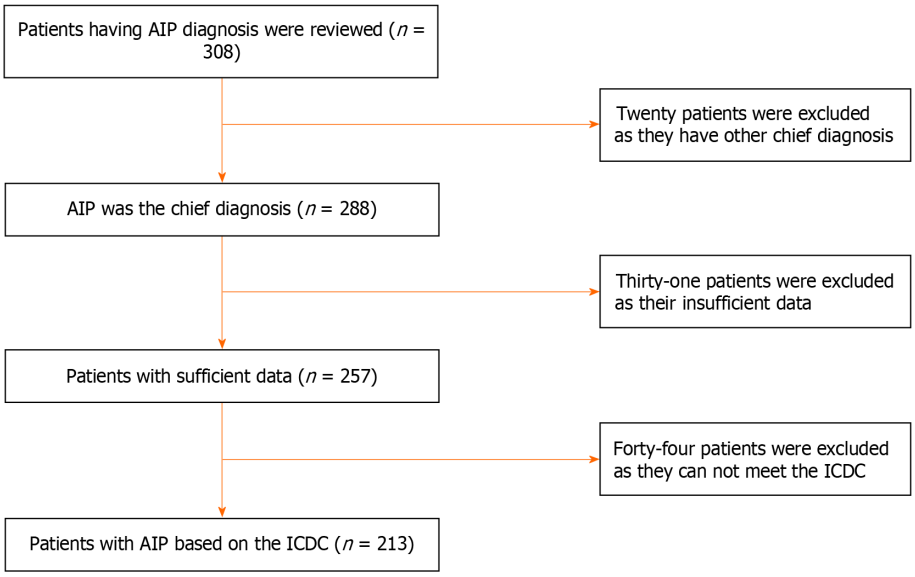
Different therapies for AIP were given to patients in the two groups (Table 5, *P* = 0.029). In the normal group, 26 (40.0%) patients received steroid monotherapy, 14 (21.5%) received steroids plus immunomodulators, 12 (18.5%) underwent endoscopy or surgery, and 13 (20.0%) received other therapies such as hepatic protectors. The median duration and dose of prednisolone therapy were 8 (6–9) wk and 40 (30–50) mg/d. In the abnormal group, 81 (54.7%) patients received steroid monotherapy, 30 (20.3%) received steroids plus immunomodulators, nine (6.1%) underwent endoscopy or surgery, and 28 (18.9%) received other therapies. The median duration and dose of prednisolone therapy were 8 (6–9) wk (*P* = 0.200) and 42.5 (40–100) mg/d (*P* = 0.750). Only three patients in the abnormal group did not achieve remission; all of whom received steroid monotherapy: one patient had persistent symptoms and two had prolonged abnormal transaminase levels.

During the median follow-up period of 53 mo, 30 patients experienced at least one episode of relapse in the normal and abnormal groups [4 (6.9%) *vs* 26 (19.1%), *P* = 0.031]. Of the 26 patients in the abnormal group, five (19.2%) had a relapse in extrapancreatic organs (*P* = 0.337). The cumulative relapse rates at 1 and 3 years were 3.8% and 11.0%, respectively, for the abnormal group and 2.0% and 6.9%, respectively, for the normal group (log-rank test, *P* = 0.023, Figure 2). Among the 30 patients with relapse, one (25.0%) of four in the normal group and 15 (57.7%) of 26 in the abnormal group received steroid monotherapy as their initial treatment (*P* = 0.129). Four (15.4%) of 26 relapse cases in the abnormal group

Table 4 Radiological results of patients in the two groups (*n*, %)

	Normal group (*n* = 65)	Abnormal group (*n* = 127)	*P* value
Parenchymal imaging			
Diffuse type	33 (56.9)	86 (67.7)	0.154
Focal type	16 (27.6)	24 (18.9)	0.227
Normal	9 (15.5)	17 (13.4)	0.699
Capsule-like rim	10 (17.2)	30 (23.6)	0.328
Others			
Bile duct enhancement	15 (25.9)	44 (34.7)	0.234
Hypo-dense lesion in kidney	4 (6.9)	11 (8.7)	0.683
Pancreatic atrophy	5 (8.6)	2 (1.6)	0.020[a]
Retroperitoneal fibrosis	3 (5.2)	1 (0.8)	0.057
Pancreatic pseudocyst	1 (1.7)	3 (2.4)	0.782
Pancreatic ductal imaging			
Stricture or dilatation	22 (37.9)	30 (23.6)	0.045[a]
Normal	36 (62.1)	97 (76.4)	
SUV-max	4.55 (3.725-6.25)	5.35 (4.025-6.475)	0.260

[a]$P < 0.05$ *vs* normal group. SUV-max: Maximum standard uptake value.



DOI: 10.3748/wjg.v29.i35.5125 **Copyright** ©The Author(s) 2023.

Figure 1 Flow diagram of the study design. A total of 308 patients were reviewed. Ninety-five patients were excluded due to other chief diagnoses (*n* = 20), insufficient data (*n* = 31), and non-fulfillment of the international consensus diagnostic criteria (*n* = 44). AIP: Autoimmune pancreatitis; ICDC: International consensus diagnostic criteria.

experienced more than one relapse ($P = 0.399$). The median relapse duration in the normal and abnormal groups was 25 (13.5-52.3) and 43 (16.3-72) mo, respectively ($P = 0.442$). Three (75.0%) of four cases in the normal group and 20 (76.9%) of 26 cases in the abnormal group received corticosteroids for relapse ($P = 0.410$). All patients responded well to treatment.

Univariate and multivariate analyses

Univariate and multivariate Cox regression models were performed to predict the risk factors for AIP relapse (Figure 3). Univariate analyses revealed an association between relapse and age > 55 years [hazard ratio (HR): 2.254; 95% confidence interval (CI): 1.074-4.731; $P = 0.032$)]. Similarly, serum IgG4 levels (> 402 mg/dL, 2 × ULN) and IgA levels (> 400 mg/dL,

Table 5 Remission and relapse of patients in the two groups (*n*, %)

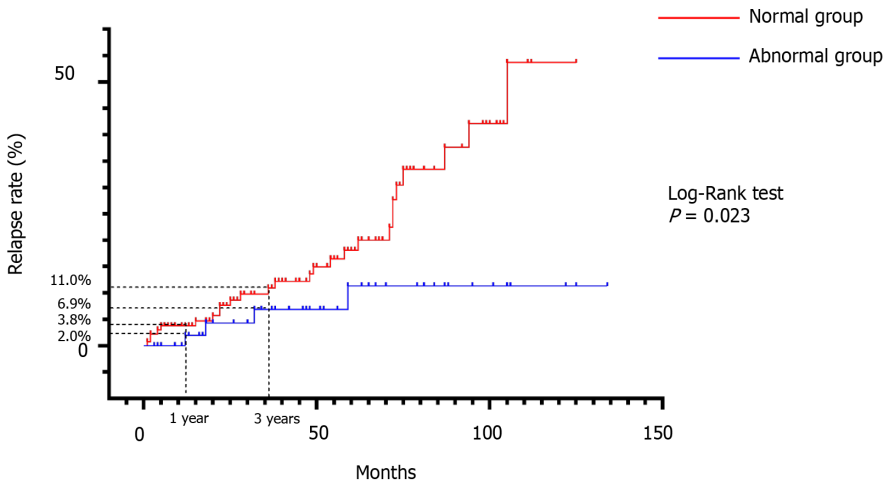
	Normal group (*n* = 65)	Abnormal group (*n* = 148)	*P* value
Managements			
Methods			
Steroid monotherapy	26 (40.0)	81 (54.7)	0.029[a]
Steroid and immunomodulator	14 (21.5)	30 (20.3)	
Endoscope or surgery	12 (18.5)	9 (6.1)	
Others[1]	13 (20.0)	28 (18.9)	
Duration of steroid (wk)	8 (6-9)	8 (6-9)	0.750
Dose of steroid (prednisolone, mg/d)	42.5 (40-100)	40 (30-50)	0.200
Remission	65 (100.0)	145 (98.0)	0.555
	Normal group (*n* = 4)	**Abnormal group (*n* = 26)**	***P* value**
Relapse			
Relapse rate	4/58 (6.2)	26/135 (17.6)	0.030[a]
Relapse duration (mo)	25 (13.5-52.3)	43 (16.3-72)	0.442
Lesions of relapse			
Pancreas	4 (100.0)	21 (80.8)	0.337
Extrapancreatic organs	0 (0.0)	5 (19.2)	
Times of relapse			
Once	4 (100.0)	22 (84.6)	0.399
More than one time	0 (0.0)	4 (15.4)	
Initial therapies			
Steroid monotherapy	1 (25.0)	15 (57.7)	0.129
Steroid and immunomodulator	2 (50.0)	2 (7.70)	
Endoscope or surgery	0 (0.00)	2 (7.70)	
Others[1]	1 (25.0)	7 (26.9)	
Therapies for relapse			
Steroid monotherapy	2 (50.0)	18 (69.2)	0.410
Steroid and immunomodulator	1 (25.0)	2 (7.70)	
Endoscope or surgery	1 (25.0)	2 (7.70)	
Others[1]	0 (0.00)	4 (15.4)	

[a]$P < 0.05$ *vs* normal group.
[1]Others: Hepatic protectors, antibiotics and proton pump inhibitors.

1 × ULN) were significant contributors to relapse (IgG4, HR: 3.381, 95%CI: 1.176–9.726, $P = 0.024$; IgA, HR: 6.271, 95%CI: 1.294–30.389, $P = 0.023$). Patients with a thickened bile duct seen on imaging scans also showed a higher risk of relapse (HR: 2.619; 95%CI: 1.096–6.258, $P = 0.030$). The presence of some clinical symptoms such as abdominal pain, type of parenchymal imaging, type of managements, initial dose of steroid and absence of maintenance therapy, were not significantly different between the relapse and non-relapse groups. Using multivariate analyses, we identified three significant independent predictors of relapse, IgG4 levels (> 402 mg/dL; HR: 3.583, 95%CI: 1.218-10.545; $P = 0.020$), IgA levels (> 400 mg/dL; HR: 5.908; 95%CI: 1.199–29.120; $P = 0.029$), and age > 55 years (HR: 2.383, 95%CI: 1.056–5.378; $P = 0.036$).

DISCUSSION

AIP is characterized by elevated IgG4 levels in the blood and abundant infiltration of IgG4-positive plasma cells and



DOI: 10.3748/wjg.v29.i35.5125 **Copyright** ©The Author(s) 2023.

Figure 2 Cumulative relapse rates in the normal and abnormal groups. The cumulative relapse rates at 1 and 3 years were 3.8% and 11.0%, respectively, for the abnormal group and 2.0% and 6.9%, respectively, for the normal group (Log-Rank test, $P = 0.023$).

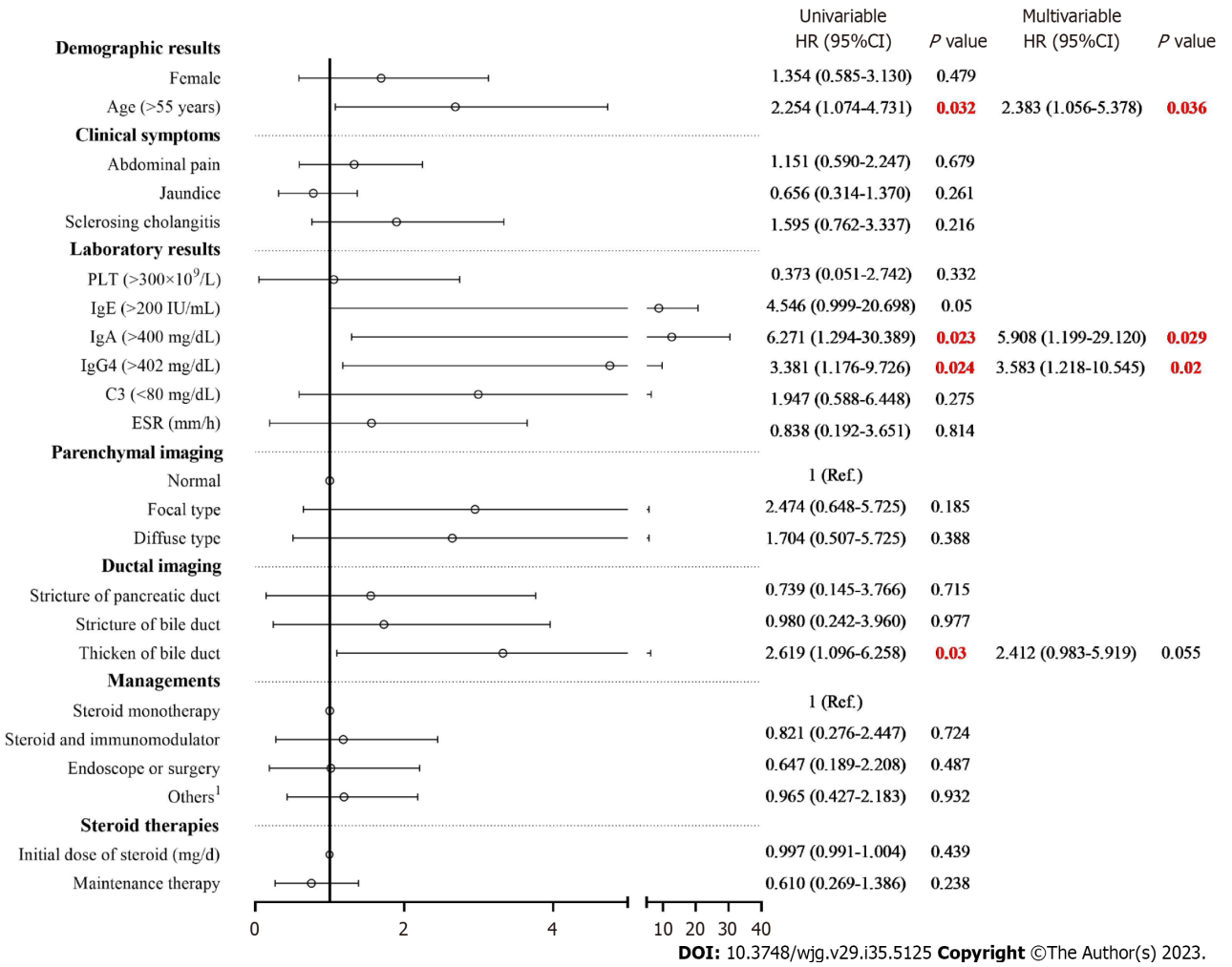
lymphocytes in tissues. Serum IgG4 has been recognized as an established diagnostic biomarker for AIP[1,2,18]. In 2011, the ICDC formally defined a cut-off with 2 × ULN of IgG4 as a diagnostic criterion for AIP. A sensitivity of 53%-81% and specificity of 90%-99% were reported in studies adopting this cutoff criterion[16,19-21]. Considering the unique features of IgG4, patients with high IgG4 levels may have a unique clinical profile and prognosis. Previous studies have shown that AIP had a favorable but short-term prognosis following steroid therapy, with a relapse rate of 24%-63%[22-25]. Patients at a higher risk of relapse had higher serum IgG4 and alkaline phosphatase concentrations. The involvement of other organs, such as the bile duct and salivary glands, are also recognized as risk factors[12,23,26].

Epidemiological studies revealed that AIP mainly affected elderly adults, especially those > 60 years, with a male predominance, which was also seen in our study[1,27]. In the abnormal group, the average age of male patients was higher compared with the normal group. No significant differences were noted among women with AIP. Similar findings were reported in previous studies[28,29]. Despite the unclear mechanism, a positive correlation was noted between age and serum IgG4 level with gender preference, which may partly explain the higher incidence rate of AIP in elderly men.

Similar to acute pancreatitis, the enlargement of the pancreas stimulates nerve endings on its capsule, leading the most common symptom of abdominal pain in patients. In addition, jaundice was obvious in patients due to the involvement of other organs, such as the bile duct, or the compression by swollen pancreatic parenchyma. Patients in the normal group had a higher incidence of jaundice with no significant differences. Although little is known about its actual mechanism, it reminds us that patients with obstructive jaundice and normal IgG4 levels are likely to be diagnosed with AIP rather than pancreatic carcinoma. Seven patients in the abnormal group had a rare initial symptom of diarrhea, which partly attributes to the abnormal digestive function of the pancreas.

Analysis of the serological results revealed that patients in the abnormal group had a significantly higher total protein level and lower albumin level, indicating a high globulin concentration, along with higher IgG and IgE levels. IgG is a major component of globulin and can be divided into four subclasses based on its structure. It activates the complement system and regulates phagocytosis[30]. In the abnormal group, except for IgG4, the levels of three subclasses of IgG were significantly higher. Some studies have demonstrated an association between IgG1 and the immunopathogenesis of AIP [31,32]. Further studies about the specific mechanism and the relation between each subclass and AIP are required. A strong relationship between allergic diseases and AIP has been identified[33]. Considering the role of IgE in allergic disorders and high levels noted in AIP, especially in the abnormal group, IgE may play a role in the pathogenesis of AIP [13,30,34]. Patients in the abnormal group also had a higher level of two FLC subtypes (FLC-κ and FLC-λ). FLCs are produced during immunoglobulin synthesis and can be detected under normal physiological conditions as they are not bound to the heavy chains. It is speculated that the accumulation of FLC is attributed to the polyclonal activation of B cells. Previous studies have also proposed their role in other autoimmune disorders; thus, FLCs may be a biomarker for AIP[35]. Additionally, those patients with high serum IgG4 levels had a faster erythrocyte sedimentation rate and a lower complement level. Overall, these immunological findings suggest enhanced antibody biosynthesis and a more active immune system in the patient with high IgG4 levels.

Pancreatic findings such as diffuse enlargement or focal low-density mass in radiology are often the typical features indicative of AIP. Although unusual, a low-attenuating rim-like capsule is also regarded as a specific characteristic of AIP. The proportion of different radiological types was similar between the two groups, which implies that there is no relationship between serum IgG4 levels and radiological types, as reported in a previous study[36]. Imaging scans of the pancreatic duct showed that AIP may have diffuse narrowing of the duct with long or multifocal strictures[12,16]. Unexpectedly, the proportion of patients with an abnormality in the pancreatic duct was higher in the normal group, probably due to the limited sample size. A higher rate of atrophy was seen in the normal group, which requires careful attention to avoid the replacement of parenchyma cells by fibrous tissue as the disease progresses and leads to pancreatic dysfunction.



DOI: 10.3748/wjg.v29.i35.5125 **Copyright** ©The Author(s) 2023.

Figure 3 Univariate and multivariate Cox regression analysis for relapse of autoimmune pancreatitis. Univariate Cox regression analysis indicated that age (> 55 years), immunoglobulin (Ig)A (> 400 mg/dL), IgG4 (> 402 mg/dL), presence of thickened bile duct were risk factors of relapse of autoimmune pancreatitis. Multivariate Cox regression analysis identified three risk factors of relapse, including age (> 55 years), IgA (> 400 mg/dL) and IgG4 (> 402 mg/dL). [1]Others: Hepatic protectors, antibiotics and proton pump inhibitors. PLT: Hemoglobin; Ig: Immunoglobulin; ESR: Erythrocyte sedimentation rate; C3: Complement C3.

Patients in the two groups received varied treatments. In the abnormal group, a higher number of patients received steroid monotherapy, whereas endoscopy or surgery was more common in the normal group. It is possible that the physician's choice of endoscopy or surgery is for biopsy when patients have normal IgG4 levels to exclude cancer diagnosis. Thus, we need simpler and more accurate methods for diagnosis of AIP and to better distinguish it from cancer. To date, the relationship between serum IgG4 level and relapse is controversial. Some studies have demonstrated that an elevated serum IgG4 level is a predictor for relapse[37-39], whereas other studies have reported contrasting findings[23,40]. In the present study, patients in the abnormal group were significantly more likely to experience relapse. Additionally, approximately 20% of patients in the abnormal group had one relapse in the extrapancreatic organs and > 15% of patients had at least two relapses, higher than the normal group. This necessitates further attention to investigate the relationship between high IgG4 levels and AIP.

Previous studies have revealed some controversial predictors of relapse, such as pancreatic enlargement, initial prednisolone dose, and involvement of extrapancreatic organs[1,15,23,41,42]. According to a UK-based study, the relapse rate of patients with elevated serum levels of IgG4 (> 2 × ULN) was twice than that of another group (IgG4 ≤ 2 × ULN) [33]. Similar results were also reported in subsequent studies[42-44]. In the present study, serum IgG4 levels seemed to be an independent risk factor for relapse. Although the specific mechanism remains unclear, the focus on IgG4 should increase owing to its potential effect on the pathogenesis, diagnosis, and prognosis. The concentration of IgA was recognized as an independent risk factor for relapse, which emphasized the association between an active immune system and relapse. IgA is the predominant antibody present at mucosal surfaces, supporting its prominent role in host defense against pathogens. Augmented presence of IgA immune complexes can result in excessive neutrophil activation, potentially leading to severe tissue damage in autoimmune diseases like IgA nephropathy and inflammatory bowel disease[45-47]. A higher IgA level was also reported in IgG4-related disease or calcific pancreatitis[48-50]. However, the elevated serum IgA levels were associated with a lower incidence of relapse of IgG4-related disease in a Japanese study. Multicenter and large sample studies are required to clarify the association between these potential risk factors and AIP. AIP is known to occur more commonly among elderly people. In our analyses, patients over the age of 55 years presented a higher risk of relapse. Maintenance therapy was recommended in various studies to prevent relapse[1,51], while in our

study, the absence of maintenance therapy did not seem to be a predictor of relapse.

There were several limitations to our study. Firstly, it was a single-center retrospective study. Secondly, we only analyzed clinical factors to predict relapse. The possible genetic and environmental factors that may contribute to relapse were not considered. Additionally, the long duration of follow-up increased the risk of recall bias.

CONCLUSION

Patients with high IgG4 levels have a unique clinical profile and are at a higher risk of relapse of AIP. Normal IgG4 levels rendered diagnosis challenging, thereby reinforcing the need for a thorough understanding of the disease. Relapse of AIP is related to age and serum IgG4 and IgA levels. An active immune system is strongly related to high IgG4 levels and the risk of relapse. Long-term and multicenter studies are needed to confirm the risk factors for relapse.

ARTICLE HIGHLIGHTS

Research background

The role of immunoglobulin (Ig) G4 in the pathogenesis, diagnosis and prognosis of autoimmune pancreatitis (AIP) has received attention and patients with high levels of IgG4 have unique properties. There is still controversy about the predictors of AIP relapse, such as high IgG4 level, radiological type and steroid use.

Research motivation

To predict the relapse of AIP and identify the properties of patients with different IgG4 level, especially those with normal IgG4 level.

Research objectives

We determined some predictors of relapse and identified unique characteristics of patients with different IgG4 levels. Further studies about improving the diagnosis algorithm of AIP and predicting the relapse are needed.

Research methods

We conducted a retrospective cohort study, including patients with normal IgG4 level (n = 65) and high IgG4 level (n = 148), and compared their clinical characteristics. We also performed univariate and multivariate Cox regression models to investigate the risk factors of relapse.

Research results

Patients with high IgG4 levels had a higher average male age; a higher level of serum total protein, IgG4, and IgE; and a lower level of serum complement C3. In addition, a lower number of cases with abnormal pancreatic duct and pancreatic atrophy and a higher rate of relapse were noted in the abnormal group. Multivariate analyses revealed that serum IgG4 (> 2 × upper limit of normal, ULN) and IgA (> 1 × ULN) and age > 55 years were independent risk factors of relapse.

Research conclusions

Patients with high IgG4 levels had different clinical features including a more active immune system and a higher relapse rate. Some factors were identified as risk factors of relapse, such as age > 55 years, high IgG4 (> 2 × ULN) and IgA level (> 1 × ULN).

Research perspectives

Further research with large samples should be conducted to verify the predictors of relapse.

FOOTNOTES

Author contributions: Pan F contributed to study conceptualization and reviewed the manuscript; Zhou GZ and Zeng JQ drafted the initial manuscript and reviewed the manuscript; Wang L and Liu M contributed to methodology and formal analysis; Zhou GZ, Yan B and Meng K contributed to data collection; Wang ZK, Zhang XL and Peng LH reviewed the manuscript; All authors approved the final manuscript as submitted, all authors had full access to the data in the present study and accept responsibility to submit for publication.

Supported by Young Scholar Independent Innovation Science Fund of Chinese PLA General Hospital, No. 22QNCZ020; National Key Research and Development Program, No. 2022YFC2504003.

Institutional review board statement: The study was reviewed and approved for publication by our Institutional Reviewer.

Informed consent statement: As the study used anonymous and pre-existing data, the requirement for the informed consent from patients was waived.

Conflict-of-interest statement: All the Authors have no conflict of interest related to the manuscript.

Data sharing statement: The original anonymous dataset is available on request from the corresponding author at panfei@plagh.org.

STROBE statement: The authors have read the STROBE Statement-checklist of items, and the manuscript was prepared and revised according to the STROBE Statement-checklist of items.

Open-Access: This article is an open-access article that was selected by an in-house editor and fully peer-reviewed by external reviewers. It is distributed in accordance with the Creative Commons Attribution NonCommercial (CC BY-NC 4.0) license, which permits others to distribute, remix, adapt, build upon this work non-commercially, and license their derivative works on different terms, provided the original work is properly cited and the use is non-commercial. See: https://creativecommons.org/Licenses/by-nc/4.0/

Country/Territory of origin: China

ORCID number: Guan-Zhou Zhou 0009-0002-8667-4593; Jia-Qi Zeng 0000-0002-9270-6259; Lei Wang 0000-0002-2827-3903; Ke Meng 0000-0002-2460-4728; Zi-Kai Wang 0000-0002-6293-7179; Li-Hua Peng 0000-0002-8549-6994; Bin Yan 0000-0003-4924-1326; Fei Pan 0000-0002-3307-7931.

S-Editor: Qu XL
L-Editor: Kerr C
P-Editor: Zhao S

REFERENCES

1 **Masamune A**, Kikuta K, Hamada S, Tsuji I, Takeyama Y, Shimosegawa T, Okazaki K; Collaborators. Nationwide epidemiological survey of autoimmune pancreatitis in Japan in 2016. *J Gastroenterol* 2020; **55**: 462-470 [PMID: 31872350 DOI: 10.1007/s00535-019-01658-7]
2 **Kanno A**, Masamune A, Okazaki K, Kamisawa T, Kawa S, Nishimori I, Tsuji I, Shimosegawa T; Research Committee of Intractable Diseases of the Pancreas. Nationwide epidemiological survey of autoimmune pancreatitis in Japan in 2011. *Pancreas* 2015; **44**: 535-539 [PMID: 25815647 DOI: 10.1097/MPA.0000000000000325]
3 **Yoshida K**, Toki F, Takeuchi T, Watanabe S, Shiratori K, Hayashi N. Chronic pancreatitis caused by an autoimmune abnormality. Proposal of the concept of autoimmune pancreatitis. *Dig Dis Sci* 1995; **40**: 1561-1568 [PMID: 7628283 DOI: 10.1007/BF02285209]
4 **Hamano H**, Kawa S, Horiuchi A, Unno H, Furuya N, Akamatsu T, Fukushima M, Nikaido T, Nakayama K, Usuda N, Kiyosawa K. High serum IgG4 concentrations in patients with sclerosing pancreatitis. *N Engl J Med* 2001; **344**: 732-738 [PMID: 11236777 DOI: 10.1056/NEJM200103083441005]
5 **Maslinska M**, Dmowska-Chalaba J, Jakubaszek M. The Role of IgG4 in Autoimmunity and Rheumatic Diseases. *Front Immunol* 2021; **12**: 787422 [PMID: 35145508 DOI: 10.3389/fimmu.2021.787422]
6 **WITEBSKY E**, ROSE NR, TERPLAN K, PAINE JR, EGAN RW. Chronic thyroiditis and autoimmunization. *J Am Med Assoc* 1957; **164**: 1439-1447 [PMID: 13448890 DOI: 10.1001/jama.1957.02980130015004]
7 **Rose NR**, Bona C. Defining criteria for autoimmune diseases (Witebsky's postulates revisited). *Immunol Today* 1993; **14**: 426-430 [PMID: 8216719 DOI: 10.1016/0167-5699(93)90244-F]
8 **Yu KH**, Chan TM, Tsai PH, Chen CH, Chang PY. Diagnostic Performance of Serum IgG4 Levels in Patients With IgG4-Related Disease. *Medicine (Baltimore)* 2015; **94**: e1707 [PMID: 26469909 DOI: 10.1097/MD.0000000000001707]
9 **Okazaki K**, Uchida K. Current Concept of Autoimmune Pancreatitis and IgG4-related Disease. *Am J Gastroenterol* 2018; **113**: 1412-1416 [PMID: 30002467 DOI: 10.1038/s41395-018-0184-7]
10 **Nista EC**, De Lucia SS, Manilla V, Schepis T, Pellegrino A, Ojetti V, Pignataro G, Zileri Dal Verme L, Franceschi F, Gasbarrini A, Candelli M. Autoimmune Pancreatitis: From Pathogenesis to Treatment. *Int J Mol Sci* 2022; **23** [PMID: 36293522 DOI: 10.3390/ijms232012667]
11 **Yoshikawa T**, Watanabe T, Kamata K, Hara A, Minaga K, Kudo M. Intestinal Dysbiosis and Autoimmune Pancreatitis. *Front Immunol* 2021; **12**: 621532 [PMID: 33833754 DOI: 10.3389/fimmu.2021.621532]
12 **Nagpal SJS**, Sharma A, Chari ST. Autoimmune Pancreatitis. *Am J Gastroenterol* 2018; **113**: 1301 [PMID: 29910463 DOI: 10.1038/s41395-018-0146-0]
13 **Maurer M**, Altrichter S, Schmetzer O, Scheffel J, Church MK, Metz M. Immunoglobulin E-Mediated Autoimmunity. *Front Immunol* 2018; **9**: 689 [PMID: 29686678 DOI: 10.3389/fimmu.2018.00689]
14 **Matsubayashi H**, Sawai H, Kimura H, Yamaguchi Y, Tanaka M, Kakushima N, Takizawa K, Kadooka M, Takao T, Hebbar S, Ono H. Characteristics of autoimmune pancreatitis based on serum IgG4 level. *Dig Liver Dis* 2011; **43**: 731-735 [PMID: 21515099 DOI: 10.1016/j.dld.2011.03.006]
15 **Huggett MT**, Culver EL, Kumar M, Hurst JM, Rodriguez-Justo M, Chapman MH, Johnson GJ, Pereira SP, Chapman RW, Webster GJM, Barnes E. Type 1 autoimmune pancreatitis and IgG4-related sclerosing cholangitis is associated with extrapancreatic organ failure, malignancy, and mortality in a prospective UK cohort. *Am J Gastroenterol* 2014; **109**: 1675-1683 [PMID: 25155229 DOI: 10.1038/ajg.2014.223]
16 **Shimosegawa T**, Chari ST, Frulloni L, Kamisawa T, Kawa S, Mino-Kenudson M, Kim MH, Klöppel G, Lerch MM, Löhr M, Notohara K, Okazaki K, Schneider A, Zhang L; International Association of Pancreatology. International consensus diagnostic criteria for autoimmune pancreatitis: guidelines of the International Association of Pancreatology. *Pancreas* 2011; **40**: 352-358 [PMID: 21412117 DOI: 10.1097/MPA.0b013e3182142fd2]
17 **Umehara H**, Okazaki K, Masaki Y, Kawano M, Yamamoto M, Saeki T, Matsui S, Yoshino T, Nakamura S, Kawa S, Hamano H, Kamisawa T, Shimosegawa T, Shimatsu A, Ito T, Notohara K, Sumida T, Tanaka Y, Mimori T, Chiba T, Mishima M, Hibi T, Tsubouchi H, Inui K, Ohara H. Comprehensive diagnostic criteria for IgG4-related disease (IgG4-RD), 2011. *Mod Rheumatol* 2012; **22**: 21-30 [PMID: 22218969 DOI: 10.1007/s10165-011-0571-z]

18 **Hara A**, Watanabe T, Minaga K, Yoshikawa T, Kamata K, Kudo M. Biomarkers in autoimmune pancreatitis and immunoglobulin G4-related disease. *World J Gastroenterol* 2021; **27**: 2257-2269 [PMID: 34040320 DOI: 10.3748/wjg.v27.i19.2257]

19 **Chari ST**, Takahashi N, Levy MJ, Smyrk TC, Clain JE, Pearson RK, Petersen BT, Topazian MA, Vege SS. A diagnostic strategy to distinguish autoimmune pancreatitis from pancreatic cancer. *Clin Gastroenterol Hepatol* 2009; **7**: 1097-1103 [PMID: 19410017 DOI: 10.1016/j.cgh.2009.04.020]

20 **Ghazale A**, Chari ST, Smyrk TC, Levy MJ, Topazian MD, Takahashi N, Clain JE, Pearson RK, Pelaez-Luna M, Petersen BT, Vege SS, Farnell MB. Value of serum IgG4 in the diagnosis of autoimmune pancreatitis and in distinguishing it from pancreatic cancer. *Am J Gastroenterol* 2007; **102**: 1646-1653 [PMID: 17555461 DOI: 10.1111/j.1572-0241.2007.01264.x]

21 **Pak LM**, Schattner MA, Balachandran V, D'Angelica MI, DeMatteo RP, Kingham TP, Jarnagin WR, Allen PJ. The clinical utility of immunoglobulin G4 in the evaluation of autoimmune pancreatitis and pancreatic adenocarcinoma. *HPB (Oxford)* 2018; **20**: 182-187 [PMID: 29033025 DOI: 10.1016/j.hpb.2017.09.001]

22 **Lee HW**, Moon SH, Kim MH, Cho DH, Jun JH, Nam K, Song TJ, Park DH, Lee SS, Seo DW, Lee SK. Relapse rate and predictors of relapse in a large single center cohort of type 1 autoimmune pancreatitis: long-term follow-up results after steroid therapy with short-duration maintenance treatment. *J Gastroenterol* 2018; **53**: 967-977 [PMID: 29362937 DOI: 10.1007/s00535-018-1434-6]

23 **Hart PA**, Kamisawa T, Brugge WR, Chung JB, Culver EL, Czakó L, Frulloni L, Go VL, Gress TM, Kim MH, Kawa S, Lee KT, Lerch MM, Liao WC, Löhr M, Okazaki K, Ryu JK, Schleinitz N, Shimizu K, Shimosegawa T, Soetikno R, Webster G, Yadav D, Zen Y, Chari ST. Long-term outcomes of autoimmune pancreatitis: a multicentre, international analysis. *Gut* 2013; **62**: 1771-1776 [PMID: 23232048 DOI: 10.1136/gutjnl-2012-303617]

24 **Kamisawa T**, Okazaki K, Kawa S, Ito T, Inui K, Irie H, Nishino T, Notohara K, Nishimori I, Tanaka S, Nishiyama T, Suda K, Shiratori K, Tanaka M, Shimosegawa T; Working Committee of the Japan Pancreas Society and the Research Committee for Intractable Pancreatic Disease supported by the Ministry of Health, Labour and Welfare of Japan. Amendment of the Japanese Consensus Guidelines for Autoimmune Pancreatitis, 2013 III. Treatment and prognosis of autoimmune pancreatitis. *J Gastroenterol* 2014; **49**: 961-970 [PMID: 24639058 DOI: 10.1007/s00535-014-0945-z]

25 **Maruyama M**, Watanabe T, Kanai K, Oguchi T, Asano J, Ito T, Ozaki Y, Muraki T, Hamano H, Arakura N, Kawa S. Autoimmune pancreatitis can develop into chronic pancreatitis. *Orphanet J Rare Dis* 2014; **9**: 77 [PMID: 24884922 DOI: 10.1186/1750-1172-9-77]

26 **Majumder S**, Mohapatra S, Lennon RJ, Piovezani Ramos G, Postier N, Gleeson FC, Levy MJ, Pearson RK, Petersen BT, Vege SS, Chari ST, Topazian MD, Witzig TE. Rituximab Maintenance Therapy Reduces Rate of Relapse of Pancreaticobiliary Immunoglobulin G4-related Disease. *Clin Gastroenterol Hepatol* 2018; **16**: 1947-1953 [PMID: 29526692 DOI: 10.1016/j.cgh.2018.02.049]

27 **Notohara K**, Kamisawa T, Uchida K, Zen Y, Kawano M, Kasashima S, Sato Y, Shiokawa M, Uehara T, Yoshifuji H, Hayashi H, Inoue K, Iwasaki K, Kawano H, Matsubayashi H, Moritani Y, Murakawa K, Oka Y, Tateno M, Okazaki K, Chiba T. Gastrointestinal manifestation of immunoglobulin G4-related disease: clarification through a multicenter survey. *J Gastroenterol* 2018; **53**: 845-853 [PMID: 29222587 DOI: 10.1007/s00535-017-1420-4.]

28 **Aucouturier P**, Danon F, Daveau M, Guillou B, Sabbah A, Besson J, Preud'homme JL. Measurement of serum IgG4 levels by a competitive immunoenzymatic assay with monoclonal antibodies. *J Immunol Methods* 1984; **74**: 151-162 [PMID: 6438233 DOI: 10.1016/0022-1759(84)90376-4]

29 **Gonzalez-Quintela A**, Alende R, Gude F, Campos J, Rey J, Meijide LM, Fernandez-Merino C, Vidal C. Serum levels of immunoglobulins (IgG, IgA, IgM) in a general adult population and their relationship with alcohol consumption, smoking and common metabolic abnormalities. *Clin Exp Immunol* 2008; **151**: 42-50 [PMID: 18005364 DOI: 10.1111/j.1365-2249.2007.03545.x]

30 **Schroeder HW Jr**, Cavacini L. Structure and function of immunoglobulins. *J Allergy Clin Immunol* 2010; **125**: S41-S52 [PMID: 20176268 DOI: 10.1016/j.jaci.2009.09.046]

31 **Minaga K**, Watanabe T, Hara A, Kamata K, Omoto S, Nakai A, Otsuka Y, Sekai I, Yoshikawa T, Yamao K, Takenaka M, Chiba Y, Kudo M. Identification of serum IFN-α and IL-33 as novel biomarkers for type 1 autoimmune pancreatitis and IgG4-related disease. *Sci Rep* 2020; **10**: 14879 [PMID: 32938972 DOI: 10.1038/s41598-020-71848-4]

32 **Shiokawa M**, Kodama Y, Kuriyama K, Yoshimura K, Tomono T, Morita T, Kakiuchi N, Matsumori T, Mima A, Nishikawa Y, Ueda T, Tsuda M, Yamauchi Y, Minami R, Sakuma Y, Ota Y, Maruno T, Kurita A, Sawai Y, Tsuji Y, Uza N, Matsumura K, Watanabe T, Notohara K, Tsuruyama T, Seno H, Chiba T. Pathogenicity of IgG in patients with IgG4-related disease. *Gut* 2016; **65**: 1322-1332 [PMID: 26964842 DOI: 10.1136/gutjnl-2015-310336]

33 **Kamisawa T**, Chari ST, Lerch MM, Kim MH, Gress TM, Shimosegawa T. Recent advances in autoimmune pancreatitis: type 1 and type 2. *Gut* 2013; **62**: 1373-1380 [PMID: 23749606 DOI: 10.1136/gutjnl-2012-304224]

34 **Zhang L**, Guo L, Huang Y, Wang T, Shi X, Chang H, Yao W, Huang X. Allergic diseases, immunoglobulin E, and autoimmune pancreatitis: a retrospective study of 22 patients. *Chin Med J (Engl)* 2014; **127**: 4104-4109 [PMID: 25430457]

35 **Ikemune M**, Uchida K, Tsukuda S, Ito T, Nakamaru K, Tomiyama T, Ikeura T, Naganuma M, Okazaki K. Serum free light chain assessment in type 1 autoimmune pancreatitis. *Pancreatology* 2021; **21**: 658-665 [PMID: 33741268 DOI: 10.1016/j.pan.2021.03.001]

36 **Lv H**, Liu A, Zhao Y, Qian J. Comparison of clinical characteristics of radiological forms of autoimmune pancreatitis. *HPB (Oxford)* 2018; **20**: 1021-1027 [PMID: 29843984 DOI: 10.1016/j.hpb.2018.04.009]

37 **Culver EL**, Sadler R, Simpson D, Cargill T, Makuch M, Bateman AC, Ellis AJ, Collier J, Chapman RW, Klenerman P, Barnes E, Ferry B. Elevated Serum IgG4 Levels in Diagnosis, Treatment Response, Organ Involvement, and Relapse in a Prospective IgG4-Related Disease UK Cohort. *Am J Gastroenterol* 2016; **111**: 733-743 [PMID: 27091321 DOI: 10.1038/ajg.2016.40]

38 **Pelkmans LG**, Hendriksz TR, Westenend PJ, Vermeer HJ, van Bommel EFH. Elevated serum IgG4 levels in diagnosis and treatment response in patients with idiopathic retroperitoneal fibrosis. *Clin Rheumatol* 2017; **36**: 903-912 [PMID: 28105551 DOI: 10.1007/s10067-017-3542-8]

39 **Kubota K**, Watanabe S, Uchiyama T, Kato S, Sekino Y, Suzuki K, Mawatari H, Iida H, Endo H, Fujita K, Yoneda M, Takahashi H, Kirikoshi H, Kobayashi N, Saito S, Sugimori K, Hisatomi K, Matsuhashi N, Sato H, Tanida E, Sakaguchi T, Fujisawa N, Nakajima A. Factors predictive of relapse and spontaneous remission of autoimmune pancreatitis patients treated/not treated with corticosteroids. *J Gastroenterol* 2011; **46**: 834-842 [PMID: 21491208 DOI: 10.1007/s00535-011-0393-y]

40 **Yamamoto M**, Nojima M, Takahashi H, Yokoyama Y, Ishigami K, Yajima H, Shimizu Y, Tabeya T, Matsui M, Suzuki C, Naishiro Y, Takano K, Himi T, Imai K, Shinomura Y. Identification of relapse predictors in IgG4-related disease using multivariate analysis of clinical data at the first visit and initial treatment. *Rheumatology (Oxford)* 2015; **54**: 45-49 [PMID: 24907151 DOI: 10.1093/rheumatology/keu228]

41 **Zhu L**, Xue HD, Zhang W, Wang Q, Tan B, Lai YM, Zheng WY, Asbach P, Hamm B, Denecke T, Jin ZY. Pancreaticobiliary involvement in treated type 1 autoimmune pancreatitis: Imaging pattern and risk factors for disease relapse. *Eur J Radiol* 2019; **120**: 108673 [PMID: 31550640

DOI: 10.1016/j.ejrad.2019.108673]

42 **Kamisawa T**, Shimosegawa T, Okazaki K, Nishino T, Watanabe H, Kanno A, Okumura F, Nishikawa T, Kobayashi K, Ichiya T, Takatori H, Yamakita K, Kubota K, Hamano H, Okamura K, Hirano K, Ito T, Ko SB, Omata M. Standard steroid treatment for autoimmune pancreatitis. *Gut* 2009; **58**: 1504-1507 [PMID: 19398440 DOI: 10.1136/gut.2008.172908]

43 **Maire F**, Le Baleur Y, Rebours V, Vullierme MP, Couvelard A, Voitot H, Sauvanet A, Hentic O, Lévy P, Ruszniewski P, Hammel P. Outcome of patients with type 1 or 2 autoimmune pancreatitis. *Am J Gastroenterol* 2011; **106**: 151-156 [PMID: 20736934 DOI: 10.1038/ajg.2010.314]

44 **Frulloni L**, Scattolini C, Falconi M, Zamboni G, Capelli P, Manfredi R, Graziani R, D'Onofrio M, Katsotourchi AM, Amodio A, Benini L, Vantini I. Autoimmune pancreatitis: differences between the focal and diffuse forms in 87 patients. *Am J Gastroenterol* 2009; **104**: 2288-2294 [PMID: 19568232 DOI: 10.1038/ajg.2009.327]

45 **Breedveld A**, van Egmond M. IgA and FcαRI: Pathological Roles and Therapeutic Opportunities. *Front Immunol* 2019; **10**: 553 [PMID: 30984170 DOI: 10.3389/fimmu.2019.00553]

46 **Aleyd E**, Heineke MH, van Egmond M. The era of the immunoglobulin A Fc receptor FcαRI; its function and potential as target in disease. *Immunol Rev* 2015; **268**: 123-138 [PMID: 26497517 DOI: 10.1111/imr.12337]

47 **Woof JM**, Kerr MA. The function of immunoglobulin A in immunity. *J Pathol* 2006; **208**: 270-282 [PMID: 16362985 DOI: 10.1002/path.1877]

48 **Bank S**, Novis BH, Petersen E, Dowdle E, Marks IN. Serum immunoglobulins in calcific pancreatitis. *Gut* 1973; **14**: 723-725 [PMID: 4752035 DOI: 10.1136/gut.14.9.723]

49 **Zhang J**, Cen XM, Zhao H, Yang M, Liu Y, Xie QB. [Diagnosis and Treatment of 43 Patients with IgG4-related Disease]. *Sichuan Da Xue Xue Bao Yi Xue Ban* 2020; **51**: 714-719 [PMID: 32975090 DOI: 10.12182/20200960604]

50 **Tsuge S**, Mizushima I, Horita M, Kawahara H, Sanada H, Yoshida M, Takahashi Y, Zoshima T, Nishioka R, Hara S, Suzuki Y, Ito K, Kawano M. High serum IgA levels in patients with IgG4-related disease (IgG4-RD) are associated with mild inflammation, sufficient disease-specific features, and favorable responses to treatments. *Mod Rheumatol* 2023 [PMID: 37307433 DOI: 10.1093/mr/road056]

51 **Masamune A**, Nishimori I, Kikuta K, Tsuji I, Mizuno N, Iiyama T, Kanno A, Tachibana Y, Ito T, Kamisawa T, Uchida K, Hamano H, Yasuda H, Sakagami J, Mitoro A, Taguchi M, Kihara Y, Sugimoto H, Hirooka Y, Yamamoto S, Inui K, Inatomi O, Andoh A, Nakahara K, Miyakawa H, Hamada S, Kawa S, Okazaki K, Shimosegawa T; Research Committee of Intractable Pancreas Diseases in Japan. Randomised controlled trial of long-term maintenance corticosteroid therapy in patients with autoimmune pancreatitis. *Gut* 2017; **66**: 487-494 [PMID: 27543430 DOI: 10.1136/gutjnl-2016-312049]

World Journal of Gastroenterology

Submit a Manuscript: https://www.f6publishing.com

World J Gastroenterol 2023 September 21; 29(35): 5138-5153

DOI: 10.3748/wjg.v29.i35.5138

ISSN 1007-9327 (print) ISSN 2219-2840 (online)

ORIGINAL ARTICLE

Retrospective Study

Machine learning-based decision tool for selecting patients with idiopathic acute pancreatitis for endosonography to exclude a biliary aetiology

Simon Sirtl, Michal Żorniak, Eric Hohmann, Georg Beyer, Miriam Dibos, Annika Wandel, Veit Phillip, Christoph Ammer-Herrmenau, Albrecht Neesse, Christian Schulz, Jörg Schirra, Julia Mayerle, Ujjwal Mukund Mahajan

Specialty type: Gastroenterology and hepatology

Provenance and peer review: Unsolicited article; Externally peer reviewed.

Peer-review model: Single blind

Peer-review report's scientific quality classification

Grade A (Excellent): 0
Grade B (Very good): B
Grade C (Good): C, C
Grade D (Fair): 0
Grade E (Poor): 0

P-Reviewer: Kitamura K, Japan; Liu C, China; Zhao CF, China

Received: June 28, 2023
Peer-review started: June 28, 2023
First decision: July 23, 2023
Revised: August 6, 2023
Accepted: August 28, 2023
Article in press: August 28, 2023
Published online: September 21, 2023

Simon Sirtl, Michal Żorniak, Eric Hohmann, Georg Beyer, Christian Schulz, Jörg Schirra, Julia Mayerle, Ujjwal Mukund Mahajan, Department of Medicine II, LMU University Hospital, Munich 81377, Germany

Michal Żorniak, Department of Endoscopy, Maria Sklodowska-Curie National Research Institute of Oncology, Gliwice 44-113, Poland

Miriam Dibos, Annika Wandel, Veit Phillip, Department of Internal Medicine II, School of Medicine, University Hospital Rechts der Isar, Technical University of Munich, Munich 81675, Germany

Christoph Ammer-Herrmenau, Albrecht Neesse, Department of Gastroenterology, Gastrointestinal Oncology and Endocrinology, University Medical Center, Göttingen 37075, Germany

Corresponding author: Julia Mayerle, MD, Professor, Department of Medicine II, LMU University Hospital, Marchioninistraße 15, Munich 81377, Germany. julia.mayerle@med.uni-muenchen.de

Abstract

BACKGROUND

Biliary microlithiasis/sludge is detected in approximately 30% of patients with idiopathic acute pancreatitis (IAP). As recurrent biliary pancreatitis can be prevented, the underlying aetiology of IAP should be established.

AIM

To develop a machine learning (ML) based decision tool for the use of endosonography (EUS) in pancreatitis patients to detect sludge and microlithiasis.

METHODS

We retrospectively used routinely recorded clinical and laboratory parameters of 218 consecutive patients with confirmed AP admitted to our tertiary care hospital between 2015 and 2020. Patients who did not receive EUS as part of the diagnostic work-up and whose pancreatitis episode could be adequately explained by other causes than biliary sludge and microlithiasis were excluded. We trained supervised ML classifiers using H_2O.ai automatically selecting the best suitable

predictor model to predict microlithiasis/sludge. The predictor model was further validated in two independent retrospective cohorts from two tertiary care centers (117 patients).

RESULTS

Twenty-eight categorized patients' variables recorded at admission were identified to compute the predictor model with an accuracy of 0.84 [95% confidence interval (CI): 0.791-0.9185], positive predictive value of 0.84, and negative predictive value of 0.80 in the identification cohort (218 patients). In the validation cohort, the robustness of the prediction model was confirmed with an accuracy of 0.76 (95%CI: 0.673-0.8347), positive predictive value of 0.76, and negative predictive value of 0.78 (117 patients).

CONCLUSION

We present a robust and validated ML-based predictor model consisting of routinely recorded parameters at admission that can predict biliary sludge and microlithiasis as the cause of AP.

Key Words: Acute pancreatitis; Idiopathic acute pancreatitis; Biliary pancreatitis; Microlithiasis; Sludge; Endosonography

©The Author(s) 2023. Published by Baishideng Publishing Group Inc. All rights reserved.

Core Tip: Occult biliary lithiasis represents the largest monocausally treatable aetiology group within idiopathic acute pancreatitis cases. The identification of this subgroup protects patients from pancreatitis recurrences and over- or underdiagnosis. Based on 28 easy-to-collect and widely available patient variables, a machine learning-based prediction score can be used to predict the presence or absence of biliary sludge or microlithiasis in the context of pancreatitis hospitalisation. We provide a web-based prediction tool to select patients for endosonography to investigate microlithiasis or sludge as the cause of pancreatitis and treat them accordingly.

Citation: Sirtl S, Żorniak M, Hohmann E, Beyer G, Dibos M, Wandel A, Phillip V, Ammer-Herrmenau C, Neesse A, Schulz C, Schirra J, Mayerle J, Mahajan UM. Machine learning-based decision tool for selecting patients with idiopathic acute pancreatitis for endosonography to exclude a biliary aetiology. *World J Gastroenterol* 2023; 29(35): 5138-5153
URL: https://www.wjgnet.com/1007-9327/full/v29/i35/5138.htm
DOI: https://dx.doi.org/10.3748/wjg.v29.i35.5138

INTRODUCTION

Pancreatitis is a high incidence disease and the underlying cause for the highest number of patients admitted to hospital admission of all benign gastrointestinal-disorders[1]. In approximately 25% of patients with acute pancreatitis (AP), aetiology cannot be established during the first episode of pancreatitis[2,3]. If the aetiology of AP cannot be identified by history, laboratory chemistry, and imaging, it is classified as "idiopathic" [idiopathic AP (IAP)]. Unclassified or idiopathic pancreatitis represents the third largest group of pancreatitis and is therefore of great importance from both a medical and a socioeconomic point of view requiring thorough workup[3,4]. All efforts should be made to elucidate a treatable aetiology to prevent further episodes of AP. A recent meta-analysis has shown that biliary aetiology is the most common cause of idiopathic pancreatitis with a prevalence of 30%[5]. Specifically, in light of morbidity and mortality of AP, it is crucial to differentiate the potentially treatable aetiology of AP triggered by biliary sludge and microlithiasis from idiopathic or other causes of AP. Unfortunately, due to a lack of unifying definition of biliary sludge and microlithiasis, it is currently impossible to assess the risk of sludge and/or microlithiasis as the cause of AP. In the absence of clear evidence, guidelines suggest to treat those patients by cholecystectomy and maybe biliary sphincterotomy. In line, the diagnostic IAP workup requires excluding biliary microconcrements as it is believed that detection and concrement removal and/or cholecystectomy can prevent further episodes of pancreatitis in over 85% of cases[6,7]. To facilitate decision-making on whether the patient should be referred to endosonography (EUS) followed by endoscopic retrograde cholangiopancreatography (ERCP) or cholecystectomy, we developed a predictive tool using a machine learning (ML)-based approach to estimate the probability of the presence of biliary sludge and/or microlithiasis at the time of presentation to the emergency department. The ML tool, which is based on routine laboratory values, will help clinicians to enrich the likelihood to detect microlithiasis or sludge at admission on EUS and hereby reduce the number of EUS exams in presumed acute idiopathic pancreatitis.

MATERIALS AND METHODS

Study design

We retrospectively studied 1340 confirmed and hospitalized patient cases of AP treated at LMU University Hospital

Munich (tertiary care hospital) between January 1, 2015 and October 1, 2020 (ICD-10 codes used: K85.00-K85.91). Patient cohorts with identical inclusion criteria from the University Hospital of the Technical University Munich and the University Medical Center Goettingen served as the validation cohort. The study was conducted in accordance with the updated STARD guideline of 2015[8].

Participants

Only patients meeting the diagnostic criteria for AP as set in the APA/IAP guidelines and adapted in the German S3-Guideline were enrolled in the analysis[9,10]. The first classifier used was whether patients received an EUS during their initial hospital stay, reducing the number of patients for further analysis to 360. The endosonographies were each performed by an experienced endoscopist. In the majority (79%) of pancreatitis stays, EUS was performed on days 1-3. Of the 360 patients with EUS, a total of 142 cases were excluded from further analysis due to incomplete records or missing coding. Two hundred and eighteen patient cases with AP and EUS were then further stratified into a cohort (47 patients) with no other cause of pancreatitis than endosonographically detected biliary microconcrements (biliary sludge/microlithiasis; detection of concrements in the common bile duct or gallbladder and common bile duct) and 171 patients with other causes of AP (Figure 1). In the two study groups [AP + EUS: 47 × microlithiasis *vs* 171 × non-microlithiasis (other cause); Supplementary Table 1], history, alcohol consumption, sonography, ERCP, or EUS findings, start or change of existing medication, known hereditary pancreatitis (available genetic testing of most prevalent susceptibility genes), and laboratory findings [lipase levels, immunoglobulin G subclasses, liver enzymes, triglycerides, and calcium level (corrected for blood serum albumin level)] were retrospectively evaluated. In the context of the laboratory value analyses, the values from the first blood analysis after admission of the respective patient stay was used in each case. The aim was to select patients in which microlithiasis/sludge was likely to subject them to EUS to reduce the number of EUS as an invasive, expensive procedure burdened with complications. To independently validate our machine-based algorithm, we obtained identical clinical data and inclusion criteria from two high volume German pancreas centers (University Hospital of the Technical University Munich: 22 × microlithiasis-AP, 51 × other-AP; University Medical Center Goettingen: 14 × microlithiasis-AP, 30 × other-AP; Supplementary Table 1). The definitions of the entities "biliary sludge" and "biliary microlithiasis" were taken from the endoscopic reports during the retrospective data evaluation and were not re-evaluated due to the current lack of an accepted unifying definition. Due to the differences between the participating centers in the use and partial equation of the two terms biliary sludge and microlithiasis, sludge-triggered pancreatitis was subsumed as biliary AP caused by microlithiasis.

Test methods

All aspects of data reporting, predictive modeling, and validation reporting were performed in accordance with the TRIPOD guidelines[11]. A diagnostic reference standard for laboratory or imaging-based prediction of biliary sludge or microlithiasis in the context of AP has not yet been published. To derive the ML-based predictor model (index test), the following steps were performed (Figure 2): (1) Baseline variables (n = 192) were filtered leaving out variables with zero and near zero variance; (2) All numeric variables were classified into within limit, above upper limit, and below lower limit, based on clinical reference limits. All categorised variables were retained; (3) The training cohort was divided into a training (80%) and a test set (20%). Endpoint balancing was achieved by stratifying the classes by inducing the sampling rate of patients with microlithiasis and reducing the sampling rate of patients with other-AP. ML was performed based on all filtered baseline variables and data from the training set, resulting in a predictor based on all variables (base predictor model); and (4) To improve robustness and interpretability, low-impact variables were iteratively removed. An iterative predictive model with a reduced number of variables (n = 26) was obtained based on the performance in the test set.

All predictor models were constructed using the H_2O.ai platform (https://www.h2o.ai) selecting (with h2o.automl) the best suitable ML method in the training set. The parameters of each method were optimized by employing an internal ten-fold cross-validation on the training set. The optimal method was then applied to the test set to assess the final performance. In each loop, the best performing predictor model was identified from all predicted outcomes obtained using the performance measure logloss. Variables with a higher proportion of missing data (> 25% missing data) were also not excluded *per se* in order to base the final model on the broadest possible number of routinely available variables in the early phase of AP. The iterative predictive model obtained was externally validated in an independent retrospective dataset.

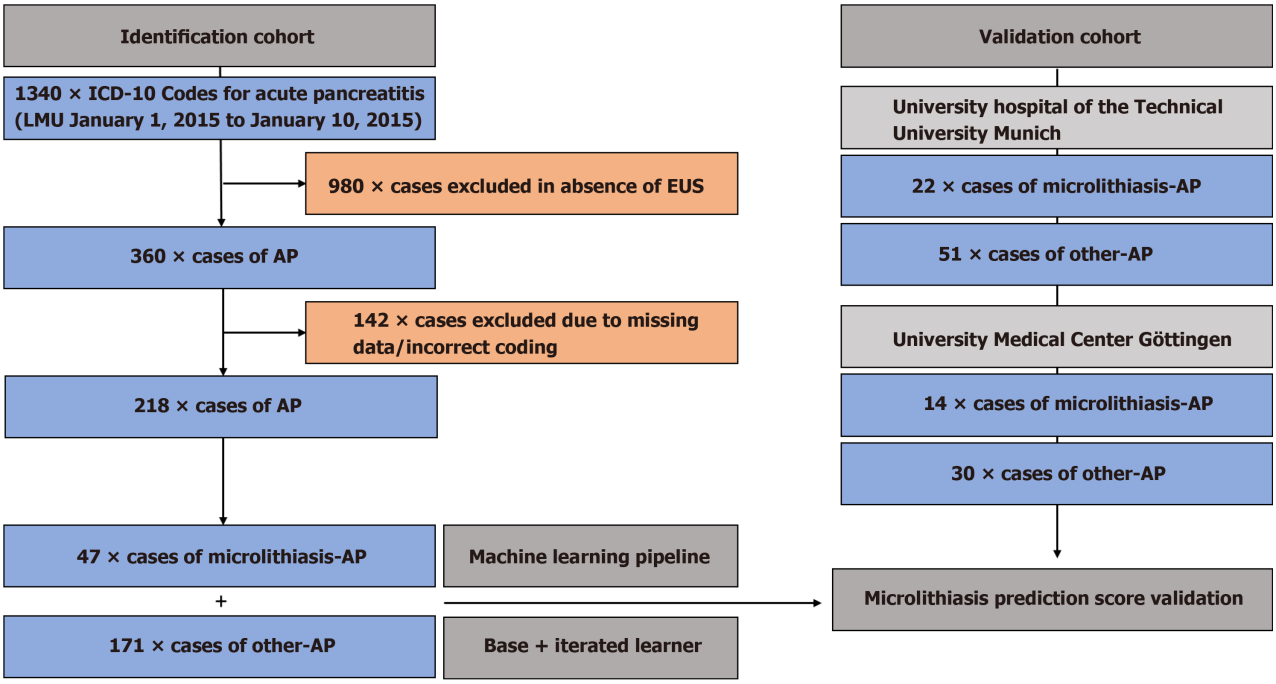
Statistical analysis

All data processing, modeling, and assessment of performances were done using R [version 4.0.4 (2021-02-15, "Lost Library Book")] and visualized in R-studio (version 1.3.9.59). No unique algorithm was developed for this study. All data R scripts or functions are available online at the following link: https://github.com/mayerlelab/microlithiasisPredict. P values of < 0.05 were considered statistically significant if appropriate for the tests used.

RESULTS

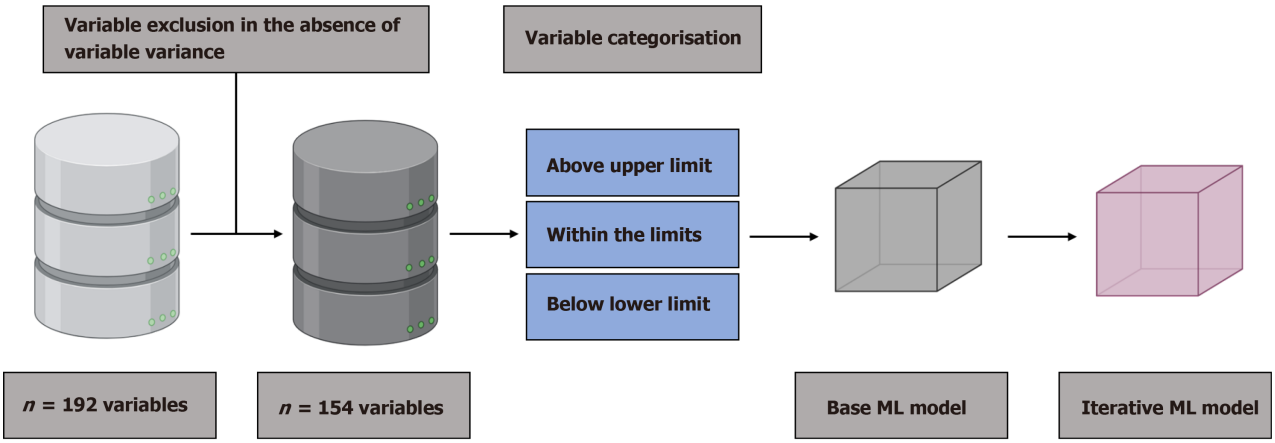
Microlithiasis predictive score - results of the identification cohort

Between January 1, 2015 and October 1, 2020, 218 patients with AP received an EUS during their initial admission with AP at LMU University Hospital meeting the study inclusion criteria (Figure 1). In 47 of 218 pancreatitis patients, no causal



DOI: 10.3748/wjg.v29.i35.5138 **Copyright** ©The Author(s) 2023.

Figure 1 Flow chart for development and external independent validation of microlithiasis prediction score. In the Ludwig-Maximilians-Universität in Munich identification cohort, 218 acute pancreatitis patients treated as inpatients between 2015-2020 were included in the final machine learning-based score survey. The validation cohort, consisting of 117 pancreatitis cases, was composed of patient data from the University Hospital of Göttingen and Technical University Munich. The microlithiasis predictive model was trained using data from both biliary sludge and biliary microlithiasis patients to cover the entirety of biliary microconcrements and to reflect the current lack of uniform definitions of biliary sludge and biliary microlithiasis in clinical practice. EUS: Endosonography; AP: Acute pancreatitis.



DOI: 10.3748/wjg.v29.i35.5138 **Copyright** ©The Author(s) 2023.

Figure 2 Machine-learning based model for the prediction of biliary sludge and microlithiasis in the context of acute (presumed) idiopathic acute pancreatitis. Of the initial 192 variables analysed, 154 were included in the categorisation step after excluding those variables without evidence of variable variance. Using an auto-machine learning approach, the final (iterative) predictive model was developed *via* the base model step. ML: Machine learning.

pancreatitis aetiology other than endosonographically detected biliary microconcrements/sludge was found during the respective inpatient stay. Among 171 out of 218 pancreatitis patients with EUS, 52.6% (90/171) were classified as 'idiopathic', 21.6% (37/171) as acute on chronic, and 15.2% (27/171) with macrolithiasis as of biliary aetiology (Supplementary Table 1). Mean age in the microlithiasis/sludge cohort was 59.1 (SD 18.8) years in comparison to that of patients with AP of other aetiologies [54.6 (SD 17.1) years; $P = 0.122$]. Gender distribution was not statistically different in the two cohorts, with a male predominance in both cohorts [31/47 (66%) of microlithiasis patients and 103/171 (60.2%); $P = 0.475$] (Table 1). 76.6% of microlithiasis-AP patients were assessed as mild pancreatitis cases according to the revised Atlanta classification [36/47; 19.1% moderate (9/47) and 4.3% severe (2/47)]. In the other-AP cohort, 71.9% of patients were assessed as mild pancreatitis cases according to the revised Atlanta classification [123/171; 25.7% moderate (44/171) and 2.3% severe (4/171)]. A total of 29 variables from serum samples and 5 from urine were used to develop the ML-based

Table 1 Variables distribution at the Ludwig-Maximilians-Universität University Hospital Munich (identification cohort)

Variable	Microlithiasis (*n* = 47)	Other (*n* = 171)	Total (*n* = 218)	*P* value
Age (yr)				0.122
mean ± SD	59.1 ± 18.8	54.6 ± 17.1	55.6 ± 17.6	
Range	30-92	24-90	24-92	
Sex				0.474
Female	16/47 (34%)	68/171 (39.8%)	84/218 (38.5%)	
Male	31/47 (66%)	103/171 (60.2%)	134/218 (61.5%)	
Albumin				0.706
N-Miss	32/47 (68%)	90/171 (52.6%)	122/218 (55.9%)	
LLN	2/47 (4.2%)	14/171 (8.1%)	16/218 (7.3%)	
WL	13/47 (27.6%)	67/171 (39.1%)	80/218 (36.6%)	
Alkaline phosphatase				0.667
N-Miss	1/47 (2.1%)	5/171 (2.9%)	6/218 (2.7%)	
LLN	0/47 (0%)	1/171 (0.5%)	1/218 (0.4%)	
ULN	22/47 (46.8%)	69/171 (40.3%)	91/218 (41.7%)	
WL	24/47 (51.0%)	96/171 (56.1%)	120/218 (55.0%)	
Total bilirubin				0.110
N-Miss	0/47 (0%)	2/171 (1.1%)	2/218 (0.9%)	
ULN	23/47 (48.9%)	61/171 (35.6%)	84/218 (38.5%)	
WL	24/47 (51.0%)	108/171 (63.1%)	132/218 (60.5%)	
Calcium				0.033
N-Miss	20/47 (42.5%)	60/171 (35.0%)	80/218 (36.6%)	
LLN	6/47 (12.7%)	7/171 (4.0%)	13/218 (5.9%)	
ULN	0/47 (0%)	2/171 (1.1.%)	2/218 (0.9%)	
WL	21/47 (44.6%)	102/171 (59.6%)	123/218 (56.4%)	
Creatine kinase				0.073
N-Miss	29/47 (61.7%)	107/171 (62.5%)	136/218 (62.3%)	
ULN	0/47 (0%)	10/171 (5.8%)	10/218 (4.5%)	
WL	18/47 (38.2%)	54/171 (31.5%)	72/218 (33%)	
CRP				0.391
ULN	37/47 (78.7%)	124/171 (72.5%)	161/218 (73.9%)	
WL	10/47 (21.3%)	47/171 (27.5%)	57/218 (26.1%)	
Total protein				0.743
N-Miss	30/47 (63.8%)	104/171 (60.8%)	134/218 (61.4%)	
LLN	0/47 (0%)	1/171 (0.5%)	1/218 (0.4%)	
ULN	3/47 (6.3%)	16/171 (9.3%)	19/218 (8.7%)	
WL	14/47 (29.7%)	50/171 (29.2%)	64/218 (29.3%)	
Erythrocytes				0.880
N-Miss	1/47 (2.1%)	0/171 (0%)	1/218 (0.4%)	
LLN	14/47 (29.7%)	53/171 (30.9%)	67/218 (30.7%)	
ULN	3/47 (6.3%)	8/171 (4.6%)	11/218 (5.0%)	
WL	29/47 (61.7%)	110/171 (64.3%)	139/218 (63.7%)	

Gamma-GT				0.108
N-Miss	0/47 (0%)	1/171 (0.5%)	1/218 (0.4%)	
ULN	37/47 (78.7%)	113/171 (66%)	150/218 (68.8%)	
WL	10/47 (21.3%)	57/171 (33.3%)	67/218 (30.7%)	
AST/GOT				0.444
N-Miss	17/47 (36.1%)	51/171 (29.8%)	68/218 (31.1%)	
ULN	21/47 (44.6%)	75/171 (43.8%)	96/218 (44.0%)	
WL	9/47 (19.1%)	45/171 (26.3%)	54/218 (24.7%)	
ALT/GPT				0.016
ULN	34/47 (72.3%)	90/171 (52.6%)	124/218 (56.9%)	
WL	13/47 (27.7%)	81/171 (47.4%)	94/218 (43.1%)	
Urea				0.429
N-Miss	31/47 (65.9%)	80/171 (46.7%)	111/218 (50.9%)	
LLN	0/47 (0%)	7/171 (4%)	7/218 (3.2%)	
ULN	3/47 (6.3%)	11/171 (6.4%)	14/218 (6.4%)	
WL	13/47 (27.6%)	73/171 (42.6%)	86/218 (39.4%)	
Hematocrit				0.304
N-Miss	1/47 (2.1%)	0/171 (0%)	1/218 (0.4%)	
LLN	0/47 (0%)	2/171 (1.1%)	2/218 (0.9%)	
ULN	41/47 (87.2%)	160/171 (93.5%)	201/218 (92.2%)	
WL	5/47 (10.6%)	9/171 (5.2%)	14/218 (6.4%)	
Haemoglobin				0.574
N-Miss	1/47 (2.1%)	0/171 (0%)	1/218 (0.4%)	
LLN	12/47 (25.5%)	45/171 (26.3%)	57/218 (26.1%)	
ULN	0/47 (0%)	4/171 (2.3%)	4/218 (1.8%)	
WL	34/47 (72.3%)	122/171 (71.3%)	156/218 (71.5%)	
INR				0.443
N-Miss	3/47 (6.3%)	9/171 (1.1%)	12/218 (5.5%)	
ULN	8/47 (17.0%)	22/171 (12.8%)	30/218 (13.7%)	
WL	36/47 (76.5%)	140/171 (81.8%)	176/218 (80.7%)	
Potassium				0.270
N-Miss	9/47 (19.1%)	2/171 (1.1%)	11/218 (5%)	
LLN	1/47 (2.1%)	7/171 (4%)	8/218 (3.6%)	
ULN	0/47 (0%)	10/171 (5.8%)	10/218 (4.5%)	
WL	37/47 (78.7%)	152/171 (88.8%)	189/218 (86.6%)	
Serum creatinine				0.738
N-Miss	6/47 (12.7%)	0/171 (0%)	6/218 (2.7%)	
LLN	1/47 (2.1%)	5/171 (2.9%)	6/218 (2.7%)	
ULN	5/47 (10.6%)	29/171 (16.9%)	34/218 (15.5%)	
WL	35/47 (74.4%)	137/171 (80.1%)	172/218 (78.8%)	
LDH				0.020
N-Miss	7/47 (14.8%)	19/171 (11.1%)	26/218 (11.9%)	
ULN	30/47 (63.8%)	83/171 (48.5%)	112/218 (51.8%)	

WL	10/47 (21.2%)	69/171 (40.3%)	79/218 (36.2%)	
Leukocytes				0.347
N-Miss	1/47 (2.1%)	0/171 (0%)	1/218 (0.4%)	
LLN	1/47 (2.1%)	3/171 (1.7%)	4/218 (1.8%)	
ULN	16/47 (34%)	80/171 (46.7%)	96/218 (44%)	
WL	29/47 (61.7%)	88/171 (51.5%)	117/218 (53.6%)	
Lipase				0.653
N-Miss	0/47 (0%)	1/171 (0.5%)	1/218 (0.4%)	
LLN	0/47 (0%)	3/171 (1.7%)	3/218 (1.3%)	
ULN	44/47 (93.6%)	157/171 (91.8%)	201/218 (92.2%)	
WL	3/47 (6.4%)	10/171 (5.8%)	13/218 (5.9%)	
MCH				0.498
N-Miss	1/47 (2.1%)	0/171 (0%)	1/218 (0.4%)	
LLN	3/47 (6.3%)	20/171 (11.6%)	23/218 (10.5%)	
ULN	4/47 (8.5%)	10/171 (5.8%)	14/218 (6.4%)	
WL	39/47 (82.9%)	141/171 (82.4%)	180/218 (82.5%)	
MCHC				0.108
N-Miss	1/47 (2.1%)	0/171 (0%)	1/218 (0.4%)	
LLN	0/47 (0%)	13/171 (7.6%)	13/218 (5.9%)	
ULN	1/47 (2.1%)	8/171 (4.6%)	9/218 (4.1%)	
WL	45/47 (95.7%)	150/171 (87.7%)	195/218 (89.4%)	
Triglycerides				0.004
N-Miss	27/47 (57.4%)	110/171 (64.3%)	137/218 (62.8%)	
ULN	1/47 (2.1%)	24/171 (14%)	25/218 (11.4%)	
WL	19/47 (40.4%)	37/171 (21.6%)	56/218 (25.6%)	
RDW				0.329
N-Miss	5/47 (10.6%)	36/171 (21%)	41/218 (18.8%)	
LLN	1/47 (2.1%)	11/171 (6.3%)	12/218 (5.5%)	
ULN	5/47 (10.6%)	21/171 (12.2%)	26/218 (11.9%)	
WL	36/47 (76.5%)	103/171 (60.2%)	139/218 (63.7%)	
MCV				0.893
N-Miss	1/47 (2.1%)	0/171 (0%)	1/218 (0.4%)	
LLN	4/47 (8.5%)	13/171 (7.6%)	17/218 (7.7%)	
ULN	4/47 (8.5%)	12/171 (7.0%)	16/218 (7.3%)	
WL	38/47 (80.8%)	146/171 (85.3%)	184/218 (84.4%)	
Sodium				0.020
N-Miss	8/47 (17.0%)	1/171 (0.5%)	9/218 (4.1%)	
LLN	1/47 (2.1%)	29/171 (16.9%)	30/218 (13.7%)	
WL	38/47 (80.8%)	141/171 (82.4%)	179/218 (82.1%)	
Quick's value				0.479
N-Miss	3/47 (6.3%)	7/171 (4%)	10/218 (4.5%)	
LLN	8/47 (17%)	23/171 (13.4%)	31/218 (14.2%)	
ULN	20/47 (42.5%)	65/171 (38%)	85/218 (38.9%)	

WL	16/47 (34%)	76/171 (44.4%)	92/218 (42.2%)	
Thrombocytes				0.434
N-Miss	1/47 (2.1%)	0/171 (0%)	1/218 (0.4%)	
LLN	8/47 (17%)	22/171 (12.8%)	30/218 (13.7%)	
ULN	4/47 (8.5%)	26/171 (15.2%)	30/218 (13.7%)	
WL	34/47 (72.3%)	123/171 (71.9%)	157/218 (72%)	
TSH				0.567
N-Miss	27/47 (57.4%)	118/171 (69%)	145/218 (66.5%)	
LLN	2/47 (4.2%)	4/171 (2.3%)	6/218 (2.7%)	
ULN	4/47 (8.5%)	6/171 (3.5%)	10/218 (4.5%)	
WL	14/47 (29.7%)	43/171 (25.1%)	57/218 (26.1%)	
Bilirubin-urine				0.027
N-Miss	26/47 (55.3%)	102/171 (59.6%)	128/218 (58.7%)	
Normal	8/47 (17%)	45/171 (26.3%)	53/218 (24.3%)	
Abnormal	13/47 (27.6%)	24/171 (14.0%)	37/218 (16.9%)	
Total protein-urine				0.231
N-Miss	26/47 (55.3%)	102/171 (59.6%)	128/218 (58.7%)	
Normal	10/47 (21.3%)	43/171 (25.1%)	53/218 (24.3%)	
Abnormal	11/47 (23.4%)	26/171 (15.2%)	37/218 (16.9%)	
Ketones-urine				0.020
N-Miss	26/47 (55.3%)	106/171 (61.9%)	132/218 (60.5%)	
Normal	21/47 (44.6%)	51/171 (29.8%)	72/218 (33%)	
Abnormal	0/47 (0%)	14/171 (8.1%)	14/218 (6.4%)	
Leukocytes-urine				0.162
N-Miss	26/47 (55.3%)	102/171 (59.6%)	128/218 (58.7%)	
Normal	7/47 (14.8%)	35/171 (20.4%)	42/218 (19.2%)	
Abnormal	14/47 (29.7%)	34/171 (19.8%)	48/218 (22%)	
Specific gravity-urine				0.918
N-Miss	29/47 (61.7%)	113/171 (66%)	142/218 (65.1%)	
mean ± SD	1018.33 ± 5.941	1018.103 ± 8.777	1018.158 ± 8.159	
Range	1005.000-1025.000	1005.000-1030.000	1005.000-1030.000	

All variables that were used for the final predictive model are listed. For laboratory or urine values, the first available value during the inpatient stay was used. For the investigated groups of microlithiasis-induced acute pancreatitis (n = 47) *vs* the group of pancreatitis induced by other aetiologies (n = 171), the variables were categorised as whether collected or not (N-Miss), in the case of laboratory values whether below the lower limit value, within the limit values, or above the upper limit value. For urine values, in addition to the rate of missing variables (N-Miss), it was categorised whether normal or abnormal. For the P value calculation using χ^2 test, variables with missing data shares of > 25% were not excluded. LLN: Lower limit value; WL: Within the limit value; ULN: Upper limit value; CRP: C-reactive protein; Gamma-GT: Gamma-glutamyl transpeptidase; AST: Aspartate aminotransferase; GOT: Glutamic oxalacetic transaminases; ALT: Alanine transaminase; GPT: Glutamic pyruvic transaminase; INR: International normalized ratio; LDH: Lactate dehydrogenase; MCH: Mean corpuscular hemoglobin; MCHC: Mean corpuscular hemoglobin concentration; RDW: Red blood cell distribution width; MCV: Mean corpuscular volume; TSH: Thyrotropin.

microlithiasis prediction algorithm. All variables listed corresponded to the values measured at admission for each individual pancreatitis inpatient (see Table 1 for the list of variables used). To move from the base ML to the iterated ML model, weighting was done, taking scale variance into account. For the LMU identification cohort, age, triglycerides, sodium, glutamic pyruvic transaminase, erythrocytes, potassium, thyrotropin, protein (total), and leukocytes in descending order were of greatest importance in predicting microlithiasis/sludge. Using the iterated learner-based model, an accuracy of 0.8361 [95% confidence interval (CI): 0.791-0.9185; odds ratio = 20.88 (95%CI: 2.08-209.27)] with a sensitivity of 97.92% and positive predictive value (PPV) of 83.93% could be achieved for the prediction of microlithiasis as the trigger of pancreatitis [negative predictive value (NPV) = 0.80; specificity: 0.31; Table 2].

Table 2 Performance matrix (identification cohort *vs* validation cohort)

Accuracy	Sensitivity	Specificity	PPV	NPV
ID: 0.8361; 95%CI: 0.7191-0.9185	ID: 0.9792	ID: 0.3077	ID: 0.8393	ID: 0.800
VD: 0.7607; 95%CI: 0.673-0.8347	VD: 0.9630	VD: 0.3056	VD: 0.7573	VD: 0.7857

The performance values for the auto-machine-learning-based predictive model are listed. The identification cohort of the Ludwig-Maximilians-Universität in Munich University Hospital (ID) *vs* the data of the predictive models from the validation cohort with patient data from the University Hospital Göttingen and the Klinikum Rechts der Isar (VD). CI: Confidence interval; PPV: Positive predictive value; NPV: Negative predictive value.

Microlithiasis predictive score - results of the validation cohort

Data from two large-volume university pancreas centers were used for score validation. In total, a validation cohort of 36 patients with microlithiasis and 81 non-microlithiasis AP patients were retrieved from the clinical database at the University Hospital of the Technical University Munich (22 × microlithiasis-AP, 51 × other-AP) as well as the University Hospital Göttingen (14 × microlithiasis-AP, 30 × other-AP; Figure 1 and Table 3). In the Technical University Munich cohort, the group of other-AP patients was mainly alcohol-related [31/51 (60.8%)], while in the Göttingen cohort biliary macrolithiasis was held responsible for the majority of AP patients [16/33 (53.3%)]. Idiopathic aetiology was named as the second most frequent aetiology group in both external cohorts with about 30% each [Technical University Munich 17/51 (33.3%), Göttingen 10/33 (33.3%)] (Supplementary Table 1). Microlithiasis patients in the validation cohort were on average 60.1 (SD 18.4) years old, while patients from the other-AP cohort were 55.3 (SD 16.8) years old. In both groups (microlithiasis + other-AP), the majority of patients were male [24/36 (66.7%) and 46/81 (56.8%), respectively], resembling the identification cohort. 63.9% of microlithiasis-AP patients were assessed as mild pancreatitis cases according to the revised Atlanta classification [23/36; 27.7% moderate (10/36) and 8.3% severe (3/36)]. In the other-AP cohort, 59.2% of patients were assessed as mild pancreatitis cases according to the revised Atlanta classification [48/81; 27.2% moderate (22/81) and 12.5% severe (11/81)]. Using automated ML, the best-fitting model for iterative reduction of variables was used to achieve external validation of the microlithiasis predictive score using the optimized iterative ML model. For the validation cohort, based on the variables ordered by scaled importance in Figure 3, an accuracy of 0.7607 (95%CI: 0.673-0.8347), PPV of 0.7573, and NPV of 0.7857 were achieved (sensitivity: 0.96, specificity: 0.31; Table 2). The robustness of the model is shown in the alluvial plot in Figure 3, with only 3 out of 81 patients being misclassified as having microlithiasis and not as having other-AP, corresponding to the discretely higher NPV (compared to the PPV) in the validation cohort (Table 2).

DISCUSSION

Previous and more recent studies on idiopathic pancreatitis still report a proportion of idiopathic pancreatitis stably at 20%-30%[12,13]. However, it has been suspected for decades and is increasingly supported by evidence that a large proportion of pancreatitis patients classified primarily as idiopathic actually suffer from a biliary aetiology and that detecting these patients during the first episode of pancreatitis is restricted due to the lack of availability of timely and high quality EUS exams[14]. Furthermore, there is a lack of reliable data on when, during an inpatient stay of an IAP-labeled patient, an EUS could detect biliary microconcrements as the trigger for pancreatitis without causing an unnecessary burden for the patient through overdiagnosis. This is an important question as we know from Oría *et al*[15] that common bile duct stones usually pass within 48 h, suggesting that microconcrements might even pass more rapidly and might not be detected on EUS. Prospective study data showed a corresponding variance of EUS-based biliary concrement detection rate of 19% in the low risk group, but 58% in the moderate risk group and 50% in the high risk group (grouping according to ASGE recommendation[16]). Risk stratification in terms of pre-test probability for EUS use < 48 h after hospital admission to rule in or out the presence of biliary concrements is warranted before intervention to overcome the lack of availability and reduce costs and side effects[12]. Diagnostic evaluation is complicated by the fact that biliary microconcrements could be a coincidental finding in the context of pancreatitis-induced gallbladder hypomotility, and therefore must always be understood in the individual patient's setting, taking into account a PPV of a biliary pancreatitis origin greater than 85% with elevation of the alanine transaminase (ALT) above three times the upper limit of normal [17]. However, no causally effective drug for pancreatitis therapy is available in 2023 and the detection of causally remediable pancreatitis causes such as biliary microlithiasis or sludge will continue to play a decisive role in the prevention of further pancreatitis attacks. The efficacy of cholecystectomy in the cohort of IAP patients was shown in a meta-analysis with a recurrence rate of 11% compared to 38.9% in conservatively treated patients (risk ratio = 0.41; 95%CI: 0.16-1.07) [18]. Our ML-based approach of predicting biliary microlithiasis and sludge should therefore be understood as an approach to make up for the lack of evidence from prospective studies on the optimal timing of EUS in IAP patients as this score is based on widely available laboratory values and can be used to determine the probability of the presence of biliary microconcrements at admission. Our score helps to select patients for EUS with a high sensitivity and very high NPV and thus will reduce costs and complications of unnecessary EUS exams as well as allow to subject patients to further treatment to prevent recurrence of biliary pancreatitis at the time of presentation in the emergency department. Preliminary work on ML-based algorithms and prediction models in the context of AP has focused on severity assessment and prediction of complications[15]. A multicenter retrospective study used an auto-ML-based approach to

Table 3 Variable distribution in the validation cohort (UMG + Technical University Munich)

Variable	Microlithiasis (*n* = 36)	Other (*n* = 81)	Total (*n* = 117)	*P* value
Age (yr)				0.162
mean ± SD	60.1 ± 18.4	55.3 ± 16.8	56.8 ± 17.4	
Range	23-93	21-87	21-93	
Sex				0.315
Female	12/36 (33.3%)	35/81 (43.2%)	47/117 (40.2%)	
Male	24/36 (66.7%)	46/81 (56.8%)	70/117 (59.8%)	
Alkaline phosphatase				0.032
N-Miss	1/36 (2.7%)	12/81 (14.8%)	13/117 (11.1%)	
ULN	23/36 (63.8%)	30/81 (37%)	53/117 (45.2%)	
WL	12/36 (33.2%)	39/81 (48.1%)	51/117 (43.5%)	
Total bilirubin				0.003
ULN	21/36 (58.3%)	24/81 (29.6%)	45/117 (38.5%)	
WL	15/36 (41.7%)	57/81 (70.4%)	72/117 (61.5%)	
Creatine kinase				0.498
N-Miss	8/36 (22.2%)	32/81 (39.5%)	40/117 (34.1%)	
ULN	5/36 (13.8%)	6/81 (7.4%)	11/117 (9.4%)	
WL	23/36 (63.8%)	43/81 (53%)	66/117 (56.4%)	
CRP				0.199
ULN	32/36 (88.9%)	64/81 (79%)	96/117 (88.8%)	
WL	4/36 (11.1%)	17/81 (21%)	21/117 (17.9%)	
Total protein				0.405
N-Miss	31/36 (86.1%)	73/81 (90.1%)	104/117 (88.8%)	
WL	5/36 (13.8%)	8/81 (9.8%)	13/117 (11.1%)	
Erythrocytes				0.650
N-Miss	0/36 (0%)	1/81 (1.2%)	1/117 (0.8%)	
LLN	10/36 (27.7%)	25/81 (30.8%)	35/117 (29.9%)	
ULN	4/36 (11.1%)	5/81 (6.1%)	9/117 (7.6%)	
WL	22/36 (61.1%)	50/81 (61.7%)	72/117 (61.5%)	
Gamma-GT				0.082
N-Miss	0/36 (0%)	2/81 (2.4%)	2/117 (1.7%)	
ULN	32/36 (88.8%)	59/81 (72.8%)	91/117 (77.7%)	
WL	4/36 (11.1%)	20/81 (24.6%)	24/117 (20.5%)	
AST/GOT				0.079
N-Miss	0/36 (0%)	4/81 (4.9%)	4/117 (3.4%)	
ULN	28/36 (77.8%)	47/81 (58%)	75/117 (64.1%)	
WL	8/36 (22.2%)	30/81 (37%)	38/117 (32.4%)	
ALT/GPT				0.052
N-Miss	0/36 (0%)	2/81 (2.4%)	2/117 (1.7%)	
ULN	28/36 (77.8%)	43/81 (53%)	71/117 (60.6%)	
WL	8/36 (22.2%)	30/81 (37%)	38/117 (32.4%)	
Urea				

N-Miss	7/36 (19.4%)	20/81 (24.6%)	27/117 (23%)	
LLN	13/36 (36.1%)	41/81 (50.6%)	54/117 (46.1%)	
ULN	0/36 (0%)	1/81 (1.2%)	1/117 (0.8%)	
WL	16/36 (44.4%)	19/81 (23.4%)	35/117 (29.9%)	
Hematocrit				< 0.001
N-Miss	0/36 (0%)	1/81 (1.2%)	1/117 (0.8%)	
ULN	36/36 (100%)	80/81 (98.7%)	116/117 (99.1%)	
Haemoglobin				0.725
N-Miss	0/36 (0%)	1/81 (1.2%)	1/117 (0.8%)	
LLN	9/36 (25%)	18/81 (22.2%)	27/117 (23%)	
ULN	3/36 (8.3%)	4/81 (4.9%)	7/117 (5.9%)	
WL	32/36 (88.9%)	64/81 (79.0%)	96/117 (82%)	
INR				0.440
ULN	2/36 (5.5%)	8/81 (9.8%)	10/117 (8.5%)	
WL	34/36 (94.4%)	73/81 (90.1%)	107/117 (91.4%)	
Potassium				0.985
LLN	2/36 (5.5%)	4/81 (4.9%)	6/117 (5.1%)	
ULN	1/36 (2.7%)	2/81 (2.4%)	3/117 (2.5%)	
WL	33/36 (91.6%)	75/81 (92.5%)	108/117 (92.3%)	
Serum creatinine				0.909
LLN	2/36 (5.5%)	6/81 (7.4%)	8/117 (6.8%)	
ULN	7/36 (19.4%)	14/81 (17.2%)	21/117 (17.9%)	
WL	27/36 (75%)	61/81 (75.3%)	88/117 (75.2%)	
LDH				0.018
N-Miss	6/36 (16.6%)	28/81 (34.5%)	34/117 (29%)	
ULN	26/36 (72.2%)	33/81 (40.7%)	59/117 (50.4%)	
WL	4/36 (11.1%)	20/81 (24.6%)	24/117 (20.5%)	
Leukocytes				0.143
N-Miss	0/36 (0%)	1/81 (1.2%)	1/117 (0.8%)	
LLN	1/36 (2.7%)	0/81 (0%)	1/117 (0.8%)	
ULN	16/36 (44.4%)	47/81 (58%)	63/117 (53.8%)	
WL	19/36 (52.7%)	33/81 (40.7%)	52/117 (44.4%)	
Lipase				0.237
N-Miss	0/36 (0%)	2/81 (2.4%)	2/117 (1.7%)	
ULN	32/36 (88.9%)	75/81 (92.5%)	107/117 (91.4%)	
WL	4/36 (11.1%)	4/81 (4.9%)	8/117 (6.8%)	
MCV				0.315
N-Miss	0/36 (0%)	1/81 (1.2%)	1/117 (0.8%)	
LLN	3/36 (8.3%)	7/81 (8.6%)	10/117 (8.5%)	
ULN	1/36 (2.7%)	9/81 (11.1%)	10/117 (8.5%)	
WL	32/36 (88.9%)	64/81 (79%)	96/117 (82%)	
Triglycerides				0.582
N-Miss	26/36 (72.2%)	43/81 (53%)	69/117 (58.9%)	

ULN	3/36 (8.3%)	15/81 (18.5%)	18/117 (15.3%)	
WL	7/36 (19.4%)	23/81 (28.3%)	30/117 (25.6%)	
RDW				
N-Miss	36/36 (100%)	81/81 (100%)	117/117 (100%)	
False	0/36 (0%)	0/81 (0%)	0/117 (0%)	
True	0/36 (0%)	0/81 (0%)	0/117 (0%)	
Sodium				0.154
LLN	2/36 (5.5%)	12/81 (14.8%)	14/117 (11.9%)	
WL	34/36 (94.4%)	69/81 (85.1%)	103/117 (88%)	
Quick's value				0.130
LLN	2/36 (5.5%)	6/81 (7.4%)	8/117 (6.8%)	
ULN	13/36 (36.1%)	44/81 (54.3%)	57/117 (48.7%)	
WL	21/36 (58.3%)	31/81 (38.2%)	52/117 (44.4%)	
Thrombocytes				0.627
N-Miss	22/36 (61.1%)	51/81 (62.9%)	73/117 (62.3%)	
LLN	2/36 (5.5%)	3/81 (3.7%)	5/117 (4.2%)	
ULN	2/36 (5.5%)	2/81 (2.4%)	4/117 (3.4%)	
WL	10/36 (27.7%)	25/81 (30.8%)	35/117 (29.9%)	
TSH				0.773
N-Miss	6/36 (16.6%)	13/81 (16%)	19/117 (16.2%)	
LLN	0/36 (0%)	1/81 (1.2%)	1/117 (0.8%)	
ULN	1/36 (2.7%)	3/81 (3.7%)	4/117 (3.4%)	
WL	29/36 (80.5%)	64/81 (79%)	93/117 (79.4%)	

All variables that were used for the final predictive model are listed. For laboratory or urine values, the first available value during the inpatient stay was used. For the investigated groups of microlithiasis-induced acute pancreatitis (n = 36) *vs* the group of pancreatitis induced by other aetiologies (n = 81), the variables were categorised as whether collected or not (N-Miss), in the case of laboratory values whether below the lower limit value, within the limit values, or above the upper limit value. For the P value calculation using χ^2 test, variables with missing data shares of > 25% were not excluded. LLN: Lower limit value; WL: Within the limit value; ULN: Upper limit value; CRP: C-reactive protein; Gamma-GT: Gamma-glutamyl transpeptidase; AST: Aspartate aminotransferase; GOT: Glutamic oxalacetic transaminases; ALT: Alanine transaminase; GPT: Glutamic pyruvic transaminase; INR: International normalized ratio; LDH: Lactate dehydrogenase; MCH: Mean corpuscular hemoglobin; MCHC: Mean corpuscular hemoglobin concentration; RDW: Red blood cell distribution width; MCV: Mean corpuscular volume; TSH: Thyrotropin.

predict pancreatitis severity, comparable to our ML approach, and achieved an area under the curve (AUC) of > 0.90 in the GBM model with a specificity and accuracy of both > 0.95 in the early detection of patients with a subsequently severe course of pancreatitis[19], outperforming clinically established non-ML-based scoring systems such as BISAP or Ranson underlying the relevance of ML approach over an educated guess[20,21]. ML-based prediction scores with regard to biliary microconcrements have not yet been published. Non-ML-based multivariate logistic regression models using widely available laboratory values have previously shown that an ALT level more than three times above the norm at patients' admission [specificity of 82%, sensitivity of 60%, receiver operating characteristic (ROC)-AUC 0.733; P < 0.001] and age > 69.5 years (specificity 92%, sensitivity 57%, ROC-AUC 0.759; P < 0.001) act as the best predictors of biliary aetiology[17,22]. Here, our ML-based prediction score achieves a higher sensitivity (96.30%), whereby ALT and, above all, age also rank 4th and 1st in the weighting of our score, thus confirming the existing evidence in the area of non-ML laboratory value-based prediction of biliary aetiology of pancreatitis (Figure 3). Contrary to previously published studies on laboratory-based prediction of biliary pancreatitis aetiology, our prediction tool is based specifically on microlithiasis and sludge and not primarily on gallstones and occult microlithiasis/sludge subsumed in this cohort.

Our study has several limitations. First, the retrospective study approach did not allow us to generate a uniform definition of the two entities microlithiasis and sludge. Even after extensive literature research, we were unable to delineate a uniform but distinct definition of biliary microlithiasis and sludge. We thus decided to use the terms as synonyms between the endoscopy centers of the three participating university hospitals. This might impose a significant bias. The macrolithiasis, which was again clearly listed in the endoscopy findings across the universities, ensured quality of EUS. Likewise, the patient cohort declared as other-AP in terms of aetiology varied greatly between the participating centers (Supplementary Table 1). Ultimately, this probably reflects the individual diagnostic scope and the question of

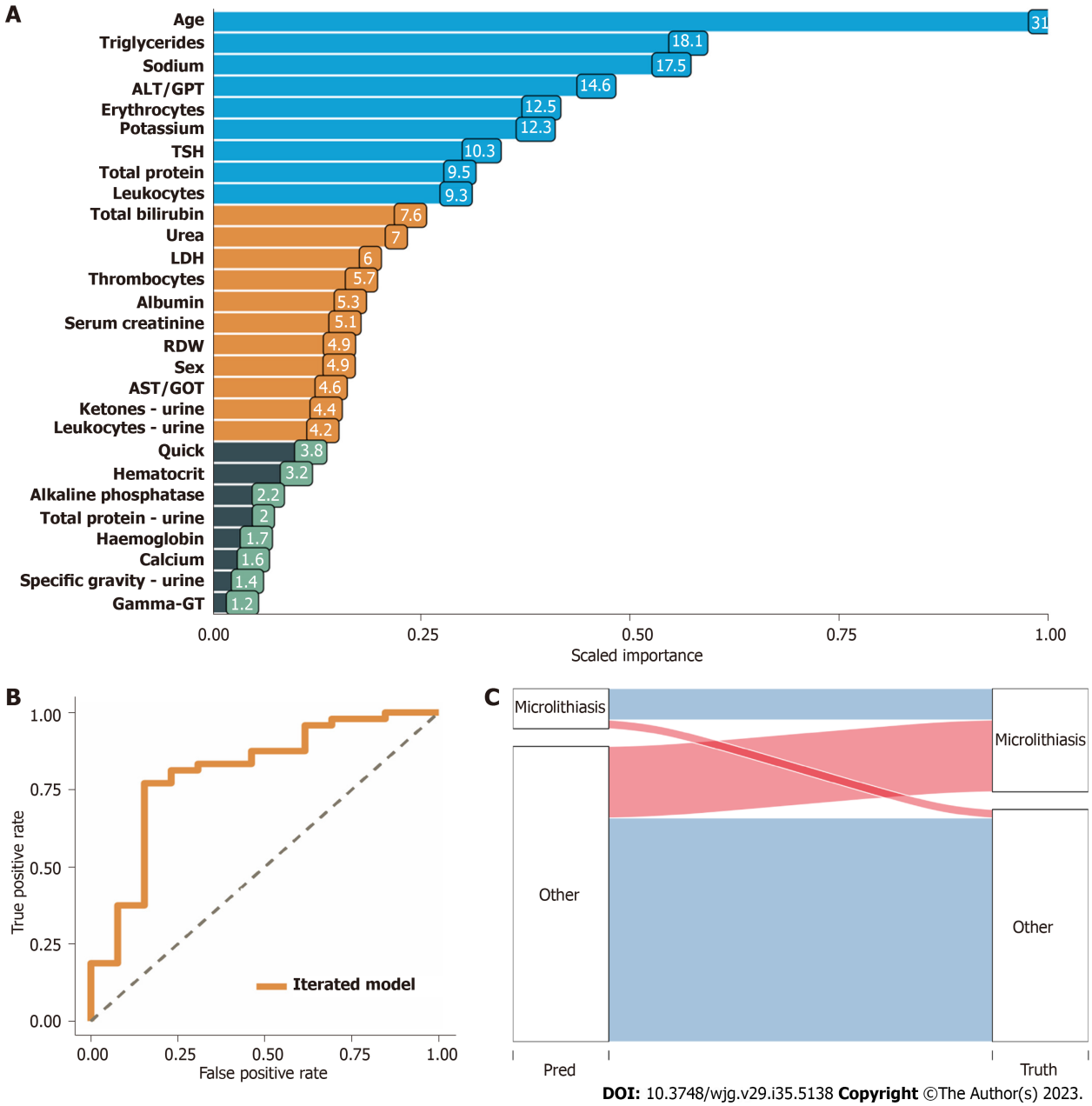


Figure 3 Graphical representation of the prediction model variables according to importance of scale. A: Variables of the final (iterated) auto-machine learning prediction model are ordered by scale of importance; B and C: Precoat diagram showing robust positive and negative prediction (3/81 patient cases were misclassified as microlithiasis and not other-acute pancreatitis). Gamma-GT: Gamma-glutamyl transpeptidase; AST: Aspartate aminotransferase; GOT: Glutamic oxalacetic transaminases; ALT: Alanine transaminase; GPT: Glutamic pyruvic transaminase; LDH: Lactate dehydrogenase; RDW: Red blood cell distribution width.

whether EUS can generate added value in the context of the individual patient. Also, due to the retrospective study design, no attempt could be made to increase the degree of purity of biliary (microlithiasis and sludge) triggered pancreatitis by uniformly fulfilling laboratory chemistry tests prior to EUS. This resulted in a proportion of patients of 36.6% with, for example, missing calcium values in the laboratory chemistry pancreatitis workup.

Our study is convincing in presenting for the first time a robust ML-based and externally validated prediction model for pancreatitis patients declared idiopathic early in the diagnostic workup and may be helpful as a noninvasive decision tool by combining simple and widely used laboratory values to decide for or against EUS. In order to make the microlithiasis predictive score and the relatively high number of underlying variables usable, a user-friendly interface is available online at the following link for use in the research context: https://github.com/mayerlelab/microlithiasisPredict. To illustrate the performance of the microlithiasis predictive score, we designed a graphical user interface for a quick entry of the values of the necessary patient variables, followed by the prediction of the need for EUS. The user-friendly interface (Video core tip, currently not deployed on Web) provides the user with the model-based estimated probability of the patient stratification to microlithiasis/sludge and other-pancreatitis. Moreover, it provides several graphical presentations to illustrate the impact of the specific variables on the decision. A multicenter prospective score validation with harmonised predefinition of biliary sludge and microlithiasis is currently being planned.

CONCLUSION

We present for the first time an ML-based tool, externally validated in two sets of data from tertiary pancreatic referral centers, to predict the presence of biliary sludge and microlithiasis in patients with an initial label of idiopathic pancreatitis with an accuracy of 0.7607 (95%CI: 0.673-0.8347), PPV of 0.7573, and NPV of 0.7857. Upon prospective validation, the prediction score will aid in decision-making on which patient to subject to EUS for diagnostic workup at a first episode of pancreatitis.

ARTICLE HIGHLIGHTS

Research background

About 30% of acute pancreatitis (AP) cases classified as idiopathic actually have a biliary and thus monocausally treatable origin.

Research motivation

To date, there is no predictive score to differentiate between idiopathic and sludge- and microlithiasis-triggered acute biliary pancreatitis. Undiagnosed biliary pancreatitis aetiology poses the risk of overdiagnosis and additional patient burden. AP triggered by small biliary concrements (microlithiasis and sludge) is a particularly challenging diagnosis.

Research objectives

The aim of this study was to develop a machine-learning based prediction score for the presence of microlithiasis and sludge in AP patients. External score validation was performed at two university pancreas centres.

Research methods

The clinical and laboratory parameters of 218 AP patients were used to calculate a machine-learning based prediction model for the presence of sludge and microlithiasis. Forty-seven patients with endosonographic evidence of sludge and microlithiasis (and no other possible underlying pancreatitis aetiology) were used in the identification cohort and compared with 171 AP patients without endosonographic evidence of sludge and microlithiasis. We trained supervised machine learning classifiers using H_2O.ai automatically selecting the best suitable predictor model to predict microlithiasis/sludge. An external pancreatitis cohort from two university pancreas centres with 117 patients was used for validation.

Research results

The score, constructed from a total of 28 simple variables to be collected in the early phase of pancreatitis-associated hospitalisation and validated externally at two university pancreas centres, can predict the presence of biliary sludge and microlithiasis with an accuracy of 0.7607 (95% confidence interval: 0.673-0.8347), positive predictive value of 0.7573, and negative predictive value of 0.7857.

Research conclusions

For the first time, we present a machine-learning based prediction score to differentiate between sludge- and microlithiasis-triggered AP and idiopathic pancreatitis. By using it in the early phase of pancreatitis-related hospitalisation, patient selection for or against the use of endosonography can support clinical decision-making.

Research perspectives

Upon prospective validation, the prediction score will aid in decision-making on which patient to subject to endosonography for diagnostic workup at a first episode of pancreatitis specifically to differentiate between sludge/microlithiasis-triggered and idiopathic AP.

FOOTNOTES

Author contributions: Sirtl S, Żorniak M, Beyer G, Schulz C, Schirra J, Mayerle J, and Mahajan UM designed this study; Sirtl S, Żorniak M, Hohmann E, Dibos M, Wandel A, Phillip V, Ammer-Herrmenau C, Neesse A, Mayerle J, and Mahajan UM contributed to the data acquisition; Sirtl S, Żorniak M, Mayerle J, and Mahajan UM were involved in the data analysis, and manuscript and figure preparation; Mahajan UM participated in the algorithmic programming and statistical analysis; Beyer G, Schulz C, and Schirra J contributed to the technical advice; and all authors approved the final version of the manuscript.

Supported by the Deutsche Forschungsgemeinschaft (German Research Foundation), No. 413635475 to Sirtl S; the LMU Munich Clinician Scientist Program; Żorniak M is supported by the United European Gastroenterology Research Fellowship.

Institutional review board statement: The study was approved by the Ethics Committee at LMU Munich (Project no.21 - 0126) and was conducted ethically in accordance with the World Medical Association Declaration of Helsinki. The Ethics Committees of the Technical University of Munich and the University Hospital of Göttingen gave their approval for the study to be conducted under the reference

numbers 2022-628-S-KH (TUM) and 14/12/22 Ü (UMG).

Informed consent statement: Not necessary due to the retrospective study design.

Conflict-of-interest statement: All the authors report no relevant conflicts of interest for this article.

Data sharing statement: All data relevant to the study are included in the article or uploaded as supplementary information.

Open-Access: This article is an open-access article that was selected by an in-house editor and fully peer-reviewed by external reviewers. It is distributed in accordance with the Creative Commons Attribution NonCommercial (CC BY-NC 4.0) license, which permits others to distribute, remix, adapt, build upon this work non-commercially, and license their derivative works on different terms, provided the original work is properly cited and the use is non-commercial. See: https://creativecommons.org/Licenses/by-nc/4.0/

Country/Territory of origin: Germany

ORCID number: Simon Sirtl 0000-0002-6047-334X; Georg Beyer 0000-0002-7607-8264; Julia Mayerle 0000-0002-3666-6459.

S-Editor: Wang JJ
L-Editor: Wang TQ
P-Editor: Wang JJ

REFERENCES

1 **Iannuzzi JP**, King JA, Leong JH, Quan J, Windsor JW, Tanyingoh D, Coward S, Forbes N, Heitman SJ, Shaheen AA, Swain M, Buie M, Underwood FE, Kaplan GG. Global Incidence of Acute Pancreatitis Is Increasing Over Time: A Systematic Review and Meta-Analysis. *Gastroenterology* 2022; **162**: 122-134 [PMID: 34571026 DOI: 10.1053/j.gastro.2021.09.043]

2 **Lee JK**, Enns R. Review of idiopathic pancreatitis. *World J Gastroenterol* 2007; **13**: 6296-6313 [PMID: 18081217 DOI: 10.3748/wjg.v13.i47.6296]

3 **Roberts SE**, Morrison-Rees S, John A, Williams JG, Brown TH, Samuel DG. The incidence and aetiology of acute pancreatitis across Europe. *Pancreatology* 2017; **17**: 155-165 [PMID: 28159463 DOI: 10.1016/j.pan.2017.01.005]

4 **Hallensleben ND**, Umans DS, Bouwense SA, Verdonk RC, Romkens TE, Witteman BJ, Schwartz MP, Spanier MB, Laheij R, van Santvoort HC, Besselink MG, van Hooft JE, Bruno MJ; Dutch Pancreatitis Study Group. The diagnostic work-up and outcomes of 'presumed' idiopathic acute pancreatitis: A post-hoc analysis of a multicentre observational cohort. *United European Gastroenterol J* 2020; **8**: 340-350 [PMID: 32213015 DOI: 10.1177/2050640619890462]

5 **Umans DS**, Rangkuti CK, Sperna Weiland CJ, Timmerhuis HC, Bouwense SAW, Fockens P, Besselink MG, Verdonk RC, van Hooft JE; Dutch Pancreatitis Study Group. Endoscopic ultrasonography can detect a cause in the majority of patients with idiopathic acute pancreatitis: a systematic review and meta-analysis. *Endoscopy* 2020; **52**: 955-964 [PMID: 32557477 DOI: 10.1055/a-1183-3370]

6 **Lee YS**, Kang BK, Hwang IK, Kim J, Hwang JH. Long-term Outcomes of Symptomatic Gallbladder Sludge. *J Clin Gastroenterol* 2015; **49**: 594-598 [PMID: 25127114 DOI: 10.1097/MCG.0000000000000202]

7 **Chebli JM**, Duarte Gaburri P, Meirelles de Souza AF, de Castro Ferreira LE, Andrade Chebli L, Ferrari AP Jr, Martins das Neves M. "Idiopathic" acute pancreatitis due to biliary sludge: prevention of relapses by endoscopic biliary sphincterotomy in high-risk patients. *Am J Gastroenterol* 2000; **95**: 3008-3009 [PMID: 11051405 DOI: 10.1111/j.1572-0241.2000.03232.x]

8 **Cohen JF**, Korevaar DA, Altman DG, Bruns DE, Gatsonis CA, Hooft L, Irwig L, Levine D, Reitsma JB, de Vet HC, Bossuyt PM. STARD 2015 guidelines for reporting diagnostic accuracy studies: explanation and elaboration. *BMJ Open* 2016; **6**: e012799 [PMID: 28137831 DOI: 10.1136/bmjopen-2016-012799]

9 **Working Group IAP/APA Acute Pancreatitis Guidelines**. IAP/APA evidence-based guidelines for the management of acute pancreatitis. *Pancreatology* 2013; **13**: e1-15 [PMID: 24054878 DOI: 10.1016/j.pan.2013.07.063]

10 **Beyer G**, Hoffmeister A, Michl P, Gress TM, Huber W, Algül H, Neesse A, Meining A, Seufferlein TW, Rosendahl J, Kahl S, Keller J, Werner J, Friess H, Bufler P, Löhr MJ, Schneider A, Lynen Jansen P, Esposito I, Grenacher L, Mössner J, Lerch MM, Mayerle J; Collaborators:. S3-Leitlinie Pankreatitis – Leitlinie der Deutschen Gesellschaft für Gastroenterologie, Verdauungs- und Stoffwechselkrankheiten (DGVS) – September 2021 – AWMF Registernummer 021-003. *Z Gastroenterol* 2022; **60**: 419-521 [PMID: 35263785 DOI: 10.1055/a-1735-3864]

11 **Collins GS**, Reitsma JB, Altman DG, Moons KG. Transparent reporting of a multivariable prediction model for individual prognosis or diagnosis (TRIPOD): the TRIPOD Statement. *BMC Med* 2015; **13**: 1 [PMID: 25563062 DOI: 10.1186/s12916-014-0241-z]

12 **Kim HJ**, Kim MH, Bae JS, Lee SS, Seo DW, Lee SK. Idiopathic acute pancreatitis. *J Clin Gastroenterol* 2003; **37**: 238-250 [PMID: 12960724 DOI: 10.1097/00004836-200309000-00010]

13 **Del Vecchio Blanco G**, Gesuale C, Varanese M, Monteleone G, Paoluzi OA. Idiopathic acute pancreatitis: a review on etiology and diagnostic work-up. *Clin J Gastroenterol* 2019; **12**: 511-524 [PMID: 31041651 DOI: 10.1007/s12328-019-00987-7]

14 **Umans DS**, Timmerhuis HC, Hallensleben ND, Bouwense SA, Anten MG, Bhalla A, Bijlsma RA, Boermeester MA, Brink MA, Hol L, Bruno MJ, Curvers WL, van Dullemen HM, van Eijck BC, Erkelens GW, Fockens P, van Geenen EJM, Hazen WL, Hoge CV, Inderson A, Kager LM, Kuiken SD, Perk LE, Poley JW, Quispel R, Römkens TE, van Santvoort HC, Tan AC, Thijssen AY, Venneman NG, Vleggaar FP, Voorburg AM, van Wanrooij RL, Witteman BJ, Verdonk RC, Besselink MG, van Hooft JE; Dutch Pancreatitis Study Group. Role of endoscopic ultrasonography in the diagnostic work-up of idiopathic acute pancreatitis (PICUS): study protocol for a nationwide prospective cohort study. *BMJ Open* 2020; **10**: e035504 [PMID: 32819938 DOI: 10.1136/bmjopen-2019-035504]

15 **Oría A**, Alvarez J, Chiapetta L, Fontana JJ, Iovaldi M, Paladino A, Bianchi R, Frider B. Risk factors for acute pancreatitis in patients with migrating gallstones. *Arch Surg* 1989; **124**: 1295-1296 [PMID: 2818183 DOI: 10.1001/archsurg.1989.01410110049010]

16 **ASGE Standards of Practice Committee**, Maple JT, Ben-Menachem T, Anderson MA, Appalaneni V, Banerjee S, Cash BD, Fisher L, Harrison ME, Fanelli RD, Fukami N, Ikenberry SO, Jain R, Khan K, Krinsky ML, Strohmeyer L, Dominitz JA. The role of endoscopy in the evaluation of suspected choledocholithiasis. *Gastrointest Endosc* 2010; **71**: 1-9 [PMID: 20105473 DOI: 10.1016/j.gie.2009.09.041]

17 **Phillip V**, Huber W, Hagemes F, Lorenz S, Matheis U, Preinfalk S, Schuster T, Lippl F, Saugel B, Schmid RM. Incidence of acute pancreatitis does not increase during Oktoberfest, but is higher than previously described in Germany. *Clin Gastroenterol Hepatol* 2011; **9**: 995-1000.e3 [PMID: 21723238 DOI: 10.1016/j.cgh.2011.06.016]

18 **Umans DS**, Hallensleben ND, Verdonk RC, Bouwense SAW, Fockens P, van Santvoort HC, Voermans RP, Besselink MG, Bruno MJ, van Hooft JE; Dutch Pancreatitis Study Group. Recurrence of idiopathic acute pancreatitis after cholecystectomy: systematic review and meta-analysis. *Br J Surg* 2020; **107**: 191-199 [PMID: 31875953 DOI: 10.1002/bjs.11429]

19 **Yin M**, Zhang R, Zhou Z, Liu L, Gao J, Xu W, Yu C, Lin J, Liu X, Xu C, Zhu J. Automated Machine Learning for the Early Prediction of the Severity of Acute Pancreatitis in Hospitals. *Front Cell Infect Microbiol* 2022; **12**: 886935 [PMID: 35755847 DOI: 10.3389/fcimb.2022.886935]

20 **Jin X**, Ding Z, Li T, Xiong J, Tian G, Liu J. Comparison of MPL-ANN and PLS-DA models for predicting the severity of patients with acute pancreatitis: An exploratory study. *Am J Emerg Med* 2021; **44**: 85-91 [PMID: 33582613 DOI: 10.1016/j.ajem.2021.01.044]

21 **Choi HW**, Park HJ, Choi SY, Do JH, Yoon NY, Ko A, Lee ES. Early Prediction of the Severity of Acute Pancreatitis Using Radiologic and Clinical Scoring Systems With Classification Tree Analysis. *AJR Am J Roentgenol* 2018; **211**: 1035-1043 [PMID: 30160978 DOI: 10.2214/AJR.18.19545]

22 **Zarnescu NO**, Costea R, Zarnescu Vasiliu EC, Neagu S. Clinico-biochemical factors to early predict biliary etiology of acute pancreatitis: age, female gender, and ALT. *J Med Life* 2015; **8**: 523-526 [PMID: 26664483]

World Journal of Gastroenterology

Submit a Manuscript: https://www.f6publishing.com

World J Gastroenterol 2023 September 21; 29(35): 5154-5165

DOI: 10.3748/wjg.v29.i35.5154

ISSN 1007-9327 (print) ISSN 2219-2840 (online)

ORIGINAL ARTICLE

Clinical Trials Study

Heparanase inhibition leads to improvement in patients with acute gastrointestinal injuries induced by sepsis

Ting-Ting Chen, Jia-Jun Lv, Ling Chen, Min Li, Li-Ping Liu

Specialty type: Gastroenterology and hepatology

Provenance and peer review: Unsolicited article; Externally peer reviewed.

Peer-review model: Single blind

Peer-review report's scientific quality classification

Grade A (Excellent): A
Grade B (Very good): 0
Grade C (Good): C
Grade D (Fair): 0
Grade E (Poor): 0

P-Reviewer: Ghimire R, Nepal; Leowattana W, Thailand

Received: July 5, 2023
Peer-review started: July 5, 2023
First decision: August 10, 2023
Revised: August 23, 2023
Accepted: September 5, 2023
Article in press: September 5, 2023
Published online: September 21, 2023

Ting-Ting Chen, Jia-Jun Lv, The First Clinical Medical School of Lanzhou University, Lanzhou University, Lanzhou 730000, Gansu Province, China

Ling Chen, Min Li, Li-Ping Liu, Department of Emergency Critical Care Medicine, The First Hospital of Lanzhou University, Lanzhou 730000, Gansu Province, China

Corresponding author: Li-Ping Liu, MD, PhD, Doctor, Department of Emergency Critical Care Medicine, The First Hospital of Lanzhou University, No. 1 West Road, Donggang, Chengguan District, Lanzhou 730000, Gansu Province, China. liulipingldyy@126.com

Abstract

BACKGROUND

Patients with sepsis are at high risk for acute gastrointestinal injury (AGI), but the diagnosis and treatment of AGI due to sepsis are unsatisfactory. Heparanase (HPA) plays an important role in septic AGI (S-AGI), but its specific mechanism is not completely understood, and few clinical reports are available.

AIM

To explore the effect and mechanism of HPA inhibition in S-AGI patients.

METHODS

In our prospective clinical trial, 48 patients with S-AGI were randomly assigned to a control group to receive conventional treatment, whereas 47 patients were randomly assigned to an intervention group to receive conventional treatment combined with low molecular weight heparin. AGI grade, sequential organ failure assessment score, acute physiology and chronic health evaluation II score, D-dimer, activated partial thromboplastin time (APTT), anti-Xa factor, interleukin-6, tumour necrosis factor-α, HPA, syndecan-1 (SDC-1), LC3B (autophagy marker), intestinal fatty acid binding protein, D-lactate, motilin, gastrin, CD4/CD8, length of intensive care unit (ICU) stay, length of hospital stay and 28-d survival on the 1st, 3rd and 7th d after treatment were compared. Correlations between HPA and AGI grading as well as LC3B were compared. Receiver operator characteristic (ROC) curves were generated to evaluate the diagnostic value of HPA, intestinal fatty acid binding protein and D-lactate in S-AGI.

RESULTS

Serum HPA and SCD-1 levels were significantly reduced in the intervention group compared with the control group ($P < 0.05$). In addition, intestinal fatty

acid-binding protein, D-lactate, AGI grade, motilin, and gastrin levels and sequential organ failure assessment score were significantly decreased ($P < 0.05$) in the intervention group. However, LC3B, APTT, anti-Xa factor, and CD4/CD8 were significantly increased ($P < 0.05$) in the intervention group. No significant differences in interleukin-6, tumour necrosis factor-α, d-dimer, acute physiology and chronic health evaluation II score, length of ICU stay, length of hospital stay, or 28-d survival were noted between the two groups ($P > 0.05$). Correlation analysis revealed a significant negative correlation between HPA and LC3B and a significant positive correlation between HPA and AGI grade. ROC curve analysis showed that HPA had higher specificity and sensitivity in diagnosis of S-AGI.

CONCLUSION

HPA has great potential as a diagnostic marker for S-AGI. Inhibition of HPA activity reduces SDC-1 shedding and alleviates S-AGI symptoms. The inhibitory effect of HPA in gastrointestinal protection may be achieved by enhanced autophagy.

Key Words: Sepsis; Acute gastrointestinal injury; Heparanase; Autophagy

©The Author(s) 2023. Published by Baishideng Publishing Group Inc. All rights reserved.

Core Tip: Heparanase (HPA) plays an important role in the occurrence and development of septic acute gastrointestinal injury (S-AGI). Our experimental results show that HPA has great potential as a diagnostic marker for S-AGI. Inhibition of HPA activity reduces syndecan-1 shedding, reduces inflammatory response, improves coagulation and immune function, and alleviates S-AGI symptoms. The inhibitory effect of HPA on gastrointestinal protection may be achieved by increasing the level of autophagy.

Citation: Chen TT, Lv JJ, Chen L, Li M, Liu LP. Heparanase inhibition leads to improvement in patients with acute gastrointestinal injuries induced by sepsis. *World J Gastroenterol* 2023; 29(35): 5154-5165
URL: https://www.wjgnet.com/1007-9327/full/v29/i35/5154.htm
DOI: https://dx.doi.org/10.3748/wjg.v29.i35.5154

INTRODUCTION

Sepsis, a life-threatening condition caused by the host's dysfunctional response to infection, is a common condition in the intensive care unit (ICU) and is associated with acute organ dysfunction and a high risk of death[1]. Sepsis has become an important public health problem worldwide due to its extremely high prevalence and mortality[2-4]. The intestine is one of the organs most vulnerable to dysfunction caused by sepsis[5]. It has been reported that sepsis causes acute gastrointestinal injury (AGI) in more than 90% of patients[6] and that gastrointestinal function is an important determinant of outcome in ICU patients[7]. Thus, AGI is the central link of sepsis. During sepsis, increased cytokine levels lead to increased intestinal mucosal permeability, in which activated myosin light streptokinase increases paracellular permeability and leads to contraction or opening of tight junctions in the apical region. Increased intestinal permeability subsequently leads to increased systemic inflammation through a positive feedback loop, forming a vicious cycle[8,9]. Treatment of septic AGI (S-AGI) currently consists mainly of prevention and correction of intestinal flora disorders, administration of intestinal mototropic agents, and early restoration of intestinal nutrition. However, these treatments do not necessarily have satisfactory therapeutic results[10]. Therefore, it is of great significance to explore treatment for S-AGI.

Heparanase (HPA) is the only enzyme in the body that can degrade heparin/heparin sulfate. HPA exists in lysosomes in the form of protonase and is widely activated in the context of tumours, inflammation, injury, hypertrophic lesions and immune reactions[11,12]. HPA degrades the heparin sulfate side chain of heparan sulfate proteoglycan (HSPG) and destroys the extracellular matrix and basement membrane, thereby damaging the structural integrity of cells[13]. In addition, HPA exhibits nonenzymatic functions, including cell signaling, adhesion, and differentiation[14]. HPA plays an important role in sepsis. A recent study demonstrated that HPA expression increases during sepsis and is associated with mortality[15]. In our previous review, we reasonably hypothesized that HPA is involved in the occurrence and development of S-AGI[16]. However, the mechanism is unclear, especially in clinical practice, and needs further investigation.

Low molecular weight heparin (LMWH) derived from common heparin is widely used due to its excellent efficacy, good predictability, low risk of bleeding, and reduced number of side effects[17]. With deepening of research, LMWH has been used in other applications in addition to anticoagulation as an anti-inflammatory, anti-fibrosis, antitumour, or antiviral agent[18-20]. These actions are all achieved by inhibiting HPA. As an inhibitor of HPA, LMWH is widely used in sepsis and inflammatory bowel disease[21,22]. Therefore, LMWH was selected as the intervention drug for the intervention group. In this study, we aimed to explore whether the gastrointestinal symptoms of S-AGI patients improve after HPA suppression and whether indicators of inflammation, coagulation, immunity, and survival status improve. The

possible mechanism was also explored.

MATERIALS AND METHODS

Patients

This study was a prospective double-blind randomized controlled trial approved by the Ethics Committee of the First Hospital of Lanzhou University. The ethics number is LDYYLL2022-270. S-AGI patients in the ICU of the First Hospital of Lanzhou University were selected from March 2022 to February 2023. The flow chart is presented in Figure 1, and 95 patients were finally included in the study.

Inclusion criteria: (1) Age ≥ 18 years old, sex unrestricted; (2) Patient meets the diagnostic criteria for sepsis 3.0 [positive or suspected infection with Sequential Organ Failure Assessment (SOFA) ≥ 2 points][1]; (3) Patient meets the AGI diagnostic criteria [(ESICM) 2012 recommendation AGI severity rating][6]; and (4) Informed consent signed by the patient or his or her family.

Exclusion criteria: (1) Combined with underlying gastrointestinal diseases (tumour, tuberculosis, inflammatory diseases, *etc.*); (2) Gastrointestinal surgery; (3) Patients with terminal disease expected to die within 24 h; (4) Patients with neurogenic shock, cerebrovascular accident, or craniocerebral trauma; and (5) Patients with definite haemorrhagic disease.

Groups and treatment

Patients who met the inclusion criteria were randomly assigned to the control group or the intervention group by hierarchical randomization generated by SAS statistical software. A letter for each random number was prepared in duplicate in a blind manner and sealed. At the time of statistical analysis, the blinding was exposed twice, the first blinding involved dividing the patients into groups, and the specific drugs in each group were determined at the second blinding. However, if the patient's condition recurred or haemodynamic instability affected the patient's prognosis during the study, it was terminated, and the blinding was urgently removed.

The control group included 48 patients who received conventional treatment; 47 patients in the intervention group were treated with LMWH in addition to conventional treatment. The control group received special intensive care as needed, including oxygen or mechanical ventilation, antimicrobial therapy, vasopressor administration, fluid resuscitation, blood glucose control, nutritional support, analgesia, sedation, or renal replacement therapy. The control group did not receive heparin as the standard of care for S-AGI patients. In the intervention group, patients were administered LMWH sodium (4000 U qd, subcutaneous injection) for 7 consecutive days in addition to receiving standard treatment as described above. The control group was given the same dose of saline (subcutaneous injection) for 7 consecutive days.

Research indicators and outcome measurement

Baseline data, such as age, sex, body mass index, source of infection, indicators of infection, AGI grade, SOFA score, and Acute Physiology And Chronic Health Evaluation II (APACHE II) score, of all patients were collected at admission. Gastrointestinal functional status was observed at 1, 3 and 7 d after treatment. Specifically, AGI grading assessment, SOFA score, APACHE II score, D-dimer, activated partial thromboplastin time (APTT), and anti-Xa factor coagulation index data were collected. Serum interleukin-6 (IL-6), tumour necrosis factor-α (TNF-α), HPA, syndecan-1 (SDC-1), LC3B, intestinal fatty acid binding protein (IFABP), D-lactate, motilin and gastrin levels were measured by enzyme-linked immunosorbent assay (ELISA). CD4 and CD8 T cells were detected by flow cytometry. The length of ICU stay and length of hospital stay were assessed, as was survival status at 28 d of all patients.

ELISA

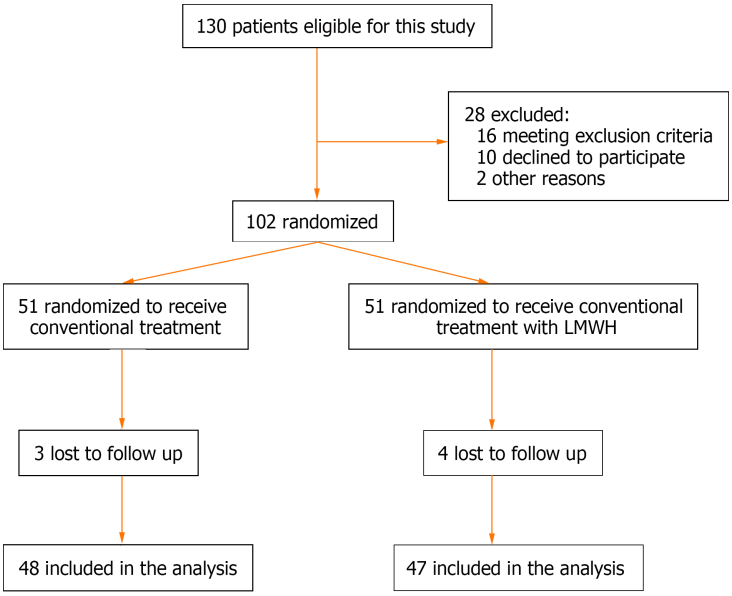
Serum samples were diluted at an appropriate ratio, and the standard working solution was configured according to the kit instructions (Elabscience, Shanghai, China). Standard, blank and sample wells were established. Then, 100 μL of standard, standard and sample diluent and serum samples to be tested were added and incubated at 37 °C for 90 min. The biotinylated antibody working solution, enzyme binding working solution, substrate solution and termination solution were added successively. After the reaction was terminated, the optical density (OD value) of each well was immediately measured based on an enzyme label at 450 nm.

Flow cytometry

FITC-labelled (the reagents were purchased from Boster, Wuhan, China) mouse anti-human CD3 antibody (2 μL), APC-labelled mouse anti-human CD4 antibody (1 μL), and PerCP/Cy5.5 mouse anti-CD8B monoclonal antibody (1 μL) were placed into flow cytometry test tubes. One hundred microlitres of whole peripheral blood was obtained and incubated at room temperature for 15 min after shaking and mixing. Then, 500 μL of haemolysin, 200 μL of phosphate buffered saline and 100 μL of fully mixed microspheres were added, and the specimens were assessed by flow cytometry. Cells were analysed by Kaluza Analysis software to obtain CD4 and CD8 T-cell counts.

Statistical analysis

Normally distributed data are expressed as the mean ± standard deviation (SD) and were compared with a t test. Nonnormally distributed data are expressed as the median (interquartile range) and were compared using the Mann-



DOI: 10.3748/wjg.v29.i35.5154 **Copyright** ©The Author(s) 2023.

Figure 1 Flow diagram of the participant selection. LMWH: Low molecular weight heparin.

Whitney *U* test. Counting data were tested using χ^2 tests. The Kolmogorov-Smirnov test was used to test the normal distribution of data. To take into account the repeated nature of the variables, analysis of variance for repeated measurements of the general linear model was implemented. Correlations were analysed using the Pearson method. The Kaplan-Meier method was used to generate a survival curve within 28 d after inclusion. The diagnostic value of HPA was evaluated by receiver operator characteristic (ROC) curve analysis. Graphs were generated using GraphPad Prism 8.0.2 software (SYSTAT, United States), and $P < 0.05$ was considered statistically significant.

RESULTS

A total of 130 patients were screened during the trial (Figure 1). Regarding loss to follow-up, 7 patients were transferred to hospitals for treatment or contact was lost after discharge and could not be followed up. In total, 95 patients with S-AGI were finally included. Of these patients, 48 were randomly assigned to the control group and 47 to the intervention group. The baseline data and clinical parameters of the patients at admission are presented in Table 1. The mean age of the control group was 59.90 ± 18.81 years old, and 68.75% were male. The mean age of patients in the intervention group was 60.98 ± 14.10 years old, and 70.21% were male. In the control group, 9 patients (18.75%) were classified as having AGI grade I, 13 patients (27.08%) as having AGI grade II, 20 patients (41.67%) as having AGI grade III, and 6 patients (12.50%) as having AGI grade IV. In the intervention group, 8 cases (17.02%), 10 cases (21.28%), 22 cases (46.81%) and 7 cases (14.89%) were classified as AGI grades I, II, III and IV, respectively. No significant differences in serum white blood cell counts or procalcitonin, HPA and SDC-1 levels were noted between the two groups ($P > 0.05$). Overall, the two groups were well balanced in terms of baseline characteristics.

LMWH effectively inhibits serum HPA and SDC-1 in S-AGI patients

The serum HPA concentration in the control group was significantly higher than that in the intervention group on the 3rd and 7th d of treatment (Figure 2A) ($P < 0.05$). Serum SDC-1 also showed a difference between the two groups on the 7th d of treatment (Figure 2B) ($P < 0.05$). The above data indicate that serum HPA and SDC-1 levels were effectively inhibited in S-AGI patients in the intervention group.

HPA inhibition improves gastrointestinal function in S-AGI patients

AGI ratings were assessed on the 1st, 3rd and 7th d after treatment (Figure 3A). The AGI grades of both groups decreased and were significantly lower in the intervention group than in the control group on the 7th d ($P < 0.05$). As shown in Table 2, the number of AGI II, III and IV patients in the intervention group was significantly lower after 7 d of treatment than after 1 and 3 d of treatment. In addition, the number of AGI II, III and IV patients were significantly lower in the intervention group than in the control group. IFABP and D-lactate are intestinal barrier biomarkers. Figures 3B and C shows that serum IFABP and D-lactate concentrations on the 7th d were significantly lower than those on the 1st d, with the concentrations in the intervention group being significantly lower than those in the control group ($P < 0.05$). Motilin and gastrin are indicators of gastrointestinal motility. As shown in Figures 3D and E, motilin and gastrin levels increased significantly in the intervention group after 7 d of treatment ($P < 0.05$). All the above data indicate that inhibition of HPA significantly improved gastrointestinal function, the intestinal barrier and gastrointestinal dynamics in S-AGI patients.

Table 1 Changes in the acute gastrointestinal injury grades of the patients in the two groups

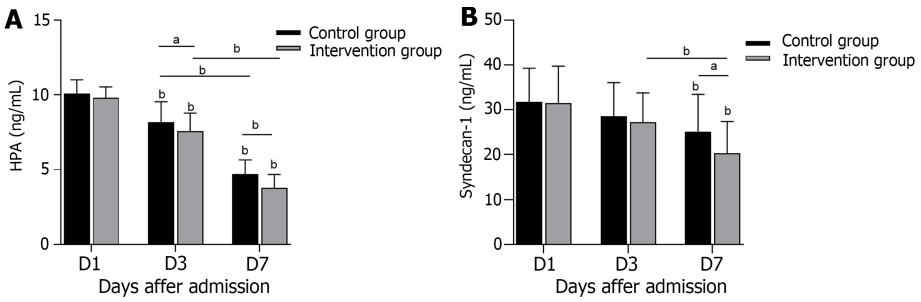
Variable	Control group (*n* = 48)	Intervention group (*n* = 47)	*P* value
Age, mean (SD), yr	59.90 (18.81)	60.98 (14.10)	0.752
Sex, male, *n* (%)	33 (68.75)	33 (70.21)	0.877
BMI, mean (SD), kg/m^2	22.62 (4.08)	23.89 (5.10)	0.788
MODS, *n* (%)	33 (68.75)	34 (72.34)	0.701
Septic shock, *n* (%)	32 (66.67)	31 (65.96)	0.942
APACHE II score, median (IQR)	22 (19, 29)	23 (19, 35)	0.966
SOFA score, median (IQR)	9 (7,10.75)	9 (7, 13)	0.871
Infection score, *n* (%)			
Lung	10 (20.83)	16 (34.04)	0.149
Urinary tract	2 (4.17)	1 (2.13)	0.57
Intra-abdominal	14 (29.17)	16 (34.04)	0.609
Central nervous system	13 (27.08)	7 (14.89)	0.145
Blood/vascular access	3 (6.25)	4 (8.51)	0.673
Other	5 (10.42)	2 (4.26)	0.25
Confirmed unknown	1 (2.08)	1 (2.13)	0.988
Initial AGI grade, *n* (%)			
I	9 (18.75)	8 (17.02)	0.826
II	13 (27.08)	10 (21.28)	0.509
III	20 (41.67)	22 (46.81)	0.614
IV	6 (12.50)	7 (14.89)	0.734
WBC, mean (SD), (10^9/L)	19.20 (9.91)	15.92 (9.65)	0.424
PCT, mean (SD), (ng/mL)	10.77 (21.64)	11.19 (17.58)	0.919
HPA, mean (SD), (ng/mL)	10.10 (0.91)	9.81 (0.72)	0.095
Syndecan-1, mean (SD), (ng/mL)	31.77 (7.49)	31.45 (8.29)	0.845

BMI: Body mass index; MODS: Multiple organ dysfunction syndrome; APACHE II: Acute physiology and chronic health evaluation II; SOFA: Sequential organ failure assessment; AGI: Acute gastrointestinal injury; HPA: Heparanase; WBC: Blood cell count; PCT: Procalcitonin; IQR: Interquartile range.

Table 2 Changes in the acute gastrointestinal injury grades of the patients in the two groups

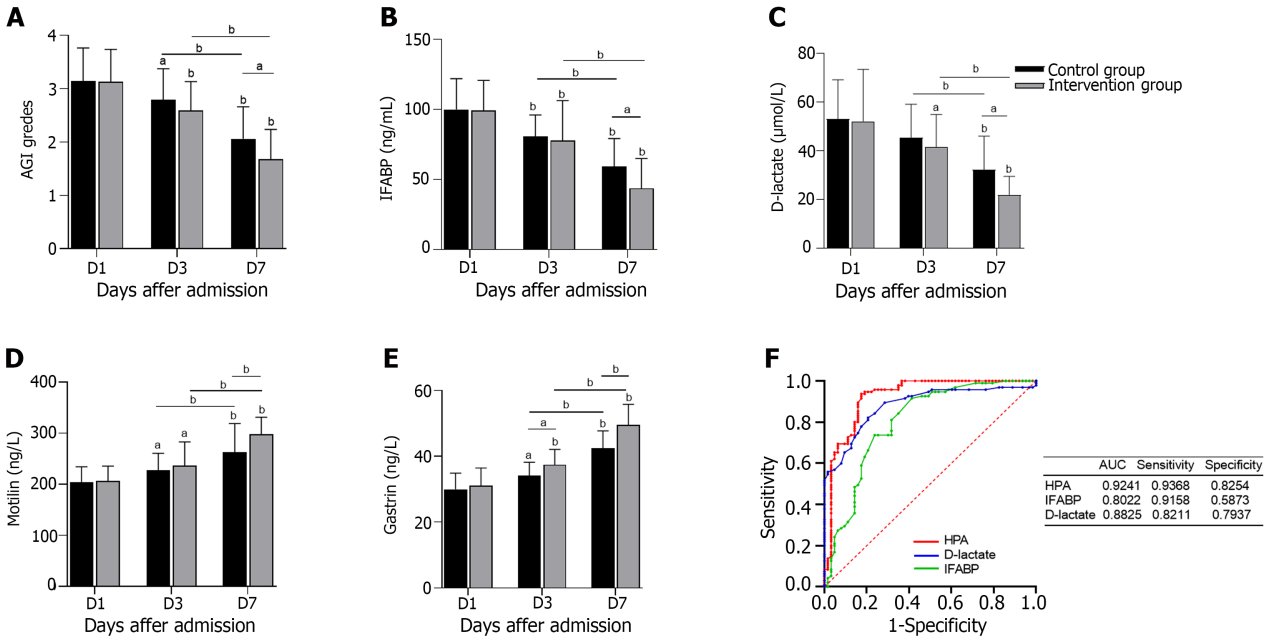
	AGI I, n (%)		AGI II, n (%)		AGI III, n (%)		AGI IV, n (%)	
	Control group	Intervention group	Control group	Intervention group	Control group	Intervention group	Control group	Intervention group
Day 1	0 (0)	0 (0)	6 (12.50)	6 (12.77)	29 (60.42)	29 (61.70)	13 (27.08)	12 (25.53)
Day 3	0 (0)	0 (0)	14 (29.17)	20 (42.55)	30 (62.50)	26 (55.32)	4 (8.33)	1 (2.13)
Day 7	7 (14.58)	17 (36.17)	31 (64.58)	28 (59.57)	10 (20.83)	2 (4.26)	0 (0)	0 (0)

AGI: Acute gastrointestinal injury.



DOI: 10.3748/wjg.v29.i35.5154 **Copyright** ©The Author(s) 2023.

Figure 2 Comparisons of heparanase and syndecan-1 levels between the two groups. A: Heparanase; B: Syndecan-1. $^{a}P < 0.05$, $^{b}P < 0.001$. HPA: Heparanase.



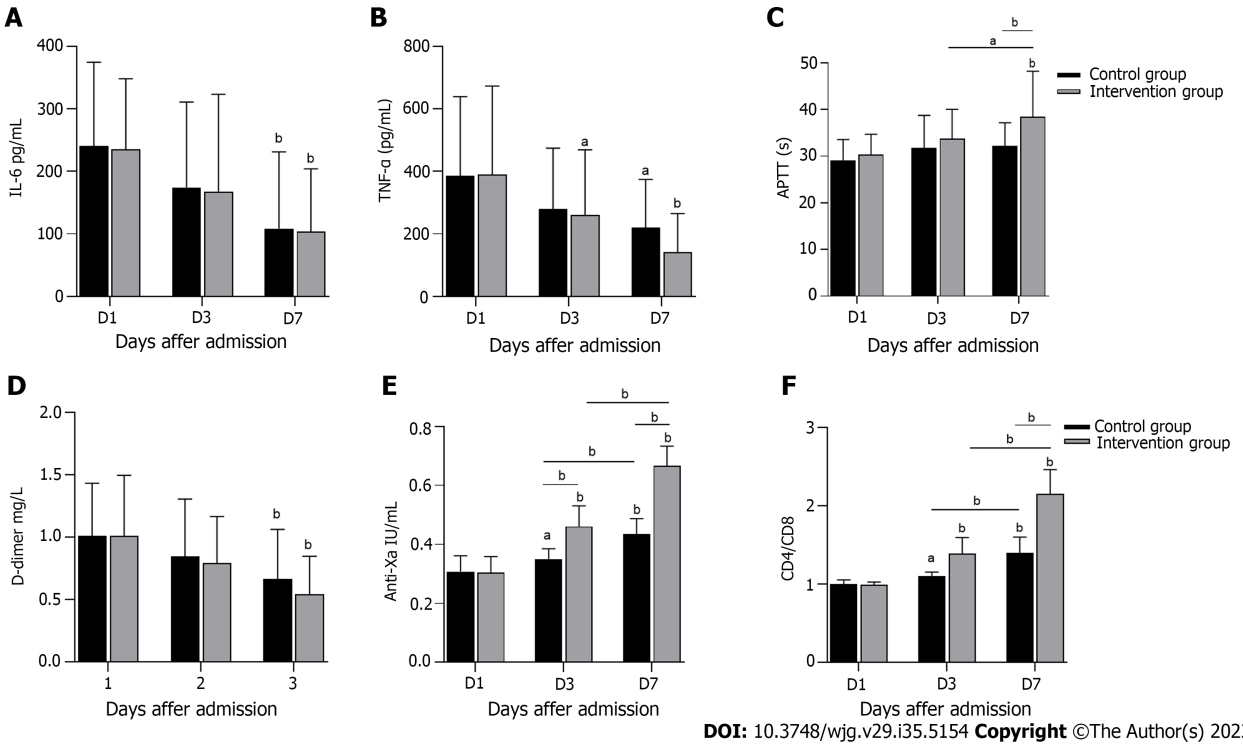
DOI: 10.3748/wjg.v29.i35.5154 **Copyright** ©The Author(s) 2023.

Figure 3 Comparisons of acute gastrointestinal injury grades, intestinal fatty acid binding protein, D-lactate, motilin, and gastrin levels between the two groups. Receiver operating characteristic curves of heparanase, D-lactate and intestinal fatty acid binding protein. A: Acute gastrointestinal injury grades; B: Intestinal fatty acid binding protein; C: D-lactate; D: Motilin; E: Gastrin; F: Receiver operating characteristic curves of heparanase, D-lactate and intestinal fatty acid binding protein. $^{a}P < 0.05$, $^{b}P < 0.001$. AGI: acute gastrointestinal injury; HPA: Heparanase; IFABP: Intestinal fatty acid binding protein; AUC: Area under the curve.

As shown in Figure 3F, we plotted ROC curves for HPA, IFABP and D-lactate and calculated their AUC values. IFABP and D-lactate are biomarkers of septic AGI, but the AUC for HPA of 0.9241 (95% confidence interval: 0.8690-0.9707) was the largest of the three. The sensitivity and specificity of HPA were 93.68% and 82.54%, respectively, and compared with the sensitivity of D-lactate (82.11% and 79.37%) and the sensitivity of IFABP (91.58% and 58.73%), HPA was still highest. These results indicate that HPA has better diagnostic efficacy in S-AGI. Overall, HPA exhibits great potential as a biomarker for S-AGI.

HPA inhibition induces anticoagulant effects and enhances immune function

Figure 4 shows the inflammation, coagulation and immune indices of the two groups after treatment. As illustrated in Figures 4A and B, IL-6 and TNF-α serum levels decreased significantly on the 7th d of treatment compared with on the 1st d ($P < 0.05$). Despite the lack of a significant difference between the two groups, levels of inflammatory cytokines in the intervention group were reduced. After 7 d of treatment, APTT and anti-Xa factor levels in the two groups increased significantly compared with those on the 1st d of treatment ($P < 0.05$), whereas D-dimer levels decreased significantly ($P < 0.05$). APTT and anti-Xa factor levels increased significantly in the intervention group compared with the control group ($P < 0.05$) (Figures 4C-E). The anticoagulation effect in the intervention group was better than that in the control group. As shown in Figure 4F, the intervention group exhibited significantly more CD4/CD8 cells than the control group ($P < 0.05$). In conclusion, compared with the control group, the intervention group exhibited better anticoagulant effects and immune enhancement effects.



DOI: 10.3748/wjg.v29.i35.5154 **Copyright** ©The Author(s) 2023.

Figure 4 Comparisons of interleukin-6, tumor necrosis factor-α, activated partial thromboplastin time, D-dimer, anti-Xa, and CD4/CD8 levels between the two groups. A: Interleukin-6; B: Tumor necrosis factor-α; C: Activated partial thromboplastin time; D: D-dimer; E: Anti-Xa; F: CD4/CD8. $^{a}P < 0.05$, $^{b}P < 0.001$. IL-6: Interleukin-6; TNF-α: Tumor necrosis factor-α; APTT: Activated partial thromboplastin time.

HPA inhibition improves gastrointestinal function in S-AGI patients through modulation of autophagy

To explore the possible mechanism by which HPA inhibition improves gastrointestinal symptoms in S-AGI patients, autophagy was assessed (Figure 5). The LC3B level of the intervention group was significantly higher than that of the control group ($P < 0.05$). As shown in Table 3, a significant negative correlation was noted between HPA and LC3B and a significant positive correlation between HPA and AGI grade. Thus, the decrease in serum HPA and SDC-1 is critical for S-AGI patients, and HPA correlates significantly with autophagy and gastrointestinal functional status.

HPA inhibition partially improves the severity score of S-AGI patients but does not shorten the length of hospital stay or improve the survival status

Within 7 d of ICU treatment, the APACHE II score and SOFA score of the two groups had significantly decreased compared to those before ICU treatment ($P < 0.05$), and the SOFA score of the intervention group was significantly lower than that of the control group on the 7th d ($P < 0.05$). However, APACHE II scores did not significantly differ between the two groups (Figures 6A and B). Figures 6C and D shows the length of ICU stay and the length of hospital stay. Although no significant difference was noted between the control group and the intervention group, both stays were shorter in the intervention group. The 28-d survival curve presented in Figure 6E demonstrates no significant difference between the two groups ($P > 0.05$). These results indicated that HPA inhibition improves the clinical severity score of patients but does not significantly improve the length of hospital stay or survival rate.

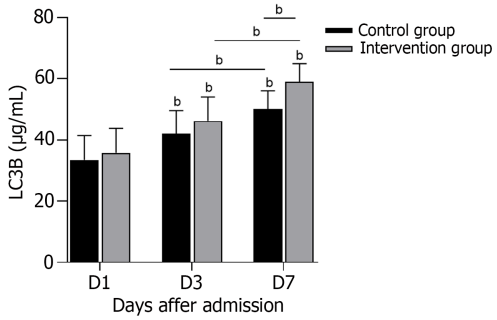
DISCUSSION

S-AGI is easily missed clinically. Complex assessment of AGI grading is not based on specific symptoms but rather includes subjective assessment of the overall development of the patient's disease. The ideal approach is to replace this grading system with one or two biomarkers[23]. Therefore, it is important to explore potential biomarkers and effective therapeutic agents for S-AGI. In this study, we selected LMWH as an intervention drug to reduce HPA levels (Figure 2). Our results indicate that HPA inhibition significantly improved the gastrointestinal functional status of S-AGI patients, reduced the AGI score, improved the intestinal mucosal barrier and gastrointestinal dynamics of patients (Figure 3 and Table 2), and contributed to their early recovery. Regarding the specific mechanism of LMWH in treatment of S-AGI, we hypothesized that LMWH inhibits HPA, protects the glycocalyx, and alleviates damage to the intestinal barrier, thus improving symptoms. This activity is not related to the direct anticoagulant properties of LMWH. Similarly, Tang *et al*[24] reported that heparin prevents caspase-11-dependent coagulation activation and reduces mortality in sepsis, regardless of its direct anticoagulant properties.

Table 3 Correlation between heparanase and LC3B and acute gastrointestinal injury grade in the two groups

		Control group				Intervention group			
		LC3B (μg/mL)		AGI grade		LC3B (μg/mL)		AGI grade	
HPA (ng/mL)	Day 1	r = -0.8394	P < 0.001	r = 0.8441	P < 0.001	r = -0.8456	P < 0.001	r = 0.7106	P < 0.001
	Day 3	r = -0.9545	P < 0.001	r = 0.7670	P < 0.001	r = -0.8882	P < 0.001	r = 0.8135	P < 0.001
	Day 7	r = -0.8258	P < 0.001	r =0.7657	P < 0.001	r = -0.8724	P < 0.001	r = 0.7839	P < 0.001

AGI: Acute gastrointestinal injury; HPA: Heparanase.



DOI: 10.3748/wjg.v29.i35.5154 **Copyright** ©The Author(s) 2023.

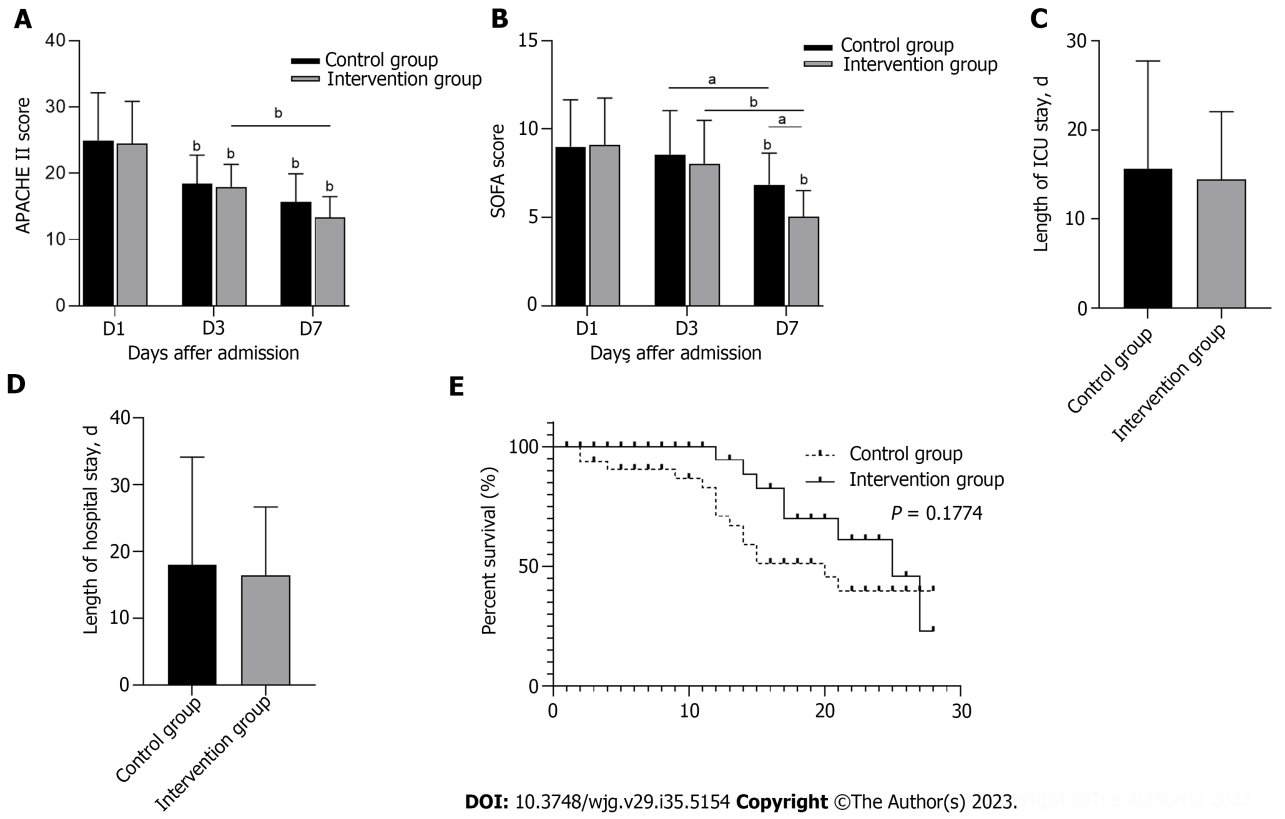
Figure 5 Comparisons of LC3B levels between the two groups. ^{b}P < 0.001.

The glycocalyx is a complex, negatively charged gel layer on one side of the lumen of endothelial cells. During sepsis, the glycocalyx becomes degraded through activation of various enzymes and/or release of reactive oxygen species[25,26]. A degraded glycocalyx induces white blood cell binding and extravasation as well as platelet recruitment, resulting in increased inflammation and increased risk of thrombosis. In addition, loss of calyx can lead to capillary leakage, which leads to oedema and reduced blood volume throughout the body. Together with thrombosis, these effects lead to tissue hydroperitoneum and organ failure[27,28]. Thus, protection of glycocalyx integrity and the intestinal barrier is essential for treatment of S-AGI. SDC-1 is a biomarker for the glycocalyx and is a transmembrane HSPG that is expressed primarily by intestinal epithelial cells; this protein is strongly associated with inflammatory processes and the integrity of the intestinal mucosa[18]. A recent meta-analysis showed that SDC-1 levels may be a useful predictor of sepsis-related complications and mortality[29]. Therefore, SDC-1 plays a crucial role in S-AGI. HPA is closely related to SDC-1, which degrades the heparin sulfate side chain of HSPG[13], accelerates shedding of SDC-1 from endothelial cells, and increases serum SDC-1 concentrations. LMWH inhibits HPA activity and prevents endothelial cell injury[28]. Therefore, our intervention results also revealed high HPA and SDC-1 levels in the context of decreased S-AGI after treatment. As HPA was significantly inhibited after conventional treatment combined with LMWH treatment, the concentrations of HPA and SDC-1 decreased more significantly (Figures 2A and B). This finding is consistent with previously reported conclusions [15,30].

Our correlation analysis revealed a significant positive correlation between HPA and AGI levels, with AGI levels decreasing significantly after LMWH inhibited HPA (Tables 2 and 3). Additionally, ROC curve analysis suggested that HPA may serve as a biomarker for S-AGI given that HPA is more specific and sensitive than IFABP and D-lactate (Figure 3F). In conclusion, our results indicate that the gastrointestinal symptoms of S-AGI patients are improved and AGI scores are reduced after HPA inhibition. HPA is expected to serve as a diagnostic biomarker for S-AGI.

In sepsis, extensive cross-talk occurs between inflammatory and clotting pathways, accompanied by overactivity and immunosuppression of the inflammatory and clotting responses, which interferes with microcirculation perfusion and leads to organ failure[31,32]. Patients with S-AGI also exhibit excessive inflammation, hypercoagulability, and immunosuppression, and these conditions improve after treatment, as shown in Figure 4. Unfortunately, there was no significant difference in inflammation between the two groups. HPA activates macrophages, leading to secretion of monocyte chemoattractant protein-1, TNF-α, and IL-1β, independent of heparin sulfate degradation activity[33], and these cytokines appear to be elevated in coronavirus disease 2019 patients[34]. It is worth mentioning that LMWH targets factor Xa to play an anticoagulant role and exhibits high anti-Xa activity[35]; hence, the anticoagulant effect in the intervention group was significantly better than that in the control group. In addition, according to the LMWH dose in our treatment plan, no associated bleeding risk was noted during patient treatment, indicating that LMWH is safe and effective. In this study, we found that CD4/CD8 levels in the intervention group were significantly increased. Therefore, HPA inhibition inhibits hypercoagulability and improves immune function in S-AGI patients.

To further investigate the possible mechanism by which HPA is reduced to improve S-AGI, we measured changes in serum LC3B levels in patients during treatment. The intervention results showed that the LC3B level was increased in the intervention group after treatment, with a significant negative correlation noted between HPA and LC3B (Figure 5,



DOI: 10.3748/wjg.v29.i35.5154 **Copyright** ©The Author(s) 2023.

Figure 6 Comparisons of Acute Physiology and Chronic Health Evaluation score, Sequential Organ Failure Assessment score, length of intensive care unit stay, length of hospital stay, and survival probability within 28 d between the two groups. A: Acute Physiology and Chronic Health Evaluation score; B: Sequential Organ Failure Assessment score; C: Length of intensive care unit stay; D: Length of hospital stay; E: Survival probability within 28 d. $^{a}P < 0.05$, $^{b}P < 0.001$. APACHE II: Acute Physiology and Chronic Health Evaluation II; SOFA: Sequential Organ Failure Assessment; ICU: Intensive care unit.

Table 3). LC3B is a marker of autophagy. Autophagy is the process by which bacteria and viruses that have escaped from phagosomes or damaged mitochondria are enclosed in vesicles, which fuse with lysosomes to form autophagosomes, followed by degradation of the contents[36]. In the early stage of sepsis, autophagy occurs in the heart, brain, lung, liver, kidney and other important organs and plays a protective role in the body. With the progression of sepsis, the body enters a period of continuous immunosuppression, and autophagy activity decreases[37]. This finding is consistent with our results. However, the results for LC3B are only indirect evidence and cannot directly show that HPA correlates completely with autophagy. Therefore, we hypothesize that HPA might aggravate S-AGI by inhibiting autophagy, and we are performing further basic experiments to test this hypothesis. LMWH inhibits HPA, thus enhancing the level of autophagy and playing a protective role in the gastrointestinal tract.

Although HPA inhibition offers many advantages, it did not significantly reduce the length of hospital stay or increase the 28-d survival rate of S-AGI patients (Figure 6). We hypothesize that the reason may be the complex aetiology of ICU patients, critical conditions, mixed interference factors during treatment, and/or the small study sample. Thus, the intervention group did not achieve our expected effect.

Finally, our experiment has some limitations: (1) Given our single-centre design and small sample size, the results may not be generalizable, and the conclusion needs to be confirmed by large-scale clinical prospective trials; (2) LMWH is not a specific HPA inhibitor, but a safe and effective specific HPA inhibitor is currently not available in clinical practice. Therefore, further development of new drugs is needed; and (3) Inhibition of HPA may enhance the level of autophagy and thus protect the gastrointestinal tract in sepsis, and this mechanism needs to be verified by basic experiments.

CONCLUSION

Our intervention results showed that LMWH inhibits HPA activity in S-AGI, reduces SDC-1 shedding, prevents endothelial cell damage, maintains intestinal epithelial cell integrity and barrier function, actively exerts anticoagulant effects, improves patients' immune function and gastrointestinal symptoms, and reduces SOFA scores. Mechanistically, HPA inhibition may play a protective role in the gastrointestinal tract by enhancing the level of autophagy. HPA represents a potential biomarker of S-AGI, and HPA inhibitors may also serve as drugs for treatment of S-AGI.

ARTICLE HIGHLIGHTS

Research background

Patients with sepsis are at high risk for acute gastrointestinal injury (AGI), heparanase (HPA) plays an important role in septic AGI (S-AGI), but its specific mechanism is not completely understood, and few clinical reports are available.

Research motivation

This study is to explore the effect and mechanism of HPA inhibition in S-AGI patients.

Research objectives

To prove the role of HPA in S-AGI and search for effective biomarkers and therapeutic targets for the diagnosis of S-AGI.

Research methods

The therapeutic effect of S-AGI patients in control group and low molecular weight heparin group was compared by a prospective double-blind randomized controlled trial. To evaluate the feasibility of HPA as a diagnostic biomarker for S-AGI.

Research results

HPA inhibitors can significantly improve AGI score, gastrointestinal function, coagulation function and immune function in S-AGI patients. The inhibitory effect of HPA in gastrointestinal protection may be achieved by enhanced autophagy.

Research conclusions

HPA has great potential as a diagnostic marker for S-AGI. Inhibition of HPA activity reduces syndecan-1 shedding and alleviates S-AGI symptoms. The inhibitory effect of HPA in gastrointestinal protection may be achieved by enhanced autophagy.

Research perspectives

HPA has great potential as a diagnostic biomarker for S-AGI, and its inhibitor is a good therapeutic drug choice in clinical practice.

FOOTNOTES

Author contributions: Chen TT collected the clinical data for data analysis and mapping and drafted the manuscript; Lv JJ collected the blood samples from the patients and performed the flow cytometry; Chen L collected blood from the patients and completed the enzyme-linked immunosorbent assays; Li M screened the research subjects and carried out clinical interventions; Liu LP participated in the experimental design, supervised the experimental process and reviewed the experimental results; and all the authors have read and approved the final manuscript.

Supported by the Science and Technology Department of Gansu Province, No. 20JR5RA35; Science and Technology Project of Gansu Province, No. 22JR10KA009; Talent Innovation and Entrepreneurship Project of Science and Technology Bureau of Chengguan District, Lanzhou, No. 2020RCCX0030; and Lanzhou Science and Technology Development Guiding Plan Project, No. 2019-ZD-37.

Institutional review board statement: The study was reviewed and approved by the Ethics Committee of Clinical Research (drugs, devices) of The First Hospital of Lanzhou University.

Clinical trial registration statement: This study is registered at Chinese Clinical Trial Registry (https://www.chictr.org.cn/). The registration identification number is ChiCTR2300072241.

Informed consent statement: All study participants or their legal guardians agreed to be enrolled in the study and provided consent (written or oral).

Conflict-of-interest statement: All the authors report no relevant conflicts of interest for this article.

Data sharing statement: This study is registered at Chinese Clinical Trial Registry (https://www.chictr.org.cn/), and the data is shared on this platform.

CONSORT 2010 statement: The authors have read the CONSORT 2010 Statement, and the manuscript was prepared and revised according to the CONSORT 2010 Statement.

Open-Access: This article is an open-access article that was selected by an in-house editor and fully peer-reviewed by external reviewers. It is distributed in accordance with the Creative Commons Attribution NonCommercial (CC BY-NC 4.0) license, which permits others to distribute, remix, adapt, build upon this work non-commercially, and license their derivative works on different terms, provided the original work is properly cited and the use is non-commercial. See: https://creativecommons.org/Licenses/by-nc/4.0/

Country/Territory of origin: China

ORCID number: Li-Ping Liu 0000-0002-8339-0256.

S-Editor: Wang JJ
L-Editor: A
P-Editor: Cai YX

REFERENCES

1 **Singer M**, Deutschman CS, Seymour CW, Shankar-Hari M, Annane D, Bauer M, Bellomo R, Bernard GR, Chiche JD, Coopersmith CM, Hotchkiss RS, Levy MM, Marshall JC, Martin GS, Opal SM, Rubenfeld GD, van der Poll T, Vincent JL, Angus DC. The Third International Consensus Definitions for Sepsis and Septic Shock (Sepsis-3). *JAMA* 2016; **315**: 801-810 [PMID: 26903338 DOI: 10.1001/jama.2016.0287]

2 **Angus DC**, Linde-Zwirble WT, Lidicker J, Clermont G, Carcillo J, Pinsky MR. Epidemiology of severe sepsis in the United States: analysis of incidence, outcome, and associated costs of care. *Crit Care Med* 2001; **29**: 1303-1310 [PMID: 11445675 DOI: 10.1097/00003246-200107000-00002]

3 **Liu V**, Escobar GJ, Greene JD, Soule J, Whippy A, Angus DC, Iwashyna TJ. Hospital deaths in patients with sepsis from 2 independent cohorts. *JAMA* 2014; **312**: 90-92 [PMID: 24838355 DOI: 10.1001/jama.2014.5804]

4 **Cecconi M**, Evans L, Levy M, Rhodes A. Sepsis and septic shock. *Lancet* 2018; **392**: 75-87 [PMID: 29937192 DOI: 10.1016/S0140-6736(18)30696-2]

5 **Rudd KE**, Johnson SC, Agesa KM, Shackelford KA, Tsoi D, Kievlan DR, Colombara DV, Ikuta KS, Kissoon N, Finfer S, Fleischmann-Struzek C, Machado FR, Reinhart KK, Rowan K, Seymour CW, Watson RS, West TE, Marinho F, Hay SI, Lozano R, Lopez AD, Angus DC, Murray CJL, Naghavi M. Global, regional, and national sepsis incidence and mortality, 1990-2017: analysis for the Global Burden of Disease Study. *Lancet* 2020; **395**: 200-211 [PMID: 31954465 DOI: 10.1016/S0140-6736(19)32989-7]

6 **Reintam Blaser A**, Malbrain ML, Starkopf J, Fruhwald S, Jakob SM, De Waele J, Braun JP, Poeze M, Spies C. Gastrointestinal function in intensive care patients: terminology, definitions and management. Recommendations of the ESICM Working Group on Abdominal Problems. *Intensive Care Med* 2012; **38**: 384-394 [PMID: 22310869 DOI: 10.1007/s00134-011-2459-y]

7 **Hu B**, Sun R, Wu A, Ni Y, Liu J, Guo F, Ying L, Ge G, Ding A, Shi Y, Liu C, Xu L, Jiang R, Lu J, Lin R, Zhu Y, Wu W, Xie B. Severity of acute gastrointestinal injury grade is a predictor of all-cause mortality in critically ill patients: a multicenter, prospective, observational study. *Crit Care* 2017; **21**: 188 [PMID: 28709443 DOI: 10.1186/s13054-017-1780-4]

8 **Sun J**, Zhang J, Wang X, Ji F, Ronco C, Tian J, Yin Y. Gut-liver crosstalk in sepsis-induced liver injury. *Crit Care* 2020; **24**: 614 [PMID: 33076940 DOI: 10.1186/s13054-020-03327-1]

9 **Yoseph BP**, Klingensmith NJ, Liang Z, Breed ER, Burd EM, Mittal R, Dominguez JA, Petrie B, Ford ML, Coopersmith CM. Mechanisms of Intestinal Barrier Dysfunction in Sepsis. *Shock* 2016; **46**: 52-59 [PMID: 27299587 DOI: 10.1097/SHK.0000000000000565]

10 **Chen FQ**, Xu WZ, Gao HY, Wu LJ, Zhang H, Cheng L, Mei JQ. Clinical effect of Changweishu on gastrointestinal dysfunction in patients with sepsis. *J Int Med Res* 2020; **48**: 300060520919579 [PMID: 32847444 DOI: 10.1177/0300060520919579]

11 **Vlodavsky I**, Friedmann Y, Elkin M, Aingorn H, Atzmon R, Ishai-Michaeli R, Bitan M, Pappo O, Peretz T, Michal I, Spector L, Pecker I. Mammalian heparanase: gene cloning, expression and function in tumor progression and metastasis. *Nat Med* 1999; **5**: 793-802 [PMID: 10395325 DOI: 10.1038/10518]

12 **Lerner I**, Hermano E, Zcharia E, Rodkin D, Bulvik R, Doviner V, Rubinstein AM, Ishai-Michaeli R, Atzmon R, Sherman Y, Meirovitz A, Peretz T, Vlodavsky I, Elkin M. Heparanase powers a chronic inflammatory circuit that promotes colitis-associated tumorigenesis in mice. *J Clin Invest* 2011; **121**: 1709-1721 [PMID: 21490396 DOI: 10.1172/JCI43792]

13 **Fernandes CL**, Escouto GB, Verli H. Structural glycobiology of heparinase II from Pedobacter heparinus. *J Biomol Struct Dyn* 2014; **32**: 1092-1102 [PMID: 23808670 DOI: 10.1080/07391102.2013.809604]

14 **Masola V**, Bellin G, Gambaro G, Onisto M. Heparanase: A Multitasking Protein Involved in Extracellular Matrix (ECM) Remodeling and Intracellular Events. *Cells* 2018; **7** [PMID: 30487472 DOI: 10.3390/cells7120236]

15 **Eustes AS**, Campbell RA, Middleton EA, Tolley ND, Manne BK, Montenont E, Rowley JW, Krauel K, Blair A, Guo L, Kosaka Y, Medeiros-de-Moraes IM, Lacerda M, Hottz ED, Neto HCF, Zimmerman GA, Weyrich AS, Petrey A, Rondina MT. Heparanase expression and activity are increased in platelets during clinical sepsis. *J Thromb Haemost* 2021; **19**: 1319-1330 [PMID: 33587773 DOI: 10.1111/jth.15266]

16 **Chen TT**, Lv JJ, Chen L, Gao YW, Liu LP. Role of heparinase in the gastrointestinal dysfunction of sepsis (Review). *Exp Ther Med* 2022; **23**: 119 [PMID: 34970342 DOI: 10.3892/etm.2021.11042]

17 **Kaczor-Kamińska M**, Stalińska K, Kamiński K, Pisarek A, Maziarz U, Feldman A, Wróbel M. Murine cellular model of mucopolysaccharidosis, type IIIB (MPS IIIB) - A preliminary study with particular emphasis on the non-oxidative l-cysteine metabolism. *Biochimie* 2020; **174**: 84-94 [PMID: 32335228 DOI: 10.1016/j.biochi.2020.04.015]

18 **Yan Y**, Ji Y, Su N, Mei X, Wang Y, Du S, Zhu W, Zhang C, Lu Y, Xing XH. Non-anticoagulant effects of low molecular weight heparins in inflammatory disorders: A review. *Carbohydr Polym* 2017; **160**: 71-81 [PMID: 28115102 DOI: 10.1016/j.carbpol.2016.12.037]

19 **Du S**, Yu Y, Xu C, Xiong H, Yang S, Yao J. LMWH and its derivatives represent new rational for cancer therapy: construction strategies and combination therapy. *Drug Discov Today* 2019; **24**: 2096-2104 [PMID: 31228613 DOI: 10.1016/j.drudis.2019.06.011]

20 **Kwon PS**, Oh H, Kwon SJ, Jin W, Zhang F, Fraser K, Hong JJ, Linhardt RJ, Dordick JS. Sulfated polysaccharides effectively inhibit SARS-CoV-2 in vitro. *Cell Discov* 2020; **6**: 50 [PMID: 32714563 DOI: 10.1038/s41421-020-00192-8]

21 **Huang Y**, Kong C. Low-molecular-weight heparin alleviates sepsis-induced renal inflammatory response and improves kidney function. *Minerva Med* 2020; **111**: 292-295 [PMID: 31282138 DOI: 10.23736/S0026-4806.19.06188-3]

22 **Ahmad A**, Vaghasiya K, Kumar A, Alam P, Raza SS, Verma RK, Khan R. Enema based therapy using liposomal formulation of low molecular weight heparin for treatment of active ulcerative colitis: New adjunct therapeutic opportunity. *Mater Sci Eng C Mater Biol Appl* 2021; **121**: 111851 [PMID: 33579485 DOI: 10.1016/j.msec.2020.111851]

23 **Reintam Blaser A**, Padar M, Mändul M, Elke G, Engel C, Fischer K, Giabicani M, Gold T, Hess B, Hiesmayr M, Jakob SM, Loudet CI, Meesters DM, Mongkolpun W, Paugam-Burtz C, Poeze M, Preiser JC, Renberg M, Rooijackers O, Tamme K, Wernerman J, Starkopf J. Development of the Gastrointestinal Dysfunction Score (GIDS) for critically ill patients - A prospective multicenter observational study (iSOFA study). *Clin Nutr* 2021; **40**: 4932-4940 [PMID: 34358839 DOI: 10.1016/j.clnu.2021.07.015]

24 **Tang Y**, Wang X, Li Z, He Z, Yang X, Cheng X, Peng Y, Xue Q, Bai Y, Zhang R, Zhao K, Liang F, Xiao X, Andersson U, Wang H, Billiar TR, Lu B. Heparin prevents caspase-11-dependent septic lethality independent of anticoagulant properties. *Immunity* 2021; **54**: 454-467.e6 [PMID: 33561388 DOI: 10.1016/j.immuni.2021.01.007]

25 **Belousoviene E**, Kiudulaite I, Pilvinis V, Pranskunas A. Links between Endothelial Glycocalyx Changes and Microcirculatory Parameters in Septic Patients. *Life (Basel)* 2021; **11** [PMID: 34440534 DOI: 10.3390/life11080790]

26 **Patterson EK**, Cepinskas G, Fraser DD. Endothelial Glycocalyx Degradation in Critical Illness and Injury. *Front Med (Lausanne)* 2022; **9**: 898592 [PMID: 35872762 DOI: 10.3389/fmed.2022.898592]

27 **Uchimido R**, Schmidt EP, Shapiro NI. The glycocalyx: a novel diagnostic and therapeutic target in sepsis. *Crit Care* 2019; **23**: 16 [PMID: 30654825 DOI: 10.1186/s13054-018-2292-6]

28 **Iba T**, Levy JH. Derangement of the endothelial glycocalyx in sepsis. *J Thromb Haemost* 2019; **17**: 283-294 [PMID: 30582882 DOI: 10.1111/jth.14371]

29 **Sun T**, Wang Y, Wu X, Cai Y, Zhai T, Zhan Q. Prognostic Value of Syndecan-1 in the Prediction of Sepsis-Related Complications and Mortality: A Meta-Analysis. *Front Public Health* 2022; **10**: 870065 [PMID: 35480580 DOI: 10.3389/fpubh.2022.870065]

30 **Anand D**, Ray S, Srivastava LM, Bhargava S. Evolution of serum hyaluronan and syndecan levels in prognosis of sepsis patients. *Clin Biochem* 2016; **49**: 768-776 [PMID: 26953518 DOI: 10.1016/j.clinbiochem.2016.02.014]

31 **Juffermans NP**, van den Brom CE, Kleinveld DJB. Targeting Endothelial Dysfunction in Acute Critical Illness to Reduce Organ Failure. *Anesth Analg* 2020; **131**: 1708-1720 [PMID: 33186159 DOI: 10.1213/ANE.0000000000005023]

32 **van der Poll T**, Shankar-Hari M, Wiersinga WJ. The immunology of sepsis. *Immunity* 2021; **54**: 2450-2464 [PMID: 34758337 DOI: 10.1016/j.immuni.2021.10.012]

33 **Blich M**, Golan A, Arvatz G, Sebbag A, Shafat I, Sabo E, Cohen-Kaplan V, Petcherski S, Avniel-Polak S, Eitan A, Hammerman H, Aronson D, Axelman E, Ilan N, Nussbaum G, Vlodavsky I. Macrophage activation by heparanase is mediated by TLR-2 and TLR-4 and associates with plaque progression. *Arterioscler Thromb Vasc Biol* 2013; **33**: e56-e65 [PMID: 23162016 DOI: 10.1161/ATVBAHA.112.254961]

34 **Coperchini F**, Chiovato L, Croce L, Magri F, Rotondi M. The cytokine storm in COVID-19: An overview of the involvement of the chemokine/chemokine-receptor system. *Cytokine Growth Factor Rev* 2020; **53**: 25-32 [PMID: 32446778 DOI: 10.1016/j.cytogfr.2020.05.003]

35 **Park J**, Byun Y. Recent advances in anticoagulant drug delivery. *Expert Opin Drug Deliv* 2016; **13**: 421-434 [PMID: 26612251 DOI: 10.1517/17425247.2016.1125880]

36 **Ho J**, Yu J, Wong SH, Zhang L, Liu X, Wong WT, Leung CC, Choi G, Wang MH, Gin T, Chan MT, Wu WK. Autophagy in sepsis: Degradation into exhaustion? *Autophagy* 2016; **12**: 1073-1082 [PMID: 27172163 DOI: 10.1080/15548627.2016.1179410]

37 **Wen X**, Xie B, Yuan S, Zhang J. The "Self-Sacrifice" of ImmuneCells in Sepsis. *Front Immunol* 2022; **13**: 833479 [PMID: 35572571 DOI: 10.3389/fimmu.2022.833479]

World Journal of Gastroenterology

Submit a Manuscript: https://www.f6publishing.com

World J Gastroenterol 2023 September 21; 29(35): 5166-5177

DOI: 10.3748/wjg.v29.i35.5166

ISSN 1007-9327 (print) ISSN 2219-2840 (online)

ORIGINAL ARTICLE

Observational Study

Lowering the threshold of alanine aminotransferase for enhanced identification of significant hepatic injury in chronic hepatitis B patients

Hong-Sheng Yu, Hao Jiang, Ming-Kai Li, Bi-Lan Yang, Abdukyamu Smayi, Jian-Ning Chen, Bin Wu, Yi-Dong Yang

Specialty type: Gastroenterology and hepatology

Provenance and peer review: Unsolicited article; Externally peer reviewed.

Peer-review model: Single blind

Peer-review report's scientific quality classification

Grade A (Excellent): 0
Grade B (Very good): B, B
Grade C (Good): 0
Grade D (Fair): 0
Grade E (Poor): 0

P-Reviewer: Marchesini G, Italy; Sirli RLD, Romania

Received: July 2, 2023
Peer-review started: July 2, 2023
First decision: July 14, 2023
Revised: July 22, 2023
Accepted: August 31, 2023
Article in press: August 31, 2023
Published online: September 21, 2023

Hong-Sheng Yu, Hao Jiang, Ming-Kai Li, Bi-Lan Yang, Abdukyamu Smayi, Bin Wu, Yi-Dong Yang, Department of Gastroenterology, The Third Affiliated Hospital of Sun Yat-Sen University, Guangzhou 510630, Guangdong Province, China

Hong-Sheng Yu, Hao Jiang, Ming-Kai Li, Bi-Lan Yang, Abdukyamu Smayi, Bin Wu, Yi-Dong Yang, Department of Liver Disease, Guangdong Provincial Key Laboratory of Liver Disease Research, Guangzhou 510630, Guangdong Province, China

Jian-Ning Chen, Department of Pathology, The Third Affiliated Hospital of Sun Yat-Sen University, Guangzhou 510630, Guangdong Province, China

Corresponding author: Yi-Dong Yang, PhD, Associate Professor, Department of Gastroenterology, The Third Affiliated Hospital of Sun Yat-sen University, No. 600 Tianhe Road, Tianhe District, Guangzhou 510630, Guangdong Province, China. yangyd6@mail.sysu.edu.cn

Abstract

BACKGROUND

The clinical and histological features of chronic hepatitis B (CHB) patients who fall into the "grey zone (GZ)" and do not fit into conventional natural phases are unclear.

AIM

To explore the impact of varying the threshold of alanine aminotransferase (ALT) levels in identifying significant liver injury among GZ patients.

METHODS

This retrospective analysis involved a cohort of 1617 adult patients diagnosed with CHB who underwent liver biopsy. The clinical phases of CHB patients were determined based on the European Association for the Study of the Liver 2017 Clinical Practice Guidelines. GZ CHB patients were classified into four groups: GZ-A (HBeAg positive, normal ALT levels, and HBV DNA ≤ 10^7 IU/mL), GZ-B (HBeAg positive, elevated ALT levels, and HBV DNA < 10^4 or > 10^7 IU/mL), GZ-C (HBeAg negative, normal ALT levels, and HBV DNA ≥ 2000 IU/mL), and GZ-D (HBeAg negative, elevated ALT levels, and HBV DNA ≤ 2000 IU/mL). Significant hepatic injury (SHI) was defined as the presence of notable liver inflammation (≥

G2) and/or significant fibrosis (≥ S2).

RESULTS

The results showed that 50.22% of patients were classified as GZ, and 63.7% of GZ patients developed SHI. The study also found that lowering the ALT treatment thresholds to the American Association for the Study of Liver Diseases 2018 treatment criteria (35 U/L for men and 25 U/L for women) can more accurately identify patients with significant liver damage in the GZ phases. In total, the proportion of patients with ALT ≤ 40 U/L who required antiviral therapy was 64.86% [(221 + 294)/794]. When we lowered the ALT treatment threshold to the new criteria (30 U/L for men and 19 U/L for women), the same outcome was revealed, and the proportion of patients with ALT ≤ 40 U/L who required antiviral therapy was 75.44% [(401 + 198)/794]. Additionally, the proportion of SHI was 49.1% in patients under 30 years old and increased to 55.3% in patients over 30 years old (P = 0.136).

CONCLUSION

These findings suggest the importance of redefining the natural phases of CHB and using new ALT treatment thresholds for better diagnosis and management of CHB patients in the GZ phases.

Key Words: Chronic hepatitis B; Grey zone; Indeterminate phase; Alanine aminotransferase; Antiviral therapy

©The Author(s) 2023. Published by Baishideng Publishing Group Inc. All rights reserved.

Core Tip: In clinical practice, 27.8%-55% of chronic hepatitis B patients fall into the "grey zone" or "indeterminate phase" that does not meet the diagnostic criteria of the traditional stages. Additionally, there is still debate regarding how best to treat these grey zone (GZ) patients and the advantages of antiviral therapy. Hence, we evaluated the clinical and histological characteristics, and additionally explored the impact of adjusting the threshold of alanine aminotransferase (ALT) in identifying significant liver injury among GZ patients. Based on these data, lowering ALT thresholds can more accurately identify patients with significant hepatic injury at an earlier stage and reduce the need for unnecessary liver biopsies.

Citation: Yu HS, Jiang H, Li MK, Yang BL, Smayi A, Chen JN, Wu B, Yang YD. Lowering the threshold of alanine aminotransferase for enhanced identification of significant hepatic injury in chronic hepatitis B patients. *World J Gastroenterol* 2023; 29(35): 5166-5177

URL: https://www.wjgnet.com/1007-9327/full/v29/i35/5166.htm

DOI: https://dx.doi.org/10.3748/wjg.v29.i35.5166

INTRODUCTION

Hepatitis B poses a significant global public health challenge, as evidenced by the estimated 316 million individuals worldwide who were afflicted with the hepatitis B virus (HBV) in 2019. The impact of HBV-related diseases is substantial, as they result in approximately 555000 fatalities globally, which constitutes 48.8% of all hepatitis-related deaths. Notably, hepatitis B stands as the primary cause of mortality in cases of liver cancer and ranks as the third leading cause of death in cirrhosis cases[1]. The progression of chronic hepatitis B (CHB) is a multifaceted interplay involving viral, host, and environmental factors. HBV interacts with the immune system of the host, and the infection status undergoes continuous changes as the disease progresses[2,3]. According to the European Association for the Study of the Liver (EASL) 2017 Clinical Practice Guidelines, CHB can be categorized into five phases: HBeAg-positive chronic HBV infection, HBeAg-positive CHB, HBeAg-negative chronic HBV infection, HBeAg-negative CHB and HBsAg-negative phase[4]. Antiviral treatment is recommended for patients with HBeAg-positive and HBeAg-negative CHB, while regular monitoring is suggested in HBeAg-positive and HBeAg-negative chronic HBV infection phases[4-6].

Nevertheless, in clinical practice, a considerable proportion of CHB patients (27.8%-55%) fall into the "grey zone (GZ)" or "indeterminate phase" that does not meet the diagnostic criteria for the five stages previously indicated[7-9]. Additionally, there is still debate regarding how best to treat these GZ patients and the advantages of antiviral therapy. A study from the United States showed the incidence of hepatocellular carcinoma (HCC) is higher in GZ patients than in HBeAg-negative chronic HBV infection patients (2.67% *vs* 0.61%)[7]. Furthermore, Huang *et al*[10] demonstrated a significant decrease in the risk of HCC among GZ patients who underwent antiviral therapy[10]. In contrast, another study found that none of the patients progressed to advanced fibrosis or cirrhosis, and only a small proportion (6.3%) of GZ patients transitioned to HBeAg-negative CHB, necessitating the use of antiviral therapy[11].

There is a crucial indication for receiving antiviral therapy when patients with CHB have significant liver fibrosis and/or inflammation, which are risk factors for HCC and liver-related mortality[4-6]. However, few studies have explored liver histological injury in the GZ phase[12]. Therefore, assessing the clinical and histological features may provide useful recommendations for managing the GZ phase. Moreover, an issue that complicates the management of CHB is the disagreement regarding the appropriate treatment threshold for alanine aminotransferase (ALT) levels. The American Association for the Study of Liver Diseases (AASLD) guidelines suggest that the upper normal limit (ULN) for ALT

should be 35 U/L for men and 25 U/L for women, while the EASL guidelines consider 40 U/L as the ULN[4,5]. In China, a recent publication titled "Expert opinion on expanding anti-HBV treatment for chronic hepatitis B" proposed a lower ALT threshold (30 U/L for males and 19 U/L for females) as initiating antiviral therapy in CHB patients[13]. However, the efficacy of reducing ALT thresholds in accurately identifying patients with significant liver damage at an earlier stage and mitigating the necessity for superfluous liver biopsy remains uncertain.

Therefore, using a retrospective cohort of treatment-naive CHB patients who underwent liver biopsy, we evaluated the clinical and histological characteristics, and additionally explored the impact of adjusting the threshold of ALT in identifying significant liver injury among GZ patients.

MATERIALS AND METHODS

Methods

Patient selection: Between January 2008 and December 2020, a total of 1617 consecutive adult patients (age, ≥ 18 years) diagnosed with CHB (hepatitis B surface antigen positive > 6 mo) who had undergone liver biopsy at the Third Affiliated Hospital of Sun Yat-Sen University were included in this retrospective analysis. The exclusion criteria were as follows: (1) Viral coinfection (hepatitis C virus, hepatitis D virus, or HIV); (2) Alcohol abuse (≥ 30 g of alcohol per day for men, ≥ 20 g of alcohol per day for women), nonalcoholic fatty liver disease (diagnosed by liver biopsy) and autoimmune liver disease; (3) Decompensated cirrhosis, HCC, and nonliver cancer; (4) Liver transplantation; and (5) Prior or current antiviral treatment (Supplementary Figure 1). The study was approved by the Ethics Committee of The Third Affiliated Hospital of Sun Yat-sen University. Written informed consent was obtained from each participant prior to the liver biopsy.

Definitions: The clinical phases of patients with CHB were determined in accordance with the EASL 2017 clinical practice guidelines, taking into consideration the highest HBV-DNA levels and ALT levels observed in at least two determinations within the 12 mo preceding enrolment (Supplementary Table 1)[4]. Patients who did not meet the criteria for any of the five phases were classified as GZ, with subcategories including GZ-A (HBeAg positive, normal ALT levels, and HBV DNA ≤ 10^7 IU/mL), GZ-B (HBeAg positive, elevated ALT levels, and HBV DNA < 10^4 or > 10^7 IU/mL), GZ-C (HBeAg negative, normal ALT levels, and HBV DNA ≥ 2000 IU/mL), and GZ-D (HBeAg negative, elevated ALT levels, and HBV DNA ≤ 2000 IU/mL)[9,12]. We used ALT and gamma-glutamyl transpeptidase (GGT) levels of 40 U/L and 60 U/L as the ULN, respectively[4]. The calculations were formulated as follows: Aspartate aminotransferase (AST)-to-platelet ratio index (APRI) = [AST (U/L)/ULN]/[PLT (10^9/L)] × 100; fibrosis score based on four factors (FIB-4) = [age (years) × AST (U/L)]/[PLT (10^9/L) × √ALT (U/L)]; GGT-to-platelet ratio (GPR) = [GGT (U/L)/ULN]/[PLT (10^9/L)] × 100.

Histological assessment: Ultrasonography-guided percutaneous liver biopsy was conducted using a 16-gauge disposable needle. The minimum sample length required was 15 mm, with a minimum inclusion of 6 portal tracts. Inflammation grade (G0-G4) and fibrosis stage (S0-S4) were estimated according to Scheuer's classification[14]. In accordance with the pathological staging system, significant liver inflammation and significant fibrosis were defined as ≥ G2 and ≥ S2, respectively. Significant hepatic injury (SHI) was defined as ≥ G2 and/or ≥ S2[12,15]. The biopsy samples were subjected to blind and independent observation and interpretation by two proficient pathologists. In cases where discordance arose between the two pathologists, a third pathologist, Jianning Chen, was consulted for additional evaluation, leading to a consensus being achieved through subsequent discussion.

Statistical analysis

SPSS version 25.0 software (SPSS Inc., Chicago, IL, United States) was used for statistical analyses. Continuous variables are expressed as the median and interquartile range, and categorical data are expressed as counts and percentages. Kruskal-Wallis tests and Pearson's chi-squared tests were applied to compare variables that were significantly different between groups. The independent predictors of SHI were determined by univariate and multiple logistic regression analyses. Areas under the receiver operating characteristic curve (AUROC) were calculated to investigate the diagnostic performance of the noninvasive scores and were compared by the Delong test. All P values were two-sided, and $P < 0.05$ was deemed statistically significant.

RESULTS

Distribution, clinical characteristics, and liver histological features of patients in different immune states

The baseline characteristics of the 1617 treatment-naive patients are presented in Table 1. Based on the defined criteria, 161 (9.96%) patients were classified as having HBeAg-positive chronic HBV infection, 203 (12.55%) patients were categorized as HBeAg-positive CHB, 171 (10.58%) patients were identified as having HBeAg-negative chronic HBV infection, and 270 (16.70%) patients were classified as HBeAg-negative CHB. Interestingly, 812 (50.22%) patients did not meet the criteria for any of the aforementioned phases and were therefore designated as GZ. Notably, there were significant variations in clinical characteristics across the different phases. The average age of patients with GZ was 36.0 years, with 74.1% being male. These patients had a mean HBV DNA level of 5.24 Log_{10} IU/mL and an intermediate ALT level of 37.0 U/L.

Table 1 Baseline characteristics of chronic hepatitis B patients among different immune phases

Clinical characteristics	HBeAg-positive chronic infection (*n* = 161)	HBeAg-positive chronic hepatitis (*n* = 203)	HBeAg-negative chronic infection (*n* = 171)	HBeAg-negative chronic hepatitis (*n* = 270)	Grey zone (*n* = 812)	*P* value
Age (year)	31.0 (26.0-36.0)	33.0 (27.0-39.0)	37.0 (32.0-42.0)	39.0 (33.0-45.0)	36.0 (30.0-42.0)	< 0.001
Male (%)	97 (60.2)	168 (82.8)	133 (77.8)	221 (81.9)	602 (74.1)	< 0.001
BMI (kg/m^2)	21.3 (19.1-23.0)	22.5 (20.3-24.9)	22.6 (20.3-24.5)	22.8 (20.4-25.1)	22.0 (20.0-24.4)	< 0.001
Diabetes (%)	0 (0)	3 (1.5)	4 (2.4)	10 (3.7)	14 (1.7)	0.071
HBV DNA (log_{10} IU/mL)	8.12 (7.60-8.23)	6.17 (5.38-6.61)	2.52 (2.00-2.89)	5.47 (4.50-6.31)	5.24 (3.92-7.50)	< 0.001
PLT (10^9/L)	211.0 (179.5-238.0)	185.0 (144.0-217.0)	191.0 (156.0-230.0)	185.0 (154.8-219.3)	199.0 (160.0-234.0)	< 0.001
ALT (U/L)	27.0 (21.0-33.0)	69.0 (51.0-111.0)	25.0 (19.0-31.0)	61.5 (50.0-100.3)	37.0 (27.0-59.0)	< 0.001
AST (U/L)	24.0 (21.0-31.0)	48.0 (36.0-73.0)	24.0 (20.0-29.0)	44.0 (33.0-66.0)	31.0 (24.0-45.0)	< 0.001
GGT (U/L)	18.0 (14.0-30.0)	51.0 (30.0-93.0)	25.0 (17.0-36.0)	40.0 (27.8-80.5)	29.0 (20.0-50.0)	< 0.001
Tbil (μmol/L)	12.7 (9.3-17.6)	14.1 (11.0-19.5)	12.6 (9.9-16.5)	14.4 (10.3-21.6)	13.0 (9.6-18.0)	< 0.001
ALB (g/L)	45.2 (43.3-47.6)	44.1 (41.0-46.2)	45.8 (43.7-48.0)	44.5 (41.2-46.9)	44.9 (42.3-47.0)	< 0.001
AFP (ng/mL)	2.4 (1.7-3.5)	5.1 (3.1-14.6)	2.3 (1.6-3.8)	3.8 (2.5-8.0)	3.1 (2.1-5.3)	< 0.001
PT (s)	13.4 (13.0-13.8)	13.4 (12.8-14.1)	13.4 (12.9-14.0)	13.5 (12.9-14.1)	13.4 (12.9-14.0)	0.073
APRI	0.29 (0.24-0.39)	0.69 (0.47-1.12)	0.32 (0.24-0.43)	0.63 (0.42-0.99)	0.40 (0.28-1.27)	< 0.001
FIB-4	0.72- (0.55-1.08)	1.05 (0.71-1.55)	0.92 (0.71-1.33)	1.18 (0.77-1.81)	0.93 (0.67-1.40)	< 0.001
GPR	0.23 (0.16-0.30)	0.71 (0.39-1.44)	0.32 (0.22-0.52)	0.56 (0.34-1.23)	0.37 (0.23-0.68)	< 0.001
Inflammation						< 0.001
G0-1	103 (64.0%)	35 (17.2%)	94 (55.0%)	76 (28.1%)	351 (43.2%)	
≥ G2	58 (36.0%)	168 (82.8%)	77 (45.0%)	194 (71.9%)	461 (56.8%)	
Fibrosis						< 0.001
S0-1	119 (73.9%)	64 (31.5%)	95 (55.6%)	98 (36.3%)	378 (46.6%)	
≥ S2	42 (26.1%)	139 (68.5%)	76 (44.4%)	172 (63.7%)	434 (53.4%)	
SHI						< 0.001
No	95 (59.0%)	32 (15.8%)	80 (46.8%)	63 (23.3%)	295 (36.3%)	
Yes	66 (41.0%)	171 (84.2%)	91 (53.2%)	207 (76.7%)	517 (63.7%)	

PLT: Platelet; ALT: Alanine aminotransferase; AST: Aspartate aminotransferase; BMI: Body mass index; GGT: Gamma-glutamyl transpeptidase; Tbil: Total bilirubin; ALB: Albumin; AFP: α-fetoprotein; PT: Prothrombin time; APRI: Aspartate aminotransferase-to-platelet ratio index; FIB-4: Fibrosis score based on four factors; GPR: Gamma-glutamyl transpeptidase-to-platelet ratio; SHI: Significant hepatic injury.

The clinical and liver histological characteristics are presented in Table 1 and Figure 1. In the GZ group, the proportion of significant liver inflammation (≥ G2) was 56.8%, and the proportion of significant fibrosis (≥ S2) was 53.4%. Among GZ patients, 63.7% had SHI. Higher proportions of SHI were observed in HBeAg-positive (84.2%) and HBeAg-negative (76.7%) CHB patients. However, HBeAg-positive (41.0%) and HBeAg-negative chronic HBV infection (53.2%) had lower but still relatively high proportions of SHI.

Distribution, clinical characteristics, and liver histological characteristics of patients in different GZs

The clinical characteristics of 812 GZ patients are shown in Supplementary Table 2. Among these patients, the proportion of GZ-C was the highest (41.1%), followed by GZ-B (34.6%), GZ-A (15.8%), and GZ-D (8.5%). Notably, patients in the GZ-A (35.0 years) and GZ-B (31.0 years) subgroups were younger than those in the GZ-C (40.0 years) and GZ-D (36.0 years) subgroups. Furthermore, higher HBV DNA levels were observed in GZ-B (7.86 Log10 IU/mL), followed by GZ-A (5.39 Log10 IU/mL), GZ-C (4.40 Log10 IU/mL), and GZ-D (2.40 Log10 IU/mL).

As shown in Supplementary Figure 2, HBeAg-positive GZ patients exhibited a significantly higher rate of significant liver inflammation (≥ G2) (66.1% *vs* 47.4%, $P < 0.001$) and SHI (70.4% *vs* 56.8%, $P < 0.001$) than HBeAg-negative GZ patients. However, there was no statistically significant difference in fibrosis stages between HBeAg-positive and HBeAg-

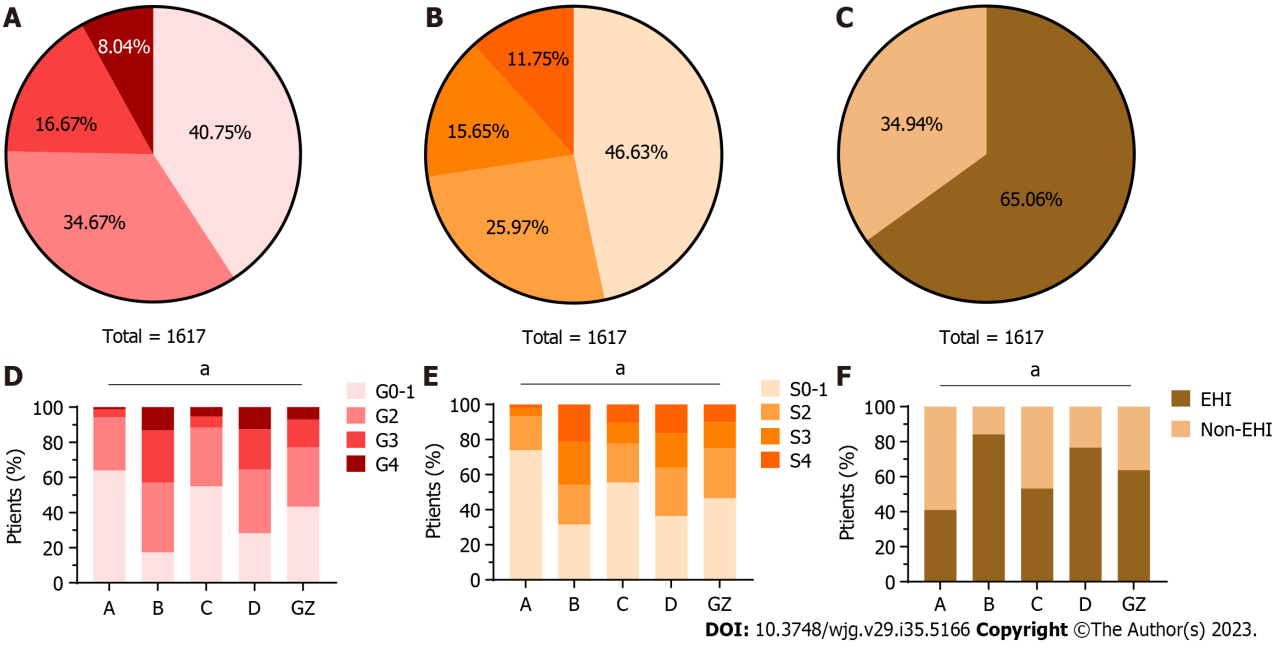


Figure 1 Distribution and liver histological features of chronic hepatitis B patients in different immune states. A and D: Proportions of liver inflammation grades in different immune status groups; B and E: Proportions of fibrosis stages in different immune status groups; C and F: Proportions of significant hepatic injury in different immune status groups. A: HBeAg-positive chronic hepatitis B virus (HBV) infection; B: HBeAg-positive chronic hepatitis B; C: HBeAg-negative chronic HBV infection; D: HBeAg-negative chronic hepatitis B; GZ: Grey zone; EHI: Evidenced hepatic injury. $^{a}P < 0.001$.

negative GZ patients (55.8% *vs* 51.2%, $P = 0.186$). The distributions of liver inflammation grades, fibrosis stages, and SHI are shown in Supplementary Table 2 and Supplementary Figure 2. The highest prevalence of significant liver inflammation (≥ G2) was observed in GZ-B (66.5%), while GZ-D (62.3%) had the highest proportion of significant fibrosis (≥ S2). In terms of SHI, the highest proportion was found in patients from GZ-B (70.5%), followed by GZ-A (70.3%), GA-D (69.6%), and GZ-C (54.2%).

Diagnostic performance of APRI, FIB-4, and GPR to detect SHI in patients with GZ

SHI was observed in 517 (63.7%) GZ patients. Of those, 288 were HBeAg-positive GZ patients, and 229 were HBeAg-negative GZ patients. In the HBeAg-positive cohort, univariate analysis indicated that PLT, ALT, AST, GGT, total bilirubin (Tbil), albumin (ALB), and prothrombin time(PT) were associated with SHI. However, multiple logistic regression analysis indicated that only PLT, AST, GGT, and ALB remained significantly associated with SHI. For the HBeAg-negative cohort, female sex, HBV-DNA, ALT, AST, GGT, Tbil, and PT were associated with higher SHI, whereas PLT and ALB were negatively associated with this event by univariate analysis. By multiple logistic regression analysis, female sex, HBV-DNA, GGT, and PLT were associated with SHI (Supplementary Table 3 and Figure 2).

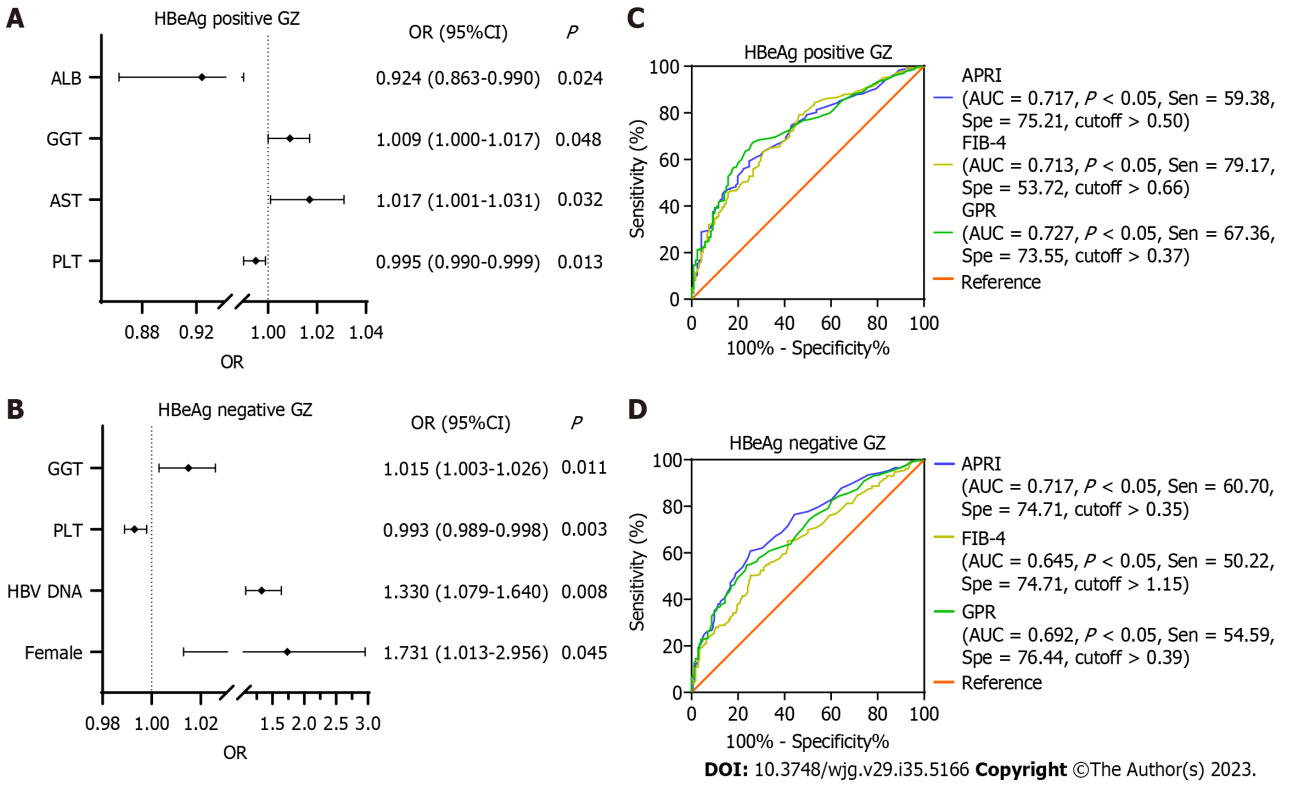
Further investigation was conducted to assess the diagnostic efficacy of established scoring systems such as APRI, FIB-4, and GPR in predicting SHI (Figure 2). The AUROCs for these three tests showed no significant difference in the HBeAg-positive GZ ($P > 0.05$). However, in HBeAg-negative GZ, APRI demonstrated superior performance compared to FIB-4 ($P < 0.001$) and was comparable to GPR ($P = 0.30$).

Effect of lowering the treatment threshold of ALT on identifying SHI

To examine the significance of lowering the treatment threshold for ALT, a total of 794 patients with normal ALT levels (ULN ≤ 40 U/L) were chosen for further investigation. The distribution of their immune states was as follows: 161 (20.28%) patients had HBeAg-positive chronic HBV infection, 128 (16.12%) patients fell within GZ-A, 171 (21.54%) patients had HBeAg-negative chronic HBV infection, and 334 (42.07%) patients were categorized under GZ-C.

Based on the AASLD 2018 criteria of the ALT antiviral treatment threshold (35 U/L for males and 25 U/L for females), we subsequently evaluated the ratio of SHI in different groups. Among the 794 chronic HBV infections, more than one-quarter of them (221/794, 27.8%) were above the AASLD criteria (Figure 3A). Of these 221 individuals, 29.2% (47/161) with HBeAg-positive chronic HBV infection, 36.7% (47/128) with GZ-A, 21.1% (36/171) with HBeAg-negative chronic HBV infection, and 27.2% (91/334) with GZ-C were above this ALT threshold (Figure 3B). It is worth noting that 54.8% (121/221) of patients had significant liver inflammation (≥ G2), which was significantly higher than that of patients below the ALT threshold (43.1%, 247/573) ($P = 0.003$) (Figure 3C). In addition, the proportion of SHI in the high ALT group was significantly higher than that in the low ALT group (60.6% *vs* 51.3%, $P = 0.018$). In total, the proportion of patients with ALT ≤ 40 U/L who required antiviral therapy was 64.86% [(221 + 294)/794] according to the AASLD 2018 Clinical Practice Guidelines.

Obviously, the SHI value in patients with HBeAg-positive chronic HBV infection below the new ALT threshold was substantially lower than that of GZ-A patients above the ALT threshold (36.8% *vs* 57.4%, $P = 0.016$). The former was in the



DOI: 10.3748/wjg.v29.i35.5166 **Copyright** ©The Author(s) 2023.

Figure 2 Multiple logistic regression analysis. A: Multiple logistic regression analysis of clinical parameters of chronic hepatitis B patients in HBeAg-positive grey zones associated with significant hepatic injury; B: Multiple logistic regression analysis of clinical parameters of chronic hepatitis B patients in HBeAg-negative grey zones associated with significant hepatic injury; C: Receiver operating characteristic (ROC) curves of aspartate aminotransferase-to-platelet ratio index (APRI), fibrosis score based on four factors (FIB-4), and gamma-glutamyl transpeptidase-to-platelet ratio (GPR) in the prediction of significant hepatic injury (SHI) in HBeAg-positive grey zones; D: ROC curves of APRI, FIB-4, and GPR in the prediction of SHI in HBeAg-negative grey zones. PLT: Platelet; AST: Aspartate aminotransferase; GGT: Gamma-glutamyl transpeptidase; ALB: Albumin; APRI: Aspartate aminotransferase-to-platelet ratio index; FIB-4: Fibrosis score based on four factors; GPR: Gamma-glutamyl transpeptidase-to-platelet ratio.

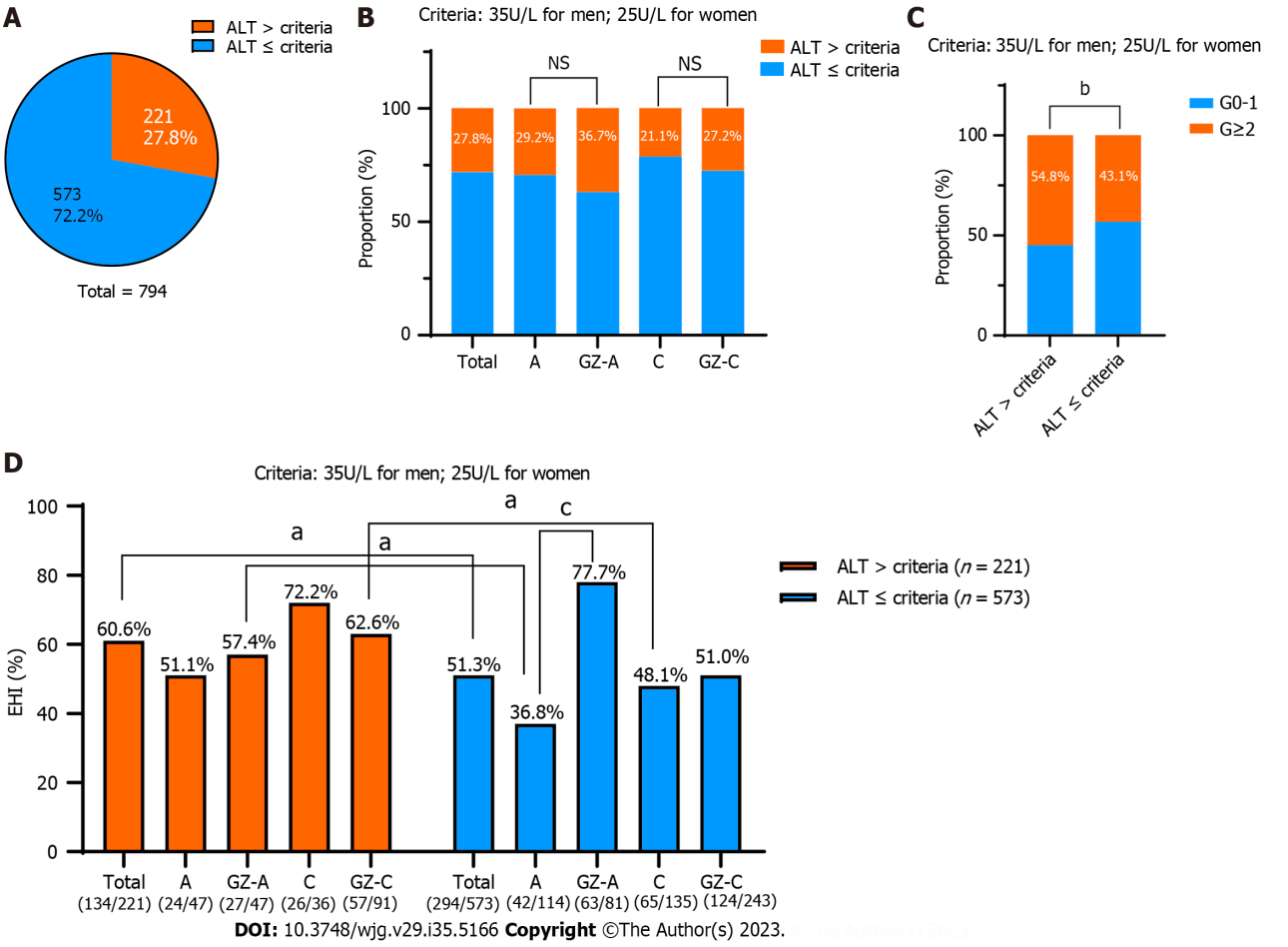
"truly" HBeAg-positive chronic HBV infection group due to high HBV DNA levels and low ALT levels. Similarly, GZ-C patients had a significantly higher SHI ratio than the "truly" HBeAg-negative chronic HBV infection patients (62.6% *vs* 48.1%, $P = 0.032$) (Figure 3D).

According to the new recommendations for the treatment threshold of ALT (30 U/L for males and 19 U/L for females), we investigated the rate of SHI in different groups separately. Among the 794 chronic HBV infections, nearly half of them (393/794, 49.5%) were below the new criteria (Figure 4A). Among these 393 patients, 46.0% (74/161) with HBeAg-positive chronic HBV infection, 36.7% (47/128) with GZ-A, 64.9% (111/171) with HBeAg-negative chronic HBV infection and 48.2% (161/334) with GZ-C were below this ALT threshold (Figure 4B). Notably, the proportions of significant liver inflammation (≥ G2) and SHI in patients above the ALT threshold were significantly higher than those in patients below the ALT threshold (50.9% *vs* 41.7%, $P = 0.01$; 57.4% *vs* 50.4%, $P = 0.049$) (Figure 4C). In total, the proportion of patients with ALT ≤ 40 U/L who required antiviral therapy was 75.44% [(401 + 198)/794] according to the "expert opinion on expanding anti-HBV treatment for chronic hepatitis B" in China.

The SHI values in patients with HBeAg-positive chronic HBV infection below the new ALT threshold was 36.4%. However, higher SHI values of 67.9% were seen in the GZ-A patients above the new ALT threshold, and the difference was statistically significant ($P < 0.001$). However, there was no significant difference in the proportion of SHI between patients with HBeAg-negative chronic HBV infection below the new ALT threshold and GZ-C patients above the new ALT threshold (45.0% *vs* 54.9%, $P = 0.105$) (Figure 4D).

An age > 30 years may not be a limitation for initiating antiviral therapy

The median age was 31, 35, 37, and 40 years for HBeAg-positive chronic HBV infection, GZ-A, HBeAg-negative chronic HBV infection, and GZ-C patients, respectively. There was an increasing trend of age in these states (Figure 5A). Among 794 patients, 76.7% (609/794) were > 30 years old, and almost 70% were HBeAg-negative patients, including 77.8% with HBeAg-negative chronic HBV infection and 88.3% with GZ-C (Figure 5B). The ratio of SHI in patients ≤ 30 years old was 49.1%, and it increased to 55.3% for those patients > 30 years old. However, there was no significant difference ($P = 0.136$). A similar result was observed in all states regardless of whether they were older or younger than 30 years old ($P > 0.05$) (Figure 5C).



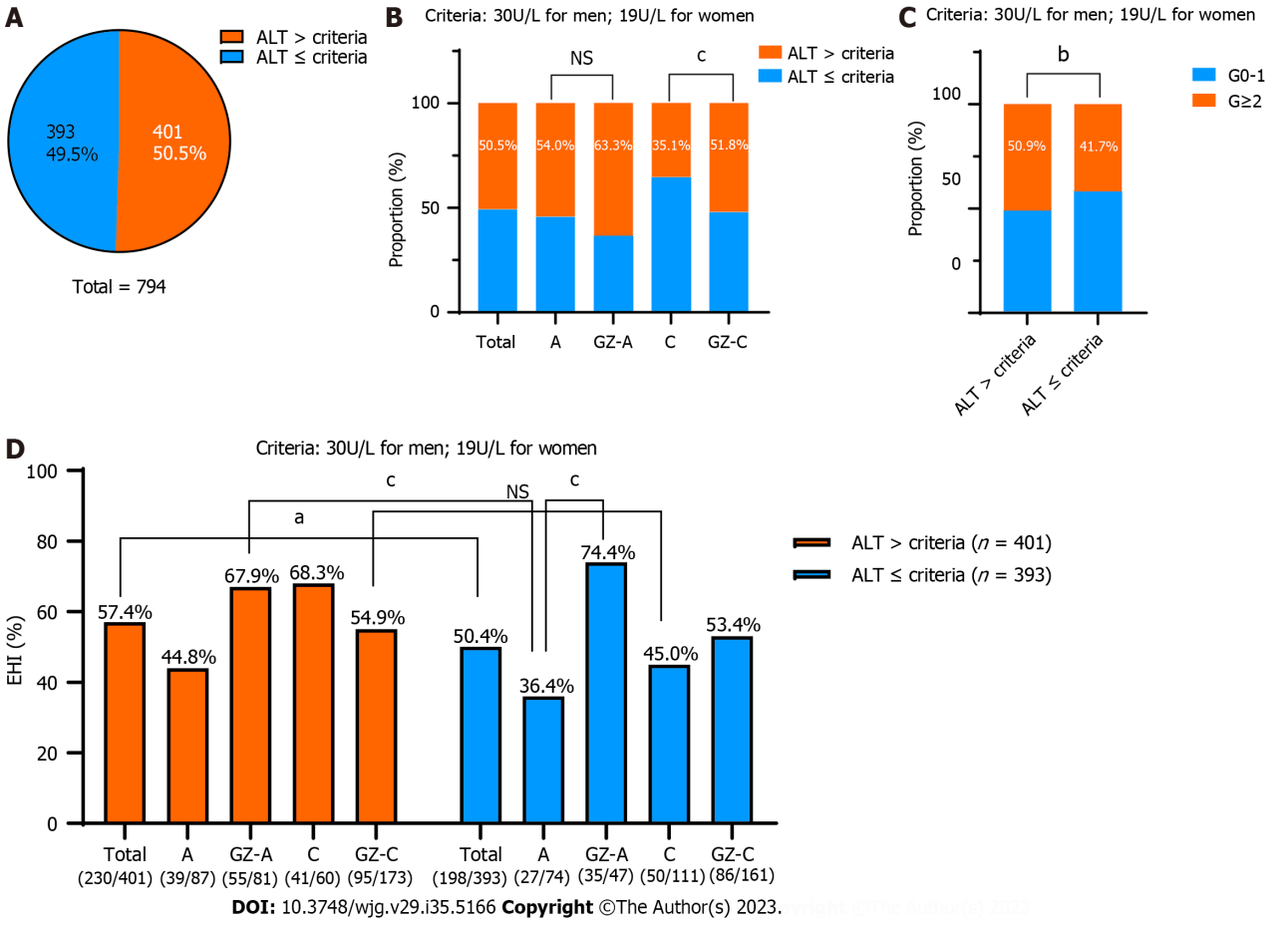
DOI: 10.3748/wjg.v29.i35.5166 **Copyright** ©The Author(s) 2023.

Figure 3 The alanine aminotransferase treatment threshold was lowered to the American Association for the Study of Liver Diseases 2018 treatment criteria (35 U/L for males and 25 U/L for females). A: Among the 794 chronic hepatitis B virus infections, 27.8% (221/794) of patients were above the American Association for the Study of Liver Diseases criteria; B: Comparison of the proportions of patients exceeding the alanine aminotransferase (ALT) threshold in different groups; C: A total of 43.1% (247/573) of patients below the ALT threshold had significant liver inflammation (≥ G2); D: The proportion of significant hepatic injury (SHI) in patients below the ALT threshold was 51.3%. Comparison of the proportions of SHI in each group. ALT: Alanine aminotransferase; NS: Not significant. $^{a}P < 0.05$, $^{b}P < 0.01$, $^{c}P < 0.001$.

DISCUSSION

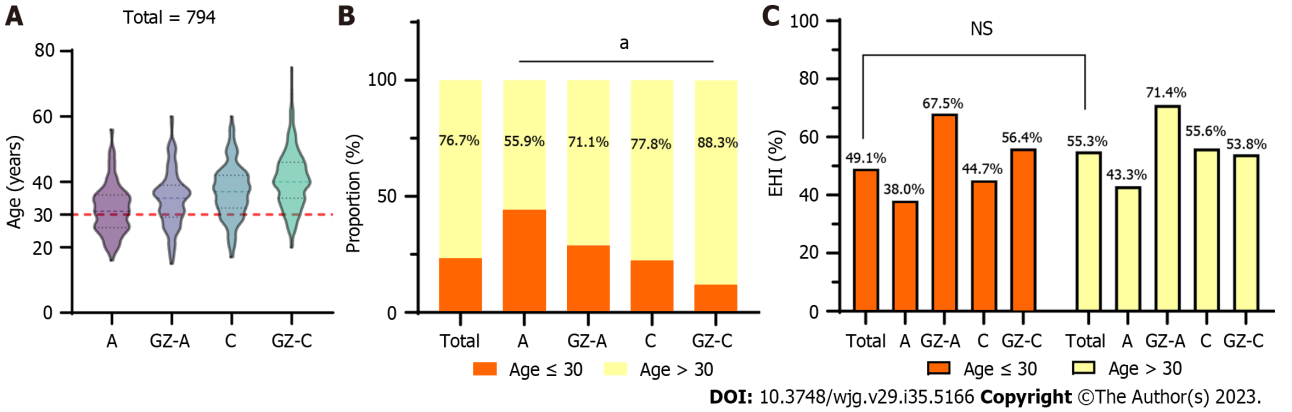
This retrospective cohort study examined a group of CHB patients who underwent liver biopsy at the Third Affiliated Hospital of Sun Yat-Sen University. The study showed that 50.22% of the patients with HBV infection fell into the GZ category, with 56.8% and 53.4% having significant liver inflammation (≥ G2) and fibrosis (≥ S2), respectively. More than half of the patients (63.7%) in the GZ category exhibited SHI, which was less than the proportion observed in HBeAg-positive and HBeAg-negative chronic hepatitis patients but more severe than those in the HBeAg-positive and HBeAg-negative chronic infection categories. While current guidelines do not require urgent antiviral therapy for GZ patients[4-6], the study findings indicated that HBeAg-positive and HBeAg-negative chronic HBV infections had relatively high proportions of SHI. The proportions were higher than those of a meta-analysis, which indicated the prevalence of significant fibrosis for chronic HBV infection as 16.9% (95%CI: 7.8-26.1) for HBeAg-positive and 24.8% (95%CI: 4.5-45.1) for HBeAg-negative chronic HBV infection[16]. This may be because the population included in the study is Asian and the genotypes are mainly B and C. Therefore, noninvasive methods, including liver biopsy, should be considered to evaluate liver inflammation and fibrosis in these individuals[17-19].

To better direct clinical diagnosis and treatment strategies, we analysed the risk factors for SHI in GZ patients. In the HBeAg-positive cohort, multiple logistic regression analysis indicated that PLT, AST, GGT, and ALB were associated with SHI. For the HBeAg-negative cohort, female sex, HBV-DNA, GGT, and PLT were associated with SHI by multiple logistic regression analysis. Based on these risk factors, we compared the diagnostic performance of APRI, FIB-4, and GPR in predicting SHI. The AUROCs of APRI, FIB-4, and GPR were 0.717, 0.713, and 0.727, respectively, in the HBeAg-positive GZ phases and 0.717, 0.645, and 0.692, respectively, in the HBeAg-negative GZ phases. Previous studies have shown that GPR provided a significantly higher AUROC than APRI and FIB-4, implying the superiority of GPR in predicting significant liver fibrosis and cirrhosis. For diagnosing significant fibrosis, the AUROCs of GPR were 0.66-0.86 and the cut-off was 0.32-0.43[20-22]. Thus, for simplicity of use in clinical practice, we advised utilizing a GPR cut-off of 0.37 as the optimal cut-off for predicting SHI in GZ patients. Treatment should be individualized for GZ patients, especially those who are over 40 years of old, HBeAg positive, and exhibit high ALT and HBV DNA levels. The state of



DOI: 10.3748/wjg.v29.i35.5166 **Copyright** ©The Author(s) 2023.

Figure 4 Lowering the alanine aminotransferase treatment threshold to new criteria (30 U/L for men and 19 U/L for women). A: Among the 794 chronic hepatitis B virus infections, 50.5% (401/794) of patients were above the new criteria; B: Comparison of the proportions of patients exceeding the alanine aminotransferase (ALT) threshold in different groups; C: A total of 41.7% (164/393) of patients below the ALT threshold had significant liver inflammation (≥ G2); D: The proportion of significant hepatic injury (SHI) in patients below the ALT threshold was 50.4%. Comparison of the proportions of SHI in each group. NS: Not significant. $^{a}P < 0.05$, $^{b}P < 0.01$, $^{c}P < 0.001$.



DOI: 10.3748/wjg.v29.i35.5166 **Copyright** ©The Author(s) 2023.

Figure 5 Comparison in different groups. A: Comparison of age in different groups; B: Comparison of the proportions of patients older than 30 years in different groups; C: The proportion of significant hepatic injury (SHI) in patients ≤ 30 years of age was 49.1%. Comparison of the proportions of SHI in each group. NS: Not significant. $^{a}P < 0.05$.

the GZ is not constant but should be dynamic. Periodic monitoring is particularly important.

The main purpose of this study was to investigate the effect of lowering the treatment threshold of ALT according to different clinical guidelines in identifying SHI patients with CHB virus infection in the GZ. A total of 794 patients with normal ALT levels (ULN ≤ 40 U/L) were selected for further investigation; of these patients, 53.90% (428/794) necessitated antiviral therapy. The proportion of patients with ALT ≤ 40 U/L who required antiviral therapy was 64.86% [(221 + 294)/794] according to the AASLD 2018 Clinical Practice Guidelines. Furthermore, the proportion of patients with

ALT ≤ 40 U/L who required antiviral therapy was 75.44% [(401 + 198)/794] according to the "expert opinion on expanding anti-HBV treatment for chronic hepatitis B" in China.

The current criteria for determining "normal" ALT levels were established based on populations that encompassed individuals with subclinical liver disease. Prati *et al*[23] propose that it is prudent to reconsider the established thresholds for ALT levels in patients diagnosed with chronic HCV infection or nonalcoholic fatty liver disease[23]. Previous studies have shown that even if the ALT level is within the normal range, the ALT level correlates with the degree of liver inflammation and fibrosis. Sonneveld *et al*[24] showed that 52% of 168 patients without liver fibrosis and 82% of 66 patients with significant liver fibrosis with normal ALT levels had mild and moderate inflammation[24]. More importantly, even if the ALT level is within the normal range, higher ALT levels have a higher incidence of decompensated cirrhosis and HCC. Compared to patients with ALT levels < 0.5 × ULN (53 U/L and 31 U/L for males and females, respectively), patients with ALT levels of 0.5-1 × ULN had an increased risk for the development of complications including ascites, spontaneous bacterial peritonitis, oesophageal varices, encephalopathy and HCC[25]. Similarly, REVEAL-HBV research demonstrated that compared to ALT < 15 U/L, patients with ALT 15-44 U/L had an increased risk of cirrhosis (aHR = 1.97, 95%CI: 1.56-2.48) and HCC (aHR = 2.45, 95%CI: 1.74-2.48)[26]. Therefore, lowering the ALT threshold in CHB patients is conducive to early initiation of antiviral therapy, which in turn reduces the incidence of cirrhosis and HCC, especially in the GZ phases.

Current studies and guidelines recommend that age > 30 years old is an independent risk factor for disease progression and can be an indication for initiating antiviral therapy. A linear correlation between age and the mortality risk of primary liver cancer, chronic liver disease and cirrhosis, and viral hepatitis was found in those whose ages ranged from 15 years to 74 years[27]. Among 794 individuals in our study with normal ALT levels (ULN ≤ 40 U/L), 23.3% of the patients were under 30 years old. The ratio of SHI in patients ≤ 30 years old was 49.1%, and it increased to 55.3% for those patients > 30 years old. However, the difference was not significant. Huang *et al*[7] showed that among patients who remained indeterminate, an age ≥ 40 years (aHR = 9.06) and ≥ 45 years (aHR = 18.40) were independently associated with HCC development[7]. This suggested that setting 30 years old as a threshold is not suitable for GZ patients. We noticed that a large proportion of CHB patients ≤ 30 years old with normal ALT levels still had inflammation and fibrosis. This finding was consistent with a previous study that noted that among 432 CHB patients with normal or mildly elevated ALT who underwent liver biopsy, the inflammation and fibrosis scores increased with age. Of these patients < 30 years old, G ≥ 2 accounted for approximately 50%, and S ≥ 2 accounted for approximately 40%[28]. Hence, age may not be a limitation for initiating antiviral therapy in patients with CHB who have normal ALT levels. Instead, more individualized attention should be given to the patient's liver inflammation and fibrosis, with the aim of reducing misdiagnosis and underdiagnosis. Additionally, patients with hepatitis B who need treatment and are at risk of disease progression should be placed on antiviral therapy in a timely manner.

Nevertheless, our study has several limitations. First, selection bias could not be ruled out because this was a retrospective and cross-sectional study. Second, the proportion of patients with SHI in this cohort may be higher than the natural population because the patients were sourced from tertiary care hospitals rather than the community, and there may be a bias in the enrolled patients. Third, because the follow-up of patients after liver biopsy was insufficient, the phase transition, benefits of antiviral therapy, and prognosis of GZ patients could not be assessed. Fourth, the study was unable to obtain information on the genotypes of all hepatitis B patients, and the limited data suggest a predominance of genotype B (65%) and genotype C (33%).

CONCLUSION

In conclusion, this study showed that 50.22% of CHB patients were in the GZ, and over half of GZ patients (63.7%) had SHI. Lowering ALT thresholds can more accurately identify patients with significant liver damage at an earlier stage and reduce the need for some unnecessary liver biopsies. Furthermore, age may not be a limitation for initiating antiviral therapy in patients with CHB who have normal ALT levels. This may have significance for refining the natural history of CHB and providing supporting evidence of lowering the antiviral therapy threshold for ALT.

ARTICLE HIGHLIGHTS

Research background

In clinical practice, a considerable proportion of chronic hepatitis B (CHB) patients (27.8%-55%) fall into the "grey zone (GZ)" or "indeterminate phase". Additionally, there is still debate regarding how best to treat these GZ patients and the advantages of antiviral therapy. Moreover, an issue that complicates the management of CHB is the disagreement regarding the appropriate treatment threshold for alanine aminotransferase (ALT) levels.

Research motivation

To explore the impact of varying the threshold of ALT levels in identifying significant hepatic injury (SHI) among GZ patients.

Research objectives

Our research evaluated the clinical and histological characteristics and additionally explored the impact of adjusting the threshold of ALT in identifying significant liver injury among GZ patients.

Research methods

This retrospective analysis involved a cohort of 1617 adult patients diagnosed with CHB who underwent liver biopsy. Significant hepatic injury was defined as the presence of notable liver inflammation (≥ G2) and/or significant fibrosis (≥ S2). Kruskal-Wallis tests and Pearson's chi-squared tests were applied to compare variables that were significantly different between groups.

Research results

The study showed that 50.22% of the patients with HBV infection fell into the GZ category, and more than half of the patients (63.7%) in the GZ category exhibited SHI. The areas under the receiver operating characteristic curves of Aspartate aminotransferase-to-platelet ratio index, fibrosis score based on four factors, and gamma-glutamyl transpeptidase-to-platelet ratio in predicting SHI were 0.717, 0.713, and 0.727, respectively, in the HBeAg-positive GZ phases and 0.717, 0.645, and 0.692, respectively, in the HBeAg-negative GZ phases. Lowering the ALT treatment thresholds to the American Association for the Study of Liver Diseases 2018 treatment criteria can more accurately identify patients with significant liver damage in the GZ phases. When we lowered the ALT treatment threshold to the new criteria, the same outcome was revealed.

Research conclusions

This study showed that 50.22% of CHB patients were in the GZ, and over half of GZ patients (63.7%) had SHI. Lowering ALT thresholds can more accurately identify patients with significant liver damage at an earlier stage and reduce the need for some unnecessary liver biopsies. Furthermore, age may not be a limitation for initiating antiviral therapy in patients with CHB who have normal ALT levels.

Research perspectives

Further investigation is needed to determine the assessment and treatment strategy for CHB patients in the GZ phases.

ACKNOWLEDGEMENTS

We would like to thank all the participants in this study.

FOOTNOTES

Author contributions: Yu HS and Jiang H have contributed equally to this work; Yu HS and Jiang H designed the study, performed the statistical analysis, and drafted the manuscript; Li MK, Yang BL, Smayi A and Chen JN collected the clinical data and then reviewed the data; Wu B and Yang YD revised the manuscript; Yang YD and Wu B were responsible for the study conception, design, data, analysis; All authors have read and approved the manuscript.

Supported by The Natural Science Foundation of Guangdong Province for Distinguished Young Scholar, No. 2022B1515020024; National Natural Science Foundation of China, No. 82070574; and The Natural Science Foundation Team Project of Guangdong Province, No. 2018B030312009.

Institutional review board statement: The study was reviewed and approved by the Third Affiliated Hospital of Sun Yat-Sen University. No. [2019]02-530-01.

Informed consent statement: All study participants provided informed written consent prior to study enrollment.

Conflict-of-interest statement: There are no conflicts of interest to report.

Data sharing statement: No additional data are available.

STROBE statement: The authors have read the STROBE Statement-checklist of items, and the manuscript was prepared and revised according to the STROBE Statement-checklist of items.

Open-Access: This article is an open-access article that was selected by an in-house editor and fully peer-reviewed by external reviewers. It is distributed in accordance with the Creative Commons Attribution NonCommercial (CC BY-NC 4.0) license, which permits others to distribute, remix, adapt, build upon this work non-commercially, and license their derivative works on different terms, provided the original work is properly cited and the use is non-commercial. See: https://creativecommons.org/Licenses/by-nc/4.0/

Country/Territory of origin: China

ORCID number: Jian-Ning Chen 0000-0002-0770-0697; Bin Wu 0000-0001-9039-9681; Yi-Dong Yang 0000-0002-3892-1687.

S-Editor: Fan JR
L-Editor: A
P-Editor: Zhao S

REFERENCES

1 **GBD 2019 Hepatitis B Collaborators**. Global, regional, and national burden of hepatitis B, 1990-2019: a systematic analysis for the Global Burden of Disease Study 2019. *Lancet Gastroenterol Hepatol* 2022; **7**: 796-829 [PMID: 35738290 DOI: 10.1016/S2468-1253(22)00124-8]
2 **Croagh CM**, Lubel JS. Natural history of chronic hepatitis B: phases in a complex relationship. *World J Gastroenterol* 2014; **20**: 10395-10404 [PMID: 25132755 DOI: 10.3748/wjg.v20.i30.10395]
3 **Fattovich G**, Bortolotti F, Donato F. Natural history of chronic hepatitis B: special emphasis on disease progression and prognostic factors. *J Hepatol* 2008; **48**: 335-352 [PMID: 18096267 DOI: 10.1016/j.jhep.2007.11.011]
4 **European Association for the Study of the Liver**. EASL 2017 Clinical Practice Guidelines on the management of hepatitis B virus infection. *J Hepatol* 2017; **67**: 370-398 [PMID: 28427875 DOI: 10.1016/j.jhep.2017.03.021]
5 **Terrault NA**, Lok ASF, McMahon BJ, Chang KM, Hwang JP, Jonas MM, Brown RS Jr, Bzowej NH, Wong JB. Update on prevention, diagnosis, and treatment of chronic hepatitis B: AASLD 2018 hepatitis B guidance. *Hepatology* 2018; **67**: 1560-1599 [PMID: 29405329 DOI: 10.1002/hep.29800]
6 **Sarin SK**, Kumar M, Lau GK, Abbas Z, Chan HL, Chen CJ, Chen DS, Chen HL, Chen PJ, Chien RN, Dokmeci AK, Gane E, Hou JL, Jafri W, Jia J, Kim JH, Lai CL, Lee HC, Lim SG, Liu CJ, Locarnini S, Al Mahtab M, Mohamed R, Omata M, Park J, Piratvisuth T, Sharma BC, Sollano J, Wang FS, Wei L, Yuen MF, Zheng SS, Kao JH. Asian-Pacific clinical practice guidelines on the management of hepatitis B: a 2015 update. *Hepatol Int* 2016; **10**: 1-98 [PMID: 26563120 DOI: 10.1007/s12072-015-9675-4]
7 **Huang DQ**, Li X, Le MH, Le AK, Yeo YH, Trinh HN, Zhang J, Li J, Wong C, Cheung RC, Yang HI, Nguyen MH. Natural History and Hepatocellular Carcinoma Risk in Untreated Chronic Hepatitis B Patients With Indeterminate Phase. *Clin Gastroenterol Hepatol* 2022; **20**: 1803-1812.e5 [PMID: 33465482 DOI: 10.1016/j.cgh.2021.01.019]
8 **Spradling PR**, Xing J, Rupp LB, Moorman AC, Gordon SC, Teshale ET, Lu M, Boscarino JA, Schmidt MA, Trinacty CM, Holmberg SD; Chronic Hepatitis Cohort Study Investigators. Distribution of disease phase, treatment prescription and severe liver disease among 1598 patients with chronic hepatitis B in the Chronic Hepatitis Cohort Study, 2006-2013. *Aliment Pharmacol Ther* 2016; **44**: 1080-1089 [PMID: 27640985 DOI: 10.1111/apt.13802]
9 **Yao K**, Liu J, Wang J, Yan X, Xia J, Yang Y, Wu W, Liu Y, Chen Y, Zhang Z, Li J, Huang R, Wu C. Distribution and clinical characteristics of patients with chronic hepatitis B virus infection in the grey zone. *J Viral Hepat* 2021; **28**: 1025-1033 [PMID: 33797145 DOI: 10.1111/jvh.13511]
10 **Huang DQ**, Tran A, Yeh ML, Yasuda S, Tsai PC, Huang CF, Dai CY, Ogawa E, Ishigami M, Ito T, Kozuka R, Enomoto M, Suzuki T, Yoshimaru Y, Preda CM, Marin RI, Sandra I, Tran S, Quek SXZ, Khine HHTW, Itokawa N, Atsukawa M, Uojima H, Watanabe T, Takahashi H, Inoue K, Maeda M, Hoang JK, Trinh L, Barnett S, Cheung R, Lim SG, Trinh HN, Chuang WL, Tanaka Y, Toyoda H, Yu ML, Nguyen MH. Antiviral therapy substantially reduces HCC risk in patients with chronic hepatitis B infection in the indeterminate phase. *Hepatology* 2023 [PMID: 37184202 DOI: 10.1097/HEP.0000000000000459]
11 **Bonacci M**, Lens S, Mariño Z, Londoño MC, Rodríguez-Tajes S, Mas A, García-López M, Pérez-Del-Pulgar S, Sánchez-Tapias JM, Forns X. Anti-viral therapy can be delayed or avoided in a significant proportion of HBeAg-negative Caucasian patients in the Grey Zone. *Aliment Pharmacol Ther* 2018; **47**: 1397-1408 [PMID: 29577350 DOI: 10.1111/apt.14613]
12 **Wang J**, Yan X, Zhu L, Liu J, Qiu Y, Li Y, Liu Y, Xue R, Zhan J, Jiang S, Geng Y, Wan Y, Li M, Mao M, Gao D, Yin S, Tong X, Xia J, Ding W, Chen Y, Li J, Zhu C, Huang R, Wu C. Significant histological disease of patients with chronic hepatitis B virus infection in the grey zone. *Aliment Pharmacol Ther* 2023; **57**: 464-474 [PMID: 36324235 DOI: 10.1111/apt.17272]
13 **Chinese Society of Hepatology**; Chinese Medical Association. [Expert opinion on expanding anti-HBV treatment for chronic hepatitis B]. *Zhonghua Gan Zang Bing Za Zhi* 2022; **30**: 131-136 [PMID: 35359064 DOI: 10.3760/cma.j.cn501113-20220209-00060]
14 **Desmet VJ**. Knodell RG, Ishak KG, Black WC, Chen TS, Craig R, Kaplowitz N, Kiernan TW, Wollman J. Formulation and application of a numerical scoring system for assessing histological activity in asymptomatic chronic active hepatitis [Hepatology 1981;1:431-435]. *J Hepatol* 2003; **38**: 382-386 [PMID: 12663226 DOI: 10.1016/s0168-8278(03)00005-9]
15 **Ren S**, Wang W, Lu J, Wang K, Ma L, Zheng Y, Zheng S, Chen X. Effect of the change in antiviral therapy indication on identifying significant liver injury among chronic hepatitis B virus infections in the grey zone. *Front Immunol* 2022; **13**: 1035923 [PMID: 36389814 DOI: 10.3389/fimmu.2022.1035923]
16 **Lin MH**, Li HQ, Zhu L, Su HY, Peng LS, Wang CY, He CP, Liang XE, Wang Y. Liver Fibrosis in the Natural Course of Chronic Hepatitis B Viral Infection: A Systematic Review with Meta-Analysis. *Dig Dis Sci* 2022; **67**: 2608-2626 [PMID: 34008117 DOI: 10.1007/s10620-021-07009-y]
17 **Lee HW**, Chan HL. Unresolved issues of immune tolerance in chronic hepatitis B. *J Gastroenterol* 2020; **55**: 383-389 [PMID: 32016713 DOI: 10.1007/s00535-020-01665-z]
18 **Howell J**, Chan HLY, Feld JJ, Hellard ME, Thompson AJ. Closing the Stable Door After the Horse Has Bolted: Should We Be Treating People With Immune-Tolerant Chronic Hepatitis B to Prevent Hepatocellular Carcinoma? *Gastroenterology* 2020; **158**: 2028-2032 [PMID: 32088205 DOI: 10.1053/j.gastro.2020.02.027]
19 **Kawanaka M**, Nishino K, Kawamoto H, Haruma K. Hepatitis B: Who should be treated?-managing patients with chronic hepatitis B during the immune-tolerant and immunoactive phases. *World J Gastroenterol* 2021; **27**: 7497-7508 [PMID: 34887645 DOI: 10.3748/wjg.v27.i43.7497]
20 **Lemoine M**, Shimakawa Y, Nayagam S, Khalil M, Suso P, Lloyd J, Goldin R, Njai HF, Ndow G, Taal M, Cooke G, D'Alessandro U, Vray M, Mbaye PS, Njie R, Mallet V, Thursz M. The gamma-glutamyl transpeptidase to platelet ratio (GPR) predicts significant liver fibrosis and cirrhosis in patients with chronic HBV infection in West Africa. *Gut* 2016; **65**: 1369-1376 [PMID: 26109530 DOI:

10.1136/gutjnl-2015-309260]

21 **Li Q**, Li W, Huang Y, Chen L. The gamma-glutamyl transpeptidase-to-platelet ratio predicts liver fibrosis and cirrhosis in HBeAg-positive chronic HBV infection patients with high HBV DNA and normal or mildly elevated alanine transaminase levels in China. *J Viral Hepat* 2016; **23**: 912-919 [PMID: 27375134 DOI: 10.1111/jvh.12563]

22 **Liu X**, Li H, Wei L, Tang Q, Hu P. Optimized cutoffs of gamma-glutamyl transpeptidase-to-platelet ratio, aspartate aminotransferase-to-platelet ratio index, and fibrosis-4 scoring systems for exclusion of cirrhosis in patients with chronic hepatitis B. *Hepatol Commun* 2022; **6**: 1664-1672 [PMID: 35312182 DOI: 10.1002/hep4.1938]

23 **Prati D**, Taioli E, Zanella A, Della Torre E, Butelli S, Del Vecchio E, Vianello L, Zanuso F, Mozzi F, Milani S, Conte D, Colombo M, Sirchia G. Updated definitions of healthy ranges for serum alanine aminotransferase levels. *Ann Intern Med* 2002; **137**: 1-10 [PMID: 12093239 DOI: 10.7326/0003-4819-137-1-200207020-00006]

24 **Sonneveld MJ**, Brouwer WP, Hansen BE, Chan HL, Piratvisuth T, Jia JD, Zeuzem S, Chien RN, Choi H, de Knegt RJ, Wat C, Pavlovic V, Gaggar A, Xie Q, Buti M, de Man RA, Janssen HLA; SONIC-B Study Group. Very low probability of significant liver inflammation in chronic hepatitis B patients with low ALT levels in the absence of liver fibrosis. *Aliment Pharmacol Ther* 2020; **52**: 1399-1406 [PMID: 32886813 DOI: 10.1111/apt.16067]

25 **Yuen MF**, Yuan HJ, Wong DK, Yuen JC, Wong WM, Chan AO, Wong BC, Lai KC, Lai CL. Prognostic determinants for chronic hepatitis B in Asians: therapeutic implications. *Gut* 2005; **54**: 1610-1614 [PMID: 15871997 DOI: 10.1136/gut.2005.065136]

26 **Lee MH**, Yang HI, Liu J, Batrla-Utermann R, Jen CL, Iloeje UH, Lu SN, You SL, Wang LY, Chen CJ; R. E.V.E.A.L.-HBV Study Group. Prediction models of long-term cirrhosis and hepatocellular carcinoma risk in chronic hepatitis B patients: risk scores integrating host and virus profiles. *Hepatology* 2013; **58**: 546-554 [PMID: 23504622 DOI: 10.1002/hep.26385]

27 **Sun Y**, Chang J, Liu X, Liu C. Mortality trends of liver diseases in mainland China over three decades: an age-period-cohort analysis. *BMJ Open* 2019; **9**: e029793 [PMID: 31712333 DOI: 10.1136/bmjopen-2019-029793]

28 **Zhao Q**, Liu K, Zhu X, Yan L, Ding Y, Xu Y, Lou S, Zhao G, Xie Q, Gao Y, Bao S, Wang H. Anti-viral effect in chronic hepatitis B patients with normal or mildly elevated alanine aminotransferase. *Antiviral Res* 2020; **184**: 104953 [PMID: 33065138 DOI: 10.1016/j.antiviral.2020.104953]

World Journal of Gastroenterology

Submit a Manuscript: https://www.f6publishing.com

World J Gastroenterol 2023 September 21; 29(35): 5178-5179

DOI: 10.3748/wjg.v29.i35.5178

ISSN 1007-9327 (print) ISSN 2219-2840 (online)

CORRECTION

Correction to "Role of prebiotics, probiotics, and synbiotics in management of inflammatory bowel disease: Current perspectives"

Supriya Roy, Suneela Dhaneshwar

Specialty type: Gastroenterology and hepatology

Provenance and peer review: Invited article; Externally peer reviewed.

Peer-review model: Single blind

Peer-review report's scientific quality classification

Grade A (Excellent): A, A
Grade B (Very good): 0
Grade C (Good): 0
Grade D (Fair): 0
Grade E (Poor): 0

P-Reviewer: Salvadori M, Italy; Zhu L, China

Received: August 16, 2023
Peer-review started: August 16, 2023
First decision: August 25, 2023
Revised: August 25, 2023
Accepted: September 1, 2023
Article in press: September 1, 2023
Published online: September 21, 2023

Supriya Roy, Department of Pharmacology, Amity Institute of Pharmacy, Lucknow, Amity University Uttar Pradesh, Noida 201303, Uttar Pradesh, India

Suneela Dhaneshwar, Department of Pharmaceutical Chemistry, Amity Institute of Pharmacy, Amity University Maharashtra, Mumbai 410206, Maharashtra, India

Corresponding author: Suneela Dhaneshwar, PhD, Academic Research, Director, Pharmacist, Professor, Department of Pharmaceutical Chemistry, Amity Institute of Pharmacy, Amity University Maharashtra, Mumbai-Pune Expressway, Bhatan, Post-Somathne, Panvel, Mumbai 410206, Maharashtra, India. suneeladhaneshwar@rediffmail.com

Abstract

Correction to "Roy S, Dhaneshwar S. Role of prebiotics, probiotics, and synbiotics in management of inflammatory bowel disease: Current perspectives. *World J Gastroenterol* 2023; 29: 2078-2100 [PMID: 37122604 DOI: 10.3748/wjg.v29.i14.2078]". In this article, a correction note is to be added.

Key Words: Ulcerative colitis; Crohn's disease; Pouchitis; Dysbiosis; Microbiota; Inflammation

©The Author(s) 2023. Published by Baishideng Publishing Group Inc. All rights reserved.

Core Tip: This manuscript is to add a "correction note" to "Roy S, Dhaneshwar S. Role of prebiotics, probiotics, and synbiotics in management of inflammatory bowel disease: Current perspectives. *World J Gastroenterol* 2023; 29: 2078-2100 [PMID: 37122604 DOI: 10.3748/wjg.v29.i14.2078]".

Citation: Roy S, Dhaneshwar S. Correction to "Role of prebiotics, probiotics, and synbiotics in management of inflammatory bowel disease: Current perspectives". *World J Gastroenterol* 2023; 29(35): 5178-5179
URL: https://www.wjgnet.com/1007-9327/full/v29/i35/5178.htm
DOI: https://dx.doi.org/10.3748/wjg.v29.i35.5178

TO THE EDITOR

Correction to: Roy S, Dhaneshwar S. Role of prebiotics, probiotics, and synbiotics in management of inflammatory bowel disease: Current perspectives. *World J Gastroenterol* 2023; 29(14): 2078-2100.

In this article, a correction note is to be added[1]. The corresponding author received a mail from Dr. Claudio De Simone sharing his concern about a probiotic formulation VSL#3 which is mentioned in this review article. Dr. Claudio wishes us to publish a corrigendum. It is an earnest request that please incorporate the following correction note and publish a corrigendum regarding the same.

Correction note: This review article includes references to several studies that investigated a probiotic formulation formerly marketed as VSL#3 which is currently, generically referred to as the "De Simone Formulation". It is important to note that the current product marketed as VSL#3 differs from the De Simone Formulation as also stated by the federal court of Maryland in the Civil Action, No. TDC-15-1356. They are distinct probiotic formulations with different compositions and characteristics. Currently, the De Simone Formulation is accessible under Vivomixx (in Europe) and Visbiome (in the United States) brand names.

FOOTNOTES

Author contributions: Dhaneshwar S conceived the idea and designed the review article protocol, edited the final draft of the manuscript; Roy S collected the data and wrote the paper; and all authors reviewed and approved the manuscript.

Conflict-of-interest statement: All the authors report no relevant conflicts of interest for this article.

Open-Access: This article is an open-access article that was selected by an in-house editor and fully peer-reviewed by external reviewers. It is distributed in accordance with the Creative Commons Attribution NonCommercial (CC BY-NC 4.0) license, which permits others to distribute, remix, adapt, build upon this work non-commercially, and license their derivative works on different terms, provided the original work is properly cited and the use is non-commercial. See: https://creativecommons.org/Licenses/by-nc/4.0/

Country/Territory of origin: India

ORCID number: Supriya Roy 0000-0002-8676-5113; Suneela Dhaneshwar 0000-0001-7646-642X.

S-Editor: Fan JR
L-Editor: A
P-Editor: Fan JR

REFERENCES

1 **Roy S**, Dhaneshwar S. Role of prebiotics, probiotics, and synbiotics in management of inflammatory bowel disease: Current perspectives. *World J Gastroenterol* 2023; **29**: 2078-2100 [PMID: 37122604 DOI: 10.3748/wjg.v29.i14.2078]



Published by **Baishideng Publishing Group Inc**
7041 Koll Center Parkway, Suite 160, Pleasanton, CA 94566, USA
Telephone: +1-925-3991568
E-mail: bpgoffice@wjgnet.com
Help Desk: https://www.f6publishing.com/helpdesk
https://www.wjgnet.com



© 2023 Baishideng Publishing Group Inc. All rights reserved.

ISSN 1007-9327 (print)
ISSN 2219-2840 (online)

World Journal of *Gastroenterology*

World J Gastroenterol 2023 September 28; 29(36): 5180-5267



Published by Baishideng Publishing Group Inc

World Journal of Gastroenterology

Contents

Weekly Volume 29 Number 36 September 28, 2023

REVIEW

5180 Liver metastases: The role of magnetic resonance imaging

Maino C, Vernuccio F, Cannella R, Cortese F, Franco PN, Gaetani C, Giannini V, Inchingolo R, Ippolito D, Defeudis A, Pilato G, Tore D, Faletti R, Gatti M

MINIREVIEWS

5198 Clinical approach to indeterminate biliary strictures: Clinical presentation, diagnosis, and workup

Yadlapati S, Mulki R, Sánchez-Luna SA, Ahmed AM, Kyanam Kabir Baig KR, Peter S

5211 Integration and implementation of precision medicine in the multifaceted inflammatory bowel disease

Jagirdhar GSK, Perez JA, Perez AB, Surani S

ORIGINAL ARTICLE

Basic Study

5226 Curcumin alleviated dextran sulfate sodium-induced colitis by recovering memory Th/Tfh subset balance

Zheng LX, Guo KE, Huang JQ, Liu MH, Deng BL, Liu DY, Zhou BG, Zhou W, Zhong YB, Zhao HM

META-ANALYSIS

5240 Diagnostic value of methylated branched chain amino acid transaminase 1/IKAROS family zinc finger 1 for colorectal cancer

Xu K, Yu AR, Pan SB, He J

SCIENTOMETRICS

5254 Intestinal barrier in inflammatory bowel disease: A bibliometric and knowledge-map analysis

Zhou F, Wu NZ, Xie Y, Zhou XJ

World Journal of Gastroenterology

Weekly Volume 29 Number 36 September 28, 2023

Contents

ABOUT COVER

Editorial Board Member of *World Journal of Gastroenterology*, Pietro Fusaroli, MD, Associate Professor, Department of Medical and Surgical Sciences, University of Bologna/Hospital of Imola, Imola (BO), via Montericco 4, Bologna 40026, Italy. pietro.fusaroli@unibo.it

AIMS AND SCOPE

The primary aim of *World Journal of Gastroenterology* (*WJG*, *World J Gastroenterol*) is to provide scholars and readers from various fields of gastroenterology and hepatology with a platform to publish high-quality basic and clinical research articles and communicate their research findings online. *WJG* mainly publishes articles reporting research results and findings obtained in the field of gastroenterology and hepatology and covering a wide range of topics including gastroenterology, hepatology, gastrointestinal endoscopy, gastrointestinal surgery, gastrointestinal oncology, and pediatric gastroenterology.

INDEXING/ABSTRACTING

The *WJG* is now abstracted and indexed in Science Citation Index Expanded (SCIE), MEDLINE, PubMed, PubMed Central, Scopus, Reference Citation Analysis, China Science and Technology Journal Database, and Superstar Journals Database. The 2023 edition of Journal Citation Reports® cites the 2022 impact factor (IF) for *WJG* as 4.3; Quartile category: Q2. The *WJG*'s CiteScore for 2021 is 8.3.

RESPONSIBLE EDITORS FOR THIS ISSUE

Production Editor: *Yu-Xi Chen*; **Production Department Director:** *Xu Guo*; **Editorial Office Director:** *Jia-Ru Fan*.

NAME OF JOURNAL

World Journal of Gastroenterology

ISSN

ISSN 1007-9327 (print) ISSN 2219-2840 (online)

LAUNCH DATE

October 1, 1995

FREQUENCY

Weekly

EDITORS-IN-CHIEF

Andrzej S Tarnawski

EXECUTIVE ASSOCIATE EDITORS-IN-CHIEF

Xian-Jun Yu (Pancreatic Oncology), Jian-Gao Fan (Chronic Liver Disease), Hou-Bao Liu (Biliary Tract Disease), Naohisa Yoshida (Gastrointestinal Endoscopy)

EDITORIAL BOARD MEMBERS

http://www.wjgnet.com/1007-9327/editorialboard.htm

PUBLICATION DATE

September 28, 2023

COPYRIGHT

© 2023 Baishideng Publishing Group Inc

PUBLISHING PARTNER

Shanghai Pancreatic Cancer Institute and Pancreatic Cancer Institute, Fudan University
Biliary Tract Disease Institute, Fudan University

INSTRUCTIONS TO AUTHORS

https://www.wjgnet.com/bpg/gerinfo/204

GUIDELINES FOR ETHICS DOCUMENTS

https://www.wjgnet.com/bpg/GerInfo/287

GUIDELINES FOR NON-NATIVE SPEAKERS OF ENGLISH

https://www.wjgnet.com/bpg/gerinfo/240

PUBLICATION ETHICS

https://www.wjgnet.com/bpg/GerInfo/288

PUBLICATION MISCONDUCT

https://www.wjgnet.com/bpg/gerinfo/208

POLICY OF CO-AUTHORS

https://www.wjgnet.com/bpg/GerInfo/310

ARTICLE PROCESSING CHARGE

https://www.wjgnet.com/bpg/gerinfo/242

STEPS FOR SUBMITTING MANUSCRIPTS

https://www.wjgnet.com/bpg/GerInfo/239

ONLINE SUBMISSION

https://www.f6publishing.com

PUBLISHING PARTNER's OFFICIAL WEBSITE

https://www.shca.org.cn
https://www.zs-hospital.sh.cn

© 2023 Baishideng Publishing Group Inc. All rights reserved. 7041 Koll Center Parkway, Suite 160, Pleasanton, CA 94566, USA

E-mail: bpgoffice@wjgnet.com https://www.wjgnet.com

World Journal of Gastroenterology

Submit a Manuscript: https://www.f6publishing.com

World J Gastroenterol 2023 September 28; 29(36): 5180-5197

DOI: 10.3748/wjg.v29.i36.5180

ISSN 1007-9327 (print) ISSN 2219-2840 (online)

REVIEW

Liver metastases: The role of magnetic resonance imaging

Cesare Maino, Federica Vernuccio, Roberto Cannella, Francesco Cortese, Paolo Niccolò Franco, Clara Gaetani, Valentina Giannini, Riccardo Inchingolo, Davide Ippolito, Arianna Defeudis, Giulia Pilato, Davide Tore, Riccardo Faletti, Marco Gatti

Specialty type: Gastroenterology and hepatology

Provenance and peer review: Invited article; Externally peer reviewed.

Peer-review model: Single blind

Peer-review report's scientific quality classification

Grade A (Excellent): 0
Grade B (Very good): 0
Grade C (Good): C, C
Grade D (Fair): 0
Grade E (Poor): 0

P-Reviewer: Xiao B, China; Zhang H, China

Received: July 30, 2023
Peer-review started: July 30, 2023
First decision: August 15, 2023
Revised: August 28, 2023
Accepted: September 11, 2023
Article in press: September 11, 2023
Published online: September 28, 2023

Cesare Maino, Paolo Niccolò Franco, Davide Ippolito, Department of Radiology, Fondazione IRCCS San Gerardo dei Tintori, Monza 20900, Italy

Federica Vernuccio, University Hospital of Padova, Institute of Radiology, Padova 35128, Italy

Roberto Cannella, Giulia Pilato, Department of Biomedicine, Neuroscience and Advanced Diagnostics (BiND), University of Palermo, Palermo 90127, Italy

Francesco Cortese, Riccardo Inchingolo, Unit of Interventional Radiology, F Miulli Hospital, Acquaviva delle Fonti 70021, Italy

Clara Gaetani, Valentina Giannini, Arianna Defeudis, Davide Tore, Riccardo Faletti, Marco Gatti, Department of Surgical Sciences, University of Turin, Turin 10126, Italy

Davide Ippolito, School of Medicine, University of Milano Bicocca, Milano 20100, Italy

Corresponding author: Marco Gatti, MD, Assistant Professor, Doctor, Department of Surgical Sciences, University of Turin, Via Genova 3, Turin 10126, Italy. marcogatti17@gmail.com

Abstract

The liver is one of the organs most commonly involved in metastatic disease, especially due to its unique vascularization. It's well known that liver metastases represent the most common hepatic malignant tumors. From a practical point of view, it's of utmost importance to evaluate the presence of liver metastases when staging oncologic patients, to select the best treatment possible, and finally to predict the overall prognosis. In the past few years, imaging techniques have gained a central role in identifying liver metastases, thanks to ultrasonography, contrast-enhanced computed tomography (CT), and magnetic resonance imaging (MRI). All these techniques, especially CT and MRI, can be considered the non-invasive reference standard techniques for the assessment of liver involvement by metastases. On the other hand, the liver can be affected by different focal lesions, sometimes benign, and sometimes malignant. On these bases, radiologists should face the differential diagnosis between benign and secondary lesions to correctly allocate patients to the best management. Considering the above-mentioned principles, it's extremely important to underline and refresh the broad spectrum of liver metastases features that can occur in everyday clinical practice. This review aims to summarize the most common imaging features of liver metastases, with a special focus on typical and atypical appearance, by using MRI.

Key Words: Liver metastases; Magnetic resonance imaging; Gadolinium; Gd-EOB-DTPA; Gadoxetate disodium; Liver specific contrast agents; Hepatobiliary contrast agents

©The Author(s) 2023. Published by Baishideng Publishing Group Inc. All rights reserved.

Core Tip: To better detect liver metastases, magnetic resonance imaging (MRI) protocol should be correctly performed, using extra-cellular or hepatobiliary contrast agents. Even if conventional non-enhanced techniques can help depict focal liver lesions, contras-enhanced sequences are mandatory, to evaluate their behavior in comparison to the healthy liver parenchyma. These aspects allow to determine liver and hepatic lesions' vascularization over time and increase radiologists' diagnostic values. The typical appearance of liver metastases can be easily recognized as hypovascular lesions. However, some primary tumors can produce liver metastases with atypical appearances, such as hypervascular ones, or within calcification, mucin, or other proteins. The multiparametric nature of MRI, combined with the administration of contrast agents, can strongly increase radiologists' confidence in the final diagnosis.

Citation: Maino C, Vernuccio F, Cannella R, Cortese F, Franco PN, Gaetani C, Giannini V, Inchingolo R, Ippolito D, Defeudis A, Pilato G, Tore D, Faletti R, Gatti M. Liver metastases: The role of magnetic resonance imaging. *World J Gastroenterol* 2023; 29(36): 5180-5197
URL: https://www.wjgnet.com/1007-9327/full/v29/i36/5180.htm
DOI: https://dx.doi.org/10.3748/wjg.v29.i36.5180

INTRODUCTION

The liver is one of the most common sites of metastatic disease, accounting for up to 25% of all secondary lesions to solid organs due to its unique architectural and vascular composition that provides fertile soil for different primary neoplasms to spread. Consequently, metastases represent the most frequent malignant liver tumors, being about 18-40 times more frequent than primary hepatic neoplasms[1]. Cancers from the gastrointestinal tract, breast, lung, pancreas, neuroendocrine tumors, and melanomas commonly spread to the liver[2,3]. Specifically, colorectal cancers (CRCs) are widespread, as 50% of such patients presenting with metastatic liver disease at diagnosis or during the follow-up after surgery[4].

Metastatic spread to the liver represents one of the major prognostic factors, determining the clinical outcome[5,6]. Surgical resection is considered the treatment option with the best curative potential for liver metastases. In the case of unresectable disease, besides systemic chemotherapy, many liver-directed approaches have been developed, including local therapies, such as stereotactic body radiation therapy or radiofrequency ablation, and regional therapies, like peptide receptor radionuclide therapy, hepatic artery directed infusional chemotherapy, trans-arterial chemoembolization and trans-arterial radioembolization (TARE)[7]. Hence, accurate detection and assessment of secondary liver lesions are pivotal to select the most tailored management approach for each patient and to determine in whom an improved overall survival rate may be expected.

Magnetic resonance imaging (MRI) represents the reference standard radiological technique for the detection of liver metastases, with its higher sensitivity and specificity compared to computed tomography (CT) and fluoro-2-deoxyglucose positron emission tomography (FDG-PET)[8,9]. The evaluation of secondary liver lesions is one of the most common clinical indications for liver MRI in radiologists' daily practice.

On these bases, the aim of this review is to summarize the role of MRI in the detection and assessment of liver metastases, describing their main imaging features and focusing on the added value of the most recent imaging tools.

MAGNETIC RESONANCE PROTOCOLS

A comprehensive MRI protocol for liver metastases detection and follow-up after systemic, surgical or locoregional treatments should include the acquisition of T1- and T2W (T1W and T2W) sequences, diffusion weighted imaging (DWI) sequences, dynamic multiphase and/or delayed sequence after intravenous administration of gadolinium-based contrast agents (GBCAs). GBCAs, with intravascular-interstitial distribution, are generally used with T1W sequences, with or without fat suppression techniques. Dynamic contrast enhanced acquisitions improve the identification and characterization of liver metastases depending on their enhancement behavior[10].

The introduction of hepatocyte-specific GBCAs, notably Gd-BOPTA (gadobenate dimeglumine-MultiHance®, Bracco) and Gd-EOB-DTPA (Gadoxetic acid, disodium-Primovis®/Eovist®, Bayer), has increased more and more MRI sensibility and specificity for liver metastases imaging. These GBCAs are taken up by hepatocytes and excreted in the biliary system and they are extremely valuable in follow-up after locoregional or systemic treatments. These molecules present a biphasic enhancement pattern; the first phase, immediately after intravenous injection, is similar to CT dynamic enhancement after iodine contrast injection while a delayed phase occurs after 10 to 120 min after injection[10,11]. Lesions

not containing hepatocytes cannot take up such molecules; therefore, metastasis appear hypointense compared with surrounding healthy liver parenchyma[12].

Super paramagnetic iron oxide (SPIO) iron-based nanoparticles contrast media were withdrawn from the market in western countries even if they are still used in clinical practice in some oriental countries such as Japan; the target of this class of contrast agents are reticuloendothelial cells (RES)[10].

In clinical practice, MRI liver protocols must be adapted to the patient's specific clinical questions and characteristics [13].

It is recommended to acquire slices as thin as possible (*i.e.* 3-5 mm), with rectangular field of view (FOV) appropriated to the habitus of the patient. Acquisition plans must include at least axial and coronal. Matrices may vary depending on the sequences used; they should be as high as possible bearing in mind contrast-to-noise ratio. A higher spatial and contrast resolution may be obtained employing 2D and 3D T1W sequences. Temporal resolution is related to the length of acquisition time of a single MRI scan, according to patient's compliance[10].

With modern MRI scanners, the possibility to acquire multiple arterial phases allows either to improve spatial resolution or to reduce scanning time, which is important in case of patients with limited breath-hold capacity or in pediatric ones[10,11].

Non-contrast acquisition

Gradient-echo T1 in-phase and out-of-phase: Gradient-echo (GRE) sequences are prone to susceptibility and chemical shift artifacts and such property may be used to detect and quantify iron and fat deposition within liver parenchyma or in focal lesions[14]. Chemical shift artifacts are due to the lower precession frequency of fat protons compared to water ones [15]. Such differences result in periodic phase coherence (in-phase), where every voxel signal is the sum of water and fat signal or opposition (out-of-phase) of water and fat signals, whereas the two signals have a phase difference of 180°, and thus nulling each other out[16]. Such sequences permit the detection of intracellular fat, either in hepatic lesions or in the hepatic parenchyma[14,16].

Fast spin-echo or turbo spin-echo T2 sequences, with or without fat-suppression: They are very rapid sequences; at present also acquired by breath-hold technique. They are characterized by a 90° excitation pulse followed by a train of several 180° refocusing pulses to fill several K-space lines (echo train) during a repetition time. Fluid content is the predominant information obtained from this kind of sequences, thus allowing to discriminate between solid and cystic-like focal lesions. Fat-suppression should be regularly used to increase contrast resolution[16].

Diffusion-weighted imaging: They are basically T2W images, acquired with single shot, echo-planar imaging (EPI) technique and fat-suppression. They are crucial to rapidly acquire the diffusion signal before it nulls[10,17]. Different series of diffusion-weighted images are obtained by modifying the gradient strength and magnitude (b-value). One series must be acquired with a b-value of 0, so that no gradient is applied and consequently no diffusion information is present, providing similar information as T2 fat-sat sequences. Other series must be acquired with increasing b-values (b50, b400, b800)[18]. These are fundamental for secondary lesion detection, as there is a "black-blood" effect, which increases conspicuity of lesions located next to the vessels. Series acquired with a high b-value (b800) are essential for liver lesion characterization: Highly cellular tissues, such as metastases, present restriction to diffusion thus appearing hyperintense in DWI images[17,18]. EPI sequences are prone to motion artifacts: Breath-hold scans have the advantage of reduced blurring and ghosting artifacts, however their short acquisition times limit spatial resolution, the number of excitations, and number of possible b-values[17,18]. On the other hand, navigator or respiratory-triggered techniques improve image signal-to-noise ratio (SNR) at higher b-values, reducing motion artifacts and blurring[14].

Post-contrast acquisition

Dynamic evaluation: GRE 2D or 3D T1 sequences with or without fat-suppression, acquired before and after GBCA administration[19]. T1W sequences are very sensitive to susceptibility artifacts thus enabling to detect iron, calcium, air or metal[16]. 3D sequences are being used more and more frequently, they are acquired with a modified Dixon technique, that explores the chemical shift effect of fat and water, allowing to separate fat and water peaks allowing to improve the homogeneity of the images, fat-suppression, and providing thinner slice thickness and slice overlap[16]. GRE 3D T1W fat-sat sequences (LAVA, VIBE, THRIVE, *etc.*) are the classical sequences used for dynamic contrast-enhanced studies to evaluate the vascularization pattern of the lesion, usually acquiring one dynamic phase for each breath-hold, about every 25-30 s[19].

At present time, some techniques (CAIPIRINHA, TWIST-VIBE, DISCO or THRIVE 4D sequences, *etc.*), based on parallel imaging and compressed sensing, allow to obtain multi-arterial acquisition in one breath-hold[20]. Non-Cartesian acquisition schemes, for example radial sampling, may be performed for dynamic studies jointly with compressed sensing and parallel imaging, further increasing temporal resolution permitting free-breathing dynamic evaluation (Siemens GRASP VIBE sequences), with reduced motion artifacts, in a sort of continuous acquisition[19,20].

Hepatobiliary-reticuloendothelial phases are T1W sequences, with or without fat-sat, if Gd-BOPTA or Gd-EOB-DTPA, both increasing T1 relaxivity, have been administered[12,19]. Proton density or T2W sequences are used with SPIOs contrast agents[12,19]. For Gd-BOPTA, hepatobiliary phase (HBP) imaging is recommended after 90-120 min, thus requiring the patient to return to the scanner for final T1W imaging of the liver and bile ducts[11,12]. For Gd-EOB-DTPA, HBP acquisition may be performed after 20 min, while the patient is still on the scanner[5,12]. On HBP there is an increase in signal intensity of the hepatic normal parenchyma compared to a non-hepatocytic lesion, thus improving Magnetic resonance (MR) sensibility in detection and characterization of different types of liver lesion[5,10,12]. Furthermore, increasing the flip angle of a T1W 3D sequence from 10° to 30° (Siemens scanner 1.5 T) in the HBP, visually and quantit-

atively improves the visualization of the biliary ducts, obtaining high quality hepatobiliary images[21].

Additional sequences: Half-Fourier Acquisition Single-shot Turbo spin Echo (HASTE), heavily T2W, with a rapid acquisition time, and acquired *via* breath-hold technique. They are used mainly to evaluate lesions or structures with prominent fluid content: They are the basic sequences for the evaluation of biliary tree and pancreatic ducts (MR colangiopancreatography)[22].

Balanced steady-state GRE (true FISP, FIESTA, balanced fast field echo). They tend to highlight fluid content providing a highly accurate morphologic imaging as well as a good delineation of vessels and ductal structures. Furthermore, due to their extremely rapid acquisition time (200 ms), these sequences can tolerate optimally motion artifacts.

Other additional sequences might be added on a case-by-case basis (sequences for fat and iron overload quantification) [8,9,11].

EXTRA-CELLULAR AND HEPATOBILIARY CONTRAST AGENTS: HOW, WHEN, AND WHY?

Contrast-enhanced sequences are mandatory to correctly characterize focal liver abnormalities to assess the vascular behavior of liver parenchyma and lesions.

Extra-cellular contrast agents (ECAs) have historically represented the reference standard for liver-enhanced MRI. All ECAs are distributed within the extra-cellular interstitial space, and despite manufacturers or chemical formulations, they shorten T1 relaxation time, producing a signal intensity enhancement during their biodistribution. From a practical point of view, enhancement proprieties are similar to iodinated contrast media for CT, firstly with the opacification of hepatic arteries and hypervascular lesions (arterial phase, 30-40 s after bolus administration), then liver parenchyma and portal vein (portal-venous phase, 60-80 s after bolus administration), and finally by moving into the interstitial space (delayed phase, 180-300 s after bolus administration). After whole-body distribution, the excretion is entirely through the kidneys [23].

More recently, the introduction of hepatobiliary contrast agents (HBAs) added relevant information to the previous clinical practice, showing some degree of biliary excretion. Due to their ability to bind specific receptors regularly expressed in healthy hepatocytes [organic anion transporter (OATP)], HBAs allow the acquisition of the so-called HBP and consequently can increase the diagnostic accuracy for different focal liver lesions. In fact, after the administration of contrast medium bolus, the initial biodistribution is similar to those of ECAs, providing multi-phase dynamic post-contrast imaging. Moreover, after a specific time, healthy hepatocytes start the uptake of HBAs, which will then be excreted into the biliary ducts. Consequently, in the HBP images, both the liver and the biliary tree are significantly enhanced, while liver vessel and non-hepatocellular lesions show a low signal intensity[24].

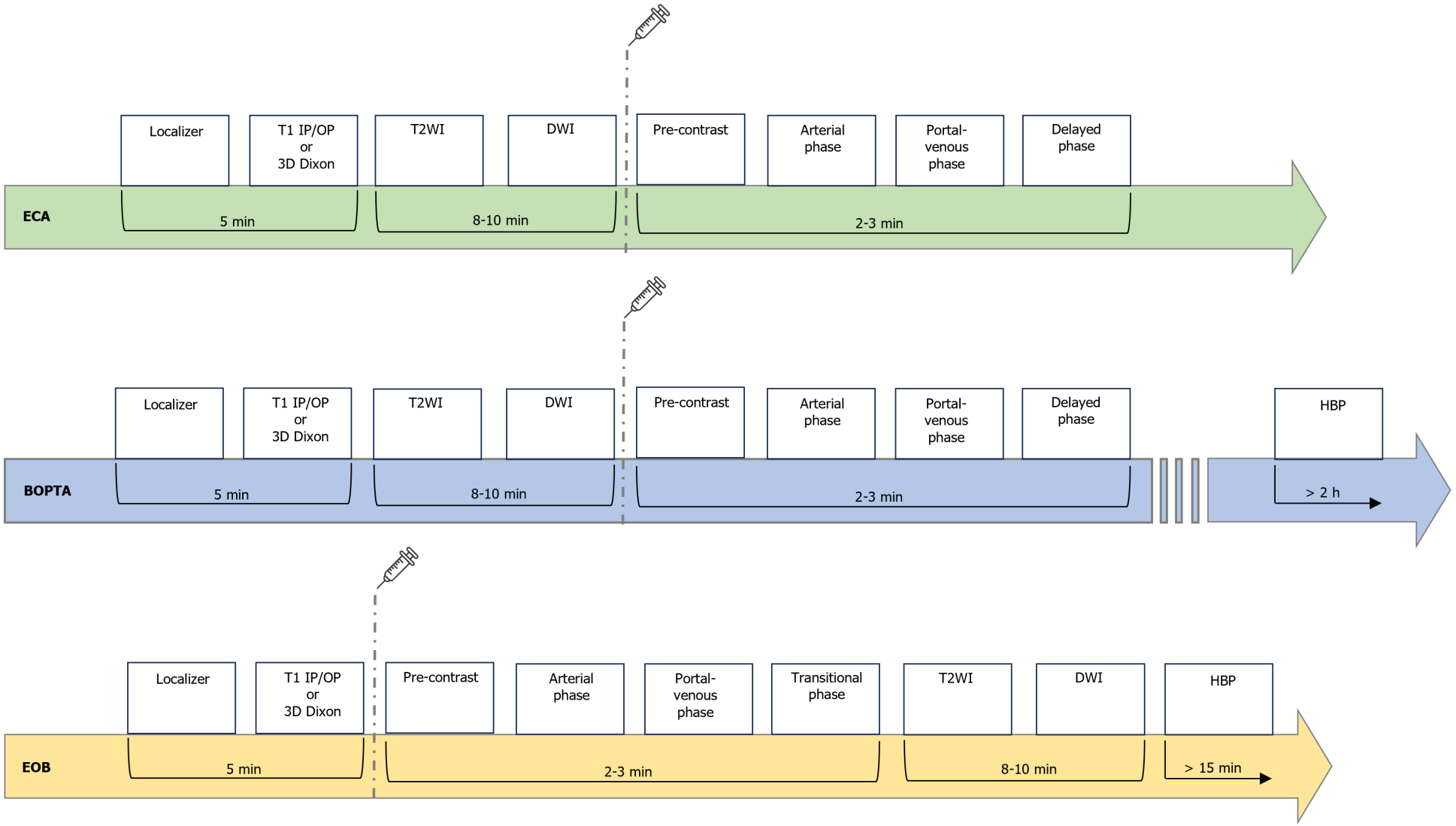
Only two HBAs are approved for the clinical practice: Gd-BOPTA and Gd-EOB-DTPA[25]. When using Gd-BOPTA, about 3%-5% of the contrast dose is eliminated by biliary excretion. In contrast, with Gd-EOB-DTPA, about half of the dose is taken up by hepatocytes and excreted with the bile. Thus, these two contrast media need different acquisition times to obtain diagnostic HBP images, which are acquired about 1.5-3 h after Gd-BOPTA injection and about 15-20 min after Gd-EOB-DTPA administration in non-cirrhotic livers. Consequently, the HBP can be acquired at the end of the liver MRI protocol in the case of Gd-EOB-DTPA, while in a second step in the case of Gd-BOPTA[26,27]. Figure 1 summarizes MRI protocols by using ECAs and HBAs.

Choosing the best contrast media when acquiring a liver MR protocol cannot be straightforward, considering that both ECAs and HBAs present advantages and disadvantages. It's well-known that arterial phase acquisition during ECAs' administration can be more robust in comparison with Gd-EOB-DTPA because the latter leads to a lower enhancement of healthy parenchyma (reducing the lesion to liver contrast) and the higher frequency of artifacts[28]. Moreover, ECAs allow better detection of lesion washout over time, while the rapid uptake of Gd-EOB-DTPA precludes its evaluation during the transitional phase (acquired 180'' to 300'' after injection).

On the other hand, the evaluation of HBP can increase contrast resolution between liver parenchyma and secondary lesions. Mainly, one of the most relevant advantages of HBAs is the easy detection of non-hepatocellular lesions and lesions with non-functioning hepatocytes, including hepatic adenomas, hepatocellular carcinoma (HCC), and metastases. Indeed, when impaired hepatocytes are present, the whole lesion or part of it can be easily depictable as hypointense during the HBP images. Moreover, HBAs can increase diagnostic accuracy in the case of focal nodular hyperplasia (FNH), where functioning hepatocytes increase the uptake of contrast agents, resulting in a hyperintense lesion during the HBP [29].

Due to the high specificity and sensitivity in detecting hepatic focal lesions, HBAs should always be preferred in oncologic patients with known extra-hepatic primary cancer, especially in cases of increased risk of the disease's spread to the liver. The number and location of liver secondary lesions can significantly modify the patient's management and is crucial for treatment strategies' success[30].

Considering that patients with known primary tumors should undergo different follow-up examinations, abbreviated MRI (AMRI) protocols-composed of DWI, T2W, and HBP - have been proposed. In a recently published review, the Authors summarize the advantages and disadvantages of these new approaches. Even if not recommended nor approved by either international society, AMRI could increase the availability of MRI examinations and therefore facilitate strict surveillance of liver metastases, preserving an acceptable accuracy in their detection and characterization[31].



DOI: 10.3748/wjg.v29.i36.5180 **Copyright** ©The Author(s) 2023.

Figure 1 Schematic summary of magnetic resonance imaging protocols by using ECAs and hepatobiliary contrast agents (Gd-BOPTA and Gd-EOB-DTPA). ECA: Extra-cellular; BOPTA: Gadobenate dimeglumine; EOB: Gadoxetic acid, disodium; T1 IP: T1-weighted in-phase imaging; T1 OP: T1-weighted out-of-phase imaging; DWI: Diffusion weighted imaging; HBP: Hepatobiliary phase; T2WI: T2-weighted imaging; HBP: Hepatobiliary phase.

CONVENTIONAL MRI FEATURES OF LIVER METASTASES

Typical appearance

Liver metastases typically occur as multifocal nodular lesions but less frequently they can occur as a solitary lesion, large confluent masses, or have an infiltrative appearance with multiple small lesions spread in the hepatic parenchyma (Figure 2). Two other rare patterns of distribution include the miliary diffusion which can be observed in lung, breast carcinomas, uveal melanoma, and neuroendocrine tumors and metastases situated in the gallbladder fossa in gallbladder cancer due to peculiar venous drainage[32]. Liver metastases from extrahepatic carcinomas usually have ill-defined margins and can present variable sizes, ranging from small nodules to bulky masses. MRI sequences like DWI and HBP images are particularly useful to identify small lesions, especially those with diameters < 1 cm[33].

The typical appearance of liver metastases is variable depending on the primary cancer, the lesions size, the extent of the disease, and background liver tissue (Figure 3). On non-contrast MRI, liver metastases are classically hypointense compared to the surrounding liver parenchyma. A slightly hypointense rim can be observed at the periphery of the lesions, reflecting the most viable tissue. Radiologists should be aware that some metastases can demonstrate various degrees of spontaneous hyperintensity on T1W images, suggesting the presence of high protein concentration (mucinous tumors), necrosis (colorectal adenocarcinomas), melanin (melanoma) or methemoglobin (hemorrhage)[34]. Fat in mass is not observed in hepatic metastases with few exceptions on fat-containing tumors such as liposarcomas or malignant teratomas[35,36]. On T2W images, liver metastases can demonstrate variable mild to moderate T2 hyperintensity, reflecting the variable amount of hypercellularity and internal desmoplastic fibrotic stroma. Elevated signal on T2W images is related to cystic or necrotic changes in larger metastatic lesions, whereas smaller lesions may appear isointense. Marked hyperintensity on T2W sequences may be detected in metastases from neuroendocrine tumors, which can resemble the imaging appearance of small hemangiomas. Up to 25% of liver metastases can demonstrate a targetoid appearance on T2W images, also known as target sign, which is characterized by a mild central T2 hyperintensity surrounded by a peripheral rim of moderate-to-marked T2 hyperintensity[32]. DWI and the apparent diffusion coefficient (ADC) map are useful to detect liver metastases, showing a restricted diffusion with ADC values lower than those of the parenchyma because of increased cellularity of the lesions. Targetoid appearance can be observed also on DWI, with a peripheral rim of marked diffusion restriction indicating the peripheral proliferative area of the metastases as opposed to the central necrotic region[37].

On post-contrast images, liver metastases can be classified according to the enhancement pattern on the late hepatic arterial phase as hypovascular or hypervascular metastases, as detailed below. On the portal-venous phase, hepatic metastases show washout, either complete or more prominent at the lesion's periphery. The peripheral washout sign, in which a peripheral rim is hypointense compared to the lesion's center and to surrounding parenchyma, can be present in both hypervascular and hypovascular metastases, but it's observed more frequently in hypervascular ones[38]. Histopathologically, peripheral washout might reflect perfusion alterations at the peripheral area of the lesions, which presents good arterial supply and good venous drainage of contrast[37]. It is important to note that washout appearance should be assessed on portal-venous and delayed phases when using ECAs, while it can be evaluated exclusively on portal-venous phase when Gd-EOB-DTPA is administered, as its uptake by functional hepatocytes starts at approximately 90 s after the contrast injection[39].

Liver metastases are typically hypointense compared to the background liver tissue on the HBP acquired after the administration of HBAs. However, metastases can also demonstrate a targetoid appearance on the HBP with marked hypointensity at the periphery of the lesion as opposed to the central cloud of enhancement likely due to contrast accumulation in the extracellular space or central fibrotic stroma[40,41]. Aberrant expression of OATP transporters has also been occasionally reported in CRC liver metastases[42]. Compared to FDG-PET and CT, EOB-MRI demonstrated the highest sensitivity (93.1%) in detecting liver secondary lesions with improved specificity (87.3%) in comparison with CT [43]. Moreover, MRI can significantly improve liver metastases detection in patients with hepatic steatosis, which can be easily overlooked on CT especially when small in size[44].

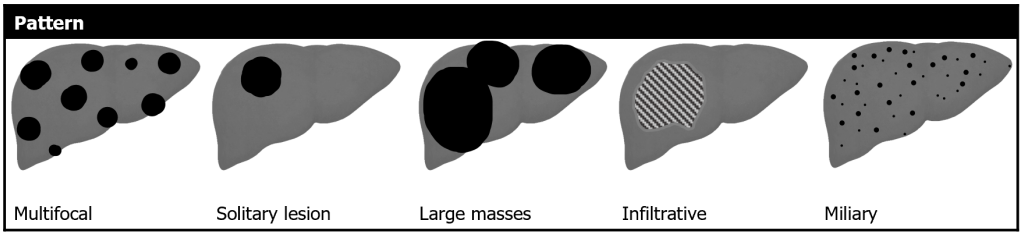
Hypovascular metastases

Hypovascular metastases are lesions in which the arterial phase enhancement is inferior or similar compared to that of the healthy liver and therefore appear hypointense on the late hepatic arterial phase. Arterial phase hypoenhancement is the most frequent pattern in liver metastases and it can be typically observed in gastrointestinal carcinomas, bladder, prostate, and lung cancers. These lesions typically demonstrate persistent hypoenhancement on the post-arterial phases and are hypointense on the HBP (Figure 4).

Hypervascular metastases

Hypervascular metastases manifest as lesions in which the arterial phase enhancement is higher compared to that of the liver parenchyma and therefore appear as hyperintense on the late hepatic arterial phase. The arterial phase hyperenhancement can be heterogenous and it can be observed in the whole or part of the lesions or be more pronounced at the periphery (*e.g.* rim arterial phase hyperenhancement). Hypervascular liver metastases with whole lesion hyperenhancement typically arise from hypervascular primary cancers such as neuroendocrine ones, renal cancer, melanoma, and thyroid cancer. These lesions can demonstrate early wash-out on the portal-venous phase or, more rarely, fading or persistent enhancement on post-arterial phases (Figures 5 and 6).

Metastases with peripheral arterial phase hyperenhancement are characterized by a targetoid appearance on post-contrast phases, showing rim hyperenhancement on arterial phase with washout on portal-venous or delayed phases, reflecting the increased cellularity at the lesion's periphery, in comparison with the central hypo-perfused area[37,45].



DOI: 10.3748/wjg.v29.i36.5180 **Copyright** ©The Author(s) 2023.

Figure 2 Schematic representation of morphological liver metastases appearance.

MRI can improve the detection of arterial phase hyperenhancement by acquiring multiple arterial phases. This technique allows to detect early enhancement that can be missed on late arterial phase with improvement in enhancement detection compared to single-phase acquisition[46,47]. However, its usefulness for differential diagnosis between liver metastases and other liver lesions needs to be validated. Finally, subtraction images should always be considered to detect the arterial phase hyperenhancement in lesions showing hyperintensity on pre-contrast T1W images.

Atypical appearance

In current clinical practice, unusual radiologic features of liver metastases may be found thus making it challenging to discriminate metastases from other focal liver lesions. Detailed knowledge of atypical imaging features of liver metastases with a good understanding of the histopathologic background is crucial for accurate differential diagnosis. Among these, metastases with cystic appearance, calcifications, or fat are herein discussed.

Cystic liver metastases: Cystic liver metastases usually appear on MRI as strongly hyperintense on T2W sequences, hypointense on non-contrast T1W images, with lack or rim enhancement on contrast-enhanced T1W images. They may occur mainly from CRC, pancreatic cancer, neuroendocrine tumors (NETs), ovarian cancer, gastrointestinal stromal tumors (GISTs), melanoma and sarcomas. The causative mechanisms of cystic appearance of liver metastases may vary [37,48]:

(1) Rapid growth beyond hepatic arterial blood supply of the lesion, thus causing central necrosis, such as in NETs, GISTs, sarcomas, melanomas, angiosarcomas, testicular carcinomas, or squamous cell carcinomas;

(2) Mucinous components of the primary tumor, such as in mucinous CRCs or ovarian carcinomas;

(3) Marked T2W hyperintensity due to the primary histological features;

And (4) Changes after chemotherapy, including necrosis or cystic or mucinous regression.

Mucinous metastases from CRC are particularly challenging in daily practice because, in addition to marked T2W hyperintensity, they show a lack of diffusion restriction in about 81% of cases, thus making the differential diagnosis with benign cysts very challenging[49].

Calcified liver metastases: Calcified liver metastases usually show small or diffuse calcifications appearing hypointense on both T1- and T2W imaging, and are better demonstrated on CT. Calcified liver metastases may occur mainly from CRC liver metastases, bone-forming tumors (osteosarcoma and chondrosarcoma), lung, breast, prostate, stomach, ovary, thyroid, neuroendocrine tumors, GISTs, neuroblastoma, and melanoma[50-52].

The causative mechanisms of the calcified appearance of liver metastases may vary:

(1) Dystrophic calcifications resulting from necrosis and/or hemorrhage within the tumor;

(2) Mucoid calcifications related to the presence of mucin produced by mucinous adenocarcinomas;

(3) Proper production due to the intrinsic nature of the primary metastasizing malignancies;

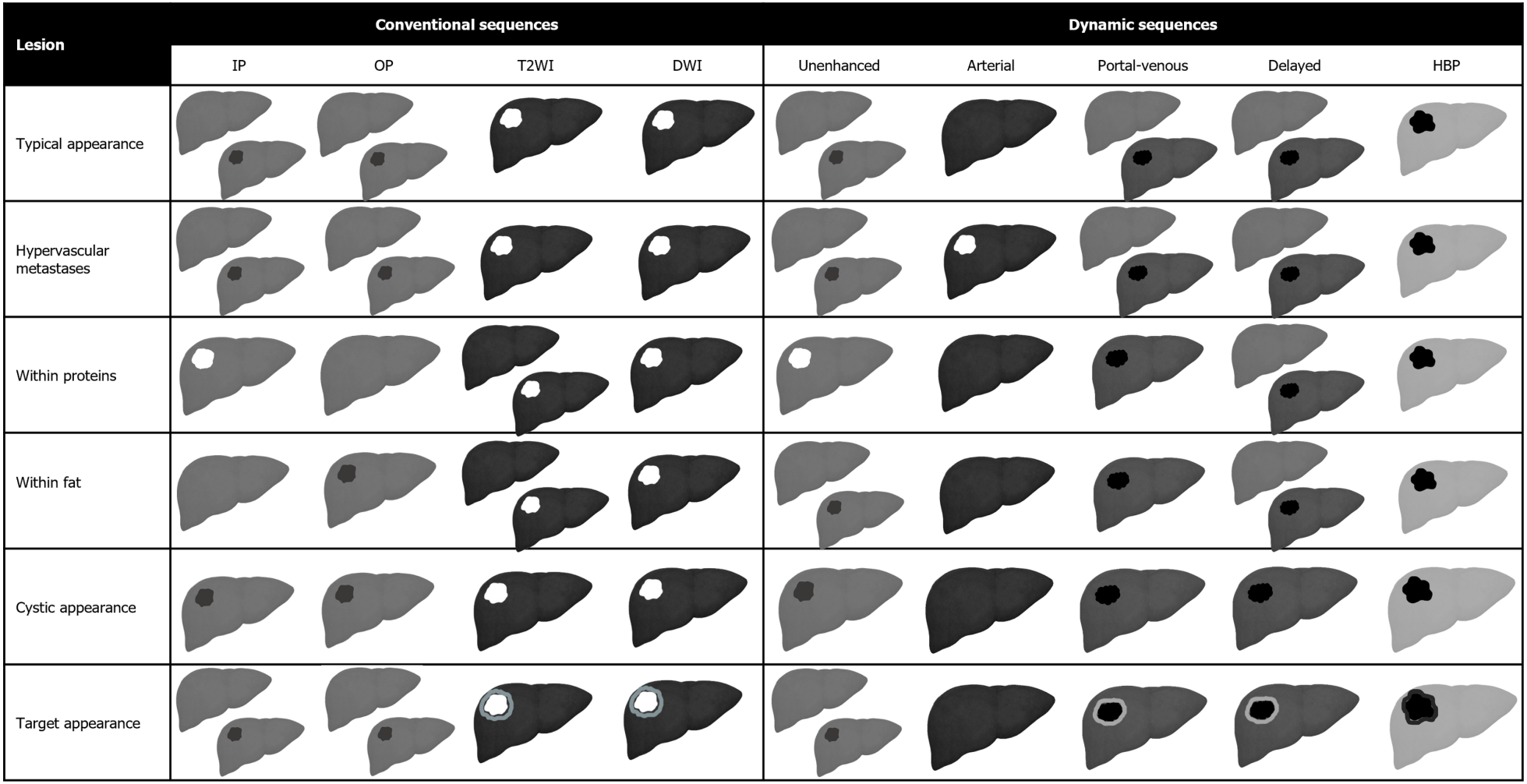
And (4) Changes after chemotherapy, including mineralization of necrotic tissue.

The occurrence of calcifications in CRC is well-known since the first years of the 1960s when Engel and Dockerty[53] described their occurrence in the primary tumor at pathology and Miele and Edmonds[54] identified them in liver metastases on abdominal radiographies in four patients, with pathology confirmation in three of the four patients. In patients with CRC, calcifications may be present in up to 11% of cases before chemotherapy[51] and in about 5% of cases after chemotherapy usually – though not always – indicating tumor response[55].

Fat-containing liver metastases: The occurrence of fat in liver metastases may be distinguished based on the fat distribution and type of fat into three different scenarios. First, intralesional macroscopic fat may be encountered in metastases from liposarcoma and will show hyperintensity on T2W non-fat-sat sequences, and heterogenous appearance on T1W images with moderate signal loss on opposed-phase and increased signal on in-phase images, indicating the presence of macroscopic fat. Second, intralesional intracellular fat may be encountered very rarely having been described in liver metastases from renal cancer[56]. Third, liver metastases from malignant teratomas can contain extracellular fat, calcifications, and necrotic components[35,36].

The role of MR in too small to characterize lesions

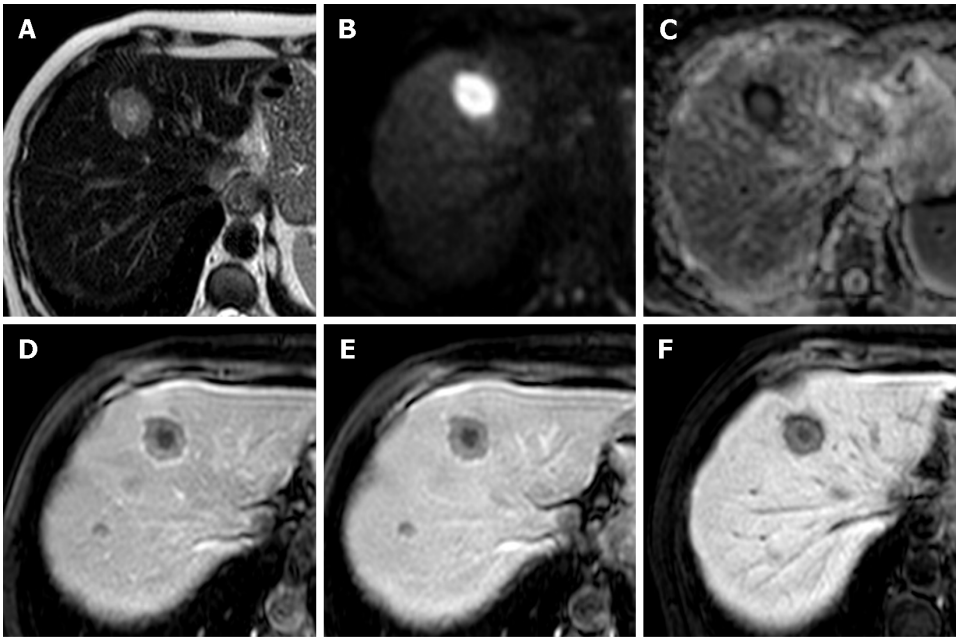
Too small to characterize (TSTC) liver lesions are defined as those small liver lesions - typically 1.5 cm in diameter or smaller - that cannot be confidently characterized on CT by the interpreting radiologist on the available images. In most cases, TSTCs are benign[57], and this is particularly true for solitary hepatic lesions up to 1 cm, that therefore do not



DOI: 10.3748/wjg.v29.i36.5180 **Copyright** ©The Author(s) 2023.

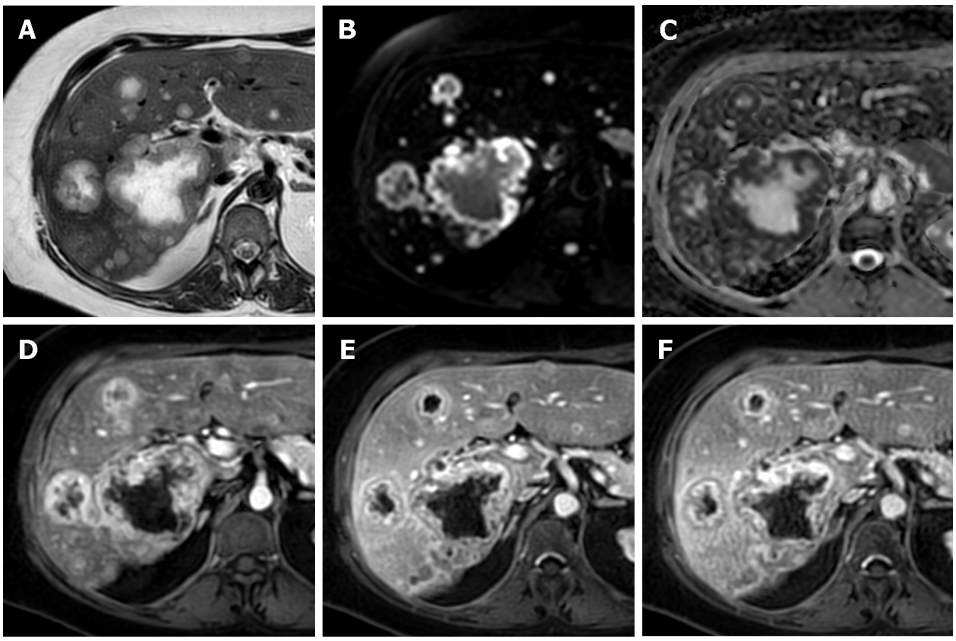
Figure 3 Graphical representation of liver metastases appearance on pre-contrast sequences and during the administration of hepatobiliary contrast agents. IP: In-phase imaging; OP: Out-of-phase imaging; DWI: Diffusion weighted imaging; T2WI: T2-weighted imaging; HBP: Hepatobiliary phase.

require any follow-up if identified in low-risk patients including patients with no known primary cancer, hepatic risk factors or hepatic failure[58,59].



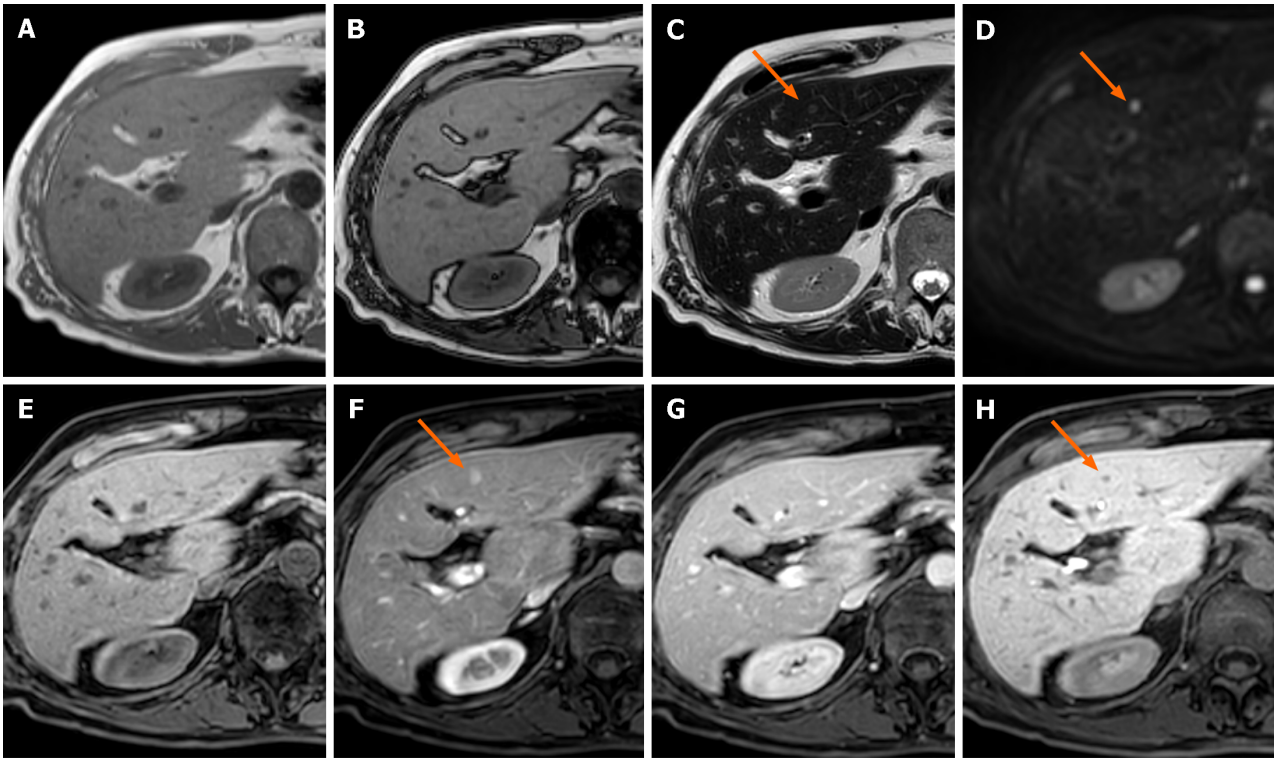
DOI: 10.3748/wjg.v29.i36.5180 **Copyright** ©The Author(s) 2023.

Figure 4 Liver metastases from colorectal cancer. A: EOB-magnetic resonance imaging of a 62-year-old woman demonstrates a liver lesion with hyperintensity on T2-weighted images; B: On diffusion weighted imaging the lesion appears markedly hyperintense; C: Apparent diffusion coefficient map demonstrates a peripheral hypointensity of the lesion; D: On the post-contrast arterial phase the lesion demonstrate reduced enhancement compared to the surrounding liver parenchyma with typical targetoid hypointensity; E: On the portal-venous phase the lesion remain hypovascular with targetoid appearance; F: On the hepatobiliary phase the lesion shows persistent hypoenhancement. Multiple other metastases were present in the liver parenchyma (not shown).



DOI: 10.3748/wjg.v29.i36.5180 **Copyright** ©The Author(s) 2023.

Figure 5 Multiple liver metastases from breast cancer. A: ECA-magnetic resonance imaging of a 51-year-old woman shows multiple liver lesions with central marker hyperintensity on T2-weighted images; B: Diffusion weighted imaging sequence demonstrates lesions' peripheral restricted diffusion; C: Apparent diffusion coefficient map shows a corresponding peripheral hypointensity of the lesions; D: On post-contrast arterial phase the lesions demonstrate a peripheral hyperenhancement rim with a central hypo-perfused area; E: On portal venous a corresponding peripheral washout is observed; F: On delayed post-contrast phase the peripheral hypoenhancement persists.



DOI: 10.3748/wjg.v29.i36.5180 **Copyright** ©The Author(s) 2023.

Figure 6 Liver metastases from ileal neuroendocrine tumor. A: EOB-magnetic resonance imaging of a 55-year-old female patient shows a focal liver lesion isointense on in-phase images; B: On out-of-phase images, the lesions persist isointense compared to the healthy liver parenchyma; C: On T2-weighted images the lesion appears slightly hyperintense (orange arrow); D: Diffusion weighted imaging reveal restriction of diffusion of the lesion (orange arrow); E: Before contrast administration the lesion is isointense; F: During the post-contrast late hepatic arterial phase the lesion appears hypervascular (orange arrow); G: The lesion is isointense on the portal-venous phase; H: On the hepatobiliary phase lesion's low signal intensity is observed (orange arrow).

Indications to MRI for TSTC: TSTC lesions up to 1 cm identified on CT need follow-up with MRI at 3-6 mo whenever identified in high-risk patients, including patients with known primary cancer with a propensity for liver diffusion, cirrhosis, and/or other hepatic risk factors[58,59].

Characterization with MRI of TSTC lesions between 1 and 1.5 cm is indicated whenever suspicious imaging features are present or if "flash-filling" imaging features are identified in high-risk patients[58,59]. Suspicion imaging features embrace blurred margins, heterogeneous density, nodularity or mural thickening, thick septa, intermediate-to-high attenuation on portal venous–phase acquisitions, and enhancement of at least 20 HU between precontrast and post-contract CT[59].

In addition to the previous settings, MRI characterization or follow-up should be considered[58]:

(1) If an incidental TSTC lesion smaller than 1 cm is newly detected on CT follow-up even in low-risk patients;

(2) If a small cystic lesion is encountered in patients with ovarian cancer or GISTs;

And (3) In case of small TSTC growing over time.

MRI characterization of TSTC: MRI with and without injection of contrast media is oftentimes regarded as the problem solver for the characterization of hepatic TSTC. To date, contrast-enhanced MRI allows to permit a conclusive diagnosis in 95% of liver lesions, with only 1.5% of patients with MRIs requiring further exams[60]. The MRI diagnostic accuracy depends on the sequences acquired and type of contrast agent used, as well as the lesion itself. A step-by-step approach to MRI is mandatory for the characterization of hepatic TSTC. Non-contrast enhanced MRI sequences allow to identify some key imaging clues for the diagnosis of small benign lesions that should be regarded before looking at contrast-enhanced images. The analysis of T2W images and DWI are oftentimes sufficient to characterize small liver cysts and small hemangiomas which are the most common incidental liver lesions; indeed, both lesions will show a lack of diffusion restriction or the so-called "T2-shine through" phenomenon, and then cysts will be as bright as the cerebrospinal fluid on T2W sequences while hemangiomas will show a slightly lower hyperintensity as compared to the cerebrospinal fluid on T2W images[61]. A clear knowledge of these pre-contrast characteristics allows to avoid misdiagnosis if a "pseudo-washout" is identified on the 3-min phase with Gd-EOB-DTPA[62]. Dual-phase sequence, with in- and opposed-phase images, may allow to identify focal fat accumulation or focal fat sparing that may occasionally mimic a true liver lesion[63]. MRI without intravenous contrast agent may therefore answer the clinical question between benignity and malignancy in some cases. In addition, as Moosavi *et al*[64] demonstrated in their study on newly discovered indeterminate focal liver lesions in non-cirrhotic subjects, the information obtained from the HBP does not necessarily modify the diagnosis or the diagnostic confidence. Therefore, in selected cases if the radiologist is confident with the lesion characterization on non-contrast sequences (*e.g.* cyst, hemangioma), the routine use of intravenous contrast agent

may not be necessary[65]. Some TSTC lesions remain indeterminate after the assessment of non-contrast MRI sequences. In these cases, post-contrast images may prove to be helpful, and the choice of the contrast agent should be tailored on a per-patient and per-lesion bases. Contrast-enhanced MRI with ECAs may be particularly helpful if the slow-filling hemangioma is the most likely diagnosis and the acquisition of pure extracellular phases would allow to capture complete filling of the lesion. On the other hand, Gd-BOPTA MRI allows to obtain both pure delayed extracellular phases and HBP images although requiring acquisition at 2 h from contrast agent injection, and may be helpful if obtaining information from both delayed extracellular and HBP is deemed necessary. Finally, Gd-EOB-DTPA MRI allows to obtain an HBP at 10-20 min from contrast agent injection. For the differentiation between hepatocellular adenoma and FNH, the acquisition of the HBP may be very helpful in the majority of cases demonstrating iso-to-hyperintensity or a donut-like appearance on HBP in case of FNH and hypointensity on HBP in most cases of hepatocellular adenomas[66]. However, hepatocellular adenomas may occasionally demonstrate inhomogeneous iso-to-hyperintensity on HBP, thus leaving the final diagnosis to pathology for confirmation[41].

USEFULNESS OF DWI

The most sensitive MRI sequences to detect liver metastases are DWI and HBP images. Diffusion restriction and HBP hypointensity are typical features of liver secondary lesions[67] (Figure 7).

DWI technical principles are based on the evaluation of water molecules' motion and is currently used in clinical practice to assess lesions and tissue properties[67,68]. Specifically, b-values are DWI-related parameters able to assess the degree of diffusion of a specific lesion or tissue[69].

Considering that water diffusion in highly cellular tumors is more restricted compared to healthy tissues, a higher b-value might null signals from healthy tissues, resulting in marked cancer-to-healthy tissue contrast, thus leading to lesion hyperintense signals[68,69]. The diagnostic values of high b-values have been investigated and reported in several tumors, including liver metastases[70]. An important meta-analysis reported 87.1% (95%CI, 83.2%-90.1%) sensitivity for DWI in liver metastases detection[33]. Moreover, different studies showed that DWI was more sensitive than T2W images for CRC liver metastases[71-73]. In particular, it has been underlined the essential role of DWI, despite the very low spatial resolution, in the detection of small (≤ 1 cm) lesions[74].

The second most important parameter obtained by DWI is the ADC map, which correlates with tissue cellularity, relying on the mono-exponential model[69]. ADC values can help not only to characterize lesions but also to predict prognosis. Two meta-analyses established that ADC values might contribute to response to chemotherapy evaluation and prediction in CRC liver metastases[75,76]. Specifically, Drewes *et al*[76] demonstrated that the pre-treatment mean ADC in responder group was lower compared to the non-responder group (1.15×10^{-3} *vs* 1.37×10^{-3} mm^2/s, respectively). Similarly, Sobeh *et al*[75] demonstrated that the most robust response predictor to therapy was a lower baseline ADC value with a pooled mean difference of -0.12×10^{-3} mm^2/s among responders and non-responders. To strengthen these data, a systematic review confirmed that ADC value might be a promising tool for response to chemotherapy prediction in CRC liver metastases[77].

Moreover, the assessment of ADC values might be useful for the earlier evaluation of chemotherapy response in comparison with the RECIST criteria[76,78].

Indeed, Cui *et al*[79] reported an prompt increase in ADC values (on day 3 or day 7 after chemo) in responding lesions, thus representing the change in tissue composition: This aspect may allow clinicians to prevent overtreatment, thus avoiding adverse effects[78].

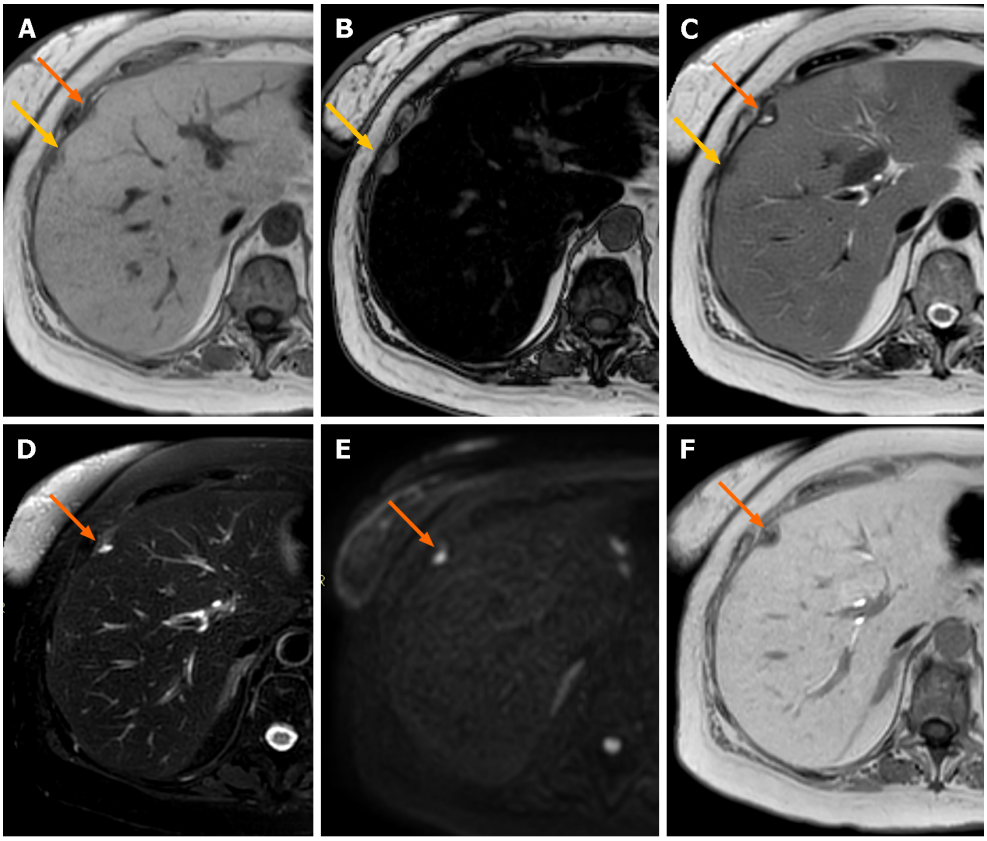
However, the ADC map may not be a sufficient diagnostic imaging method itself but needs to be integrated with other MRI sequences[80].

To move forward, it's important to highlight that the ADC map relies on the mono-exponential model based on the Gaussian movement of water molecules. However, considering that tumor heterogeneity affects the non-Gaussian diffusion behavior, two new diffusion techniques, namely intravoxel incoherent motion (IVIM) and diffusion kurtosis imaging (DKI), were introduced[78].

IVIM evaluates both diffusion and microcapillary perfusion modifications, analyzing the signal decay curve obtained from multiple b-values[81], while DKI is a straightforward extension of DWI providing a sensible measure of tissue structure depending on a probability distribution function[69,82]. Both modalities were analyzed by different studies, with a special focus as a predictor tool for response to therapy. In particular, Zhang *et al*[83] demonstrated the possible role of IVIM and DKI in predicting response to therapy in CRC liver metastases: At baseline, lower D values on IVIM map and higher *K* values on DKI map were independently associated with a good response to chemotherapy.

However, in clinical practice, DWI sequences are sometimes affected by artifacts, especially due to motions (cardiac pulsations and peristaltic movements) or magnetic susceptibility (especially at the boundary surfaces)[84].

Different techniques were developed to avoid or at least reduce the amount of artifacts, firstly to increase reader's confidence for the final diagnosis. In fact in 2021, some Authors aimed to compare the clinical utility of single-shot EPI using different breathing schemes and readout-segmented EPI (RS-EPI). The Authors found out that RS-EPI has the higher SNR, suggesting it as an emerging technique to be applied in everyday clinical practice[85]. More details regarding the usefulness of advanced DWI techniques are out of the scope of the present review; more details can be found in the review by Saito *et al*[84].



DOI: 10.3748/wjg.v29.i36.5180 **Copyright** ©The Author(s) 2023.

Figure 7 Liver metastases from pancreatic adenocarcinoma. A: EOB-magnetic resonance imaging (MRI) of a 64-year-old woman shows two adjacent focal liver lesions (yellow and orange arrows) in the subcapsular region on the in-phase imaging; B: On out-phase imaging, one lesion (yellow arrow) shows hyperintensity, while the other one shows slight hypointensity. The liver is characterized by severe steatosis, considering the important signal drop-off between in-phase and out-of-phase imaging; C: On T2-weighted (T2W) imaging, one lesion (yellow arrow) is hypointense, while the other one (orange arrow) demonstrates inhomogeneous hyperintense signal; D: On fat-sat T2W sequence the low signal of the first lesion and the inhomogeneous high signal of the second one (orange arrow) are confirmed; E: Diffusion weighted imaging reveals focal restriction of diffusion corresponding to only one of the two lesions (orange arrow); F: On the hepatobiliary phase one lesion is isointense to liver parenchyma, while the second lesion shows a hypointense aspect. The final diagnosis for the lesion tagged by the orange arrow was liver metastasis from pancreatic adenocarcinoma, while the MRI characteristics of the lesion tagged by the yellow arrow are consistent with a focal fatty-sparing area.

THE ADDED VALUE OF GD-EOB-DTPA

Since its introduction, Gd-EOB-DTPA acquired a key role in characterization of malignant liver lesions, especially metastasis, and in evaluating response to therapy. One of the most important published randomized multicenter trials[86] demonstrated the superior diagnostic accuracy of Gd-EOB-DTPA, compared to ECAs-MRI and CT, in patients with suspected CRC liver metastases. The Authors demonstrated that no additional imaging was required for all patients who underwent EOB-MRI, while for patients who underwent ECA-MRI and CT further confirms were needed (in 17% and 39% of cases, respectively, $P < 0.0001$)[86].

An important systematic review and meta-analysis showed the higher per-lesion sensitivity of Gd-EOB-DTPA MRI in comparison to CT (median 94.9% *vs* 74.2%, respectively, $P < 0.001$). Higher diagnostic values of EOB-MRI were also demonstrated for small lesions (with an axial diameter < 1 cm), with a per-lesion sensitivity of 85.7% (*vs* 50%, $P < 0.001$) [87].

Vilgrain *et al*[33] published a meta-analysis regarding 1989 patients with 3854 Liver metastases to analyze diagnostic values of DWI and HPB acquired with Gd-EOB-DTPA alone and a combination of both. When considered singularly, HBP was more sensitive than DWI to detect liver metastases (90.6% *vs* 87.1%). However, the combination of both sequences showed the highest per-lesion sensitivity (95%, $P < 0.0001$).

Interestingly, Zech *et al*[88] evaluated the cost of the diagnostic workup of CRC liver metastases patients, three different imaging approaches were compared: EOB-MRI, ECA-MRI, and CT. Overall costs were lower when using Gd-EOB-DTPA as the first line imaging technique compared to different strategies. Indeed, no patient in the EOB-MRI group required supplementary imaging to decide on treatment as compared to 18.1% and 39.7% for patients who underwent ECAs-MRI and CT, respectively. To endorse these aspects, Renzulli *et al*[89] suggested that EOB-MRI should be the initial imaging modality of choice for patients pre-operatively evaluation.

Kim *et al*[90] studied the importance of EOB-MRI compared to CT in CRC patients with synchronous liver secondary lesions. They found out that EOB-MRI increased the detection of liver secondary lesions, helping a more fitted treatment,

with an overall increase in survival rate (estimated 5-year survival of 70.8% for EOB-MRI *vs* 48.1% for CT).

EOB-MRI has also proved useful for predicting therapeutic responses. Recently, Gu *et al*[91] evaluated whether some HBP parameters, such as the relative tumor enhancement (RTE) and the standard deviation value of signal intensity ratio (SDR), can predict the pathological response to systemic therapy in CRC liver metastases. RTE and SDR values were significantly higher in the responder group in comparison with the non-responder one ($P < 0.001$).

Similarly, Murata *et al*[92] demonstrated that the mean pre-treatment RTE was significantly higher in responders in comparison with the non-responder group (37.2% ± 10.9% *vs* 17.9% ± 10.5%, $P = 0.0006$). Larger and prospective studies should aim to better evaluate the usefulness of EOB-MRI as a prognostic factor in patients with liver metastases.

Finally, EOB-MRI is even worthwhile in the assessment of chemotherapy-induced liver disease, as in the case of sinusoidal obstruction syndrome, especially during the early stages. The under-expression of OATP by centrilobular hepatocytes reflects the reticular hypointensity appearance on HBP which can be more easily detected than with conventional MRI sequences[89,93].

ADVANCED TOOLS: RADIOMICS AND ARTIFICIAL INTELLIGENCE

Radiomics, which uses artificial intelligence (AI) techniques to extract and analyze quantitative features from medical images, has been proven as an effective tool in medical imaging to improve detection and characterization of diseases in terms of diagnosis and prognosis. These algorithms can analyze image patterns, extract meaningful features, and make predictions based on the data, providing valuable insights to clinicians. Among different clinical applications, radiomics has been proposed by researchers to face different challenges regarding liver metastases, mostly using CT images. Different algorithms have been proposed for diagnosis, prediction of development of liver metastases, response to therapy, recurrence, and survival[94].

AI applied to CT images has shown excellent results in detecting liver metastases with a sensitivity of 93%[95] and in making differential diagnosis between liver metastases from other liver lesions, reaching an accuracy of 92%[96]. Moreover, some studies assessed the feasibility of using radiomics for response prediction to therapy at lesion level also demonstrating the superiority of radiomic features compared to the standard biomarkers, such as size and RECIST[97].

Despite CT being the diagnostic tool most often used during staging and follow-up, and consequently, the one for which it is easier to develop radiomics tools, MRI is the only technique that allows providing quantitative data to assess morphological and functional information useful for tumor characterization and prediction of response to treatment. Therefore, efforts have been made to correlate MRI-based radiomics data to clinical outcomes. Zhang *et al*[98] demonstrated that radiomics features derived from pre-treatment T2W images can correlate with response to chemotherapy, *e.g.*, responding lesions showed a lower angular second moment and higher variance (two homogeneity measures) compared to non-responding ones. Similarly, but using post-treatment MRI features, Reimer *et al*[99] demonstrated that higher kurtosis on arterial and portal-venous images and higher skewness in portal-venous phase could identify patients undergoing TARE with a progressive disease earlier compared to standard RECIST criteria. However, when radiomics features are combined into statistical classifiers, *e.g.*, in a multivariate analysis, predictive performances are boosted. For example, Granata *et al*[100] proven that combining some radiomics features obtained from T2W images into a statistical classifier, such as the KNN, allows predicting the tumor growth with an area under the curve (AUC) of 0.9 in the validation set. Han *et al*[101] developed a model to preoperatively identify Histopathological Growth Patterns of CRC liver metastases, analyzing the tumor-liver interface zone on MR, reaching an AUC of 0.91 in the cohort of internal validation.

Radiomics has also shown promising results on MRI in the diagnostic field of research, distinguishing different types of liver lesions, and differentiating secondary lesions from benign lesions and primary liver cancer[102]. Finally, an important objective that has been pursued with radiomics is the correlation between radiomics and genomics through an approach called radiogenomics. Using MR-based radiomics features, Granata *et al*[103] assessed the RAS mutation status, a robust prognostic and predictive biomarker among subjects undergoing liver CRC metastases resection. They performed a multivariate analysis using features extracted from MRI, obtaining an accuracy of 87.5% with 91.7% of sensitivity and 83.3% of specificity on an external validation cohort in predicting RAS mutational status. Despite these promising results, further studies should be conducted to face important challenges such as the instability of radiomic features among different devices and acquisition protocols, especially for MRI images, lack of fully automatic segmentation tools and user-friendly interfaces[104], and shortage of well-annotated multicenter datasets. The latter can be overcome by designing clinical trials enhancing the cooperation between institutions and collaborations between clinicians and medical imaging experts.

CONCLUSION

Liver metastases are the most common malignant hepatic tumors occurring in everyday clinical practice, particularly during MR examinations. MRI, thanks to its multiparametric approach, can help radiologists to correctly evaluate and characterize liver metastases, reaching a fitted approach for each patient. The wide spectrum of liver metastases should be well-known, especially in the case of atypical appearance. The usefulness of HBAs, especially Gd-EOB-DTPA, has been widely demonstrated in the international literature and should be adopted whenever a liver MRI in patients with known primary tumors is required. Finally, MRI diagnostic accuracy can reach high values, representing nowadays the non-invasive reference standard technique to stage, re-stage and evaluate the prognosis of cancer patients with secondary

liver involvement.

Future directions should be focused firstly on the usefulness of MR as a prognostic tool in patients with liver metastases. Moreover, the integration of AI techniques, especially machine and deep learning models, should be considered to identify liver metastases and to enhance radiologists' confidence in the final diagnosis.

FOOTNOTES

Author contributions: All Authors equally contributed to this paper with the conception and design of the study, literature review and analysis, drafting and critical revision, and editing; All authors gave final approval of the final version.

Conflict-of-interest statement: All the authors report no relevant conflicts of interest for this article.

Open-Access: This article is an open-access article that was selected by an in-house editor and fully peer-reviewed by external reviewers. It is distributed in accordance with the Creative Commons Attribution NonCommercial (CC BY-NC 4.0) license, which permits others to distribute, remix, adapt, build upon this work non-commercially, and license their derivative works on different terms, provided the original work is properly cited and the use is non-commercial. See: https://creativecommons.org/Licenses/by-nc/4.0/

Country/Territory of origin: Italy

ORCID number: Cesare Maino 0000-0002-5742-802X; Federica Vernuccio 0000-0003-0350-1794; Roberto Cannella 0000-0002-3808-0785; Francesco Cortese 0000-0002-2731-3766; Paolo Niccolò Franco 0000-0001-8280-3787; Clara Gaetani 0000-0001-9303-4397; Valentina Giannini 0000-0001-5052-8231; Riccardo Inchingolo 0000-0002-0253-5936; Davide Ippolito 0000-0003-3870-0371; Arianna Defeudis 0000-0002-1745-3044; Giulia Pilato 0009-0004-6265-2079; Davide Tore 0000-0002-5087-5740; Riccardo Faletti 0000-0002-8865-8637; Marco Gatti 0000-0001-8168-5280.

S-Editor: Li L
L-Editor: A
P-Editor: Chen YX

REFERENCES

1 **Namasivayam S**, Martin DR, Saini S. Imaging of liver metastases: MRI. *Cancer Imaging* 2007; **7**: 2-9 [PMID: 17293303 DOI: 10.1102/1470-7330.2007.0002]
2 **Centeno BA**. Pathology of liver metastases. *Cancer Control* 2006; **13**: 13-26 [PMID: 16508622 DOI: 10.1177/107327480601300103]
3 **Tsilimigras DI**, Brodt P, Clavien PA, Muschel RJ, D'Angelica MI, Endo I, Parks RW, Doyle M, de Santibañes E, Pawlik TM. Liver metastases. *Nat Rev Dis Primers* 2021; **7**: 27 [PMID: 33859205 DOI: 10.1038/s41572-021-00261-6]
4 **Alberts SR**, Wagman LD. Chemotherapy for colorectal cancer liver metastases. *Oncologist* 2008; **13**: 1063-1073 [PMID: 18838438 DOI: 10.1634/theoncologist.2008-0142]
5 **Imam K**, Bluemke DA. MR imaging in the evaluation of hepatic metastases. *Magn Reson Imaging Clin N Am* 2000; **8**: 741-756 [PMID: 11149677 DOI: 10.1016/S1064-9689(21)00641-3]
6 **Horn SR**, Stoltzfus KC, Lehrer EJ, Dawson LA, Tchelebi L, Gusani NJ, Sharma NK, Chen H, Trifiletti DM, Zaorsky NG. Epidemiology of liver metastases. *Cancer Epidemiol* 2020; **67**: 101760 [PMID: 32562887 DOI: 10.1016/j.canep.2020.101760]
7 **Zane KE**, Cloyd JM, Mumtaz KS, Wadhwa V, Makary MS. Metastatic disease to the liver: Locoregional therapy strategies and outcomes. *World J Clin Oncol* 2021; **12**: 725-745 [PMID: 34631439 DOI: 10.5306/wjco.v12.i9.725]
8 **Niekel MC**, Bipat S, Stoker J. Diagnostic imaging of colorectal liver metastases with CT, MR imaging, FDG PET, and/or FDG PET/CT: a meta-analysis of prospective studies including patients who have not previously undergone treatment. *Radiology* 2010; **257**: 674-684 [PMID: 20829538 DOI: 10.1148/radiol.10100729]
9 **Floriani I**, Torri V, Rulli E, Garavaglia D, Compagnoni A, Salvolini L, Giovagnoni A. Performance of imaging modalities in diagnosis of liver metastases from colorectal cancer: a systematic review and meta-analysis. *J Magn Reson Imaging* 2010; **31**: 19-31 [PMID: 20027569 DOI: 10.1002/jmri.22010]
10 **Baghdadi A**, Mirpour S, Ghadimi M, Motaghi M, Hazhirkarzar B, Pawlik TM, Kamel IR. Imaging of Colorectal Liver Metastasis. *J Gastrointest Surg* 2022; **26**: 245-257 [PMID: 34664191 DOI: 10.1007/s11605-021-05164-1]
11 **Karaosmanoglu AD**, Onur MR, Ozmen MN, Akata D, Karcaaltincaba M. Magnetic Resonance Imaging of Liver Metastasis. *Semin Ultrasound CT MR* 2016; **37**: 533-548 [PMID: 27986172 DOI: 10.1053/j.sult.2016.08.005]
12 **Koh DM**. Liver-specific contrast agents. *Cancer Imaging* 2012; **12**: 363-364 [PMID: 23023233 DOI: 10.1102/1470-7330.2012.9022]
13 **Fiorentini G**, Sarti D, Aliberti C, Carandina R, Mambrini A, Guadagni S. Multidisciplinary approach of colorectal cancer liver metastases. *World J Clin Oncol* 2017; **8**: 190-202 [PMID: 28638789 DOI: 10.5306/wjco.v8.i3.190]
14 **Chandarana H**, Feng L, Ream J, Wang A, Babb JS, Block KT, Sodickson DK, Otazo R. Respiratory Motion-Resolved Compressed Sensing Reconstruction of Free-Breathing Radial Acquisition for Dynamic Liver Magnetic Resonance Imaging. *Invest Radiol* 2015; **50**: 749-756 [PMID: 26146869 DOI: 10.1097/RLI.0000000000000179]
15 **Hood MN**, Ho VB, Smirniotopoulos JG, Szumowski J. Chemical shift: the artifact and clinical tool revisited. *Radiographics* 1999; **19**: 357-371 [PMID: 10194784 DOI: 10.1148/radiographics.19.2.g99mr07357]
16 **Agostini A**, Kircher MF, Do RK, Borgheresi A, Monti S, Giovagnoni A, Mannelli L. Magnetic Resonanance Imaging of the Liver (Including Biliary Contrast Agents)-Part 2: Protocols for Liver Magnetic Resonanance Imaging and Characterization of Common Focal Liver Lesions. *Semin Roentgenol* 2016; **51**: 317-333 [PMID: 27743568 DOI: 10.1053/j.ro.2016.05.016]

17 **Baliyan V**, Das CJ, Sharma R, Gupta AK. Diffusion weighted imaging: Technique and applications. *World J Radiol* 2016; **8**: 785-798 [PMID: 27721941 DOI: 10.4329/wjr.v8.i9.785]

18 **Qayyum A**. Diffusion-weighted imaging in the abdomen and pelvis: concepts and applications. *Radiographics* 2009; **29**: 1797-1810 [PMID: 19959522 DOI: 10.1148/rg.296095521]

19 **Frydrychowicz A**, Lubner MG, Brown JJ, Merkle EM, Nagle SK, Rofsky NM, Reeder SB. Hepatobiliary MR imaging with gadolinium-based contrast agents. *J Magn Reson Imaging* 2012; **35**: 492-511 [PMID: 22334493 DOI: 10.1002/jmri.22833]

20 **Qu J**, Han S, Zhang H, Liu H, Wang Z, Kamel IR, Berthold K, Dominik NM, Zhang J, Zhang S, Dong Y, Jiang L, Liu C, Li H. Arterial Phase with CAIPIRINHA-Dixon-TWIST (CDT)-Volume-Interpolated Breath-Hold Examination (VIBE) in Detecting Hepatic Metastases. *Transl Oncol* 2017; **10**: 46-53 [PMID: 27940372 DOI: 10.1016/j.tranon.2016.11.005]

21 **Okada M**, Wakayama T, Yada N, Hyodo T, Numata K, Kagawa Y, Nishiyama D, Miyakoshi K, Murakami T. Optimal flip angle of Gd-EOB-DTPA-enhanced MRI in patients with hepatocellular carcinoma and liver metastasis. *Abdom Imaging* 2014; **39**: 694-701 [PMID: 24562726 DOI: 10.1007/s00261-014-0096-y]

22 **Jhan SR**, Wu YY, Chang PY, Chai JW, Su TC. Comparison of ability of lesion detection of two MRI sequences of T2WI HASTE and T2WI BLADE for hepatocellular carcinoma. *Medicine (Baltimore)* 2023; **102**: e32890 [PMID: 36820556 DOI: 10.1097/MD.0000000000032890]

23 **Gandhi SN**, Brown MA, Wong JG, Aguirre DA, Sirlin CB. MR contrast agents for liver imaging: what, when, how. *Radiographics* 2006; **26**: 1621-1636 [PMID: 17102040 DOI: 10.1148/rg.266065014]

24 **Matos AP**, Velloni F, Ramalho M, AlObaidy M, Rajapaksha A, Semelka RC. Focal liver lesions: Practical magnetic resonance imaging approach. *World J Hepatol* 2015; **7**: 1987-2008 [PMID: 26261689 DOI: 10.4254/wjh.v7.i16.1987]

25 **Welle CL**, Guglielmo FF, Venkatesh SK. MRI of the liver: choosing the right contrast agent. *Abdom Radiol (NY)* 2020; **45**: 384-392 [PMID: 31392396 DOI: 10.1007/s00261-019-02162-5]

26 **Neri E**, Bali MA, Ba-Ssalamah A, Boraschi P, Brancatelli G, Alves FC, Grazioli L, Helmberger T, Lee JM, Manfredi R, Martì-Bonmatì L, Matos C, Merkle EM, Op De Beeck B, Schima W, Skehan S, Vilgrain V, Zech C, Bartolozzi C. ESGAR consensus statement on liver MR imaging and clinical use of liver-specific contrast agents. *Eur Radiol* 2016; **26**: 921-931 [PMID: 26194455 DOI: 10.1007/s00330-015-3900-3]

27 **Wang C**, Yuan XD, Wu N, Sun WR, Tian Y. Optimization of hepatobiliary phase imaging in gadoxetic acid-enhanced magnetic resonance imaging: a narrative review. *Quant Imaging Med Surg* 2023; **13**: 1972-1982 [PMID: 36915322 DOI: 10.21037/qims-22-916]

28 **Kalor A**, Girometti R, Maheshwari E, Kierans AS, Pugliesi RA, Buros C, Furlan A. Update on MR Contrast Agents for Liver Imaging: What to Use and When. *Radiol Clin North Am* 2022; **60**: 679-694 [PMID: 35989037 DOI: 10.1016/j.rcl.2022.04.005]

29 **Reimer P**, Schneider G, Schima W. Hepatobiliary contrast agents for contrast-enhanced MRI of the liver: properties, clinical development and applications. *Eur Radiol* 2004; **14**: 559-578 [PMID: 14986050 DOI: 10.1007/s00330-004-2236-1]

30 **Chen L**, Zhang J, Zhang L, Bao J, Liu C, Xia Y, Huang X, Wang J. Meta-analysis of gadoxetic acid disodium (Gd-EOB-DTPA)-enhanced magnetic resonance imaging for the detection of liver metastases. *PLoS One* 2012; **7**: e48681 [PMID: 23144927 DOI: 10.1371/journal.pone.0048681]

31 **Winder M**, Grabowska S, Hitnarowicz A, Barczyk-Gutkowska A, Gruszczyńska K, Steinhof-Radwańska K. The application of abbreviated MRI protocols in malignant liver lesions surveillance. *Eur J Radiol* 2023; **164**: 110840 [PMID: 37141846 DOI: 10.1016/j.ejrad.2023.110840]

32 **Ozaki K**, Higuchi S, Kimura H, Gabata T. Liver Metastases: Correlation between Imaging Features and Pathomolecular Environments. *Radiographics* 2022; **42**: 1994-2013 [PMID: 36149824 DOI: 10.1148/rg.220056]

33 **Vilgrain V**, Esvan M, Ronot M, Caumont-Prim A, Aubé C, Chatellier G. A meta-analysis of diffusion-weighted and gadoxetic acid-enhanced MR imaging for the detection of liver metastases. *Eur Radiol* 2016; **26**: 4595-4615 [PMID: 26883327 DOI: 10.1007/s00330-016-4250-5]

34 **Furlan A**, Marin D, Bae KT, Lagalla R, Agnello F, Bazzocchi M, Brancatelli G. Focal liver lesions hyperintense on T1-weighted magnetic resonance images. *Semin Ultrasound CT MR* 2009; **30**: 436-449 [PMID: 19842568 DOI: 10.1053/j.sult.2009.07.002]

35 **Costa AF**, Thipphavong S, Arnason T, Stueck AE, Clarke SE. Fat-Containing Liver Lesions on Imaging: Detection and Differential Diagnosis. *AJR Am J Roentgenol* 2018; **210**: 68-77 [PMID: 29064755 DOI: 10.2214/AJR.17.18136]

36 **Porrello G**, Cannella R, Randazzo A, Badalamenti G, Brancatelli G, Vernuccio F. CT and MR Imaging of Retroperitoneal Sarcomas: A Practical Guide for the Radiologist. *Cancers (Basel)* 2023; **15** [PMID: 37296946 DOI: 10.3390/cancers15112985]

37 **Paulatto L**, Dioguardi Burgio M, Sartoris R, Beaufrère A, Cauchy F, Paradis V, Vilgrain V, Ronot M. Colorectal liver metastases: radiopathological correlation. *Insights Imaging* 2020; **11**: 99 [PMID: 32844319 DOI: 10.1186/s13244-020-00904-4]

38 **Danet IM**, Semelka RC, Leonardou P, Braga L, Vaidean G, Woosley JT, Kanematsu M. Spectrum of MRI appearances of untreated metastases of the liver. *AJR Am J Roentgenol* 2003; **181**: 809-817 [PMID: 12933487 DOI: 10.2214/ajr.181.3.1810809]

39 **Dahlqvist Leinhard O**, Dahlström N, Kihlberg J, Sandström P, Brismar TB, Smedby O, Lundberg P. Quantifying differences in hepatic uptake of the liver specific contrast agents Gd-EOB-DTPA and Gd-BOPTA: a pilot study. *Eur Radiol* 2012; **22**: 642-653 [PMID: 21984449 DOI: 10.1007/s00330-011-2302-4]

40 **Hui CL**, Mautone M. Patterns of enhancement in the hepatobiliary phase of gadoxetic acid-enhanced MRI. *Br J Radiol* 2020; **93**: 20190989 [PMID: 32462892 DOI: 10.1259/bjr.20190989]

41 **Vernuccio F**, Gagliano DS, Cannella R, Ba-Ssalamah A, Tang A, Brancatelli G. Spectrum of liver lesions hyperintense on hepatobiliary phase: an approach by clinical setting. *Insights Imaging* 2021; **12**: 8 [PMID: 33432491 DOI: 10.1186/s13244-020-00928-w]

42 **Park SH**, Kim H, Kim EK, Choi DK, Chung YE, Kim MJ, Choi JY. Aberrant expression of OATP1B3 in colorectal cancer liver metastases and its clinical implication on gadoxetic acid-enhanced MRI. *Oncotarget* 2017; **8**: 71012-71023 [PMID: 29050339 DOI: 10.18632/oncotarget.20295]

43 **Choi SH**, Kim SY, Park SH, Kim KW, Lee JY, Lee SS, Lee MG. Diagnostic performance of CT, gadoxetate disodium-enhanced MRI, and PET/CT for the diagnosis of colorectal liver metastasis: Systematic review and meta-analysis. *J Magn Reson Imaging* 2018; **47**: 1237-1250 [PMID: 28901685 DOI: 10.1002/jmri.25852]

44 **Nakai H**, Arizono S, Isoda H, Togashi K. Imaging Characteristics of Liver Metastases Overlooked at Contrast-Enhanced CT. *AJR Am J Roentgenol* 2019; **212**: 782-787 [PMID: 30779660 DOI: 10.2214/AJR.18.20526]

45 **Cannella R**, Cunha GM, Catania R, Chupetlovska K, Borhani AA, Fowler KJ, Furlan A. Magnetic Resonance Imaging of Nonhepatocellular Malignancies in Chronic Liver Disease. *Magn Reson Imaging Clin N Am* 2021; **29**: 404-418 [PMID: 34243926 DOI: 10.1016/j.mric.2021.05.009]

46 **Ikram NS**, Yee J, Weinstein S, Yeh BM, Corvera CU, Monto A, Hope TA. Multiple arterial phase MRI of arterial hypervascular hepatic lesions: improved arterial phase capture and lesion enhancement. *Abdom Radiol (NY)* 2017; **42**: 870-876 [PMID: 27770162 DOI:

10.1007/s00261-016-0948-8]
47 **Hong S**, Choi SH, Hong SB, Kim SY, Lee SS. Clinical usefulness of multiple arterial-phase images in gadoxetate disodium-enhanced magnetic resonance imaging: a systematic review and meta-analysis. *Eur Radiol* 2022; **32**: 5413-5423 [PMID: 35192009 DOI: 10.1007/s00330-022-08620-x]
48 **Borhani AA**, Wiant A, Heller MT. Cystic hepatic lesions: a review and an algorithmic approach. *AJR Am J Roentgenol* 2014; **203**: 1192-1204 [PMID: 25415696 DOI: 10.2214/AJR.13.12386]
49 **Lee JE**, Kim SH, Lee S, Choi SY, Hwang JA, Woo SY. Differentiating metastatic mucinous colorectal adenocarcinomas from simple cysts of the liver using contrast-enhanced and diffusion-weighted MRI. *Br J Radiol* 2018; **91**: 20180303 [PMID: 30040437 DOI: 10.1259/bjr.20180303]
50 **Patnana M**, Menias CO, Pickhardt PJ, Elshikh M, Javadi S, Gaballah A, Shaaban AM, Korivi BR, Garg N, Elsayes KM. Liver Calcifications and Calcified Liver Masses: Pattern Recognition Approach on CT. *AJR Am J Roentgenol* 2018; **211**: 76-86 [PMID: 29667888 DOI: 10.2214/AJR.18.19704]
51 **Hale HL**, Husband JE, Gossios K, Norman AR, Cunningham D. CT of calcified liver metastases in colorectal carcinoma. *Clin Radiol* 1998; **53**: 735-741 [PMID: 9817090 DOI: 10.1016/s0009-9260(98)80315-2]
52 **Kim SJ**, Choi JA, Lee SH, Choi JY, Hong SH, Chung HW, Kang HS. Imaging findings of extrapulmonary metastases of osteosarcoma. *Clin Imaging* 2004; **28**: 291-300 [PMID: 15246481 DOI: 10.1016/S0899-7071(03)00206-7]
53 **Engel S**, Dockerty MB. Calcification and ossification in rectal malignant processes. *JAMA* 1962; **179**: 347-350 [PMID: 13890226 DOI: 10.1001/jama.1962.03050050037006]
54 **Miele AJ**, Edmonds HW. Calcified liver metastases: a specific roentgen diagnostic sign. *Radiology* 1963; **80**: 779-785 [PMID: 13935630 DOI: 10.1148/80.5.779]
55 **Zhou Y**, Zhang J, Dan Pu, Bi F, Chen Y, Liu J, Li Q, Gou H, Wu B, Qiu M. Tumor calcification as a prognostic factor in cetuximab plus chemotherapy-treated patients with metastatic colorectal cancer. *Anticancer Drugs* 2019; **30**: 195-200 [PMID: 30570508 DOI: 10.1097/CAD.0000000000000726]
56 **Nakayama T**, Yoshimitsu K, Irie H, Aibe H, Tajima T, Shinozaki K, Nishie A, Kakihara D, Honda H. Fat in liver metastasis from renal cell carcinoma detected by chemical shift MR imaging. *Abdom Imaging* 2003; **28**: 657-659 [PMID: 14628870 DOI: 10.1007/s00261-003-0001-6]
57 **Khalil HI**, Patterson SA, Panicek DM. Hepatic lesions deemed too small to characterize at CT: prevalence and importance in women with breast cancer. *Radiology* 2005; **235**: 872-878 [PMID: 15833992 DOI: 10.1148/radiol.2353041099]
58 **Bird JR**, Brahm GL, Fung C, Sebastian S, Kirkpatrick IDC. Recommendations for the Management of Incidental Hepatobiliary Findings in Adults: Endorsement and Adaptation of the 2017 and 2013 ACR Incidental Findings Committee White Papers by the Canadian Association of Radiologists Incidental Findings Working Group. *Can Assoc Radiol J* 2020; **71**: 437-447 [PMID: 32515993 DOI: 10.1177/0846537120928349]
59 **Gore RM**, Pickhardt PJ, Mortele KJ, Fishman EK, Horowitz JM, Fimmel CJ, Talamonti MS, Berland LL, Pandharipande PV. Management of Incidental Liver Lesions on CT: A White Paper of the ACR Incidental Findings Committee. *J Am Coll Radiol* 2017; **14**: 1429-1437 [PMID: 28927870 DOI: 10.1016/j.jacr.2017.07.018]
60 **Margolis NE**, Shaver CM, Rosenkrantz AB. Indeterminate liver and renal lesions: comparison of computed tomography and magnetic resonance imaging in providing a definitive diagnosis and impact on recommendations for additional imaging. *J Comput Assist Tomogr* 2013; **37**: 882-886 [PMID: 24270109 DOI: 10.1097/RCT.0b013e3182aace0d]
61 **Holzapfel K**, Bruegel M, Eiber M, Ganter C, Schuster T, Heinrich P, Rummeny EJ, Gaa J. Characterization of small (≤10 mm) focal liver lesions: value of respiratory-triggered echo-planar diffusion-weighted MR imaging. *Eur J Radiol* 2010; **76**: 89-95 [PMID: 19501995 DOI: 10.1016/j.ejrad.2009.05.014]
62 **Vernuccio F**, Bruno A, Costanzo V, Bartolotta TV, Vieni S, Midiri M, Salvaggio G, Brancatelli G. Comparison of the Enhancement Pattern of Hepatic Hemangioma on Magnetic Resonance Imaging Performed With Gd-EOB-DTPA Versus Gd-BOPTA. *Curr Probl Diagn Radiol* 2020; **49**: 398-403 [PMID: 31253462 DOI: 10.1067/j.cpradiol.2019.06.006]
63 **Dioguardi Burgio M**, Bruno O, Agnello F, Torrisi C, Vernuccio F, Cabibbo G, Soresi M, Petta S, Calamia M, Papia G, Gambino A, Ricceri V, Midiri M, Lagalla R, Brancatelli G. The cheating liver: imaging of focal steatosis and fatty sparing. *Expert Rev Gastroenterol Hepatol* 2016; **10**: 671-678 [PMID: 27027652 DOI: 10.1586/17474124.2016.1169919]
64 **Moosavi B**, Shenoy-Bhangle AS, Tsai LL, Reuf R, Mortele KJ. MRI characterization of focal liver lesions in non-cirrhotic patients: assessment of added value of gadoxetic acid-enhanced hepatobiliary phase imaging. *Insights Imaging* 2020; **11**: 101 [PMID: 32960337 DOI: 10.1186/s13244-020-00894-3]
65 **Chernyak V**, Horowitz JM, Kamel IR, Arif-Tiwari H, Bashir MR, Cash BD, Farrell J, Goldstein A, Grajo JR, Gupta S, Hindman NM, Kamaya A, McNamara MM, Porter KK, Solnes LB, Srivastava PK, Zaheer A, Carucci LR, Expert Panel on Gastrointestinal Imaging. ACR Appropriateness Criteria® Liver Lesion-Initial Characterization. *J Am Coll Radiol* 2020; **17**: S429-S446 [PMID: 33153555 DOI: 10.1016/j.jacr.2020.09.005]
66 **Zech CJ**, Grazioli L, Breuer J, Reiser MF, Schoenberg SO. Diagnostic performance and description of morphological features of focal nodular hyperplasia in Gd-EOB-DTPA-enhanced liver magnetic resonance imaging: results of a multicenter trial. *Invest Radiol* 2008; **43**: 504-511 [PMID: 18580333 DOI: 10.1097/RLI.0b013e3181705cd1]
67 **Ablefoni M**, Surup H, Ehrengut C, Schindler A, Seehofer D, Denecke T, Meyer HJ. Diagnostic Benefit of High b-Value Computed Diffusion-Weighted Imaging in Patients with Hepatic Metastasis. *J Clin Med* 2021; **10** [PMID: 34830572 DOI: 10.3390/jcm10225289]
68 **Hazhirkarzar B**, Khoshpouri P, Shaghaghi M, Ghasabeh MA, Pawlik TM, Kamel IR. Current state of the art imaging approaches for colorectal liver metastasis. *Hepatobiliary Surg Nutr* 2020; **9**: 35-48 [PMID: 32140477 DOI: 10.21037/hbsn.2019.05.11]
69 **Tang L**, Zhou XJ. Diffusion MRI of cancer: From low to high b-values. *J Magn Reson Imaging* 2019; **49**: 23-40 [PMID: 30311988 DOI: 10.1002/jmri.26293]
70 **Kele PG**, van der Jagt EJ. Diffusion weighted imaging in the liver. *World J Gastroenterol* 2010; **16**: 1567-1576 [PMID: 20355235 DOI: 10.3748/wjg.v16.i13.1567]
71 **Coenegrachts K**, Delanote J, Ter Beek L, Haspeslagh M, Bipat S, Stoker J, Van Kerkhove F, Steyaert L, Rigauts H, Casselman JW. Improved focal liver lesion detection: comparison of single-shot diffusion-weighted echoplanar and single-shot T2 weighted turbo spin echo techniques. *Br J Radiol* 2007; **80**: 524-531 [PMID: 17510250 DOI: 10.1259/bjr/33156643]
72 **Parikh T**, Drew SJ, Lee VS, Wong S, Hecht EM, Babb JS, Taouli B. Focal liver lesion detection and characterization with diffusion-weighted MR imaging: comparison with standard breath-hold T2W imaging. *Radiology* 2008; **246**: 812-822 [PMID: 18223123 DOI: 10.1148/radiol.2463070432]

73 **Bruegel M**, Rummeny EJ. Hepatic metastases: use of diffusion-weighted echo-planar imaging. *Abdom Imaging* 2010; **35**: 454-461 [PMID: 19471997 DOI: 10.1007/s00261-009-9541-8]

74 **Mainenti PP**, Romano F, Pizzuti L, Segreto S, Storto G, Mannelli L, Imbriaco M, Camera L, Maurea S. Non-invasive diagnostic imaging of colorectal liver metastases. *World J Radiol* 2015; **7**: 157-169 [PMID: 26217455 DOI: 10.4329/wjr.v7.i7.157]

75 **Sobeh T**, Inbar Y, Apter S, Soffer S, Anteby R, Kraus M, Konen E, Klang E. Diffusion-weighted MRI for predicting and assessing treatment response of liver metastases from CRC - A systematic review and meta-analysis. *Eur J Radiol* 2023; **163**: 110810 [PMID: 37075628 DOI: 10.1016/j.ejrad.2023.110810]

76 **Drewes R**, Pech M, Powerski M, Omari J, Heinze C, Damm R, Wienke A, Surov A. Apparent Diffusion Coefficient Can Predict Response to Chemotherapy of Liver Metastases in Colorectal Cancer. *Acad Radiol* 2021; **28** Suppl 1: S73-S80 [PMID: 33008734 DOI: 10.1016/j.acra.2020.09.006]

77 **Beckers RCJ**, Lambregts DMJ, Lahaye MJ, Rao SX, Kleinen K, Grootscholten C, Beets GL, Beets-Tan RGH, Maas M. Advanced imaging to predict response to chemotherapy in colorectal liver metastases - a systematic review. *HPB (Oxford)* 2018; **20**: 120-127 [PMID: 29196021 DOI: 10.1016/j.hpb.2017.10.013]

78 **Caruso M**, Stanzione A, Prinster A, Pizzuti LM, Brunetti A, Maurea S, Mainenti PP. Role of advanced imaging techniques in the evaluation of oncological therapies in patients with colorectal liver metastases. *World J Gastroenterol* 2023; **29**: 521-535 [PMID: 36688023 DOI: 10.3748/wjg.v29.i3.521]

79 **Cui Y**, Zhang XP, Sun YS, Tang L, Shen L. Apparent diffusion coefficient: potential imaging biomarker for prediction and early detection of response to chemotherapy in hepatic metastases. *Radiology* 2008; **248**: 894-900 [PMID: 18710982 DOI: 10.1148/radiol.2483071407]

80 **Nalaini F**, Shahbazi F, Mousavinezhad SM, Ansari A, Salehi M. Diagnostic accuracy of apparent diffusion coefficient (ADC) value in differentiating malignant from benign solid liver lesions: a systematic review and meta-analysis. *Br J Radiol* 2021; **94**: 20210059 [PMID: 34111960 DOI: 10.1259/bjr.20210059]

81 **Kim JH**, Joo I, Kim TY, Han SW, Kim YJ, Lee JM, Han JK. Diffusion-Related MRI Parameters for Assessing Early Treatment Response of Liver Metastases to Cytotoxic Therapy in Colorectal Cancer. *AJR Am J Roentgenol* 2016; **207**: W26-W32 [PMID: 27303858 DOI: 10.2214/AJR.15.15683]

82 **Jensen JH**, Helpern JA, Ramani A, Lu H, Kaczynski K. Diffusional kurtosis imaging: the quantification of non-gaussian water diffusion by means of magnetic resonance imaging. *Magn Reson Med* 2005; **53**: 1432-1440 [PMID: 15906300 DOI: 10.1002/mrm.20508]

83 **Zhang H**, Li W, Fu C, Grimm R, Chen Z, Zhang W, Qiu L, Wang C, Zhang X, Yue L, Hu X, Guo W, Tong T. Comparison of intravoxel incoherent motion imaging, diffusion kurtosis imaging, and conventional DWI in predicting the chemotherapeutic response of colorectal liver metastases. *Eur J Radiol* 2020; **130**: 109149 [PMID: 32659615 DOI: 10.1016/j.ejrad.2020.109149]

84 **Saito K**, Tajima Y, Harada TL. Diffusion-weighted imaging of the liver: Current applications. *World J Radiol* 2016; **8**: 857-867 [PMID: 27928467 DOI: 10.4329/wjr.v8.i11.857]

85 **Xie S**, Masokano IB, Liu W, Long X, Li G, Pei Y, Li W. Comparing the clinical utility of single-shot echo-planar imaging and readout-segmented echo-planar imaging in diffusion-weighted imaging of the liver at 3 tesla. *Eur J Radiol* 2021; **135**: 109472 [PMID: 33370640 DOI: 10.1016/j.ejrad.2020.109472]

86 **Zech CJ**, Korpraphong P, Huppertz A, Denecke T, Kim MJ, Tanomkiat W, Jonas E, Ba-Ssalamah A; VALUE study group. Randomized multicentre trial of gadoxetic acid-enhanced MRI versus conventional MRI or CT in the staging of colorectal cancer liver metastases. *Br J Surg* 2014; **101**: 613-621 [PMID: 24652690 DOI: 10.1002/bjs.9465]

87 **Vreugdenburg TD**, Ma N, Duncan JK, Riitano D, Cameron AL, Maddern GJ. Comparative diagnostic accuracy of hepatocyte-specific gadoxetic acid (Gd-EOB-DTPA) enhanced MR imaging and contrast enhanced CT for the detection of liver metastases: a systematic review and meta-analysis. *Int J Colorectal Dis* 2016; **31**: 1739-1749 [PMID: 27682648 DOI: 10.1007/s00384-016-2664-9]

88 **Zech CJ**, Justo N, Lang A, Ba-Ssalamah A, Kim MJ, Rinde H, Jonas E. Cost evaluation of gadoxetic acid-enhanced magnetic resonance imaging in the diagnosis of colorectal-cancer metastasis in the liver: Results from the VALUE Trial. *Eur Radiol* 2016; **26**: 4121-4130 [PMID: 26905871 DOI: 10.1007/s00330-016-4271-0]

89 **Renzulli M**, Clemente A, Ierardi AM, Pettinari I, Tovoli F, Brocchi S, Peta G, Cappabianca S, Carrafiello G, Golfieri R. Imaging of Colorectal Liver Metastases: New Developments and Pending Issues. *Cancers (Basel)* 2020; **12** [PMID: 31936319 DOI: 10.3390/cancers12010151]

90 **Kim C**, Kim SY, Kim MJ, Yoon YS, Kim CW, Lee JH, Kim KP, Lee SS, Park SH, Lee MG. Clinical impact of preoperative liver MRI in the evaluation of synchronous liver metastasis of colon cancer. *Eur Radiol* 2018; **28**: 4234-4242 [PMID: 29691635 DOI: 10.1007/s00330-018-5422-2]

91 **Gu XL**, Cui Y, Wang K, Xing Q, Li XT, Zhu HT, Li ZW, Sun YS. Qualitative and quantitative parameters on hepatobiliary phase of gadoxetic acid-enhanced MR imaging for predicting pathological response to preoperative systemic therapy in colorectal liver metastases. *Eur J Radiol* 2022; **157**: 110572 [PMID: 36327859 DOI: 10.1016/j.ejrad.2022.110572]

92 **Murata S**, Matsushima S, Sato Y, Yamaura H, Kato M, Hasegawa T, Muro K, Inaba Y. Predicting chemotherapeutic response for colorectal liver metastases using relative tumor enhancement of gadoxetic acid disodium-enhanced magnetic resonance imaging. *Abdom Radiol (NY)* 2018; **43**: 3301-3306 [PMID: 29666951 DOI: 10.1007/s00261-018-1615-z]

93 **Yoneda N**, Matsui O, Ikeno H, Inoue D, Yoshida K, Kitao A, Kozaka K, Kobayashi S, Gabata T, Ikeda H, Nakamura K, Ohta T. Correlation between Gd-EOB-DTPA-enhanced MR imaging findings and OATP1B3 expression in chemotherapy-associated sinusoidal obstruction syndrome. *Abdom Imaging* 2015; **40**: 3099-3103 [PMID: 26187715 DOI: 10.1007/s00261-015-0503-z]

94 **Rompianesi G**, Pegoraro F, Ceresa CD, Montalti R, Troisi RI. Artificial intelligence in the diagnosis and management of colorectal cancer liver metastases. *World J Gastroenterol* 2022; **28**: 108-122 [PMID: 35125822 DOI: 10.3748/wjg.v28.i1.108]

95 **Hamm CA**, Wang CJ, Savic LJ, Ferrante M, Schobert I, Schlachter T, Lin M, Duncan JS, Weinreb JC, Chapiro J, Letzen B. Deep learning for liver tumor diagnosis part I: development of a convolutional neural network classifier for multi-phasic MRI. *Eur Radiol* 2019; **29**: 3338-3347 [PMID: 31016442 DOI: 10.1007/s00330-019-06205-9]

96 **Liu Y**, Kohlberger T, Norouzi M, Dahl GE, Smith JL, Mohtashamian A, Olson N, Peng LH, Hipp JD, Stumpe MC. Artificial Intelligence-Based Breast Cancer Nodal Metastasis Detection: Insights Into the Black Box for Pathologists. *Arch Pathol Lab Med* 2019; **143**: 859-868 [PMID: 30295070 DOI: 10.5858/arpa.2018-0147-OA]

97 **Rao SX**, Lambregts DM, Schnerr RS, Beckers RC, Maas M, Albarello F, Riedl RG, Dejong CH, Martens MH, Heijnen LA, Backes WH, Beets GL, Zeng MS, Beets-Tan RG. CT texture analysis in colorectal liver metastases: A better way than size and volume measurements to assess response to chemotherapy? *United European Gastroenterol J* 2016; **4**: 257-263 [PMID: 27087955 DOI: 10.1177/2050640615601603]

98 **Zhang H**, Li W, Hu F, Sun Y, Hu T, Tong T. MR texture analysis: potential imaging biomarker for predicting the chemotherapeutic response

of patients with colorectal liver metastases. *Abdom Radiol (NY)* 2019; **44**: 65-71 [PMID: 29967982 DOI: 10.1007/s00261-018-1682-1]

99 **Reimer RP**, Reimer P, Mahnken AH. Assessment of Therapy Response to Transarterial Radioembolization for Liver Metastases by Means of Post-treatment MRI-Based Texture Analysis. *Cardiovasc Intervent Radiol* 2018; **41**: 1545-1556 [PMID: 29881933 DOI: 10.1007/s00270-018-2004-2]

100 **Granata V**, Fusco R, De Muzio F, Cutolo C, Setola SV, Grassi R, Grassi F, Ottaiano A, Nasti G, Tatangelo F, Pilone V, Miele V, Brunese MC, Izzo F, Petrillo A. Radiomics textural features by MR imaging to assess clinical outcomes following liver resection in colorectal liver metastases. *Radiol Med* 2022; **127**: 461-470 [PMID: 35347583 DOI: 10.1007/s11547-022-01477-6]

101 **Han Y**, Chai F, Wei J, Yue Y, Cheng J, Gu D, Zhang Y, Tong T, Sheng W, Hong N, Ye Y, Wang Y, Tian J. Identification of Predominant Histopathological Growth Patterns of Colorectal Liver Metastasis by Multi-Habitat and Multi-Sequence Based Radiomics Analysis. *Front Oncol* 2020; **10**: 1363 [PMID: 32923388 DOI: 10.3389/fonc.2020.01363]

102 **Jansen MJA**, Kuijf HJ, Veldhuis WB, Wessels FJ, Viergever MA, Pluim JPW. Automatic classification of focal liver lesions based on MRI and risk factors. *PLoS One* 2019; **14**: e0217053 [PMID: 31095624 DOI: 10.1371/journal.pone.0217053]

103 **Granata V**, Fusco R, Avallone A, De Stefano A, Ottaiano A, Sbordone C, Brunese L, Izzo F, Petrillo A. Radiomics-Derived Data by Contrast Enhanced Magnetic Resonance in RAS Mutations Detection in Colorectal Liver Metastases. *Cancers (Basel)* 2021; **13** [PMID: 33504085 DOI: 10.3390/cancers13030453]

104 **Fiz F**, Viganò L, Gennaro N, Costa G, La Bella L, Boichuk A, Cavinato L, Sollini M, Politi LS, Chiti A, Torzilli G. Radiomics of Liver Metastases: A Systematic Review. *Cancers (Basel)* 2020; **12** [PMID: 33036490 DOI: 10.3390/cancers12102881]

World Journal of Gastroenterology

Submit a Manuscript: https://www.f6publishing.com

World J Gastroenterol 2023 September 28; 29(36): 5198-5210

DOI: 10.3748/wjg.v29.i36.5198

ISSN 1007-9327 (print) ISSN 2219-2840 (online)

MINIREVIEWS

Clinical approach to indeterminate biliary strictures: Clinical presentation, diagnosis, and workup

Sujani Yadlapati, Ramzi Mulki, Sergio A Sánchez-Luna, Ali M Ahmed, Kondal Rao Kyanam Kabir Baig, Shajan Peter

Specialty type: Gastroenterology and hepatology

Provenance and peer review: Invited article; Externally peer reviewed.

Peer-review model: Single blind

Peer-review report's scientific quality classification

Grade A (Excellent): 0
Grade B (Very good): B, B, B
Grade C (Good): 0
Grade D (Fair): 0
Grade E (Poor): 0

P-Reviewer: Khalil MTASH, Egypt; Kim HJ, South Korea; Wang LM, China

Received: April 25, 2023
Peer-review started: April 25, 2023
First decision: July 9, 2023
Revised: July 23, 2023
Accepted: August 21, 2023
Article in press: August 21, 2023
Published online: September 28, 2023

Sujani Yadlapati, Department of Gastroenterology and Hepatology, Indiana University Hospital, Indianapolis, IN 46202, USA

Ramzi Mulki, Sergio A Sánchez-Luna, Ali M Ahmed, Kondal Rao Kyanam Kabir Baig, Shajan Peter, Department of Gastroenterology and Hepatology, University of Alabama at Birmingham, Birmingham, AL 35294, USA

Corresponding author: Sujani Yadlapati, MD, Doctor, Department of Gastroenterology and Hepatology, Indiana University Hospital, 500 N University Blvd, Indianapolis, IN 46202, United States. syadlapati@iuhealth.org

Abstract

Despite advances in cross-sectional imaging and endoscopic technology, bile duct strictures remain a challenging clinical entity. It is crucial to make an early determination of benign or malignant nature of biliary strictures. Early diagnosis not only helps with further management but also minimizes mortality and morbidity associated with delayed diagnosis. Conventional imaging and endoscopic techniques, particularly endoscopic retrograde cholangiopancreatography (ERCP) and tissue sampling techniques play a key in establishing a diagnosis. Indeterminate biliary strictures (IDBSs) have no definite mass on imaging or absolute histopathological diagnosis and often warrant utilization of multiple diagnostics to ascertain an etiology. In this review, we discuss possible etiologies, clinical presentation, diagnosis, and management of IDBSs. Based on available data and expert opinion, we depict an evidence based diagnostic algorithm for management of IDBSs. Areas of focus include use of traditional tissue sampling techniques such as ERCP with brush cytology, intraductal biopsies, fluorescence *in situ* hybridization and flow cytometry. We also describe the role of endoscopic ultrasound (EUS)-guided fine needle aspiration and biopsies, cholangioscopy, confocal laser endomicroscopy, and intraductal EUS in management of IDBSs.

Key Words: Biliary strictures; Indeterminate strictures; Biliary sampling; Cholangioscopy; Benign strictures; Malignant strictures; Indeterminate biliary strictures

©The Author(s) 2023. Published by Baishideng Publishing Group Inc. All rights reserved.

Core Tip: Despite advances in imaging and endoscopy, bile duct strictures remain challenging. Timely detection of malignant strictures is crucial. Conventional techniques play a crucial role in diagnosis, but indeterminate biliary strictures (IDBSs) require multiple diagnostic tools. This review discusses etiology, diagnosis, and workup of IDBSs, presenting an evidence-based algorithm focusing on traditional tissue sampling techniques and innovative technologies. The importance of future research is emphasized.

Citation: Yadlapati S, Mulki R, Sánchez-Luna SA, Ahmed AM, Kyanam Kabir Baig KR, Peter S. Clinical approach to indeterminate biliary strictures: Clinical presentation, diagnosis, and workup. *World J Gastroenterol* 2023; 29(36): 5198-5210
URL: https://www.wjgnet.com/1007-9327/full/v29/i36/5198.htm
DOI: https://dx.doi.org/10.3748/wjg.v29.i36.5198

INTRODUCTION

Bile duct strictures are commonly encountered in clinical practice and pose a diagnostic challenge to endoscopists. The diagnostic difficulty lies in differentiating malignant strictures from benign strictures. Failure to diagnose malignant strictures or subjecting patients with benign strictures to unwarranted surgery can result in increased morbidity and mortality. Biliary strictures are characterized as indeterminate when no overt mass or differentiating characteristics are seen on cross-sectional imaging or after performing endoscopic retrograde cholangiopancreatography (ERCP) with standard diagnostic tools[1]. At present, up to 20% of biliary strictures are indeterminate. These strictures include both benign and malignant conditions. Biliary strictures may result from intrinsic biliary pathology as well as from extrinsic compression or infiltration from benign or malignant lesions.

Based on previous observational studies, up to one-third of biliary strictures are benign, and two-thirds are malignant in nature[2]. Inflammatory strictures, particularly those related to primary sclerosing cholangitis (PSC), often mimic malignant strictures. Close to 25% of suspected neoplastic strictures are ultimately found to be benign after surgical intervention[2]. Treatment of benign strictures typically involves medical and endoscopic therapy, with only a few patients requiring surgical intervention. Alternatively, malignant strictures often require surgical resection or palliative biliary drainage.

Establishing histological diagnosis is key in determining further management of biliary strictures. ERCP with traditional diagnostics such as brush cytology and forceps biopsies have limited sensitivity in establishing a definitive diagnosis[3]. In some cases, it may be necessary to use additional diagnostic tools such as endoscopic ultrasound (EUS)-guided sampling or cholangioscopy to improve diagnostic yield. Our review aims to explore potential causes of indeterminate biliary strictures (IDBSs) and provide guidance on how to use diagnostic testing and technologies to confirm a diagnosis and plan further management. Based on the available data and expert opinion, we depict an evidence based diagnostic algorithm for management of IDBSs.

ETIOLOGY AND CLINICAL PRESENTATION OF BILIARY STRICTURES

Clinical presentation in these patients is often variable. Strictures may be found incidentally on cross sectional imaging in asymptomatic patients undergoing testing for other reasons or in those who are symptomatic with abdominal pain or jaundice. Clinical presentation can range from lack of symptoms to fulminant cholangitis or sepsis. A detailed history can help determine underlying etiology to some extent. Painless jaundice and rapid weight loss raise suspicion of underlying malignancy, whereas a more progressive course is seen in those with benign strictures.

Biliary strictures can have benign or malignant origins and may arise from either intraductal pathology or external compression on the biliary tract (Table 1). The most frequent causes of benign biliary strictures include postoperative strictures and those associated with chronic pancreatitis. Postoperative strictures can develop after cholecystectomy, bile duct surgery, or liver transplant (Figure 1). These strictures may be caused by several factors: ischemic injury, mechanical injury, anastomotic leakage, and postoperative infections causing inflammation, underlying autoimmune disease, or malignancy. Chronic inflammation and fibrosis of the pancreatic ducts (PDs) in chronic pancreatitis can cause scarring and narrowing of the adjacent bile ducts, leading to the development of biliary strictures. In some cases, chronic inflammation may result in extrinsic compression of bile ducts due to adhesions and fibrosis.

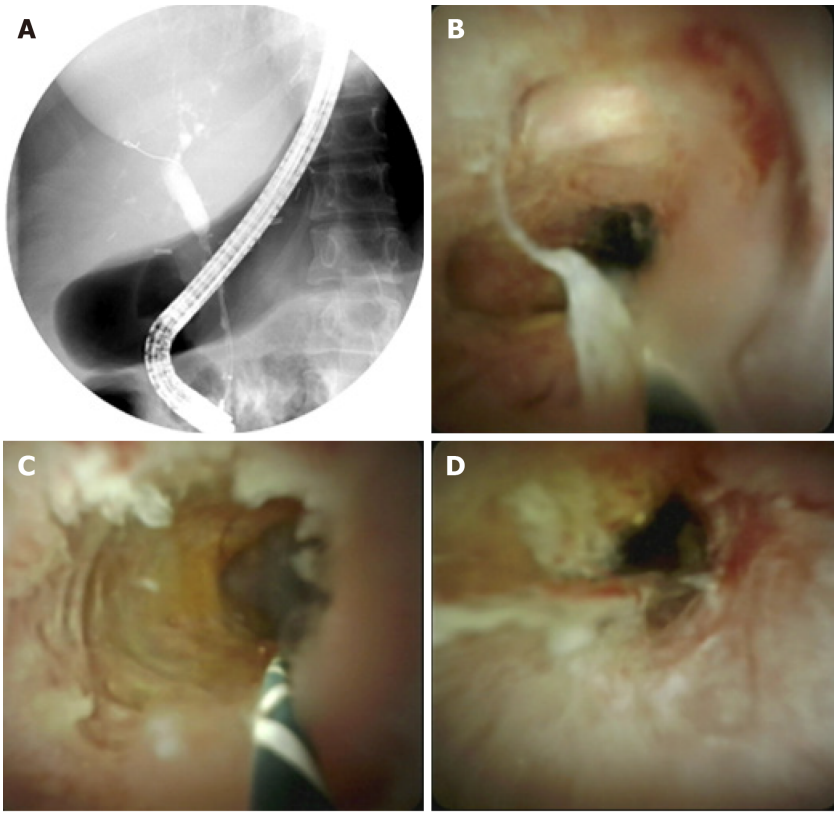
Other causes of benign strictures include systemic or inflammatory diseases such as acquired immunodeficiency syndrome, PSC or IgG4 cholangiopathy. PSC is an inflammatory disorder characterized by focal biliary strictures and dilations involving both intra- and extrahepatic bile ducts. Close to 13% of patients with PSC eventually develop cholangiocarcinoma (CCA). Biliary strictures in PSC can be managed with endoscopic therapy. Oncological treatment is warranted in those with CCA and this highlights the importance of endoscopic tissue acquisition for management of biliary stricture[3]. IgG4 disease is a fibroinflammatory condition characterized by the infiltration of IgG4 plasma cells into the bile duct wall and pancreas, leading to the development of sclerosing cholangitis and autoimmune pancreatitis.

Malignant biliary strictures are commonly associated with pancreatic cancer, CCA, gallbladder cancer, and metastatic cancer. Cross-sectional imaging can detect a mass lesion involving surrounding structures, such as the pancreas, liver, gallbladder, or regional lymph nodes. In some cases of malignant biliary obstruction, a stricture may be visible without

Table 1 Etiologies of biliary strictures

Benign	Malignant
Postoperative or iatrogenic strictures: After cholecystectomy, liver transplantation or surgical procedures involving pancreas. Local cancer treatment including radiation therapy, chemoembolization, and microwave ablation	Pancreatic adenocarcinoma
Chronic pancreatitis	Cholangiocarcinoma
Primary sclerosing cholangitis	Gallbladder malignancy
Trauma	Hepatocellular carcinoma
Infection: Recurrent pyogenic cholangitis, AIDS cholangiopathy	Ampullary carcinoma
Autoimmune: IgG4 related sclerosing cholangitis, sarcoidosis	Metastatic tumors or perihilar malignant nodes (colon cancer, breast cancer, renal cell cancer, squamous cell carcinoma)
Vascular: Ischemia, portal hypertensive biliopathy	Less common: Lymphomas or neuroendocrine tumors
Primary biliary cirrhosis	
Rarely COVID-19 cholangiopathy, gallstones, inflammatory bowel disease or medications	

IgG4: Immunoglobulin G4; AIDS: Acquired immunodeficiency syndrome; COVID-19: Coronavirus disease 2019.



DOI: 10.3748/wjg.v29.i36.5198 **Copyright** ©The Author(s) 2023.

Figure 1 Fluoroscopy and Spyglass images of a patient with benign biliary stricture who previously underwent a liver transplant for primary sclerosing cholangitis/primary biliary cirrhosis. A: Fluoroscopy imaging during endoscopic retrograde cholangiopancreatography showing common bile duct stricture; B–D: Cholangioscopy images showing concentric stricture with scarring and minimal erythema.

an obvious mass in the early stages of the disease. Although rare, malignant biliary strictures can also be caused by biliary lymphoma, sarcoma, or intraductal papillary neoplasm of the bile duct. Biliary strictures in the setting of malignancy occur due to tumor growth and invasion into bile ducts or surrounding structures, inflammation and scarring, or metastases.

DIAGNOSTIC TESTING

Initial testing often involves a combination of laboratory markers and cross-sectional imaging. This is followed by endoscopic procedures for tissue sampling. Although many tests are available to determine the nature of biliary strictures, no single test is considered absolute. A combination of tests may need to be utilized to evaluate indeterminate strictures. Serum markers play a limited role in detection and diagnosis of CCA and pancreatic adenocarcinoma. Carbohydrate antigen (CA) 19-9 is commonly used but has variable sensitivity and specificity. It is worth noting that CA 19-9 can also be elevated in certain benign conditions that lead to cholestasis, such as biliary tract inflammation, infection, or diabetes. Carcinoembryonic antigen was previously used for colorectal cancer diagnosis but has limited performance in CCA. Elevated IgG4 levels are associated with IgG4-related sclerosing cholangitis and can aid in diagnosis when used in conjunction with other tests. Other potential tumor markers, such as interleukin-6, transthyretin, mitochondrial-mediated apoptotic pathway-7, mucin-5AC, and miRNA-16 and 21, require further validation through larger studies to determine their clinical utility.

IMAGING

Ultrasound

Transabdominal US is typically performed early in work up of biliary obstruction. US is highly sensitive for detecting biliary dilation however has limited ability to identify biliary strictures. Therefore, follow up cross sectional imaging is generally required. Transabdominal US is readily available in all institutions, cost-effective, easy to perform, and lacks exposure to radiation, which makes it an optimal screening test.

Computed tomography

Computed tomography (CT) has a higher sensitivity for detecting biliary strictures and pancreaticobiliary malignancies. The sensitivity of CT in detecting malignant strictures is 40%–77%[4-6]. With the advent of enhanced detectors and contrast agents, the performance of CT scans has dramatically improved. In initial stages, CCA can present as a biliary stricture without an obvious mass. CT findings in such cases include a hypoenhancing biliary lesion during the arterial phase and hyperenhancement during the delayed phase. Several studies have concluded that multidetector CT is nearly 100% sensitive in detecting hilar malignancies, but it has low specificity (60%–80%) for identifying malignant *versus* biliary strictures.

Magnetic resonance imaging/magnetic resonance cholangiopancreatography

Magnetic resonance imaging/magnetic resonance cholangiopancreatography (MRI/MRCP) can provide high-quality cholangiograms, making them an ideal choice for evaluating biliary strictures. The cholangiogram performed during MRCP is similar in diagnostic quality to that performed at the time of ERCP. MRCP can help determine the location and extent of a biliary stricture. A large meta-analysis looking at the performance found a sensitivity of 91% and specificity of 98% in determining the presence of biliary obstruction and ~98% combined sensitivity and specificity in the ability to detect the location of a biliary stricture. The sensitivity and specificity in the ability to delineate benign from malignant strictures were 88% and 95%, respectively[7]. Diffusion-weighted imaging allows for an improvement in the ability to determine the nature of biliary strictures. Compared to ERCP, this test eliminates several risks, including pancreatitis and cholangitis. However, it is not readily available, expensive, and does not allow for tissue sampling.

ENDOSCOPIC MANAGEMENT OF IDBSS

ERCP with fluoroscopic imaging, biliary brush cytology and intraductal biopsies

With the increasing availability of MRI, the diagnostic utility of ERCP in detecting strictures has significantly decreased. Nonetheless, ERCP continues to serve as a valuable diagnostic tool for tissue acquisition to determine the nature of these strictures. Cholangiogram performed after successful biliary cannulation is used to evaluate location, anatomy, and extent of strictures. Physical characteristics of a biliary stricture, although indicative, are often inadequate to definitively differentiate between malignant and benign etiologies. Double duct sign, dilation of common bile duct and PD, is more likely to be seen in malignancy. Malignant strictures are often long and irregular with abrupt cut off "shouldering" resulting in upstream biliary dilation (Figure 2A). However, benign biliary strictures often appear smoother[2]. Brush cytology and intraductal biopsies during ERCP are routinely performed to establish histological diagnosis. A recent meta-analysis by Navaneethan *et al*[8] showed that brush cytology and biopsies during ERCP had limited sensitivity of 45% and 48%, respectively, in establishing diagnosis of strictures. Combining both diagnostic modalities only increased sensitivity to 59% [95% confidence interval (CI): 54%–65%], however, specificity for confirming malignancy was close to 100% (95%CI: 90%–100%)[8]. In this regard, patients may need multiple ERCPs with brushings and biopsies to establish a conclusive diagnosis.

Several techniques have been proposed to enhance tissue acquisition during ERCP, such as the use of novel brushes, biliary stricture dilation followed by biopsies and brushing, and repetitive brushings. Pörner *et al*[9] have suggested that balloon dilation of the stricture before forceps biopsies can improve sensitivity from 40% to > 70% without increasing the complication rate. In another study by Sugimoto *et al*[10] post brushing biliary lavage fluid was obtained by injecting



DOI: 10.3748/wjg.v29.i36.5198 **Copyright** ©The Author(s) 2023.

Figure 2 Fluoroscopy images. A: A malignant biliary stricture; B: Intraductal brushings; C: Freehand biopsies.

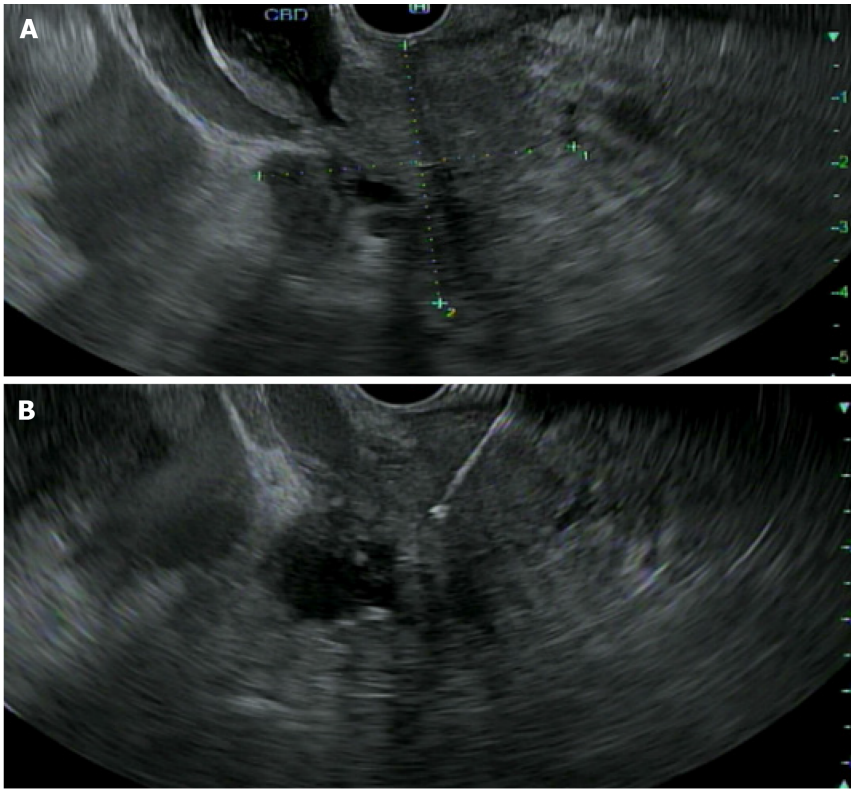
small amount of saline into bile duct. This increased cumulative sensitivity by > 24%. Submucosal tumor growth and presence of extrinsic malignancy with biliary involvement are difficult to detect with standard biliary brushings. Inadequate brushings or biopsy specimens are primary reason for nondiagnostic samples. At present wire-guided endobiliary forceps, free-hand biopsies, and endoscopic scrapers are available to obtain tissue. Free-hand biopsies are performed by using forceps to grasp the stricture and obtain a tissue sample, while wire-guided endobiliary biopsies use a wire guide to navigate to the stricture and obtain a tissue sample. There is no clear consensus on whether free-hand biopsies have a greater yield than wire-guided endobiliary biopsies. Some studies have suggested that free-hand biopsies may have a higher yield, while others have found no significant difference in yield between the two methods. The choice between the two techniques may depend on individual factors such as the location and characteristics of the stricture, as well as the expertise and experience of the endoscopist. Endoscopic devices with scraping loops have recently been proposed for sampling of biliary strictures. This type of device can be considered in institutions where cholangioscopy is unavailable. A recent study compared one endoscopic scraper device to cholangioscopy guided tissue acquisition. Sufficient samples were obtained in 87.5% of cases with endoscopic scraping loops compared to 90% with cholangioscopy forceps. This study described 83% sensitivity and 86% specificity with endoscopic scrapers compared to 90% sensitivity and specificity with samples obtained during cholangioscopy[11]. Endoscopic sphincterotomy was less frequently needed when sampling was done with endoscopic scrapers[11].

Fluorescence *in situ* hybridization (FISH) is a tissue-based diagnostic tool that uses fluorescent-labeled DNA probes to detect chromosomal abnormalities in cells. It has been found that about 80% of pancreaticobiliary malignancies exhibit abnormalities such as aneuploidy or polysomy of chromosomes[12]. FISH probes typically target chromosomes 3, 7, 9 and 17. FISH has shown a sensitivity of 89% and specificity of 97% for detecting malignancy, especially when combined with other techniques like biopsies and cytology[13,14]. However, false-positive results can occur in chronic inflammatory conditions. Flow cytometry has lower sensitivity (42%) and moderate specificity (77%) for detecting neoplastic cells in cytology samples[15]. Bile aspirate analysis for mutations and proteomic profiling may aid in distinguishing CCA from benign strictures, but further validation is required for routine use.

EUS-guided fine-needle aspiration and biopsy and EUS/ERCP combination

EUS can play a pivotal role in evaluation of IDBSs. EUS allows for high-resolution imaging of the pancreaticobiliary system and tissue acquisition by fine-needle aspiration and biopsy (FNA/FNB) at the same time (Figure 3). This has been proven to be safe and is considered a primary modality of tissue acquisition from biliary lesions. An overall sensitivity ranging from 47% to 87% has been reported in several studies looking at role of EUS-FNA in work up of hilar strictures [16-18]. EUS has some benefits over ERCP in determining etiology of extrahepatic biliary strictures. In a single center study, EUS-FNA was found to be superior to ERCP with brush cytology and transpapillary biopsies with a sensitivity of 93.8% *versus* 60% and accuracy of 94% *versus* 62% (P = 0.034)[19]. However, when ERCP and EUS were combined during a single session, the two procedures reached a sensitivity and accuracy of > 97%[19]. Zaheer *et al*[20] noted diagnostic accuracy of both procedures was > 90% for both benign and malignant strictures. Similarly, in a multicenter retrospective study of 263 patients with suspected malignant biliary strictures, combining EUS/ERCP had diagnostic sensitivity and accuracy of 85.8% and 87.1% respectively[21]. This approach has better outcomes for distal bile duct strictures and those > 15 mm[19]. No significant difference in combination procedure *versus* EUS-FNA alone was noted in patients with large biliary or pancreatic mass of ≥ 4 cm. One advantage of performing both procedures during same session is being able to better triage the need for ERCP in patients with biliary obstruction.

Lee *et al*[16] concluded that sonographic features could provide clues in determining etiology of indeterminate strictures. The presence of pancreatic mass or irregular bile duct wall is suggestive of malignancy. Bile duct wall thickness of ≥ 3 mm has a sensitivity and specificity close to 79%. EUS-FNA may have low sensitivity but is highly specific for diagnosis of malignancy. One drawback of EUS-FNA in diagnosis of CCA is concern for potential seeding along the needle tract. A small-scale study by Heimbach *et al*[22] revealed peritoneal metastasis was noted in 83% of patients with positive transperitoneal biopsies for CCA. Metastasis was not found in those with negative biopsies and only 8% of patients who did not undergo FNA had peritoneal metastasis. In contrast, no difference in overall survival was noted



DOI: 10.3748/wjg.v29.i36.5198 **Copyright** ©The Author(s) 2023.

Figure 3 Use of endoscopic ultrasound in evaluation of a biliary stricture. A: Linear array endoscopic ultrasound image of a pancreatic head mass, extending into the bile duct resulting in biliary stricture/obstruction and abutting the portal vein; B: Linear array endoscopic ultrasound image of a 22G fine needle biopsy of a pancreatic head mass.

among patients who did or did not undergo EUS-FNA. Seeding after EUS-FNA of pancreatic adenocarcinoma is rare with an estimated incidence ~2%[23]. No large-scale studies are available to investigate EUS-FNA related peritoneal carcinomatosis in cases of CCA. Patients being considered for liver transplant should ideally not undergo EUS-FNA.

Intraductal US

A high frequency (12–30 MHz) US probe is typically placed into extrahepatic bile duct during ERCP to perform intraductal US (IDUS). This allows for real time imaging of bile ducts and surrounding structures. Features suggestive of malignancy include hypoechoic mass or evidence of infiltration to adjacent structures, interruption of three-layer architecture of a bile duct, eccentric wall thickening, heterogenous or irregular margins, malignant appearing perihilar or periductal lymph nodes or periportal vascular invasion. A cohort study of 397 patients undergoing IDUS concluded that IDUS could differentiate benign from malignant biliary strictures with a sensitivity of 93%, specificity of 90%, and accuracy of ~91%[24]. Other studies have concluded ERCP with IDUS significantly improved diagnostic accuracy in identifying malignant strictures compared to ERCP alone. In addition, IDUS was also found to be superior in sensitivity (91% *vs* 76%), specificity (80% *vs* 75%), accuracy (89% *vs* 76%) and cancer staging (78% *vs* 54%) compared to EUS alone [25]. Limitations of IDUS include inability to obtain tissue to confirm histopathological diagnosis. Adverse events associated with IDUS include pancreatitis, bleeding, cholangitis, and perforation of the bile duct. It is also challenging to evaluate proximal biliary tree as advancing IDUS probe may be technically difficult.

Cholangioscopy

Cholangioscopy was first introduced in 1976 and has undergone significant technological advancement since its inception [26]. Cholangioscopy allows for direct visualization and targeted biopsies of bile ducts. This technique failed to gain popularity a few decades ago due to poor reliability and need for two operators to manipulate the mother–baby endoscopies. Traditional peroral cholangioscopy requires insertion of a dedicated video-cholangioscope through an accessory channel of the duodenoscope and requires two skilled endoscopists to operate the system. However, with development of single operator cholangioscopy (SOC) systems, cholangioscopy has gained renewed interest. At present there are two SOC system: duodenoscope-assisted SOC called Spyglass and peroral direct cholangioscopy using an ultrathin gastroscope.

Chen *et al*[27] concluded that sensitivity and specificity of SOC in determining etiology of biliary strictures was 78% and 82% respectively, compared to 51% and 54% with ERCP alone. A meta-analysis conducted by Navaneethan *et al*[28] concluded that pooled sensitivity and specificity for detection of CCA using cholangioscopy was 60% and 98% respectively. Another meta-analysis performed by Korrapati *et al*[29] compared diagnostic accuracy of SOC based on visual images to histology and reported overall accuracy of 89% for making a phenotypic diagnosis and 79% for making a

histopathological diagnosis. Similar results of higher diagnostic yield with visual impression compared to visually targeted biopsies was seen in multiple other studies[30,31]. This may be a result of sampling error at time of biopsy. Cholangioscopy has also been found useful to differentiate PSC related strictures from those of IgG-4 disease[32].

Cholangioscopy-guided biopsies improve diagnosis of IDBSs in patients with negative ERCP brushings and biopsies (Figure 2B and 2C). In two meta-analyses performed by Navaneethan *et al*[28] and Wen *et al*[33] pooled sensitivity and specificity of cholangioscopy-guided biopsies were 60% and 98%, and 74% and 98% respectively. Mean number of biopsies performed in these studies were 2–5. A recent prospective trial looking at rapid on-site evaluation (ROSE) of the biopsy specimen in these patients did not significantly alter diagnostic accuracy[34]. Two prior cost analysis studies have shown that cholangioscopy was more cost efficient for establishing CCA diagnosis compared to conventional ERCP[35, 36]. One study showed a reduction in number of procedures by over 30% and cost by 5% when cholangioscopy was utilized[36].

Interobserver variability is often noted when it comes to performing a visual diagnosis during cholangioscopy. This variability exists due to a lack of consensus on what constitutes a malignant stricture. The Mendoza criteria are a set of guidelines used to describe high-risk features during cholangioscopy, and these features have been found to be statistically associated with presence of malignancy. Based on this criteria, high risk features include presence of neovascularization or dilated tortuous vessels, irregular or nodular biliary mucosa, tumors or masses, irregular surface with ulcerated, infiltrative, or friable appearance (Figure 4). Biopsies obtained from malignant strictures often reveal malignant cells arranged in inflamed desmoplastic stroma; moreover, immunostaining for CK7 on the biopsy specimen exhibits positive results in tumor cells with appropriate control (Figure 5). Diagnostic accuracy using this method has been found to be close to 77%[37].

Limitations to the use of the Spyglass Visualization System include cost, specialized training requirements for endoscopists and technical staff, and associated risks. An extended biliary sphincterotomy is required to allow for cholangioscopy equipment to advance into biliary tree and this increases risk of cholangitis, pancreatitis, and bleeding. Sethi *et al*[38] reported an increase in overall complication rate to 7% with use of cholangioscopy compared with 2.9% with ERCP alone. Rate of cholangitis was significantly higher in patients undergoing cholangioscopy in this study. Similar data were also reported by Korrapati *et al*[29]. Risk of infection after cholangioscopy is attributed to bacterial accumulation in setting of biliary obstruction and disruption of microbial flora with introduction of cholangioscopy. For this reason, prophylactic antibiotics are usually given prior to the procedure. Cholangioscopy should therefore be used in conjunction to ERCP when conventional techniques fail to provide a diagnosis despite high suspicion for malignancy.

Confocal laser endomicroscopy

Confocal laser endomicroscopy (CLE) is an imaging technique that allows for real-time optical biopsies during ERCP. A contrast agent is typically injected intravenously, and the biliary tissue is imaged with a CLE probe. This technique results in specific patterns that correlate with histology and help differentiate between malignant and normal biliary mucosa. Miami classification is used to differentiate probe-based CLE visual findings as benign or malignant strictures. Presence of thick dark bands (> 40 m), thick white bands (> 20 m), dark clumps, epithelial strictures, villous glands, and contrast leakage can differentiate nature of strictures[39]. Paris classification is a newer classification which includes additional features like vascular congestion, dark glandular patterns, interglandular spaces and thickened reticular structures[40]. A multicenter study found that CLE provided higher diagnostic accuracy (90% *vs* 73%) for identifying malignant biliary strictures than conventional ERCP[41].

Use of CLE in clinical practice is limited by several factors. One limitation is that CLE quires specialized equipment and trained personnel to operate it. Cost of the equipment can be prohibitive for some healthcare facilities. Another limitation is the need for specialized training for endoscopists to ensure that the procedure is performed correctly and safely.

Investigational and less widely used techniques: chromoendoscopy, narrow-band imaging, autofluorescence, and optical coherence tomography

During chromoendoscopy different stains are applied to surface of biliary mucosa at time of cholangioscopy. Methylene blue can be used to delineate malignant lesions and ischemic strictures. High-risk lesions concerning for malignancy such as increased vascularity and infiltrative or irregular mucosal surface can be better examined using narrow-band imaging. Initial studies looking at use of autofluorescence during cholangioscopy have been less promising given lack of specificity and high false-positive rates seen with this method of testing. This technique is not widely use.

Optical coherence tomography (OCT) is an imaging technique that allows acquisition of high-resolution images of the intra- and extrahepatic bile ducts. OCT is performed by advancing a probe through accessory channel of a duodenoscope. Disturbed bile duct layers and nonreflective areas, indicating presence of tumor vessels are indicative of malignant strictures. A second-generation OCT system using volumetric laser endomicroscopy was recently introduced. Tyberg *et al* [42] reported findings of epithelial thickening, hyper-reflective surfaces with shadowing and haziness of inner mucosal layers in patients with CCA. A pilot study noted at least one such finding in 79% of study population[43]. However, large, randomized trials are necessary to confirm clinical utility of adding this technique to ERCP and conventional tissue acquisition techniques.

OUR APPROACH TO MANAGEMENT OF IDBSS

Management of biliary strictures can be complex and requires a personalized approach that considers the specific clinical presentation and the diagnostic techniques available at the institution (Table 2). Biliary strictures can have a variable

Table 2 Tissue sampling techniques in evaluation of indeterminate biliary strictures

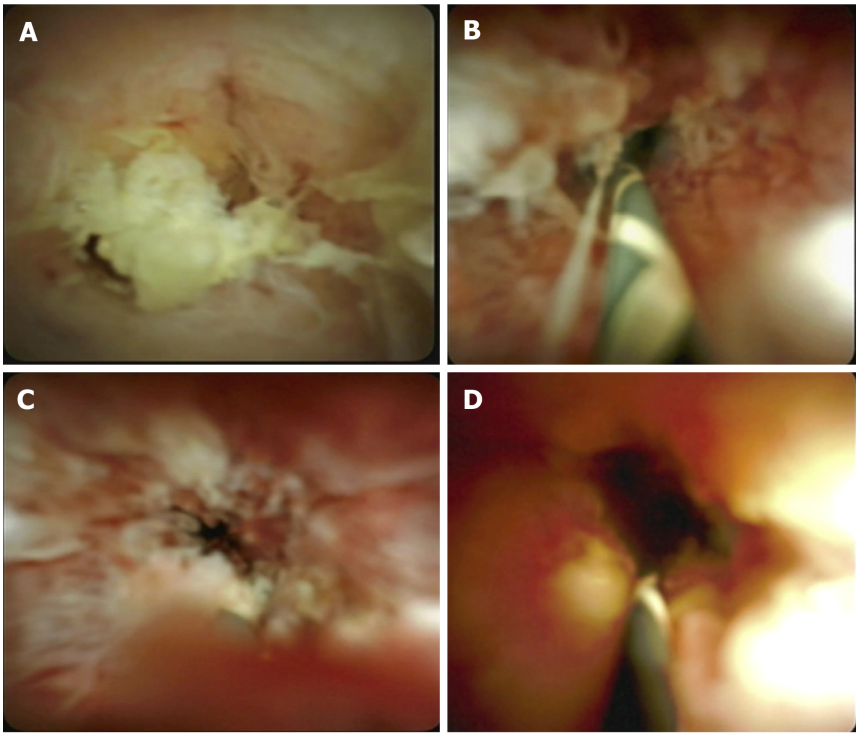
Tissue acquisition technique	Advantages	Disadvantages	Comments
ERCP-guided techniques			
Intraductal biopsy	Direct sampling of larger tissue samples	Risk of bleeding, perforation, pancreatitis	Used in conjunction to other techniques to maximize yield
Brush cytology	Less invasive. Can be used in cases of advanced liver or pancreatic disease	Smaller tissues sample. Low diagnostic yield	Used in conjunction to other techniques to maximize yield
FISH	Can detect genetic abnormalities associated with malignancy	Requires specialized equipment for analysis. Limited sensitivity and specificity	Used in conjunction with biopsies or brushings to improve diagnostic yield
Flow cytometry	Can detect abnormal cellular DNA associated with malignancy	Requires specialized equipment for analysis. Limited sensitivity and specificity	Used in conjunction with other techniques
Cholangioscopy with biopsy	Direct visualization of stricture and targeted biopsies	Requires specialized equipment and expertise. Associated with higher risk of complications such as cholangitis, pancreatitis, and bleeding. More expensive than conventional ERCP	Can perform interventions under direct visualization
Intraductal ultrasound	High-resolution imaging of the biliary tract and surrounding structures, can detect structural abnormalities associated with malignancy	Invasive, requires specialized equipment and expertise	Not available in every institution
Risks associated with ERCP - bleeding, perforation, pancreatitis, infection			
EUS guided sampling			
EUS with FNA	High diagnostic yield, ability to sample adjacent lymph nodes or lesions	Invasive, risk of bleeding and infection, requires expertise	Can be used as a complementary technique to ERCP or alone. Should be used with ROSE if available and if malignancy suspected
EUS with FNB	High diagnostic yield, ability to sample lymph nodes, larger tissue	Invasive, risk of bleeding and infection, requires expertise	Can be used as a complementary technique to ERCP or alone
EUS/ERCP combination	Ability to obtain tissue samples and perform therapeutic interventions in the same encounter	Invasive, requires specialized equipment and expertise	Used in complex cases and in cases where biliary drainage is needed
Confocal laser endomicroscopy	Real-time *in vivo* imaging of biliary tissue at the cellular level	Limited availability and expertise, expensive	Can be used to improve diagnostic accuracy and guide targeted biopsies
Optical coherence tomography	High-resolution imaging of biliary tissue, can detect structural abnormalities associated with malignancy	Limited availability and expertise, expensive	Can be useful in cases where other techniques have failed or when precise localization of the stricture is necessary

ERCP: Endoscopic retrograde cholangiopancreatography; EUS: Endoscopic ultrasound; FNA: Fine-needle aspiration; FNB: Fine-needle biopsy; ROSE: Rapid onsite evaluation; FISH: Fluorescent *in situ* hybridization.

presentation and can be caused by a variety of underlying conditions, which can make it difficult to have a standardized approach to their management. Drawing on the data available, we propose an approach to address IDBSs (Figure 6). Additionally, it can be challenging to rule out neoplastic biliary strictures prior to surgery, despite the evolution of endoscopic techniques for diagnosis and treatment. It is important for healthcare providers to carefully evaluate each patient and consider the complete clinical picture to develop an appropriate plan of care.

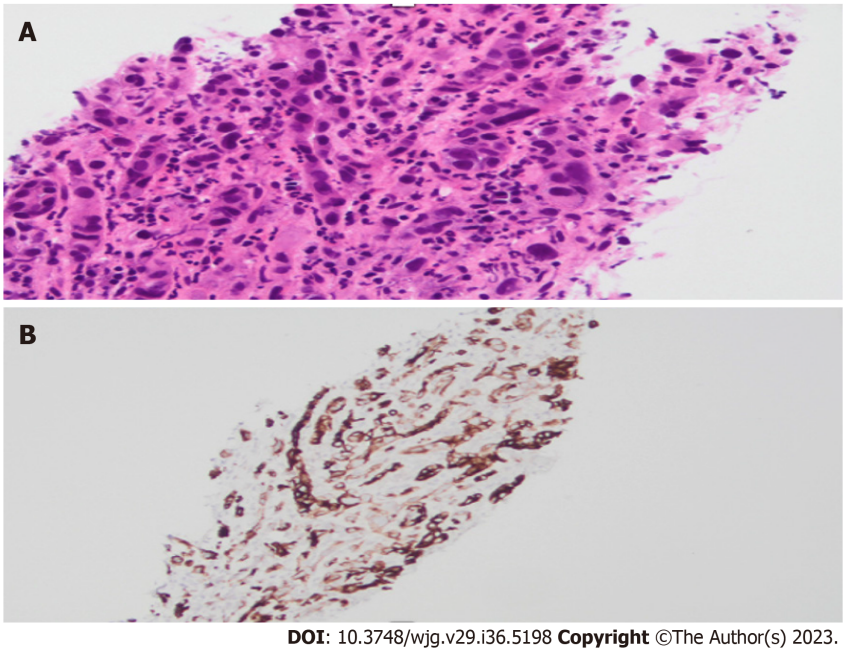
During the initial evaluation of biliary strictures, it is important to obtain a detailed history and physical examination to assess the patient's risk factors and determine the type of biliary stricture. Basic laboratory tests, particularly liver function tests, should be performed. In cases with clinical suspicion of certain conditions such as PSC, IgG4 or human immunodeficiency virus (HIV), additional testing for tumor markers, HIV antibodies, and IgG4 levels may be necessary. Imaging studies, such as US and CT with IV contrast, can be useful in the evaluation of biliary strictures. If intra- and extrahepatic biliary dilation is visualized on US, this is more suggestive of a distal bile duct stricture, which may be caused by an ampullary or pancreatic mass. CT with intravenous contrast is the preferred imaging modality in such cases. If intrahepatic biliary dilation is seen on US, this is more suggestive of a proximal biliary stricture, for which MRI/MRCP is the preferred imaging modality.

In instances where extrahepatic biliary strictures are suspected to be a result of a pancreatic mass, EUS-guided fine-needle sampling is the preferred method to assess for presence of malignancy. EUS-guided FNB or EUS with FNA plus ROSE is recommended over EUS with FNA without ROSE. EUS can help identify minute lesions, in about 40% of cases that may not be readily visible on CT. Single session EUS and ERCP may be warranted in cases where biliary



DOI: 10.3748/wjg.v29.i36.5198 **Copyright** ©The Author(s) 2023.

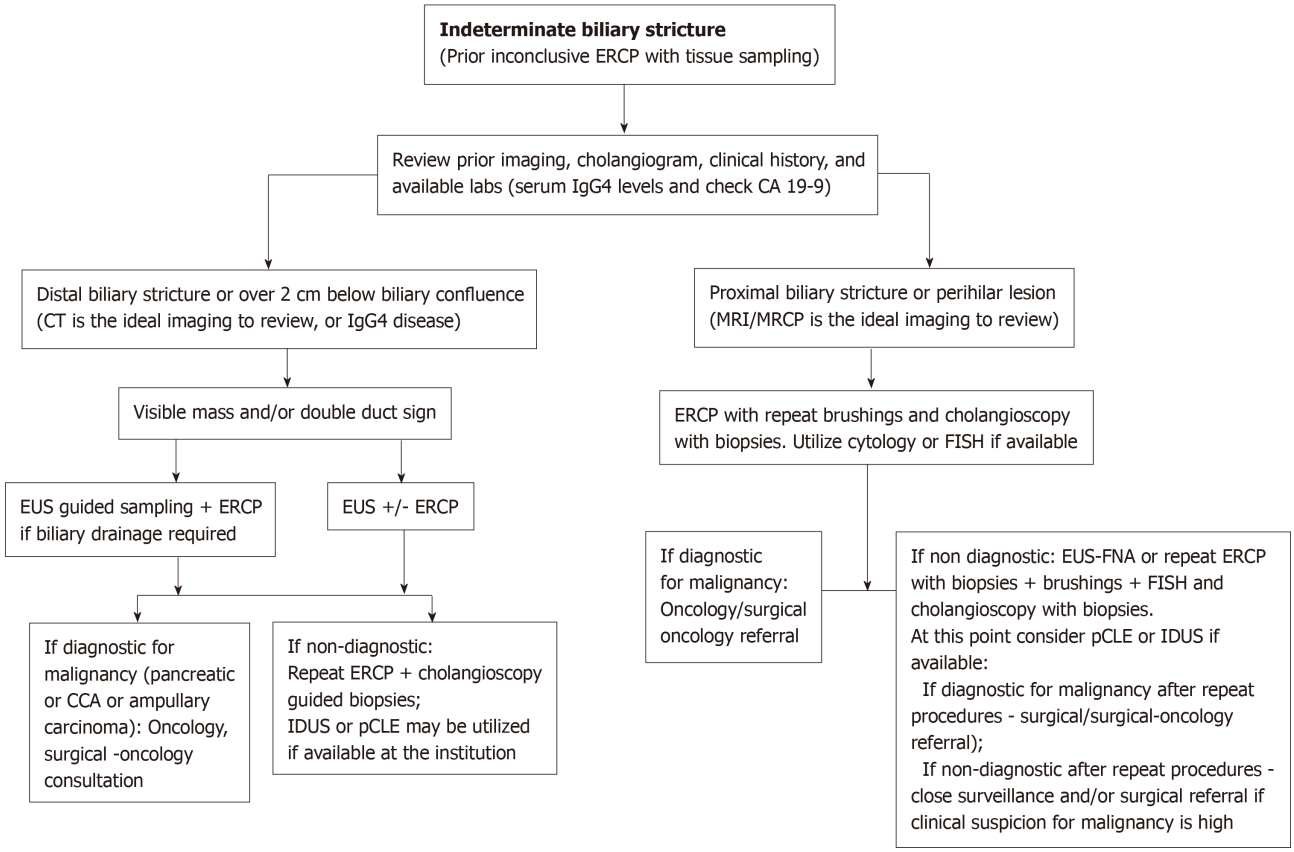
Figure 4 Cholangioscopy images of malignant biliary strictures. A–D: Infiltrative stricture with finger like projections and friable, nodular elevated surface.



DOI: 10.3748/wjg.v29.i36.5198 **Copyright** ©The Author(s) 2023.

Figure 5 Biliary stricture biopsy. A: Microscopic examination (hematoxylin and eosin) reveals medium sized malignant cells arranged in clusters and single cell units. Tumor cells are diffusely distributed in an inflamed desmoplastic stroma; B: Immunostaining for CK7 performed on the biopsy specimen is positive in tumor cells with appropriate control.

decompression is warranted in addition to establishing diagnosis. Cholangioscopy-guided biopsies or IDUS may be needed if conventional ERCP is unable to determine nature of stricture. Maintaining stable positioning of cholangioscope is key to performing targeted biopsies and this can often be challenging if there is a distal bile duct stricture. Endoscopists may use techniques such as balloon dilation to widen the stricture and improve access to the bile ducts. In cases of proximal or hilar lesions, ERCP is often the primary diagnostic and therapeutic procedure. In the assessment of hilar strictures, multimodal sampling during ERCP is preferred over relying solely on brush cytology. EUS may be warranted if ERCP and traditional sampling techniques, cytology and FISH are inconclusive. Since the location of proximal biliary strictures tends to be more intra-hepatic and away from duodenal wall, it may be challenging to adequately visualize



DOI: 10.3748/wjg.v29.i36.5198 **Copyright** ©The Author(s) 2023.

Figure 6 Approach to indeterminate biliary strictures. ERCP: Endoscopic retrograde cholangiopancreatography; EUS: Endoscopic ultrasound; CT: Computerized tomography; MRI: Magnetic resonance imaging; MRCP: Magnetic resonance cholangiopancreatography; FISH: Fluorescence *in situ* hybridization; IDUS: Intraductal ultrasound; pCLE: Probe based confocal laser micro-endoscopy; CCA: Cholangiocarcinoma; IgG4: Immunoglobulin G4; CA 19-9: Carbohydrate antigen 19-9; FNA: Fine needle aspiration.

using EUS and obtain biopsies. In cases that are being considered for liver transplant, caution should be exercised before perming biopsies of biliary or hilar lesions. Lymph nodes may be biopsied safely with low concern for seeding.

Lee *et al*[16] conducted a study of 181 patients with suspected malignant biliary strictures. Accuracy of cholangioscopy in diagnosis of malignancy in proximal strictures was 93.6% whereas accuracy of EUS-FNA or biopsy in diagnosis malignant biliary strictures was 96.3%. Currently there are no randomized control trials comparing cholangioscopy guided biopsies and EUS-FNA in cases of IDBSs where conventional ERCP based tissue sampling is inconclusive. However, based on available data and expert opinions this could be considered a diagnostic approach.

CONCLUSION

Despite advancement in diagnostic testing, nonsurgical evaluation of biliary strictures is often challenging. Management of IDBSs often involves a multidisciplinary approach and multiple diagnostic modalities. The entire clinical picture should be considered to come up with a management strategy. Goal of management should be early establishment of diagnosis in cases of malignant strictures and avoidance of unnecessary surgical exploration in cases of benign biliary strictures. A single test may be inadequate to diagnose IDBSs. However, a combination of validated serum or bile-based markers, imaging and endoscopic testing will improve diagnostic yield.

ACKNOWLEDGEMENTS

We thank Leona Council, MD. Department of Pathology, University of Alabama at Birmingham.

FOOTNOTES

Author contributions: Yadlapati S and Mulki R contributed to the literature review and drafting the manuscript; Sánchez-Luna SA and

Ahmed AM provided valuable assistance in manuscript preparation; Kyanam Kabir Baig KR and Peter S played a role in conceptualization and final review; Yadlapati S lead author responsible for conducting the, organizing the paper's structure.

Conflict-of-interest statement: All the authors report no relevant conflicts of interest for this article.

Open-Access: This article is an open-access article that was selected by an in-house editor and fully peer-reviewed by external reviewers. It is distributed in accordance with the Creative Commons Attribution NonCommercial (CC BY-NC 4.0) license, which permits others to distribute, remix, adapt, build upon this work non-commercially, and license their derivative works on different terms, provided the original work is properly cited and the use is non-commercial. See: https://creativecommons.org/Licenses/by-nc/4.0/

Country/Territory of origin: United States

ORCID number: Sujani Yadlapati 0000-0002-3904-6730; Ali M Ahmed 0000-0002-8940-6757; Kondal Rao Kyanam Kabir Baig 0000-0003-1550-4853; Shajan Peter 0000-0003-3214-2989.

S-Editor: Wang JJ
L-Editor: Kerr C
P-Editor: Wang JJ

REFERENCES

1 **Oleas R**, Alcívar-Vasquez J, Robles-Medranda C. New technologies for indeterminate biliary strictures. *Transl Gastroenterol Hepatol* 2022; **7**: 22 [PMID: 35548472 DOI: 10.21037/tgh.2020.03.05]
2 **Novikov A**, Kowalski TE, Loren DE. Practical Management of Indeterminate Biliary Strictures. *Gastrointest Endosc Clin N Am* 2019; **29**: 205-214 [PMID: 30846149 DOI: 10.1016/j.giec.2018.12.003]
3 **Sun B**, Moon JH, Cai Q, Rerknimitr R, Ma S, Lakhtakia S, Ryozawa S, Kutsumi H, Yasuda I, Shiomi H, Li X, Li W, Zhang X, Itoi T, Wang HP, Qian D, Wong Lau JY, Yang Z, Ji M, Hu B; Asia-Pacific ERCP Club. Review article: Asia-Pacific consensus recommendations on endoscopic tissue acquisition for biliary strictures. *Aliment Pharmacol Ther* 2018; **48**: 138-151 [PMID: 29876948 DOI: 10.1111/apt.14811]
4 **Tillich M**, Mischinger HJ, Preisegger KH, Rabl H, Szolar DH. Multiphasic helical CT in diagnosis and staging of hilar cholangiocarcinoma. *AJR Am J Roentgenol* 1998; **171**: 651-658 [PMID: 9725291 DOI: 10.2214/ajr.171.3.9725291]
5 **Heinzow HS**, Kammerer S, Rammes C, Wessling J, Domagk D, Meister T. Comparative analysis of ERCP, IDUS, EUS and CT in predicting malignant bile duct strictures. *World J Gastroenterol* 2014; **20**: 10495-10503 [PMID: 25132767 DOI: 10.3748/wjg.v20.i30.10495]
6 **Rösch T**, Meining A, Frühmorgen S, Zillinger C, Schusdziarra V, Hellerhoff K, Classen M, Helmberger H. A prospective comparison of the diagnostic accuracy of ERCP, MRCP, CT, and EUS in biliary strictures. *Gastrointest Endosc* 2002; **55**: 870-876 [PMID: 12024143 DOI: 10.1067/mge.2002.124206]
7 **Romagnuolo J**, Bardou M, Rahme E, Joseph L, Reinhold C, Barkun AN. Magnetic resonance cholangiopancreatography: a meta-analysis of test performance in suspected biliary disease. *Ann Intern Med* 2003; **139**: 547-557 [PMID: 14530225 DOI: 10.7326/0003-4819-139-7-200310070-00006]
8 **Navaneethan U**, Njei B, Lourdusamy V, Konjeti R, Vargo JJ, Parsi MA. Comparative effectiveness of biliary brush cytology and intraductal biopsy for detection of malignant biliary strictures: a systematic review and meta-analysis. *Gastrointest Endosc* 2015; **81**: 168-176 [PMID: 25440678 DOI: 10.1016/j.gie.2014.09.017]
9 **Pörner D**, Kaczmarek DJ, Heling D, Hausen A, Mohr R, Hüneburg R, Matthaei H, Glowka TR, Manekeller S, Fischer HP, Toma M, Nattermann J, Strassburg CP, Gonzalez-Carmona MA, Weismüller TJ. Transpapillary tissue sampling of biliary strictures: balloon dilatation prior to forceps biopsy improves sensitivity and accuracy. *Sci Rep* 2020; **10**: 17423 [PMID: 33060723 DOI: 10.1038/s41598-020-74451-9]
10 **Sugimoto S**, Matsubayashi H, Kimura H, Sasaki K, Nagata K, Ohno S, Uesaka K, Mori K, Imai K, Hotta K, Takizawa K, Kakushima N, Tanaka M, Kawata N, Ono H. Diagnosis of bile duct cancer by bile cytology: usefulness of post-brushing biliary lavage fluid. *Endosc Int Open* 2015; **3**: E323-E328 [PMID: 26357678 DOI: 10.1055/s-0034-1391666]
11 **Kato M**, Onoyama T, Takeda Y, Kawata S, Kurumi H, Koda H, Yamashita T, Hamamoto W, Sakamoto Y, Matsumoto K, Isomoto H. Peroral Cholangioscopy-Guided Forceps Biopsy and Endoscopic Scraper for the Diagnosis of Indeterminate Extrahepatic Biliary Stricture. *J Clin Med* 2019; **8** [PMID: 31248095 DOI: 10.3390/jcm8060873]
12 **Levy MJ**, Baron TH, Clayton AC, Enders FB, Gostout CJ, Halling KC, Kipp BR, Petersen BT, Roberts LR, Rumalla A, Sebo TJ, Topazian MD, Wiersema MJ, Gores GJ. Prospective evaluation of advanced molecular markers and imaging techniques in patients with indeterminate bile duct strictures. *Am J Gastroenterol* 2008; **103**: 1263-1273 [PMID: 18477350 DOI: 10.1111/j.1572-0241.2007.01776.x]
13 **Gonda TA**, Glick MP, Sethi A, Poneros JM, Palmas W, Iqbal S, Gonzalez S, Nandula SV, Emond JC, Brown RS, Murty VV, Stevens PD. Polysomy and p16 deletion by fluorescence in situ hybridization in the diagnosis of indeterminate biliary strictures. *Gastrointest Endosc* 2012; **75**: 74-79 [PMID: 22100297 DOI: 10.1016/j.gie.2011.08.022]
14 **Nanda A**, Brown JM, Berger SH, Lewis MM, Barr Fritcher EG, Gores GJ, Keilin SA, Woods KE, Cai Q, Willingham FF. Triple modality testing by endoscopic retrograde cholangiopancreatography for the diagnosis of cholangiocarcinoma. *Therap Adv Gastroenterol* 2015; **8**: 56-65 [PMID: 25729431 DOI: 10.1177/1756283X14564674]
15 **Ryan ME**, Baldauf MC. Comparison of flow cytometry for DNA content and brush cytology for detection of malignancy in pancreaticobiliary strictures. *Gastrointest Endosc* 1994; **40**: 133-139 [PMID: 8013809 DOI: 10.1016/s0016-5107(94)70154-7]
16 **Lee JH**, Salem R, Aslanian H, Chacho M, Topazian M. Endoscopic ultrasound and fine-needle aspiration of unexplained bile duct strictures. *Am J Gastroenterol* 2004; **99**: 1069-1073 [PMID: 15180727 DOI: 10.1111/j.1572-0241.2004.30223.x]
17 **Eloubeidi MA**, Chen VK, Jhala NC, Eltoum IE, Jhala D, Chhieng DC, Syed SA, Vickers SM, Mel Wilcox C. Endoscopic ultrasound-guided fine needle aspiration biopsy of suspected cholangiocarcinoma. *Clin Gastroenterol Hepatol* 2004; **2**: 209-213 [PMID: 15017604 DOI: 10.1016/s1542-3565(04)00005-9]
18 **Rösch T**, Hofrichter K, Frimberger E, Meining A, Born P, Weigert N, Allescher HD, Classen M, Barbur M, Schenck U, Werner M. ERCP or

EUS for tissue diagnosis of biliary strictures? A prospective comparative study. *Gastrointest Endosc* 2004; **60**: 390-396 [PMID: 15332029 DOI: 10.1016/s0016-5107(04)01732-8]

19 **Moura DTH**, de Moura EGH, Matuguma SE, Dos Santos ME, Moura ETH, Baracat FI, Artifon E, Cheng S, Bernardo WM, Chacon D, Tanigawa R, Jukemura J. EUS-FNA versus ERCP for tissue diagnosis of suspect malignant biliary strictures: a prospective comparative study. *Endosc Int Open* 2018; **6**: E769-E777 [PMID: 29876515 DOI: 10.1055/s-0043-123186]

20 **Zaheer A**, Anwar MM, Donohoe C, O'Keeffe S, Mushtaq H, Kelleher B, Clarke E, Kirca M, McKiernan S, Mahmud N, Keeling N, MacMathuna P, O'Toole D. The diagnostic accuracy of endoscopic ultrasound in suspected biliary obstruction and its impact on endoscopic retrograde cholangiopancreatography burden in real clinical practice: a consecutive analysis. *Eur J Gastroenterol Hepatol* 2013; **25**: 850-857 [PMID: 23411866 DOI: 10.1097/MEG.0b013e32835ee5d0]

21 **Jo JH**, Cho CM, Jun JH, Chung MJ, Kim TH, Seo DW, Kim J, Park DH; Research Group for Endoscopic Ultrasonography in KSGE. Same-session endoscopic ultrasound-guided fine needle aspiration and endoscopic retrograde cholangiopancreatography-based tissue sampling in suspected malignant biliary obstruction: A multicenter experience. *J Gastroenterol Hepatol* 2019; **34**: 799-805 [PMID: 30378169 DOI: 10.1111/jgh.14528]

22 **Heimbach JK**, Sanchez W, Rosen CB, Gores GJ. Trans-peritoneal fine needle aspiration biopsy of hilar cholangiocarcinoma is associated with disease dissemination. *HPB (Oxford)* 2011; **13**: 356-360 [PMID: 21492336 DOI: 10.1111/j.1477-2574.2011.00298.x]

23 **Micames C**, Jowell PS, White R, Paulson E, Nelson R, Morse M, Hurwitz H, Pappas T, Tyler D, McGrath K. Lower frequency of peritoneal carcinomatosis in patients with pancreatic cancer diagnosed by EUS-guided FNA vs. percutaneous FNA. *Gastrointest Endosc* 2003; **58**: 690-695 [PMID: 14595302 DOI: 10.1016/s0016-5107(03)02009-1]

24 **Meister T**, Heinzow HS, Woestmeyer C, Lenz P, Menzel J, Kucharzik T, Domschke W, Domagk D. Intraductal ultrasound substantiates diagnostics of bile duct strictures of uncertain etiology. *World J Gastroenterol* 2013; **19**: 874-881 [PMID: 23430958 DOI: 10.3748/wjg.v19.i6.874]

25 **Menzel J**, Poremba C, Dietl KH, Domschke W. Preoperative diagnosis of bile duct strictures--comparison of intraductal ultrasonography with conventional endosonography. *Scand J Gastroenterol* 2000; **35**: 77-82 [PMID: 10672839 DOI: 10.1080/003655200750024579]

26 **Turowski F**, Hügle U, Dormann A, Bechtler M, Jakobs R, Gottschalk U, Nötzel E, Hartmann D, Lorenz A, Kolligs F, Veltzke-Schlieker W, Adler A, Becker O, Wiedenmann B, Bürgel N, Tröger H, Schumann M, Daum S, Siegmund B, Bojarski C. Diagnostic and therapeutic single-operator cholangiopancreatoscopy with SpyGlassDS™: results of a multicenter retrospective cohort study. *Surg Endosc* 2018; **32**: 3981-3988 [PMID: 29532224 DOI: 10.1007/s00464-018-6141-0]

27 **Chen YK**, Parsi MA, Binmoeller KF, Hawes RH, Pleskow DK, Slivka A, Haluszka O, Petersen BT, Sherman S, Devière J, Meisner S, Stevens PD, Costamagna G, Ponchon T, Peetermans JA, Neuhaus H. Single-operator cholangioscopy in patients requiring evaluation of bile duct disease or therapy of biliary stones (with videos). *Gastrointest Endosc* 2011; **74**: 805-814 [PMID: 21762903 DOI: 10.1016/j.gie.2011.04.016]

28 **Navaneethan U**, Hasan MK, Lourdusamy V, Njei B, Varadarajulu S, Hawes RH. Single-operator cholangioscopy and targeted biopsies in the diagnosis of indeterminate biliary strictures: a systematic review. *Gastrointest Endosc* 2015; **82**: 608-14.e2 [PMID: 26071061 DOI: 10.1016/j.gie.2015.04.030]

29 **Korrapati P**, Ciolino J, Wani S, Shah J, Watson R, Muthusamy VR, Klapman J, Komanduri S. The efficacy of peroral cholangioscopy for difficult bile duct stones and indeterminate strictures: a systematic review and meta-analysis. *Endosc Int Open* 2016; **4**: E263-E275 [PMID: 27004242 DOI: 10.1055/s-0042-100194]

30 **Nishikawa T**, Tsuyuguchi T, Sakai Y, Sugiyama H, Miyazaki M, Yokosuka O. Comparison of the diagnostic accuracy of peroral video-cholangioscopic visual findings and cholangioscopy-guided forceps biopsy findings for indeterminate biliary lesions: a prospective study. *Gastrointest Endosc* 2013; **77**: 219-226 [PMID: 23231758 DOI: 10.1016/j.gie.2012.10.011]

31 **Ramchandani M**, Reddy DN, Gupta R, Lakhtakia S, Tandan M, Darisetty S, Sekaran A, Rao GV. Role of single-operator peroral cholangioscopy in the diagnosis of indeterminate biliary lesions: a single-center, prospective study. *Gastrointest Endosc* 2011; **74**: 511-519 [PMID: 21737076 DOI: 10.1016/j.gie.2011.04.034]

32 **Itoi T**, Kamisawa T, Igarashi Y, Kawakami H, Yasuda I, Itokawa F, Kishimoto Y, Kuwatani M, Doi S, Hara S, Moriyasu F, Baron TH. The role of peroral video cholangioscopy in patients with IgG4-related sclerosing cholangitis. *J Gastroenterol* 2013; **48**: 504-514 [PMID: 22948487 DOI: 10.1007/s00535-012-0652-6]

33 **Wen LJ**, Chen JH, Xu HJ, Yu Q, Liu K. Efficacy and Safety of Digital Single-Operator Cholangioscopy in the Diagnosis of Indeterminate Biliary Strictures by Targeted Biopsies: A Systematic Review and Meta-Analysis. *Diagnostics (Basel)* 2020; **10** [PMID: 32887436 DOI: 10.3390/diagnostics10090666]

34 **Guvendir I**, Zemheri IE, Ozdil K. Impact of rapid on-site evaluation on diagnostic accuracy of EUS-guided fine-needle aspiration of solid pancreatic lesions: experience from a single center. *BMC Gastroenterol* 2022; **22**: 264 [PMID: 35624440 DOI: 10.1186/s12876-022-02330-w]

35 **Njei B**, McCarty TR, Varadarajulu S, Navaneethan U. Cost utility of ERCP-based modalities for the diagnosis of cholangiocarcinoma in primary sclerosing cholangitis. *Gastrointest Endosc* 2017; **85**: 773-781.e10 [PMID: 27590963 DOI: 10.1016/j.gie.2016.08.020]

36 **Deprez PH**, Garces Duran R, Moreels T, Furneri G, Demma F, Verbeke L, Van der Merwe SW, Laleman W. The economic impact of using single-operator cholangioscopy for the treatment of difficult bile duct stones and diagnosis of indeterminate bile duct strictures. *Endoscopy* 2018; **50**: 109-118 [PMID: 29172216 DOI: 10.1055/s-0043-121268]

37 **Kahaleh M**, Gaidhane M, Shahid HM, Tyberg A, Sarkar A, Ardengh JC, Kedia P, Andalib I, Gress F, Sethi A, Gan SI, Suresh S, Makar M, Bareket R, Slivka A, Widmer JL, Jamidar PA, Alkhiari R, Oleas R, Kim D, Robles-Medranda CA, Raijman I. Digital single-operator cholangioscopy interobserver study using a new classification: the Mendoza Classification (with video). *Gastrointest Endosc* 2022; **95**: 319-326 [PMID: 34478737 DOI: 10.1016/j.gie.2021.08.015]

38 **Sethi A**, Chen YK, Austin GL, Brown WR, Brauer BC, Fukami NN, Khan AH, Shah RJ. ERCP with cholangiopancreatoscopy may be associated with higher rates of complications than ERCP alone: a single-center experience. *Gastrointest Endosc* 2011; **73**: 251-256 [PMID: 21106195 DOI: 10.1016/j.gie.2010.08.058]

39 **Meining A**, Shah RJ, Slivka A, Pleskow D, Chuttani R, Stevens PD, Becker V, Chen YK. Classification of probe-based confocal laser endomicroscopy findings in pancreaticobiliary strictures. *Endoscopy* 2012; **44**: 251-257 [PMID: 22261749 DOI: 10.1055/s-0031-1291545]

40 **Caillol F**, Filoche B, Gaidhane M, Kahaleh M. Refined probe-based confocal laser endomicroscopy classification for biliary strictures: the Paris Classification. *Dig Dis Sci* 2013; **58**: 1784-1789 [PMID: 23314855 DOI: 10.1007/s10620-012-2533-5]

41 **Meining A**, Chen YK, Pleskow D, Stevens P, Shah RJ, Chuttani R, Michalek J, Slivka A. Direct visualization of indeterminate pancreaticobiliary strictures with probe-based confocal laser endomicroscopy: a multicenter experience. *Gastrointest Endosc* 2011; **74**: 961-968 [PMID: 21802675 DOI: 10.1016/j.gie.2011.05.009]

42 **Tyberg A**, Xu MM, Gaidhane M, Kahaleh M. Second generation optical coherence tomography: Preliminary experience in pancreatic and biliary strictures. *Dig Liver Dis* 2018; **50**: 1214-1217 [PMID: 29937365 DOI: 10.1016/j.dld.2018.05.019]

43 **Arvanitakis M**, Hookey L, Tessier G, Demetter P, Nagy N, Stellke A, De Maertelaer V, Devière J, Le Moine O. Intraductal optical coherence tomography during endoscopic retrograde cholangiopancreatography for investigation of biliary strictures. *Endoscopy* 2009; **41**: 696-701 [PMID: 19618343 DOI: 10.1055/s-0029-1214950]

World Journal of Gastroenterology

Submit a Manuscript: https://www.f6publishing.com

World J Gastroenterol 2023 September 28; 29(36): 5211-5225

DOI: 10.3748/wjg.v29.i36.5211

ISSN 1007-9327 (print) ISSN 2219-2840 (online)

MINIREVIEWS

Integration and implementation of precision medicine in the multifaceted inflammatory bowel disease

Gowthami Sai Kogilathota Jagirdhar, Jose Andres Perez, Andrea Belen Perez, Salim Surani

Specialty type: Gastroenterology and hepatology

Provenance and peer review: Invited article; Externally peer reviewed.

Peer-review model: Single blind

Peer-review report's scientific quality classification

Grade A (Excellent): 0
Grade B (Very good): B, B
Grade C (Good): C
Grade D (Fair): D
Grade E (Poor): 0

P-Reviewer: Duan SL, China; Wen XL, China; Yang JS, China

Received: July 1, 2023
Peer-review started: July 1, 2023
First decision: July 10, 2023
Revised: July 31, 2023
Accepted: September 6, 2023
Article in press: September 6, 2023
Published online: September 28, 2023

Gowthami Sai Kogilathota Jagirdhar, Department of Medicine, Saint Francis Health Science Center, Newark, NJ 07107, United States

Jose Andres Perez, Department of Medicine, Saint Francis Health Systems, Tulsa, OK 74133, United States

Andrea Belen Perez, Department of Research, Columbia University, New York, NY 10027, United States

Salim Surani, Department of Medicine and Pharmacology, Texas A&M University, College Station, TX 77413, United States

Corresponding author: Salim Surani, FCCP, MD, MHSc, Academic Editor, Professor, Department of Medicine and Pharmacology, Texas A&M University, 400 Bizzell Street, College Station, TX 77413, United States. srsurani@hotmail.com

Abstract

Inflammatory bowel disease (IBD) is a complex disease with variability in genetic, environmental, and lifestyle factors affecting disease presentation and course. Precision medicine has the potential to play a crucial role in managing IBD by tailoring treatment plans based on the heterogeneity of clinical and temporal variability of patients. Precision medicine is a population-based approach to managing IBD by integrating environmental, genomic, epigenomic, transcriptomic, proteomic, and metabolomic factors. It is a recent and rapidly developing medicine. The widespread adoption of precision medicine worldwide has the potential to result in the early detection of diseases, optimal utilization of healthcare resources, enhanced patient outcomes, and, ultimately, improved quality of life for individuals with IBD. Though precision medicine is promising in terms of better quality of patient care, inadequacies exist in the ongoing research. There is discordance in study conduct, and data collection, utilization, interpretation, and analysis. This review aims to describe the current literature on precision medicine, its multiomics approach, and future directions for its application in IBD.

Key Words: Precision medicine; Multiomics; Inflammatory bowel disease; Crohn's disease; Ulcerative colitis; Data integration

©The Author(s) 2023. Published by Baishideng Publishing Group Inc. All rights reserved.

Core Tip: Precision medicine holds significant promise in managing inflammatory bowel disease (IBD) by aiming to customize treatments based on the unique biological characteristics of patients. Despite advancements in biological and small-molecule therapies offering new therapeutic options for IBD; however, the is a large gap in understanding the clinical course of IBD, the durability of treatment response, and enhancing available and new therapeutic options. Integrating multiomics into patient care can help in early diagnosis, predict disease course, deliver targeted treatments based on unique patient profiles, and evaluate prognosis.

Citation: Jagirdhar GSK, Perez JA, Perez AB, Surani S. Integration and implementation of precision medicine in the multifaceted inflammatory bowel disease. *World J Gastroenterol* 2023; 29(36): 5211-5225
URL: https://www.wjgnet.com/1007-9327/full/v29/i36/5211.htm
DOI: https://dx.doi.org/10.3748/wjg.v29.i36.5211

INTRODUCTION

Understanding precision medicine requires knowing two important concepts. (1) The definition of precision medicine; and (2) The role it plays in inflammatory bowel disease (IBD).

According to the National Cancer Institute, precision medicine is a form of therapy that utilizes knowledge about an individual's genetic makeup or specific proteins to prevent, diagnose, or treat diseases[1]. Liu *et al*[2] state the term was first proposed in 2011, and over the years, this term has gained more importance. The strategy of precision medicine is to classify patients with shared characteristics into the same subgroup based on specific and similar clinical features, treatment, and prognostic factors[2].

The pathophysiology of ulcerative colitis (UC) and Crohn's disease (CD) is increasingly evolving, mainly focusing on its genome, exposome, microbiome, immunome, and many other omics approaches. Thomas *et al*[3] noted that the development of IBD is attributed to an aberrant immune reaction resulting from intricate interactions among various genetic risk factors, imbalanced gut flora, and environmental influences. Unlike rare and clearly defined monogenic disorders, IBD arises from mutations in multiple genes rather than a single gene[3]. In this sense, precision medicine is pivotal in creating personalized therapies combining these various aspects into a multiomics approach[4]. If we target only the immune part of it without addressing the genome, the microbiome can result in treatment-limited success[2]. By treating IBD patients with the same and limited therapies, we assume that the underlying gastrointestinal inflammatory process is the same in all patients. Precision medicine in IBD aims to utilize specific clinical and biological characteristics of patients to predict disease and therefore use the correct treatment at the right time for the right patient[5].

The three priority areas of the precision medicine approach to IBD are: (1) Understanding the vulnerability, severity, and behavioral aspects of disease; (2) forecasting the response to medications; and (3) enhancing existing and creating novel molecular technologies to facilitate precision medicine.

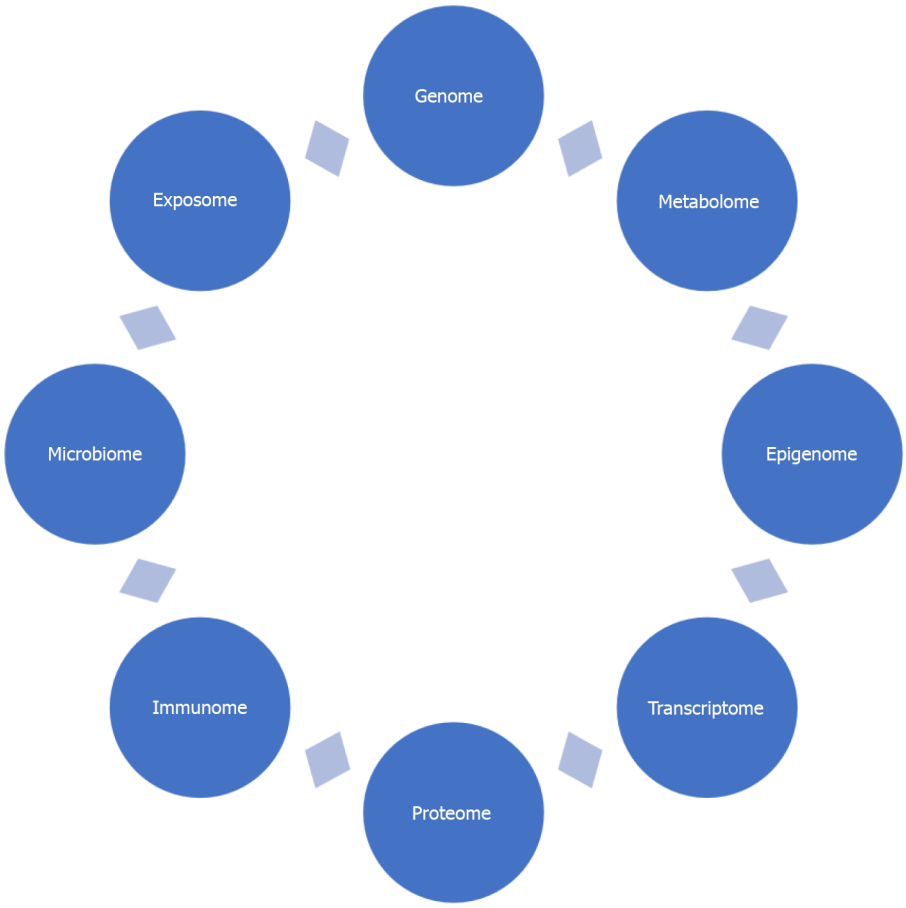
We can achieve this through advances in multiomics in IBD. Figure 1 shows the various omics in IBD management. Using this approach, we could better understand disease pathogenesis, model predictive biomarkers, and facilitate early diagnosis and treatment.

LITERATURE SEARCH

We conducted a review of existing literature in PubMed and Google Scholar to find relevant studies with information on multiomics in IBD and integrating various IBD therapies. We included studies from inception to May 2023. We created search criteria using a combination of free text words, including precision medicine, IBD, Genome, epigenome, epigenetics, proteome, transcriptome, immunome, microbiome, and integration. We examined studies that were published in the English language as part of our review. Pertinent articles were analyzed and incorporated into the review.

GENOMICS

Genetic factors stratify IBD into UC and CD. The utilization of genome-wide association studies (GWASs) has enabled the identification of notable genetic risk regions and IBD phenotypes to classify the disease into ileal Crohn's, colonic Crohn's, and UC compared to the current classification[6]. The genetic mechanisms implicated in IBD encompass various pathways, including microbial sensing (*NOD2, CARD9* and *RIPK2*), maintenance of intestinal barrier function (*C1orf106* and *HNF4A*), signaling within the innate and adaptive immune systems (*NLRP7, IL18RAP, CD28, IFNG, PTPN22, STAT4, IL6ST, IL23R, RORC and IL17RA*), fibrosis development (*OSMR* and *SMAD3*), and cellular homeostasis (*ATG16L1, RNF186* and *ERGIC1*)[7]. Despite the advances in genetic pathways, few relate to treatment response, prognosis, or clinical outcomes. Over 230 genetic loci have been identified to be involved in IBD[2,6,8]. However, in one of the largest phenotype-genotype GWASs of 29838 patients by Cleynen *et al*[6], over 163 loci related to IBD were studied, and genetic



DOI: 10.3748/wjg.v29.i36.5211 **Copyright** ©The Author(s) 2023.

Figure 1 The interplay of various omics in inflammatory bowel disease.

risk scores were created for CD and UC separately. On cross-validation of the data, the predictive accuracy for phenotypic variance in the adult population was low. These genetic predictors, along with smoking, could only explain 6.8% of the disease location with CD and only 1.1% with UC emphasizing that research using an interdisciplinary approach is required to provide the best risk assessment and aid diagnosis[6].

GWASs have been used in investigating pathways like the *NOD2/CARD15*, which are involved in pattern recognition and receptor signaling in response to microbial signaling. It has been associated with an ileal fibrostenotic disease phenotype that needs surgery and has a complicated disease course[9]. There is another study of the ATG16L1, T300A, an autophagy pathway reported to give an enhanced risk of CD[10]. Another autophagy gene *IGRM* is associated with penetrating disease in CD[11]. Interleukin (IL)-3 receptor has become a therapeutic agent for CD[12]. Studies have utilized genome basis to identify patients that benefit from hematopoietic stem cell transplantation (HSCT) and mesenchymal stem cell transplantation in patients with early-onset IBD and those with inborn errors of immunity[13-16]. Patients with genetic deficiencies such as IL-10, IL-10 receptor, and *XIAP* deficiencies benefitted from HSCT[13,17,18]. It also identifies mutations such as *STXBP2, TTC7A*, and *EPCAM* genes that will not benefit from particular therapies[19-21]. IBD is a polygenic disease, and research on the utilization of genome pathway-specific therapies to correct genetic defects is still developing. Thus, understanding genetic mechanisms helps personalized medicine in IBD.

EPIGENOMICS

Epigenetics is the study of inheritable changes in gene expression that are not caused by alterations in the DNA sequence.

Environmental factors cause alterations in DNA methylation, histone modifications, and miRNA synthesis, thus changing the phenotypic expression of genes and response to treatment. Parenteral exposure influences epigenetic alterations that are transmissible across generations. Epigenetics factors are potentially modifiable and preventable. Maternal protein restriction and maternal high fat intake were associated with DNA methylation changes that led to increased steatosis, impaired glucose tolerance, diabetes, and obesity in offspring[22,23]. Pan *et al*[24] describe gut microbiota alteration that causes changes in DNA methylation and transcriptome changes in intestinal epithelial cells postnatally in newborns[24]. A prospective study by Sun *et al*[25] describes a 12-year follow-up of CD and UC patients. Patients with unhealthy lifestyles had a hazard ratio (HR) of 1.94 and 1.98 for CD and UC. Patients with increased genetic risk for IBD but healthy lifestyles had a lower risk of developing IBD than those with increased genetic risk and

unhealthy lifestyles (HR: 2.23 *vs* 4.40)[25]. Yang and Jostins-Dean[26] published data using the information of IBD patients from a United Kingdom biobank. They analyzed 24 dietary exposures, perinatal childhood exposures, and lifestyle factors in individuals. They showed that multiple factors interacted, causing polygenic risk in predicting IBD occurrence. Factors such as appendectomy, smoking, childhood antibiotic use, exposure to the sun in winter, socio-economic factors, and oral contraceptive use played a role in IBD pathogenesis[26]. Ryan *et al*[27] found that inflamed and non-inflamed colonic mucosa in IBD patients had different microbiota composition and epigenetic profiles. Using machine learning to classify disease status and inflammation, the authors found that epigenomics and microbiota could classify UC, CD, and health status with an AUROC of 0.87[27]. Thus, epigenetics plays a role in defining IBD risk.

EXPOSOME

The exposome is defined as all encountered exposures in the lifetime of an individual beginning from conception. There are endogenous and exogenous exposomes in IBD. Microbiota is an endogenous exposome. Evidence suggests that mode of delivery at birth (cesarean *vs* vaginal, breastfeeding *vs* formula feeding) and early exposure to antibiotics in life are associated with intestinal colonization of bacteria early in life[28,29]. They contribute to intestinal immune homeostasis and are associated with UC and CD development[28]. Direct effects of infections, stress, diet, air and water pollutants, food additives, antibiotics, vitamin D deficiency, and physical activity on intestinal mucosal cells and indirect effects through alterations in the microbiome and immunomodulation influence IBD occurrence, presentation, course, and response to treatment[30,31]. These factors have been shown in animal models to induce DNA methylation and alteration in RNA and histone proteins, promoting the development of IBD[31]. Notably, Borg Bartolo states that industrialized nations exhibit the highest incidence of IBD[4]. According to Lamb *et al*[32], it is the environmental factors that influence IBD pathogenesis. A western diet of fast and processed foods, high-fat content, ultra-processed food consumption, and meat increases the risk of developing disease. In contrast, mitigating elements comprise elevated consumption of dietary fiber, caffeine, fruits, vegetables, olive oil, seafood, cereals, and nuts; all of which play a crucial role in safeguarding against certain conditions[32]. Initial investigations have demonstrated that exclusive enteral nutrition (EEN) diets based on specific formulas can effectively trigger remission in individuals with CD. As per the findings of Svolos *et al*[33], a customized food-based diet has been developed, sharing a similar composition with EEN. This personalized diet has exhibited favorable tolerability, notable enhancements in disease activity, significant alterations in the gut microbiome, and a metabolome profile comparable to that achieved with EEN[33]. Smoking, for example, is a risk factor in the progression of CD[34]. The relationship between IBD and smoking varies for CD and UC. Chemicals contained in the smoke generate carcinogenic and mutagenic components that can affect the immune system in the gastrointestinal mucosa. Smoking releases reactive metabolites that can cause DNA methylation, thus affecting gene regulation and expression[28]. Epigenome and exposome are closely interlinked in IBD pathogenesis.

IMMUNOME AND PROTEOME

The gut is the main barrier that controls the immunological interface and maintains the immunological balance by appropriately recognizing and tolerating bacteria, food antigens, and self-antigens. Proteomics studies can develop targeted therapy for IBD and find biomarkers to monitor drug response in IBD patients. Yau *et al*[35] describe that blood tests can identify epithelial component proteins that help in early predicting intestinal complications in IBD, such as stricturing and fistulizing disease[35]. Deeke *et al*[36] describe the identification of active IBD and pancolitis based on a panel of proteins in IBD stool samples[36]. IBD tissue samples can be classified into UC or CD based on proteomic analysis[37-39]. Protein analysis also helps to understand the response to treatment therapies[40]. Calprotectin is a marker that can be used for mucosal healing and clinical remission in IBD[41,42]. Tumor necrosis factor-like ligand 1A (TL1A) is involved in colonic inflammation and fibrosis through epithelial-to-mesenchymal cell transition and immune response mechanisms. It was detected in high levels in IBD patients. This is a potential target for IBD treatment[43]. Since IBD is an immune-mediated disease, both CD and UC have primarily immune targets for treatment. Masoodi *et al*[44] described altered polyunsaturated-fatty-acid-derived lipid mediators (eicosanoids), such as PGE2, PGD2, TXB2, 5-HETE, 11-HETE, 12-HETE and 15-HETE, that are elevated in inflamed mucosa in IBD patients and correlated with the severity of inflammation. These can assist in diagnosing inflammation in IBD[44,45]. Bennike *et al*[46] describe increased levels of neutrophils and neutrophil extracellular traps and several other proteins in UC patients' normal-appearing colon tissue, suggesting the role of innate immune system in IBD[46]. Titz *et al*[45] identified 18 studies on proteomics and lipidomics to identify biomarkers for IBD. Through the utilization of blood, serum samples, and colonic mucosal biopsies, these studies aided in diagnosis, patient stratification, treatment categorization, and response[45].

MICROBIOME

The microbiome is a critical factor in initiating and perpetuating the inflammatory response of IBD. Studies conducted on patients initiating treatment with vedolizumab have observed a higher prevalence of *Roseburia inlinivorans* and a species belonging to Burkholderiales among individuals with CD who successfully achieved remission by week 14[47]. Furthermore, a study indicated that neural networking modeling demonstrated superior predictive capability for

remission when utilizing microbial metadata compared to relying solely on clinical metadata. In 232 patients in the CERTIFIED study treated with ustekinumab, *Faecalibacterium* and *Bacteroides* were found in baseline stool in CD patients who achieved remission[47]. Microbiome has also helped identify high-risk individuals. Gevers *et al*[48] discovered that specific microbial patterns in the ileum could accurately predict the occurrence of CD, even in cases where inflammation was not present[48]. Vázquez-Baeza *et al*[49] describes that microbes play an important role in altering the response to medications, indicating that altering them could modify a patient's response to treatments. This can be a future target in microbiomics research[49].

Precision medicine needs to be applied by taking each of the above aspects and unifying them. The concept is to integrate data and generate patient profiles that could predict disease risk, onset, progression, complications, prognosis, and treatment in multi populations based on multiomics. Figure 2 describes a simplified pathway for utilizing multi-omics in IBD.

PRECISION MEDICINE TO PREDICT DISEASE SUSCEPTIBILITY, DIAGNOSIS, AND CLINICAL PHENOTYPE

The true power of precision medicine resides in the vast possibilities presented by multiomics data and its ability to merge effectively with clinical information. This concept is already applied in the field of oncology, where accurate biomarkers are utilized to forecast prognosis and anticipate the response to treatment[10]. The field of medicine has shifted from a treatment-oriented approach to a personalized and preventive approach. Biological data acquisition and digitization techniques have advanced, producing large amounts of high-specificity data. To examine and interpret these data, new databases, algorithms, and user-friendly applications are being designed to facilitate the analysis by bioinformatics specialists and physicians[5,50]. Table 1 shows studies utilizing multiomics in IBD for diagnosis and treatment.

To enhance transparency and accessibility of bio-sample data, standardization and harmonization of data frameworks are needed at a global level. A Data Commons should be established to facilitate global collaboration and provide access to biospecimens and data before and after treatment with established and novel therapies[3,51].

Cleynen *et al*[6] conducted a large genotype association study in patients with IBD using genotype-phenotype associations from 156-154 gene variants. They found ileal CD, colonic CD, and ulcerative colitis as distinct groups based on genetic risk scores of 29 838 patients. The application and utilization of these groups in clinical practice and patient treatment is not yet studied in detail[6]. Epigenetic studies by authors like Sun *et al*[25] prove the importance of genome-wide associations and gene–environment studies in IBD[25]. There is a need for biobanks such as the Dutch IBD biobank [52] and the GETECCU Eneida registry to be established globally since genetic predisposition, varied environmental exposures, and population differences can create different genetic susceptibilities based on location[53]. These can create population-specific effects that are not generalizable to all IBD patients[28]. This will create patient profiling that can be distinct based on geographic location. Studies conducted using biobank information also need to be standardized with quality control and the establishment of core validation guidelines so that generated results are comparable across studies and can be utilized to further precision medicine in IBD. Multiple studies analyzing biomarkers in IBD have been published, but the results have not been translated to clinical practice. We are lagging in terms of translation of the discovered research[45].

Screening programs such as DNA or RNA sequencing can inform healthy people with a family history of cancer about their health status. For example, mutations in the BRCA genes can be detected to identify the familial risk of breast cancer [54]. Disease monitoring using a combination of clinical data, biomarkers, imaging, therapeutic drug monitoring, modeling, and simulation is essential. The objective is to administer the appropriate treatment to each patient precisely when it is needed, based on their unique disease pattern and progression. By doing so, aiming to minimize long-term complications and improve patient outcomes[55]. The ability to identify the correct personalized therapies should also result in an earlier clinical response compared to current treatment strategies.

Omics are fields of study that analyze biological molecules and systems on a large scale. They aim to understand the complex interactions and functions of these molecules and systems and how they contribute to the health and disease of organisms. The study of genomics and transcriptomics is crucial for discovering disease pathways and designing effective drugs. Understanding these areas can help treat diseases that do not respond to current treatments. Nucleic acid sequencing methods, particularly next-generation sequencing technologies, are essential for studying genomics and transcriptomics. Various studies have explored individual differences in patients with the same condition at the genome level, including the human genome project, single nucleotide polymorphism detection, and GWASs. For the transcriptome, splicing, alternative splicing, and RNA sequencing are critical areas because many human genes undergo alternative splicing, and changes at this level can be difficult (and usually impossible) to detect at the genome level[54].

IBD omics investigate particular characteristics associated with IBD, emphasizing the importance of using methods that thoroughly explore and model the various interactions at play, enabling the acquisition of comprehensive knowledge. The use of molecular markers or molecular disease profiles can eliminate the interpretive aspects of response and remission definition and can guide more accurate drug selection and monitoring of immune modulators, biologics, and small molecule therapy[3,51,56].

The primary obstacle in the development and validation of precision medicine interventions for IBD lies in the extensive variability observed in disease progression, coupled with the current inability to accurately predict its course. Predictive models need to account for environmental influences and the heterogeneous response to treatment over time. Although mucosal healing serves as a substantial indicator for predicting future relapse, complications, and the

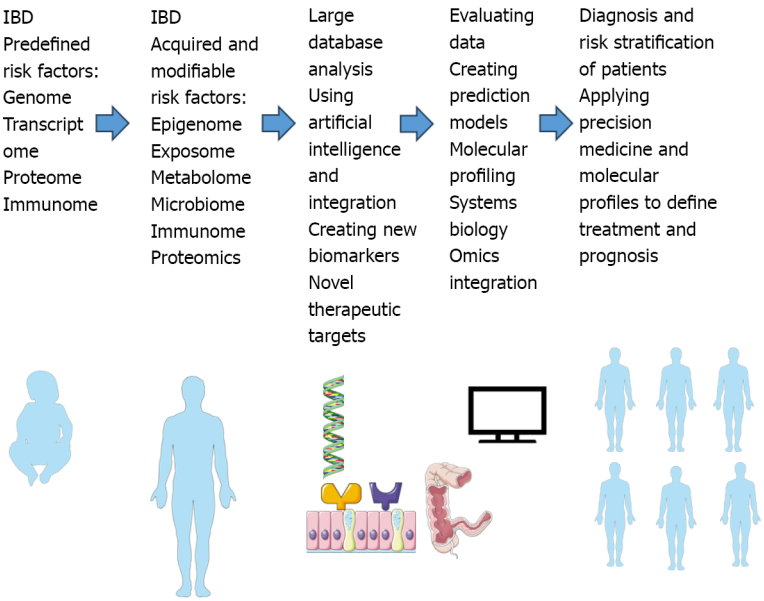
Table 1 Studies utilizing multiomics in inflammatory bowel disease

No.	Ref.	Type of study	Number of participants	Type of omics utilized	Results
1	Lloyd-Price *et al* [75]	Cohort study	132 IBD	Microbiome; genome; metagenome; meta; transcriptome; metabolome profiles; proteome	Found functional dysbiosis in the gut microbiome, changes in metabolite pools, and increased levels of antibodies in serum during periods of inflammatory bowel disease activity
2	Mills *et al* [83]	Cohort study	-40 UC, -validation cohort: 73 UC, 117 CD, 20 controls	Proteome; metaproteome; metabolome; metagenome; meta peptidome	UC patients with active disease had increased protease activity that originated from the bacterium *Bacteroides vulgatus*
3	Zhang *et al* [84]	Cohort study	25 CD, 22 UC, 24 controls	Metaproteome; microbiome	Identified functional alterations of microbiome and associated microbial proteins in the intestinal mucosa in new-onset pediatric IBD patients which contributed to abnormal host-microbiota interactions
4	Lee *et al* [74]	Prospective study	108 CD, 77 UC	Metabolome; microbiome; metagenome; proteome	Microbial, metagenomic diversity and metabolomics (serum secondary bile acid concentrations) predicted response in moderate-to-severe Crohn's disease or ulcerative colitis patients initiating anti-cytokine therapy (anti-TNF or -IL12/23) or anti-integrin therapy
5	Dai *et al* [85]	Prospective study	5956 CD, 21770 controls	Genome; epigenome; transcriptome	Identified strongly associated CD genes involved in immune response, MHC class II receptor activity, and immunological disorders. Involvement of constitutive photomorphogenesis 9 signalosome in CD pathogenesis. Interactions among CD genes with CD drug target genes
6	Suskind *et al*[86]	Randomized controlled trial	10 CD	Microbiome; metagenome; metaproteome; metabolome	Diet had a positive effect on CD patient symptoms and inflammation; Specific exclusionary diets were associated with a better resolution of inflammation
7	Borren *et al* [87]	Cohort study	108 CD, 56 UC	Proteome; metabolome; microbiome	Identified proteomic, metabolomic, and microbiome biomarkers that characterized a proinflammatory state in quiescent IBD patients and predicted clinical relapse
8	Liu *et al* [88]	Prospective study	42 UC, 11 controls	Metabonome; microbiome	Identified that the combination of Verrucomicrobiota, butyric acid, and isobutyric acid improved the prediction of early remission to anti-integrin therapy
9	Huang *et al*[89]	Cohort study	140 CD, 73 UC, 86 controls	Metagenome; meta transcriptome; proteome; metabolome; virome; microbiome	Established artificial intelligence models that can subtype IBD with high accuracy using simple noninvasive fecal biomarkers and avoiding invasive procedures
10	Mishra *et al*[60]	Cohort study	37 IBD	Genome; epigenome	Identified biomarkers of early shifts in gene expression and DNA methylation for early prediction of anti-TNF treatment success
11	Gonzalez *et al*[90]	Cohort study	200 IBD	Microbiome; metabolome; metaproteome; metagenome	Identified colonic- and ileal-isolated CD subtypes had different pathologies. Colonic CD was similar to ulcerative colitis with neutrophil and Bacteroides vulgatus involvement while Ileal-isolated CD had a bile acid-driven profile
12	Xu *et al*[91]	Cohort study	Discovery: 6 datasets, Validation: 46 CD, 44 controls	Genome; transcriptome; Epigenome; microbiome	Identified that CD onset results from a number of oxidative stress genes through DNA methylation, gene expression, and host-microbiota interactions
13	Gao *et al* [92]	Cohort study	30 CD, 5 controls	Proteome; microbiome; metagenome	Identified alterations in proteins, microbiome, and metabolic processes across multi-tissues in CD patients that are imprinted in serum and fecal samples as potential diagnostic biomarkers, allowing a non-invasive precision diagnosis
14	Baran *et al* [93]	Cohort study	18 IBD	Epigenome; transcriptome; genome	Therapeutic response causes transcriptional changes in the mucosa and early changes in gene expression in peripheral blood that are regulated epigenetically

IBD: Inflammatory bowel disease; UC: Ulcerative colitis; CD: Crohn's Disease; IL: Interleukin; TNF: Tumor necrosis factor.

likelihood of surgery, the requirement for frequent endoscopic examinations can be resource-intensive and may not be well-received by patients. To address this, patient-reported outcomes, and noninvasive biomarkers like fecal calprotectin (FC) and C-reactive protein (CRP) are highly utilized to assess treatment response in both research studies and clinical practice. However, the lack of universally agreed-upon definitions for treatment response and remission poses challenges in interpreting the usefulness of these measures[4,32].

A systematic analysis of six studies showed that two consecutive elevated FC levels predicted disease relapse within the next 2-3 mo, but an optimal cutoff for monitoring could not be defined. However, it was discovered that setting a cutoff value of no more than 250 μg/g for FC could effectively predict the achievement of endoscopic remission.



DOI: 10.3748/wjg.v29.i36.5211 **Copyright** ©The Author(s) 2023.

Figure 2 Simplified pathway to precision medicine in inflammatory bowel disease. IBD: Inflammatory bowel disease. Parts of Figure 2 were drawn by using pictures from Servier Medical Art. Servier Medical Art by Servier is licensed under a Creative Commons Attribution 3.0 Unported License (https://creativecommons.org/Licenses/by/3.0/).

Likewise, it was observed that CRP exhibits a correlation with both clinical disease activity and endoscopic inflammation. However, it is important to note that CRP levels can also be elevated in other clinical situations, such as infections. Glycoprotein acetylation (GlycA) is a new biomarker that has been investigated as a potential disease activity biomarker in patients with IBD. GlycA presents a potential advantage over CRP due to its composition as a composite marker derived from various acute-phase proteins. This characteristic renders GlycA more stable compared to CRP[4].

Two studies in 2021 shed light on the development and treatment of IBD[50]. The first study investigated the role of *NOD2* variants in the pathogenesis of CD and found that loss-of-function mutations in *NOD2* were associated with the activation of a macrophage–fibroblast niche, which is involved in the development of the disease. The study also identified a potential signaling pathway involving the gp130-STAT3 axis, which may contribute to the pathogenesis of CD. Furthermore, the study found that the gp130 inhibitor bazedoxifene could alleviate pathogenicity in zebrafish models of IBD. The second study aimed to predict the effectiveness of treatments for patients with IBD by analyzing microbial community profiles, baseline clinical features, and serum inflammatory markers. The study found that patients who started with anticytokine therapy had higher remission rates compared to those who began with anti-integrin therapy. Additionally, the study demonstrated the potential for using multiple types of data, including metagenomic, metabolomic, and proteomic features, to predict therapeutic efficacy for patients with IBD[5,50]. Rapid advances in human microbiome research suggest that profiling and manipulating the human microbiome can offer significant opportunities for diagnosis, intervention, risk management, and risk stratification[2].

Discussions about the integration of research and clinical care have focused more on human genetic and genomic data than human microbiome data. In 2014, working groups were established to explore the storage and display of genetic information in electronic medical records, which revealed differences in how genetic information was documented across institutions and the need to develop effective clinical support mechanisms for standardized clinically actionable genetic information that can be shared across health systems.

Through research, we have been able to identify environmental exposures in IBD, but we need to improve integrating it into patient profiles. Planned investigations with multinational studies in the field of both basic laboratory science and epidemiological studies will help create extensive patient profiling that can be used in understanding disease processes and further patient care[28]. According to Valles-Colomer *et al*[57], the use of microbiology (metaomics) has allowed the analysis of bacteria present in people with IBD. In normal flora, the use of 16S rRNA sequencing identified Bacteroidetes and Firmicutes, interestingly in people with IBD, gastrointestinal biopsies have found decreased levels of these bacteria [57].

According to a study by Stankovic *et al*[58], the use of machine learning approaches by using artificial intelligence (AI) and algorithms creates patterns not seen before in the management of IBD[58]. By creating big datasets and then using linear regressions, logistic regressions, and fitting models to characterize risk factors, patient baseline characteristics, treatment plans, and prognosis can be predefined. To date, the largest database available for IBD is the IBD genomic database, which allowed the discovery of more than 200 IBD-related loci[57].

PRECISION MEDICINE TO PREDICT TREATMENT RESPONSE AND PROGNOSIS

The ability to predict if a treatment will fail is important as well, as it allows for early switching of therapy and improves the chances and cost-effectiveness of recapturing a positive response. The Personalized Anti-tumor necrosis factor (TNF) Therapy in CD Study (PANTS) followed 1610 patients on anti-TNF therapy for 12 mo or until therapy was withdrawn. The presence of low drug concentrations at week 14 demonstrated a connection to both primary nonresponse and the absence of remission at week 54. Patients on infliximab were more likely to have immunogenicity than those on adalimumab (62.8% *vs* 28.5%). Obesity at baseline was linked to nonremission at week 54 for adalimumab only, while smoking and immunomodulator use affected infliximab. HLA variants and glycosylation also affected anti-TNF therapy immunogenicity. Colonic biopsies obtained from patients diagnosed with UC revealed reduced levels of branched N-glycans, which served as an indicator of the inability to respond effectively to standard therapy. High levels of CRP were identified as the sole additional independent predictor in this context[59]. Single-cell gene expression technologies have been used to gain insights into the molecular mechanisms underlying drug response to comprehend the pathophysiology of this process. In cases of active UC, there is a distinct decrease in the expression of mitochondrial genes in the epithelial cells. Conversely, an exclusive cellular module in CD is observed in inflamed tissues, which is linked to the inability to achieve long-lasting remission with corticosteroids and anti-TNF therapy[4]. Not surprisingly, one study by Mishra *et al* [60], which analyzed the early shifts of gene expression and DNA methylation, found that patients resistant to TNF treatment lacked such signatures[60].

Single-cell profiling techniques can help identify and measure different cell populations and their transformations over time and location. Changes in cell behavior can disrupt the balance in IBD, and studying these changes using techniques like single-cell RNA-seq and ATAC-seq can help understand the complex spectrum of cell types that contribute to IBD pathogenesis[50]. In 2021, researchers developed yeast-based probiotics for the treatment of IBD. The engineered probiotics expressed a human P2Y2 purinergic receptor that senses extracellular ATP, a molecule involved in intestinal inflammation. Activation of the receptor led to the secretion of the ATP-degrading enzyme apyrase, which created a self-feedback mechanism to maintain extracellular ATP at normal levels. The engineered probiotics did not cause unwanted adverse effects such as inflammation-driven fibrosis or gut microbiota dysbiosis. This shows promise for the development of new therapies for IBD based on precision medicine approaches that target the gut microbiota[5,50].

Multiomics projects are currently underway to investigate the heterogeneity of IBD and improve precision management. However, these high-throughput data require advanced computational techniques, such as machine learning to model and analyze them. Machine learning includes supervised and unsupervised algorithms that could be used for patient clustering, predictions, and to detect novel biomarkers. These strategies have been successfully applied to integrated multiomics data in cancer therapy[2]. Incorporating the increasing array of biomarkers, prediction tools, and treatments into the field of IBD presents a notable difficulty. The combination of early intervention and these novel tools may provide the greatest opportunity for delivering precision medicine in IBD. Additionally, powerful tools and equipment are required to store and share a vast amount of data. The use of mobile phones and app technology is one of the significant advances in this field for collecting and sharing big data. However, knowledge and expertise are necessary to standardize the collection of data and translate the archived data into clinical applications. It is our responsibility to contribute to big data in IBD and practice high-quality biomarker-driven care to enable the provision of truly individualized patient care in the future[4,54,55].

Molecular profiling is another technique that can provide information on the genes involved in IBD. It is based on tissue and blood and can predict specific patterns. For example, one study showed which patients were responders *versus* nonresponders to anti-TNF induction using single transcripts such as the OSM, OSMR or TREM[61]. A study also differentiated responders *versus* nonresponders to vedolizumab based on the expression of *RGS13, DCHS2, MAATS1* and *P1Wil1*[56]. The PROFILE trial marks a groundbreaking advancement in medical research, being the inaugural prospective randomized control trial that used T-cell signatures to categorize patients at the time of diagnosis[62].

Deep learning models using convolutional neural networks, computer image analysis systems, and machine learning can predict disease severity and remission comparable to that of gastroenterologists and radiologists[63-65].

Waljee *et al*[66] used machine learning to predict steroid use and the risk of hospital admission in IBD patients. Developing such models can help in the therapeutic management of IBD patients[66]. Lee *et al*[67] describes 170 disease susceptibility loci in IBD and found that loci associated with the risk of developing IBD were not predictive of disease prognosis. This emphasizes the need to reassess GWASs based on patient phenotypes, response to treatment, and prognosis[67].

Finally, treatment with biologics can alter the transcriptome profiles of CD patients distinguishing naïve from exposed patients undergoing ileocolic resection. This knowledge can be used by clinicians in medical therapy decision-making postoperatively in adjunct to clinical factors and endoscopy[68].

Integrative approaches combining multiple omics to create a framework that assesses the complex factors that interplay in IBD are required. This should be established from the initial risk assessment, prevention of disease, disease categorization, subcategorization, treatment during the changing disease course, prognostication, and follow-up.

MULTIOMICS

In recent decades, advances in technology have enabled the comprehensive profiling of the human gut microbiome through metaomics methodologies. The power of functional metaomics lies in its potential to identify molecular biomarkers that can assist with noninvasive screening and diagnosis, and treatment response. Data integration is the

process of combining multiomics data[69,70]. Table 1 describes studies consulting using multiple layers of multiomics data. Recent comprehensive human omics studies have substantiated findings from murine models and enhanced our comprehension of the connections between bile acids, their microbial progenitors, intestinal inflammation, and tumorigenesis. However, a significant portion of these human omics studies predominantly focus on either metagenomics or bile-acid-related metabolomics rather than combining this data to elucidate the associations between fluctuations in the abundance or function of gut microbiota and bile acid concentrations[71]. There is an essential need for additional investigations to delineate the role of bile acids in the adaptive immune system, thereby facilitating the evolution of therapeutic agents and diagnostic tools for IDB and colorectal cancer (CRC). Targeting the gut microbiota–bile acid axis offers significant potential for CRC and IBD treatment and prognosis but requires extensive research to deepen our understanding of the mechanistic links and clinical implications[71].

The intestinal microbiota is increasingly viewed as a potentially influential factor in the onset of IBD and CRC. IBD and its association with CRC suggest a potentially shared etiology between these two conditions. It is suggested that genetic, environmental, and immunological factors play a role in the onset of these diseases; however, the mechanisms through which they exert their influence remain complex and ambiguous. Additionally, functional metaomics has revealed similar metabolic dysregulation in both IBD and CRC, suggesting a disruption in host–microbiota interaction leading to abnormal immune responses and inflammation[72].

In another study, omics data were utilized to profile prospective patients undergoing either anticytokine or anti-integrin therapy. Certain bacterial species linked to a decrease in inflammation, often by creating a beneficial fecal short-chain fatty acid profile, were associated with patients more likely to achieve remission with anticytokine therapy. Moreover, these patients had an increased presence of colonic-butyrate-producing species that promoted intestinal balance. Those undergoing anti-integrin therapy who successfully achieved remission demonstrated increased abundances of different bacterial species, such as *Bifidobacterium longum* and *Bacteroides* species. Interestingly, some of these bacteria have previously shown effectiveness in independent microbiome-based therapies. However, the correlation between the microbiome and clinical response was more significant in week 14 of remission than in week 52 outcomes, suggesting the microbiome's influence may be on early response[73]. In this study, it was demonstrated that metabolomic profiling also contributed to understanding patient responses to treatment, with a strong association found between serum secondary bile acid concentrations and the likelihood of achieving remission with anti-cytokine therapy[74].

The Integrated Bowel Disease Microbiome Database study, part of the Human Microbiome Project Phase 2, investigated the gut microbiome of IBD. They used various measurement methods to analyze the microbiome's molecular components in CD and UC. The study found unique molecular features associated with dysbiosis in IBD, including previously known and new findings. The stability of the microbiome varied across IBD phenotypes and disease activity. The study identified potential targets for further investigation and highlighted the need to translate the findings into clinical applications, such as predictive biomarkers and new treatments for IBD[75].

The Danish IBD biobank project on 840 patients naïve to biologics started on biological therapy. It is an ongoing 3-year study utilizing clinical patient data, transcriptomic, proteomic, and microbiomic data. The study aims to identify biomarkers for response to biological therapy and understanding disease courses in IBD patients. The IBD prognosis study, 1000 IBD project, Swedish IBD quality register, and the Dutch IBD biobank are similar multi-omics integration studies and datasets for IBD[52,76,77].

The expansion of advanced platforms and tools for omics analysis signifies a change in molecular epidemiological research. Although the current omics data of IBD development is limited, the field is rapidly growing and presents immense possibilities. Various human cohorts, including those involving diverse births, at-risk individuals, and prediagnostic stages, have been established. Ongoing multiomics studies aim to characterize the pathways associated with IBD, incorporating the use of novel biomarkers. Rigorous statistical analyses, long-term monitoring of omics patterns in individuals before and after the onset of IBD, and replication of findings in independent cohorts are expected to provide valuable insights. To draw reliable conclusions from individual studies and facilitate the integration of data from multiple studies, it is crucial to collect detailed clinical information and follow standardized sampling, storage, and analysis protocols.

Availability of the knowledge acquired from precision medicine across all socioeconomic statuses is essential. Current data on precision medicine is not diverse and is restricted to some groups of populations. In a systematic review by Norris *et al*[78], those with low socioeconomic status were 17% less likely to be treated with novel precision medicine therapies for cancer[78]. Spratt *et al*[79] describes in his study of 5729 genomic sequencing samples that only 12% were African American and 3% were Hispanic and 3% were Asian. This over-represents the white population and under-represents other communities[79]. The results of such research can have an impact on the understanding of disease pathogenesis and the generalizability of results globally[80]. In a study by Yeh *et al*[81], African Americans and Hispanics questioned the benefits of precision medicine to their population due to the current inequalities in health care access and quality[81]. Another example of such a difference was seen by Lynch *et al*[82] in their study on Medicare patients with lung cancer. The authors observed racial, income, and regional disparities in EGFR testing and underutilization of guideline-recommended testing in certain populations. Precision medicine is advancing in terms of the complexity of disease management. The benefits of precision medicine need to be available to everyone equally, and a conscious effort to not increase the existing gap in health care is necessary[82].

Advancements in analysis techniques of omics data hold the potential to revolutionize the molecular epidemiology of IBD and other diseases, especially as more high-quality studies are conducted. This could lead to improved prediction of IBD onset and the development of treatment and preventive strategies. Furthermore, the findings in such studies can serve as a foundation to unravel pathways relevant to other immune-mediated and chronic diseases, contributing to advancements in public health as a whole[65].

FUTURE DIRECTIONS

With the upcoming evolution of AI to develop algorithms to diagnose and treat diseases, using databases will be the pillar of collecting information and analyzing trends with the help of statistical systems. It is essential to combine these individual databases so that by documenting known patient factors, specific profiles that will allow us to treat patients with specific patterns are generated. The complexity and heterogeneity of IBD make it a challenge because it is an evolving disease, and one treatment will not fit all patients. The future of IBD relies on these multiomics databases and the integration of profiles targeting different omics layers.

Establishing a checklist for future studies on precision medicine in IBD to regulate the methodology, quality, model validation, external validation, and algorithmic bias. Utilizing checklists to ensure reproducibility from study conduction to analysis and study data presentation will allow a better understanding of study outcomes and allow its applicability globally.

Efforts to minimize the current socioeconomic and racial gap in health care and precision medicine by ensuring further research include minority groups in diagnostics, drug discovery, and disease management.

Information about barriers to participation based on sex, race, and socioeconomic status is essential to help in the recruitment of underrepresented samples and ensure results are generalizable.

Precision medicine is promising, but the cost of genomic sequencing and creating patient profiles is not affordable to all patients. This could lead to further disparities in health care and is a barrier to its widespread adoption.

Large complex data needs to be standardized and integrated to achieve the full benefit of precision medicine. Establishing standards for collecting widely variable genomic data to allow comparison across studies is necessary.

Another important concept is the ethical aspects of utilizing genetic and patient data, ensuring patient privacy, and preventing data misuse.

There is a wide gap from creation to translation of the extensive research that is being generated on omics data. The complex information generated needs to be integrated and translated to patient care. This process involves rigorous clinical evidence, standardization, cost-benefit assessment, and regulations.

Summary of key points

Defining and understanding IBD requires a multidisciplinary approach by taking the genome, exposome, microbiome, immunome, proteome, transcriptome, epigenome, and metabolome concepts as a unit.

The development of GWASs has allowed the identification of notable genetic risk regions and IBD phenotypes. Other pathways have been developed, including microbial sensing, the maintenance of intestinal barrier function, signaling within the innate and adaptive immune system, fibrosis development, and cellular homeostasis.

Regarding the environmental risk factors, databases like the United Kingdom Biobank have allowed the recognition of polygenic risk factors like smoking, childhood antibiotic use, sun exposure in the winter, socioeconomic factors, and oral contraceptive use to be related to IBD occurrence.

The study of proteins has always been a target for diagnosis and treatment. One example is the TL1A, which has been involved in colonic inflammation and fibrosis through epithelial-to-mesenchymal cell transition and immune response mechanisms.

The interaction of our gut with the microorganisms that form part of the habitat in our intestine has also been the target of studies like the CERTIFIED study, where patients treated with ustekinumab, bacteria like *Faecalibacterium* and *Bacteroides* were found in baseline stool in CD patients who achieved remission.

The use of databases and AI creates the possibility of algorithms not seen before for the treatment and management of IBD, with the use of linear, logistic regressions and fitting models to characterize risk factors, baseline characteristics, treatment plans, and prognosis.

CONCLUSION

IBD is a complex longitudinal disease that utilizes multiple omics such as genomics, epigenomics, microbiomics, proteomics and immunomics. Utilizing mutiomics to further IBD management and deliver precision medicine with next-level care in IBD patients for the current and future should be targeted.

FOOTNOTES

Author contributions: Jagirdhar GSK, Perez JA, and Perez AB performed the literature review, wrote the original manuscript; Surani S wrote the original manuscript, revised the paper, and approved the final version.

Conflict-of-interest statement: None of the co-authors declared any conflicts of interest.

Open-Access: This article is an open-access article that was selected by an in-house editor and fully peer-reviewed by external reviewers. It is distributed in accordance with the Creative Commons Attribution NonCommercial (CC BY-NC 4.0) license, which permits others to distribute, remix, adapt, build upon this work non-commercially, and license their derivative works on different terms, provided the original work is properly cited and the use is non-commercial. See: https://creativecommons.org/Licenses/by-nc/4.0/

Country/Territory of origin: United States

ORCID number: Gowthami Sai Kogilathota Jagirdhar 0000-0003-1855-0863; Jose Andres Perez 0009-0007-2337-6317; Andrea Belen Perez 0009-0002-1547-3516; Salim Surani 0000-0001-7105-4266.

Corresponding Author's Membership in Professional Societies: Society of Critical Care Medicine; American College of Physician.

S-Editor: Fan JR
L-Editor: Kerr C
P-Editor: Fan JR

REFERENCES

1 **Definition of precision medicine**. NCI Dictionary of Cancer Terms-NCI. Available from: https://www.cancer.gov/publications/dictionaries/cancer-terms/def/precision-medicine

2 **Liu XY**, Tang H, Zhou QY, Zeng YL, Chen D, Xu H, Li Y, Tan B, Qian JM. Advancing the precision management of inflammatory bowel disease in the era of omics approaches and new technology. *World J Gastroenterol* 2023; **29**: 272-285 [PMID: 36687128 DOI: 10.3748/wjg.v29.i2.272]

3 **Thomas JP**, Modos D, Korcsmaros T, Brooks-Warburton J. Network Biology Approaches to Achieve Precision Medicine in Inflammatory Bowel Disease. *Front Genet* 2021; **12**: 760501 [PMID: 34745229 DOI: 10.3389/fgene.2021.760501]

4 **Borg-Bartolo SP**, Boyapati RK, Satsangi J, Kalla R. Precision medicine in inflammatory bowel disease: concept, progress and challenges. *F1000Res* 2020; **9** [PMID: 32047622 DOI: 10.12688/f1000research.20928.1]

5 **Denson LA**, Curran M, McGovern DPB, Koltun WA, Duerr RH, Kim SC, Sartor RB, Sylvester FA, Abraham C, de Zoeten EF, Siegel CA, Burns RM, Dobes AM, Shtraizent N, Honig G, Heller CA, Hurtado-Lorenzo A, Cho JH. Challenges in IBD Research: Precision Medicine. *Inflamm Bowel Dis* 2019; **25**: S31-S39 [PMID: 31095701 DOI: 10.1093/ibd/izz078]

6 **Cleynen I**, Boucher G, Jostins L, Schumm LP, Zeissig S, Ahmad T, Andersen V, Andrews JM, Annese V, Brand S, Brant SR, Cho JH, Daly MJ, Dubinsky M, Duerr RH, Ferguson LR, Franke A, Gearry RB, Goyette P, Hakonarson H, Halfvarson J, Hov JR, Huang H, Kennedy NA, Kupcinskas L, Lawrance IC, Lee JC, Satsangi J, Schreiber S, Théâtre E, van der Meulen-de Jong AE, Weersma RK, Wilson DC; International Inflammatory Bowel Disease Genetics Consortium, Parkes M, Vermeire S, Rioux JD, Mansfield J, Silverberg MS, Radford-Smith G, McGovern DP, Barrett JC, Lees CW. Inherited determinants of Crohn's disease and ulcerative colitis phenotypes: a genetic association study. *Lancet* 2016; **387**: 156-167 [PMID: 26490195 DOI: 10.1016/S0140-6736(15)00465-1]

7 **Graham DB**, Xavier RJ. Pathway paradigms revealed from the genetics of inflammatory bowel disease. *Nature* 2020; **578**: 527-539 [PMID: 32103191 DOI: 10.1038/s41586-020-2025-2]

8 **Ellinghaus D**, Jostins L, Spain SL, Cortes A, Bethune J, Han B, Park YR, Raychaudhuri S, Pouget JG, Hübenthal M, Folseraas T, Wang Y, Esko T, Metspalu A, Westra HJ, Franke L, Pers TH, Weersma RK, Collij V, D'Amato M, Halfvarson J, Jensen AB, Lieb W, Degenhardt F, Forstner AJ, Hofmann A; International IBD Genetics Consortium (IIBDGC); International Genetics of Ankylosing Spondylitis Consortium (IGAS); International PSC Study Group (IPSCSG); Genetic Analysis of Psoriasis Consortium (GAPC); Psoriasis Association Genetics Extension (PAGE), Schreiber S, Mrowietz U, Juran BD, Lazaridis KN, Brunak S, Dale AM, Trembath RC, Weidinger S, Weichenthal M, Ellinghaus E, Elder JT, Barker JN, Andreassen OA, McGovern DP, Karlsen TH, Barrett JC, Parkes M, Brown MA, Franke A. Analysis of five chronic inflammatory diseases identifies 27 new associations and highlights disease-specific patterns at shared loci. *Nat Genet* 2016; **48**: 510-518 [PMID: 26974007 DOI: 10.1038/ng.3528]

9 **Girardin SE**, Hugot JP, Sansonetti PJ. Lessons from Nod2 studies: towards a link between Crohn's disease and bacterial sensing. *Trends Immunol* 2003; **24**: 652-658 [PMID: 14644139 DOI: 10.1016/j.it.2003.10.007]

10 **Ashton JJ**, Mossotto E, Ennis S, Beattie RM. Personalising medicine in inflammatory bowel disease-current and future perspectives. *Transl Pediatr* 2019; **8**: 56-69 [PMID: 30881899 DOI: 10.21037/tp.2018.12.03]

11 **Latiano A**, Palmieri O, Cucchiara S, Castro M, D'Incà R, Guariso G, Dallapiccola B, Valvano MR, Latiano T, Andriulli A, Annese V. Polymorphism of the IRGM gene might predispose to fistulizing behavior in Crohn's disease. *Am J Gastroenterol* 2009; **104**: 110-116 [PMID: 19098858 DOI: 10.1038/ajg.2008.3]

12 **Deepak P**, Sandborn WJ. Ustekinumab and Anti-Interleukin-23 Agents in Crohn's Disease. *Gastroenterol Clin North Am* 2017; **46**: 603-626 [PMID: 28838418 DOI: 10.1016/j.gtc.2017.05.013]

13 **Meena S**, Varla H, Swaminathan VV, Chandar R, Jayakumar I, Ramakrishnan B, Uppuluri R, Raj R. Hematopoietic stem cell Transplantation in Children with very Early Onset Inflammatory Bowel Disease Secondary to Monogenic Disorders of immune-dysregulation. *Indian J Hematol Blood Transfus* 2023; **39**: 183-190 [PMID: 37006985 DOI: 10.1007/s12288-022-01586-2]

14 **Moser LM**, Fekadu J, Willasch A, Rettinger E, Sörensen J, Jarisch A, Kirwil M, Lieb A, Holzinger D, Calaminus G, Bader P, Bakhtiar S. Treatment of inborn errors of immunity patients with inflammatory bowel disease phenotype by allogeneic stem cell transplantation. *Br J Haematol* 2023; **200**: 595-607 [PMID: 36214981 DOI: 10.1111/bjh.18497]

15 **Lightner AL**, Dadgar N, Matyas C, Elliott K, Fulmer C, Khaitan N, Ream J, Nachand D, Steele SR. A phase IB/IIA study of remestemcel-L, an allogeneic bone marrow-derived mesenchymal stem cell product, for the treatment of medically refractory ulcerative colitis: an interim analysis. *Colorectal Dis* 2022; **24**: 1358-1370 [PMID: 35767384 DOI: 10.1111/codi.16239]

16 **Ye Z**, Zhou Y, Huang Y, Wang Y, Lu J, Tang Z, Miao S, Dong K, Jiang Z. Phenotype and Management of Infantile-onset Inflammatory Bowel Disease: Experience from a Tertiary Care Center in China. *Inflamm Bowel Dis* 2017; **23**: 2154-2164 [PMID: 29140941 DOI: 10.1097/MIB.0000000000001269]

17 **Engelhardt KR**, Shah N, Faizura-Yeop I, Kocacik Uygun DF, Frede N, Muise AM, Shteyer E, Filiz S, Chee R, Elawad M, Hartmann B, Arkwright PD, Dvorak C, Klein C, Puck JM, Grimbacher B, Glocker EO. Clinical outcome in IL-10- and IL-10 receptor-deficient patients with or without hematopoietic stem cell transplantation. *J Allergy Clin Immunol* 2013; **131**: 825-830 [PMID: 23158016 DOI: 10.1016/j.jaci.2012.09.025]

18 **Ono S**, Takeshita K, Kiridoshi Y, Kato M, Kamiya T, Hoshino A, Yanagimachi M, Arai K, Takeuchi I, Toita N, Imamura T, Sasahara Y, Sugita J, Hamamoto K, Takeuchi M, Saito S, Onuma M, Tsujimoto H, Yasui M, Taga T, Arakawa Y, Mitani Y, Yamamoto N, Imai K, Suda W, Hattori M, Ohara O, Morio T, Honda K, Kanegane H. Hematopoietic Cell Transplantation Rescues Inflammatory Bowel Disease and Dysbiosis of Gut Microbiota in XIAP Deficiency. *J Allergy Clin Immunol Pract* 2021; **9**: 3767-3780 [PMID: 34246792 DOI: 10.1016/j.jaip.2021.05.045]

19 **Fujikawa H**, Shimizu H, Nambu R, Takeuchi I, Matsui T, Sakamoto K, Gocho Y, Miyamoto T, Yasumi T, Yoshioka T, Arai K. Monogenic inflammatory bowel disease with STXBP2 mutations is not resolved by hematopoietic stem cell transplantation but can be alleviated *via* immunosuppressive drug therapy. *Clin Immunol* 2023; **246**: 109203 [PMID: 36503158 DOI: 10.1016/j.clim.2022.109203]

20 **Kammermeier J**, Drury S, James CT, Dziubak R, Ocaka L, Elawad M, Beales P, Lench N, Uhlig HH, Bacchelli C, Shah N. Targeted gene panel sequencing in children with very early onset inflammatory bowel disease--evaluation and prospective analysis. *J Med Genet* 2014; **51**: 748-755 [PMID: 25194001 DOI: 10.1136/jmedgenet-2014-102624]

21 **Kammermeier J**, Lamb CA, Jones KDJ, Anderson CA, Baple EL, Bolton C, Braggins H, Coulter TI, Gilmour KC, Gregory V, Hambleton S, Hartley D, Hawthorne AB, Hearn S, Laurence A, Parkes M, Russell RK, Speight RA, Travis S, Wilson DC, Uhlig HH. Genomic diagnosis and care co-ordination for monogenic inflammatory bowel disease in children and adults: consensus guideline on behalf of the British Society of Gastroenterology and British Society of Paediatric Gastroenterology, Hepatology and Nutrition. *Lancet Gastroenterol Hepatol* 2023; **8**: 271-286 [PMID: 36634696 DOI: 10.1016/S2468-1253(22)00337-5]

22 **Dominguez-Salas P**, Moore SE, Baker MS, Bergen AW, Cox SE, Dyer RA, Fulford AJ, Guan Y, Laritsky E, Silver MJ, Swan GE, Zeisel SH, Innis SM, Waterland RA, Prentice AM, Hennig BJ. Maternal nutrition at conception modulates DNA methylation of human metastable epialleles. *Nat Commun* 2014; **5**: 3746 [PMID: 24781383 DOI: 10.1038/ncomms4746]

23 **Fernandez-Twinn DS**, Constância M, Ozanne SE. Intergenerational epigenetic inheritance in models of developmental programming of adult disease. *Semin Cell Dev Biol* 2015; **43**: 85-95 [PMID: 26135290 DOI: 10.1016/j.semcdb.2015.06.006]

24 **Pan WH**, Sommer F, Falk-Paulsen M, Ulas T, Best P, Fazio A, Kachroo P, Luzius A, Jentzsch M, Rehman A, Müller F, Lengauer T, Walter J, Künzel S, Baines JF, Schreiber S, Franke A, Schultze JL, Bäckhed F, Rosenstiel P. Exposure to the gut microbiota drives distinct methylome and transcriptome changes in intestinal epithelial cells during postnatal development. *Genome Med* 2018; **10**: 27 [PMID: 29653584 DOI: 10.1186/s13073-018-0534-5]

25 **Sun Y**, Yuan S, Chen X, Sun J, Kalla R, Yu L, Wang L, Zhou X, Kong X, Hesketh T, Ho GT, Ding K, Dunlop M, Larsson SC, Satsangi J, Chen J, Wang X, Li X, Theodoratou E, Giovannucci EL. The Contribution of Genetic Risk and Lifestyle Factors in the Development of Adult-Onset Inflammatory Bowel Disease: A Prospective Cohort Study. *Am J Gastroenterol* 2023; **118**: 511-522 [PMID: 36695739 DOI: 10.14309/ajg.0000000000002180]

26 **Yang AZ**, Jostins-Dean L. Environmental variables and genome-environment interactions predicting IBD diagnosis in large UK cohort. *Sci Rep* 2022; **12**: 10890 [PMID: 35764673 DOI: 10.1038/s41598-022-13222-0]

27 **Ryan FJ**, Ahern AM, Fitzgerald RS, Laserna-Mendieta EJ, Power EM, Clooney AG, O'Donoghue KW, McMurdie PJ, Iwai S, Crits-Christoph A, Sheehan D, Moran C, Flemer B, Zomer AL, Fanning A, O'Callaghan J, Walton J, Temko A, Stack W, Jackson L, Joyce SA, Melgar S, DeSantis TZ, Bell JT, Shanahan F, Claesson MJ. Colonic microbiota is associated with inflammation and host epigenomic alterations in inflammatory bowel disease. *Nat Commun* 2020; **11**: 1512 [PMID: 32251296 DOI: 10.1038/s41467-020-15342-5]

28 **Noble CL**, Abbas AR, Lees CW, Cornelius J, Toy K, Modrusan Z, Clark HF, Arnott ID, Penman ID, Satsangi J, Diehl L. Characterization of intestinal gene expression profiles in Crohn's disease by genome-wide microarray analysis. *Inflamm Bowel Dis* 2010; **16**: 1717-1728 [PMID: 20848455 DOI: 10.1002/ibd.21263]

29 **van der Sloot KWJ**, Weersma RK, Alizadeh BZ, Dijkstra G. Identification of Environmental Risk Factors Associated With the Development of Inflammatory Bowel Disease. *J Crohns Colitis* 2020; **14**: 1662-1671 [PMID: 32572465 DOI: 10.1093/ecco-jcc/jjaa114]

30 **Rogler G**, Vavricka S. Exposome in IBD: recent insights in environmental factors that influence the onset and course of IBD. *Inflamm Bowel Dis* 2015; **21**: 400-408 [PMID: 25358064 DOI: 10.1097/MIB.0000000000000229]

31 **Vieujean S**, Caron B, Haghnejad V, Jouzeau JY, Netter P, Heba AC, Ndiaye NC, Moulin D, Barreto G, Danese S, Peyrin-Biroulet L. Impact of the Exposome on the Epigenome in Inflammatory Bowel Disease Patients and Animal Models. *Int J Mol Sci* 2022; **23** [PMID: 35886959 DOI: 10.3390/ijms23147611]

32 **Lamb CA**, Saifuddin A, Powell N, Rieder F. The Future of Precision Medicine to Predict Outcomes and Control Tissue Remodeling in Inflammatory Bowel Disease. *Gastroenterology* 2022; **162**: 1525-1542 [PMID: 34995532 DOI: 10.1053/j.gastro.2021.09.077]

33 **Svolos V**, Hansen R, Nichols B, Quince C, Ijaz UZ, Papadopoulou RT, Edwards CA, Watson D, Alghamdi A, Brejnrod A, Ansalone C, Duncan H, Gervais L, Tayler R, Salmond J, Bolognini D, Klopfleisch R, Gaya DR, Milling S, Russell RK, Gerasimidis K. Treatment of Active Crohn's Disease With an Ordinary Food-based Diet That Replicates Exclusive Enteral Nutrition. *Gastroenterology* 2019; **156**: 1354-1367.e6 [PMID: 30550821 DOI: 10.1053/j.gastro.2018.12.002]

34 **To N**, Gracie DJ, Ford AC. Systematic review with meta-analysis: the adverse effects of tobacco smoking on the natural history of Crohn's disease. *Aliment Pharmacol Ther* 2016; **43**: 549-561 [PMID: 26749371 DOI: 10.1111/apt.13511]

35 **Yau YY**, Leong RWL, Pudipeddi A, Redmond D, Wasinger VC. Serological Epithelial Component Proteins Identify Intestinal Complications in Crohn's Disease. *Mol Cell Proteomics* 2017; **16**: 1244-1257 [PMID: 28490445 DOI: 10.1074/mcp.M116.066506]

36 **Deeke SA**, Starr AE, Ning Z, Ahmadi S, Zhang X, Mayne J, Chiang CK, Singleton R, Benchimol EI, Mack DR, Stintzi A, Figeys D. Mucosal-luminal interface proteomics reveals biomarkers of pediatric inflammatory bowel disease-associated colitis. *Am J Gastroenterol* 2018; **113**: 713-724 [PMID: 29531307 DOI: 10.1038/s41395-018-0024-9]

37 **Seeley EH**, Washington MK, Caprioli RM, M'Koma AE. Proteomic patterns of colonic mucosal tissues delineate Crohn's colitis and ulcerative colitis. *Proteomics Clin Appl* 2013; **7**: 541-549 [PMID: 23382084 DOI: 10.1002/prca.201200107]

38 **M'Koma AE**, Seeley EH, Washington MK, Schwartz DA, Muldoon RL, Herline AJ, Wise PE, Caprioli RM. Proteomic profiling of mucosal and submucosal colonic tissues yields protein signatures that differentiate the inflammatory colitides. *Inflamm Bowel Dis* 2011; **17**: 875-883 [PMID: 20806340 DOI: 10.1002/ibd.21442]

39 **Starr AE**, Deeke SA, Ning Z, Chiang CK, Zhang X, Mottawea W, Singleton R, Benchimol EI, Wen M, Mack DR, Stintzi A, Figeys D. Proteomic analysis of ascending colon biopsies from a paediatric inflammatory bowel disease inception cohort identifies protein biomarkers that differentiate Crohn's disease from UC. *Gut* 2017; **66**: 1573-1583 [PMID: 27216938 DOI: 10.1136/gutjnl-2015-310705]

40 **Magnusson MK**, Strid H, Isaksson S, Bajor A, Lasson A, Ung KA, Öhman L. Response to infliximab therapy in ulcerative colitis is associated with decreased monocyte activation, reduced CCL2 expression and downregulation of Tenascin C. *J Crohns Colitis* 2015; **9**: 56-65 [PMID: 25518051 DOI: 10.1093/ecco-jcc/jju008]

41 **De Vos M**, Dewit O, D'Haens G, Baert F, Fontaine F, Vermeire S, Franchimont D, Moreels T, Staessen D, Terriere L, Vander Cruyssen B, Louis E; behalf of BIRD. Fast and sharp decrease in calprotectin predicts remission by infliximab in anti-TNF naïve patients with ulcerative colitis. *J Crohns Colitis* 2012; **6**: 557-562 [PMID: 22398050 DOI: 10.1016/j.crohns.2011.11.002]

42 **Facciorusso A**, Ramai D, Ricciardelli C, Paolillo R, Maida M, Chandan S, Mohan BP, Domislovic V, Sacco R. Prognostic Role of Post-Induction Fecal Calprotectin Levels in Patients with Inflammatory Bowel Disease Treated with Biological Therapies. *Biomedicines* 2022; **10** [PMID: 36140408 DOI: 10.3390/biomedicines10092305]

43 **Wenxiu J**, Mingyue Y, Fei H, Yuxin L, Mengyao W, Chenyang L, Jia S, Hong Z, Shih DQ, Targan SR, Xiaolan Z. Effect and Mechanism of TL1A Expression on Epithelial-Mesenchymal Transition during Chronic Colitis-Related Intestinal Fibrosis. *Mediators Inflamm* 2021; **2021**: 5927064 [PMID: 34257516 DOI: 10.1155/2021/5927064]

44 **Masoodi M**, Pearl DS, Eiden M, Shute JK, Brown JF, Calder PC, Trebble TM. Altered colonic mucosal Polyunsaturated Fatty Acid (PUFA) derived lipid mediators in ulcerative colitis: new insight into relationship with disease activity and pathophysiology. *PLoS One* 2013; **8**: e76532 [PMID: 24204637 DOI: 10.1371/journal.pone.0076532]

45 **Titz B**, Gadaleta RM, Lo Sasso G, Elamin A, Ekroos K, Ivanov NV, Peitsch MC, Hoeng J. Proteomics and Lipidomics in Inflammatory Bowel Disease Research: From Mechanistic Insights to Biomarker Identification. *Int J Mol Sci* 2018; **19** [PMID: 30223557 DOI: 10.3390/ijms19092775]

46 **Bennike TB**, Carlsen TG, Ellingsen T, Bonderup OK, Glerup H, Bøgsted M, Christiansen G, Birkelund S, Stensballe A, Andersen V. Neutrophil Extracellular Traps in Ulcerative Colitis: A Proteome Analysis of Intestinal Biopsies. *Inflamm Bowel Dis* 2015; **21**: 2052-2067 [PMID: 25993694 DOI: 10.1097/MIB.0000000000000460]

47 **Ananthakrishnan AN**, Luo C, Yajnik V, Khalili H, Garber JJ, Stevens BW, Cleland T, Xavier RJ. Gut Microbiome Function Predicts Response to Anti-integrin Biologic Therapy in Inflammatory Bowel Diseases. *Cell Host Microbe* 2017; **21**: 603-610.e3 [PMID: 28494241 DOI: 10.1016/j.chom.2017.04.010]

48 **Gevers D**, Kugathasan S, Denson LA, Vázquez-Baeza Y, Van Treuren W, Ren B, Schwager E, Knights D, Song SJ, Yassour M, Morgan XC, Kostic AD, Luo C, González A, McDonald D, Haberman Y, Walters T, Baker S, Rosh J, Stephens M, Heyman M, Markowitz J, Baldassano R, Griffiths A, Sylvester F, Mack D, Kim S, Crandall W, Hyams J, Huttenhower C, Knight R, Xavier RJ. The treatment-naive microbiome in new-onset Crohn's disease. *Cell Host Microbe* 2014; **15**: 382-392 [PMID: 24629344 DOI: 10.1016/j.chom.2014.02.005]

49 **Vázquez-Baeza Y**, Callewaert C, Debelius J, Hyde E, Marotz C, Morton JT, Swafford A, Vrbanac A, Dorrestein PC, Knight R. Impacts of the Human Gut Microbiome on Therapeutics. *Annu Rev Pharmacol Toxicol* 2018; **58**: 253-270 [PMID: 28968189 DOI: 10.1146/annurev-pharmtox-042017-031849]

50 **Mao R**, Chen M. Precision medicine in IBD: genes, drugs, bugs and omics. *Nat Rev Gastroenterol Hepatol* 2022; **19**: 81-82 [PMID: 34785787 DOI: 10.1038/s41575-021-00555-w]

51 **Dovrolis N**, Filidou E, Kolios G. Systems biology in inflammatory bowel diseases: on the way to precision medicine. *Ann Gastroenterol* 2019; **32**: 233-246 [PMID: 31040620 DOI: 10.20524/aog.2019.0373]

52 **Spekhorst LM**, Imhann F, Festen EAM, van Bodegraven AA, de Boer NKH, Bouma G, Fidder HH, d'Haens G, Hoentjen F, Hommes DW, de Jong DJ, Löwenberg M, Maljaars PWJ, van der Meulen-de Jong AE, Oldenburg B, Pierik MJ, Ponsioen CY, Stokkers PC, Verspaget HW, Visschedijk MC, van der Woude CJ, Dijkstra G, Weersma RK; Parelsnoer Institute (PSI) and the Dutch Initiative on Crohn and Colitis (ICC). Cohort profile: design and first results of the Dutch IBD Biobank: a prospective, nationwide biobank of patients with inflammatory bowel disease. *BMJ Open* 2017; **7**: e016695 [PMID: 29122790 DOI: 10.1136/bmjopen-2017-016695]

53 **Chaparro M**, Ramas M, Benítez JM, López-García A, Juan A, Guardiola J, Mínguez M, Calvet X, Márquez L, Fernández Salazar LI, Bujanda L, García C, Zabana Y, Lorente R, Barrio J, Hinojosa E, Iborra M, Cajal MD, Van Domselaar M, García-Sepulcre MF, Gomollón F, Piqueras M, Alcaín G, García-Sánchez V, Panés J, Domènech E, García-Esquinas E, Rodríguez-Artalejo F, Gisbert JP. Extracolonic Cancer in Inflammatory Bowel Disease: Data from the GETECCU Eneida Registry. *Am J Gastroenterol* 2017; **112**: 1135-1143 [PMID: 28534520 DOI: 10.1038/ajg.2017.96]

54 **Khodadadian A**, Darzi S, Haghi-Daredeh S, Sadat Eshaghi F, Babakhanzadeh E, Mirabutalebi SH, Nazari M. Genomics and Transcriptomics: The Powerful Technologies in Precision Medicine. *Int J Gen Med* 2020; **13**: 627-640 [PMID: 32982380 DOI: 10.2147/IJGM.S249970]

55 **Noor NM**, Sousa P, Paul S, Roblin X. Early Diagnosis, Early Stratification, and Early Intervention to Deliver Precision Medicine in IBD. *Inflamm Bowel Dis* 2022; **28**: 1254-1264 [PMID: 34480558 DOI: 10.1093/ibd/izab228]

56 **Verstockt B**, Verstockt S, Veny M, Dehairs J, Arnauts K, Van Assche G, De Hertogh G, Vermeire S, Salas A, Ferrante M. Expression Levels of 4 Genes in Colon Tissue Might Be Used to Predict Which Patients Will Enter Endoscopic Remission After Vedolizumab Therapy for Inflammatory Bowel Diseases. *Clin Gastroenterol Hepatol* 2020; **18**: 1142-1151.e10 [PMID: 31446181 DOI: 10.1016/j.cgh.2019.08.030]

57 **Valles-Colomer M**, Darzi Y, Vieira-Silva S, Falony G, Raes J, Joossens M. Meta-omics in Inflammatory Bowel Disease Research: Applications, Challenges, and Guidelines. *J Crohns Colitis* 2016; **10**: 735-746 [PMID: 26802086 DOI: 10.1093/ecco-jcc/jjw024]

58 **Stankovic B**, Kotur N, Nikcevic G, Gasic V, Zukic B, Pavlovic S. Machine Learning Modeling from Omics Data as Prospective Tool for Improvement of Inflammatory Bowel Disease Diagnosis and Clinical Classifications. *Genes (Basel)* 2021; **12** [PMID: 34573420 DOI: 10.3390/genes12091438]

59 **Kennedy NA**, Heap GA, Green HD, Hamilton B, Bewshea C, Walker GJ, Thomas A, Nice R, Perry MH, Bouri S, Chanchlani N, Heerasing NM, Hendy P, Lin S, Gaya DR, Cummings JRF, Selinger CP, Lees CW, Hart AL, Parkes M, Sebastian S, Mansfield JC, Irving PM, Lindsay J, Russell RK, McDonald TJ, McGovern D, Goodhand JR, Ahmad T; UK Inflammatory Bowel Disease Pharmacogenetics Study Group. Predictors of anti-TNF treatment failure in anti-TNF-naive patients with active luminal Crohn's disease: a prospective, multicentre, cohort study. *Lancet Gastroenterol Hepatol* 2019; **4**: 341-353 [PMID: 30824404 DOI: 10.1016/S2468-1253(19)30012-3]

60 **Mishra N**, Aden K, Blase JI, Baran N, Bordoni D, Tran F, Conrad C, Avalos D, Jaeckel C, Scherer M, Sørensen SB, Overgaard SH, Schulte B, Nikolaus S, Rey G, Gasparoni G, Lyons PA, Schultze JL, Walter J, Andersen V; SYSCID Consortium, Dermitzakis ET, Schreiber S, Rosenstiel P. Longitudinal multi-omics analysis identifies early blood-based predictors of anti-TNF therapy response in inflammatory bowel disease. *Genome Med* 2022; **14**: 110 [PMID: 36153599 DOI: 10.1186/s13073-022-01112-z]

61 **West NR**, Hegazy AN, Owens BMJ, Bullers SJ, Linggi B, Buonocore S, Coccia M, Görtz D, This S, Stockenhuber K, Pott J, Friedrich M, Ryzhakov G, Baribaud F, Brodmerkel C, Cieluch C, Rahman N, Müller-Newen G, Owens RJ, Kühl AA, Maloy KJ, Plevy SE; Oxford IBD Cohort Investigators, Keshav S, Travis SPL, Powrie F. Oncostatin M drives intestinal inflammation and predicts response to tumor necrosis factor-neutralizing therapy in patients with inflammatory bowel disease. *Nat Med* 2017; **23**: 579-589 [PMID: 28368383 DOI: 10.1038/nm.4307]

62 **Parkes M**, Noor NM, Dowling F, Leung H, Bond S, Whitehead L, Upponi S, Kinnon P, Sandham AP, Lyons PA, McKinney EF, Smith KGC,

Lee JC. PRedicting Outcomes For Crohn's dIsease using a moLecular biomarkEr (PROFILE): protocol for a multicentre, randomised, biomarker-stratified trial. *BMJ Open* 2018; **8**: e026767 [PMID: 30523133 DOI: 10.1136/bmjopen-2018-026767]

63 **Stidham RW**, Liu W, Bishu S, Rice MD, Higgins PDR, Zhu J, Nallamothu BK, Waljee AK. Performance of a Deep Learning Model *vs* Human Reviewers in Grading Endoscopic Disease Severity of Patients With Ulcerative Colitis. *JAMA Netw Open* 2019; **2**: e193963 [PMID: 31099869 DOI: 10.1001/jamanetworkopen.2019.3963]

64 **Stidham RW**, Enchakalody B, Waljee AK, Higgins PDR, Wang SC, Su GL, Wasnik AP, Al-Hawary M. Assessing Small Bowel Stricturing and Morphology in Crohn's Disease Using Semi-automated Image Analysis. *Inflamm Bowel Dis* 2020; **26**: 734-742 [PMID: 31504540 DOI: 10.1093/ibd/izz196]

65 **Reddy BK**, Delen D, Agrawal RK. Predicting and explaining inflammation in Crohn's disease patients using predictive analytics methods and electronic medical record data. *Health Informatics J* 2019; **25**: 1201-1218 [PMID: 29320910 DOI: 10.1177/1460458217751015]

66 **Waljee AK**, Lipson R, Wiitala WL, Zhang Y, Liu B, Zhu J, Wallace B, Govani SM, Stidham RW, Hayward R, Higgins PDR. Predicting Hospitalization and Outpatient Corticosteroid Use in Inflammatory Bowel Disease Patients Using Machine Learning. *Inflamm Bowel Dis* 2017; **24**: 45-53 [PMID: 29272474 DOI: 10.1093/ibd/izx007]

67 **Lee JC**, Biasci D, Roberts R, Gearry RB, Mansfield JC, Ahmad T, Prescott NJ, Satsangi J, Wilson DC, Jostins L, Anderson CA; UK IBD Genetics Consortium, Traherne JA, Lyons PA, Parkes M, Smith KG. Genome-wide association study identifies distinct genetic contributions to prognosis and susceptibility in Crohn's disease. *Nat Genet* 2017; **49**: 262-268 [PMID: 28067912 DOI: 10.1038/ng.3755]

68 **Cushing KC**, Mclean R, McDonald KG, Gustafsson JK, Knoop KA, Kulkarni DH, Sartor RB, Newberry RD. Predicting Risk of Postoperative Disease Recurrence in Crohn's Disease: Patients With Indolent Crohn's Disease Have Distinct Whole Transcriptome Profiles at the Time of First Surgery. *Inflamm Bowel Dis* 2019; **25**: 180-193 [PMID: 29982468 DOI: 10.1093/ibd/izy228]

69 **Gligorijević V**, Pržulj N. Methods for biological data integration: perspectives and challenges. *J R Soc Interface* 2015; **12** [PMID: 26490630 DOI: 10.1098/rsif.2015.0571]

70 **Argelaguet R**, Velten B, Arnol D, Dietrich S, Zenz T, Marioni JC, Buettner F, Huber W, Stegle O. Multi-Omics Factor Analysis-a framework for unsupervised integration of multi-omics data sets. *Mol Syst Biol* 2018; **14**: e8124 [PMID: 29925568 DOI: 10.15252/msb.20178124]

71 **Cai J**, Sun L, Gonzalez FJ. Gut microbiota-derived bile acids in intestinal immunity, inflammation, and tumorigenesis. *Cell Host Microbe* 2022; **30**: 289-300 [PMID: 35271802 DOI: 10.1016/j.chom.2022.02.004]

72 **Pratt M**, Forbes JD, Knox NC, Bernstein CN, Van Domselaar G. Microbiome-Mediated Immune Signaling in Inflammatory Bowel Disease and Colorectal Cancer: Support From Meta-omics Data. *Front Cell Dev Biol* 2021; **9**: 716604 [PMID: 34869308 DOI: 10.3389/fcell.2021.716604]

73 **Zhuang X**, Tian Z, Li N, Mao R, Li X, Zhao M, Xiong S, Zeng Z, Feng R, Chen M. Gut Microbiota Profiles and Microbial-Based Therapies in Post-operative Crohn's Disease: A Systematic Review. *Front Med (Lausanne)* 2020; **7**: 615858 [PMID: 33585513 DOI: 10.3389/fmed.2020.615858]

74 **Lee JWJ**, Plichta D, Hogstrom L, Borren NZ, Lau H, Gregory SM, Tan W, Khalili H, Clish C, Vlamakis H, Xavier RJ, Ananthakrishnan AN. Multi-omics reveal microbial determinants impacting responses to biologic therapies in inflammatory bowel disease. *Cell Host Microbe* 2021; **29**: 1294-1304. e4 [PMID: 34297922 DOI: 10.1016/j.chom.2021.06.019]

75 **Lloyd-Price J**, Arze C, Ananthakrishnan AN, Schirmer M, Avila-Pacheco J, Poon TW, Andrews E, Ajami NJ, Bonham KS, Brislawn CJ, Casero D, Courtney H, Gonzalez A, Graeber TG, Hall AB, Lake K, Landers CJ, Mallick H, Plichta DR, Prasad M, Rahnavard G, Sauk J, Shungin D, Vázquez-Baeza Y, White RA 3rd; IBDMDB Investigators, Braun J, Denson LA, Jansson JK, Knight R, Kugathasan S, McGovern DPB, Petrosino JF, Stappenbeck TS, Winter HS, Clish CB, Franzosa EA, Vlamakis H, Xavier RJ, Huttenhower C. Multi-omics of the gut microbial ecosystem in inflammatory bowel diseases. *Nature* 2019; **569**: 655-662 [PMID: 31142855 DOI: 10.1038/s41586-019-1237-9]

76 **Imhann F**, Van der Velde KJ, Barbieri R, Alberts R, Voskuil MD, Vich Vila A, Collij V, Spekhorst LM, Van der Sloot KWJ, Peters V, Van Dullemen HM, Visschedijk MC, Festen EAM, Swertz MA, Dijkstra G, Weersma RK. The 1000IBD project: multi-omics data of 1000 inflammatory bowel disease patients; data release 1. *BMC Gastroenterol* 2019; **19**: 5 [PMID: 30621600 DOI: 10.1186/s12876-018-0917-5]

77 **Ludvigsson JF**, Andersson E, Ekbom A, Feychting M, Kim JL, Reuterwall C, Heurgren M, Olausson PO. External review and validation of the Swedish national inpatient register. *BMC Public Health* 2011; **11**: 450 [PMID: 21658213 DOI: 10.1186/1471-2458-11-450]

78 **Norris RP**, Dew R, Sharp L, Greystoke A, Rice S, Johnell K, Todd A. Are there socio-economic inequalities in utilization of predictive biomarker tests and biological and precision therapies for cancer? A systematic review and meta-analysis. *BMC Med* 2020; **18**: 282 [PMID: 33092592 DOI: 10.1186/s12916-020-01753-0]

79 **Spratt DE**, Chan T, Waldron L, Speers C, Feng FY, Ogunwobi OO, Osborne JR. Racial/Ethnic Disparities in Genomic Sequencing. *JAMA Oncol* 2016; **2**: 1070-1074 [PMID: 27366979 DOI: 10.1001/jamaoncol.2016.1854]

80 **Martin AR**, Kanai M, Kamatani Y, Okada Y, Neale BM, Daly MJ. Clinical use of current polygenic risk scores may exacerbate health disparities. *Nat Genet* 2019; **51**: 584-591 [PMID: 30926966 DOI: 10.1038/s41588-019-0379-x]

81 **Yeh VM**, Bergner EM, Bruce MA, Kripalani S, Mitrani VB, Ogunsola TA, Wilkins CH, Griffith DM. Can Precision Medicine Actually Help People Like Me? African American and Hispanic Perspectives on the Benefits and Barriers of Precision Medicine. *Ethn Dis* 2020; **30**: 149-158 [PMID: 32269456 DOI: 10.18865/ed.30.S1.149]

82 **Lynch JA**, Berse B, Rabb M, Mosquin P, Chew R, West SL, Coomer N, Becker D, Kautter J. Underutilization and disparities in access to EGFR testing among Medicare patients with lung cancer from 2010 - 2013. *BMC Cancer* 2018; **18**: 306 [PMID: 29554880 DOI: 10.1186/s12885-018-4190-3]

83 **Mills RH**, Dulai PS, Vázquez-Baeza Y, Sauceda C, Daniel N, Gerner RR, Batachari LE, Malfavon M, Zhu Q, Weldon K, Humphrey G, Carrillo-Terrazas M, Goldasich LD, Bryant M, Raffatellu M, Quinn RA, Gewirtz AT, Chassaing B, Chu H, Sandborn WJ, Dorrestein PC, Knight R, Gonzalez DJ. Multi-omics analyses of the ulcerative colitis gut microbiome link Bacteroides vulgatus proteases with disease severity. *Nat Microbiol* 2022; **7**: 262-276 [PMID: 35087228 DOI: 10.1038/s41564-021-01050-3]

84 **Zhang X**, Deeke SA, Ning Z, Starr AE, Butcher J, Li J, Mayne J, Cheng K, Liao B, Li L, Singleton R, Mack D, Stintzi A, Figeys D. Metaproteomics reveals associations between microbiome and intestinal extracellular vesicle proteins in pediatric inflammatory bowel disease. *Nat Commun* 2018; **9**: 2873 [PMID: 30030445 DOI: 10.1038/s41467-018-05357-4]

85 **Dai Y**, Pei G, Zhao Z, Jia P. A Convergent Study of Genetic Variants Associated With Crohn's Disease: Evidence From GWAS, Gene Expression, Methylation, eQTL and TWAS. *Front Genet* 2019; **10**: 318 [PMID: 31024628 DOI: 10.3389/fgene.2019.00318]

86 **Suskind DL**, Lee D, Kim YM, Wahbeh G, Singh N, Braly K, Nuding M, Nicora CD, Purvine SO, Lipton MS, Jansson JK, Nelson WC. The Specific Carbohydrate Diet and Diet Modification as Induction Therapy for Pediatric Crohn's Disease: A Randomized Diet Controlled Trial. *Nutrients* 2020; **12** [PMID: 33291229 DOI: 10.3390/nu12123749]

87 **Borren NZ**, Plichta D, Joshi AD, Bonilla G, Sadreyev R, Vlamakis H, Xavier RJ, Ananthakrishnan AN. Multi-"-Omics" Profiling in Patients With Quiescent Inflammatory Bowel Disease Identifies Biomarkers Predicting Relapse. *Inflamm Bowel Dis* 2020; **26**: 1524-1532 [PMID: 32766830 DOI: 10.1093/ibd/izaa183]

88 **Liu J**, Fang H, Hong N, Lv C, Zhu Q, Feng Y, Wang B, Tian J, Yu Y. Gut Microbiome and Metabonomic Profile Predict Early Remission to Anti-Integrin Therapy in Patients with Moderate to Severe Ulcerative Colitis. *Microbiol Spectr* 2023; **11**: e0145723 [PMID: 37199618 DOI: 10.1128/spectrum.01457-23]

89 **Huang Q**, Zhang X, Hu Z. Application of Artificial Intelligence Modeling Technology Based on Multi-Omics in Noninvasive Diagnosis of Inflammatory Bowel Disease. *J Inflamm Res* 2021; **14**: 1933-1943 [PMID: 34017190 DOI: 10.2147/JIR.S306816]

90 **Gonzalez CG**, Mills RH, Zhu Q, Sauceda C, Knight R, Dulai PS, Gonzalez DJ. Location-specific signatures of Crohn's disease at a multi-omics scale. *Microbiome* 2022; **10**: 133 [PMID: 35999575 DOI: 10.1186/s40168-022-01331-x]

91 **Xu S**, Li X, Zhang S, Qi C, Zhang Z, Ma R, Xiang L, Chen L, Zhu Y, Tang C, Bourgonje AR, Li M, He Y, Zeng Z, Hu S, Feng R, Chen M. Oxidative stress gene expression, DNA methylation, and gut microbiota interaction trigger Crohn's disease: a multi-omics Mendelian randomization study. *BMC Med* 2023; **21**: 179 [PMID: 37170220 DOI: 10.1186/s12916-023-02878-8]

92 **Gao X**, Sun R, Jiao N, Liang X, Li G, Gao H, Wu X, Yang M, Chen C, Sun X, Chen L, Wu W, Cong Y, Zhu R, Guo T, Liu Z. Integrative multi-omics deciphers the spatial characteristics of host-gut microbiota interactions in Crohn's disease. *Cell Rep Med* 2023; **4**: 101050 [PMID: 37172588 DOI: 10.1016/j.xcrm.2023.101050]

93 **Baran NM**, Aden K, Tran F, Ira Blasé J, Conrad3 C, Nikolaus S, Schreiber S, Rosenstiel P. Early Molecular Signatures of Therapeutic Response To Vedolizumab Therapy In Inflammatory Bowel Disease Patients Identified Using A Longitudinal Multi-Omics Approach. *United European Gastroenterol J* 2022; **10** [DOI: 10.1016/s0016-5085(22)61889-4]

World Journal of Gastroenterology

Submit a Manuscript: https://www.f6publishing.com

World J Gastroenterol 2023 September 28; 29(36): 5226-5239

DOI: 10.3748/wjg.v29.i36.5226

ISSN 1007-9327 (print) ISSN 2219-2840 (online)

ORIGINAL ARTICLE

Basic Study

Curcumin alleviated dextran sulfate sodium-induced colitis by recovering memory Th/Tfh subset balance

Lin-Xin Zheng, Kai-En Guo, Jia-Qi Huang, Miao-Hua Liu, Bai-Ling Deng, Duan-Yong Liu, Bu-Gao Zhou, Wen Zhou, You-Bao Zhong, Hai-Mei Zhao

Specialty type: Pharmacology and pharmacy

Provenance and peer review: Unsolicited article; Externally peer reviewed.

Peer-review model: Single blind

Peer-review report's scientific quality classification

Grade A (Excellent): 0
Grade B (Very good): B, B
Grade C (Good): 0
Grade D (Fair): 0
Grade E (Poor): 0

P-Reviewer: Balbaa ME, Egypt; Song XY, China

Received: August 16, 2023
Peer-review started: August 16, 2023
First decision: August 25, 2023
Revised: August 26, 2023
Accepted: September 7, 2023
Article in press: September 7, 2023
Published online: September 28, 2023

Lin-Xin Zheng, Kai-En Guo, Jia-Qi Huang, Miao-Hua Liu, Department of Postgraduate, Jiangxi University of Chinese Medicine, Nanchang 330004, Jiangxi Province, China

Bai-Ling Deng, Hai-Mei Zhao, College of Traditional Chinese Medicine, Jiangxi University of Chinese Medicine, Nanchang 330004, Jiangxi Province, China

Duan-Yong Liu, Bu-Gao Zhou, Formula-Pattern Research Center, Jiangxi University of Chinese Medicine, Nanchang 330004, Jiangxi Province, China

Wen Zhou, Nanchang Medical College, Nanchang 330052, Jiangxi Province, China

You-Bao Zhong, Laboratory Animal Research Center for Science and Technology, Jiangxi University of Chinese Medicine, Nanchang 330004, Jiangxi Province, China

Corresponding author: Wen Zhou, MD, Associate Professor, Nanchang Medical College, No. 689 Huiren Road, Nanchang 330052, Jiangxi Province, China. zw1103380809@163.com

Abstract

BACKGROUND

Restoration of immune homeostasis by targeting the balance between memory T helper (mTh) cells and memory follicular T helper (mTfh) cells is a potential therapeutic strategy against ulcerative colitis (UC). Because of its anti-inflammatory and immunomodulatory properties, curcumin (Cur) is a promising drug for UC treatment. However, fewer studies have demonstrated whether Cur can modulate the mTh/mTfh subset balance in mice with colitis.

AIM

To explore the potential mechanism underlying Cur-mediated alleviation of colitis induced by dextran sulfate sodium (DSS) in mice by regulating the mTh and mTfh immune homeostasis.

METHODS

Balb/c mice were administered 3% and 2% DSS to establish the UC model and treated with Cur (200 mg/kg/d) by gavage on days 11-17. On the 18th d, all mice were anesthetized and euthanized, and the colonic length, colonic weight, and colonic weight index were evaluated. Histomorphological changes in the mouse colon were observed through hematoxylin-eosin staining. Levels of Th/mTh and

Tfh/mTfh cell subsets in the spleen were detected through flow cytometry. Western blotting was performed to detect SOCS-1, SOCS-3, STAT3, p-STAT3, JAK1, p-JAK1, and NF-κB p65 protein expression levels in colon tissues.

RESULTS

Cur effectively mitigates DSS-induced colitis, facilitates the restoration of mouse weight and colonic length, and diminishes the colonic weight and colonic weight index. Simultaneously, it hinders ulcer development and inflammatory cell infiltration in the colonic mucous membrane. While the percentage of Th1, mTh1, Th7, mTh7, Th17, mTh17, Tfh1, mTfh1, Tfh7, mTfh7, Tfh17, and mTfh17 cells decreased after Cur treatment of the mice for 7 d, and the frequency of mTh10, Th10, mTfh10, and Tfh10 cells in the mouse spleen increased. Further studies revealed that Cur administration prominently decreased the SOCS-1, SOCS-3, STAT3, p-STAT3, JAK1, p-JAK1, and NF-κB p65 protein expression levels in the colon tissue.

CONCLUSION

Cur regulated the mTh/mTfh cell homeostasis to reduce DSS-induced colonic pathological damage, potentially by suppressing the JAK1/STAT3/SOCS signaling pathway.

Key Words: Curcumin; Ulcerative colitis; Memory T helper; Memory follicular T helper; JAK1/STAT3/SOCS

©The Author(s) 2023. Published by Baishideng Publishing Group Inc. All rights reserved.

Core Tip: Memory T cells (mTh) are formed by the differentiation of initial T cells following antigenic stimulation and have a long lifespan. The dysfunction and out-of-balance of mTh and their subsets destroy immune homeostasis to induce autoimmune diseases including inflammatory bowel disease. Finding new drugs for inflammatory bowel disease (IBD) treatment from natural plant medicine and traditional Chinese medicine is a research hotspot. Cur can regulate memory B cells and other immune cells to effectively treat experimental colitis. However, whether Cur can regulate mTh cell- and mfTh cell-mediated homeostasis to treat IBD remains unclear. We here indicated that Cur regulates the mTh/memory follicular T helper cell homeostasis to reduce dextran sulfate sodium-induced colonic pathological injury, which may be achieved by inhibiting the JAK1/STAT3/SOCS signaling pathway.

Citation: Zheng LX, Guo KE, Huang JQ, Liu MH, Deng BL, Liu DY, Zhou BG, Zhou W, Zhong YB, Zhao HM. Curcumin alleviated dextran sulfate sodium-induced colitis by recovering memory Th/Tfh subset balance. *World J Gastroenterol* 2023; 29(36): 5226-5239
URL: https://www.wjgnet.com/1007-9327/full/v29/i36/5226.htm
DOI: https://dx.doi.org/10.3748/wjg.v29.i36.5226

INTRODUCTION

As a common and traditional drug and food additive, turmeric (*Curcuma longa L)* is widely used for thousand years. It has been largely cultivated in China, India, and Arabia. Being among the main active ingredients of turmeric, curcumin (Cur) is used in various applications and is closely related to our daily lives[1]. Cur is currently among the world's largest-selling natural food colorings and is recognized by the World Health Organization as an international food additive, often used as a culinary spice, food flavoring agent, and coloring agent[2]. Cur, as an active polyphenol extracted from Traditional Chinese medicine Curcuma longa (turmeric)[3], was popularly used as medicine and food to treat ulcer-like diseases including inflammatory bowel disease (IBD) and gastric ulcer. According to many clinical studies, Cur has a wide range of pharmacological effects such as anti-inflammatory[3], antioxidant, and immunomodulatory effects, and has a good safety profile for immune diseases such as IBD [including Crohn's disease and ulcerative colitis (UC)] and systemic lupus erythematosus[4-6]. Recent UC treatment with Cur in clinical practices revealed that patients are well tolerated Cur without any post-Cur intervention severe side effects[3,7,8]. Animal experiments have demonstrated that Cur remarkably enhanced survival, increased body weight, and improved diarrhea and rectal bleeding, thereby effectively treating dextran sulfate sodium (DSS)-induced colitis in mice[9]. Many of our previous study results have indicated that Cur can effectively improve DSS-induced colonic pathological injury by regulating memory T cells, memory B cells, and Breg differentiation and function; inhibiting IL-1β, IL-6, IL-33, CCL-2, IFN-γ, and TNF-α, production; and promoting the secretion of IL-4, IL-10, IL-13, and IgA. All of these were probably achieved by regulating the Bcl-6-Syk-BLNK signaling pathway and inhibiting the TLR/MyD88 pathway[10-12]. The aforementioned studies have indicated that Cur can regulate memory immune cells to treat experimental colitis. In the immune system, initial T cells differentiate into memory T cells after receiving antigenic stimulation. These memory T cells have a long lifespan. When an organism is first attacked by foreign substances, the body has a small number of activated memory T cells, which then trigger an antigenic response[13]. When the secondary antigenic response is activated, even in the absence of foreign stimuli, memory T cells are activated, respond rapidly, and continue to differentiate and promote cytokine expression. Memory T cells can differentiate into Th cells and Tfh cells, with most of these helper cells in the peripheral circulation being memory T helper (mTh) cells and memory follicular T helper (mTfh) cells[14,15]. During the induction

of immunity, a part of memory T lymphocytes rapidly evolves into effector T cells such as Th1, Tfh1, Th7, and Tfh7, releasing numerous inflammatory factors such as IL-1, IL-7, IL-17, and TNF-α, which are involved in mediating tissue damage. Another type of memory T cells rapidly transforms into anti-inflammatory cells such as Treg, Th10, and Tfh10, enhancing the protection of the organism[16]. When the balance between the two is disrupted, homeostasis is altered, inducing autoimmune diseases, including IBD[17]. UC is a type of IBD, characterized by autoimmune pathology that primarily affects the rectum and sigmoid colon. Clinical manifestations of IBD include abdominal pain, diarrhea, mucopurulent stools, and varying degrees of systemic and extraintestinal symptoms, such as weakness, weight loss, fever, and vomiting[18,19]. Although UC pathogenesis is unknown, disturbances in immune function and systemic immune homeostasis within the intestinal mucosa are believed to be key contributing factors to IBD development[20].

However, the regulatory effects of Cur on colonic mucosa damage by modulating the balance of mTh and mTfh cell subsets, including mTh1, mTh7, mTh10, and mTh17 as well as mTfh1, mTfh7, mTfh10, and mTfh17 subsets, remain to be elucidated. Therefore, we evaluated the efficacy and possible action mechanisms of Cur in UC treatment by using a mouse model of DSS-induced UC. Flow cytometry and other experimental methods were used to investigate the differentiation and function of mTh/mTfh cell subsets.

MATERIALS AND METHODS

Drugs

Cur was provided by Chengdu Purifa Technology Development Co., Ltd. (relative molecular mass: 368.39, purity: 98%, No. 458377), and DSS (M.W.36000-50000, No. 160110) was purchased from MP Biomedicals (Irvine, CA, United States).

Mice

Forty SPF-grade male Balb/c mice (age: 6-9 wk, weight: 21 g ± 1 g) were purchased from Hunan Silaike Jingda Experimental Animal Co. Ltd (Changsha, Hunan Province, China) [Animal Certificate No: SCXK (Xiang) 2019-0004]. These mice were placed in the barrier of the Laboratory Animal Science and Technology Center at the Jiangxi University of Chinese Medicine for 7 d for adaptation. When in the barrier, they were subjected to consistent temperature and humidity conditions and had unrestricted access to food and water. The animal study protocol (identification code: JZLLSC2021-17-9; date of approval: May 9, 2021) was approved by the Institutional Animal Care and Use Committee of Jiangxi University of Chinese Medicine. The mice were randomly allocated to the I control group, Ctrl + Cur group, DSS group, or DSS + Cur group at the end of adaptive feeding.

DSS-induced colitis

Following adaptive feeding, the DSS and DSS + Cur groups were given 3% DSS solution to drink freely for 6 d, followed by sterile drinking water for 6 d and 2% DSS solution for 6 d (Figure 1A). During this period, the control and Ctrl + Cur groups drank standard drinking water. An occult blood (OB) test paper was used to evaluate the situation of intestinal hemorrhage. An OB score equal to or greater than 2 (positive fecal OB) indicated bleeding in the colonic mucosa and the formation of ulcers. Thus, the colitis model was successfully replicated.

Treatment protocols

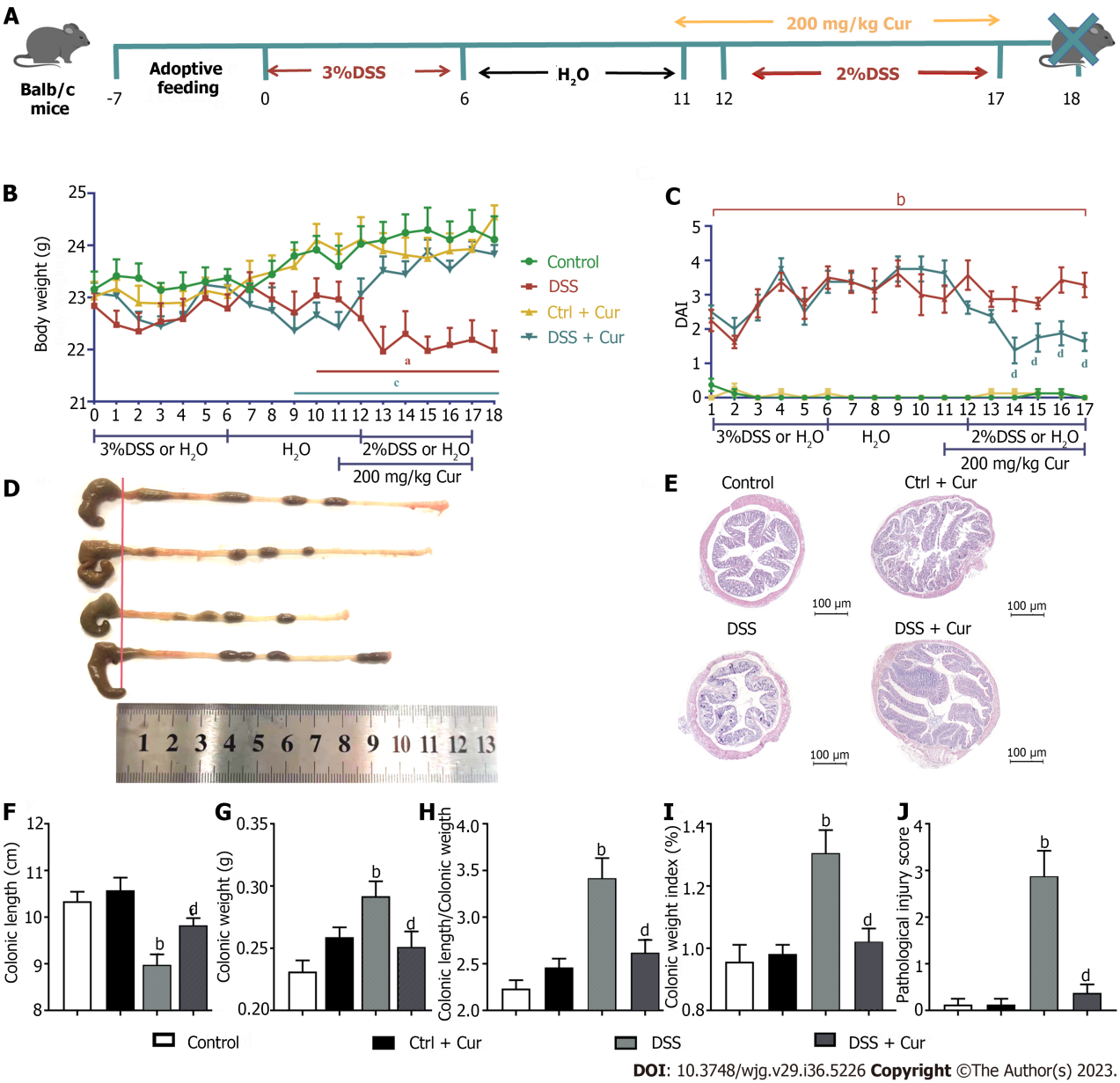
The first 3% DSS administration was counted as the first day, and the Ctrl + Cur group was gavaged with Cur solution (200 mg/kg/d). The DSS + Cur group was administered the same Cur dose from the 11th d, and the control and DSS groups received the same volume of saline for 7 consecutive days (Figure 1A). The body weight, fecal character, and bleeding in the mouse stool were evaluated and recorded daily to evaluate the disease activity index (DAI).

Sample collection

After the last administration was completed, all mice were fasted without access to water. After 10 h of fasting was completed, the mice were weighed on the morning of the 18th d. Subsequently, pentobarbital sodium (20 mg/kg) was administered intraperitoneally to induce anesthesia before euthanizing the mice. The spleen and colon were collected from the euthanized mice on an ice platform. The spleen was placed in a 2-mL Eppendorf (EP) tube containing 0.5 mL of 1640 medium and stored at 4 °C for subsequent use. The colon was separated, placed on an ice platform, and photographed, and its length was measured. The intestinal contents were cleaned, washed with phosphate-buffered saline, aspirated, and weighed. Approximately 1 cm of the colon (2 cm below the ileocecal region) was placed in a 2-mL EP tube containing 4% paraformaldehyde. The remaining part was placed in a lyophilization tube and stored at -80 °C in the refrigerator for subsequent experiments.

Macroscopic observation and DAI

During the experiment, the general conditions of the mice were observed and recorded daily at the same period: Body weight, mental status, activity, fecal consistency, and OB score. The DAI was assessed during the treatment period according to the following criteria: Body weight (no significant reduction, 0; 1%-5% decrease, 1; 6%-10% decrease, 2; 11%-20% decrease, 3; and a decrease of > 20%, 4), consistency of stools [normal stools, 0; loose stools (dry), 2; and loose stools or diarrhea (watery stools), 4], and presence of bleeding (absence of bleeding, 0; OB detection in stool, 2; visible blood in the stool, 3; and anal bleeding, 4)[21].



DOI: 10.3748/wjg.v29.i36.5226 **Copyright** ©The Author(s) 2023.

Figure 1 Curcumin effectively improved the symptoms of dextran sulfate sodium-induced ulcerative colitis mice. A: Dextran sulfate sodium (DSS)-induced ulcerative colitis model replication and Cur administration; B: Body weight changes of mice from days 0 to 18; C: Disease activity indexes of mice in each group from days 0 to 18; D: Specific colonic lengths of mice in each group; E: Pathological sections of the colon of each group of mice (HE staining, 50 × magnification; scale bar = 100 μm); F: The colonic length of mice in each group on day 18; G: Colon weights of mice in each group on day 18; H: The colonic length/colonic weight of mice in each group on day 18; I: The colonic weight index of mice in each group on day 18; J: Pathological injury scores of mice in each group. Data are expressed as the mean ± SD (n = 8). The differences were statistically significant when compared with the Ctrl group ($^aP < 0.05$, $^bP < 0.01$). Differences were statistically significant with the DSS group ($^cP < 0.05$, $^dP < 0.01$). Cur: Curcumin; DSS: Dextran sulfate sodium.

Histopathological observation

After the mouse colon tissues were soaked and fixed, they were placed in a 4% paraformaldehyde solution for 72 h. A 3-4 mm length of colonic tissue was cut and placed in ethanol for stepwise dehydration, followed by xylene for dehydration and clearing and liquid paraffin for soaking and embedding. The sections were then further cut into 4-μm posterior slices, rehydrated, and stained with hematoxylin-eosin (HE). The stained sections were histopathologically examined under a light microscope (Lecia, Wetzlar, Germany). A double-blind approach was used to score the pathological damage: (1) Degree of inflammatory cell infiltration (none 0, mild 1, moderate 2, and more severe 3); (2) degree of tissue damage (none 0, damage to mucosa 1, damage to mucosa and mucosa 2, and already transmural 3); and (3) tissue regeneration (normal tissue or complete regeneration 0, almost complete regeneration 1, and crypt regeneration 2).

Flow cytometry

To identify immune cell populations in mouse spleen, a 1640 culture medium (Procell Life, Wuhan, Hubei Province, China) was added to the spleen samples. The samples were placed on ice for grinding, passed through a 70-μm cell strainer, and continued to be washed with a 1640 culture medium. The samples were immediately centrifuged at 500 g for

5 min, and the supernatant was discarded. After the samples were washed and resuspended, 2-3 mL of lysis buffer (BD Biosciences, Franklin Lakes, NJ, United States) was added to each sample and incubated in the dark for 15 min for erythrocyte removals. These single-cell suspensions were first added to the Leukocyte Activation Cocktail (BD Biosciences, Franklin Lakes, NJ, United States) and incubated at room temperature for 2.5 h with light protection. Then, an Fcγ receptor-blocking monoclonal antibody (CD16/32; BioLegend, San Diego, CA, United States) was added to the cell suspensions and incubated at 4 °C for 15 min. The cells were assessed for surface antigens, shielded from light, and labeled with BV510 rat anti-mouse CD4 (NO. 563106), AF647 rat anti-mouse CCR7 (NO. 560766), FITC rat anti-mouse CXCR5 (NO. 560577), PE rat anti-mouse CXCR3 (NO. 562152), PE-Cy7 rat anti-mouse IL-10 (NO. 505026), and BV421 rat anti-mouse IL-7R (NO. 566377) antibodies. After the Cytofix/Cytoperm Fixation/Permeabilization Kit (BD Biosciences, Franklin Lakes, NJ, United States) was applied, intracellular antigens were detected by incubating the cells with PE rat anti-mouse IL-17A antibody (NO. 506904) and shielded from light. All of the aforementioned flow cytometry antibodies were obtained from BD Biosciences. Gates were established for the quadrant markers based on negative populations and isotype controls. Data were analyzed using FlowJo software V10 (TreeStar, Ashland, Oregon, United States).

Western blotting

Western blotting was performed to evaluate JAK1, p-JAK1, STAT3, p-STAT3, SOCS-1, SOCS-3, and NF-κB p65 protein levels in colon tissue. First, 100 mg of colon tissue was accurately weighed, cut into small pieces, and added to 1000 μL of radio immunoprecipitation assay buffer. The mixture was homogenized with a tissue homogenizer (Xinzhi Biotechnology Co., Ningbo, Zhejiang Province, China) and incubated at 4 °C for 30 min. The lysed sample was centrifuged at 13000 rpm for 10 min, and the resulting supernatant was used to determine the total protein content in the tissue. Subsequently, the protein concentration was quantified through the bicinchoninic acid (BCA) assay. Polyacrylamide gel electrophoresis was performed to extract equivalent protein quantities from the colonic mucosa samples. The extracted proteins were subsequently transferred onto PVDF membranes, treated with a 5% solution of bovine serum albumin for 2 h at room temperature, and incubated overnight at 4°C with primary antibodies, including JAK1 (Abcam, ab32101, 1:1000), p-JAK1 (Abcam, ab32101, 1:1000), STAT3 (Abcam, ab131103, 1:1000), p-STAT3 (Abcam, ab194732, 1:1000), SOCS-1 (Abcam, ab9870, 1:1000), SOCS-3 (Abcam, ab16030, 1:1000), NF-κB p65 (Abcam, ab16502, 1:1000), and tubulin (Abcam, ab7291, 1:5000). After the membranes were washed, the secondary antibody goat anti-rabbit lgG (HRP) (Abcam, ab205718, 1:10000) was added, and the membranes were incubated at room temperature for 1 h. Finally, the membranes were transferred to a gel imager (Bio-Rad, Hercules, California, United States) for exposure and imaging. For semi-quantitative analysis, the target protein grayscale values were analyzed using Image J software.

Statistical analysis

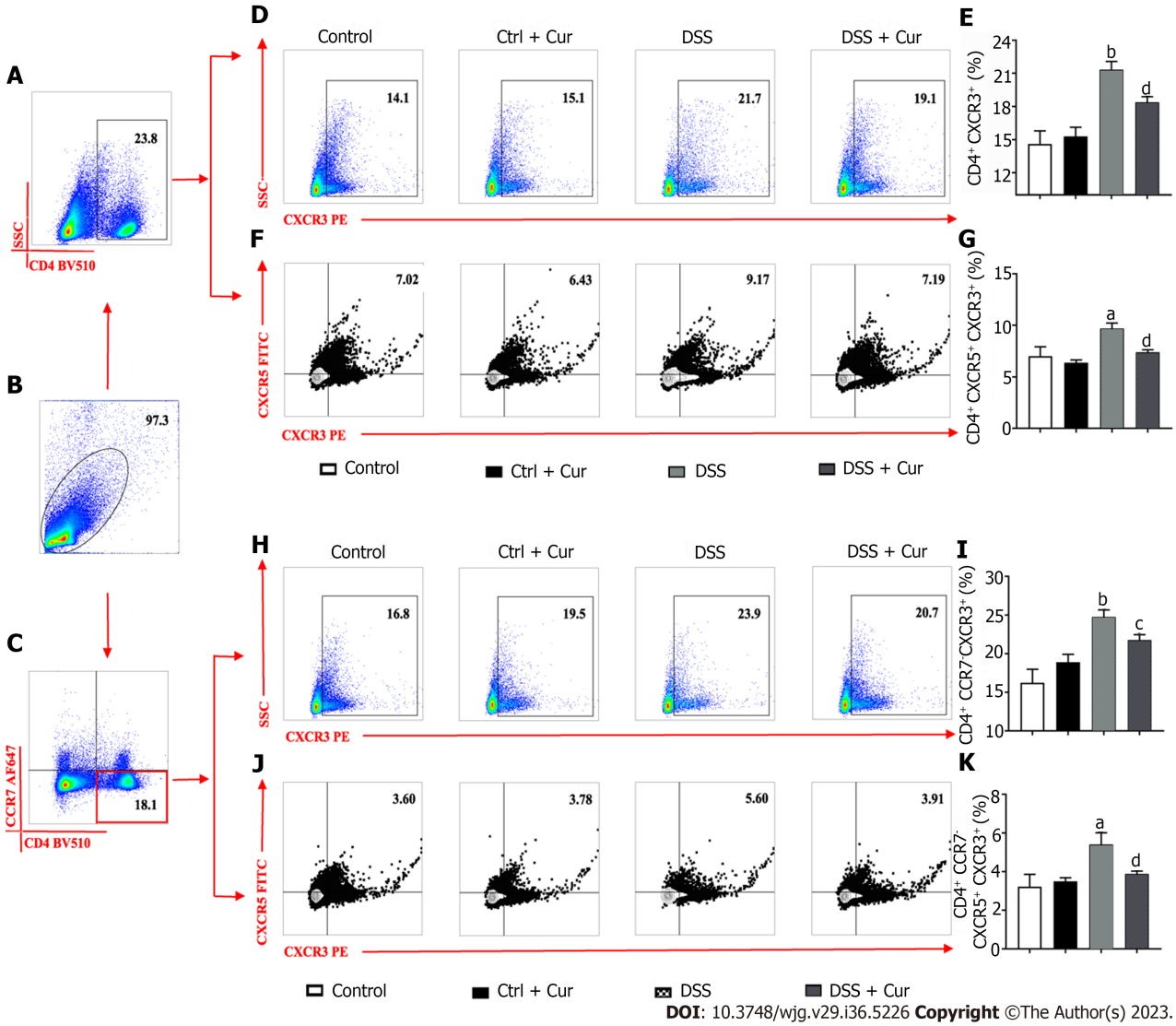
All data were analyzed using GraphPad Prism software version 8.0. The data were expressed as mean ± SD. One-way analysis of variance was performed between multiple groups, followed by Tukey's test for multiple comparisons. Statistical significance was determined for differences at $P < 0.05$ or $P < 0.01$.

RESULTS

Cur effectively alleviates DSS-induced UC mice

The symptoms in animal models of DSS-induced IBD are similar to those of clinical cases. The symptoms include abdominal pain, diarrhea, blood in the stool, weight loss, and depression. After the autopsy was performed, the colon became shorter and heavier, and multiple bleeding spots were observed in the intestine[22]. In this study, weight changes, DAI, and general signs of the mice were noted during the experimental cycle to evaluate the therapeutic effect of Cur on colitis in mice. The mice in the model group exhibited a dull coat after DSS induction, were mentally dull and less active, and liked to gather and huddle. The body weight (Figure 1B) of the mice decreased, colon length shortened (Figure 1D and F), colonic weight increased (Figure 1G), the ratio of the colonic weight/colonic length (Figure 1H) and the colonic weight index (Figure 1I) increased ($P < 0.05$ or $P < 0.01$). When the DAI results (Figure 1C) were compared, from days 1 to 17, the DAI scores of the model group were notably higher than those of the control group. The aforementioned results suggest that the mice exhibit significant UC symptoms after DSS induction. Surprisingly, these manifestations changed significantly after Cur treatment. The colonic length (Figure 1D and F) in the DSS + Cur group was restored after Cur treatment, and the colonic weight (Figure 1G), the ratio of the colonic weight/colonic length (Figure 1H) and Colonic weight index (Figure 1I) in this group were notedly lower than those in the DSS group ($P < 0.05$ or $P < 0.01$). After the drug was administered from days 12 to 17, the DAI score (Figure 1B) sharply lowered in the DSS + Cur group than in the DSS group, while the body weight (Figure 1B) regained gradually.

The histological pathological sections of DSS-induced UC mice mostly exhibited increased plasma cells in the mucosal lamina propria, inflammatory cell infiltration, progressive crypt destruction, and increased vesicular ulcers[23]. HE staining exhibited that the epithelial tissue of the colonic mucosa was intact in the control and Ctrl + Cur groups, and the crypt structure was clear, without congestion and edema. The epithelial tissue of the colonic mucosa in the DSS group was absent, congested, and edematous. Multiple ulcers were observed. The mucosa and crypt structures were severely damaged. Inflammatory cell infiltration appeared (Figure 1E). The pathological injury score (Figure 1J) was remarkably higher in the DSS group than in all groups. This is because Cur effectively reverses DSS-induced colonic tissue damage. A small amount of congestion and edema was observed in the DSS + Cur group, with epithelial tissue repair, less pronounced ulcers (Figure 1E), and a reduced pathological damage score (Figure 1J). The aforementioned data indicate that Cur effectively relieved the clinical symptoms of DSS-induced colitis mice, restored colonic epithelial tissues, and



DOI: 10.3748/wjg.v29.i36.5226 **Copyright** ©The Author(s) 2023.

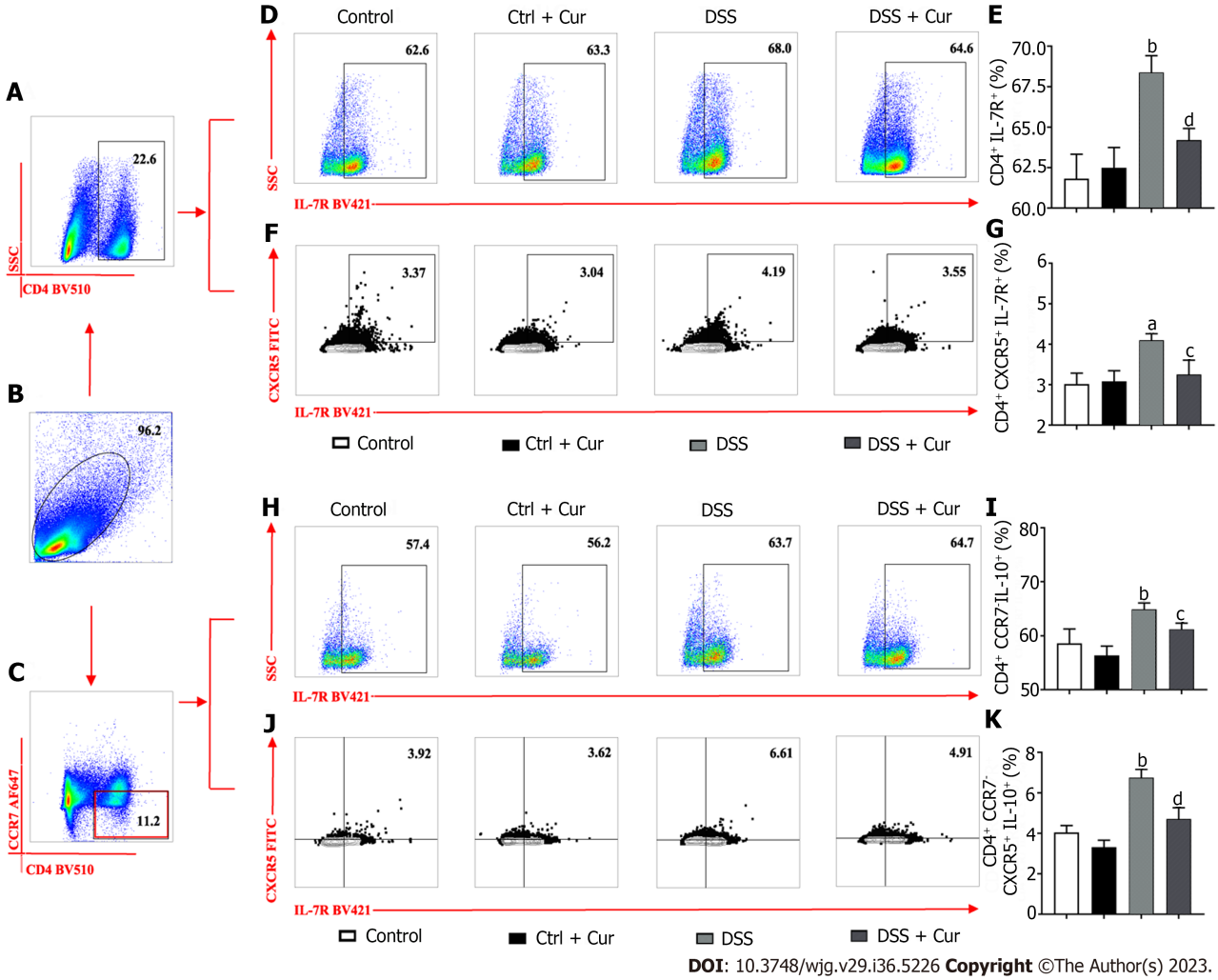
Figure 2 Memory T helper 1/memory follicular T helper 1 cell subpopulation levels in ulcerative colitis mice. A: Typical flow cytometry patterns of $CD4^+$ cells; B: Typical flow cytometry patterns were observed in the spleen; C: Typical flow cytometry patterns and histograms of $CD4^+$ $CCR7^-$ cells; D and E: Typical flow cytometry patterns and histograms of $CD4^+$ $CXCR3^+$ (Th1) cells; F and G: $CD4^+$ $CXCR5^+$ $CXCR3^+$ (Tfh1) cells; H and I: $CD4^+$ $CCR7^-CXCR3^+$ (mTh1) cells; J and K: $CD4^+$ $CCR7^-$ $CXCR5^+$ $CXCR3^+$ (mTfh1) cells. Data are expressed as the mean ± SD (n = 8). The differences were statistically significant when compared with the Ctrl group ($^aP < 0.05$, $^bP < 0.01$). Differences were statistically significant with the dextran sulfate sodium group ($^cP < 0.05$, $^dP < 0.01$). Cur: Curcumin; DSS: Dextran sulfate sodium.

accelerated ulcer healing.

Cur regulated $CD4^+$ Th cell subpopulation in UC mice

Memory $CD4^+$ T helper cells are a highly heterogeneous group of cells mainly involved in the adaptive immune response, aiding in the clearing of pathogens and constituting a crucial defense mechanism of the body against microbial pathogens and toxins[24]. When activated by T cell receptors, these cells differentiate into specific mTh lineages such as Th1, Th7, Th17, and Th10. Aberrant activation and differentiation of these Th-cell subpopulations have a critical impact on UC development[25]. In this study, Th cells were labeled by gating $CD4^+$ cells (Figures 2-4; Figure 5A and B) and effector memory T cell ($CD4^+CCR7^-$T) (Figures 2-4; Figure 5B and C) According to the results, the $CD4^+$ $IL\text{-}10^+$ (Th10) (Figure 4D and E) and $CD4^+$ $CCR7^-IL\text{-}10^+$ (mTh10) (Figure 4H and I) cell levels significantly decreased ($P < 0.05$ or $P < 0.01$) in the spleen of the DDS group. By contrast, the $CD4^+$ $CXCR3^+$ (Th1) (Figure 2D and E), $CD4^+$ $CCR7^-CXCR3^+$ (mTh1) (Figure 2H and I), $CD4^+$ $IL\text{-}7R^+$ (Th7) (Figure 3D and E), $CD4^+$ $CCR7^-$ $IL\text{-}7R^+$ (mTh7) (Figure 3H and I), $CD4^+$ $IL\text{-}17A^+$ (Th17) (Figure 5D and E), and $CD4^+$ $CCR7^-IL\text{-}17A^+$ (mTh17) (Figure 5H and I) cell levels increased ($P < 0.05$ or $P < 0.01$). After treatment with Cur, Th1/mTh1, Th7/mTh7, and Th17/mTh17 cell levels in the UC mouse spleen were effectively downregulated ($P < 0.05$ or $P < 0.01$), whereas Th10/mTh10 cell levels were upregulated ($P < 0.01$). These results suggest that Cur can effectively regulate the balance among Th cell subsets in UC mice.

According to most experts, Tfh cell-mediated immune dysfunction is widely accepted to significantly contribute to the onset, progression, and recovery of UC[26,27]. To investigate whether abnormal cell expression and dysfunctional balance between Th and Tfh cell subpopulations in UC mice are closely related to UC pathogenesis. we determined the



DOI: 10.3748/wjg.v29.i36.5226 **Copyright** ©The Author(s) 2023.

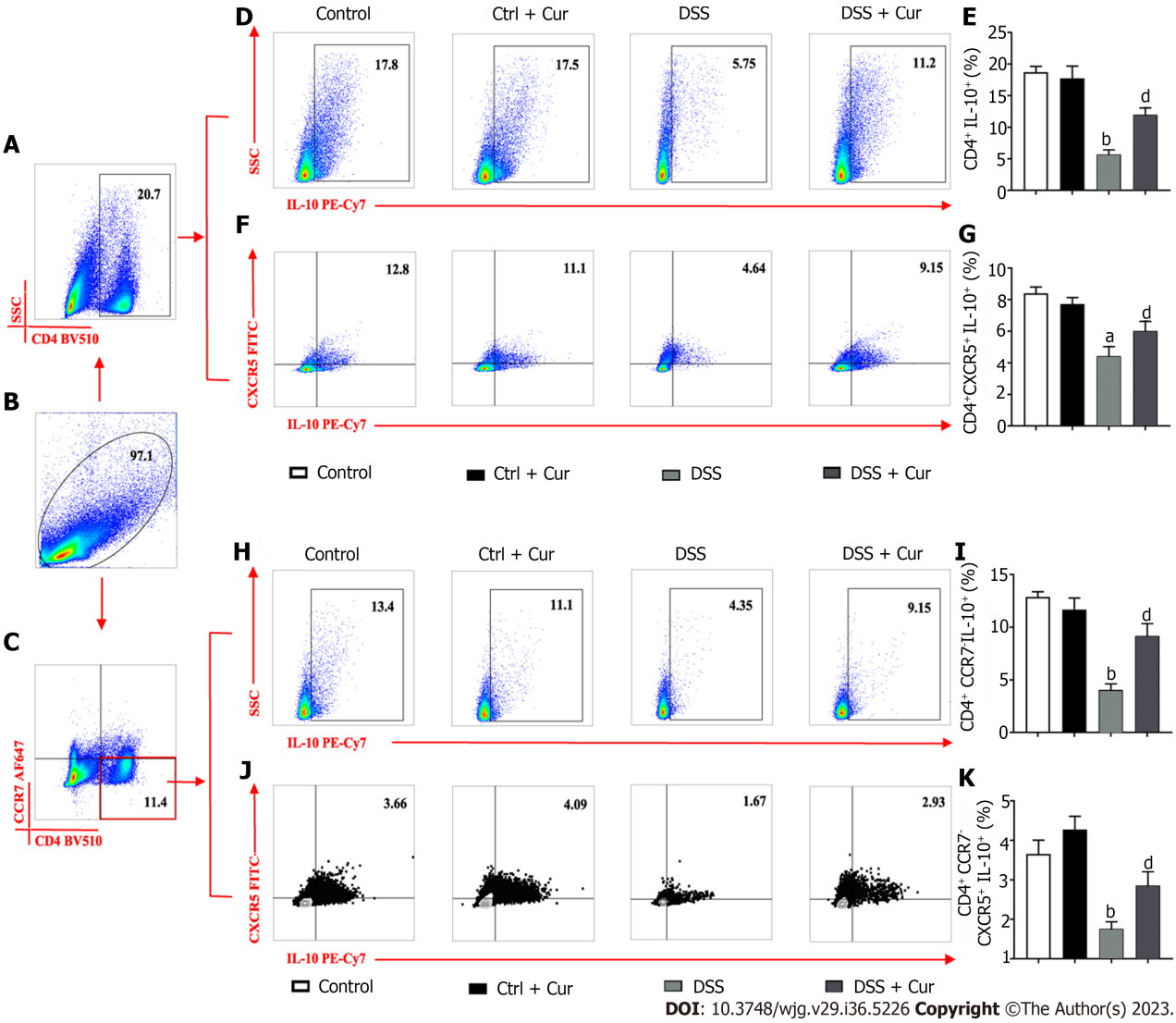
Figure 3 Memory T helper 7/memory follicular T helper 7 cell subpopulation levels in ulcerative colitis mice. A: Typical flow cytometry patterns of the spleen CD4$^+$ cells in the spleen; B: Typical flow cytometry patterns were observed in the spleen; C: Typical flow cytometry patterns and histograms in the spleen of CD4$^+$ CCR7$^-$ cells; D and E: CD4$^+$ IL-7R$^+$ (Th7) cells; F and G: CD4$^+$ CXCR5$^+$ IL-7R$^+$ (Tfh7) cells; H and I: CD4$^+$ CCR7$^-$IL-7R$^+$ (mTh7) cells; J and K: CD4$^+$ CCR7$^-$CXCR5$^+$ IL-7R$^+$ (mTfh7) cells. Data are expressed as the mean ± SD (n = 8). The differences were statistically significant when compared with the Ctrl group ($^a P < 0.05$, $^b P < 0.01$). Differences were statistically significant with the dextran sulfate sodium group ($^c P < 0.05$, $^d P < 0.01$). DSS: Dextran sulfate sodium. Cur: Curcumin; DSS: Dextran sulfate sodium.

expression levels of Tfh1/mTfh1, Tfh7/mTfh7, Tfh10/mTfh10, and Tfh17/mTfh17 cells in each group. The results revealed that the CD4$^+$ CXCR5$^+$ IL-10$^+$ (Tfh10) (Figure 4F and G) and CD4$^+$ CCR7$^-$CXCR5$^+$ IL-10$^+$ (mTfh10) (Figure 4J and K) cell levels were downregulated in the spleen of mice with DSS-induced colitis ($P < 0.05$ or $P < 0.01$). By contrast, CD4$^+$ CXCR5$^+$ CXCR3$^+$ (Tfh1) (Figure 2F and G), CD4$^+$ CCR7$^-$CXCR5$^+$ CXCR3$^+$ (mTfh1) (Figure 2J and K), CD4$^+$ CXCR5$^+$ IL-7R$^+$ (Tfh7) (Figure 3F and G), CD4$^+$ CCR7$^-$CXCR5$^+$ IL-7R$^+$ (mTfh7) (Figure 3J and K), CD4$^+$ CXCR5$^+$ IL-17A$^+$ (Tfh17) (Figure 5F and G), and CD4$^+$ CCR7$^-$CXCR5$^+$ IL-17A$^+$ (mTfh17) (Figure 5J and K) cell levels were remarkably increased ($P < 0.05$ or $P < 0.01$). Surprisingly, Cur treatment successfully reversed this result. The flow cytometry results of the Cur group exhibited a significant rebound in the proportion of Tfh10 and mTfh10 cells, followed by a decrease in the proportion of Tfh1/mTfh1, Tfh7/mTfh7, and Tfh17/mTfh17 cells.

The aforementioned results revealed that Cur treatment effectively regulated mTh/mTfh intercellular overexpression and differentiation in UC mice and promoted the establishment of immune homeostasis.

Cur inhibits the JAK1/STAT3/SOCS signaling pathway in UC mice

The JAK1/STAT3/SOCS signaling pathway is involved in cell development, differentiation, proliferation, and apoptosis and can participate in the inflammatory response in autoimmune diseases by influencing the differentiation of memory T cells, including mTh and mTfh[28-30]. The study findings indicate that SOCS-1 (Figure 6A and I) and SOCS-3 (Figure 6A and J) protein levels were noticeably reduced in the DSS group compared with the control group ($P < 0.05$ or $P < 0.01$). By contrast, p-STAT3 (Figure 6A and I), STAT3 (Figure 6A and I), JAK1 (Figure 6A and B), p-JAK1 (Figure 6A and C), and NF-κB p65 (Figure 6A and H) protein expression levels and the ratio of p-JAK/JAK (Figure 6A and D) were significantly increased ($P < 0.05$ or $P < 0.01$). Following treatment with Cur, SOCS-1 (Figure 6A and I), and SOCS-3 (Figure 6A and J) protein expression levels obviously increased ($P < 0.01$), whereas p-STAT3 (Figure 6A and I), STAT3 (Figure 6A and I), JAK1 (Figure 6A and B), p-JAK1 (Figure 6A and C), and NF-κB p65 (Figure 6A and H) protein expression levels and the



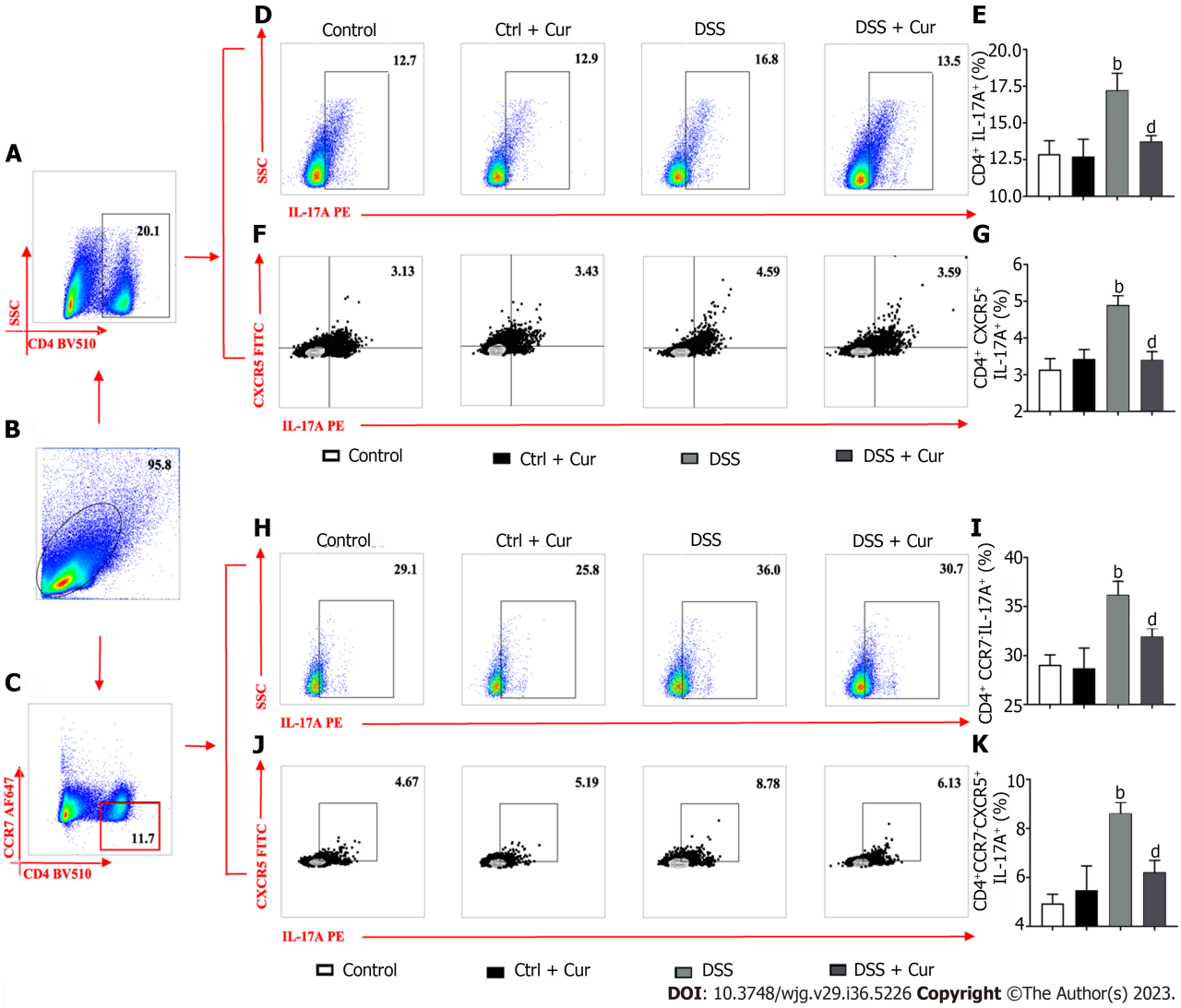
DOI: 10.3748/wjg.v29.i36.5226 **Copyright** ©The Author(s) 2023.

Figure 4 Memory T helper 10/memory follicular T helper 10 cell subpopulation levels in ulcerative colitis mice. A: Typical flow cytometry patterns of the spleen CD4$^+$ cells; B: Typical flow cytometry patterns were observed in the spleen; C: Typical flow cytometry patterns and histograms in the spleen of CD4$^+$ CCR7$^-$ cells; D and E: CD4$^+$ IL-10$^+$ (Th10) cells; F and G: CD4$^+$ CXCR5$^+$ IL-10$^+$ (Tfh10) cells; H and I: CD4$^+$ CCR7$^-$IL-10$^+$ (mTh10) cells; J and K: CD4$^+$ CCR7$^-$ CXCR5$^+$ IL-10$^+$ (mTfh10) cells. Data are expressed as the mean ± SD (n = 8). The differences were statistically significant when compared with the Ctrl group (^aP < 0.05, ^bP < 0.01). Differences were statistically significant with the dextran sulfate sodium group (^cP < 0.05, ^dP < 0.01). Cur: Curcumin; DSS: Dextran sulfate sodium.

ratio of p-JAK/JAK (Figure 6A and D) were downregulated (P < 0.05 or P < 0.01) in the colon tissues of mice.

DISCUSSION

The mouse model of DSS-induced UC exhibits pathogenesis characteristics closely resembling those of human UC patients. Thus, this is a well-established experimental UC model widely used for developing novel therapeutic interventions against UC. We here found that mTh and mTfh cells exhibited significant abnormalities, as observed through increased levels of mTh1/mTfh1, mTh7/mTfh7, and mTh17/mTfh17 cells, decreased levels of mTh10/mTfh10 cells, and their evolving into an imbalance in the effector Th and Tfh cell levels. This indicated that the disruption of the balance of Th/Tfh immune cells and immune homeostasis are pivotal players in the pathogenesis of DSS-induced colitis, which is consistent with the results of Zhong *et al*[31], Xue *et al*[32], Zhu *et al*[33], and Xiao *et al*[34]. Cur effectively regulated the balance between total Th/Tfh cells and mTh/mTfh cells, and their subsets. The mTh1/mTfh1 (Th1/Tfh1), mTh7/mTfh7 (Th7/Tfh7), and mTh17/mTfh17 (Th17/Tfh17) cell levels decreased. For example, the expression level of CXCR3, a biomarker of Th1 and mTh1 cells, decreased in the two cells. Additionally, a reduction in IL-7 and IL-17A production was noted, which could be attributable to suppressed activation that leads to differentiation from memory to effector phenotypes[35]. Meanwhile, the levels of IL-10-secreting mTh10/mTfh10 and Th10/Tfh10 cells noticeably increased, and this increase plays a role in suppressing inflammation development[36]; similar results were observed in the present study. Second, the levels of mTh/mTfh cells were also effectively suppressed or restored, thus maintaining immune homeostasis and enhancing the adaptive immune response[37]. Our study findings align with the notion that

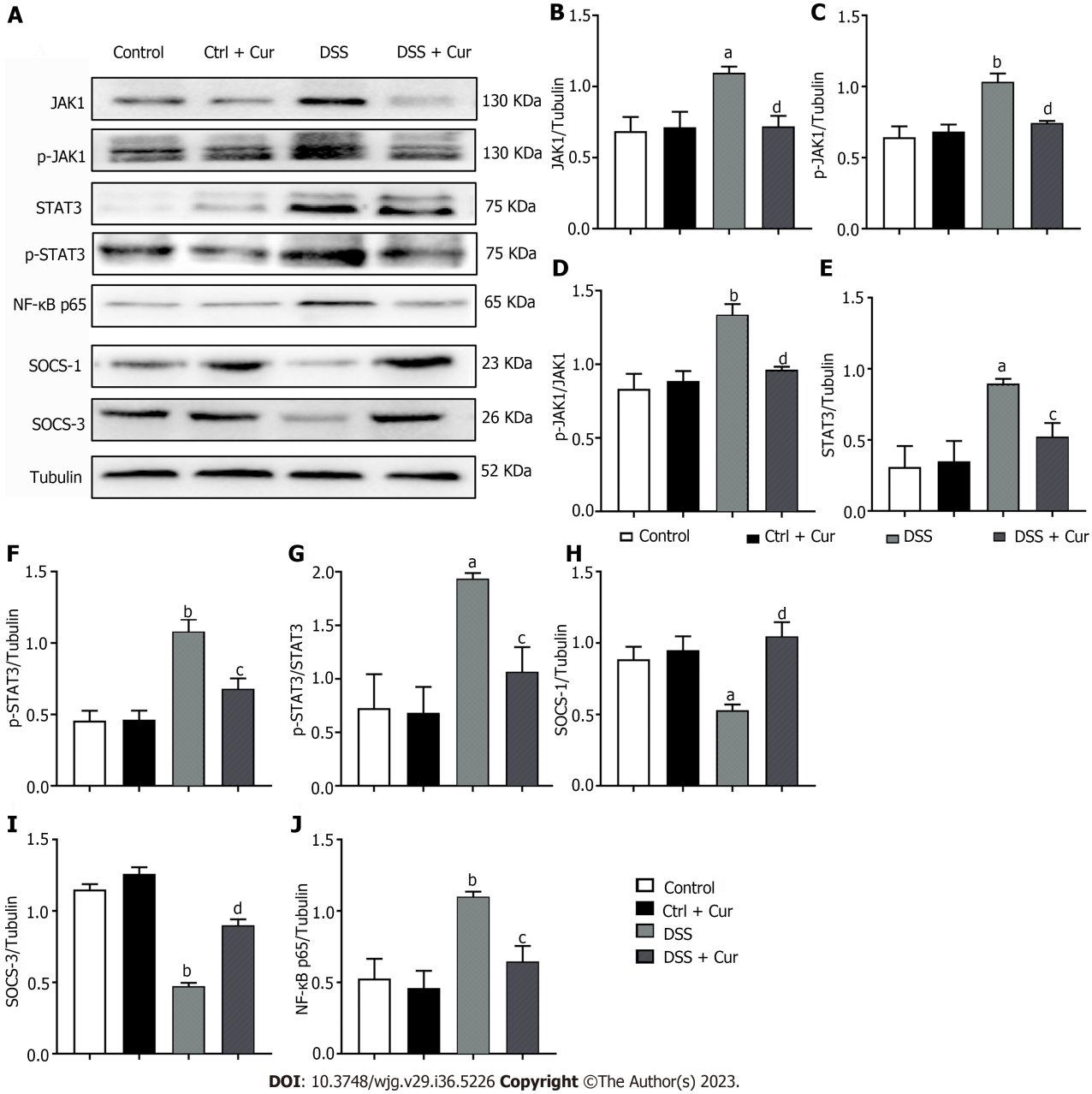


DOI: 10.3748/wjg.v29.i36.5226 **Copyright** ©The Author(s) 2023.

Figure 5 Memory T helper 17/memory follicular T helper 17 cell subpopulation levels in ulcerative colitis mice. A: Typical flow cytometry patterns of the spleen $CD4^+$ cells; B: Typical flow cytometry patterns were observed in the spleen; C: Typical flow cytometry patterns and histograms in the spleen of $CD4^+$ $CCR7^-$ cells; D and E: $CD4^+$ $IL\text{-}17A^+$ (Th17) cells; F and G: $CD4^+$ $CXCR5^+$ $IL\text{-}17A^+$ (Tfh17) cells; H and I: $CD4^+$ $CCR7^-IL\text{-}17A^+$ (mTh17) cells; J and K: $CD4^+$ $CCR7^-CXCR5^+$ $IL\text{-}17A^+$ (mTfh17) cells. Data are expressed as the mean ± SD (n = 8). The differences were statistically significant when compared with the Ctrl group ($^aP < 0.05$, $^bP < 0.01$). Differences were statistically significant with the dextran sulfate sodium group ($^cP < 0.05$, $^dP < 0.01$). Cur: Curcumin; DSS: Dextran sulfate sodium.

Cur exerts a therapeutic effect on DSS-induced colitis by effectively ameliorating its pathological state in mice[12]. In our study, Cur significantly increased mouse body weight and colonic length, whereas markedly reduced the DAI score, colonic weight, colonic weight/colonic length, and colon weight index in mice with colitis. It also improved the pathological damage to the colon while significantly decreasing the pathological damage score. Notably, in our study, Cur exhibited remarkable effectiveness in mitigating DSS-induced colitis in the mice while simultaneously exerting a modulatory influence on mTh/mTfh cells. These indications suggest that Cur effectively addresses DSS-induced colitis in mice, potentially by modulating the mTh/mTfh cell-mediated immune homeostasis. However, the probable mechanism underlying the Cur-modulated balance of the mTh/mTfh cells and their subsets must be explored.

We emphatically examined the changes in the JAK1/STAT3/SOCS signaling pathway in mouse colon tissues through western blotting. Without treatment, JAK1 and STAT3 proteins were activated and the downstream protein SOCS was inhibited in the mice with colitis, indicating that this signaling pathway was activated and closely related to the pathogenesis of DSS-induced colitis. In the presence of various cytokine stimuli, the JAK1/STAT3/SOCS pathway has a crucial regulatory role in the development, differentiation, proliferation, apoptosis, and functionality of immune cells such as memory T cells and memory follicular T cells[38,39]. Upon stimulation with certain hetero antigens, specific cytokines upregulate *SOCS-1* and *SOCS-3* gene expression. Consequently, these gene products inhibit the JAK1/STAT3 pathway and decrease the levels of inflammatory factors and apoptosis-inducing genes, thereby creating a negative feedback loop that aids in sustaining the body's immune homeostasis[40]. The JAK1/STAT3/SOCS pathway mainly regulates the differentiation of T cells, including mTh/mTfh cells and other memory T cell subsets[41]. Initial $CD4^+$ T cells can activate STAT3 and induce RORγt expression in the presence of low IL-6 concentrations, thus contributing to Th17 cell differentiation[42]. IL-6 can also indirectly promote Th17 cell differentiation by activating STAT3, inhibiting T-bet and



DOI: 10.3748/wjg.v29.i36.5226 **Copyright** ©The Author(s) 2023.

Figure 6 Curcumin inhibits JAK1/STAT3/SOCS signaling pathway-related proteins in ulcerative colitis mice. A: Western blotting of the major proteins in the JAK1/STAT3/SOCS signaling pathway, such as JAK1, p-JAK1, STAT3, p-STAT3, NF-κB p65, SOCS-1, and SOCS-3. Tubulin served as the reference protein in this study; B-J: Quantitative evaluations of JAK1 (B), p-JAK1 (C), JAK1/p-JAK1 (D), STAT3 (E), p-STAT3 (F), STAT3/p-STAT3 (G), SOCS-1 (H), SOCS-3 (I), and NF-κB p65 (J). Data of each group are expressed as the mean ± SD. The differences were statistically significant when compared with the Ctrl group ($^{a}P < 0.05$, $^{b}P < 0.01$). Differences were statistically significant with the dextran sulfate sodium group ($^{c}P < 0.05$, $^{d}P < 0.01$). Cur: Curcumin; DSS: Dextran sulfate sodium.

Treg expression, and reducing Th1 cell differentiation[43-45]. Furthermore, increasing evidence has shown that *SOCS-1/SOCS-3* gene overexpression can inhibit Th1, Th2, and Th17 cell differentiation[46-48]. When Cur was administered, JAK1 and STAT3 protein expression was inhibited and SOCS protein levels increased, which indicated that Cur can effectively inhibit the activation of this signaling pathway. Combined with the results of the aforementioned efficacy evaluation, we inferred that the ability of Cur to effectively treat mouse colitis and to inhibit the JAK1/STAT3/SOCS signaling pathway are closely related.

Based on the aforementioned inferences, the present results thus offer us many vital hints. First, Cur can promote the differentiation of mTh10/mTfh10 to Th10/Tfh10 to increase IL-10 Levels by inhibiting this JAK1/STAT3/SOCS signaling pathway, while inhibiting the differentiation of mTh1/mTfh1 to Th1/Tfh1, mTh7/mTfh7 to Th7/Tfh7, and mTh17/mTfh17 to Th17/Tfh17, thus regulating the balance between different Th/Tfh cell subpopulations. Finally, it decreases the secretion of pro-inflammatory cytokines such as INF-γ, IL-7, and IL-17A, ultimately maintaining the body's immune homeostasis[24,49]. Second, Cur may also regulate the crosstalk between Th and Tfh, mTh and mTfh cells by inhibiting the activation of the JAK1/STAT3/SOCS signaling pathway; the Th and Tfh, mTh, and mTfh cells may undergo interconversion[50]. In summary, Cur can effectively treat DSS-induced colitis by preserving the immune homeostasis mediated by mTh/mTfh cells and their subsets, which is possibly realized by inhibiting the JAK1/STAT3/SOCS signaling

pathway. We are here to provide a shred of indirect evidence. However, we believe that Cur-mediated regulation of this signaling pathway creates the environment and conditions for the transformation, communication, and dialog between mTfh and mTh cells. In our future work, we intend to use flow cytometry or other methods to induce and isolate mTh and mTfh cells, and then use Cur intervention to evaluate their differentiation levels. We will also use lentiviral transfection to overexpress or under express the *JAK1* gene and use inhibitors or agonists to accurately evaluate whether Cur can interfere with the JAK1/STAT3/SOCS signaling pathway to interfere with the crosstalk between mTh and mTfh cells, which would be very interesting work.

CONCLUSION

Cur regulated the mTh/mTfh cell homeostasis to reduce DSS-induced colonic pathological damage, potentially by suppressing the JAK1/STAT3/SOCS signaling pathway.

ARTICLE HIGHLIGHTS

Research background

Maintaining immune homeostasis by targeting memory immune cells is a crucial treatment strategy for autoimmune diseases. Discovering new drugs from natural plant medicine and traditional Chinese medicine to treat inflammatory bowel disease (IBD) is a research hotspot. Many researches had shown that curcumin (Cur) can effectively treat patients and animals with ulcerative colitis (UC). Although Cur can regulate the function of immune cells to alleviate UC in mice, whether Cur can regulate the memory T helper (mTh) cell- and memory follicular T helper (mTfh) cell-mediated homeostasis to treat IBD remains unknown.

Research motivation

To further widen the category of the immunopharmacological action of Cur and supply increasing scientific evidence for promoting the clinical application of Cur in IBD treatment.

Research objectives

To explore the potential mechanism underlying Cur-mediated alleviation of dextran sulfate sodium (DSS)-induced colonic pathological damage by observing changes in mTh and mTfh cells and their subsets and function.

Research methods

DSS was used to induce experimental colitis, and colitis was treated with Cur for 7 consecutive days. The therapeutic effect of Cur was evaluated through macroscopic and microscopic observations. The levels of mTh and mTfh cells and their subsets were detected through flow cytometry. SOCS-1, SOCS-3, STAT3, p-STAT3, JAK1, p-JAK1, and NF-κB p65 protein expression levels were measured through Western blotting.

Research results

Cur effectively alleviates DSS-induced colitis in mice, promotes the recovery of mouse weight and colonic length, and reduces colonic weight and the colonic weight index. Meanwhile, Cur inhibits ulcer formation and inflammatory cell infiltration in the colonic mucosa. The percentage of Th1, mTh1, Th7, mTh7, Th17, mTh17, Tfh1, mTfh1, Tfh7, mTfh7, Tfh17, and mTfh17 cells decreased after the mice with colitis were treated with Cur for 7 d, whereas the frequency of mTh10, Th10, mTfh10, and Tfh10 cells in the spleen of these mice increased. Additional studies revealed that the SOCS-1, SOCS-3, STAT3, p-STAT3, JAK1, p-JAK1, and NF-κB p65 protein expression levels significantly decreased in the colon tissue after Cur administration.

Research conclusions

Cur effectively alleviated DSS-induced colitis in mice by regulating mTh/Tfh cells, which was potentially realized by inhibiting the JAK1/STAT3/SOCS signaling pathway.

Research perspectives

Cur is a commonly used food additive and the main effective constituent of traditional Chinese medicine. Cur regulates the immune homeostasis mediated by memory T and B cells. This is a very promising and significant effect of Cur that can be used to develop the value of Cur as a healthcare product for preventing many chronic and recurrent diseases.

FOOTNOTES

Author contributions: Zheng LX, Guo KE, Huang JQ, Liu MH, Deng BL, Liu DY, and Zhou BG performed the experiments; Zhou W and Zhao HM contributed reagents/materials/analytical tools; Zhao HM, Liu DY, and Zhong YB analyzed the data; Zheng LX, Guo KE, and Zhong YB wrote the paper; Zhou W, Zhong YB, and Zhao HM designed the experiments.

Supported by the National Natural Science Foundation of China, No. 81760808 and No. 82260863; Scientific and Technological Project of Education Department of Jiangxi Province, No. GJJ181582; Jiangxi University of Chinese Medicine Science and Technology Innovation Team Development Program, No. CXTD22008; and Key Laboratory of Pharmacodynamics and Quality Evaluation on anti-Inflammatory Chinese Herbs, Jiangxi Administration of Traditional Chinese Medicine, No. 202208.

Institutional animal care and use committee statement: All procedures involving animals were reviewed and approved by the Experimental Animal Science and Technology Center of Jiangxi University of Traditional Chinese Medicine (Approval No. JZLLSC2021-196).

Conflict-of-interest statement: The authors declare no conflicts of interest.

Data sharing statement: The data presented in this study are available from the corresponding author upon reasonable request.

ARRIVE guidelines statement: The authors have read the ARRIVE Guidelines, and the manuscript was prepared and revised according to the ARRIVE Guidelines.

Open-Access: This article is an open-access article that was selected by an in-house editor and fully peer-reviewed by external reviewers. It is distributed in accordance with the Creative Commons Attribution NonCommercial (CC BY-NC 4.0) license, which permits others to distribute, remix, adapt, build upon this work non-commercially, and license their derivative works on different terms, provided the original work is properly cited and the use is non-commercial. See: https://creativecommons.org/Licenses/by-nc/4.0/

Country/Territory of origin: China

ORCID number: Duan-Yong Liu 0000-0003-2855-2811; Hai-Mei Zhao 0000-0001-8767-5251.

S-Editor: Chen YL
L-Editor: A
P-Editor: Cai YX

REFERENCES

1 **Liu S**, Liu J, He L, Liu L, Cheng B, Zhou F, Cao D, He Y. A Comprehensive Review on the Benefits and Problems of Curcumin with Respect to Human Health. *Molecules* 2022; **27** [PMID: 35889273 DOI: 10.3390/molecules27144400]
2 **Xiang DB**, Zhang KQ, Zeng YL, Yan QZ, Shi Z, Tuo QH, Lin LM, Xia BH, Wu P, Liao DF. Curcumin: From a controversial "panacea" to effective antineoplastic products. *Medicine (Baltimore)* 2020; **99**: e18467 [PMID: 31914018 DOI: 10.1097/MD.0000000000018467]
3 **Yin J**, Wei L, Wang N, Li X, Miao M. Efficacy and safety of adjuvant curcumin therapy in ulcerative colitis: A systematic review and meta-analysis. *J Ethnopharmacol* 2022; **289**: 115041 [PMID: 35091013 DOI: 10.1016/j.jep.2022.115041]
4 **Zeng L**, Yang T, Yang K, Yu G, Li J, Xiang W, Chen H. Curcumin and Curcuma longa Extract in the Treatment of 10 Types of Autoimmune Diseases: A Systematic Review and Meta-Analysis of 31 Randomized Controlled Trials. *Front Immunol* 2022; **13**: 896476 [PMID: 35979355 DOI: 10.3389/fimmu.2022.896476]
5 **Sarawi WS**, Alhusaini AM, Fadda LM, Alomar HA, Albaker AB, Aljrboa AS, Alotaibi AM, Hasan IH, Mahmoud AM. Curcumin and Nano-Curcumin Mitigate Copper Neurotoxicity by Modulating Oxidative Stress, Inflammation, and Akt/GSK-3β Signaling. *Molecules* 2021; **26** [PMID: 34577062 DOI: 10.3390/molecules26185591]
6 **Cui X**, Lin L, Sun X, Wang L, Shen R. Curcumin Protects against Renal Ischemia/Reperfusion Injury by Regulating Oxidative Stress and Inflammatory Response. *Evid Based Complement Alternat Med* 2021; **2021**: 8490772 [PMID: 34812266 DOI: 10.1155/2021/8490772]
7 **Memarzia A**, Khazdair MR, Behrouz S, Gholamnezhad Z, Jafarnezhad M, Saadat S, Boskabady MH. Experimental and clinical reports on anti-inflammatory, antioxidant, and immunomodulatory effects of Curcuma longa and curcumin, an updated and comprehensive review. *Biofactors* 2021; **47**: 311-350 [PMID: 33606322 DOI: 10.1002/biof.1716]
8 **Zheng T**, Wang X, Chen Z, He A, Zheng Z, Liu G. Efficacy of adjuvant curcumin therapy in ulcerative colitis: A meta-analysis of randomized controlled trials. *J Gastroenterol Hepatol* 2020; **35**: 722-729 [PMID: 31696975 DOI: 10.1111/jgh.14911]
9 **Zhang L**, Xue H, Zhao G, Qiao C, Sun X, Pang C, Zhang D. Curcumin and resveratrol suppress dextran sulfate sodiuminduced colitis in mice. *Mol Med Rep* 2019; **19**: 3053-3060 [PMID: 30816479 DOI: 10.3892/mmr.2019.9974]
10 **Wei SY**, Wu TT, Huang JQ, Kang ZP, Wang MX, Zhong YB, Ge W, Zhou BG, Zhao HM, Wang HY, Liu DY. Curcumin alleviates experimental colitis *via* a potential mechanism involving memory B cells and Bcl-6-Syk-BLNK signaling. *World J Gastroenterol* 2022; **28**: 5865-5880 [PMID: 36353208 DOI: 10.3748/wjg.v28.i40.5865]
11 **Huang J**, Wu T, Zhong Y, Huang J, Kang Z, Zhou B, Zhao H, Liu D. Effect of curcumin on regulatory B cells in chronic colitis mice involving TLR/MyD88 signaling pathway. *Phytother Res* 2023; **37**: 731-742 [PMID: 36196887 DOI: 10.1002/ptr.7656]
12 **Zhong YB**, Kang ZP, Wang MX, Long J, Wang HY, Huang JQ, Wei SY, Zhou W, Zhao HM, Liu DY. Curcumin ameliorated dextran sulfate sodium-induced colitis *via* regulating the homeostasis of DCs and Treg and improving the composition of the gut microbiota. *J Function Foods* 2021; **86**: 104716 [DOI: 10.1016/j.jff.2021.104716]
13 **Corrado M**, Pearce EL. Targeting memory T cell metabolism to improve immunity. *J Clin Invest* 2022; **132** [PMID: 34981777 DOI: 10.1172/JCI148546]
14 **Duan X**, Sun P, Lan Y, Shen C, Zhang X, Hou S, Chen J, Ma B, Xia Y, Su C. (1)IFN-α Modulates Memory Tfh Cells and Memory B Cells in Mice, Following Recombinant FMDV Adenoviral Challenge. *Front Immunol* 2020; **11**: 701 [PMID: 32411135 DOI: 10.3389/fimmu.2020.00701]

15 **Foucher ED**, Blanchard S, Preisser L, Descamps P, Ifrah N, Delneste Y, Jeannin P. IL-34- and M-CSF-induced macrophages switch memory T cells into Th17 cells *via* membrane IL-1α. *Eur J Immunol* 2015; **45**: 1092-1102 [PMID: 25545357 DOI: 10.1002/eji.201444606]

16 **Xiao QP**, Zhong YB, Kang ZP, Huang JQ, Fang WY, Wei SY, Long J, Li SS, Zhao HM, Liu DY. Curcumin regulates the homeostasis of Th17/Treg and improves the composition of gut microbiota in type 2 diabetic mice with colitis. *Phytother Res* 2022; **36**: 1708-1723 [PMID: 35234309 DOI: 10.1002/ptr.7404]

17 **Long Y**, Zhao X, Xia C, Li X, Fan C, Liu C, Wang C. Upregulated IL-17A secretion and CCR6 co-expression in Treg subsets are related to the imbalance of Treg/Th17 cells in active UC patients. *Scand J Immunol* 2020; **91**: e12842 [PMID: 31660620 DOI: 10.1111/sji.12842]

18 **Zhang L**, Yu L, Wei Y. Oral Administration of Cryptotanshinone-Encapsulated Nanoparticles for the Amelioration of Ulcerative Colitis. *Cell Mol Bioeng* 2022; **15**: 129-136 [PMID: 35096188 DOI: 10.1007/s12195-021-00711-x]

19 **Li C**, Zhu F, Wang S, Wang J, Wu B. Danggui Buxue Decoction Ameliorates Inflammatory Bowel Disease by Improving Inflammation and Rebuilding Intestinal Mucosal Barrier. *Evid Based Complement Alternat Med* 2021; **2021**: 8853141 [PMID: 33531923 DOI: 10.1155/2021/8853141]

20 **Peng W**, Zhao X, Li X. Helicobacter bilis Contributes to the Occurrence of Inflammatory Bowel Disease by Inducing Host Immune Disorders. *Biomed Res Int* 2022; **2022**: 1837850 [PMID: 35983246 DOI: 10.1155/2022/1837850]

21 **Zhou XL**, Yang J, Qu XJ, Meng J, Miao RR, Cui SX. M10, a Myricetin-3-O-b-D-Lactose Sodium Salt, Prevents Ulcerative Colitis Through Inhibiting Necroptosis in Mice. *Front Pharmacol* 2020; **11**: 557312 [PMID: 33041798 DOI: 10.3389/fphar.2020.557312]

22 **Yang HJ**, Jeong SJ, Ryu MS, Ha G, Jeong DY, Park YM, Lee HY, Bae JS. Protective effect of traditional Korean fermented soybean foods (doenjang) on a dextran sulfate sodium-induced colitis mouse model. *Food Funct* 2022; **13**: 8616-8626 [PMID: 35894596 DOI: 10.1039/d2fo01347a]

23 **Cheng Y**, Li J, Zhang X, Li Y, Shi X, Shi R, Mao T, Kou F, Shi L. Protective Effect of Qingchang Wenzhong Decoction on Colitis and Colitis-Related Carcinogenesis by Regulating Inflammation and Intestinal Fibrosis. *J Inflamm Res* 2023; **16**: 1479-1495 [PMID: 37056910 DOI: 10.2147/JIR.S402395]

24 **Basu A**, Ramamoorthi G, Albert G, Gallen C, Beyer A, Snyder C, Koski G, Disis ML, Czerniecki BJ, Kodumudi K. Differentiation and Regulation of T(H) Cells: A Balancing Act for Cancer Immunotherapy. *Front Immunol* 2021; **12**: 669474 [PMID: 34012451 DOI: 10.3389/fimmu.2021.669474]

25 **Zhu J**, Paul WE. CD4 T cells: fates, functions, and faults. *Blood* 2008; **112**: 1557-1569 [PMID: 18725574 DOI: 10.1182/blood-2008-05-078154]

26 **Law H**, Venturi V, Kelleher A, Munier CML. Tfh Cells in Health and Immunity: Potential Targets for Systems Biology Approaches to Vaccination. *Int J Mol Sci* 2020; **21** [PMID: 33198297 DOI: 10.3390/ijms21228524]

27 **Gu-Trantien C**, Migliori E, Buisseret L, de Wind A, Brohée S, Garaud S, Noël G, Dang Chi VL, Lodewyckx JN, Naveaux C, Duvillier H, Goriely S, Larsimont D, Willard-Gallo K. CXCL13-producing TFH cells link immune suppression and adaptive memory in human breast cancer. *JCI Insight* 2017; **2** [PMID: 28570278 DOI: 10.1172/jci.insight.91487]

28 **Andoh A**, Shioya M, Nishida A, Bamba S, Tsujikawa T, Kim-Mitsuyama S, Fujiyama Y. Expression of IL-24, an activator of the JAK1/STAT3/SOCS3 cascade, is enhanced in inflammatory bowel disease. *J Immunol* 2009; **183**: 687-695 [PMID: 19535621 DOI: 10.4049/jimmunol.0804169]

29 **Zongfei J**, Rongyi C, Xiaomeng C, Lili M, Lingying M, Xiufang K, Xiaomin D, Zhuojun Z, Huiyong C, Ying S, Lindi J. In vitro IL-6/IL-6R Trans-Signaling in Fibroblasts Releases Cytokines That May Be Linked to the Pathogenesis of IgG4-Related Disease. *Front Immunol* 2020; **11**: 1272 [PMID: 32733444 DOI: 10.3389/fimmu.2020.01272]

30 **Fukuta M**, Suzuki K, Kojima S, Yabe Y, Iida K, Yamada H, Makino S, Iwata A, Tanaka S, Iwamoto T, Suto A, Nakagomi D, Wakashin H, Maezawa Y, Takemoto M, Asanuma K, Nakajima H. Suppressor of cytokine signalling 3 (SOCS3) expressed in podocytes attenuates glomerulonephritis and suppresses autoantibody production in an imiquimod-induced lupus model. *Lupus Sci Med* 2021; **8** [PMID: 34016718 DOI: 10.1136/lupus-2020-000426]

31 **Zhong Y**, Liu W, Xiong Y, Li Y, Wan Q, Zhou W, Zhao H, Xiao Q, Liu D. Astragaloside IV alleviates ulcerative colitis by regulating the balance of Th17/Treg cells. *Phytomedicine* 2022; **104**: 154287 [PMID: 35752072 DOI: 10.1016/j.phymed.2022.154287]

32 **Xue G**, Zhong Y, Hua L, Zhong M, Liu X, Chen X, Gao D, Zhou N. Aberrant alteration of follicular T helper cells in ulcerative colitis patients and its correlations with interleukin-21 and B cell subsets. *Medicine (Baltimore)* 2019; **98**: e14757 [PMID: 30855475 DOI: 10.1097/MD.0000000000014757]

33 **Zhu Q**, Zheng P, Zhou J, Chen X, Feng Y, Wang W, Zhou F, He Q. Andrographolide affects Th1/Th2/Th17 responses of peripheral blood mononuclear cells from ulcerative colitis patients. *Mol Med Rep* 2018; **18**: 622-626 [PMID: 29749556 DOI: 10.3892/mmr.2018.8992]

34 **Xiao J**, Wang J, Chen Y, Zhou Z, Gao C, Guo Z. Sauchinone ameliorates intestinal inflammation and promotes Th17 cell production of IL-10 *via* Blimp-1. *Biochem Biophys Res Commun* 2020; **522**: 435-441 [PMID: 31771884 DOI: 10.1016/j.bbrc.2019.11.122]

35 **Jeger-Madiot R**, Vaineau R, Heredia M, Tchitchek N, Bertrand L, Pereira M, Konza O, Gouritin B, Hoareau-Coudert B, Corneau A, Blanc C, Savier E, Buffet P, Six A, Klatzmann D, Moris A, Graff-Dubois S. Naive and memory CD4(+) T cell subsets can contribute to the generation of human Tfh cells. *iScience* 2022; **25**: 103566 [PMID: 34984326 DOI: 10.1016/j.isci.2021.103566]

36 **Liu XK**, Zhao HM, Wang HY, Ge W, Zhong YB, Long J, Liu DY. Regulatory Effect of Sishen Pill on Tfh Cells in Mice With Experimental Colitis. *Front Physiol* 2020; **11**: 589 [PMID: 32581849 DOI: 10.3389/fphys.2020.00589]

37 **Tsai LM**, Yu D. Follicular helper T-cell memory: establishing new frontiers during antibody response. *Immunol Cell Biol* 2014; **92**: 57-63 [PMID: 24189164 DOI: 10.1038/icb.2013.68]

38 **Chetoui N**, Boisvert M, Gendron S, Aoudjit F. Interleukin-7 promotes the survival of human CD4+ effector/memory T cells by up-regulating Bcl-2 proteins and activating the JAK/STAT signalling pathway. *Immunology* 2010; **130**: 418-426 [PMID: 20465565 DOI: 10.1111/j.1365-2567.2009.03244.x]

39 **Betts BC**, Bastian D, Iamsawat S, Nguyen H, Heinrichs JL, Wu Y, Daenthanasanmak A, Veerapathran A, O'Mahony A, Walton K, Reff J, Horna P, Sagatys EM, Lee MC, Singer J, Chang YJ, Liu C, Pidala J, Anasetti C, Yu XZ. Targeting JAK2 reduces GVHD and xenograft rejection through regulation of T cell differentiation. *Proc Natl Acad Sci U S A* 2018; **115**: 1582-1587 [PMID: 29382747 DOI: 10.1073/pnas.1712452115]

40 **Kopalli SR**, Annamneedi VP, Koppula S. Potential Natural Biomolecules Targeting JAK/STAT/SOCS Signaling in the Management of Atopic Dermatitis. *Molecules* 2022; **27** [PMID: 35889539 DOI: 10.3390/molecules27144660]

41 **Vahed H**, Agrawal A, Srivastava R, Prakash S, Coulon PA, Roy S, BenMohamed L. Unique Type I Interferon, Expansion/Survival Cytokines, and JAK/STAT Gene Signatures of Multifunctional Herpes Simplex Virus-Specific Effector Memory CD8(+) T(EM) Cells Are Associated

with Asymptomatic Herpes in Humans. *J Virol* 2019; **93** [PMID: 30487281 DOI: 10.1128/JVI.01882-18]

42 **Tang Z**, Wang Y, Xing R, Zeng S, Di J, Xing F. Deltex-1 is indispensible for the IL-6 and TGF-β treatment-triggered differentiation of Th17 cells. *Cell Immunol* 2020; **356**: 104176 [PMID: 32736174 DOI: 10.1016/j.cellimm.2020.104176]

43 **Yang Y**, Xu J, Niu Y, Bromberg JS, Ding Y. T-bet and eomesodermin play critical roles in directing T cell differentiation to Th1 versus Th17. *J Immunol* 2008; **181**: 8700-8710 [PMID: 19050290 DOI: 10.4049/jimmunol.181.12.8700]

44 **Serada S**, Fujimoto M, Mihara M, Koike N, Ohsugi Y, Nomura S, Yoshida H, Nishikawa T, Terabe F, Ohkawara T, Takahashi T, Ripley B, Kimura A, Kishimoto T, Naka T. IL-6 blockade inhibits the induction of myelin antigen-specific Th17 cells and Th1 cells in experimental autoimmune encephalomyelitis. *Proc Natl Acad Sci U S A* 2008; **105**: 9041-9046 [PMID: 18577591 DOI: 10.1073/pnas.0802218105]

45 **Aqel SI**, Kraus EE, Jena N, Kumari V, Granitto MC, Mao L, Farinas MF, Zhao EY, Perottino G, Pei W, Lovett-Racke AE, Racke MK, Fuchs JR, Li C, Yang Y. Novel small molecule IL-6 inhibitor suppresses autoreactive Th17 development and promotes T(reg) development. *Clin Exp Immunol* 2019; **196**: 215-225 [PMID: 30615197 DOI: 10.1111/cei.13258]

46 **Liao SX**, Chen J, Zhang LY, Zhang J, Sun PP, Ou-Yang Y. Effects of SOCS1-overexpressing dendritic cells on Th17- and Treg-related cytokines in COPD mice. *BMC Pulm Med* 2022; **22**: 145 [PMID: 35428280 DOI: 10.1186/s12890-022-01931-1]

47 **Bachus H**, McLaughlin E, Lewis C, Papillion AM, Benveniste EN, Hill DD, Rosenberg AF, Ballesteros-Tato A, León B. IL-6 prevents Th2 cell polarization by promoting SOCS3-dependent suppression of IL-2 signaling. *Cell Mol Immunol* 2023; **20**: 651-665 [PMID: 37046042 DOI: 10.1038/s41423-023-01012-1]

48 **Shao YY**, Zhou YM, Hu M, Li JZ, Chen CJ, Wang YJ, Shi XY, Wang WJ, Zhang TT. The Anti-Allergic Rhinitis Effect of Traditional Chinese Medicine of Shenqi by Regulating Mast Cell Degranulation and Th1/Th2 Cytokine Balance. *Molecules* 2017; **22** [PMID: 28327534 DOI: 10.3390/molecules22030504]

49 **Wang Q**, Li J, Yu TS, Liu Y, Li K, Liu S, Feng Q, Zhang L, Li GS, Shao LL, Peng J, Hou M, Liu XG. Disrupted balance of CD4(+) T-cell subsets in bone marrow of patients with primary immune thrombocytopenia. *Int J Biol Sci* 2019; **15**: 2798-2814 [PMID: 31853219 DOI: 10.7150/ijbs.33779]

50 **Crotty S**. Do Memory CD4 T Cells Keep Their Cell-Type Programming: Plasticity versus Fate Commitment? Complexities of Interpretation due to the Heterogeneity of Memory CD4 T Cells, Including T Follicular Helper Cells. *Cold Spring Harb Perspect Biol* 2018; **10** [PMID: 28432129 DOI: 10.1101/cshperspect.a032102]

World Journal of Gastroenterology

Submit a Manuscript: https://www.f6publishing.com

World J Gastroenterol 2023 September 28; 29(36): 5240-5253

DOI: 10.3748/wjg.v29.i36.5240

ISSN 1007-9327 (print) ISSN 2219-2840 (online)

META-ANALYSIS

Diagnostic value of methylated branched chain amino acid transaminase 1/IKAROS family zinc finger 1 for colorectal cancer

Ke Xu, Ai-Ru Yu, Shen-Bin Pan, Jie He

Specialty type: Gastroenterology and hepatology

Provenance and peer review: Unsolicited article; Externally peer reviewed.

Peer-review model: Single blind

Peer-review report's scientific quality classification
Grade A (Excellent): 0
Grade B (Very good): B, B
Grade C (Good): C
Grade D (Fair): 0
Grade E (Poor): 0

P-Reviewer: Dauyey K, Kazakhstan; Fabozzi M, Italy; Ridder MD, Belgium

Received: June 20, 2023
Peer-review started: June 20, 2023
First decision: August 26, 2023
Revised: September 1, 2023
Accepted: September 7, 2023
Article in press: September 7, 2023
Published online: September 28, 2023

Ke Xu, Ai-Ru Yu, Shen-Bin Pan, Jie He, Clinical Medical College, Chengdu Medical College, Chengdu 610500, Sichuan Province, China

Ke Xu, Ai-Ru Yu, Shen-Bin Pan, Department of Oncology, The First Affiliated Hospital of Chengdu Medical College, Chengdu 610500, Sichuan Province, China

Jie He, Department of Pulmonary and Critical Care Medicine, The First Affiliated Hospital of Chengdu Medical College, Chengdu 610500, Sichuan Province, China

Corresponding author: Jie He, PhD, Doctor, Department of Pulmonary and Critical Care Medicine, The First Affiliated Hospital of Chengdu Medical College, No. 278 Baoguang Street, Chengdu 610500, Sichuan Province, China. 2325@cmc.edu.cn

Abstract

BACKGROUND

The diagnostic value of combined methylated branched chain amino acid transaminase 1 (BCAT1)/IKAROS family zinc finger 1 (IKZF1) in plasma for colorectal cancer (CRC) has been explored since 2015. Recently, several related studies have published their results and showed its diagnostic efficacy.

AIM

To analyze the diagnostic value of methylated BCAT1/IKZF1 in plasma for screening and postoperative follow-up of CRC.

METHODS

The candidate studies were identified by searching the PubMed, Embase, Cochrane Library, CNKI, and Wanfang databases from May 31, 2003 to June 1, 2023. Sensitivity, specificity, and diagnostic accuracy were calculated by merging ratios or means.

RESULTS

Twelve eligible studies were included in the analysis, involving 6561 participants. The sensitivity of methylated BCAT1/IKZF1 in plasma for CRC diagnosis was 60% [95% confidence interval (CI) 53-67] and specificity was 92% (95%CI: 90-94). The positive and negative likelihood ratios were 8.0 (95%CI: 5.8-11.0) and 0.43 (95%CI: 0.36-0.52), respectively. Diagnostic odds ratio was 19 (95%CI: 11-30) and area under the curve was 0.88 (95%CI: 0.85-0.91). The sensitivity and specificity for CRC screening were 64% (95%CI: 59-69) and 92% (95%CI: 91-93), respectively. The sensitivity and specificity for recurrence detection during follow-up were 54%

(95%CI: 42-67) and 93% (95%CI: 88-96), respectively.

CONCLUSION
The detection of methylated BCAT1/IKZF1 in plasma, as a non-invasive detection method of circulating tumor DNA, has potential CRC diagnosis, but the clinical application prospect needs to be further explored.

Key Words: Branched chain amino acid transaminase 1; IKAROS family zinc finger 1; Methylation; Liquid biopsy; Colorectal cancer

©The Author(s) 2023. Published by Baishideng Publishing Group Inc. All rights reserved.

Core Tip: DNA methylation, a commonly used target for detecting ctDNA in plasma, is often explored as diagnostic biomarker of cancer. Here, the present study systematically analyzed 12 studies including 6561 individuals to assess the diagnostic value of methylated branched chain amino acid transaminase 1 (BCAT1)/ IKAROS family zinc finger 1 (IKZF1) in plasma for colorectal cancer (CRC) through meta-analysis. The sensitivity and specificity of methylated BCAT1/IKZF1 in plasma for CRC diagnosis were 60% [95% confidence interval (CI) 53-67] and 92% (95%CI: 90-94), respectively. The detection of methylated BCAT1/IKZF1 has potential in CRC diagnosis, but the clinical application prospect needs to be explored.

Citation: Xu K, Yu AR, Pan SB, He J. Diagnostic value of methylated branched chain amino acid transaminase 1/IKAROS family zinc finger 1 for colorectal cancer. *World J Gastroenterol* 2023; 29(36): 5240-5253
URL: https://www.wjgnet.com/1007-9327/full/v29/i36/5240.htm
DOI: https://dx.doi.org/10.3748/wjg.v29.i36.5240

INTRODUCTION

Colorectal cancer (CRC) is the most common malignancy of the digestive system worldwide, with more than 18 million cases each year[1]. During long-term follow-up, 25%-40% of patients with CRC show disease recurrence even if after receiving radical treatment[2,3]. As is well known, early diagnosis and treatment are crucial for secondary cancer prevention. Both initial diagnosis and diagnosis of relapse after radical treatment have a major impact on the overall survival of patients. Currently, the diagnostic accuracy of CRC has greatly improved through the wide application of carcinoembryonic antigen (CEA) testing, colonoscopy, and imaging examination. However, the poor sensitivity of CEA detection, invasiveness of colonoscopy, high cost and radiation problems of imaging examination warrant safer, more convenient, economical, and accurate diagnostic methods in the future.

In recent years, liquid biopsy technology is being increasingly applied to disease diagnosis and treatment, owing to its characteristics such as less trauma, convenience, high speed, and cost efficiency. In the field of oncology, liquid biopsy technology has already been used for the diagnosis, prognosis, and treatment response prediction of diseases. During tumor development, because of the aggressiveness of the tumor and biological phenomena of cell necrosis and apoptosis, circulating tumor DNA (ctDNA) may enter the circulation in the early stages of disease development. Therefore, tumor markers based on ctDNA may play an important role in the early diagnosis of tumors[4,5]. DNA methylation, mutation, and chromosomal copy number alteration are the most commonly used targets for detecting ctDNA in plasma, and are often explored as biomarkers[6]. The identification of biomarkers can promote the development of liquid biopsy technology, and mining ctDNA-based biomarkers is considered a promising research direction.

In the field of CRC, the accumulation of genetic and epigenetic changes begins more than 10 years before the onset of the disease[7]. Among these changes, genetic mutation and DNA methylation are the most commonly used biomarkers for the diagnosis and clinical prediction of CRC. As a biomarker, DNA methylation is more advantageous than genetic mutation, because DNA methylation is more common and gene mutation is more susceptible to tumor heterogeneity[8-12]. In 2016, the first DNA-methylated tumor diagnostic marker, SEPT9, was approved by the United States Food and Drug Administration (FDA) for CRC screening, which promoted research in this area[13]. To date, several DNA methylation diagnostic markers have been explored for CRC, including APC, BCAT1, IKZF1, ALX4, LINE-1, SDC2, MGMT, RASSF1A, and WIF1[14-24]. Among them, the diagnostic value of the combination of branched chain amino acid transaminase 1 (BCAT1)/IKAROS family zinc finger 1 (IKZF1) for CRC has been explored since 2015[25]. Recently, several clinical studies on the diagnostic accuracy of methylated BCAT1/IKZF1 in plasma for CRC have published their results. Methylated BCAT1/IKZF1 detection in plasma has similar or better diagnostic efficacy. In particular, a study also found that in the follow-up after radical treatment, some patients without imaging evidence have a recent recurrence event after the occurrence of BCAT1/IKZF1 hypermethylation, implying that methylated BCAT1/IKZF1 in plasma may have good timeliness in diagnosis[26]. To fully understand the diagnostic value of BCAT1/IKZF1 hypermethylation in initial diagnosis and postoperative recurrence of CRC, in the present study, we systematically analyzed the sensitivity, specificity, and other diagnostic indicators of methylated BCAT1/IKZF1 detection through meta-analysis, with the aim to provide a theoretical reference for its future clinical application in CRC diagnosis.

MATERIALS AND METHODS

This meta-analysis was performed using the Preferred Reporting Items for Systematic Reviews and Meta-analysis of Diagnostic Test Accuracy Studies as the standard. Before performing this meta-analysis, a preliminary plan was developed and registered at https://www.crd.york.ac.uk/PROSPERO/.

Literature search strategy

A Computer search of PubMed, Embase, Cochrane Library, CNKI, and Wanfang databases was performed. Studies on the diagnostic accuracy of methylated BCAT1/IKZF1 in plasma for CRC were collected. The search period was from May 31, 2003, to June 1, 2023. In addition, references in the included literature were traced to supplement and obtain relevant literature. The method of free word retrieval was adopted. The search formula was (BCAT1 or IKZF1) and (methylation or methylated) and (colorectal or colon or rectal) and (cancer or tumor or carcinoma).

Inclusion and exclusion criteria

The inclusion criteria were as follows. Patients with CRC confirmed by pathological examination were included in the case group and healthy volunteers without CRC were included in the control group. Methylated BCAT1 and/or IKZF1 in plasma were used as diagnostic markers, and a positive diagnosis was defined as the presence of methylation in either BCAT1 or IKZF1. The exclusion criteria were as follows: reviews, letters, reviews, and conference papers; non-human research; lack of data or incomplete information; and data required for the four-grid statistical table could not be directly or indirectly extracted.

Literature screening and data extraction

Two researchers independently performed literature screening and data extraction, and then cross-checked the data. After removing duplicate references, the titles and abstracts of the remaining articles were screened for inclusion and exclusion criteria to exclude irrelevant studies. Eligible articles were then reviewed in full to filter again and a final inclusion was arrived. The main data extracted included the following: (1) Basic information: First author, publication time, country, design type (prospective or retrospective), detection method, and diagnostic standard; (2) Test subjects: Subject selection and number of subjects; and (3) Test indicators: number of true positive, false positive, true negative, and false negative cases. Any differences in the data extraction process were assessed independently by a third researcher.

Quality assessment

All studies were subjected to quality assessment according to the Cochrane Collaboration's Diagnostic Accuracy Studies Quality Assessment 2 (QUADAS-2). Similarly, two researchers independently assessed the quality of each study. If there was any disagreement, it was discussed with and decided by a third researcher.

Statistical analysis

Meta-Disc 1.4 and Stata 11.0 software were used for meta-analysis. The spearman correlation coefficient was used to explore whether there was a threshold effect, and the I^2 statistic was used to explore whether there was heterogeneity due to non-threshold effects. If the I^2 was greater than 50%, it indicated obvious heterogeneity among studies, and the random effects model was used for fitting. Otherwise, the fixed effect model was used. The combined statistics were expressed by sensitivity, specificity, positive likelihood ratio, negative likelihood ratio, diagnostic odds ratio (DOR), and 95% confidence interval (CI). A summary receiver operating characteristic curve was plotted and area under the curve (AUC) was calculated. Subgroup analysis and meta-regression analysis were used to explore the sources of heterogeneity. In addition, publication bias was visually assessed using a funnel plot and quantitatively assessed using Deeks' funnel plot asymmetric linear regression test. In full-text statistics, results with $P < 0.05$ were considered statistically significant.

RESULTS

Characteristics of the included studies

Among the 310 papers obtained through the search formula, 12 papers (11 prospective studies and 1 retrospective study) were included by excluding irrelevant literatures, duplicate studies, basic experimental studies, case reports, and other ineligible literatures[26-36]. The specific process of inclusion and exclusion is shown in Figure 1, and the detailed information of each included study is shown in Table 1. Next, we assessed the quality of the included studies using the QUADAS-2 tool, and none of the included studies were assessed as having a high-risk bias (Figure 2) (Supplementary Table 1).

Extraction of literature data

The 12 studies involved 6561 participants. The number of true positives, false positives, true negatives, and false negatives of BCAT1/IKZF1 methylation in plasma for CRC diagnosis was clearly described by each study. Among them, 5 studies included CRC screening populations, and 7 studies included follow-up populations after radical treatment for CRC. Quantitative polymerase chain reaction (PCR) was used for assessment in all studies, but the diagnostic criteria for positive results were different among the studies. Six studies set at least one PCR replicate as positive, whereas the other 6

Table 1 Information on the studies eligible for enrollment (%)

Ref.	Year	Country	Trial design	Disease	Detection method	Total volunteers	Cases (CRC)	Controls (non-CRC)	Sensitivity (95%CI)	Specificity (95%CI)	Sensitivity (95%CI)				Definition of a positive
											Stage I	Stage II	Stage III	Stage IV	
Symonds *et al*[27]	2016	Australia	Prospective observational study	CRC screening	Real-time PCR	1381	66	1315	62 (49–74)	92 (90–93)	41 (18-67)	76 (55–91)	59 (33–82)	71 (29–96)	At least one PCR replicate was positive
Pedersen *et al*[32]	2015	Australia	Prospective observational study	CRC screening	Real-time PCR	218	74	144	77 (66-86)	92 (86-96)	50 (7-93)	68 (48-84)	87 (66-97)	100 (63-100)	A total change in fluorescence intensity above background levels was measured within 50 PCR amplification cycles
Winter *et al*[30]	2022	Australia	Prospective observational study	CRC screening	Real-time PCR	896	290	606	60 (54-66)	92 (89-94)	24 (14-37)	62 (51-72)	68 (58-77)	91 (78-97)	Methylation levels of 10% or more
Pedersen *et al*[32]	2015	Australia	Prospective observational study	CRC screening	Real-time PCR	967	129	838	66 (57-74)	94 (92-95)	38 (57-74)	69 (53-82)	73 (56-85)	94 (70-100)	At least one PCR replicate was positive
Saluja *et al* [35]	2021	Australia	Retrospective case–control study	CRC screening	Real-time PCR	1593	114	1479	61 (52-70)	91 (90-93)	NA	NA	NA	NA	At least one PCR replicate was positive
Young *et al* [28]	2016	Australia	Prospective observational study	Recurrent CRC detection	Real-time PCR	122	28	94	68 (48-84)	87 (79-93)	0/0	75 (35-97)	71 (44-90)	33 (1-91)	At least one PCR replicate was positive
Symonds *et al*[29]	2020	Australia	Prospective observational study	Recurrent CRC detection	Real-time PCR	144	50	94	66 (57-69)	98; (93 -100)	0/0	69 (39-91)	70 (51-85)	43 (10-82)	COLVERA (Clinical Genomics Pty, Ltd, North Ryde, New South Wales Australia) detectability of ctDNA
Pedersen *et al*[26]	2023	Australia	Prospective observational study	Recurrent CRC detection	Real-time PCR	142	33	109	27 (13-46)	91 (84-96)	NA	NA	NA	NA	0.07%
Pedersen *et al*[31]	2022	Australia	Prospective observational study	Recurrent CRC detection	Real-time PCR	549	77	472	64 (52-74)	98 (96-99)	NA	NA	NA	NA	0.07%
Musher *et al*[33]	2020	United States	Prospective observational study	Recurrent CRC detection	Real-time PCR	322	27	295	63 (42-81)	92 (88-94)	NA	NA	NA	NA	COLVERA (clinical Genomics Pathology Inc., NJ, United States) detectability of ctDNA
Symonds *et al*[34]	2022	Australia	Prospective observational study	Recurrent CRC detection	Real-time PCR	55	10	45	70 (35-93)	87 (73-95)	NA	NA	NA	NA	At least one PCR replicate was positive
Murray *et al*[36]	2018	Australia	Prospective observational	recurrent CRC	real-time PCR	172	23	149	30 (13-53)	86 (79-91)	NA	NA	NA	NA	At least one PCR replicate

	study	detection

CRC: Colorectal cancer; CI: Confidence interval; PCR: Polymerase chain reaction; ctDNA: Circulating tumor DNA; NA: Not available.

studies defined positive by setting a threshold of methylation rate.

Threshold effect analysis

As different thresholds can lead to different sensitivity, specificity, and DOR of diagnostic tests, resulting in threshold effects, it is necessary to first detect whether the diagnostic method has a threshold effect. Spearman correlation analysis carried out using Meta-Disc 1.4 software showed that the correlation coefficient among the included studies was r = -0.287 (P = 0.366), there was no significant threshold effect and the results were pooled for analysis.

Pooled analysis

The pooled sensitivity and specificity of the 12 studies were 60% (95%CI: 53-67) and 92% (95%CI: 90-94), respectively. The positive likelihood ratio and negative likelihood ratio were 8.0 (95%CI: 5.8-11.0) and 0.43 (95%CI: 0.36-0.52), respectively. The DOR was 19 (95%CI: 11-30) and AUC was 0.88 (95%CI: 0.85-0.91) (Figure 3). Furthermore, to explore the diagnostic ability of methylated BCAT1/IKZF1 detection for early CRC, we investigated the diagnostic accuracy in patients with different stages of CRC. The diagnostic sensitivity in patients with stage I, II, III, and IV disease was 32% (95%CI: 22-43), 66% (95%CI: 59-73), 71% (95%CI: 63-78), and 91% (95%CI: 81-96), respectively (Figure 4).

Subgroup analysis

To further explore the source of heterogeneity, we conducted a subgroup analysis according to the purpose of testing and positive result definition. The results of the subgroup analysis showed that when methylated BCAT1/IKZF1 in plasma was used for CRC screening, the sensitivity was 64% (95%CI: 59-69), specificity was 92% (95%CI: 91-93), positive likelihood ratio was 8.5 (95%CI: 7.1-10.1), negative likelihood ratio was 0.39 (95%CI: 0.33-0.45), DOR was 22 (95%CI: 16-30) and AUC was 0.92 (95%CI: 0.89-0.94). When the method was applied to postoperative follow-up and assessment of disease recurrence, the sensitivity was 54% (95%CI: 42-67), specificity was 93% (95%CI: 88-96), positive likelihood ratio was 7.4 (95%CI: 3.9-14.2). Negative likelihood ratio was 0.49 (95%CI: 0.37-0.66), DOR was 15 (95%CI: 6-37) and AUC was 0.85 (95%CI: 0.81-0.88). The subgroup analysis based on the purpose of testing effectively reduced heterogeneity, especially in the subgroup of CRC screening, where no significant heterogeneity was detected in both sensitivity and specificity analyses (I^2 = 48.58, I^2 = 26.75). As the method of evaluating results could directly affect the accuracy of diagnosis, the included studies were divided according to the definition of positive results. The two subgroups were defined as follows: At least one PCR replicate was positive, and exceeding the set threshold was considered positive. When at least one PCR replicate was positive, the sensitivity was 59% (95%CI: 50-67), specificity was 91% (95%CI: 89-93), and AUC was = 0.87 (95%CI: 0.84-0.90). When result exceeding the set threshold was defined as positive, the sensitivity was 61% (95%CI: 49-72), specificity was 94% (95%CI: 87-96), and AUC was = 0.91 (95%CI: 0.88-0.93). Combining the principle of real-time PCR and the results of the comprehensive analysis, setting a threshold to define positive result may improve the diagnostic accuracy (Table 2).

Sensitivity and publication bias analysis

To test the robustness of the results, we conducted a sensitivity analysis. The sensitivity analysis showed that after

Table 2 Subgroup analysis of the included studies based on the differences of the purpose of testing and the positive result definition (95% CI, %)

	Pooled sensitivity	Pooled specificity	Pooled positive likelihood ratio	Pooled negative likelihood ratio	Pooled diagnostic DOR	AUC
Overall	60 (53-67)	92 (90-94)	8.0 (5.8-11.0)	0.43 (0.36-0.52)	19 (11-30)	0.88 (0.85-0.91)
The purpose of testing						
CRC screening	64 (59-69)	92 (91-93)	8.5 (7.1-10.1)	0.39 (0.33-0.45)	22 (16-30)	0.92 (0.89-0.94)
Assessment of recurrence	54 (42-67)	93 (88-96)	7.4 (3.9-14.2)	0.49 (0.37-0.66)	15 (6-37)	0.85 (0.81-0.88)
The definition of positive results						
At least one PCR replicate	59 (50-67)	91 (89-93)	6.6 (4.6-9.5)	0.45 (0.36-0.56)	15 (8-26)	0.87 (0.84-0.90)
Set a specific threshold	61 (49-72)	94 (87-96)	10.5 (6.1-17.9)	0.42 (0.31-0.57)	25 (12-55)	0.91 (0.88-0.93)

AUC: Area under the curve; CRC: Colorectal cancer; CI: Confidence interval; PCR: Polymerase chain reaction.

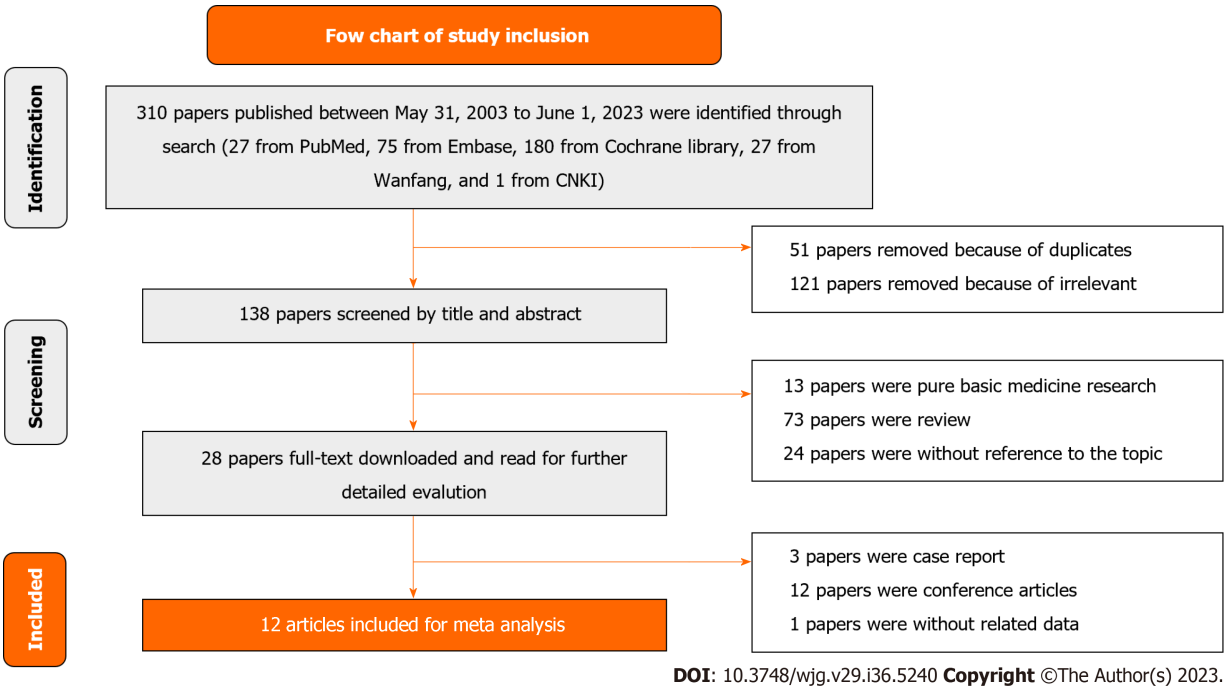
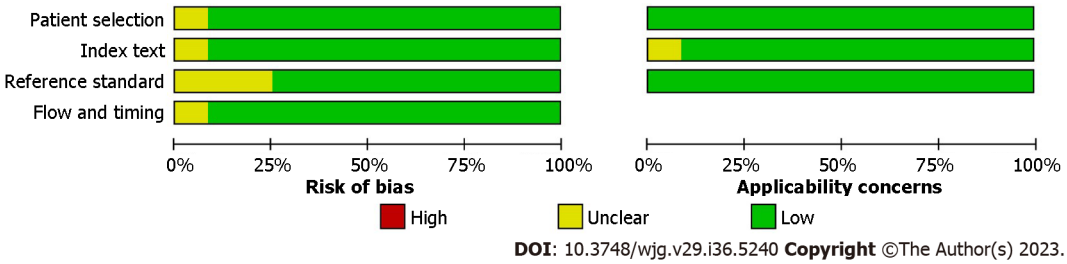


Figure 1 Detailed process of literature identification and screening.

omitting each study one by one, the main results of the meta-analysis did not change significantly, indicating that there was no significant bias in the included studies, and the results were reliable and stable (Figure 5). Deeks' funnel plot was used to assess publication bias, and no significant publication bias was observed (P = 0.604) (Figure 6).

DISCUSSION

Screening and post-treatment follow-up methods for CRC vary worldwide. Currently, the main methods include fecal sample-based testing, colonoscopy, blood sample-based testing, and computed tomography or magnetic resonance imaging colonography. The tests based on fecal samples include fecal occult blood tests, fecal immunochemical tests (FIT), gut microbe analysis, and FIT-DNA tests. Among the fecal sample-based tests, Multi-Target Stool DNA test, approved by the FDA in 2014 for CRC screening is noteworthy. In this test, CRC is diagnosed using the methylation

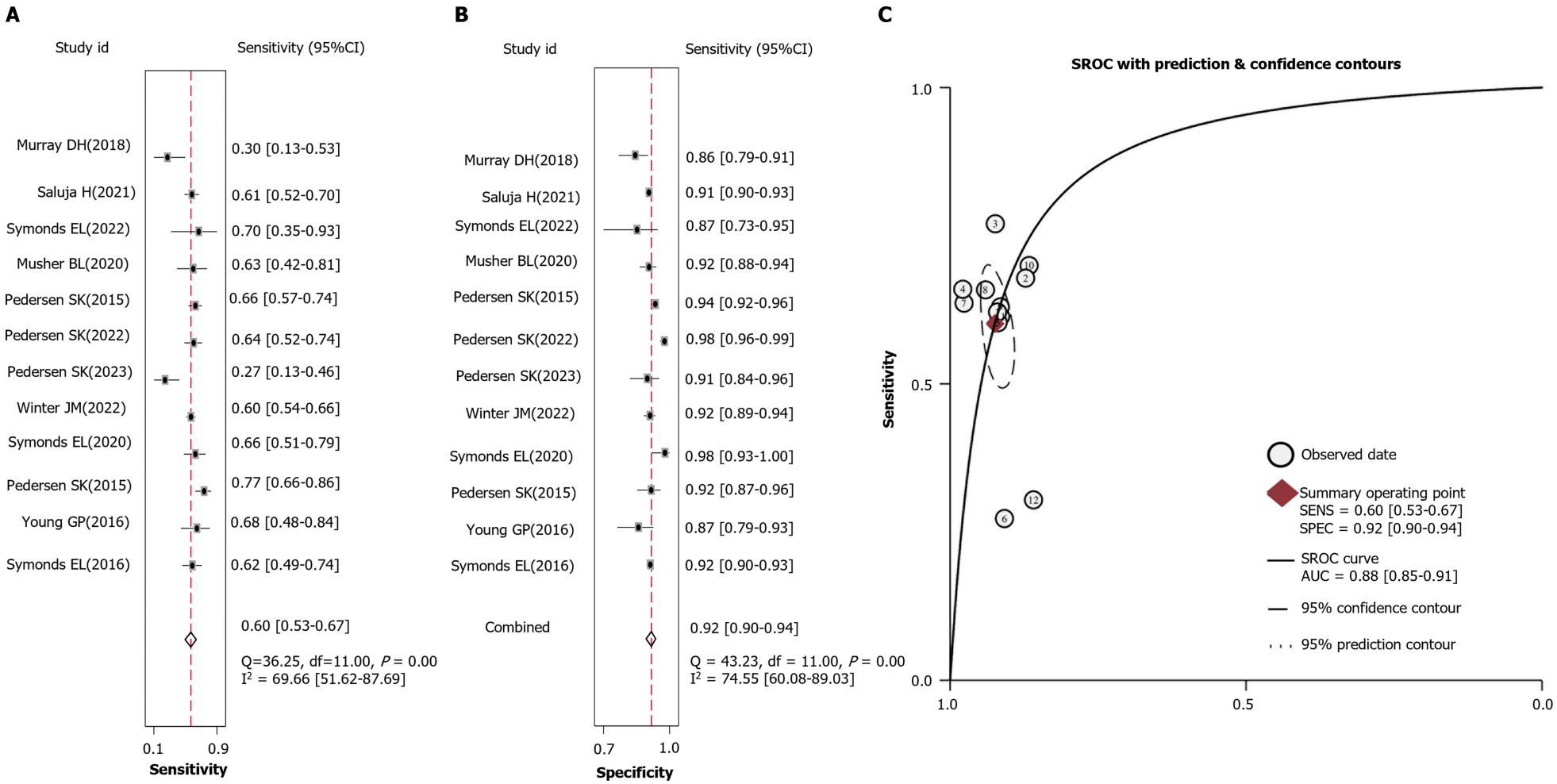


DOI: 10.3748/wjg.v29.i36.5240 Copyright ©The Author(s) 2023.

Figure 2 Overview of applicability concerns and the risk of bias of included studies according to the Cochrane Collaboration's Diagnostic Accuracy Studies Quality Assessment 2 tool.

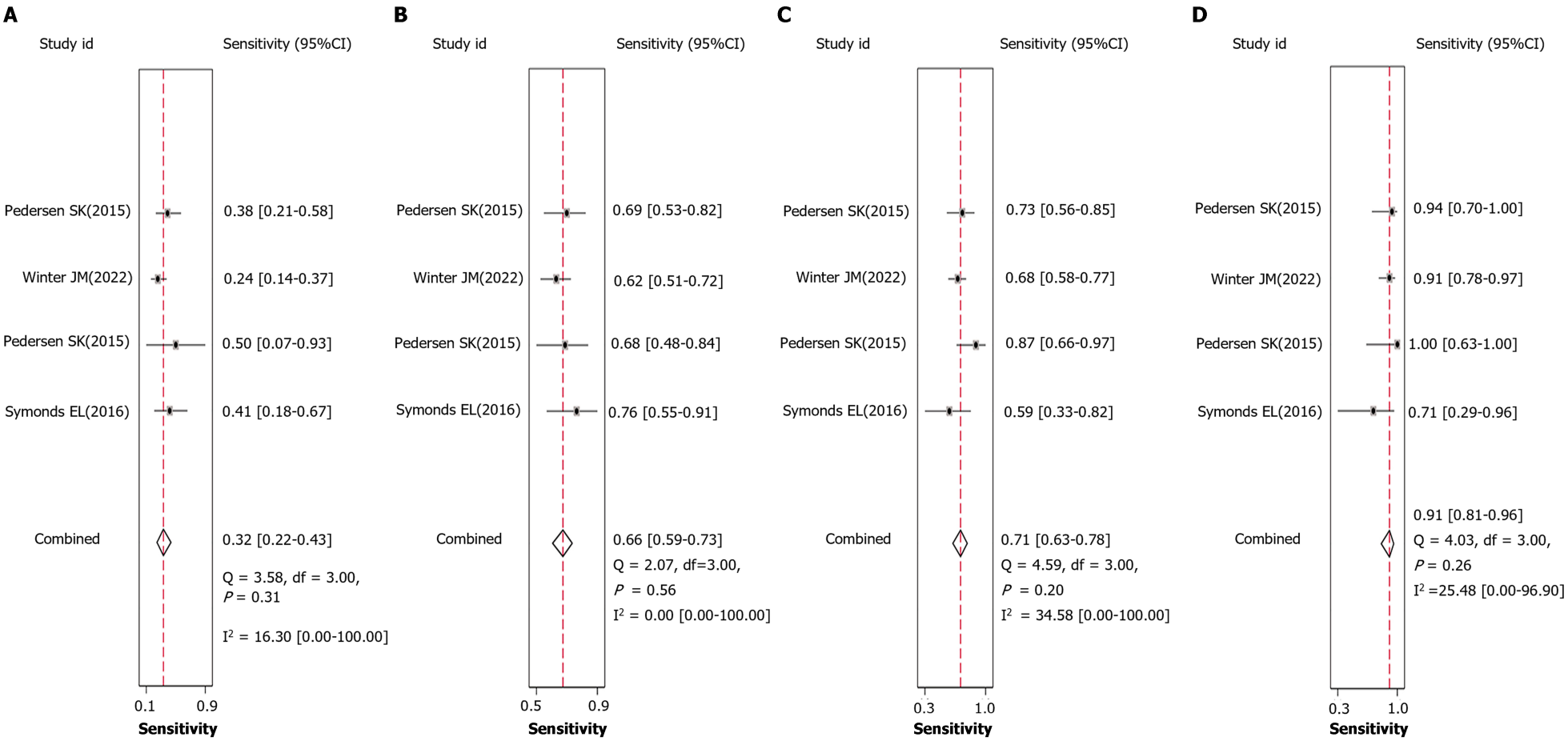
markers NDRG4, BMP3, VIM, and TFP12, combined with mutant KRAS and fecal hemoglobin level. Its sensitivity for CRC screening was 92% and its specificity was 87%[37-39]. Owing to the high diagnostic accuracy of the Multi-Target Stool DNA test, it is recommended for screening high-risk populations[40]. However, its widespread application still has challenges, such as high cost and commercialization issues[41]. Blood sample assay was vital for non-invasive detection, and the diagnostic markers mainly included DNA mutation, DNA methylation, cfDNA, tumor-derived circulating cells, circular RNA, P-element-induced wimpy testis, microRNA, and exosomal microRNA. Researchers have gradually realized the advantages of DNA methylation as a biomarker for tumor diagnosis. Because its changes occur even before the occurrence of tumors, it is theoretically ideal for early screening of tumors[10,42]. SEPT9 methylation was the first methylated marker approved by the FDA for screening CRC using plasma samples, with a diagnostic sensitivity of 0.679 (95%CI: 0.622-0.732) and specificity of 0.904 (95%CI: 0.881-0.923)[43]. However, it is no longer recommended by most guidelines because it is less sensitive than other current tests[44]. Recently, scholars have tried to find other DNA methylation markers with better accuracy for the diagnosis of CRC, such as BCAT1, IKZF1, APC, ALX4, LINE-1, SDC2, MGMT, RASSF1A, and WIF1. They have been used to establish a variety of combinations of diagnostic panels, but there is no sufficient evidence to effectively show their application prospects[14-24]. Owing to the wide application of machine learning in biomedicine, studies on multi-omics and pan-cancer screening products have gradually expanded in the exploration of tumor marker screening based on blood samples. For example, CanerSEEK was a multi-omics tool for detecting ctDNA and proteins for screening various cancers, with a diagnostic sensitivity of up to 84% for CRC[45]. Another new method for pan-cancer screening is GRAIL, which has a diagnostic sensitivity of 82% for CRC, 43.3%, 85.0%, 87.9%, and 95.3% for stage I, II, III, and IV CRC, respectively[46]. It is worth noting that the establishment of most pan-cancer detection methods is still based on DNA methylation as the main diagnostic marker. In the future, more new detection methods will be introduced for the initial diagnosis of CRC and post-treatment follow-up, which will further improve the overall prognosis of CRC.

Recently, multiple studies on the use of methylated BCAT1/IKZF1 in plasma for the diagnosis of CRC have been reported. Overall, its diagnostic accuracy is good, and it may be affected by fewer clinical variables. Based on the results, Clinical Genomics has already completed the commercialization of this detection method, named COLVERA®. At present, it is approved for use in postoperative follow-up detection and assessment of recurrence risk in patients with CRC in the United States and Australia[31]. According to the results of this meta-analysis, methylated BCAT1/IKZF1 in plasma has a sensitivity of 60% (95%CI: 53-67) and specificity of 92% (95%CI: 91-93) for CRC screening. The results are better than those for CEA detection, and its accuracy is similar to that of SETP9 methylation detection. To further confirm the diagnostic value of methylated BCAT1/IKZF1 detection, a direct cross-over study with methods such as FIT and Multi-Target Stool DNA test is needed. As a postoperative follow-up diagnostic method for CRC, the sensitivity of methylated BCAT1/IKZF1 detection 54% (95%CI: 42-67), specificity 93% (95%CI: 88-96), and AUC was 0.85 (95%CI: 0.81-0.88). A study has reported that the sensitivity of this method in the diagnosis of recurrence is as high as 75%, while the sensitivity of the CEA index commonly used in the clinical diagnosis of postoperative recurrence is just 32.1%. It can be seen that it has a major advantage in the postoperative assessment of recurrence. Additionally, some reports suggest that changes in methylated BCAT1/IKZF1 level in plasma occur before imaging changes, which also has the diagnostic timeliness of recurrence[26]. Recently, it has been reported that ctDNA detection using a 15-gene mutation panel can be used to monitor the recurrence of postoperative CRC[47]. Some studies have also found that mesenchymal circulating tumor cell with phosphatase of regenerating liver-3+ is associated with recurrence, which is likely to have a monitoring effect on disease recurrence[48]. However, from the perspective of detection time point, methylated BCAT1/IKZF1 in plasma has major advantages in postoperative follow-up. Earlier, gene mutation indicator detection often required 4-10 wk after surgery, otherwise the sensitivity may decrease, and the method discussed here is not affected by the detection time point [8,49,50]. For the stability and reliability of the results, a subgroup analysis was conducted. The Subgroup analysis based on the purpose of detection could effectively reduce the heterogeneity of the results, especially in the CRC screening group. However, there was still some heterogeneity in the postoperative follow-up group, considering this was most likely caused by different time points of monitoring and the different tumor stages. Owing to the limitations of data, further in-depth analysis could not be conducted in this group. From another perspective of grouping, there were differences in the definition of how to determine a positive result. Seven of the included studies defined at least one PCR replicate as positive. In the past two years, it has been found that setting a specific threshold based on this method could substantially improve the specificity of diagnosis without affecting the sensitivity of diagnosis. In this meta-analysis, it was also found that when at least one PCR replicate was positive, the diagnostic sensitivity was 59% (95%CI: 50-67) and



DOI: 10.3748/wjg.v29.i36.5240 **Copyright** ©The Author(s) 2023.

Figure 3 Pooled analysis of the diagnostic accuracy of methylated branched chain amino acid transaminase 1/IKAROS family zinc finger 1 in plasma for patients with colorectal cancer. A: Sensitivity; B: Specificity; C: Summary receiver operating characteristic curve. SROC: Summary receiver operating characteristics.



DOI: 10.3748/wjg.v29.i36.5240 **Copyright** ©The Author(s) 2023.

Figure 4 The Sensitivity of methylated branched chain amino acid transaminase 1/IKAROS family zinc finger 1 in plasma for patients with colorectal cancer at different stages. A: I stage; B: II stage; C: III stage; D: IV stage.

specificity was 91% (95%CI: 89-93). When thresholds were set, diagnostic sensitivity was 61% (95%CI: 49-72), specificity was 94% (95%CI: 87-96), and AUC was 0.91 (95%CI: 0.88-0.93). In the future application of this method, setting a threshold value may further improve the diagnostic accuracy. In terms of diagnostic sensitivity for patients with different stages of CRC, the detection of the methylated BCAT1/IKZF1 in plasma, similar to other detection methods, has a poor diagnostic sensitivity for patients with early-stage CRC, which may limit its clinical application in CRC screening. In the future, the clinical application value of methylated BCAT1/IKZF1 in plasma can be enhanced by combining it with other

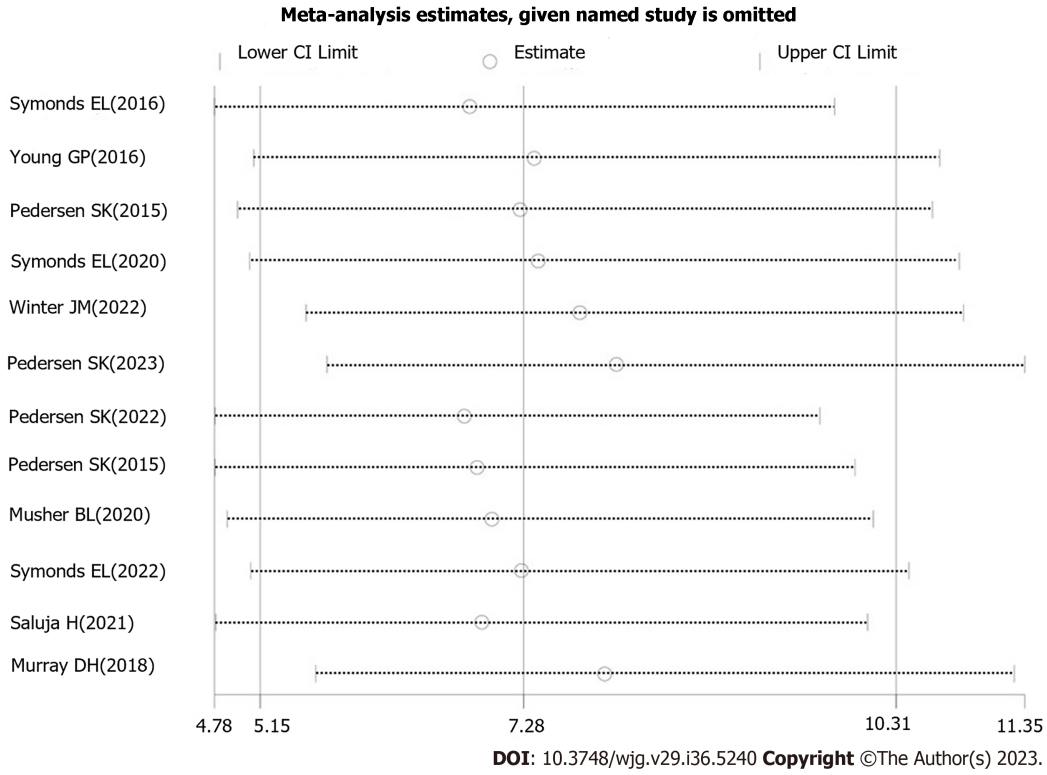


Figure 5 Sensitivity analysis of the included studies.

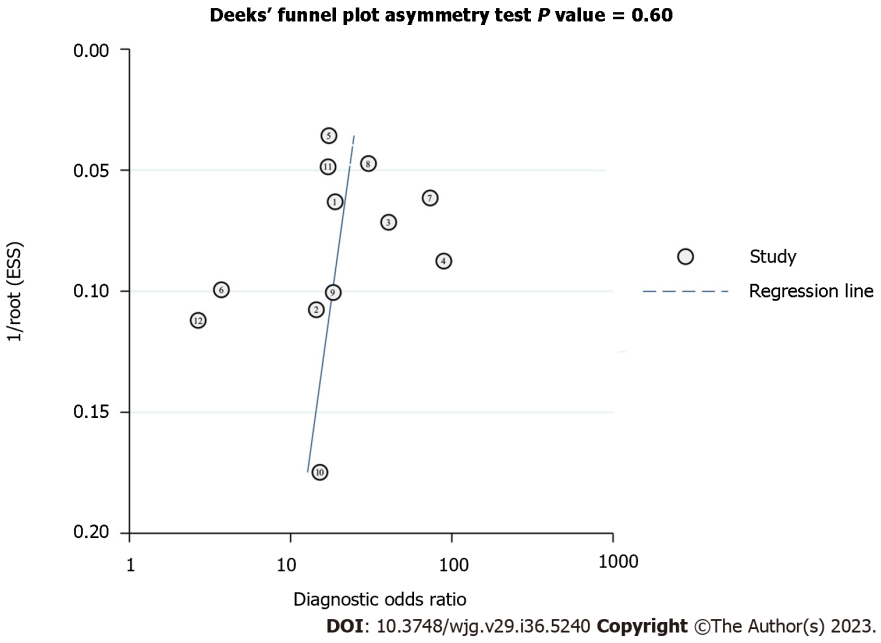


Figure 6 Publication bias analysis of the included studies by Deeks' funnel plot asymmetric linear regression test.

tests. Overall, in this meta-analysis, we systematically analyzed the diagnostic accuracy of methylated BCAT1/IKZF1 in plasma for CRC. These results can provide a basis for further research and clinical application of BCAT1/IKZF1 methylation in the diagnosis of CRC in the future.

In recent years, researchers have found that methylated BCAT1/IKZF1 in plasma may also be valuable in the prognostic prediction of CRC, suggesting that methylated BCAT1/IKZF1 in plasma is more likely to be found in patients with postoperative incisal margin deficiency, lymph node invasion or distant metastasis[36]. Another study analyzed the 3-year recurrence free survival (RFS) of postoperative patients with CRC and found the RFS of patients with methylation was 56.5%, that of patients without methylation was 83.3%[26].

The multivariate analysis showed that the presence of methylated BCAT1/IKZF1 in plasma was an independent factor for poor RFS in CRC. The value of this method in prognostic prediction may be related to its role in the diagnosis of relapse. The above results suggest that patients with consistently positive BCAT1/IKZF1 methylation in plasma after surgery should be followed up cautiously, and the methylation level should be dynamically monitored. At present, some scholars believe that the cause of positive results after surgery may be related to the existence of minimal residual disease (MRD). However, as there is no gold standard for the diagnosis of MRD in CRC; further research is needed to confirm this hypothesis.

There were some limitations to this meta-analysis. As all included studies were conducted in Australia or the United States, the ability of methylated BCAT1/IKZF1 testing to diagnose CRC in other ethnic groups and regions needs to be further investigated. In addition, not all studies clearly recorded the diagnostic sensitivity for patients with different stages of disease; the diagnostic sensitivity analyzed by stratification needs to be explored. Owing to the limitation of data, the diagnostic efficacy of methylated BCAT1/IKZF1 for patients with different genotypes could not be analyzed separately. Finally, it was not possible to perform a pooled analysis of data on the prognosis, because only two studies recorded prognostic results for this approach.

CONCLUSION

The detection of methylated BCAT1/IKZF1 in plasma, as a non-invasive detection method of ctDNA, has potential CRC diagnosis, but the clinical application prospect needs to be further explored.

ARTICLE HIGHLIGHTS

Research background

Currently, DNA methylation is one of the most commonly used detection targets for circulating tumor DNA (ctDNA) in plasma, and is often explored as a diagnostic biomarker for cancer. The diagnostic value of combined methylated branched chain amino acid transaminase 1 (BCAT1)/IKAROS family zinc finger 1 (IKZF1) in plasma for colorectal cancer (CRC) has been explored since 2015. Recently, several related studies have published their results and showed its diagnostic efficacy.

Research motivation

To fully understand the diagnostic value of methylated BCAT1/IKZF1 in initial diagnosis and postoperative recurrence of CRC.

Research objectives

To evaluate the diagnostic accuracy of methylated BCAT1/IKZF1 in plasma for screening and postoperative follow-up of patients with CRC.

Research methods

We searched the PubMed, Embase, Cochrane Library, CNKI, and Wanfang databases. Studies on the diagnostic accuracy of methylated BCAT1/IKZF1 in plasma for CRC were retrieved. Data extraction, pooled analysis, subgroup analysis, sensitivity analysis, and publication bias analysis were performed.

Research results

The pooled sensitivity and specificity of methylated BCAT1/IKZF1 for CRC diagnosis were 60% [95% confidence interval (CI) 53-67] and 92% (95%CI: 90-94), respectively. The positive likelihood ratio and negative likelihood ratio were 8.0 (95%CI: 5.8-11.0) and 0.43 (95%CI: 0.36-0.52), respectively. The diagnostic odds ratio and area under the curve were 19 (95%CI: 11-30) and 0.88 (95%CI: 0.85-0.91), respectively.

Research conclusions

The detection of methylated BCAT1/IKZF1 in plasma, as a non-invasive detection method of ctDNA, has potential in the diagnosis of CRC, but the clinical application value still needs to be explored.

Research perspectives

The detection of methylated BCAT1/IKZF1 in plasma, similar to other detection methods, has poor diagnostic sensitivity for early-stage disease, which may limit its clinical application in CRC screening. In the future, the clinical application of methylated BCAT1/IKZF1 in plasma can be promoted by combining it with other tests.

FOOTNOTES

Author contributions: He J conceived and designed the study; Xu K, He J, Yu AR, and Pan SB performed the collection and assembly of data; Xu K, He J, and Yu AR performed study quality evaluation; Xu K and He J performed data analysis and interpretation; Xu K and Pan SB wrote the initial draft; All authors revised the manuscript, read and approved the final version of the manuscript.

Supported by Natural Science Foundation of Sichuan Province, No. 2023NSFSC0729; Wu Jieping Foundation Special Fund for Clinical Research, No. 320.6750.2022-19-100; Foundation of Key Clinical Specialty of Sichuan Province, No. 2022; School Foundation of Chengdu Medical College, No. CYZYB21-05.

Conflict-of-interest statement: The authors deny any conflict of interest.

PRISMA 2009 Checklist statement: The authors have read the PRISMA 2009 Checklist, and the manuscript was prepared and revised according to the PRISMA 2009 Checklist.

Open-Access: This article is an open-access article that was selected by an in-house editor and fully peer-reviewed by external reviewers. It is distributed in accordance with the Creative Commons Attribution NonCommercial (CC BY-NC 4.0) license, which permits others to distribute, remix, adapt, build upon this work non-commercially, and license their derivative works on different terms, provided the original work is properly cited and the use is non-commercial. See: https://creativecommons.org/Licenses/by-nc/4.0/

Country/Territory of origin: China

ORCID number: Ke Xu 0000-0002-5520-5754; Jie He 0000-0003-4466-9251.

S-Editor: Qu XL
L-Editor: A
P-Editor: Chen YX

REFERENCES

1 **Sung H**, Ferlay J, Siegel RL, Laversanne M, Soerjomataram I, Jemal A, Bray F. Global Cancer Statistics 2020: GLOBOCAN Estimates of Incidence and Mortality Worldwide for 36 Cancers in 185 Countries. *CA Cancer J Clin* 2021; **71**: 209-249 [PMID: 33538338 DOI: 10.3322/caac.21660]

2 **Kunst N**, Alarid-Escudero F, Aas E, Coupé VMH, Schrag D, Kuntz KM. Estimating Population-Based Recurrence Rates of Colorectal Cancer over Time in the United States. *Cancer Epidemiol Biomarkers Prev* 2020; **29**: 2710-2718 [PMID: 32998946 DOI: 10.1158/1055-9965.EPI-20-0490]

3 **Figueredo A**, Rumble RB, Maroun J, Earle CC, Cummings B, McLeod R, Zuraw L, Zwaal C; Gastrointestinal Cancer Disease Site Group of Cancer Care Ontario's Program in Evidence-based Care. Follow-up of patients with curatively resected colorectal cancer: a practice guideline. *BMC Cancer* 2003; **3**: 26 [PMID: 14529575 DOI: 10.1186/1471-2407-3-26]

4 **Spindler KL**, Pallisgaard N, Andersen RF, Brandslund I, Jakobsen A. Circulating free DNA as biomarker and source for mutation detection in metastatic colorectal cancer. *PLoS One* 2015; **10**: e0108247 [PMID: 25875772 DOI: 10.1371/journal.pone.0108247]

5 **Avanzini S**, Kurtz DM, Chabon JJ, Moding EJ, Hori SS, Gambhir SS, Alizadeh AA, Diehn M, Reiter JG. A mathematical model of ctDNA shedding predicts tumor detection size. *Sci Adv* 2020; **6** [PMID: 33310847 DOI: 10.1126/sciadv.abc4308]

6 **Bach S**, Sluiter NR, Beagan JJ, Mekke JM, Ket JCF, van Grieken NCT, Steenbergen RDM, Ylstra B, Kazemier G, Tuynman JB. Circulating Tumor DNA Analysis: Clinical Implications for Colorectal Cancer Patients. A Systematic Review. *JNCI Cancer Spectr* 2019; **3**: pkz042 [PMID: 32328554 DOI: 10.1093/jncics/pkz042]

7 **Noffsinger AE**. Serrated polyps and colorectal cancer: new pathway to malignancy. *Annu Rev Pathol* 2009; **4**: 343-364 [PMID: 19400693 DOI: 10.1146/annurev.pathol.4.110807.092317]

8 **Reinert T**, Henriksen TV, Christensen E, Sharma S, Salari R, Sethi H, Knudsen M, Nordentoft I, Wu HT, Tin AS, Heilskov Rasmussen M, Vang S, Shchegrova S, Frydendahl Boll Johansen A, Srinivasan R, Assaf Z, Balcioglu M, Olson A, Dashner S, Hafez D, Navarro S, Goel S, Rabinowitz M, Billings P, Sigurjonsson S, Dyrskjøt L, Swenerton R, Aleshin A, Laurberg S, Husted Madsen A, Kannerup AS, Stribolt K, Palmelund Krag S, Iversen LH, Gotschalck Sunesen K, Lin CJ, Zimmermann BG, Lindbjerg Andersen C. Analysis of Plasma Cell-Free DNA by Ultradeep Sequencing in Patients With Stages I to III Colorectal Cancer. *JAMA Oncol* 2019; **5**: 1124-1131 [PMID: 31070691 DOI: 10.1001/jamaoncol.2019.0528]

9 **Parikh AR**, Van Seventer EE, Siravegna G, Hartwig AV, Jaimovich A, He Y, Kanter K, Fish MG, Fosbenner KD, Miao B, Phillips S, Carmichael JH, Sharma N, Jarnagin J, Baiev I, Shah YS, Fetter IJ, Shahzade HA, Allen JN, Blaszkowsky LS, Clark JW, Dubois JS, Franses JW, Giantonio BJ, Goyal L, Klempner SJ, Nipp RD, Roeland EJ, Ryan DP, Weekes CD, Wo JY, Hong TS, Bordeianou L, Ferrone CR, Qadan M, Kunitake H, Berger D, Ricciardi R, Cusack JC, Raymond VM, Talasaz A, Boland GM, Corcoran RB. Minimal Residual Disease Detection using a Plasma-only Circulating Tumor DNA Assay in Patients with Colorectal Cancer. *Clin Cancer Res* 2021; **27**: 5586-5594 [PMID: 33926918 DOI: 10.1158/1078-0432.CCR-21-0410]

10 **Weisenberger DJ**. Characterizing DNA methylation alterations from The Cancer Genome Atlas. *J Clin Invest* 2014; **124**: 17-23 [PMID: 24382385 DOI: 10.1172/JCI69740]

11 **Vogelstein B**, Papadopoulos N, Velculescu VE, Zhou S, Diaz LA Jr, Kinzler KW. Cancer genome landscapes. *Science* 2013; **339**: 1546-1558 [PMID: 23539594 DOI: 10.1126/science.1235122]

12 **Markowitz SD**, Bertagnolli MM. Molecular origins of cancer: Molecular basis of colorectal cancer. *N Engl J Med* 2009; **361**: 2449-2460 [PMID: 20018966 DOI: 10.1056/NEJMra0804588]

13 **Beltrán-García J**, Osca-Verdegal R, Mena-Mollá S, García-Giménez JL. Epigenetic IVD Tests for Personalized Precision Medicine in Cancer. *Front Genet* 2019; **10**: 621 [PMID: 31316555 DOI: 10.3389/fgene.2019.00621]

14 **He Q**, Chen HY, Bai EQ, Luo YX, Fu RJ, He YS, Jiang J, Wang HQ. Development of a multiplex MethyLight assay for the detection of multigene methylation in human colorectal cancer. *Cancer Genet Cytogenet* 2010; **202**: 1-10 [PMID: 20804913 DOI: 10.1016/j.cancergencyto.2010.05.018]

15 **Rasmussen SL**, Krarup HB, Sunesen KG, Johansen MB, Stender MT, Pedersen IS, Madsen PH, Thorlacius-Ussing O. Hypermethylated DNA, a circulating biomarker for colorectal cancer detection. *PLoS One* 2017; **12**: e0180809 [PMID: 28700744 DOI: 10.1371/journal.pone.0180809]

16 **Ebert MP**, Model F, Mooney S, Hale K, Lograsso J, Tonnes-Priddy L, Hoffmann J, Csepregi A, Röcken C, Molnar B, Schulz HU, Malfertheiner P, Lofton-Day C. Aristaless-like homeobox-4 gene methylation is a potential marker for colorectal adenocarcinomas. *Gastroenterology* 2006; **131**: 1418-1430 [PMID: 17101318 DOI: 10.1053/j.gastro.2006.08.034]

17 **Herbst A**, Rahmig K, Stieber P, Philipp A, Jung A, Ofner A, Crispin A, Neumann J, Lamerz R, Kolligs FT. Methylation of NEUROG1 in serum is a sensitive marker for the detection of early colorectal cancer. *Am J Gastroenterol* 2011; **106**: 1110-1118 [PMID: 21326223 DOI: 10.1038/ajg.2011.6]

18 **Salehi R**, Atapour N, Vatandoust N, Farahani N, Ahangari F, Salehi AR. Methylation pattern of ALX4 gene promoter as a potential biomarker for blood-based early detection of colorectal cancer. *Adv Biomed Res* 2015; **4**: 252 [PMID: 26918234 DOI: 10.4103/2277-9175.170677]

19 **Erdem B**, Küçükyıldırım S, Sağlar E, Polat Z, Mergen H. Promoter hypermethylation of p16 and APC in gastrointestinal cancer patients. *Turk J Gastroenterol* 2014; **25**: 512-517 [PMID: 25417611 DOI: 10.5152/tjg.2014.4791]

20 **Pack SC**, Kim HR, Lim SW, Kim HY, Ko JY, Lee KS, Hwang D, Park SI, Kang H, Park SW, Hong GY, Hwang SM, Shin MG, Lee S. Usefulness of plasma epigenetic changes of five major genes involved in the pathogenesis of colorectal cancer. *Int J Colorectal Dis* 2013; **28**: 139-147 [PMID: 22990173 DOI: 10.1007/s00384-012-1566-8]

21 **Matthaios D**, Balgkouranidou I, Karayiannakis A, Bolanaki H, Xenidis N, Amarantidis K, Chelis L, Romanidis K, Chatzaki A, Lianidou E, Trypsianis G, Kakolyris S. Methylation status of the APC and RASSF1A promoter in cell-free circulating DNA and its prognostic role in patients with colorectal cancer. *Oncol Lett* 2016; **12**: 748-756 [PMID: 27347211 DOI: 10.3892/ol.2016.4649]

22 **Mitchell SM**, Ho T, Brown GS, Baker RT, Thomas ML, McEvoy A, Xu ZZ, Ross JP, Lockett TJ, Young GP, LaPointe LC, Pedersen SK, Molloy PL. Evaluation of Methylation Biomarkers for Detection of Circulating Tumor DNA and Application to Colorectal Cancer. *Genes (Basel)* 2016; **7** [PMID: 27983717 DOI: 10.3390/genes7120125]

23 **Shalaby SM**, El-Shal AS, Abdelaziz LA, Abd-Elbary E, Khairy MM. Promoter methylation and expression of DNA repair genes MGMT and ERCC1 in tissue and blood of rectal cancer patients. *Gene* 2018; **644**: 66-73 [PMID: 29080834 DOI: 10.1016/j.gene.2017.10.056]

24 **Nagai Y**, Sunami E, Yamamoto Y, Hata K, Okada S, Murono K, Yasuda K, Otani K, Nishikawa T, Tanaka T, Kiyomatsu T, Kawai K, Nozawa H, Ishihara S, Hoon DS, Watanabe T. LINE-1 hypomethylation status of circulating cell-free DNA in plasma as a biomarker for colorectal cancer. *Oncotarget* 2017; **8**: 11906-11916 [PMID: 28060757 DOI: 10.18632/oncotarget.14439]

25 **Pedersen SK**, Baker RT, McEvoy A, Murray DH, Thomas M, Molloy PL, Mitchell S, Lockett T, Young GP, LaPointe LC. A two-gene blood test for methylated DNA sensitive for colorectal cancer. *PLoS One* 2015; **10**: e0125041 [PMID: 25928810 DOI: 10.1371/journal.pone.0125041]

26 **Pedersen SK**, Symonds EL, Roy AC, Cornthwaite KJ, LaPointe LC, Young GP. Detection of methylated BCAT1 and IKZF1 after curative-intent treatment as a prognostic indicator for colorectal cancer recurrence. *Cancer Med* 2023; **12**: 1319-1329 [PMID: 35822405 DOI: 10.1002/cam4.5008]

27 **Symonds EL**, Pedersen SK, Baker RT, Murray DH, Gaur S, Cole SR, Gopalsamy G, Mangira D, LaPointe LC, Young GP. A Blood Test for Methylated BCAT1 and IKZF1 vs. a Fecal Immunochemical Test for Detection of Colorectal Neoplasia. *Clin Transl Gastroenterol* 2016; **7**: e137 [PMID: 26765125 DOI: 10.1038/ctg.2015.67]

28 **Young GP**, Pedersen SK, Mansfield S, Murray DH, Baker RT, Rabbitt P, Byrne S, Bambacas L, Hollington P, Symonds EL. A cross-sectional study comparing a blood test for methylated BCAT1 and IKZF1 tumor-derived DNA with CEA for detection of recurrent colorectal cancer. *Cancer Med* 2016; **5**: 2763-2772 [PMID: 27726312 DOI: 10.1002/cam4.868]

29 **Symonds EL**, Pedersen SK, Murray D, Byrne SE, Roy A, Karapetis C, Hollington P, Rabbitt P, Jones FS, LaPointe L, Segelov E, Young GP. Circulating epigenetic biomarkers for detection of recurrent colorectal cancer. *Cancer* 2020; **126**: 1460-1469 [PMID: 31909823 DOI: 10.1002/cncr.32695]

30 **Winter JM**, Sheehan-Hennessy L, Yao B, Pedersen SK, Wassie MM, Eaton M, Chong M, Young GP, Symonds EL. Detection of hypermethylated BCAT1 and IKZF1 DNA in blood and tissues of colorectal, breast and prostate cancer patients. *Cancer Biomark* 2022; **34**: 493-503 [PMID: 35253733 DOI: 10.3233/CBM-210399]

31 **Pedersen SK**, Musher BL, LaPointe LC, Tuck MK, Symonds EL, Loayza N, Young GP. Detection of recurrent colorectal cancer with high specificity using a reporting threshold for circulating tumor DNA methylated in BCAT1 and IKZF1. *Cancer* 2022; **128**: 1921-1928 [PMID: 35290664 DOI: 10.1002/cncr.34159]

32 **Pedersen SK**, Symonds EL, Baker RT, Murray DH, McEvoy A, Van Doorn SC, Mundt MW, Cole SR, Gopalsamy G, Mangira D, LaPointe LC, Dekker E, Young GP. Evaluation of an assay for methylated BCAT1 and IKZF1 in plasma for detection of colorectal neoplasia. *BMC Cancer* 2015; **15**: 654 [PMID: 26445409 DOI: 10.1186/s12885-015-1674-2]

33 **Musher BL**, Melson JE, Amato G, Chan D, Hill M, Khan I, Kochuparambil ST, Lyons SE, Orsini J Jr, Pedersen SK, Robb B, Saltzman J, Silinsky J, Gaur S, Tuck MK, LaPointe LC, Young GP. Evaluation of Circulating Tumor DNA for Methylated BCAT1 and IKZF1 to Detect Recurrence of Stage II/Stage III Colorectal Cancer (CRC). *Cancer Epidemiol Biomarkers Prev* 2020; **29**: 2702-2709 [PMID: 32958500 DOI: 10.1158/1055-9965.EPI-20-0574]

34 **Symonds EL**, Pedersen SK, Yeo B, Al Naji H, Byrne SE, Roy A, Young GP. Assessment of tumor burden and response to therapy in patients with colorectal cancer using a quantitative ctDNA test for methylated BCAT1/IKZF1. *Mol Oncol* 2022; **16**: 2031-2041 [PMID: 35000264 DOI: 10.1002/1878-0261.13178]

35 **Saluja H**, Young GP, Kholmurodova F, Symonds EL. Variables Associated with Detection of Methylated BCAT1 or IKZF1 in Blood from Patients Without Colonoscopically Evident Colorectal Cancer. *Cancer Epidemiol Biomarkers Prev* 2021; **30**: 774-781 [PMID: 33500319 DOI: 10.1158/1055-9965.EPI-20-1609]

36 **Murray DH**, Symonds EL, Young GP, Byrne S, Rabbitt P, Roy A, Cornthwaite K, Karapetis CS, Pedersen SK. Relationship between post-surgery detection of methylated circulating tumor DNA with risk of residual disease and recurrence-free survival. *J Cancer Res Clin Oncol* 2018; **144**: 1741-1750 [PMID: 29992492 DOI: 10.1007/s00432-018-2701-x]

37 **Ahlquist DA**. Multi-target stool DNA test: a new high bar for noninvasive screening. *Dig Dis Sci* 2015; **60**: 623-633 [PMID: 25492503 DOI:

10.1007/s10620-014-3451-5]

38 **Prince M**, Lester L, Chiniwala R, Berger B. Multitarget stool DNA tests increases colorectal cancer screening among previously noncompliant Medicare patients. *World J Gastroenterol* 2017; **23**: 464-471 [PMID: 28210082 DOI: 10.3748/wjg.v23.i3.464]

39 **Imperiale TF**, Ransohoff DF, Itzkowitz SH, Levin TR, Lavin P, Lidgard GP, Ahlquist DA, Berger BM. Multitarget stool DNA testing for colorectal-cancer screening. *N Engl J Med* 2014; **370**: 1287-1297 [PMID: 24645800 DOI: 10.1056/NEJMoa1311194]

40 **Levin TR**, Corley DA, Jensen CD, Schottinger JE, Quinn VP, Zauber AG, Lee JK, Zhao WK, Udaltsova N, Ghai NR, Lee AT, Quesenberry CP, Fireman BH, Doubeni CA. Effects of Organized Colorectal Cancer Screening on Cancer Incidence and Mortality in a Large Community-Based Population. *Gastroenterology* 2018; **155**: 1383-1391.e5 [PMID: 30031768 DOI: 10.1053/j.gastro.2018.07.017]

41 **Ladabaum U**, Mannalithara A. Comparative Effectiveness and Cost Effectiveness of a Multitarget Stool DNA Test to Screen for Colorectal Neoplasia. *Gastroenterology* 2016; **151**: 427-439.e6 [PMID: 27311556 DOI: 10.1053/j.gastro.2016.06.003]

42 **Hong SN**. Genetic and epigenetic alterations of colorectal cancer. *Intest Res* 2018; **16**: 327-337 [PMID: 30090031 DOI: 10.5217/ir.2018.16.3.327]

43 **Min L**, Chen J, Yu M, Liu D. Using Circulating Tumor DNA as a Novel Biomarker to Screen and Diagnose Colorectal Cancer: A Meta-Analysis. *J Clin Med* 2023; **12** [PMID: 36675337 DOI: 10.3390/jcm12020408]

44 **US Preventive Services Task Force**, Davidson KW, Barry MJ, Mangione CM, Cabana M, Caughey AB, Davis EM, Donahue KE, Doubeni CA, Krist AH, Kubik M, Li L, Ogedegbe G, Owens DK, Pbert L, Silverstein M, Stevermer J, Tseng CW, Wong JB. Screening for Colorectal Cancer: US Preventive Services Task Force Recommendation Statement. *JAMA* 2021; **325**: 1965-1977 [PMID: 34003218 DOI: 10.1001/jama.2021.6238]

45 **Cohen JD**, Li L, Wang Y, Thoburn C, Afsari B, Danilova L, Douville C, Javed AA, Wong F, Mattox A, Hruban RH, Wolfgang CL, Goggins MG, Dal Molin M, Wang TL, Roden R, Klein AP, Ptak J, Dobbyn L, Schaefer J, Silliman N, Popoli M, Vogelstein JT, Browne JD, Schoen RE, Brand RE, Tie J, Gibbs P, Wong HL, Mansfield AS, Jen J, Hanash SM, Falconi M, Allen PJ, Zhou S, Bettegowda C, Diaz LA Jr, Tomasetti C, Kinzler KW, Vogelstein B, Lennon AM, Papadopoulos N. Detection and localization of surgically resectable cancers with a multi-analyte blood test. *Science* 2018; **359**: 926-930 [PMID: 29348365 DOI: 10.1126/science.aar3247]

46 **Klein EA**, Richards D, Cohn A, Tummala M, Lapham R, Cosgrove D, Chung G, Clement J, Gao J, Hunkapiller N, Jamshidi A, Kurtzman KN, Seiden MV, Swanton C, Liu MC. Clinical validation of a targeted methylation-based multi-cancer early detection test using an independent validation set. *Ann Oncol* 2021; **32**: 1167-1177 [PMID: 34176681 DOI: 10.1016/j.annonc.2021.05.806]

47 **Tie J**, Wang Y, Cohen J, Li L, Hong W, Christie M, Wong HL, Kosmider S, Wong R, Thomson B, Choi J, Fox A, Field K, Burge M, Shannon J, Kotasek D, Tebbutt NC, Karapetis C, Underhill C, Haydon A, Schaeffer J, Ptak J, Tomasetti C, Papadopoulos N, Kinzler KW, Vogelstein B, Gibbs P. Circulating tumor DNA dynamics and recurrence risk in patients undergoing curative intent resection of colorectal cancer liver metastases: A prospective cohort study. *PLoS Med* 2021; **18**: e1003620 [PMID: 33939694 DOI: 10.1371/journal.pmed.1003620]

48 **Su P**, Lai W, Liu L, Zeng Y, Xu H, Lan Q, Chu Z. Mesenchymal and Phosphatase of Regenerating Liver-3 Status in Circulating Tumor Cells May Serve as a Crucial Prognostic Marker for Assessing Relapse or Metastasis in Postoperative Patients With Colorectal Cancer. *Clin Transl Gastroenterol* 2020; **11**: e00265 [PMID: 33512811 DOI: 10.14309/ctg.0000000000000265]

49 **Tie J**, Wang Y, Tomasetti C, Li L, Springer S, Kinde I, Silliman N, Tacey M, Wong HL, Christie M, Kosmider S, Skinner I, Wong R, Steel M, Tran B, Desai J, Jones I, Haydon A, Hayes T, Price TJ, Strausberg RL, Diaz LA Jr, Papadopoulos N, Kinzler KW, Vogelstein B, Gibbs P. Circulating tumor DNA analysis detects minimal residual disease and predicts recurrence in patients with stage II colon cancer. *Sci Transl Med* 2016; **8**: 346ra92 [PMID: 27384348 DOI: 10.1126/scitranslmed.aaf6219]

50 **Tie J**, Cohen JD, Wang Y, Christie M, Simons K, Lee M, Wong R, Kosmider S, Ananda S, McKendrick J, Lee B, Cho JH, Faragher I, Jones IT, Ptak J, Schaeffer MJ, Silliman N, Dobbyn L, Li L, Tomasetti C, Papadopoulos N, Kinzler KW, Vogelstein B, Gibbs P. Circulating Tumor DNA Analyses as Markers of Recurrence Risk and Benefit of Adjuvant Therapy for Stage III Colon Cancer. *JAMA Oncol* 2019; **5**: 1710-1717 [PMID: 31621801 DOI: 10.1001/jamaoncol.2019.3616]

World Journal of Gastroenterology

Submit a Manuscript: https://www.f6publishing.com

World J Gastroenterol 2023 September 28; 29(36): 5254-5267

DOI: 10.3748/wjg.v29.i36.5254

ISSN 1007-9327 (print) ISSN 2219-2840 (online)

SCIENTOMETRICS

Intestinal barrier in inflammatory bowel disease: A bibliometric and knowledge-map analysis

Feng Zhou, Nan-Zhen Wu, Yong Xie, Xiao-Jiang Zhou

Specialty type: Gastroenterology and hepatology

Provenance and peer review: Unsolicited article; Externally peer reviewed.

Peer-review model: Single blind

Peer-review report's scientific quality classification

Grade A (Excellent): A
Grade B (Very good): B, B
Grade C (Good): 0
Grade D (Fair): 0
Grade E (Poor): 0

P-Reviewer: Iizuka M, Japan; Wu H, United States

Received: July 20, 2023
Peer-review started: July 20, 2023
First decision: August 5, 2023
Revised: August 11, 2023
Accepted: September 8, 2023
Article in press: September 8, 2023
Published online: September 28, 2023

Feng Zhou, Yong Xie, Xiao-Jiang Zhou, Department of Gastroenterology, The First Affiliated Hospital of Nanchang University, Nanchang 330000, Jiangxi Province, China

Nan-Zhen Wu, Department of Gastrointestinal Surgery, Fengcheng People's Hospital, Fengcheng 331100, Jiangxi Province, China

Corresponding author: Xiao-Jiang Zhou, MD, PhD, Academic Research, Chief Physician, Professor, Department of Gastroenterology, The First Affiliated Hospital of Nanchang University, No. 17 Yongwaizheng Street, Nanchang 330000, Jiangxi Province, China.
yfyzxj1970@163.com

Abstract

BACKGROUND

Barrier surfaces composed of specialized epithelial cells separate the host body from the external environment, and are essential for maintaining proper intestinal physiologic and immune homeostasis.

AIM

To explore the development trends and research hotspots of intestinal barrier research in inflammatory bowel disease (IBD).

METHODS

The publications related to the intestinal barrier in IBD were obtained from the Web of Science Core Collection database. Bibliometric analysis and visualization were conducted using VOSviewer, CiteSpace and R software.

RESULTS

A total of 4482 articles published between 2002 and 2022 were identified. The United States is dominant in intestinal barrier research, whereas the University of Chicago is the most active institution. Jerrold from Harvard Medical School was the most productive authors with the most citations. The journals Inflammatory Bowel Disease and Gastroenterology have made significant contributions in this field. The keywords appearing at high frequency related to the intestinal barrier in IBD were detected, including nuclear factor kappa B, tumor necrosis factor-α, apoptosis, oxidative stress and probiotics. Among them, antioxidants, *Akkermansia muciniphila*, nanoparticles, short-chain fatty acids and extracellular vesicles have received growing interest in recent research.

CONCLUSION

The intestinal barrier field is developing rapidly with extensive cooperation. Targeting the gut microbiota and dietary metabolism to regulate the intestinal barrier has shown promising prospective applications and has generated broad interest. The importance of the intestinal barrier in IBD is gradually being fully recognized, providing a new therapeutic perspective for improving inflammation and prognosis.

Key Words: Intestinal barrier; Inflammatory bowel disease; Bibliometrics; Visualization; Hotspots

©The Author(s) 2023. Published by Baishideng Publishing Group Inc. All rights reserved.

Core Tip: The complete composition and function of the intestinal mucosal barrier are essential for maintaining proper intestinal physiological and immune homeostasis. The study evaluated the developmental trends and research hotspots of intestinal barrier research in inflammatory bowel disease (IBD) using bibliometric methods. The results showed that Intestinal barrier field is developing rapidly with extensive cooperation. Targeting the gut microbiota and dietary metabolism to regulate intestinal barrier shown promising prospective applications. This may provide guidance and new insights for further research into improving IBD by modulating the intestinal barrier.

Citation: Zhou F, Wu NZ, Xie Y, Zhou XJ. Intestinal barrier in inflammatory bowel disease: A bibliometric and knowledge-map analysis. *World J Gastroenterol* 2023; 29(36): 5254-5267
URL: https://www.wjgnet.com/1007-9327/full/v29/i36/5254.htm
DOI: https://dx.doi.org/10.3748/wjg.v29.i36.5254

INTRODUCTION

Specialized epithelial cells constitute barrier surfaces that separate host body from the external environment. The complete composition and function of intestinal mucosal barrier is essential for maintaining proper intestinal physiologic and immune homeostasis[1]. There is growing evidence that a deficit of in the intestinal barrier contributes to inflammation activation, especially in inflammatory bowel disease (IBD).

The intestinal barrier is mainly composed of intestinal epithelial cells, tight junctions and mucous layers. Genetic predisposition and environmental influences generally lead to disruption of the intestinal barrier in IBD, including tight junction changes, mucous layer defects, reduced antimicrobial peptide expression, and autophagy dysregulation[2,3]. This imbalance in the intestinal barrier allows external antigens to invade the body through damaged intestinal barrier, causing inappropriate immune activation. A series of studies have shown that mucosal healing and reestablishment of barrier integrity are significantly associated with clinical remission and improved patient outcomes[4-6]. Knowledge of the research status and focus hotpots of the current field is helpful to further explore the pathogenesis of IBD and search for potential therapeutic targets.

Bibliometrics has become an important methodology for researchers to actively accumulate knowledge and collect evidence. The bibliographic and visual analysis provides new angles to identify development trends and predict research prospects of this field by mathematics and statistics[7-9]. Therefore, this study aimed to explore the knowledge landscape of the intestinal barrier in IBD, hoping to provide guidance and new insights for further research in the field of IBD.

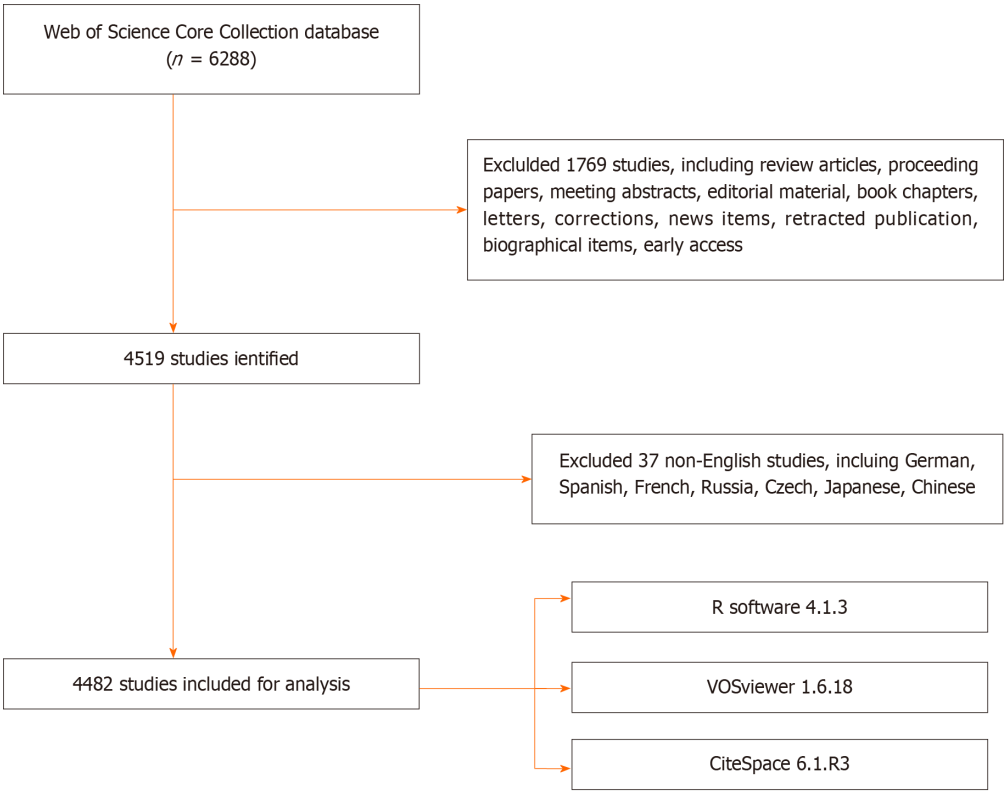
MATERIALS AND METHODS

Search strategies

Bibliometric and visualization analyses were conducted through the Web of Science Core Collection (WoSCC) database, which is one of the most widely used source for academic and bibliometric analysis. The WoS database covers a broad spectrum of academic disciplines and offers precise citation data, facilitating in-depth evaluation of topic development and trend evolution[10-12]. The search strategy was as follows: TS (Topic) = ("inflammatory bowel disease" OR "ulcerative colitis" OR "crohn's disease") AND TS = (intestin* OR gut OR bowel) AND TS = (barrier OR integrity OR permeability). The publication period was between 2001 and 2021 with the publication type limited to original articles written in English (Figure 1).

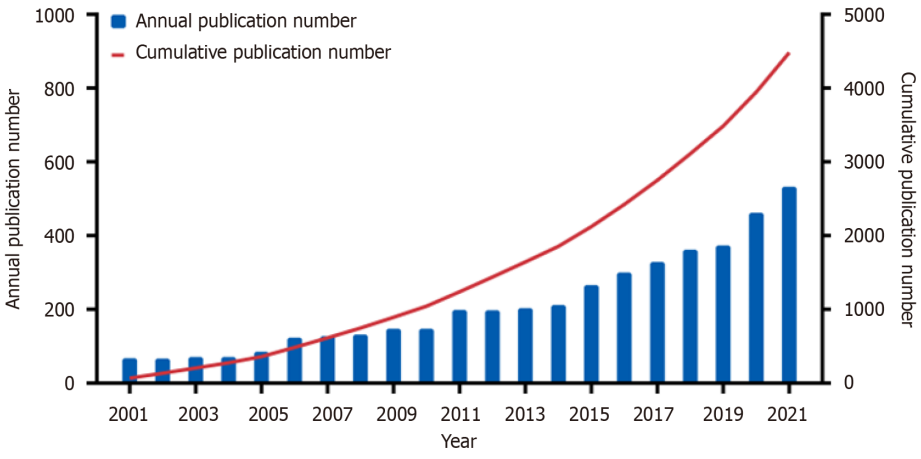
Data collection

Bibliometric indicators were extracted from selected publications to quantitatively evaluate the characteristics of the literature and its trends, including titles, publication years, authors, affiliations, countries/regions, journals, abstracts, keywords, citations and references. The H-index of scholars, impact factor (IF) and Journal Citation Reports division of journals were also obtained from the Web of Science. Inappropriate formulations of elements were modified and multiple phrases with the same meaning were merged into a single element. The author's significant publications were obtained from the *Reference Citation Analysis* (*RCA*, https://referencecitationanalysis.com/) database. RCA is an open citation



DOI: 10.3748/wjg.v29.i36.5254 **Copyright** ©The Author(s) 2023.

Figure 1 Flowchart of the literature screening.



DOI: 10.3748/wjg.v29.i36.5254 **Copyright** ©The Author(s) 2023.

Figure 2 Annual and cumulative growth trends of publications.

analysis database covering various fields and is owned by Baishideng Publishing Group Inc., situated in Pleasanton, CA 94566, United States[13-15]. Scientific data were searched and collected independently by two researchers to ensure the reliability of the results.

Bibliometric analysis

Bibliometric analysis is a quantitative research method that is widely employed to evaluate academic development in a specific field. VOSviewer, CiteSpace and R package were used for constructing the scientometric network and knowledge visualization. VOSviewer was adopted to conduct co-authorship analysis of authors and countries/regions, co-occurrence analysis of keywords and co-citation analysis of journals. Co-authorship and co-occurrence relationships were defined as the simultaneous occurrence of two items, while co-citation relationships referred to two items being cited simultaneously by a third item[16,17]. The network graph generated by VOSviewer displays the size of nodes based on the number of publications, and the connection represents the relationship between nodes. Closely related nodes were

Table 1 The top 10 countries/regions and institutions in the intestinal barrier field relevant to inflammatory bowel disease

Country	Centrality	Count	Citation	CPR	Institution	Centrality	Count	Citation	CPR
United States	0.30	1534	90667	59.1	University of Chicago	0.08	87	8288	95.3
China	0.26	1383	25867	18.7	University of Calgary	0.06	84	4051	48.2
Germany	0.18	533	37129	69.7	Emory University	0.09	83	6183	74.5
Canada	0.09	352	17335	49.2	Shanghai Jiao Tong University	0.07	74	2323	31.4
United Kingdom	0.28	336	23096	68.7	University of Toronto	0.05	68	3125	46.0
Italy	0.12	266	12121	45.6	Harvard Medical School	0.07	62	1883	30.4
Japan	0.10	244	8467	34.7	Chinese Academy of Sciences	0.04	62	1600	25.8
France	0.16	226	11080	49.0	University of California San Diego	0.07	59	6034	102.3
Sweden	0.02	178	11089	62.3	University of Alberta	0.06	58	3310	57.1
Netherlands	0.03	168	7693	45.8	McMaster University	0.05	58	4047	69.8

CPR: Citations per publication.

divided into clusters of the same color.

CiteSpace was used to calculate the node centrality and keyword burst trends. Centrality measures the quantity of all the shortest paths passing through a node in a network, with nodes having centrality greater than 0.1 identified as key nodes of significant importance. Burst detection was employed to identify keywords that experienced a sudden surge in their frequency of appearance during a specific time frame. The green line indicates the occurrence and development of keywords, while the red line represents the duration of the burst.

In addition, R software was used to develop the distribution of scientific productivity among authors and different countries/regions. Lotka's Law demonstrates the relationship between the frequency of scientific paper authorship and the number of publications, revealing an unbalanced distribution of author productivity.

RESULTS

Growth trend of publications

A total of 4482 publications related to the intestinal barrier in IBD were published between 2002-2022. There were only a small number of studies in the early stage, with less than 100 articles each year (Figure 2). During the middle period from 2006 to 2014, the number of publications showed a slow increase. Subsequently, annual publications have grown rapidly, with 53.8% of all publications occurring in the past two decades. Increasing attention to the intestinal barrier in IBD from researchers has driven further development of this field.

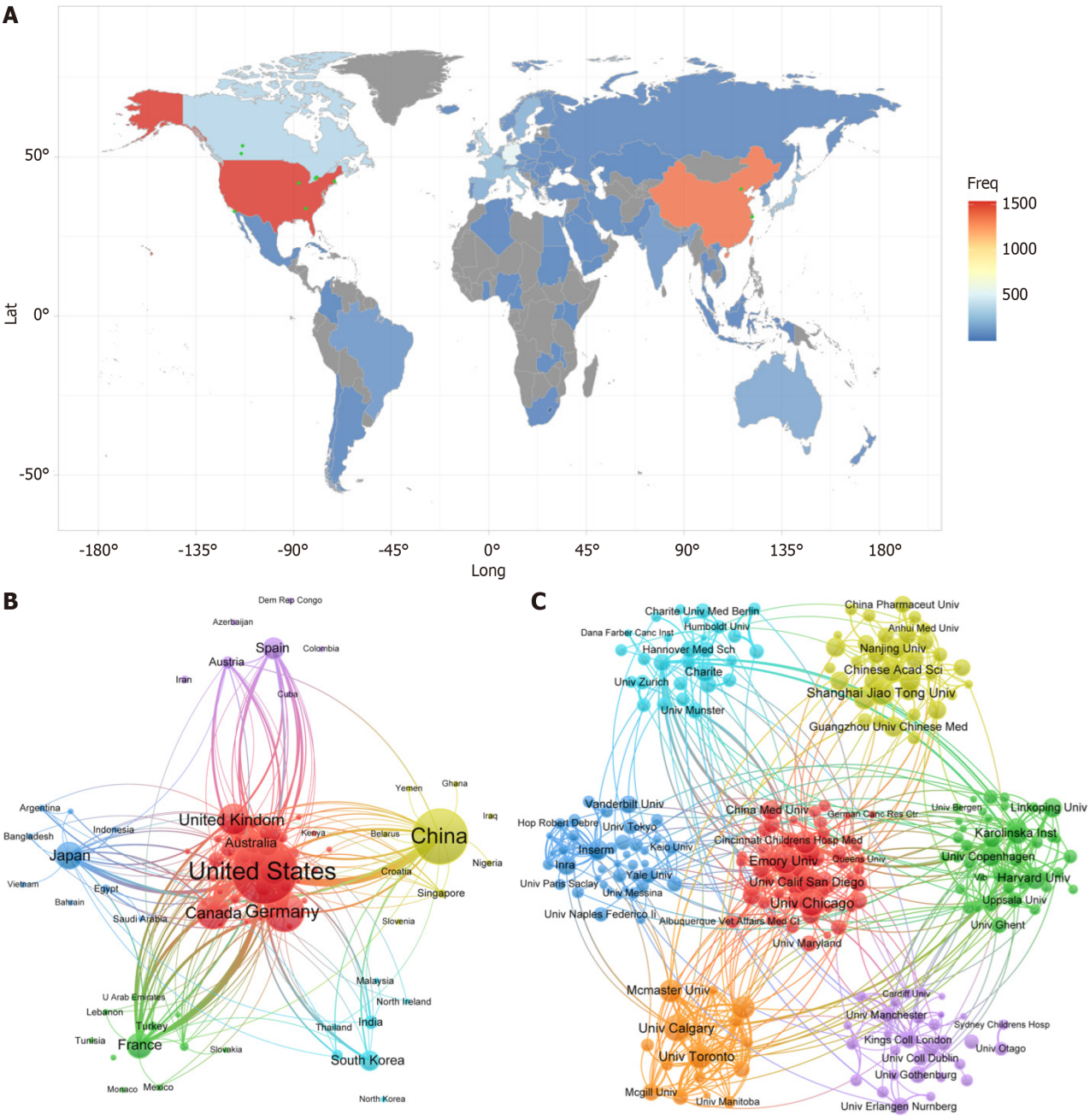
Countries/regions and institutions

Intestinal barrier research in IBD has been carried out at 4650 institutions from 89 countries/regions (Figure 3A). The United States is dominant in this field with the highest number of publications (n = 1426) and citations (n = 89615). The next most productive countries/regions were China and Germany (Table 1). In addition, Germany achieved the highest citations per publication at 73.2. These countries were divided into seven clusters to show the extensive cooperation between nodes (Figure 3B). Multiple nodes played a strong bridging role in the collaboration, most notably for the United States, the United Kingdom and China.

The University of Chicago conducted the largest number of studies (n = 8236), followed by Emory University (n = 6437) and the University of Calgary (n = 4064). Among them, the University of California San Diego exhibited the highest average citations of 102.3. Cooperation between institutions is more evident than that between countries, which enables further exploration and collaboration on the subject (Figure 3C).

Authors and cited authors

A total of 26245 authors have participated in the field of intestinal barrier research in IBD. Seventy-six percent of the authors contributed one article, whereas only 6.0% contributed more than 3 articles (Figure 4A). Turner[18] (n = 35), Söderholm *et al*[19-21] (n = 32) and Keshavarzian *et al*[22-25] (n = 28) were the most productive authors (Table 2). Although Turner[18] from Harvard Medical School also has the most citations (n = 3399), the nodes of these scholars were more dispersed across different clusters rather than being aggregated (Figure 4B). Close communication and similar research directions exist in the nodes of the same cluster. In addition, the clusters displaying different colors are not entirely independent and exhibit a relatively low level of connections.



DOI: 10.3748/wjg.v29.i36.5254 **Copyright** ©The Author(s) 2023.

Figure 3 Network visualization map of countries/regions and institutions. A: Geographic distribution map based on the total publications; B: Cooperation map of countries/regions; C: Cooperation map of institutions. The nodes in the network map represent countries/regions, and the node size is proportional to the number of publications. The thickness of the connecting line between nodes indicates the strength of the co-authorship relationships.

Journals and cited academic journals

There were 1045 journals involved in the publication of intestinal barrier research in IBD. IBDs contributed the most articles (n = 258), while Gastroenterology received the most citations (Table 3). The next most productive journals were PLoS One (n = 145) and the American Journal of Physiology-Gastrointestinal and Liver Physiology (n = 119). Articles published in established journals exhibit a higher average citation count, which is consistent with the IF of the journal.

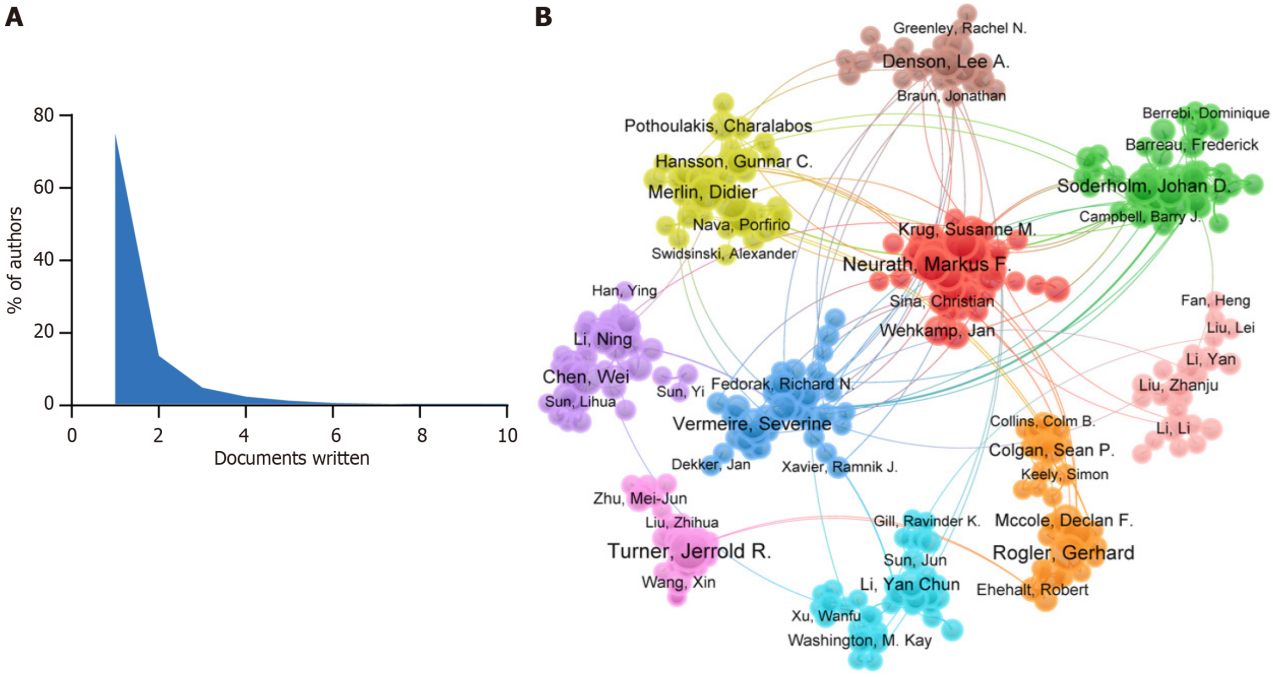
Among them, the majority of journals had an early initiation into this field (Figure 5A). Despite being relatively new to the field, Frontiers in Immunology, Food & Function and Scientific Reports demonstrated rapid development. As shown in Figure 5B, these journals were divided into five clusters based on the similarity of their themes. The higher the number of co-citations between two journals, the stronger is the link between the two nodes.

Keywords co-occurrence, clusters and bursts

Keywords were extracted for multidimensional analysis to determine the research hotspot and exploration direction in the specific field. The keywords appearing at high frequency related with intestinal barrier in IBD were identified, including molecules, pathological processes and treatments (Table 4). Nuclear factor kappa B (NF-κB) (n = 418), tumor

Table 2 The top 10 productive authors and cited authors in the intestinal barrier field relevant to inflammatory bowel disease

Ref.	Count	H-index	Ref.	Count	H-index
Turner[18]	35	78	Turner[18]	3399	78
Söderholm *et al*[19-21]	32	46	Neurath[35]	3257	87
Keshavarzian *et al*[22-25]	28	77	Ma *et al*[40]	2811	26
Rogler[59]	26	66	Hansson[60]	2785	71
Neurath[35]	25	87	Johansson *et al*[61]	2725	47
Schulzke *et al*[62]	23	58	Al-Sadi *et al*[63]	2489	21
Merlin *et al*[64]	23	62	Danese and Fiocchi[46]	2440	96
Ma *et al*[40]	22	26	Becker *et al*[44]	2319	61
Fromm *et al*[34]	21	66	Schulzke *et al*[62]	1852	58
Vermeire *et al*[51]	21	122	Nusrat *et al*[33]	1838	47



DOI: 10.3748/wjg.v29.i36.5254 **Copyright** ©The Author(s) 2023.

Figure 4 Network visualization map of authors. A: Scientific productivity of authors based on Lotka's Law; B: Cooperation map of authors. Each node represents a different author, and the connections between the nodes reflect the co-authorship relationships.

necrosis factor-α (TNF-α) (n = 329) and interferon (IFN)-γ (n = 173) were the most commonly implicated molecules. Apoptosis (n = 292), oxidative stress (n = 232) and metabolism (n = 88) were widely involved in research on the intestinal barrier. Regarding treatments, probiotics (n = 237), nanoparticles (n = 77) and antioxidant (n = 73) have attracted extensive attention.

The network map was classified into four clusters by co-occurrence analysis, which portrayed the fundamental knowledge structure of related research fields (Figure 6). Based on the closeness between nodes, the largest blue cluster contains keywords associated with clinical characteristics, such as risk, children and therapy. The red cluster was mainly composed of tight junctions, permeability and transport, which drew attention to barrier function in IBD. The yellow cluster mainly focused on the gut microbiota, including probiotics, metabolism and dysbiosis. The green cluster was involved in the regulation of inflammation, with keywords such as apoptosis, NF-κB and oxidative stress.

The visual keyword burst trend was constructed to show the major research interests in the intestinal barrier field (Figure 7). Early keyword bursts were mainly concentrated on intestinal barrier function and related inflammatory molecules, where intestinal permeability showed strong bursts. During the middle period, only a limited number of keywords exhibited an outbreak trend, such as autophagy, matrix metalloproteinase, and vitamin D. In contrast, targeted intestinal barrier therapy has been receiving growing interest from researchers, with a particular focus on antioxidants, *Akkermansia muciniphila*, nanoparticles, short-chain fatty acids, and extracellular vesicles as recent areas of research

Table 3 The top 10 journals and co-cited journals in the intestinal barrier field relevant to inflammatory bowel disease

Journal	Count	IF (2022)	JCR (2022)	Cited journal	Citation	IF (2022)	JCR (2022)
Inflammatory Bowel Diseases	258	7.290	Q1	*Gastroenterology*	14345	33.883	Q1
PLos One	145	3.752	Q2	*Gut*	12840	31.793	Q1
American Journal of Physiology-Gastrointestinal and Liver Physiology	119	4.871	Q1/Q2	*Inflammatory Bowel Diseases*	10188	69.504	Q1
Gastroenterology	118	33.883	Q1	*American Journal of Physiology-Gastrointestinal and Liver Physiology*	8962	4.871	Q1/Q2
World Journal of Gastroenterology	107	5.374	Q2	*Plos One*	6557	3.752	Q2
Gut	94	31.793	Q1	*Proceedings of the National Academy of Sciences of the United States of America*	6250	12.779	Q1
Frontiers in Immunology	86	8.786	Q1	*Nature*	4978	69.504	Q1
Food & Function	83	6.317	Q1	*World Journal of Gastroenterology*	4509	5.374	Q2
Digestive Diseases and Sciences	78	3.487	Q3	*Journal of Immunology*	4142	5.426	Q2
Scientific Reports	74	4.996	Q2	*Journal of Clinical Investigation*	3390	19.456	Q1

IF: Impact factor; JCR: Journal Citation Reports.

Table 4 The top 10 molecules, pathological processes and disease in the intestinal barrier field relevant to inflammatory bowel disease

Molecule	Count	Pathological process	Count	Treatment	Count
NF-kB	418	Apoptosis	292	Probiotic	237
TNF-α	329	Oxidative stress	232	Nanoparticles	77
IFN-gamma	173	Metabolism	88	Antioxidant	73
Mucin	100	Dysbiosis	83	Butyrate	70
Occludin	90	Autophagy	82	Infliximab	66
Nitric oxide	87	Infection	80	Polysaccharide	48
ZO-1	55	Bacterial translocation	68	Prebiotic	40
Claudin-2	54	Endoplasmic reticulum stress	65	Fecal microbiota transplantation	37
E-cadherin	51	Transport	59	Lactobacillus	32
Antimicrobial peptide	50	Absorption	50	Vitamin D	26

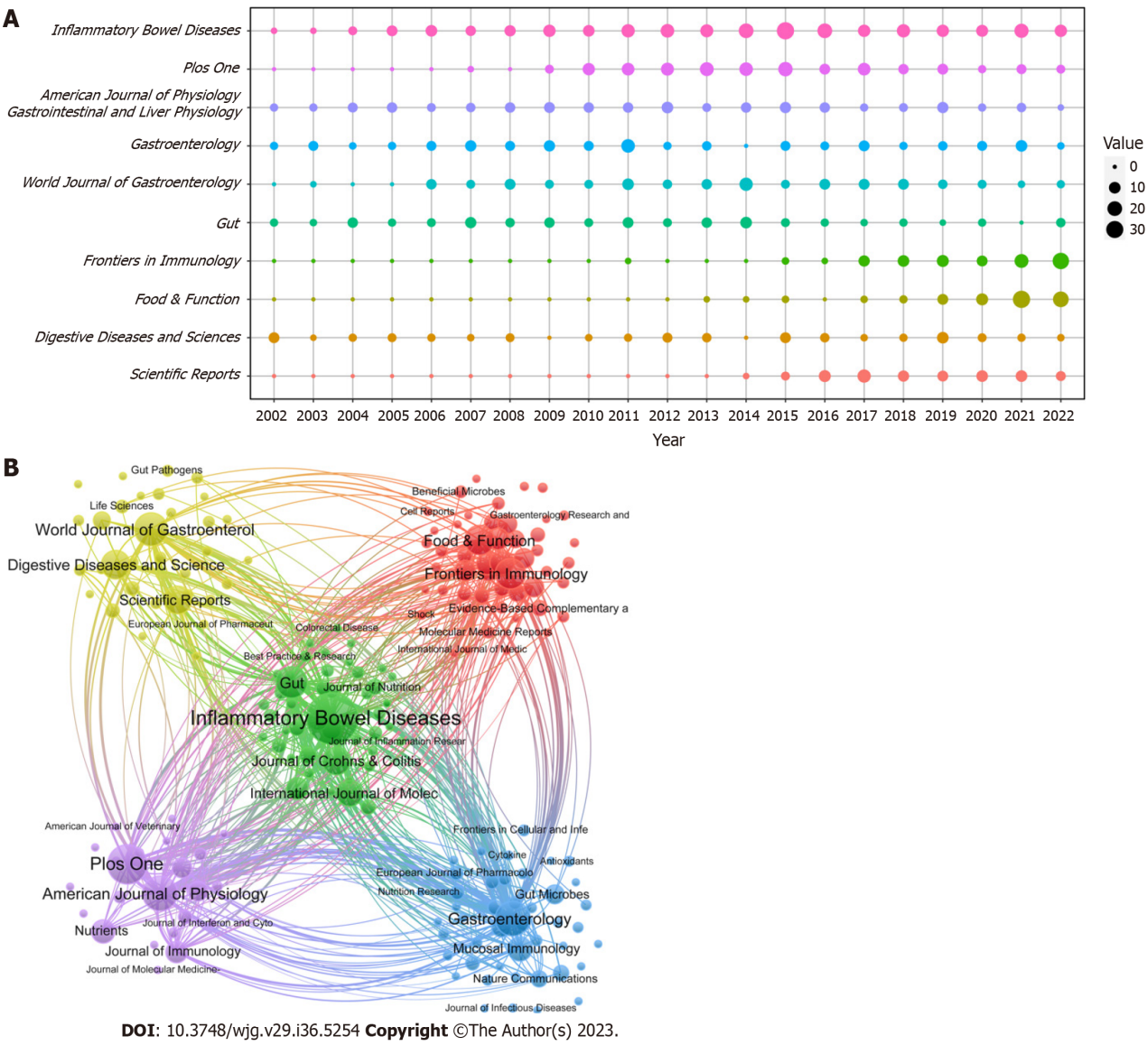
NF-kB: Nuclear factor kappa B; TNF-α: Tumor necrosis factor-α; IFN: Interferon.

attention.

DISCUSSION

The intestinal barrier refers to the physiological barrier composed of intestinal epithelial cells and mucous layers, which plays a crucial role in the onset and progression of IBD[26-28]. The disruption of the intestinal barrier in IBD patients is closely related to the severity of intestinal inflammation and immune response. The significant increase in the number of annual publications indicates a rapidly growing interest and recognition of the intestinal barrier field.

The United States occupied the dominant places in the intestinal barrier field with the highest number of publications and citations. Although China is developing rapidly in this field, it exhibits lower average citation rates. Other countries such as Germany and the United Kingdom have conducted more in-depth research and have the highest average citation rates. It is necessary to increase the depth and influence of research to address the imbalance between the number of publications and citations. Extensive collaboration is observed in countries such as the United States and the United Kingdom, however, institutional collaboration tends to show a trend of geographic alignment in terms of its distribution.



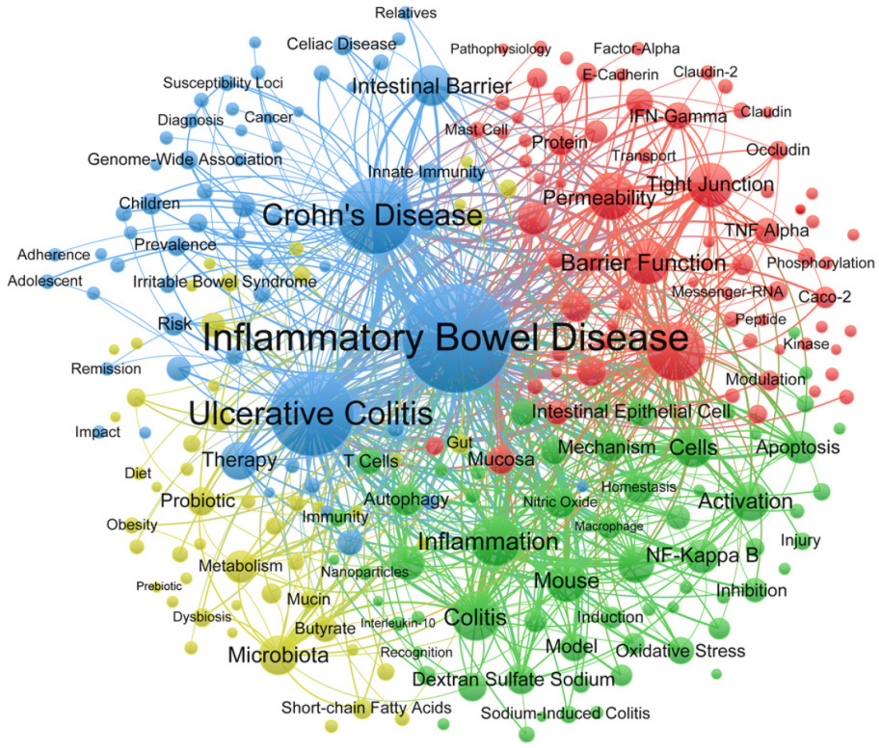
DOI: 10.3748/wjg.v29.i36.5254 **Copyright** ©The Author(s) 2023.

Figure 5 Network visualization map of authors. A: Annual number of publications for the top 10 journals; B: Cooperation map of Journals. The nodes in the graph represented journals, and the connections between the nodes reflect the co-authorship relationships.

The author's productivity is consistent with Lotka's Law. Turner[18] from Harvard Medical School has made significant contributions to intestinal barrier research. He and His group found that MLCK-dependent tight junction dysfunction can cause immune system activation and experimental colitis induction[18,29]. Söderholm *et al*[19-21] mainly investigated how chronic stress triggers intestinal inflammation, which is closely associated with mast cells. In contrast, Keshavarzian *et al*[22-25] focused on the connections between colitis and other systemic diseases, such as Alzheimer's disease. These findings demonstrate the feasibility of improving IBD through barrier repair, which could become a strong candidate for nonimmune suppressive methods to achieve or maintain disease remission.

Intestinal barrier research was initially published in gastroenterology journals, particularly in IBD. The exploration of the intestinal barrier has revealed extensive relationships between this field and several other research areas, such as physiology, biochemistry and immunology. As a result, there has been an increase in the number of interdisciplinary journals to better cater to the needs of this rapidly expanding field. Comprehensive journals have a wide readership and are more conducive to interdisciplinary collaboration.

The integrity of the intestinal barrier has been found to be closely associated with host defense and regulates the progression of IBD. Keywords in the field of the intestinal barrier mainly revolve around four aspects, encompassing clinical characteristics, barrier function, the gut microbiota, and inflammation regulation. Studies have reported that disruptions in the intestinal barrier lead to persistent intestinal symptoms and poor prognosis in IBD patients[30,31]. The increase in intestinal permeability is a marker of intestinal barrier dysfunction. The tight junction between intestinal epithelial cells are dynamic structures capable of swift adjustments, which determine the mucosal permeability[32-34]. The active transcellular transport of ions and water relies on the presence of intact tight junction barriers. Damage to epithelial cells triggers the release of inflammatory cytokines such as TNF and IFN-γ[35-37]. Stimulation of TNF downregulates the expression of tight junction proteins and changes their localization in colonic epithelial cells[38-40]. Insufficiency of interleukin (IL)-10, excessive production of nitric oxide, and impaired autophagy can also induce an



DOI: 10.3748/wjg.v29.i36.5254 **Copyright** ©The Author(s) 2023.

Figure 6 The network map of keywords in the intestinal barrier field relevant to inflammatory bowel disease. The network map displays the size of nodes based on the number of publications, and the connection represents the co-occurrence relationships between nodes. Closely related nodes were divided into clusters of the same color.

overactive immune system and enhance barrier loss[41-44], which in turn causes further leakage of luminal substances and amplifies local inflammation. The homeostasis of intestinal barrier can be affected either directly by inducing intracellular signaling pathways, or indirectly by the gut microbiota as an interacting partner to a greater extent[45,46]. Reduced intestinal community richness in patients with IBD leads to loss of intestinal homeostasis and inappropriate immune activation, which is characterized by a decrease in Firmicutes and proliferation of facultative anaerobic *Enterobacteriaceae* and adherent invasive *Escherichia coli*[47-49].

Recently, there has been widespread research interest in improving the intestinal barrier by targeting gut microbiota and dietary metabolism. Exogenous administration of probiotics can influence the composition and characteristics of the intestinal microbiota to exert intervention effects, typically in combination with prebiotics. The colonization of the beneficial bacterium *Akkermansia muciniphila* increased the number of goblet cells and upregulated the expression of genes encoding mucin[50]. Although fecal microbiota transplantation (FMT) has been shown to induce clinical remission of ulcerative colitis, the long-term effects of FMT as maintenance therapy have not been validated in IBD[51,52]. Microbial and dietary metabolites also demonstrate a regulatory influence on the intestinal barrier. Short-chain fatty acids produced by dietary fiber fermentation are the main energy source of colon cells, promoting the integrity of epithelial tight junctions and mucus secretion, which may be related to the activation of AMPK and STAT3[53,54]. The observed abnormality in bile acid metabolism may contribute to an enhanced epithelial inflammatory response. The reduction in secondary bile acids weakens the inhibition of IL-8 secretion[55] and the activation of TGR5 receptors in intestinal stem cells[56]. In addition, extracellular vesicles produced by host cells and microorganisms are also involved in cellular communication. Immune cells such as mast cells can secrete extracellular vesicles containing miR-223 to regulate intestinal permeability with downregulation of tight junction proteins[57]. Notably, extracellular vesicles themselves also represent a natural nanomaterial for drug delivery, that can improve the therapeutic effect and reduce systemic exposure in healthy tissues to promote remission of IBD[58].

The bibliometric analysis offers novel and objective insights into evolving intestinal barrier research hotspots and trends across multiple dimensions. Inevitably, there were several limitations to this study. The data were extracted from the WoSCC database, potentially omitting some information from other sources. Furthermore, while bibliometric methods based on natural language processing are susceptible to biases from subject categorization and citation behavior, a sufficient sample size helps ensure the accuracy of research findings to some extent.

CONCLUSION

In conclusion, the intestinal barrier field is developing rapidly with extensive cooperation. Targeting the gut microbiota and dietary metabolism to regulate the intestinal barrier shown promising prospective applications and has generated

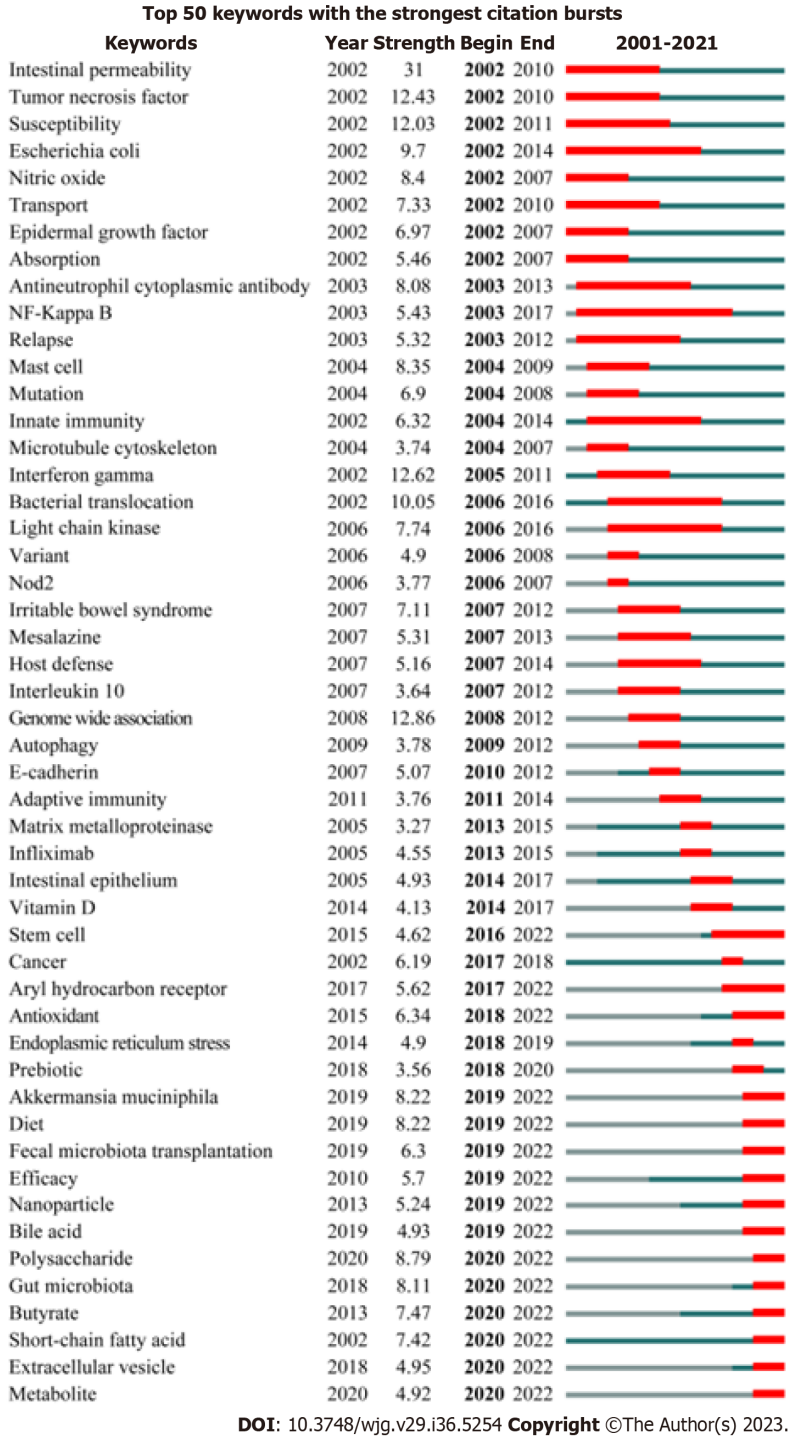


Figure 7 The top 50 keywords with the strongest citation bursts in the intestinal barrier field relevant to inflammatory bowel disease. The green line indicates the occurrence and development of keywords, while the red line represents the duration of the burst.

broad interest. The importance of the intestinal barrier in IBD is gradually being fully recognized, providing a new therapeutic perspective for improving inflammation.

ARTICLE HIGHLIGHTS

Research background

Barrier surfaces composed of specialized epithelial cells separate the host body from the external environment, and are essential for maintaining proper intestinal physiologic and immune homeostasis. There is growing evidence that the mucosal healing and reestablishment of barrier integrity are significantly associated with clinical remission and improved patient outcomes.

Research motivation

With the rapid expansion of research topics, it has become challenging for researchers to accumulate knowledge and actively collect evidence in specific field. The bibliographic and visual analysis provides new angles to identify development trends and predict research prospects of this field by mathematics and statistics.

Research objectives

The purpose of this study was to provide a comprehensive overview of the knowledge structure and research hotspots of intestinal barrier in inflammatory bowel disease (IBD).

Research methods

The publications related to intestinal barrier in IBD were obtained from the Web of Science Core Collection database. Bibliometric analysis and visualization were conducted using VOSviewer, CiteSpace and R software.

Research results

A comprehensive analysis of 4482 articles published between 2002 and 2022 has revealed significant insights in the realm of intestinal barrier research. Intestinal barrier research mainly focuses on four aspects, including clinical characteristics, barrier function, gut microbiota, and inflammation regulation. The keywords appearing at high frequency related with intestinal barrier in IBD were detected, including nuclear factor kappa B, tumor necrosis factor-α, apoptosis, oxidative stress and probiotics. Among them, antioxidants, Akkermansia muciniphila, nanoparticles, short-chain fatty acids and extracellular vesicles have received extensive interest in current research.

Research conclusions

The intestinal barrier field is developing rapidly with extensive cooperation. Targeting the gut microbiota and dietary metabolism to regulate intestinal barrier shown promising applied prospective and has generated broad interest.

Research perspectives

The importance of the intestinal barrier in IBD is gradually being fully recognized, providing a new therapeutic perspective for improving inflammation.

FOOTNOTES

Author contributions: Zhou XJ and Xie Y designed the study; Zhou F and Wu NZ conducted data extraction; Zhou F performed data analysis and drafted the manuscript; Zhou XJ and Xie Y interpreted the data and revised the manuscript; All authors have read and approve the final manuscript.

Supported by National Natural Science Foundation of China, No. 8186030315 and No. 81760105; and Natural Science Foundation of Jiangxi Province, China, No. 20202ACBL206009.

Conflict-of-interest statement: None of the authors have any conflicts of interest or financial ties to disclose.

PRISMA 2009 Checklist statement: The authors have read the PRISMA 2009 Checklist, and the manuscript was prepared and revised according to the PRISMA 2009 Checklist.

Open-Access: This article is an open-access article that was selected by an in-house editor and fully peer-reviewed by external reviewers. It is distributed in accordance with the Creative Commons Attribution NonCommercial (CC BY-NC 4.0) license, which permits others to distribute, remix, adapt, build upon this work non-commercially, and license their derivative works on different terms, provided the original work is properly cited and the use is non-commercial. See: https://creativecommons.org/Licenses/by-nc/4.0/

Country/Territory of origin: China

ORCID number: Yong Xie 0000-0002-5290-5579; Xiao-Jiang Zhou 0000-0003-4622-6040.

S-Editor: Fan JR
L-Editor: A
P-Editor: Zhao S

REFERENCES

1 **Villablanca EJ**, Selin K, Hedin CRH. Mechanisms of mucosal healing: treating inflammatory bowel disease without immunosuppression? *Nat Rev Gastroenterol Hepatol* 2022; **19**: 493-507 [PMID: 35440774 DOI: 10.1038/s41575-022-00604-y]

2 **Ramos GP**, Papadakis KA. Mechanisms of Disease: Inflammatory Bowel Diseases. *Mayo Clin Proc* 2019; **94**: 155-165 [PMID: 30611442 DOI: 10.1016/j.mayocp.2018.09.013]

3 **Chen Y**, Cui W, Li X, Yang H. Interaction Between Commensal Bacteria, Immune Response and the Intestinal Barrier in Inflammatory Bowel Disease. *Front Immunol* 2021; **12**: 761981 [PMID: 34858414 DOI: 10.3389/fimmu.2021.761981]

4 **Schoultz I**, Keita ÅV. Cellular and Molecular Therapeutic Targets in Inflammatory Bowel Disease-Focusing on Intestinal Barrier Function. *Cells* 2019; **8** [PMID: 30813280 DOI: 10.3390/cells8020193]

5 **Michaels M**, Madsen KL. Immunometabolism and microbial metabolites at the gut barrier: Lessons for therapeutic intervention in inflammatory bowel disease. *Mucosal Immunol* 2023; **16**: 72-85 [PMID: 36642380 DOI: 10.1016/j.mucimm.2022.11.001]

6 **Otte ML**, Lama Tamang R, Papapanagiotou J, Ahmad R, Dhawan P, Singh AB. Mucosal healing and inflammatory bowel disease: Therapeutic implications and new targets. *World J Gastroenterol* 2023; **29**: 1157-1172 [PMID: 36926666 DOI: 10.3748/wjg.v29.i7.1157]

7 **Agarwal A**, Durairajanayagam D, Tatagari S, Esteves SC, Harlev A, Henkel R, Roychoudhury S, Homa S, Puchalt NG, Ramasamy R, Majzoub A, Ly KD, Tvrda E, Assidi M, Kesari K, Sharma R, Banihani S, Ko E, Abu-Elmagd M, Gosalvez J, Bashiri A. Bibliometrics: tracking research impact by selecting the appropriate metrics. *Asian J Androl* 2016; **18**: 296-309 [PMID: 26806079 DOI: 10.4103/1008-682X.171582]

8 **Chen C**, Song M. Visualizing a field of research: A methodology of systematic scientometric reviews. *PLoS One* 2019; **14**: e0223994 [PMID: 31671124 DOI: 10.1371/journal.pone.0223994]

9 **Chen C**. Searching for intellectual turning points: progressive knowledge domain visualization. *Proc Natl Acad Sci U S A* 2004; **101** Suppl 1: 5303-5310 [PMID: 14724295 DOI: 10.1073/pnas.0307513100]

10 **Cheng K**, Guo Q, Shen Z, Yang W, Wang Y, Sun Z, Wu H. Bibliometric Analysis of Global Research on Cancer Photodynamic Therapy: Focus on Nano-Related Research. *Front Pharmacol* 2022; **13**: 927219 [PMID: 35784740 DOI: 10.3389/fphar.2022.927219]

11 **Cheng K**, Zhang H, Guo Q, Zhai P, Zhou Y, Yang W, Wang Y, Lu Y, Shen Z, Wu H. Emerging trends and research foci of oncolytic virotherapy for central nervous system tumors: A bibliometric study. *Front Immunol* 2022; **13**: 975695 [PMID: 36148235 DOI: 10.3389/fimmu.2022.975695]

12 **Yeung AWK**. Web of Science, PubMed and publishers for mislabelled review papers. *Curr Sci* 2019; **116**: 1909-1914 [DOI: 10.18520/cs/v116/i11/1909-1914]

13 **Wang JL**, Ma YJ, Ma L, Ma N, Guo DM, Ma LS. Baishideng's Reference Citation Analysis database announces the first Journal Article Influence Index of 101 core journals and a list of high-quality academic journals in gastroenterology and hepatology. *World J Gastroenterol* 2022; **28**: 5383-5394 [PMID: 36312837 DOI: 10.3748/wjg.v28.i37.5383]

14 **Wang JL**, Ma YJ, Ma L, Ma N, Guo DM, Ma LS. Baishideng's Reference Citation Analysis database announces the first Journal Article Influence Index of 104 core journals and a list of high-quality academic journals in orthopedics. *World J Orthop* 2022; **13**: 891-902 [PMID: 36312521 DOI: 10.5312/wjo.v13.i10.891]

15 **Wang JL**, Ma YJ, Ma L, Ma N, Guo DM, Ma LS. Baishideng's Reference Citation Analysis database announces the first Article Influence Index of multidisciplinary scholars. *World J Clin Cases* 2022; **10**: 10391-10398 [PMID: 36312463 DOI: 10.12998/wjcc.v10.i29.10391]

16 **Wu Z**, Cheng K, Shen Z, Lu Y, Wang H, Wang G, Wang Y, Yang W, Sun Z, Guo Q, Wu H. Mapping knowledge landscapes and emerging trends of sonodynamic therapy: A bibliometric and visualized study. *Front Pharmacol* 2022; **13**: 1048211 [PMID: 36699067 DOI: 10.3389/fphar.2022.1048211]

17 **Wu H**, Cheng K, Tong L, Wang Y, Yang W, Sun Z. Knowledge structure and emerging trends on osteonecrosis of the femoral head: a bibliometric and visualized study. *J Orthop Surg Res* 2022; **17**: 194 [PMID: 35346273 DOI: 10.1186/s13018-022-03068-7]

18 **Turner JR**. Molecular basis of epithelial barrier regulation: from basic mechanisms to clinical application. *Am J Pathol* 2006; **169**: 1901-1909 [PMID: 17148655 DOI: 10.2353/ajpath.2006.060681]

19 **Söderholm JD**, Yang PC, Ceponis P, Vohra A, Riddell R, Sherman PM, Perdue MH. Chronic stress induces mast cell-dependent bacterial adherence and initiates mucosal inflammation in rat intestine. *Gastroenterology* 2002; **123**: 1099-1108 [PMID: 12360472 DOI: 10.1053/gast.2002.36019]

20 **Söderholm JD**, Yates DA, Gareau MG, Yang PC, MacQueen G, Perdue MH. Neonatal maternal separation predisposes adult rats to colonic barrier dysfunction in response to mild stress. *Am J Physiol Gastrointest Liver Physiol* 2002; **283**: G1257-G1263 [PMID: 12388189 DOI: 10.1152/ajpgi.00314.2002]

21 **Söderholm JD**. Mast cells and mastocytosis. *Dig Dis* 2009; **27** Suppl 1: 129-136 [PMID: 20203509 DOI: 10.1159/000268133]

22 **Keshavarzian A**, Farhadi A, Forsyth CB, Rangan J, Jakate S, Shaikh M, Banan A, Fields JZ. Evidence that chronic alcohol exposure promotes intestinal oxidative stress, intestinal hyperpermeability and endotoxemia prior to development of alcoholic steatohepatitis in rats. *J Hepatol* 2009; **50**: 538-547 [PMID: 19155080 DOI: 10.1016/j.jhep.2008.10.028]

23 **Keshavarzian A**, Green SJ, Engen PA, Voigt RM, Naqib A, Forsyth CB, Mutlu E, Shannon KM. Colonic bacterial composition in Parkinson's disease. *Mov Disord* 2015; **30**: 1351-1360 [PMID: 26179554 DOI: 10.1002/mds.26307]

24 **Keshavarzian A**, Mutlu E, Guzman JP, Forsyth C, Banan A. Phosphodiesterase 4 inhibitors and inflammatory bowel disease: emerging therapies in inflammatory bowel disease. *Expert Opin Investig Drugs* 2007; **16**: 1489-1506 [PMID: 17714033 DOI: 10.1517/13543784.16.9.1489]

25 **Keshavarzian A**, Engen P, Bonvegna S, Cilia R. The gut microbiome in Parkinson's disease: A culprit or a bystander? *Prog Brain Res* 2020; **252**: 357-450 [PMID: 32247371 DOI: 10.1016/bs.pbr.2020.01.004]

26 **Mehandru S**, Colombel JF. The intestinal barrier, an arbitrator turned provocateur in IBD. *Nat Rev Gastroenterol Hepatol* 2021; **18**: 83-84 [PMID: 33318680 DOI: 10.1038/s41575-020-00399-w]

27 **Odenwald MA**, Turner JR. The intestinal epithelial barrier: a therapeutic target? *Nat Rev Gastroenterol Hepatol* 2017; **14**: 9-21 [PMID: 27848962 DOI: 10.1038/nrgastro.2016.169]

28 **Yu LC**. Microbiota dysbiosis and barrier dysfunction in inflammatory bowel disease and colorectal cancers: exploring a common ground hypothesis. *J Biomed Sci* 2018; **25**: 79 [PMID: 30413188 DOI: 10.1186/s12929-018-0483-8]

29 **Graham WV**, He W, Marchiando AM, Zha J, Singh G, Li HS, Biswas A, Ong MLDM, Jiang ZH, Choi W, Zuccola H, Wang Y, Griffith J, Wu J, Rosenberg HJ, Snapper SB, Ostrov D, Meredith SC, Miller LW, Turner JR. Intracellular MLCK1 diversion reverses barrier loss to restore mucosal homeostasis. *Nat Med* 2019; **25**: 690-700 [PMID: 30936544 DOI: 10.1038/s41591-019-0393-7]

30 **Chang J**, Leong RW, Wasinger VC, Ip M, Yang M, Phan TG. Impaired Intestinal Permeability Contributes to Ongoing Bowel Symptoms in Patients With Inflammatory Bowel Disease and Mucosal Healing. *Gastroenterology* 2017; **153**: 723-731.e1 [PMID: 28601482 DOI: 10.1053/j.gastro.2017.05.056]

31 **Turpin W**, Lee SH, Raygoza Garay JA, Madsen KL, Meddings JB, Bedrani L, Power N, Espin-Garcia O, Xu W, Smith MI, Griffiths AM, Moayyedi P, Turner D, Seidman EG, Steinhart AH, Marshall JK, Jacobson K, Mack D, Huynh H, Bernstein CN, Paterson AD; Crohn's and Colitis Canada Genetic Environmental Microbial Project Research Consortium; CCC GEM Project recruitment site directors include Maria

Abreu, Croitoru K. Increased Intestinal Permeability Is Associated With Later Development of Crohn's Disease. *Gastroenterology* 2020; **159**: 2092-2100.e5 [PMID: 32791132 DOI: 10.1053/j.gastro.2020.08.005]

32 **Slifer ZM**, Blikslager AT. The Integral Role of Tight Junction Proteins in the Repair of Injured Intestinal Epithelium. *Int J Mol Sci* 2020; **21** [PMID: 32024112 DOI: 10.3390/ijms21030972]

33 **Nusrat A**, Turner JR, Madara JL. Molecular physiology and pathophysiology of tight junctions. IV. Regulation of tight junctions by extracellular stimuli: nutrients, cytokines, and immune cells. *Am J Physiol Gastrointest Liver Physiol* 2000; **279**: G851-G857 [PMID: 11052980 DOI: 10.1152/ajpgi.2000.279.5.G851]

34 **Fromm M**, Krug SM, Zeissig S, Richter JF, Rosenthal R, Schulzke JD, Günzel D. High-resolution analysis of barrier function. *Ann N Y Acad Sci* 2009; **1165**: 74-81 [PMID: 19538291 DOI: 10.1111/j.1749-6632.2009.04047.x]

35 **Neurath MF**. Targeting cytokines in inflammatory bowel disease. *Sci Transl Med* 2022; **14**: eabq4473 [PMID: 36516267 DOI: 10.1126/scitranslmed.abq4473]

36 **Abraham C**, Abreu MT, Turner JR. Pattern Recognition Receptor Signaling and Cytokine Networks in Microbial Defenses and Regulation of Intestinal Barriers: Implications for Inflammatory Bowel Disease. *Gastroenterology* 2022; **162**: 1602-1616.e6 [PMID: 35149024 DOI: 10.1053/j.gastro.2021.12.288]

37 **Luissint AC**, Parkos CA, Nusrat A. Inflammation and the Intestinal Barrier: Leukocyte-Epithelial Cell Interactions, Cell Junction Remodeling, and Mucosal Repair. *Gastroenterology* 2016; **151**: 616-632 [PMID: 27436072 DOI: 10.1053/j.gastro.2016.07.008]

38 **Al-Sadi R**, Guo S, Ye D, Rawat M, Ma TY. TNF-α Modulation of Intestinal Tight Junction Permeability Is Mediated by NIK/IKK-α Axis Activation of the Canonical NF-κB Pathway. *Am J Pathol* 2016; **186**: 1151-1165 [PMID: 26948423 DOI: 10.1016/j.ajpath.2015.12.016]

39 **Yu M**, Wang Q, Ma Y, Li L, Yu K, Zhang Z, Chen G, Li X, Xiao W, Xu P, Yang H. Aryl Hydrocarbon Receptor Activation Modulates Intestinal Epithelial Barrier Function by Maintaining Tight Junction Integrity. *Int J Biol Sci* 2018; **14**: 69-77 [PMID: 29483826 DOI: 10.7150/ijbs.22259]

40 **Ma TY**, Iwamoto GK, Hoa NT, Akotia V, Pedram A, Boivin MA, Said HM. TNF-alpha-induced increase in intestinal epithelial tight junction permeability requires NF-kappa B activation. *Am J Physiol Gastrointest Liver Physiol* 2004; **286**: G367-G376 [PMID: 14766535 DOI: 10.1152/ajpgi.00173.2003]

41 **Koelink PJ**, Bloemendaal FM, Li B, Westera L, Vogels EWM, van Roest M, Gloudemans AK, van 't Wout AB, Korf H, Vermeire S, Te Velde AA, Ponsioen CY, D'Haens GR, Verbeek JS, Geiger TL, Wildenberg ME, van den Brink GR. Anti-TNF therapy in IBD exerts its therapeutic effect through macrophage IL-10 signalling. *Gut* 2020; **69**: 1053-1063 [PMID: 31506328 DOI: 10.1136/gutjnl-2019-318264]

42 **Cross RK**, Wilson KT. Nitric oxide in inflammatory bowel disease. *Inflamm Bowel Dis* 2003; **9**: 179-189 [PMID: 12792224 DOI: 10.1097/00054725-200305000-00006]

43 **Larabi A**, Barnich N, Nguyen HTT. New insights into the interplay between autophagy, gut microbiota and inflammatory responses in IBD. *Autophagy* 2020; **16**: 38-51 [PMID: 31286804 DOI: 10.1080/15548627.2019.1635384]

44 **Becker C**, Dornhoff H, Neufert C, Fantini MC, Wirtz S, Huebner S, Nikolaev A, Lehr HA, Murphy AJ, Valenzuela DM, Yancopoulos GD, Galle PR, Karow M, Neurath MF. Cutting edge: IL-23 cross-regulates IL-12 production in T cell-dependent experimental colitis. *J Immunol* 2006; **177**: 2760-2764 [PMID: 16920909 DOI: 10.4049/jimmunol.177.5.2760]

45 **Iyer N**, Corr SC. Gut Microbial Metabolite-Mediated Regulation of the Intestinal Barrier in the Pathogenesis of Inflammatory Bowel Disease. *Nutrients* 2021; **13** [PMID: 34959809 DOI: 10.3390/nu13124259]

46 **Danese S**, Fiocchi C. Etiopathogenesis of inflammatory bowel diseases. *World J Gastroenterol* 2006; **12**: 4807-4812 [PMID: 16937461 DOI: 10.3748/wjg.v12.i30.4807]

47 **Schirmer M**, Garner A, Vlamakis H, Xavier RJ. Microbial genes and pathways in inflammatory bowel disease. *Nat Rev Microbiol* 2019; **17**: 497-511 [PMID: 31249397 DOI: 10.1038/s41579-019-0213-6]

48 **Palmela C**, Chevarin C, Xu Z, Torres J, Sevrin G, Hirten R, Barnich N, Ng SC, Colombel JF. Adherent-invasive Escherichia coli in inflammatory bowel disease. *Gut* 2018; **67**: 574-587 [PMID: 29141957 DOI: 10.1136/gutjnl-2017-314903]

49 **Glassner KL**, Abraham BP, Quigley EMM. The microbiome and inflammatory bowel disease. *J Allergy Clin Immunol* 2020; **145**: 16-27 [PMID: 31910984 DOI: 10.1016/j.jaci.2019.11.003]

50 **Everard A**, Belzer C, Geurts L, Ouwerkerk JP, Druart C, Bindels LB, Guiot Y, Derrien M, Muccioli GG, Delzenne NM, de Vos WM, Cani PD. Cross-talk between Akkermansia muciniphila and intestinal epithelium controls diet-induced obesity. *Proc Natl Acad Sci U S A* 2013; **110**: 9066-9071 [PMID: 23671105 DOI: 10.1073/pnas.1219451110]

51 **Vermeire S**, Joossens M, Verbeke K, Wang J, Machiels K, Sabino J, Ferrante M, Van Assche G, Rutgeerts P, Raes J. Donor Species Richness Determines Faecal Microbiota Transplantation Success in Inflammatory Bowel Disease. *J Crohns Colitis* 2016; **10**: 387-394 [PMID: 26519463 DOI: 10.1093/ecco-jcc/jjv203]

52 **Tan P**, Li X, Shen J, Feng Q. Fecal Microbiota Transplantation for the Treatment of Inflammatory Bowel Disease: An Update. *Front Pharmacol* 2020; **11**: 574533 [PMID: 33041818 DOI: 10.3389/fphar.2020.574533]

53 **Miao W**, Wu X, Wang K, Wang W, Wang Y, Li Z, Liu J, Li L, Peng L. Sodium Butyrate Promotes Reassembly of Tight Junctions in Caco-2 Monolayers Involving Inhibition of MLCK/MLC2 Pathway and Phosphorylation of PKCβ2. *Int J Mol Sci* 2016; **17** [PMID: 27735862 DOI: 10.3390/ijms17101696]

54 **Zheng L**, Kelly CJ, Battista KD, Schaefer R, Lanis JM, Alexeev EE, Wang RX, Onyiah JC, Kominsky DJ, Colgan SP. Microbial-Derived Butyrate Promotes Epithelial Barrier Function through IL-10 Receptor-Dependent Repression of Claudin-2. *J Immunol* 2017; **199**: 2976-2984 [PMID: 28893958 DOI: 10.4049/jimmunol.1700105]

55 **Duboc H**, Rajca S, Rainteau D, Benarous D, Maubert MA, Quervain E, Thomas G, Barbu V, Humbert L, Despras G, Bridonneau C, Dumetz F, Grill JP, Masliah J, Beaugerie L, Cosnes J, Chazouillères O, Poupon R, Wolf C, Mallet JM, Langella P, Trugnan G, Sokol H, Seksik P. Connecting dysbiosis, bile-acid dysmetabolism and gut inflammation in inflammatory bowel diseases. *Gut* 2013; **62**: 531-539 [PMID: 22993202 DOI: 10.1136/gutjnl-2012-302578]

56 **Sorrentino G**, Perino A, Yildiz E, El Alam G, Bou Sleiman M, Gioiello A, Pellicciari R, Schoonjans K. Bile Acids Signal *via* TGR5 to Activate Intestinal Stem Cells and Epithelial Regeneration. *Gastroenterology* 2020; **159**: 956-968.e8 [PMID: 32485177 DOI: 10.1053/j.gastro.2020.05.067]

57 **Li M**, Zhao J, Cao M, Liu R, Chen G, Li S, Xie Y, Xie J, Cheng Y, Huang L, Su M, Xu Y, Zheng M, Zou K, Geng L, Xu W, Gong S. Mast cells-derived MiR-223 destroys intestinal barrier function by inhibition of CLDN8 expression in intestinal epithelial cells. *Biol Res* 2020; **53**: 12 [PMID: 32209121 DOI: 10.1186/s40659-020-00279-2]

58 **Li DF**, Yang MF, Xu J, Xu HM, Zhu MZ, Liang YJ, Zhang Y, Tian CM, Nie YQ, Shi RY, Wang LS, Yao J. Extracellular Vesicles: The Next

Generation Theranostic Nanomedicine for Inflammatory Bowel Disease. *Int J Nanomedicine* 2022; **17**: 3893-3911 [PMID: 36092245 DOI: 10.2147/IJN.S370784]

59 **Rogler G**. The effects of NOD2/CARD15 mutations on the function of the intestinal barrier. *J Crohns Colitis* 2007; **1**: 53-60 [PMID: 21172185 DOI: 10.1016/j.crohns.2007.08.008]

60 **Hansson GC**. Mucins and the Microbiome. *Annu Rev Biochem* 2020; **89**: 769-793 [PMID: 32243763 DOI: 10.1146/annurev-biochem-011520-105053]

61 **Johansson ME**, Gustafsson JK, Holmén-Larsson J, Jabbar KS, Xia L, Xu H, Ghishan FK, Carvalho FA, Gewirtz AT, Sjövall H, Hansson GC. Bacteria penetrate the normally impenetrable inner colon mucus layer in both murine colitis models and patients with ulcerative colitis. *Gut* 2014; **63**: 281-291 [PMID: 23426893 DOI: 10.1136/gutjnl-2012-303207]

62 **Schulzke JD**, Siegmund B, Günzel D. New insights into intestinal secretion. *Gut* 2014; **63**: 1371-1372 [PMID: 23868326 DOI: 10.1136/gutjnl-2013-305214]

63 **Al-Sadi R**, Dharmaprakash V, Nighot P, Guo S, Nighot M, Do T, Ma TY. Bifidobacterium bifidum Enhances the Intestinal Epithelial Tight Junction Barrier and Protects against Intestinal Inflammation by Targeting the Toll-like Receptor-2 Pathway in an NF-κB-Independent Manner. *Int J Mol Sci* 2021; **22** [PMID: 34360835 DOI: 10.3390/ijms22158070]

64 **Merlin D**, Sitaraman S, Liu X, Eastburn K, Sun J, Kucharzik T, Lewis B, Madara JL. CD98-mediated links between amino acid transport and beta 1 integrin distribution in polarized columnar epithelia. *J Biol Chem* 2001; **276**: 39282-39289 [PMID: 11507094 DOI: 10.1074/jbc.M105077200]



Published by **Baishideng Publishing Group Inc**
7041 Koll Center Parkway, Suite 160, Pleasanton, CA 94566, USA
Telephone: +1-925-3991568
E-mail: bpgoffice@wjgnet.com
Help Desk: https://www.f6publishing.com/helpdesk
https://www.wjgnet.com



© 2023 Baishideng Publishing Group Inc. All rights reserved.

ISSN 1007-9327 (print)
ISSN 2219-2840 (online)

World Journal of *Gastroenterology*

World J Gastroenterol 2023 October 7; 29(37): 5268-5360



Published by Baishideng Publishing Group Inc

World Journal of Gastroenterology

Contents

Weekly Volume 29 Number 37 October 7, 2023

REVIEW

5268 Acute pancreatitis: A review of diagnosis, severity prediction and prognosis assessment from imaging technology, scoring system and artificial intelligence

Hu JX, Zhao CF, Wang SL, Tu XY, Huang WB, Chen JN, Xie Y, Chen CR

5292 New insights into the pathogenesis of primary biliary cholangitis asymptomatic stage

Reshetnyak VI, Maev IV

MINIREVIEWS

5305 Sequence of events leading to primary biliary cholangitis

Lenci I, Carnì P, Milana M, Bicaj A, Signorello A, Baiocchi L

ORIGINAL ARTICLE

Case Control Study

5313 Leukocyte immunoglobulin-like receptor B2 overexpression as a promising therapeutic target and noninvasive screening biomarker for colorectal cancer

Wang QQ, Zhou L, Qin G, Tan C, Zhou YC, Yao SK

META-ANALYSIS

5327 Efficacy and safety of semaglutide in non-alcoholic fatty liver disease

Zhu K, Kakkar R, Chahal D, Yoshida EM, Hussaini T

SCIENTOMETRICS

5339 Global trends and hotspots of treatment for nonalcoholic fatty liver disease: A bibliometric and visualization analysis (2010-2023)

Dai JJ, Zhang YF, Zhang ZH

World Journal of Gastroenterology

Weekly Volume 29 Number 37 October 7, 2023

Contents

ABOUT COVER

Editorial Board of *World Journal of Gastroenterology*, Gregory Christodoulidis, MD, PhD, Senior Consultant in General Surgery, Department of General Surgery, University hospital of Larissa, Mezourlo 41110, Larissa, Greece. gregsurg09@gmail.com

AIMS AND SCOPE

The primary aim of *World Journal of Gastroenterology* (*WJG*, *World J Gastroenterol*) is to provide scholars and readers from various fields of gastroenterology and hepatology with a platform to publish high-quality basic and clinical research articles and communicate their research findings online. *WJG* mainly publishes articles reporting research results and findings obtained in the field of gastroenterology and hepatology and covering a wide range of topics including gastroenterology, hepatology, gastrointestinal endoscopy, gastrointestinal surgery, gastrointestinal oncology, and pediatric gastroenterology.

INDEXING/ABSTRACTING

The *WJG* is now abstracted and indexed in Science Citation Index Expanded (SCIE), MEDLINE, PubMed, PubMed Central, Scopus, Reference Citation Analysis, China Science and Technology Journal Database, and Superstar Journals Database. The 2023 edition of Journal Citation Reports® cites the 2022 impact factor (IF) for *WJG* as 4.3; Quartile category: Q2. The *WJG*'s CiteScore for 2021 is 8.3.

RESPONSIBLE EDITORS FOR THIS ISSUE

Production Editor: *Hua-Ge Yu*; **Production Department Director:** *Xiang Li*; **Editorial Office Director:** *Jia-Ru Fan.*

NAME OF JOURNAL

World Journal of Gastroenterology

ISSN

ISSN 1007-9327 (print) ISSN 2219-2840 (online)

LAUNCH DATE

October 1, 1995

FREQUENCY

Weekly

EDITORS-IN-CHIEF

Andrzej S Tarnawski

EXECUTIVE ASSOCIATE EDITORS-IN-CHIEF

Xian-Jun Yu (Pancreatic Oncology), Jian-Gao Fan (Chronic Liver Disease), Hou-Bao Liu (Biliary Tract Disease), Naohisa Yoshida (Gastrointestinal Endoscopy)

EDITORIAL BOARD MEMBERS

http://www.wjgnet.com/1007-9327/editorialboard.htm

PUBLICATION DATE

October 7, 2023

COPYRIGHT

© 2023 Baishideng Publishing Group Inc

PUBLISHING PARTNER

Shanghai Pancreatic Cancer Institute and Pancreatic Cancer Institute, Fudan University
Biliary Tract Disease Institute, Fudan University

INSTRUCTIONS TO AUTHORS

https://www.wjgnet.com/bpg/gerinfo/204

GUIDELINES FOR ETHICS DOCUMENTS

https://www.wjgnet.com/bpg/GerInfo/287

GUIDELINES FOR NON-NATIVE SPEAKERS OF ENGLISH

https://www.wjgnet.com/bpg/gerinfo/240

PUBLICATION ETHICS

https://www.wjgnet.com/bpg/GerInfo/288

PUBLICATION MISCONDUCT

https://www.wjgnet.com/bpg/gerinfo/208

POLICY OF CO-AUTHORS

https://www.wjgnet.com/bpg/GerInfo/310

ARTICLE PROCESSING CHARGE

https://www.wjgnet.com/bpg/gerinfo/242

STEPS FOR SUBMITTING MANUSCRIPTS

https://www.wjgnet.com/bpg/GerInfo/239

ONLINE SUBMISSION

https://www.f6publishing.com

PUBLISHING PARTNER's OFFICIAL WEBSITE

https://www.shca.org.cn
https://www.zs-hospital.sh.cn

© 2023 Baishideng Publishing Group Inc. All rights reserved. 7041 Koll Center Parkway, Suite 160, Pleasanton, CA 94566, USA

E-mail: bpgoffice@wjgnet.com https://www.wjgnet.com

World Journal of Gastroenterology

Submit a Manuscript: https://www.f6publishing.com

World J Gastroenterol 2023 October 7; 29(37): 5268-5291

DOI: 10.3748/wjg.v29.i37.5268

ISSN 1007-9327 (print) ISSN 2219-2840 (online)

REVIEW

Acute pancreatitis: A review of diagnosis, severity prediction and prognosis assessment from imaging technology, scoring system and artificial intelligence

Jian-Xiong Hu, Cheng-Fei Zhao, Shu-Ling Wang, Xiao-Yan Tu, Wei-Bin Huang, Jun-Nian Chen, Ying Xie, Cun-Rong Chen

Specialty type: Gastroenterology and hepatology

Provenance and peer review: Unsolicited article; Externally peer reviewed.

Peer-review model: Single blind

Peer-review report's scientific quality classification

Grade A (Excellent): A
Grade B (Very good): B, B
Grade C (Good): C
Grade D (Fair): 0
Grade E (Poor): 0

P-Reviewer: Akbulut S, Turkey; Kitamura K, Japan; Tsoulfas G, Greece

Received: May 1, 2023
Peer-review started: May 1, 2023
First decision: July 9, 2023
Revised: July 31, 2023
Accepted: September 14, 2023
Article in press: September 14, 2023
Published online: October 7, 2023

Jian-Xiong Hu, Intensive Care Unit, The Affiliated Hospital of Putian University, Putian 351100, Fujian Province, China

Cheng-Fei Zhao, School of Pharmacy and Medical Technology, Putian University, Putian 351100, Fujian Province, China

Cheng-Fei Zhao, Key Laboratory of Pharmaceutical Analysis and Laboratory Medicine, Putian University, Putian 351100, Fujian Province, China

Shu-Ling Wang, Xiao-Yan Tu, Wei-Bin Huang, Jun-Nian Chen, Cun-Rong Chen, Department of Critical Care Medicine, Fujian Medical University Union Hospital, Fuzhou 350001, Fujian Province, China

Ying Xie, School of Mechanical, Electrical and Information Engineering, Putian University, Putian 351100, Fujian Province, China

Corresponding author: Cun-Rong Chen, MD, PhD, Chief Physician, Doctor, Professor, Department of Critical Care Medicine, Fujian Medical University Union Hospital, No. 29 Xinquan Road, Gulou District, Fuzhou 350001, Fujian Province, China. chcr789@139.com

Abstract

Acute pancreatitis (AP) is a potentially life-threatening inflammatory disease of the pancreas, with clinical management determined by the severity of the disease. Diagnosis, severity prediction, and prognosis assessment of AP typically involve the use of imaging technologies, such as computed tomography, magnetic resonance imaging, and ultrasound, and scoring systems, including Ranson, Acute Physiology and Chronic Health Evaluation II, and Bedside Index for Severity in AP scores. Computed tomography is considered the gold standard imaging modality for AP due to its high sensitivity and specificity, while magnetic resonance imaging and ultrasound can provide additional information on biliary obstruction and vascular complications. Scoring systems utilize clinical and laboratory parameters to classify AP patients into mild, moderate, or severe categories, guiding treatment decisions, such as intensive care unit admission, early enteral feeding, and antibiotic use. Despite the central role of imaging technologies and scoring systems in AP management, these methods have

limitations in terms of accuracy, reproducibility, practicality and economics. Recent advancements of artificial intelligence (AI) provide new opportunities to enhance their performance by analyzing vast amounts of clinical and imaging data. AI algorithms can analyze large amounts of clinical and imaging data, identify scoring system patterns, and predict the clinical course of disease. AI-based models have shown promising results in predicting the severity and mortality of AP, but further validation and standardization are required before widespread clinical application. In addition, understanding the correlation between these three technologies will aid in developing new methods that can accurately, sensitively, and specifically be used in the diagnosis, severity prediction, and prognosis assessment of AP through complementary advantages.

Key Words: Acute pancreatitis; Imaging technology; Scoring system; Artificial intelligence; Severity prediction; Prognosis assessment

©The Author(s) 2023. Published by Baishideng Publishing Group Inc. All rights reserved.

Core Tip: In this review, we comprehensively analyzed, discussed, and summarized the latest progress in the diagnosis, severity prediction, and prognosis assessment of acute pancreatitis from the aspects of imaging technologies, scoring systems, and artificial intelligence. This review provided comprehensive guidance and suggestions with clinical value for the diagnosis and treatment of acute pancreatitis.

Citation: Hu JX, Zhao CF, Wang SL, Tu XY, Huang WB, Chen JN, Xie Y, Chen CR. Acute pancreatitis: A review of diagnosis, severity prediction and prognosis assessment from imaging technology, scoring system and artificial intelligence. *World J Gastroenterol* 2023; 29(37): 5268-5291
URL: https://www.wjgnet.com/1007-9327/full/v29/i37/5268.htm
DOI: https://dx.doi.org/10.3748/wjg.v29.i37.5268

INTRODUCTION

Acute pancreatitis (AP) is an inflammatory disorder resulting from intracellular activation and leakage of improper proteolytic enzymes, including active inflammation and pancreatic injury[1,2]. AP can result in nausea, vomiting, severe upper abdominal pain, abnormal release of pancreatic juice, or a systemic inflammatory response syndrome with fever, low blood pressure, and in some cases failure of one or more organs[2]. AP is one of the most common causes of hospitalization from gastrointestinal diseases, with a global incidence rate ranging from 13 to 45 cases per 100000 individuals annually[2,3]. Globally, the incidence of AP varies, with the North America and Western Pacific regions (as defined by the World Health Organization) experiencing the highest rates, surpassing 34 cases per 100000 individuals annually[4]. The incidence of AP has steadily increased over time in most countries of the Western world[5]. In the United States, the rate of AP-related hospitalization increased from 65.4 to 81.9 per 100000 adults from 2001 to 2014[6].

Classification of AP based on severity

AP, often worsened by comorbidities and demographic factors such as obesity, type 2 diabetes, cardiovascular and renal diseases, alcohol use disorder, and age over 45, is classified by severity into three categories: Mild AP (MAP), moderately severe AP (MSAP), and severe AP (SAP)[7]. SAP typically results in pancreatic necrosis, systematic inflammation, and multi-organ dysfunction and failure. Its mortality rate, ranging from 20%-40%, significantly surpasses those of MAP and MSAP[8]. The volume of extrapancreatic necrosis positively correlates with the complication rate of SAP, potentially serving as an indicator for predicting adverse outcomes in AP[9]. Early prediction of SAP with high mortality remains a challenge due to the limited accuracy of current predictive tools and the complex clinical features of SAP[10].

MSAP is characterized by transient organ failure, local complications, or exacerbation of comorbid disease, and SAP is defined by persistent organ failure lasting more than 48 h[11]. MSAP is linked to transient organ failure, while SAP involves persistent organ failure, often necessitating intensive care management[7]. The early identification of SAP is critical for the stratification and treatment of patients. Additionally, for SAP, it is crucial to avoid interventions that are either excessive and premature or insufficient and delayed; instead, a progressive intervention approach should be implemented at the appropriate time. The development of risk stratification tools that meet clinical needs and guide clinicians in terms of resource allocation, patient consultation and clinical audit, and the multidisciplinary approaches including evidence-based care are essential to achieve optimal clinical outcomes[12]. Therefore, early assessment of the etiology and severity of AP is essential for prompt treatment and close monitoring of severe patients.

Pathophysiology of AP

The pathophysiology of AP involves acinar cell damage, resulting in premature intrapancreatic activation of digestive proteases[13]. The pathological factors of AP includes calcium (Ca^{2+}) overload, mitochondrial dysfunction, impaired autophagy, endoplasmic reticulum stress, unfolded protein response, intraductal fluid stasis, genetic mutations (*e.g.*,

PRSS1 or *CTFR* gene), unsaturated fatty acids, and exosomes, which mainly lead to inappropriate activation of trypsinogen, infiltration of inflammatory cells, and destruction of secretory cells[14,15]. Ca^{2+} overload is a prevalent mechanism causing cell damage in the body[15]. Intracellular Ca^{2+} overload and mitochondrial dysfunction, induced by cholecystokinin, excessive alcohol consumption, and bile acids, have been identified as key steps in SAP development caused by acinar cell dysfunction[15]. Mitochondrial dysfunction hinders cell autophagy, leading to increased production of reactive oxygen species and cytokines, which exacerbates pancreatic cell damage[15]. Mitochondrial injury exacerbates endoplasmic reticulum stress and lysosomal damage, promoting the release and activation of cathepsinogen and trypsinogen, which results in cytoplasmic protein degradation and cell necrosis[15].

Uncertainty of serum amylase and lipase in diagnosing AP

Common biochemistry markers used in clinical practice include amylase and lipase in serum, but clinicians must be aware of the difference in half-life between the two[12]. In serum, amylase returns to normal limits within 3-5 d, and lipase returns to normal limits within 8-14 d[12]. Elevated serum amylase and/or lipase levels support the clinical suspicion of AP, and the measurement of amylase is more widely used[16]. However, about 40% of serum amylase is derived from the pancreas, with the rest primarily from the salivary glands[16]. Therefore, the elevation of serum total amylase is not specific for pancreatitis, and other intra-abdominal diseases should be considered[16]. For example, Gumaste *et al*[17] reported that the sensitivity of serum amylase in detecting AP was 72% and the specificity was 99%. In a prospective study including 500 patients with acute abdominal pain, the serum amylase assay had a sensitivity of 85% (with a cutoff value of 300 U/L for the upper reference limit) and a specificity of 91%[18]. Another prospective study showed that the sensitivity and specificity of total amylase in serum were 45% and 97%, respectively, at the calculated diagnostic threshold of 175 U/L[19].

In some non-pancreatic diseases, there is also a false elevation of serum amylase. For example, Hu *et al*[20] reported a case of hyperamylasemia with an average serum amylase value of 881 U/L, significantly exceeding the reference range of 10-220 U/L. In addition, elevated levels of amylase and lipase, while indicative, are not exclusive to AP and may result from conditions such as bowel obstruction, infarction, cholecystitis, or perforated ulcer[21]. However, the sensitivity of serum lipase ranges from 85%-100%; while some studies reported it was less sensitive than serum amylase, others contended it surpassed amylase in sensitivity[22].

Current clinical diagnosis of AP

The definition of severity in AP is pivotal for determining the therapeutic approach. Patients with MAP typically respond to conservative treatment, while those patients with necrotizing pancreatitis often experience organic dysfunction, necessitating intensive care and regular therapeutic interventions, with a more uncertain prognosis[1]. Currently, the clinical diagnosis of AP necessitates meeting two of the following three criteria: (1) Abdominal pain consistent with AP; (2) Serum levels of amylase or lipase exceeding three times the upper normal limit; and (3) Cross-sectional abdominal imaging findings consistent with AP[23]. It is important to note that two of these criteria alone may fail to identify one-quarter of AP patients and misdiagnose it in one-tenth of patients[23].

At present, there is still no single scoring system that can cover all the issues related to the management and evaluation of AP. AP continues to be one of the most intricate digestive disorders in terms of clinical course and outcome, and its inherent variability in each case makes it both challenging and captivating[24]. Meanwhile, to predict the severity and mortality of AP, clinicians evaluate clinical data, including assessing organ function, conducting laboratory tests and imaging, and utilizing severity-of-the-disease rating systems, such as Ranson, Acute Physiology and Chronic Health Evaluation (APACHE) II, Balthazar's computed tomography severity index (CTSI), modified Mortele's CTSI (MCTSI), Bedside Index for Severity in AP (BISAP), harmless AP score (HAPS), and the first artificial intelligence (AI) model, EASY-APP[25]. In addition to these, the latest imaging studies and clinical scoring systems for the early diagnosis, prognosis assessment, and severity prediction of AP have been extensively studied and reported. In this review, we provided a detailed discussion and analysis of the latest imaging examinations and some scoring systems applied in this field to afford more valuable guidance to more accurately diagnose, predict, and assess AP.

IMAGING TECHNOLOGY

Imaging technology still plays a fundamental role in the initial evaluation, identification of severe cases, prognosis prediction, and decision-making for the treatment and management of AP patients[1]. An accurate description of imaging findings is crucial in all diseases, particularly in diseases like AP where the appropriate therapy depends on precise diagnosis[26]. The manifestations of pancreatic diseases are variable, and imaging plays an important role in the diagnosis and treatment of pancreatic diseases[27]. Imaging evaluation is still essential to validate the clinical diagnosis, ascertain the etiology, exclude other causes of pain related to elevated levels of amylase and/or lipase, and assess the severity and extent of AP[1].

Imaging modalities for the pancreas encompass plain X-ray, ultrasonography (US), endoscopic ultrasound (EUS), endoscopic retrograde cholangiopancreaticography (ERCP), computed tomography (CT), magnetic resonance imaging (MRI), and magnetic resonance cholangiopancreatography[27]. US is usually considered to be the only appropriate modality in the early phase of AP with typical presentations and is used for the detection of gallstones. CT and MRI are suitable for patients in the early phase of AP with equivocal presentation[28]. In emergency situations, CT and US are the preferred imaging modalities due to their advantages of accessibility, speed, and lower cost[29]. Early detection of CT imaging may influence the diagnosis or treatment in up to 15% of AP patients presenting to the emergency department,

particularly in older patients with a history of pancreatitis and biliary interventions.

However, abdominal US may offer a more precise screening for biliary etiologies and provide a more informed direction for subsequent treatment[30]. Based on the fact that US often shows a regular pancreatic structure, the main role of transabdominal US in AP is to identify gallstones and/or choledocholithiasis, which is useful especially for the evaluation of biliary tract[31,32]. However, because of the presence and overlap of bowel gas, US is not possible to visualize pancreatic distal abnormality in the detection of AP[31,32].

In the late phase, typically 48-72 h post-presentation, CT and MRI serve as primary imaging modalities for AP patients, facilitating the assessment of etiology, complications, disease extent, interventions, and subsequent follow-up[28]. For example, as early as 2007, Stimac *et al*[33] reported that non-enhanced MRI was comparable to contrast-enhanced CT (CECT) in the early assessment of AP severity, with both methods demonstrating equal efficacy in predicting local and systemic complications of AP. MRI of the pancreas serves as both a problem-solving tool following CT or US evaluations and an initial imaging examination of choice. Furthermore, magnetic resonance cholangiopancreatography is valuable for detecting and evaluating pancreatic ductal anomalies, such as pancreas divisum and annular pancreas[34].

Abdominal CT

Radiological evaluation, especially by CT, plays a pivotal role in the definition of managing severe cases, particularly in characterizing local complications that impact the prognosis and dictate the therapeutic approach[1]. CT is an outstanding noninvasive diagnostic tool for discerning the origins of endocrine and exocrine pancreatic insufficiencies in most patients, and its significance has grown considerably in the diagnosis, treatment, and follow-up of AP patients[21,27,35]. CT is commonly used to assess the severity of the inflammatory process, ascertain the presence and extent of pancreatic necrosis, and identify local complications[21]. CT with high spatial resolution and rapid acquisition is the preferred for diagnosing AP and associated local complications[36]. Moreover, CT can clearly display the pancreas and adjacent tissues and is more precise than US in diagnosing and delineating the extent of pancreatic disease[36,37].

CECT plays a pivotal role in assessing the scope and progression of AP and stands as the primary imaging modality for initially pinpointing local complications. Typical cross-sectional imaging features encompass pancreatic enlargement, pancreatic edema, uneven density, peripancreatic fat stranding, and fluid collection[15,38]. For example, on CECT, SAP patients typically exhibit larger amounts of peripancreatic retroperitoneal fluid[39]. Approximately 7 d after the onset of AP, initial CECT plays a significant role in predicting infected pancreatic necrosis, which underscores the significance for clinicians to contemplate the initial imaging of the pancreas[40]. In addition, CT is regarded as the gold standard for imaging evaluation of AP due to its satisfactory effectiveness, outstanding timeliness, and widespread availability[1]. A lack of clinical response to appropriate conservative treatment within 48-72 h often indicates the necessity for a CT scan to verify the initial diagnosis, assess the severity of the onset, and identify any complications[41].

In 1990, Balthazar *et al*[42] developed CTSI by integrating observations of peripancreatic inflammation, phlegmon, and the degree of pancreatic necrosis evident in initial CT examinations. To enhance the accuracy in predicting the prognosis of AP patients, Mortele *et al*[43] simplified the assessment of fluid collections and the extent of pancreatic necrosis in CTSI and added features that reflect organ failure and extrapancreatic complications, leading to the development of MCTSI. MCTSI grading of AP was significantly associated with duration of hospitalization, requirements for intensive care unit (ICU), necessity for intervention, and organ failure[44]. CTSI is an easy-to-calculate and informative tool and is considered to be a good predictor of mortality and severity of AP[45].

A prospective study including 50 patients evaluated prognostic correlation and clinical outcome of AP using both Balthazar's CTSI and modified Mortele's CTSI[27]. In this study, Raghuwanshi *et al*[27] concluded that the scores derived from the modified Mortele's CTSI exhibited a more robust correlation for all outcome parameters in all the patients compared to Balthazar's index. They asserted that CECT served as an outstanding diagnostic tool for staging the inflammatory process, identifying pancreatic necrosis, detecting local complications, and grading the severity of AP[27]. Contrary to expectation, the 2012 Revised Atlanta Classification (RAC) demonstrated greater accuracy than the modified Mortele's and Balthazar's CTSI in assessing mortality and organ failure among AP patients[27].

In a study including 178 patients with interstitial edematous pancreatitis, Song *et al*[46] indicated that the initial CECT findings of peripancreatic fluid and heterogeneous enhancement in the pancreatic parenchyma could serve as useful predictors for the progression to necrotizing pancreatitis (NP) in patients initially diagnosed with interstitial edematous pancreatitis. However, it was disconcerting that the early CT scan might not conclusively diagnose NP[46]. Tasu *et al*[47] demonstrated that a pancreatic enhancement threshold of less than 30 UH on post-contrast CT images during the portal phase provided an accurate and consistent criterion for diagnosing NP. Badat *et al*[48] highlighted that using the 2012 RAC to categorize pancreatic and peripancreatic collections by CT yielded moderate interobserver agreement, underscoring the potential necessity to either devise a new semiology for characterizing peripancreatic collections by CT or to employ alternative imaging modalities like MRI for more precise analysis of collection contents.

However, the latest relevant clinical research also has encouraging results. A retrospective cross-sectional study enrolled 1924 patients experiencing their first episode of AP from three tertiary referral centers in three different prefecture-level cities of Sichuan Province in China and revealed a positive rate of 96.7% (1860/1924) for CT findings in AP diagnosis based on CECT[49]. Among these 1860 AP patients with affirmative CT results, MCTSI exhibited positive correlations with both the 2012 RAC and APACHE II, as evidenced by Spearman's rank correlation coefficients[49].

However, there remains a puzzling contradiction, *i.e.*, CTSI and MCTSI remain inconsistent in assessing the severity and clinical outcome of AP. Bollen *et al*[50] determined that there was no notable distinction between CTSI and MCTSI in assessing AP severity. Both CT indexes were more accurate for diagnosing AP severity and had a better correlation with the need for intervention and pancreatic infection in comparison with APACHE II. Sahu *et al*[51] concluded that both CTSI and MCTSI significantly correlated with the clinical outcome of AP and aligned well with RAC grading of severity. MCTSI demonstrated higher sensitivity albeit with lower specificity than CTSI in differentiating MAP from MSAP/SAP.

Alberti *et al*[52] determined that CT indexes surpassed APACHE II in assessing the severity in AP, with CTSI holding a slight advantage over MCTSI. Additionally, CTSI precisely predicted pancreatic infections and intervention requirements. Liao *et al*[53] indicated that both CTSI and MCTSI were significantly associated with clinical prognosis, offering higher accuracy in predicting infectious pancreatic necrosis but less precision in predicting persistent organ failure compared to APACHE II.

Another important factor affecting the effectiveness of CECT in assessing AP severity is the appropriate timing. Dachs *et al*[54] indicated that early abdominal CT did not offer benefits to afebrile patients experiencing their first episodes of AP. The evidence-based guidelines from the International Association of Pancreatology/American Pancreatic Association recommend that the optimal timing for an initial CT assessment should be between 72-96 h following the onset of symptoms[55]. However, until now, the appropriate point in time for when CECT should be performed to provide an accurate assessment for AP has not been well established in clinical practice. For example, in a retrospective study with 309 SAP patients, Huang *et al*[56] highlighted that the optimal timeframe for CECT evaluation of SAP-associated complications was between 72 h and 1 wk following the onset of SAP, particularly for SAP patients with infection. Their findings revealed that the severity of the disease and its alterations manifested as expanded areas of acute peripancreatic fluid collection (APFC) and increased exudation of pleural effusion within the first 1 wk of SAP onset[56]. However, the former showed a decrease after 4 wk or more, while the latter reduced after 2 wk or more[56].

Pocard and Soyer[57] found that a meticulous review of the current literature failed to offer compelling evidence regarding a specific interval between symptom onset and CT examination, suggesting that the pertinent matter of timely CT examination in AP patients remains inadequately addressed by the existing studies. In this regard, an important and outstanding issue is that the optimal time point for CECT to evaluate SAP patients' needs to be determined by larger multicenter clinical studies to improve accuracy of disease diagnosis, avoid unnecessary CECT tests, promote early intervention, and thus improve prognosis.

Chest CT

In AP patients, thoracic complications encompass pleural effusion, pulmonary consolidation, atelectasis, pulmonary embolism, cardiac tamponade, pericardial effusion, elevated diaphragms, mediastinal pseudocysts, and acute respiratory distress syndrome (ARDS), the first two of which are common in AP[58-65]. In AP patients, pleural effusion accounted for 50% on admission, and the emergence of pulmonary consolidation was associated with the onset of respiratory failure [66]. A retrospective study from three Chinese Acute Pancreatitis Centers showed that 232 out of 465 AP patients had positive pleural effusion, accounting for 49.9%[67]. In a study including 358 AP patients from seven European centers, more than half of the patients had pleural effusion, with the proportion of 54.4% (195/358), and pleural effusion appeared mostly bilaterally (150/195, 76.9%)[64]. It has been reported that AP patients with bilateral pleural effusion had a significantly worse 1-year survival[64]. Bilateral pleural effusion/pulmonary consolidation was suggestive of SAP to a certain extent, and it was considered that measurement of these two parameters has certain clinical value in assessing the severity and prognosis of AP[68]. Moreover, the early onset of pleural effusion highlights its clinical significance and predicts a poor prognosis in AP[63].

In a single center study with 309 AP patients, Peng *et al*[65] explored the predictive significance of semiquantitative pleural effusion and pulmonary consolidation in determining AP severity using chest CT. In AP patients without organ failure, the values of pleural effusion and pulmonary consolidation were 25.4 ± 23.5 mL and 0.8 ± 1.0 points, respectively, which were lower than the corresponding values of 137.4 ± 116.9 mL and 2.4 ± 1.2 points observed in AP patients with organ failure[65]. Simultaneously, the values of pleural effusion and pulmonary consolidation in AP patients without death were 39.0 ± 36.0 mL and 1.0 ± 1.1 points, respectively, and were lower than the corresponding values of 144.0 ± 140.3 mL and 3.0 ± 1.1 points in the patients who died[65]. In addition, in predicting SAP, the accuracy of pleural effusion volume (mean value of 41.7 ± 38.0 mL, range of 1-1079 mL) and pulmonary consolidation score (mean value of 1.0 ± 1.2 points, range of 0-5 points) was similar to that of CTSI, APACHE II, and BISAP. For predicting organ failure, both the parameters had the same accuracy with the three scores, suggesting that the two parameters could provide prediction of SAP occurrences and organ failure in the early stage[65]. More importantly, this clinical study may increase the application value of CT due to the important role of these two parameters in predicting AP severity.

In a retrospective study from three medical centers, Yan *et al*[67] reported that the mean volume of pleural effusion was 98.8 ± 113.2 mL in 465 AP patients. The volume of pleural effusion exhibited significant and robust correlations with C-reactive protein (CRP), duration of hospital stay, and scoring systems, such as Ranson, BISAP, Marshall, APACHE II, CTSI, and extrapancreatic inflammation on CT, and displayed considerable accuracy in predicting outcomes like severity, infection, mortality, procedural needs, ICU admission, and organ failure[67]. Luiken *et al*[64] categorized the volume of pleural effusion in 195 AP patients as low (48.2%, 94/195), moderate (30.3%, 59/195), and severe (21.5%, 42/195). Their findings suggest that the presence of bilateral and/or moderate to severe amounts of pleural effusion in the early phase of AP could independently predict SAP[64].

Thus, the volume of pleural effusion can serve as a dependable radiological biomarker to predict the severity and clinical outcome of AP. In addition, larger and more multi-center prospective studies need to be conducted to promote the clinical application of pleural effusion in the prediction of AP severity. So far, there is an absence of an established quantitative grading system for pleural effusion, meriting attention in forthcoming clinical research.

Practical problems in the application of CT in AP

Based on advances in predicting and diagnosing AP severity, CECT is considered the diagnostic criterion for assessing AP. However, there is a non-negligible situation where contrast CT is contraindicated in patients with renal dysfunction and in pregnant women, and it is not possible to replicate follow-up studies due to cost and radiation exposure. When uncomplicated AP is diagnosed both clinically and biochemically, CT is superfluous; minimizing its overuse will not only

curtail healthcare costs but also diminish radiation exposure to patients[69]. CT on admission to predict outcome does not appear to have an advantage compared with the simpler and more readily available clinical scoring systems. Therefore, CT on the day of admission to assess severity is not recommended[70]. Improvement measures aimed at curbing the overuse of early imaging in AP patients may diminish superfluous imaging, elevate quality of care, and curtail wastage [71].

In addition, CT possesses limitations in assessing the severity of AP, and it is difficult to distinguish between necrosis and local effusion in small nonenhanced areas of the pancreas[36]. Without pancreatic parenchymal necrosis, small organized peripancreatic fluid collections might be misconstrued as pseudocysts on CT, leading to an underestimation of extrapancreatic necrosis[72]. These disadvantages limit the use of CT in some situations, and there is a need to develop other methods that can be used for the diagnosis and prognosis evaluation of AP. Furthermore, it is recommended that future studies should incorporate reliable non-radiological and laboratory-based categorization tests to enhance the precision in determining and assessing the severity and prognosis of AP, thereby reducing morbidity and mortality associated with post-necrotic inflammation of the pancreas.

MRI

While CT remains the prevalent choice for evaluating AP, MRI has demonstrated greater sensitivity than CT in detecting AP[34]. MRI, a noninvasive technology boasting high tissue contrast and multiple acquisition sequences, effectively aids in determining the diagnosis, complications, and severity of AP[36]. When CT yields negative results but there remains a strong clinical suspicion of AP, fat-saturated turbo spin echo T2-weighted or diffusion-weighted imaging sequences can reveal nuanced pancreatic and/or peripancreatic inflammation[73]. MRI holds a pivotal role in the diagnosis of AP and is instrumental in assessing and characterizing extrapancreatic necrosis, inflammation, splenomegaly, and tissue involvement, including vascular, transverse-mesocolon, interfascial plane, and the gastrointestinal tract, in AP patients [21,74-80]. MRI can effectively capture the intra-abdominal inflammatory spread that affects mesenteric and omental fatty regions, indicative of a pathological manifestation of intra-abdominal fat edema combined with fat necrosis resulting from AP[81].

MRI is particularly beneficial for imaging of patients with iodine allergies or renal insufficiency, characterizing fluid collections and evaluating abnormalities or disconnections in the pancreatic duct[38]. As an alternate method for diagnosing AP, MRI shows great potential in clinical applications. MRI offers superior capabilities in diagnosing early extrapancreatic necrosis compared to CT, without the need for radiation, making it suitable for repeated follow-up assessments[74]. MRI more adeptly identifies the subtlest changes in AP and can delineate the constituents of mild extrapancreatic inflammatory effusions that might be missed on CT[82]. Fat-saturated T2-weighted MRI offers superior sensitivity in detecting fluid and no liquefied material in extrapancreatic collections compared to CT, while T1-weighted MRI is beneficial for identifying pancreatic or peripancreatic hemorrhage[74].

MRI in hemorrhage, tissue necrosis, and APFC

Compared to CT, MRI demonstrates superior sensitivity in visualizing hemorrhages, which appear hyperintense on T1-weighted imaging during the acute phase and maintain their signal intensity longer than on CT[36]. In necrotizing pancreatitis, MRI offers superior soft tissue contrast compared to CT and excels in visualizing hemorrhage and tissue necrosis[36]. A retrospective study including 539 AP patients demonstrated that MRI was superior in detecting hemorrhage associated with AP compared to CT, even when CT showed no signs of hemorrhage[83]. This study revealed that pancreatitis in AP patients with accompanying hemorrhage presented with greater clinical severity, increased susceptibility to organ failure, and prolonged hospital stays, suggesting that early hemorrhage detection on MRI could serve as a novel severity indicator in AP associated with poorer prognosis[83]. Additionally, due to its enhanced tissue resolution, MRI is poised as the frontline imaging technology for evaluating AP and its complications, notably the identification of hemorrhage[83].

In a retrospective analysis including 301 AP patients, MRI revealed that 24.9% exhibited at least one peripancreatic vascular abnormality related to AP, and the incidence of peripancreatic vascular involvement was notably more pronounced in necrotizing pancreatitis compared to edematous pancreatitis[76]. The common manifestations of early AP on MRI were splenic vein phlebitis and splenic artery involvement/arteritis, and 6.3% of the patients had splenic artery arteritis complicated with hemorrhage in the early phase of AP[76]. The findings highlighted the efficacy of MRI in delineating the progression of inflammatory processes and associated vascular changes during treatment, and early-stage vascular involvement detected by MRI might serve as a valuable indicator of AP severity[76].

Since the introduction of abdominal US and CT in the early 1970s, there has been a marked increase in the identification of acute fluid collections in AP, accompanied by a deeper insight into their natural progression and management [84]. APFC can complicate acute interstitial edematous pancreatitis, manifesting in approximately 30%-50% of such cases [85]. If APFC was associated with high BISAP (≥ 3) and CRP levels (≥ 150 mg/L) after 48 h from admission or with persistent clinical symptoms reflecting prolonged inflammatory responses, SAP patients with APFC were more likely to develop late complications[86]. Acute necrotic collections, observed exclusively in necrotic pancreatitis within the first 4 wk of onset, comprise varying amounts of fluid and necrosis, with the latter potentially affecting the pancreatic parenchyma or peripancreatic tissues, or both[36]. Pancreatic necrosis, characterized by focal, multifocal, or diffuse devitalized tissue within the pancreas, either superficial or deep, is deemed a critical imaging indicator of necrotizing pancreatitis[81]. A significant correlation exists between the presence of pancreatic necrosis and extrapancreatic fluid collections in relation to the clinical parameters, with an increase in extrapancreatic fluid collections aligning with the escalating severity of AP[87].

While CT has emerged as the primary noninvasive tool for identifying local complications in AP, it is difficult to distinguish between APFC and acute necrotic collection in the early phase due to its limited sensitivity in revealing the necrosis debris of peripancreatic tissue[81]. Given its exceptional resolution for soft tissues, MRI surpasses CT in delineating pancreatic/peripancreatic fluid collections, especially in quantifying solid debris and fat necrosis, serving as an alternative in cases with CT contraindications[88]. In MRI findings, hemorrhage in the pancreas and/or surrounding tissues may intermingle with necrosis of these same regions, manifesting as spotted, patchy, or extensive regions of hyperintensity on T1-weighted fat-suppressed images[81]. In a retrospective study including 70 AP patients, Zhou *et al* [74] discovered that MRI characteristics of extrapancreatic collections, particularly its extent and amount, could differentiate early extrapancreatic necrosis from peripancreatic fluid collections, suggesting the presence of extrapancreatic necrosis. Moreover, the more extensive the extrapancreatic collections and the broader the scope of extrapancreatic inflammation associated with hemorrhage in AP on MRI, the higher the likelihood of extrapancreatic necrosis[74].

In a meta-analysis encompassing a total of 566 patients, MRI demonstrated superior accuracy and sensitivity compared to CT for diagnosing AP[89]. While no study has yet shown that MRI can decrease AP mortality or enhance prognosis, MRI serves as an invaluable diagnostic tool for distinguishing individuals with suspected AP and is regarded as the premier imaging choice for the clinical diagnosis of AP[89]. Tang *et al*[82], utilizing MRI and APACHE II, devised a novel model through logistic regression for the early prediction of AP severity and ascertained that the combined model of extrapancreatic inflammation on MRI (EPIM) and APACHE II excelled in predicting AP severity, surpassing individual parameters. This retrospective analysis including 363 AP patients suggested that merging MRI and APACHE II for gauging AP severity was both viable and more accurate than other scoring mechanisms, potentially facilitating the creation of tailored treatment and management[82].

MRI severity index in AP

MRI severity index (MRSI), derived from CTSI, evaluates the severity of AP by integrating both peripancreatic inflammation and pancreatic parenchymal necrosis, achieving an effect comparable to that of CTSI in assessing AP severity[36]. In patients with pancreatitis, MRSI outperformed APACHE II in assessing local complications, while APACHE II demonstrated superiority in determining systemic complications[90]. MRSI is pivotal for the initial assessment, staging, and prognosis of AP. The clinical relevance of MRSI allows for prediction of the severity of AP based on initial MRI findings in the early phase, and it holds a significant correlation with APACHE II, incidence of systemic complication, duration of hospital stay, and overall clinical outcome[81]. In a retrospective study including 337 AP patients, Zhou *et al* [75] reported that in the early stages of AP EPIM based on MRI proved more effective in assessing the severity than extrapancreatic inflammation on CT . Moreover, the predictive accuracies of EPIM for SAP and organ failure aligned with those of APACHE II and BISAP, surpassing the accuracy of MRSI[75].

Overall, MRI serves as an excellent instrument for identifying and distinguishing prevalent local complications subsequent to AP. MRI offers diagnostic and prognostic value on par with CT, though it presents certain limitations in clinical practice. The scans necessitate greater cooperation of the patient, including prolonged immobility and apnea, and are more time-consuming and costly[1]. Additionally, MRI has the limitation of a restricted field of view, preventing it from capturing extensive regions of the chest and pelvic cavity simultaneously, as CT can[81].

US

Based on its quick, simple, repeatable, radiation-free, bedside applicability, US is the first-line imaging method in most medical centers to confirm the diagnosis of AP and exclude other causes of acute abdomen. In the early period, the advantages of US are its capability of assessing the gallbladder and biliary tract, detecting gallstones, and identifying bile duct dilatation[21]. However, US may show normal pancreas in MAP patients and is not able to differentiate the diagnosis between interstitial and necrotizing pancreatitis because of not allowing the assessment of parenchymal perfusion[21]. EUS can identify choledocholithiasis and hidden pancreatic tumors that remain elusive on CT or MRI in recurrent AP patients. EUS-guided fine needle puncture biopsy can distinguish focal pancreatitis from a pancreatic tumor, and color Doppler US can be used to assess vascular complications such as false arterial aneurysms or portal vein thrombosis[21]. Xu *et al*[91] reported that EUS outperformed CT in accurately categorizing symptomatic peripancreatic fluid collections and emerged as a preferred imaging modality for detecting solid necrotic debris. EUS-guided lumen-apposing metal stents for pancreatic fluid collections were feasible and effective with preferable technical and clinical success rates[92].

In a retrospective analysis with a cohort of 6069 patient, Froes *et al*[93] evaluated the impact of abdominal ultrasound (AUS) on the length of service (LOS) for patients hospitalized for AP who lacked radiographic evidence of AP on CT of the abdomen and pelvis (CTAP). Additionally, they further assessed how AUS affected the probability of subsequent interventions, such as ERCP or cholecystectomy[93]. In patients with AP, undergoing AUS within 48 h resulted in a reduced LOS by 1.099 d. Those who underwent AUS were 1.126 times more likely to proceed with subsequent ERCP compared to those who only had CTAP; patients receiving AUS after CTAP had a 2.711 times higher likelihood of undergoing subsequent cholecystectomy[93]. In this cohort of patients admitted for AP, conducting AUS within 48 h after negative CTAP correlated with reduced LOS. Moreover, patients undergoing AUS were not only more inclined to undergo ERCP but also exhibited a higher likelihood of undergoing cholecystectomy[93].

In a study with a total of 196 patients, Cai *et al*[94] investigated the diagnostic accuracy of US and contrast-enhanced US (CEUS) for AP. They demonstrated that CEUS outperformed US in diagnosing AP and SAP and produced excellent results in the staging of AP severity[94]. In this study, compared to results from CECT, the diagnostic rates for pancreatic swelling using US and CEUS were 121% (148/122) and 91% (111/122), respectively, while for peripancreatic fluid collection, they were 84.8% (151/178) and 96.6% (172/178), respectively[94]. The findings confirmed that CEUS surpassed US in specificity when visualizing pancreatic parenchyma edema, pancreatic border-capsula, collection fluid of

peripancreas, and peripancreatic necrosis. This discrepancy between US and CEUS might arise from the ability of CEUS to visualize vessels upon contrast agent injection[94]. The conclusion drawn was that CEUS serves as a trustworthy method for diagnosing and monitoring AP and SAP, potentially acting as an alternative to CECT[94].

Summary

The application of imaging in patients with AP is an essential aspect of modern clinical management. While there are challenges associated with their use, continuous research, technological advances, and thoughtful implementation of guidelines can optimize their role in patient management.

Imaging technologies for diagnosing and managing AP have made great strides, but inappropriate imaging tests can increase economic costs to the health system, subject patients to excess radiation, and elevate complication rates without benefiting patients. The choice of appropriate imaging modality for AP depends exactly on available time, technique, and clinical situation of the patient. Although imaging examination is widely used and carefully evaluated during the diagnosis process of AP, it remains unclear when imaging should be performed, especially given the economic costs associated with imaging and the financial burden on patients. In terms of the economic and financial implications of diagnostic imaging for AP patients, early imaging may not be advisable for those presenting with characteristic clinical symptoms and pronounced laboratory results. However, when clinical manifestations are unclear, early imaging examination is often used to identify suspected AP, discover potential etiology, diagnose complications, assess severity, implement risk stratification, and guide treatment. For AP patients, imaging technologies remain pivotal in initial diagnosis, identification of severe cases, assessment of prognosis, and decision of therapeutic management.

Radiomics is a data science technique that extracts a large number of quantitative features from medical images using advanced algorithms. These features capture subtle differences in the texture, shape, and intensity of image regions, which may be difficult for human observers to discern. By extracting these features, radiomics can transform images into high-dimensional data that can be analyzed and mined using machine learning and other data science techniques. This allows for more objective and precise diagnosis, treatment planning, and prognosis evaluation in AP. Therefore, radiomics has the potential to revolutionize medical imaging and improve patient outcomes in the 21st century.

CLINICAL SCORING SYSTEMS

Over the decades, many clinical scoring systems have been developed and applied, and their efficacy and accuracy have been compared. Clinically, an ideal scoring system should be responsive, simple, reliable, and universally applicable across diverse patient populations and geographical areas, maintaining its relevance over time. Such clinical scoring systems are imperative to predict complications, severity, mortality, and ICU admission requirements in AP patients[95]. Numerous "traditional" multifactorial clinical scoring systems, such as APACHE II, Ranson, Glasgow, Systemic Inflammatory Response Syndrome (SIRS), HAPS, Japanese Severity Score (JSS), CTSI, Sequential Organ Failure Assessment (SOFA) and BISAP, provide insights into systemic complications to some extent and possess commendable predictive capabilities for severity and mortality of disease[12,82,96-98]. Based on the 2012 RAC, these scoring systems primarily stratified the severity of AP into MAP, MSAP, and SAP[99].

Development of the original APACHE severity-of-illness classification system began in 1978, and APACHE II was derived from the results of a simplified effort based on the 12 most commonly used physiological measures included in the original APACHE system[100]. APACHE II, initially designed for intensive care applications, necessitates the aggregation of numerous parameters, some of which might not be pertinent to the prognosis in AP, while it overlooks key indicators such as pancreatic injury and significant regional complications[101,102].

Ranson was first used to assess the severity of AP in 1974 and has been used for nearly 50 years[103]. Ranson is relatively accurate in classifying the severity of AP patients; however, its limitation is the 48-h duration required for completion, thereby missing a crucial early therapeutic opportunity[102]. The main limitation of Glasgow, much like Ranson, is the need for a 48-h duration to finalize the calculation[96]. However, based on the local characteristics of CT examinations, CTSI mainly emphasizes local complications but falls short in representing the systemic inflammatory response[42]. In addition, for SAP, MCTSI demonstrates prognostic value for short-term mortality, while CTSI effectively predicts the necessity for intervention[104]. SOFA, similar to APACHE II, is a detailed scoring system that takes into account acute and chronic illness, signs, and laboratory values in patients[12].

Comparison of different scoring systems used in AP

For a more thorough understanding of the various attributes inherent in distinct scoring systems, we will embark on a comprehensive discussion and detailed analysis of the utilization of commonly employed clinical scoring systems within the context of AP in the following sections.

In two independent, prospectively enrolled cohorts [training (n = 256) and validation (n = 397)] of AP patients, Mounzer *et al*[105] compared the accuracy of the scoring systems including APACHE II, BISAP, Glasgow, HAPS, JSS, Ranson, and SIRS in predicting persistent organ failure. In this study, they discovered that these scoring systems exhibited moderate accuracy, with area under the curve (AUC) at admission ranging from 0.62-0.84 in the training cohort and 0.57-0.74 in the validation cohort. Notably, Glasgow emerged as the superior classifier at admission in both cohorts [105]. In a retrospective study including 161 patients, statistically significant cutoff values in predicting SAP were APACHE II ≥ 8, Ranson ≥ 3, BISAP ≥ 2, CTSI ≥ 3, and CRP_{24} ≥ 21.4 mg/dL. APACHE II had the highest accuracy in predicting SAP[106].

Confusingly, different studies have shown that these scoring systems vary widely in accuracy, sensitivity, and specificity for the desired purpose of prediction, as follows. In a retrospective study including 326 patients diagnosed with hyperlipidemic AP (HLAP), the predictive abilities of APACHE II, BISAP, Ranson, and MCTSI were compared for assessing MSAP and SAP, local complications, and HLAP mortality[107]. The results showed that the four scoring systems have their own advantages and characteristics. For example, Ranson lacked a distinct advantage in predicting severity and prognosis of HLAP compared to other three scoring systems. APACHE II excelled in predicting HLAP severity but fell short in predicting local complications. MCTSI demonstrated exceptional prowess in predicting local complications yet was less adept in predicting severity and mortality. BISAP offered a commendable accuracy in evaluating the severity, local complications, and mortality of HLAP, yet there remains room for refining its precision in future assessments[107].

In a prospective study including 50 AP patients, Kumar and Griwan[108] assessed the accuracy of APACHE II, BISAP, Ranson and MCTSI in predicting the severity of AP, referencing the 2012 RAC. In this study, MCTSI demonstrated the highest AUC values for predicting SAP (0.919), pancreatic necrosis (0.993), organ failure (0.893), and ICU admission (0.993); meanwhile, APACHE II ranked second in accuracy for predicting SAP (0.834) and organ failure (0.831)[108]. The findings indicated that APACHE II demonstrated a high sensitivity in predicting pancreatic necrosis (93.33%), organ failure (92.86%), and ICU admission (92.31%) while also maintaining a substantial negative predictive value (NPV) for predicting pancreatic necrosis (96.15%), organ failure (96.15%), and ICU admission (95.83%)[108].

Keskin *et al*[109] retrospectively investigated 690 patients who had been admitted due to AP by five scoring systems including HAPS, Ranson, BISAP, Glasgow, and JSS. In this study, NPV of each score was notably superior to their respective positive predictive value (PPV)[109]. Of the five scoring systems, JSS exhibited the highest value of AUC across all endpoints (0.80 for in-hospital major adverse events, 0.94 for in-hospital mortality, 0.91 for 30-d mortality); nevertheless, none of the five scoring systems effectively predicted 30-d readmission[109].

Li *et al*[110] conducted a retrospective assessment of four scoring systems (Ranson, BISAP, Glasgow, and APACHE II) to predict AP outcomes in 918 patients, categorizing them into two age groups: The elderly (≥ 60-years-old) and the younger (< 60-years-old). In this study, they drew several following conclusions: BISAP effectively predicted the severity, pancreatic necrosis, and mortality in elderly AP patients; APACHE II was more suitable for assessing severity in younger patients; both Ranson and Glasgow were generally applicable for evaluating most AP patients; and Ranson demonstrated heightened efficacy in assessing severity among younger patients[110]. In this study, the criterion of predicting SAP was different between the elderly and the younger (the elderly: Ranson ≥ 4, Glasgow ≥ 3, APACHE II ≥ 9, BISAP ≥ 3; the younger: Ranson ≥ 3, Glasgow ≥ 2, APACHE II ≥ 8, BISAP ≥ 2), suggesting that the scoring cutoffs for the elderly were consistently one point higher than those for the younger[110]. The variation in the cutoff value for predicting SAP enhanced the specificity of the four scoring systems albeit with a marginal reduction in their sensitivity to SAP[110].

In a retrospective analysis including 653 AP patients, Teng *et al*[111] investigated and compared the characteristics of six scores in predicting SAP, ICU admission, and mortality, including Ranson, Glasgow, APACHE II, BISAP, HAPS, and SOFA. In predicting SAP, SOFA exhibited the lowest sensitivity at 13.6% but boasted the highest specificity at 99.7%. Conversely, Ranson maintained the highest sensitivity at 92.6% but had one of the lowest specificities at 51.9%, with only HAPS registering a slightly lower specificity at 49.7%[111]. In predicting ICU admission, APACHE II and Ranson displayed a sensitivity at 100.0%, BISAP demonstrated the lowest sensitivity at 25.0% and a specificity at 93.4%, and SOFA demonstrated the highest specificity at 99.2%[111]. In predicting mortality, APACHE II and Ranson displayed a sensitivity at 100.0%, BISAP showcased the lowest sensitivity at 25.0%, and SOFA had the highest specificity at 98.9%, similar to ICU admission[111]. All scores had high and comparable NPVs in the prediction of SAP, ICU admission, and mortality in AP patients[111]. In this study, they concluded that SOFA and 48-h Ranson outperformed other clinical scorings (Glasgow, APACHE II, BISAP, HAPS) in predicting severity, ICU admission, and mortality[111].

In a prospective observational study including 164 patients, Venkatesh *et al*[112] reported that, based on receiver operating characteristic (ROC) curves, Ranson at admission demonstrated superior diagnostic accuracy in predicting severity, organ failure, and mortality and outperformed the other three scores (APACHE II, BISAP, and modified Glasgow) in predicting AP severity. In addition, this study revealed that while BISAP might be calculated within 24 h of admission, both APACHE II and modified Glasgow demonstrated superior diagnostic accuracy, with APACHE II exhibiting the strongest association with mortality in SAP patients[112].

Asfuroğlu Kalkan *et al*[113] retrospectively analyzed 1150 AP patients, and reported that these scoring systems including BISAP, Ranson, HAPS, APACHE II, and Glasgow were capable of predicting mortality. However, APACHE II predicted mortality with a sensitivity of 90% and specificity of 92%[113].

Drawing on the insights gleaned from the aforementioned body of literature, we have meticulously synthesized a detailed appraisal of the application of various clinical scoring systems in prognosticating severity, local complications, organ failure, and mortality rates associated with AP. These summarizations are comprehensively depicted in Table 1. Various scoring systems exhibited diverse levels of sensitivity, specificity, and accuracy in forecasting the severity, local complications, organ failure, and associated mortality. Further, it is noteworthy that numerous studies have indicated the existence of substantial differences among these scoring systems, highlighting their lack of uniform standards and, in some instances, a concerning degree of inconsistency in their projections. Given the variability in accuracy among diverse scoring systems for predicting the severity, local complications, organ failure, and mortality associated with AP, there is a plausible need for further refinement and design optimization of each scoring system to enhance the precision of these predictions. Moreover, another potential area of research could be the amalgamation of multiple existing scoring systems to boost the predictive accuracy for AP through a more comprehensive scoring approach.

To enhance a more comprehensive understanding of the clinical utility of prevalent scoring systems, such as BISAP, SOFA, and qSOFA, in predicting AP outcomes, we conducted independent discussions and analyses on the latest advancements of these tools to provide invaluable reference and guidance for their practical application in clinical

Table 1 Comparison of existing clinical scoring systems used in patients with acute pancreatitis for predicting the severity of acute pancreatitis, such as severe acute pancreatitis, mortality, organ failure, intensive care unit admission, location complications, in-hospital adverse events, and pancreatic necrosis

Prediction	Scoring system (cutoff value)	Sensitivity, %	Specificity, %	Accuracy, %	PPV, %	NPV, %	AUC	No. of patients	Ref.
MSAP and SAP[1]	BISAP (≥ 3)	54	86	-	68	-	0.795	326	[107]
	Ranson (≥ 3)	46	84	-	54	-	0.766		
	APACHE II (≥ 8)	57	89	-	67	-	0.814		
	MCTSI (≥ 4)	36	94	-	66	-	0.654		
SAP[1]	Ranson (≥ 3)	85.7	44.3	-	18.8	95.3	0.69	161	[106]
	BISAP (≥ 2)	61.9	72.1	-	25.0	92.7	0.74		
	APACHE II (≥ 8)	81.0	65.7	-	26.2	95.8	0.78		
	CTSI (≥ 3)	66.7	67.1	-	23.3	93.1	0.69		
SAP[1,2]	Ranson (≥ 4/≥ 3)	81.4/92.0	84.2/92.8	-	28.9/37.7	98.3/99.6	0.867/0.964	368/550	[110]
	BISAP (≥ 3/≥ 2)	88.9/96.0	86.5/88.0	-	34.3/27.6	99.0/99.8	0.922/0.942		
	APACHE II (≥ 9/≥ 8)	85.2/96.0	61.0/93.0	-	14.7/42.9	98.1/99.8	0.784/0.951		
	Glasgow (≥ 3/≥ 2)	85.2/80.0	84.2/88.2	-	29.9/24.4	98.6/98.9	0.913/0.881		
SAP	HAPS (≥ 1)	79.0	49.7	53.3	18.2	94.4	0.687	653	[111]
	BISAP (≥ 3)	24.7	95.3	86.5	42.6	89.9	-		
	APACHE II (≥ 8)	80.2	63.3	65.4	23.6	95.8	-		
	Ranson (≥ 3)	92.6	51.9	57.0	21.4	98.0	0.857		
	Glasgow (≥ 3)	76.5	68.5	69.5	25.6	95.4	-		
	SOFA (≥ 7)	13.6	99.7	89.0	84.6	89.1	0.966		
SAP[3]	APACHE II (≥ 6)	50	100	68.3	100	53.57	0.771	164	[112]
	BISAP (≥ 2)	25.96	100	53.1	100	43.80	0.640		
	Modified Glasgow ≥ 3)	75.96	100	84.8	100	70.59	0.649		
	Ranson (≥ 2)	32.69/58.65	100/100	57.3/73.8	100/100	46.15/58.25	0.848/0.817		
SAP[3,4]	APACHE II (≥ 6)	63.7	77.1	68.2	84.6	51.9	-	69	[112]
	BISAP (≥ 2)	31.8	85.7	50.0	81.4	38.9	-		
	Modified Glasgow (≥ 3)	79.9	31.4	63.4	69.6	44.0	-		
	Ranson (≥ 2)	44.9/63.7	91.4/51.4	60.5/59.6	91.1/72.1	45.7/41.8	-		
Mortality[1]	BISAP (≥ 3)	89	80	-	15	-	0.867	326	[107]
	Ranson (≥ 3)	78	77	-	9	-	0.842		
	APACHE II (≥ 8)	89	78	-	10	-	0.854		
	MCTSI (≥ 4)	78	86	-	14	-	0.839		
Mortality in AP	HAPS (≥ 1)	83.3	46.6	29.9	2.8	99.3	-	653	[111]

	BISAP (≥ 3)	25	93.1	91.9	6.4	98.5	-		
	APACHE II (≥ 8)	100	58.7	59.1	3.6	100	-		
	Ranson (≥ 3)	100	47.3	48.2	3.4	100	0.917		
	Glasgow ≥ 3)	75.0	63.8	64.2	4.1	99.5	-		
	SOFA (≥ 7)	50.0	98.9	98.0	46.2	99.1	0.968		
Mortality[1]	BISAP (≥ 2.5)	92.0	90.0	-	-	-	0.92	106	[113]
	HAPS (≥ 1.5)	49.0	98.0	-	-	-	0.83		
	Ranson (≥ 3.5)	75.0	71.0	-	-	-	0.78		
	JSS (≥ 3.5)	84.0	94.0	-	-	-	0.92		
	Glasgow (≥ 2.5)	89.0	86.0	-	-	-	0.91		
	APACHE II (≥ 5.5)	90.0	92.0	-	-	-	0.94		
Persistent organ failure[1,5]	APACHE II (≥ 7)	84/94	71/44	-	49/14	93/99	0.77/0.71	256/397	[105]
	BISAP (≥ 2)	61/62	84/76	-	54/20	87/96	0.72/0.69		
	Glasgow (≥ 2)	85/65	83/82	-	61/22	95/97	0.84/0.74		
	HAPS (≥ 1)	70/73	53/58	-	32/12	85/97	0.62/0.66		
	JSS (≥ 2)	59/42	92/89	-	70/23	88/95	0.76/0.66		
	Ranson (≥ 2)	66/46	78/80	-	49/16	88/95	0.72/0.63		
	SIRS (≥ 2)	70/69	71/58	-	43/11	88/96	0.70/0.64		
Organ failure[1]	Ranson (≥ 3)	88.89	96.67	-	88.89	96.67	0.757	50	[108]
	BISAP (≥ 3)	90.00	83.87	-	64.29	96.30	0.762		
	APACHE II (≥ 8)	92.86	69.44	-	54.17	96.15	0.831		
	MCTSI (> 4)	92.86	75.00	-	59.09	96.43	0.893		
Association with organ failure[3]	APACHE II (≥ 6)	48.5	36.2	40.3	27.8	28.1		164	[112]
	BISAP (≥ 2)	8.5	55	39.4	8.8	54.2	0.640		
	Modified Glasgow (≥ 3)	68.5	20.2	36.5	30.3	56	0.649		
	Ranson (≥ 2)	14.2/22.8	68.1/36.2	50/31.7	18.5/15.3	61/48	0.848/0.817		
ICU admission[1]	Ranson (≥ 3)	80.00	96.55	-	88.89	93.33	0.910	50	[108]
	BISAP (≥ 3)	90.91	86.67	-	71.43	96.30	0.877		
	APACHE II (≥ 8)	92.31	65.71	-	50.00	95.83	0.885		
	MCTSI (> 4)	92.86	75.00	-	59.09	96.43	0.993		
ICU admission	HAPS ≥ 1	90.0	47.2	29.9	5.1	99.3	-	653	[111]
	BISAP ≥ 3	25.0	93.4	91.3	10.6	97.5	-		
	APACHE II ≥ 8	100	59.6	60.5	6.6	100	-		
	Ranson ≥ 3	100	47.9	49.5	5.7	100	0.946		
	Glasgow ≥ 3	75.0	64.5	65.1	7.0	99.3	-		
	SOFA ≥ 7	40.0	99.2	97.4	61.5	98.1	0.943		
Location complications[1]	BISAP (≥ 3)	54	81	-	21	-	0.731	326	[107]
	Ranson (≥ 3)	57	79	-	20	-	0.698		

	APACHE II (≥ 8)	43	78	-	15	-	0.580		
	MCTSI (≥ 4)	68	90	-	38	-	0.791		
In-hospital adverse events[1,6]	HAPS ≥ 2	66.2	70.6		36.0	89.1	0.70	690	[109]
	Ranson ≥ 3	66.9	62.8	-	31.2	88.3	0.68		
	BISAP ≥ 2	61.9	75.9	-	39.3	88.7	0.74		
	Glasgow ≥ 2	51.8	83.7	-	44.0	87.3	0.71		
	JSS[7]	81.9	66.0	-	38.2	93.4	0.80		
Pancreatic necrosis[1]	Ranson (≥ 3)	80.00	96.55	-	88.89	93.33	0.910	50	[108]
	BISAP (≥ 3)	81.82	83.33	-	64.29	92.59	0.822		
	APACHE II (≥ 8)	93.33	71.43	-	58.33	96.15	0.855		
	MCTSI (> 4)	93.33	77.14	-	63.64	96.43	0.993		

[1]The predictive accuracy of each scoring system was measured by the area under the curve.
[2]In this study, 918 patients with were divided into two groups, namely the elderly group (368 patients who were ≥ 60-years-old) and the younger group (550 patients who were < 60-years-old). The former value corresponds to the elderly group, and the latter value corresponds to the younger group.
[3]The Ranson score in this study involved two time points: at admission and 48-h after admission. For Ranson, the former value corresponds to at admission, and the latter value corresponds to 48-h after admission.
[4]Computed tomography (CT) abdomen in 69 patients showed modified CT severity index ≥ 8 in all 69 (100%) patients.
[5]In this study, two prospective cohorts were involved, namely the training cohort and the validation cohort. The former value corresponds to the training cohort, and the latter value corresponds to the validation cohort.
[6]In-hospital adverse events included all in-hospital complications, pancreatic necrosis, and in-hospital mortality.
[7]Severe acute pancreatitis according to the Japanese Severity Score was defined if the prognostic factor was ≥ 3 or CT grade ≥ 2.
AP: Acute pancreatitis; APACHE: Acute Physiology and Chronic Health Evaluation; AUC: Area under the curve; BISAP: Bedside Index for Severity in Acute Pancreatitis; CTSI: Computed tomography severity index; HAPS: Harmless acute pancreatitis score; ICU: Intensive care unit; JSS: Japanese Severity Score; MCTSI: Modified Mortele's computed tomography severity index; MSAP: Moderately severe acute pancreatitis; NPV: Negative predictive value; PPV: Positive predictive value; SAP: Severe acute pancreatitis; SIRS: Systemic Inflammatory Response Syndrome; SOFA: Sequential Organ Failure Assessment.

settings.

BISAP

In a large population-based study, Wu *et al*[101] identified five variables for prediction of in-hospital mortality by Classification and Regression Tree analysis to derive a prognostic scoring system (BISAP) including blood urea nitrogen (> 25 mg/dL), age (> 60 years), SIRS, pleural effusion, and impaired mental status. Blood urea nitrogen emerged as the most efficient primary discriminative variable, age and SIRS further distinguished between high-risk and low-risk cases, and mental status and pleural effusion further refined the categorization of intermediate-risk patients[101]. Introduced in 2008, BISAP, with its advantages of simplicity and precision, had been employed for the early identification of AP patients with an elevated risk of in-hospital mortality[101]. BISAP is adept at identifying AP patients at heightened risk of mortality, representing the advancement of intermediate markers of severity within 24 h of onset, and its risk stratification ability could hold potential for enhancing clinical care and streamlining enrollment in clinical trials[114]. BISAP was considered to be as good as APACHE II in predicting severity, death, and especially organ failure in AP. It outperformed Ranson, CTSI, CRP, hematocrit, and body mass index, with a score of 2 being a statistically significant cutoff value[115]. BISAP is a streamlined scoring system designed to predict the severity of AP and is instrumental in early risk stratification of AP.

A prospective study of 87 patients experiencing their first episode of AP revealed that BISAP (≥ 2) demonstrated comparability to both APACHE II (≥ 8) and MCTSI (≥ 8) in metrics of accuracy, sensitivity, specificity, and NPV[116]. In a systematic review and meta-analysis, a pooled analysis from 12 prospective cohorts showcased the exemplary performance of BISAP in predicting SAP across diverse patient populations and disease severity[117]. Furthermore, the performance of BISAP was notably superior when severe pancreatitis was characterized by the persistence of organ failure for 48 h or more[117]. A European cohort study indicated that BISAP effectively predicted SAP, mortality, and ICU admission, making it invaluable for triaging patients toward ICU care[118].

Chen *et al*[119] assessed the accuracy of BISAP in predicting the severity and prognoses of AP in Chinese patients. In this study, they retrospectively analyzed clinical data from 497 AP patients comparing BISAP with APACHE II, Ranson, and CTSI regarding their predictive capacities for the severity of AP and the occurrence of mortality, pancreatic necrosis, and organ failure in SAP patients[119]. They highlighted that BISAP outperformed traditional scoring systems in terms of simplicity and speed, and maintained a performance comparable to other scoring systems in predicting both SAP and its associated prognoses[119].

Zhang *et al*[120] evaluated the efficacy of BISAP, APACHE II, and Ranson in predicting the severity, mortality, and pancreatic necrosis of AP based on the 2012 RAC at a tertiary care center in China. From their study involving 155 patients, they determined that BISAP might serve as a reliable tool for risk stratification and prognostic assessment in Chinese AP patients[120]. Gao *et al*[121] conducted a meta-analysis to systematically assess the accuracy of BISAP in predicting mortality and SAP and affirmed that BISAP served as a dependable tool for identifying AP patients at elevated risk for adverse outcomes. While BISAP demonstrated superior specificity compared to Ranson and APACHE II, it exhibited a slightly diminished sensitivity for both mortality and SAP[121].

An Indian study with 119 AP patients showed that BISAP was an accurate means of risk stratification, and patients with BISAP ≥ 4 invariably developed SAP or pancreatic necrosis and had high mortality[122]. The available studies collectively demonstrated that BISAP performs very well in predicting SAP, and the simplicity and accuracy of the calculation make BISAP a valuable tool for clinical care of AP patients. Additionally, before confidently advocating for the adoption of BISAP, its integration into clinical practice should be evaluated to determine its potential to enhance outcomes in AP.

BISAP, an easily computed clinical prediction scale, leverages data from initial assessment of patients and routine laboratory results, demonstrating excellent performance in predicting SAP. BISAP is less cumbersome to calculate and more economical, which makes it an ideal scoring system. It is considered that BISAP should be popularized at primary and secondary care institutions for severity classification and risk stratification of early AP. Therefore, SAP patients can be referred to higher-level medical centers for more reasonable clinical intervention.

However, as more and more clinical studies have been conducted, BISAP has shown inconsistent predictive power and results in predicting SAP, as reported in the next studies. A prospective study including 51 patients showed that BISAP was inferior to APACHE II in predicting the severity of AP, especially for SAP[123]. In a meta-analysis including 1972 subjects, Yang and Li evaluated the diagnostic performance of BISAP in predicting SAP[124]. They concluded that despite its high specificity BISAP was not the optimal standalone method for assessing AP severity due to its low sensitivity[124].

In a prospective study including 50 AP patients, the accuracy of BISAP in predicting SAP was 84%, surpassing that of serum procalcitonin (PCT) (≥ 3.29 ng/mL) at 76%, which was on par with APACHE II; moreover, in logistic regression analysis, BISAP demonstrated greater statistical significance than serum PCT[125]. They determined that BISAP outperformed serum PCT, APACHE II, Glasgow, and BCTSI in accurately predicting AP severity, positioning it as a promising tool for gauging the clinical progression of AP[125]. Hagjer *et al*[126] evaluated the usefulness of BISAP and PCT for AP prediction in a prospective observational study including 60 patients. Based on this study, in predicting severity, mortality, and organ failure, they finally concluded that BISAP was as effective as APACHE II and surpassed Ranson, CTSI, CRP, hematocrit, and body mass index in evaluating AP patients. PCT was a good independent prognostic marker and was comparable with BISAP and APACHE II in accuracy[126].

A multicenter validation study is essential to corroborate these findings and further elucidate the role of BISAP in AP. Meanwhile, further well-designed prospective studies are warranted to investigate the conditions under which BISAP can be used to more accurately, sensitively, and specifically assess severity and prognosis in AP.

Combination of BISAP and other diagnostic indicators

In a retrospective analysis including 114 cases, the severity and mortality of AP escalated with the increase of BISAP, and BISAP exhibited a positive correlation with CRP, D-dimer, and serum glucose and negatively correlated with serum Ca^{2+} [127]. Based on the positive correlation between CRP and APACHE-II, Ranson, BISAP, and CTSI, when CRP was included into BISAP, the AUC of predicting SAP and death were 0.873 and 0.909, respectively, showing that the combination of BISAP and CRP had better predictive value for severity and death of AP[127]. In a study including 117 SAP patients, Wu *et al*[128] reported that combining BISAP with miR-155 yielded a superior AUC compared to individual predictions, suggesting that this combination could enhance the clinical predictive accuracy for AP severity.

Early diagnosis and timely assessment of the severity are critical because early aggressive treatment reduces morbidity and mortality of AP. However, an ideal multifactor scoring system for early assessment of AP severity has not been determined. Based on an analysis of the available data and evidence, we recommend that BISAP as a multifactor scoring system is combined with characteristic biochemical markers present at 48 h, in order to achieve optimal early assessment of AP severity.

SOFA

In October 1994, the European Society of Intensive Care Medicine convened in Paris to establish the SOFA score, aiming to quantitatively and objectively describe the degree of organ dysfunction/failure over time in patient groups or even in individual cases[129]. Although SOFA is primarily designed for patients with sepsis, it was deemed necessary to expand its application beyond this specific patient group[129]. At present, SOFA is widely utilized in the ICU to evaluate, prognosticate, and assess patients; since its validation, it has been applied in diverse medical settings, including trauma, surgical, cardiac, and neurological ICUs[130].

Minne *et al*[131] conducted a systematic review on the utility of SOFA-based models for predicting the risk of mortality in ICU patients and recommended an integration of a traditional model derived from data within the initial 24 h post-ICU admission with sequential SOFA. SOFA could be easily integrated into contemporary cardiac ICU through an electronic algorithm, and the day 1 SOFA demonstrated strong predictive capability for short-term mortality among a broad spectrum of patients in the cardiac ICU[132]. Among the critical care systems, SOFA has distinct benefits, including its simplicity in computation, incorporation of therapeutic needs, and facilitation of comparisons of AP with other critical care diseases[24].

Adam *et al*[133] retrospectively evaluated the efficacy of APACHE II, SOFA, and modified Ranson in predicting mortality among 43 SAP patients as well as other factors influencing mortality in patients admitted to the ICU and concluded that SOFA was superior to Ranson and APACHE II in determining prognosis. In this study, SOFA had a significant correlation with mortality, and all patients with SOFA ≥ 11 at any point during the ICU stay exhibited a heightened mortality risk, with a sensitivity of 80% and a specificity of 79%[133].

Tee *et al*[134] retrospectively obtained serial measurements of Ranson, APACHE II, and SOFA in 159 patients with SAP, assessing the efficacy of serial measurement using these three scoring systems. In this study, besides acquiring Ranson and APACHE II on admission and at 48 h, they took serial weekly measurements of SOFA, including data from admission, 48 h, and days 7, 14, and 21[134]. The three scoring systems reliably predicted both overall and ICU mortality. However, the SOFA on day 7 exhibited the largest AUC, with any increase or lack of change in SOFA on day 7 of hospitalization correlating with elevated mortality[134]. They concluded that both APACHE II and SOFA were sensitive in predicting mortality for AP. Serial SOFA proved reliable for guiding clinical decisions, and day 7 of hospitalization was a reasonable time for SOFA reassessment to predict late mortality in SAP[134].

A retrospective study enrolling 146 AP patients demonstrated that an increase in SOFA independently heightened the likelihood of adverse outcomes during hospitalization for AP patients, and SOFA > 5 was highly predictive of in-hospital mortality compared to other scores[135]. Utilizing a straightforward tool like SOFA, validated in intensive care settings, could enhance the stratification of in-hospital mortality risk and clinical deterioration among AP patients admitted to medical wards. Teng *et al*[111] reported that both SOFA and 48-h Ranson effectively predicted the severity, ICU admission, and mortality associated with AP, with SOFA showing particularly favorable results.

qSOFA

The qSOFA includes respiratory rate (breaths per minute), systolic blood pressure (mm Hg), and Glasgow Coma Scale score[136]. In a 17-year observation study including 1059 patients, the ROC curve analysis revealed that the AUC values of APACHE II, SOFA, and qSOFA scores in predicting the prognosis of infected patients were 0.713, 0.744, and 0.662, respectively[137]. In this study, Qin *et al*[137] posited that qSOFA, due to its advantages of rapid acquisition, would serve as an efficient tool for assessing the prognosis of ICU patients with infections. Given its extraordinary simplicity, qSOFA would be an appropriate score particularly for the initial patient evaluation in the emergency department and was considered to be a rapidly available prognostic score in AP with limited prognostic validity[138]. In a cohort study including 203 patients, Rasch *et al*[138] reported that qSOFA could predict ICU admission and multiple organ dysfunction syndrome in AP.

In a retrospective cohort study involving 161 patients with the diagnosis of alcohol-induced AP, a qSOFA score of 2 or higher both upon admission and 48 h post-admission exhibited a specificity of 94% or greater and sensitivity of 33% or higher for assessing pancreatitis severity and determining the necessity for intensive care admission, intubation, or vasopressor[139]. In a 3-year cohort study from the United States, Hallac *et al*[140] evaluated the ability of qSOFA and SIRS in predicting extended hospital stays among patients presenting with AP to the emergency department and hospital ward. A qSOFA of 2 or higher was linked to a diagnosis of significant AP with a specificity of 99% and a sensitivity of 4%. In contrast, a SIRS score of 2 displayed a specificity of 61% and a sensitivity of 80% in detecting patients with significant AP[140]. Based on their findings, they inferred that relying solely on qSOFA for triaging AP patients could lead to under recognition and potential undertreatment[140].

HAPS

HAPS was calculated rapidly from the following three parameters: presence or absence of rebound tenderness or guarding; hematocrit (> 43 mg/dL for males or > 39.6 mg/dL for females); and serum creatinine (> 2 mg/dL)[105,141]. Oskarsson *et al*[142] reported that HAPS predicting nonsevere AP progression had a specificity of 96.3% and a corresponding PPV of 98.7% in 531 patients experiencing either a first-time or a recurrent attack of AP, emphasizing HAPS as a highly specific scoring algorithm predicting nonsevere AP progression[142]. In a prospective pilot study with 103 AP patients from India, the sensitivity, specificity, PPV, NPV, and AUC of HAPS as a predictor of nonsevere disease were 76.3%, 85.7%, 93.8%, 56.6%, and 0.848, respectively[143]. In a study including 703 AP patients from China, the sensitivity, specificity, PPV, NPV, and AUC of HAPS on admission for predicting MAP was 48.2%, 97.7%, 95.6%, 64.1%, and 0.749, respectively[97]. These studies validated the utility of HAPS at admission in predicting nonsevere AP in India and MAP in China, respectively. Maisonneuve *et al*[144] evaluated the PPV of HAPS by performing a meta-analysis of 20 reports covering 6374 patients. They concluded that HAPS accurately identified patients with nonsevere AP who would not require ICU care, enabling the pinpointing of patients suitable for brief general ward stays or home-based care[144].

HAPS may offer significant advantages in the triage of AP patients when compared to other scoring systems, underscoring its potential utility in optimizing patient classification and guiding treatment strategies. In a study including 60 patients with the first attack of AP, Gupta *et al*[145] reported that the sensitivity, specificity, PPV, NPV, and AUC of HAPS predicting SAP were 90.91%, 59.81%, 33.33%, 96.67%, and 0.75, respectively. The high NPV indicated that HAPS could very accurately identify within the first hour of admission patients who had a mild course of disease, did not require intensive management, and were not at risk of dying from the disease[145]. Based on this result, they argued that the patient typically tended to experience a milder course of illness if the evaluation of HAPS yielded a negative result [145]. Conversely, in instances where the score was positive, the patient's clinical progression could unfold in any direction, demonstrating the uncertainty associated with such an outcome[145]. In this same study, the sensitivity, specificity, PPV, NPV, and AUC of BISAP in the prediction of SAP were 63.64%, 100%, 100%, 92.45%, and 0.82, respectively[145]. In comparison to BISAP in this study, HAPS demonstrated a heightened sensitivity towards processes predicting mortality and severity and played a pivotal role in determining whether patients necessitated costly imaging procedures, thereby potentially enabling significant hospital cost savings[145]. In a study with 116 patients, Al-Qahtani *et*

al[146] compared HAPS with Ranson in predicting the severity of AP and concluded that HAPS was effective in rapidly identifying patients likely to experience a nonsevere course of the disease.

Of significant importance is the fact that assessment of HAPS can be accomplished within the first hour of a patient visit, offering a distinct advantage in terms of time efficiency. In contrast, while Ranson might offer superior accuracy, it necessitates a full 48 h to reach completion, highlighting a potential trade-off between speed and precision in these scoring systems. Considering that the substantial majority of individuals diagnosed with AP typically exhibit a milder form of the disease, the capacity to accurately distinguish these patients of MAP is of utmost significance. Drawing upon the aforementioned analysis and discussion, HAPS appears to be a commendable choice for assisting physicians in evaluating the severity of AP. Furthermore, HAPS could potentially be perceived as a gold standard for facilitating both the early identification and cost-effective management of this disease. In addition, due to the readily accessible parameters required for its computation, HAPS can be effectively utilized in a wide range of healthcare facilities, including those located in developing countries. This ease of implementation makes HAPS an inclusive and practical tool for global health contexts.

Other recent clinical scoring systems

Hong *et al*[147] developed a prognostic score termed SABP, encompassing systemic inflammatory response syndrome, serum albumin, blood urea nitrogen, and pleural effusion. The SABP score could serve as an instrumental tool to categorize patients at risk of developing SAP as per the latest revised Atlanta criteria. Its application on admission may enhance clinical care and refine management approaches for AP[147]. He *et al*[148] retrospectively analyzed the clinical data of 469 patients with AP, and selected seven prognostic indicators to establish an unweighted predictive score and weighted predictive score for MSAP and SAP. The early multi-indicator prediction models for MSAP and SAP demonstrated robust predictive efficacy, offering a meaningful clinical benchmark for diagnosis and treatment[148].

In a retrospective analysis encompassing a total of 1295 AP patients, Feng *et al*[149] developed an independent predictive tool, known as a nomogram, to predict the likelihood of sepsis occurrence in this patient population. In this study, the predictive performance and clinical utility of the newly established nomogram surpassed those of other scoring systems such as SIRS, BISAP, SOFA, and qSOFA[149]. The innovative risk-prediction system could precisely estimate the likelihood of sepsis in AP patients, assisting clinicians in formulating personalized treatment strategies for the patients. By doing so, it not only alleviated the disease burden of the patients but also facilitated the reasonable distribution of medical resources, which was a crucial aspect of tertiary prevention[149]. The nomogram incorporated all the independent prognostic factors, including body temperature, phosphate, Ca^{2+}, sodium, lactate, albumin, platelet count, urinary output, mean blood pressure, Glasgow Coma Scale, and Charlson Comorbidity Index[149]. These diverse elements collectively contributed to its predictive strength.

Summary

Score systems, utilizing 4-25 factors, have been developed to predict severity, yet they frequently rely on multiple parameters not measurable daily and often require over 24 h to finalize, leading to critical time loss[150]. While these scores can predict failure or severity of specific organs, their reliance on dichotomous parameters leads to information loss, limiting their practical application in clinical settings[150]. Based on the current literature, here are the identified problems and potential solutions for applying clinical scoring systems to the diagnosis, severity prediction, and prognosis assessment of AP.

Inconsistency: Different scoring systems like Ranson, Glasgow, BISAP, and CTSI may yield inconsistent results, leading to confusion in clinical decision-making.

Solution: Research to validate and compare different scoring systems can help identify the most accurate and reliable ones. Standardizing the use of a particular scoring system across healthcare settings can reduce inconsistency.

Complexity: Some scoring systems are complex and require multiple parameters, making them time-consuming to calculate. This complexity can hinder their practical application in urgent care settings.

Solution: Creating simplified and user-friendly scoring systems that maintain accuracy can make them more practical for clinicians to use, especially in urgent care settings.

Lack of sensitivity and specificity: Some scoring systems may lack sensitivity or specificity in predicting the severity and prognosis of AP, leading to inaccurate assessments.

Solution: Combining scoring systems with comprehensive clinical assessment can lead to more accurate care. This solution is more of a clinical recommendation rather than a documented research finding.

Lack of personalization: Scoring systems are often based on population-level data and may not account for characteristics of individual patient, leading to generalized predictions that may not be applicable to all patients.

Solution: Considering patient-specific factors, such as comorbidities, lifestyle, and preferences, in conjunction with scoring systems, can lead to more personalized and effective care.

Over-reliance on scoring systems: Sole reliance on scoring systems without considering clinical judgment and other patient-specific factors may lead to suboptimal care.

Solution: Providing education and training to healthcare professionals on how to effectively use scoring systems, including their limitations, can enhance their application in clinical practice.

In conclusion, while clinical scoring systems are valuable tools in managing AP, they present challenges that are recognized both in clinical practice and in the research literature. The solutions outlined above, grounded in current research and clinical wisdom, can enhance the effectiveness of these systems in providing accurate and personalized treatment for patients with AP.

AI

In the era of AI, machine learning algorithms have been devised to accurately predict the severity, complications, recurrence, mortality, and even the optimal timing of surgery for AP patients. However, the quality of research evaluating the accuracy of AI is still low and lacks studies comparing AI with these commonly used clinical scores. Therefore, more research is needed before we can routinely use AI in our daily clinical practice. Prior to this, the easy-to-calculate and applicable scoring systems seems to be the most reasonable choice.

Recently, AI applications, utilizing machine learning, have been progressively integrated into the medical field, demonstrating superior performance in predicting complications compared to logistic regression analysis[151]. AI-based machine learning is booming and creating a technological revolution, especially in the healthcare industry[152]. Machine learning, a subset of AI, employs statistical methods to train algorithms for predictions, enabling a computer system to self-learn and enhance its performance based on experience[150]. Machine learning has garnered significant attention and recognition from clinicians, driven by advancements in statistical theory and computer technology[153]. Machine learning adeptly discerns intricate relationships between diseases and variables, categorizes variables based on specific criteria, predicts outcomes from foundational features, and recognizes objects with analogous patterns[152]. Innovative machine learning technologies have been extensively employed in predictive models for a spectrum of diseases, consistently demonstrating superior performance over traditional logistic regression or Cox regression analyses[153].

In this age of technological advancement, AI stands as a pinnacle of innovation, proficiently discerning the intricate non-linear proficiently between numerous biochemical parameters and their associated disease outcomes[150]. For example, a retrospective study demonstrated that when juxtaposed with the traditional logistic regression model machine learning models [extreme gradient boosting (XGBoost) and random forest (RF)] utilizing readily accessible features upon admission exhibited superior performance in predicting acute kidney injury among AP patients[151]. Leveraging such machine learning algorithms in predictive models could enable clinicians to foresee acute kidney injury at an early stage, potentially mitigating further renal damage[151].

Based on an international cohort of 1184 patients and a validation cohort of 3543 patients, Kui *et al*[154] devised a user-friendly web application named EASY-APP, which employs multiple continuous variables accessible at admission. The EASY prediction score serves as an effective tool for pinpointing patients at elevated risk for severe AP within hours of hospitalization, and the web application was made available to clinicians, enhancing the utility and precision of the model[154].

Zhou *et al*[155] demonstrated that the XGBoost algorithm possesses the capability to precisely predict the severity of AP, offering clinicians valuable assistance in identifying severe AP at an early stage. In a prospective cohort study integrating necrosis prediction with AI, the XGBoost machine learning algorithm was employed to analyze the data from 2387 AP patients[156]. This model in the predictive capability rivals those existing clinical scoring systems, and its performance is anticipated to improve with continued use[156]. In the United States, Thapa *et al*[7] applied machine learning algorithms to predict which AP patients need SAP treatment and developed three models using logistic regression, neural networks, and XGBoost. In this study, machine learning models were trained and tested to utilize data from 61894 patients, with the XGBoost model surpassing the performance of both logistic regression and neural network-based models[7]. Furthermore, the XGBoost model achieved a superior AUROC compared to both HAPS and BISAP in identifying patients likely to be diagnosed with SAP[7]. They concluded that machine learning has the potential to refine the precision of AP risk stratification methods, facilitating prompter treatment and intervention initiation[7].

In a large retrospective study enrolling 5460 patients, Yuan *et al*[157] developed and validated a novel machine learning tool, APCU, leveraging clinical, laboratory, and radiologic data to predict ICU admission among AP patients. They showed that the APCU effectively categorized AP patients into high-risk and low-risk groups, demonstrating a superior discriminative capability compared to other risk scores like Ranson, APACHE II, SIRS, and NEWS in predicting ICU admission for AP patients and specific subgroups within 48 h of hospitalization[157]. Notably, this study marked the inaugural application of a machine learning algorithm for the predictions of ICU admission in AP patients within 48 h of hospitalization, relying on widely accessible clinical, laboratory, and radiologic data[157].

In a retrospective analysis involving 648 AP patients, Hong *et al*[158] developed RF and logistic regression models using a training sample; the RF model, notable for its interpretability, showcased the most superior discriminative performance in predicting SAP. In a retrospective study involving 631 AP patients, Luo *et al*[159] developed a machine learning model, culminating in a nomogram designed for the early identification of SAP during the progression of AP. Their findings indicated that the RF model delivered optimal predictive performance, with the nomogram offering a visual scoring model suitable for clinical application[159]. Such models have the potential to act as functional tools, enabling personalized treatment choices and enhancing clinical results by stratifying AP patients prior to treatment[159]. In a study with a total of 1012 patients, Yin *et al*[160] developed a series of effective models for early prediction of SAP based on automated machine learning (AutoML) platform, and these models outperformed the existing scoring systems, which might offer insights into AutoML applications in future medical studies. The AutoML model based on the GBM algorithm for early prediction of SAP showed evident clinical practicability[160].

In a recent retrospective study involving a cohort of 460 AP patients to predict ARDS in these patients at admission, Zhang *et al*[161] constructed and optimized four machine learning models, including support vector machine, ensembles of decision trees (EDTs), Bayesian classifier (BC), and nomogram models, based on 31 features with significant differences between the groups with and without ARDS. Among the four models, the BC algorithm exhibited superior predictive performance with the highest AUC (0.891), surpassing support vector machine (0.870), EDTs (0.813), and the nomogram (0.874) in the test set[161]. Concurrently, the EDT algorithm achieved the highest accuracy at 0.891, precision at 0.800, and F1 score at 0.615 but registered the lowest FDR at 0.200 and the second-highest NPV at 0.902[161]. In terms of predictive performance for ARDS as a complication of AP, they concluded that BC was the superior predictive model in the test set, and EDTs exhibited promising potential for predicting large samples[161].

Summary

The application of AI in the diagnosis, severity prediction, and prognosis assessment of AP represents an exciting development in the field of medicine. However, based on these current studies, we recognize several limitations and potential challenges that must be addressed to fully leverage the capabilities of AI in this context.

Data quality and availability: AI algorithms require high-quality, comprehensive, and diverse data to build robust and accurate models. In the context of AP, such data sets may not be readily available, especially for rare subtypes of the disease or patient populations with specific comorbidities. Furthermore, incomplete or inconsistent data can lead to biased or flawed results.

Interpretability: AI models, especially those employing complex algorithms like deep learning, often operate as 'black boxes,' providing outputs without clear, understandable reasons for their decisions. This can limit their acceptance in the clinical setting, as healthcare professionals typically prefer to understand the reasoning behind a diagnosis or prediction.

Standardization: AI algorithms are typically designed and validated on specific datasets. Their generalizability to other populations or healthcare settings, especially those that are vastly different from the original context, is not guaranteed. This lack of standardization can lead to inconsistent results when the models are used in different settings.

Generalizability: Models trained on a specific set of data may not perform well when applied to different datasets, especially if there are demographic or geographical differences. For example, an AI model trained on data from a high-income country might not work as well in a low-income setting due to differences in healthcare infrastructure, disease prevalence, and patient characteristics.

Regulation: The use of patient data to develop and apply AI models raises significant concerns around data privacy, consent, and security. It is crucial that these concerns are addressed to ensure ethical usage and maintain public trust. For instance, who is responsible if an AI system makes an incorrect diagnosis or prognosis? How is patient data privacy ensured?

Implementation: The successful implementation of AI in healthcare settings requires clinicians to have a certain level of understanding and trust in the technology. This can be challenging due to varying levels of digital literacy among healthcare providers and resistance to change.

Given these challenges, ongoing research is critical to improve the reliability, interpretability, and generalizability of AI tools in healthcare and to address the ethical, legal, and workflow integration issues associated with their use. It is important that as we move forward, these tools are developed and used in a manner that complements the expertise of healthcare professionals rather than seeking to replace it.

CONCLUSION

Early aggressive treatment of AP has been proven to reduce the incidence and mortality rates. Therefore early diagnosis and severity assessment of AP are extremely necessary, and there is a particular need for early technological approaches to evaluate and predict the progression of AP.

In recent years, there has been heightened interest in leveraging imaging technologies, scoring systems, and AI to improve the diagnosis, severity prediction, and prognosis evaluation of AP. Different imaging modalities, such as CT, MRI, and US, are used to assess the severity and extent of pancreatic inflammation and detect any complications that may arise. Several scoring systems have been developed to assess the severity of AP and predict the risk of complications, such as Ranson, APACHE II, BISAP, SOFA, and HAPS. These scoring systems take into account various clinical and laboratory parameters, such as age, blood pressure, serum glucose, and white blood cell count, to provide a numerical score that reflects the severity of the disease. AI is a rapidly developing field that has the potential to revolutionize the diagnosis and management of AP. AI algorithms can be trained to analyze large datasets of imaging and clinical data to predict the severity and prognosis of AP. AI algorithms have been developed to analyze CT scans of patients with AP to predict the risk of complications such as pancreatic necrosis, abscess, or pseudocyst. The algorithms can detect subtle changes in the pancreas that may be missed by human radiologists and can provide more accurate and timely predictions of the risk of complications.

The integration of imaging technologies, scoring systems, and AI in the diagnosis, severity prediction, and prognosis assessment of AP has several advantages, including: (1) More accurate diagnosis. Imaging technologies and AI algorithms can provide more accurate diagnoses, reducing the risk of misdiagnosis and unnecessary treatment; (2)

Improved risk assessment. Scoring systems and AI algorithms can provide more accurate risk assessments, which can help healthcare providers make more informed treatment decisions; (3) Personalized treatment. The combination of imaging technologies, scoring systems, and AI can provide a more personalized approach to treatment, taking into account each patient's unique circumstances; and (4) Improved patient outcomes. The earlier and more accurate diagnosis, as well as the more personalized treatment options, can lead to improved patient outcomes and reduced healthcare costs.

Despite these advantages, there are several challenges that need to be addressed when integrating imaging technologies, scoring systems, and AI in the management of AP. These challenges include the need for standardized imaging protocols and scoring systems, the need for large datasets of imaging and clinical data to train AI algorithms, and ethical and legal challenges associated with the use of AI in healthcare. In conclusion, the integration of imaging technologies, scoring systems, and AI has the potential to revolutionize the diagnosis, severity prediction, and prognosis assessment of AP.

FOOTNOTES

Author contributions: Hu JX and Zhao CF wrote this paper and contributed equally to this work; Chen CR designed this paper; Wang SL and Tu XY checked and proofread this paper; Huang WB, Chen JN, and Xie Y searched related literature and information for this paper; all authors have read and approved the final manuscript.

Supported by Fujian Provincial Health Technology Project, No. 2020GGA079; Natural Science Foundation of Fujian Province, No. 2021J011380; and National Natural Science Foundation of China, No. 62276146.

Conflict-of-interest statement: All the authors in this article declare there are no conflicts of interest.

Open-Access: This article is an open-access article that was selected by an in-house editor and fully peer-reviewed by external reviewers. It is distributed in accordance with the Creative Commons Attribution NonCommercial (CC BY-NC 4.0) license, which permits others to distribute, remix, adapt, build upon this work non-commercially, and license their derivative works on different terms, provided the original work is properly cited and the use is non-commercial. See: https://creativecommons.org/Licenses/by-nc/4.0/

Country/Territory of origin: China

ORCID number: Jian-Xiong Hu 0000-0003-0810-2696; Cheng-Fei Zhao 0000-0002-6646-6327; Cun-Rong Chen 0009-0002-4693-8726.

S-Editor: Yan JP
L-Editor: Filipodia
P-Editor: Cai YX

REFERENCES

1 **Cunha EF**, Rocha Mde S, Pereira FP, Blasbalg R, Baroni RH. Walled-off pancreatic necrosis and other current concepts in the radiological assessment of acute pancreatitis. *Radiol Bras* 2014; **47**: 165-175 [PMID: 25741074 DOI: 10.1590/0100-3984.2012.1565]

2 **Ouyang G**, Pan G, Liu Q, Wu Y, Liu Z, Lu W, Li S, Zhou Z, Wen Y. The global, regional, and national burden of pancreatitis in 195 countries and territories, 1990-2017: a systematic analysis for the Global Burden of Disease Study 2017. *BMC Med* 2020; **18**: 388 [PMID: 33298026 DOI: 10.1186/s12916-020-01859-5]

3 **Siregar GA**, Siregar GP. Management of Severe Acute Pancreatitis. *Open Access Maced J Med Sci* 2019; **7**: 3319-3323 [PMID: 31949538 DOI: 10.3889/oamjms.2019.720]

4 **Petrov MS**, Yadav D. Global epidemiology and holistic prevention of pancreatitis. *Nat Rev Gastroenterol Hepatol* 2019; **16**: 175-184 [PMID: 30482911 DOI: 10.1038/s41575-018-0087-5]

5 **Iannuzzi JP**, King JA, Leong JH, Quan J, Windsor JW, Tanyingoh D, Coward S, Forbes N, Heitman SJ, Shaheen AA, Swain M, Buie M, Underwood FE, Kaplan GG. Global Incidence of Acute Pancreatitis Is Increasing Over Time: A Systematic Review and Meta-Analysis. *Gastroenterology* 2022; **162**: 122-134 [PMID: 34571026 DOI: 10.1053/j.gastro.2021.09.043]

6 **Gapp J**, Hall AG, Walters RW, Jahann D, Kassim T, Reddymasu S. Trends and Outcomes of Hospitalizations Related to Acute Pancreatitis: Epidemiology From 2001 to 2014 in the United States. *Pancreas* 2019; **48**: 548-554 [PMID: 30946239 DOI: 10.1097/MPA.0000000000001275]

7 **Thapa R**, Iqbal Z, Garikipati A, Siefkas A, Hoffman J, Mao Q, Das R. Early prediction of severe acute pancreatitis using machine learning. *Pancreatology* 2022; **22**: 43-50 [PMID: 34690046 DOI: 10.1016/j.pan.2021.10.003]

8 **Lou D**, Shi K, Li HP, Zhu Q, Hu L, Luo J, Yang R, Liu F. Quantitative metabolic analysis of plasma extracellular vesicles for the diagnosis of severe acute pancreatitis. *J Nanobiotechnology* 2022; **20**: 52 [PMID: 35090480 DOI: 10.1186/s12951-022-01239-6]

9 **Fu B**, Feng H, Gao F, Fu X. Role of Extrapancreatic Necrosis Volume in Assessing the Severity and Predicting the Outcomes of Severe Acute Pancreatitis. *Int J Gen Med* 2021; **14**: 9515-9521 [PMID: 34916833 DOI: 10.2147/IJGM.S338658]

10 **Lee PJ**, Papachristou GI. Management of Severe Acute Pancreatitis. *Curr Treat Options Gastroenterol* 2020; **18**: 670-681 [PMID: 33230385 DOI: 10.1007/s11938-020-00322-x]

11 **Banks PA**, Bollen TL, Dervenis C, Gooszen HG, Johnson CD, Sarr MG, Tsiotos GG, Vege SS; Acute Pancreatitis Classification Working Group. Classification of acute pancreatitis--2012: revision of the Atlanta classification and definitions by international consensus. *Gut* 2013;

62: 102-111 [PMID: 23100216 DOI: 10.1136/gutjnl-2012-302779]
12 **Chan KS**, Shelat VG. Diagnosis, severity stratification and management of adult acute pancreatitis-current evidence and controversies. *World J Gastrointest Surg* 2022; **14**: 1179-1197 [PMID: 36504520 DOI: 10.4240/wjgs.v14.i11.1179]
13 **Purschke B**, Bolm L, Meyer MN, Sato H. Interventional strategies in infected necrotizing pancreatitis: Indications, timing, and outcomes. *World J Gastroenterol* 2022; **28**: 3383-3397 [PMID: 36158258 DOI: 10.3748/wjg.v28.i27.3383]
14 **Jia YC**, Ding YX, Mei WT, Wang YT, Zheng Z, Qu YX, Liang K, Li J, Cao F, Li F. Extracellular vesicles and pancreatitis: mechanisms, status and perspectives. *Int J Biol Sci* 2021; **17**: 549-561 [PMID: 33613112 DOI: 10.7150/ijbs.54858]
15 **Zheng Z**, Ding YX, Qu YX, Cao F, Li F. A narrative review of acute pancreatitis and its diagnosis, pathogenetic mechanism, and management. *Ann Transl Med* 2021; **9**: 69 [PMID: 33553362 DOI: 10.21037/atm-20-4802]
16 **Forsmark CE**, Baillie J; AGA Institute Clinical Practice and Economics Committee; AGA Institute Governing Board. AGA Institute technical review on acute pancreatitis. *Gastroenterology* 2007; **132**: 2022-2044 [PMID: 17484894 DOI: 10.1053/j.gastro.2007.03.065]
17 **Gumaste VV**, Roditis N, Mehta D, Dave PB. Serum lipase levels in nonpancreatic abdominal pain versus acute pancreatitis. *Am J Gastroenterol* 1993; **88**: 2051-2055 [PMID: 7504396]
18 **Kemppainen EA**, Hedström JI, Puolakkainen PA, Sainio VS, Haapiainen RK, Perhoniemi V, Osman S, Kivilaakso EO, Stenman UH. Rapid measurement of urinary trypsinogen-2 as a screening test for acute pancreatitis. *N Engl J Med* 1997; **336**: 1788-1793 [PMID: 9187069 DOI: 10.1056/NEJM199706193362504]
19 **Treacy J**, Williams A, Bais R, Willson K, Worthley C, Reece J, Bessell J, Thomas D. Evaluation of amylase and lipase in the diagnosis of acute pancreatitis. *ANZ J Surg* 2001; **71**: 577-582 [PMID: 11552931 DOI: 10.1046/j.1445-2197.2001.02220.x]
20 **Hu J**, Chen J, Xu G. Hyperamylasemia of Abnormally Elevated Serum Amylase: Macroamylasemia in a Healthy Individual. *Clin Lab* 2021; **67**: 1091-1094 [PMID: 33865250 DOI: 10.7754/Clin.Lab.2020.200827]
21 **Türkvatan A**, Erden A, Türkoğlu MA, Seçil M, Yener Ö. Imaging of acute pancreatitis and its complications. Part 1: acute pancreatitis. *Diagn Interv Imaging* 2015; **96**: 151-160 [PMID: 24512896 DOI: 10.1016/j.diii.2013.12.017]
22 **Yadav D**, Agarwal N, Pitchumoni CS. A critical evaluation of laboratory tests in acute pancreatitis. *Am J Gastroenterol* 2002; **97**: 1309-1318 [PMID: 12094843 DOI: 10.1111/j.1572-0241.2002.05766.x]
23 **Szatmary P**, Grammatikopoulos T, Cai W, Huang W, Mukherjee R, Halloran C, Beyer G, Sutton R. Acute Pancreatitis: Diagnosis and Treatment. *Drugs* 2022; **82**: 1251-1276 [PMID: 36074322 DOI: 10.1007/s40265-022-01766-4]
24 **Alsfasser G**, Rau BM, Klar E. Scoring of human acute pancreatitis: state of the art. *Langenbecks Arch Surg* 2013; **398**: 789-797 [PMID: 23680979 DOI: 10.1007/s00423-013-1087-0]
25 **Walkowska J**, Zielinska N, Karauda P, Tubbs RS, Kurtys K, Olewnik Ł. The Pancreas and Known Factors of Acute Pancreatitis. *J Clin Med* 2022; **11**: 5565 [PMID: 36233433 DOI: 10.3390/jcm11195565]
26 **Bollen TL**, van Santvoort HC, Besselink MG, van Es WH, Gooszen HG, van Leeuwen MS. Update on acute pancreatitis: ultrasound, computed tomography, and magnetic resonance imaging features. *Semin Ultrasound CT MR* 2007; **28**: 371-383 [PMID: 17970553 DOI: 10.1053/j.sult.2007.06.002]
27 **Raghuwanshi S**, Gupta R, Vyas MM, Sharma R. CT Evaluation of Acute Pancreatitis and its Prognostic Correlation with CT Severity Index. *J Clin Diagn Res* 2016; **10**: TC06-TC11 [PMID: 27504376 DOI: 10.7860/JCDR/2016/19849.7934]
28 **Expert Panel on Gastrointestinal Imaging**, Porter KK, Zaheer A, Kamel IR, Horowitz JM, Arif-Tiwari H, Bartel TB, Bashir MR, Camacho MA, Cash BD, Chernyak V, Goldstein A, Grajo JR, Gupta S, Hindman NM, Kamaya A, McNamara MM, Carucci LR. ACR Appropriateness Criteria® Acute Pancreatitis. *J Am Coll Radiol* 2019; **16**: S316-S330 [PMID: 31685100 DOI: 10.1016/j.jacr.2019.05.017]
29 **Brizi MG**, Perillo F, Cannone F, Tuzza L, Manfredi R. The role of imaging in acute pancreatitis. *Radiol Med* 2021; **126**: 1017-1029 [PMID: 33982269 DOI: 10.1007/s11547-021-01359-3]
30 **Lohse MR**, Ullah K, Seda J, Thode HC Jr, Singer AJ, Morley EJ. The role of emergency department computed tomography in early acute pancreatitis. *Am J Emerg Med* 2021; **48**: 92-95 [PMID: 33866269 DOI: 10.1016/j.ajem.2021.04.026]
31 **Vacca G**, Reginelli A, Urraro F, Sangiovanni A, Bruno F, Di Cesare E, Cappabianca S, Vanzulli A. Magnetic resonance severity index assessed by T1-weighted imaging for acute pancreatitis: correlation with clinical outcomes and grading of the revised Atlanta classification-a narrative review. *Gland Surg* 2020; **9**: 2312-2320 [PMID: 33447582 DOI: 10.21037/gs-20-554]
32 **Stevens KJ**, Lisanti C. Pancreas Imaging. 2023 Mar 6. In: StatPearls [Internet]. Treasure Island (FL): StatPearls Publishing; 2023 Jan [PMID: 31613505]
33 **Stimac D**, Miletić D, Radić M, Krznarić I, Mazur-Grbac M, Perković D, Milić S, Golubović V. The role of nonenhanced magnetic resonance imaging in the early assessment of acute pancreatitis. *Am J Gastroenterol* 2007; **102**: 997-1004 [PMID: 17378903 DOI: 10.1111/j.1572-0241.2007.01164.x]
34 **O'Neill E**, Hammond N, Miller FH. MR imaging of the pancreas. *Radiol Clin North Am* 2014; **52**: 757-777 [PMID: 24889170 DOI: 10.1016/j.rcl.2014.02.006]
35 **Zhou Y**, Hao N, Duan Z, Kong M, Xu M, Zhang D, Xu X, Yuan Q, Li C. Assessment of Acute Pancreatitis Severity and Prognosis with CT-Measured Body Composition. *Int J Gen Med* 2021; **14**: 3971-3980 [PMID: 34349546 DOI: 10.2147/IJGM.S322589]
36 **Sun H**, Zuo HD, Lin Q, Yang DD, Zhou T, Tang MY, Wáng YXJ, Zhang XM. MR imaging for acute pancreatitis: the current status of clinical applications. *Ann Transl Med* 2019; **7**: 269 [PMID: 31355236 DOI: 10.21037/atm.2019.05.37]
37 **Williford ME**, Foster WL Jr, Halvorsen RA, Thompson WM. Pancreatic pseudocyst: comparative evaluation by sonography and computed tomography. *AJR Am J Roentgenol* 1983; **140**: 53-57 [PMID: 6600325 DOI: 10.2214/ajr.140.1.53]
38 **Türkvatan A**, Erden A, Türkoğlu MA, Seçil M, Yüce G. Imaging of acute pancreatitis and its complications. Part 2: complications of acute pancreatitis. *Diagn Interv Imaging* 2015; **96**: 161-169 [PMID: 24703377 DOI: 10.1016/j.diii.2013.12.018]
39 **Morgan DE**. Imaging of acute pancreatitis and its complications. *Clin Gastroenterol Hepatol* 2008; **6**: 1077-1085 [PMID: 18928934 DOI: 10.1016/j.cgh.2008.07.012]
40 **Ding L**, Yu C, Deng F, He WH, Xia L, Zhou M, Lan GL, Huang X, Lei YP, Zhou XJ, Zhu Y, Lu NH. New Risk Factors for Infected Pancreatic Necrosis Secondary to Severe Acute Pancreatitis: The Role of Initial Contrast-Enhanced Computed Tomography. *Dig Dis Sci* 2019; **64**: 553-560 [PMID: 30465178 DOI: 10.1007/s10620-018-5359-y]
41 **Balthazar EJ**, Freeny PC, vanSonnenberg E. Imaging and intervention in acute pancreatitis. *Radiology* 1994; **193**: 297-306 [PMID: 7972730 DOI: 10.1148/radiology.193.2.7972730]
42 **Balthazar EJ**, Robinson DL, Megibow AJ, Ranson JH. Acute pancreatitis: value of CT in establishing prognosis. *Radiology* 1990; **174**: 331-

336 [PMID: 2296641 DOI: 10.1148/radiology.174.2.2296641]
43 **Mortele KJ**, Wiesner W, Intriere L, Shankar S, Zou KH, Kalantari BN, Perez A, vanSonnenberg E, Ros PR, Banks PA, Silverman SG. A modified CT severity index for evaluating acute pancreatitis: improved correlation with patient outcome. *AJR Am J Roentgenol* 2004; **183**: 1261-1265 [PMID: 15505289 DOI: 10.2214/ajr.183.5.1831261]
44 **Saneesh PS**, Garga UC, Gupta AK, Yelamanchi R. Role of multi-detector computed tomography in severity assessment of cases of acute pancreatitis. *Wien Klin Wochenschr* 2021; **133**: 654-660 [PMID: 33914151 DOI: 10.1007/s00508-021-01870-7]
45 **Mikó A**, Vigh É, Mátrai P, Soós A, Garami A, Balaskó M, Czakó L, Mosdósi B, Sarlós P, Erőss B, Tenk J, Rostás I, Hegyi P. Computed Tomography Severity Index vs. Other Indices in the Prediction of Severity and Mortality in Acute Pancreatitis: A Predictive Accuracy Meta-analysis. *Front Physiol* 2019; **10**: 1002 [PMID: 31507427 DOI: 10.3389/fphys.2019.01002]
46 **Song YS**, Park HS, Yu MH, Kim YJ, Jung SI. Prediction of Necrotizing Pancreatitis on Early CT Based on the Revised Atlanta Classification. *Taehan Yongsang Uihakhoe Chi* 2020; **81**: 1436-1447 [PMID: 36237716 DOI: 10.3348/jksr.2020.0012]
47 **Tasu JP**, Guen RL, Rhouma IB, Guerrab A, Beydoun N, Bergougnoux B, Ingrand P, Herpe G. Accuracy of a CT density threshold enhancement to identify pancreatic parenchyma necrosis in acute pancreatitis during the first week. *Diagn Interv Imaging* 2022; **103**: 266-272 [PMID: 34991994 DOI: 10.1016/j.diii.2021.12.003]
48 **Badat N**, Millet I, Corno L, Khaled W, Boulay-Coletta I, Zins M. Revised Atlanta classification for CT pancreatic and peripancreatic collections in the first month of acute pancreatitis: interobserver agreement. *Eur Radiol* 2019; **29**: 2302-2310 [PMID: 30631920 DOI: 10.1007/s00330-018-5906-0]
49 **Du J**, Zhang J, Zhang X, Jiang R, Fu Q, Yang G, Fan H, Tang M, Chen T, Li X. Computed tomography characteristics of acute pancreatitis based on different etiologies at different onset times: a retrospective cross-sectional study. *Quant Imaging Med Surg* 2022; **12**: 4448-4461 [PMID: 36060601 DOI: 10.21037/qims-21-1231]
50 **Bollen TL**, Singh VK, Maurer R, Repas K, van Es HW, Banks PA, Mortele KJ. Comparative evaluation of the modified CT severity index and CT severity index in assessing severity of acute pancreatitis. *AJR Am J Roentgenol* 2011; **197**: 386-392 [PMID: 21785084 DOI: 10.2214/AJR.09.4025]
51 **Sahu B**, Abbey P, Anand R, Kumar A, Tomer S, Malik E. Severity assessment of acute pancreatitis using CT severity index and modified CT severity index: Correlation with clinical outcomes and severity grading as per the Revised Atlanta Classification. *Indian J Radiol Imaging* 2017; **27**: 152-160 [PMID: 28744075 DOI: 10.4103/ijri.IJRI_300_16]
52 **Alberti P**, Pando E, Mata R, Vidal L, Roson N, Mast R, Armario D, Merino X, Dopazo C, Blanco L, Caralt M, Gomez C, Balsells J, Charco R. Evaluation of the modified computed tomography severity index (MCTSI) and computed tomography severity index (CTSI) in predicting severity and clinical outcomes in acute pancreatitis. *J Dig Dis* 2021; **22**: 41-48 [PMID: 33184988 DOI: 10.1111/1751-2980.12961]
53 **Liao Q**, He WH, Li TM, Lai C, Yu L, Xia LY, Luo Y, Zhu P, Liu H, Zeng Y, Zhu NH, Lyu N. Evaluation of severity and prognosis of acute pancreatitis by CT severity index and modified CT severity index. *Zhonghua Yi Xue Za Zhi* 2022; **102**: 2011-2017 [PMID: 35817726 DOI: 10.3760/cma.j.cn112137-20220424-00914]
54 **Dachs RJ**, Sullivan L, Shanmugathasan P. Does early ED CT scanning of afebrile patients with first episodes of acute pancreatitis ever change management? *Emerg Radiol* 2015; **22**: 239-243 [PMID: 25239388 DOI: 10.1007/s10140-014-1266-5]
55 **Working Group IAP/APA Acute Pancreatitis Guidelines**. IAP/APA evidence-based guidelines for the management of acute pancreatitis. *Pancreatology* 2013; **13**: e1-e15 [PMID: 24054878 DOI: 10.1016/j.pan.2013.07.063]
56 **Huang H**, Chen W, Tang G, Liang Z, Qin M, Tang Y, Qin H, Chang R. Optimal timing of contrast-enhanced computed tomography in an evaluation of severe acute pancreatitis-associated complications. *Exp Ther Med* 2019; **18**: 1029-1038 [PMID: 31363364 DOI: 10.3892/etm.2019.7700]
57 **Pocard M**, Soyer P. CT of acute pancreatitis: a matter of time. *Diagn Interv Imaging* 2015; **96**: 129-131 [PMID: 25617113 DOI: 10.1016/j.diii.2015.01.001]
58 **Kumar P**, Gupta P, Rana S. Thoracic complications of pancreatitis. *JGH Open* 2019; **3**: 71-79 [PMID: 30834344 DOI: 10.1002/jgh3.12099]
59 **Song LJ**, Xiao B. Medical imaging for pancreatic diseases: Prediction of severe acute pancreatitis complicated with acute respiratory distress syndrome. *World J Gastroenterol* 2022; **28**: 6206-6212 [PMID: 36504558 DOI: 10.3748/wjg.v28.i44.6206]
60 **Liao YT**, Chiu NC, Chen CK, Su KC. Acute-on-chronic pancreatitis complicated with mediastinal pseudocysts and cardiac tamponade: A case report and literature review. *Respirol Case Rep* 2022; **10**: e0929 [PMID: 35309959 DOI: 10.1002/rcr2.929]
61 **Kozlov A**, Becher MU, Schlecker S. Hypertriglyceridemic pancreatitis and cardiac tamponade in a 26-year-old woman. *Inn Med (Heidelb)* 2023; **64**: 88-92 [PMID: 36418500 DOI: 10.1007/s00108-022-01434-5]
62 **Dąbkowski K**, Białek A, Kukla M, Wójcik J, Smereczyński A, Kołaczyk K, Grodzki T, Starzyńska T. Mediastinal Pancreatic Pseudocysts. *Clin Endosc* 2017; **50**: 76-80 [PMID: 27641151 DOI: 10.5946/ce.2016.089]
63 **Browne GW**, Pitchumoni CS. Pathophysiology of pulmonary complications of acute pancreatitis. *World J Gastroenterol* 2006; **12**: 7087-7096 [PMID: 17131469 DOI: 10.3748/wjg.v12.i44.7087]
64 **Luiken I**, Eisenmann S, Garbe J, Sternby H, Verdonk RC, Dimova A, Ignatavicius P, Ilzarbe L, Koiva P, Penttilä AK, Regnér S, Dober J, Wohlgemuth WA, Brill R, Michl P, Rosendahl J, Damm M. Pleuropulmonary pathologies in the early phase of acute pancreatitis correlate with disease severity. *PLoS ONE* 2022; **17**: e0263739 [PMID: 35130290 DOI: 10.1371/journal.pone.0263739]
65 **Peng R**, Zhang L, Zhang ZM, Wang ZQ, Liu GY, Zhang XM. Chest computed tomography semi-quantitative pleural effusion and pulmonary consolidation are early predictors of acute pancreatitis severity. *Quant Imaging Med Surg* 2020; **10**: 451-463 [PMID: 32190570 DOI: 10.21037/qims.2019.12.14]
66 **Raghu MG**, Wig JD, Kochhar R, Gupta D, Gupta R, Yadav TD, Agarwal R, Kudari AK, Doley RP, Javed A. Lung complications in acute pancreatitis. *JOP* 2007; **8**: 177-185 [PMID: 17356240]
67 **Yan G**, Li H, Bhetuwal A, McClure MA, Li Y, Yang G, Zhao L, Fan X. Pleural effusion volume in patients with acute pancreatitis: a retrospective study from three acute pancreatitis centers. *Ann Med* 2021; **53**: 2003-2018 [PMID: 34727802 DOI: 10.1080/07853890.2021.1998594]
68 **Liu D**, Song B, Huang ZX, Yuan F, Li WM. The value of chest CT features evaluating the severity and prognosis for acute pancreatitis. *Sichuan Da Xue Xue Bao Yi Xue Ban* 2013; **44**: 319-322 [PMID: 23745281]
69 **Kothari S**, Kalinowski M, Kobeszko M, Almouradi T. Computed tomography scan imaging in diagnosing acute uncomplicated pancreatitis: Usefulness vs cost. *World J Gastroenterol* 2019; **25**: 1080-1087 [PMID: 30862996 DOI: 10.3748/wjg.v25.i9.1080]
70 **Bollen TL**, Singh VK, Maurer R, Repas K, van Es HW, Banks PA, Mortele KJ. A comparative evaluation of radiologic and clinical scoring systems in the early prediction of severity in acute pancreatitis. *Am J Gastroenterol* 2012; **107**: 612-619 [PMID: 22186977 DOI:

10.1038/ajg.2011.438]
71 **Shinagare AB**, Ip IK, Raja AS, Sahni VA, Banks P, Khorasani R. Use of CT and MRI in emergency department patients with acute pancreatitis. *Abdom Imaging* 2015; **40**: 272-277 [PMID: 25078061 DOI: 10.1007/s00261-014-0210-1]
72 **Kamal A**, Singh VK, Akshintala VS, Kawamoto S, Tsai S, Haider M, Fishman EK, Kamel IR, Zaheer A. CT and MRI assessment of symptomatic organized pancreatic fluid collections and pancreatic duct disruption: an interreader variability study using the revised Atlanta classification 2012. *Abdom Imaging* 2015; **40**: 1608-1616 [PMID: 25425489 DOI: 10.1007/s00261-014-0303-x]
73 **Bastati N**, Kristic A, Poetter-Lang S, Messner A, Herold A, Hodge JC, Schindl M, Ba-Ssalamah A. Imaging of inflammatory disease of the pancreas. *Br J Radiol* 2021; **94**: 20201214 [PMID: 34111970 DOI: 10.1259/bjr.20201214]
74 **Zhou T**, Tang MY, Deng Y, Wu JL, Sun H, Chen Y, Chen TW, Zhang XM. MR Imaging for Early Extrapancreatic Necrosis in Acute Pancreatitis. *Acad Radiol* 2021; **28** Suppl 1: S225-S233 [PMID: 31767534 DOI: 10.1016/j.acra.2019.10.023]
75 **Zhou T**, Chen Y, Wu JL, Deng Y, Zhang J, Sun H, Lan C, Zhang XM. Extrapancreatic Inflammation on Magnetic Resonance Imaging for the Early Prediction of Acute Pancreatitis Severity. *Pancreas* 2020; **49**: 46-52 [PMID: 31856079 DOI: 10.1097/MPA.0000000000001425]
76 **Jiang ZQ**, Xiao B, Zhang XM, Xu HB. Early-phase vascular involvement is associated with acute pancreatitis severity: a magnetic resonance imaging study. *Quant Imaging Med Surg* 2021; **11**: 1909-1920 [PMID: 33936974 DOI: 10.21037/qims-20-280]
77 **Xie CL**, Zhang M, Chen Y, Hu R, Tang MY, Chen TW, Xue HD, Jin ZY, Zhang XM. Spleen and splenic vascular involvement in acute pancreatitis: an MRI study. *Quant Imaging Med Surg* 2018; **8**: 291-300 [PMID: 29774182 DOI: 10.21037/qims.2018.03.04]
78 **Chi XX**, Zhang XM, Chen TW, Huang XH, Yang L, Tang W, Xiao B. The normal transverse mesocolon and involvement of the mesocolon in acute pancreatitis: an MRI study. *PLoS ONE* 2014; **9**: e93687 [PMID: 24705446 DOI: 10.1371/journal.pone.0093687]
79 **Chi XX**, Chen TW, Huang XH, Yang L, Tang W, Wáng YX, Xiao B, Zhang XM. Magnetic resonance imaging of retroperitoneal interfascial plane involvement in acute pancreatitis. *Quant Imaging Med Surg* 2016; **6**: 250-258 [PMID: 27429909 DOI: 10.21037/qims.2016.06.09]
80 **Ji YF**, Zhang XM, Mitchell DG, Li XH, Chen TW, Li Y, Bao ZG, Tang W, Xiao B, Huang XH, Yang L. Gastrointestinal tract involvement in acute pancreatitis: initial findings and follow-up by magnetic resonance imaging. *Quant Imaging Med Surg* 2017; **7**: 641-653 [PMID: 29312869 DOI: 10.21037/qims.2017.12.03]
81 **Xiao B**, Xu HB, Jiang ZQ, Zhang J, Zhang XM. Current concepts for the diagnosis of acute pancreatitis by multiparametric magnetic resonance imaging. *Quant Imaging Med Surg* 2019; **9**: 1973-1985 [PMID: 31929970 DOI: 10.21037/qims.2019.11.10]
82 **Tang MY**, Zhou T, Ma L, Huang XH, Sun H, Deng Y, Wang SY, Ji YF, Xiao B, Zhang XM. A new logistic regression model for early prediction of severity of acute pancreatitis using magnetic resonance imaging and Acute Physiology and Chronic Health Evaluation II scoring systems. *Quant Imaging Med Surg* 2022; **12**: 4424-4434 [PMID: 36060575 DOI: 10.21037/qims-22-158]
83 **Tang MY**, Chen TW, Bollen TL, Wang YX, Xue HD, Jin ZY, Huang XH, Xiao B, Li XH, Ji YF, Zhang XM. MR imaging of hemorrhage associated with acute pancreatitis. *Pancreatology* 2018; **18**: 363-369 [PMID: 29615311 DOI: 10.1016/j.pan.2018.03.004]
84 **Brun A**, Agarwal N, Pitchumoni CS. Fluid collections in and around the pancreas in acute pancreatitis. *J Clin Gastroenterol* 2011; **45**: 614-625 [PMID: 21750432 DOI: 10.1097/MCG.0b013e318213ef3e]
85 **Ahmed A**, Gibreel W, Sarr MG. Recognition and Importance of New Definitions of Peripancreatic Fluid Collections in Managing Patients with Acute Pancreatitis. *Dig Surg* 2016; **33**: 259-266 [PMID: 27216496 DOI: 10.1159/000445005]
86 **Lee DW**, Kim HG, Cho CM, Jung MK, Heo J, Cho KB, Kim SB, Kim KH, Kim TN, Han J, Kim H. Natural Course of Early Detected Acute Peripancreatic Fluid Collection in Moderately Severe or Severe Acute Pancreatitis. *Medicina (Kaunas)* 2022; **58**: 1131 [PMID: 36013598 DOI: 10.3390/medicina58081131]
87 **Lankisch PG**, Struckmann K, Lehnick D. Presence and extent of extrapancreatic fluid collections are indicators of severe acute pancreatitis. *Int J Pancreatol* 1999; **26**: 131-136 [PMID: 10732289 DOI: 10.1385/IJGC:26:3:131]
88 **Dhaka N**, Samanta J, Kochhar S, Kalra N, Appasani S, Manrai M, Kochhar R. Pancreatic fluid collections: What is the ideal imaging technique? *World J Gastroenterol* 2015; **21**: 13403-13410 [PMID: 26730150 DOI: 10.3748/wjg.v21.i48.13403]
89 **Sun H**, Jian S, Peng B, Hou J. Comparison of magnetic resonance imaging and computed tomography in the diagnosis of acute pancreatitis: a systematic review and meta-analysis of diagnostic test accuracy studies. *Ann Transl Med* 2022; **10**: 410 [PMID: 35530935 DOI: 10.21037/atm-22-812]
90 **Tang W**, Zhang XM, Xiao B, Zeng NL, Pan HS, Feng ZS, Xu XX. Magnetic resonance imaging versus Acute Physiology And Chronic Healthy Evaluation II score in predicting the severity of acute pancreatitis. *Eur J Radiol* 2011; **80**: 637-642 [PMID: 20843620 DOI: 10.1016/j.ejrad.2010.08.020]
91 **Xu N**, Li L, Zhao D, Wang Z, Wang X, Wang R, Zeng Y, Zhang L, Zhong N, Lv Y, Linghu E, Chai N. A preferable modality for the differentiation of peripancreatic fluid collections: Endoscopic ultrasound. *Endosc Ultrasound* 2022; **11**: 291-295 [PMID: 35083982 DOI: 10.4103/EUS-D-21-00130]
92 **Li J**, Zhang Q, Zhou A, Zhao G, Li P. Comparative outcomes of endoscopic ultrasound-guided lumen-apposing mental stents drainage for pancreatic pseudocysts and walled-off necrosis: Case series and meta-analysis. *Chronic Dis Transl Med* 2021; **7**: 157-168 [PMID: 34505016 DOI: 10.1016/j.cdtm.2021.07.001]
93 **Froes CD**, Gosal K, Singh P, Collier V. The Utility of Abdominal Ultrasound Following Negative Computed Tomography in Diagnosing Acute Pancreatitis. *Cureus* 2022; **14**: e27752 [PMID: 36106274 DOI: 10.7759/cureus.27752]
94 **Cai D**, Parajuly SS, Wang H, Wang X, Ling W, Song B, Li Y, Luo Y. Accuracy of contrast-enhanced ultrasound compared with conventional ultrasound in acute pancreatitis: Diagnosis and complication monitoring. *Exp Ther Med* 2016; **12**: 3189-3194 [PMID: 27882136 DOI: 10.3892/etm.2016.3760]
95 **Juneja D**. Ideal scoring system for acute pancreatitis: Quest for the Holy Grail. *World J Crit Care Med* 2022; **11**: 198-200 [PMID: 36331986 DOI: 10.5492/wjccm.v11.i3.198]
96 **Silva-Vaz P**, Abrantes AM, Castelo-Branco M, Gouveia A, Botelho MF, Tralhão JG. Multifactorial Scores and Biomarkers of Prognosis of Acute Pancreatitis: Applications to Research and Practice. *Int J Mol Sci* 2020; **21**: 338 [PMID: 31947993 DOI: 10.3390/ijms21010338]
97 **Ma X**, Li L, Jin T, Xia Q. Harmless acute pancreatitis score on admission can accurately predict mild acute pancreatitis. *Nan Fang Yi Ke Da Xue Xue Bao* 2020; **40**: 190-195 [PMID: 32376542 DOI: 10.12122/j.issn.1673-4254.2020.02.09]
98 **Ueda T**, Takeyama Y, Yasuda T, Kamei K, Satoi S, Sawa H, Shinzeki M, Ku Y, Kuroda Y, Ohyanagi H. Utility of the new Japanese severity score and indications for special therapies in acute pancreatitis. *J Gastroenterol* 2009; **44**: 453-459 [PMID: 19308309 DOI: 10.1007/s00535-009-0026-x]
99 **Lin F**, Lu R, Han D, Fan Y, Zhang Y, Pan P. A prediction model for acute respiratory distress syndrome among patients with severe acute pancreatitis: a retrospective analysis. *Ther Adv Respir Dis* 2022; **16**: 17534666221122592 [PMID: 36065909 DOI:

10.1177/17534666221122592]
100 **Wagner DP**, Draper EA. Acute physiology and chronic health evaluation (APACHE II) and Medicare reimbursement. *Health Care Financ Rev* 1984; **1984** (Suppl): 91-105 [PMID: 10311080]
101 **Wu Bu**, Johannes RS, Sun X, Tabak Y, Conwell DL, Banks PA. The early prediction of mortality in acute pancreatitis: a large population-based study. *Gut* 2008; **57**: 1698-1703 [PMID: 18519429 DOI: 10.1136/gut.2008.152702]
102 **Papachristou GI**, Muddana V, Yadav D, O'Connell M, Sanders MK, Slivka A, Whitcomb DC. Comparison of BISAP, Ranson's, APACHE-II, and CTSI scores in predicting organ failure, complications, and mortality in acute pancreatitis. *Am J Gastroenterol* 2010; **105**: 435-441 [PMID: 19861954 DOI: 10.1038/ajg.2009.622]
103 **Ranson JH**, Rifkind KM, Roses DF, Fink SD, Eng K, Localio SA. Objective early identification of severe acute pancreatitis. *Am J Gastroenterol* 1974; **61**: 443-451 [PMID: 4835417]
104 **Avanesov M**, Löser A, Smagarynska A, Keller S, Guerreiro H, Tahir E, Karul M, Adam G, Yamamura J. Clinico-radiological comparison and short-term prognosis of single acute pancreatitis and recurrent acute pancreatitis including pancreatic volumetry. *PLoS ONE* 2018; **13**: e0206062 [PMID: 30359398 DOI: 10.1371/journal.pone.0206062]
105 **Mounzer R**, Langmead CJ, Wu BU, Evans AC, Bishehsari F, Muddana V, Singh VK, Slivka A, Whitcomb DC, Yadav D, Banks PA, Papachristou GI. Comparison of existing clinical scoring systems to predict persistent organ failure in patients with acute pancreatitis. *Gastroenterology* 2012; **142**: 1476-1482 [PMID: 22425589 DOI: 10.1053/j.gastro.2012.03.005]
106 **Cho JH**, Kim TN, Chung HH, Kim KH. Comparison of scoring systems in predicting the severity of acute pancreatitis. *World J Gastroenterol* 2015; **21**: 2387-2394 [PMID: 25741146 DOI: 10.3748/wjg.v21.i8.2387]
107 **Yang L**, Liu J, Xing Y, Du L, Chen J, Liu X, Hao J. Comparison of BISAP, Ranson, MCTSI, and APACHE II in Predicting Severity and Prognoses of Hyperlipidemic Acute Pancreatitis in Chinese Patients. *Gastroenterol Res Pract* 2016; **2016**: 1834256 [PMID: 27882045 DOI: 10.1155/2016/1834256]
108 **Harshit Kumar A**, Singh Griwan M. A comparison of APACHE II, BISAP, Ranson's score and modified CTSI in predicting the severity of acute pancreatitis based on the 2012 revised Atlanta Classification. *Gastroenterol Rep (Oxf)* 2018; **6**: 127-131 [PMID: 29780601 DOI: 10.1093/gastro/gox029]
109 **Biberci Keskin E**, Taşlıdere B, Koçhan K, Gülen B, İnce AT, Şentürk H. Comparison of scoring systems used in acute pancreatitis for predicting major adverse events. *Gastroenterol Hepatol* 2020; **43**: 193-199 [PMID: 31924368 DOI: 10.1016/j.gastrohep.2019.10.008]
110 **Li Y**, Zhang J, Zou J. Evaluation of four scoring systems in prognostication of acute pancreatitis for elderly patients. *BMC Gastroenterol* 2020; **20**: 165 [PMID: 32487074 DOI: 10.1186/s12876-020-01318-8]
111 **Teng TZJ**, Tan JKT, Baey S, Gunasekaran SK, Junnarkar SP, Low JK, Huey CWT, Shelat VG. Sequential organ failure assessment score is superior to other prognostic indices in acute pancreatitis. *World J Crit Care Med* 2021; **10**: 355-368 [PMID: 34888161 DOI: 10.5492/wjccm.v10.i6.355]
112 **Venkatesh NR**, Vijayakumar C, Balasubramaniyan G, Chinnakkulam Kandhasamy S, Sundaramurthi S, G S S, Srinivasan K. Comparison of Different Scoring Systems in Predicting the Severity of Acute Pancreatitis: A Prospective Observational Study. *Cureus* 2020; **12**: e6943 [PMID: 32190494 DOI: 10.7759/cureus.6943]
113 **Asfuroğlu Kalkan E**, Kalkan Ç, Kaçar S, Barutçu S, Yüksel M, Güçbey Türker Ö, Göre B, Canlı T, Asfuroğlu U, Barutçu Asfuroğlu B, Hamamcı M, Kılıç V, Köseoğlu T, Özaslan E, Ödemiş B, Kılıç M, Yüksel İ, Ersoy O, Altıparmak E, Ateş İ, Soykan İ. Similarities and Differences Between Gerontal and Young Patients with Acute Pancreatitis: Evaluation of Clinical Characteristics and Outcomes. *Turk J Gastroenterol* 2022; **33**: 874-884 [PMID: 36205509 DOI: 10.5152/tjg.2022.22227]
114 **Singh VK**, Wu BU, Bollen TL, Repas K, Maurer R, Johannes RS, Mortele KJ, Conwell DL, Banks PA. A prospective evaluation of the bedside index for severity in acute pancreatitis score in assessing mortality and intermediate markers of severity in acute pancreatitis. *Am J Gastroenterol* 2009; **104**: 966-971 [PMID: 19293787 DOI: 10.1038/ajg.2009.28]
115 **Park JY**, Jeon TJ, Ha TH, Hwang JT, Sinn DH, Oh TH, Shin WC, Choi WC. Bedside index for severity in acute pancreatitis: comparison with other scoring systems in predicting severity and organ failure. *Hepatobiliary Pancreat Dis Int* 2013; **12**: 645-650 [PMID: 24322751 DOI: 10.1016/s1499-3872(13)60101-0]
116 **Chatterjee R**, Parab N, Sajjan B, Nagar VS. Comparison of Acute Physiology and Chronic Health Evaluation II, Modified Computed Tomography Severity Index, and Bedside Index for Severity in Acute Pancreatitis Score in Predicting the Severity of Acute Pancreatitis. *Indian J Crit Care Med* 2020; **24**: 99-103 [PMID: 32205940 DOI: 10.5005/jp-journals-10071-23343]
117 **Chandra S**, Murali A, Bansal R, Agarwal D, Holm A. The Bedside Index for Severity in Acute Pancreatitis: a systematic review of prospective studies to determine predictive performance. *J Community Hosp Intern Med Perspect* 2017; **7**: 208-213 [PMID: 29046745 DOI: 10.1080/20009666.2017.1361292]
118 **Valverde-López F**, Matas-Cobos AM, Alegría-Motte C, Jiménez-Rosales R, Úbeda-Muñoz M, Redondo-Cerezo E. BISAP, RANSON, lactate and others biomarkers in prediction of severe acute pancreatitis in a European cohort. *J Gastroenterol Hepatol* 2017; **32**: 1649-1656 [PMID: 28207167 DOI: 10.1111/jgh.13763]
119 **Chen L**, Lu G, Zhou Q, Zhan Q. Evaluation of the BISAP score in predicting severity and prognoses of acute pancreatitis in Chinese patients. *Int Surg* 2013; **98**: 6-12 [PMID: 23438270 DOI: 10.9738/0020-8868-98.1.6]
120 **Zhang J**, Shahbaz M, Fang R, Liang B, Gao C, Gao H, Ijaz M, Peng C, Wang B, Niu Z, Niu J. Comparison of the BISAP scores for predicting the severity of acute pancreatitis in Chinese patients according to the latest Atlanta classification. *J Hepatobiliary Pancreat Sci* 2014; **21**: 689-694 [PMID: 24850587 DOI: 10.1002/jhbp.118]
121 **Gao W**, Yang HX, Ma CE. The Value of BISAP Score for Predicting Mortality and Severity in Acute Pancreatitis: A Systematic Review and Meta-Analysis. *PLoS ONE* 2015; **10**: e0130412 [PMID: 26091293 DOI: 10.1371/journal.pone.0130412]
122 **Yadav J**, Yadav SK, Kumar S, Baxla RG, Sinha DK, Bodra P, Besra RC, Baski BM, Prakash O, Anand A. Predicting morbidity and mortality in acute pancreatitis in an Indian population: a comparative study of the BISAP score, Ranson's score and CT severity index. *Gastroenterol Rep (Oxf)* 2016; **4**: 216-220 [PMID: 25733696 DOI: 10.1093/gastro/gov009]
123 **Bezmarević M**, Kostić Z, Jovanović M, Micković S, Mirković D, Soldatović I, Trifunović B, Pejović J, Vujanić S. Procalcitonin and BISAP score versus C-reactive protein and APACHE II score in early assessment of severity and outcome of acute pancreatitis. *Vojnosanit Pregl* 2012; **69**: 425-431 [PMID: 22764546]
124 **Yang YX**, Li L. Evaluating the Ability of the Bedside Index for Severity of Acute Pancreatitis Score to Predict Severe Acute Pancreatitis: A Meta-Analysis. *Med Princ Pract* 2016; **25**: 137-142 [PMID: 26613249 DOI: 10.1159/000441003]
125 **Kim BG**, Noh MH, Ryu CH, Nam HS, Woo SM, Ryu SH, Jang JS, Lee JH, Choi SR, Park BH. A comparison of the BISAP score and serum

procalcitonin for predicting the severity of acute pancreatitis. *Korean J Intern Med* 2013; **28**: 322-329 [PMID: 23682226 DOI: 10.3904/kjim.2013.28.3.322]

126 **Hagjer S**, Kumar N. Evaluation of the BISAP scoring system in prognostication of acute pancreatitis - A prospective observational study. *Int J Surg* 2018; **54**: 76-81 [PMID: 29684670 DOI: 10.1016/j.ijsu.2018.04.026]

127 **Zheng J**, Zhang J, Gao J. Early evaluations of BISAP plus C-reactive protein in predicting the severity of acute pancreatitis. *Zhonghua Yi Xue Za Zhi* 2015; **95**: 925-928 [PMID: 26081056]

128 **Wu B**, Yang J, Dai Y, Xiong L. Combination of the BISAP Score and miR-155 is Applied in Predicting the Severity of Acute Pancreatitis. *Int J Gen Med* 2022; **15**: 7467-7474 [PMID: 36187163 DOI: 10.2147/IJGM.S384068]

129 **Vincent JL**, Moreno R, Takala J, Willatts S, De Mendonça A, Bruining H, Reinhart CK, Suter PM, Thijs LG. The SOFA (Sepsis-related Organ Failure Assessment) score to describe organ dysfunction/failure. On behalf of the Working Group on Sepsis-Related Problems of the European Society of Intensive Care Medicine. *Intensive Care Med* 1996; **22**: 707-710 [PMID: 8844239 DOI: 10.1007/BF01709751]

130 **Kashyap R**, Sherani KM, Dutt T, Gnanapandithan K, Sagar M, Vallabhajosyula S, Vakil AP, Surani S. Current Utility of Sequential Organ Failure Assessment Score: A Literature Review and Future Directions. *Open Respir Med J* 2021; **15**: 1-6 [PMID: 34249175 DOI: 10.2174/1874306402115010001]

131 **Minne L**, Abu-Hanna A, de Jonge E. Evaluation of SOFA-based models for predicting mortality in the ICU: A systematic review. *Crit Care* 2008; **12**: R161 [PMID: 19091120 DOI: 10.1186/cc7160]

132 **Jentzer JC**, Bennett C, Wiley BM, Murphree DH, Keegan MT, Gajic O, Wright RS, Barsness GW. Predictive Value of the Sequential Organ Failure Assessment Score for Mortality in a Contemporary Cardiac Intensive Care Unit Population. *J Am Heart Assoc* 2018; **7**: e008169 [PMID: 29525785 DOI: 10.1161/JAHA.117.008169]

133 **Adam F**, Bor C, Uyar M, Demırağ K, Çankayalı İ. Severe acute pancreatitis admitted to intensive care unit: SOFA is superior to Ranson's criteria and APACHE II in determining prognosis. *Turk J Gastroenterol* 2013; **24**: 430-435 [PMID: 24557967 DOI: 10.4318/tjg.2013.0761]

134 **Tee YS**, Fang HY, Kuo IM, Lin YS, Huang SF, Yu MC. Serial evaluation of the SOFA score is reliable for predicting mortality in acute severe pancreatitis. *Medicine (Baltimore)* 2018; **97**: e9654 [PMID: 29443733 DOI: 10.1097/MD.0000000000009654]

135 **Para O**, Caruso L, Savo MT, Antonielli E, Blasi E, Capello F, Ciarambino T, Corbo L, Curto A, Giampieri M, Maddaluni L, Zaccagnini G, Nozzoli C. The challenge of prognostic markers in acute pancreatitis: internist's point of view. *J Genet Eng Biotechnol* 2021; **19**: 77 [PMID: 34036463 DOI: 10.1186/s43141-021-00178-3]

136 **Seymour CW**, Liu VX, Iwashyna TJ, Brunkhorst FM, Rea TD, Scherag A, Rubenfeld G, Kahn JM, Shankar-Hari M, Singer M, Deutschman CS, Escobar GJ, Angus DC. Assessment of Clinical Criteria for Sepsis: For the Third International Consensus Definitions for Sepsis and Septic Shock (Sepsis-3). *JAMA* 2016; **315**: 762-774 [PMID: 26903335 DOI: 10.1001/jama.2016.0288]

137 **Qin X**, Lin H, Liu T, Zhao L, Li H. Evaluation value of the quick sequential organ failure assessment score on prognosis of intensive care unit adult patients with infection: a 17-year observation study from the real world. *Zhonghua Wei Zhong Bing Ji Jiu Yi Xue* 2018; **30**: 544-548 [PMID: 30009728 DOI: 10.3760/cma.j.issn.2095-4352.2018.06.008]

138 **Rasch S**, Pichlmeier EM, Phillip V, Mayr U, Schmid RM, Huber W, Lahmer T. Prediction of Outcome in Acute Pancreatitis by the qSOFA and the New ERAP Score. *Dig Dis Sci* 2022; **67**: 1371-1378 [PMID: 33770328 DOI: 10.1007/s10620-021-06945-z]

139 **Wagner J**, Hernández Blanco YY, Yu A, Garcia-Rodriguez V, Mohajir W, Goodman C, DuPont AW, Cash BD, Farooq A. The Quick Sepsis-Related Organ Failure Assessment Score Is Prognostic of Pancreatitis Severity in Patients With Alcohol-Induced Pancreatitis. *Pancreas* 2022; **51**: 694-699 [PMID: 36206471 DOI: 10.1097/MPA.0000000000002095]

140 **Hallac A**, Puri N, Applebury D, Myers K, Dhumal P, Thatte A, Srikureja W. The Value of Quick Sepsis-Related Organ Failure Assessment Scores in Patients With Acute Pancreatitis Who Present to Emergency Departments: A Three-Year Cohort Study. *Gastroenterology Res* 2019; **12**: 67-71 [PMID: 31019615 DOI: 10.14740/gr1132]

141 **Lankisch PG**, Weber-Dany B, Hebel K, Maisonneuve P, Lowenfels AB. The harmless acute pancreatitis score: a clinical algorithm for rapid initial stratification of nonsevere disease. *Clin Gastroenterol Hepatol* 2009; **7**: 702-705 [PMID: 19245846 DOI: 10.1016/j.cgh.2009.02.020]

142 **Oskarsson V**, Mehrabi M, Orsini N, Hammarqvist F, Segersvärd R, Andrén-Sandberg A, Sadr Azodi O. Validation of the harmless acute pancreatitis score in predicting nonsevere course of acute pancreatitis. *Pancreatology* 2011; **11**: 464-468 [PMID: 21968430 DOI: 10.1159/000331502]

143 **Talukdar R**, Sharma M, Deka A, Teslima S, Dev Goswami A, Goswami A, Baro A, Nageshwar Reddy D. Utility of the "harmless acute pancreatitis score" in predicting a non-severe course of acute pancreatitis: a pilot study in an Indian cohort. *Indian J Gastroenterol* 2014; **33**: 316-321 [PMID: 24671724 DOI: 10.1007/s12664-014-0452-4]

144 **Maisonneuve P**, Lowenfels AB, Lankisch PG. The harmless acute pancreatitis score (HAPS) identifies non-severe patients: A systematic review and meta-analysis. *Pancreatology* 2021; **21**: 1419-1427 [PMID: 34629293 DOI: 10.1016/j.pan.2021.09.017]

145 **Gupta D**, Mandal NS, Arora JK, Soni RK. Comparative Evaluation of Harmless Acute Pancreatitis Score (HAPS) and Bedside Index of Severity in Acute Pancreatitis (BISAP) Scoring System in the Stratification of Prognosis in Acute Pancreatitis. *Cureus* 2022; **14**: e32540 [PMID: 36654581 DOI: 10.7759/cureus.32540]

146 **Al-Qahtani HH**, Alam MKh, Waheed M. Comparison of Harmless Acute Pancreatitis Score with Ranson's Score in Predicting the Severity of Acute Pancreatitis. *J Coll Physicians Surg Pak* 2017; **27**: 75-79 [PMID: 28292382]

147 **Hong W**, Lillemoe KD, Pan S, Zimmer V, Kontopantelis E, Stock S, Zippi M, Wang C, Zhou M. Development and validation of a risk prediction score for severe acute pancreatitis. *J Transl Med* 2019; **17**: 146 [PMID: 31068202 DOI: 10.1186/s12967-019-1903-6]

148 **He SS**, Li D, He QY, Chen XP, Lin YX, Yu YW, Chen FL, Ding J. Establishment of Early Multi-Indicator Prediction Models of Moderately Severe Acute Pancreatitis and Severe Acute Pancreatitis. *Gastroenterol Res Pract* 2022; **2022**: 5142473 [PMID: 35419053 DOI: 10.1155/2022/5142473]

149 **Feng A**, Ao X, Zhou N, Huang T, Li L, Zeng M, Lyu J. A Novel Risk-Prediction Scoring System for Sepsis among Patients with Acute Pancreatitis: A Retrospective Analysis of a Large Clinical Database. *Int J Clin Pract* 2022; **2022**: 5435656 [PMID: 35685488 DOI: 10.1155/2022/5435656]

150 **Tarján D**, Hegyi P. Acute Pancreatitis Severity Prediction: It Is Time to Use Artificial Intelligence. *J Clin Med* 2023; **12**: 290 [PMID: 36615090 DOI: 10.3390/jcm12010290]

151 **Qu C**, Gao L, Yu XQ, Wei M, Fang GQ, He J, Cao LX, Ke L, Tong ZH, Li WQ. Machine Learning Models of Acute Kidney Injury Prediction in Acute Pancreatitis Patients. *Gastroenterol Res Pract* 2020; **2020**: 3431290 [PMID: 33061958 DOI: 10.1155/2020/3431290]

152 **Yu X**, Wu R, Ji Y, Huang M, Feng Z. Identifying Patients at Risk of Acute Kidney Injury among Patients Receiving Immune Checkpoint Inhibitors: A Machine Learning Approach. *Diagnostics (Basel)* 2022; **12**: 3157 [PMID: 36553164 DOI: 10.3390/diagnostics12123157]

153 **Yue S**, Li S, Huang X, Liu J, Hou X, Zhao Y, Niu D, Wang Y, Tan W, Wu J. Machine learning for the prediction of acute kidney injury in patients with sepsis. *J Transl Med* 2022; **20**: 215 [PMID: 35562803 DOI: 10.1186/s12967-022-03364-0]

154 **Kui B**, Pintér J, Molontay R, Nagy M, Farkas N, Gede N, Vincze Á, Bajor J, Gódi S, Czimmer J, Szabó I, Illés A, Sarlós P, Hágendorn R, Pár G, Papp M, Vitális Z, Kovács G, Fehér E, Földi I, Izbéki F, Gajdán L, Fejes R, Németh BC, Török I, Farkas H, Mickevicius A, Sallinen V, Galeev S, Ramírez-Maldonado E, Párniczky A, Erőss B, Hegyi PJ, Márta K, Váncsa S, Sutton R, Szatmary P, Latawiec D, Halloran C, de-Madaria E, Pando E, Alberti P, Gómez-Jurado MJ, Tantau A, Szentesi A, Hegyi P; Hungarian Pancreatic Study Group. EASY-APP: An artificial intelligence model and application for early and easy prediction of severity in acute pancreatitis. *Clin Transl Med* 2022; **12**: e842 [PMID: 35653504 DOI: 10.1002/ctm2.842]

155 **Zhou Y**, Han F, Shi XL, Zhang JX, Li GY, Yuan CC, Lu GT, Hu LH, Pan JJ, Xiao WM, Yao GH. Prediction of the severity of acute pancreatitis using machine learning models. *Postgrad Med* 2022; **134**: 703-710 [PMID: 35801388 DOI: 10.1080/00325481.2022.2099193]

156 **Kiss S**, Pintér J, Molontay R, Nagy M, Farkas N, Sipos Z, Fehérvári P, Pecze L, Földi M, Vincze Á, Takács T, Czakó L, Izbéki F, Halász A, Boros E, Hamvas J, Varga M, Mickevicius A, Faluhelyi N, Farkas O, Váncsa S, Nagy R, Bunduc S, Hegyi PJ, Márta K, Borka K, Doros A, Hosszúfalusi N, Zubek L, Erőss B, Molnár Z, Párniczky A, Hegyi P, Szentesi A; Hungarian Pancreatic Study Group. Early prediction of acute necrotizing pancreatitis by artificial intelligence: a prospective cohort-analysis of 2387 cases. *Sci Rep* 2022; **12**: 7827 [PMID: 35552440 DOI: 10.1038/s41598-022-11517-w]

157 **Yuan L**, Ji M, Wang S, Wen X, Huang P, Shen L, Xu J. Machine learning model identifies aggressive acute pancreatitis within 48 h of admission: a large retrospective study. *BMC Med Inform Decis Mak* 2022; **22**: 312 [PMID: 36447180 DOI: 10.1186/s12911-022-02066-3]

158 **Hong W**, Lu Y, Zhou X, Jin S, Pan J, Lin Q, Yang S, Basharat Z, Zippi M, Goyal H. Usefulness of Random Forest Algorithm in Predicting Severe Acute Pancreatitis. *Front Cell Infect Microbiol* 2022; **12**: 893294 [PMID: 35755843 DOI: 10.3389/fcimb.2022.893294]

159 **Luo Z**, Shi J, Fang Y, Pei S, Lu Y, Zhang R, Ye X, Wang W, Li M, Li X, Zhang M, Xiang G, Pan Z, Zheng X. Development and evaluation of machine learning models and nomogram for the prediction of severe acute pancreatitis. *J Gastroenterol Hepatol* 2023; **38**: 468-475 [PMID: 36653317 DOI: 10.1111/jgh.16125]

160 **Yin M**, Zhang R, Zhou Z, Liu L, Gao J, Xu W, Yu C, Lin J, Liu X, Xu C, Zhu J. Automated Machine Learning for the Early Prediction of the Severity of Acute Pancreatitis in Hospitals. *Front Cell Infect Microbiol* 2022; **12**: 886935 [PMID: 35755847 DOI: 10.3389/fcimb.2022.886935]

161 **Zhang M**, Pang M. Early prediction of acute respiratory distress syndrome complicated by acute pancreatitis based on four machine learning models. *Clinics (Sao Paulo)* 2023; **78**: 100215 [PMID: 37196588 DOI: 10.1016/j.clinsp.2023.100215]

World Journal of Gastroenterology

Submit a Manuscript: https://www.f6publishing.com

World J Gastroenterol 2023 October 7; 29(37): 5292-5304

DOI: 10.3748/wjg.v29.i37.5292

ISSN 1007-9327 (print) ISSN 2219-2840 (online)

REVIEW

New insights into the pathogenesis of primary biliary cholangitis asymptomatic stage

Vasiliy Ivanovich Reshetnyak, Igor Veniaminovich Maev

Specialty type: Gastroenterology and hepatology

Provenance and peer review: Invited article; Externally peer reviewed.

Peer-review model: Single blind

Peer-review report's scientific quality classification

Grade A (Excellent): 0
Grade B (Very good): B, B
Grade C (Good): 0
Grade D (Fair): 0
Grade E (Poor): 0

P-Reviewer: Bredt LC, Brazil; Tsoulfas G, Greece

Received: July 19, 2023
Peer-review started: July 19, 2023
First decision: August 5, 2023
Revised: August 10, 2023
Accepted: September 14, 2023
Article in press: September 14, 2023
Published online: October 7, 2023

Vasiliy Ivanovich Reshetnyak, Igor Veniaminovich Maev, Department of Propaedeutics of Internal Diseases and Gastroenterology, A.I. Yevdokimov Moscow State University of Medicine and Dentistry, Moscow 127473, Russia

Corresponding author: Vasiliy Ivanovich Reshetnyak, DSc, MD, PhD, Full Professor, Department of Propaedeutics of Internal Diseases and Gastroenterology, A.I. Yevdokimov Moscow State University of Medicine and Dentistry, No. 20 Delegatskaya St, Moscow 127473, Russia. vasiliy.reshetnyak@yandex.ru

Abstract

Primary biliary cholangitis (PBC) is a chronic cholestatic progressive liver disease and one of the most important progressive cholangiopathies in adults. Damage to cholangiocytes triggers the development of intrahepatic cholestasis, which progresses to cirrhosis in the terminal stage of the disease. Accumulating data indicate that damage to biliary epithelial cells [(BECs), cholangiocytes] is most likely associated with the intracellular accumulation of bile acids, which have potent detergent properties and damaging effects on cell membranes. The mechanisms underlying uncontrolled bile acid intake into BECs in PBC are associated with pH change in the bile duct lumen, which is controlled by the bicarbonate (HCO_3^-) buffer system "biliary HCO_3^- umbrella". The impaired production and entry of HCO_3^- from BECs into the bile duct lumen is due to epigenetic changes in expression of the X-linked microRNA 506. Based on the growing body of knowledge on the molecular mechanisms of cholangiocyte damage in patients with PBC, we propose a hypothesis explaining the pathogenesis of the first morphologic (ductulopenia), immunologic (antimitochondrial autoantibodies) and clinical (weakness, malaise, rapid fatigue) signs of the disease in the asymptomatic stage. This review focuses on the consideration of these mechanisms.

Key Words: Primary biliary cholangitis; Antimitochondrial autoantibodies; MicroRNA 506; Inositol-1,4,5-trisphosphate receptor type 3; Chloride/bicarbonate anion exchanger 2; Biliary bicarbonate umbrella; Dihydrolipoyl transacetylase (E2 subunit); Pyruvate dehydrogenase complex

©The Author(s) 2023. Published by Baishideng Publishing Group Inc. All rights reserved.

Core Tip: This review considers the mechanisms contributing to the damage of the E2 subunit of the pyruvate dehydrogenase complex, formation of antimitochondrial autoantibodies (AMAs), and the development of ductulopenia in primary biliary cholangitis asymptomatic stage. A hypothesis explaining the pathogenesis of the initial morphological (ductulopenia), immunologic (AMAs), and clinical (weakness, malaise, rapid fatigue) signs of the disease in the asymptomatic stage is proposed.

Citation: Reshetnyak VI, Maev IV. New insights into the pathogenesis of primary biliary cholangitis asymptomatic stage. *World J Gastroenterol* 2023; 29(37): 5292-5304
URL: https://www.wjgnet.com/1007-9327/full/v29/i37/5292.htm
DOI: https://dx.doi.org/10.3748/wjg.v29.i37.5292

INTRODUCTION

Primary biliary cholangitis (PBC) is a chronic cholestatic progressive liver disease of autoimmune etiology, characterized by the destruction, necrosis, and apoptosis of small bile duct epithelial cells, in the terminal stage of which cirrhosis develops[1-3]. PBC development is preceded by a long asymptomatic period[1,2], during which time there are no physical signs of the disease. The earliest and most common symptoms are fatigue, weakness, and malaise. Detection of serum antimitochondrial autoantibodies (AMAs) at a titer ≥ 1: 40 during this period serves as a pathognomonic marker of PBC development. AMAs are detectable months to years before PBC manifests clinically, indicating their primary immunopathogenetic role rather than a secondary phenomenon occurring as a consequence of cholestasis[4,5]. However, AMAs titer does not correlate with disease activity or duration[4-7]. Identifying the causes and mechanisms of AMAs formation may contribute to understanding the pathogenesis of the development of clinical, morphologic, biochemical, and immunologic signs of PBC.

AMAs are not strictly specific for PBC[4]. They are classified as immunoglobulin (Ig) M which reacts with multiple antigens in mitochondria, designated M1-M9[8]. The highly sensitive and most frequent (> 95%) AMAs found in PBC are anti-M2 IgM[8]. In patients with classical PBC, the antigenic components of AMAs are related to the dihydrolipoyl transacetylase (E2 subunit) of the pyruvate dehydrogenase (PDC) complex (E2 PDC), which localizes to the inner mitochondrial membrane[8]. Immunization of laboratory animals with E2 PDC recombinant polypeptide leads to AMAs formation but not cholangiocyte damage[9], indicating that AMAs do not trigger the destruction of biliary epithelial cells [(BECs), cholangiocytes].

It is critical to understand how the E2 PDC antigen of BECs, located on the inner membrane of mitochondria in small and medium-sized bile ducts, can be a target of immune effector mechanisms[4]. The theory of antigenic mimicry is discussed below.

AMAs AND THE THEORY OF ANTIGENIC MIMICRY

The PDC in prokaryotes is structurally similar to that of eukaryotes[10]. Antibodies from the serum of patients with PBC have been shown to react with yeast and bacterial proteins[11,12]. Therefore, it has been suggested that AMAs in PBC arise due to cross-reactivity to exogenous bacterial antigens (antigenic mimicry)[13,14] and that the disease may have a bacterial origin[15]. However, there is no clear evidence of an infectious agent[4]. In classic bacterial antigenic exposure, IgM is the first antibody secreted by the adaptive immune system, and after 3-4 wk, IgG is produced. IgM can persist in the blood for up to 3 mo, followed by its decline. However, in PBC, the level of IgM-related AMAs does not decline over the course of the disease, which does not align with the bacterial nature of antigens triggering the production of AMAs. With continuous exposure to thymus-independent antigens and decreased immune tolerance to them, IgM synthesis can become stable[16]. However, there is low likelihood that bacterial antigen is constantly present in patients with PBC and triggers the production of AMAs[10]. It is more logical to assume that the antigen is from the patients' own tissues, namely the epithelium of the biliary tract. The production of AMAs in patients with PBC is initiated once E2 PDC becomes an immunomodified antigen, leaves the mitochondria, exits the cholangiocyte, enters the blood, and meets immunocompetent T and B lymphocytes which recognize it as a foreign antigen. To date, the triggers and mechanisms that initiate these processes in cholangiocytes remain unknown.

In the last decade, scientific data have shown that the "protective umbrella" of bicarbonate (HCO_3^-) protects cholangiocytes from the toxic effects of bile acids. In PBC, the production of HCO_3^- decreases, which leads to increased bile acid intake into cholangiocytes (theory of defective "biliary HCO_3^- umbrella"). Based on these data, we hypothesize that the gradual accumulation of bile acids in BECs may serve as a trigger mechanism for AMAs formation, ductulopenia development, and one of the early clinical signs of PBC, namely weakness in the asymptomatic stage.

AGGRESSIVE AND DEFENSE FACTORS OF CHOLANGIOCYTES

Bile is an aggressive medium for cholangiocytes, which are epithelial cells lining the intrahepatic and extrahepatic bile ducts. The presence of bile acids in bile, which have potent detergent properties, can cause damage to the cell membranes of cholangiocytes. Hydrophobic bile acids are cytotoxic to many cell types[17]. However, BECs under physiological conditions are exposed to very high (millimolar) concentrations of hydrophobic bile acids without signs of cytotoxicity [18], indicating the presence of mechanisms protecting cholangiocytes from the toxic effects of bile acids.

The conjugation of bile acids and formation of mixed micelles with cholesterol and phospholipids are considered defense mechanisms at the levels of hepatocytes, bile capillaries, and Hering's canals[18]. Defense factors that enter the bile during its passage through bile ducts include the production and secretion of mucin and HCO_3^-[19]. Under physiological conditions, the main function of cholangiocytes is biliary secretion of HCO_3^-[20]. HCO_3^- is produced by cholangiocytes lining the biliary tree. Mucin glycoprotein is produced by peribiliary glands (PBGs)[21], which are located in the wall of large intrahepatic and extrahepatic bile ducts and are directly connected with the bile duct lumen. Experimental evidence indicates that the glycocalyx, which covers the apical surface of large cholangiocyte membranes with glycosylated mucins and other glycan-containing membrane glycoproteins, stabilizes the biliary HCO_3^- umbrella, thereby helping to protect human large cholangiocytes from bile acid toxicity[22]. In addition, the mucin produced by PBGs protects the cholangiocytes of only large bile ducts[19]. Thus, the cholangiocytes of large intrahepatic and extrahepatic bile ducts have dual protection: The mucin produced by PBGs and HCO_3^-. Intralobular, interlobular, and septal bile ducts do not contain PBGs, which is accompanied by the absence of mucin in them[21]. As a result, only HCO_3^- serves as a factor of BEC defense at the levels of intralobular, interlobular, and septal ducts. Under physiological conditions, there is a balance between aggressive factors (bile acids) and defense factors (HCO_3^- and/or mucin secretion).

CHOLANGIOCYTE DEFENSE MECHANISMS

Cholangiocytes are polarized epithelial cells that line the intrahepatic and extrahepatic bile ducts and are responsible for regulating bile volume, modifying bile, and maintaining bile pH (alkalinity)[23,24]. They play an important role in modifying the composition of primary bile by secreting water, chloride (Cl^-), and HCO_3^-[25], and by absorbing bile acid salts, amino acids, and glucose. Small and large cholangiocytes are distinguished depending on their size and location in small and large bile ducts[26]. They are differently involved in the processes of secretion and absorption[27]. The secretion of HCO_3^- with human bile accounts for 25%-40% of the total volume of secreted bile and maintains physiologic pH in the lumen of bile ducts[17,28,29].

In the process of bile formation, predominantly conjugated bile acids and a minimal amount of unconjugated bile acids enter the bile capillary. Under physiological conditions, both conjugated and unconjugated bile acids are secreted into bile by hepatocytes in anionic (deprotonated, ionized, negatively charged) form[30]. HCO_3^-, which is secreted by cholangiocytes into the lumen of the bile duct, creates a slightly alkaline pH of hepatic bile due to its buffering properties, keeping bile acids in a deprotonated state. The ionized form of bile acids are impermeable to BECs due to the presence of negatively charged HCO_3^- molecules on the apical surface of the cytoplasmic membrane of cholangiocytes[30]. Thus, the secretion of HCO_3^- ions protects cholangiocytes from uncontrolled transmembrane bile acid entrance and their cytotoxicity. This protective mechanism, which preserves cholangiocytes and normal bile flow along the biliary tree, is called the biliary HCO_3^- umbrella.

MAIN REGULATORS OF HCO_3^- PRODUCTION AND SECRETION BY CHOLANGIOCYTES

The pH fluctuation in bile ducts depends on the rate of HCO_3^- production by cholangiocytes. The signaling pathways regulating HCO_3^- secretion differ in large and small cholangiocytes[31]. In small cholangiocytes, activation of HCO_3^- secretion is due to biliary adenosine triphosphate (ATP) secreted from upstream hepatocytes of Hering's canals (Figure 1). Cholangiocytes express apical membrane proteins of the purinergic receptor (P2YR) family, which are stimulated by ATP[32]. Luminal ATP binds to P2YR, stimulating intracellular calcium (Ca^{2+}) release *via* inositol-1,4,5-trisphosphate receptor type 3 ($InsP_3R3$)[33]. In cholangiocytes, $InsP_3R3$ is the major receptor isoform localized in the apical region[31,34]; it is involved in $InsP_3R3$-mediated cell signaling and Ca^{2+} secretion[35]. $InsP_3R3$ is the only receptor that promotes the opening of intracellular Ca^{2+} channels and release of Ca^{2+} ions[34]. Ca^{2+} is one of the second messengers in cholangiocytes that modulates and regulates diverse cellular functions such as ion channel activation, secretion, cell proliferation, and apoptosis[34,36]. Ca^{2+} release from subapical stores in the endoplasmic reticulum triggers and locally activates transmembrane 16A Cl^- channels (TMEM16A) on the apical membrane of cholangiocytes (Figure 1)[36-38]. The appearing Cl^- concentration gradient on the apical membrane activates the Cl^-/HCO_3^- anion exchanger 2 (AE2), also Slc4A2, which leads to the secretion of HCO_3^- into the lumen of the bile duct.

In large cholangiocytes, with the exception of the Ca^{2+}-dependent pathway of HCO_3^- secretion, there is an additional mechanism involving the hormones secretin and somatostatin[39] (Figure 1). Secretin is produced by the S cells of the duodenal mucosa, and stimulates the production of HCO_3^- by the intestinal mucosa itself as well as by cholangiocytes and pancreatic ductular epithelial cells[39]. Secretin regulates the secretion of HCO_3^- and Cl^- into bile by large cholangiocytes through interaction with secretin receptors (SRs) located on the basolateral membrane of BECs[39-42] (Figure 1).

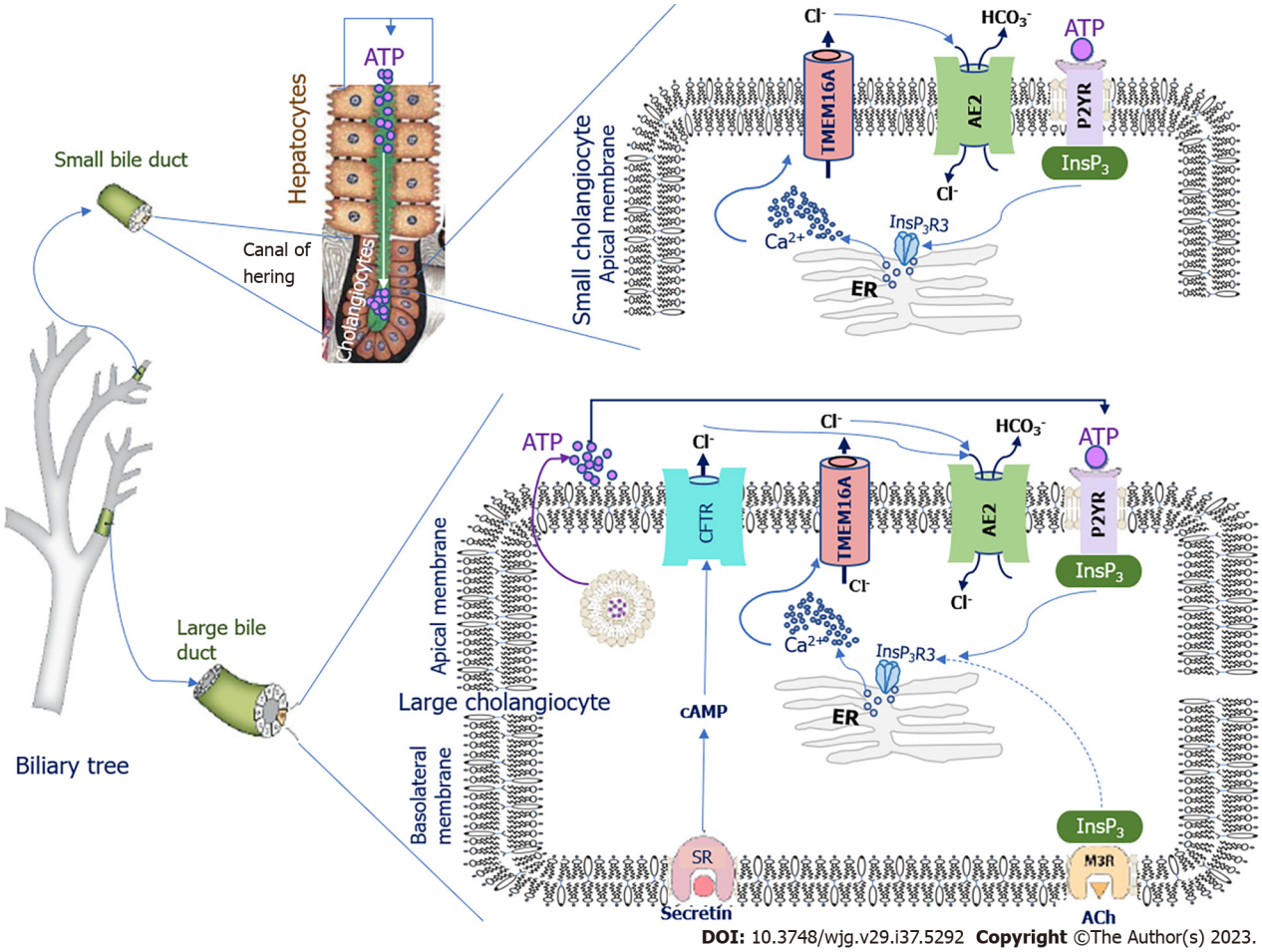


Figure 1 Schematic of bicarbonate secretion by small and large cholangiocytes. AE2: Chloride/bicarbonate anion exchanger 2; TMEM16A: Transmembrane 16A chloride channels; ATP: Adenosine triphosphate; P2YR: Purinergic receptor family; $InsP_3$: Inositol-1,4,5-trisphosphate; $InsP_3R3$: Inositol-1,4,5-trisphosphate receptor type 3; ER: Endoplasmic reticulum; SR: Secretin receptor; cAMP: Cyclic adenosine monophosphate; Ach: Acetylcholine; CFTR: Cystic fibrosis transmembrane conductance regulator; M3R: Muscarinic acetylcholine M3 receptor; HCO_3^-: Bicarbonate; Cl^-: Chloride; Ca^{2+}: Calcium.

As a result of this interaction, the formation of cyclic adenosine monophosphate (cAMP) is stimulated *via* G proteins. cAMP activates the cystic fibrosis transmembrane conductance regulator (CFTR) through adenylate cyclase, resulting in the secretion of Cl^- ions into the bile duct[28]. The appearing Cl^- concentration gradient on the apical membrane of cholangiocytes activates AE2, which leads to the secretion of HCO_3^- into the bile duct lumen in exchange for the intracellular entry of Cl^- ions into the cholangiocytes[20,24,26,43]. In parallel, ATP from cholangiocytes enters the bile duct lumen by exocytosis, which stimulates the secretion of HCO_3^- *via* a Ca^{2+}-dependent mechanism[44]. SRs and CFTR are not found in small cholangiocytes; therefore, secretin is unable to stimulate the secretion and entry of HCO_3^- and Cl^- into bile in small cholangiocytes[24]. However, a Ca^{2+}-dependent mechanism of HCO_3^- secretion is present in both small and large cholangiocytes (Figure 1)[20,24]. Somatostatin, which binds to the somatostatin receptor, counteracts the stimulating effect of secretin, inhibits fluid secretion, and slows the production and entry of HCO_3^- from cholangiocytes into the lumen of the bile duct[45].

MECHANISMS OF BILE ACID PROTONATION-DEPROTONATION AND THEIR ENTRY INTO CHOLANGIOCYTES

Uncontrolled, carrier-independent, passive diffusion of unconjugated primary bile acids into BECs is determined by their polarity and degree of protonation[18,46,47]. Protonation of bile acids is an exponential function of pH. When the pH of hepatic bile acidifies, bile acids may undergo protonation. The degree of protonation of bile acids depends on both their dissociation constant (pKa) and the pH of the bile. The pKa values for unconjugated primary bile acids are 5-6[48-50]. Conjugation of primary bile acids with amino acids reduces pKa values to 4-5 for conjugates with glycine and to 1-2 for conjugates with taurine, which improves their solubility in water and reduces their lipophilicity[48-50]. The low pKa values of the taurine conjugates of primary bile acids indicate that they are stronger acids than glycine conjugates. Therefore, taurine-conjugated bile acids are in a dissociated (deprotonated) form even at acidic bile pH values. Whereas glycine conjugates, with higher pKa values, are weak acids and will quickly change to a protonated state at the slightest

acidification of bile[50].

Ionized (deprotonated, negatively charged) bile acids are unable to overcome the biliary HCO_3^- umbrella on the outer hemi leaflet of the apical cytoplasmic membrane of cholangiocytes[18,47]. Under normal physiological conditions, a small amount of unconjugated protonated primary bile acids is taken up by cholangiocytes. The neutral intracellular pH further promotes the transport of unconjugated protonated primary bile acids into the peribiliary vascular plexus with subsequent return to hepatocytes and re-release into biliary capillaries[51]. Such a biliary-hepatic shunt aims to prevent the accumulation of toxic bile acids with strong detergent properties in cholangiocytes[18,47].

Conjugated bile acids can be transported through the apical and basolateral membranes of cholangiocytes with the aid of specific transporters[26,52-56]. Conjugates of bile acids with glycine in human hepatic bile account for three-quarters of all conjugated bile acids and have a pKa close to 4[57]. At physiologic pH (approximately 7.4), glycine conjugates of primary bile acids, as relatively weak acids, are partially protonated (nonpolar), which promotes their absorption by cholangiocytes in micromolar amounts. Small shifts in local pH to an acidic region in biliary ducts lead to an increase in protonated glycine conjugates of primary bile acids. A significant increase in the ratio of protonated:deprotonated glycine-conjugated bile acids will lead to increased absorption by cholangiocytes.

Bile acid conjugates with taurine in hepatic bile account for one-quarter of all conjugated bile acids. They are stronger acids and have a pKa of 1-2[57,58]. Therefore, changes in biliary pH have little effect on their protonation. Most of the taurine conjugates of bile acids are in anionic form and thus are not able to enter cholangiocytes. Therefore, taurine conjugates of primary bile acids are less toxic to cholangiocytes.

Active functioning of bile acid transporters in the basolateral membrane of cholangiocytes, as a rule, leads to the rapid removal of hydrophobic bile acids from the intracellular space and their delivery back into hepatocytes[59]. Therefore, the accumulation of toxic bile acids with detergent properties in cholangiocytes does not occur under normal conditions.

THEORY OF DEFECTIVE BILIARY HCO_3^- UMBRELLA IN PBC

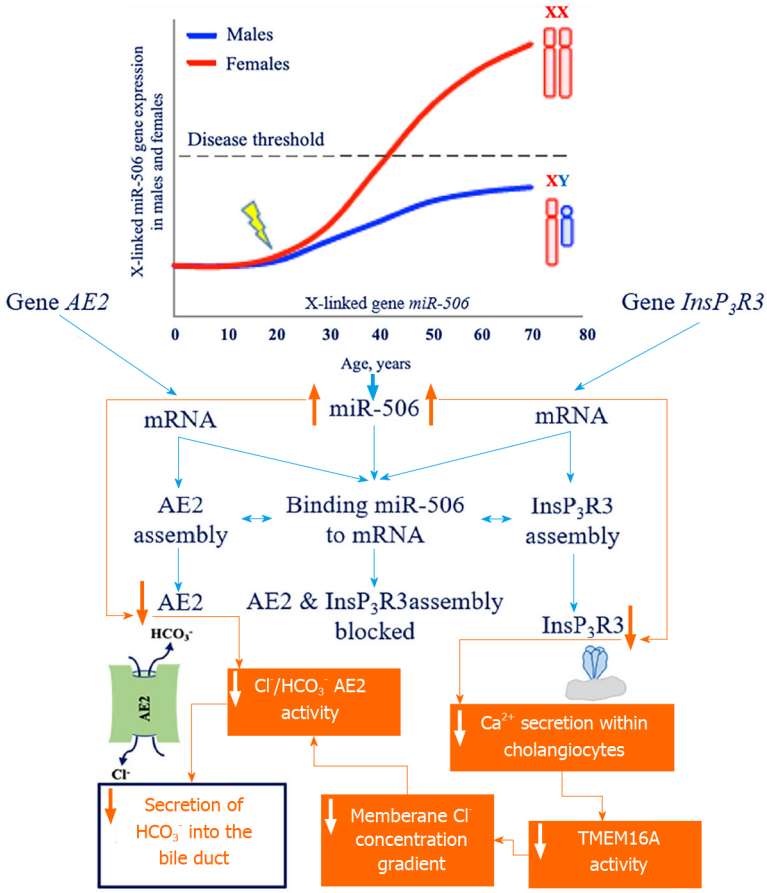
In PBC, there is a reduction in the protective role of HCO_3^- for cholangiocytes. The theory of defective "biliary HCO_3^- umbrella" has been extensively discussed[1,17,22]. This theory is based on a number of clinical and experimental works showing insufficient HCO_3^- supply to the bile ducts in PBC, which leads to a shift in the pH of intraductal (hepatic) bile to the slightly acidic region and an increase of pH in cholangiocytes to the slightly alkaline region. The reasons for the insufficient production of HCO_3^- by cholangiocytes are unknown. The involvement of $InsP_3R3$ and AE2 in this process is discussed. The expression of $InsP_3R3$ and AE2 genes is reduced in the liver biopsy specimens and blood mononuclear cells of patients with PBC, indicating their dysfunction and involvement in the pathogenesis of this disease[60,61]. The decreased expression and activity of $InsP_3R3$ and AE2 is associated with increased microRNA 506 (miR-506) expression in cholangiocytes[62]. MiRNAs are small noncoding RNAs 22-23 nucleotides long that inhibit gene expression by full or partial pairing with initial sequences located in the 3′-untranslated region (3′-UTR) of mRNA[62].

The 3′-UTR region of the mRNA of $InsP_3R3$[62] and the 3′-UTR region of the mRNA of AE2[63] contain binding sites for miR-506. MiR-506 binding to the 3′-UTR regions of the mRNA of $InsP_3R3$ and AE2 prevents the translation of these proteins. In this way, miR-506 is a regulator of $InsP_3R3$ and AE2 expression (Figure 2). The expression of miR-506 likely undergoes epigenetic regulation and can vary by individual as a result of polymorphisms in nuclear factor kappa B[30].

An increase in the amount and activity of X-linked miR-506 has been reported in the cholangiocytes of patients with PBC[63], which leads to the decreased expression and activity of $InsP_3R3$ and AE2, potentially explaining the prevalence of this disease in women[30] (Figure 2).

Decreased expression and activity of $InsP_3R3$ in cholangiocytes in PBC[64] impairs intracellular Ca^{2+} secretion and its use as a messenger in signaling to the transmembrane Cl^- channel TMEM16A[44]. Impaired Ca^{2+} signaling in cholangiocytes in PBC is evidenced by the absence of ATP stimulation of P2YRs on the apical membrane[36]. Decreased Ca^{2+}-dependent activity of TMEM16A on the apical membrane of cholangiocytes leads to the decreased secretion of Cl^- ions into the lumen of bile ducts, which is accompanied by decreased activity of the chlorine/HCO_3^- anion exchanger and impaired secretion of biliary HCO_3^-. In models of cholangiocytes expressing miR-506, $InsP_3R3$-mediated reduction in intracellular Ca^{2+} release and decreased fluid and HCO_3^- secretion into bile ducts has been shown[36,44]. Binding of miR-506 to the 3′-UTR of AE2 mRNA also contributes to decreased Cl^-/HCO_3^- anion exchanger activity and decreased HCO_3^- secretion by cholangiocytes (Figure 2). Human cholangiocytes isolated from biopsy specimens of patients with PBC show decreased AE2 activity[65]. Thus, the homeostasis of intracellular pH (pHi) in cholangiocytes and bile duct pH in patients with PBC may undergo changes[30]. Changes in intra- and extracellular pH in PBC associated with the loss of $InsP_3R3$ and decreased activity of AE2 promote the protonation of bile acids, their entry into cholangiocytes, and the development of damage to the latter[44].

Destruction of biliary epithelium of small intrahepatic bile ducts during the early asymptomatic stage of PBC is most likely related to the imbalance between the aggressive factors (bile acids) and defense factors (biliary HCO_3^- umbrella) of cholangiocytes. Because intralobular, interlobular, and septal bile ducts, which are damaged in PBC, do not contain PBGs producing mucin glycoproteins (mucin supraepithelial layer)[21], this defense mechanism for small cholangiocytes most likely does not play a pathogenetic role in the development of PBC.



DOI: 10.3748/wjg.v29.i37.5292 **Copyright** ©The Author(s) 2023.

Figure 2 Mechanism of inositol-1,4,5-trisphosphate receptor type 3 and chloride/carbonate (chloride/bicarbonate) anion exchanger 2 gene expression reduction due to the increase in the amount of micro-RNA 506 and its activity. $InsP_3R3$: Inositol-1,4,5-trisphosphate receptor type 3; AE2: Chloride/bicarbonate anion exchanger 2; miR-506: Micro-RNA 506; TMEM16A: Transmembrane 16A chloride channels; HCO_3^-: Bicarbonate; Cl^-: Chloride.

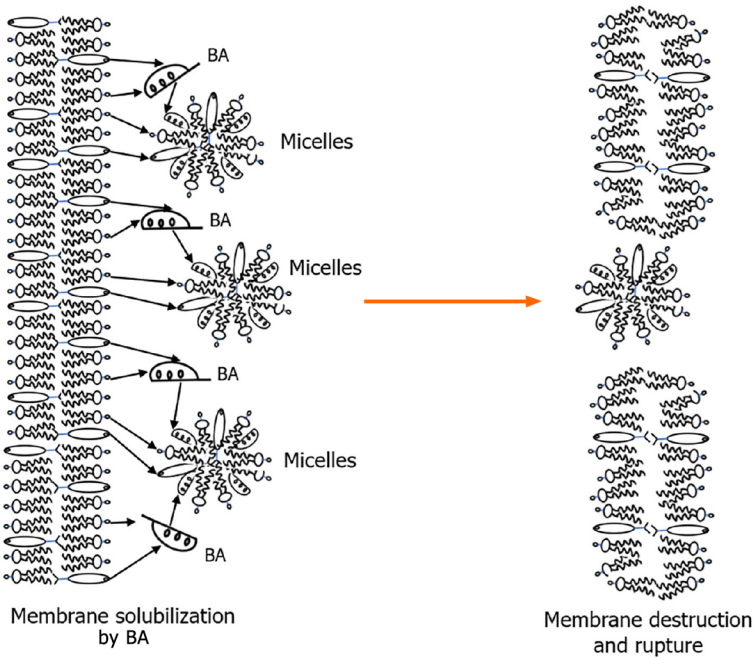
MECHANISM OF CHOLANGIOCYTE DAMAGE AND DESTABILIZATION OF BILIARY HCO_3^- UMBRELLA

Decrease of HCO_3^- supply to bile ducts, due to a decrease in $InsP_3R3$ and AE2 activity, will shift pH in the bile duct lumen to an acidic region[66]. Simultaneously, due to the retention and accumulation of HCO_3^- in the cytosol of cholangiocytes, there is gradual alkalinization of intracellular pHi in patients with PBC[30,65,67]. Complete AE2 deficiency will lead to intracellular alkalosis of cholangiocytes[61]. However, the reduced (rather than absent) expression of $InsP_3R3$ and AE2 genes has been observed in patients with PBC[61].

A shift of pH to a slightly acidic region in the lumen of bile ducts will increase the amount of protonated unconjugated and glycine-conjugated primary bile acids. This will lead to their increased entry into the small cholangiocytes (intralobular, interlobular, septal) of the bile ducts. Once in the slightly alkaline pHi within the cholangiocytes, the protonated bile acids will undergo deprotonation. Alkalinization of pHi and ionization of glycine-conjugated and unconjugated primary bile acids within cholangiocytes reduces the process of their difundation from intracellular to peribiliary space. As a result, there is a delayed and gradual accumulation of glycine-conjugated and unconjugated primary bile acids in small cholangiocytes. The theory of defective biliary HCO_3^- umbrella helps to explain the intracellular uncontrolled increased entry and accumulation of bile acids in small BECs.

The presence of the mucin-containing glycocalyx layer on the apical surface of large cholangiocytes protects them from penetration and the damaging effect of protonated conjugated and unconjugated bile acids. Intracellular accumulation of hydrophobic bile acids is a prerequisite for their cytotoxic effects[68]. As strong detergents, they are able to solubilize phospholipids and cholesterol from membrane structures of cholangiocytes, which leads to damage and destruction of cytoplasmic membrane and membranes of cell organelles (Figure 3). Thus, the entry and accumulation of unconjugated bile acids with stronger detergent properties in small cholangiocytes is more toxic for the cell than the accumulation of conjugated bile acids.

The chronic damaging effect of bile acids on membrane structures triggers accelerated senescence, necrosis, and/or apoptosis of BECs[69]. Bile acids destroy the membranes of cell organelles and nuclear membrane of cholangiocytes with the release of apoptogenic factors. The barrier function of the biliary epithelium is impaired, resulting in concomitant damage, inflammation, and oxidative stress. Cytokines, chemokines, and pro-inflammatory mediators released by cholangiocytes probably stimulate apoptotic and proliferative responses as well as activate fibrogenesis[70]. Bile acids



DOI: 10.3748/wjg.v29.i37.5292 **Copyright** ©The Author(s) 2023.

Figure 3 Solubilization of phospholipids and cholesterol from membrane structures by bile acids. BA: Bile acids.

also mediate their toxic, apoptotic effects through specific signaling pathways at the intracellular level. The intrinsic apoptotic pathway is activated, including mitochondrial translocation of B-cell lymphoma 2-associated X protein, release of cytochrome C from mitochondria, activation of caspase 3, cleavage of poly (ADP-ribose) polymerase, and DNA fragmentation[71]. There is evidence that miR-506 activates the apoptosis pathway upon stimulation with toxic bile acids [66].

Proinflammatory cytokines additionally increase miR-506 expression[30]. A vicious circle develops that supports senescence, apoptosis, and proliferation of cholangiocytes. Ultimately, ductulopenia develops[30]. Together, this reflects the direct effects of bile acids on cholangiocytes rather than the nonspecific effects resulting from periportal inflammation [31].

From a pathophysiologic point of view, common to all cholangiopathies is the coexistence of cholangiocyte death and proliferation, as well as various degrees of portal inflammation and fibrosis[70]. Cell death induces the activation of inflammatory and profibrogenic pathways that trigger the development and progression of fibrosis, which gradually leads to small bile duct ductulopenia[72]. The conceptual mechanisms of these processes have been described in reviews [69,72].

Disruption of apoptosis is considered a trigger of PBC and already in the asymptomatic stage leads to the development of small bile duct ductulopenia, one of the early morphologic signs of the disease[73]. Apoptosis depends on mitochondrial permeabilization associated with excessive intracellular accumulation of bile acids[74-76]. In addition, bile acids and incomplete apoptosis of BECs diverted to necrosis can lead to pathogenic effects on intracellular components with subsequent generation of AMAs[77].

MECHANISM OF MITOCHONDRIAL PERMEABILIZATION AND AMAs FORMATION

Solubilization of phospholipids and cholesterol from the outer membrane of mitochondria by bile acids leads to their permeabilization[78]. There is an increase in the permeability of the mitochondrial outer membrane to ions and solutes [71,78]. There is leakage of the contents of the intermembrane space into the cytosol and loss of membrane potential. Mitochondria swell, their outer membrane swells, and the release of apoptogenic factors occurs[78]. The inner mitochondrial membrane, the main target for AMA formation, is opened. Further solubilization by bile acids of phospholipids and cholesterol from the inner membrane and destruction of mitochondria can lead to the release and degradation of PDC. The latter includes three enzymes: E1 PDC, E2 PDC, and E3 PDC[73]. Each of these enzymes, in addition to the protein part, has cofactors: E1 PDC contains thiamine pyrophosphate as a cofactor; E2 PDC contains lipoic acid and coenzyme A; and E3 PDC contains flavin adenine dinucleotide and nicotinamide adenine dinucleotide. E1 and E3 PDC are protein complexes that do not contain lipid components. Therefore, they are unlikely to be affected by bile acids accumulated in cholangiocytes, since they have an effect on lipid components. Sera from PBC patients do not show serologically detectable reactivity against the E1 and E3 components of PDC[79].

E2 PDC is a lipoprotein with two lipoic acid binding sites[8]. E2 PDCs contain an essential lysine residue in the lipoyl domain to which lipoic acid is covalently attached[8]. The lipoic-lysine bond at position 173 is highly conserved across species and is essential for antigen recognition[80]. AMAs target immunodominant epitopes containing lipoic acid.

The importance of chemical xenobiotics capable of modifying lipoic acid in E2 PDC has been previously shown for the appearance of serologic reactivity of this complex[81,82]. Alteration of the conformational structure of the lipoyl domain of E2 PDC, due to chemical modification of lipoic acid may contribute to the loss of immune tolerance[83,84]. Most likely, such chemical modifiers in PBC are bile acids accumulating in cholangiocytes upon loss of the protective properties of the biliary HCO_3^- umbrella. Bile acids can interact with the lipoic acid of the antigen-recognized E2 PDC. The result of such an interaction may be immunomodification of the E2 PDC complex with acquisition of autoantigenic properties and loss of immune tolerance[66]. This assumption is supported by a number of studies performed at the end of the last century. In these works, it was shown that the main immunogenic region on E2 PDC recognized by sera from patients with PBC is localized in the lipoyl-containing domain[85-87]. The lipoic acid content of E2 PDC is thought to play a role as a potent adjuvant[88]. The presentation of immunomodified E2 PDC complex to lymphocytes can lead to stimulation of the T-cell subpopulation and specific production of AMAs[66,88,89].

A defective biliary HCO_3^- umbrella triggers a continuous and endless process of accumulation and detergent action of bile acids on small cholangiocytes with the formation of AMAs. Since the disruption of HCO_3^- entry into the lumen of the bile duct is constant, the production of AMAs will be continuous. As a result, an elevated level of IgM (M2) will be constantly maintained in the plasma of PBC patients. The appearance of AMAs in serum is another early immunologic pathognomonic sign of PBC, which occurs in the asymptomatic stage of the disease.

DYSFUNCTION OF THE PDC COMPLEX AND THE FIRST CLINICAL SIGNS OF THE ASYMPTOMATIC STAGE OF PBC

AMAs detection in the asymptomatic stage of the disease is accompanied by the appearance of the first subjective clinical signs, namely weakness, malaise, fatigue, and decreased performance[90]. Fatigue is the most common symptom of PBC in the asymptomatic and early stage of the disease[91-93], occurring in about 40%-80% of patients[94,95]. However, there is no correlation between fatigue and the severity or duration of the disease[95-98].

The mechanism underlying fatigue development is closely related to gradually progressive energy deficiency[99]. The latter is most likely related to the involvement of the PDC in the pathologic process of PBC development. The PDC is a very important metabolic enzyme. PDC functions in every cell and is required for the conversion of pyruvate to acetyl-CoA, which is incorporated into the Krebs cycle and is essential for the body to obtain energy in the form of ATP[73]. As mitochondria in cholangiocytes permeabilize and PDC becomes involved in AMAs production, there is a gradual decrease in ATP synthesis. This leads to the development of local energy deficiency, which in turn, enhances the senescence and apoptosis processes of small BECs initiated by bile acids. A vicious cycle occurs, contributing to the progression of ductulopenia and AMAs formation. In this case, AMAs are able to react with polypeptides including E2 PDC in the mitochondria of almost any cell. It has been shown that antibodies to PBC cross-react with polypeptides in the mitochondria of beef heart, presumably related to E2 PDC[100]. ATP production decreases and energy deficiency develops throughout the organism.

The development of energy deficiency is accompanied by an increase in glycogenolysis and a decrease in glycogenogenesis. The study by Green *et al*[101] showed that in the initial stages of PBC, there was a gradual decrease in glycogen stores in the liver associated with increased glycogenolysis and decreased glycogenogenesis. The authors also demonstrated that glucokinase activity significantly dropped (down to zero) in patients with PBC, indicating a decrease in glycogen formation in the liver[101]. At the same time, hexokinase (phosphorylates hexoses), which is responsible for glycogen synthesis mainly in muscles, was significantly increased in patients with PBC during this period compared to healthy individuals[101]. As a result of the developing energy deficiency in the asymptomatic stage of the disease, the first clinical signs of expressed weakness, rapid fatigue, decreased performance, functional status, and quality of life appear in patients with PBC[90,102-104].

CONCLUSION

Based on the growing body of knowledge on the molecular mechanisms underlying the development of cholangiocyte damage in patients with PBC, we proposed a hypothesis to explain the pathogenesis of the initial morphologic (ductulopenia), immunologic (AMAs) and clinical (weakness, malaise, rapid fatigue) signs of the disease in the asymptomatic stage (Figure 4).

Evidence suggests that in susceptible individuals, an unknown initial trigger causes an X-linked epigenetic change that leads to gene reactivation and increased expression of miR-506[30]. The increased synthesis and activation of miR-506 leads to inhibition of $InsP_3R3$ and AE2 translation[105]. As a result, HCO_3^- entry into the bile duct lumen is reduced and HCO_3^- accumulation in the cytosol of cholangiocytes occurs[30]. Changes in extra- and intracellular pH alter the protonation (in the lumen of the bile duct) and deprotonation (intracholangiocyte) of bile acids, leading to an increase in the uncontrolled entry and accumulation of unconjugated and glycine-conjugated bile acids into the BECs.

The detergent properties of bile acids trigger cell membrane disruption, senescence and apoptosis of cholangiocytes, mitochondrial permeabilization, destruction and immunomodification of E2 PDC, followed by AMAs formation. Senescence, apoptosis, and proliferation of cholangiocytes lead to the gradual development of ductulopenia. The involvement of PDC in the pathological process contributes to insufficient ATP synthesis, development of energy deficiency, and occurrence of the nonspecific clinical sign of fatigue. The development of ductulopenia is accompanied by

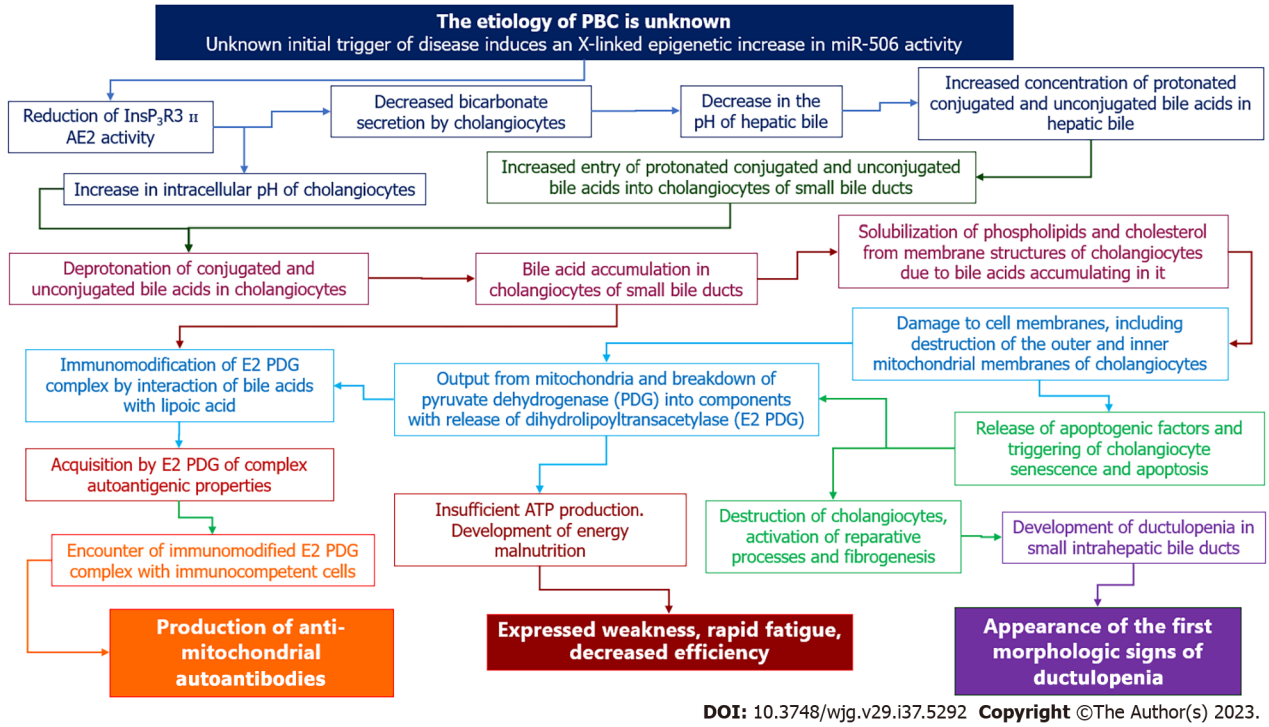


Figure 4 Mechanism of anti-mitochondrial antibody formation, development of ductulopenia, weakness, fatigue and malaise in the asymptomatic stage of primary biliary cholangitis: hypothesis. $InsP_3R3$: Inositol-1,4,5-trisphosphate receptor type 3; AE2: Chloride/bicarbonate anion exchanger 2; PDG: Pyruvate dehydrogenase; ATP: Adenosine triphosphate.

the development of intrahepatic cholestasis. Cholangiocytes are the main target in the initial stage of PBC. However, as soon as cholestasis develops, hepatocytes are also involved in the pathological process, which leads to their damage[30].

FOOTNOTES

Author contributions: Reshetnyak VI and Maev IV have equally contributed to the study conception and design, literature review and analysis, drafting, critical revision and editing, and approval of the final version.

Conflict-of-interest statement: Authors declare no conflict of interests for this article.

Open-Access: This article is an open-access article that was selected by an in-house editor and fully peer-reviewed by external reviewers. It is distributed in accordance with the Creative Commons Attribution NonCommercial (CC BY-NC 4.0) license, which permits others to distribute, remix, adapt, build upon this work non-commercially, and license their derivative works on different terms, provided the original work is properly cited and the use is non-commercial. See: https://creativecommons.org/Licenses/by-nc/4.0/

Country/Territory of origin: Russia

ORCID number: Vasiliy Ivanovich Reshetnyak 0000-0003-3614-5052; Igor Veniaminovich Maev 0000-0001-6114-564X.

S-Editor: Qu XL
L-Editor: Webster JR
P-Editor: Yu HG

REFERENCES

1 **Prieto J**, Banales JM, Medina JF. Primary biliary cholangitis: pathogenic mechanisms. *Curr Opin Gastroenterol* 2021; **37**: 91-98 [PMID: 33332913 DOI: 10.1097/MOG.0000000000000703]
2 **Reshetnyak VI**. Primary biliary cirrhosis: Clinical and laboratory criteria for its diagnosis. *World J Gastroenterol* 2015; **21**: 7683-7708 [PMID: 26167070 DOI: 10.3748/wjg.v21.i25.7683]
3 **de Veer RC**, van Hooff MC, da Silva G, Harms MH, Metselaar HJ, Willemse J, Utomo E, van der Meer AJ. Quality of life in Dutch patients with primary biliary cholangitis: Discrepancies between patients' perspectives and objective disease parameters. *Hepatol Res* 2023; **53**: 401-408 [PMID: 36635224 DOI: 10.1111/hepr.13880]

4 **Neuberger J**, Thomson R. PBC and AMA--what is the connection? *Hepatology* 1999; **29**: 271-276 [PMID: 9862877 DOI: 10.1002/hep.510290126]

5 **Chen R**, Tang R, Ma X, Gershwin ME. Immunologic Responses and the Pathophysiology of Primary Biliary Cholangitis. *Clin Liver Dis* 2022; **26**: 583-611 [PMID: 36270718 DOI: 10.1016/j.cld.2022.06.003]

6 **Mutimer DJ**, Fussey SP, Yeaman SJ, Kelly PJ, James OF, Bassendine MF. Frequency of IgG and IgM autoantibodies to four specific M2 mitochondrial autoantigens in primary biliary cirrhosis. *Hepatology* 1989; **10**: 403-407 [PMID: 2673968 DOI: 10.1002/hep.1840100402]

7 **Van Norstrand MD**, Malinchoc M, Lindor KD, Therneau TM, Gershwin ME, Leung PS, Dickson ER, Homburger HA. Quantitative measurement of autoantibodies to recombinant mitochondrial antigens in patients with primary biliary cirrhosis: relationship of levels of autoantibodies to disease progression. *Hepatology* 1997; **25**: 6-11 [PMID: 8985257 DOI: 10.1002/hep.510250103]

8 **Coppel RL**, McNeilage LJ, Surh CD, Van de Water J, Spithill TW, Whittingham S, Gershwin ME. Primary structure of the human M2 mitochondrial autoantigen of primary biliary cirrhosis: dihydrolipoamide acetyltransferase. *Proc Natl Acad Sci U S A* 1988; **85**: 7317-7321 [PMID: 3174635 DOI: 10.1073/pnas.85.19.7317]

9 **Krams SM**, Surh CD, Coppel RL, Ansari A, Ruebner B, Gershwin ME. Immunization of experimental animals with dihydrolipoamide acetyltransferase, as a purified recombinant polypeptide, generates mitochondrial antibodies but not primary biliary cirrhosis. *Hepatology* 1989; **9**: 411-416 [PMID: 2920998 DOI: 10.1002/hep.1840090311]

10 **Fussey SP**, Lindsay JG, Fuller C, Perham RN, Dale S, James OF, Bassendine MF, Yeaman SJ. Autoantibodies in primary biliary cirrhosis: analysis of reactivity against eukaryotic and prokaryotic 2-oxo acid dehydrogenase complexes. *Hepatology* 1991; **13**: 467-474 [PMID: 1999318 DOI: 10.1002/hep.1840130314]

11 **Lindenborn-Fotinos J**, Baum H, Berg PA. Mitochondrial antibodies in primary biliary cirrhosis: species and nonspecies specific determinants of M2 antigen. *Hepatology* 1985; **5**: 763-769 [PMID: 2411647 DOI: 10.1002/hep.1840050510]

12 **Frazer IH**, Mackay IR, Jordan TW, Whittingham S, Marzuki S. Reactivity of anti-mitochondrial autoantibodies in primary biliary cirrhosis: definition of two novel mitochondrial polypeptide autoantigens. *J Immunol* 1985; **135**: 1739-1745 [PMID: 2410503]

13 **Stemerowicz R**, Hopf U, Möller B, Wittenbrink C, Rodloff A, Reinhardt R, Freudenberg M, Galanos C. Are antimitochondrial antibodies in primary biliary cirrhosis induced by R(rough)-mutants of enterobacteriaceae? *Lancet* 1988; **2**: 1166-1170 [PMID: 2903378 DOI: 10.1016/s0140-6736(88)90235-8]

14 **Khor SS**, Ueno K, Nishida N, Kawashima M, Kawai Y, Aiba Y, Hitomi Y, Nagasaki M, Nakamura M, Tokunaga K. Novel HLA allele associations with susceptibility, staging, symptomatic state, autoimmune hepatitis and hepatocellular carcinoma events for primary biliary cholangitis in the Japanese population. *Front Immunol* 2023; **14**: 1151502 [PMID: 37325616 DOI: 10.3389/fimmu.2023.1151502]

15 **Burroughs AK**, Rosenstein IJ, Epstein O, Hamilton-Miller JM, Brumfitt W, Sherlock S. Bacteriuria and primary biliary cirrhosis. *Gut* 1984; **25**: 133-137 [PMID: 6363217 DOI: 10.1136/gut.25.2.133]

16 **Loginov AS**, Tsaregorodtseva TM, Zotina MM. The immune system and digestive diseases. Moscow: Meditsina Publishers, 1986: 42-65 Available from: https://search.rsl.ru/ru/record/01008480564?ysclid=llov5y33xp23524599

17 **Hohenester S**, Wenniger LM, Paulusma CC, van Vliet SJ, Jefferson DM, Elferink RP, Beuers U. A biliary HCO3- umbrella constitutes a protective mechanism against bile acid-induced injury in human cholangiocytes. *Hepatology* 2012; **55**: 173-183 [PMID: 21932391 DOI: 10.1002/hep.24691]

18 **Hofmann AF**. The enterohepatic circulation of bile acids in mammals: form and functions. *Front Biosci (Landmark Ed)* 2009; **14**: 2584-2598 [PMID: 19273221 DOI: 10.2741/3399]

19 **Matsubara T**, Kozaka K, Matsui O, Nakanuma Y, Uesaka K, Inoue D, Yoneda N, Yoshida K, Kitao A, Yokka A, Koda W, Gabata T, Kobayashi S. Peribiliary glands: development, dysfunction, related conditions and imaging findings. *Abdom Radiol (NY)* 2020; **45**: 416-436 [PMID: 31707436 DOI: 10.1007/s00261-019-02298-4]

20 **Banales JM**, Prieto J, Medina JF. Cholangiocyte anion exchange and biliary bicarbonate excretion. *World J Gastroenterol* 2006; **12**: 3496-3511 [PMID: 16773707 DOI: 10.3748/wjg.v12.i22.3496]

21 **Carpino G**, Cardinale V, Onori P, Franchitto A, Berloco PB, Rossi M, Wang Y, Semeraro R, Anceschi M, Brunelli R, Alvaro D, Reid LM, Gaudio E. Biliary tree stem/progenitor cells in glands of extrahepatic and intraheptic bile ducts: an anatomical in situ study yielding evidence of maturational lineages. *J Anat* 2012; **220**: 186-199 [PMID: 22136171 DOI: 10.1111/j.1469-7580.2011.01462.x]

22 **Maillette de Buy Wenniger LJ**, Hohenester S, Maroni L, van Vliet SJ, Oude Elferink RP, Beuers U. The Cholangiocyte Glycocalyx Stabilizes the 'Biliary HCO3 Umbrella': An Integrated Line of Defense against Toxic Bile Acids. *Dig Dis* 2015; **33**: 397-407 [PMID: 26045275 DOI: 10.1159/000371864]

23 **Esteller A**. Physiology of bile secretion. *World J Gastroenterol* 2008; **14**: 5641-5649 [PMID: 18837079 DOI: 10.3748/wjg.14.5641]

24 **Hrncir HR**, Gracz AD. Cellular and transcriptional heterogeneity in the intrahepatic biliary epithelium. *Gastro Hep Adv* 2023; **2**: 108-120 [PMID: 36593993 DOI: 10.1016/j.gastha.2022.07.015]

25 **Hirata K**, Nathanson MH. Bile duct epithelia regulate biliary bicarbonate excretion in normal rat liver. *Gastroenterology* 2001; **121**: 396-406 [PMID: 11487549 DOI: 10.1053/gast.2001.26280]

26 **Tabibian JH**, Masyuk AI, Masyuk TV, O'Hara SP, LaRusso NF. Physiology of cholangiocytes. *Compr Physiol* 2013; **3**: 541-565 [PMID: 23720296 DOI: 10.1002/cphy.c120019]

27 **Marzioni M**, Glaser SS, Francis H, PHinizy JL, LeSage G, Alpini G. Functional heterogeneity of cholangiocytes. *Semin Liver Dis* 2002; **22**: 227-240 [PMID: 12360417 DOI: 10.1055/s-2002-34501]

28 **Kanno N**, LeSage G, Glaser S, Alpini G. Regulation of cholangiocyte bicarbonate secretion. *Am J Physiol Gastrointest Liver Physiol* 2001; **281**: G612-G625 [PMID: 11518673 DOI: 10.1152/ajpgi.2001.281.3.G612]

29 **Masyuk AI**, Masyuk TV, Tietz PS, Splinter PL, LaRusso NF. Intrahepatic bile ducts transport water in response to absorbed glucose. *Am J Physiol Cell Physiol* 2002; **283**: C785-C791 [PMID: 12176735 DOI: 10.1152/ajpcell.00118.2002]

30 **Chang JC**, Go S, Verhoeven AJ, Beuers U, Oude Elferink RPJ. Role of the bicarbonate-responsive soluble adenylyl cyclase in cholangiocyte apoptosis in primary biliary cholangitis; a new hypothesis. *Biochim Biophys Acta Mol Basis Dis* 2018; **1864**: 1232-1239 [PMID: 28962898 DOI: 10.1016/j.bbadis.2017.09.022]

31 **Rodrigues MA**, Gomes DA, Nathanson MH. Calcium Signaling in Cholangiocytes: Methods, Mechanisms, and Effects. *Int J Mol Sci* 2018; **19** [PMID: 30563259 DOI: 10.3390/ijms19123913]

32 **Dranoff JA**, Masyuk AI, Kruglov EA, LaRusso NF, Nathanson MH. Polarized expression and function of P2Y ATP receptors in rat bile duct epithelia. *Am J Physiol Gastrointest Liver Physiol* 2001; **281**: G1059-G1067 [PMID: 11557527 DOI: 10.1152/ajpgi.2001.281.4.G1059]

33 **Nathanson MH**, Burgstahler AD, Mennone A, Boyer JL. Characterization of cytosolic Ca2+ signaling in rat bile duct epithelia. *Am J Physiol* 1996; **271**: G86-G96 [PMID: 8760111 DOI: 10.1152/ajpgi.1996.271.1.G86]

34 **Lemos FO**, Florentino RM, Lima Filho ACM, Dos Santos ML, Leite MF. Inositol 1,4,5-trisphosphate receptor in the liver: Expression and function. *World J Gastroenterol* 2019; **25**: 6483-6494 [PMID: 31802829 DOI: 10.3748/wjg.v25.i44.6483]

35 **Berridge MJ**, Bootman MD, Roderick HL. Calcium signalling: dynamics, homeostasis and remodelling. *Nat Rev Mol Cell Biol* 2003; **4**: 517-529 [PMID: 12838335 DOI: 10.1038/nrm1155]

36 **Trampert DC**, Nathanson MH. Regulation of bile secretion by calcium signaling in health and disease. *Biochim Biophys Acta Mol Cell Res* 2018; **1865**: 1761-1770 [PMID: 29787781 DOI: 10.1016/j.bbamcr.2018.05.010]

37 **Li Q**, Dutta A, Kresge C, Bugde A, Feranchak AP. Bile acids stimulate cholangiocyte fluid secretion by activation of transmembrane member 16A Cl(-) channels. *Hepatology* 2018; **68**: 187-199 [PMID: 29360145 DOI: 10.1002/hep.29804]

38 **Dutta AK**, Khimji AK, Kresge C, Bugde A, Dougherty M, Esser V, Ueno Y, Glaser SS, Alpini G, Rockey DC, Feranchak AP. Identification and functional characterization of TMEM16A, a Ca2+-activated Cl- channel activated by extracellular nucleotides, in biliary epithelium. *J Biol Chem* 2011; **286**: 766-776 [PMID: 21041307 DOI: 10.1074/jbc.M110.164970]

39 **Afroze S**, Meng F, Jensen K, McDaniel K, Rahal K, Onori P, Gaudio E, Alpini G, Glaser SS. The physiological roles of secretin and its receptor. *Ann Transl Med* 2013; **1**: 29 [PMID: 25332973 DOI: 10.3978/j.issn.2305-5839.2012.12.01]

40 **Boyer JL**. Bile duct epithelium: frontiers in transport physiology. *Am J Physiol* 1996; **270**: G1-G5 [PMID: 8772494 DOI: 10.1152/ajpgi.1996.270.1.G1]

41 **Alpini G**, PHinizy JL, Glaser S, Francis H, Benedetti A, Marucci L, LeSage G. Development and characterization of secretin-stimulated secretion of cultured rat cholangiocytes. *Am J Physiol Gastrointest Liver Physiol* 2003; **284**: G1066-G1073 [PMID: 12540366 DOI: 10.1152/ajpgi.00260.2002]

42 **Banales JM**, Arenas F, Rodríguez-Ortigosa CM, Sáez E, Uriarte I, Doctor RB, Prieto J, Medina JF. Bicarbonate-rich choleresis induced by secretin in normal rat is taurocholate-dependent and involves AE2 anion exchanger. *Hepatology* 2006; **43**: 266-275 [PMID: 16440368 DOI: 10.1002/hep.21042]

43 **Alvaro D**, Cho WK, Mennone A, Boyer JL. Effect of secretion on intracellular pH regulation in isolated rat bile duct epithelial cells. *J Clin Invest* 1993; **92**: 1314-1325 [PMID: 8397224 DOI: 10.1172/JCI116705]

44 **Minagawa N**, Nagata J, Shibao K, Masyuk AI, Gomes DA, Rodrigues MA, Lesage G, Akiba Y, Kaunitz JD, Ehrlich BE, Larusso NF, Nathanson MH. Cyclic AMP regulates bicarbonate secretion in cholangiocytes through release of ATP into bile. *Gastroenterology* 2007; **133**: 1592-1602 [PMID: 17916355 DOI: 10.1053/j.gastro.2007.08.020]

45 **Tietz PS**, Alpini G, Pham LD, Larusso NF. Somatostatin inhibits secretin-induced ductal hypercholeresis and exocytosis by cholangiocytes. *Am J Physiol* 1995; **269**: G110-G118 [PMID: 7631787 DOI: 10.1152/ajpgi.1995.269.1.G110]

46 **Amelsberg A**, Schteingart CD, Ton-Nu HT, Hofmann AF. Carrier-mediated jejunal absorption of conjugated bile acids in the guinea pig. *Gastroenterology* 1996; **110**: 1098-1106 [PMID: 8612999 DOI: 10.1053/gast.1996.v110.pm8612999]

47 **Masyuk AI**, Masyuk TV, Larusso NF. Physiology of Cholangiocytes. *Physiology of the Gastrointestinal Tract (Fourth Edition)* 2006; **2**: 1505-1533 [DOI: 10.1016/B978-012088394-3/50022-2]

48 **Fini A**, Ferocia G, Roda A. Acidity in bile acid systems. *Polyhedron* 2002; **21**: 1421-1427 [DOI: 10.1016/s0277-5387(02)00968-3]

49 **Bortolini O**, Bernardi T, Fantin G, Ferretti V, Fogagnolo M. Relative acidity scale of glycine- and taurine-conjugated bile acids through ESI-MS measurements. *Steroids* 2011; **76**: 596-602 [PMID: 21371488 DOI: 10.1016/j.steroids.2011.02.028]

50 **Pavlović N**, Goločorbin-Kon S, Đanić M, Stanimirov B, Al-Salami H, Stankov K, Mikov M. Bile Acids and Their Derivatives as Potential Modifiers of Drug Release and Pharmacokinetic Profiles. *Front Pharmacol* 2018; **9**: 1283 [PMID: 30467479 DOI: 10.3389/fphar.2018.01283]

51 **Dawson PA**, Shneider BL, Hofmann AF. CHAPTER 56 - Bile Formation and the Enterohepatic Circulation. *Physiology of the Gastrointestinal Tract (Fourth Edition)* **2006**: 1437-1462 [DOI: 10.1016/B978-012088394-3/50059-33]

52 **Alpini G**, Glaser SS, Rodgers R, PHinizy JL, Robertson WE, Lasater J, Caligiuri A, Tretjak Z, LeSage GD. Functional expression of the apical Na+-dependent bile acid transporter in large but not small rat cholangiocytes. *Gastroenterology* 1997; **113**: 1734-1740 [PMID: 9352879 DOI: 10.1053/gast.1997.v113.pm9352879]

53 **Benedetti A**, Di Sario A, Marucci L, Svegliati-Baroni G, Schteingart CD, Ton-Nu HT, Hofmann AF. Carrier-mediated transport of conjugated bile acids across the basolateral membrane of biliary epithelial cells. *Am J Physiol* 1997; **272**: G1416-G1424 [PMID: 9227477 DOI: 10.1152/ajpgi.1997.272.6.G1416]

54 **Hirohashi T**, Suzuki H, Takikawa H, Sugiyama Y. ATP-dependent transport of bile salts by rat multidrug resistance-associated protein 3 (Mrp3). *J Biol Chem* 2000; **275**: 2905-2910 [PMID: 10644759 DOI: 10.1074/jbc.275.4.2905]

55 **Lazaridis KN**, Pham L, Tietz P, Marinelli RA, deGroen PC, Levine S, Dawson PA, LaRusso NF. Rat cholangiocytes absorb bile acids at their apical domain *via* the ileal sodium-dependent bile acid transporter. *J Clin Invest* 1997; **100**: 2714-2721 [PMID: 9389734 DOI: 10.1172/JCI119816]

56 **Lazaridis KN**, Tietz P, Wu T, Kip S, Dawson PA, LaRusso NF. Alternative splicing of the rat sodium/bile acid transporter changes its cellular localization and transport properties. *Proc Natl Acad Sci U S A* 2000; **97**: 11092-11097 [PMID: 10984521 DOI: 10.1073/pnas.200325297]

57 **Carey MC**. Physical-chemical properties of bile acids and their salts. *New Comprehensive Biochemistry* 1985; **12**: 345-403 [DOI: 10.1016/S0167-7306(08)60689-4]

58 **Hofmann AF**. Bile acids: trying to understand their chemistry and biology with the hope of helping patients. *Hepatology* 2009; **49**: 1403-1418 [PMID: 19296471 DOI: 10.1002/hep.22789]

59 **Luo ZL**, Cheng L, Wang T, Tang LJ, Tian FZ, Xiang K, Cui L. Bile Acid Transporters Are Expressed and Heterogeneously Distributed in Rat Bile Ducts. *Gut Liver* 2019; **13**: 569-575 [PMID: 30919600 DOI: 10.5009/gnl18265]

60 **Prieto J**, Qian C, García N, Díez J, Medina JF. Abnormal expression of anion exchanger genes in primary biliary cirrhosis. *Gastroenterology* 1993; **105**: 572-578 [PMID: 8335211 DOI: 10.1016/0016-5085(93)90735-u]

61 **Medina JF**, Martínez-Ansó, Vazquez JJ, Prieto J. Decreased anion exchanger 2 immunoreactivity in the liver of patients with primary biliary cirrhosis. *Hepatology* 1997; **25**: 12-17 [PMID: 8985258 DOI: 10.1002/hep.510250104]

62 **Ananthanarayanan M**, Banales JM, Guerra MT, Spirli C, Munoz-Garrido P, Mitchell-Richards K, Tafur D, Saez E, Nathanson MH. Post-translational regulation of the type III inositol 1,4,5-trisphosphate receptor by miRNA-506. *J Biol Chem* 2015; **290**: 184-196 [PMID: 25378392 DOI: 10.1074/jbc.M114.587030]

63 **Banales JM**, Sáez E, Uriz M, Sarvide S, Urribarri AD, Splinter P, Tietz Bogert PS, Bujanda L, Prieto J, Medina JF, LaRusso NF. Up-regulation of microRNA 506 leads to decreased Cl-/HCO3- anion exchanger 2 expression in biliary epithelium of patients with primary biliary

cirrhosis. *Hepatology* 2012; **56**: 687-697 [PMID: 22383162 DOI: 10.1002/hep.25691]

64 **Shibao K**, Hirata K, Robert ME, Nathanson MH. Loss of inositol 1,4,5-trisphosphate receptors from bile duct epithelia is a common event in cholestasis. *Gastroenterology* 2003; **125**: 1175-1187 [PMID: 14517800 DOI: 10.1016/s0016-5085(03)01201-0]

65 **Melero S**, Spirlì C, Zsembery A, Medina JF, Joplin RE, Duner E, Zuin M, Neuberger JM, Prieto J, Strazzabosco M. Defective regulation of cholangiocyte Cl-/HCO3(-) and Na+/H+ exchanger activities in primary biliary cirrhosis. *Hepatology* 2002; **35**: 1513-1521 [PMID: 12029638 DOI: 10.1053/jhep.2002.33634]

66 **Erice O**, Munoz-Garrido P, Vaquero J, Perugorria MJ, Fernandez-Barrena MG, Saez E, Santos-Laso A, Arbelaiz A, Jimenez-Agüero R, Fernandez-Irigoyen J, Santamaria E, Torrano V, Carracedo A, Ananthanarayanan M, Marzioni M, Prieto J, Beuers U, Oude Elferink RP, LaRusso NF, Bujanda L, Marin JJG, Banales JM. MicroRNA-506 promotes primary biliary cholangitis-like features in cholangiocytes and immune activation. *Hepatology* 2018; **67**: 1420-1440 [PMID: 28922472 DOI: 10.1002/hep.29533]

67 **Concepcion AR**, Lopez M, Ardura-Fabregat A, Medina JF. Role of AE2 for pHi regulation in biliary epithelial cells. *Front Physiol* 2013; **4**: 413 [PMID: 24478713 DOI: 10.3389/fphys.2013.00413]

68 **Komichi D**, Tazuma S, Nishioka T, Hyogo H, Une M, Chayama K. Unique inhibition of bile salt-induced apoptosis by lecithins and cytoprotective bile salts in immortalized mouse cholangiocytes. *Dig Dis Sci* 2003; **48**: 2315-2322 [PMID: 14714619 DOI: 10.1023/b:ddas.0000007869.67105.27]

69 **Borkham-Kamphorst E**, Weiskirchen R. The PDGF system and its antagonists in liver fibrosis. *Cytokine Growth Factor Rev* 2016; **28**: 53-61 [PMID: 26547628 DOI: 10.1016/j.cytogfr.2015.10.002]

70 **Strazzabosco M**. Transport systems in cholangiocytes: their role in bile formation and cholestasis. *Yale J Biol Med* 1997; **70**: 427-434 [PMID: 9626763]

71 **Chang JC**, Go S, de Waart DR, Munoz-Garrido P, Beuers U, Paulusma CC, Oude Elferink R. Soluble Adenylyl Cyclase Regulates Bile Salt-Induced Apoptosis in Human Cholangiocytes. *Hepatology* 2016; **64**: 522-534 [PMID: 26991014 DOI: 10.1002/hep.28550]

72 **Trautwein C**, Friedman SL, Schuppan D, Pinzani M. Hepatic fibrosis: Concept to treatment. *J Hepatol* 2015; **62**: S15-S24 [PMID: 25920084 DOI: 10.1016/j.jhep.2015.02.039]

73 **Saipiyeva D**, Askarov M, Tuganbekov T, Rustemova K, Grigorevsky V, Dossatayeva G, Tostanovskaya N. Antimitochondrial and antinuclear antibodies in primary biliary cholangitis. *Journal of Clinical Medicine of Kazakhstan* 2019; **2**: 16-23 [DOI: 10.23950/1812-2892-JCMK-00681]

74 **Szalai G**, Krishnamurthy R, Hajnóczky G. Apoptosis driven by IP(3)-linked mitochondrial calcium signals. *EMBO J* 1999; **18**: 6349-6361 [PMID: 10562547 DOI: 10.1093/emboj/18.22.6349]

75 **Csordás G**, Thomas AP, Hajnóczky G. Quasi-synaptic calcium signal transmission between endoplasmic reticulum and mitochondria. *EMBO J* 1999; **18**: 96-108 [PMID: 9878054 DOI: 10.1093/emboj/18.1.96]

76 **Ichas F**, Jouaville LS, Mazat JP. Mitochondria are excitable organelles capable of generating and conveying electrical and calcium signals. *Cell* 1997; **89**: 1145-1153 [PMID: 9215636 DOI: 10.1016/s0092-8674(00)80301-3]

77 **Berg CP**, Stein GM, Keppeler H, Gregor M, Wesselborg S, Lauber K. Apoptosis-associated antigens recognized by autoantibodies in patients with the autoimmune liver disease primary biliary cirrhosis. *Apoptosis* 2008; **13**: 63-75 [PMID: 18060504 DOI: 10.1007/s10495-007-0157-6]

78 **Halestrap AP**, Richardson AP. The mitochondrial permeability transition: a current perspective on its identity and role in ischaemia/reperfusion injury. *J Mol Cell Cardiol* 2015; **78**: 129-141 [PMID: 25179911 DOI: 10.1016/j.yjmcc.2014.08.018]

79 **Surh CD**, Roche TE, Danner DJ, Ansari A, Coppel RL, Prindiville T, Dickson ER, Gershwin ME. Antimitochondrial autoantibodies in primary biliary cirrhosis recognize cross-reactive epitope(s) on protein X and dihydrolipoamide acetyltransferase of pyruvate dehydrogenase complex. *Hepatology* 1989; **10**: 127-133 [PMID: 2473022 DOI: 10.1002/hep.1840100202]

80 **Gulamhusein AF**, Hirschfield GM. Pathophysiology of primary biliary cholangitis. *Best Pract Res Clin Gastroenterol* 2018; **34-35**: 17-25 [PMID: 30343706 DOI: 10.1016/j.bpg.2018.05.012]

81 **Ge S**, Xu Q, Li H, Shao T, Zhong F, Leung PSC, Shuai Z. Differential immune response to xenobiotic-modified self-molecule in simple and connective tissue disease-associated primary biliary cholangitis. *Liver Int* 2022; **42**: 2204-2215 [PMID: 35791754 DOI: 10.1111/liv.15360]

82 **Rieger R**, Gershwin ME. The X and why of xenobiotics in primary biliary cirrhosis. *J Autoimmun* 2007; **28**: 76-84 [PMID: 17360156 DOI: 10.1016/j.jaut.2007.02.003]

83 **Wang J**, Budamagunta MS, Voss JC, Kurth MJ, Lam KS, Lu L, Kenny TP, Bowlus C, Kikuchi K, Coppel RL, Ansari AA, Gershwin ME, Leung PS. Antimitochondrial antibody recognition and structural integrity of the inner lipoyl domain of the E2 subunit of pyruvate dehydrogenase complex. *J Immunol* 2013; **191**: 2126-2133 [PMID: 23894195 DOI: 10.4049/jimmunol.1301092]

84 **Naiyanetr P**, Butler JD, Meng L, Pfeiff J, Kenny TP, Guggenheim KG, Reiger R, Lam K, Kurth MJ, Ansari AA, Coppel RL, López-Hoyos M, Gershwin ME, Leung PS. Electrophile-modified lipoic derivatives of PDC-E2 elicits anti-mitochondrial antibody reactivity. *J Autoimmun* 2011; **37**: 209-216 [PMID: 21763105 DOI: 10.1016/j.jaut.2011.06.001]

85 **Rahmatullah M**, Gopalakrishnan S, Andrews PC, Chang CL, Radke GA, Roche TE. Subunit associations in the mammalian pyruvate dehydrogenase complex. Structure and role of protein X and the pyruvate dehydrogenase component binding domain of the dihydrolipoyl transacetylase component. *J Biol Chem* 1989; **264**: 2221-2227 [PMID: 2914903]

86 **Fussey SP**, Bassendine MF, James OF, Yeaman SJ. Characterisation of the reactivity of autoantibodies in primary biliary cirrhosis. *FEBS Lett* 1989; **246**: 49-53 [PMID: 2468528 DOI: 10.1016/0014-5793(89)80251-0]

87 **Surh CD**, Coppel R, Gershwin ME. Structural requirement for autoreactivity on human pyruvate dehydrogenase-E2, the major autoantigen of primary biliary cirrhosis. Implication for a conformational autoepitope. *J Immunol* 1990; **144**: 3367-3374 [PMID: 1691756]

88 **Ohmori Hnt**, Yamauchi T, Yamamoto I. Augmentation of the antibody response by lipoic acid in mice. I. Analysis of the mode of action in an in vitro cultures system. *Jpn J Pharmacol* 1986; **42**: 135-140 [PMID: 2948041 DOI: 10.1254/jjp.42.135]

89 **Colapietro F**, Lleo A, Generali E. Antimitochondrial Antibodies: from Bench to Bedside. *Clin Rev Allergy Immunol* 2022; **63**: 166-177 [PMID: 34586589 DOI: 10.1007/s12016-021-08904-y]

90 **Sogolow ED**, Lasker JN, Short LM. Fatigue as a major predictor of quality of life in women with autoimmune liver disease: the case of primary biliary cirrhosis. *Womens Health Issues* 2008; **18**: 336-342 [PMID: 18420421 DOI: 10.1016/j.whi.2007.12.005]

91 **Kremer AE**, Mayo MJ, Hirschfield G, Levy C, Bowlus CL, Jones DE, Steinberg A, McWherter CA, Choi YJ. Seladelpar improved measures of pruritus, sleep, and fatigue and decreased serum bile acids in patients with primary biliary cholangitis. *Liver Int* 2022; **42**: 112-123 [PMID: 34403559 DOI: 10.1111/liv.15039]

92 **Shamshtein D**, Liwinski T. Pathogenesis and management of fatigue in primary biliary cholangitis. *Fatigue: Biomedicine, Health & Behavior*

2022; **10**: 1-25 [DOI: 10.1080/21641846.2022.2034473]

93 **Abbas G**, Jorgensen RA, Lindor KD. Fatigue in primary biliary cirrhosis. *Nat Rev Gastroenterol Hepatol* 2010; **7**: 313-319 [PMID: 20458334 DOI: 10.1038/nrgastro.2010.62]

94 **Witt-Sullivan H**, Heathcote J, Cauch K, Blendis L, Ghent C, Katz A, Milner R, Pappas SC, Rankin J, Wanless IR. The demography of primary biliary cirrhosis in Ontario, Canada. *Hepatology* 1990; **12**: 98-105 [PMID: 2197212 DOI: 10.1002/hep.1840120116]

95 **Galoosian A**, Hanlon C, Zhang J, Holt EW, Yimam KK. Clinical Updates in Primary Biliary Cholangitis: Trends, Epidemiology, Diagnostics, and New Therapeutic Approaches. *J Clin Transl Hepatol* 2020; **8**: 49-60 [PMID: 32274345 DOI: 10.14218/JCTH.2019.00049]

96 **Newton JL**, Gibson GJ, Tomlinson M, Wilton K, Jones D. Fatigue in primary biliary cirrhosis is associated with excessive daytime somnolence. *Hepatology* 2006; **44**: 91-98 [PMID: 16800007 DOI: 10.1002/hep.21230]

97 **Biagini MR**, Tozzi A, Milani S, Grippo A, Amantini A, Capanni M, Galli A, Surrenti C. Fatigue in primary biliary cirrhosis: a possible role of comorbidities. *Eur J Gastroenterol Hepatol* 2008; **20**: 122-126 [PMID: 18188032 DOI: 10.1097/MEG.0b013e3282f1cbda]

98 **Newton JL**. Fatigue in primary biliary cirrhosis. *Clin Liver Dis* 2008; **12**: 367-83; ix [PMID: 18456186 DOI: 10.1016/j.cld.2008.02.010]

99 **Reshetnyak VI**, Maev IV. Mechanism for development of malnutrition in primary biliary cholangitis. *World J Meta-Anal* 2022; **10**: 81-98 [DOI: 10.13105/wjma.v10.i3.81]

100 **Flannery GR**, Burroughs AK, Butler P, Chelliah J, Hamilton-Miller J, Brumfitt W, Baum H. Antimitochondrial antibodies in primary biliary cirrhosis recognize both specific peptides and shared epitopes of the M2 family of antigens. *Hepatology* 1989; **10**: 370-374 [PMID: 2474482 DOI: 10.1002/hep.1840100321]

101 **Green JH**, Bramley PN, Losowsky MS. Are patients with primary biliary cirrhosis hypermetabolic? A comparison between patients before and after liver transplantation and controls. *Hepatology* 1991; **14**: 464-472 [PMID: 1874491]

102 **Jopson L**, Jones DE. Fatigue in Primary Biliary Cirrhosis: Prevalence, Pathogenesis and Management. *Dig Dis* 2015; **33** Suppl 2: 109-114 [PMID: 26641884 DOI: 10.1159/000440757]

103 **Parikh-Patel A**, Gold EB, Utts J, Worman H, Krivy KE, Gershwin ME. Functional status of patients with primary biliary cirrhosis. *Am J Gastroenterol* 2002; **97**: 2871-2879 [PMID: 12425562 DOI: 10.1111/j.1572-0241.2002.07055.x]

104 **Griffiths L**, Jones DE. Pathogenesis of primary biliary cirrhosis and its fatigue. *Dig Dis* 2014; **32**: 615-625 [PMID: 25034296 DOI: 10.1159/000360515]

105 **Mardones P**, Medina JF, Elferink RP. Activation of cyclic AMP Signaling in Ae2-deficient mouse fibroblasts. *J Biol Chem* 2008; **283**: 12146-12153 [PMID: 18319251 DOI: 10.1074/jbc.M710590200]

World Journal of Gastroenterology

Submit a Manuscript: https://www.f6publishing.com

World J Gastroenterol 2023 October 7; 29(37): 5305-5312

DOI: 10.3748/wjg.v29.i37.5305

ISSN 1007-9327 (print) ISSN 2219-2840 (online)

MINIREVIEWS

Sequence of events leading to primary biliary cholangitis

Ilaria Lenci, Paola Carnì, Martina Milana, Agreta Bicaj, Alessandro Signorello, Leonardo Baiocchi

Specialty type: Gastroenterology and hepatology

Provenance and peer review: Invited article; Externally peer reviewed.

Peer-review model: Single blind

Peer-review report's scientific quality classification

Grade A (Excellent): A
Grade B (Very good): B, B
Grade C (Good): C
Grade D (Fair): D
Grade E (Poor): 0

P-Reviewer: He YH, China; Kordzaia D, Georgia; Pan Y, China; Wang XL, China

Received: July 7, 2023
Peer-review started: July 7, 2023
First decision: August 15, 2023
Revised: August 22, 2023
Accepted: September 11, 2023
Article in press: September 11, 2023
Published online: October 7, 2023

Ilaria Lenci, Paola Carnì, Martina Milana, Agreta Bicaj, Alessandro Signorello, Leonardo Baiocchi, Hepatology Unit, University of Tor Vergata, Rome 00133, Italy

Paola Carnì, Agreta Bicaj, Leonardo Baiocchi, Postgraduate School in Hepato/Gastroenterology, Catholic University Our Lady of Good Counsel, Tirana 1004, Albania

Corresponding author: Leonardo Baiocchi, MD, PhD, Associate Professor, Senior Scientist, Hepatology Unit, University of Tor Vergata, No. 81 Viale Oxford, Rome 00133, Italy. baiocchi@uniroma2.it

Abstract

Primary biliary cholangitis (PBC) is a chronic cholestatic liver disease that is observed more frequently in middle-aged women. This disorder is considered an autoimmune disease, since liver injury is sustained by the presence of self-directed antimitochondrial antibodies targeting the bile duct cells. The prognosis may vary depending on an early diagnosis and response to therapy. However, nearly a third of patients can progress to liver cirrhosis, thus requiring a liver transplant. Traditional immunosuppressive therapies, commonly employed for other autoimmune diseases, have limited effects on PBC. In fact, dramatic functional changes that occur in the biliary epithelium in the course of inflammation play a major role in perpetuating the injury. In this minireview, after a background on the disease and possible predisposing factors, the sequential cooperation of cellular/molecular events leading to end-stage PBC is discussed in detail. The rise and maintenance of the autoimmune process, as well as the response of the biliary epithelia during inflammatory injury, are key factors in the progression of the disease. The so-called "ductular reaction (DR)", intended as a reactive expansion of cells with biliary phenotype, is a process frequently observed in PBC and partially understood. However, recent findings suggest a strict relationship between this pathological picture and the progression to liver fibrosis, cell senescence, and loss of biliary ducts. All these issues (onset of chronic inflammation, changes in secretive and proliferative biliary functions, DR, and its relationship with other pathological events) are discussed in this manuscript in an attempt to provide a snapshot, for clinicians and researchers, of the most relevant and sequential contributors to the progression of this human cholestatic disease. We believe that interpreting this disorder as a multistep process may help identify possible therapeutic targets to prevent evolution to severe disease.

Key Words: Primary biliary cholangitis; Cholangiocyte; Biliary secretion; Biliary proliferation; Ductular reaction; Antimitochondrial antibody; Cellular senescence; Liver fibrosis

©The Author(s) 2023. Published by Baishideng Publishing Group Inc. All rights reserved.

Core Tip: Primary biliary cholangitis is a chronic cholestatic human disease. The pathological processes that favor the evolution toward end-stage liver disease during this disorder are only partially elucidated. The aim of this minireview is to summarize the sequential pathological contributors, supporting the progression of liver injury, in the course of this disease.

Citation: Lenci I, Carnì P, Milana M, Bicaj A, Signorello A, Baiocchi L. Sequence of events leading to primary biliary cholangitis. *World J Gastroenterol* 2023; 29(37): 5305-5312
URL: https://www.wjgnet.com/1007-9327/full/v29/i37/5305.htm
DOI: https://dx.doi.org/10.3748/wjg.v29.i37.5305

INTRODUCTION

Primary biliary cholangitis (PBC), previously named primary biliary cirrhosis[1], was probably already described in the middle of the nineteenth century. In fact, important similarities with PBC were reported in a clinical case observed at Guy's Hospital in 1851[2]. Almost one century later, a description of the clinical course of the disease was reported in a group of patients, mainly achieving diagnosis after a surgical approach[3]. The etiology of PBC remains elusive today, even if the pathogenesis is related to the onset of an autoimmune response characterized by the presence of anti-mitochondrial antibodies (AMA) in the sera of affected patients[4]. The target of the immune response is represented by the intrahepatic biliary tract, thereby determining progressive chronic cholestasis, fibrosis, and a possible evolution toward liver cirrhosis[5]. Women are prevalently affected by PBC, with an age of onset that usually falls within the fourth or fifth decade[5]. The prevalence can change among different countries, accounting in general for 20-30/100.000 inhabitants in United States and Europe[5,6]. Liver biopsy is generally not required for diagnosis since AMA positivity, coupled with increased cholestasis indexes in the absence of biliary obstruction, represents a specific and characteristic presentation[7]. Ursodeoxycholic acid (UDCA), 13-15 mg/kg daily is the main and mandatory treatment to slow the progression in patients affected by PBC. The use of obeticholic acid (OCA) should help increase the response to UDCA or in subjects UDCA intolerant[8]. Despite the identification of effective medical treatments for PBC, a third of patients have a scarce response, thus evolving toward liver cirrhosis that may also require liver transplantation[9]. This problem and uncertainty about the mechanisms of onset and progression of the disease suggest that further research is needed to decipher the natural/molecular history of PBC. In this review, which also describes possible predisposing factors, we examine current knowledge on sequential molecular and cellular mechanisms in the onset of PBC. Reversion of these chain processes may possibly prevent the most severe sequelae of this chronic cholestatic disorder. The manuscript was prepared on the base of a literature search (PubMed, Scopus, Web of Science) using several key words (alone or in combination) such as: PBC, primary biliary cirrhosis, cholangiocyte, bile duct cells, secretion, proliferation, cholestasis, molecular mechanism, risk factors, pathology, antibody, immunology, and others.

Before PBC (predisposing factors)

Some generic risk factors, such as female sex and age, have been identified in patients with PBC. More interestingly, and suggesting a genetic predisposition, studies examine the prevalence of autoimmune disorders in patients with PBC and their relatives[10]. The family history of PBC seems, in fact, to be the strongest predisposing factor for the disease with an odds ratio of nearly 10 compared to controls. Furthermore, this familiar occurrence also increases the possibility of developing other autoimmune disorders such as polymyositis, systemic lupus erythematosus, and others[10]. These observations claim a possible similar genetic background between PBC and other autoimmune disorders, as also suggested by a clinical study focusing on this category of diseases[11]. However, we must emphasize that in PBC, such as other complex disorders, genetics represents only a permissive trait, which requires exposure to possible environmental/external factors for the development of injury[12]. Human leukocyte antigens (HLA) have long been investigated for their possible relationship with the onset of immune diseases[13]. Similarly, early data suggested an association between PBC and HLA DRB1*08[12]. This finding was later expanded, demonstrating an opposite protective effect of DRB1*11 and DRB1*13 and not only with regard to PBC, but also extended to other hepatic diseases such as viral B and C hepatitis[14]. The approach of genome-wide association studies has more recently allowed to identify other genetic changes in PBC, including several non-HLA variants[15]. These may affect the interleukin-12/JAK-STAT pathway, the B cell response, and other steps of inflammatory signalling. However, the trigger factors that may cause disease in the presence of a favourable genetic background are still not clearly defined. Smoking or drinking habits have been associated with the development of PBC, as well as recurrent urinary infections, hair dye, and hormonal replacement therapy in women[10]. The large diffusion of these conditions, together with the limited prevalence of PBC, allow us to foresee the scarce utility of possible preventive strategies for this disease, at present.

The beginning of injury: the antimitochondrial antibody

In parallel with what has been observed in other autoimmune disorders, the presence of self-directed antibodies (AMA) is the basis of the physio-pathological process in PBC. The main target of AMA is represented by the mitochondrial E2

subunits of the pyruvate dehydrogenase complexes (PDC-E2)[4]. Since E2 is a highly preserved portion in other species and bacteria, the possible origin of AMA by molecular mimicry (cross-reaction with self-antigen after a previous exposure to exogenous pathogens with similar moieties) has long been suggested[16]. Several agents have been proposed in the past to induce AMA formation, including microorganisms or environmental substances[17]. Among bacteria, *Escherichia coli (E. Coli)* has long been suggested as a possible important actor in eliciting the immune response in PBC[18]. The contribution of *E. Coli* may also explain the frequent association between the onset of PBC and recurrent urinary tract infection, as this microorganism is an important causative agent of this latter disorder. More recently, exposure to *Novosphingobium aromaticivorans (N. Aromaticivorans)*, a ubiquitous gram-negative bacteria capable of metabolizing xenobiotics, has been suggested as a possible trigger factor in PBC. In fact, the immune reactivity of sera from patients with PBC is 100 times stronger for *N. Aromaticivorans* compared to *E. Coli* and the ubiquity of this bacteria is demonstrated by its presence in 25% of fecal samples from both PBC patients or control[19]. Regarding the mechanism linking bacteria to PBC progression, also a role for intestinal dysbiosis has been claimed[20]. This may increase intestinal permeability and lipopolysaccharide flux toward the liver, thus resulting in an enhanced immune/inflammatory response. Interestingly and supporting this view, UDCA treatment was reported to attenuate the difference in intestinal microbioma between PBC patients and normal controls[21]. However, to underscore that studies on gut microbial composition are particularly complex, affected by individual, environmental and dietary factors as well as by sampling procedure, so that a conclusive picture on this issue is not available at present. The development of an AMA titer in blood has been considered in the clinic to play an important causal role in the following biliary damage. However, in this regard, while some authors suggest that the onset of this antibody is an important predictive factor for the development of PBC[22], others underscore the higher prevalence (1/1000) of AMA compared to PBC (0.4/1000), therefore suggesting that some subjects may be healthy for life despite displaying these autoantibodies in blood[4]. With this regard, some data show that AMA does not seem pathogenic by itself, and its complex with the corresponding antigen is needed to prompt immunity. However, why the formation of immune complexes occurs in PBC patients is a question that remains unanswered at present[23]. The AMA target within PDC-E2 is represented by the lipoyl domain, and the different degradations of this epitope seem related to the reason that the antibodies mainly target bile duct cells (*i.e.*, cholangiocytes). In fact, PDC-E2 is ubiquitously present in cells; however, it appears that after the apoptotic death of cholangiocytes, differently from other epithelial cells, the epitope is released in its intact form, thus maintaining the immune response and lymphocyte homing[17]. This pattern appears to be also followed by the salivary and lacrimal glands, explaining the frequent association between PBC and Sjögren syndrome[24], being the latter a disease that presents characteristically with dryness in the mouth and eyes and also recognizing an autoimmune origin[25]. Finally, from a clinical point of view, the AMA titer does not have a significant relationship with the prognosis or extent of liver damage in PBC[26] while some patients with this disease exhibit an antinuclear antibody (ANA) instead of AMA (AMA negative PBC)[27].

Onset of chronic inflammation

Biliary cell apoptosis is a critical event in maintaining the injury since the early stages of PBC. This process allows exposure to specific epitopes that support the autoimmune response[28]. The possible contribution of innate immunity to the inflammatory process of PBC remains an argument for debate. Destruction of biliary cells has been described after toll-like receptor 4 stimulation of natural killer cells (NK) in the presence of interferon alpha[29]. Interestingly, biliary damage is proportional to the degree of NK infiltration of the biliary tract[30]. In fact, when the ratio of NK/bile duct cells is low, no biliary damage occurs. On the contrary, high NK infiltration is associated with extensive cholangiocyte damage and epitope exposure. These are targeted by T cells, which in turn maintain chronic injury realizing the adaptive immune response[30]. In this perspective, the activity of NK cells would be the main determinant of the evolution from an innate to an adaptive immunological response, during the onset of PBC. Anti-PDC $E2_{163-176}$ specific T cells then expand and are preferentially located in the lymph nodes and liver. These cells are recovered only in patients with PBC, and their specific location in the liver supports their pathogenic role in chronic injury involving this organ[31]. Once the inflammatory process is established, changes that occur in the activities of bile duct cells further contribute to injury, as reported in the following paragraphs.

Changes in biliary physiology

Several changes occur in the function of cholangiocytes when the PBC inflammatory damage is established. These involve the secretory and proliferative processes of the biliary epithelium and other aspects. These issues are discussed in the following paragraphs, including their contribution to perpetuating and worsening the damage.

Impairment of secretive processes

Several studies in recent decades have elucidated the paramount importance of biliary epithelia in bile secretion and the physiopathological changes that occur in this system in cholestatic disorders (when the bile does not reach the intestine) such as PBC[32]. Differently from hepatocytes, in which bile secretion is constant and is driven by canalicular bile acids (BA) transfer, the cholangiocyte bile output can change significantly according to exposure to different gastro-intestinal hormones or peptides[32]. Moreover, endogenous (inflammatory) or exogenous stimuli (bacterial, toxic, drug-induced, and others) altering the ductal microenvironment can change cholangiocyte secretory response[33]. The classical molecular process that stimulates biliary bile secretion recognizes as a first step the stimulation by secretin (Sec) of a specific sec receptor (SR) expressed only in cholangiocytes within the liver[34]. Sec/SR binding activates a cascade of molecular events involving, in turn: (1) Increased intracellular cyclic adenosine 3',5'-monophosphate (cAMP); (2) phosphorylation of protein kinase A (PKA); (3) Cl^- extrusion in canalicular space by cystic fibrosis transmembrane

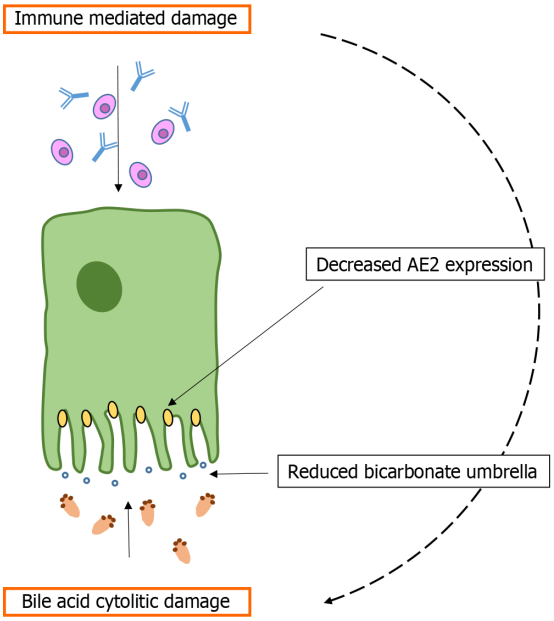
regulator; and (4) reabsorption of Cl^- and its replacement with bicarbonate operated by the chloride-bicarbonate exchanger (AE2)[34]. This determines the realization of a BA-independent bicarbonate-enriched choleresis that may contribute, under some conditions, to more than 50% of total bile flow. Several human and experimental evidences demonstrated impaired AE2 activity in PBC. In 1993, a decrease in AE2 mRNA was first described in the liver of PBC patients[35]. In a subsequent human study, a reduction in AE2 was also demonstrated with respect to protein synthesis, employing the immune staining technique[36]. Finally, the same group demonstrated with positron emission tomography reduced (both basal and Sec-stimulated) bicarbonate biliary secretion in patients with PBC[37]. Further evidence supporting the impairment of AE2 in PBC came from the Ae2 knockout mouse model, which resembles several features of this human disease[38]. The mechanism at the base of the down-regulation of AE2, in the course of PBC, is not clear at present. However, research demonstrated epigenetic changes in the AE2 promoter region (both in liver and peripheral blood mononuclear cells of PBC patients) characterized by enhanced methylation, thus determining reduced mRNA transcription[39]. Despite the uncertainty with respect to the chain of events that leads to decreased AE2 activity, the outcome of this occurrence is well evidenced by the impairment of bicarbonate-enriched choleresis after Sec stimulation[37]. The fall in biliary bile flow and, in particular, of bicarbonate secretion, opens the door to BA-induced cytolitic damage, according to the theory of bicarbonate umbrella[40]. In agreement with this view, given the decreased AE2 activity, the delicate bicarbonate film (bicarbonate umbrella), laying on the luminal side of the cholangiocyte, would be altered, allowing cellular damage by hydrophobic BA monomers. The main determinants of this process are shown in Figure 1. In this perspective, two pathological components would contribute to chronic biliary damage during PBC: (1) The autoimmune inflammatory process; and (2) the cytotoxic BA-related injury. The role of hydrophobic BA accumulation, in perpetuating PBC damage, is also indirectly supported by the beneficial results obtained when the BA pool is supplemented with less detergent and more hydrophilic BA such as UDCA or when their synthesis is inhibited with OCA.

Changes in proliferative processes

Bile duct proliferation is a complex process, characterized by important changes during pathological conditions. As observed with respect to the secretive process, intracellular cAMP levels also play a key role in modulating biliary growth [41]. After enhanced cAMP formation, the PKA/Sc/MEK/ERK1/2 axis is activated in order to stimulate cellular proliferation[42]. Several gastro-intestinal hormones and neuropeptides may enhance cholangiocyte proliferation using the cAMP route (such as Sec, acetylcholine, serotonin, histamine, *etc.*), while others (such as gastrin and somatostatin) may negatively regulate this pathway, obtaining the opposite effect[43]. Finally, BA are also important key molecules for biliary growth[44], interacting with specific cholangiocyte receptors. For example, the interaction of BA with the cholangiocyte Takeda G protein-coupled receptor 5 modulates proliferation, with an opposite effect in ciliated and nonciliated cells[45]. From a morphological point of view, three different proliferative pictures can be recognized in the biliary tree [46]. Type I 'typical' proliferation is observed in humans after high-grade acute biliary obstruction or in the early phase of chronic cholestatic disease, including PBC. In Type I, biliary proliferation is restricted to portal spaces and characterized by ducts with a preserved architecture and orientation. In Type 2 'atypical' proliferation, the extension of truncated, poorly organized, and possibly nonfunctional ducts, with an indefinite lumen, is observed in the liver parenchima, usually coupled with enhanced inflammatory processes. Type II proliferation is generally observed in the more advanced stage of PBC and may represent the introductive step toward the progressive loss of bile ducts (ductopenia) found in the late phase of the disease. Finally, Type III 'oval cell' proliferation is also reported. This irregular proliferation (distorted duct with architectural changes in the liver parenchima) is observed in the early phase of experimental carcinogenesis and may have a relationship with the onset of cholangiocarcinoma, as it originates from multipotent (oval) cells[44,46]. As mentioned above and according to this morphological classification, the repairing process during PBC: (1) Would stimulate biliary growth that; (2) may evolve from a typical phase to an atypical phase, and possibly; and (3) may lead to a ductopenic end stage. This complex cellular/molecular process is morphologically recapitulated in the so-called 'ductular reaction (DR)', which probably promotes the evolution towards liver fibrosis and duct loss, both characteristic features of end-stage PBC.

Mixing biliary proliferation, fibrosis, and cellular senescence(CS): The DR

The term DR was coined and is generally preferred to proliferation in liver pathology, since it implies a reactive expansion of the ductular phenotype that may or may not derive from a ductal origin[47]. This suggested definition comes from evidence reporting the presence of inflammatory cells, as well as cells with an intermediate progenitor phenotype, in the DR microenvironment. Although DR may be detected in various liver disorders, it seems particularly frequent and widespread in chronic cholestatic diseases, compared to the normal liver[48,49]. The pathogenetic role of DR in the course of chronic cholestatic diseases has not yet been fully elucidated. However, some experimental data suggest that inhibition of biliary growth in bile duct ligated mice also negatively regulates hepatic stellate cells (HSC) activation and fibrous tissue deposition, suggesting a close link between DR and the onset of liver fibrosis[50]. On the other hand, DR has also been associated with CS[51]. CS refers to a cell that shows permanent G1 phase growth arrest. This cell acquires a so-called senescence-associated secretory phenotype that has been implicated in the pathogenesis of cholangiopathies[52]. With regard to PBC, CS is largely observed within biliary cells and its occurrence (since the possible replacement of vital cells with senescent ones) has been related to the evolution toward ductopenia[53]. In agreement with this view, CS has generally been observed in the late stage of PBC. On the other hand, autophagy, likely supported by the impairment of the bicarbonate umbrella[54], is more frequent in the early phase of the disease, suggesting that this last cellular event may be a possible trigger for CS[55].



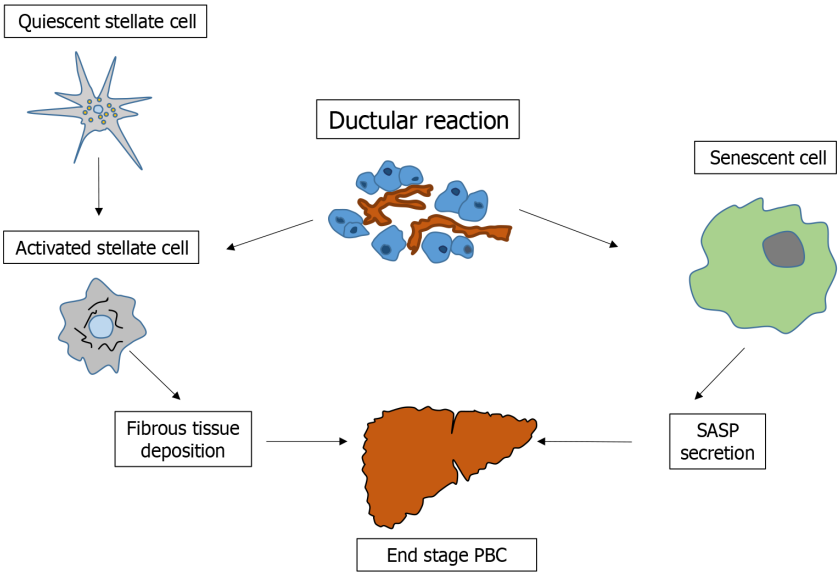
DOI: 10.3748/wjg.v29.i37.5305 **Copyright** ©The Author(s) 2023.

Figure 1 From immune mediated damage to bile acids injury. In primary biliary cholangitis the inflammatory process induces a decrease in chloride-bicarbonate exchangerexpression. This in turn determines a reduction of bicarbonate film (bicarbonate umbrella) on the canalicular portion of bile duct cells, exposing them to hydrophobic bile acids injury. AE2: Chloride-bicarbonate exchanger.

As described above, it is clear how the PBC liver represents a pathology compendium in which several cellular/molecular determinants (inflammation, changes in biliary secretion, HSC activation, CS, autophagy, *etc.*) combine to support the injury. The common field in which all these events are recapitulated or prompted could possibly be represented by DR. In this perspective, we emphasize that DR began to attract the attention of pathologists more than 60 years ago, due to its characteristic features and its relationship with human liver injury[56]. In PBC, a recent clinical study again demonstrated DR as the most relevant pathological characteristic in predicting the stage of the disease, fibrosis progression, and response to UDCA therapy[57]. Unfortunately, most of the research focusing on DR and its relationship with other liver pathological features (such as fibrosis or cell senescence) is mainly descriptive. Mechanistic studies are needed to reveal the molecular pathways that trigger the sequential cascade of pathological events in PBC. In Figure 2 the relationship between DR and other pathological processes during PBC, is depicted.

CONCLUSION

Several sequential molecular/cellular events may occur to develop end-stage PBC. While the presence of the principal predisposing factors (family inheritance or gender) should not be modified, a deep knowledge of the mechanisms involved in the onset and perpetuation of the disease can reveal possible therapeutic targets. However, to decipher the progression of injury during PBC, research cannot be restricted to the study of the immune-inflammatory process, since important physiological and pathological changes in cholangiocytes also contribute to liver damage. To support this view, clinical studies approaching PBC with immunosuppressive or anti-inflammatory drugs, which are usually effective in other autoimmune disorders, gave limited results in these patients[8]. In this perspective and as observed in other liver diseases (such as alcoholic and nonalcoholic steato-hepatitis)[58], multiple hits are likely needed in PBC to develop severe liver damage. Therefore, in an attempt to design a possible pathological route leading to this disorder, a series of events linking together should be considered. As reported in Figure 1 and described in this minireview, the autoimmune process not only promotes inflammation, but also radically changes the secretive and proliferative activities of bile duct cells. Regarding biliary secretion, decreased expression of AE2 negatively regulates biliary flow and bicarbonate secretion. This in turn allows BA cytolitic damage from the impairment of the bicarbonate umbrella. Parallel to this, biliary growth is enhanced in an attempt to balance cellular loss. The chronic enhancement of proliferative activities is recapitulated in the pathological finding of the DR. This represents a microenvironment in which CS and profibrotic processes originate, leading to ductopenic/fibrotic end-stage liver injury (Figure 2). While previous reviews consist in a conventional broad description of PBC or consider a specific aspect of the disorder (genetic, immunology, diagnosis, therapy, *etc.*), in this manuscript we aimed: (1) To design with clarity the sequential steps allowing the PBC evolution from liver inflammation to end-stage fibrosis; and (2)to examine and define in detail the key consecutive molecular/cellular events supporting this path. We believe that deciphering the natural history of PBC as a step by step route, may facilitate the identification of important therapeutic targets. It is clear that several pieces are still lacking to complete the pathogenetic puzzle of this disease. In this sense, studies that examine in detail the molecular pathways that lead to different changes/responses of cholangiocytes may improve our knowledge of PBC and should be helpful in developing new pharmacological



DOI: 10.3748/wjg.v29.i37.5305 **Copyright** ©The Author(s) 2023.

Figure 2 Central role of ductular reaction in the progression of primary biliary cholangitis. Ductular reaction contributes to the activation of hepatic stellate cells and simultaneously favours a cell senescent phenotype. These events support the ductopenic/cirrhotic evolution of liver tissue during this cholestatic disease. PBC: Primary biliary cholangitis; SASP: Senescence-associated secretory phenotype.

treatments.

FOOTNOTES

Author contributions: Lenci I acquisition of data, analysis and interpretation, drafting of manuscript, critical revision; Carnì P, Milana M, Bicaj A, and Signorello A acquisition of data, critical revision; Baiocchi L proposal of study, study conception, correction of manuscript, critical revision.

Conflict-of-interest statement: There is no conflict of interest associated with any of the senior author or other coauthors contributed their efforts in this manuscript.

Open-Access: This article is an open-access article that was selected by an in-house editor and fully peer-reviewed by external reviewers. It is distributed in accordance with the Creative Commons Attribution NonCommercial (CC BY-NC 4.0) license, which permits others to distribute, remix, adapt, build upon this work non-commercially, and license their derivative works on different terms, provided the original work is properly cited and the use is non-commercial. See: https://creativecommons.org/Licenses/by-nc/4.0/

Country/Territory of origin: Italy

ORCID number: Ilaria Lenci 0000-0001-5704-9890; Paola Carnì 0009-0008-0092-5456; Martina Milana 0000-0003-2027-0481; Agreta Bicaj 0000-0002-5332-7643; Alessandro Signorello 0000-0002-3831-7244; Leonardo Baiocchi 0000-0003-3672-4505.

S-Editor: Qu XL
L-Editor: A
P-Editor: Zhao S

REFERENCES

1 **Beuers U**, Gershwin ME, Gish RG, Invernizzi P, Jones DE, Lindor K, Ma X, Mackay IR, Parés A, Tanaka A, Vierling JM, Poupon R. Changing Nomenclature for PBC: From 'Cirrhosis' to 'Cholangitis'. *Am J Gastroenterol* 2015; **110**: 1536-1538 [PMID: 26416194 DOI: 10.1038/ajg.2015.312]
2 **Heathcote EJ**. Primary biliary cirrhosis: historical perspective. *Clin Liver Dis* 2003; **7**: 735-740 [PMID: 14594128 DOI: 10.1016/s1089-3261(03)00098-9]
3 **Sherlock S**. Primary billiary cirrhosis (chronic intrahepatic obstructive jaundice). *Gastroenterology* 1959; **37**: 574-586 [PMID: 14445875]
4 **Colapietro F**, Lleo A, Generali E. Antimitochondrial Antibodies: from Bench to Bedside. *Clin Rev Allergy Immunol* 2022; **63**: 166-177 [PMID: 34586589 DOI: 10.1007/s12016-021-08904-y]
5 **Younossi ZM**, Bernstein D, Shiffman ML, Kwo P, Kim WR, Kowdley KV, Jacobson IM. Diagnosis and Management of Primary Biliary Cholangitis. *Am J Gastroenterol* 2019; **114**: 48-63 [PMID: 30429590 DOI: 10.1038/s41395-018-0390-3]

6 **Gazda J**, Drazilova S, Janicko M, Jarcuska P. The Epidemiology of Primary Biliary Cholangitis in European Countries: A Systematic Review and Meta-Analysis. *Can J Gastroenterol Hepatol* 2021; **2021**: 9151525 [PMID: 34239845 DOI: 10.1155/2021/9151525]

7 **European Association for the Study of the Liver**. EASL Clinical Practice Guidelines: The diagnosis and management of patients with primary biliary cholangitis. *J Hepatol* 2017; **67**: 145-172 [PMID: 28427765 DOI: 10.1016/j.jhep.2017.03.022]

8 **Medford A**, Childs J, Little A, Chakraborty S, Baiocchi L, Alpini G, Glaser S. Emerging Therapeutic Strategies in The Fight Against Primary Biliary Cholangitis. *J Clin Transl Hepatol* 2023; **11**: 949-957 [PMID: 37408803 DOI: 10.14218/JCTH.2022.00398]

9 **Shah RA**, Kowdley KV. Current and potential treatments for primary biliary cholangitis. *Lancet Gastroenterol Hepatol* 2020; **5**: 306-315 [PMID: 31806572 DOI: 10.1016/S2468-1253(19)30343-7]

10 **Gershwin ME**, Selmi C, Worman HJ, Gold EB, Watnik M, Utts J, Lindor KD, Kaplan MM, Vierling JM; USA PBC Epidemiology Group. Risk factors and comorbidities in primary biliary cirrhosis: a controlled interview-based study of 1032 patients. *Hepatology* 2005; **42**: 1194-1202 [PMID: 16250040 DOI: 10.1002/hep.20907]

11 **Yamamoto K**, Okada Y. Shared genetic factors and their causality in autoimmune diseases. *Ann Rheum Dis* 2019; **78**: 1449-1451 [PMID: 30842123 DOI: 10.1136/annrheumdis-2019-215099]

12 **Juran BD**, Lazaridis KN. Genetics and genomics of primary biliary cirrhosis. *Clin Liver Dis* 2008; **12**: 349-65; ix [PMID: 18456185 DOI: 10.1016/j.cld.2008.02.007]

13 **Dendrou CA**, Petersen J, Rossjohn J, Fugger L. HLA variation and disease. *Nat Rev Immunol* 2018; **18**: 325-339 [PMID: 29292391 DOI: 10.1038/nri.2017.143]

14 **Invernizzi P**. Human leukocyte antigen in primary biliary cirrhosis: an old story now reviving. *Hepatology* 2011; **54**: 714-723 [PMID: 21563204 DOI: 10.1002/hep.24414]

15 **Gerussi A**, Carbone M, Corpechot C, Schramm C, Asselta R, Invernizzi P. The genetic architecture of primary biliary cholangitis. *Eur J Med Genet* 2021; **64**: 104292 [PMID: 34303876 DOI: 10.1016/j.ejmg.2021.104292]

16 **Baum H**. Mitochondrial antigens, molecular mimicry and autoimmune disease. *Biochim Biophys Acta* 1995; **1271**: 111-121 [PMID: 7541246 DOI: 10.1016/0925-4439(95)00017-x]

17 **Kaplan MM**, Gershwin ME. Primary biliary cirrhosis. *N Engl J Med* 2005; **353**: 1261-1273 [PMID: 16177252 DOI: 10.1056/NEJMra043898]

18 **Butler P**, Hamilton-Miller JM, McIntyre N, Burroughs AK. Natural history of bacteriuria in women with primary biliary cirrhosis and the effect of antimicrobial therapy in symptomatic and asymptomatic groups. *Gut* 1995; **36**: 931-934 [PMID: 7615287 DOI: 10.1136/gut.36.6.931]

19 **Selmi C**, Balkwill DL, Invernizzi P, Ansari AA, Coppel RL, Podda M, Leung PS, Kenny TP, Van De Water J, Nantz MH, Kurth MJ, Gershwin ME. Patients with primary biliary cirrhosis react against a ubiquitous xenobiotic-metabolizing bacterium. *Hepatology* 2003; **38**: 1250-1257 [PMID: 14578864 DOI: 10.1053/jhep.2003.50446]

20 **Zhang L**, Yang L, Chu H. Targeting Gut Microbiota for the Treatment of Primary Biliary Cholangitis: From Bench to Bedside. *J Clin Transl Hepatol* 2023; **11**: 958-966 [PMID: 37408823 DOI: 10.14218/JCTH.2022.00408]

21 **Tang R**, Wei Y, Li Y, Chen W, Chen H, Wang Q, Yang F, Miao Q, Xiao X, Zhang H, Lian M, Jiang X, Zhang J, Cao Q, Fan Z, Wu M, Qiu D, Fang JY, Ansari A, Gershwin ME, Ma X. Gut microbial profile is altered in primary biliary cholangitis and partially restored after UDCA therapy. *Gut* 2018; **67**: 534-541 [PMID: 28213609 DOI: 10.1136/gutjnl-2016-313332]

22 **Milkiewicz M**, Caballería L, Smyk DS, Milkiewicz P. Predicting and preventing autoimmunity: the case of anti-mitochondrial antibodies. *Auto Immun Highlights* 2012; **3**: 105-112 [PMID: 26000133 DOI: 10.1007/s13317-012-0038-z]

23 **Prieto J**, Banales JM, Medina JF. Primary biliary cholangitis: pathogenic mechanisms. *Curr Opin Gastroenterol* 2021; **37**: 91-98 [PMID: 33332913 DOI: 10.1097/MOG.0000000000000703]

24 **Deng X**, Li J, Hou S, Ci B, Liu B, Xu K. Prevalence and impact of Sjögren's syndrome in primary biliary cholangitis: a systematic review and meta-analysis. *Ann Hepatol* 2022; **27**: 100746 [PMID: 35970319 DOI: 10.1016/j.aohep.2022.100746]

25 **Mariette X**, Criswell LA. Primary Sjögren's Syndrome. *N Engl J Med* 2018; **378**: 931-939 [PMID: 29514034 DOI: 10.1056/NEJMcp1702514]

26 **Dahlqvist G**, Gaouar F, Carrat F, Meurisse S, Chazouillères O, Poupon R, Johanet C, Corpechot C; French network of Immunology Laboratories. Large-scale characterization study of patients with antimitochondrial antibodies but nonestablished primary biliary cholangitis. *Hepatology* 2017; **65**: 152-163 [PMID: 27688145 DOI: 10.1002/hep.28859]

27 **Chascsa DM**, Lindor KD. Antimitochondrial Antibody-Negative Primary Biliary Cholangitis: Is It Really the Same Disease? *Clin Liver Dis* 2018; **22**: 589-601 [PMID: 30259855 DOI: 10.1016/j.cld.2018.03.009]

28 **Li H**, Guan Y, Han C, Zhang Y, Liu Q, Wei W, Ma Y. The pathogenesis, models and therapeutic advances of primary biliary cholangitis. *Biomed Pharmacother* 2021; **140**: 111754 [PMID: 34044277 DOI: 10.1016/j.biopha.2021.111754]

29 **Shimoda S**, Harada K, Niiro H, Shirabe K, Taketomi A, Maehara Y, Tsuneyama K, Nakanuma Y, Leung P, Ansari AA, Gershwin ME, Akashi K. Interaction between Toll-like receptors and natural killer cells in the destruction of bile ducts in primary biliary cirrhosis. *Hepatology* 2011; **53**: 1270-1281 [PMID: 21400555 DOI: 10.1002/hep.24194]

30 **Shimoda S**, Hisamoto S, Harada K, Iwasaka S, Chong Y, Nakamura M, Bekki Y, Yoshizumi T, Shirabe K, Ikegami T, Maehara Y, He XS, Gershwin ME, Akashi K. Natural killer cells regulate T cell immune responses in primary biliary cirrhosis. *Hepatology* 2015; **62**: 1817-1827 [PMID: 26264889 DOI: 10.1002/hep.28122]

31 **Shimoda S**, Van de Water J, Ansari A, Nakamura M, Ishibashi H, Coppel RL, Lake J, Keeffe EB, Roche TE, Gershwin ME. Identification and precursor frequency analysis of a common T cell epitope motif in mitochondrial autoantigens in primary biliary cirrhosis. *J Clin Invest* 1998; **102**: 1831-1840 [PMID: 9819369 DOI: 10.1172/JCI4213]

32 **Wu N**, Baiocchi L, Zhou T, Kennedy L, Ceci L, Meng F, Sato K, Wu C, Ekser B, Kyritsi K, Kundu D, Chen L, Meadows V, Franchitto A, Alvaro D, Onori P, Gaudio E, Lenci I, Francis H, Glaser S, Alpini G. Functional Role of the Secretin/Secretin Receptor Signaling During Cholestatic Liver Injury. *Hepatology* 2020; **72**: 2219-2227 [PMID: 32737904 DOI: 10.1002/hep.31484]

33 **Cai X**, Tacke F, Guillot A, Liu H. Cholangiokines: undervalued modulators in the hepatic microenvironment. *Front Immunol* 2023; **14**: 1192840 [PMID: 37261338 DOI: 10.3389/fimmu.2023.1192840]

34 **Alpini G**, Roberts S, Kuntz SM, Ueno Y, Gubba S, Podila PV, LeSage G, LaRusso NF. Morphological, molecular, and functional heterogeneity of cholangiocytes from normal rat liver. *Gastroenterology* 1996; **110**: 1636-1643 [PMID: 8613073 DOI: 10.1053/gast.1996.v110.pm8613073]

35 **Prieto J**, Qian C, García N, Díez J, Medina JF. Abnormal expression of anion exchanger genes in primary biliary cirrhosis. *Gastroenterology* 1993; **105**: 572-578 [PMID: 8335211 DOI: 10.1016/0016-5085(93)90735-u]

36 **Medina JF**, Martínez-Ansó, Vazquez JJ, Prieto J. Decreased anion exchanger 2 immunoreactivity in the liver of patients with primary biliary

cirrhosis. *Hepatology* 1997; **25**: 12-17 [PMID: 8985258 DOI: 10.1002/hep.510250104]

37 **Prieto J**, García N, Martí-Climent JM, Peñuelas I, Richter JA, Medina JF. Assessment of biliary bicarbonate secretion in humans by positron emission tomography. *Gastroenterology* 1999; **117**: 167-172 [PMID: 10381924 DOI: 10.1016/s0016-5085(99)70564-0]

38 **Salas JT**, Banales JM, Sarvide S, Recalde S, Ferrer A, Uriarte I, Oude Elferink RP, Prieto J, Medina JF. Ae2a,b-deficient mice develop antimitochondrial antibodies and other features resembling primary biliary cirrhosis. *Gastroenterology* 2008; **134**: 1482-1493 [PMID: 18471521 DOI: 10.1053/j.gastro.2008.02.020]

39 **Arenas F**, Hervías I, Sáez E, Melero S, Prieto J, Parés A, Medina JF. Promoter hypermethylation of the AE2/SLC4A2 gene in PBC. *JHEP Rep* 2019; **1**: 145-153 [PMID: 32039364 DOI: 10.1016/j.jhepr.2019.05.006]

40 **van Niekerk J**, Kersten R, Beuers U. Role of Bile Acids and the Biliary HCO(3)(-) Umbrella in the Pathogenesis of Primary Biliary Cholangitis. *Clin Liver Dis* 2018; **22**: 457-479 [PMID: 30259847 DOI: 10.1016/j.cld.2018.03.013]

41 **Baiocchi L**, Lenci I, Milana M, Kennedy L, Sato K, Zhang W, Ekser B, Ceci L, Meadows V, Glaser S, Alpini G, Francis H. Cyclic AMP Signaling in Biliary Proliferation: A Possible Target for Cholangiocarcinoma Treatment? *Cells* 2021; **10** [PMID: 34359861 DOI: 10.3390/cells10071692]

42 **Francis H**, Glaser S, Ueno Y, Lesage G, Marucci L, Benedetti A, Taffetani S, Marzioni M, Alvaro D, Venter J, Reichenbach R, Fava G, Phinizy JL, Alpini G. cAMP stimulates the secretory and proliferative capacity of the rat intrahepatic biliary epithelium through changes in the PKA/Src/MEK/ERK1/2 pathway. *J Hepatol* 2004; **41**: 528-537 [PMID: 15464232 DOI: 10.1016/j.jhep.2004.06.009]

43 **Hall C**, Sato K, Wu N, Zhou T, Kyritsi K, Meng F, Glaser S, Alpini G. Regulators of Cholangiocyte Proliferation. *Gene Expr* 2017; **17**: 155-171 [PMID: 27412505 DOI: 10.3727/105221616X692568]

44 **Franchitto A**, Onori P, Renzi A, Carpino G, Mancinelli R, Alvaro D, Gaudio E. Recent advances on the mechanisms regulating cholangiocyte proliferation and the significance of the neuroendocrine regulation of cholangiocyte pathophysiology. *Ann Transl Med* 2013; **1**: 27 [PMID: 25332971 DOI: 10.3978/j.issn.2305-5839.2012.10.03]

45 **Masyuk AI**, Huang BQ, Radtke BN, Gajdos GB, Splinter PL, Masyuk TV, Gradilone SA, LaRusso NF. Ciliary subcellular localization of TGR5 determines the cholangiocyte functional response to bile acid signaling. *Am J Physiol Gastrointest Liver Physiol* 2013; **304**: G1013-G1024 [PMID: 23578785 DOI: 10.1152/ajpgi.00383.2012]

46 **Alvaro D**, Gigliozzi A, Attili AF. Regulation and deregulation of cholangiocyte proliferation. *J Hepatol* 2000; **33**: 333-340 [PMID: 10952254 DOI: 10.1016/s0168-8278(00)80377-3]

47 **Roskams TA**, Theise ND, Balabaud C, Bhagat G, Bhathal PS, Bioulac-Sage P, Brunt EM, Crawford JM, Crosby HA, Desmet V, Finegold MJ, Geller SA, Gouw AS, Hytiroglou P, Knisely AS, Kojiro M, Lefkowitch JH, Nakanuma Y, Olynyk JK, Park YN, Portmann B, Saxena R, Scheuer PJ, Strain AJ, Thung SN, Wanless IR, West AB. Nomenclature of the finer branches of the biliary tree: canals, ductules, and ductular reactions in human livers. *Hepatology* 2004; **39**: 1739-1745 [PMID: 15185318 DOI: 10.1002/hep.20130]

48 **Crosby HA**, Hubscher S, Fabris L, Joplin R, Sell S, Kelly D, Strain AJ. Immunolocalization of putative human liver progenitor cells in livers from patients with end-stage primary biliary cirrhosis and sclerosing cholangitis using the monoclonal antibody OV-6. *Am J Pathol* 1998; **152**: 771-779 [PMID: 9502419]

49 **Kinugasa Y**, Nakashima Y, Matsuo S, Shono K, Suita S, Sueishi K. Bile ductular proliferation as a prognostic factor in biliary atresia: an immunohistochemical assessment. *J Pediatr Surg* 1999; **34**: 1715-1720 [PMID: 10591578 DOI: 10.1016/s0022-3468(99)90652-8]

50 **Wu N**, Meng F, Zhou T, Venter J, Giang TK, Kyritsi K, Wu C, Alvaro D, Onori P, Mancinelli R, Gaudio E, Francis H, Alpini G, Glaser S, Franchitto A. The Secretin/Secretin Receptor Axis Modulates Ductular Reaction and Liver Fibrosis through Changes in Transforming Growth Factor-β1-Mediated Biliary Senescence. *Am J Pathol* 2018; **188**: 2264-2280 [PMID: 30036520 DOI: 10.1016/j.ajpath.2018.06.015]

51 **Sato K**, Marzioni M, Meng F, Francis H, Glaser S, Alpini G. Ductular Reaction in Liver Diseases: Pathological Mechanisms and Translational Significances. *Hepatology* 2019; **69**: 420-430 [PMID: 30070383 DOI: 10.1002/hep.30150]

52 **Meng L**, Quezada M, Levine P, Han Y, McDaniel K, Zhou T, Lin E, Glaser S, Meng F, Francis H, Alpini G. Functional role of cellular senescence in biliary injury. *Am J Pathol* 2015; **185**: 602-609 [PMID: 25619959 DOI: 10.1016/j.ajpath.2014.10.027]

53 **Sasaki M**, Ikeda H, Haga H, Manabe T, Nakanuma Y. Frequent cellular senescence in small bile ducts in primary biliary cirrhosis: a possible role in bile duct loss. *J Pathol* 2005; **205**: 451-459 [PMID: 15685690 DOI: 10.1002/path.1729]

54 **Sasaki M**, Sato Y, Nakanuma Y. An impaired biliary bicarbonate umbrella may be involved in dysregulated autophagy in primary biliary cholangitis. *Lab Invest* 2018; **98**: 745-754 [PMID: 29540861 DOI: 10.1038/s41374-018-0045-4]

55 **Sasaki M**, Miyakoshi M, Sato Y, Nakanuma Y. Autophagy may precede cellular senescence of bile ductular cells in ductular reaction in primary biliary cirrhosis. *Dig Dis Sci* 2012; **57**: 660-666 [PMID: 21989821 DOI: 10.1007/s10620-011-1929-y]

56 **POPPER H**, KENT G, STEIN R. Ductular cell reaction in the liver in hepatic injury. *J Mt Sinai Hosp N Y* 1957; **24**: 551-556 [PMID: 13476145]

57 **Overi D**, Carpino G, Cristoferi L, Onori P, Kennedy L, Francis H, Zucchini N, Rigamonti C, Viganò M, Floreani A, D'Amato D, Gerussi A, Venere R, Alpini G, Glaser S, Alvaro D, Invernizzi P, Gaudio E, Cardinale V, Carbone M. Role of ductular reaction and ductular-canalicular junctions in identifying severe primary biliary cholangitis. *JHEP Rep* 2022; **4**: 100556 [PMID: 36267871 DOI: 10.1016/j.jhepr.2022.100556]

58 **Glaser T**, Baiocchi L, Zhou T, Francis H, Lenci I, Grassi G, Kennedy L, Liangpunsakul S, Glaser S, Alpini G, Meng F. Pro-inflammatory signalling and gut-liver axis in non-alcoholic and alcoholic steatohepatitis: Differences and similarities along the path. *J Cell Mol Med* 2020; **24**: 5955-5965 [PMID: 32314869 DOI: 10.1111/jcmm.15182]

World Journal of Gastroenterology

Submit a Manuscript: https://www.f6publishing.com

World J Gastroenterol 2023 October 7; 29(37): 5313-5326

DOI: 10.3748/wjg.v29.i37.5313

ISSN 1007-9327 (print) ISSN 2219-2840 (online)

ORIGINAL ARTICLE

Case Control Study

Leukocyte immunoglobulin-like receptor B2 overexpression as a promising therapeutic target and noninvasive screening biomarker for colorectal cancer

Qian-Qian Wang, Lei Zhou, Geng Qin, Chang Tan, Yuan-Chen Zhou, Shu-Kun Yao

Specialty type: Gastroenterology and hepatology

Provenance and peer review: Unsolicited article; Externally peer reviewed.

Peer-review model: Single blind

Peer-review report's scientific quality classification

Grade A (Excellent): 0
Grade B (Very good): B, B
Grade C (Good): 0
Grade D (Fair): 0
Grade E (Poor): 0

P-Reviewer: Herold Z, Hungary; Vega KJ, United States

Received: June 15, 2023
Peer-review started: June 15, 2023
First decision: August 26, 2023
Revised: September 8, 2023
Accepted: September 14, 2023
Article in press: September 14, 2023
Published online: October 7, 2023

Qian-Qian Wang, Chang Tan, Yuan-Chen Zhou, Shu-Kun Yao, Department of Gastroenterology, Peking University China-Japan Friendship School of Clinical Medicine, Beijing 100029, China

Lei Zhou, Department of General Surgery, China-Japan Friendship Hospital, Beijing 100029, China

Geng Qin, Department of Gastroenterology, China-Japan Friendship Hospital, Beijing 100029, China

Corresponding author: Shu-Kun Yao, MD, PhD, Professor, Department of Gastroenterology, Peking University China-Japan Friendship School of Clinical Medicine, No. 2 Yinghua East Road, Chaoyang District, Beijing 100029, China. shukunyao@126.com

Abstract

BACKGROUND

Colorectal cancer (CRC) has become the second most deadly malignancy in the world, and the exploration of screening markers and precise therapeutic targets is urgent. Our previous research identified leukocyte immunoglobulin-like receptor B2 (LILRB2) protein as a characteristic protein of CRC, but the association between LILRB2 expression and clinicopathological features, the internal mechanism related to CRC progression, and screening diagnostic efficacy are not clear. Therefore, we hypothesized that LILRB2 is significantly highly expressed in CRC tissues, correlated with advanced stage and a poor prognosis, and could be used as a therapeutic target and potential screening biomarker for CRC.

AIM

To explore whether LILRB2 can be used as a potential therapeutic target and noninvasive screening biomarker for CRC.

METHODS

Patients who underwent radical surgery for CRC at China-Japan Friendship Hospital between February 2021 and October 2022 were included. Cancer and paracancerous tissues were collected to verify LILRB2 expression, and the association between LILRB2 expression and clinicopathological features was analysed. Serum was collected from CRC patients, adenoma patients and healthy controls during the same period to assess the diagnostic value of LILRB2 as a

noninvasive screening biomarker, and its diagnostic value was further compared with that of the traditional markers carcinoembryonic antigen (CEA) and carbohydrate antigen 19-9 (CA19-9).

RESULTS

A total of 58 CRC patients were included, and LILRB2 protein was significantly overexpressed in cancer tissues compared with paracancerous tissues ($P < 0.001$). Angiopoietin-like protein 2 (ANGPTL2) protein, as the ligand of LILRB2, was synergistically overexpressed in CRC tissues ($P < 0.001$), and overexpression of LILRB2 and ANGPTL2 protein was significantly correlated with poor to moderate differentiation, vascular involvement, lymph node metastasis, distant metastasis, advanced tumor-node-metastasis stage and a poor prognosis ($P < 0.05$), which suggested that LILRB2 and ANGPTL2 are closely associated with CRC progression. In addition, serum LILRB2 concentrations increased stepwise in healthy individuals, adenoma patients and CRC patients with statistically significant differences. The sensitivity of serum LILRB2 for the diagnosis of CRC was 89.74%, the specificity was 88.89%, the area under the curve was 0.95, and the diagnostic efficacy was better than that of conventional CEA and CA19-9.

CONCLUSION

LILRB2 protein can be used as a potential novel therapeutic target and noninvasive screening biomarker for CRC, which is beneficial for early screening and precise treatment.

Key Words: Colorectal cancer; Leukocyte immunoglobulin-like receptor B2; Angiopoietin-like protein 2; Therapeutic target; Noninvasive screening biomarker

©The Author(s) 2023. Published by Baishideng Publishing Group Inc. All rights reserved.

Core Tip: Based on prior proteomic research rather than simple data mining, this study innovatively proposed and validated that leukocyte immunoglobulin-like receptor B2 (LILRB2) and its ligand, the angiopoietin-like protein 2 protein, are significantly overexpressed in colorectal cancer (CRC) and closely associated with tumour progression and a poor prognosis. In addition, this study is the first to propose that serum LILRB2 concentration can be used as a novel screening biomarker with a sensitivity of 89.74%, a specificity of 88.89% and an accuracy rate of 89.63% for the diagnosis of CRC. The sensitivity and accuracy were significantly higher than those of carcinoembryonic antigen and carbohydrate antigen 19-9. Therefore, LILRB2 could be a promising therapeutic target and noninvasive screening biomarker for CRC.

Citation: Wang QQ, Zhou L, Qin G, Tan C, Zhou YC, Yao SK. Leukocyte immunoglobulin-like receptor B2 overexpression as a promising therapeutic target and noninvasive screening biomarker for colorectal cancer. *World J Gastroenterol* 2023; 29(37): 5313-5326

URL: https://www.wjgnet.com/1007-9327/full/v29/i37/5313.htm

DOI: https://dx.doi.org/10.3748/wjg.v29.i37.5313

INTRODUCTION

The latest cancer statistics show that more than 1.9 million new cases of colorectal cancer (CRC) and 935000 deaths occurred in 2020, accounting for approximately one-tenth of all new cancer cases and deaths. CRC has become the third ranked malignancy worldwide in terms of incidence and the second ranked in terms of mortality, second only to lung cancer[1-3]. The 5-year overall survival (OS) rate for early-stage CRC can be as high as 80%-90%, while the prognosis for advanced-stage patients is poor, with a 5-year survival rate of less than 20%[4,5]. Although targeted therapy or immunotherapy has improved the OS of CRC patients, limited treatment options, moderate response rates and drug resistance remain major challenges for CRC treatment. Therefore, the exploration of novel therapeutic targets and noninvasive screening biomarkers is essential to improve the outcomes of CRC patients.

Proteomics has been widely used in cancer research[6,7]. In preliminary research, we screened leukocyte immunoglobulin-like receptor B2 (LILRB2) protein as a characteristic protein of CRC[8]. LILRB2 is a transmembrane glycoprotein with a structure similar to immune checkpoint protein programmed cell death protein-1 (PD-1)/PD-ligand 1; it has four extracellular immunoglobulin-like structural domains and intracellular tyrosine-based immune receptor inhibitory motifs (ITIMs); it is widely expressed on the surface of dendritic cells, macrophages, and other myeloid cells and can inhibit immune cell function and participate in important pathological processes such as tumour immune microenvironment (TME), immune escape, and promotion of tumour progression[9]. Angiopoietin-like proteins (ANGPTLs) are a family of seven secreted glycoproteins that play an important role in angiogenesis, the inflammatory response, and tumour progression[10]. In recent years, it has been revealed that LILRB2 is a receptor for ANGPTLs, with the strongest affinity for ANGPTL2, ending the status of ANGPTLs as "orphan ligands"[11]. The interaction of the LILRB2 receptor with the ANGPTL2 ligand has been reported to promote the progression of tumours such as acute leukaemia and non-small cell

lung cancer (NSCLC)[10,12,13]. However, such interactions have not been reported in CRC.

Therefore, this study hypothesized that LILRB2 could be a potential novel therapeutic target and screening biomarker for CRC, but validation of LILRB2 and ANGPTL2 protein expression and interaction in CRC tissues is first needed to further explore the feasibility of LILRB2 protein as a noninvasive screening biomarker.

MATERIALS AND METHODS

Study subjects

Patients who underwent radical surgery for CRC at China-Japan Friendship Hospital between February 2021 and October 2022 were recruited. Inclusion criteria were as follows: patients diagnosed with CRC by the department of pathology who intended to undergo radical resection. The exclusion criteria were as follows: (1) Patients with familial adenomatous polyposis, hereditary nonpolyposis CRC (lynch syndrome), synchronous multiple tumours, inflammatory bowel disease-related CRC; (2) CRC with neuroendocrine manifestations; (3) Patients who received radiotherapy, targeted therapy, immunotherapy, *etc.*, within 6 mo prior to radical surgery; and (4) Patients who lacked informed consent or patients with missing information.

Colorectal adenoma patients and healthy controls were recruited at the Endoscopy Center of China-Japan Friendship Hospital during the same period. Inclusion criteria for adenoma patients were as follows: Patients with pathologically confirmed colorectal adenoma who were intended to undergo elective endoscopic mucosal resection. The exclusion criteria were as follows: (1) Severe atypical hyperplasia, high-grade intraepithelial neoplasia or carcinoma in situ; (2) Familial adenomatous polyposis or inflammatory bowel disease-associated colorectal polyps; and (3) Refusal to sign the informed consent form. Patients with no abnormalities according to colonoscopy were included in the healthy control group. The study was approved by the ethics committee of China-Japan Friendship Hospital and conducted in accordance with the Declaration of Helsinki.

Sample collection

Cancer and paracancerous tissues (> 5 cm from the cancer margin) were collected from CRC patients after surgical resection, and the samples were rinsed with ice-cold saline, soaked in 10% formalin solution with a volume ratio of 1:7, fixed for 24 h, rinsed under running water, dehydrated and waxed at 55 °C and embedded in paraffin. The paraffin blocks were stored at room temperature and subsequently used for immunohistochemical staining.

Fresh whole blood samples were collected from CRC patients before (within 7 d) and after (within 24 h) surgery, adenoma patients before surgery (within 7 d) and healthy controls and centrifuged at 2-8 °C and 3000 r/min for 15 min at room temperature. The supernatant serum was collected into 2 mL freezing tubes, transferred to a -80 °C refrigerator in liquid nitrogen for freezing and storage, and subsequently used for enzyme-linked immunosorbent assay (ELISA), and the samples avoided repeated thawing before the examination.

Data collection

In the electronic medical record system, applications were made to view the medical records of the enrolled patients and collect clinical information (age, sex), tumour markers [carcinoembryonic antigen (CEA), carbohydrate antigen 19-9 (CA19-9)], histopathological features [tumour location, size, pathological type, degree of differentiation, vascular involvement, nerve involvement, lymph node metastasis, and tumor-node-metastasis (TNM) stage] and molecular pathology (KRAS, NRAS, PIK3CA, BRAF, MS). The normal reference ranges were CEA < 5 ng/mL and CA19-9 ≤ 30 U/mL. TNM staging was based on the American Joint Committee on Cancer 8th edition TNM staging system.

Immunohistochemistry

Paraffin blocks were cut into 4-μm-thick sections, and the sections were sequentially placed in dewaxing solution I for 15 min, dewaxing solution II for 15 min, dewaxing solution III for 15 min, anhydrous ethanol I for 5 min, anhydrous ethanol II for 5 min, 85% alcohol for 5 min, and 75% alcohol for 5 min and then washed with distilled water. The slides were placed in a repair box filled with EDTA antigen repair buffer (pH 9.0) in a microwave oven for antigen repair, and after natural cooling, the slides were placed in phosphate buffered saline (PBS) (pH = 7.4) on a decolorization shaker and washed 3 times for 5 min each. Sections were placed in 3% hydrogen peroxide solution, incubated for 25 min at room temperature and protected from light, and the slides were placed in PBS (pH = 7.4) on a decolorizing shaker and washed three times for 5 min each time to block endogenous peroxidase. The tissue slides were covered uniformly with 3% BSA in a dropwise manner and then blocked at room temperature for 30 min; the slide was gently shaked to remove the blocking solution, and a primary antibody (anti-LILRB2, LSBio, Cat No. LS-B9762-50, 1:150; anti-ANGPTL2, Proteintech, Cat No. 12316-1-AP, 1:200) in a certain ratio of PBS was added dropwise onto the section. Sections were incubated flat in a wet box overnight at 4 °C. After washing and shaking the slides dry, HRP-labelled goat anti-rabbit secondary antibody (Servicebio, GB23303, 1:200) was added dropwise in the circle to cover the tissue and incubated at room temperature for 50 min. After washing and shaking the slides dry, freshly prepared DAB colour development solution was added dropwise, the colour development time was controlled under the microscope, and the positive colour was brownish yellow. Haematoxylin was used to restain the nuclei for approximately 3 min, and the sections were washed with tap water. Finally, microscopic examination was performed, and images were acquired for analysis. Image-Pro Plus image analysis software was used to quantify the immunohistochemical images; five fields of view were randomly selected after magnification of each section at 200 × to assess the integrated optical density and area, and the average optical density

value was calculated.

Correlation and survival analysis

The Gene Expression Profiling Interactive Analysis (GEPIA) platform can analyse differentially expressed genes or mRNAs between normal and cancer tissues online for survival and correlation analysis in a variety of tumours. In this study, we used GEPIA V2.0 (http://gepia2.cancer-pku.cn/) for survival analysis and correlation analysis of CRC at the mRNA level as a complement to proteomics and immunohistochemistry (IHC) at the protein level.

ELISA

The assay was performed according to the instructions of the Human LILRB2 ELISA Kit (Abcam, Cat No. ab269551). Prepare blank wells and wells with multiply diluted standards, add 100 μL of properly diluted serum samples to be tested in the reaction wells, seal the plate with sealing film and incubate at 37 °C for 1-2 h. Discard the liquid, add 300 μL of washing solution to each well, soak for 1-2 min, pat dry on absorbent paper and repeat 3-5 times. Then, 100 μL of diluted biotinylated antibody working solution was added to each well, the plate was sealed with sealing film and incubated at 37 °C for 1 h. The liquid was discarded, 300 μL of washing solution was added to each well, and the washing was repeated. Then, 100 μL of diluted enzyme conjugate working solution was added to each well, the plate was sealed with sealing film and incubated for 30 min at 37 °C, and the washing process was repeated. TMB substrate solution (100 μL) was added to each well and incubated for 10-30 min at 37 °C, protected from light, until a clear colour gradient appeared in the wells of the standards diluted in multiples. The reaction was terminated by adding 100 μL of 2 M sulfuric acid to each well, and the colour changed from blue to yellow. The OD value of each well, including wells with enzyme standards and blank wells, was measured at 450 nm. The blank control wells were adjusted to zero. A standard curve was made according to the concentration and OD value of the standards, and then the sample concentration was calculated according to the equation of the standard curve, and the result was multiplied by the dilution factor for the sample.

Statistical analysis

SPSS 25.0 was used for statistical analysis. Quantitative data are expressed as the mean ± SD, and an independent sample *t* test was used for comparisons between two groups. If the quantitative data did not obey a normal distribution or the variance was not uniform, the median (quartiles) was used, the Mann-Whitney *U* test was used for two-group comparisons, the Kruskal-Wallis *H* test was used for multigroup comparisons, and the Bonferroni method was required to correct the significance level for multiple two-group comparisons. Categorical data were expressed as percentages, and two or more groups were compared using the χ^2 test or Fisher's exact test. Quantitative data correlation analysis was performed using Pearson correlation or Spearman correlation analysis (nonnormally distributed). OS curves and progression-free survival (PFS) curves were constructed using the Kaplan-Meier method and analysed using the log rank test. $P < 0.05$ was considered to indicate a significant difference.

RESULTS

LILRB2 and ANGPTL2 protein expression in CRC tissues and paracancerous tissues

From February 2021 to October 2022, a total of 58 CRC patients met the criteria, and 58 pairs of tissues were successfully collected. Figure 1 demonstrates the actual expression of LILRB2 and ANGPTL2 proteins in primary CRC tissues and paracancerous tissues. Figure 1A shows that LILRB2 protein expression significantly higher in CRC tissues than in paracancerous tissues ($P < 0.001$), and ANGPTL2 protein was significantly overexpressed in CRC tissues compared with paracancerous tissues ($P < 0.001$) (Figure 1B).

Association between LILRB2 and ANGPTL2 protein expression and clinicopathological features of CRC

The associations between LILRB2 and ANGPTL2 protein expression and clinicopathological characteristics of CRC are shown in Table 1. The results showed that the overexpression of LILRB2 protein and ANGPTL2 protein was significantly correlated with poor to moderate tumour differentiation, vascular involvement, lymph node metastasis and advanced TNM stage. In addition, high LILRB2 protein expression was significantly correlated with nerve involvement ($P = 0.019$), confirming that LILRB2 and ANGPTL2 protein are closely associated with the progression of CRC.

Correlation of LILRB2 and ANGPTL2 expression at the mRNA and protein levels in CRC

Figure 2 demonstrates the correlation between *LILRB2* and *ANGPTL2* expression at the mRNA and protein levels in primary CRC tissues. The correlation between *LILRB2* and *ANGPTL2* expression at the mRNA level was first analysed using the GEPIA database, and the results showed that *LILRB2* mRNA expression was significantly and positively correlated with *ANGPTL2* mRNA expression in CRC tissues ($r = 0.63$, $P = 0$) (Figure 2A); similarly, LILRB2 protein expression was significantly and positively correlated with ANGPTL2 protein expression ($r = 0.63$, $P < 0.0001$) (Figure 2B).

Observation of IHC images showed that LILRB2 protein was expressed in the cell membrane, cytoplasm or both in CRC cells, and inflammatory cells also showed brown staining/positive expression, while ANGPTL2 protein was mainly expressed in the cytoplasm of CRC cells. LILRB2 protein was highly expressed in 67.2% of CRC tissues, and ANGPTL2 protein was highly expressed in 48.3% of CRC tissues. However, in the paracancerous tissues, LILRB2 protein and ANGPTL2 protein expression was significantly lower or not detected (Figures 2C-H).

Table 1 Associations between leukocyte immunoglobulin-like receptor B2 and angiopoietin-like protein 2 protein expression and clinicopathological features of colorectal cancer

	LILRB2		*P* value	ANGPTL2		*P* value
	Low (*n* = 19)	High (*n* = 39)		Low (*n* = 30)	High (*n* = 28)	
Clinical features						
Age (yr)			0.670			0.986
≤ 50	4 (21.1%)	5 (12.8%)		14 (46.7%)	13 (46.4%)	
> 50	15 (78.9%)	34 (87.2%)		16 (53.3%)	15 (53.6%)	
Sex			1.000			0.473
Male	10 (52.6%)	21 (53.8%)		24 (80.0%)	25 (89.3%)	
Female	9 (47.4%)	18 (46.2%)		6 (20.0%)	3 (10.7%)	
Histopathological features						
Location			0.737			0.065
Right-side colon	2 (10.5%)	7 (17.9%)		2 (6.60%)	7 (25.0%)	
Left-side colon	6 (31.6%)	9 (23.1%)		11 (36.7%)	4 (14.3%)	
Rectum	11 (57.9%)	23 (59.0%)		17 (56.7%)	17 (60.7%)	
Size (cm)			0.224			0.436
> 4.9	7 (36.8%)	21 (53.8%)		13 (43.3%)	15 (53.6%)	
≤ 4.9	12 (63.2%)	18 (46.2%)		17 (56.7%)	13 (46.4%)	
Pathological type			0.287			0.589
Ulcer	12 (63.2%)	29 (74.4%)		23 (76.7%)	18 (64.3%)	
Bulge	6 (31.6%)	5 (12.8%)		5 (16.7%)	6 (21.4%)	
Mix	1 (5.20%)	5 (12.8%)		2 (6.60%)	4 (14.3%)	
Differentiation			0.009			0.013
Poor	0 (0.00%)	10 (25.6%)		1 (3.40%)	9 (32.1%)	
Moderate	15 (78.9%)	27 (69.2%)		25 (83.3%)	17 (60.7%)	
High	4 (21.1%)	2 (5.20%)		4 (13.3%)	2 (7.20%)	
Vascular involvement			0.001			0.016
Yes	1 (5.30%)	19 (48.7%)		6 (20.0%)	14 (50.0%)	
No	18 (94.7%)	20 (51.3%)		24 (80.0%)	14 (50.0%)	
Nerve involvement			0.019			0.754
Yes	7 (36.8%)	27 (69.2%)		17 (56.7%)	17 (60.7%)	
No	12 (63.2%)	12 (30.8%)		13 (43.3%)	11 (39.3%)	
Lymph node metastasis			< 0.001			0.008
Yes	2 (10.5%)	29 (74.4%)		11 (36.7%)	20 (71.4%)	
No	17 (89.5%)	10 (25.6%)		19 (63.3%)	8 (28.6%)	
Molecular pathology						
KRAS			0.186			0.249
+	6 (31.6%)	19 (48.7%)		11 (36.7%)	14 (50.0%)	
-	13 (68.4%)	20 (51.3%)		19 (63.3%)	14 (50.0%)	
NRAS			0.594			0.613
+	2 (10.5%)	2 (5.10%)		3 (10.0%)	1 (3.60%)	
-	17 (89.5%)	37 (94.9%)		27 (90.0%)	27 (96.4%)	

PIK3CA			1.000			1.000
+	0 (0.0%)	1 (2.60%)		1 (3.30%)	0 (0.0%)	
-	19 (100%)	38 (97.4%)		29 (96.7%)	28 (100%)	
BRAF			0.548			1.000
+	0 (0.0%)	2 (5.10%)		1 (3.30%)	1 (3.60%)	
-	19 (100%)	37 (94.9%)		29 (96.7%)	27 (96.4%)	
MS			1.000			1.000
MSS	18 (94.7%)	37 (94.9%)		28 (93.3%)	27 (96.4%)	
MSI-H	1 (5.30%)	2 (5.10%)		2 (6.70%)	1 (3.60%)	
Clinical stage						
pT			0.001			0.006
T1	0 (0.0%)	0 (0.0%)		0 (0.0%)	0 (0.0%)	
T2	7 (36.8%)	1 (2.60%)		7 (23.3%)	1 (3.60%)	
T3	11 (57.9%)	27 (69.2%)		21 (70.0%)	17 (60.7%)	
T4	1 (5.30%)	11 (28.2%)		2 (6.70%)	10 (35.7%)	
pN			< 0.001			0.001
N0	19 (100%)	11 (28.2%)		22 (73.3%)	8 (28.6%)	
N1	0 (0.0%)	15 (38.5%)		6 (20.0%)	9 (32.1%)	
N2	0 (0.0%)	13 (33.3%)		2 (6.70%)	11 (39.3%)	
pM			0.044			0.002
M0	19 (100%)	31 (79.5%)		30 (100%)	20 (71.4%)	
M1	0 (0.0%)	8 (20.5%)		0 (0.0%)	8 (28.6%)	
pTNM stage			< 0.001			< 0.001
I-II	18 (94.7%)	10 (25.6%)		22 (73.3%)	6 (21.4%)	
III-IV	1 (5.30%)	29 (74.4%)		8 (26.7%)	22 (78.6%)	

LILRB2: Leukocyte immunoglobulin-like receptor B2; ANGPTL2: Angiopoietin-like protein 2; CRC: Colorectal cancer; MS: Microsatellite state; MSS: Microsatellite stability; MSI-H: Microsatellite instability-high.

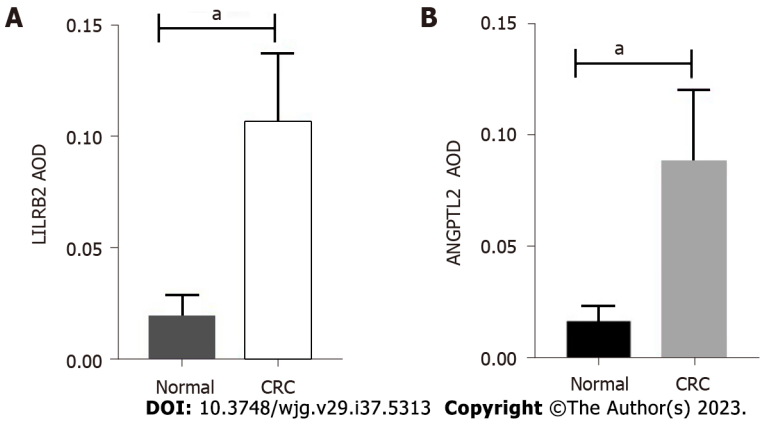
Associations between LILRB2 and ANGPTL2 expression and the prognosis of CRC

ANGPTL2 mRNA was significantly negatively correlated with the OS (P = 0.0042) and PFS (P = 0.0013) of CRC patients, while no association was found at the protein level (Figures 3A and B). In contrast, *LILRB2* mRNA expression was not associated with the OS or PFS of CRC patients (P > 0.05) (Figure 3C), while LILRB2 protein overexpression was significantly associated with reduced OS (P = 0.045) (Figure 3D), suggesting a poor prognosis in CRC patients and indicating the procancer role of LILRB2 protein in CRC progression.

Screening and diagnostic efficacy of serum LILRB2 concentration

From February 2021 to October 2022, 313 serum samples were collected, including 117 preoperative and 85 postoperative serum samples from CRC patients, 93 serum samples from adenoma patients and 18 serum samples from healthy controls.

Comparison of the differences in serum LILRB2 concentrations among CRC patients, adenoma patients and healthy controls showed that serum LILRB2 concentrations were not identical in the three groups, and the differences were statistically significant (H = 75.25, P < 0.001). The Bonferroni method was used to correct for significance levels, and a two-by-two comparison showed that serum LILRB2 concentrations in patients with CRC (7074.69 pg/mL *vs* 3931.33 pg/mL, adjusted P < 0.001) and in adenoma patients (4855.88 pg/mL *vs* 3931.33 pg/mL, adjusted P = 0.036) were significantly higher than those in healthy controls (Figure 4A). The serum LILRB2 concentration in CRC was again significantly higher than that in the adenoma group (7074.69 pg/mL *vs* 4855.88 pg/mL, adjusted P < 0.001). When compared before and after CRC radical surgery, postoperative serum LILRB2 concentrations were significantly lower than preoperative concentrations (5665.30 pg/mL *vs* 7074.69 pg/mL, adjusted P < 0.001) (Figure 4B), and this result was consistent with the analysis of 50 paired serum samples (5431.44 pg/mL *vs* 6579.17 pg/mL, P = 0.002).



DOI: 10.3748/wjg.v29.i37.5313 **Copyright** ©The Author(s) 2023.

Figure 1 Leukocyte immunoglobulin-like receptor B2 and angiopoietin-like protein 2 protein expression in colorectal cancer tissues and paracancerous tissues. A: Comparison of leukocyte immunoglobulin-like receptor B2 protein expression in colorectal cancer (CRC) and paired normal tissues; B: Comparison of angiopoietin-like protein 2 protein expression in CRC and paired normal tissues. Quantification of protein expression using immunohistochemistry and Image-Pro Plus software. LILRB2: Leukocyte immunoglobulin-like receptor B2; ANGPTL2: Angiopoietin-like protein 2; CRC: Colorectal cancer; AOD: Average option density. $^{a}P < 0.001$.

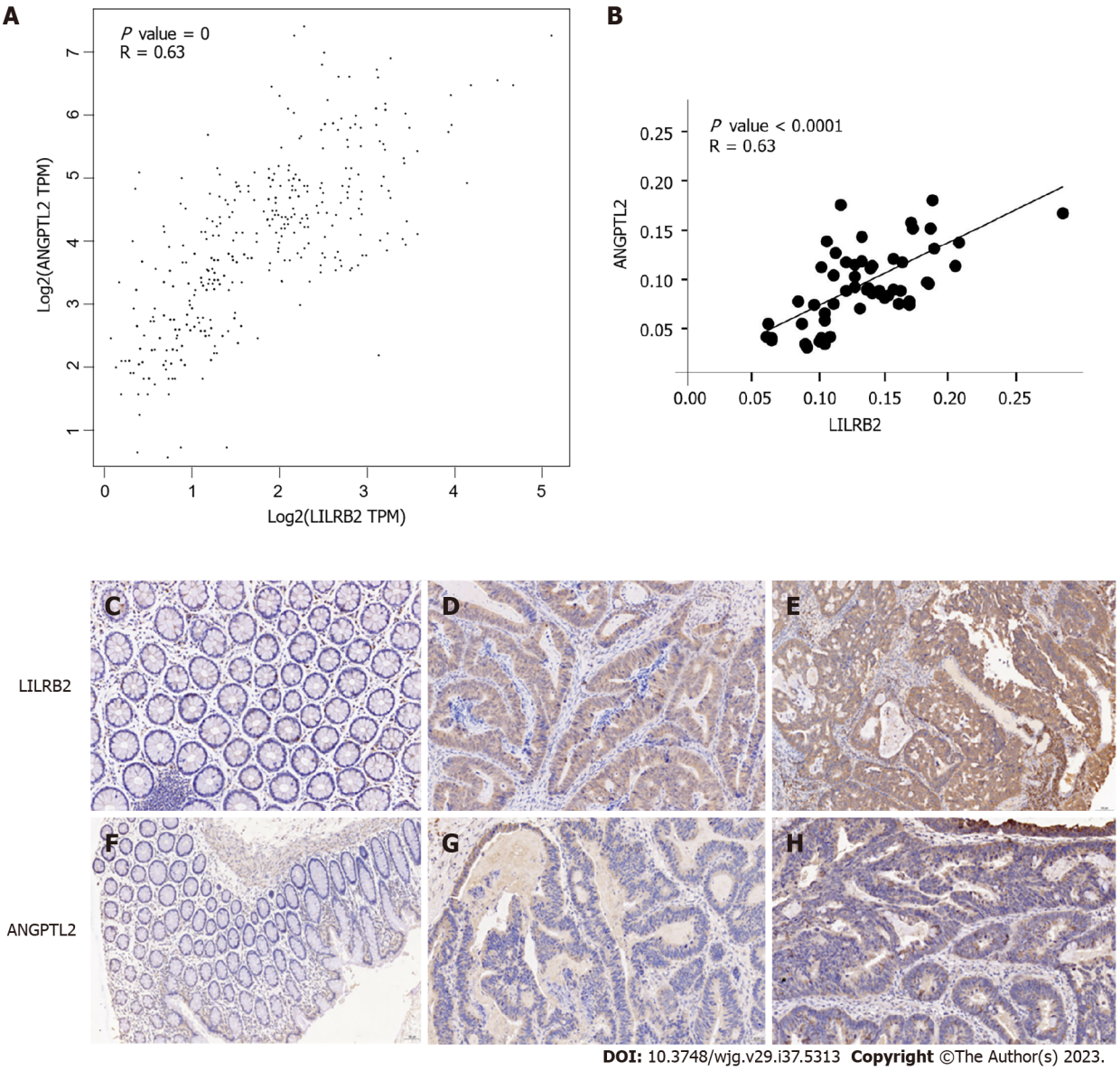
Further stratified analysis of CRC patients showed significant differences in serum LILRB2 concentrations between tumours with different infiltration depths ($H = 42.13$, $P < 0.001$). Compared with those in healthy controls, serum LILRB2 concentrations at pT2 (adjusted $P = 0.004$), pT3 (adjusted $P < 0.001$) and pT4 (adjusted $P < 0.001$) were significantly higher (Figure 4C). LILRB2 concentrations were significantly higher in pT1-T2 stage (adjusted $P = 0.002$) and pT3-T4 stage (adjusted $P < 0.001$) patients than in healthy controls (Figure 4D). There was also a significant difference between samples with different degrees of differentiation ($H = 38.525$, $P < 0.001$), with significantly higher serum LILRB2 concentrations in both the poor differentiation (adjusted $P < 0.001$) and moderate differentiation groups (adjusted $P < 0.001$) than in the healthy controls (Figure 4E).

The recommended cut-off value of serum LILRB2 concentration for screening CRC was 5256 pg/mL, with a sensitivity of 89.74% (105/117), a specificity of 88.89% (16/18), an accuracy rate of 89.63% (121/135), an area under the curve (AUC) of 0.95 (0.89, 1.00) and $P < 0.0001$ (Figure 4F). The diagnostic efficacy of LILRB2 was superior to that of the traditional serum markers CEA and CA19-9 (Figure 4G).

DISCUSSION

The high morbidity and mortality of CRC has created a more urgent clinical need for novel therapeutic targets and screening biomarkers. Preliminary high-throughput proteomics research identified LILRB2 as a signature protein for CRC. In this study, IHC was used to confirm that LILRB2 protein was significantly highly expressed in CRC and that increased LILRB2 protein expression was significantly associated with clinicopathological features such as poor to moderate degree of differentiation, lymph node metastasis, advanced TNM stage and poor prognosis. ANGPTL2, as the ligand for LILRB2, was significantly highly expressed in CRC tissues and synergistically overexpressed with LILRB2 at both the mRNA and protein levels, suggesting that their overexpression and interaction are associated with CRC progression. In addition, serum LILRB2 concentrations increased in healthy controls, adenoma patients and CRC patients sequentially with statistically significant differences; the sensitivity for the diagnosis of CRC was 89.74%, the specificity was 88.89%, and the AUC value was 0.95, and these results were superior to those of traditional CEA and CA19-9 in terms of diagnostic efficacy. Therefore, we believe that LILRB2 protein can be used as a potential therapeutic target and noninvasive screening biomarker for CRC; the biomarker could facilitate early screening and precise treatment and improve the prognosis of CRC patients.

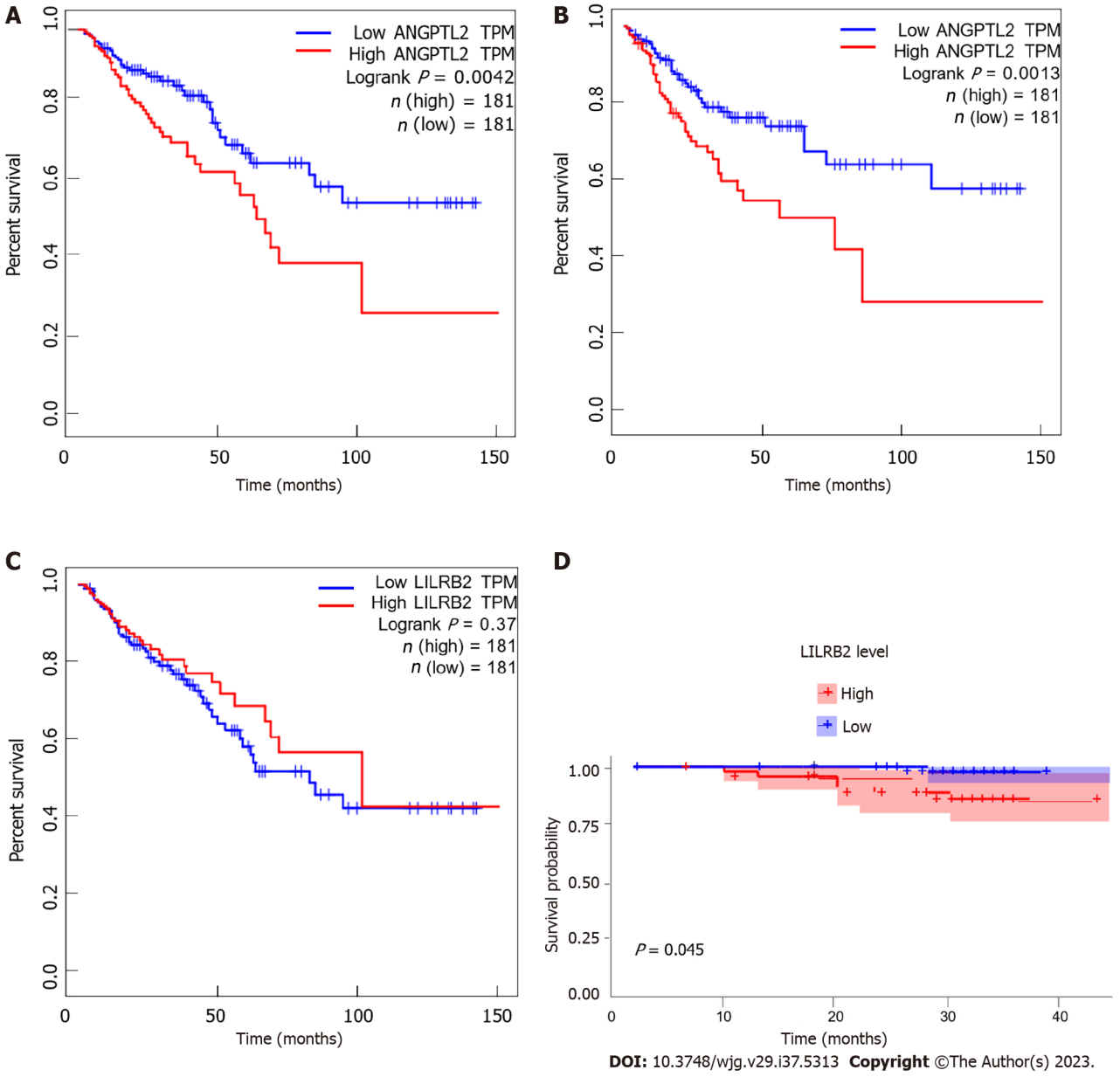
At present, there are relatively few basic experimental or clinical studies on the relevance of LILRB2 to CRC. One study explored the expression of LILRB2 in human normal colorectal mucosal cells and various CRC cell lines, and the results showed that LILRB2 was significantly highly expressed in CRC cell lines, and the malignant biological behaviour of cancer cells was inhibited after blocking LILRB2, suggesting that LILRB2 is involved in and regulates the proliferation, migration and invasion of CRC cells and promotes cancer development[14,15]. The results of this cellular assay complement and validate the results of our clinical study. In addition to the basal cell assay, another study analysed clinical samples from CRC patients, but unlike our study using IHC, the researchers prepared cell suspensions from frozen CRC tissues and analysed the immune checkpoint protein LILRB2 by flow cytometry; the results showed that LILRB2 expression was associated with distant lymph node metastasis, advanced stage, and shorter survival and that LILRB2 overexpression may be an independent prognostic risk factor for CRC patients[15]. This study used flow cytometry analysis, and the study technique is innovative, but because flow cytometry requires fresher of tissue samples, prolonged cryopreservation may affect the accuracy of LILRB2 expression detection by flow cytometry. Our used traditional immunohistochemical staining, and the findings with the two study methods corroborated each other. Ultimately, the findings further supported that LILRB2 promotes colorectal carcinogenesis and development.



DOI: 10.3748/wjg.v29.i37.5313 **Copyright** ©The Author(s) 2023.

Figure 2 Correlation of leukocyte immunoglobulin-like receptor B2 and angiopoietin-like protein 2 expression at the mRNA and protein levels in colorectal cancer. A: Correlation at the mRNA level in colorectal cancer (CRC); B: Correlation at the protein level in CRC; C: Immunohistochemical staining of leukocyte immunoglobulin-like receptor B2 (LILRB2) in paracancerous tissue; D: Low expression of LILRB2 in CRC tissue; E: High expression of LILRB2 in CRC tissue; F: Immunohistochemical staining of angiopoietin-like protein 2 (ANGPTL2) in paracancerous tissue; G: Low expression of ANGPTL2 in CRC; H: Overexpression of ANGPTL2 in CRC. LILRB2: Leukocyte immunoglobulin-like receptor B2; ANGPTL2: Angiopoietin-like protein 2; CRC: Colorectal cancer.

Since the discovery of the LILRB2 receptor, ANGPTLs have lost their designation as "orphan ligands"; the LILRB2 receptor interacts with the highest affinity with ANGPTL2 to support the development of a variety of malignancies, such as CRC, acute myeloid leukaemia (AML)[12] and NSCLC[13]. The present study confirmed the synergistic expression of LILRB2 and ANGPTL2 in CRC: There was a significant positive correlation between their expression at both the mRNA and protein levels and a significant association with clinicopathological parameters, suggesting that LILRB2 receptor and ANGPTL2 ligand interactions are closely associated with the development of CRC. A study analysing more than 9000 human leukaemia samples revealed that *LILRB2* mRNA levels could be elevated several-fold in human AML cells. In a mouse leukaemia model, defects in the mouse immunoglobulin-like receptor (PirB), a homologue of human LILRB2, led to increased differentiation of leukaemic stem cells and significant downregulation of the expression of many pro-oncogenes, suggesting that PirB promotes leukaemia development[10]. Another study further indicated that the LILRB2 receptor accelerated leukaemia development by binding to overexpressed ANGPTL2, and the binding of both induced activation of tyrosine phosphatases SHP-1/SHP-2 and calmodulin-dependent protein kinase downstream of iTIMs, stimulating leukaemia development, and suggested that targeting ANGPTL2 ligands could serve as a certain type of AML as a potential disruption strategy[12,16]. LILRB2 is significantly highly expressed in NSCLC tissues and correlates with a poor prognosis[17]. There have been corresponding advances in the study of the mechanisms by which LILRB2 promotes NSCLC development and immunotherapy tolerance, which are expected to bring new therapeutic opportunities to NSCLC patients. On the one hand, tumour cell-derived ANGPTL2 overexpression, by acting on LILRB2 receptors, promotes increased tumour angiogenesis, epithelial mesenchymal transition, reduced intercellular adhesion,

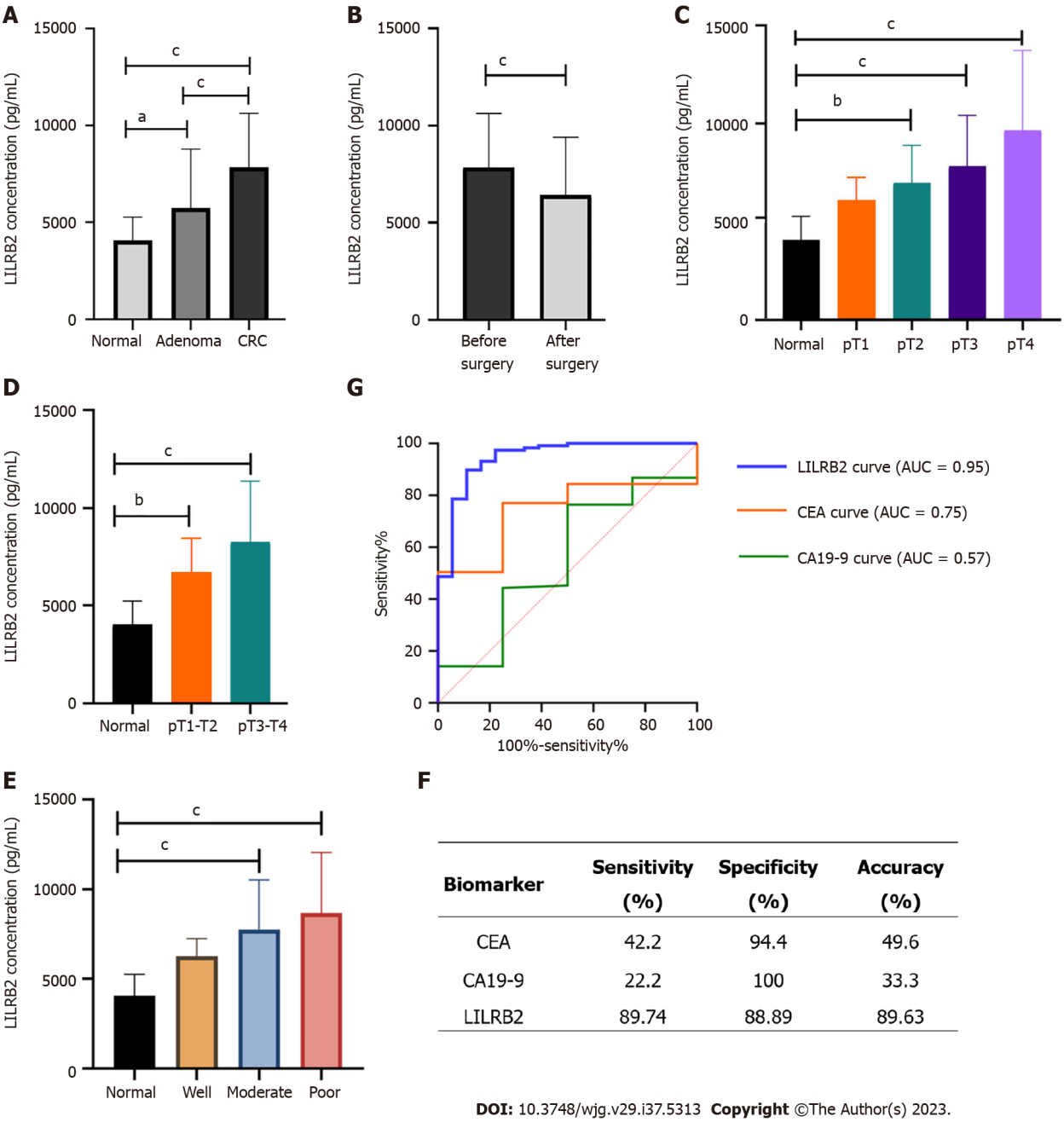


DOI: 10.3748/wjg.v29.i37.5313 **Copyright** ©The Author(s) 2023.

Figure 3 Association between leukocyte immunoglobulin-like receptor B2 and angiopoietin-like protein 2 expression and the prognosis of colorectal cancer. A: Angiopoietin-like protein 2 (*ANGPTL2*) mRNA expression and overall survival of colorectal cancer (CRC); B: *ANGPTL2* mRNA expression and progression-free survival of CRC; C: Leukocyte immunoglobulin-like receptor B2 (*LILRB2*) mRNA expression and overall survival of CRC; D: LILRB2 protein expression and overall survival of CRC. LILRB2: Leukocyte immunoglobulin-like receptor B2; ANGPTL2: Angiopoietin-like protein 2; CRC: Colorectal cancer.

and enhanced cell motility, thus conferring high invasive and metastatic potential to tumour cells[18]. On the other hand, in NSCLC cells, activation of epidermal growth factor receptor-protein kinase B and extracellular signal-related kinases 1 and 2 signalling induces LILRB2 production, and LILRB2 overexpression reprograms the TME, recruits tumour-associated macrophages of the M2-like phenotype, inhibits dendritic cell maturation and antigen presentation, and promotes the progression of NSCLC[13]. In addition, LILRB2 expression was also significantly increased in hepatocellular carcinoma and breast cancer, but the underlying mechanisms by which LILRB2 regulates the progression of hepatocellular carcinoma and breast cancer need to be further investigated[19,20].

In the last three years, several LILRB-targeted therapies have entered clinical trials, but most are in phase I and phase II clinical trials. JTX-8064 is a specific antibody targeting LILRB2 that exerts antitumour effects by blocking the binding of the receptor to MHC-I class molecules, ANGPTLs and other relevant ligands in the TME, and its combination therapy with the PD-1 inhibitor pablizumab has also been conducted in clinical trials[21]. IO-108 is a novel inhibitory antibody that specifically binds LILRB2 with high affinity and blocks the binding of the receptor to ligands in the TME while reprogramming immunosuppressed myeloid cells to exhibit a proinflammatory phenotype, thereby enhancing the antitumour effects of both intrinsic and adaptive immunity[22]. In addition to LILRB2, the targeting of other LILRB family members has been a hot topic of research in recent years. For example, BND-22, a new class of humanized immunoglobulin G4 monoclonal antibodies targeting the LILRB1 receptor, can be targeted for the treatment of solid tumours; this blocks immunosuppression caused by the binding of the LILRB1 receptor and HLA-G ligand, which in turn



Biomarker	Sensitivity (%)	Specificity (%)	Accuracy (%)
CEA	42.2	94.4	49.6
CA19-9	22.2	100	33.3
LILRB2	89.74	88.89	89.63

DOI: 10.3748/wjg.v29.i37.5313 **Copyright** ©The Author(s) 2023.

Figure 4 Screening and diagnostic efficacy of serum leukocyte immunoglobulin-like receptor B2 concentration. A: Comparison of serum leukocyte immunoglobulin-like receptor B2 (LILRB2) concentrations among colorectal cancer (CRC) patients, adenoma patients and healthy controls; B: Comparison of serum LILRB2 concentrations before and after radical surgery; C and D: Comparison of serum LILRB2 concentrations between samples with different infiltration depths; E: Comparison of serum LILRB2 concentrations between samples with different degrees of differentiation; F: Sensitivity, specificity and accuracy of serum LILRB2, carcinoembryonic antigen (CEA), and carbohydrate antigen 19-9 (CA19-9) for the diagnosis of CRC; G: The receiver operating characteristic curve and area under the curve of serum LILRB2, CEA and CA19-9 concentrations in the diagnosis of CRC. LILRB2: Leukocyte immunoglobulin-like receptor B2; CRC: Colorectal cancer; CEA: Carcinoembryonic antigen; CA19-9: Carbohydrate antigen 19-9; ROC: Receiver operating characteristic curve; AUC: Area under the curve. $^{a}P < 0.05$; $^{b}P < 0.01$; $^{c}P < 0.001$.

activates T-cell-mediated innate and adaptive immunity and acts as a tumour killer[23,24]. IO-202 is a monoclonal antibody targeting the inhibition of LILRB4 for the indications of AML and chronic granulocytic leukaemia and has been granted orphan drug status by the United States Food and Drug Administration for the treatment of AML[25]. In terms of the latest progress of several clinical trials, the indications are broad, and no drugs targeting LILRBs have had breakthrough therapeutic effects in tumours; the present study provides a theoretical basis for assessing LILRB2 expression in CRC to guide immune checkpoint blockade therapy to achieve early screening and precision medicine.

Based on this study, we proposed for the first time that serum LILRB2 concentration could be used as a noninvasive screening biomarker for CRC with better diagnostic efficacy than traditional serum tumour markers to facilitate early diagnosis and treatment of CRC[26,27]. We analysed the source of serum LILRB2, since LILRB2 molecules are expressed on the surface of myeloid cells and tumour cells, and we hypothesized that serum LILRB2 may originate from circulating exfoliated cells of CRC, inflammatory cells or immune cells associated with CRC. Postoperative serum LILRB2 concen-

trations were significantly lower than preoperative serum concentrations in CRC, indicating a strong association between serum LILRB2 source and CRC; to further verify the relationship, a comparison of paired serum from 50 patients before and after surgery was performed and revealed that serum LILRB2 concentrations were significantly lower after surgery than before surgery, confirming that serum LILRB2 level is associated with tumour burden in CRC. It was hypothesized that serum LILRB2 might originate from circulating tumour cells shed in the blood and that the decreased LILRB2 concentration is associated with a reduced CRC cell load in the blood after surgery. Another source is hypothesized to be CRC-associated immune cells because tumorigenesis is closely related to the chronic inflammatory state in the body and during tumour development, chemotaxis and infiltration of myeloid cells, including neutrophils, dendritic cells, and tumour-associated macrophages, which are common cell types with LILRB2 expression[28,29]. There are no relevant studies on the source of serum LILRB2 globally, this study can only make reasonable speculations on its source. However, considering the half-life of protein, the time is not long enough to detect the serum LILRB2 concentration only 24 h after operation, and this is also not long enough for the immune cells to disappear gradually from circulation. Therefore, follow-up after the surgical removal, including measurements of the serum LILRB2 concentration, circulating tumor cell load and immune cell infiltration, is necessary. It is more meaningful that the serum LILRB2 decreases after 2 wk or longer of follow-up and increases when the tumor progresses or recurs.

There are advantages but also limitations to this study. The advantages are as follows: First, this study is based on the results of preliminary high-throughput proteomics screening and further protein expression validation and correlation analysis, with a solid prior experimental foundation, rather than through mere database mining. Second, this study confirms that LILRB2 can be a novel therapeutic target for CRC with high potential for clinical translation, providing new therapeutic opportunities for CRC. Third, this study is the first to suggest that ELISA of serum LILRB2 concentration can be used as a noninvasive screening method for CRC, with better diagnostic efficacy than traditional serum tumour markers. The shortcomings of this study are that further testing and analysis of circulating tumour cell load and immune cell infiltration in the blood of CRC patients are needed in the future to clarify the source of serum LILRB2. Furthermore, LILRB2 levels could be confounded by the presence of other tumors concurrently, such as NSCLC, hepatocellular and breast cancer, which needs to be excluded. In addition, although the results of this study corroborate those of previous basic studies, the single center study type and small sample size are still limitations of this study, and more efforts are needed in the future to eventually achieve the goal of translation to clinical treatment.

CONCLUSION

In conclusion, LILRB2 protein is significantly highly expressed in CRC tissues, and high LILRB2 protein expression is significantly correlated with tumour progression and a poor prognosis. The LILRB2 receptor is synergistically expressed with the ANGPTL2 ligand, and their binding and interaction are closely related to CRC development. Serum LILRB2 concentration showed higher diagnostic efficacy than traditional markers, highlight its potential as an innovative screening marker for CRC. Therefore, LILRB2 protein is a potential novel therapeutic target and noninvasive screening biomarker, which could be beneficial for early screening and precise treatment and is important for the development of new therapeutic strategies for CRC.

ARTICLE HIGHLIGHTS

Research background

The incidence and mortality of colorectal cancer (CRC) have been rising continuously. CRC has become the second leading cause of cancer-related death worldwide, and the 5-year survival rate of patients with advanced CRC is below 20%.

Research motivation

Early screening and precise targeted therapy are very important to improve the prognosis of CRC patients. Therefore, identifying novel therapeutic targets and early screening biomarkers is urgent for clinical practice.

Research objectives

To explore whether leukocyte immunoglobulin-like receptor B2 (LILRB2) can be used as a potential therapeutic target and noninvasive screening biomarker for CRC.

Research methods

On the basis of previous proteomics, immunohistochemical staining was used to verify the expression of LILRB2 protein and its ligand angiopoietin-like protein 2 (ANGPTL2) protein in CRC cancer tissues and paired paracarcinoma tissues, and to explore the association between their expression and the clinicopathological features. Enzyme-linked immunosorbent assay was used to detect serum LILRB2 concentration and explore the diagnostic efficacy for CRC.

Research results

LILRB2 protein is significantly overexpressed in CRC cancer tissues and is closely associated with peritumoral infilt-

ration, distant metastasis and poor prognosis. LILRB2 may bind to the ligand ANGPTL2 protein, and the synergistic expression and interaction of the two proteins promotes CRC progression and metastasis. Serum LILRB2 concentration has high sensitivity, specificity and accuracy in screening CRC, which is better than traditional carcinoembryonic antigen and carbohydrate antigen 19-9.

Research conclusions

Therefore, LILRB2 protein can be used as a potential novel therapeutic target and noninvasive screening biomarker.

Research perspectives

Novel LILRB2 protein is beneficial for early screening and precise treatment, which provides new opportunities to improve the prognosis of CRC patients.

ACKNOWLEDGEMENTS

We thank all medical staff and patients who agreed to participate in this study.

FOOTNOTES

Author contributions: Wang QQ analyzed the data and drafted the manuscript; Tan C and Zhou YC collected samples and clinical data; Zhou L and Qin G provided guidance on experimental procedures; Yao SK supervised the study performance, revised the manuscript, and obtained the funding; and all authors read and approved the final manuscript.

Supported by the National Key Development Plan for Precision Medicine Research, No. 2017YFC0910002.

Institutional review board statement: This study was approved by the Ethics Committee of China-Japan Friendship Hospital (No. 2018-116-K85).

Informed consent statement: All study participants, or their legal guardian, provided informed written consent prior to study enrollment.

Conflict-of-interest statement: All the authors report no relevant conflicts of interest for this article.

Data sharing statement: No additional data are available.

STROBE statement: The authors have read the STROBE Statement-checklist of items, and the manuscript was prepared and revised according to the STROBE Statement-checklist of items.

Open-Access: This article is an open-access article that was selected by an in-house editor and fully peer-reviewed by external reviewers. It is distributed in accordance with the Creative Commons Attribution NonCommercial (CC BY-NC 4.0) license, which permits others to distribute, remix, adapt, build upon this work non-commercially, and license their derivative works on different terms, provided the original work is properly cited and the use is non-commercial. See: https://creativecommons.org/Licenses/by-nc/4.0/

Country/Territory of origin: China

ORCID number: Qian-Qian Wang 0000-0002-7709-2121; Lei Zhou 0000-0002-5540-4120; Geng Qin 0000-0002-1197-2011; Chang Tan 0000-0002-0969-1851; Yuan-Chen Zhou 0000-0001-6024-6246; Shu-Kun Yao 0000-0002-8512-2589.

S-Editor: Wang JJ
L-Editor: A
P-Editor: Yu HG

REFERENCES

1 **Siegel RL**, Miller KD, Jemal A. Cancer statistics, 2020. *CA Cancer J Clin* 2020; **70**: 7-30 [PMID: 31912902 DOI: 10.3322/caac.21590]
2 **Sung H**, Ferlay J, Siegel RL, Laversanne M, Soerjomataram I, Jemal A, Bray F. Global Cancer Statistics 2020: GLOBOCAN Estimates of Incidence and Mortality Worldwide for 36 Cancers in 185 Countries. *CA Cancer J Clin* 2021; **71**: 209-249 [PMID: 33538338 DOI: 10.3322/caac.21660]
3 **Siegel RL**, Wagle NS, Cercek A, Smith RA, Jemal A. Colorectal cancer statistics, 2023. *CA Cancer J Clin* 2023; **73**: 233-254 [PMID: 36856579 DOI: 10.3322/caac.21772]
4 **Biller LH**, Schrag D. Diagnosis and Treatment of Metastatic Colorectal Cancer: A Review. *JAMA* 2021; **325**: 669-685 [PMID: 33591350 DOI: 10.1001/jama.2021.0106]
5 **Shen C**, Tannenbaum D, Horn R, Rogers J, Eng C, Zhou S, Johnson B, Kopetz S, Morris V, Overman M, Parseghian C, Chang GJ, Lopez-

Olivo MA, Kanwal R, Ellis LM, Dasari A. Overall Survival in Phase 3 Clinical Trials and the Surveillance, Epidemiology, and End Results Database in Patients With Metastatic Colorectal Cancer, 1986-2016: A Systematic Review. *JAMA Netw Open* 2022; **5**: e2213588 [PMID: 35608860 DOI: 10.1001/jamanetworkopen.2022.13588]

6 **Mani DR**, Krug K, Zhang B, Satpathy S, Clauser KR, Ding L, Ellis M, Gillette MA, Carr SA. Cancer proteogenomics: current impact and future prospects. *Nat Rev Cancer* 2022; **22**: 298-313 [PMID: 35236940 DOI: 10.1038/s41568-022-00446-5]

7 **Li C**, Sun YD, Yu GY, Cui JR, Lou Z, Zhang H, Huang Y, Bai CG, Deng LL, Liu P, Zheng K, Wang YH, Wang QQ, Li QR, Wu QQ, Liu Q, Shyr Y, Li YX, Chen LN, Wu JR, Zhang W, Zeng R. Integrated Omics of Metastatic Colorectal Cancer. *Cancer Cell* 2020; **38**: 734-747.e9 [PMID: 32888432 DOI: 10.1016/j.ccell.2020.08.002]

8 **Wang Q**, Zhou Y, Zhou G, Qin G, Tan C, Yin T, Zhao D, Yao S. Age-stratified proteomic characteristics and identification of promising precise clinical treatment targets of colorectal cancer. *J Proteomics* 2023; **277**: 104863 [PMID: 36870673 DOI: 10.1016/j.jprot.2023.104863]

9 **Chen HM**, van der Touw W, Wang YS, Kang K, Mai S, Zhang J, Alsina-Beauchamp D, Duty JA, Mungamuri SK, Zhang B, Moran T, Flavell R, Aaronson S, Hu HM, Arase H, Ramanathan S, Flores R, Pan PY, Chen SH. Blocking immunoinhibitory receptor LILRB2 reprograms tumor-associated myeloid cells and promotes antitumor immunity. *J Clin Invest* 2018; **128**: 5647-5662 [PMID: 30352428 DOI: 10.1172/JCI97570]

10 **Zheng J**, Umikawa M, Cui C, Li J, Chen X, Zhang C, Huynh H, Kang X, Silvany R, Wan X, Ye J, Cantó AP, Chen SH, Wang HY, Ward ES, Zhang CC. Inhibitory receptors bind ANGPTLs and support blood stem cells and leukaemia development. *Nature* 2012; **485**: 656-660 [PMID: 22660330 DOI: 10.1038/nature11095]

11 **Deng M**, Lu Z, Zheng J, Wan X, Chen X, Hirayasu K, Sun H, Lam Y, Chen L, Wang Q, Song C, Huang N, Gao GF, Jiang Y, Arase H, Zhang CC. A motif in LILRB2 critical for Angptl2 binding and activation. *Blood* 2014; **124**: 924-935 [PMID: 24899623 DOI: 10.1182/blood-2014-01-549162]

12 **Kang X**, Cui C, Wang C, Wu G, Chen H, Lu Z, Chen X, Wang L, Huang J, Geng H, Zhao M, Chen Z, Müschen M, Wang HY, Zhang CC. CAMKs support development of acute myeloid leukemia. *J Hematol Oncol* 2018; **11**: 30 [PMID: 29482582 DOI: 10.1186/s13045-018-0574-8]

13 **Chen X**, Gao A, Zhang F, Yang Z, Wang S, Fang Y, Li J, Wang J, Shi W, Wang L, Zheng Y, Sun Y. ILT4 inhibition prevents TAM- and dysfunctional T cell-mediated immunosuppression and enhances the efficacy of anti-PD-L1 therapy in NSCLC with EGFR activation. *Theranostics* 2021; **11**: 3392-3416 [PMID: 33537094 DOI: 10.7150/thno.52435]

14 **Cai Z**, Wang L, Han Y, Gao W, Wei X, Gong R, Zhu M, Sun Y, Yu S. Immunoglobulinlike transcript 4 and human leukocyte antigenG interaction promotes the progression of human colorectal cancer. *Int J Oncol* 2019; **54**: 1943-1954 [PMID: 30942436 DOI: 10.3892/ijo.2019.4761]

15 **Chen QY**, Chen YX, Han QY, Zhang JG, Zhou WJ, Zhang X, Ye YH, Yan WH, Lin A. Prognostic Significance of Immune Checkpoints HLA-G/ILT-2/4 and PD-L1 in Colorectal Cancer. *Front Immunol* 2021; **12**: 679090 [PMID: 34054869 DOI: 10.3389/fimmu.2021.679090]

16 **Huang D**, Sun G, Hao X, He X, Zheng Z, Chen C, Yu Z, Xie L, Ma S, Liu L, Zhou BO, Cheng H, Zheng J, Cheng T. ANGPTL2-containing small extracellular vesicles from vascular endothelial cells accelerate leukemia progression. *J Clin Invest* 2021; **131** [PMID: 33108353 DOI: 10.1172/JCI138986]

17 **Zhang P**, Guo X, Li J, Yu S, Wang L, Jiang G, Yang D, Wei Z, Zhang N, Liu J, Sun Y. Immunoglobulin-like transcript 4 promotes tumor progression and metastasis and up-regulates VEGF-C expression *via* ERK signaling pathway in non-small cell lung cancer. *Oncotarget* 2015; **6**: 13550-13563 [PMID: 25948790 DOI: 10.18632/oncotarget.3624]

18 **Endo M**, Nakano M, Kadomatsu T, Fukuhara S, Kuroda H, Mikami S, Hato T, Aoi J, Horiguchi H, Miyata K, Odagiri H, Masuda T, Harada M, Horio H, Hishima T, Nomori H, Ito T, Yamamoto Y, Minami T, Okada S, Takahashi T, Mochizuki N, Iwase H, Oike Y. Tumor cell-derived angiopoietin-like protein ANGPTL2 is a critical driver of metastasis. *Cancer Res* 2012; **72**: 1784-1794 [PMID: 22345152 DOI: 10.1158/0008-5472.CAN-11-3878]

19 **Li X**, Wei X, Xu H, Sha Z, Gao A, Sun Y, Li J, Xu L. Expression of leukocyte immunoglobulin-like receptor B2 in hepatocellular carcinoma and its clinical significance. *J Cancer Res Ther* 2018; **14**: 1655-1659 [PMID: 30589055 DOI: 10.4103/jcrt.JCRT_542_18]

20 **Liu J**, Wang L, Gao W, Li L, Cui X, Yang H, Lin W, Dang Q, Zhang N, Sun Y. Inhibitory receptor immunoglobulin-like transcript 4 was highly expressed in primary ductal and lobular breast cancer and significantly correlated with IL-10. *Diagn Pathol* 2014; **9**: 85 [PMID: 24762057 DOI: 10.1186/1746-1596-9-85]

21 **Umiker B**, Hashambhoy-Ramsay Y, Smith J, Rahman T, Mueller A, Davidson R, Meyer C, Patankar G, Alam MM, Jaffe S, Krukenberg K, Goodman A, Spaulding V, Priess M, Dhaneshwar A, Wong M, Diiorio A, O'Malley K, McGrath L, Willer M, Pepper L, Gostissa M, Kis-Toth K, Wiederschain D, Cohen H, Shaffer DR. Inhibition of LILRB2 by a Novel Blocking Antibody Designed to Reprogram Immunosuppressive Macrophages to Drive T-Cell Activation in Tumors. *Mol Cancer Ther* 2023; **22**: 471-484 [PMID: 36780212 DOI: 10.1158/1535-7163.MCT-22-0351]

22 **Taylor MH**, Patel MR, Powderly JD, Woodard P, Chung L, Tian H, Hong X, Hong K, Valencia D, Huang T, Schebye XM, Liao C, Naing A. Abstract CT040: A first-in-human phase 1 trial of IO-108, an antagonist antibody targeting LILRB2 (ILT4), as monotherapy and in combination with pembrolizumab in adult patients with advanced relapsed or refractory solid tumors: Dose escalation study. *Cancer Res* 2023; **83**: CT040 [DOI: 10.1158/1538-7445.AM2023-CT040]

23 **Mandel I**, Haves Ziv D, Goldshtein I, Peretz T, Alishekevitz D, Fridman Dror A, Hakim M, Hashmueli S, Friedman I, Sapir Y, Greco R, Qu H, Nestle F, Wiederschain D, Pao L, Sharma S, Ben Moshe T. BND-22, a first-in-class humanized ILT2-blocking antibody, promotes antitumor immunity and tumor regression. *J Immunother Cancer* 2022; **10** [PMID: 36096532 DOI: 10.1136/jitc-2022-004859]

24 **Barkal AA**, Weiskopf K, Kao KS, Gordon SR, Rosental B, Yiu YY, George BM, Markovic M, Ring NG, Tsai JM, McKenna KM, Ho PY, Cheng RZ, Chen JY, Barkal LJ, Ring AM, Weissman IL, Maute RL. Engagement of MHC class I by the inhibitory receptor LILRB1 suppresses macrophages and is a target of cancer immunotherapy. *Nat Immunol* 2018; **19**: 76-84 [PMID: 29180808 DOI: 10.1038/s41590-017-0004-z]

25 **Anami Y**, Deng M, Gui X, Yamaguchi A, Yamazaki CM, Zhang N, Zhang CC, An Z, Tsuchikama K. LILRB4-targeting Antibody-Drug Conjugates for the Treatment of Acute Myeloid Leukemia. *Mol Cancer Ther* 2020; **19**: 2330-2339 [PMID: 32879051 DOI: 10.1158/1535-7163.MCT-20-0407]

26 **Gao Y**, Wang J, Zhou Y, Sheng S, Qian SY, Huo X. Evaluation of Serum CEA, CA19-9, CA72-4, CA125 and Ferritin as Diagnostic Markers and Factors of Clinical Parameters for Colorectal Cancer. *Sci Rep* 2018; **8**: 2732 [PMID: 29426902 DOI: 10.1038/s41598-018-21048-y]

27 **Chen F**, Dai X, Zhou CC, Li KX, Zhang YJ, Lou XY, Zhu YM, Sun YL, Peng BX, Cui W. Integrated analysis of the faecal metagenome and serum metabolome reveals the role of gut microbiome-associated metabolites in the detection of colorectal cancer and adenoma. *Gut* 2022; **71**: 1315-1325 [PMID: 34462336 DOI: 10.1136/gutjnl-2020-323476]

28 **Coussens LM**, Werb Z. Inflammation and cancer. *Nature* 2002; **420**: 860-867 [PMID: 12490959 DOI: 10.1038/nature01322]

29 **Diakos CI**, Charles KA, McMillan DC, Clarke SJ. Cancer-related inflammation and treatment effectiveness. *Lancet Oncol* 2014; **15**: e493-e503 [PMID: 25281468 DOI: 10.1016/S1470-2045(14)70263-3]

World Journal of Gastroenterology

Submit a Manuscript: https://www.f6publishing.com

World J Gastroenterol 2023 October 7; 29(37): 5327-5338

DOI: 10.3748/wjg.v29.i37.5327

ISSN 1007-9327 (print) ISSN 2219-2840 (online)

META-ANALYSIS

Efficacy and safety of semaglutide in non-alcoholic fatty liver disease

Kai Zhu, Rohan Kakkar, Daljeet Chahal, Eric M Yoshida, Trana Hussaini

Specialty type: Gastroenterology and hepatology

Provenance and peer review: Unsolicited article; Externally peer reviewed.

Peer-review model: Single blind

Peer-review report's scientific quality classification

Grade A (Excellent): A, A, A
Grade B (Very good): 0
Grade C (Good): 0
Grade D (Fair): 0
Grade E (Poor): 0

P-Reviewer: Du Y, China; Morozov S, Russia; Ren WR, China

Received: June 28, 2023
Peer-review started: June 28, 2023
First decision: August 15, 2023
Revised: August 23, 2023
Accepted: September 12, 2023
Article in press: September 12, 2023
Published online: October 7, 2023

Kai Zhu, Rohan Kakkar, Internal Medicine, University of British Columbia, Vancouver V5Z 1M9, BC, Canada

Daljeet Chahal, Eric M Yoshida, Department of Gastroenterology, University of British Columbia, Vancouver V5Z 1M9, BC, Canada

Daljeet Chahal, Eric M Yoshida, Trana Hussaini, BC Liver Transplant Program, Vancouver General Hospital, Vancouver V5Z 1M9, BC, Canada

Trana Hussaini, Pharmaceutical Sciences, University of British Columbia, Vancouver V5Z 1M9, BC, Canada

Corresponding author: Trana Hussaini, BPharm, MHSc, PharmD, Associate Professor, Pharmacist, BC Liver Transplant Program, Vancouver General Hospital, 899 West 12th Avenue, Vancouver V5Z 1M9, BC, Canada. trana.hussaini@vch.ca

Abstract

BACKGROUND

Non-alcoholic fatty liver disease (NAFLD) is the leading cause of chronic liver disease. The prevalence and disease burden of NAFLD are projected to exponentially increase resulting in significant healthcare expenditures and lower health-related quality of life. To date, there are no approved pharmacotherapies for NAFLD or non-alcoholic steatohepatitis (NASH). Semaglutide has glycemic and weight loss benefits that may be advantageous for patients with NAFLD.

AIM

To investigate the efficacy and safety of semaglutide in patients with NAFLD.

METHODS

MEDLINE, CENTRAL, and EMBASE were searched from inception to May 1, 2023, to identify eligible randomized controlled trials (RCTs). Meta-analysis was performed using random effects model expressing continuous outcomes as mean differences (MD) or standardized MDs (SMD), and dichotomous outcomes as odds ratios (OR) with 95% confidence intervals (CI). Statistical heterogeneity was assessed using the Cochran's *Q* test and *I2* statistic.

RESULTS

Three RCTs involving 458 patients were included. Semaglutide increased the likelihood of NASH resolution (OR: 3.18, 95%CI: 1.70, 5.95; $P < 0.001$), impro-

vement in steatosis (OR: 2.83, 95%CI: 1.19, 6.71; P = 0.03), lobular inflammation (OR: 1.81, 95%CI: 1.11, 2.96; P = 0.02), and hepatocellular ballooning (OR: 2.92, 95%CI: 1.83, 4.65; P < 0.001), but not fibrosis stage (OR: 0.71, 95%CI: 0.15, 3.41; P = 0.67). Radiologically, semaglutide reduced liver stiffness (SMD: -0.48, 95%CI: -0.86, -0.11; P = 0.01) and steatosis (MD: -4.96%, 95%CI: -9.92, 0.01; P = 0.05). It also reduced alanine aminotransferase (MD: -14.06 U/L, 95%CI: -22.06, -6.07; P < 0.001) and aspartate aminotransferase (MD: -11.44 U/L, 95%CI: -17.23, -5.65; P < 0.001). Semaglutide led to improved cardiometabolic outcomes, including decreased HgA1c (MD: -0.77%, 95%CI: -1.18, -0.37; P < 0.001) and weight loss (MD: -6.53 kg, 95%CI: -11.21, -1.85; P = 0.006), but increased the occurrence of GI-related side effects (OR: 3.72, 95%CI: 1.68, 8.23; P = 0.001). Overall risk of serious adverse events was similar compared to placebo (OR: 1.40, 95%CI: 0.75, 2.62; P < 0.29).

CONCLUSION

Semaglutide is effective in the treatment of NAFLD while maintaining a well-tolerated safety profile. Future studies are required to evaluate its effects on fibrosis regression and different phases of NAFLD.

Key Words: Non-alcoholic fatty liver disease; Fatty liver; Metabolic-associated fatty liver; Semaglutide

©The Author(s) 2023. Published by Baishideng Publishing Group Inc. All rights reserved.

Core Tip: Semaglutide demonstrates significant histologic improvements, with a higher likelihood of non-alcoholic steatohepatitis resolution and improved steatosis, lobular inflammation, and hepatocellular ballooning, but it does not significantly improve fibrosis stage compared to placebo. Furthermore, semaglutide results in radiologic improvements in liver stiffness and steatosis, liver enzymes, as well as cardiometabolic effects on body weight and HgA1c, while maintaining a well-tolerated safety profile.

Citation: Zhu K, Kakkar R, Chahal D, Yoshida EM, Hussaini T. Efficacy and safety of semaglutide in non-alcoholic fatty liver disease. *World J Gastroenterol* 2023; 29(37): 5327-5338
URL: https://www.wjgnet.com/1007-9327/full/v29/i37/5327.htm
DOI: https://dx.doi.org/10.3748/wjg.v29.i37.5327

INTRODUCTION

Non-alcoholic fatty liver disease (NAFLD) is the leading cause of chronic liver disease, with an estimated worldwide prevalence of 32.4%[1,2]. The prevalence and disease burden of NAFLD are projected to exponentially increase, with mathematical models forecasting a 168% increase in the incidence of decompensated cirrhosis and a 178% increase in NAFLD-related deaths between 2015 and 2030. These projections highlight the significant healthcare expenditures and lower health-related quality of life associated with the disease[3-5].

NAFLD is a spectrum of liver disease characterized by hepatic steatosis in the absence of excessive alcohol consumption[6]. The majority of patients with NAFLD have NAFL, of which approximately 20% will develop non-alcoholic steatohepatitis (NASH) and have a risk of further progression to cirrhosis, hepatocellular carcinoma, and end-stage liver disease[3]. Although lean NAFLD is increasingly recognized, the majority of patients with NAFLD have one or more components of metabolic syndrome, which is also independently strongly associated with fibrosis progression[7,8].

GLP-1 receptor agonists (RAs) offer promising therapeutic options in NAFLD due to their beneficial glycemic and weight loss effects. GLP-1 receptors have been detected on human hepatocytes, and it is hypothesized that their activation by GLP-1 RAs can have positive effects on hepatic steatosis, lipotoxicity, fatty acid oxidation, and cytokines involved in hepatic inflammation and fibrosis[9,10]. Moreover, GLP-1 RAs may have indirect hepatoprotective benefits through increased insulin secretion in response to hyperglycemia, decreased glucagon secretion, delayed gastric emptying, and significant weight loss[11,12].

Among the GLP-1 RAs, semaglutide has demonstrated the greatest glycemic and weight loss benefits[13]. In a recent phase three trial of patients with overweight or obesity, semaglutide showed a significant decrease in body weight by 14.9% compared to 2.4% with placebo[14]. Additionally, semaglutide has shown reduced rates of major adverse cardiovascular events and a lower risk of adverse renal outcomes in patients with type 2 diabetes (T2DM)[15]. It has since been approved for the treatment of T2DM and chronic weight management.

Several randomized clinical trials have also demonstrated the beneficial effects of semaglutide in patients with NAFLD. A previous systematic review with meta-analysis was conducted to assess the impact of semaglutide on biochemical and radiologic measures of NAFLD[16]. However, more than 85% of the study's patients had diabetes or obesity rather than confirmed NAFLD. Additionally, no histological outcomes were reported, which are considered the gold standard for diagnosing and managing NAFLD. Since its publication, a recent randomized controlled trial (RCT) by Loomba *et al*[17] has been performed, focusing on semaglutide in patients with NASH and compensated cirrhosis. The purpose of this systematic review and meta-analysis is to provide an updated review on the efficacy and safety of semaglutide, focusing on patients with NAFLD, in order to more specifically reflect the NAFLD population and expand the current

understanding of semaglutide in NAFLD.

MATERIALS AND METHODS

Search strategy and study selection

The systematic review was conducted in accordance with the Preferred Reporting Items for Systematic Reviews and Meta-analyses guidelines and was registered prospectively on the PROSPERO database (ID: CRD42023422487). Two independent reviewers (K.Z. and R.K.) evaluated the titles and abstracts of all identified studies based on predetermined inclusion and exclusion criteria (Supplementary Table 1). Any discrepancies were resolved through discussion with a third reviewer (T.H.).

Multiple databases, including MEDLINE, CENTRAL, EMBASE, and grey literature sources such as Clinicaltrials.gov and the World Health Organization International Clinical Trials Registries, were searched from inception to May 1, 2023 using a predefined search strategy (Supplementary Table 2). Additionally, a forward and backward citation search was performed on eligible studies using CitationChaser.

Data extraction and outcome measures

Two reviewers (K.Z. and R.K.) independently extracted the data using predetermined data collection forms. Any discrepancies were resolved through consultation with a third reviewer (T.H.).

The primary outcomes of interest for this study were histological improvement in NAFLD activity score, resolution of NASH with no worsening of liver fibrosis, and improvement in liver fibrosis without worsening of NASH, as defined by the NASH Clinical Research Network Criteria (CRN).

The secondary outcomes of interest included radiologic improvement in liver stiffness and steatosis, measured using either magnetic resonance elastography (MRE) or Fibroscan; changes in liver enzymes [alanine aminotransferase (ALT) and aspartate aminotransferase (AST)]; cardiometabolic parameters such as body weight, HgA1c, total cholesterol, non-HDL cholesterol, and LDL cholesterol; as well as adverse events, including gastrointestinal-related side effects and serious adverse events.

Quality assessment

The risk of bias was independently conducted by two reviewers (K.Z. and R.K.) using the Cochrane risk-of-bias 2 tool for randomized trials. Due to the limited number of included studies, a funnel plot was not generated to assess publication bias. Finally, the quality of the evidence was evaluated using the Grading of Recommendations Assessment, Development, and Evaluation (GRADE) framework.

Missing data

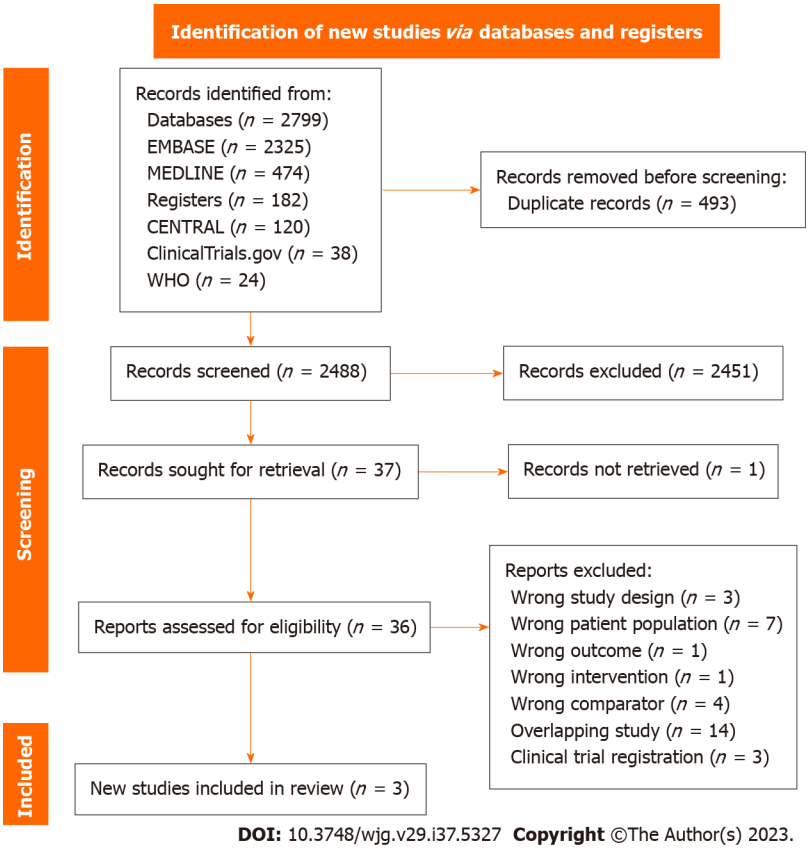
To address missing data, attempts were made to contact the study authors for the necessary information. In cases where the data could not be obtained, relevant values were extracted from figures, using the PlotDigitizer software, following Cochrane methodology. If the data was unavailable anywhere in the study, it was excluded from the analysis. Missing standard deviations (SD) for continuous outcomes were estimated using the available standard error, 95% confidence interval (CI), or P value. If these values were not available, SDs were imputed from other studies, as outlined by Furukawa *et al*[18].

Data synthesis and analysis

Continuous outcomes were presented as mean differences (MD) in change scores with corresponding 95%CI. The DerSimonian and Laird random-effects model was used given expected clinical and methodological diversity between the included studies. When outcomes were measured on different scales that could not be converted to a common scale, such as Fibroscan and MRE measurements, they were reported as standardized MDs (SMD) using Hedges' G. A correlation coefficient of $r = 0.4$, which is consistent with previous meta-analyses of liraglutide in NAFLD, was utilized [19].

Dichotomous outcomes were expressed as odds ratios (OR) with 95%CI. Statistical heterogeneity was assessed using Cochran's Q statistic and I^2 statistic, where $P < 0.10$ and $I^2 > 50\%$ were considered significant indicators of heterogeneity. The significance level for all other statistical tests was set at $P < 0.05$. RevMan version 5.4 (Copenhagen, Denmark) was used for all statistical analyses.

Sensitivity analysis was conducted using the leave-one-out method to evaluate the influence of each individual study on the overall estimate. Additional sensitivity analysis was performed comparing the outcomes using a fixed-effect model *vs* random-effect model. Subgroup analysis was performed by stratifying participants within the included studies based on their T2DM status. However, due to the limited number of included studies, additional sensitivity and subgroup analyses were not performed.



DOI: 10.3748/wjg.v29.i37.5327 **Copyright** ©The Author(s) 2023.

Figure 1 PRISMA flow diagram of study selection. WHO: World health organization.

RESULTS

Search results

A total of 2981 potentially eligible studies were identified, of which 493 duplicates were removed prior to screening. An additional 2451 studies were excluded based on titles and abstracts screening. Full text was obtained for 36 out of the 37 eligible studies. From these, we identified three studies that met our inclusion criteria and were included in the meta-analysis[17,20,21] (Figure 1).

Study characteristics

The study characteristics of the included summaries are outlined in Table 1. A total of 458 patients were included, with 321 receiving semaglutide and 137 receiving placebo. All studies were RCTs ranging from 48 wk to 72 wk in duration. Various doses of semaglutide were utilized. Newsome *et al*[20] compared daily doses of 0.1 mg, 0.2 mg, and 0.4 mg of semaglutide, whereas Flint *et al*[21] and Loomba *et al*[17] used daily doses of 0.4 mg and weekly doses of 2.4 mg, respectively. Furthermore, Flint *et al*[21] focused exclusively on patients with NAFL, while the other two studies only included patients with biopsy confirmed NASH. Both Newsome *et al*[20] and Loomba *et al*[17] conducted histological assessments. All studies included patients with and without T2DM.

Risk of bias assessment

The methodological qualities of the studies are summarized in the appendix, Supplementary Figure 1. The trial of Newsome *et al*[20] was classified as having a low risk of bias, while the other trials raised some concerns. Specifically, the study of Loomba *et al*[17] had concerns related to randomization, as a higher proportion of patients in the semaglutide group had an Ishak fibrosis score of 6, while more patients receiving placebo had a score of 4 or 5. Additionally, baseline measurements of MRE, hepatic collagen proportion, liver enzymes, and pro-C3 were slightly higher in the semaglutide group. Flint *et al*[21] raised concerns regarding missing data, as seven out of 34 patients in the semaglutide group discontinued treatment, and no sensitivity analysis was performed, or analysis conducted to address the resulting bias. The quality of the evidence was evaluated using the GRADE framework as illustrated in Table 2.

Outcome evaluation

Effect of semaglutide on histological parameters: Two studies, involving 391 patients, evaluated histological outcomes (Figure 2). Semaglutide was associated with a significantly higher likelihood of NASH resolution with no worsening of liver fibrosis (OR: 3.18, 95%CI: 1.70, 5.95; I^2 = 0%) (Figure 2A). However, there was no significant improvement in liver fibrosis stage without worsening of NASH (OR: 0.71, 95%CI: 0.15, 3.41; I^2 = 80%) (Figure 2B). Significant improvements

Table 1 Baseline characteristics of included studies

Ref.	Location sponsor	Study design	Sample size (*n*)	Demographics (%)	Intervention/comparator(s)	Outcomes assessed
Newsome *et al*[20], 2021	16 countrie, 143 sites; Novo Nordisk	MC, DB, four-arm parallel-group RCT; duration: 72 wk; randomization: 3:3:3:1:1:1	320	Age (SD): 55.0 (10.6); male/female: 125(39)/195(61); T2DM: 199 (62)	Semaglutide: 0.1 mg SQ OD (*n* = 80); 0.2 mg SQ OD (*n* = 78); 0.4 mg SQ OD (*n* = 82); and placebo (*n* = 80)	Primary: Resolution of NASH; secondary: Liver fibrosis stage, total and component of NAS, ALT, AST, liver stiffness, liver steatosis, cardiometabolic parameters, adverse events
Flint *et al* [21], 2021	Germany, 2 sites; Novo Nordisk	Two-centre, DB, two-arm parallel-group RCT; duration: 72 wk; randomization: 1:1	67	Age (SD): 60.0 (9.3); male/female: 47(70)/20(30); T2DM: 49 (73)	Semaglutide: 0.4 mg SQ OD (*n* = 34); placebo (*n* = 33)	Primary: Liver stiffness MRE at week 48; secondary: Liver stiffness at week 24 and 72, liver steatosis, ALT, AST, cardiometabolic parameters, adverse events
Loomba *et al*[17], 2023	5 countries, 38 sites; Novo Nordisk	MC, DB, two-arm-parallel group RCT; duration: 48 wk; randomization: 2:1	71	Age (SD): 59.5 (8.0); male/female: 22(31)/49(61); T2DM: 53 (75)	Semaglutide: 2.4 mg SQ qw (*n* = 47); Placebo (*n* = 24)	Primary: Liver fibrosis stage; secondary: Liver stiffness, liver steatosis, NASH resolution, total and component of NAS, ALT, AST, cardiometabolic parameters, adverse events

MC: Multi-centre; DB: Double-blind; RCT: Randomized controlled trial; SD: Standard deviation; T2DM: Type 2 diabetes mellitus; SQ: Subcutaneous; OD: Once daily; qw: Weekly; NASH: Non-alcoholic steatohepatitis; NAS: NAFLD activity score; ALT: Alanine aminotransferase; AST: Aspartate aminotransferase; MRE: Magnetic resonance elastography.

were observed in all NAFLD Activity Score (NAS) components with OR 2.83 (95%CI: 1.19, 6.71; I^2 = 57%) for steatosis, 1.81 (95%CI: 1.11, 2.96; I^2 = 0%) for lobular inflammation, and 2.92 (95%CI: 1.83, 4.65; I^2 = 0%) for hepatocellular ballooning (Figure 2C-E). Significant heterogeneity was noted for improvement in liver fibrosis stage.

Effect of semaglutide on radiologic parameters: All three studies reported radiologic parameters and semaglutide demonstrated a significant reduction in liver stiffness on MRE or Fibroscan, with a standardized MD of -0.48 (95%CI: -0.86, -0.11; I^2 = 57%) (Figure 3A). Additionally, a significant reduction in liver steatosis on MRI proton density fat fraction (MRI-PDFF) was observed, with a MD of -4.96% (95%CI: -9.92, 0.01; I^2 = 64%), although significant heterogeneity was noted (Figure 3B).

Effect of semaglutide on liver enzymes: All three studies evaluated ALT and AST, which showed a significant reduction of 14.06 U/L (95%CI: -22.06, -6.07; I^2 = 0%) and 11.44 U/L (95%CI: -17.23, -5.65; I^2 = 0%), respectively, compared to placebo. No significant heterogeneity was observed (Figure 4).

Effect of semaglutide on cardiometabolic parameters: All three studies evaluated total body weight, which revealed a significant reduction of 6.53 kg (95%CI: -11.21, -1.85; I^2 = 0%) compared to placebo, with no significant heterogeneity observed (Figure 5A).

Overall, semaglutide also significantly decreased HgA1c by 0.77% (95%CI: -1.18, -0.37; I^2 = 75%) compared to placebo (Figure 5B). Subgroup analysis of participants within the studies, stratified by T2DM status, showed a significant reduction in HgA1c among patients with T2DM (MD: -1.10%, 95%CI: -1.48, -0.72; I^2 = 29%), but not among those without (MD: -0.37%, 95%CI: -0.79, 0.06; I^2 = 61%). Heterogeneity was no longer significant with the subgroup analysis.

Regarding lipid panel results, semaglutide was not associated with a significant difference in triglycerides (MD: -24.03 mg/dL, 95%CI: -60.94, 12.88; I^2 = 42%), total cholesterol (MD: -7.31 mg/dL, 95%CI: -51.66, 37.03; I^2 = 87%), non-HDL cholesterol (MD: -7.52 mg/dL, 95%CI: -49.32, 34.27; I^2 = 84%), and LDL cholesterol (MD: -4.72 mg/dL, 95%CI: -56.23, 46.79; I^2 = 92%), although significant heterogeneity was observed (Supplementary Figure 2).

Adverse events with semaglutide: Semaglutide was associated with a significantly higher occurrence of gastrointestinal-related side effects compared to placebo (OR: 3.72, 95%CI: 1.68, 8.23; I^2 = 49%) (Figure 6A). However, the overall risk of serious adverse events was comparable between the two groups (OR: 1.40, 95%CI: 0.75, 2.62; I^2 = 0%) (Figure 6B).

Sensitivity and subgroup analysis

Each article was individually excluded to examine the influence of each study on the overall effect-size estimate (Supplementary Table 3). Most of the outcomes remained unchanged; however, when Newsome *et al*[20] was removed, the effect size for resolution of NASH, steatosis, lobular inflammation, and hepatocellular ballooning became non-significant. The effect estimates for liver stiffness when restricted to MRE and excluding Fibroscan as used in the study by Newsome *et al*[20], also became non-significant. However, there was no longer any heterogeneity observed.

Regarding cardiometabolic outcomes, the significant effect of semaglutide on body weight was no longer sustained when the trial by Flint *et al*[21] was excluded. Furthermore, when Newsome *et al*[20] was removed, there was a significant

Table 2 Grading of recommendations assessment, development, and evaluation summary of findings table

Outcomes	Anticipated absolute effects[1] (95%CI)		Relative effect (95%CI)	Number of participants (studies)	Certainty of the evidence (GRADE)
	Risk with placebo	Risk with semaglutide			
Resolution of NASH with no worsening of liver fibrosis assessed with: Liver biopsy	183 per 1000	416 per 1000 (276 to 571)	OR 3.18 (1.70 to 5.95)	301 (2 RCTs)	+++O: Moderate[2]
Improvement in liver fibrosis stage without worsening of NASH assessed with: Liver biopsy	317 per 1000	248 per 1000 (65 to 613)	OR 0.71 (0.15 to 3.41)	301 (2 RCTs)	++OO: Low[2,3,4]
Liver stiffness assessed with: MRI-PDFF or Fibroscan	-	SMD 0.48 lower (0.86 lower to 0.11 lower)	-	350 (3 RCTs)	++++: High
Liver steatosis assessed with: MRE	The mean liver steatosis ranged from -0.57% to -2.57%	MD 4.96 % lower (9.92 lower to 0.01 higher)	-	138 (2 RCTs)	+++O: Moderate[3]
ALT	The mean ALT ranged from 1.90 U/L to -11.22 U/L	MD 14.06 U/L lower (22.06 lower to 6.07 lower)	-	458 (3 RCTs)	++++: High
AST	The mean AST ranged from 1.50 U/K to -5.76 U/K	MD 11.44 U/K lower (17.23 lower to 5.65 lower)	-	458 (3 RCTs)	++++: High
Serious adverse events	109 per 1000	147 per 1000 (84 to 244)	OR 1.40 (0.75 to 2.62)	456 (3 RCTs)	+++O: Moderate[2,4]

[1]The risk in the intervention group [and its 95% confidence interval (95%CI)] is based on the assumed risk in the comparison group and the relative effect of the intervention (and its 95%CI).
[2]Few events.
[3]Possibly substantial heterogeneity.
[4]Wide confidence interval including no effect and does not exclude appreciable benefit or harm.
GRADE Working Group grades of evidence. High certainty: We are very confident that the true effect lies close to that of the estimate of the effect. Moderate certainty: We are moderately confident in the effect estimate: The true effect is likely to be close to the estimate of the effect, but there is a possibility that it is substantially different. Low certainty: Our confidence in the effect estimate is limited: The true effect may be substantially different from the estimate of the effect. Very low certainty: We have very little confidence in the effect estimate: The true effect is likely to be substantially different from the estimate of effect. CI: Confidence interval; MD: Mean difference; OR: Odds ratio; SMD: Standardised mean difference; MRI-PDFF: MRI proton density fat fraction; MRE: Magnetic resonance elastography.

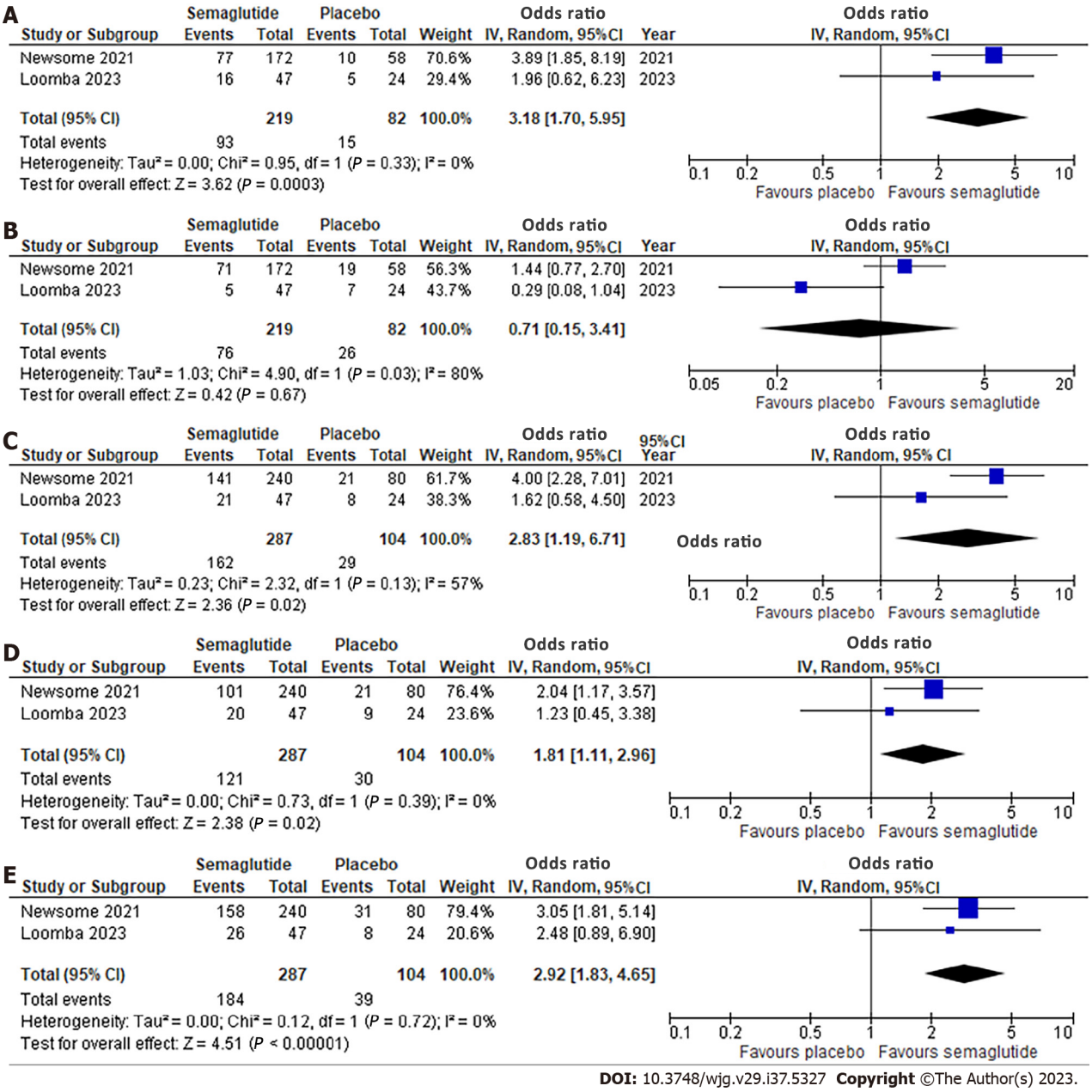
decrease in triglycerides, total cholesterol, and non-HDL cholesterol. Additionally, the exclusion of Newsome *et al*[20] led to a significant reduction in LDL-cholesterol, whereas the exclusion of Loomba *et al*[17] resulted in significant increases. No significant differences were observed in the sensitivity analysis when comparing the fixed-effect model to the random-effect model (Supplementary Table 4).

DISCUSSION

In this systematic review and meta-analysis, semaglutide demonstrated significant histologic improvements, with a higher likelihood of NASH resolution and improved NAS components, but it did not significantly improve fibrosis stage compared to placebo. Furthermore, semaglutide resulted in radiologic improvements in liver stiffness and steatosis, liver enzymes, as well as cardiometabolic effects on body weight and HgA1c, while maintaining a well-tolerated safety profile.

In the systematic review with meta-analysis on the impact of semaglutide on biochemical and radiologic measures of NAFLD conducted by Dutta *et al*[16], the majority of included patients did not have confirmed NAFLD. Out of the four RCTs included, only two involved patients with NAFLD. The other two trials focused on the cardiovascular outcomes of semaglutide in patients with type 2 diabetes and the efficacy of semaglutide in weight loss for patients with obesity. Since these two trials did not separately report outcomes for the NAFLD subgroup, they were not included in our systematic review and meta-analysis. Furthermore, the meta-analysis did not include any histological outcomes, which are considered the gold standard for NAFLD diagnosis and management. In contrast, our paper exclusively focuses on the NAFLD population, reports histological outcomes, and provides an updated review that includes the recent RCT conducted by Loomba *et al*[17].

Previous studies have demonstrated an association between histological resolution of NASH and decrease in NAS components with improvement in fibrosis stage[22,23]. However, despite improvements in other histologic outcomes, our meta-analysis did not observe an improvement in liver fibrosis. Of note, Loomba *et al*[17] had an imbalance in baseline characteristics, with a higher proportion of patients in the semaglutide group exhibiting higher grade fibrosis and non-invasive markers of inflammation compared to the placebo group. This imbalance may have reduced the treatment effect



DOI: 10.3748/wjg.v29.i37.5327 **Copyright** ©The Author(s) 2023.

Figure 2 Effect of semaglutide on histologic parameters. A: Resolution of non-alcoholic steatohepatitis (NASH) with no worsening of liver fibrosis; B: Improvement in liver fibrosis stage without worsening of NASH; C: Improvement in steatosis; D: Improvement in lobular inflammation; E: Improvement in hepatocellular ballooning. 95%CI: 95% confidence intervals.

estimate and resulted in the observed heterogeneity. Furthermore, the proportion of patients with improved fibrosis in the placebo group in the trial of Newsome *et al*[20] (33%) was higher than that reported in the LEAN trial (14%) or the pooled placebo outcomes of 23 RCTs involving patients with NAFLD (21%), possibly contributing to the non-significant treatment effect estimate[24,25]. Despite no difference in the improvement of fibrosis, Newsome's trial observed that a smaller proportion of patients in the semaglutide group (5%) experienced worsening of fibrosis compared to the placebo group (19%), suggesting a potential benefit[20]. It is possible that a longer follow-up time may be required to achieve improvements in fibrosis, particularly since most of the patients had advanced fibrosis, and the timeline for improvement in fibrosis remains unclear.

Although liver biopsy remains the gold standard for diagnosing and staging NAFLD, MRE and MRI-PDFF are effective non-invasive assessments of liver stiffness and steatosis, respectively. MRI-PDFF is significantly associated with histological NASH CRN steatosis grade, independent of age, sex, and other NASH parameters[26]. This correlation has been demonstrated in several other studies[27,28]. Both MRE and MRI-PDFF are considered more accurate than ultrasound-based transient elastography in detecting fibrosis and steatosis, respectively, and remain effective in patients with obesity, which is a common comorbidity in patients with NAFLD[29].

However, the accuracy of MRI-PDFF is limited by the extent of hepatic fibrosis. Permutt *et al*[30] demonstrated that the association between MRI and histology-determined steatosis remained relatively stable at fibrosis stages 0-3 but significantly dropped at stage 4. Similarly, Idilman *et al*[27] showed that the correlation between liver biopsy and MRI-

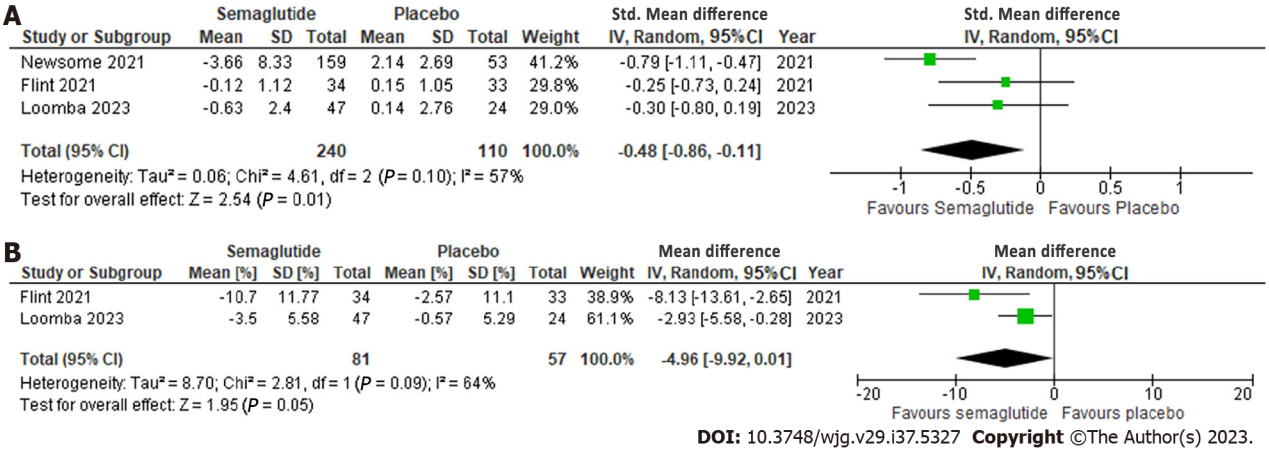


Figure 3 Effect of semaglutide on radiologic parameters. A: Liver stiffness assessed by magnetic resonance enterography or Fibroscan; B: Liver steatosis assessed by MRI proton density fat fraction. 95%CI: 95% confidence intervals.

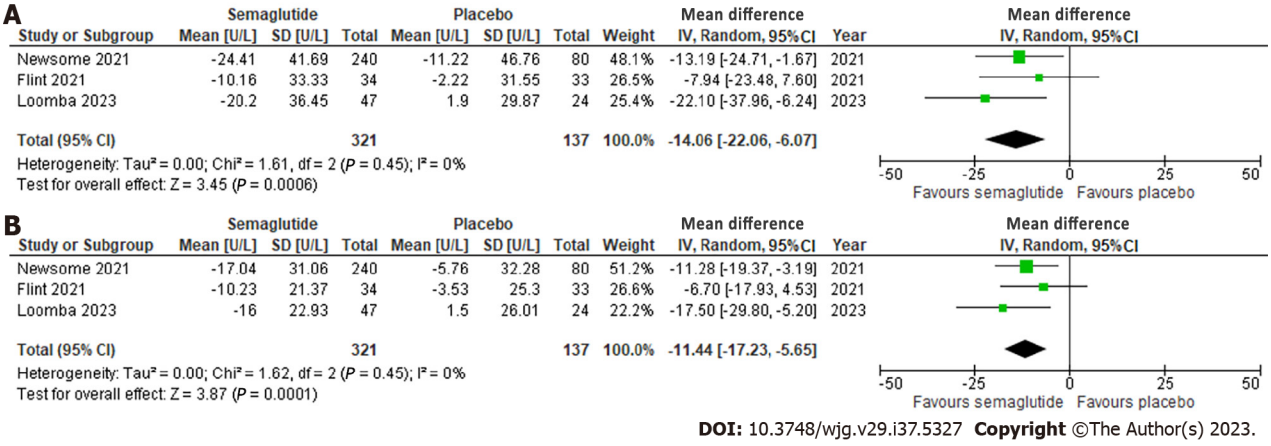


Figure 4 Effect of semaglutide on liver enzymes. A: Alanine aminotransferase; B: Aspartate aminotransferase. 95%CI: 95% confidence intervals.

determined steatosis was less pronounced when fibrosis was present (r = 0.60) than when fibrosis was absent (r = 0.86). In contrast, liver stiffness measured using MRE is less influenced by fibrosis and provides a more accurate prediction of liver fibrosis in patients with more advanced fibrosis[31]. The decreased reproducibility and accuracy of MRI PDFF in higher fibrosis stages may explain the substantial heterogeneity observed in liver steatosis in our study, especially considering that the population of the included studies had advanced fibrosis. Heterogeneity in liver stiffness, although not statistically significant, became negligible when Fibroscan was removed and only MRE was utilized to measure liver stiffness.

Semaglutide showed a significant association with moderate decreases in ALT and AST, which have previously been correlated with histologic response, fibrosis regression, and reduced progression in NAFLD[22,32]. However, both the LEAN trial and a meta-analysis of liraglutide in NAFLD did not observe significant reductions in liver enzymes[24,33]. Despite being in the same drug class with similar mechanisms of action, there may be intrinsic differences between effect of semaglutide and liraglutide. Furthermore, our study demonstrated a significant improvement in HgA1c and a reduction of 6.53 kg in body weight in the semaglutide compared to placebo group. The superior metabolic outcomes associated with semaglutide, compared to liraglutide, may lead to a more effective reduction in hepatocellular stress and injury, resulting in a significant decrease in liver enzymes. Vilar-Gomez *et al*[34] previously demonstrated that patients with weight losses ≥ 10% had the highest rates of NAS reduction, NASH resolution and fibrosis regression. Therefore, semaglutide appears to be particularly beneficial for patients with both NAFLD and features of metabolic syndrome.

The safety profile of semaglutide was comparable to that reported in the recent phase 3 trial with once-weekly dosing in patients with obesity and trials from the SUSTAIN (Semaglutide Unabated Sustainability in Treatment of Type 2 Diabetes) programs[14,35]. Gastrointestinal-related side effects, including nausea, constipation, vomiting, and abdominal pain, were significantly more prevalent in patients receiving semaglutide compared to placebo. These side effects are well-documented among the GLP-1 RA class. In all RCTs included in our review, adverse events mostly occurred during treatment initiation or the dose-escalation period. These symptoms become less pronounced with gradual up-titration and are often self-limiting, subsiding after a few weeks. Furthermore, the risks of serious adverse events were not different between semaglutide and placebo.

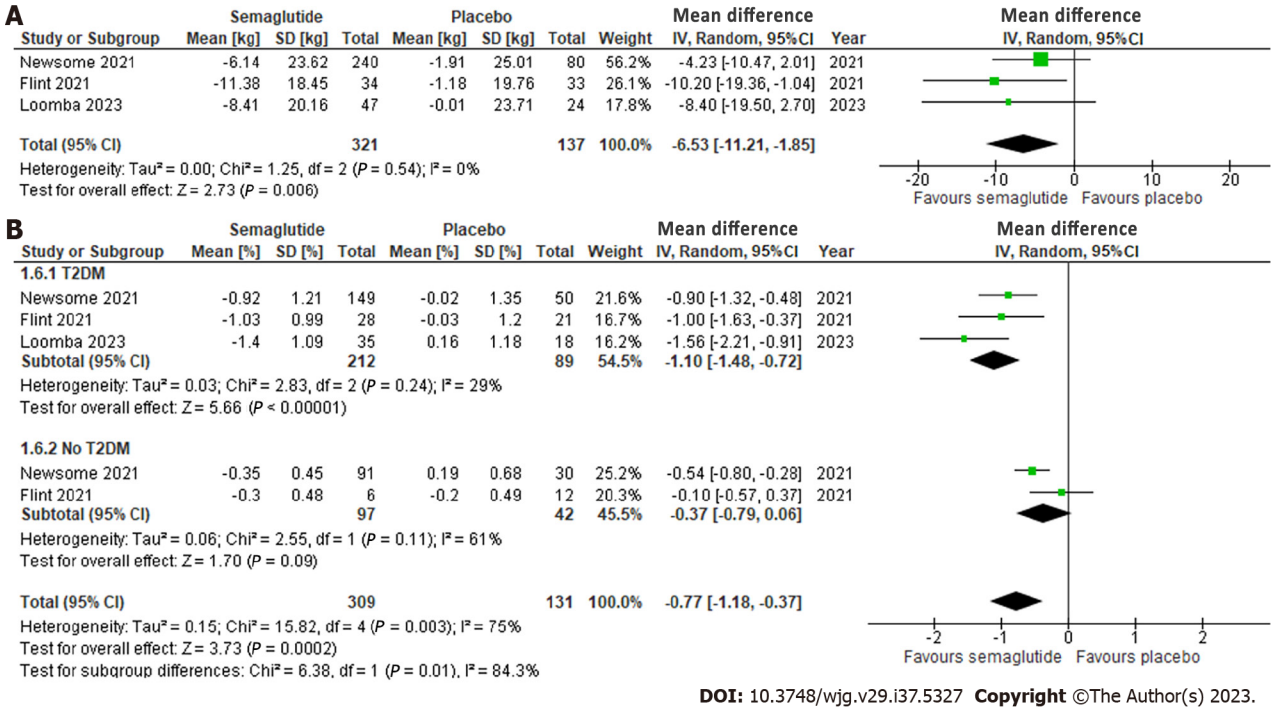


Figure 5 Effect of semaglutide on cardiometabolic parameters. A: Body weight; B: HgA1c in patients with type 2 diabetes (T2DM) *vs* without T2DM. 95%CI: 95% confidence intervals.

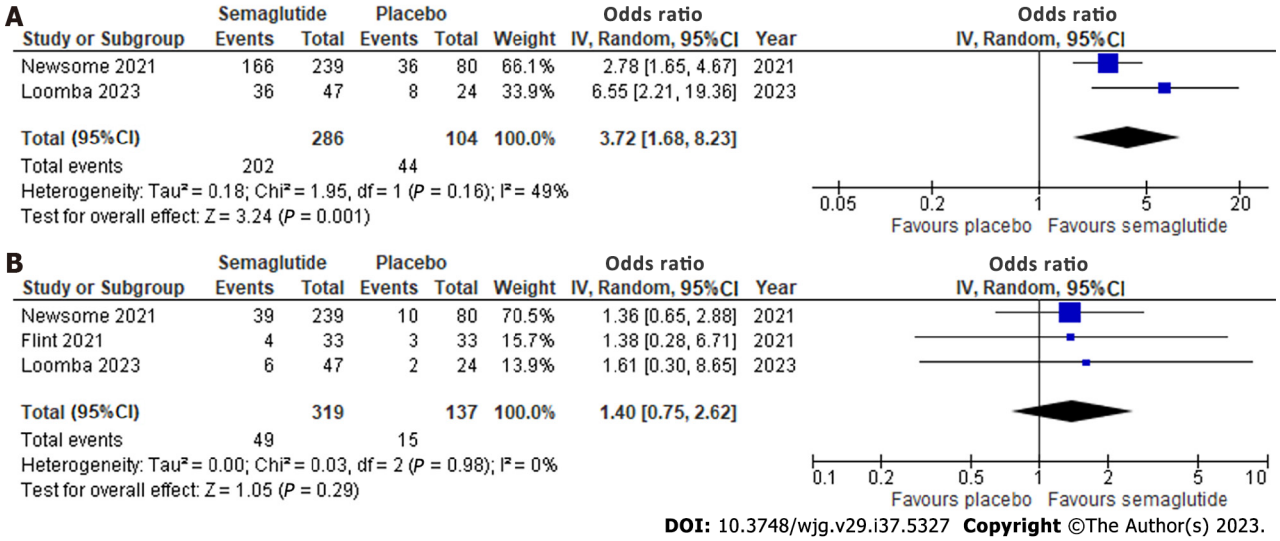


Figure 6 Adverse events with semaglutide. A: Gastrointestinal related side effects; B: Serious adverse events. 95%CI: 95% confidence intervals.

Our study has several limitations. The included RCTs are clinically heterogeneous from each other, with patients across the spectrum of NAFLD. Flint *et al*[21] recruited patients with NAFL, whereas Newsome and Loomba's trials involved patients with NASH and NASH-related cirrhosis, respectively. The heterogeneous patient population limits the applicability of the results, as treatment and response across the spectrum of NAFLD may differ. Additionally, a range of doses of semaglutide was used across the trials, including 0.1 mg, 0.2 mg, 0.4 mg once daily, and 2.4 mg weekly. However, this is less of a concern as once-weekly dosing has been shown to be comparably effective in the obesity population, and unpublished data suggests similar plasma concentrations to daily dosing[14,17]. Furthermore, histologic outcomes were only reported for patients with NASH or NASH-related cirrhosis, but not for patients with NAFL. Therefore, the effect of semaglutide on histologic outcomes in the NAFL population remains unclear. Lastly, the limited number of eligible studies restricted our ability to perform subgroup analysis comparing outcomes in NAFL, NASH, and NASH-related cirrhosis populations, or meta-regression to investigate heterogeneity and the effect of covariates on the effect sizes.

CONCLUSION

In conclusion, our meta-analysis of RCTs demonstrates that semaglutide has beneficial histologic, radiologic, liver enzyme, and cardiometabolic effects in patients with NAFLD, with a well-tolerated safety profile. Semaglutide is particularly beneficial for patients with NAFLD and features of metabolic syndrome, given its notable effects on lowering HbA1c and promoting weight loss. However, the results are limited by the small number of included studies and clinical heterogeneity, which restricts the generalizability these findings across the spectrum of NAFLD. Additional RCTs with larger sample sizes and longer durations are required to characterize the effects of semaglutide on fibrosis regression and its role in the different phases of NAFLD.

ARTICLE HIGHLIGHTS

Research background

Non-alcoholic fatty liver disease (NAFLD) is the leading cause of chronic liver disease. The prevalence and disease burden of NAFLD are projected to exponentially increase resulting in significant healthcare expenditures and lower health-related quality of life. To date, there are no approved pharmacotherapies for NAFLD or non-alcoholic steatohepatitis (NASH).

Research motivation

Several randomized clinical trials have demonstrated the beneficial effects of semaglutide in patients with NAFLD. Prior systematic review with meta-analysis assessing the impact of semaglutide did not report histological outcomes and were not focused on a NAFLD specific population.

Research objectives

This study aimed to review the efficacy and safety of semaglutide, focusing on patients with NAFLD, in order to more specifically reflect the NAFLD population and expand the current understanding of semaglutide in NAFLD.

Research methods

MEDLINE, CENTRAL, EMBASE, and grey literature sources were searched from inception to May 1, 2023, to identify eligible randomized controlled trials (RCTs) using a predefined search strategy. Predetermined outcomes were extracted, and quality assessment was performed using the Cochrane risk-of-bias 2 tool and GRADE framework. Meta-analysis was performed using random effects model expressing continuous outcomes as mean differences (MD) or standardized MDs (SMD), and dichotomous outcomes as odds ratios (OR) with 95% confidence intervals (CI). Statistical heterogeneity was assessed using the Cochran's Q test and I^2 statistic.

Research results

A total of three RCTs involving 458 patients were included. Semaglutide increased the likelihood of NASH resolution (OR: 3.18, 95%CI: 1.70, 5.95; $P < 0.001$), improvement in steatosis (OR: 2.83, 95%CI: 1.19, 6.71; $P = 0.03$), lobular inflammation (OR: 1.81, 95%CI: 1.11, 2.96; $P = 0.02$), and hepatocellular ballooning (OR: 2.92, 95%CI: 1.83, 4.65; $P < 0.001$), but not fibrosis stage (OR: 0.71, 95%CI: 0.15, 3.41; $P = 0.67$). Radiologically, semaglutide reduced liver stiffness (SMD: -0.48, 95%CI: -0.86, -0.11; $P = 0.01$) and steatosis (MD: -4.96%, 95%CI: -9.92, 0.01; $P = 0.05$). It also reduced ALT (MD: -14.06 U/L, 95%CI: -22.06, -6.07; $P < 0.001$) and AST (MD: -11.44 U/L, 95%CI: -17.23, -5.65; $P < 0.001$).

Semaglutide led to improved cardiometabolic outcomes, including decreased HgA1c (MD: -0.77%, 95%CI: -1.18, -0.37; $P < 0.001$) and weight loss (MD: -6.53 kg, 95%CI: -11.21, -1.85; $P = 0.006$), but increased the occurrence of GI-related side effects (OR: 3.72, 95%CI: 1.68, 8.23; $P = 0.001$). Overall risk of serious adverse events was similar compared to placebo (OR: 1.40, 95%CI: 0.75, 2.62; $P < 0.29$).

Research conclusions

Semaglutide demonstrated significant histologic improvements, with a higher likelihood of NASH resolution and improved NAS components, but it did not significantly improve fibrosis stage compared to placebo. Furthermore, semaglutide resulted in radiologic improvements in liver stiffness and steatosis, liver enzymes, as well as cardiometabolic effects on body weight and HgA1c, while maintaining a well-tolerated safety profile.

Research perspectives

Additional RCTs with larger sample sizes and longer durations are required to characterize the effects of semaglutide on fibrosis regression and its role in the different phases of NAFLD.

ACKNOWLEDGEMENTS

The authors thank Dr. Lorri Puil for her advice and assistance with the statistical analysis.

FOOTNOTES

Author contributions: Zhu K contributed to conception and design, analysis and interpretation of data, drafting the article, and final approval; Rohan K contributed to acquisition of data, analysis and interpretation of data, drafting the article; Chahal D contributed to revising the article and final approval; Yoshida E contributed to conception and design, revising the article, and final approval; Hussaini T contributed to conception and design, revising the article, and final approval.

Conflict-of-interest statement: Zhu K, Kakkar R and Chahal D have no conflicts of interests to declare; Yoshida EM is an investigator of clinical trials sponsored by Gilead Sciences, Pfizer, Genfit, Intercept, Celgene, Allergan, and Madrigal; Yoshida EM has received research funding from Paladin Labs Inc; Hussaini T has received research funding from Transplant Research Foundation of BC, and Paladin Labs Inc.

PRISMA 2009 Checklist statement: The authors have read the PRISMA 2009 Checklist, and the manuscript was prepared and revised according to the PRISMA 2009 Checklist.

Open-Access: This article is an open-access article that was selected by an in-house editor and fully peer-reviewed by external reviewers. It is distributed in accordance with the Creative Commons Attribution NonCommercial (CC BY-NC 4.0) license, which permits others to distribute, remix, adapt, build upon this work non-commercially, and license their derivative works on different terms, provided the original work is properly cited and the use is non-commercial. See: https://creativecommons.org/Licenses/by-nc/4.0/

Country/Territory of origin: Canada

ORCID number: Kai Zhu 0000-0002-2883-5486; Daljeet Chahal 0000-0003-2486-1449; Eric M Yoshida 0000-0003-2910-7461; Trana Hussaini 0000-0002-6463-6847.

S-Editor: Chen YL
L-Editor: A
P-Editor: Yu HG

REFERENCES

1 **Riazi K**, Azhari H, Charette JH, Underwood FE, King JA, Afshar EE, Swain MG, Congly SE, Kaplan GG, Shaheen AA. The prevalence and incidence of NAFLD worldwide: a systematic review and meta-analysis. *Lancet Gastroenterol Hepatol* 2022; **7**: 851-861 [PMID: 35798021 DOI: 10.1016/S2468-1253(22)00165-0]
2 **Cheemerla S**, Balakrishnan M. Global Epidemiology of Chronic Liver Disease. *Clin Liver Dis (Hoboken)* 2021; **17**: 365-370 [PMID: 34136143 DOI: 10.1002/cld.1061]
3 **Estes C**, Razavi H, Loomba R, Younossi Z, Sanyal AJ. Modeling the epidemic of nonalcoholic fatty liver disease demonstrates an exponential increase in burden of disease. *Hepatology* 2018; **67**: 123-133 [PMID: 28802062 DOI: 10.1002/hep.29466]
4 **Golabi P**, Otgonsuren M, Cable R, Felix S, Koenig A, Sayiner M, Younossi ZM. Non-alcoholic Fatty Liver Disease (NAFLD) is associated with impairment of Health Related Quality of Life (HRQOL). *Health Qual Life Outcomes* 2016; **14**: 18 [PMID: 26860700 DOI: 10.1186/s12955-016-0420-z]
5 **Younossi ZM**, Blissett D, Blissett R, Henry L, Stepanova M, Younossi Y, Racila A, Hunt S, Beckerman R. The economic and clinical burden of nonalcoholic fatty liver disease in the United States and Europe. *Hepatology* 2016; **64**: 1577-1586 [PMID: 27543837 DOI: 10.1002/hep.28785]
6 **Chalasani N**, Younossi Z, Lavine JE, Diehl AM, Brunt EM, Cusi K, Charlton M, Sanyal AJ; American Gastroenterological Association; American Association for the Study of Liver Diseases; American College of Gastroenterologyh. The diagnosis and management of non-alcoholic fatty liver disease: practice guideline by the American Gastroenterological Association, American Association for the Study of Liver Diseases, and American College of Gastroenterology. *Gastroenterology* 2012; **142**: 1592-1609 [PMID: 22656328 DOI: 10.1053/j.gastro.2012.04.001]
7 **Rinella ME**. Nonalcoholic fatty liver disease: a systematic review. *JAMA* 2015; **313**: 2263-2273 [PMID: 26057287 DOI: 10.1001/jama.2015.5370]
8 **Ma J**, Hwang SJ, Pedley A, Massaro JM, Hoffmann U, Chung RT, Benjamin EJ, Levy D, Fox CS, Long MT. Bi-directional analysis between fatty liver and cardiovascular disease risk factors. *J Hepatol* 2017; **66**: 390-397 [PMID: 27729222 DOI: 10.1016/j.jhep.2016.09.022]
9 **Gupta NA**, Mells J, Dunham RM, Grakoui A, Handy J, Saxena NK, Anania FA. Glucagon-like peptide-1 receptor is present on human hepatocytes and has a direct role in decreasing hepatic steatosis in vitro by modulating elements of the insulin signaling pathway. *Hepatology* 2010; **51**: 1584-1592 [PMID: 20225248 DOI: 10.1002/hep.23569]
10 **Dichtel LE**. The Glucagon-Like Peptide-1 Receptor Agonist, Semaglutide, for the Treatment of Nonalcoholic Steatohepatitis. *Hepatology* 2021; **74**: 2290-2292 [PMID: 33960005 DOI: 10.1002/hep.31886]
11 **Davies MJ**, Aroda VR, Collins BS, Gabbay RA, Green J, Maruthur NM, Rosas SE, Del Prato S, Mathieu C, Mingrone G, Rossing P, Tankova T, Tsapas A, Buse JB. Management of Hyperglycemia in Type 2 Diabetes, 2022. A Consensus Report by the American Diabetes Association (ADA) and the European Association for the Study of Diabetes (EASD). *Diabetes Care* 2022; **45**: 2753-2786 [PMID: 36148880 DOI: 10.2337/dci22-0034]
12 **Targher G**, Mantovani A, Byrne CD. Mechanisms and possible hepatoprotective effects of glucagon-like peptide-1 receptor agonists and other incretin receptor agonists in non-alcoholic fatty liver disease. *Lancet Gastroenterol Hepatol* 2023; **8**: 179-191 [PMID: 36620987 DOI: 10.1016/S2468-1253(22)00338-7]
13 **Nauck MA**, Meier JJ. MANAGEMENT OF ENDOCRINE DISEASE: Are all GLP-1 agonists equal in the treatment of type 2 diabetes? *Eur J Endocrinol* 2019; **181**: R211-R234 [PMID: 31600725 DOI: 10.1530/EJE-19-0566]

14 **Wilding JPH**, Batterham RL, Calanna S, Davies M, Van Gaal LF, Lingvay I, McGowan BM, Rosenstock J, Tran MTD, Wadden TA, Wharton S, Yokote K, Zeuthen N, Kushner RF; STEP 1 Study Group. Once-Weekly Semaglutide in Adults with Overweight or Obesity. *N Engl J Med* 2021; **384**: 989-1002 [PMID: 33567185 DOI: 10.1056/NEJMoa2032183]

15 **Marso SP**, Bain SC, Consoli A, Eliaschewitz FG, Jódar E, Leiter LA, Lingvay I, Rosenstock J, Seufert J, Warren ML, Woo V, Hansen O, Holst AG, Pettersson J, Vilsbøll T; SUSTAIN-6 Investigators. Semaglutide and Cardiovascular Outcomes in Patients with Type 2 Diabetes. *N Engl J Med* 2016; **375**: 1834-1844 [PMID: 27633186 DOI: 10.1056/NEJMoa1607141]

16 **Dutta D**, Kumar M, Shivaprasad KS, Kumar A, Sharma M. Impact of semaglutide on biochemical and radiologic measures of metabolic-dysfunction associated fatty liver disease across the spectrum of glycaemia: A meta-analysis. *Diabetes Metab Syndr* 2022; **16**: 102539 [PMID: 35709586 DOI: 10.1016/j.dsx.2022.102539]

17 **Loomba R**, Abdelmalek MF, Armstrong MJ, Jara M, Kjær MS, Krarup N, Lawitz E, Ratziu V, Sanyal AJ, Schattenberg JM, Newsome PN; NN9931-4492 investigators. Semaglutide 2·4 mg once weekly in patients with non-alcoholic steatohepatitis-related cirrhosis: a randomised, placebo-controlled phase 2 trial. *Lancet Gastroenterol Hepatol* 2023; **8**: 511-522 [PMID: 36934740 DOI: 10.1016/S2468-1253(23)00068-7]

18 **Furukawa TA**, Barbui C, Cipriani A, Brambilla P, Watanabe N. Imputing missing standard deviations in meta-analyses can provide accurate results. *J Clin Epidemiol* 2006; **59**: 7-10 [PMID: 16360555 DOI: 10.1016/J.JCLINEPI.2005.06.006]

19 **Kalogirou MS**, Patoulias D, Haidich AB, Akriviadis E, Sinakos E. Liraglutide in patients with non-alcoholic fatty liver disease: a systematic review and meta-analysis of randomized controlled trials. *Clin Res Hepatol Gastroenterol* 2021; **45**: 101568 [PMID: 33309563 DOI: 10.1016/j.clinre.2020.10.012]

20 **Newsome PN**, Buchholtz K, Cusi K, Linder M, Okanoue T, Ratziu V, Sanyal AJ, Sejling AS, Harrison SA; NN9931-4296 Investigators. A Placebo-Controlled Trial of Subcutaneous Semaglutide in Nonalcoholic Steatohepatitis. *N Engl J Med* 2021; **384**: 1113-1124 [PMID: 33185364 DOI: 10.1056/NEJMoa2028395]

21 **Flint A**, Andersen G, Hockings P, Johansson L, Morsing A, Sundby Palle M, Vogl T, Loomba R, Plum-Mörschel L. Randomised clinical trial: semaglutide versus placebo reduced liver steatosis but not liver stiffness in subjects with non-alcoholic fatty liver disease assessed by magnetic resonance imaging. *Aliment Pharmacol Ther* 2021; **54**: 1150-1161 [PMID: 34570916 DOI: 10.1111/apt.16608]

22 **Kleiner DE**, Brunt EM, Wilson LA, Behling C, Guy C, Contos M, Cummings O, Yeh M, Gill R, Chalasani N, Neuschwander-Tetri BA, Diehl AM, Dasarathy S, Terrault N, Kowdley K, Loomba R, Belt P, Tonascia J, Lavine JE, Sanyal AJ; Nonalcoholic Steatohepatitis Clinical Research Network. Association of Histologic Disease Activity With Progression of Nonalcoholic Fatty Liver Disease. *JAMA Netw Open* 2019; **2**: e1912565 [PMID: 31584681 DOI: 10.1001/jamanetworkopen.2019.12565]

23 **Brunt EM**, Kleiner DE, Wilson LA, Sanyal AJ, Neuschwander-Tetri BA; Nonalcoholic Steatohepatitis Clinical Research Network. Improvements in Histologic Features and Diagnosis Associated With Improvement in Fibrosis in Nonalcoholic Steatohepatitis: Results From the Nonalcoholic Steatohepatitis Clinical Research Network Treatment Trials. *Hepatology* 2019; **70**: 522-531 [PMID: 30549292 DOI: 10.1002/hep.30418]

24 **Armstrong MJ**, Gaunt P, Aithal GP, Barton D, Hull D, Parker R, Hazlehurst JM, Guo K; LEAN trial team, Abouda G, Aldersley MA, Stocken D, Gough SC, Tomlinson JW, Brown RM, Hübscher SG, Newsome PN. Liraglutide safety and efficacy in patients with non-alcoholic steatohepatitis (LEAN): a multicentre, double-blind, randomised, placebo-controlled phase 2 study. *Lancet* 2016; **387**: 679-690 [PMID: 26608256 DOI: 10.1016/S0140-6736(15)00803-X]

25 **Han MAT**, Altayar O, Hamdeh S, Takyar V, Rotman Y, Etzion O, Lefebvre E, Safadi R, Ratziu V, Prokop LJ, Murad MH, Noureddin M. Rates of and Factors Associated With Placebo Response in Trials of Pharmacotherapies for Nonalcoholic Steatohepatitis: Systematic Review and Meta-analysis. *Clin Gastroenterol Hepatol* 2019; **17**: 616-629.e26 [PMID: 29913275 DOI: 10.1016/j.cgh.2018.06.011]

26 **Tang A**, Tan J, Sun M, Hamilton G, Bydder M, Wolfson T, Gamst AC, Middleton M, Brunt EM, Loomba R, Lavine JE, Schwimmer JB, Sirlin CB. Nonalcoholic fatty liver disease: MR imaging of liver proton density fat fraction to assess hepatic steatosis. *Radiology* 2013; **267**: 422-431 [PMID: 23382291 DOI: 10.1148/radiol.12120896]

27 **Idilman IS**, Aniktar H, Idilman R, Kabacam G, Savas B, Elhan A, Celik A, Bahar K, Karcaaltincaba M. Hepatic steatosis: quantification by proton density fat fraction with MR imaging versus liver biopsy. *Radiology* 2013; **267**: 767-775 [PMID: 23382293 DOI: 10.1148/radiol.13121360]

28 **Bannas P**, Kramer H, Hernando D, Agni R, Cunningham AM, Mandal R, Motosugi U, Sharma SD, Munoz del Rio A, Fernandez L, Reeder SB. Quantitative magnetic resonance imaging of hepatic steatosis: Validation in ex vivo human livers. *Hepatology* 2015; **62**: 1444-1455 [PMID: 26224591 DOI: 10.1002/hep.28012]

29 **Park CC**, Nguyen P, Hernandez C, Bettencourt R, Ramirez K, Fortney L, Hooker J, Sy E, Savides MT, Alquiraish MH, Valasek MA, Rizo E, Richards L, Brenner D, Sirlin CB, Loomba R. Magnetic Resonance Elastography vs Transient Elastography in Detection of Fibrosis and Noninvasive Measurement of Steatosis in Patients With Biopsy-Proven Nonalcoholic Fatty Liver Disease. *Gastroenterology* 2017; **152**: 598-607.e2 [PMID: 27911262 DOI: 10.1053/j.gastro.2016.10.026]

30 **Permutt Z**, Le TA, Peterson MR, Seki E, Brenner DA, Sirlin C, Loomba R. Correlation between liver histology and novel magnetic resonance imaging in adult patients with non-alcoholic fatty liver disease - MRI accurately quantifies hepatic steatosis in NAFLD. *Aliment Pharmacol Ther* 2012; **36**: 22-29 [PMID: 22554256 DOI: 10.1111/j.1365-2036.2012.05121.x]

31 **Jayakumar S**, Middleton MS, Lawitz EJ, Mantry PS, Caldwell SH, Arnold H, Mae Diehl A, Ghalib R, Elkhashab M, Abdelmalek MF, Kowdley KV, Stephen Djedjos C, Xu R, Han L, Mani Subramanian G, Myers RP, Goodman ZD, Afdhal NH, Charlton MR, Sirlin CB, Loomba R. Longitudinal correlations between MRE, MRI-PDFF, and liver histology in patients with non-alcoholic steatohepatitis: Analysis of data from a phase II trial of selonsertib. *J Hepatol* 2019; **70**: 133-141 [PMID: 30291868 DOI: 10.1016/j.jhep.2018.09.024]

32 **Loomba R**, Sanyal AJ, Kowdley KV, Terrault N, Chalasani NP, Abdelmalek MF, McCullough AJ, Shringarpure R, Ferguson B, Lee L, Chen J, Liberman A, Shapiro D, Neuschwander-Tetri BA. Factors Associated With Histologic Response in Adult Patients With Nonalcoholic Steatohepatitis. *Gastroenterology* 2019; **156**: 88-95.e5 [PMID: 30222962 DOI: 10.1053/j.gastro.2018.09.021]

33 **Song T**, Jia Y, Li Z, Wang F, Ren L, Chen S. Effects of Liraglutide on Nonalcoholic Fatty Liver Disease in Patients with Type 2 Diabetes Mellitus: A Systematic Review and Meta-Analysis. *Diabetes Ther* 2021; **12**: 1735-1749 [PMID: 34002333 DOI: 10.1007/s13300-021-01072-4]

34 **Vilar-Gomez E**, Martinez-Perez Y, Calzadilla-Bertot L, Torres-Gonzalez A, Gra-Oramas B, Gonzalez-Fabian L, Friedman SL, Diago M, Romero-Gomez M. Weight Loss Through Lifestyle Modification Significantly Reduces Features of Nonalcoholic Steatohepatitis. *Gastroenterology* 2015; **149**: 367-78.e5; quiz e14 [PMID: 25865049 DOI: 10.1053/j.gastro.2015.04.005]

35 **Aroda VR**, Ahmann A, Cariou B, Chow F, Davies MJ, Jódar E, Mehta R, Woo V, Lingvay I. Comparative efficacy, safety, and cardiovascular outcomes with once-weekly subcutaneous semaglutide in the treatment of type 2 diabetes: Insights from the SUSTAIN 1-7 trials. *Diabetes Metab* 2019; **45**: 409-418 [PMID: 30615985 DOI: 10.1016/j.diabet.2018.12.001]

World Journal of Gastroenterology

Submit a Manuscript: https://www.f6publishing.com

World J Gastroenterol 2023 October 7; 29(37): 5339-5360

DOI: 10.3748/wjg.v29.i37.5339

ISSN 1007-9327 (print) ISSN 2219-2840 (online)

SCIENTOMETRICS

Global trends and hotspots of treatment for nonalcoholic fatty liver disease: A bibliometric and visualization analysis (2010-2023)

Jin-Jin Dai, Ya-Fei Zhang, Zhen-Hua Zhang

Specialty type: Gastroenterology and hepatology

Provenance and peer review: Unsolicited article; Externally peer reviewed.

Peer-review model: Single blind

Peer-review report's scientific quality classification

Grade A (Excellent): 0
Grade B (Very good): B, B
Grade C (Good): 0
Grade D (Fair): 0
Grade E (Poor): 0

P-Reviewer: Gutierrez-Castrellon P, Mexico; Zamani M, Iran

Received: June 25, 2023
Peer-review started: June 25, 2023
First decision: July 23, 2023
Revised: July 26, 2023
Accepted: September 4, 2023
Article in press: September 4, 2023
Published online: October 7, 2023

Jin-Jin Dai, Department of Infectious Diseases, Suzhou Hospital of Anhui Medical University, Suzhou 234000, Anhui Province, China

Jin-Jin Dai, Ya-Fei Zhang, Zhen-Hua Zhang, Department of Infectious Diseases, The Second Affiliated Hospital of Anhui Medical University, Hefei 230601, Anhui Province, China

Corresponding author: Zhen-Hua Zhang, MD, Professor, Department of Infectious Diseases, The Second Affiliated Hospital of Anhui Medical University, No. 678 Furong Road, Hefei 230601, Anhui Province, China. zzh1974cn@163.com

Abstract

BACKGROUND

Nonalcoholic fatty liver disease (NAFLD) is chronic, with its progression leading to liver fibrosis and end-stage cirrhosis. Although NAFLD is increasingly common, no treatment guideline has been established. Many mechanistic studies and drug trials have been conducted for new drug development to treat NAFLD. An up-to-date overview on the knowledge structure of NAFLD through bibliometrics, focusing on research hotspots, is necessary to reveal the rational and timely directions of development in this field.

AIM

To research the latest literature and determine the current trends in treatment for NAFLD.

METHODS

Publications related to treatment for NAFLD were searched on the Web of Science Core Collection database, from 2010 to 2023. VOSviewers, CiteSpace, and R package "bibliometrix" were used to conduct this bibliometric analysis. The key information was extracted, and the results of the cluster analysis were based on network data for generating and investigating maps for country, institution, journal, and author. Historiography analysis, bursts and cluster analysis, co-occurrence analysis, and trend topic revealed the knowledge structure and research hotspots in this field. GraphPad Prism 9.5.1.733 and Microsoft Office Excel 2019 were used for data analysis and visualization.

RESULTS

In total, 10829 articles from 120 countries (led by China and the United States) and 8785 institutions were included. The number of publications related to treatment for NAFLD increased annually. While China produced the most publications, the

United States was the most cited country, and the United Kingdom collaborated the most from an international standpoint. The University of California-San Diego, Shanghai Jiao Tong University, and Shanghai University of Traditional Chinese Medicine produced the most publications of all the research institutions. The International Journal of Molecular Sciences was the most frequent journal out of the 1523 total journals, and Hepatology was the most cited and co-cited journal. Sanyal AJ was the most cited author, the most co-cited author was Younossi ZM, and the most influential author was Loomba R. The most studied topics included the epidemiology and mechanism of NAFLD, the development of accurate diagnosis, the precise management of patients with NAFLD, and the associated metabolic comorbidities. The major cluster topics were "emerging drug," "glucagon-like peptide-1 receptor agonist," "metabolic dysfunction-associated fatty liver disease," "gut microbiota," and "glucose metabolism."

CONCLUSION

The bibliometric study identified recent research frontiers and hot directions, which can provide a valuable reference for scholars researching treatments for NAFLD.

Key Words: Bibliometrics; Treatment; Therapy; Nonalcoholic fatty liver disease; Metabolic dysfunction-associated fatty liver disease; Historiography analysis

©The Author(s) 2023. Published by Baishideng Publishing Group Inc. All rights reserved.

Core Tip: A total of 10829 articles published between 2010-2023 were identified through a bibliometric analysis to explore the trends and hotspots of treatment for nonalcoholic fatty liver disease (NAFLD). Replacing NAFLD/nonalcoholic steatohepatitis with metabolic dysfunction-associated fatty liver disease has been shown to greatly promote transformation of the treatment strategy of the disease. Research on gut microbiomes and traditional medicine will continue to be a short-term research hotspot. Obeticholic acid (phase 3 clinical validation) and semaglutide (under study) are likely to become the first approved drugs for NAFLD treatment.

Citation: Dai JJ, Zhang YF, Zhang ZH. Global trends and hotspots of treatment for nonalcoholic fatty liver disease: A bibliometric and visualization analysis (2010-2023). *World J Gastroenterol* 2023; 29(37): 5339-5360
URL: https://www.wjgnet.com/1007-9327/full/v29/i37/5339.htm
DOI: https://dx.doi.org/10.3748/wjg.v29.i37.5339

INTRODUCTION

Nonalcoholic fatty liver disease (NAFLD) was first proposed by Ludwig *et al*[1] in 1980 to describe fatty liver disease without a history of alcoholism. NAFLD is further divided histologically into nonalcoholic fatty liver and nonalcoholic steatohepatitis (NASH)[2]. NASH can progress to fibrosis, eventually leading to cirrhosis and cirrhosis-related complications such as end-stage liver disease and hepatocellular carcinoma (HCC)[3]. In the United States, NASH cirrhosis is the leading indicator and fastest-growing cause of candidates waiting for liver transplantation (LT)[4] and is expected to become the prevalent indication for LT by 2030[5]. Currently, NAFLD is an epidemic among chronic diseases, threatening the health of nearly 1.7 billion people worldwide and placing a huge burden on individuals, families, and healthcare systems[6].

The clinical burden of NAFLD extends beyond liver-related morbidity and mortality as there is growing evidence suggesting its association with various metabolic comorbidities, including obesity, type 2 diabetes, cardiovascular disease, chronic kidney disease, hypertension, and hypercholesterolemia[7]. The global epidemics of obesity, diabetes, and metabolic syndrome (MetS) have led to an increasing prevalence of NAFLD[8]. The presence of multiple metabolic comorbidities increases the risk of NAFLD and the risk of progressive liver disease. The primary liver pathology in NAFLD affects liver structure and function, increasing the risk of morbidity and mortality associated with cirrhosis, end-stage liver disease, and HCC, with cardiovascular disease accounting for the most deaths in patients with NAFLD[9]. Therefore, Eslam *et al*[10], representing the International Consensus Group in 2020, recommended renaming NAFLD/NASH to metabolic dysfunction-associated fatty liver disease (MAFLD) to more accurately reflect its pathogenesis and accelerate the transition to novel therapeutics.

The most effective strategy for addressing chronic disease is to reduce the disease burden through prevention. However, this goal has not been achieved for NAFLD. Lifestyle changes focused on weight loss remain the cornerstone of NASH treatment, with a 10% weight loss able to resolve steatohepatitis or improve fibrosis and portal vein inflammation [11]. Nonetheless, achieving significant weight loss in clinical practice is challenging, as its effects are slow and can easily be reversed. Studies have shown that only 30% of patients can lose more than 5% of their weight through lifestyle changes after 13 mo[12].

New drug research and development for NAFLD treatment has been slow. Currently, clinical phase 2b and phase 3 studies have achieved certain efficacy. It is anticipated that new drugs will be available in the near future. However, no drugs have been approved yet, and the efficacy of the various compounds under development is not deemed satisfactory. The response rates for the investigational drugs in current studies range from 20%-40%, with no significant difference from the placebo response rate of 10%-20%[10].

Bibliometric analysis is a statistical method of literature analysis that examines the publication status of studies in a specific field from both quantitative and qualitative perspectives. It includes various factors such as authorship, country of origin, affiliated institutions, journal publications, and keywords[13]. Bibliometric tools such as VOSviewer, the R package "bibliometrix"[14], and CiteSpace[15] were used to visualize the results of this literature analysis, and these tools are gradually being used more frequently in the medical field. The application of bibliometrics to analyze research in the treatment of NAFLD/MAFLD is exceedingly helpful for identifying hotspots and research trends in this field of study, and in identifying those countries, institutions, and researchers that contribute the most. The advantages of this research methodology also include the possibility of analyzing and summarizing the evolution of research directions and content for a given institution or individual, as well as of quantitatively analyzing the collaboration between them. However, there are not many bibliometric statistical analyses in the field of liver disease, with few articles related to NAFLD[16-20]. In analyzing research that focuses on the possible causes of classical liver diseases, the research hotspots are mainly viral hepatitis and alcoholic liver disease. In recent years, with the overall decline in the prevalence of viral hepatitis and the annual increase in the incidence of NAFLD, there has been a growing interest in the latter. Indeed, the collective research and resultant advancement in knowledge of the disease from the proposal of "NAFLD" in 1980[1], to the proposed renaming of the disease to "MAFLD" in 2020[10], to the recent publication of the "multi-society Delphi consensus statement on new fatty liver disease nomenclature"[21] is serving as a signal to the end of the diagnosis and research into NAFLD and the entry into a brand new era of the more accurately termed "metabolic dysfunction-associated steatotic liver disease (MASLD)". Therefore, at the time of this new naming of the disease, it is necessary to analyze and summarize the research results for the treatment of this disease through the method of bibliometric statistical analysis, so as to accurately analyze the research hotspots and the trend of future development through a more objective approach and global perspective.

As mentioned earlier, NAFLD is widespread and harmful, and new treatment strategies are urgently needed to halt the progression of hepatic steatosis and fibrosis[22]. Since the renaming of NAFLD to MAFLD in 2020, a major shift has been observed in the direction of its treatment. With the publication of research results in the past 2 years, it is crucial to conduct a statistical analysis of relevant literature, identify key contributors and the current research status in this field, pinpoint current research areas of focus, and outline future research trends and development prospects.

MATERIALS AND METHODS

Search strategy

We conducted a literature search on the Web of Science Core Collection database (https://www.webofscience.com/wos/woscc/basic-search) on April 10, 2023 to collect all literature data related to therapy for NAFLD. We completed the search and retrieval of data within 1 d in order to reduce the bias caused by frequent database updates. The search formula was set to [TS = (nonalcoholic fatty liver) or (non-alcoholic fatty liver disease) or (NAFLD) or (MAFLD) or (metabolic dysfunction-associated fatty liver disease) or (metabolic associated fatty liver disease)] and TS = [(therapy) or (treatment)] and LA = (English). The type of documents was set to "articles" and "review" (editorials, proceeding papers, abstracts, and book chapters articles were excluded) with a timespan ranging from January 1, 2010 to April 12, 2023 (Figure 1).

Bibliometric analysis

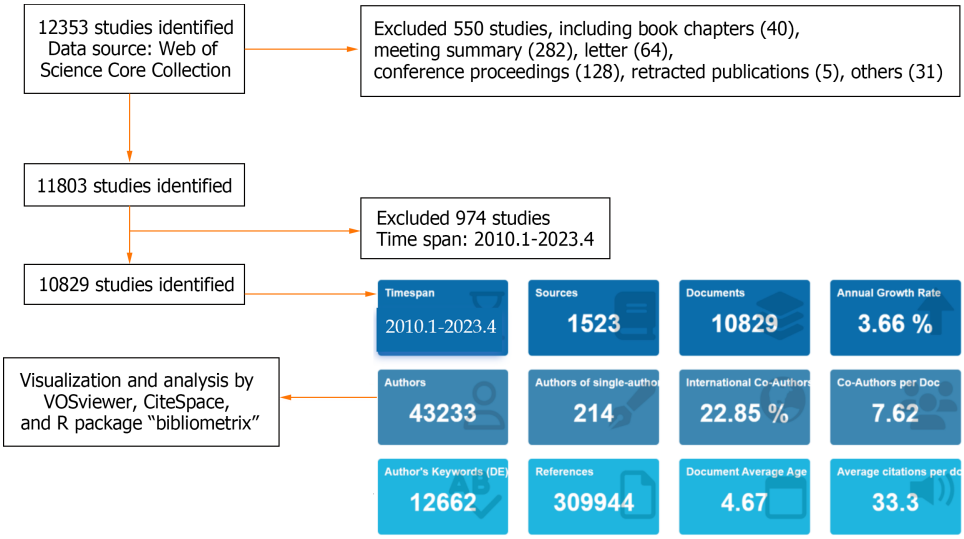
VOSviewer (version 1.6.19) is a bibliometric analysis software released in 2010 by van Eck and Waltman[23]. VOSviewer can extract the key information and show the results of cluster analysis based on network data for generating and investigating maps[24,25]. Country and institution analysis, journal and co-cited journal analysis, author and co-cited author analysis, and author keywords co-occurrence analysis were performed by the VOSviewer software[26]. Of note, reference co-citation cluster and keyword co-occurrence analysis have the ability to recognize the knowledge structure and research hotspots in a field[27].

The R package "bibliometrix"[28] (version 3.2.1) (https://www.bibliometrix.org) was applied for a thematic evolution analysis and to construct a global distribution network of publications of therapy for NAFLD. CiteSpace (version 6.2.R2 Advanced) is the most popular and recognized bibliometric visualization tool[29] developed by Synnestvedt *et al*[15]. In our study, the CiteSpace map primarily completed the dual-map overlay of journals' analysis and the timeline cluster analysis of keywords. GraphPad Prism 9.5.1.733 and Microsoft Office Excel 2019 were used for data analysis and visualization.

RESULTS

Quantitative analysis of publication

According to our search strategy, there were a total of 10829 studies on therapy or treatment for NAFLD since 2010, including 7826 articles and 3003 reviews. The annual number of publication increased year over year, and it showed



DOI: 10.3748/wjg.v29.i37.5339 **Copyright** ©The Author(s) 2023.

Figure 1 Flowchart for publication screening.

explosive growth from 2019 to 2022. Although only a quarter of 2023 was available, there were more than 352 articles, suggesting a continuation of the upward trend (Figure 2A).

Country and institution analysis

These publications came from 120 countries and 8785 institutions. More than half of the publications came from China and the United States (54.9%). The United States had the most publications until 2020 when publications from China increased massively (Figure 2B and C). The top 10 countries were distributed in Europe, Asia, and North America (Figure 2D).

China had the highest single-country publications (SCP) ratio of all countries (total of 3160 papers; SCP: 2763; SCP ratio: 87.4%). The SCP ratio in the United States was 75.0%, with 1978 papers. Of note, there was an abundance of active cooperation between different countries and regions (Figure 2E). Germany and the United Kingdom placed the greatest emphasis on international cooperation; their multiple country publication ratios were 42.1% and 43.3%, respectively (Figure 2D).

Subsequently, we filtered and visualized 76 countries based on the minimum number of five publications and constructed a collaborative network based on the number and relationship of publications in each country. In 2018, the United States was the most important and biggest research center in the world, which was transferred to China in 2020 (Figure 2F).

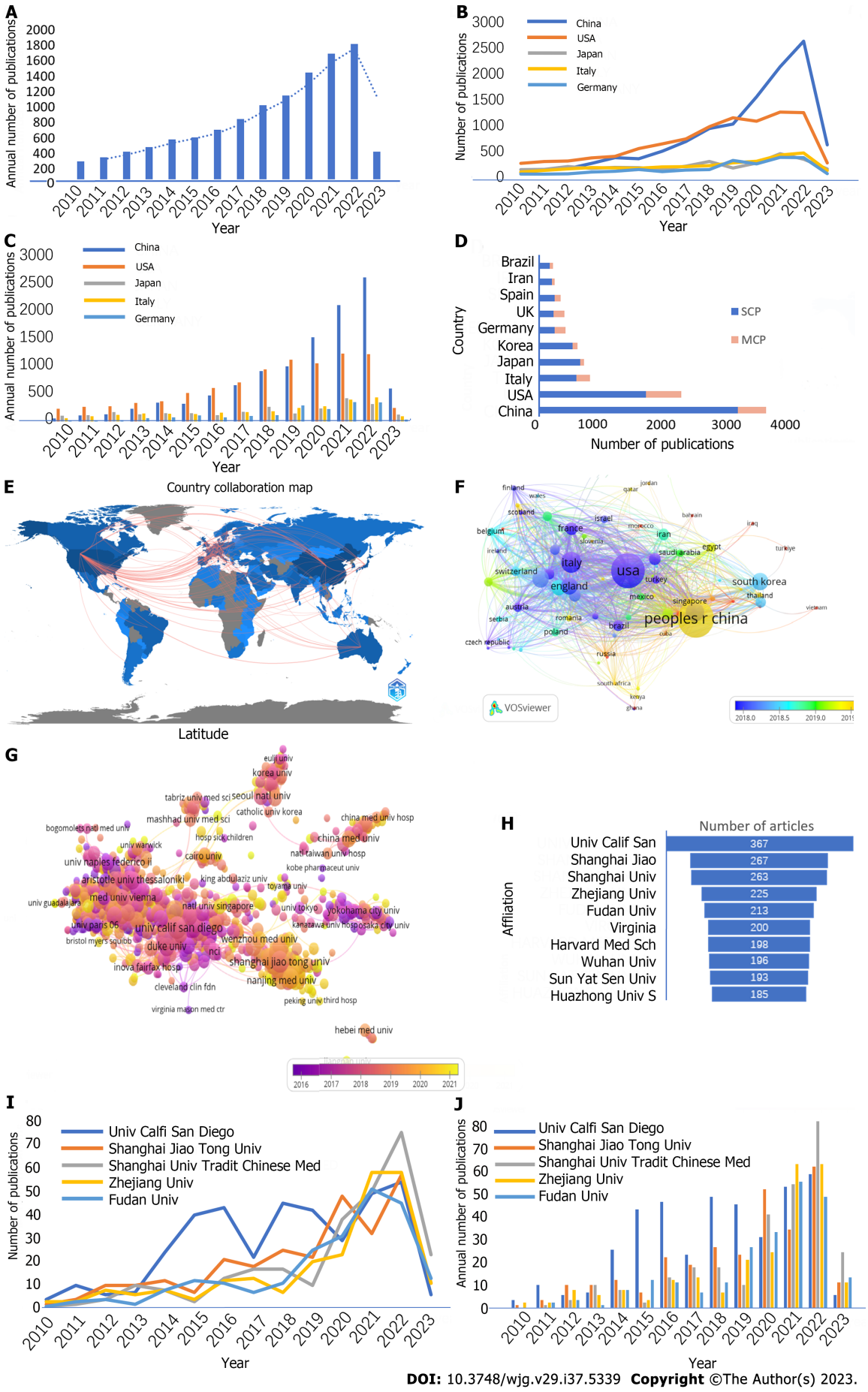
Then, we selected 1173 institutions based on the minimum number of five publications for visualization and constructed a collaborative network based on the number and relationship of publications of each institution (Figure 2G). The top 10 institutions were located in two countries; seven of the institutions were located in China (Figure 2H). The three institutions that published the most relevant papers were University of California-San Diego, Shanghai Jiao Tong University, and Shanghai University of Traditional Chinese Medicine. University of California-San Diego was the leader in publication output and maintained a high level of publications in recent years (Figure 2I and J). In the past 3 years, Chinese institutions have increasingly published NAFLD research. In particular, Shanghai Jiao Tong University ranked second and Shanghai University of Traditional Chinese Medicine ranked third, publishing frequently since 2020 and showing expansive growth in 2022.

Journals and cited and co-cited journals

Publications related to therapy for NAFLD were published in 1523 journals. The International Journal of Molecular Sciences published the most papers (n = 281, 2.6%). The top three journals with the most citations were Hepatology (n = 21451), Journal of Hepatology (n = 20843), and the World Journal of Gastroenterology (n = 12454). Among the top 20 journals of total link strength, the journal with the highest impact factor (IF) was Nature Reviews Gastroenterology and Hepatology (IF = 73.082).

Among the top 20 co-cited journals, five journals were cited more than 10000 times. Hepatology (co-citation = 49058) was the most cited journal, followed by the Journal of Hepatology (co-citation = 26782), Gastroenterology (co-citation = 21448), Journal of Biological Chemistry (co-citation = 12220), and PLOS ONE (co-citation = 12083). In addition, the IF of The Lancet was the highest (IF = 202.731) followed by the New England Journal of Medicine (IF = 176.079).

The dual-map overlay of journals can show the citation relationships between citing journals on the left and the clusters of co-cited journals on the right through the colored paths[29]. As shown in Figure 3A, the orange path is the main citation path, which represents the studies published in molecular/biology/immunology journals primarily cited by literature in molecular/biology/gene and health nursing/medicine journals. The green path is the main document flow path, which represents the research published in molecular/biology/gene and health nursing/medicine journals



DOI: 10.3748/wjg.v29.i37.5339 **Copyright** ©The Author(s) 2023.

Figure 2 Quantitative analysis of publication. A: Annual output of therapy for nonalcoholic fatty liver disease; B: Country production over time; C: Annual output by country; D: Corresponding authors' countries; E: Country collaboration world map; F: Visualization of countries; G: Visualization of institutions on nonalcoholic fatty liver disease research; H: Most relevant affiliations; I: Institution production over time; J: Annual output by institution. MCP: Multiple country publication; SCP: Single country publication.

primarily cited by studies published in medicine/medical clinical journals.

Historiography analysis

Through historiography analysis by R package "bibliometrix," we observed that the publications with the highest importance in chronological order in the dataset were Sanyal *et al*[30], Neuschwander-Tetri *et al*[31], Rinella[32], and Younossi *et al*[33] (Figure 3B and Table 1). Table 1 clearly showed that the vast majority of important studies (local cited documents and global cited documents were both high) were randomized controlled trials[30,31,34-36]. In addition, two important reviews in 2018 were "mechanisms of NAFLD development and therapeutic strategies"[37] and "global burden of NAFLD and NASH: Trends, predictions, risk factors and prevention"[33].

Reference with citation bursts and cluster analysis

Reference with citation bursts refers to those references that are frequently cited by scholars in a certain field over a period of time. In our study, the details of 25 references with strong citation bursts by R package "bibliometrix" were listed in Table 2. As shown in Table 2, every bar represents a year, and the red bar represents strong citation burstiness. Citation bursts for references appeared as early as 2010 and as late as 2023. The burst strength of these 25 references ranged from 49.79 to 161.62, and endurance strength was from 2-5 years.

A total of eight major clusters (Q = 0.519; S = 0.8789; Q/S = 0.6532) were generated from the co-citation networks of references after cluster analysis by CiteSpace (Figure 3C). The cluster nomenclature may reflect the study hotspots and frontiers in treatment of NAFLD. The largest cluster was emerging drug, followed by glucagon-like peptide-1 (GLP-1) receptor agonist, liver diseases, MAFLD, gut microbiota, hepatologists points, glucose-induced glucagon-like peptide, and glucose metabolism.

Authors and cited and co-cited authors

A total of 51987 authors participated in research on the therapy for NAFLD. Among the top 10 authors, 5 (who were from the United States, the United Kingdom, Italy, and France) each published more than 50 papers (Figure 3D). We built a collaborative network based on authors whose number of published papers was ≥ 5 (Figure 3E). Sanyal *et al*[30], Loomba *et al*[38], and Ratziu *et al*[22] had the largest nodes due to publishing the most related publications. In addition, we observed close collaboration among multiple authors.

Sanyal *et al*[30] was considered one of the most distinguished scholars because of his prolific research output (Figure 3D) and the highest number of citations (Figure 3E). His research on fatty liver encompassed a multidisciplinary interactive approach, covering areas such as apoptosis, cancer research, obesity, and microRNA. He hypothesized that NASH was associated with altered liver microRNA expression and alterations in the human gut microbiome were associated with cirrhosis and its complications[39]. He has committed to the field of effective therapeutic development for NASH and has provided summaries of new drugs under development or key ongoing research[40]. These include highly anticipated treatments such as farnesoid X receptor agonists, peroxisome proliferator-activated receptor agonists, GLP-1 receptor agonists, C-C chemokine receptor type 2 and 5 inhibitors, caspase inhibitors, lysyl oxidase-like 2 inhibitors, galectin-3 inhibitors, and others.

According to the H-index, which is a measure used to assess the scientific productivity and impact of researchers, the most influential scientists in this field of NAFLD are Loomba *et al*[38], Sanyal *et al*[30]. Loomba *et al*[38] has focused on various aspects of NAFLD, including aging, epidemiology, genetic and environmental susceptibility, natural history, and the treatment of NASH. His research has also explored the efficacy of metformin[40], ezetimibe[41], obeticholic acid (OCA)[31], sitagliptin[42], cenicriviroc[43], selonsert[44], polyethylene glycol[45], and semaglutide[46] in the treatment of NAFLD.

Among the 163234 co-cited authors, five authors were co-cited more than 2000 times. The most co-cited author was Younossi *et al*[33] (n = 4007) followed by Chalasani *et al*[3] (n = 2363) and Sanyal *et al*[30] (n = 2088). Younossi *et al*[33] concluded that lifestyle modifications to achieve weight loss remains a first-line intervention for patients with NAFLD [47]. He also found that a dosage of 25 mg of OCA significantly improved fibrosis and NASH disease activity scores in patients with NASH[34,48]. Chalasani *et al*[3] suggested that bariatric surgery may be a viable option for patients with cirrhosis and extreme obesity[49]. Furthermore, Chalasani *et al*[3]was involved in research on the treatment of NASH using saroglitazar[50], belapectin[51], and OCA[34,48].

Co-cited references

There are 309771 co-cited references on research on the therapy for NAFLD over the past 12 years. In the top 10 co-cited references, all references were co-cited more than 550 times. We selected references with co-citation ≥ 20 for the construction of the co-citation network map (Figure 3F). Four articles occupied an important position and became the center of the co-citation network diagram. They were Kleiner *et al*[52], Younossi *et al*[33], Sanyal *et al*[30], and Chalasani *et al*[3]. The most cited country is the United States (Figure 3G).

Table 1 Reported clinical results of neoadjuvant immunotherapy for resectable esophageal squamous cell carcinoma

Ref.	Year	Title	LCS	GCS
Musso *et al*[93]	2010	A meta-analysis of randomized trials for the treatment of nonalcoholic fatty liver disease	213	410
Sanyal *et al*[30]	2010	Pioglitazone, vitamin E, or placebo for nonalcoholic steatohepatitis	986	2063
Promrat *et al*[35]	2010	Randomized controlled trial testing the effects of weight loss on nonalcoholic steatohepatitis	426	832
Ratziu *et al*[22]	2010	A position statement on NAFLD/NASH based on the EASL 2009 special conference	245	731
Lavine *et al*[94]	2011	Effect of vitamin E or metformin for treatment of nonalcoholic fatty liver disease in children and adolescents: the toninc randomized controlled trial	363	711
Musso *et al*[105]	2012	Impact of current treatments on liver disease, glucose metabolism and cardiovascular risk in non-alcoholic fatty liver disease: A systematic review and meta-analysis of randomised trials	224	435
Mudaliar *et al*[96]	2013	Efficacy and safety of the farnesoid X receptor agonist obeticholic acid in patients with type 2 diabetes and nonalcoholic fatty liver disease	234	631
Neuschwander-Tetri *et al*[31]	2015	Farnesoid X nuclear receptor ligand obeticholic acid for non-cirrhotic, non-alcoholic steatohepatitis (FLINT): a multicentre, randomised, placebo-controlled trial	586	1416
Rinella *et al*[32]	2015	Nonalcoholic fatty liver disease: A systematic review	403	1443
Buzzetti *et al*[97]	2016	The multiple-hit pathogenesis of NAFLD	538	1386
Boursier *et al*[98]	2016	The severity of nonalcoholic fatty liver disease is associated with gut dysbiosis and shift in the metabolic function of the gut microbiota	213	717
Cusi *et al*[106]	2016	Long-term pioglitazone treatment for patients with nonalcoholic steatohepatitis and prediabetes or type 2 diabetes mellitus: A randomized trial	277	525
Ratziu *et al*[107]	2016	Elafibranor, an agonist of the peroxisome proliferator-activated receptor-α and-δ, induces resolution of nonalcoholic steatohepatitis without fibrosis worsening	350	642
Armstrong *et al*[36]	2016	Liraglutide safety and efficacy in patients with non-alcoholic steatohepatitis (LEAN): A multicentre, double-blind, randomised, placebo-controlled phase 2 study	529	1006
Friedman *et al*[37]	2018	Mechanisms of NAFLD development and therapeutic strategies	550	1526
Younossi *et al*[33]	2018	Global burden of NAFLD and NASH: Trends, predictions, risk factors and prevention	739	2379
Younossi[56]	2019	Non-alcoholic fatty liver disease-a global public health perspective	243	906
Younossi *et al*[6]	2019	Global perspectives on nonalcoholic fatty liver disease and nonalcoholic steatohepatitis	254	808
Younossi *et al*[34]	2019	Obeticholic acid for the treatment of non-alcoholic steatohepatitis: interim analysis from a multicentre, randomised, placebo-controlled phase 3 trial	263	541

EASL: European association for the study of the liver; GCS: Global cited documents; LCS: Local cited documents; NAFLD: Nonalcoholic fatty liver disease; NASH: Nonalcoholic steatohepatitis.

Keywords with citation bursts and clustered network

Keywords with citation bursts refers to those keywords or topics that are frequently discussed in a certain field over a period of time. In our study, 25 keywords with strong citation bursts were identified by R package "bibliometrix" (Figure 4A). Judging from the top 25 keywords with the strongest citation bursts, the whole period can be divided into two: Period I (2010-2017) and period II (2019-2023). Keywords in period I primarily included MetS, insulin resistance, lifestyle intervention, and focus on pathogenesis such as lipid peroxidation. Subsequently, keywords in period II primarily included traditional Chinese medicine, network pharmacology, lifestyle modification, autophagy, and gut microbiota. Cluster analysis of the keyword timeline graph built by CiteSpace showed the evolution of high-frequency keywords (Figure 4B).

Co-occurrence analysis of author keywords

Through the co-occurrence analysis of author keywords (n = 12665), we could quickly capture research hotspots in a certain field. Table 3 showed the top 20 high-frequency keywords excluding the name of the disease (such as NAFLD, MAFLD, NASH, *etc*) for publications regarding therapy for NAFLD. Among these keywords, obesity, insulin resistance, inflammation, and MetS appeared more than 500 times, which represented the main research direction of therapy for NAFLD. We filtered keywords with the number of occurrences ≥ 20 and performed cluster analysis through VOSviewer (Figure 4C). We obtained five clusters representing five research directions. The keywords in red clusters consisted of inflammation, oxidative stress, lipid metabolism, high-fat diet, lipogenesis, macrophages, *etc*. The keywords in yellow clusters consisted of gut microbiota, probiotics, bile acids, *etc*. The keywords in blue clusters consisted of vitamin E, weight loss, diet, *etc*. The keywords in purple clusters consisted of obesity, MetS, insulin resistance, metformin, adiponectin, diabetes, liraglutide, *etc*. The keywords in green clusters consisted of HCC, fibrosis, cirrhosis, live

Table 2 Top 25 references with strong citations

Rank	Ref.	Year	Primary research content	Strength	Beginning	Ending
1	Sanyal *et al*[30]	2010	Vitamin E showed improvement in nonalcoholic steatohepatitis in adults without diabetes	161.62	2010	2015
2	Chalasani *et al*[3]	2018	The diagnosis and management of nonalcoholic fatty liver disease practice guideline	150.14	2013	2017
3	Neuschwander-Tetri *et al*[31]	2015	Obeticholic acid improved the histological features of nonalcoholic steatohepatitis	102.84	2016	2020
4	Vernon *et al*[111]	2011	Systematic review: The epidemiology and natural history of NAFDL and NASH in adults	97.78	2012	2016
5	Chalasani *et al*[2]	2012	A practice guideline of the diagnosis and management of NAFLD	87.88	2013	2017
6	Williams *et al*[116]	2011	Prevalence of NAFLD was higher than estimated, especially in hispanics and diabetes patients	82.64	2012	2016
7	Promrat *et al*[35]	2010	Weight reduction achieved through lifestyle intervention led to improvements in liver histology in NASH	80.62	2011	2015
8	Vilar-Gomez *et al*[11]	2015	NASH resolution/fibrosis regression occurred in patients with ≥ 10% weight loss induced by lifestyle changes	77.63	2016	2020
9	Lavine *et al*[94]	2011	Neither vitamin E nor metformin was effective in reducing ALT in patients with pediatric NAFLD	76.39	2012	2016
10	Rinella *et al*[32]	2015	A systematic review of NAFLD	73.68	2016	2020
11	Cohen *et al*[101]	2011	NAFLD is strongly associated with obesity and insulin resistance	72.23	2012	2016
12	Angulo *et al*[110]	2015	Fibrosis stage was associated with long-term overall mortality, liver transplantation, and liver-related events	71.71	2016	2020
13	Ratziu *et al*[22]	2010	Collaboration between hepatologists and specialists in the endocrine, nutritional, and cardiology fields should be encouraged to optimize clinical management	62.53	2011	2015
14	Targher *et al*[7]	2010	NAFLD was associated with an increased risk of cardiovascular disease	58.16	2011	2015
15	Byrne *et al*[5]	2015	NAFLD is a multisystem disease, affecting extrahepatic organs and regulatory pathways	57.94	2016	2020
16	Ekstedt *et al*[108]	2015	Fibrosis stage predicted both overall and disease-specific mortality	57.38	2016	2020
17	Wong *et al*[109]	2015	NASH has been predicted to become the leading indication for liver transplantation	54.86	2016	2020
18	Anstee *et al*[112]	2013	NAFLD is associated with liver-related morbidity and mortality and an increased risk of developing cardiovascular disease and T2DM	50.86	2014	2018
19	Younossi *et al*[53]	2016	As the global epidemic of obesity fuels metabolic conditions, the clinical and economic burden of NAFLD will become enormous	125.36	2018	2021
20	Loomba *et al*[114]	2013	The epidemiology and demographic characteristics of NAFLD vary worldwide	63.19	2015	2018
21	Tilg *et al*[115]	2010	Many parallel hits derived from the gut and/or the adipose tissue may promote liver inflammation. endoplasmic reticulum stress and related signaling networks, (adipo) cytokines, and innate immunity are emerging as central pathways that regulate key features of NASH	58.39	2012	2015
22	Buzzetti *et al*[97]	2016	The multiple-hit pathogenesis of NAFLD	49.79	2018	2021
23	Eslam *et al*[102]	2020	A diagnosis of MAFLD requires positive criteria	75.68	2021	2023
24	Eslam *et al*[10]	2020	Renaming NAFLD to MAFLD was proposed to accelerate the translational path to new treatments	68.10	2021	2023
25	Newsome *et al*[103]	2021	Treatment with semaglutide resulted in a higher percentage of NASH resolution than placebo	55.16	2021	2023

ALT: Alanine aminotransferase; MAFLD: Metabolic dysfunction-associated fatty liver disease; NAFLD: Nonalcoholic fatty liver disease; NASH: Nonalcoholic steatohepatitis; T2DM: Type 2 diabetes mellitus.

transplantation, immunotherapy, *etc*.

Trend topic analysis

The trend topic analysis of the keywords showed that from 2010 to 2016, the research focused on diet, lifestyle intervention, vitamin E, *etc*. Since 2017, researchers have begun to focus on MetS and actively explore the precise

Table 3 Top 20 high-frequency keywords (excluding the name of disease)

Rank	Keyword	Occurrence
1	Obesity	898
2	Insulin resistance	684
3	Inflammation	670
4	Metabolic syndrome	547
5	Oxidative stress	444
6	Steatosis	418
7	Fibrosis	414
8	Hepatocellular carcinoma	306
9	Lipid metabolism	304
10	Gut microbiota	260
11	Diabetes	258
12	Cirrhosis	241
13	Treatment	177
14	Autophagy	165
15	High-fat diet	141
16	Bariatric surgery	124
17	Cardiovascular disease	123
18	Metformin	121
19	Apoptosis	118
20	Lipogenesis	118

diagnosis and effective treatment for NAFLD. Since the suggestion of renaming NAFLD to MAFLD in 2020, the main keywords were insulin resistance, obesity, inflammation, microbiome, OCA, *etc*. It is worth noting that gut microbiota, gut-liver axis, and traditional Chinese medicine are the latest trending topics (Figure 4D).

DISCUSSION

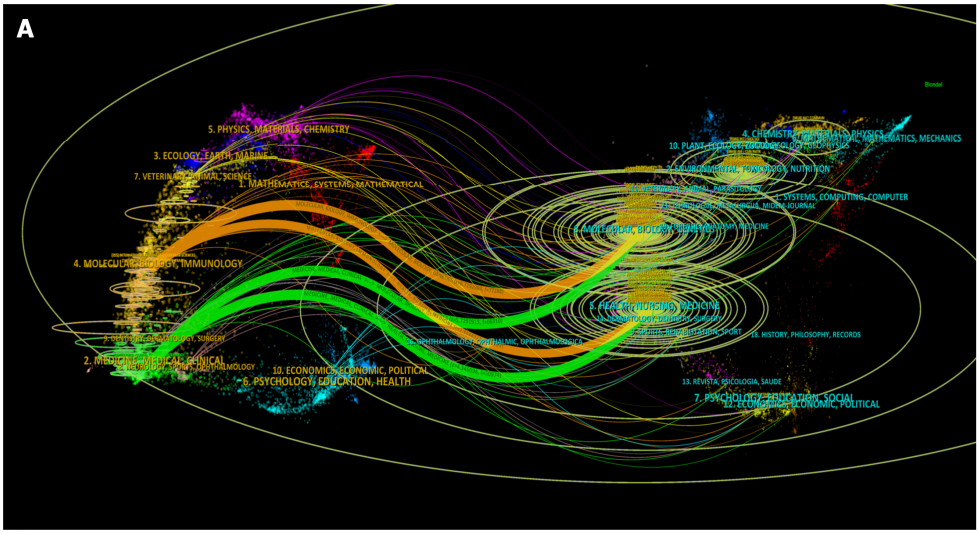
General information

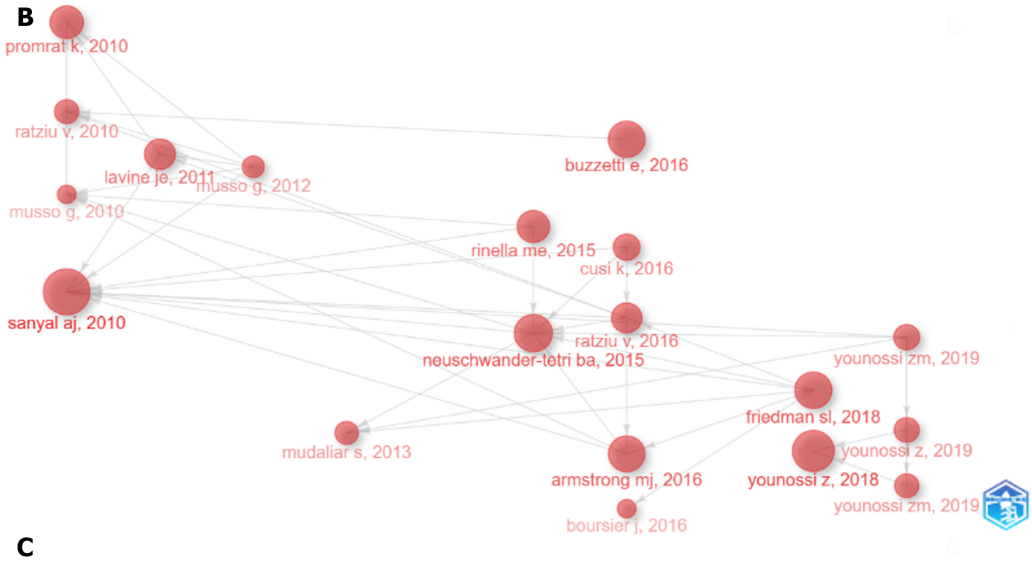
Since 2010, the annual publications regarding NAFLD treatment have increased, particularly in the past 5 years. The number of related studies has also grown rapidly, indicating that research on NAFLD treatment is in an explosive period, and China and the United States are the leading countries studying the treatment of NAFLD. The United States has been the largest center for publications on the treatment of NAFLD worldwide. However, 2020 was a turning point when the number of publications from China exploded. The cumulative number of publications from China surpassed those from the United States in 2022. China accounts for 70% of the top 10 research institutions regarding publication volume, and the remaining institutions are in the United States. University of California San Diego has been a leader in the NAFLD field; however, research institutions in China have developed rapidly in recent years.

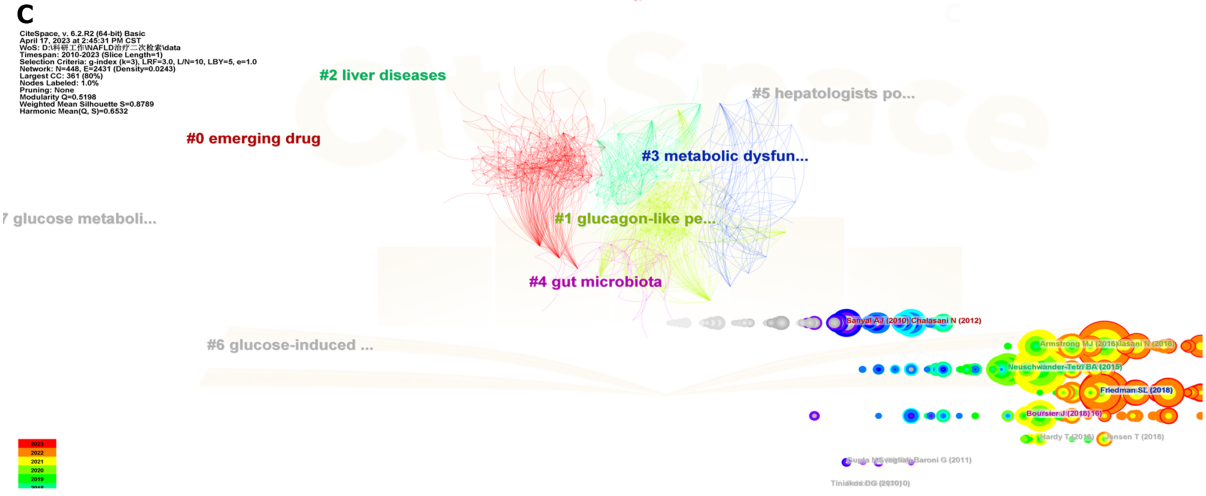
China is developing rapidly in the NAFLD field, surpassing the United States in the number of related publications. There are several reasons for this, which we analyzed below.

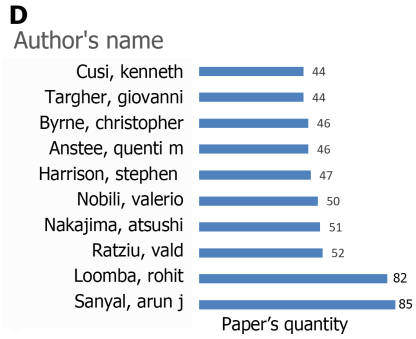
The first reason is that the incidence of NAFLD is increasing in China. The global prevalence of NAFLD is 25.2%[53] and 29.2% in China. This has increased rapidly (2008-2010: 25.4%; 2015-2018: 32.3%)[54]. Over the past 20 years, the economic development, urbanization, and dietary patterns in China have changed (*e.g.*, increased consumption of animal-derived foods, refined grains, and highly processed, high-sugar, and high-fat foods)[55]. This has led to sedentary lifestyles and overnutrition, undergirding obesity and the NAFLD epidemic[56].

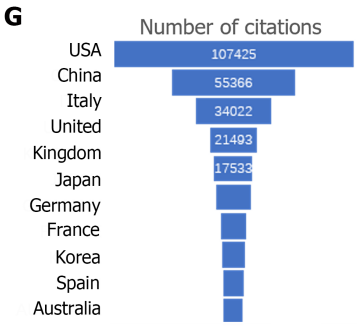
The second reason is that the burden of NAFLD in China will continue to increase. With the development of the global economy, the global prevalence of NASH will increase by 15%-56%, and the highest prevalence of NAFLD is expected to occur in China[6]. The Chinese population is large, and the burden of the disease increases exponentially[57,58]. In a NAFLD disease burden modeling analysis, it was estimated that by 2030, the NASH population in China is expected to increase by 48% compared to that in 2016 (48.26 million), with an 86% increase in HCC (14090)[59].

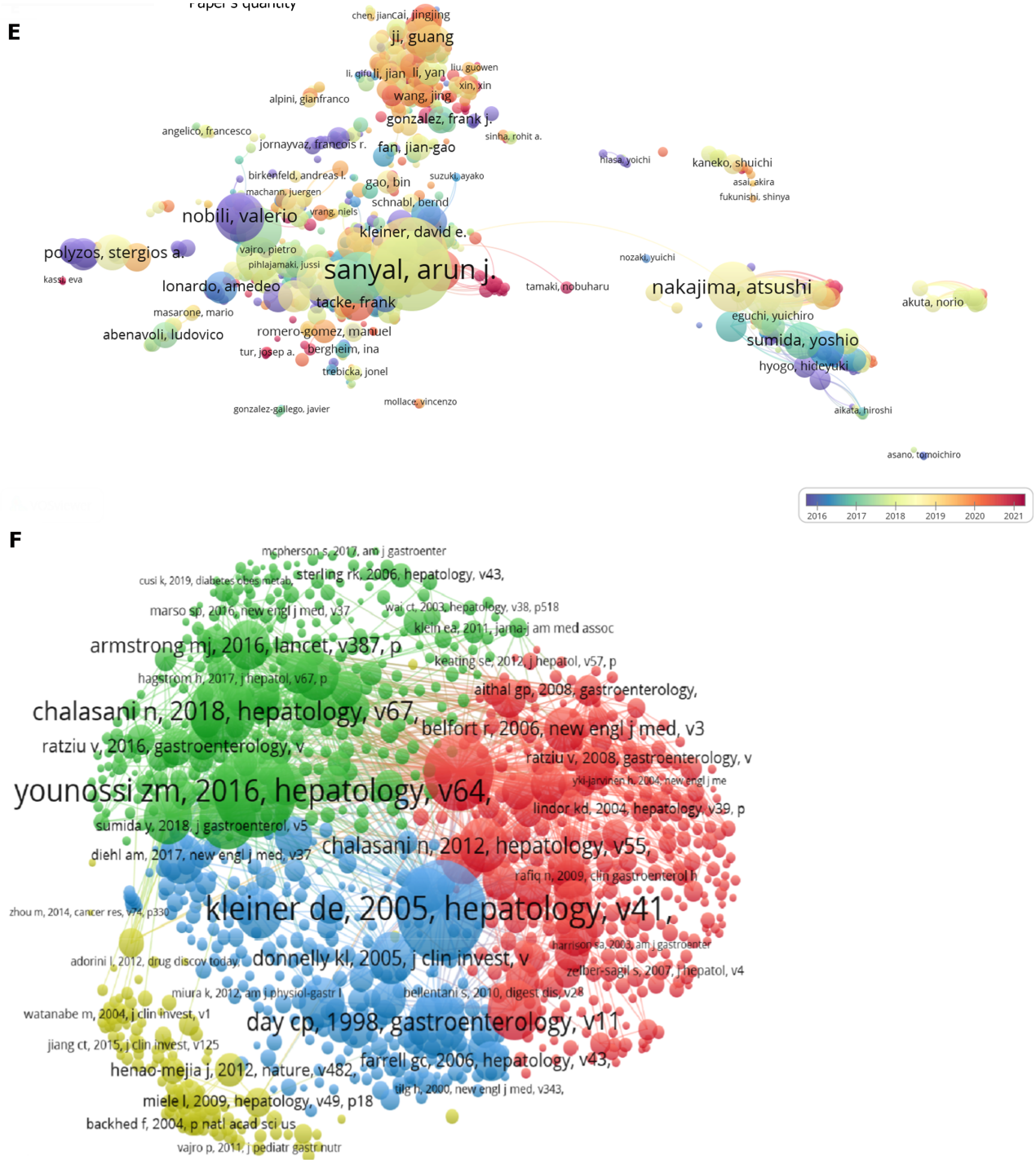

A
5. PHYSICS, MATERIALS, CHEMISTRY
3. ECOLOGY, EARTH, MARINE
7. VETERINARY, ANIMAL, SCIENCE
1. MATHEMATICS, SYSTEMS, MATHEMATICAL
4. MOLECULAR, BIOLOGY, IMMUNOLOGY
2. MEDICINE, MEDICAL, CLINICAL
10. ECONOMICS, ECONOMIC, POLITICAL
6. PSYCHOLOGY, EDUCATION, HEALTH
4. CHEMISTRY, MATERIALS, PHYSICS, MATHEMATICS, MECHANICS
10. PLANT, ECOLOGY, ZOOLOGY, BIOLOGY, MICROBIOLOGY
2. ENVIRONMENTAL, TOXICOLOGY, NUTRITION
1. SYSTEMS, COMPUTING, COMPUTER
4. MOLECULAR, BIOLOGY, IMMUNOLOGY, MEDICINE
8. HEALTH, NURSING, MEDICINE
18. HISTORY, PHILOSOPHY, RECORDS
13. REVISTA, SOCIOLOGIA, SAUDE
7. PSYCHOLOGY, EDUCATION, SOCIAL
10. ECONOMICS, ECONOMIC, POLITICAL


B
promrat k, 2010
ratziu v, 2010
lavine je, 2011
musso g, 2012
musso g, 2010
sanyal aj, 2010
buzzetti e, 2016
rinella me, 2015
cusi k, 2016
ratziu v, 2016
neuschwander-tetri ba, 2015
younossi zm, 2019
friedman sl, 2018
younossi z, 2019
younossi z, 2018
younossi zm, 2019
mudaliar s, 2013
armstrong mj, 2016
boursier j, 2016


C
CiteSpace, v. 6.2.R2 (64-bit) Basic
April 17, 2023 at 2:45:31 PM CST
Timespan: 2010-2023 (Slice Length=1)
Selection Criteria: g-index (k=3), LRF=3.0, L/N=10, LBY=5, e=1.0
Network: N=448, E=2431 (Density=0.0243)
Largest CC: 361 (80%)
Nodes Labeled: 1.0%
Pruning: None
Modularity Q=0.5198
Weighted Mean Silhouette S=0.8789
Harmonic Mean(Q, S)=0.6532
#2 liver diseases
#5 hepatologists po...
#0 emerging drug
#3 metabolic dysfun...
7 glucose metaboli...
#1 glucagon-like pe...
#4 gut microbiota
#6 glucose-induced ...
Sanyal AJ (2010) Chalasani N (2012)
Armstrong MJ (2016) Hasani N (2016)
Neuschwander-Tetri BA (2015)
Friedman SL (2018)
Boursier J (2016)
Vilar-Gomez E (2015)
Younossi ZM (2019)
Hansen T (2018)
Younossi Z (2018)
Vilar-Gomez E (2015)
Baroni G (2011)
Tiniakos DG (2010)


D
Author's name
Cusi, kenneth 44
Targher, giovanni 44
Byrne, christopher 46
Anstee, quenti m 46
Harrison, stephen 47
Nobili, valerio 50
Nakajima, atsushi 51
Ratziu, vald 52
Loomba, rohit 82
Sanyal, arun j 85
Paper's quantity


G
Number of citations
USA 107425
China 55366
Italy 34022
United Kingdom 21493
Japan 17533
Germany
France
Korea
Spain
Australia



DOI: 10.3748/wjg.v29.i37.5339 **Copyright** ©The Author(s) 2023.

Figure 3 Research trends. A: Dual-map overlay of journals publishing studies on the therapy for nonalcoholic fatty liver disease; B: Historiograph; C: Co-citation network of reference cluster analysis; D: Paper's quantity of most relevant authors; E: Visualization of relevant authors; F: Visualization of co-cited references; G: Most cited country.

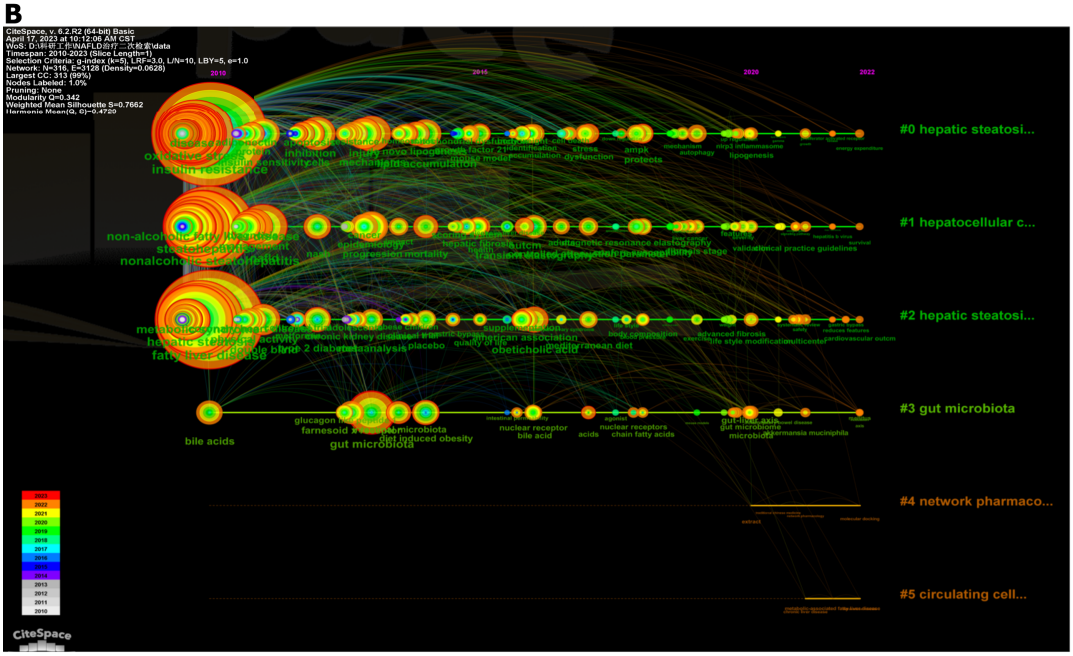
The third reason is that MetS is a significant public health problem in China[60]. MetS is the strongest risk factor for NAFLD and NASH. The association between NAFLD and MetS may be bidirectional, particularly for diabetes and systemic hypertension, while traditional Chinese culinary culture (high in fat, salt, and fiber) adversely affects these diseases. Given the two-way causal relationship between NAFLD and type 2 diabetes mellitus, a rapid increase in diabetes and obesity rates directly leads to an increase in the prevalence of NAFLD[61].

The fourth reason is that the prevalence of hepatitis B in China has decreased. China has the highest prevalence of hepatitis B. However, government control measures, effective hepatitis B virus vaccination, and standardized anti-hepatitis B virus treatment have had a positive impact on decreasing the prevalence. Hepatitis B in China has been largely controlled, making chronic liver disease caused by NAFLD increasingly prominent.

A

Keywords	Year	Strength	Begin	End	2010-2023
Metabolic syndrome	2010	63.88	2010	2013	
Placebo controlled trial	2010	35.06	2010	2016	
Natural history	2010	31.34	2010	2015	
Term follow up	2010	23.89	2010	2016	
Life style intervention	2010	23.74	2010	2014	
Risk factors	2010	22.99	2010	2015	
Randomized controlled trial	2010	20.1	2010	2017	
Alanine aminotransferase	2010	16.9	2010	2013	
Necrosis factor alpha	2010	16.51	2010	2016	
Chronic hepatitis C	2010	15.92	2010	2016	
Coronary heart disease	2010	15.55	2010	2015	
Vitamin E	2010	15.44	2010	2014	
Cryptogenic cirrhosis	2010	15.35	2010	2016	
Gamma glutamyl transferase	2010	15.35	2010	2016	
Follow up	2010	15.24	2010	2016	
Activated protein kinase	2010	14.62	2010	2016	
Nonalcoholic steatohepatitis	2010	14.39	2010	2011	
Ursodeoxycholie acid	2010	12.86	2010	2014	
Fatty liver	2010	19.87	2011	2013	
Magnetic resonancs clastography	2018	13.27	2018	2020	
Gut microbiota	2013	23.85	2021	2023	
Traditional chinese medicine	2021	13.75	2021	2023	
Network pharmacology	2021	13.59	2021	2023	
Obeticholic acid	2016	12.88	2021	2023	
Clinical practice guidelines	2021	12.82	2021	2023	

B



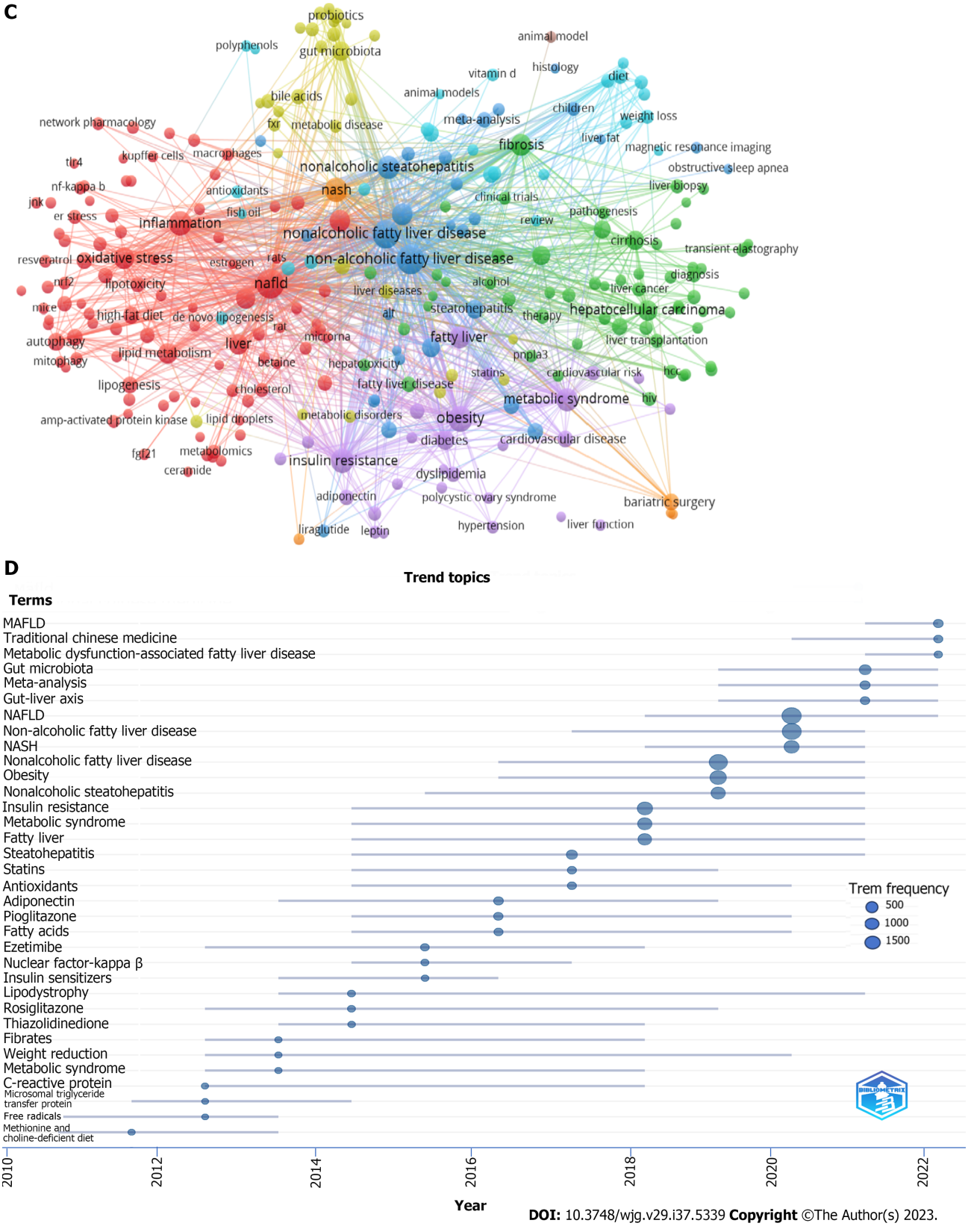


Figure 4 Research hotspots. A: Keywords with the strongest burst strength; B: Timeline cluster analysis; C: Co-occurrence author keyword; D: Trend topics.

The fifth reason is that the government attached importance to scientific research and improved the level of scientific research. In 2010, China spent less than half the amount on research and development as the United States (208280000 USD *vs* 444709000 USD) (https://data.oecd.org/rd/gross-domestic-spending-on-r-d.htm). Recently, due to economic development and robust government support, China has become the world's second-largest industry research and development center, with its total research and development expenditure reaching 80% of that of the United States' research and development expenditure (631845000 USD) in 2019 (https://www.oecd.org/sti/msti-highlights-march-

2021.pdf). Over the years, basic and clinical research on liver disease in China has been listed as a priority investment area by the National Natural Science Foundation of China (NSFC). From 2010 to 2022, the total number of research projects related to fatty liver funded by the NSFC was 7515, with a total funding of 535000000 USD. The number of projects and funding provided by the NSFC has increased annually. During the same period the National Institutes of Health in the United States funded 3304 projects (1267000000 USD) in the field of fatty liver disease. Although the investment gap between China and the United States is still significant, the number of NSFC-funded projects has surpassed that of the United States.

The final reason is the emphasis on traditional medicine. The NSFC has funded 960 projects related to traditional Chinese medicine and integrated traditional Chinese medicine and western medicine, while there are few funded projects related to traditional medicine in the United States. This also reflects the advantages and characteristics of the fatty liver research field in China. For example, Shanghai University of Traditional Chinese Medicine systematically and comprehensively analyzes the multitarget mechanism of action of traditional Chinese medicine compounds[62-64] and explores the metabolite-target-disease network of traditional Chinese medicine[65-67] in the treatment of NAFLD. The concept of multitarget therapy with traditional Chinese medicine compounds is consistent with the multiple pathogeneses of NAFLD. It is challenging for a single drug to address the diversity of the pathogenesis of NAFLD. Therefore, traditional Chinese medicine and compound multitarget active ingredients may usher in a new era in the treatment of NAFLD.

Although the number of publications in China has grown rapidly in recent years, the citation volume is still relatively low. Possible causes are: (1) Insufficient international cooperation in China. China's SCP ratio was as high as 87.4%, the highest among all countries; (2) the international discourse of China in this field needs to be improved. The top experts in this field are all American scholars who have decades of experience in the field. Their research directions are focused and deep, which allows the publication of their research in top journals. Conversely, researchers in China lack international academic authority and have few articles published in top journals; and (3) the quality and innovation of publications needs to be improved. Research in China is primarily basic, and there is a lack of multicenter randomized controlled trials and large-sample prospective cohort studies with high clinical evidence levels.

Although Chinese scientists are not ranked high regarding personal influence, they are ranked second only to the United States in the ranking of cited countries, which indicates that the overall scientific research strength in China cannot be underestimated. The top 30 cited Chinese studies focused on epidemiology[59,61,68,69], basic research, particularly pathogenesis[70-76], the search for therapeutic targets[77-89], in vitro tests[76,82,86], animal experiments[87-89], and review articles[81,83]. At present, most data on drug treatment originate from foreign research, and there is a lack of research on the Chinese population. This is an important direction that needs to be addressed in future research on NAFLD treatments in China.

Most studies on NAFLD treatment have been published in the International Journal of Molecular Sciences (IF = 6.208, second quartile), indicating that it is currently the most popular journal in this field of research. Among the top 20 journals, Nature Reviews Gastroenterology and Hepatology (IF = 73.082) had the highest IF. For co-cited journals, we found that most were high-impact top quartile journals. These high-quality international journals provide research support for the treatment of NAFLD. Among them, Hepatology and Journal of Hepatology are the most popular co-cited journals, indicating the high quality of the journal in the field of NAFLD research. Additionally, the research results in molecular/biology/immunology journals mainly flow to molecular/biology/genetic and health care/medical journals, which also indicates that the development of therapeutics is inseparable from basic research fields such as molecular biology, genetics, and immunity. The articles in the field of NAFLD treatment research have been cited by medical/clinical journals, which illustrates the clinical application value of treatment research.

Historiography analysis

Co-cited references are regarded as the basis of research in a certain field, and the development and evolutionary dynamics of a discipline can be explored by studying co-cited networks[90,91]. We selected the 10 most co-cited articles to determine the research basis for the treatment of NAFLD. Among the 309771 cited publications, the design and validation of the histology scoring system for NAFLD published by Kleiner *et al*[52] in 2005 was the most cited study. The top 10 citations covered five main topics: diagnosis; epidemiology[33,53]; pathogenesis; therapeutic drug development[30,31]; and review of NAFLD[92]. Epidemiology is the exploration of disease prevalence and incidence[33], global burden trend prediction and prevention[53], and the overall understanding of the disease. The standardization of diagnostic methods [3,52] is a prerequisite for disease management and guiding treatment. The exploration of pathogenesis[37,92] is conducive to the development of new drugs and individualized and precise treatment. Vitamin E, pioglitazone[30], and OCA[31] are the most promising NAFLD therapeutics in development. These main topics also reflect the evolution of NAFLD drug research directions.

Historiography analysis is commonly described as "the history of history" and seeks to explain origins and evolution providing a clearer understanding of the future. Results from the first randomized controlled trial in 2010 of adult NASH patients using lifestyle modification as an active therapeutic intervention suggested that lifestyle changes focused on diet, exercise, and behavioral changes could successfully improve overall histological activity, degree of steatosis, and liver chemistry of NASH[35]. Weight loss, physical activity, reduction of a sedentary lifestyle, and dietary changes should be treated as the first-line treatment of NAFLD/NASH and assessed after 6 mo. If this is not effective, then additional treatment options, such as medication, may be considered[30].

Simultaneously, it was hypothesized that oxidative stress dealt a second "blow" to the liver, and there was a strong correlation between the severity of NASH and the degree of oxidative stress. However, the results from antioxidant treatment are inconsistent in the treatment of NAFLD[93]. Only vitamin E, through inhibiting fatty acid oxidation, is superior to placebo in the treatment of NAFLD[30]. NAFLD/NASH is closely related to the global diabetes and obesity epidemics. Some hypoglycemic drugs, such as metformin, can improve aminotransferase levels, and pioglitazone can

improve steatohepatitis (recommended NASH regimen: pioglitazone or vitamin E combined with high-dose ursodeoxycholic acid)[30]. However, in 2011, it was found that neither vitamin E nor metformin was superior to placebo for the primary outcome of a sustained reduction in alanine aminotransferase levels in children with NAFLD[94]. A 2012 meta-analysis noted that vitamin E improved histological indices after 2 years of use, but increased insulin resistance and plasma triacylglycerol were observed. Long-term use may increase the risk of prostate cancer, and there is a lack of efficacy in reducing liver fibrosis[37]. In patients who did not respond to lifestyle interventions, pioglitazone improved histological disease activity, slowed fibrosis progression, and broadly improved the cardiometabolic endpoints[95]. However, the use of thiazolidinediones has been limited by adverse effects, such as weight gain, fluid retention, increased risk of fractures (particularly in older women), and bladder cancer.

OCA is a semi-synthetic derivative of human cholic acid, which is a natural agonist of farnesoid X receptors. Farnesoid X receptors are nuclear hormone receptors that regulate glycolipid metabolism, can block the conversion of cholesterol to bile acids, increase serum cholesterol concentration, and promote the reverse transport of cholesterol from tissues. A phase 2 trial in 2013[96] and a multicenter randomized controlled trial in 2015 confirmed that OCA was well tolerated in the treatment of NAFLD, increased insulin sensitivity and weight loss, and reduced markers of liver inflammation and fibrosis[31]. An interim analysis of a phase 3 clinical trial in 2019 concluded that 25 mg/day of OCA resulted in significant histological improvements in NASH[34] and unfortunately in itching and a moderate increase in low-density lipoprotein cholesterol.

The 2016 "two-hit" hypothesis became obsolete, and the "multiple blows" hypothesis more accurately explained the pathogenesis of NAFLD, which includes insulin resistance, hormones secreted by adipose tissue, nutritional factors, gut microbiota, and genetic and epigenetic factors[97]. In 2016, Buzzetti *et al*[97] evaluated the association between intestinal dysbiosis and liver fibrosis in human NAFLD and found that animal diets favor the accumulation of branched-chain fatty acids of *Bacteroides*, thereby promoting insulin resistance and increasing the risk of NASH. The diet of agricultural societies is rich in fiber, starch, and plant polysaccharides, which promotes the abundance of *Prevobacterium*, and its abundance decreases with an increase in liver lesions. A gut microbiota analysis provided a theoretical basis for NAFLD patients to regulate diet structure and intestinal microbial preparations[98].

In 2018, probiotics containing endotoxin antibodies and bovine colostrum were evaluated for their efficacy in the treatment of NASH by enhancing brown adipose tissue to burn glucose and ameliorate obesity and glucose abnormalities [37]. Insulin resistance has long been considered an important component of the pathogenesis of NAFLD and worsens as the disease progresses. GLP-1 analogs reduce hepatic steatosis, liver enzyme concentrations, and insulin resistance by inducing insulin secretion and reducing glucagon secretion in a glucose-dependent manner. Armstrong *et al*[36] reported the effects of GLP-1 analogs on liver histology in patients with NASH in a randomized, placebo-controlled trial. Liraglutide was well tolerated in this study, improving several key components of MetS, including weight and glycemic control, and improving NASH histology.

The pathogenesis of NAFLD involves multiple drivers, and no more than 40% of patients in clinical trials have shown benefits from monotherapy, which is likely insufficient to prompt regulatory approval of monotherapy for long-term treatment of NAFLD. Current research favors combination therapies including drug combinations, single-agent searches for multitarget effects[99], and comorbidities in patients with NAFLD. We hypothesize that NAFLD has progressed to become the most common cause of chronic liver disease worldwide[57]. The global burden of NAFLD and NASH is growing rapidly. Future research should focus on accurate non-invasive measurement of biomarkers and clarification of pathogenic pathways, which will facilitate the development and effective evaluation of the efficacy of new drugs. Simultaneously, we continue to actively explore effective treatments, including the development of effective treatments for patients with NASH and prevention methods for individuals at high risk of progression[56].

Research trends and hotspots

Citation bursts represent emerging topics in a particular field of study[100]. Based on the main research content[5,30,97,100,101] of the strongly cited burst references (Table 2), we found that renaming NAFLD to MAFLD[10,102] and the development of semaglutide for NAFLD treatment[103] may represent the main hotspots of current NAFLD treatment research. Both of these topics were cited in 2021. As shown in Table 2, 16 of the 25 citations were reviewed, and high-quality reviews reflected understanding of the disease at a certain time. With the exploration of the pathogenesis of NAFLD, the naming and diagnosis of the disease have been gradually updated and standardized[104], and its treatment strategy has gradually evolved from vitamin E, weight loss, and lifestyle interventions[105] for the management of metabolism-related diseases[106,107].

In addition to citation bursts, keywords can also quickly capture the distribution and evolution of hot topics in our research field. The top keywords from the last 2 years included gut microbiota, traditional Chinese medicine, network pharmacology, OCA, and clinical practice guideline. In keyword trend topic analysis, it was evident that MAFLD, traditional Chinese medicine, gut-liver axis, and gut microbiota were the most frequently discussed keywords. Interestingly, insulin sensitizers such as pioglitazone for the treatment of fatty liver were popular in 2012, reached their peak from 2014 to 2016, and gradually faded in 2020.

Due to the complex pathogenesis of NAFLD, it is challenging to treat[108-110]. Effective treatment requires precise localization based on the patients' phenotype[111] and genetic background[10]. The study of treatment strategies[112,113], epidemiological knowledge[114], pathogenesis[115], and precise diagnosiss[116] (including non-invasive diagnostic techniques) may all be integrated into the consideration of heterogeneity in disease treatment. The current mainstream view is to replace the diagnosis of NAFLD/NASH with MAFLD. Hence, this name change has greatly promoted the transformation of the treatment strategy of the disease. The previous treatment plan mainly included two directions: (1) Correction of insulin resistance and reduction of fat mass with a focus on lifestyle changes for weight loss, including physical activity, diet, insulin sensitizers, and anti-obesity surgery; and (2) prevention/reversal of lipotoxicity-induced

hepatocellular damage by inhibiting lipid peroxidation and oxidative stress or by using anti-inflammatory, anti-apoptotic, or other hepatoprotective agents.

Future therapeutic research on NAFLD/MAFLD should focus on comprehensive therapies tailored to individual patients, considering the above two therapeutic directions, and targeting multitarget and multiaction mechanisms[29]. Research on gut microbiomes and traditional medicine will continue to be a short-term research hotspot. With the official name change to MASLD[117], more emphasis was given to the management of associated comorbid, particularly metabolic abnormalities. OCA, which has entered phase 3 clinical validation, and semaglutide, which is currently under study, are likely to become the first approved drugs for the treatment of NAFLD. A clinical trial called Semaglutide treatment in the real-world for fibrosis due to NAFLD in obesity and type 2 diabetes mellitus (SAMARA) to evaluate the efficacy of semaglutide in improving liver scarring associated with NAFLD is currently ongoing in the US. Once SAMARA is completed, a larger multi-centred global trial may follow.

Advantages and shortcomings: This study had several advantages. First, we systematically analyzed the research on NAFLD/MAFLD treatment through bibliometrics, which provided comprehensive guidance for scholars who are interested in related research. Second, we used three bibliometric tools simultaneously for the survey, hence our data analysis process was objective. Third, bibliometric analysis provided a more complete insight into hot topics and frontiers than traditional reviews.

This study also had some shortcomings. First, the data for this study was extracted from the Web of Science Core Collection database only. Other databases were not searched, and some relevant studies may have been missed. This may increase the risk of bias in the selection of the literature. Second, we filtered studies published in English, which means that non-English language papers were underestimated. In addition, the 2023 publication data was not fully included, resulting in insufficient statistics for 2023. The research directions of NAFLD/MAFLD therapeutic research, cluster analysis, and trend topic analysis may not be comprehensive and may not cover marginal and emerging topics. Last but not least, bibliometric analysis is an analytical method of bibliometrics that focuses on the analysis of measures such as the number of articles issued, cited and quoted, with particular consideration of research countries, institutions and individuals, but pays less attention to the content of the articles themselves; as such, it may not be able to detect and temporally count research for a new type of topic, especially for the beginning stage of a certain research field that may become a hot spot in the future.

CONCLUSION

The treatment of NAFLD has important research value and application prospects, as indicated by the rapidly increasing number of documents. The study of treatments and therapies for NAFLD, particularly NASH, is highly valued worldwide. The leading countries publishing NAFLD research are the United States and China. NAFLD research in China is developing rapidly, with their number of published articles quickly surpassing the United States in recent years. However, it is worth noting that most of the top scientists in the field are from the United States. Conducting an in-depth study of the pathogenesis can foster the development and research of new drugs, while accurate diagnosis, specifically through non-invasive diagnostic technology, contributes to better patient management and efficacy evaluation. The multiple-hit pathogenesis of NAFLD and the renaming of NAFLD to MAFLD require enhanced multidisciplinary and multicenter cooperation. Mechanism studies provide guidance for therapeutic strategies, while clinical application and treatment research represent the transformation of basic research.

ARTICLE HIGHLIGHTS

Research background

Nonalcoholic fatty liver disease (NAFLD) is a chronic disease that threatens the lives of numerous people globally. However, there are limited bibliometric statistical analyses on NAFLD. In this study, we conducted a bibliometric analysis to examine previous research on NAFLD, aiming to identify key contributors and assess the current research status in the field of liver health. Moreover, we identified prospects for future research trends and development.

Research motivation

The progression of NAFLD leads to liver fibrosis and end-stage cirrhosis. However, no treatment has been established. Many mechanistic studies and drug trials have been undertaken for the development of new drugs for NAFLD treatment. In particular, NAFLD was renamed metabolic dysfunction-associated fatty liver disease (MAFLD), and there was a major shift in treatment strategy. It is necessary to understand the knowledge structure of NAFLD through bibliometrics, focusing on research hotspots in order to explore the direction of development in this field.

Research objectives

The treatment of NAFLD has important research value and application prospects. It is anticipated that drugs may become available in the near future. However, no drugs are currently approved. Clinical phase 2b and phase 3 studies have achieved certain efficacy. While trends and hotspots can be clearly studied through bibliometric analysis, clues can reveal possible future therapeutic strategies for scholars in the field.

Research methods

Bibliometric analysis was applied to provide a comprehensive understanding of the knowledge structure of a research field, and visualization analysis was used to visualize the results. Historiography analysis, bursts and cluster analysis, co-occurrence analysis, and trend topic analysis were also utilized to reveal the knowledge structure and research hotspots in this field.

Research results

The bibliometric study identified recent research frontiers and hotspot directions, which will provide a valuable reference for scholars researching treatments for NAFLD. The leading countries publishing NAFLD research are the United States and China. The NAFLD research field in China has developed rapidly in the past 3 years.

Research conclusions

Research on the treatment and therapeutics of NAFLD, especially nonalcoholic steatohepatitis, is highly valued by the global academic community. It is likely that obeticholic acid, which has entered phase 3 clinical validation, and semaglutide, which is currently under study, will become the first approved drugs for the treatment of NAFLD.

Research perspectives

The multiple-hit pathogenesis of NAFLD and the renaming of NAFLD to MAFLD requires enhanced multidisciplinary and multicenter cooperation. More clinical trials are needed to verify the safety and efficacy of drugs and to discover new ones.

ACKNOWLEDGEMENTS

We would like to thank Hao Xing from Hefei Third Hospital and Xiaodan Hong, MD from the Second Hospital of Anhui Medical University for their comments on drafting the manuscript.

FOOTNOTES

Author contributions: Zhang ZH and Dai JJ conceived and designed the study; Dai JJ performed the research, analyzed the data and wrote the manuscript; Zhang ZH and Zhang YF supervised the study; All authors have read and approved the final manuscript as submitted.

Supported by National Science Foundation of China, No. 81273142; Anhui Provincial Natural Science Foundation, No. 2108085MH298; University Scientific Research Project of Anhui Provincial Education Department, No. KJ2021A0323; Fund of Anhui Medical University, No. 2021xkj196; Clinical Medicine project of Anhui Medical University, No. 2021LCXK027; The Second Hospital of Anhui Medical University Natural Science Foundation, No. 2019GMFY02.

Conflict-of-interest statement: The authors declare that they have no conflict of interest.

PRISMA 2009 Checklist statement: The authors have read the PRISMA 2009 Checklist, and the manuscript was prepared and revised according to the PRISMA 2009 Checklist.

Open-Access: This article is an open-access article that was selected by an in-house editor and fully peer-reviewed by external reviewers. It is distributed in accordance with the Creative Commons Attribution NonCommercial (CC BY-NC 4.0) license, which permits others to distribute, remix, adapt, build upon this work non-commercially, and license their derivative works on different terms, provided the original work is properly cited and the use is non-commercial. See: https://creativecommons.org/Licenses/by-nc/4.0/

Country/Territory of origin: China

ORCID number: Jin-Jin Dai 0009-0009-2072-9046; Ya-Fei Zhang 0000-0003-4594-186X; Zhen-Hua Zhang 0000-0002-8480-9004.

S-Editor: Qu XL
L-Editor: A
P-Editor: Cai YX

REFERENCES

1 **Ludwig J**, Viggiano TR, McGill DB, Oh BJ. Nonalcoholic steatohepatitis: Mayo Clinic experiences with a hitherto unnamed disease. *Mayo Clin Proc* 1980; **55**: 434-438 [PMID: 7382552]

2 **Chalasani N**, Younossi Z, Lavine JE, Diehl AM, Brunt EM, Cusi K, Charlton M, Sanyal AJ; American Gastroenterological Association; American Association for the Study of Liver Diseases; American College of Gastroenterologyh. The diagnosis and management of non-

alcoholic fatty liver disease: practice guideline by the American Gastroenterological Association, American Association for the Study of Liver Diseases, and American College of Gastroenterology. *Gastroenterology* 2012; **142**: 1592-1609 [PMID: 22656328 DOI: 10.1053/j.gastro.2012.04.001]

3 **Chalasani N**, Younossi Z, Lavine JE, Charlton M, Cusi K, Rinella M, Harrison SA, Brunt EM, Sanyal AJ. The diagnosis and management of nonalcoholic fatty liver disease: Practice guidance from the American Association for the Study of Liver Diseases. *Hepatology* 2018; **67**: 328-357 [PMID: 28714183 DOI: 10.1002/hep.29367]

4 **Stepanova M**, Kabbara K, Mohess D, Verma M, Roche-Green A, AlQahtani S, Ong J, Burra P, Younossi ZM. Nonalcoholic steatohepatitis is the most common indication for liver transplantation among the elderly: Data from the United States Scientific Registry of Transplant Recipients. *Hepatol Commun* 2022; **6**: 1506-1515 [PMID: 35224886 DOI: 10.1002/hep4.1915]

5 **Byrne CD**, Targher G. NAFLD: a multisystem disease. *J Hepatol* 2015; **62**: S47-S64 [PMID: 25920090 DOI: 10.1016/j.jhep.2014.12.012]

6 **Younossi Z**, Tacke F, Arrese M, Chander Sharma B, Mostafa I, Bugianesi E, Wai-Sun Wong V, Yilmaz Y, George J, Fan J, Vos MB. Global Perspectives on Nonalcoholic Fatty Liver Disease and Nonalcoholic Steatohepatitis. *Hepatology* 2019; **69**: 2672-2682 [PMID: 30179269 DOI: 10.1002/hep.30251]

7 **Targher G**, Day CP, Bonora E. Risk of cardiovascular disease in patients with nonalcoholic fatty liver disease. *N Engl J Med* 2010; **363**: 1341-1350 [PMID: 20879883 DOI: 10.1056/NEJMra0912063]

8 **Flegal KM**, Carroll MD, Kit BK, Ogden CL. Prevalence of obesity and trends in the distribution of body mass index among US adults, 1999-2010. *JAMA* 2012; **307**: 491-497 [PMID: 22253363 DOI: 10.1001/jama.2012.39]

9 **Golabi P**, Fukui N, Paik J, Sayiner M, Mishra A, Younossi ZM. Mortality Risk Detected by Atherosclerotic Cardiovascular Disease Score in Patients With Nonalcoholic Fatty Liver Disease. *Hepatol Commun* 2019; **3**: 1050-1060 [PMID: 31388626 DOI: 10.1002/hep4.1387]

10 **Eslam M**, Sanyal AJ, George J; International Consensus Panel. MAFLD: A Consensus-Driven Proposed Nomenclature for Metabolic Associated Fatty Liver Disease. *Gastroenterology* 2020; **158**: 1999-2014.e1 [PMID: 32044314 DOI: 10.1053/j.gastro.2019.11.312]

11 **Vilar-Gomez E**, Martinez-Perez Y, Calzadilla-Bertot L, Torres-Gonzalez A, Gra-Oramas B, Gonzalez-Fabian L, Friedman SL, Diago M, Romero-Gomez M. Weight Loss Through Lifestyle Modification Significantly Reduces Features of Nonalcoholic Steatohepatitis. *Gastroenterology* 2015; **149**: 367-78.e5; quiz e14 [PMID: 25865049 DOI: 10.1053/j.gastro.2015.04.005]

12 **Hallsworth K**, Adams LA. Lifestyle modification in NAFLD/NASH: Facts and figures. *JHEP Rep* 2019; **1**: 468-479 [PMID: 32039399 DOI: 10.1016/j.jhepr.2019.10.008]

13 **Ke L**, Lu C, Shen R, Lu T, Ma B, Hua Y. Knowledge Mapping of Drug-Induced Liver Injury: A Scientometric Investigation (2010-2019). *Front Pharmacol* 2020; **11**: 842 [PMID: 32581801 DOI: 10.3389/fphar.2020.00842]

14 **Arruda H**, Silva ER, Lessa M, Proença D Jr, Bartholo R. VOSviewer and Bibliometrix. *J Med Libr Assoc* 2022; **110**: 392-395 [PMID: 36589296 DOI: 10.5195/jmla.2022.1434]

15 **Synnestvedt MB**, Chen C, Holmes JH. CiteSpace II: visualization and knowledge discovery in bibliographic databases. *AMIA Annu Symp Proc* 2005; **2005**: 724-728 [PMID: 16779135]

16 **Zhang TS**, Qin HL, Wang T, Li HT, Li H, Xia SH, Xiang XH. Global publication trends and research hotspots of nonalcoholic fatty liver disease: a bibliometric analysis and systematic review. *Springerplus* 2015; **4**: 776 [PMID: 26697286 DOI: 10.1186/s40064-015-1542-1]

17 **Zhang TS**, Qin HL, Wang T, Li HT, Li H, Xia SH, Xiang XH. Bibliometric analysis of top 100 cited articles in nonalcoholic fatty liver disease research. *World J Hepatol* 2016; **8**: 1478-1488 [PMID: 27957247 DOI: 10.4254/wjh.v8.i33.1478]

18 **Trifan A**, Stanciu C, Jurcău M, Zenovia S, Frunzuc G, Timofte D. Nonalcoholic steatohepatitis: A scientometric analysis of publications during 1980-2018. *Medicine (Baltimore)* 2019; **98**: e18221 [PMID: 31852081 DOI: 10.1097/MD.0000000000018221]

19 **Li Z**, Cao S, Zhao S, Kang N. A bibliometric analysis and visualization of nonalcoholic fatty liver disease from 2012 to 2021. *Clin Exp Med* 2023 [PMID: 36795238 DOI: 10.1007/s10238-023-01023-2]

20 **Yang S**, Yu D, Liu J, Qiao Y, Gu S, Yang R, Chai X, Wang W. Global publication trends and research hotspots of the gut-liver axis in NAFLD: A bibliometric analysis. *Front Endocrinol (Lausanne)* 2023; **14**: 1121540 [PMID: 36967792 DOI: 10.3389/fendo.2023.1121540]

21 **Rinella ME**, Lazarus JV, Ratziu V, Francque SM, Sanyal AJ, Kanwal F, Romero D, Abdelmalek MF, Anstee QM, Arab JP, Arrese M, Bataller R, Beuers U, Boursier J, Bugianesi E, Byrne C, Narro GEC, Chowdhury A, Cortez-Pinto H, Cryer D, Cusi K, El-Kassas M, Klein S, Eskridge W, Fan J, Gawrieh S, Guy CD, Harrison SA, Kim SU, Koot B, Korenjak M, Kowdley K, Lacaille F, Loomba R, Mitchell-Thain R, Morgan TR, Powell E, Roden M, Romero-Gómez M, Silva M, Singh SP, Sookoian SC, Spearman CW, Tiniakos D, Valenti L, Vos MB, Wong VW, Xanthakos S, Yilmaz Y, Younossi Z, Hobbs A, Villota-Rivas M, Newsome PN (senior); NAFLD Nomenclature consensus group. A multi-society Delphi consensus statement on new fatty liver disease nomenclature. *Ann Hepatol* 2023; 101133 [PMID: 37364816 DOI: 10.1016/j.aohep.2023.101133]

22 **Ratziu V**, Bellentani S, Cortez-Pinto H, Day C, Marchesini G. A position statement on NAFLD/NASH based on the EASL 2009 special conference. J Hepatol 2010; 53: 372-384 [PMID: 20494470 DOI: 10.1016/j.jhep.2010.04.008]

23 **van Eck NJ**, Waltman L. Software survey: VOSviewer, a computer program for bibliometric mapping. *Scientometrics* 2010; **84**: 523-538 [PMID: 20585380 DOI: 10.1007/s11192-009-0146-3]

24 **Yeung AWK**, Mozos I. The Innovative and Sustainable Use of Dental Panoramic Radiographs for the Detection of Osteoporosis. *Int J Environ Res Public Health* 2020; **17** [PMID: 32260243 DOI: 10.3390/ijerph17072449]

25 **Zhang XL**, Zheng Y, Xia ML, Wu YN, Liu XJ, Xie SK, Wu YF, Wang M. Knowledge Domain and Emerging Trends in Vinegar Research: A Bibliometric Review of the Literature from WoSCC. *Foods* 2020; **9** [PMID: 32050682 DOI: 10.3390/foods9020166]

26 **Wu H**, Cheng K, Guo Q, Yang W, Tong L, Wang Y, Sun Z. Mapping Knowledge Structure and Themes Trends of Osteoporosis in Rheumatoid Arthritis: A Bibliometric Analysis. *Front Med (Lausanne)* 2021; **8**: 787228 [PMID: 34888333 DOI: 10.3389/fmed.2021.787228]

27 **Chen Y**, Zhang Q, Ma J, Yu Y. Mapping research trends of insulin resistance in polycystic ovary syndrome from 2017 to 2021: A bibliometric analysis. *Front Endocrinol (Lausanne)* 2022; **13**: 963213 [PMID: 36589816 DOI: 10.3389/fendo.2022.963213]

28 **Aria M**, Cuccurullo C. bibliometrix: An R-Tool for Comprehensive Science Mapping Analysis. *Journal of Informetrics* 2018; **11**: 959-975 [DOI: 10.1016/j.joi.2017.08.007]

29 **Chen C**. Searching for intellectual turning points: progressive knowledge domain visualization. *Proc Natl Acad Sci U S A* 2004; **101** Suppl 1: 5303-5310 [PMID: 14724295 DOI: 10.1073/pnas.0307513100]

30 **Sanyal AJ**, Chalasani N, Kowdley KV, McCullough A, Diehl AM, Bass NM, Neuschwander-Tetri BA, Lavine JE, Tonascia J, Unalp A, Van Natta M, Clark J, Brunt EM, Kleiner DE, Hoofnagle JH, Robuck PR; NASH CRN. Pioglitazone, vitamin E, or placebo for nonalcoholic steatohepatitis. *N Engl J Med* 2010; **362**: 1675-1685 [PMID: 20427778 DOI: 10.1056/NEJMoa0907929]

31 **Neuschwander-Tetri BA**, Loomba R, Sanyal AJ, Lavine JE, Van Natta ML, Abdelmalek MF, Chalasani N, Dasarathy S, Diehl AM, Hameed B, Kowdley KV, McCullough A, Terrault N, Clark JM, Tonascia J, Brunt EM, Kleiner DE, Doo E; NASH Clinical Research Network. Farnesoid X nuclear receptor ligand obeticholic acid for non-cirrhotic, non-alcoholic steatohepatitis (FLINT): a multicentre, randomised, placebo-controlled trial. *Lancet* 2015; **385**: 956-965 [PMID: 25468160 DOI: 10.1016/S0140-6736(14)61933-4]

32 **Rinella ME**. Nonalcoholic fatty liver disease: a systematic review. *JAMA* 2015; **313**: 2263-2273 [PMID: 26057287 DOI: 10.1001/jama.2015.5370]

33 **Younossi Z**, Anstee QM, Marietti M, Hardy T, Henry L, Eslam M, George J, Bugianesi E. Global burden of NAFLD and NASH: trends, predictions, risk factors and prevention. *Nat Rev Gastroenterol Hepatol* 2018; **15**: 11-20 [PMID: 28930295 DOI: 10.1038/nrgastro.2017.109]

34 **Younossi ZM**, Ratziu V, Loomba R, Rinella M, Anstee QM, Goodman Z, Bedossa P, Geier A, Beckebaum S, Newsome PN, Sheridan D, Sheikh MY, Trotter J, Knapple W, Lawitz E, Abdelmalek MF, Kowdley KV, Montano-Loza AJ, Boursier J, Mathurin P, Bugianesi E, Mazzella G, Olveira A, Cortez-Pinto H, Graupera I, Orr D, Gluud LL, Dufour JF, Shapiro D, Campagna J, Zaru L, MacConell L, Shringarpure R, Harrison S, Sanyal AJ; REGENERATE Study Investigators. Obeticholic acid for the treatment of non-alcoholic steatohepatitis: interim analysis from a multicentre, randomised, placebo-controlled phase 3 trial. *Lancet* 2019; **394**: 2184-2196 [PMID: 31813633 DOI: 10.1016/S0140-6736(19)33041-7]

35 **Promrat K**, Kleiner DE, Niemeier HM, Jackvony E, Kearns M, Wands JR, Fava JL, Wing RR. Randomized controlled trial testing the effects of weight loss on nonalcoholic steatohepatitis. *Hepatology* 2010; **51**: 121-129 [PMID: 19827166 DOI: 10.1002/hep.23276]

36 **Armstrong MJ**, Gaunt P, Aithal GP, Barton D, Hull D, Parker R, Hazlehurst JM, Guo K; LEAN trial team, Abouda G, Aldersley MA, Stocken D, Gough SC, Tomlinson JW, Brown RM, Hübscher SG, Newsome PN. Liraglutide safety and efficacy in patients with non-alcoholic steatohepatitis (LEAN): a multicentre, double-blind, randomised, placebo-controlled phase 2 study. *Lancet* 2016; **387**: 679-690 [PMID: 26608256 DOI: 10.1016/S0140-6736(15)00803-X]

37 **Friedman SL**, Neuschwander-Tetri BA, Rinella M, Sanyal AJ. Mechanisms of NAFLD development and therapeutic strategies. *Nat Med* 2018; **24**: 908-922 [PMID: 29967350 DOI: 10.1038/s41591-018-0104-9]

38 **Loomba R**, Lutchman G, Kleiner DE, Ricks M, Feld JJ, Borg BB, Modi A, Nagabhyru P, Sumner AE, Liang TJ, Hoofnagle JH. Clinical trial: pilot study of metformin for the treatment of non-alcoholic steatohepatitis. *Aliment Pharmacol Ther* 2009; **29**: 172-182 [PMID: 18945255 DOI: 10.1111/j.1365-2036.2008.03869.x]

39 **Albhaisi SAM**, Bajaj JS, Sanyal AJ. Role of gut microbiota in liver disease. *Am J Physiol Gastrointest Liver Physiol* 2020; **318**: G84-G98 [PMID: 31657225 DOI: 10.1152/ajpgi.00118.2019]

40 **Albhaisi SAM**, Sanyal AJ. New drugs for NASH. *Liver Int* 2021; **41** Suppl 1: 112-118 [PMID: 34155794 DOI: 10.1111/liv.14844]

41 **Loomba R**, Sirlin CB, Ang B, Bettencourt R, Jain R, Salotti J, Soaft L, Hooker J, Kono Y, Bhatt A, Hernandez L, Nguyen P, Noureddin M, Haufe W, Hooker C, Yin M, Ehman R, Lin GY, Valasek MA, Brenner DA, Richards L; San Diego Integrated NAFLD Research Consortium (SINC). Ezetimibe for the treatment of nonalcoholic steatohepatitis: assessment by novel magnetic resonance imaging and magnetic resonance elastography in a randomized trial (MOZART trial). *Hepatology* 2015; **61**: 1239-1250 [PMID: 25482832 DOI: 10.1002/hep.27647]

42 **Cui J**, Philo L, Nguyen P, Hofflich H, Hernandez C, Bettencourt R, Richards L, Salotti J, Bhatt A, Hooker J, Haufe W, Hooker C, Brenner DA, Sirlin CB, Loomba R. Sitagliptin vs. placebo for non-alcoholic fatty liver disease: A randomized controlled trial. *J Hepatol* 2016; **65**: 369-376 [PMID: 27151177 DOI: 10.1016/j.jhep.2016.04.021]

43 **Friedman SL**, Ratziu V, Harrison SA, Abdelmalek MF, Aithal GP, Caballeria J, Francque S, Farrell G, Kowdley KV, Craxi A, Simon K, Fischer L, Melchor-Khan L, Vest J, Wiens BL, Vig P, Seyedkazemi S, Goodman Z, Wong VW, Loomba R, Tacke F, Sanyal A, Lefebvre E. A randomized, placebo-controlled trial of cenicriviroc for treatment of nonalcoholic steatohepatitis with fibrosis. *Hepatology* 2018; **67**: 1754-1767 [PMID: 28833331 DOI: 10.1002/hep.29477]

44 **Loomba R**, Lawitz E, Mantry PS, Jayakumar S, Caldwell SH, Arnold H, Diehl AM, Djedjos CS, Han L, Myers RP, Subramanian GM, McHutchison JG, Goodman ZD, Afdhal NH, Charlton MR; GS-US-384-1497 Investigators. The ASK1 inhibitor selonsertib in patients with nonalcoholic steatohepatitis: A randomized, phase 2 trial. *Hepatology* 2018; **67**: 549-559 [PMID: 28892558 DOI: 10.1002/hep.29514]

45 **Sanyal A**, Charles ED, Neuschwander-Tetri BA, Loomba R, Harrison SA, Abdelmalek MF, Lawitz EJ, Halegoua-DeMarzio D, Kundu S, Noviello S, Luo Y, Christian R. Pegbelfermin (BMS-986036), a PEGylated fibroblast growth factor 21 analogue, in patients with non-alcoholic steatohepatitis: a randomised, double-blind, placebo-controlled, phase 2a trial. Lancet 2019; 392: 2705-2717 [PMID: 30554783 DOI: 10.1016/S0140-6736(18)31785-9]

46 **Loomba R**, Abdelmalek MF, Armstrong MJ, Jara M, Kjær MS, Krarup N, Lawitz E, Ratziu V, Sanyal AJ, Schattenberg JM, Newsome PN; NN9931-4492 investigators. Semaglutide 2·4 mg once weekly in patients with non-alcoholic steatohepatitis-related cirrhosis: a randomised, placebo-controlled phase 2 trial. *Lancet Gastroenterol Hepatol* 2023; **8**: 511-522 [PMID: 36934740 DOI: 10.1016/S2468-1253(23)00068-7]

47 **Younossi ZM**, Corey KE, Lim JK. AGA Clinical Practice Update on Lifestyle Modification Using Diet and Exercise to Achieve Weight Loss in the Management of Nonalcoholic Fatty Liver Disease: Expert Review. *Gastroenterology* 2021; **160**: 912-918 [PMID: 33307021 DOI: 10.1053/j.gastro.2020.11.051]

48 **Ratziu V**, Sanyal AJ, Loomba R, Rinella M, Harrison S, Anstee QM, Goodman Z, Bedossa P, MacConell L, Shringarpure R, Shah A, Younossi Z. REGENERATE: Design of a pivotal, randomised, phase 3 study evaluating the safety and efficacy of obeticholic acid in patients with fibrosis due to nonalcoholic steatohepatitis. *Contemp Clin Trials* 2019; **84**: 105803 [PMID: 31260793 DOI: 10.1016/j.cct.2019.06.017]

49 **Vuppalanchi R**, McCabe ME 4th, Tandra SR, Parcha SP, Ghafoor A, Schuh L, Inman MM, Selzer DJ, Stefanidis D, Chalasani N. Safety and Efficacy of Bariatric Surgery in Cirrhosis Patients With Extreme Obesity. *Ann Surg* 2022; **275**: e174-e180 [PMID: 32925171 DOI: 10.1097/SLA.0000000000003891]

50 **Gawrieh S**, Noureddin M, Loo N, Mohseni R, Awasty V, Cusi K, Kowdley KV, Lai M, Schiff E, Parmar D, Patel P, Chalasani N. Saroglitazar, a PPAR-α/γ Agonist, for Treatment of NAFLD: A Randomized Controlled Double-Blind Phase 2 Trial. *Hepatology* 2021; **74**: 1809-1824 [PMID: 33811367 DOI: 10.1002/hep.31843]

51 **Chalasani N**, Abdelmalek MF, Garcia-Tsao G, Vuppalanchi R, Alkhouri N, Rinella M, Noureddin M, Pyko M, Shiffman M, Sanyal A, Allgood A, Shlevin H, Horton R, Zomer E, Irish W, Goodman Z, Harrison SA, Traber PG; Belapectin (GR-MD-02) Study Investigators. Effects of Belapectin, an Inhibitor of Galectin-3, in Patients With Nonalcoholic Steatohepatitis With Cirrhosis and Portal Hypertension. *Gastroenterology* 2020; **158**: 1334-1345.e5 [PMID: 31812510 DOI: 10.1053/j.gastro.2019.11.296]

52 **Kleiner DE**, Brunt EM, Van Natta M, Behling C, Contos MJ, Cummings OW, Ferrell LD, Liu YC, Torbenson MS, Unalp-Arida A, Yeh M, McCullough AJ, Sanyal AJ; Nonalcoholic Steatohepatitis Clinical Research Network. Design and validation of a histological scoring system for nonalcoholic fatty liver disease. *Hepatology* 2005; **41**: 1313-1321 [PMID: 15915461 DOI: 10.1002/hep.20701]

53 **Younossi ZM**, Koenig AB, Abdelatif D, Fazel Y, Henry L, Wymer M. Global epidemiology of nonalcoholic fatty liver disease-Meta-analytic

assessment of prevalence, incidence, and outcomes. *Hepatology* 2016; **64**: 73-84 [PMID: 26707365 DOI: 10.1002/hep.28431]

54 **Lee HW**, Wong VW. Changing NAFLD Epidemiology in China. *Hepatology* 2019; **70**: 1095-1098 [PMID: 31298746 DOI: 10.1002/hep.30848]

55 **Pan XF**, Wang L, Pan A. Epidemiology and determinants of obesity in China. *Lancet Diabetes Endocrinol* 2021; **9**: 373-392 [PMID: 34022156 DOI: 10.1016/S2213-8587(21)00045-0]

56 **Younossi ZM**. Non-alcoholic fatty liver disease - A global public health perspective. *J Hepatol* 2019; **70**: 531-544 [PMID: 30414863 DOI: 10.1016/j.jhep.2018.10.033]

57 **Estes C**, Razavi H, Loomba R, Younossi Z, Sanyal AJ. Modeling the epidemic of nonalcoholic fatty liver disease demonstrates an exponential increase in burden of disease. *Hepatology* 2018; **67**: 123-133 [PMID: 28802062 DOI: 10.1002/hep.29466]

58 **Wang FS**, Fan JG, Zhang Z, Gao B, Wang HY. The global burden of liver disease: the major impact of China. *Hepatology* 2014; **60**: 2099-2108 [PMID: 25164003 DOI: 10.1002/hep.27406]

59 **Estes C**, Anstee QM, Arias-Loste MT, Bantel H, Bellentani S, Caballeria J, Colombo M, Craxi A, Crespo J, Day CP, Eguchi Y, Geier A, Kondili LA, Kroy DC, Lazarus JV, Loomba R, Manns MP, Marchesini G, Nakajima A, Negro F, Petta S, Ratziu V, Romero-Gomez M, Sanyal A, Schattenberg JM, Tacke F, Tanaka J, Trautwein C, Wei L, Zeuzem S, Razavi H. Modeling NAFLD disease burden in China, France, Germany, Italy, Japan, Spain, United Kingdom, and United States for the period 2016-2030. *J Hepatol* 2018; **69**: 896-904 [PMID: 29886156 DOI: 10.1016/j.jhep.2018.05.036]

60 **Du LJ**, He ZY, Gu X, Hu X, Zhang XX, Yang LJ, Li J, Pan LY, Li YQ, Yang B, Gu XJ. Inverse Association of Fruit and Vegetable Consumption with Nonalcoholic Fatty Liver Disease in Chinese Patients with Type 2 Diabetes Mellitus. *Nutrients* 2022; **14** [PMID: 36364821 DOI: 10.3390/nu14214559]

61 **Xiao J**, Wang F, Wong NK, He J, Zhang R, Sun R, Xu Y, Liu Y, Li W, Koike K, He W, You H, Miao Y, Liu X, Meng M, Gao B, Wang H, Li C. Global liver disease burdens and research trends: Analysis from a Chinese perspective. *J Hepatol* 2019; **71**: 212-221 [PMID: 30871980 DOI: 10.1016/j.jhep.2019.03.004]

62 **Zhang Q**, Zhang L, Liu K, Shang H, Ruan J, Yu Z, Meng S, Liang F, Wang T, Zhang H, Peng W, Wang Y, Chen J, Xiao T, Wang B. A Network Pharmacology Study on the Active Components and Targets of the Radix Ginseng and Radix Bupleuri Herb Pair for Treating Nonalcoholic Fatty Liver Disease. *Evid Based Complement Alternat Med* 2022; **2022**: 1638740 [PMID: 35178098 DOI: 10.1155/2022/1638740]

63 **Liu H**, Xu J, Li H, Zhang L, Xu P. Network pharmacology-based investigation to explore the effect and mechanism of Erchen decoction against the nonalcoholic fatty liver disease. *Anat Rec (Hoboken)* 2021; **304**: 2605-2619 [PMID: 34536264 DOI: 10.1002/ar.24770]

64 **Jia W**, Wang K, Zhang S, Lu W, Du A, Li J, Ji L, Xu H. Integrating network pharmacology and *in vivo* experimental validation to reveal the alleviation of mailuoning oral liquid on non-alcoholic fatty liver disease. *Phytomedicine* 2022; **104**: 154326 [PMID: 35853303 DOI: 10.1016/j.phymed.2022.154326]

65 **Zhao L**, Zhang H, Li N, Chen J, Xu H, Wang Y, Liang Q. Network pharmacology, a promising approach to reveal the pharmacology mechanism of Chinese medicine formula. *J Ethnopharmacol* 2023; **309**: 116306 [PMID: 36858276 DOI: 10.1016/j.jep.2023.116306]

66 **Zhou W**, Zhu Z, Xiao X, Li C, Zhang L, Dang Y, Ge G, Ji G, Zhu M, Xu H. Jiangzhi Granule attenuates non-alcoholic steatohepatitis by suppressing TNF/NFκB signaling pathway-a study based on network pharmacology. *Biomed Pharmacother* 2021; **143**: 112181 [PMID: 34649337 DOI: 10.1016/j.biopha.2021.112181]

67 **Mao FF**, Gao SS, Huang YJ, Zhou N, Feng JK, Liu ZH, Zhang YQ, Yuan LY, Wei G, Cheng SQ. Network pharmacology-based analysis of Resinacein S against non-alcoholic fatty liver disease by modulating lipid metabolism. *Front Nutr* 2023; **10**: 1076569 [PMID: 36866057 DOI: 10.3389/fnut.2023.1076569]

68 **Ye Q**, Zou B, Yeo YH, Li J, Huang DQ, Wu Y, Yang H, Liu C, Kam LY, Tan XXE, Chien N, Trinh S, Henry L, Stave CD, Hosaka T, Cheung RC, Nguyen MH. Global prevalence, incidence, and outcomes of non-obese or lean non-alcoholic fatty liver disease: a systematic review and meta-analysis. *Lancet Gastroenterol Hepatol* 2020; **5**: 739-752 [PMID: 32413340 DOI: 10.1016/S2468-1253(20)30077-7]

69 **Zhou J**, Zhou F, Wang W, Zhang XJ, Ji YX, Zhang P, She ZG, Zhu L, Cai J, Li H. Epidemiological Features of NAFLD From 1999 to 2018 in China. *Hepatology* 2020; **71**: 1851-1864 [PMID: 32012320 DOI: 10.1002/hep.31150]

70 **Liu YZ**, Wang YX, Jiang CL. Inflammation: The Common Pathway of Stress-Related Diseases. *Front Hum Neurosci* 2017; **11**: 316 [PMID: 28676747 DOI: 10.3389/fnhum.2017.00316]

71 **Wang GX**, Zhao XY, Meng ZX, Kern M, Dietrich A, Chen Z, Cozacov Z, Zhou D, Okunade AL, Su X, Li S, Blüher M, Lin JD. The brown fat-enriched secreted factor Nrg4 preserves metabolic homeostasis through attenuation of hepatic lipogenesis. *Nat Med* 2014; **20**: 1436-1443 [PMID: 25401691 DOI: 10.1038/nm.3713]

72 **Li R**, Xin T, Li D, Wang C, Zhu H, Zhou H. Therapeutic effect of Sirtuin 3 on ameliorating nonalcoholic fatty liver disease: The role of the ERK-CREB pathway and Bnip3-mediated mitophagy. *Redox Biol* 2018; **18**: 229-243 [PMID: 30056271 DOI: 10.1016/j.redox.2018.07.011]

73 **Xu B**, Jiang M, Chu Y, Wang W, Chen D, Li X, Zhang Z, Zhang D, Fan D, Nie Y, Shao F, Wu K, Liang J. Gasdermin D plays a key role as a pyroptosis executor of non-alcoholic steatohepatitis in humans and mice. *J Hepatol* 2018; **68**: 773-782 [PMID: 29273476 DOI: 10.1016/j.jhep.2017.11.040]

74 **Yang L**, Roh YS, Song J, Zhang B, Liu C, Loomba R, Seki E. Transforming growth factor beta signaling in hepatocytes participates in steatohepatitis through regulation of cell death and lipid metabolism in mice. *Hepatology* 2014; **59**: 483-495 [PMID: 23996730 DOI: 10.1002/hep.26698]

75 **Li L**, Chen L, Hu L, Liu Y, Sun HY, Tang J, Hou YJ, Chang YX, Tu QQ, Feng GS, Shen F, Wu MC, Wang HY. Nuclear factor high-mobility group box1 mediating the activation of Toll-like receptor 4 signaling in hepatocytes in the early stage of nonalcoholic fatty liver disease in mice. *Hepatology* 2011; **54**: 1620-1630 [PMID: 21809356 DOI: 10.1002/hep.24552]

76 **Cao J**, Dai DL, Yao L, Yu HH, Ning B, Zhang Q, Chen J, Cheng WH, Shen W, Yang ZX. Saturated fatty acid induction of endoplasmic reticulum stress and apoptosis in human liver cells *via* the PERK/ATF4/CHOP signaling pathway. *Mol Cell Biochem* 2012; **364**: 115-129 [PMID: 22246806 DOI: 10.1007/s11010-011-1211-9]

77 **Jiang C**, Xie C, Li F, Zhang L, Nichols RG, Krausz KW, Cai J, Qi Y, Fang ZZ, Takahashi S, Tanaka N, Desai D, Amin SG, Albert I, Patterson AD, Gonzalez FJ. Intestinal farnesoid X receptor signaling promotes nonalcoholic fatty liver disease. *J Clin Invest* 2015; **125**: 386-402 [PMID: 25500885 DOI: 10.1172/JCI76738]

78 **Zhang CY**, Yuan WG, He P, Lei JH, Wang CX. Liver fibrosis and hepatic stellate cells: Etiology, pathological hallmarks and therapeutic targets. *World J Gastroenterol* 2016; **22**: 10512-10522 [PMID: 28082803 DOI: 10.3748/wjg.v22.i48.10512]

79 **Ma YY**, Li L, Yu CH, Shen Z, Chen LH, Li YM. Effects of probiotics on nonalcoholic fatty liver disease: a meta-analysis. *World J*

Gastroenterol 2013; **19**: 6911-6918 [PMID: 24187469 DOI: 10.3748/wjg.v19.i40.6911]
80 **Wang RH**, Kim HS, Xiao C, Xu X, Gavrilova O, Deng CX. Hepatic Sirt1 deficiency in mice impairs mTorc2/Akt signaling and results in hyperglycemia, oxidative damage, and insulin resistance. *J Clin Invest* 2011; **121**: 4477-4490 [PMID: 21965330 DOI: 10.1172/JCI46243]
81 **Xu Y**, Wang N, Tan HY, Li S, Zhang C, Feng Y. Function of Akkermansia muciniphila in Obesity: Interactions With Lipid Metabolism, Immune Response and Gut Systems. *Front Microbiol* 2020; **11**: 219 [PMID: 32153527 DOI: 10.3389/fmicb.2020.00219]
82 **Dai J**, Liang K, Zhao S, Jia W, Liu Y, Wu H, Lv J, Cao C, Chen T, Zhuang S, Hou X, Zhou S, Zhang X, Chen XW, Huang Y, Xiao RP, Wang YL, Luo T, Xiao J, Wang C. Chemoproteomics reveals baicalin activates hepatic CPT1 to ameliorate diet-induced obesity and hepatic steatosis. *Proc Natl Acad Sci U S A* 2018; **115**: E5896-E5905 [PMID: 29891721 DOI: 10.1073/pnas.1801745115]
83 **Xu MQ**, Cao HL, Wang WQ, Wang S, Cao XC, Yan F, Wang BM. Fecal microbiota transplantation broadening its application beyond intestinal disorders. *World J Gastroenterol* 2015; **21**: 102-111 [PMID: 25574083 DOI: 10.3748/wjg.v21.i1.102]
84 **Wang PX**, Ji YX, Zhang XJ, Zhao LP, Yan ZZ, Zhang P, Shen LJ, Yang X, Fang J, Tian S, Zhu XY, Gong J, Zhang X, Wei QF, Wang Y, Li J, Wan L, Xie Q, She ZG, Wang Z, Huang Z, Li H. Targeting CASP8 and FADD-like apoptosis regulator ameliorates nonalcoholic steatohepatitis in mice and nonhuman primates. *Nat Med* 2017; **23**: 439-449 [PMID: 28218919 DOI: 10.1038/nm.4290]
85 **Li S**, Liao X, Meng F, Wang Y, Sun Z, Guo F, Li X, Meng M, Li Y, Sun C. Therapeutic role of ursolic acid on ameliorating hepatic steatosis and improving metabolic disorders in high-fat diet-induced non-alcoholic fatty liver disease rats. *PLoS One* 2014; **9**: e86724 [PMID: 24489777 DOI: 10.1371/journal.pone.0086724]
86 **Zhao XJ**, Yu HW, Yang YZ, Wu WY, Chen TY, Jia KK, Kang LL, Jiao RQ, Kong LD. Polydatin prevents fructose-induced liver inflammation and lipid deposition through increasing miR-200a to regulate Keap1/Nrf2 pathway. *Redox Biol* 2018; **18**: 124-137 [PMID: 30014902 DOI: 10.1016/j.redox.2018.07.002]
87 **Xiao J**, Ho CT, Liong EC, Nanji AA, Leung TM, Lau TY, Fung ML, Tipoe GL. Epigallocatechin gallate attenuates fibrosis, oxidative stress, and inflammation in non-alcoholic fatty liver disease rat model through TGF/SMAD, PI3 K/Akt/FoxO1, and NF-kappa B pathways. *Eur J Nutr* 2014; **53**: 187-199 [PMID: 23515587 DOI: 10.1007/s00394-013-0516-8]
88 **Zhang P**, Wang PX, Zhao LP, Zhang X, Ji YX, Zhang XJ, Fang C, Lu YX, Yang X, Gao MM, Zhang Y, Tian S, Zhu XY, Gong J, Ma XL, Li F, Wang Z, Huang Z, She ZG, Li H. The deubiquitinating enzyme TNFAIP3 mediates inactivation of hepatic ASK1 and ameliorates nonalcoholic steatohepatitis. *Nat Med* 2018; **24**: 84-94 [PMID: 29227477 DOI: 10.1038/nm.4453]
89 **Liu D**, Wong CC, Fu L, Chen H, Zhao L, Li C, Zhou Y, Zhang Y, Xu W, Yang Y, Wu B, Cheng G, Lai PB, Wong N, Sung JJY, Yu J. Squalene epoxidase drives NAFLD-induced hepatocellular carcinoma and is a pharmaceutical target. *Sci Transl Med* 2018; **10** [PMID: 29669855 DOI: 10.1126/scitranslmed.aap9840]
90 **Barlow P**, McKee M, Basu S, Stuckler D. The health impact of trade and investment agreements: a quantitative systematic review and network co-citation analysis. *Global Health* 2017; **13**: 13 [PMID: 28274238 DOI: 10.1186/s12992-017-0240-x]
91 **Chen C**. CiteSpace II: Detecting and visualizing emerging trends and transient patterns in scientific literature. *Journal of the Association for Information Science and Technology* 2006; **57**: 359-377 [DOI: 10.1002/asi.20317]
92 **Angulo P**. Nonalcoholic fatty liver disease. *N Engl J Med* 2002; **346**: 1221-1231 [PMID: 11961152 DOI: 10.1056/NEJMra011775]
93 **Musso G**, Gambino R, Cassader M, Pagano G. A meta-analysis of randomized trials for the treatment of nonalcoholic fatty liver disease. *Hepatology* 2010; **52**: 79-104 [PMID: 20578268 DOI: 10.1002/hep.23623]
94 **Lavine JE**, Schwimmer JB, Van Natta ML, Molleston JP, Murray KF, Rosenthal P, Abrams SH, Scheimann AO, Sanyal AJ, Chalasani N, Tonascia J, Ünalp A, Clark JM, Brunt EM, Kleiner DE, Hoofnagle JH, Robuck PR; Nonalcoholic Steatohepatitis Clinical Research Network. Effect of vitamin E or metformin for treatment of nonalcoholic fatty liver disease in children and adolescents: the TONIC randomized controlled trial. *JAMA* 2011; **305**: 1659-1668 [PMID: 21521847 DOI: 10.1001/jama.2011.520]
95 **Bellanti F**, Lo Buglio A, Dobrakowski M, Kasperczyk A, Kasperczyk S, Aich P, Singh SP, Serviddio G, Vendemiale G. Impact of sodium glucose cotransporter-2 inhibitors on liver steatosis/fibrosis/inflammation and redox balance in non-alcoholic fatty liver disease. *World J Gastroenterol* 2022; **28**: 3243-3257 [PMID: 36051336 DOI: 10.3748/wjg.v28.i26.3243]
96 **Mudaliar S**, Henry RR, Sanyal AJ, Morrow L, Marschall HU, Kipnes M, Adorini L, Sciacca CI, Clopton P, Castelloe E, Dillon P, Pruzanski M, Shapiro D. Efficacy and safety of the farnesoid X receptor agonist obeticholic acid in patients with type 2 diabetes and nonalcoholic fatty liver disease. *Gastroenterology* 2013; **145**: 574-82.e1 [PMID: 23727264 DOI: 10.1053/j.gastro.2013.05.042]
97 **Buzzetti E**, Pinzani M, Tsochatzis EA. The multiple-hit pathogenesis of non-alcoholic fatty liver disease (NAFLD). *Metabolism* 2016; **65**: 1038-1048 [PMID: 26823198 DOI: 10.1016/j.metabol.2015.12.012]
98 **Boursier J**, Mueller O, Barret M, Machado M, Fizanne L, Araujo-Perez F, Guy CD, Seed PC, Rawls JF, David LA, Hunault G, Oberti F, Calès P, Diehl AM. The severity of nonalcoholic fatty liver disease is associated with gut dysbiosis and shift in the metabolic function of the gut microbiota. *Hepatology* 2016; **63**: 764-775 [PMID: 26600078 DOI: 10.1002/hep.28356]
99 **Promrat K**, Longato L, Wands JR, de la Monte SM. Weight loss amelioration of non-alcoholic steatohepatitis linked to shifts in hepatic ceramide expression and serum ceramide levels. *Hepatol Res* 2011; **41**: 754-762 [PMID: 21794038 DOI: 10.1111/j.1872-034X.2011.00815.x]
100 **Amjad T**, Shahid N, Daud A, Khatoon A. Citation burst prediction in a bibliometric network. *Scientometrics* 2022; **127**: 2773-2790 [DOI: 10.1007/s11192-022-04344-3]
101 **Cohen JC**, Horton JD, Hobbs HH. Human fatty liver disease: old questions and new insights. *Science* 2011; **332**: 1519-1523 [PMID: 21700865 DOI: 10.1126/science.1204265]
102 **Eslam M**, Newsome PN, Sarin SK, Anstee QM, Targher G, Romero-Gomez M, Zelber-Sagi S, Wai-Sun Wong V, Dufour JF, Schattenberg JM, Kawaguchi T, Arrese M, Valenti L, Shiha G, Tiribelli C, Yki-Järvinen H, Fan JG, Grønbæk H, Yilmaz Y, Cortez-Pinto H, Oliveira CP, Bedossa P, Adams LA, Zheng MH, Fouad Y, Chan WK, Mendez-Sanchez N, Ahn SH, Castera L, Bugianesi E, Ratziu V, George J. A new definition for metabolic dysfunction-associated fatty liver disease: An international expert consensus statement. *J Hepatol* 2020; **73**: 202-209 [PMID: 32278004 DOI: 10.1016/j.jhep.2020.03.039]
103 **Newsome PN**, Buchholtz K, Cusi K, Linder M, Okanoue T, Ratziu V, Sanyal AJ, Sejling AS, Harrison SA; NN9931-4296 Investigators. A Placebo-Controlled Trial of Subcutaneous Semaglutide in Nonalcoholic Steatohepatitis. *N Engl J Med* 2021; **384**: 1113-1124 [PMID: 33185364 DOI: 10.1056/NEJMoa2028395]
104 **Eslam M**, Sanyal AJ, George J. Toward More Accurate Nomenclature for Fatty Liver Diseases. *Gastroenterology* 2019; **157**: 590-593 [PMID: 31158374 DOI: 10.1053/j.gastro.2019.05.064]
105 **Musso G**, Cassader M, Rosina F, Gambino R. Impact of current treatments on liver disease, glucose metabolism and cardiovascular risk in non-alcoholic fatty liver disease (NAFLD): a systematic review and meta-analysis of randomised trials. *Diabetologia* 2012; **55**: 885-904

[PMID: 22278337 DOI: 10.1007/s00125-011-2446-4]

106 **Cusi K**, Orsak B, Bril F, Lomonaco R, Hecht J, Ortiz-Lopez C, Tio F, Hardies J, Darland C, Musi N, Webb A, Portillo-Sanchez P. Long-Term Pioglitazone Treatment for Patients With Nonalcoholic Steatohepatitis and Prediabetes or Type 2 Diabetes Mellitus: A Randomized Trial. *Ann Intern Med* 2016; **165**: 305-315 [PMID: 27322798 DOI: 10.7326/M15-1774]

107 **Ratziu V**, Harrison SA, Francque S, Bedossa P, Lehert P, Serfaty L, Romero-Gomez M, Boursier J, Abdelmalek M, Caldwell S, Drenth J, Anstee QM, Hum D, Hanf R, Roudot A, Megnien S, Staels B, Sanyal A; GOLDEN-505 Investigator Study Group. Elafibranor, an Agonist of the Peroxisome Proliferator-Activated Receptor-α and -δ, Induces Resolution of Nonalcoholic Steatohepatitis Without Fibrosis Worsening. *Gastroenterology* 2016; **150**: 1147-1159.e5 [PMID: 26874076 DOI: 10.1053/j.gastro.2016.01.038]

108 **Ekstedt M**, Hagström H, Nasr P, Fredrikson M, Stål P, Kechagias S, Hultcrantz R. Fibrosis stage is the strongest predictor for disease-specific mortality in NAFLD after up to 33 years of follow-up. *Hepatology* 2015; **61**: 1547-1554 [PMID: 25125077 DOI: 10.1002/hep.27368]

109 **Wong RJ**, Aguilar M, Cheung R, Perumpail RB, Harrison SA, Younossi ZM, Ahmed A. Nonalcoholic steatohepatitis is the second leading etiology of liver disease among adults awaiting liver transplantation in the United States. *Gastroenterology* 2015; **148**: 547-555 [PMID: 25461851 DOI: 10.1053/j.gastro.2014.11.039]

110 **Angulo P**, Kleiner DE, Dam-Larsen S, Adams LA, Bjornsson ES, Charatcharoenwitthaya P, Mills PR, Keach JC, Lafferty HD, Stahler A, Haflidadottir S, Bendtsen F. Liver Fibrosis, but No Other Histologic Features, Is Associated With Long-term Outcomes of Patients With Nonalcoholic Fatty Liver Disease. Gastroenterology 2015; 149: 389-97.e10 [PMID: 25935633 DOI: 10.1053/j.gastro.2015.04.043]

111 **Vernon G**, Baranova A, Younossi ZM. Systematic review: the epidemiology and natural history of non-alcoholic fatty liver disease and non-alcoholic steatohepatitis in adults. *Aliment Pharmacol Ther* 2011; **34**: 274-285 [PMID: 21623852 DOI: 10.1111/j.1365-2036.2011.04724.x]

112 **Anstee QM**, Targher G, Day CP. Progression of NAFLD to diabetes mellitus, cardiovascular disease or cirrhosis. Nat Rev Gastroenterol Hepatol 2013; 10: 330-344 [PMID: 23507799 DOI: 10.1038/nrgastro.2013.41]

113 **Anstee QM**, Day CP. A lipid to treat non-alcoholic fatty liver disease - the dawn of 'lipo-rehabilitation'? *J Hepatol* 2012; **56**: 987-989 [PMID: 22015962 DOI: 10.1016/j.jhep.2011.10.002]

114 **Loomba R**, Sanyal AJ. The global NAFLD epidemic. *Nat Rev Gastroenterol Hepatol* 2013; **10**: 686-690 [PMID: 24042449 DOI: 10.1038/nrgastro.2013.171]

115 **Tilg H**, Moschen AR. Evolution of inflammation in nonalcoholic fatty liver disease: the multiple parallel hits hypothesis. *Hepatology* 2010; **52**: 1836-1846 [PMID: 21038418 DOI: 10.1002/hep.24001]

116 **Williams CD**, Stengel J, Asike MI, Torres DM, Shaw J, Contreras M, Landt CL, Harrison SA. Prevalence of nonalcoholic fatty liver disease and nonalcoholic steatohepatitis among a largely middle-aged population utilizing ultrasound and liver biopsy: a prospective study. *Gastroenterology* 2011; **140**: 124-131 [PMID: 20858492 DOI: 10.1053/j.gastro.2010.09.038]

117 **Rinella ME**, Lazarus JV, Ratziu V, Francque SM, Sanyal AJ, Kanwal F, Romero D, Abdelmalek MF, Anstee QM, Arab JP, Arrese M, Bataller R, Beuers U, Boursier J, Bugianesi E, Byrne C, Castro Narro GE, Chowdhury A, Cortez-Pinto H, Cryer D, Cusi K, El-Kassas M, Klein S, Eskridge W, Fan J, Gawrieh S, Guy CD, Harrison SA, Kim SU, Koot B, Korenjak M, Kowdley K, Lacaille F, Loomba R, Mitchell-Thain R, Morgan TR, Powell E, Roden M, Romero-Gómez M, Silva M, Singh SP, Sookoian SC, Spearman CW, Tiniakos D, Valenti L, Vos MB, WaiSun Wong V, Xanthakos S, Yilmaz Y, Younossi Z, Hobbs A, Villota-Rivas M, Newsome PN; NAFLD Nomenclature consensus group. A multi-society Delphi consensus statement on new fatty liver disease nomenclature. *J Hepatol* 2023; **20**: S0168-8278(23)00418-X [PMID: 37364790 DOI: 10.1016/j.jhep.2023.06.003]



Published by **Baishideng Publishing Group Inc**
7041 Koll Center Parkway, Suite 160, Pleasanton, CA 94566, USA
Telephone: +1-925-3991568
E-mail: bpgoffice@wjgnet.com
Help Desk: https://www.f6publishing.com/helpdesk
https://www.wjgnet.com



© 2023 Baishideng Publishing Group Inc. All rights reserved.

ISSN 1007-9327 (print)
ISSN 2219-2840 (online)

World Journal of *Gastroenterology*

World J Gastroenterol 2023 October 14; 29(38): 5361-5434



Published by Baishideng Publishing Group Inc

World Journal of Gastroenterology

Contents

Weekly Volume 29 Number 38 October 14, 2023

MINIREVIEWS

5361 Intraductal papillary neoplasm of the bile duct: The new frontier of biliary pathology

Mocchegiani F, Vincenzi P, Conte G, Nicolini D, Rossi R, Cacciaguerra AB, Vivarelli M

ORIGINAL ARTICLE

Basic Study

5374 Expression and functional study of cholecystokinin-A receptors on the interstitial Cajal-like cells of the guinea pig common bile duct

Xu D, Ma SL, Huang ML, Zhang H

Retrospective Study

5383 Impressive recompensation in transjugular intrahepatic portosystemic shunt-treated individuals with complications of decompensated cirrhosis based on Baveno VII criteria

Gao L, Li MB, Li JY, Liu Y, Ren C, Feng DP

Observational Study

5395 Hepatitis D virus dual-infection among Chinese hepatitis B patient related to hepatitis B surface antigen, hepatitis B virus DNA and age

Zi J, Li YH, Wang XM, Xu HQ, Liu WH, Cui JY, Niu JQ, Chi XM

SYSTEMATIC REVIEWS

5406 Scoping review on health-related physical fitness in patients with inflammatory bowel disease: Assessment, interventions, and future directions

Demers K, Bak MTJ, Bongers BC, de Vries AC, Jonkers DMAE, Pierik MJ, Stassen LPS

CASE REPORT

5428 Dose escalation of adalimumab as a strategy to overcome anti-drug antibodies: A case report of infantile-onset inflammatory bowel disease

Ancona S, Signa S, Longo C, Cangemi G, Carfora R, Drago E, La Rosa A, Crocco M, Chiaro A, Gandullia P, Arrigo S

ABOUT COVER

Editorial Board Member of *World Journal of Gastroenterology*, Emilio De Raffele, MD, PhD, Assistant Professor, Consultant Surgeon, Dipartimento Medico Chirurgico delle Malattie Digestive, Epatiche ed Endocrino-metaboliche, IRCCS Azienda Ospedaliero-Universitaria di Bologna, Via Albertoni 15, Bologna 40138, Italy.

AIMS AND SCOPE

The primary aim of *World Journal of Gastroenterology* (*WJG*, *World J Gastroenterol*) is to provide scholars and readers from various fields of gastroenterology and hepatology with a platform to publish high-quality basic and clinical research articles and communicate their research findings online. *WJG* mainly publishes articles reporting research results and findings obtained in the field of gastroenterology and hepatology and covering a wide range of topics including gastroenterology, hepatology, gastrointestinal endoscopy, gastrointestinal surgery, gastrointestinal oncology, and pediatric gastroenterology.

INDEXING/ABSTRACTING

The *WJG* is now abstracted and indexed in Science Citation Index Expanded (SCIE), MEDLINE, PubMed, PubMed Central, Scopus, Reference Citation Analysis, China Science and Technology Journal Database, and Superstar Journals Database. The 2023 edition of Journal Citation Reports® cites the 2022 impact factor (IF) for *WJG* as 4.3; Quartile category: Q2. The *WJG*'s CiteScore for 2021 is 8.3.

RESPONSIBLE EDITORS FOR THIS ISSUE

Production Editor: *Ying-Yi Yuan*; **Production Department Director:** *Xu Guo*; **Editorial Office Director:** *Jia-Ru Fan*.

NAME OF JOURNAL
World Journal of Gastroenterology

ISSN
ISSN 1007-9327 (print) ISSN 2219-2840 (online)

LAUNCH DATE
October 1, 1995

FREQUENCY
Weekly

EDITORS-IN-CHIEF
Andrzej S Tarnawski

EXECUTIVE ASSOCIATE EDITORS-IN-CHIEF
Xian-Jun Yu (Pancreatic Oncology), Jian-Gao Fan (Chronic Liver Disease), Hou-Bao Liu (Biliary Tract Disease), Naohisa Yoshida (Gastrointestinal Endoscopy)

EDITORIAL BOARD MEMBERS
http://www.wjgnet.com/1007-9327/editorialboard.htm

PUBLICATION DATE
October 14, 2023

COPYRIGHT
© 2023 Baishideng Publishing Group Inc

PUBLISHING PARTNER
Shanghai Pancreatic Cancer Institute and Pancreatic Cancer Institute, Fudan University
Biliary Tract Disease Institute, Fudan University

INSTRUCTIONS TO AUTHORS
https://www.wjgnet.com/bpg/gerinfo/204

GUIDELINES FOR ETHICS DOCUMENTS
https://www.wjgnet.com/bpg/GerInfo/287

GUIDELINES FOR NON-NATIVE SPEAKERS OF ENGLISH
https://www.wjgnet.com/bpg/gerinfo/240

PUBLICATION ETHICS
https://www.wjgnet.com/bpg/GerInfo/288

PUBLICATION MISCONDUCT
https://www.wjgnet.com/bpg/gerinfo/208

POLICY OF CO-AUTHORS
https://www.wjgnet.com/bpg/GerInfo/310

ARTICLE PROCESSING CHARGE
https://www.wjgnet.com/bpg/gerinfo/242

STEPS FOR SUBMITTING MANUSCRIPTS
https://www.wjgnet.com/bpg/GerInfo/239

ONLINE SUBMISSION
https://www.f6publishing.com

PUBLISHING PARTNER's OFFICIAL WEBSITE
https://www.shca.org.cn
https://www.zs-hospital.sh.cn

© 2023 Baishideng Publishing Group Inc. All rights reserved. 7041 Koll Center Parkway, Suite 160, Pleasanton, CA 94566, USA
E-mail: bpgoffice@wjgnet.com https://www.wjgnet.com

World Journal of Gastroenterology

Submit a Manuscript: https://www.f6publishing.com

World J Gastroenterol 2023 October 14; 29(38): 5361-5373

DOI: 10.3748/wjg.v29.i38.5361

ISSN 1007-9327 (print) ISSN 2219-2840 (online)

MINIREVIEWS

Intraductal papillary neoplasm of the bile duct: The new frontier of biliary pathology

Federico Mocchegiani, Paolo Vincenzi, Grazia Conte, Daniele Nicolini, Roberta Rossi, Andrea Benedetti Cacciaguerra, Marco Vivarelli

Specialty type: Gastroenterology and hepatology

Provenance and peer review: Invited article; Externally peer reviewed.

Peer-review model: Single blind

Peer-review report's scientific quality classification

Grade A (Excellent): 0
Grade B (Very good): 0
Grade C (Good): C, C
Grade D (Fair): 0
Grade E (Poor): 0

P-Reviewer: Kawabata H, Japan; Saengboonmee C, Thailand

Received: May 31, 2023
Peer-review started: May 31, 2023
First decision: July 23, 2023
Revised: August 7, 2023
Accepted: August 31, 2023
Article in press: August 31, 2023
Published online: October 14, 2023

Federico Mocchegiani, Andrea Benedetti Cacciaguerra, Marco Vivarelli, Department of Experimental and Clinical Medicine, Polytechnic University of Marche, Ancona 60126, Italy

Paolo Vincenzi, Grazia Conte, Daniele Nicolini, Roberta Rossi, Department of Gastroenterology and Transplant, United Hospital of Marche, Ancona 60126, Italy

Corresponding author: Federico Mocchegiani, MD, Associate Professor, Department of Experimental and Clinical Medicine, Polytechnic University of Marche, Via Tronto 10 a, Ancona 60126, Italy. federico.mocchegiani@ospedaliriuniti.marche.it

Abstract

Intraductal papillary neoplasms of the bile duct (IPNBs) represent a rare variant of biliary tumors characterized by a papillary growth within the bile duct lumen. Since their first description in 2001, several classifications have been proposed, mainly based on histopathological, radiological and clinical features, although no specific guidelines addressing their management have been developed. Bile duct neoplasms generally develop through a multistep process, involving different precursor pathways, ranging from the initial lesion, detectable only microscopically, *i.e.* biliary intraepithelial neoplasia, to the distinctive grades of IPNB until the final stage represented by invasive cholangiocarcinoma. Complex and advanced investigations, mainly relying on magnetic resonance imaging (MRI) and cholangioscopy, are required to reach a correct diagnosis and to define an adequate bile duct mapping, which supports proper treatment. The recently introduced subclassifications of types 1 and 2 highlight the histopathological and clinical aspects of IPNB, as well as their natural evolution with a particular focus on prognosis and survival. Aggressive surgical resection, including hepatectomy, pancreaticoduodenectomy or both, represents the treatment of choice, yielding optimal results in terms of survival, although several endoscopic approaches have been described. IPNBs are newly recognized preinvasive neoplasms of the bile duct with high malignant potential. The novel subclassification of types 1 and 2 defines the histological and clinical aspects, prognosis and survival. Diagnosis is mainly based on MRI and cholangioscopy. Surgical resection represents the mainstay of treatment, although endoscopic resection is currently applied to nonsurgically fit patients. New frontiers in genetic research have identified the processes underlying the carcinogenesis of IPNB, to identify targeted therapies.

Key Words: Intraductal neoplasm of the bile duct; Bile duct neoplasms; Cholangiocarcinoma; Intraductal papilloma; Classification; Treatment

©The Author(s) 2023. Published by Baishideng Publishing Group Inc. All rights reserved.

Core Tip: Intraductal papillary neoplasms of the bile duct are rare premalignant lesions, which are especially prevalent in East Asia. Due to the lack of specific guidelines addressing their management, recent subclassification of types 1 and 2 clarifies several aspects, particularly histopathological, clinical and prognostic features. Magnetic resonance imaging and cholangioscopy occupy a central role in diagnosis and treatment. Surgery is the most appropriate treatment, yielding optimal results in terms of survival, although endoscopic techniques have been used, particularly in nonsurgically fit patients. Lastly, recent genetic research has focused on identifying targeted therapies acting on the stepwise progression of neoplastic biliary epithelium.

Citation: Mocchegiani F, Vincenzi P, Conte G, Nicolini D, Rossi R, Cacciaguerra AB, Vivarelli M. Intraductal papillary neoplasm of the bile duct: The new frontier of biliary pathology. *World J Gastroenterol* 2023; 29(38): 5361-5373
URL: https://www.wjgnet.com/1007-9327/full/v29/i38/5361.htm
DOI: https://dx.doi.org/10.3748/wjg.v29.i38.5361

INTRODUCTION

Intraductal papillary neoplasms of the bile duct (IPNBs), first described by Chen *et al*[1] in 2001, are a type of biliary tumors with a distinctive papillary growth inside the common bile duct lumen, and typically develop along the biliary tree. IPNBs are identified macroscopically, according to bile duct dilatation and intraductal masses apparent upon radiologic imaging[2-4]. Together with biliary intraepithelial neoplasia (BilIN)[5], IPNBs were first recognized as a premalignant lesion of invasive cholangiocarcinoma (CCA) in the 2010 World Health Organization (WHO) classification of tumors of the digestive system[6]. The term IPNB was introduced because of the similarities with intraductal papillary mucinous neoplasms (IPMNs) of the pancreas (IPMN-Ps). IPNBs are considered the biliary counterparts of IPMN-Ps[3,7,8], even though the simultaneous occurrence of both types is rare[9-19].

IPNBs are complex and generally require extensive multidisciplinary investigation. Accurate diagnosis of IPNB is mandatory to guide the therapeutic approach, with aggressive surgical resection being the treatment of choice, particularly in early stages. Endoscopic management has been described as a potential alternative in nonsurgically fit patients [20-24]. This review summarizes the current and latest concepts regarding IPNB, discusses the various morphological features of IPNB and its mimickers, and describes clinical approaches in the diagnosis and treatment that are useful for multidisciplinary management.

DEFINITION, EPIDEMIOLOGY AND CLINICAL FEATURES

Definition

Invasive bile duct neoplasms, *e.g.*, CCA[25], always develop through a multistep process, involving the two above-mentioned precursors: BilIN and IPNB[5]. While BilIN is a flat or low-papillary growth of dysplastic biliary epithelium, detected only microscopically, IPNB consists of an intraductal papillary growth of neoplastic biliary epithelium that can be identified macroscopically and is therefore visible on imaging[3,5].

BilINs have been classified into three grades described as mild, moderate and severe dysplasia, or as low-grade dysplasia, high-grade dysplasia and carcinoma *in situ*[26]. Recently, several cytological features, namely detailed cellular and nuclear changes, glandular involvement, mitosis, nuclear location and intraepithelial neutrophils, have been incorporated into the categorization of BilINs, allowing the identification of three histological grades: BilIN-1, BilIN-2 and BilIN-3 (including the so-called carcinoma *in situ*)[26].

IPNBs are typically represented by a papillary or villous tumor growing inside the bile duct lumen and composed of papillary stalks with fine vascular cores that can develop anywhere along the biliary tree, involving both the intrahepatic and extrahepatic bile ducts[2-4]. Although already described in 2001[1], the term IPNB was introduced by the revised WHO Classification of Tumors of the Digestive System in 2010[6], incorporating different entities; for example, the previously named mucin-producing CCA, papillary CCA (PCC), mucin-hypersecreting bile duct tumor, IPMN of the bile duct, biliary papilloma or papillomatosis, papillary adenocarcinoma of the bile duct, and intraductal growth type CCA[5,6].

Epidemiology, risk factors and clinical features

IPNB is an uncommon disease, with a prevalence of 5%-15% among bile duct tumors and mainly reported in series from East Asia[22,27-30]. It is reported in relation to specific and common risk factors identified such as hepatolithiasis and

liver parasitic infections (*Clonorchis sinensis* and *Opistorchis viverrini*)[2,4]. Other series described the association of IPNB with hepatocellular carcinoma[31], primary sclerosing cholangitis[32] and mixed adenoneuroendocrine carcinoma[33]. Conversely, IPNBs have been described only in isolated reports from Europe, with a propensity of a more invasive course and an extrahepatic location in comparison to those reported in eastern centers[5,34-36]. Similarly, previous reports describing the association of IPNBs with IPMN-Ps are sporadic, as summarized in Table 1[9-19].

IPNB tends to be more frequent in men aged > 65 years, presenting clinically with right upper abdominal discomfort/pain, jaundice, and cholangitis. It has been demonstrated that 5%-29% of patients might be asymptomatic[2,37]. Elevation of total and direct bilirubin, alkaline phosphatase, -glutamyl transferase, alanine aminotransferase and aspartate aminotransferase are common laboratory findings. Increased levels of tumor markers, *i.e.* carcinoembryonic antigen (CEA) and carbohydrate antigen (CA)19-9, have been documented in approximately 25% and 40% of patients, respectively[37].

Although the mucin produced by IPNBs is usually retained inside the neoplastic cells, in up to one-third of cases, elevated quantities of mucin are secreted into the bile duct lumen, leading to intermittent obstruction of the bile flow with consequent upstream and downstream duct dilatation[5]. This particular type of IPNB has been named by some authors as IPMNs of the bile duct[5].

HISTOLOGIC AND MACROSCOPIC FEATURES

Histologic aspects

No precise criteria for grading the biliary epithelium dysplasia within IPNBs have been established. Some authors have divided IPNBs into four types based on the worsening degree of dysplasia, ranging from type 1, low grade, to type 4, stromal invasion of adenocarcinoma[2,5]. Others have classified IPNBs into noninvasive and invasive lesions, including adenoma, borderline tumor, and carcinoma *in situ* in the first group and tubular or mucinous adenocarcinoma in the other group[30,37]. Invasive carcinomas arising from IPNBs have been described in 30%-75% of cases, according to the different surgical series, with a 9%-15% rate of lymph node metastasis at the time of surgical resection[2,27-29,38] and an overall better prognosis when compared to normal CCA[2,21,22,28,39].

Anatomical location and geographical distribution of IPNBs have been correlated with the risk of stromal invasion. Stromal invasion is higher in tumors originating in the extrahepatic bile ducts, and in those affecting Caucasian patients, suggesting a more indolent course of intrahepatic IPNBs (I-IPNBs) and in those occurring in Asian countries[2,3,28,38,40]. Nakanuma *et al*[41] recently reviewed the pathological features of invasive carcinoma associated with IPNB, identifying three different patterns of increasing invasiveness, A, B and C. The first showed a favorable postoperative overall survival (OS) similar to that of noninvasive types, in contrast to the latter two that might be considered clinically advanced entities.

The neoplastic epithelia of IPNB is categorized into four histological phenotypes according to hematoxylin and eosin staining: pancreatobiliary (PB), intestinal, gastric and oncocytic[3,4,42] (Figure 1). The PB type consists of columnar or cuboidal cells with eosinophilic cytoplasm, round hyperchromatic nuclei and scarce mucinous appearance. This variant is usually immunohistochemically positive for mucin (MUC)1, MUC5AC, cytokeratin (CK)7 and S100P[3,4,42]. The intestinal type resembles a colorectal villous neoplasm, showing columnar cells with cigar-shaped nuclei, basophilic cytoplasm, and variable amount of sopranuclear mucin. Immunohistochemically, the cells express MUC2 and MUC5AC but not MUC1[3,4,42]. The gastric type features the gastric foveolar epithelium, consisting of tall columnar cells with basally oriented nuclei and abundant cytoplasmic mucin, generally associated with pyloric glands. While the latter are typically positive for MUC6, the foveolar portions frequently express MUC5AC and CK7 but rarely MUC1 and MUC2[3,4,42]. The oncocytic type presents with convoluted and branching papillae lined by one or different layers of cuboidal/columnar cells with hyperchromatic, round and large nuclei, and abundant, intensely eosinophilic cytoplasm, consistently expressing MUC5AC and focally MUC1 and/or MUC2[3,4,42].

The PB and intestinal patterns are the most common and usually associated with invasive lesions. The remaining two histological types are uncommon and generally present with an indolent course[3,4,42] (Figure 2).

Macroscopic and radiological aspects

Four morphological subtypes have been recognized based on the gross pathological picture: polypoid, superficial-spreading, cystic, and cast-like[5,42]. The polypoid type describes an intraductal lesion, pedunculated or sessile, sometimes reaching great dimensions. Differential diagnosis involves typical CCA and bile duct stones when tumor pieces disintegrate inside the bile ducts[5,42].

The superficial spreading type depicts a tumor barely visible on imaging that spreads along varying lengths of the bile ducts. Radiologically, it appears as isolated bile duct dilatation without an obvious obstructing lesion, secondary to copious mucin production by the tumor. Any biliary obstruction leading to bile duct dilatation can mimic this form, although a real stricture cannot generally be identified in this variant of IPNB[5,42].

The cystic type develops as a focal cystic dilatation of a bile duct that maintains the communication with the lumen of the adjacent bile duct, thus configuring the pattern of a pseudocyst. This feature allows differentiation of the cystic type IPNB from the mucinous cystic neoplasms, *i.e.* cystadenomas and cystadenocarcinomas, where in the absence of a luminal communication, mucin secretion is confined within the neoplastic cyst. In addition, the presence of ovarian-like stroma is necessary to diagnose mucinous cystic neoplasms[5,42]. Lastly, mural nodules or mucin aggregates are common findings in this form of IPNB[5].

Table 1 Summary of reported synchronous intraductal papillary neoplasms of the bile duct and pancreas

Refs	Age (yr)	Sex	IPNB			IPMN-P			Treatment
			Site	Size (cm)	Histology	Site	Size (cm)	Histology	
Joo *et al*[9]	60	M	LL	1.5 × 1.5	Benign	T	2.5 × 2.5	Benign	LH + SPDP
Ishida *et al*[10]	67	M	S1	4 × 3	Benign	UP	3.5 × 3	Benign	LH + S1 segmentectomy + resection of uncinate process
Yamaguchi *et al*[11]	69	M	S2-3	6.5 × 3.5	Malignant	H	3 × 2.5	Malignant	S2-3 segmentectomy + PPPD
Zalinski *et al*[12]	65	F	LL	10 × 10	Malignant	H	NR	High-grade dysplasia	NR
Park *et al*[13]	67	M	S2-3	NR	Medium-grade dysplasia	T	2.5 × 1	Medium-grade dysplasia	S2-3 segmentectomy + DP + splenectomy
Xu *et al*[14]	68	F	S2-3	5 × 4	Benign	T	0.5:1	Benign	laparoscopic S2-3 segmentectomy + SPDP
Valente *et al*[15]	76	F	CBD + LHD + RHD	2.5 × 1.8	Malignant	UP + T	1:1.3	Malignant	CHT + RT
Ren *et al*[16]	52	M	Distal CBD	NR	Malignant	EP	NR	Benign	PPTP
Luvira *et al*[17]	53	M	CBD + LHD + RHD	NR	Malignant	EP	NR	Low-grade dysplasia	L trisectionectomy + PPTP + splenectomy
Moon *et al*[18]	66	F	LL	NR	Malignant	EP	NR	Malignant	LH + TP + splenectomy
Tarantino *et al*[19]	55	F	CBD	NR	NR	H	11	Malignant	NR

IPNB: Intraductal papillary neoplasm of the bile duct; IPMN-P: Intraductal papillary mucinous neoplasm-pancreatic; M: Male; F: Female; LL: Left lobe; T: Tail; LH: Left hepatectomy; SPDP: Spleen preserving distal pancreatectomy; EP: Entire pancreas; UP: Uncinate process; H: Head; PPPD: Pylorus preserving pancreaticoduodenectomy; NR: Not reported; DP: Distal pancreatectomy; CBD: Common bile duct; LHD: Left hepatic duct; RHD: Right hepatic duct; CHT: Chemotherapy; RT: Radiotherapy; PPTP: Pylorus preserving total pancreatectomy; TP: Total pancreatectomy.

In the cast-like type, the tumor occupies the lumen of the bile duct, expanding along the longitudinal axis. Although radiologically it appears as a cast-like lesion, histologically it presents as a polyp, with only a small attachment to the biliary epithelium[5,42].

This macroscopic classification presents some common elements with the classification of mucin-producing CCA proposed by Sakamoto *et al*[43] in 1997, which included the duct-ectatic, cystic and intermediate types. In the first group, papillary tumors developed within diffusely dilated intrahepatic ducts. In the second, large cystic lesions with papillary projections were found inside the liver, communicating with intrahepatic bile ducts. In the latter pattern, large cystic lesions were intermingled with solid tumors invading the liver parenchyma[43]. Histologically, all the CCAs were papillary adenocarcinoma, demonstrating a superficial spread along the bile duct mucosa in almost half of the cases[43].

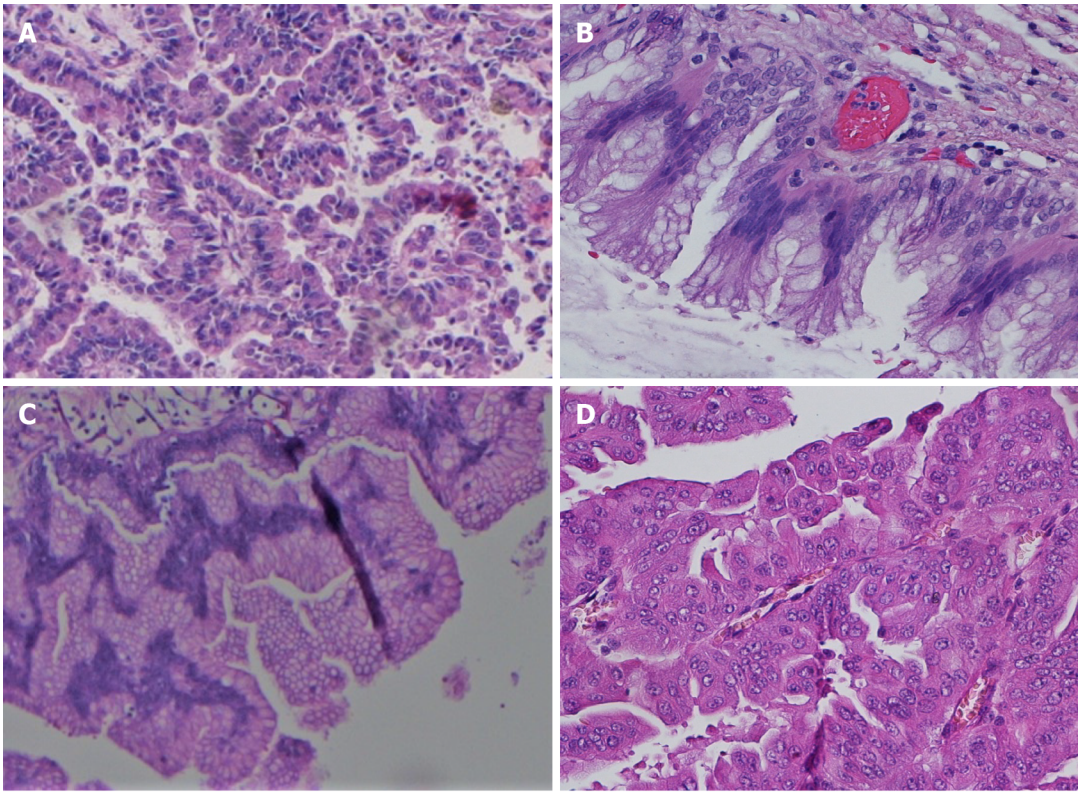
CLASSIFICATIONS

Recently, Kim *et al*[44] resumed the duct-ectatic and cystic subgroups of I-IPNBs that together accounted for most tumors in their surgical series (68.5%), while the remaining were extrahepatic (26.6%) and diffuse (4.1%) types. The latter included lesions diffusely affecting both the intrahepatic and extrahepatic bile ducts. In this modified anatomical classification, as named by the authors, no significant difference in terms of OS was recorded among the three groups[44].

Another radiological-pathological classification was introduced by Luvira *et al*[45] in 2017. Five different categories of IPNB were described in their series of 103 patients: (1) Classical I-IPNB with an intraductal tumor determining unilateral duct dilatation; (2) extrahepatic IPNB (E-IPNB) with an intraductal tumor producing bilateral intrahepatic duct dilatation; (3) cystic lesion with a papillary tumor inside, communicating with the lumen of the bile duct; (4) micropapillary tumor causing disproportionate bile duct dilatation without a clear lesion radiologically evident; and (5) mass-forming tumor with macroinvasion[45]. Their analysis concluded that the category of IPNB and the presence of lymph node metastasis represented the only significant prognostic factors, with class II and V showing worse OS[45].

Novel subclassification of types 1 and 2 IPNBs

In 2020, the Japan Biliary Association and the Korean Association of Hepato-Biliary-Pancreatic Surgery, after retro-



DOI: 10.3748/wjg.v29.i38.5361 **Copyright** ©The Author(s) 2023.

Figure 1 Histological subtypes of intraductal papillary neoplasms of the bile duct. A: Pancreatobiliary; B: Intestinal; C: Gastric; D: Oncocytic. Hematoxylin and eosin staining.

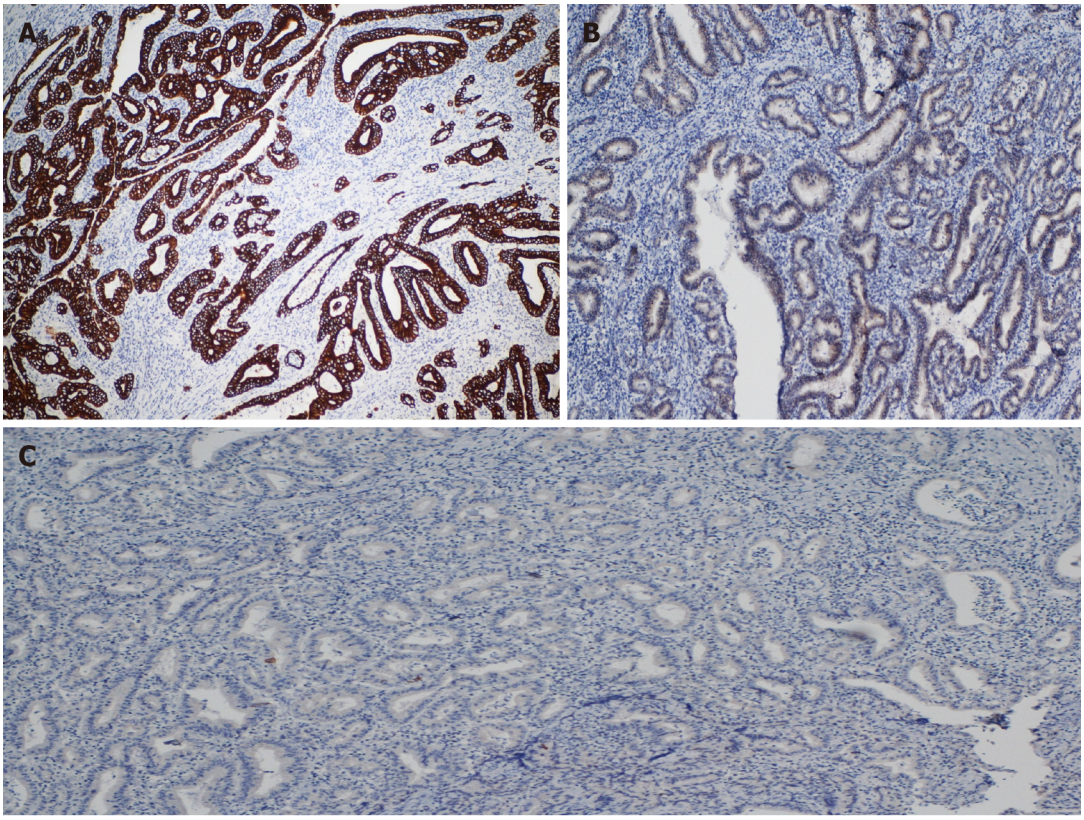
spectively reviewing the clinicopathological data of 694 patients who had undergone surgery for IPNB over a 20-year period, proposed new histopathological diagnostic criteria and identified types 1 and 2 IPNB[28]. Type 1 showed a regular growth with papillary, villous or tubular homogenous structures, thin papillary fibrovascular stalks and a large amount of mucin, and type 2 displayed a heterogenous appearance and an irregular growth with complicated structures, such as cribriform, compact tubular, solid or large cystic components and rare mucin overproduction[28] (Figure 3). In addition, associated invasive carcinoma was reported in almost all cases of type 2 lesions (93.6%), while low-intermediate- or high-grade dysplasia was observed in 9.7% and 40.2% of type 1 lesions, respectively, with ~50% of these exhibiting stromal invasion[28]. The intestinal and gastric histological subtypes were generally associated with type 1, while incidence of the PB subtype was significantly higher in the second group[28].

Clinically, type 1, representing the majority (75%) of tumors reviewed in that multicenter analysis, tended to be more frequent at the level of intrahepatic bile ducts. Conversely, the type 2 tended to develop inside the extrahepatic ducts leading to significantly higher levels of bilirubin, alkaline phosphatase, -glutamyl transferase, alanine aminotransferase, aspartate aminotransferase and tumor markers (CEA and CA19-9), with increased occurrences of liver dysfunction, jaundice and pain[28].

Radiologically, type 1 IPNB typically presented with the aspects of extensive cystic duct dilatation or intraductal cauliflower-like lesion, whereas an intraductal solid mass determining upstream duct dilatation was the classic pattern of type 2[46]. The above-mentioned study highlighted that bile duct margin status after surgical resection did not affect OS and disease-free survival (DFS) in both groups, and there was no significant difference in recurrence rate (RR) observed between types 1 and 2, although lymph node metastasis rate was significantly higher in type 2[28]. Nevertheless, patients with type 2 IPNBs had significantly lower OS and DFS at 1, 3 and 5 years when compared to those with type 1 IPNBs, leading the authors to conclude that their new classification might be strongly predictive of the patient outcome[28].

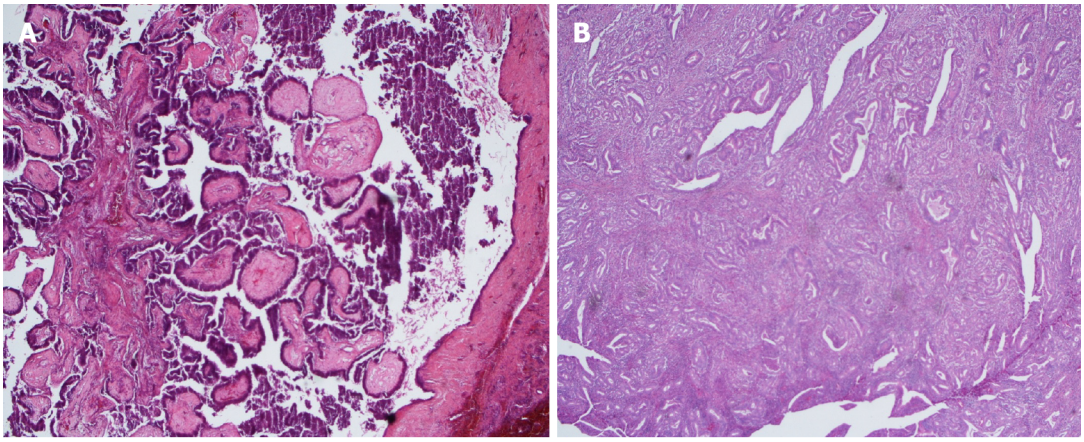
Although the above-mentioned binary classification was included in the most recent WHO classification of digestive system tumors[47], the differential diagnosis between these two types of IPNBs has been challenging, particularly in the hands of unexperienced pathologists. Accordingly, Onoe *et al*[30] developed a scoring system based on six pathological features aimed at differentiating between type 1 and 2 IPNBs. Lesions scoring a total of 5 or 6 were categorized as type 1, whereas those scoring 0 or 1 and 2-4 were categorized as type 2 or unclassifiable, respectively. The authors confirmed the findings of a prevalent intrahepatic location of type 1 IPNB in comparison to the extrahepatic site for type 2, and the survival rates were higher in the first group compared to type 2 or unclassifiable lesions[30].

As other authors have suggested[2,46], type 1 IPNBs might be considered the real biliary counterpart of IPMN-Ps, particularly the main duct variant, while type 2 might be identified as PCC, indicating that papillary bile duct tumors occupy a single continuous spectrum, ranging from less advanced forms, *i.e.* type 1, to more advanced forms, *i.e.* type unclassifiable and type 2. The geographic distribution is divergent between types 1 and 2, with the former being predominant in Asia and the latter in Europe and the USA[46,48].



DOI: 10.3748/wjg.v29.i38.5361 **Copyright** ©The Author(s) 2023.

Figure 2 Histological features of intraductal papillary neoplasms of the bile duct with irregular growth pattern and foci of invasive carcinoma (pancreatobiliary type). A: Immunostaining positive for cytokeratin (CK)19; B: Immunostaining negative for CDX2; C: Immunostaining negative for CK20.

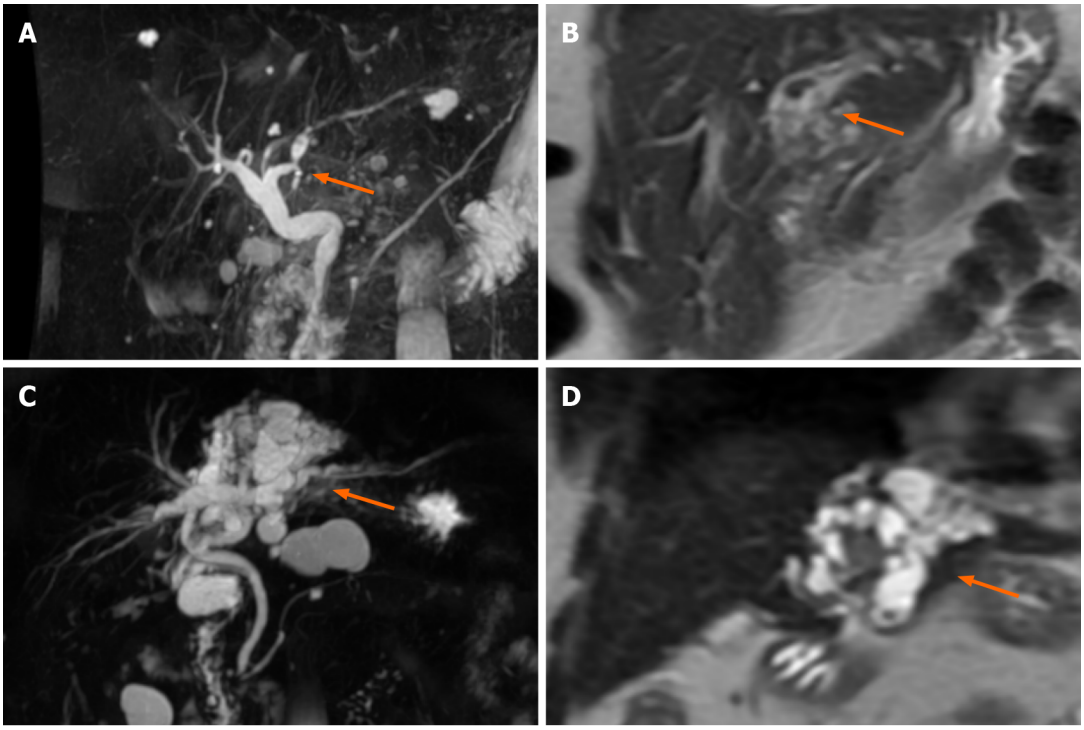


DOI: 10.3748/wjg.v29.i38.5361 **Copyright** ©The Author(s) 2023.

Figure 3 Subclassification of intraductal papillary neoplasms of the bile duct according to the Japan Biliary Association and the Korean Association of Hepato-Biliary-Pancreatic Surgery. A: Type 1 consists of papillary, villous or tubular homogenous structures with thin papillary fibrovascular stalks; B: Type 2 consists of thick papillary glands with irregular branching, often intermingled with solid irregular components. Hematoxylin and eosin staining.

DIAGNOSIS: CROSS-SECTIONAL IMAGING, ENDOSCOPY AND CHOLANGIOSCOPY

Routine diagnostic methods used in IPNBs are represented by computed tomography (CT) and magnetic resonance imaging (MRI), commonly showing intraductal masses associated with bile duct dilatation[42]. On CT, IPNBs generally present an enhancement pattern of isointensity or hyperintensity during the late arterial phase with an occasional intense rim enhancement at the base of the lesions. On MRI, IPNBs tend to be hypointense on T1-weighted images and hyperintense on T2-weighted images, which has the advantage of identifying small intraductal or multiple tumors[2,4,37] (Figure 4).



DOI: 10.3748/wjg.v29.i38.5361 **Copyright** ©The Author(s) 2023.

Figure 4 Magnetic resonance imaging of intraductal papillary neoplasms of the bile duct. A: Magnetic resonance cholangiopancreatography showed an intraductal lesion of the left hepatic duct with upstream bile duct dilatation; B: Diffuse dilatation of the intrahepatic left lobe bile ducts with low intensity tumors (T2 weighted image, coronal section); C: Magnetic resonance cholangiopancreatography showed a cystic type intraductal papillary neoplasm of the bile duct; D: Cystic type intraductal papillary neoplasm of the bile duct (T2 weighted image, coronal section).

Lee *et al*[20] recognized significant features on MRI that are useful in differentiating IPNBs with an associated invasive carcinoma from noninvasive forms. They included an intraductal visible mass, tumor size ≥ 2.5 cm, tumor multiplicity, adjacent organ invasion, and bile duct wall thickening. Bile duct wall thickening had the highest diagnostic accuracy. However, the superficial spread and progression of IPNBs along the bile duct mucosa might be underestimated by conventional imaging[21]. For this reason, intraductal ultrasonography and direct cholangioscopy play a central role in assessing these parameters; that is, the depth and extent of invasion, and in performing a biopsy of the lesion[2,21].

Nevertheless, the discrepancy between the preoperative biopsy and the definitive histology after surgical resection might be notable, particularly in E-IPNB, with a reported negative predictive value of ~40%. This means that ~60% of patients with a preoperative diagnosis of nonmalignancy actually have an invasive carcinoma by definitive pathology [40]. Since these two methods have been widely applied in the evaluation of IPNBs, the current applications of endoscopic retrograde cholangiography are limited, apart from determining the presence of mucobilia or direct communication between a cystic lesion and the bile duct[4] (Figure 5). Therefore, classifications of IPNBs based on their cholangiographic patterns, such as the one proposed by Yeh *et al*[49], no longer have a significant clinical utilization.

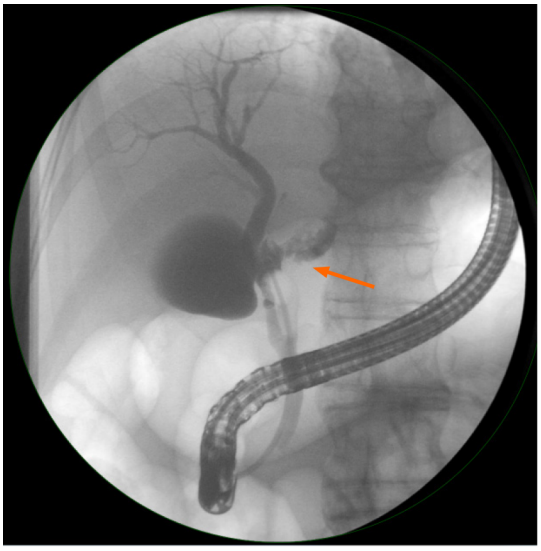
High-risk stigmata of malignancy

Few studies have focused on the analysis of features that might anticipate the risk of invasiveness and/or malignant degeneration in IPNBs[29,40]. In a recent large surgical series, the presence of CEA > 5 IU/mL, CA19-9 > 37 IU/L, a mural nodule > 12 mm, intrahepatic calculi and lymph node enlargement were identified as potential predictors of malignancy in I-IPNB, while total bilirubin > 3 mg/dL, enhancement of mural nodules and CA19-9 > 37 IU/L were potential risk factors in E-IPNB[40].

However, after multivariate analysis, mural nodule > 12 mm [relative risk (RR): 5.33, 95% confidence interval (CI): 1.05-26.89, P = 0.043] and the enhancement of mural nodules (RR: 19.08, 95% CI: 1.08-335.5, P = 0.044) were confirmed as the only significant predictors of malignancy in I-IPNB and E-IPNB, respectively[40]. These two features were identified as absolute surgical indications in IPMN-Ps, according to the 2018 European Guidelines and the 2017 International Consensus Guidelines[50,51].

TREATMENT

Based on the remarkable frequency of high-grade dysplasia or invasive carcinoma and of symptoms reported in IPNBs and on the poor sensitivity of preoperative biopsy, particularly in invasive forms, treatment should be considered mandatory, with surgery representing the main therapeutic option[21].



DOI: 10.3748/wjg.v29.i38.5361 **Copyright** ©The Author(s) 2023.

Figure 5 Endoscopic retrograde cholangiopancreatography of an intrahepatic intraductal papillary neoplasm of the bile duct showed a direct communication between the cystic lesion and the bile duct.

Surgical resection

The type and extent of surgical resection depends on the location of the IPNB, with bile duct resection or pancreaticoduodenectomy applied to E-IPNB and hepatic resection to I-IPNB. Regional lymphadenectomy should always be carried out since the incidence of regional lymph node metastasis is estimated to be 9%-15%[2,27-29].

R0 resection has been reportedly achieved in 90% of patients[4], and the presence of residual disease, including dysplasia, in the resection margin should indicate further resection, although specific guidelines are not available[21]. According to Uemura *et al*[52] and Luvira *et al*[53], only the bile duct margin positive for carcinoma represented a significant poor prognostic factor. Jung *et al*[54] reported the presence of any dysplasia, even if low, in the bile duct margin as having a significant impact on OS and DFS to the same extent as carcinoma *in situ* or invasive carcinoma. Similarly, Youn *et al*[29] identified R1 resection (although, not specifying any dysplasia or carcinoma) as the most important factor for poor outcome in terms of OS and RR, together with high serum levels of CA19-9 (> 37 IU/mL). Conversely, Kubota *et al*[28] in a large surgical series, found that the status of the surgical margin (positive *vs* negative) did not influence the OS, DFS or RR in types 1 and 2 IPNBs, indicating that this parameter does not affect the prognosis.

Role of liver transplantation

Liver transplantation might be considered the only definitive and curative treatment in patients with extensive superficial spread along the bile duct mucosa, bilobar disease or with positive surgical margins, even after multiple resections. However, only limited experience has been described in the literature so far[55-58].

Other therapeutic approaches

In nonsurgically fit patients, some palliative treatments, such as percutaneous transhepatic biliary drainage, biliary stenting and endoscopic approaches (including cholangioscopic electrocoagulation, submucosal resection, argon plasma coagulation, radiofrequency ablation, and transpapillary intraluminal radiotherapy), have been reported[24,59-61].

Among the endoscopic treatments described, the IPNB lesion can be resected *via* electrocoagulation using a high-frequency electric needle knife that directly targets and destroys the tumor tissue[61], through either the classical method of submucosal resection by using polypectomy snares[23], the argon plasma coagulation method that dehydrates the tissue by blocking the blood flow into the lesion and dries the surrounding area[59,62,63], or the radiofrequency ablation method that induces coagulative necrosis of the neoplastic tissue[24]. In particular, the advantage of electrocoagulation relies on its concomitant utilization with cholangioscopy[61], with the ability to reach intrahepatic lesions, which is different from the other techniques that are used by classical endoscopy. Alternatively, transpapillary intraluminal radiotherapy with a high dose of iridium-192 can be delivered directly into the lesion by using an ultrathin flexible probe. Response to treatment can be easily monitored through conventional imaging, and sessions can be repeated according to treatment response[60].

PROGNOSIS AND SURVIVAL

Few reports exist in the literature investigating the natural evolution of untreated IPNBs. In the series of 196 patients with IPNBs by Han *et al*[40], only 16 (9 I-IPNB and 7 E-IPNB) did not undergo surgery and were observed during a median period of ~3 years. Of those with intrahepatic lesions, 55.5% experienced a malignant transformation *versus* 28.5% of those

belonging to the other group. In addition, 33.3% were admitted due to cholangitis *versus* 57.0% of the patients with E-IPNB. The remaining patients did not develop either malignancy or any type of symptoms related to their IPNBs.

Although survival data have varied widely among different series, the studies generally agree on the concept of a significantly improved OS and DFS for surgically resected IPNBs compared to conventional CCAs, with associated decreased rates of lymph node and distant metastases[2,22,36,37,39]. Several factors have been reported to be significant predictors of outcome after surgical resection of IPNBs, although most of them have not been well established or are still considered controversial[27,28,39,44,52].

For example, Rocha *et al*[7] reported depth of invasion (≥ 5 mm, < 5 mm, or none) and percentage of invasive carcinoma components (≥ 10%, < 10%, or none) as the main significant prognostic factors, with patient OS inversely proportional to the grade of invasion and to the proportion of malignancy detected in the IPNB. Similarly, Onoe *et al*[64] investigated 184 patients with PCCs and documented the presence of > 50% invasive components, defined as PCC-4, as an independent predictor of survival that approached the 5-year OS of patients with non-PCCs. The authors concluded that, although IPNBs might be nosologically applied only for PCC cases with < 50% invasive component, their prognostic classification of PCCs according to the proportion of invasive components indicated that all subgroups belonged to a singular disease group[64].

The classification of IPNBs into types 1 and 2, according to their clinical and histopathological features, has been generally recognized as a significant predictor of survival[27,28,52], independent from the grade of dysplasia and/or presence of invasive carcinoma. The 1-, 3-, 5- and 10-year OS rates for type 1 IPNB were 96.1%, 85.2%, 75.2% and 58.5%, respectively, and for type 2 IPNB were 94.6%, 69.1%, 50.9% and 26.8%, respectively ($P < 0.0001$). The 1-, 3-, 5- and 10-year DFS rates for type 1 were 88.3%, 73.8%, 64.1%, and 52.2%, respectively, and for type 2 IPNB were 81.0%, 48.0%, 35.3% and 25.8%, respectively ($P < 0.0001$)[28].

For all these features, type 1 IPNB might be considered the real biliary counterpart of IPMN-Ps, while PCCs might be included in the subgroup of type 2 IPNB, as stated above[2,46]. Likewise, Matsumoto *et al*[38] identified I-IPNB as those with more regular histopathological characteristics and favorable prognosis similar to type 1 in comparison with E-IPNB that might resemble type 2. Another significant poor prognostic factor recognized in several studies was lymph node metastasis, which carried an increased risk of locoregional recurrence[27,28,44,52,53]. Controversial results in terms of prognosis and survival have emerged from the analysis of other distinctive features of IPNBs, such as macroscopic appearance, histological subtype, immunohistochemical phenotype, and level of CA19-9[27,28,39,52,53].

IPNB GENETIC CHANGES AND TARGETED THERAPIES: THE NEW FRONTIERS

Recent genetic analyses of IPNBs have identified several mutations involving different oncogenes and oncosuppressor genes, such as *KRAS*, *BRAF*, *GNAS*, *RNF43*, *TP53*, *APC*, *CTNNB1*, *ZNRF3*, *CDKNZA* and *SMAD4*. The altered expression is strictly related to the different immunohistochemical patterns observed[65-68]. Accordingly, at least three main signaling pathways have been identified in the carcinogenesis of IPNBs: RAS-MAPK, controlled by the *KRAS* and *BRAF* oncogenes; WNT-β-catenin, regulated by the oncogene *CTNNB1* and by two oncosuppressor genes, *APC* and *ZNRF43*; and GPCR-CAMP, activated by mutations of the oncogene *GNAS*[65-68].

In particular, since mutations affecting the *APC* and *CTNNB1* genes have been rarely detected in IPMN-Ps, the WNT-β-catenin pathway appears to have a unique role in the molecular alterations underlying the neoplastic transformation of the biliary epithelium, acting in the early phases of carcinogenesis. Dysregulation of other signaling pathways, particularly the RAS-MAPK pathway, has been described in different neoplasms, such as colorectal, pancreatic and lung cancers[65-68]. In addition, *KRAS* and *GNAS* mutations were frequently identified in type 1 IPNB, often of the intestinal subtype, which share several clinicopathological features with IPMN-Ps, while mutations in the *APC* oncosuppressor gene and in the *CTNNB1* oncogene, that is, the WNT-β-catenin pathway, were generally described in type 2, often associated with the PB subtype[65-68].

These genetic studies confirmed that IPNBs consist of at least two distinct entities, and that the type 1 and 2 subclassifications, recently introduced by the Japan Biliary Association and the Korean Association of Hepato-Biliary-Pancreatic Surgery, may reflect these genetic subcategorizations[65-68]. For all these reasons, recent research has focused its attention on these dysregulated signaling pathways, especially the WNT-β-catenin pathway, identifying several target agents that are currently under evaluation in clinical trials and preclinical studies of application to solid and hematological neoplasms[69,70]. Recently, preliminary valuable results have emerged from the NCT02675946 and NCT03507998 clinical trials evaluating the efficacy and safety of the WNT pathway porcupine inhibitor CGX1321 in advanced gastrointestinal neoplasms, including CCAs. However, at the time of this writing, none of these targeted therapies have been adopted in the field of IPNB management[71].

CONCLUSION

IPNBs are newly recognized preinvasive neoplasms of the bile duct with high malignant potential and a tendency to evolve to invasive CCAs. Although several classifications have been proposed over the past 10 years, the recently introduced subclassification of types 1 and 2 highlights the histopathological and clinical aspects of IPNBs, their natural evolution with a particular focus on prognosis, OS, DFS and similarities/discrepancies with IPMN-Ps. In relation to their complexity, advanced techniques used in a multimodal approach are needed for correct diagnosis and precise identification of their locations, extension and pathological extent.

Surgery with a radical intent represents the most appropriate treatment, although different methods, mainly consisting of endoscopic approaches, can be considered in nonsurgically fit patients. Genetic analysis of the specific mutations driving the stepwise progression of neoplastic biliary epithelium might represent an innovative research field in terms of targeted therapies, particularly those implicating the WNT-β-catenin pathway.

FOOTNOTES

Author contributions: Mocchegiani F and Vincenzi P wrote and revised the paper; Benedetti Cacciaguerra A and Rossi R performed the research; Conte G and Nicolini D analyzed the data; Vivarelli M revised the paper.

Conflict-of-interest statement: The authors declare having no conflicts of interest.

Open-Access: This article is an open-access article that was selected by an in-house editor and fully peer-reviewed by external reviewers. It is distributed in accordance with the Creative Commons Attribution NonCommercial (CC BY-NC 4.0) license, which permits others to distribute, remix, adapt, build upon this work non-commercially, and license their derivative works on different terms, provided the original work is properly cited and the use is non-commercial. See: https://creativecommons.org/Licenses/by-nc/4.0/

Country/Territory of origin: Italy

ORCID number: Federico Mocchegiani 0000-0002-8833-5360; Paolo Vincenzi 0000-0002-5446-2556; Grazia Conte 0000-0002-3877-7355; Daniele Nicolini 0000-0002-5477-3346; Roberta Rossi 0000-0003-3643-6298; Andrea Benedetti Cacciaguerra 0000-0001-6886-8138; Marco Vivarelli 0000-0003-0500-9461.

S-Editor: Lin C
L-Editor: Kerr C
P-Editor: Yuan YY

REFERENCES

1 **Chen TC**, Nakanuma Y, Zen Y, Chen MF, Jan YY, Yeh TS, Chiu CT, Kuo TT, Kamiya J, Oda K, Hamaguchi M, Ohno Y, Hsieh LL, Nimura Y. Intraductal papillary neoplasia of the liver associated with hepatolithiasis. *Hepatology* 2001; **34**: 651-658 [PMID: 11584359 DOI: 10.1053/jhep.2001.28199]

2 **Nakanuma Y**, Uesaka K, Kakuda Y, Sugino T, Kubota K, Furukawa T, Fukumura Y, Isayama H, Terada T. Intraductal Papillary Neoplasm of Bile Duct: Updated Clinicopathological Characteristics and Molecular and Genetic Alterations. *J Clin Med* 2020; **9** [PMID: 33317146 DOI: 10.3390/jcm9123991]

3 **Nakanuma Y**, Kakuda Y, Uesaka K. Characterization of Intraductal Papillary Neoplasm of the Bile Duct with Respect to the Histopathologic Similarities to Pancreatic Intraductal Papillary Mucinous Neoplasm. *Gut Liver* 2019; **13**: 617-627 [PMID: 30982236 DOI: 10.5009/gnl18476]

4 **Gordon-Weeks AN**, Jones K, Harriss E, Smith A, Silva M. Systematic Review and Meta-analysis of Current Experience in Treating IPNB: Clinical and Pathological Correlates. *Ann Surg* 2016; **263**: 656-663 [PMID: 26501712 DOI: 10.1097/SLA.0000000000001426]

5 **Mondal D**, Silva MA, Soonawalla Z, Wang LM, Bungay HK. Intraductal papillary neoplasm of the bile duct (IPN-B): also a disease of western Caucasian patients. A literature review and case series. *Clin Radiol* 2016; **71**: e79-e87 [PMID: 26493757 DOI: 10.1016/j.crad.2015.09.004]

6 **Bosman FT**, Carneiro F, Hruban RH, Theise ND. WHO classification of tumours of the digestive system. 4th ed. Geneva: World Health Organization, 2010

7 **Rocha FG**, Lee H, Katabi N, DeMatteo RP, Fong Y, D'Angelica MI, Allen PJ, Klimstra DS, Jarnagin WR. Intraductal papillary neoplasm of the bile duct: a biliary equivalent to intraductal papillary mucinous neoplasm of the pancreas? *Hepatology* 2012; **56**: 1352-1360 [PMID: 22504729 DOI: 10.1002/hep.25786]

8 **Zaccari P**, Cardinale V, Severi C, Pedica F, Carpino G, Gaudio E, Doglioni C, Petrone MC, Alvaro D, Arcidiacono PG, Capurso G. Common features between neoplastic and preneoplastic lesions of the biliary tract and the pancreas. *World J Gastroenterol* 2019; **25**: 4343-4359 [PMID: 31496617 DOI: 10.3748/wjg.v25.i31.4343]

9 **Joo YH**, Kim MH, Lee SK, Seo DW, Yoo KS, Min YI, Chang JJ, Yu E. A case of mucin-hypersecreting intrahepatic bile duct tumor associated with pancreatic intraductal papillary mucinous tumor. *Gastrointest Endosc* 2000; **52**: 409-412 [PMID: 10968862 DOI: 10.1067/mge.2000.108294]

10 **Ishida M**, Seki K, Honda K, Kimura T, Katayama K, Hirose K, Dojo M, Azuma T, Imamura Y, Hutchins RR, Yamaguchi A. Intraductal mucinous tumors occurring simultaneously in the liver and pancreas. *J Gastroenterol* 2002; **37**: 1073-1078 [PMID: 12522542 DOI: 10.1007/s005350200181]

11 **Yamaguchi Y**, Abe N, Imase K, Mizuno H, Chinen K, Mori H, Sugiyama M, Atomi Y, Ishida H, Takahashi S. A case of mucin hypersecreting intraductal papillary carcinomas occurring simultaneously in liver and pancreas. *Gastrointest Endosc* 2005; **61**: 330-334 [PMID: 15729259 DOI: 10.1016/s0016-5107(04)02635-5]

12 **Zalinski S**, Paradis V, Valla D, Belghiti J. Intraductal papillary mucinous tumors of both biliary and pancreatic ducts. *J Hepatol* 2007; **46**: 978-979 [PMID: 17391800 DOI: 10.1016/j.jhep.2007.02.005]

13 **Park BH**, Suh JH, Cha HJ, Kim YM, Choi HJ. Intraductal Papillary Mucinous Tumor Simultaneously Involving the Liver and Pancreas: A Case Report. *Korean J Pathol* 2010; **44**: 83-86 [DOI: 10.4132/KoreanJPathol.2010.44.1.83]

14 **Xu XW**, Li RH, Zhou W, Wang J, Zhang RC, Chen K, Mou YP. Laparoscopic resection of synchronous intraductal papillary mucinous neoplasms: a case report. *World J Gastroenterol* 2012; **18**: 6510-6514 [PMID: 23197900 DOI: 10.3748/wjg.v18.i44.6510]

15 **Valente R**, Capurso G, Pierantognetti P, Iannicelli E, Piciucchi M, Romiti A, Mercantini P, Larghi A, Federici GF, Barucca V, Osti MF, Di

Giulio E, Ziparo V, Delle Fave G. Simultaneous intraductal papillary neoplasms of the bile duct and pancreas treated with chemoradiotherapy. *World J Gastrointest Oncol* 2012; **4**: 22-25 [PMID: 22403738 DOI: 10.4251/wjgo.v4.i2.22]

16 **Ren X**, Zhu CL, Qin XF, Jiang H, Xia T, Qu YP. Co-occurrence of IPMN and malignant IPNB complicated by a pancreatobiliary fistula: A case report and review of the literature. *World J Clin Cases* 2019; **7**: 102-108 [PMID: 30637259 DOI: 10.12998/wjcc.v7.i1.102]

17 **Luvira V**, Pugkhem A, Tipwaratorn T, Chamgramol Y, Pairojkul C, Bhudhisawasdi V. Simultaneous Extensive Intraductal Papillary Neoplasm of the Bile Duct and Pancreas: A Very Rare Entity. *Case Rep Surg* 2016; **2016**: 1518707 [PMID: 26925284 DOI: 10.1155/2016/1518707]

18 **Moon DB**, Lee SG, Jung DH, Park GC, Park YH, Park HW, Kim MH, Lee SK, Yu ES, Kim JH. Synchronous malignant intraductal papillary mucinous neoplasms of the bile duct and pancreas requiring left hepatectomy and total pancreatectomy. *Korean J Gastroenterol* 2014; **63**: 129-133 [PMID: 24561701 DOI: 10.4166/kjg.2014.63.2.129]

19 **Tarantino I**, Mocciaro F, Barresi L, Vitulo P, Liotta R, Curcio G, Granata A, Pisa MD, Traina M. Synchronous extrapancreatic malignant papillary mucinous neoplasms in a patient with intraductal papillary mucinous neoplasm of the pancreas: a rare case of simultaneous pancreatic, hepatic, and pulmonary involvement. *Pancreas* 2012; **41**: 501-502 [PMID: 22415674 DOI: 10.1097/MPA.0b013e3182320bf7]

20 **Lee S**, Kim MJ, Kim S, Choi D, Jang KT, Park YN. Intraductal papillary neoplasm of the bile duct: Assessment of invasive carcinoma and long-term outcomes using MRI. *J Hepatol* 2019; **70**: 692-699 [PMID: 30553839 DOI: 10.1016/j.jhep.2018.12.005]

21 **Sakai Y**, Ohtsuka M, Sugiyama H, Mikata R, Yasui S, Ohno I, Iino Y, Kato J, Tsuyuguchi T, Kato N. Current status of diagnosis and therapy for intraductal papillary neoplasm of the bile duct. *World J Gastroenterol* 2021; **27**: 1569-1577 [PMID: 33958844 DOI: 10.3748/wjg.v27.i15.1569]

22 **Wu X**, Li B, Zheng C. Clinicopathologic characteristics and long-term prognosis of intraductal papillary neoplasm of the bile duct: a retrospective study. *Eur J Med Res* 2023; **28**: 132 [PMID: 36945047 DOI: 10.1186/s40001-023-01102-w]

23 **Yaghnam I**, Syed N, Peng J, Moyer M. Endoscopic treatment of a large intraductal papillary mucinous neoplasm of the bile duct: tips and tricks learned during multiple treatments of a difficult case. *VideoGIE* 2023; **8**: 141-143 [PMID: 37095840 DOI: 10.1016/j.vgie.2022.12.005]

24 **Natov NS**, Horton LC, Hegde SR. Successful endoscopic treatment of an intraductal papillary neoplasm of the bile duct. *World J Gastrointest Endosc* 2017; **9**: 238-242 [PMID: 28572878 DOI: 10.4253/wjge.v9.i5.238]

25 **Lendvai G**, Szekerczés T, Illyés I, Dóra R, Kontsek E, Gógl A, Kiss A, Werling K, Kovalszky I, Schaff Z, Borka K. Cholangiocarcinoma: Classification, Histopathology and Molecular Carcinogenesis. *Pathol Oncol Res* 2020; **26**: 3-15 [PMID: 30448973 DOI: 10.1007/s12253-018-0491-8]

26 **Geramizadeh B**. Precursor Lesions of Cholangiocarcinoma: A Clinicopathologic Review. *Clin Pathol* 2020; **13**: 2632010X20925045 [PMID: 32596664 DOI: 10.1177/2632010X20925045]

27 **Aoki Y**, Mizuma M, Hata T, Aoki T, Omori Y, Ono Y, Mizukami Y, Unno M, Furukawa T. Intraductal papillary neoplasms of the bile duct consist of two distinct types specifically associated with clinicopathological features and molecular phenotypes. *J Pathol* 2020; **251**: 38-48 [PMID: 32100878 DOI: 10.1002/path.5398]

28 **Kubota K**, Jang JY, Nakanuma Y, Jang KT, Haruyama Y, Fukushima N, Furukawa T, Hong SM, Sakuraoka Y, Kim H, Matsumoto T, Lee KB, Zen Y, Kim J, Miyazaki M, Choi DW, Heo JS, Endo I, Hwang S, Nakamura M, Han HS, Uemoto S, Park SJ, Hong EK, Nanashima A, Kim DS, Kim JY, Ohta T, Kang KJ, Fukumoto T, Nah YW, Seo HI, Inui K, Yoon DS, Unno M. Clinicopathological characteristics of intraductal papillary neoplasm of the bile duct: a Japan-Korea collaborative study. *J Hepatobiliary Pancreat Sci* 2020; **27**: 581-597 [PMID: 32511838 DOI: 10.1002/jhbp.785]

29 **Youn JM**, Hwang S, Ahn CS, Moon DB, Ha TY, Song GW, Jung DH, Hong SM. Clinicopathological Features and Long-Term Outcomes of Intraductal Papillary Neoplasms of the Bile Duct of the Liver: Single-Institution Experience with 146 Patients. *J Gastrointest Surg* 2022; **26**: 1394-1405 [PMID: 35141839 DOI: 10.1007/s11605-022-05268-2]

30 **Onoe S**, Ebata T, Yokoyama Y, Igami T, Mizuno T, Yamaguchi J, Watanabe N, Otsuka S, Nakamura S, Shimoyama Y, Nagino M. A clinicopathological reappraisal of intraductal papillary neoplasm of the bile duct (IPNB): a continuous spectrum with papillary cholangiocarcinoma in 181 curatively resected cases. *HPB (Oxford)* 2021; **23**: 1525-1532 [PMID: 33832834 DOI: 10.1016/j.hpb.2021.03.004]

31 **Xu J**, Sato Y, Harada K, Yoneda N, Ueda T, Kawashima A, Nakanuma Y. Intraductal papillary neoplasm of the bile duct in liver cirrhosis with hepatocellular carcinoma. *World J Gastroenterol* 2011; **17**: 1923-1926 [PMID: 21528069 DOI: 10.3748/wjg.v17.i14.1923]

32 **Hachiya H**, Kita J, Shiraki T, Iso Y, Shimoda M, Kubota K. Intraductal papillary neoplasm of the bile duct developing in a patient with primary sclerosing cholangitis: a case report. *World J Gastroenterol* 2014; **20**: 15925-15930 [PMID: 25400480 DOI: 10.3748/wjg.v20.i42.15925]

33 **Onishi I**, Kitagawa H, Harada K, Maruzen S, Sakai S, Makino I, Hayashi H, Nakagawara H, Tajima H, Takamura H, Tani T, Kayahara M, Ikeda H, Ohta T, Nakanuma Y. Intraductal papillary neoplasm of the bile duct accompanying biliary mixed adenoneuroendocrine carcinoma. *World J Gastroenterol* 2013; **19**: 3161-3164 [PMID: 23716999 DOI: 10.3748/wjg.v19.i20.3161]

34 **Apostolopoulos P**, Ekmektzoglou KA, Paraskeva K, Dimopoulos K, Paparaskeva K, Alexandrakis G. Intraductal papillary neoplasm of the bile duct: case report and review of the literature. *Acta Gastroenterol Belg* 2018; **81**: 97-99 [PMID: 29562383]

35 **Le A**, Mathew A, Khrais A, Khmelnitsky I, Vossough S. Intraductal Papillary Neoplasm of the Bile Duct: A Rare Disease and Presentation. *Cureus* 2023; **15**: e34556 [PMID: 36879718 DOI: 10.7759/cureus.34556]

36 **Schlitter AM**, Born D, Bettstetter M, Specht K, Kim-Fuchs C, Riener MO, Jeliazkova P, Sipos B, Siveke JT, Terris B, Zen Y, Schuster T, Höfler H, Perren A, Klöppel G, Esposito I. Intraductal papillary neoplasms of the bile duct: stepwise progression to carcinoma involves common molecular pathways. *Mod Pathol* 2014; **27**: 73-86 [PMID: 23828315 DOI: 10.1038/modpathol.2013.112]

37 **Krawczyk M**, Ziarkiewicz-Wróblewska B, Podgórska J, Grzybowski J, Gierej B, Krawczyk P, Grąt M, Kornasiewicz O, Skalski M, Wróblewski T. Intraductal papillary neoplasm of the bile duct - A comprehensive review. *Adv Med Sci* 2021; **66**: 138-147 [PMID: 33556909 DOI: 10.1016/j.advms.2021.01.005]

38 **Matsumoto T**, Kubota K, Hachiya H, Sakuraoka Y, Shiraki T, Shimizu T, Mori S, Iso Y, Kato M, Yamagishi H, Imai Y, Aoki T. Impact of Tumor Location on Postoperative Outcome of Intraductal Papillary Neoplasm of the Bile Duct. *World J Surg* 2019; **43**: 1313-1322 [PMID: 30659344 DOI: 10.1007/s00268-019-04913-3]

39 **Harada F**, Matsuyama R, Mori R, Kumamoto T, Morioka D, Taguri M, Yamanaka S, Endo I. Outcomes of surgery for 2010 WHO classification-based intraductal papillary neoplasm of the bile duct: Case-control study of a single Japanese institution's experience with special attention to mucin expression patterns. *Eur J Surg Oncol* 2019; **45**: 761-768 [PMID: 30389302 DOI: 10.1016/j.ejso.2018.10.532]

40 **Han SY**, Kim DU, Nam HS, Kang DH, Jang SI, Lee DK, Shin DW, Cho KB, Yang MJ, Hwang JC, Kim JH, So H, Bang SJ, Sung MJ, Kwon CI, Lee DW, Cho CM, Cho JH. Comparison of the Malignant Predictors in Intrahepatic and Extrahepatic Intraductal Papillary Neoplasm of the

Bile Duct. *J Clin Med* 2022; **11** [PMID: 35407592 DOI: 10.3390/jcm11071985]

41 **Nakanuma Y**, Sugino T, Kakuda Y, Okamura Y, Uesaka K, Nomura Y, Watanabe H, Terada T, Fukumura Y, Ohnishi Y, Sato Y. Pathologic patterns of invasive carcinoma associated with intraductal papillary neoplasms of bile duct (IPNB). *Ann Diagn Pathol* 2022; **61**: 152055 [PMID: 36279801 DOI: 10.1016/j.anndiagpath.2022.152055]

42 **Park HJ**, Kim SY, Kim HJ, Lee SS, Hong GS, Byun JH, Hong SM, Lee MG. Intraductal Papillary Neoplasm of the Bile Duct: Clinical, Imaging, and Pathologic Features. *AJR Am J Roentgenol* 2018; **211**: 67-75 [PMID: 29629808 DOI: 10.2214/AJR.17.19261]

43 **Sakamoto E**, Nimura Y, Hayakawa N, Kamiya J, Kondo S, Nagino M, Kanai M, Miyachi M. Clinicopathological studies of mucin-producing cholangiocarcinoma. *J Hepatobiliary Pancreat Sci* 1997; **4**: 157-62 [DOI: 10.1007/BF02489781]

44 **Kim JR**, Lee KB, Kwon W, Kim E, Kim SW, Jang JY. Comparison of the Clinicopathologic Characteristics of Intraductal Papillary Neoplasm of the Bile Duct according to Morphological and Anatomical Classifications. *J Korean Med Sci* 2018; **33**: e266 [PMID: 30310366 DOI: 10.3346/jkms.2018.33.e266]

45 **Luvira V**, Somsap K, Pugkhem A, Eurboonyanun Ch, Luvira V, Bhudhisawasdi V, Pairojkul Ch, Kamsa Ard S. Morphological Classification of Intraductal Papillary Neoplasm of the Bile Duct with Survival Correlation. *Asian Pac J Cancer Prev* 2017; **18**: 207-213 [PMID: 28240521 DOI: 10.22034/APJCP.2017.18.1.207]

46 **Zen Y**, Akita M. Neoplastic Progression in Intraductal Papillary Neoplasm of the Bile Duct. *Arch Pathol Lab Med* 2023 [PMID: 36800543 DOI: 10.5858/arpa.2022-0407-RA]

47 **Bosman FT**, Carneiro F, Hruban RH, Theise ND. Digestive System Tumours, WHO Classification of Tumours. 5th ed. Geneva: World Health, 2019

48 **Goeppert B**, Stichel D, Toth R, Fritzsche S, Loeffler MA, Schlitter AM, Neumann O, Assenov Y, Vogel MN, Mehrabi A, Hoffmann K, Köhler B, Springfeld C, Weichenhan D, Plass C, Esposito I, Schirmacher P, von Deimling A, Roessler S. Integrative analysis reveals early and distinct genetic and epigenetic changes in intraductal papillary and tubulopapillary cholangiocarcinogenesis. *Gut* 2022; **71**: 391-401 [PMID: 33468537 DOI: 10.1136/gutjnl-2020-322983]

49 **Yeh TS**, Tseng JH, Chiu CT, Liu NJ, Chen TC, Jan YY, Chen MF. Cholangiographic spectrum of intraductal papillary mucinous neoplasm of the bile ducts. *Ann Surg* 2006; **244**: 248-253 [PMID: 16858187 DOI: 10.1097/01.sla.0000217636.40050.54]

50 **Tanaka M**, Fernández-Del Castillo C, Kamisawa T, Jang JY, Levy P, Ohtsuka T, Salvia R, Shimizu Y, Tada M, Wolfgang CL. Revisions of international consensus Fukuoka guidelines for the management of IPMN of the pancreas. *Pancreatology* 2017; **17**: 738-753 [PMID: 28735806 DOI: 10.1016/j.pan.2017.07.007]

51 **European Study Group on Cystic Tumours of the Pancreas**. European evidence-based guidelines on pancreatic cystic neoplasms. *Gut* 2018; **67**: 789-804 [PMID: 29574408 DOI: 10.1136/gutjnl-2018-316027]

52 **Uemura S**, Higuchi R, Yazawa T, Izumo W, Matsunaga Y, Shiihara M, Ota T, Furukawa T, Yamamoto M. Prognostic Factors for Surgically Resected Intraductal Papillary Neoplasm of the Bile Duct: A Retrospective Cohort Study. *Ann Surg Oncol* 2021; **28**: 826-834 [PMID: 32651697 DOI: 10.1245/s10434-020-08835-6]

53 **Luvira V**, Pugkhem A, Bhudhisawasdi V, Pairojkul C, Sathitkarnmanee E, Luvira V, Kamsa-Ard S. Long-term outcome of surgical resection for intraductal papillary neoplasm of the bile duct. *J Gastroenterol Hepatol* 2017; **32**: 527-533 [PMID: 27356284 DOI: 10.1111/jgh.13481]

54 **Jung G**, Park KM, Lee SS, Yu E, Hong SM, Kim J. Long-term clinical outcome of the surgically resected intraductal papillary neoplasm of the bile duct. *J Hepatol* 2012; **57**: 787-793 [PMID: 22634127 DOI: 10.1016/j.jhep.2012.05.008]

55 **Vibert E**, Dokmak S, Belghiti J. Surgical strategy of biliary papillomatosis in Western countries. *J Hepatobiliary Pancreat Sci* 2010; **17**: 241-245 [PMID: 19649560 DOI: 10.1007/s00534-009-0151-1]

56 **Imvrios G**, Papanikolaou V, Lalountas M, Patsiaoura K, Giakoustidis D, Fouzas I, Anagnostara E, Antoniadis N, Takoudas D. Papillomatosis of intra- and extrahepatic biliary tree: Successful treatment with liver transplantation. *Liver Transpl* 2007; **13**: 1045-1048 [PMID: 17600352 DOI: 10.1002/Lt.21207]

57 **Ferraro D**, Levi Sandri GB, Vennarecci G, Santoro R, Colasanti M, Meniconi RL, Lepiane P, Ettorre GM. Successful Orthotopic Liver Transplant for Diffuse Biliary Papillomatosis With Malignant Transformation: A Case Report With Long-Term Follow-Up. *Exp Clin Transplant* 2019; **17**: 835-837 [PMID: 29534660 DOI: 10.6002/ect.2017.0134]

58 **Caso Maestro Ó**, Justo Alonso I, Rodríguez Gil Y, Marcacuzco Quinto A, Calvo Pulido J, Jiménez Romero C. Tumor recurrence after liver transplantation for diffuse biliary papillomatosis in the absence of invasive carcinoma. *Rev Esp Enferm Dig* 2018; **110**: 526-528 [PMID: 29938516 DOI: 10.17235/reed.2018.5557/2018]

59 **Syed AR**, Kumar U, Garg M, Dhawan M, Thakkar S. Argon plasma coagulation treatment of intraductal papillary neoplasm of biliary tract: an alternative approach. *VideoGIE* 2018; **3**: 234-235 [PMID: 30128400 DOI: 10.1016/j.vgie.2018.03.006]

60 **Lu XL**, Itoi T, Kubota K. Cholangioscopy by using narrow-band imaging and transpapillary radiotherapy for mucin-producing bile duct tumor. *Clin Gastroenterol Hepatol* 2009; **7**: e34-e35 [PMID: 19061973 DOI: 10.1016/j.cgh.2008.11.001]

61 **Wu C**, Yang JF, Zhang Q, Liu W, Liao K, Hu B. Successful cholangioscopic electrocoagulation for biliary papillomatosis: Report covering six cases (with video). *Gastroenterol Hepatol* 2021; **44**: 546-551 [PMID: 33617929 DOI: 10.1016/j.gastrohep.2020.12.012]

62 **Brauer BC**, Fukami N, Chen YK. Direct cholangioscopy with narrow-band imaging, chromoendoscopy, and argon plasma coagulation of intraductal papillary mucinous neoplasm of the bile duct (with videos). *Gastrointest Endosc* 2008; **67**: 574-576 [PMID: 18207145 DOI: 10.1016/j.gie.2007.07.031]

63 **Cha B**, Park JS, Jeong S, Lee DH, Kim JM. Direct cholangioscopy with argon plasma coagulation of an intraductal papillary mucinous neoplasm of the bile duct. *Korean J Intern Med* 2019; **34**: 940-941 [PMID: 29761795 DOI: 10.3904/kjim.2017.301]

64 **Onoe S**, Shimoyama Y, Ebata T, Yokoyama Y, Igami T, Sugawara G, Nakamura S, Nagino M. Prognostic delineation of papillary cholangiocarcinoma based on the invasive proportion: a single-institution study with 184 patients. *Surgery* 2014; **155**: 280-291 [PMID: 24287144 DOI: 10.1016/j.surg.2013.08.011]

65 **Yang CY**, Huang WJ, Tsai JH, Cheng A, Chen CC, Hsu HP, Jeng YM. Targeted next-generation sequencing identifies distinct clinicopathologic and molecular entities of intraductal papillary neoplasms of the bile duct. *Mod Pathol* 2019; **32**: 1637-1645 [PMID: 31231124 DOI: 10.1038/s41379-019-0306-9]

66 **Xian ZH**, Qin C, Cong WM. KRAS mutation and immunohistochemical profile in intraductal papillary neoplasm of the intrahepatic bile ducts. *Pathol Res Pract* 2018; **214**: 105-111 [PMID: 29103773 DOI: 10.1016/j.prp.2017.10.017]

67 **Fujikura K**, Akita M, Ajiki T, Fukumoto T, Itoh T, Zen Y. Recurrent Mutations in APC and CTNNB1 and Activated Wnt/β-catenin Signaling in Intraductal Papillary Neoplasms of the Bile Duct: A Whole Exome Sequencing Study. *Am J Surg Pathol* 2018; **42**: 1674-1685 [PMID:

30212390 DOI: 10.1097/PAS.0000000000001155]

68 **Tsai JH**, Liau JY, Yuan CT, Cheng ML, Yuan RH, Jeng YM. RNF43 mutation frequently occurs with GNAS mutation and mucin hypersecretion in intraductal papillary neoplasms of the bile duct. *Histopathology* 2017; **70**: 756-765 [PMID: 27864998 DOI: 10.1111/his.13125]

69 **Zhang Y**, Wang X. Targeting the Wnt/β-catenin signaling pathway in cancer. *J Hematol Oncol* 2020; **13**: 165 [PMID: 33276800 DOI: 10.1186/s13045-020-00990-3]

70 **Wang W**, Cho U, Yoo A, Jung CL, Kim B, Kim H, Lee J, Jo H, Han Y, Song MH, Lee JO, Kim SI, Lee M, Ku JL, Lee C, Song YS. Wnt/β-Catenin Inhibition by CWP232291 as a Novel Therapeutic Strategy in Ovarian Cancer. *Front Oncol* 2022; **12**: 852260 [PMID: 35646632 DOI: 10.3389/fonc.2022.852260]

71 **Giannakis M**, Le DT, Pishvaian MJ, Weinberg BA, Papadopoulos KP, Shen L, Gong J, Li J, Strickler JH, Zhou A, Zhang W, Parikh AR, Deming DA, Falchook GS, Cai J, Rosenstein L, Dorr A, An MM. Phase 1 study of WNT pathway Porcupine inhibitor CGX1321 and phase 1b study of CGX1321 + pembrolizumab (pembro) in patients (pts) with advanced gastrointestinal (GI) tumors. *J Clin Oncol* 2023; **41**: 3514-3514 [DOI: 10.1200/JCO.2023.41.16_suppl.3514]

World Journal of Gastroenterology

Submit a Manuscript: https://www.f6publishing.com

World J Gastroenterol 2023 October 14; 29(38): 5374-5382

DOI: 10.3748/wjg.v29.i38.5374

ISSN 1007-9327 (print) ISSN 2219-2840 (online)

ORIGINAL ARTICLE

Basic Study

Expression and functional study of cholecystokinin-A receptors on the interstitial Cajal-like cells of the guinea pig common bile duct

Dan Xu, Song-Lin Ma, Man-Lin Huang, Heng Zhang

Specialty type: Gastroenterology and hepatology

Provenance and peer review: Unsolicited article; Externally peer reviewed.

Peer-review model: Single blind

Peer-review report's scientific quality classification

Grade A (Excellent): 0
Grade B (Very good): B
Grade C (Good): C
Grade D (Fair): 0
Grade E (Poor): 0

P-Reviewer: de Haas RJ, Netherlands; Venkat V, United States

Received: July 27, 2023
Peer-review started: July 27, 2023
First decision: August 8, 2023
Revised: September 16, 2023
Accepted: September 26, 2023
Article in press: September 26, 2023
Published online: October 14, 2023

Dan Xu, Song-Lin Ma, Man-Lin Huang, Heng Zhang, Department of Gastroenterology, The Central Hospital of Wuhan, Tongji Medical College, Huazhong University of Science and Technology, Wuhan 430014, Hubei Province, China

Dan Xu, Song-Lin Ma, Man-Lin Huang, Heng Zhang, Key Laboratory for Molecular Diagnosis of Hubei Province, The Central Hospital of Wuhan, Tongji Medical College, Huazhong University of Science and Technology, Wuhan 430014, Hubei Province, China

Corresponding author: Heng Zhang, PhD, Doctor, Department of Gastroenterology, The Central Hospital of Wuhan, Tongji Medical College, Huazhong University of Science and Technology, No. 26 Shengli Street, Jiang'an District, Wuhan 430014, Hubei Province, China.
xqzr@sohu.com

Abstract

BACKGROUND

Many studies have shown that interstitial Cajal-like cell (ICLC) abnormalities are closely related to a variety of dynamic gastrointestinal disorders. ICLCs are pacemaker cells for gastrointestinal movement and are involved in the transmission of nerve impulses.

AIM

To elucidate the expression profile and significance of cholecystokinin-A (CCK-A) receptors in ICLCs in the common bile duct (CBD), as well as the role of CCK in regulating CBD motility through CCK-A receptors on CBD ICLCs.

METHODS

The levels of tyrosine kinase receptor (c-kit) and CCK-A receptors in CBD tissues and isolated CBD cells were quantified using the double immunofluorescence labeling technique. The CCK-mediated enhancement of the movement of CBD muscle strips through CBD ICLCs was observed by a muscle strip contraction test.

RESULTS

Immunofluorescence showed co-expression of c-kit and CCK-A receptors in the CBD muscularis layer. Observations of isolated CBD cells showed that c-kit was expressed on the surface of ICLCs, the cell body and synapse were colored and polygonal, and some cells presented protrusions and formed networks adjacent to the CBD while others formed filaments at the synaptic terminals of local cells. CCK-A receptors were also expressed on CBD ICLCs. At concentrations ranging

from 10^{-6} mol/L to 10^{-10} mol/L, CCK promoted CBD smooth muscle contractility in a dose-dependent manner. In contrast, after ICLC removal, the contractility mediated by CCK in CBD smooth muscle decreased.

CONCLUSION
CCK-A receptors are highly expressed on CBD ICLCs, and CCK may regulate CBD motility through the CCK-A receptors on ICLCs.

Key Words: Interstitial Cajal-like cells; Tyrosine kinase receptor; Common bile duct; Cholecystokinin-A receptors

©The Author(s) 2023. Published by Baishideng Publishing Group Inc. All rights reserved.

Core Tip: Interstitial Cajal-like cells (ICLCs) are pacemaker cells for gastrointestinal movement and are involved in the transmission of nerve impulses. This projects intends to elucidate the expression profiling and significance of cholecystokinin-A (CCK-A) receptors in ICLCs of common bile duct (CBD), as well as the role of CCK in regulating CBD motility through CCK-A receptors on CBD ICLCs.

Citation: Xu D, Ma SL, Huang ML, Zhang H. Expression and functional study of cholecystokinin-A receptors on the interstitial Cajal-like cells of the guinea pig common bile duct. *World J Gastroenterol* 2023; 29(38): 5374-5382
URL: https://www.wjgnet.com/1007-9327/full/v29/i38/5374.htm
DOI: https://dx.doi.org/10.3748/wjg.v29.i38.5374

INTRODUCTION

Cholecystokinin (CCK) was first found in the gastrointestinal tract (GIT) and was named for its function of stimulating gallbladder contraction. Endothelial cells in the proximal small intestine release CCK after food intake[1]. CCK was thought to directly stimulate gallbladder smooth muscle cells (SMCs) to cause gallbladder contraction[2]. In recent years, the existence of CCK receptors has been confirmed by isolating gallbladder SMCs and radioimmunoassays[3]. CCK, classified into either the CCK-A subtype or CCK-B subtype, can bind to receptors and participate in modulating a series of physiological functions, such as gallbladder contraction, pancreatic enzyme secretion and gastric acid secretion[4]. CCKs in the blood circulation are present as four peptides with chains of different lengths, namely, CCK octapeptide (CCK-8), CCK-33, CCK-39 and CCK-58, among which CCK-8 has the greatest physiological effect on gallbladder contraction[2]. CCK has been reported to regulate guinea pig ileal contraction *via* CCK-A and CCK-B receptors[5], but CCK modulates guinea pig gallbladder contraction through only CCK-A receptors[6].

CCK regulates biliary system motility in two ways: By neural mechanisms and through receptor binding. Abundant intrinsic and extrinsic nerve plexuses are distributed around the biliary system, with cholinergic and adrenergic fibers and a large number of peptidergic fibers containing various neuropeptides, such as CCK peptidergic fibers. The neural mechanism by which CCK is involved in gallbladder contraction is its direct action on presynaptic neurons and promotion of the release of the neurotransmitter acetylcholine, thus enhancing gallbladder smooth muscle contraction. In addition, CCK directly boosts gallbladder smooth muscle contractility by binding to specific CCK-A receptors on gallbladder smooth muscle[7].

Interstitial Cajal cells (ICCs) are interstitial cells that exist in the GIT and are related to the basic electric rhythm (BER). The tyrosine kinase receptor (c-kit) expressed by ICCs can activate a tyrosine kinase, trigger intracellular signal transduction and maintain the ICC phenotype[7], making c-kit a specific marker for gastrointestinal ICCs. Essentially, ICCs are a kind of BER pacemaker cell, and the network formed by their processes can assist in spreading BER[8]. In recent years, interstitial Cajal-like cells (ICLCs) or ICCs outside the GIT have become a research hotspot[9], with evidence indicating the presence of ICLCs in mice[7], guinea pigs[10] and human gallbladder[11]. ICLCs have also been reported in the common bile duct (CBD) of guinea pigs[12].

From these research directions, this study aims to preliminarily investigate the pathogenesis of biliary tract diseases to deepen our understanding of biliary tract dynamics and provide novel ideas for the pathogenesis and clinical treatment of related dynamic diseases by determining the following: (1) The distribution, expression, morphology and ultrastructure of CBD ICLCs; (2) The expression and function of CCK-A receptors on CBD ICLCs; (3) The pathogenesis of biliary tract dynamics and related dynamic diseases such as choledocholithiasis; (4) The expression of CCK-A receptors on CBD ICLCs; and (5) How CCK regulates biliary tract dynamics through CBD ICLCs.

MATERIALS AND METHODS

Materials

The experimental animals were adult guinea pigs of both sexes weighing 250-300 g and were supplied by the Center for

Animal Experiment of Wuhan University. All protocols were approved by the Institutional Animal Care and Use Committee of The Central Hospital of Wuhan, Tongji Medical College, Huazhong University of Science and Technology.

Methods

Expression of c-kit and CCK-A receptors in CBD sections: Preparation of CBD tissue. The guinea pigs were fasted overnight and euthanized *via* CO_2 inhalation[13] in the morning (10 a.m.) of the following day. The CBD tissue was collected from the guinea pigs and immediately placed in a Ca^{2+}-free physiological saline solution (PSS) petri dish, which was continuously oxygenated with 95% O_2: 5% CO_2. The CBD blood vessels were then peeled off under a microscope, and the CBD tissue was washed with Ca^{2+}-free PSS (20 mL). All experimental procedures conformed to the guidelines from the Committee on the Ethics of Animal Experiments of the Central Hospital of Wuhan.

Immunohistochemistry: The collected tissues were immersed in 4% paraformaldehyde fixative overnight (4 °C, 16-18 h). After the samples were dehydrated and made transparent using different concentration gradients of ethanol and xylene according to routine procedures followed by embedding, slicing and conventional dehydration. The tissue was then cultivated with 3% hydrogen peroxide for 10 min before rinsing with distilled water, followed by washing with phosphate buffered saline (PBS) (3 min each). Diluted normal goat serum was added dropwise to block the samples at room temperature for 10 min. Then, the following diluted primary antibodies were added dropwise: Anti-c-kit monoclonal (1:100) and anti-CCK-A receptor (1:8000), and the sample was placed in a wet box sealed and kept at 4 °C overnight. Subsequently, FITC-labeled rabbit anti-rat IgG (1:50) and Cy3-labeled goat anti-rabbit antibody (1:50) were added for 1 h of incubation at room temperature away from light, followed by washing with PBS and mounting with 50% glycerol. The CBD tissue was finally observed under a laser confocal microscope and photographed. Confocal fluorescence images were captured using an electron multiplying charge-coupled device camera (EMCCD, iXon Ultra, Andor, Tokyo, Japan) mounted onto an inverted microscope (IX83, Olympus), and the fluorescence intensity was quantified using capture software (iQ3, Andor).

Immunofluorescence determination of c-kit and CCK-A receptors in CBD-cultured cells

Preparation of the CBD ICLC single-cell suspension: Guinea pig CBD tissue was collected in the same way as described above. Then, the CBD tissue was fixed for longitudinal and horizontal dissection, and the mucous layer was stripped. Next, the muscle strips were cut into pieces, and 1-2 mm^3 pieces were placed into a beaker to which 5 mL of type II collagenase digestive solution was added with slight oscillation and digestion at 37 °C for 23 min. Then, the strips were rinsed five times with Ca^{2+}-free PSS. After that, the tissue blocks were mixed with a wide-mouth fire-polished pipette to produce a cell suspension, which was then added to an equal volume of Ficoll 400 gradient solution for 10 min of centrifugation (30 g). The cells at the interface of the liquid surface were precipitated and plated.

Cell inoculation: First, cells were suspended in M199 culture medium to adjust the concentration to 1×10^6/mL, followed by seeding the cell suspension into the wells of a 6-well culture plate, in which a rat tail collagen-coated (2 ng/cm^2) cover glass was placed in advance. The plate was then put into an incubator to culture under 5% CO_2 at 37 °C.

Expression of c-kit and CCK-A receptors on ICLCs determined by immunofluorescence. The culture medium in the petri dish was removed, and the nonadherent cells were washed away after 24 h of cell culture. The remaining cells were rinsed with PBS three times, fixed at room temperature for 10 min with acetone, washed again with PBS, and sheep serum was added for 30 min of blocking at ambient temperature. Then, anti-c-kit monoclonal antibody (1:100) and anti-CCK-A receptor polyclonal antibody (1:8000) were added for incubation overnight at 4 °C. Finally, FITC-labeled rabbit anti-rat IgG (1:50) and Cy3-labeled goat anti-rabbit IgG (1:50) were added for 1 h of incubation at room temperature away from light, followed by washing with PBS and mounting with 50% glycerol. The cells were observed under a laser confocal microscope and photographs were taken.

Contractile response of guinea pig CBD muscle strips to CCK-8

Preparation of guinea pig CBD muscle strips: Muscle strips (8 mm × 2 mm) were used to prepare two types of smooth muscle strips: (1) CBD muscle strips with ICLCs; and (2) Muscle strips with damaged CBD ICLCs.

Damaged CBD ICLCs: ICLCs were selectively damaged by 50 μmol of methylene blue (MB) + 50 mW/cm light irradiation. Using an adjustable 540 nm spotlight, the tissue sample was placed 315 cm away from the light source and irradiated on the tissue surface for 5 min. A digital photometer was used to measure light intensity. This approach damaged only the ICLC structure and not the CBD intermuscular neural network or SMCs[14].

Contractile response of CCK-8 to CBD muscle strips: Four prepared CBD muscle strips were placed in tissue chambers with one strip per chamber. One end of the CBD muscle strip was fixed on the hook at the bottom of the tissue chamber, and the other end was fixed on the tension sensor. The input signal was input into the physiological recorder to record the spontaneous contractive activity of the CBD muscle strip. Each tissue chamber contained 5 mL of Krebs solution at 37 °C and was continuously filled with mixed gas composed of 5% CO_2 and 95% O_2. The muscle strips were incubated for approximately 1 h under a 1 g preload, and after the spontaneous contraction of the muscle strips was observed to be smooth, atropine (10^{-6} mol/L) and tetrodotoxin (TTX) (3×10^{-7} mol/L) were added to observe the contractile activity of the CBD muscle strips. Subsequently, CCK-8 at concentrations ranging from 10^{-8} to 10^{-6} mol/L was added to observe the reaction after ICLC removal. The test procedure was performed as described above.

Identification of damaged CBD ICLCs: After the muscle strip experiment, a 1 mm^3 section of the CBD tissue was put into buffered glutaraldehyde fixative (2.5%, 2 h), rinsed with PBS, and refixed with 1% OsO_4 (1 h). Then, the samples were

dehydrated with a gradient series of alcohol and acetone and embedded in Epon 812 resin. Following ultrathin sectioning, the tissue was double-stained with uranyl acetate and lead citrate to be observed and photographed using an FEI Tecnai G^2 12 transmission electron microscope.

Statistical analysis

Experiments were repeated at least three times, and the measured data were averaged.

RESULTS

Expression of c-kit and CCK-A receptors on CBD tissue sections determined by co-immunofluorescence

c-kit-positive cells were mainly distributed in the muscularis layer of the CBD co-expressing CCK-A receptors. These cells aggregated in a network and were distributed parallel to the circular muscle, as shown in Figure 1. The optimal concentration of CCK-A receptor primary antibody was 1:8000; below this concentration, the CCK-A receptors were hardly expressed in CBD SMCs, but once the antibody concentration was above 1:8000, CCK-A receptor immunopositivity was observed in CBD SMCs (Figure 1).

Expression of c-kit and CCK-A receptors on CBD cultured cells determined by co-immunofluorescence

The CBD ICLCs of guinea pigs after immunofluorescence staining were observed under a laser confocal microscope. It was found that the ICLCs were polygonal and c-kit positive with well-stained cell bodies and synapses. Some cells presented long and thin protrusions, while others had more slender synaptic terminals that formed filaments. There were few CBD ICLCs, and they were distributed roughly parallel to the circular muscle and clustered in a network. Moreover, CCK-A receptors were highly expressed in CBD ICLCs. In ICLCs with multiple synapses, the synapses extended into adjacent SMCs, with very large hyperchromatic nuclei in most of the cells, scattered chromatin, and relatively little cytoplasm. However, the organelles were abundant, including well-developed perinuclear endoplasmic reticulum and rough endoplasmic reticulum, which were closely arranged in the cytoplasm. Mitochondria and free ribosomes were also abundant, and the cells had many filaments and intermediate filaments but no myofilaments, distinguishing them from peripheral SMCs. The characteristic structure that distinguished ICLCs from fibrocytes, glial cells and macrophages was caveolae. ICLCs were surrounded by collagen fibers and formed cellular junctions with surrounding SMCs (Figure 2).

Response of guinea pig CBD muscle strips to CCK-8

The response of CBD muscle strips with ICLCs to CCK: Figure 3A shows the contractile response curve of guinea pig CBD muscle strips treated with CCK-8 at concentrations ranging from 10^{-10} to 10^{-6} mol/L. CCK-8 dose dependently enhanced the contractile amplitude of the CBD muscle strips. Pre-addition of atropine (10^{-6} mol/L) and TTX (3×10^{-7} mol/L) was performed to eliminate nervous system contraction of the CBD strips in guinea pigs and did not affect contraction of the CBD muscle strips by CCK-8 in guinea pigs.

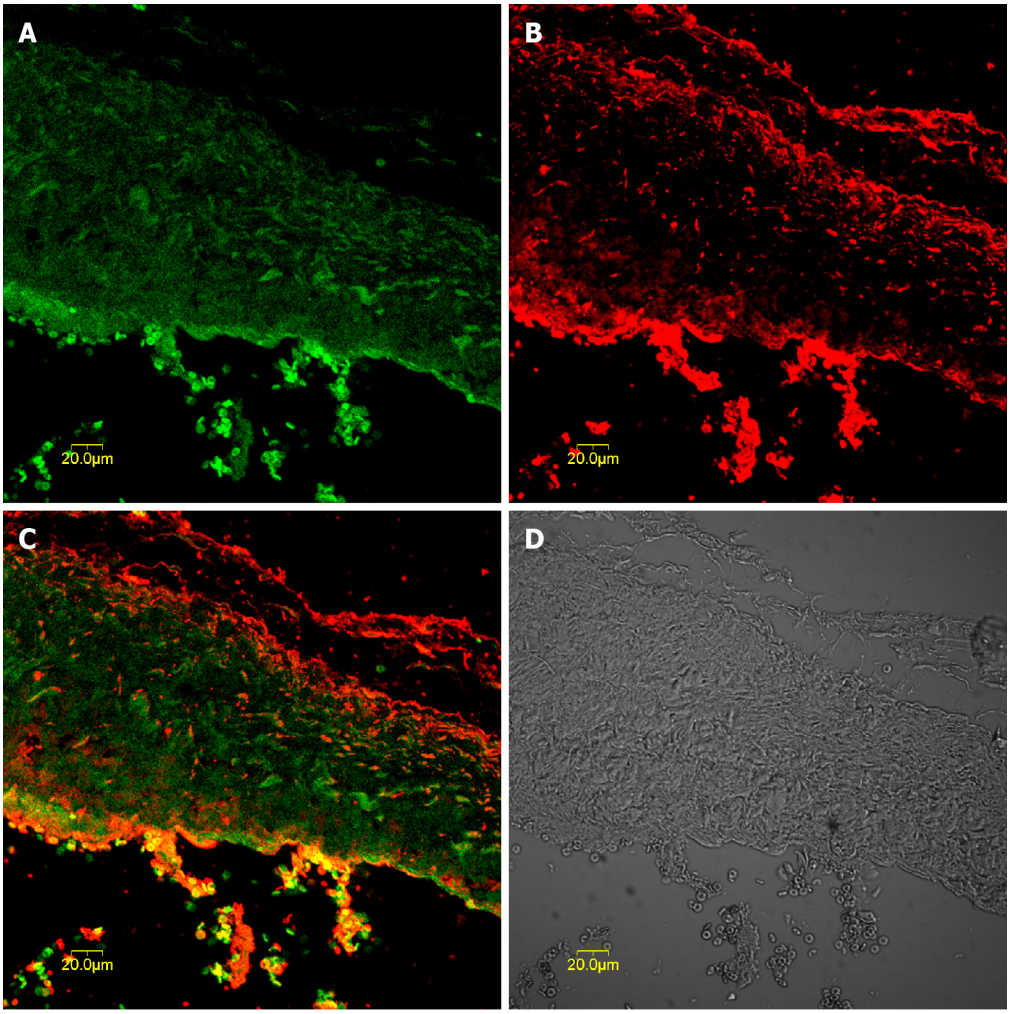
Response of ICLC-removed CBD muscle strips to CCK-8: Figure 3B shows the contractile response curve of guinea pig CBD after ICLC removal to CCK-8 (concentration range: 10^{-6} to 10^{-10} mol/L), which showed a rightward shift.

Electron microscopy images of the damaged CBD ICLCs: The following features were observed in CBD ICLCs damaged by MB plus light irradiation under an electron microscope: Incomplete cell membrane, nuclear swelling, chromatin homogenization, partial expansion of the endoplasmic reticulum, unrecognizable mitochondrial damage, and a reduction in or even the disappearance of the characteristic caveolae. However, and no damage was observed to CBD SMCs after treatment with MB plus light (Figure 4).

DISCUSSION

Biliary tract motility includes the movements of the gallbladder and bile duct[15]. The motility of the CBD is regulated by autonomic nerves as well as joint regulation by gastrointestinal hormones (CCK, motilin, *etc.*) and neuromediators. Together with nerve regulation, these substances coordinate the contraction and relaxation of the CBD[16]. In contrast, biliary system dysfunction causes cholestasis, which is an important precursor of choledocholithiasis. There are few intrahepatic bile duct SMCs. The distribution of extrahepatic bile duct SMCs also varies, with SMC detection rates in the common hepatic duct, upper duodenum of the CBD, and pancreatic segment being 24%, 53%, and 87%, respectively. There are only a few longitudinal or circular SMCs in the upper segment of the CBD, which form the CBD sphincter (the CBD and pancreatic duct end and ampullary around the ring of the sphincter, collectively known as the Oddi sphincter [17]) at the ampulla[7]. In the bile duct wall, no obvious intramural nerve plexus formed, although there were many nerve cells. CBD motility can be divided into active lengthening and shortening movements for bile transportation[18].

ICCs, which are involved in transmitting nerve impulses to mediate gastrointestinal motility, are the pacemakers of gastrointestinal motility. Extra-gastrointestinal ICLCs share similar functions with gastrointestinal pacemaker cells. These ICLCs lack contractile activity but have morphological characteristics similar to ICCs, including elongated and abundant protrusions, intermediate filaments, mitochondria, and characteristic caveolae that can form network structures. ICLCs also function similarly to ICCs in the GIT. Studies have shown that there are special pacemaker cells in the rabbit urethra;



DOI: 10.3748/wjg.v29.i38.5374 **Copyright** ©The Author(s) 2023.

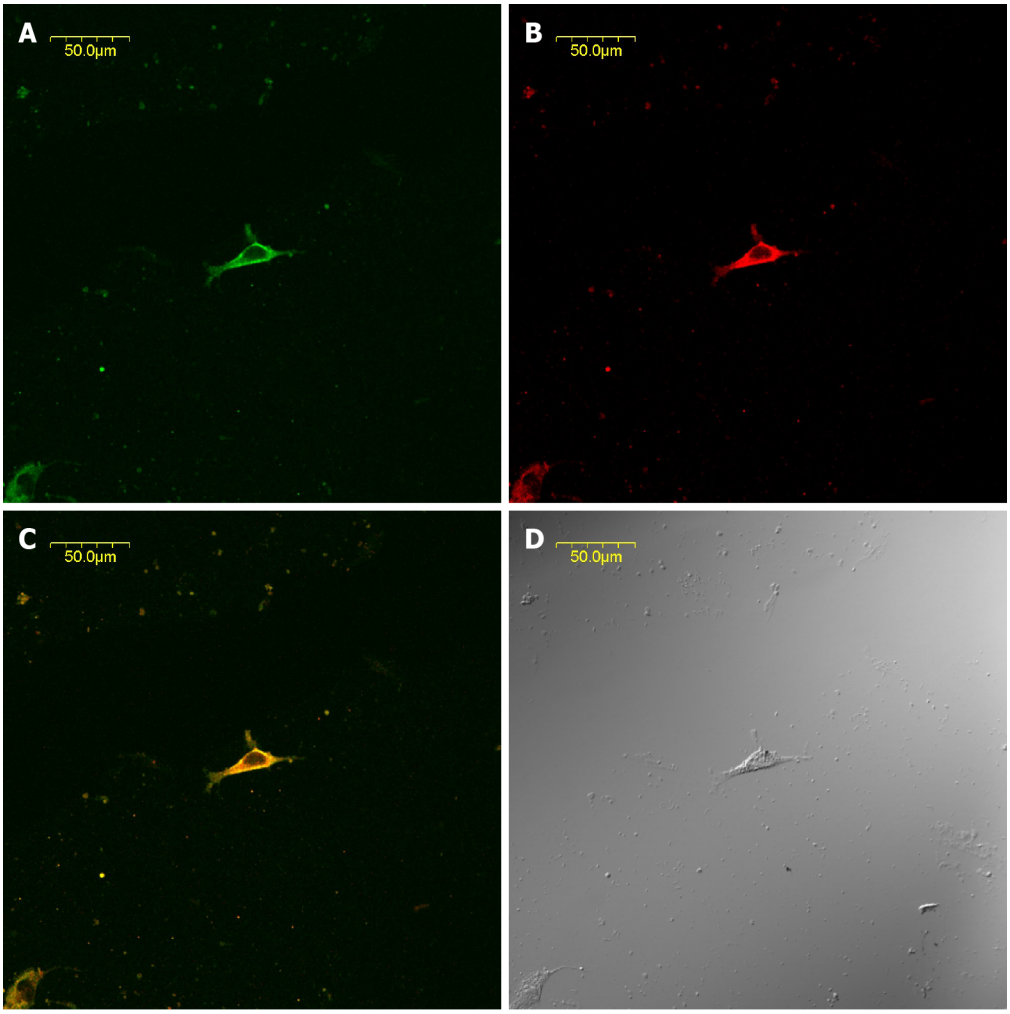
Figure 1 Expression of tyrosine kinase receptor and cholecystokinin-A receptors in gallbladder tissue sections determined by immunofluorescence. A: Tyrosine kinase receptor-positive cells (green) in the muscularis layer of the gallbladder; B: Cholecystokinin-A receptor-positive cells (red) were mainly located in the muscularis layer of the gallbladder; C: Synthetic micrographs of A and B; D: Phase-contrast micrograph of A and B.

such ICLCs are similar to rabbit intestinal ICCs and generate slow waves[19]. ICLCs are also present in the CBD sphincter [20].

In this study, it was found that guinea pig CBD ICLCs had abundant mitochondria, which were active and provided energy for slow-wave pacemaker cells. The CBD ICLCs contained a large amount of endoplasmic reticulum, especially rough endoplasmic reticulum, which explains their active synthesis and secretion functions. In addition, the cellular junctions formed between ICLCs and SMCs may act as an intermediary regulating nervous system-mediated control of the movement of CBD SMCs.

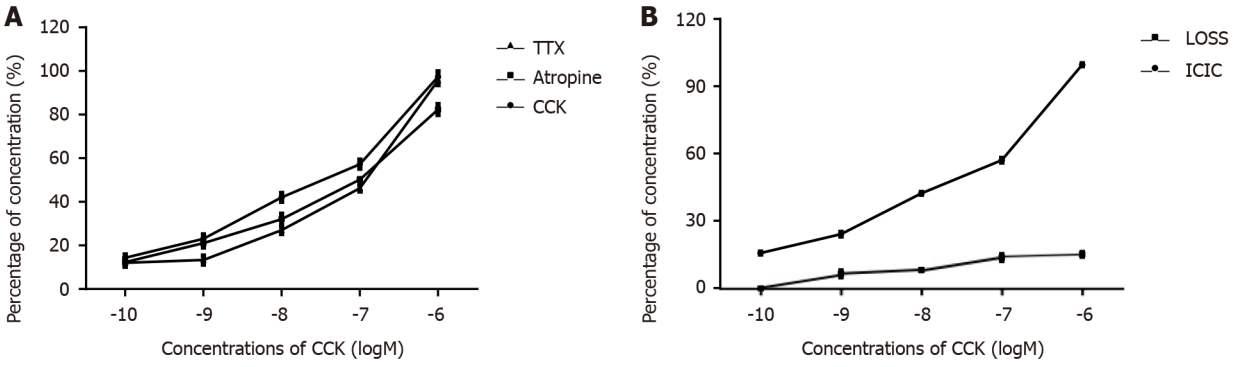
Cholecystic contractile function is enhanced as the CCK level increases; a decrease in the CCK level and its concomitant gallbladder contraction dysfunction are important pathological mechanisms leading to the formation of gallstones[21]. CCK-A receptors are found in gallbladder smooth muscle, and CCK binding to CCK-A receptors plays a vital role in gallbladder motility. The conventional view is that CCK regulates gallbladder contraction through a neural mechanism that acts on presynaptic neurons to increase the release of acetylcholine, which affects smooth muscle contraction. CCK can also directly contract gallbladder smooth muscle, mainly through specific binding with CCK-A receptors on gallbladder smooth muscle, activating non-G protein-mediated signaling pathways and G protein-coupled signaling pathways to promote signal transduction, thus causing relevant physiological effects[22].

The expression of CCK-A receptors on isolated cultured ICLC slides was confirmed in guinea pig CBD ICLCs by choledochal histology and immunofluorescence. In the choledochal tissue section, clear immunofluorescence was observed, and CCK-A receptors were distributed in the choledochal smooth muscle layer. A CCK-A receptor antibody concentration higher than 1:8000 was initially used in the immunofluorescence assay of CBD tissue sections and revealed no difference in fluorescence intensity between CBD smooth muscle and ICLCs. When the antibody concentration was 1:8000, the SMCs in the CBD tissue sections were not detected, while the ICLC fluorescence intensity was strongly positive. Therefore, CCK-A receptors were expressed in both SMCs and ICLCs of the guinea pig CBD, with a higher concentration in the former.



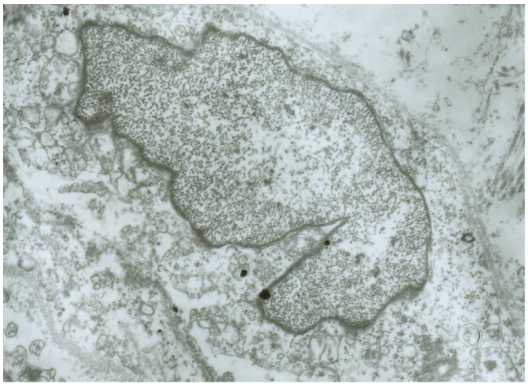
DOI: 10.3748/wjg.v29.i38.5374 **Copyright** ©The Author(s) 2023.

Figure 2 Expression of tyrosine kinase receptor and cholecystokinin-A receptors in common bile duct cultured cells determined by immunofluorescence. A: Interstitial Cajal-like cells (ICLCs) are tyrosine kinase receptor-positive (green); B: ICLCs express cholecystokinin-A receptors (red); C: Synthetic micrographs of A and B; D: Phase-contrast micrographs of A and B.



DOI: 10.3748/wjg.v29.i38.5374 **Copyright** ©The Author(s) 2023.

Figure 3 Response of common bile duct muscle strips with interstitial Cajal-like cells and interstitial Cajal-like cell-removed common bile duct muscle strips to cholecystokinin octapeptide. A: Response of common bile duct muscle strips with interstitial Cajal-like cells (ICLCs) to cholecystokinin octapeptide (CCK-8); B: Response of ICLC-removed common bile duct muscle strips to CCK-8. ICLC: Interstitial Cajal-like cell; CCK: Cholecystokinin; TTX: Tetrodotoxin.



DOI: 10.3748/wjg.v29.i38.5374 **Copyright** ©The Author(s) 2023.

Figure 4 Electron microscopy images of damaged interstitial Cajal-like cells. Interstitial Cajal-like cells (ICLCs) in common bile duct notably changed after incubation with methylene blue and light treatment. The ICLCs were swollen, the cytoplasm was loose, the number of mitochondria was reduced, the caveolae disappeared, and the cell membrane was damaged.

CCK-A was also found to be expressed on CBD ICLCs in this study. Therefore, how does CCK regulate CBD motility? Is it through CCK-A receptors on ICLCs in addition to directly binding with CCK-A receptors to promote CBD motility? We found that guinea pig CBD ICLCs strongly expressed CCK-A receptors, suggesting the important role of ICCs in CCK-induced CBD smooth muscle contraction. Thus, CCK may regulate biliary system pressure through CCK-A receptors on CBD ICLCs.

In this experiment, CCK-8 notably and dose-dependently increased the contraction of CBD muscle strips. Following the removal of ICLCs, however, we observed a significant rightward shift in the contractile dose-response curve of the CBD smooth muscle strips induced by CCK-8. After light + MB treatment, the guinea pig ICLCs were clearly altered. The electron microscopy images of CBD ICLCs showed swollen cell bodies, loose cytoplasm, notably fewer mitochondria, disappearance of the characteristic caveolae, and destroyed cell membranes. Light + MB treatment specifically damages only the ICLCs but not the SMCs that are closely connected to them[17]. These findings suggest that CBD ICLCs are crucial in initiating SMC contraction. After the ICLCs were removed, CCK caused a significant decrease in the contractility of the CBD muscle strips, indicating that CCK may partially induce the contraction of guinea pig CBD smooth muscle through the CCK-A receptors on the CBD ICLCs.

CONCLUSION

This research demonstrates the dose-dependent contraction of smooth muscle by CCK at concentrations ranging from 10^{-10} to 10^{-6} mol/L and reduced responses of ICLC-removed CBD smooth muscle to CCK. These data suggest that ICLCs not only regulate CBD smooth muscle motility through the slow wave potentials caused by the known pacemaker current pathway but also mediate CCK-induced CBD smooth muscle contraction through chemical excitation. In addition to acting on CCK-A receptors on CBD SMCs, CCK may also regulate CBD contraction by binding to CCK-A receptors on ICLCs. CBD ICLCs not only excite smooth muscle slow wave potentials and modulate enteric neurotransmitters but also regulate CBD contraction by regulating hormones such as CCK in blood circulation.

ARTICLE HIGHLIGHTS

Research background

Interstitial Cajal cells (ICCs) are a kind of interstitial cells existing in the gastrointestinal tract, which are related to basic electric rhythm. Many studies have shown that Interstitial Cajal-like cells (ICLCs) abnormalities are closely related to a variety of gastrointestinal dynamic disorders. ICLCs are pacemaker cells for gastrointestinal movement and are involved in the transmission of nerve impulses.

Research motivation

This study aims to preliminarily investigate the pathogenesis of biliary tract diseases to deepen our understanding of biliary tract dynamics and provide novel ideas for the pathogenesis and clinical treatment of related dynamic diseases.

Research objectives

Figure out the pathogenesis of biliary tract dynamics and related dynamic diseases such as choledocholithiasis. As well as the expression of cholecystokinin-A (CCK-A) receptors on common bile duct (CBD) ICLCs. Investigate how CCK regulates biliary tract dynamics through CBD ICLCs

Research methods

Of 250-300g adult guinea pigs of either sex were used to obtain CBD tissue. Then, the levels of tyrosine kinase receptor and CCK-A receptors in CBD tissues and CBD isolated cells were quantified using the double immunofluorescence labeling technique. The enhancement effect of CCK on the movement of CBD muscle strips through CBD ICLCs was observed by muscle strip contraction test.

Research results

The guinea pig CBD ICLCs had abundant mitochondria, which were active in function and provided energy for slow-wave pacemaker cells. The expression of CCK-A receptors was confirmed on guinea pig CBD ICLCs by choledochal histology and immunofluorescence method of isolated ICLC-cultured slides.

Research conclusions

This research demonstrates a dose-dependent contraction of smooth muscle by CCK with a concentration ranging 10^{-10} to 10^{-6} mol/L, and reduced responses of ICLC-removed CBD smooth muscle to CCK, suggesting that ICLCs not only regulate CBD smooth muscle motility by slow wave potentials caused by the known pacemaker current pathway, but also mediate CCK-induced CBD smooth muscle contraction through chemical excitation.

Research perspectives

Investigate the distribution, expression, morphology and ultrastructure of CBD ICLCs. Also, the expression and function of CCK-A receptors on CBD ICLCs.

FOOTNOTES

Co-first authors: Dan Xu and Song-Lin Ma.

Author contributions: Xu D and Ma SL contributed equally to this work and are co-first authors, including design of the study, acquiring and analyzing data from experiments, and writing of the actual manuscript. Xu D, Ma SL, and Zhang H conceived and designed the experiments, wrote the paper, contributed to the statistical analysis; Xu D, Ma SL, Huang ML, and Zhang H performed the experiments; and all authors read and approved the final manuscript.

Institutional animal care and use committee statement: All experiments were conducted in accordance with the institutional guidelines of the Central Hospital of Wuhan for the care and use of laboratory animals.

Conflict-of-interest statement: All the authors report no relevant conflicts of interest for this article.

Data sharing statement: No additional data are available.

ARRIVE guidelines statement: The authors have read the ARRIVE guidelines, and the manuscript was prepared and revised according to the ARRIVE guidelines.

Open-Access: This article is an open-access article that was selected by an in-house editor and fully peer-reviewed by external reviewers. It is distributed in accordance with the Creative Commons Attribution NonCommercial (CC BY-NC 4.0) license, which permits others to distribute, remix, adapt, build upon this work non-commercially, and license their derivative works on different terms, provided the original work is properly cited and the use is non-commercial. See: https://creativecommons.org/Licenses/by-nc/4.0/

Country/Territory of origin: China

ORCID number: Man-Lin Huang 0000-0001-7991-0979; Heng Zhang 0000-0002-2725-6562.

S-Editor: Wang JJ
L-Editor: A
P-Editor: Yuan YY

REFERENCES

1 **Liu Y**, Fan Y, Wu S. Developments in research on interstitial Cajal-like cells in the biliary tract. *Expert Rev Gastroenterol Hepatol* 2021; **15**: 159-164 [PMID: 32933347 DOI: 10.1080/17474124.2021.1823214]
2 **Nadella S**, Ciofoaia V, Cao H, Kallakury B, Tucker RD, Smith JP. Cholecystokinin Receptor Antagonist Therapy Decreases Inflammation and Fibrosis in Chronic Pancreatitis. *Dig Dis Sci* 2020; **65**: 1376-1384 [PMID: 31598921 DOI: 10.1007/s10620-019-05863-5]
3 **Wang HH**, Portincasa P, Liu M, Tso P, Wang DQ. An Update on the Lithogenic Mechanisms of Cholecystokinin a Receptor (CCKAR), an Important Gallstone Gene for Lith13. *Genes (Basel)* 2020; **11** [PMID: 33260332 DOI: 10.3390/genes11121438]
4 **Zeng Q**, Ou L, Wang W, Guo DY. Gastrin, Cholecystokinin, Signaling, and Biological Activities in Cellular Processes. *Front Endocrinol (Lausanne)* 2020; **11**: 112 [PMID: 32210918 DOI: 10.3389/fendo.2020.00112]

5 **Wang DQ**. Emerging Trends in Deciphering the Pathogenesis of Human Diseases through Genetic Analysis. *Genes (Basel)* 2021; **12** [PMID: 33451126 DOI: 10.3390/genes12010096]

6 **Tang C**, Biemond I, Lamers CB. Cholecystokinin receptors in human pancreas and gallbladder muscle: a comparative study. *Gastroenterology* 1996; **111**: 1621-1626 [PMID: 8942742 DOI: 10.1016/s0016-5085(96)70025-2]

7 **Sun X**, Yu B, Xu L, Dong W, Luo H. Interstitial cells of Cajal in the murine gallbladder. *Scand J Gastroenterol* 2006; **41**: 1218-1226 [PMID: 16990209 DOI: 10.1080/00365520600708800]

8 **Chen L**, Yu B. Telocytes and interstitial cells of Cajal in the biliary system. *J Cell Mol Med* 2018; **22**: 3323-3329 [PMID: 29700981 DOI: 10.1111/jcmm.13643]

9 **Huizinga JD**, Faussone-Pellegrini MS. About the presence of interstitial cells of Cajal outside the musculature of the gastrointestinal tract. *J Cell Mol Med* 2005; **9**: 468-473 [PMID: 15963266 DOI: 10.1111/j.1582-4934.2005.tb00372.x]

10 **Lavoie B**, Balemba OB, Nelson MT, Ward SM, Mawe GM. Morphological and physiological evidence for interstitial cell of Cajal-like cells in the guinea pig gallbladder. *J Physiol* 2007; **579**: 487-501 [PMID: 17204499 DOI: 10.1113/jphysiol.2006.122861]

11 **Hinescu ME**, Ardeleanu C, Gherghiceanu M, Popescu LM. Interstitial Cajal-like cells in human gallbladder. *J Mol Histol* 2007; **38**: 275-284 [PMID: 17541711 DOI: 10.1007/s10735-007-9099-0]

12 **Xu D**, Liu J, Huang M, Zhang H, Ma S. Kit-positive cells in the murine common bile duct. *AQCH* 2021

13 **Greulich S**, de Wiza DH, Preilowski S, Ding Z, Mueller H, Langin D, Jaquet K, Ouwens DM, Eckel J. Secretory products of guinea pig epicardial fat induce insulin resistance and impair primary adult rat cardiomyocyte function. *J Cell Mol Med* 2011; **15**: 2399-2410 [PMID: 21143387 DOI: 10.1111/j.1582-4934.2010.01232.x]

14 **Liu LW**, Thuneberg L, Huizinga JD. Selective lesioning of interstitial cells of Cajal by methylene blue and light leads to loss of slow waves. *Am J Physiol* 1994; **266**: G485-G496 [PMID: 8166287 DOI: 10.1152/ajpgi.1994.266.3.g485]

15 **Feng H**, Wang F, Wang C. C-Kit expression in the gallbladder of guinea pig with chronic calculous cholecystitis and the effect of Artemisia capillaris Thunb on interstitial cells of Cajal. *Iran J Basic Med Sci* 2016; **19**: 720-725 [PMID: 27635195]

16 **Zhou M**, Guo YT, Chang YB, Zhong ZH. Effects of anisodamine and gabexate on biliary dynamics in patients after biliary operation. *World Chin J Dig* 2009; **17**: 2748-2751 [DOI: 10.11569/wcjd.v17.i26.2748]

17 **Woods CM**, Mawe GM, Toouli J, Saccone GT. The sphincter of Oddi: understanding its control and function. *Neurogastroenterol Motil* 2005; **17** Suppl 1: 31-40 [PMID: 15836453 DOI: 10.1111/j.1365-2982.2005.00658.x]

18 **Fratantoni ME**, Giuffrida P, Di Menno J, Ardiles V, de Santibañes M, Clariá RS, Palavecino M, de Santibañes E, Pekolj J, Mazza O. Prevalence of Persistent Common Bile Duct Stones in Acute Biliary Pancreatitis Remains Stable Within the First Week of Symptoms. *J Gastrointest Surg* 2021; **25**: 3178-3187 [PMID: 34159556 DOI: 10.1007/s11605-021-05068-0]

19 **Sergeant GP**, Hollywood MA, McCloskey KD, Thornbury KD, McHale NG. Specialised pacemaking cells in the rabbit urethra. *J Physiol* 2000; **526** Pt 2: 359-366 [PMID: 10896724 DOI: 10.1111/j.1469-7793.2000.t01-2-00359.x]

20 **Park CG**, Wu MJ, Hong C, Jo JY, Jiao HY, Park H, Jun JY, Choi S. Regulation of Intracellular Calcium by Endoplasmic Reticulum Proteins in Small Intestinal Interstitial Cells of Cajal. *J Neurogastroenterol Motil* 2018; **24**: 128-137 [PMID: 28774158 DOI: 10.5056/jnm16212]

21 **Fu BB**, Zhao JN, Wu SD, Fan Y. Cholesterol gallstones: Focusing on the role of interstitial Cajal-like cells. *World J Clin Cases* 2021; **9**: 3498-3505 [PMID: 34046450 DOI: 10.12998/wjcc.v9.i15.3498]

22 **Sato N**, Miyasaka K, Suzuki S, Kanai S, Ohta M, Kawanami T, Yoshida Y, Takiguchi S, Noda T, Takata Y, Funakoshi A. Lack of cholecystokinin-A receptor enhanced gallstone formation: a study in CCK-A receptor gene knockout mice. *Dig Dis Sci* 2003; **48**: 1944-1947 [PMID: 14627338 DOI: 10.1016/s0016-5085(08)80889-x]

World Journal of Gastroenterology

Submit a Manuscript: https://www.f6publishing.com

World J Gastroenterol 2023 October 14; 29(38): 5383-5394

DOI: 10.3748/wjg.v29.i38.5383

ISSN 1007-9327 (print) ISSN 2219-2840 (online)

ORIGINAL ARTICLE

Retrospective Study

Impressive recompensation in transjugular intrahepatic portosystemic shunt-treated individuals with complications of decompensated cirrhosis based on Baveno VII criteria

Long Gao, Man-Biao Li, Jin-Yu Li, Yang Liu, Chao Ren, Dui-Ping Feng

Specialty type: Gastroenterology and hepatology

Provenance and peer review: Unsolicited article; Externally peer reviewed.

Peer-review model: Single blind

Peer-review report's scientific quality classification

Grade A (Excellent): 0
Grade B (Very good): B
Grade C (Good): C
Grade D (Fair): D
Grade E (Poor): 0

P-Reviewer: Batta A, India; Karagiannakis DS, Greece

Received: July 7, 2023
Peer-review started: July 7, 2023
First decision: August 8, 2023
Revised: August 15, 2023
Accepted: September 20, 2023
Article in press: September 20, 2023
Published online: October 14, 2023

Long Gao, Jin-Yu Li, Dui-Ping Feng, Department of Oncological and Vascular Intervention, First Hospital of Shanxi Medical University, Taiyuan 030001, Shanxi Province, China

Long Gao, Jin-Yu Li, Dui-Ping Feng, Shanxi Provincial Clinical Research Center for Interventional Medicine, First Hospital of Shanxi Medical University, Taiyuan 030001, Shanxi Province, China

Man-Biao Li, Yang Liu, Chao Ren, College of Medical Imaging, Shanxi Medical University, Taiyuan 030001, Shanxi Province, China

Corresponding author: Dui-Ping Feng, MD, Chief Doctor, Department of Oncological and Vascular Intervention, First Hospital of Shanxi Medical University, No. 85 Jiefang South Road, Yingze District, Taiyuan 030001, Shanxi Province, China. fengdp@sxmu.edu.cn

Abstract

BACKGROUND

Transjugular intrahepatic portosystemic shunt (TIPS) is the standard second-line treatment option for individuals with complications of decompensated cirrhosis, such as variceal bleeding and refractory ascites.

AIM

To investigate whether recompensation existed in TIPS-treated patients with decompensated cirrhosis according to Baveno VII criteria.

METHODS

This retrospective analysis was performed on 64 patients who received TIPS for variceal bleeding or refractory ascites. The definition of recompensation referred to Baveno VII criteria and previous study. Clinical events, laboratory tests, and radiological examinations were regularly conducted during a preset follow-up period. The recompensation ratio in this cohort was calculated. Beyond that, univariate and multivariate regression models were conducted to identify the predictors of recompensation.

RESULTS

Of the 64 patients with a 12-mo follow-up, 20 (31%) achieved recompensation. Age [odds ratio (OR): 1.124; 95% confidence interval (CI): 1.034-1.222] and post-

TIPS portal pressure gradient < 12 mmHg (OR: 0.119; 95%CI: 0.024-0.584) were identified as independent predictors of recompensation in patients with decompensated cirrhosis after TIPS.

CONCLUSION

The present study demonstrated that nearly one-third of the TIPS-treated patients achieved recompensation within this cohort. According to our findings, recompensation is more likely to be achieved in younger patients. In addition, postoperative portal pressure gradient reduction below 12 mmHg contributes to the occurrence of recompensation.

Key Words: Liver cirrhosis; Cirrhosis recompensation; Complications; Portal hypertension; Transjugular intrahepatic portosystemic shunt; Predictors

©The Author(s) 2023. Published by Baishideng Publishing Group Inc. All rights reserved.

Core Tip: Decompensated cirrhosis with complications of portal hypertension is often considered the end-stage of cirrhosis, with little chance of improvement. Despite this, recent studies have put forward the concept of recompensation. However, it remains unknown whether transjugular intrahepatic portosystemic shunts (TIPS) can achieve recompensation. Herein, we demonstrated that almost one-third of patients treated with TIPS achieved recompensation. Therefore, TIPS should be given greater priority in the treatment of decompensated cirrhosis with complications of portal hypertension, and prospective studies are necessary. In summary, the role of TIPS in achieving recompensation warrants further examination.

Citation: Gao L, Li MB, Li JY, Liu Y, Ren C, Feng DP. Impressive recompensation in transjugular intrahepatic portosystemic shunt-treated individuals with complications of decompensated cirrhosis based on Baveno VII criteria. *World J Gastroenterol* 2023; 29(38): 5383-5394

URL: https://www.wjgnet.com/1007-9327/full/v29/i38/5383.htm

DOI: https://dx.doi.org/10.3748/wjg.v29.i38.5383

INTRODUCTION

Liver cirrhosis ranks as the 14th most common cause of adult deaths worldwide, causing 1.03 million deaths annually. Most cirrhotic complications and subsequent deaths result from portal hypertension rather than hepatocyte failure[1]. Serious health threats, such as variceal bleeding and refractory ascites, are common complications of portal hypertension, and they create a significant burden on healthcare economics[2-4]. Unlike liver fibrosis, cirrhosis has been considered an end-stage disease with limited chances of improvement in clinical practice. The therapeutic goals for cirrhosis are typically focused on symptom relief and avoiding liver transplantation, if possible[5].

However, recent studies have introduced the concept of recompensation, although there is currently no agreement on its definition[6]. The Baveno VII consensus proposed criteria for recompensation, but specific cutoff values for stable improvement of liver function have not yet been established[7]. More recently, Wang *et al*[8] validated the Baveno VII criteria for recompensation in entecavir-treated individuals with hepatitis B-related decompensated cirrhosis and proposed laboratory criteria to define recompensation. Nevertheless, it is still unclear whether this threshold can be applied to other treatments.

Transjugular intrahepatic portosystemic shunts (TIPS) is an effective treatment for cirrhosis patients who experience variceal bleeding or refractory ascites[9]. In cases of variceal bleeding, TIPS is typically used as a salvage therapy after the failure of standard medication combined with endoscopic therapy, with the goal of preventing rebleeding[10]. Studies have shown that early implantation of TIPS is recommended to improve survival in patients with acute variceal bleeding and high risk of early rebleeding who fulfill any of the following criteria: Child-Pugh class C < 14 points or Child-Pugh class B > 7 with active bleeding at initial endoscopy or hepatic venous pressure gradient > 20 mmHg at the time of hemorrhage[11-13].

For patients with refractory ascites, TIPS has been shown to effectively clear ascites, leading to nutritional improvement and even normalization of renal function[14]. In a prospective randomized trial involving 62 patients with cirrhosis and recurrent ascites, TIPS was found to increase the proportion of patients who survived transplantation-free for 1 year compared to patients who underwent repeated large-volume paracenteses and albumin (ALB) infusion. This supports TIPS as a first-line intervention in this scenario[15]. Despite these advantages, the role of TIPS in the treatment of portal hypertension complications in cirrhosis remains secondary, and it is often considered only as a bridge to liver transplantation. Additionally, it is still unknown whether TIPS can further achieve recompensation.

Based on the above analysis, we hypothesized that TIPS can aid in recompensation to some extent based on Baveno VII criteria for recompensation[7] and the laboratory threshold from Wang *et al*[8]. To verify our assumption, we retrospectively collected relative data and outcomes of TIPS-treated patients over a 12-mo follow-up.

MATERIALS AND METHODS

Study population

This single-center, retrospective, single-arm study was conducted at the First Hospital of Shanxi Medical University between April 2019 and August 2022, which complied with the ethical guidelines of the 2013 Declaration of Helsinki and was approved by the ethics committee of the First Hospital of Shanxi Medical University (approval No. K-K231). Prior to enrolling the subjects, all participants or their legal guardian gave written informed consent.

The inclusion criteria were as follows: (1) 18-75 years of age; (2) receipt of etiological treatment before or immediately after enrollment; (3) meeting of clinical, biochemical, hematological, radiological, or histological diagnostic criteria for cirrhosis; (4) fulfillment of indication for TIPS; and (5) agreement to be treated with TIPS for variceal bleeding or refractory ascites. The exclusion criteria were as follows: (1) Concomitant hepatocellular carcinoma or other malignancies; (2) previous history of hepatic encephalopathy (HE), hepatorenal syndrome, or hepatopulmonary syndrome; (3) prothrombin time > 20 s or international normalized ratio (INR) > 2.0; (4) creatinine > 3 mg/dL; (5) comorbidity of any malignancy (excluding cured); (6) previous history of heart, lung, kidney, brain, blood, or other vital organ dysfunction; and (7) Other scenarios that did not meet the inclusion criteria.

TIPS procedure and follow-up

All TIPS procedures were performed by three interventional radiologists with more than 10 years of TIPS experience. No participant had active variceal bleeding at the time of the procedure. The TIPS procedure was performed under local anesthesia as previously described[10,16,17]. The portosystemic pressure gradient (PPG) values were recorded before and after stent placement. In all patients, 8-mm expanded e-polytetrafluoroethylene-covered stent grafts (VIATORR; W.L. Gore and Associates, Inc, Newark, NJ, United States) were used. The varices were embolized with coils (Interlock; Boston Scientific, Marlborough, MA, United States) and N-butyl cyanoacrylate (B. Braun Melsungen AG, Melsungen, Germany), mixed with iodine oil (Guerbet, Villepinte, France) at a 1:2 ratio.

At baseline (1-7 d prior to TIPS), the patient's demographics, clinical features, biochemical and radiological findings, and other related data were collected. After that, all patients were re-examined at 3-d, 1-mo, 3-mo, and 6-mo postoperative, and then every 6 mo thereafter. At each time point, data from laboratory tests, radiological examinations, and reports of clinical events were collected *via* outpatient follow-up or inpatient follow-up if necessary.

Etiological treatment

Besides TIPS treatment, all patients received necessary medication or lifestyle interventions for treating their respective causes according to the Guidelines of the European Association for the Study of the Liver study on chronic hepatitis B [18], hepatitis C[19], alcoholic liver disease[20], nonalcoholic fatty liver disease[21], autoimmune liver disease[22], and cholestatic liver disease[23]. These interventions were aimed at achieving the removal/suppression of the primary cause of cirrhosis.

Definition of recompensation and research endpoints

Based on the Baveno VII consensus[7] and a previous report[8], the definition of recompensation in this study fulfilled three items: (1) Removal of etiology of cirrhosis; (2) regression of ascites or resolution of ascites (off diuretics) and encephalopathy (off lactulose/rifaximin), and absence of recurrent variceal bleeding (for at least 12 mo); and (3) stable improvement of liver function tests, such as model for end-stage liver disease (MELD) score < 10 and/or liver function tests within Child-Pugh A [ALB > 35 g/L, INR < 1.50, and total bilirubin (TBIL) < 34 μmol/L].

The primary endpoint was the clinical occurrence of recompensation in TIPS-treated patients according to the above criteria. The secondary endpoints were changes in Child-Pugh scores, MELD scores, abdominal ultrasound parameters, PPG values, and the predictors of recompensation.

Abdominal ultrasound measurement methods

The ultrasound measurement procedures were performed by the same observer with more than 10 years of experience in ultrasound examinations. All patients were examined after an overnight fast. Operations were performed in strict accordance with standards using a convex array probe (Resona 6W; Mindray, Mahwah, NJ, United States) or a LFP5-1U probe (Resona 6W; Mindray) for real-time grey-scale imaging and measurement and sound touch quantification (STQ) [24]. The portal vein diameter and peak flow velocity were measured approximately 1-2 cm in front of the branches emanating from the portal vein trunk. The formula for calculating spleen volume was: (Maximum length × maximum width × maximum thickness × 0.52)[25]. Severity of ascites were measured as: Grade 1 (mild), < 3 cm depth of ascites; grade 2 (moderate), 3-10 cm; and grade 3 (severe), ≥ 10 cm [26]. All measurements were repeated three times and averaged.

Statistical analysis

All analyses were conducted using SPSS statistical software (version 26.0; IBM Corp., Armonk, NY, United States) and GraphPad Prism (version 8.0). Sankey diagram was performed on the Tutools platform (https://www.cloudtutu.com). Before analysis, normality tests or P-P plots were used to check the normality of the variables. Continuous variables were expressed as mean ± SD or median interquartile range (IQR), while categorical variables were expressed as frequency (proportion). Comparison of two groups for quantitative variables was performed with a Student's *t*-test or with the Mann-Whitney U test. Categorical variables for comparison of two groups was performed with a χ^2 test or Fisher's exact test. Differences in biochemistry, ultrasound parameters, MELD scores, and Child-Pugh scores were compared at each

time point using paired samples *t*-test/independent samples *t*-test or repeated measures analysis of variance. Sankey plots were generated to represent the change in Child-Pugh scores from baseline to month 12 of treatment. A univariate logistic regression analysis was used to investigate the factors of recompensation. Covariates with a *P* value less than 0.1 were further included in the multivariate logistic analysis with stepwise method (likelihood ratio) to test the association. In all cases, bilateral *P* values < 0.05 were considered statistically significant.

RESULTS

Baseline characteristics of the enrolled patients

Eligibility screening of 163 patients undergoing TIPS for cirrhotic decompensated events was retrospective conducted. After excluding 93 patients for various reasons, 70 patients were enrolled. We further excluded 6 patients with new hepatic malignancies. For the remaining 64 patients, data were collected (Figure 1).

The baseline characteristics of the patients are shown in Table 1. The mean age was 56 ± 13 years, of which 53% (34/64) were male. The mean alanine aminotransferase (ALT) level was 19 (IQR 16-27) IU/L, with 4.7% (3/64) having elevated ALT (> 40 IU/L). Prior to TIPS insertion, the median PPG was 25.50 (IQR 22.00-28.25) mmHg. The median Child-Pugh score was 7.50 (IQR 6.00-8.25), and the mean MELD score was 10.60 ± 4.13. All patients were successfully stented, and the mean PPG for the entire cohort decreased to 14.21 ± 4.59 mmHg postoperatively.

Follow-up of major laboratory test parameters and Child-Pugh and MELD scores after TIPS

Liver function tests changed significantly after TIPS (Figure 2, Supplementary Table 1). ALT increased significantly in the 12th month [from a median of 19 (IQR 16-27) IU/L to 30 (IQR 20-36) IU/L, $P < 0.001$] (Figure 2A). Similarly, aspartate aminotransferase level also increased significantly from baseline in the 12th month ($P < 0.001$) (Figure 2B). ALB levels were not different from baseline levels ($P = 0.060$) (Figure 2C). TBIL level continued to rise from baseline levels and reached a maximum in the 3rd postoperative month ($P < 0.001$). Then, the TBIL level decreased to level similar to baseline (Figure 2D). Creatinine continued to decrease postoperatively [baseline 67.18 ± 16.20 μmol/L *vs* 44.47 (IQR 40.08- 48.58) μmol/L in the 12th month, $P < 0.001$] (Figure 2E). Platelet level increased significantly from baseline in the 12th month ($P < 0.001$) (Figure 2F). The INR increased to a maximum in the 6th postoperative month ($P < 0.001$) and then returned to baseline levels (Figure 2G). Child-Pugh scores increased on the 3rd postoperative day then decreased in the 12th postoperative month ($P < 0.001$) (Figure 2H). MELD scores remained high from baseline for 6 mo ($P < 0.001$) and then decreased to baseline levels in the 12th postoperative month (Figure 2I).

Follow-up of abdominal ultrasound after TIPS

As shown in Supplementary Table 2, portal vein blood flow velocity was faster than at baseline ($P < 0.001$) and reached a maximum flow velocity of 33.69 ± 12.37 cm/s in the 6th postoperative month, accompanied by a maximum portal vein inner diameter of 1.45 ± 0.42 cm ($P < 0.001$) in the 6th postoperative month (Figure 3A and B). Liver STQ and spleen STQ decreased from baseline in the 12th postoperative month ($P < 0.001$) (Figure 3C and D). Spleen length decreased by 10.8% in the 6th postoperative month ($P < 0.001$) (Figure 3E). Similarly, spleen volume shrank to 75% of baseline in the 3rd postoperative month ($P = 0.035$) (Figure 3F).

Baseline and on-treatment characteristics in patients with and without recompensation

According to whether recompensation had occurred, the patients were divided into a recompensated group ($n = 20$) or a no recompensation group ($n = 44$). The baseline characteristics of the two groups are presented in Supplementary Table 3. The difference in Child-Pugh scores between the two groups at baseline was not statistically significant [6.5 (IQR 6.0-8.0) *vs* 8.0 (IQR 6.0-9.0), $P = 0.174$]. The patients without recompensation had higher MELD scores than patients with recompensation (11.41 ± 4.04 *vs* 8.81 ± 3.85, $P = 0.019$). In addition, the patients without recompensation tended to have higher TBIL, portal vein velocity, spleen length, spleen volume, and post-TIPS PPG, although they were not statistically different ($P > 0.05$).

There was a more profound improvement in Child-Pugh and MELD scores from the 6th postoperative month to the 12th postoperative month in the patients with recompensation compared to the patients without recompensation (Figure 4A and B). We plotted Sankey plots to represent the change in Child-Pugh scores from baseline to the 12th postoperative month, and the results showed significantly more favorable outcomes in the group with recompensation (Figure 4C-E). Although there was no statistical difference between the two groups at baseline, the proportion of patients with Child-Pugh A increased significantly over time in the recompensation group (Figure 4D).

Univariate and multivariate logistic analyses of predictors for recompensation

All baseline data were first analyzed using the univariate logistic regression model, which revealed no statistical differences between the two groups in terms of etiology and sex (Supplementary Table 4). Only age and post-TIPS PPG < 12 mmHg were significant ($P < 0.05$) and included in the multivariate regression model (Figure 5A). In the multivariate analysis, age [odds ratio (OR): 1.124; 95% confidence interval (CI): 1.034-1.222] and post-TIPS PPG < 12 mmHg (OR: 0.119; 95%CI: 0.024-0.584) were independent predictors of recompensation after TIPS (Figure 5B).

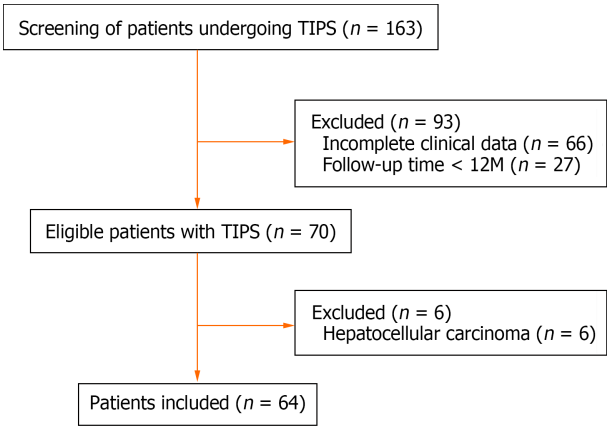
Characteristics in patients with or without new-onset HE

In general, 19 patients had HE within 12 mo and no patients had variceal bleeding. The baseline characteristics of those 19

Table 1 Characteristics of patients

Variables	Value
Age in yr	56 ± 13
Male sex	34 (53.1)
Etiology	
Viral	32 (50.0)
Alcohol	10 (15.6)
Other	22 (34.4)
PLT as 10^9/L	68.5 (44.5, 114.8)
INR	1.36 (1.23, 1.52)
ALT in IU/L	19 (16, 27)
AST in IU/L	29 (22, 35)
ALB in g/L	32.28 ± 4.46
TBIL in μmol/L	30.3 (18.2, 43.9)
MELD score	10.60 ± 4.13
Child-Pugh score	7.5 (6.0, 8.3)
PPG in mmHg	
Pre-TIPS	25.5 (22.0, 28.3)
Post-TIPS	14.21 ± 4.59
Post-TIPS PPG < 12 mmHg	15 (23.4)
PPG reduction by TIPS	9 (7, 14)

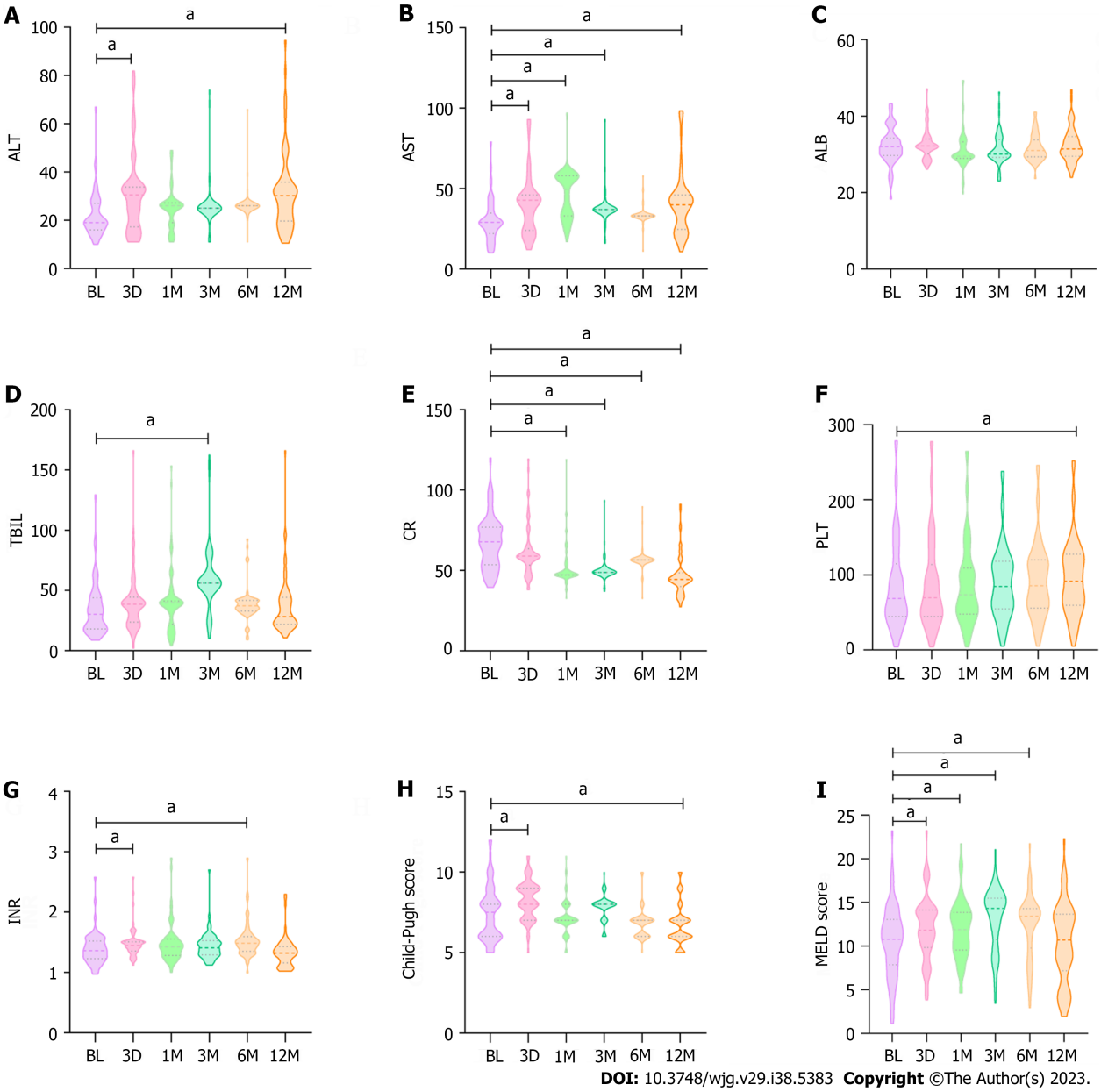
Data are mean ± SD, *n* (%), or median (interquartile range). ALB: Albumin; ALT: Alanine aminotransferase; AST: Aspartate aminotransferase; INR: International normalized ratio; MELD: Model for end-stage liver disease; PLT: Platelets; PPG: Portosystemic pressure gradient; TBIL: Total bilirubin; TIPS: Transjugular intrahepatic portosystemic shunt.



DOI: 10.3748/wjg.v29.i38.5383 **Copyright** ©The Author(s) 2023.

Figure 1 Flow chart of patient inclusion. TIPS: Transjugular intrahepatic portosystemic shunt.

patients with new-onset HE and 45 patients without new-onset HE are shown in Supplementary Table 5. Compared with patients without new-onset HE, patients with new-onset HE had higher age (53 ± 11 years *vs* 64 ± 13 years, $P = 0.002$) and pre-TIPS PPG [27.00 (IQR 25.50-29.50) mmHg *vs* 23.00 (IQR 21.00-26.25) mmHg, $P = 0.031$].



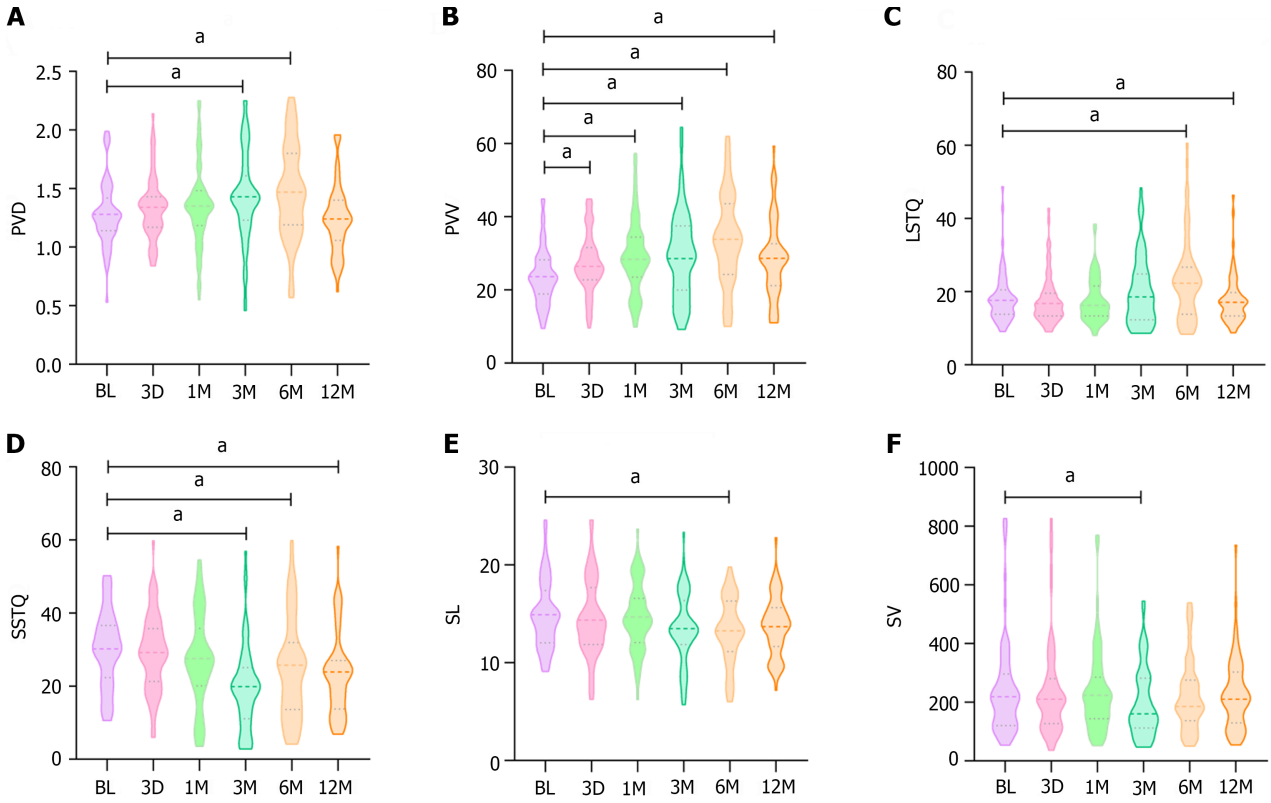
DOI: 10.3748/wjg.v29.i38.5383 **Copyright** ©The Author(s) 2023.

Figure 2 Dynamic changes of major laboratory test parameters and Child-Pugh/model for end-stage liver disease scores during the 12-mo follow-up. A: Alanine aminotransferase; B: Aspartate aminotransferase; C: Albumin; D: Total bilirubin; E: Creatinine; F: Platelets; G: International normalized ratio; H: Child-Pugh score; I: Model for end-stage liver disease score. [a]*P* < 0.05. BL: Baseline; 3D: Postoperative day 3; 1M: One month postoperatively; 3M: Three months postoperatively; 6M: Six months postoperatively; 12M: Twelve months postoperatively; ALT: Alanine aminotransferase; AST: Aspartate aminotransferase; ALB: Albumin; TBIL: Total bilirubin; CR: Creatinine; PLT: Platelets; INR: International normalized ratio; MELD: Model for end-stage liver disease.

DISCUSSION

It is unknown whether the TIPS procedure is able to achieve recompensation. Our present study showed 31% of patients (*n* = 20/64) achieved recompensation after TIPS. Beyond that, we found that age and post-TIPS PPG < 12 mmHg were independent predictors of recompensation (Figure 5). Therefore, we suggest that TIPS should be given more priority for treatment of decompensated cirrhosis with complications of portal hypertension in the above scenarios. To the best of our knowledge, this is the first study to examine recompensation after TIPS based on the Baveno VII definition of recompensation[7] and recent research[8].

Baveno VII proposed criteria to define recompensation, including the elimination or control of the underlying cause, absence of recurrent events for at least 12 mo, and stable improvement in liver function tests. However, the detailed criteria for stable improvement of liver function tests were still absent. Fortunately, a recent study validated the Baveno VII definition of recompensation and precisely defined the cutoff values for stable improvement of liver function tests, which require a MELD score < 10 and/or a liver function test in the Child-Pugh A range (ALB > 35 g/L, INR < 1.50, and TBIL < 34 μmol/L).



DOI: 10.3748/wjg.v29.i38.5383 **Copyright** ©The Author(s) 2023.

Figure 3 Dynamic changes in abdominal ultrasound measurement results during the 12-mo follow-up. A: Portal vein inner diameter; B: Portal vein velocity; C: Liver sound touch quantification; D: Spleen sound touch quantification; E: Spleen length; F: Spleen volume. $^{a}P < 0.05$. BL: Baseline; 3D: Postoperative day 3; 1M: One month postoperatively; 3M: Three months postoperatively; 6M: Six months postoperatively; 12M: Twelve months postoperatively; PVD: Portal vein inner diameter; PVV: Portal vein velocity; LSTQ: Liver sound touch quantification; SSTQ: Spleen sound touch quantification; SL: Spleen length; SV: Spleen volume.

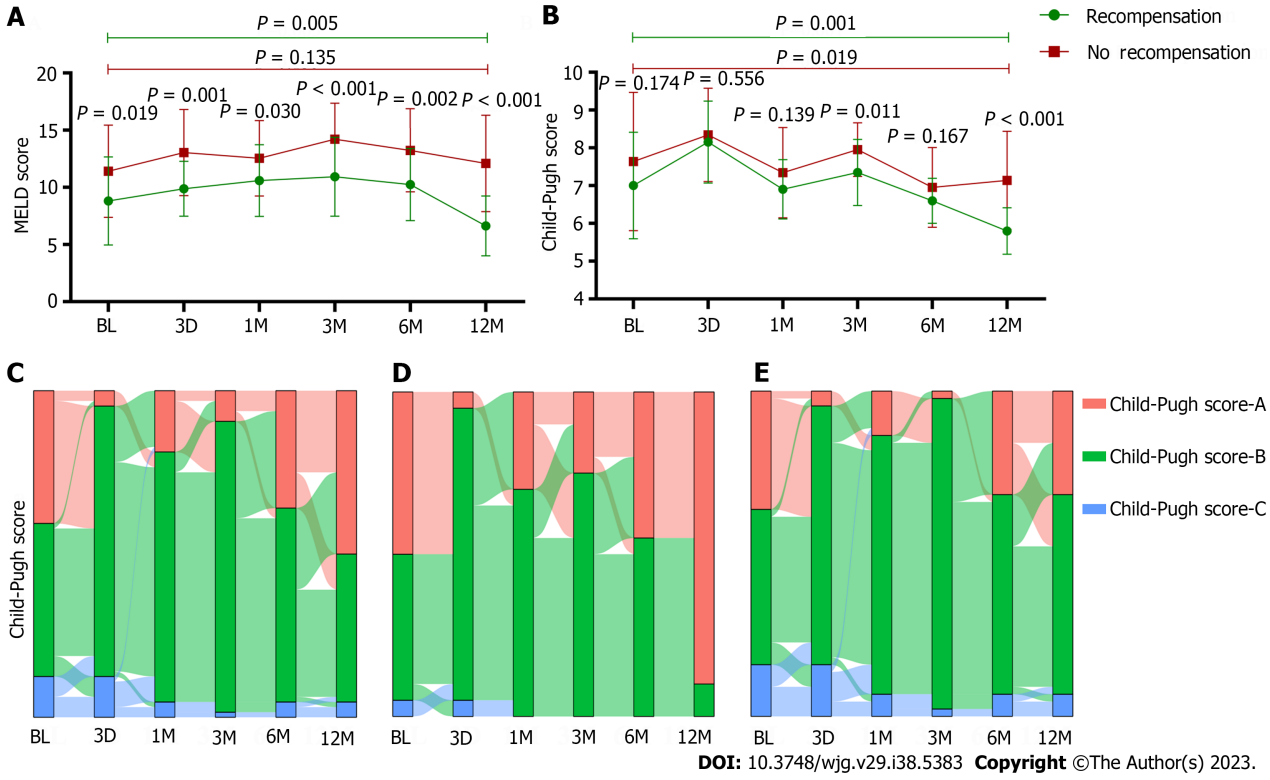
We chose the above criteria to conduct our current study for several reasons. First, it was easier to draw credible conclusions from mostly similar etiology and demographic backgrounds. Second, the nature of multicenter prospective clinical research determined the high evidence-based value. Third, the explanations of threshold setting (such as using INR instead of prothrombin time) was logical and acceptable.

TIPS is regarded as the bridge before liver transplantation and remains the second-line option either for gastrointestinal hemorrhage or refractory ascites[10,16], mainly attributed to the larger trauma of TIPS and postoperative HE[27,28]. However, since a previous milestone study reported that early use of TIPS in patients with cirrhosis and variceal bleeding at high risk for treatment failure was associated with significant reductions in treatment failure and in mortality[13], more and more studies have confirmed that TIPS provides significant survival benefits over traditional first-line treatment (*i.e.* endoscopic therapy or medication) in selected patients[29-31]. Lv *et al*[11] revealed that early TIPS could improve transplantation-free survival in selected patients with advanced cirrhosis and acute variceal bleeding compared to standard first-line treatment with no significant difference in adverse events. Furthermore, Wang *et al*[32] showed that TIPS with 8-mm covered stents achieved similar shunt function to 10-mm covered stents and halved the risk of spontaneous overt HE and reduced hepatic impairment.

In addition, a more recent meta-analysis of data from 1327 patients with cirrhosis reconfirmed that preemptive TIPS increased the proportion who survived for 1 year compared with drugs plus endoscopy in both subgroups separately [30]. Nevertheless, none of these studies clarified the detailed mechanism for the survival benefits associated with TIPS, such as cirrhosis recompensation.

Our current study indicated that nearly one-third of patients achieved recompensation after TIPS during the 12-mo follow-up, which was impressive and encouraging for TIPS practitioners. As previous research confirmed, the stiffness of the liver and spleen had a good correlation with hepatic vein pressure gradient, which served as the gold standard for assessing severity of portal hypertension. However, in our cohort, we were unable to draw the same conclusion. Although the stiffness of the liver and spleen decreased 12 mo after TIPS compared to baseline (Figure 3C and D), it did not show statistical significance in predicting recompensation in univariate and multivariate logistic regression analysis (Supplementary Table 4). This may be due to the fact that the patients included in our study had not responded to repeated medical treatment, indicating that their cirrhosis was more severe and could not be easily reversed[5].

Previous research had shown that low MELD score and high platelet levels at admission predicted delisting after improvement[33]. Accordingly, we originally believed that the MELD score could predict recompensation, and it did show statistical significance in univariate analysis. However, surprisingly, there was no statistical significance in multivariate analysis for MELD score to predict recompensation (Figure 5). This finding highlights the possible impact



DOI: 10.3748/wjg.v29.i38.5383 **Copyright** ©The Author(s) 2023.

Figure 4 Dynamic changes of liver function classification in patients with and without recompensation during the 12-mo follow-up. A and B: Mean Child-Pugh/model for end-stage liver disease (MELD) scores at baseline (BL) and follow-up in patients with or without recompensation (bars represent standard error of the mean). The differences in Child-Pugh/MELD scores in these two groups at each time point were compared using the Student's *t*-test. The difference in Child-Pugh/MELD scores between BL and 12 mo after transjugular intrahepatic portosystemic shunt was compared separately for each group. Sankey diagrams were used to show the major transfers or flows of patients. The colors of the columns represent patients with different Child-Pugh classifications, with red representing Child-Pugh A, green representing Child-Pugh B, and blue representing Child-Pugh C. The length of the column represents the proportion of patients. The thicker the line, the greater the number of patients involved; C: Entire cohort (n = 64); D: Patients with recompensation (n = 20); E: Patients without recompensation (n = 44). BL: Baseline; 3D: Postoperative day 3; 1M: One month postoperatively; 3M: Three months postoperatively; 6M: Six months postoperatively; 12M: Twelve months postoperatively.

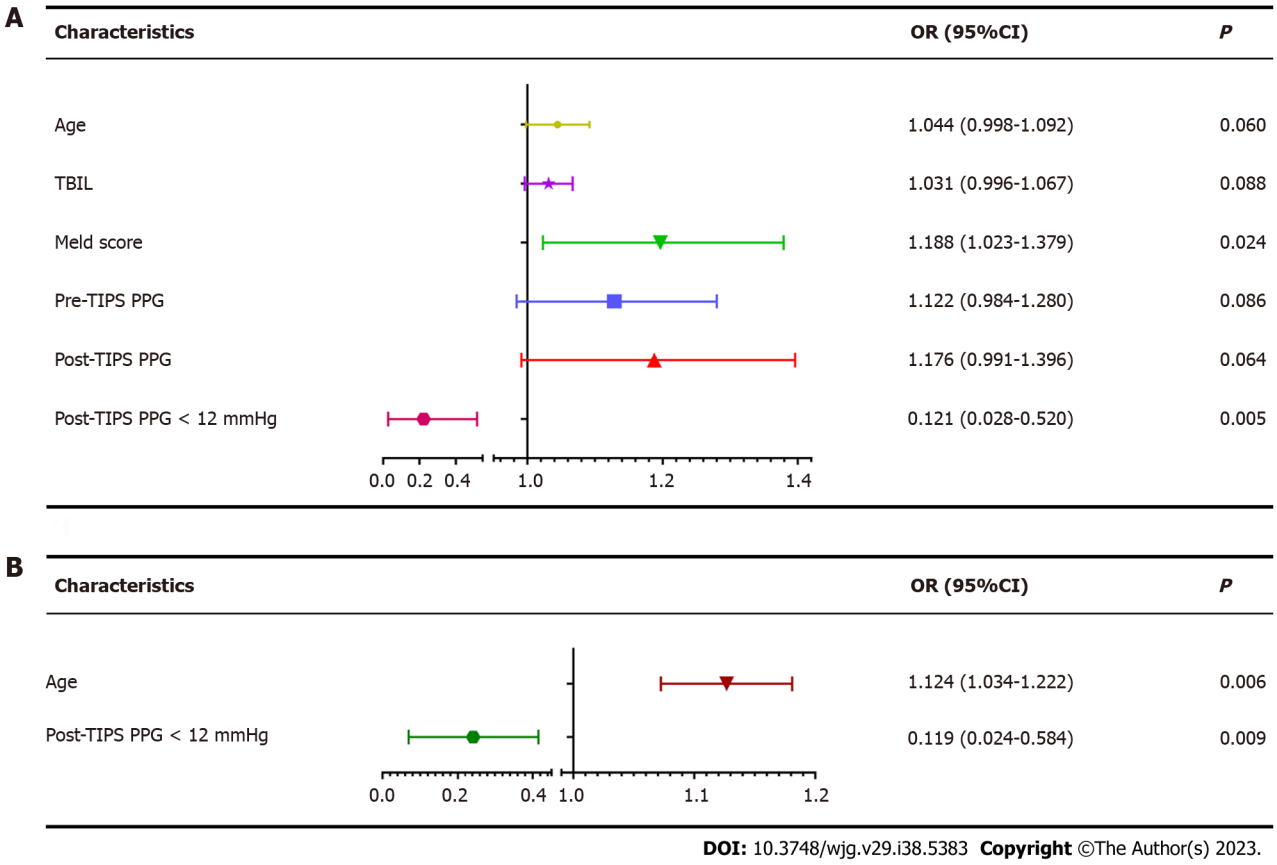
that a small sample size can have on studies and the importance of replicative investigations with large sample sizes for validation. Additionally, we found that older patients were more likely to develop new-onset HE (Supplementary Table 5), which was consistent with previous research[2,34].

To examine possible causes, we further compared relevant characteristics of patients with or without new-onset HE and found that the preoperative PPG of the former was significantly higher than that of the latter (Supplementary Table 5). This may be attributed to the fact that higher PPG predicted poorer liver function and therefore greater susceptibility to HE. Although preoperative PPG itself cannot predict the risk of HE, it can still be considered as a risk factor for early onset HE after TIPS, as evidenced by other studies[17,34].

While it had been documented that addressing the underlying causes can lead to cirrhosis recompensation, the severity of decompensation in the cirrhosis patients involved in these studies was reported to be mild[8,35]. However, in our study, the enrolled patients had already met the indications for TIPS, indicating an already advanced stage of liver cirrhosis in these individuals. Consequently, relying solely on etiological treatment proved woefully insufficient in suppressing the recurrence of life-threatening portal hypertension complications, not to mention facilitating cirrhosis recompensation. Given this context, we firmly believed that in our study, the pivotal factor driving liver cirrhosis recompensation was the reversal of portal hypertension achieved through TIPS, rather than the sole emphasis on etiological treatment.

There are several rational explanations for postoperative recompensation after TIPS. First, since predisposition for decompensation in cirrhosis was mainly due to the progress of portal hypertension, radically reduced portal pressure after TIPS was a prerequisite for recompensation[36]. Second, TIPS increased the cardiac output and thereby the effective blood volume, which further improved perfusion of vital organs, especially that of the kidneys and liver[37]. Finally, portal hypertension is highly correlated with systemic inflammation. As a result, the reduction of portal vein pressure can in turn reduce systemic inflammation to some extent, especially the inflammation of hepatic sinuses[33]. In this regard, the reversal of abnormal intestinal flora, attributed to intestinal congestion of portal hypertension, also led to an improvement in systemic and logical inflammation[34]. In addition, the improvement in nutritional status after TIPS, especially in sarcopenia, was beneficial to recompensation and further reduced the risk of death[2].

Our study had certain limitations. First, the nature of retrospective research determined that the level of evidence-based medical evidence for our present work was not high enough. Second, the relatively small sample size limited the credibility of this study. Third, this work was performed in our single-center, which inevitably leads to selection bias. In



DOI: 10.3748/wjg.v29.i38.5383 **Copyright** ©The Author(s) 2023.

Figure 5 Univariate and multivariate logistic regression analysis identified independent predictors of recompensation after transjugular intrahepatic portosystemic shunt. A: Univariate logistic regression analysis; B: Multivariate logistic regression analysis. Age and post-transjugular intrahepatic portosystemic shunt portosystemic pressure gradient < 12 mmHg could be identified as independent predictors of recompensation. All parameters with a *P* value < 0.1 in the univariate analysis were included in the multivariate logistic regression analysis. CI: Confidence interval; TIPS: Transjugular intrahepatic portosystemic shunt; OR: Odds ratio; PPG: Portosystemic pressure gradient; TBIL: Total bilirubin.

addition, the etiology of cirrhosis in the enrolled patients was not entirely hepatitis B. Consequently, the laboratory criteria we selected to define recompensation may not be entirely accurate. Last but not the least, this study did not incorporate a control group for ethical and practical considerations, since etiological treatment such as antiviral therapy or alcohol abstinence had become the standard of care. In other words, once a patient met the indications for TIPS, it would have been both ethically and clinically inappropriate to administer treatment focused solely on either the underlying causes or TIPS in isolation.

CONCLUSION

For the first time, our study demonstrated that nearly one-third of individuals achieved recompensation after TIPS according to the Baveno VII definition of recompensation and previous research. Postoperative PPG < 12 mmHg and age were demonstrated as independent predictors of recompensation. Additional prospective trials are warranted to further validate our findings.

ARTICLE HIGHLIGHTS

Research background

Decompensated cirrhosis with complications of portal hypertension is often considered the end-stage of cirrhosis, with little chance of improvement. Despite this, recent studies have put forward the concept of recompensation.

Research motivation

Transjugular intrahepatic portosystemic shunts (TIPS) are the standard second-line treatment option for individuals with complications of decompensated cirrhosis, such as variceal bleeding and refractory ascites. However, it remains unknown whether TIPS can achieve recompensation.

Research objectives
Herein, we investigated whether recompensation existed in TIPS-treated patients with decompensated cirrhosis according to the Baveno VII criteria.

Research methods
This retrospective analysis was performed on 64 patients who received TIPS for variceal bleeding or refractory ascites. The definition of recompensation referred to the Baveno VII criteria and a previous study. Clinical events, laboratory tests, and radiological examinations were regularly conducted during the follow-up period. The recompensation ratio in this cohort was calculated. Beyond that, univariate and multivariate regression models were conducted to identify the predictors of recompensation.

Research results
In this present cohort, nearly one-third of the TIPS-treated patients achieved recompensation. TIPS-treated patients will benefit from recompensation if portosystemic pressure gradient (PPG) drops below 12 mmHg. Age is recommended as the observation index of recompensation. PPG and age were identified as the independent predictors of recompensation in TIPS-treated patients with decompensated cirrhosis.

Research conclusions
Therefore, TIPS should be given greater priority in the treatment of decompensated cirrhosis with complications of portal hypertension, and prospective studies are necessary.

Research perspectives
In summary, the role of TIPS in achieving recompensation warrants further examination.

FOOTNOTES

Author contributions: Gao L, Li MB, and Li JY contributed equally to this manuscript; Gao L, Li MB, Li JY and Feng DP contributed to study conception and design; Li MB, Liu Y, and Ren C contributed to data acquisition; Li MB, Gao L, Li JY, and Feng DP contributed to analysis and interpretation of data; Gao L, Li MB, Li JY, and Feng DP contributed to manuscript writing, critical revision of the manuscript, and statistical analysis; All authors vouch for the veracity and completeness of the data and analyses presented, the final version of the manuscript has been reviewed and approved by all authors.

Supported by Natural Science Foundation of China, No. 82200650; Key Research and Development (R and D) Projects of Shanxi Province, No. 202102130501014; Shanxi Provincial Clinical Research Center for Interventional Medicine, No. 202204010501004; Natural Science Foundation of Shanxi Province, No. 202203021211021; Natural Science Foundation of Shanxi Province, No. 202203021212046; Natural Science Foundation of Shanxi Province, No. 20210302123258.

Institutional review board statement: The study was reviewed and approved by the Ethics Committee of the First Hospital of Shanxi Medical University.

Informed consent statement: All study participants, or their legal guardian, provided informed written consent prior to study enrollment.

Conflict-of-interest statement: We have no financial relationships to disclose.

Data sharing statement: No additional data are available.

Open-Access: This article is an open-access article that was selected by an in-house editor and fully peer-reviewed by external reviewers. It is distributed in accordance with the Creative Commons Attribution NonCommercial (CC BY-NC 4.0) license, which permits others to distribute, remix, adapt, build upon this work non-commercially, and license their derivative works on different terms, provided the original work is properly cited and the use is non-commercial. See: https://creativecommons.org/Licenses/by-nc/4.0/

Country/Territory of origin: China

ORCID number: Long Gao 0000-0002-2803-3416; Man-Biao Li 0000-0001-5563-5052; Jin-Yu Li 0000-0003-2563-5937; Yang Liu 0009-0007-4532-3304; Chao Ren 0009-0007-4810-4086; Dui-Ping Feng 0000-0003-4516-3797.

S-Editor: Qu XL
L-Editor: A
P-Editor: Cai YX

REFERENCES

1 **Tsochatzis EA**, Bosch J, Burroughs AK. Liver cirrhosis. *Lancet* 2014; **383**: 1749-1761 [PMID: 24480518 DOI: 10.1016/S0140-6736(14)60121-5]

2 **Engelmann C**, Clària J, Szabo G, Bosch J, Bernardi M. Pathophysiology of decompensated cirrhosis: Portal hypertension, circulatory dysfunction, inflammation, metabolism and mitochondrial dysfunction. *J Hepatol* 2021; **75** Suppl 1: S49-S66 [PMID: 34039492 DOI: 10.1016/j.jhep.2021.01.002]

3 **Magaz M**, Baiges A, Hernández-Gea V. Precision medicine in variceal bleeding: Are we there yet? *J Hepatol* 2020; **72**: 774-784 [PMID: 31981725 DOI: 10.1016/j.jhep.2020.01.008]

4 **Mezzano G**, Juanola A, Cardenas A, Mezey E, Hamilton JP, Pose E, Graupera I, Ginès P, Solà E, Hernaez R. Global burden of disease: acute-on-chronic liver failure, a systematic review and meta-analysis. *Gut* 2022; **71**: 148-155 [PMID: 33436495 DOI: 10.1136/gutjnl-2020-322161]

5 **Rudler M**, Savier E, Alioua I, Sultanik P, Thabut D. TIPS and liver transplantation should always be discussed together. *J Hepatol* 2021; **75**: 1000-1001 [PMID: 34051330 DOI: 10.1016/j.jhep.2021.05.012]

6 **Reiberger T**, Hofer BS. The Baveno VII concept of cirrhosis recompensation. *Dig Liver Dis* 2023; **55**: 431-441 [PMID: 36646527 DOI: 10.1016/j.dld.2022.12.014]

7 **de Franchis R**, Bosch J, Garcia-Tsao G, Reiberger T, Ripoll C; Baveno VII Faculty. Baveno VII - Renewing consensus in portal hypertension. *J Hepatol* 2022; **76**: 959-974 [PMID: 35120736 DOI: 10.1016/j.jhep.2021.12.022]

8 **Wang Q**, Zhao H, Deng Y, Zheng H, Xiang H, Nan Y, Hu J, Meng Q, Xu X, Fang J, Xu J, Wang X, You H, Pan CQ, Xie W, Jia J. Validation of Baveno VII criteria for recompensation in entecavir-treated patients with hepatitis B-related decompensated cirrhosis. *J Hepatol* 2022; **77**: 1564-1572 [PMID: 36038017 DOI: 10.1016/j.jhep.2022.07.037]

9 **Rössle M**. TIPS: 25 years later. *J Hepatol* 2013; **59**: 1081-1093 [PMID: 23811307 DOI: 10.1016/j.jhep.2013.06.014]

10 **Tripathi D**, Stanley AJ, Hayes PC, Travis S, Armstrong MJ, Tsochatzis EA, Rowe IA, Roslund N, Ireland H, Lomax M, Leithead JA, Mehrzad H, Aspinall RJ, McDonagh J, Patch D. Transjugular intrahepatic portosystemic stent-shunt in the management of portal hypertension. *Gut* 2020; **69**: 1173-1192 [PMID: 32114503 DOI: 10.1136/gutjnl-2019-320221]

11 **Lv Y**, Yang Z, Liu L, Li K, He C, Wang Z, Bai W, Guo W, Yu T, Yuan X, Zhang H, Xie H, Yao L, Wang J, Li T, Wang Q, Chen H, Wang E, Xia D, Luo B, Li X, Yuan J, Han N, Zhu Y, Niu J, Cai H, Xia J, Yin Z, Wu K, Fan D, Han G; AVB-TIPS Study Group. Early TIPS with covered stents versus standard treatment for acute variceal bleeding in patients with advanced cirrhosis: a randomised controlled trial. *Lancet Gastroenterol Hepatol* 2019; **4**: 587-598 [PMID: 31153882 DOI: 10.1016/S2468-1253(19)30090-1]

12 **Liu J**, Shi Q, Xiao S, Zhou C, Zhou B, Yuan F, Zheng C, Lin S, Qian K, Feng G, Xiong B. Using transjugular intrahepatic portosystemic shunt as the first-line therapy in secondary prophylaxis of variceal hemorrhage. *J Gastroenterol Hepatol* 2020; **35**: 278-283 [PMID: 31222830 DOI: 10.1111/jgh.14761]

13 **García-Pagán JC**, Caca K, Bureau C, Laleman W, Appenrodt B, Luca A, Abraldes JG, Nevens F, Vinel JP, Mössner J, Bosch J; Early TIPS (Transjugular Intrahepatic Portosystemic Shunt) Cooperative Study Group. Early use of TIPS in patients with cirrhosis and variceal bleeding. *N Engl J Med* 2010; **362**: 2370-2379 [PMID: 20573925 DOI: 10.1056/NEJMoa0910102]

14 **Adebayo D**, Neong SF, Wong F. Refractory Ascites in Liver Cirrhosis. *Am J Gastroenterol* 2019; **114**: 40-47 [PMID: 29973706 DOI: 10.1038/s41395-018-0185-6]

15 **Bureau C**, Thabut D, Oberti F, Dharancy S, Carbonell N, Bouvier A, Mathurin P, Otal P, Cabarrou P, Péron JM, Vinel JP. Transjugular Intrahepatic Portosystemic Shunts With Covered Stents Increase Transplant-Free Survival of Patients With Cirrhosis and Recurrent Ascites. *Gastroenterology* 2017; **152**: 157-163 [PMID: 27663604 DOI: 10.1053/j.gastro.2016.09.016]

16 **Lv Y**, Fan D, Han G. Transjugular intrahepatic portosystemic shunt for portal hypertension: 30 years experience from China. *Liver Int* 2023; **43**: 18-33 [PMID: 35593016 DOI: 10.1111/liv.15313]

17 **Liu J**, Ma J, Zhou C, Yang C, Huang S, Shi Q, Xiong B. Potential Benefits of Underdilation of 8-mm Covered Stent in Transjugular Intrahepatic Portosystemic Shunt Creation. *Clin Transl Gastroenterol* 2021; **12**: e00376 [PMID: 34140457 DOI: 10.14309/ctg.0000000000000376]

18 **European Association for the Study of the Liver**. EASL 2017 Clinical Practice Guidelines on the management of hepatitis B virus infection. *J Hepatol* 2017; **67**: 370-398 [PMID: 28427875 DOI: 10.1016/j.jhep.2017.03.021]

19 **European Association for Study of Liver**. EASL Clinical Practice Guidelines: management of hepatitis C virus infection. *J Hepatol* 2014; **60**: 392-420 [PMID: 24331294 DOI: 10.1016/j.jhep.2013.11.003]

20 **European Association for the Study of the Liver**. EASL Clinical Practice Guidelines: Management of alcohol-related liver disease. *J Hepatol* 2018; **69**: 154-181 [PMID: 29628280 DOI: 10.1016/j.jhep.2018.03.018]

21 **European Association for the Study of the Liver (EASL)**; European Association for the Study of Diabetes (EASD); European Association for the Study of Obesity (EASO). EASL-EASD-EASO Clinical Practice Guidelines for the management of non-alcoholic fatty liver disease. *Diabetologia* 2016; **59**: 1121-1140 [PMID: 27053230 DOI: 10.1007/s00125-016-3902-y]

22 **European Association for the Study of the Liver**. EASL Clinical Practice Guidelines: Autoimmune hepatitis. *J Hepatol* 2015; **63**: 971-1004 [PMID: 26341719 DOI: 10.1016/j.jhep.2015.06.030]

23 **European Association for the Study of the Liver**. EASL Clinical Practice Guidelines: management of cholestatic liver diseases. *J Hepatol* 2009; **51**: 237-267 [PMID: 19501929 DOI: 10.1016/j.jhep.2009.04.009]

24 **Zhu H**, Guo H, Yin X, Yang J, Yin Q, Xiao J, Wang Y, Zhang M, Han H, Zhuge Y, Zhang F. Spleen Stiffness Predicts Survival after Transjugular Intrahepatic Portosystemic Shunt in Cirrhotic Patients. *Biomed Res Int* 2020; **2020**: 3860390 [PMID: 33282945 DOI: 10.1155/2020/3860390]

25 **Huang Y**, Zheng Y, Zhang C, Zhong S. Ultrasound Assessment of the Relevance of Liver, Spleen, and Kidney Dimensions with Body Parameters in Adolescents. *Comput Math Methods Med* 2022; **2022**: 9150803 [PMID: 35832132 DOI: 10.1155/2022/9150803]

26 **Aithal GP**, Palaniyappan N, China L, Härmälä S, Macken L, Ryan JM, Wilkes EA, Moore K, Leithead JA, Hayes PC, O'Brien AJ, Verma S. Guidelines on the management of ascites in cirrhosis. *Gut* 2021; **70**: 9-29 [PMID: 33067334 DOI: 10.1136/gutjnl-2020-321790]

27 **Lee HL**, Lee SW. The role of transjugular intrahepatic portosystemic shunt in patients with portal hypertension: Advantages and pitfalls. *Clin Mol Hepatol* 2022; **28**: 121-134 [PMID: 34571587 DOI: 10.3350/cmh.2021.0239]

28 **Patel RK**, Chandel K, Tripathy TP, Mukund A. Complications of transjugular intrahepatic portosystemic shunt (TIPS) in the era of the stent graft - What the interventionists need to know? *Eur J Radiol* 2021; **144**: 109986 [PMID: 34619618 DOI: 10.1016/j.ejrad.2021.109986]

29 **Kumar R**, Kerbert AJC, Sheikh MF, Roth N, Calvao JAF, Mesquita MD, Barreira AI, Gurm HS, Ramsahye K, Mookerjee RP, Yu D, Davies NH, Mehta G, Agarwal B, Patch D, Jalan R. Determinants of mortality in patients with cirrhosis and uncontrolled variceal bleeding. *J Hepatol* 2021; **74**: 66-79 [PMID: 32561318 DOI: 10.1016/j.jhep.2020.06.010]

30 **Nicoară-Farcău O**, Han G, Rudler M, Angrisani D, Monescillo A, Torres F, Casanovas G, Bosch J, Lv Y, Thabut D, Fan D, Hernández-Gea V, García-Pagán JC; Preemptive TIPS Individual Data Metanalysis, International Variceal Bleeding Study and Baveno Cooperation Study groups. Effects of Early Placement of Transjugular Portosystemic Shunts in Patients With High-Risk Acute Variceal Bleeding: a Meta-analysis of Individual Patient Data. *Gastroenterology* 2021; **160**: 193-205.e10 [PMID: 32980344 DOI: 10.1053/j.gastro.2020.09.026]

31 **Trebicka J**, Gu W, Ibáñez-Samaniego L, Hernández-Gea V, Pitarch C, Garcia E, Procopet B, Giráldez Á, Amitrano L, Villanueva C, Thabut D, Silva-Junior G, Martinez J, Genescà J, Bureau C, Llop E, Laleman W, Palazon JM, Castellote J, Rodrigues S, Gluud L, Ferreira CN, Barcelo R, Cañete N, Rodríguez M, Ferlitsch A, Mundi JL, Gronbaek H, Hernández-Guerra M, Sassatelli R, Dell'Era A, Senzolo M, Abraldes JG, Romero-Gómez M, Zipprich A, Casas M, Masnou H, Primignani M, Weiss E, Catalina MV, Erasmus HP, Uschner FE, Schulz M, Brol MJ, Praktiknjo M, Chang J, Krag A, Nevens F, Calleja JL, Robic MA, Conejo I, Albillos A, Rudler M, Alvarado E, Guardascione MA, Tantau M, Bosch J, Torres F, Pavesi M, Garcia-Pagán JC, Jansen C, Bañares R; International Variceal Bleeding Observational Study Group and Baveno Cooperation. Rebleeding and mortality risk are increased by ACLF but reduced by pre-emptive TIPS. *J Hepatol* 2020; **73**: 1082-1091 [PMID: 32339602 DOI: 10.1016/j.jhep.2020.04.024]

32 **Wang Q**, Lv Y, Bai M, Wang Z, Liu H, He C, Niu J, Guo W, Luo B, Yin Z, Bai W, Chen H, Wang E, Xia D, Li X, Yuan J, Han N, Cai H, Li T, Xie H, Xia J, Wang J, Zhang H, Wu K, Fan D, Han G. Eight millimetre covered TIPS does not compromise shunt function but reduces hepatic encephalopathy in preventing variceal rebleeding. *J Hepatol* 2017; **67**: 508-516 [PMID: 28506905 DOI: 10.1016/j.jhep.2017.05.006]

33 **Liu J**, Ma J, Yang C, Chen M, Shi Q, Zhou C, Huang S, Chen Y, Wang Y, Li T, Xiong B. Sarcopenia in Patients with Cirrhosis after Transjugular Intrahepatic Portosystemic Shunt Placement. *Radiology* 2022; **303**: 711-719 [PMID: 35289658 DOI: 10.1148/radiol.211172]

34 **Trebicka J**. Does Transjugular Intrahepatic Portosystemic Shunt Stent Differentially Improve Survival in a Subset of Cirrhotic Patients? *Semin Liver Dis* 2018; **38**: 87-96 [PMID: 29471569 DOI: 10.1055/s-0038-1627457]

35 **Hofer BS**, Simbrunner B, Hartl L, Jachs M, Balcar L, Paternostro R, Schwabl P, Semmler G, Scheiner B, Trauner M, Mandorfer M, Reiberger T. Hepatic recompensation according to Baveno VII criteria is linked to a significant survival benefit in decompensated alcohol-related cirrhosis. *Liver Int* 2023; **43**: 2220-2231 [PMID: 37469291 DOI: 10.1111/liv.15676]

36 **Gracia-Sancho J**, Marrone G, Fernández-Iglesias A. Hepatic microcirculation and mechanisms of portal hypertension. *Nat Rev Gastroenterol Hepatol* 2019; **16**: 221-234 [PMID: 30568278 DOI: 10.1038/s41575-018-0097-3]

37 **Gedgaudas R**, Bajaj JS, Skieceviciene J, Varkalaite G, Jurkeviciute G, Gelman S, Valantiene I, Zykus R, Pranculis A, Bang C, Franke A, Schramm C, Kupcinskas J. Circulating microbiome in patients with portal hypertension. *Gut Microbes* 2022; **14**: 2029674 [PMID: 35130114 DOI: 10.1080/19490976.2022.2029674]

World Journal of Gastroenterology

Submit a Manuscript: https://www.f6publishing.com

World J Gastroenterol 2023 October 14; 29(38): 5395-5405

DOI: 10.3748/wjg.v29.i38.5395

ISSN 1007-9327 (print) ISSN 2219-2840 (online)

ORIGINAL ARTICLE

Observational Study

Hepatitis D virus dual-infection among Chinese hepatitis B patient related to hepatitis B surface antigen, hepatitis B virus DNA and age

Jun Zi, Yu-Huan Li, Xiao-Mei Wang, Hong-Qin Xu, Wen-Hui Liu, Jia-Yue Cui, Jun-Qi Niu, Xiu-Mei Chi

Specialty type: Infectious diseases

Provenance and peer review: Unsolicited article; Externally peer reviewed.

Peer-review model: Single blind

Peer-review report's scientific quality classification

Grade A (Excellent): 0
Grade B (Very good): B, B, B
Grade C (Good): C
Grade D (Fair): 0
Grade E (Poor): 0

P-Reviewer: Kao JT, Taiwan; Senousy M, Egypt; Yoshioka K, Japan

Received: June 6, 2023
Peer-review started: June 6, 2023
First decision: August 8, 2023
Revised: August 21, 2023
Accepted: September 26, 2023
Article in press: September 26, 2023
Published online: October 14, 2023

Jun Zi, Yu-Huan Li, Xiu-Mei Chi, Gene Therapy Laboratory, Center for Pathogen Biology and Infectious Diseases, First Hospital of Jilin University, Changchun 130061, Jilin Province, China

Xiao-Mei Wang, Hong-Qin Xu, Jun-Qi Niu, Department of Hepatology, Center for Pathogen Biology and Infectious Diseases, First Hospital of Jilin University, Changchun 130061, Jilin Province, China

Wen-Hui Liu, Jia-Yue Cui, Department of Histology and Embryology, College of Basic Medical Sciences, Jilin University, Changchun 130061, Jilin Province, China

Corresponding author: Xiu-Mei Chi, PhD, Assistant Professor, Gene Therapy Laboratory, Center for Pathogen Biology and Infectious Diseases, First Hospital of Jilin University, No. 519 of East Minzhu Street, Changchun 130061, Jilin Province, China. chixm@jlu.edu.cn

Abstract

BACKGROUND

The screening practices for hepatitis D virus (HDV) are diverse and non-standardized worldwide, and the exact prevalence of HDV is uncertain.

AIM

To estimate HDV prevalence and investigate viral marker quantity trends in patients with hepatitis D.

METHODS

We collected 5594 serum samples from patients with hepatitis B in Jilin Province, China (3293 males and 2301 females, age range of 2 to 89 years). We then conducted tests for hepatitis B surface antigen (HBsAg), hepatitis B Virus (HBV) DNA, anti-hepatitis D antigen (HDAg), and HDV RNA.

RESULTS

We found that the prevalence of anti-HDAg and HDV RNA among hepatitis B patient were 3.6% (3.2-4.2%) and 1.2% (0.9-1.5%), respectively, 87.69% of hepatitis D patients were 51-70 years old. HDV infection screening positive rate of patients with HBV DNA levels below 2000 IU/mL (2.0%) was higher than those above 2000 IU/mL (0.2%). Among anti-HDAg positive patients, the HDV RNA positive rate was positively correlated with the HBsAg level and anti-HDAg level. There was a weak correlation between HBsAg and anti-HDAg levels among hepatitis D patients.

CONCLUSION
Our study highlights the importance of considering multiple factors when assessing the severity of HDV infection, comprehensive evaluation of patients' clinical and laboratory parameters is necessary for proper diagnosis and treatment.

Key Words: Hepatitis D virus; Hepatitis B virus; Epidemiology; Anti-hepatitis D antigen; Hepatitis D virus RNA

©The Author(s) 2023. Published by Baishideng Publishing Group Inc. All rights reserved.

Core Tip: The screening practices for hepatitis D virus (HDV) are diverse and non-standardized worldwide, the exact prevalence of HDV is uncertain. To estimating HDV prevalence and investigate viral marker quantity trends in patients with hepatitis D, we collected serum samples from patients with hepatitis B, and tested hepatitis B surface antigen, hepatitis B virus (HBV) DNA, anti-hepatitis D antigen (HDAg), and HDV RNA. We found that the prevalence of anti-HDAg and HDV RNA among hepatitis B patient in Jilin Province were 3.6% and 1.2%, respectively. HDV infection screening positive rate was higher in patients with lower HBV DNA levels, and with higher anti-HDAg levels.

Citation: Zi J, Li YH, Wang XM, Xu HQ, Liu WH, Cui JY, Niu JQ, Chi XM. Hepatitis D virus dual-infection among Chinese hepatitis B patient related to hepatitis B surface antigen, hepatitis B virus DNA and age. *World J Gastroenterol* 2023; 29(38): 5395-5405
URL: https://www.wjgnet.com/1007-9327/full/v29/i38/5395.htm
DOI: https://dx.doi.org/10.3748/wjg.v29.i38.5395

INTRODUCTION

Hepatitis D virus (HDV) has a diameter of 35-37 nm[1] and is composed of RNA, hepatitis D antigen (HDAg), and an envelope containing hepatitis B surface antigen (HBsAg)[2]. HDV is a satellite virus of hepatitis B virus (HBV), co-infection of HBV and HDV results in extensive liver tissue damage and severe fulminant hepatitis. Patients with chronic hepatitis B who are super-infected with HDV experience an accelerated progression of the disease to cirrhosis and an increased risk of developing hepatocellular carcinoma[3]. Chronic hepatitis D (CHD) is the most severe form of viral hepatitis[4].

According to the World Health Organization (WHO), an estimated 296 million people were living with chronic hepatitis B infection globally in 2019[5]. China has the highest number of hepatitis B patients in the world, about 86 million people were living with HBsAg[6,7]. Since 1992, China has provided free HBV vaccination to newborns[8], at that time, the HBsAg carrier rates among general population was about 9.75%, which declined to about 7.18% in 2006[9], and was about 6.1% in 2016[7].

HDV is widespread worldwide, and its prevalence varies by geography[10]. The screening practices for HDV are diverse and non-standardized. Guidelines from the European Association for the Study of the Liver and the Asia Pacific Association for the Study of Liver (EASL/APASL) recommend HDV screening for all individuals who are positive for HBsAg[11]. The American Association for the Study of Liver Diseases recommends HDV screening for certain high-risk groups, with the recommended screening test being anti-HDAg. If the test is positive, HDV RNA testing should be performed[12,13]. In many endemic areas, the screening rate is inaccessible.

The global prevalence of HDV remains uncertain due to deficiencies in screening, especially HDV RNA testing. Different meta-analyses have estimated varying prevalence rates. Chen *et al*[14] estimated the prevalence of HDV to be 0.98% (0.61-1.42) among the general population and 14.57% (12.93-16.27) among HBsAg-positive individuals. Miao *et al*[15] estimated the prevalence of HDV to be 0.80% (0.63-1.00) among the general population and 13.02% (11.96-14.11) among HBV carriers. Stockdale *et al*[16] estimated the prevalence of anti-HDAg to be 0.16% (0.11-0.25) among the general population and 4.5% (3.6-5.7) among HBsAg-positive individuals, and the prevalence of HDV RNA to be 0.09% (0.07-0.15) among the general population.

China has the highest number of hepatitis D patients in the world, with estimated HDV prevalence rates of 0.69% (0.24-1.36) among the general population and 10.16% (8.50-11.95) among HBsAg-positive individuals[15]. Regional studies had conducted and reported prevalence rates of HDV RNA among HBV carriers ranging from 0.0% (Beijing, Tibet, *etc*) to 13.55% (Inner Mongolia)[17-22].

This study aims to estimate the prevalence of HDV in Jilin Province, China. Promoting research on the prevalence of HDV can help raise awareness of CHD, improve screening rate and identify hepatitis D patients as early as possible to reduce HDV transmission. We also studied the trend in the quantity of HBsAg, HBV DNA, anti-HDAg, and HDV RNA among hepatitis D patients. This information may provide some guidance for screening practices: Hepatitis B patients with quantitatively characteristic viral markers are more likely to be dual-infected with HDV, and hence should be screened for HDV infection.

MATERIALS AND METHODS

Study specimens

Form April 2021 to August 2022, a total of 5594 hepatitis B serum samples were collected from outpatient center of the First Hospital of Jilin University, comprising 3293 males and 2301 females, with an age range of 2 to 89 years. Fasting venous blood was centrifuged at 4000 rpm for 10 min to obtain serum. This study was approved by the Ethics Committee of the First Hospital of Jilin University (AF-IRB-029-06). The serum samples were separated into several aliquots of approximately 400 μL each and stored at -80 °C for the detection of HBV DNA, HBsAg, anti-HDAg, and HDV RNA. The basic information of the patients was recorded, and the specimen inclusion criteria were HBsAg positive or HBV DNA positive.

Detection of hepatitis B surface antigen

We used the Architect i2000SR platform and Abbott Architect reagents (Abbott Laboratories, Abbott Park, IL, United States) to detect HBsAg, as previously described (Chemiluminescence Microparticle Immunoassay, CMIA)[23]. HBsAg levels were measured with a dynamic range of 0-250 IU/mL. If the detection value of the original sample was higher than 250 IU/mL, it was properly diluted to obtain the final data.

Detection of hepatitis B virus DNA

Serum (400 μL) were used to detect HBV DNA by the Roche COBAS AmpliPrep/COBAS TaqMan system (Roche Diagnostics, Basel, Switzerland), as previously described (Quantitative Polymerase Chain Reaction, qPCR)[23]. The lowest detection limit was 20 IU/mL.

Detection of anti-hepatitis D antigen

We used the HDV IgG Antibody Detection Kit (Wantai, Beijing, China) to detect anti-HDAg IgG (hereinafter referred to as anti-HDAg), according to the manufacturer's instructions (Enzyme Linked Immunosorbent Assay, ELISA). The absorbance at 450 nm was measured using an SBYMB-001 microplate reader system (Thermo, Waltham, MA, United States), and the cut-off value was 0.12 plus the mean of the negative control.

Detection of HDV RNA

We selected anti-HDAg-positive specimens and used a nucleic acid extraction reagent (Jianwei, Shandong Province, China) to extract nucleic acid from 400 μL of serum, following the manufacturer's instructions. The extraction was performed on an EZ Bead nucleic acid extraction instrument (Jianwei, Shandong Province, China).

We used the RoboGene HDV RNA Quantification Kit 2.0 (AJ Roboscreen GmbH, Leipzig, Germany) to detect HDV RNA, according to the manufacturer's instructions (real time qPCR, RT-qPCR). The RT-qPCR was performed on an Mx3005P system (Agilent, Santa Clara, CA, United States), and the lowest detection limit was 6 IU/mL.

Statistical analysis

All statistical analyses were performed using SPSS version 26.0. Categorical variables were expressed as percentages and 95% confidence intervals (CI), and compared using the χ^2 test. Continuous variables with a normal distribution were expressed as mean ± SD. Continuous variables with non-normally distribution was expressed as median and interquartile range (IQR), Mann-Whitney *U* test was used for comparison of two groups, and Kruskal-Wallis test was used for comparison of multiple groups. Correlations between viral markers were assessed using simple linear regression models and Pearson's correlation coefficient (*r*). All tests were two-tailed, and a *P* value of less than 0.05 was considered statistically significant. Graphs were generated using GraphPad Prism 8.0.

RESULTS

Prevalence of HDV among hepatitis B patients in Jilin Province, China

Among hepatitis B patients in Jilin Province, China, the prevalence of anti-HDAg was 3.6% (203/5594, 95%CI: 3.2%-4.2%), and the prevalence of HDV RNA was 1.2% (65/5594, 95%CI: 0.9%-1.5%). Among anti-HDAg positive patients, the HDV RNA positive rate was 32.0% (65/203, 95%CI: 25.7%-38.9%). We divided these 5594 hepatitis B patients into three infection groups: 5391 patients were anti-HDAg negative and HDV RNA negative (HBV mono-infected patients); 138 patients were anti-HDAg positive and HDV RNA negative (indicating resolved hepatitis D, persistent infection with very low viraemia, or a false negative PCR test result[24]. Hereinafter referred to as HDV-resolved patients); and 65 patients were anti-HDAg positive and HDV RNA positive (HBV-HDV dual-infected patients).

Gender

Among the 5594 patients, there were 3168 males and 2223 females in the HBV mono-infected group, 86 males and 52 females in the HDV-resolved group, and 39 males and 26 females in the HBV-HDV dual-infected group. The differences in gender distribution among the three groups were not statistically significant ($P > 0.05$, $\chi^2 = 0.737$).

Among the 3293 male and 2301 female hepatitis B patients, there was no significant difference in the anti-HDAg screening positive rates [3.8% (male) *vs* 3.4% (female), $P > 0.05$, $\chi^2 = 0.639$] or the HDV RNA screening positive rates [1.2% (male) *vs* 1.1% (female), $P > 0.05$, $\chi^2 = 0.035$]. Among male and female anti-HDAg positive patients, there was also no

significant difference in the HDV RNA positive rates [31.2% (male) *vs* 33.3% (female), $P > 0.05$, $\chi^2 = 0.100$] (Table 1).

Age

The age range of HBV mono-infected patients was from 2 years to 89 years, with a median of 50 years (IQR: 41-58 years). HDV-resolved patients had an age range from 32 years to 72 years, with a mean of 57.9 years ± 0.7 years. For HBV-HDV dual-infected patients, the age range was from 35 years to 72 years, with a mean of 57.0 years ± 0.9 years. Statistically significant differences were detected among their age ($P < 0.05$, H = 99.902), the age of HBV mono-infected patients was found to be lower than that of HDV-resolved patients and HBV-HDV dual-infected patients ($P < 0.05$), and there was no significant difference in age between HDV-resolved patients and HBV-HDV dual-infected patients ($P > 0.05$) (Figure 1A).

Among the Hepatitis B patients, those who were 30 years old or younger (323 patients) and those who were over 80 years old (13 patients) were all negative for anti-HDAg and HDV RNA. The remaining 5258 patients (aged 31-80) were divided into five groups based on age: 31-40, 41-50, 51-60, 61-70, and 71-80 years old, respectively. The screening positive rates of anti-HDAg in the five age groups were 0.7% (7/1009, 95%CI: 0.3%-1.4%), 1.5% (21/1412, 95%CI: 0.9%-2.3%), 6.1% (107/1762, 95%CI: 5.0%-7.3%), 6.4% (59/928, 95%CI: 4.9%-8.1%), and 6.1% (9/147, 95%CI: 2.8%-11.3%), respectively. Similarly, the screening positive rates of HDV RNA in the five age groups were 0.2% (2/1009, 95%CI: 0.0%-0.7%), 0.3% (4/1412, 95%CI: 0.1%-0.7%), 2.4% (42/1762, 95%CI: 1.7%-3.2%), 1.6% (15/928, 95%CI: 0.9%-2.7%), and 1.4% (2/147, 95%CI: 0.2%-4.8%), respectively (Figure 1B).

Based on preliminary observations, the screening positive rates of anti-HDAg and HDV RNA in the 31-40 and 41-50 age groups appear to be lower than those in the 51-60, 61-70, and 71-80 age groups. Upon combining the corresponding age groups, the anti-HDAg screening positive rate in patients aged 31-50 years old (1.2%, 95%CI: 0.8%-1.7%) was found to be lower than in patients aged 51-80 years old (6.2%, 95%CI: 5.3%-7.1%, $P < 0.05$, $\chi^2 = 88.403$). Similarly, the HDV RNA screening positive rate in patients aged 31-50 years old (0.2%, 95%CI: 0.1%-0.5%) was lower than in patients aged 51-80 years old (2.1%, 95%CI: 1.6%-2.7%, $P < 0.05$, $\chi^2 = 35.902$).

Among the five age groups of patients who tested positive for anti-HDAg, the HDV RNA positive rates were 28.6% (2/7, 95%CI: 3.7%-71.0%), 19.0% (4/21, 95%CI: 5.4%-41.9%), 39.3% (42/107, 95%CI: 30.0%-49.2%), 25.4% (15/59, 95%CI: 15.0%-38.4%), and 22.2% (2/9, 95%CI: 2.8%-60.0%), respectively (Supplementary Figure 1A). However, the differences in these HDV RNA positive rates were not statistically significant ($P > 0.05$, $\chi^2 = 5.809$).

Hepatitis B surface antigen

In HBV mono-infected patients, the quantity of HBsAg ranged from 0 to 123935.00 IU/mL, with a median of 881.41 IU/mL (IQR: 0.01-3651.62 IU/mL). Among these patients, 38.6% had quantities ranging from 0 to 2.5×10^2 IU/mL, 13.2% had quantities ranging from 2.5×10^2 IU/mL to 1.0×10^3 IU/mL, 37.8% had quantities ranging from 1.0×10^3 IU/mL to 1.0×10^4 IU/mL, and 10.4% had quantities ranging from 1.0×10^4 IU/mL to 1.3×10^5 IU/mL (Figure 2A).

For HDV-resolved patients, the HBsAg quantity ranged from 0 to 20685.00 IU/mL, with a median of 65.83 IU/mL (IQR: 0.00-1245.30 IU/mL). Among these patients, 61.8% had quantities ranging from 0 to 2.5×10^2 IU/mL, 13.0% had quantities ranging from 2.5×10^2 IU/mL to 1.0×10^3 IU/mL, 13.0% had quantities ranging from 1.0×10^3 IU/mL to 1.0×10^4 IU/mL, and 12.2% had quantities ranging from 1.0×10^4 IU/mL to 1.3×10^5 IU/mL (Figure 2A).

For HBV-HDV dual-infected patients, the HBsAg quantity ranged from 0 to 22070.00 IU/mL, with a median of 892.90 IU/mL (IQR: 37.26-5525.50 IU/mL). Among these patients, 41.3% had quantities ranging from 0 to 2.5×10^2 IU/mL, 11.1% had quantities ranging from 2.5×10^2 IU/mL to 1.0×10^3 IU/mL, 33.3% had quantities ranging from 1.0×10^3 IU/mL to 1.0×10^4 IU/mL, and 14.3% had quantities ranging from 1.0×10^4 IU/mL to 1.3×10^5 IU/mL (Figure 2A).

Statistically significant differences were detected among their HBsAg quantity ($P < 0.05$, H = 14.639), the quantity of HBsAg in HDV-resolved patients was found to be lower than that in HBV mono-infected patients and HBV-HDV dual-infected patients ($P < 0.05$), and there was no statistically significant difference in HBsAg quantity between HBV mono-infected patients and HBV-HDV dual-infected patients ($P > 0.05$) (Figure 2A).

Hepatitis B patients were categorized into four groups based on their HBsAg quantity: 0-2.5×10^2, 2.5×10^2-1.0×10^3, 1.0×10^2-1.0×10^4, and 1.0×10^4-1.3×10^5 IU/mL, respectively. The anti-HDAg screening positive rates in these four HBsAg groups were 6.4% (102/1589, 95%CI: 5.3%-7.7%), 4.3% (23/531, 95%CI: 2.8%-6.4%), 2.5% (37/1491, 95%CI: 1.8%-3.4%), and 5.6% (24/426, 95%CI: 3.6%-8.3%), respectively. The HDV RNA screening positive rates were 1.6% (26/1589, 95%CI: 1.1%-2.4%), 1.3% (7/531, 95%CI: 0.5%-2.7%), 1.4% (21/1491, 95%CI: 0.9%-2.1%), and 2.1% (9/426, 95%CI: 1.0%-4.0%), respectively (Figure 2B).

Among the four HBsAg groups with anti-HDAg positive patients, the HDV RNA positive rates were 25.5% (26/102, 95%CI: 17.4%-35.1%), 30.4% (7/23, 95%CI: 13.2%-52.9%), 56.8% (21/37, 95%CI: 39.5%-72.9%), and 37.5% (9/24, 95%CI: 18.8%-59.4%), respectively (Supplementary Figure 1B).

Hepatitis B virus DNA

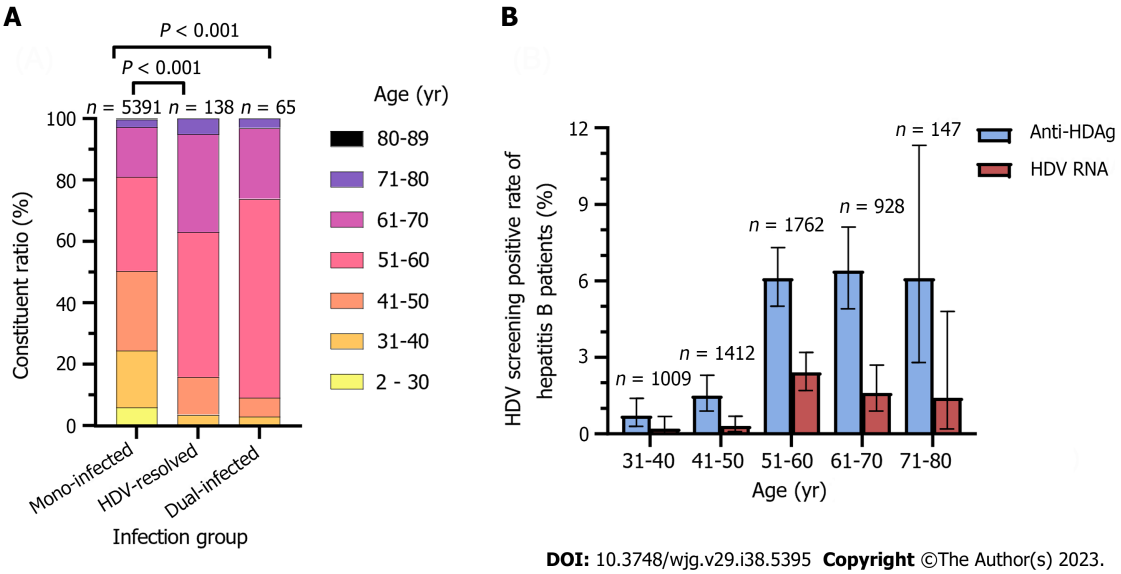
In HBV mono-infected patients, the quantity of HBV DNA ranged from 0 to 1.10×10^9 IU/mL, with a median of 3.38×10^2 IU/mL (IQR: 5.05×10^1 IU/mL-6.69×10^3 IU/mL). Among these patients, 24.9% had quantities ranging from 0 to 5×10^1 IU/mL, 42.5% had quantities ranging from 5×10^1 IU/mL to 2×10^3 IU/mL, 12.3% had quantities ranging from 2×10^3 IU/mL to 2×10^4 IU/mL, 15.4% had quantities ranging from 2×10^4 IU/mL to 2×10^7 IU/mL, and 4.9% had quantities ranging from 2×10^7 IU/mL to 2×10^9 IU/mL (Figure 3A).

For HDV-resolved patients, the median of the HBV DNA quantity was 1.41×10^1 IU/mL (IQR: 0-1.10×10^2 IU/mL), ranging from 0 to 3.33×10^7 IU/mL. Among them, 67.2% of patients had a range of 0 to 5×10^1 IU/mL, 25.4% had a range of 5×10^1 IU/mL to 2×10^3 IU/mL, 3.3% had a range of 2×10^3 IU/mL to 2×10^4 IU/mL, 3.3% had a range of 2×10^4 IU/mL to 2×10^7 IU/mL, and 0.8% had a range of 2×10^7 IU/mL to 2×10^9 IU/mL (Figure 3A).

Table 1 Differences in the positive rate of hepatitis D virus between gender

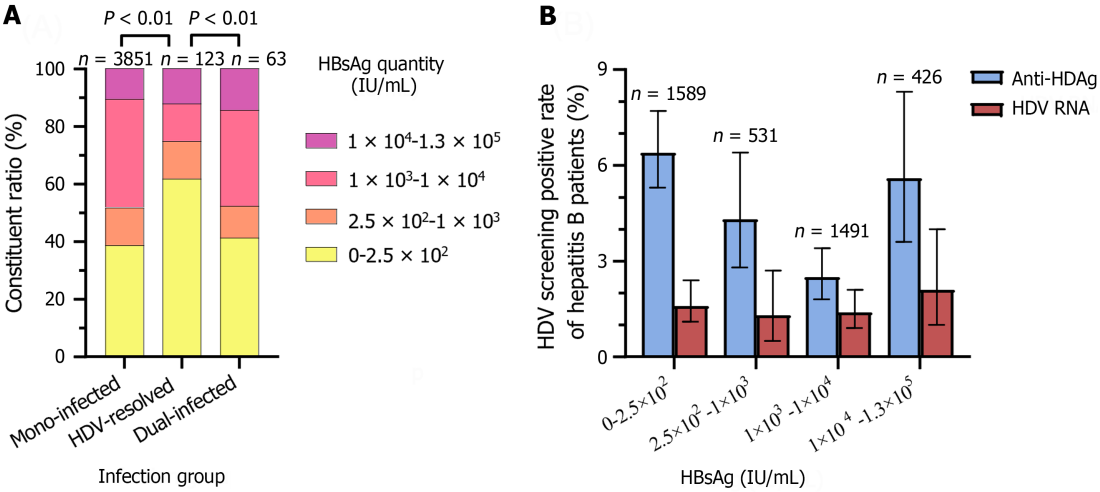
	Male			Female		
	+/total	%	95%CI	+/total	%	95%CI
Anti-HDAg screening positive rate among hepatitis B patients	125/3293	3.8	3.2-4.5	78/2301	3.4	2.7-4.2
HDV RNA screening positive rate among hepatitis B patients	39/3293	1.2	0.8-1.6	26/2301	1.1	0.7-1.7
HDV RNA positive rate among anti-HDAg positive patients	39/125	31.2	23.2-40.1	26/78	33.3	23.1-44.9

HDAg: Hepatitis D antigen; HBV: Hepatitis B virus; HDV: Hepatitis D virus; 95%CI: 95% confidence interval.



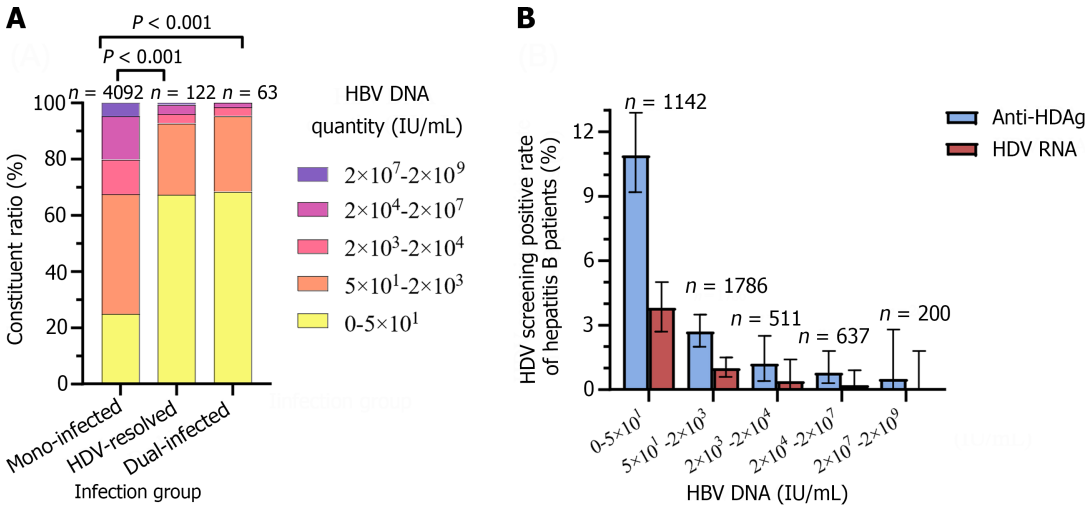
DOI: 10.3748/wjg.v29.i38.5395 **Copyright** ©The Author(s) 2023.

Figure 1 Constituent ratio of age among three infection groups' patients and the hepatitis D virus screening positive rate of hepatitis B patients with different age. A and B: Age was compared using Kruskal-Wallis test, error bars represent 95% confidence interval. Note: The screening positive rate of hepatitis D virus in patients who were 30 years old or younger, and who were over 80 years old were 0.0%, and not shown in figure 1B. HDAg: Hepatitis D antigen; HDV: Hepatitis D virus.



DOI: 10.3748/wjg.v29.i38.5395 **Copyright** ©The Author(s) 2023.

Figure 2 Constituent ratio of hepatitis B surface antigen among three infection groups' patients and the hepatitis D virus screening positive rate of hepatitis B patients with different hepatitis B surface antigen. A and B: Hepatitis B surface antigen (HBsAg) was compared using Kruskal-Wallis test, error bars represent 95% confidence interval. HBsAg: Hepatitis B surface antigen; HDAg: Hepatitis D antigen; HDV: Hepatitis D virus.



DOI: 10.3748/wjg.v29.i38.5395 **Copyright** ©The Author(s) 2023.

Figure 3 Constituent ratio of hepatitis B virus DNA among three infection groups' patients and the hepatitis D virus screening positive rate of hepatitis B patients with different hepatitis B virus DNA. A and B: Hepatitis B virus DNA was compared using Kruskal-Wallis test, error bars represent 95% confidence interval. HBV: Hepatitis B virus; HDV: Hepatitis D virus.

In the HBV-HDV dual-infected patients, the median of the HBV DNA quantity was 1.86 × 10^1 IU/mL (IQR: 2.06-7.07 × 10^1 IU/mL), ranging from 0 to 1.80 × 10^4 IU/mL. Among them, 68.3% of patients had a range of 0 to 5 × 10^1 IU/mL, 27.0% had a range of 5 × 10^1 IU/mL to 2 × 10^3 IU/mL, 3.2% had a range of 2 × 10^3 IU/mL to 2 × 10^4 IU/mL, and 1.6% had a range of 2 × 10^4 IU/mL to 2 × 10^7 IU/mL (Figure 3A).

Statistically significant differences were detected among their HBV DNA quantity ($P < 0.05$, H = 190.771), the HBV DNA quantity of HBV mono-infected patients was higher than that of HDV-resolved patients and HBV-HDV dual-infected patients ($P < 0.05$), and there was no statistically significant difference in the HBV DNA quantity between HDV-resolved patients and HBV-HDV dual-infected patients ($P > 0.05$) (Figure 3A).

Hepatitis B patients were classified into five groups according to their HBV DNA quantity: 0-5 × 10^1, 5 × 10^1-2 × 10^3, 2 × 10^3-2 × 10^4, 2 × 10^4-2 × 10^7, and 2 × 10^7-2 × 10^9 IU/mL, respectively. The anti-HDAg screening positive rates of the five HBV DNA groups were 10.9% (125/1142, 95%CI: 9.2%-12.9%), 2.7% (48/1786, 95%CI: 2.0%-3.5%), 1.2% (6/511, 95%CI: 0.4%-2.5%), 0.8% (5/637, 95%CI: 0.3%-1.8%), and 0.5% (1/200, 95%CI: 0.0%-2.8%), respectively. The HDV RNA screening positive rates were 3.8% (43/1142, 95%CI: 2.7%-5.0%), 1.0% (17/1786, 95%CI: 0.6%-1.5%), 0.4% (2/511, 95%CI: 0.0%-1.4%), 0.2% (1/637, 95%CI: 0.0%-0.9%), and 0.0% (0/200, 95%CI: 0.0%-1.8%), respectively (Figure 3B).

According to preliminary observations, the anti-HDAg and HDV RNA screening positive rates of the first two HBV DNA quantity groups (0-2 × 10^3 IU/mL) appeared to be higher than the last three groups (2 × 10^3 IU/mL-2 × 10^9 IU/mL). After combining the corresponding groups, the anti-HDAg screening positive rate of patients with HBV DNA quantity between 0-2 × 10^3 IU/mL (5.9%, 95%CI: 5.1%-6.8%) was higher than that of patients with 2 × 10^3 IU/mL-2 × 10^9 IU/mL (0.9%, 95%CI: 0.5%-1.5%, $P < 0.05$, $\chi^2 = 56.157$), and the HDV RNA screening positive rate of 0-2 × 10^3 IU/mL patients (2.0%, 95%CI: 1.6%-2.6%) was also higher than that of 2 × 10^3 IU/mL-2 × 10^9 IU/mL patients (0.2%, 95%CI: 0.0%-0.6%, $P < 0.05$, $\chi^2 = 21.216$).

Among the five HBV DNA groups, the HDV RNA positive rates of anti-HDAg positive patients were 34.4% (43/125, 95%CI: 26.1%-43.4%), 35.4% (17/48, 95%CI: 22.2%-50.5%), 33.3% (2/6, 95%CI: 4.3%-77.7%), 20.0% (1/5, 95%CI: 0.5%-71.6%), and 0.0% (0/1, 95%CI: 0.0%-97.5%) respectively (Supplementary Figure 1C).

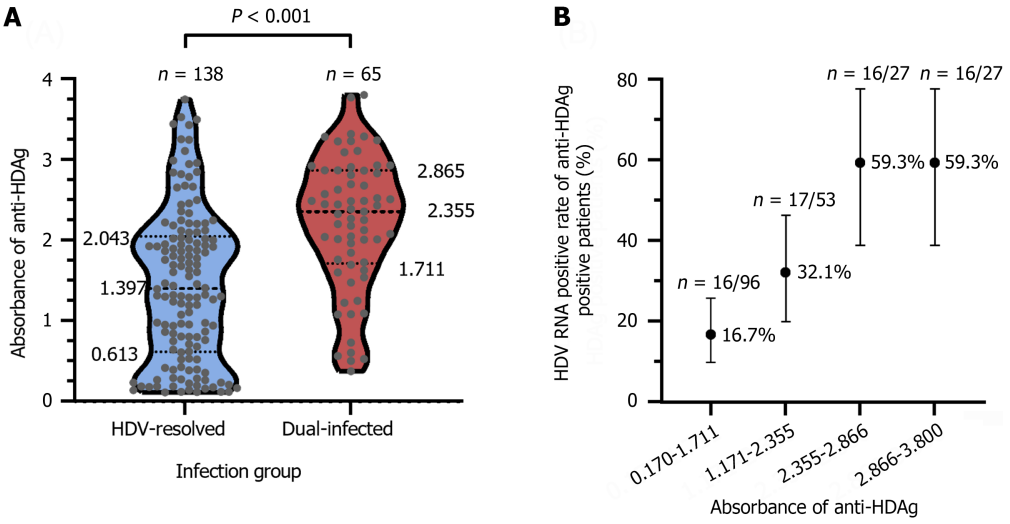
Anti-hepatitis D antigen

In HDV-resolved patients, the absorbance of anti-HDAg ranged from 0.170 to 3.740, with a median of 1.397 (IQR: 0.613-2.043). Among HBV-HDV dual-infected patients, the absorbance of anti-HDAg ranged from 0.370 to 3.800, with a mean of 2.219 ± 0.103. The absorbance of anti-HDAg in HDV-resolved patients was lower than that in HBV-HDV dual-infected patients ($P < 0.05$, $Z = -5.461$) (Figure 4A).

Anti-HDAg positive patients were categorized into four groups based on the absorbance of anti-HDAg: 0.170-1.711, 1.711-2.355, 2.355-2.865, and 2.865-3.800. The HDV RNA positive rates for the four anti-HDAg groups were 16.7% (16/96, 95%CI: 9.8%-25.6%), 32.1% (17/53, 95%CI: 19.9%-46.3%), 59.3% (16/27, 95%CI: 38.8%-77.6%), and 59.3% (16/27, 95%CI: 38.8%-77.6%) respectively (Figure 4B).

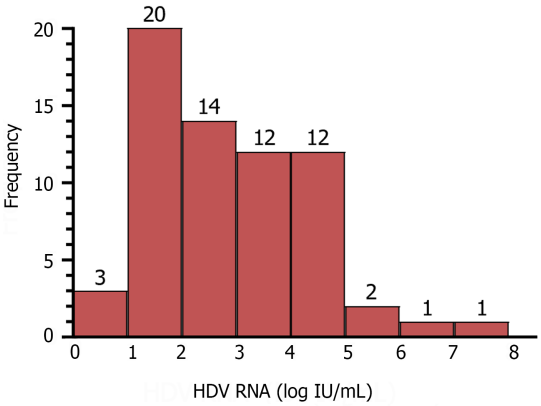
Hepatitis D virus RNA

Among HBV-HDV dual-infected patients, the HDV RNA quantity ranged from 7.10 to 2.35 × 10^7 IU/mL, the median was 4.61 × 10^2 IU/mL (IQR: 4.95 × 10^1 IU/mL-8.99 × 10^3 IU/mL) (Figure 5). The HDV RNA quantity of 3 (4.62%) patients ranged from 0 to 10^1 IU/mL, 20 (30.77%) patients ranged from 10^1 to 10^2 IU/mL, 14 (21.54%) patients ranged from 10^2 to 10^3 IU/mL, 12 (18.46%) patients ranged from 10^3 to 10^4 IU/mL, 12 (19.46%) patients ranged from 10^4 to 10^5 IU/mL, 2 (3.08%) patients ranged from 10^5 to 10^6 IU/mL, 1 (1.54%) patient ranged from 10^6 to 10^7 IU/mL, 1 (1.54%) patient ranged



DOI: 10.3748/wjg.v29.i38.5395 **Copyright** ©The Author(s) 2023.

Figure 4 Distribution of anti-hepatitis D antigen among two infection groups' patients and hepatitis D virus RNA positive rate of patients with different anti-HDAg. A and B: Anti-hepatitis D antigen was compared using Mann-Whitney *U* test, error bars represent 95% confidence interval. HDAg: Hepatitis D antigen; HDV: Hepatitis D virus.



DOI: 10.3748/wjg.v29.i38.5395 **Copyright** ©The Author(s) 2023.

Figure 5 Distribution of the hepatitis D virus RNA among hepatitis B virus-hepatitis D virus dual-infected patients. HDV: Hepatitis D virus.

from 10^7 to 10^8 IU/mL.

Correlations between viral markers

The Pearson's correlation coefficients among the viral markers of HBV-HDV dual-infected patients were analyzed. The *R* values suggest that the correlations between the viral markers were weak, with all coefficients being less than 0.3. HBsAg and anti-HDAg had a weak correlation ($r = 0.256$, $P = 0.043$), but there were no significant correlations between HBsAg and HBV DNA, HBsAg and HDV RNA, or anti-HDAg and HDV RNA ($r = 0.151$, $P = 0.241$; $r = 0.101$, $P = 0.431$; $r = 0.224$, $P = 0.073$, respectively). The correlations between HBV DNA and anti-HDAg, and HBV DNA and HDV RNA were even weaker ($r = 0.082$, $P = 0.529$; $r = 0.041$, $P = 0.750$, respectively).

DISCUSSION

The prevalence of anti-HDAg among hepatitis B patients in Jilin Province, China was 3.6%, which is lower than the estimated prevalence in China (10.16%)[15] and worldwide (4.50%-14.57%)[14-16]. The prevalence of HDV RNA was 1.2%, which is slightly higher than the global meta-analysis estimates (0.09%)[14-16], and similar to other provinces in China (0%-13.55%)[17-22]. Gender did not seem to influence the spread of HDV in Jilin Province, as the HDV screening positive rates were similar between different genders.

According to China Center for Disease Control, HBsAg prevalence among 1-4, 5-14, and 15-29 years old general population was 9.9%, 10.6%, and 9.8%, respectively in 1992. Which declined to 0.3%, 0.9%, and 4.4%, respectively in 2014 [25]. Before China offering free HBV vaccination to newborns, the prevalence of HBV was similar across different age

groups, and the vaccine has been effective in preventing HBV transmission to newborns. Our data indirectly verifies this conclusion, the majority (91.19%) of HBV mono-infected patients falling between 31 years old and 70 years old, among which distributed relatively even.

The ages of HDV-resolved patients and HBV-HDV dual-infected patients were mainly (78.83% and 87.69%, respectively) between 51 and 70 years old, and the anti-HDAg and HDV RNA screening positive rates were higher in patients aged 51-80 than in those aged 31-50. Before 1992, the health, medical and hygiene conditions of China were suboptimal, and the awareness about viral hepatitis prevention was poor. HDV infected Chinese adults (currently in the 51-80 years age group) severely through risk behaviors such as unsafe sexual contact and injection, and infected minors (currently in the 31-50 years age group) occasionally through intrafamilial transmission. In 1992, along with HBV vaccination widespread and economic development, the suboptimal conditions and the awareness about viral hepatitis prevention were improved too. When HBV patients aged 31-50 became adults, the decline of risk behaviors might be one of the reasons for their relatively low HDV positive rate. Since HDV requires HBV for secretion and infection[26], HBV vaccination is effective in preventing HDV transmission to newborns.

The positive rate of HDV RNA among anti-HDAg positive patients was 32.0%, and there were no statistically significant differences between genders or age groups. A previous meta-analysis estimated that approximately one-third of anti-HDAg positive patients have undetectable HDV RNA[24], while another estimated that the pooled proportion of anti-HDAg positive patients with HDV RNA detection was 58.5%[16]. The positive rate of HDV RNA among anti-HDAg positive patients in Jilin Province seems relatively low. More research is needed to understand it, one possible reason was, as we previously reported, most hepatitis D patients in Jilin Province were infected with HDV Genotype 1[18], which secretes high virus titers with extremely delayed kinetics[27]. The delay of HDV secretion providing patients' immune system with more time to respond to the HDV before it proliferates extensively and widespread.

We observed that the HBsAg level of HBV-HDV dual-infected patients and HBV mono-infected patients were similar, but the HBV DNA level of the former was significantly lower than the latter. This conclusion was consistent with previous studies that showed HBV DNA were significantly decreased after HDV infection, without decrease in HBsAg levels[28-32].

Before the study, we hypothesized that the HBsAg and HBV DNA levels of HDV-resolved patients and HBV mono-infected patients would be similar, due to minor HDV replication and interference in both groups of patients. But the study data showed that the levels of the former were both significantly lower than the latter. Additionally, we found that among anti-HDAg positive patients, the HDV RNA positive rate was positively correlated with the HBsAg level, except for an abnormal decrease in the 1×10^4-1×10^5 group. According to previous research results, the HBsAg level kept relatively stable in hepatitis B patients before and after HDV infection[28-32]. We speculate that, before HDV acute infecting those HDV-resolved patients, their immune systems maintain the HBsAg on low level already, and were more capable of resolving HDV acute infection than those who with high level HBsAg. Otherwise, HDV-resolved patients might eliminate HDV alone with some HBV after HDV acute infection, leading to decrease in HBsAg and HBV DNA.

Our study data suggests that to effectively screen HDV and save medical resources, screening hepatitis B patients for HDV infection whose HBV DNA quantity is lower than 2×10^3 IU/mL. Additionally, hepatitis B patients whose HBV DNA quantity is between 2×10^3 IU/mL-2×10^7 IU/mL can be screened for HDV infection if clinical symptoms imply HDV infection, while those whose HBV DNA quantity is higher than 2×10^7 IU/mL seem don't need HDV screening. For anti-HDAg positive patients, those with a higher HBsAg level have a higher possibility of dual-infection with HDV, but patients with a low HBsAg level should also be screened for HDV infection. Finally, using the Wantai kit (mentioned in 2.4), we found that patients with anti-HDAg level lower than 0.370 were HDV RNA negative and may have undetectable HDV RNA according to the patient's condition.

The quantity of HDV RNA in HBV-HDV dual-infected patients from Jilin Province was mainly between 1×10^1 IU/mL to 1×10^5 IU/mL (92.06%), with a significant proportion (30.77%) concentrated between 1×10^1 IU/mL to 1×10^2 IU/mL. These findings suggested that the HDV RNA level was not very high and may not accurately reflect the severity of the disease.

In our study, we investigated the correlations between HBsAg, HBV DNA, anti-HDAg, and HDV RNA in HBV-HDV dual-infected patients. Our analysis revealed a weak correlation between HBsAg and anti-HDAg, while the correlations between other viral markers were not statistically significant. The complex physiological process underlying HDV generation may contribute to the lack of strong quantitative correlation between viral markers. Additionally, other factors such as the patient's health status, medication use, and viral load fluctuations can influence viral marker level.

We used the HDV IgG antibody detection kit produced by Wantai company in Beijing, which has a high market share in China. The test is easy to perform and can be conducted in conventional hospitals, ensuring the authenticity of the data. Despite good quality, it is an indirect ELISA kit and other components in the serum may competitively bind to HDAg, the cross-reactivity may lead to false positive results or overestimation[33]. Further, we only detected anti-HDAg IgG, which present in the serum of individuals after resolution of acute HDV infection, or who have developed CHD[34]. The absence of IgM (indicates acute or active infection[35]) detection may result in missing some patients with HDV acute infection, and lead to underestimation of HDV positivity rates. In addition, all samples were from Jilin Province, which may not fully reflect the overall situation in China.

CONCLUSION

In Jilin Province, China, the prevalence of anti-HDAg was 3.6% and the prevalence of HDV RNA was 1.2% among hepatitis B patients. These rates were related to age, and the majority of hepatitis D patients were 51-70 years old. The

experimental data suggests that screening for HDV infection is more likely to yield positive results in hepatitis B patients with lower HBV DNA level. Patients with lower HBsAg levels appear to resolve HDV acute infection, while those with higher anti-HDAg levels are more likely to test positive for HDV RNA. A weak correlation was observed between HBsAg and anti-HDAg in hepatitis D patients. Overall, our study highlights the importance of considering multiple factors when assessing the severity of HDV infection, comprehensive evaluation of patients' clinical and laboratory parameters is necessary for proper diagnosis and treatment.

ARTICLE HIGHLIGHTS

Research background

The screening practices for hepatitis D virus (HDV) are diverse and non-standardized worldwide, and the exact prevalence of HDV is uncertain.

Research motivation

To estimate the prevalence of HDV in Jilin Province, China.

Research objectives

Promoting research on the prevalence of HDV can help raise awareness of chronic hepatitis D, improve screening rate and identify hepatitis D patients as early as possible to reduce HDV transmission.

Research methods

We collected 5594 serum samples from patients with hepatitis B in Jilin Province, China (3293 males and 2301 females, age range of 2 to 89 years) and then conducted tests for hepatitis B surface antigen (HBsAg), hepatitis B virus (HBV) DNA, anti-hepatitis D antigen (HDAg), and HDV RNA.

Research results

The prevalence of anti-HDAg and HDV RNA among hepatitis B patient were 3.6% (3.2%-4.2%) and 1.2% (0.9%-1.5%), respectively, 87.69% of hepatitis D patients were 51-70 years old. HDV infection screening positive rate of patients with HBV DNA levels below 2000 IU/mL (2.0%) was higher than those above 2000 IU/mL (0.2%). Among anti-HDAg positive patients, the HDV RNA positive rate was positively correlated with the HBsAg level and anti-HDAg level. There was a weak correlation between HBsAg and anti-HDAg levels among hepatitis D patients.

Research conclusions

Our study highlights the importance of considering multiple factors when assessing the severity of HDV infection, comprehensive evaluation of patients' clinical and laboratory parameters is necessary for proper diagnosis and treatment.

Research perspectives

From the perspective of medical institutions.

ACKNOWLEDGEMENTS

We thank the Department of Biobank, Division of Clinical Research for the providing of human sera.

FOOTNOTES

Author contributions: Chi XM and Li YH obtained fundings and designed the study; Chi XM, Zi J, Li YH, Wang XM, and Liu WH collected and diagnosed the specimens; Zi J and Xu HQ analyzed the data; Zi J and Li YH wrote this manuscript; Chi XM, Niu JQ, Cui JY, and Xu HQ revised the manuscript.

Supported by the National Natural Science Foundation of Jilin Provence, No. YDZJ202201ZTYS016; and Jilin Provincial Health Commission, No. 2022JC053.

Institutional review board statement: This study was approved by the Ethics Committee of the First Hospital of Jilin University (Approval No. AF-IRB-029-06).

Informed consent statement: All study participants, or their legal guardian, provided informed written consent prior to study enrollment.

Conflict-of-interest statement: No potential conflict of interest was reported by the authors.

Data sharing statement: Technical appendix, statistical code, and dataset available from the corresponding author at chixm@jlu.edu.cn.

STROBE statement: The authors have read the STROBE Statement—checklist of items, and the manuscript was prepared and revised according to the STROBE Statement—checklist of items.

Open-Access: This article is an open-access article that was selected by an in-house editor and fully peer-reviewed by external reviewers. It is distributed in accordance with the Creative Commons Attribution NonCommercial (CC BY-NC 4.0) license, which permits others to distribute, remix, adapt, build upon this work non-commercially, and license their derivative works on different terms, provided the original work is properly cited and the use is non-commercial. See: https://creativecommons.org/Licenses/by-nc/4.0/

Country/Territory of origin: China

ORCID number: Xiao-Mei Wang 0000-0003-2606-4013; Hong-Qin Xu 0000-0002-7022-7732; Jun-Qi Niu 0000-0001-5415-2024; Xiu-Mei Chi 0000-0002-6291-8496.

S-Editor: Chen YL
L-Editor: A
P-Editor: Cai YX

REFERENCES

1 **Mentha N**, Clément S, Negro F, Alfaiate D. A review on hepatitis D: From virology to new therapies. *J Adv Res* 2019; **17**: 3-15 [PMID: 31193285 DOI: 10.1016/j.jare.2019.03.009]
2 **Lempp FA**, Ni Y, Urban S. Hepatitis delta virus: insights into a peculiar pathogen and novel treatment options. *Nat Rev Gastroenterol Hepatol* 2016; **13**: 580-589 [PMID: 27534692 DOI: 10.1038/nrgastro.2016.126]
3 **Botelho-Souza LF**, Vasconcelos MPA, Dos Santos AO, Salcedo JMV, Vieira DS. Hepatitis delta: virological and clinical aspects. *Virol J* 2017; **14**: 177 [PMID: 28903779 DOI: 10.1186/s12985-017-0845-y]
4 **Elbahrawy A**, Atalla H, Alboraie M, Alwassief A, Madian A, El Fayoumie M, Tabll AA, Aly HH. Recent Advances in Protective Vaccines against Hepatitis Viruses: A Narrative Review. *Viruses* 2023; **15** [PMID: 36680254 DOI: 10.3390/v15010214]
5 **World Orgnazation Health**. Hepatitis B. [cited 24 June 2022]. Available from: https://www.who.int/en/news-room/fact-sheets/detail/hepatitis-b.
6 **Yao X**, Huang S, Zhou H, Tang SH, Qin JP. Clinical efficacy of antiviral therapy in patients with hepatitis B-related cirrhosis after transjugular intrahepatic portosystemic shunt. *World J Gastroenterol* 2021; **27**: 5088-5099 [PMID: 34497437 DOI: 10.3748/wjg.v27.i30.5088]
7 **Polaris Observatory Collaborators**. Global prevalence, treatment, and prevention of hepatitis B virus infection in 2016: a modelling study. *Lancet Gastroenterol Hepatol* 2018; **3**: 383-403 [PMID: 29599078 DOI: 10.1016/S2468-1253(18)30056-6]
8 **Cao WW**, Zhou RR, Ou X, Shi LX, Xiao CQ, Chen TY, Tan H, Fan XG, Li BJ, Li N. Prevalence of hepatitis B virus, hepatitis C virus, human immunodeficiency virus and Treponema pallidum infections in hospitalized patients before transfusion in Xiangya hospital Central South University, China from 2011 to 2016. *BMC Infect Dis* 2018; **18**: 145 [PMID: 29606088 DOI: 10.1186/s12879-018-3051-7]
9 **Wang FS**, Fan JG, Zhang Z, Gao B, Wang HY. The global burden of liver disease: the major impact of China. *Hepatology* 2014; **60**: 2099-2108 [PMID: 25164003 DOI: 10.1002/hep.27406]
10 **Sahin A**, Gurocak S, Tunc N, Demirel U, Poyrazoglu OK, Akbulut H, Yalniz M, Toraman ZA, Bahcecioglu IH. Anti-HDV seroprevalance among patients with previous HBV infection. *North Clin Istanb* 2018; **5**: 132-138 [PMID: 30374479 DOI: 10.14744/nci.2018.01328]
11 **Lee AU**, Lee C. Hepatitis D Review: Challenges for the Resource-Poor Setting. *Viruses* 2021; **13** [PMID: 34696341 DOI: 10.3390/v13101912]
12 **Da BL**, Rahman F, Lai WC, Kleiner DE, Heller T, Koh C. Risk Factors for Delta Hepatitis in a North American Cohort: Who Should Be Screened? *Am J Gastroenterol* 2021; **116**: 206-209 [PMID: 33027083 DOI: 10.14309/ajg.0000000000000954]
13 **Terrault NA**, Lok ASF, McMahon BJ, Chang KM, Hwang JP, Jonas MM, Brown RS Jr, Bzowej NH, Wong JB. Update on prevention, diagnosis, and treatment of chronic hepatitis B: AASLD 2018 hepatitis B guidance. *Hepatology* 2018; **67**: 1560-1599 [PMID: 29405329 DOI: 10.1002/hep.29800]
14 **Chen HY**, Shen DT, Ji DZ, Han PC, Zhang WM, Ma JF, Chen WS, Goyal H, Pan S, Xu HG. Prevalence and burden of hepatitis D virus infection in the global population: a systematic review and meta-analysis. *Gut* 2019; **68**: 512-521 [PMID: 30228220 DOI: 10.1136/gutjnl-2018-316601]
15 **Miao Z**, Zhang S, Ou X, Li S, Ma Z, Wang W, Peppelenbosch MP, Liu J, Pan Q. Estimating the Global Prevalence, Disease Progression, and Clinical Outcome of Hepatitis Delta Virus Infection. *J Infect Dis* 2020; **221**: 1677-1687 [PMID: 31778167 DOI: 10.1093/infdis/jiz633]
16 **Stockdale AJ**, Kreuels B, Henrion MYR, Giorgi E, Kyomuhangi I, de Martel C, Hutin Y, Geretti AM. The global prevalence of hepatitis D virus infection: Systematic review and meta-analysis. *J Hepatol* 2020; **73**: 523-532 [PMID: 32335166 DOI: 10.1016/j.jhep.2020.04.008]
17 **Wang Y**. Survey of HDV Infection and Molecular Characterization of HDV, HBV and HIV-1 among Chronic Hepatitis B Patients in China. Doctoral Thesis, National Center for AIDS/STD Control and Prevention, China, 2019. [cited 24 June 2022]. Available from: https://kns.cnki.net/kcms2/article/abstract?v=3uoqIhG8C447WN1SO36whLpCgh0R0Z-ia63qwICAcC3-s4XdRlECrREwcOYYpgWONc6mn6bnC_SrOpFUE5RYCbnC4qu_UDxq&uniplatform=NZKPT
18 **Roggenbach I**, Chi X, Lempp FA, Qu B, Walter L, Wu R, Gao X, Schnitzler P, Ding Y, Urban S, Niu J. HDV Seroprevalence in HBsAg-Positive Patients in China Occurs in Hotspots and Is Not Associated with HCV Mono-Infection. *Viruses* 2021; **13** [PMID: 34578380 DOI: 10.3390/v13091799]
19 **Chang SY**, Yang CL, Ko WS, Liu WC, Lin CY, Wu CH, Su YC, Chang SF, Chen MY, Sheng WH, Hung CC, Chang SC. Molecular epidemiology of hepatitis D virus infection among injecting drug users with and without human immunodeficiency virus infection in Taiwan. *J Clin Microbiol* 2011; **49**: 1083-1089 [PMID: 21191061 DOI: 10.1128/JCM.01154-10]

20 **Zhou L**, Wei Q, Huang H, Huang W. Investigation and molecular characteristics of mixed infection of Hepatitis B virus and Hepatitis D virus in Zhuhai South China. *J Prev Med* 2021; **47**: 753-756 [DOI: 10.12183/j.scjpm.2021.0753]

21 **Chen F**, Zhang J, Guo F, Wen B, Luo S, Yuan D, Lin Y, Ou W, Tang P, Dai G, Li F, Liu W, Qu X. Hepatitis B, C, and D virus infection showing distinct patterns between injection drug users and the general population. *J Gastroenterol Hepatol* 2017; **32**: 515-520 [PMID: 27248508 DOI: 10.1111/jgh.13460]

22 **Wu S**, Zhang Y, Tang Y, Yao T, Lv M, Tang Z, Zang G, Yu Y, Chen X. Molecular epidemiology and clinical characteristics of hepatitis delta virus (HDV) infected patients with elevated transaminases in Shanghai, China. *BMC Infect Dis* 2020; **20**: 565 [PMID: 32746807 DOI: 10.1186/s12879-020-05275-1]

23 **Chi XM**, Wang XM, Wang ZF, Wu RH, Gao XZ, Xu HQ, Ding YH, Niu JQ. Serum hepatitis B core-related antigen as a surrogate marker of hepatitis B e antigen seroconversion in chronic hepatitis B. *World J Gastroenterol* 2021; **27**: 6927-6938 [PMID: 34790015 DOI: 10.3748/wjg.v27.i40.6927]

24 **Shen DT**, Goyal H, Xu HG. Differences in delta virus hepatitis diagnosis methods and its effect on the hepatitis D prevalence. *Gut* 2020; **69**: 1893 [PMID: 31719130 DOI: 10.1136/gutjnl-2019-320159]

25 **Cui F**, Shen L, Li L, Wang H, Wang F, Bi S, Liu J, Zhang G, Zheng H, Sun X, Miao N, Yin Z, Feng Z, Liang X, Wang Y. Prevention of Chronic Hepatitis B after 3 Decades of Escalating Vaccination Policy, China. *Emerg Infect Dis* 2017; **23**: 765-772 [PMID: 28418296 DOI: 10.3201/eid2305.161477]

26 **Zi J**, Gao X, Du J, Xu H, Niu J, Chi X. Multiple Regions Drive Hepatitis Delta Virus Proliferation and Are Therapeutic Targets. *Front Microbiol* 2022; **13**: 838382 [PMID: 35464929 DOI: 10.3389/fmicb.2022.838382]

27 **Wang W**, Lempp FA, Schlund F, Walter L, Decker CC, Zhang Z, Ni Y, Urban S. Assembly and infection efficacy of hepatitis B virus surface protein exchanges in 8 hepatitis D virus genotype isolates. *J Hepatol* 2021; **75**: 311-323 [PMID: 33845061 DOI: 10.1016/j.jhep.2021.03.025]

28 **Alfaiate D**, Lucifora J, Abeywickrama-Samarakoon N, Michelet M, Testoni B, Cortay JC, Sureau C, Zoulim F, Dény P, Durantel D. HDV RNA replication is associated with HBV repression and interferon-stimulated genes induction in super-infected hepatocytes. *Antiviral Res* 2016; **136**: 19-31 [PMID: 27771387 DOI: 10.1016/j.antiviral.2016.10.006]

29 **Lütgehetmann M**, Mancke LV, Volz T, Helbig M, Allweiss L, Bornscheuer T, Pollok JM, Lohse AW, Petersen J, Urban S, Dandri M. Humanized chimeric uPA mouse model for the study of hepatitis B and D virus interactions and preclinical drug evaluation. *Hepatology* 2012; **55**: 685-694 [PMID: 22031488 DOI: 10.1002/hep.24758]

30 **Wu JC**, Chen PJ, Kuo MY, Lee SD, Chen DS, Ting LP. Production of hepatitis delta virus and suppression of helper hepatitis B virus in a human hepatoma cell line. *J Virol* 1991; **65**: 1099-1104 [PMID: 1847439 DOI: 10.1128/jvi.65.3.1099-1104.1991]

31 **Pollicino T**, Raffa G, Santantonio T, Gaeta GB, Iannello G, Alibrandi A, Squadrito G, Cacciola I, Calvi C, Colucci G, Levrero M, Raimondo G. Replicative and transcriptional activities of hepatitis B virus in patients coinfected with hepatitis B and hepatitis delta viruses. *J Virol* 2011; **85**: 432-439 [PMID: 20962099 DOI: 10.1128/JVI.01609-10]

32 **Schaper M**, Rodriguez-Frias F, Jardi R, Tabernero D, Homs M, Ruiz G, Quer J, Esteban R, Buti M. Quantitative longitudinal evaluations of hepatitis delta virus RNA and hepatitis B virus DNA shows a dynamic, complex replicative profile in chronic hepatitis B and D. *J Hepatol* 2010; **52**: 658-664 [PMID: 20346531 DOI: 10.1016/j.jhep.2009.10.036]

33 **Escrivá L**, Font G, Manyes L, Berrada H. Studies on the Presence of Mycotoxins in Biological Samples: An Overview. *Toxins (Basel)* 2017; **9** [PMID: 28820481 DOI: 10.3390/toxins9080251]

34 **Koh C**, Heller T, Glenn JS. Pathogenesis of and New Therapies for Hepatitis D. *Gastroenterology* 2019; **156**: 461-476.e1 [PMID: 30342879 DOI: 10.1053/j.gastro.2018.09.058]

35 **Miao Z**, Xie Z, Ren L, Pan Q. Hepatitis D: advances and challenges. *Chin Med J (Engl)* 2022; **135**: 767-773 [PMID: 35234694 DOI: 10.1097/CM9.0000000000002011]

World Journal of Gastroenterology

Submit a Manuscript: https://www.f6publishing.com

World J Gastroenterol 2023 October 14; 29(38): 5406-5427

DOI: 10.3748/wjg.v29.i38.5406

ISSN 1007-9327 (print) ISSN 2219-2840 (online)

SYSTEMATIC REVIEWS

Scoping review on health-related physical fitness in patients with inflammatory bowel disease: Assessment, interventions, and future directions

Karlijn Demers, Michiel T J Bak, Bart C Bongers, Annemarie C de Vries, Daisy M A E Jonkers, Marieke J Pierik, Laurents P S Stassen

Specialty type: Gastroenterology and hepatology

Provenance and peer review: Unsolicited article; Externally peer reviewed.

Peer-review model: Single blind

Peer-review report's scientific quality classification

Grade A (Excellent): 0
Grade B (Very good): B, B
Grade C (Good): 0
Grade D (Fair): 0
Grade E (Poor): 0

P-Reviewer: Shalaby MN, Egypt; Stogov MV, Russia

Received: July 28, 2023
Peer-review started: July 28, 2023
First decision: August 25, 2023
Revised: September 6, 2023
Accepted: September 12, 2023
Article in press: September 12, 2023
Published online: October 14, 2023

Karlijn Demers, Laurents P S Stassen, Department of Surgery, Maastricht University Medical Center+, Maastricht 6229 HX, Netherlands

Karlijn Demers, Marieke J Pierik, Department of Internal Medicine, Division of Gastroenterology-Hepatology, Maastricht University Medical Center+, Maastricht 6229 HX, Netherlands

Karlijn Demers, Daisy M A E Jonkers, Marieke J Pierik, Department of Internal Medicine, Division of Gastroenterology-Hepatology, School of Nutrition and Translational Research in Metabolism, Maastricht University, Maastricht 6229 ER, Netherlands

Karlijn Demers, Bart C Bongers, Laurents P S Stassen, Department of Surgery, School of Nutrition and Translational Research in Metabolism, Maastricht University, Maastricht 6229 ER, Netherlands

Michiel T J Bak, Annemarie C de Vries, Department of Gastroenterology and Hepatology, Erasmus University Medical Center Rotterdam, Rotterdam 3015 GD, Netherlands

Bart C Bongers, Department of Nutrition and Movement Sciences, School of Nutrition and Translational Research in Metabolism, Maastricht University, Maastricht 6229 ER, Netherlands

Corresponding author: Karlijn Demers, MD, MSc, Department of Surgery, Maastricht University Medical Center+, Maastricht 6229 HX, Netherlands.
k.demers@maastrichtuniversity.nl

Abstract

BACKGROUND

Reaching the Selecting Therapeutic Targets in Inflammatory Bowel Disease-II (STRIDE-II) therapeutic targets for inflammatory bowel disease (IBD) requires an interdisciplinary approach. Lifestyle interventions focusing on enhancing and preserving health-related physical fitness (HRPF) may aid in improving subjective health, decreasing disability, or even controlling inflammation. However, ambiguity remains about the status and impact of HRPF (*i.e.* body composition, cardiorespiratory fitness, muscular strength, muscular endurance, and flexibility) in IBD patients, hindering the development of physical activity and physical exercise training guidelines.

AIM
To review HRPF components in IBD patients and the impact of physical activity and physical exercise training interventions on HRPF.

METHODS
A systematic search in multiple databases was conducted for original studies that included patients with IBD, assessed one or more HRPF components, and/or evaluated physical activity or physical exercise training interventions.

RESULTS
Sixty-eight articles were included. No study examined the complete concept of HRPF, and considerable heterogeneity existed in assessment methods, with frequent use of non-validated tests. According to studies that used gold standard tests, cardiorespiratory fitness seemed to be reduced, but findings on muscular strength and endurance were inconsistent. A limited number of studies that evaluated physical activity or physical exercise training interventions reported effects on HRPF, overall showing a positive impact.

CONCLUSION
We performed a scoping review using a systematic and iterative approach to identify and synthesize an emerging body of literature on health-related physical fitness in patients with IBD, highlighting several research gaps and opportunities for future research. Findings of this review revealed a gap in the literature regarding the accurate assessment of HRPF in patients with IBD and highlighted important methodological limitations of studies that evaluated physical activity or physical exercise training interventions. This scoping review is a step towards performing studies and systematic reviews in the future, which was not possible at present given the heterogeneity in endpoints and designs of the available studies on this topic. Future well-designed studies are required to determine the optimal training paradigm for improving HRPF in patients with IBD before guidelines can be developed and integrated into the therapeutic strategy.

Key Words: Inflammatory bowel disease; Physical fitness; Assessment; Intervention; Physical activity; Exercise

©The Author(s) 2023. Published by Baishideng Publishing Group Inc. All rights reserved.

Core Tip: Lifestyle interventions focusing on enhancing and preserving health-related physical fitness (HRPF) may aid in improving subjective health, decreasing disability, or even controlling inflammation in patients with inflammatory bowel disease (IBD). This scoping review encompassed a comprehensive exploration of the available literature on the assessment of HRPF components in patients with IBD, summarized the effects of physical activity and physical exercise training interventions on these components in this specific patient population, and provided valuable recommendations for future research directions.

Citation: Demers K, Bak MTJ, Bongers BC, de Vries AC, Jonkers DMAE, Pierik MJ, Stassen LPS. Scoping review on health-related physical fitness in patients with inflammatory bowel disease: Assessment, interventions, and future directions. *World J Gastroenterol* 2023; 29(38): 5406-5427
URL: https://www.wjgnet.com/1007-9327/full/v29/i38/5406.htm
DOI: https://dx.doi.org/10.3748/wjg.v29.i38.5406

INTRODUCTION

Inflammatory bowel disease (IBD), including Crohn's disease (CD) and ulcerative colitis (UC), are chronic inflammatory diseases of the gastrointestinal tract[1,2]. The disease course is characterized by recurrent episodes of mucosal inflammation. Besides a genetic predisposition, an altered immune response and intestinal microbiota perturbations as well as psychosocial and lifestyle factors underlie the recurrent inflammation of IBD. As a result, substantial variation exists between patients for disease course and treatment outcomes. Since the disease course is unfavorable for many patients and a significant proportion requires surgery to manage the disease or its complications[3], novel drugs have been introduced and tight control of mucosal inflammation has been added to the traditional treatment goal of steroid-free clinical remission[4,5]. In addition to intestinal symptoms caused by mucosal inflammation or intestinal complications, patients frequently experience impaired subjective well-being due to symptoms such as fatigue, or impaired social functioning or emotional health[6-8]. This often persists even in the absence of mucosal inflammation and contributes to a high physical and psychological disease burden with a significant impact on quality of life.

The treat-to-target strategy for IBD, according to the Selecting Therapeutic Targets in Inflammatory Bowel Disease-II (STRIDE-II) recommendations, aims for endoscopic healing, absence of disability, and optimal subjective health, and

warrants a multidisciplinary treatment approach[9]. Lifestyle interventions involving physical activity or physical exercise training to improve or preserve physical fitness might improve the outcome of IBD. In general, such interventions are key factors in health promotion and disease prevention programs[10,11]. Beneficial effects include a reduced risk of all-cause mortality, reduced risk of developing noncommunicable diseases (*e.g.* cardiovascular diseases, diabetes, cancer, neurodegenerative diseases) and postoperative complications, and better mental health and subjective well-being[12-16]. In addition, the anti-inflammatory benefits of regular physical activity and physical exercise training (*e.g.* the release of myokines, reduction in visceral fat, and subsequent decrease of adipokine release) are well documented [17,18].

The use of standardized nomenclature is necessary to understand and optimally target the concepts of physical fitness, physical activity, physical exercise training, and their interrelationships. Physical fitness can be considered an integrated measure of bodily functions involved in daily physical activity. The physical fitness components that have a relationship with health are referred to as health-related physical fitness (HRPF), which includes body composition, cardiorespiratory fitness, muscular strength, muscular endurance, and flexibility[19-21]. Physical activity and physical exercise training are often used interchangeably but are physiologically different, resulting in unique local and systemic responses[19,22-24]. While physical activity is defined as any bodily movement produced by skeletal muscles that requires energy expenditure, physical exercise training is considered a subcategory of physical activity that is planned, structured, and repetitive with the final or intermediate purpose of maintaining or improving one or more physical fitness components.

To date, the status of several components of HRPF and their impact on inflammation and subjective health in IBD is not clear, which hinders the development of (inter)national guidelines regarding physical activity and physical exercise training for this population. Due to a sedentary lifestyle in general, lack of physical activity as a consequence of illness as well as corticosteroid use is likely to cause patients with IBD to suffer from an impaired HRPF[25-27]. Furthermore, malnutrition and the direct effect of proinflammatory cytokines can negatively influence muscle quality and function[28, 29]. The need for such guidelines to improve HRPF is further highlighted by a potential link between impaired components of HRPF in patients with IBD and subjective well-being in terms of fatigue and health-related quality of life [30,31].

Accurate assessment of HRPF components is necessary to obtain more insight into the state of HRPF in patients with IBD as well as to clearly define endpoints in intervention studies to determine whether physical activity or physical exercise training can improve HRPF components in these patients. Therefore, the first objective of this scoping review was to provide an overview of studies on the assessment of HRPF components in patients with IBD using a systematic and iterative approach. As the literature on body composition in patients with IBD was recently reviewed systematically [32-34], the current review focused on the remaining components of HRPF (*i.e.* cardiorespiratory fitness, muscular strength, muscular endurance, and flexibility). The second objective was to review the effects of physical activity and physical exercise training interventions on HRPF in patients with IBD. The ultimate goal of this scoping review was to identify and synthesize an emerging body of literature on health-related physical fitness in patients with IBD, highlighting several research gaps and opportunities for future research.

MATERIALS AND METHODS

This scoping review was performed and reported according to the Preferred Reporting Items for Systematic reviews and Meta-Analyses Extension for Scoping Reviews guideline[35].

Search strategy

A comprehensive search was performed in MEDLINE, EMBASE, Cochrane Central Register of Controlled Trials (CENTRAL), CINAHL, Web of Science, and PEDro for articles published through November 5, 2022. The literature search was performed in collaboration with the medical librarian of Maastricht University. An overview of the search strategy is presented in Supplementary material.

Study selection

Eligible studies were those that fulfilled the following criteria: (1) Inclusion of children and/or adults diagnosed with IBD; and (2) Addressing at least one of the following two elements: Assessing one or more of the four HRPF components (*i.e.* cardiorespiratory fitness, muscular strength, muscular endurance, and flexibility); and/or Assessing the effects of any frequency, intensity, time, and type of physical activity or physical exercise training interventions.

All original studies performed in humans from any geographical setting were eligible for inclusion. Letters, case reports, study protocols, animal studies, reviews, (conference) abstracts, and studies written in languages other than Dutch or English were excluded. In cases where the full-text article was not available, the corresponding authors were contacted. After the removal of duplicates, all unique studies were screened by title and abstract based on the predefined inclusion criteria by two reviewers (Demers K and Bak MTJ). Subsequently, these reviewers independently evaluated the full texts of all potentially relevant records to determine eligibility. Any disagreements between the reviewers were solved through discussion until a consensus was reached. Reasons for exclusion at this stage were documented. Furthermore, a snowball method was administered for the included studies to identify other relevant studies that were not identified within the search strategy.

Data extraction

The two independent reviewers extracted data in duplicate. For each study, the following data were collected (if

applicable) using a standardized registration form: First author; year of publication; study design; study location; population (number of participants, sex, age, disease entity, disease duration, disease location, disease activity, IBD medication, previous IBD-related surgery); control group or reference values; assessment methods (*e.g.* tests, test protocols) and corresponding outcomes; and physical activity intervention or physical exercise training intervention and comparator intervention (*e.g.* frequency, intensity, time, type, compliance, adverse events) and the reported effects.

Data synthesis

First, an overview was provided of the assessment methods used to assess HRPF in the included studies, classified according to the four different components of HRPF. A distinction was made between gold standard tests (*i.e.* laboratory-based tests) and practical field tests. Then, studies that used gold standard tests to assess HRPF were selected and considered key publications and used to report HRPF outcomes of patients with IBD in comparison with healthy control subjects or reference values, if applicable. Finally, the effects of physical activity interventions and physical exercise training interventions on HRPF components were reviewed.

Gold standard tests

The objective assessment of maximal oxygen uptake (VO_2max) or oxygen uptake at peak exercise (VO_2peak) using the cardiopulmonary exercise test (CPET), at which the patient performs a maximal effort, is considered the gold standard measurement method for assessing cardiorespiratory fitness[11,36]. If no true VO_2max (*i.e.* leveling-off of oxygen uptake despite further increases in exercise intensity) is achieved, the VO_2peak is often recorded. In that case, a respiratory exchange ratio at peak exercise, which represents the ratio of carbon dioxide production and oxygen uptake, ≥ 1.10 is indicative of a maximal or near-maximal effort. Isokinetic (*i.e.* dynamic) and isometric (*i.e.* static) peak torque measurements performed on an electromechanical dynamometer (*e.g.* Cybex, Biodex) are considered the most accurate and the gold standard tests for muscular strength and endurance examination[37-39]. The assessment of a single joint-specific range of motion using goniometers or fleximeters is considered the gold standard test for testing flexibility. However, publications describing compound flexibility measures, which involve the assessment of more than one joint, were also considered key publications[40,41].

RESULTS

Search results

The search yielded 7323 records. After removing duplicates, screening for eligibility, and snowballing, 68 studies were included in the review (Figure 1) with 4412 unique patients. The median sample size of the included studies was 42 [interquartile range (IQR): 24-77]. In total, 53 studies were conducted in adults and 15 studies in children or adolescents. Most studies (n = 32) evaluated patients with CD, followed by studies that included both patients with CD and UC (n = 30) and studies that included only patients with UC (n = 6). In total, 59 studies (86.8%) reported on disease activity. Although definitions varied across studies, 2410 unique patients were considered to be in remission, and 1147 patients were considered to have active disease, according to 48 studies that reported the number of patients in each group.

In total, 56 studies assessed one or more of the four HRPF components (*i.e.* cardiorespiratory fitness, muscular strength, muscular endurance, and flexibility) in a total number of 3949 unique patients with IBD. Physical activity or physical exercise interventions were evaluated in 22 studies, including 740 unique patients with IBD. Only 10 of these 22 studies (45.5%) reported the effects of the intervention on one or more HRPF component. The sample size distribution of the studies included is shown in Figure 2. The median sample size of the studies that assessed HRPF components in patients with IBD (*i.e.* assessment studies) was 42 (IQR: 24-75). The median sample size of the studies examining physical activity or physical exercise training interventions in patients with IBD (*i.e.* intervention studies) was 34 (IQR: 21-58).

Assessment of HRPF

Of all studies that assessed HRPF (n = 56), none assessed all components of HRPF within its IBD study population, and no single study assessed flexibility. Most studies (n = 42) examined only one component, including cardiorespiratory fitness (n = 13), muscular strength (n = 28), and muscular endurance (n = 1). Two or more components were assessed in 14 studies. Of these, 13 studies assessed two components of HRPF [muscular strength and muscular endurance (n = 8) and cardiorespiratory fitness and muscular strength (n = 5)]. One study assessed three components of HRPF (cardiorespiratory fitness, muscular strength, and muscular endurance). In total, cardiorespiratory fitness was assessed in 19 studies, muscular strength in 42 studies, and muscular endurance in 10 studies.

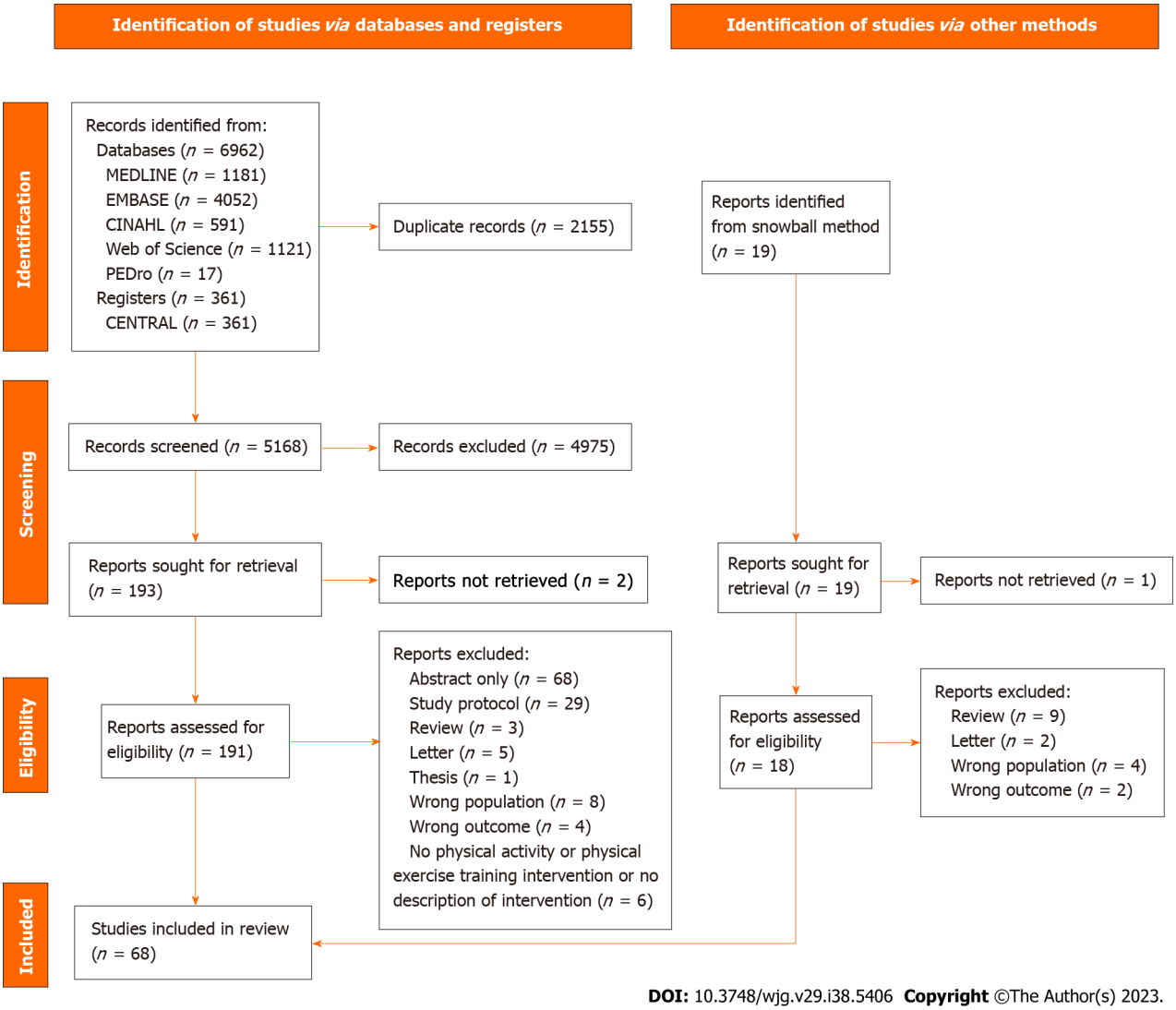
Methods used to assess HRPF

Table 1 shows an overview of the assessment methods used to assess HRPF components in patients with IBD, distinguishing between gold standard tests and practical field tests. Significant heterogeneity was observed in the assessment methodologies applied for the various components of HRPF, with frequent use of non-validated practical field tests such as a cycle ergometer test or a 6-min walk test for cardiorespiratory fitness, handgrip strength or jumping mechanography for muscular strength, and handgrip endurance or the chair-stand-test for muscular endurance. Overall, gold standard tests were used in 19 studies (33.9%). Cardiorespiratory fitness was assessed by CPET performance in eight out of nineteen studies (42.1%). However, only seven studies reported the gold standard VO_2max/VO_2peak. Muscular strength was examined by the gold standard peak torque measurement performed on a dynamometer in 12 out of 42 studies

Table 1 Overview of methods used to assess health-related physical fitness components in patients with inflammatory bowel disease

Health-related physical fitness component	Gold standard or practical field test	Assessment method	Outcome	Number of studies
Cardiorespiratory fitness	Gold standard test	CPET on a cycle ergometer	VO_2max/VO_2peak	7[28,43-45,57,59,61]
			WRpeak	1[71]
	Practical field test	Incremental cycle ergometer test	Submaximal heart rate	2[42,72]
			WRpeak	1[73]
		6-min walk test	Distance	2[28,53]
			Speed	1[74]
		Incremental shuttle walk test	Distance	2[75,76]
		CAFT step test	Estimated VO_2max	1[60]
		Bruce treadmill stress test	Duration of exercise and heart rate recovery index	1[77]
		Rockport 1-mile walk test	Estimated VO_2max	1[56]
		Duke activity status index	Points	1[78]
Muscular strength	Gold standard test	Isometric dynamometry	Peak torque	7[30,42,46-49,72]
		Isokinetic dynamometry	Peak torque	5[28,50-52,79]
	Practical field test	Handgrip strength	Peak torque	31[42,49,51,55,58,72,74-76,80-101]
		Jumping mechanography	P_{max}, F_{max}, jump height	4[99,102-104]
		Finger pinching strength	Peak torque	2[42,72]
		Isometric leg-press strength	Peak torque	1[98]
		Isometric HHD	Peak torque	1[58]
		Respiratory muscle strength	MIP, MEP	1[76]
			Peak expiratory flow	1[93]
Muscular endurance	Gold standard test	Isometric dynamometry	Slope of median muscle activation frequency	1[48]
			Decrement in peak torque	1[30]
	Practical field test	Handgrip endurance	Decrement in peak torque	2[86,87]
			Mean peak torque	1[98]
		Chair-stand test/sit-to-stand test	Repetitions	1[51]
			Time	4[49,51,55,74,98]
		3-meter walk test	Speed	1[55]
		Leg-press endurance	Mean force	1[98]
		Arm-curl test	Repetitions	1[51]
		Sit-ups	Repetitions	1[54]
		Back extensions	Repetitions	1[54]
		Push-ups	Repetitions	1[54]
		Squats	Repetitions	1[54]
		Plank position	Time	1[54]
Flexibility		N/A	N/A	0

CAFT: Canadian aerobic fitness test; CPET: Cardiopulmonary exercise testing; F_{max}: Maximum force; HHD: Hand-held dynamometry; MEP: Maximal expiratory pressure; MIP: Maximal inspiratory pressure; N/A: Not available; P_{max}: Maximum power; VO_2max: Maximal oxygen uptake; VO_2peak: Oxygen uptake at peak exercise; WRpeak: Work rate at peak exercise.



DOI: 10.3748/wjg.v29.i38.5406 **Copyright** ©The Author(s) 2023.

Figure 1 Preferred reporting items for systematic reviews and meta-analyses flow diagram of the literature search and selection process.

(28.6%). However, in one study, muscular strength was reported as a composite outcome combining dynamometry peak torque and practical field test results[42]. Muscular endurance was assessed by the gold standard method in two out of ten studies (20.0%).

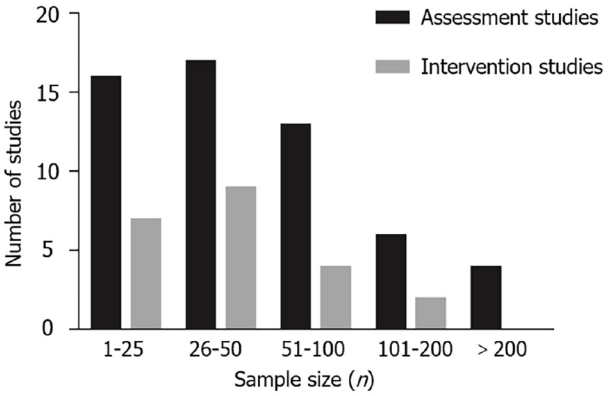
HRPF outcomes

Comprehensive descriptions and main outcomes of the included studies assessing cardiorespiratory fitness, muscular strength, and muscular endurance with the gold standard as well as practical field tests are presented in Supplementary Tables 1-3.

Cardiorespiratory fitness: The seven studies that assessed cardiorespiratory fitness by VO_2max/VO_2peak measurement during CPET performance are summarized in Table 2. A true VO_2max was reported in one study, while six studies reported VO_2peak. However, the achieved respiratory exchange ratio at peak exercise was only reported in two studies, indicating maximal achieved performance at the group level in both studies[28,43]. Four studies compared the cardiorespiratory fitness of patients with IBD to a healthy control group or reference values. All studies showed a diminished VO_2 peak in children or adolescents with CD and UC in remission or with mildly active disease[43,44], in adult patients with CD and UC in remission[28], and in patients with CD and UC awaiting colorectal surgery[45].

Muscular strength: The 11 studies that assessed muscular strength by isokinetic or isometric peak torque measurements performed on a dynamometer are listed in Table 3. Nine studies compared the muscular strength of patients with IBD to a healthy control group or reference values, with inconsistent results. However, it is crucial to note that testing methodologies and population characteristics varied throughout these studies, making comparison challenging. Two studies assessed muscular strength in pediatric and adolescent patients with CD, and seven evaluated adult patients with CD and/or UC.

Regarding pediatric and adolescent patients, reduced strength of the ankle dorsiflexion muscles was found in a prospective cohort of CD patients with low bone density in remission or with active disease and in a cross-sectional



DOI: 10.3748/wjg.v29.i38.5406 **Copyright** ©The Author(s) 2023.

Figure 2 Distribution of sample sizes of the studies that assessed health-related physical fitness components (*n* = 56) and that investigated physical activity or physical exercise training interventions (*n* = 22).

cohort of patients with new-onset CD experiencing moderate-to-severe disease activity[46,47]. However, reduced strength of the ankle dorsiflexion muscles was not observed in patients with new-onset CD experiencing mild disease activity in the cross-sectional cohort[47].

Of the seven studies that assessed muscular strength in adult patients with CD and/or UC, three studies showed reduced muscular strength of the lower limbs, two studies found both decreased and equivalent strength with regard to different muscle groups, and two studies found an equal strength of the lower limbs as compared to healthy control groups. The three studies that showed reduced muscular strength of the lower limbs were conducted in CD patients in remission with prior small bowel resection and musculoskeletal pain or weakness[48], in a cohort of fatigued and non-fatigued CD and UC patients in remission[28], and in sedentary female patients with UC and varying disease activity severity[49]. Both a decreased and equivalent strength in different muscle groups was demonstrated by Geerling *et al*[50] and Jones *et al*[51]. Geerling *et al*[50] showed a diminished strength of the knee flexor muscles but not the knee extensor muscles in a cohort of patients with longstanding CD, and Jones *et al*[51] demonstrated a reduced strength of the knee extensor muscles but no difference in elbow flexor strength in a group of CD patients in remission and with active disease. An equivalent strength of the lower limb muscles compared to healthy control groups was observed in recently diagnosed patients with CD and UC and in patients with CD in remission or with active disease[30,52].

Muscular endurance: Two studies assessed muscular endurance of the lower limbs by isometric endurance measurements on a dynamometer in patients with CD as compared to healthy control groups (Table 3), also with conflicting results. Salacinski *et al*[48] showed significantly better endurance of the rectus femoris muscle and an equivalent endurance of the vastus lateralis muscle in patients with CD in remission with prior small bowel resection and musculoskeletal pain or weakness as compared to healthy control subjects. van Langenberg *et al*[30] demonstrated worse endurance of the knee extensor muscles in patients with CD in remission or with active disease in comparison with a healthy control group.

Physical activity and physical exercise training interventions

Different types of physical activity and physical exercise training interventions have been published (*e.g.* walking, running, cycling, resistance exercises, video gameplay, yoga) ranging from low-intensity to high-intensity. Detailed tables with the study characteristics and main findings of all interventions are presented in Supplementary Table 4. In total, 10 studies investigated the effect of a physical activity or physical exercise training intervention on one or more HRPF components (Table 4), of which the majority used non-validated practical field tests. The remaining studies examined other outcomes, such as feasibility, acceptability, or safety of the interventions as well as their effects on other health outcomes concerning disease activity and subjective well-being (*e.g.* quality of life, fatigue, depression, anxiety, sleep, stress).

Two studies focused on pediatric patients with IBD, and both demonstrated beneficial effects of their intervention on HRPF components[53,54]. Mählmann *et al*[53] demonstrated that an 8-wk aerobic exercise training intervention with active video gameplay increased the distance reached on the 6-min walk test, a practical field test for assessing cardiorespiratory fitness, in children with IBD in remission and with active disease. The effects of a home-based resistance exercise training program for 6 mo on HRPF components in children and adolescents with IBD in remission were investigated by Trivić *et al*[54]. Lean body mass significantly improved, whereas lean body mass age-based and sex-based z-scores did not. Furthermore, they found a significant improvement in muscular endurance as measured by using various practical field tests.

Eight studies examined the effect of a physical activity or physical exercise training intervention on HRPF components in adult patients with IBD – three were randomized controlled trials[51,55,56], four were pilot studies[57-60], and one involved a secondary analysis[61]. Seven studies included patients in remission or with mildly active disease activity, and one study included patients in remission as well as patients with mild to severely active disease. Two pilot studies and a secondary analysis investigated the effects of aerobic exercise and showed favorable effects on cardiorespiratory fitness

Table 2 Description and main findings of studies examining cardiorespiratory fitness by objective maximal oxygen uptake or oxygen uptake at peak exercise assessment in patients with inflammatory bowel disease

Ref.	Study design, country	Sample size (*n*)	Sample features	CD, UC, IBD-U (*n*)	Female sex, (%)	Age in yr, mean (SD)	Disease activity	Control group	Test protocol	Main findings, mean (SD), or median (IQR)
Ploeger *et al*[43], 2011	Cross-sectional study, Canada	29	N/A	19, 10, 0	41%	13.7 (2.3)	Remission (*n* = N/A) or mildly active disease (*n* = N/A)	Healthy age-matched and sex-matched youth	Incremental ramp cycle ergometer test: Height-based increase of work rate every 2 min until exhaustion (pedaling frequency < 50 rpm)	VO_2peak: CD, 34.9 (6.5) mL/kg/min; UC, 37.8 (7.7) mL/kg/min; Total, 36.0 (7.0) mL/kg/min; VO_2peak CD, UC, total < VO_2 peak ref (P < 0.05, P < 0.001)
Nguyen *et al*[44], 2013	Cross-sectional study, Canada	7	N/A	7, 0, 0	N/A	15.2 (2.3)	Remission (*n* = 7)	Healthy age-matched and sex-matched CG (*n* = 7)	Incremental ramp cycle ergometer test: Height-based increase of work rate every 2 min until exhaustion (pedaling frequency < 50 rpm)	VO_2peak: CD, 43.1 (6.5) mL/kg/min; CG, 53.5 (4.6) mL/kg/min; VO_2 peak CD < VO_2peak CG (P < 0.01)
Otto *et al* [45], 2012	Retrospective study, United Kingdom	100	Patients awaiting colorectal surgery	54, 46, 0	N/A	41.1 (14.9)	Active disease requiring surgery (*n* = 100)	Reference values[105]	Incremental ramp cycle ergometer test (8-12 min): Work rate increments based on prediction quotation and PA until exhaustion (pedaling frequency < 40 rpm)	VO_2peak: CD, 20.0 (7.9) mL/kg/min;UC, 21.9 (7.1) mL/kg/min; Total, 20.9 (7.6) mL/kg/min; VO_2peak total; VO_2peak ref (P < 0.0001)
Vogelaar *et al*[28], 2015	Cross-sectional study, The Netherlands	20	With fatigue (*n* = 10), without fatigue (*n* = 10)	15, 5, 0	50%	37.3 (11.4)	Remission (*n* = 20)	Reference values[106]	Incremental ramp cycle ergometer test (8-12 min): Work rate starting at 20 W, which increased by 15-20 W/min until exhaustion (pedaling frequency < 60 rpm)	VO_2peak: IBD with fatigue, 1.99 (0.44) L/min; IBD without fatigue, 2.43 (0.75) L/min; VO_2peak IBD < VO_2peak ref (P = N/A)
Tew *et al* [59], 2019	Pilot RCT, United Kingdom	36	N/A	36, 0, 0	53%	36.9 (11.2)	Remission (*n* = 32) or mildly active disease (*n* = 4)	N/A	Incremental ramp cycle ergometer test: Work rate starting at 0 W, which increased by 15-20 W/min until exhaustion (pedaling frequency < 60 rpm)[107]	VO_2peak[1]: CD, 28.2 (8.6) mL/kg/min
Bottoms *et al*[61], 2019	Secondary analysis of Tew *et al*[59], United Kingdom	25	HIIT group (*n* = 12), MICT group (*n* = 13)	25, 0, 0	60%	N/A for total sample	Remission (*n* = 32) or mildly active disease (*n* = 4)	N/A	Incremental ramp cycle ergometer test: Work rate starting at 0 W, which increased by 15-20 W/min until exhaustion (pedaling frequency < 60 rpm)[107]	VO_2peak[1]: N/A for total sample; CD HIIT group, 27.3 (7.7) mL/kg/min; CD MICT group, 28.7 (8.6) mL/kg/min
van Erp *et al*[57], 2021	Pilot study, The Netherlands	25	With severe fatigue	21, 3, 1	40%	45 (2.6)	Remission (*n* = 25)	N/A	Incremental ramp cycle ergometer test: Protocol N/A	VO_2max[1]: IBD, 28 (25-31) mL/kg/min

[1]Baseline values are shown.

CD: Crohn's disease; CG: Control group; HIIT: High-intensity interval training; IBD: Inflammatory bowel disease; IBD-U: Inflammatory bowel disease unclassified; IQR: Interquartile range; MICT: Moderate-intensity continuous training; N/A: Not available; PA: Physical activity; RCT: Randomized controlled trial; ref: Reference; SD: Standard deviation; UC: Ulcerative colitis; VO_2max: Maximal oxygen uptake; VO_2peak: Oxygen uptake at peak exercise.

Table 3 Description and main findings of studies examining muscular strength and muscular endurance by isokinetic or isometric strength or endurance assessment on a dynamometer in patients with inflammatory bowel disease

Ref.	Study design, country	Sample size (*n*)	Sample features	CD, UC (*n*)	Female sex, (%)	Age in yr, mean (SD), mean (95%CI), or median (IQR)	Disease activity	Control group	Test protocol	Main findings, mean (SD), mean (95%CI), or median (IQR)
Lee *et al*[47], 2015	Cross-sectional study, United States	64	Recently diagnosed	64, 0	41%	12.8 (2.7)	Remission to mild active disease (*n* = 26), moderate-to-severe active disease (*n* = 38)	Healthy subjects (*n* = 264)	Isometric muscular strength dynamometry (Biodex): AD peak torque (20° plantar flexion)	AD peak torque: CD, 14.7 (10.1-18.8) ft/lbs; CG, 17.9 (11.2-24.8) ft/lbs; AD peak torque CD (remission-mild activity) = AD peak torque CG (*P* = 0.72); AD peak torque CD (moderate-to-severe activity) < AD peak torque CG (*P* = 0.05)
Lee *et al*[46], 2018	Prospective study, United States	138	With low bone density	138, 0	52%	14.2 (2.8)	Remission (*n* = 85), or mild (*n* = 46), or moderate-to-severe (*n* = 7) active disease	Healthy subjects (*n* = 264)	Isometric muscular strength dynamometry (Biodex): AD peak torque (20° plantar flexion)	AD peak torque Z-score[1] (relative to age, sex, race, adjusted for tibia length): CD, -0.43 (0.90); AD peak torque CD < AD peak torque ref (*P* < 0.0001)
Geerling *et al* [50], 1998	Cross-sectional study, The Netherlands	32	With longstanding disease	32, 0	56%	40.0 (34.3-54.0)	Remission (*n* = 17) or active disease (*n* = 15)	Healthy age-matched and sex-matched CG (*n* = 32)	Isokinetic muscular strength dynamometry (Cybex II): KE and KF peak torque (60°/s, 180°/s)	**KE peak torque:** CD 60°/s, 123.1 (27.4) Nm; CD 180°/s, 81.5 (18.5) Nm; CG 60°/s, 136.5 (53.8) Nm; CG 180°/s, 88.7 (39.7) Nm; KE peak torque CD = KE peak torque CG (*P* = N/A); **KF peak torque:** CD 60°/s, 71.6 (22.3) Nm; CD 180°/s, 45.6 (15.2) Nm; CG 60°/s, 87.6 (33.4) Nm; CG 180°/s, 59.3 (31.9) Nm; KF peak torque CD (60°, 180°/s) < KF peak torque CG (*P* < 0.02, *P* < 0.05)
Geerling *et al* [52], 2000	Cross-sectional study, The Netherlands	69	Recently diagnosed	23, 46	52%	35.4 (13.6)	Remission (*n* = 61) or active disease (*n* = 8)	Healthy age-matched and sex-matched CG (*n* = 69)	Isokinetic muscular strength dynamometry (Cybex II): KE and KF peak torque (60°/s, 180°/s)	**KE peak torque:** N/A for total sample; CD 60°/s, 127.5 (33.4) Nm; CD 180°/s, 81.5 (25.7) Nm; CG for CD 60°/s, 142.4 (33.2) Nm; CG for CD 180°/s, 93.2 (37.2) Nm; UC 60°/s, 148.8 (44.6)

										Nm; UC 180°/s, 96.1 (30.7) Nm; CG for UC 60°/s, 155.7 (50.0) Nm; CG for UC 180°/s, 100.5 (38.4) Nm; KE peak torque CD and UC = KE peak torque CG (*P* = N/A); **KF peak torque:** N/A for total sample; CD 60°/s, 74.9 (23.5) Nm; CD 180°/s, 46.8 (25.3) Nm; CG for CD 60°/s, 86.8 (19.8) Nm; CG for CD 180°/s, 57.8 (22.0) Nm; UC 60°/s, 89.7 (31.9) Nm; UC 180°/s, 58.6 (21.3) Nm; CG for UC 60°/s, 98.5 (37.3) Nm; CG for UC 180°/s, 64.8 (30.4) Nm; KF peak torque CD and UC = KF peak torque CG (*P* = N/A)
Jensen *et al* [72], 2002	Follow-up study of Kissmeyer-Nielsen *et al* [42], Denmark	20	Patients who accepted follow-up 4-6 yr after J-pouch surgery	0, 20	60%	38 (9)	N/A	N/A	Isometric muscular strength dynamometry (Metitur): KE peak torque (60° knee flexion), AF peak torque (90° elbow flexion)	**KE peak torque:** UC preoperative, 475 (187) N; UC 4-6 yr postoperative, 532 (179) N (*P* = 0.080); **AF peak torque:** UC preoperative, 258 (93) N; UC 4-6 yr postoperative, 275 (83) N (*P* = 0.017)
Salacinski *et al*[48], 2013	Cross-sectional study, United States	19	≥ 1 small bowel resection and idiopathic musculoskeletal pain or weakness	19, 0	53%	44.2 (10.3)	Remission (*n* = 19)	Healthy age-matched and sex-matched CG (*n* = 19)	Isometric muscular strength dynamometry (customized): KE and KF peak torque (45° knee flexion)	**KE peak torque/KE peak torque normalized to BW:** CD, 75.2 (45.4) Nm/0.06 (0.03) Nm/kg; CG, 105.6 (40.7) Nm/0.07 (0.03) Nm/kg; KE peak torque CD < KE peak torque CG (*P* = 0.013, normalized to BW *P* = 0.039); **KF peak torque/KF peak torque normalized to BW:** CD, 27.2 (10.7) Nm/0.02 (0.01) Nm/kg, CG, 53.7 (27.3) Nm/0.09 (0.02) Nm/kg; KF peak torque CD < KF peak torque CG (*P* = 0.001, normalized to BW *P* = 0.022)
									Isometric muscular endurance dynamometry (customized): Slope of median VL and RF muscle activation frequency measured with EMG during 60-s submaximal (60% of maximum) contraction (45° knee flexion)	RF fatigue rate: CD, -0.069 (0.06) Hz/s; CG, -0.142 (0.09) Hz/s; RF fatigue rate CD < FR fatigue rate CG (*P* = 0.015); VL fatigue rate: CD, -0.028 (0.042) Hz/s; CG, -0.027 (0.085) Hz/s; VL fatigue rate CD = VL fatigue rate CG (*P* = 0.969)

van Langenberg *et al*[30], 2014	Cross-sectional study, Australia	27	N/A	27, 0	56%	43 (38, 48)	Remission (n = 19) or active disease (n = 8)	Healthy age-matched and sex-matched CG (n = 22)	Isometric muscular strength dynamometry (Biodex): KE peak torque (60° knee flexion)	KE peak torque: CD 60°, 148.8 (130, 168) Nm; CG 60°, 133.6 (111, 156) Nm; KE peak torque CD = KE peak torque CG (P = 0.29)
									Isometric muscular endurance dynamometry (Biodex): Fatigue rate as decrement of KE peak torque from maximal peak torque (repetition 2 or 3) to peak torque at the end of 30 maximal contractions (at 60° knee flexion)	KE fatigue rate: CD, -5.2 (-8.2, -2.2) Nm/min; CG, -1.3 (-3.9, 1.4) Nm/min; KE fatigue rate CD > KE fatigue rate CG (P = 0.047)
Zaltman *et al* [49], 2014	Case-control study, Brazil	23	Sedentary	0, 23	100%	43.9 (10.0)	Remission (n = 8), mild (n = 9), or moderate (n = 5), or severe (n = 1) active disease	Healthy age-matched, sex-matched, and BMI-matched CG (n = 23)	Isometric muscular strength dynamometry (IsoTeste): KE peak torque (angle N/A)	KE peak torque: UC, 38.6 (4.4) Kgf; CG, 41.0 (1.1) Kgf; KE peak torque UC < KE peak torque CG (P = 0.012)
Subramaniam *et al*[79], 2015	Prospective study, Australia	19	Starting with IFX	19, 0	42%	33.2 (10.7)	Active disease (n = 19)	N/A	Isokinetic muscular strength dynamometry (Cybex/HUMAC Norm): KE peak torque (30°/s, 60°/s, 90°/s)	KE peak torque[1]: CD 30°/s left leg, 166.5 (93.4) Nm, right leg 184.8 (96.6) Nm; CD 60°/s left leg, 172.8 (103.5) Nm, right leg 183.5 (116.4) Nm; CD 90°/s left leg, 128.5 (55.9) Nm, right leg 139.4 (54.4) Nm
Vogelaar *et al* [28], 2015	Cross-sectional study, The Netherlands	20	With fatigue (n = 10), without fatigue (n = 10)	15, 5	50%	37.3 (11.4)	Remission	Reference values	Isokinetic muscular strength dynamometry (Biodex): KE and KF peak torque (60°/s, 180°/s)	**KE peak torque:** N/A for total sample; IBD with fatigue 60°/s, 107.1 (25.4) Nm; IBD with fatigue 180°/s, 60.7 (12.3) Nm; IBD without fatigue 60°/s, 123.7 (38.0) Nm; IBD without fatigue 180°/s, 73.5 (21.4) Nm; KE peak torque IBD with and without fatigue < KE peak torque ref (P = N/A); **KF peak torque:** N/A for total sample; IBD with fatigue 60°/s, 51.7 (14.3) Nm; IBD with fatigue 180°/s, 31.1 (8.0) Nm; IBD without fatigue 60°/s, 63.0 (20.1) Nm; IBD without fatigue 180°/s, 38.9 (14.2) Nm; KF peak torque IBD with and without fatigue < KF peak torque ref (P = N/A)
Jones *et al* [51], 2020	RCT, United Kingdom	47	N/A	47, 0	68%	49.3 (13.0)	Remission (n = 31) or	Healthy age-	Isokinetic muscular strength	**KE peak torque[1]:** CD 60°/s, 72.6

		mild active disease (*n* = 16)	matched, sex-matched, PA-matched, BMI-matched, and ethnicity-matched CG (*n* = 33)	dynamometry (Biodex): KE peak torque (60°/s, 180°/s), EF peak torque (60°/s, 120°/s)	(33.3) Nm; CD 180°/s, 46.2 (23.0) Nm; CG 60°/s, 94.6 (46.6) Nm; CG 180°/s, 60.1 (34.9) Nm; KE peak torque CD < KE peak torque CG (*P* = 0.001, *P* = 0.011); **EF peak torque[1]:** CD 60°/s, 25.4 (11.2) Nm; CD 120°/s, 22.3 (9.1) Nm; CG 60°/s, 26.0 (12.4) Nm; CG 120°/s, 22.2 (11.2) Nm; EF peak torque CD = EF peak torque CG (*P* = 0.664, *P* = 0.747)

[1]Baseline values are shown.

95%CI: 95% confidence interval; AD: Ankle dorsiflexor; AF: Arm flexor; BMI: Body mass index; BW: Body weight; CD: Crohn's disease; CG: Control group; EF: Elbow flexor; EMG: Electromyography; IBD: Inflammatory bowel disease; IFX: Infliximab; IQR: Interquartile range; KE: Knee extensor; KF: Knee flexor; N/A: Not available; PA: Physical activity; RCT: Randomized controlled trial; RF: Rectus femoris; ref: Reference; SD: Standard deviation; UC: Ulcerative colitis; VL: Vastus lateralis.

[59-61].

A 12-wk walking program in physically inactive patients with CD resulted in a significant improvement in cardiorespiratory fitness as determined by a practical field test[60]. Improvements in cardiorespiratory fitness, as measured by VO_2 peak during CPET, were also observed in patients with CD who completed a 3-mo program of high-intensity interval training (HIIT) or moderate-intensity continuous training[59]. A greater increase in VO_2peak was found in CD patients who followed the HIIT program than in CD patients who followed the moderate-intensity continuous training program compared with CD patients who received usual care. A secondary analysis of this study showed that the work rate at peak exercise increased only in those patients who underwent the HIIT program[61].

The effect of resistance training on HRPF components was studied by two randomized controlled trials[51,55]. Jones *et al*[51] found that a 6-mo impact (*e.g.* rope skipping, jumps) and resistance training program in patients with CD significantly improved upper and lower limb muscular strength as measured with gold standard tests (*i.e.* knee extensor and elbow flexor muscular strength testing with isokinetic dynamometry) as well as upper and lower limb muscular endurance measured with practical field tests (*i.e.* handgrip strength, chair-stand test, and arm-curl test). In contrast, Zhao *et al*[55] did not observe significant changes in various practical field tests for muscular strength and muscular endurance after an 8-wk resistance training program with either protein supplementation or placebo in patients with IBD diagnosed with sarcopenia.

Two studies investigated interventions that included both aerobic and resistance training for the duration of 8 wk and 12 wk[56,57]. Cronin *et al*[56] demonstrated favorable changes in body fat and lean tissue mass as well as in cardiorespiratory fitness measured by the Rockport 1-mile test in physically inactive patients with IBD after an 8-wk intervention as compared to physically inactive patients with IBD receiving usual care. However, the intervention study by van Erp *et al*[57], conducted in severely fatigued patients with IBD, failed to demonstrate improvements in the gold standard outcome for cardiorespiratory fitness (*i.e.* VO_2max achieved during CPET) after 12 wk. Yet, they did report an improvement in work rate at peak exercise. The effects of aerobic exercise and resistance exercise were compared in a randomized pilot study by Seeger *et al*[58]. After 12 wk, both patients with CD who performed aerobic exercise and patients with CD who performed resistance exercise showed a gain in muscular strength as determined by practical field tests.

DISCUSSION

This scoping review aimed to provide an overview of studies on the assessment of HRPF components in patients with IBD and to review the effects of physical activity and physical exercise training interventions on HRPF components in patients with IBD. Accurate measurement of the HRPF concept is the first step towards the investigation and implementation of targeted physical activity or physical exercise training interventions to improve clinical outcomes and patient-reported outcomes in IBD. The findings of this scoping review indicated a shortcoming in the present literature regarding the accurate assessment of the HRPF concept, as most studies considered only one or two HRPF components, and no single study assessed flexibility. In addition, large heterogeneity existed in assessment methods, with frequent use of non-validated tests. According to limited studies that used gold standard tests, cardiorespiratory fitness seemed to be reduced in patients with IBD, but findings on muscular strength and endurance were inconsistent. An overall positive effect on HRPF components was present for physical activity or physical exercise training interventions. Important insights and research gaps that resulted from the thematic mapping of the evidence are outlined below, along with

Table 4 Description and main findings of studies examining the effect of physical activity and physical exercise training interventions on health-related physical fitness components in patients with inflammatory bowel disease

Ref.	Study design, country	Sample size, *n*	Sample features	CD, UC, IBD-U (*n*)	Female sex, (%)	Age in yr, mean (SD)	Disease activity	Healthy control group	Intervention, IG	Comparator, CG	HRPF components assessed	Effect on HRPF components
Mählmann *et al*[53], 2017	Pilot study, Switzerland	21	Pediatric patients	12, 7, 3	48%	13.88	Remission (*n* = 14) or active disease (*n* = 7)	Age-matched and sex-matched HC (*n* = 23)	Moderate-intensity aerobic exercise training with active video gameplay (*n* = 21), 5 sessions/wk (30 min) for 8 wk	N/A	Cardiorespiratory fitness with 6-min walk test (practical field test) at wk 8	Distance reached in 6 min increased in patients with active disease from 655 (95%CI: 542-769) m to 758 (95%CI: 610-906) m, and in patients in remission from 655 (95%CI: 542-769) m to 758 (95%CI: 610-906) m, and in CG from 678 (95%CI: 640-715) m to 727 (95%CI: 74-93) m, without between-group differences (*P* = N/A)
Trivić *et al* [54], 2022	Intervention study, Croatia	42	Pediatric patients	22, 18, 2	40%	N/A for total sample	Remission (*n* = 42)	N/A	Personalized home-based structured resistance training (*n* = 42), 3 sessions/wk for 6 mo	N/A	Body composition (LBM) with DEXA; muscular endurance 30 s sit-ups, push-ups, back extensions, squats, and holding a plank position for as long as possible (practical field tests), all at 6 mo	Improvement in LBM from 37.12 (SD: 1.43) kg to 38.75 (SD: 1.61) kg, (*P* = 0.012) but not in LBM z-score. Improvement in muscular endurance tasks: Number of sit-up repetitions from 19.32 (SD: 5.82) to 21.00 (SD: 6.53) (*P* = 0.024), back extension repetitions from 27.39 (SD: 12.09) to 38.27 (SD: 16.10) (*P* < 0.001), push-up repetitions from 17.37 (SD: 6.67) to 24.59 (SD: 7.58) (*P* < 0.001), squat repetitions from 22.10 (SD: 4.87) to 24.88 (SD: 6.23) (*P* < 0.001), and time holding the plank position from 81.0 (SD: 46.26) s to 114.34 (SD: 74.06) s (*P* < 0.001)
Loudon *et al*[60], 1999	Pilot study, Canada	16	Sedentary adult patients	16, 0, 0	83%	38.3 (7.5)	Remission or mild active disease (*n* = N/A)	N/A	Supervised indoor (group) walking program, 3 sessions/wk (of 20-35 min) for 12 wk	N/A	Cardiorespiratory fitness with CAFT step test (practical field test) at wk 12	Improvement in estimated VO_2max from 30.6 (SD: 4.7) mL/kg/min to 32.4 (SD: 4.8) mL/kg/min (*P* = 0.0013)
Bottoms *et al*[61], 2019	Secondary analysis of Tew *et al*[59], United Kingdom	25	Adult patients	25, 0, 0	60%	N/A for total sample	Remission or mild active disease (*n* = N/A)	N/A	HIIT (*n* = 13) or MICT (*n* = 12), 3 sessions/wk for 3 mo	N/A	Cardiorespiratory fitness with CPET (gold standard test) at week 4, 8, and 12	Increase in WRpeak after HIIT from baseline to week 4 with mean difference of 20.5 (SD: 10.8) W (*P* = 0.03), and from week 4 to week 12 with 12.30 (SD: 6.32) W, (*P* = 0.02); No change in WRpeak after MICT
Cronin *et al* [56], 2019	Cross-over RCT, Ireland	17	Physically inactive adult patients	N/A for total sample	N/A for total sample	25 (6.5)	Remission (*n* = 17)	N/A	Combined aerobic and resistance exercise program (*n* = 13, of which 7 crossed-over), 3 sessions/wk (of 60	Usual care (*n* = 7)	Body composition (body fat and lean tissue mass) with DEXA, cardiores-piratory fitness with Rockport 1-mile walk test (practical field test), all at	Total body fat decreased in the IG with 2.1% (IQR: -2.15 to -0.45) but increased in the CG with 0.1% (IQR: -0.4-1), (*P* = 0.022); total lean tissue mass increased in the IG with 1.59 (IQR: 0.68-2.69) kg but decreased in the CG with 1.38 (IQR: -2.45-

									min) for 8 wk		week 8	0.26) kg, (P = 0.003); improvement of estimated VO_2max in the IG from 43.41 mL/kg/min to 46.01 mL/kg/min, (P = 0.03)
Tew *et al* [59], 2019	Pilot RCT, United Kingdom	36	Adult patients	36, 0, 0	53%	36.9 (11.2)	Remission (n = 32) or mildly active disease (n = 4)	N/A	HIIT (n = 13) or MICT (n = 12), 3 sessions/wk for 3 mo	Usual care (n = 11)	Cardiorespiratory fitness with CPET (gold standard test) at 3 mo	Change in VO_2peak from 27.3 (SD: 7.7) mL/kg/min to 29.7 (SD: 8.2) mL/kg/min after HIIT. Change in VO_2peak from 28.7 (SD: 8.6) mL/kg/min to 29.3 (SD: 6.6) mL/kg/min after MICT. Change in VO_2 peak from 28.6 (SD: 10.0) mL/kg/min to 28.5 (SD: 9.2) mL/kg/min after usual care. Mean change in VO_2peak from baseline to 3 mo relative to the usual care was greater following HIIT than MICT (+2.4 *vs* +0.7 mL/kg/min) (P = N/A)
Jones *et al* [51], 2020	RCT, United Kingdom	47	Adult patients	47, 0, 0	68%	49.3 (13.0)	Remission (n = 31) or mild active disease (n = 16)	Age-matched, sex-matched, PA-matched, BMI-matched, and ethnicity-matched HC (n = 33)	Combined impact and resistance exercise training (n = 23), 3 sessions/wk (of 60 min) for 6 mo	Usual care (n = 24)	Muscular strength and endurance with isokinetic dynamometry (gold standard test) as well as with HGS, chair-stand test, and arm-curl test (practical field tests), all at 6 mo	Improvement of all muscular strength and endurance tests in the IG compared to the CG: mean difference KE peak torque 60°/s, 22.4 (95%CI: 12.1-32.8) Nm; KE peak torque 180°/s, 16.8 (95%CI: 9.0-24.5) Nm; EF peak torque 60°/s, 6.8 (95%CI: 3.9-9.6) Nm; EF peak torque 180°/s, 6.3 (95%CI: 3.3-9.3) Nm; HGS, 8.3 (95%CI: 6.2-10.5) kg; Chair-stand test, 4 (95%CI: 3-6) repetitions; arm-curl test, 7 (95%CI: 5-8) repetitions; All P < 0.001
Seeger *et al* [58], 2020	Pilot RCT, Germany	45	Adult patients	45, 0, 0	63%	N/A for total sample	Remission or mild active disease (n = N/A)	N/A	Moderate endurance training (n = 17, only n = 9 were analyzed), or moderate muscle training (n = 15, only n = 13 analyzed), 3 sessions/wk (of 30-40 min) for 12 wk	Usual care (n = 13)	Muscular strength with HGS and isometric HHD (practical field tests) at week 12	Improvement of HGS and QS in both endurance training IG (P = 0.01, P = 0.035) and muscle training IG (P = 0.01, P = 0.002), while HGS decreased and QS did not change in CG (P = 0.01, P = 0.23)
Van Erp *et al*[57], 2021	Pilot study, The Netherlands	25	Adult patients with severe fatigue	21, 3, 1	40%	45 (2.6)	Remission (n = 25)	N/A	Aerobic and progressive resistance training, 3 sessions/wk (of 60 min) for 12 wk	N/A	Cardiorespiratory fitness with a CPET (gold standard test) at week 12	No significant change in VO_2max. A significant change in WRpeak from 2.4 (SD: 0.5) W/kg to 2.7 (SD: 0.5) W/kg (P = 0.002)
Zhao *et al* [55], 2022	RCT, China	28	Adult patients with low nutritional risk state [RT + WP intervention (n = 15), RT + placebo intervention (n = 13)]	N/A	31%	44.1	Remission (n = 3), or mild (n = 12), moderate (n = 9), or severe (n = 4) active disease	N/A	Unsupervised resistance training (n = 28), 3 sessions/wk for 8 wk		Muscular strength with HGS and muscular endurance with 3-m walk speed and 5-time chair-stand-test (all practical field tests), all at week 8	HGS changed from 36.7 (SD: 10.8) kg to 42.6 (SD: 8.4) kg in the RT + WP group and from 31.7 (SD: 12.6) kg to 32.9 (SD: 12.5) kg in the RT + placebo group. 3-m walk speed changed from 1.0 (SD: 0.3) m/s to 0.9 (SD: 0.1) m/s in the RT + WP group and from 1.1 (SD: 0.2) m/s to 1.0 (SD: 0.2) m/s in the RT + placebo group. Time to perform the 5-time chair-stand test changed from 7.0 (SD: 1.5) s to 6.2

									(SD: 1.4) s in the RT + WP group and from 6.6 (SD: 1.6) s to 6.2 (SD: 1.3) s in the RT + placebo group. All are not statistically significant (P = N/A)

95%CI: 95% confidence interval; BMI: Body mass index; CAFT: Canadian aerobic fitness test; CD: Crohn's disease; CG: Control group; CPET: Cardiopulmonary exercise test; DEXA: Dual-energy X-ray absorptiometry; EF: Elbow flexor; HC: Healthy controls; HGS: Handgrip strength; HHD: Hand-held dynamometry; HIIT: High-intensity interval training, HRPF: Health-related physical fitness; IBD-U: Inflammatory bowel disease unclassified; IG: Intervention group; IQR: Interquartile range; KE: Knee extensor; LBM: Lean body mass; MICT: Moderate-intensity continuous training; N/A: Not available; PA: Physical activity; QS: Quadriceps strength; RCT: Randomized controlled trial; RT: Resistance training; SD: Standard deviation; UC: Ulcerative colitis; VO_2max: Maximal oxygen uptake; VO_2peak: Oxygen uptake at peak exercise; WP: Whey protein; WRpeak: Work rate at peak exercise.

recommendations for future research.

Current evidence for an impaired HRPF in patients with IBD is limited, which is partially attributable to a lack of accurate assessment methodology in a significant proportion of the studies as well as the inclusion of small sample sizes and different populations. Cardiorespiratory fitness, as determined by direct measurement of VO_2max/VO_2peak, seems to be reduced in pediatric and adult patients with IBD. However, this is based on only four studies that made comparisons with healthy control subjects or reference values. Controversial findings emerged from studies that assessed muscular strength and endurance by gold standard assessment methods. This might indicate that it depends on, for example, the specific muscle group examined, test protocol, patient- or disease-specific factors, and/or the control group or reference values used for comparison, as to whether muscular strength and endurance are affected. Better-designed studies are warranted to objectively assess the components of HRPF in patients with IBD and to subsequently investigate their associations with patient-specific and disease-specific factors as well as with clinical and patient-reported outcomes to ascertain whether any particular components are insufficient or below normal values (*e.g.* in certain patient subgroups) and could be improved with appropriate interventions. Due to the heterogeneity of the disease, large patient populations are required for these studies to ensure that relevant patient subgroups are adequately represented.

This review showed substantial heterogeneity in assessment methods used for the different components of HRPF in the included studies. As gold standard assessment methods are often too complex to implement on a large scale, there is a need for less demanding alternative assessment methods. To enable the assessment of HRPF in routine clinical practice and to perform studies in large populations with long-term follow-up, future research should focus on determining the validity and reliability of screening instruments and easily applicable practical field tests for HRPF within the IBD population. It is crucial to investigate these aspects, as patients with IBD frequently experience fatigue or joint arthralgia, which may limit the capacity to undertake exercise tests, or patients may avoid or give up exercise for fear of exacerbating bowel symptoms[62]. For instance, clinical implementation of a validated practical patient-reported screening tool (*e.g.* the Duke activity status index for cardiorespiratory fitness) may serve in identifying patients at risk for impaired HRPF [63]. These patients could then be offered a comprehensive objective assessment using validated practical field tests by dedicated physical therapists or exercise physiologists to evaluate the specific intolerance with regard to the different components of HRPF. Subsequently, a personalized physical exercise training program may then be proposed to those patients with an impaired HRPF.

Overall, a positive effect of physical activity or physical exercise training interventions on HRPF components was present in patients with IBD in remission or with mild active disease. However, these findings should be interpreted with caution given the important methodological limitations of the studies. Studies were often underpowered to detect true statistically significant effects. Even though pilot research is necessary to explore the feasibility, acceptability, and safety of an intervention preliminary to the subsequent implementation of a full-scale trial, large high-quality methodology randomized controlled trials or quasi-experiments are warranted to establish the benefits of physical activity or physical

exercise training in patients with IBD. In addition to high methodological quality, future trials should also consider the quality of the exercise therapy program to ensure therapeutic potential. Quality of the exercise therapy program involves patient selection, type and timing of the outcome assessment, the dosage and type of the exercise program, trained supervision, safety, and adherence[64].

Patients in remission or with mild disease activity have been the main focus of the current intervention studies, often excluding patients with moderate to severe disease. In addition, research on the effectiveness of physical activity or physical exercise training in the context of preoperative optimization in patients with IBD is virtually absent[65]. Since preoperative optimization of cardiorespiratory fitness and muscular strength has been shown to reduce postoperative complications and enhance recovery in unfit patients undergoing abdominal surgery, it seems likely that patients with IBD would benefit from these interventions as well[66,67]. Future trials involving participants with moderate to severely active disease or those awaiting surgery are warranted. Furthermore, current studies were limited by a lack of proper preselection based on the pre-existing fitness level of participants receiving an intervention. Patient selection based on HRPF components that align with the purpose of the study is required to evaluate the true effectiveness of the intervention. For instance, if the intervention purpose is to improve cardiorespiratory fitness, then those patients with reduced cardiorespiratory fitness should be included to ensure optimal effects of the intervention[64]. Current studies are frequently limited by the inclusion of patients who have adequate cardiorespiratory fitness or muscular strength, leaving little opportunity for improvement.

The type and timing of the primary outcome assessment is another major limitation among current intervention studies. The majority of studies lack accurate assessment of HRPF components over time with validated assessment methods as a primary endpoint, making it difficult to assess the true effects of the intervention. Only 10 of 22 studies reported the effects of the intervention on HRPF components, with frequent use of non-validated practical field tests. Physical exercise training is, by definition, intended to improve components of HRPF, in contrast to physical activity. Hence, an accurate assessment of HRPF is imperative to ascertain the true effects of physical exercise training in patients with IBD. Since not all studies reported a clear rationale towards the (direct or indirect) improvement of HRPF components within the purpose of the study, which is an important part of the definition of physical exercise training in contrast to physical activity, it was not possible to differentiate between physical activity interventions and physical exercise training interventions in this review. To study the effects of both types of interventions separately from one another, future studies should provide a more detailed description of the chosen interventions, along with the congruent outcome measure. Furthermore, future trials should also include longer follow-ups to determine whether these potential beneficial effects persist after the intervention.

Other frequently reported endpoints were quality of life, fatigue, depression, anxiety, and stress, which are multifactorial by origin and often influenced by other factors such as social support, medication use, and bowel symptoms. Especially for subjective outcomes, the Hawthorn effect (*i.e.* change due to received attention or assessment) instead of the intervention under examination can explain the observed effects of these trials[68]. A better understanding of the exact mechanism by which physical activity or physical exercise training may help to improve such parameters of subjective well-being (*e.g.* as an indirect effect of the improvement of HRPF components) is warranted.

Large variability was observed in the dosage and type of physical activity and physical exercise training programs in the included studies. To ensure high therapeutic potential of an intervention in patients with IBD, the underlying framework of the intervention (*i.e.* the 'Frequency, Intensity, Time, Type' principle) should be based on a potential or proven rationale (based on anatomical, physiological, or behavioral relevance) towards the purpose of the intervention, and should preferably be individually tailored to a patient's needs[64]. Most studies implemented interventions of low-to-moderate intensities and showed that these were feasible and well tolerated in patients with IBD in remission or with mild disease activity. In general, high-intensity training is usually not recommended in patients with IBD as this may lead to an increase in inflammation and an exacerbation of symptoms[69]. However, existing evidence does not provide much support for these recommendations.

Only one study examined the effect of a high-intensity training intervention in patients with IBD as compared to moderate-continuous training[59]. The findings of this study showed that neither mode of training intensity increased bowel symptoms and that high-intensity training caused a greater change in cardiorespiratory fitness than moderate-continuous training. Furthermore, Ploeger *et al*[70] showed that a single bout of HIIT did not cause an acute exacerbation of inflammation parameters in youth with CD. More research on the safety and efficacy of different training dosages and types for patients with IBD is needed to elucidate the optimal training paradigm.

Many studies conducted physical activity or physical exercise training interventions that were (partly) home-based and unsupervised. Although interventions under the supervision of trained professionals can positively influence the impact of the intervention by encouraging adherence, unsupervised interventions might better reflect non-research contexts where supervised programs will not always be feasible due to expense or a lack of trained personnel.

To our knowledge, this is the first review dedicated to HRPF in pediatric and adult patients with IBD, with an emphasis on the assessment of the various HRPF components and the effect of physical activity and physical exercise training interventions on HRPF components. The major strengths of this review were its broad scope and the extensive systematic search across multiple databases. This review revealed a large volume of research and identified several research gaps that give rise to new research opportunities. This review also had some limitations. First, the classification of studies to the different components of HRPF that were assessed was based on the researchers' judgment and thus may have been influenced by their interpretation. Second, as a traditional scoping review approach was used, all published literature was considered, regardless of study quality. This precluded the weighting of higher-quality studies *vs* lower-quality studies in formulating conclusions.

CONCLUSION

This review revealed a gap in the present literature concerning the assessment of the complete HRPF concept as well as significant heterogeneity in assessment methods used to assess the components of HRPF. Cardiorespiratory fitness seems to be diminished in patients with IBD, yet conflicting evidence exists with regard to muscular strength and endurance. More well-designed large-scale studies are warranted to assess the status of the various components of HRPF in patients with IBD using validated assessment methods and to subsequently investigate their association with patient-specific and disease-specific factors as well as clinical and patient-reported outcomes. Furthermore, an overall favorable impact of physical activity and physical exercise training interventions on HRPF components was present. However, important methodological limitations were identified. Future well-designed studies on the effect of such interventions on disease outcomes are required to determine the optimal training paradigm before (inter)national guidelines regarding physical activity and physical exercise training can be integrated into the holistic therapeutic care for patients with IBD.

ARTICLE HIGHLIGHTS

Research background

Reaching the Selecting Therapeutic Targets in Inflammatory Bowel Disease-II (STRIDE-II) therapeutic targets for inflammatory bowel disease (IBD) requires an interdisciplinary approach. Lifestyle interventions to enhance and maintain health-related physical fitness (HRPF) could potentially aid in improving subjective health, decreasing disability, or even controlling inflammation. However, ambiguity remains about the status and impact of HRPF (encompassing body composition, cardiorespiratory fitness, muscular strength, muscular endurance, and flexibility) in IBD patients, hindering the development of physical activity and physical exercise training guidelines.

Research motivation

Accurate evaluation of HRPF components is imperative for a deeper understanding of the state of HRPF in IBD patients as well as to clearly define endpoints in intervention studies to determine whether physical activity or physical exercise training can improve HRPF components in patients with IBD. Hence, accurate assessment of the HRPF concept is the initial step toward investigating and implementing targeted physical activity or physical exercise training interventions, aiming to improve clinical outcomes and patient-reported outcomes in IBD.

Research objectives

The primary objective of this scoping review was to provide an overview of studies on the assessment of HRPF components in patients with IBD. The second objective was to review the effects of physical activity and physical exercise training interventions on HRPF in patients with IBD.

Research methods

A systematic search was conducted in multiple databases for original studies that included patients with IBD, assessed one or more HRPF components, and/or evaluated physical activity or physical exercise training interventions.

Research results

Sixty-eight articles were included. No study examined the complete concept of HRPF, and considerable heterogeneity existed in assessment methods, with frequent use of non-validated tests. According to studies that used gold standard tests, cardiorespiratory fitness seemed to be reduced, but findings on muscular strength and endurance were inconsistent. A limited number of studies that evaluated physical activity or physical exercise training interventions reported effects on HRPF, overall showing a positive impact.

Research conclusions

The findings of this scoping review indicated a shortcoming in the present literature regarding the accurate assessment of the HRPF concept, as most studies considered only one or two HRPF components, and no single study assessed flexibility. Important methodological limitations of studies that evaluated physical activity or physical exercise training interventions were identified.

Research perspectives

More well-designed large-scale studies are warranted to assess the status of the various components of HRPF in patients with IBD using validated assessment methods and to subsequently investigate their association with patient-specific and disease-specific factors as well as clinical and patient-reported outcomes. Furthermore, more research on the effect of physical activity or physical exercise training interventions on disease outcomes is required to determine the optimal training paradigm before (inter)national guidelines regarding physical activity and physical exercise training can be integrated in the holistic therapeutic care for patients with IBD.

FOOTNOTES

Author contributions: Demers K, Bak MTJ, Bongers BC, Jonkers DMAE, de Vries AC, Pierik MJ, and Stassen LPS contributed to the conception and design of this review; Demers K performed the literature search; Demers K and Bak MTJ performed study selection and data acquisition; Demers K drafted the manuscript; Bak MTJ, Bongers BC, Jonkers DMAE, de Vries AC, Pierik MJ, and Stassen LPS critically revised the manuscript for important intellectual content; All authors revised the manuscript and approved the final version.

Conflict-of-interest statement: Karlijn Demers, Michiel TJ Bak, and Bart C Bongers declare no conflicts of interest. Daisy MAE Jonkers reports grant from the public-private partnership grants of Dutch Top Institute of Food and Nutrition (TIFN), Top Knowledge Institute (TKI) Agri&Food and Health Holland, by the Carbokinetics program as part of the NWO-CCC Partnership Program, by Organic A2BV/Mothersfinest BV and, EU/FP7 SysmedIBD/305564, BIOM/305479 and Character/305676, H2020 DISCOvERIE/848228, all outside the submitted work. Annemarie C de Vries has served on advisory boards for Takeda, Janssen, Bristol Myers Squibb, Abbvie, Pfizer, and Galapagos and has received unrestricted research grants from Takeda, Janssen, and Pfizer outside the submitted work. Marieke J Pierik reports grants and non-financial support from Falk Pharma, grants from European commission, grants from ZONMW (Dutch national research fund), grants and non-financial support from Takeda, grants and non-financial support from Johnson and Johnson, grants and non-financial support from Abbvie, non-financial support from Ferring, non-financial support from Immunodiagnostics, non-financial support from MSD, all outside the submitted work. Laurents PS Stassen has served as a speaker and received research support from Takeda, outside the submitted work.

PRISMA 2009 Checklist statement: The authors have read the PRISMA 2009 Checklist, and the manuscript was prepared and revised according to the PRISMA 2009 Checklist.

Open-Access: This article is an open-access article that was selected by an in-house editor and fully peer-reviewed by external reviewers. It is distributed in accordance with the Creative Commons Attribution NonCommercial (CC BY-NC 4.0) license, which permits others to distribute, remix, adapt, build upon this work non-commercially, and license their derivative works on different terms, provided the original work is properly cited and the use is non-commercial. See: https://creativecommons.org/Licenses/by-nc/4.0/

Country/Territory of origin: Netherlands

ORCID number: Karlijn Demers 0000-0003-3709-9959; Michiel TJ Bak 0000-0001-8515-425X; Bart C Bongers 0000-0002-1948-9788; Annemarie C de Vries 0000-0002-3988-9201; Daisy MAE Jonkers 0000-0001-8981-8965; Marieke J Pierik 0000-0001-6981-6516; Laurents PS Stassen 0000-0002-3383-9035.

S-Editor: Lin C
L-Editor: Webster JR
P-Editor: Yu HG

REFERENCES

1 **Baumgart DC**, Sandborn WJ. Crohn's disease. *Lancet* 2012; **380**: 1590-1605 [PMID: 22914295 DOI: 10.1016/S0140-6736(12)60026-9]
2 **Ordás I**, Eckmann L, Talamini M, Baumgart DC, Sandborn WJ. Ulcerative colitis. *Lancet* 2012; **380**: 1606-1619 [PMID: 22914296 DOI: 10.1016/S0140-6736(12)60150-0]
3 **Tsai L**, Ma C, Dulai PS, Prokop LJ, Eisenstein S, Ramamoorthy SL, Feagan BG, Jairath V, Sandborn WJ, Singh S. Contemporary Risk of Surgery in Patients With Ulcerative Colitis and Crohn's Disease: A Meta-Analysis of Population-Based Cohorts. *Clin Gastroenterol Hepatol* 2021; **19**: 2031-2045.e11 [PMID: 33127595 DOI: 10.1016/j.cgh.2020.10.039]
4 **Raine T**, Bonovas S, Burisch J, Kucharzik T, Adamina M, Annese V, Bachmann O, Bettenworth D, Chaparro M, Czuber-Dochan W, Eder P, Ellul P, Fidalgo C, Fiorino G, Gionchetti P, Gisbert JP, Gordon H, Hedin C, Holubar S, Iacucci M, Karmiris K, Katsanos K, Kopylov U, Lakatos PL, Lytras T, Lyutakov I, Noor N, Pellino G, Piovani D, Savarino E, Selvaggi F, Verstockt B, Spinelli A, Panis Y, Doherty G. ECCO Guidelines on Therapeutics in Ulcerative Colitis: Medical Treatment. *J Crohns Colitis* 2022; **16**: 2-17 [PMID: 34635919 DOI: 10.1093/ecco-jcc/jjab178]
5 **Torres J**, Bonovas S, Doherty G, Kucharzik T, Gisbert JP, Raine T, Adamina M, Armuzzi A, Bachmann O, Bager P, Biancone L, Bokemeyer B, Bossuyt P, Burisch J, Collins P, El-Hussuna A, Ellul P, Frei-Lanter C, Furfaro F, Gingert C, Gionchetti P, Gomollon F, González-Lorenzo M, Gordon H, Hlavaty T, Juillerat P, Katsanos K, Kopylov U, Krustins E, Lytras T, Maaser C, Magro F, Marshall JK, Myrelid P, Pellino G, Rosa I, Sabino J, Savarino E, Spinelli A, Stassen L, Uzzan M, Vavricka S, Verstockt B, Warusavitarne J, Zmora O, Fiorino G. ECCO Guidelines on Therapeutics in Crohn's Disease: Medical Treatment. *J Crohns Colitis* 2020; **14**: 4-22 [PMID: 31711158 DOI: 10.1093/ecco-jcc/jjz180]
6 **Burisch J**, Jess T, Martinato M, Lakatos PL; ECCO -EpiCom. The burden of inflammatory bowel disease in Europe. *J Crohns Colitis* 2013; **7**: 322-337 [PMID: 23395397 DOI: 10.1016/j.crohns.2013.01.010]
7 **Romberg-Camps MJ**, Bol Y, Dagnelie PC, Hesselink-van de Kruijs MA, Kester AD, Engels LG, van Deursen C, Hameeteman WH, Pierik M, Wolters F, Russel MG, Stockbrügger RW. Fatigue and health-related quality of life in inflammatory bowel disease: results from a population-based study in the Netherlands: the IBD-South Limburg cohort. *Inflamm Bowel Dis* 2010; **16**: 2137-2147 [PMID: 20848468 DOI: 10.1002/ibd.21285]
8 **Lönnfors S**, Vermeire S, Greco M, Hommes D, Bell C, Avedano L. IBD and health-related quality of life -- discovering the true impact. *J Crohns Colitis* 2014; **8**: 1281-1286 [PMID: 24662394 DOI: 10.1016/j.crohns.2014.03.005]
9 **Turner D**, Ricciuto A, Lewis A, D'Amico F, Dhaliwal J, Griffiths AM, Bettenworth D, Sandborn WJ, Sands BE, Reinisch W, Schölmerich J, Bemelman W, Danese S, Mary JY, Rubin D, Colombel JF, Peyrin-Biroulet L, Dotan I, Abreu MT, Dignass A; International Organization for

the Study of IBD. STRIDE-II: An Update on the Selecting Therapeutic Targets in Inflammatory Bowel Disease (STRIDE) Initiative of the International Organization for the Study of IBD (IOIBD): Determining Therapeutic Goals for Treat-to-Target strategies in IBD. *Gastroenterology* 2021; **160**: 1570-1583 [PMID: 33359090 DOI: 10.1053/j.gastro.2020.12.031]

10 **Bouchard C SR**. Physical activity, fitness and health: the model and key concepts. In: Bouchard C, Shepard RJ, Stephens T, editors: Physical activity, fitness and health, International Proceedings and Concensus Statement. Illinois: Human Kinetics, 1994

11 **Ross R**, Blair SN, Arena R, Church TS, Després JP, Franklin BA, Haskell WL, Kaminsky LA, Levine BD, Lavie CJ, Myers J, Niebauer J, Sallis R, Sawada SS, Sui X, Wisløff U; American Heart Association Physical Activity Committee of the Council on Lifestyle and Cardiometabolic Health; Council on Clinical Cardiology; Council on Epidemiology and Prevention; Council on Cardiovascular and Stroke Nursing; Council on Functional Genomics and Translational Biology; Stroke Council. Importance of Assessing Cardiorespiratory Fitness in Clinical Practice: A Case for Fitness as a Clinical Vital Sign: A Scientific Statement From the American Heart Association. *Circulation* 2016; **134**: e653-e699 [PMID: 27881567 DOI: 10.1161/CIR.0000000000000461]

12 **Lee IM**, Shiroma EJ, Lobelo F, Puska P, Blair SN, Katzmarzyk PT; Lancet Physical Activity Series Working Group. Effect of physical inactivity on major non-communicable diseases worldwide: an analysis of burden of disease and life expectancy. *Lancet* 2012; **380**: 219-229 [PMID: 22818936 DOI: 10.1016/S0140-6736(12)61031-9]

13 **Han M**, Qie R, Shi X, Yang Y, Lu J, Hu F, Zhang M, Zhang Z, Hu D, Zhao Y. Cardiorespiratory fitness and mortality from all causes, cardiovascular disease and cancer: dose-response meta-analysis of cohort studies. *Br J Sports Med* 2022; **56**: 733-739 [PMID: 35022163 DOI: 10.1136/bjsports-2021-104876]

14 **Chekroud SR**, Gueorguieva R, Zheutlin AB, Paulus M, Krumholz HM, Krystal JH, Chekroud AM. Association between physical exercise and mental health in 1·2 million individuals in the USA between 2011 and 2015: a cross-sectional study. *Lancet Psychiatry* 2018; **5**: 739-746 [PMID: 30099000 DOI: 10.1016/S2215-0366(18)30227-X]

15 **Berkel AEM**, van Wijk L, van Dijk DPJ, Prins SN, van der Palen J, van Meeteren NLU, Olde Damink SWM, Klaase JM, Bongers BC. The association between preoperative body composition and aerobic fitness in patients scheduled for colorectal surgery. *Colorectal Dis* 2022; **24**: 93-101 [PMID: 34612581 DOI: 10.1111/codi.15941]

16 **Cuijpers ACM**, Heldens AFJM, Bours MJL, van Meeteren NLU, Stassen LPS, Lubbers T, Bongers BC. Relation between preoperative aerobic fitness estimated by steep ramp test performance and postoperative morbidity in colorectal cancer surgery: prospective observational study. *Br J Surg* 2022; **109**: 155-159 [PMID: 34536001 DOI: 10.1093/bjs/znab292]

17 **Beavers KM**, Brinkley TE, Nicklas BJ. Effect of exercise training on chronic inflammation. *Clin Chim Acta* 2010; **411**: 785-793 [PMID: 20188719 DOI: 10.1016/j.cca.2010.02.069]

18 **Gleeson M**, Bishop NC, Stensel DJ, Lindley MR, Mastana SS, Nimmo MA. The anti-inflammatory effects of exercise: mechanisms and implications for the prevention and treatment of disease. *Nat Rev Immunol* 2011; **11**: 607-615 [PMID: 21818123 DOI: 10.1038/nri3041]

19 **Caspersen CJ**, Powell KE, Christenson GM. Physical activity, exercise, and physical fitness: definitions and distinctions for health-related research. *Public Health Rep* 1985; **100**: 126-131 [PMID: 3920711]

20 **American College of Sports Medicine**. ACSM's health-related physical fitness assessment manual. 5nd ed. Philadelphia: Wolters Kluwer, 2014

21 **Gibson AL**, Wagner DR, Heyward VH. Advanced Fitness Assessment and Exercise Prescription. 8nd ed. Illinois: Human Kinetics, 2018

22 **Dasso NA**. How is exercise different from physical activity? A concept analysis. *Nurs Forum* 2019; **54**: 45-52 [PMID: 30332516 DOI: 10.1111/nuf.12296]

23 WHO Guidelines on Physical Activity and Sedentary Behaviour. Geneva: World Health Organization; 2020– [PMID: 33369898]

24 **Elia J**, Kane S. Adult Inflammatory Bowel Disease, Physical Rehabilitation, and Structured Exercise. *Inflamm Bowel Dis* 2018; **24**: 2543-2549 [PMID: 29850914 DOI: 10.1093/ibd/izy199]

25 **van Langenberg DR**, Papandony MC, Gibson PR. Sleep and physical activity measured by accelerometry in Crohn's disease. *Aliment Pharmacol Ther* 2015; **41**: 991-1004 [PMID: 25783784 DOI: 10.1111/apt.13160]

26 **Mack DE**, Wilson PM, Gilmore JC, Gunnell KE. Leisure-time physical activity in Canadians living with Crohn disease and ulcerative colitis: population-based estimates. *Gastroenterol Nurs* 2011; **34**: 288-294 [PMID: 21814062 DOI: 10.1097/SGA.0b013e3182248732]

27 **Schakman O**, Gilson H, Thissen JP. Mechanisms of glucocorticoid-induced myopathy. *J Endocrinol* 2008; **197**: 1-10 [PMID: 18372227 DOI: 10.1677/JOE-07-0606]

28 **Vogelaar L**, van den Berg-Emons R, Bussmann H, Rozenberg R, Timman R, van der Woude CJ. Physical fitness and physical activity in fatigued and non-fatigued inflammatory bowel disease patients. *Scand J Gastroenterol* 2015; **50**: 1357-1367 [PMID: 25966749 DOI: 10.3109/00365521.2015.1046135]

29 **Dhaliwal A**, Quinlan JI, Overthrow K, Greig C, Lord JM, Armstrong MJ, Cooper SC. Sarcopenia in Inflammatory Bowel Disease: A Narrative Overview. *Nutrients* 2021; **13** [PMID: 33671473 DOI: 10.3390/nu13020656]

30 **van Langenberg DR**, Della Gatta P, Warmington SA, Kidgell DJ, Gibson PR, Russell AP. Objectively measured muscle fatigue in Crohn's disease: correlation with self-reported fatigue and associated factors for clinical application. *J Crohns Colitis* 2014; **8**: 137-146 [PMID: 23938210 DOI: 10.1016/j.crohns.2013.07.006]

31 **Cioffi I**, Imperatore N, Di Vincenzo O, Santarpia L, Rispo A, Marra M, Testa A, Contaldo F, Castiglione F, Pasanisi F. Association between Health-Related Quality of Life and Nutritional Status in Adult Patients with Crohn's Disease. *Nutrients* 2020; **12** [PMID: 32168964 DOI: 10.3390/nu12030746]

32 **Bryant RV**, Trott MJ, Bartholomeusz FD, Andrews JM. Systematic review: body composition in adults with inflammatory bowel disease. *Aliment Pharmacol Ther* 2013; **38**: 213-225 [PMID: 23763279 DOI: 10.1111/apt.12372]

33 **Thangarajah D**, Hyde MJ, Konteti VK, Santhakumaran S, Frost G, Fell JM. Systematic review: Body composition in children with inflammatory bowel disease. *Aliment Pharmacol Ther* 2015; **42**: 142-157 [PMID: 26043941 DOI: 10.1111/apt.13218]

34 **Ding NS**, Tassone D, Al Bakir I, Wu K, Thompson AJ, Connell WR, Malietzis G, Lung P, Singh S, Choi CR, Gabe S, Jenkins JT, Hart A. Systematic Review: The Impact and Importance of Body Composition in Inflammatory Bowel Disease. *J Crohns Colitis* 2022; **16**: 1475-1492 [PMID: 35325076 DOI: 10.1093/ecco-jcc/jjac041]

35 **Tricco AC**, Lillie E, Zarin W, O'Brien KK, Colquhoun H, Levac D, Moher D, Peters MDJ, Horsley T, Weeks L, Hempel S, Akl EA, Chang C, McGowan J, Stewart L, Hartling L, Aldcroft A, Wilson MG, Garritty C, Lewin S, Godfrey CM, Macdonald MT, Langlois EV, Soares-Weiser K, Moriarty J, Clifford T, Tunçalp Ö, Straus SE. PRISMA Extension for Scoping Reviews (PRISMA-ScR): Checklist and Explanation. *Ann Intern Med* 2018; **169**: 467-473 [PMID: 30178033 DOI: 10.7326/M18-0850]

36 **American Thoracic Society**; American College of Chest Physicians. ATS/ACCP Statement on cardiopulmonary exercise testing. *Am J Respir Crit Care Med* 2003; **167**: 211-277 [PMID: 12524257 DOI: 10.1164/rccm.167.2.211]

37 **Drouin JM**, Valovich-mcLeod TC, Shultz SJ, Gansneder BM, Perrin DH. Reliability and validity of the Biodex system 3 pro isokinetic dynamometer velocity, torque and position measurements. *Eur J Appl Physiol* 2004; **91**: 22-29 [PMID: 14508689 DOI: 10.1007/s00421-003-0933-0]

38 **Abernethy P**, Wilson G, Logan P. Strength and power assessment. Issues, controversies and challenges. *Sports Med* 1995; **19**: 401-417 [PMID: 7676101 DOI: 10.2165/00007256-199519060-00004]

39 **Ly LP**, Handelsman DJ. Muscle strength and ageing: methodological aspects of isokinetic dynamometry and androgen administration. *Clin Exp Pharmacol Physiol* 2002; **29**: 37-47 [PMID: 11917904 DOI: 10.1046/j.1440-1681.2002.03606.x]

40 **Corbin CB**, Noble L. Flexibility. *Journal of Physical Education and Recreation* 1980; 51: 23-60 [DOI: 10.1080/00971170.1980.10622349]

41 **American College of Sports Medicine**. ACSM's Resource Manual for Guidelines for Exercise Testing and prescription. 7nd ed. Philadelphia: Wolters Kluwer, 2013

42 **Kissmeyer-Nielsen P**, Jensen MB, Laurberg S. Perioperative growth hormone treatment and functional outcome after major abdominal surgery: a randomized, double-blind, controlled study. *Ann Surg* 1999; **229**: 298-302 [PMID: 10024114 DOI: 10.1097/00000658-199902000-00020]

43 **Ploeger HE**, Takken T, Wilk B, Issenman RM, Sears R, Suri S, Timmons BW. Exercise capacity in pediatric patients with inflammatory bowel disease. *J Pediatr* 2011; **158**: 814-819 [PMID: 21146188 DOI: 10.1016/j.jpeds.2010.10.020]

44 **Nguyen T**, Ploeger HE, Obeid J, Issenman RM, Baker JM, Takken T, Parise G, Timmons BW. Reduced fat oxidation rates during submaximal exercise in adolescents with Crohn's disease. *Inflamm Bowel Dis* 2013; **19**: 2659-2665 [PMID: 24105390 DOI: 10.1097/01.MIB.0000436958.54663.4f]

45 **Otto JM**, O'Doherty AF, Hennis PJ, Mitchell K, Pate JS, Cooper JA, Grocott MP, Montgomery HE. Preoperative exercise capacity in adult inflammatory bowel disease sufferers, determined by cardiopulmonary exercise testing. *Int J Colorectal Dis* 2012; **27**: 1485-1491 [PMID: 22842663 DOI: 10.1007/s00384-012-1533-4]

46 **Lee D**, Lewis JD, Shults J, Baldassano RN, Long J, Herskovitz R, Zemel B, Leonard MB. The Association of Diet and Exercise With Body Composition in Pediatric Crohn's Disease. *Inflamm Bowel Dis* 2018; **24**: 1368-1375 [PMID: 29718224 DOI: 10.1093/ibd/izy024]

47 **Lee DY**, Wetzsteon RJ, Zemel BS, Shults J, Organ JM, Foster BJ, Herskovitz RM, Foerster DL, Leonard MB. Muscle torque relative to cross-sectional area and the functional muscle-bone unit in children and adolescents with chronic disease. *J Bone Miner Res* 2015; **30**: 575-583 [PMID: 25264231 DOI: 10.1002/jbmr.2375]

48 **Salacinski AJ**, Regueiro MD, Broeder CE, McCrory JL. Decreased neuromuscular function in Crohn's disease patients is not associated with low serum vitamin D levels. *Dig Dis Sci* 2013; **58**: 526-533 [PMID: 22949179 DOI: 10.1007/s10620-012-2372-4]

49 **Zaltman C**, Braulio VB, Outeiral R, Nunes T, de Castro CL. Lower extremity mobility limitation and impaired muscle function in women with ulcerative colitis. *J Crohns Colitis* 2014; **8**: 529-535 [PMID: 24315794 DOI: 10.1016/j.crohns.2013.11.006]

50 **Geerling BJ**, Badart-Smook A, Stockbrügger RW, Brummer RJ. Comprehensive nutritional status in patients with long-standing Crohn disease currently in remission. *Am J Clin Nutr* 1998; **67**: 919-926 [PMID: 9583850 DOI: 10.1093/ajcn/67.5.919]

51 **Jones K**, Baker K, Speight RA, Thompson NP, Tew GA. Randomised clinical trial: combined impact and resistance training in adults with stable Crohn's disease. *Aliment Pharmacol Ther* 2020; **52**: 964-975 [PMID: 33119156 DOI: 10.1111/apt.16002]

52 **Geerling BJ**, Badart-Smook A, Stockbrügger RW, Brummer RJ. Comprehensive nutritional status in recently diagnosed patients with inflammatory bowel disease compared with population controls. *Eur J Clin Nutr* 2000; **54**: 514-521 [PMID: 10878655 DOI: 10.1038/sj.ejcn.1601049]

53 **Mählmann L**, Gerber M, Furlano RI, Legeret C, Kalak N, Holsboer-Trachsler E, Brand S. Aerobic exercise training in children and adolescents with inflammatory bowel disease: Influence on psychological functioning, sleep and physical performance – An exploratory trial. *Ment Health Phys Act* 2017; **13**: 30-39 [DOI: 10.1016/j.mhpa.2017.09.002]

54 **Trivić I**, Sila S, Mišak Z, Niseteo T, Batoš AT, Hojsak I, Kolaček S. Impact of an exercise program in children with inflammatory bowel disease in remission. *Pediatr Res* 2023; **93**: 1999-2004 [PMID: 36319697 DOI: 10.1038/s41390-022-02362-8]

55 **Zhao J**, Huang Y, Yu X. Effects of nutritional supplement and resistance training for sarcopenia in patients with inflammatory bowel disease: A randomized controlled trial. *Medicine (Baltimore)* 2022; **101**: e30386 [PMID: 36042627 DOI: 10.1097/MD.0000000000030386]

56 **Cronin O**, Barton W, Moran C, Sheehan D, Whiston R, Nugent H, McCarthy Y, Molloy CB, O'Sullivan O, Cotter PD, Molloy MG, Shanahan F. Moderate-intensity aerobic and resistance exercise is safe and favorably influences body composition in patients with quiescent Inflammatory Bowel Disease: a randomized controlled cross-over trial. *BMC Gastroenterol* 2019; **19**: 29 [PMID: 30755154 DOI: 10.1186/s12876-019-0952-x]

57 **van Erp LW**, Roosenboom B, Komdeur P, Dijkstra-Heida W, Wisse J, Horjus Talabur Horje CS, Liem CS, van Cingel REH, Wahab PJ, Groenen MJM. Improvement of Fatigue and Quality of Life in Patients with Quiescent Inflammatory Bowel Disease Following a Personalized Exercise Program. *Dig Dis Sci* 2021; **66**: 597-604 [PMID: 32239380 DOI: 10.1007/s10620-020-06222-5]

58 **Seeger WA**, Thieringer J, Esters P, Allmendinger B, Stein J, Schulze H, Dignass A. Moderate endurance and muscle training is beneficial and safe in patients with quiescent or mildly active Crohn's disease. *United European Gastroenterol J* 2020; **8**: 804-813 [PMID: 32580666 DOI: 10.1177/2050640620936383]

59 **Tew GA**, Leighton D, Carpenter R, Anderson S, Langmead L, Ramage J, Faulkner J, Coleman E, Fairhurst C, Seed M, Bottoms L. High-intensity interval training and moderate-intensity continuous training in adults with Crohn's disease: a pilot randomised controlled trial. *BMC Gastroenterol* 2019; **19**: 19 [PMID: 30696423 DOI: 10.1186/s12876-019-0936-x]

60 **Loudon CP**, Corroll V, Butcher J, Rawsthorne P, Bernstein CN. The effects of physical exercise on patients with Crohn's disease. *Am J Gastroenterol* 1999; **94**: 697-703 [PMID: 10086654 DOI: 10.1111/j.1572-0241.1999.00939.x]

61 **Bottoms L**, Leighton D, Carpenter R, Anderson S, Langmead L, Ramage J, Faulkner J, Coleman E, Fairhurst C, Seed M, Tew G. Affective and enjoyment responses to 12 wk of high intensity interval training and moderate continuous training in adults with Crohn's disease. *PLoS One* 2019; **14**: e0222060 [PMID: 31539378 DOI: 10.1371/journal.pone.0222060]

62 **Fagan G**, Osborne H, Schultz M. Physical Activity in Patients with Inflammatory Bowel Disease: A Cross-Sectional Study. *Inflamm Intest Dis* 2021; **6**: 61-69 [PMID: 34124177 DOI: 10.1159/000511212]

63 **Hlatky MA**, Boineau RE, Higginbotham MB, Lee KL, Mark DB, Califf RM, Cobb FR, Pryor DB. A brief self-administered questionnaire to determine functional capacity (the Duke Activity Status Index). *Am J Cardiol* 1989; **64**: 651-654 [PMID: 2782256 DOI: 10.1016/0002-9149(89)90496-7]

64 **Hoogeboom TJ**, Kousemaker MC, van Meeteren NL, Howe T, Bo K, Tugwell P, Ferreira M, de Bie RA, van den Ende CH, Stevens-Lapsley JE. i-CONTENT tool for assessing therapeutic quality of exercise programs employed in randomised clinical trials. *Br J Sports Med* 2021; **55**: 1153-1160 [PMID: 33144350 DOI: 10.1136/bjsports-2019-101630]

65 **Bak MTJ**, Ruiterkamp MFE, van Ruler O, Campmans-Kuijpers MJE, Bongers BC, van Meeteren NLU, van der Woude CJ, Stassen LPS, de Vries AC. Prehabilitation prior to intestinal resection in Crohn's disease patients: An opinion review. *World J Gastroenterol* 2022; **28**: 2403-2416 [PMID: 35979261 DOI: 10.3748/wjg.v28.i22.2403]

66 **Berkel AEM**, Bongers BC, Kotte H, Weltevreden P, de Jongh FHC, Eijsvogel MMM, Wymenga M, Bigirwamungu-Bargeman M, van der Palen J, van Det MJ, van Meeteren NLU, Klaase JM. Effects of Community-based Exercise Prehabilitation for Patients Scheduled for Colorectal Surgery With High Risk for Postoperative Complications: Results of a Randomized Clinical Trial. *Ann Surg* 2022; **275**: e299-e306 [PMID: 33443905 DOI: 10.1097/SLA.0000000000004702]

67 **Barberan-Garcia A**, Ubré M, Roca J, Lacy AM, Burgos F, Risco R, Momblán D, Balust J, Blanco I, Martínez-Pallí G. Personalised Prehabilitation in High-risk Patients Undergoing Elective Major Abdominal Surgery: A Randomized Blinded Controlled Trial. *Ann Surg* 2018; **267**: 50-56 [PMID: 28489682 DOI: 10.1097/SLA.0000000000002293]

68 **Sedgwick P**, Greenwood N. Understanding the Hawthorne effect. *BMJ* 2015; **351**: h4672 [PMID: 26341898 DOI: 10.1136/bmj.h4672]

69 **Bilski J**, Brzozowski B, Mazur-Bialy A, Sliwowski Z, Brzozowski T. The role of physical exercise in inflammatory bowel disease. *Biomed Res Int* 2014; **2014**: 429031 [PMID: 24877092 DOI: 10.1155/2014/429031]

70 **Ploeger H**, Obeid J, Nguyen T, Takken T, Issenman R, de Greef M, Timmons B. Exercise and inflammation in pediatric Crohn's disease. *Int J Sports Med* 2012; **33**: 671-679 [PMID: 22562735 DOI: 10.1055/s-0032-1304323]

71 **Ohrström M**, Jansson O, Wohlfart B, Ekelund M. Working capacity and resting energy expenditure after ileal pouch-anal anastomosis. *Br J Surg* 2004; **91**: 618-624 [PMID: 15122615 DOI: 10.1002/bjs.4519]

72 **Jensen MB**, Houborg KB, Vestergaard P, Kissmeyer-Nielsen P, Mosekilde L, Laurberg S. Improved physical performance and increased lean tissue and fat mass in patients with ulcerative colitis four to six years after ileoanal anastomosis with a J-pouch. *Dis Colon Rectum* 2002; **45**: 1601-1607 [PMID: 12473882 DOI: 10.1007/s10350-004-7246-1]

73 **Brevinge H**, Berglund B, Bosaeus I, Tölli J, Nordgren S, Lundholm K. Exercise capacity in patients undergoing proctocolectomy and small bowel resection for Crohn's disease. *Br J Surg* 1995; **82**: 1040-1045 [PMID: 7648147 DOI: 10.1002/bjs.1800820813]

74 **Zhang Y**, Zhang L, Gao X, Dai C, Huang Y, Wu Y, Zhou W, Cao Q, Jing X, Jiang H, Zhu W, Wang X. Validation of the GLIM criteria for diagnosis of malnutrition and quality of life in patients with inflammatory bowel disease: A multicenter, prospective, observational study. *Clin Nutr* 2022; **41**: 1297-1306 [PMID: 35537380 DOI: 10.1016/j.clnu.2022.04.016]

75 **Cabalzar AL**, Azevedo FM, Lucca FA, Reboredo MM, Malaguti C, Chebli JMF. Physical activity in daily life, exercise capacity and quality of life in patients with crohn's disease on infliximab-induced remission: a preliminary study. *Arq Gastroenterol* 2019; **56**: 351-356 [PMID: 31618395 DOI: 10.1590/S0004-2803.201900000-65]

76 **Cabalzar AL**, Oliveira DJF, de Moura Reboredo M, Lucca FA, Chebli JMF, Malaguti C. Muscle function and quality of life in the Crohn's disease. *Fisioterapia em Movimento* 2017; **30**: 337-345

77 **Sarli B**, Dogan Y, Poyrazoglu O, Baktir AO, Eyvaz A, Altinkaya E, Tok A, Donudurmaci E, Ugurlu M, Ortakoyluoglu A, Saglam H, Arinc H. Heart Rate Recovery Is Impaired in Patients with Inflammatory Bowel Diseases. *Med Princ Pract* 2016; **25**: 363-367 [PMID: 27164968 DOI: 10.1159/000446318]

78 **Fiorindi C**, Cuffaro F, Piemonte G, Cricchio M, Addasi R, Dragoni G, Scaringi S, Nannoni A, Ficari F, Giudici F. Effect of long-lasting nutritional prehabilitation on postoperative outcome in elective surgery for IBD. *Clin Nutr* 2021; **40**: 928-935 [PMID: 32684485 DOI: 10.1016/j.clnu.2020.06.020]

79 **Subramaniam K**, Fallon K, Ruut T, Lane D, McKay R, Shadbolt B, Ang S, Cook M, Platten J, Pavli P, Taupin D. Infliximab reverses inflammatory muscle wasting (sarcopenia) in Crohn's disease. *Aliment Pharmacol Ther* 2015; **41**: 419-428 [PMID: 25580985 DOI: 10.1111/apt.13058]

80 **Altowati MMA**, Shepherd S, McMillan M, McGrogan P, Russell R, Ahmed SF, Wong SC. Persistence of Muscle-bone Deficits Following Anti-tumour Necrosis Factor Therapy in Adolescents With Crohn Disease. *J Pediatr Gastroenterol Nutr* 2018; **67**: 738-744 [PMID: 30052566 DOI: 10.1097/MPG.0000000000002099]

81 **Asscher VER**, Waars SN, van der Meulen-de Jong AE, Stuyt RJL, Baven-Pronk AMC, van der Marel S, Jacobs RJ, Haans JJL, Meijer LJ, Klijnsma-Slagboom JD, Duin MH, Peters MER, Lee-Kong FVYL, Provoost NE, Tijdeman F, van Dijk KT, Wieland MWM, Verstegen MGM, van der Meijs ME, Maan ADI, van Deudekom FJ, Mooijaart SP, Maljaars PWJ. Deficits in Geriatric Assessment Associate With Disease Activity and Burden in Older Patients With Inflammatory Bowel Disease. *Clin Gastroenterol Hepatol* 2022; **20**: e1006-e1021 [PMID: 34153476 DOI: 10.1016/j.cgh.2021.06.015]

82 **Bin CM**, Flores C, Alvares-da-Silva MR, Francesconi CF. Comparison between handgrip strength, subjective global assessment, anthropometry, and biochemical markers in assessing nutritional status of patients with Crohn's disease in clinical remission. *Dig Dis Sci* 2010; **55**: 137-144 [PMID: 19229617 DOI: 10.1007/s10620-008-0692-1]

83 **Bryant RV**, Ooi S, Schultz CG, Goess C, Grafton R, Hughes J, Lim A, Bartholomeusz FD, Andrews JM. Low muscle mass and sarcopenia: common and predictive of osteopenia in inflammatory bowel disease. *Aliment Pharmacol Ther* 2015; **41**: 895-906 [PMID: 25753216 DOI: 10.1111/apt.13156]

84 **Casanova MJ**, Chaparro M, Molina B, Merino O, Batanero R, Dueñas-Sadornil C, Robledo P, Garcia-Albert AM, Gómez-Sánchez MB, Calvet X, Trallero MDR, Montoro M, Vázquez I, Charro M, Barragán A, Martínez-Cerezo F, Megias-Rangil I, Huguet JM, Marti-Bonmati E, Calvo M, Campderá M, Muñoz-Vicente M, Merchante A, Ávila AD, Serrano-Aguayo P, De Francisco R, Hervías D, Bujanda L, Rodriguez GE, Castro-Laria L, Barreiro-de Acosta M, Van Domselaar M, Ramirez de la Piscina P, Santos-Fernández J, Algaba A, Torra S, Pozzati L, López-Serrano P, Arribas MDR, Rincón ML, Peláez AC, Castro E, García-Herola A, Santander C, Hernández-Alonso M, Martín-Noguerol E, Gómez-Lozano M, Monedero T, Villoria A, Figuerola A, Castaño-García A, Banales JM, Díaz-Hernández L, Argüelles-Arias F, López-Díaz J, Pérez-Martínez I, García-Talavera N, Nuevo-Siguairo OK, Riestra S, Gisbert JP. Prevalence of Malnutrition and Nutritional Characteristics of Patients With Inflammatory Bowel Disease. *J Crohns Colitis* 2017; **11**: 1430-1439 [PMID: 28981652 DOI: 10.1093/ecco-jcc/jjx102]

85 **Cioffi I**, Marra M, Imperatore N, Pagano MC, Santarpia L, Alfonsi L, Testa A, Sammarco R, Contaldo F, Castiglione F, Pasanisi F. Assessment of bioelectrical phase angle as a predictor of nutritional status in patients with Crohn's disease: A cross sectional study. *Clin Nutr* 2020; **39**: 1564-1571 [PMID: 31303525 DOI: 10.1016/j.clnu.2019.06.023]

86 **Davies A**, Nixon A, Tsintzas K, Stephens FB, Moran GW. Skeletal muscle anabolic and insulin sensitivity responses to a mixed meal in adult patients with active Crohn's disease. *Clin Nutr ESPEN* 2021; **41**: 305-313 [PMID: 33487282 DOI: 10.1016/j.clnesp.2020.11.014]

87 **Davies A**, Nixon A, Muhammed R, Tsintzas K, Kirkham S, Stephens FB, Moran GW. Reduced skeletal muscle protein balance in paediatric Crohn's disease. *Clin Nutr* 2020; **39**: 1250-1257 [PMID: 31178247 DOI: 10.1016/j.clnu.2019.05.017]

88 **Jansen I**, Prager M, Valentini L, Büning C. Inflammation-driven malnutrition: a new screening tool predicts outcome in Crohn's disease. *Br J Nutr* 2016; **116**: 1061-1067 [PMID: 27546478 DOI: 10.1017/S0007114516003044]

89 **Knudsen AW**, Naver A, Bisgaard K, Nordgaard-Lassen I, Becker U, Krag A, Slinde F. Nutrition impact symptoms, handgrip strength and nutritional risk in hospitalized patients with gastroenterological and liver diseases. *Scand J Gastroenterol* 2015; **50**: 1191-1198 [PMID: 25876708 DOI: 10.3109/00365521.2015.1028994]

90 **Lee N**, Radford-Smith GL, Forwood M, Wong J, Taaffe DR. Body composition and muscle strength as predictors of bone mineral density in Crohn's disease. *J Bone Miner Metab* 2009; **27**: 456-463 [PMID: 19333683 DOI: 10.1007/s00774-009-0059-5]

91 **Lu ZL**, Wang TR, Qiao YQ, Zheng Q, Sun Y, Lu JT, Han XX, Fan ZP, Ran ZH. Handgrip Strength Index Predicts Nutritional Status as a Complement to Body Mass Index in Crohn's Disease. *J Crohns Colitis* 2016; **10**: 1395-1400 [PMID: 27402912 DOI: 10.1093/ecco-jcc/jjw121]

92 **Marra M**, Di Vincenzo O, Cioffi I, Sammarco R, Scalfi L, Pasanisi F. The Relationship between Body Composition and Physical Activity in Patients with Crohn's Disease. In: 7th International Conference on Sport Sciences Research and Technology Support; 2019 Sep 20-21; Austria

93 **Norman K**, Kirchner H, Lochs H, Pirlich M. Malnutrition affects quality of life in gastroenterology patients. *World J Gastroenterol* 2006; **12**: 3380-3385 [PMID: 16733855 DOI: 10.3748/wjg.v12.i21.3385]

94 **Tsiountsioura M**, Wong JE, Upton J, McIntyre K, Dimakou D, Buchanan E, Cardigan T, Flynn D, Bishop J, Russell RK, Barclay A, McGrogan P, Edwards C, Gerasimidis K. Detailed assessment of nutritional status and eating patterns in children with gastrointestinal diseases attending an outpatients clinic and contemporary healthy controls. *Eur J Clin Nutr* 2014; **68**: 700-706 [PMID: 24424079 DOI: 10.1038/ejcn.2013.286]

95 **Ünal NG**, Oruç N, Tomey O, Ömer Özütemiz A. Malnutrition and sarcopenia are prevalent among inflammatory bowel disease patients with clinical remission. *Eur J Gastroenterol Hepatol* 2021; **33**: 1367-1375 [PMID: 33470696 DOI: 10.1097/MEG.0000000000002044]

96 **Valentini L**, Schaper L, Buning C, Hengstermann S, Koernicke T, Tillinger W, Guglielmi FW, Norman K, Buhner S, Ockenga J, Pirlich M, Lochs H. Malnutrition and impaired muscle strength in patients with Crohn's disease and ulcerative colitis in remission. *Nutrition* 2008; **24**: 694-702 [PMID: 18499398 DOI: 10.1016/j.nut.2008.03.018]

97 **Werkstetter KJ**, Ullrich J, Schatz SB, Prell C, Koletzko B, Koletzko S. Lean body mass, physical activity and quality of life in paediatric patients with inflammatory bowel disease and in healthy controls. *J Crohns Colitis* 2012; **6**: 665-673 [PMID: 22398103 DOI: 10.1016/j.crohns.2011.11.017]

98 **Wiroth JB**, Filippi J, Schneider SM, Al-Jaouni R, Horvais N, Gavarry O, Bermon S, Hébuterne X. Muscle performance in patients with Crohn's disease in clinical remission. *Inflamm Bowel Dis* 2005; **11**: 296-303 [PMID: 15735436 DOI: 10.1097/01.mib.0000160810.76729.9c]

99 **Steell L**, Johnston BA, Dewantoro D, Foster JE, Gaya DR, Macdonald J, McMillan M, Russell RK, Seenan JP, Ahmed SF, Gray SR, Wong SC. Muscle deficits with normal bone microarchitecture and geometry in young adults with well-controlled childhood-onset Crohn's disease. *Eur J Gastroenterol Hepatol* 2020; **32**: 1497-1506 [PMID: 32675776 DOI: 10.1097/MEG.0000000000001838]

100 **Yamamoto H**, Takeshima F, Haraguchi M, Akazawa Y, Matsushima K, Kitayama M, Ogihara K, Tabuchi M, Hashiguchi K, Yamaguchi N, Miyaaki H, Kondo H, Nakao K. High serum concentrations of growth differentiation factor-15 and their association with Crohn's disease and a low skeletal muscle index. *Sci Rep* 2022; **12**: 6591 [PMID: 35449185 DOI: 10.1038/s41598-022-10587-0]

101 **Bian D**, Liu X, Wang C, Jiang Y, Gu Y, Zhong J, Shi Y. Association between Dietary Inflammatory Index and Sarcopenia in Crohn's Disease Patients. *Nutrients* 2022; **14** [PMID: 35215553 DOI: 10.3390/nu14040901]

102 **Hradsky O**, Soucek O, Maratova K, Matyskova J, Copova I, Zarubova K, Bronsky J, Sumnik Z. Supplementation with 2000 IU of Cholecalciferol Is Associated with Improvement of Trabecular Bone Mineral Density and Muscle Power in Pediatric Patients with IBD. *Inflamm Bowel Dis* 2017; **23**: 514-523 [PMID: 28267045 DOI: 10.1097/MIB.0000000000001047]

103 **Maratova K**, Hradsky O, Matyskova J, Copova I, Soucek O, Sumnik Z, Bronsky J. Musculoskeletal system in children and adolescents with inflammatory bowel disease: normal muscle force, decreased trabecular bone mineral density and low prevalence of vertebral fractures. *Eur J Pediatr* 2017; **176**: 1355-1363 [PMID: 28840427 DOI: 10.1007/s00431-017-2988-7]

104 **Ward LM**, Ma J, Rauch F, Benchimol EI, Hay J, Leonard MB, Matzinger MA, Shenouda N, Lentle B, Cosgrove H, Scharke M, Konji VN, Mack DR. Musculoskeletal health in newly diagnosed children with Crohn's disease. *Osteoporos Int* 2017; **28**: 3169-3177 [PMID: 28791436 DOI: 10.1007/s00198-017-4159-0]

105 **Koch B**, Schäper C, Ittermann T, Spielhagen T, Dörr M, Völzke H, Opitz CF, Ewert R, Gläser S. Reference values for cardiopulmonary exercise testing in healthy volunteers: the SHIP study. *Eur Respir J* 2009; **33**: 389-397 [PMID: 18768575 DOI: 10.1183/09031936.00074208]

106 **Fairbarn MS**, Blackie SP, McElvaney NG, Wiggs BR, Paré PD, Pardy RL. Prediction of heart rate and oxygen uptake during incremental and maximal exercise in healthy adults. *Chest* 1994; **105**: 1365-1369 [PMID: 8181321 DOI: 10.1378/chest.105.5.1365]

107 **Tew GA**, Carpenter R, Seed M, Anderson S, Langmead L, Fairhurst C, Bottoms L. Feasibility of high-intensity interval training and moderate-intensity continuous training in adults with inactive or mildly active Crohn's disease: study protocol for a randomised controlled trial. *Pilot Feasibility Stud* 2017; **3**: 17 [PMID: 28373911 DOI: 10.1186/s40814-017-0133-z]

World Journal of Gastroenterology

Submit a Manuscript: https://www.f6publishing.com

World J Gastroenterol 2023 October 14; 29(38): 5428-5434

DOI: 10.3748/wjg.v29.i38.5428

ISSN 1007-9327 (print) ISSN 2219-2840 (online)

CASE REPORT

Dose escalation of adalimumab as a strategy to overcome anti-drug antibodies: A case report of infantile-onset inflammatory bowel disease

Silvana Ancona, Sara Signa, Chiara Longo, Giuliana Cangemi, Roberta Carfora, Enrico Drago, Alessandro La Rosa, Marco Crocco, Andrea Chiaro, Paolo Gandullia, Serena Arrigo

Specialty type: Gastroenterology and hepatology

Provenance and peer review: Unsolicited article; Externally peer reviewed.

Peer-review model: Single blind

Peer-review report's scientific quality classification

Grade A (Excellent): 0
Grade B (Very good): B, B, B
Grade C (Good): 0
Grade D (Fair): 0
Grade E (Poor): 0

P-Reviewer: Dauyey K, Kazakhstan; Knudsen T, Denmark; Lee WS, Malaysia

Received: June 7, 2023
Peer-review started: June 7, 2023
First decision: July 7, 2023
Revised: July 21, 2023
Accepted: July 27, 2023
Article in press: July 27, 2023
Published online: October 14, 2023

Silvana Ancona, Chiara Longo, Roberta Carfora, Enrico Drago, Alessandro La Rosa, Dipartimento di Neuroscienze, Riabilitazione, Oftalmologia, Genetica e Scienze Materno-Infantili (DINOGMI), Università degli Studi di Genova, Genova 16126, Italy

Sara Signa, Chiara Longo, Alessandro La Rosa, Marco Crocco, Andrea Chiaro, Paolo Gandullia, Serena Arrigo, Pediatric Gastroenterology and Endoscopy Unit, IRCCS Istituto Giannina Gaslini, Genova 16147, Italy

Giuliana Cangemi, Chromatography and Mass Spectrometry Section, Central Laboratory of Analysis, IRCCS Istituto Giannina Gaslini, Genova 16147, Italy

Corresponding author: Serena Arrigo, MD, Staff Physician, Pediatric Gastroenterology and Endoscopy Unit, IRCCS Istituto Giannina Gaslini, 5 Via Gerolamo Gaslini, Genova 16147, Italy. serenaarrigo@gaslini.org

Abstract

BACKGROUND

Treatment of infantile-onset inflammatory bowel disease (IO-IBD) is often challenging due to its aggressive disease course and failure of standard therapies with a need for biologics. Secondary loss of response is frequently caused by the production of anti-drug antibodies, a well-known problem in IBD patients on biologic treatment. We present a case of IO-IBD treated with therapeutic drug monitoring (TDM)-guided high-dose anti-tumor necrosis factor therapy, in which dose escalation monitoring was used as a strategy to overcome anti-drug antibodies.

CASE SUMMARY

A 5-mo-old boy presented with a history of persistent hematochezia from the 10th d of life, as well as relapsing perianal abscess and growth failure. Hypoalbuminemia, anemia, and elevated inflammatory markers were also present. Endoscopic assessment revealed skip lesions with deep colic ulcerations, inflammatory anal sub-stenosis, and deep fissures with persistent abscess. A diagnosis of IO-IBD Crohn-like was made. The patient was initially treated with oral steroids and fistulotomy. After the perianal abscess healed, adalimumab (ADA) was administered with concomitant gradual tapering of steroids. Clinical and biochemical

steroid-free remission was achieved with good trough levels. After 3 mo, antibodies to ADA (ATA) were found with undetectable trough levels; therefore, we optimized the therapy schedule, first administering 10 mg weekly and subsequently up to 20 mg weekly (2.8 mg/kg/dose). After 2 mo of high-dose treatment, ATA disappeared, with concomitant high trough levels and stable clinical and biochemical remission of the disease.

CONCLUSION
TDM-guided high-dose ADA treatment as a monotherapy overcame ATA production. This strategy could be a good alternative to combination therapy, especially in very young patients.

Key Words: Infantile-onset inflammatory bowel disease; Adalimumab; Loss of response; Dose escalation; Anti-drug antibodies; Case report

©The Author(s) 2023. Published by Baishideng Publishing Group Inc. All rights reserved.

Core Tip: Infantile-onset inflammatory bowel disease (IBD) frequently has a more severe course and a greater resistance to standard therapy than IBD in older children. Anti-tumor necrosis factor agents often lead to the production of anti-drug antibodies, resulting in loss of clinical response and disease progression. For this reason, the early detection of anti-drug antibodies is important, which may be possible with therapeutic drug monitoring. To date, commonly used strategies to overcome anti-drug antibodies are switching drugs or adding an immunomodulator, but a better option may be dose escalation.

Citation: Ancona S, Signa S, Longo C, Cangemi G, Carfora R, Drago E, La Rosa A, Crocco M, Chiaro A, Gandullia P, Arrigo S. Dose escalation of adalimumab as a strategy to overcome anti-drug antibodies: A case report of infantile-onset inflammatory bowel disease. *World J Gastroenterol* 2023; 29(38): 5428-5434
URL: https://www.wjgnet.com/1007-9327/full/v29/i38/5428.htm
DOI: https://dx.doi.org/10.3748/wjg.v29.i38.5428

INTRODUCTION

Inflammatory bowel disease (IBD) is a chronic inflammatory disorder of the gastrointestinal tract, and its incidence and prevalence in the pediatric population are rising in most countries[1]. Patients with IBD can be categorized by age at diagnosis: IBD cases diagnosed before 6 years of age are classified as very early onset IBD (VEO-IBD), whereas those with onset by 2 years of age are classified as infantile onset IBD (IO-IBD)[2]. Children with VEO-IBD and IO-IBD tend to have a more severe disease course[3,4] and higher rates of treatment resistance to standard therapy, including biologics[5-8]. Therefore, treatment of IO-IBD is challenging and frequently requires an aggressive approach[9].

Anti-tumor necrosis factor (TNF) agents are highly effective drugs for the treatment of pediatric IBD; however, some patients do not respond to induction therapy (primary non-responders) and some initial responders later experience loss of response (LOR; secondary non-responders). Primary and secondary non-responses are often the result of low trough concentration or high levels of anti-drug antibodies[10]. The use of therapeutic drug monitoring (TDM) has modified the biologic therapeutic approach in pediatric IBD by allowing the measurement of drug and anti-drug antibody serum concentrations[11,12]. Trough and antibody levels can guide appropriate dosing and interval schedules, allowing the development of an individualized treatment plan and leading to higher remission rates[13]. TDM has consequently resulted in higher treatment intensification rates, making it useful for guiding high-dose therapy in IO-IBD. A recent case series by Assa *et al*[14] suggested that an accelerated high-dose anti-TNF induction protocol could help recapture the response in children with IO-IBD who experienced an initial non-response or secondary LOR with infliximab (IFX).

Herein, we present a patient with IO-IBD who experienced secondary LOR due to anti-drug antibodies, and was successfully treated with TDM-guided high-dose anti-TNF therapy.

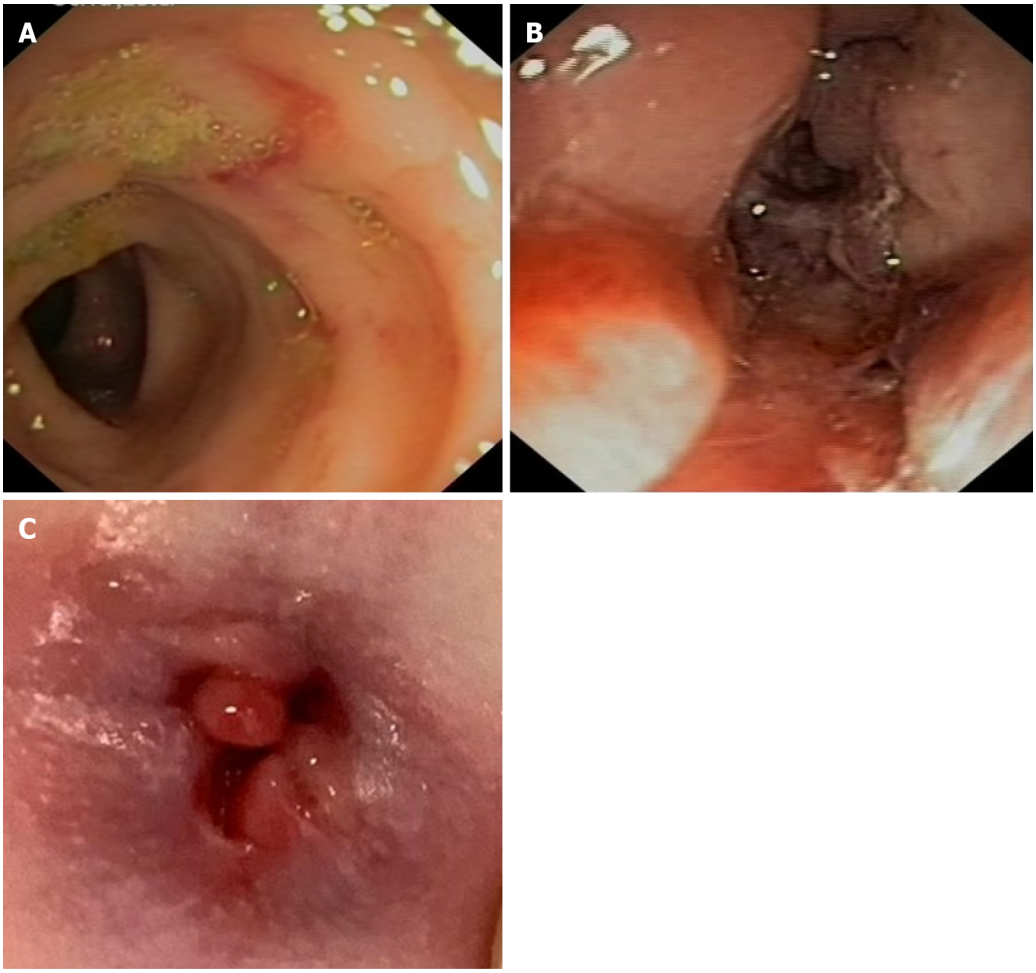
CASE PRESENTATION

Chief complaints

A 5-mo-old boy presented with a history of persistent hematochezia from the 10th d of life, as well as relapsing perianal abscess and growth failure.

Imaging examinations

The ileocolonoscopy revealed skip lesions with deep colic ulcerations, especially in the descending colon, and inflammatory anal sub-stenosis with deep fissures and tags (Figure 1). Histological findings demonstrated patchy severe chronic active colitis, characterized by crypt distortion and abscesses, loss of glands, and basal plasma cell expansion, all of which



DOI: 10.3748/wjg.v29.i38.5428 **Copyright** ©The Author(s) 2023.

Figure 1 Endoscopic images. A: A deep ulceration in the descending colon; B: A deep ulceration in the anal canal; C: Deep anal fissures and micropolyps.

strongly suggested IBD. Pelvic magnetic resonance imaging was performed, and no additional perianal lesions were discovered.

Laboratory examinations

Blood tests revealed microcytic anemia (hemoglobin 7.4 g/dL, normal range: 11-13 g/dL; mean corpuscular volume 67.5 fL, normal range: 77-101 fL) and hypoalbuminemia (2740 mg/dL). Inflammatory markers were moderately increased [C-reactive protein (CRP) 3.61 mg/dL]. Total immunoglobulin levels and immunological screening results were normal. Stool cultures and the *Clostridium difficile* test were negative.

Physical examination

On physical examination, the infant was pale and mildly hyporeactive, with adequate hydration. A perianal fistula, without drainage, and an anal fissure were found. No abdominal tenderness or mass was found. An auxological evaluation demonstrated growth failure. The rest of the examination was unremarkable.

Personal and family history

His parents denied a family history of autoimmune or gastrointestinal diseases.

History of past illness

At the age of 6 wk, he presented for the first time to the Emergency Department of our hospital with complaint of a perianal abscess and a history of persistent hematochezia from the 10th d of life. He was also unresponsive to a cow's milk protein-free diet. His growth was regular, and his psychomotor development was normal. Blood tests showed elevated inflammatory markers (CRP: 2.38 mg/dL, normal range: < 0.46 mg/dL) and mild hypoalbuminemia (2970 mg/dL, normal range: 3800-5400 mg/dL). Stool cultures were negative. A rectosigmoidoscopy was performed and showed macroscopic signs of unspecific proctocolitis, without hypereosinophilia at the histological exam. Intravenous antibiotic therapy led to transient resolution of hematochezia and improvement of the perianal abscess.

Two months later, the patient was readmitted to the hospital due to the recurrence of perianal abscess and bloody stools, so a second rectosigmoidoscopy was performed, which showed evidence of a macroscopic micronodular

proctosigmoiditis. No specific histological alterations were found and blood tests were normal. The patient was discharged with topical steroid therapy.

History of present illness

In the last several weeks before hospital admission, his clinical condition worsened: he developed diarrhea, characterized by more than eight completely unformed bloody stools, and had painful defecation.

FINAL DIAGNOSIS

Taking into consideration the endoscopic assessment and perianal disease, a diagnosis of IO-IBD Crohn-like was made. Targeted IO-IBD next-generation sequencing panel was negative, and whole exome sequencing results are pending; an eventual pathogenic mutation for a monogenic IBD could explain the severity of the disease course in a very young child and may suggest a more targeted treatment.

TREATMENT

The patient was initially treated with oral steroids (prednisone 1.5 mg/kg/d) with a clinical response and fistulotomy. After the perianal abscess healed, adalimumab (ADA) was administered [20 mg (3.3 mg/kg) for the first two doses, and then 10 mg (1.6 mg/kg) every 2 wk] with concomitant gradual steroid tapering. Of note, ADA has currently been approved for the treatment of moderate-to-severe Crohn's disease in children from six years of age; in particular, for patients < 40 kg, the drug label recommends 80 mg at the first dose (week 0), 40 mg at week 2 and 20 mg every two weeks (from week 4 onwards). IFX was avoided due to extremely difficult venous access. Clinical and biochemical steroid-free remission was achieved with good trough levels.

After 3 mo, antibodies to ADA (ATA) were found with undetectable trough levels: therefore, we decided to optimize the therapy schedule, first administering 10 mg weekly and subsequently up to 20 mg weekly (2.8 mg/kg/dose). After 2 mo of high-dose treatment, the ATA disappeared, with concomitant high trough levels and stable clinical and biochemical remission of the disease. In Figure 2, ADA dosage and trough levels are shown, which correlated with ATA and disease activity, as assessed with the Pediatric Crohn's Disease Activity Index.

OUTCOME AND FOLLOW-UP

Four months after the ATA disappearance, the child is still in clinical and biochemical remission. No adverse events have been reported, and the high dose of ADA has been well tolerated.

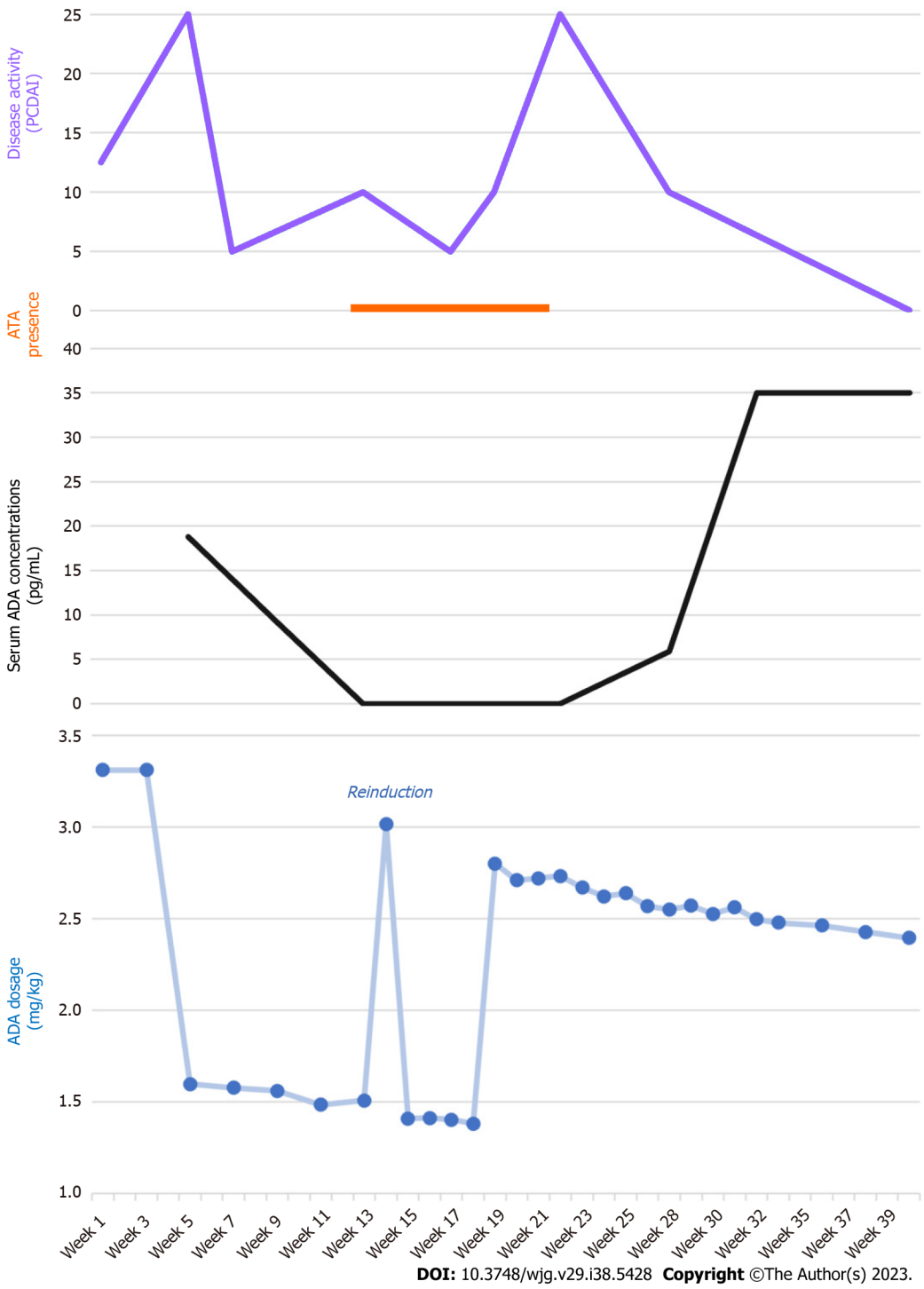
DISCUSSION

We describe a case of successful TDM-guided high-dose ADA treatment of a patient with IO-IBD. He experienced secondary LOR due to ATA production, which was overcome with dose intensification of ADA in monotherapy, reaching high trough levels.

Treatment of pediatric IBD with anti-TNF agents can result in immunogenicity and the formation of anti-drug antibodies[15], which are associated with loss of clinical response and worsening disease. Similar to adults[16,17], studies in the pediatric population have demonstrated that the combination of anti-TNF with an immunomodulator, such as azathioprine or methotrexate, lowers the risk of antibody formation and associated secondary LOR[18-20]. In line with these findings, the 2020 ECCO-ESPGHAN guidelines recommend combination therapy in patients with pediatric Crohn's disease, starting with IFX, and prudentially suggest a concomitant immunomodulator when starting ADA in patients previously sensitized to IFX or in high-risk patients when used as a primary anti-TNF agent[10]. However, long-term treatment with immunomodulators, especially thiopurines, is controversial because of the risk of malignancy[21,22].

To date, the management of patients who develop antibodies to IFX or ADA is often empiric. In our case, we administered accelerated high-dose ADA treatment, which overcame ATA production, resulting in stable clinical and biochemical remission after a period of transient LOR. This strategy of dose optimization has been previously suggested in adults[23]. Regarding the pediatric IBD literature, Cohen *et al*[24] showed suppression of antibodies in pediatric IBD patients with lower antibody levels (< 10 U/mL)[24].

Although a stable clinical remission has been achieved for almost a year, a recurrence of ATA could happen again in the future. Indeed, it is important to continue a strict trough levels and antibodies monitoring, in order to adjust ADA dosage and prevent ATA production. Other possible therapeutic approaches in the case of a recurrence of LOR, could be a combination with an immunomodulator, such as azathioprine or methotrexate, or a switch to another off-label biologic drug, like ustekinumab or vedolizumab. IFX has been previously avoided for the extremely difficult venous access, but a more stable venous device could be placed for making an attempt with IFX.



DOI: 10.3748/wjg.v29.i38.5428 **Copyright** ©The Author(s) 2023.

Figure 2 Disease activity, laboratory findings, and therapy. ADA: Adalimumab; ATA: Antibodies to adalimumab; PCDAI: Pediatric Crohn's Disease Activity Index.

CONCLUSION

We describe the first case of successful TDM-guided high-dose ADA treatment of a patient with IO-IBD. We overcame ATA production and subsequent transient LOR with a combination of interval shortening and dose escalation of ADA in monotherapy, reaching high trough levels. This strategy may be a good alternative to combination therapy, particularly in IO-IBD where an underlying primary immunodeficiency needs to be considered.

FOOTNOTES

Author contributions: Ancona S, Signa S, Longo C, Carfora R, and Drago E contributed to manuscript writing and editing, and data

collection; Cangemi G contributed to therapeutic drug monitoring and data collection; Arrigo S, Gandullia P, Crocco M, La Rosa A, and Chiaro A contributed to conceptualization and supervision; and all authors read and approved the final manuscript.

Informed consent statement: Informed written consent was obtained from the patients for the publication of this report and any accompanying images.

Conflict-of-interest statement: The authors have no conflicts of interest to declare.

CARE Checklist (2016) statement: The authors have read the CARE Checklist (2016), and the manuscript was prepared and revised according to the CARE Checklist (2016).

Open-Access: This article is an open-access article that was selected by an in-house editor and fully peer-reviewed by external reviewers. It is distributed in accordance with the Creative Commons Attribution NonCommercial (CC BY-NC 4.0) license, which permits others to distribute, remix, adapt, build upon this work non-commercially, and license their derivative works on different terms, provided the original work is properly cited and the use is non-commercial. See: https://creativecommons.org/Licenses/by-nc/4.0/

Country/Territory of origin: Italy

ORCID number: Marco Crocco 0000-0001-7277-4767; Serena Arrigo 0000-0002-5564-7018.

S-Editor: Chen YL
L-Editor: A
P-Editor: Yuan YY

REFERENCES

1 **Kuenzig ME**, Fung SG, Marderfeld L, Mak JWY, Kaplan GG, Ng SC, Wilson DC, Cameron F, Henderson P, Kotze PG, Bhatti J, Fang V, Gerber S, Guay E, Kotteduwa Jayawarden S, Kadota L, Maldonado D F, Osei JA, Sandarage R, Stanton A, Wan M; InsightScope Pediatric IBD Epidemiology Group, Benchimol EI. Twenty-first Century Trends in the Global Epidemiology of Pediatric-Onset Inflammatory Bowel Disease: Systematic Review. *Gastroenterology* 2022; **162**: 1147-1159.e4 [PMID: 34995526 DOI: 10.1053/j.gastro.2021.12.282]

2 **Arai K**. Very Early-Onset Inflammatory Bowel Disease: A Challenging Field for Pediatric Gastroenterologists. *Pediatr Gastroenterol Hepatol Nutr* 2020; **23**: 411-422 [PMID: 32953636 DOI: 10.5223/pghn.2020.23.5.411]

3 **Kelsen JR**, Sullivan KE, Rabizadeh S, Singh N, Snapper S, Elkadri A, Grossman AB. North American Society for Pediatric Gastroenterology, Hepatology, and Nutrition Position Paper on the Evaluation and Management for Patients With Very Early-onset Inflammatory Bowel Disease. *J Pediatr Gastroenterol Nutr* 2020; **70**: 389-403 [PMID: 32079889 DOI: 10.1097/MPG.0000000000002567]

4 **Kelsen JR**, Conrad MA, Dawany N, Patel T, Shraim R, Merz A, Maurer K, Sullivan KE, Devoto M. The Unique Disease Course of Children with Very Early onset-Inflammatory Bowel Disease. *Inflamm Bowel Dis* 2020; **26**: 909-918 [PMID: 31560377 DOI: 10.1093/ibd/izz214]

5 **Ouahed J**, Spencer E, Kotlarz D, Shouval DS, Kowalik M, Peng K, Field M, Grushkin-Lerner L, Pai SY, Bousvaros A, Cho J, Argmann C, Schadt E, Mcgovern DPB, Mokry M, Nieuwenhuis E, Clevers H, Powrie F, Uhlig H, Klein C, Muise A, Dubinsky M, Snapper SB. Very Early Onset Inflammatory Bowel Disease: A Clinical Approach With a Focus on the Role of Genetics and Underlying Immune Deficiencies. *Inflamm Bowel Dis* 2020; **26**: 820-842 [PMID: 31833544 DOI: 10.1093/ibd/izz259]

6 **Kelsen JR**, Grossman AB, Pauly-Hubbard H, Gupta K, Baldassano RN, Mamula P. Infliximab therapy in pediatric patients 7 years of age and younger. *J Pediatr Gastroenterol Nutr* 2014; **59**: 758-762 [PMID: 25419596 DOI: 10.1097/MPG.0000000000000533]

7 **Kerur B**, Fiedler K, Stahl M, Hyams J, Stephens M, Lu Y, Pfefferkorn M, Alkhouri R, Strople J, Kelsen J, Siebold L, Goyal A, Rosh JR, LeLeiko N, Van Limbergen J, Guerrerio AL, Maltz RM, Karam L, Crowley E, Griffiths AM, Heyman MB, Deneau M, Benkov K, Noe J, Moulton D, Pappa H, Galanko J, Snapper S, Muise AM, Kappelman MD, Benchimol EI. Utilization of Antitumor Necrosis Factor Biologics in Very Early Onset Inflammatory Bowel Disease: A Multicenter Retrospective Cohort Study From North America. *J Pediatr Gastroenterol Nutr* 2022; **75**: 64-69 [PMID: 35622080 DOI: 10.1097/MPG.0000000000003464]

8 **Shim JO**. Recent Advance in Very Early Onset Inflammatory Bowel Disease. *Pediatr Gastroenterol Hepatol Nutr* 2019; **22**: 41-49 [PMID: 30671372 DOI: 10.5223/pghn.2019.22.1.41]

9 **Kammermeier J**, Dziubak R, Pescarin M, Drury S, Godwin H, Reeve K, Chadokufa S, Huggett B, Sider S, James C, Acton N, Cernat E, Gasparetto M, Noble-Jamieson G, Kiparissi F, Elawad M, Beales PL, Sebire NJ, Gilmour K, Uhlig HH, Bacchelli C, Shah N. Phenotypic and Genotypic Characterisation of Inflammatory Bowel Disease Presenting Before the Age of 2 years. *J Crohns Colitis* 2017; **11**: 60-69 [PMID: 27302973 DOI: 10.1093/ecco-jcc/jjw118]

10 **van Rheenen PF**, Aloi M, Assa A, Bronsky J, Escher JC, Fagerberg UL, Gasparetto M, Gerasimidis K, Griffiths A, Henderson P, Koletzko S, Kolho KL, Levine A, van Limbergen J, Martin de Carpi FJ, Navas-López VM, Oliva S, de Ridder L, Russell RK, Shouval D, Spinelli A, Turner D, Wilson D, Wine E, Ruemmele FM. The Medical Management of Paediatric Crohn's Disease: an ECCO-ESPGHAN Guideline Update. *J Crohns Colitis* 2020 [PMID: 33026087 DOI: 10.1093/ecco-jcc/jjaa161]

11 **Kapoor A**, Crowley E. Advances in Therapeutic Drug Monitoring in Biologic Therapies for Pediatric Inflammatory Bowel Disease. *Front Pediatr* 2021; **9**: 661536 [PMID: 34123968 DOI: 10.3389/fped.2021.661536]

12 **van Hoeve K**, Hoffman I, Vermeire S. Therapeutic drug monitoring of anti-TNF therapy in children with inflammatory bowel disease. *Expert Opin Drug Saf* 2018; **17**: 185-196 [PMID: 29202588 DOI: 10.1080/14740338.2018.1413090]

13 **Conrad MA**, Kelsen JR. The Treatment of Pediatric Inflammatory Bowel Disease with Biologic Therapies. *Curr Gastroenterol Rep* 2020; **22**: 36 [PMID: 32542562 DOI: 10.1007/s11894-020-00773-3]

14 **Assa A**, Dorfman L, Shouval DS, Shamir R, Cohen S. Therapeutic Drug Monitoring-guided High-dose Infliximab for Infantile-onset Inflammatory Bowel Disease: A Case Series. *J Pediatr Gastroenterol Nutr* 2020; **71**: 516-520 [PMID: 32639454 DOI: 10.1097/MPG.0000000000002832]

15 **Aardoom MA**, Veereman G, de Ridder L. A Review on the Use of Anti-TNF in Children and Adolescents with Inflammatory Bowel Disease. *Int J Mol Sci* 2019; **20** [PMID: 31126015 DOI: 10.3390/ijms20102529]

16 **Colombel JF**, Sandborn WJ, Reinisch W, Mantzaris GJ, Kornbluth A, Rachmilewitz D, Lichtiger S, D'Haens G, Diamond RH, Broussard DL, Tang KL, van der Woude CJ, Rutgeerts P; SONIC Study Group. Infliximab, azathioprine, or combination therapy for Crohn's disease. *N Engl J Med* 2010; **362**: 1383-1395 [PMID: 20393175 DOI: 10.1056/NEJMoa0904492]

17 **Cosnes J**, Sokol H, Bourrier A, Nion-Larmurier I, Wisniewski A, Landman C, Marteau P, Beaugerie L, Perez K, Seksik P. Adalimumab or infliximab as monotherapy, or in combination with an immunomodulator, in the treatment of Crohn's disease. *Aliment Pharmacol Ther* 2016; **44**: 1102-1113 [PMID: 27666569 DOI: 10.1111/apt.13808]

18 **Kansen HM**, van Rheenen PF, Houwen RHJ, Tjon A Ten W, Damen GM, Kindermann A, Escher JC, Wolters VM; Kids with Crohn's, Colitis (KiCC) Working Group for Collaborative Paediatric IBD Research in the Netherlands. Less Anti-infliximab Antibody Formation in Paediatric Crohn Patients on Concomitant Immunomodulators. *J Pediatr Gastroenterol Nutr* 2017; **65**: 425-429 [PMID: 28945207 DOI: 10.1097/MPG.0000000000001551]

19 **Chi LY**, Zitomersky NL, Liu E, Tollefson S, Bender-Stern J, Naik S, Snapper S, Bousvaros A. The Impact of Combination Therapy on Infliximab Levels and Antibodies in Children and Young Adults With Inflammatory Bowel Disease. *Inflamm Bowel Dis* 2018; **24**: 1344-1351 [PMID: 29718278 DOI: 10.1093/ibd/izy010]

20 **Grossi V**, Lerer T, Griffiths A, LeLeiko N, Cabrera J, Otley A, Rick J, Mack D, Bousvaros A, Rosh J, Grossman A, Saeed S, Kay M, Boyle B, Oliva-Hemker M, Keljo D, Pfefferkorn M, Faubion W, Kappelman MD, Sudel B, Markowitz J, Hyams JS. Concomitant Use of Immunomodulators Affects the Durability of Infliximab Therapy in Children With Crohn's Disease. *Clin Gastroenterol Hepatol* 2015; **13**: 1748-1756 [PMID: 25911120 DOI: 10.1016/j.cgh.2015.04.010]

21 **Hyams JS**, Dubinsky MC, Baldassano RN, Colletti RB, Cucchiara S, Escher J, Faubion W, Fell J, Gold BD, Griffiths A, Koletzko S, Kugathasan S, Markowitz J, Ruemmele FM, Veereman G, Winter H, Masel N, Shin CR, Tang KL, Thayu M. Infliximab Is Not Associated With Increased Risk of Malignancy or Hemophagocytic Lymphohistiocytosis in Pediatric Patients With Inflammatory Bowel Disease. *Gastroenterology* 2017; **152**: 1901-1914.e3 [PMID: 28193515 DOI: 10.1053/j.gastro.2017.02.004]

22 **Biancone L**, Onali S, Petruzziello C, Calabrese E, Pallone F. Cancer and immunomodulators in inflammatory bowel diseases. *Inflamm Bowel Dis* 2015; **21**: 674-698 [PMID: 25545375 DOI: 10.1097/MIB.0000000000000243]

23 **Dreesen E**, Van Stappen T, Ballet V, Peeters M, Compernolle G, Tops S, Van Steen K, Van Assche G, Ferrante M, Vermeire S, Gils A. Anti-infliximab antibody concentrations can guide treatment intensification in patients with Crohn's disease who lose clinical response. *Aliment Pharmacol Ther* 2018; **47**: 346-355 [PMID: 29226370 DOI: 10.1111/apt.14452]

24 **Cohen RZ**, Schoen BT, Kugathasan S, Sauer CG. Management of Anti-drug Antibodies to Biologic Medications in Children With Inflammatory Bowel Disease. *J Pediatr Gastroenterol Nutr* 2019; **69**: 551-556 [PMID: 31335833 DOI: 10.1097/MPG.0000000000002440]



Published by **Baishideng Publishing Group Inc**
7041 Koll Center Parkway, Suite 160, Pleasanton, CA 94566, USA
Telephone: +1-925-3991568
E-mail: bpgoffice@wjgnet.com
Help Desk: https://www.f6publishing.com/helpdesk
https://www.wjgnet.com



© 2023 Baishideng Publishing Group Inc. All rights reserved.

ISSN 1007-9327 (print)
ISSN 2219-2840 (online)

World Journal of *Gastroenterology*

World J Gastroenterol 2023 October 21; 29(39): 5435-5525



Published by Baishideng Publishing Group Inc

World Journal of Gastroenterology

Contents

Weekly Volume 29 Number 39 October 21, 2023

REVIEW

5435 Function and biomedical implications of exosomal microRNAs delivered by parenchymal and nonparenchymal cells in hepatocellular carcinoma

Wang HC, Yin WX, Jiang M, Han JY, Kuai XW, Sun R, Sun YF, Ji JL

ORIGINAL ARTICLE

Basic Study

5452 Prostaglandin $F_{2\alpha}$ synthase promotes oxaliplatin resistance in colorectal cancer through prostaglandin $F_{2\alpha}$-dependent and $F_{2\alpha}$-independent mechanism

Wang YJ, Xie XL, Liu HQ, Tian H, Jiang XY, Zhang JN, Chen SX, Liu T, Wang SL, Zhou X, Jin XX, Liu SM, Jiang HQ

5471 Enhanced glucose homeostasis *via Clostridium symbiosum*-mediated glucagon-like peptide 1 inhibition of hepatic gluconeogenesis in mid-intestinal bypass surgery

Luo X, Tao F, Tan C, Xu CY, Zheng ZH, Pang Q, He XA, Cao JQ, Duan JY

Retrospective Cohort Study

5483 Development and validation of a nomogram for preoperative prediction of tumor deposits in colorectal cancer

Zheng HD, Hu YH, Ye K, Xu JH

Observational Study

5494 Risk assessment of venous thromboembolism in inflammatory bowel disease by inherited risk in a population-based incident cohort

Rifkin AS, Shi Z, Wei J, Zheng SL, Helfand BT, Cordova JS, Biank VF, Tafur AJ, Khan O, Xu J

SYSTEMATIC REVIEWS

5503 Diagnostic role of transient elastography in patients with autoimmune liver diseases: A systematic review and meta-analysis

Chen H, Shen Y, Wu SD, Zhu Q, Weng CZ, Zhang J, Wang MX, Jiang W

World Journal of Gastroenterology

Weekly Volume 29 Number 39 October 21, 2023

Contents

ABOUT COVER

Editorial Board Member of *World Journal of Gastroenterology*, Serag M Esmat, MD, Professor, Department of Internal Medicine, Faculty of Medicine, Cairo University, Cairo 11562, Egypt. Seragesmat@yahoo.com

AIMS AND SCOPE

The primary aim of *World Journal of Gastroenterology* (*WJG*, *World J Gastroenterol*) is to provide scholars and readers from various fields of gastroenterology and hepatology with a platform to publish high-quality basic and clinical research articles and communicate their research findings online. *WJG* mainly publishes articles reporting research results and findings obtained in the field of gastroenterology and hepatology and covering a wide range of topics including gastroenterology, hepatology, gastrointestinal endoscopy, gastrointestinal surgery, gastrointestinal oncology, and pediatric gastroenterology.

INDEXING/ABSTRACTING

The *WJG* is now abstracted and indexed in Science Citation Index Expanded (SCIE), MEDLINE, PubMed, PubMed Central, Scopus, Reference Citation Analysis, China Science and Technology Journal Database, and Superstar Journals Database. The 2023 edition of Journal Citation Reports® cites the 2022 impact factor (IF) for *WJG* as 4.3; Quartile category: Q2. The *WJG*'s CiteScore for 2021 is 8.3.

RESPONSIBLE EDITORS FOR THIS ISSUE

Production Editor: *Yi-Xuan Cai*; **Production Department Director:** *Xiang Li*; **Editorial Office Director:** *Jia-Ru Fan.*

NAME OF JOURNAL
World Journal of Gastroenterology

ISSN
ISSN 1007-9327 (print) ISSN 2219-2840 (online)

LAUNCH DATE
October 1, 1995

FREQUENCY
Weekly

EDITORS-IN-CHIEF
Andrzej S Tarnawski

EXECUTIVE ASSOCIATE EDITORS-IN-CHIEF
Xian-Jun Yu (Pancreatic Oncology), Jian-Gao Fan (Chronic Liver Disease), Hou-Bao Liu (Biliary Tract Disease), Naohisa Yoshida (Gastrointestinal Endoscopy)

EDITORIAL BOARD MEMBERS
http://www.wjgnet.com/1007-9327/editorialboard.htm

PUBLICATION DATE
October 21, 2023

COPYRIGHT
© 2023 Baishideng Publishing Group Inc

PUBLISHING PARTNER
Shanghai Pancreatic Cancer Institute and Pancreatic Cancer Institute, Fudan University
Biliary Tract Disease Institute, Fudan University

INSTRUCTIONS TO AUTHORS
https://www.wjgnet.com/bpg/gerinfo/204

GUIDELINES FOR ETHICS DOCUMENTS
https://www.wjgnet.com/bpg/GerInfo/287

GUIDELINES FOR NON-NATIVE SPEAKERS OF ENGLISH
https://www.wjgnet.com/bpg/gerinfo/240

PUBLICATION ETHICS
https://www.wjgnet.com/bpg/GerInfo/288

PUBLICATION MISCONDUCT
https://www.wjgnet.com/bpg/gerinfo/208

POLICY OF CO-AUTHORS
https://www.wjgnet.com/bpg/GerInfo/310

ARTICLE PROCESSING CHARGE
https://www.wjgnet.com/bpg/gerinfo/242

STEPS FOR SUBMITTING MANUSCRIPTS
https://www.wjgnet.com/bpg/GerInfo/239

ONLINE SUBMISSION
https://www.f6publishing.com

PUBLISHING PARTNER's OFFICIAL WEBSITE
https://www.shca.org.cn
https://www.zs-hospital.sh.cn

© 2023 Baishideng Publishing Group Inc. All rights reserved. 7041 Koll Center Parkway, Suite 160, Pleasanton, CA 94566, USA
E-mail: bpgoffice@wjgnet.com https://www.wjgnet.com

World Journal of Gastroenterology

Submit a Manuscript: https://www.f6publishing.com

World J Gastroenterol 2023 October 21; 29(39): 5435-5451

DOI: 10.3748/wjg.v29.i39.5435

ISSN 1007-9327 (print) ISSN 2219-2840 (online)

REVIEW

Function and biomedical implications of exosomal microRNAs delivered by parenchymal and nonparenchymal cells in hepatocellular carcinoma

Hai-Chen Wang, Wen-Xuan Yin, Meng Jiang, Jia-Yi Han, Xing-Wang Kuai, Rui Sun, Yu-Feng Sun, Ju-Ling Ji

Specialty type: Gastroenterology and hepatology

Provenance and peer review: Invited article; Externally peer reviewed.

Peer-review model: Single blind

Peer-review report's scientific quality classification

Grade A (Excellent): A
Grade B (Very good): B, B, B, B, B
Grade C (Good): 0
Grade D (Fair): 0
Grade E (Poor): 0

P-Reviewer: Ghazy A, Egypt; Granito A, Italy; Haque N, Bangladesh; Tsai HW, Taiwan; Wang YG, China

Received: May 26, 2023
Peer-review started: May 26, 2023
First decision: July 23, 2023
Revised: August 13, 2023
Accepted: October 16, 2023
Article in press: October 16, 2023
Published online: October 21, 2023

Hai-Chen Wang, Wen-Xuan Yin, Meng Jiang, Jia-Yi Han, Xing-Wang Kuai, Rui Sun, Yu-Feng Sun, Ju-Ling Ji, Department of Pathology, Medical School of Nantong University, Nantong 226001, Jiangsu Province, China

Meng Jiang, Jia-Yi Han, Xing-Wang Kuai, Rui Sun, Yu-Feng Sun, Ju-Ling Ji, Key Laboratory of Microenvironment and Translational Cancer Research, Science and Technology Bureau of Nantong City, Nantong 226001, Jiangsu Province, China

Ju-Ling Ji, Department of Pathology, The Affiliated Hospital of Nantong University, Nantong 226001, Jiangsu Province, China

Corresponding author: Ju-Ling Ji, MD, PhD, Professor, Department of Pathology, Medical School of Nantong University, No. 19 Qixiu Road, Nantong 226001, Jiangsu Province, China. jijuling@ntu.edu.cn

Abstract

Small extracellular vesicles (exosomes) are important components of the tumor microenvironment. They are small membrane-bound vesicles derived from almost all cell types and play an important role in intercellular communication. Exosomes transmit biological molecules obtained from parent cells, such as proteins, lipids, and nucleic acids, and are involved in cancer development. MicroRNAs (miRNAs), the most abundant contents in exosomes, are selectively packaged into exosomes to carry out their biological functions. Recent studies have revealed that exosome-delivered miRNAs play crucial roles in the tumorigenesis, progression, and drug resistance of hepatocellular carcinoma (HCC). In addition, exosomes have great industrial prospects in the diagnosis, treatment, and prognosis of patients with HCC. This review summarized the composition and function of exosomal miRNAs of different cell origins in HCC and highlighted the association between exosomal miRNAs from stromal cells and immune cells in the tumor microenvironment and the progression of HCC. Finally, we described the potential applicability of exosomal miRNAs derived from mesenchymal stem cells in the treatment of HCC.

Key Words: Hepatocellular carcinoma; MicroRNA; Exosomes; Extracellular vesicles; Nonparenchymal cells

©The Author(s) 2023. Published by Baishideng Publishing Group Inc. All rights reserved.

Core Tip: Hepatocellular carcinoma (HCC) is one of the most serious cancers in adults, and microRNAs (miRNAs) in small extracellular vesicles (exosomes) play a vital role in the pathological processes of HCC. Recent studies on exosomal miRNAs in HCC mainly focus on miRNA profiling but place little emphasis on where miRNAs come from and what target cells they act on. This review focused on the origin of exosomal miRNAs according to their parent cells in the tumor microenvironment and their role in HCC pathogenesis, contributing to a better understanding of exosomal miRNAs in the tumor microenvironment.

Citation: Wang HC, Yin WX, Jiang M, Han JY, Kuai XW, Sun R, Sun YF, Ji JL. Function and biomedical implications of exosomal microRNAs delivered by parenchymal and nonparenchymal cells in hepatocellular carcinoma. *World J Gastroenterol* 2023; 29(39): 5435-5451
URL: https://www.wjgnet.com/1007-9327/full/v29/i39/5435.htm
DOI: https://dx.doi.org/10.3748/wjg.v29.i39.5435

INTRODUCTION

In 2020, liver cancer was ranked the sixth most frequent malignant solid cancer globally. It was also the third-leading cause of cancer-related deaths in the world[1]. Hepatocellular carcinoma (HCC) is the primary histological type of liver cancer, comprising 80% of primary liver cancer cases[2]. It is characterized by the high degree of malignancy and poor prognosis. It is a threat to the health of humans. The symptoms of incipient-stage HCC are strong concealment, and it is challenging to diagnose HCC early. In addition, approximately 70% of patients undergo recurrence and experience metastasis within 5 years after surgical resection[3].

The tumor microenvironment (TME) is important in the development of HCC[3] and primarily comprises host cells, both resident and recruited, along with the secreted molecules and extracellular matrix (ECM) proteins[4]. Nonparenchymal cells in the liver, such as sinusoidal endothelial cells, hepatic stellate cells (HSCs), and macrophages, have a critical role in establishing the TME and mediating tumorigenesis by paracrine communication *via* cytokines and/or angiocrine factors[5]. Accumulating investigations on the TME have revealed novel perceptions of tumor growth as well as metastasis therein exosomes play a crucial function[6-8].

Small extracellular vesicles, also known as exosomes, refer to a specific type of extracellular vesicles with a size of 40-160 nm that originate from multivesicular bodies (MVBs), which act as carriers for biological information exchange to shape the cellular microenvironment[9]. To maintain consistency in nomenclature across studies published at different stages, we will use the name exosome for the rest of this review. Studies have shown that exosomes contain various cargoes including DNA, lipids, proteins, and RNA such as microRNAs (miRNAs), circular RNAs (circRNAs), long noncoding RNAs, and messenger RNAs, which are involved in intercellular communication[10,11].

More and more molecules of different classes carried by exosomes have been reported. Based on data retrieved from the ExoCarta database (http://www.exocarta.org), the identified components within exosomes consist of 9769 unique proteins, 3408 distinct messenger RNAs, 2838 different miRNAs, and 1116 lipids. Initially, exosomes were considered carriers of cellular waste, and their functions were underestimated[12]. Over the past few decades, the crucial functions of exosomes in facilitating intercellular communication in both physiological and pathological processes have been extensively studied and validated[13].

In 1996, exosomes derived from murine and human B lymphocytes were proven to execute a crucial function in transporting MHC molecules and eliciting MHC-II restricted T-cell responses[14]. Later, cancer cells and non-tumor cells in the TME were also found to be able to deliver exosomes and thereby participate in the malignant progression of tumors through molecular exchanges mediated by them[15,16]. Exosomes, hence, are recognized as important contributors to cancer initiation and progression[17-19].

MiRNAs represent an extensive collection of post-transcriptional gene expression regulators in eukaryotes. These regulatory molecules typically consist of 20-24 nucleotides and exert their function over various developmental and cellular processes[20]. Due to their essential role in gene expression, exosomal miRNAs have also been widely studied. In 2007, Valadi *et al*[21] reported that exosomes contained miRNAs, which could be delivered to other cells and exert their functions. Studies have demonstrated that exosomes are loaded with a high abundance of miRNAs, which play a crucial role in immune modulation, resistance to chemotherapy, and metastasis in diverse malignancies[22]. These miRNAs can promote tumor development in a paracrine manner in the surrounding microenvironment[23-25]. Furthering the comprehension of cancer mechanisms will require the identification of exosomal miRNAs, which are abnormally expressed in pathological states.

Numerous scientific studies have demonstrated that exosomes play a critical role in the genesis and malignant progression of tumors by transmitting signals between cells and regulating the TME[26]. This paper summarizes the studies of exosomal miRNAs released from nonparenchymal cells in the TME of HCC and discusses the association between these exosomal miRNAs and HCC. This study will help researchers in the field to better understand the role of exosomal miRNAs from stromal cells and immune cells in HCC and develop innovative strategies for HCC prevention

and treatment.

FORMATION, COMPOSITION, AND FUNCTION OF EXOSOMES

Unlike other types of vesicles, exosomes have a different formation mechanism. First, the plasma membrane germinates inwards to form early endosomes (membrane-bound vacuoles)[27,28]. By further inwards budding of early endosomes encompassing miRNAs, proteins, and other selected substances, late endosomes called MVBs are formed[29]. Following this, the MVBs undergo fusion with the cell membrane, and the intraluminal endosomal vesicles are released into the extracellular area. These vesicles subsequently form exosomes[30] or fuse with the lysosome to decompose the biological information[31].

Studies revealed that the essential system involved in the biogenesis of exosomes is the endosomal sorting complex required for transport[32]. The endosomal sorting complex required for transport- identifies the ubiquitin-labeled "cargo" protein, guides it to MVBs, and subsequently separates the MVB from the peripheral membrane in a highly conserved process similar to the process of cytokinesis and virus budding[33].

Exosomes can be produced by any cell under normal or pathological conditions and might be taken up by other cells, hereby executing their designated tasks[34,35]. Exosomes transport multiple biologically active substances, such as proteins, RNA, DNA, and cholesterol[36-38]. The sucrose gradient density range in which exosomes float is 1.13-1.19 g/mL[39]. Of note, the composition of exosomes varies depending on their cellular origin[40], and different cell-derived exosomes or even the same cell-derived exosomes contain different components in different physiological or pathological states[41]. The amount of exosomal miRNAs secreted by hepatoma cells could also vary under different stimuli[42]. Research has shown that 55 miRNAs in Heb3B cell-derived exosomes were expressed at levels that were four times higher than those in donor cells, while 30 miRNAs were expressed at lower levels, and 11 miRNAs were expressed only in exosomes[43]. These changes may be a potential mechanism for disease progression.

EXOSOMAL MIRNAS AND LIVER CANCER

In the past few years, exosomes have been shown to be crucial mediators of intercellular material and information exchange that can modulate the TME by transmitting nucleic acids and proteins between cells; hence, they are involved in tumor cell proliferation and migration, immune regulation, and drug resistance[44,45]. As an essential component of exosomes, exosomal miRNAs exert crucial functions in HCC tumorigenesis and progression.

First, we will review the function of exosomal miRNAs derived from HCC cells. MiR-122, which proved to be the most enriched miRNA in the human liver, is found to be decreased in the liver of HCC patients[46-48]. It is expressed and delivered by Huh7 cells (human HCC cell line) and can be transferred into HepG2 cells (human HCC cell line, of which the basal expression of miR-122 is low) in the form of exosomes, reducing the growth and proliferation of recipient HepG2 cells. The restoration of miR-122 inhibits HCC growth and enhances HCC sensitivity to chemotherapeutic drugs [49]. In addition, exosomes delivered by liver cancer cells can affect nonparenchymal cells in the microenvironment, promoting the malignant progression of tumors, which will be discussed in subsequent sections.

On the other hand, exosomal miRNAs secreted by tumor cells other than liver cancer cells can also promote the formation of premetastatic niches in the liver. Colon cancer cell-derived exosomes are able to deliver miR-21, miR-192, and miR-221 to hepatoma cells[50]. Exosomal miR-25-3p delivered by colon cancer cells promotes premetastatic niche formation in the liver by improving vascular permeability and angiogenesis[51]. Exosomes from colorectal cancer highly expressed miR-135a-5p, which could be transmitted to hepatic Kupffer cells to regulate the LATS2-YAP1/TEAD1-matrix metalloproteinase (MMP) 7 pathway and promote cell adhesion, forming premetastatic niches[52]. These results showed that exosomes could communicate between different types of cancers, even remodeling the microenvironment to boost liver metastasis[53].

Exosomal miRNAs might also be linked to different etiology of liver disease related to HCC. The connection between miRNAs and different liver diseases covering hepatitis B virus (HBV) infection, hepatitis C virus (HCV) infection, alcohol-associated liver disease (ALD), nonalcoholic steatohepatitis (NASH), nonalcoholic fatty liver disease, autoimmune hepatitis, and drug-induced liver injury has been discussed in-depth in previous high-quality reviews[54-56]. In the liver of ALD, NASH, and HCC patients, the level of hepatocyte-specific miR-122 exhibits a remarkable decrease. This specific miRNA directly targets distinct regions at the 5′-UTR of the HCV RNA genome, thereby facilitating the replication of HCV RNA[57]. When it comes to HBV replication, miR-122 functions oppositely. It acts as an inhibitor by downregulating the cyclin G1-p53 complex and preventing the specific interaction between p53 and HBV enhancers[58].

In simple steatosis, the liver shows an increase in the expression of miR-192, which is enriched in hepatocytes. However, this elevation is not observed in NASH[59]. On the other hand, the expression of miR-192 is decreased in HCC [60]. It is the most significantly downregulated miRNA in hepatic cancer stem cells and plays a role in the activation of cancer stem cells. Due to the anti-tumor property of miR-192, administering miR-192 to individuals with HCC can be a potential strategy for HCC therapy[60].

The expression of miR-155, a highly abundant miRNA in immune cells, including macrophages, is elevated in the liver tissues of patients with ALD, autoimmune hepatitis, and HCC. It is an oncogenic miRNA that links inflammation with tumorigenesis[61,62]. The activation of NF-κB signaling was reported to induce an upregulation in miR-155 levels in hepatocytes and liver cancer when mice were fed a choline-deficient and amino acid-defined diet[61] or in HCV infection

in patients[62]. However, few studies have focused on the etiology of HCC and miRNAs delivered by exosomes.

According to a recent investigation, extracellular vesicles derived from neutrophils have the capability to transfer miR-223 to macrophages, stimulating the resolution of liver fibrosis[63]. Neutrophil/myeloid-specific miR-223 has been extensively studied for its anti-inflammatory properties. Its function involves the suppression of IL-6 expression, effectively reducing the activation of the IL-6-p47phox-ROS pathway within neutrophils[64]. The upregulation of miR-223 is observed in the serum and/or liver of patients or mouse models experiencing ALD or NASH, both diseases characterized by significant hepatic neutrophil infiltration. Consequently, the compensatory increase in miR-223 expression is a protective mechanism against ALD[64] and NASH[65]. At the same time, the reduction of miR-223 in HCC might be a causal factor in promoting HCC progression[66]. Therefore, the administration of miR-223 is thought to be a potent treatment in murine models of acute hepatitis and NASH[67]. Future studies of the above-reported miRNAs associated with different etiologies of liver diseases underlying HCC could be extended to the area of exosomes.

THE INTERACTIONS BETWEEN TME AND TUMOR CELLS *VIA* EXOSOMAL MIRNAS IN HCC

Since Stephen Paget proposed the "seed-soil" theory of tumor metastasis in 1889 to explain the organ specificity of tumor metastasis, there has been increasing evidence that tumor metastasis requires coordination between tumor cells and the TME, which has been identified as an evolutionary and ecological process characterized by constant, dynamic, and reciprocal action upon each other. Nonparenchymal cells in the liver cancer TME, such as HSCs, cancer-associated fibroblasts (CAFs), immune cells [T lymphocytes, B lymphocytes, natural killer (NK) cells, NK T cells, and tumor-associated macrophages (TAMs)], and endothelial cells, are pivotal in mediating tumor-stromal communications, thus regulating the biological processes of HCC[68]. Noncellular components are composed of growth factors like transforming growth factor-β (TGF-β), insulin-like growth factor, fibroblast growth factor, hepatocyte growth factor, vascular endothelial growth factor, proteolytic enzymes, ECM, and inflammatory cytokines. These components create a beneficial environment for the formation and proliferation of HCCs. Exosomal miRNAs, a crucial element of the TME, play a significant role in transmitting signals between cells and contribute to the development and advancement of tumors. In the next section, the role of the exosomal miRNAs from different nonparenchymal cells in HCC formation and metastasis is thoroughly discussed. The related investigations are paving the way for novel strategies in clinical diagnosis and treatments aimed at HCC (Figure 1).

Exosome-mediated cell-cell communication between activated HSCs and HCC cells

HSCs can be observed in the space of Disse, located between liver sinusoidal endothelial cells and hepatocytes. These cells are responsible for storing lipid droplets containing vitamin A[69,70]. When there is damage to the liver, quiescent HSCs transform to activated HSCs, which resemble myofibroblasts and produce excessive fibrotic ECM[70]. The migration and accumulation of myofibroblasts are thought to be the key events that initiate liver fibrosis. Although many cell types, such as HSCs[71-73], portal fibroblasts[71,72], mesenchymal stem cell (MSC)-like cells[74], mesothelial cells[75] and bone marrow-derived cells[76], have been reported to contribute to the myofibroblast pool, recently researchers have evidence that 82%-96% of myofibroblasts in models with toxic, cholestatic, and fatty liver diseases are generated from activated HSCs[73].

The initiation and promotion of liver cancer are significantly correlated to the existence of liver fibrosis[70]. Activated HSC is a major factor mediating liver fibrosis and promotes liver cancer progression. Activated HSCs cocultured with HCC cells promoted tumor growth and invasiveness in nude mice[77]. In 2022, Zhang *et al*[78] reported that reducing activated HSC-delivered exosomal miR-148a-3p inhibited HCC initiation through the ITGA5/PI3K/Akt pathway. Another group found that HSC-HCC cell coculture reduced intracellular miR-335-5p expression in both types of cells. Additionally, *in vitro* and *in vivo* experiments showed that miR-335-5p-loaded HSC exosomes inhibited cancer growth and invasion[79]. In summary, activated HSCs can promote the development of HCC *via* various miRNAs delivered by exosomes, and targeting activated HSC-exosome miRNAs represents an innovative therapeutic strategy in HCC. At the same time, exosomes derived from HCC cells also promote the activation of HSCs. The HCC cell-derived exosome-miRNA-21, which targets the *PTEN* gene in HSCs, activates the PDK1/AKT pathway and converts HSCs to CAFs[80]. The progression of cancer was further accelerated by the activation of CAFs, which release angiogenic cytokines such as vascular endothelial growth factor, basic fibroblast growth factor, TGF-β, MMP2, and MMP9[80]. Another study suggested that a high level of serum exosomal miRNA-21 is associated with increased activation of CAFs and a higher vessel density in patients with HCC[80].

Exosome-mediated cell-cell communication between CAFs and HCC cells

CAFs are an important component of the TME[81]. However, the concepts of HSCs and CAFs in early literature sometimes need to be clarified. Researchers used to believe that in the HCC microenvironment, HSCs frequently differentiated into CAFs, which have been extensively reported to influence HCC progression[81-84]. In the latest study, Zhu *et al*[85] successfully identified five CAF subtypes within HCC tumors through single-cell RNA sequencing data obtained from both mouse and human HCC tumors. The subtypes include vascular CAFs, matrix CAFs, lipid processing-matrix CAFs (also known as $CD36^+$ CAFs), lipid-processing CAFs, and antigen-presenting CAFs. In these cells, CD36+ CAFs are derived from HSCs[85]. Another group also showed that Tcf21 was explicitly expressed in HSCs in mouse and human livers. Tcf21-positive HSCs, representing approximately 10% of all HSCs, can transdifferentiate into the majority of myofibroblasts in fibrotic liver and CAFs in HCC[86].

As crucial contributors to the alterations of the ECM that contribute to the development of HCC, CAFs have the potential to stimulate the progression of HCC through communication mediated by exosomes. A recent study found that the miR-320a level was remarkably decreased in CAF-derived exosomes compared with corresponding para-neoplastic fibroblast-derived exosomes in HCC patients. *In vitro* and *in vivo* experiments showed the anti-tumor effects of miR-320a when it was delivered to malignant cells through exosomes. The anti-tumor effect of miR-320a might be achieved by effectively targeting PBX3, thereby impeding the activation of the MAPK pathway[87]. Another study confirmed that miR-150-3p was lost in exosomes released by CAFs. CAF-delivered exosomes potently accelerate the malignant progression of HCC due to the absence of anti-tumoral miR-150-3p. Restoring the expression level of miR-150-3p by delivering miR-150-3p-loaded exosomes to HCC cells can effectively suppress their migration and invasiveness. Therefore, exosomal miR-150-3p can serve as a prognostic biomarker for HCC, and a supplement with exosomal miR-150-3p might be a potential treatment option[88].

Apart from those underexpressed anti-tumor miRNAs found in CAF-derived exosomes, the oncogenic miR-20a-5p was enriched in CAFs compared to HCC cells. MiR-20a-5p can be transferred from CAFs to HCC cells through exosomes and thereby suppress the expression of the tumor suppressor LIM domain and actin binding 1, which in turn inhibits the Wnt/β-catenin signaling pathway in HCC[89]. Thus, the distinct expression of exosomal miRNAs in CAFs plays a crucial part in the malignant progression of HCC. Therefore, potential therapeutic implications can be expected from anti-CAF medications that aim at certain exosomal miRNAs.

However, exosomal noncoding RNAs other than miRNAs also participate in the CAF-tumor cell communication. Chemoresistance in HCC can be influenced by CAF-exosomal circRNAs. Circular RNA ZFR is highly expressed in CAFs and CAF exosomes. CAF-exosomes transfer circular RNA ZFR to tumor cells, suppress the STAT3/NF-κB signaling pathway, and consequently enhance the growth of HCC cells as well as stimulate chemoresistance to cisplatin[90]. In addition, the migration, invasion, and glycolytic abilities of HCC cells were enhanced by long noncoding RNA TUG1 loaded in CAF-exosomes by targeting the miR-524-5p/SIX1 axis[91].

Exosome-mediated cell-cell communication between adipocytes and HCC cells

The involvement of adipose tissue in tumor progression has long been recognized[92]. Adipocytes play a crucial role in the hepatic microenvironment of nonalcoholic fatty liver disease, which is also a proven risk factor for HCC[44]. There is a close association between the adipocyte-HCC cell interaction and the risk of HCC development and progression[93]. Adipocyte-derived exosomes can affect the gene expression of liver cancer cells. In 2014, Koeck *et al*[94] found that exosomes from obese donors' visceral adipose tissues caused dysregulation of genes involved in the TGF-β pathway in HepG2 cells. Recently, Liu *et al*[95] found that the levels of miR-23a/b in serum exosomes and tumor tissues were significantly elevated in high-body fat ratio (BFR) HCC patients compared to their low-BFR counterparts. In tumor tissues, it is highly probable that miR-23a/b can be transported from adipocytes into cancer cells *via* exosomes, thus promoting the malignant progression of HCC[95]. Moreover, exosomal miR-23a/b affects the von Hippel-Lindau/hypoxia-inducible factor pathway, thus promoting chemoresistance[95]. Exosomal circRNAs also play a role. Adipocyte exosomal circDB can suppress miR-34a expression in HCC cells and subsequently activate the deubiquitination-related USP7/cyclin A2 signaling pathway and promote tumor growth of HCC[96]. These studies provided evidence that high BFR-related exosomal miRNA could be valuable therapeutic targets for HCC.

On the other hand, HCC cell-derived exosomes can educate adjacent adipocytes and generate a microenvironment that promotes tumor formation and progression. HepG2-exosomes induced an inflammatory phenotype in adipocytes by activating several phosphorylated kinases (p-AKT, p-Erk1/2, p-GSKb, p-stat5a, and p-p38) and the NF-kB signaling pathway[44]. Adipocytes treated by tumor-derived exosomes enhance tumor development, angiogenesis, and macrophage recruitment in a mouse xenograft model[44]. The specific exosomal miRNAs that play a role in the process remain to be revealed.

In addition, it was observed in experimental models and human studies that the exposure to the adipocyte exosome increased the expression of various profibrotic molecules in HSCs, including tissue inhibitor of metal protease 1 and 4, Smad-3, integrins αvβ-5 and αvβ-8, and MMP-9[94].

Exosome-mediated cell-cell communication between vascular endothelial cells and HCC cells

It is widely acknowledged that angiogenic factors from tumor cells activate vascular endothelial cells, promote their proliferation and migration, and contribute to aberrant tumor angiogenesis[97]. HCC is a typical hypervascular tumor, and understanding the mechanisms of angiogenesis in HCC is very important[98]. In an early study, Shih *et al*[99] discovered that the decrease of miR-214 in HCC cells contributed to the upregulation of hepatoma-derived growth factor, stimulating vascular endothelial cells to promote angiogenesis and tumor growth. Therefore, miR-214 is a potent suppressor of angiogenesis. It was also shown that exosomes derived from HCC cells are able to induce the formation of lumens of human umbilical vein endothelial cells[98].

Recently, several HCC cell-derived exosomal miRNAs were found to be vital to angiogenesis. Fang *et al*[100] reported that hepatoma cell-derived exosomal miR-103 can be internalized by endothelial cells and damage the integrity of endothelial junctions and a subsequent elevation in vascular permeability that facilitates tumor metastasis. The underlying mechanism involves the specific targeting of crucial endothelial junction proteins, such as vascular endothelial-cadherin and p120-catenin, by exosomal miR-103[100]. Exosomal miR-210, derived from HCC cells, can be delivered to endothelial cells and lead to the promotion of tumor angiogenesis. This effect is mediated by the specific targeting of SMAD4 and STAT6, key regulators involved in modulating angiogenic processes[101]. Exosomal miRNAs (miR-638, miR-663a, miR-3648, and miR-4258) from HuH-7M (which is established from luciferase-expressing human hepatoma Huh-7 and deemed as a new, highly intrahepatic metastatic cell line) are able to attenuate the integrity of endothelial junctions, thus enhancing permeability by reducing vascular endothelial cadherin and zonula occludens-1

expression[102]. These findings revealed that HCC-exosomal miRNAs could be delivered to endothelial cells to promote HCC progression.

On the other hand, the exosomes released by endothelial cells might also affect tumor cells. A recent study showed that engineered human cerebral endothelial cell-derived exosomes containing increased miR-214 (hCEC-Exo-214) could enhance the sensitivity of HCC cells to anticancer drugs, such as oxaliplatin and sorafenib[103]. However, how endothelial cell-derived exosomes and exosomal miRNAs act on HCC cells is poorly studied. It is worth paying attention to in the follow-up studies.

Exosome-mediated cell-cell communication between immune cells and HCC cells

The tumor immune microenvironment (TIME) is an important part of the TME[104]. The complicated interactions between cancer cells and host immune cells significantly influence TIME[105]. In HCC, the poor overall survival outcome arises as a result of immune surveillance disruption, which is strongly associated with the suppression of host immune reactions[105-107]. The growing evidence shows that the intricate interplay of exosome exchange-based cancer immunity shapes the tumor microenvironment, causing immune suppression and immune tolerance.

TAM presents the major leukocyte component infiltrating the HCC TIME[107]. Hepatic macrophages, also known as Kupffer cells, are the most abundant immune cells in the liver[108]. During the early stages of carcinogenesis, proinflammatory activation of Kupffer cells is important in tumor development. Once the primary tumor is established, the liver-infiltrating macrophages play a more critical role than Kupffer cells in HCC progression[109]. M2-polarized TAMs promote HCC progression by preventing T cells from recognizing and killing cancer cells, promoting tumor growth, angiogenesis, invasion, metastasis, and evasion of immune attack[110,111].

The role of TAM-derived exosomes is now attracting more and more attention. Liu *et al*[112] found a role of exosomal miR-92a-2-5p derived from M2 macrophages in promoting HCC cell invasion. This process is mediated through the regulation of the AR/PHLPP/p-AKT/β-catenin signaling pathway by miR-92a-2-5p. Increased expression of miR-27a-3p and miR-660-5p in M2 macrophage-derived exosomes facilitates HCC development by downregulating thioredoxin-interacting protein and KLF Transcription Factor 3 (KLF3)[113,114]. Exosomes derived from TAMs exhibit a reduction of miR-125a and miR-125b expression, which have been proven to promote HCC cell proliferation, sphere cell formation, and metastasis. MiR-125a/b exerts inhibitory effects on the HCC proliferation and attenuates their stem cell-like characteristics by specifically targeting CD90, a recognized stem cell marker in HCC[115].

Modulating TAM exosomal miRNAs provides a new way to suppress HCC. A tumor suppressor miRNA, miR-375, which is enriched in exosomes from IL-2 modulated TAMs, can ameliorate HCC development[116]. Moreover, propofol can stimulate TAMs to secrete exosomes overexpressing miR-142-3p. When miR-142-3p exosomes are transferred to HCC cells, they can inhibit HCC cell invasion[117]. Conversely, M1 macrophages contribute to proinflammatory and anti-tumor effects. M1 macrophage-derived exosomal miR-628-5p suppresses HCC development by restraining the m6A modification of circFUT8[118]. Peripheral blood monocyte-derived exosomal miR-142 and miR-223 can directly inhibit the proliferation of HCC[119].

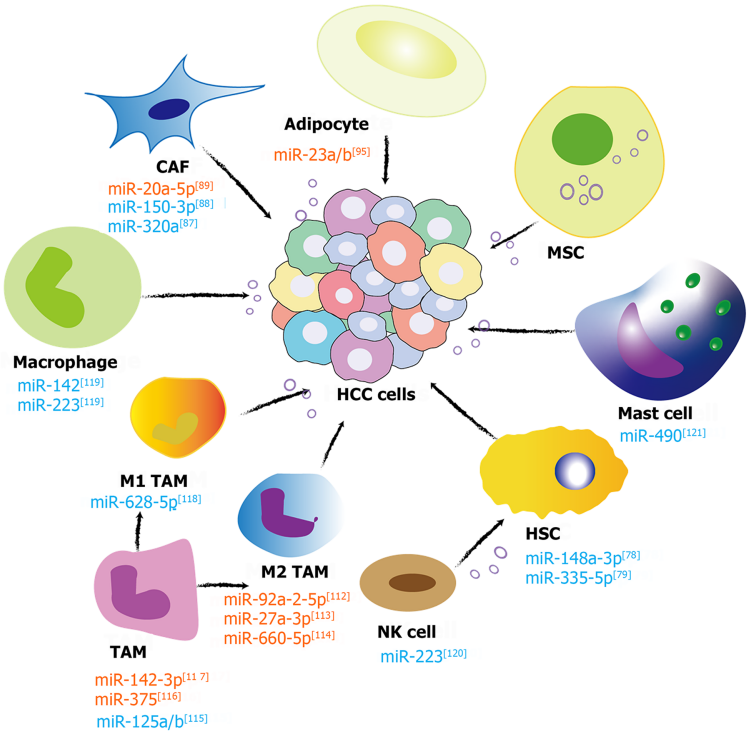
The exosomes from other immune cells are also involved in HCC. In mice, NK-exosomes rich in miR-223 inhibited carbon tetrachloride-induced liver fibrosis by inhibiting TGF-β1 induced HSC activation by directly targeting ATG7. Therefore, the overexpression of ATG7 in HSCs abolished the HSC activation-suppressive effect of NK cell exosomes [120]. Hepatitis C virus E2 envelope glycoprotein can stimulate mast cells, which in turn secrete a considerable amount of miR-490 enriched exosomes. When these exosomes are transferred into HCC cells, they inhibit tumor cell metastasis through the ERK1/2 pathway[121]. In addition, miR-150-5p and miR-142-3p can be transferred from regulatory T cells (Tregs) to dendritic cells *via* exosomes, resulting in the induction of a tolerant phenotype in these cells, characterized by elevated IL-10 production and decreased IL-6 production upon lipopolysaccharide stimulation[122].

On the other hand, tumor-derived exosomal miRNAs also affect the distribution and function of immune cells. Tregs constitute the most prominent subset of suppressor cells in the TME and release immunosuppressive factors, including IL-10 and TGF-β, contributing to tumor progression. Tregs also present various chemokine receptors and surface molecules like CTLA4 and PD-1, which make them susceptible to immune checkpoint inhibitor immunotherapy. The development of immune-related adverse events may partly be attributed to Treg destabilization[123]. Tumor cell-delivered miR-214 has the potential to augment the population of CD4+CD25highFoxp3+ Treg by reducing the expression of PTEN in CD4+ T cells, which results in the suppression of the host immune response and accelerates tumor development[124]. Indeed, the expansion of Treg populations through tumor-secreted miR-214 is believed to be a shared mechanism employed by various cancer cells to establish an immune-tolerant environment. This miRNA is crucial in modulating immune responses and promoting immune tolerance within the tumor microenvironment. Consequently, the inhibition of tumor-secreted miR-214 transportation to immune cells shows potential as an innovative approach to counteract tumor-induced immune tolerance[124].

In summary, exosome-delivered miRNAs from immune cells were intensely involved in the biological processes of HCC, and HCC-derived exosomal miRNAs also affect the distribution and function of immune cells.

CLINICAL APPLICATIONS OF EXOSOME-DELIVERED MIRNAS IN HCC

Radical resection and transarterial chemoembolization remain the most efficacious therapeutic approaches for patients with early-stage liver cancer. Still, the treatment efficacy remains unsatisfactory due to the compensatory effect of vascular proliferation after hypoxia[125,126]. For patients with advanced liver cancer, targeted therapy and traditional chemotherapy can only prolong the survival of these patients to a certain extent. Innovative and alternative therapies are



DOI: 10.3748/wjg.v29.i39.5435 **Copyright** ©The Author(s) 2023.

Figure 1 Schematic of exosomal microRNAs in the tumor microenvironment of hepatocellular carcinoma. Orange represents the promoting effect of microRNA (miR) on hepatocellular carcinoma (HCC) proliferation, and blue represents the inhibitory effect of miR on HCC proliferation. CAF: Cancer-associated fibroblast; HSC: Hepatic stellate cell; MSC: Mesenchymal stem cell; NK: Natural killer; TAM: Tumor-associated macrophage.

continuously needed to improve the prognosis of HCC patients.

Studies have recently confirmed that specific miRNAs can be transported through exosomes, thereby controlling tumor growth and achieving therapeutic effects[127]. Since exosomes exhibit distinct characteristics as a vehicle for drug transport, encompassing diminished immunogenicity, enhanced biocompatibility, reduced toxicity, and the capacity to traverse the blood-brain barrier, exosomes have garnered considerable attention as an innate delivery vector for conveying miRNA molecules[128]. Among the various cell types recognized for their ability to produce exosomes, MSCs are a promising choice for the large-scale production of exosomes for drug delivery. It has been shown in regenerative medicine and tumor treatment studies that MSC-derived exosomes can serve as effective vehicles for drug delivery[129, 130]. Based on the above findings, engineered MSC-derived exosomes loaded with specific miRNAs present a novel therapeutic approach for HCC treatment.

Exosomal miRNAs have been utilized to enhance the chemosensitivity of tumor cells[131,132]. Recent research demonstrated that miR-122 overexpression could sensitize the response of HCC cells to chemotherapy drugs by suppressing multidrug resistance-associated genes, the anti-apoptotic gene *Bcl-w*, and the cell cycle-related gene cyclin B1 [47]. The miR-122 overexpression amniotic membrane MSCs (AMSCs) can effectively encapsulate miR-122 to secreted exosomes, which are in turn delivered to HCC cells and further increase the sensitivity of HCC cells to sorafenib[133]. The miR-199a loaded AMSC exosomes produced through miR-199a overexpression lentivirus infection and subsequent puromycin selection are able to potently transport miR-199a and enhance the sensitivity of HCC cells towards doxorubicin by specifically targeting the mTOR pathway. Furthermore, tumor tissue can be effectively targeted by AMSC exosomal miRNA-199a through intravenous injection, thereby enhancing the therapeutic effect of Dox on HCC *in vivo* [134].

Liver fibrosis is the precursor stage of cirrhosis and liver cancer. MSC-derived exosomes alleviated carbon tetrachloride-induced liver fibrosis in mice through the expression of miR-148a. MiR-148a directly targets KLF transcription factor 6 and successfully converts the M1 macrophages to M2 macrophages *in vitro* and liver fibrosis models [135]. *In vitro* studies have shown that transplanted human chorionic plate-derived MSCs reduce lung and liver fibrosis in murine models[136,137]. One study supported that chorionic plate-derived MSCs released exosomes containing miRNA-125b into hedgehog-responsive HSCs and restrained the activation of hedgehog signaling by blocking the expression of smoothened receptors, consequently reducing the severity of hepatic fibrosis[138]. As a new candidate therapeutic strategy, MSC exosomes have excellent application prospects for HCC.

In addition, human liver stem cell-derived exosomes are loaded with multiple antitumor miRNAs (miR451, miR223, miR24, miR31, miR214, and miR122), which can downregulate multi-drug resistance 1, migration inhibitory factor, ras-associated protein 14, and E2F transcription factor 1. These exosomes have been proven to be able to inhibit the growth of hepatoma cells both *in vitro* and *in vivo*[139].

Table 1 Function of exosomal microRNAs from interstitial cells in the liver

miRNA species in exosomes	Exosome secreting cells	Exosome isolation methods	Target cells	miRNA expression of exosome	Downstream targets	Functions of miRNA	Additional information	Ref.	Year
miR-148a-3p	Primary fibroblasts (the HSC cell line LX-2)	The ExoQuick-TC kit	Human HCC cell lines PLC, HCCLM3, and SMMC-7721	Reduced in the exosomes of HSCs after cocultivation with primary liver cancer-associated fibroblasts	ITGA5/PI3K/Akt axis	Inhibited HCC cell malignancy	Primary fibroblasts were isolated from primary HCC tumor and paired peritumor tissues in 17 primary HCC patient samples	[78]	2022
miR-335-5p	The HSC cell line LX-2	Ultracentrifugation	Human HCC cell lines MHCC97H, MHCC97L, HepG2, and Huh7	Reduced in the exosomes of fibroblasts as well as in HCC cells after cocultivation	CDC42? CDK2?	Inhibited neighboring cancer cell proliferation, invasion, and motility	-	[79]	2019
miR-320a	CAFs	Life Technology exosome precipitation solution	Human HCC cell lines MHCC97-H, SMMC-7721, Huh7, and the human normal liver cell line 7702	Reduced in the exosomes of CAFs derived from human HCC patients	PBX3	Inhibited HCC cell proliferation and metastasis ability	PAFs and CAFs derived from 6 pairs of matched primary hepatocarcinoma and adjacent tumor-free tissues (5 cm from the cut edge of the tumor edge)	[87]	2017
miR-150-3p	CAFs	0.22-μm PVDF filter and Total Exosome Isolation Reagent	Human HCC cell lines Huh7 and Hep3B	Decreased in CAF-derived exosomes	-	Inhibited HCC proliferation and metastasis	Stromal fibroblasts isolated from tumor tissue and adjacent (> 5 cm from the tumor edge) tissues from 6 HCC patients	[88]	2021
miR-20a-5p	CAFs	Centrifuged and filtered through a 0.22-μm PVDF membrane	Human HCC cell lines SMMC7721, Huh7, YY8103, Hep3B, Focus, HepG2, and HCCLM3 and a normal liver cell line MIHA, WRL68	Higher in exosomes from cancer tissues than in matched adjacent para-tumoral tissues	LIMA1	Contributed to HCC cell proliferation, metastasis, and EMT	CAFs were from the HCC tissues and NFs in paired adjacent normal tissues from 92 HCC patients	[89]	2022
miR-214	hCECs	Centrifuged and filtered through a 0.22-μm PVDF membrane and ultracentrifugation	Human HCC cell lines HepG2, Hep3B, the human liver epithelial cell line THLE-2	Lower levels in HCC cells than in normal human liver epithelial cells	P-gp/SF3B3	Reduced cancer cell viability and invasion compared with monotherapy with oxaliplatin or sorafenib	-	[103]	2021
miR-23a/b	Adipose cell mouse preadipocyte 3T3-L1 cells	Differential centrifugation	The human HCC cell lines BEL-7402 and BEL-7402/5-Fu murine hepatoma cell line Hepa1-6	High in exosomes from HCC patients with high BFR	VHL/HIF-1α	Promoted HCC cell growth and migration	Adipose cells were isolated from human tumor tissues from obese and nonobese patients	[95]	2019
miR-142,	Monocyte-derived	Microfiltration and	The human HCC	High when cocultured	STMN-1	Inhibited HCC	PBMCs were isolated from lymphocyte cones	[119]	2013

miR-223	macrophages; human acute monocytic leukemia THP-1, B-lymphoblastoid 721.221, and murine lymphoblast-like mastocytoma P815 cell lines	ultracentrifugation	cell lines Huh7 and HepG2	with HCC cells		proliferation	or fresh blood by density gradient centrifugation and were incubated for 2 h in plastic plates before the flask was washed intensively to remove any nonadherent cells. After 4 d of incubation in serum-free medium supplemented with 1% autologous serum, adherent cells were washed with PBS and cultured in standard DMEM-based medium for 3-6 extra days to generate monocyte-derived macrophages phenotyped to be $CD14^+$, $CD11a^+$, $CD3^-$, $CD56^-$, and $CD19^-$		
miR-490	Human MC line HMC-1 (treated with HCV-E2)	Total exosome separation reagent from Invitrogen	The human HCC cell lines HepG2 and HepG3b	High when HCV-E2-stimulated MC-derived exosomes were incubated with the two types of HCC cells for 24 h compared with the incubation with normal MC-derived exosomes	ERK1/2	Inhibited HCC proliferation		[121]	2017
miR-223	Human NK cell line NK92-MI	Differential centrifugation	The human HSC line LX-2	Higher in exosomes derived from NK cells than in parental NK-92MI cells	AGT7	Attenuated TGF-β1-induced HSC activation and inhibited liver fibrosis	LX-2 cells were treated with TGF-β1 (5 ng/mL) for 24 h to stimulate HSC activation. LX-2 cells in the exosomes derived from NK cells-treated groups were pretreated with exosomes derived from NK cells (10 μg/mL) before TGF-β1 treatment. LX-2 cells in the rapamycin-treated groups were pretreated with the autophagy activator rapamycin (2 mM) in DMSO for 12 h before TGF-β1 treatment	[120]	2020
miR-125a/b	TAMs	ExoQuick exosome precipitation solution	The human HCC cell lines Huh7, HepG2, and BEL-7404	Downregulated in exosomes from HCC-associated macrophages	CD90	Suppressed HCC cell growth and sphere formation	TAMs and nontumor macrophages were isolated from primary human HCC, adjacent nontumor liver tissues from 6 patients with HCC	[115]	2019
miR-628-5p	M1 macrophage	-	The human HCC cell lines Huh7, HCCLM3, Hep3B, and MHCC97H, immortalized human liver epithelial THLE-3 cell line	High in M1-exosomes	METTL14/circFUT4/CHMP14B	Inhibited HCC cell progression	THP-1 cells were differentiated into M0 macrophages by a 24 h incubation with 150 nM phorbol 12-myristate 13-acetate followed by a 24 h incubation in RPMI medium. M0 macrophages were polarized to M1 macrophages by incubation with 20 ng/mL IFN-γ and 10 pg/mL lipopolysaccharide	[118]	2022
miR-92a-2-5p	M2 macrophage (monocytic leukemia cell line THP-1)	Centrifuged and filtered through a 0.22-μm PVDF membrane and ultracentrifugation	Human liver cancer SK-HEP-1 and HepG2 cell lines, HA22T cell line, and murine HCC Hepa 1-6 cell line	Increased after coculture with liver cancer cells	AR/PHLPP/p-AKT/β-catenin signaling	Promoted HCC growth and invasiveness	To induce differentiation into macrophages, THP-1 cells were cultured with 100 ng/mL PMA (Sigma) for 48 h, and the macrophage was cultured with the addition of DMSO to promote M2 polarization	[112]	2020
miR-660-5p	M2 macrophage	Differential centrifu-	Human HCC cell	High	KLF3	Augmented the	THP-1 monocytes were stimulated by 100 ng	[114]	2021

	(monocytic leukemia cell line THP-1)	gation	lines HepG2 and Bel-7402			tumorigenic ability of HCC cells	of phorbol 12-myristate 13-acetate (Sigma-Aldrich, MO, United States) for 48 h, thus differentiating into M0 macrophages. Then, M0 macrophages were treated with 20 ng/mL interleukin 4 (AF-200–04-5, PeproTech, NJ, United States) for 72 h to polarize into M2 macrophages		
miR-27a-3p	M2 macrophage (monocytic leukemia cell line THP-1)	SBI ExoQuick-TC Kit	Human HCC cell lines Huh7, 97H, HepG2, LM3, and SMMC-7721	-	TXNIP	Induced the cancer stemness of HCC	Differentiation of THP-1 cells to macrophages was performed using 200 ng/mL phorbol myristic acetate, and the cells were then cultured with 20 ng/mL interleukin-4 for 72 h to induce M2-type polarization	[113]	2021
miR-142-3p	TAMs treated by propofol (the murine macrophage cell line Raw 264.7 cells)	Differential centrifu-gation	The murine HCC cell line Hepa1-6	Dose-dependent increase when treated with propofol	RAC1	Enhanced the antitumor activity of propofol	Raw 264.7 cells were cultured in complete RPMI 1640 with 10% FBS and treated with propofol (dissolved in RPMI 1640) in complete medium. TAMs were isolated from tumor-bearing mice treated with 0 mg/kg, 20 mg/kg, and 50 mg/kg propofol by i.p. injection	[117]	2014
miR-375	TAMs (IL-2 induced)	Total exosome isolation reagent	The human HCC cell lines HepG2 and QJY–7703	High	-	Ameliorated HCC development and progression	Primary human HCC specimens were collected from patients who suffered from hepatectomy. The macrophages were isolated and cultured by Percoll (GE Healthcare) density gradient centrifugation. TAMs were treated with IL-2 for 24 h before the supernatants were collected. The treatment concentration was 20 ng/mL	[116]	2022

AGT7: Autophagy-related 7; AR: Androgen receptor; BFR: Body fat ratio; CAFs: Cancer-associated fibroblasts; CDC42: Cell division cycle 42; CDK2: Cyclin dependent kinase 2; EMT: Epithelial-mesenchymal transition; ERK1/2: Extracellular regulated protein kinases 1/2; Exos: Exosomes; HCC: Hepatocellular carcinoma; hCECs: Human cerebral endothelial cells; HCV-E2: Hepatitis C virus E2 envelope glycoprotein; HIF-1α: Hypoxia-inducible factor 1α; HSCs: Hepatic stellate cells; i.p.: Intraperitoneal; ITGA5: Integrin α5; KLF3: Kruppel-like factor 3; LIMA1: LIM domain and actin binding 1; MCs: Mast cells; METTL14: Methyltransferase-like 14; miR: MicroRNA; NK: Natural killer; PAFs: Paraneoplastic fibroblasts; PBMCs: Peripheral blood mononuclear cells; PBX3: Pre-B-cell leukemia homeobox 3; P-gp: P-glycoprotein; PI3K: Phosphoinositide 3-kinase; RAC1: Rac family small GTPase 1; SF3B3: Splicing factor 3b subunit 3; STMN1: Stathmin-1; TAMs: Tumor-associated macrophages; TXNIP: thioredoxin-interacting protein; VHL: Von Hippel-Lindau.

CONCLUSION

Despite significant advances in diagnosis and therapeutics, HCC remains exceedingly fatal. In most cases, HCC develops from chronic liver inflammation, which provides a tumor-promoting microenvironment composed of immune and stromal cells. As a novel cellular communicator in TME, exosomes mediate the intricate interaction of nonparenchymal cells (including immune and stromal cells) with cancer cells. They are involved in the etiology of HCC and multiple processes related to tumor initiation, development, metastasis, and drug resistance. Exosome cargoes, especially miRNAs, are key communication factors in the complicated cross-talk, indicating that they are promising prognostic markers and therapeutic targets for HCC. In this review, we emphasized the function and mechanism of exosomal miRNAs from nonparenchymal cells for the initiation and malignant progression of HCC. Also, we introduced the influences of exosomal miRNAs delivered by tumor cells on nonparenchymal cells. The functions of the exosomal miRNAs in HCC were also summarized (Table 1). Finally, the therapeutic potential of exosomes for HCC was discussed. With the

development of nanoengineering technology, exosomes can be modified to carry specific miRNAs and target specific cells, thus enabling precision and individualized treatment of HCC.

Although significant progress has been achieved in elucidating the functions of exosomes and their miRNA cargoes in HCC, some challenges remain. Sometimes, different investigators reported different experimental observations for the same exosomal miRNAs. The inconsistency of experimental subjects and study designs might cause these discrepancies. Therefore, factors such as the environment, age and sex of the subjects, cause of HCC occurrence, and data collection from multiple centers should be considered to produce more accurate results. Moreover, different techniques can lead to the isolation of varied subtypes of extracellular vesicles, each exhibiting unique miRNA profiles, protein compositions, and biological functions[140-142]. In clinical applications, problems include low targeting efficiency and easily phagocytosed by the immune system. The exosome separation and purification method also have limitations and could be time-consuming and laborious. Therefore, further research must be done to address these problems and determine more feasible and effective clinical translational applications of exosomes. The integration of nanoengineering and molecular biology allows for the utilization of exosome-mediated miRNAs in precision nanomedicine, presenting novel approaches for the diagnosis and treatment of HCC.

ACKNOWLEDGEMENTS

The authors would like to thank the anonymous reviewers whose feedback substantially improved the quality of this article.

FOOTNOTES

Author contributions: Ji JL designed the review; Wang HC and Ji JL drafted the paper; Wang HC prepared the figure; Yin WX, Jiang M, Han JY, and Sun YF researched the background of the study; Ji JL, Kuai XW, and Sun R reviewed and revised the paper; all authors read and approved the final manuscript.

Supported by the National Natural Science Foundation of China, No. 81761128018 and No. 81572871; the Natural Science Foundation of Jiangsu Province, No. BK20151277; and the Undergraduate Training Programs for Innovation and Entrepreneurship of Jiangsu Province, No. 202110304035Z.

Conflict-of-interest statement: The authors declare having no conflicts of interest for this article.

Open-Access: This article is an open-access article that was selected by an in-house editor and fully peer-reviewed by external reviewers. It is distributed in accordance with the Creative Commons Attribution NonCommercial (CC BY-NC 4.0) license, which permits others to distribute, remix, adapt, build upon this work non-commercially, and license their derivative works on different terms, provided the original work is properly cited and the use is non-commercial. See: https://creativecommons.org/Licenses/by-nc/4.0/

Country/Territory of origin: China

ORCID number: Hai-Chen Wang 0000-0003-0352-630X; Wen-Xuan Yin 0000-0002-2266-7514; Meng Jiang 0000-0003-2070-0082; Jia-Yi Han 0000-0001-7983-6844; Xing-Wang Kuai 0000-0003-0527-7108; Yu-Feng Sun 0000-0003-3873-175X; Ju-Ling Ji 0000-0001-6500-8052.

S-Editor: Yan JP
L-Editor: Filipodia
P-Editor: Cai YX

REFERENCES

1 **Sung H**, Ferlay J, Siegel RL, Laversanne M, Soerjomataram I, Jemal A, Bray F. Global Cancer Statistics 2020: GLOBOCAN Estimates of Incidence and Mortality Worldwide for 36 Cancers in 185 Countries. *CA Cancer J Clin* 2021; **71**: 209-249 [PMID: 33538338 DOI: 10.3322/caac.21660]

2 **Rumgay H**, Ferlay J, de Martel C, Georges D, Ibrahim AS, Zheng R, Wei W, Lemmens VEPP, Soerjomataram I. Global, regional and national burden of primary liver cancer by subtype. *Eur J Cancer* 2022; **161**: 108-118 [PMID: 34942552 DOI: 10.1016/j.ejca.2021.11.023]

3 **Villanueva A**. Hepatocellular Carcinoma. *N Engl J Med* 2019; **380**: 1450-1462 [PMID: 30970190 DOI: 10.1056/NEJMra1713263]

4 **Anderson NM**, Simon MC. The tumor microenvironment. *Curr Biol* 2020; **30**: R921-R925 [PMID: 32810447 DOI: 10.1016/j.cub.2020.06.081]

5 **Lu C**, Rong D, Zhang B, Zheng W, Wang X, Chen Z, Tang W. Current perspectives on the immunosuppressive tumor microenvironment in hepatocellular carcinoma: challenges and opportunities. *Mol Cancer* 2019; **18**: 130 [PMID: 31464625 DOI: 10.1186/s12943-019-1047-6]

6 **Wu Q**, Zhou L, Lv D, Zhu X, Tang H. Exosome-mediated communication in the tumor microenvironment contributes to hepatocellular carcinoma development and progression. *J Hematol Oncol* 2019; **12**: 53 [PMID: 31142326 DOI: 10.1186/s13045-019-0739-0]

7 **Luo C**, Xin H, Zhou Z, Hu Z, Sun R, Yao N, Sun Q, Borjigin U, Wu X, Fan J, Huang X, Zhou S, Zhou J. Tumor-derived exosomes induce immunosuppressive macrophages to foster intrahepatic cholangiocarcinoma progression. *Hepatology* 2022; **76**: 982-999 [PMID: 35106794

DOI: 10.1002/hep.32387]

8 **Martínez-Reyes I**, Chandel NS. Cancer metabolism: looking forward. *Nat Rev Cancer* 2021; **21**: 669-680 [PMID: 34272515 DOI: 10.1038/s41568-021-00378-6]

9 **Théry C**, Witwer KW, Aikawa E, Alcaraz MJ, Anderson JD, Andriantsitohaina R, Antoniou A, Arab T, Archer F, Atkin-Smith GK, Ayre DC, Bach JM, Bachurski D, Baharvand H, Balaj L, Baldacchino S, Bauer NN, Baxter AA, Bebawy M, Beckham C, Bedina Zavec A, Benmoussa A, Berardi AC, Bergese P, Bielska E, Blenkiron C, Bobis-Wozowicz S, Boilard E, Boireau W, Bongiovanni A, Borràs FE, Bosch S, Boulanger CM, Breakefield X, Breglio AM, Brennan MÁ, Brigstock DR, Brisson A, Broekman ML, Bromberg JF, Bryl-Górecka P, Buch S, Buck AH, Burger D, Busatto S, Buschmann D, Bussolati B, Buzás EI, Byrd JB, Camussi G, Carter DR, Caruso S, Chamley LW, Chang YT, Chen C, Chen S, Cheng L, Chin AR, Clayton A, Clerici SP, Cocks A, Cocucci E, Coffey RJ, Cordeiro-da-Silva A, Couch Y, Coumans FA, Coyle B, Crescitelli R, Criado MF, D'Souza-Schorey C, Das S, Datta Chaudhuri A, de Candia P, De Santana EF, De Wever O, Del Portillo HA, Demaret T, Deville S, Devitt A, Dhondt B, Di Vizio D, Dieterich LC, Dolo V, Dominguez Rubio AP, Dominici M, Dourado MR, Driedonks TA, Duarte FV, Duncan HM, Eichenberger RM, Ekström K, El Andaloussi S, Elie-Caille C, Erdbrügger U, Falcón-Pérez JM, Fatima F, Fish JE, Flores-Bellver M, Försönits A, Frelet-Barrand A, Fricke F, Fuhrmann G, Gabrielsson S, Gámez-Valero A, Gardiner C, Gärtner K, Gaudin R, Gho YS, Giebel B, Gilbert C, Gimona M, Giusti I, Goberdhan DC, Görgens A, Gorski SM, Greening DW, Gross JC, Gualerzi A, Gupta GN, Gustafson D, Handberg A, Haraszti RA, Harrison P, Hegyesi H, Hendrix A, Hill AF, Hochberg FH, Hoffmann KF, Holder B, Holthofer H, Hosseinkhani B, Hu G, Huang Y, Huber V, Hunt S, Ibrahim AG, Ikezu T, Inal JM, Isin M, Ivanova A, Jackson HK, Jacobsen S, Jay SM, Jayachandran M, Jenster G, Jiang L, Johnson SM, Jones JC, Jong A, Jovanovic-Talisman T, Jung S, Kalluri R, Kano SI, Kaur S, Kawamura Y, Keller ET, Khamari D, Khomyakova E, Khvorova A, Kierulf P, Kim KP, Kislinger T, Klingeborn M, Klinke DJ 2nd, Kornek M, Kosanović MM, Kovács ÁF, Krämer-Albers EM, Krasemann S, Krause M, Kurochkin IV, Kusuma GD, Kuypers S, Laitinen S, Langevin SM, Languino LR, Lannigan J, Lässer C, Laurent LC, Lavieu G, Lázaro-Ibáñez E, Le Lay S, Lee MS, Lee YXF, Lemos DS, Lenassi M, Leszczynska A, Li IT, Liao K, Libregts SF, Ligeti E, Lim R, Lim SK, Linē A, Linnemannstöns K, Llorente A, Lombard CA, Lorenowicz MJ, Lörincz ÁM, Lötvall J, Lovett J, Lowry MC, Loyer X, Lu Q, Lukomska B, Lunavat TR, Maas SL, Malhi H, Marcilla A, Mariani J, Mariscal J, Martens-Uzunova ES, Martin-Jaular L, Martinez MC, Martins VR, Mathieu M, Mathivanan S, Maugeri M, McGinnis LK, McVey MJ, Meckes DG Jr, Meehan KL, Mertens I, Minciacchi VR, Möller A, Møller Jørgensen M, Morales-Kastresana A, Morhayim J, Mullier F, Muraca M, Musante L, Mussack V, Muth DC, Myburgh KH, Najrana T, Nawaz M, Nazarenko I, Nejsum P, Neri C, Neri T, Nieuwland R, Nimrichter L, Nolan JP, Nolte-'t Hoen EN, Noren Hooten N, O'Driscoll L, O'Grady T, O'Loghlen A, Ochiya T, Olivier M, Ortiz A, Ortiz LA, Osteikoetxea X, Østergaard O, Ostrowski M, Park J, Pegtel DM, Peinado H, Perut F, Pfaffl MW, Phinney DG, Pieters BC, Pink RC, Pisetsky DS, Pogge von Strandmann E, Polakovicova I, Poon IK, Powell BH, Prada I, Pulliam L, Quesenberry P, Radeghieri A, Raffai RL, Raimondo S, Rak J, Ramirez MI, Raposo G, Rayyan MS, Regev-Rudzki N, Ricklefs FL, Robbins PD, Roberts DD, Rodrigues SC, Rohde E, Rome S, Rouschop KM, Rughetti A, Russell AE, Saá P, Sahoo S, Salas-Huenuleo E, Sánchez C, Saugstad JA, Saul MJ, Schiffelers RM, Schneider R, Schøyen TH, Scott A, Shahaj E, Sharma S, Shatnyeva O, Shekari F, Shelke GV, Shetty AK, Shiba K, Siljander PR, Silva AM, Skowronek A, Snyder OL 2nd, Soares RP, Sódar BW, Soekmadji C, Sotillo J, Stahl PD, Stoorvogel W, Stott SL, Strasser EF, Swift S, Tahara H, Tewari M, Timms K, Tiwari S, Tixeira R, Tkach M, Toh WS, Tomasini R, Torrecilhas AC, Tosar JP, Toxavidis V, Urbanelli L, Vader P, van Balkom BW, van der Grein SG, Van Deun J, van Herwijnen MJ, Van Keuren-Jensen K, van Niel G, van Royen ME, van Wijnen AJ, Vasconcelos MH, Vechetti IJ Jr, Veit TD, Vella LJ, Velot É, Verweij FJ, Vestad B, Viñas JL, Visnovitz T, Vukman KV, Wahlgren J, Watson DC, Wauben MH, Weaver A, Webber JP, Weber V, Wehman AM, Weiss DJ, Welsh JA, Wendt S, Wheelock AM, Wiener Z, Witte L, Wolfram J, Xagorari A, Xander P, Xu J, Yan X, Yáñez-Mó M, Yin H, Yuana Y, Zappulli V, Zarubova J, Žėkas V, Zhang JY, Zhao Z, Zheng L, Zheutlin AR, Zickler AM, Zimmermann P, Zivkovic AM, Zocco D, Zuba-Surma EK. Minimal information for studies of extracellular vesicles 2018 (MISEV2018): a position statement of the International Society for Extracellular Vesicles and update of the MISEV2014 guidelines. *J Extracell Vesicles* 2018; **7**: 1535750 [PMID: 30637094 DOI: 10.1080/20013078.2018.1535750]

10 **Isaac R**, Reis FCG, Ying W, Olefsky JM. Exosomes as mediators of intercellular crosstalk in metabolism. *Cell Metab* 2021; **33**: 1744-1762 [PMID: 34496230 DOI: 10.1016/j.cmet.2021.08.006]

11 **Krylova SV**, Feng D. The Machinery of Exosomes: Biogenesis, Release, and Uptake. *Int J Mol Sci* 2023; **24** [PMID: 36674857 DOI: 10.3390/ijms24021337]

12 **Johnstone RM**, Adam M, Hammond JR, Orr L, Turbide C. Vesicle formation during reticulocyte maturation. Association of plasma membrane activities with released vesicles (exosomes). *J Biol Chem* 1987; **262**: 9412-9420 [PMID: 3597417]

13 **Kalluri R**, LeBleu VS. The biology, function, and biomedical applications of exosomes. *Science* 2020; **367** [PMID: 32029601 DOI: 10.1126/science.aau6977]

14 **Raposo G**, Nijman HW, Stoorvogel W, Liejendekker R, Harding CV, Melief CJ, Geuze HJ. B lymphocytes secrete antigen-presenting vesicles. *J Exp Med* 1996; **183**: 1161-1172 [PMID: 8642258 DOI: 10.1084/jem.183.3.1161]

15 **Rak J**. Microparticles in cancer. *Semin Thromb Hemost* 2010; **36**: 888-906 [PMID: 21049390 DOI: 10.1055/s-0030-1267043]

16 **Hood JL**, San RS, Wickline SA. Exosomes released by melanoma cells prepare sentinel lymph nodes for tumor metastasis. *Cancer Res* 2011; **71**: 3792-3801 [PMID: 21478294 DOI: 10.1158/0008-5472.CAN-10-4455]

17 **Zhang L**, Yu D. Exosomes in cancer development, metastasis, and immunity. *Biochim Biophys Acta Rev Cancer* 2019; **1871**: 455-468 [PMID: 31047959 DOI: 10.1016/j.bbcan.2019.04.004]

18 **Rupaimoole R**, Slack FJ. MicroRNA therapeutics: towards a new era for the management of cancer and other diseases. *Nat Rev Drug Discov* 2017; **16**: 203-222 [PMID: 28209991 DOI: 10.1038/nrd.2016.246]

19 **Kim SB**. Function and therapeutic development of exosomes for cancer therapy. *Arch Pharm Res* 2022; **45**: 295-308 [PMID: 35604532 DOI: 10.1007/s12272-022-01387-1]

20 **Krol J**, Loedige I, Filipowicz W. The widespread regulation of microRNA biogenesis, function and decay. *Nat Rev Genet* 2010; **11**: 597-610 [PMID: 20661255 DOI: 10.1038/nrg2843]

21 **Valadi H**, Ekström K, Bossios A, Sjöstrand M, Lee JJ, Lötvall JO. Exosome-mediated transfer of mRNAs and microRNAs is a novel mechanism of genetic exchange between cells. *Nat Cell Biol* 2007; **9**: 654-659 [PMID: 17486113 DOI: 10.1038/ncb1596]

22 **Qiu S**, Xie L, Lu C, Gu C, Xia Y, Lv J, Xuan Z, Fang L, Yang J, Zhang L, Li Z, Wang W, Xu H, Li B, Xu Z. Gastric cancer-derived exosomal miR-519a-3p promotes liver metastasis by inducing intrahepatic M2-like macrophage-mediated angiogenesis. *J Exp Clin Cancer Res* 2022; **41**: 296 [PMID: 36217165 DOI: 10.1186/s13046-022-02499-8]

23 **Nallasamy P**, Nimmakayala RK, Parte S, Are AC, Batra SK, Ponnusamy MP. Tumor microenvironment enriches the stemness features: the architectural event of therapy resistance and metastasis. *Mol Cancer* 2022; **21**: 225 [PMID: 36550571 DOI: 10.1186/s12943-022-01682-x]

24 **Yuan X**, Qian N, Ling S, Li Y, Sun W, Li J, Du R, Zhong G, Liu C, Yu G, Cao D, Liu Z, Wang Y, Qi Z, Yao Y, Wang F, Liu J, Hao S, Jin X,

Zhao Y, Xue J, Zhao D, Gao X, Liang S, Song J, Yu S. Breast cancer exosomes contribute to pre-metastatic niche formation and promote bone metastasis of tumor cells. *Theranostics* 2021; **11**: 1429-1445 [PMID: 33391543 DOI: 10.7150/thno.45351]

25 **Chen B**, Sang Y, Song X, Zhang D, Wang L, Zhao W, Liang Y, Zhang N, Yang Q. Exosomal miR-500a-5p derived from cancer-associated fibroblasts promotes breast cancer cell proliferation and metastasis through targeting USP28. *Theranostics* 2021; **11**: 3932-3947 [PMID: 33664871 DOI: 10.7150/thno.53412]

26 **Han QF**, Li WJ, Hu KS, Gao J, Zhai WL, Yang JH, Zhang SJ. Exosome biogenesis: machinery, regulation, and therapeutic implications in cancer. *Mol Cancer* 2022; **21**: 207 [PMID: 36320056 DOI: 10.1186/s12943-022-01671-0]

27 **Tan S**, Xia L, Yi P, Han Y, Tang L, Pan Q, Tian Y, Rao S, Oyang L, Liang J, Lin J, Su M, Shi Y, Cao D, Zhou Y, Liao Q. Exosomal miRNAs in tumor microenvironment. *J Exp Clin Cancer Res* 2020; **39**: 67 [PMID: 32299469 DOI: 10.1186/s13046-020-01570-6]

28 **Shao H**, Im H, Castro CM, Breakefield X, Weissleder R, Lee H. New Technologies for Analysis of Extracellular Vesicles. *Chem Rev* 2018; **118**: 1917-1950 [PMID: 29384376 DOI: 10.1021/acs.chemrev.7b00534]

29 **Han J**, Zhang Y, Ge P, Dakal TC, Wen H, Tang S, Luo Y, Yang Q, Hua B, Zhang G, Chen H, Xu C. Exosome-derived CIRP: An amplifier of inflammatory diseases. *Front Immunol* 2023; **14**: 1066721 [PMID: 36865547 DOI: 10.3389/fimmu.2023.1066721]

30 **Sun Z**, Shi K, Yang S, Liu J, Zhou Q, Wang G, Song J, Li Z, Zhang Z, Yuan W. Effect of exosomal miRNA on cancer biology and clinical applications. *Mol Cancer* 2018; **17**: 147 [PMID: 30309355 DOI: 10.1186/s12943-018-0897-7]

31 **Fei X**, Li Z, Yang D, Kong X, Lu X, Shen Y, Li X, Xie S, Wang J, Zhao Y, Sun Y, Zhang J, Ye Z, Cai Z. Neddylation of Coro1a determines the fate of multivesicular bodies and biogenesis of extracellular vesicles. *J Extracell Vesicles* 2021; **10**: e12153 [PMID: 34623756 DOI: 10.1002/jev2.12153]

32 **Lee YJ**, Shin KJ, Jang HJ, Ryu JS, Lee CY, Yoon JH, Seo JK, Park S, Lee S, Je AR, Huh YH, Kong SY, Kwon T, Suh PG, Chae YC. GPR143 controls ESCRT-dependent exosome biogenesis and promotes cancer metastasis. *Dev Cell* 2023; **58**: 320-334 [PMID: 36800996 DOI: 10.1016/j.devcel.2023.01.006]

33 **Shinde SR**, Mick DU, Aoki E, Rodrigues RB, Gygi SP, Nachury MV. The ancestral ESCRT protein TOM1L2 selects ubiquitinated cargoes for retrieval from cilia. *Dev Cell* 2023; **58**: 677-693.e9 [PMID: 37019113 DOI: 10.1016/j.devcel.2023.03.003]

34 **Hirsova P**, Ibrahim SH, Verma VK, Morton LA, Shah VH, LaRusso NF, Gores GJ, Malhi H. Extracellular vesicles in liver pathobiology: Small particles with big impact. *Hepatology* 2016; **64**: 2219-2233 [PMID: 27628960 DOI: 10.1002/hep.28814]

35 **Yokoi A**, Yoshioka Y, Yamamoto Y, Ishikawa M, Ikeda SI, Kato T, Kiyono T, Takeshita F, Kajiyama H, Kikkawa F, Ochiya T. Malignant extracellular vesicles carrying MMP1 mRNA facilitate peritoneal dissemination in ovarian cancer. *Nat Commun* 2017; **8**: 14470 [PMID: 28262727 DOI: 10.1038/ncomms14470]

36 **Wang Y**, Balaji V, Kaniyappan S, Krüger L, Irsen S, Tepper K, Chandupatla R, Maetzler W, Schneider A, Mandelkow E, Mandelkow EM. The release and trans-synaptic transmission of Tau *via* exosomes. *Mol Neurodegener* 2017; **12**: 5 [PMID: 28086931 DOI: 10.1186/s13024-016-0143-y]

37 **Chivet M**, Javalet C, Hemming F, Pernet-Gallay K, Laulagnier K, Fraboulet S, Sadoul R. Exosomes as a novel way of interneuronal communication. *Biochem Soc Trans* 2013; **41**: 241-244 [PMID: 23356290 DOI: 10.1042/BST20120266]

38 **Kowal J**, Arras G, Colombo M, Jouve M, Morath JP, Primdal-Bengtson B, Dingli F, Loew D, Tkach M, Théry C. Proteomic comparison defines novel markers to characterize heterogeneous populations of extracellular vesicle subtypes. *Proc Natl Acad Sci U S A* 2016; **113**: E968-E977 [PMID: 26858453 DOI: 10.1073/pnas.1521230113]

39 **Pužar Dominkuš P**, Stenovec M, Sitar S, Lasič E, Zorec R, Plemenitaš A, Žagar E, Kreft M, Lenassi M. PKH26 labeling of extracellular vesicles: Characterization and cellular internalization of contaminating PKH26 nanoparticles. *Biochim Biophys Acta Biomembr* 2018; **1860**: 1350-1361 [PMID: 29551275 DOI: 10.1016/j.bbamem.2018.03.013]

40 **Mathivanan S**, Lim JW, Tauro BJ, Ji H, Moritz RL, Simpson RJ. Proteomics analysis of A33 immunoaffinity-purified exosomes released from the human colon tumor cell line LIM1215 reveals a tissue-specific protein signature. *Mol Cell Proteomics* 2010; **9**: 197-208 [PMID: 19837982 DOI: 10.1074/mcp.M900152-MCP200]

41 **Ruan Z**, Liang Y, Chen Z, Yin J, Li C, Pan P, Zhang Q, Wu J, Luo Z. Enterovirus 71 non-structural protein 3A hijacks vacuolar protein sorting 25 to boost exosome biogenesis to facilitate viral replication. *Front Microbiol* 2022; **13**: 1024899 [PMID: 36274707 DOI: 10.3389/fmicb.2022.1024899]

42 **Lin H**, Zhang R, Wu W, Lei L. miR-4454 Promotes Hepatic Carcinoma Progression by Targeting Vps4A and Rab27A. *Oxid Med Cell Longev* 2021; **2021**: 9230435 [PMID: 34777698 DOI: 10.1155/2021/9230435]

43 **Kogure T**, Lin WL, Yan IK, Braconi C, Patel T. Intercellular nanovesicle-mediated microRNA transfer: a mechanism of environmental modulation of hepatocellular cancer cell growth. *Hepatology* 2011; **54**: 1237-1248 [PMID: 21721029 DOI: 10.1002/hep.24504]

44 **Wang S**, Xu M, Li X, Su X, Xiao X, Keating A, Zhao RC. Exosomes released by hepatocarcinoma cells endow adipocytes with tumor-promoting properties. *J Hematol Oncol* 2018; **11**: 82 [PMID: 29898759 DOI: 10.1186/s13045-018-0625-1]

45 **Zhang H**, Deng T, Liu R, Ning T, Yang H, Liu D, Zhang Q, Lin D, Ge S, Bai M, Wang X, Zhang L, Li H, Yang Y, Ji Z, Wang H, Ying G, Ba Y. CAF secreted miR-522 suppresses ferroptosis and promotes acquired chemo-resistance in gastric cancer. *Mol Cancer* 2020; **19**: 43 [PMID: 32106859 DOI: 10.1186/s12943-020-01168-8]

46 **Bandiera S**, Pfeffer S, Baumert TF, Zeisel MB. miR-122--a key factor and therapeutic target in liver disease. *J Hepatol* 2015; **62**: 448-457 [PMID: 25308172 DOI: 10.1016/j.jhep.2014.10.004]

47 **Xu Y**, Xia F, Ma L, Shan J, Shen J, Yang Z, Liu J, Cui Y, Bian X, Bie P, Qian C. MicroRNA-122 sensitizes HCC cancer cells to adriamycin and vincristine through modulating expression of MDR and inducing cell cycle arrest. *Cancer Lett* 2011; **310**: 160-169 [PMID: 21802841 DOI: 10.1016/j.canlet.2011.06.027]

48 **Girard M**, Jacquemin E, Munnich A, Lyonnet S, Henrion-Caude A. miR-122, a paradigm for the role of microRNAs in the liver. *J Hepatol* 2008; **48**: 648-656 [PMID: 18291553 DOI: 10.1016/j.jhep.2008.01.019]

49 **Basu S**, Bhattacharyya SN. Insulin-like growth factor-1 prevents miR-122 production in neighbouring cells to curtail its intercellular transfer to ensure proliferation of human hepatoma cells. *Nucleic Acids Res* 2014; **42**: 7170-7185 [PMID: 24813441 DOI: 10.1093/nar/gku346]

50 **Chiba M**, Kimura M, Asari S. Exosomes secreted from human colorectal cancer cell lines contain mRNAs, microRNAs and natural antisense RNAs, that can transfer into the human hepatoma HepG2 and lung cancer A549 cell lines. *Oncol Rep* 2012; **28**: 1551-1558 [PMID: 22895844 DOI: 10.3892/or.2012.1967]

51 **Zeng Z**, Li Y, Pan Y, Lan X, Song F, Sun J, Zhou K, Liu X, Ren X, Wang F, Hu J, Zhu X, Yang W, Liao W, Li G, Ding Y, Liang L. Cancer-derived exosomal miR-25-3p promotes pre-metastatic niche formation by inducing vascular permeability and angiogenesis. *Nat Commun* 2018; **9**: 5395 [PMID: 30568162 DOI: 10.1038/s41467-018-07810-w]

52 **Sun H**, Meng Q, Shi C, Yang H, Li X, Wu S, Familiari G, Relucenti M, Aschner M, Wang X, Chen R. Hypoxia-Inducible Exosomes Facilitate Liver-Tropic Premetastatic Niche in Colorectal Cancer. *Hepatology* 2021; **74**: 2633-2651 [PMID: 34110633 DOI: 10.1002/hep.32009]

53 **Xie Z**, Gao Y, Ho C, Li L, Jin C, Wang X, Zou C, Mao Y, Li Q, Fu D, Zhang YF. Exosome-delivered CD44v6/C1QBP complex drives pancreatic cancer liver metastasis by promoting fibrotic liver microenvironment. *Gut* 2022; **71**: 568-579 [PMID: 33827783 DOI: 10.1136/gutjnl-2020-323014]

54 **Xie KL**, Zhang YG, Liu J, Zeng Y, Wu H. MicroRNAs associated with HBV infection and HBV-related HCC. *Theranostics* 2014; **4**: 1176-1192 [PMID: 25285167 DOI: 10.7150/thno.8715]

55 **Wang X**, He Y, Mackowiak B, Gao B. MicroRNAs as regulators, biomarkers and therapeutic targets in liver diseases. *Gut* 2021; **70**: 784-795 [PMID: 33127832 DOI: 10.1136/gutjnl-2020-322526]

56 **Hochreuter MY**, Dall M, Treebak JT, Barrès R. MicroRNAs in non-alcoholic fatty liver disease: Progress and perspectives. *Mol Metab* 2022; **65**: 101581 [PMID: 36028120 DOI: 10.1016/j.molmet.2022.101581]

57 **Sarnow P**, Sagan SM. Unraveling the Mysterious Interactions Between Hepatitis C Virus RNA and Liver-Specific MicroRNA-122. *Annu Rev Virol* 2016; **3**: 309-332 [PMID: 27578438 DOI: 10.1146/annurev-virology-110615-042409]

58 **Wang S**, Qiu L, Yan X, Jin W, Wang Y, Chen L, Wu E, Ye X, Gao GF, Wang F, Chen Y, Duan Z, Meng S. Loss of microRNA 122 expression in patients with hepatitis B enhances hepatitis B virus replication through cyclin G(1) -modulated P53 activity. *Hepatology* 2012; **55**: 730-741 [PMID: 22105316 DOI: 10.1002/hep.24809]

59 **Pirola CJ**, Fernández Gianotti T, Castaño GO, Mallardi P, San Martino J, Mora Gonzalez Lopez Ledesma M, Flichman D, Mirshahi F, Sanyal AJ, Sookoian S. Circulating microRNA signature in non-alcoholic fatty liver disease: from serum non-coding RNAs to liver histology and disease pathogenesis. *Gut* 2015; **64**: 800-812 [PMID: 24973316 DOI: 10.1136/gutjnl-2014-306996]

60 **Gu Y**, Wei X, Sun Y, Gao H, Zheng X, Wong LL, Jin L, Liu N, Hernandez B, Peplowska K, Zhao X, Zhan QM, Feng XH, Tang ZY, Ji J. miR-192-5p Silencing by Genetic Aberrations Is a Key Event in Hepatocellular Carcinomas with Cancer Stem Cell Features. *Cancer Res* 2019; **79**: 941-953 [PMID: 30530815 DOI: 10.1158/0008-5472.CAN-18-1675]

61 **Wang B**, Majumder S, Nuovo G, Kutay H, Volinia S, Patel T, Schmittgen TD, Croce C, Ghoshal K, Jacob ST. Role of microRNA-155 at early stages of hepatocarcinogenesis induced by choline-deficient and amino acid-defined diet in C57BL/6 mice. *Hepatology* 2009; **50**: 1152-1161 [PMID: 19711427 DOI: 10.1002/hep.23100]

62 **Zhang Y**, Wei W, Cheng N, Wang K, Li B, Jiang X, Sun S. Hepatitis C virus-induced up-regulation of microRNA-155 promotes hepatocarcinogenesis by activating Wnt signaling. *Hepatology* 2012; **56**: 1631-1640 [PMID: 22610915 DOI: 10.1002/hep.25849]

63 **Calvente CJ**, Tameda M, Johnson CD, Del Pilar H, Lin YC, Adronikou N, De Mollerat Du Jeu X, Llorente C, Boyer J, Feldstein AE. Neutrophils contribute to spontaneous resolution of liver inflammation and fibrosis *via* microRNA-223. *J Clin Invest* 2019; **129**: 4091-4109 [PMID: 31295147 DOI: 10.1172/JCI122258]

64 **Li M**, He Y, Zhou Z, Ramirez T, Gao Y, Ross RA, Cao H, Cai Y, Xu M, Feng D, Zhang P, Liangpunsakul S, Gao B. MicroRNA-223 ameliorates alcoholic liver injury by inhibiting the IL-6-p47(phox)-oxidative stress pathway in neutrophils. *Gut* 2017; **66**: 705-715 [PMID: 27679493 DOI: 10.1136/gutjnl-2016-311861]

65 **He Y**, Hwang S, Cai Y, Kim SJ, Xu M, Yang D, Guillot A, Feng D, Seo W, Hou X, Gao B. MicroRNA-223 Ameliorates Nonalcoholic Steatohepatitis and Cancer by Targeting Multiple Inflammatory and Oncogenic Genes in Hepatocytes. *Hepatology* 2019; **70**: 1150-1167 [PMID: 30964207 DOI: 10.1002/hep.30645]

66 **Wong QW**, Lung RW, Law PT, Lai PB, Chan KY, To KF, Wong N. MicroRNA-223 is commonly repressed in hepatocellular carcinoma and potentiates expression of Stathmin1. *Gastroenterology* 2008; **135**: 257-269 [PMID: 18555017 DOI: 10.1053/j.gastro.2008.04.003]

67 **Jimenez Calvente C**, Del Pilar H, Tameda M, Johnson CD, Feldstein AE. MicroRNA 223 3p Negatively Regulates the NLRP3 Inflammasome in Acute and Chronic Liver Injury. *Mol Ther* 2020; **28**: 653-663 [PMID: 31585800 DOI: 10.1016/j.ymthe.2019.09.013]

68 **Ogunwobi OO**, Harricharran T, Huaman J, Galuza A, Odumuwagun O, Tan Y, Ma GX, Nguyen MT. Mechanisms of hepatocellular carcinoma progression. *World J Gastroenterol* 2019; **25**: 2279-2293 [PMID: 31148900 DOI: 10.3748/wjg.v25.i19.2279]

69 **Jenne CN**, Kubes P. Immune surveillance by the liver. *Nat Immunol* 2013; **14**: 996-1006 [PMID: 24048121 DOI: 10.1038/ni.2691]

70 **Tsuchida T**, Friedman SL. Mechanisms of hepatic stellate cell activation. *Nat Rev Gastroenterol Hepatol* 2017; **14**: 397-411 [PMID: 28487545 DOI: 10.1038/nrgastro.2017.38]

71 **Lua I**, Li Y, Zagory JA, Wang KS, French SW, Sévigny J, Asahina K. Characterization of hepatic stellate cells, portal fibroblasts, and mesothelial cells in normal and fibrotic livers. *J Hepatol* 2016; **64**: 1137-1146 [PMID: 26806818 DOI: 10.1016/j.jhep.2016.01.010]

72 **Iwaisako K**, Jiang C, Zhang M, Cong M, Moore-Morris TJ, Park TJ, Liu X, Xu J, Wang P, Paik YH, Meng F, Asagiri M, Murray LA, Hofmann AF, Iida T, Glass CK, Brenner DA, Kisseleva T. Origin of myofibroblasts in the fibrotic liver in mice. *Proc Natl Acad Sci U S A* 2014; **111**: E3297-E3305 [PMID: 25074909 DOI: 10.1073/pnas.1400062111]

73 **Mederacke I**, Hsu CC, Troeger JS, Huebener P, Mu X, Dapito DH, Pradere JP, Schwabe RF. Fate tracing reveals hepatic stellate cells as dominant contributors to liver fibrosis independent of its aetiology. *Nat Commun* 2013; **4**: 2823 [PMID: 24264436 DOI: 10.1038/ncomms3823]

74 **Kramann R**, Schneider RK, DiRocco DP, Machado F, Fleig S, Bondzie PA, Henderson JM, Ebert BL, Humphreys BD. Perivascular Gli1+ progenitors are key contributors to injury-induced organ fibrosis. *Cell Stem Cell* 2015; **16**: 51-66 [PMID: 25465115 DOI: 10.1016/j.stem.2014.11.004]

75 **Li Y**, Wang J, Asahina K. Mesothelial cells give rise to hepatic stellate cells and myofibroblasts *via* mesothelial-mesenchymal transition in liver injury. *Proc Natl Acad Sci U S A* 2013; **110**: 2324-2329 [PMID: 23345421 DOI: 10.1073/pnas.1214136110]

76 **Kisseleva T**, Uchinami H, Feirt N, Quintana-Bustamante O, Segovia JC, Schwabe RF, Brenner DA. Bone marrow-derived fibrocytes participate in pathogenesis of liver fibrosis. *J Hepatol* 2006; **45**: 429-438 [PMID: 16846660 DOI: 10.1016/j.jhep.2006.04.014]

77 **Amann T**, Bataille F, Spruss T, Mühlbauer M, Gäbele E, Schölmerich J, Kiefer P, Bosserhoff AK, Hellerbrand C. Activated hepatic stellate cells promote tumorigenicity of hepatocellular carcinoma. *Cancer Sci* 2009; **100**: 646-653 [PMID: 19175606 DOI: 10.1111/j.1349-7006.2009.01087.x]

78 **Zhang X**, Chen F, Huang P, Wang X, Zhou K, Zhou C, Yu L, Peng Y, Fan J, Zhou J, Lu Z, Hu J, Wang Z. Exosome-depleted MiR-148a-3p derived from Hepatic Stellate Cells Promotes Tumor Progression *via* ITGA5/PI3K/Akt Axis in Hepatocellular Carcinoma. *Int J Biol Sci* 2022; **18**: 2249-2260 [PMID: 35414782 DOI: 10.7150/ijbs.66184]

79 **Wang F**, Li L, Piontek K, Sakaguchi M, Selaru FM. Exosome miR-335 as a novel therapeutic strategy in hepatocellular carcinoma. *Hepatology* 2018; **67**: 940-954 [PMID: 29023935 DOI: 10.1002/hep.29586]

80 **Zhou Y**, Ren H, Dai B, Li J, Shang L, Huang J, Shi X. Hepatocellular carcinoma-derived exosomal miRNA-21 contributes to tumor progression by converting hepatocyte stellate cells to cancer-associated fibroblasts. *J Exp Clin Cancer Res* 2018; **37**: 324 [PMID: 30591064 DOI: 10.1186/s13046-018-0965-2]

81 **Song M**, He J, Pan QZ, Yang J, Zhao J, Zhang YJ, Huang Y, Tang Y, Wang Q, Gu J, Li Y, Chen S, Zeng J, Zhou ZQ, Yang C, Han Y, Chen H, Xiang T, Weng DS, Xia JC. Cancer-Associated Fibroblast-Mediated Cellular Crosstalk Supports Hepatocellular Carcinoma Progression. *Hepatology* 2021; **73**: 1717-1735 [PMID: 33682185 DOI: 10.1002/hep.31792]

82 **Song T**, Dou C, Jia Y, Tu K, Zheng X. TIMP-1 activated carcinoma-associated fibroblasts inhibit tumor apoptosis by activating SDF1/CXCR4 signaling in hepatocellular carcinoma. *Oncotarget* 2015; **6**: 12061-12079 [PMID: 25909286 DOI: 10.18632/oncotarget.3616]

83 **Fang T**, Lv H, Lv G, Li T, Wang C, Han Q, Yu L, Su B, Guo L, Huang S, Cao D, Tang L, Tang S, Wu M, Yang W, Wang H. Tumor-derived exosomal miR-1247-3p induces cancer-associated fibroblast activation to foster lung metastasis of liver cancer. *Nat Commun* 2018; **9**: 191 [PMID: 29335551 DOI: 10.1038/s41467-017-02583-0]

84 **Zheng X**, Xu M, Yao B, Wang C, Jia Y, Liu Q. IL-6/STAT3 axis initiated CAFs *via* up-regulating TIMP-1 which was attenuated by acetylation of STAT3 induced by PCAF in HCC microenvironment. *Cell Signal* 2016; **28**: 1314-1324 [PMID: 27297362 DOI: 10.1016/j.cellsig.2016.06.009]

85 **Zhu GQ**, Tang Z, Huang R, Qu WF, Fang Y, Yang R, Tao CY, Gao J, Wu XL, Sun HX, Zhou YF, Song SS, Ding ZB, Dai Z, Zhou J, Ye D, Wu DJ, Liu WR, Fan J, Shi YH. CD36(+) cancer-associated fibroblasts provide immunosuppressive microenvironment for hepatocellular carcinoma *via* secretion of macrophage migration inhibitory factor. *Cell Discov* 2023; **9**: 25 [PMID: 36878933 DOI: 10.1038/s41421-023-00529-z]

86 **Wang SS**, Tang XT, Lin M, Yuan J, Peng YJ, Yin X, Shang G, Ge G, Ren Z, Zhou BO. Perivenous Stellate Cells Are the Main Source of Myofibroblasts and Cancer-Associated Fibroblasts Formed After Chronic Liver Injuries. *Hepatology* 2021; **74**: 1578-1594 [PMID: 33817801 DOI: 10.1002/hep.31848]

87 **Zhang Z**, Li X, Sun W, Yue S, Yang J, Li J, Ma B, Wang J, Yang X, Pu M, Ruan B, Zhao G, Huang Q, Wang L, Tao K, Dou K. Loss of exosomal miR-320a from cancer-associated fibroblasts contributes to HCC proliferation and metastasis. *Cancer Lett* 2017; **397**: 33-42 [PMID: 28288874 DOI: 10.1016/j.canlet.2017.03.004]

88 **Yugawa K**, Yoshizumi T, Mano Y, Itoh S, Harada N, Ikegami T, Kohashi K, Oda Y, Mori M. Cancer-associated fibroblasts promote hepatocellular carcinoma progression through downregulation of exosomal miR-150-3p. *Eur J Surg Oncol* 2021; **47**: 384-393 [PMID: 32883551 DOI: 10.1016/j.ejso.2020.08.002]

89 **Qi Y**, Wang H, Zhang Q, Liu Z, Wang T, Wu Z, Wu W. CAF-Released Exosomal miR-20a-5p Facilitates HCC Progression *via* the LIMA1-Mediated β-Catenin Pathway. *Cells* 2022; **11** [PMID: 36497115 DOI: 10.3390/cells11233857]

90 **Zhou Y**, Tang W, Zhuo H, Zhu D, Rong D, Sun J, Song J. Cancer-associated fibroblast exosomes promote chemoresistance to cisplatin in hepatocellular carcinoma through circZFR targeting signal transducers and activators of transcription (STAT3)/ nuclear factor -kappa B (NF-κB) pathway. *Bioengineered* 2022; **13**: 4786-4797 [PMID: 35139763 DOI: 10.1080/21655979.2022.2032972]

91 **Lu L**, Huang J, Mo J, Da X, Li Q, Fan M, Lu H. Exosomal lncRNA TUG1 from cancer-associated fibroblasts promotes liver cancer cell migration, invasion, and glycolysis by regulating the miR-524-5p/SIX1 axis. *Cell Mol Biol Lett* 2022; **27**: 17 [PMID: 35193488 DOI: 10.1186/s11658-022-00309-9]

92 **Chang KS**, Ng PN, Lee MM, Chan SJ. Sexual maturation of chinese boys in Hong Kong. *Pediatrics* 1966; **37**: 804-811 [PMID: 5932630]

93 **Fujiwara N**, Nakagawa H, Kudo Y, Tateishi R, Taguri M, Watadani T, Nakagomi R, Kondo M, Nakatsuka T, Minami T, Sato M, Uchino K, Enooku K, Kondo Y, Asaoka Y, Tanaka Y, Ohtomo K, Shiina S, Koike K. Sarcopenia, intramuscular fat deposition, and visceral adiposity independently predict the outcomes of hepatocellular carcinoma. *J Hepatol* 2015; **63**: 131-140 [PMID: 25724366 DOI: 10.1016/j.jhep.2015.02.031]

94 **Koeck ES**, Iordanskaia T, Sevilla S, Ferrante SC, Hubal MJ, Freishtat RJ, Nadler EP. Adipocyte exosomes induce transforming growth factor beta pathway dysregulation in hepatocytes: a novel paradigm for obesity-related liver disease. *J Surg Res* 2014; **192**: 268-275 [PMID: 25086727 DOI: 10.1016/j.jss.2014.06.050]

95 **Liu Y**, Tan J, Ou S, Chen J, Chen L. Adipose-derived exosomes deliver miR-23a/b to regulate tumor growth in hepatocellular cancer by targeting the VHL/HIF axis. *J Physiol Biochem* 2019; **75**: 391-401 [PMID: 31321740 DOI: 10.1007/s13105-019-00692-6]

96 **Zhang H**, Deng T, Ge S, Liu Y, Bai M, Zhu K, Fan Q, Li J, Ning T, Tian F, Li H, Sun W, Ying G, Ba Y. Exosome circRNA secreted from adipocytes promotes the growth of hepatocellular carcinoma by targeting deubiquitination-related USP7. *Oncogene* 2019; **38**: 2844-2859 [PMID: 30546088 DOI: 10.1038/s41388-018-0619-z]

97 **Viallard C**, Larrivée B. Tumor angiogenesis and vascular normalization: alternative therapeutic targets. *Angiogenesis* 2017; **20**: 409-426 [PMID: 28660302 DOI: 10.1007/s10456-017-9562-9]

98 **Yukawa H**, Suzuki K, Aoki K, Arimoto T, Yasui T, Kaji N, Ishikawa T, Ochiya T, Baba Y. Imaging of angiogenesis of human umbilical vein endothelial cells by uptake of exosomes secreted from hepatocellular carcinoma cells. *Sci Rep* 2018; **8**: 6765 [PMID: 29713019 DOI: 10.1038/s41598-018-24563-0]

99 **Shih TC**, Tien YJ, Wen CJ, Yeh TS, Yu MC, Huang CH, Lee YS, Yen TC, Hsieh SY. MicroRNA-214 downregulation contributes to tumor angiogenesis by inducing secretion of the hepatoma-derived growth factor in human hepatoma. *J Hepatol* 2012; **57**: 584-591 [PMID: 22613005 DOI: 10.1016/j.jhep.2012.04.031]

100 **Fang JH**, Zhang ZJ, Shang LR, Luo YW, Lin YF, Yuan Y, Zhuang SM. Hepatoma cell-secreted exosomal microRNA-103 increases vascular permeability and promotes metastasis by targeting junction proteins. *Hepatology* 2018; **68**: 1459-1475 [PMID: 29637568 DOI: 10.1002/hep.29920]

101 **Lin XJ**, Fang JH, Yang XJ, Zhang C, Yuan Y, Zheng L, Zhuang SM. Hepatocellular Carcinoma Cell-Secreted Exosomal MicroRNA-210 Promotes Angiogenesis In Vitro and In Vivo. *Mol Ther Nucleic Acids* 2018; **11**: 243-252 [PMID: 29858059 DOI: 10.1016/j.omtn.2018.02.014]

102 **Yokota Y**, Noda T, Okumura Y, Kobayashi S, Iwagami Y, Yamada D, Tomimaru Y, Akita H, Gotoh K, Takeda Y, Tanemura M, Murakami T, Umeshita K, Doki Y, Eguchi H. Serum exosomal miR-638 is a prognostic marker of HCC *via* downregulation of VE-cadherin and ZO-1 of endothelial cells. *Cancer Sci* 2021; **112**: 1275-1288 [PMID: 33426736 DOI: 10.1111/cas.14807]

103 **Semaan L**, Zeng Q, Lu Y, Zhang Y, Zreik MM, Chamseddine MB, Chopp M, Zhang ZG, Moonka D. MicroRNA-214 enriched exosomes from human cerebral endothelial cells (hCEC) sensitize hepatocellular carcinoma to anti-cancer drugs. *Oncotarget* 2021; **12**: 185-198 [PMID: 33613846 DOI: 10.18632/oncotarget.27879]

104 **Binnewies M**, Roberts EW, Kersten K, Chan V, Fearon DF, Merad M, Coussens LM, Gabrilovich DI, Ostrand-Rosenberg S, Hedrick CC, Vonderheide RH, Pittet MJ, Jain RK, Zou W, Howcroft TK, Woodhouse EC, Weinberg RA, Krummel MF. Understanding the tumor immune

microenvironment (TIME) for effective therapy. *Nat Med* 2018; **24**: 541-550 [PMID: 29686425 DOI: 10.1038/s41591-018-0014-x]

105 **Ma L**, Hernandez MO, Zhao Y, Mehta M, Tran B, Kelly M, Rae Z, Hernandez JM, Davis JL, Martin SP, Kleiner DE, Hewitt SM, Ylaya K, Wood BJ, Greten TF, Wang XW. Tumor Cell Biodiversity Drives Microenvironmental Reprogramming in Liver Cancer. *Cancer Cell* 2019; **36**: 418-430.e6 [PMID: 31588021 DOI: 10.1016/j.ccell.2019.08.007]

106 **Zhang Q**, He Y, Luo N, Patel SJ, Han Y, Gao R, Modak M, Carotta S, Haslinger C, Kind D, Peet GW, Zhong G, Lu S, Zhu W, Mao Y, Xiao M, Bergmann M, Hu X, Kerkar SP, Vogt AB, Pflanz S, Liu K, Peng J, Ren X, Zhang Z. Landscape and Dynamics of Single Immune Cells in Hepatocellular Carcinoma. *Cell* 2019; **179**: 829-845.e20 [PMID: 31675496 DOI: 10.1016/j.cell.2019.10.003]

107 **Lu Y**, Yang A, Quan C, Pan Y, Zhang H, Li Y, Gao C, Lu H, Wang X, Cao P, Chen H, Lu S, Zhou G. A single-cell atlas of the multicellular ecosystem of primary and metastatic hepatocellular carcinoma. *Nat Commun* 2022; **13**: 4594 [PMID: 35933472 DOI: 10.1038/s41467-022-32283-3]

108 **Ju C**, Tacke F. Hepatic macrophages in homeostasis and liver diseases: from pathogenesis to novel therapeutic strategies. *Cell Mol Immunol* 2016; **13**: 316-327 [PMID: 26908374 DOI: 10.1038/cmi.2015.104]

109 **Wu J**, Li J, Salcedo R, Mivechi NF, Trinchieri G, Horuzsko A. The proinflammatory myeloid cell receptor TREM-1 controls Kupffer cell activation and development of hepatocellular carcinoma. *Cancer Res* 2012; **72**: 3977-3986 [PMID: 22719066 DOI: 10.1158/0008-5472.CAN-12-0938]

110 **Chanmee T**, Ontong P, Konno K, Itano N. Tumor-associated macrophages as major players in the tumor microenvironment. *Cancers (Basel)* 2014; **6**: 1670-1690 [PMID: 25125485 DOI: 10.3390/cancers6031670]

111 **Mantovani A**, Marchesi F, Malesci A, Laghi L, Allavena P. Tumour-associated macrophages as treatment targets in oncology. *Nat Rev Clin Oncol* 2017; **14**: 399-416 [PMID: 28117416 DOI: 10.1038/nrclinonc.2016.217]

112 **Liu G**, Ouyang X, Sun Y, Xiao Y, You B, Gao Y, Yeh S, Li Y, Chang C. The miR-92a-2-5p in exosomes from macrophages increases liver cancer cells invasion *via* altering the AR/PHLPP/p-AKT/β-catenin signaling. *Cell Death Differ* 2020; **27**: 3258-3272 [PMID: 32587378 DOI: 10.1038/s41418-020-0575-3]

113 **Li W**, Xin X, Li X, Geng J, Sun Y. Exosomes secreted by M2 macrophages promote cancer stemness of hepatocellular carcinoma via the miR-27a-3p/TXNIP pathways. *Int Immunopharmacol* 2021; **101**: 107585 [PMID: 34601333 DOI: 10.1016/j.intimp.2021.107585]

114 **Tian B**, Zhou L, Wang J, Yang P. miR-660-5p-loaded M2 macrophages-derived exosomes augment hepatocellular carcinoma development through regulating KLF3. *Int Immunopharmacol* 2021; **101**: 108157 [PMID: 34673296 DOI: 10.1016/j.intimp.2021.108157]

115 **Wang Y**, Wang B, Xiao S, Li Y, Chen Q. miR-125a/b inhibits tumor-associated macrophages mediated in cancer stem cells of hepatocellular carcinoma by targeting CD90. *J Cell Biochem* 2019; **120**: 3046-3055 [PMID: 30536969 DOI: 10.1002/jcb.27436]

116 **Chen H**, Tang C, Tan C, Wu F, Li Z, Ji W, Lu L, Xu C, Shen Z, Huang Y. IL-2 Modulates TAMs Derived Exosomal MiRNAs to Ameliorate Hepatocellular Carcinoma Development and Progression. *J Oncol* 2022; **2022**: 3445350 [PMID: 36284632 DOI: 10.1155/2022/3445350]

117 **Zhang J**, Shan WF, Jin TT, Wu GQ, Xiong XX, Jin HY, Zhu SM. Propofol exerts anti-hepatocellular carcinoma by microvesicle-mediated transfer of miR-142-3p from macrophage to cancer cells. *J Transl Med* 2014; **12**: 279 [PMID: 25292173 DOI: 10.1186/s12967-014-0279-x]

118 **Wang L**, Yi X, Xiao X, Zheng Q, Ma L, Li B. Exosomal miR-628-5p from M1 polarized macrophages hinders m6A modification of circFUT8 to suppress hepatocellular carcinoma progression. *Cell Mol Biol Lett* 2022; **27**: 106 [PMID: 36474147 DOI: 10.1186/s11658-022-00406-9]

119 **Aucher A**, Rudnicka D, Davis DM. MicroRNAs transfer from human macrophages to hepato-carcinoma cells and inhibit proliferation. *J Immunol* 2013; **191**: 6250-6260 [PMID: 24227773 DOI: 10.4049/jimmunol.1301728]

120 **Wang L**, Wang Y, Quan J. Exosomal miR-223 derived from natural killer cells inhibits hepatic stellate cell activation by suppressing autophagy. *Mol Med* 2020; **26**: 81 [PMID: 32873229 DOI: 10.1186/s10020-020-00207-w]

121 **Xiong L**, Zhen S, Yu Q, Gong Z. HCV-E2 inhibits hepatocellular carcinoma metastasis by stimulating mast cells to secrete exosomal shuttle microRNAs. *Oncol Lett* 2017; **14**: 2141-2146 [PMID: 28781655 DOI: 10.3892/ol.2017.6433]

122 **Tung SL**; Boardman DA, Sen M, Letizia M, Peng Q, Cianci N, Dioni L, Carlin LM, Lechler R, Bollati V, Lombardi G, Smyth LA. Regulatory T cell-derived extracellular vesicles modify dendritic cell function. *Sci Rep* 2018; **8**: 6065 [PMID: 29666503 DOI: 10.1038/s41598-018-24531-8]

123 **Granito A**, Muratori L, Lalanne C, Quarneti C, Ferri S, Guidi M, Lenzi M, Muratori P. Hepatocellular carcinoma in viral and autoimmune liver diseases: Role of CD4+ CD25+ Foxp3+ regulatory T cells in the immune microenvironment. *World J Gastroenterol* 2021; **27**: 2994-3009 [PMID: 34168403 DOI: 10.3748/wjg.v27.i22.2994]

124 **Yin Y**, Cai X, Chen X, Liang H, Zhang Y, Li J, Wang Z, Zhang W, Yokoyama S, Wang C, Li L, Hou D, Dong L, Xu T, Hiroi T, Yang F, Ji H, Zhang J, Zen K, Zhang CY. Tumor-secreted miR-214 induces regulatory T cells: a major link between immune evasion and tumor growth. *Cell Res* 2014; **24**: 1164-1180 [PMID: 25223704 DOI: 10.1038/cr.2014.121]

125 **Kudo M**, Ueshima K, Ikeda M, Torimura T, Tanabe N, Aikata H, Izumi N, Yamasaki T, Nojiri S, Hino K, Tsumura H, Kuzuya T, Isoda N, Yasui K, Aino H, Ido A, Kawabe N, Nakao K, Wada Y, Yokosuka O, Yoshimura K, Okusaka T, Furuse J, Kokudo N, Okita K, Johnson PJ, Arai Y; TACTICS study group. Randomised, multicentre prospective trial of transarterial chemoembolisation (TACE) plus sorafenib as compared with TACE alone in patients with hepatocellular carcinoma: TACTICS trial. *Gut* 2020; **69**: 1492-1501 [PMID: 31801872 DOI: 10.1136/gutjnl-2019-318934]

126 **Chan SL**, Yeo W, Mo F, Chan AWH, Koh J, Li L, Hui EP, Chong CCN, Lai PBS, Mok TSK, Yu SCH. A phase 2 study of the efficacy and biomarker on the combination of transarterial chemoembolization and axitinib in the treatment of inoperable hepatocellular carcinoma. *Cancer* 2017; **123**: 3977-3985 [PMID: 28640364 DOI: 10.1002/cncr.30825]

127 **Inoue J**, Inazawa J. Cancer-associated miRNAs and their therapeutic potential. *J Hum Genet* 2021; **66**: 937-945 [PMID: 34088973 DOI: 10.1038/s10038-021-00938-6]

128 **Liao W**, Du Y, Zhang C, Pan F, Yao Y, Zhang T, Peng Q. Exosomes: The next generation of endogenous nanomaterials for advanced drug delivery and therapy. *Acta Biomater* 2019; **86**: 1-14 [PMID: 30597259 DOI: 10.1016/j.actbio.2018.12.045]

129 **Shi Y**, Du L, Lin L, Wang Y. Tumour-associated mesenchymal stem/stromal cells: emerging therapeutic targets. *Nat Rev Drug Discov* 2017; **16**: 35-52 [PMID: 27811929 DOI: 10.1038/nrd.2016.193]

130 **Zhang Z**, Mi T, Jin L, Li M, Zhanghuang C, Wang J, Tan X, Lu H, Shen L, Long C, Wei G, He D. Comprehensive proteomic analysis of exosome mimetic vesicles and exosomes derived from human umbilical cord mesenchymal stem cells. *Stem Cell Res Ther* 2022; **13**: 312 [PMID: 35841000 DOI: 10.1186/s13287-022-03008-6]

131 **Jayaraj R**, Raymond G, Krishnan S, Tzou KS, Baxi S, Ram MR, Govind SK, Chandramoorthy HC, Abu-Khzam FN, Shaw P. Clinical Theragnostic Potential of Diverse miRNA Expressions in Prostate Cancer: A Systematic Review and Meta-Analysis. *Cancers (Basel)* 2020; **12** [PMID: 32397507 DOI: 10.3390/cancers12051199]

132 **Zuo Y**, Zheng W, Liu J, Tang Q, Wang SS, Yang XS. MiR-34a-5p/PD-L1 axis regulates cisplatin chemoresistance of ovarian cancer cells. *Neoplasma* 2020; **67**: 93-101 [PMID: 31777260 DOI: 10.4149/neo_2019_190202N106]

133 **Lou G**, Song X, Yang F, Wu S, Wang J, Chen Z, Liu Y. Exosomes derived from miR-122-modified adipose tissue-derived MSCs increase chemosensitivity of hepatocellular carcinoma. *J Hematol Oncol* 2015; **8**: 122 [PMID: 26514126 DOI: 10.1186/s13045-015-0220-7]

134 **Lou G**, Chen L, Xia C, Wang W, Qi J, Li A, Zhao L, Chen Z, Zheng M, Liu Y. MiR-199a-modified exosomes from adipose tissue-derived mesenchymal stem cells improve hepatocellular carcinoma chemosensitivity through mTOR pathway. *J Exp Clin Cancer Res* 2020; **39**: 4 [PMID: 31898515 DOI: 10.1186/s13046-019-1512-5]

135 **Tian S**, Zhou X, Zhang M, Cui L, Li B, Liu Y, Su R, Sun K, Hu Y, Yang F, Xuan G, Ma S, Zheng X, Guo C, Shang Y, Wang J, Han Y. Mesenchymal stem cell-derived exosomes protect against liver fibrosis *via* delivering miR-148a to target KLF6/STAT3 pathway in macrophages. *Stem Cell Res Ther* 2022; **13**: 330 [PMID: 35858897 DOI: 10.1186/s13287-022-03010-y]

136 **Lee MJ**, Jung J, Na KH, Moon JS, Lee HJ, Kim JH, Kim GI, Kwon SW, Hwang SG, Kim GJ. Anti-fibrotic effect of chorionic plate-derived mesenchymal stem cells isolated from human placenta in a rat model of CCl(4)-injured liver: potential application to the treatment of hepatic diseases. *J Cell Biochem* 2010; **111**: 1453-1463 [PMID: 20830742 DOI: 10.1002/jcb.22873]

137 **Cargnoni A**, Gibelli L, Tosini A, Signoroni PB, Nassuato C, Arienti D, Lombardi G, Albertini A, Wengler GS, Parolini O. Transplantation of allogeneic and xenogeneic placenta-derived cells reduces bleomycin-induced lung fibrosis. *Cell Transplant* 2009; **18**: 405-422 [PMID: 19622228 DOI: 10.3727/096368909788809857]

138 **Hyun J**, Wang S, Kim J, Kim GJ, Jung Y. MicroRNA125b-mediated Hedgehog signaling influences liver regeneration by chorionic plate-derived mesenchymal stem cells. *Sci Rep* 2015; **5**: 14135 [PMID: 26370741 DOI: 10.1038/srep14135]

139 **Fonsato V**, Collino F, Herrera MB, Cavallari C, Deregibus MC, Cisterna B, Bruno S, Romagnoli R, Salizzoni M, Tetta C, Camussi G. Human liver stem cell-derived microvesicles inhibit hepatoma growth in SCID mice by delivering antitumor microRNAs. *Stem Cells* 2012; **30**: 1985-1998 [PMID: 22736596 DOI: 10.1002/stem.1161]

140 **Nordin JZ**, Lee Y, Vader P, Mäger I, Johansson HJ, Heusermann W, Wiklander OP, Hällbrink M, Seow Y, Bultema JJ, Gilthorpe J, Davies T, Fairchild PJ, Gabrielsson S, Meisner-Kober NC, Lehtiö J, Smith CI, Wood MJ, El Andaloussi S. Ultrafiltration with size-exclusion liquid chromatography for high yield isolation of extracellular vesicles preserving intact biophysical and functional properties. *Nanomedicine* 2015; **11**: 879-883 [PMID: 25659648 DOI: 10.1016/j.nano.2015.01.003]

141 **Van Deun J**, Mestdagh P, Sormunen R, Cocquyt V, Vermaelen K, Vandesompele J, Bracke M, De Wever O, Hendrix A. The impact of disparate isolation methods for extracellular vesicles on downstream RNA profiling. *J Extracell Vesicles* 2014; **3** [PMID: 25317274 DOI: 10.3402/jev.v3.24858]

142 **Nawaz M**, Camussi G, Valadi H, Nazarenko I, Ekström K, Wang X, Principe S, Shah N, Ashraf NM, Fatima F, Neder L, Kislinger T. The emerging role of extracellular vesicles as biomarkers for urogenital cancers. *Nat Rev Urol* 2014; **11**: 688-701 [PMID: 25403245 DOI: 10.1038/nrurol.2014.301]

World Journal of Gastroenterology

Submit a Manuscript: https://www.f6publishing.com

World J Gastroenterol 2023 October 21; 29(39): 5452-5470

DOI: 10.3748/wjg.v29.i39.5452

ISSN 1007-9327 (print) ISSN 2219-2840 (online)

ORIGINAL ARTICLE

Basic Study

Prostaglandin $F_{2\alpha}$ synthase promotes oxaliplatin resistance in colorectal cancer through prostaglandin $F_{2\alpha}$-dependent and $F_{2\alpha}$-independent mechanism

Yi-Jun Wang, Xiao-Li Xie, Hong-Qun Liu, Hui Tian, Xiao-Yu Jiang, Jiu-Na Zhang, Sheng-Xiong Chen, Ting Liu, Shu-Ling Wang, Xue Zhou, Xiao-Xu Jin, Shi-Mao Liu, Hui-Qing Jiang

Specialty type: Gastroenterology and hepatology

Provenance and peer review: Unsolicited article; Externally peer reviewed.

Peer-review model: Single blind

Peer-review report's scientific quality classification

Grade A (Excellent): 0
Grade B (Very good): B, B
Grade C (Good): 0
Grade D (Fair): 0
Grade E (Poor): E

P-Reviewer: Liao Z, Singapore; Liu H, United States; Sahin TT, Turkey

Received: July 3, 2023
Peer-review started: July 3, 2023
First decision: August 25, 2023
Revised: September 14, 2023
Accepted: September 26, 2023
Article in press: September 26, 2023
Published online: October 21, 2023

Yi-Jun Wang, Xiao-Li Xie, Hui Tian, Xiao-Yu Jiang, Xue Zhou, Xiao-Xu Jin, Hui-Qing Jiang, Department of Gastroenterology, The Second Hospital of Hebei Medical University, Shijiazhuang 050000, Hebei Province, China

Hong-Qun Liu, Liver Unit, University of Calgary, Calgary T1W0K6, Canada

Jiu-Na Zhang, Department of Gastroenterology, The Affiliated Hospital of Hebei Engineering University, Handan 056000, Hebei Province, China

Sheng-Xiong Chen, Department of Hepatobiliary Surgery, The Second Hospital of Hebei Medical University, Shijiazhuang 050000, Hebei Province, China

Ting Liu, Shu-Ling Wang, Department of Gastroenterology, The First Hospital of Hebei Medical University, Shijiazhuang 050000, Hebei Province, China

Shi-Mao Liu, Department of Gastroenterology, Hebei Youfu Hospital, Shijiazhuang 050000, Hebei Province, China

Corresponding author: Hui-Qing Jiang, Doctor, Chief Physician, Director, Department of Gastroenterology, The Second Hospital of Hebei Medical University, No. 215 Heping West Road, Shijiazhuang 050000, Hebei Province, China. jianghuiqing1959@sina.com

Abstract

BACKGROUND

Oxaliplatin (Oxa) is the first-line chemotherapy drug for colorectal cancer (CRC), and Oxa resistance is crucial for treatment failure. Prostaglandin $F_{2\alpha}$ synthase (PG-$F_{2\alpha}$) (PGFS), an enzyme that catalyzes the production of $PGF_{2\alpha}$, is involved in the proliferation and growth of a variety of tumors. However, the role of PGFS in Oxa resistance in CRC remains unclear.

AIM

To explore the role and related mechanisms of PGFS in mediating Oxa resistance in CRC.

METHODS

The PGFS expression level was examined in 37 pairs of CRC tissues and paracancerous tissues at both the mRNA and protein levels. Overexpression or knockdown of PGFS was performed in CRC cell lines with acquired Oxa resistance (HCT116-OxR and HCT8-OxR) and their parental cell lines (HCT116 and HCT8) to assess its influence on cell proliferation, chemoresistance, apoptosis, and DNA damage. For determination of the underlying mechanisms, CRC cells were examined for platinum-DNA adducts and reactive oxygen species (ROS) levels in the presence of a PGFS inhibitor or its products.

RESULTS

Both the protein and mRNA levels of PGFS were increased in the 37 examined CRC tissues compared to the adjacent normal tissues. Oxa induced PGFS expression in the parental HCT116 and HCT8 cells in a dose-dependent manner. Furthermore, overexpression of PGFS in parental CRC cells significantly attenuated Oxa-induced proliferative suppression, apoptosis, and DNA damage. In contrast, knockdown of PGFS in Oxa-resistant HCT116 and HCT8 cells (HCT116-OxR and HCT8-OxR) accentuated the effect of Oxa treatment *in vitro* and *in vivo*. The addition of the PGFS inhibitor indomethacin enhanced the cytotoxicity caused by Oxa. Treatment with the PGFS-catalyzed product $PGF_{2\alpha}$ reversed the effect of PGFS knockdown on Oxa sensitivity. Interestingly, PGFS inhibited the formation of platinum-DNA adducts in a $PGF_{2\alpha}$-independent manner. $PGF_{2\alpha}$ exerts its protective effect against DNA damage by reducing ROS levels.

CONCLUSION

PGFS promotes resistance to Oxa in CRC *via* both $PGF_{2\alpha}$-dependent and $PGF_{2\alpha}$-independent mechanisms.

Key Words: Prostaglandin $F_{2\alpha}$synthase; Colorectal cancer; Oxaliplatin; Drug resistance; DNA damage

©The Author(s) 2023. Published by Baishideng Publishing Group Inc. All rights reserved.

Core Tip: Prostaglandin $F_{2\alpha}$ synthase ($PGF_{2\alpha}$) (PGFS) is an enzymatic catalyst responsible for the biosynthesis of $PGF_{2\alpha}$. Our study revealed that PGFS exerts an inhibitory effect on the generation of reactive oxygen species by means of its downstream product $PGF_{2\alpha}$, and consequently facilitates resistance to oxaliplatin in colorectal cancer. Simultaneously, PGFS suppresses the formation of platinum-DNA adducts in a manner that is not reliant on $PGF_{2\alpha}$, which is rarely reported.

Citation: Wang YJ, Xie XL, Liu HQ, Tian H, Jiang XY, Zhang JN, Chen SX, Liu T, Wang SL, Zhou X, Jin XX, Liu SM, Jiang HQ. Prostaglandin $F_{2\alpha}$ synthase promotes oxaliplatin resistance in colorectal cancer through prostaglandin $F_{2\alpha}$-dependent and $F_{2\alpha}$-independent mechanism. *World J Gastroenterol* 2023; 29(39): 5452-5470
URL: https://www.wjgnet.com/1007-9327/full/v29/i39/5452.htm
DOI: https://dx.doi.org/10.3748/wjg.v29.i39.5452

INTRODUCTION

Colorectal cancer (CRC) is one of the most frequently diagnosed cancers and a leading cause of cancer death worldwide [1]. In China, CRC is the third most common cancer, and the incidence rate also exceeds that of liver cancer, ranking third in cancer[2]. The current clinical treatment regimen for CRC involves surgical resection followed by chemotherapy, radiotherapy and combination therapy. For prevention of tumor recurrence, surgery alone or combined with adjuvant chemotherapy remains the cornerstone of the treatment of nonmetastatic CRC[3]. Adjuvant oxaliplatin (Oxa)-based fluorouracil, leucovorin, and Oxa (FOLFOX) or capecitabine plus Oxa chemotherapy is the standard for patients with stage II or III colon cancer following surgery, as recommended by several treatment guidelines[4,5].

Oxa, as an alternative to cisplatin, is a third-generation platinum agent. Several multicenter clinical trials have been conducted on the therapies with Oxa shown in preclinical and single-center trials to have beneficial anticancer effects. Oxa can significantly reduce the risk of recurrence and mortality of CRC and prolong disease-free survival and overall survival[6,7]. However, resistance to chemotherapy remains a major clinical issue in the treatment of CRC[8]. However, only half of CRC patients respond to FOLFOX, and this half of chemotherapy-resistant patients also develop resistance during chemotherapy, a type of resistance known as secondary resistance. That is, cancer drug resistance includes two types: Intrinsic (also called innate or primary resistance) and acquired (also called avoidant, adaptive, or secondary resistance).

Cisplatin resistance likely occurs for complex reasons, including increased drug efflux, drug breakdown, increased repair of damaged DNA, and increased activation of prosurvival pathways or inhibition of pathways that promote cell death[9]. Several studies have also shown that for Oxa resistance, the reduction in damage formation rather than the increase in damage repair is the main factor in the acquired resistance to Oxa[10]. Compared with cisplatin, Oxa has a large platinum atom ring, which can bind more DNA molecules to form platinum-DNA complexes and cause DNA damage to cells. Then, the DNA repair mechanism is activated. Once the repair is successful, Oxa will be excreted from the body, resulting in drug resistance. If DNA damage repair fails, the cell will undergo apoptosis[11]. Several studies

have shown that although Oxa has greater cell lethality than cisplatin, side effects such as ototoxicity and nephrotoxicity are weaker than those of cisplatin, and this drug can treat cisplatin-resistant tumors, but Oxa more easily results in resistance than cisplatin[12,13]. Therefore, studying the resistance to Oxa has important clinical value.

Prostaglandins (PGs) are a group of biologically active lipid mediators derived from the cyclooxygenase (COX) pathway of the arachidonic acid cascade[14]. PGs are involved in growth and development, inflammation, and cancer progression by binding to their respective receptors[15]. Prostaglandin $F_{2\alpha}$ ($PGF_{2\alpha}$) is one of the main PGs produced by the COX pathway. $PGF_{2\alpha}$ is synthesized by $PGF_{2\alpha}$ synthase (PGFS), which is a member of the aldo-keto reductase (AKR) family and a key enzyme in steroid metabolism[16]. PGFS converts prostaglandin D2 (PGD2) into 11β-$PGF_{2\alpha}$[17,18]. Recently, the cancer-promoting effects of PGFS in prostate cancer, gastric cancer, lung cancer, and other tumors have been confirmed[19,20].

Oxidative stress is related to the occurrence and development of tumors, with reactive oxygen species (ROS) playing an important role in inducing oxidative stress. Excessive ROS production is caused by the imbalance between defense and metabolic mechanisms. Low concentrations of ROS induce cell proliferation and regulate the activation of several signaling pathways[21]; however, high concentrations of ROS induce changes in gene expression and promote the accumulation of mutations and DNA damage[22]. ROS can promote the generation of PGD2 and $PGF_{2\alpha}$[3,23], but the relationship between $PGF_{2\alpha}$ and ROS and CRC treatment remains unclear.

In CRC, PGFS overexpression was reported to reduce the DNA damage caused by oxidative stress and thereby induce cisplatin resistance[24]. However, studies on the drug resistance of Oxa are scarce. Moreover, the role and mechanism of PGFS in CRC drug resistance and the relationship between $PGF_{2\alpha}$ and DNA damage require further study. In this study, Oxa-resistant CRC cell lines with PGFS overexpression and knockdown were evaluated, revealing its mediating effect on Oxa resistance. Thus, this study provides novel ideas for the diagnosis and treatment of CRC.

MATERIALS AND METHODS

Patients and samples

Fresh CRC tissues and adjacent nontumor tissue samples were acquired from 37 patients with CRC who underwent surgical resection at the Second Hospital of Hebei Medical University, Shijiazhuang, China. This study was approved by the Ethics Committee of the Second Hospital of Hebei Medical University (approval No. 2021-R441). Each tissue was divided into three parts: one part was directly snap-frozen in liquid nitrogen and stored at -80 ℃ for western blotting, a second part was immediately frozen with TRIzol and stored at -80 °C for RNA extraction, and the third part was immersed in 4% paraformaldehyde and stored at 4 ℃ for further paraffin embedding.

Resistance signature analysis

The different gene expression levels were compared between the nonresponse and response groups. The data on the expression of PGFS in CRC patients with or without response to an Oxa-containing regimen are available in the cancer treatment response gene signature database (http://ctrdb.ncpsb.org.cn/)[25]. Data were generated from the merged dataset of CTR_Microarray_35 and CTR_Microarray_90. We found that 29 out of 45 patients were nonresponsive, and the remaining 16 were responsive. The expression levels of PGFS in the two groups of patients were calculated using the website tool.

Histology and immunohistochemical analysis

Sections were stained for hematoxylin and eosin and immunofluorescence staining. Immunohistochemistry (IHC) was performed as previously described[26]. Briefly, the slides were routinely deparaffinized, rehydrated, subjected to antigen retrieval, and incubated in 3% hydrogen peroxide to block endogenous peroxidase. Subsequently, the slides were blocked and incubated with primary antibodies against PGFS (diluted 1:1000, Proteintech, Wuhan, China) and proliferating cell nuclear antigen (PCNA) (diluted 1:500, Proteintech, Wuhan China) at 4 ℃ overnight, followed by incubation with polymer-horseradish peroxidase-conjugated anti-rabbit secondary antibody the next day. Then, the section was stained with 3,3′-diaminobenzidine and counterstained with hematoxylin, dehydrated and coverslipped.

Cell culture

The human CRC HCT116 cell line was obtained from the Shanghai Institute of Biochemistry and Cell Biology, Chinese Academy of Sciences (Shanghai, China). Oxa-resistant cell lines (HCT116-OxR and HCT8-OxR) and HCT8 cells were purchased from Oulu Biotechnology (Shanghai, China). HCT116 and HCT8 cells were cultured in roswell park memorial institute (RPMI) 1640 medium (Gibco BRL, Rockville, MD, United States), which was supplemented with 10% fetal bovine serum (Gibco BRL), 100 U/mL penicillin, and 100 μg/mL streptomycin at 37 ℃ in a humidified incubator with 5% CO_2. HCT116-OxR and HCT8-OxR cells were cultured in Oxa-containing RPMI 1640 medium. HCT116, HCT116-OxR, HCT8, and HCT8-OxR cells were certified by Viva Cell Biosciences Ltd. (Shanghai, China). The reagents used in this study were Oxa (Selleck, Shanghai, China), indomethacin (MCE, Shanghai, China), and PGF2α (Merck, Jiangsu Province, China).

Western blot analysis

Proteins were extracted from CRC and adjacent tissues and cells using radio immunoprecipitation assay lysis buffer with proteinase inhibitors. Protein concentrations were measured using bicinchoninic acid (Sigma-Aldrich St. Louis, MO,

United States). The primary antibodies used included anti-PGFS antibody (diluted 1:500, Abways, Shanghai, China), anti-β-actin antibody (diluted 1:1000, Abways), anti-cleaved-caspase 3 antibody (diluted 1:200, Abways), anti-cleaved poly ADP-ribose polymerase (PARP) antibody (diluted 1:500, Abways), anti-PCNA (diluted 1:500, Abways), and anti-[γ-H2A histone family member X (γ-H2AX), diluted 1:500, Abways]. Briefly, protein purification was confirmed using electrophoresis on a sodium dodecyl sulfate-polyacrylamide gel, which was then transferred onto a polyvinylidene difluoride membrane. Membranes were incubated in 5% milk for 1 h before incubation with primary antibodies at 4 ℃ overnight. The following day, the membrane was washed three times with TBS with Tween-20. Secondary antibodies were incubated for 1 h at room temperature. The bands were visualized using an Odyssey infrared imaging system (LI-COR Biosciences), and protein quantification was performed using ImageJ software (National Institutes of Health, Bethesda, MD, United States).

Virus and small interfering RNA (siRNA) transfection

For generation of stable reporter lines, HCT116 and HCT8 cells were infected with lentiviral particles expressing PGFS, and the empty vector was used as a control. Lentiviruses for PGFS knockdown were infected into the Oxa-resistant cell lines HCT116-OxR and HCT8-OxR following the manufacturer's instructions. Subsequently, transfected cells were selected for 14-d incubations in 5 ng/mL puromycin. The construction of PGFS knockdown and overexpression lentiviruses was completed by GeneChem Co., Ltd. (Shanghai, China).

RNA extraction and real-time polymerase chain reaction (RT-PCR)

Total RNA was extracted from tissues using TRIzol reagent (Tiangen). Complementary DNA (cDNA) was synthesized from total RNA through reverse transcription using the PrimeScript RT reagent kit from TaKaRa Biomedical Technology Co., Ltd. (Beijing, China). cDNA was used for RT-PCR using the above PrimeScript RT reagent kit on a StepOnePlus™ RT-PCR system (Applied Biosystems, MS). Glyceraldehyde 3-phosphate dehydrogenase (GAPDH) was used as an internal control. Specific primer sequences were designed as follows: PGFS-forward: *5′-GTC ATC CGT ATT TCA ACC GGAG-3′*; PGFS-reverse: *5′-CCA CCC ATC GTT TGT CTC GTT-3′*; GAPDH-forward: *5′-AGG GGG GAG CCA AAA GGG TCA-3′*; GAPDH-reverse: *5′-TGG GTG GCA GTG ATG GCA TGG A-3′*.

Cell viability assay

Cell viability was determined using a cell counting kit-8 (CCK-8) kit (Dojindo Laboratories, Kumamoto, Japan) following the manufacturer's instructions. Briefly, CCK-8 solution (10 μL) was added to each well and incubated for 2 h at 37 ℃. Absorbance was measured at 450 nm using a plate reader (BioTek, Winooski, VT, United States). CCK-8 assays were used to examine the half-inhibitory concentration (IC_{50}). The inhibition concentration (%) was calculated as [(anegative - blank) - (Aexp - blank)]/(anegative-blank) × 100%. The IC_{50} was calculated from the survival curves using GraphPad Prism 7 (Version X; La Jolla, CA, United States). Each assay was performed in triplicate.

Colony formation assays

Cells stably transfected with lentiviruses were reseeded (3×10^3 cells per well) in 6-well plates and cultured for two weeks. The colonies were subsequently stained with 0.05% crystal violet for visualization. After routine culture for 2 wk, colony numbers were counted under a microscope.

Apoptosis assays

For analysis of early/late apoptotic or necrotic cell death, cells were measured with the Annexin V-FITC apoptosis detection kit (Beyotime, Shanghai, China) using flow cytometric analysis. We also detected total apoptosis by a terminal deoxynucleotidyl transferase dUTP nick end labeling (TUNEL) assay (Beyotime, Shanghai, China).

Immunofluorescence assay

Stably transfected cells were seeded onto cover glasses in 24-well plates. After 24 h of intervention, cells were fixed in 4% paraformaldehyde for 30 min, permeabilized with 0.1% Triton X-100, diluted in phosphate-buffered saline (PBS) for 10 min, and blocked with 5% normal goat serum for 30 min at room temperature. The cells were incubated with rabbit anti-PGFS or rabbit anti-γ-H2AX overnight at 4 ℃. After washing with PBS, the cells were incubated with the secondary antibody (594 goat anti-rabbit immunoglobulin G) for 1 h at room temperature. After washing, the slides were counterstained with 4′6′-diamidino-2-phenylindole dihydrochloride (Sigma-Aldrich) for 5 min. Images were acquired using a laser scanning confocal microscope (Olympus, Tokyo, Japan).

Assays for intracellular ROS levels

Intracellular ROS levels were evaluated using a ROS assay kit (KGAF019, KeyGEN Biotech, Nanjing, China) following the manufacturer's instructions. Briefly, cells were stained with dihydroethidium (DHE) for 30 min and analyzed for intracellular ROS levels under a fluorescence microscope (Olympus, Tokyo, Japan). The mean fluorescence intensity, as an index of the amount of ROS, was measured using ImageJ software.

Platinum-DNA adduct determination

The DNA concentration was determined using a nanodrop spectrophotometer (Thermo Fisher Scientific), and the DNA-bound platinum content was quantified using inductively coupled plasma-mass spectrometry.

Alkaline comet assay

DNA damage was detected using a comet assay. CRC cells were administered different drug concentrations and had different exposure times. The comet assay was performed according to the alkaline comet assay protocol (KeyGEN Biotech, Nanjing, China). Nuclear DNA and migrating DNA (comet tail) labeled with propidium iodide appeared red and were observed at 515-560 nm using a fluorescence microscope (Olympus, Tokyo, Japan). Comet tail length and tail moment (percentage of DNA in the tail to the total DNA) were analyzed using ImageJ software.

Animal study

Nude mice were implanted subcutaneously with HCT8-OXR cells. When the average volume of the tumors reached approximately 100 mm^3. The nude mice in the LV-shNC + Oxa and LV-shPGFS + Oxa groups were treated with Oxa by gavage at a dosage of 10 mg/kg/d for 14 d, and the volume of tumors was measured. We sacrificed the nude mice when the treatment was completed, and the tissues were fixed with 4% paraformaldehyde or immediately placed at -80 ℃. The animal protocol was designed to minimize pain and discomfort to animals. The nude mice were acclimatized to laboratory conditions for 1 wk prior to our experiment. Intragastric gavage administration was conducted by using straight gavage needles (22 gauge). All the animals in our study received humane care, and the ethics committee of the Second Hospital of Hebei Medical University approved our study (approval letter No. 2022-AE010).

Statistical analyses

Data are presented as the mean ± SD. The association between PGFS expression and clinicopathological features was evaluated using a nonparametric test. The statistical analyses included analysis of variance (ANOVA) with the Student-Newman-Keuls post hoc test and a standard two-tailed Student's *t* test. Student's *t* test was used for comparisons between two groups, while comparisons between three or more groups were conducted using one or two-way ANOVA with the Brown-Forsythe test for equality of group variances. Statistical analysis was performed using SPSS software version 25.0 (Chicago, IL, United States). $P < 0.05$ was considered statistically significant.

RESULTS

PGFS expression is elevated in CRC tissues

We first tested the expression of PGFS in 37 pairs of CRC tissues and matched paracarcinoma tissues. PGFS was significantly upregulated at both the protein and RNA levels in cancerous tissues compared with adjacent nontumor tissues (Figure 1A and B). IHC analysis showed that the strong positive PGFS signals were mainly detected in the nuclei of the cancerous epithelial cells. In contrast, the normal tissue samples showed low expression of PGFS homogenously distributed in the nuclei and cytoplasm (Figure 1C). Then, we investigated the relationship between PGFS and clinicopathological features. High PGFS expression was associated with advanced T stage (Tables 1 and 2). Moreover, PGFS expression was higher in the Oxa-nonresponsive group than in the Oxa-responsive group (Figure 1D).

PGFS is upregulated in Oxa-resistant CRC cells

To assess the role of PGFS in Oxa resistance in CRC cells, we used two Oxa-resistant CRC cell lines derived from HCT116 and HCT8 (hereafter named HCT116-OxR and HCT8-OxR). The resistance of the two Oxa-resistant cell lines was determined by measuring the resistance index (RI), which was calculated as the IC_{50} ratio of drug-resistant cells to their parent cells. Both HCT116-OxR and HCT8-OxR cells showed moderate Oxa resistance, with RIs of 10.1 and 5.86, respectively (IC_{50}-HCT116-OxR *vs.* IC_{50}-HCT116: 64.2 μM *vs.* 6.315 μM; IC_{50}-HCT8-OxR *vs.* IC_{50}-HCT8: 6.241 μM *vs.* 1.064 μM; Supplementary Figure 1A). Colony formation assays revealed increased colony formation efficiency in the two Oxa-resistant cell lines (Supplementary Figure 1B). PGFS expression was significantly increased in HCT116-OxR and HCT8-OxR cells compared with their parent cells (HCT116 and HCT8) (Supplementary Figure 1C). The elevated PGFS expression in the resistant cells was confirmed using immunofluorescence staining and was largely localized in the cytoplasm and nuclei (Supplementary Figure 1D). Furthermore, Oxa induced PGFS expression in a dose-dependent manner, peaking at 24 h, in both parent and Oxa-resistant cells (Supplementary Figure 1E-H). Therefore, upregulated PGFS is associated with acquired Oxa resistance in CRC cells.

PGFS attenuates Oxa-induced proliferation inhibition, apoptosis, and DNA damage in CRC cells

To further confirm the role of PGFS in Oxa resistance, we performed lentivirus-mediated overexpression of PGFS in HCT116 and HCT8 cells, which showed low levels of PGFS. Overexpression of PGFS was verified by western blotting (Supplementary Figure 2A). Stable overexpression of PGFS induced a significant right shift of the IC_{50} value for Oxa, which indicated a reduction in sensitivity to Oxa (Figure 2A). To validate this result, we designed three siRNAs to target PGFS and evaluated their knockdown efficiency in Oxa-resistant cells with high PGFS expression. The short hairpin RNA (shRNA) sequence that caused an obvious reduction in PGFS expression was cloned and inserted into a lentiviral vector for the stable knockdown of PGFS (Supplementary Figure 2B and C). Lentiviral shRNA-mediated knockdown of PGFS decreased the IC_{50} value for Oxa in HCT116-OxR and HCT8-OxR cells (Figure 2B). We then examined the effect of PGFS on the expression of PCNA (a marker of cell proliferation). Treatment with Oxa resulted in a decrease in PCNA expression, which was diminished by overexpression of PGFS in HCT116 and HCT8 cells (Figure 2C). In contrast, knockdown of PGFS further exacerbated the Oxa-induced reduction in PCNA expression in HCT116-OxR and HCT8-OxR cells (Figure 2D). Additionally, overexpression of PGFS restored the colony-forming capacity of CRC cells treated with

Table 1 Correlation between prostaglandin $F_{2\alpha}$ synthase expression level and clinicopathological characteristics in 37 colorectal cancer patients, *n* (%)

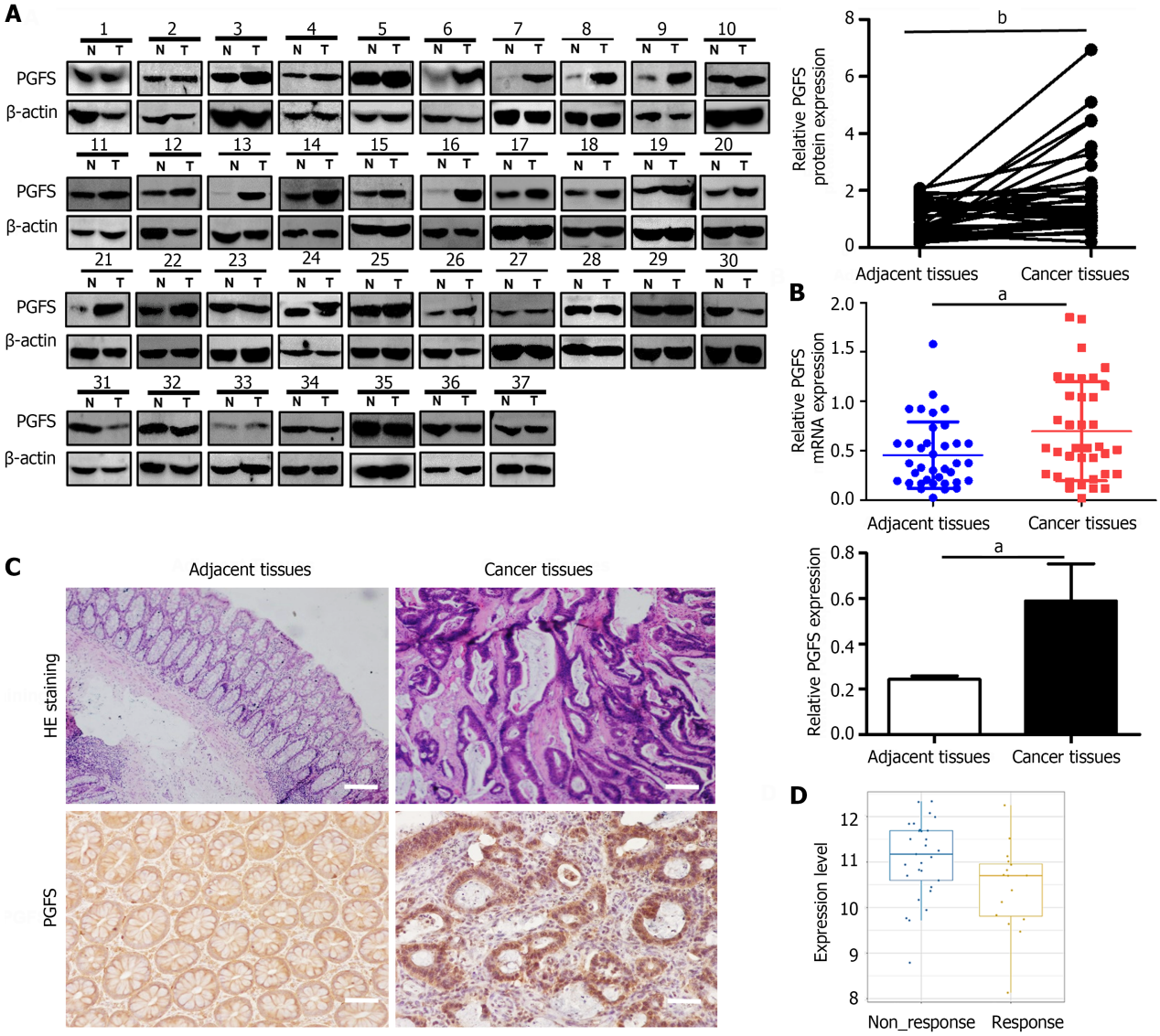
Variables	No. of patients	Relatives PGFS expressions (mean ± SD)	*P* value
All cases	37 (100)		
Gender			0.376
Male	22 (59)	1.84 ± 1.67	
Female	15 (41)	1.68 ± 1.02	
Age (yr)			0.495
≥ 60	19 (51)	1.40 ± 0.8	
< 60	18 (49)	2.12 ± 1.8	
Tumor location			0.066
Colon	15 (41)	1.71 ± 1.2	
Rectum	22 (59)	1.84 ± 1.65	
Differentiations			0.437
Well and Moderately	26 (70)	1.65 ± 1.29	
Poorly	11 (30)	1.81 ± 1.08	
T stage			0.023[a]
T1 or T2	25 (68)	1.26 ± 0.52	
T3 or T4	12 (32)	2.47 ± 0.87	
Lymph node metastasis			0.063
No	25 (68)	1.17 ± 0.56	
Yes	12 (32)	2.09 ± 1.69	
AJCC stage			0.069
I or II	29 (78)	1.44 ± 0.89	
III or IV	8 (22)	3.09 ± 2.69	

[a]*P* < 0.05 concluded that T stage was correlated with prostaglandin F2α synthase expression level. PGFS: Prostaglandin $F_{2\alpha}$ synthase; AJCC: American Joint Committee on Cancer.

Table 2 Spearman analysis of the correlation between prostaglandin $F_{2\alpha}$ synthase expression level with clinicopathological, *n* (%)

Variables	No. of patients	PGFS expression level Spearman correlation	*P* value
T stage		0.666	0[a]
T1 or T2	25 (68)		
T3 or T4	12 (32)		
AJCC stage		0.113	0.504
I or II	29 (78)		
III or IV	8 (22)		

[a]*P* < 0.05 indicates that there is a significant relationship between T stage and prostaglandin F2α synthase (PGFS) expression level in tissues. The Spearman correlation of PGFS expression level, also known as the sample correlation coefficient, was 0.666, that is, the significance relationship was moderately correlated and passed the significance test. PGFS: Prostaglandin $F_{2\alpha}$ synthase; AJCC: American Joint Committee on Cancer.



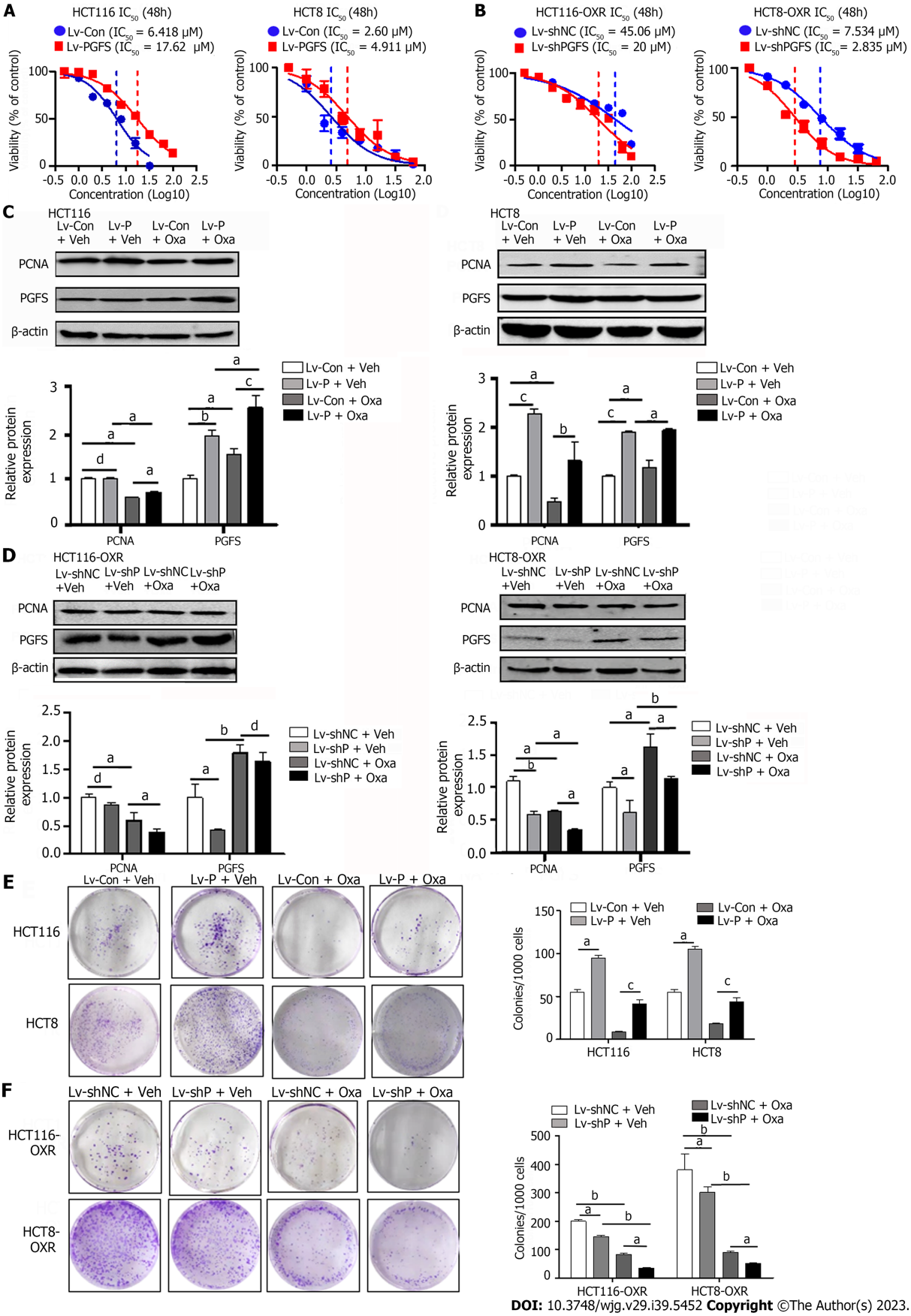
DOI: 10.3748/wjg.v29.i39.5452 **Copyright** ©The Author(s) 2023.

Figure 1 Prostaglandin $F_{2\alpha}$ synthase is upregulation in patients with colorectal cancer. A: Prostaglandin $F_{2\alpha}$ synthase (PGFS) protein expression was verified using western blot in 37 pairs of colorectal cancer (CRC) and adjacent normal tissues; B: Real-time polymerase chain reaction analysis of PGFS mRNA expression in 37 pairs of CRC and adjacent normal tissues; C: Hematoxylin and eosin staining and immunohistochemistry for PGFS expression (scale bar, 50 μm); D: PGFS expression in non-response and response patients analyzed by the Cancer Treatment Response gene signature DataBase (http://ctrdb.ncpsb.org.cn/). $^{a}P < 0.05$, $^{b}P < 0.01$. T: Tumor; N: Adjacent normal tissues; PGFS: Prostaglandin $F_{2\alpha}$ synthase; HE: Hematoxylin and eosin.

Oxa. However, knockdown of PGFS caused a further decrease in clonogenic capacity (Figure 2E and F). In summary, PGFS attenuates Oxa-induced proliferation suppression.

We then tested the effect of PGFS on apoptosis induced by Oxa. Western blotting showed that treatment with Oxa elevated the levels of cleaved PARP and cleaved caspase 3 in HCT116 and HCT8 cells. However, overexpression of PGFS inhibited the Oxa-induced increase in the two proteins (Figure 3A). Conversely, silencing PGFS in HCT116-OxR and HCT8-OxR cells led to a further increase in the two apoptosis markers caused by Oxa (Figure 3B). Furthermore, we examined apoptosis by TUNEL staining. We observed that PGFS overexpression reduced the increase in TUNEL-positive cells induced by Oxa treatment. In contrast, the number of apoptotic cells was further increased by infection with lentivirus expressing sh-PGFS (Figure 3C and D). In addition, we performed flow cytometry as further evidence of apoptosis. The percentage of apoptotic cells was decreased in the PGFS-overexpressing CRC cells but increased in the Oxa-resistant cells with PGFS knockdown (Figure 3E and F). These observations suggested that PGFS protects CRC cells against Oxa-induced apoptosis.

Oxa induces DNA damage by directly binding to DNA. We investigated the role of PGFS in DNA damage caused by Oxa by detecting the expression of γ-H2AX (a marker for DNA damage). The γ-H2AX level was increased by treatment with Oxa, which was diminished by PGFS overexpression in the parental CRC cells, while it was elevated by knockdown of PGFS in the Oxa-resistant CRC cells (Figure 4A and B). We then examined DNA double-strand breaks (DSBs) by γ-H2AX immunofluorescence staining. Overexpression of PGFS in HCT116 and HCT8 cells led to a reduction in the number of γ-H2AX-positive DNA damage foci induced by Oxa treatment. Conversely, the number of γ-H2AX foci was



DOI: 10.3748/wjg.v29.i39.5452 **Copyright** ©The Author(s) 2023.

Figure 2 Prostaglandin $F_{2\alpha}$ synthase resists the inhibitory effect of oxaliplatin on colorectal cancer cell proliferation. A: The effects of prostaglandin $F_{2\alpha}$ synthase (PGFS) overexpression on cell viability in HCT116 and HCT8 cells; B: The effects of PGFS knockdown on cell viability in HCT116-OxR and HCT8-OxR cells; C and D: Western blot analysis showed proliferating cell nuclear antigen levels in parental and oxaliplatin-resistant (OR) colorectal cancer (CRC) cells; E and F: Plate colony formation assay in parental and OR CRC cells. $^{a}P < 0.05$, $^{b}P < 0.01$, $^{c}P < 0.001$, ^{d}No significance. PCNA: Proliferating cell nuclear

antigen; PGFS: Prostaglandin $F_{2\alpha}$ synthase; Oxa: Oxaliplatin; IC_{50}: Half-inhibitory concentration.

increased in the drug-resistant CRC cells upon PGFS knockdown (Figure 4C). In addition, we used a comet assay to determine DNA damage. Tail length and DNA content percentage (tail DNA%) were significantly increased after incubation with Oxa in HCT116 and HCT8 cells, and these changes were attenuated by overexpression of PGFS. Moreover, PGFS knockdown resulted in enhanced DNA damage induced by Oxa (Figure 4D and E). These results showed that PGFS is resistant to Oxa-induced DNA damage. Collectively, these findings indicated that PGFS promotes Oxa resistance in CRC cell lines.

PGFS knockdown enhances the efficiency of Oxa in vivo

HCT8-OxR cells with stable PGFS knockdown were inoculated subcutaneously into nude mice. Treatment with Oxa caused a decrease in tumor volume and weight, which were further decreased by knockdown of PGFS (Figure 5A-C). Immunohistochemical staining was used to evaluate PCNA expression in the xenograft tumors. Knockdown of PGFS further exacerbated the Oxa-induced reduction in PCNA expression (Figure 5D). These data indicated that PGFS knockdown enhances the sensitivity of CRC to Oxa.

PGFS exerts an Oxa-resistant effect through its $PGF_{2\alpha}$ synthase activity

PGFS catalyzed synthesis of $PGF_{2\alpha}$. To clarify whether the Oxa-resistant effect of PGFS is dependent on its enzymatic action, we blocked PGFS activity by its inhibitor indomethacin. PCNA expression was upregulated by PGFS overexpression in CRC cells treated with Oxa, and this effect was inhibited after indomethacin administration. Moreover, overexpression of PGFS attenuated the upregulation of cleaved PARP and cleaved caspase-3 caused by Oxa treatment, while indomethacin treatment reversed the effect of PGFS overexpression on the expression of apoptotic proteins (Supplementary Figure 3A). Flow cytometric analysis showed that Oxa-induced apoptosis was suppressed by infecting CRC cells with a lentivirus expressing PGFS. Treatment with indomethacin abolished the ability of PGFS to resist Oxa-induced apoptosis (Supplementary Figure 3B). Western blot analysis revealed that overexpression of PGFS inhibited the upregulation of γ-H2AX caused by Oxa, which was diminished by indomethacin incubation (Supplementary Figure 3C). A comet assay further revealed that overexpression of PGFS in CRC cells inhibited the increase in comet DNA tail length and percentage of DNA in the tail induced by Oxa, while the inhibitory function of PGFS was attenuated by indomethacin (Supplementary Figure 3D). These findings suggested that the effect of PGFS on increasing CRC resistance to Oxa depends on its $PGF_{2\alpha}$ synthase activity.

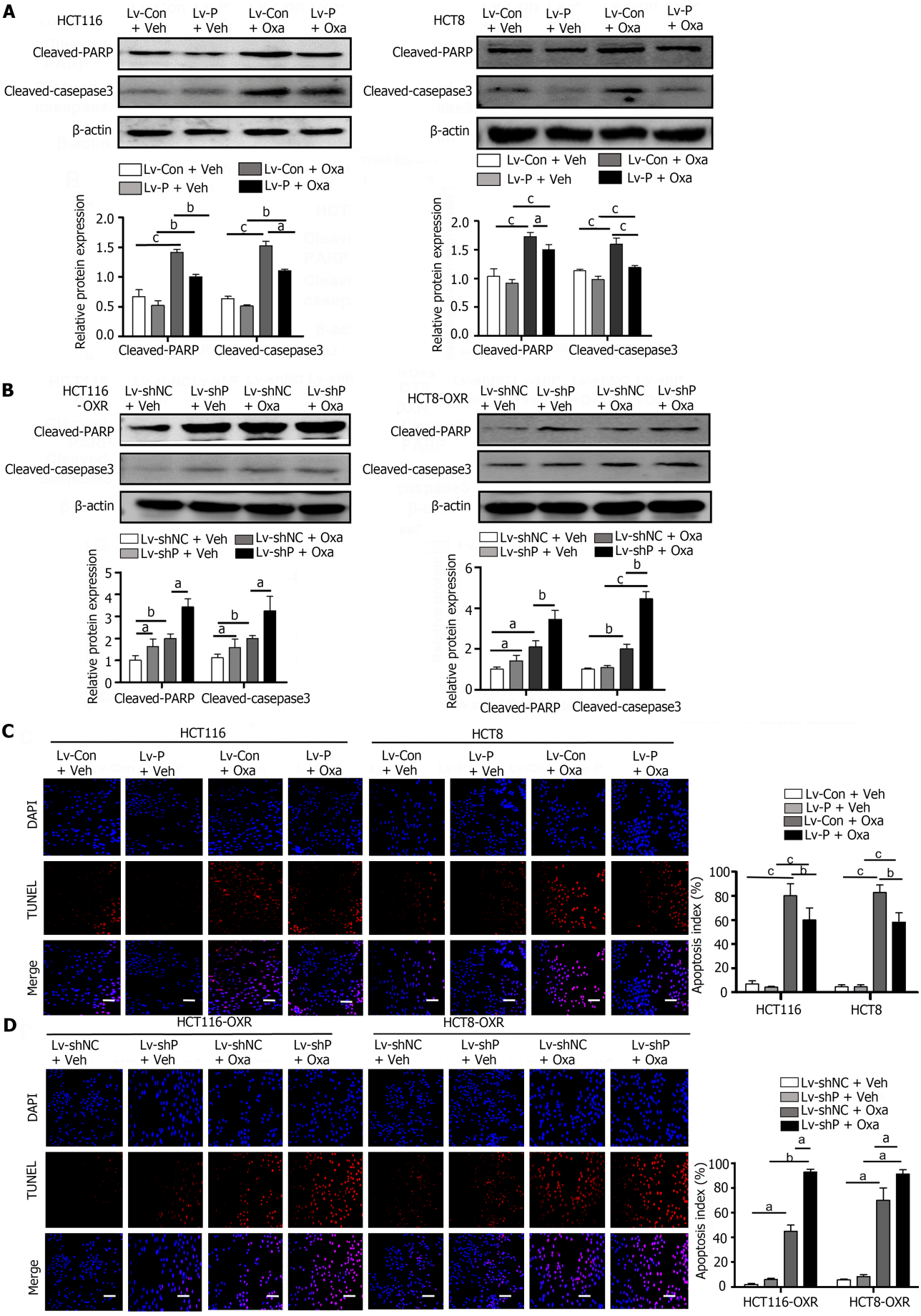
PGFS promotes resistance to Oxa through its product $PGF_{2\alpha}$

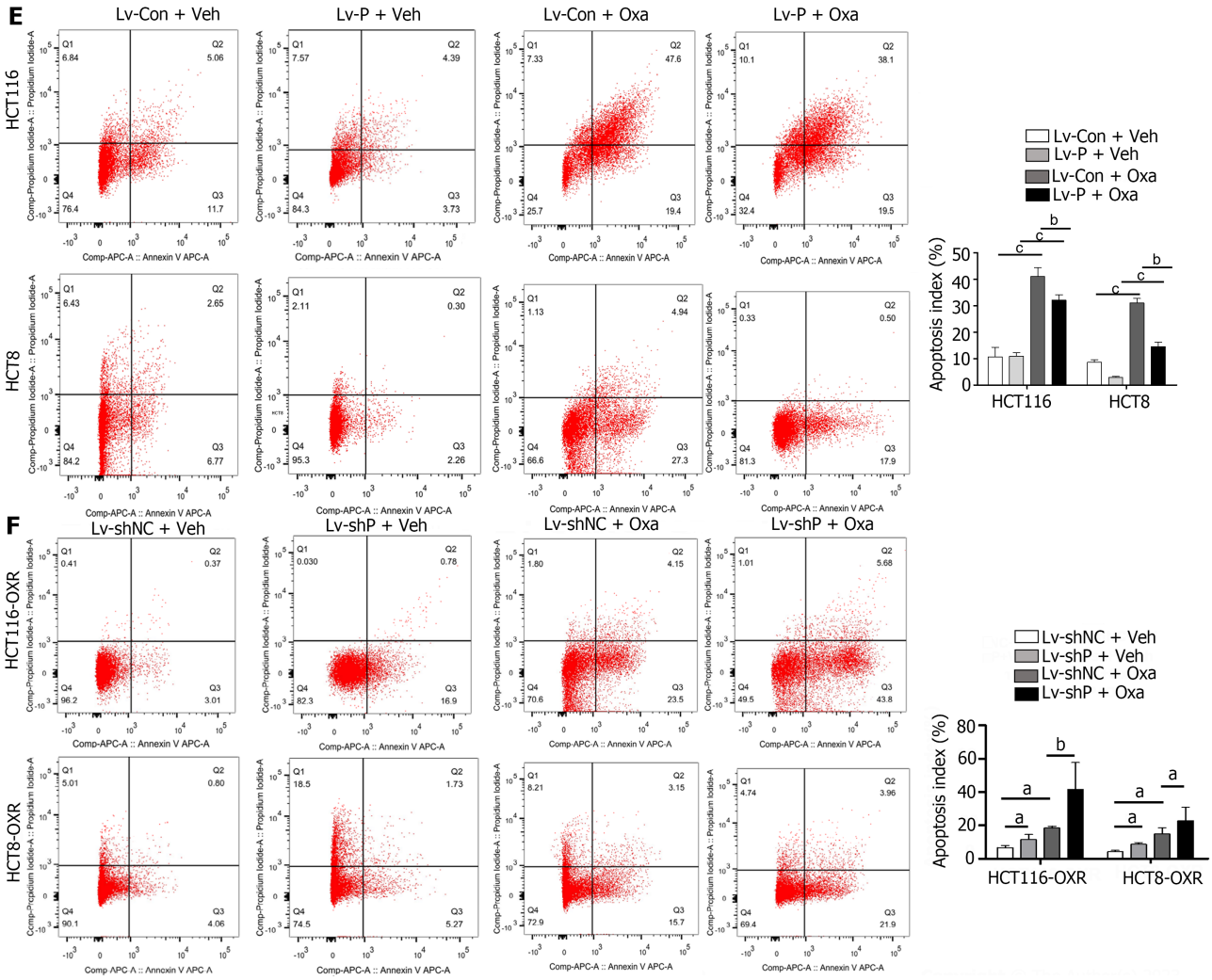
PGFS catalyzes the reduction of PGD2 to $PGF_{2\alpha}$. To confirm the role of PGF2α in PGFS-mediated Oxa resistance, we performed rescue experiments by introducing $PGF_{2\alpha}$ to HCT116-OxR and HCT8-OxR cells with PGFS knockdown. Western blot analysis revealed that PCNA expression was further decreased by the depletion of PGFS in HCT116 and HCT8 cells treated with Oxa, which was alleviated by the addition of $PGF_{2\alpha}$. Knockdown of PGFS further increased Oxa-induced elevation of cleaved PARP and cleaved caspase 3, which was partially rescued by $PGF_{2\alpha}$ supplementation (Figure 6A). TUNEL staining results showed that the percentage of apoptotic cells was increased after the knockdown of PGFS in Oxa-treated cells, while the addition of $PGF_{2\alpha}$ decreased apoptosis (Figure 6B). Moreover, knockdown of PGFS further increased the upregulation of γ-H2AX expression caused by Oxa, while supplementation with $PGF_{2\alpha}$ attenuated the effect of PGFS depletion (Figure 6C). Similarly, comet assays showed that the percentage of comet tail DNA and tail length were elevated by Oxa stimulation and were further increased in HCT116-OxR and HCT8-OxR cells with PGFS knockdown, which was alleviated by the addition of $PGF_{2\alpha}$ (Figure 6D). These data indicate that $PGF_{2\alpha}$, the product catalyzed by PGFS, plays an important role in PGFS-mediated Oxa resistance.

PGFS promotes Oxa resistance through both $PGF_{2\alpha}$-dependent and $PGF_{2\alpha}$-independent mechanisms

Oxa exerts its cytotoxic effect by forming platinum-DNA adducts or by generating a large amount of ROS, thereby causing DNA damage. To explore the role of PGFS in the formation of platinum-DNA adducts, we measured the amount of platinum on DNA after treatment with Oxa by inductively coupled plasma mass spectrometry. Overexpression of PGFS did not affect the platinum concentrations in HCT116 and HCT8 cells (Figure 7A). In contrast, knockdown of PGFS induced an increase in the platinum concentrations in HCT116-OxR and HCT8-OxR cells (Figure 7B). However, the addition of $PGF_{2\alpha}$ did not affect the formation of platinum-DNA adducts in HCT8-OxR cells with knockdown of PGFS (Figure 7C). These findings suggested that PGFS may suppress the formation of platinum-DNA adducts in a $PGF_{2\alpha}$-independent manner.

As Oxa exerts its antitumor effect through the induction of ROS, we explored the role of PGFS in the generation of ROS by DHE staining. Compared with that of the parent CRC cells, ROS production was reduced in drug-resistant cells (Figure 7D). In addition, overexpression of PGFS led to a decrease in Oxa-induced ROS (Figure 7E). Conversely, the increased ROS induced by Oxa was further elevated by knockdown of PGFS (Figure 7F), which was alleviated by supplementation with $PGF_{2\alpha}$ (Figure 7G). These data indicated that PGFS inhibits the generation of ROS in a $PGF_{2\alpha}$-dependent manner.


A
HCT116
Lv-Con + Veh
Lv-P + Veh
Lv-Con + Oxa
Lv-P + Oxa
Cleaved-PARP
Cleaved-casepase3
β-actin
Relative protein expression
HCT8
B
HCT116 -OXR
Lv-shNC + Veh
Lv-shP + Veh
Lv-shNC + Oxa
Lv-shP + Oxa
HCT8-OXR
C
DAPI
TUNEL
Merge
Apoptosis index (%)
D



DOI: 10.3748/wjg.v29.i39.5452 **Copyright** ©The Author(s) 2023.

Figure 3 Prostaglandin $F_{2\alpha}$ synthase suppresses apoptosis induced by oxaliplatin in colorectal cancer cell lines. A and B: Western blot analysis showed cleaved poly ADP-ribose polymerase and cleaved caspase-3 were assessed in colorectal cancer (CRC) cells or in oxaliplatin-resistant (OR) CRC cells; C and D: Apoptosis of parental and OR CRC cells evaluation by terminal deoxynucleotidyl transferase dUTP nick end labeling assay, scale bar 100 μm; E and F: Apoptosis was measured by the Annexin V-PI staining in parental and OR CRC cells. $^{a}P < 0.05$, $^{b}P < 0.01$, $^{c}P < 0.001$. Oxa: Oxaliplatin; PARP: Poly ADP-ribose polymerase.

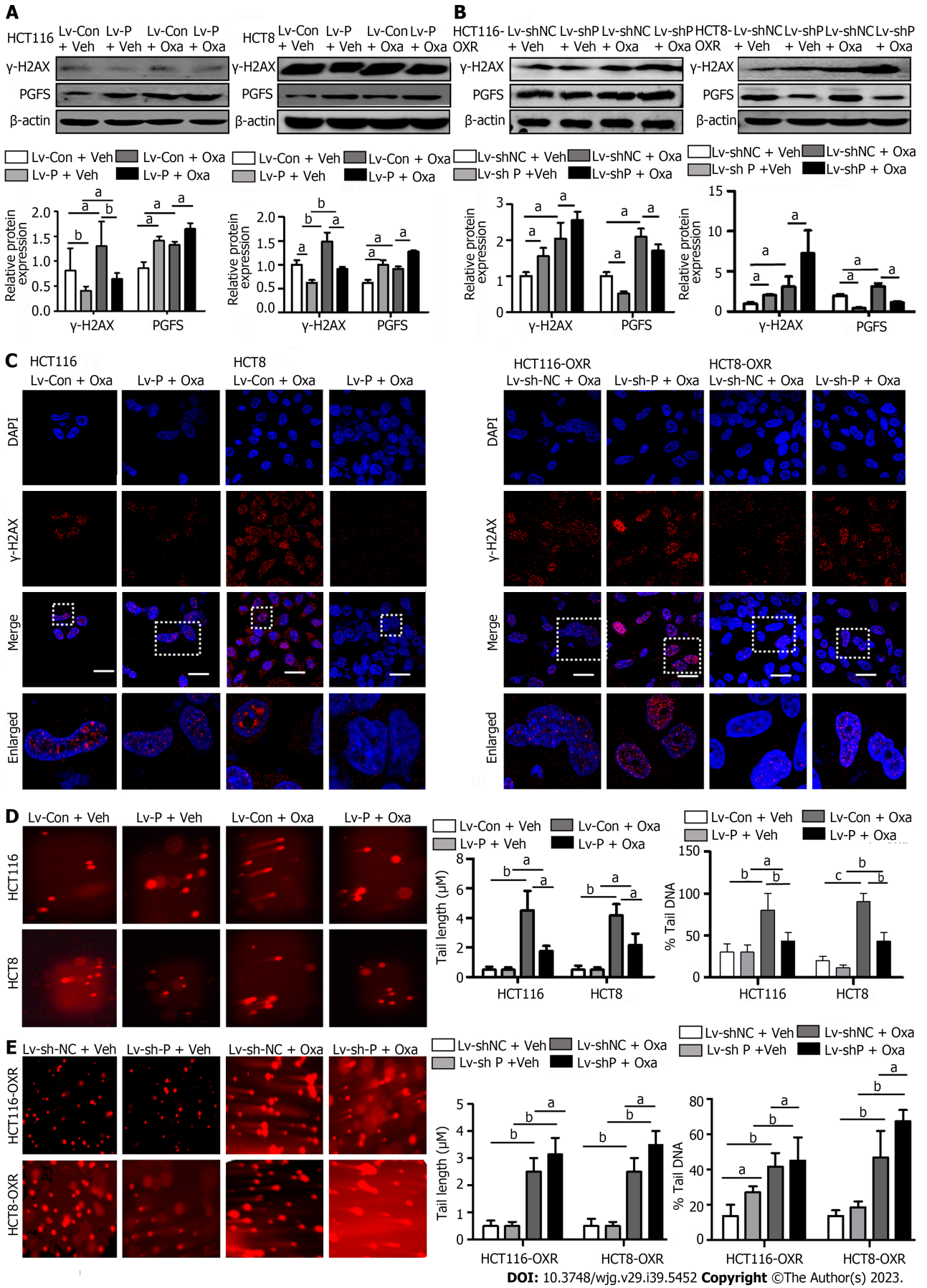
DISCUSSION

PGFS belongs to the AKR superfamily of NADP (H)-dependent enzymes, which play central roles in the proinflammation [20,27], proliferation[15,28] and drug resistance of tumors[29-31]. Previous studies have shown that Oxa suppresses cell proliferation and induces apoptosis in CRC cells[32]. The involvement of PGFS in resistance to cisplatin has been reported previously[24]. However, the role of PGFS in Oxa resistance in CRC and its molecular mechanism remain unclear.

Our study revealed that PGFS expression was significantly higher in human CRC tissues than in adjacent normal tissues, and PGFS may be correlated with tumor stage[28] and lymph node metastasis[33]. Therefore, how PGFS regulates CRC progression and metastasis warrants further investigation.

Induction of cell death is one of the challenges for chemotherapy. Any factors that enhance the effect of Oxa on cell proliferation and apoptosis may improve the therapeutic effect of Oxa on tumors[34,35]. PGFS-$PGF_{2\alpha}$ may be a target in tumor chemotherapy. Zhou *et al*[33] recently found that PGFS activates nuclear factor kappaB and promotes hepatocellular carcinoma proliferation and metastasis. Other studies found that $PGF_{2\alpha}$ enhances mitogen-activated protein kinase signaling and inhibits peroxisome proliferator-activated receptor-gamma, a cancer inhibitor; therefore, $PGF_{2\alpha}$ promotes cancer cell proliferation and inhibits differentiation[36-38]. The present study found that PGFS was induced by Oxa in a dose-dependent manner. These findings indicated that PGFS was related to Oxa resistance in CRC. In our *in vitro* study, we constructed PGFS-overexpressing and PGFS knockdown cells in both parental and Oxa-resistant CRC cell lines. We proved that the effect of Oxa on apoptosis and proliferation was suppressed by PGFS overexpression and enhanced by PGFS knockdown. These results indicated that PGFS was involved in Oxa resistance in CRC.

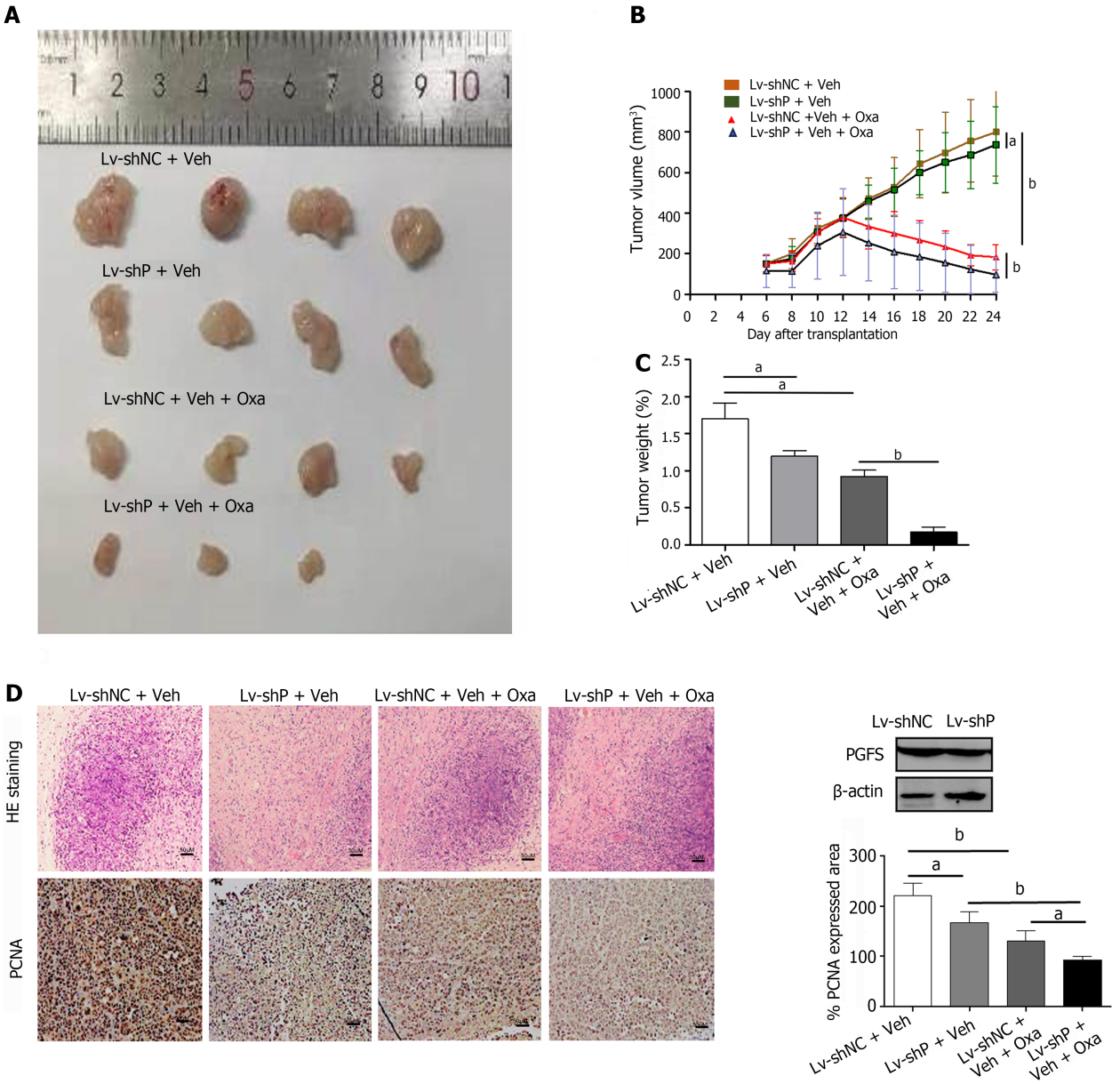
The main mechanism of DNA damage caused by Oxa is the direct combination of platinum with DNA, ultimately destroying tumors[39]. Oxa is a platinum-based chemotherapy that induces a complex spectrum of DNA damage, including DSBs, single-strand breaks, and DNA crosslinks[40], and oxidized bases elicit DNA damage[41]. Indomethacin, a PGFS-specific inhibitor, has additive/synergistic effects on Oxa-induced proliferative inhibition, apoptosis, and DNA



DOI: 10.3748/wjg.v29.i39.5452 **Copyright** ©The Author(s) 2023.

Figure 4 The protective effect of prostaglandin $F_{2\alpha}$ synthase on DNA damage induced by oxaliplatin in colorectal cancer cells. A and B: DNA damage marker protein γ-H2A histone family member X (γ-H2AX) was determined using western blot in HCT116 and HCT8 cells and HCT116-OxR and HCT8-OxR

cells; C: γ-H2AX fluorescent spots were detected using immunofluorescence staining; D and E: Detection of DNA damage using single-cell gel electrophoresis (comet assay) in parent and drug-resistant cells (scale bar, 50 μm). [a]*P* < 0.05, [b]*P* < 0.01, [c]*P* < 0.001. PGFS: Prostaglandin $F_{2\alpha}$ synthase; Oxa: Oxaliplatin; γ-H2AX: γ-H2A histone family member X.



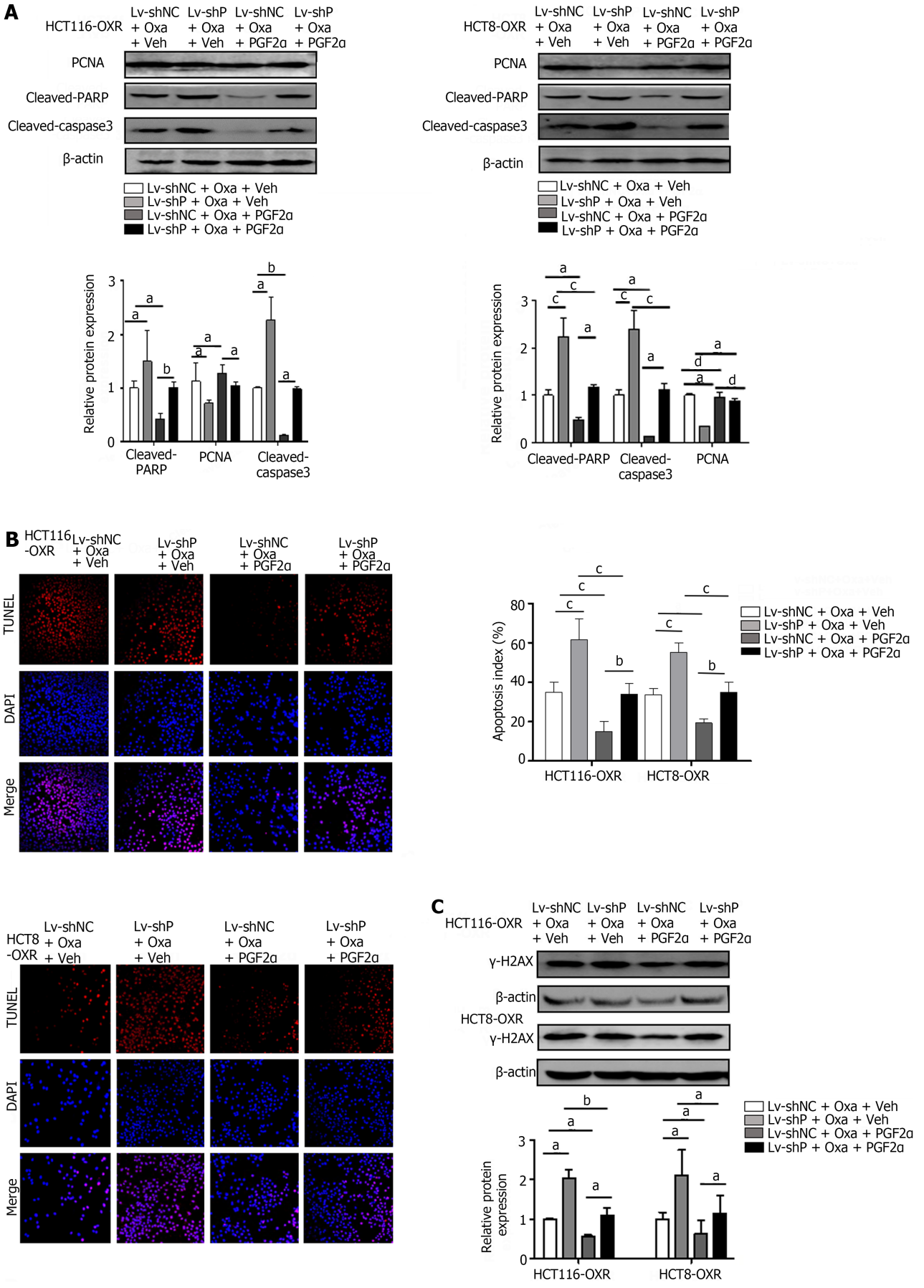
DOI: 10.3748/wjg.v29.i39.5452 **Copyright** ©The Author(s) 2023.

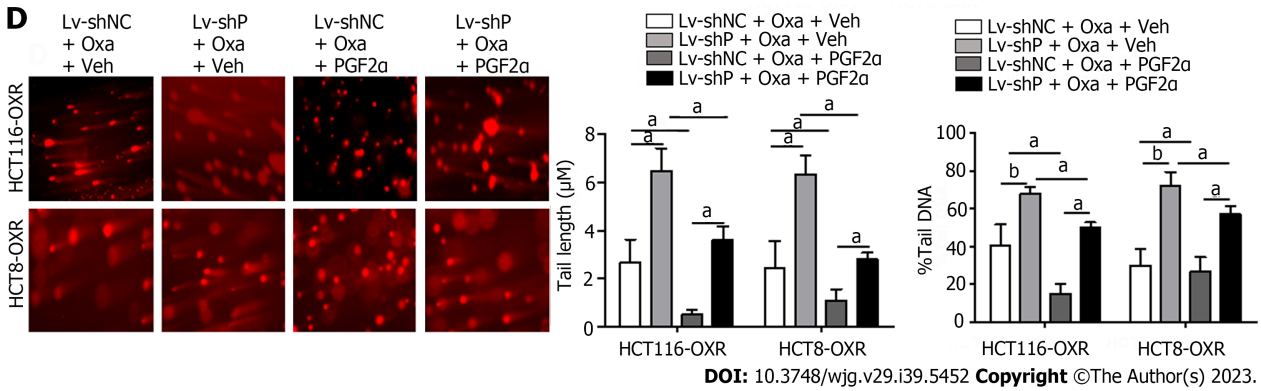
Figure 5 Prostaglandin $F_{2\alpha}$ synthase knockdown improves oxaliplatin efficiency *in vivo*. A: Morphologies of collected tumors in subcutaneous HCT8-OxR xenografts in nude mice; B: Curves of tumor growth in each group; C: Tumor weights were measured after collection; D: Hematoxylin-eosin (upper panel; magnification, × 200) and immunohistochemical staining for proliferating cell nuclear antigen (bottom panel; magnification, × 200) using xenograft tumor samples from each group. [a]*P* < 0.05, [b]*P* < 0.01. PCNA: Proliferating cell nuclear antigen; PGFS: Prostaglandin $F_{2\alpha}$ synthase; HE: Hematoxylin and eosin; Oxa: Oxaliplatin.

damage, whereas the administration of $PGF_{2\alpha}$ partially alleviated the above effects[42]. In summary, our data implied that the effect of PGFS on resistance in CRC is $PGF_{2\alpha}$ dependent. The knockdown of PGFS sensitizes CRC to Oxa treatment.

Several studies have demonstrated that Oxa-resistant cells can modulate the cellular resistance capacity to oxidative stress by regulating key detoxification enzymes[43,44]. The present study found that PGFS inhibited the effect of Oxa on DNA damage and thereby promoted Oxa resistance in CRC.

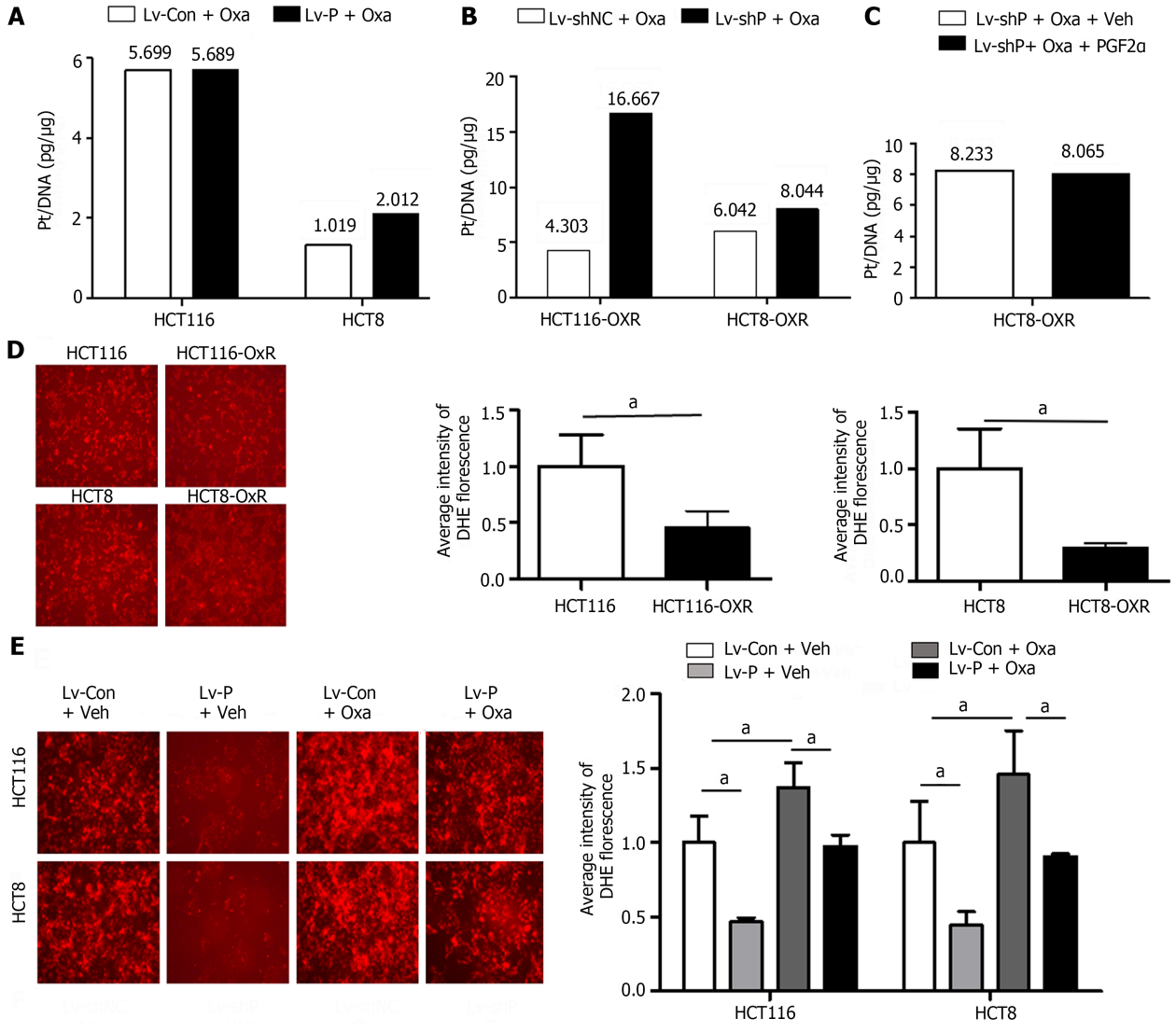
In the present study, PGFS was significantly increased in CRC tissues, PGFS overexpression inhibited the cytotoxic effect of Oxa on CRC cells, and downregulation of PGFS improved the efficacy of Oxa in the treatment of CRC. PGFS promotes CRC resistance to Oxa in a $PGF_{2\alpha}$-dependent manner; therefore, the PGFS-$PGF_{2\alpha}$ pathway may be a potential target for the treatment of CRC patients with Oxa resistance.

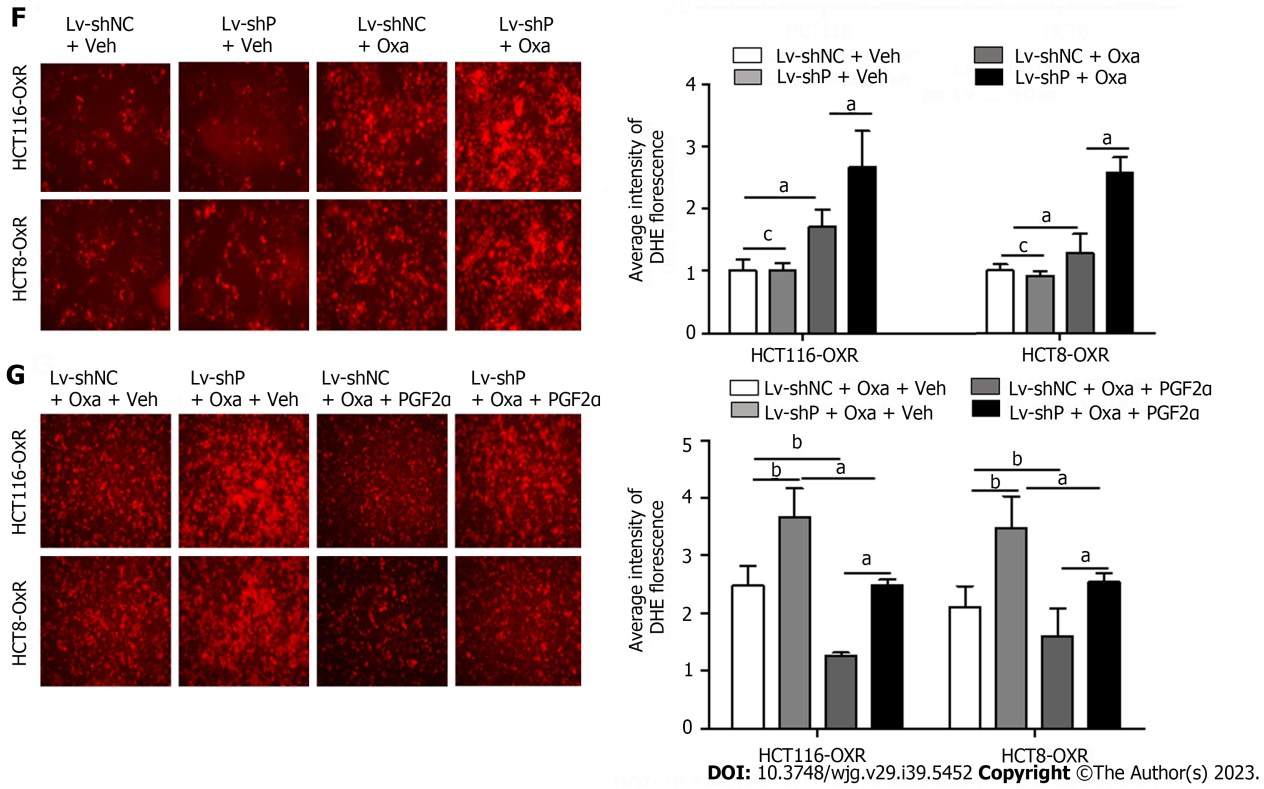

A
HCT116-OXR
Lv-shNC + Oxa + Veh
Lv-shP + Oxa + Veh
Lv-shNC + Oxa + PGF2α
Lv-shP + Oxa + PGF2α
PCNA
Cleaved-PARP
Cleaved-caspase3
β-actin
Lv-shNC + Oxa + Veh
Lv-shP + Oxa + Veh
Lv-shNC + Oxa + PGF2α
Lv-shP + Oxa + PGF2α
Relative protein expression
Cleaved-PARP
PCNA
Cleaved-caspase3
HCT8-OXR
Lv-shNC + Oxa + Veh
Lv-shP + Oxa + Veh
Lv-shNC + Oxa + PGF2α
Lv-shP + Oxa + PGF2α
PCNA
Cleaved-PARP
Cleaved-caspase3
β-actin
Lv-shNC + Oxa + Veh
Lv-shP + Oxa + Veh
Lv-shNC + Oxa + PGF2α
Lv-shP + Oxa + PGF2α
Relative protein expression
Cleaved-PARP
Cleaved-caspase3
PCNA
B
HCT116-OXR
Lv-shNC + Oxa + Veh
Lv-shP + Oxa + Veh
Lv-shNC + Oxa + PGF2α
Lv-shP + Oxa + PGF2α
TUNEL
DAPI
Merge
Apoptosis index (%)
Lv-shNC + Oxa + Veh
Lv-shP + Oxa + Veh
Lv-shNC + Oxa + PGF2α
Lv-shP + Oxa + PGF2α
HCT116-OXR
HCT8-OXR
HCT8-OXR
Lv-shNC + Oxa + Veh
Lv-shP + Oxa + Veh
Lv-shNC + Oxa + PGF2α
Lv-shP + Oxa + PGF2α
TUNEL
DAPI
Merge
C
HCT116-OXR
Lv-shNC + Oxa + Veh
Lv-shP + Oxa + Veh
Lv-shNC + Oxa + PGF2α
Lv-shP + Oxa + PGF2α
γ-H2AX
β-actin
HCT8-OXR
γ-H2AX
β-actin
Lv-shNC + Oxa + Veh
Lv-shP + Oxa + Veh
Lv-shNC + Oxa + PGF2α
Lv-shP + Oxa + PGF2α
Relative protein expression
HCT116-OXR
HCT8-OXR



DOI: 10.3748/wjg.v29.i39.5452 **Copyright** ©The Author(s) 2023.

Figure 6 The inhibitory effect of prostaglandin $F_{2\alpha}$ on oxaliplatin-induced cytotoxicity. A: Western blots showed the effect of prostaglandin F2α synthase ($PGF_{2\alpha}$) (PGFS) on the expressions of proliferating cell nuclear antigen, cleaved-poly ADP-ribose polymerase, and γ-H2A histone family member X (γ-H2AX) in PGFS knockdown, oxaliplatin-resistant (OR) cells; B: The effect of PGF2α on apoptosis in PGFS knockdown, OR cells evaluated by immunofluorescence. scale bar 100 uM; C: The effect of PGF2α on the cleavage of γ-H2AX protein expressions in PGFS knockdown, OR cells; D: The effect of PGF2α on DNA damage in PGFs knockdown, OR cells evaluated by single-cell gel electrophoresis. scale bar 50 μm). $^{a}P < 0.05$, $^{b}P < 0.01$, $^{c}P < 0.001$, ^{d}No significance. PCNA: Proliferating cell nuclear antigen; PARP: Poly ADP-ribose polymerase; γ-H2AX: γ-H2A histone family member X; TUNEL: Terminal deoxynucleotidyl transferase dUTP nick end labeling.





DOI: 10.3748/wjg.v29.i39.5452 **Copyright** ©The Author(s) 2023.

Figure 7 Prostaglandin $F_{2\alpha}$ synthase may suppresses the formation of platinum-DNA adducts. A: The effect of Prostaglandin $F_{2\alpha}$ synthase (PGF2α) (PGFS) overexpression on the formation of platinum-DNA adducts was determined using inductively coupled plasma mass spectrometry in colorectal cancer (CRC) cells; B: The effect of PGFS knockdown on the formation of platinum-DNA adducts in oxaliplatin-resistant (OR) CRC cells; C: The effect of PGF2α on the formation of platinum-DNA adducts in OR CRC cells; D: The reactive oxygen species (ROS) content were significantly decreased in OR CRC cells; E: PGFS overexpression significantly decreased ROS content in CRC cells; F: PGFS knockdown significantly decreased ROS content in OR CRC cells; G: PGFS knockdown significantly decreased ROS content in OR CRC cells (scale bar, 50 μm). $^{a}P < 0.05$, $^{b}P < 0.01$; ^{c}No significance. $PGF_{2\alpha}$: Prostaglandin $F_{2\alpha}$; Oxa: Oxaliplatin.

CONCLUSION

PGFS knockdown effectively inhibited the resistance of CRC to Oxa. Mechanistically, PGFS knockdown increased DNA and platinum binding. Moreover, the downstream product PGF2α of PGFS was reduced. The production of ROS was increased. In summary, the above function causes reduced cell death. Hence, we surmise that downregulation of PGFS could improve the efficacy of Oxa in the treatment of CRC.

ARTICLE HIGHLIGHTS

Research background

Chemoresistance is a major obstacle in colorectal cancer (CRC) therapy. Therefore, characterizing mechanisms of chemoresistance is beneficial to improve the treatment efficacy and survival rate of CRC patients. In this study, we identify the role and potential mechanism of prostaglandin $F2_{\alpha}$ synthase ($PGF_{2\alpha}$) (PGFS) in drug resistance to CRC, providing a novel therapeutic target against cancer drug resistance in the treatment of CRC.

Research motivation

The new theory of this study is that PGFS resistance to oxaliplatin (Oxa) has two effects, one is to reduce the production of reactive oxygen species (ROS) through the generation of $PGF_{2\alpha}$ products, and the other is the direct protective effect of PGFS on CRC nucleus. The new method in this study is the application of comet experiment to detect DNA damage, and the other is the application of inductively coupled plasma mass spectrometry (ICP-MS) to directly detect the platinum content of DNA in the nucleus, so as to directly detect the effect of PGFS on the binding of platinum and DNA.

Research objectives

This study was designed to exploit the function and mechanism of PGFS in chemoresistance in CRC. Our study reveals the different ways in which PGFS promotes chemoresistance in CRC, and provides a potential target for predicting and reversing chemoresistance of CRC.

Research methods

The expression level of PGFS is assessed in 37 pairs of CRC tissues and para-cancer tissues by as detected by quantitative polymerase chain reaction and western blot. We examined the influence of PGFS overexpression or knockdown in acquired Oxa-resistant CRC cell lines (HCT116-OxR and HCT8-OxR) and their parental cell lines (HCT116 and HCT8). In order to analyze how PGFS affects colon cancer cell proliferation, A cholecystokinin octapeptide assay was utilized to determine the half-inhibitory concentration value of the cells, a plate clone formation assay was used to determine the clonogenesis ability, and an analysis of proliferating cell nuclear antigen expression was performed to determine the growth rate. Transferase dUTP nick end labeling and Annexin V/propidium iodide stainings, as well as the apoptotic markers cleaved-poly ADP-ribose polymerase and cleaved-caspase 3, were used to detect apoptosis. Western blot and cellular immunofluorescence were used to detect the expression and morphology of the DNA damage marker γ-H2AX. The DNA damage was detected by single-cell gel electrophoresis. Indomethacin, an inhibitor of prostaglandin synthase of PGFS, was used to elucidate the underlying mechanisms. Rescue experiments were conducted by introducing $PGF_{2\alpha}$, the product of PGFS, subsequent to the knockdown of PGFS. The platinum-DNA adducts were quantified using ICP-MS, and intracellular ROS levels were measured using a kit for measuring reactive oxygen species.

Research results

We found that PGFS reduced the production of ROS through its downstream product $PGF_{2\alpha}$, and thereby promotes Oxa resistance in CRC, meanwhile, it inhibited the formation of platinum-DNA adducts in a $PGF_{2\alpha}$-independent manner. The suppressive role of PGFS in the formation of platinum-DNA adducts has never been reported before. However, some questions need to be further clarified, for example, by what mechanism does PGFS suppress the formation of platinum-DNA adducts?

Research conclusions

This study aims to explore the relationship between PGFS and the occurrence and development of CRC, and the relationship between PGFS and Oxa resistance in CRC as well as the related mechanisms. In the future, it is hoped to predict whether patients with CRC are resistant to Oxa by detecting PGFS genes.

Research perspectives

Further work will be needed to clarify the function of PGFS in the nucleus and its mechanisms of action. Moreover, the inhibition mechanism of PGFS in the formation of platinum-DNA adducts needs to be further elucidated.

FOOTNOTES

Author contributions: Wang YJ, Xie XL, and Jiang HQ conceived, and designed the study; Wang YJ, Xie XL, Zhang JN, Zhou X, Chen SX, and Liu T performed most experiments, analyzed the data, wrote the manuscript and edited the paper; Xie XL and Jiang HQ helped to supervise the study; Tian H, Jiang XY, Wang SL, Zhang JN, Jin XX, and Liu SM helped to perform the experiments and analyzed the data; Xie XL, Liu HQ, and Jiang HQ helped to edit the paper; All authors have read and approved the final manuscript.

Supported by the S and T Program of Hebei, No. 22377704D; Medical Science Research Project of Hebei Province, No. 20190510; Postgraduate's Innovation Fund Project of Hebei Province, No. CXZZBS2021077.

Institutional review board statement: This study was reviewed and approved by the Ethics Committee of the Second Hospital of Hebei Medical University (No. 2021-R441).

Institutional animal care and use committee statement: All animal experiments conformed to the internationally accepted principles for the care and use of laboratory animals (The Animal Experiments Inspectorate, Second Hospital of Hebei Medical University; protocol no. 2022-AE010, The Institutional Animal Care and Use Committee at the Second Hospital of Hebei Medical University, Hebei Province, China).

Informed consent statement: All study participants or their legal guardian provided informed written consent about personal and medical data collection prior to study enrolment.

Conflict-of-interest statement: The authors declare that there are no conflicts of interest in our study.

Data sharing statement: No additional data are available.

ARRIVE guidelines statement: The authors have read the ARRIVE guidelines, and the manuscript was prepared and revised according to the ARRIVE guidelines.

Open-Access: This article is an open-access article that was selected by an in-house editor and fully peer-reviewed by external reviewers. It is distributed in accordance with the Creative Commons Attribution NonCommercial (CC BY-NC 4.0) license, which permits others to distribute, remix, adapt, build upon this work non-commercially, and license their derivative works on different terms, provided the original work is properly cited and the use is non-commercial. See: https://creativecommons.org/Licenses/by-nc/4.0/

Country/Territory of origin: China

ORCID number: Yi-Jun Wang 0000-0002-3918-1051; Xiao-Li Xie 0000-0001-5910-0231; Hong-Qun Liu 0000-0002-6805-5177; Hui Tian 0000-0003-3125-3820; Xiao-Yu Jiang 0000-0003-3592-9197; Jiu-Na Zhang 0000-0003-3813-9369; Sheng-Xiong Chen 0000-0002-1566-3064; Ting Liu 0000-0002-0874-9775; Shu-Ling Wang 0000-0002-9798-1604; Xue Zhou 0000-0002-5683-1861; Xiao-Xu Jin 0000-0002-2307-9888; Shi-Mao Liu 0000-0003-2535-2638; Hui-Qing Jiang 0000-0001-8706-0943.

S-Editor: Qu XL
L-Editor: A
P-Editor: Cai YX

REFERENCES

1 **Sung H**, Ferlay J, Siegel RL, Laversanne M, Soerjomataram I, Jemal A, Bray F. Global Cancer Statistics 2020: GLOBOCAN Estimates of Incidence and Mortality Worldwide for 36 Cancers in 185 Countries. *CA Cancer J Clin* 2021; **71**: 209-249 [PMID: 33538338 DOI: 10.3322/caac.21660]

2 **Yang Y**, Wang HY, Chen YK, Chen JJ, Song C, Gu J. Current status of surgical treatment of rectal cancer in China. *Chin Med J (Engl)* 2020; **133**: 2703-2711 [PMID: 32889914 DOI: 10.1097/CM9.0000000000001076]

3 **Taieb J**, Shi Q, Pederson L, Alberts S, Wolmark N, Van Cutsem E, de Gramont A, Kerr R, Grothey A, Lonardi S, Yoshino T, Yothers G, Sinicrope FA, Zaanan A, André T. Prognosis of microsatellite instability and/or mismatch repair deficiency stage III colon cancer patients after disease recurrence following adjuvant treatment: results of an ACCENT pooled analysis of seven studies. *Ann Oncol* 2019; **30**: 1466-1471 [PMID: 31268130 DOI: 10.1093/annonc/mdz208]

4 **Glynne-Jones R**, Wyrwicz L, Tiret E, Brown G, Rödel C, Cervantes A, Arnold D; ESMO Guidelines Committee. Rectal cancer: ESMO Clinical Practice Guidelines for diagnosis, treatment and follow-up. *Ann Oncol* 2018; **29**: iv263 [PMID: 29741565 DOI: 10.1093/annonc/mdy161]

5 **Benson AB**, Venook AP, Al-Hawary MM, Arain MA, Chen YJ, Ciombor KK, Cohen S, Cooper HS, Deming D, Garrido-Laguna I, Grem JL, Gunn A, Hoffe S, Hubbard J, Hunt S, Kirilcuk N, Krishnamurthi S, Messersmith WA, Meyerhardt J, Miller ED, Mulcahy MF, Nurkin S, Overman MJ, Parikh A, Patel H, Pedersen K, Saltz L, Schneider C, Shibata D, Skibber JM, Sofocleous CT, Stoffel EM, Stotsky-Himelfarb E, Willett CG, Johnson-Chilla A, Gurski LA. NCCN Guidelines Insights: Rectal Cancer, Version 6.2020. *J Natl Compr Canc Netw* 2020; **18**: 806-815 [PMID: 32634771 DOI: 10.6004/jnccn.2020.0032]

6 **Tougeron D**, Mouillet G, Trouilloud I, Lecomte T, Coriat R, Aparicio T, Des Guetz G, Lécaille C, Artru P, Sickersen G, Cauchin E, Sefrioui D, Boussaha T, Ferru A, Matysiak-Budnik T, Silvain C, Karayan-Tapon L, Pagès JC, Vernerey D, Bonnetain F, Michel P, Taïeb J, Zaanan A. Efficacy of Adjuvant Chemotherapy in Colon Cancer With Microsatellite Instability: A Large Multicenter AGEO Study. *J Natl Cancer Inst* 2016; **108** [PMID: 26839356 DOI: 10.1093/jnci/djv438]

7 **de Gramont A**, Schmoll HJ, Cervantes A, Tournigand C. The evolving role of oxaliplatin in the management of colorectal cancer. *Colorectal Dis* 2003; **5** Suppl 3: 10-19 [PMID: 23573556 DOI: 10.1046/j.1463-1318.5.s3.3.x]

8 **Rödel C**, Graeven U, Fietkau R, Hohenberger W, Hothorn T, Arnold D, Hofheinz RD, Ghadimi M, Wolff HA, Lang-Welzenbach M, Raab HR, Wittekind C, Ströbel P, Staib L, Wilhelm M, Grabenbauer GG, Hoffmanns H, Lindemann F, Schlenska-Lange A, Folprecht G, Sauer R, Liersch T; German Rectal Cancer Study Group. Oxaliplatin added to fluorouracil-based preoperative chemoradiotherapy and postoperative chemotherapy of locally advanced rectal cancer (the German CAO/ARO/AIO-04 study): final results of the multicentre, open-label, randomised, phase 3 trial. *Lancet Oncol* 2015; **16**: 979-989 [PMID: 26189067 DOI: 10.1016/S1470-2045(15)00159-X]

9 **Galluzzi L**, Senovilla L, Vitale I, Michels J, Martins I, Kepp O, Castedo M, Kroemer G. Molecular mechanisms of cisplatin resistance. *Oncogene* 2012; **31**: 1869-1883 [PMID: 21892204 DOI: 10.1038/onc.2011.384]

10 **Vaughn CM**, Selby CP, Yang Y, Hsu DS, Sancar A. Genome-wide single-nucleotide resolution of oxaliplatin-DNA adduct repair in drug-sensitive and -resistant colorectal cancer cell lines. *J Biol Chem* 2020; **295**: 7584-7594 [PMID: 32299912 DOI: 10.1074/jbc.RA120.013347]

11 **Assaf KI**, Nau WM. Cucurbiturils: from synthesis to high-affinity binding and catalysis. *Chem Soc Rev* 2015; **44**: 394-418 [PMID: 25317670 DOI: 10.1039/c4cs00273c]

12 **Stordal BK**, Davey MW, Davey RA. Oxaliplatin induces drug resistance more rapidly than cisplatin in H69 small cell lung cancer cells. *Cancer Chemother Pharmacol* 2006; **58**: 256-265 [PMID: 16283310 DOI: 10.1007/s00280-005-0148-7]

13 **Ekblad L**, Kjellström J, Johnsson A. Reduced drug accumulation is more important in acquired resistance against oxaliplatin than against cisplatin in isogenic colon cancer cells. *Anticancer Drugs* 2010; **21**: 523-531 [PMID: 20168208 DOI: 10.1097/CAD.0b013e328337b867]

14 **Chu C**, Wei H, Zhu W, Shen Y, Xu Q. Decreased Prostaglandin D2 Levels in Major Depressive Disorder Are Associated with Depression-Like Behaviors. *Int J Neuropsychopharmacol* 2017; **20**: 731-739 [PMID: 28582515 DOI: 10.1093/ijnp/pyx044]

15 **Wang MT**, Honn KV, Nie D. Cyclooxygenases, prostanoids, and tumor progression. *Cancer Metastasis Rev* 2007; **26**: 525-534 [PMID: 17763971 DOI: 10.1007/s10555-007-9096-5]

16 **Wang S**, Yang Q, Fung KM, Lin HK. AKR1C2 and AKR1C3 mediated prostaglandin D2 metabolism augments the PI3K/Akt proliferative signaling pathway in human prostate cancer cells. *Mol Cell Endocrinol* 2008; **289**: 60-66 [PMID: 18508192 DOI: 10.1016/j.mce.2008.04.004]

17 **Sinreih M**, Anko M, Kene NH, Kocbek V, Rižner TL. Expression of AKR1B1, AKR1C3 and other genes of prostaglandin F2α biosynthesis and action in ovarian endometriosis tissue and in model cell lines. *Chem Biol Interact* 2015; **234**: 320-331 [PMID: 25446850 DOI: 10.1016/j.cbi.2014.11.009]

18 **Watanabe K**. Recent reports about enzymes related to the synthesis of prostaglandin (PG) F(2) (PGF(2α) and 9α, 11β-PGF(2)). *J Biochem* 2011; **150**: 593-596 [PMID: 21926128 DOI: 10.1093/jb/mvr116]

19 **Fung KM**, Samara EN, Wong C, Metwalli A, Krlin R, Bane B, Liu CZ, Yang JT, Pitha JV, Culkin DJ, Kropp BP, Penning TM, Lin HK. Increased expression of type 2 3alpha-hydroxysteroid dehydrogenase/type 5 17beta-hydroxysteroid dehydrogenase (AKR1C3) and its relationship with androgen receptor in prostate carcinoma. *Endocr Relat Cancer* 2006; **13**: 169-180 [PMID: 16601286 DOI: 10.1677/erc.1.01048]

20 **Wang HW**, Lin CP, Chiu JH, Chow KC, Kuo KT, Lin CS, Wang LS. Reversal of inflammation-associated dihydrodiol dehydrogenases (AKR1C1 and AKR1C2) overexpression and drug resistance in nonsmall cell lung cancer cells by wogonin and chrysin. *Int J Cancer* 2007;

120: 2019-2027 [PMID: 17266043 DOI: 10.1002/ijc.22402]
21 **Baraibar MA**, Liu L, Ahmed EK, Friguet B. Protein oxidative damage at the crossroads of cellular senescence, aging, and age-related diseases. *Oxid Med Cell Longev* 2012; **2012**: 919832 [PMID: 23125894 DOI: 10.1155/2012/919832]
22 **Srinivas US**, Tan BWQ, Vellayappan BA, Jeyasekharan AD. ROS and the DNA damage response in cancer. *Redox Biol* 2019; **25**: 101084 [PMID: 30612957 DOI: 10.1016/j.redox.2018.101084]
23 **Sugino N**, Karube-Harada A, Kashida S, Takiguchi S, Kato H. Reactive oxygen species stimulate prostaglandin F2 alpha production in human endometrial stromal cells in vitro. *Hum Reprod* 2001; **16**: 1797-1801 [PMID: 11527878 DOI: 10.1093/humrep/16.9.1797]
24 **Matsunaga T**, Hojo A, Yamane Y, Endo S, El-Kabbani O, Hara A. Pathophysiological roles of aldo-keto reductases (AKR1C1 and AKR1C3) in development of cisplatin resistance in human colon cancers. *Chem Biol Interact* 2013; **202**: 234-242 [PMID: 23165153 DOI: 10.1016/j.cbi.2012.09.024]
25 **Liu Z**, Liu J, Liu X, Wang X, Xie Q, Zhang X, Kong X, He M, Yang Y, Deng X, Yang L, Qi Y, Li J, Liu Y, Yuan L, Diao L, He F, Li D. CTR-DB, an omnibus for patient-derived gene expression signatures correlated with cancer drug response. *Nucleic Acids Res* 2022; **50**: D1184-D1199 [PMID: 34570230 DOI: 10.1093/nar/gkab860]
26 **Tan Z**, Gao L, Wang Y, Yin H, Xi Y, Wu X, Shao Y, Qiu W, Du P, Shen W, Fu L, Jia R, Zhao C, Zhang Y, Zhao Z, Sun Z, Chen H, Hu X, Xu J. PRSS contributes to cetuximab resistance in colorectal cancer. *Sci Adv* 2020; **6**: eaax5576 [PMID: 31911942 DOI: 10.1126/sciadv.aax5576]
27 **Schiffer L**, Bossey A, Kempegowda P, Taylor AE, Akerman I, Scheel-Toellner D, Storbeck KH, Arlt W. Peripheral blood mononuclear cells preferentially activate 11-oxygenated androgens. *Eur J Endocrinol* 2021; **184**: 353-363 [PMID: 33444228 DOI: 10.1530/EJE-20-1077]
28 **Nakarai C**, Osawa K, Akiyama M, Matsubara N, Ikeuchi H, Yamano T, Hirota S, Tomita N, Usami M, Kido Y. Expression of AKR1C3 and CNN3 as markers for detection of lymph node metastases in colorectal cancer. *Clin Exp Med* 2015; **15**: 333-341 [PMID: 24934327 DOI: 10.1007/s10238-014-0298-1]
29 **Zhao J**, Xiang Y, Xiao C, Guo P, Wang D, Liu Y, Shen Y. AKR1C3 overexpression mediates methotrexate resistance in choriocarcinoma cells. *Int J Med Sci* 2014; **11**: 1089-1097 [PMID: 25170291 DOI: 10.7150/ijms.9239]
30 **Minotti G**, Menna P, Salvatorelli E, Cairo G, Gianni L. Anthracyclines: molecular advances and pharmacologic developments in antitumor activity and cardiotoxicity. *Pharmacol Rev* 2004; **56**: 185-229 [PMID: 15169927 DOI: 10.1124/pr.56.2.6]
31 **Heibein AD**, Guo B, Sprowl JA, Maclean DA, Parissenti AM. Role of aldo-keto reductases and other doxorubicin pharmacokinetic genes in doxorubicin resistance, DNA binding, and subcellular localization. *BMC Cancer* 2012; **12**: 381 [PMID: 22938713 DOI: 10.1186/1471-2407-12-381]
32 **Rixe O**, Ortuzar W, Alvarez M, Parker R, Reed E, Paull K, Fojo T. Oxaliplatin, tetraplatin, cisplatin, and carboplatin: spectrum of activity in drug-resistant cell lines and in the cell lines of the National Cancer Institute's Anticancer Drug Screen panel. *Biochem Pharmacol* 1996; **52**: 1855-1865 [PMID: 8951344 DOI: 10.1016/s0006-2952(97)81490-6]
33 **Zhou Q**, Tian W, Jiang Z, Huang T, Ge C, Liu T, Zhao F, Chen T, Cui Y, Li H, Yao M, Li J, Tian H. A Positive Feedback Loop of AKR1C3-Mediated Activation of NF-κB and STAT3 Facilitates Proliferation and Metastasis in Hepatocellular Carcinoma. *Cancer Res* 2021; **81**: 1361-1374 [PMID: 33361392 DOI: 10.1158/0008-5472.CAN-20-2480]
34 **Ruan Y**, Wang L, Lu Y. HDAC6 inhibitor, ACY1215 suppress the proliferation and induce apoptosis of gallbladder cancer cells and increased the chemotherapy effect of gemcitabine and oxaliplatin. *Drug Dev Res* 2021; **82**: 598-604 [PMID: 33428788 DOI: 10.1002/ddr.21780]
35 **Hsu HH**, Chen MC, Baskaran R, Lin YM, Day CH, Lin YJ, Tu CC, Vijaya Padma V, Kuo WW, Huang CY. Oxaliplatin resistance in colorectal cancer cells is mediated *via* activation of ABCG2 to alleviate ER stress induced apoptosis. *J Cell Physiol* 2018; **233**: 5458-5467 [PMID: 29247488 DOI: 10.1002/jcp.26406]
36 **Sales KJ**, List T, Boddy SC, Williams AR, Anderson RA, Naor Z, Jabbour HN. A novel angiogenic role for prostaglandin F2alpha-FP receptor interaction in human endometrial adenocarcinomas. *Cancer Res* 2005; **65**: 7707-7716 [PMID: 16140938 DOI: 10.1158/0008-5472.CAN-05-0101]
37 **Suzuki-Yamamoto T**, Nishizawa M, Fukui M, Okuda-Ashitaka E, Nakajima T, Ito S, Watanabe K. cDNA cloning, expression and characterization of human prostaglandin F synthase. *FEBS Lett* 1999; **462**: 335-340 [PMID: 10622721 DOI: 10.1016/s0014-5793(99)01551-3]
38 **Qualtrough D**, Kaidi A, Chell S, Jabbour HN, Williams AC, Paraskeva C. Prostaglandin F(2alpha) stimulates motility and invasion in colorectal tumor cells. *Int J Cancer* 2007; **121**: 734-740 [PMID: 17437271 DOI: 10.1002/ijc.22755]
39 **Zhang Y**, Xie C, Li A, Liu X, Xing Y, Shen J, Huo Z, Zhou S, Xie Y, Cao W, Ma Y, Xu R, Cai S, Tang X, Ma D. PKI-587 enhances chemosensitivity of oxaliplatin in hepatocellular carcinoma through suppressing DNA damage repair pathway (NHEJ and HR) and PI3K/AKT/mTOR pathway. *Am J Transl Res* 2019; **11**: 5134-5149 [PMID: 31497229]
40 **Liu J**, Fu XQ, Zhou W, Yu HG, Yu JP, Luo HS. LY294002 potentiates the anti-cancer effect of oxaliplatin for gastric cancer *via* death receptor pathway. *World J Gastroenterol* 2011; **17**: 181-190 [PMID: 21245990 DOI: 10.3748/wjg.v17.i2.181]
41 **Deb S**, Xu H, Tuynman J, George J, Yan Y, Li J, Ward RL, Mortensen N, Hawkins NJ, McKay MJ, Ramsay RG, Fox SB. RAD21 cohesin overexpression is a prognostic and predictive marker exacerbating poor prognosis in KRAS mutant colorectal carcinomas. *Br J Cancer* 2014; **110**: 1606-1613 [PMID: 24548858 DOI: 10.1038/bjc.2014.31]
42 **Liedtke AJ**, Adeniji AO, Chen M, Byrns MC, Jin Y, Christianson DW, Marnett LJ, Penning TM. Development of potent and selective indomethacin analogues for the inhibition of AKR1C3 (Type 5 17β-hydroxysteroid dehydrogenase/prostaglandin F synthase) in castrate-resistant prostate cancer. *J Med Chem* 2013; **56**: 2429-2446 [PMID: 23432095 DOI: 10.1021/jm3017656]
43 **Marzano C**, Gandin V, Folda A, Scutari G, Bindoli A, Rigobello MP. Inhibition of thioredoxin reductase by auranofin induces apoptosis in cisplatin-resistant human ovarian cancer cells. *Free Radic Biol Med* 2007; **42**: 872-881 [PMID: 17320769 DOI: 10.1016/j.freeradbiomed.2006.12.021]
44 **Rudin CM**, Yang Z, Schumaker LM, VanderWeele DJ, Newkirk K, Egorin MJ, Zuhowski EG, Cullen KJ. Inhibition of glutathione synthesis reverses Bcl-2-mediated cisplatin resistance. *Cancer Res* 2003; **63**: 312-318 [PMID: 12543781]

World Journal of Gastroenterology

Submit a Manuscript: https://www.f6publishing.com

World J Gastroenterol 2023 October 21; 29(39): 5471-5482

DOI: 10.3748/wjg.v29.i39.5471

ISSN 1007-9327 (print) ISSN 2219-2840 (online)

ORIGINAL ARTICLE

Basic Study

Enhanced glucose homeostasis *via Clostridium symbiosum*-mediated glucagon-like peptide 1 inhibition of hepatic gluconeogenesis in mid-intestinal bypass surgery

Xin Luo, Fang Tao, Cai Tan, Chi-Ying Xu, Zhi-Hua Zheng, Qiang Pang, Xiang-An He, Jia-Qing Cao, Jin-Yuan Duan

Specialty type: Gastroenterology and hepatology

Provenance and peer review: Unsolicited article; Externally peer reviewed.

Peer-review model: Single blind

Peer-review report's scientific quality classification

Grade A (Excellent): 0
Grade B (Very good): B
Grade C (Good): C
Grade D (Fair): 0
Grade E (Poor): 0

P-Reviewer: Mata-Torres G, Mexico; Thongon N, Thailand

Received: July 14, 2023
Peer-review started: July 14, 2023
First decision: September 6, 2023
Revised: September 11, 2023
Accepted: October 11, 2023
Article in press: October 11, 2023
Published online: October 21, 2023

Xin Luo, Fang Tao, Chi-Ying Xu, Jin-Yuan Duan, Department of General Surgery, The First Affiliated Hospital of Nanchang University, Nanchang 330000, Jiangxi Province, China

Cai Tan, Department of Women's Health, Jiangxi Maternal and Child Health Hospital, Nanchang 330000, Jiangxi Province, China

Zhi-Hua Zheng, Qiang Pang, Xiang-An He, Jia-Qing Cao, Department of General Surgery, The Second Affiliated Hospital of Nanchang University, Nanchang 330000, Jiangxi Province, China

Corresponding author: Jin-Yuan Duan, PhD, Associate Chief Physician, Department of General Surgery, The First Affiliated Hospital of Nanchang University, No. 1519 Dongyue Avenue, Nanchang 330000, Jiangxi Province, China. duanjy2022@outlook.com

Abstract

BACKGROUND

The small intestine is known to play a crucial role in the development and remission of diabetes mellitus (DM). However, the exact mechanism by which mid-small intestinal bypass improves glucose metabolism in diabetic rats is not fully understood.

AIM

To elucidate the mechanisms by which mid-small intestinal bypass improves glucose metabolism.

METHODS

Streptozotocin (STZ) was used to induce DM in Sprague-Dawley (SD) rats at a dose of 60 mg/kg. The rats were then randomly divided into two groups: The mid-small intestine bypass (MSIB) group and the sham group (underwent switch laparotomy). Following a 6-wk recovery period post-surgery, the rats underwent various assessments, including metabolic parameter testing, analysis of liver glycogen levels, measurement of key gluconeogenic enzyme activity, characterization of the gut microbiota composition, evaluation of hormone levels, determination of bile acid concentrations, and assessment of the expression of the intestinal receptors Takeda G protein-coupled receptor 5 and farnesoid X receptor.

RESULTS
The MSIB group of rats demonstrated improved glucose metabolism and lipid metabolism, along with increased hepatic glycogen content. Furthermore, there was a decrease in the expression of the key gluconeogenic enzymes phosphoenolpyruvate carboxykinase 1 and glucose-6-phosphatase. Importantly, the MSIB group exhibited a substantial increase in the abundances of intestinal *Lactobacillus*, *Clostridium symbiosum*, *Ruminococcus gnavus*, and *Bilophila*. Moreover, higher levels of secondary bile acids, such as intestinal lithocholic acid, were observed in this group. Remarkably, the changes in the gut microbiota showed a significant correlation with the expression of key gluconeogenic enzymes and glucagon-like peptide 1 (GLP-1) at 6 wk postoperatively, highlighting their potential role in glucose regulation. These findings highlight the beneficial effects of mid-small intestine bypass on glucose metabolism and the associated modulation of the gut microbiota.

CONCLUSION
The findings of this study demonstrate that the introduction of postoperative intestinal *Clostridium symbiosum* in the mid-small intestine contributes to the enhancement of glucose metabolism in nonobese diabetic rats. This improvement is attributed to the increased inhibition of hepatic gluconeogenesis mediated by GLP-1, resulting in a favorable modulation of glucose homeostasis.

Key Words: Gut micobiome; Glucagon-like peptide-1; Glucose metablism; Bile acid; Bariatric surgery; Gluconeogenesis

©The Author(s) 2023. Published by Baishideng Publishing Group Inc. All rights reserved.

Core Tip: Intestinal function plays a pivotal role in the onset, progression, and alleviation of diabetes. However, research on surgical procedures and functions involving the mid-small intestine is limited. The precise mechanisms by which the mid-small intestine improves glucose metabolism in diabetic rats remain largely unclear. This study explores the effects of mid-small intestine bypass surgery on diabetic rats. Post-surgery, there was an increase in the abundance of *Clostridium symbiosum* in the rat gut, which contributed to improved glucose metabolism through the inhibition of hepatic gluconeogenesis mediated by glucagon-like peptide 1. These findings provide a theoretical basis for non-surgical interventions in the treatment of metabolic disorders associated with diabetes.

Citation: Luo X, Tao F, Tan C, Xu CY, Zheng ZH, Pang Q, He XA, Cao JQ, Duan JY. Enhanced glucose homeostasis *via Clostridium symbiosum*-mediated glucagon-like peptide 1 inhibition of hepatic gluconeogenesis in mid-intestinal bypass surgery. *World J Gastroenterol* 2023; 29(39): 5471-5482
URL: https://www.wjgnet.com/1007-9327/full/v29/i39/5471.htm
DOI: https://dx.doi.org/10.3748/wjg.v29.i39.5471

INTRODUCTION

Diabetes and obesity have become global health concerns, and their strong association has been widely recognized[1,2]. Bariatric surgery has gained considerable attention as a therapeutic approach for obesity and diabetes improvement[3]. The small intestine, a pivotal organ in dietary metabolism, plays a crucial role in the development of diabetes[4]. Each segment of the small intestine exhibits distinct functions[5], including the "ileal brake" mechanism at the distal ileum[6,7]. Additionally, the gut microbiota composition varies among different segments of the small intestine. While gastric bypass, a commonly employed bariatric surgery, involves bypassing a portion of the upper small intestine[8], less research has focused on the procedure and function of the middle small intestine. To investigate the role of the middle small intestine in glucose metabolism, we utilized a STZ-induced nonobese diabetic SD rat model[9] and conducted middle small intestinal bypass surgery to assess the changes in metabolic function and related factors postoperatively. This study aimed to elucidate the metabolic function and underlying mechanisms of the mid-segment small intestine, with the ultimate goal of providing a theoretical foundation for nonsurgical interventions targeting glucose metabolism disorders.

MATERIALS AND METHODS

Experimental animals

In this study, 8-wk-old male SD rats were used to investigate the metabolic improvement effect of mid-small intestine bypass (MSIB). The rats were obtained from Shanghai Slaughter Laboratory Animal Co., Ltd. and were fed a normal diet. After a one-week acclimatization period, a diabetic rat model was established by intraperitoneal administration of STZ at a dose of 60 mg/kg, divided into two doses administered on the same day. Following successful model establishment, the

rats were randomly assigned to undergo either MSIB or sham surgery (sham). The rats were maintained under identical environmental conditions for 6 wk until euthanasia. Glucose tolerance [oral glucose tolerance test (OGTT)] and insulin sensitivity [insulin tolerance test (ITT)] were assessed at 2 and 6 wk postoperatively. Venous blood, liver tissue, ileal tissue, and fecal samples were collected for analysis at 6 wk postoperatively.

The rats were individually housed in well-ventilated cages with ad libitum access to water and food. Weekly measurements of body weight and food intake were recorded. All animal experiments adhered to the relevant ethical guidelines for animal research and were approved by the Animal Ethics Committee of Nanchang University. Standard animal care and laboratory protocols were followed in accordance with the ARRIVE guidelines.

Animal operations

The rats were fasted for approximately 14 h and underwent surgery after anesthesia (isoflurane, 2% for maintenance and 4% for induction). The abdomen was prepared, and a 4-cm median incision was made to access the abdominal cavity.

In the MSIB group, the point close to the ileocecal flap was used as the reference point. Approximately 60% of the small bowel was bypassed, starting 20 cm proximal to this point and extending 20 cm distal to the flexural ligament. Intestinal continuity was restored through a lateral anastomosis between the distal and proximal small bowel segments. The lumen of the bypassed segment was occluded by silk ligation at the site of the lateral anastomosis. For the sham group, the bowel was gently manipulated upon entering the abdominal cavity. The abdominal cavity was closed with 3-0 silk sutures. The duration of the surgery was approximately 45 min. Subsequently, the rats were subcutaneously injected with 10 mL of sterile saline for fluid resuscitation and placed individually in cages to recover from anesthesia.

Biochemical tests and enzyme-linked immunosorbent assay

Blood was collected from the rat tail vein, and the blood glucose level was measured using an electronic glucometer (Accu-Chek Performa, Roche Diagnostics, Switzerland). The blood was then centrifuged at 3000 rpm for 15 min at 4 °C, and the resulting sera were immediately transferred to new tubes and stored at -80 °C until assay analysis was performed. Serum concentrations of triglycerides (TG), total cholesterol, high-density lipoprotein (HDL), low-density lipoprotein, non-HDL, and free fatty acids were determined using a fully automated biochemical analyzer. The analysis and testing procedures were conducted by the Biochemistry Laboratory at the Second Affiliated Hospital of Nanchang University. Insulin concentrations in serum were measured using an enzyme-linked immunosorbent assay (ELISA) kit (Millipore, Billerica, MA, United States). Additionally, serum concentrations of glucagon-like peptide-1 (GLP-1), peptide tyrosine tyrosine, leptin, ghrelin, and fibroblast growth factor 21 (FGF21) were determined using ELISA kits (Uscn Life Sciences, Wuhan, China).

OGTT and ITT

The OGTT and ITT were conducted at 2 and 6 wk postoperatively, respectively. The rats were fasted for 14 h prior to the tests. The OGTT was performed at 8 am by measuring the initial blood glucose level from the tail vein. Subsequently, a gavage of 20% glucose solution (1 g/kg) was administered to the rats with STZ-induced diabetes mellitus (STZ-DM). Blood glucose measurements were taken at 0, 15, 30, 60, 90, and 120 min after glucose administration, and the area under the curve (AUC) of the glucose tolerance test was calculated. Furthermore, six hours after fasting, the rats underwent ITT. After measuring the initial blood glucose level, 0.5 IU/kg human insulin (Wanbang Biopharmaceuticals, Jiangsu, China) was injected intraperitoneally, and blood glucose levels were measured at 0, 15, 30, 60, 90, and 180 min. Insulin sensitivity was assessed by calculating the ratio of blood glucose to basal blood glucose at each time point, and the AUC of the ITT was calculated.

Metabolomics

After 6 wk of surgery, each rat was placed in an individual collection box, and fecal samples were collected within 48 h. The collected samples were immediately frozen in a -80 °C freezer. Bile acid extraction was performed using methanol. For each sample, methanol (5 mL/g) was added, and the mixture was shaken and incubated at room temperature for a specified period. Subsequently, the mixture was centrifuged at 1200 rpm for 2 min at room temperature, and the supernatant was carefully transferred into a new centrifuge tube. High-performance liquid chromatography (HPLC) was employed for bile acid determination. The filtered supernatant was injected into the HPLC apparatus and passed through the separation column. Gradient elution was performed using an appropriate mobile phase, and the absorbance of bile acids was detected by an ultraviolet detector. The concentration of bile acids in rat feces was determined by referencing a known concentration of bile acids in the standard curve.

Quantitative real-time polymerase chain reaction

RNA extraction from the collected liver and ileal samples was performed using the TRIzol Plus RNA Purification Kit (Thermo Fisher) following the manufacturer's instructions. The extracted RNA samples were assessed for quantity and quality using a nanophotometer (NanoDrop-2000, Thermo Fisher Scientific, Massachusetts, United States). Reverse transcription reactions were carried out using the Reverse Transcription Kit (XYZ Company, Country) to convert RNA into cDNA, utilizing SuperScript™ III First-Strand Synthesis SuperMix (Thermo Fisher). The reverse transcription reaction mixture consisted of RNA template, reverse transcriptase, random primers, and reverse transcription buffer. The reaction conditions involved incubation at 37 °C for 30 min, followed by heat inactivation at 95 °C for 5 min. To amplify the target genes, preamplification reactions were performed using the Preamplification Kit (XYZ Company, Country). The preamplification reaction mixture included cDNA template, target gene-specific primer mixture, and preamplification buffer. The reaction conditions consisted of initial denaturation at 95 °C for 2 min, followed by 14 cycles of

denaturation (95 °C, 15 s), annealing (60 °C, 1 min), and extension (72 °C, 30 s), with a final extension at 72 °C for 5 min. Real-time fluorescent quantitative polymerase chain reaction (PCR) analysis was performed using an ABI Prism 7700 sequence detector system (Applied Biosystems, Foster City, CA, United States). The PCR mixture consisted of the preamplified product, primer mix, fluorescent probe, and PCR Master Mix. The concentrations of primers and probes were adjusted based on optimization experiments. The reaction conditions included initial denaturation at 95 °C for 2 min, followed by 40 cycles of denaturation (95 °C, 15 s) and annealing (60 °C, 1 min).

16S rRNA sequencing

Microbial DNA was extracted from frozen fecal samples using the MagPure Fecal DNA KF Kit B (Magen, China). The extraction process was performed following the manufacturer's instructions, and the concentration and purity of the DNA were measured using a nanophotometer with the Qubit dsDNA BR Analysis Kit (Invitrogen, United States). The V3-V4 region of the 16S rRNA gene was selected as the target for amplification. The PCR amplification reaction consisted of 10 ng of template DNA, 2.5 μM of each primer, and KAPA HiFi HotStart ReadyMix PCR Master Mix (Kapa Biosystems, United States). The PCR amplification conditions were as follows: Predenaturation at 95 °C for 3 min, followed by 30 cycles of denaturation at 95 °C for 30 s, annealing at 55 °C for 30 s, extension at 72 °C for 30 s, and a final extension step at 72 °C for 5 min.

The PCR products were verified by gel electrophoresis and then purified using Ampure XP beads (Beckman Coulter, United States). The purified products underwent secondary PCR amplification using Illumina aptamers and sample-specific index sequences. The secondary PCR products were again validated by gel electrophoresis and purified using Ampure XP beads.

Sequencing was performed on the PacBio Sequel platform (UW Genetics, Shenzhen, China), and the obtained sequences were assigned to operational taxonomic units (OTUs) based on 97% sequence similarity. Clean tags were clustered into OTUs using USEARCH software (v7.0.1090), and species classification of the OTUs was completed. The representative sequences of the OTUs were compared to the Greengene_2013_5_99 database using RDP classifier (v2.2) software for species annotation, with a confidence threshold set to 0.5[10]. Diversity indices of the gut flora were calculated, and the beta diversity index of the gut microbiota was visualized using principal coordinate analysis, with the Shannon index representing the alpha diversity index. The differences in OTU abundance between groups were compared, and significantly different flora were identified using the linear discriminant analysis effect sizes (LEfSe) method, available on the Galaxy (harvard.edu) website.

Quantification and statistical analysis

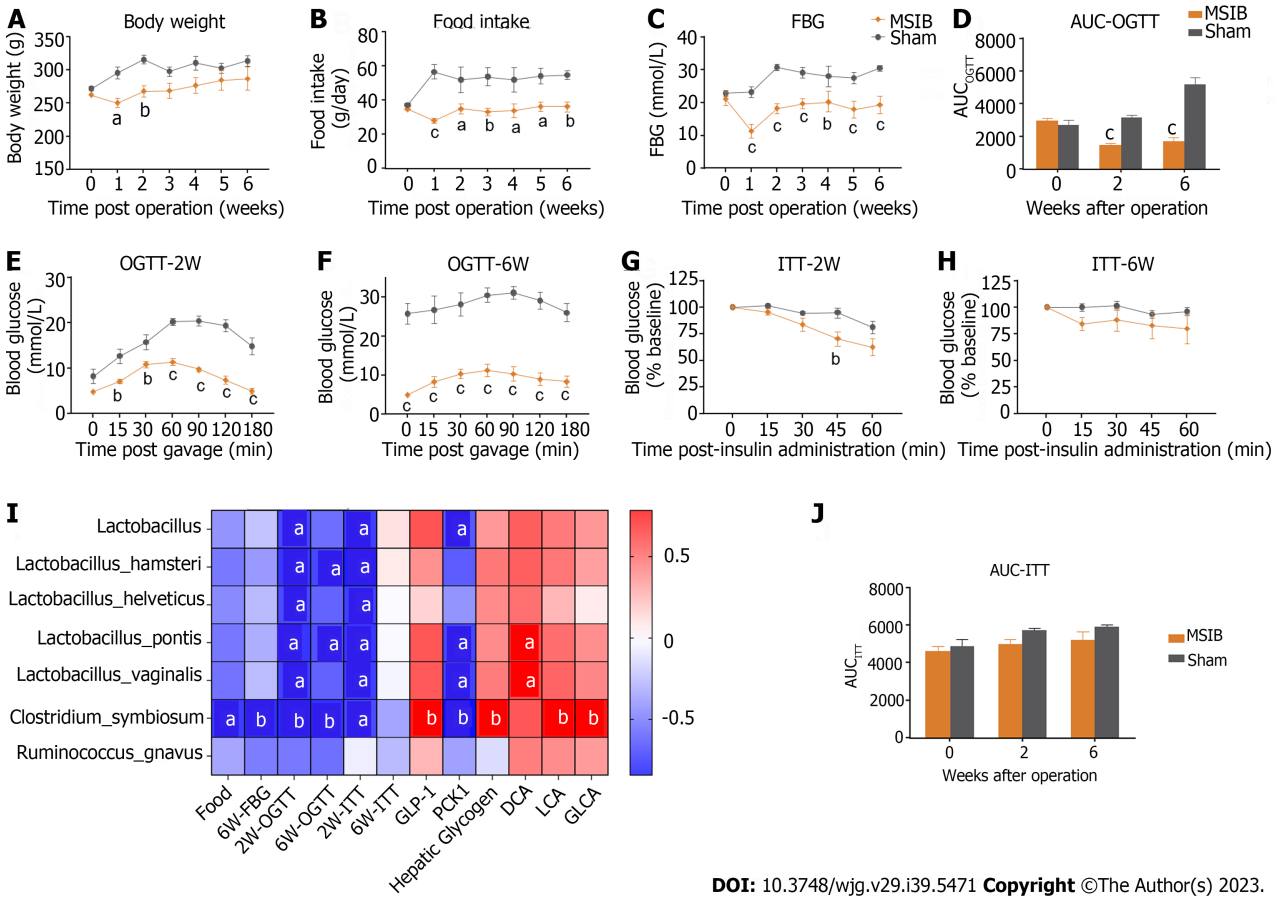
Graphical data are presented as the mean ± SEM. All analyses were performed using R software version 4.1.3 and GraphPad Prism version 8.4 (GraphPad Software, San Diego, CA, United States), with a significance level set at 0.05. The AUC was calculated using trapezoidal integration. Differences between the two groups were analyzed using a *t* test. Changes in body weight, food intake, fasting blood glucose, OGTT, and ITT over time were analyzed using a two-way analysis of variance (ANOVA). Student's *t* test was used for pairwise comparisons between the groups. Statistical significance was defined as follows: $^{a}P < 0.05$, $^{b}P < 0.01$, and $^{c}P < 0.001$.

RESULTS

Significant metabolic improvements were observed after MSIB (Figures 1 and 2). At 2 wk after surgery, the body weight of rats in the MSIB group decreased compared to that of rats in the sham group (Figure 1A). Additionally, mean blood glucose levels were significantly lower in the MSIB group than in the sham group after surgery (Figure 1C). The OGTT results showed a significant decrease in both the OGTT values and the area under the OGTT curve (OGTT-AUC) in the MSIB group compared to the sham group (Figure 1D-F). Moreover, the MSIB group exhibited a significant reduction in food intake compared to the sham group (Figure 1B). However, there was no significant improvement in insulin sensitivity (ITT) in the MSIB group compared to the sham group, except for the 45-min mark in the ITT test two weeks after surgery and the 60-min mark in the ITT test six weeks after surgery (Figures 1G, H and J). In conclusion, these findings suggest that MSIB has a significant positive effect on glucose metabolism in diabetic rats.

After MSIB, there was an observed increase in hepatic glycogen stores, a reduction in gluconeogenic key enzymes, and a decrease in the expression of transcription factors (Figure 3C). These changes were significantly correlated with glucose metabolism. Examination of liver tissue sections at 6 wk postoperatively revealed a higher hepatic glycogen content in the MSIB group than in the sham group (Figures 3A and B). Furthermore, the MSIB group showed reduced expression of phosphoenolpyruvate carboxykinase 1 (PCK1) and glucose-6-phosphatase (G6PC), which are key enzymes involved in hepatic gluconeogenesis. Additionally, there was a decrease in the expression of Forkhead box O1 (FOXO1) and peroxisome proliferator-activated receptor gamma coactivator 1 alpha (PGC-1α), which are transcription factors that regulate gluconeogenesis (Figure 3C).

The gut microbiome of rats in the MSIB group exhibited notable alterations compared to that of the sham group following surgery, resulting in discernible differences in beta diversity between the two groups (Figure 4A). Specifically, there was a significant increase in the abundances of several *Lactobacillus spp.* at the species level, including *Lactobacillus hamsteri*, *Lactobacillus helveticus*, *Lactobacillus pontis*, and *Lactobacillus vaginalis*. Additionally, there was a significant increase in the abundances of *Clostridium symbiosum*, *Bilophila* and *Ruminococcus gnavus* in the gut microbiome of rats in the MSIB group (Figures 4B and C). Notably, these upregulated microbial species were correlated with changes in key enzymes involved in gluconeogenesis and bile acid metabolism.



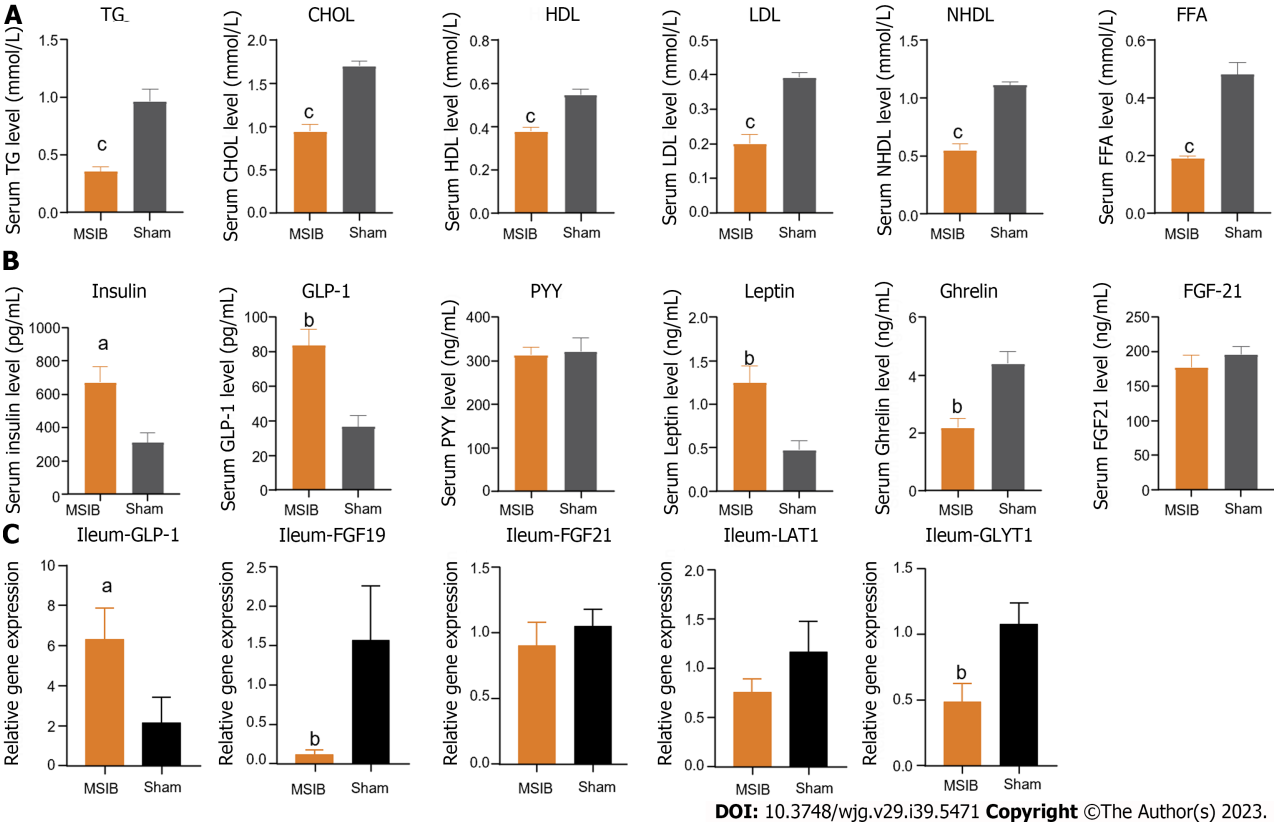
DOI: 10.3748/wjg.v29.i39.5471 **Copyright** ©The Author(s) 2023.

Figure 1 Glucose metabolism improved after mid-small intestine bypass and was significantly correlated with postoperative increased abundance of gut microbiota. A: Postoperative body weight changes in rats; B: Postoperative food intake in rats; C: Postoperative mean random blood glucose changes in rats; D-F: Glucose tolerance test and area under the curve in rats; G-J: Insulin sensitivity test and area under the curve in rats (G, H, and J); analysis of the correlation between postoperative abundance of rising gut microbiota and glucose metabolism and bile acids (I). Data are expressed as mean ± SEM and statistical significance was determined by two-tailed Student's test or two-way ANOVA, $^{a}P < 0.05$, $^{b}P < 0.01$, $^{c}P < 0.001$. FBG: Fasting blood glucose; AUC: Area under the curve; OGTT: Oral glucose tolerance test; MSIB: Mid-small intestine bypass; ITT: Insulin tolerance test; PCK1: Phosphoenolpyruvate carboxykinase 1; DCA: Deoxycholic acid; LCA: Lithocholic acid; GLCA: Glycolithocholic acid.

After surgery, the MSIB group exhibited increased expression of farnesoid X receptor (FXR) and Takeda G protein-coupled receptor 5 (TGR5) (Figure 5E), as well as elevated levels of fecal bile acids and secondary bile acids (Figure 5B). Metabolomics analysis revealed a significant increase in fecal bile acids in the MSIB group compared to the sham group (Figure 5). Specifically, there was an increase in secondary bile acids, including chenodeoxycholic acid, deoxycholic acid (DCA), glyco-deoxycholic acid, lithocholic acid (LCA), glycolithocholic acid (GLCA), and ursodeoxycholic acid. Correlation analysis further demonstrated a significant positive correlation between the levels of the intestinal secondary bile acids LCA and GLCA and the abundance of *Clostridium_symbiosum* in the intestines (Figure 5C). Moreover, LCA showed a significant positive correlation with intestinal GLP-1 expression and a significant negative correlation with the key hepatic gluconeogenic enzyme PCK1 (Figures 5C and F).

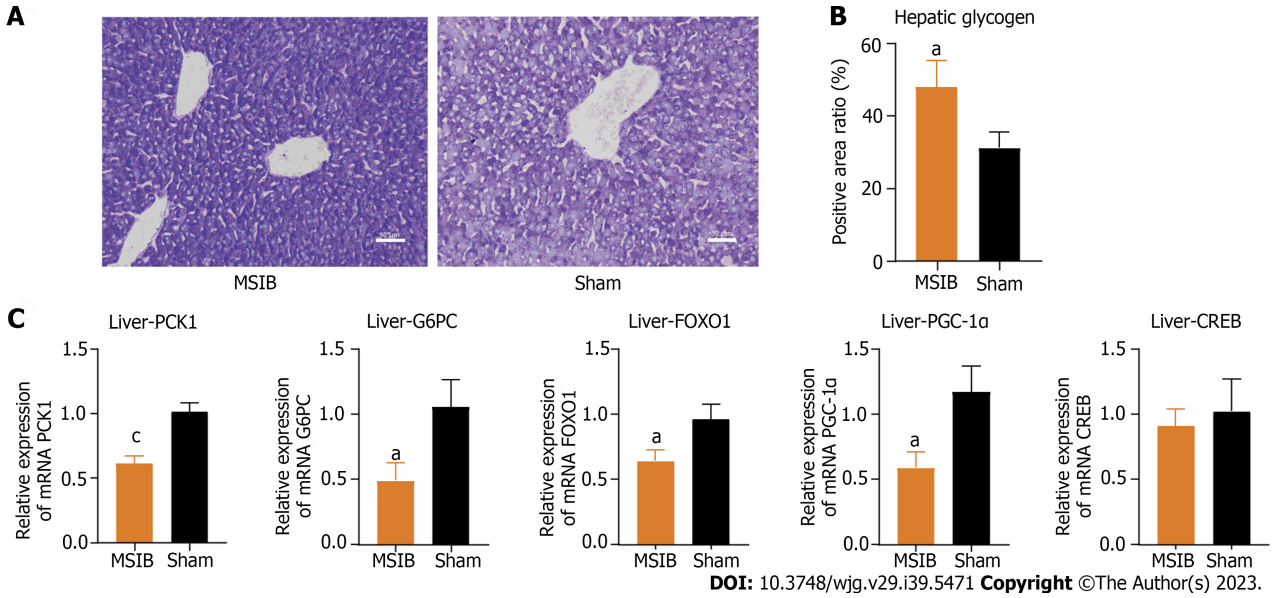
DISCUSSION

The decrease in serum glucose levels after MSIB is associated with the inhibition of hepatic gluconeogenesis. At 6 wk post-MSIB, diabetic rats in the MSIB group exhibited a significant decrease in blood glucose levels compared to those in the sham group, as well as a significant difference in the OGTT-AUC. These findings confirmed that a 60% small intestinal resection could still improve glucose metabolism, although the effect on reducing body weight was not significant. To explore the underlying mechanism of improved glucose metabolism after MSIB, we assessed the liver tissue glycogen content of rats at 6 wk post-surgery. The results revealed a significantly higher hepatic glycogen content in the MSIB group than in the sham group, indicating that the improved glucose metabolism after MSIB is associated with enhanced serum glucose conversion. Previous studies have reported increased hepatic glucose uptake and decreased endogenous glucose production following metabolic surgery, which aligns with our findings of elevated hepatic glycogen levels[11]. Moreover, bariatric surgery has been shown to inhibit hepatic glucose production[12], further supporting our observation. Analysis of liver tissue also demonstrated significantly reduced expression of the key gluconeogenic enzymes PCK1 and G6PC in the MSIB group compared to the sham group, along with decreased



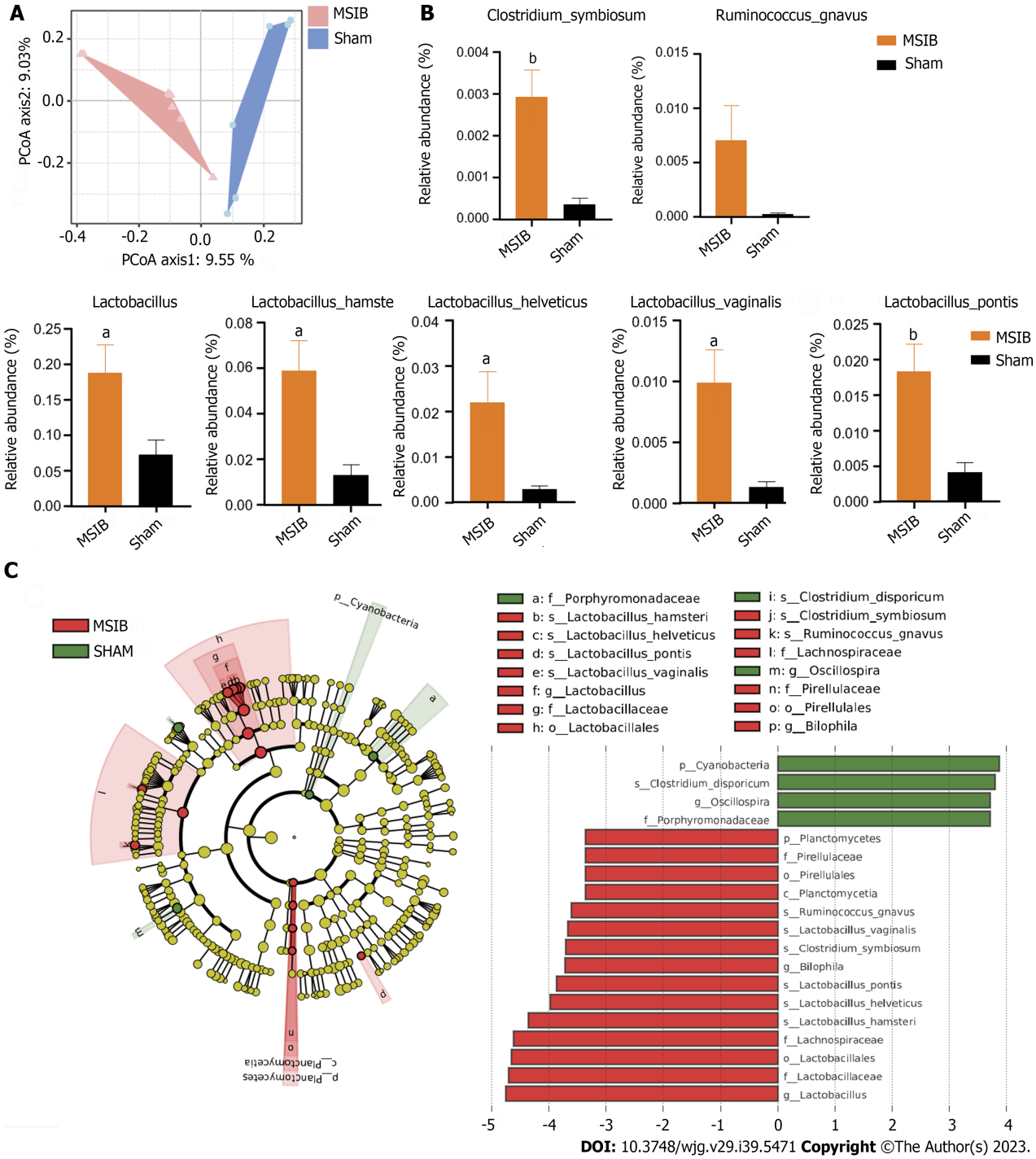
DOI: 10.3748/wjg.v29.i39.5471 **Copyright** ©The Author(s) 2023.

Figure 2 The serum lipid metabolism was improved, serum glucagon-like peptide 1 level was increased and intestinal glucagon-like peptide 1 transcript was increased in rats after mid-small intestine bypass. A: Changes in serum triglycerides, total cholesterol, high-density lipoprotein, low-density lipoprotein, non-high-density lipoprotein, and free fatty acids levels in rats after surgery; B: Changes in serum gastrointestinal hormones in rats after surgery; C: Changes in intestinal glucagon-like peptide 1, fibroblast growth factor 19, fibroblast growth factor 21, LAT1, glycine transporter 1 transcript in rats after surgery. Data are expressed as mean ± SEM and statistical significance was determined by two-tailed Student's test or two-way ANOVA, $^{a}P < 0.05$, $^{b}P < 0.01$, $^{c}P < 0.001$. TG: Triglycerides; CHOL: Cholesterol; HDL: High-density lipoprotein; LDL: Low-density lipoprotein; NHDL: Non-high-density lipoprotein; FFA: Free fatty acid; GLP-1: Glucagon-like peptide 1; PYY: Peptide tyrosine tyrosine; FGF21: Fibroblast growth factor 21; GLYT1: Glycine transporter 1.



DOI: 10.3748/wjg.v29.i39.5471 **Copyright** ©The Author(s) 2023.

Figure 3 Increased glycogen reserves and decreased expression of gluconeogenesis-related enzymes and transcription factors in rat liver after mid-small intestine bypass. A and B: Glycogen staining and comparison of liver tissue sections; C: Expression of key gluconeogenesis enzymes and regulatory-related transcription factors. Data are expressed as mean ± SEM and statistical significance was determined by two-tailed Student's test or two-way ANOVA, $^{a}P < 0.05$, $^{c}P < 0.001$. MSIB: Mid-small intestine bypass; PCK1: Phosphoenolpyruvate carboxykinase 1; G6PC: Glucose-6-phosphatase; FOXO1: Forkhead box O1; PGC1α: Peroxisome proliferator-activated receptor gamma coactivator 1 alpha; CREB: cAMP response element-binding protein.

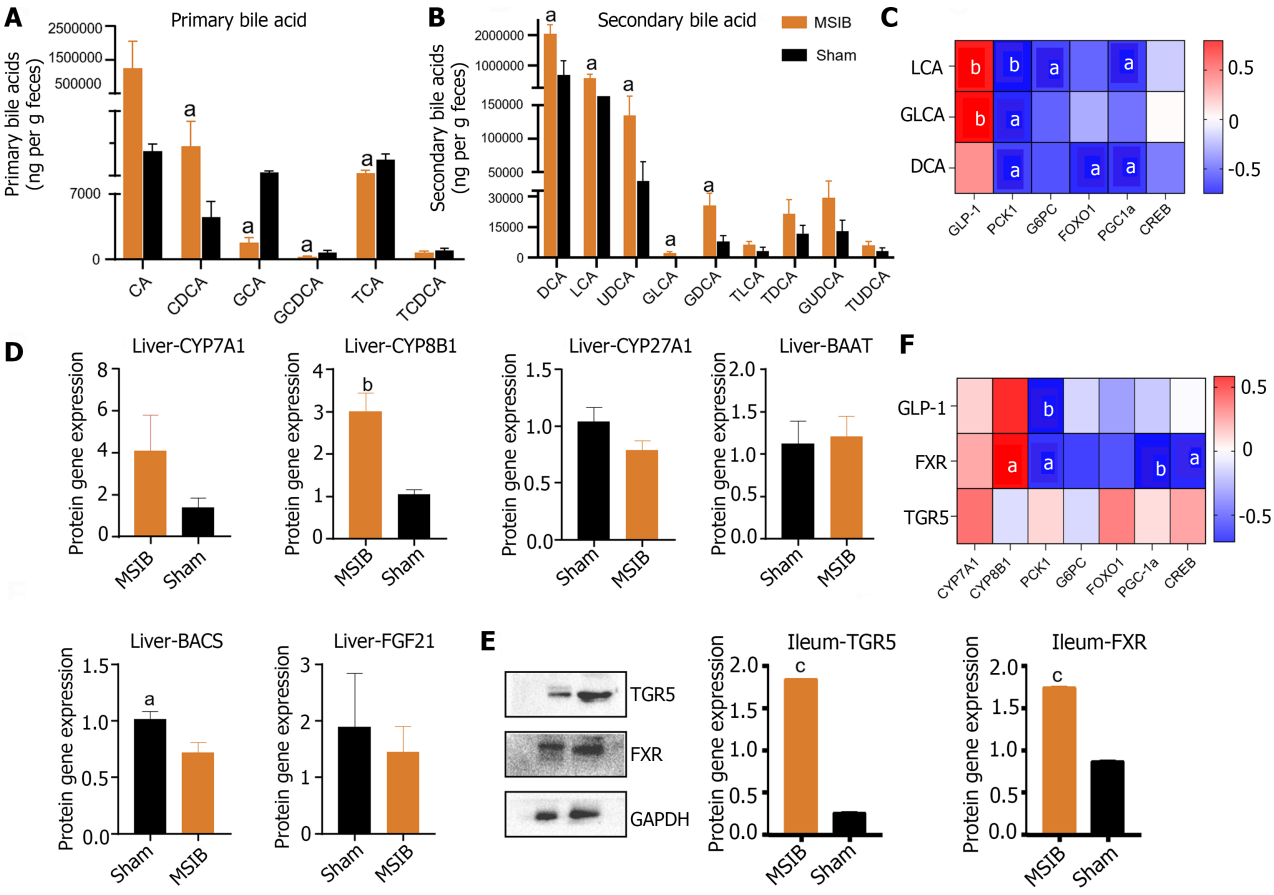


DOI: 10.3748/wjg.v29.i39.5471 **Copyright** ©The Author(s) 2023.

Figure 4 Changes in gut microbiota after mid-small intestine bypass. A: Principal coordinate analysis of gut microbiota based on OUT data from mid-small intestine bypass (MSIB) and sham groups; B: Bacteria with increased intestinal abundance in rats after MSIB; C: Phylogenetic tree for comparison of linear discriminant analysis (LDA) effect sizes of gut microbiota in MSIB and sham groups, bacteria with significantly enriched LDA scores taxa are marked with the colours shown. Data are expressed as mean ± SEM and statistical significance was determined by two-tailed Student's test or two-way ANOVA, $^{a}P < 0.05$, $^{b}P < 0.01$. MSIB: Mid-small intestine bypass; LDA: Linear discriminant analysis; PCoA: Principal coordinate analysis.

expression of the transcription factors FOXO1 and PGC-1α, which regulate gluconeogenesis. Correlation analysis revealed a significant positive correlation between PCK1, G6PC, and glucose levels. Based on these findings, we conclude that the decrease in serum glucose levels after MSIB is attributed to the inhibition of gluconeogenesis.

The gut microbiome of rats underwent significant changes after MSIB, as revealed by LEfSe analysis. Specifically, there was a significant increase in the abundance of *Lactobacillus spp*., including specific species such as *Lactobacillus hamsteri*, *Lactobacillus helveticus*, *Lactobacillus pontis*, *Lactobacillus vaginalis*, and *Ruminococcus gnavus*. Additionally, the abundances of *Bilophila* and *Clostridium symbiosum*, which are known to metabolize bile acids, also increased significantly. Our experiments demonstrated an increase in the fecal levels of various secondary bile acids in the MSIB group compared to the sham group. Correlation analysis revealed a significant positive correlation between the levels of LCA and GLCA and the abundance of intestinal *Clostridium symbiosum*, suggesting the involvement of the intestinal flora in metabolic



DOI: 10.3748/wjg.v29.i39.5471 **Copyright** ©The Author(s) 2023.

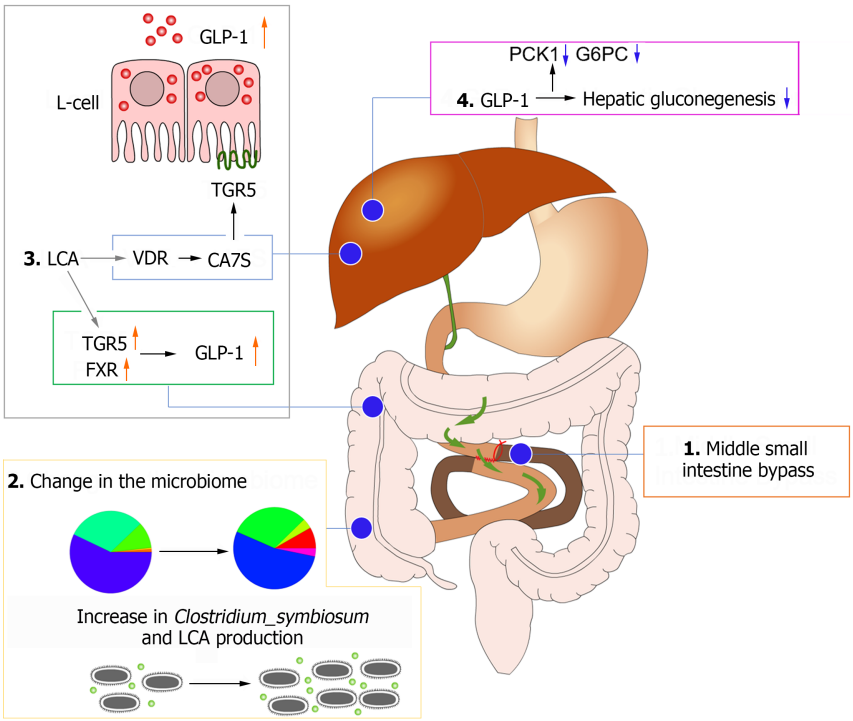
Figure 5 Changes in intestinal bile acid profile in rats after mid-small intestine bypass, correlating significantly with intestinal hormones and key enzymes of gluconeogenesis. A: Changes in primary bile acid profile in rats; B: Changes in secondary bile acid profile in rats; C: Correlation analysis of bile acid with glucagon-like peptide 1 and factors regulating gluconeogenesis; D: Expression of bile acid synthase and transcription factor, fibroblast growth factor 21. E: Takeda G protein-coupled receptor 5 and farnesoid X receptor WB results. F: Correlation analysis. Data are expressed as mean ± SEM and statistical significance was determined by two-tailed Student's test or two-way ANOVA, $^{a}P < 0.05$, $^{b}P < 0.01$, $^{c}P < 0.001$. PCK1: Phosphoenolpyruvate carboxykinase 1; DCA: Deoxycholic acid; LCA: Lithocholic acid; GLCA: Glycolithocholic acid; GLP-1: Glucagon-like peptide 1; TGR5: Takeda G protein-coupled receptor 5; FXR: Farnesoid X receptor; G6PC: Glucose-6-phosphatase; CA: Cholic acid; CDCA: Chenodeoxycholic acid; GCA: Glycocholic acid; GCDCA: Glycochenodeoxycholic acid; TCA: Taurocholic acid; TCDCA: Taurochenodeoxycholic acid; UDCA: Ursodeoxycholic acid; GDCA: Glyco-deoxycholic acid; TLCA: Taurolithocholic acid; TDCA: Taurodeoxycholic acid; GUDCA: Glycoursodeoxycholic acid; TUDCA: Tauroursodeoxycholic acid; FOXO1: Forkhead box O1; PGC1α: Peroxisome proliferator-activated receptor gamma coactivator 1 alpha; CREB: cAMP response element-binding protein; MSIB: Mid-small intestine bypass; CYP: Cytochrome P450; BAAT: Bile acid-CoA amino acid N-acyltransferase; BACS: Bile acid-CoA synthetase; FGF21: Fibroblast growth aactor 21; TGR5: Takeda G protein-coupled receptor 5; FXR: Farnesol X receptor.

regulation through the catabolic production of secondary bile acids.

Remarkably, the expression levels of cytochrome P450 family 8 subfamily B member 1, an enzyme involved in bile acid synthesis, were significantly increased in the experimental group, suggesting that the elevated bile acid levels after MSIB may be attributed to augmented classical bile acid pathway synthesis. Bile acids play a crucial role in metabolic regulation as important signaling molecules. Previous studies by Steenackers *et al*[8] demonstrated that LCA can bind to hepatic vitamin D receptors, thereby promoting GLP-1 secretion from intestinal L cells (Figure 6). In our experiments, we also observed an increase in intestinal LCA levels and GLP-1 transcription in rats following MSIB surgery.

Moreover, bile acids can modulate metabolic homeostasis by activating the nuclear receptor FXR and the membrane receptor TGR5[13-15]. TGR5 receptor activation is generally believed to confer metabolic benefits, while the precise role of FXR in metabolic regulation remains to be fully elucidated. Pathak *et al*[16] demonstrated that the dual agonist INT-767 induces GLP-1 secretion from cells, which aligns with our observations. We found increased transcript levels of TGR5 and FXR in the MSIB group of rats after surgery, along with elevated GLP-1 transcript levels. GLP-1, as a gastrointestinal hormone, reduces blood glucose levels and improves insulin resistance. Importantly, we observed a positive correlation between insulin sensitivity and GLP-1 in the experimental group of rats. Based on these findings, we propose that secondary bile acids promote GLP-1 secretion through the activation of TGR5 and FXR, thus benefiting glucose metabolism in rats after MSIB. Additionally, the gut microbiota plays a crucial role as an important mediator of this process.

There was a significant negative correlation between GLP-1 levels and the transcript levels of the key enzymes PCK1 and G6PC after MSIB. We observed increased glycogen stores in liver tissue and a significant decrease in the expression



DOI: 10.3748/wjg.v29.i39.5471 **Copyright** ©The Author(s) 2023.

Figure 6 Diagram of the mechanism of improved glucose metabolism after mid-small intestine bypass. GLP-1: Glucagon-like peptide 1; TGR5: Takeda G protein-coupled receptor 5; FXR: Farnesoid X receptor; LCA: Lithocholic acid; PCK1: Phosphoenolpyruvate carboxykinase 1; G6PC: Glucose-6-phosphatase.

of the gluconeogenic enzymes PCK1 and G6PC in the MSIB group compared to the sham group after surgery. Additionally, the transcription factors FOXO1 and CREB, which regulate gluconeogenesis, were also found to be inhibited. These findings suggest that the inhibition of gluconeogenesis played a significant role in the reduction in blood glucose levels in rats after MSIB.

Furthermore, correlation analysis revealed a significant negative correlation between PCK1 expression and GLP-1 levels, indicating that GLP-1 may be involved in the inhibition of gluconeogenesis. However, further experimental evidence is required to confirm this relationship. Previous studies by Lee *et al*[17] demonstrated that GLP-1 gene therapy reduces hepatic gluconeogenesis. Other scholars have suggested that GLP-1 may inhibit hepatic gluconeogenesis through FGF21[18] and regulate hepatic glucose production through neural circuits[19]. Additionally, intraperitoneal injection of GLP-1 has been shown to inhibit gluconeogenesis and related enzyme activity in obese mice[20]. These studies support the notion that GLP-1 can influence hepatic gluconeogenesis to improve blood glucose levels, which aligns with our observation of the decreased expression of key gluconeogenic enzymes. Therefore, we conclude that the increased levels of GLP-1 were responsible for the inhibition of postoperative gluconeogenesis in the MSIB group of rats.

In summary, our findings suggest that hepatic gluconeogenesis is inhibited by the decrease in serum glucose levels in rats after MSIB. Increased GLP-1 secretion, attributed to the elevated abundance of intestinal *Clostridium symbiosum*, serves as a potential pathway mediating these effects.

The study has some limitations, including a small sample size and a relatively short observation period. To further investigate the relationship between the intestinal *Clostridium symbiosum* abundance, bile acids, and GLP-1, future studies should consider conducting microbiota transplantation experiments and cell-based assays. Additionally, the cellular pathways connecting GLP-1 and gluconeogenesis still require further investigation.

CONCLUSION

Postoperative intestinal bypass of the midsection small intestine in nonobese diabetic rats improves glucose metabolism by increasing GLP-1 levels and inhibiting hepatic gluconeogenesis through the increased abundance of intestinal *Clostridium symbiosum*.

ARTICLE HIGHLIGHTS

Research background

The exact mechanism by which mid-small intestinal bypass (MSIB) improves glucose metabolism in diabetic rats is not fully understood.

Research motivation

To explore the role of the mid-small intestine in the onset and progression of diabetes.

Research objectives

The aim of this study was to elucidate the mechanisms by which MSIB improves glucose metabolism.

Research methods

Streptozotocin was used to induce diabetes mellitus in Sprague-Dawley rats at a dose of 60 mg/kg. The rats were then randomly divided into two groups: The MSIB group and the sham group (underwent switch laparotomy). Following a 6-wk recovery period post-surgery, the rats underwent various assessments, including metabolic parameter testing, analysis of liver glycogen levels, measurement of key gluconeogenic enzyme activity, characterization of the gut microbiota composition, evaluation of hormone levels, determination of bile acid concentrations, and assessment of the expression of the intestinal receptors Takeda G protein-coupled receptor 5 and farnesoid X receptor.

Research results

The MSIB group of rats exhibited improved glucose and lipid metabolism, increased hepatic glycogen content, and decreased expression of key gluconeogenic enzymes (phosphoenolpyruvate carboxykinase 1 and glucose-6-phosphatase). Notably, this group showed a substantial rise in specific intestinal bacteria, including *Lactobacillus*, *Clostridium symbiosum*, *Ruminococcus gnavus*, and *Bilophila*. Additionally, elevated levels of secondary bile acids, such as lithocholic acid, were observed. Importantly, changes in the gut microbiota were significantly correlated with the expression of gluconeogenic enzymes and glucagon-like peptide 1 (GLP-1) at 6 wk post-surgery, suggesting their potential involvement in regulating glucose. These findings underscore the beneficial impact of mid-small intestine bypass on glucose metabolism and its modulation of the gut microbiota.

Research conclusions

This study shows that postoperative introduction of intestinal *Clostridium symbiosum* in the mid-small intestine improves glucose metabolism in non-obese diabetic rats. This enhancement is linked to increased inhibition of hepatic gluconeogenesis mediated by GLP-1, leading to a positive impact on glucose regulation.

Research perspectives

This study explores partial mechanisms of the interaction between gut microbiota and host metabolism, providing a theoretical foundation for non-surgical interventions in diabetes-related metabolic disorders.

FOOTNOTES

Author contributions: Luo X, Tan C, Cao JQ, and Duan JY contributed to the conception of the study; Luo X, Tan C, Zheng ZH, and Pang Q performed the experiment; Luo X, Tan C, and Duan JY contributed significantly to analysis and manuscript preparation; Luo X, Tao F, Xu CY, Zheng ZH, Pang Q, He XA, Cao JQ, and Duan JY helped perform the analysis with constructive discussions; Luo X, Tan C, and Duan JY performed the data analyses and wrote the manuscript.

Supported by National Natural Science Foundation of China, No. 82060161, 81960154, and 81760156; Jiangxi Provincial Youth Science Foundation, No. 2018ACB21040; Natural Science Foundation of Jiangxi Province, No. 20212BAB206020; and Foundation of Health commission of Jiangxi Province, No. SKJP220225830.

Institutional animal care and use committee statement: The study was reviewed and approved by the the Animal Ethics Committee of Nanchang University.

Conflict-of-interest statement: All the authors report no relevant conflicts of interest for this article.

Data sharing statement: Technical appendix, statistical code, and dataset available from the corresponding author at duanjy2022@outlook.com.

ARRIVE guidelines statement: The authors have read the ARRIVE Guidelines, and the manuscript was prepared and revised according to the ARRIVE Guidelines.

Open-Access: This article is an open-access article that was selected by an in-house editor and fully peer-reviewed by external reviewers. It is distributed in accordance with the Creative Commons Attribution NonCommercial (CC BY-NC 4.0) license, which permits others to

distribute, remix, adapt, build upon this work non-commercially, and license their derivative works on different terms, provided the original work is properly cited and the use is non-commercial. See: https://creativecommons.org/Licenses/by-nc/4.0/

Country/Territory of origin: China

ORCID number: Xin Luo 0009-0002-9361-8178; Fang Tao 0009-0003-0464-9595; Cai Tan 0009-0009-4338-1505; Chi-Ying Xu 0009-0006-2150-762X; Zhi-Hua Zheng 0009-0007-7695-6921; Qiang Pang 0009-0007-0511-3580; Xiang-An He 0009-0007-9231-7652; Jia-Qing Cao 0000-0002-7270-2779; Jin-Yuan Duan 0000-0002-7772-7844.

S-Editor: Wang JJ
L-Editor: A
P-Editor: Cai YX

REFERENCES

1 **NCD Risk Factor Collaboration (NCD-RisC)**. Worldwide trends in body-mass index, underweight, overweight, and obesity from 1975 to 2016: a pooled analysis of 2416 population-based measurement studies in 128·9 million children, adolescents, and adults. *Lancet* 2017; **390**: 2627-2642 [PMID: 29029897 DOI: 10.1016/S0140-6736(17)32129-3]

2 **Molina-Montes E**, Coscia C, Gómez-Rubio P, Fernández A, Boenink R, Rava M, Márquez M, Molero X, Löhr M, Sharp L, Michalski CW, Farré A, Perea J, O'Rorke M, Greenhalf W, Iglesias M, Tardón A, Gress TM, Barberá VM, Crnogorac-Jurcevic T, Muñoz-Bellvís L, Dominguez-Muñoz JE, Renz H, Balcells J, Costello E, Ilzarbe L, Kleeff J, Kong B, Mora J, O'Driscoll D, Poves I, Scarpa A, Yu J, Hidalgo M, Lawlor RT, Ye W, Carrato A, Real FX, Malats N; PanGenEU Study Investigators. Deciphering the complex interplay between pancreatic cancer, diabetes mellitus subtypes and obesity/BMI through causal inference and mediation analyses. *Gut* 2021; **70**: 319-329 [PMID: 32409590 DOI: 10.1136/gutjnl-2019-319990]

3 **Fink J**, Seifert G, Blüher M, Fichtner-Feigl S, Marjanovic G. Obesity Surgery. *Dtsch Arztebl Int* 2022; **119**: 70-80 [PMID: 34819222 DOI: 10.3238/arztebl.m2021.0359]

4 **Cummings BP**, Strader AD, Stanhope KL, Graham JL, Lee J, Raybould HE, Baskin DG, Havel PJ. Ileal interposition surgery improves glucose and lipid metabolism and delays diabetes onset in the UCD-T2DM rat. *Gastroenterology* 2010; **138**: 2437-2446, 2446.e1 [PMID: 20226188 DOI: 10.1053/j.gastro.2010.03.005]

5 **Zhang X**, Young RL, Bound M, Hu S, Jones KL, Horowitz M, Rayner CK, Wu T. Comparative Effects of Proximal and Distal Small Intestinal Glucose Exposure on Glycemia, Incretin Hormone Secretion, and the Incretin Effect in Health and Type 2 Diabetes. *Diabetes Care* 2019; **42**: 520-528 [PMID: 30765429 DOI: 10.2337/dc18-2156]

6 **Soper NJ**, Chapman NJ, Kelly KA, Brown ML, Phillips SF, Go VL. The 'ileal brake' after ileal pouch-anal anastomosis. *Gastroenterology* 1990; **98**: 111-116 [PMID: 2293569 DOI: 10.1016/0016-5085(90)91298-k]

7 **Jarvie BC**, Knight ZA. Breaking down a gut-to-brain circuit that prevents malabsorption. *Cell* 2022; **185**: 2393-2395 [PMID: 35803241 DOI: 10.1016/j.cell.2022.06.012]

8 **Steenackers N**, Vanuytsel T, Augustijns P, Tack J, Mertens A, Lannoo M, Van der Schueren B, Matthys C. Adaptations in gastrointestinal physiology after sleeve gastrectomy and Roux-en-Y gastric bypass. *Lancet Gastroenterol Hepatol* 2021; **6**: 225-237 [PMID: 33581761 DOI: 10.1016/S2468-1253(20)30302-2]

9 **Reed MJ**, Meszaros K, Entes LJ, Claypool MD, Pinkett JG, Gadbois TM, Reaven GM. A new rat model of type 2 diabetes: the fat-fed, streptozotocin-treated rat. *Metabolism* 2000; **49**: 1390-1394 [PMID: 11092499 DOI: 10.1053/meta.2000.17721]

10 **Bokulich NA**, Subramanian S, Faith JJ, Gevers D, Gordon JI, Knight R, Mills DA, Caporaso JG. Quality-filtering vastly improves diversity estimates from Illumina amplicon sequencing. *Nat Methods* 2013; **10**: 57-59 [PMID: 23202435 DOI: 10.1038/nmeth.2276]

11 **Immonen H**, Hannukainen JC, Iozzo P, Soinio M, Salminen P, Saunavaara V, Borra R, Parkkola R, Mari A, Lehtimäki T, Pham T, Laine J, Kärjä V, Pihlajamäki J, Nelimarkka L, Nuutila P. Effect of bariatric surgery on liver glucose metabolism in morbidly obese diabetic and non-diabetic patients. *J Hepatol* 2014; **60**: 377-383 [PMID: 24060855 DOI: 10.1016/j.jhep.2013.09.012]

12 **Ben-Haroush Schyr R**, Al-Kurd A, Moalem B, Permyakova A, Israeli H, Bardugo A, Arad Y, Hefetz L, Bergel M, Haran A, Azar S, Magenheim I, Tam J, Grinbaum R, Ben-Zvi D. Sleeve Gastrectomy Suppresses Hepatic Glucose Production and Increases Hepatic Insulin Clearance Independent of Weight Loss. *Diabetes* 2021; **70**: 2289-2298 [PMID: 34341005 DOI: 10.2337/db21-0251]

13 **Sayin SI**, Wahlström A, Felin J, Jäntti S, Marschall HU, Bamberg K, Angelin B, Hyötyläinen T, Orešič M, Bäckhed F. Gut microbiota regulates bile acid metabolism by reducing the levels of tauro-beta-muricholic acid, a naturally occurring FXR antagonist. *Cell Metab* 2013; **17**: 225-235 [PMID: 23395169 DOI: 10.1016/j.cmet.2013.01.003]

14 **Duboc H**, Taché Y, Hofmann AF. The bile acid TGR5 membrane receptor: from basic research to clinical application. *Dig Liver Dis* 2014; **46**: 302-312 [PMID: 24411485 DOI: 10.1016/j.dld.2013.10.021]

15 **Yan Y**, Niu Z, Sun C, Li P, Shen S, Liu S, Wu Y, Yun C, Jiao T, Jia S, Li Y, Fang ZZ, Zhao L, Wang J, Xie C, Jiang C, Feng X, Hu C, Jiang J, Ying H. Hepatic thyroid hormone signalling modulates glucose homeostasis through the regulation of GLP-1 production *via* bile acid-mediated FXR antagonism. *Nat Commun* 2022; **13**: 6408 [PMID: 36302774 DOI: 10.1038/s41467-022-34258-w]

16 **Pathak P**, Liu H, Boehme S, Xie C, Krausz KW, Gonzalez F, Chiang JYL. Farnesoid X receptor induces Takeda G-protein receptor 5 cross-talk to regulate bile acid synthesis and hepatic metabolism. *J Biol Chem* 2017; **292**: 11055-11069 [PMID: 28478385 DOI: 10.1074/jbc.M117.784322]

17 **Lee YS**, Shin S, Shigihara T, Hahm E, Liu MJ, Han J, Yoon JW, Jun HS. Glucagon-like peptide-1 gene therapy in obese diabetic mice results in long-term cure of diabetes by improving insulin sensitivity and reducing hepatic gluconeogenesis. *Diabetes* 2007; **56**: 1671-1679 [PMID: 17369525 DOI: 10.2337/db06-1182]

18 **Liu J**, Yang K, Yang J, Xiao W, Le Y, Yu F, Gu L, Lang S, Tian Q, Jin T, Wei R, Hong T. Liver-derived fibroblast growth factor 21 mediates effects of glucagon-like peptide-1 in attenuating hepatic glucose output. *EBioMedicine* 2019; **41**: 73-84 [PMID: 30827929 DOI: 10.1016/j.ebiom.2019.02.037]

19 **Yang M**, Wang J, Wu S, Yuan L, Zhao X, Liu C, Xie J, Jia Y, Lai Y, Zhao AZ, Boden G, Li L, Yang G. Duodenal GLP-1 signaling regulates hepatic glucose production through a PKC-δ-dependent neurocircuitry. *Cell Death Dis* 2017; **8**: e2609 [PMID: 28182013 DOI: 10.1038/cddis.2017.28]

20 **Ip W**, Shao W, Chiang YT, Jin T. GLP-1-derived nonapeptide GLP-1(28-36)amide represses hepatic gluconeogenic gene expression and improves pyruvate tolerance in high-fat diet-fed mice. *Am J Physiol Endocrinol Metab* 2013; **305**: E1348-E1358 [PMID: 24085036 DOI: 10.1152/ajpendo.00376.2013]

World Journal of Gastroenterology

Submit a Manuscript: https://www.f6publishing.com

World J Gastroenterol 2023 October 21; 29(39): 5483-5493

DOI: 10.3748/wjg.v29.i39.5483

ISSN 1007-9327 (print) ISSN 2219-2840 (online)

ORIGINAL ARTICLE

Retrospective Cohort Study

Development and validation of a nomogram for preoperative prediction of tumor deposits in colorectal cancer

Hui-Da Zheng, Yun-Huang Hu, Kai Ye, Jian-Hua Xu

Specialty type: Gastroenterology and hepatology

Provenance and peer review: Unsolicited article; Externally peer reviewed.

Peer-review model: Single blind

Peer-review report's scientific quality classification

Grade A (Excellent): A
Grade B (Very good): B
Grade C (Good): 0
Grade D (Fair): 0
Grade E (Poor): 0

P-Reviewer: Camacho S, Mexico; Ekine-Afolabi B, United Kingdom

Received: July 11, 2023
Peer-review started: July 11, 2023
First decision: September 18, 2023
Revised: September 21, 2023
Accepted: September 28, 2023
Article in press: September 28, 2023
Published online: October 21, 2023

Hui-Da Zheng, Yun-Huang Hu, Kai Ye, Jian-Hua Xu, Department of Gastrointestinal Surgery, The Second Affiliated Hospital of Fujian Medical University, Quanzhou 362000, Fujian Province, China

Corresponding author: Jian-Hua Xu, MD, Chief Physician, Dean, Research Dean, Surgeon, Surgical Oncologist, Department of Gastrointestinal Surgery, The Second Affiliated Hospital of Fujian Medical University, No. 950 Donghai Street, Fengze District, Quanzhou 362000, Fujian Province, China. xjh630913@126.com

Abstract

BACKGROUND

Based on the clinical data of colorectal cancer (CRC) patients who underwent surgery at our institution, a model for predicting the formation of tumor deposits (TDs) in this patient population was established.

AIM

To establish an effective model for predicting TD formation, thus enabling clinicians to identify CRC patients at high risk for TDs and implement personalized treatment strategies.

METHODS

CRC patients (n = 645) who met the inclusion criteria were randomly divided into training (n = 452) and validation (n = 193) cohorts using a 7:3 ratio in this retrospective analysis. Least absolute shrinkage and selection operator regression was employed to screen potential risk factors, and multivariable logistic regression analysis was used to identify independent risk factors. Subsequently, a predictive model for TD formation in CRC patients was constructed based on the independent risk factors. The discrimination ability of the model, its consistency with actual results, and its clinical applicability were evaluated using receiver-operating characteristic curves, area under the curve (AUC), calibration curves, and decision curve analysis (DCA).

RESULTS

Thirty-four (7.5%) patients with TDs were identified in the training cohort based on postoperative pathological specimens. Multivariate logistic regression analysis identified female sex, preoperative intestinal obstruction, left-sided CRC, and lymph node metastasis as independent risk factors for TD formation. The AUCs of the nomogram models constructed using these variables were 0.839 and 0.853 in

the training and validation cohorts, respectively. The calibration curve demonstrated good consistency, and the training cohort DCA yielded a threshold probability of 7%-78%.

CONCLUSION
This study developed and validated a nomogram with good predictive performance for identifying TDs in CRC patients. Our predictive model can assist surgeons in making optimal treatment decisions.

Key Words: Colorectal cancer; Tumor deposits; Nomogram

©The Author(s) 2023. Published by Baishideng Publishing Group Inc. All rights reserved.

Core Tip: This article retrospectively analyzed the risk factors for tumor deposits (TDs) in colorectal cancer (CRC) and established a nomogram that included female sex, preoperative intestinal obstruction, left-sided CRC, and lymph node metastasis. This model enabled clinicians to identify high-risk populations for TDs in CRC patients and implement personalized treatment strategies.

Citation: Zheng HD, Hu YH, Ye K, Xu JH. Development and validation of a nomogram for preoperative prediction of tumor deposits in colorectal cancer. *World J Gastroenterol* 2023; 29(39): 5483-5493
URL: https://www.wjgnet.com/1007-9327/full/v29/i39/5483.htm
DOI: https://dx.doi.org/10.3748/wjg.v29.i39.5483

INTRODUCTION

Colorectal cancer (CRC) is the third most common cancer worldwide, with over 1 million new cases each year, making it the second leading cause of cancer death[1]. The current management of CRC is based on the tumor, lymph node, and metastasis (TNM) staging system. Initially developed to predict cancer prognosis, this system has evolved and now serves as the basis for determining treatment strategies and enrolling patients in clinical studies[2]. The TNM system has evolved continuously throughout scientific advancements, and its latest edition, the 8th edition of the TNM classification, was published in 2017[3]. However, the current TNM staging system exhibits limited ability to evaluate prognosis and clinical outcomes for patients with stage III CRC[4]. To improve the accuracy of staging systems in CRC, it is important to consider several key prognostic markers, including lymphatic invasion, neural invasion, and tumor deposits (TDs)[5]. TDs are defined as isolated tumor lesions found in the fat around the colon or rectum or adjacent mesentery (colon mesentery fat) far from the edge of tumor infiltration without evidence of residual lymphatic tissue[6]. Previous studies have shown that TDs are associated with early metastasis and poor prognosis[6,7]. No consensus has been reached on whether TDs should be considered positive lymph nodes in the TNM staging of CRC, leading to modifications and changes in the TNM staging system over time. Since 1997, TDs have been considered in the TNM classification[8]. In the 7th and 8th versions of the TNM staging systems, the presence of TDs without any positive lymph nodes is classified as "N1c"[9]. Some studies suggest that TDs may indicate a worse prognosis than lymph node metastasis, highlighting the importance of recognizing the role of TDs in prognostic assessment within the TNM staging system[6,10,11].

Limited research has investigated preoperative risk factors associated with TDs, particularly in the development of reliable predictive models. As a result, accurately assessing the presence of TDs before surgery remains challenging. This study aimed to address that gap by constructing a nomogram that can accurately and effectively predict the likelihood of TDs in patients with CRC. The nomogram aimed to identify individuals at high risk of recurrence, providing valuable insights for personalized treatment strategies and ultimately enhancing prognosis.

MATERIALS AND METHODS

Patients

This retrospective study was conducted at a single center and received approval from the Ethics Committee of the Second Affiliated Hospital of Fujian Medical University (2023-266). The study included a total of 645 patients diagnosed with CRC who underwent surgery between July 2019 and October 2022. The inclusion criteria were as follows: (1) Pathological confirmation of CRC; (2) undergoing surgical treatment; and (3) CRC being the primary malignant tumor. The exclusion criteria were as follows: (1) Presence of distant metastasis; (2) history of treatment with preoperative neoadjuvant radiotherapy and chemotherapy; and (3) incomplete clinical data.

The definition of TDs

TDs are characterized by the presence of tumor cells within the adipose tissue surrounding the colon or rectum, situated at a distance from the leading edge of tumor invasion. Importantly, there is no indication of residual lymph node tissue

within the lymphatic drainage region of the tumor[12]. As shown in Figure 1, we found nodular formations consisting of tumor cell extensions in the surrounding structures of the colon and rectum, which do not appear to meet the criteria for classification as lymph nodes.

Variables

In the present study, certain variables were reclassified based on specific criteria. Age was divided into two groups: ≤ 64 years old and > 64 years old. Sex was categorized as male and female. Body mass index records were classified as ≤ 25 and > 25. Tumor size was grouped as ≤ 3 cm and > 3 cm. The tumor site was divided into the right side (cecum, ascending colon, hepatic flexure, and transverse colon) and the left side (splenic flexure, descending colon, sigmoid colon, and rectum). Tumor circumference was categorized as ≤ 1/2 bowel circumference and > 1/2 bowel circumference. T staging was classified as T1-2 and T3-4. N staging was grouped as N0 and N1-2. The degree of differentiation was divided into "highly differentiated/moderately differentiated" and "poorly differentiated/undifferentiated" stages. The cutoff values for certain variables were determined using receiver-operating characteristic (ROC) curves and the Youden index[13]. For instance, the preoperative carcinoembryonic antigen (CEA) level variables were divided into ≤ 5 ng/mL and > 5 ng/mL based on the cutoff value. Similarly, the carbohydrate antigen 19-9 (CA199) level variables were categorized as ≤ 18 U/mL and > 18 U/mL. The tumor size variables were grouped as ≤ 3 cm and > 3 cm. The preoperative neutrophil-to-lymphocyte ratio was divided into ≤ 3 and > 3. Other variables, such as preoperative intestinal obstruction, hypertension, diabetes, smoking history, and previous surgery history, were classified as "yes" or "no" based on their presence or absence in the patients' medical records.

Statistical analysis

Before conducting the statistical analysis, we randomly divided the 645 patients into two cohorts: A training cohort and a validation cohort, using a 7:3 ratio. The statistical analysis was performed using IBM SPSS software (version 27.0). For normally distributed measurement data, *t* tests were employed, while the Mann-Whitney U test was used for nonnormally distributed measurement data. Chi-square tests were conducted to analyze count data. Least absolute shrinkage and selection operator (LASSO) regression, incorporating Lambda's penalty coefficient, was employed to reduce the regression coefficient of variables to zero. Variables with zero regression coefficients were excluded, while those without zero regression coefficients were recognized as being associated with TDs. Multivariate logistic analysis was performed on the selected variables to determine the most relevant variable, which formed the basis for developing a nomogram. The validation cohort was utilized to assess the predictive ability of the developed nomogram, including discrimination and calibration. Calibration curves were generated to illustrate any potential disparities between the training cohort and the validation cohort, encompassing both the original and recalibrated nomograms. The discriminative ability of the model was evaluated through ROC curve analysis, with the area under the curve (AUC) serving as a measure. The predictive ability of the final model was evaluated by comparing the observed incidence of TDs. Additionally, decision curve analysis (DCA) was performed to assess the clinical application value of the model, calculating the net benefit under various risk threshold probabilities. R version 4.2.1 software was used for statistical analysis of the predictive models, with a P value < 0.05 considered indicative of statistical significance.

RESULTS

Clinicopathologic characteristics

A total of 645 CRC patients who met the eligibility criteria were included in this study and randomly divided into a training cohort (452 individuals) and a validation cohort (193 individuals). Among the patients, 372 were male and 273 were female, indicating a higher proportion of males (57.7%). Preoperative intestinal obstruction was present in 73 cases, while 572 cases showed no symptoms of bowel obstruction. Tumors were located on the left side in 487 patients and on the right side in 158 patients. Additionally, 239 patients had tumors occupying ≤ 1/2 of the intestinal canal circumference; 137 patients had a maximum tumor diameter of ≤ 3 cm, while 508 patients had a diameter > 3 cm. Pathological staging revealed T1-2 in 109 cases and T3-4 in 536 cases. Lymph node metastasis (pN1-2) was observed in 294 patients, while 351 patients had no lymph node metastasis (pN0). Moreover, 41 patients had poor differentiation, and 604 patients had moderate and good differentiation. All patients were divided into two groups based on the presence of TDs: The TD group (n = 51) and the non-TD group (n = 594).

Upon analyzing the clinical baseline characteristics of the included patients, significant differences were observed in sex, preoperative intestinal obstruction, tumor size, serum CEA level, serum CA199 level, pathological T stage, pathological N stage, and differentiation degree (P < 0.05). However, no significant differences were observed in other factors. The basic demographics and clinicopathological characteristics can be found in Table 1.

Predictor selection and identification

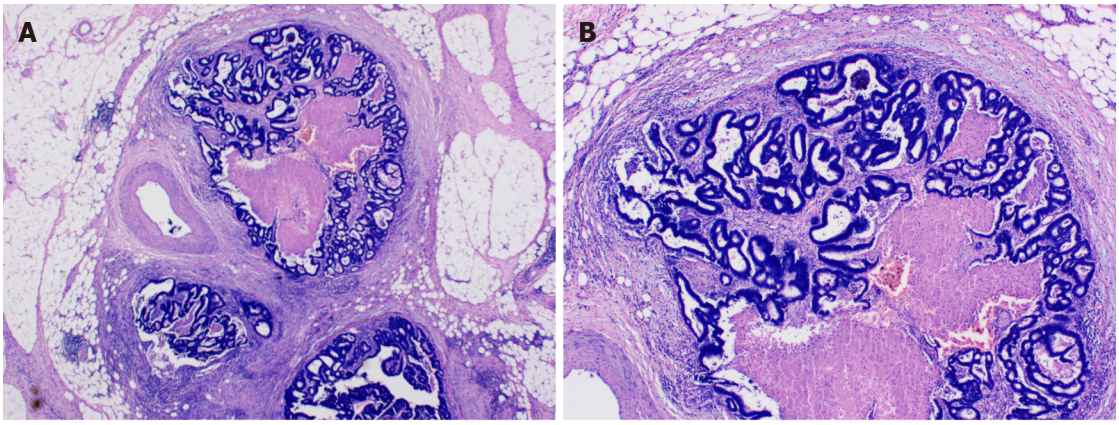
In the training cohort, we employed the LASSO regression algorithm to perform feature selection. This approach helps minimize the impact of multicollinearity and offers strong predictability and stability. We selected features based on the partial likelihood binomial deviance reaching its minimum value, and eight variables with nonzero coefficients were retained in the LASSO regression (Figure 2). These variables were considered significantly associated with TDs. The identified variables included sex, preoperative intestinal obstruction, diabetes, tumor location, tumor size, serum CEA level, pathological N stage, and degree of differentiation.

Table 1 Characteristics of patients, *n* (%)

Variables	No TD	TD	Total	*P* value
Age (yr)				0.906
≤ 64	321 (54.0)	28 (54.9)	349 (54.1)	
> 64	273 (46.0)	23 (45.1)	296 (45.9)	
Sex				0.029
Male	350 (58.9)	22 (43.1)	372 (57.7)	
Female	244 (41.1)	29 (56.9)	273 (42.3)	
Preoperative obstruction				< 0.001
No	535 (90.1)	37 (72.5)	572 (88.7)	
Yes	59 (9.9)	14 (27.5)	73 (11.3)	
Hypertension				0.106
No	440 (74.1)	43 (84.3)	483 (74.9)	
Yes	154 (25.9)	8 (15.7)	162 (25.1)	
Diabetes				0.459
No	522 (87.9)	43 (84.3)	565 (87.6)	
Yes	72 (12.1)	8 (15.7)	80 (12.4)	
BMI (kg/m^2)				0.970
≤ 25	502 (84.5)	43 (84.3)	545 (84.5)	
>25	92 (15.5)	8 (15.7)	100 (15.5)	
Smoking history				0.581
No	533 (89.7)	47 (92.2)	580 (89.9)	
Yes	61 (10.3)	4 (7.8)	65 (10.1)	
Abdominal surgery				1.000
No	542 (91.2)	47 (92.2)	589 (91.3)	
Yes	52 (8.8)	4 (7.8)	56 (8.7)	
Tumor position				0.236
Right	149 (25.1)	9 (17.6)	158 (24.5)	
Left	445 (74.9)	42 (82.4)	487 (75.5)	
Occupied intestinal circumference				0.139
≤ 1/2	225 (37.9)	14 (27.5)	239 (37.1)	
> 1/2	369 (62.1)	37 (72.5)	406 (62.9)	
Tumor size (cm)				0.015
≤ 3	133 (22.4)	4 (7.8)	137 (21.2)	
> 3	461 (77.6)	47 (92.2)	508 (78.8)	
NLR				0.925
≤ 3	423 (71.2)	36 (70.6)	459 (71.2)	
> 3	171 (28.8)	15 (29.4)	186 (28.8)	
CA-199 (U/mL)				0.037
≤ 18	400 (67.3)	27 (52.9)	427 (66.2)	
> 18	194 (32.7)	24 (47.1)	218 (33.8)	
CEA (ng/mL)				0.01
≤ 5	355 (59.8)	21 (41.2)	376 (58.3)	

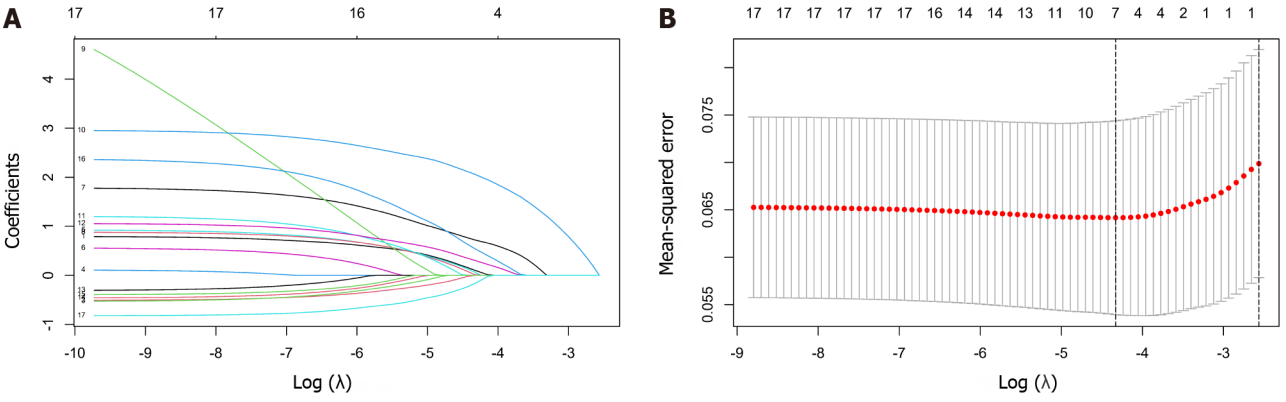
> 5	239 (40.2)	30 (58.8)	269 (41.7)	
T stage				0.003
T0-T2	108 (18.2)	1 (2.0)	109 (16.9)	
T3-T4	486 (81.8)	50 (98.0)	536 (83.1)	
N stage				< 0.001
N0	349 (58.8)	2 (3.9)	351 (54.4)	
N1-N2	245 (41.2)	49 (96.1)	294 (45.6)	
Differentiation				0.011
Poor	33 (5.6)	8 (15.7)	41 (6.4)	
Well/moderate	561 (94.4)	43 (84.3)	604 (93.6)	

TD: Tumor deposit; BMI: Body mass index; NLR: Neutrophil-to-lymphocyte ratio; CEA: Carcinoembryonic antigen; CA-199: Carbohydrate antigen 199.



DOI: 10.3748/wjg.v29.i39.5483 **Copyright** ©The Author(s) 2023.

Figure 1 Hematoxylin-eosin staining of tumor deposits. A: Magnification (× 20); B: Magnification (× 40).



DOI: 10.3748/wjg.v29.i39.5483 **Copyright** ©The Author(s) 2023.

Figure 2 The Lasso regression method is used to screen for predictable variables. A: The coefficient distribution of 17 baseline features; B: In Lasso regression, 10-fold cross-validation was used to select predictive variables using the minimum criterion (dashed line on the left).

To further investigate their predictive significance, we conducted a multivariate logistic regression analysis using these eight variables. The results demonstrated that sex (female) [odds ratio (OR) = 2.404; 95% confidence interval (CI) = 1.249-4.626; P = 0.009], preoperative intestinal obstruction (OR = 3.119; 95%CI = 1.427-6.818; P = 0.004), tumor location (left side) (OR = 2.511; 95%CI = 1.088-5.795; P = 0.031), and pathological N stage (OR = 29.658; 95%CI = 7.051-124.744; P < 0.001) were all significant predictors of TDs. The detailed results of the multivariate logistic regression analysis can be found in Table 2.

Table 2 The multivariate logistic regression results

Variables	Odds ratio	95%CI	*P* value
Sex			
Male	1		
Female	2.404	1.249-4.626	0.009
Preoperative obstruction			
No	1		
Yes	3.119	1.427-6.818	0.004
Diabetes			
No	1		
Yes	1.485	0.602-3.663	0.391
Tumor position			
Right	1		
Left	2.511	1.088-5.795	0.031
Tumor size (cm)			
≤ 3	1		
> 3	2.631	0.867-7.977	0.088
CEA			
≤ 5	1		
> 5	1.889	0.983-3.632	0.056
N stage			
N0	1		
N1-N2	29.658	7.051-124.744	< 0.001
Differentiation			
Poor	1		
Well/moderate	0.476	0.179-1.260	0.135

CEA: Carcinoembryonic antigen; CI: Confidence interval.

Construction and evaluation of the nomogram

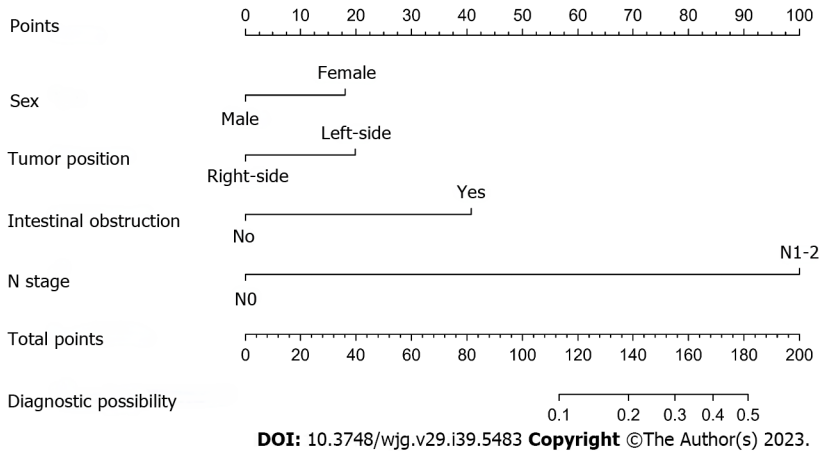
A nomogram was developed based on the four independent risk factors identified through multivariable logistic regression analysis (Figure 3). Each risk factor was assigned a specific score to calculate the total risk score for predicting TDs in CRC patients. The risk score for lymph node metastasis had the highest weightage (100 points), followed by preoperative symptoms of bowel obstruction (40 points). By summing the scores of the four risk factors, the total risk score can be obtained, indicating the likelihood of TDs in the patient.

To assess the predictive accuracy of the nomogram, ROC curves were generated, yielding an AUC of 0.839 for the training cohort and 0.853 for the validation cohort (Figure 4). These values indicated that the nomogram had good predictive ability. The calibration curves (Figure 5) demonstrated excellent agreement between the predicted TDs and the actual observations in both the training and validation cohorts.

Furthermore, the DCA curve was plotted for the training cohort (Figure 6). The curve showed that within a threshold probability range of 7% to 78%, using this predictive model to identify the presence of TDs in CRC patients can lead to net clinical benefits.

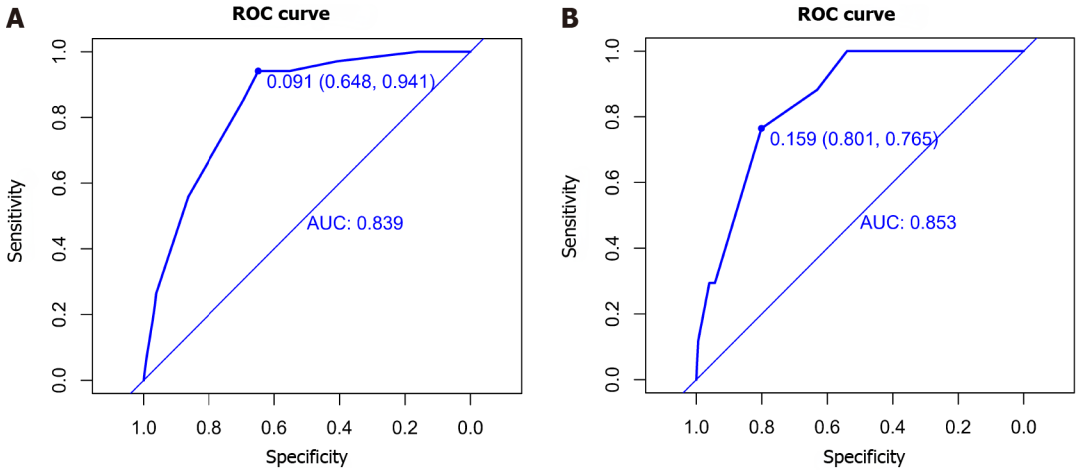
DISCUSSION

CRC, as one of the most common malignant tumors worldwide, has attracted significant attention in clinical and scientific research in recent years[1]. Notably, the prognosis of CRC patients has become a key area of concern for clinical practitioners. With research progress achieved on prognostic factors, emerging evidence suggests that tumor pathological characteristics play a crucial role in the prognosis of CRC patients[14]. Among these characteristics, TNM staging is



DOI: 10.3748/wjg.v29.i39.5483 **Copyright** ©The Author(s) 2023.

Figure 3 A nomogram was used to predict the risk of tumor deposits in colorectal cancer patients. The predictors included sex, tumor position, preoperative intestinal obstruction, and lymph node metastasis.



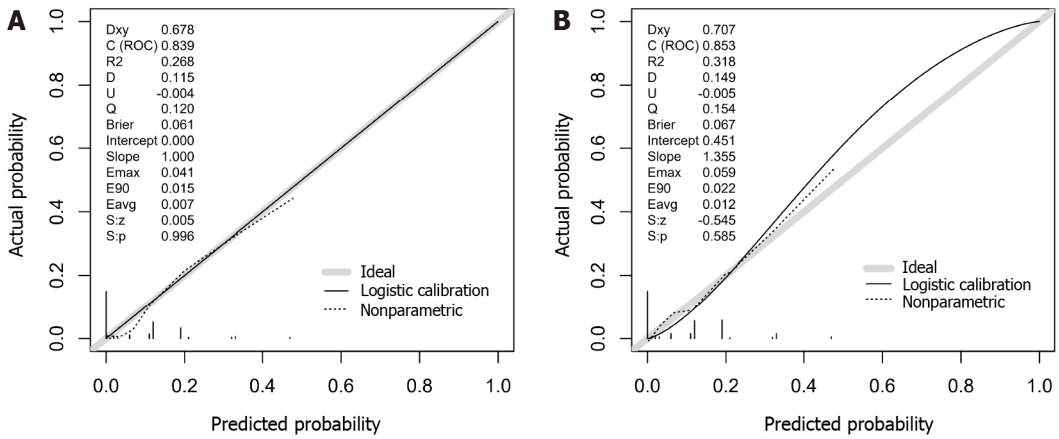
DOI: 10.3748/wjg.v29.i39.5483 **Copyright** ©The Author(s) 2023.

Figure 4 The receiver-operating characteristic curves of the nomogram for predicting tumor deposits. A: Receiver operating characteristic (ROC) curve for the nomogram based on the training cohort. The area under the curve (AUC) is 0.839; B: ROC curve for the nomogram based on the validation cohort. The AUC is 0.853. ROC: Receiver operating characteristic; AUC: Area under the curve.

widely recognized as the most crucial prognostic indicator[15]. The significance of TDs has grown in subsequent revisions of the TNM classification, with their inclusion in TNM-8 and classification as "N1c" when accompanied by lymph node negativity[9,16]. Importantly, in the 8th edition of TNM, tumor nodules with venous, lymphatic vessel, or perineural infiltration are considered distinct entities[7]. An increasing body of literature suggests that TDs carry a worse prognosis than N1 or N2 involvement[7,11,16,17]. Therefore, accurately predicting the presence of TDs in CRC patients before surgery holds immense value in guiding personalized staging, preoperative treatment decisions, and prognosis assessment. Currently, limited research exists on the risk factors associated with TDs in CRC patients. Most studies have focused on comparing TDs with the prognosis of lymph node metastasis, and only a few have established effective clinical prediction models. Our study included comprehensive baseline and pathological information and incorporated patient symptoms such as intestinal obstruction. This approach enhanced the sensitivity and specificity of the model, enabling clinicians to identify high-risk populations for TDs in CRC patients and implement personalized treatment strategies.

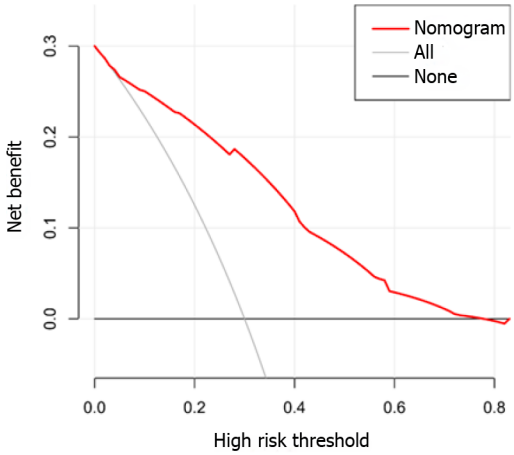
Nomograms are valuable tools for predicting outcomes in clinical practice. They provide a visual representation of the impact of various predictors on the outcome, offering a practical and intuitive explanation of their influence[18]. In our study, we developed a nomogram to predict the risk of TDs in CRC patients. The nomogram was constructed based on important clinical characteristics identified through LASSO regression and multivariate logistic regression. The calibration curve demonstrated high agreement between the predicted and observed TD incidence, indicating reliable prediction performance. Moreover, the AUC values exceeded 0.8 for both the training and validation cohorts, indicating good prediction model accuracy and discrimination.

Previous studies have reported that the incidence rate of TDs in CRC patients is approximately 10%[19], which is slightly higher than that in the present study. The exploration of clinical risk factors for TDs in CRC patients remains limited. However, there have been some notable studies in this field. Hong *et al*[20] investigated predictive factors for TDs



DOI: 10.3748/wjg.v29.i39.5483 **Copyright** ©The Author(s) 2023.

Figure 5 Calibration curve for the nomogram in the cohort. A: Calibration curve of the training cohort; B: Calibration curve of the validation cohort. ROC: Receiver operating characteristic.



DOI: 10.3748/wjg.v29.i39.5483 **Copyright** ©The Author(s) 2023.

Figure 6 Decision curve analysis of the nomogram. The Y-axis represents net income, and the red line represents the risk nomogram. When the threshold probability is > 7% and < 78%, this predictive model can achieve net clinical benefits.

in rectal cancer using a radiomics signature and developed a predictive model based on imaging features. They identified tumor location and two imaging features (D*, α) as accurate predictors of TDs. Chen *et al*[19] extracted data from the Surveillance, Epidemiology, and End Results database and found that poor tumor differentiation, positive CEA, higher T staging, tumor location, and increased lymph node metastasis were risk factors for TDs in CRC patients. In our study, we conducted intergroup comparisons and identified age, preoperative intestinal obstruction, tumor size, serum CEA, serum CA199, pathological T stage, pathological N stage, and degree of differentiation as factors associated with TDs, which aligns with the aforementioned research. However, after applying LASSO regression and multivariable logistic regression, we determined that tumor location (left side), preoperative intestinal obstruction, female sex, and N stage were independent predictive variables. Notably, the association between sex and TDs has not been extensively explored, and our finding of a higher risk of TDs in female patients has not yet been documented. This may suggest that female patients are more susceptible to lymph node metastasis[21], but further investigation is required to clarify this relationship. We also found a significant correlation between tumor location and TDs, with the left side being prone to TDs, especially in rectal cancer cases. This discrepancy in TD location can be attributed to variations in lymphatic vessel involvement and lymph node metastasis between left-sided and right-sided colon cancers[19,22]. CRC patients often experience intestinal obstruction at advanced stages, sometimes requiring emergency surgery or the placement of an intestinal stent[23]. Previous studies have indicated that preoperative intestinal obstruction in CRC patients is associated with elevated CEA levels, poorly differentiated tumors, advanced T stage, left-sided primary tumor location, and nerve invasion, which may explain the significant association between preoperative intestinal obstruction and TDs[24-26]. Furthermore, a higher number of lymph node metastases increases the likelihood of TDs, potentially due to the involvement of peripheral nerves, lymphatic vessels, and blood vessels[19]. The fifth edition of TNM staging distinguished between TDs and lymph node metastasis based on size, classifying all nodules with a diameter larger than 3 mm as lymph node metastasis, thus highlighting the strong relationship between TDs and lymph nodes[27].

The current TNM staging only considers TDs in the absence of lymph node metastasis, which may not fully reflect the important role of TDs in prognosis and may lead to incorrect treatment strategies[3,9]. Liang *et al*[11] conducted a large retrospective study with a large sample size and found that TDs were an independent prognostic factor for gastric cancer patients after radical resection, suggesting that TDs should be included in the N staging system. In Liu *et al*'s study[28], after combining TDs and lymph node metastasis, it was observed that the prognosis of N1 patients with TD positivity was similar to that of N2 patients, while the prognosis of N2 patients with TD positivity was much worse than that of N2 patients without TDs. The researchers believe that in the presence of lymph node metastasis, TDs should also be considered in the TNM system. However, when evaluating the role of TDs, ignoring the number of TDs does not seem to be a correct decision[14]. A previous multicenter study demonstrated a significant correlation between the number of TDs and prognosis, with patients with ≥ 4 TDs experiencing a significantly worse prognosis than those with < 4 TDs under the same conditions[7]. In summary, it is necessary to fully evaluate the prognosis of CRC patients, regardless of the presence or absence of lymph node metastasis, by considering TDs and their quantity.

In conclusion, our study integrated preoperative predictive factors into a model and achieved favorable results supported by a sufficient sample size and robust testing efficacy. However, there are some limitations to consider. First, this study has a retrospective design, which may introduce inherent biases. Second, the absence of imaging data for the preoperative predictors is a limitation, and future prospective cohort studies incorporating radiomics signatures may help support our findings.

CONCLUSION

In summary, our study identified female sex, preoperative intestinal obstruction, left-sided CRC, and lymph node metastasis as predictors of TDs in CRC. Assessing these factors before surgery is crucial for accurately determining the presence of TDs. Consideration of the impact of these predictors on clinical decision-making and patient prognosis, especially for high-risk individuals, is essential for making informed decisions and obtaining optimal outcomes.

ARTICLE HIGHLIGHTS

Research background

Colorectal cancer (CRC) poses a serious threat to human life and health. Previous studies have shown that tumor deposits (TDs) are significantly associated with early metastasis and poor prognosis. However, research on related risk factors is limited, and accurate prediction of TDs remains challenging. We developed a model based on preoperative clinical and pathological features to accurately predict the likelihood of TDs in CRC patients.

Research motivation

At present, the diagnosis of TDs in CRC requires postoperative pathology, which is passive for clinicians. If TDs can be accurately identified before patients receive treatment, it is of great importance for evaluating clinical staging, selecting reasonable treatment plans, and judging the prognosis of CRC patients.

Research objectives

To develop and validate a nomogram with good predictive ability for the preoperative prediction of TDs in patients with CRC.

Research methods

We retrospectively collected the data of 645 eligible patients with CRC. SPSS 27.0 and R (version 4.2.1) were used for statistical analysis, and a prediction model for TDs in CRC patients was established.

Research results

A total of 51 patients with CRC had TDs in this study. The areas under the curve of the training cohort and the validation cohort were 0.839 and 0.853, respectively. The model showed good accuracy and discrimination ability and has broad clinical practicability. The results of this study suggest the value of preoperative indicators in predicting TDs in CRC patients and can assist in guiding clinical decision making.

Research conclusions

This nomogram based on preoperative indicators can effectively predict the preoperative TD status of CRC.

Research perspectives

In the future, we will try to apply radiomics combined with clinical indicators to construct a model to predict the status of TDs in CRC patients.

FOOTNOTES

Author contributions: Zheng HD designed/planned the study and wrote the paper; Zheng HD, Hu YH and Ye K acquired and analyzed data and performed computational modeling; Xu JH participated in discussion of related data; All authors read and approved the final manuscript.

Supported by Fujian Province Science and Technology Innovation Joint Fund Project, No. 2021Y9029.

Institutional review board statement: The study was reviewed and approved for publication by our Institutional Reviewer.

Informed consent statement: As the study used anonymous and pre-existing data, the requirement for the informed consent from patients was waived.

Conflict-of-interest statement: All the Authors have no conflict of interest related to the manuscript.

Data sharing statement: The datasets used and/or analyzed during the current study are available from the corresponding author on reasonable request.

STROBE statement: The authors have read the STROBE Statement-checklist of items, and the manuscript was prepared and revised according to the STROBE Statement-checklist of items.

Open-Access: This article is an open-access article that was selected by an in-house editor and fully peer-reviewed by external reviewers. It is distributed in accordance with the Creative Commons Attribution NonCommercial (CC BY-NC 4.0) license, which permits others to distribute, remix, adapt, build upon this work non-commercially, and license their derivative works on different terms, provided the original work is properly cited and the use is non-commercial. See: https://creativecommons.org/Licenses/by-nc/4.0/

Country/Territory of origin: China

ORCID number: Hui-Da Zheng 0000-0002-4986-8770; Jian-Hua Xu 0000-0001-5147-292X.

S-Editor: Qu XL
L-Editor: A
P-Editor: Yuan YY

REFERENCES

1 **Sung H**, Ferlay J, Siegel RL, Laversanne M, Soerjomataram I, Jemal A, Bray F. Global Cancer Statistics 2020: GLOBOCAN Estimates of Incidence and Mortality Worldwide for 36 Cancers in 185 Countries. *CA Cancer J Clin* 2021; **71**: 209-249 [PMID: 33538338 DOI: 10.3322/caac.21660]

2 **Quirke P**, Williams GT, Ectors N, Ensari A, Piard F, Nagtegaal I. The future of the TNM staging system in colorectal cancer: time for a debate? *Lancet Oncol* 2007; **8**: 651-657 [PMID: 17613427 DOI: 10.1016/S1470-2045(07)70205-X]

3 **Delattre JF**, Selcen Oguz Erdogan A, Cohen R, Shi Q, Emile JF, Taieb J, Tabernero J, André T, Meyerhardt JA, Nagtegaal ID, Svrcek M. A comprehensive overview of tumour deposits in colorectal cancer: Towards a next TNM classification. *Cancer Treat Rev* 2022; **103**: 102325 [PMID: 34954486 DOI: 10.1016/j.ctrv.2021.102325]

4 **Moon JY**, Lee MR, Ha GW. Prognostic value of tumor deposits for long-term oncologic outcomes in patients with stage III colorectal cancer: a systematic review and meta-analysis. *Int J Colorectal Dis* 2022; **37**: 141-151 [PMID: 34595585 DOI: 10.1007/s00384-021-04036-z]

5 **Wu W**, Zeng S, Zhang X, Liu P, Qiu T, Li S, Gong P. The value of tumor deposits in evaluating colorectal cancer survival and metastasis: a population-based retrospective cohort study. *World J Surg Oncol* 2022; **20**: 41 [PMID: 35189906 DOI: 10.1186/s12957-022-02501-9]

6 **Bouquot M**, Creavin B, Goasguen N, Chafai N, Tiret E, André T, Flejou JF, Parc Y, Lefevre JH, Svrcek M. Prognostic value and characteristics of N1c colorectal cancer. *Colorectal Dis* 2018; **20**: O248-O255 [PMID: 29894583 DOI: 10.1111/codi.14289]

7 **Cohen R**, Shi Q, Meyers J, Jin Z, Svrcek M, Fuchs C, Couture F, Kuebler P, Ciombor KK, Bendell J, De Jesus-Acosta A, Kumar P, Lewis D, Tan B, Bertagnolli MM, Philip P, Blanke C, O'Reilly EM, Shields A, Meyerhardt JA. Combining tumor deposits with the number of lymph node metastases to improve the prognostic accuracy in stage III colon cancer: a post hoc analysis of the CALGB/SWOG 80702 phase III study (Alliance)(☆). *Ann Oncol* 2021; **32**: 1267-1275 [PMID: 34293461 DOI: 10.1016/j.annonc.2021.07.009]

8 **von Winterfeld M**, Hoffmeister M, Ingold-Heppner B, Jansen L, Tao S, Herpel E, Schirmacher P, Dietel M, Chang-Claude J, Autschbach F, Brenner H, Bläker H. Frequency of therapy-relevant staging shifts in colorectal cancer through the introduction of pN1c in the 7th TNM edition. *Eur J Cancer* 2014; **50**: 2958-2965 [PMID: 25281526 DOI: 10.1016/j.ejca.2014.09.002]

9 **Lord A**, Brown G, Abulafi M, Bateman A, Frankel W, Goldin R, Gopal P, Kirsch R, Loughrey MB, Märkl B, Moran B, Puppa G, Rasheed S, Shimada Y, Snaebjornsson P, Svrcek M, Washington K, West N, Wong N, Nagtegaal I. Histopathological diagnosis of tumour deposits in colorectal cancer: a Delphi consensus study. *Histopathology* 2021; **79**: 168-175 [PMID: 33511676 DOI: 10.1111/his.14344]

10 **Wu WX**, Zhang DK, Chen SX, Hou ZY, Sun BL, Yao L, Jie JZ. Prognostic impact of tumor deposits on overall survival in colorectal cancer: Based on Surveillance, Epidemiology, and End Results database. *World J Gastrointest Oncol* 2022; **14**: 1699-1710 [PMID: 36187391 DOI: 10.4251/wjgo.v14.i9.1699]

11 **Liang Y**, Wu L, Liu L, Ding X, Wang X, Liu H, Meng J, Xu R, He D, Liang H. Impact of extranodal tumor deposits on prognosis and N stage in gastric cancer. *Surgery* 2019; **166**: 305-313 [PMID: 31221435 DOI: 10.1016/j.surg.2019.04.027]

12 **Jhuang YH**, Chou YC, Lin YC, Hu JM, Pu TW, Chen CY. Risk factors predict microscopic extranodal tumor deposits in advanced stage III

colon cancer patients. *World J Gastroenterol* 2023; **29**: 1735-1744 [PMID: 37077516 DOI: 10.3748/wjg.v29.i11.1735]

13 **Böhning D**, Holling H, Patilea V. A limitation of the diagnostic-odds ratio in determining an optimal cut-off value for a continuous diagnostic test. *Stat Methods Med Res* 2011; **20**: 541-550 [PMID: 20639268 DOI: 10.1177/0962280210374532]

14 **Arrichiello G**, Pirozzi M, Facchini BA, Facchini S, Paragliola F, Nacca V, Nicastro A, Canciello MA, Orlando A, Caterino M, Ciardiello D, Della Corte CM, Fasano M, Napolitano S, Troiani T, Ciardiello F, Martini G, Martinelli E. Beyond N staging in colorectal cancer: Current approaches and future perspectives. *Front Oncol* 2022; **12**: 937114 [PMID: 35928863 DOI: 10.3389/fonc.2022.937114]

15 **Chen K**, Collins G, Wang H, Toh JWT. Pathological Features and Prognostication in Colorectal Cancer. *Curr Oncol* 2021; **28**: 5356-5383 [PMID: 34940086 DOI: 10.3390/curroncol28060447]

16 **Li X**, An B, Zhao Q, Qi J, Wang W, Zhang D, Li Z, Qin C. Impact of tumor deposits on the prognosis and chemotherapy efficacy in stage III colorectal cancer patients with different lymph node status: A retrospective cohort study in China. *Int J Surg* 2018; **56**: 188-194 [PMID: 29936197 DOI: 10.1016/j.ijsu.2018.06.029]

17 **Pu H**, Pang X, Fu J, Zheng R, Chen Y, Zhang D, Fang X. Significance of tumor deposits combined with lymph node metastasis in stage III colorectal cancer patients: a retrospective multi-center cohort study from China. *Int J Colorectal Dis* 2022; **37**: 1411-1420 [PMID: 35595975 DOI: 10.1007/s00384-022-04149-z]

18 **Park SY**. Nomogram: An analogue tool to deliver digital knowledge. *J Thorac Cardiovasc Surg* 2018; **155**: 1793 [PMID: 29370910 DOI: 10.1016/j.jtcvs.2017.12.107]

19 **Chen J**, Zhang Z, Ni J, Sun J, Ren W, Shen Y, Shi L, Xue M. Predictive and Prognostic Assessment Models for Tumor Deposit in Colorectal Cancer Patients With No Distant Metastasis. *Front Oncol* 2022; **12**: 809277 [PMID: 35251979 DOI: 10.3389/fonc.2022.809277]

20 **Hong Y**, Song G, Jia Y, Wu R, He R, Li A. Predicting tumor deposits in patients with rectal cancer: Using the models of multiple mathematical parameters derived from diffusion-weighted imaging. *Eur J Radiol* 2022; **157**: 110573 [PMID: 36347167 DOI: 10.1016/j.ejrad.2022.110573]

21 **Naito A**, Iwamoto K, Ohtsuka M, Imasato M, Nakahara Y, Mikamori M, Furukawa K, Moon J, Asaoka T, Kishi K, Akamatsu H. Risk Factors for Lymph Node Metastasis in Pathological T1b Colorectal Cancer. *In Vivo* 2021; **35**: 987-991 [PMID: 33622893 DOI: 10.21873/invivo.12341]

22 **Xiong X**, Wang C, Cao J, Gao Z, Ye Y. Lymph node metastasis in T1-2 colorectal cancer: a population-based study. *Int J Colorectal Dis* 2023; **38**: 94 [PMID: 37055602 DOI: 10.1007/s00384-023-04386-w]

23 **Zahid A**, Young CJ. How to decide on stent insertion or surgery in colorectal obstruction? *World J Gastrointest Surg* 2016; **8**: 84-89 [PMID: 26843916 DOI: 10.4240/wjgs.v8.i1.84]

24 **Katoh H**, Yamashita K, Wang G, Sato T, Nakamura T, Watanabe M. Prognostic significance of preoperative bowel obstruction in stage III colorectal cancer. *Ann Surg Oncol* 2011; **18**: 2432-2441 [PMID: 21369738 DOI: 10.1245/s10434-011-1625-3]

25 **Nozawa H**, Morikawa T, Kawai K, Hata K, Tanaka T, Nishikawa T, Sasaki K, Shuno Y, Kaneko M, Hiyoshi M, Emoto S, Murono K, Sonoda H, Fukayama M, Ishihara S. Obstruction is associated with perineural invasion in T3/T4 colon cancer. *Colorectal Dis* 2019; **21**: 917-924 [PMID: 31017742 DOI: 10.1111/codi.14655]

26 **Lv X**, Yu H, Gao P, Song Y, Sun J, Chen X, Wang Y, Wang Z. A nomogram for predicting bowel obstruction in preoperative colorectal cancer patients with clinical characteristics. *World J Surg Oncol* 2019; **17**: 21 [PMID: 30658652 DOI: 10.1186/s12957-019-1562-3]

27 **Ueno H**, Nagtegaal ID, Quirke P, Sugihara K, Ajioka Y. Tumor deposits in colorectal cancer: Refining their definition in the TNM system. *Ann Gastroenterol Surg* 2023; **7**: 225-235 [PMID: 36998291 DOI: 10.1002/ags3.12652]

28 **Liu F**, Zhao J, Li C, Wu Y, Song W, Guo T, Chen S, Cai S, Huang D, Xu Y. The unique prognostic characteristics of tumor deposits in colorectal cancer patients. *Ann Transl Med* 2019; **7**: 769 [PMID: 32042785 DOI: 10.21037/atm.2019.11.69]

World Journal of Gastroenterology

Submit a Manuscript: https://www.f6publishing.com

World J Gastroenterol 2023 October 21; 29(39): 5494-5502

DOI: 10.3748/wjg.v29.i39.5494

ISSN 1007-9327 (print) ISSN 2219-2840 (online)

ORIGINAL ARTICLE

Observational Study

Risk assessment of venous thromboembolism in inflammatory bowel disease by inherited risk in a population-based incident cohort

Andrew S Rifkin, Zhuqing Shi, Jun Wei, Siqun Lilly Zheng, Brian T Helfand, Jonathan S Cordova, Vincent F Biank, Alfonso J Tafur, Omar Khan, Jianfeng Xu

Specialty type: Gastroenterology and hepatology

Provenance and peer review: Unsolicited article; Externally peer reviewed.

Peer-review model: Single blind

Peer-review report's scientific quality classification

Grade A (Excellent): A
Grade B (Very good): 0
Grade C (Good): C
Grade D (Fair): 0
Grade E (Poor): 0

P-Reviewer: Huang JG, Singapore; Yasuda H, Japan

Received: June 5, 2023
Peer-review started: June 5, 2023
First decision: August 8, 2023
Revised: August 18, 2023
Accepted: September 28, 2023
Article in press: September 28, 2023
Published online: October 21, 2023

Andrew S Rifkin, Zhuqing Shi, Jun Wei, Siqun Lilly Zheng, Brian T Helfand, Jianfeng Xu, Program for Personalized Cancer Care, NorthShore University HealthSystem, Evanston, IL 60201, United States

Brian T Helfand, Jianfeng Xu, Department of Surgery, NorthShore University HealthSystem, Evanston, IL 60201, United States

Brian T Helfand, Jianfeng Xu, Pritzker School of Medicine, University of Chicago, Chicago, IL 60637, United States

Jonathan S Cordova, Vincent F Biank, Department of Pediatrics, NorthShore University HealthSystem, Evanston, IL 60201, United States

Alfonso J Tafur, Cardiovascular Institute, NorthShore University HealthSystem, Evanston, IL 60201, United States

Omar Khan, Department of Medicine, NorthShore University HealthSystem, Evanston, IL 60201, United States

Corresponding author: Jianfeng Xu, MD, DrPH, Professor, Program for Personalized Cancer Care, NorthShore University HealthSystem, 1001 University Place, Evanston, IL 60201, United States. jxu@northshore.org

Abstract

BACKGROUND

Inflammatory bowel disease (IBD), including Crohn's disease (CD) and ulcerative colitis (UC), is a chronic inflammatory disease of the digestive tract with increasing prevalence globally. Although venous thromboembolism (VTE) is a major complication in IBD patients, it is often underappreciated with limited tools for risk stratification.

AIM

To estimate the proportion of VTE among IBD patients and assess genetic risk factors (monogenic and polygenic) for VTE.

METHODS
Incident VTE was followed for 8465 IBD patients in the UK Biobank (UKB). The associations of VTE with *F5* factor V leiden (FVL) mutation, *F2* G20210A prothrombin gene mutation (PGM), and polygenic score (PGS003332) were tested using Cox hazards regression analysis, adjusting for age at IBD diagnosis, gender, and genetic background (top 10 principal components). The performance of genetic risk factors for discriminating VTE diagnosis was estimated using the area under the receiver operating characteristic curve (AUC).

RESULTS
The overall proportion of incident VTE was 4.70% in IBD patients and was similar for CD (4.46%), UC (4.49%), and unclassified (6.42%), and comparable to that of cancer patients (4.66%) who are well-known at increased risk for VTE. Mutation carriers of *F5*/*F2* had a significantly increased risk for VTE compared to non-mutation carriers, hazard ratio (HR) was 1.94, 95% confidence interval (CI): 1.42-2.65. In contrast, patients with the top PGS decile had a considerably higher risk for VTE compared to those with intermediate scores (middle 8 deciles), HR was 2.06 (95%CI: 1.57-2.71). The AUC for differentiating VTE diagnosis was 0.64 (95%CI: 0.61-0.67), 0.68 (95%CI: 0.66-0.71), and 0.69 (95%CI: 0.66-0.71), respectively, for *F5*/*F2* mutation carriers, PGS, and combined.

CONCLUSION
Similar to cancer patients, VTE complications are common in IBD patients. PGS provides more informative risk information than *F5*/*F2* mutations (FVL and PGM) for personalized thromboprophylaxis.

Key Words: Inflammatory bowel disease; Venous thromboembolism; Polygenic score; Factor V leiden; Prothrombin gene mutation

©The Author(s) 2023. Published by Baishideng Publishing Group Inc. All rights reserved.

Core Tip: Based on 8475 inflammatory bowel disease (IBD) patients from a population-based biobank, we showed they have an elevated risk for venous thromboembolism (VTE), with the overall proportion of incident VTE at 4.70%, similar to 4.66% observed in cancer patients. Polygenic score (PGS) is a significant predictor for VTE events, stronger than the well-known *F5* factor V leiden mutation and *F2* G20210A prothrombin gene mutation. The overall proportion of incident VTE is 8.53% in patients at the top 10 PGS percentile. These findings highlight the importance of VTE complications in IBD patients and provide genetic tools for personalized thromboprophylaxis.

Citation: Rifkin AS, Shi Z, Wei J, Zheng SL, Helfand BT, Cordova JS, Biank VF, Tafur AJ, Khan O, Xu J. Risk assessment of venous thromboembolism in inflammatory bowel disease by inherited risk in a population-based incident cohort. *World J Gastroenterol* 2023; 29(39): 5494-5502
URL: https://www.wjgnet.com/1007-9327/full/v29/i39/5494.htm
DOI: https://dx.doi.org/10.3748/wjg.v29.i39.5494

INTRODUCTION

Inflammatory bowel disease (IBD), including Crohn's disease (CD) and ulcerative colitis (UC), is a disease characterized by chronic inflammation of the digestive tract. Its prevalence was estimated at 1.3% (3 million adults) in the United States in 2015 and is expected to increase globally[1,2]. IBD is associated with several adverse complications, including venous thromboembolism (VTE). IBD patients have a 2 to 3-fold higher risk of developing a VTE as compared to the general population[3]. Although the pathophysiology underlying this observation remains largely unknown, it may involve changes in the coagulation system, increased platelet count and reactivity, and altered fibrinolysis[4]. The importance of elevated VTE risk in IBD patients is emphasized in a recent international consensus on the prevention of venous and arterial thrombotic events in patients with IBD, which encourages screening for VTE risk factors. Statement 2 of the consensus states that "Patients with IBD should be screened for VTE risk factors" (consensus reached 100%)[4].

Several inherited factors are associated with risk for VTE, including relatively common gain of function mutations in genes for coagulation factors: Factor V leiden (FVL) mutation in the *F5* gene and the G20210A prothrombin gene mutation (PGM) in the *F2* gene[5]. Recent advances in genome-wide association studies (GWAS) have also revealed multiple common single nucleotide polymorphisms (SNPs) that are associated with increased VTE risk[6]. Polygenic scores (PGS) based on these SNPs have been shown to be effective to stratify VTE risk in the general population. While the consensus recognizes several genetic factors such as *F5* and *F2* for VTE risk among IBD patients, it does not mention PGS[4].

The objectives of this study are to utilize a large population-based cohort to: (1) Estimate the proportion of VTE among IBD patients and compare it to that in cancer patients who are well-known to have an increased risk for VTE; (2) test the association of inherited risk factors (*F5*/*F2* mutations and PGS) and VTE among IBD patients; and (3) assess the

performance of PGS for predicting VTE among IBD patients, alone or in combination with *F5*/*F2* mutations. Results from this study may provide needed evidence for PGS to be included in the updated international consensus for VTE prevention among IBD patients.

MATERIALS AND METHODS

Subjects in this study were patients who had a diagnosis of IBD in the UK Biobank (UKB), a population-based study of 500000 volunteers from the United Kingdom[7]. IBD diagnoses were obtained based on International Classification of Diseases-10 (ICD-10) codes (K50 for CD and K51 for UC) of primary care, death register, inpatient diagnosis, and self-report. Incident VTE after IBD diagnosis were identified based on the inclusion criteria described by Klarin *et al*[8] Briefly, subjects were defined as a VTE case based on at least one of the following criteria: (1) VTE (deep vein thrombosis and pulmonary embolism) ascertained at baseline by self-report; (2) Hospitalization for ICD-10 Code I80.1, I80.2, I82.2, I26.0, or I26.9; and (3) Hospitalization for Office of Population and Censuses and Survey-4 Procedures Codes L79.1 or L90.2. Only incident VTE, *i.e.*, those that occurred after a diagnosis of IBD were included in the analysis. As a comparison, VTE events after a cancer diagnosis were also estimated among cancer patients (ICD-10: C00-C96) in the UKB[9].

Genotypes for the *F5* FVL mutation (c.1601G>A, rs6025) and the *F2* PGM (c.*97G>A, rs1799963) as well as genome-wide SNPs were obtained from the UKB Axiom SNP genotype array (genotyped or imputed). A published pan-ancestry PGS for VTE (PGS003332) was selected from the PGS catalog for the study because it was developed from the largest GWAS of VTE with 81190 cases and 1419671 controls sampled from six cohorts[6,10]. Based on the scoring file of the PGS, raw PGS was first calculated by taking the product of the count of risk alleles and the risk allele weight at each locus in the PGS (1092045 SNPs) and then summing across available risk loci. Ancestry-adjusted PGS was calculated based on the first four principal components using a previously described method[11]. To remove the contribution of SNPs from the *F5* and *F2* genes to the score, a modified PGS ($PGS_{nonF5/F2}$) was also calculated by removing 1515 SNPs in these two genes (chr1: 168519049-170519049 for *F5* and chr11: 45761055-47761055 for *F2*).

The proportion of incident VTE was calculated as (number of patients with incident VTE)/(number of patients with IBD). The difference in VTE proportion among groups of patients was tested using a χ^2 test. Time to VTE diagnosis from the time of IBD diagnosis was estimated using Kaplan-Meier survival analysis and its difference among various groups of IBD patients was tested using and log-rank test. Association of genetic risk factors (PGS and *F5*/*F2* mutations) and other known risk factors with VTE among IBD patients were tested using the Cox proportional hazards regression analysis, adjusting for gender, body mass index at study recruitment, and genetic background (top 10 principal components). In addition, the performance of genetic risk factors for discriminating VTE was estimated using the area under the receiver operating characteristic curve (AUC). All statistical analyses were performed using R-package.

RESULTS

As of the last UKB accession date (October 7, 2022), 8465 (1.68%) IBD patients were identified from 501095 subjects in the UKB, including 2267 (0.45%), 5233 (1.05%), and 965 (0.19%) patients with CD only, UC only, and IBD unclassified (IBD-U) (diagnosed with both CD and UC), respectively (Table 1). The median age at diagnosis was 49.60, 51.34, and 44.09 years for CD only, UC only, and IBD-U, respectively. Among these IBD patients, 398 developed VTE events after IBD diagnosis, with the overall proportion of incident VTE of 4.70%. The proportion of VTE was statistically different among patients with CD only (4.46%), UC only (4.49%), and IBD-U colitis (6.42%), χ^2 = 7.22, degree of freedom = 2, P = 0.03. It is noted that the overall proportion of incident VTE in these IBD patients was similar to that of 107520 cancer patients (4.66%) in the UKB who are well-known to have an increased risk for VTE. However, a different pattern of VTE events during the follow-up was noticed; VTE events occurred continuously throughout the follow-up period for IBD patients where a disproportionally higher number of VTE events occurred in the first several years in cancer patients (Figure 1).

Among the 8210 IBD patients with genetic data, 509 (6.20%) were carriers of *F5*/*F2* mutations, including 351 (4.28%) carriers of *F5* FVL and 163 (1.99%) carriers of *F2* PGM (Table 2). The overall proportion of incident VTE among mutation carriers was 9.04%, higher than that of non-mutation carriers (4.31%) (Table 2 and Figure 2A). In comparison, PGS was more informative in differentiating VTE events and the proportion of incident VTE increased with increasing decile of $PGS_{nonF5/F2}$, P_{trend} = 1.60E-18 (Figure 2B). For example, the proportion of incident VTE was 1.58% for IBD patients at the bottom of $PGS_{nonF5/F2}$ decile, which was considerably lower than that of non-mutation carriers of *F5*/*F2*. On the other hand, the proportion of incident VTE was 8.53% for IBD patients at the top of $PGS_{nonF5/F2}$ decile, which was higher than that of mutation carriers of *F5*/*F2*. As expected, original PGS (including SNPs in the *F5*/*F2* regions) performed well in stratifying VTE risk and is slightly better than that of $PGS_{nonF5/F2}$ (Figure 2C). For example, the proportion of incident VTE was 1.10% and 10.17% for IBD patients at the bottom and top decile, respectively.

Compared to non-mutation carriers of *F5*/*F2*, mutation carriers were at a marginally increased risk for VTE, with a hazard ratio (HR) of 1.94, 95% confidence interval (CI): 1.42-2.65 (Table 2). For $PGS_{nonF5/F2}$, patients at the top decile had a considerably higher risk for VTE compared to IBD patients with intermediate scores (middle 8 deciles), HR was 1.98 (95%CI: 1.52-2.57). Furthermore, $PGS_{nonF5/F2}$ can also identify patients at lower risk for VTE, HR was 0.36 (95%CI: 0.21-0.63) for patients at the bottom decile. In a multivariable analysis where both *F5*/*F2* mutation carrier status and $PGS_{nonF5/F2}$ (continuous variable) were included, both were significantly associated with VTE risk, P < 0.001.

Table 1 Characteristics of inflammatory bowel disease patients and incident venous thromboembolism in the UK Biobank

	Subjects, *n* (%)	Age dx, median (IQR), yr	Incident VTE, *n* (%)
IBD, all	8465 (1.68)	50.08 (35.24-61.76)	398 (4.7)
Crohn's disease	2267 (0.45)	49.68 (32.48-62.37)	101 (4.46)
Ulcerative colitis	5233 (1.05)	51.38 (36.87-62.50)	235 (4.49)
Indeterminate colitis	965 (0.19)	44.26 (31.56-54.92)	62 (6.42)

IBD: Inflammatory bowel disease; VTE: Venous thromboembolism.

Table 2 Association of venous thromboembolism risk with *F5/F2* mutations and polygenic score in the UK Biobank

	IBD patients, *n* (%)	Incident VTE, *n* (%)	HR (95%CI)[1]	*P* value
FVL/F2 carrier status				
Non-carriers	7701/8210 (93.8)	332/7701 (4.31)	Ref.	
FVL carriers	351/8210 (4.28)	37/351 (10.54)	2.27 (1.61-3.21)	2.84E-06
F2 carriers	163/8210 (1.99)	10/163 (6.13)	1.29 (0.69-2.43)	0.43
Any *FVL/F2* carriers	509/8210 (6.2)	46/509 (9.04)	1.94 (1.42-2.65)	3.27E-05
$PGS_{non\text{-}F5/F2}$ decile				
Bottom	821/8210 (10)	13/821 (1.58)	0.36 (0.21-0.63)	3.12E-04
Intermediate	6568/8210 (80)	295/6568 (4.49)	Ref.	
Top	821/8210 (10)	70/821 (8.53)	1.98 (1.52-2.57)	3.26E-07

[1]HR adjusted for gender, body mass index, and genetic background. The time in survival analysis was from inflammatory bowel disease to event.
IBD: Inflammatory bowel disease; VTE: Venous thromboembolism; 95%CI: 95% confidence interval; HR: Hazard ratio.

$PGS_{nonF5/F2}$ also had a significantly better discriminative performance for VTE diagnosis than *F5/F2* mutations, with the AUC estimated at 0.68 (95%CI: 0.65-0.71) and 0.64 (95%CI: 0.61-0.67), respectively, $P = 0.05$ (Table 3). Combining these two risk factors increased the AUC to 0.69 (95%CI: 0.66-0.71), which was also significantly higher than that of *F5/F2* mutations, $P = 0.01$. Interestingly, the original PGS for VTE, which includes SNPs in the *F5/F2* gene regions, had a similar AUC (0.69, 95%CI: 0.67-0.72) to that of combined $PGS_{nonF5/F2}$ and *F5/F2* mutations.

DISCUSSION

By following incident VTE events among 8465 IBD patients from a population-based biobank, three major findings that have potentially translational implications were obtained from our study. First, VTE was a common complication among IBD patients, with a proportion similar to diseases commonly considered at elevated risk for VTE such as cancer. This elevated VTE risk among IBD patients was also reported in previously published studies[12,13]. In a cohort of 2811 IBD patients recruited from 14 referral centers in Austria, a VTE prevalence of 5.6% was reported, similar to that in our study [12]. In another large cohort study of hospitalized and ambulatory IBD patients ($n = 13756$), as well as matched controls ($n = 71672$) from the General Practice Research Database in the United Kingdom, a higher VTE rate compared to the general population was also reported[13]. For hospitalized patients with IBD, HR for VTE was 3.2, 95%CI: 1.7-6.3. Similarly, for ambulatory patients with IBD, the HR was 8.4, 95%CI: 5.5-12.8. In addition, several studies have also indicated that there is a high risk of recurrent VTE following hospital discharge[13,14]. Interestingly, this increased VTE risk seems to be unique to IBD, setting it apart from other autoimmune diseases like rheumatoid arthritis or celiac disease where this association is not commonly observed[15]. Despite the consistent research observation of an association between IBD and VTE, VTE complication in IBD patients is commonly overlooked in clinical practice. Adherence to VTE prophylaxis among IBD patients is low and inconsistent, with only 68% of hospitalized UC patients prescribed prophylaxis[16]. Even when prescribed, one-third of the doses were not actually administered. Factors contributing to low adherence could include patient noncompliance, physician unawareness, fragmented care, and bleeding risk concerns.

Second, results from our study suggest the VTE risk conferred by *F5/F2* mutations (FVL and PGM) in IBD patients was modest and considerably lower than previously reported. For *F5* FVL, two meta-analyses published in 2011 reported a combined OR of 4.0 and 5.3, respectively, for VTE in IBD patients[17,18]. These ORs, however, were likely over-estimated due to a combination of several factors, including small sample sizes, study designs (the vast majority was case-control

Table 3 Discriminative performance of venous thromboembolism by inherited risk factors

	AUC (95%CI)[1]
F5/F2 mutations	0.64 (0.61-0.67)
$PGS_{non\text{-}F5/F2}$	0.68 (0.65-0.71)
F5/F2 mutations + $PGS_{non\text{-}F5/F2}$	0.69 (0.66-0.71)
PGS	0.69 (0.67-0.72)

[1]Model also included age, gender, body mass index and genetic background.

AUC: Area under the receiver operating characteristic curve; PGS: Polygenic score; 95%CI: 95% confidence interval.

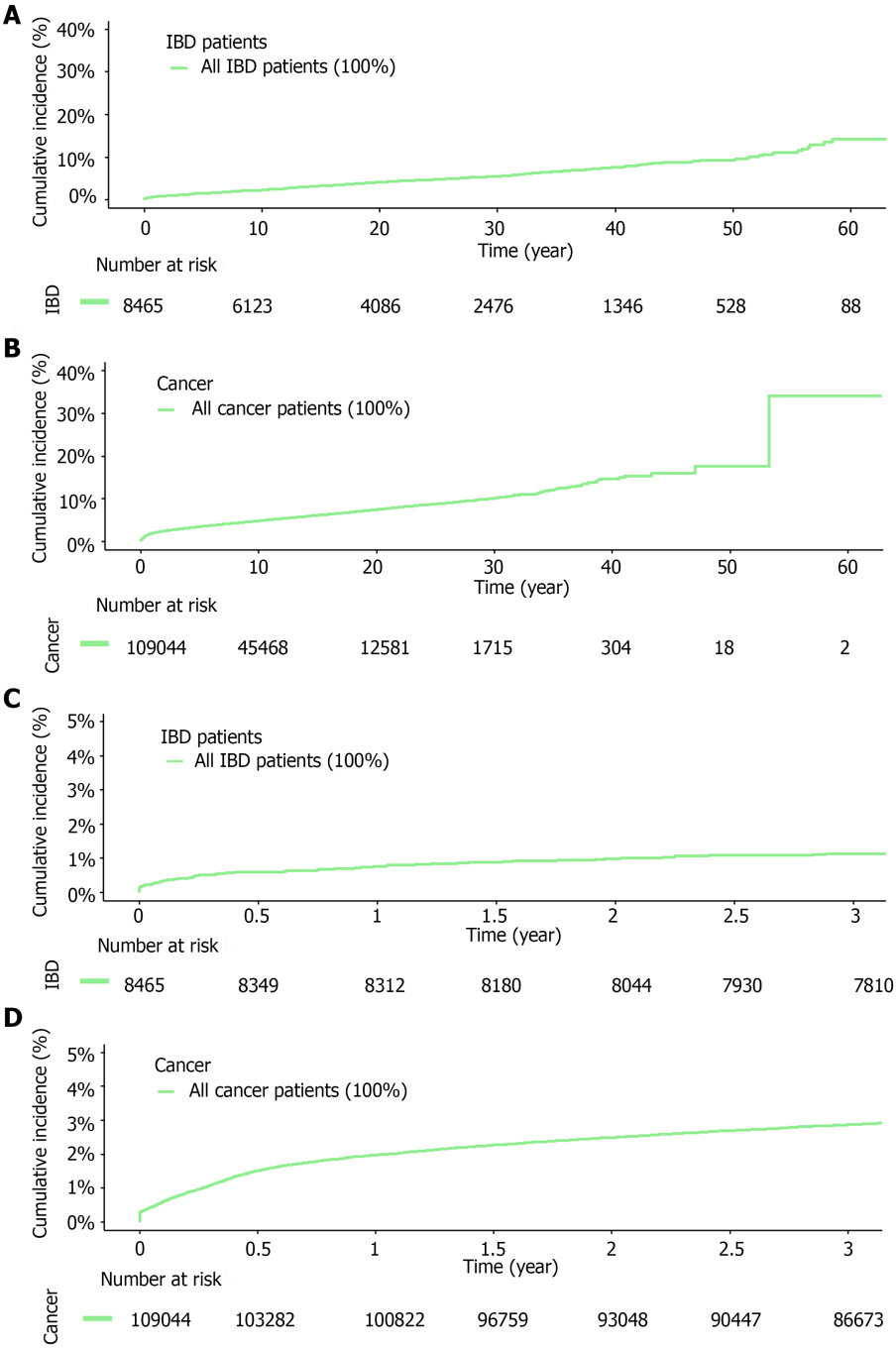
studies), genetic heterogeneity (ancestry and genetic background were not accounted for), and publication bias (positive finding were more likely to be published). For example, in the meta-analysis performed by Zhong *et al*[17], the total sample size of IBD patients from 10 individual studies published before 2008 was 938, including 124 (13%) with VTE. In particular, 9 of the 10 studies had fewer than 80 IBD patients. The only relatively large study (477 IBD patients, including 14 (2.9%) with VTE) failed to observe a significant association between FVL and VTE, OR = 1.28, 95%CI: 0.16-10.17[19]. For *F2* PGM, its association with VTE in IBD patients was inconclusive from two small studies published prior to 2007, with fewer than 100 IBD patients in each study[20,21]. In comparison, the association results and OR estimates from our study were more reliable because the study was based on a large cohort of 8300 IBD patients whose VTE diagnosis was uniformly followed. Furthermore, our association test was performed adjusted for genetic background, therefore, reduced the confounder of genetic heterogeneity. However, additional large cohorts of IBD patients with follow-up information for VTE are still needed to validate our findings.

Third, compared to *F5/F2* mutations, we showed new PGS was more informative for stratifying VTE risk and performs better in discriminating VTE diagnosis after IBD. The better performance of PGS is consistent with the strong genetic basis for VTE where about 60% of the variance in VTE incidence is attributable to genetic effects[22]. Our finding is also consistent with a previous polygenic risk score study in 792 IBD patients where the score was based on 265 established VTE risk-associated SNPs[23]. However, the PGS used in the current study differs from the published study in that it includes many more SNPs (more than a million) and captures both established risk-associated SNPs implicated in GWAS and many more SNPs in the genome that did not reach the GWAS significance level individually (due to either modest-effect or low allele frequency)[6,23,24]. Consequently, the performance of PGS for stratifying VTE risk is improved. Additionally, our PGS not only identified patients at high-risk for VTE, but also identified patients at considerably low risk for VTE. This information is important for considering the need, dosage and duration for anticoagulant treatment to balance its potential benefits and harms. Importantly, it is worth noting that the PGS evaluated in this study was developed and validated in large external study populations with over a million subjects[6]. Our study simply assessed its performance in IBD patients, therefore, is not susceptible to issues related to model development such as overfitting and multiple testing. Furthermore, the risk estimate for PGS is not susceptible to potential observer bias because neither physicians nor patients are aware of their PGS for VTE.

Considering the similar AUC performance for the combined $PGS_{nonF5/F2}$ and *F5/F2* mutations and the original PGS, either approach may be used for VTE risk assessment in IBD patients in the clinic. While the first approach has the advantage of integrating well-known *F5/F2* mutations with new PGS, the latter approach is simpler to use (single scoring file) and easier to interpret (risk estimate derived from a large number of subjects is more reliable with a narrow CI). Furthermore, as a pan-ancestry PGS, PGS is applicable to patients of various ancestry populations. The added value of PGS over *F5/F2* mutations is more relevant in non-European ancestries because of their relatively low *F5/F2* mutation carrier rates (carrier rate of *F5/F2* mutations was 6.31% and 4.16% in European and non-European IBD patients, respectively). However, considering this PGS was developed and validated primarily in subjects of European ancestry, its performance in other ancestries is less certain. As shown in Supplementary Table 1 for the performance of PGS in 409 non-European IBD patients, compared to patients with intermediate scores, those at the top decile had HR of 1.48 (95%CI: 0.17-13.11) for VTE. Additional data for non-European IBD patients are urgently needed.

Our findings have potential clinical utilities. Genetic risk assessment using $PGS_{nonF5/F2}$ and *F5/F2* mutations may be integrated into clinical presentations to develop personalized strategies for thromboprophylaxis. For example, IBD patients with high genetic risk may consider higher dosage and longer duration of anticoagulation therapy. On the other hand, patients with low PGS and without *F5/F2* mutations may consider lower dosages and shorter duration to minimize risk for bleeding events.

Several limitations of our study are noted. Considering possible under-diagnosis of VTE (especially deep vein thrombosis) in subjects without IBD or other major diseases requiring hospitalization and intensive clinical care, we did not compare the VTE proportion between IBD and non-IBD subjects. Furthermore, due to the difficulty in obtaining detailed clinical variables related to the clinical characteristics of IBD and treatment, we were unable to include key clinical variables to assess the independent and added value of PGS in existing clinical risk assessment models. Another major limitation of our study is a lack of ancestral diversity in study subjects (96% of IBD patients in our study are of European ancestry), therefore it is critical to validate our findings in other diverse ancestry groups in future studies. Lastly, we did not include other known major genes for VTE (*SERPINC1*, *PROC*, and *PROS1*) in this study. Mutations in these genes are rare and can only be detected by whole exome sequencing (WES) which is currently available in only 40%



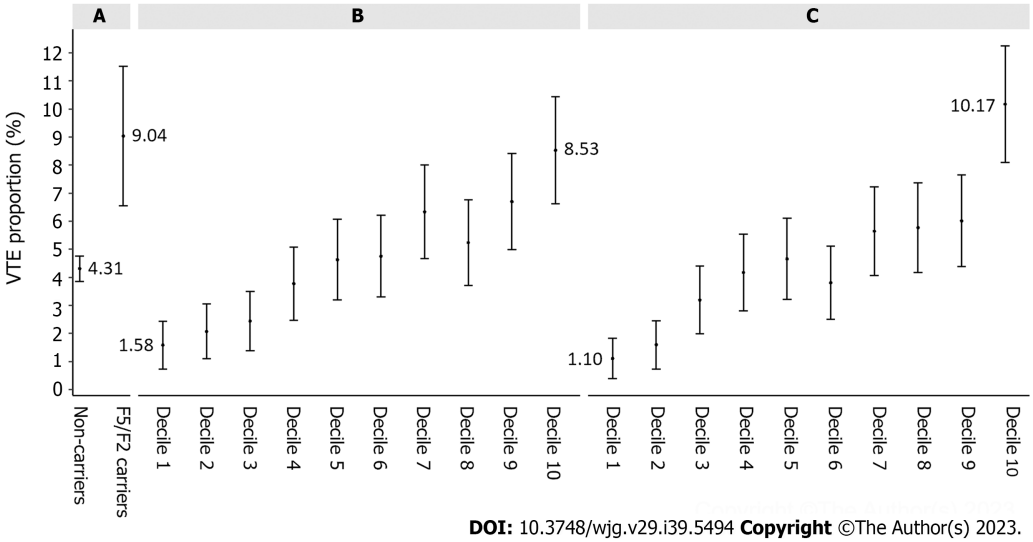
DOI: 10.3748/wjg.v29.i39.5494 **Copyright** ©The Author(s) 2023.

Figure 1 Kaplan-Meier analysis. A and B: Kaplan-Meier analysis for time to incident venous thromboembolism in the UK Biobank during the entire follow-up period for inflammatory bowel disease (IBD) patients (A) and cancer patients (B); C and D: Within the 3 years after IBD diagnosis for IBD patients (C) and cancer patients (D). IBD: Inflammatory bowel disease.

of subjects in the UKB[7]. Among 3227 IBD patients with WES data, only 6 (0.19%), 2 (0.06%), and 2 (0.06%) carriers of loss of function mutations were identified, 2 (20%) of whom developed VTE. Larger studies with WES data are required to test these genetic risk factors.

CONCLUSION

In conclusion, we demonstrated that VTE complications are common in IBD patients with the proportion similar to diseases known at increased VTE risk. Furthermore, we showed SNP-based PGS is more informative and superior to *F5*/*F2* mutations in identifying IBD patients at high risk for VTE. These results may have potential implications for developing personalized anticoagulant treatment.



DOI: 10.3748/wjg.v29.i39.5494 **Copyright** ©The Author(s) 2023.

Figure 2 Proportion of incident venous thromboembolism in the UK Biobank by carrier status of *F5* factor V leiden and/or *F2* prothrombin gene mutation, decile of polygenic score$_{nonF5/F2}$, and decile of original polygenic score. Dot and vertical line indicate mean and 95% confidence interval, respectively. A: Carrier status of *F5* factor V leiden and/or *F2* prothrombin gene mutation; B: Decile of polygenic score (PGS)$_{nonF5/F2}$; C: Decile of original PGS. Dot and vertical line indicate mean and 95% confidence interval, respectively. VTE: Venous thromboembolism.

ARTICLE HIGHLIGHTS

Research background

Venous thromboembolism (VTE) is a major complication in patients with inflammatory bowel disease (IBD). However, it is often underappreciated among physicians and patients. Furthermore, limited VTE risk stratification tools are available for personalized thromboprophylaxis.

Research motivation

A large IBD patient cohort is available from the UK Biobank (UKB). Its long-term clinical follow-up data and genome-wide genetic data provide a rare and efficient opportunity to address these two major challenges.

Research objectives

To estimate the prevalence of VTE complications among IBD patients and assess the performance of known and novel genetic predictors of VTE risk stratification in these patients.

Research methods

We retrospectively followed the incident VTE complication among 8465 IBD patients in the UKB. The associations of VTE with factor V leiden (FVL) mutation in the *F5* gene, G20210A prothrombin gene mutation (PGM) in the *F2* gene, and polygenic score (PGS) were tested using Cox hazards regression analysis, adjusting for age at IBD diagnosis, gender, and genetic background (top 10 principal components). The performance of genetic risk factors for discriminating VTE complications was estimated using the area under the receiver operating characteristic curve (AUC).

Research results

The overall prevalence of VTE complication after an IBD diagnosis was 4.70%. This prevalence was comparable to that of cancer patients (4.66%) who are well-known at increased risk for VTE. A novel genetic predictor (PGS) was significantly associated with VTE risk and was independent of known genetic predictors (FVL/PGM). The AUC of differentiating VTE complication was significantly higher for PGS [0.68, 95% confidence interval (CI): 0.66-0.71] than that of FVL/PGM (0.64, 95%CI: 0.61-0.67) and was highest by combining these two genetic predictors (0.69, 95%CI: 0.66-0.71).

Research conclusions

VTE complication is common in IBD patients and is similar to that of cancer patients. Newly developed PGS provides a more informative VTE risk stratification tool than known mutations (FVL/PGM).

Research perspectives

Findings from this large study of IBD patients have potential clinical utilities. It not only highlights the significance of VTE complications in IBD patients, but also provides an informative VTE risk assessment tool for developing personalized thromboprophylaxis strategies.

ACKNOWLEDGEMENTS

We are grateful to the Ellrodt-Schweighauser family for establishing Endowed Chair of Cancer Genomic Research (Xu), and Chez and Melman families for establishing Endowed Chairs of Personalized Prostate Cancer Care (Helfand).

FOOTNOTES

Author contributions: Xu J contributed to the concept and design; Shi Z, and Wei J performed the data analysis; Rifkin AS, and Xu J drafted the manuscript; Rifkin AS, Shi Z, Wei J, Zheng SL, Helfand BT, Cordova JS, Biank VF, Tafur AJ, Khan O, and Xu J contributed to the critical revision of the manuscript for important intellectual content; Xu J performed the supervision.

Institutional review board statement: The UK Biobank was approved by North West-Haydock Research Ethics Committee (REC reference: 16/NW/0274; IRAS project ID: 200778).

Informed consent statement: Data from the UK Biobank was accessed through a Material Transfer Agreement under Application Reference Number: 50295. This study was performed in accordance with the Declaration of Helsinki.

Conflict-of-interest statement: NorthShore University HealthSystem has an agreement with GoPath Laboratories and GenomicMD for genetic tests of polygenic risk score.

Data sharing statement: The data used in this study is available in the UK Biobank, a publicly available repository. Data was accessed through a Material Transfer Agreement under Application Reference Number: 50295. For additional information, please feel free to contact the corresponding author, Jianfeng Xu, DrPH.

STROBE statement: The authors have read the STROBE Statement—checklist of items, and the manuscript was prepared and revised according to the STROBE Statement—checklist of items.

Open-Access: This article is an open-access article that was selected by an in-house editor and fully peer-reviewed by external reviewers. It is distributed in accordance with the Creative Commons Attribution NonCommercial (CC BY-NC 4.0) license, which permits others to distribute, remix, adapt, build upon this work non-commercially, and license their derivative works on different terms, provided the original work is properly cited and the use is non-commercial. See: https://creativecommons.org/Licenses/by-nc/4.0/

Country/Territory of origin: United States

ORCID number: Jianfeng Xu 0000-0002-1343-8752.

S-Editor: Fan JR
L-Editor: A
P-Editor: Cai YX

REFERENCES

1 **Dahlhamer JM**, Zammitti EP, Ward BW, Wheaton AG, Croft JB. Prevalence of Inflammatory Bowel Disease Among Adults Aged ≥18 Years - United States, 2015. *MMWR Morb Mortal Wkly Rep* 2016; **65**: 1166-1169 [PMID: 27787492 DOI: 10.15585/mmwr.mm6542a3]

2 **Ng SC**, Shi HY, Hamidi N, Underwood FE, Tang W, Benchimol EI, Panaccione R, Ghosh S, Wu JCY, Chan FKL, Sung JJY, Kaplan GG. Worldwide incidence and prevalence of inflammatory bowel disease in the 21st century: a systematic review of population-based studies. *Lancet* 2017; **390**: 2769-2778 [PMID: 29050646 DOI: 10.1016/S0140-6736(17)32448-0]

3 **Grainge MJ**, West J, Card TR. Venous thromboembolism during active disease and remission in inflammatory bowel disease: a cohort study. *Lancet* 2010; **375**: 657-663 [PMID: 20149425 DOI: 10.1016/S0140-6736(09)61963-2]

4 **Olivera PA**, Zuily S, Kotze PG, Regnault V, Al Awadhi S, Bossuyt P, Gearry RB, Ghosh S, Kobayashi T, Lacolley P, Louis E, Magro F, Ng SC, Papa A, Raine T, Teixeira FV, Rubin DT, Danese S, Peyrin-Biroulet L. International consensus on the prevention of venous and arterial thrombotic events in patients with inflammatory bowel disease. *Nat Rev Gastroenterol Hepatol* 2021; **18**: 857-873 [PMID: 34453143 DOI: 10.1038/s41575-021-00492-8]

5 **Rosendaal FR**, Reitsma PH. Genetics of venous thrombosis. *J Thromb Haemost* 2009; **7** Suppl 1: 301-304 [PMID: 19630821 DOI: 10.1111/j.1538-7836.2009.03394.x]

6 **Ghouse J**, Tragante V, Ahlberg G, Rand SA, Jespersen JB, Leinøe EB, Vissing CR, Trudsø L, Jonsdottir I, Banasik K, Brunak S, Ostrowski SR, Pedersen OB, Sørensen E, Erikstrup C, Bruun MT, Nielsen KR, Køber L, Christensen AH, Iversen K, Jones D, Knowlton KU, Nadauld L, Halldorsson GH, Ferkingstad E, Olafsson I, Gretarsdottir S, Onundarson PT, Sulem P, Thorsteinsdottir U, Thorgeirsson G, Gudbjartsson DF, Stefansson K, Holm H, Olesen MS, Bundgaard H. Genome-wide meta-analysis identifies 93 risk loci and enables risk prediction equivalent to monogenic forms of venous thromboembolism. *Nat Genet* 2023; **55**: 399-409 [PMID: 36658437 DOI: 10.1038/s41588-022-01286-7]

7 **Bycroft C**, Freeman C, Petkova D, Band G, Elliott LT, Sharp K, Motyer A, Vukcevic D, Delaneau O, O'Connell J, Cortes A, Welsh S, Young A, Effingham M, McVean G, Leslie S, Allen N, Donnelly P, Marchini J. The UK Biobank resource with deep phenotyping and genomic data. *Nature* 2018; **562**: 203-209 [PMID: 30305743 DOI: 10.1038/s41586-018-0579-z]

8 **Klarin D**, Emdin CA, Natarajan P, Conrad MF; INVENT Consortium, Kathiresan S. Genetic Analysis of Venous Thromboembolism in UK

Biobank Identifies the ZFPM2 Locus and Implicates Obesity as a Causal Risk Factor. *Circ Cardiovasc Genet* 2017; **10** [PMID: 28373160 DOI: 10.1161/CIRCGENETICS.116.001643]

9 **Shi Z**, Wei J, Rifkin AS, Wang CH, Billings LK, Woo JSH, Talamonti MS, Vogel TJ, Moore E, Brockstein BE, Khandekar JD, Dunnenberger HM, Hulick PJ, Duggan D, Zheng SL, Lee CJ, Helfand BT, Tafur AJ, Xu J. Cancer-associated thrombosis by cancer sites and inherited factors in a prospective population-based cohort. *Thromb Res* 2023; **229**: 69-72 [PMID: 37419004 DOI: 10.1016/j.thromres.2023.06.023]

10 **Lambert SA**, Gil L, Jupp S, Ritchie SC, Xu Y, Buniello A, McMahon A, Abraham G, Chapman M, Parkinson H, Danesh J, MacArthur JAL, Inouye M. The Polygenic Score Catalog as an open database for reproducibility and systematic evaluation. *Nat Genet* 2021; **53**: 420-425 [PMID: 33692568 DOI: 10.1038/s41588-021-00783-5]

11 **Khera AV**, Chaffin M, Zekavat SM, Collins RL, Roselli C, Natarajan P, Lichtman JH, D'Onofrio G, Mattera J, Dreyer R, Spertus JA, Taylor KD, Psaty BM, Rich SS, Post W, Gupta N, Gabriel S, Lander E, Ida Chen YD, Talkowski ME, Rotter JI, Krumholz HM, Kathiresan S. Whole-Genome Sequencing to Characterize Monogenic and Polygenic Contributions in Patients Hospitalized With Early-Onset Myocardial Infarction. *Circulation* 2019; **139**: 1593-1602 [PMID: 30586733 DOI: 10.1161/CIRCULATIONAHA.118.035658]

12 **Papay P**, Miehsler W, Tilg H, Petritsch W, Reinisch W, Mayer A, Haas T, Kaser A, Feichtenschlager T, Fuchssteiner H, Knoflach P, Vogelsang H, Platzer R, Tillinger W, Jaritz B, Schmid A, Blaha B, Dejaco C, Sobala A, Weltermann A, Eichinger S, Novacek G. Clinical presentation of venous thromboembolism in inflammatory bowel disease. *J Crohns Colitis* 2013; **7**: 723-729 [PMID: 23127785 DOI: 10.1016/j.crohns.2012.10.008]

13 **McCurdy JD**, Israel A, Hasan M, Weng R, Mallick R, Ramsay T, Carrier M. A clinical predictive model for post-hospitalisation venous thromboembolism in patients with inflammatory bowel disease. *Aliment Pharmacol Ther* 2019; **49**: 1493-1501 [PMID: 31066471 DOI: 10.1111/apt.15286]

14 **Faye AS**, Hung KW, Cheng K, Blackett JW, Mckenney AS, Pont AR, Li J, Lawlor G, Lebwohl B, Freedberg DE. Minor Hematochezia Decreases Use of Venous Thromboembolism Prophylaxis in Patients with Inflammatory Bowel Disease. *Inflamm Bowel Dis* 2020; **26**: 1394-1400 [PMID: 31689354 DOI: 10.1093/ibd/izz269]

15 **Miehsler W**, Reinisch W, Valic E, Osterode W, Tillinger W, Feichtenschlager T, Grisar J, Machold K, Scholz S, Vogelsang H, Novacek G. Is inflammatory bowel disease an independent and disease specific risk factor for thromboembolism? *Gut* 2004; **53**: 542-548 [PMID: 15016749 DOI: 10.1136/gut.2003.025411]

16 **Tinsley A**, Naymagon S, Enomoto LM, Hollenbeak CS, Sands BE, Ullman TA. Rates of pharmacologic venous thromboembolism prophylaxis in hospitalized patients with active ulcerative colitis: results from a tertiary care center. *J Crohns Colitis* 2013; **7**: e635-e640 [PMID: 23706933 DOI: 10.1016/j.crohns.2013.05.002]

17 **Zhong M**, Dong XW, Zheng Q, Tong JL, Ran ZH. Factor V Leiden and thrombosis in patients with inflammatory bowel disease (IBD): a meta-analysis. *Thromb Res* 2011; **128**: 403-409 [PMID: 21831411 DOI: 10.1016/j.thromres.2011.07.014]

18 **Liang J**, Wu S, Feng B, Lei S, Luo G, Wang J, Li K, Li X, Xie H, Zhang D, Wang X, Wu K, Miao D, Fan D. Factor V Leiden and inflammatory bowel disease: a systematic review and meta-analysis. *J Gastroenterol* 2011; **46**: 1158-1166 [PMID: 21805067 DOI: 10.1007/s00535-011-0441-7]

19 **Bernstein CN**, Sargent M, Vos HL, Rosendaal FR. Mutations in clotting factors and inflammatory bowel disease. *Am J Gastroenterol* 2007; **102**: 338-343 [PMID: 17156138 DOI: 10.1111/j.1572-0241.2006.00974.x]

20 **Guédon C**, Le Cam-Duchez V, Lalaude O, Ménard JF, Lerebours E, Borg JY. Prothrombotic inherited abnormalities other than factor V Leiden mutation do not play a role in venous thrombosis in inflammatory bowel disease. *Am J Gastroenterol* 2001; **96**: 1448-1454 [PMID: 11374681 DOI: 10.1111/j.1572-0241.2001.03797.x]

21 **Koutroubakis IE**, Sfiridaki A, Tsiolakidou G, Theodoropoulou A, Livadiotaki A, Paspatis G, Kouroumalis EA. Genetic risk factors in patients with inflammatory bowel disease and vascular complications: case-control study. *Inflamm Bowel Dis* 2007; **13**: 410-415 [PMID: 17206678 DOI: 10.1002/ibd.20076]

22 **Heit JA**, Phelps MA, Ward SA, Slusser JP, Petterson TM, De Andrade M. Familial segregation of venous thromboembolism. *J Thromb Haemost* 2004; **2**: 731-736 [PMID: 15099278 DOI: 10.1111/j.1538-7933.2004.00660.x]

23 **Naito T**, Botwin GJ, Haritunians T, Li D, Yang S, Khrom M, Braun J; NIDDK IBD Genetics Consortium, Abbou L, Mengesha E, Stevens C, Masamune A, Daly M, McGovern DPB. Prevalence and Effect of Genetic Risk of Thromboembolic Disease in Inflammatory Bowel Disease. *Gastroenterology* 2021; **160**: 771-780.e4 [PMID: 33098885 DOI: 10.1053/j.gastro.2020.10.019]

24 **Klarin D**, Busenkell E, Judy R, Lynch J, Levin M, Haessler J, Aragam K, Chaffin M, Haas M, Lindström S, Assimes TL, Huang J, Min Lee K, Shao Q, Huffman JE, Kabrhel C, Huang Y, Sun YV, Vujkovic M, Saleheen D, Miller DR, Reaven P, DuVall S, Boden WE, Pyarajan S, Reiner AP, Trégouët DA, Henke P, Kooperberg C, Gaziano JM, Concato J, Rader DJ, Cho K, Chang KM, Wilson PWF, Smith NL, O'Donnell CJ, Tsao PS, Kathiresan S, Obi A, Damrauer SM, Natarajan P; INVENT Consortium; Veterans Affairs' Million Veteran Program. Genome-wide association analysis of venous thromboembolism identifies new risk loci and genetic overlap with arterial vascular disease. *Nat Genet* 2019; **51**: 1574-1579 [PMID: 31676865 DOI: 10.1038/s41588-019-0519-3]

World Journal of Gastroenterology

Submit a Manuscript: https://www.f6publishing.com

World J Gastroenterol 2023 October 21; 29(39): 5503-5525

DOI: 10.3748/wjg.v29.i39.5503

ISSN 1007-9327 (print) ISSN 2219-2840 (online)

SYSTEMATIC REVIEWS

Diagnostic role of transient elastography in patients with autoimmune liver diseases: A systematic review and meta-analysis

Hong Chen, Yue Shen, Sheng-Di Wu, Qin Zhu, Cheng-Zhao Weng, Jun Zhang, Mei-Xia Wang, Wei Jiang

Specialty type: Gastroenterology and hepatology

Provenance and peer review: Invited article; Externally peer reviewed.

Peer-review model: Single blind

Peer-review report's scientific quality classification
Grade A (Excellent): 0
Grade B (Very good): B, B
Grade C (Good): C, C, C
Grade D (Fair): 0
Grade E (Poor): 0

P-Reviewer: Granito A, Italy; Tai DI, Taiwan; Yoshioka K, Japan; Jian-Gao Fan, China

Received: July 2, 2023
Peer-review started: July 2, 2023
First decision: August 30, 2023
Revised: September 9, 2023
Accepted: October 11, 2023
Article in press: October 11, 2023
Published online: October 21, 2023

Hong Chen, Sheng-Di Wu, Cheng-Zhao Weng, Jun Zhang, Mei-Xia Wang, Wei Jiang, Department of Gastroenterology and Hepatology, Zhongshan Hospital (Xiamen), Fudan University, Xiamen 361015, Fujian Province, China

Hong Chen, Yue Shen, Sheng-Di Wu, Qin Zhu, Wei Jiang, Department of Gastroenterology and Hepatology, Zhongshan Hospital of Fudan University, Shanghai 200032, China

Hong Chen, Yue Shen, Sheng-Di Wu, Qin Zhu, Wei Jiang, Shanghai Institute of Liver Diseases, Fudan University Shanghai Medical College, Shanghai 200032, China

Corresponding author: Wei Jiang, MD, PhD, Academic Research, Chief Doctor, Professor, Department of Gastroenterology and Hepatology, Zhongshan Hospital (Xiamen), Fudan University, No. 666 Jinhu Road, Huli District, Xiamen 361015, Fujian Province, China.
jiang.wei@zs-hospital.sh.cn

Abstract

BACKGROUND

Noninvasive methods have been developed to detect fibrosis in many liver diseases due to the limits of liver biopsy. However, previous studies have focused primarily on chronic viral hepatitis and nonalcoholic fatty liver disease. The diagnostic value of transient elastography for autoimmune liver diseases (AILDs) is worth studying.

AIM

To compare the diagnostic accuracy of imaging techniques with serum biomarkers of fibrosis in AILD.

METHODS

The PubMed, Cochrane Library and EMBASE databases were searched. Studies evaluating the efficacy of noninvasive methods in the diagnosis of AILDs [autoimmune hepatitis (AIH), primary biliary cholangitis (PBC) and primary sclerosing cholangitis (PSC)] were included. The summary area under the receiver operating characteristic curve (AUROC), diagnostic odds ratio, sensitivity and specificity were used to assess the accuracy of these noninvasive methods for staging fibrosis.

RESULTS

A total of 60 articles were included in this study, and the number of patients with AIH, PBC and PSC was 1594, 3126 and 501, respectively. The summary AUROC

of transient elastography in the diagnosis of significant fibrosis, advanced fibrosis and cirrhosis in patients with AIH were 0.84, 0.88 and 0.90, respectively, while those in patients with PBC were 0.93, 0.93 and 0.91, respectively. The AUROC of cirrhosis for patients with PSC was 0.95. However, other noninvasive indices (aspartate aminotransferase to platelet ratio index, aspartate aminotransferase/alanine aminotransferase ratio, fibrosis-4 index) had corresponding AUROCs less than 0.80.

CONCLUSION

Transient elastography exerts better diagnostic accuracy in AILD patients, especially in PBC patients. The appropriate cutoff values for staging advanced fibrosis and cirrhosis ranged from 9.6 to 10.7 and 14.4 to 16.9 KPa for PBC patients.

Key Words: Liver stiffness; Serum parameter; Liver fibrosis; Noninvasive diagnosis; Transient elastography; Autoimmune liver disease

©The Author(s) 2023. Published by Baishideng Publishing Group Inc. All rights reserved.

Core Tip: Onset of autoimmune liver diseases is frequently insidious, and immune cell infiltration and continuous inflammation drive hepatic fibrosis, which gradually progresses to cirrhosis, causing poorer long-term outcomes. Liver biopsy as the reference standard is an invasive procedure. Thus, repeated biopsies are difficult to implement. Consequently, appropriate noninvasive methods are essential to dynamically monitor the degree of liver fibrosis. Our meta-analysis compared the diagnostic accuracy of imaging techniques with serum biomarkers of fibrosis in autoimmune liver diseases.

Citation: Chen H, Shen Y, Wu SD, Zhu Q, Weng CZ, Zhang J, Wang MX, Jiang W. Diagnostic role of transient elastography in patients with autoimmune liver diseases: A systematic review and meta-analysis. *World J Gastroenterol* 2023; 29(39): 5503-5525
URL: https://www.wjgnet.com/1007-9327/full/v29/i39/5503.htm
DOI: https://dx.doi.org/10.3748/wjg.v29.i39.5503

INTRODUCTION

The incidence of autoimmune liver diseases (AILDs), including autoimmune hepatitis (AIH), primary biliary cholangitis (PBC), primary sclerosing cholangitis (PSC), and multiple overlap syndromes, a group of autoimmune diseases associated with the liver and bile duct is increasing[1,2]. Onset is frequently insidious, with nonspecific symptoms. Immune cell infiltration and continuous inflammation drive hepatic fibrosis, which gradually progresses to cirrhosis, causing poorer long-term outcomes in patients[3-5]. Accordingly, accurate identification of high-risk patients for such conditions is essential in clinical care to guide timely treatment and delay disease progression.

For years, liver biopsy has been recognized as the reference standard for the assessment of liver fibrosis. However, biopsy area restrictions, sampling errors, and interobserver variability may affect the diagnostic accuracy[6,7]. Moreover, because biopsy is an invasive procedure with potentially hazardous complications ranging from pain to more severe events and even death, many patients are reluctant to undergo repeat biopsies[8,9]. Consequently, an increasing number of studies have focused on noninvasive methods to identify the ideal approach for dynamically monitoring the degree of liver fibrosis[10].

In recent years, some noninvasive methods, including biochemical tests and imaging techniques, have been widely developed, including the aspartate aminotransferase to platelet ratio index (APRI), aspartate aminotransferase/alanine aminotransferase (ALT) ratio (AAR), fibrosis-4 index (FIB-4), red cell distribution width to platelet ratio (RPR), Mac-2 binding protein (M2BP), platelet count to spleen diameter (PC/SD) ratio, transient elastography (TE), shear wave elastography (SWE), acoustic radiation force impulse (ARFI), magnetic resonance spectroscopy (MRS) and magnetic resonance elastography (MRE). Previous studies have validated that elastography is a reliable method with a diagnostic accuracy higher than that of blood tests for staging liver fibrosis in chronic viral hepatitis[11-13], nonalcoholic fatty liver disease[14] and AIH[15]; however, no studies have explored the diagnostic accuracy of noninvasive methods for the other two types of AILDs (PBC and PSC).

Therefore, the present meta-analysis aimed to compare the diagnostic accuracy of biochemical tests and imaging techniques for detecting liver fibrosis in patients with AILD, determine whether the same noninvasive methods show different diagnostic values in the three types of AILDs and recommend appropriate cutoff values for different fibrosis stages.

MATERIALS AND METHODS

Literature search strategy

Studies on the diagnosis of AILD published between January 2006 and December 2022 were searched in PubMed, Cochrane Library and EMBASE databases using the following keywords: AIH, PSC, PBC, liver fibrosis, TE, SWE, MRE, APRI, FIB-4 and AAR. The detailed search strategy is presented in Supplementary Table 1.

Study selection criteria

Original studies that fulfilled the following criteria were enrolled: (1) Studies with patient populations with AIH, PBC or PSC with discrete data that could be separately extracted from the mixed liver disease study cohort; (2) Studies in which liver biopsy was used as the gold standard to assess fibrosis based on the Metavir score or another score that could be converted to the Metavir score; (3) Studies assessing the performance and utility of APRI, AAR, FIB-4, RPR, M2BP, ARFI, PC/SD ratio, TE, SWE, MRE or MRS for staging liver fibrosis; and (4) Studies directly reporting the true-positive, false-positive, false-negative and true-negative values or provided data by which they could be calculated to allow the construction of a 2 × 2 table for each test.

The following studies were excluded: (1) Studies exploring the prognostic value of liver stiffness measurement (LSM) for patients with AILD; (2) Animal experiments, reviews, protocols, guidelines, case reports or meta-analyses; (3) Studies on liver fibrosis due to other etiologies, including nonalcoholic fatty liver disease, chronic hepatitis B, or chronic hepatitis C; and (4) Studies without sufficient data for further analysis or with the same or overlapping group of participants.

Data extraction and quality assessment

Two investigators (Chen H and Shen Y) independently evaluated the eligibility and quality of the included studies and extracted the data. Any disagreements were resolved by a senior researcher (Wu SD). We collated the following parameters in Microsoft Excel 2010: authors; year of publication; country; study period and design; pathological type; diagnostic methods; sample size; patient characteristics [age, sex, body mass index (BMI), ALT level, treatment condition]; quality of liver biopsy; and performance of the index test, including cutoff values, sensitivity, specificity, positive predictive value, negative predictive value, and area under the receiver operating characteristic curve (AUROC). Two reviewers (Chen H and Shen Y) independently assessed the risk of bias using the Quality Assessment of Diagnostic Accuracy Studies-2 tool[16].

Data synthesis and statistical analysis

According to the Metavir, Batts-Ludwig and Scheuer scores, liver fibrosis was classified into five stages (F0, F1, F2, F3 and F4), whereas there were seven stages according to the Ishak score. Given that Shiha *et al*[17] proposed that an Ishak score of 3 corresponds to METAVIR score of F2, significant fibrosis (SF), advanced fibrosis (AF) and cirrhosis were defined as stages F2-F4, F3-F4, and F4, respectively. For the data analysis, we constructed 2 × 2 contingency tables with true-positive, false-positive, false-negative and true-negative values based on data directly extracted from the original studies or calculated from indirect variables (sensitivity, specificity and sample size). A bivariate random effects model was subsequently applied to calculate the diagnostic test accuracy variables, including summary sensitivity, summary specificity, positive likelihood ratio, negative likelihood ratio and diagnostic odds ratio (DOR) with their associated 95% confidence intervals (95%CIs). We also performed meta-analyses using hierarchical models to produce summary ROC curves, from which we obtained summary AUROC values to evaluate the diagnostic accuracy of the different noninvasive methods. The method was considered to have excellent accuracy if the summary AUROC value was above 0.90, moderate accuracy if it was greater than 0.80, and poor accuracy if it was less than 0.80[18].

The heterogeneity was assessed using multiple methods. Spearman's correlation coefficient was calculated to evaluate the threshold heterogeneity of the included studies, whereas Cochran's Q and I^2 values were used to assess nonthreshold heterogeneity. If an I^2 value > 50% or P < 0.05 indicated distinct statistical heterogeneity, a random effects model was used to combine the data. A fixed effect model was chosen when the I^2 value ≤ 50% or P ≤ 0.05. However, the number of original studies was sufficient to perform a meta-regression to explore the potential heterogeneity of certain index tests. In addition, we conducted a subgroup analysis according to the sample size, treatment conditions and cutoff value. Deeks' funnel plots were used to evaluate the possible publication bias. The meta-analysis was performed using Stata 12.0, Reviewer Manager Version 5.3 and Meta-Disc Version 1.4.

RESULTS

Characteristics of the included studies and patients

The study selection process is illustrated in Figure 1. A total of 1386 studies were retrieved through our search strategy, of which 427 were excluded as duplicates and 602 were removed following the screening of titles, abstracts and reviews. The remaining 355 potentially eligible studies were selected for further evaluation. Of these, 60 articles were included in the evaluation and analysis. Among them, 22, 29 and 6 studies were regarding AIH, PBC and PSC, respectively (2 studies focused on both AIH and PBC[19,20], while 1 study focused on both PBC and PSC[21]). In total, they included 11 noninvasive index tests. The basic characteristics of the included studies are presented in Table 1. We selected articles published between 2006 and 2022, of which 46 (76.7%) were published between 2016 and 2022. There were 31 (51.7%) retrospective studies, 17 (28.3%) prospective studies, 10 (16.7%) unknown studies and 2 studies with both designs. Most

Table 1 Characteristics of studies included in this study

No.	Ref.	Country	Disease	Study time	Study design	Diagnostic model[1]	Sample size	Mean age in yr	Sex, F/M	Mean BMI in kg/m^2	Mean, ALT in IU/mL	Treatment condition	Scoring system	Interval
1	Youssef *et al*[40], 2013	Egypt	AIH	NA	Retrospective	5	16	NA	NA	NA	NA	NA	Metavir	NA
2	Kim *et al*[41], 2014	Korea	AIH	2008-2014	Retrospective	5	47	NA	41/6	NA	NA	NA	Metavir	NA
3	Abdollahi *et al* [42], 2015	Iran	AIH	2011-2013	NA	1, 2, 3	80	34.75	51/29	NA	106.49	NA	Ishak	NA
4	Harrison *et al*[43], 2016	United Kingdom	AIH	2013-2015	Prospective	5	27	56	25/2	NA	21	Post	Ishak	The same day
5	Hartl *et al*[44], 2016	Germany	AIH	2007-2010	Prospective	5	34	53	28/6	NA	48.5	Post	Scheuer	Within 3 mo
	Hartl *et al*[44], 2016	Germany	AIH	2008-2015	Retrospective	5	60	52	50/10	NA	35	Post	Scheuer	Within 4 mo
6	Nishikawa *et al*[45], 2016	Japan	AIH	2005-2015	Prospective	1, 2, 3, 11	84	64	69/15	NA	57.5	Pre	Scheuer	NA
7	E Anastasiou *et al* [46], 2016	Germany	AIH	2008-2013	Retrospective	1, 2, 3, 5	53	47.3	31/22	NA	606.42	Pre 35 + post 18	Metavir	Within 3 wk
8	Piwczyńska *et al* [47], 2016	Poland	AIH	NA	Prospective	4	46	14.5	33/13	NA	NA	NA	Batts-Ludwig	NA
9	Sheptulina *et al* [48], 2016	Russian	AIH	2008-2014	Prospective	1, 2, 3, 9	76	40	65/11	25	54.4	Pre 22 + post 54	Metavir	Within 7 d
10	Guo *et al*[29], 2017	China	AIH	2012-2017	Retrospective	1, 3, 5	108	46.54	88/20	23.52	146.51	NA	Metavir	Within 3 d
11	Paranagua-Vezozzo *et al*[49], 2016	Brazil	AIH	2012-2015	Prospective	4, 5	33	NA	28/5	28.6	NA	Post	Metavir	The same day
12	Puustinen *et al* [50], 2017	Finland	AIH	NA	Prospective	8	12	42.8	10/2	NA	28.5	NA	Metavir	Within 1 mo
13	Wang *et al*[22], 2017	China	AIH	2007-2015	Retrospective	1, 2, 3, 7	36	51.6	NA	27.7	217.4	Pre 17 + post 19	Metavir	Within 3 mo
14	Xu *et al*[51], 2017	China	AIH	2014-2016	Prospective	1, 3, 5	100	45	81/19	NA	131.5	Pre	Metavir	The same day
15	Zeng *et al*[52], 2017	China	AIH	2011-2016	Prospective	6	62	45.6	NA	21.6	78.5	Pre	Metavir	3 d
16	Liu *et al*[53], 2019	China	AIH	2008-2018	Retrospective	2, 3	45	54.29	37/8	NA	NA	NA	Metavir	The same day

17	Park *et al*[19], 2019	South Korea	AIH	2014-2017	NA	4	49	56	42/7	23.7	163	NA	Metavir	The same day
			PBC				41	55.3	35/6	25.5	45	NA		
18	Li *et al*[54], 2020	China	AIH	2010-2019	Retrospective	1, 2, 3, 10	72	54	64/8	NA	137.55	Post	Metavir	NA
19	Wang *et al*[55], 2020	China	AIH	2016-2019	Retrospective	1, 3, 10	119	52.5	99/20	NA	81.6	Pre	Scheuer	Within 7 d
20	Xing *et al*[30], 2020	China	AIH	2016-2019	Retrospective	1, 3, 6	103	54	81/22	22.5	163	NA	Scheuer	Within 7 d
21	Janik *et al*[31], 2021	Poland	AIH	2015-2020	Prospective	6	63	37	15/48	23.9	130	Post	Batts-Ludwig	Within 3 mo
22	Zachou *et al*[20], 2021	Greece	AIH	2009-2016	Retrospective	5	78	57	54/24	NA	68	Pre 47 + post 31	Metavir	The same day
			PBC				56	52	48/8	NA	47	Pre 37 + post 19		
23	Ferronato *et al*[56], 2022	Italy	AIH	NA	Retrospective	1, 2, 3	122	59	90/32	NA	481.8	Pre	Ishak	Within 23 d
24	Soh *et al*[57], 2022	Korea	AIH	2014-2021	Retrospective	6	69	59.7	60/9	NA	187.1	Pre 44 + post 25	Metavir	The same day
25	Nyblom *et al*[58], 2006	Sweden	PBC	1976-2000	Retrospective	2	121	54	NA	NA	189.9	NA	Metavir	NA
26	Gómez-Dominguez *et al*[59], 2008	Spain	PBC	NA	Prospective	5	80	54	64/16	NA	NA	Post	Metavir	Within 9 mo
27	Alempijevic *et al*[60], 2009	Serbia	PBC	2006	NA	1, 2	112	53.88	104/8	NA	NA	Post	Scheuer	Within 1 wk
28	Ferrara *et al*[61], 2009	Italy	PBC	NA	NA	1, 3	248	52	233/15	NA	NA	NA	Scheuer	The same day
29	Su *et al*[62], 2009	China	PBC	1985-2006	Retrospective	2	46	53.3	34/12	NA	140.6	NA	Scheuer	Within 1 mo
30	Floreani *et al*[63], 2011	Italy	PBC	2009	NA	5	114	58	96/24	24	44	NA	Metavir	Within 6 mo
31	Corpechot *et al*[64], 2012	France	PBC	2004-2010	Prospective	5	103	56	87/16	23.9	76	Post	Metavir	Within 9 mo
32	Zhang *et al*[34], 2014	China	PBC	2011-2013	NA	4	56	45	46/10	NA	NA	NA	Batts-Ludwig	Within 3 d
33	Sheptulina *et al*[21], 2015	Russian	PBC	2008-2014	Retrospective	9	82	54.5	78/4	NA	NA	NA	Metavir	NA
			PSC			3	22	38	6/16	NA	NA	NA		NA
34	Umemura *et al*[65], 2015	Japan	PBC	1981-2014	Retrospective	11	137	57	111/26	NA	41	Post	Metavir	The same day

35	Nishikawa *et al* [66], 2016	Japan	PBC	2005-2014	Prospective	1, 3, 11	57	59	49/8	NA	35	Pre	Scheuer	NA
36	Olmez *et al*[67], 2016	Turkey	PBC	1995-2013	Retrospective	1, 3	40	49.6	40/0	NA	54.5	NA	Scheuer	Within 1 wk
37	Wang *et al*[68], 2016	China	PBC	2010-2015	Retrospective	1, 3, 10	73	52.4	62/11	NA	89.3	Pre	Ludwing and Scheuer	The day before
38	Koizumi *et al*[23], 2017	Japan	PBC	2012-2015	Prospective	1, 2, 3, 5	44	60.5	41/3	NA	65.9	Post	Metavir	Within 1 wk
39	Wang *et al*[69], 2017	China	PBC	2009-2016	Retrospective	1, 3	261	52	230/31	NA	NA	NA	Metavir	NA
40	Jiang *et al*[70], 2018	China	PBC	2009-2015	Retrospective	3, 10	77	62.4	64/13	NA	81.2	Pre	Scheuer	NA
41	Kamal *et al*[71], 2018	Netherlands	PBC	1979-2010	Retrospective	1, 2, 3	85	50	75/10	NA	NA	NA	Ishak	NA
42	Meng *et al*[72], 2018	China	PBC	2013-2017	Retrospective	1, 3, 10	94	51.02	NA	NA	116.58	Pre	Ludwing and Scheuer	Within 1 wk
43	Milovanović *et al* [73], 2018	Serbia	PBC	2009-2011	Prospective	1, 2, 5	122	57.4	NA	NA	50.8	Post	Metavir	Within 1 mo
44	Wang *et al*[74], 2018	China	PBC	2010-2016	Retrospective	1, 3, 10	58	53.3	51/7	NA	90.4	Pre	Ludwing and Scheuer	Within 1 wk
45	Jiang *et al*[75], 2020	China	PBC	2008-2018	Prospective	1, 2, 3, 10	78	52	71/7	NA	NA	Pre 39 + post 39	Scheuer	Within 2 wk
	Jiang *et al*[75], 2020	China b	PBC	2008-2018	Retrospective	1, 3, 10	40	51	35/5	NA	NA	Pre 20 + post 20	Scheuer	Within 2 wk
46	Joshita *et al*[76], 2020	Japan	PBC	2015-2019	NA	5, 11	74	64	62/12	NA	48	Pre	Scheuer	The same day
47	Rossi *et al*[77], 2020	Italy	PBC	NA	NA	5	92	NA	NA	NA	NA	NA	Scheuer	Within 1 mo
48	Yan *et al*[32], 2020	China	PBC	2016-2019	Retrospective	1, 2, 3, 6	157	53	136/21	22.2	72	NA	Scheuer	NA
49	Cristoferi *et al*[78], 2021	Italy	PBC	2006-2019	Prospective	1, 5	126	52	114/12	22.3	52.8	Pre	Batts-Ludwig	Within 12 wk
50	Fujinaga *et al*[79], 2021	Japan	PBC	2000-2019	Retrospective	1, 3, 11	102	61	89/13	NA	68.4	Pre	Scheuer	NA
51	Manesis *et al*[80], 2021	Greece	PBC	2010-2018	Retrospective	6	53	62.6	46/7	25.7	30	Pre 30 + post 23	Scheuer	Within 3 mo
52	Osman *et al*[33], 2021	United States	PBC	2007-2019	Retrospective	5	63	60.95	NA	NA	31.2	NA	Batts-Ludwig	Within 1 yr

						7	98	60.21	NA	NA	36.4	NA		
53	Avcioğlu *et al*[81], 2022	Turkey	PBC	2008-2020	Retrospective	1, 3	35	49.6	33/2	NA	50.6	Pre	Scheuer	Within 1 wk
54	Garrido *et al*[82], 2022	Portugal	PBC	2010-2021	NA	5	79	52	NA	NA	NA	Pre 40 + post 39	Batts-Ludwig	Within 2 mo
55	Corpechot *et al* [83], 2014	France	PSC	2005-20210	Prospective	5	59	40.7	24/35	NA	145.7	Post	Metavir	Within 6 mo
56	Bowlus *et al*[84], 2016,	France	PSC	NA	NA	5	56	43	22/34	NA	255	NA	Ishak	NA
57	Eaton *et al*[85], 2016	United States	PSC	2007-2013	Retrospective	1, 7	266	46.12	81/185	26	48	Pre	Batts-Ludwig	Within 1 yr
58	Ehlken *et al*[86], 2016	Germany	PSC	2006-2014	Retrospective	5	62	38	63/77	NA	38	NA	Scheuer	NA
59	Krawczyk *et al* [87], 2017	Poland	PSC	2014-2016	Prospective	5	30	33	12/18	NA	50	NA	Metavir	NA
60	Umetsu *et al*[88], 2018	Japan	PSC	2007-2016	Retrospective	1, 2, 3, 11	28	14	8/20	NA	56.5	NA	Batts-Ludwig	The same day

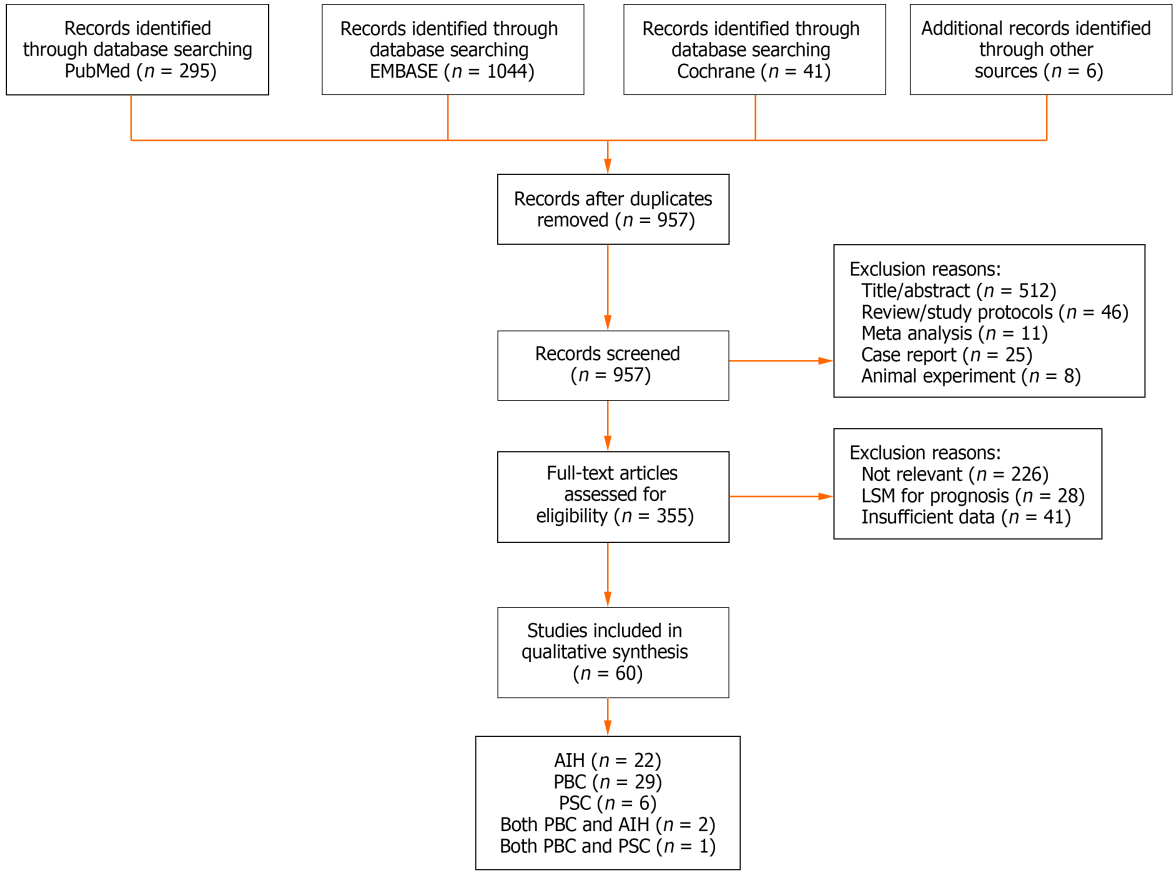
[1]Diagnostic models are represented by the following numbers: 1 = Aspartate aminotransferase to platelet ratio index; 2 = caspartate aminotransferase to alanine aminotransferase ratio; 3 = Fibrosis-4 index; 4 = Acoustic radiation force impulse; 5 = Transient elastography; 6 = Shear wave elastography; 7 = Magnetic resonance elastography; 8 = Magnetic resonance spectroscopy; 9 = Platelet count to spleen diameter ratio; 10 = Red cell distribution width to platelet ratio ; 11 = Mac-2-binding protein. AIH: Autoimmune hepatitis; ALT: Alanine aminotransferase; BMI: Body mass index; F: Female; M: Male; NA: Not available; PBC: Primary biliary cholangitis; PSC: Primary sclerosing cholangitis.

included studies were conducted in Asia (28 studies) or Europe (24 studies). A total of 27 studies utilized the Metavir score, 8 studies used the Batts-Ludwig score, 17 studies used the Scheuer score, 5 studies used the Ishak score, and 3 studies used the Ludwig-Scheuer score.

A total of 1594, 3126 and 501 patients with AIH, PBC, and PSC, respectively, were included to analyze the diagnostic performance of noninvasive methods in staging liver fibrosis. Most patients with AIH and PBC were female (72.4% and 87.6%, respectively). In contrast, patients with PSC were predominantly male (73.7%). The average ages of patients with AIH, PBC and PSC were 47.0, 55.2 and 41.5 years, respectively. Patients with AIH (160.29 IU/mL) had higher ALT levels than patients with PBC (69.81 IU/mL).

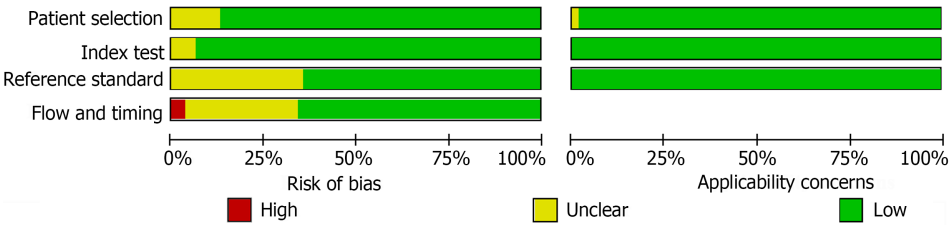
Quality assessment of the included studies

The results of the quality assessment based on the Quality Assessment of Diagnostic Accuracy Studies-2 scale for all 60 eligible studies are shown in Figure 2 and Supplementary Figure 1. Regarding patient selection, eight studies had an unclear risk of bias owing to the lack of information on whether patients were enrolled randomly or consecutively. Regarding the index test, four studies were determined to have an unclear risk of bias because the results of the index test were interpreted without blinded information on the results of the reference standard. Likewise, 22 studies were regarded as having an unclear risk of bias because the results of the reference standard were interpreted without blinded information regarding the results of the index test. In terms of flow and timing, two studies were considered high-risk because not every subject received a reference standard, while 19 studies were considered unclear risk because of an



DOI: 10.3748/wjg.v29.i39.5503 **Copyright** ©The Author(s) 2023.

Figure 1 Flowchart of study identification and selection process. AIH: Autoimmune hepatitis; LSM: Liver stiffness measurement; PBC: Primary biliary cholangitis; PSC: Primary sclerosing cholangitis.



DOI: 10.3748/wjg.v29.i39.5503 **Copyright** ©The Author(s) 2023.

Figure 2 Quality assessment of included studies by Quality Assessment of Diagnostic Accuracy Studies-2. Risk of bias and applicability concerns graph.

unknown time interval between the index and reference tests.

Performance of noninvasive methods in diagnosing SF (F ≥ 2)

Diagnosis of SF for AIH: Fifteen studies (n = 1001) evaluated eight noninvasive methods for detecting SF in patients with AIH. Of these, five (n = 459), two (n = 129), five (n = 459), nine (n = 523) and three (n = 234) studies focused on APRI, AAR, FIB-4, TE and SWE separately, whereas only one study each utilized the ARFI, PC/SD ratio and RPR.

The APRI had moderate summary sensitivity (exceeding 70%) with poor summary specificity (less than 50%), whereas the FIB-4 had the opposite result (Table 2). Interestingly, TE had a relatively greater diagnostic performance than the other laboratory tests, with summary sensitivity and specificity values of 0.82 and 0.73, respectively, and cutoff values ranging from 5.8–7.0 KPa. The summary sensitivity of SWE (0.89; 95%CI: 0.83–0.93) was significantly higher than that of the other six noninvasive methods and slightly greater than that of TE (0.83; 95%CI: 0.78–0.87).

Diagnosis of SF for PBC: Thirteen studies (n = 1389) evaluated nine noninvasive methods for diagnosing SF in patients with PBC. Among them, four (n = 584), three (n = 323), three (n = 462), two (n = 87), five (n = 446) and two (n = 210) studies focused on APRI, AAR, FIB-4, ARFI, TE and SWE, respectively; however, only one study each utilized the PC/SD ratio, MRE and M2BP.

Table 2 Summary sensitivities, specificities, positive likelihood ratio and negative likelihood ratio of noninvasive methods at various diagnostic thresholds for prediction of significant fibrosis, advanced fibrosis and cirrhosis in autoimmune liver diseases patients

Disease	Diagnostic model/Stage	Cutoff values	No. of patients (*n*)	Summary sensitivity	Summary specificity	Summary PLR	Summary NLR
AIH	APRI						
	SF	0.27-0.70	2 (195)	0.80 (0.72-0.86)	0.35 (0.23-0.48)	1.46 (0.55-3.89)	0.36 (0.061-2.09)
		0.88-1.55	3 (264)	0.74 (0.68-0.80)	0.51 (0.38-0.63)	1.52 (1.18-1.96)	0.50 (0.36-0.69)
	AF	0.38-0.90	4 (379)	0.86 (0.81-0.90)	0.48 (0.41-0.56)	1.60 (1.18-2.15)	0.33 (0.24-0.47)
		1.12-3.40	6 (538)	0.80 (0.72-0.86)	0.35 (0.23-0.48)	0.57 (0.51-0.64)	0.68 (0.62-0.73)
	Cirrhosis	0.55-1.81	3 (330)	0.65 (0.56-0.74)	0.47 (0.40-0.54)	1.49 (0.93-2.39)	0.62 (0.46-0.83)
		1.85-2.00	3 (213)	0.70 (0.57-0.81)	0.73 (0.65-0.79)	2.48 (1.75-3.52)	0.42 (0.28-0.62)
	AAR						
	SF	0.72-0.93	2 (129)	0.67 (0.57-0.77)	0.68 (0.49-0.83)	2.22 (1.32-3.72)	0.46 (0.23-0.90)
	AF	0.76-1.18	7 (532)	0.61 (0.54-0.68)	0.72 (0.66-0.77)	2.01 (1.59-2.53)	0.58 (0.46-0.73)
	Cirrhosis	0.94-1.40	3 (213)	0.61 (0.47-0.74)	0.83 (0.76-0.88)	3.31 (1.96-5.59)	0.49 (0.36-0.69)
	FIB-4						
	SF	1.95-2.90	3 (303)	0.64 (0.58-0.71)	0.71 (0.61-0.81)	2.20 (1.48-3.27)	0.50 (0.38-0.65)
		3.20-5.07	2 (156)	0.60 (0.51-0.69)	0.77 (0.60-0.90)	2.66 (1.44-4.92)	0.52 (0.39-0.69)
	AF	1.75-2.37	6 (476)	0.66 (0.59-0.72)	0.63 (0.57-0.69)	2.05 (1.56-2.70)	0.40 (0.20-0.81)
		3.21-5.60	5 (486)	0.47 (0.41-0.54)	0.73 (0.67-0.79)	1.83 (1.24-2.71)	0.68 (0.50-0.92)
	Cirrhosis	2.21-3.40	5 (440)	0.75 (0.67-0.82)	0.56 (0.50-0.62)	2.06 (1.53-2.77)	0.37 (0.19-0.71)
		6.44	1 (103)	0.68	0.64	1.88	0.51
	TE						
	SF	5.80-7.00	7 (423)	0.83 (0.78-0.87)	0.73 (0.65-0.80)	2.89 (2.23-3.76)	0.23 (0.12-0.42)
		9.10-10.05	2 (100)	0.77 (0.67-0.86)	0.94 (0.70-1.00)	7.65 (1.66-35.32)	0.18 (0.02-1.47)
	AF	8.18-9.00	3 (286)	0.80 (0.72-0.87)	0.80 (0.73-0.86)	4.09 (2.64-6.33)	0.24 (0.17-0.35)
		10.40-12.10	4 (174)	0.73 (0.60-0.83)	0.93 (0.86-0.97)	7.67 (2.89-20.31)	0.27 (0.12-0.61)
	Cirrhosis	11.00-12.67	4 (213)	0.89 (0.82-0.94)	0.88 (0.81-0.93)	6.89 (4.38-10.85)	0.14 (0.09-0.23)
		16.00-19.00	3 (147)	0.88 (0.74-0.96)	0.97 (0.92-0.99)	22.08 (5.35-91.22)	0.16 (0.08-0.33)
	2D-SWE						
	SF	8.20-10.00	3 (234)	0.89 (0.83-0.93)	0.72 (0.59-0.83)	3.25 (1.67-6.32)	0.17 (0.11-0.28)
	AF	12.20-15.80	3 (234)	0.82 (0.73-0.89)	0.79 (0.72-0.86)	3.92 (2.79-5.52)	0.24 (0.13-0.44)
	Cirrhosis	14.30-19.30	4 (297)	0.83 (0.74-0.90)	0.86 (0.81-0.91)	5.85 (4.09-8.37)	0.21 (0.13-0.34)
PBC	APRI						
	SF	0.26-1.20	4 (584)	0.84 (0.80-0.87)	0.63 (0.56-0.70)	1.98 (1.54-2.55)	0.34 (0.23-0.51)
	AF	0.3.0-0.75	8 (858)	0.62 (0.57-0.68)	0.54 (0.50-0.58)	1.39 (1.09-1.79)	0.68 (0.48-0.98)
		0.93-2.00	7 (731)	0.73 (0.68-0.78)	0.68 (0.64-0.72)	2.68 (1.80-3.97)	0.46 (0.36-0.58)
	Cirrhosis	0.65-1.39	6 (852)	0.75 (0.67-0.83)	0.51 (0.48-0.55)	2.19 (1.38-3.50)	0.31 (0.10-0.99)
	AAR						
	SF	0.92-1.00	3 (323)	0.69 (0.61-0.76)	0.56 (0.48-0.63)	1.61 (1.33-1.95)	0.52 (0.31-0.87)
	AF	0.81-1.01	5 (559)	0.54 (0.47-0.62)	0.73 (0.68-0.77)	2.15 (1.52-3.03)	0.63 (0.44-0.91)
	Cirrhosis	1.00-1.10	4 (407)	0.81 (0.70-0.90)	0.77 (0.72-0.82)	4.55 (1.98-10.49)	0.28 (0.10-0.79)
	FIB-4						

	SF	1.39-3.90	3 (462)	0.85 (0.81-0.89)	0.77 (0.69-0.83)	2.89 (2.10-3.98)	0.26 (0.10-0.66)
	AF	2.05-2.63	7 (865)	0.77 (0.72-0.81)	0.57 (0.53-0.61)	1.95 (1.51-2.52)	0.31 (0.16-0.61)
		2.81-4.60	6 (431)	0.63 (0.55-0.71)	0.80 (0.75-0.85)	3.25 (1.78-5.94)	0.49 (0.30-0.81)
	Cirrhosis	2.05-4.60	6 (852)	0.87 (0.80-0.93)	0.61 (0.58-0.65)	2.79 (1.92-4.07)	0.16 (0.05-0.52)
	TE						
	SF	5.90-8.80	4 (402)	0.81 (0.76-0.85)	0.95 (0.89-0.98)	10.51 (2.03-54.36)	0.23 (0.12-0.44)
		16.00	1 (44)	0.94	0.81	4.90	0.07
	AF	6.75-7.60	4 (377)	0.80 (0.73-0.86)	0.81 (0.76-0.86)	4.19 (2.35-7.46)	0.19 (0.05-0.79)
		9.60-10.70	3 (317)	0.91 (0.84-0.95)	0.82 (0.77-0.87)	5.68 (2.55-12.69)	0.12 (0.07-0.21)
		11.90-17.90	3 (180)	0.75 (0.60-0.86)	0.94 (0.88-0.97)	11.76 (2.29-60.48)	0.22 (0.06-0.80)
	Cirrhosis	11.40-14.40	3 (256)	0.84 (0.69-0.93)	0.94 (0.90-0.97)	13.46 (7.66-23.65)	0.19 (0.10-0.38)
		15.60-25.10	3 (227)	0.90 (0.74-0.98)	0.93 (0.89-0.96)	22.8 (0.81-639.69)	0.12 (0.04-0.34)
	RPR						
	AF	0.10-0.14	4 (362)	0.49 (0.40-0.58)	0.89 (0.84-0.92)	4.27 (2.22-8.22)	0.59 (0.47-0.74)
	M2BP						
	AF	1.00-1.40	4 (370)	0.68 (0.59-0.77)	0.80 (0.75-0.85)	4.26 (1.82-9.96)	0.32 (0.14-0.75)
PSC	TE						
	SF	8.80	2 (121)	0.76 (0.62-0.87)	0.88 (0.79-0.95)	6.34 (3.25-12.37)	0.29 (0.18-0.46)
	AF	9.60	3 (177)	0.82 (0.70-0.91)	0.83 (0.75-0.89)	4.75 (2.21-10.19)	0.15 (0.02-1.04)
	Cirrhosis	13.70-14.40	4 (207)	0.82 (0.68-0.91)	0.89 (0.83-0.94)	7.46 (3.74-14.88)	0.25 (0.15-0.43)

2D-SWE: Two-dimensional shear wave elastography; AAR: Aspartate aminotransferase to alanine aminotransferase ratio; AF: Advanced fibrosis; AIH: Autoimmune hepatitis; APRI: Aspartate aminotransferase to platelet ratio index; FIB-4: Fibrosis-4 index; M2BP: Mac-2-binding protein; NLR: Negative likelihood ratio; PLR: Positive likelihood ratio; PBC: Primary biliary cholangitis; PSC: Primary sclerosing cholangitis; RPR: Red cell distribution width to platelet ratio; SF: Significant fibrosis; TE: Transient elastography.

As shown in Table 2, the APRI and FIB-4 index had relatively good summary sensitivities of 0.84 and 0.85, respectively, with mild summary specificities of 0.63 and 0.77, respectively. The corresponding values for sensitivity and specificity of the AAR were poor (0.69, 0.56). In contrast, both the summary sensitivity (0.81; 95%CI: 0.76–0.85) and specificity (0.95; 95%CI: 0.89–0.98) of TE were significantly higher than those of the other five noninvasive methods for predicting SF with cutoff values ranging from 5.9–8.8 KPa.

Furthermore, Table 3 shows that the summary DORs of APRI, FIB-4 and TE were 3.9 (95%CI: 2.1–7.3), 5.1 (95%CI: 3.1–8.5) and 16.8 (95%CI: 8.8–32.2), respectively, in patients with AIH, while the summary DORs of APRI and TE were 6.3 (95%CI: 3.5–11.2) and 74.5 (95%CI: 12.2–455.5), respectively, in patients with PBC. Additionally, the summary AUROC value of TE in patients with PBC (0.93, 95%CI: 0.91–0.95) was relatively higher than that of TE in patients with AIH (0.84, 95%CI: 0.80–0.87) but significantly higher than that of FIB-4 (0.74) and APRI (0.67) in patients with AIH and APRI (0.77) in patients with PBC (Table 3 and Figure 3).

Performance of noninvasive methods in diagnosing AF (F ≥ 3)

Diagnosis of AF for AIH: Twenty studies (n = 1435) evaluated 11 noninvasive methods for detecting AF in patients with AIH. Among them, 10 (n = 917), 7 (n = 532), 11 (n = 962), 7 (n = 460), 3 (n = 234) and 2 (n = 191) studies focused on APRI, AAR, FIB-4, TE, SWE and RPR, respectively; however, only one study each utilized the ARFI, MRS, PC/SD ratio, MRE and M2BP methods.

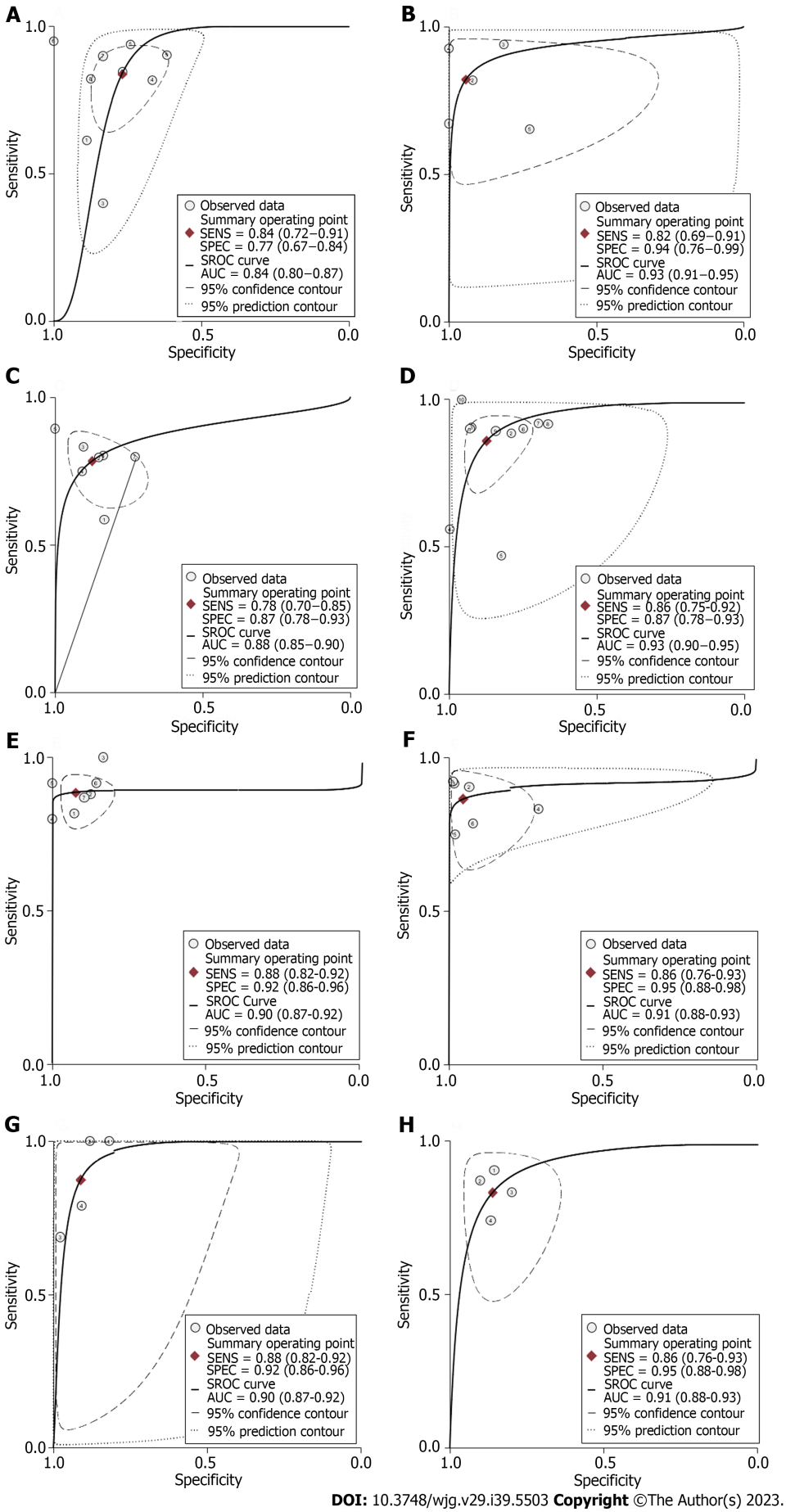
As shown in Table 2, with a cutoff value of 8.2–9.0 KPa, both the summary sensitivity and specificity exceeded 80% when TE was used for predicting AF, whereas with a cutoff value of 10.4–12.1 KPa, there was a better summary specificity (0.93; 95%CI: 0.86–0.97) with a mild summary sensitivity (0.73; 95%CI: 0.60–0.83). Regarding SWE, MRE and the PC/SD ratio, the summary sensitivity and specificity also exceeded 80%. The specificity of MRE was 1.00, but only one study assessed it[22]. For AAR and FIB-4 index, there was a relatively modest summary specificity (< 0.80) and poor summary sensitivity (< 0.60).

Diagnosis of AF for PBC: Twenty-eight studies (n = 2737) evaluated 11 noninvasive methods for detecting AF in patients with PBC. Of these, 15 (n = 1589), 6 (n = 559), 13 (n = 1296), 2 (n = 97), 10 (n = 874), 5 (n = 362), 4 (n = 370) and 2 (n = 210) studies were focused on APRI, AAR, FIB-4, ARFI, TE, RPR, M2BP and SWE, respectively. Only one study each utilized the methods of MRE and RLR.

Table 3 Summary area under the receiver operator curve and diagnostic odds ratio of noninvasive methods for prediction of significant fibrosis, advanced fibrosis and cirrhosis in autoimmune liver diseases patients

Disease	Diagnostic model/Stage	No. of studies (patients)	AUROC (95%CI)	DOR (95%CI)
AIH	APRI			
	SF	4 (383)	0.67 (0.63-0.71)	3.87 (2.1-7.3)
	AF	10 (917)	0.71 (0.67-0.75)	3.85 (2.8-5.3)
	Cirrhosis	6 (543)	0.71 (0.67-0.75)	3.77 (2.2-6.4)
	FIB-4			
	SF	5 (459)	0.74 (0.70-0.78)	5.11 (3.1-8.5)
	AF	11 (962)	0.73 (0.69-0.76)	4.04 (2.4-6.8)
	Cirrhosis	6 (543)	0.72 (0.68-0.76)	5.48 (2.4-12.6)
	TE			
	SF	9 (523)	0.84 (0.80-0.87)	16.83 (8.8-32.2)
	AF	7 (460)	0.88 (0.85-0.90)	25.14 (9.7-65.3)
	Cirrhosis	7 (415)	0.90 (0.87-0.92)	91.77 (40.1-201.2)
	AAR			
	AF	6 (410)	0.73 (0.69-0.77)	4.94 (3.2-7.8)
	2D-SWE			
	Cirrhosis	4 (297)	0.91 (0.89-0.94)	30.68 (15.7-59.9)
PBC	APRI			
	SF	4 (584)	0.77 (0.73-0.80)	6.27 (3.5-11.2)
	AF	15 (1589)	0.70 (0.66-0.74)	3.67 (2.3-5.9)
	Cirrhosis	6 (852)	0.83 (0.79-0.86)	14.55 (1.9-113.8)
	FIB-4			
	AF	13 (1296)	0.79 (0.75-0.82)	7.13 (4.0-12.8)
	Cirrhosis	6 (852)	0.88 (0.85-0.91)	29.79 (5.9-150.3)
	TE			
	SF	5 (446)	0.93 (0.91-0.95)	74.45 (12.2-455.5)
	AF	10 (880)	0.93 (0.90-0.95)	41.84 (19.3-91.0)
	Cirrhosis	6 (483)	0.91 (0.88-0.93)	134.83 (33.0-551.8)
	AAR			
	AF	6 (559)	0.74 (0.70-0.78)	4.13 (2.0-8.6)
	Cirrhosis	4 (407)	0.88 (0.84-0.90)	25.29 (9.0-70.9)
	RPR			
	AF	4 (362)	0.53 (0.49-0.58)	7.98 (4.0-15.8)
	M2BP			
	AF	4 (370)	0.86 (0.82-0.88)	13.17 (4.1-42.4)
PSC	TE			
	Cirrhosis	4 (207)	0.95 (0.93-0.97)	70.59 (15.4-322.7)

2D-SWE: Two-dimensional shear wave elastography; 95%CI: 95% confidence interval; AAR: Aspartate aminotransferase to alanine aminotransferase ratio; AF: Advanced fibrosis; AIH: Autoimmune hepatitis; APRI: Aspartate aminotransferase to platelet ratio index; AUROC: Area under the receiver operator curve; DOR: Diagnostic odds ratio; FIB-4: Fibrosis-4 index; PBC: Primary biliary cholangitis; PSC: Primary sclerosing cholangitis; RPR: Red cell distribution width to platelet ratio; SF: Significant fibrosis; TE: Transient elastography.



DOI: 10.3748/wjg.v29.i39.5503 **Copyright** ©The Author(s) 2023.

Figure 3 The summary receiver operating characteristic curve plots of transient elastography in autoimmune liver disease patients. A and

B: Transient elastography (TE) for detecting significant fibrosis in autoimmune hepatitis (AIH, A) and primary biliary cholangitis (PBC, B) patients; C and D: TE for detecting advanced fibrosis in AIH (C) and PBC (D) patients; E-G: TE for detecting cirrhosis in AIH (E), PBC (F) and primary sclerosing cholangitis (G) patients; H: Shear wave elastography for detecting cirrhosis in AIH patients. AUC: Area under the curve; SENS: Sensitivity; SPEC: Specificity; SROC: Summary receiver operating characteristic.

As shown in Table 2, TE had a good summary sensitivity and specificity (0.91, 0.82) with a cutoff value of 9.6–10.7 KPa, while RPR and M2BP had good summary specificity (0.89 and 0.80, respectively) with poor summary sensitivity (0.49 and 0.68, respectively). Regardless of the cutoff values, the summary sensitivities and specificities of the AAR, APRI and FIB-4 were less than 0.80.

Furthermore, Table 3 shows that the summary DORs of AAR, APRI, FIB-4 and TE were 4.9 (95%CI: 3.2–7.8), 3.9 (95%CI: 2.8–5.3), 4.0 (95%CI: 2.4–6.8) and 25.1 (95%CI: 9.7–65.3), respectively, in patients with AIH and 4.1 (95%CI: 2.0–8.6), 3.7 (95%CI: 2.3–6.0), 7.1 (95%CI: 4.0–12.8) and 41.8 (95%CI: 19.3–91.0), respectively, in patients with PBC. Moreover, the summary DORs of RPR and M2BP in patients with PBC were 8.0 (95%CI: 4.0–15.8) and 13.2 (95%CI: 4.1–42.4), respectively. As shown in Table 3 and Figure 3, the summary AUROC value of TE for detecting AF was 0.88 (95%CI: 0.85–0.90) and 0.93 (95%CI: 0.90–0.95) in patients with AIH and PBC, respectively. The value of M2BP was 0.86 (95%CI: 0.82–0.88) in patients with PBC, whereas the summary AUROC values for AAR, APRI and FIB-4 were less than 0.80 in both patients with AIH and PBC, and the value for RPR in patients with PBC was less than 0.60.

Performance of noninvasive methods in diagnosing cirrhosis (F = 4)

Diagnosis of cirrhosis for AIH: Sixteen studies (n = 1076) evaluated ten noninvasive methods for detecting cirrhosis in patients with AIH. Of these, six (n = 543), three (n = 213), six (n = 543), two (n = 82), seven (n = 415) and four (n = 297) studies focused on APRI, AAR, FIB-4, ARFI, TE and SWE, respectively. Only one study each utilized the PC/SD ratio, MRE, RPR and M2BP.

As shown in Table 2, the summary sensitivities and specificities of APRI and FIB-4 were less than 75%, and those of AAR were 0.61 and 0.83, respectively. Moreover, the summary sensitivity and specificity of TE (cutoff value ranging from 11.0–12.7 KPa) were significantly higher for predicting cirrhosis, with 0.89 (95%CI: 0.82–0.94) and 0.88 (95%CI: 0.81–0.93), respectively, while the summary sensitivity and specificity of SWE (0.83, 0.86) were close to those of TE. Surprisingly, the summary specificity dramatically rose to 0.97 (95%CI 0.92–0.99) with a cutoff value ranging from 16.0–19.0 KPa.

Diagnosis of cirrhosis for PBC: Sixteen studies (n = 1568) evaluated nine noninvasive methods for detecting cirrhosis in patients with PBC. Among them, six (n = 852), four (n = 407), six (n = 852), six (n = 483), two (n = 210) and two (n = 194) studies focused on APRI, AAR, FIB-4, TE, SWE and M2BP, respectively. However, only one study utilized the ARFI and MRE methods.

As listed in Table 2, the summary sensitivities of APRI, AAR and FIB-4 for predicting cirrhosis were 0.75, 0.81 and 0.87, respectively, and their corresponding summary specificities were 0.51, 0.77 and 0.61, respectively. In contrast, TE had higher summary sensitivity (0.90; 95%CI: 0.74–0.98) and specificity (0.93; 95%CI: 0.89–0.96) with a cutoff value ranging from 15.6–25.1 KPa.

Diagnosis of cirrhosis for PSC: Four studies (n = 207) evaluated TE as a predictor of cirrhosis in patients with PSC. Because the diagnosis of PSC does not rely on liver biopsy, few related studies have been conducted. As listed in Table 2, the summary sensitivity and specificity of TE were 0.82 (95%CI: 0.68–0.91) and 0.89 (95%CI: 0.83–0.94), respectively.

Furthermore, Table 3 shows that the summary DORs of APRI and FIB-4 were 3.8 (95%CI: 2.2–6.4) and 5.5 (95%CI: 2.4–12.6) in patients with AIH and 14.6 (95%CI: 1.9–113.8) and 29.8 (95%CI: 5.9–150.3) in patients with PBC. In addition, the summary DOR of TE was highest in patients with PBC, with values of 91.8 (95%CI: 40.1–201.2), 134.8 (95%CI: 33.0–551.8) and 70.6 (95%CI: 15.4–322.7) in patients with AIH, PBC and PSC, respectively. The summary AUROC values of TE for detecting cirrhosis in patients with AIH, PBC and PSC were 0.90 (95%CI: 0.87–0.92), 0.91 (95%CI: 0.88–0.93) and 0.95 (95%CI: 0.93–0.97), respectively, while the summary AUROC values for APRI and FIB-4 were less than 0.80 in patients with AIH and 0.90 in patients with PBC (Table 3 and Figure 3).

Methodological heterogeneity, subgroup analysis and publication bias

As shown in Table 4, threshold heterogeneity was observed only in APRI F2 in both patients with AIH and PBC, whereas nonthreshold heterogeneity was observed in most groups (Figure 4, Supplementary Figures 2 and 3). Because meta-regression to explore the source of heterogeneity requires the number of original studies to exceed 10, we only conducted a meta-regression for AF in patients with AIH and PBC. The heterogeneity of APRI, FIB-4 and TE accuracy was mainly affected by the cutoff value with regard to specificity, whereas FIB-4 and TE were affected by sample size with regard to sensitivity, according to the meta-regression analysis (Supplementary Figure 4).

Subgroup analyses of TE according to sample size, cutoff value and treatment status are shown in Table 5. Because of the limited data, we only conducted an analysis for posttreatment combined with original data for pretreatment (Supplementary Table 2).

Deeks' funnel plot of these noninvasive methods was generated to assess publication bias. There was a publication bias for APRI in detecting SF (P = 0.06) and cirrhosis (P = 0.08) in patients with PBC but not in other methods for detecting SF, AF and cirrhosis (Figure 5, Supplementary Figure 5). Moreover, no publication bias was observed for any noninvasive method in patients with AIH (Figure 5, Supplementary Figure 6).

Table 4 Heterogeneity of all the included studies

		Fibrosis stage	Threshold heterogeneity		Non-threshold heterogeneity	
			r	*P* value	I^2 (%)	*P* value
AIH	TE	SF	0.176	0.651	82.9	0
		AF	-0.429	0.337	93.8	0
		Cirrhosis	0.321	0.482	56.59	0.03
	APRI	SF	1.0	0	62.34	0.05
		AF	0.717	0.02	71.94	0
		Cirrhosis	0.714	0.111	90.93	0
	FIB-4	SF	0.70	0.188	46.81	0.11
		AF	0.627	0.039	98.29	0
		Cirrhosis	-0.029	0.957	88.98	0
	AAR	AF	0.857	0.014	36.46	0.16
	SWE	Cirrhosis	0	1.0	61.97	0.05
PBC	TE	SF	-0.10	0.873	99.99	0
		AF	0.195	0.590	100	0
		Cirrhosis	-0.726	0.027	93.77	0
	APRI	SF	1.0	0	99.9	0
		AF	0.209	0.454	100	0
		Cirrhosis	-0.657	0.156	100	0
	FIB-4	AF	0.418	0.156	100	0
		Cirrhosis	0.029	0.957	100	0
	AAR	AF	0.60	0.208	96.05	0
		Cirrhosis	0.40	0.60	95.37	0
	M2BP	AF	0	1.0	99.24	0
	RPR	AF	0	1.0	94.49	0
PSC	TE	Cirrhosis	0.80	0.20	50.07	0.11

AAR: Aspartate aminotransferase to alanine aminotransferase ratio; AF: Advanced fibrosis; AIH: Autoimmune hepatitis; APRI: Aspartate aminotransferase to platelet ratio index; FIB-4: Fibrosis-4 index; M2BP: Mac-2-binding protein; PBC: Primary biliary cholangitis; PSC: Primary sclerosing cholangitis; RPR: Red cell distribution width to platelet ratio; SF: Significant fibrosis; SWE: Shear wave elastography; TE: Transient elastography.

DISCUSSION

In our review, a total of 60 studies (including 1594, 3126 and 501 patients with AIH, PBC and PSC, respectively) were included to evaluate the diagnostic accuracy of noninvasive methods for predicting SF, AF and cirrhosis in patients with AILDs. TE had excellent accuracy with summary AUROC values of 0.93, 0.93 and 0.91 for SF, AF and cirrhosis, respectively, in patients with PBC, while TE had a moderate to excellent accuracy of 0.84, 0.88 and 0.90, respectively, in patients with AIH. Moreover, the summary AUROC was 0.95 for cirrhosis in patients with PSC. In contrast, other noninvasive methods, such as AAR, APRI, FIB-4 and RPR, had poor accuracy, with summary AUROC values of < 0.80. In addition, the pooled sensitivity and specificity of TE were higher than those of the other noninvasive methods. Our results indicated that LSM using TE had a better diagnostic performance for staging hepatic fibrosis in AILDs, especially in patients with PBC. Moreover, our results showed that TE had mostly higher specificity and relatively low sensitivity for the diagnosis of AILDs. Koizumi *et al*[23] found that TE had high sensitivity and relatively low specificity for the diagnosis of PBC. However, the optimal cutoff values were higher and the range was wider than those in other studies, indicating that different optimal cutoff values may have an effect on diagnostic accuracy.

Meta-regression analysis is a reliable method for screening heterogeneity. In our study, the sample size, cutoff values, prevalence of SF and scoring system provided heterogeneity in summarizing the test results, consistent with previous studies[24,25]. We conducted subgroup analyses based on the sample size and cutoff values. Our results revealed that TE had a better predictive effect in a larger sample of patients with PBC. LSM by TE is the best surrogate marker for staging in SF and AF with a cutoff ranging from 6.4–9.1 KPa and 9.0–11.0 KPa, respectively, in patients with AIH and staging in

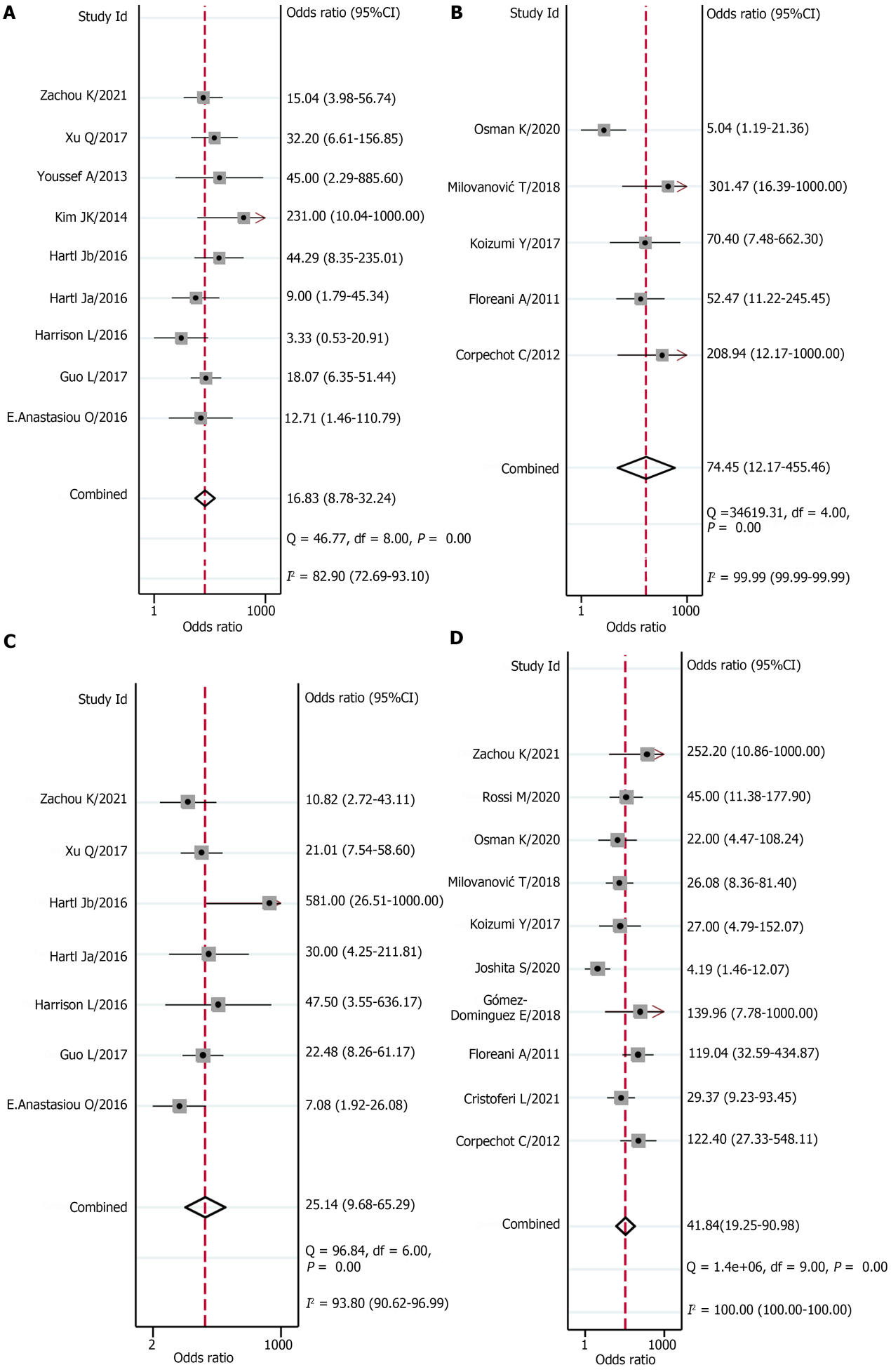
Table 5 Subgroup analysis of sample size and treatment status in prediction of significant fibrosis, advanced fibrosis and cirrhosis in autoimmune hepatitis and primary biliary cholangitis patients

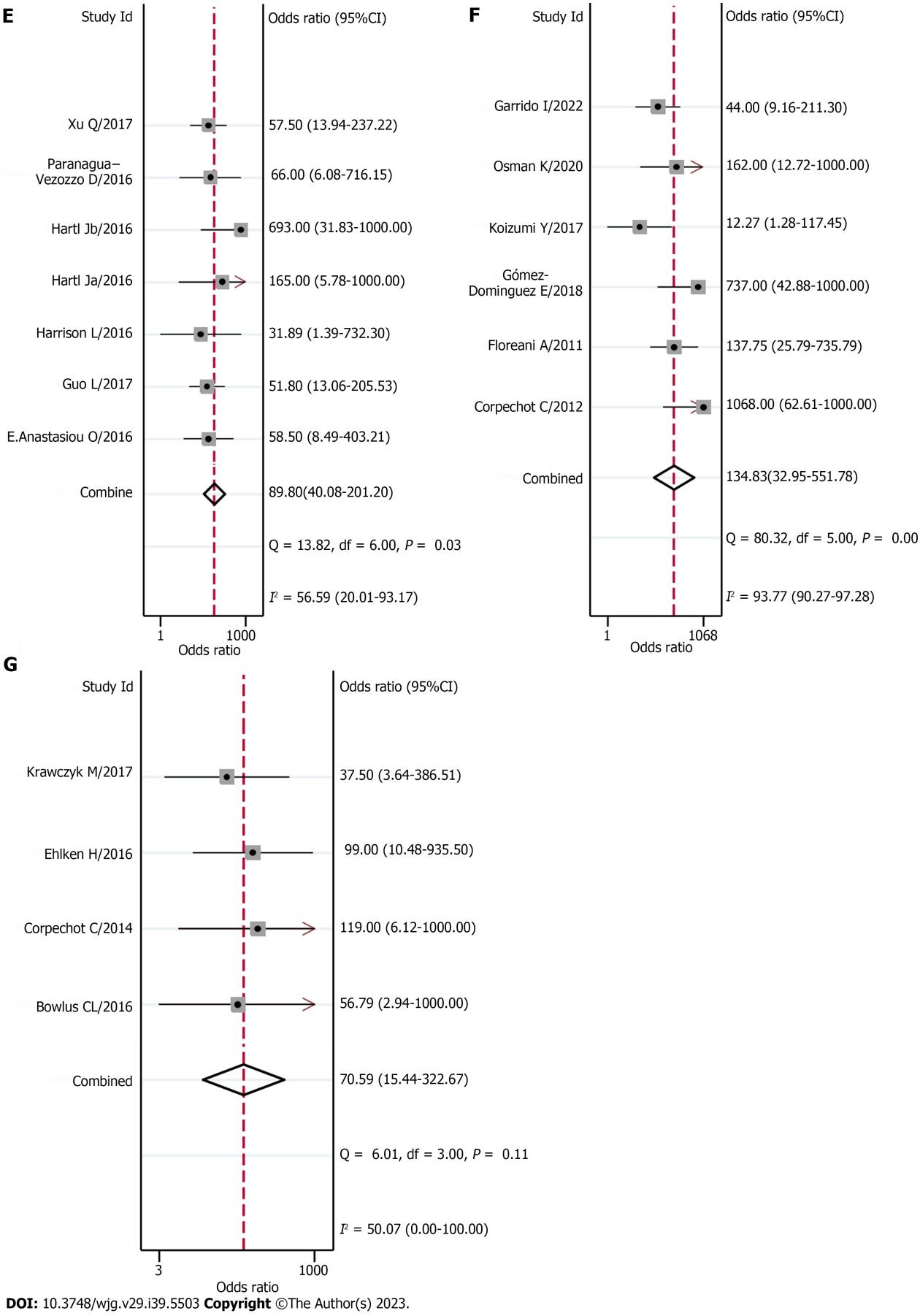
Disease	Parameter	Stage	Subgroup	Sensitivity (95%CI)	Specificity (95%CI)	AUROC (95%CI)
AIH	Sample size	SF	$n < 50$	0.83 (0.55-0.95)	0.82 (0.65-0.92)	0.85 (0.82-0.88)
			$n > 50$	0.84 (0.73-0.91)	0.77 (0.63-0.87)	0.87 (0.84-0.90)
		AF	$n < 50$	0.78 (0.54-0.91)	0.91 (0.78-0.96)	0.92 (0.89-0.94)
			$n > 50$	0.78 (0.68-0.86)	0.87 (0.73-0.94)	0.88 (0.84-0.90)
		Cirrhosis	$n < 50$	0.90 (0.65-0.98)	0.92 (0.74-0.98)	0.96 (0.94-0.97)
			$n > 50$	0.88 (0.82-0.93)	0.93 (0.86-0.96)	0.92 (0.89-0.94)
	Treatment status	SF	Post	0.78 (0.44-0.94)	0.76 (0.60-0.86)	0.79 (0.75-0.82)
		AF	Post	0.83 (0.66-0.93)	0.96 (0.84-0.99)	0.93 (0.91-0.95)
		Cirrhosis	Post	0.91(0.77-0.97)	0.97 (0.73-1.00)	0.94 (0.91-0.95)
	Cutoff value	SF	5.80-6.27	0.87 (0.81-0.92)	0.69 (0.60-0.77)	0.86 (0.83-0.89)
			6.40-9.10	0.82 (0.75-0.88)	0.89 (0.74-0.96)	0.92 (0.89-0.94)
		AF	9.00-11.00	0.83 (0.69-0.91)	0.92 (0.73-0.98)	0.88 (0.85-0.91)
			8.18-12.10	0.77 (0.71-0.83)	0.85 (0.80-0.89)	0.88 (0.85-0.90)
		Cirrhosis	11.00-12.67	0.89 (0.82-0.94)	0.88 (0.81-0.93)	0.92 (0.94-0.96)
			11.00-19.00	0.88 (0.82-0.93)	0.92 (0.88-0.95)	0.90 (0.87-0.92)
PBC	Sample size	SF	$n < 100$	0.81 (0.48-0.95)	0.78 (0.60-0.89)	0.82 (0.79-0.86)
			$n > 100$	0.83 (0.68-0.92)	0.98 (0.74-1.00)	0.97 (0.95-0.98)
		AF	$n < 100$	0.90 (0.85-0.94)	0.88 (0.78-0.94)	0.91 (0.88-0.93)
			$n > 100$	0.81 (0.64-0.91)	0.88 (0.75-0.94)	0.91 (0.88-0.93)
		Cirrhosis	$n < 100$	0.82 (0.67-0.91)	0.94 (0.80-0.99)	0.86 (0.82-0.89)
			$n > 100$	0.91 (0.76-0.97)	0.97 (0.90-0.99)	0.94 (0.92-0.96)
	Treatment status	SF	Post	0.89 (0.70-0.97)	0.98 (0.41-1.00)	0.97 (0.95-0.98)
		AF	Post	0.85 (0.68-0.94)	0.92 (0.63-0.99)	0.93 (0.91-0.95)
		Cirrhosis	Post	0.90 (0.71-0.97)	0.96 (0.74-1.00)	0.94 (0.92-0.96)
	Cutoff value	AF	6.75-7.60	0.80 (0.73-0.86)	0.81 (0.76-0.86)	0.88 (0.85-0.91)
			9.60-10.70	0.91 (0.84-0.95)	0.82 (0.77-0.87)	0.92 (0.89-0.94)
			11.90-17.90	0.75 (0.60-0.86)	0.94 (0.88-0.97)	0.93 (0.91-0.95)
		Cirrhosis	11.40-14.40	0.84 (0.69-0.93)	0.94 (0.90-0.97)	0.96 (0.94-0.97)
			14.40-16.90	0.88 (0.72-0.97)	0.99 (0.96-1.00)	0.99 (0.98-1.00)

95%CI: 95% confidence interval; AF: Advanced fibrosis; AIH: Autoimmune hepatitis; AUROC: Area under the receiver operator curve; PBC: Primary biliary cholangitis; SF: Significant fibrosis.

AF and cirrhosis with a cutoff ranging from 9.6–10.7 KPa and 14.4–16.9 KPa, respectively, in patients with PBC.

Several previous studies have demonstrated that inflammation in the liver (reflected by elevated ALT levels)[26] and extrahepatic cholestasis (reflected by total bilirubin)[27] may increase the stiffness value, causing a decrease in the diagnostic accuracy of TE, whereas ALT and bilirubin levels decline after treatment. Because a limited number of studies have reported results for the ALT subgroup, we only conducted a subgroup analysis of treatment conditions, which showed that the diagnostic accuracy for staging liver fibrosis was comparable between pretreatment and posttreatment in patients with both PBC and AIH. In other words, this may indicate that ALT levels have no significant effect on diagnostic accuracy. Meanwhile, two scoring systems [International Autoimmune Hepatitis Group (IAIHG) 1999 and IAIHG 2008] proposed by Granito *et al*[28] for the diagnosis of AIH are not interchangeable. According to our subgroup analysis regarding diagnostic criteria, the IAIHG 2008 showed diagnostic accuracy comparable to that of the IAIHG 1999 in distinguishing patients with AIH (Supplementary Tables 3 and 4). However, due to the limited number of studies, further investigation is required to confirm these results.

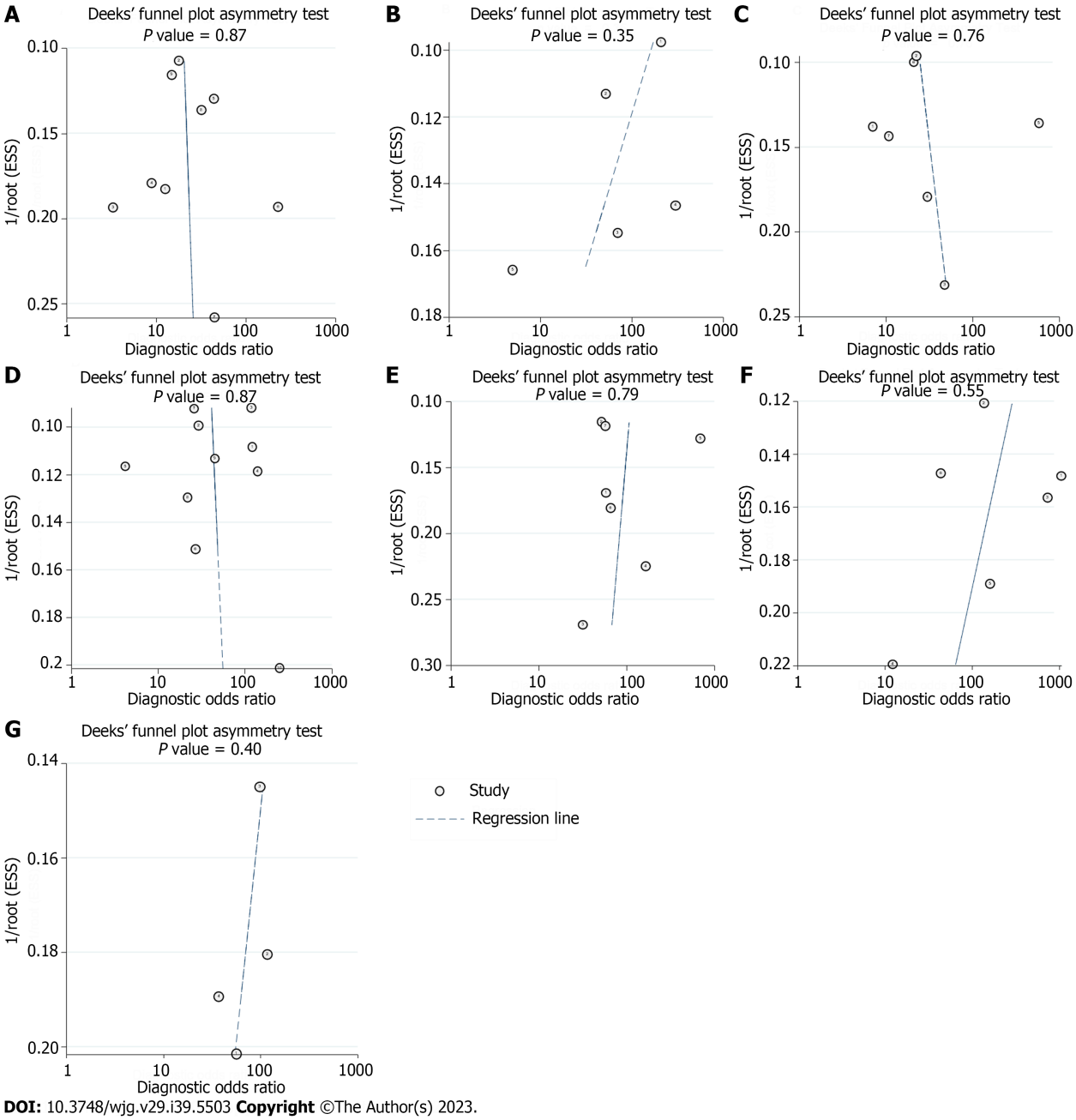

A
Study Id
Odds ratio (95%CI)
Zachou K/2021
15.04 (3.98-56.74)
Xu Q/2017
32.20 (6.61-156.85)
Youssef A/2013
45.00 (2.29-885.60)
Kim JK/2014
231.00 (10.04-1000.00)
Hartl Jb/2016
44.29 (8.35-235.01)
Hartl Ja/2016
9.00 (1.79-45.34)
Harrison L/2016
3.33 (0.53-20.91)
Guo L/2017
18.07 (6.35-51.44)
E.Anastasiou O/2016
12.71 (1.46-110.79)
Combined
16.83 (8.78-32.24)
Q = 46.77, df = 8.00, P = 0.00
I² = 82.90 (72.69-93.10)
1
1000
Odds ratio
B
Study Id
Odds ratio (95%CI)
Osman K/2020
5.04 (1.19-21.36)
Milovanović T/2018
301.47 (16.39-1000.00)
Koizumi Y/2017
70.40 (7.48-662.30)
Floreani A/2011
52.47 (11.22-245.45)
Corpechot C/2012
208.94 (12.17-1000.00)
Combined
74.45 (12.17-455.46)
Q =34619.31, df = 4.00, P = 0.00
I² = 99.99 (99.99-99.99)
1
1000
Odds ratio
C
Study Id
Odds ratio (95%CI)
Zachou K/2021
10.82 (2.72-43.11)
Xu Q/2017
21.01 (7.54-58.60)
Hartl Jb/2016
581.00 (26.51-1000.00)
Hartl Ja/2016
30.00 (4.25-211.81)
Harrison L/2016
47.50 (3.55-636.17)
Guo L/2017
22.48 (8.26-61.17)
E.Anastasiou O/2016
7.08 (1.92-26.08)
Combined
25.14 (9.68-65.29)
Q = 96.84, df = 6.00, P = 0.00
I² = 93.80 (90.62-96.99)
2
1000
Odds ratio
D
Study Id
Odds ratio (95%CI)
Zachou K/2021
252.20 (10.86-1000.00)
Rossi M/2020
45.00 (11.38-177.90)
Osman K/2020
22.00 (4.47-108.24)
Milovanović T/2018
26.08 (8.36-81.40)
Koizumi Y/2017
27.00 (4.79-152.07)
Joshita S/2020
4.19 (1.46-12.07)
Gómez-Dominguez E/2018
139.96 (7.78-1000.00)
Floreani A/2011
119.04 (32.59-434.87)
Cristoferi L/2021
29.37 (9.23-93.45)
Corpechot C/2012
122.40 (27.33-548.11)
Combined
41.84(19.25-90.98)
Q = 1.4e+06, df = 9.00, P = 0.00
I² = 100.00 (100.00-100.00)
1
1000
Odds ratio



DOI: 10.3748/wjg.v29.i39.5503 **Copyright** ©The Author(s) 2023.

Figure 4 Forest plots of diagnostic odds ratio of transient elastography in autoimmune liver disease patients. A and B: Transient elastography (TE) for detecting significant fibrosis in autoimmune hepatitis (AIH, A) and primary biliary cholangitis (PBC, B) patients, respectively; C and D: TE for detecting

advanced fibrosis in AIH (C) and PBC (D) patients; E-G: TE for detecting cirrhosis in AIH (E), PBC (F) and primary sclerosing cholangitis (G) patients. 95%CI: 95% confidence interval.



DOI: 10.3748/wjg.v29.i39.5503 **Copyright** ©The Author(s) 2023.

Figure 5 Deeks' funnel plot asymmetry test for publication bias of transient elastography in autoimmune liver disease patients. A and B: Transient elastography (TE) for detecting significant fibrosis in autoimmune hepatitis (AIH, A) and primary biliary cholangitis (PBC, B) patients; C and D: TE for detecting advanced fibrosis in AIH (C) and PBC (D) patients; E-G: TE for detecting cirrhosis in AIH (E), PBC (F) and primary sclerosing cholangitis (G) patients.

In addition, some studies have shown that other imaging technologies, including two-dimensional-SWE (2D-SWE)[29-32], MRE[22,33] and ARFI[19,34], also perform well in staging liver fibrosis (Supplementary Table 5). Further, 2D-SWE had excellent accuracy, with a summary AUROC of 0.91 for cirrhosis in patients with AIH (Table 3). In comparison, our findings indicated that 2D-SWE and ARFI had good accuracy with higher sensitivity, specificity and AUROC for AF and cirrhosis in patients with PBC, while the AUROC of MRE was higher in patients with AIH. Interestingly, compared with TE, 2D-SWE produces a two-dimensional grayscale image so that interference from the gallbladder, ascites and large tubular structures in the liver can be effectively avoided. However, the number of studies on 2D-SWE, MRE and ARFI included in our analysis was small. Indeed, the diagnostic accuracies of 2D-SWE and MRE require further studies with larger sample sizes to determine the best method for staging fibrosis in patients with AILDs.

However, the overlap syndrome, one of the AILDs, also deserves attention because it exhibits significantly higher rates of various complications, progresses to cirrhosis more rapidly and has a poor treatment response to ursodeoxycholic acid [35,36]. Hence, the development of noninvasive methods is beneficial for this disease. Wu *et al*[37] reported that the AUROCs of TE for SF, AF and cirrhosis were 0.837, 0.910 and 0.996, respectively. Yan *et al*[38] reported that the AUROCs of SWE were 0.91, 0.97 and 0.96, respectively. These results show that noninvasive imaging techniques have excellent accuracy for overlap syndrome, although more studies are required for further validation.

Our study had some limitations. First, we only included studies published in the English language; therefore, a language bias may have influenced the results. Second, we did not consider the confounding factors such as obesity, whereas a previous study proposed that a high BMI may reduce the efficiency of ultrasound-based elastography techniques in detecting fibrosis[39]. However, only a limited number of studies have provided sufficient data to conduct subgroup analyses to explore the potential impact of BMI on the diagnostic effects. Third, it is unknown whether ALT level is responsible for the difference in the diagnosis of TE between patients with AIH and PBC due to a lack of sufficient data. Moreover, the treatment conditions before inclusion in the study were unknown, and the lack of pretreatment studies made it impossible to compare the effects of treatment on outcomes. Finally, the number of studies on SWE, MRE and ARFI was inadequate to compare the effects of these imaging technologies and TE.

CONCLUSION

In conclusion, LSM using TE had better diagnostic performance for staging hepatic fibrosis in patients with AILDs compared to other serum biomarkers, especially in patients with PBC. The appropriate cutoff value for staging in AF and cirrhosis ranged from 9.6 to 10.7 KPa and 14.4 to 16.9 KPa, respectively, for patients with PBC. Additional recommended optimal cutoff values warrant further investigation to provide a better reference for clinical applications.

ARTICLE HIGHLIGHTS

Research background

Noninvasive criteria are needed for autoimmune liver diseases (AILDs) to assess liver fibrosis stage for prognosis and treatment decisions.

Research motivation

Results of individual diagnostic test accuracy studies assessing the diagnostic accuracy of transient elastography (TE) for the diagnosis of AILD appear promising. However, previous systematic review and meta-analyses have focused primarily on other liver diseases, which is still lacking in AILD.

Research objectives

To compare the diagnostic accuracy of imaging techniques with serum biomarkers of fibrosis in AILD.

Research methods

The PubMed, Cochrane and EMBASE databases were searched for literature. The Quality Assessment of Diagnostic Accuracy Studies-2 tool was used to evaluate the quality. Meta-Disc 1.4 and STATA 12.0 software were used to analyze the combined statistics: sensitivity; specificity; positive likelihood ratio; negative likelihood ratio; diagnostic odds ratio; and area under the curve fitted to the total receiver operating characteristic curve (AUROC).

Research results

A total of 60 studies were included in the meta-analysis. The AUROC curve values were 0.93, 0.93 and 0.91 for significant fibrosis, advanced fibrosis and cirrhosis, respectively, in primary biliary cholangitis patients, while the AUROC curve values were 0.84, 0.88 and 0.90, respectively, in autoimmune hepatitis patients.

Research conclusions

TE is a reliable method for diagnosis in AILD patients, especially in primary biliary cholangitis patients. The appropriate cutoff value for staging advanced fibrosis and cirrhosis ranged from 9.6 to 10.7 KPa and 14.4 to 16.9 KPa, respectively.

Research perspectives

We propose a suitable diagnostic threshold for TE in PBC patients. However, future prospective multicenter studies with TE and histopathology protocol are required to validate our results.

FOOTNOTES

Author contributions: Jiang W conceived and designed the study; Chen H and Shen Y contributed to acquiring the data; Wang MX and

Weng CZ contributed statistical analysis support; Chen H, Shen Y, Wu SD and Zhu Q contributed to analysis and interpretation of the data; Chen H wrote the manuscript; Wu SD and Zhang J contributed to manuscript revision; All authors read and approved the submitted version and are accountable for all aspects of the work.

Supported by Natural Science and Technology Major Project of Fujian Province, No. 2021D033; Natural Science Foundation of Shanghai, No. 20ZR1410900; Medical Innovation Project of Fujian Province, No. 2022CXB020; National Science and Technology Major Project, No. 2017ZX 10203202-003-002.

Conflict-of-interest statement: The authors declare that the research was conducted in the absence of any commercial or financial relationships that could be construed as a potential conflict of interest.

PRISMA 2009 Checklist statement: The authors have read the PRISMA 2009 Checklist, and the manuscript was prepared and revised according to the PRISMA 2009 Checklist.

Open-Access: This article is an open-access article that was selected by an in-house editor and fully peer-reviewed by external reviewers. It is distributed in accordance with the Creative Commons Attribution NonCommercial (CC BY-NC 4.0) license, which permits others to distribute, remix, adapt, build upon this work non-commercially, and license their derivative works on different terms, provided the original work is properly cited and the use is non-commercial. See: https://creativecommons.org/Licenses/by-nc/4.0/

Country/Territory of origin: China

ORCID number: Hong Chen 0000-0002-3966-5355; Yue Shen 0000-0002-4771-9114; Sheng-Di Wu 0000-0002-3829-2999; Qin Zhu 0000-0002-6661-8343; Cheng-Zhao Weng 0009-0005-5168-8751; Jun Zhang 0009-0008-9410-2011; Mei-Xia Wang 0000-0002-3139-1847; Wei Jiang 0000-0002-9354-6699.

S-Editor: Lin C
L-Editor: Filipodia
P-Editor: Cai YX

REFERENCES

1 **Boonstra K**, Beuers U, Ponsioen CY. Epidemiology of primary sclerosing cholangitis and primary biliary cirrhosis: a systematic review. *J Hepatol* 2012; **56**: 1181-1188 [PMID: 22245904 DOI: 10.1016/j.jhep.2011.10.025]
2 **Tanaka A**, Ma X, Yokosuka O, Weltman M, You H, Amarapurkar DN, Kim YJ, Abbas Z, Payawal DA, Chang ML, Efe C, Ozaslan E, Abe M, Mitchell-Thain R, Zeniya M, Han KH, Vierling JM, Takikawa H. Autoimmune liver diseases in the Asia-Pacific region: Proceedings of APASL symposium on AIH and PBC 2016. *Hepatol Int* 2016; **10**: 909-915 [PMID: 27649967 DOI: 10.1007/s12072-016-9767-9]
3 **Manns MP**, Czaja AJ, Gorham JD, Krawitt EL, Mieli-Vergani G, Vergani D, Vierling JM; American Association for the Study of Liver Diseases. Diagnosis and management of autoimmune hepatitis. *Hepatology* 2010; **51**: 2193-2213 [PMID: 20513004 DOI: 10.1002/hep.23584]
4 **Beringer A**, Miossec P. IL-17 and IL-17-producing cells and liver diseases, with focus on autoimmune liver diseases. *Autoimmun Rev* 2018; **17**: 1176-1185 [PMID: 30321671 DOI: 10.1016/j.autrev.2018.06.008]
5 **Carbone M**, Neuberger JM. Autoimmune liver disease, autoimmunity and liver transplantation. *J Hepatol* 2014; **60**: 210-223 [PMID: 24084655 DOI: 10.1016/j.jhep.2013.09.020]
6 **Poynard T**, Halfon P, Castera L, Charlotte F, Le Bail B, Munteanu M, Messous D, Ratziu V, Benhamou Y, Bourlière M, De Ledinghen V; FibroPaca Group. Variability of the area under the receiver operating characteristic curves in the diagnostic evaluation of liver fibrosis markers: impact of biopsy length and fragmentation. *Aliment Pharmacol Ther* 2007; **25**: 733-739 [PMID: 17311607 DOI: 10.1111/j.1365-2036.2007.03252.x]
7 **Castera L**, Forns X, Alberti A. Non-invasive evaluation of liver fibrosis using transient elastography. *J Hepatol* 2008; **48**: 835-847 [PMID: 18334275 DOI: 10.1016/j.jhep.2008.02.008]
8 **Piccinino F**, Sagnelli E, Pasquale G, Giusti G. Complications following percutaneous liver biopsy. A multicentre retrospective study on 68,276 biopsies. *J Hepatol* 1986; **2**: 165-173 [PMID: 3958472 DOI: 10.1016/s0168-8278(86)80075-7]
9 **Zein CO**, Angulo P, Lindor KD. When is liver biopsy needed in the diagnosis of primary biliary cirrhosis? *Clin Gastroenterol Hepatol* 2003; **1**: 89-95 [PMID: 15017500 DOI: 10.1053/cgh.2003.50014]
10 **Czaja AJ**. Review article: The prevention and reversal of hepatic fibrosis in autoimmune hepatitis. *Aliment Pharmacol Ther* 2014; **39**: 385-406 [PMID: 24387318 DOI: 10.1111/apt.12592]
11 **Friedrich-Rust M**, Ong MF, Herrmann E, Dries V, Samaras P, Zeuzem S, Sarrazin C. Real-time elastography for noninvasive assessment of liver fibrosis in chronic viral hepatitis. *AJR Am J Roentgenol* 2007; **188**: 758-764 [PMID: 17312065 DOI: 10.2214/AJR.06.0322]
12 **Li Y**, Huang YS, Wang ZZ, Yang ZR, Sun F, Zhan SY, Liu XE, Zhuang H. Systematic review with meta-analysis: the diagnostic accuracy of transient elastography for the staging of liver fibrosis in patients with chronic hepatitis B. *Aliment Pharmacol Ther* 2016; **43**: 458-469 [PMID: 26669632 DOI: 10.1111/apt.13488]
13 **Johannessen A**, Stockdale AJ, Henrion MYR, Okeke E, Seydi M, Wandeler G, Sonderup M, Spearman CW, Vinikoor M, Sinkala E, Desalegn H, Fall F, Riches N, Davwar P, Duguru M, Maponga T, Taljaard J, Matthews PC, Andersson M, Mboup S, Sombie R, Shimakawa Y, Lemoine M. Systematic review and individual-patient-data meta-analysis of non-invasive fibrosis markers for chronic hepatitis B in Africa. *Nat Commun* 2023; **14**: 45 [PMID: 36596805 DOI: 10.1038/s41467-022-35729-w]
14 **Xiao G**, Zhu S, Xiao X, Yan L, Yang J, Wu G. Comparison of laboratory tests, ultrasound, or magnetic resonance elastography to detect fibrosis in patients with nonalcoholic fatty liver disease: A meta-analysis. *Hepatology* 2017; **66**: 1486-1501 [PMID: 28586172 DOI: 10.1002/hep.29302]

15 **Wu S**, Yang Z, Zhou J, Zeng N, He Z, Zhan S, Jia J, You H. Systematic review: diagnostic accuracy of non-invasive tests for staging liver fibrosis in autoimmune hepatitis. *Hepatol Int* 2019; **13**: 91-101 [PMID: 30443702 DOI: 10.1007/s12072-018-9907-5]

16 **Whiting PF**, Rutjes AW, Westwood ME, Mallett S, Deeks JJ, Reitsma JB, Leeflang MM, Sterne JA, Bossuyt PM; QUADAS-2 Group. QUADAS-2: a revised tool for the quality assessment of diagnostic accuracy studies. *Ann Intern Med* 2011; **155**: 529-536 [PMID: 22007046 DOI: 10.7326/0003-4819-155-8-201110180-00009]

17 **Shiha G**, Zalata K. Ishak versus METAVIR: Terminology, Convertibility and Correlation with Laboratory Changes in Chronic Hepatitis C. *Liver Biopsy* 2011; **10**: 155-170 [DOI: 10.5772/20110]

18 **Swets JA**. Measuring the accuracy of diagnostic systems. *Science* 1988; **240**: 1285-1293 [PMID: 3287615 DOI: 10.1126/science.3287615]

19 **Park DW**, Lee YJ, Chang W, Park JH, Lee KH, Kim YH, Kang NK, Chung JW, Jang HY, Ahn S, Kim H, Jeong SH, Kim JW, Jang ES. Diagnostic performance of a point shear wave elastography (pSWE) for hepatic fibrosis in patients with autoimmune liver disease. *PLoS One* 2019; **14**: e0212771 [PMID: 30856201 DOI: 10.1371/journal.pone.0212771]

20 **Zachou K**, Lygoura V, Arvaniti P, Giannoulis G, Gatselis NK, Koukoulis GK, Dalekos GN. FibroMeter scores for the assessment of liver fibrosis in patients with autoimmune liver diseases. *Ann Hepatol* 2021; **22**: 100285 [PMID: 33157268 DOI: 10.1016/j.aohep.2020.10.013]

21 **Sheptulina A**, Shirokova E, Ivashkin V. The diagnostic performance of non-invasive serum markers to identify significant liver fibrosis in patients with primary biliary cirrhosis and primary sclerosing cholangitis. In: UEG Week 2015 Poster Presentations. *United European Gastroenterol J* 2015; **3**: 146-687 [DOI: 10.1177/2050640615601623]

22 **Wang J**, Malik N, Yin M, Smyrk TC, Czaja AJ, Ehman RL, Venkatesh SK. Magnetic resonance elastography is accurate in detecting advanced fibrosis in autoimmune hepatitis. *World J Gastroenterol* 2017; **23**: 859-868 [PMID: 28223730 DOI: 10.3748/wjg.v23.i5.859]

23 **Koizumi Y**, Hirooka M, Abe M, Tokumoto Y, Yoshida O, Watanabe T, Nakamura Y, Imai Y, Yukimoto A, Kumagi T, Takeshita E, Ikeda Y, Hiasa Y. Comparison between real-time tissue elastography and vibration-controlled transient elastography for the assessment of liver fibrosis and disease progression in patients with primary biliary cholangitis. *Hepatol Res* 2017; **47**: 1252-1259 [PMID: 28044427 DOI: 10.1111/hepr.12861]

24 **Coco B**, Oliveri F, Maina AM, Ciccorossi P, Sacco R, Colombatto P, Bonino F, Brunetto MR. Transient elastography: a new surrogate marker of liver fibrosis influenced by major changes of transaminases. *J Viral Hepat* 2007; **14**: 360-369 [PMID: 17439526 DOI: 10.1111/j.1365-2893.2006.00811.x]

25 **Xu X**, Su Y, Song R, Sheng Y, Ai W, Wu X, Liu H. Performance of transient elastography assessing fibrosis of single hepatitis B virus infection: a systematic review and meta-analysis of a diagnostic test. *Hepatol Int* 2015; **9**: 558-566 [PMID: 26187292 DOI: 10.1007/s12072-015-9643-z]

26 **Xu XY**, Kong H, Song RX, Zhai YH, Wu XF, Ai WS, Liu HB. The effectiveness of noninvasive biomarkers to predict hepatitis B-related significant fibrosis and cirrhosis: a systematic review and meta-analysis of diagnostic test accuracy. *PLoS One* 2014; **9**: e100182 [PMID: 24964038 DOI: 10.1371/journal.pone.0100182]

27 **Millonig G**, Reimann FM, Friedrich S, Fonouni H, Mehrabi A, Büchler MW, Seitz HK, Mueller S. Extrahepatic cholestasis increases liver stiffness (FibroScan) irrespective of fibrosis. *Hepatology* 2008; **48**: 1718-1723 [PMID: 18836992 DOI: 10.1002/hep.22577]

28 **Granito A**, Muratori P, Ferri S, Pappas G, Quarneti C, Lenzi M, Bianchi FB, Muratori L. Diagnosis and therapy of autoimmune hepatitis. *Mini Rev Med Chem* 2009; **9**: 847-860 [PMID: 19519509 DOI: 10.2174/138955709788452676]

29 **Guo L**, Zheng L, Hu L, Zhou H, Yu L, Liang W. Transient Elastography (FibroScan) Performs Better Than Non-Invasive Markers in Assessing Liver Fibrosis and Cirrhosis in Autoimmune Hepatitis Patients. *Med Sci Monit* 2017; **23**: 5106-5112 [PMID: 29073121 DOI: 10.12659/msm.907300]

30 **Xing X**, Yan Y, Shen Y, Xue M, Wang X, Luo X, Yang L. Liver fibrosis with two-dimensional shear-wave elastography in patients with autoimmune hepatitis. *Expert Rev Gastroenterol Hepatol* 2020; **14**: 631-638 [PMID: 32510248 DOI: 10.1080/17474124.2020.1779589]

31 **Janik MK**, Kruk B, Szczepankiewicz B, Kostrzewa K, Raszeja-Wyszomirska J, Górnicka B, Lammert F, Milkiewicz P, Krawczyk M. Measurement of liver and spleen stiffness as complementary methods for assessment of liver fibrosis in autoimmune hepatitis. *Liver Int* 2021; **41**: 348-356 [PMID: 33159831 DOI: 10.1111/liv.14726]

32 **Yan Y**, Xing X, Lu Q, Wang X, Luo X, Yang L. Assessment of biopsy proven liver fibrosis by two-dimensional shear wave elastography in patients with primary biliary cholangitis. *Dig Liver Dis* 2020; **52**: 555-560 [PMID: 32111390 DOI: 10.1016/j.dld.2020.02.002]

33 **Osman KT**, Maselli DB, Idilman IS, Rowan DJ, Viehman JK, Harmsen WS, Harnois DM, Carey EJ, Gossard AA, LaRusso NF, Lindor KD, Venkatesh SK, Eaton JE. Liver Stiffness Measured by Either Magnetic Resonance or Transient Elastography Is Associated With Liver Fibrosis and Is an Independent Predictor of Outcomes Among Patients With Primary Biliary Cholangitis. *J Clin Gastroenterol* 2021; **55**: 449-457 [PMID: 32976197 DOI: 10.1097/MCG.0000000000001433]

34 **Zhang DK**, Chen M, Liu Y, Wang RF, Liu LP, Li M. Acoustic radiation force impulse elastography for non-invasive assessment of disease stage in patients with primary biliary cirrhosis: A preliminary study. *Clin Radiol* 2014; **69**: 836-840 [PMID: 24837697 DOI: 10.1016/j.crad.2014.03.019]

35 **Park Y**, Cho Y, Cho EJ, Kim YJ. Retrospective analysis of autoimmune hepatitis-primary biliary cirrhosis overlap syndrome in Korea: characteristics, treatments, and outcomes. *Clin Mol Hepatol* 2015; **21**: 150-157 [PMID: 26157752 DOI: 10.3350/cmh.2015.21.2.150]

36 **To U**, Silveira M. Overlap Syndrome of Autoimmune Hepatitis and Primary Biliary Cholangitis. *Clin Liver Dis* 2018; **22**: 603-611 [PMID: 30259856 DOI: 10.1016/j.cld.2018.03.010]

37 **Wu HM**, Sheng L, Wang Q, Bao H, Miao Q, Xiao X, Guo CJ, Li H, Ma X, Qiu DK, Hua J. Performance of transient elastography in assessing liver fibrosis in patients with autoimmune hepatitis-primary biliary cholangitis overlap syndrome. *World J Gastroenterol* 2018; **24**: 737-743 [PMID: 29456412 DOI: 10.3748/wjg.v24.i6.737]

38 **Yan YL**, Xing X, Wang Y, Wang XZ, Wang Z, Yang L. Clinical utility of two-dimensional shear-wave elastography in monitoring disease course in autoimmune hepatitis-primary biliary cholangitis overlap syndrome. *World J Gastroenterol* 2022; **28**: 2021-2033 [PMID: 35664960 DOI: 10.3748/wjg.v28.i18.2021]

39 **Petitclerc L**, Sebastiani G, Gilbert G, Cloutier G, Tang A. Liver fibrosis: Review of current imaging and MRI quantification techniques. *J Magn Reson Imaging* 2017; **45**: 1276-1295 [PMID: 27981751 DOI: 10.1002/jmri.25550]

40 **Youssef A**, Abdel Ghaffar TY, Esmat G, Wanis AAA. Non invasive assessment of hepatic fibrosis in children: Performance of liver stiffness measurement and aspartate transaminase to platelet ratio. *Hepatology* 2013; **58**: 815A [DOI: 10.1002/hep.26862]

41 **Kim JK**, Kim HW, Lee JI, Lee KS. Analysis of liver stiffness measured by transient elastography in autoimmune hepatitis. *Hepatology* 2014; **60**: 364A-365A [DOI: 10.1002/hep.27496]

42 **Abdollahi M**, Pouri A, Ghojazadeh M, Estakhri R, Somi M. Non-invasive serum fibrosis markers: A study in chronic hepatitis. *Bioimpacts* 2015; **5**: 17-23 [PMID: 25901293 DOI: 10.15171/bi.2015.05]

43 **Harrison L**, McFarlane E, Dube A, Gleeson D. Accuracy of transient elastography in predicting histological fibrosis severity in treated autoimmune hepatitis? *Gut* 2016; **65**: A268-A269 [DOI: 10.1136/gutjnl-2016-312388.505]

44 **Hartl J**, Denzer U, Ehlken H, Zenouzi R, Peiseler M, Sebode M, Hübener S, Pannicke N, Weiler-Normann C, Quaas A, Lohse AW, Schramm C. Transient elastography in autoimmune hepatitis: Timing determines the impact of inflammation and fibrosis. *J Hepatol* 2016; **65**: 769-775 [PMID: 27238753 DOI: 10.1016/j.jhep.2016.05.023]

45 **Nishikawa H**, Enomoto H, Iwata Y, Hasegawa K, Nakano C, Takata R, Nishimura T, Yoh K, Aizawa N, Sakai Y, Ikeda N, Takashima T, Iijima H, Nishiguchi S. Clinical significance of serum Wisteria floribunda agglutinin positive Mac-2-binding protein level and high-sensitivity C-reactive protein concentration in autoimmune hepatitis. *Hepatol Res* 2016; **46**: 613-621 [PMID: 26406984 DOI: 10.1111/hepr.12596]

46 **E Anastasiou O**, Büchter M, A Baba H, Korth J, Canbay A, Gerken G, Kahraman A. Performance and Utility of Transient Elastography and Non-Invasive Markers of Liver Fiibrosis in Patients with Autoimmune Hepatitis: A Single Centre Experience. *Hepat Mon* 2016; **16**: e40737 [PMID: 28070199 DOI: 10.5812/hepatmon.40737]

47 **Piwczyńska K**, Marek W, Maciej D, Małgorzata W. APRI as a fibrosis marker in children with autoimmune hepatitis(AIH). In: ESPGHAN 49th ANNUAL MEETING of the European Society for Paediatric Gastroenterology, Hepatology and Nutrition. *Journal of Pediatric Gastroenterology and Nutrition* 2016; **62**: 1-890 [DOI: 10.1097/01.mpg.0000484500.48517.e7]

48 **Sheptulina A**, Shirokova E, Nekrasova T, Blum H, Ivashkin V. Platelet count to spleen diameter ratio non-invasively identifies severe fibrosis and cirrhosis in patients with autoimmune hepatitis. *J Gastroenterol Hepatol* 2016; **31**: 1956-1962 [PMID: 27059170 DOI: 10.1111/jgh.13407]

49 **Paranagua-Vezozzo D**, Terrabuio DR, Moutinho RD, Ono S, Salas V, Carrilho F, Alves VF, Cancado EL. Transient elastography (TE) and acoustic radiation force impulse imaging (ARFI) can predict degree of advanced fibrosis for autoimmune hepatitis in biochemical remission. *Hepatology* 2017; **66**: 187A

50 **Puustinen L**, Hakkarainen A, Kivisaari R, Boyd S, Nieminen U, Färkkilä M, Lundbom N, Arkkila P. (31) Phosphorus magnetic resonance spectroscopy of the liver for evaluating inflammation and fibrosis in autoimmune hepatitis. *Scand J Gastroenterol* 2017; **52**: 886-892 [PMID: 28415898 DOI: 10.1080/00365521.2017.1315738]

51 **Xu Q**, Sheng L, Bao H, Chen X, Guo C, Li H, Ma X, Qiu D, Hua J. Evaluation of transient elastography in assessing liver fibrosis in patients with autoimmune hepatitis. *J Gastroenterol Hepatol* 2017; **32**: 639-644 [PMID: 27505153 DOI: 10.1111/jgh.13508]

52 **Zeng J**, Huang ZP, Zheng J, Wu T, Zheng RQ. Non-invasive assessment of liver fibrosis using two-dimensional shear wave elastography in patients with autoimmune liver diseases. *World J Gastroenterol* 2017; **23**: 4839-4846 [PMID: 28765706 DOI: 10.3748/wjg.v23.i26.4839]

53 **Liu L**, Cao J, Zhong Z, Guo Z, Jiang Y, Bai Y, Xu J. Noninvasive indicators predict advanced liver fibrosis in autoimmune hepatitis patients. *J Clin Lab Anal* 2019; **33**: e22922 [PMID: 31115929 DOI: 10.1002/jcla.22922]

54 **Li X**, Xu H, Gao P. Red Blood Cell Distribution Width-to-Platelet Ratio and Other Laboratory Indices Associated with Severity of Histological Hepatic Fibrosis in Patients with Autoimmune Hepatitis: A Retrospective Study at a Single Center. *Med Sci Monit* 2020; **26**: e927946 [PMID: 33180750 DOI: 10.12659/MSM.927946]

55 **Wang H**, Wang J, Xia J, Yan X, Feng Y, Li L, Chen J, Liu D, Ding W, Yang Y, Huang R, Wu C. Red cell distribution width to platelet ratio predicts liver fibrosis in patients with autoimmune hepatitis. *Medicine (Baltimore)* 2020; **99**: e21408 [PMID: 32846758 DOI: 10.1097/MD.0000000000021408]

56 **Ferronato M**, Lenzi M, Muratori P, Muratori L. Blood-Based Non-Invasive Tests of Hepatic Fibrosis in Autoimmune Hepatitis: Application among Selected Patients Leads to Higher Accuracy. *Gastroenterology Insights* 2022; **13**: 286-295 [DOI: 10.3390/gastroent13030029]

57 **Soh EG**, Lee YH, Kim YR, Yoon KH, Choi KH. Usefulness of 2D shear wave elastography for the evaluation of hepatic fibrosis and treatment response in patients with autoimmune hepatitis. *Ultrasonography* 2022; **41**: 740-749 [PMID: 36195317 DOI: 10.14366/usg.21266]

58 **Nyblom H**, Björnsson E, Simrén M, Aldenborg F, Almer S, Olsson R. The AST/ALT ratio as an indicator of cirrhosis in patients with PBC. *Liver Int* 2006; **26**: 840-845 [PMID: 16911467 DOI: 10.1111/j.1478-3231.2006.01304.x]

59 **Gómez-Dominguez E**, Mendoza J, García-Buey L, Trapero M, Gisbert JP, Jones EA, Moreno-Otero R. Transient elastography to assess hepatic fibrosis in primary biliary cirrhosis. *Aliment Pharmacol Ther* 2008; **27**: 441-447 [PMID: 18081731 DOI: 10.1111/j.1365-2036.2007.03585.x]

60 **Alempijevic T**, Krstic M, Jesic R, Jovanovic I, Sokic Milutinovic A, Kovacevic N, Krstic S, Popovic D. Biochemical markers for non-invasive assessment of disease stage in patients with primary biliary cirrhosis. *World J Gastroenterol* 2009; **15**: 591-594 [PMID: 19195061 DOI: 10.3748/wjg.15.591]

61 **Ferrara F**, Caroli D, Antoniazzi S, Variola A, Cazzagon N, Baldo V, Floreani A. Performance of surrogate markers of hepatic fibrosis in primary biliary cirrhosis. *J Hepatol* 2009; **50**: S243 [DOI: 10.1016/S1590-8658(09)60099-2]

62 **Su CW**, Chan CC, Hung HH, Huo TI, Huang YH, Li CP, Lin HC, Tsay SH, Lee PC, Lee SD, Wu JC. Predictive value of aspartate aminotransferase to alanine aminotransferase ratio for hepatic fibrosis and clinical adverse outcomes in patients with primary biliary cirrhosis. *J Clin Gastroenterol* 2009; **43**: 876-883 [PMID: 19247208 DOI: 10.1097/MCG.0b013e31818980ac]

63 **Floreani A**, Cazzagon N, Martines D, Cavalletto L, Baldo V, Chemello L. Performance and utility of transient elastography and noninvasive markers of liver fibrosis in primary biliary cirrhosis. *Dig Liver Dis* 2011; **43**: 887-892 [PMID: 21783442 DOI: 10.1016/j.dld.2011.06.011]

64 **Corpechot C**, Carrat F, Poujol-Robert A, Gaouar F, Wendum D, Chazouillères O, Poupon R. Noninvasive elastography-based assessment of liver fibrosis progression and prognosis in primary biliary cirrhosis. *Hepatology* 2012; **56**: 198-208 [PMID: 22271046 DOI: 10.1002/hep.25599]

65 **Umemura T**, Joshita S, Sekiguchi T, Usami Y, Shibata S, Kimura T, Komatsu M, Matsumoto A, Ota M, Tanaka E. Serum Wisteria floribunda Agglutinin-Positive Mac-2-Binding Protein Level Predicts Liver Fibrosis and Prognosis in Primary Biliary Cirrhosis. *Am J Gastroenterol* 2015; **110**: 857-864 [PMID: 25916223 DOI: 10.1038/ajg.2015.118]

66 **Nishikawa H**, Enomoto H, Iwata Y, Hasegawa K, Nakano C, Takata R, Nishimura T, Yoh K, Aizawa N, Sakai Y, Ikeda N, Takashima T, Ishii A, Iijima H, Nishiguchi S. Impact of serum Wisteria floribunda agglutinin positive Mac-2-binding protein and serum interferon-γ-inducible protein-10 in primary biliary cirrhosis. *Hepatol Res* 2016; **46**: 575-583 [PMID: 26418076 DOI: 10.1111/hepr.12595]

67 **Olmez S**, Sayar S, Avcioglu U, Tenlik İ, Ozaslan E, Koseoglu HT, Altiparmak E. The relationship between liver histology and noninvasive markers in primary biliary cirrhosis. *Eur J Gastroenterol Hepatol* 2016; **28**: 773-776 [PMID: 27092904 DOI: 10.1097/MEG.0000000000000637]

68 **Wang H**, Xu H, Wang X, Wu R, Gao X, Jin Q, Niu J. Red Blood Cell Distribution Width to Platelet Ratio is Related to Histologic Severity of Primary Biliary Cirrhosis. *Medicine (Baltimore)* 2016; **95**: e3114 [PMID: 26986159 DOI: 10.1097/MD.0000000000003114]

69 **Wang X**, Han Z, Chen Y, Guo C, Han Y. Validity analysis based on non-invasive methods for the assessment of liver fibrosis in primary biliary cholangitis. In: Abstracts of the 26th Annual Conference of APASL. *Hepatol Int* 2017; **11**: S590 [DOI: 10.1007/s12072-016-9783-9]

70 **Jiang X**, Wang Y, Su Z, Yang F, Lv H, Lin L, Sun C. Red blood cell distribution width to platelet ratio levels in assessment of histologic severity in patients with primary biliary cholangitis. *Scand J Clin Lab Invest* 2018; **78**: 258-263 [PMID: 29533114 DOI: 10.1080/00365513.2018.1449011]

71 **Kamal N**, Surana P, Noureddin M, Kleiner D, Hoofnagle J, Heller T, Koh C. Bile Duct Damage and Cirrhosis in Primary Biliary Cholangitis: An Investigation of Non-Invasive Biomarkers. *Gastroenterology* 2018; **154**: S1209 [DOI: 10.1016/s0016-5085(18)33995-7]

72 **Meng J**, Xu H, Liu X, Wu R, Niu J. Increased red cell width distribution to lymphocyte ratio is a predictor of histologic severity in primary biliary cholangitis. *Medicine (Baltimore)* 2018; **97**: e13431 [PMID: 30508955 DOI: 10.1097/MD.0000000000013431]

73 **Milovanović T**, Copertino A, Boričić I, Miličić B, Marković AP, Krstić M, Matović V, Popović D. Transient elastography for noninvasive assessment of liver fibrosis in patients with primary biliary cirrhosis. *Vojnosanitetski Pregled* 2018; **75**: 374-379 [DOI: 10.2298/VSP160409337A]

74 **Wang Z**, Liu X, Xu H, Qu L, Zhang D, Gao P. Platelet count to spleen thickness ratio is related to histologic severity of primary biliary cholangitis. *Medicine (Baltimore)* 2018; **97**: e9843 [PMID: 29443746 DOI: 10.1097/MD.0000000000009843]

75 **Jiang M**, Yan X, Song X, Yan Q, Zhao Y, Wang L, Gao P. Total bile acid to platelet ratio: A noninvasive index for predicting liver fibrosis in primary biliary cholangitis. *Medicine (Baltimore)* 2020; **99**: e20502 [PMID: 32481469 DOI: 10.1097/MD.0000000000020502]

76 **Joshita S**, Yamashita Y, Sugiura A, Uehara T, Usami Y, Yamazaki T, Fujimori N, Matsumoto A, Tanaka E, Umemura T. Clinical utility of FibroScan as a non-invasive diagnostic test for primary biliary cholangitis. *J Gastroenterol Hepatol* 2020; **35**: 1208-1214 [PMID: 31724755 DOI: 10.1111/jgh.14929]

77 **Rossi M**, Alessi N, Cabibi A, Fichera A, Zarcone A, Bianco AL, Marco VD, Cammà C, Craxì A. High rate of misclassification of fibrosis stage using Transient Elastography in patients with Primary Biliary Cholangitis. *Digestive and Liver Disease* 2020; **52**: e34 [DOI: 10.1016/j.dld.2019.12.122]

78 **Cristoferi L**, Calvaruso V, Overi D, Viganò M, Rigamonti C, Degasperi E, Cardinale V, Labanca S, Zucchini N, Fichera A, Di Marco V, Leutner M, Venere R, Picciotto A, Lucà M, Mulinacci G, Palermo A, Gerussi A, D'Amato D, Elisabeth O'Donnell S, Cerini F, De Benedittis C, Malinverno F, Ronca V, Mancuso C, Cazzagon N, Ciaccio A, Barisani D, Marzioni M, Floreani A, Alvaro D, Gaudio E, Invernizzi P, Carpino G, Nardi A, Carbone M; Italian PBC Registry. Accuracy of Transient Elastography in Assessing Fibrosis at Diagnosis in Naïve Patients With Primary Biliary Cholangitis: A Dual Cut-Off Approach. *Hepatology* 2021; **74**: 1496-1508 [PMID: 33724515 DOI: 10.1002/hep.31810]

79 **Fujinaga Y**, Namisaki T, Takaya H, Tsuji Y, Suzuki J, Shibamoto A, Kubo T, Iwai S, Tomooka F, Takeda S, Fujimoto Y, Enomoto M, Murata K, Ishida K, Ogawa H, Takagi H, Ozutsumi T, Furukawa M, Nishimura N, Sawada Y, Kitagawa K, Sato S, Kaji K, Kawaratani H, Moriya K, Noguchi R, Akahane T, Mitoro A, Yoshiji H. Enhanced liver fibrosis score as a surrogate of liver-related complications and mortality in primary biliary cholangitis. *Medicine (Baltimore)* 2021; **100**: e27403 [PMID: 34596167 DOI: 10.1097/MD.0000000000027403]

80 **Manesis EK**, Schina M, Vafiadis I, Gatos I, Theotokas J, Zoumpoulis P, Drazinos P, Ketikoglou J, Delladetsima IK, Tiniakos DG. Liver stiffness measurements by 2-dimensional shear wave elastography compared to histological and ultrasound parameters in primary biliary cholangitis. *Scand J Gastroenterol* 2021; **56**: 1187-1193 [PMID: 34375562 DOI: 10.1080/00365521.2021.1928277]

81 **Avcioğlu U**, Eruzun H, Ustaoğlu M. The gamma-glutamyl transferase to platelet ratio for noninvasive evaluation of liver fibrosis in patients with primary biliary cholangitis. *Medicine (Baltimore)* 2022; **101**: e30626 [PMID: 36221370 DOI: 10.1097/MD.0000000000030626]

82 **Garrido I**, Liberal R, Macedo G. Perfomance of vibrationcontrolled transient elastography in primary biliary cholangitis. *Hepatology* 2022; **76**: S1483-S1483 [DOI: 10.1002/hep.32697]

83 **Corpechot C**, Gaouar F, El Naggar A, Kemgang A, Wendum D, Poupon R, Carrat F, Chazouillères O. Baseline values and changes in liver stiffness measured by transient elastography are associated with severity of fibrosis and outcomes of patients with primary sclerosing cholangitis. *Gastroenterology* 2014; **146**: 970-9; quiz e15 [PMID: 24389304 DOI: 10.1053/j.gastro.2013.12.030]

84 **Bowlus CL**, Montano-Loza AJ, Invernizzi P, Chazouillères O, Hirschfield G, Metselaar HJ, Goodman Z, Myers RP, Aguilar R, Subramanian GM, McHutchison JG, Chapman R, Muir AJ, Eksteen B, Levy C. Liver stiffness measurement by transient elastography for the prediction of fibrosis in patients with primary sclerosing cholangitis in a randomized trial of simtuzumab. *J Hepatol* 2016; **64**: S434

85 **Eaton JE**, Dzyubak B, Venkatesh SK, Smyrk TC, Gores GJ, Ehman RL, LaRusso NF, Gossard AA, Lazaridis KN. Performance of magnetic resonance elastography in primary sclerosing cholangitis. *J Gastroenterol Hepatol* 2016; **31**: 1184-1190 [PMID: 26691631 DOI: 10.1111/jgh.13263]

86 **Ehlken H**, Wroblewski R, Corpechot C, Arrivé L, Rieger T, Hartl J, Lezius S, Hübener P, Schulze K, Zenouzi R, Sebode M, Peiseler M, Denzer UW, Quaas A, Weiler-Normann C, Lohse AW, Chazouilleres O, Schramm C. Validation of Transient Elastography and Comparison with Spleen Length Measurement for Staging of Fibrosis and Clinical Prognosis in Primary Sclerosing Cholangitis. *PLoS One* 2016; **11**: e0164224 [PMID: 27723798 DOI: 10.1371/journal.pone.0164224]

87 **Krawczyk M**, Ligocka J, Ligocki M, Raszeja-Wyszomirska J, Milkiewicz M, Szparecki G, Ilczuk T, Górnicka B, Zieniewicz K, Krawczyk M, Lammert F, Milkiewicz P. Does transient elastography correlate with liver fibrosis in patients with PSC? Laennec score-based analysis of explanted livers. *Scand J Gastroenterol* 2017; **52**: 1407-1412 [PMID: 28851259 DOI: 10.1080/00365521.2017.1370009]

88 **Umetsu S**, Inui A, Sogo T, Komatsu H, Fujisawa T. Usefulness of serum Wisteria floribunda agglutinin-positive Mac-2 binding protein in children with primary sclerosing cholangitis. *Hepatol Res* 2018; **48**: 355-363 [PMID: 29168311 DOI: 10.1111/hepr.13004]



Published by **Baishideng Publishing Group Inc**
7041 Koll Center Parkway, Suite 160, Pleasanton, CA 94566, USA
Telephone: +1-925-3991568
E-mail: bpgoffice@wjgnet.com
Help Desk: https://www.f6publishing.com/helpdesk
https://www.wjgnet.com

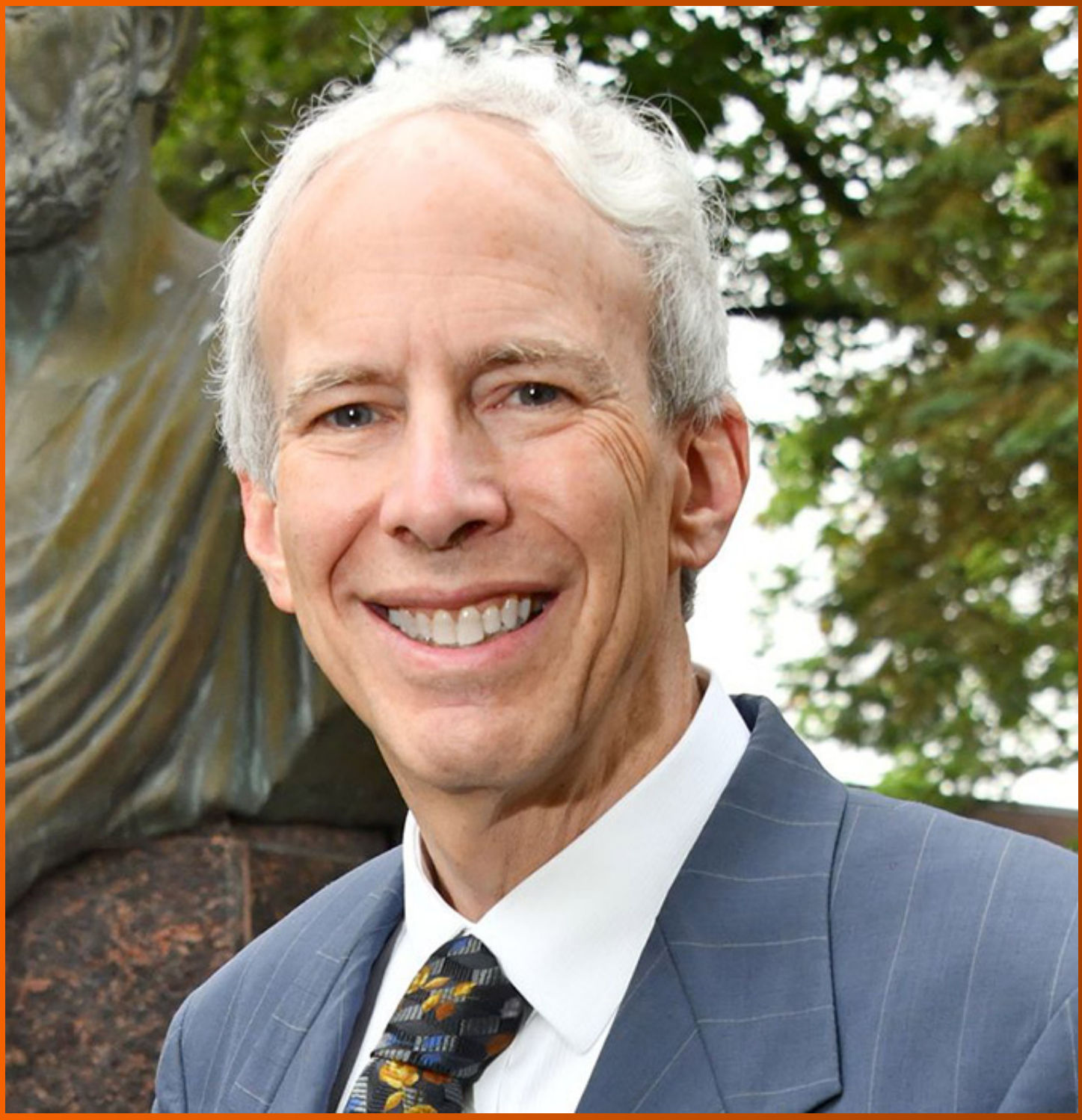


© 2023 Baishideng Publishing Group Inc. All rights reserved.

ISSN 1007-9327 (print)
ISSN 2219-2840 (online)

World Journal of *Gastroenterology*

World J Gastroenterol 2023 October 28; 29(40): 5526-5617



Published by Baishideng Publishing Group Inc

World Journal of Gastroenterology

Contents

Weekly Volume 29 Number 40 October 28, 2023

REVIEW

5526 Overview on the endoscopic treatment for obesity: A review

Abdulla M, Mohammed N, AlQamish J

ORIGINAL ARTICLE

Basic Study

5543 Roles of phosphatidylinositol-3-kinases signaling pathway in inflammation-related cancer: Impact of rs10889677 variant and buparlisib in colitis-associated cancer

Razali NN, Raja Ali RA, Muhammad Nawawi KN, Yahaya A, Mohd Rathi ND, Mokhtar NM

Retrospective Study

5557 Endoscopic transgastric fenestration versus percutaneous drainage for management of (peri)pancreatic fluid collections adjacent to gastric wall (with video)

Zhang HM, Ke HT, Ahmed MR, Li YJ, Nabi G, Li MH, Zhang JY, Liu D, Zhao LX, Liu BR

5566 Clinical significance of programmed cell death-ligand expression in small bowel adenocarcinoma is determined by the tumor microenvironment

Hoshimoto A, Tatsuguchi A, Hamakubo R, Nishimoto T, Omori J, Akimoto N, Tanaka S, Fujimori S, Hatori T, Shimizu A, Iwakiri K

Observational Study

5582 Expression characteristics of peripheral lymphocyte programmed death 1 and FoxP3^{+} Tregs in gastric cancer during surgery and chemotherapy

Li H, Cao GM, Gu GL, Li SY, Yan Y, Fu Z, Du XH

SCIENTOMETRICS

5593 Advances and key focus areas in gastric cancer immunotherapy: A comprehensive scientometric and clinical trial review (1999-2023)

Li YN, Xie B, Zhang Y, He MH, Xing Y, Mu DM, Wang H, Guo R

World Journal of Gastroenterology

Weekly Volume 29 Number 40 October 28, 2023

Contents

ABOUT COVER

Associate Editor of *World Journal of Gastroenterology*, Marc D Basson, MD, PhD, MBA, Professor, Departments of Surgery and Anatomy and Neurobiology, and Dean, College of Medicine, Northeast Ohio Medical University, Rootstown, OH 44272, United States. mbasson@neomed.edu

AIMS AND SCOPE

The primary aim of *World Journal of Gastroenterology* (*WJG*, *World J Gastroenterol*) is to provide scholars and readers from various fields of gastroenterology and hepatology with a platform to publish high-quality basic and clinical research articles and communicate their research findings online. *WJG* mainly publishes articles reporting research results and findings obtained in the field of gastroenterology and hepatology and covering a wide range of topics including gastroenterology, hepatology, gastrointestinal endoscopy, gastrointestinal surgery, gastrointestinal oncology, and pediatric gastroenterology.

INDEXING/ABSTRACTING

The *WJG* is now abstracted and indexed in Science Citation Index Expanded (SCIE), MEDLINE, PubMed, PubMed Central, Scopus, Reference Citation Analysis, China Science and Technology Journal Database, and Superstar Journals Database. The 2023 edition of Journal Citation Reports® cites the 2022 impact factor (IF) for *WJG* as 4.3; Quartile category: Q2. The *WJG*'s CiteScore for 2021 is 8.3.

RESPONSIBLE EDITORS FOR THIS ISSUE

Production Editor: *Yu-Xi Chen*; **Production Department Director:** *Xu Guo*; **Editorial Office Director:** *Jia-Ru Fan*.

NAME OF JOURNAL

World Journal of Gastroenterology

ISSN

ISSN 1007-9327 (print) ISSN 2219-2840 (online)

LAUNCH DATE

October 1, 1995

FREQUENCY

Weekly

EDITORS-IN-CHIEF

Andrzej S Tarnawski

EXECUTIVE ASSOCIATE EDITORS-IN-CHIEF

Xian-Jun Yu (Pancreatic Oncology), Jian-Gao Fan (Chronic Liver Disease), Hou-Bao Liu (Biliary Tract Disease), Naohisa Yoshida (Gastrointestinal Endoscopy)

EDITORIAL BOARD MEMBERS

http://www.wjgnet.com/1007-9327/editorialboard.htm

PUBLICATION DATE

October 28, 2023

COPYRIGHT

© 2023 Baishideng Publishing Group Inc

PUBLISHING PARTNER

Shanghai Pancreatic Cancer Institute and Pancreatic Cancer Institute, Fudan University
Biliary Tract Disease Institute, Fudan University

INSTRUCTIONS TO AUTHORS

https://www.wjgnet.com/bpg/gerinfo/204

GUIDELINES FOR ETHICS DOCUMENTS

https://www.wjgnet.com/bpg/GerInfo/287

GUIDELINES FOR NON-NATIVE SPEAKERS OF ENGLISH

https://www.wjgnet.com/bpg/gerinfo/240

PUBLICATION ETHICS

https://www.wjgnet.com/bpg/GerInfo/288

PUBLICATION MISCONDUCT

https://www.wjgnet.com/bpg/gerinfo/208

POLICY OF CO-AUTHORS

https://www.wjgnet.com/bpg/GerInfo/310

ARTICLE PROCESSING CHARGE

https://www.wjgnet.com/bpg/gerinfo/242

STEPS FOR SUBMITTING MANUSCRIPTS

https://www.wjgnet.com/bpg/GerInfo/239

ONLINE SUBMISSION

https://www.f6publishing.com

PUBLISHING PARTNER's OFFICIAL WEBSITE

https://www.shca.org.cn
https://www.zs-hospital.sh.cn

© 2023 Baishideng Publishing Group Inc. All rights reserved. 7041 Koll Center Parkway, Suite 160, Pleasanton, CA 94566, USA

E-mail: bpgoffice@wjgnet.com https://www.wjgnet.com

World Journal of Gastroenterology

Submit a Manuscript: https://www.f6publishing.com

World J Gastroenterol 2023 October 28; 29(40): 5526-5542

DOI: 10.3748/wjg.v29.i40.5526

ISSN 1007-9327 (print) ISSN 2219-2840 (online)

REVIEW

Overview on the endoscopic treatment for obesity: A review

Maheeba Abdulla, Nafeesa Mohammed, Jehad AlQamish

Specialty type: Gastroenterology and hepatology

Provenance and peer review: Unsolicited article; Externally peer reviewed.

Peer-review model: Single blind

Peer-review report's scientific quality classification

Grade A (Excellent): 0
Grade B (Very good): B, B
Grade C (Good): 0
Grade D (Fair): D
Grade E (Poor): 0

P-Reviewer: Rabago LR, Spain; Seretis C, Greece; Osera S, Japan

Received: August 3, 2023
Peer-review started: August 3, 2023
First decision: September 5, 2023
Revised: September 15, 2023
Accepted: October 23, 2023
Article in press: October 23, 2023
Published online: October 28, 2023

Maheeba Abdulla, Jehad AlQamish, Department of Internal Medicine, Ibn Al Nafees Hospital, Manama 54533, Bahrain

Nafeesa Mohammed, Department of Intensive Care Unit, Salmaniya Medical Complex, Manama 5616, Bahrain

Corresponding author: Maheeba Abdulla, MD, MRCP, Consultant Physician, Gastroenterologist & Hepatologist, Department of Internal Medicine, Ibn Al Nafees Hospital, No. 3302 Road, Manama 54533, Bahrain. amaheeba@hotmail.com

Abstract

Obesity rates have increased, and so has the need for more specific treatments. This trend has raised interest in non-surgical weight loss techniques that are novel, safe, and straightforward. Thus, the present review describes the endoscopic bariatric treatment for obesity, its most recent supporting data, the questions it raises, and its future directions. Various endoscopic bariatric therapies for weight reduction, such as intragastric balloons (IGBs), aspiration therapy (AT), small bowel endoscopy, endoscopic sleeve gastroplasty, endoluminal procedures, malabsorption endoscopic procedures, and methods of regulating gastric emptying, were explored through literature sourced from different databases. IGBs, AT, and small bowel endoscopy have short-term effects with a possibility of weight regain. Minor adverse events have occurred; however, all procedures reduce weight. Vomiting and nausea are common side effects, although serious complications have also been observed.

Key Words: Overweight; Gastric bypass; Malabsorption; Intragastric balloons

©The Author(s) 2023. Published by Baishideng Publishing Group Inc. All rights reserved.

Core Tip: To enhance endoscopic intervention effectiveness and patent satisfaction, the research recommends device design, procedures, patient selection, and personalized therapy. Endoscopists, bariatric surgeons, and researchers must collaborate to solve problems, improve patient comfort, and reduce treatment risks. Effective weight maintenance through endoscopic methods and patient education requires comprehensive and long-term follow-up. Robotic-assisted endoscopy and tissue-engineered implants may revolutionize obesity treatment and patient outcomes in five to ten years.

Citation: Abdulla M, Mohammed N, AlQamish J. Overview on the endoscopic treatment for obesity: A review. *World J Gastroenterol* 2023; 29(40): 5526-5542
URL: https://www.wjgnet.com/1007-9327/full/v29/i40/5526.htm
DOI: https://dx.doi.org/10.3748/wjg.v29.i40.5526

INTRODUCTION

Obesity prevalence has increased dramatically over the last thirty years, now approaching 35% in men and 40% in women[1]. Obesity affects 39 million children, 340 million teenagers, and 650 million adults worldwide. This figure is still rising; by 2025, 167 million children and adults will have suffered as a result of being obese or overweight[2]. As a multi-faceted illness with pandemic proportions, obesity is prevalent nowadays. Since 1975, obesity prevalence has virtually tripled during the last three decades globally, primarily due to an increase in sedentary behavior and intake of less nutrient-dense foods[3]. There are severe public health issues with obesity[4]. Such as diabetes, hyperlipidemia, mortality all-causes, and all-cause cardiovascular mortality[5]. In 2015, the World Obesity Federation established World Obesity Day as a day of commitment and action to promote an integrated, cross-sector approach to combating obesity[6]. A new index for Obesity-Non-Communicable Disease Preparedness is presented in the World Obesity Federation report; worries about the consequences of inactivity for already vulnerable people have grown. The top 30 most prepared countries are all high-income countries, whereas the least prepared 30 are all lower-middle and low-income countries[7]. Obesity-related yearly healthcare costs are predicted to total 1.2 trillion USD globally by 2025[6].

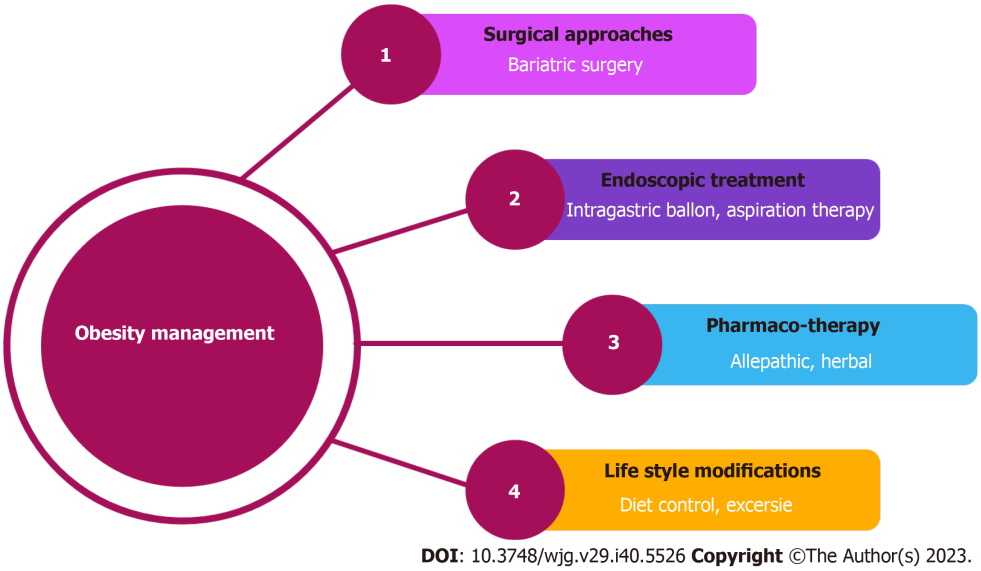
A bio-socio-ecological framework, in which biological predisposition, environmental factors, and socioeconomic factors interact to promote the deposition and proliferation of adipose tissue, can explain the process of persistence and development of obesity[8]. In wealthy nations, poverty and obesity appear to be related. However, a more thorough examination of the empirical literature leads one to believe that the relationship between income and obesity is more nuanced because it can be either positive or negative, or it can alter as nations grow older[9]. Among the numerous therapies for obesity, pharmaceutical substances, surgical procedures, and lifestyle changes can be used[10] as shown in Figure 1.

Despite being the least invasive and expensive approach, lifestyle changes have been demonstrated to be the least effective[11]. Adults with obesity can lose > 5% of their body weight with many sessions of intensive behavioral interventions, such as identification of different barriers, peer support, and self-monitoring of weight, combined with dietary plans, lifestyle modifications, and increased exercise[12]. The central nervous system, adipose tissue, gastrointestinal hormones, liver, kidney, and skeletal muscle are only a few of the systems and tissues that are now modulated by some anti-obesity drugs under investigation[13]. Bariatric surgery is currently the only treatment that causes significant and long-lasting decrease in body weight[14]. However, even if there are clinically significant comorbidities (metabolic, psychological, *etc.*), patients with a body mass index (BMI) of 35 kg/m^2 or over are not suitable for bariatric surgery. Only a small number of eligible patients can potentially benefit from bariatric surgery[15]. This may be due to various reasons, such as a less favorable risk-benefit profile, as higher BMI levels often correlate with increased surgical complications, postoperative mortality, and reduced success rates[16]. Additionally, the potential benefits of surgery, such as weight loss and improvement in comorbidities, might be outweighed by the surgical risks and associated challenges in this specific BMI range. Moreover, alternative interventions, including lifestyle modifications, pharmacotherapy, and non-surgical interventions, might be considered more appropriate due to the complexities posed by the patient's heightened obesity levels. However, carefully assessing individual risks and benefits remains essential in determining the most suitable treatment approach[17]. Lastly, advanced studies have questioned the longevity of bariatric surgery due to the regular occurrence of weight regain and adverse effects[17].

Endoscopic procedures can be used in a multidisciplinary approach to managing obesity. Endoscopists should become familiar with the gastrointestinal pathology that might develop after bariatric surgery, such as malnutrition, anastomotic stenosis, acid reflux, gallstone disease, leaks, fistulas, and weight gain[17]. The creation of new obesity treatment modalities without a high operational risk is the current area of research; thus, obesity endoscopic management is garnering major attention. Endoscopy has an indisputable role in the assessment and management of bariatric surgery complications as well as the evaluation of patients in the preoperative stage of the procedure[18]. Additionally, in order to lower the risks associated with surgery connected to obesity, endoscopic techniques have been employed as a "bridge to surgery"[19]. Thus, the present review describes the present endoscopic treatment for obesity, the most recent data supporting it, the questions, and the future directions the field will face in the next ten years.

BARIATRIC ENDOSCOPY

Endoscopic weight loss therapies have been developed as a result of increased interest and innovation in the fields of gastroenterology and endoscopy, as well as the proven results of bariatric surgery for weight loss[20]. Although surgery is a successful approach for weight loss, it is constrained by its high resource requirements and low patient acceptance [21]. However, endoscopic bariatric therapy (EBT) may be more effective than anti-obesity medicines[22]. Endoscopic weight loss procedures are becoming more popular in Western countries where obesity has escalated rapidly[23]. Indeed, EBT has demonstrated outstanding results in the treatment of obesity and associated surgical consequences[24], therefore, must be included in the arsenal in the battle against obesity[25]. In fact, EBT has evolved into a significant tool for exami-



DOI: 10.3748/wjg.v29.i40.5526 **Copyright** ©The Author(s) 2023.

Figure 1 Different approaches for the management of obesity.

nation, diagnosis, surgical complication management[26] and even primary bariatric therapies[27]. It can also be a more effective alternative than dietary and lifestyle changes[28]. Additionally, EBTs are being used increasingly as a treatment therapy option for obesity in different settings due to their minimally intrusive nature and ease of administration. These treatments induce weight loss primarily by reducing meal volume and promoting early satiety[29]. Currently, a wide range of endoscopic procedures, based on the principles of stomach volume reduction, small bowel or gastric bypass, and size restriction, are being investigated, with a few being used in daily practice[30]. Innovative endoscopic therapies, such as double-pigtail stents, septostomy, and endoscopic vacuum therapy, have been developed[31]. Newer endoscopic approaches, such as intragastric balloons (IGBs), aspiration therapy (AT), small bowel devices, and endoscopic plication and suturing techniques, have been developed[32] and show significant effects.

Space occupying techniques

Space-occupying devices limit stomach capacity, thus reducing hunger and food intake as a result. There are various versions of silicon-made balloons that can be filled with liquid or air. Because of its reduced likelihood for issues, the most popular type is the non-adjustable liquid-filled balloon. The mechanism of action is multifaceted, with neurohormonal and physiological alterations involved[33]. Generally, there are two types of space-occupying techniques: Intragastric fluid filled balloons, and intragastric air or gas filled balloons.

IGBs (fluid filled)

Over 20000 papers have been published in the previous 20 years covering a wide range of topics connected to the effects of the IGBs, including weight reduction outcomes, complications, hormonal impacts, quality of life (QoL), and other aspects[34]. IGBs are invasive therapies that are used to enhance satiety by neuroendocrine and mechanical mechanisms [35] as well as limiting stomach capacity as a space-occupying device, resulting in decreased food intake and hunger[33]. The Bubble (Garren-Edwards) was the first-developed IGB in 1985. The Food and Drug Administration (FDA) of the United States approved it as a temporary weight loss device[36]. IGB therapy is helpful in decreasing weight and improving depression, anxiety, symptoms of eating disorders, and overall QoL in obese individuals primarily within 6 mo of device placement and when used in tandem with conventional therapies[37] and found to be more effective in pre-obese individuals[38]. Although significant morbidity is possible, it is a useful way to lose weight when implemented in conjunction with dietary modifications and physical exercise[39]. However, due to the consequent regain of weight, different methods are now favored in adults. Balloons may be an option for less reversible operations in teens, who are more open to lifestyle modification[40]. The drawbacks of IGBs, such as risks during insertion and removal, and unknown long-term weight loss benefits, prevent their widespread use[41]. Considering conscious sedation *vs* general anesthesia during balloon withdrawal, with or without anesthetic intubation, is pivotal due to its potential implications for procedural complications[42]. The choice between these approaches hinges on patient health status, procedure complexity, and anticipated discomfort. Utilizing conscious sedation may offer benefits like reduced risks associated with intubation but could lead to patient discomfort or inadequate sedation levels, potentially increasing complications[43]. In contrast, employing general anesthesia with intubation might mitigate patient discomfort but could introduce intubation-related risks. Balancing these considerations is essential to optimize patient comfort and procedural safety during balloon withdrawal, and a comprehensive understanding of the relationship between sedation choices and associated complications is critical for informed decision-making. Meanwhile, utilizing a dual-channel gastroscope, specialized foreign body forceps, and a symmetrical snare designed for polyp removal enables a secure, efficient, and straightforward extraction of the balloon. This approach ensures the balloon is removed without any misplacement risk while maintaining patient comfort throughout the procedure[44].

Endoscopically-placed balloons are normally placed in the stomach for no longer than 6 mo, after which they are removed, as they can cause complications[45]. A meta-analysis of 5668 participants found there was moderate indication of improvement in most metabolic markers in participants (IGB therapy *vs* standard non-surgical therapy)[46]. In another review, the total body weight loss (TBWL) of the IGBs after 6-mo implantation was 6.8%-13.2% at 12 mo *i.e.*, 7.6%-11.3% TBWL[47]. Furthermore, 20 randomized controlled trials (RCTs) were used in a meta-analysis involving 1195 patients, indicating significant effects following IGB use[48]. Another similar meta-analysis was comprised of thirteen RCTs with a total of 1523 subjects. At follow-up, the difference in mean % excess weight loss (EWL) was 17.98% [total weight loss (TWL) was 4.40%] and was substantially larger in the IGB group. This concluded that, in overweight and obese individuals, IGB therapy is more effective than lifestyle change alone for weight loss[49]. Additionally, in the RCT, 288 patients were assigned at random to one of two groups: IGB or control group. At 32 wk, the mean TWL in the IGB group was 15% [95% confidence interval (CI): 13.9-16.1] against 3.3% (2-4.6) in the second group which remained as a control without any intervention ($P < 0.0001$). Seven (4%) patients experienced major adverse events (AEs) associated with the device, with no deaths. When therapy was combined with lifestyle changes, substantial weight loss was obtained and sustained for 6 mo after IGB removal[50]. A 10-year review was performed and initially, 49 patients (IGB *vs* control group) were included with a 51.6% follow-up rate. TBWL favored the IGB group at 6 mo [9.75 *vs* 7.48 kg ($P = 0.03$)], at 12 mo [6.52 *vs* 4.42 kg ($P = 0.05$)], at 18 mo [5.42 *vs* 3.57 ($P = 0.32$)], and 24 mo [4.07 *vs* 2.93 kg ($P = 0.56$)]. TWL at 10 years was 0.03 *vs* -2.32 kg ($P = 0.05$) and %TWL was -0.16% ± 12.8% *vs* -2.84% ± 5.6% ($P = 0.39$), which were not statistically different between groups. BMI at follow-up [30.97 ± 1.6 *vs* 30.38 ± 1.8 kg/m^2 ($P = 1.00$)] was comparable and it was concluded that IGB provides weight loss for up to two years and is superior to the control[51]. In contrast, in one of the studies only 2910 (0.4%) of the 652927 individuals identified received IGB treatment. Patients who received IGB therapy were older, had a lower BMI at baseline (37.0 ± 6.2 kg/m^2 *vs* 45.3 ± 7.8 kg/m^2), and had a greater rate of early non-operative re-intervention (7.7% *vs* 1.1%; $P < 0.0001$). Between 2016 and 2019, according to the Metabolic and Bariatric Surgery Accreditation and Quality Improvement Program the number of IGB procedures reported decreased considerably [953 (0.62%) *vs* 418 (0.25%); $P < 0.0001$]. Given the safety and efficacy of current bariatric surgery and novel pharmaceutical treatments for weight loss, the function of IGBs in treating obesity remains uncertain[52]. In another study, the mean preoperative BMI for all 20680 IGBs, encompassing 12 distinct models, was 34.05 kg/m^2. On average 17.66% ± 2.5% of TBWL was noted. There were 3.62% early removals because of intolerance. Consensual management had an AE rate of 0.70% and 6.37% for major and mild problems, respectively. Only one death was reported[53]. In short, many patients have benefited from the IGBs, which bridges the gap between clinical management of obesity, medications, and bariatric surgery while also helping thousands of patients lose weight and improve their comorbidities[34]. A summary is also described in Table 1.

The United States FDA has approved three IGBs. Orbera is an endoscopically implanted single balloon[54]. ReShape is a duo balloon system, connected in the middle by a tube. The third balloon, Obalon (Figure 2), is filled with nitrogen gas and is part of a three-balloon treatment. All systems require endoscopic placement and removal after 6 mo[55].

A single balloon (Orbera IGB)

The Orbera IGB (OIB) is a single fluid filled IGB authorized for weight loss induction and obesity treatment[56]. The FDA-approved Orbera is a single 13 cm silicone-made balloon that arrives commercially deflated and is inflated at the end by a filling tube connected to a radiopaque self-sealing valve. Following a diagnostic endoscopy, the balloon implantation assembly is inserted directly into the stomach, and a volume of 500 to 700 mL saline solution [this volume range (500 to 700 mL) is chosen based on optimal balloon expansion and effective positioning within the stomach] with 5 mL of methylene blue used for balloon inflation *via* a closed infusion system, with the entire procedure being performed under direct endoscopic observation[57,58]. The FDA has approved Orbera for a 6-mo placement in people with a BMI of 30-40 kg/m^2. To rule out contraindications, such as a big hiatal hernia or a stomach ulcer, an endoscopy should be performed before or concurrently with placement[54].

Orbera® meets the obesity therapy "preservation and incorporation of valuable endoscopic innovations" thresholds of 5% TBWL and 15% EWL over control, respectively[59]. Similarly, a review of a database of individuals who had the OIB endoscopically placed revealed that it was effective, safe at inducing weight loss, and reduced complications related to obesity[56]. There were no spontaneous deflations observed in employing the OIB system. In this device, deflation can be detected through weight changes or patient-reported loss of satiety; however, current practice mandates a very simple method of detection through observing any irregular change in urine output[60].

A double balloon system (ReShape Integrated Dual Balloon System)

The ReShape IGB is a temporary implantation of a fluid-filled balloon that is designed to encourage weight loss by occupying space in the stomach. Endoscopy is utilized to deliver the balloon trans-orally. After positioning, inflation is done with saline (sterile) and methylene blue, which is used as an indicator in case the balloon mistakenly leaks or deflates. The balloon can remain in the stomach for six months[61].

In one study, total body weight was found to be lowered by 6.8% ± 7.3% ($P < 0.001$) and BMI was reduced by 2.7 ± 2.9 kg/m^2 ($P < 0.001$) in all patients who had the ReShape IGB implanted, with completed follow-up of 6 mo. According to subgroup analyses, patients with > 40 kg/m^2 BMIs reported significant reductions in TBWL and BMI[61].

A three-balloon system

The three-balloon system is made up of three distinct balloons. These are placed through the mouth and subsequently filled with gas nitrogen to a capacity of roughly 250 mL by a connected catheter. One balloon is implanted monthly, with a maximum of three balloons. All balloons are removed endoscopically six months after the placement of the first balloon. The anticipated TBWL is 7.1%[62]. In one study, a swallowable gas-filled IGB device was deemed safe after six months

Table 1 A summary of endoscopic procedures for reducing weight in obese patients

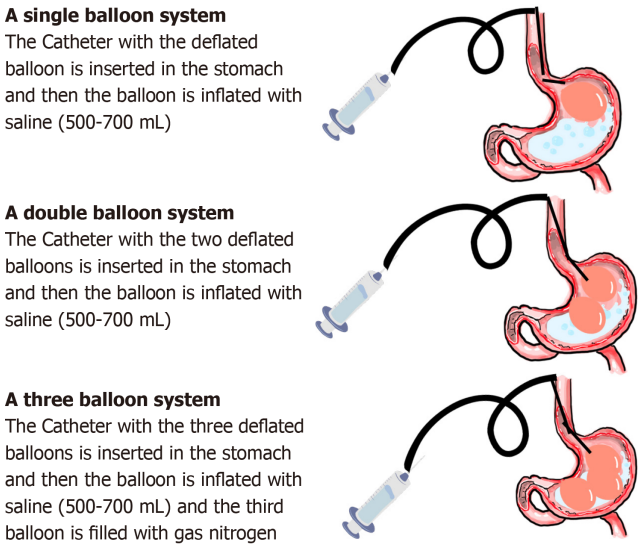
Method	Indication (BMI)	Duration	Efficacy	Adverse events	Limitations	Ref.
IGBs	30-40 kg/m^2	6 mo	IGB therapy is a successful short-term weight loss strategy	Nausea/vomiting and stomach pain were the most common consequences, but mortality and gastric perforation were unusual. Other serious problems included dehydration, which required hospitalization, and intestinal obstruction due to balloon deflation, which required surgery	Short-term effects and weight regain	[45, 48, 50, 54, 87]
AT	35-55 kg/m^2	Long term usage	AT is an implantable device that drains a portion of the stomach contents after each meal, removing up to 30% of the calories consumed	Postoperative peristomal granulation tissue and peristomal irritation, cardiac arrhythmias, hypokalemia, hypochloremic hypokalemic metabolic alkalosis, rather than gastric botox and eating problems	It cannot be used for patients with eating disorders. For this technology to be effective and long-lasting, significant patient commitment, motivation, and adherence are necessary. In addition to adhering to correct device operation, chewing food thoroughly is a significant crucial aspect in attaining successful weight reduction using this device; thus, patients who fail to stick to thoroughly chewing their meal are unlikely to get ideal outcomes	[91, 94, 99]
Small bowel endoscopic procedures	41.5 kg/m^2	6-12 mo	10.6% TBWL and 40.2% EWL after one year	There were no AEs, and the nausea and diarrhea were self-limiting	Short-term efficacy, no small bowel EBTs are currently FDA-approved	[32, 83, 102, 103, 150]
Endoscopic sleeve gastroplasty	> 30 kg/m^2	6-24 mo	%TBWL 12%-19% [150]	Leaks, perforation, hemorrhage, improved depth perception, improved visualization, severe stomach discomfort, and perigastric collection are all possible AEs	Required expertise and skills	[105, 111, 119, 150]
Endoluminal procedures	30-40 kg/m^2	6-12 mo	41.5 kg/m^2, which reduced to 33.1 kg/m^2	Pain, nausea, and vomiting	N/A	[129, 130]
DJBS	> 35 kg/m^2	6-12 mo	Effective patients lost 15% of their body weight at 12 mo, compared to 4% of controls	Nausea, vomiting, pancreatitis, GI bleeds, hepatic abscess, obstruction of the sleeve	As the common channel length shortens, so do diarrhea and severe vitamin A and D deficits	[132, 135, 137-139]
GJBS	30-40 kg/m^2	N/A	Patients reduced 39.7% of their excess	N/A	N/A	[140, 141]
Regulation gastric emptying	N/A	N/A	Weight loss was within 10% of their optimum weight	N/A	Hormonal imbalance and weight regain	[148, 149]

IGBs: Intragastric balloons; AT: Aspiration therapy; TBWL: Total body weight loss; EWL: Excess weight loss; N/A: Not applicable; GJBS: Gastroduodenal jejunal bypass sleeve; DJBS: Duodenal-jejunal bypass sleeve; GI: Gastrointestinal; AEs: Adverse events; EBT: Endoscopic bariatric therapy; FDA: Food and Drug Administration; BMI: Body mass index.

and resulted in double the weight loss than a sham control, with significant weight loss maintenance at 48 wk[63]. However, a study with 87 individuals who were successfully implanted with IGBs (gas-filled IGB; fluid-filled IGB) showed no differences in %TBWL between balloon systems at removal and 12 mo (P = 0.39). Although both gastric balloon systems were equally effective, the gas filled IGB had fewer significant side effects[64].

Orbera 365 balloon

The revolutionary ORBERA 365® balloon, made by Apollo Endosurgery, can remain within the stomach for a full year, hence its name[65,66]. Up to this point, limited studies with clinical data have been published. In one study, 97 individuals had an Orbera365 implanted. Prior to the treatment, the average weight and BMI of participants were 93.8 kg and 35.2 kg/m^2, respectively. After the procedure, these values decreased to 80.6 kg and 29.8 kg/m^2 after 8.2 mo and to 82.4 kg and 30.4 kg/m^2 on the last day of follow-up after 12.9 mo[62]. In another study, the weight reduction at IGB (Orbera) removal after 6 mo and at IGB (Orbera 365) removal after 12 mo was retrospectively examined. Mean TBWL was 15.2 and 15.8 kg in patients undergoing IGB placement for 6 and 12 mo, respectively. In patients receiving IGB placement for 6 or 12 mo, there was no discernible change in the mean %TBWL (15.3% *vs* 14.7%, P = 0.7)[67].



DOI: 10.3748/wjg.v29.i40.5526 **Copyright** ©The Author(s) 2023.

Figure 2 Different types of intra-gastric balloon system.

IGBS (AIR-FILLED)

IGBs, like air-filled balloons, as a temporary endoscopic treatment for obesity, have the potential to play an important role for the obese population[54]. They can also be used as a preoperative test before doing restricted bariatric surgery on patients. Furthermore, an intragastric device can be used as a "bridge treatment" before major surgery in individuals with severe obesity to lower the risk of operation-related complications[68]. Furthermore, IG balloons play a pivotal role as a transitional measure before bariatric surgery by serving as a bridge to reduce BMI and potentially mitigate the associated surgical risks. IGBs help patients achieve a lower BMI by facilitating initial weight loss, which may lead to improved overall health and decreased comorbidities. This reduction in BMI can also contribute to decreased surgical complications during subsequent bariatric procedures. Acting as a preoperative intervention, IGBs offer a safer trajectory for individuals with high BMI, allowing them to undergo bariatric surgery with potentially reduced morbidity and an enhanced surgical outcome. According to research, the air-filled balloon is effective and well tolerated, with weight reduction comparable to other types of balloons[69].

The air-filled IGB has not been shown to be harmful. It appears to have the same effect on weight loss as other balloons. After removal of the balloon, 30% of the patients in one study sustained a weight decrease of more than 10%[70]. However, in a comparative study, patients undergoing saline-filled balloon therapy (4.66 ± 4.75) lost considerably more weight than patients undergoing air-filled balloon surgery ($P < 0.001$). The variation in early withdrawal rates between the two groups, on the other hand, was minor ($P = 0.21$)[71]. With the air-filled IGB, the balloon is inflated with a specific gas, such as air or a mixture of air and nitrogen, using a catheter or a small tube connected to the balloon. The gas inflates the balloon, causing it to expand and take up space within the stomach[41].

Obalon

The United States FDA approved Obalon for the treatment of obesity[72]. This device, which is swallowed as a gel at the end of thin tubing, can be used anywhere. The device is then filled with a gas, and fluoroscopy is used to ensure proper installation. As a result, removal requires only one endoscopic treatment[73].

In one study, patients were randomly assigned to receive 3 balloon capsules (Obalon) or three sugar filled dummy capsules in a RCT with 15 facilities in the United States. A licensed dietician provided lifestyle advice to all subjects every three weeks. The treatment group's %TBWL was 6.81% ± 5.1%, while the control group's TBWL was 3.59% ± 5.0%. In the therapy group, the responder rate was 64.3%, defined as %TBWL > 5%. Minor AEs, such as abdominal pain and nausea, occurred in most patients, with only one serious AE, which was a gastric ulcer in a patient who violated the research protocol by using a nonsteroidal anti-inflammatory medicine[71]. Mion *et al*[74] reported a prospective feasibility study, and all balloons were retrieved *via* upper gastrointestinal (GI) endoscopy 12 wk after the ingestion of the first balloon. Of the 44 balloon swallowing attempts, 43 (98%) were successful. Nausea and stomach pain were the most common AEs. Significant weight reduction was reported as well[64].

Heliosphere

The Heliosphere Bag is a silicone-encased air-filled polymer balloon[74]. When compared to fluid-filled balloons, this endoscopy-inserted device weighs less than 30 g, shows a 30-fold weight reduction, and it is certified for 6-mo use[41]. This device demonstrates a high effectiveness and tolerance profile. Loss of weight seems to be comparable to that of other types of balloons. In contrast, technical issues, particularly during removal, are most likely related to the device's substance and create a low safety profile[74].

In one study, the average weight reduction and BMI drop were 14.5 ± 8.2 kg and 5.3 ± 2.8 kg/m^2, respectively (P < 0.001). During the first week after Heliosphere Bag implantation, 7.4% of patients experienced nausea and vomiting[75]. Even though mid/long-term follow-up may result in some weight gain, Heliosphere® BAG allows for short-term loss of weight with few AEs[76]. Furthermore, De Castro *et al*[77] showed comparable weight reduction outcomes. Meanwhile, fluid-filled balloons are found to be more beneficial for weight loss[77]. In addition, a life-threatening complication was also reported in a patient using Heliosphere Bag[78].

Elipse

The Elipse balloon is a unique non-endoscopic weight loss approach[79]. At 16 wk, the Elipse IGB is naturally excreted out as it is a swallowable balloon[80]. Although Elipse has a shorter residence period in the stomach than other standard IGBs that need endoscopy, the procedure appears to have identical results[81]. Vomiting and nausea are the most common AEs. There were no major AEs[82].

In prospective research, 51 Elipse insertions were performed, and the patients' total weight reduction was 8.84 kg, %EWL 40.84%, %TBWL 10.44%, and change in BMI 3.42 kg/m^2. The device was proven to be effective; however, several limits were discovered that must be overcome for improved results[83]. Furthermore, a meta-analysis showed that the Elipse IGB is effective in weight reduction, safe, and is an efficient obesity technology with a low AE profile. A study conducted in Italy found early results after 4 mo with a mean %EWL of 26%. There were no balloon passage issues in the included patients[84].

COMPLICATIONS WITH IGBS

Despite the extremely low rates of difficulties and death linked with IGBs, AEs and complications can occur, and they can range from mild to severe[85]. The most prevalent AEs reported were vomiting, nausea, and stomach pain, while fatalities and gastric perforation were uncommon[86]. However, a 58-year-old Pakistani female presented with 2 wk of vomiting and abdominal bloating. While the external pigtail catheter and blue clasp for retrieval were stretching into D1/D2, the balloon was impacted at the antrum and pylorus. This is a relatively uncommon IGB complication[87]. Other severe complications included dehydration, which necessitated hospitalization, and intestinal blockage induced by balloon deflation, requiring surgery[88].

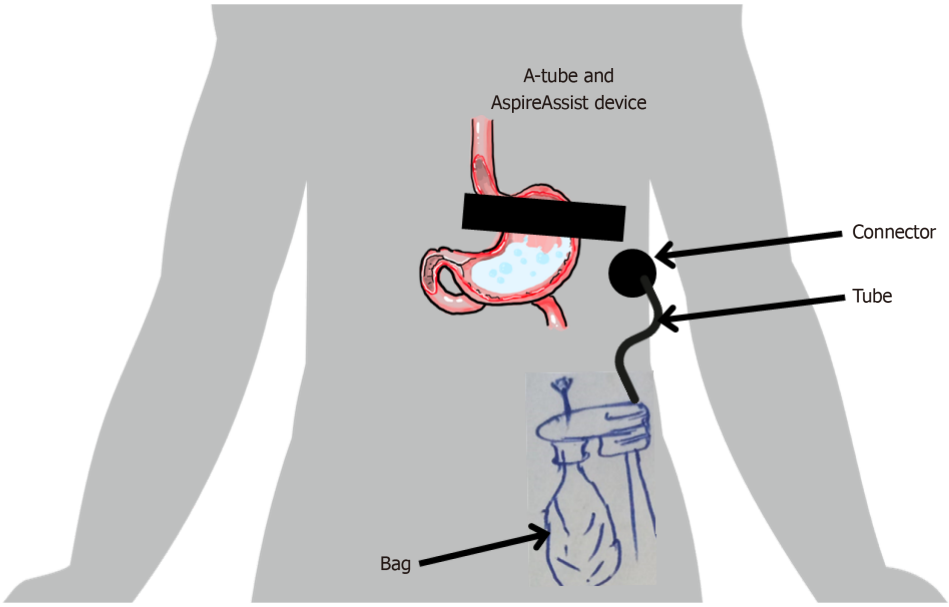
In conclusion, fluid-filled balloons are much more likely to result in weight loss than gas-filled balloons. They may, however, be associated with a higher likelihood of intolerance and removal. This data will assist clinicians in selecting devices and engaging patients in collaborative decision-making[89].

AT

The AspireAssist AT is the first FDA-approved device for the treatment of class II and III obesity[90]. AT comprises an endoscopic placement of a gastrostomy tube (A-tube) and an AspireAssist siphon component to aspirate gastric contents 20 min after meal consumption[91] (Figure 3), in conjunction with lifestyle modifications and an external device to allow drainage of around 30% of the calories taken in a meal[92]. It is approved for long-term usage in persons with BMIs of 35-55 kg/m^2 in the United States[93].

Studies show 14.2% to 21.5% TBWL in participants who complete one year of treatment and weight loss maintenance when treated for two years[94]. A pilot study was conducted, and patients in the AT group dropped 18.6% ± 2.3% of their body weight with 49.0% ± 7.7% EWL after one year, while in the lifestyle therapy group patients lost 5.9% ± 5.0% and 14.9% ± 12.2% EWL (P < 0.04). AT was found to be effective and safe as a long-term obesity weight loss therapy[95]. Similarly, a multicenter study with 82 individuals was carried out where the patients' average baseline BMI was 41.6 ± 4.5 kg/m^2. At the conclusion of the first year, participants had 34.1 ± 5.4 kg/m^2 BMI and 18.3% ± 8.0% TWL. Patients experienced 15.3% TWL after 2 years, 16.6% after 3 years and 18.7% TWL after 4 years with a significant difference (P < 0.01). The safety profile of AT was found to be satisfactory, effective, and approved for long-term weight loss treatment. Additionally, AT was found to be a safe and effective therapy for reducing weight as the mean percent total weight reduction was 18.2% ± 9.4%, 19.8% ± 11.3%, 21.3% ± 9.6%, and 19.2% ± 13.1%, at 1, 2, 3, and 4 years, respectively[96]. Similarly, a study with 25 obese participants was undertaken, and after 2 years of AT, BMI was 31.0 ± 5.1 kg/m^2, P < 0.01, and EWL was 61.5% ± 28.5%, P < 0.01. It was concluded that AT is a safe and efficient treatment for obesity, and weight loss enhances QoL[97]. Furthermore, the effects were not limited to obesity; comorbidities related to obesity, such as diabetes, blood pressure, triglycerides, and lipoproteins, were significantly improved with AT[98].

However, the most commonly observed AEs with AT were perioperative discomfort and stomach pain as well as postoperative peristomal granulation tissue and peristomal irritation[91]. This can cause more serious hypokalemia, cardiac arrhythmias, and hypochloremic hypokalemic metabolic alkalosis than gastric botox. Some eating disorders can also be caused by AT[99]. Indeed, gastric irrigation and aspiration may result in persistent loss of chloride and hydrogen ions. The physiologic response is renal potassium ion secretion and hydrogen ion resorption; hypochloremic hypokalemic metabolic alkalosis may occur[100].



DOI: 10.3748/wjg.v29.i40.5526 **Copyright** ©The Author(s) 2023.

Figure 3 Schematic illustration of aspire assist device when in place.

SMALL BOWEL ENDOSCOPIC BARIATRIC TECHNIQUE

Endoscopic bariatric therapies for the small bowel include incisionless anastomosis devices (IAS), bypass sleeves and duodenal mucosal resurfacing. Endoscopic bariatric treatments can be performed safely and efficiently for weight loss and metabolic improvement, according to clinical evidence, employing tiny intestinal devices[98]. These therapies focus on foregut and hindgut processes to achieve weight loss and enhance glucose homeostasis[101]. When fully deployed, the IAS magnets form an octagonal shape. Pairs of IAS magnets are inserted into distinct segments of the small bowel, *via* simultaneous enteroscopy and colonoscopy, and are connected under endoscopic and fluoroscopic view[102].

In a research pilot, ten patients with a 41 kg/m^2 mean BMI had the operation. Laparoscopy was performed in this pilot study to establish appropriate magnet coupling and to validate limb lengths. The anastomosis developed in about a week, and the magnets were ejected without any pain or hindrance. At the 2 and 6-mo follow-up endoscopies, all anastomoses were patented. After six months, the patient had a 10.6% TBWL and 40.2% EWL after one year, and all anastomosis endured a patent[103]. There were no AEs. Diarrhea and nausea were self-limiting[102], as shown in Table 1.

ENDOSCOPIC SLEEVE GASTROPLASTY

Endoscopic sleeve gastroplasty (ESG) is a newer type of noninvasive weight loss procedure that uses a suturing device [104]. The endoscopist uses sutures to form a tube-like configuration in the stomach to promote restriction. If diet and exercise are not working and one is extremely overweight (BMI of 30 or higher), this treatment may be possible (Table 1). The technique is minimally invasive, which reduces the risk of operational impediments and allows for a speedy return to normal activities[105]. Additionally, the overstitch system also includes a double-channel endoscope with a suturing platform attached to it. A tissue grasper device is used to mobilize and capture the desired position of the suture on the stomach wall, after which the tissue is retracted into the device's suturing arm [106].

A recent study discovered that a customized running suture adopting a Z-pattern had a good effect on producing a homogeneous distribution of the suture's disruptive force across all stitch positions[107] and a "U" stitch pattern was also used[108]. Furthermore, a review of seven of the eight trials with adequate data revealed a weight loss which was statistically significant ($P < 0.05$). In an RCT, for the ESG group, the primary endpoint of mean %EWL was 49.2%, and for the control group, it was 32% at 52 wk ($P < 0.00001$). ESG had a significant weight loss, which was sustained at 104 wk and is also safe, with significant improvements in metabolic comorbidities[109]. Similarly, in another study, 435 patients from various obesity classes were included. At all-time intervals, ESG had a significantly higher %TBWL, TBWL, and BMI decrease in class III obesity compared to obesity of classes I and II ($P < 0.001$). In all types of obesity, ESG causes considerable weight loss[110]. Furthermore, efficacy was well established in a multicenter study conducted with 91 patients, and after treatment, BMI reduction after 3 mo was 7.3, after 6 mo 9.3, and after 12 mo 8.6 from baseline. EBWL was 17.3% after one month, 29.2% after three months, and 35.6% after six months with significant difference ($P < 0.000$)[111]. In addition, a meta-analysis was performed, the ESG resulted in around 15% TBWL or 58% EWL at 6-mo, and there was sustainability in weight loss at 12, 18, and 24 mo[112]. However, a study found laparoscopic sleeve gastrectomy (LSG) to be more efficient than ESG as it improved weight related QoL significantly[113]. Seven studies in a meta-analysis encompassed 6775 patients, with 3413 undergoing ESG and 3362 undergoing LSG procedures. Notable disparities were observed in the percentage of %TBWL, all of which favored LSG over ESG. While there was a tendency towards a decreased occurrence

of AEs with ESG compared to LSG, this distinction did not achieve statistical significance [risk ratio (RR) = 0.51, 95%CI: 0.23-1.11, P = 0.09]. The frequency of new-onset gastroesophageal reflux disease was markedly lower following ESG as opposed to LSG, at 1.3% compared to 17.9%, respectively (RR = 0.10, 95%CI: 0.02-0.53, P = 0.006)[114]. Moreover, a total of 2188 patients (1429 for LSG and 759 for ESG) from sixteen studies were included in another meta-analysis. The mean percentage of %EWL was 80.32% (± 12.20%; 95%CI; P = 0.001; I^2 = 98.88) for the LSG group and 62.20% (± 4.38%; 95%CI; P = 0.005; I^2 = 65.52) for the ESG group. This represents an absolute difference of 18.12% (± 0.89%; 95%CI, P = 0.0001) between the two groups. The variation in the average rate of AEs was 0.19% (± 0.37%; 95%CI; χ^2 = 1.602; P = 0.2056)[115]. Similarly, ESG results in weight loss comparable to LSG, with similar improvements in comorbidity resolution and safety profiles was shown in another study[116].

Meanwhile, around 2.3% of patients had serious post-procedure issues; nevertheless, no deaths were documented [117]. Leaks, perforation, bleeding[112], better depth perception, better visualization[118], severe abdominal pain and a perigastric collection[119] have all been reported. Intraabdominal collection, refractory symptoms requiring ESG reversal, hemorrhage requiring transfusion or endoscopic intervention, pneumoperitoneum and pneumothorax and pulmonary embolism[120] are among the serious AEs that have been documented.

In conclusion, as with any weight loss intervention, the success of the ESG procedure can be influenced by factors such as patient adherence to lifestyle changes, dietary habits, and individual metabolic factors. Comparing the lasting utility of ESG with LSG, a surgical procedure, the latter has a longer track record and more established data on long-term outcomes. LSG has demonstrated sustained weight loss and metabolic improvements over several years. However, it is essential to note that LSG is a more invasive procedure with potential surgical risks and complications. When evaluating the choice between ESG and LSG, patients and healthcare providers should consider the balance between the invasiveness of the procedure and the expected long-term outcomes, as well as individual patient preferences and medical considerations.

ENDOLUMINAL PROCEDURES

Endoluminal procedures performed exclusively using gastrointestinal flexible endoscopy provide safer and more cost-effective alternatives to currently used surgical techniques for obesity management. However, endoscopic gastroplasty is one of the promising applications of endoluminal procedures in the field of metabolic obesity disorder[121]. Several endoluminal treatments for the loss of weight in obese patients have been developed, claiming to be as effective as surgery but safer[122]. Endoluminal obesity treatments show promise, and recent technology breakthroughs have been amazing. However, new therapies have had to meet the same requirements as present surgical treatments[123]. In fact, until the success of endoluminal treatments was proven, most surgeons were unwilling to consider them for their patients [124].

The transoral gastroplasty (TOGA) method conducts a vertical gastroplasty along the smaller curvature of the stomach using transoral endoscopy[125]. As a result, a gastric pouch forms, which restricts the food quantity or liquids that the patient can intake, resulting in an early feeling of fullness[126]. Another technique is the incisionless operating platform (IOP) which is used in primary obesity surgery endoluminal (POSE). The IOP is a four-part device used to regulate a full-thickness plication system endoscopically. It delivers a series of anchors into the stomach to encourage gastric imbrication [127].

In a systematic review, it was concluded that endoluminal plication devices were more successful in 91.8% of patients with 5.02% lower recurrence rates than sclerotherapy and Argon Plasma coagulation, which also had 46.8% success and 21.5% recurrence rates, respectively[128]. The same findings were reported in a multicenter trial with a one-year follow-up that included 67 patients with a mean BMI of 41.5 kg/m^2, which decreased to 33.1 kg/m^2 at 6 mo after TOGA treatment, with consequences including respiratory insufficiency and an asymptomatic pneumoperitoneum[129]. In a 12-mo multicenter RCT in the United States, 221 patients got the POSE surgery in conjunction with low-intensity lifestyle interventions. They attained a TBWL of 4.95% ± 7.04% against 1.38% ± 5.58% in the sham group with complications such as pain, nausea, and vomiting also reported[130].

The POSE and ESG methods are distinct endoscopic approaches for obesity control. Meanwhile, the POSE method involves the creation of tissue folds within the stomach to reduce its size and restrict food intake without removing tissue. In contrast, the ESG method involves suturing and narrowing the stomach's capacity, resembling a sleeve, to induce weight loss. While both methods are minimally invasive and avoid surgical incisions, the POSE method focuses on tissue folding, while the ESG method centers on suturing, leading to different mechanisms of action. The choice between these techniques depends on individual patient characteristics, preferences, and specific weight loss goals.

MALABSORPTIVE ENDOSCOPIC PROCEDURES

Malabsorptive endoscopic procedures may potentially provide an opportunity for an ambulatory technique that is both safer and less expensive than laparoscopic surgery. Endoscopic malabsorptive treatments can result in weight loss and have improved metabolic parameters associated with obesity[131].

Duodenal-jejunal bypass sleeve

The Duodenal-jejunal bypass sleeve (DJBS), known as DJBS is introduced using endoscopic and fluoroscopic methods. This implant consists of a non-porous fluoropolymer sleeve, temporarily anchored within the duodenal bulb and

extending approximately 80 cm into the small intestine, typically ending in the proximal jejunum[132,133]. It allows chyme to move from the stomach to the jejunum without contacting the duodenum. By not allowing mixing with pancreatic exocrine secretions and bile in the jejunum, it replicates a duodenal-jejunal bypass and promotes weight reduction through malabsorption[123]. Which has similarities to Roux-en-Y gastric bypass (RYGB) and this combined mechanism aims to achieve weight loss by reducing calorie intake and altering nutrient absorption patterns. The DJBS procedure offers a potentially reversible option for individuals with obesity seeking to manage their weight and improve metabolic health[134].

In a cohort trial, after 6 mo of DJBS treatment, there was a substantial rise in EWL and a drop in weight[135]. Similarly, a blinded, randomized, prospective clinical trial was carried out to assess the safety and efficacy of a new device for obese weight loss. The DJBS device was successfully implanted. At the end of the three-month research period, the device was removed endoscopically. The patient's TBWL was 9.09 kg[136]. Additionally, in another multicenter study, RCT was conducted with 41 patients and the EndoBarrier Gastrointestinal Liner device was implanted. After 3 mo, the mean EWL for the intervention group was 19% *vs* 6.9% for control patients ($P < 0.002$). The BMI absolute change was 5.5 and 1.9 kg/m^2, respectively. The device was discovered to be a practical and safe noninvasive weight loss device with outstanding short-term weight loss results[133]. Similar to previous research, in a multicenter open-label RCT, 24% of DJBS patients lost 15% of their body weight at 12 mo, compared to 4% of controls (odds ratio = 8.3, 95%CI: 1.8-39; $P = 0.007$). The inclusion of the DJBS to intense medical care was linked to greater weight loss and improvements in QoL[137]. However, significant weight recovery happens during long-term follow-up after device removal, particularly in people with BMIs larger than 35 kg/m^2[138].

In total, 3.7% of patients experienced serious AEs such as pancreatitis (2 cases), GI bleeds (7 cases), hepatic abscess, obstruction of the sleeve, and esophageal tears[139]. There were no reported fatalities. Mild AEs primarily comprised nausea, vomiting, and anchor ulceration. Meanwhile, the attachment point of the DJBL was responsible for inducing or potentially inducing 85% of the SAEs[140].

Gastroduodenal-jejunal bypass sleeve

The gastroduodenal jejunal bypass sleeve (GJBS) treatment can help patients lose weight while also managing comorbidities such as diabetes, hypertension, and obstructive sleep apnea[15]. In theory, this device is the same as the EndoBarrier®. Its sleeve, on the contrary, is attached at the esophagogastric junction and continues about 120 cm through the stomach into the small bowel, imitating the ultimate anatomical structure in RYGB surgery. As a result, food passes immediately from the esophagus to the intestine, with no nutritional absorption occurring in the stomach, duodenum, or jejunum[141].

In one study, the GJBS was implanted in 24 patients. These patients reduced 39.7% of their excess weight by the end of the study. AEs were limited and resolved after the endoscopic device was removed[142]. Similarly, the implementation and retrieval were both safe. It is generally tolerated and has a favorable safety profile. It provides effective weight loss results, with more than 70% of all comorbidities cured or improved[143].

REGULATING GASTRIC EMPTYING

Changes in gastrointestinal motility, which are critical in food absorption and digestion in the gastrointestinal tract, may be one of the reasons why obesity develops[144]. The functions of incretins, particularly glucagon-like peptide-1, gastric inhibitory polypeptide, peptide tyrosine-tyrosine, glucagon, the duodenal and pancreatic hormones motilin, amylin, motilin, and the gastric orexigenic hormones ghrelin have the greatest impact on stomach emptying. Except for ghrelin and motilin, which accelerate stomach emptying, all these hormones delay gastric emptying[144]. The vagus nerve regulates the change in fundic compliance (also known as accommodation) once food enters the stomach, allowing the stomach to develop a reservoir with just a slight increase in intragastric pressure, boosting food intake[145,146]. Changes in circulating gut hormone concentrations activate a variety of pathways, especially in the brain stem and hypothalamus, which influence eating behavior and a variety of metabolic progressions[147]. In addition, gastric emptying inhibition may contribute to a decrease in energy intake. Mechanoreceptor activation caused by stomach distension may restrict additional food intake *via* neuronal reflex arcs[148]. However, diet-induced weight reduction causes long-term alterations in gut hormones for appetite, which are thought to favor increased desire and weight regain[149].

In an experimental study, the subjects were all subjected to quantitative fluid/solid gastric emptying experiments using a dual radionuclide method. In the solid phase, obese patients had a faster emptying rate than nonobese subjects ($P < 0.05$). Repeat gastric emptying investigations on four obese participants whose weight loss was within 10% of their optimum weight found no change in liquid or solid emptying rates. Obese patients have an abnormally fast rate of solid stomach emptying[150].

FUTURE DIRECTIONS

The future directions as follows: (1) A customized step-up approach aimed at improving and sustaining health performance is ideal, such as lifestyle therapies, nutrition modification, psychiatric treatment, medication and, if necessary, bariatric surgery; (2) In obese patients, EBTs successfully control metabolic comorbidities, improve overall weight loss and lower adverse risk events; (3) There should be some proper peer-reviewed guidelines for the implementation of

EBTs; (4) Studies should be conducted to increase the efficacy of EBTs as they are effective for a short time, and the problem of weight regain is also observed in EBTs, which should also be addressed; (5) Due to the vast variety of accessible therapies, the majority of which are not FDA-approved, first, there is a need to follow FDA and other quality control organizations to get approval; (6) There is a lack of a consistent therapeutic strategy, as well as a lack of training programs, which has limited their distribution and usage, short training programs should be organized and, if possible, should be added in the curriculum of medical schools; (7) Sophisticated endoscopy is now becoming a major component of minimally invasive fellowships, preparing surgeons to take on the role of bariatric endoscopists; (8) Cost benefits analysis should be made for a better understanding of the total expenditure on the use of therapy; and (9) Longer follow-up and larger multicenter RCTs are required to confirm current outcomes and improve the standardization process of these procedures.

CONCLUSION

Obesity is a chronic systemic disease that requires a multidisciplinary approach for prevention, treatment, and management. Proper treatment must be personalized and tailored to the degree of the patient's obesity and the combination of comorbidities. According to different studies, lifestyle changes and medicines can only achieve moderate weight loss results. Despite the fact that bariatric surgery has been shown to be a game-changing strategy in obesity, many patients find it unappealing due to its adverse effect profile and potential long-term difficulties. Compared to standard surgical treatments, bariatric endoscopic therapies may offer a valuable armamentarium in the therapy of obesity because their success in loss of weight is accompanied by being less intrusive, reversible, cost-effective and having a positive safety profile. It may become increasingly popular in the coming years because, when compared to surgery, it has a lower chance of AEs. Long-term efficacy is unknown at this moment. Additional research on long-term efficacy, metabolic disease outcomes, and RCTs is required. However, the future of obesity treatment lies in a multidisciplinary strategy requiring various treatment methods.

FOOTNOTES

Author contributions: Abdulla M, Mohammed N, and AlQamish J contributed to the colleting the data, review, editing, and finalizing the manuscript; Abdulla M designed the review and wrote the manuscript.

Conflict-of-interest statement: All the authors report no relevant conflicts of interest for this article.

Open-Access: This article is an open-access article that was selected by an in-house editor and fully peer-reviewed by external reviewers. It is distributed in accordance with the Creative Commons Attribution NonCommercial (CC BY-NC 4.0) license, which permits others to distribute, remix, adapt, build upon this work non-commercially, and license their derivative works on different terms, provided the original work is properly cited and the use is non-commercial. See: https://creativecommons.org/Licenses/by-nc/4.0/

Country/Territory of origin: Bahrain

ORCID number: Maheeba Abdulla 0000-0001-5319-2892; Nafeesa Mohammed 0000-0003-4718-9325; Jehad AlQamish 0000-0001-8597-9913.

S-Editor: Wang JJ
L-Editor: A
P-Editor: Wang JJ

REFERENCES

1 **Flegal KM**, Kruszon-Moran D, Carroll MD, Fryar CD, Ogden CL. Trends in Obesity Among Adults in the United States, 2005 to 2014. *JAMA* 2016; **315**: 2284-2291 [PMID: 27272580 DOI: 10.1001/jama.2016.6458]

2 **World Health Organization**. World Obesity Day 2022–Accelerating action to stop obesity. [cited 15 June 2023]. Available from: https://www.who.int/news/item/04-03-2022-world-obesity-day-2022-accelerating-action-to-stop-obesity

3 **Boutari C**, Mantzoros CS. A 2022 update on the epidemiology of obesity and a call to action: as its twin COVID-19 pandemic appears to be receding, the obesity and dysmetabolism pandemic continues to rage on. *Metabolism* 2022; **133**: 155217 [PMID: 35584732 DOI: 10.1016/j.metabol.2022.155217]

4 **Wang L**, Zhou B, Zhao Z, Yang L, Zhang M, Jiang Y, Li Y, Zhou M, Wang L, Huang Z, Zhang X, Zhao L, Yu D, Li C, Ezzati M, Chen Z, Wu J, Ding G, Li X. Body-mass index and obesity in urban and rural China: findings from consecutive nationally representative surveys during 2004-18. *Lancet* 2021; **398**: 53-63 [PMID: 34217401 DOI: 10.1016/S0140-6736(21)00798-4]

5 **Adams KF**, Schatzkin A, Harris TB, Kipnis V, Mouw T, Ballard-Barbash R, Hollenbeck A, Leitzmann MF. Overweight, obesity, and mortality in a large prospective cohort of persons 50 to 71 years old. *N Engl J Med* 2006; **355**: 763-778 [PMID: 16926275 DOI: 10.1056/NEJMoa055643]

6 **Peng W**, Zhang J, Zhou H, Zhang A, Wang Y, Tian X, Wen D. Obesity intervention efforts in China and the 2022 World Obesity Day. *Globa Health J* 2002; **6**: 118-121 [DOI: 10.1016/j.glohj.2022.07.007]

7 **Lobstein T**, Brinsden H, Neveux M. World Obesity Atlas 2022. London: World Obesity Federation, 2022

8 **Jebeile H**, Kelly AS, O'Malley G, Baur LA. Obesity in children and adolescents: epidemiology, causes, assessment, and management. *Lancet Diabetes Endocrinol* 2022; **10**: 351-365 [PMID: 35248172 DOI: 10.1016/S2213-8587(22)00047-X]

9 **Mathieu-Bolh N**. The elusive link between income and obesity. *J Econ Surv* 2022; **36**: 935-968 [DOI: 10.1111/joes.12458]

10 **Fisher BL**, Schauer P. Medical and surgical options in the treatment of severe obesity. *Am J Surg* 2002; **184**: 9S-16S [PMID: 12527344 DOI: 10.1016/s0002-9610(02)01173-x]

11 **Wing RR**, Goldstein MG, Acton KJ, Birch LL, Jakicic JM, Sallis JF Jr, Smith-West D, Jeffery RW, Surwit RS. Behavioral science research in diabetes: lifestyle changes related to obesity, eating behavior, and physical activity. *Diabetes Care* 2001; **24**: 117-123 [PMID: 11194216 DOI: 10.2337/diacare.24.1.117]

12 **US Preventive Services Task Force**, Curry SJ, Krist AH, Owens DK, Barry MJ, Caughey AB, Davidson KW, Doubeni CA, Epling JW Jr, Grossman DC, Kemper AR, Kubik M, Landefeld CS, Mangione CM, Phipps MG, Silverstein M, Simon MA, Tseng CW, Wong JB. Behavioral Weight Loss Interventions to Prevent Obesity-Related Morbidity and Mortality in Adults: US Preventive Services Task Force Recommendation Statement. *JAMA* 2018; **320**: 1163-1171 [PMID: 30326502 DOI: 10.1001/jama.2018.13022]

13 **Angelidi AM**, Belanger MJ, Kokkinos A, Koliaki CC, Mantzoros CS. Novel Noninvasive Approaches to the Treatment of Obesity: From Pharmacotherapy to Gene Therapy. *Endocr Rev* 2022; **43**: 507-557 [PMID: 35552683 DOI: 10.1210/endrev/bnab034]

14 **Albaugh VL**, Abumrad NN. Surgical treatment of obesity. *F1000Res* 2018; **7** [PMID: 29904577 DOI: 10.12688/f1000research.13515.1]

15 **Buchwald H**, Avidor Y, Braunwald E, Jensen MD, Pories W, Fahrbach K, Schoelles K. Bariatric surgery: a systematic review and meta-analysis. *JAMA* 2004; **292**: 1724-1737 [PMID: 15479938 DOI: 10.1001/jama.292.14.1724]

16 **Ri M**, Aikou S, Seto Y. Obesity as a surgical risk factor. *Ann Gastroenterol Surg* 2018; **2**: 13-21 [PMID: 29863119 DOI: 10.1002/ags3.12049]

17 **McCarty TR**, Kumar N. Revision Bariatric Procedures and Management of Complications from Bariatric Surgery. *Dig Dis Sci* 2022; **67**: 1688-1701 [PMID: 35347535 DOI: 10.1007/s10620-022-07397-9]

18 **Asge Standards of Practice Committee**, Anderson MA, Gan SI, Fanelli RD, Baron TH, Banerjee S, Cash BD, Dominitz JA, Harrison ME, Ikenberry SO, Jagannath SB, Lichtenstein DR, Shen B, Lee KK, Van Guilder T, Stewart LE. Role of endoscopy in the bariatric surgery patient. *Gastrointest Endosc* 2008; **68**: 1-10 [PMID: 18577471 DOI: 10.1016/j.gie.2008.01.028]

19 **Behary J**, Kumbhari V. Advances in the Endoscopic Management of Obesity. *Gastroenterol Res Pract* 2015; **2015**: 757821 [PMID: 26106413 DOI: 10.1155/2015/757821]

20 **Mccarty TR**, Thompson CC. Bariatric endoscopy. In: Wang TC, Camilleri M, Lebwohl B, Wang KK, LOK AS, Wu GD, Sandborn WJ, editors. Yamada's Textbook of Gastroenterology, 3 Volume Set, 7th ed. New Jersey: Willey-Blackwell, 2022

21 **Staudenmann DA**, Sui Z, Saxena P, Kaffes AJ, Marinos G, Kumbhari V, Aepli P, Sartoretto A. Endoscopic bariatric therapies for obesity: a review. *Med J Aust* 2021; **215**: 183-188 [PMID: 34333788 DOI: 10.5694/mja2.51179]

22 **Saunders KH**, Igel LI, Saumoy M, Sharaiha RZ, Aronne LJ. Devices and Endoscopic Bariatric Therapies for Obesity. *Curr Obes Rep* 2018; **7**: 162-171 [PMID: 29667157 DOI: 10.1007/s13679-018-0307-x]

23 **Tawadros A**, Makar M, Kahaleh M, Sarkar A. Overview of bariatric and metabolic endoscopy interventions. *Ther Adv Gastrointest Endosc* 2020; **13**: 2631774520935239 [PMID: 32964206 DOI: 10.1177/2631774520935239]

24 **Reja D**, Zhang C, Sarkar A. Endoscopic bariatrics: current therapies and future directions. *Transl Gastroenterol Hepatol* 2022; **7**: 21 [PMID: 35548475 DOI: 10.21037/tgh.2020.03.09]

25 **de Moura DTH**, Dantas ACB, Ribeiro IB, McCarty TR, Takeda FR, Santo MA, Nahas SC, de Moura EGH. Status of bariatric endoscopy-what does the surgeon need to know? A review. *World J Gastrointest Surg* 2022; **14**: 185-199 [PMID: 35317547 DOI: 10.4240/wjgs.v14.i2.185]

26 **De Moura DTH**, Jirapinyo P, Thompson CC. 2022b. Training in Bariatric Endoscopy. In: Cohen J. Successful Training in Gastrointestinal Endoscopy, 2nd ed. New Jersey: John Wiley & Sons Ltd, 2022

27 **Malli CP**, Sioulas AD, Emmanouil T, Dimitriadis GD, Triantafyllou K. Endoscopy after bariatric surgery. *Ann Gastroenterol* 2016; **29**: 249-257 [PMID: 27366025 DOI: 10.20524/aog.2016.0034]

28 **Mehta A**, Sharaiha RZ. Bariatric and metabolic endoscopy: impact on obesity and related comorbidities. *Ther Adv Gastrointest Endosc* 2021; **14**: 26317745211019156 [PMID: 34179778 DOI: 10.1177/26317745211019156]

29 **Negi A**, Asokkumar R, Ravi R, Lopez-Nava G, Bautista-Castaño I. Nutritional Management and Role of Multidisciplinary Follow-Up after Endoscopic Bariatric Treatment for Obesity. *Nutrients* 2022; **14** [PMID: 36014956 DOI: 10.3390/nu14163450]

30 **Král J**, Machytka E, Horká V, Selucká J, Doleček F, Špičák J, Kovářová V, Haluzík M, Bužga M. Endoscopic Treatment of Obesity and Nutritional Aspects of Bariatric Endoscopy. *Nutrients* 2021; **13** [PMID: 34959819 DOI: 10.3390/nu13124268]

31 **Castro M**, Guerron AD. Bariatric endoscopy: current primary therapies and endoscopic management of complications and other related conditions. *Mini-invasive Sur* 2020; **4**: 47 [DOI: 10.20517/2574-1225.2020.14]

32 **Dolan RD**, Schulman AR. Endoscopic Approaches to Obesity Management. *Annu Rev Med* 2022; **73**: 423-438 [PMID: 34554827 DOI: 10.1146/annurev-med-042320-125832]

33 **Silva LB**, Neto MG. Intragastric balloon. *Minim Invasive Ther Allied Technol* 2022; **31**: 505-514 [PMID: 33571068 DOI: 10.1080/13645706.2021.1874420]

34 **Neto MG**, Silva LB, Usuy Jr EN, Campos JM. Intragastric Balloon for Weight Management: A Practical Guide. Switzerland: Springer International, 2020

35 **Lari E**, Burhamah W, Lari A, Alsaeed T, Al-Yaqout K, Al-Sabah S. Intra-gastric balloons - The past, present and future. *Ann Med Surg (Lond)* 2021; **63**: 102138 [PMID: 33664941 DOI: 10.1016/j.amsu.2021.01.086]

36 **Gleysteen JJ**. A history of intragastric balloons. *Surg Obes Relat Dis* 2016; **12**: 430-435 [PMID: 26775045 DOI: 10.1016/j.soard.2015.10.074]

37 **Pietrabissa G**, Bertuzzi V, Simpson S, Guerrini Usubini A, Cattivelli R, Bertoli S, Mozzi E, Roviaro G, Castelnuovo G, Molinari E. Psychological Aspects of Treatment with Intragastric Balloon for Management of Obesity: A Systematic Review of the Literature. *Obes Facts* 2022; **15**: 1-18 [PMID: 34818229 DOI: 10.1159/000518200]

38 **Carvalho GL**, Barros CB, Moraes CE, Okazaki M, Ferreira Mde N, Silva JS, de Albuquerque PP, Coelho Rde M. The use of an improved intragastric balloon technique to reduce weight in pre-obese patients--preliminary results. *Obes Surg* 2011; **21**: 924-927 [PMID: 19756895 DOI: 10.1007/s11695-009-9947-y]

39 **Zafar S**, Haque I, Farooq M, Bashir H, Khan GM, Chaudry NU. Intra-gastric balloon for weight loss: preliminary analysis of efficacy & tolerability. *P J M H S* 2014; **8**: 224-229

40 **Sachdev P**, Reece L, Thomson M, Natarajan A, Copeland RJ, Wales JK, Wright NP. Intragastric balloon as an adjunct to lifestyle programme in severely obese adolescents: impact on biomedical outcomes and skeletal health. *Int J Obes (Lond)* 2018; **42**: 115-118 [PMID: 28871150 DOI: 10.1038/ijo.2017.215]

41 **Choi SJ**, Choi HS. Various Intragastric Balloons Under Clinical Investigation. *Clin Endosc* 2018; **51**: 407-415 [PMID: 30257544 DOI: 10.5946/ce.2018.140]

42 **Messina T**, Genco A, Favaro R, Maselli R, Torchia F, Guidi F, Razza R, Aloi N, Piattelli M, Lorenzo M. Intragastric balloon positioning and removal: sedation or general anesthesia? *Surg Endosc* 2011; **25**: 3811-3814 [PMID: 21656325 DOI: 10.1007/s00464-011-1794-y]

43 **Tsaousi G**, Fyntanidou B, Stavrou G, Papakostas P, Kotzampassi K, Grosomanidis V. Propofol Sedation for Intragastric Balloon Removal: Looking for the Optimal Body Weight Descriptor. *Obes Surg* 2019; **29**: 3882-3890 [PMID: 31290110 DOI: 10.1007/s11695-019-04075-0]

44 **Galloro G**, Sivero L, Magno L, Diamantis G, Pastore A, Karagiannopulos P, Inzirillo M, Formisano C, Iovino P. New technique for endoscopic removal of intragastric balloon placed for treatment of morbid obesity. *Obes Surg* 2007; **17**: 658-662 [PMID: 17658026 DOI: 10.1007/s11695-007-9110-6]

45 **Sioulas AD**, Polymeros D, Kourikou A, Papanikolaou IS, Triantafyllou K. Intragastric balloon left in the stomach for more than a year: two case reports. *Obes Facts* 2012; **5**: 436-439 [PMID: 22797371 DOI: 10.1159/000341134]

46 **Popov VB**, Ou A, Schulman AR, Thompson CC. The Impact of Intragastric Balloons on Obesity-Related Co-Morbidities: A Systematic Review and Meta-Analysis. *Am J Gastroenterol* 2017; **112**: 429-439 [PMID: 28117361 DOI: 10.1038/ajg.2016.530]

47 **Vargas EJ**, Rizk M, Bazerbachi F, Abu Dayyeh BK. Medical Devices for Obesity Treatment: Endoscopic Bariatric Therapies. *Med Clin North Am* 2018; **102**: 149-163 [PMID: 29156183 DOI: 10.1016/j.mcna.2017.08.013]

48 **Saber AA**, Shoar S, Almadani MW, Zundel N, Alkuwari MJ, Bashah MM, Rosenthal RJ. Efficacy of First-Time Intragastric Balloon in Weight Loss: a Systematic Review and Meta-analysis of Randomized Controlled Trials. *Obes Surg* 2017; **27**: 277-287 [PMID: 27465936 DOI: 10.1007/s11695-016-2296-8]

49 **Kotinda APST**, de Moura DTH, Ribeiro IB, Singh S, da Ponte Neto AM, Proença IM, Flor MM, de Souza KL, Bernardo WM, de Moura EGH. Efficacy of Intragastric Balloons for Weight Loss in Overweight and Obese Adults: a Systematic Review and Meta-analysis of Randomized Controlled Trials. *Obes Surg* 2020; **30**: 2743-2753 [PMID: 32300945 DOI: 10.1007/s11695-020-04558-5]

50 **Abu Dayyeh BK**, Maselli DB, Rapaka B, Lavin T, Noar M, Hussan H, Chapman CG, Popov V, Jirapinyo P, Acosta A, Vargas EJ, Storm AC, Bazerbachi F, Ryou M, French M, Noria S, Molina D, Thompson CC. Adjustable intragastric balloon for treatment of obesity: a multicentre, open-label, randomised clinical trial. *Lancet* 2021; **398**: 1965-1973 [PMID: 34793746 DOI: 10.1016/S0140-6736(21)02394-1]

51 **Chan DL**, Cruz JR, Mui WL, Wong SKH, Ng EKW. Outcomes with Intra-gastric Balloon Therapy in BMI < 35 Non-morbid Obesity: 10-Year Follow-Up Study of an RCT. *Obes Surg* 2021; **31**: 781-786 [PMID: 33034015 DOI: 10.1007/s11695-020-04986-3]

52 **Chow A**, Mocanu V, Verhoeff K, Switzer N, Birch D, Karmali S. Trends in the Utilization of Intragastric Balloons: a 5-Year Analysis of the MBSAQIP Registry. *Obes Surg* 2022; **32**: 1649-1657 [PMID: 35290611 DOI: 10.1007/s11695-022-06005-z]

53 **Espinet Coll E**, Del Pozo García AJ, Turró Arau R, Nebreda Durán J, Cortés Rizo X, Serrano Jiménez A, Escartí Usó MÁ, Muñoz Tornero M, Carral Martínez D, Bernabéu López J, Sierra Bernal C, Martínez-Ares D, Espinel Díez J, Marra-López Valenciano C, Sola Vera J, Sanchis Artero L, Domínguez Jiménez JL, Carreño Macián R, Juanmartiñena Fernández JF, Fernández Zulueta A, Consiglieri Alvarado C, Grecco E, Bezerra Silva L, Galvao Neto M. Spanish Intragastric Balloon Consensus Statement (SIBC): practical guidelines based on experience of over 20 000 cases. *Rev Esp Enferm Dig* 2023; **115**: 22-34 [PMID: 36426855 DOI: 10.17235/reed.2022.9322/2022]

54 **Kumar N**, Sullivan S, Thompson CC. The role of endoscopic therapy in obesity management: intragastric balloons and aspiration therapy. *Diabetes Metab Syndr Obes* 2017; **10**: 311-316 [PMID: 28740414 DOI: 10.2147/DMSO.S95118]

55 **Abu Dayyeh BK**. Intragastric Balloons for Obesity Management. *Gastroenterol Hepatol (N Y)* 2017; **13**: 737-739 [PMID: 29339949]

56 **Vargas EJ**, Pesta CM, Bali A, Ibegbu E, Bazerbachi F, Moore RL, Kumbhari V, Sharaiha RZ, Curry TW, DosSantos G, Schmitz R, Agnihotri A, Novikov AA, Pitt T, Dunlap MK, Herr A, Aronne L, Ledonne E, Kadouh HC, Cheskin LJ, Mundi MS, Acosta A, Gostout CJ, Abu Dayyeh BK. Single Fluid-Filled Intragastric Balloon Safe and Effective for Inducing Weight Loss in a Real-World Population. *Clin Gastroenterol Hepatol* 2018; **16**: 1073-1080.e1 [PMID: 29425781 DOI: 10.1016/j.cgh.2018.01.046]

57 **Giardiello C**, Borrelli A, Silvestri E, Antognozzi V, Iodice G, Lorenzo M. Air-filled vs water-filled intragastric balloon: a prospective randomized study. *Obes Surg* 2012; **22**: 1916-1919 [PMID: 23054576 DOI: 10.1007/s11695-012-0786-x]

58 **Cho JH**, Bilal M, Kim MC, Cohen J; Study Group for Endoscopic Bariatric and Metabolic Therapies of the Korean Society of Gastrointestinal Endoscopy. The Clinical and Metabolic Effects of Intragastric Balloon on Morbid Obesity and Its Related Comorbidities. *Clin Endosc* 2021; **54**: 9-16 [PMID: 33684281 DOI: 10.5946/ce.2020.302]

59 **Abu Dayyeh BK**, Eaton LL, Woodman GF, Fusco M, Shayani V, Billy HT, Courcoulas A, Pambianco DJ, Gostout CJ. A randomized, multi-center study to evaluate the safety and effectiveness of an intragastric balloon as an adjunct to a behavioral modification program, in comparison with a behavioral modification program alone in the weight management of obese subjects. *Gastrointest Endosc* 2015; **81**: AB147 [DOI: 10.1016/j.gie.2015.03.1235]

60 **Vyas D**, Deshpande K, Pandya Y. Advances in endoscopic balloon therapy for weight loss and its limitations. *World J Gastroenterol* 2017; **23**: 7813-7817 [PMID: 29209122 DOI: 10.3748/wjg.v23.i44.7813]

61 **Suchartlikitwong S**, Laoveeravat P, Mingbunjerdsuk T, Vutthikraivit W, Ismail A, Islam S, Islam E. Usefulness of the ReShape intragastric balloon for obesity. *Proc (Bayl Univ Med Cent)* 2019; **32**: 192-195 [PMID: 31191125 DOI: 10.1080/08998280.2018.1559397]

62 **Gollisch KSC**, Raddatz D. Endoscopic intragastric balloon: a gimmick or a viable option for obesity? *Ann Transl Med* 2020; **8**: S8 [PMID: 32309412 DOI: 10.21037/atm.2019.09.67]

63 **Sullivan S**, Swain J, Woodman G, Edmundowicz S, Hassanein T, Shayani V, Fang JC, Noar M, Eid G, English WJ, Tariq N, Larsen M, Jonnalagadda SS, Riff DS, Ponce J, Early D, Volckmann E, Ibele AR, Spann MD, Krishnan K, Bucobo JC, Pryor A. Randomized sham-controlled trial of the 6-month swallowable gas-filled intragastric balloon system for weight loss. *Surg Obes Relat Dis* 2018; **14**: 1876-1889 [PMID: 30545596 DOI: 10.1016/j.soard.2018.09.486]

64 **Swei E**, Almuhaidb A, Sullivan S, Al-Shahrani A, D'Souza FR, Altayar O, Bell S, Maday R, Wagh MS, Mullady D, Bennett M, Early D, Kushnir V. Comparison of the Efficacy and Safety of the FDA-approved Intragastric Balloon Systems in a Clinical Setting. *J Clin Gastroenterol* 2023; **57**: 578-585 [PMID: 35604348 DOI: 10.1097/MCG.0000000000001718]

65 **Jamal MH**, Al-Kanawati N, ElAbd R, Al-Haddad M, AlKhadher T, Hamshari F, Akrouf S. A Study Examining the Orbera365 Intragastric Balloon Safety and Effects on Weight Loss. *Obes Surg* 2021; **31**: 5342-5347 [PMID: 34591263 DOI: 10.1007/s11695-021-05729-8]

66 **Genco A**, Ernesti I, Gualtieri L. Intragastric Occupying Space Devices. In: Testoni PA, Inoue H, Wallace MB. Gastrointestinal and

Pancreatico-Biliary Diseases: Advanced Diagnostic and Therapeutic Endoscopy. Cham: Springer, 2021

67 **Kozłowska-Petriczko K**, Pawlak KM, Wojciechowska K, Reiter A, Błaszczyk Ł, Szełemej J, Petriczko J, Wiechowska-Kozłowska A. The Efficacy Comparison of Endoscopic Bariatric Therapies: 6-Month Versus 12-Month Intragastric Balloon Versus Endoscopic Sleeve Gastroplasty. *Obes Surg* 2023; **33**: 498-505 [PMID: 36525237 DOI: 10.1007/s11695-022-06398-x]

68 **Giuricin M**, Nagliati C, Palmisano S, Simeth C, Urban F, Buri L, Balani A, de Manzini N. Short- and long-term efficacy of intragastric air-filled balloon (Heliosphere® BAG) among obese patients. *Obes Surg* 2012; **22**: 1686-1689 [PMID: 22820924 DOI: 10.1007/s11695-012-0700-6]

69 **Falcão M**, Martins MC. Air-Filled Intragastric Balloon Implant. In: Galvao Neto M, Silva LB, Usuy Jr, EN, Campos JM. Intragastric Balloon for Weight Management: A Practical Guide. Cham: Springer, 2020

70 **Mion F**, Gincul R, Roman S, Beorchia S, Hedelius F, Claudel N, Bory RM, Malvoisin E, Trepo F, Napoleon B. Tolerance and efficacy of an air-filled balloon in non-morbidly obese patients: results of a prospective multicenter study. *Obes Surg* 2007; **17**: 764-769 [PMID: 17879576 DOI: 10.1007/s11695-007-9141-z]

71 **Abdelbadie M**, Hashem M, Fawzy M, Lababidi R, Abbsi S, Nabil M, Fathy A, Almahdy A, Subei I. Air-Filled versus Water-Filled Intragastric Balloon: A Comparative Retrospective Study 1033. *Am J Gastroenterol* 2018; **113**: S587-S589

72 **Tate CM**, Geliebter A. Intragastric Balloon Treatment for Obesity: Review of Recent Studies. *Adv Ther* 2017; **34**: 1859-1875 [PMID: 28707286 DOI: 10.1007/s12325-017-0562-3]

73 **Kazi D**, Khaitan L. Endoscopic Bariatric/Metabolic Surgery. *Digest Dis Interven* 2018; **2**: 375-382

74 **Mion F**, Ibrahim M, Marjoux S, Ponchon T, Dugardeyn S, Roman S, Deviere J. Swallowable Obalon® gastric balloons as an aid for weight loss: a pilot feasibility study. *Obes Surg* 2013; **23**: 730-733 [PMID: 23512445 DOI: 10.1007/s11695-013-0927-x]

75 **Trande P**, Mussetto A, Mirante VG, De Martinis E, Olivetti G, Conigliaro RL, De Micheli EA. Efficacy, tolerance and safety of new intragastric air-filled balloon (Heliosphere BAG) for obesity: the experience of 17 cases. *Obes Surg* 2010; **20**: 1227-1230 [PMID: 19082675 DOI: 10.1007/s11695-008-9786-2]

76 **Lecumberri E**, Krekshi W, Matía P, Hermida C, de la Torre NG, Cabrerizo L, Rubio MÁ. Effectiveness and safety of air-filled balloon Heliosphere BAG® in 82 consecutive obese patients. *Obes Surg* 2011; **21**: 1508-1512 [PMID: 21221835 DOI: 10.1007/s11695-010-0314-9]

77 **De Castro ML**, Morales MJ, Del Campo V, Pineda JR, Pena E, Sierra JM, Arbones MJ, Prada IR. Efficacy, safety, and tolerance of two types of intragastric balloons placed in obese subjects: a double-blind comparative study. *Obes Surg* 2010; **20**: 1642-1646 [PMID: 20390374 DOI: 10.1007/s11695-010-0128-9]

78 **Caglar E**, Dobrucali A, Bal K. Gastric balloon to treat obesity: filled with air or fluid? *Dig Endosc* 2013; **25**: 502-507 [PMID: 23369002 DOI: 10.1111/den.12021]

79 **Drozdowski R**, Wyleżoł M, Frączek M, Hevelke P, Giaro M, Sobański P. Small bowel necrosis as a consequence of spontaneous deflation and migration of an air-filled intragastric balloon - a potentially life-threatening complication. *Wideochir Inne Tech Maloinwazyjne* 2014; **9**: 292-296 [PMID: 25097704 DOI: 10.5114/wiitm.2011.38177]

80 **Ienca R**, Al Jarallah M, Caballero A, Giardiello C, Rosa M, Kolmer S, Sebbag H, Hansoulle J, Quartararo G, Zouaghi SAS, Juneja G, Murcia S, Turro R, Pagan A, Badiuddin F, Dargent J, Urbain P, Paveliu S, di Cola RS, Selvaggio C, Al Kuwari M. The Procedureless Elipse Gastric Balloon Program: Multicenter Experience in 1770 Consecutive Patients. *Obes Surg* 2020; **30**: 3354-3362 [PMID: 32279182 DOI: 10.1007/s11695-020-04539-8]

81 **Ramai D**, Singh J, Mohan BP, Madedor O, Brooks OW, Barakat M, Ofosu A, Khan SR, Chandan S, Dhindsa B, Dhaliwal A, Facciorusso A, McDonough S, Adler DG. Influence of the Elipse Intragastric Balloon on Obesity and Metabolic Profile: A Systematic Review and Meta-Analysis. *J Clin Gastroenterol* 2021; **55**: 836-841 [PMID: 33394629 DOI: 10.1097/MCG.0000000000001484]

82 **Raftopoulos I**, Giannakou A. The Elipse Balloon, a swallowable gastric balloon for weight loss not requiring sedation, anesthesia or endoscopy: a pilot study with 12-month outcomes. *Surg Obes Relat Dis* 2017; **13**: 1174-1182 [PMID: 28372952 DOI: 10.1016/j.soard.2017.02.016]

83 **Machytka E**, Chuttani R, Bojkova M, Kupka T, Buzga M, Stecco K, Levy S, Gaur S. Elipse™, a Procedureless Gastric Balloon for Weight Loss: a Proof-of-Concept Pilot Study. *Obes Surg* 2016; **26**: 512-516 [PMID: 26253980 DOI: 10.1007/s11695-015-1783-7]

84 **Al-Subaie S**, Khalifa S, Buhaimed W, Al-Rashidi S. A prospective pilot study of the efficacy and safety of Elipse intragastric balloon: A single-center, single-surgeon experience. *Int J Surg* 2017; **48**: 16-22 [PMID: 28989057 DOI: 10.1016/j.ijsu.2017.10.001]

85 **Genco A**, Ernesti I, Ienca R, Casella G, Mariani S, Francomano D, Soricelli E, Lorenzo M, Monti M. Safety and Efficacy of a New Swallowable Intragastric Balloon Not Needing Endoscopy: Early Italian Experience. *Obes Surg* 2018; **28**: 405-409 [PMID: 28871497 DOI: 10.1007/s11695-017-2877-1]

86 **Ribeiro IB**, Kotinda APST, Sánchez-Luna SA, de Moura DTH, Mancini FC, de Souza TF, Matuguma SE, Sakai CM, Rocha RSP, Luz GO, Lera Dos Santos ME, Chaves DM, Franzini TAP, de Moura ETH, de Moura EGH. Adverse Events and Complications with Intragastric Balloons: a Narrative Review (with Video). *Obes Surg* 2021; **31**: 2743-2752 [PMID: 33788158 DOI: 10.1007/s11695-021-05352-7]

87 **Yorke E**, Switzer NJ, Reso A, Shi X, de Gara C, Birch D, Gill R, Karmali S. Intragastric Balloon for Management of Severe Obesity: a Systematic Review. *Obes Surg* 2016; **26**: 2248-2254 [PMID: 27444806 DOI: 10.1007/s11695-016-2307-9]

88 **Mujtaba G**, Zehra R, Balkhi F, Shaikh N. Impact of Intragastric Balloon: A Rare Complication. *J Coll Physicians Surg Pak* 2022; **32**: S89-S91 [PMID: 36210657 DOI: 10.29271/jcpsp.2022.Supp2.S89]

89 **Mathus-Vliegen EM**, Alders PR, Chuttani R, Scherpenisse J. Outcomes of intragastric balloon placements in a private practice setting. *Endoscopy* 2015; **47**: 302-307 [PMID: 25479562 DOI: 10.1055/s-0034-1390860]

90 **Bazerbachi F**, Haffar S, Sawas T, Vargas EJ, Kaur RJ, Wang Z, Prokop LJ, Murad MH, Abu Dayyeh BK. Fluid-Filled Versus Gas-Filled Intragastric Balloons as Obesity Interventions: a Network Meta-analysis of Randomized Trials. *Obes Surg* 2018; **28**: 2617-2625 [PMID: 29663250 DOI: 10.1007/s11695-018-3227-7]

91 **Thompson CC**, Abu Dayyeh BK, Kushner R, Sullivan S, Schorr AB, Amaro A, Apovian CM, Fullum T, Zarrinpar A, Jensen MD, Stein AC, Edmundowicz S, Kahaleh M, Ryou M, Bohning JM, Ginsberg G, Huang C, Tran DD, Glaser JP, Martin JA, Jaffe DL, Farraye FA, Ho SB, Kumar N, Harakal D, Young M, Thomas CE, Shukla AP, Ryan MB, Haas M, Goldsmith H, McCrea J, Aronne LJ. Percutaneous Gastrostomy Device for the Treatment of Class II and Class III Obesity: Results of a Randomized Controlled Trial. *Am J Gastroenterol* 2017; **112**: 447-457 [PMID: 27922026 DOI: 10.1038/ajg.2016.500]

92 **Sullivan S**, Stein R, Jonnalagadda S, Mullady D, Edmundowicz S. Aspiration therapy leads to weight loss in obese subjects: a pilot study. *Gastroenterology* 2013; **145**: 1245-52.e1 [PMID: 24012983 DOI: 10.1053/j.gastro.2013.08.056]

93 **Thompson CC**, Abu Dayyeh BK, Kushnir V, Kushner RF, Jirapinyo P, Schorr AB, Aronne LJ, Amaro A, Jaffe DL, Schulman AR, Early D,

Stein AC, Sharaiha R, Edmundowicz SA, Bohning JM, Jensen MD, Shukla AP, Apovian C, Kim DW, Tran D, Zarrinpar A, Ryan MB, Young M, Lowe A, Haas M, Goldsmith H, McCrea J, Sullivan S. Aspiration therapy for the treatment of obesity: 4-year results of a multicenter randomized controlled trial. *Surg Obes Relat Dis* 2019; **15**: 1348-1354 [PMID: 31302000 DOI: 10.1016/j.soard.2019.04.026]

94 PMA P150024: FDA Summary of safety and effectiveness data (SSED). [cited 15 June 2023]. Available from: https://www.accessdata.fda.gov/cdrh_docs/pdf15/p150024b.pdf

95 **Sullivan S**. Aspiration Therapy for Obesity. *Gastrointest Endosc Clin N Am* 2017; **27**: 277-288 [PMID: 28292406 DOI: 10.1016/j.giec.2016.12.001]

96 **Nyström M**, Machytka E, Norén E, Testoni PA, Janssen I, Turró Homedes J, Espinos Perez JC, Turro Arau R. Aspiration Therapy As a Tool to Treat Obesity: 1- to 4-Year Results in a 201-Patient Multi-Center Post-Market European Registry Study. *Obes Surg* 2018; **28**: 1860-1868 [PMID: 29388050 DOI: 10.1007/s11695-017-3096-5]

97 **Norén E**, Forssell H. Aspiration therapy for obesity; a safe and effective treatment. *BMC Obes* 2016; **3**: 56 [PMID: 28035287 DOI: 10.1186/s40608-016-0134-0]

98 **Jirapinyo P**, de Moura DTH, Horton LC, Thompson CC. Effect of Aspiration Therapy on Obesity-Related Comorbidities: Systematic Review and Meta-Analysis. *Clin Endosc* 2020; **53**: 686-697 [PMID: 32106362 DOI: 10.5946/ce.2019.181]

99 **Ülger TG**, Tayfur M, Çakıroğlu FP. The role of aspiration therapy and intragastric botulinum toxin A injection in obesity treatment. *Obes Med* 2021; **26**: 100367 [DOI: 10.1016/j.obmed.2021.100367]

100 **Gennari FJ**. Pathophysiology of metabolic alkalosis: a new classification based on the centrality of stimulated collecting duct ion transport. *Am J Kidney Dis* 2011; **58**: 626-636 [PMID: 21849227 DOI: 10.1053/j.ajkd.2011.06.004]

101 **Gong EJ**, Kim DH. Small Bowel Endoscopic Bariatric Therapies. *Clin Endosc* 2018; **51**: 425-429 [PMID: 30257545 DOI: 10.5946/ce.2018.153]

102 **Machytka E**, Bužga M, Zonca P, Lautz DB, Ryou M, Simonson DC, Thompson CC. Partial jejunal diversion using an incisionless magnetic anastomosis system: 1-year interim results in patients with obesity and diabetes. *Gastrointest Endosc* 2017; **86**: 904-912 [PMID: 28716404 DOI: 10.1016/j.gie.2017.07.009]

103 **Machytka E**, Buzga M, Ryou M, Lautz DB, Thompson CCJG. Endoscopic dual-path enteral anastomosis using self-assembling magnets: first-in-human clinical feasibility. *Gastroenterology* 2016; **150**: S232 [DOI: 10.1016/S0016-5085(16)30848-4]

104 **Abu Dayyeh BK**, Acosta A, Camilleri M, Mundi MS, Rajan E, Topazian MD, Gostout CJ. Endoscopic Sleeve Gastroplasty Alters Gastric Physiology and Induces Loss of Body Weight in Obese Individuals. *Clin Gastroenterol Hepatol* 2017; **15**: 37-43 [PMID: 26748219 DOI: 10.1016/j.cgh.2015.12.030]

105 **Sujka J**, Teixeira A, Galvao Neto M. Endoscopic Sleeve Gastroplasty for Obesity. In: Agrawal, S. editor. Obesity, Bariatric and Metabolic Surgery: A Comprehensive Guide. Cham: Springer, 2020

106 **Bazerbachi F**, Vargas Valls EJ, Abu Dayyeh BK. Recent Clinical Results of Endoscopic Bariatric Therapies as an Obesity Intervention. *Clin Endosc* 2017; **50**: 42-50 [PMID: 28147472 DOI: 10.5946/ce.2017.013]

107 **Graus Morales J**, Crespo Pérez L, Marques A, Marín Arribas B, Bravo Arribas R, Ramo E, Escalada C, Arribas C, Himpens J. Modified endoscopic gastroplasty for the treatment of obesity. *Surg Endosc* 2018; **32**: 3936-3942 [PMID: 29492709 DOI: 10.1007/s00464-018-6133-0]

108 **Barrichello S**, Hourneaux de Moura DT, Hourneaux de Moura EG, Jirapinyo P, Hoff AC, Fittipaldi-Fernandez RJ, Baretta G, Felício Lima JH, Usuy EN, de Almeida LS, Ramos FM, Matz F, Galvão Neto MDP, Thompson CC. Endoscopic sleeve gastroplasty in the management of overweight and obesity: an international multicenter study. *Gastrointest Endosc* 2019; **90**: 770-780 [PMID: 31228432 DOI: 10.1016/j.gie.2019.06.013]

109 **Jain D**, Bhandari BS, Arora A, Singhal S. Endoscopic Sleeve Gastroplasty - A New Tool to Manage Obesity. *Clin Endosc* 2017; **50**: 552-561 [PMID: 28607328 DOI: 10.5946/ce.2017.032]

110 **Abu Dayyeh BK**, Bazerbachi F, Vargas EJ, Sharaiha RZ, Thompson CC, Thaemert BC, Teixeira AF, Chapman CG, Kumbhari V, Ujiki MB, Ahrens J, Day C; MERIT Study Group, Galvao Neto M, Zundel N, Wilson EB. Endoscopic sleeve gastroplasty for treatment of class 1 and 2 obesity (MERIT): a prospective, multicentre, randomised trial. *Lancet* 2022; **400**: 441-451 [PMID: 35908555 DOI: 10.1016/S0140-6736(22)01280-6]

111 **Lopez-Nava G**, Laster J, Negi A, Fook-Chong S, Bautista-Castaño I, Asokkumar R. Endoscopic sleeve gastroplasty (ESG) for morbid obesity: how effective is it? *Surg Endosc* 2022; **36**: 352-360 [PMID: 33492503 DOI: 10.1007/s00464-021-08289-1]

112 **Sarkar A**, Tawadros A, Andalib I, Shahid HM, Tyberg A, Alkhiari R, Gaidhane M, Kedia P, John ES, Bushe B, Martinez GM, Zamarripa F, Carames MC, Carames JC, Casarodriguez F, Bove V, Costamagna G, Boskoski I, Kahaleh M. Safety and efficacy of endoscopic sleeve gastroplasty for obesity management in new bariatric endoscopy programs: a multicenter international study. *Ther Adv Gastrointest Endosc* 2022; **15**: 26317745221093883 [PMID: 35694412 DOI: 10.1177/26317745221093883]

113 **Hedjoudje A**, Abu Dayyeh BK, Cheskin LJ, Adam A, Neto MG, Badurdeen D, Morales JG, Sartoretto A, Nava GL, Vargas E, Sui Z, Fayad L, Farha J, Khashab MA, Kalloo AN, Alqahtani AR, Thompson CC, Kumbhari V. Efficacy and Safety of Endoscopic Sleeve Gastroplasty: A Systematic Review and Meta-Analysis. *Clin Gastroenterol Hepatol* 2020; **18**: 1043-1053.e4 [PMID: 31442601 DOI: 10.1016/j.cgh.2019.08.022]

114 **Beran A**, Matar R, Jaruvongvanich V, Rapaka BB, Alalwan A, Portela R, Ghanem O, Dayyeh BKA. Comparative Effectiveness and Safety Between Endoscopic Sleeve Gastroplasty and Laparoscopic Sleeve Gastrectomy: a Meta-analysis of 6775 Individuals with Obesity. *Obes Surg* 2022; **32**: 3504-3512 [PMID: 36053446 DOI: 10.1007/s11695-022-06254-y]

115 **Marincola G**, Gallo C, Hassan C, Raffaelli M, Costamagna G, Bove V, Pontecorvi V, Orlandini B, Boškoski I. Laparoscopic sleeve gastrectomy versus endoscopic sleeve gastroplasty: a systematic review and meta-analysis. *Endosc Int Open* 2021; **9**: E87-E95 [PMID: 33403240 DOI: 10.1055/a-1300-1085]

116 **Carr P**, Keighley T, Petocz P, Blumfield M, Rich GG, Cohen F, Soni A, Maimone IR, Fayet-Moore F, Isenring E, Marshall S. Efficacy and safety of endoscopic sleeve gastroplasty and laparoscopic sleeve gastrectomy with 12+ months of adjuvant multidisciplinary support. *BMC Prim Care* 2022; **23**: 26 [PMID: 35123409 DOI: 10.1186/s12875-022-01629-7]

117 **Sharaiha R**. Managing Obesity With Endoscopic Sleeve Gastroplasty. *Gastroenterol Hepatol (N Y)* 2017; **13**: 547-549 [PMID: 29038645]

118 **Afonso M**, Soares R, Ramos R, Balkesthahl J, Andrade E, Machado L. Three-Dimensional (3D) Endoxcopic Sleeve Gastroplasty: Single center case series. *Endoscopy* 2022

119 **Manos T**, Costil V, Karsenty L, Costil P, Noel P, Carandina S, Nedelcu M. Safety of Endoscopic Sleeve Gastroplasty with a Single-Channel Endoscope. *Obes Surg* 2022; **32**: 3074-3078 [PMID: 35857182 DOI: 10.1007/s11695-022-06210-w]

120 **Storm AC**, Abu Dayyeh BK. Endoscopic sleeve gastroplasty for obesity: defining the risk and reward after more than 1600 procedures.

Gastrointest Endosc 2019; **89**: 1139-1140 [PMID: 31104746 DOI: 10.1016/j.gie.2019.02.025]

121 **Choi HS**, Chun HJ. Recent Trends in Endoscopic Bariatric Therapies. *Clin Endosc* 2017; **50**: 11-16 [PMID: 28147471 DOI: 10.5946/ce.2017.007]

122 Recent Advances in Laparoscopic Surgery. [cited 15 June 2023]. Available from: http://dx.doi.org/10.5772/intechopen.78455

123 **Coté GA**, Edmundowicz SA. Emerging technology: endoluminal treatment of obesity. *Gastrointest Endosc* 2009; **70**: 991-999 [PMID: 19879407 DOI: 10.1016/j.gie.2009.09.016]

124 **Brethauer SA**, Pryor AD, Chand B, Schauer P, Rosenthal R, Richards W, Bessler M; American Society for Metabolic and Bariatric Surgery Emerging Technologies Committee. Endoluminal procedures for bariatric patients: expectations among bariatric surgeons. *Surg Obes Relat Dis* 2009; **5**: 231-236 [PMID: 19136306 DOI: 10.1016/j.soard.2008.09.019]

125 **Moreno C**, Closset J, Dugardeyn S, Baréa M, Mehdi A, Collignon L, Zalcman M, Baurain M, Le Moine O, Devière J. Transoral gastroplasty is safe, feasible, and induces significant weight loss in morbidly obese patients: results of the second human pilot study. *Endoscopy* 2008; **40**: 406-413 [PMID: 18459077 DOI: 10.1055/s-2007-995748]

126 **ASGE Technology Committee**, Kethu SR, Banerjee S, Barth BA, Desilets DJ, Kaul V, Pedrosa MC, Pfau PR, Pleskow DK, Tokar JL, Wang A, Song LM, Rodriguez SA. Endoluminal bariatric techniques. *Gastrointest Endosc* 2012; **76**: 1-7 [PMID: 22579259 DOI: 10.1016/j.gie.2012.02.020]

127 **Brunaldi VO**, Galvao Neto M. Endoscopic techniques for weight loss and treating metabolic syndrome. *Curr Opin Gastroenterol* 2019; **35**: 424-431 [PMID: 31219828 DOI: 10.1097/MOG.0000000000000561]

128 **Goh YM**, James NE, Goh EL, Khanna A. The use of endoluminal techniques in the revision of primary bariatric surgery procedures: a systematic review. *Surg Endosc* 2020; **34**: 2410-2428 [PMID: 32112253 DOI: 10.1007/s00464-020-07468-w]

129 **Familiari P**, Costamagna G, Bléro D, Le Moine O, Perri V, Boskoski I, Coppens E, Barea M, Iaconelli A, Mingrone G, Moreno C, Devière J. Transoral gastroplasty for morbid obesity: a multicenter trial with a 1-year outcome. *Gastrointest Endosc* 2011; **74**: 1248-1258 [PMID: 22136774 DOI: 10.1016/j.gie.2011.08.046]

130 **Sullivan S**, Swain JM, Woodman G, Antonetti M, De La Cruz-Muñoz N, Jonnalagadda SS, Ujiki M, Ikramuddin S, Ponce J, Ryou M, Reynoso J, Chhabra R, Sorenson GB, Clarkston WK, Edmundowicz SA, Eagon JC, Mullady DK, Leslie D, Lavin TE, Thompson CC. Randomized sham-controlled trial evaluating efficacy and safety of endoscopic gastric plication for primary obesity: The ESSENTIAL trial. *Obesity (Silver Spring)* 2017; **25**: 294-301 [PMID: 28000425 DOI: 10.1002/oby.21702]

131 **Park JM**. Role of Malabsorptive Endoscopic Procedures in Obesity Treatment. *Clin Endosc* 2017; **50**: 26-30 [PMID: 28147470 DOI: 10.5946/ce.2017.004]

132 **Ruban A**, Miras AD, Glaysher MA, Goldstone AP, Prechtl CG, Johnson N, Chhina N, Al-Najim W, Aldhwayan M, Klimowska-Nassar N, Smith C, Lord J, Li JV, Flores L, Al-Lababidi M, Dimitriadis GK, Patel M, Moore M, Chahal H, Ahmed AR, Cousins J, Aldubaikhi G, Glover B, Falaschetti E, Ashrafian H, Roux CWL, Darzi A, Byrne JP, Teare JP. Duodenal-Jejunal Bypass Liner for the management of Type 2 Diabetes Mellitus and Obesity: A Multicenter Randomized Controlled Trial. *Ann Surg* 2022; **275**: 440-447 [PMID: 34647708 DOI: 10.1097/SLA.0000000000004980]

133 **Schouten R**, Rijs CS, Bouvy ND, Hameeteman W, Koek GH, Janssen IM, Greve JW. A multicenter, randomized efficacy study of the EndoBarrier Gastrointestinal Liner for presurgical weight loss prior to bariatric surgery. *Ann Surg* 2010; **251**: 236-243 [PMID: 19858703 DOI: 10.1097/SLA.0b013e3181bdfbff]

134 **Chen JH**, Yu ZH, Liu QF, Meng QG, Chen X. Research Progress of Duodenal-Jejunal Bypass Liner in the Treatment of Obesity and Type 2 Diabetes Mellitus. *Diabetes Metab Syndr Obes* 2022; **15**: 3319-3327 [PMID: 36329806 DOI: 10.2147/DMSO.S382324]

135 **van Rijn S**, Betzel B, de Jonge C, van Dijk DPJ, Janssen IM, Berends FJ, Bouvy ND, Greve JWM. The Effect of 6 and 12 months Duodenal-Jejunal Bypass Liner Treatment on Obesity and Type 2 Diabetes: a Crossover Cohort Study. *Obes Surg* 2018; **28**: 1255-1262 [PMID: 29110244 DOI: 10.1007/s11695-017-2997-7]

136 **Gersin KS**, Keller JE, Stefanidis D, Simms CS, Abraham DD, Deal SE, Kuwada TS, Heniford BT. Duodenal- jejunal bypass sleeve: a totally endoscopic device for the treatment of morbid obesity. *Surg Innov* 2007; **14**: 275-278 [PMID: 18178916 DOI: 10.1177/1553350607312901]

137 **Boonchaya-Anant P**, Bueter M, Gubler C, Gerber PA. Sustained weight loss after duodenal-jejunal bypass liner treatment in patients with body mass index below, but not above 35 kg/m(2) : A retrospective cohort study. *Clin Obes* 2023; **13**: e12561 [PMID: 36239531 DOI: 10.1111/cob.12561]

138 **Betzel B**, Koehestanie P, Aarts EO, Dogan K, Homan J, Janssen IM, Wahab PJ, Groenen MJ, Berends FJ. Safety experience with the duodenal-jejunal bypass liner: an endoscopic treatment for diabetes and obesity. *Gastrointest Endosc* 2015; **82**: 845-852 [PMID: 25952090 DOI: 10.1016/j.gie.2015.03.1911]

139 **Betzel B**, Drenth JPH, Siersema PD. Adverse Events of the Duodenal-Jejunal Bypass Liner: a Systematic Review. *Obes Surg* 2018; **28**: 3669-3677 [PMID: 30121857 DOI: 10.1007/s11695-018-3441-3]

140 **Sandler BJ**, Rumbaut R, Swain CP, Torres G, Morales L, Gonzales L, Schultz S, Talamini M, Horgan S. Human experience with an endoluminal, endoscopic, gastrojejunal bypass sleeve. *Surg Endosc* 2011; **25**: 3028-3033 [PMID: 21487876 DOI: 10.1007/s00464-011-1665-6]

141 **Sandler BJ**, Rumbaut R, Swain CP, Torres G, Morales L, Gonzales L, Schultz S, Talamini MA, Jacobsen GR, Horgan S. One-year human experience with a novel endoluminal, endoscopic gastric bypass sleeve for morbid obesity. *Surg Endosc* 2015; **29**: 3298-3303 [PMID: 25631114 DOI: 10.1007/s00464-015-4081-5]

142 **Fu XY**, Li Z, Zhang N, Yu HT, Wang SR, Liu JR. Effects of gastrointestinal motility on obesity. *Nutr Metab (Lond)* 2014; **11**: 3 [PMID: 24398016 DOI: 10.1186/1743-7075-11-3]

143 **Camilleri M**. Gastrointestinal hormones and regulation of gastric emptying. *Curr Opin Endocrinol Diabetes Obes* 2019; **26**: 3-10 [PMID: 30418188 DOI: 10.1097/MED.0000000000000448]

144 **Jahnberg T**, Martinson J, Hultén L, Fasth S. Dynamic gastric response to expansion before and after vagotomy. *Scand J Gastroenterol* 1975; **10**: 593-598 [PMID: 1179152 DOI: 10.1080/00365521.1975.12097017]

145 **Kuiken SD**, Vergeer M, Heisterkamp SH, Tytgat GN, Boeckxstaens GE. Role of nitric oxide in gastric motor and sensory functions in healthy subjects. *Gut* 2002; **51**: 212-218 [PMID: 12117882 DOI: 10.1136/gut.51.2.212]

146 **Adamska E**, Ostrowska L, Górska M, Krętowski A. The role of gastrointestinal hormones in the pathogenesis of obesity and type 2 diabetes. *Prz Gastroenterol* 2014; **9**: 69-76 [PMID: 25061485 DOI: 10.5114/pg.2014.42498]

147 **Chaudhri O**, Small C, Bloom S. Gastrointestinal hormones regulating appetite. *Philos Trans R Soc Lond B Biol Sci* 2006; **361**: 1187-1209 [PMID: 16815798 DOI: 10.1098/rstb.2006.1856]

148 **Lean ME**, Malkova D. Altered gut and adipose tissue hormones in overweight and obese individuals: cause or consequence? *Int J Obes (Lond)* 2016; **40**: 622-632 [PMID: 26499438 DOI: 10.1038/ijo.2015.220]

149 **Wright RA**, Krinsky S, Fleeman C, Trujillo J, Teague E. Gastric emptying and obesity. *Gastroenterology* 1983; **84**: 747-751 [PMID: 6825986 DOI: 10.1016/0016-5085(83)90141-5]

150 **Dixon JB**, Eaton LL, Vincent V, Michaelson R. LAP-BAND for BMI 30-40: 5-year health outcomes from the multicenter pivotal study. *Int J Obes (Lond)* 2016; **40**: 291-298 [PMID: 26283140 DOI: 10.1038/ijo.2015.156]

World Journal of Gastroenterology

Submit a Manuscript: https://www.f6publishing.com

World J Gastroenterol 2023 October 28; 29(40): 5543-5556

DOI: 10.3748/wjg.v29.i40.5543

ISSN 1007-9327 (print) ISSN 2219-2840 (online)

ORIGINAL ARTICLE

Basic Study

Roles of phosphatidylinositol-3-kinases signaling pathway in inflammation-related cancer: Impact of rs10889677 variant and buparlisib in colitis-associated cancer

Nurul Nadirah Razali, Raja Affendi Raja Ali, Khairul Najmi Muhammad Nawawi, Azyani Yahaya, Norshafila Diana Mohd Rathi, Norfilza Mohd Mokhtar

Specialty type: Gastroenterology and hepatology

Provenance and peer review: Unsolicited article; Externally peer reviewed.

Peer-review model: Single blind

Peer-review report's scientific quality classification

Grade A (Excellent): 0
Grade B (Very good): B
Grade C (Good): C, C
Grade D (Fair): 0
Grade E (Poor): 0

P-Reviewer: Qin J, China; Sahin TT, Turkey; Sheykhhasan M, Iran

Received: July 20, 2023
Peer-review started: July 20, 2023
First decision: August 25, 2023
Revised: September 5, 2023
Accepted: October 11, 2023
Article in press: October 11, 2023
Published online: October 28, 2023

Nurul Nadirah Razali, Norshafila Diana Mohd Rathi, Norfilza Mohd Mokhtar, Department of Physiology, Faculty of Medicine, Universiti Kebangsaan Malaysia, Cheras 56000, Kuala Lumpur, Malaysia

Raja Affendi Raja Ali, School of Medical and Life Sciences, Sunway University, Sunway City 47500, Malaysia

Raja Affendi Raja Ali, Khairul Najmi Muhammad Nawawi, Norfilza Mohd Mokhtar, GUT Research Group, Faculty of Medicine, Universiti Kebangsaan Malaysia, Cheras 56000, Kuala Lumpur, Malaysia

Raja Affendi Raja Ali, Khairul Najmi Muhammad Nawawi, Gastroenterology Unit, Department of Medicine, Faculty of Medicine, Universiti Kebangsaan Malaysia, Cheras 56000, Kuala Lumpur, Malaysia

Azyani Yahaya, Department of Pathology, Faculty of Medicine, Universiti Kebangsaan Malaysia, Cheras 56000, Kuala Lumpur, Malaysia

Corresponding author: Norfilza Mohd Mokhtar, PhD, Professor, Department of Physiology, Faculty of Medicine, Universiti Kebangsaan Malaysia, Jalan Yaacob Latif, Bandar Tun Razak, Cheras 56000, Kuala Lumpur, Malaysia. norfilza@ppukm.ukm.edu.my

Abstract

BACKGROUND

Phosphatidylinositol-3-kinases (PI3K) is a well-known route in inflammation-related cancer. Recent discovery on PI3K-related genes revealed a potential variant that links ulcerative colitis (UC) and colorectal cancer (CRC) with colitis-associated cancer (CAC). PI3K/AKT pathway has been recommended as a potential additional therapeutic option for CRC due to its substantial role in modifying cellular processes. Buparlisib is a pan-class I PI3K inhibitor previously shown to reduce tumor growth.

AIM

To investigate the regulation of rs10889677 and the role of buparlisib in the PI3K signaling pathway in CAC pathogenesis.

METHODS
Genomic DNA from 32 colonic samples, including CAC (n = 7), UC (n = 10) and CRC (n = 15), was sequenced for the rs10889677 mutation. The mutant and wildtype fragments were amplified and cloned in the pmirGLO vector. The luciferase activity of cloned vectors was assessed after transfection into the HT29 cell line. CAC mice were induced by a mixture of a single azoxymethane injection and three cycles of dextran sulphate sodium, then buparlisib was administered after 14 d. The excised colon was subjected to immunohistochemistry for Ki67 and Cleaved-caspase-3 markers and quantitative real-time polymerase chain reaction analysis for *Pdk1* and *Sgk2*.

RESULTS
Luciferase activity decreased by 2.07-fold in the rs10889677 mutant, confirming the hypothesis that the variant disrupted miRNA binding sites, which led to an increase in *IL23R* expression and the activation of the PI3K signaling pathway. Furthermore, CAC-induced mice had a significantly higher disease activity index ($P < 0.05$). Buparlisib treatment significantly decreased mean weight loss in CAC-induced mice ($P < 0.05$), reduced the percentage of proliferating cells by 5%, and increased the number of apoptotic cells. The treatment also caused a downward trend of *Pdk1* expression and significantly decreased *Sgk2* expression.

CONCLUSION
Our findings suggested that the rs10889677 variant as a critical initiator of the PI3K signaling pathway, and buparlisib had the ability to prevent PI3K-non-AKT activation in the pathophysiology of CAC.

Key Words: Colitis-associated cancer; Colorectal cancer; Phosphatidylinositol 3-kinase; Animal model; Luciferases; Renilla; Phosphatidylinositol 3-kinase inhibitor

©The Author(s) 2023. Published by Baishideng Publishing Group Inc. All rights reserved.

Core Tip: The role of phosphatidylinositol-3-kinases (PI3K) in promoting cancer progression has been widely acknowledged due to its crucial involvement in regulating the survival, differentiation, and proliferation of cancer cells. Here, we investigate the role of PI3K signaling in colitis-associated cancer (CAC) pathogenesis by studying the regulation of potential variant in PI3K-related gene in the colorectal cancer cell line and the utilization of PI3K inhibitor, buparlisib, in the CAC-induced mice model. We suggested that rs10889677 variant plays a crucial role in initiating the PI3K signaling pathway, and buparlisib has the capability to inhibit PI3K-non-AKT activation in the pathophysiology of CAC.

Citation: Razali NN, Raja Ali RA, Muhammad Nawawi KN, Yahaya A, Mohd Rathi ND, Mokhtar NM. Roles of phosphatidylinositol-3-kinases signaling pathway in inflammation-related cancer: Impact of rs10889677 variant and buparlisib in colitis-associated cancer. *World J Gastroenterol* 2023; 29(40): 5543-5556
URL: https://www.wjgnet.com/1007-9327/full/v29/i40/5543.htm
DOI: https://dx.doi.org/10.3748/wjg.v29.i40.5543

INTRODUCTION

Inflammatory bowel disease (IBD), a chronic inflammatory disorder that goes into remission and then recurs, eventually leading to the development of colitis-associated cancer (CAC), is a kind of colorectal cancer (CRC)[1,2]. Crohn's disease and ulcerative colitis (UC), the two main subtypes of IBD, had CAC risks of 1.4% and 0.8%, respectively[3,4]. The rising trend of IBD incidence and prevalence among Asians increased from 1.3% to 7.2% per 100000 population among Malaysian-Singaporeans[5]. Rapid urbanization, adoption of a Western diet, antibiotics use, personal hygiene standards, microbiological exposures, and pollution are all risk factors for developing IBD[6]. In Malaysia, the average annual incidence of IBD has risen to 1.46 per 100000 people over the last decade[7]. CAC accounted for 10%-15% of IBD fatality cases among Westerners, accounting for only 1% to 2% of CRC incidence in Malaysia[4,8].

CAC develops through the inflammation–dysplasia–carcinoma pathway[9]. Immune cells, including cytokines, chemokines, epithelial cells, and stromal cells, are among the cell types contributing to the inflammatory processes in the CAC development[10]. Moreover, inflammatory mediators had a substantial impact on the control of pre-neoplastic growth during CAC development, and their release is more likely to target multiple carcinogenesis-related signaling pathways involved, such as NFkB, PI3K, JAK/STAT and Wnt/B-catenin[11,12].

Phosphatidylinositol-3-kinases (PI3K) signaling pathway is an essential intracellular signaling mechanism in regulating the cell cycle[13]. Growth factors, cytokines, and other stimulatory chemicals activate *PI3K via* their receptors. The *AKT-mTOR* and *SGK* families receive signals from activated *PI3K*, which controls cell growth, proliferation, and apoptosis[14]. PI3K enzymatic activity has been linked to the aetiology of various diseases, including chronic inflammation and cancer [12,15]. Our earlier research identified *PI3K* as one of the critical pathways in long-duration UC associated with an increased risk of developing CAC[16]. A recent study on mutational analysis in CAC patients identified several potential

variants, including rs10889677, in the *IL23R*, a cytokine-induced PI3K-related gene that may link inflammation to an increased risk of cancer[17].

PI3K/AKT pathway has been proposed as a viable therapeutic target for CRC due to its significant role in modulating cellular processes by targeting the downstream pathway[18]. Buparlisib is an oral pan-class I PI3K inhibitor that targets all four class I PI3K catalytic isoforms (p110α, p110β, p110δ and p110γ)[19,20]. This drug is the most clinically advanced medication to have passed a phase II clinical trial in the cancer[21,22]. Buparlisib treatment in *in vivo* study showed encouraging outcomes by enormously lowering the quantity of phosphorylated *AKT* and slowing tumor growth in tumor-bearing mouse models[19,23]. Therefore, the objective of this study was to study the regulation of the PI3K-related variant, rs10889677, in the CRC cell line and to investigate whether buparlisib may affect the non-AKT-independent branch of the PI3K signaling pathway, which was one of the keys signaling pathways implicated in cancer development and progression, using a mouse model.

MATERIALS AND METHODS

Sample collection and preparation

The Universiti Kebangsaan Malaysia Research Ethics Committee (UKM/PPI/111/8/JEP-2019-572) approved this study. A total of 32 fresh frozen and archival samples (ranging from the year 2014 to 2019) from patients with long-standing UC, CAC, and CRC were collected from the Endoscopy Unit at Universiti Kebangsaan Malaysia Medical Centre, Kuala Lumpur, Malaysia. Upon admission, all patients provided informed consent. All tissues were collected by December 2020, stored in RNAlater, and frozen at -80 °C until further processing. The hematoxylin and eosin-stained tissue sections were evaluated by an experienced pathologist for confirmation of diagnosis, inflammation, and metastatic status. The genomic DNA was extracted from fresh frozen tissues using the AllPrep DNA/RNA/miRNA Universal Kit (Qiagen, United States) according to the manufacturer's protocol. Meanwhile, GENEREAD DNA FFPE Kit (Qiagen, United States) was used to extract DNA from formalin-fixed paraffin-embedded blocks of archival samples. DNA concentration was measured using DeNovix DS11+ Spectrophotometer (DeNovix Inc., United States).

Sanger sequencing

Primers were designed using the NCBI Primer Tool (National Center for Biotechnology Information, United States) and Primer3Plus[24] based on the location of the somatic variant. The predesigned primers were as follows: *IL23R*, forward 5'-TCT GTG CTC CTA CCA TCA CC-3', and reverse 5'-TGT GCC TGT ATG TGT GAC CA-3'. SnapGene Viewer 5.3.2 was used to analyze the sequencing results.

Fragment amplification

The fragments containing the wildtype and mutant rs10889677 variant on the 3' untranslated region of *IL23R* were amplified from the genotyped DNA samples. The predesigned primers were added with the target sequences of the *Xba*I and *Xho*I restriction enzymes. The primers were as follows: Forward 5'-ATC GCT CGA GGC TGC CTT GCA ATC TGA ACT-3' and reverse 5'-ATC GTC TAG ATC TGC CTT CCT GGT TCA AGT-3'. The polymerase chain reaction for fragment amplification was carried out using GoTaq® Green Master Mix (Promega, United States) with a pre-denaturation step at 95 °C for eight minutes, followed by 35-40 cycles of 95 °C for 30 s, 60 °C for 30 s and 72 °C for 30 s, with an additional final elongation step at 72 °C for five minutes. Then, the polymerase chain reaction (PCR) products were run on gel electrophoresis to check for fragment bands, followed by the gel purification step using the QIAquick® Gel Extraction Kit (Qiagen, United States).

Plasmid preparation and cloning

A total of 1 μg of pmirGLO (Promega, United States) vector was digested with the following enzymes: *Xba*1 (NEB, United Kingdom) and *Xho*I (NEB, United Kingdom) according to the manufacturer's instructions. The ligation reactions were prepared using a T4 DNA Ligase kit (NEB, United Kingdom) with a molar ratio of 1:3 vector to insert. The ligated products were transformed utilizing the heat-shock technique with an *E.coli* competent cell (NEB, United Kingdom). Colonies from prior successful transformations were screened, and positive transformant plasmid was purified using PureYield™ Plasmid Miniprep System (Promega, United States).

Transfection and luciferase assay

The CRC cell line, HT29, was routinely cultured in a RPMI-1640 (Elabscience, United States) supplemented with 10% fetal bovine serum (Gibco, United States) and 1% of Penicillin/Streptomycin (Gibco, United States) and cultivated in 5% of CO_2 level incubator at 37 °C. Before transfection, 5.0 × 10^4 HT29 cells were seeded into a 96-well white plate in 100 μL antibiotic-free growth media. Cultures were performed in triplicate. A total of 0.25 μg of wildtype, mutant and empty plasmids were transfected using Lipofectamine 2000 (Invitrogen, United States) transfection reagent according to the manufacturer's protocol. Afterwards, the luciferase activity was measured 48 h after post-transfection using the Dual-Glo® Luciferase Assay system (Promega, United States) following the manufacturer's protocol. Firefly and Renilla luciferase activity were measured using the GloMax® 20/20 Luminometer (Promega, United States). The assay was performed in triplicate, and all results were normalized with the internal control reading.

Animals

Forty male Balb/c mice (seven to eight weeks old, weighing 25-30 g) were purchased from the Animal Unit, Faculty of Science and Technology, Universiti Kebangsaan Malaysia, Bangi, Malaysia. The mice were housed in individual cages with kenaf bedding and maintained on a 12 h light/dark cycle with controlled humidity at 25 °C kept in the animal laboratory unit, Faculty of Medicine, Universiti Kebangsaan Malaysia. Regular food and water were supplied ad libitum. All mice were acclimatized for ten days before the start of the treatment. The animal handling and protocol was approved by the Animal Ethics Committee of Universiti Kebangsaan Malaysia (PPUKM/2019/NORFILZA/25-SEPT./1035-SEPT.-2019-DEC.-2021).

Chemical induction and PI3K inhibitor administration

The mice were randomly divided into four groups (n = 10 each): Control, dextran sodium sulphate (DSS) induced, azoxymethane (AOM) induced, and AOM/DSS combination induced[25]. A single intraperitoneal injection of AOM (10 mg/kg body weight) (Sigma-Aldrich Chemicals, United States) was administered to the AOM and AOM/DSS-induced group. A week after injection, AOM/DSS and DSS-induced groups received 2.5% DSS (40kDa; Sigma-Aldrich Chemicals, United States) in their drinking water for seven days in three cycles (each cycle consisting of one-week DSS, followed by two weeks of sterile water). The control and AOM-induced groups were only provided with sterile water throughout the treatment. Beginning in week eight, mice from the AOM/DSS-induced group were treated daily for 14 d with a PI3K inhibitor buparlisib (NVP-BKM120, MedChemExpress, United States) at 30 mg/kg *via* oral administration (Figure 1).

Disease activity index scoring

Daily observations and records were made of body weight, bowel consistency, and rectal bleeding throughout ten weeks. Changes in these factors will be scored to determine the disease activity index (DAI), which is based on the rating of each component. Scores were assigned for weight loss (0: 0-1%, 1: 1%-5%, 2: 5%-10%, 3: 10%-20%, 4: > 20%), stool consistency (0: Normal, 2: Loose stool, 4: Diarrhea), and presence of blood in the stool (0: Negative, 2: Visual blood in stool, 4: Fresh rectal bleeding)[26]. A total score was determined, ranging from 0 to 12.

Histological examination

Colons were removed, cleaned, and flushed with sterile phosphate buffer saline and cut into two parts: Proximal and distal colon. The proximal colon was stored in RNAlater solution (ThermoFisher, United States), and the distal colons were rolled, placed in the tissue cassette, and soaked in 10% neutral-buffered formalin for at least one night. Then, the tissues were processed, embedded in paraffin, and sectioned for hematoxylin and eosin staining. Histological structures were assessed and scored (0: Healthy colon, 1: Minimal inflammation with minimal to no separation of crypts, 2: Mild inflammation with mild separation of crypts, 3: Moderate inflammation with separation of crypts, with or without focal effacement of crypts, 4: Extensive inflammation with marked separation and effacement of crypts, 5: Diffuse inflammation with marked separation and effacement of crypts)[27]. The pathologist used an inverted microscope to examine all slides.

Immunohistochemistry

Immunohistochemistry (IHC) staining was performed using the Rabbit-specific HRP/DAB Detection IHC Detection kit Micro-polymer, as instructed by the manufacturer (ab236469; Abcam, United States). Slides were incubated in primary antibodies: Rabbit monoclonal Cleaved caspase-3 (CC-3) (1:5000, ab214430; Abcam, United Kingdom) and rabbit monoclonal Ki67 (1:100, ab16667; Abcam, United Kingdom) for 30 minutes. The secondary antibody was goat anti-rabbit HRP Conjugate, included in the same kit. Images were obtained using an Olympus light microscope (Japan). Qualitative and quantitative scoring were scored blindly by the experienced pathologist.

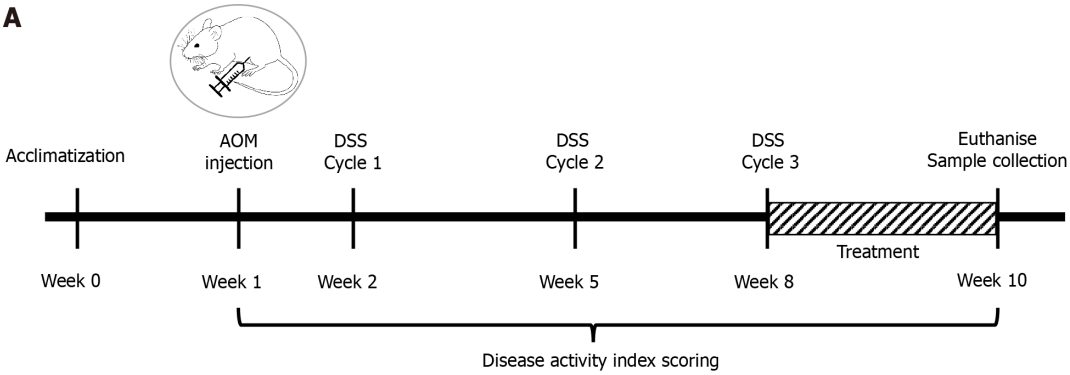
Quantitative real-time PCR

The excised proximal colon was sectioned into smaller fragments and placed in different tubes at -80 °C. RNA was prepared using AllPrep DNA/RNA/miRNA Universal Kit (Qiagen, United States) following the manufacturer's instructions. The total RNA yield was quantified using a DS-11 spectrophotometer (DeNovix Inc., United States). cDNA conversion was conducted using QuantiNova Reverse Transcription Kit (Qiagen, United States) from 1 µg RNA following the manufacturer's instructions. Quantitative PCR amplifications were prepared with approximately 100 ng cDNA using the QuantiNova SYBR Green PCR Kit (Qiagen, United States) and mouse primer sets (IDT, United States). The predesigned primers were as follows: *Ppia*, forward 5′-CAA ACA CAA ACG GTT AG-3′ and reverse 5′-TTC ACC TTC CCA AAG ACC AC-3′; *Sgk2*, forward, 5′-GCA TAG AGC CTA CCT GAT CAC-3′ and reverse 5′-CCC AGG TTG ATG TTC CCA TT-3′ and *Pdk1*, forward 5′-CAT GCA CAT CCA GAT CAC AGA-3′ and reverse 5′- CTT TTA CAC GCC GAC TTC TCT-3′. The gene expression was normalized to the reference gene, *Ppia* and all reactions were prepared in triplicate.

Statistical analysis

Normally distributed variables are presented as the mean ± standard error mean. For statistical significance, the Student T-test and ANOVA tests were performed. At $P < 0.05$, the differences between groups were considered significant. Statistical analyses were performed using the GraphPad Prism Version 9.3.1 (GraphPad Software Inc., United States).

A



B

		Week									
		1	2	3	4	5	6	7	8	9	10
Group	Control	PBS	Water								
	CAC	AOM	DSS	Water		DSS	Water		DSS	Water	
	CRC	AOM	Water								
	Colitis	PBS	DSS	Water		DSS	Water		DSS	Water	

DOI: 10.3748/wjg.v29.i40.5543 **Copyright** ©The Author(s) 2023.

Figure 1 Animal induction procedure. A: The experimental design for the chemical induction procedure; B: The schematic diagram of mice model grouping. DSS: Dextran sodium sulphate; AOM: Azoxymethane; CAC: Colitis-associated cancer; CRC: Colorectal cancer.

RESULTS

Information in clinical samples

Table 1 displays demographic data for all samples. The median age of all samples was 63 years old (IQR:11.5). Malays made up the majority of the samples (56%) and were followed by Chinese (28%) and Indians (15%). The gender distribution was equal between males and females. Most patients' smoking status was non-smoker (91%) instead of smoker/ex-smoker (9%). Most UC patients were diagnosed with left-sided colitis or pancolitis, with a Mayo index score of 1 to 3 and a Geboes score of Grade 2A.1 to 2A.2. The majority of CRC and CAC patients were at stages 1 and 3, and the rectosigmoid and distal colon were the sites of the malignancies. Histologically, most CRCs were moderately differentiated, whereas tumors from CAC patients were categorized as poor, moderate and well differentiated. There was no reported familial history of CRC among any of the patients.

PI3K-related somatic variant rs10889677 exhibited a reduced trend of luciferase activity in CRC cell line

To understand the significance of the PI3K signaling pathway in the formation of CAC, the functional role of PI3K-related somatic variants that potentially correlate CAC with UC and CRC was investigated to gain insight into the role. Somatic variant rs10889677C>A has been successfully sequenced in CAC, UC and CRC samples. The proportion of homozygous CC (wildtype) was discovered to be the highest in CRC samples (60%), while the proportion of homozygous AA (mutant) was highest in CAC samples (85%). We discovered mutant rs10889677 had a 2.07-fold lower luciferase activity (2.35 ± 0.85) than the wildtype construct (4.42 ± 0.86). However, the difference was not statistically significant (Figure 2).

Combination of AOM + DSS produced a successful CAC-induced mice model

In a CAC mouse model, chemical induction of a single AOM injection with three cycles of 2.5% DSS was considered successful. The assessment of a successful CAC induction was based on observing body weight loss, the condition of the stool and the occurrence of any rectal bleeding. The CAC mice group endured reduced body weight, watery stools, and rectal bleeding for ten weeks. In light of this, the CAC mice group scored significantly higher on the DAI than the colitis and control groups, with a mean score of 1.25 ± 0.22 ($P < 0.05$) (Figure 3A). The DAI score of the CAC mice group began to rise dramatically after the second DSS induction (Figure 3B). On the other hand, the colitis group had a low DAI score, while the control group had none.

Buparlisib therapy was able to reverse the weight loss in the CAC-induced mice model

Due to ongoing DSS exposure, the colitis and CAC-induced mice group's body weights have fluctuated (Figure 4). At every DSS induction cycle, weight loss was predicted to occur. Following each cycle, mice had a two-weeks recovery period to help them regain any lost weight. However, starting with the third cycle of DSS induction, the CAC mice group had substantial weight loss, losing about 5% of their total body weight. This significant body weight reduction in the CAC group explained why they had a higher DAI score than other groups. Meanwhile, the mice in the other groups

Table 1 Clinical and demographic details of the recruited patients

	CRC (*n* = 15)	CAC (*n* = 7)	UC (*n* = 10)
Median age (range)	63 (39-67)	58 (20-71)	65 (52-69)
Race			
Malay	11	2	5
Chinese	4	2	3
Indian	-	3	2
Gender			
Male	9	3	4
Female	6	4	6
Smoking status			
Smoker/Ex-smoker	2	1	-
Non-smoker	13	6	10
Stage[1]			
I	2	1	Not applicable
II	-	-	
III	7	4	
Adenocarcinoma types[1]			
Poorly differentiated	-	1	Not applicable
Moderately differentiated	7	1	
Well differentiated	1	3	
Mayo score (range)[1]	Not applicable	Data unavailable	1-3
Geboes score (range)[1]	Not applicable	Data unavailable	2A.1-2A.2
Presentation	Rectal bleeding	Rectal bleeding, abdominal pain, severe diarrhea	Diarrhea, loss of appetite

[1]Some data are unavailable.

All data are expressed as n except where indicated in the table. UC: Ulcerative colitis; CRC: Colorectal cancer; CAC: Colitis-associated cancer.

recovered and kept their body weight throughout the treatment (Figure 4A).

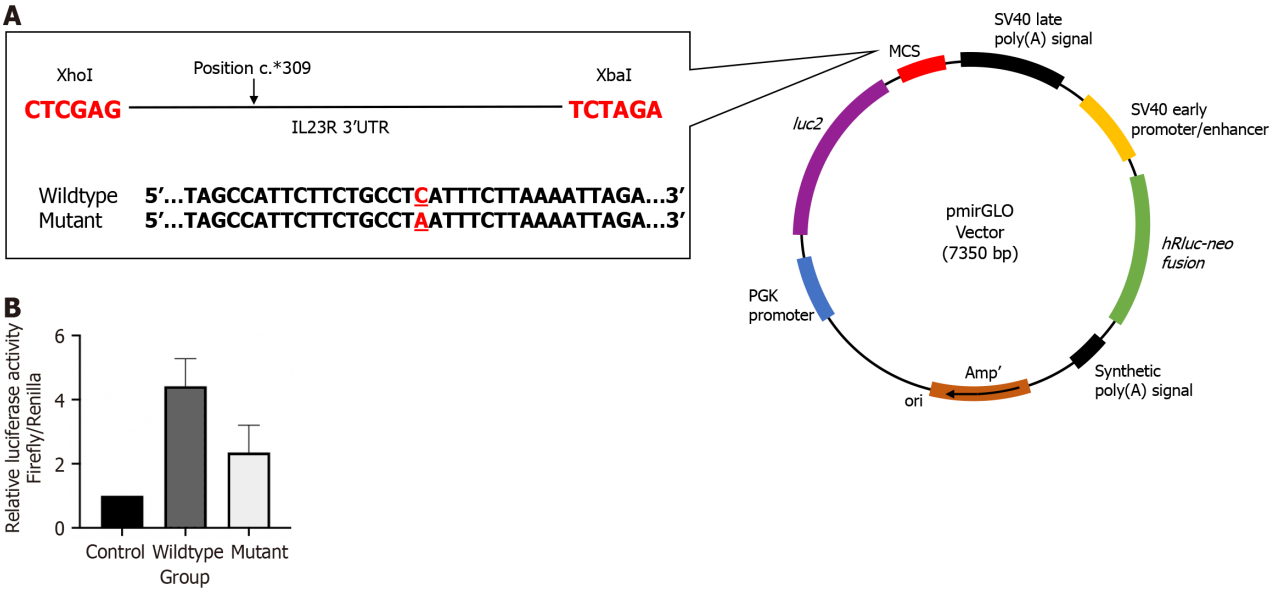
PI3K inhibitor (buparlisib) supplementation, started in the eight week of treatment, was used to perform additional research on the relationship between PI3K and the advancement of CAC. PI3K oral inhibitor dosage was calculated depending on the body weight of CAC mice. After receiving daily treatment for 14 d, the mean weight loss (g) in the CAC-induced mice was significantly lower (2.0 ± 0.0) than in the CAC group that had not received any treatment (2.6 ± 1.07) ($P < 0.05$) (Figure 4B).

CAC-induced animals exhibited inflammation and tumor growth characteristics

The distal colon underwent histological evaluation to check for any morphological alterations, and the results were reported in Figure 5. No diffuse inflammation was observed in any of the tissues in the present study, which ranged from 0 (no inflammation/healthy), 1 (minimal inflammation), 2 (mild inflammation), 3 (moderate inflammation), and 4 (extensive inflammation). Most control group mice had healthy colons with uniformly shaped glands and minimal inflammation. In the colon tissues of the colitis mice group, mild to moderate inflammation with separation of crypts, with or without focal effacement of crypts, and various gland shapes were seen. On the other hand, at least 50% of CAC-induced mice had tumors and varying degrees of mild to severe inflammation. These tumors had enlarged nuclei, reactive cellular changes, moderate inflammatory response, depleted glands, and an elevated neutrophil count. The scoring on colitis and CAC mice colon tissue were scored depending on the inflamed area (chronic) or specifically at the tumor location (Figure 6).

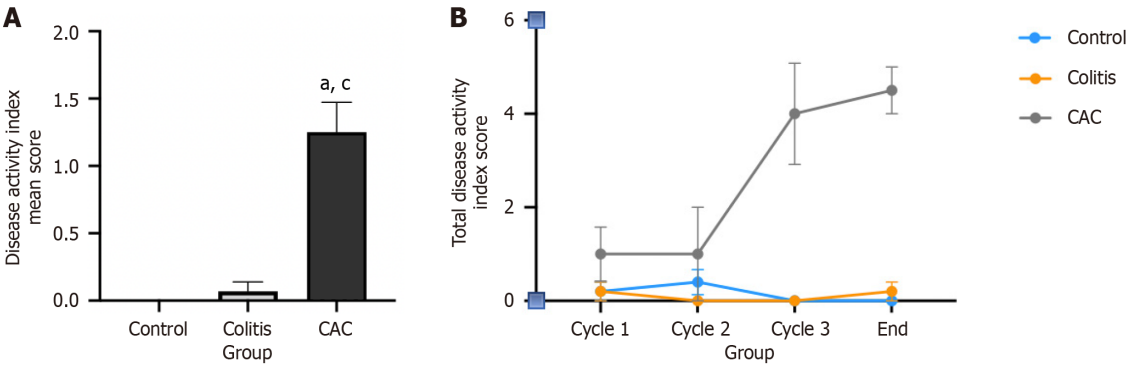
Buparlisib treatment had anti-proliferative and pro-apoptotic actions in the CAC-induced mice model

The apoptotic marker (CC-3) and the proliferative marker (Ki67) were both subjected (Figure 7). Every type of tissue, even the healthy tissue, had proliferating cells. The proliferative cells' distribution might vary depending on the different tissue types. In the control group, the healthy colon exhibited 30% of Ki67-positive cells, with the proliferating cells predominating in the basal regions of the glands. In contrast, more than 50% and 80% of Ki67-positive cells had irregular



DOI: 10.3748/wjg.v29.i40.5543 **Copyright** ©The Author(s) 2023.

Figure 2 Dual-luciferase reporter assay for rs10889677 construct. A: The structure of luciferase vector, pmirGLO, with wildtype and mutant constructs; B: Luciferase activity of HT29 cell line transfected with a construct containing wildtype and mutant variant of rs10889677. Data are presented as mean ± SEM; one-way ANOVA was employed; *n* = 3.



DOI: 10.3748/wjg.v29.i40.5543 **Copyright** ©The Author(s) 2023.

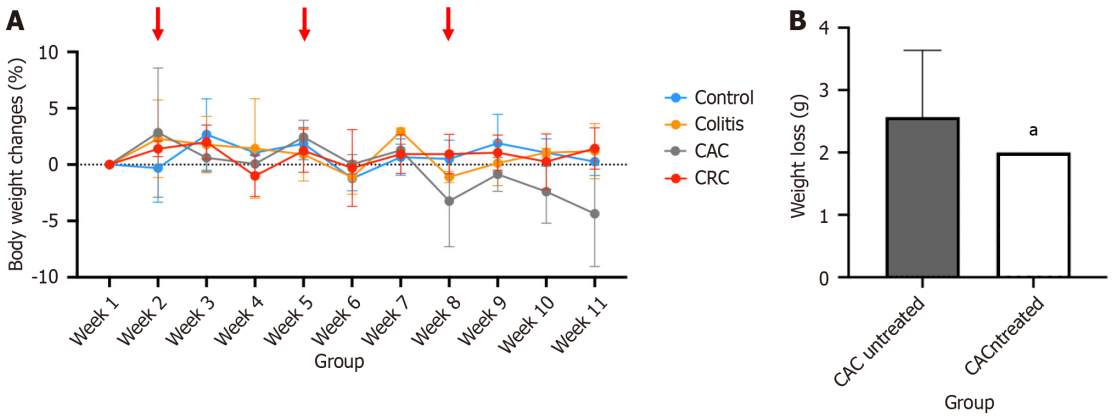
Figure 3 The disease activity index score. A: The total average disease activity index (DAI) score per group at the end of treatment. [a]*P* < 0.05 (compared to the control group); [c]*P* < 0.05 (compared to the colitis group); data are presented as mean ± SEM; one-way ANOVA was used; *n* = 8; B: The total average DAI score per group at each dextran sodium sulphate-induction cycle. Two-way ANOVA was used. CAC: Colitis-associated cancer.

distribution in the colitis and CAC mice groups, respectively. The uneven distribution of proliferative cells, particularly in the upper section of the glands, suggested the cells were highly proliferating. Buparlisib administration to the CAC mice group reduced about 5% of the positive cells compared to the untreated CAC mice group (Figure 7).

CC-3 was assessed as an apoptotic marker based on its intensity and the number of positive cells. Most tissues from the control, colitis and CAC mice group have moderate intensity of CC-3. In contrast to the control group, which had fewer than 50% positive cells, most colitis and CAC mice had more than 75% CC-3 positive cells. Based on the PI3K inhibitor treatment evaluation, buparlisib-treated CAC mice achieved a high overall score of CC3-intensity and -positive cells (6/8) (Figure 7).

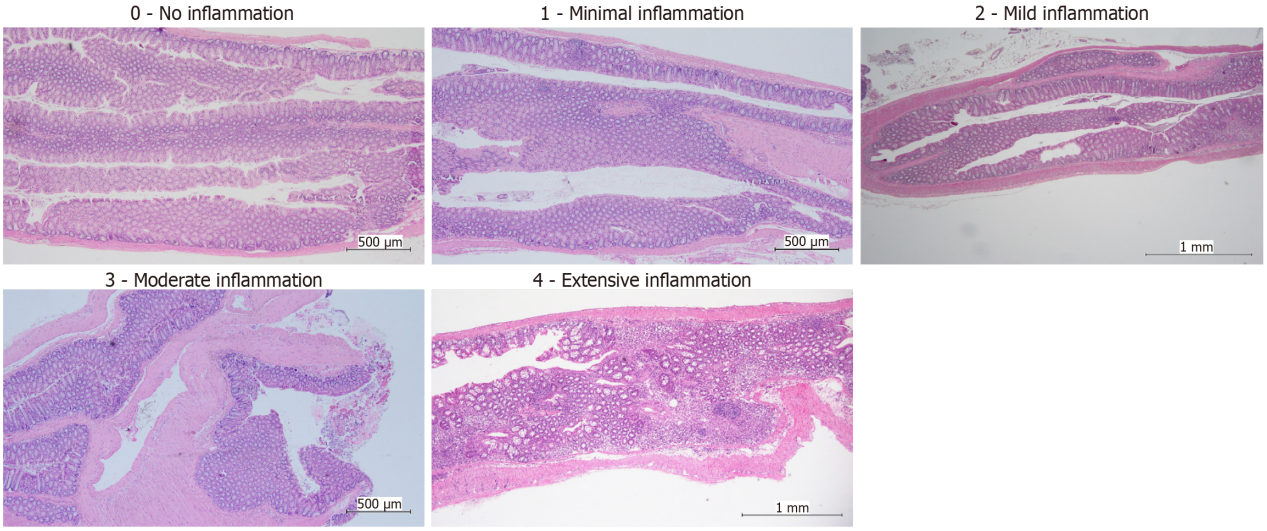
Buparlisib was successful in reducing the activity of PI3K-non-AKT-associated genes

The relative gene expression of the downstream PI3K-non-AKT pathway genes *Pdk1* and *Sgk2*, which are involved in CAC progression, was assessed to study further the impact of the PI3K inhibitor on CAC development. Buparlisib treatment showed a downward trend in the expression of *Pdk1* (2.04 ± 1.17) in the CAC-induced mice group, however, it is not significant compared to the untreated group (Figure 8). Only *Sgk2* expression showed a significant reduction in treated CAC-induced mice (2.56 ± 1.09) in comparison to the untreated CAC mice (5.61 ± 0.79) ($P < 0.05$).



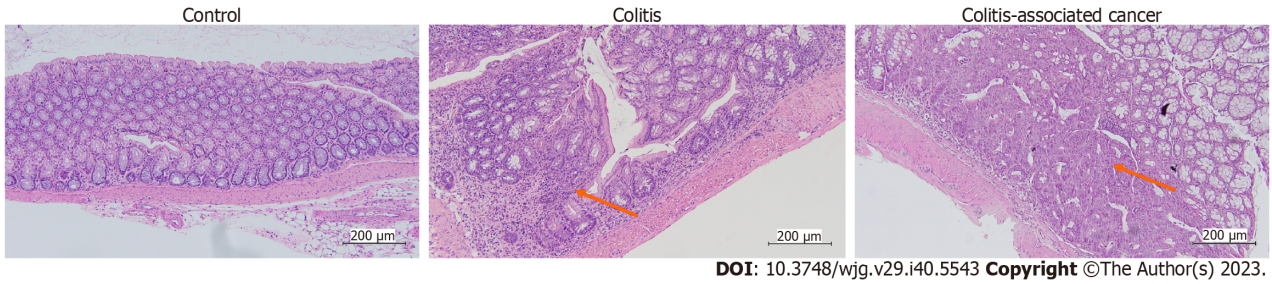
DOI: 10.3748/wjg.v29.i40.5543 **Copyright** ©The Author(s) 2023.

Figure 4 The body weight changes. A: Percentage of weight loss (%) in all groups. A drop in body weight was seen in the colitis-associated cancer (CAC) group after every cycle of dextran sodium sulphate (DSS) induction. Red arrows indicate the cycle of DSS induction. Two-way ANOVA was employed; $n = 8$; B: Total mean body weight loss (g) between buparlisib-treated and -untreated CAC-induced mice group. $^{a}P < 0.05$ (compared to the CAC untreated group); data are presented as mean ± SEM; student T-test was employed; $n = 4$. CAC: Colitis-associated cancer; CRC: Colorectal cancer.



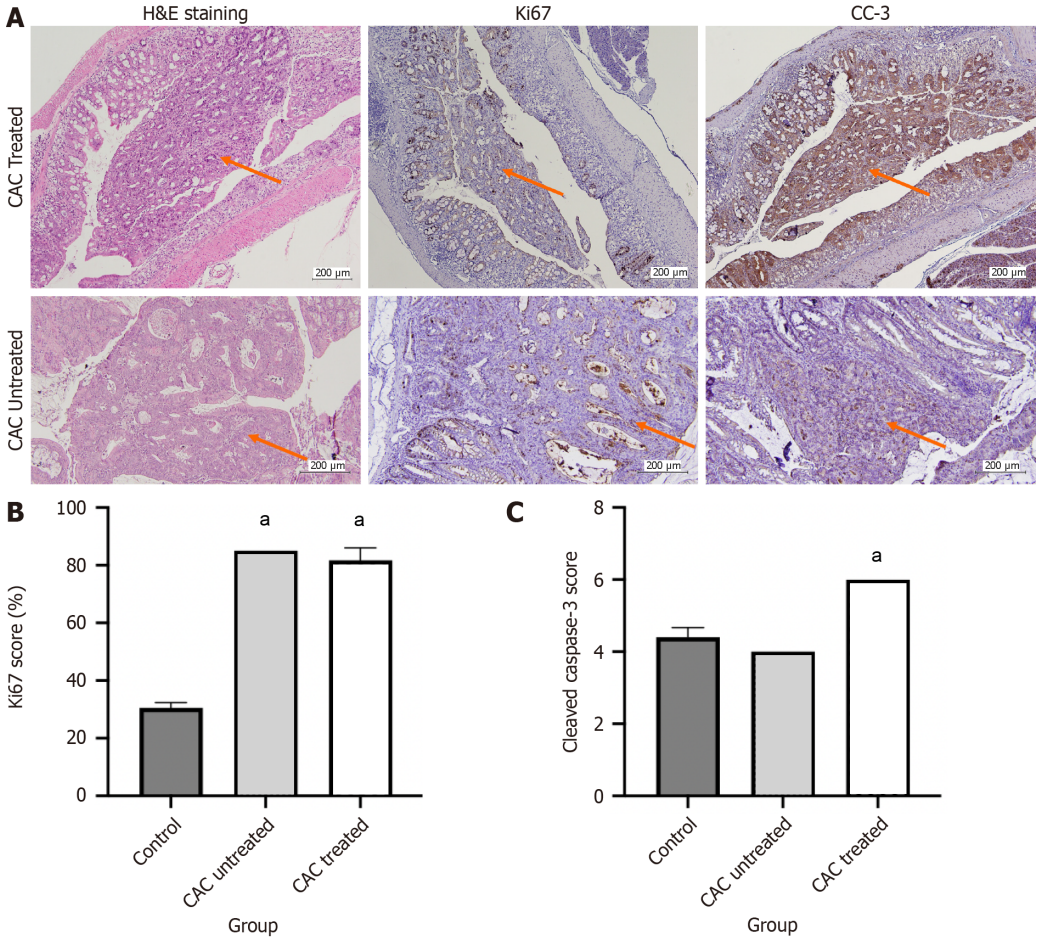
DOI: 10.3748/wjg.v29.i40.5543 **Copyright** ©The Author(s) 2023.

Figure 5 Histological structure assessment. The range of the histologic scores varied from 0 (no inflammation) to 4 (extensive inflammation). Magnification is 40 ×.



DOI: 10.3748/wjg.v29.i40.5543 **Copyright** ©The Author(s) 2023.

Figure 6 Histological examination of the control, colitis and colitis-associated cancer mice model. The control group exhibited a healthy colon with a uniform gland shape. Meanwhile, the colitis mice group showed mild to moderate inflammation. The tumor was only found in the colitis-associated cancer-induced mice group. Red arrows indicate the inflamed area and tumor sites. Magnification is 100 ×.



DOI: 10.3748/wjg.v29.i40.5543 **Copyright** ©The Author(s) 2023.

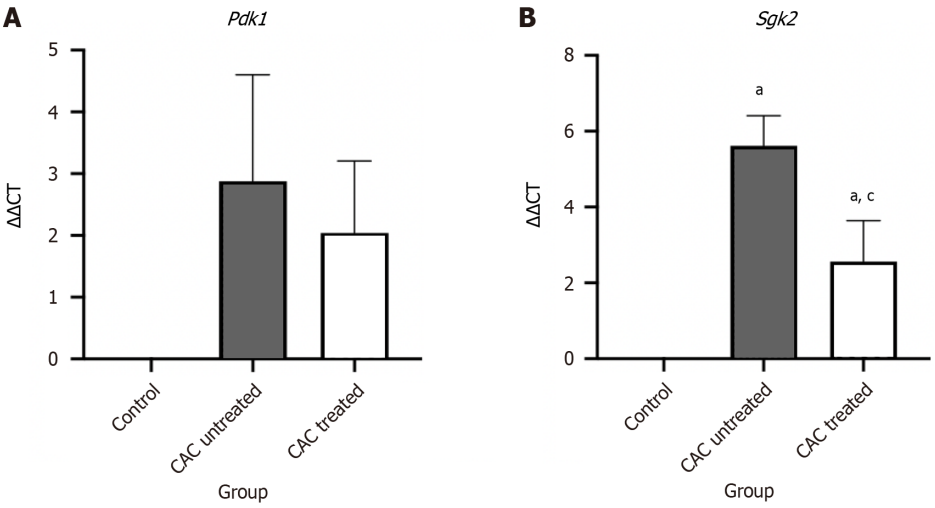
Figure 7 Immunohistochemistry analysis on Ki67 and cleaved caspase-3 markers on colitis-associated cancer-mice model. A: H&E staining, Ki67 and cleaved caspase-3 (CC-3) staining; B and C: Ki67 and CC-3 staining exhibited lower proliferative and higher apoptotic cells on the buparlisib-treated colitis-associated cancer (CAC) mice model compared to the untreated CAC mice. [a]*P* < 0.05 (compared to the control group); data are presented as mean ± SEM; one-way ANOVA was employed; *n* = 4-8. The red arrow showed the tumor area. Magnification is 100 ×. CAC: Colitis-associated cancer; CC-3: Cleaved caspase-3.

DISCUSSION

A well-known pathway in the emergence of inflammation-related cancer is the PI3K pathway. Dysregulation of the PI3K signaling pathway may affect cellular development, metabolism, proliferation, and apoptosis[28]. Recent research on the function of cytokine-induced PI3K-related genes in CAC patients led to the discovery of possible mutations that might connect CAC with UC and CRC[17]. We are, therefore, interested in learning more about the pathophysiology of CAC and how the PI3K signaling pathway is involved. In this study, we utilized dual luciferase assay to investigate the functional significance of rs10889677, a somatic mutation related to PI3K, and we generated CAC in mice to assess the function and regulation of PI3K inhibitor in the modulation of PI3K-non-AKT signaling pathway.

The single nucleotide polymorphism (SNP) rs10889677 is a genetic variant identified in the IL23R, one of the cytokine-induced PI3K-related genes. This particular SNP is a variation in the DNA sequence of the *IL23R*, where a single nucleotide (cytosine, C) is replaced by another nucleotide (adenine, A). The rs10889677 SNP is situated precisely in the 3′ untranslated region of *IL23R*, which is also a miRNA binding site[29]. Any SNPs present in the miRNA binding site may affect how miRNA-mRNA interacts, changing the stability or translation efficiency of the mRNA[30]. This, in turn, may influence the expression of the IL23R protein, which is involved in immune response and inflammation, and may increase the susceptibility to certain diseases, such as CRC. The rs10889677 mutation has been linked strongly to IBD and several other cases, including breast, lung, bladder and colorectal[31-33]. In our recent publication, we have successfully predicted a notable decrease in the stability of mRNA secondary structure for the rs10889677 variant construct compared to the wildtype[17]. This finding supported the hypothesis that genetic mutations resulted in mRNA structural instability and disrupted the binding sites[17].

About 60%-70% of human CRC s were associated with activating the PI3K pathway, increased *AKT* signaling and *PTEN* inactivation[34]. Furthermore, PI3K inhibitors have been proposed as another effective targeted therapy for solid tumors, including CRC[35,36]. Nevertheless, further elucidation regarding the utilization of PI3K inhibitors in the context of CAC is warranted. Balb/c male mice were chosen because they are more susceptible and prone to grow tumors than other strains, and tumors were induced in them with a combination of AOM injection and repeated DSS cycles[37,38]. The application of combined AOM and DSS is a potent, reproducible, and reasonably priced initiation-promotion



DOI: 10.3748/wjg.v29.i40.5543 **Copyright** ©The Author(s) 2023.

Figure 8 The relative gene expression for *Pdk1* and *Sgk2*. A: The relative gene expression of *Pdk1* in colitis-associated cancer (CAC)-induced mice showed no significant difference between buparlisib treated and untreated group; B: In CAC-induced mice, buparlisib treatment demonstrated a significantly reduced expression of *Sgk2*. [a]*P* < 0.05 (compared to the control group); [c]*P* < 0.05 (compared to the CAC untreated group); data are presented as mean ± SEM; one-way ANOVA was employed; *n* = 4-8. CAC: Colitis-associated cancer; DDCT: Delta-delta CT; *Pdk1*: Phosphoinositide-dependent kinase 1; *Sgk2*: Serum/glucocorticoid regulated kinase 2.

paradigm that has been widely used in CAC-related research[25,39]. A high DAI score indicates that the mouse CAC model is successful. The CAC-induced mice model manifested similar symptoms as CAC patients, where the mice were experiencing rectal bleeding, watering stool and body weight loss[40]. According to a previous study, symptoms including bloody stools, began to manifest between days 13 and 21 after the mice received DSS[41]. Similar results were shown in this study, where disease activity in CAC-induced mice began to increase dramatically following the second cycle of DSS, which occurred just 21 d after the first induction of DSS.

Histologically, three cycles of 2.5% DSS induced mild to moderate inflammatory response in the colitis group. No tumor formation was observed along the digestive system in the CRC group. Hence, no additional evaluation of those tissues was done. On the other hand, 50% of the CAC-induced mice group were found to have moderate inflammation. No diffuse inflammation was observed in the colonic mucosal of CAC-induced mice, even though it was reported that signs of diffuse inflammation can appear as early as third to fourth weeks after treatment[42]. Furthermore, compared to a prior study, where submucosal tumor infiltrations were sporadically seen in 20%–24% of AOM-DSS mice at week ten, the percentage of CAC-induced mice with tumors in this study was considered high[43]. The selection of the mouse strain may have affected the percentage of tumor occurrence because different strains of mice have varying susceptibilities.

Buparlisib was given daily for 14 d to the CAC-induced mice group to perform additional research on the function of PI3K inhibitors. Buparlisib is a potent oral pan-PI3K inhibitor that targets all four catalytic isoforms of class I PI3K (p110α, p110β, p110δ and p110γ)[44]. Buparlisib has been tested in clinical trials phase I and II in several solid tumors, including breast, brain, and lung cancer[20]. The preclinical studies showed buparlisib's inhibitory action against numerous PI3K isoforms and anti-proliferative effects in various *in vitro* cell lines[19]. Additionally, the authors provided the outcomes of *in vivo* studies with mouse xenograft models that demonstrate the effectiveness of buparlisib in reducing tumor growth [19]. Our findings showed that buparlisib treatment significantly decreased weight loss in CAC-induced mice. Another study supported this finding in which buparlisib therapy inhibited the growth of established patient-derived glioblastoma multiforme xenografts and increased survival in nude rats[45].

Additionally, buparlisib treatment in CAC-induced mice resulted in a slight rise in apoptotic cell activity and decreased cell proliferation. This result was consistent with several studies that found buparlisib to have the ability to induce apoptosis and reduce tumor growth in a variety of malignancies[44,46]. Buparlisib's effectiveness was also examined in CRC cell lines, where it was discovered that the drug had a considerable impact on the process of apoptosis induction, which progressed from AKT inhibition *via* FoxO3a-dependent p53 upregulated modulator of apoptosis induction[47].

Additionally, buparlisib treatment has been demonstrated to inhibit the PI3K/Akt signaling pathway, which causes apoptosis and slows tumor growth in medulloblastoma cells[44]. The most frequent downstream targets of buparlisib are *AKT* and *mTOR*. Studies have demonstrated that buparlisib effectively inhibited at serine 473 and threonine 308 and suppressed the phosphorylation of proteins downstream from mTORC1, including *S6K* and *4E-BP1* in bone and soft tissue sarcomas[48]. Despite that, there has been limited research conducted on the correlation between buparlisib and PI3K-non-AKT downstream pathways. Our results revealed that the non-AKT downstream of PI3K, *Pdk1* and *Sgk2* also showed a similar down-regulation tendency with buparlisib treatment. The expression of two PI3K-non-AKT downstream genes was previously found to be higher in malignant tissues than in healthy mucosa[49,50]. *PDK1* is a gene that plays a critical role in regulating cell proliferation and survival through its ability to curb signal propagation to the downstream targets such as *AKT* and *SGK2*. *PDK1* was discovered to interact with a specific protein known as HuR (human antigen R), which is known to attach to the mRNA of PI3K and stabilize it, enhancing the production of PI3K[51].

Meanwhile, *SGK* is activated by the same signaling cascade as *AKT*, and its inhibitor has been created and demonstrated encouraging results in preclinical tests as a possible therapeutic target in cancer[52]. The therapeutic potential of *SGK1 i*nhibition in cancer treatment has been demonstrated in preclinical studies using a variety of small molecule inhibitors and RNAi-based strategies that target *SGK1*[53]. Buparlisib and wortmannin, both of which are PI3K inhibitors, decreased the stimulatory impact of insulin on hOAT4 transport activity, aided by *SGK2*[54]. This showed that PI3K inhibition, whether by buparlisib or wortmannin, can lessen the stimulatory effect of insulin on hOAT4 transport activity and that *SGK2* may mediate this effect[54].

There are a few limitations in this study. There were only male mice used in the animal experiment. The AOM/DSS-induced mice model has been widely used in research, with a focus on male mice[42]. This preference for male mice is primarily caused by behavioural changes in female mice that can be altered by hormone cycles[55]. Additional studies using female balb/c mice will be required to establish that gender does not interfere with generalization of findings. Another limitation of this study is that the gene expression analysis was only performed on mouse tissues derived from inflammatory and malignant regions. It would be beneficial to include surrounding normal tissue in the analysis to observe and analyse any potential differences.

CONCLUSION

We investigated the functional relevance of the cytokine-induced PI3K-related gene variation, rs10889677, and it is hypothesized that this variant was a mediating factor in the beginning of the PI3K signaling pathway. Buparlisib, a PI3K inhibitor, was also administered, and it showed promise in preventing PI3K-non-AKT activation in the CAC-induced mice model. Overall, our research may offer a fresh perspective on how PI3K is used in the pathophysiology of CAC.

ARTICLE HIGHLIGHTS

Research background

The phosphatidylinositol-3-kinases (PI3K)/AKT pathway has emerged as a potential new approach in the complicated landscape of inflammation-related cancer, providing new hope for patients with colitis-associated cancer (CAC). A recent discovery in the investigation of PI3K-related genes revealed a promising association between ulcerative colitis (UC), colorectal cancer (CRC), and the elusive rs10889677 mutation.

Research motivation

Understanding the involvement of the PI3K signalling pathway in the development and progression of CAC. Genetic Variants and CAC Susceptibility: Investigating the impact of genetic variants, such as the rs10889677 variant, on CAC susceptibility and their contribution to PI3K pathway activation. The potential of the pan-class I PI3K inhibitor buparlisib as a potential therapeutic option for the treatment of CAC was being examined.

Research objectives

To investigate the role of PI3K-related gene variation in CAC pathogenesis and to evaluate the therapeutic potential of buparlisib, a powerful pan-class I PI3K inhibitor with tumor-suppressive properties.

Research methods

The study examined the genomic DNA from 32 colonic samples from cases of CAC, UC, and CRC. The rs10889677 mutation was highlighted, which was amplified and cloned for both mutant and wild-type fragments in the pmirGLO vector. Luciferase activity was measured using the HT29 cell line. CAC was induced using a precise protocol that included azoxymethane and sodium dextran sulphate. Buparlisib was administered after 14 d. Immunohistochemistry for Ki67 and Cleaved-caspase-3 markers as well as quantitative real-time polymerase chain reaction for *Pdk1* and *Sgk2* were performed on excised colonic tissues.

Research results

Buparlisib significantly reduced the mean weight loss in these mice, indicating an increase in general health and well-being. It has an effect in slowing cancer cell development and promoting cell death in CAC-induced mice. It also had an effect on the expression of particular genes involved in the PI3K pathway, with significantly decreased *Sgk2* expression and a decreasing trend in *Pdk1* expression.

Research conclusions

Our study discovered that a specific genetic variant (rs10889677 variation) is critical in the activation of a cancer-promoting pathway known as PI3K. We also discovered that a drug called buparlisib can prevent this route from being triggered, which is great news for those fighting cancer (CAC).

Research perspectives

Patient stratification: Future research could look into whether the rs10889677 variant can be used as a biomarker to

predict CAC development in UC patients. This could help with early detection and personalised treatment initiatives. Mechanism Elucidation: The mechanisms by which the rs10889677 variation alters the PI3K pathway should be studied further in the future.

ACKNOWLEDGEMENTS

Special thanks to the Jameel Education Foundation for the student financial assistance. We also would like to thank Mrs Nazierah Abd Ghani from the Department of Physiology, Faculty of Medicine, UKM, for her assistance in animal handling; staff of Laboratory Animal Resource Unit (LARU), UKM, for providing the animal facilities; Mr Muaatamarulain Mustangin from Department of Pathology, Faculty of Medicine, UKM for his assistance in histology optimization and Dr Saiful Effendi Syafruddin from UMBI, UKM for his assistance in cloning works.

FOOTNOTES

Author contributions: Mokhtar NM and Raja Ali RA contributed to the conceptualization; Mokhtar NM, Raja Ali RA, Muhammad Nawawi KN, and Razali NN contributed to the methodology and participant recruitments; Razali NN, and Mohd Rathi ND contributed to the animal handling; Razali NN, Yahaya A, and Mokhtar NM performed the validation; Razali NN, and Mokhtar NM contributed to the data analysis; Razali NN wrote the original draft preparation; Mokhtar NM, Raja Ali RA, and Muhammad Nawawi KN wrote the review and editing; Mokhtar NM, Raja Ali RA, and Muhammad Nawawi KN contributed to the supervision; All authors have read and agreed to the published version of the manuscript.

Supported by The Fundamental Research Grant Scheme, Ministry of Higher Education, Malaysia, No. FRGS/1/2018/SKK06/UKM/02/4.

Institutional review board statement: The human study has been approved under the Universiti Kebangsaan Malaysia Research Ethics Committee with a reference number: UKM/PPI/111/8/JEP-2019-572.

Institutional animal care and use committee statement: The animal study has been approved under the Animal Ethics Committee of Universiti Kebangsaan Malaysia with a reference number: PPUKM/2019/NORFILZA/25-SEPT./1035-SEPT.-2019-DEC.-2021 has approved the animal handling protocol.

Informed consent statement: Written informed consent was obtained from all the patients.

Conflict-of-interest statement: There is no conflict of interest.

Data sharing statement: Our raw data will be shared upon official request.

ARRIVE guidelines statement: The authors have read the ARRIVE guidelines, and the manuscript was prepared and revised according to the ARRIVE guidelines.

Open-Access: This article is an open-access article that was selected by an in-house editor and fully peer-reviewed by external reviewers. It is distributed in accordance with the Creative Commons Attribution NonCommercial (CC BY-NC 4.0) license, which permits others to distribute, remix, adapt, build upon this work non-commercially, and license their derivative works on different terms, provided the original work is properly cited and the use is non-commercial. See: https://creativecommons.org/Licenses/by-nc/4.0/

Country/Territory of origin: Malaysia

ORCID number: Nurul Nadirah Razali 0000-0002-7725-0353; Raja Affendi Raja Ali 0000-0003-4995-3868; Khairul Najmi Muhammad Nawawi 0000-0002-5309-5301; Norfilza Mohd Mokhtar 0000-0002-4863-100X.

S-Editor: Fan JR
L-Editor: A
P-Editor: Zhao S

REFERENCES

1 **Grivennikov SI**, Cominelli F. Colitis-Associated and Sporadic Colon Cancers: Different Diseases, Different Mutations? *Gastroenterology* 2016; **150**: 808-810 [PMID: 26924087 DOI: 10.1053/j.gastro.2016.02.062]
2 **Liverani E**, Scaioli E, Digby RJ, Bellanova M, Belluzzi A. How to predict clinical relapse in inflammatory bowel disease patients. *World J Gastroenterol* 2016; **22**: 1017-1033 [PMID: 26811644 DOI: 10.3748/wjg.v22.i3.1017]
3 **Laukoetter MG**, Mennigen R, Hannig CM, Osada N, Rijcken E, Vowinkel T, Krieglstein CF, Senninger N, Anthoni C, Bruewer M. Intestinal cancer risk in Crohn's disease: a meta-analysis. *J Gastrointest Surg* 2011; **15**: 576-583 [PMID: 21152994 DOI: 10.1007/s11605-010-1402-9]
4 **Zhou Q**, Shen ZF, Wu BS, Xu CB, He ZQ, Chen T, Shang HT, Xie CF, Huang SY, Chen YG, Chen HB, Han ST. Risk of Colorectal Cancer in

Ulcerative Colitis Patients: A Systematic Review and Meta-Analysis. *Gastroenterol Res Pract* 2019; **2019**: 5363261 [PMID: 31781191 DOI: 10.1155/2019/5363261]

5 **Zhiqin W**, Palaniappan S, Raja Ali RA. Inflammatory Bowel Disease-related Colorectal Cancer in the Asia-Pacific Region: Past, Present, and Future. *Intest Res* 2014; **12**: 194-204 [PMID: 25349593 DOI: 10.5217/ir.2014.12.3.194]

6 **Ananthakrishnan AN**, Bernstein CN, Iliopoulos D, Macpherson A, Neurath MF, Ali RAR, Vavricka SR, Fiocchi C. Environmental triggers in IBD: a review of progress and evidence. *Nat Rev Gastroenterol Hepatol* 2018; **15**: 39-49 [PMID: 29018271 DOI: 10.1038/nrgastro.2017.136]

7 **Mokhtar NM**, Nawawi KNM, Verasingam J, Zhiqin W, Sagap I, Azman ZAM, Mazlan L, Hamid HA, Yaacob NY, Rose IM, Den ELN, Wan MS, Raja Ali RA. A four-decade analysis of the incidence trends, sociodemographic and clinical characteristics of inflammatory bowel disease patients at single tertiary centre, Kuala Lumpur, Malaysia. *BMC Public Health* 2019; **19**: 550 [PMID: 31196184 DOI: 10.1186/s12889-019-6858-2]

8 **Kameyama H**, Nagahashi M, Shimada Y, Tajima Y, Ichikawa H, Nakano M, Sakata J, Kobayashi T, Narayanan S, Takabe K, Wakai T. Genomic characterization of colitis-associated colorectal cancer. *World J Surg Oncol* 2018; **16**: 121 [PMID: 29966533 DOI: 10.1186/s12957-018-1428-0]

9 **Hartnett L**, Egan LJ. Inflammation, DNA methylation and colitis-associated cancer. *Carcinogenesis* 2012; **33**: 723-731 [PMID: 22235026 DOI: 10.1093/carcin/bgs006]

10 **Axelrad JE**, Lichtiger S, Yajnik V. Inflammatory bowel disease and cancer: The role of inflammation, immunosuppression, and cancer treatment. *World J Gastroenterol* 2016; **22**: 4794-4801 [PMID: 27239106 DOI: 10.3748/wjg.v22.i20.4794]

11 **Zundler S**, Neurath MF. Integrating Immunologic Signaling Networks: The JAK/STAT Pathway in Colitis and Colitis-Associated Cancer. *Vaccines (Basel)* 2016; **4** [PMID: 26938566 DOI: 10.3390/vaccines4010005]

12 **Qu X**, Tang Y, Hua S. Immunological Approaches Towards Cancer and Inflammation: A Cross Talk. *Front Immunol* 2018; **9**: 563 [PMID: 29662489 DOI: 10.3389/fimmu.2018.00563]

13 **Fruman DA**, Chiu H, Hopkins BD, Bagrodia S, Cantley LC, Abraham RT. The PI3K Pathway in Human Disease. *Cell* 2017; **170**: 605-635 [PMID: 28802037 DOI: 10.1016/j.cell.2017.07.029]

14 **Hoxhaj G**, Manning BD. The PI3K-AKT network at the interface of oncogenic signalling and cancer metabolism. *Nat Rev Cancer* 2020; **20**: 74-88 [PMID: 31686003 DOI: 10.1038/s41568-019-0216-7]

15 **Ciraolo E**, Gulluni F, Hirsch E. Methods to measure the enzymatic activity of PI3Ks. *Methods Enzymol* 2014; **543**: 115-140 [PMID: 24924130 DOI: 10.1016/B978-0-12-801329-8.00006-4]

16 **Low END**, Mokhtar NM, Wong Z, Raja Ali RA. Colonic Mucosal Transcriptomic Changes in Patients with Long-Duration Ulcerative Colitis Revealed Colitis-Associated Cancer Pathways. *J Crohns Colitis* 2019; **13**: 755-763 [PMID: 30954025 DOI: 10.1093/ecco-jcc/jjz002]

17 **Razali NN**, Raja Ali RA, Muhammad Nawawi KN, Yahaya A, Mokhtar NM. Targeted Sequencing of Cytokine-Induced PI3K-Related Genes in Ulcerative Colitis, Colorectal Cancer and Colitis-Associated Cancer. *Int J Mol Sci* 2022; **23** [PMID: 36232773 DOI: 10.3390/ijms231911472]

18 **Pons-Tostivint E**, Thibault B, Guillermet-Guibert J. Targeting PI3K Signaling in Combination Cancer Therapy. *Trends Cancer* 2017; **3**: 454-469 [PMID: 28718419 DOI: 10.1016/j.trecan.2017.04.002]

19 **Maira SM**, Pecchi S, Huang A, Burger M, Knapp M, Sterker D, Schnell C, Guthy D, Nagel T, Wiesmann M, Brachmann S, Fritsch C, Dorsch M, Chène P, Shoemaker K, De Pover A, Menezes D, Martiny-Baron G, Fabbro D, Wilson CJ, Schlegel R, Hofmann F, García-Echeverría C, Sellers WR, Voliva CF. Identification and characterization of NVP-BKM120, an orally available pan-class I PI3-kinase inhibitor. *Mol Cancer Ther* 2012; **11**: 317-328 [PMID: 22188813 DOI: 10.1158/1535-7163.MCT-11-0474]

20 **Mishra R**, Patel H, Alanazi S, Kilroy MK, Garrett JT. PI3K Inhibitors in Cancer: Clinical Implications and Adverse Effects. *Int J Mol Sci* 2021; **22** [PMID: 33801659 DOI: 10.3390/ijms22073464]

21 **Zhao W**, Qiu Y, Kong D. Class I phosphatidylinositol 3-kinase inhibitors for cancer therapy. *Acta Pharm Sin B* 2017; **7**: 27-37 [PMID: 28119806 DOI: 10.1016/j.apsb.2016.07.006]

22 **Janku F**, Yap TA, Meric-Bernstam F. Targeting the PI3K pathway in cancer: are we making headway? *Nat Rev Clin Oncol* 2018; **15**: 273-291 [PMID: 29508857 DOI: 10.1038/nrclinonc.2018.28]

23 **Ni J**, Ramkissoon SH, Xie S, Goel S, Stover DG, Guo H, Luu V, Marco E, Ramkissoon LA, Kang YJ, Hayashi M, Nguyen QD, Ligon AH, Du R, Claus EB, Alexander BM, Yuan GC, Wang ZC, Iglehart JD, Krop IE, Roberts TM, Winer EP, Lin NU, Ligon KL, Zhao JJ. Combination inhibition of PI3K and mTORC1 yields durable remissions in mice bearing orthotopic patient-derived xenografts of HER2-positive breast cancer brain metastases. *Nat Med* 2016; **22**: 723-726 [PMID: 27270588 DOI: 10.1038/nm.4120]

24 **Untergasser A**, Nijveen H, Rao X, Bisseling T, Geurts R, Leunissen JA. Primer3Plus, an enhanced web interface to Primer3. *Nucleic Acids Res* 2007; **35**: W71-W74 [PMID: 17485472 DOI: 10.1093/nar/gkm306]

25 **Parang B**, Barrett CW, Williams CS. AOM/DSS Model of Colitis-Associated Cancer. *Methods Mol Biol* 2016; **1422**: 297-307 [PMID: 27246042 DOI: 10.1007/978-1-4939-3603-8_26]

26 **Hidalgo-Cantabrana C**, Algieri F, Rodriguez-Nogales A, Vezza T, Martínez-Camblor P, Margolles A, Ruas-Madiedo P, Gálvez J. Effect of a Ropy Exopolysaccharide-Producing Bifidobacterium animalis subsp. lactis Strain Orally Administered on DSS-Induced Colitis Mice Model. *Front Microbiol* 2016; **7**: 868 [PMID: 27375589 DOI: 10.3389/fmicb.2016.00868]

27 **Rogers R**, Eastham-Anderson J, DeVoss J, Lesch J, Yan D, Xu M, Solon M, Hotzel K, Diehl L, Webster JD. Image Analysis-Based Approaches for Scoring Mouse Models of Colitis. *Vet Pathol* 2016; **53**: 200-210 [PMID: 25907770 DOI: 10.1177/0300985815579998]

28 **Papadatos-Pastos D**, Rabbie R, Ross P, Sarker D. The role of the PI3K pathway in colorectal cancer. *Crit Rev Oncol Hematol* 2015; **94**: 18-30 [PMID: 25591826 DOI: 10.1016/j.critrevonc.2014.12.006]

29 **Moschen AR**, Tilg H, Raine T. IL-12, IL-23 and IL-17 in IBD: immunobiology and therapeutic targeting. *Nat Rev Gastroenterol Hepatol* 2019; **16**: 185-196 [PMID: 30478416 DOI: 10.1038/s41575-018-0084-8]

30 **Bhaumik P**, Gopalakrishnan C, Kamaraj B, Purohit R. Single nucleotide polymorphisms in microRNA binding sites: implications in colorectal cancer. *ScientificWorldJournal* 2014; **2014**: 547154 [PMID: 25654126 DOI: 10.1155/2014/547154]

31 **Duerr RH**, Taylor KD, Brant SR, Rioux JD, Silverberg MS, Daly MJ, Steinhart AH, Abraham C, Regueiro M, Griffiths A, Dassopoulos T, Bitton A, Yang H, Targan S, Datta LW, Kistner EO, Schumm LP, Lee AT, Gregersen PK, Barmada MM, Rotter JI, Nicolae DL, Cho JH. A genome-wide association study identifies IL23R as an inflammatory bowel disease gene. *Science* 2006; **314**: 1461-1463 [PMID: 17068223 DOI: 10.1126/science.1135245]

32 **Zheng J**, Jiang L, Zhang L, Yang L, Deng J, You Y, Li N, Wu H, Li W, Lu J, Zhou Y. Functional genetic variations in the IL-23 receptor gene

are associated with risk of breast, lung and nasopharyngeal cancer in Chinese populations. *Carcinogenesis* 2012; **33**: 2409-2416 [PMID: 23042301 DOI: 10.1093/carcin/bgs307]

33 **Peng LL**, Wang Y, Zhu FL, Xu WD, Ji XL, Ni J. IL-23R mutation is associated with ulcerative colitis: A systemic review and meta-analysis. *Oncotarget* 2017; **8**: 4849-4863 [PMID: 27902482 DOI: 10.18632/oncotarget.13607]

34 **Pandurangan AK**. Potential targets for prevention of colorectal cancer: a focus on PI3K/Akt/mTOR and Wnt pathways. *Asian Pac J Cancer Prev* 2013; **14**: 2201-2205 [PMID: 23725112 DOI: 10.7314/apjcp.2013.14.4.2201]

35 **Janku F**. Phosphoinositide 3-kinase (PI3K) pathway inhibitors in solid tumors: From laboratory to patients. *Cancer Treat Rev* 2017; **59**: 93-101 [PMID: 28779636 DOI: 10.1016/j.ctrv.2017.07.005]

36 **Fernandes MS**, Sanches JM, Seruca R. Targeting the PI3K Signalling as a Therapeutic Strategy in Colorectal Cancer. *Adv Exp Med Biol* 2018; **1110**: 35-53 [PMID: 30623365 DOI: 10.1007/978-3-030-02771-1_4]

37 **Suzuki R**, Kohno H, Sugie S, Nakagama H, Tanaka T. Strain differences in the susceptibility to azoxymethane and dextran sodium sulfate-induced colon carcinogenesis in mice. *Carcinogenesis* 2006; **27**: 162-169 [PMID: 16081511 DOI: 10.1093/carcin/bgi205]

38 **Rosenberg DW**, Giardina C, Tanaka T. Mouse models for the study of colon carcinogenesis. *Carcinogenesis* 2009; **30**: 183-196 [PMID: 19037092 DOI: 10.1093/carcin/bgn267]

39 **Greten FR**, Eckmann L, Greten TF, Park JM, Li ZW, Egan LJ, Kagnoff MF, Karin M. IKKbeta links inflammation and tumorigenesis in a mouse model of colitis-associated cancer. *Cell* 2004; **118**: 285-296 [PMID: 15294155 DOI: 10.1016/j.cell.2004.07.013]

40 **Moazzami B**, Moazzami K, Rezaei N. Early onset inflammatory bowel disease: manifestations, genetics and diagnosis. *Turk J Pediatr* 2019; **61**: 637-647 [PMID: 32104994 DOI: 10.24953/turkjped.2019.05.001]

41 **Tanaka T**, Kohno H, Suzuki R, Yamada Y, Sugie S, Mori H. A novel inflammation-related mouse colon carcinogenesis model induced by azoxymethane and dextran sodium sulfate. *Cancer Sci* 2003; **94**: 965-973 [PMID: 14611673 DOI: 10.1111/j.1349-7006.2003.tb01386.x]

42 **De Robertis M**, Massi E, Poeta ML, Carotti S, Morini S, Cecchetelli L, Signori E, Fazio VM. The AOM/DSS murine model for the study of colon carcinogenesis: From pathways to diagnosis and therapy studies. *J Carcinog* 2011; **10**: 9 [PMID: 21483655 DOI: 10.4103/1477-3163.78279]

43 **Tanimura Y**, Fukui T, Horitani S, Matsumoto Y, Miyamoto S, Suzuki R, Tanaka T, Tomiyama T, Ikeura T, Ando Y, Nishio A, Okazaki K. Long-term model of colitis-associated colorectal cancer suggests tumor spread mechanism and nature of cancer stem cells. *Oncol Lett* 2021; **21**: 7 [PMID: 33240413 DOI: 10.3892/ol.2020.12268]

44 **Zhao P**, Hall J, Durston M, Voydanoff A, VanSickle E, Kelly S, Nagulapally AB, Bond J, Saulnier Sholler G. BKM120 induces apoptosis and inhibits tumor growth in medulloblastoma. *PLoS One* 2017; **12**: e0179948 [PMID: 28662162 DOI: 10.1371/journal.pone.0179948]

45 **Netland IA**, Førde HE, Sleire L, Leiss L, Rahman MA, Skeie BS, Miletic H, Enger PØ, Goplen D. Treatment with the PI3K inhibitor buparlisib (NVP-BKM120) suppresses the growth of established patient-derived GBM xenografts and prolongs survival in nude rats. *J Neurooncol* 2016; **129**: 57-66 [PMID: 27283525 DOI: 10.1007/s11060-016-2158-1]

46 **Li X**, Dai D, Chen B, Tang H, Xie X, Wei W. Efficacy of PI3K/AKT/mTOR pathway inhibitors for the treatment of advanced solid cancers: A literature-based meta-analysis of 46 randomised control trials. *PLoS One* 2018; **13**: e0192464 [PMID: 29408858 DOI: 10.1371/journal.pone.0192464]

47 **Yang S**, Li X, Guan W, Qian M, Yao Z, Yin X, Zhao H. NVP-BKM120 inhibits colon cancer growth *via* FoxO3a-dependent PUMA induction. *Oncotarget* 2017; **8**: 83052-83062 [PMID: 29137323 DOI: 10.18632/oncotarget.20943]

48 **Anderson JL**, Park A, Akiyama R, Tap WD, Denny CT, Federman N. Evaluation of In Vitro Activity of the Class I PI3K Inhibitor Buparlisib (BKM120) in Pediatric Bone and Soft Tissue Sarcomas. *PLoS One* 2015; **10**: e0133610 [PMID: 26402468 DOI: 10.1371/journal.pone.0133610]

49 **Liu T**, Yin H. PDK1 promotes tumor cell proliferation and migration by enhancing the Warburg effect in non-small cell lung cancer. *Oncol Rep* 2017; **37**: 193-200 [PMID: 27878287 DOI: 10.3892/or.2016.5253]

50 **Chen JB**, Zhang M, Zhang XL, Cui Y, Liu PH, Hu J, Li HH, Jin H, Liu LF, Chen MF, Chen HQ, Liang CZ, Zu XB. Glucocorticoid-Inducible Kinase 2 Promotes Bladder Cancer Cell Proliferation, Migration and Invasion by Enhancing β-catenin/c-Myc Signaling Pathway. *J Cancer* 2018; **9**: 4774-4782 [PMID: 30588263 DOI: 10.7150/jca.25811]

51 **Dieterle AM**, Böhler P, Keppeler H, Alers S, Berleth N, Drießen S, Hieke N, Pietkiewicz S, Löffler AS, Peter C, Gray A, Leslie NR, Shinohara H, Kurosaki T, Engelke M, Wienands J, Bonin M, Wesselborg S, Stork B. PDK1 controls upstream PI3K expression and PIP3 generation. *Oncogene* 2014; **33**: 3043-3053 [PMID: 23893244 DOI: 10.1038/onc.2013.266]

52 **Bruhn MA**, Pearson RB, Hannan RD, Sheppard KE. Second AKT: the rise of SGK in cancer signalling. *Growth Factors* 2010; **28**: 394-408 [PMID: 20919962 DOI: 10.3109/08977194.2010.518616]

53 **Sang Y**, Kong P, Zhang S, Zhang L, Cao Y, Duan X, Sun T, Tao Z, Liu W. SGK1 in Human Cancer: Emerging Roles and Mechanisms. *Front Oncol* 2020; **10**: 608722 [PMID: 33542904 DOI: 10.3389/fonc.2020.608722]

54 **Wang H**, Zhang J, You G. The mechanistic links between insulin and human organic anion transporter 4. *Int J Pharm* 2019; **555**: 165-174 [PMID: 30453017 DOI: 10.1016/j.ijpharm.2018.11.040]

55 **Meziane H**, Ouagazzal AM, Aubert L, Wietrzych M, Krezel W. Estrous cycle effects on behavior of C57BL/6J and BALB/cByJ female mice: implications for phenotyping strategies. *Genes Brain Behav* 2007; **6**: 192-200 [PMID: 16827921 DOI: 10.1111/j.1601-183X.2006.00249.x]

World Journal of Gastroenterology

Submit a Manuscript: https://www.f6publishing.com

World J Gastroenterol 2023 October 28; 29(40): 5557-5565

DOI: 10.3748/wjg.v29.i40.5557

ISSN 1007-9327 (print) ISSN 2219-2840 (online)

ORIGINAL ARTICLE

Retrospective Study

Endoscopic transgastric fenestration versus percutaneous drainage for management of (peri)pancreatic fluid collections adjacent to gastric wall (with video)

Hong-Mei Zhang, Hui-Ting Ke, Md Robin Ahmed, Ya-Juan Li, Ghulam Nabi, Mu-Han Li, Ji-Yu Zhang, Dan Liu, Li-Xia Zhao, Bing-Rong Liu

Specialty type: Gastroenterology and hepatology

Provenance and peer review: Unsolicited article; Externally peer reviewed.

Peer-review model: Single blind

Peer-review report's scientific quality classification

Grade A (Excellent): A
Grade B (Very good): B, B
Grade C (Good): 0
Grade D (Fair): D
Grade E (Poor): 0

P-Reviewer: Kitamura K, Japan; Shelat VG, Singapore; Thandassery RB, United States; Sharma S, India

Received: July 24, 2023
Peer-review started: July 24, 2023
First decision: September 18, 2023
Revised: October 1, 2023
Accepted: October 23, 2023
Article in press: October 23, 2023
Published online: October 28, 2023

Hong-Mei Zhang, Md Robin Ahmed, Ya-Juan Li, Mu-Han Li, Ji-Yu Zhang, Dan Liu, Li-Xia Zhao, Bing-Rong Liu, Department of Gastroenterology and Hepatology, The First Affiliated Hospital of Zhengzhou University, Zhengzhou 450000, Henan Province, China

Hui-Ting Ke, Department of Ultrasound, Ezhou Central Hospital, Ezhou 436099, Hubei Province, China

Ghulam Nabi, Institute of Nature Conservation, Polish Academy of Sciences, Krakow 31120, Poland

Bing-Rong Liu, State Key Laboratory of Esophageal Cancer Prevention and Treatment, Zhengzhou University, Zhengzhou 450052, Henan Province, China

Corresponding author: Bing-Rong Liu, PhD, Chief Physician, Department of Gastroenterology and Hepatology, The First Affiliated Hospital of Zhengzhou University, No. 1 Eastern Jianshe Road, Zhengzhou 450000, Henan Province, China. fccliubr@zzu.edu.cn

Abstract

BACKGROUND

Percutaneous drainage (PCD) and endoscopic approaches have largely replaced surgical drainage as the initial approach for (peri) pancreatic fluid collections (PFC)s, while complications associated with endoscopic stent implantation are common.

AIM

To introduce a novel endoscopic therapy named endoscopic transgastric fenestration (ETGF), which involves resection of tissue by endoscopic accessory between gastric and PFCs without stent implantation, and to evaluate its efficacy and safety compared with PCD for the management of PFCs adjacent to the gastric wall.

METHODS

Patients diagnosed with PFCs adjacent to the gastric wall and who subsequently received ETGF or PCD were restrospectively enrolled. Indications for intervention were consistent with related guidelines. We analyzed patients baseline character-

istics, technical and clinical success rate, recurrence and reintervention rate, procedure-related complications and adverse events.

RESULTS
Seventy-two eligible patients were retrospectively identified (ETGF = 34, PCD = 38) from October 2017 to May 2021. Patients in the ETGF group had a significantly higher clinical success rate than those in the PCD group (97.1 *vs* 76.3%, P = 0.01). There were no statistically significant differences regarding recurrence, reintervention and incidence of complication between the two groups. While long-term catheter drainage was very common in the PCD group.

CONCLUSION
Compared with PCD, ETGF has a higher clinical success rate in the management of PFCs adjacent to the gastric wall. ETGF is an alternative effective strategy for the treatment of PFCs adjacent to the gastric wall.

Key Words: (Peri) Pancreatic fluid collections; Endoscopic transgastric fenestration; Percutaneous drainage

©The Author(s) 2023. Published by Baishideng Publishing Group Inc. All rights reserved.

Core Tip: Inspired by endoscopic full-thickness resection, we proposed the concept of endoscopic transgastric fenestration (ETGF), which involves resection of connect tissue between the gastric wall and (peri) pancreatic fluid collections (PFCs) with the assistance of endoscopic accessory to treat PFCs secondary to pancreatitis adjacent to the gastric wall, avoiding the stent implantation. In the current study, we evaluate the efficacy and safety of ETGF by comparing with percutaneous drainage for the management of PFCs adjacent to the gastric wall.

Citation: Zhang HM, Ke HT, Ahmed MR, Li YJ, Nabi G, Li MH, Zhang JY, Liu D, Zhao LX, Liu BR. Endoscopic transgastric fenestration versus percutaneous drainage for management of (peri)pancreatic fluid collections adjacent to gastric wall (with video). *World J Gastroenterol* 2023; 29(40): 5557-5565
URL: https://www.wjgnet.com/1007-9327/full/v29/i40/5557.htm
DOI: https://dx.doi.org/10.3748/wjg.v29.i40.5557

INTRODUCTION

Pancreatic and peripancreatic fluid collections (PFCs) are causes of fluid leakage or liquefaction of pancreatic necrosis following acute pancreatitis, chronic pancreatitis, surgery or abdominal trauma[1]. Collections usually forms 4 wk after the onset of acute pancreatitis and the majority resolve spontaneously[1]. Indications to intervene PFCs include infection and symptomatic sterile necrosis, while persistent collections that are asymptomatic may be observed[1-3]. Percutaneous drainage (PCD) and an endoscopic approach with stent implantation have replaced surgical drainage as the initial treatment for PFCs which reduce the complications and costs of hospitalization[3-7]. The European Society of Gastrointestinal Endoscopy recommends endoscopy or PCD as the first interventional method for PFCs[8]. PCD is an attractive and conventional approach that appears to be safe and the least invasive. However, inability to remove necrotic debris in the cavity has restricted its use[5,6,9]. Commonly, transluminal endoscopic drainage with stent implantation is an effective method[4,7]. However, embedding, displacement, and bleeding related to stent implantation are common complications, which leads to multi-interventions, and hence resulting in additional cost[10-12]. In addition, application of stent has been limited due to its high cost and is not commercial in some tertiary hospitals in China. Inspired by endoscopic full-thickness resection (EFTR), Liu *et al*[13] first conducted endoscopic transgastric fenestration (ETGF), an innovative endoscopic treatment avoiding the implantation of a stent to manage PFCs. ETGF involves endoscopic resection of connected tissues between gastric and pancreatic lesions with the assistance of endoscopic accessory, which can drain the collection of fluid in the cavity and debride the necrotic debris inside. In this retrospective study, the primary objective was to assess the availability of ETGF by comparing the rate of technical and clinical success, recurrence and reintervention with patients who received PCD. The secondary objective was to assess its safety by evaluating complications related to the procedure.

MATERIALS AND METHODS

Patient enrollment

Patients diagnosed with PFCs at the First Affiliated Hospital of Zhengzhou University between October 2017 and May 2021 were enrolled in this study. Inclusion criteria included patients diagnosed with PFCs that was adjacent to the gastric wall and who subsequently received ETGF or PCD. Indications to intervene PFCs were consistent with related guidelines

[1,8]. Patients with incomplete clinical data and who were lost to follow-up were excluded. All patients underwent ultrasonography (USG), computed tomography (CT) scan or magnetic resonance cholangiopancreatography to evaluate the lesion prior to the procedure. Patients in the ETGF group underwent endoscopy at least twice to observe the absorption of the cavity and the natural healing of the artificial fistula between the gastric wall and the cavity, the majority of which almost healed within 1 mo. CT or USG was reviewed within 6 mo after treatment. The study was approved by the institutional ethics committee and all patients were provided written informed consent to undergo the procedures (KY-2021-00642).

Definitions

PFCs were defined according to the revised Atlanta consensus related to acute pancreatitis[1]. Technical success was defined as the ability to access the lesion. Clinical success was defined as symptom relief with PFCs reduced to < 2 cm within 6 mo without another alternative drainage procedure.

ETGF technique

Endoscopic drainages were performed under general anesthesia with endotracheal intubation as follows: (1) Endoscopic ultrasonography (EUS) was used to determine the lesion location, whether a large vessel was hidden in the operative region and marked the site of fenestration using a Hook knife (KD-620LR, Olympus); (2) then the mucosal layer of the fenestration site was then removed with an endoscopic snare and full-thickness incision was subsequently made with the Hook knife, fluid in the collection was seen to pour out spontaneously; (3) re-evaluation of the fistula between the stomach and cavity; (4) the gastric-collections incision was enlarged to a diameter of approximately 2 cm to the facilitate the operation and drainage by EFTR; (5) coagulating styptic forcep was used for hemostasis (Coagrasper, FD-410LR; Olympus); (6) the endoscope was advanced into the collection, and the content of the PFCs was further cleaned with saline rinse and vacuum suction, debris was removed by snare assistance, and (7) nasocystic tube (18 Fr) was indwelled if necessary (large or complicated with infection) and endoscopy was undertaken twice to observe the healing of the artificial fistula, most of which closed within one month (Figures 1 and 2, Video).

PCD technique

Under local anesthesia using lignocaine, an 18-gauge needle was placed into the PFCs percutaneously with the guidance of USG or CT scan and the fluid was aspirated. A guidewire was then advanced into the collection. The tract was dilated and then a pigtail catheter of 8 or 10 Fr was inserted into the lesion. The catheter was replaced when the drainage tube failed due to obstruction and eventually removed when the collections was < 2 cm in length.

Statistical analysis

Statistical analysis was performed using SPSS Statistics v26.0. For continuous variables, the mean ± SD was used to describe data that fitted a normal distribution and quartiles were used for data that did not conform to normal distribution. Statistical significance was analyzed by the t-test and nonparametric test respectively. Counting card information was described by percentage and performed by the chi-square test. $P < 0.05$ was considered statistically significant.

RESULTS

Between October 2017 and May 2021, a total of 72 patients were enrolled in this study (ETGF = 34, PCD = 38, Figure 3). There were no statistically differences regarding sex and size of the lesion between the two groups. Patients in the ETGF group were younger than in PCD group (36.8 ± 12.9 years *vs* 46.0 ± 16.8years, $P = 0.01$). The clinical success rate in the ETGF group was significantly higher than that in the PCD group (97.1 *vs* 76.3%, $P = 0.01$). There were no statistically significant differences regarding recurrence and reintervention between the two groups. Although the complication rate was similar in the two groups, catheter related adverse events were common in the PCD group (2.9 *vs* 34.3 %, $P = 0.001$). Patients were followed up by the electronic medical record system combined with telephone consultation for a median follow-up of 35 wk (9-85 wk). There was no procedure related mortality in either groups. The largest lesion was encountered in the endoscopic group with a length of 220 mm. Baseline characteristics and patient demographics are shown in Table 1. Primary and secondary outcomes are shown in Table 2.

ETGF approach

Six of 34 patients had previous therapeutic history in another hospital: one received ETGF, one received surgical treatment, and the other four received PCD. The average age of the participants was 36.8 ± 12.9 years old. The mean length of PFCs was 109.4 ± 7.8 mm. The average total interventions were 1.03 sessions. The total duration of hospital stays and total cost was 14.5 d and 4852 $ respectively. Clinical success was achieved in 33 patients (97.1%). One recurrence was observed in this group. With regard to reintervention, 9 cases received a second therapeutic endoscopy for infection in the cavity, and another patient transferred to PCD as a result of inadequate drainage due to small caliber of the fenestration. Procedure related bleeding occurred in 4 patients (11.76%) and was resolved by endoscopy. An nasocystic tube was inserted in seven patients for pus or necrosis collection, and the mean duration of the indwelling nasocystic tube was 8.6 d.

Table 1 Baseline characteristics

	ETGF (%)	PCD (%)	*P* value
Total	34	38	
Male	24 (70.6)	26 (68.4)	0.84
Mean age	36.8 ± 12.9	46.0 ± 16.8	0.01
Mean length of lesions (mm)	109.4 ± 7.8	94.8 (80.8-133.2)	0.89
Cause of pancreastitis			
Hyperlipidemia	10 (29.4)	8 (21.1)	
Gallstone	8 (23.5)	8 (21.1)	
Alcohol	9 (26.5)	6 (15.8)	
Trauma	1 (2.9)	4 (10.5)	
Autoimmunity	1 (2.9)	3 (7.9)	
Pancreatic duct stones	3 (8.8)		
Choledochocyst		1 (2.6)	
Idiopathic	1 (2.9)	8 (21.1)	
Clinical symptoms[1]			
Abdominal pain (%)	24 (70.6)	27 (71.1)	
Abdominal distention (%)	6 (17.65)	5 (13.2)	
Nausea or vomiting	5	3	
Fever	6	1	
Asymptomatic	1	2	
Preintervention	6	4	
PCD	4	3	
ETGF	1		
Surgery	1	1	
Opportunity of intervention[2]			0.381
< 4 wk	7	13	
> 4 wk	21	24	
Total interventions	1.03 ± 0.03	1.32 ± 0.09	0.003
Total hospital visits	1.0 (0)	1.0 (1.0)	0.278
Total hospital stays(days)	14.5 (10.25)	19.0 (20.5)	0.177
Total cost ($)	4852 (3877)	5206 (8377)	0.955

[1]Multiple symptoms may coexist in one patient, so we didn't calculate percentages of each item.
[2]Here, we excluded patients that preintervention was inconsistent with original treatment in our hospital.
ETGF: Endoscopic transgastric fenestration; PCD: Percutaneous drainage.

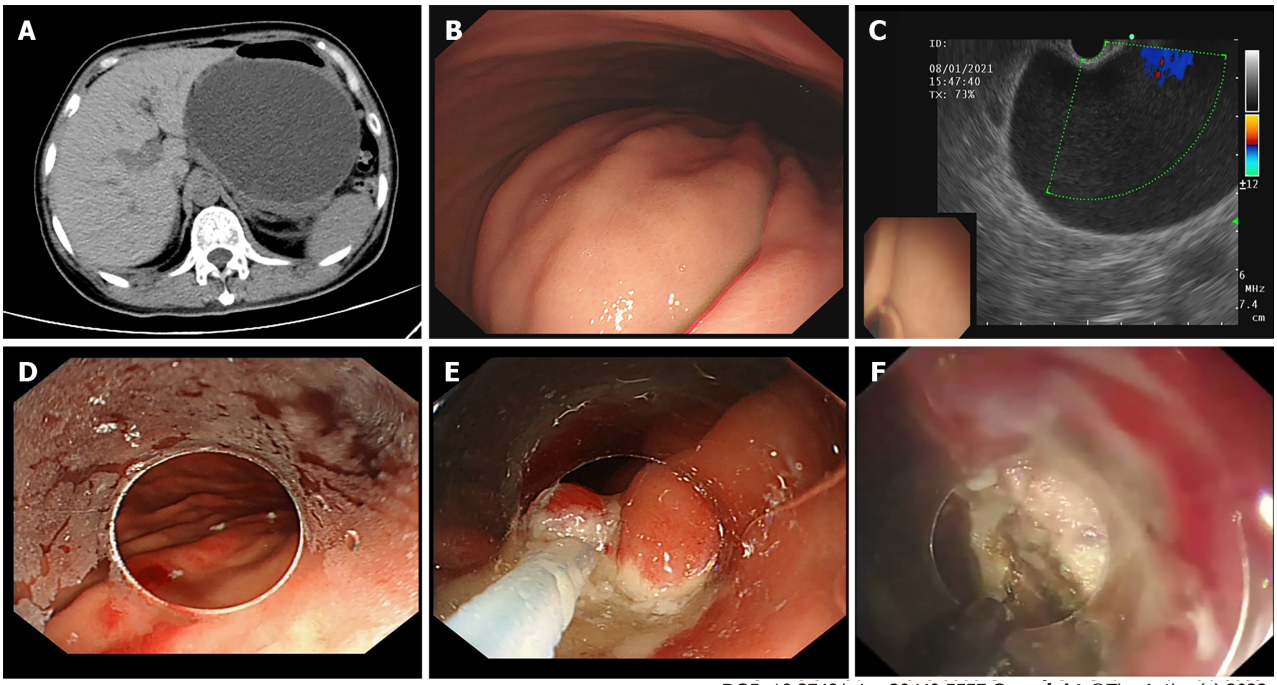
PCD approach

Four of 38 patients received preintervention but failed, which included one open surgery and 3 cases of PCD. The average age of the participants was 46.0 ± 16.8 years old with more male patients than female patients (26 *vs* 12). Approximately three quarters of patients suffered from abdominal pain (27/38). The average length of PFCs was 94.8 mm (80.8-133.2 mm). Hyperlipidemia, gallstones, and alcohol-related pancreatitis were the etiologies in 57.9% of patients (22/38). The average total interventions was 1.32 sessions. The total duration of hospital stays and total cost was 19 days and 5206 $ respectively. Clinical success was achieved in 29 patients (76.3%). Four patients showed recurrence (10.5%) and reintervention occurred in 17 of 38 patients (44.7%). With regard to adverse events, two patients developed bleeding which stopped spontaneously, two had local infection, and one had drainage adhesion to surrounding tissue. In 11 patients, the duration of catheterization was more than 8 wk. Drainage obstruction was encountered in 5 cases.

Table 2 Endoscopic transgastric fenestration *vs* percutaneous drainage for management of (peri) pancreatics, *n* (%)

	ETGF	PCD	*P* value
Technical success	34 (100)	38 (100)	
Clinical success	33/34 (97.1)	29/38 (76.3)	0.01
Recurrence	1/34 (2.94)	4/38 (10.5)	0.42
Reintervention	10/34 (29.4)	17[1]/38 (44.7)	0.18
Complication			1.00
		Bleeding 2 (5.26)	
		Local infection 2 (5.26)	
		Adhesion to surrounding tissue 1 (2.63)	
Catheter related adverse events			0.001
		Intubation time > 8 wk 11 (28.9)	
		Drainage obstruction 5 (13.2)	

[1]There were 8 patients who received a twice percutaneous drainage (PCD) and another 3 required no less than three times of PCD, 2 transferred to endoscopic transgastric fenestration and 7 to surgery after PCD failure. ETGF: Endoscopic transgastric fenestration; PCD: Percutaneous drainage.

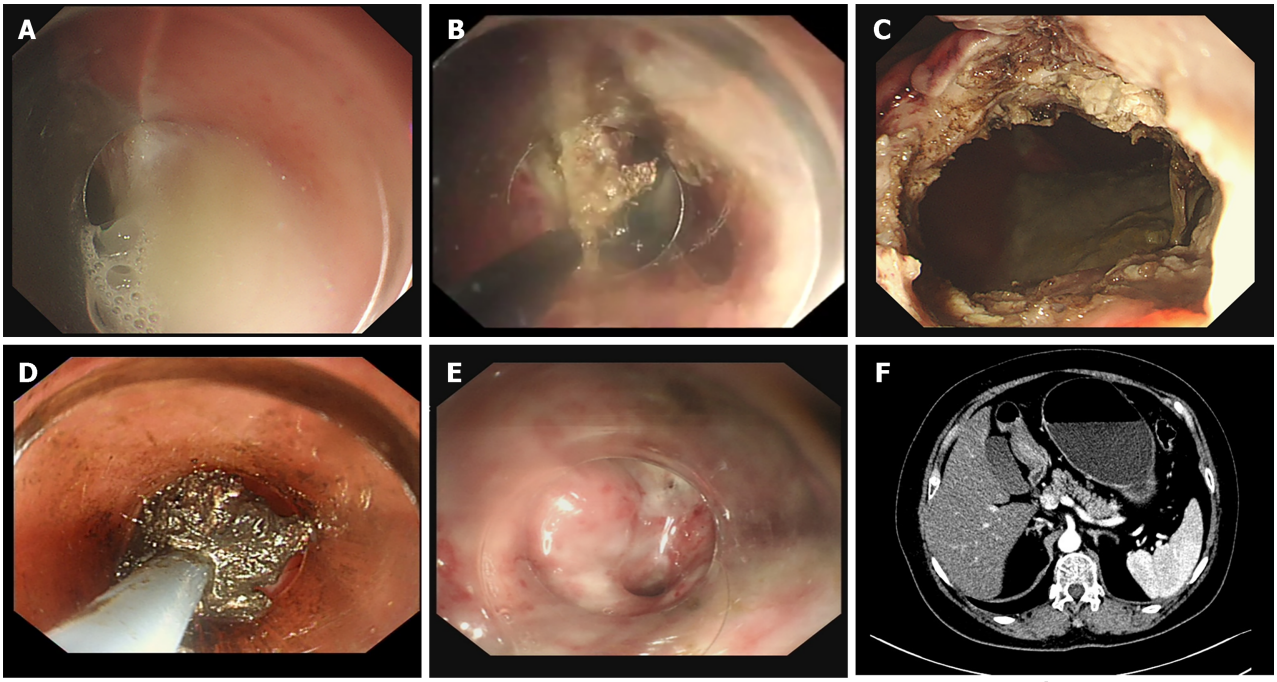


DOI: 10.3748/wjg.v29.i40.5557 **Copyright** ©The Author(s) 2023.

Figure 1 Endoscopic transgastric fenestration: From location to endoscopic full-thickness resection. A: Preoperative computed tomography scan of (peri) pancreatic collections; B: Gastric bulge caused by (peri) pancreatic collections under upper endoscope view; C: Assessment of fenestration site under endoscopic ultrasound; D: Marked the mucous layer; E: Resect the mucosal layer by endoscopic mucosal resection; F: Full-thickness incision was operated.

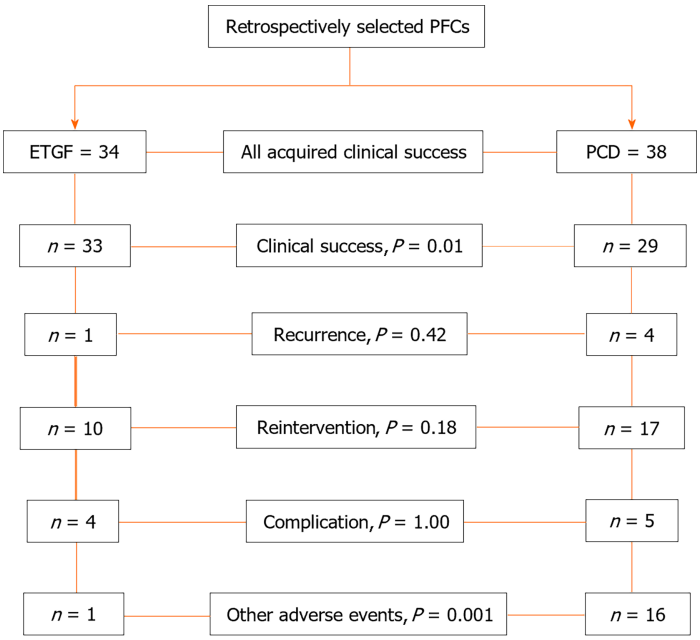
DISCUSSION

Surgical treatment has been traditionally used for PFCs[3]. Recently, PCD and endoscopic management have replaced surgery as the main treatment for PFCs due to their minimal invasiveness[6,8]. However, PCD cannot debride necrosis and an external drainage tube affects quality of life, which has limited its clinical use[5,14-16]. Endoscopic treatment can not only drainage the pus inside but also remove debris in the cavity and is beneficial to patient's health[5,6,14,17]. While previously endoscopic therapy involved stent implantation, embedding, displacement, and bleeding were inevitable[10-12]. Different to conventional endoscopic management, ETGF was conducted by means of ETFR to drain and debride PFCs adherent to the gastric wall, avoiding stent implantation.



DOI: 10.3748/wjg.v29.i40.5557 **Copyright** ©The Author(s) 2023.

Figure 2 Endoscopic transgastric fenestration: Enlarge the aperture of opening and debridement. A: Collections inflowing *via* the artificial fistula; B: Enlarged the aperture of opening with hook knife; C: The artificial fistula (about 2 cm in diameter) between the gastric wall and the cavity was made; D: Debridement of necrotic tissue under endoscopic direct vision; E: Endoscopic review of the fistula showed fistula almost healed one months later; F: The reviewed computed tomography scan one month after endoscopic transgastric fenestration.



DOI: 10.3748/wjg.v29.i40.5557 **Copyright** ©The Author(s) 2023.

Figure 3 Flow-chart for this retrospective study. ETGF: Endoscopic transgastric fenestration; PFCs: (peri) Pancreatic collections; PCD: Percutaneous drainage.

Our findings are basically consistent with previous studies on conventional endoscopic drainage which actually involves plastic or metal stent implantation and the PCD approach[16,18-20]. A respective study from the United States reported that the technical and clinical success rate of EUS-guided drainage of PFCs was 100% and 97% respectively[18]. Similarly, ETGF had a relatively favorable effect with 100% technical success and 97.1% clinical success. Jianhua *et al* performed a comparative study on drainage of PFCs and initial clinical success was considerably higher in patients who received transluminal endoscopic drainage than those in the PCD group (94.9% *vs* 65.0%)[20]. In our study, the clinical success rate in the PCD group was 65.8% which was also lower than that in the ETGF group.

PCD was associated with a high rate of reintervention and the endoscopic stent implantation approach was shown to significantly reduce the rate of retreatment, which resulted in short hospital stay, low cost and a reduced number of follow-up abdominal imaging studies[9,15]. In the present study, the total cost and reintervention rate following ETGF was lower than that in PCD, but was not statistically significantly different.

Keane *et al*[15] agreed that there was no difference between PCD and transluminal endoscopic drainage of PFCs in terms of recurrence. In another study, endoscopic drainage with stent implantation was an effective and appropriate method with the advantage of fewer recurrences compared to PCD[19]. In the present study, we found that there was no difference in the recurrence rate between two groups. In a long-term follow up study about PFCs, the recurrence of transluminal endoscopic drainage reported by Nabi *et al* was 6.7%[11]. In this study, one recurrence was encountered in ETGF group (2.94%).

The procedural adverse events rate was high in the PCD group compared with the transluminal endoscopic drainage with stent implantation group[20]. In the current study, the rate of complications in the ETGF group was similar with that in the PCD. Bleeding was encountered in ETGF patients and was managed by conservative treatment totally , which was consistent with previous studies[21].

Research by Storm *et al*[18] on endoscopic drainage of PFCs discovered that size of collections > 100 mm was correlated with an increased risk of adverse events. The size of PFCs was an independent risk factor for infection related to the cavity, and large PFCs with a diameter > 150 mm were more likely to become infected[22]. In the present study, seven patients had nasocystic tube implanted due to pus and necrosis in the cavity, of which 3 lesions were more than 150 mm and another 3 lesions were > 100 mm. A study on ETGF found that there were 3 of 5 patients received a nasocystic tube and the mean catheterization time was 10 d, which was longer than that in our study (8.6 d)[23]. We also recommended an indwelling nasocystic tube for large lesion or lesions combined with infection.

A previous study reported that the average length of time the drainage catheter in place was as long as 44.5 d in PCD [14]. Similarly, in our study, there were 28.9% of patients (11/38) whose underwent drainage for more than 8 wk. In addition, drainage obstruction occurred in 5 patients due to pus or necrosis, all of which led to further discomfort. Furthermore, an external catheter requires long-term care, as well as reminding the patient of their underlying disease state, and results in significant patient discomfort and compromised the quality of life[14]. During ETGF we used a natural orifice as the access route, avoiding an external catheter and scarring, which was beneficial to mental health and improved quality of life.

The limitations of this study were as follows. Firstly, we didn't examine how different types of PFCs affected the therapeutic efficacy. Secondly, prognostic factors associated with postoperative infection (size of PFCs, the area of fenestration) were not been identified in ETGF. A quality of life scale was not used in this study, thus, how the two different methods affected the quality of life is not known. A large, prospective, multicenter study is necessary to confirm our results.

CONCLUSION

Both PCD and ETGF can be used effectively for the treatment of PFCs, although ETGF is superior to PCD as it has a higher rate of clinical success and a lower rate of adverse events. ETGF is an innovative, effective, safe and scarless strategy for the management of PFCs adherent to the gastric wall. However, further studies especially clinical trials are needed before final recommendations are made.

ARTICLE HIGHLIGHTS

Research background

Percutaneous drainage (PCD) and endoscopic approaches with stent implantation have largely replaced surgical drainage as the initial approach for (peri) pancreatic fluid collections (PFCs). While stent implantation guided by endoscopic ultrasound has been mature and preferred treatment, but stent displacement, bleeding and embedding should not be neglected.

Research motivation

Inspired by endoscopic full-thickness resection, we conducted endoscopic transgastric fenestration (ETGF), which involves resection of connected tissues between gastric wall and PFCs, so as to drain the collection of fluid in the cavity and debride the necrosis inside.

Research objectives

The study aimed to evaluate the efficacy and safety of ETGF by accessing its success and complication rate compared with PCD.

Research methods

This retrospective analysis enrolled patients diagnosed with PFCs adjacent to the gastric wall and subsequently received ETGF or PCD during 4 years, analyzed patients baseline characteristics, technical and clinical success rate, recurrence and

reintervention rate, procedure related complication and adverse events.

Research results

Seventy-two eligible patients were retrospectively identified (ETGF = 34, PCD = 38). Patients in the ETGF group acquired significantly higher clinical success rate than that in PCD (97.1 *vs* 76.3%, P = 0.01). There was no statistical difference about recurrence, reintervention and incidence of complication between the two groups.

Research conclusions

ETGF would be an alternative effective and safe strategy for the treatment of PFCs adjacent to the gastric wall.

Research perspectives

ETGF can drainage fluid inside and debride necrosis, which improves its clinical success. Therefore, in our opinion ETGF may be an alternative treatment for PFCs adjacent to gastric, especially for large lesions or leions that associated with infection or necrosis.

ACKNOWLEDGEMENTS

We express our gratitude to Professor Shi Niu, Department of Gastroenterology and Hepatology, Inner Mongolia People's Hospital, China, for his encouragement and assistance in preparing the audio and revising the manuscript.

FOOTNOTES

Co-first authors: Hong-Mei Zhang and Hui-Ting Ke.

Author contributions: Zhang HM, Ke HT and Li YJ contributed to the design of the study, collected data and drafted the manuscript; Ke HT and Nabi G performed the data analysis; Ahmed MR, Liu D and Zhao LX conceived the work; Zhang JY and Li MH contributed to video clip of endoscopic transgastric fenestration; Liu BR revised the manuscript; All authors issued final approval for the version to be submitted. Here are the reasons for designating Zhang HM and Ke HT as co-first authors: During the period of the study, Ke HT was a postgraduate student of the First Affiliated Hospital of Zhengzhou University and fully participated in the study. Ke HT graduated one year ago and worded in Ezhou Central Hospital. Zhang HM and Ke HT proposed the concept of this study, searched relevant literature and then discussed the research design together, and finally determined the research idea. Before the paper was drafted, they collected the research data together, and carried out the collation, statistical analysis and later verification work. They worked together on the first draft. Zhang HM explained the data charts and graphs and Ke HT selected typical case pictures and illustrated them.

Supported by Zhongyuan Talent Program, No. ZYYCYU202012113; The Key R and D Program of Henan Province, No. 222102310038.

Institutional review board statement: This study was reviewed and approved by the Ethics Committee of the First Affiliated Hospital of Zhengzhou University.

Informed consent statement: All study participants or their legal guardian provided informed written consent regarding personal and medical data collection prior to study enrollment.

Conflict-of-interest statement: We have no financial relationships to disclose.

Data sharing statement: No additional data are available.

Open-Access: This article is an open-access article that was selected by an in-house editor and fully peer-reviewed by external reviewers. It is distributed in accordance with the Creative Commons Attribution NonCommercial (CC BY-NC 4.0) license, which permits others to distribute, remix, adapt, build upon this work non-commercially, and license their derivative works on different terms, provided the original work is properly cited and the use is non-commercial. See: https://creativecommons.org/Licenses/by-nc/4.0/

Country/Territory of origin: China

ORCID number: Ghulam Nabi 0000-0001-5256-0083; Mu-Han Li 0000-0003-0064-8942; Ji-Yu Zhang 0000-0003-1919-4418; Dan Liu 0000-0001-8313-4343; Li-Xia Zhao 0000-0002-1114-9754; Bing-Rong Liu 0000-0001-6101-8675.

S-Editor: Qu XL
L-Editor: A
P-Editor: Chen YX

REFERENCES

1 **Banks PA**, Bollen TL, Dervenis C, Gooszen HG, Johnson CD, Sarr MG, Tsiotos GG, Vege SS; Acute Pancreatitis Classification Working Group. Classification of acute pancreatitis--2012: revision of the Atlanta classification and definitions by international consensus. *Gut* 2013; **62**: 102-111 [PMID: 23100216 DOI: 10.1136/gutjnl-2012-302779]

2 **Hines OJ**, Pandol SJ. Management of severe acute pancreatitis. *BMJ* 2019; **367**: l6227 [PMID: 31791953 DOI: 10.1136/bmj.l6227]

3 **Saftoiu A**, Vilmann A, Vilmann P. Endoscopic ultrasound-guided drainage of pancreatic pseudocysts. *Endosc Ultrasound* 2015; **4**: 319-323 [PMID: 26643700 DOI: 10.4103/2303-9027.170424]

4 **Singhal S**, Rotman SR, Gaidhane M, Kahaleh M. Pancreatic fluid collection drainage by endoscopic ultrasound: an update. *Clin Endosc* 2013; **46**: 506-514 [PMID: 24143313 DOI: 10.5946/ce.2013.46.5.506]

5 **Kawakami H**, Itoi T, Sakamoto N. Endoscopic ultrasound-guided transluminal drainage for peripancreatic fluid collections: where are we now? *Gut Liver* 2014; **8**: 341-355 [PMID: 25071899 DOI: 10.5009/gnl.2014.8.4.341]

6 **Baron TH**, DiMaio CJ, Wang AY, Morgan KA. American Gastroenterological Association Clinical Practice Update: Management of Pancreatic Necrosis. *Gastroenterology* 2020; **158**: 67-75.e1 [PMID: 31479658 DOI: 10.1053/j.gastro.2019.07.064]

7 **Bang JY**, Arnoletti JP, Holt BA, Sutton B, Hasan MK, Navaneethan U, Feranec N, Wilcox CM, Tharian B, Hawes RH, Varadarajulu S. An Endoscopic Transluminal Approach, Compared With Minimally Invasive Surgery, Reduces Complications and Costs for Patients With Necrotizing Pancreatitis. *Gastroenterology* 2019; **156**: 1027-1040.e3 [PMID: 30452918 DOI: 10.1053/j.gastro.2018.11.031]

8 **Arvanitakis M**, Dumonceau JM, Albert J, Badaoui A, Bali MA, Barthet M, Besselink M, Deviere J, Oliveira Ferreira A, Gyökeres T, Hritz I, Hucl T, Milashka M, Papanikolaou IS, Poley JW, Seewald S, Vanbiervliet G, van Lienden K, van Santvoort H, Voermans R, Delhaye M, van Hooft J. Endoscopic management of acute necrotizing pancreatitis: European Society of Gastrointestinal Endoscopy (ESGE) evidence-based multidisciplinary guidelines. *Endoscopy* 2018; **50**: 524-546 [PMID: 29631305 DOI: 10.1055/a-0588-5365]

9 **Akshintala VS**, Saxena P, Zaheer A, Rana U, Hutfless SM, Lennon AM, Canto MI, Kalloo AN, Khashab MA, Singh VK. A comparative evaluation of outcomes of endoscopic versus percutaneous drainage for symptomatic pancreatic pseudocysts. *Gastrointest Endosc* 2014; **79**: 921-8 [PMID: 24315454 DOI: 10.1016/j.gie.2013.10.032]

10 **Bang JY**, Navaneethan U, Hasan MK, Sutton B, Hawes R, Varadarajulu S. Non-superiority of lumen-apposing metal stents over plastic stents for drainage of walled-off necrosis in a randomised trial. *Gut* 2019; **68**: 1200-1209 [PMID: 29858393 DOI: 10.1136/gutjnl-2017-315335]

11 **Nabi Z**, Lakhtakia S, Basha J, Chavan R, Gupta R, Ramchandani M, Kalapala R, Pal P, Darisetty S, Rao GV, Nageshwar Reddy D. Endoscopic drainage of pancreatic fluid collections: Long-term outcomes in children. *Dig Endosc* 2017; **29**: 790-797 [PMID: 28374894 DOI: 10.1111/den.12884]

12 **Yang J**, Chen YI, Friedland S, Holmes I, Paiji C, Law R, Hosmer A, Stevens T, Matheus F, Pawa R, Mathur N, Sejpal D, Inamdar S, Berzin TM, DiMaio CJ, Gupta S, Yachimski PS, Anderloni A, Repici A, James T, Jamil LH, Ona M, Lo SK, Gaddam S, Dollhopf M, Alammar N, Shieh E, Bukhari M, Kumbhari V, Singh V, Brewer O, Sanaei O, Fayad L, Ngamruengphong S, Shin EJ, Baron TH, Khashab MA. Lumen-apposing stents versus plastic stents in the management of pancreatic pseudocysts: a large, comparative, international, multicenter study. *Endoscopy* 2019; **51**: 1035-1043 [PMID: 30536255 DOI: 10.1055/a-0759-1353]

13 **Liu BR**, Song JT, Zhang XY. Video of the Month: Emergency Endoscopic Fenestration for Treatment of a Recurrence Pancreatic Pseudocyst. *Am J Gastroenterol* 2015; **110**: 644 [PMID: 25942297 DOI: 10.1038/ajg.2015.13]

14 **Kwon YM**, Gerdes H, Schattner MA, Brown KT, Covey AM, Getrajdman GI, Solomon SB, D'Angelica MI, Jarnagin WR, Allen PJ, Dimaio CJ. Management of peripancreatic fluid collections following partial pancreatectomy: a comparison of percutaneous versus EUS-guided drainage. *Surg Endosc* 2013; **27**: 2422-2427 [PMID: 23361258 DOI: 10.1007/s00464-012-2752-z]

15 **Keane MG**, Sze SF, Cieplik N, Murray S, Johnson GJ, Webster GJ, Thorburn D, Pereira SP. Endoscopic versus percutaneous drainage of symptomatic pancreatic fluid collections: a 14-year experience from a tertiary hepatobiliary centre. *Surg Endosc* 2016; **30**: 3730-3740 [PMID: 26675934 DOI: 10.1007/s00464-015-4668-x]

16 **Fabbri C**, Luigiano C, Lisotti A, Cennamo V, Virgilio C, Caletti G, Fusaroli P. Endoscopic ultrasound-guided treatments: are we getting evidence based--a systematic review. *World J Gastroenterol* 2014; **20**: 8424-8448 [PMID: 25024600 DOI: 10.3748/wjg.v20.i26.8424]

17 **Varadarajulu S**, Bang JY, Sutton BS, Trevino JM, Christein JD, Wilcox CM. Equal efficacy of endoscopic and surgical cystogastrostomy for pancreatic pseudocyst drainage in a randomized trial. *Gastroenterology* 2013; **145**: 583-90.e1 [PMID: 23732774 DOI: 10.1053/j.gastro.2013.05.046]

18 **Storm AC**, Levy MJ, Kaura K, Abu Dayyeh BK, Cleary SP, Kendrick ML, Truty MJ, Vargas EJ, Topazian M, Chandrasekhara V. Acute and early EUS-guided transmural drainage of symptomatic postoperative fluid collections. *Gastrointest Endosc* 2020; **91**: 1085-1091.e1 [PMID: 31843369 DOI: 10.1016/j.gie.2019.11.045]

19 **Xie LT**, Zhao QY, Gu JH, Ying HJ, Tian G, Jiang TA. Endoscopic Ultrasonography-Guided Versus Percutaneous Drainage for the Recurrent Pancreatic Fluid Collections. *Med Sci Monit* 2019; **25**: 5785-5794 [PMID: 31377748 DOI: 10.12659/MSM.915193]

20 **Wan J**, Wu D, He W, Zhu Y, Zeng H, Liu P, Xia L, Lu N. Comparison of percutaneous *vs* endoscopic drainage in the management of pancreatic fluid collections: A prospective cohort study. *J Gastroenterol Hepatol* 2020; **35**: 2170-2175 [PMID: 32473080 DOI: 10.1111/jgh.15121]

21 **Künzli HT**, Timmer R, Schwartz MP, Witteman BJ, Weusten BL, van Oijen MG, Siersema PD, Vleggaar FP. Endoscopic ultrasonography-guided drainage is an effective and relatively safe treatment for peripancreatic fluid collections in a cohort of 108 symptomatic patients. *Eur J Gastroenterol Hepatol* 2013; **25**: 958-963 [PMID: 23571613 DOI: 10.1097/MEG.0b013e3283612f03]

22 **Guo J**, Feng L, Sun S, Ge N, Liu X, Wang S, Wang G, Sun B. Risk factors for infection after endoscopic ultrasonography-guided drainage of specific types of pancreatic and peripancreatic fluid collections (with video). *Surg Endosc* 2016; **30**: 3114-3120 [PMID: 26801793 DOI: 10.1007/s00464-015-4557-3]

23 **Liu F**, Wu L, Wang XD, Xiao JG, Li W. Endoscopic gastric fenestration of debriding pancreatic walled-off necrosis: A pilot study. *World J Gastroenterol* 2020; **26**: 6431-6441 [PMID: 33244203 DOI: 10.3748/wjg.v26.i41.6431]

World Journal of Gastroenterology

Submit a Manuscript: https://www.f6publishing.com

World J Gastroenterol 2023 October 28; 29(40): 5566-5581

DOI: 10.3748/wjg.v29.i40.5566

ISSN 1007-9327 (print) ISSN 2219-2840 (online)

ORIGINAL ARTICLE

Retrospective Study

Clinical significance of programmed cell death-ligand expression in small bowel adenocarcinoma is determined by the tumor microenvironment

Aitoshi Hoshimoto, Atsushi Tatsuguchi, Ryohei Hamakubo, Takayoshi Nishimoto, Jun Omori, Naohiko Akimoto, Shu Tanaka, Shunji Fujimori, Tsutomu Hatori, Akira Shimizu, Katsuhiko Iwakiri

Specialty type: Gastroenterology and hepatology

Provenance and peer review: Unsolicited article; Externally peer reviewed.

Peer-review model: Single blind

Peer-review report's scientific quality classification

Grade A (Excellent): 0
Grade B (Very good): B, B
Grade C (Good): C
Grade D (Fair): 0
Grade E (Poor): 0

P-Reviewer: Qin J, China; Zhe MM, China; Tsoulfas G, Greece

Received: August 14, 2023
Peer-review started: August 14, 2023
First decision: September 19, 2023
Revised: October 4, 2023
Accepted: October 23, 2023
Article in press: October 23, 2023
Published online: October 28, 2023

Aitoshi Hoshimoto, Atsushi Tatsuguchi, Ryohei Hamakubo, Takayoshi Nishimoto, Jun Omori, Naohiko Akimoto, Shu Tanaka, Shunji Fujimori, Katsuhiko Iwakiri, Department of Gastroenterology, Nippon Medical School, Tokyo 113-8603, Japan

Aitoshi Hoshimoto, Atsushi Tatsuguchi, Akira Shimizu, Department of Analytic Human Pathology, Nippon Medical School, Tokyo 113-8603, Japan

Tsutomu Hatori, Department of Pathology, Nippon Medical School, Chiba Hokusoh Hospital, Chiba 270-1694, Japan

Corresponding author: Atsushi Tatsuguchi, MD, PhD, Associate Professor, Department of Gastroenterology, Nippon Medical School, 1-1-5 Sendagi, Bunkyo-ku, Tokyo 113-8603, Japan. tachan@nms.ac.jp

Abstract

BACKGROUND

Comprehensive genomic analysis has shown that small bowel adenocarcinoma (SBA) has different genomic profiles from gastric and colorectal cancers. Hence, it is essential to establish chemotherapeutic regimens based on SBA characteristics. The expression of programmed cell death-ligand 1 (PD-L1) and programmed cell death-ligand 2 (PD-L2) in SBA is not fully understood. Anti-PD-L1/PD-1 therapy uses tumor-infiltrating lymphocytes (TILs); therefore, the status of TILs in the tumor microenvironment (TME) may influence their efficacy. The ratio of FoxP3+ to CD8+ T cells has been reported to be useful in predicting the prognosis of digestive system cancers.

AIM

To investigate the clinicopathological significance of PD-L1/2 expression according to the status of TILs in SBA tissues.

METHODS

We performed immunohistochemical analysis for PD-L1, PD-L2, CD8, FoxP3, and DNA mismatch repair (MMR) proteins using formalin-fixed, paraffin-embedded tissues from 50 patients diagnosed with primary SBA. The immunoreactivities of PD-L1 and PD-L2 were determined separately in tumor cells and tumor-infilt-

rating immune cells throughout the tumor center and invasive margins, and finally evaluated using the combined positive score (CPS). We assessed CD8+ and FoxP3+ T cells in the intratumoral and tumor-surrounding stroma. Subsequently, we calculated and summed the ratio of FoxP3 to CD8+ T cell counts. Immune-related cell densities were graded as low or high. Immunohistochemical results were compared with clinicopathological factors and patient prognosis. The distribution of cancer-specific survival (CSS) was estimated using the Kaplan–Meier method, and the log-rank test was used to test for significant differences in CSS. A Cox proportional hazard model was also used to assess the effect of tumor variables on CSS.

RESULTS

PD-L1 expression was positive in 34% in tumor cells (T-PD-L1) and 54% in tumor-infiltrating immune cells (I-PD-L1) of the cases examined. T-PD-L2 was positive in 34% and I-PD-L2 was positive in 42% of the cases. PD-L1 CPS ≥ 10 and PD-L2 CPS ≥ 10 were observed in 50% and 56% of the cases, respectively. Deficient MMR (dMMR) was 14% of the cases. T-PD-L1, I-PD-L1 and PD-L1 CPS ≥ 10 were all significantly associated with dMMR (P = 0.037, P = 0.009, and P = 0.005, respectively). T-PD-L1, I-PD-L1, and PD-L1 CPS ≥ 10 were all associated with deeper depth of invasion (P = 0.001, P = 0.024, and P = 0.002, respectively). I-PD-L2 expression and PD-L2 CPS ≥ 10 were significantly higher in the differentiated histological type (P = 0.015 and P = 0.030, respectively). The I-PD-L1 and I-PD-L2 levels were significantly associated with better CSS (P = 0.037 and P = 0.015, respectively). CD8-high was significantly associated with less lymph node metastasis (P = 0.047), less distant metastasis (P = 0.024), less peritoneal dissemination (P = 0.034), and earlier TNM stage (P = 0.047). The CD8-high group had better prognosis than the CD8-low group (P = 0.018). FoxP3 expression was not associated with any clinicopathological factors or prognosis. We found that patients with PD-L2 CPS ≥ 10 tended to have worse prognosis in the FoxP3/CD8-low group (P = 0.088).

CONCLUSION

The clinicopathological significance of PD-L1/2 expression may differ depending on the TME status. Immune checkpoint inhibitors may improve the prognosis of SBA patients with low FoxP3/CD8 ratio and PD-L2 expression.

Key Words: Small bowel adenocarcinoma; Programmed cell death-ligand 1; Programmed cell death-ligand 2; Tumor microenvironment; Tumor-infiltrating lymphocytes; Regulatory T-cells

©The Author(s) 2023. Published by Baishideng Publishing Group Inc. All rights reserved.

Core Tip: We investigated the clinicopathological significance of programmed cell death-ligand 1 (PD-L1) and programmed cell death-ligand 2 (PD-L2) expression in association with the infiltration of FoxP3+ and CD8+ T cells into the tumor microenvironment (TME) to identify PD-L/PD-1 immunotherapy candidates among patients with small bowel adenocarcinoma (SBA). We demonstrated that the status of the TME affects the clinical significance of PD-L1 and PD-L2. PD-L2 may be associated with poor prognosis of SBA patients with a high immune cell infiltration.

Citation: Hoshimoto A, Tatsuguchi A, Hamakubo R, Nishimoto T, Omori J, Akimoto N, Tanaka S, Fujimori S, Hatori T, Shimizu A, Iwakiri K. Clinical significance of programmed cell death-ligand expression in small bowel adenocarcinoma is determined by the tumor microenvironment. *World J Gastroenterol* 2023; 29(40): 5566-5581
URL: https://www.wjgnet.com/1007-9327/full/v29/i40/5566.htm
DOI: https://dx.doi.org/10.3748/wjg.v29.i40.5566

INTRODUCTION

Small bowel adenocarcinoma (SBA) is an uncommon condition, accounting for less than 3% of all gastrointestinal neoplasms; however, the small intestine accounts for 95% of the surface area of the entire gastrointestinal tract[1]. According to a recent report from the United States, the incidence of small bowel cancer has been increasing, with an annual increase of 1.8% between 2006 and 2015[2]. Although there are no definitive risk factors for SBA, diets containing high volumes of animal fat and protein have been reported to increase the risk, which may be related to an increase in the number of SBA[3]. SBA accounts for 30%–50% of all small bowel malignancies, and limited data exist on its molecular and clinicopathological features[4]. SBA has a high probability of being discovered at an advanced stage owing to a delay in diagnosis. No effective chemotherapy has been established for unresectable SBAs, and the regimens for colorectal cancer are palliatively administered. However, comprehensive genomic analyses have revealed that SBA and colorectal cancer have different genomic profiles, and it is assumed that the molecular pathways leading to carcinogenesis may also be different[3,5,6]. Therefore, it is essential to establish chemotherapeutic regimens based on the specific characteristics of SBA.

The small bowel is the largest organ of the human immune system. Lymphoid tissues in the lamina propria and various immune-related cells are prevalent in the small intestine and contribute to immune surveillance. Programmed cell death-ligand 1 (PD-L1) is the primary PD-1 Ligand that is upregulated in various solid tumors, and plays a pivotal role in modulating the tumor microenvironment (TME) to inhibit cytokine production and the cytolytic activity of PD-1+ tumor-infiltrating CD4+ and CD8+ T cells[7]. Several studies have demonstrated the efficacy of blocking the PD-1/PD-L1 signaling pathway in gastrointestinal cancers with high microsatellite instability (MSI-high)[8-11], and recent studies have demonstrated a significant association between MSI-high and PD-L1 expression in SBA[12,13]. PD-L1 expression has been reported to be associated with gastrointestinal cancer prognosis, despite several conflicting reports. While some studies have reported that PD-L1 expression is associated with favorable prognosis in gastric and colorectal cancers[14-18], others have reported that PD-L1 expression is associated with poorer prognosis in these cancers[19-22]. Considering the role of PD-1/PD-L1 in the TME, PD-L1 expression is predicted to be associated with worse prognosis in cancer patients.

Programmed cell death-ligand 2 (PD-L2) was discovered as a second ligand for PD-1 and has been reported to inhibit T cell proliferation by blocking cell cycle progression, similar to PD-L1[23,24]. PD-L2 suppresses the proliferation and cytokine production of CD4+ T cells through T cell receptors[23]. Its expression is significantly associated with PD-L1 expression in melanoma, non-small cell lung cancer, head and neck squamous cell carcinoma, renal cell carcinoma, bladder cancer, gastric cancer, and triple-negative breast cancer[25]. Although the function and expression pattern of PD-L2 are considered to be similar to those of PD-L1, PD-L2 has not received much attention, and its role in modulating tumor immunity remains undetermined.

Anti-PD-L1/PD-1 therapy utilizes tumor-infiltrating lymphocytes (TILs). Therefore, the status of TILs in the TME may influence their efficacy. Although TILs are mainly composed of CD8+ T cells, they are heterogeneous cell populations that also contain regulatory T cells (Tregs), which are believed to inhibit CD8+ T cells[26]. Tregs are an immunosuppressive subset of CD4+ T cells that orchestrate cellular and molecular networks to induce an immunosuppressive environment favorable to tumorigenesis[27]. Tregs are characterized by the expression of the master regulatory transcription factor FoxP3[28]. A high ratio of FoxP3+ to CD8+ T cells is associated with poor clinical outcomes in digestive system cancers [29-31].

This study investigated the clinicopathological significance of PD-L1 and PD-L2 expression in association with the infiltration of FoxP3+ and CD8+ T cells into the TME to identify PD-L/PD-1 immunotherapy candidates among SBA patients.

MATERIALS AND METHODS

Patients and tissue samples

We obtained 50 duodenal, jejunal, and ileal adenocarcinoma tissue samples from the archives of the Department of Pathology at Nippon Medical School Hospital for immunohistochemical analysis of PD-L1, PD-L2, CD8, FoxP3, and DNA mismatch repair (MMR) protein expression. Samples from patients with predisposing conditions, including Lynch syndrome, familial adenomatous polyposis, celiac disease, and Crohn's disease, were excluded to focus on sporadic SBA. Furthermore, samples from patients with ampullary adenocarcinoma or metastatic cancer were excluded. Cancer-specific survival (CSS) was defined as the interval from the date of the first surgery until death due to SBA; patients who died due to other causes were excluded. All patients provided informed written consent prior to study enrollment, and the study was approved by the Ethics Committee of Nippon Medical School (approval no. B-2020-164). All staging criteria were defined following the International Union for Cancer TNM classification.

Immunohistochemical analysis

Specimens were fixed in 10% formalin, embedded in paraffin wax, and immersed in 0.5% H_2O_2–methanol for 10 min to block endogenous peroxidase activity. Subsequently, the sections were microwaved in 0.01 mol/L citrate phosphate buffer (pH = 6.0) or EDTA (pH = 9.0) for antigen retrieval and incubated with 10% normal horse or goat serum for 10 min at 37°C to block nonspecific IgG binding. Thereafter, the sections were incubated for 18 h at 4°C with the primary antibodies listed in Supplementary Table 1. Next, they were treated with their respective biotinylated antibodies, namely anti-mouse IgG or anti-rabbit IgG (1:200; Vector) for 30 min at 25°C, followed by treatment with avidin-biotin-peroxidase complex for 30 min at 25°C. The reaction products were developed by immersing the sections in a 3,3′-diaminobenzidine tetrahydrochloride solution containing 0.03% H_2O_2.

Evaluation of immunohistochemical staining

Each patient was blindly evaluated by two independent observers (A.H. and A.T.). Any disagreements were resolved using a multi-headed microscope. The immunoreactivities of PD-L1 and PD-L2 were determined separately in tumor cells and tumor-infiltrating immune cells, such as lymphocytes and macrophages, throughout the tumor center and invasive margins. Tumor samples were defined as PD-L1 and PD-L2 positive when ≥ 1% of the tumor cells and/or tumor-infiltrating immune cells were immunoreactive with unequivocal intensity. Subsequently, for PD-L1 and PD-L2 expression, a combined positive score (CPS) was calculated by dividing the total number of both tumor cells and immune cells above the positive threshold by the total number of viable tumor cells[32,33]. We set the PD-L1 and PD-L2 CPS cutoffs at ≥ 10% [34].

We assessed CD8+ T cells in ten randomly selected microscopic areas, including the intratumoral and tumor-surrounding stroma, no further than one high-power field from the tumor edge, by light microscopy (400 ×; BX63; Olympus, Tokyo, Japan). FoxP3+ T cells were assessed in the same ten high-power fields. Cell counts were determined

using CellSens Dimension software (Olympus, Tokyo, Japan). Immune-related cell densities were graded as low (≤ median cell counts/mm^2 tumor area) or high (> median cell counts/mm^2 tumor area).

MMR status was defined by immunostaining for MLH1, MSH2, MLH6, and PMS2. Tumors were considered negative when there was a complete absence of nuclear staining of neoplastic cells in the presence of an internal positive control assessed on a whole slide. Tumors with negative staining for one of the MMR proteins were considered deficient MMR (dMMR), and all others were considered proficient MMR (pMMR). Each section was evaluated microscopically (400 ×; BX63; Olympus, Tokyo, Japan).

Statistical analysis

The immunostaining results for each protein were compared with the clinicopathological factors using the chi-square test or Fisher's exact test. Association between protein immunostaining was assessed using the chi-square test or Fisher's exact test, as appropriate. The distribution of CSS was estimated using the Kaplan–Meier method and the log-rank test was used to test for significant differences in CSS. A Cox proportional hazards model was used to assess the effects of tumor variables on CSS. In the multivariate analysis, variables with $P < 0.05$ in the univariate analysis were included. Statistical significance was set at $P < 0.05$.

RESULTS

Demographic data of patients

Demographic and baseline clinicopathological characteristics are listed in Table 1. The study included 35 men and 15 women ranging in age from 32 to 84 years (mean age, 65 years; median age, 68 years). At the time of analysis, 18 patients had died. The overall 5-year survival rate was 64%. The median follow-up duration for the entire series was 36 mo (mean, 45.1 mo; range, 5–124 mo). Twenty-three patients with stages III and IV disease received chemotherapy after surgery.

PD-L1, PD-L2, CD8, and FoxP3 Localization in SBA

PD-L1 immunoreactivity was observed in both tumor cells (T-PD-L1) and tumor-infiltrating immune cells (I-PD-L1), including lymphocytes and macrophages (Figure 1A and B). PD-L1 immunostaining was membranous and cytoplasmic in tumor cells and membranous in macrophages. The clinicopathological correlation of PD-L1 and PD-L2 expression are summarized in Table 2. T-PD-L1 was positive in 34% and I-PD-L1 was positive in 54% of cases. T-PD-L1 expression was associated with deeper depth of invasion ($P = 0.001$), but not with lymph node metastasis or distant metastasis. I-PD-L1 expression was associated with deeper depth of invasion ($P = 0.024$) and less peritoneal metastasis ($P = 0.019$). Both T-PD-L1 and I-PD-L1 expression were more common in stage II tumors compared to stage I tumors. PD-L2 immunoreactivity was observed in tumor cells (T-PD-L2) and tumor-infiltrating immune cells (I-PD-L2), including lymphocytes and macrophages (Figure 1C and D). The apical membrane showed a predominant PD-L2 staining pattern in tumor cells (Figure 1C). T-PD-L2 was positive in 34% and I-PD-L2 was positive in 42% of cases. T-PD-L2 expression was significantly higher in differentiated histological type ($P = 0.015$).

Then, we assessed PD-L1 and PD-L2 expression in a mixture of tumor and immune cells using CPS. Patients with PD-L1 CPS ≥ 10% and PD-L2 CPS ≥ 10% were observed in 50% and 56% of cases, respectively. In patients with PD-L1 CPS ≥ 10% of tumors were associated with deeper depth of invasion ($P = 0.002$), less peritoneal metastasis ($P = 0.034$), and more common in stage II compared to stage I (Table 2). Patients with PD-L2 CPS ≥ 10% were significantly correlated with younger age ($P = 0.027$) and more differentiated histological type ($P = 0.030$) (Table 2).

Representative micrographs of CD8 and FoxP3 staining are shown in Figure 2. CD8-high was significantly associated with less lymph node metastasis ($P = 0.047$), less distant metastasis ($P = 0.024$), less peritoneal dissemination ($P = 0.034$), and earlier TNM stage ($P = 0.047$) (Table 3). FoxP3 immunoreactivities were not associated with any clinicopathological factors, including age, sex, localization, histological type, lymph node metastasis, distant metastasis, peritoneal dissemination, or TNM stage. FoxP3-high tumors had deeper depth of invasion, although the difference was not statistically significant ($P = 0.059$) (Table 3).

Then, we calculated and summed the ratio of FoxP3 to CD8 positive T cell counts in ten high-power fields. FoxP3/CD8-high was significantly associated with lymph node metastasis ($P = 0.002$), distant metastasis ($P = 0.004$), peritoneal dissemination ($P = 0.005$), and TNM stage ($P = 0.002$) (Table 3).

dMMR was 14% of the cases identified using MLH1, MSH2, MLH6, and PMS2 immunostaining. T-PD-L1, I-PD-L1, and PD-L1 CPS ≥ 10% were significantly higher in the dMMR tumors than in the pMMR tumors. No PD-L2 positivity rate was associated with MMR status (Table 2).

Mutual relationship between *PD-L1, PD-L2, CD8, and FoxP3 expression*

Mutual relationship between PD-L1, PD-L2, CD8, and FoxP3 expression levels are shown in Table 4. A significant positive relationship was observed between PD-L1 and PD-L2 expression in both tumor and immune cells. A significant positive relationship was observed between CD8-high and T-PD-L1, I-PD-L1, and I-PD-L2 expression. FoxP3-high expression was associated with I-PD-L1 expression, but not with T-PD-L1, T-PD-L2, or I-PD-L2 expression.

Comparative survival analysis

Both I-PD-L1 and I-PD-L2 expression were significantly associated with better CSS ($P = 0.037$ and $P = 0.015$, respectively) (Figure 3). There was no significant association between T-PD-L1 expression or PD-L1 CPS ≥ 10% and patients' survival. There was no significant association between T-PD-L2 expression or PD-L2 CPS ≥ 10% and patients' survival. Patients in

Table 1 Clinicopathological data of patients with small bowel adenocarcinoma

	No. of cases (%)
Age	
≤ 68	27 (54.0)
> 68	23 (46.0)
Sex	
Female	15 (30.0)
Male	35 (70.0)
Site	
Duodenum and jejunum	45 (90.0)
Ileum	5 (10.0)
Histology	
WD, MD	41 (82.0)
PD, Muc	9 (18.0)
Depth of invasion	
pT1-2	14 (28.0)
pT3-4	36 (72.0)
Lymph node metastasis	
Absence	27 (54.0)
Presence	23 (46.0)
Distant metastasis	
Absence	37 (74.0)
Presence	13 (26.0)
Peritoneal seeding	
Absence	40 (80.0)
Presence	10 (20.0)
Chemotherapy	
Absence	27 (54.0)
Presence	23 (46.0)
TNM stage	
I	14 (28.0)
II	13 (26.0)
III	10 (20.0)
IV	13 (26.0)

WD: Well differentiated; MD: Moderately differentiated; PD: Poorly differentiated; Muc: Mucinous adenocarcinoma.

the CD8-high group had better prognosis than those in the CD8-low group (P = 0.018) (Figure 4). There was no significant association between FoxP3+ T cells and patients' survival. In contrast, the FoxP3/CD8-low group had significantly better prognosis than the FoxP3/CD8-high group (P = 0.004). We performed a survival analysis for PD-L1 and PD-L2 expression stratified by the FoxP3/CD8 ratio, and found that patients with PD-L2 CPS ≥ 10 in the FoxP3/CD8-low group had worse prognosis, although the difference was not significant (P = 0.088) (Figure 5).

In the univariate analysis using the Cox proportional hazards model for CSS, lymph node status and I-PD-L1, I-PD-L2, CD8, and FoxP3/CD8 ratios had significant prognostic value (Table 5). In the multivariate analysis performed by introducing all the above variables into the Cox proportional hazards model, lymph node status and I-PD-L2 expression retained independent prognostic significance.

Table 2 Clinicopathological correlation of programmed cell death-ligand 1 and programmed cell death-ligand 2 expression

	No.	T-PD-L1		I-PD-L1		PD-L1 CPS ≥ 10		T-PD-L2		I-PD-L2		PD-L2 CPS ≥ 10	
		N (%)	*P* value	*N* (%)	*P* value	*N* (%)	*P* value	*N* (%)	*P* value	*N* (%)	*P* value	*N* (%)	*P* value
Age													
≤ 68	27	10 (37.0)	NS	16 (59.3)	NS	14 (51.9)	NS	12 (44.4)	NS	14 (51.9)	NS	19 (70.4)	0.027
> 68	23	7 (30.4)		11 (47.8)		11 (47.8)		5 (21.7)		7 (30.4)		9 (39.1)	
Sex													
Female	15	4 (26.7)	NS	7 (46.7)	NS	7 (46.7)	NS	6 (40.0)	NS	8 (53.3)	NS	8 (53.3)	NS
Male	35	13 (37.1)		20 (57.1)		18 (51.4)		11 (31.4)		13 (37.1)		20 (57.1)	
Site													
Duodenum and jejunum	45	16 (35.6)	NS	25 (55.6)	NS	24 (53.3)	NS	16 (35.6)	NS	20 (44.4)	NS	26 (57.8)	NS
Ileum	5	1 (20.0)		2 (40.0)		1 (20.0)		1 (20.0)		1 (20.0)		2 (40.0)	
Histology													
WD, MD	41	13 (31.7)	NS	24 (58.5)	NS	21 (51.2)	NS	17 (41.5)	0.015	19 (46.3)	NS	26 (63.4)	0.030
PD, Muc	9	4 (44.4)		3 (33.3)		4 (44.4)		0 (0.0)		2 (22.2)		2 (22.2)	
Depth of invasion													
pT1-2	14	0 (0.0)	0.001	4 (28.6)	0.024	2 (14.3)	0.002	5 (35.7)	NS	6 (42.9)	NS	6 (42.9)	0.068
pT3-4	36	17 (47.2)		23 (63.9)		23 (63.9)		12 (33.3)		15 (41.7)		22 (61.1)	
Lymph node metastasis													
Absence	27	8 (29.6)	NS	16 (59.3)	NS	13 (48.1)	NS	8 (29.6)	NS	13 (48.1)	NS	15 (55.6)	NS
Presence	23	9 (39.1)		11 (47.8)		12 (52.2)		9 (39.1)		8 (34.8)		13 (56.5)	
Distant metastasis													
Absence	37	12 (32.4)	NS	22 (59.5)	NS	20 (54.1)	NS	13 (35.1)	NS	18 (48.6)	NS	23 (62.2)	0.095
Presence	13	5 (38.5)		5 (38.5)		5 (38.5)		4 (30.8)		3 (23.1)		5 (38.5)	
Peritoneal seeding													
Absence	40	14 (35.0)	NS	25 (62.5)	0.019	23 (57.5)	0.034	14 (35.0)	NS	19 (47.5)	NS	25 (62.5)	NS
Presence	10	3 (30.0)		2 (20.0)		2 (20.0)		3 (30.0)		2 (20.0)		3 (30.0)	
TNM stage													

I	14	0 (0.0)	0.008	4 (28.6)	0.005	2 (14.3)	0.001	5 (35.7)	NS	6 (42.9)	NS	6 (42.9)	NS
II	13	8 (61.5)		12 (92.3)		11 (84.6)		3 (23.1)		7 (53.8)		9 (69.2)	
III	10	4 (40.0)		6 (60.0)		7 (70.0)		5 (50.0)		5 (50.0)		8 (80.0)	
IV	13	5 (38.5)		5 (38.5)		5 (38.5)		4 (30.8)		3 (23.1)		5 (38.5)	
MMR status													
Proficient	43	12 (27.9)	0.037	20 (46.5)	0.009	18 (41.9)	0.005	15 (34.9)	NS	16 (37.2)	NS	22 (51.2)	NS
Deficient	7	5 (71.4)		7 (100.0)		7 (100.0)		2 (28.6)		5 (71.4)		6 (85.7)	

PD-L1: Programmed cell death-ligand 1; PD-L2: Programmed cell death-ligand 2; CPS: Combined positive score; WD: Well differentiated; MD: Moderately differentiated; PD: Poorly differentiated; Muc: Mucinous adenocarcinoma; NS: Not significant.

DISCUSSION

In this study, we performed immunostaining for PD-L1 and PD-L2 to investigate their clinicopathological significance in SBA. Since PD-L1 is expressed in both tumor cells and tumor-infiltrating immune cells, we examined the clinicopathological significance of their expression separately to clarify whether there were differences in their roles in tumor progression. Although there were several similarities and correlations, some differences in association with clinicopathological factors were observed. T-PD-L1 expression was associated with deeper depth of invasion, but not with lymph node metastasis, distant metastasis, or prognosis. These results suggest that T-PD-L1 contributes to the local invasion of tumor cells but not to metastasis; consequently, it is not associated with prognosis. I-PD-L1 expression is associated with deeper depth of invasion, less peritoneal metastasis, and favorable prognosis. We speculated that I-PD-L1 expression might be influenced by peritumoral infiltrating T cells, which correlates with favorable prognosis. Indeed, we found a positive relationship between I-PD-L1 expression and the CD8+ T cell count, and a high density of CD8+ TILs was associated with favorable prognosis. The main similarity between T-PD-L1 and I-PD-L1 expression was that both were associated with deeper depth of invasion and were more common in stage II compared to stage I tumors. These results suggest that the clinical significance of PD-L1 does not differ following the cell type in which it is expressed. Based on the above findings, we adopted the CPS to evaluate PD-L1 expression. The CPS was calculated by summing the number of PD-L1–stained cells (tumor cells, lymphocytes, and macrophages) and dividing the result by the total number of viable tumor cells, and multiplying by 100. Based on the observed response rate and response durability, the U.S. Food and Drug Administration granted pembrolizumab accelerated approval for the treatment of recurrent locally advanced, metastatic gastric or gastro-esophageal junction adenocarcinoma that expresses PD-L1 CPS ≥ 1. Thus, the CPS is now becoming a standard method for the assessment of PD-L1 expression. Because the CPS is a scoring system characterized by collectively quantifying positivity for tumor cells and positivity for surrounding immune cells, it may be possible to optimize the presence or absence of PD-L1 expression in carcinomas accompanied by inflammatory or immune cell infiltration. We examined the relationship between PD-L1 expression and clinicopathological factors using the CPS ≥ 10 as a cut-off in this study, resulting in that no significant association between PD-L1 expression and prognosis was found.

It has been demonstrated that PD-L2 is a second ligand for PD-1 and can be expressed by immune, stromal, or tumor cells, mainly through Th2-associated cytokines depending on tumor microenvironmental stimuli[35]. To date, a few studies have reported the significance of PD-L2 expression in gastrointestinal carcinomas[36,37]. To our knowledge, this

Table 3 Clinicopathological correlation of CD8, FoxP3, and FoxP3/CD8

	No.	FoxP3		CD8		FoxP3/CD8	
		N (%)	*P* value	*N* (%)	*P* value	*N* (%)	*P* value
Age							
≤ 68	27	14 (51.9)	NS	14 (51.9)	NS	14 (51.9)	NS
> 68	23	11 (47.8)		11 (47.8)		11 (47.8)	
Sex							
Female	15	7 (46.7)	NS	8 (53.3)	NS	8 (53.3)	NS
Male	35	18 (51.4)		17 (48.6)		17 (48.6)	
Site							
Duodenum and jejunum	45	22 (48.9)	NS	23 (51.1)	NS	22 (48.9)	NS
Ileum	5	3 (60.0)		2 (40.0)		3 (60.0)	
Histology							
WD, MD	41	21 (51.2)	NS	21 (51.2)	NS	20 (48.8)	NS
PD, Muc	9	4 (44.4)		4 (44.4)		5 (55.6)	
Depth							
pT1-2	14	4 (28.6)	0.059	7 (50.0)	NS	4 (28.6)	0.059
pT3-4	36	21 (58.3)		18 (50.0)		21 (58.3)	
Lymph node metastasis							
Absence	27	11 (40.7)	NS	17 (63.0)	0.047	8 (29.6)	0.002
Presence	23	14 (60.9)		8 (34.8)		17 (73.9)	
Distant metastasis							
Absence	37	16 (43.2)	NS	22 (59.5)	0.024	14 (37.8)	0.004
Presence	13	9 (69.2)		3 (23.1)		11 (84.6)	
Peritoneal seeding							
Absence	40	19 (47.5)	NS	23 (57.5)	0.034	16 (40.0)	0.005
Presence	10	6 (60.0)		2 (20.0)		9 (90.0)	
TNM stage							
I	14	4 (28.6)	NS	7 (50.0)	NS	4 (28.6)	0.011
II	13	7 (53.8)		10 (76.9)		4 (30.8)	
III	10	5 (50.0)		5 (50.0)		6 (60.0)	
IV	13	9 (69.2)		3 (23.1)		11 (84.6)	
MMR status							
Proficient	43	19 (44.2)	0.049	20 (46.5)	NS	22 (51.2)	NS
Deficient	7	6 (85.7)		5 (71.4)		3 (42.9)	

WD: Well differentiated; MD: Moderately differentiated; PD: Poorly differentiated; Muc: Mucinous adenocarcinoma; NS: Not significant.

is the first study to examine the relationship between PD-L2 expression and the clinicopathological characteristics of SBA patients. Since PD-L2 is expressed in both tumor cells and tumor-infiltrating immune cells, we examined the clinicopathological significance of its expression in both cell types, as we did for PD-L1. T-PD-L2 expression was not associated with any clinicopathological factors except for histological type and prognosis. I-PD-L2 expression was significantly associated with better CSS, suggesting that I-PD-L2 expression may be influenced by peritumoral infiltrating T cells that correlate with favorable prognosis. Then, we evaluated the PD-L2 expression using the CPS. PD-L2 CPS ≥ 10 was associated with younger age and was more common in differentiated histological type, but not with prognosis. It has been reported that PD-L2 expression was associated with poor prognosis in gastric and colorectal cancers[36,37]. These findings are intuitively understandable, considering that PD-L2 expression suppresses tumor immunity as well as PD-L1 does.

Table 4 Mutual relationship of programmed cell death-ligand 1, programmed cell death-ligand 2, CD8 and FoxP3 (*n* = 50)

	I-PD-L1	PD-L1 CPS ≥ 10	T-PD-L2	I-PD-L2	PD-L2 CPS ≥ 10	FoxP3	CD8	FoxP3/CD8
T-PD-L1	0.002	< 0.001	0.042	0.003	0.001	NS	0.007	NS
I-PD-L1		< 0.001	NS	0.019	0.002	0.005	0.047	NS
PD-L1 CPS ≥ 10			NS	0.010	0.004	0.048	0.011	NS
T-PD-L2				< 0.001	< 0.001	NS	NS	NS
I-PD-L2					< 0.001	NS	0.002	0.045[1]
PD-L2 CPS ≥ 10						NS	0.004	NS
FoxP3							NS	0.002
CD8								< 0.001[1]

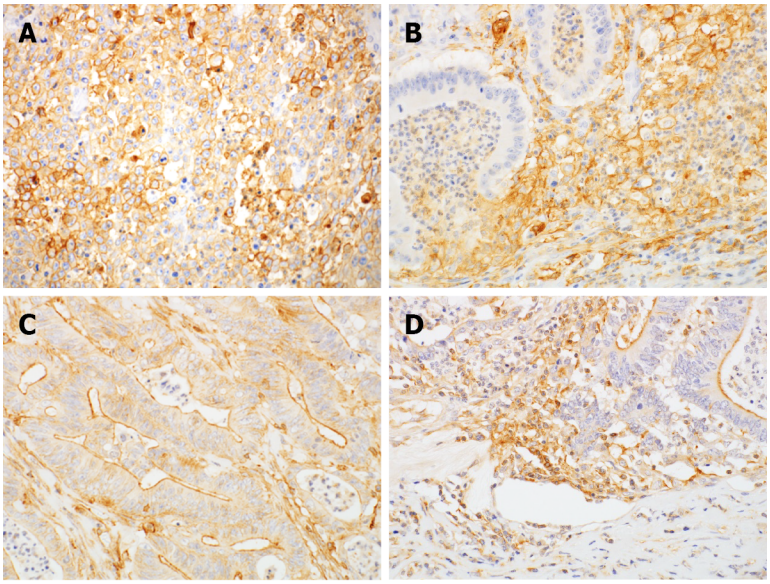
[1]An inverse relationship.
PD-L1: Programmed cell death-ligand 1; PD-L2: Programmed cell death-ligand 2; NS: Not significant.

Table 5 Univariate and multivariate Cox proportional hazards analysis for cancer-specific survival (*n* = 50)

Variables	Categories	Univariate analysis		Multivariate analysis	
		HR (95%CI)	*P* value	HR (95%CI)	*P* value
Histological type	PD, Muc *vs*. WD, MD	2.252 (0.799-6.348)	NS		
Depth	pT3-4 *vs*. pT1-2	39.308 (0.661-2337.048)	NS		
Lymph node metastasis	Positive *vs*. negative	42.764 (5.639-324.314)	< 0.001	66.320 (7.494-586.923)	< 0.001
T-PD-L1	Positive *vs*. negative	0.733 (0.261-2.059)	NS		
I-PD-L1	Positive *vs*. negative	0.367 (0.137-0.980)	0.046	1.156 (0.231-5.769)	NS
PD-L1 CPS ≥ 10	Positive *vs*. negative	0.621 (0.240-1.606)	NS		
T-PD-L2	Positive *vs*. negative	0.702 (0.249-1.981)	NS		
I-PD-L2	Positive *vs*. negative	0.243 (0.070-0.840)	0.025	0.113 (0.020-0.650)	0.015
PD-L2 CPS ≥ 10	Positive *vs*. negative	0.493 (0.191-1.276)	NS		
FoxP3	High *vs*. low	1.067 (0.423-2.694)	NS		
CD8	High *vs*. low	0.311 (0.111-0.872)	0.026	1.922 (0.164-22.481)	NS
FoxP3/CD8	High *vs*. low	4.490 (1.476-13.660)	0.008	1.476 (0.138-15.769)	NS

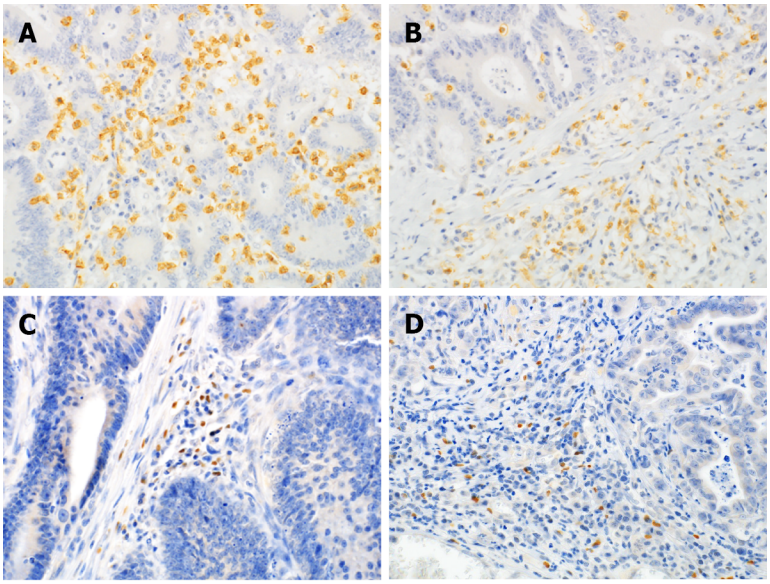
HR: Hazard ratio; 95%CI: 95% confidence interval; PD-L1: Programmed cell death-ligand 1; PD-L2: Programmed cell death-ligand 2; NS: Not significant.

However, several studies have demonstrated that both PD-L2 and PD-L1 expression are favorable prognostic indicators for gastric and colorectal cancer[25,38]. To date, such discrepancies have been explained by differences in scoring methods, cutoff values of immunostaining, heterogeneities of carcinoma, and any bias originating from the inclusion of an insufficient number of cases. To resolve this, we investigated the clinical significance of PD-L1 and PD-L2 expression according to TME status. CD8+ TILs are associated with the tumor immune response and can be used to predict the response to immunotherapy and survival outcomes in CRC[39]. It has been reported a high density of CD8+ TILs is associated with favorable prognosis in CRC[40-42]. We found that CD8-high was negatively associated with lymph node metastasis, distant metastasis, and peritoneal dissemination in SBA patients. We also found that the CD8-high group had better prognosis than the CD8-low group, which is consistent with the findings of previous reports. These results suggest that CD8+ TILs have an anti-tumor effect in SBA as well as in CRC and that CD8+ TILs play an important role in improving patient survival. Then, we analyzed the association between FoxP3+ Tregs and clinicopathological factors. CD4+ Tregs expressing the transcription factor FoxP3 are highly immunosuppressive and play a central role in maintaining self-tolerance and immune homeostasis. FoxP3+ T cells promote tumor progression by suppressing effective anti-tumor immunity by inactivating or reducing the proliferation of cytotoxic CD8+ T cells and CD4+ T effector cells in tumors[27,28]. To the best of our knowledge, this is the first study to examine the relationship between the density of FoxP3+ T cells and the clinicopathological characteristics in SBA patients. We found that FoxP3-high tumors tended to have deeper depth of invasion but were not associated with lymph node metastasis, distant metastasis, and peritoneal dissemination. No association was observed between FoxP3+ T cell density and CSS. This is due to the functional hetero-



DOI: 10.3748/wjg.v29.i40.5566 **Copyright** ©The Author(s) 2023.

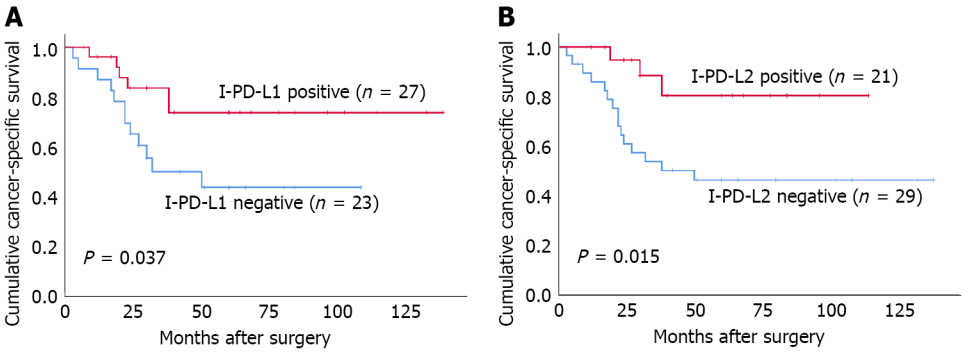
Figure 1 Immunohistochemical localization of programmed cell death-ligand 1 and programmed cell death-ligand 2 in small bowel adenocarcinoma. Magnification 400×. A: T-programmed cell death-ligand 1 expression was membranous and cytoplasmic; B: I-programmed cell death-ligand 1 (I-PD-L1) was positive in peritumoral lymphocytes and macrophages; C: The predominant pattern of T-programmed cell death-ligand 2 expression was in the apical membrane; D: I-programmed cell death-ligand 2 expression was positive in peritumoral lymphocytes and macrophages, similar to that of I-PD-L1.



DOI: 10.3748/wjg.v29.i40.5566 **Copyright** ©The Author(s) 2023.

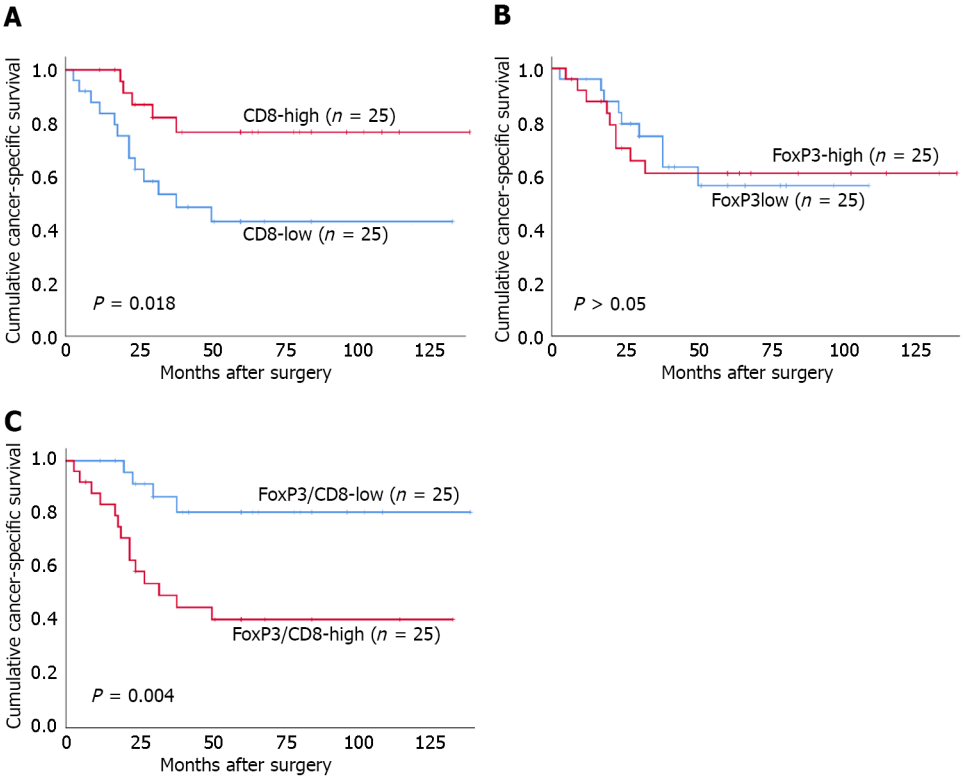
Figure 2 Immunohistochemical localization of CD8 and FoxP3 in small bowel adenocarcinoma. A: CD8+ T cells in the intratumoral stroma; B: CD8+ T cells in the tumor-surrounding stroma; C: FoxP3+ T cells in the intratumoral stroma; D: FoxP3+ T cells in tumor-surrounding stroma. Magnification 400 ×.

geneity of FoxP3+ T cells, as FoxP3+ non-Tregs are secreted depending on inflammatory cytokines such as TGF-β and IL-12[43]. While some studies have reported that high density of FoxP3+ T cells in the TME is associated with poor prognosis in lung cancer, others have reported that high density of FoxP3+ T cells is associated with favorable prognosis in CRC, bladder cancer, and head and neck cancers[44]. Thus, it has been reported that the amount of FoxP3+ T cells infiltration does not always serve as a poor prognostic indicator in the case of carcinoma accompanied by inflammatory cell infiltration, including CRC[43]. Then, we estimated the ratio of FoxP3+ T cells to CD8+ T cells in 10 HPF selected from the same site in the same section. FoxP3/CD8-high was significantly associated with deeper depth of invasion, lymph node metastasis, distant metastasis, peritoneal dissemination, and TNM stage progression. Patients with higher FoxP3+/CD8+ T cells ratios have poor prognosis for gastrointestinal cancers[29-31]. Similarly, we observed that the prognostic value of this ratio was better than that of FoxP3+ or CD8+ T cells alone, which partly reflects the interactions between anti-tumor CD8+ T cells and immunosuppressive FoxP3+ T cells in tumors[45,46]. These results indicate that assessing both FoxP3+ and CD8+ T cells is more useful for understanding TME status than assessing FoxP3 or CD8 + T cells alone.



DOI: 10.3748/wjg.v29.i40.5566 **Copyright** ©The Author(s) 2023.

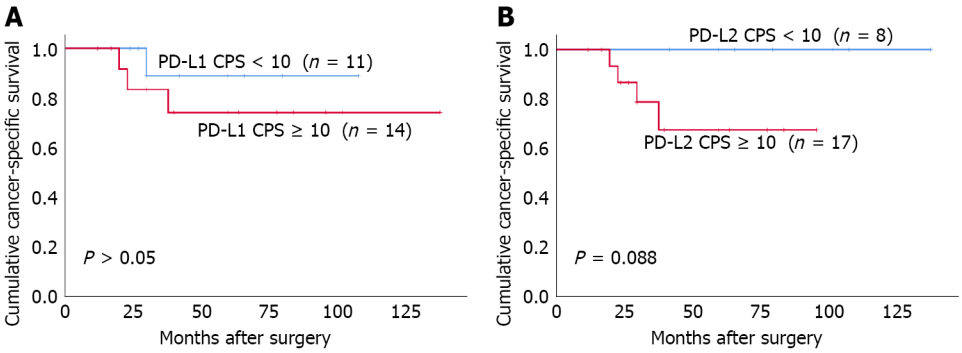
Figure 3 Kaplan–Meier analysis of cancer-specific survival according to programmed cell death-ligand 1 and programmed cell death-ligand 2 expressions in small bowel adenocarcinoma evaluated by log-rank tests. A: Survival based on I-programmed cell death-ligand 1 expression in overall cases; B: Survival based on I-programmed cell death-ligand 2 expression in overall cases. I-PD-L1: I-programmed cell death-ligand 1; I-PD-L2: I-programmed cell death-ligand 2.



DOI: 10.3748/wjg.v29.i40.5566 **Copyright** ©The Author(s) 2023.

Figure 4 Kaplan–Meier analysis of cancer-specific survival according to CD8+ and FoxP3+ T cell counts in small bowel adenocarcinoma evaluated by log-rank tests. A: Survival based on CD8+ T cell counts in overall cases; B: Survival based on FoxP3+ T cell counts in overall cases; C: Survival based on FoxP3+/CD8+ T cell counts in overall cases.

Both PD-L1 CPS ≥ 10 and PD-L2 CPS ≥ 10 significantly correlated with increased CD8+ T cells infiltration. Furthermore, I-PD-L2 expression was more frequent in FoxP3/CD8-low tumors. These results may explain why I-PD-L2 expression is associated with favorable outcomes. To determine the effect of PD-L1 and PD-L2 on the prognosis of patients with SBA, excluding the effect of the TME, we divided the patients into FoxP3/CD8-low and FoxP3/CD8-high groups. We investigated the correlation between PD-L1 and PD-L2 expression and the prognosis in the two patient groups. We found that patients with PD-L2 CPS ≥ 10 tended to have poorer prognosis than those with PD-L2 CPS < 10 in the FoxP3/CD8-low group, although the difference was not statistically significant. Furthermore, there were no deaths among patients with a PD-L2 CPS < 10 in the FoxP3/CD8-low group. Generally, cases in which the infiltration of CD8 is dominant over FoxP3 are predicted to have favorable prognosis due to the anti-tumor immune effect of T cells; nevertheless, patients showing poor prognosis are also included within the group. The PD-L2 pathway may contribute to poor prognosis in patients with FoxP3/CD8-low tumors. The results of this study also indicate that PD-L2 may be a better



DOI: 10.3748/wjg.v29.i40.5566 **Copyright** ©The Author(s) 2023.

Figure 5 Kaplan–Meier analysis of cancer-specific survival according to PD-L1 and PD-L2 expression in small bowel adenocarcinoma patients with FoxP3/CD8-low tumors. A: Survival based on PD-L1 combined positive score (CPS) among patients in the FoxP3/CD8-low group; B: Survival based on PD-L2 CPS among patients in the FoxP3/CD8-low group.

predictive factor for prognosis in these cases than PD-L1.

Recent studies have demonstrated that the tumor mutation burden (TMB) could be a biomarker in patients with cancer treated with immune checkpoint inhibitors (ICIs), in which high TMB is significantly correlated with better survival[47]. Although the efficacy of ICIs in patients with cancer with TMB-high or MSI-high/dMMR has been confirmed, patients with MSI-high have a favorable prognosis, and generally, only a small number of patients require chemotherapy. In fact, none of the patients with dMMR died in our cohort, and only two of seven patients received chemotherapy. Most patients with SBA have microsatellite stable (MSS)/pMMR or TMB-low, and it is necessary to identify useful biomarkers for ICI therapy in patients with MSS/pMMR. Previous studies have shown that TMB-high tumors are immunogenic and that TMB-high tumors are also present in SBA[48]. In small bowel cancer, TMB-high has been reported to be associated with dMMR, CD8-high, and PD-L1 expression, but it has been shown that TMB-high cases are also present in cases of pMMR [49,50]. Our results indicate that PD-L2 positive and FoxP3/CD8-low patients with pMMR may benefit from ICI therapy. Although we did not examine the TMB in this study, it may stratify the outcomes of patients with SBA with PD-L2 positive and FoxP3/CD8-low.

This study has several limitations. First, the sample size is small. In addition, there was a bias in tumor localization. Second, MMR status was determined based solely on the results of immunohistochemical staining for MMR proteins. Third, there were no deaths among the patients with dMMR tumors. Therefore, we could not analyze patients' prognosis based on the MMR status.

CONCLUSION

We elucidated a discrepancy in the previously reported clinical significance of PD-L1 expression in SBA. Several studies have reported that PD-L1 expression, which should be involved in tumorigenesis, is associated with favorable prognosis. This contradictory finding may originate from the fact that all patients are equally included in the analysis without considering the TME status and the type of cells in which PD-L1 is expressed. We demonstrated that the clinical significance of PD-L2 may be affected by TME status. Although SBA patients with high immune cell infiltration generally have better prognosis, some of these patients have poorer prognosis. PD-L2 may contribute to poorer prognosis of these patients. ICIs may improve the patients' prognosis in the FoxP3/CD8-low group through blocking the binding of the PD-1 to PD-L2 and activating locally infiltrated T cells.

ARTICLE HIGHLIGHTS

Research background

According to a recent report from the United States, the incidence of small bowel adenocarcinoma (SBA) has been increasing, with an annual increase of 1.8% between 2006 and 2015. Comprehensive genomic analyses revealed that SBA and colorectal cancer have different genomic profiles, and it is assumed that the molecular pathways leading to carcinogenesis may also be different. Therefore, it is essential to establish chemotherapeutic regimens based on the specific characteristics of SBA.

Research motivation

The clinicopathological significance of programmed cell death-ligand 1 (PD-L1) and programmed cell death-ligand 2 (PD-L2) expression in SBA is not yet fully understood. There are several conflicting reports regarding the clinicopathological significance of PD-L1 expression in gastrointestinal cancers. To resolve this discrepancy, we investigated the clinical

significance of PD-L1 and PD-L2 expression according to tumor microenvironment (TME) status stratified by the density of FoxP3+ and CD8+ T cells.

Research objectives

In this study, we investigated the clinicopathological significance of PD-L1 and PD-L2 expression in association with the infiltration of FoxP3+ and CD8+ T cells in the TME to identify PD-L/PD-1 immunotherapy candidates among patients with SBA. We elucidated the discrepancy in previously reported clinical significance of PD-L1 expression in SBA.

Research methods

The immunoreactivities of PD-L1 and PD-L2 were determined separately in tumor cells and tumor-infiltrating immune cells, such as lymphocytes and macrophages, and evaluated using the combined positive score (CPS). To our knowledge, this is the first study to examine the relationship between PD-L2 expression, and the density of FoxP3+ T cells, and the clinicopathological characteristics of patients with SBA.

Research results

PD-L1 expression was positive in 34% in tumor cells (T-PD-L1) and 54% in tumor-infiltrating immune cells (I-PD-L1) of the cases examined. T-PD-L2 was positive in 34% and I-PD-L2 was positive in 42% of the cases, respectively. PD-L1 CPS ≥ 10 and PD-L2 CPS ≥ 10 were observed in 50% and 56% of cases, respectively. I-PD-L1 and I-PD-L2 Levels were significantly associated with better prognosis. We speculated that I-PD-L1 expression might be influenced by peritumoral infiltrating T cells, which correlates with favorable prognosis. We found that patients with PD-L2 CPS ≥ 10 tended to have worse prognosis in the FoxP3/CD8-low group. Although SBA patients with high immune cell infiltration, such as those in the FoxP3/CD8-low group, generally have better prognosis, some have poorer prognosis. Therefore, PD-L2 may contribute to the poor prognosis of these patients.

Research conclusions

We identified a discrepancy in the previously reported clinical significance of PD-L1 expression in SBA. Several studies have reported that PD-L1 expression, which is involved in tumorigenesis, is associated with favorable prognosis. This contradictory finding may originate from the fact that all patients were equally included in the analysis without considering the TME status and the type of cells in which PD-L1 was expressed. To identify PD-L/PD-1 immunotherapy candidates, not only PD-L1 expression and DNA mismatch repair/microsatellite instability but also PD-L2 expression and the density of tumor-infiltrating lymphocytes, such as FoxP3+ and CD8+ T cells, in the TME should be considered.

Research perspectives

In this study, we did not consider tumor mutation burden (TMB). TMB-high has been proposed as a predictive biomarker for the response to immune checkpoint inhibitors based on the assumption that increasing the number of mutant proteins will create antigenic peptides, allowing for enhanced immunogenicity. In the future, we may be able to analyze TMB status in SBA and combine it with PD-L1/2 expression and TME status to generate powerful biomarkers for identifying immunotherapy candidates.

ACKNOWLEDGEMENTS

We thank Mrs. Akiko Takeda for her technical assistance.

FOOTNOTES

Author contributions: Hoshimoto A designed and performed the research and wrote the paper; Tatsuguchi A designed the research and contributed to the analysis; Hamakubo R, Nishimoto T, Omori J, Akimoto N, Tanaka S, Fujimori S, and Hatori T provided clinical advice; Shimizu A and Iwakiri K supervised the report; All authors have read and approve the final manuscript.

Institutional review board statement: The study was reviewed and approved by the Nippon Medical School Institutional Review Board (Approval No. B-2020-164).

Informed consent statement: All study participants, or their legal guardian, provided informed written consent prior to study enrollment.

Conflict-of-interest statement: The authors declare no conflicts of interest.

Data sharing statement: Technical appendix, statistical code, and dataset available from the corresponding author at tachan@nms.ac.jp. Participants gave informed consent for data sharing.

Open-Access: This article is an open-access article that was selected by an in-house editor and fully peer-reviewed by external reviewers. It is distributed in accordance with the Creative Commons Attribution NonCommercial (CC BY-NC 4.0) license, which permits others to

distribute, remix, adapt, build upon this work non-commercially, and license their derivative works on different terms, provided the original work is properly cited and the use is non-commercial. See: https://creativecommons.org/Licenses/by-nc/4.0/

Country/Territory of origin: Japan

ORCID number: Aitoshi Hoshimoto 0000-0002-6883-4795; Atsushi Tatsuguchi 0000-0002-8499-8837; Ryohei Hamakubo 0000-0003-1205-3866; Takayoshi Nishimoto 0000-0002-5147-0665; Jun Omori 0000-0002-4375-5070; Naohiko Akimoto 0000-0001-9880-4143; Shu Tanaka 0000-0003-4121-5553; Shunji Fujimori 0000-0002-6214-2595; Tsutomu Hatori 0009-0003-0780-6904; Akira Shimizu 0000-0002-4364-9251; Katsuhiko Iwakiri 0000-0002-5558-6104.

S-Editor: Lin C
L-Editor: A
P-Editor: Lin C

REFERENCES

1 **Siegel RL**, Miller KD, Jemal A. Cancer statistics, 2019. *CA Cancer J Clin* 2019; **69**: 7-34 [PMID: 30620402 DOI: 10.3322/caac.21551]
2 **Benson AB**, Venook AP, Al-Hawary MM, Arain MA, Chen YJ, Ciombor KK, Cohen SA, Cooper HS, Deming DA, Garrido-Laguna I, Grem JL, Hoffe SE, Hubbard J, Hunt S, Kamel A, Kirilcuk N, Krishnamurthi S, Messersmith WA, Meyerhardt J, Miller ED, Mulcahy MF, Nurkin S, Overman MJ, Parikh A, Patel H, Pedersen KS, Saltz LB, Schneider C, Shibata D, Skibber JM, Sofocleous CT, Stoffel EM, Stotsky-Himelfarb E, Willett CG, Johnson-Chilla A, Gregory KM, Gurski LA. Small Bowel Adenocarcinoma, Version 1.2020, NCCN Clinical Practice Guidelines in Oncology. *J Natl Compr Canc Netw* 2019; **17**: 1109-1133 [PMID: 31487687 DOI: 10.6004/jnccn.2019.0043]
3 **Fujimori S**, Hamakubo R, Hoshimoto A, Nishimoto T, Omori J, Akimoto N, Tanaka S, Tatsuguchi A, Iwakiri K. Risk factors for small intestinal adenocarcinomas that are common in the proximal small intestine. *World J Gastroenterol* 2022; **28**: 5658-5665 [PMID: 36338888 DOI: 10.3748/wjg.v28.i39.5658]
4 **Bilimoria KY**, Bentrem DJ, Wayne JD, Ko CY, Bennett CL, Talamonti MS. Small bowel cancer in the United States: changes in epidemiology, treatment, and survival over the last 20 years. *Ann Surg* 2009; **249**: 63-71 [PMID: 19106677 DOI: 10.1097/SLA.0b013e31818e4641]
5 **Schrock AB**, Devoe CE, McWilliams R, Sun J, Aparicio T, Stephens PJ, Ross JS, Wilson R, Miller VA, Ali SM, Overman MJ. Genomic Profiling of Small-Bowel Adenocarcinoma. *JAMA Oncol* 2017; **3**: 1546-1553 [PMID: 28617917 DOI: 10.1001/jamaoncol.2017.1051]
6 **Tatsuguchi A**, Yamada T, Ueda K, Furuki H, Hoshimoto A, Nishimoto T, Omori J, Akimoto N, Gudis K, Tanaka S, Fujimori S, Shimizu A, Iwakiri K. Genetic analysis of Japanese patients with small bowel adenocarcinoma using next-generation sequencing. *BMC Cancer* 2022; **22**: 723 [PMID: 35778698 DOI: 10.1186/s12885-022-09824-6]
7 **Brahmer JR**, Tykodi SS, Chow LQM, Hwu WJ, Topalian SL, Hwu P, Drake CG, Camacho LH, Kauh J, Odunsi K, Pitot HC, Hamid O, Bhatia S, Martins R, Eaton K, Chen SM, Salay TM, Alaparthy S, Grosso JF, Korman AJ, Parker SM, Agrawal S, Goldberg SM, Pardoll DM, Gupta A, Wigginton JM. Safety and Activity of Anti-PD-L1 Antibody in Patients with Advanced Cancer. *N Engl J Med* 2012; **366** (26): 2455-2465 [DOI: 10.1056/NEJMoa1200694]
8 **Fuchs CS**, Doi T, Jang RW, Muro K, Satoh T, Machado M, Sun W, Jalal SI, Shah MA, Metges JP, Garrido M, Golan T, Mandala M, Wainberg ZA, Catenacci DV, Ohtsu A, Shitara K, Geva R, Bleeker J, Ko AH, Ku G, Philip P, Enzinger PC, Bang YJ, Levitan D, Wang J, Rosales M, Dalal RP, Yoon HH. Safety and Efficacy of Pembrolizumab Monotherapy in Patients With Previously Treated Advanced Gastric and Gastroesophageal Junction Cancer: Phase 2 Clinical KEYNOTE-059 Trial. *JAMA Oncol* 2018; **4**: e180013 [PMID: 29543932 DOI: 10.1001/jamaoncol.2018.0013]
9 **Muro K**, Chung HC, Shankaran V, Geva R, Catenacci D, Gupta S, Eder JP, Golan T, Le DT, Burtness B, McRee AJ, Lin CC, Pathiraja K, Lunceford J, Emancipator K, Juco J, Koshiji M, Bang YJ. Pembrolizumab for patients with PD-L1-positive advanced gastric cancer (KEYNOTE-012): a multicentre, open-label, phase 1b trial. *Lancet Oncol* 2016; **17**: 717-726 [PMID: 27157491 DOI: 10.1016/S1470-2045(16)00175-3]
10 **Overman MJ**, McDermott R, Leach JL, Lonardi S, Lenz HJ, Morse MA, Desai J, Hill A, Axelson M, Moss RA, Goldberg MV, Cao ZA, Ledeine JM, Maglinte GA, Kopetz S, André T. Nivolumab in patients with metastatic DNA mismatch repair-deficient or microsatellite instability-high colorectal cancer (CheckMate 142): an open-label, multicentre, phase 2 study. *Lancet Oncol* 2017; **18**: 1182-1191 [PMID: 28734759 DOI: 10.1016/S1470-2045(17)30422-9]
11 **Fashoyin-Aje L**, Donoghue M, Chen H, He K, Veeraraghavan J, Goldberg KB, Keegan P, McKee AE, Pazdur R. FDA Approval Summary: Pembrolizumab for Recurrent Locally Advanced or Metastatic Gastric or Gastroesophageal Junction Adenocarcinoma Expressing PD-L1. *Oncologist* 2019; **24**: 103-109 [PMID: 30120163 DOI: 10.1634/theoncologist.2018-0221]
12 **Thota R**, Gonzalez RS, Berlin J, Cardin DB, Shi C. Could the PD-1 Pathway Be a Potential Target for Treating Small Intestinal Adenocarcinoma? *Am J Clin Pathol* 2017; **148**: 208-214 [PMID: 28821192 DOI: 10.1093/AJCP/AQX070]
13 **Noh BJ**, Hong SM, Jun SY, Eom DW. Prognostic implications of immune classification in a multicentre cohort of patients with small intestinal adenocarcinoma. *Pathology* 2020; **52**: 228-235 [PMID: 31685233 DOI: 10.1016/j.pathol.2019.09.004]
14 **Böger C**, Behrens HM, Mathiak M, Krüger S, Kalthoff H, Röcken C. PD-L1 is an independent prognostic predictor in gastric cancer of Western patients. *Oncotarget* 2016; **7**: 24269-24283 [PMID: 27009855 DOI: 10.18632/oncotarget.8169]
15 **Seo AN**, Kang BW, Kwon OK, Park KB, Lee SS, Chung HY, Yu W, Bae HI, Jeon SW, Kang H, Kim JG. Intratumoural PD-L1 expression is associated with worse survival of patients with Epstein-Barr virus-associated gastric cancer. *Br J Cancer* 2017; **117**: 1753-1760 [PMID: 29073638 DOI: 10.1038/bjc.2017.369]
16 **Li Y**, Liang L, Dai W, Cai G, Xu Y, Li X, Li Q, Cai S. Prognostic impact of programed cell death-1 (PD-1) and PD-ligand 1 (PD-L1) expression in cancer cells and tumor infiltrating lymphocytes in colorectal cancer. *Mol Cancer* 2016; **15**: 55 [PMID: 27552968 DOI: 10.1186/s12943-016-0539-x]
17 **Droeser RA**, Hirt C, Viehl CT, Frey DM, Nebiker C, Huber X, Zlobec I, Eppenberger-Castori S, Tzankov A, Rosso R, Zuber M, Muraro MG,

Amicarella F, Cremonesi E, Heberer M, Iezzi G, Lugli A, Terracciano L, Sconocchia G, Oertli D, Spagnoli GC, Tornillo L. Clinical impact of programmed cell death ligand 1 expression in colorectal cancer. *Eur J Cancer* 2013; **49**: 2233-2242 [PMID: 23478000 DOI: 10.1016/j.ejca.2013.02.015]

18 **Wang W**, Jing H, Liu J, Bu D, Zhang Y, Zhu T, Lu K, Xu Y, Cheng M, Yao J, Huang S, Wang L. Correlation between schistosomiasis and CD8+ T cell and stromal PD-L1 as well as the different prognostic role of CD8+ T cell and PD-L1 in schistosomal-associated colorectal cancer and non-schistosomal-associated colorectal cancer. *World J Surg Oncol* 2021; **19**: 321 [PMID: 34743724 DOI: 10.1186/s12957-021-02433-w]

19 **Gu L**, Chen M, Guo D, Zhu H, Zhang W, Pan J, Zhong X, Li X, Qian H, Wang X. PD-L1 and gastric cancer prognosis: A systematic review and meta-analysis. *PLoS One* 2017; **12**: e0182692 [PMID: 28796808 DOI: 10.1371/journal.pone.0182692]

20 **Koganemaru S**, Inoshita N, Miura Y, Miyama Y, Fukui Y, Ozaki Y, Tomizawa K, Hanaoka Y, Toda S, Suyama K, Tanabe Y, Moriyama J, Fujii T, Matoba S, Kuroyanagi H, Takano T. Prognostic value of programmed death-ligand 1 expression in patients with stage III colorectal cancer. *Cancer Sci* 2017; **108**: 853-858 [PMID: 28267224 DOI: 10.1111/cas.13229]

21 **Shi SJ**, Wang LJ, Wang GD, Guo ZY, Wei M, Meng YL, Yang AG, Wen WH. B7-H1 expression is associated with poor prognosis in colorectal carcinoma and regulates the proliferation and invasion of HCT116 colorectal cancer cells. *PLoS One* 2013; **8**: e76012 [PMID: 24124529 DOI: 10.1371/journal.pone.0076012]

22 **Lee LH**, Cavalcanti MS, Segal NH, Hechtman JF, Weiser MR, Smith JJ, Garcia-Aguilar J, Sadot E, Ntiamoah P, Markowitz AJ, Shike M, Stadler ZK, Vakiani E, Klimstra DS, Shia J. Patterns and prognostic relevance of PD-1 and PD-L1 expression in colorectal carcinoma. *Mod Pathol* 2016; **29**: 1433-1442 [PMID: 27443512 DOI: 10.1038/modpathol.2016.139]

23 **Latchman Y**, Wood CR, Chernova T, Chaudhary D, Borde M, Chernova I, Iwai Y, Long AJ, Brown JA, Nunes R, Greenfield EA, Bourque K, Boussiotis VA, Carter LL, Carreno BM, Malenkovich N, Nishimura H, Okazaki T, Honjo T, Sharpe AH, Freeman GJ. PD-L2 is a second ligand for PD-1 and inhibits T cell activation. *Nat Immunol* 2001; **2**: 261-268 [PMID: 11224527 DOI: 10.1038/85330]

24 **Rodig N**, Ryan T, Allen JA, Pang H, Grabie N, Chernova T, Greenfield EA, Liang SC, Sharpe AH, Lichtman AH, Freeman GJ. Endothelial expression of PD-L1 and PD-L2 down-regulates CD8+ T cell activation and cytolysis. *Eur J Immunol* 2003; **33**: 3117-3126 [PMID: 14579280 DOI: 10.1002/eji.200324270]

25 **Yearley JH**, Gibson C, Yu N, Moon C, Murphy E, Juco J, Lunceford J, Cheng J, Chow LQM, Seiwert TY, Handa M, Tomassini JE, McClanahan T. PD-L2 Expression in Human Tumors: Relevance to Anti-PD-1 Therapy in Cancer. *Clin Cancer Res* 2017; **23**: 3158-3167 [PMID: 28619999 DOI: 10.1158/1078-0432.CCR-16-1761]

26 **Aristin Revilla S**, Kranenburg O, Coffer PJ. Colorectal Cancer-Infiltrating Regulatory T Cells: Functional Heterogeneity, Metabolic Adaptation, and Therapeutic Targeting. *Front Immunol* 2022; **13**: 903564 [PMID: 35874729 DOI: 10.3389/fimmu.2022.903564]

27 **Saleh R**, Elkord E. FoxP3(+) T regulatory cells in cancer: Prognostic biomarkers and therapeutic targets. *Cancer Lett* 2020; **490**: 174-185 [PMID: 32721551 DOI: 10.1016/j.canlet.2020.07.022]

28 **Takeuchi Y**, Nishikawa H. Roles of regulatory T cells in cancer immunity. *Int Immunol* 2016; **28**: 401-409 [PMID: 27160722 DOI: 10.1093/intimm/dxw025]

29 **Kiryu S**, Ito Z, Suka M, Bito T, Kan S, Uchiyama K, Saruta M, Hata T, Takano Y, Fujioka S, Misawa T, Yamauchi T, Yanagisawa H, Sato N, Ohkusa T, Sugiyama H, Koido S. Prognostic value of immune factors in the tumor microenvironment of patients with pancreatic ductal adenocarcinoma. *BMC Cancer* 2021; **21**: 1197 [PMID: 34758773 DOI: 10.1186/s12885-021-08911-4]

30 **Zhu Y**, Li M, Mu D, Kong L, Zhang J, Zhao F, Li Z, Liu X, Bo C, Yu J. CD8+/FOXP3+ ratio and PD-L1 expression associated with survival in pT3N0M0 stage esophageal squamous cell cancer. *Oncotarget* 2016; **7**: 71455-71465 [PMID: 27683115 DOI: 10.18632/oncotarget.12213]

31 **Suzuki H**, Chikazawa N, Tasaka T, Wada J, Yamasaki A, Kitaura Y, Sozaki M, Tanaka M, Onishi H, Morisaki T, Katano M. Intratumoral CD8(+) T/FOXP3 (+) cell ratio is a predictive marker for survival in patients with colorectal cancer. *Cancer Immunol Immunother* 2010; **59**: 653-661 [PMID: 19908042 DOI: 10.1007/s00262-009-0781-9]

32 **Shitara K**, Van Cutsem E, Bang YJ, Fuchs C, Wyrwicz L, Lee KW, Kudaba I, Garrido M, Chung HC, Lee J, Castro HR, Mansoor W, Braghiroli MI, Karaseva N, Caglevic C, Villanueva L, Goekkurt E, Satake H, Enzinger P, Alsina M, Benson A, Chao J, Ko AH, Wainberg ZA, Kher U, Shah S, Kang SP, Tabernero J. Efficacy and Safety of Pembrolizumab or Pembrolizumab Plus Chemotherapy *vs* Chemotherapy Alone for Patients With First-line, Advanced Gastric Cancer: The KEYNOTE-062 Phase 3 Randomized Clinical Trial. *JAMA Oncol* 2020; **6**: 1571-1580 [PMID: 32880601 DOI: 10.1001/jamaoncol.2020.3370]

33 **Kulangara K**, Zhang N, Corigliano E, Guerrero L, Waldroup S, Jaiswal D, Ms MJ, Shah S, Hanks D, Wang J, Lunceford J, Savage MJ, Juco J, Emancipator K. Clinical Utility of the Combined Positive Score for Programmed Death Ligand-1 Expression and the Approval of Pembrolizumab for Treatment of Gastric Cancer. *Arch Pathol Lab Med* 2019; **143**: 330-337 [PMID: 30028179 DOI: 10.5858/arpa.2018-0043-OA]

34 **Wainberg ZA**, Fuchs CS, Tabernero J, Shitara K, Muro K, Van Cutsem E, Bang YJ, Chung HC, Yamaguchi K, Varga E, Chen JS, Hochhauser D, Thuss-Patience P, Al-Batran SE, Garrido M, Kher U, Shih CS, Shah S, Bhagia P, Chao J. Efficacy of Pembrolizumab Monotherapy for Advanced Gastric/Gastroesophageal Junction Cancer with Programmed Death Ligand 1 Combined Positive Score ≥10. *Clin Cancer Res* 2021; **27**: 1923-1931 [PMID: 33446564 DOI: 10.1158/1078-0432.CCR-20-2980]

35 **Masugi Y**, Nishihara R, Hamada T, Song M, da Silva A, Kosumi K, Gu M, Shi Y, Li W, Liu L, Nevo D, Inamura K, Cao Y, Liao X, Nosho K, Chan AT, Giannakis M, Bass AJ, Hodi FS, Freeman GJ, Rodig SJ, Fuchs CS, Qian ZR, Nowak JA, Ogino S. Tumor PDCD1LG2 (PD-L2) Expression and the Lymphocytic Reaction to Colorectal Cancer. *Cancer Immunol Res* 2017; **5**: 1046-1055 [PMID: 29038297 DOI: 10.1158/2326-6066.CIR-17-0122]

36 **Wang H**, Yao H, Li C, Liang L, Zhang Y, Shi H, Zhou C, Chen Y, Fang JY, Xu J. PD-L2 expression in colorectal cancer: Independent prognostic effect and targetability by deglycosylation. *Oncoimmunology* 2017; **6**: e1327494 [PMID: 28811964 DOI: 10.1080/2162402X.2017.1327494]

37 **Gao Y**, Li S, Xu D, Chen S, Cai Y, Jiang W, Zhang X, Sun J, Wang K, Chang B, Wang F, Hong M. Prognostic value of programmed death-1, programmed death-ligand 1, programmed death-ligand 2 expression, and CD8(+) T cell density in primary tumors and metastatic lymph nodes from patients with stage T1-4N+M0 gastric adenocarcinoma. *Chin J Cancer* 2017; **36**: 61 [PMID: 28754154 DOI: 10.1186/s40880-017-0226-3]

38 **Pyo JS**, Son BK, Chung KH, Oh IH. Clinicopathological significance and prognostic implication of programmed death-1 Ligand 2 expression in colorectal cancer. *Int J Biol Markers* 2019; **34**: 276-283 [PMID: 31337259 DOI: 10.1177/1724600819858753]

39 **Zou Q**, Wang X, Ren D, Hu B, Tang G, Zhang Y, Huang M, Pai RK, Buchanan DD, Win AK, Newcomb PA, Grady WM, Yu H, Luo Y. DNA methylation-based signature of CD8+ tumor-infiltrating lymphocytes enables evaluation of immune response and prognosis in colorectal cancer. *J Immunother Cancer* 2021; **9** [PMID: 34548385 DOI: 10.1136/jitc-2021-002671]

40 **Mei Z**, Liu Y, Liu C, Cui A, Liang Z, Wang G, Peng H, Cui L, Li C. Tumour-infiltrating inflammation and prognosis in colorectal cancer: systematic review and meta-analysis. Br J Cancer 2014; 110(6): 1595-1605 [DOI: 10.1038/bjc.2014.46]

41 **Wang E**, Shibutani M, Nagahara H, Fukuoka T, Iseki Y, Okazaki Y, Kashiwagi S, Tanaka H, Maeda K. Prognostic value of the density of tumor-infiltrating lymphocytes in colorectal cancer liver metastases. *Oncol Lett* 2021; **22**: 837 [PMID: 34712361 DOI: 10.3892/ol.2021.13098]

42 **Topalian SL**, Taube JM, Anders RA, Pardoll DM. Mechanism-driven biomarkers to guide immune checkpoint blockade in cancer therapy. *Nat Rev Cancer* 2016; **16**: 275-287 [PMID: 27079802 DOI: 10.1038/nrc.2016.36]

43 **Saito T**, Nishikawa H, Wada H, Nagano Y, Sugiyama D, Atarashi K, Maeda Y, Hamaguchi M, Ohkura N, Sato E, Nagase H, Nishimura J, Yamamoto H, Takiguchi S, Tanoue T, Suda W, Morita H, Hattori M, Honda K, Mori M, Doki Y, Sakaguchi S. Two FOXP3(+)CD4(+) T cell subpopulations distinctly control the prognosis of colorectal cancers. *Nat Med* 2016; **22**: 679-684 [PMID: 27111280 DOI: 10.1038/nm.4086]

44 **Fridman WH**, Pagès F, Sautès-Fridman C, Galon J. The immune contexture in human tumours: impact on clinical outcome. *Nat Rev Cancer* 2012; **12**: 298-306 [PMID: 22419253 DOI: 10.1038/nrc3245]

45 **Roychoudhuri R**, Eil RL, Restifo NP. The interplay of effector and regulatory T cells in cancer. *Curr Opin Immunol* 2015; **33**: 101-111 [PMID: 25728990 DOI: 10.1016/j.coi.2015.02.003]

46 **Vignali DA**, Collison LW, Workman CJ. How regulatory T cells work. *Nat Rev Immunol* 2008; **8**: 523-532 [PMID: 18566595 DOI: 10.1038/nri2343]

47 **Li DD**, Tang YL, Wang X. Challenges and exploration for immunotherapies targeting cold colorectal cancer. *World J Gastrointest Oncol* 2023; **15**: 55-68 [PMID: 36684057 DOI: 10.4251/wjgo.v15.i1.55]

48 **Chan TA**, Yarchoan M, Jaffee E, Swanton C, Quezada SA, Stenzinger A, Peters S. Development of tumor mutation burden as an immunotherapy biomarker: utility for the oncology clinic. *Ann Oncol* 2019; **30**: 44-56 [PMID: 30395155 DOI: 10.1093/annonc/mdy495]

49 **Wirta EV**, Szeto S, Hänninen U, Ahtiainen M, Böhm J, Mecklin JP, Aaltonen LA, Seppälä TT. Prognostic Value of Immune Environment Analysis in Small Bowel Adenocarcinomas with Verified Mutational Landscape and Predisposing Conditions. *Cancers (Basel)* 2020; **12** [PMID: 32718028 DOI: 10.3390/cancers12082018]

50 **Pedersen KS**, Foster NR, Overman MJ, Boland PM, Kim SS, Arrambide KA, Jaszewski BL, Bekaii-Saab T, Graham RP, Welch J, Wilson RH, McWilliams RR. ZEBRA: A Multicenter Phase II Study of Pembrolizumab in Patients with Advanced Small-Bowel Adenocarcinoma. *Clin Cancer Res* 2021; **27**: 3641-3648 [PMID: 33883178 DOI: 10.1158/1078-0432.CCR-21-0159]

World Journal of Gastroenterology

Submit a Manuscript: https://www.f6publishing.com

World J Gastroenterol 2023 October 28; 29(40): 5582-5592

DOI: 10.3748/wjg.v29.i40.5582

ISSN 1007-9327 (print) ISSN 2219-2840 (online)

ORIGINAL ARTICLE

Observational Study

Expression characteristics of peripheral lymphocyte programmed death 1 and FoxP3+ Tregs in gastric cancer during surgery and chemotherapy

Hao Li, Guan-Mei Cao, Guo-Li Gu, Song-Yan Li, Yang Yan, Ze Fu, Xiao-Hui Du

Specialty type: Gastroenterology and hepatology

Provenance and peer review: Unsolicited article; Externally peer reviewed.

Peer-review model: Single blind

Peer-review report's scientific quality classification

Grade A (Excellent): 0
Grade B (Very good): B
Grade C (Good): C
Grade D (Fair): 0
Grade E (Poor): 0

P-Reviewer: Cho JY, South Korea; Toshimori A, Japan

Received: August 7, 2023
Peer-review started: August 7, 2023
First decision: August 28, 2023
Revised: August 31, 2023
Accepted: October 11, 2023
Article in press: October 11, 2023
Published online: October 28, 2023

Hao Li, Ze Fu, Graduate School, Medical School of Chinese People's Liberation Army, Beijing 100039, China

Hao Li, Guo-Li Gu, Department of General Surgery, Air Force Medical Center, Air Force Medical University, Beijing 100142, China

Guan-Mei Cao, Department of Radiology, Beijing Tiantan Hospital, Capital Medical University, Beijing 100070, China

Song-Yan Li, Yang Yan, Xiao-Hui Du, Department of General Surgery, Chinese PLA General Hospital, Beijing 100039, China

Corresponding author: Xiao-Hui Du, MD, PhD, Chief Doctor, Deputy Director, Professor, Surgeon, Department of General Surgery, Chinese PLA General Hospital, No. 28 Fuxing Road, Haidian District, Beijing 100039, China. duxiaohui3011@sina.com

Abstract

BACKGROUND

Programmed death 1 (PD-1) and $CD4^+CD25^+FoxP3^+$ expression in peripheral blood T-cells has been previously reported in various types of cancer. However, the specific variation tendency during surgery and chemotherapy, as well as their relationship in gastric cancer patients, still remain unclear. Understanding this aspect may provide some novel insights for future studies on tumor recurrence and tumor immune escape, and also serve as a reference for determining the optimal timing and dose of clinical anti-PD-1 antibodies.

AIM

To observe and analyze the expression characteristics of peripheral lymphocyte PD-1 and $FoxP3^+$ regulatory T cells ($FoxP3^+$ Tregs) before and after surgery or chemotherapy in gastric cancer patients.

METHODS

Twenty-nine stomach cancer patients undergoing chemotherapy after a D2 gastrectomy provided 10 mL peripheral blood samples at each phase of the perioperative period and during chemotherapy. This study also included 29 age-matched healthy donors as a control group. PD-1 expression was detected on

lymphocytes, including CD4$^+$CD8$^+$CD45RO$^+$, CD4$^+$CD45RO$^+$, and CD8$^+$CD45RO$^+$ lymphocytes as well as regulatory T cells.

RESULTS

We observed a significant increase of PD-1 expression on immune subsets and a larger number of FoxP3$^+$ Tregs in gastric cancer patients ($P < 0.05$). Following D2 gastrectomy, peripheral lymphocytes PD-1 expression and the number of FoxP3$^+$ Tregs notably decrease ($P < 0.05$). However, during postoperative chemotherapy, we only observed a decrease in PD-1 expression on lymphocytes in the CD8$^+$CD45RO$^+$ and CD8$^+$CD45RO$^+$ populations. Additionally, linear correlation analysis indicated a positive correlation between PD-1 expression and the number of CD4$^+$CD45RO$^+$FoxP3^{high} activated Tregs (aTregs) on the total peripheral lymphocytes ($r = 0.5622$, $P < 0.0001$).

CONCLUSION

The observed alterations in PD-1 expression and the activation of regulatory T cells during gastric cancer treatment may offer novel insights for future investigations into tumor immune evasion and the clinical application of anti-PD-1 antibodies in gastric cancer.

Key Words: Programmed death 1; Active regulatory T cells; Stomach cancer; Peripheral lymphocyte

©The Author(s) 2023. Published by Baishideng Publishing Group Inc. All rights reserved.

Core Tip: In short, this paper shows that programmed death 1 (PD-1) expression on immune subsets and the number of FoxP3$^+$ Treg were higher in peripheral blood of patients with gastric cancer than healthy donors. PD-1 expression and the number of FoxP3$^+$ Treg decrease notably after D2 gastrectomy. PD-1 expression declines on lymphocytes, CD8$^+$, CD45RO$^+$ and CD8$^+$CD45RO$^+$ populations during postoperative chemotherapy. PD-1 expression correlates with the number of CD4$^+$ CD45RO$^+$FoxP3 high activated Treg in peripheral lymphocytes. This paper is particularly timely, as the studies of PD-1 expression on immune subsets in peripheral blood are of expanding interest. As well as providing some novel insight for future studies of tumor recurrence and tumor immune escape, our results might also be a reference to determining the timing and dose of clinical anti-PD-1 antibodies, and we anticipate that this study will be widely cited.

Citation: Li H, Cao GM, Gu GL, Li SY, Yan Y, Fu Z, Du XH. Expression characteristics of peripheral lymphocyte programmed death 1 and FoxP3$^+$ Tregs in gastric cancer during surgery and chemotherapy. *World J Gastroenterol* 2023; 29(40): 5582-5592
URL: https://www.wjgnet.com/1007-9327/full/v29/i40/5582.htm
DOI: https://dx.doi.org/10.3748/wjg.v29.i40.5582

INTRODUCTION

Global cancer statistics have revealed that there were 1089103 newly diagnosed gastric cancer cases in 2020, resulting in a significant number of newly diagnosed gastric cancer cases and deaths worldwide[1]. Specifically, the National Cancer Centre of China estimated that 679000 new gastric cancer cases and 498000 gastric cancer-related deaths would occur in China in 2015[2]. Further compounding this issue is the fact that almost 70% of newly diagnosed cases are advanced gastric cancer, with the overall five-year survival rate being less than 30%[3].

With the advances of Chimeric antigen receptor T-cells, genetically engineered T cells, cytotoxic T-lymphocyte-associated antigen-4, and the programmed death-1/programmed death-ligand (PD-1/PD-L) pathway, tumor immunotherapy has rapidly emerged as a field of advanced research[4].

Multiple clinical trials have confirmed the efficacy and safety of PD-1 monoclonal antibody[5,6], and PD-1 monoclonal antibody was already approved for advanced gastric cancer in the United States and Japan. However, a recently randomized and open Phase III trial, Keymat-61[7], showed no significant improvement on objective response rate or progression-free survival (PFS) from paclitaxel. Meanwhile, in the randomized III trials, JAVELIN Gastric 300, reported by Bang *et al*[8], Avelumab in the treatment of advanced gastric/gastroesophageal joint cancer patients did not improve OS and PFS compared with the third-line treatment.

A growing body of evidence suggests that Tregs might be involved in the treatment of PD-1/PD-L1 blockade and PD-1/PD-L1 axis could influence Treg differentiation and function. However, the complex relationship between PD-1/PD-L1 pathway and Tregs is yet to be fully elucidated[9,10].

Although research into peripheral PD-1 expression in patients with gastric cancer has been reported previously, few studies have sequentially investigated such expression from the time of surgery to the completion of postoperative chemotherapy[11]. Furthermore, studies investigating the relationship between peripheral PD-1 expression and FoxP3$^+$ Tregs in gastric cancer patients are largely lacking.

In this study, we detected PD-1 expression on peripheral blood T cell subsets and the population of FoxP3$^+$ Tregs in gastric cancer from surgery to the completion of postoperative chemotherapy to analyse how these indexes change in expectation of being helpful to decide when and how the anti-PD-1 antibodies should be applied and deeper under-

standing on the mechanism of tumor immune escape in gastric cancer in the future.

MATERIALS AND METHODS

Human subjects

Patients with a histologically confirmed diagnosis of gastric adenocarcinoma following a D2 gastrectomy and treated with postoperative adjuvant chemotherapy, as well as age-matched healthy donors were eligible for this prospective observational study. Other inclusion criteria consisted of: (1) A healthy physical examination of the donors performed within the past three months; and (2) the age of patients and donors within the range of 18-75 years old. The exclusion criteria consisted of: (1) Patients diagnosed with other types of cancer within five years; (2) patients that received preoperative adjuvant chemotherapy, radiotherapy, or immunotherapy; (3) patients and donors who were diagnosed with chronic hepatitis, human immunodeficiency virus, syphilis, or any other acute infectious disease; (4) patients and donors who suffered from rheumaimmune systemic diseases (*e.g.*, systemic lupus erythematosus or hyperthyroidism); (5) patients with any other severe disease that might render them incapable of completing the entire course of chemotherapy; and (6) patients suffered gastric cancer recurrence or failed to finish the entire course of chemotherapy.

At the beginning of this study, 33 patients (alongside 33 age-matched donors) were enrolled from February 2020 to February 2021 in the Chinese People's Liberation Army General Hospital (PLAGH). However, one patient experienced tumor recurrence and three who failed to complete the entire cycles were excluded. A total of 29 patients (15 men and 14 women; mean age: 59.72 years) and 29 age-matched donors (17 men and 12 women; mean age: 59.62 years) were ultimately included in this study.

This study received approval from the ethics commission of the General Hospital of PLA, and all patients and donors provided signed informed consent.

Treatment strategy for patients

The treatment strategy for the enrolled patients consisted of MDT and a D2 gastrectomy performed by a chief physician at the General Hospital of PLA. The patients were treated with the following doses of chemotherapy and affiliated schedules: Oral capecitabine (1000 mg/m^2 twice daily on days 1-14 of each cycle) plus intravenous oxaliplatin (130 mg/m^2 on day 1 of each cycle) for eight three-week cycles.

Flow cytometry analysis

A sample volume of 10 mL peripheral blood was obtained from the patients into ananticoagulation tube on the day before surgery, the first and fourth cycles of chemotherapy and the day after chemotherapy. All blood samples were analysed within 6 h. Each sample was divided into two tubes and the detection of PD-1 expression and CD4$^+$CD25$^+$ FoxP3$^+$ regulatory T cells was performed separately on Accuri C6, a four-channel flow cytometer form BD ACCURI (Franklin Lakes, NJ, United States).

The detection of PD-1 expression involved staining the cells from the whole blood with fluorescently labelled antibodies, including anti-CD4-PerCP-Cy5.5 (clone RPA-4), anti-CD8-FITC (clone RPA-T8), anti-CD45RO-PE (clone UCHL-1) and anti-CD279 (PD-1)-APC (clone MIH4), from BD Biosciences (Franklin Lakes, NJ, United States) for the detection of PD-1 expression.

The detection of CD4$^+$CD25$^+$FoxP3$^+$ regulatory T cells was performed by staining PBMCs with anti-CD3-APC (clone SP34-2), anti-CD4-Percp (clone RPA-T4), anti-CD25-FITC (clone M-A251) andanti-CD45RO-PE (clone UCHL-1) from BD Biosciences (Franklin Lakes, NJ, United States) first, followed by anti-FoxP3-PE (clone 236A/E7, BD Biosciences) was added after permeabilizing the cell and nuclear membranes.

Statistical analysis

Data in this paper is represented as the mean ± SD. Comparisons of the differences in the continuous variables between the patients and donors were made using a Student's *t*-test or Wilcoxon rank sum test. A Chi-square test was performed for the categorical data. A paired-*t* test was adopted to compare the measurement data before and after the operation. Changes in the measurement data during chemotherapy were evaluated by an analysis of variance repeated-measures function. A Pearson correlation analysis was applied to dispose of the relativity between PD-1 expression and a population of FoxP3$^+$ Tregs. *P* values were based on two-tailed tests, with a value of $P < 0.05$ considered to be statistically significant.

RESULTS

Human characteristics

Statistical analysis revealed no significant difference in age (59.72 ± 15.33 *vs* 59.62 ± 15.64, $P = 0.9798$), gender (15/14 *vs* 17/12, $P = 0.7918$), and body mass index (23.90 ± 5.00 *vs* 25.10 ± 3.18, $P = 0.2824$) between the patients and healthy donors. We also assessed the daily life activity of both patients and donors using the Karnofsky score; all patients scored above 60 (indicating occasional care required for most needs), which is a score above the threshold at which patients with advanced gastric cancer are advised to transition from systemic therapy to supportive therapy according to the NCCN Guidelines. The descriptive statistics for CEA levels, TNM stages, and tumor differentiation are detailed in Table 1.

Table 1 Characteristics of patients and donors

Characteristics	Patients (*n* = 29)	Donors (*n* = 29)
Age (mean ± SD)	59.72 ± 15.33	59.62 ± 15.64[1]
Sex (M/F)	15/14	17/12[1]
BMI (kg/m^2, mean ± SD)	23.90 ± 5.00	25.10 ± 3.18[1]
KPs score		
≥ 60	29	29[1]
< 60	0	0
CEA (μg/L, mean ± SD)	95.26 ± 58.06	-
TNM stage		-
I	2	
II	12	
III	15	
Differentiation		-
High	2	
Moderate	18	
Low	9	

[1]The donors exhibited no differences from the patients at $P > 0.05$.
BMI: Body mass index; CEA: Carcinoembryonic antigen; KPs: Karnofsky performance status.

PD-1 expression between preoperative patients and donors

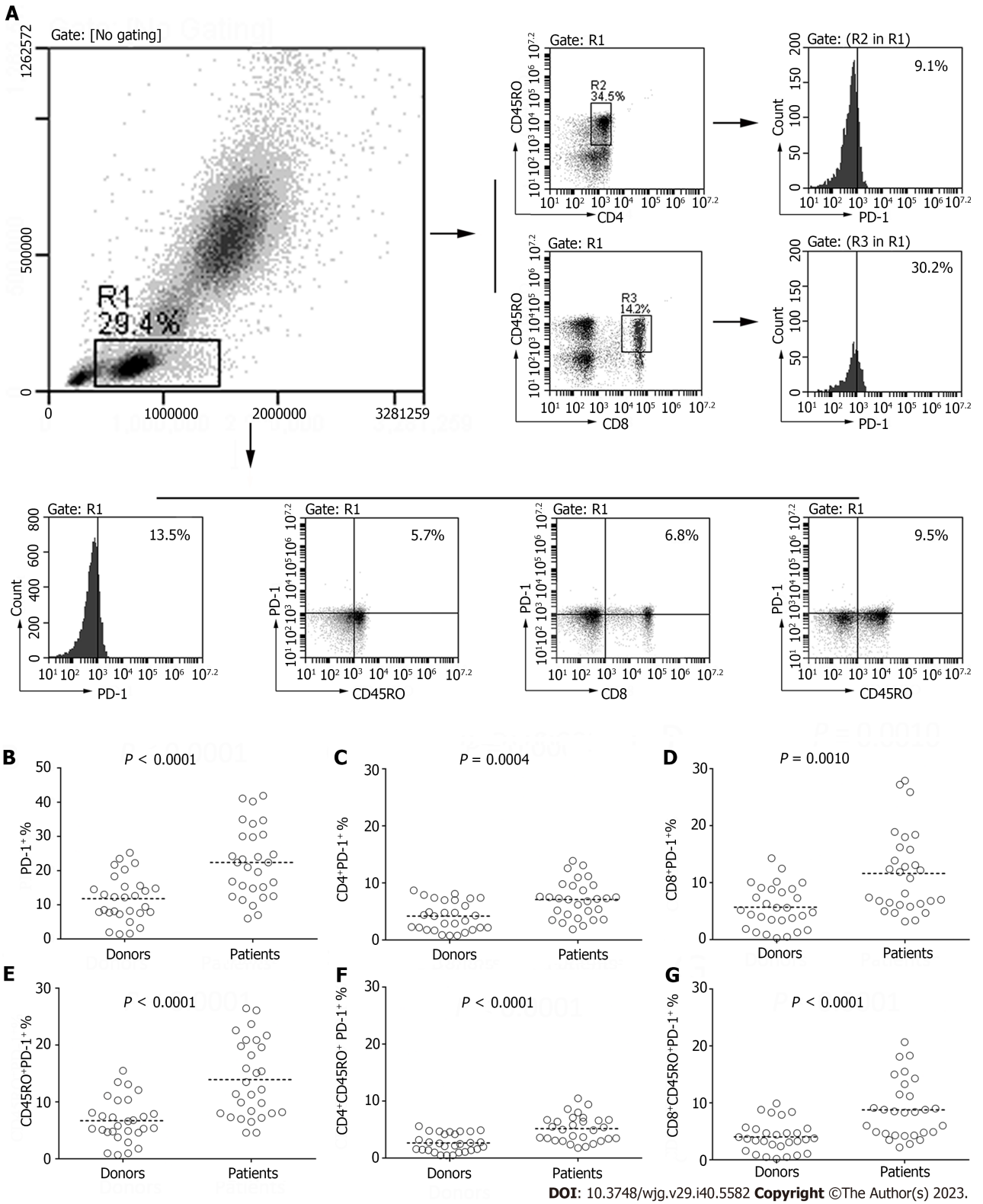
We performed an analysis of PD-1 expression on fresh peripheral blood sample subsets using flow cytometry (Figure 1A). The PD-1 expression on lymphocytes obtained from patients was significantly higher than those derived from donors (22.37% ± 10.35% *vs* 11.77% ± 6.67%, $P < 0.0001$; Figure 1B-G). Similarly, PD-1 expression on the CD4$^+$ and CD8$^+$ lymphocytes was notably higher in the patient group compared to the donor group (7.10% ± 3.27% *vs* 4.18% ± 2.53%, $P = 0.0004$; 11.63% ± 7.06% *vs* 5.71% ± 3.74%, $P = 0.001$; Figure 1B-G). Further, we assessed the PD-1 expression in lymphocytes through CD45RO phenotyping, a crucial marker utilized to distinguish memory T cells from naive T cells. This analysis revealed a significant difference between the patients and donors (13.94% ± 6.75% *vs* 6.71% ± 3.86%, $P < 0.0001$; Figure 1B-G). Moreover, PD-1 expression on CD4$^+$CD45RO$^+$ and CD8$^+$CD45RO$^+$ lymphocytes was also markedly higher in the gastric cancer patients (5.16% ± 2.31% *vs* 2.67% ± 1.57%, $P < 0.0001$; 8.79% ± 5.15% *vs* 4.05% ± 2.67%, $P < 0.0001$; Figure 1B-G).

PD-1 expression before and after the D2 gastrectomy

In this part, we detected the expression of PD-1 on the lymphocytes from blood samples drawn from postoperative patients. Blood samples were drawn on average of 27.24 d ± 5.06 d (range: 19-35 d) following surgery. A paired-*t* test was applied to compare the frequency of PD-1 on lymphocytes between the preoperative and operative blood samples. Strikingly, we found that surgery might be able to reduce the level of PD-1 expression on T cells. There was a significant decline in the PD-1 expression on lymphocytes from postoperative peripheral blood (22.37% ± 10.35% *vs* 16.00% ± 6.29%, $P = 0.0001$; Figure 2). A significant decrease was also observed for the level of PD-1 expression on CD4$^+$ and CD8$^+$ lymphocytes (7.10% ± 3.27% *vs* 5.26% ± 2.62%, $P = 0.0008$; 11.63% ± 7.06% *vs* 8.05% ± 3.60%, $P = 0.001$; Figure 2). The frequency of PD-1 expression on CD4$^+$CD45RO$^+$ and CD8$^+$CD45RO$^+$ lymphocytes from postoperative patients was also significantly lower than that derived from preoperative patients (5.16% ± 2.31% *vs* 3.67% ± 1.80%, $P = 0.0085$; 8.79% ± 5.15% *vs* 6.19% ± 3.20%, $P < 0.0001$; Figure 2). Similarly, the PD-1 expression on CD45RO$^+$ lymphocytes was also significantly lower (13.94% ± 6.75% *vs* 9.86% ± 4.41%, $P < 0.0001$; Figure 2). Since the increase of PD-1 expression is dependent on antigen stimulation, one explanation for the observed results might be the lack of stimulation from tumor antigens following surgery.

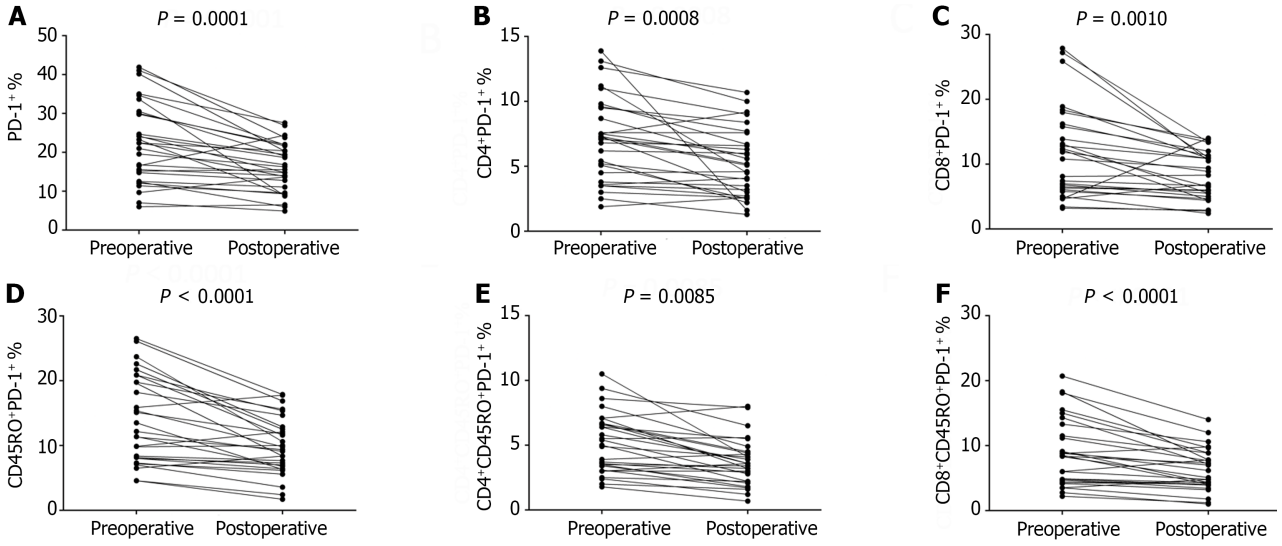
PD-1 expression during chemotherapy

A total of 29 patients in the trial accepted an eight three-week cycles course of chemotherapy with oxaliplatin and capecitabine following a D2 gastrectomy. We drew peripheral blood samples on the day before the first cycle of chemotherapy (an average of 27.24 d ± 5.06 d after surgery), fourth cycle of chemotherapy (an average of 97.90 d ± 6.64 d after surgery) and the day after the eighth cycle of chemotherapy (an average of 171.14 d ± 8.73 d after surgery). There was a statistically significant decrease in PD-1 expression on the total lymphocytes (16.00% ± 6.29%, 13.62% ± 6.43% *vs* 13.33% ± 6.35%, $P = 0.031$; Figure 3) and CD8$^+$T cells (8.05% ± 3.60%, 6.39% ± 3.59% *vs* 6.56% ± 3.64%, $P = 0.009$; Figure 3).



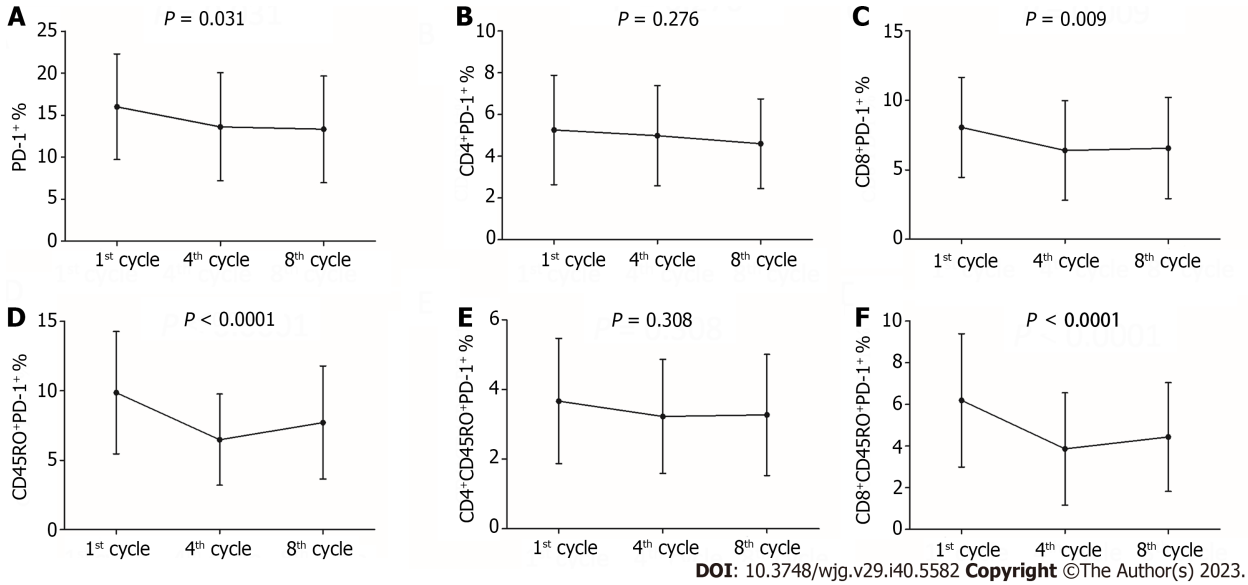
DOI: 10.3748/wjg.v29.i40.5582 **Copyright** ©The Author(s) 2023.

Figure 1 Programmed death 1 expression on all T cell subsets of healthy donors and preoperative patients with gastric cancer. A: The scatter and histogram plots of one representative patient are illustrated. The relationships between the diagrams are indicated by arrows and gates (R1, R2, and R3); B-G: The percentages of total programmed death 1⁺ (PD-1⁺) cells (B), CD4⁺PD-1⁺ (C), CD8⁺PD-1⁺ (D), CD45RO⁺PD-1⁺ (E), CD4⁺CD45RO⁺PD-1⁺ (F), and CD8⁺CD45RO⁺PD-1⁺ (G) cells out of the total peripheral lymphocytes from patients and healthy donors are shown. The *P* value was calculated using a Student's *t*-test or Wilcoxon rank sum test.



DOI: 10.3748/wjg.v29.i40.5582 **Copyright** ©The Author(s) 2023.

Figure 2 Changes in programmed death 1 expression on all subsets before and after the D2 gastrectomy. A-F: The percentage of total programmed death 1⁺ (PD-1⁺) cells (A), CD4⁺PD-1⁺ (B), CD8⁺PD-1⁺ (C), CD45RO⁺PD-1⁺ (D), CD4⁺CD45RO⁺PD-1⁺ (E), and CD8⁺CD45RO⁺PD-1⁺ (F) cells of the peripheral lymphocytes derived from patients before and after the D2 gastrectomy are shown. The *P* value was calculated using an analysis of variance repeated-measures function.



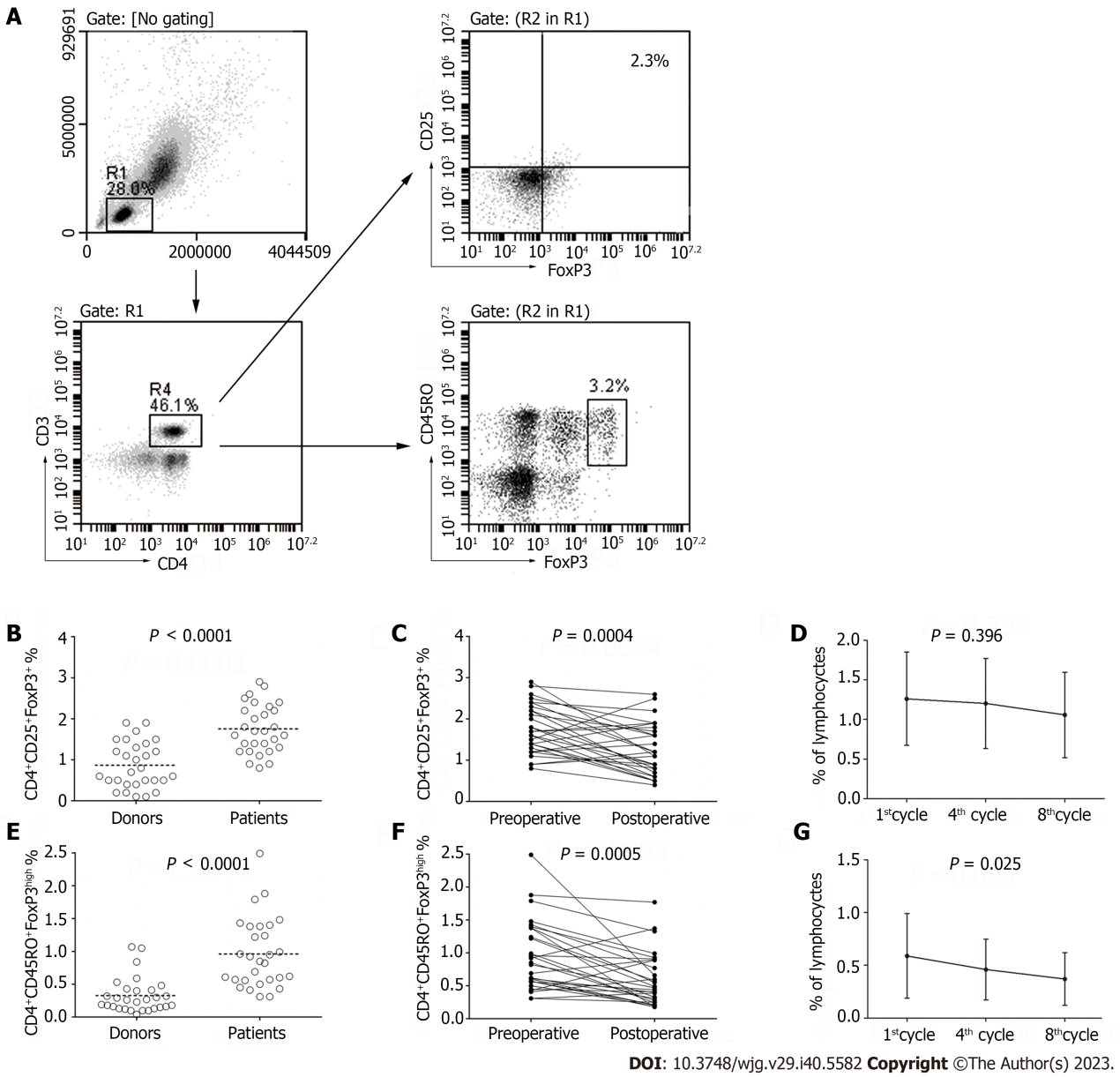
DOI: 10.3748/wjg.v29.i40.5582 **Copyright** ©The Author(s) 2023.

Figure 3 Changes in programmed death 1 expression on all subsets during chemotherapy. A-F: The percentage of total programmed death 1⁺ (PD-1⁺) cells (A), CD4⁺PD-1⁺ (B), CD8⁺PD-1⁺ (C), CD45RO⁺PD-1⁺ (D), CD4⁺CD45RO⁺PD-1⁺ (E), and CD8⁺CD45RO⁺PD-1⁺ (F) cells of the peripheral lymphocytes derived from patients during chemotherapy are shown. The *P* value was calculated using an analysis of variance repeated-measures function.

A notably significant decline was also observed for the PD-1 expression on CD45RO⁺ lymphocytes (9.86% ± 4.41%, 6.48% ± 3.28% *vs* 7.71% ± 4.07%, $P < 0.0001$; Figure 3) and CD8⁺CD45RO⁺ lymphocytes (6.19% ± 3.20%, 3.86% ± 2.69% *vs* 4.44% ± 2.61%, $P < 0.0001$; Figure 3). However, the difference in PD-1 expression on CD4⁺ lymphocytes (5.26% ± 2.62%, 4.98% ± 2.40% *vs* 4.60% ± 2.15%, $P = 0.276$; Figure 3) and CD4⁺CD45RO⁺ lymphocytes (3.67% ± 1.80%, 3.23% ± 1.64% *vs* 3.27% ± 1.74%, $P = 0.308$; Figure 3) was not statistically significant.

Changes in theFoxP3⁺ Tregs in patients with gastric cancer

While analyzing the PD-1 expression on lymphocytes, we also detected the frequency of CD4⁺CD25⁺FoxP3⁺ T cells and CD4⁺CD45RO⁺FoxP3^{high} T cellsin the lymphocyte population (Figure 4A). The frequency of FoxP3⁺T cells and CD4⁺ CD45RO⁺FoxP3^{high} T cellswas higher in the patients than in the healthy donors (1.76% ± 0.59% *vs* 0.87% ± 0.56%, $P < 0.0001$; 0.92% ± 0.45% *vs* 0.33% ± 0.27%, $P < 0.0001$; Figure 4B-G) and declined after the D2 gastrectomy was performed (1.76% ± 0.59% *vs* 1.26% ± 0.62%, $P = 0.0004$; 0.92% ± 0.45% *vs* 0.59% ± 0.40%, $P = 0.0005$; Figure 4B-G). Statistical difference was also observed in the frequency of CD4⁺CD45RO⁺FoxP3^{high} T cells in the peripheral lymphocytes during



DOI: 10.3748/wjg.v29.i40.5582 **Copyright** ©The Author(s) 2023.

Figure 4 Treg and activated Treg cells in the peripheral blood of donors and patients. A: Scatter plots are shown from one representative patient. Relationships of the diagrams are denoted with arrows and gates; B-G: The percent of TCD4⁺CD25⁺FoxP3⁺ and CD4⁺CD45RO⁺FoxP3^{high} cells in the peripheral lymphocytes from the donors and patients during treatment were shown and the *P* value was calculated using an analysis of variance repeated-measures function.

chemotherapy (0.59% ± 0.40%, 0.46% ± 0.29% *vs*0.37% ± 0.25%, $P = 0.025$; Figure 4B-G).

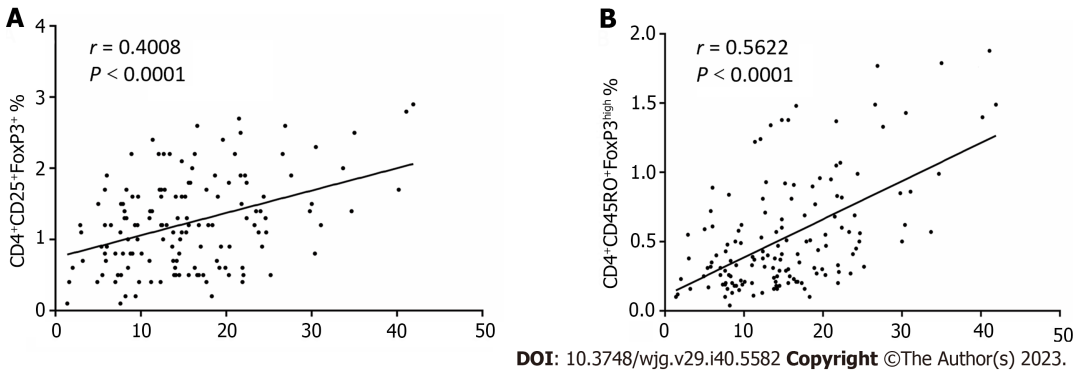
Relativity between PD-1 expression and FoxP3⁺ Tregs

Previous research has suggested that PD-1⁺ T cells and Tregs arecorrelative in the tumor tissues and tumor-involved lymph nodes in both breast and papillary thyroid cancer[12,13]. However, no clear correlations between the frequency of PD-1 expression and the number of CD4⁺CD25⁺FoxP3⁺ T cellsobserved in the peripheral blood of preoperative patients ($r = 0.4008$, $P < 0.0001$; Figure 5) but significant correlation between CD4⁺CD45RO⁺FoxP3^{high} T cells and PD-1 expression ($r = 0.5622$, $P < 0.0001$; Figure 5) were observed in our study.

DISCUSSION

Studies have shown that the PD-1/PD-L1 pathway plays a critical role in promoting T cell exhaustion[14]. In many types of tumor tissues, overexpression of PD-L1 has been found, with a similar pattern of PD-1 overexpression observed on tumor-infiltrating lymphocytes[15,16].

Supported by T-helper cells, CD8⁺ T cells can be activated, leading to the destruction of tumor cells through the perforin/granzyme and Fas/Fas ligand (FasL) apoptosis pathways. However, tumor cells have been found to inhibit the function of CD4⁺ and CD8⁺ T cells by boosting PD-1 expression[17,18]. This scenario has been observed in the peripheral



DOI: 10.3748/wjg.v29.i40.5582 **Copyright** ©The Author(s) 2023.

Figure 5 Relative programmed death 1 expression on lymphocytes and the percent of Treg and activated Treg cells. A and B: Programmed death 1 expression on lymphocytes and the percent of $CD4^+CD25^+FoxP3^+$ (A) and $CD4^+CD45RO^+FoxP3^{high}$ (B) cells in the peripheral blood. PD-1: Programmed death 1.

blood of various cancer types, such as non-small cell lung cancers, actinic cheilitis, oral squamous cell carcinoma, and head and neck cancer[19-22].

Our analysis unveiled a notable increase in PD-1 expression on $CD45RO^+$ lymphocytes in gastric cancer. CD45RO is a surface antigen employed to differentiate memory T cells from naive T cells. When antigens are reintroduced, $CD4^+$ $CD45RO^+$ T cells are seen to respond rapidly and robustly, migrating to the antigen source and aiding B cells in antibody production[23,24].

Several studies have suggested that $CD8^+CD45RO^+$ T cells serve as a more effective independent prognostic factor for metastatic colorectal cancer in Cox regression multivariate analysis compared to traditional markers like CEA and LDH [25-27]. Given this evidence, it seems likely that the upregulation of PD-1 on $CD45RO^+$ T cells is a consequence of tumor cell stimulation, thereby facilitating tumor immune escape from memory T cells.

PD-1/PD-L1 expression can be induced or maintained by many cytokines, such as type I IFn and IFNγ. Research has shown that tumor-associated plasmacytoid DCs produce large amounts of type I IFn[28], which can in turn induce PD-1/PD-L1 expression[29]. The decline in these cytokines following tumor resection might be the underlying cause of the observed reduction in PD-1 expression.

Research conducted by Maeda *et al*[30] found that the populations of $CD4^+$, $CD8^+$ and NK cells in the peripheral blood of patients with metastatic colorectal cancer remained stable following FOLFOX administration, yet the number of regulatory cells exhibited a significant decline. A similar drop in the Tregs population was observed in patients treated with paclitaxel-based chemotherapy[31]. Data from our present study reveal a trend of significant decline or reduction in PD-1 expression and population of $FoxP3^+$ Tregs in patients undergoing surgery and chemotherapy.

We observed that the population of regulatory T cells was higher in patients compared to donors, which is consistent with prior findings in prostate, lung, pancreatic, and breast cancer studies[32,33]. The increased population of Tregs in tumor-bearing patients could potentially arise from the secretion of TGF-β, IL-10, and H-ferritin, which have been known to induce $CD4^+CD25^-$ T cells to transition into $CD4^+CD25^+$ T cells and upregulate the expression of FoxP3[34-36].

Interestingly, this mechanism might also be responsible for the observed decrease in the number of peripheral Tregs following tumor tissue removal. Moreover, several studies have indicated that drugs like cyclophosphamide, fludarabine, and paclitaxel could down-regulate the quantity and function of Tregs in cancer patients[37,38].

These findings provide a theoretical foundation for the treatment of tumors with PD-1/PDL-1 blockers in combination with chemotherapy drugs, offering a potential strategy to optimize cancer immunotherapy.

In this study, $CD4^+CD45RO^+FoxP3^+$ appears to have a stronger correlation to PD-1 expression than Tregs in peripheral blood. Previous detection of FoxP3 at both the mRNA and protein levels has shown that human $CD25^{high}CD4^+$ T cells indeed express FoxP3[39,40], indicating that the population of $CD4^+CD45RO^+FoxP3^+$ cells can serve as a reflection of $CD25^{high}CD45RA^-FoxP3^{high}$ activated Treg cells (aTreg cells).

Moreover, the $CD4^+FoxP3^+$T cells in peripheral blood comprise three subpopulations, distinguished by differing levels of FoxP3 and cell surface molecules CD45RA and CD25. Notably, only $CD25^{high}CD45RA^-FoxP3^{high}$ cells (aTregs) are terminally differentiated and exhibit high suppressive capacities[41].

CONCLUSION

The exploration of PD-1 expression impacts on immune subsets and the abundance of $FoxP3^+$ Tregs in peripheral blood could provide invaluable insights for future research on the PD-1/PDL-1 axis, tumor recurrence, and tumor immune escape. Additionally, these findings may also serve as potential biomarkers for studies involving the timing and dosing of clinical anti-PD-1 antibodies.

ARTICLE HIGHLIGHTS

Research background

Programmed death 1 (PD-1) and CD4$^+$CD25$^+$FoxP3$^+$ expression in peripheral blood T-cells have been identified in multiple cancer types, but their variation during surgery and chemotherapy in gastric cancer remains elusive. Understanding this could illuminate tumor recurrence mechanisms and guide optimal anti-PD-1 antibody treatment strategies.

Research motivation

Despite known PD-1 and CD4$^+$CD25$^+$FoxP3$^+$ expression in various cancers, the specific changes during surgery and chemotherapy, and their relationship in gastric cancer, remain undefined. This study seeks to shed light on these variations, potentially offering insights into tumor recurrence, immune evasion, and the clinical application of anti-PD-1 antibodies in gastric cancer.

Research objectives

The study aims to observe and analyze the expression characteristics of peripheral lymphocyte PD-1 and FoxP3$^+$ regulatory T cells (FoxP3$^+$Tregs) in gastric cancer patients, both prior to and following surgery or chemotherapy, to better understand their roles and implications in gastric cancer treatment.

Research methods

In this study, 29 gastric cancer patients, post-D2 gastrectomy and undergoing chemotherapy, provided 10 mL peripheral blood samples during various perioperative phases. PD-1 expression was analyzed on specific lymphocyte subsets, with an additional 29 age-matched healthy donors serving as a control group.

Research results

The study found a significant elevation in PD-1 expression and FoxP3$^+$ Tregs in gastric cancer patients, which decreased notably post-D2 gastrectomy. A positive correlation was identified between PD-1 expression and the number of activated FoxP3high Tregs in peripheral lymphocytes, especially during postoperative chemotherapy.

Research conclusions

Alterations in PD-1 expression and regulatory T cell activation during gastric cancer treatment could provide valuable insights for understanding tumor immune evasion. These findings may also influence the clinical application of anti-PD-1 antibodies in gastric cancer therapy.

Research perspectives

The changes observed in PD-1 expression and regulatory T cell activation during gastric cancer treatments pave the way for deeper exploration into tumor immune evasion mechanisms. These findings could also shape the future clinical application and optimization of anti-PD-1 antibodies in treating gastric cancer.

FOOTNOTES

Co-first authors: Hao Li and Guan-Mei Cao.

Author contributions: Li H, Cao GM, and Du XH were the guarantor of integrity of entire study, and contributed to the study concepts; Li H, Cao GM, Gu GL, Li SY, and Du XH designed the study; Li H, Cao GM, Gu GL, and Li SY involved in the literature research; Li H and Cao GM contributed to the data acquisition; Li H, Cao GM, and Fu Z contributed to the statistical analysis/interpretation and manuscript preparation; Li H, Cao GM, Gu GL, Li SY, Fu Z, and Du XH contributed to the manuscript definition of intellectual content; Li H, Cao GM, Gu GL, and Du XH edited the manuscript; Li H and Cao GM contributed equally to this work as co-first authors; Li H and Cao GM are designated as co-first authors due to their equal and substantial contributions to the study conception, design, data acquisition, and analysis, as well as manuscript preparation and editing, each playing pivotal roles in ensuring the integrity and quality of the research.

Supported by the National Natural Science Foundation of China, No. 81871317; and Military Medical Innovation Project, No. 18CXZ025.

Institutional review board statement: The study was reviewed and approved by the Ethics Commission of the General Hospital of PLA (Approval No. S2009-051-02).

Informed consent statement: All patients and donors provided signed informed consent.

Conflict-of-interest statement: There are no conflicts of interest to report.

Data sharing statement: The datasets generated and/or analyzed during the current study are available from the corresponding author on reasonable request.

STROBE statement: The authors have read the STROBE Statement—checklist of items, and the manuscript was prepared and revised according to the STROBE Statement—checklist of items.

Open-Access: This article is an open-access article that was selected by an in-house editor and fully peer-reviewed by external reviewers. It is distributed in accordance with the Creative Commons Attribution NonCommercial (CC BY-NC 4.0) license, which permits others to distribute, remix, adapt, build upon this work non-commercially, and license their derivative works on different terms, provided the original work is properly cited and the use is non-commercial. See: https://creativecommons.org/Licenses/by-nc/4.0/

Country/Territory of origin: China

ORCID number: Hao Li 0000-0002-5502-8786; Guo-Li Gu 0000-0002-9998-047X; Song-Yan Li 0000-0001-7094-5913; Yang Yan 0000-0001-8019-7314; Ze Fu 0009-0002-0465-2009; Xiao-Hui Du 0000-0001-7083-2046.

S-Editor: Chen YL
L-Editor: A
P-Editor: Cai YX

REFERENCES

1 **Sung H**, Ferlay J, Siegel RL, Laversanne M, Soerjomataram I, Jemal A, Bray F. Global Cancer Statistics 2020: GLOBOCAN Estimates of Incidence and Mortality Worldwide for 36 Cancers in 185 Countries. *CA Cancer J Clin* 2021; **71**: 209-249 [PMID: 33538338 DOI: 10.3322/caac.21660]

2 **Chen W**, Zheng R, Baade PD, Zhang S, Zeng H, Bray F, Jemal A, Yu XQ, He J. Cancer statistics in China, 2015. *CA Cancer J Clin* 2016; **66**: 115-132 [PMID: 26808342 DOI: 10.3322/caac.21338]

3 **Cunningham SC**, Schulick RD. Palliative management of gastric cancer. *Surg Oncol* 2007; **16**: 267-275 [PMID: 17881220 DOI: 10.1016/j.suronc.2007.08.004]

4 **Yao S**, Zhu Y, Chen L. Advances in targeting cell surface signalling molecules for immune modulation. *Nat Rev Drug Discov* 2013; **12**: 130-146 [PMID: 23370250 DOI: 10.1038/nrd3877]

5 **Bang YJ**, Muro K, Fuchs CS, Golan T, Geva R, Hara H, Jalal SI, Borg C, Doi T, Wainberg ZA, Wang JD, Koshiji M, Dalal RP, Chung HC. Keynote-059 cohort2: safety and efficacy of pembrolizumab (pembro) plus 5-fluorouracil (5-Fu) and cisplatin for first-line (1L) treatment of advanced gastric cancer. *J Clini Onco* 2017; **35** Suppl 15: 4012-4012 [DOI: 10.1200/jco.2017.35.15_suppl.4012]

6 **Kang YK**, Boku N, Satoh T, Ryu MH, Chao Y, Kato K, Chung HC, Chen JS, Muro K, Kang WK, Yeh KH, Yoshikawa T, Oh SC, Bai LY, Tamura T, Lee KW, Hamamoto Y, Kim JG, Chin K, Oh DY, Minashi K, Cho JY, Tsuda M, Chen LT. Nivolumab in patients with advanced gastric or gastro-oesophageal junction cancer refractory to, or intolerant of, at least two previous chemotherapy regimens (ONO-4538-12, ATTRACTION-2): a randomised, double-blind, placebo-controlled, phase 3 trial. *Lancet* 2017; **390**: 2461-2471 [PMID: 28993052 DOI: 10.1016/S0140-6736(17)31827-5]

7 **Shitara K**, Özgüroğlu M, Bang YJ, Di Bartolomeo M, Mandalà M, Ryu MH, Fornaro L, Olesiński T, Caglevic C, Chung HC, Muro K, Goekkurt E, Mansoor W, McDermott RS, Shacham-Shmueli E, Chen X, Mayo C, Kang SP, Ohtsu A, Fuchs CS; KEYNOTE-061 investigators. Pembrolizumab versus paclitaxel for previously treated, advanced gastric or gastro-oesophageal junction cancer (KEYNOTE-061): a randomised, open-label, controlled, phase 3 trial. *Lancet* 2018; **392**: 123-133 [PMID: 29880231 DOI: 10.1016/S0140-6736(18)31257-1]

8 **Bang YJ**, Ruiz EY, Van Cutsem E, Lee KW, Wyrwicz L, Schenker M, Alsina M, Ryu MH, Chung HC, Evesque L, Al-Batran SE, Park SH, Lichinitser M, Boku N, Moehler MH, Hong J, Xiong H, Hallwachs R, Conti I, Taieb J. Phase III, randomised trial of avelumab versus physician's choice of chemotherapy as third-line treatment of patients with advanced gastric or gastro-oesophageal junction cancer: primary analysis of JAVELIN Gastric 300. *Ann Oncol* 2018; **29**: 2052-2060 [PMID: 30052729 DOI: 10.1093/annonc/mdy264]

9 **Cai J**, Wang D, Zhang G, Guo X. The Role Of PD-1/PD-L1 Axis In Treg Development And Function: Implications For Cancer Immunotherapy. *Onco Targets Ther* 2019; **12**: 8437-8445 [PMID: 31686860 DOI: 10.2147/OTT.S221340]

10 **Woods DM**, Ramakrishnan R, Laino AS, Berglund A, Walton K, Betts BC, Weber JS. Decreased Suppression and Increased Phosphorylated STAT3 in Regulatory T Cells are Associated with Benefit from Adjuvant PD-1 Blockade in Resected Metastatic Melanoma. *Clin Cancer Res* 2018; **24**: 6236-6247 [PMID: 30131384]

11 **Saito H**, Kuroda H, Matsunaga T, Osaki T, Ikeguchi M. Increased PD-1 expression on CD4+ and CD8+ T cells is involved in immune evasion in gastric cancer. *J Surg Oncol* 2013; **107**: 517-522 [PMID: 23129549 DOI: 10.1002/jso.23281]

12 **Ghebeh H**, Barhoush E, Tulbah A, Elkum N, Al-Tweigeri T, Dermime S. FOXP3+ Tregs and B7-H1+/PD-1+ T lymphocytes co-infiltrate the tumor tissues of high-risk breast cancer patients: Implication for immunotherapy. *BMC Cancer* 2008; **8**: 57 [PMID: 18294387 DOI: 10.1186/1471-2407-8-57]

13 **French JD**, Kotnis GR, Said S, Raeburn CD, McIntyre RC Jr, Klopper JP, Haugen BR. Programmed death-1+ T cells and regulatory T cells are enriched in tumor-involved lymph nodes and associated with aggressive features in papillary thyroid cancer. *J Clin Endocrinol Metab* 2012; **97**: E934-E943 [PMID: 22466343 DOI: 10.1210/jc.2011-3428]

14 **Zajac AJ**, Blattman JN, Murali-Krishna K, Sourdive DJ, Suresh M, Altman JD, Ahmed R. Viral immune evasion due to persistence of activated T cells without effector function. *J Exp Med* 1998; **188**: 2205-2213 [PMID: 9858507 DOI: 10.1084/jem.188.12.2205]

15 **Zou W**, Chen L. Inhibitory B7-family molecules in the tumour microenvironment. *Nat Rev Immunol* 2008; **8**: 467-477 [PMID: 18500231 DOI: 10.1038/nri2326]

16 **Dong H**, Strome SE, Salomao DR, Tamura H, Hirano F, Flies DB, Roche PC, Lu J, Zhu G, Tamada K, Lennon VA, Celis E, Chen L. Tumor-associated B7-H1 promotes T-cell apoptosis: a potential mechanism of immune evasion. *Nat Med* 2002; **8**: 793-800 [PMID: 12091876 DOI: 10.1038/nm730]

17 **Ahmadzadeh M**, Johnson LA, Heemskerk B, Wunderlich JR, Dudley ME, White DE, Rosenberg SA. Tumor antigen-specific CD8 T cells infiltrating the tumor express high levels of PD-1 and are functionally impaired. *Blood* 2009; **114**: 1537-1544 [PMID: 19423728 DOI:

10.1182/blood-2008-12-195792]
18 **Wu X**, Zhang H, Xing Q, Cui J, Li J, Li Y, Tan Y, Wang S. PD-1(+) CD8(+) T cells are exhausted in tumours and functional in draining lymph nodes of colorectal cancer patients. *Br J Cancer* 2014; **111**: 1391-1399 [PMID: 25093496 DOI: 10.1038/bjc.2014.416]
19 **Zhang Y**, Huang S, Gong D, Qin Y, Shen Q. Programmed death-1 upregulation is correlated with dysfunction of tumor-infiltrating CD8+ T lymphocytes in human non-small cell lung cancer. *Cell Mol Immunol* 2010; **7**: 389-395 [PMID: 20514052 DOI: 10.1038/cmi.2010.28]
20 **Malaspina TS**, Gasparoto TH, Costa MR, de Melo EF Jr, Ikoma MR, Damante JH, Cavassani KA, Garlet GP, da Silva JS, Campanelli AP. Enhanced programmed death 1 (PD-1) and PD-1 ligand (PD-L1) expression in patients with actinic cheilitis and oral squamous cell carcinoma. *Cancer Immunol Immunother* 2011; **60**: 965-974 [PMID: 21442435 DOI: 10.1007/s00262-011-1007-5]
21 **Baruah P**, Lee M, Odutoye T, Williamson P, Hyde N, Kaski JC, Dumitriu IE. Decreased levels of alternative co-stimulatory receptors OX40 and 4-1BB characterise T cells from head and neck cancer patients. *Immunobiology* 2012; **217**: 669-675 [PMID: 22204816 DOI: 10.1016/j.imbio.2011.11.005]
22 **Waki K**, Yamada T, Yoshiyama K, Terazaki Y, Sakamoto S, Matsueda S, Komatsu N, Sugawara S, Takamori S, Itoh K, Yamada A. PD-1 expression on peripheral blood T-cell subsets correlates with prognosis in non-small cell lung cancer. *Cancer Sci* 2014; **105**: 1229-1235 [PMID: 25117757 DOI: 10.1111/cas.12502]
23 **Clement LT**, Vink PE, Bradley GE. Novel immunoregulatory functions of phenotypically distinct subpopulations of CD4+ cells in the human neonate. *J Immunol* 1990; **145**: 102-108 [PMID: 1694200 DOI: 10.4049/jimmunol.145.1.102]
24 **Lanzavecchia A**, Sallusto F. Understanding the generation and function of memory T cell subsets. *Curr Opin Immunol* 2005; **17**: 326-332 [PMID: 15886125 DOI: 10.1016/j.coi.2005.04.010]
25 **Formica V**, Massara MC, Portarena I, Fiaschetti V, Grenga I, Del Vecchio Blanco G, Sileri P, Tosetto L, Skoulidis F, Pallone F, Roselli M. Role of CA19.9 in predicting bevacizumab efficacy for metastatic colorectal cancer patients. *Cancer Biomark* 2009; **5**: 167-175 [PMID: 19729826 DOI: 10.3233/CBM-2009-0101]
26 **Ferroni P**, Palmirotta R, Spila A, Martini F, Formica V, Portarena I, Del Monte G, Buonomo O, Roselli M, Guadagni F. Prognostic value of carcinoembryonic antigen and vascular endothelial growth factor tumor tissue content in colorectal cancer. *Oncology* 2006; **71**: 176-184 [PMID: 17652942 DOI: 10.1159/000106072]
27 **Formica V**, Cereda V, di Bari MG, Grenga I, Tesauro M, Raffaele P, Ferroni P, Guadagni F, Roselli M. Peripheral CD45RO, PD-1, and TLR4 expression in metastatic colorectal cancer patients treated with bevacizumab, fluorouracil, and irinotecan (FOLFIRI-B). *Med Oncol* 2013; **30**: 743 [PMID: 24114613 DOI: 10.1007/s12032-013-0743-0]
28 **Gupta S**, Maheshwari A, Parab P. Reply to V.G. Gupta *et al* and W. Zou *et al*. *J Clin Oncol* 2018; **36**: 2813-2814 [PMID: 29897828 DOI: 10.1200/JCO.2018.79.2622]
29 **Curiel TJ**, Wei S, Dong H, Alvarez X, Cheng P, Mottram P, Krzysiek R, Knutson KL, Daniel B, Zimmermann MC, David O, Burow M, Gordon A, Dhurandhar N, Myers L, Berggren R, Hemminki A, Alvarez RD, Emilie D, Curiel DT, Chen L, Zou W. Blockade of B7-H1 improves myeloid dendritic cell-mediated antitumor immunity. *Nat Med* 2003; **9**: 562-567 [PMID: 12704383 DOI: 10.1038/nm863]
30 **Ma C**, Dong X. Colorectal cancer-derived Foxp3(+) IL-17(+) T cells suppress tumour-specific CD8+ T cells. *Scand J Immunol* 2011; **74**: 47-51 [PMID: 21352252 DOI: 10.1111/j.1365-3083.2011.02539.x]
31 **Zhang L**, Dermawan K, Jin M, Liu R, Zheng H, Xu L, Zhang Y, Cai Y, Chu Y, Xiong S. Differential impairment of regulatory T cells rather than effector T cells by paclitaxel-based chemotherapy. *Clin Immunol* 2008; **129**: 219-229 [PMID: 18771959 DOI: 10.1016/j.clim.2008.07.013]
32 **Baecher-Allan C**, Anderson DE. Regulatory cells and human cancer. *Semin Cancer Biol* 2006; **16**: 98-105 [PMID: 16378733 DOI: 10.1016/j.semcancer.2005.11.003]
33 **Loskog A**, Ninalga C, Paul-Wetterberg G, de la Torre M, Malmström PU, Tötterman TH. Human bladder carcinoma is dominated by T-regulatory cells and Th1 inhibitory cytokines. *J Urol* 2007; **177**: 353-358 [PMID: 17162090 DOI: 10.1016/j.juro.2006.08.078]
34 **Lu L**, Ma J, Li Z, Lan Q, Chen M, Liu Y, Xia Z, Wang J, Han Y, Shi W, Quesniaux V, Ryffel B, Brand D, Li B, Liu Z, Zheng SG. All-trans retinoic acid promotes TGF-β-induced Tregs *via* histone modification but not DNA demethylation on Foxp3 gene locus. *PLoS One* 2011; **6**: e24590 [PMID: 21931768 DOI: 10.1371/journal.pone.0024590]
35 **Fuss IJ**, Boirivant M, Lacy B, Strober W. The interrelated roles of TGF-beta and IL-10 in the regulation of experimental colitis. *J Immunol* 2002; **168**: 900-908 [PMID: 11777988 DOI: 10.4049/jimmunol.168.2.900]
36 **Gray CP**, Arosio P, Hersey P. Heavy chain ferritin activates regulatory T cells by induction of changes in dendritic cells. *Blood* 2002; **99**: 3326-3334 [PMID: 11964300 DOI: 10.1182/blood.v99.9.3326]
37 **Ghiringhelli F**, Menard C, Puig PE, Ladoire S, Roux S, Martin F, Solary E, Le Cesne A, Zitvogel L, Chauffert B. Metronomic cyclophosphamide regimen selectively depletes CD4+CD25+ regulatory T cells and restores T and NK effector functions in end stage cancer patients. *Cancer Immunol Immunother* 2007; **56**: 641-648 [PMID: 16960692 DOI: 10.1007/s00262-006-0225-8]
38 **Beyer M**, Kochanek M, Darabi K, Popov A, Jensen M, Endl E, Knolle PA, Thomas RK, von Bergwelt-Baildon M, Debey S, Hallek M, Schultze JL. Reduced frequencies and suppressive function of CD4+CD25hi regulatory T cells in patients with chronic lymphocytic leukemia after therapy with fludarabine. *Blood* 2005; **106**: 2018-2025 [PMID: 15914560 DOI: 10.1182/blood-2005-02-0642]
39 **Roncador G**, Brown PJ, Maestre L, Hue S, Martínez-Torrecuadrada JL, Ling KL, Pratap S, Toms C, Fox BC, Cerundolo V, Powrie F, Banham AH. Analysis of FOXP3 protein expression in human CD4+CD25+ regulatory T cells at the single-cell level. *Eur J Immunol* 2005; **35**: 1681-1691 [PMID: 15902688 DOI: 10.1002/eji.200526189]
40 **Yagi H**, Nomura T, Nakamura K, Yamazaki S, Kitawaki T, Hori S, Maeda M, Onodera M, Uchiyama T, Fujii S, Sakaguchi S. Crucial role of FOXP3 in the development and function of human CD25+CD4+ regulatory T cells. *Int Immunol* 2004; **16**: 1643-1656 [PMID: 15466453 DOI: 10.1093/intimm/dxh165]
41 **Miyara M**, Yoshioka Y, Kitoh A, Shima T, Wing K, Niwa A, Parizot C, Taflin C, Heike T, Valeyre D, Mathian A, Nakahata T, Yamaguchi T, Nomura T, Ono M, Amoura Z, Gorochov G, Sakaguchi S. Functional delineation and differentiation dynamics of human CD4+ T cells expressing the FoxP3 transcription factor. *Immunity* 2009; **30**: 899-911 [PMID: 19464196 DOI: 10.1016/j.immuni.2009.03.019]

World Journal of Gastroenterology

Submit a Manuscript: https://www.f6publishing.com

World J Gastroenterol 2023 October 28; 29(40): 5593-5617

DOI: 10.3748/wjg.v29.i40.5593

ISSN 1007-9327 (print) ISSN 2219-2840 (online)

SCIENTOMETRICS

Advances and key focus areas in gastric cancer immunotherapy: A comprehensive scientometric and clinical trial review (1999-2023)

Yao-Nan Li, Bin Xie, Ying Zhang, Ming-Hua He, Yang Xing, Dong-Mei Mu, Hong Wang, Rui Guo

Specialty type: Gastroenterology and hepatology

Provenance and peer review: Unsolicited article; Externally peer reviewed.

Peer-review model: Single blind

Peer-review report's scientific quality classification

Grade A (Excellent): 0
Grade B (Very good): B, B
Grade C (Good): C
Grade D (Fair): 0
Grade E (Poor): 0

P-Reviewer: Fu L, China; Nishida T, Japan

Received: August 28, 2023
Peer-review started: August 28, 2023
First decision: September 11, 2023
Revised: September 25, 2023
Accepted: October 17, 2023
Article in press: October 17, 2023
Published online: October 28, 2023

Yao-Nan Li, Rui Guo, Clinical Laboratory, The First Hospital of Jilin University, Changchun 130012, Jilin Province, China

Bin Xie, Ying Zhang, Yang Xing, Hong Wang, Cancer Center, The First Hospital of Jilin University, Changchun 130012, Jilin Province, China

Ming-Hua He, College of Computer Science and Technology, Jilin University, Changchun 130012, Jilin Province, China

Dong-Mei Mu, Division of Clinical Research, The First Hospital of Jilin University, Changchun 130012, Jilin Province, China

Corresponding author: Rui Guo, MD, Associate Professor, Clinical Laboratory, The First Hospital of Jilin University, No. 1 Xinmin Street, Chaoyang District, Changchun 130012, Jilin Province, China. guoruijdyy@jlu.edu.cn

Abstract

BACKGROUND

Gastric cancer (GC) is the sixth most common cancer and third leading cause of cancer-related deaths worldwide. Current treatments mainly rely on surgery- and chemotherapy-based systemic; however, the prognosis remains poor for advanced disease. Recent studies have suggested that immunotherapy has significant potential in cancer therapy; thus, GC immunotherapy may improve quality of life and survival for patients with this disease.

AIM

To provide a comprehensive overview of the knowledge structure and research hotspots of GC immunotherapy.

METHODS

We conducted a bibliometric analysis of publications on immunotherapy related to GC in the Web of Science Core Collection database. We analyzed 2013 publications from 1999 to February 1, 2023, using the VOSviewer and CiteSpace software. We assessed publication and citation distributions using the WoS platform and explored research countries, institutions, journals, authors, references, and keywords (co-occurrence, timeline view, and burst analysis). In addition, we examined 228 trials on immunotherapy, 137 on adoptive cell therapy, 274 on immune checkpoint inhibitors (ICIs), and 23 on vaccines from ClinicalTrials.gov and the International Clinical Trials Registry Platform. The

Impact Index Per Article for the top ten high-cited papers collected from *Reference Citation Analysis* (*RCA*) are presented.

RESULTS

Our bibliometric analysis revealed that the study of immunotherapy in GC has developed rapidly in recent years. China accounted for almost half the publications, followed by the United States. The number of publications in recent years has been growing continuously, and most institutions and authors with the most publications are from China. The main keywords or clusters identified were "tumor microenvironment", "adoptive immunotherapy", "dendritic therapy", and "microsatellite instability".

CONCLUSION

Our analysis of 2013 publications indicated that immunotherapy for GC has led to several new developments in recent years. Considerable progress has been made in vaccinations, immune checkpoint therapy, and adoptive cellular therapy. In particular, ICIs and chimeric antigen receptor T-cells are novel options for the treatment of GC. We suggest that the combination of ICIs, chemotherapy, targeted therapy, and other immunotherapies should be the primary research direction in the future.

Key Words: Immunotherapy; Gastric cancer; Clinical trials; Scientometric analysis; Visualization

©The Author(s) 2023. Published by Baishideng Publishing Group Inc. All rights reserved.

Core Tip: In this study, we systematically analyzed studies related to immunotherapy for gastric cancer (GC). We used scientometrics to explore research hotspots in the field and summarize the current developmental status of GC immunotherapy, as well as the advantages and disadvantages of different immunotherapy modalities. We also compiled information on ongoing clinical trials and predicted future developmental trends in this field based on the direction and stage of these trials. This research can help advance our understanding of the latest progress and future development trends in the field, as well as provide scientific research recommendations.

Citation: Li YN, Xie B, Zhang Y, He MH, Xing Y, Mu DM, Wang H, Guo R. Advances and key focus areas in gastric cancer immunotherapy: A comprehensive scientometric and clinical trial review (1999-2023). *World J Gastroenterol* 2023; 29(40): 5593-5617

URL: https://www.wjgnet.com/1007-9327/full/v29/i40/5593.htm

DOI: https://dx.doi.org/10.3748/wjg.v29.i40.5593

INTRODUCTION

Gastric cancer (GC) is the sixth most prevalent cancer and the third leading cause of cancer-related fatalities worldwide, thus presenting a significant global health concern[1]. The incidence rates of GC are highest in Eastern Europe and Eastern Asia, and it remains the most prevalent cancer and the leading cause of cancer-related deaths in specific regions of South and Central Asia[2]. Despite a trend toward decreasing morbidity and mortality rates in several countries and regions, GC continues to be a substantial health burden[3]. Numerous factors have been established to contribute to the pathogenesis of GC, including family history, dietary habits, smoking, and *Helicobacter pylori* or Epstein-Barr virus (EBV) infection[4]. GC can be categorized into four distinct molecular subgroups based on the patterns of molecular alterations, with each subgroup corresponding to a different disease progression and prognosis: (1) Microsatellite stable/epithelial-mesenchymal transition; (2) Microsatellite instability (MSI); (3) Tumor protein 53 (TP53)-active; and (4) TP53-inactive types[5].

Owing to its predominantly asymptomatic nature, early detection of GC poses a significant challenge, with > 50% of patients being diagnosed after the cancer has already metastasized[6,7]. The prognosis of advanced GC remains dismal; the five-year overall survival (OS) rate is < 5% and the median OS is approximately 8 mo[8-10]. Although surgery remains the primary curative approach, chemotherapy forms the foundation of treatment for metastatic GC, with multimodal therapy employed to enhance survival outcomes[9]. However, the efficacy of conventional treatments, including surgery, radiotherapy, chemotherapy, and anti-human epidermal growth factor receptor-2 (HER2) therapy, in combating this lethal disease[11].

Surgery, chemotherapy, radiation therapy, and targeted therapy have long been considered the four pillars of GC management; however, immunotherapy has recently emerged as a promising "fifth pillar", and its use is rapidly expanding[12]. For cases of unresectable locally advanced, recurrent, or metastatic GC, a combination therapy of anti-HER2, chemotherapy, and optional pembrolizumab is preferred for HER2-positive diseases, with the inclusion of pembrolizumab demonstrating a high objective response rate (ORR)[13]. Irrespective of HER2 status, nivolumab [for programmed death-ligand 1 (PD-L1) CPS ≥ 5] is recommended as part of systemic treatment regimens[14]. Currently, there are four principal strategies for tumor immunotherapy: Immune checkpoint inhibitors (ICIs), tumor vaccines,

adoptive immunotherapy, and nonspecific immunomodulators. With advancements in the understanding of the tumor microenvironment (TME), immunotherapy for advanced GC has evolved rapidly, demonstrating superior efficacy and tolerable toxicity compared to traditional therapies, leading to the rapidly increasing use of ICIs[7]. As most GCs are relatively resistant to ICI monotherapy, patients may benefit from combination therapy to achieve enhanced therapeutic effects[15]. Multiple studies have demonstrated that immunotherapy combined with conventional therapy provides superior efficacy compared with monotherapy[16]. Although immunotherapy holds promise for the treatment of GC, the complexity of the immune microenvironment and the heterogeneity of immunogenicity present significant challenges that require further investigation[17].

Chemotherapies for patients with locally advanced or metastatic GC include S-1 + oxaliplatin, docetaxel + oxaliplatin + fluorouracil, docetaxel + oxaliplatin + S-1 (DOS), capecitabine + oxaliplatin (XELOX), and folinic acid/5-fluorouracil/oxaliplatin chemotherapy (FOLFOX). Trastuzumab or pembrolizumab should be added to first-line chemotherapy for patients with HER2 overexpression-positive GC[18,19]. There are two commonly used combinations: Trastuzumab combined with a fluoropyrimidine and a platinum agent and a combination of trastuzumab, pembrolizumab, and XELOX/PF. Regimens for HER2-negative disease include nivolumab, cindilimab, and tislelizumab combined with first-line chemotherapy[20]. Docetaxel, cisplatin, 5-fluorouracil (DCF), modified DCF, and POF also exhibit promising activity. The selection of regimens for second-line or subsequent therapy depends on prior therapy and performance status. Ramucirumab combined with paclitaxel is the preferred second-line or subsequent therapy[19]. Single-agent docetaxel, paclitaxel, irinotecan, albumin-paclitaxel, pembrolizumab, nivolumab, vedicitumab, and apatinib mesylate have also been used as second-line or subsequent therapies. Although there is currently a relatively complete treatment plan, the OS of patients remains short. Therefore, more effective treatment options are required. Based on traditional treatment, explore combination therapy with immunotherapy, subdivide the population, and improve curative effects.

Recent phase I/II trials focusing on the perioperative use of ICIs in combination with chemotherapy for resectable locally advanced gastric/gastroesophageal junction cancer (GC/GEJC) have yielded positive results, thus expanding the potential applications of ICIs in GC management[21]. The addition of sintilimab to chemotherapy has demonstrated encouraging pathological complete response (pCR) and major pathological response rates as a perioperative treatment for resectable locally advanced GC/GEJC with manageable safety profiles. In a phase II study, durvalumab combined with DOS as neoadjuvant chemotherapy reached its primary efficacy endpoint, confirming a pCR in 29.0% of the patients (9 of 31) with acceptable toxicity (safety endpoint < 20%)[22]. In a separate multicenter, single-arm, multi-cohort, phase II trial of tremelimumab and durvalumab as neoadjuvant treatments in patients with MSI-high (MSI-H) resectable gastric adenocarcinoma/gastroesophageal junction adenocarcinoma (GAC/GEJAC; NCT04817826), a pCR rate of 60% (9 of 15) and a major-complete pathological response rate of 18% (< 10% viable cells) were achieved[23].

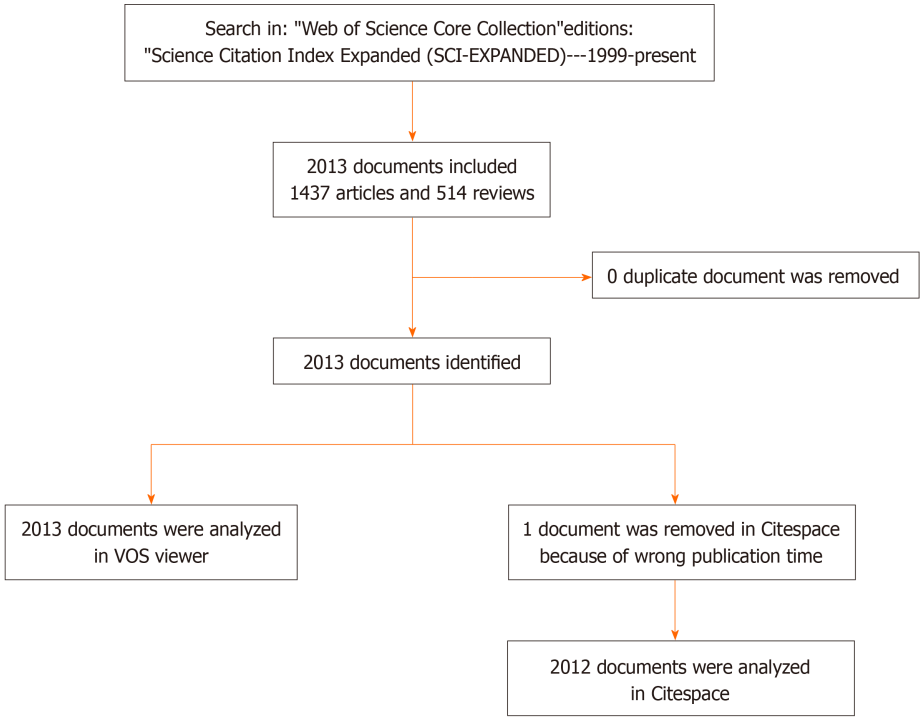
Bibliometrics is a methodological approach that encompasses the analysis and summary of data produced within a specific timeframe. It offers invaluable insights into scientific productivity, behavior, and advancements within the research domain[24]. The objective of this study was to employ bibliometric analysis to elucidate the current status and emergent trends in the field of GC immunotherapy research.

MATERIALS AND METHODS

This analysis was conducted on February 1, 2023, and searched the Web of Science Core Collection (WoSCC) and Science Citation Index Expanded. The retrieval terms in the topic: ("gastric cancer" OR "gastric adenocarcinoma" OR "gastric neoplasm" OR "gastric tumor" OR "stomach cancer" OR "stomach adenocarcinoma" OR "stomach neoplasm" OR "stomach tumor" OR "gastric cancers" OR "gastric adenocarcinoma" OR "gastric neoplasms" OR "gastric tumors" OR "stomach cancers" OR "stomach adenocarcinoma" OR "stomach neoplasms" OR "stomach tumors" OR "tumor of stomach") AND ("immunotherapeutic" OR "immunotherapy" OR "immunotherapies" OR "immunotherapeutics"). Types of documents: Article and review. Finally, the information for a total of 2013 documents was downloaded as Plain Text Files and Tab Delimited Files, and full records and cited references were included. All duplicate records were removed. All documents published in 2013 were included in the analysis.

We searched ClinicalTrials. gov and the International Clinical Trials Registry Platform (ICTRP) (clinical). The retrieval terms: ("gastric cancer" OR "gastric adenocarcinoma" OR "gastric neoplasm" OR "gastric tumor" OR "stomach cancer" OR "stomach adenocarcinoma" OR "stomach neoplasm" OR "stomach tumor") AND ("immunotherapy"). There were 228 registered clinical trials, 25 of which were completed, and 113 were recruiting or not yet recruiting. We searched for some of the main immunotherapies in clinical trials using these two platforms. The research strategy: ("dendritic cells" OR "DNA vaccine" OR "RNA vaccine") AND "gastric cancer" for vaccine clinical trials; (ACT OR TIL OR TCR-T OR CAR-T OR TCR T OR CAR T OR NK OR CIK) AND "gastric cancer" for ACT clinical trials; (ICI OR PD-1 OR PD-L1 OR CTLA-4) AND "gastric cancer" for ICI clinical trials. In total, 274, 137, and 23 clinical trials were incorporated, respectively. These retrievals were conducted on February 19, 2023.

We used CiteSpace (6.1.6) and VOSviewer (1.6.18) to analyze the data. Plain Text Files were analyzed using CiteSpace, and Tab Delimited Files were analyzed using the VOSviewer. CiteSpace made time slicings for the original files from January 1999 to December 2023 with 1 year per slice, and qualified records from 2012 were analyzed. The literature search and screening processes are illustrated in Figure 1. The Citation Report of WoS on February 1, 2023, provided the number of publications and citations annually. The figures used in this study were mapped using CiteSpace, VOSviewer, and Excel.



DOI: 10.3748/wjg.v29.i40.5593 **Copyright** ©The Author(s) 2023.

Figure 1 Flow chart of literature search and screening.

RESULTS

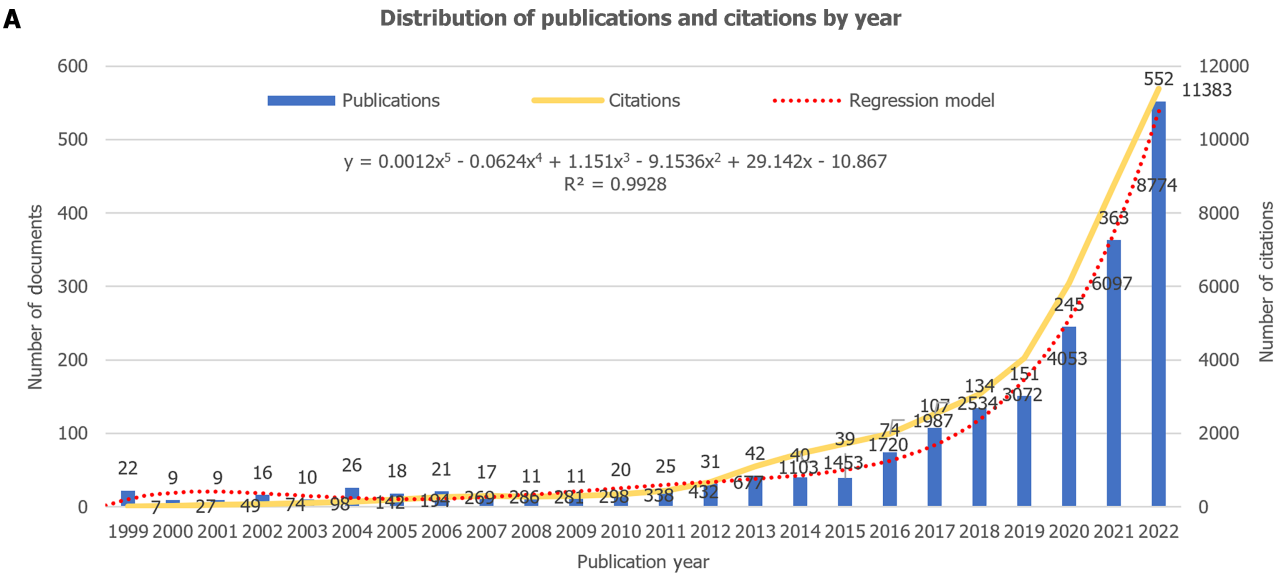
Bibliometric analysis

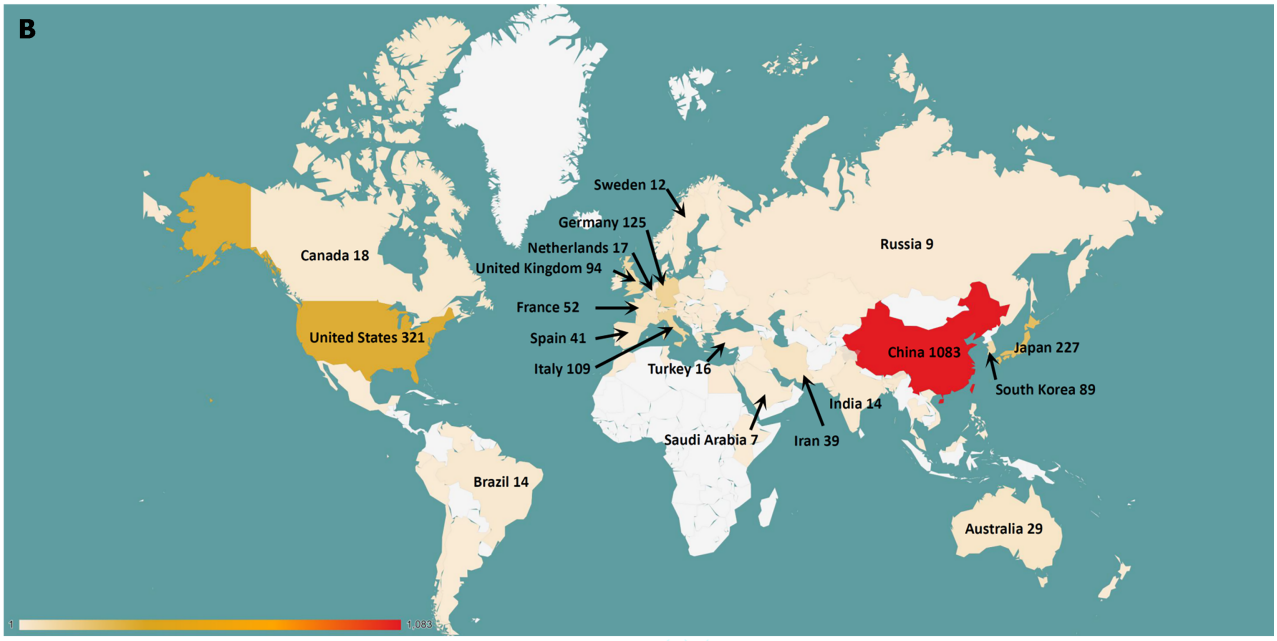
Annual distribution of publications and citations: The spatial-temporal distribution of scholarly publications has been demonstrating a noteworthy ascending trajectory. As per the WoSCC, the 2013 documents collectively garnered 45700 citations, averaging 22.7 citations per document until February 1, 2023. The H-index was 86, indicating that 86 documents each received over 86 citations. Figure 2A illustrates the annual distribution of publications and citations. Only 22 publications were released in 1999, with the number fluctuating between 9 and 42 from 1999 to 2015. However, starting in 2016, the number of publications experienced steady and significant growth, reaching 552 in 2022. Although there were only seven citations in 1999, this figure escalated to 11382 in 2022, marking 23 years of consistent growth. We adopted the regression model $y = 0.0012x^5 - 0.0624x^4 + 1.151x^3 - 9.1536x^2 + 29.142x - 10.867$ ($R^2 = 0.9928$) to show how the number of publications in this field changed over time and forecast it in the following year.

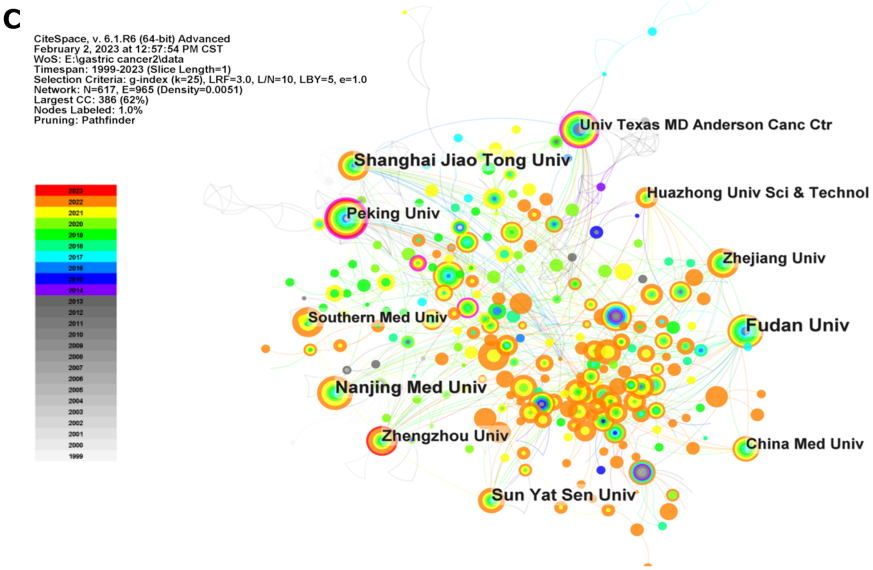
Related countries and institutions: The CiteSpace analysis revealed that contributions to publications in this field originated from 72 countries and 617 institutions, as depicted in Figures 2B and C. Of these, 26 countries and 58 institutions contributed ten or more publications. China had the highest number of publications ($n = 1070$), representing 53.2% of the total, which was significantly higher than that of other countries. The United States was second with 321 publications (16.0 %), followed by Japan ($n = 227$, 11.3%), Germany ($n = 125$, 6.2%), and Italy ($n = 109$, 5.4%). The top ten institutions with the highest number of publications were located in China, five of which were Fudan University ($n = 85$), Nanjing Medical University ($n = 64$), Shanghai Jiao Tong University ($n = 64$), Sun Yat-sen University ($n = 52$), and Zhengzhou University ($n = 43$).

Journals: The 2013 analyzed documents were disseminated across 532 journals, with those comprising at least five documents incorporated into Figure 3A using the VOSviewer. The nodes exhibiting high brightness in this figure denote a higher frequency of occurrence. *Frontiers in Oncology* led the list with 104 documents, followed by *Frontiers in Immunotherapy* ($n = 78$) and *Cancers* ($n = 69$). Additionally, we conducted a co-citation analysis of the cited journals. These articles cited 5445 journals, and we analyzed 102 journals that received at least 200 citations (Figure 3B). The *Journal of Clinical Oncology* garnered the highest number of citations ($n = 5044$), followed by *Cancer Research*, with 3018 citations.

Authors: After excluding documents coauthored by more than 25 authors, we identified 11730 authors across the documents. Only authors with at least five publications were considered, resulting in an analysis of 212 authors who fulfilled the criteria (Figure 4A). In the VOSviewer analysis, Lin Shen had the highest number of publications (525 citations across 25 documents), followed by Hao Liu coming with the second highest number (444 citations across 24 documents). Regarding citations, Sakamoto Junichi had the most citations (810 citations across 6 documents), followed by Xin Wang (705 citations across seven documents). Thirty authors had at least 10 publications in this field, and 17 authors garnered over 400 citations.



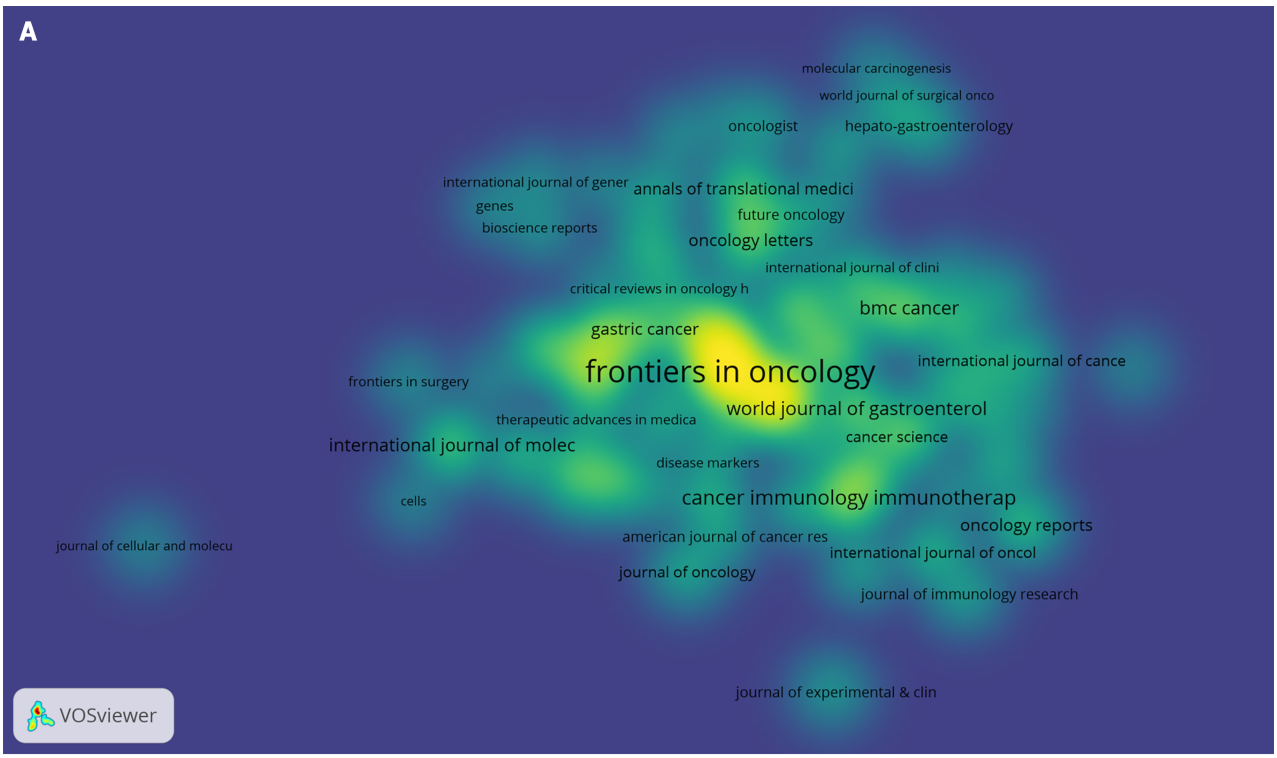




DOI: 10.3748/wjg.v29.i40.5593 **Copyright** ©The Author(s) 2023.

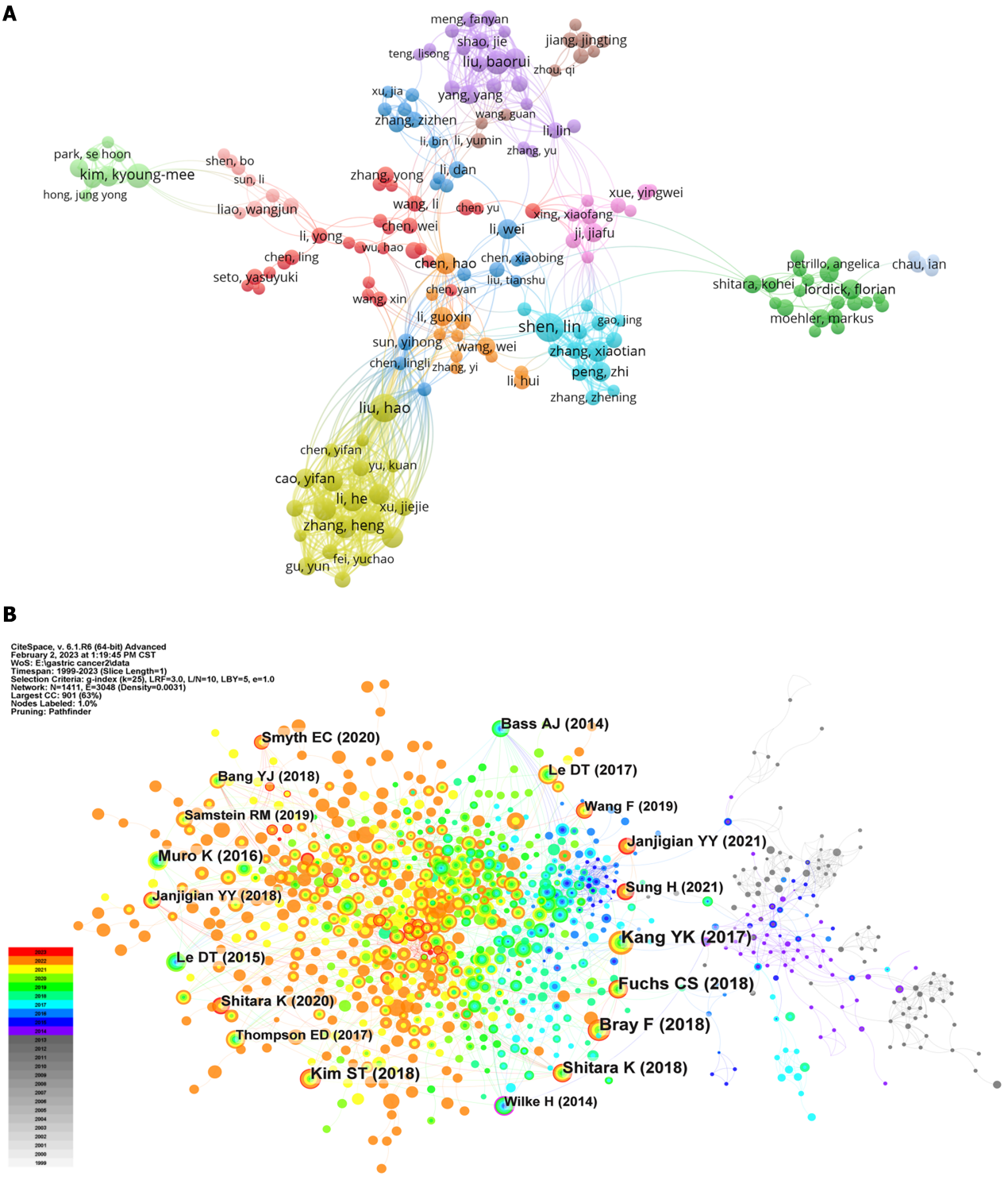
Figure 2 Annual distribution of publications and citations, geographical visualization, and institutions analysis. A: Distribution of publications

and citations by year. The regression formula is $y = 0.0012x^5 - 0.0624x^4 + 1.151x^3 - 9.1536x^2 + 29.142x - 10.867$, $R^2 = 0.9928$; B: Geographical visualization of publications for immunotherapy in gastric cancer; C: Co-occurrence map of the research institutions.



DOI: 10.3748/wjg.v29.i40.5593 **Copyright** ©The Author(s) 2023.

Figure 3 The visualization of journals. A: Journals with at least five publications in this field; B: Highly cited journals in this field.



DOI: 10.3748/wjg.v29.i40.5593 **Copyright** ©The Author(s) 2023.

Figure 4 The visualization of authors. A: Network map of researching authors who had at least five publications; B: Citation analysis of references. Highly cited references are marked by author and publication year.

References: Table 1 shows the ten most frequently co-cited articles based on citation frequency data retrieved from WoS as of February 1, 2023. Seven of these articles were disseminated in the past seven years, and the majority of the highly cited documents had recent publication dates, suggesting a swift progression in this field (Figure 4B). The clinical trial spearheaded by Brahmer *et al*[25], illustrating the induction of tumor regression through an antibody-mediated PD-L1 blockade, amassed 5555 citations, which is significantly more than that of all other articles. This trial, published in the *New England Journal of Medicine* in 2012, experienced a citation surge from 2014 to 2017, exhibiting a strength of 15.45 (Figure 5A). Two additional articles focused on programmed cell death protein 1 (PD-1) or PD-L1, a topic that continues to garner significant attention[26,27]. The second most cited article, also a clinical trial, validated the efficacy of pembrolizumab in patients with advanced triple-negative breast cancer by evaluating its safety and antitumor activity[28]. The

Table 1 The top ten co-cited documents

	Title	Year	Type	First author	Journal	IF (2021)	JCR	Co-citation	DOI	Impact index per article
1	Safety and Activity of Anti-PD-L1 Antibody in Patients with Advanced Cancer	2012	Clinical trial	Brahmer JR	*N Engl J Med*	176.08	Q1	5555	10.1056/NEJMoa1200694	524.5
2	Pembrolizumab in Patients With Advanced Triple-Negative Breast Cancer: Phase Ib KEYNOTE-012 Study	2016	Clinical trial	Nanda R	*J Clin Oncol*	50.72	Q1	1297	10.1200/JCO.2015.64.8931	133.7
3	Benefit of Adjuvant Chemotherapy for Resectable Gastric Cancer A Meta-analysis	2010	Review	Paoletti X	*JAMA*	157.34	Q1	604	10.1001/jama.2010.534	47.9
4	Progress in the treatment of advanced gastric cancer	2017	Review	Song ZY	*Tumour Biol*	3.65 (2016)	Q2	490	10.1177/1010428317714626	75.7
5	m(6)A regulator-mediated methylation modification patterns and tumor microenvironment infiltration characterization in gastric cancer	2020	Article	Zhang B	*Mol Cancer*	41.44	Q1	442	10.1186/s12943-020-01170-0	134.0
6	PD-1(+) regulatory T cells amplified by PD-1 blockade promote hyperprogression of cancer	2019	Article	Kamada T	*Proc Natl Acad Sci U S A*	12.78	Q1	428	10.1073/pnas.1822001116	106.8
7	Tumor Microenvironment Characterization in Gastric Cancer Identifies Prognostic and Immunotherapeutically Relevant Gene Signatures	2019	Article	Zeng DQ	*Cancer Immunol Res*	12.02	Q1	418	10.1158/2326-6066.CIR-18-0436	93.7
8	PD-L1 expression in human cancers and its association with clinical outcomes	2016	Review	Wang X	*Onco Targets Ther*	4.35	Q2	412	10.2147/OTT.S105862	59.0
9	Deep learning can predict microsatellite instability directly from histology in gastrointestinal cancer	2019	Article	Kather JN	*Nat Med*	87.24	Q1	400	10.1038/s41591-019-0462-y	114.0
10	The trifunctional antibody catumaxomab for the treatment of malignant ascites due to epithelial cancer: results of a prospective randomized phase II/III trial	2010	Clinical trial	Heiss MM	*Int J Cancer*	7.32	Q1	349	10.1002/ijc.25423	30.8

JCR: Journal Citation Reports; IF: Impact Factor.

remaining articles in this table pertained to the TME, adjuvant chemotherapy, or review articles. The impact index per article of the top ten articles ranged from 30.8 to 524.5, which is also shown in Table 1.

Figure 5B presents an overlay map of journals, illustrating aspects such as the distribution, citation trajectory, and shift in the center of gravity of papers across each discipline. The label on the left represents the discipline of the cited journal, whereas the label on the right indicates the discipline of the journal in which the cited paper was published. In the figure on the left, the vertical axis of the ellipse extends as the number of papers published by a journal increases, whereas the horizontal axis increases as the number of authors increases. Our analysis revealed that most publications appeared in journals associated with molecular biology, genetics, health, nursing, and medicine. Furthermore, most publications have been cited in journals pertaining to molecular biology, immunology, and medicine. The orange and green citation trajectories suggest that research journals in the molecular/biology/genetics domain garner frequent citations in molecular/biology/immunology and medicine/medical/clinical journals.

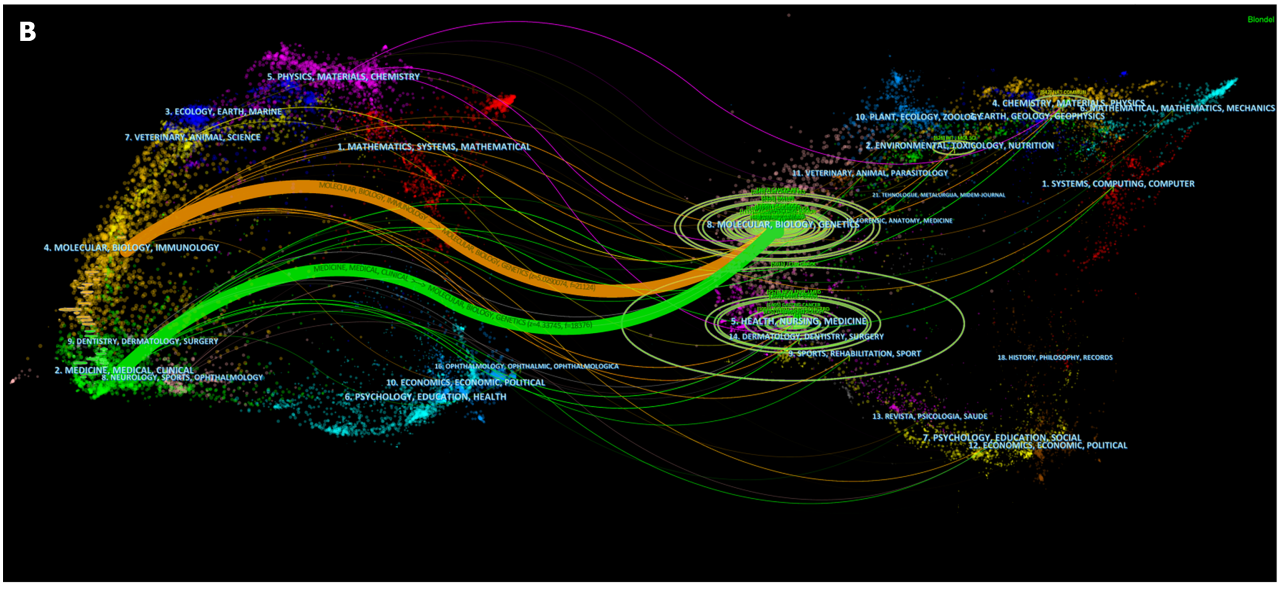
Co-occurrence analysis of keywords: Keywords play a pivotal role in encapsulating scientific research trends. To identify the most prevalent keywords, we used the VOSviewer tool for keyword co-occurrence analysis. From the 6337 keywords, we focused on 152 keywords that appeared 25 times or more (Figure 6A). "Gastric cancer" emerged as the most recurrent keyword, appearing 1257 times. The top ten most frequently occurring keywords included GC (n = 1257), immunotherapy (n = 988), expression (n = 394), chemotherapy (n = 320), prognosis (n = 253), open label (n = 206), survival (n = 194), cancer (n = 190), double-blind (n = 177), and TME (n = 174).

Timeline view of keywords: Following cluster analysis, the keywords were segregated into ten clusters and subsequently subjected to a timeline view analysis in CiteSpace (Figure 6B): #0 MSI, #1 targeted therapy, #2 dendritic cells (DCs), #3 breast cancer, #4 adoptive immunotherapy, #5 TME, #6 immune infiltration, #7 GC, #8 stomach adenocar-

A

Top 25 references with the strongest citation bursts

References	Year	Strength	Begin	End	1999 - 2023
Bass AJ, 2014, NATURE, V513, P202, DOI 10.1038/nature13480, DOI	2014	**65.39**	2015	2019	
Le DT, 2015, NEW ENGL J MED, V372, P2509, DOI 10.1056/NEJMoa1500596, DOI	2015	**39**	2016	2020	
Wilke H, 2014, LANCET ONCOL, V15, P1224, DOI 10.1016/S1470-2045(14)70420-6, DOI	2014	**36.68**	2015	2019	
Fuchs CS, 2014, LANCET, V383, P31, DOI 10.1016/S0140-6736(13)61719-5, DOI	2014	**33.57**	2015	2019	
Muro K, 2016, LANCET ONCOL, V17, P717, DOI 10.1016/S1470-2045(16)00175-3, DOI	2016	**28.91**	2017	2020	
Cristescu R, 2015, NAT MED, V21, P449, DOI 10.1038/nm.3850, DOI	2015	**25.57**	2016	2020	
Ferlay J, 2015, INT J CANCER, V136, PE359, DOI 10.1002/ijc.29210, DOI	2015	**23.61**	2016	2020	
Waddell T, 2013, LANCET ONCOL, V14, P481, DOI 10.1016/S1470-2045(13)70096-2, DOI	2013	**16.35**	2015	2018	
Lordick F, 2013, LANCET ONCOL, V14, P490, DOI 10.1016/S1470-2045(13)70102-5, DOI	2013	**15.84**	2015	2018	
Topalian SL, 2012, NEW ENGL J MED, V366, P2443, DOI 10.1056/NEJMoa1200690, DOI	2012	**15.52**	2013	2017	
Brahmer JR, 2012, NEW ENGL J MED, V366, P2455, DOI 10.1056/NEJMoa1200694, DOI	2012	**15.45**	2015	2017	
Torre LA, 2015, CA-CANCER J CLIN, V65, P87, DOI 10.3322/caac.21262, DOI	2015	**15.39**	2015	2019	
Boger C, 2016, ONCOTARGET, V7, P24269, DOI 10.18632/oncotarget.8169, DOI	2016	**15.25**	2017	2020	
Rizvi NA, 2015, SCIENCE, V348, P124, DOI 10.1126/science.aaa1348, DOI	2015	**14.52**	2016	2020	
Shi LR, 2012, CANCER IMMUNOL IMMUN, V61, P2251, DOI 10.1007/s00262-012-1289-2, DOI	2012	**14.37**	2013	2017	
Smyth EC, 2016, ANN ONCOL, V27, Pv38, DOI 10.1093/annonc/mdw350, DOI	2016	**14.22**	2018	2021	
Jemal A, 2011, CA-CANCER J CLIN, V61, P134, DOI 10.3322/caac.20107, DOI	2011	**13.67**	2012	2016	
Tumeh PC, 2014, NATURE, V515, P568, DOI 10.1038/nature13954, DOI	2014	**13.63**	2015	2019	
Satoh T, 2014, J CLIN ONCOL, V32, P2039, DOI 10.1200/JCO.2013.53.6136, DOI	2014	**13.62**	2016	2019	
Derks S, 2016, ONCOTARGET, V7, P32925, DOI 10.18632/oncotarget.9076, DOI	2016	**13.6**	2017	2018	
Larkin J, 2015, NEW ENGL J MED, V373, P23, DOI 10.1056/NEJMoa1504030, DOI	2015	**13.54**	2016	2020	
Herbst RS, 2014, NATURE, V515, P563, DOI 10.1038/nature14011, DOI	2014	**12.75**	2015	2019	
Hontscha C, 2011, J CANCER RES CLIN, V137, P305, DOI 10.1007/s00432-010-0887-7, DOI	2011	**12.43**	2012	2016	
Ford HER, 2014, LANCET ONCOL, V15, P78, DOI 10.1016/S1470-2045(13)70549-7, DOI	2014	**12.31**	2015	2019	
Lin SJ, 2015, GUT, V64, P1721, DOI 10.1136/gutjnl-2014-308252, DOI	2015	**11.93**	2016	2020	

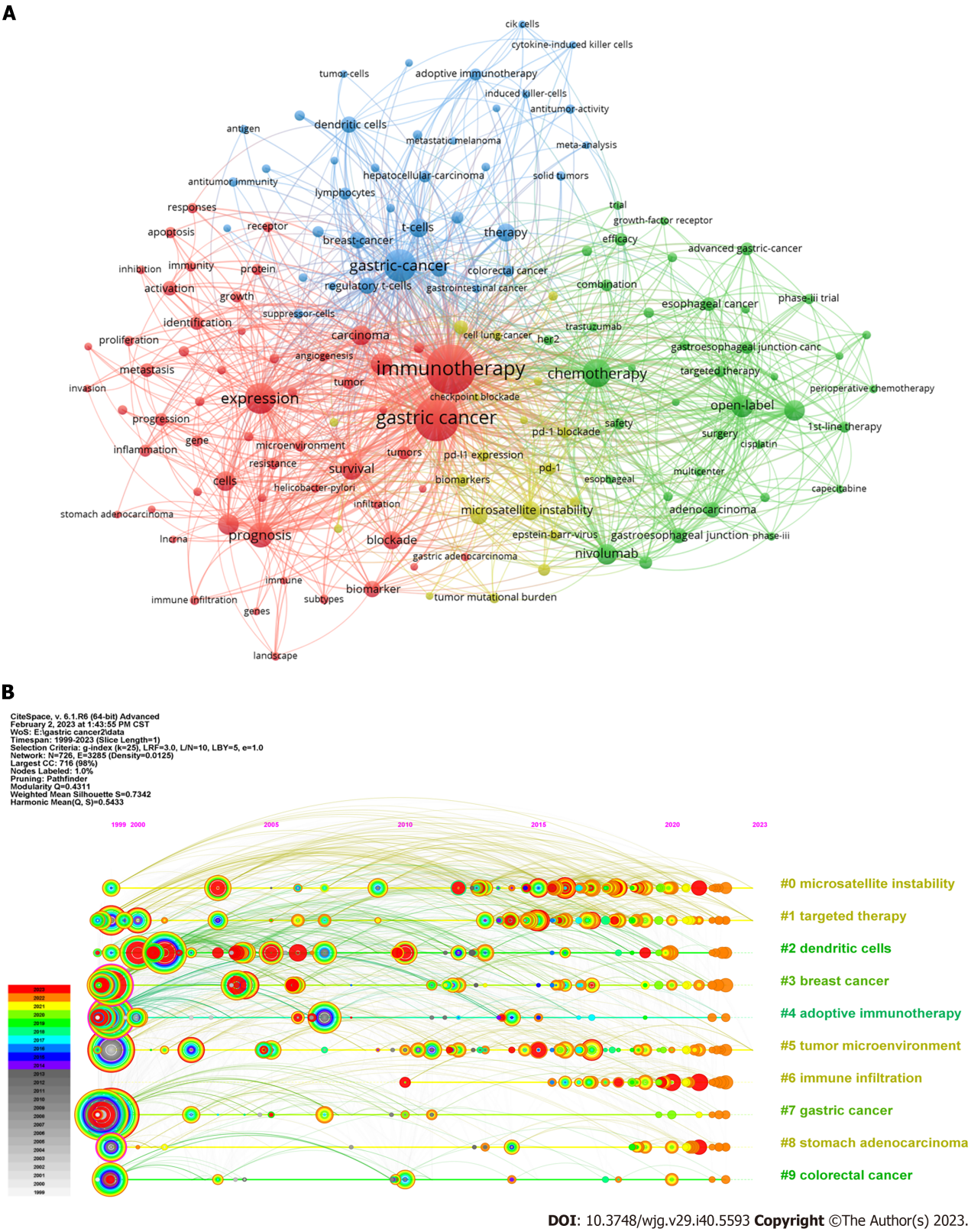


DOI: 10.3748/wjg.v29.i40.5593 **Copyright** ©The Author(s) 2023.

Figure 5 References burst analysis and dual-map overlay of journals. A: Top 25 references with the strongest citation bursts are sorted by strength; B: Dual-map overlay of journals. The colored curve represents the reference path; the nature of each region is defined by the journal of the corresponding region.

cinoma, and #9 colorectal cancer. Each cluster comprised multiple closely associated words with smaller ranks or cluster numbers that contained more keywords. The premier cluster (#0) had the largest number of keywords, showing minimal past activity with two minor bursts but became more active in the recent decade. Cluster #1 followed a trend akin to that of cluster #0, signifying that MSI and targeted therapy have drawn significant interest. Clusters #2, #3, and #4 were notably active around 2000 and have undergone minor bursts in recent years. The term "tumor microenvironment" first appeared in 2010 in cluster #5 and has maintained activity in recent years.

Burst analysis of keywords: Following the burst analysis, we selected 25 keywords from the burst keywords based on burst strength and initiation time (Figures 7A and B). The keywords exhibiting the highest burst strengths included "Adoptive immunotherapy" (strength = 17.37), "dendritic cells" (strength = 16.79), and "carcinoma" (strength = 12.14). Three keywords that initiated bursting in the past 5 years and were identified as hotspots encompassed "mismatch repair deficiency" (initiated in 2018), "tumors" (initiated in 2019), and "plus chemotherapy" (initiated in 2021). The emergence of new burst keywords and prevalence of strong bursts in recent years have led to rapid developments in this field.



DOI: 10.3748/wjg.v29.i40.5593 **Copyright** ©The Author(s) 2023.

Figure 6 Keywords occurrences and timeline view analysis. A: Co-occurrence map of the keywords with at least 25 occurrences; B: Timeline view of keywords with the ten leading clusters.

Clinical trials

The clinical trial with the earliest enrolment commenced in 1987, and was a randomized controlled trial predicated on preoperative serum glycoproteins assessing the efficacy of immunotherapy in GC (JPRN-UMIN000037472). The annual distribution of clinical trials (Figure 8A) indicated a sharp recent progress in the study of GC immunotherapy. The peak in the number of clinical trials occurred in 2019 (n = 37), with high numbers observed in the subsequent three years (2020 n = 32, 2021 n = 35, 2022 n = 30). The trials were predominantly in phase I (n = 46), phase I/II (n = 44), or phase II (n = 75)

A

Top 25 keywords with the strongest citation bursts

Keywords	Year	Strength	Begin	End	1999 - 2023
adoptive immunotherapy	1999	17.37	1999	2016	
monoclonal antibody	1999	11.36	1999	2015	
breast cancer	1999	11.13	1999	2017	
metastatic melanoma	1999	7.78	1999	2016	
interleukin 2	1999	6.91	1999	2006	
carcinoma	1999	12.14	2000	2013	
identification	2000	10.28	2000	2014	
dendritic cells	2001	16.79	2001	2013	
antigen	2001	8.94	2001	2014	
cytotoxic t lymphocytes	2001	8.82	2001	2012	
tumor cells	2004	7.01	2004	2018	
in vivo	2006	10.11	2006	2017	
ovarian cancer	2006	8.5	2006	2017	
antitumor activity	2003	8.18	2009	2018	
lymphocytes	2010	11.45	2010	2018	
lung cancer	2004	10.15	2010	2017	
growth factor receptor	2011	6.95	2011	2018	
cik cells	2012	10.75	2012	2017	
t cells	1999	8.89	2012	2016	
melanoma	2005	6.87	2012	2018	
cytokine-induced killer cells	2013	11.39	2013	2017	
phase ii trial	2014	8.3	2014	2018	
mismatch repair deficiency	2018	10.82	2018	2020	
tumors	2015	7.59	2019	2021	
plus chemotherapy	2021	8.07	2021	2023	

B

Top 25 keywords with the strongest citation bursts

Keywords	Year	Strength	Begin	End	1999 - 2023
adoptive immunotherapy	1999	17.37	1999	2016	
dendritic cells	2001	16.79	2001	2013	
carcinoma	1999	12.14	2000	2013	
lymphocytes	2010	11.45	2010	2018	
cytokine-induced killer cells	2013	11.39	2013	2017	
monoclonal antibody	1999	11.36	1999	2015	
breast cancer	1999	11.13	1999	2017	
mismatch repair deficiency	2018	10.82	2018	2020	
cik cells	2012	10.75	2012	2017	
identification	2000	10.28	2000	2014	
lung cancer	2004	10.15	2010	2017	
in vivo	2006	10.11	2006	2017	
antigen	2001	8.94	2001	2014	
t cells	1999	8.89	2012	2016	
cytotoxic t lymphocytes	2001	8.82	2001	2012	
ovarian cancer	2006	8.5	2006	2017	
phase ii trial	2014	8.3	2014	2018	
antitumor activity	2003	8.18	2009	2018	
plus chemotherapy	2021	8.07	2021	2023	
metastatic melanoma	1999	7.78	1999	2016	
tumors	2015	7.59	2019	2021	
tumor cells	2004	7.01	2004	2018	
growth factor receptor	2011	6.95	2011	2018	
interleukin 2	1999	6.91	1999	2006	
melanoma	2005	6.87	2012	2018	

DOI: 10.3748/wjg.v29.i40.5593 **Copyright** ©The Author(s) 2023.

Figure 7 Analysis of keywords burst. A: Top 25 keywords with the strongest citation bursts are sorted by strength; B: Top 25 keywords with the strongest citation bursts sorted by starting year.

(Figure 9A). We have consolidated the clinical trials of phase II/III (n = 4), III (n = 4), and IV (n = 2) in Table 2, offering scholars an update on the latest advancements in this field. The status of the clinical trials is shown in Figure 9B, with a significant number of trials either recruiting (n = 92) or not yet recruiting (n = 21). The three primary immunotherapies for GC, namely adoptive cell therapy (ACT), ICI, and vaccination, were subjected to separate clinical trial searches (Supplementary material, Figures 8B and 9C).

Table 2 Clinical trials in phase 3 and phase 4 (or phase 2/3)

No.	Trial ID	Status	Phases	Start date	Title
1	NCT00503321	Terminated	Phase 2/3	October 1, 2006	Phase II Study of TS-1 Therapy and TS-1+PSK Therapy Against Advanced Gastric Carcinoma
2	EUCTR2017-004896-30-IE	Not recruiting	Phase 3	July 6, 2018	A Randomized, Active-Controlled, Blinded, Phase III Clinical Trial of BMS- 986213 (Fixed Dose Combination of Relatlimab [anti-LAG-3] and Nivolumab) in Combination with Chemotherapy versus Placebo in Combination with Chemotherapy as First-Line Treatment in Participants with Unresectable, Locally Advanced or Metastatic LAG-3 Positive Gastric or Gastroesophageal Junction Adenocarcinoma
3	NCT04078152	Active, not recruiting	Phase 4	September 5, 2019	Durvalumab Long-Term Safety and Efficacy Study
4	ChiCTR2000039110	Recruiting	Phase 4	October 14, 2020	Effect of immunotherapy combined with chemotherapy on gastric cancer
5	NCT05002686	Recruiting	Phase 2/3	August 7, 2021	Safety and Efficacy of Sintilimab in Combination With Chemoradiothrapy Followed by D2 Surgical Resection in Patients With Advanced Gastric Cancer With Retroperitoneal Lymph Node Metastasis
6	NCT05152147	Recruiting	Phase 3	December 2, 2021	A Study of Zanidatamab in Combination With Chemotherapy Plus or Minus Tislelizumab in Patients With HER2-positive Advanced or Metastatic Gastric and Esophageal Cancers
7	NCT05270824	Not yet recruiting	Phase 3	March 1, 2022	Study Evaluating Neoadjuvant Immunotherapy Increasing CD8+ Cell Infiltration in Advance Gastric Adenocarcinoma
8	NCT05325528	Recruiting	Phase 2/3	April 4, 2022	Study of Tislelizumab in Combination With SOX for the Treatment of Gastric Cancer With Liver Metastases
9	NCT05677490	Not yet recruiting	Phase 3	January 6, 2023	mFOLFIRINOX Versus mFOLFOX With or Without Nivolumab for the Treatment of Advanced, Unresectable, or Metastatic HER2 Negative Esophageal, Gastroesophageal Junction, and Gastric Adenocarcinoma
10	NCT05699655	Not yet recruiting	Phase 2/3	March 1, 2023	Tislelizumab Combined With Apatinib and Oxaliplatin Plus S1 Vs Oxaliplatin Plus S1 as Neoadjuvant Therapy for Borrmann IV, Large Borrmann III Type and Bulky N Positive Advanced Gastric Cancer

DISCUSSION

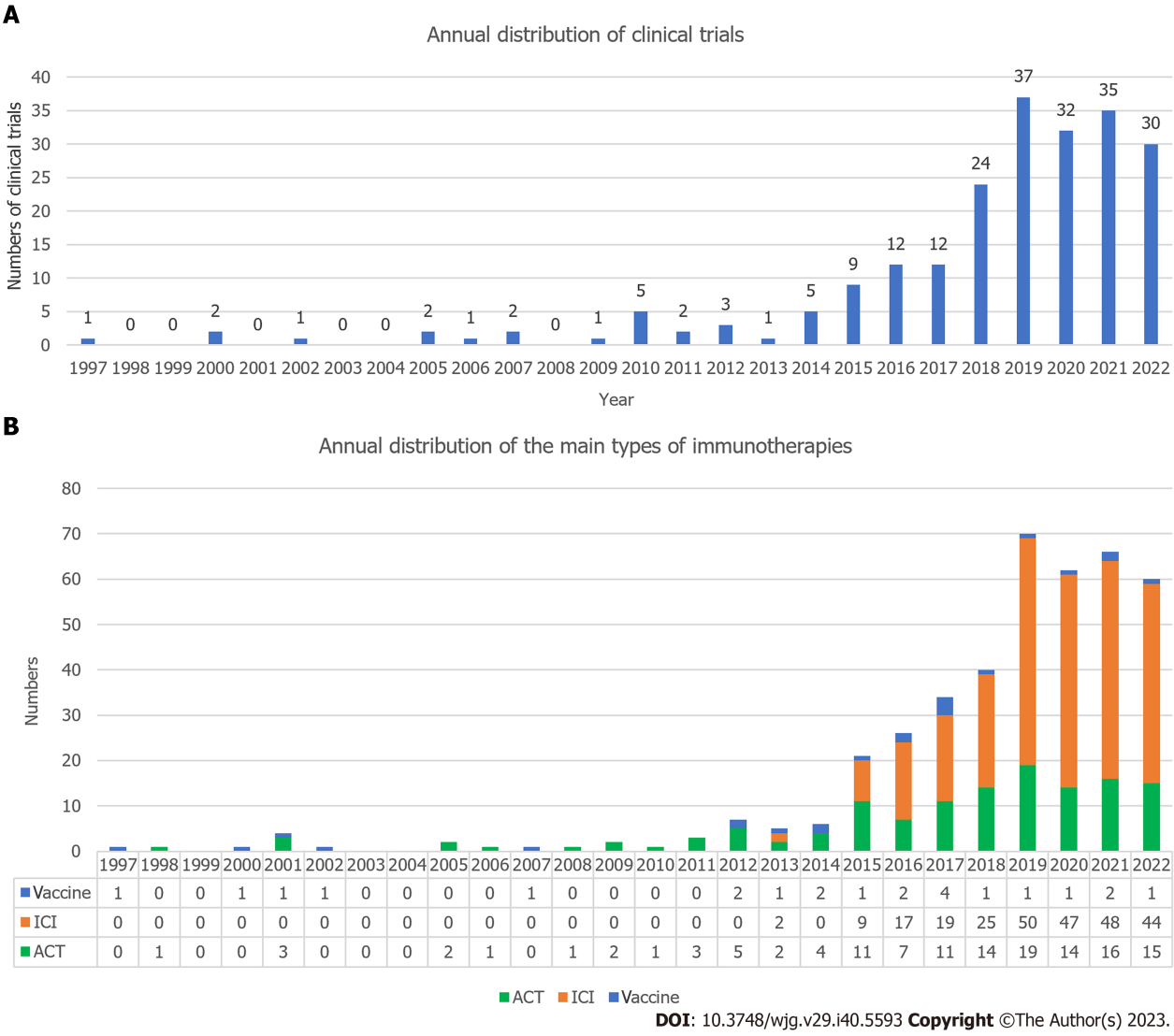
In recent years, there has been a surge in the bibliometric analysis of articles across various fields. Tools such as CiteSpace and the VOSviewer enable raw data visualization, offering comprehensive and intuitive data representation. Cancer is a persistent medical challenge that has caused researchers to work globally toward enhancing treatments to improve progression-free survival (PFS) and OS. GC is one of the most prevalent cancers and requires more effective and targeted treatments. Bibliometric analysis of documents pertaining to GC immunotherapy elucidated the current research hotspots, thereby providing researchers with insights and directions. This analysis incorporated every related article from the WoSCC database until December 31, 2022, offering a visual and systematic overview. It summarizes and analyzes the countries, institutions, authors, keywords, and references. Clinical trials included every related trial from ClinicalTrials.gov and ICTRP until February 18, 2023.

Bibliometric analysis

With regard to the volume of documents produced by each country, China held a dominant position, contributing 1070 documents, accounting for 53.2% of the total. The ten institutions with the highest publication counts were all located in China. The substantial population base of China facilitates a larger number of researchers and institutions in related fields, thereby leading to a higher volume of literature production. Furthermore, China's substantial investment in GC immunotherapy research underscores the promising future of this field. In addition to the patient count correlating with the large population base, the incidence of GC in China significantly surpasses that in the United States and United Kingdom[29]. Elevated rates of smoking and *Helicobacter pylori* infection in China could contribute to a higher incidence of GC. The extent of early cancer screening in China remains unclear.

The United States holds the second position with regard to the volume of documents produced, contributing 16.0% of the publications, and is potentially linked to factors such as obesity, alcohol consumption, and high-fat diets. Japan ranked third (11.3%). The high incidence of GC in Japan mirrors that in China, likely because of Asian dietary habits, including high salt intake and excessive nitrite consumption, which are associated with a high incidence of digestive system tumors.

Co-citation analysis revealed that Sakamoto Junichi had the highest citation count (810 citations across six documents). His research has primarily focused on immunochemotherapy or adjuvant chemotherapy, with a meta-analysis of the benefits of adjuvant chemotherapy for resectable GC with over 600 citations. Oba *et al*[30] also highlighted the therapeutic effects of polysaccharide K, lentinan, and OK-432 in GC[31,32]. This highlights the pivotal role of chemotherapy in GC treatment and ongoing advancements in research on the integration of immunotherapy and chemotherapy. Xin Wang, with 705 citations across seven documents, held the second position. His contributions include the development of



DOI: 10.3748/wjg.v29.i40.5593 **Copyright** ©The Author(s) 2023.

Figure 8 Distribution of clinical trials by year. A: Annual distribution of clinical trials in this field; B: Annual distribution of the main types of immunotherapies (vaccine, immune checkpoint inhibitor, and adoptive cell therapy). ICI: Immune checkpoint inhibitor; ACT: Adoptive cell therapy.

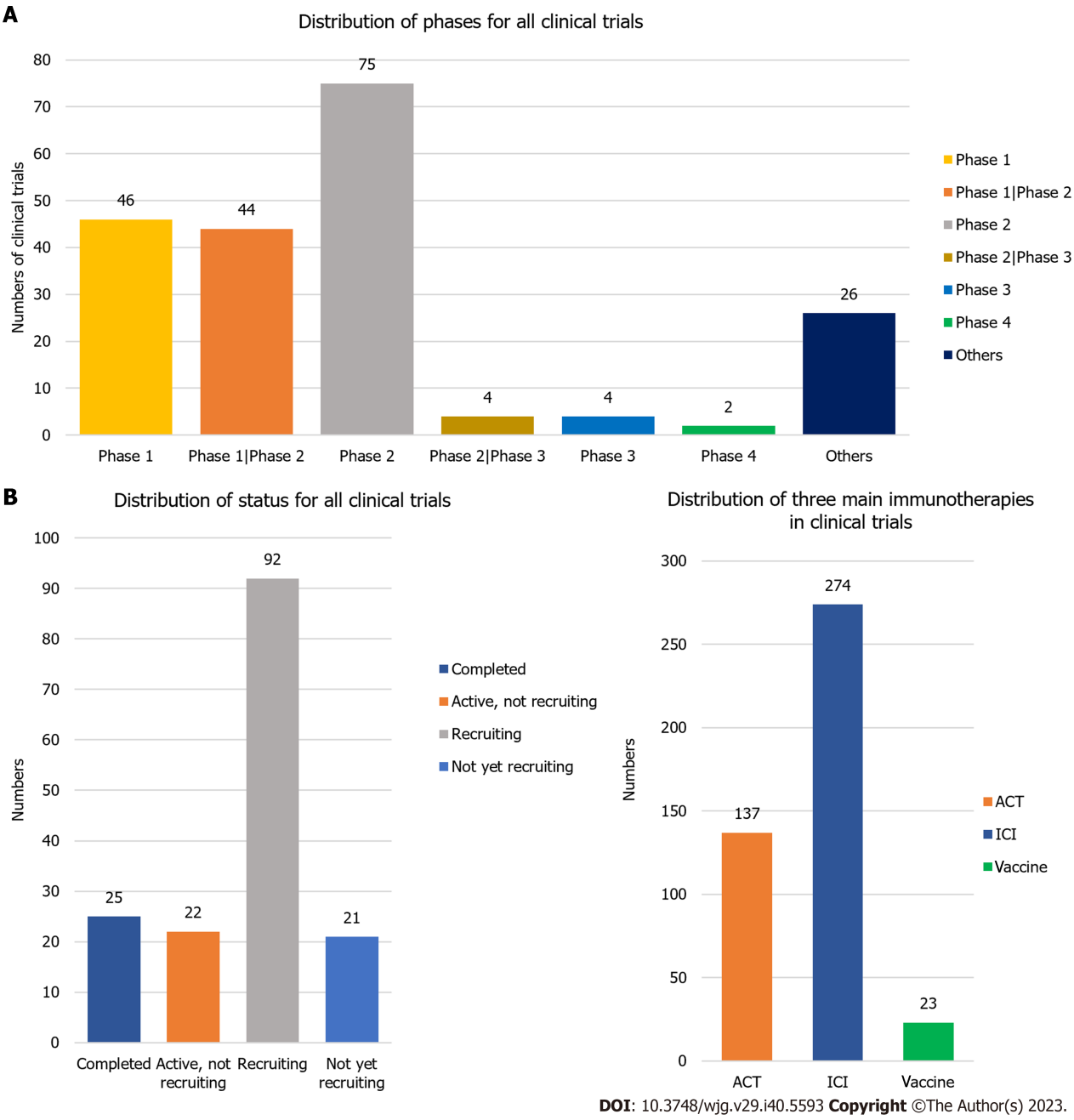
clinical guidelines for GC diagnosis and treatment and a review of PD-L1 expression in human cancers and its correlation with clinical outcomes, which has received over 400 citations. PD-L1-related research has emerged as a significant focus in recent years, offering new prospects for GC immunotherapy, which will be discussed in subsequent sections.

Keyword analysis

Keyword analysis, excluding less-specific terms, revealed several significant keywords and clusters. Notably, clusters #0 (MSI), #2 (DCs), #4 (adoptive immunotherapy), and #5 (TME) stood out; these were also keywords with notable bursts. Moreover, keyword "mismatch repair deficiencies" have garnered considerable attention. We delved into these categories in detail. Because of the substantial progress and potential of ICIs reported in recent studies, we discuss them separately.

TME (#5 TME): Among the top ten most frequently occurring keywords in this study, three only surfaced in recent years: "open label" (first appearance in 2015, 206 occurrences), "double-blind" (first appearance in 2015, 177 occurrences), and "tumor microenvironment" (first appearance in 2017, 174 occurrences). Open-label and double-blind denote two contrasting types of experiments. In open-label trials, both investigators and participants are aware of the treatment status, whereas in double-blind trials, neither party knows the treatment status. The frequent appearance of these two keywords likely reflects the growing number of immunotherapeutic drugs entering clinical trials in recent years. Pembrolizumab and nivolumab have shown efficacy against certain types of GC[33,34]. Toripalimab, currently under evaluation for its safety and efficacy in treating advanced GC resistant to chemotherapy, is also part of an ongoing phase III randomized trial assessing the combined therapy of toripalimab and XELOX[33,35].

The sixth keyword cluster, represented by "tumor microenvironment", gained prominence in 1999 and has received consistent attention since 2010. The TME refers to non-tumor cells and their metabolites and secretions within the tumor, including immune cells such as myeloid suppressor cells, tumor-infiltrating lymphocytes (TILs), macrophages, stromal fibroblasts, endothelial cells, extracellular matrix components, growth factors, and cytokines[36]. Five highly cited articles



DOI: 10.3748/wjg.v29.i40.5593 **Copyright** ©The Author(s) 2023.

Figure 9 Phases and status distribution across all clinical trials. A: Distribution of phases for all clinical trials. Phases include: Phase 1, phase 1/phase 2, phase 2, phase 2/phase 3, phase 3, phase 4, and others; B: Distribution of status for all clinical trials. The status includes: Completed, active but not recruiting, recruiting, and not yet recruiting; C: Distribution of adoptive cell therapy, immune checkpoint inhibitor, and vaccine in clinical trials. ICI: Immune checkpoint inhibitor; ACT: Adoptive cell therapy.

in this study featured "tumor microenvironment" as a keyword, focusing on tumor-associated macrophages (TAMs) or pyroptosis. Macrophages are primarily categorized into two phenotypes, classically activated (M1) and alternatively activated (M2). M1 macrophages exhibit antitumor effects; however, M2 macrophages promote angiogenesis and tumor progression. TAMs, comprising M2 and a fraction of M1 cells, foster pro-angiogenic and immunosuppressive signals in gastric tumors, thereby presenting potential therapeutic targets[37,38]. Another study highlighted the significant role of RNA N6-methyladenosine modifications in shaping the diversity and complexity of the TME[39]. Pyroptosis aids cytotoxic lymphocytes in eliminating tumor cells and reprograms the TME toward an immunostimulatory state[40]. A recent study has suggested that the GC microenvironment of patients may provide a more accurate prediction of chemotherapy sensitivity, thereby enabling improved staging and prognostic assessment of patients[41]. The role of TME in GC continues to garner interest.

MSI (#0 MSI) and defective mismatch repair (mismatch repair deficiency): MSI arises from the inability to repair replication errors in microsatellite sequences owing to defective mismatch repair (dMMR). When these errors accumulate significantly, they result in MSI-H, a subtype of GAC constituting up to 22% of the cases[42]. The keyword "mismatch repair deficiency" experienced a burst from 2018 to 2020, with a burst strength of 10.82, ranking eighth (Figure 7A). As

depicted in Figure 6B, MSI ranks first in the cluster, signifying its high association and occurrence. The MSI-driven cancer pathway prompts tumor cells to produce abnormal and potentially immunogenic neoantigens, suggesting high antigenic potential in MSI GC[43,44]. Studies have established the independent prognostic significance of dMMR (P = 0.0001), with patients with metastatic GC exhibiting defective MMR systems demonstrating improved prognoses[44]. MSI cancer, characterized by extensive expression of immune checkpoint ligands and robust immunogenicity, exhibits heightened sensitivity to immunotherapy, albeit with potential resistance to chemotherapy[45,46]. The significance of the MSI-H subtype is well established, with numerous recent studies focusing on this subtype. Both nivolumab as a standalone treatment and in combination with ipilimumab have demonstrated antitumor activity with a tolerable toxicity profile in chemotherapy-resistant gastroesophageal adenocarcinomas. Moreover, pembrolizumab has received regulatory approval as a therapeutic alternative for MSI-H tumors[47,48]. Emerging evidence indicates a potential correlation between MSI-H and PD-L1 expression in various cancers, suggesting that MMR defects may serve as predictors of ICI therapy[45].

DC (#2 DCs): "Dendritic cells" constituted the third cluster in Figure 6B, exhibiting a significant burst from 2001 to 2013, as indicated by the second highest burst strength (Figure 7A, strength = 16.79). DCs are antigen-presenting cells essential for the induction and regulation of adaptive immune responses. DCs can phagocytose and process antigens and present these antigens to naive T-cells, resulting in the activation, differentiation, and polarization of T-cells toward specific effector functions. In GC immunotherapy, DCs play a key role in the activation and regulation of antitumor immune responses[49]. DCs can be used as adjuvants or vaccine adjuvants to enhance antitumor immunity by presenting tumor-specific antigens to naïve T-cells[49,50].

DC-based vaccination and ACT are the two main types of cellular immunotherapies used in GC[50]. Our analysis revealed that 23 clinical trials have focused on GC vaccines, with new trials initiated annually since 2012, as depicted in Figures 8B and 9C. Vaccines have surfaced as a pivotal modality in cancer immunotherapy, with DC-based vaccination being the predominant approach, constituting 20 out of 23 clinical trials. In 1990, Inaba *et al*[51] demonstrated that injection of *in vitro* antigens from DCs could sensitize normal mice to protein antigens. A decade later, researchers discovered that DCs can elicit antitumor responses[52]. A study in 2015 illustrated that DCs, when loaded with tumor RNA, can stimulate lymphocytes to differentiate into effector cells that respond to tumors and are capable of eliminating tumor cells[53]. The fusion of GC cells and DCs significantly enhances their ability to stimulate anti-tumor immune responses and prevents their proliferation into newly implanted tumors *in vivo*, highlighting the potential of DCs as a safe and effective anti-tumor vaccine[54]. Recombinant adenovirus-bearing secondary lymphoid tissue chemokine-modified DCs could serve as adjuvants to induce a robust immune response against GC[55]. DCs derived from cord blood in combination with cytokine-induced killer (CIK) cells have also been clinically utilized for the treatment of GC, showing significant disease-free survival (DFS, P = 0.0448) and OS (P = 0.0646) rates[56]. As of February 6, 2023, we identified 18 trials on ClinicalTrials.gov using the keywords "gastric cancer" and "dendritic cells", with seven completed, nine with unknown status (indicating that the study had passed its completion date and its status had not been verified for over two years), one active, and one recruiting.

ACT (#4 adoptive immunotherapy): Adoptive immunotherapy was identified as the fifth cluster (Figure 6B, #4 adoptive immunotherapy) and experienced a surge in research from 1999 to 2016, as evidenced by its high strength (Figures 7A and B, strength = 17.37). A total of 137 clinical trials pertaining to ACT were initiated during this period, with relevant trials conducted almost annually for the past two decades (Figures 8B and 9C). ACTs involve the transfer of immune cells, such as lymphocytes or DCs, to a patient to enhance the antitumor immune response. In GC immunotherapy, ACTs generate effector T-cells that specifically target tumor antigens and induce long-term antitumor immunity[57]. ACTs can also enhance the function of regulatory T-cells and improve patient outcomes[50,57].

ACT has a rich history demonstrating its importance and progression in the field of immunotherapy. Currently, four types of ACTs have made significant contributions to international research: (1) TIL therapy; (2) Engineered T-cell receptor (TCR) therapy; (3) Chimeric antigen receptor T-cell (CAR-T) therapy; and (4) Natural killer (NK) cell therapy. CIK cell therapy, another form of ACT, is considered a promising approach for next-generation tumor-adaptive cell immunotherapies, with CIK cells often referred to as precision-guided missiles that target tumor cells[58].

First, we investigated TIL therapy. Unlike several types of cell immunotherapies that use blood-derived cells, TIL therapy leverages immune cells extracted directly from tumor tissues, thereby enhancing the capacity of these cells for tumor recognition. TILs play a critical role in curbing tumor growth and adjusting therapeutic response in cancer patients and could potentially act as predictive markers, providing insights into patient response to treatment and prognosticating survival outcomes[59,60]. GC can be stratified into four distinct TME subtypes based on the assessment of PD-L1 expression and TILs: (1) PD-L1+/TIL+, associated with the best PFS [Hazards ratio (HR = 2.044)] and OS (HR = 1.993); (2) PD-L1-/TIL-, linked with the poorest survival outcomes; (3) PD-L1+/TIL-; and (4) PD-L1+/TIL+[61]. Increased counts of T-bet+ TILs were found to be correlated with non-invasion of the muscle layer (P = 0.0138), smaller tumor size (P = 0.0202), and early Union for International Cancer Control stage (P = 0.0196), and studies have demonstrated that higher numbers of T-bet+ TILs are associated with longer median PFS (41 *vs* 26 mo, P = 0.0481) and median survival time (MST) (55 *vs* 32 mo, P = 0.0455)[62].

Second, we examined engineered TCR therapies. TCR-engineered T-cells require the presentation of antigens by specific major histocompatibility complex (MHC) molecules for activation, which presents certain constraints on their clinical applications[63]. Initial trials with TCR therapy showcased cancer regression; however, the associated toxicities were severe, underscoring the need for caution when implementing high-avidity TCRs[10,64]. Later clinical trials achieved efficacy without substantial toxicity by using T-cells redirected against cancer testis antigens[63,65,66]. A 2022 study profiled the hypervariable complementarity determining region 3 of the TCR beta chain in the peripheral blood of GC patients to identify new biomarkers[67].

Thirdly, we turn our attention to CAR-T therapy. Emerging over the past 30 years, CAR-T-cell therapy is a relatively novel approach, evolving from prior clinical applications of ACT, including TILs[11]. CAR-T-cells, a subset of genetically engineered T-cells, can identify specific antigens, and their cytotoxic effects operate independently of MHC interactions [50]. The first-generation CAR, constructed in 1993, comprises an extracellular antigen recognition domain-commonly a single-chain Fragment variant derived from an antibody-a transmembrane domain, and the intracellular T-cell activation domain of CD3+[68,69]. The second-generation CAR introduces a costimulatory domain, enhancing antitumor effects and promoting the establishment of immunological memory in patients with hematological tumors[69,70]. Third-generation CAR integrate two tandem costimulatory molecules[11]. The fourth-generation CAR adopts a more intricate design that aims to mitigate off-target toxicity and immunosuppression and boost the anti-tumor transport activity targeted by solid tumors[11]. Various potential targets for GC therapy, including claudin 18.2, mesothelin, ANTXR1 (TEM8), and MUC3A, have been identified, and claudine18.2-specific CAR-T-cell therapy is currently being explored in clinical trials[71,72]. As of February 6, 2023, a search of ClinicalTrials.gov using the keywords "gastric cancer" and "CAR T" yielded 37 trials, 23 of which were recruiting or not yet recruiting. Numerous related experiments will be conducted in the coming years, likely catalyzing rapid advancements in CAR-T therapy.

NK cell therapy was also considered. Patients with digestive cancers frequently demonstrate elevated PD-1 expression in both peripheral and tumor-infiltrating NK cells, and this heightened expression could potentially signify an unfavorable prognosis[73]. A decade ago, a study revealed that among patients with GAC, those with high concentrations of NK cells exhibited higher survival rates than those with low concentrations (P = 0.0027, HR = 0.343)[74]. As NK cell therapy continues to evolve, researchers have begun to integrate NK cells with other forms of immunotherapy to investigate the potential improvements in patient outcomes. A recent animal study employed a combination of interleukin (IL)-2-activated NK cells and anti-PD-1 therapy, demonstrating that this synergistic approach could hinder gastric tumor progression and promote tumor immune cell infiltration[75]. Moreover, various strategies involving CAR NK cell therapy have demonstrated efficacy in the treatment of certain tumor types[76-78].

Finally, CIK cell therapy is discussed. As illustrated in Figure 7A, the term "cytokine-induced killer cells" experienced a research publication surge from 2013 to 2017, with a burst strength of 11.39, whereas "cik cells" followed a similar trend from 2012 to 2017, with a burst strength of 10.75. CIK cells have several attributes that make them a promising therapeutic avenue for cancer treatment, including the potent antitumor capabilities of T lymphocytes and the non-MHC-restricted tumoricidal activity characteristic of NK cells. The earliest research document we obtained featuring the terms "cytokine-induced killer cells" or "CIK" dates back to a 2006 study, which indicated that the total remission rate (CR + PR + MR) in the group treated with a combination of chemotherapy and CIK cells was higher than in the group treated with chemotherapy alone (56.3% *vs* 48.0%)[79]. A clinical trial in 2010 showed that GC patients treated with CIK cell adoptive immunotherapy combined with chemotherapy had a significantly longer survival time than those treated with chemotherapy alone (MST: 49 m *vs* 27 m, $P < 0.05$; 2- and 5-year survival rates: 73.5% *vs* 52.6%, 40.4% *vs* 23.9%, $P < 0.05$). Another report evaluated 11 studies proving that adjuvant immunotherapy with CIK cells may prevent recurrence and improve the quality of life and PFS rate in patients with cancer[80,81]. However, a recent meta-analysis revealed that the incorporation of cellular immunotherapy into chemotherapy resulted in a statistically significant improvement in OS and DFS only in patients with stage III GC[82].

Despite the significant anti-tumor effects demonstrated by CAR-T therapy across various iterations, numerous challenges remain in its widespread application. Future research in this area will likely concentrate on the development of more potent CAR-T-cells with enhanced anti-tumor activity and mitigated toxicity[83]. Despite the significant anti-tumor effects demonstrated by CAR-T therapy across various iterations, there are still numerous challenges to its widespread application. Future research in this area will likely concentrate on the development of more potent CAR-T-cells with enhanced anti-tumor activity and mitigated toxicity[84]. NK cells display high anti-tumor activity and antibody-dependent cytotoxicity. However, their therapeutic application is limited by the challenge of generating large quantities of highly pure and functional NK cells[7,85]. In contrast, immunotherapies involving CIK cells and TILs have a significant potential for cancer treatment. Our analysis shows that CIK cells exhibit potent anti-tumor activity, and that combination therapies incorporating CIK cells demonstrate improved efficacy in patients with GC. TILs immunotherapy has also been extensively used in advanced GC treatment[7]. TILs offer several key advantages, including lower off-target toxicity and increased specificity, making them superior in addressing tumor heterogeneity in comparison to other ACT therapies; they can also regulate the immune response by releasing cytokines, which subsequently bolster anti-tumor immunity [86]. Moreover, TIL levels are prognostic indicators[87].

ICIs: Clinical research on ICIs is the most advanced and widespread cancer immunotherapy. These inhibitors have shown notable efficacy in the treatment of various solid and hematological cancers, often leading to durable, long-lasting responses that are typically well tolerated by patients[88].

The interaction of PD-1 (also referred to as CD279) with PD-L1 (also denoted as CD274 or B7-H1) can induce T-cell dysfunction, exhaustion, and tolerance, thereby inhibiting the PD-1/PD-L1 and cytotoxic T lymphocyte-associated antigen-4 (CTLA-4, also known as CD152) signaling pathways, T-cell function can be rejuvenated, leading to an increase in the destruction of tumor cells[17,89]. Studies over the past 20 years have indicated that inhibiting PD-L1 can boost anti-tumor immunity[90-92]. In fact, it has been demonstrated that most patients with GAC express CTLA-4 on their tumor cells (CTLA-4 86.6%, PD-L1 44.9%) and those who tested negative for CTLA-4 or PD-L1 had a significantly better mean OS than those who tested positive (CTLA-4: 62.0 *vs* 44.4 mo, P = 0.018; PD-L1: 54.2 *vs* 39.1 mo, P = 0.011)[93]. Contrary to a previous study, another study demonstrated that the expression of PD-L1 was associated with improved DFS and OS in GC (PD-L1+ *vs* PD-L1- tumors: 5-year DFS rate, 82.6% *vs* 66.9%; 5-year OS rate, 83.0% *vs* 69.1%, $P < 0.05$)[94]. These contrasting findings could be due to differences in the ethnic backgrounds of the patients (Caucasians in the first study and Asians in the second) or variations in the antibodies used in each study, indicating the need for larger studies to

clarify the roles of PD-L1 and CTLA-4 in GC.

As of February 18, 2023, 274 clinical trials were registered at ClinicalTrials.gov and ICTRP, focusing on ICIs, which is a considerably larger number than those related to ACT and vaccine therapies (Figure 9C). The first clinical trials centered on ICIs began to emerge in 2013, and their counts saw a steady increase from 2015 to 2019, maintaining a high level over the last four years (Figure 8B). ICIs have received growing academic attention and have shown robust potential in GC immunotherapy. Some PD-1 inhibitors with relatively advanced research include avelumab, pembrolizumab, nivolumab, tislelizumab, camrelizumab, atezolizumab, and ipilimumab, function in combination with CTLA-4.

Published studies indicate that therapy using ICIs may present less toxicity, better tolerance than chemotherapy, and potentially superior outcomes. In trials with GC patients, avelumab did not outperform chemotherapy in terms of OS or RFS, but it did showcase a more manageable safety profile [grade ≥ 3 treatment-related adverse events (AEs): 9.2% *vs* 31.6% and 12.8% *vs* 32.8%, NCT02625623 and NCT02625610][95,96]. Pembrolizumab, which has undergone phase III clinical trials (NCT02370498 and NCT02494583), showed promising results; compared to chemotherapy, it demonstrated a trend toward improved OS and ORR while reducing the occurrence of treatment-related AEs[97,98].

In recent years, notable advances have been made in the combination of ICIs and chemotherapy. In patients with advanced GAC, the combination of tislelizumab and chemotherapy results in sustained responses and manageable side effects[99]. Similarly, a combination of Camrelizumab and CAPOX has demonstrated encouraging anti-tumor effects and manageable toxicity in patients with metastatic or advanced GAC, having successfully completed phase II clinical trials (NCT03469557 and NCT03472365)[100]. The effectiveness of ipilimumab in combination with chemotherapy has been assessed in both phase II and III clinical trials (NCT03241173 and NCT03126110, respectively).

The HER2, also known as Neu or ErbB2, is part of the epidermal growth factor receptors family, which encodes the transmembrane glycoprotein p185. It was initially discovered to have high expression in GC in 1986 and has since become a significant focus in translational cancer research due to its role in the HER2 signaling pathway[101,102]. For HER2-positive GCs, the preferred treatment regimen often includes a combination of pembrolizumab, trastuzumab, and chemotherapy[13]. A recent clinical trial (NCT03409848) demonstrated that combination therapy with trastuzumab, nivolumab, and FOLFOX was more effective than previous treatment protocols in treating HER2-positive esophagogastric adenocarcinoma[103].

Clinical trial

We screened 228 clinical trials on GC immunotherapy identified in a preliminary search and further analyzed 174 eligible clinical trials. There were 38 phase I clinical trials, 40 phase I/phase II clinical trials, 71 phase II clinical trials, three phase II/phase III clinical trials, four phase III clinical trials, and two phase IV clinical trials. For status, 25 clinical trials were completed: 20 were active but not recruited, 72 were recruited, 17 were not yet recruited, and the others were unknown or difficult to classify.

Completed trials: There are 25 completed clinical trials were completed, all of which were in phase I or II. After some immunotherapeutic drugs have proven effective, researchers have begun to explore the potential of multiple immunotherapy combinations.

Monoclonal antibodies (mAbs) are the predominant form of immunotherapy used to manage GC. The anticipated synergies arise primarily from the combination of anti-PD-1 and anti-CTLA-4 antibodies, a therapeutic pairing that has been extensively explored by numerous researchers, as indicated by associated clinical trials (NCT02340975, NCT02983045). Moreover, the inclusion of anti-HER2 antibodies in this treatment paradigm has also been investigated (NCT03409848). Beyond ICIs, other emergent forms of immunotherapy, such as ACT, have also been initiated in clinical trials. The completed trials included an array of treatment strategies. These include the integration of autologous DC-CIK cell immunotherapy with chemotherapy (NCT01783951), implementation of CAR-T immunotherapy (NCT02850536), and combination of NK cell therapy with ICIs (NCT03319459, NCT03841110). A phase II clinical trial (ChiCTR-OCH-12002610) investigating postoperative immunotherapies involving tumor lysate-loaded DCs, *in vitro* DC-activated T-cells, and activated T-cells in conjunction with chemotherapy demonstrated significantly improved mean survival rates in patients with operable colorectal cancer (59.74 ± 3.21 years *vs* 49.99 ± 2.54 years, $P = 0.034$), though its applicability to GC has not been substantiated with published results[104].

Trials active, not recruiting: Eighteen active clinical trials that completed recruitment primarily employed a therapeutic approach involving the synergistic use of multiple ICIs alongside chemotherapy, with notable targets, including PD-1/PD-L1, CTLA-4, HER2, and LAG3 (NCT03662659, NCT03647969, NCT03443856, NCT04062656). A phase I/II clinical trial (NCT03093688) preliminarily corroborated the tolerability of an immunotherapeutic approach based on invariant NK T cells and PD-1+CD8+ T-cells for lung adenocarcinoma, suggesting their potential applicability to other solid tumors[105].

Trails in recruiting: With 66 clinical trials currently recruiting, the discovery of novel cellular immunotherapeutic approaches continues to facilitate the development of increasingly effective immune cells, and consequently, the integration of more cellular immunotherapies into clinical trials.

Four clinical trials focused on peptide vaccines (NCT03784040, KCT0005481, NCT05269381, and NCT05311176), all of which implemented treatment regimens that incorporated a combination of vaccines and ICIs or the addition of chemotherapy. Notably, a phase II clinical trial was initiated to explore the potential of IMU-131, a B-cell peptide vaccine, in combination with anti-vascular endothelial growth factor receptor (VEGFR) and anti-PD-1 antibodies (NCT05311176).

Current research indicates that, although the combination of DC-CIK with S-1 does not yield a statistically significant advantage over S-1 in combination with cisplatin ($P = 0.892$), DC-CIK exhibit good tolerability, suggesting their potential as an alternative in cases where multi-agent chemotherapy is not tolerated[106]. Therefore, researchers continue to explore more efficacious cellular immunotherapies. T-cells stimulated by Claudin18.2 peptide demonstrate potent anti-

tumor activity and are emerging as a beacon of hope and a focal point of interest in the landscape of GC cellular immunotherapy, with corresponding clinical trials already underway (NCT04683939)[107].

Zanidatamab (ZW25) is an asymmetrically structured antibody that binds to two non-overlapping HER2 epitopes. A phase III clinical trial aims to examine the efficacy of ZW25 in combination with chemotherapy, both with and without tislelizumab, as a first-line treatment for patients with advanced or metastatic HER2-positive gastroesophageal adenocarcinomas (NCT05152147). Investigations involving ZW25 as a stand-alone treatment or in conjunction with chemotherapy or ICIs are ongoing. On May 29, 2019, the United States Food and Drug Administration (FDA) approved ZW25 as a first-line treatment in conjunction with standard-of-care chemotherapy for patients with HER2-overexpressing gastroesophageal adenocarcinoma[102]. ZW49, an antibody-drug conjugate (ADC) derivative of ZW25, utilizes the proprietary cytotoxic and cleavage adapters of the Zymework. A Phase I clinical trial (NCT03821233) is currently underway to explore the potential of ZW49 in patients with HER2-positive malignancies.

IL-2 is known for its ability to foster the growth of diverse immune cell populations, modulate cellular differentiation, and depending on the cellular milieu, either promote survival or induce apoptosis. Being the first cytokine to gain FDA approval for cancer treatment, IL-2's role in strategies that synergistically enhance immune responses is garnering increasing interest. Several clinical trials have investigated the synergistic use of interleukins with other treatments, including IL-2 combined with an anti-PD-1 antibody (NCT05086692), and AU-007 (interleukin antibodies) in conjunction with aldesleukin (NCT05267626). IL-15, which is similar to IL-2, is currently under investigation in a phase II clinical trial (NCT04847466) that examines the combination of N803 (an IL-15 agonist), pembrolizumab, and PD-L1 CAR NK cells. Additionally, an ongoing investigation involves a combination of KK-LC-1 TCR-T cells and aldesleukin (NCT05483491). However, no associated literature has been published on these trials. The future utility and progress of interleukins in cancer therapy warrants further investigation.

Trails not yet recruiting: Sixteen trials have not yet started recruitment, and most of them were phase II trials, with some phase I and III trials being planned. One or more ICIs combined with chemotherapy continue to be the most frequently studied, but some new treatment strategies are also being explored.

Research has demonstrated that the addition of anti-PD-1 antibodies to anti-HER2 antibodies and chemotherapy substantially diminishes tumor size and significantly enhances the ORR to 74.4%, as opposed to 51.9% without anti-PD-1 antibodies in HER2-positive GC[13]. In recent years, simultaneous blockade of PD-1 and HER2 has emerged as a significant area of research. Studies on VEGFR continue to progress. The anti-VEGFR2 antibody, ramucirumab, has demonstrated clinical efficacy in GC, both as a standalone therapy and in combination with chemotherapy[15]. Furthermore, clinical trials have been initiated to investigate the combination of anti-VEGFR and anti-PD-1 antibodies with and without chemotherapy (NCT05585580 and NCT05721651).

Olaparib, a PARP inhibitor approved for the treatment of ovarian cancer, is currently being explored for its potential clinical utility in GC. A phase I/II clinical trial (NCT04592211) has investigated the combination of olaparib, pembrolizumab, and paclitaxel in patients with GC. Over the past decades, 5-fluorouracil has remained a mainstay in the realm of chemotherapy. Recently, researchers have introduced NUC-3373, which has demonstrated a more favorable safety profile in patients[108]. A phase I/II clinical trial is currently centered on the use of NUC-3373 in conjunction with other agents in patients with advanced solid tumors, including GC (NCT05714553). IRAK4 can induce T cell dysfunction, making it a promising and novel target for immunotherapy[109]. A phase I clinical trial (NCT05187182) is currently investigating the use of CA-4948 (an IRAK4 inhibitor) combined with chemotherapy and ICIs for untreated unresectable gastric and esophageal cancer. A phase II clinical trial (NCT05671822) focusing on SHR-A1811 (an ADC drug targeting HER2 and TOP1) combined with SHR-1701 (a PD-L1 and TGFBR2 inhibitor) and chemotherapy in advanced HER2-positive GC is being conducted, which we believe will be significant.

The trends of clinical trials: (1) Discovering novel biomarkers to subclassify patients and exploring more specific treatment options. NCT05593419, ChiCTR2100052367, NCT02757391, NCT03158571; (2) Integration of immunotherapy with surgery, radiotherapy, and chemotherapy. NCT04688801, chemotherapy ± immunotherapy ± radiotherapy after surgery; (3) Transition from single-agent to multi-agent therapy. NCT05152147, trastuzumab (anti-HER2)/ZW25 (anti-HER2) ± tislelizumab (anti-PD-1) + chemotherapy; (4) Combination therapy involving various immunotherapies such as ICI, ADC, and ACT. NCT05269381, vaccine + pembrolizumab (anti-PD-1, ICI) + chemotherapy; NCT05671822, SHR-A1811 (HER2, ADC) + SHR-1701 (PD-L1 and transforming growth factor-β double antibody) + capecitabine + oxaliplatin; NCT05313906, RC48 (HER2, ADC) + AK105 (anti-PD-1) + cisplatin; (5) Discovery of new ICIs. NCT05187182, CA-4948(IRAK4/FLT3 inhibitor) + FOLFOX + PD-1 inhibitor ± trastuzumab (anti-HER2); NCT05714553, NUC-3373 (thymine synthase inhibitors) + leucovorin+ pembrolizumab/docetaxel.

Current status and future perspectives

Through this study, we have understood that: (1) Immunotherapy has become an important treatment modality for GC, representing the greatest advancement since chemotherapy and anti-HER2 therapy; (2) Immunotherapy has evolved from a sole focus on replacing chemotherapy to a concept of combined therapy; (3) Immunotherapy has developed from a simple pursuit of efficacy to one that balances efficacy and toxicity; and (4) Immunotherapy has progressed from the use of ICIs to the exploration of CAR-T therapy. For future research, we suggest: (1) Continued exploration of new targets; (2) Investigation into new prognostic and predictive biomarkers for immunotherapy, enabling individualized precision treatment; (3) Exploration of the optimal treatment modalities for immunotherapy in combination with ADC therapy; (4) Investigation into the application scenarios for immune therapy bispecific antibodies; and (5) Further development of CAR-T therapy targets and reduction of CAR-T therapy-related toxicities.

Currently, there are many limitations and challenges in GC immunotherapy research that need to be overcome in future studies. Firstly, GC is highly heterogeneous, both inter- and intratumorally. This variability affects the response to immunotherapeutic agents and poses challenges for identifying universal targets. Comprehensive genomic and transcriptomic analyses could identify reliable biomarkers and offer a more individualized treatment approach. Secondly, current biomarkers like PD-L1 expression, and MSI are not wholly predictive of the treatment response. So the development and validation of new biomarkers or a set of biomarkers are essential for better patient stratification and response prediction. Thirdly, immunotherapies have shown limited efficacy in the late stages of GC thus far. Combining immunotherapy with other treatment modalities such as chemotherapy or targeted therapy could potentially synergize to improve outcomes. Fourthly, the use of ICIs can lead to autoimmunity and other side effects. Therefore, developing methods for early identification and management of AEs is crucial, or discovering new lower toxic agents. Fifthly, the lack of clinically relevant animal models (*e.g.*, TIL, ACT, TME/TIME) for GC hampers the pre-clinical evaluation of immunotherapeutic strategies. The development of patient-derived xenograft models and organoids could enhance the translational potential of pre-clinical findings.

Trends in publications and significant breakthroughs: As presented in Figure 2A, discernible surges in both publications and citations characterize the years 2016-2017 and 2020, with a pronounced resurgence beginning in 2020. These periods align with seminal studies and landmark events in the field. For instance, a 2015 meta-analysis reported that PD-L1 overexpression was correlated with adverse prognoses in solid tumors[110]. Furthermore, in 2016, a distinguished trial (NCT02447003) examining the antitumor efficacy and safety of pembrolizumab amassed 1298 citations, culminating in the FDA's subsequent approval for HER2-positive GC treatment on May 5, 2021[28,48]. Post-2020, propelled by technological advancements, breakthroughs such as the use of single-cell RNA sequencing in GC cells and transcriptome analysis of peritoneal cancer samples from patients with GAC have emerged, enriching our understanding of tumor biology and uncovering novel immunotherapy targets[111,112]. Notably, EBV-positive status has been identified as a potential biomarker for EBV-associated GC, paving the way for future studies[113].

Evolving clinical trial landscape: With only ten phase III or IV clinical trials and 113 in either the recruiting stage or yet to commence (Figures 9A and B), immunotherapy application in GC is rapidly evolving and requires for further investigation. Analysis of ongoing trials portends emerging directions in the field, emphasizing the continuance of surgery, chemotherapy, and radiotherapy as foundational modalities, supplemented by significant advancements in targeted therapy and immunotherapy[12,114].

Monotherapy and combination therapies: The current therapeutic armamentarium includes monotherapies with ICIs and combination regimens that demonstrate efficacy against solid tumors, including GC. Specifically, ICIs have become prevalent in the treatment of advanced GC, with all analyzed phase III and IV trials incorporating anti-PD-1 antibodies, highlighting this avenue as a focal research point[114].

Anticipated future developments: Concurrently, advancements in anti-HER2 and anti-VEGFR therapies are steadily progressing, with research anticipated to encompass a wide spectrum, including ICI monotherapies, various ICI combinations, and integration with ADCs. ADCs, which bridge the specificity of mAbs with the potency of cytotoxic agents, hold immense potential as therapeutic modalities for GC, with ongoing trials investigating their synergistic application with chemotherapy. These collective developments indicate a well-defined direction for future research, affirming a promising era for immunotherapy in the field of GC.

CONCLUSION

In conclusion, this study delineates a clear trajectory in GC therapy, from the present use of monotherapies and chemo/target therapy to future integrative and combinatorial approaches, with CAR-T technologies at the forefront. It encapsulates the potential for enhanced therapeutic paradigms and heralds a new era of precision medicine for GC treatment. The findings presented here highlight substantial progress as well as pinpoint the direction for continued research and clinical innovation, aligning with the rigorous academic standards of premier oncological journals.

Strengths and limitations

Strengths: This study offers systematic and specialized insights into the treatment and current status of GC by merging published literature with clinical research. By comprehensively articulating GC immunotherapy, readers can decode this complex subject into multiple dimensions. This inclusive approach synthesizes the current understanding and offers a valuable reference for future investigations, thereby enriching the collective knowledge of this field.

Limitations: Literature selection: Although extensive literature related to immunotherapy for GC was included, enabling comprehensive and objective conclusions, our search was restricted to articles and reviews within the WoSCC, using limited terms. Although this strategy emphasizes high-impact data, potentially enhancing the accuracy of our analysis, it may also lead to incomplete literature retrieval. Time constraints: Conducted in early 2023, our literature review spans from 1999 to the present, imposing time limitations that may create delays in reflecting the most recent advancements. Citation bias: Newly published critical research findings may lack substantial citation numbers, thereby obscuring their value in our data analysis.

In summary, the strengths of this study lie in its systematic and specialized approach, providing a multidimensional understanding of GC immunotherapy, whereas the limitations primarily pertain to literature selection, temporal

boundaries, and potential citation bias. These factors must be considered when interpreting the findings and their implications for future research and clinical practice.

ARTICLE HIGHLIGHTS

Research background

Gastric cancer (GC) ranks sixth in incidence among all cancers, and is the third leading cause of cancer-related deaths worldwide. However, there are significant limitations to the treatment of GC, and more effective and less toxic treatment options are required to prolong the survival of patients with GC. Immunotherapy has recently shown rapid development for the treatment of GC and has great potential.

Research motivation

In recent years, scientometrics has been applied to analyze literature related to certain fields to identify hotspots and predict future trends. However, to the best of our knowledge, there have been no previous studies on scientometric analyses in the field of GC immunotherapy.

Research objectives

To present a comprehensive review of the knowledge framework and research hotspots in the field of GC immunotherapy, we aimed to assist scholars in promptly understanding the current research status and latest developments in this field and provide new ideas and directions for future studies.

Research methods

Publications related to GC immunotherapy between 1999 and 2023 were retrieved from the Web of Science Core Collection database on February 1, 2023. An analysis of the 2013 relevant articles retrieved using CiteSpace and VOSviewer was conducted. We get Impact Index Per Article from *Reference Citation Analysis* (*RCA*). Additionally, we searched for clinical trials on ClinicalTrials.gov and the International Clinical Trials Registry Platform, and analyzed ongoing clinical trials in this field to predict future developmental trends.

Research results

Through a literature search, we included 2013 relevant articles in this study and used the scientometric software CiteSpace and VOSviewer to analyze 11730 authors, 617 institutions, 71 countries, 726 keywords, citations, and the emergence and timeline of certain information. We have provided specific explanations for the main keywords and analyzed the significance of these research hotspots, including "tumor microenvironment", "microsatellite instability", "mismatch repair deficiency", "dendritic cells", and "adoptive immunotherapy". Because immune checkpoint inhibitors (ICIs) play an important role in GC immunotherapy, we have also provided a separate discussion on them. Additionally, we classified the retrieved clinical trials based on the type of immunotherapy and stage of disease and further analyzed the research hotspots and trends in this field in the coming years. The integration of literature and clinical trials has enabled the production of comprehensive and objective research findings.

Research conclusions

Through the use of novel research methods, ideas, and software, we gained innovative and comprehensive insights into the current status and future trends in GC immunotherapy. Our research findings summarize the current state of development in this field and facilitate understanding and learning among scholars. Additionally, this article identifies future developmental directions and trends in this field and provides scientific research ideas for researchers to promote the development of GC immunotherapy.

Research perspectives

Burst keywords and clusters, including tumor microenvironment, microsatellite instability, mismatch repair deficiency, dendritic cells, and adoptive immunotherapy represent the current frontiers of research on immunological factors in cirrhosis. ICIs have also been studied. The combination of multiple drugs and immunotherapeutic methods has received increasing attention.

FOOTNOTES

Author contributions: Wang H and Guo R conceived the study and critically revised the manuscript; Li YN designed the study, performed statistical analyses, and drafted the manuscript; Xie B, Zhang Y, He MH, Mu DM, and Wang H designed the study and wrote the manuscript; Li YN, Guo R, and Wang H performed article retrieval and data interpretation; Mu DM conducted statistical assessment; and all the authors have read and agreed to the final version of the manuscript.

Supported by Natural Science Foundation of China, No. 81500116 and 81601449; and Jilin Science and Technique, No. 20200201472JC and YDZJ202301ZYTS092.

Conflict-of-interest statement: All the authors report no relevant conflicts of interest for this article.

PRISMA 2009 Checklist statement: The authors have read the PRISMA 2009 Checklist, and the manuscript was prepared and revised according to the PRISMA 2009 Checklist.

Open-Access: This article is an open-access article that was selected by an in-house editor and fully peer-reviewed by external reviewers. It is distributed in accordance with the Creative Commons Attribution NonCommercial (CC BY-NC 4.0) license, which permits others to distribute, remix, adapt, build upon this work non-commercially, and license their derivative works on different terms, provided the original work is properly cited and the use is non-commercial. See: https://creativecommons.org/Licenses/by-nc/4.0/

Country/Territory of origin: China

ORCID number: Yao-Nan Li 0009-0000-7864-6408; Bin Xie 0009-0001-5859-3289; Ying Zhang 0009-0000-1250-8918; Ming-Hua He 0000-0003-4439-9810; Yang Xing 0000-0001-5541-8832; Dong-Mei Mu 0000-0003-1457-303X; Hong Wang 0000-0003-0212-5379; Rui Guo 0009-0001-5756-4806.

S-Editor: Wang JJ
L-Editor: A
P-Editor: Chen YX

REFERENCES

1 **Chhikara BS**, Parang K. Global Cancer Statistics 2022: the trends projection analysis. *Chem Biol Lett* 2023; **10**: 451
2 **Sung H**, Ferlay J, Siegel RL, Laversanne M, Soerjomataram I, Jemal A, Bray F. Global Cancer Statistics 2020: GLOBOCAN Estimates of Incidence and Mortality Worldwide for 36 Cancers in 185 Countries. *CA Cancer J Clin* 2021; **71**: 209-249 [PMID: 33538338 DOI: 10.3322/caac.21660]
3 **Ferro A**, Peleteiro B, Malvezzi M, Bosetti C, Bertuccio P, Levi F, Negri E, La Vecchia C, Lunet N. Worldwide trends in gastric cancer mortality (1980-2011), with predictions to 2015, and incidence by subtype. *Eur J Cancer* 2014; **50**: 1330-1344 [PMID: 24650579 DOI: 10.1016/j.ejca.2014.01.029]
4 **Machlowska J**, Baj J, Sitarz M, Maciejewski R, Sitarz R. Gastric Cancer: Epidemiology, Risk Factors, Classification, Genomic Characteristics and Treatment Strategies. *Int J Mol Sci* 2020; **21** [PMID: 32512697 DOI: 10.3390/ijms21114012]
5 **Cristescu R**, Lee J, Nebozhyn M, Kim KM, Ting JC, Wong SS, Liu J, Yue YG, Wang J, Yu K, Ye XS, Do IG, Liu S, Gong L, Fu J, Jin JG, Choi MG, Sohn TS, Lee JH, Bae JM, Kim ST, Park SH, Sohn I, Jung SH, Tan P, Chen R, Hardwick J, Kang WK, Ayers M, Hongyue D, Reinhard C, Loboda A, Kim S, Aggarwal A. Molecular analysis of gastric cancer identifies subtypes associated with distinct clinical outcomes. *Nat Med* 2015; **21**: 449-456 [PMID: 25894828 DOI: 10.1038/nm.3850]
6 **Högner A**, Moehler M. Immunotherapy in Gastric Cancer. *Curr Oncol* 2022; **29**: 1559-1574 [PMID: 35323331 DOI: 10.3390/curroncol29030131]
7 **Jin X**, Liu Z, Yang D, Yin K, Chang X. Recent Progress and Future Perspectives of Immunotherapy in Advanced Gastric Cancer. *Front Immunol* 2022; **13**: 948647 [PMID: 35844558 DOI: 10.3389/fimmu.2022.948647]
8 **Li K**, Zhang A, Li X, Zhang H, Zhao L. Advances in clinical immunotherapy for gastric cancer. *Biochim Biophys Acta Rev Cancer* 2021; **1876**: 188615 [PMID: 34403771 DOI: 10.1016/j.bbcan.2021.188615]
9 **Charalampakis N**, Economopoulou P, Kotsantis I, Tolia M, Schizas D, Liakakos T, Elimova E, Ajani JA, Psyrri A. Medical management of gastric cancer: a 2017 update. *Cancer Med* 2018; **7**: 123-133 [PMID: 29239137 DOI: 10.1002/cam4.1274]
10 **Morgan RA**, Chinnasamy N, Abate-Daga D, Gros A, Robbins PF, Zheng Z, Dudley ME, Feldman SA, Yang JC, Sherry RM, Phan GQ, Hughes MS, Kammula US, Miller AD, Hessman CJ, Stewart AA, Restifo NP, Quezado MM, Alimchandani M, Rosenberg AZ, Nath A, Wang T, Bielekova B, Wuest SC, Akula N, McMahon FJ, Wilde S, Mosetter B, Schendel DJ, Laurencot CM, Rosenberg SA. Cancer regression and neurological toxicity following anti-MAGE-A3 TCR gene therapy. *J Immunother* 2013; **36**: 133-151 [PMID: 23377668 DOI: 10.1097/CJI.0b013e3182829903]
11 **Long B**, Qin L, Zhang B, Li Q, Wang L, Jiang X, Ye H, Zhang G, Yu Z, Jiao Z. CAR Tcell therapy for gastric cancer: Potential and perspective (Review). *Int J Oncol* 2020; **56**: 889-899 [PMID: 32319561 DOI: 10.3892/ijo.2020.4982]
12 **Kumar AR**, Devan AR, Nair B, Vinod BS, Nath LR. Harnessing the immune system against cancer: current immunotherapy approaches and therapeutic targets. *Mol Biol Rep* 2021; **48**: 8075-8095 [PMID: 34671902 DOI: 10.1007/s11033-021-06752-9]
13 **Janjigian YY**, Kawazoe A, Yañez P, Li N, Lonardi S, Kolesnik O, Barajas O, Bai Y, Shen L, Tang Y, Wyrwicz LS, Xu J, Shitara K, Qin S, Van Cutsem E, Tabernero J, Li L, Shah S, Bhagia P, Chung HC. The KEYNOTE-811 trial of dual PD-1 and HER2 blockade in HER2-positive gastric cancer. *Nature* 2021; **600**: 727-730 [PMID: 34912120 DOI: 10.1038/s41586-021-04161-3]
14 **Janjigian YY**, Shitara K, Moehler M, Garrido M, Salman P, Shen L, Wyrwicz L, Yamaguchi K, Skoczylas T, Campos Bragagnoli A, Liu T, Schenker M, Yanez P, Tehfe M, Kowalyszyn R, Karamouzis MV, Bruges R, Zander T, Pazo-Cid R, Hitre E, Feeney K, Cleary JM, Poulart V, Cullen D, Lei M, Xiao H, Kondo K, Li M, Ajani JA. First-line nivolumab plus chemotherapy versus chemotherapy alone for advanced gastric, gastro-oesophageal junction, and oesophageal adenocarcinoma (CheckMate 649): a randomised, open-label, phase 3 trial. *Lancet* 2021; **398**: 27-40 [PMID: 34102137 DOI: 10.1016/S0140-6736(21)00797-2]
15 **Smyth EC**, Nilsson M, Grabsch HI, van Grieken NC, Lordick F. Gastric cancer. *Lancet* 2020; **396**: 635-648 [PMID: 32861308 DOI: 10.1016/S0140-6736(20)31288-5]
16 **Sato H**, Okonogi N, Nakano T. Rationale of combination of anti-PD-1/PD-L1 antibody therapy and radiotherapy for cancer treatment. *Int J Clin Oncol* 2020; **25**: 801-809 [PMID: 32246277 DOI: 10.1007/s10147-020-01666-1]
17 **Zeng Z**, Yang B, Liao Z. Progress and prospects of immune checkpoint inhibitors in advanced gastric cancer. *Future Oncol* 2021; **17**: 1553-1569 [PMID: 33397136 DOI: 10.2217/fon-2020-0829]

18 **Bang YJ**, Van Cutsem E, Feyereislova A, Chung HC, Shen L, Sawaki A, Lordick F, Ohtsu A, Omuro Y, Satoh T, Aprile G, Kulikov E, Hill J, Lehle M, Rüschoff J, Kang YK; ToGA Trial Investigators. Trastuzumab in combination with chemotherapy versus chemotherapy alone for treatment of HER2-positive advanced gastric or gastro-oesophageal junction cancer (ToGA): a phase 3, open-label, randomised controlled trial. *Lancet* 2010; **376**: 687-697 [PMID: 20728210 DOI: 10.1016/S0140-6736(10)61121-X]

19 **Shah MA**, Kennedy EB, Alarcon-Rozas AE, Alcindor T, Bartley AN, Malowany AB, Bhadkamkar NA, Deighton DC, Janjigian Y, Karippot A, Khan U, King DA, Klute K, Lacy J, Lee JJ, Mehta R, Mukherjee S, Nagarajan A, Park H, Saeed A, Semrad TJ, Shitara K, Smyth E, Uboha NV, Vincelli M, Wainberg Z, Rajdev L. Immunotherapy and Targeted Therapy for Advanced Gastroesophageal Cancer: ASCO Guideline. *J Clin Oncol* 2023; **41**: 1470-1491 [PMID: 36603169 DOI: 10.1200/JCO.22.02331]

20 **Sato Y**, Okamoto K, Kida Y, Mitsui Y, Kawano Y, Sogabe M, Miyamoto H, Takayama T. Overview of Chemotherapy for Gastric Cancer. *J Clin Med* 2023; **12** [PMID: 36835872 DOI: 10.3390/jcm12041336]

21 **Ding X**, Wang X, Li B, Wang L, Guo H, Shang L, Huang W, Wu L, Ke B, Liu Y, Liu N, Wang B, Cai M, Deng J, Zhang R, Zhang J, Chai J, Zhao Q, Li L, Liang H. PERSIST: A multicenter, randomized phase II trial of perioperative oxaliplatin and S-1 (SOX) with or without sintilimab in resectable locally advanced gastric/gastroesophageal junction cancer (GC/GEJC). *J Clin Oncol* 2023; **41**: 364-364 [DOI: 10.1200/JCO.2023.41.4_suppl.364]

22 **Kim HD**, Ryu MH, Park YS, Lee JS, Kang YK. A phase 2 study of durvalumab plus DOS (docetaxel, oxaliplatin, S-1) neoadjuvant chemotherapy followed by surgery and adjuvant durvalumab plus S-1 chemotherapy in patients with resectable locally advanced gastric cancer: An interim efficacy report. *J Clin Oncol* 2023; **41**: 408-408 [DOI: 10.1200/JCO.2023.41.4_suppl.408]

23 **Pietrantonio F**, Raimondi A, Lonardi S, Murgioni S, Cardellino GG, Tamberi S, Strippoli A, Palermo F, Prisciandaro M, Randon G, Corti F, Bergamo F, Nappo F, Leone AG, Leoncini G, Sabella G, Kaneva K, Sposito C, Bartolomeo MD, Mazzaferro V. INFINITY: A multicentre, single-arm, multi-cohort, phase II trial of tremelimumab and durvalumab as neoadjuvant treatment of patients with microsatellite instability-high (MSI) resectable gastric or gastroesophageal junction adenocarcinoma (GAC/GEJAC). *J Clin Oncol* 2023; **41**: 358-358 [DOI: 10.1200/JCO.2023.41.4_suppl.358]

24 **Sur D**, Lungulescu C, Puscariu II, Volovat SR, Preda M, Mateianu EA, Lungulescu CV. Immunotherapy-Related Publications in Colorectal Cancer: A Bibliometric Analysis. *Healthcare (Basel)* 2021; **10** [PMID: 35052239 DOI: 10.3390/healthcare10010075]

25 **Brahmer JR**, Tykodi SS, Chow LQ, Hwu WJ, Topalian SL, Hwu P, Drake CG, Camacho LH, Kauh J, Odunsi K, Pitot HC, Hamid O, Bhatia S, Martins R, Eaton K, Chen S, Salay TM, Alaparthy S, Grosso JF, Korman AJ, Parker SM, Agrawal S, Goldberg SM, Pardoll DM, Gupta A, Wigginton JM. Safety and activity of anti-PD-L1 antibody in patients with advanced cancer. *N Engl J Med* 2012; **366**: 2455-2465 [PMID: 22658128 DOI: 10.1056/NEJMoa1200694]

26 **Wang X**, Teng F, Kong L, Yu J. PD-L1 expression in human cancers and its association with clinical outcomes. *Onco Targets Ther* 2016; **9**: 5023-5039 [PMID: 27574444 DOI: 10.2147/OTT.S105862]

27 **Kamada T**, Togashi Y, Tay C, Ha D, Sasaki A, Nakamura Y, Sato E, Fukuoka S, Tada Y, Tanaka A, Morikawa H, Kawazoe A, Kinoshita T, Shitara K, Sakaguchi S, Nishikawa H. PD-1(+) regulatory T cells amplified by PD-1 blockade promote hyperprogression of cancer. *Proc Natl Acad Sci U S A* 2019; **116**: 9999-10008 [PMID: 31028147 DOI: 10.1073/pnas.1822001116]

28 **Nanda R**, Chow LQ, Dees EC, Berger R, Gupta S, Geva R, Pusztai L, Pathiraja K, Aktan G, Cheng JD, Karantza V, Buisseret L. Pembrolizumab in Patients With Advanced Triple-Negative Breast Cancer: Phase Ib KEYNOTE-012 Study. *J Clin Oncol* 2016; **34**: 2460-2467 [PMID: 27138582 DOI: 10.1200/JCO.2015.64.8931]

29 **Qiu H**, Cao S, Xu R. Cancer incidence, mortality, and burden in China: a time-trend analysis and comparison with the United States and United Kingdom based on the global epidemiological data released in 2020. *Cancer Commun (Lond)* 2021; **41**: 1037-1048 [PMID: 34288593 DOI: 10.1002/cac2.12197]

30 **Oba K**, Kobayashi M, Matsui T, Kodera Y, Sakamoto J. Individual patient based meta-analysis of lentinan for unresectable/recurrent gastric cancer. *Anticancer Res* 2009; **29**: 2739-2745 [PMID: 19596954]

31 **Oba K**, Teramukai S, Kobayashi M, Matsui T, Kodera Y, Sakamoto J. Efficacy of adjuvant immunochemotherapy with polysaccharide K for patients with curative resections of gastric cancer. *Cancer Immunol Immunother* 2007; **56**: 905-911 [PMID: 17106715 DOI: 10.1007/s00262-006-0248-1]

32 **Oba MS**, Teramukai S, Ohashi Y, Ogawa K, Maehara Y, Sakamoto J. The efficacy of adjuvant immunochemotherapy with OK-432 after curative resection of gastric cancer: an individual patient data meta-analysis of randomized controlled trials. *Gastric Cancer* 2016; **19**: 616-624 [PMID: 25804300 DOI: 10.1007/s10120-015-0489-9]

33 **Qiu H**. Safety and efficacy of toripalimab in advanced gastric cancer: A new clinical trial bringing hope for immunotherapy in gastric cancer. *Cancer Commun (Lond)* 2020; **40**: 194-196 [PMID: 32277740 DOI: 10.1002/cac2.12019]

34 **Fuchs CS**, Doi T, Jang RW, Muro K, Satoh T, Machado M, Sun W, Jalal SI, Shah MA, Metges JP, Garrido M, Golan T, Mandala M, Wainberg ZA, Catenacci DV, Ohtsu A, Shitara K, Geva R, Bleeker J, Ko AH, Ku G, Philip P, Enzinger PC, Bang YJ, Levitan D, Wang J, Rosales M, Dalal RP, Yoon HH. Safety and Efficacy of Pembrolizumab Monotherapy in Patients With Previously Treated Advanced Gastric and Gastroesophageal Junction Cancer: Phase 2 Clinical KEYNOTE-059 Trial. *JAMA Oncol* 2018; **4**: e180013 [PMID: 29543932 DOI: 10.1001/jamaoncol.2018.0013]

35 **Wang F**, Wei XL, Wang FH, Xu N, Shen L, Dai GH, Yuan XL, Chen Y, Yang SJ, Shi JH, Hu XC, Lin XY, Zhang QY, Feng JF, Ba Y, Liu YP, Li W, Shu YQ, Jiang Y, Li Q, Wang JW, Wu H, Feng H, Yao S, Xu RH. Safety, efficacy and tumor mutational burden as a biomarker of overall survival benefit in chemo-refractory gastric cancer treated with toripalimab, a PD-1 antibody in phase Ib/II clinical trial NCT02915432. *Ann Oncol* 2019; **30**: 1479-1486 [PMID: 31236579 DOI: 10.1093/annonc/mdz197]

36 **Liu Y**, Li C, Lu Y, Liu C, Yang W. Tumor microenvironment-mediated immune tolerance in development and treatment of gastric cancer. *Front Immunol* 2022; **13**: 1016817 [PMID: 36341377 DOI: 10.3389/fimmu.2022.1016817]

37 **Gambardella V**, Castillo J, Tarazona N, Gimeno-Valiente F, Martínez-Ciarpaglini C, Cabeza-Segura M, Roselló S, Roda D, Huerta M, Cervantes A, Fleitas T. The role of tumor-associated macrophages in gastric cancer development and their potential as a therapeutic target. *Cancer Treat Rev* 2020; **86**: 102015 [PMID: 32248000 DOI: 10.1016/j.ctrv.2020.102015]

38 **Zhou J**, Tang Z, Gao S, Li C, Feng Y, Zhou X. Tumor-Associated Macrophages: Recent Insights and Therapies. *Front Oncol* 2020; **10**: 188 [PMID: 32161718 DOI: 10.3389/fonc.2020.00188]

39 **Zhang B**, Wu Q, Li B, Wang D, Wang L, Zhou YL. m(6)A regulator-mediated methylation modification patterns and tumor microenvironment infiltration characterization in gastric cancer. *Mol Cancer* 2020; **19**: 53 [PMID: 32164750 DOI: 10.1186/s12943-020-01170-0]

40 **Tsuchiya K**. Switching from Apoptosis to Pyroptosis: Gasdermin-Elicited Inflammation and Antitumor Immunity. *Int J Mol Sci* 2021; **22** [PMID: 33406603 DOI: 10.3390/ijms22010426]

41 **Jiang Y**, Xie J, Huang W, Chen H, Xi S, Han Z, Huang L, Lin T, Zhao LY, Hu YF, Yu J, Cai SR, Li T, Li G. Tumor Immune Microenvironment and Chemosensitivity Signature for Predicting Response to Chemotherapy in Gastric Cancer. *Cancer Immunol Res* 2019; **7**: 2065-2073 [PMID: 31615816 DOI: 10.1158/2326-6066.CIR-19-0311]

42 **Farmkiss L**, Hopkins I, Jones M. Idylla microsatellite instability assay versus mismatch repair immunohistochemistry: a retrospective comparison in gastric adenocarcinoma. *J Clin Pathol* 2021; **74**: 604-607 [PMID: 33020177 DOI: 10.1136/jclinpath-2020-207033]

43 **Colle R**, Cohen R, Cochereau D, Duval A, Lascols O, Lopez-Trabada D, Afchain P, Trouilloud I, Parc Y, Lefevre JH, Fléjou JF, Svrcek M, André T. Immunotherapy and patients treated for cancer with microsatellite instability. *Bull Cancer* 2017; **104**: 42-51 [PMID: 27979364 DOI: 10.1016/j.bulcan.2016.11.006]

44 **Giampieri R**, Maccaroni E, Mandolesi A, Del Prete M, Andrikou K, Faloppi L, Bittoni A, Bianconi M, Scarpelli M, Bracci R, Scartozzi M, Cascinu S. Mismatch repair deficiency may affect clinical outcome through immune response activation in metastatic gastric cancer patients receiving first-line chemotherapy. *Gastric Cancer* 2017; **20**: 156-163 [PMID: 26796888 DOI: 10.1007/s10120-016-0594-4]

45 **Ratti M**, Lampis A, Hahne JC, Passalacqua R, Valeri N. Microsatellite instability in gastric cancer: molecular bases, clinical perspectives, and new treatment approaches. *Cell Mol Life Sci* 2018; **75**: 4151-4162 [PMID: 30173350 DOI: 10.1007/s00018-018-2906-9]

46 **Janjigian YY**, Sanchez-Vega F, Jonsson P, Chatila WK, Hechtman JF, Ku GY, Riches JC, Tuvy Y, Kundra R, Bouvier N, Vakiani E, Gao J, Heins ZJ, Gross BE, Kelsen DP, Zhang L, Strong VE, Schattner M, Gerdes H, Coit DG, Bains M, Stadler ZK, Rusch VW, Jones DR, Molena D, Shia J, Robson ME, Capanu M, Middha S, Zehir A, Hyman DM, Scaltriti M, Ladanyi M, Rosen N, Ilson DH, Berger MF, Tang L, Taylor BS, Solit DB, Schultz N. Genetic Predictors of Response to Systemic Therapy in Esophagogastric Cancer. *Cancer Discov* 2018; **8**: 49-58 [PMID: 29122777 DOI: 10.1158/2159-8290.CD-17-0787]

47 **Janjigian YY**, Bendell J, Calvo E, Kim JW, Ascierto PA, Sharma P, Ott PA, Peltola K, Jaeger D, Evans J, de Braud F, Chau I, Harbison CT, Dorange C, Tschaika M, Le DT. CheckMate-032 Study: Efficacy and Safety of Nivolumab and Nivolumab Plus Ipilimumab in Patients With Metastatic Esophagogastric Cancer. *J Clin Oncol* 2018; **36**: 2836-2844 [PMID: 30110194 DOI: 10.1200/JCO.2017.76.6212]

48 **Joshi SS**, Badgwell BD. Current treatment and recent progress in gastric cancer. *CA Cancer J Clin* 2021; **71**: 264-279 [PMID: 33592120 DOI: 10.3322/caac.21657]

49 **Guo Z**, Yuan Y, Chen C, Lin J, Ma Q, Liu G, Gao Y, Huang Y, Chen L, Chen LZ, Huang YF, Wang H, Li B, Chen Y, Zhang X. Durable complete response to neoantigen-loaded dendritic-cell vaccine following anti-PD-1 therapy in metastatic gastric cancer. *NPJ Precis Oncol* 2022; **6**: 34 [PMID: 35661819 DOI: 10.1038/s41698-022-00279-3]

50 **Faghfuri E**, Shadbad MA, Faghfouri AH, Soozangar N. Cellular immunotherapy in gastric cancer: adoptive cell therapy and dendritic cell-based vaccination. *Immunotherapy* 2022; **14**: 475-488 [PMID: 35232264 DOI: 10.2217/imt-2021-0285]

51 **Inaba K**, Metlay JP, Crowley MT, Steinman RM. Dendritic cells pulsed with protein antigens in vitro can prime antigen-specific, MHC-restricted T cells in situ. *J Exp Med* 1990; **172**: 631-640 [PMID: 2373994 DOI: 10.1084/jem.172.2.631]

52 **Yu Z**, Restifo NP. Cancer vaccines: progress reveals new complexities. *J Clin Invest* 2002; **110**: 289-294 [PMID: 12163445 DOI: 10.1172/jci16216]

53 **Ohshita A**, Yamaguchi Y, Minami K, Okita R, Toge T. Generation of tumor-reactive effector lymphocytes using tumor RNA-introduced dendritic cells in gastric cancer patients. *Int J Oncol* 2006; **28**: 1163-1171 [PMID: 16596232]

54 **Zhang K**, Gao PF, Yu PW, Rao Y, Zhou LX. Study on biological characters of SGC7901 gastric cancer cell-dendritic cell fusion vaccines. *World J Gastroenterol* 2006; **12**: 3438-3441 [PMID: 16733866 DOI: 10.3748/wjg.v12.i21.3438]

55 **Xue G**, Cheng Y, Ran F, Li X, Huang T, Yang Y, Zhang Y. SLC gene-modified dendritic cells mediate T cell-dependent anti-gastric cancer immune responses in vitro. *Oncol Rep* 2013; **29**: 595-604 [PMID: 23229068 DOI: 10.3892/or.2012.2154]

56 **Mu Y**, Wang WH, Xie JP, Zhang YX, Yang YP, Zhou CH. Efficacy and safety of cord blood-derived dendritic cells plus cytokine-induced killer cells combined with chemotherapy in the treatment of patients with advanced gastric cancer: a randomized Phase II study. *Onco Targets Ther* 2016; **9**: 4617-4627 [PMID: 27524915 DOI: 10.2147/OTT.S107745]

57 **Park R**, Williamson S, Kasi A, Saeed A. Immune Therapeutics in the Treatment of Advanced Gastric and Esophageal Cancer. *Anticancer Res* 2018; **38**: 5569-5580 [PMID: 30275174 DOI: 10.21873/anticanres.12891]

58 **Fucikova J**, Hensler M, Kasikova L, Lanickova T, Pasulka J, Rakova J, Drozenova J, Fredriksen T, Hraska M, Hrnciarova T, Sochorova K, Rozkova D, Sojka L, Dundr P, Laco J, Brtnicky T, Praznovec I, Halaska MJ, Rob L, Ryska A, Coosemans A, Vergote I, Cibula D, Bartunkova J, Galon J, Galluzzi L, Spisek R. An Autologous Dendritic Cell Vaccine Promotes Anticancer Immunity in Patients with Ovarian Cancer with Low Mutational Burden and Cold Tumors. *Clin Cancer Res* 2022; **28**: 3053-3065 [PMID: 35536547 DOI: 10.1158/1078-0432.CCR-21-4413]

59 **Fridman WH**, Pagès F, Sautès-Fridman C, Galon J. The immune contexture in human tumours: impact on clinical outcome. *Nat Rev Cancer* 2012; **12**: 298-306 [PMID: 22419253 DOI: 10.1038/nrc3245]

60 **Yu W**, Wang S, Rong Q, Ajayi OE, Hu K, Wu Q. Profiling the Tumor-Infiltrating Lymphocytes in Gastric Cancer Reveals Its Implication in the Prognosis. *Genes (Basel)* 2022; **13** [PMID: 35741779 DOI: 10.3390/genes13061017]

61 **Cho J**, Chang YH, Heo YJ, Kim S, Kim NK, Park JO, Kang WK, Lee J, Kim KM. Four distinct immune microenvironment subtypes in gastric adenocarcinoma with special reference to microsatellite instability. *ESMO Open* 2018; **3**: e000326 [PMID: 29636988 DOI: 10.1136/esmoopen-2018-000326]

62 **Chen LJ**, Zheng X, Shen YP, Zhu YB, Li Q, Chen J, Xia R, Zhou SM, Wu CP, Zhang XG, Lu BF, Jiang JT. Higher numbers of T-bet(+) intratumoral lymphoid cells correlate with better survival in gastric cancer. *Cancer Immunol Immunother* 2013; **62**: 553-561 [PMID: 23090288 DOI: 10.1007/s00262-012-1358-6]

63 **Mandriani B**, Pelle' E, Pezzicoli G, Strosberg J, Abate-Daga D, Guarini A, Cives M, Porta C. Adoptive T-cell immunotherapy in digestive tract malignancies: Current challenges and future perspectives. *Cancer Treat Rev* 2021; **100**: 102288 [PMID: 34525422 DOI: 10.1016/j.ctrv.2021.102288]

64 **Parkhurst MR**, Yang JC, Langan RC, Dudley ME, Nathan DA, Feldman SA, Davis JL, Morgan RA, Merino MJ, Sherry RM, Hughes MS, Kammula US, Phan GQ, Lim RM, Wank SA, Restifo NP, Robbins PF, Laurencot CM, Rosenberg SA. T cells targeting carcinoembryonic antigen can mediate regression of metastatic colorectal cancer but induce severe transient colitis. *Mol Ther* 2011; **19**: 620-626 [PMID: 21157437 DOI: 10.1038/mt.2010.272]

65 **D'Angelo SP**, Melchiori L, Merchant MS, Bernstein D, Glod J, Kaplan R, Grupp S, Tap WD, Chagin K, Binder GK, Basu S, Lowther DE, Wang R, Bath N, Tipping A, Betts G, Ramachandran I, Navenot JM, Zhang H, Wells DK, Van Winkle E, Kari G, Trivedi T, Holdich T, Pandite L, Amado R, Mackall CL. Antitumor Activity Associated with Prolonged Persistence of Adoptively Transferred NY-ESO-1 (c259)T Cells in Synovial Sarcoma. *Cancer Discov* 2018; **8**: 944-957 [PMID: 29891538 DOI: 10.1158/2159-8290.CD-17-1417]

66 **Lu YC**, Parker LL, Lu T, Zheng Z, Toomey MA, White DE, Yao X, Li YF, Robbins PF, Feldman SA, van der Bruggen P, Klebanoff CA, Goff

SL, Sherry RM, Kammula US, Yang JC, Rosenberg SA. Treatment of Patients With Metastatic Cancer Using a Major Histocompatibility Complex Class II-Restricted T-Cell Receptor Targeting the Cancer Germline Antigen MAGE-A3. *J Clin Oncol* 2017; **35**: 3322-3329 [PMID: 28809608 DOI: 10.1200/JCO.2017.74.5463]

67 **Wang M**, Gao P, Ren L, Duan J, Yang S, Wang H, Sun J, Gao X, Li B, Li S, Su W. Profiling the peripheral blood T cell receptor repertoires of gastric cancer patients. *Front Immunol* 2022; **13**: 848113 [PMID: 35967453 DOI: 10.3389/fimmu.2022.848113]

68 **Eshhar Z**, Waks T, Gross G, Schindler DG. Specific activation and targeting of cytotoxic lymphocytes through chimeric single chains consisting of antibody-binding domains and the gamma or zeta subunits of the immunoglobulin and T-cell receptors. *Proc Natl Acad Sci U S A* 1993; **90**: 720-724 [PMID: 8421711 DOI: 10.1073/pnas.90.2.720]

69 **Jaspers JE**, Brentjens RJ. Development of CAR T cells designed to improve antitumor efficacy and safety. *Pharmacol Ther* 2017; **178**: 83-91 [PMID: 28342824 DOI: 10.1016/j.pharmthera.2017.03.012]

70 **Kalos M**, Levine BL, Porter DL, Katz S, Grupp SA, Bagg A, June CH. T cells with chimeric antigen receptors have potent antitumor effects and can establish memory in patients with advanced leukemia. *Sci Transl Med* 2011; **3**: 95ra73 [PMID: 21832238 DOI: 10.1126/scitranslmed.3002842]

71 **Sotoudeh M**, Shirvani SI, Merat S, Ahmadbeigi N, Naderi M. MSLN (Mesothelin), ANTXR1 (TEM8), and MUC3A are the potent antigenic targets for CAR T cell therapy of gastric adenocarcinoma. *J Cell Biochem* 2019; **120**: 5010-5017 [PMID: 30260046 DOI: 10.1002/jcb.27776]

72 **Bębnowska D**, Grywalska E, Niedźwiedzka-Rystwej P, Sosnowska-Pasiarska B, Smok-Kalwat J, Pasiarski M, Góźdź S, Roliński J, Polkowski W. CAR-T Cell Therapy-An Overview of Targets in Gastric Cancer. *J Clin Med* 2020; **9** [PMID: 32560392 DOI: 10.3390/jcm9061894]

73 **Liu Y**, Cheng Y, Xu Y, Wang Z, Du X, Li C, Peng J, Gao L, Liang X, Ma C. Increased expression of programmed cell death protein 1 on NK cells inhibits NK-cell-mediated anti-tumor function and indicates poor prognosis in digestive cancers. *Oncogene* 2017; **36**: 6143-6153 [PMID: 28692048 DOI: 10.1038/onc.2017.209]

74 **Rosso D**, Rigueiro MP, Kassab P, Ilias EJ, Castro OA, Novo NF, Lourenço LG. [Correlation of natural killer cells with the prognosis of gastric adenocarcinoma]. *Arq Bras Cir Dig* 2012; **25**: 114-117 [PMID: 23381755 DOI: 10.1590/s0102-67202012000200011]

75 **Abdolahi S**, Ghazvinian Z, Muhammadnejad S, Ahmadvand M, Aghdaei HA, Ebrahimi-Barough S, Ai J, Zali MR, Verdi J, Baghaei K. Adaptive NK Cell Therapy Modulated by Anti-PD-1 Antibody in Gastric Cancer Model. *Front Pharmacol* 2021; **12**: 733075 [PMID: 34588986 DOI: 10.3389/fphar.2021.733075]

76 **Klapdor R**, Wang S, Hacker U, Büning H, Morgan M, Dörk T, Hillemanns P, Schambach A. Improved Killing of Ovarian Cancer Stem Cells by Combining a Novel Chimeric Antigen Receptor-Based Immunotherapy and Chemotherapy. *Hum Gene Ther* 2017; **28**: 886-896 [PMID: 28836469 DOI: 10.1089/hum.2017.168]

77 **Zhang Q**, Zhang H, Ding J, Liu H, Li H, Lu M, Miao Y, Li L, Zheng J. Combination Therapy with EpCAM-CAR-NK-92 Cells and Regorafenib against Human Colorectal Cancer Models. *J Immunol Res* 2018; **2018**: 4263520 [PMID: 30410941 DOI: 10.1155/2018/4263520]

78 **Klapdor R**, Wang S, Morgan M, Dörk T, Hacker U, Hillemanns P, Büning H, Schambach A. Characterization of a Novel Third-Generation Anti-CD24-CAR against Ovarian Cancer. *Int J Mol Sci* 2019; **20** [PMID: 30717444 DOI: 10.3390/ijms20030660]

79 **Jiang J**, Xu N, Wu C, Deng H, Lu M, Li M, Xu B, Wu J, Wang R, Xu J, Nilsson-Ehle P. Treatment of advanced gastric cancer by chemotherapy combined with autologous cytokine-induced killer cells. *Anticancer Res* 2006; **26**: 2237-2242 [PMID: 16821594]

80 **Jiang JT**, Shen YP, Wu CP, Zhu YB, Wei WX, Chen LJ, Zheng X, Sun J, Lu BF, Zhang XG. Increasing the frequency of CIK cells adoptive immunotherapy may decrease risk of death in gastric cancer patients. *World J Gastroenterol* 2010; **16**: 6155-6162 [PMID: 21182234 DOI: 10.3748/wjg.v16.i48.6155]

81 **Hontscha C**, Borck Y, Zhou H, Messmer D, Schmidt-Wolf IG. Clinical trials on CIK cells: first report of the international registry on CIK cells (IRCC). *J Cancer Res Clin Oncol* 2011; **137**: 305-310 [PMID: 20407789 DOI: 10.1007/s00432-010-0887-7]

82 **Hu G**, Zhong K, Wang S, Ding Q, Xu F, Chen W, Cheng P, Huang L. Cellular immunotherapy plus chemotherapy ameliorates survival in gastric cancer patients: a meta-analysis. *Int J Clin Oncol* 2020; **25**: 1747-1756 [PMID: 32728865 DOI: 10.1007/s10147-020-01750-6]

83 **Sterner RC**, Sterner RM. CAR-T cell therapy: current limitations and potential strategies. *Blood Cancer J* 2021; **11**: 69 [PMID: 33824268 DOI: 10.1038/s41408-021-00459-7]

84 **Zhao Q**, Jiang Y, Xiang S, Kaboli PJ, Shen J, Zhao Y, Wu X, Du F, Li M, Cho CH, Li J, Wen Q, Liu T, Yi T, Xiao Z. Engineered TCR-T Cell Immunotherapy in Anticancer Precision Medicine: Pros and Cons. *Front Immunol* 2021; **12**: 658753 [PMID: 33859650 DOI: 10.3389/fimmu.2021.658753]

85 **Ishikawa T**, Okayama T, Sakamoto N, Ideno M, Oka K, Enoki T, Mineno J, Yoshida N, Katada K, Kamada K, Uchiyama K, Handa O, Takagi T, Konishi H, Kokura S, Uno K, Naito Y, Itoh Y. Phase I clinical trial of adoptive transfer of expanded natural killer cells in combination with IgG1 antibody in patients with gastric or colorectal cancer. *Int J Cancer* 2018; **142**: 2599-2609 [PMID: 29388200 DOI: 10.1002/ijc.31285]

86 **Wang S**, Sun J, Chen K, Ma P, Lei Q, Xing S, Cao Z, Sun S, Yu Z, Liu Y, Li N. Perspectives of tumor-infiltrating lymphocyte treatment in solid tumors. *BMC Med* 2021; **19**: 140 [PMID: 34112147 DOI: 10.1186/s12916-021-02006-4]

87 **Zhang D**, He W, Wu C, Tan Y, He Y, Xu B, Chen L, Li Q, Jiang J. Scoring System for Tumor-Infiltrating Lymphocytes and Its Prognostic Value for Gastric Cancer. *Front Immunol* 2019; **10**: 71 [PMID: 30761139 DOI: 10.3389/fimmu.2019.00071]

88 **Mazloom A**, Ghalehsari N, Gazivoda V, Nimkar N, Paul S, Gregos P, Rateshwar J, Khan U. Role of Immune Checkpoint Inhibitors in Gastrointestinal Malignancies. *J Clin Med* 2020; **9** [PMID: 32781500 DOI: 10.3390/jcm9082533]

89 **Xu-Monette ZY**, Zhang M, Li J, Young KH. PD-1/PD-L1 Blockade: Have We Found the Key to Unleash the Antitumor Immune Response? *Front Immunol* 2017; **8**: 1597 [PMID: 29255458 DOI: 10.3389/fimmu.2017.01597]

90 **Strome SE**, Dong H, Tamura H, Voss SG, Flies DB, Tamada K, Salomao D, Cheville J, Hirano F, Lin W, Kasperbauer JL, Ballman KV, Chen L. B7-H1 blockade augments adoptive T-cell immunotherapy for squamous cell carcinoma. *Cancer Res* 2003; **63**: 6501-6505 [PMID: 14559843]

91 **Curiel TJ**, Wei S, Dong H, Alvarez X, Cheng P, Mottram P, Krzysiek R, Knutson KL, Daniel B, Zimmermann MC, David O, Burow M, Gordon A, Dhurandhar N, Myers L, Berggren R, Hemminki A, Alvarez RD, Emilie D, Curiel DT, Chen L, Zou W. Blockade of B7-H1 improves myeloid dendritic cell-mediated antitumor immunity. *Nat Med* 2003; **9**: 562-567 [PMID: 12704383 DOI: 10.1038/nm863]

92 **Blank C**, Brown I, Peterson AC, Spiotto M, Iwai Y, Honjo T, Gajewski TF. PD-L1/B7H-1 inhibits the effector phase of tumor rejection by T cell receptor (TCR) transgenic CD8+ T cells. *Cancer Res* 2004; **64**: 1140-1145 [PMID: 14871849 DOI: 10.1158/0008-5472.can-03-3259]

93 **Schlößer HA**, Drebber U, Kloth M, Thelen M, Rothschild SI, Haase S, Garcia-Marquez M, Wennhold K, Berlth F, Urbanski A, Alakus H, Schauss A, Shimabukuro-Vornhagen A, Theurich S, Warnecke-Ebertz U, Stippel DL, Zippelius A, Büttner R, Hallek M, Hölscher AH, Zander T, Mönig SP, von Bergwelt-Baildon M. Immune checkpoints programmed death 1 ligand 1 and cytotoxic T lymphocyte associated molecule 4

in gastric adenocarcinoma. *Oncoimmunology* 2016; **5**: e1100789 [PMID: 27467911 DOI: 10.1080/2162402X.2015.1100789]

94 **Kim JW**, Nam KH, Ahn SH, Park DJ, Kim HH, Kim SH, Chang H, Lee JO, Kim YJ, Lee HS, Kim JH, Bang SM, Lee JS, Lee KW. Prognostic implications of immunosuppressive protein expression in tumors as well as immune cell infiltration within the tumor microenvironment in gastric cancer. *Gastric Cancer* 2016; **19**: 42-52 [PMID: 25424150 DOI: 10.1007/s10120-014-0440-5]

95 **Bang YJ**, Ruiz EY, Van Cutsem E, Lee KW, Wyrwicz L, Schenker M, Alsina M, Ryu MH, Chung HC, Evesque L, Al-Batran SE, Park SH, Lichinitser M, Boku N, Moehler MH, Hong J, Xiong H, Hallwachs R, Conti I, Taieb J. Phase III, randomised trial of avelumab versus physician's choice of chemotherapy as third-line treatment of patients with advanced gastric or gastro-oesophageal junction cancer: primary analysis of JAVELIN Gastric 300. *Ann Oncol* 2018; **29**: 2052-2060 [PMID: 30052729 DOI: 10.1093/annonc/mdy264]

96 **Moehler M**, Dvorkin M, Boku N, Özgüroğlu M, Ryu MH, Muntean AS, Lonardi S, Nechaeva M, Bragagnoli AC, Coşkun HS, Cubillo Gracian A, Takano T, Wong R, Safran H, Vaccaro GM, Wainberg ZA, Silver MR, Xiong H, Hong J, Taieb J, Bang YJ. Phase III Trial of Avelumab Maintenance After First-Line Induction Chemotherapy Versus Continuation of Chemotherapy in Patients With Gastric Cancers: Results From JAVELIN Gastric 100. *J Clin Oncol* 2021; **39**: 966-977 [PMID: 33197226 DOI: 10.1200/JCO.20.00892]

97 **Fuchs CS**, Özgüroğlu M, Bang YJ, Di Bartolomeo M, Mandala M, Ryu MH, Fornaro L, Olesinski T, Caglevic C, Chung HC, Muro K, Van Cutsem E, Elme A, Thuss-Patience P, Chau I, Ohtsu A, Bhagia P, Wang A, Shih CS, Shitara K. Pembrolizumab versus paclitaxel for previously treated PD-L1-positive advanced gastric or gastroesophageal junction cancer: 2-year update of the randomized phase 3 KEYNOTE-061 trial. *Gastric Cancer* 2022; **25**: 197-206 [PMID: 34468869 DOI: 10.1007/s10120-021-01227-z]

98 **Chao J**, Fuchs CS, Shitara K, Tabernero J, Muro K, Van Cutsem E, Bang YJ, De Vita F, Landers G, Yen CJ, Chau I, Elme A, Lee J, Özgüroglu M, Catenacci D, Yoon HH, Chen E, Adelberg D, Shih CS, Shah S, Bhagia P, Wainberg ZA. Assessment of Pembrolizumab Therapy for the Treatment of Microsatellite Instability-High Gastric or Gastroesophageal Junction Cancer Among Patients in the KEYNOTE-059, KEYNOTE-061, and KEYNOTE-062 Clinical Trials. *JAMA Oncol* 2021; **7**: 895-902 [PMID: 33792646 DOI: 10.1001/jamaoncol.2021.0275]

99 **Xu J**, Bai Y, Xu N, Li E, Wang B, Wang J, Li X, Wang X, Yuan X. Tislelizumab Plus Chemotherapy as First-line Treatment for Advanced Esophageal Squamous Cell Carcinoma and Gastric/Gastroesophageal Junction Adenocarcinoma. *Clin Cancer Res* 2020; **26**: 4542-4550 [PMID: 32561664 DOI: 10.1158/1078-0432.CCR-19-3561]

100 **Peng Z**, Wei J, Wang F, Ying J, Deng Y, Gu K, Cheng Y, Yuan X, Xiao J, Tai Y, Wang L, Zou J, Zhang Y, Shen L. Camrelizumab Combined with Chemotherapy Followed by Camrelizumab plus Apatinib as First-line Therapy for Advanced Gastric or Gastroesophageal Junction Adenocarcinoma. *Clin Cancer Res* 2021; **27**: 3069-3078 [PMID: 33766817 DOI: 10.1158/1078-0432.CCR-20-4691]

101 **Sakai K**, Mori S, Kawamoto T, Taniguchi S, Kobori O, Morioka Y, Kuroki T, Kano K. Expression of epidermal growth factor receptors on normal human gastric epithelia and gastric carcinomas. *J Natl Cancer Inst* 1986; **77**: 1047-1052 [PMID: 3464796]

102 **Zhu Y**, Zhu X, Wei X, Tang C, Zhang W. HER2-targeted therapies in gastric cancer. *Biochim Biophys Acta Rev Cancer* 2021; **1876**: 188549 [PMID: 33894300 DOI: 10.1016/j.bbcan.2021.188549]

103 **Stein A**, Paschold L, Tintelnot J, Goekkurt E, Henkes SS, Simnica D, Schultheiss C, Willscher E, Bauer M, Wickenhauser C, Thuss-Patience P, Lorenzen S, Ettrich T, Riera-Knorrenschild J, Jacobasch L, Kretzschmar A, Kubicka S, Al-Batran SE, Reinacher-Schick A, Pink D, Sinn M, Lindig U, Hiegl W, Hinke A, Hegewisch-Becker S, Binder M. Efficacy of Ipilimumab vs FOLFOX in Combination With Nivolumab and Trastuzumab in Patients With Previously Untreated ERBB2-Positive Esophagogastric Adenocarcinoma: The AIO INTEGA Randomized Clinical Trial. *JAMA Oncol* 2022; **8**: 1150-1158 [PMID: 35737383 DOI: 10.1001/jamaoncol.2022.2228]

104 **Du XH**, Liu HL, Li L, Xia SY, Ning N, Zou ZY, Teng D, Xiao CH, Li R, Xu YX. Clinical significance of immunotherapy with combined three kinds of cells for operable colorectal cancer. *Tumour Biol* 2015; **36**: 5679-5685 [PMID: 25764087 DOI: 10.1007/s13277-015-3242-4]

105 **Cheng X**, Wang J, Qiu C, Jin Y, Xia B, Qin R, Hu H, Yan J, Zhang X, Xu J. Feasibility of iNKT cell and PD-1+CD8+ T cell-based immunotherapy in patients with lung adenocarcinoma: Preliminary results of a phase I/II clinical trial. *Clin Immunol* 2022; **238**: 108992 [PMID: 35367396 DOI: 10.1016/j.clim.2022.108992]

106 **Qiao G**, Wang X, Zhou L, Zhou X, Song Y, Wang S, Zhao L, Morse MA, Hobeika A, Song J, Yi X, Xia X, Ren J, Lyerly HK. Autologous Dendritic Cell-Cytokine Induced Killer Cell Immunotherapy Combined with S-1 Plus Cisplatin in Patients with Advanced Gastric Cancer: A Prospective Study. *Clin Cancer Res* 2019; **25**: 1494-1504 [PMID: 30514775 DOI: 10.1158/1078-0432.CCR-18-2360]

107 **Xu B**, Chen F, Zhang X, Wang Z, Che K, Wu N, Yu L, Fan X, Liu B, Wei J. Antigen-Specific T Cell Immunotherapy Targeting Claudin18.2 in Gastric Cancer. *Cancers (Basel)* 2022; **14** [PMID: 35681738 DOI: 10.3390/cancers14112758]

108 **Bré J**, Dickson AL, Read OJ, Zhang Y, McKissock FG, Mullen P, Tang P, Zickuhr GM, Czekster CM, Harrison DJ. The novel anti-cancer fluoropyrimidine NUC-3373 is a potent inhibitor of thymidylate synthase and an effective DNA-damaging agent. *Cancer Chemother Pharmacol* 2023; **91**: 401-412 [PMID: 37000221 DOI: 10.1007/s00280-023-04528-5]

109 **Somani VK**, Zhang D, Dodhiawala PB, Lander VE, Liu X, Kang LI, Chen HP, Knolhoff BL, Li L, Grierson PM, Ruzinova MB, DeNardo DG, Lim KH. IRAK4 Signaling Drives Resistance to Checkpoint Immunotherapy in Pancreatic Ductal Adenocarcinoma. *Gastroenterology* 2022; **162**: 2047-2062 [PMID: 35271824 DOI: 10.1053/j.gastro.2022.02.035]

110 **Wu P**, Wu D, Li L, Chai Y, Huang J. PD-L1 and Survival in Solid Tumors: A Meta-Analysis. *PLoS One* 2015; **10**: e0131403 [PMID: 26114883 DOI: 10.1371/journal.pone.0131403]

111 **Wang R**, Dang M, Harada K, Han G, Wang F, Pool Pizzi M, Zhao M, Tatlonghari G, Zhang S, Hao D, Lu Y, Zhao S, Badgwell BD, Blum Murphy M, Shanbhag N, Estrella JS, Roy-Chowdhuri S, Abdelhakeem AAF, Wang Y, Peng G, Hanash S, Calin GA, Song X, Chu Y, Zhang J, Li M, Chen K, Lazar AJ, Futreal A, Song S, Ajani JA, Wang L. Single-cell dissection of intratumoral heterogeneity and lineage diversity in metastatic gastric adenocarcinoma. *Nat Med* 2021; **27**: 141-151 [PMID: 33398161 DOI: 10.1038/s41591-020-1125-8]

112 **Sathe A**, Grimes SM, Lau BT, Chen J, Suarez C, Huang RJ, Poultsides G, Ji HP. Single-Cell Genomic Characterization Reveals the Cellular Reprogramming of the Gastric Tumor Microenvironment. *Clin Cancer Res* 2020; **26**: 2640-2653 [PMID: 32060101 DOI: 10.1158/1078-0432.CCR-19-3231]

113 **Salnikov M**, Prusinkiewicz MA, Lin S, Ghasemi F, Cecchini MJ, Mymryk JS. Tumor-Infiltrating T Cells in EBV-Associated Gastric Carcinomas Exhibit High Levels of Multiple Markers of Activation, Effector Gene Expression, and Exhaustion. *Viruses* 2023; **15** [PMID: 36680216 DOI: 10.3390/v15010176]

114 **Guan WL**, He Y, Xu RH. Gastric cancer treatment: recent progress and future perspectives. *J Hematol Oncol* 2023; **16**: 57 [PMID: 37245017 DOI: 10.1186/s13045-023-01451-3]



Published by **Baishideng Publishing Group Inc**
7041 Koll Center Parkway, Suite 160, Pleasanton, CA 94566, USA
Telephone: +1-925-3991568
E-mail: bpgoffice@wjgnet.com
Help Desk: https://www.f6publishing.com/helpdesk
https://www.wjgnet.com



© 2023 Baishideng Publishing Group Inc. All rights reserved.